IENCE
C
0
4

U. of ILL. LIBRARY
JAN 3 - 1973
CHICAGO CIRCLE

NUCLEAR SCIENCE ABSTRACTS

U. OF I. LIB.
DOCUMENTS
DEC 2 0 1972
CHICAGO CIRCLE

Volume 26 Number 22

Abstracts 52893-55642

November 30, 1972

UNITED STATES ATOMIC ENERGY COMMISSION

REPORT COLLECTIONS IN THE UNITED STATES

The libraries listed below purchase and maintain microfiche collections of USAEC and foreign reports that are abstracted in *NSA*. Their collections also include *NSA* and its indexes, AEC's Technical Progress Reviews, AEC-sponsored translations, conference proceedings published by AEC, and various bibliographic tools. Most of these libraries have microfiche reader-printers or other photocopy facilities with which to reproduce enlarged copies from microfiche. Charges for reproduction services vary.

ALABAMA
Auburn, Auburn University
Tuskegee Institute, Tuskegee Institute

ALASKA
College, University of Alaska

ARIZONA
Tucson, University of Arizona

CALIFORNIA
Davis, University of California
Los Angeles, University of California
Santa Barbara, University of California

COLORADO
Boulder, University of Colorado

DISTRICT OF COLUMBIA
Washington, Library of Congress

FLORIDA
Gainesville, University of Florida

GEORGIA
Atlanta, Georgia Institute of Technology

HAWAII
Honolulu, University of Hawaii

IDAHO
Pocatello, Idaho State University

ILLINOIS
Urbana, University of Illinois

INDIANA
Lafayette, Purdue University

IOWA
Ames, Iowa State University

KANSAS
Manhattan, Kansas State University

KENTUCKY
Lexington, University of Kentucky
Louisville, University of Louisville

MARYLAND
Baltimore, Johns Hopkins University
College Park, University of Maryland

MASSACHUSETTS
Cambridge, Massachusetts Institute of Technology
Worcester, Worcester Polytechnic Institute

MICHIGAN
Ann Arbor, University of Michigan

MISSISSIPPI
State College, Mississippi State University

MISSOURI
Columbia, University of Missouri
Kansas City, Linda Hall Library

NEW JERSEY
Princeton, Princeton University

NEW MEXICO
Albuquerque, University of New Mexico

NEW YORK
Albany, New York State Library
Albany, State University at Albany
Ithaca, Cornell University
New York, Columbia University
Rochester, University of Rochester
Syracuse, Syracuse University
Troy, Rensselaer Polytechnic Institute

NORTH CAROLINA
Raleigh, North Carolina State University

OHIO
Cincinnati, University of Cincinnati
Cleveland, Cleveland Public Library

OHIO (Continued)
Columbus, Ohio State University
Toledo, University of Toledo

OKLAHOMA
Norman, University of Oklahoma

PENNSYLVANIA
Philadelphia, University of Pennsylvania
Pittsburgh, Carnegie Library
University Park, Pennsylvania State University

PUERTO RICO
San Juan, University of Puerto Rico

SOUTH CAROLINA
Columbia, University of South Carolina

TENNESSEE
Knoxville, University of Tennessee
Nashville, Joint University Libraries

TEXAS
Austin, University of Texas
College Station, Texas A & M University
Houston, Rice University

UTAH
Salt Lake City, University of Utah

VIRGINIA
Blacksburg, Virginia Polytechnic Institute
Charlottesville, University of Virginia

WASHINGTON
Pullman, Washington State University
Seattle, University of Washington

WEST VIRGINIA
Morgantown, West Virginia University

WISCONSIN
Madison, University of Wisconsin

The following governmental and international organizations offer for sale USAEC reports abstracted in *Nuclear Science Abstracts:*

National Technical Information Service, U. S. Department of Commerce
Springfield, Virginia 22151
International Atomic Energy Agency, Vienna, Austria
National Lending Library, Boston Spa, England

Volume 26, Number 22, November 30, 1972

NUCLEAR SCIENCE ABSTRACTS

A semimonthly publication of the USAEC Office of Information Services, John A. Harris, Director. Published by the USAEC Technical Information Center, Robert L. Shannon, Manager.

Nuclear Science Abstracts provides the only comprehensive abstracting and indexing coverage of international nuclear science literature. *Nuclear Science Abstracts* covers scientific and technical reports of the U. S. Atomic Energy Commission and its contractors, other U. S. Government agencies, other governments, universities, and industrial and research organizations. In addition, books, conference proceedings, individual conference papers, patents, and journal literature on a worldwide basis are abstracted and indexed. Each issue of *Nuclear Science Abstracts* includes four indexes: subject, personal author, corporate author, and report number.

The following organizations scan and abstract the nuclear science literature in their respective countries:

Atomic Energy of Canada Limited
Australian Atomic Energy Commission
Danish Atomic Energy Commission
Finnish Atomic Energy Commission
French Atomic Energy Commission
Japan Atomic Energy Bureau—Atomic Energy Research Institute
Institutt for Atomenergi (Norway)
Aktiebolaget Atomenergi (Sweden)
United Kingdom Atomic Energy Authority
Zentralstelle für Atomkernenergie-Dokumentation (West Germany)

Numerous organizations, societies, and publishers throughout the world provide *Nuclear Science Abstracts* with advance page-proof copy of their publications, e.g., in the United States the American Institute of Physics provides page-proof copy of its publications.

A list of the journals scanned regularly and the abbreviations used appears in Issue 1 (January 15) of each volume of *Nuclear Science Abstracts* and is supplemented in Issues 7, 13, and 19. Issue 1 of each volume also describes the scope and arrangement of the subject matter covered in *Nuclear Science Abstracts.* The subject matter covered is also described in TID-4552, *Subject Scope of Nuclear Science Abstracts,* available free from the USAEC Technical Information Center, P. O. Box 62, Oak Ridge, Tennessee 37830. An outline of the subject categories appears in the Contents of each issue.

AVAILABILITY OF PUBLICATIONS ABSTRACTED

Public availability of all U. S. Atomic Energy Commission reports is indicated in the report number indexes. The availability of other reports, when known, is also indicated. The availability of some unnumbered reports is given in the abstract.

Dissertations abstracted in *Dissertation Abstracts International, Part B* and included in *Nuclear Science Abstracts* are available from University Microfilms, Inc., 315 N. First Street, Ann Arbor, Michigan 48103.

Information on the availability of the published literature and unpublished conference papers abstracted in *Nuclear Science Abstracts* can be obtained from the USAEC Technical Information Center, P. O. Box 62, Oak Ridge, Tennessee 37830.

HOW TO OBTAIN NUCLEAR SCIENCE ABSTRACTS

Nuclear Science Abstracts is available to the public on a subscription basis from the Superintendent of Documents, U. S. Government Printing Office, Washington, D. C. 20402.

For the 24 regular issues, the yearly rate is $42.00 for domestic subscribers and $52.50 for foreign subscribers. A single issue costs $1.75, domestic rates, or $2.19, foreign rates. Domestic rates apply to the United States, Canada, Mexico, and Central and South American countries except Argentina, Brazil, Guyana, French Guiana, Surinam, and British Honduras.

For a yearly subscription to the cumulative indexes, the rates are $34.50 for domestic subscribers and $43.00 for foreign subscribers.

The following cumulative indexes are available:

From Johnson Reprint Corporation, 111 Fifth Avenue, New York, N. Y. 10003:
Vols. 1–4, Subjects and Authors (1948–1950), $30.00.

From Superintendent of Documents, U. S. Government Printing Office, Washington, D. C. 20402:

Vols. 5–10, Subjects and Authors (1951–1956), $5.25.

Vols. 11–15, Subjects (1957–1961), $19.00.
Vols. 11–15, Personal Authors (1957–1961), $14.25.
Vols. 11–15, Corporate Authors (1957–1961), $2.50.

Vols. 16–20, Subjects (1962–1966), $36.00.
Vols. 16–20, Personal Authors (1962–1966), $22.50.
Vols. 16–20, Corporate Authors (1962–1966), $3.75.

Vol. 21, Subjects and Authors (1967), $16.00.
Vol. 22, Subjects and Authors (1968), $26.00.
Vol. 23, Subjects and Authors (1969), $25.75.
Vol. 24, Subjects and Authors (1970), $22.50.
Vol. 24, Authors (1970), Suppl., $2.00.
Vol. 25, Subjects and Authors (1971), $27.50.

Cumulative Report Number Index, Vols. 1–15 Revised, $4.00.
Cumulative Report Number Index, Vols. 16–20 Revised, $5.50.
Cumulative Report Number Index, Vols. 21–25, $5.75.

Nuclear Science Abstracts is available on an exchange basis to universities, research institutions, industrial firms, and publishers of scientific information. Government agencies may obtain *NSA* free of charge. Inquiries should be directed to the USAEC Technical Information Center, P. O. Box 62, Oak Ridge, Tennessee 37830.

Nuclear Science Abstracts is also available on 16-mm and 35-mm microfilm in reel or cartridge from Princeton Microfilm Corporation, Alexander Road, Princeton, New Jersey 08540. The cost of Vols. 1–24 (1948–1970) including *Abstracts of Declassified Documents* (1947–1948) is $625.20. The indexes for *Nuclear Science Abstracts* Vols. 1–24 (1948–1970) are also available for $320.00. The cost of each volume (one calendar year) of *NSA* and its indexes, including that for the year 1971, is $95.

INDEXES TO NSA

Comprehensive indexes appear in each issue and are cumulated quarterly and annually. Multivolume cumulations have been issued as indicated above.

All documents abstracted are indexed by subjects and personal authors. Report literature is indexed also by corporate author and report number. Each of these indexes in every issue is preceded by an introduction explaining in detail the organization of the index and the principles by which it is compiled. The reader is referred to these explanations for information not found in the brief summary below.

Personal Authors

Each author's name is indexed in the form appearing on the document abstracted:

NEWCOMB, William A., Stability of a magnetic well, 25:1239
NEWKIRK, L. R., Superconductivity in the pseudobinary alloys V_3Si--Nb_3Al, 25:1093 (CALT-822-13)
NEWLAND, E. A., Radiation treatment of sewage, 25:140 (AAEC/LIB/Bib-254)

Subjects

The subject index consisting of specific materials, objects, and processes is arranged alphabetically. Modifying phrases specific to these subjects in turn are arranged alphabetically under the subjects.

TRANSURANIUM ELEMENTS
  determination in bone ash, radiochemical method for, 25:40 (IDO-12073, pp 28-36)
  separation by ion exchange and complex-formation elution, 25:251(P)

TRIETHYLENETETRAMINE
  complexes with cobalt(III) and rhodium(III) chlorides, radiation effects on labeled, thermal-neutron, 25:137
TRITIUM
  content in Cattaraugus Creek near West Valley Processing Plant, July through Dec. 1969, 25:258 (DOCKET-50201-48)
  content in Cattaraugus Creek near West Valley Processing Plant, Jan. to July 1970, 25:259 (DOCKET-50201-49)
  determination in luminescent material by scintillation ccunting, 25:40 (IDO-12073, pp 28-36)

Corporate Authors

Technical report literature is indexed from the name of the organization or institution responsible for the issuance of the report.

372 (UCRL-72739) CONSTRUCTION OF A UNIQUE UNDERGROUND WHOLE BODY COUNTER. Griffith, R. V.; Anderson, A. L.; Lindeken, C. L. **(California Univ., Livermore. Lawrence Radiation Lab.).** Oct 1970. 27p. (CONF-701009-1). Dep. NTIS.

is indexed as:

CALIFORNIA UNIV., LIVERMORE. LAWRENCE RADIATION LAB.
  Construction cf a unique underground whole body counter, 25:372 (UCRL-72739)

Report Numbers

Technical report literature is also indexed by report numbers. This index includes information on where individual reports may be obtained. While not reports, patents and conference papers are indexed here as a matter of convenience.

ORNL-		
4270(Vol.2)	25-614	Dep. NTIS
4606	25-1530	Dep. NTIS
ORNL-IBP-		
70-3	25-2025	Dep. NTIS
ORNL-IIC-		
21	25-261	Dep. NTIS
30(Pt.2)	25-331	Dep. NTIS
ORNL-NSIC-		
78	25-1912	Dep. NTIS

TABLE OF CONTENTS

Volume 26, Number 22, November 30, 1972

Category — *Page*

- **CHEMISTRY** 5081
  - Analytical Chemistry 5081
    - *Activation and Nuclear Reaction Procedures* 5081
    - *Chemical and Spectral Procedures* 5083
    - *Radiometric and Radiochemical Procedures* 5085
    - *Separation Procedures* 5086
  - Inorganic, Organic, and Physical Chemistry 5087
    - *Chemical and Physico-chemical Properties* 5087
    - *Isotope Effects* 5087
    - *Isotope Exchange and Isotope Separation* 5088
    - *Feed Materials Processing* 5089
  - Radiation Chemistry 5089
  - Radiochemistry and Nuclear Chemistry 5094
    - *Hot-Atom Chemistry* 5094
    - *Properties of Radioactive Materials* 5094
    - *Radioactive Waste Treatment* 5096
    - *Radioisotope Production* 5098
    - *Reactor Fuel Reprocessing* 5099

- **ENGINEERING** 5101
  - Energy Conversion 5101
  - Facilities and Equipment 5103
  - Heat Transfer and Fluid Flow 5104
  - Materials Testing 5104
  - Nuclear Explosions 5105
  - Protective Structures and Equipment 5106
  - Safety Engineering 5106
  - Vacuum Engineering 5106

- **ENVIRONMENTAL AND EARTH SCIENCES** 5107
  - Minerals and Ores 5107
  - Radioactive Effluents 5107
  - Radioactivity Transport and Monitoring 5107
    - *Atmosphere* 5108
    - *Soil* 5109
    - *Water* 5109
    - *Ecosystems and Food Cycles* 5110
  - Radiometric Techniques 5110
  - Thermal Effluents 5111

- **INSTRUMENTATION** 5113
  - Radiation Detection Instruments 5113
    - *General Detectors and Monitors* 5113
    - *Radiation Dosimeters* 5116
    - *Nuclear Spectroscopic Instrumentation* 5119
    - *High Energy Physics Instrumentation* 5120
  - Radiometric Instruments 5122
  - Radiation Effects on Instrument Components, Instruments, and Electronic Systems 5122
  - Miscellaneous Instruments and Components 5123

- **ISOTOPE AND RADIATION SOURCE TECHNOLOGY** 5127
  - Isotope Separation (Industrial) 5127
  - Isotopic Power Sources 5127
  - Radiation Sources 5128
    - *Industrial Uses* 5128

Category — *Page*

- **LIFE SCIENCES** 5130
  - Radiation Effects on Biochemicals (External Source) 5130
  - Radiation Effects on Cells (External Source) 5130
  - Radiation Effects on Microorganisms (External Source) 5132
  - Radiation Effects on Plants (External Source) 5134
  - Radiation Effects on Animals (External Source) 5135
    - *Man* 5136
    - *Vertebrates* 5141
    - *Invertebrates* 5147
  - Radionuclide Effects (Internal Source) 5148
    - *Man* 5148
    - *Animals* 5149
    - *Microorganisms* 5150
  - Nuclide Kinetics and Toxicology 5150
    - *Man* 5150
    - *Animals* 5151
    - *Plants* 5152
  - New Tracer Techniques 5153

- **MATERIALS** 5154
  - Ceramics and Cermets 5154
  - Metals and Alloys 5160
    - *Corrosion and Erosion* 5160
    - *Preparation and Fabrication* 5161
    - *Properties, Structure, and Phase Studies* 5164
    - *Radiation Effects* 5170
  - Other Materials 5172

- **NUCLEAR MATERIALS AND WASTE MANAGEMENT** 5174
  - Accountability and Safeguards 5174
  - Disposal and Storage 5174
  - Handling Equipment and Procedures 5174
  - Transportation 5175

- **PARTICLE ACCELERATORS** 5176
  - Design, Development, and Operation 5176
  - Auxiliaries and Components 5176
  - Ion Sources, Injection, and Extraction 5177
  - Ion Optics and Field Calculations 5177
  - Storage Rings 5178
  - Experimental Facilities 5179

- **PHYSICS (ASTROPHYSICS AND COSMOLOGY)** 5182
  - Cosmic Radiation 5182
  - Stars 5190
  - Quasi-Stellar, Radio, and X-Ray Sources 5194
  - Solar Phenomena 5196
  - Galaxies 5200
  - Cosmology 5203
  - Planetary Phenomena 5203

- **PHYSICS (ATMOSPHERIC)** 5205
  - Auroral and Ionospheric Phenomena 5205
  - Effects of Nuclear Detonations 5209
  - Particle Kinetics and Trapping 5209
  - Solar Wind and Cosmic Ray Interactions 5211

TABLE OF CONTENTS (continued)

Category *Page*

PHYSICS (ATOMIC AND MOLECULAR) 5214
  Atomic, Electron, Ion, and Molecular Beams and Their Reactions 5214
  Atomic and Molecular Properties 5215
  Positronium, Muonium, and Mesic Atoms and Molecules 5215
  Collision Phenomena 5216
  Atomic Theory 5220

PHYSICS (ELECTROFLUID AND MAGNETOFLUID) . . 5223

PHYSICS (HIGH-ENERGY) 5224
  Particle Interactions and Properties (Experimental) . . . 5224
    Electromagnetic 5224
    Weak 5225
    Strong (Baryon-induced) 5226
    Strong (Meson-induced) 5227
  Particle Interactions and Properties (Theoretical) 5230
    General 5230
    Electromagnetic 5231
    Weak 5234
    Strong (General) 5236
    Strong (Baryon No. = 0) 5237
    Strong (Baryon No. = 1) 5238
    Strong (Baryon No. ≥ 2) 5239
  Particle Invariance Principles and Symmetries 5240
    General 5240
    Applications (Electromagnetic and Weak) 5241
    Applications (Strong) 5241
  Field Theories 5242
    General 5242
    Quantum Field Theory 5242
    Gravitation and General Relativity 5243
    Scattering Theory 5245

PHYSICS (LOW-TEMPERATURE) 5247
  Superfluidity 5247
  Superconductivity 5248
  Equipment and Devices 5250

PHYSICS (NUCLEAR) 5252
  Neutron Interactions with Matter 5252
  Nuclear Properties and Reactions, A ≤ 5 5255
  Nuclear Properties and Reactions, 6 ≤ A ≤ 19 5257
  Nuclear Properties and Reactions, 20 ≤ A ≤ 38 5259
  Nuclear Properties and Reactions, 39 ≤ A ≤ 58 5260
  Nuclear Properties and Reactions, 59 ≤ A ≤ 89 5262
  Nuclear Properties and Reactions, 90 ≤ A ≤ 149 5263
  Nuclear Properties and Reactions, 150 ≤ A ≤ 189 . . . 5266
  Nuclear Properties and Reactions, 190 ≤ A ≤ 219 . . . 5267
  Nuclear Properties and Reactions, A ≥ 220 5268
  Nuclear Theory 5270

PHYSICS (PLASMA AND THERMONUCLEAR) 5277
  Confinement and Heating 5277
  Diagnostics 5277
  Kinetics (General) 5279
  Kinetics (Experimental) 5280
  Kinetics (Theoretical) 5280
  Production 5281
  Stability 5281
  Thermonuclear Processes 5283
  Wave Phenomena 5284

Category *Page*

PHYSICS (RADIATION AND SHIELDING) 5289
  Radiation Physics 5289
  Radiation Protection Standards 5293
  Radiation Source Calibration and Standardization . . . 5296
  Shielding Calculations and Theory 5296

PHYSICS (SOLID-STATE) 5301
  Radiation Effects 5301
  Physical Properties 5306
  Moessbauer Effects and NMR 5309
  Theory 5310

PHYSICS (THEORETICAL) 5311

REACTOR TECHNOLOGY 5313
  Power Reactor Development 5313
    Physics and Core Engineering 5314
    Control and Instrumentation 5317
    Containment Systems, Waste Processing, and Radiation Protection 5318
    Coolant System 5319
    Fuels and Fuel Elements 5322
    Auxiliary Systems and Engineered Safeguards 5324
    Operation and Economics 5324
    Safety and Siting 5324
    Steam and Power Conversion System 5325
  Commercial Power Reactors 5325
    Control and Instrumentation 5326
    Containment Systems, Waste Processing, and Radiation Protection 5326
    Coolant System 5326
    Fuels and Fuel Elements 5327
    Auxiliary Systems and Engineered Safeguards 5327
    Operation and Economics 5327
    Safety and Siting 5329
  Propulsion and Auxiliary Power Reactors 5332
  Process Heat and Desalination Reactors 5335
  Research and Test Reactors 5335
  Reactor Components, Fuels, and Accessories 5339
  Reactor Physics and Core Engineering 5339
    Physics 5340
    Core Thermal Hydraulics 5342

GENERAL 5343
  Law 5343
  Miscellaneous 5344

CORPORATE AUTHOR INDEX INDEX-1

PERSONAL AUTHOR INDEX INDEX-16

SUBJECT INDEX INDEX-78

REPORT NUMBER INDEX INDEX-182

STAFF OF NUCLEAR SCIENCE ABSTRACTS

John W. Norris
Managing Editor

Donald D. Davis
Assistant Managing Editor

David E. Bost
Production Manager

Sidney F. Lanier
Subject Heading Specialist

J. Paul Meredith
Descriptive Cataloging Specialist

Frederick E. Marsh, Jr.
Computer Index Coordinator

Clara L. Fox
Corporate Author Specialist

Helen W. White
Report Number Specialist

Section Editors

Donald D. Davis
Life Sciences

Everett J. Hoffman
Chemistry

James M. Jacobs
Reactor Technology

Robert C. Kelly
Engineering; Environmental and Earth Sciences; Isotope and Radiation Source Technology; Materials; Nuclear Materials and Waste Management

Charles E. Stuber
Instrumentation; Particle Accelerators; High Energy Physics; Theoretical Physics

Lee M. Thompson
Astrophysics and Cosmology; Atmospheric Physics; Atomic and Molecular Physics; Electrofluid and Magnetofluid Physics; Low Temperature Physics; Plasma and Thermonuclear Physics; Radiation and Shielding Physics; Solid State Physics

Lawrence T. Whitehead
Nuclear Physics

Evaluators

Thomas S. Chapman
John H. Mitchell
Mary H. Newman
Polly C. Summers

Abstractors

Ellis R. Bedford
Jane G. Buchanan
D. Lamar Cason
David C. Cunningham
Theodore F. Davis
James R. Dulaney
Helga B. Gerstner
Mary C. Grissom
Phyllis C. Hansen
Carolyn D. Houston
W. Hugh Kinser, Jr.
Lisbeth C. Lieberman
William D. Matheny
Dora H. Moneyhun
Jean F. Peckham
Henry D. Raleigh
Mona H. Raridon
Julia S. Redford
Jessie W. Rushing
Robert W. Rutkowski
Francis L. Sachs
Lila B. Smith
Anne G. Ward
Helen L. Ward
Kenneth S. Warren
Milton O. Whitson
Juanita Wilson

Charles R. Bruce
Publishing Coordinator

Communication concerning the editorial policy and content of *Nuclear Science Abstracts* should be addressed to the Managing Editor, *Nuclear Science Abstracts*, USAEC Technical Information Center, P. O. Box 62, Oak Ridge, Tennessee 37830.

Use of funds for printing this publication approved by the Director of the Office of Management and Budget, June 19, 1972.

Volume 26, Number 22 November 30, 1972

NUCLEAR SCIENCE ABSTRACTS

CHEMISTRY

52893 (EUR–4765) 2nd CONFERENCE ON MASS SPECTROMETRY, ISPRA, ITALY, 1–3 SEPTEMBER 1971. Facchetti, Sergio (comp.) (European Atomic Energy Community, Luxembourg. Center for Information and Documentation). Nov 1971. 485p. (In several languages). (CONF-710957).

Separate abstracts were prepared for 7 of the 26 papers included. The remaining 19 papers are outside the scope of NSA. (J.W.R.)

For abstracts of individual papers see: 52916–52918, 52982, 53033, 53549, and 54495.

Analytical Chemistry

Refer also to abstracts 53027, 53109, 53211, 53287, and 53330.

Activation and Nuclear Reaction Procedures

Refer also to abstracts 53121, 53212, and 53217.

52894 (CEA-R–4338) MANUFACTURE AND ANALYSIS OF SINGLE CRYSTALS OF LABELED LITHIUM HYDRIDE. Guerin, Danielle; Lefevre, Hubert (Commissariat a l'Energie Atomique, Bruyeres-le-Chatel (France). Centre d'Etudes). Jun 1972. 34p. (In French). Dep. NTIS (U. S. Sales Only).

The homogeneity of lithium hydride single crystals produced by hydrogen and lithium synthesis was investigated. The effect of freezing on the segregation of impurities was studied. Two testing methods were used: the introduction of radioactive tracers in fused Li, and the activation analysis of impurities. (France)

52895 (CONF-710959–, Paper 18) BEHAVIOUR OF FISSION AND CORROSION PRODUCTS IN SODIUM. Davies, R. A. 9p.

From Meeting on fission and corrosion product behaviour in primary systems of LMFBR's; Bensberg, Germany (20 Sep 1971).

A method for studying the solubility of elements in liquid sodium is described. A known amount of neutron activated solute in a capsule containing liquid sodium is monitored. The amount of solute actually in solution is determined by comparing the activity of the solute in the region of an absolute with that in the rest of the capsule. (J.M.J.)

52896 (CONF-720920–2) RELIABILITY IN SCIENTIFIC EVIDENCE BASED ON MULTI-TRACE FORENSIC NAA. Lyon, W. S.; Ricci, E.; Bate, L. C.; Dyer, F. F. (Oak Ridge National Lab., Tenn.). 1972. 9p. Dep. NTIS.

From 2nd international conference on forensic activation analysis; Glasgow, Scotland (27 Sep 1972).

Neutron activation analysis has been accepted in the courts and successfully used in a number of trials. Some individualistic solutions (such as hair) that once appeared to offer an easy road to criminal identification and prosecution are now viewed more realistically. It is in these areas that more care must be taken. Biological material, such as blood and hair, and many inhomogeneous organic-inorganic mixtures, such as soil, may never be amenable to complete identification by neutron activation. (auth)

52897 (CONF-721010–3) ANALYSIS OF TRACES AT ORNL'S NEW HIGH-FLUX NEUTRON ACTIVATION LABORATORY. Ricci, Enzo; Handley, T. H.; Dyer, F. F. (Oak Ridge National Lab., Tenn.). 1972. 11p. Dep. NTIS.

From International conference on modern trends in activation analysis; Saclay, France (2 Oct 1972).

A facility for neutron activation analysis (NAA) with a thermal flux of 5×10^{14} cm^{-2} sec^{-1} was recently installed at the ORNL High Flux Isotope Reactor. This unusually high flux together with a small computer and necessary software for γ spectrometry with a Ge(Li) detector makes possible shorter irradiation, faster data analysis, and more economical analysis than is possible using more conventional facilities. Features and tests of the High-Flux NAA Laboratory are discussed, as well as results of comparator and absolute NAA of several types of environmental matrices for mercury, cadmium, bromine, arsenic, chlorine, and sodium. (auth)

52898 (COO–3034-2) APPLICATION OF NUCLEAR TECHNOLOGY TO ART IDENTIFICATION PROBLEMS. Final Report. Keisch, Bernard; Miller, Holly H. (Mellon Inst., Pittsburgh, Pa.). Feb 1972. Contract AT(11-1)-3034. 89p. Dep. NTIS.

Neutron activation analyses of lapis lazuli, Italian renaissance bronze objects, and various samples of terracotta statuary are described. The limited utility of this method for purposes of identification of these materials is described. A simple procedure for determining ^{14}C context of cellulosic materials is described that can be used to detect man-made additions since the 1950's. The application of Mössbauer effect spectrometry to analytical problems of the fine arts is introduced and the potentialities of the method are explored. A brief summary of general conclusions reached regarding the use of various nuclear methods explored during the four-year research period is presented. (auth)

52899 (LA-DC–72-809) ACTIVE ^{3}He ACTIVATION ANALYSIS FOR CARBON AND OXYGEN. Sanders, Wm. Mort; Barnes, Barry K.; Holm, Dale M. (Los Alamos Scientific Lab., N. Mex.). 1970. 17p. (CONF-721010–2). Dep. NTIS.

From International conference on modern trends in activation analysis; Saclay, France (2 Oct 1972).

The surface and body concentrations of carbon and oxygen were measured in various materials using prompt ^{3}He activation techniques. Thin target excitation functions were determined for (^{3}He,p) reactions with carbon and oxygen over a ^{3}He energy range from 2.5 to 9.0 MeV. These data were used in the calculations of activation curves for various combinations of incident particle energy, impurity distributions, and material. Information on a computer code that was used in the analysis of the data is presented. (auth)

52900 (LYCEN–7236) ANALYSIS OF THIN LAYERS OF CHALCOGENIDE GLASSES FOR Te, As, Ge, AND S. USE OF THE NUCLEAR REACTIONS AND X RAYS PRODUCED BY PROTON BOMBARDMENT. Porte, Louis (Lyon Univ. (France). Institut de Physique Nucleaire). Jun 1972. 59p. (In French). Dep. NTIS (U. S. Sales Only). Thesis.

The quantitative analysis of thin layers of chalcogenide glasses for As, Ge, S, and Te was studied. Two methods were used, the first based on nuclear reactions resulting from proton bombardment of the sample. Experimental parameters for the analysis are given. X-ray fluorescence analysis was also used. The two methods gave comparable results with good precision. (J.G.B.)

52901 (UJV–2851-F,Ch) NONDESTRUCTIVE NEUTRON ACTIVATION ANALYSIS OF MINERAL MATERIALS. II. Benada, J.; Randa, Z.; Kuncir, J.; Vobecky, M. (Ceskoslovenska Akademie Ved, Rez. Ustav Jaderneho Vyzkumu). Jun 1972. 88p. Dep. NTIS (U. S. Sales Only).

The gamma spectra of 9 further elements that can be found in INAA (instrumental neutron activation analysis) of mineral materials and 41 mineral materials are included. These gamma spectra were measured after at least 9 hours cooling time. Besides these spectra of artificial radionuclides, the products of a neutron activation, gamma spectra of the natural decay products of uranium and thorium are included together with a typical background spectrum. (auth)

52902 ANALYSIS OF THIN ALUMINA FILMS OBTAINED BY REACTIVE SPUTTERING: NUCLEAR REACTIONS; I.R.; ELECTRON DIFFRACTION. Diaine, C.; Roger, J. A.; Pivot, J.; Cachard, A.; Dupuy, C. H. S. (Univ. Lyon, Villeurbanne, France). pp 377-84 of International Colloquium on the Application of Vacuum Techniques to the Semiconductor Industry, Electronic, and Microelectronic Components. Paris; Societe Francaise des Ingenieurs et Techniciens du Vide (1971). (In French).

From third international symposium on the application of vacuum techniques in semiconductor industry, electronic components, and microelectronics; Versailles, France (13 Sep 1971). See CONF-710932.

Microanalysis using simultaneously (d,p_0) nuclear reactions with ^{16}O and ^{27}Al and infrared spectrophotometry enabled the composition of aluminum oxide obtained by reactive sputtering in oxygen to be determined. The dependence of the composition on the energy conditions in the discharge was studied. The stoichiometric properties of the alumina obtained were shown to be dependent upon the sputtering voltage, high voltages being necessary to obtain a good stoichiometry. Comparisons with the electric properties enabled the results obtained to be generalized for SiO_x, the presence of a negative differential resistance (dV/dI) being related to an excess of oxygen in the oxide. (France)

52903 RADIOANALYTICAL PURIFICATION OF PROTACTINIUM BY ANION EXCHANGE IN HYDROCHLORIC ACID–HYDROFLUORIC ACID MEDIUM. Dominguez, G.; Adrada, J. (Junta de Energia Nuclear, Madrid). An. Quim.; 67: No. 6, 591-606(1971). (In Spanish).

To establish the possibility of separating Pa from interfering elements in solution resulting from the $HNO_3-HF-H_2SO_4$ attack on neutron-irradiated ores, in connection with the activation analysis for Th, the distribution coefficients of Pa, Ac, Nb, and Np in Dowex 1 resins and HCl (12 to 9N)–HF (0.003 to 1N) mixtures were determined. The separation of these elements seems to be possible; Zr and Ru interfere, but H_2SO_4 and Fe(III) can be tolerated. (Anal. Abstr.).

52904 ROUTINE DETERMINATIONS OF TRACES OF COBALT IN SOIL AND PLANT TISSUE BY INSTRUMENTAL NEUTRON ACTIVATION ANALYSIS. Johansen, O.; Steinnes, E. (Institutt for Atomenergi, Kjeller, Norway). Acta Agr. Scand.; 22: No. 2, 103-6(1972).

The determination of cobalt in soils and vegetable tissue using instrumental neutron activation analysis with a well-type NaI(Tl) detector was studied. The amount of work per sample is low, and the sensitivity is adequate for direct determination in plant samples. The precision of the method in routine application is of the order of 5%. (auth)

52905 ACTIVATION ANALYSIS FOR VANADIUM IN MINERAL OIL. Mayer, Walter A. Erdoel Kohle, Erdgas, Petrochem.; 24: No. 6, 416-17(1971). (In German).

The sample (as received or diluted with xylene) in a Zircaloy tube is irradiated for 10 min. in a neutron flux of $\simeq 3 \times 10^8$ neutrons/sq. cm/sec., then transferred to a glass container, and, 1 min. after irradiation, the γ-ray activity of the induced ^{52}V is counted for 10 min. at 1.43 MeV with a NaI(Tl) scintillation counter. Interference by the 1.6-MeV peak of ^{38}Cl produced from natural Cl in the oil is corrected by making a second 10-min. measurement 17 min. after the end of irradiation. If the counts accumulated in the second measurement are multiplied by 1.373 and subtracted from the value obtained in the first measurement, the corrected activity corresponds to the ^{52}V. Standards containing 0.1, 1, and 10 ppM of V are analyzed analogously. The detection limit is 0.02 ppM of V in the oil, and, at the 1-ppM level, the accuracy is within $\simeq 2\%$. (Anal. Abstr.)

52906 NEUTRON ACTIVATION OF SILVER, CADMIUM, INDIUM, TIN, ANTIMONY, TELLURIUM, AND IODINE: ANALYSIS OF METEORITIC, TERRESTRIAL, AND LUNAR MATERIALS. Elzie, Johnny Lee. Los Angeles; Univ. of California (1972). 135p. University Microfilms Order No. 72-22,162. Thesis.

Silver, cadmium, indium, tin, antimony, tellurium, and iodine were determined in separated meteoritic phases and terrestrial materials by neutron activation analysis. Cadmium and indium were determined in lunar materials returned by Apollo 12 and Apollo 14. The elemental separation scheme involved the separation and purification of iodine by repeated extractions into carbon tetrachloride. Tellurium was determined via ^{131}I in the purified iodine fraction. Silver was separated by AgCl precipitation, and subsequent purification involved mainly the extraction of silver diethyldithiocarbamate into carbon tetrachloride. Tin was separated and purified by repeated extractions into 0.5M thenoyltrifluoroacetone in 4-methyl-2-pentanone followed by back-extractions into tartaric acid. Antimony was separated and purified by repeated extractions of antimonic chloride into isopropyl ether followed by back-extraction of the antimonous chloride into 7M hydrochloric acid. Cadmium was separated on an anion exchange column and purified by subsequent hydroxide and sulfide precipitations. Relative errors associated with the determination of each element were 15% or less except in the case of iodine. The trace elements determined in this study were found to fall into two general categories based on the distribution coefficients between the metal and troilite phases of iron meteorites: chalcophilic elements that concentrate strongly in the troilite with only minor siderophilic (metal-seeking) tendencies (Ag, Te, and I) and those that show appreciable siderophilic as well as chalcophilic properties (Sn, Sb, and In). Cadmium and indium, both volatile elements, were found to concentrate in the lunar soil samples relative to the lunar rocks, indicating an extralunar component in the soils. The extralunar component was estimated to be about 1.1% at the Apollo 12 site and about 2.2% at the Apollo 14 site assuming a carbonaceous chondrite-like nature for the extralunar component. Concentrations of most trace elements in the ultrabasic rocks are lower than in the basalts and other igneous rock types. Antimony is exceptional, with concentrations which are nearly the same in all rock types. The observed fractionation is compatible with the hypothesis that both basalts and ultrabasics are low-melting and high-melting fractions of upper mantle material, with the basalts being formed through a partial melting process with the ultrabasics constituting the residuum. (Diss. Abstr. Int., B)

52907 DETERMINATION OF BROMINE, ARSENIC, MERCURY, AND SELENIUM IN PLANTS BY NEUTRON ACTIVATION ANALYSIS. Chun, Sea Yull. Han'guk Sikp'um Kwahakhoe Chi; 3: No. 3, 144-50(1971).

As, Br, and Hg were determined in tobacco by Bethge destructive method and subsequent neutron activation analysis. Se-77m was determined by nondestructive activation analysis. Quantities of the element determined in Korean tobaccos are: As, 0.65 ppM; Hg, 0.74 ppM; Se, 1.18 ppM; and Br, 7.1 ppM. (Korean Sci. Abstr.)

52908 STUDY BY NEUTRON ACTIVATION ANALYSIS OF THE DISTRIBUTION OF Cs IN POTASSIUM MINERALS OF GRANITIC CORSICAN ROCKS. Carron, Jean-Paul; Lagache, Martine (Ecole Normale Superieure, Paris). Bull. Soc. Fr. Miner. Crist.; 95: No. 1, 161-2(Jan 1972). (In French).

Biotite and feldspath samples were irradiated in a neutron flux of $10^{13} n \cdot cm^{-2} s^{-1}$. The ^{134}Cs was determined by γ spectrometry. The quantity of Cs, and the K/Cs and Rb/Cs ratios found in the biotites and feldspars of granites and granodiorites are given in ppM. The distribution (by weight) of Cs between these two minerals is represented graphically. (France)

52909 DETERMINATION OF VANADIUM IN SILICATE MATERIALS BY NEUTRON ACTIVATION. Decarreau, Alain (Univ. Paris, Orsay, France); Jaffrezic, Henry. Compt. Rend., Ser. D; 274: No. 18, 2553-5(3 May 1972). (In French).

An original method for determination of vanadium by neutron activation is proposed; the application of this method to silicate rocks is described. The vanadium is isolated (before irradiation) from the principal undesirable elements by paper chromatography. Determinations are then made using γ spectrometry with a Ge(Li) detector. International interlaboratory comparisons were made using standard samples. (France)

52910 DETERMINATION OF BISMUTH IN SOME MINERALS BY ACTIVATION ANALYSIS. Babaev, A.; Khaidarov, A. Dokl. Akad. Nauk Tadzh. SSR; 13: No. 11, 21-2(1970). (In Russian).

The instrumental method described for determination of Bi in galena and chalcopyrite is based on the nuclear reaction $^{209}Bi(n,\gamma)^{210}Bi$; ^{210}Bi decays by β emission to form ^{210}Po, which in turn emits α particles to form ^{206}Pb. The sample and a standard of metallic Bi are wrapped in aluminum foil and irradiated in a thermal-neutron flux of $\simeq 1.8 \times 10^{13}$ neutrons/cm^2/sec. After 15 days for accumulation of ^{210}Po and decay of interfering isotopes, the irradiated sample is spread in a uniform layer over a standard transparent plastic cup to give infinite-thickness conditions, and the α activity is measured with use of a ZnS(Ag) scintillation counter. (Referativnyi Zh.)

52911 DETERMINATION BY NEUTRON ANALYSIS OF MERCURY RESIDUES IN FOODSTUFFS. Chun, Sea Yull Han'guk Sikp'um Kwahakhoe Chi; 3: No. 3, 135-43(1971).

Neutron activation analysis was used to determine the degree of mercury contamination in common foodstuffs. Polished rice contained 0.050 ppM and rice bran had 0.095 ppM mercury. It was found in other grain in lesser amounts. Vegetables and fruits also contained 0.035 to 0.190 ppM of mercury with relatively small variations except for persimmons, which had a considerably higher amount of mercury. Soybean sprouts contained an unexpectedly high amount of mercury. Of the animal products, chicken and eggs contained more mercury than meat. (Korean Sci. Abstr.)

52912 NEUTRON ACTIVATION ANALYSIS. De Soete, D.; Gijbels, R.; Hoste, J. Chemical Analysis, Volume 34. New York; John Wiley and Sons, Inc. (1972). 856p. $39.50.

Titles of the twelve chapters are: activation analysis, general aspects in trace analysis, neutron-induced reactions, neutron sources, growth and decay of radioactivity during and after irradiation, nuclear disintegration and radiation detection, preparation of samples and standards, activation analysis with post-irradiation radiochemical separations, analysis without chemical separation, systematic errors in activation analysis, statistical interpretation of results, and, bibliographical survey of neutron activation analysis. Also included are appendixes on thermal neutron cross sections, resonance neutron cross sections, fission neutron cross sections, 14-MeV neutron cross sections, gamma energies of radionuclides formed by neutron capture and determined by Ge(Li) spectrometry, gamma mass attenuation coefficients, and chemical yield determinations. (J.G.B.)

Chemical and Spectral Procedures

Refer also to abstracts 52955 and 55170.

52913 (AEC-tr-7345) ABSOLUTE MEASUREMENT OF THE ISOTOPIC RATIO OF A WATER SAMPLE WITH A VERY LOW DEUTERIUM CONTENT. Hagemann, R.; Nief, G.; Roth, E. Translated for Savannah River Lab., Aiken, S. C., from report CEA-R-3633. 25p. Dep. NTIS.

A method was developed for the isotopic determination of hydrogen in water very depleted in deuterium. It is based on utilization of a distillation column mounted directly on the introduction line of a mass spectrometer. The latter is equipped with an isotope ratio measuring apparatus the sensitivity of which is better than 0.01 ppM. The column used permits a high separation factor, above 5000, to be obtained, so that it is possible to measure the response of the mass spectrometer for a vapor containing less than 0.001 ppM of deuterium. This method was applied for determining the isotopic ratios of three depleted waters. The results obtained allowed the assignment to the most depleted among the others an absolute value in deuterium equal to 1.71 ± 0.03 ppM. This water constitutes the primary standard used to determine the isotopic ratio of a natural water serving as a laboratory standard. (auth)

52914 (ANL-7860(Pt.3), pp 55-63) DETERMINATION OF SELECTED TRACE ELEMENTS IN NATURAL WATER SAMPLES USING SPARK SOURCE MASS SPECTROSCOPY. Wahlgren, M. A.; Edgington, D. N.; Rawlings, F. F. [nd].

In Radiological Physics Division annual report, January–December 1971.

A spark source mass spectroscopic method for analyzing water samples from the South Basin and from tributaries to the South Basin and Green Bay regions of Lake Michigan for twenty-one selected trace elements of radiological, biological, and geochemical interest is described. The elements determined include B, F, Al, Si, P, V, Cr, Mn, Ni, Cu, Zn, Se, Ag, Cd, Sn, Sb, I, Ba, Pb, Bi, and U. (D.H.M.)

52915 (CONF-720827-2) RAPID, SENSITIVE METHOD FOR THE DETERMINATION OF THE CHEMICAL OXYGEN DEMAND OF POLLUTED WATERS. Pitt, W. Wilson Jr.; Katz, Sidney; Thacker, Louis H. (Oak Ridge National Lab., Tenn.). 1972. 20p. Dep. NTIS.

From seventy-third national meeting of the American Institute of Chemical Engineers; Minneapolis, MI. (27 Aug 1972).

A rapid, sensitive cerate oxidative method for measuring the chemical oxygen demand (COD) of waters is described. The pollutants are oxidized with perchlorato-cerate reagent and the resulting cerium(III) is determined fluorometrically. Analysis requires only a few minutes for determinations at levels as low as 100 μg oxygen demand per liter. Results of tests on solutions of known organic compounds, various industrial waste streams, and natural waters show that the method compares favorably with the dichromate reflux procedure. However, the new method is considerably faster and easier to use, and is a hundred times more sensitive. An analytical system suitable for use as either a continuous COD monitor or as an analyzer for multiple samples in series is also described. (auth)

52916 (EUR-4765, pp 41-75) HIGH ACCURACY ISOTOPE ANALYSIS OF THE ELEMENTS. De Bievre, P. (Central Bureau for Nuclear Measurements, Geel, Belg.).

From 2nd conference on mass spectrometry; Ispra, Italy (1 Sep 1971).

The need and means for acquiring reliable data in the field of isotope analysis are discussed. Suggested requirements for accurate analyses are: enriched isotopes (>99% isotopic purity) of the element concerned, accurate chemical assay of these isotopes (accuracy 0.1%), accurate blending of these isotopes, calibration of the mass spectrometer with these blends, and isotopic measurement of natural samples of the element concerned. Best available estimates of natural isotope abundances for the elements are tabulated. (J.G.B.)

52917 (EUR-4765, pp 77-89) APPLICATION AND AUTOMATION OF MASS SPECTROMETRY IN THE ANALYSIS OF IRRADIATED NUCLEAR FUELS. Cricchio, A.; Gerin, F.; Koch, L.; Wilhelmi, M. (European Transuranium Inst., Karlsruhe, Ger. Gesellschaft fuer Kernforschung, Karlsruhe, Ger.). (In Italian).

From 2nd conference on mass spectrometry; Ispra, Italy (1 Sep 1971).

A procedure is given for the analysis of irradiated nuclear fuels, beginning with their dissolution in HNO_3, and the spectrometric analysis of the fission gases liberated during dissolution. Six Kr and six Xe isotopes were thus determined. Another mass spectrometer was used to assay four U isotopes and six Pu isotopes. The isotope ^{238}Pu and the isotopes of Am and Cm were determined by alpha spectrometry. The extent of burn-up was obtained from a determination of ^{148}Nd by means of an isotopic dilution technique, using ^{150}Nd as an indicator. Automation of some of the procedures and data processing by computer are described. (K.S.W.)

52918 (EUR-4765, pp 91-115) ISOTOPIC ANALYSIS OF URANIUM AS A RUNNING CONTROL OF THE EUREX PROCESS. Pozzi, F.; Trincherini, R. P. (CNEN, Vercelli, Italy). (In Italian).

From 2nd conference on mass spectrometry; Ispra, Italy (1 Sep 1971).

Preliminary tests are described that served to prepare a Varian CH_4–B spectrometer for the widest possible interval for uranium isotopes. National Bureau of Standards samples were utilized in these adjustments. The complete procedure for the determination of U and of the relative percent of the U isotopes present is given. Dissolution of the EUREX Plant product yields a solution of U enriched to 80 to 90% and a concentration between 2 and 3 g U/l. Glove-box preparation of the sample, extraction of U with methyl isobutyl ketone after complexing with tetrapropylammonium nitrate, and the pertinent calculations and statistical treatment of the data are described. Variations in the relative isotopic abundance and their relation to current control of the EUREX process are discussed. (K.S.W.)

52919 (NIM-1432) DETERMINATION OF RUTHENIUM AND OSMIUM IN THE RESIDUES RESULTING FROM THE LEACHING OF MATTES. Krueger, Magdalena M.; Robert, R. V. D. (National Inst. for Metallurgy, Johannesburg (South Africa)). 5 Jul 1972. 4p. Dep. NTIS (U. S. Sales Only).

The residue is sintered with barium peroxide, and the ruthenium and osmium distilled from the sinter. The distillates are collected separately in 6N hydrochloric acid. The ruthenium is determined by atomic absorption spectrophotometry and the osmium by a colorimetric method using thiourea. (auth)

52920 (RT/CHI-(72)3) PROGRESS IN STANDARDIZATION OF ANALYTICAL METHODS FOR MATERIALS OF NUCLEAR INTEREST. I. STANDARD METHOD FOR SPECTROPHOTOMETRIC DETERMINATION OF HEXAVALENT URANIUM IN AQUEOUS AND NON-AQUEOUS SYSTEMS BY DIBENZOYLMETHANE. Castagnola, A. M.; Guidotti, G. R.; Lorenzini, L.; Pigozzi, G. (Comitato Nazionale per l'Energia Nucleare, Rome (Italy)). 4 Mar 1972. 39p. Dep. NTIS (U. S. Sales Only).

The spectrophotometric method for determination of uranium (VI) by using dibenzoylmethane (1,3-diphenyl-1,3-propanedione) as a chromogenic reagent was revised and standardized for analytical control purposes. The method can be applied to the analysis of aqueous systems containing nitric and oxalic acid as well as thorium(IV) and stainless steel corrosion products and of TBP and tricaprylamine nonaqueous systems containing nitric acid. The applicability range in aqueous and nonaqueous systems is 0.04 to 50 and 0.01 to 2.5 g/l of uranium(VI), respectively. Limits for the mean at a level of about 0.13 mg U(VI)/25 ml and a probability of 0.05 (5% risk) in aqueous and nonaqueous systems of ±0.5 (for 15° of freedom) and ±1% (for 9° of freedom), respectively, were obtained. A statistical control was also made on the accuracy of determinations of an aqueous standard solution containing 500.0 mg/l of uranium(VI). Thirty-two measurements were made during a period of two months and upper and lower control limits of 511.8 and 488.2 mg/l were obtained respectively, without evidence of lack of control. (auth)

52921 ATOMIC ABSORPTION DETERMINATION OF ALKALINE EARTH METALS AND REFRACTORY OXIDES IN GEOCHEMICAL STANDARDS WITH A NITROUS OXIDE–ACETYLENE FLAME. Luecke, Werner (Univ., Karlsruhe, Ger.). Neues Jahrb. Mineral., Monatsh.; No. 6, 263-88(1971). (In German).

Beryllium, Mg, Ca, Sr, Ba, Ti, V, Cr, Mn, and Fe were determined by atomic absorption spectroscopy using a nitrous oxide–acetylene flame. Interference due to thermal ionization was suppressed by addition of large amounts of an easily ionized alkali metal, e.g., Cs. Silicates were decomposed for the determination of major and minor elements with $Li_2B_4O_7$ melts in platinum–gold crucibles. To determine trace elements the samples were treated with $HF-HClO_4$ under pressure in a PTFE-lined bomb followed by volatilization of Si. (Anal. Abstr.)

52922 DETERMINATION OF URANIUM IN HIGH-ALLOY STEEL. Peisteiner, E. (Schoeller-Bleckmann Stahlwerke AG, Ternitz, Austria). Radex. Rundsch.; No. 2, 442-6(1971). (In German).

A wet-chemical method was developed in order to calibrate the x-ray fluorescence determination of uranium. The steel sample is dissolved in HCl containing a few drops of HF, and the solution is oxidized with HNO_3. The uranium is extracted with tributyl phosphate–isobutyl methyl ketone. The uranium is reextracted from the organic phase by an aqueous solution of ammonium acetate and ammonium fluoride, and the pH is adjusted to 7.6. The resulting aqueous phase is extracted with 8-hydroxyquinoline solution in $CHCl_3$ and the extinction of the $CHCl_3$ layer is measured at 470 nm. Results obtained on samples containing up to 0.2% of uranium were rectilinearly related to counting rates obtained with a vacuum x-ray fluorescence spectrometer. (Anal. Abstr.)

52923 CALORIMETRIC METHODS OF ANALYSIS. Pennington, Sam N. (East Carolina Univ., Greenville, N. C.). Rev. Anal. Chem.; 1: No. 2, 113-40(1972).

The area of calorimetry considered is solution calorimetry, i.e. the heat absorbed or evolved when two solutions are mixed. The theory of thermal analysis is reviewed. Instruments, measurements, analytical determinations, kinetic measurements, and other applications are discussed. Radiochemical calibration for measurements is considered. (39 references) (M.C.G.)

52924 AMPEROMETRIC AND POTENTIOMETRIC DETERMINATION OF COPPER AND MOLYBDENUM IN ORE CONCENTRATES AND ALLOYS WITH 5-BROMO-8-MERCAPTO- AND 8-MERCAPTO-4-METHYLQUINOLINE. Berzina, V.; Jansons, E.; Priedite, R. Uch. Zap., Latv. Gos. Univ.; 117: 138-41(1970). (In Russian).

Either of these reagents (I and II, respectively) can be used as a titrant for Cu or Mo. The amperometric titration of Cu with I solution is carried out in a basal electrolyte of N H_2SO_4 and that with II solution in a basal electrolyte of HCl–KCl buffer solution (pH 2) at +0.9 V; in the presence of Pb the titration is carried out with 0.5 N H_2SO_4 as basal electrolyte. For the determination of Mo, the sample is mixed with concentrated H_3PO_4 (if W is present) and adjusted with 20% NaOH solution to pH 2, then diluted with one of the basal electrolytes specified above and titrated. Potentiometric titration is carried out similarly with use of a platinum electrode and the S.C.E. The method is suitable for the determination of Cu in bronze, brass, nickel silver, duralumin, silumin, and coinage alloy, and for the determination of Mo in steel; procedures are given. (Referativnyi Zh.)

52925 RAPID SPECTROPHOTOMETRIC DETERMINATION OF TANTALUM IN HARD-METAL ALLOY MIXTURES USING NILE BLUE. Panteleeva, M.; Dimitrova, M. (Forschungsinstitut fuer Metallkeramik, Sofia). Z. Anal. Chem.; 260: No. 4, 290-1 1972). (In German).

A sensitive method for determination of tantalum in hard metal alloys is described. The method is based on complexing the tantalum and extracting the colored compound with organic solvents. Within three hours, five samples can be analyzed. (H.B.G.)

52926 SPECTROPHOTOMETRIC STUDY OF THE REACTION OF NIOBIUM WITH ALIZARIN RED S [C.I. MORDANT RED 3]. Akhmedli, M. K.; Chan Khiem Tkham; Gambarov, D. G. Uch. Zap. Azerb. Gos. Univ., Ser. Khim. Nauk; No. 3, 46-50(1970). (In Russian).

Complex formation between Nb(Y) and Alizarin red S (I) was studied as a function of pH, concentration of I, concentration of the complex-forming substance added to prevent hydrolysis of the Nb, and presence of salts of Na^+, K^+, and NH_4^+ (which enhance the sensitivity and selectivity of the reaction). The sensitivity of the reaction diminishes in the series of systems Nb–EDTA, Nb–oxalate, Nb–tartrate and Nb–KOH. Complex formation generally attains maximum at pH 5 except for the Nb–EDTA system, for which the optimum pH is 4 (or 3 in the presence of salts). The maximum absorption of the complex is at 500 nm in the absence of salts and at 540 nm in their presence; the corresponding molecular extinction coefficients are 18,000 and 87,000. Color development takes 15 min in the absence of salts, but 4, 45, or 15 h in the presence of K^+, NH_4^+, or Na^+, respectively. (Referativnyi Zh.)

52927 SPECTROGRAPHIC DETERMINATION OF NICKEL, COBALT, SILVER, VANADIUM, TIN, MOLYBDENUM, TITANIUM, ALUMINUM, BISMUTH, IRON, LEAD, AND MANGANESE IN NATURAL WATER IN THE PRESENCE OF RELATIVELY LARGE AMOUNTS OF COPPER. Eremenko, V. Ya.; Mel'nikov, E. A. Gidrokhim. Mater.; 54: 87-90(1970). (In Russian).

The effect of Cu on the determination of heavy metals in water was studied. For Cu contents up to 120 μg per liter, all the elements named (except Ag) can be determined with an error of <20%. For >160 μg of Cu per liter, the Cu must first be separated (by extraction, as its dithizone complex, from a weak acid solution containing NH_4SCN); some Ag and Sn are extracted with the Cu. After removal of most of the Cu, the pH is adjusted to ≃5, and the other elements are extracted as their complexes with diethyldithiocarbamate and 8-hydroxquinoline. The extracts are analyzed by accepted spectrographic methods. (Referativnyi Zh.)

52928 DIRECT SPECTROPHOTOMETRIC DETERMINATION OF BORON IN ALUMINIUM ALLOYS. Pakalns, P. (Australian Atomic Energy Commission Research Establishment, Lucas Heights). Metallurgia; 39: No. 8, 308-9(Aug 1972).

A procedure is presented for the spectrophotometric determination of boron in aluminium and aluminium alloys. The sample is dissolved in a mixture of sulphuric, nitric, and hydrochloric acids, and the nitrate reduced with formic acid. An aliquot of the solution is treated with acetic anhydride, curcumin added, followed by an acetone-water mixture, and the absorbance of the boron-curcumin complex measured. (auth)

52929 TECHNIQUE FOR THE QUALITATIVE SPECTROGRAPHIC ANALYSIS OF VERY SMALL SAMPLES. Christopher, A. J. (Royal Aircraft Establishment, Farnborough, Eng.). Microchem. J.; 17: No. 4, 470-5(Aug 1972).

The sample and a small yarn of carbon fibers are stuck on a pointed graphite electrode; the gap between this and the upper electrode is bridged by the carbon fibers, which strike the arc when the dc source is switched on. Background emission is greatly reduced by enclosing the arc in an argon atmosphere. Many elements can be detected with ease in 1 μg amounts. Molybdenum was one element determined by this method. (auth)

52930 MICRODETERMINATION OF METALS IN ORGANOMETALLIC COMPOUNDS BY THE OXINE METHOD AFTER OXYGEN FLASK COMBUSTION. I. CADMIUM, MAGNESIUM, URANIUM, AND ZINC. Sakla, A. B.; Bishara, S. W.; Abo-Taleb, S. A. (Cairo Univ., Giza, Egypt). Microchem. J.; 17: No. 4, 436-42(Aug 1972).

A simple, accurate, and relatively rapid procedure for the estimation of cadmium, magnesium, uranium, and zinc in organometallic compounds is presented. The oxygen-filled flask is recommended for decomposition of the organic sample. Determination of the metal concerned is carried out by three methods using a single sample weight. Both the gravimetric and titrimetric finishes are applied. The method has the advantage of a favorable conversion factor for the gravimetric determination besides an 8- or 12-fold amplification reaction, depending on the valency of the metal, in case of the titrimetric finish. (auth)

52931 SPECTROPHOTOMETRIC DETERMINATION OF MOLYBDENUM AND PHOSPHORUS BY CARMINIC ACID METHOD. Lee, Albert; Boltz, D. F. (Wayne State Univ., Detroit). Microchem. J.; 17: No. 4, 380-7(Aug 1972).

A spectrophotometric method for the determination of molybdenum based on the use of carminic acid is proposed. Conformity to Beer's law was observed with an optimum concentration range of 1.5 to 8 ppM of molybdenum when absorbance measurements were made at 565 nm. The molar absorptivities for the determination of molybdenum are 1.4×10^4 mol l^{-1} cm^{-1} at 565 nm and 5.1×10^3 mol l^{-1} cm^{-1} at 336 nm. An indirect spectrophotometric procedure for the determination of orthophosphate based on the determination of the equivalent molybdenum in 12-molybdophosphoric acid was developed suitable for the determination of 0.03 to 0.18 ppM of phosphorus. (auth)

52932 QUANTITATIVE SPECTRAL DETERMINATION OF Nb, Ta, Fe, AND Mn IN MINERALS OF THE COLUMBITE–TANTALITE GROUP. Galibin, V. A.; Tsyina, N. V. Mineral. Geokhim.; No. 4, 77-84(1972). (In Russian).

A method of quantitative spectral determination of the composition of columbite–tantalite type minerals was developed employing a direct measurement of the ratios Nb_2O_5/Ta_2O_5 and FeO/MnO and 10 mg of sample. Preparation of the Nb, Ta, Fe, and Mn standards is described in detail. The mean arithmetic error in the oxide contents, based on the ratios determined, was 5.7% for Nb_2O_5, 6.5% for Ta_2O_5, 5.6% for FeO, and 7.0% for MnO. (K.S.W.)

Radiometric and Radiochemical Procedures

Refer also to abstracts 53256 and 54084.

52933 (JAERI-Memo-4094) APPLICATION OF ELECTROPHORESIS FOR BURNUP DETERMINATION. Hayashi, Teiji; Ito, Tadaharu; Nakayama, Shiro (Japan Atomic Energy Research Inst., Tokyo). Aug 1970. (In Japanese and English). NTIS (U. S. Sales Only).

Nuclear fuel burnup determination by electrophoresis with remote handling is described. The separation of inorganic components by electrochromatography was applied to the burnup determination. Some experiments were carried out on the separation of ^{137}Cs, one of the indicators for burnup determination, in the highly radioactive solution of an irradiated fuel specimen. The results by this method were found to be in agreement with those by a conventional radiochemical analysis. (auth)

52934 (MLM-1368) NEW TECHNIQUES FOR RELATIVE CALIBRATION OF TRITIUM SOURCES BY BREMSSTRAHLUNG COUNTING. Curtis, M. L.; Bentz, L. L. (Mound Lab., Miamisburg, Ohio). 15 May 1966. Contract AT-33-1-Gen-53. 12p. Dep. NTIS.

Where the very soft beta radiation from tritium cannot be detected and measured readily because of its chemical or physical form, the more penetrating bremsstrahlung radiation can be measured as a convenient method of analysis. Techniques are described for rapid measurement of a large number of liquid or solid samples sealed in circular polyethylene bags, using a thin window sodium iodide crystal and multichannel analyzer. Disintegration rates are determined by comparison with the bremsstrahlung counting rate of standardized tritiated water. Empirical corrections are made for the differences in bremsstrahlung intensity due to sample composition. The method was used in studies of hydrogen penetration into steel, the measurement of tritium absorbed in charcoal, the determination of tritium in contaminated and discolored pump oil, and in aqueous waste materials. It is applicable to analysis for tritium in any material that can be contained in polyethylene, in the range of one microcurie per cc or higher. (auth)

52935 (MLM-1888) MOUND LABORATORY CHEMISTRY AND PHYSICS PROGRESS REPORT: OCTOBER-DECEMBER 1971. (Mound Lab., Miamisburg, Ohio). 21 Aug 1972. Contract AT-33-1-Gen-53. 24p. Dep. NTIS.

LITHIUM SULFATES—analysis for impurities, spectrographic
NATURAL WATERS—plutonium in, possibility of pentavalent
PLUTONIUM—chemical state in solutions, effects of hydrolysis on
—content of pentavalent, in natural waters, possibility of
—determination in soil, sample size for fusion method for
—separation from uranium, residue adsorption and anion exchange methods for
PLUTONIUM-238—analysis for uranium-232 and uranium-234 by hydrolysis, residue adsorption, and α spectroscopy
SOILS—analysis for plutonium, sample size for fusion method for
TRITIUM—determination by liquid scintillation counting
URANIUM—separation from plutonium, residue adsorption and anion exchange methods for
URANIUM-232—determination in plutonium-238 and uranium-234 by hydrolysis, residue adsorption, and α spectroscopy
URANIUM-234—determination in plutonium-238 and uranium-232 by hydrolysis, residue adsorption, and α spectroscopy
—purification of, anion exchange method for (M.C.G.)

52936 (RT/EL-(72)4) ELECTRON EMISSION FROM SOLIDS BY IONIC BOMBARDMENT. Catoni, F.; Gislon, R.; Papa, C. (Comitato Nazionale per l'Energia Nucleare, Rome (Italy)). 13 Apr 1972. 31p. (In Italian). Dep. NTIS (U. S. Sales Only).

Ejection of electrons by low-energy ion bombardment is the basis of methods of surface analysis. The physical fundamentals involved are reviewed. (45 references) (auth)

52937 ANALYSIS USING SECONDARY ION EMISSION IN SEMICONDUCTORS. Blanchard, B.; Hilleret, N.; Quoirin, J. B. (CEN, Grenoble, France). pp 393-400 of International Colloquium on the Application of Vacuum Techniques to the Semiconductor Industry, Electronic, and Microelectronic Components. Paris; Societe Francaise des Ingenieurs et Techniciens du Vide (1971). (In French).

From third international symposium on the application of vacuum techniques in semiconductor industry, electronic components, and microelectronics; Versailles, France (13 Sep 1971). See CONF-710932.

The Castaing-Slodzian ion analyzer was used to determine impurity profiles in semiconductors (impurity distributions determine most of the electrical properties). The measurement methods are described in detail using the diffusion profiles of B in Si and silica as examples. This method enables curves to be rapidly obtained for the distributions. (France)

52938 RADIOCHEMICAL DETERMINATION OF VITAMIN B_{12}. Iversen, M. S. (Dr. Fuersts Medisinske Laboratorium, Oslo). Fysiokjemikeren; No. 9, 6-9(Mar 1971). (In Norwegian).

A new method for the determination of vitamin B_{12}, based on isotopic dilution and ultrafiltering, was developed. A competitive absorption between labeled and nonlabeled B_{12} to "intrinsic factor" is utilized. Vitamin B_{12} in the blood is released from serum protein by warming at pH 4.9 in the presence of cyanide. Cobalt-57-labeled B_{12} and "intrinsic factor" are added. The solution is ultrafiltered and the amount of vitamin B_{12} in the sample can be calculated from the radioactivity in the filtrate. The quality of the labeled solution and the "intrinsic factor" are important factors. Details of the procedure are given. The results give good agreement with the microbiological method and have the advantage of being available the same day the samples are taken. Batches of 40 samples, including standards and controls, prove suitable. (Norway)

52939 MICROANALYSIS OF MATERIALS BY BACKSCATTERING SPECTROMETRY. Nicolet, M.-A. (California Inst. of Tech., Pasadena); Mayer, J. W.; Mitchell, I. V. Science; 177: No. 4052, 841-9(8 Sep 1972).

A survey is presented of backscattering spectrometric analysis and its applications. This technique is sensitive to the mass of the constituents, their depth distribution, and the crystalline structure. Some of the applications include ion-implanted semiconductors, dielectric layers, metal-semiconductor contacts, metal analyses, films (such as in paper industry), etc. Sensitivity and limitations of the technique are discussed. (11 figures, 33 references) (D.L.C.)

52940 DETERMINATION OF URINARY PLUTONIUM BY RADIOCHEMICAL ANALYSIS ON ION EXCHANGER FILTERS. Clanet, F. (Laboratoire de Chimie Minerale et d'Hydrologie, Tours, France); Ballada, J.; Lucas, J.; Gil, C. Health Phys.; 23: No. 2, 244-7(Aug 1972). (In French).

Background studies and a recommended method are described for determining Pu in urine, which involves separation of Pu(IV) on an HAWP Millipore filter supporting three Amberlite SB-2 ion exchange filter papers. The detection limit claimed is 1 pCi ^{239}Pu/liter of urine. There is excellent agreement between the results of this method and the standard one involving separation of Pu on an ion exchange column, but the described method is far quicker. (UK)

52941 RADIOMETRIC METHOD FOR STANDARD URANIUM ORE SAMPLES: COMPARISON WITH STANDARD THORIUM ORE SAMPLES BY MEANS OF THE GAMMA RAYS SPECTROSCOPY. Krzuk, Jerzy (Instytut Techniki Jadrowej, Krakow). Nukleonika; 16: No. 11-12, 555-64(1971). (In Polish).

A possibility of the thorium content comparison with that of uranium in the standard samples by means of gamma spectroscopy is shown. The basis of the described method is that both ThC'' (^{208}Tl) in thorium series, and RaC (^{214}Bi) in uranium series emit gamma rays of energy ~0.6 MeV. (auth)

52942 METODE RADIOMETRICE DE ANALIZA. (Radiometric Methods of Analysis). Nascutiu, Tiberiu. Bucharest; Editura Academiei Republicii Socialiste Romania (1971). 346p. (NP-19380).

Physical fundamentals of the use of the radioactive isotopes in analytical chemistry are reviewed. Radiometric methods of analysis are described. The basic principle of each method, the necessary apparatus, the errors affecting the determinations, and achievements and outlooks at laboratory and plant level are discussed. Former methods, based on direct measurements of radioactivity, excellent methods for the determination of uranium, thorium, radium, potassium, and of other elements having natural radioactive isotopes, are also described. Methods based on the use of artificial radioactive sources are given. In the case of x-ray fluorescence analysis using such sources, advantages of the substitution of the x-ray generator tube (classical method) and possibilities of construction of a simplified, portable and cheaper apparatus for rapid, routine analysis in hard field conditions, are also exposed. Gas analysis by ionization with radioactive sources and methods based on the attenuation of nuclear radiations (absorption and back scattering), the Mössbauer effect, and the scattering of charged particles are described. Special attention was paid to neutron methods, at present widely developed as a result of nuclear reactors, charged particles accelerators, and neutrons isotopic sources improvement and marketing. Specific features of the methods of analysis by activation with thermal neutrons, with fast neutrons, with charged particles, and with photons are given. (auth)

52943 INVESTIGATIONS OF THE EQUIVALENCE BETWEEN HEAVY ELEMENTS CONCENTRATIONS IN THE ROCK: USE OF THE GAMMA–GAMMA SELECTIVE METHOD. Charbucinski, J.; Gyurcsak, J. (Instytut Techniki Jadrowej, Krakow). Nukleonika; 17: No. 1-2, 123-9(1972). (In Polish).

The relationship of the equivalence factor to Z_{eq} of matrix value, and initial energy of the source applied to the measurement as well as to the atomic number of the element that is the additive component of the rock, is also described. The equivalence factors for Fe, Mo, Ba, and Pb in the range of energy 60 keV to 661 keV were investigated. The semiempirical determination of equivalence factors is introduced. (auth)

52944 USE OF THE KNOBLOCH ELEMENTARY MICROANALYZER FOR THE COMBUSTION OF ANALYTICAL SAMPLES CONTAINING ^{14}C AS A PRESTAGE OF LIQUID SCINTILLATION MEASUREMENT. Mende, G. (Zentralinstitut fuer Kernforschung, Rossendorf, Ger.). Isotopenpraxis; 8: No. 2, 71-2(Feb 1972). (In German).

The modifications made in the procedure used with the Knobloch elementary microanalyzer so that it could be used for the combustion of analytical samples as a pre-stage of liquid scintillation measurement were described. The modifications were tested on a ^{14}C-labeled benzoic acid sample. From 41 combustions a relative standard deviation of the individual values of 0.7% was obtained. (J.S.R.)

52945 FULL-RANGE SOLUTION FOR THE MEASUREMENT OF THIN-FILM SURFACE DENSITIES WITH PROTON-EXCITED X RAYS. Reuter III, F. William; Smith, Harold P. Jr. (Univ. of California, Berkeley). J. Appl. Phys.; 43: No. 10, 4228-32 (Oct 1972).

A Fredholm-integral expression for characteristic x-ray production by proton bombardment is developed relating multicomponent elemental thin-film concentration profiles to proton-stopping power, x-ray-production cross section, and x-ray attenuation. The thickness of Al_2O_3 and Ta_2O_3 films on their respective metallic substrates were measured with 20- to 80-keV protons with an accuracy of 5% for thick films (1200 Å) and 25% for thinner films (30 Å). Nonlinear regression analysis of the data indicated that all parameters of interest, including the zero-voltage anodization potential, can be determined from the raw data. With exception to the oxygen K-shell x-ray attenuation coefficient, the parameters were determined with good to reasonable accuracy. A general concentration profile could not be determined by numerical methods as a result of insufficient variation in the kernel of the integral equation. (auth)

52946 CORRECTION OF A FORMULA USED IN THE RADIOASSAY OF ^{99m}Tc. Banerjee, Krishnadas; McAllister, John D.; DiPrimio, Joseph; Henry, Maureen L. (St. Francis General Hospital, Pittsburgh). Radiology; 104: No. 3, 711-12(Sep 1972).

A formula was derived for the radioassay of ^{99m}Tc using a ^{57}Co standard source, employing the number of usable photons produced by the decay of the respective isotopes. The activity of ^{99m}Tc, as determined with NaI (Tl) well-crystal and Ge(Li) detectors, compares favorably with that measured with two different commercially available dose calibrators. (auth)

Separation Procedures

Refer also to abstract 52954.

52947 (BM-RI-7671) SEPARATION OF COLUMBIUM, TANTALUM, TITANIUM, AND ZIRCONIUM FROM TITANIUM CHLORINATION RESIDUES. Merrill, Carl C.; Couch, D. E. (Bureau of Mines, Boulder City, Nev. Boulder City Metallurgy Research Lab.). 1972. 10p.

Niobium, tantalum, titanium, and zirconium are present in solid-waste products generated by the chlorination of rutile used for production of titanium tetrachloride ($TiCl_4$). The niobium and tantalum were separated from titanium and zirconium by liquid-liquid extraction techniques using a secondary amine. Salts of these elements are in a leach liquor produced by water leaching of mineral waste from the chlorination of rutile. This waste, produced at the rate of approximately 50,000 tons per year, is about 40 wt % water soluble. Leach liquors, separated by filtration, were further separated into a solid fraction and a liquid fraction by pressure hydrolysis. The solid fraction containing Nb, Ta, Ti, and Zr was dissolved in HCl-HF and used as a feed solution. Niobium and tantalum were removed from the organic extractant with 1 N HCl. A miniature 10-stage reactor showed that the niobium and tantalum present in solution could be separated with a continuous flow. (auth)

52948 USE OF ION EXCHANGERS IN ANALYTICAL CHEMISTRY. Inczedy, J. (Univ. of Chemical Industries, Veszprem, Hungary). Rev. Anal. Chem.; 1: No. 2, 157-74(1972).

Recent applications of ion exchange are reviewed and trends in the development of ion-exchange chromatography are shown. Topics covered include: ion exchange materials, methods based on total ion exchange, chromatographic separation, separation of metal ions by cation exchangers, separation of organic bases on cation exchange columns, separation of metal ions by anion exchange columns, separations of anions and of organic acids with anion exchangers, new techniques, liquid ion exchangers, and ion exchange papers. (135 references) (M.C.G.)

52949 CHROMATOGRAPHIC SEPARATION OF INDIUM FROM ELEMENTS THAT FORM PERIODATES OF LOW SOLUBILITY, AND ITS SUBSEQUENT DETERMINATION. Verdizade, A. A.; Mekhtiev, M. M. Uch. Zap. Azerb. Gos. Univ., Ser. Khim. Nauk; No. 3, 42-5(1970). (In Russian).

The separation of In from such elements as (Cu, Zn, Al, Bi, Pb, Mo, Cd, Fe, Cr, Sn, As, Sb, Co, Ni, and Ga) is achieved by the ion-exchange chromatography of complexes with sulfosalicylic acid on a column of KU-2 cationite (NH_4^+ form). To the aqueous test solution is added aqueous NH_3 until the color changes to orange–yellow, then the solution is diluted and passed through the column, which is washed (×3 or 4) with 4% aqueous sulfosalicylic acid (neutralized with aqueous NH_3) and then with water (×3 or 4). At this stage, there remain on the column only the complexes of In, Ga, Co, Ni and C(III). The column is then washed with 0.4 to 0.5M HCl, which elutes In, Cr, Co, and Ni; the eluate is evaporated, concentrated aqueous NH_3 is added to precipitate In and Cr, the precipitate is collected, washed with aqueous NH_3 and dissolved in 2M HNO_3, then saturated aqueous $NaIO_4$ is added, and the mixture is neutralized to 4-nitrophenol with 10% aqueous NaOH. Dilute HNO_3 is added until the pH is between 2 and 7, and the solution is heated to 80° and filtered; the precipitate is washed with hot 1% ammonium acetate solution then dissolved in M H_2SO_4, benzene and M KI are added, and the liberated iodine is titrated with $Na_2S_2O_3$ solution. The method is applicable to the determination of In in phosphate concentrates. (Referativnyi Zh.)

52950 RECOVERY OF RHENIUM AND MOLYBDENUM VALUES FROM SOLUTION. Litz, John E. (to Continental Ore Corp.). U. S. Patent 3,681,016. 1 Aug 1972. Filed 2 Dec 1970.

A process is described for recovering rhenium and molybdenum values from solution. The soluble molybdenum and rhenium values are extracted with an amine solvent, the values stripped from the amine extract with an ammonium hydroxide solution, the strip solution of copper, iron, silicon, phosphorous, and arsenic purified, the molybdenum crystallized as ammonium tetramolybdate containing a minimum of rhenium and other impurities, and the rhenium concentrated and recovered from the crystallization mother liquor by amine solvent extraction, stripping with sodium hydroxide solution, extraction into a pyridine solvent, and distillation of the pyridine away from a rhenium salt. (Official Gazette)

52951 ION-EXCHANGE BEHAVIOUR OF METALS ON DEAE-CELLULOSE IN METHANOL–THIOCYANATE–HYDROCHLORIC ACID MEDIA. Kuroda, Rokuro; Kondo, Takaaki; Oguma, Koichi (Univ. of Chiba, Japan). Talanta; 19: No. 9, 1043-8(Sep 1972).

Only a few metals can be adsorbed on DEAE-cellulose (diethylaminoethylcellulose) from aqueous thiocyanate-chloride media. However, several metal ions, including Cu(II), Zn, Cd, In, Bi and U(VI), exhibit enhanced adsorption on DEAE-cellulose from methanol-thiocyanate-hydrochloric acid mixtures. The distribution coefficients for these metals are given as functions of methanol, ammonium thiocyanate, and hydrochloric acid concentration. Differences in adsorption among metals permit many useful separations, including Ni, Cu, and Zn; mixed rare earths and hexavalent U; Cd and In; Ga and In; and Al and In, on short columns containing 1 to 1.5 g of DEAE-cellulose. (auth)

52952 SYNERGISTIC EFFECT OF TRI-n-OCTYLAMINE ON THE SOLVENT EXTRACTION OF CERIUM(III) BY THENOYLTRIFLUOROACETONE. Newman, L.; Klotz, P. (Brookhaven National Lab., Upton, N. Y.). Inorg. Chem.; 11: No. 9, 2150-4(Sep 1972).

The synergistic effect of tri-n-octylamine (R_3N) on the solvent extraction of cerium by thenoyltrifluoroacetone (HT) is shown to arise from the organic-phase reactions $CeT_3 + R_3NHCl = CeT_3R_3NHCl$, $CeT_3 + R_3NHT = CeT_3R_3NHT$, and $CeT_3 + R_3NHClHT = CeT_3R_3NHClHT$, where T^- represents the enolate ion of HT. It was ascertained that the formation constants for each of these reactions as measured in benzene are the same, and a value was found for $\log K_S = 4.83 \pm 0.15$. The synergistic effect in this system was found to be identical in kind and almost in magnitude with that observed in a previous investigation involving americium. (auth)

Inorganic, Organic, and Physical Chemistry

Refer also to abstract 53027.

Chemical and Physico-chemical Properties

Refer also to abstracts 52895, 53033, 53055, and 53664.

52953 (CONF-720716–1) SURFACE INTERACTIONS OF IODINE WITH Fe_3O_4. Hoinkis, E. (Oak Ridge National Lab., Tenn.). [nd]. 31p. Dep. NTIS.

From International conference and exhibition on vacuum instruments and methods in surface studies; Guildford, Surrey, UK (10 Jul 1972).

Surface interactions of iodine at low partial pressure with Fe_3O_4 at high temperature were studied because of interest in the mechanism that determines the transport and retention of fission-product iodine in the coolant circuits of high-temperature gas-cooled reactors. The distribution of iodine on Fe_3O_4 powder was studied as a function of the initial coverage and the temperature during adsorption. The two experimental techniques used were a pseudo-isopiestic method to expose Fe_3O_4 at high temperature to radioactive labeled gaseous iodine and thermodesorption to investigate the desorption of the adsorbed iodine into vacuum. Experiments were performed with iodine-loaded Fe_3O_4 samples with 4 different initial coverages at 250°C, then heated to 350° or 450°C. Results indicate that the temperature at the maximum desorption rate becomes independent of the initial coverage (of Fe_3O_4 with adsorbed iodine) and point to a first-order desorption process. Re-adsorption of desorbing iodine or its re-distribution on the surfaces during desorption experiments was negligible. Energy spectra are given. (J.G.B.)

52954 (NIM–1439) REACTION OF SULPHIDE MINERALS WITH THIOL COMPOUNDS. Goold, L. A. (National Inst. for Metallurgy, Johannesburg (South Africa)). 29 Jun 1972. 9p. Dep. NTIS (U. S. Sales Only).

A selected group of thiol reagents was reacted with a wide range of sulfide minerals including molybdenite for extraction of molybdenum, and products that were formed at the surface were extracted and identified by infrared spectrophotometry. Only pyrite oxidized the thiol reagent. With all other sulfide minerals for which reactions took place, the metal thiolate was formed at the mineral surface. These results agree with predictions from rest-potential measurements. (auth)

52955 (RT/CHI–(72)4) THERMOCHEMICAL REACTIONS BETWEEN ALKALINE HALIDES AND OXIDE IMPURITIES IN U_3O_8 MATRIX. Boniforti, R.; Ciancia, A.; Di Giorgio, G. (Comitato Nazionale per l'Energie Nucleare, Rome (Italy)). 21 Mar 1972. 46p. Dep. NTIS (U. S. Sales Only).

The action mechanism of alkali metal halides in the carrier distillation process was studied. The temperature data in the anodic charge allow the alkali metal halide carriers to be considered as melted; a solvent action of the carrier salt in respect to the oxide impurities containied in the U_3O_8 matrix is supposed. The possibility of some thermochemical reactions in the anodic cup was evaluated; the reaction products, formed during arcing, were identified by x-ray diffraction analysis. The x-ray diffraction data and the thermodynamic calculations generally are in rather good agreement. (auth)

52956 EARLY TRANSITION METALS. Kepert, D. L. New York; Academic Press Inc. (1972). 506p. $25.00.

Titles of the four chapters are: general properties of the early transition metals; group IV—titanium, zirconium, and hafnium; group V—vanadium, niobium, and tantalum; and, group VI—chromium, molybdenum, tungsten. References (2445), author and subject indexes are also included. (J.G.B.)

52957 CONTROLLED-POTENTIAL AND CONTROLLED-CURRENT CYCLIC VOLTAMMETER (25 Mar 1969) (Engineering Materials). (Oak Ridge National Lab., Tenn.). (CAPE–1653). 6 drawings.

This voltammeter is used in investigations of the electrochemical properties of molten-salt systems. The instrument operates in either the controlled-potential or controlled-current mode. In the controlled-potential mode it is used for linear-sweep voltammetry or chronoamperometry, and in the controlled-current mode for chronopotentiometry with control of the initial potential. (6 drawings) (For details see TID-4100 Suppl. 72) (F.S.)

Isotope Effects

Refer also to abstracts 52990 and 53009.

52958 (UR–3490-193) QUENCHING OF TYROSINE AND TRYPTOPHAN FLUORESCENCE BY H_2O AND D_2O. McGuire, Robert; Feldman, Isaac (Rochester Univ., N. Y. Dept. of Radiation Biology and Biophysics). 1971. 19p. Dep. NTIS.

The quantum yields and lifetimes of the fluorescence of tyrosine and tryptophan were determined in D_2O-H_2O and glycerol-H_2O solvent mixtures of varying composition from 10 vol.% to 100% H_2O at 15°C. For both amino acids the ratio of the quantum yields in D_2O and H_2O (i.e., q_D/q_H) was smaller than the ratio of the corresponding lifetimes (τ_D/τ_H). For tyrosine the ratio of the quantum yields in glycerol and H_2O (q_G/q_H) was also smaller than the corresponding τ_G/τ_H ratio, but for tryptophan $q_G/q_H \cong \tau_G/\tau_H$. The proximity of the q vs τ plots for tyrosine in the two solvent mixtures indicates that at 15°C neither D_2O nor glycerol, in the pure state or when diluted with H_2O, quenches tyrosine significantly. However, H_2O quenches tyrosine by a dynamic process, which increases both the radiative and the nonradiative rate constant. The quenching action is attributed to a tyrosine-H_2O exciplex, whose formation is independent of bulk viscosity and dielectric constant. Unlike tyrosine, tryptophan is quenched weakly by D_2O by a static process at 15°C, but H_2O quenches tryptophan much more efficiently by a dynamic process, which involves the nonradiative rate constant, but not the radiative constant. (auth)

52959 THEORETICAL STUDIES OF HYDROGEN KINETIC ISOTOPE EFFECTS. Schneider, Mary Elizabeth. New York,; Yeshiva Univ. (1971). 148p. University Microfilms Order No. 72-21,748.

Thesis.

Theoretical studies of hydrogen kinetic isotope effects were carried out with particular emphasis on the development of methods of analysis for the interpretation of experimental kinetic-isotope-effect data. Theoretical "exact" isotope-effect data are obtained by computer using a statistical-mechanical expression developed by Bigeleisen. "Exact" model-reaction calculations are used to determine the lower limit to the Arrhenius pre-exponential factors, A_Q, for primary hydrogen kinetic isotope effects in the harmonic approximation and in the absence of quantum mechanical tunneling. Attempts are made to force the A_Q values as low as possible solely through adjustments in the force constant changes, at the isotopic positions, between reactants and transition states. Values of A_Q lower than ~0.7 could not be achieved without making the models so mechanistically unreasonable as to render the results meaningless. This result is in excellent agreement with a prediction made by Bell on the basis of a less rigorous theoretical treatment and lends support to the common practice of interpreting experimental values of A_Q significantly lower than 0.5 as due to the operation of tunneling in the reactions. A method of using Arrhenius pre-exponential factors for secondary hydrogen kinetic isotope effects as sources of information in the elucidation of mechanisms of chemical reactions is developed. The Arrhenius intercepts associated with the individual force constant changes, from reactant to transition state at the isotopic position(s), occurring in a model reaction are found, under certain conditions, to be additive to give the intercept associated with the overall reaction. The same type of additivity is valid for the quantum mechanical contribution to the kinetic isotope effect. These additivity relationships provide a basis for a systematic method of determining force fields for real reaction systems through a combination of experimental measurements and model calculations. It is shown theoretically that low-magnitude, primary, hydrogen kinetic isotope effects may be characterized by the same types of temperature-dependence irregularities that were previously found to be expected fairly commonly for secondary hydrogen isotope effects and primary heavy-atom isotope effects. (Diss. Abstr. Int., B)

52960 MICROWAVE SPECTRUM AND RING-BENDING VIBRATION OF 3-OXETANONE. Gibson, James S.; Harris, David O. (Univ. of California, Santa Barbara). J. Chem. Phys.; 57: No. 6, 2318-28(15 Sep 1972).

The microwave rotational spectrum of 3-oxetanone was observed and assigned for the ground vibrational state, the first five excited states of the ring-bending vibrational mode, and the two carbon-13 isotopically substituted species. The features of the microwave spectrum indicate that the molecule has a single-minimum ring-bending vibrational potential and consequently a planar equilibrium configuration. Approximate models for the ring-bending vibrational mode were set up and the vibrational potential function interpreted in terms of contributions from ring-angle deformations and torsional interactions. The ^{13}C data were used to derive a partial substitution structure. Stark effect measurements yielded the dipole moment as 0.887 ± 0.005 D for the common isotopic species in the ground vibrational state. (auth)

52961 HYDRIDE ION TRANSFER AND ISOTOPE EFFECTS IN CD_4–SILANE ION MOLECULE REACTIONS. Stewart, G. W.; Henis, J. M. S.; Gaspar, P. P. (Monsanto Co., St. Louis). J. Chem. Phys.; 57: No. 6, 2247-8(15 Sep 1972). (COO–1713-29).

Hydride ion transfer is identified as an important mechanism in the reactions of methane and deuterated methane primary ions with silane. The pathway for these reactions is shown not to involve the production of a long-lived intermediate. However, it is shown that additional reactions proceeding through a long-lived intermediate show relatively little isotopic scrambling. Furthermore, it appears that the probability of losing a H atom is very much higher than that for losing a D atom from such an intermediate. (auth)

52962 HOT ATOM REACTIONS IN THE $HBr-Br_2$, $DBr-Br_2$ SYSTEMS. White, John M. (Los Alamos Scientific Lab., N. Mex.); Su, H. Y. J. Chem. Phys.; 57: No. 6, 2344-9(15 Sep 1972).

Reactions of photochemically generated hot hydrogen atoms were studied in $HBr-Br_2$ systems at 185 and 229 nm and in $DBr-Br_2$ systems at 185 nm. Kinetic analysis furnishes k_3/k_2, the rate coefficient ratio for the reactions, $H^* + Br_2 \xrightarrow{3} HBr + Br$ and $H^* + HBr \xrightarrow{2} H_2 + Br$. At 185 nm for HBr, $k_3/k_2 = 4.11 \pm 0.16$, while at 229 nm $k_3k_2 = 5.48 \pm 0.22$. For DBr at 185 nm the ratio is 5.07 ± 0.12. Complementary trajectory calculations were performed on a semiempirical potential energy surface. The results of these calculations suggest that the observed variations in k_3/k_2 arise primarily because the reaction cross section for Process (3) varies strongly with energy in the hot atom regime and is different for the HBr and DBr systems. (auth)

52963 VARIABLE TRAP PROBLEM IN ISOTOPIC MIXED CRYSTALS OF s-TRIAZINE. Fischer, Gad (Australian National Univ., Canberra). J. Chem. Phys.; 57: No. 7, 2646-52 (1 Oct 1972).

Theoretical treatments of isotopic mixed crystals, in general, assumed that the intermolecular interactions are equal and that the problem can be reduced to a consideration of the free molecule excitation energies. It is shown that for the isotopic s-triazines the intermolecular interactions are different and that now it is necessary to consider a trap depth that is both concentration and distribution dependent. This necessitated a modification of existing theories. Experimental results were obtained over the entire concentration range for the s-triazine$_{d-0}$/s-triazine$_{d-3}$ mixed crystal system, and the results are qualitatively explained in terms of a concentration dependent trap depth. (auth)

52964 KINETICS OF PROTON TRANSFER TO CYANINES. A TEMPERATURE-JUMP STUDY. Dynes, Paul J.; Chapman, Gretchen S.; Kebede, Eshetu; Schneider, Friedemann W. (Univ. of Southern California, Los Angeles). J. Amer. Chem. Soc.; 94: No. 18, 6356-63(6 Sep 1972).

A linear free energy type relationship has been obtained between the logarithm of the measured protonation rate constants of a number of substituted 2,2′-cyanines and the change in π-electron delocalization energies as a consequence of protonation. The absolute values of all rate constants measured by the T-jump technique are five to seven orders of magnitude below diffusion controlled indicating that protonation occurs on the methine carbon. Proton-transfer rate constants to the carbon from second acid-base pairs have Brønsted plots that are strongly unsymmetrical about $\Delta pK = 0$ showing saturation behavior at negative ΔpK values. Activation energies for proton transfer to pseudoisocyanine are between 8 and 9 kcal/mol, and entropies of activation are strongly negative leading to relatively low Arrhenius factors. Solvent isotope effects measured as a function of temperature for proton transfer involving acetic acid and pseudoisocyanine are large (~6). Kinetic salt effects support our assignment of relaxation times. Measurements in methanol–water solvents of varying dielectric constants suggest that the effective reaction distance for proton transfer may be relatively short. Thermodynamic parameters for proton transfer involving pseudoisocyanine are presented. (auth)

52965 H_2BH_3 AS AN INTERMEDIATE IN TETRAHYDRIDOBORATE HYDROLYSIS. Kreevoy, M. M.; Hutchins, J. E. C. (Univ. of Minnesota, Minneapolis). J. Amer. Chem. Soc.; 94: No. 18, 6371-6(6 Sep 1972).

The rate law corresponding to a simple, rate-determining, proton transfer fails to correlate rates of BH_4^- hydrolysis in basic solutions. A rate law arising from a mechanism involving an intermediate which can react with OH^- to regenerate BH_4^- successfully correlates all the observed rate constants. Under appropriate conditions BH_4^- exchanges hydrogen isotopes with the solvent. The exchange rate appears to be about half the rate of regeneration of BH_4^- from the intermediate. These observations strongly suggest an intermediate of composition BH_5 but with the added proton equivalent to only one of the original four. (auth)

52966 POTENTIAL FUNCTION FOR THE RING PUCKERING VIBRATION OF B_2H_6 AND B_2D_6. Pringle, W. C. Jr.; Meinzer, A. L. (Wesleyan Univ., Middletown, Conn.). J. Chem. Phys.; 57: No. 7, 2920-3(1 Oct 1972).

The v = 1 → 2 transition of the ring puckering mode of B_2H_6 was observed at 389.5 ± 0.5 cm^{-1} and identified on the basis of relative intensity measurements of the rotational fine structure of the overlapped v = 0 → 1 and v = 1 → 2 bands. The band center for the ring puckering fundamental was determined to be 369.3 cm^{-1} utilizing an asymmetric rotor calculation. The potential function for the ring puckering vibration based on the v = 0 → 1 and v = 1 → 2 transitions is $V(X) = 25.25(X^4 + 11.78X^2)$, where X is a reduced coordinate. The band centers for the v = 0 → 1 and v = 1 → 2 bands for B_2D_6 were assigned to the "holes" in the band envelope at 261.3 and 272.6 cm^{-1}, respectively. The rotational fine structure in the bands of the deuterated molecule was not resolved. The potential for the deuterated molecule predicted from a reduced mass model is $V(X) = 15.93(X^4 + 14.71X^2)$. (auth)

52967 ISOTOPIC MIGRATION EFFECTS OF ALKALINE IONS IN SULFURIC SOLUTIONS. Perie, Michele; Perie, Jacques (Univ., Paris). J. Chim. Phys.; 69: No. 6, 976-81(Jun 1972). (In French).

The differences between the mobilities of $^6Li-^7Li$ and $^{22}Na-^{24}Na$ ions were studied using electrophoresis on glass paper in water–sulfuric acid mixtures with the acid concentration varying between 9 and 95% (by weight). The isotopic effect increased with the sulfuric ion concentration until a maximum was reached (>0.02 for $^6Li-^7Li$) at a concentration of about 60%. This high value, which is similar to that obtained with molten salts, is probably due essentially to exchange equilibrium effects occurring between the free and associated cations. The diminution of the isotopic effect with H_2SO_4 concentrations greater than 70% may be interpreted by a different structure of the migration medium. (France)

52968 RAMAN SPECTRA OF MOLECULAR CRYSTALS: AMMONIA AND 3-DEUTERO-AMMONIA. Binbrek, O. S.; Anderson, A. (Univ. of Waterloo, Ont.). Chem. Phys. Lett.; 15: No. 3, 421-7(15 Aug 1972).

Raman and infrared spectra of polycrystalline samples of NH_3 and ND_3 were recorded at temperatures between 18 and 107°K. Features from metastable phases are identified, and assignments for the lattice and internal modes of the cubic crystals are proposed. (auth)

52969 MOLECULAR g-VALUE, MAGNETIC SUSCEPTIBILITY ANISOTROPY, MOLECULAR QUADRUPOLE MOMENT, AND SIGN OF THE ELECTRIC DIPOLE MOMENT IN CHLOROACETYLENE. Allen, W. C.; Flygare, W. H. (Univ. of Illinois, Urbana). Chem. Phys. Lett.; 15: No. 3, 461-4(15 Aug 1972).

The high-field molecular Zeeman effect was examined in $^{35}ClC_2H$ and $^{37}ClC_2H$ yielding the molecular g-values, $^{35}g_\perp = -0.00630 \pm 0.00014$ and $^{37}g_\perp = -0.00601 \pm 0.00008$; the magnetic susceptibility anisotropy, $(\chi_\parallel - \chi_\perp) = (9.3 \pm 0.5) \times 10^{-6}$ erg/G^2 mole; the quadrupole moment, $Q_\parallel = (8.8 \pm 0.4) \times 10^{-26}$ esu·cm^2, and the electric dipole moment sign of $-ClC_2H+$. (auth)

52970 TEMPERATURE DEPENDENCE OF THE HYPERFINE INTERACTIONS OF Eu^{2+} IN $SrCl_2$. Utley, H. B.; Mahendroo, P. P. (Texas Christian Univ., Fort Worth). Chem. Phys. Lett.; 15: No. 5, 553-4(1 Sep 1972).

ESR spectra of enriched $^{151}Eu^{2+}$ and $^{153}Eu^{2+}$ in a host lattice of $SrCl_2$ were observed at 9.3 GHz over the temperature range of 10 to 300°K. From the EPR spectra the Eu^{2+} hyperfine coupling constants and the Debye temperature were obtained. (auth)

52971 RAMAN SPECTRA OF ORTHORHOMBIC AND CUBIC HYDROGEN AND DEUTERIUM CHLORIDES AT TEMPERATURES ABOVE 80°K. Heastie, R. (Univ. of Waterloo, Ont.). Chem. Phys. Lett.; 15: No. 4, 613-16(1 Sep 1972).

Raman spectra of orthorhombic and cubic HCl and DCl and of liquid HCl were recorded. The significance of the measurements is discussed. (auth)

52972 OBSERVATION AND CALCULATION OF A POSITION DEPENDENT DEUTERIUM EFFECT ON THE TRIPLET LIFETIME OF ANTHRACENE-d_4. Charlton, James L.; Henry, Bryan R. (Univ. of Manitoba, Winnipeg). Chem. Phys. Lett.; 15: No. 3, 369-72(15 Aug 1972).

The lifetimes of anthracene, 1,4,5,8-anthracene-d_4 and 2,3,6,7-anthracene-d_4 were measured. The observed position dependent deuterium effect was theoretically accounted for. (auth)

Isotope Exchange and Isotope Separation

Refer also to abstracts 52996, 53052, and 53088.

52973 EFFECT OF VIBRATIONAL ANHARMONICITY ON HYDROGEN–DEUTERIUM EXCHANGE EQUILIBRIA INVOLVING AMMONIA MOLECULES. Bron, J.; Wolfsberg, Max (Univ. of California, Irvine). J. Chem. Phys.; 57: No. 7, 2862-9(1 Oct 1972).

The anharmonicity correction to the zero-point energy of isotopic ammonias was theoretically evaluated. The G_0 term, usually ignored, makes a significant contribution to this correction. Comparison of the corrections leads to the conclusion that the anharmonicity corrections to the isotopic self-exchange equilibria among the ammonias are negligible. Other correction factors to the self-exchange equilibrium constants calculated in the usual harmonic approximation are also considered and found to be quite negligible. The calculated self-exchange equilibrium constants were compared with experiment and good agreement found. Agreement was also found between theory and experiment for the isotopic exchange equilibrium constant between ammonia and hydrogen. (auth)

52974 ISOTOPIC EXCHANGE BETWEEN SOLID SILVER IODIDE AND IODINE IN p-CYMENE SOLUTION. Sugier, Henryk (Technical Univ., Lodz, Poland). Nukleonika; 17: No. 3-4, 205-6(1972).

The isotopic exchange between solid silver iodide and iodine in p-cymene solutions was studied in the temperature range 90°C to 190°C. It was found that at the temperature of $\beta-\text{AgI} \rightarrow \alpha-\text{AgI}$ phase change the rate constant of exchange increases by the factor of 13.5 but below and over this point it does not depend on the temperature. (auth)

52975 PRODUCTION OF HYDROGEN FOR DEUTERIUM EXTRACTION. Dirian, Gregoire; Leger, Daniel; Pauly, Jean (to Commissariat a l'Energie Atomique). French Patent 2,098,623. 10 Mar 1972. Filed 22 Jul 1970. (In French).

Water vapor is passed over a metal in the bulk state (Fe, Ni, or Cr), which reduces the water to hydrogen. The hydrogen formed is sent to a plant that extracts the deuterium. The metal is then regenerated by the deuterium-depleted hydrogen. Reduction of the water vapor and the regeneration of the metal are effected in two adjacent tubes. Heat exchange occurs between these tubes, a sensibly constant temperature being established in these tubes. The metal is brought to a temperature between 600 and 900°C. (France)

Feed Materials Processing

Refer also to abstract 53148.

52976 (IEA-250) PREPARATION OF CLEAR URANYL NITRATE SOLUTION BY FRACTIONAL DISSOLUTION OF SODIUM DIURANATE. Abrao, Alcidio; Franca, J. M. Jr. (Instituto de Energia Atomica, Sao Paulo (Brazil)). Nov 1971. 8p. (CONF-680571-1). Dep. NTIS (U. S. Sales Only).

From Materials technology: an inter-American approach conference; Sao Paulo, Brazil (May 1968).

A procedure for preparation of clear uranyl nitrate solutions by fractional dissolution of crude sodium diuranate (SDU) is described. The raw SDU used is obtained by industrial processing of monazite sand and contains some thorium, rare earth elements, iron, silicon and phosphorus as main impurities. With the procedure described, clear and stable uranyl nitrate solutions having 270 to 300 g/l U and exhibiting good filtration characteristics are obtained. The procedure allows a satisfactory removal of thorium, rare earth elements, phosphorus, silicon, and iron. (auth)

52977 NUCLEAR FUELS AND FUEL PROCESSING. Johari, S. S.; Bhandari, D. R. (Univ. of Jodhpur, India). Mfg. Eng.; 1: No. 4, 22-32(Jan 1971).

Extraction of thorium and uranium metal from their ores is outlined with a note on machining of materials. Three processes, solvent extraction, fluoride volatility, and oxidative slagging for fuel reprocessing, are described in detail giving the principle, procedure, advantages and disadvantages, etc. Four methods for enrichment of the fuel, gaseous diffusion process, thermal diffusion, electromagnetic method, and centrifugation, are briefly described. A short note is given on the separation of ^{233}U from thorium. (INIS)

Radiation Chemistry

Refer also to abstracts 52962, 54996, and 55018.

52978 (CEA-N-1528) PHOTOLYSIS AND RADIOLYSIS OF NITROMETHANE IN THE LIQUID PHASE. Tran-Dinh-Son (Commissariat a l'Energie Atomique, Saclay (France). Centre d'Etudes Nucleaires). Jun 1972. 119p. (In French). Dep. NTIS (U. S. Sales Only).

Thesis. Submitted to Paris Univ., Orsay, France.

The physical and chemical properties of nitromethane are summarized. The reaction of this substance with methyl radicals was studied by observing the reduction of CH_4 and C_2H_6 formed during the photolysis of acetone in aqueous nitromethane solutions of different concentrations. The photolysis and radiolysis of pure liquid nitromethane are described. All the products produced were analyzed and the existence of an important after-effect, which affects the yields of some of these products was demonstrated. The mechanisms responsible for the formation of all of these products are discussed. The differences between the reactions undergone by the ions and the primary radicals enabled the contributions of each type of dissociation to the radiolysis to be estimated. (France)

52979 (COO-1105-179) SOME PRELIMINARY PARAMAGNETIC RESONANCE STUDIES FOR DOSIMETRY RESEARCH. Fuller, G. E.; Leach, R. K.; Moran, P. R.; Fitzsimmons, W. A. (Wisconsin Univ., Madison. Dept. of Physics). [nd]. 12p. Dep. NTIS.

Paramagnetic resonance studies were made of some compounds that have potential application at room temperature as low radiation level dosimeters. Radioinduced radicals in arsenate-doped ammonium dihydrogen phosphate gave large ESR signals. The radiation yield, recombination rates, spin-lattice relaxation times, and EPR lineshapes of H atoms produced by 160-keV electron bombardment of solid H_2 in the temperature range from 1.4 to 8°K were measured. The estimated yield of 0.2 H atoms per 100 eV of ionizing radiation for low concentrations was in reasonable agreement with other experiments. (M.C.G.)

52980 (COO-3461-1) STUDY OF THE PULSE RADIOLYSIS OF GASES. Final Report. Dondes, S.; Harteck, P.; Carr, T.; Haskell, R. (Rensselaer Polytechnic Inst., Troy, N. Y.). 15 Sep 1972. Contract AT(30-1)-3821. 25p. Dep. NTIS.

The pulse radiolysis of gases and direct determination of short-lived species having lifetimes on the order of nanoseconds and longer are reported. This study is important in the determination of mechanisms and kinetics in radiation chemistry. At the inception of this work, emphasis was placed on experiments involving the wavelength range from about 2000 to 8000 angstroms, light focusing devices, elimination of noise and gamma flash interference within the signal, cell design, shielding, etc. Short-lived species were produced by the injection of high energy electrons from a 1-MeV van de Graaff Accelerator into various gaseous systems at pressures of about 20 atmospheres. Their presence was determined by analysis of their emission spectra. Lifetimes of the species, such as NO(γ) bands and NH bands, were determined using, single (0.5×10^{-6} second) pulse techniques on nitrogen—oxygen, nitrogen—nitric oxide, and helium—nitrogen mixtures. This area of the work indicated that a redesign of the Van de Graaff Electron Accelerator to produce 1×10^{-9} second pulses was necessary to determine the lifetimes of such species as the N_2^+ first negative bands, the N_2 second positive bands, etc. The available pulse widths are 1, 3, 10, 30, and 100 nanoseconds. (Changes in the Van de Graaff Electron Accelerator were enumerated in RPI-3821-5.) Use of the 1, 3, 10. and 30 nanosecond electron pulses in lifetime determinations of the N_2^+ first negative and N_2 second positive band systems was studied. The N_2 second positive band system was studied in pure nitrogen, helium—nitrogen and argon—nitrogen mixtures. The N_2^+ first negative band system was studied in helium—nitrogen mixtures. The observed radiative lifetimes for the N_2 second positive band system in pure nitrogen, Ar—0.5% N_2 and He—0.1% N_2 are 11.76, 12.23, and 13.66 nanoseconds, respectively. The observed lifetime of the N_2^+ first negative band system was found to be 18.69 nanoseconds. (auth)

52981 (COO-3571-3) RELATION BETWEEN SINGLE-STRAND DNA MASS AND SEDIMENTATION DISTANCE IN ALKALINE SUCROSE GRADIENTS. Levin, David; Hutchinson, Franklin (Yale Univ., New Haven, Conn. Dept. of Molecular Biophysics and Biochemistry). 1972. 21p. Dep. NTIS.

Single-strand breaks were introduced into T2 and B. subtilis DNA in dilute solution with gamma rays and the DNA sedimented on alkaline sucrose gradients. Assuming the number of single-strand breaks is linear with dose and the distance sedimented in alkaline sucrose gradients D is proportional to M^α (M is the single-strand DNA mass), the value of α was determined to be 0.40. (auth)

52982 (EUR-4765, pp 11-24) IONIC CHEMISTRY OF GASEOUS cC_6H_{12}. Cosandey, M.; Giardini, A.; Zocchi, F. (CNEN, Rome. Univ., Rome).

From 2nd conference on mass spectrometry; Ispra, Italy (1 Sep 1971).

Mass spectrometric studies were conducted on ion—molecule reactions in pure cyclohexane and in mixtures of cyclohexane and NH_3 and NO. The effects of small variable concentrations of several gases, including CO_2, SF_6, CO, N_2O, O_2, C_2H_2, and H_2O, on the ionic distribution in cyclohexane were also studied. Mechanisms for reactions within the systems are proposed and confirmed by comparison of results with those from γ-radiolytic studies on cyclohexane and cyclohexane—ND_3 mixtures. (J.G.B.)

52983 (EUR-4828) STUDY BY DIFFERENTIAL ABSORPTION IN INFRARED OF IRRADIATED LIPIDS AND POLYMERS.

Deschreider, A. R. (Ministere des Affaires Economiques, Brussels (Belgium)); Vigneron, J. M. (Centre National d'Assistance Technique et de Recherche Appliquee, Antwerp (Belgium)). 1972. 32p. (In French). Dep. NTIS (U. S. Sales Only).

In the case of examination by infrared spectrophotometry of gamma-irradiated substances, the differential absorption curves allow elimination of the difficulty of interpretation of normal infrared spectra. This technique was applied to irradiated frozen eggs, animal fats, and plastic packaging materials for foods. In all the cases, differential absorption bands were observed coming from typical frequential groups and, in particular for the irradiated polymers, their number was a function of the applied dose. (auth)

52984 (FRNC-TH-262) RADIATION EFFECTS ON IONIC AND MOLECULAR CRYSTALS. Dimitropoulos, Constantin (Universite Scientifique et Medicale de Grenoble (France)). 1972. 109p. (In French). Dep. NTIS (U. S. Sales Only).

Thesis.

The experimental techniques (nuclear quadrupole resonance, electron spin resonance, double resonance, optical spectroscopy, mass spectroscopy, chromatography) and the irradiation procedures used at high and low temperatures are described. $NaClO_3$ and paradichlorobenzene crystals exposed to γ and x radiations at 78°K, and paradichlorobenzene samples irradiated under different conditions (gamma rays, neutrons, dose rates, controlled atmosphere) at temperatures greater than the melting point were studied. The results obtained are discussed. (France)

52985 (NASA-TM-X-2440, pp 584-94) MICROSCOPIC OBSERVATION OF X-RAY AND γ-RAY-INDUCED DECOMPOSITION OF AMMONIUM PERCHLORATE CRYSTALS. Herley, P. J. (Picatinny Arsenal, Dover, N. J.); Levy, P. W. Jan 1972.

From Symposium on natural and manmade radiation in space; Las Vegas, Nev. (1 Mar 1971).

The x-ray- and γ-ray-induced decomposition of ammonium perchlorate (a commonly used oxidizer in solid propellents) was studied by optical, transmission, and scanning electron microscopy. In some respects the radiation-induced damage closely resembles the effects produced by thermal decomposition, but in other respects the results differ markedly. Similar radiation and thermal effects include the following: (a) irregular or ill-defined circular etch pits are formed in both cases; (b) approximately the same size pits are produced; (c) the pit density is similar, namely ~2 to 40 × 10^6/cm^2; (d) the c face is considerably more reactive than the m face; and (e) most importantly, many of the etch pits are aligned in crystallographic directions which are the same for thermal or radiolytic decomposition. Thus, dislocations play an important role in the radiolytic decomposition process. Radiolytic decomposition produces at least three effects not previously observed with ammonium perchlorate: (a) after 10^8 rad γ-ray irradiated crystals effervesce during solution in water; (b) the initial x-ray and γ-ray induced decomposition sites occur throughout the volume where energy is deposited. Once formed they continue to grow. In contrast, the initial thermal pits appear at the surface and grow. New pits are formed as the reaction zone proceeds inward; (c) x-ray irradiation produces highly strained crystals. The layer adjacent to the irradiated surface becomes extensively cracked and large crystals have pronounced convex curvature. Inasmuch as the principal decomposition is restricted to certain crystallographic sites, highly mobile energy transfer mechanisms must play an important role in the radiolytic decomposition and ammonium perchlorate. Most likely, the transfer agents are electrons, holes, excitons, or possibly protons. (auth)

52986 (ORNL-4794, pp 98-101) MISCELLANEOUS PROGRAMS. Aug 1972.

In Chemical Technology Division annual progress report for period ending March 31, 1972.

Research progress is reported on: quality assurance program, evaluation of the radiation resistance of selected protective coatings, resource studies, and environmental impact of nuclear power reactors and chemical reprocessing plants. (D.H.M.)

52987 (ORO-2968-78) RESEARCH CONCERNING IONIC AND FREE RADICAL REACTIONS IN RADIATION CHEMISTRY. Progress Report, September 15, 1971-August 15, 1972. Williams, T. Ffrancon (Tennessee Univ., Knoxville. Dept. of Chemistry). 1972. Contract AT(40-1)-2968. 106p. Dep. NTIS.

Research progress is reported on intermediate species produced in γ-irradiated organic and inorganic compounds at low temperatures and on ESR studies of radical trapping in the radiolysis of organic liquids. Project summaries are given with references to published work. Separate abstracts were prepared for 4 "in press" papers attached. (M.C.G.)

For abstracts of individual papers see: 52988-52991.

52988 (ORO-2968-78, Paper 2) ELECTRON SPIN RESONANCE STUDIES OF RADICAL TRAPPING IN THE RADIOLYSIS OF ORGANIC LIQUIDS. I. EVIDENCE FOR THE PRIMARY FORMATION OF THE METHOXY RADICAL IN METHANOL. Wargon, Jorge A.; Williams, Ffrancon. 1972. 9p.

In Research concerning ionic and free radical reactions in radiation chemistry.

Utilization of the spin trapping technique is reported in resolution of the problem of primary radical formation in the γ radiolysis of deaerated liquid methanol. Results indicated that the methoxy radical is the most abundant primary radical formed. (M.C.G.)

52989 (ORO-2968-78, Paper 4) INVESTIGATION OF THE STRUCTURE OF THE HYDRATED ELECTRON BASED ON UNPAIRED ELECTRON DENSITIES CALCULATED BY THE INDO METHOD. Kerr, Carolyn M. L.; Williams, Ffrancon. 1972. 19p.

In Research concerning ionic and free radical reactions in radiation chemistry.

Spin density distributions were calculated for a number of possible structures for the hydrated electron, and the total spin density associated with the hydrogen atoms compared with the value derived from ESR experiments. Although the agreement with experiment was not close, the best results were obtained for a planar dimeric structure containing two central hydrogens close to one another. The structure of the hydrated electron may incorporate symmetrically placed units of this type. (auth)

52990 (ORO-2968-78, Paper 5) HYDROGEN ATOM ABSTRACTION BY METHYL RADICALS IN METHANOL GLASSES AT 67 TO 77°K. Campion, Alan; Williams, Ffrancon. 1972. 20p.

In Research concerning ionic and free radical reactions in radiation chemistry.

It was shown by ESR studies that the thermal decay of $CH_3\cdot$ radicals in a methanol-d glass at 77°K proceeds with the concomitant formation of the $\cdot CH_2OD$ radical. The reaction obeys first-order kinetics over 75% of its course and there is reasonably good agreement between the rate constants as determined from $CH_3\cdot$ decay and $\cdot CH_2OD$ growth. At 77°K, the rates of H-atom abstraction by $CH_3\cdot$ from CH_3OD and CH_3OH are comparable but the rate of $CH_3\cdot$ decay in CD_3OD is slower by at least a thousandfold. This primary deuterium isotope effect confirms that abstraction occurs almost exclusively from the hydrogens of the methyl group. The apparent activation energy of 0.9 kcal mol^{-1} for the abstraction reaction in the glassy state at 67 to 77°K is much lower than the value of 8.2 ± 0.2 kcal mol^{-1} previously reported for essentially the same reaction in the gas phase above 376°K. These findings are similar to those reported for H-atom abstraction by $CH_3\cdot$ radicals from acetonitrile and methyl isocyanide, and are consistent with the proposal that these reactions proceed mainly by quantum-mechanical tunneling at low temperatures. (auth)

52991 (ORO-2968-78, Paper 6) ESR STUDIES OF ALIPHATIC RADICAL ANIONS AND RADICAL-ANION PAIRS IN γ-IRRADIATED CRYSTALLINE SOLIDS. Bonin, M. A.; Chung, Y. J.; Sprague, E. D.; Takeda, K.; Wang, J. T.; Williams, F. 1972. 19p.

In Research concerning ionic and free radical reactions in radiation chemistry.

ESR studies on γ-irradiated acetonitrile, adiponitrile, succinonitrile, acrylonitrile, tert-butyl isocyanate, and tert-butyl isothiocyanate crystals are reported. Reactions of the radical anions and radical-anion pairs are summarized. (M.C.G.)

52992 (RFP-1924) THERMAL AND RADIATION STABILITY OF POLYVINYL CHLORIDE. Kazanjian, A. R.; Horrell, D. R. (Dow Chemical Co., Denver, Colo. Rocky Flats Div.). 1 Sep 1972. Contract AT(29-1)-1106. 6p. Dep. NTIS.

A study was made of the thermal and radiation stability of the poly(vinyl chloride) bags used for plutonium storage at Rocky Flats. The poly(vinyl chloride) (PVC) was subjected to temperatures of 98 to 140°C, and gamma radiation up to doses of 2.1 × 10^6 rads. It was found that radiation and heat, applied together, significantly lowered the physical strength of the PVC, whereas applied individually to the same levels the effects were negligible. Oxygen in air was shown to be necessary for a rapid rate of degradation. It was estimated that the PVC bags could be used for almost indefinite storage periods under the usual conditions (i.e., less than 98°C and very low radiation doses) at Rocky Flats. (auth)

52993 (RRL-3238-398) QUARTERLY REPORT, APRIL 1, 1972-JUNE 30, 1972. Fundamental Research No. 6041. (Mellon Inst. of Science, Pittsburgh, Pa. Radiation Research Labs.). 27 Jul 1972. Contract AT(11-1)-3238. 17p. Dep. NTIS.

Research progress is reported on ESR spectra of radiolytic radicals and other radiation chemistry studies. Journal publications are listed and abstracts of reports issued are included. (M.C.G.)

52994 PEROXIDATION OF POLYMETHYLHYDROGENSILOXANE AND CELLULOSE BY γ-IRRADIATION IN AIR AND GRAFTING INDUCED BY THEIR DECOMPOSITION. Shimizu, Harumichi (Tokyo Metropolitan Isotope Research Center). J. Nucl. Sci. Technol. (Tokyo); 9: No. 8, 473-9(Aug 1972).

The peroxides of polymethylhydrogensiloxane, cellulose, and a mixture of both were determined by the ferrous ion method. The relation between the decomposition of the peroxide and the degree of grafting by standing at an elevated temperature after irradiation was examined. The G-value for the peroxide formation of polymethylhydrogensiloxane was found to be 8.7, and the activation energy for the peroxide decomposition was determined from calculation to be 43 kcal/mole. The ratio of G-values of silicone between those terminated by methoxy radical and by methyl radical is estimated to be about 2/1. It would thus appear certain that the rate of peroxidation is affected by the end group. The peroxidation is not a chain reaction at room temperature, and the peroxide is produced by the recombination of the peroxy radical. At least two types of peroxide are produced by irradiation in air, and one is decomposed at 80°C but the other is relatively stable. On the other hand, the G-value for the peroxide formation of cellulose is equal to 5.6. The tendency seen for the decrease of the peroxide corresponds to that of increasing degree of grafting, and it may be concluded that only 1/10 of the peroxides formed in the cellulose–silicone system results in grafting, since it was calculated that the G-value for the grafting through the peroxide is about 1.0. (auth)

52995 ESR STUDY OF AMINO ACID AND PROTEIN-FREE RADICALS IN SOLUTION. IV. AN ESR STUDY OF GAMMA-IRRADIATED AMINO ACIDS IN FROZEN AQUEOUS SOLUTIONS. Hong, Sun Joo; Holmes, D. E.; Piette, L. H. Daehan Hwahak Hwoejee; 15: No. 5, 256-65(1971).

An ESR study was made on free radicals produced in frozen aqueous solutions (ices) of glycine, DL-α-alanine, DL-serine, L-cysteine, DL-leucine, and DL-isoleucine by γ-irradiation at dry ice temperature. All free radicals induced were decayed concomitant to the successive annealing but the radical species which was believed to be dominant seems to be stable even near the melting point of the ice. These dominant species were found to be identical to those resulting from direct action of radiation in the solid at room temperature. Small but significant changes in the spectra of glycine and DL-α-alanine were observed by varying the microwave power. These results seem to support the view that the spectra obtained were a composite of more than two different resonances having different power saturation characteristics. The relative contribution of unidentified resonances to the composite spectra was greater for solutions of low concentration. These resonances are assumed to be induced by indirect effects, mainly hydrogen abstraction by radiation produced hydroxyl radicals and also C–N bond cleavage hydrated electrons. (Korean Sci. Abstr.)

52996 ELECTRON SPIN RESONANCE AND ELECTRON NUCLEAR DOUBLE RESONANCE OF SINGLE CRYSTALS OF DL-SERINE. Castleman, Bruce Wayne. Tallahassee; Florida State Univ. (1972). 151p. University Microfilms Order No. 72-21,303.

Thesis.

The free radicals produced in x-irradiated single crystals of DL-serine in the temperature range 77 to 340°K were identified using ESR and electron nuclear double resonance (ENDOR) techniques. At 77°K the primary products are molecular anions and cations. The DL-serine cation successor has been proposed as the radical $HOCH_2\dot{C}H(NH_3^+)$, produced by decarboxylation, which decays upon warming the crystal to 153°K to the species $HO\dot{C}HCH(NH_3^+)COO^-$ through an intermolecular hydrogen abstraction. It is proposed that the anion is $HOCH_2CH(NH_3^+)\dot{C}OO^{2-}$, which is neutralized by means of proton transfer and becomes $HOCH_2CH(NH_3^+)CO^-OH$. At about 153°K this species decays through deamination to the form $HOCH_2\dot{C}HCOOH$, which is stable only in the range 153 to 173°K. Above 173°K this species undergoes a molecular reorientation and persists to room temperature. It then decays at room temperature through two separate paths to yield the species $HO\dot{C}HCH(NH_3^+)COO^-$ and $HOCH_2\dot{C}(NH_3^+)COO^-$, which are stable at room temperature. Irradiation with 3-MeV x rays at 300°K yields initially the species $HOCH_2\dot{C}HCOOH$, which decays as above. Deuterated crystals after irradiation at 300°K undergo hydrogen–deuteron exchanges and eventually yield the species $DOCD_2\dot{C}DCOOD$. An ENDOR spectrometer was constructed and used to identify one of the radical species. A description of the ENDOR system is given. (Diss. Abstr. Int., B)

52997 DECOMPOSITION OF ALDRIN BY GAMMA RADIATION. II. IN LIPID SOLUTIONS. Carp, A. E.; Liska, B. J.; Ziemer, P. L. (Purdue Univ., Lafayette, Ind.). Bull. Environ. Contam. Toxicol.; 7: No. 6, 331-7(1972).

A study was made of the effects of γ irradiation on aldrin dissolved in corn oil and lard by varying conditions used in packing, irradiating, and storing the samples. The only treatment which produced any major alteration of the amounts of the isomers formed was the temperature at which irradiation was accomplished. The chromatographs of the samples irradiated without any temperature control generally showed four peaks, while those irradiated at −196°C showed only three. (D.H.M.)

52998 FORMATION OF ANTIBIOLOGICAL SUBSTANCES BY RADIATION-CHEMICAL REACTION. OCCURRENCE OF ANTIBACTERIAL ACTIVITY AFTER GAMMA IRRADIATION FROM TWO CONSTITUENT MOIETIES OF THE CHLORAMPHENICOL MOLECULE. Tamemasa, Osamu; Goto, Rensuke (Shizuoka Coll. of Pharmacy, Japan). Yakugaku Zasshi; 92: No. 1, 104-8(Jan 1972). (In Japanese).

In order to develop a new molecular species of compounds with antibiological activities by the application of radioinduced reactions, a model experiment was carried out to see whether chloramphenicol would be formed by γ irradiation of some mixtures of nitrobenzene, p-nitrophenol, or p-bromonitrobenzene, and 2-dichloroacetamidopropane-1,3-diol. The results showed that after irradiation of 100 to 200 × 10^4 R, antibacterial activities against E. coli and St. aureus of only the aqueous mixture of nitrobenzene and 2-dichloroacetamidopropane-1,3-diol were about 4 to 8 times greater than those of each irradiated component or of the mixture of each irradiated component. No formation of chloramphenicol itself was, however, confirmed in the irradiation products by means of paper chromatography, bioautography, radiopaper chromatography, or Sephadex G-10 gel filtration. (auth) (Japan)

52999 RADIATION ABSTRACTION OF HYDROGEN ATOMS IN SINGLE CRYSTALS OF THYMINE. Dulcic, A.; Herak, J. N. (Inst. Rudjer Boskovic, Zagreb). J. Chem. Phys.; 57: No. 6, 2537-40(15 Sep 1972).

Single crystals of both thymine monohydrate and anhydrous thymine were irradiated at 77°K and the radicals induced were analyzed with ESR spectroscopy. The radical species, formed by abstraction of a hydrogen atom from nitrogen, was studied in detail. Molecular orbital calculations suggest that the abstraction takes place from $N_{(1)}$. The nitrogen and the methyl proton coupling tensors are identical in both crystal systems. The $\tilde{g}$ tensor is axially symmetric ($g_{\|} = 2.0032$, $g_{\perp} = 2.0064$) with the axis of symmetry perpendicular to the ring plane. The differences between deuterated and undeuterated thymine monohydrate crystals are also discussed. (auth)

53000 FORMATION OF ACETYLENE AND METHANE IN ARGON AND XENON SENSITIZED RADIOLYSIS OF GASEOUS ETHYLENE. Gawlowski, Janusz; Niedzielski, Jan; Sobkowski, Jerzy (Univ., Warsaw). Nukleonika; 16: No. 11-12, 513-21(1971).

The radiation yields of methane and acetylene in argon- and xenon-sensitized radiolysis of gaseous ethylene were determined. $G(C_2H_2)$ and $G(CH_4)$ decreased with increasing argon pressure over the range 50 to 700 torr. $G(C_2H_2)$ was practically independent of the pressure of xenon. Results indicate that in the radiolysis of ethylene some part of the acetylene is formed in ion-molecule reactions, originating with primary vinyl and acetylene ions. Methane is formed predominantly by the dissociation of butyl ions $[C_4H_9^+]^*$. The lifetime of excited butenyl ions is approximately 5 times shorter than that of butyl ones. Charge transfer from acetylene ions to ethylene is unaffected by the changes in the pressure of a rare gas. (auth)

53001 PREPARATION OF ANHYDROUS HYDRAZINE BY THE RADIOLYSIS OF LIQUID AMMONIA. Belloni, Jacqueline Dolores Therese; Fradin de la Renaudiere, Jean Jacques Marie. French Patent 2,087,507. 31 Dec 1971. Filed 21 May 1970. (In French).

A method of preparing pure anhydrous hydrazine by the radiolysis of liquid ammonia with γ rays from ^{60}Co, or a beam of accelerated electrons, is described. The method consists of adding various salts (amide, imide, nitride, or hydride) to the liquid ammonia in order to make its pH basic. The solution is then irradiated. Fractional distillation is used to separate the hydrazine from the synthesizing medium. (France)

53002 SHOULDER OF OPTICAL ABSORPTION SPECTRUM OF THE TRAPPED ELECTRON IN GAMMA-IRRADIATED CRYSTALLINE ICE. Kawabata, Keisuke; Okabe, Shigeru; Taniguchi, Setsuo (Radiation Center, Osaka). J. Chem. Phys.; 57: No. 7, 2855-6(1 Oct 1972).

Precise measurements of the absorption spectrum and its differential of the trapped electron in crystalline ice were made. The absorption spectrum, due to a single kind of trap, has a shoulder around 5000 to 5600 Å, suggesting that it is composed of at least two components. (auth)

53003 PULSE RADIOLYSIS STUDY OF SUCCINONITRILE IN THE ROTATOR PHASE. Campion, Alan (Univ. of Tennessee, Knoxville); Ghormley, John A.; Williams, Ffrancon. Contract AT(40-1)-2968. J. Amer. Chem. Soc.; 94: No. 18, 6301-4(6 Sep 1972). (ORO-2968-71).

A transient absorption spectrum ($t_{½}$ = 0.23 μsec) was detected in the pulse radiolysis of succinonitrile, a plastic crystal at room temperature. This absorption is not produced in the presence of 1 mole % tetracyanoethylene (TCNE) and the spectrum of $TCNE^{\bar{\cdot}}$ is observed instead. The value of λ_{max} (450 nm) for the transient corresponds to the absorption maxima observed in the low-temperature spectra of monomer radical anions from acetonitrile and adiponitrile. On the basis of these results, the transient spectrum is assigned to a monomer radical anion of succinonitrile although the possibility of a dimer species similar to that observed at low temperature cannot be excluded. The first-order decay of the radical anion is attributed to the unimolecular dissociation to $\cdot CH_2CH_2CN$ and CN^-. In addition to the radical anion, a long-lived species is produced which absorbs most strongly in the ultraviolet. (auth)

53004 ELECTRON SPIN RESONANCE AND ELECTRON NUCLEAR DOUBLE RESONANCE STUDIES OF DL-SERINE. II. IDENTIFICATION OF FREE RADICALS PRODUCED IN THE RANGE 153 TO 340°K. Castleman, B. W.; Moulton, Grace C. (Florida State Univ., Tallahassee). J. Chem. Phys.; 57: No. 7, 2762-8(1 Oct 1972).

Single crystals of x-irradiated DL-serine, deuterated DL-serine, and α-D-1-DL serine were examined in the temperature range 77 to 340°K using ESR and ENDOR techniques. Six of the radical species observed were identified and the mechanisms by which these species are formed are discussed. The initial species produced at 77°K are the anion and cation radicals that decay through inter- and intramolecular processes and finally form two stable radicals at room temperature. (auth)

53005 ESR STUDY OF AN IRRADIATED SINGLE CRYSTAL OF ACETYLENE DICARBOXYLIC ACID DIHYDRATE. Muto, Hachizo; Toriyama, Kazumi; Iwasaki, Machio (Government Industrial Research Inst., Nagoya, Japan). J. Chem. Phys.; 57: No. 7, 3016-17(1 Oct 1972).

ESR spectra are shown for an irradiated single crystal of acetylenedicarboxylic acid dihydrate measured after irradiation at 77°K in the dark, after annealing at −140°C for 5 min, and after annealing at −90°C for 10 min. (M.C.G.)

53006 PULSE RADIOLYSIS OF LIQUIDS AT HIGH PRESSURES. III. HYDRATED-ELECTRON REACTIONS NOT CONTROLLED BY DIFFUSION. Hentz, Robert R.; Farhataziz; Hansen, Earl M. (Univ. of Notre Dame, Ind.). J. Chem. Phys.; 57: No. 7, 2959-63(1 Oct 1972).

Specific rates of the reactions of e_{aq}^- with hydrogen ion, formamide, acetamide, acetoxime, benzyl alcohol, and 2-chloroethanol were measured by pulse radiolysis at 29°C and six pressures from atmospheric to 6.4 kbar. The specific rates increased monotonically with increases in pressure to 6.4 kbar except that for the H_3O^+ reaction, for which there was no further significant increase above ~3.5 kbar. Results for the H_3O^+ reaction were consistent with that reaction not being diffusion controlled. The activation volume of each reaction increased with increases in pressure. Such a result is attributed to a decrease in cavity volume of the electron with increase in pressure. Activation volumes, in units of milliliters per mole, at 1 atm and 29°C are −2.7, −10.3, −7.0, −9.5, −9.3, and −8.2 for reactions with H_2O^+, formamide, acetamide, acetoxime, benzyl alcohol, and 2-chloroethanol, respectively. Interpretation of the activation volumes gives a partial molal volume of 7 ml $mole^{-1}$ and, with an electrostriction volume of 3 ml $mole^{-1}$, a cavity volume of 10 ml $mole^{-1}$ for the electron in water at 1 atm and 29°C. A previous estimate of $\overline{V}(e_{aq}^-)$ = 0 ml $mole^{-1}$, based on study of competitive reactions of e_{aq}^- by γ radiolysis at high pressures, is reconciled with the value of $\overline{V}(e_{aq}^-)$ = 7 ml $mole^{-1}$. (auth)

53007 SOLVATION OF ELECTRONS IN 3-METHYLHEXANE AT 77°K. Richards, J. T. (Univ. of Salford, Eng.); Thomas, J. K.; Klassen, N. V.; Gillis, H. A.; Walker, D. C. J. Chem. Phys.; 57: No. 7, 3025-8(1 Oct 1972).

Previous time dependence of the spectra of radiolytic solvated electrons in organic glasses was not observed in the absorption spectra of e_s^- in 3-methylhexane liquid at −78°C, but rather a decay with time of the whole spectrum. Also reported are similar absorption data in propane from 1500 to 1700 nm. (M.G.C.)

53008 POSSIBLE IDENTIFICATION OF Pb^{1+} AND PbH^{2+}: AN ELECTRON PARAMAGNETIC RESONANCE STUDY. Roberts H. C.; Eachus, R. S. (Eastman Kodak Co., Rochester, N. Y.). J. Chem. Phys.; 57: No. 7, 3022-3(1 Oct 1972).

ESR spectra tentatively assigned to Pb^+ and PbH^{2+} were obtained from x-irradiated $Pb(C_2H_3O_2)_2 \cdot 3H_2O$ powders and single crystals at 77°K. The analysis and assignments are based on the observed principal g factors and the detection of hyperfine splittings from the ^{207}Pb isotope. (M.C.G.)

53009 EFFECT OF THE STRUCTURE OF THE SOLID PHASE ON HNO_3 RADIOLYSIS. Kozlowska-Milner, Ewa (Inst. of Nuclear Research, Warsaw). Nukleonika; 17: No. 1-2, 11-22(1972).

A considerable change in ESR spectra (at 77°K) of HNO_3 and DNO_3 frozen under various conditions of crystallization and subjected to γ irradiation in a ^{60}Co source was observed. The spectrum of the acid dispersed in the xenon or chloroform matrices resembles the spectrum of rapidly frozen acid of vitreous structure. A spectrum of a type not hitherto observed was obtained for the acid crystallized slowly at a temperature near the melting point. A far more complex structure of NO_3 and NO_2 signals was observed. In contradiction to previous works it is assumed that in the HNO_3 medium the rotational motion of NO_2, observed in some other systems at 77°K, does not occur, and the g tensor is nonaxially symmetric. Splitting of individual NO_2 signals into doublets, observed for slowly crystallized acid, is presumably due to the interaction of proton through a short hydrogen bond of NO_2 in HNO_3. In nitric acid medium deformation of the NO_3 radical occurs, which is reflected in the full anisotropy of the g tensor. The spectral data for the NO_3 radical are similar to those obtained for urea nitrate. This implies the presence of a hydrogen bond of NO_3 in HNO_3 medium. The triplet structure (splitting of ~3.5 G) of the NO_3 signals is noted. Quantitative evaluation indicates a decrease of the NO_3/NO_2 ratio for the acid rapidly frozen in liquid nitrogen (vitreous structure) or for the acid dispersed in the xenon matrix. These changes are interpreted taking also into account ir data, as an effect of various structure of the associates on the radiolysis of HNO_3. (auth)

53010 RADIOTHERMOLUMINESCENCE OF CYCLOHEXENE. Rybicki, Edward; Kroh, Jerzy (Technical Univ., Lodz, Poland). Nukleonika; 17: No. 1-2, 59-67(1972).

The radiothermoluminescence (RTL) of cyclohexene, its dependence on the absorbed γ dose and the presence of various additives (CH_3OH, CCl_4, C_6H_6), was investigated. Experiments on photobleaching made possible identification of $C_6H_{10}^+$ cations. Results suggest that the recombination of cyclohexene cations and anions plays an important role in RTL of C_6H_{10}. (auth)

53011 HYDROGEN SULFIDE RADIOLYSIS SENSITIZED BY ARGON, KRYPTON, XENON, AND NITROGEN. Jezierska, Krystyna; Forys, Mieczyslaw (Univ. of Warsaw). Nukleonika; 17: No. 1-2, 23-9(1972).

Gaseous mixtures of hydrogen sulfide with argon, krypton, xenon, and nitrogen were subjected to γ radiolysis in a wide range of concentrations. The main role of charge-transfer processes in sensitized radiolysis of hydrogen sulfide is demonstrated. It is shown that a competition between charge transfer to hydrogen sulfide and formation of dimeric ions takes place, which causes the linear dependence of $G(H_2)^s$ on $[R]^2/[H_2S]$ ratio. Charge transfer rate constants were calculated: $k_{Ar^+ + H_2S}$ = 1.0 10^{-10} cm^3/molecules × s, $k_{Kr^+ + H_2S}$ = 2.6 × 10^{-11} cm^3/molecules × s, and $k_{N_2^+ + H_2S}$ = 1.1 · 10^{-9} cm^3/molecules × s. (auth)

53012 RADIATION SULFOXIDATION OF n-PARAFFINS. I. Kowalski, Antoni; Bogus, Wlodzimierz; Perkowski, Jan (Miedzyresortowy Instytut Techniki Radiacyjnej, Lodz, Poland). Nukleonika; 17: No. 1-2, 31-45(1972). (In Polish).

The radioinduced sulfoxidation process was investigated for two fractions of normal paraffins: C_{10} to C_{14} and C_{14} to C_{17} respectively. A critical review of the mechanism of radioinduced sulfoxidation as proposed by different authors is also included. Results of investigations on the following problems are presented: dependence of the rate of sulfoxidation on the purity of paraffins and methods of their purification, the influence of dose rate on reaction rate, relation between the pressure of gaseous reagents and rate of the sulfoxidation process, and the possibility of synthesis when only gases entering the reactor are irradiated. Highest reaction rates were observed with alkanes which were used in previous sulfoxidation experiments. The alkanes available contained some inhibitors of the sulfoxidation process. The reaction yields for the sulfoxidation were about 1200 for alkanes C_{10} to C_{14} and 650 for fraction C_{14} to C_{17}. It was found that the yield of sulfuric acid diminished with an increasing degree of conversion. A very low yield of sulfoxidation products was observed in the case when gases entering the reactor were irradiated but no radiation was applied to hydrocarbons. (auth)

53013 CROSSLINKED NYLON BY IRRADIATION OF A GRAFT COPOLYMER OF NYLON WITH AN ETHYLENE/ ACRYLATE OR MODIFIED COPOLYMER. Galiano, Francis R.; Thackaberry, Samuel P.; Smith, Wayne E.; Anderson, Raymond P. (to Custom Resins, Inc.). U. S. Patent 3,681,216. 1 Aug 1972. Filed 13 Jun 1969.

The nylon articles such as films and fibers are effectively crosslinked by irradiation to obtain dimensional stability, memory, and resistance to heat and solvents without significant polymer degradation by employing a graft of a nylon polymer grown on an ethylene-acrylate copolymer as initiator and restricting the dose of ionizing radiation to a low dose of about 5 to 20 megarads. Higher doses gave a highly crosslinked polymer with significantly lower degradation than with nylon homopolymers. The preferred ethylene copolymer has a portion of the acrylate converted to amide. (Official Gazette)

53014 DECOMPOSITION OF ALDRIN BY GAMMA RADIATION. I. IN ORGANIC SOLVENTS. Carp, A. E.; Liska, B. J.; Ziemer, P. L. (Purdue Univ., Lafayette, Ind.). Bull. Environ. Contam. Toxicol.; 7: No. 6, 321-30(1972).

Aldrin, dissolved in hexane in initial concentrations of 1 mg/ml and 10 mg/ml, was irradiated at three different dosages: 0.5 Mrad, 3.0 Mrad and 6.0 Mrad. As the total absorbed dose increased, the decomposition of aldrin increased. As the percent of aldrin remaining in the sample decreased, the amounts of the products formed increased. The major radiation product has a retention time relative to aldrin of 0.72. The second most intense new peak formed by irradiation of aldrin dissolved in hexane was one with a retention time relative to aldrin of 1.20. In contrast to the 0.72 peak, the percent of the 1.20 compound was greater in the 10 mg/ml sample than it was in the 1 mg/ml sample. The effects of temperature and solvent on the radiolysis were also studied. (D.H.M.)

53015 DETERMINATION OF RATE CONSTANTS FOR THE REACTIONS OF H, OH, AND e^-_{aq} WITH INDOLE-3-ACETIC ACID AND OTHER PLANT HORMONES. Shetiya, R. S.; Rao, K. N.; Shankar, J. (Bhabha Atomic Research Centre, Bombay). Radiat. Eff.; 14: No. 3-4, 185-9(Jun 1972).

In the radiolysis of aqueous solutions of indole, indole-3-acetic acid, indole-3-propionic acid, 1-naphthylacetic acid and phenylacetic acid, the absolute rate constants of their reactions with H and OH were determined by competition kinetics using 2-propanol as the competitor. Hydrated electron reaction rate constants were determined for indole, indole-3-acetic acid and indole-3-propionic acid at pH = 11 using the decay of the hydrated electron generated by the photolysis of OH^- in a H_2 saturated solution. The rate constants were compared with literature values for other indole derivatives. (auth)

53016 EFFECT OF GAMMA RADIATION ON ION EXCHANGE RESINS. IV. DEGRADATION AND CROSSLINKING IN POLYSTYRENESULFONIC CATION EXCHANGE RESIN ZEROLIT 225 OF DIFFERENT DVB CONTENT. Narebska, Anna; Mazurkiewicz, Barbara (Univ., Torun, Poland). Nukleonika; 17: No. 3-4, 169-79(1972). (In Polish).

Investigations of the degradation and crosslinking in the polystyrenesulfonic cation exchange resin Zerolit 225 (H^+, of different DVB content), irradiated in the wet state, were performed. It was found that in samples of resin containing 1 to 2% DVB a further crosslinking occurs. The significant decrease of the ion exchange capacity and a low concentration of sulfuric acid in the eluate indicate the formation of an appreciable amount of "sulfonic bridges" in the resin. In resins containing 8, 12, and 20% DVB, crosslinking is diminished and degradation processes prevail. In irradiated Zerolit 225 at least two kinds of weakly acidic groups, differing in their radiation stability, are formed. (auth)

53017 INFLUENCE OF WATER VAPOR ON THE γ-RADIOLYSIS OF CRYSTALLINE KI. Sugier, Henryk; Tilk, Stefan (Politechniki Lodzkiej, Lodz, Poland). Nukleonika; 17: No. 3-4, 181-7(1972). (In Polish).

The radiation yield of iodine $G(I_2)$ was measured for potassium iodide crystals irradiated with ^{60}Co γ-rays within the dose range up to 1600 kI/kg (160 Mrads). The yield of iodine was calculated as a sum of gaseous iodine and iodine incorporated in the crystal. $G(I_2)$ was of the range 10^{-3} to 10^{-2} for single crystals of KI and 10^{-2} for polycrystalline samples. The yield of $G(I_2)$ is enhanced by a factor of 3 to 5 in the presence of air. It was found that the increase of $G(I_2)$ was due to the presence of water vapor which promotes a set of reactions between H_2O molecules and KI as well as between their radiolysis products. (auth)

53018 KINETICS OF THE HYDRATED ELECTRON DISAPPEARANCE IN CONCENTRATED AQUEOUS ALKALI SOLUTIONS. Kabakchi, S. A.; Shubin, V. N. (Inst. of Electrochemistry, Moscow). Radiat. Eff.; 15: No. 1-2, 23-9(Jul 1972).

Investigation of the kinetics of disappearance of optical absorption arising during pulse radiolysis of 14.5M aqueous KOH solutions revealed that the laws of disappearance of absorption at $\lambda = 6500\text{Å}$ and $\lambda = 7200\text{Å}$ are different. It is suggested from the spectroscopic data obtained earlier that in the region 7200Å in addition to the hydrated electron, another short-lived particle absorbs light. The modeling of chemical processes occurring in the system by means of an analogue computer allowed to determine the extinction coefficient of this particle, which is equal to 1.0×10^4 1/mol cm, and also the rate constants of the reactions of its formation and disappearance. (auth)

53019 ESR STUDY OF THE FREE RADICAL REACTIONS OF γ-IRRADIATED POLYPROPYLENE WITH METHYL METHACRYLATE. Klinshpont, E. R.; Milinchuk, V. K.; Dmitriev, S. M.; Kurilenko, A. I. (Scientific-Research Physical-Chemical Inst., Moscow). Vysokomol. Soedin., Ser. A; 14: No. 7, 1596-1602(Jul 1972). (In Russian)

The reactions of allyl, polyene, and peroxide radicals of polypropylene with methyl methacrylate were studied by the ESR method. At 300°K the relative reactivity of the radicals decreases in the sequence allyl > polyene > peroxide radicals. The kinetics of the radical reactions occurring during the gas-phase graft postpolymerization are considered. (auth)

53020 EFFECT OF VARIOUS KINDS OF IONIZING RADIATION ON POLY(VINYL CHLORIDE). Lavrentovich, Ya. I.; Zverev, A. B.; Kovalenko, L. M.; Kabakchi, A. M. (Inst. of Physical Chemistry, Kiev). Vysokomol. Soedin., Ser. B; 14: No. 5, 373-7(May 1972). (In Russian).

The effects of ^{60}Co γ radiation, 14-MeV deuterons, and 28-MeV α particles on rigid poly(vinyl chloride) (PVC) were studied with respect to polymer crosslinking and to fading of the dye 1,4-diaminoanthraquinone (DAA) in the PVC. The accumulation of a gel fraction and a change in viscosity with radiation dose began at a dose of 30 to 35 MR. The calculated radiation yield of crosslinking was about 0.9 molecule/100 eV. DAA in PVC was reduced by radiation to the leuco-form at a rate of about 0.2 molecule/100 eV, and this ratio represented a linear dependence on dose from 1 to 12 MR. (K.S.W.)

For abstracts of individual sections see: 53022—53024 and 53352.

53021 ADVANCES IN RADIATION CHEMISTRY. VOLUME 3. Burton, Milton; Magee, John L. (eds.). New York; John Wiley and Sons, Inc. (1972). 305p. $19.95.

The book is divided into four sections, each of which has been abstracted separately for NSA. (J.G.B.)

53022 SHORT-LIVED TRANSIENTS. Ludwig, Peter K. (Univ. of Notre Dame, Ind.). Advan. Radiat. Chem.; 3: 1-74 (1972).

Optical techniques for the study of fast and ultrafast processes are surveyed. Details are given on phase and modulation fluorometry, single-photon counting technique, laser flash photolysis, mode-locked laser techniques, and pulse radiolysis. Experimental results are given for the pulse radiolysis of liquid organic systems, fast pulse radiolysis of glasses, ultrafast pulse radiolysis, luminescence-decay studies, mode-locked laser studies, and laser flash photolysis. (185 references) (J.G.B.)

53023 SOME TOPICS IN RADIATION CHEMICAL SYNTHESIS OF ORGANIC COMPOUNDS. Vereshchinskii, I. V. (Inst. of Physical Chemistry, Moscow). Advan. Radiat. Chem.; 3: 75-123(1972).

The radioinduced synthesis of organic compounds is considered under the following headings: halogenation, sulfochlorination, sulfonic acid production, oxidation of hydrocarbons, hydrohalogenation, synthesis of perchlorinated hydrocarbons, telomerization, synthesis of organosilicon compounds, fluorination, carboxylation and carbonylation, synthesis of nitrogen-containing organic compounds, synthesis of sulfur organic compounds, synthesis of organophosphorus compounds, synthesis of organotin compounds, and isomerization. (176 references) (J.G.B.)

53024 RADIATION CHEMICAL MECHANISMS IN RADIATION BIOLOGY. Adams, G. E. (Mount Vernon Hospital, Northwood, Eng.). Advan. Radiat. Chem.; 3: 125-208(1972).

Radiation chemical mechanisms in radiation biology are discussed under the following headings: appropriate techniques of radiation chemistry, amino acids and peptides, enzymes and proteins, radiation chemistry of aqueous solutions of nucleic acid derivatives, and modification of cellular radiosensitivity. (212 references) (J.G.B.)

53025 CONFIGURATION DIAGRAM OF THE SOLVATED ELECTRON. Tachiya, M. (Tokyo Univ.). Chem. Phys. Lett.; 15: No. 4, 575-8(1 Sep 1972).

The absorption line shape of the solvated electron is considered in terms of the interaction of the electron with lattice vibration. Based on this consideration, the configuration diagram of the solvated electron in liquid ammonia was constructed from the absorption spectrum of it, which was obtained experimentally. The physical meaning of the constructed diagram is discussed briefly. (auth)

53026 H_3O RADICAL? Melamud, E.; Getz, D.; Schlick, S.; Silver, Brian L. (Technion–Israel Inst. of Tech., Haifa). Chem. Phys. Lett.; 15: No. 4, 590-1(1 Sep 1972).

A report of the identification of the H_3O radical is shown to be erroneous. ESR studies of aqueous solutions enriched to over 90 atom % in ^{17}O provide no evidence for the H_3O radical. The spectrum originally assigned to H_3O is probably due to the methyl radical. (auth)

53027 ABSTRACTS OF PAPERS OF THE JOINT SOUTHEAST–SOUTHWEST REGIONAL ACS MEETING, NEW ORLEANS, LOUISIANA, DECEMBER 2–4, 1970. Washington, D. C.; American Chemistry Society (1970). 220p. (CONF-701204–(Absts)).

Radiochemistry and Nuclear Chemistry

Refer also to abstracts 53027 and 53313.

53028 (COO–584-50) DISTRIBUTION OF TRITIUM IN GLUCOSE AND STARCH LABELED BY TRITIUM ATOM BOMBARDMENT. Liang, T.; Nordin, P.; Moser, H. (Kansas State Univ., Manhattan). 1972. 17p. Dep. NTIS.

Samples of glucose and starch were labeled by tritium atom bombardment. Up to 51% incorporation as non-labile tritium was achieved with crystalline, anhydrous glucose. Distribution of tritium in the carbon skeleton of glucose was calculated from a comparison of the specific molar activity of glucose with its derivatives. Derivatives prepared were gluconic acid, glucose phenyl osatriazole, 2-phenyl-4-formyl osatriazole, 2-phenyl-4-carboxylic acid osatriazole, glucose phenyl flavazole, 1-phenyl-3-formyl flavazole and formaldehyde dimedone. The tritium distribution showed definite structural effects. Generally films of glucose and the amylose–butanol complex had random or nearly random distribution of tritium in glucose. Crystalline α-D-glucose monohydrate had zero tritium on C-2 and twice random tritium on C-5. Starch granules had zero or near zero tritium on C-3 and close to twice random tritium on C-2. (auth)

53029 LABELED IODOQUINE. Moretti, Jean-Luc; Safi, Nour. French Patent 2,081,592. 10 Dec 1971. Filed 27 Mar 1970. (In French).

A method was developed for preparing and labeling 7-iodo(131) and 7-iodo(125)-4(4-diethylamino-1-methylbutylamino)quinoline. The 7-chloroquine is treated using a radioactive iodizing reagent in order to substitute the chlorine atom with a labeled iodine atom. The labeled iodizing reagent consists of KI, sodium nitrite, HCl and a molecular iodine isotope: ^{125}I, ^{131}I or ^{134}I. (France)

Hot-Atom Chemistry

Refer also to abstract 52962.

53030 EFFECT OF SCAVENGER COMPETITION ON HOT ATOM CHEMISTRY. II. COMPUTER SIMULATION. Malcolme-Lawes, D. J. (Yale Univ., New Haven). J. Chem. Phys.; 57: No. 6, 2481-7(15 Sep 1972).

A computer model is used to simulate the effect of varying amounts of scavenger competition in a hot atom system consisting of reactant, inert moderator, and scavenger. The results were analyzed in terms of the kinetic theory of hot atom reactions. The scavenger corrected kinetic theory was tested and shown to yield adequately corrected kinetic parameters. (auth)

53031 EFFECT OF SCAVENGER COMPETITION ON HOT ATOM CHEMISTRY. I. CORRECTION TO THE KINETIC THEORY. Malcolme-Lawes, D. J. (Yale Univ., New Haven). Contract AT(30-1)-1957. J. Chem. Phys.; 57: No. 6, 2476-80 (15 Sep 1972).

The effect of scavenger reactivity in a hot reaction zone is considered using the model and symbolism of the kinetic theory of hot atom reactions. Expressions were derived, which enable the extent of scavenger interference to be estimated from experimental scavenger curves, and a simple method of correcting available kinetic theory parameters is given. (auth)

53032 LIFETIME VARIATION OF ^{64}Cu AND THE CHEMICAL STATE OF (n,γ) RECOIL COPPER IN α-COPPER PHTHALOCYANINE CRYSTALS. Auric, P.; Vargas, J. I. (CEN, Grenoble, France). Chem. Phys. Lett.; 15: No. 3, 366-8(15 Aug 1972).

The decay constant, λ, of ^{64}Cu in α copper phtalocyanine is changed by $\Delta\lambda/\lambda = (10 \pm 1.6) \times 10^{-4}$ when the electron capture decay rate in the labeled crystal is compared to that of samples in which the ^{64}Cu activity was introduced by neutron irradiation. It is shown that the (n,γ) generated recoil copper is probably lattice stabilized in the atomic state. (auth)

Properties of Radioactive Materials

Refer also to abstracts 52934, 52935, 52955, and 53548.

53033 (EUR–4765, pp 117-30) SURFACE IONIZATION APPLIED TO SOME MATERIALS OF NUCLEAR INTEREST. Facchetti, S.; Marell, A. (CCR-Euratom, Ispra, Italy). (In Italian).

From 2nd conference on mass spectrometry; Ispra, Italy (1 Sep 1971).

In working with sources of surface ionization it is difficult to obtain reproducible conditions because of the multiplicity of parameters, but the effort to do so may be justified by the results. The difficulties are discussed, and related to the ideal case of a polished surface in the absence of external electric fields when the Langmuir–Saha expression applies. The Schottky equation correlates the desorption of a given ion from a surface, and pertinent data are tabulated for the elements U and Th. Other elements referred to in connection with the surface ionization techniques are Nd, Pu, W, and Np. (K.S.W.)

53034 (MLM–1964(tr)) HYDROLYSIS OF TETRAVALENT PLUTONIUM. Mativier, H.; Guillaumont, R. Translated for Mound Lab., Miamisburg, Ohio, from Radiochem. Radioanal. Lett.; 10: No. 2, 27-35(1972). 9p. Dep. NTIS.

Hydrolysis constants for Pu^{4+} were calculated by solvent extraction of Pu(IV) in the system $HClO_4-LiClO_4-TTA$ or dibenzoylmethane–benzene with ^{238}Pu. Analysis of distribution coefficient using a computer gave: $\log K_1 = -0.45$, $\log K_2 = -0.75$, $\log K_3 = -3.3$, $\log K_4 = -6.3$. Conditions were found for stability of tetravalent plutonium in this system and the extraction of plutonium(IV) by isopropyltropolone in benzene. (See NSA 26: 30884 for abstract from original language.) (auth)

53035 (NIM–1448) POTENTIOSTATIC STUDY OF THE ANODIC DISSOLUTION OF URANIUM DIOXIDE IN AQUEOUS SOLUTIONS. Nicol, M. J.; Needes, C. R. S. (National Inst. for Metallurgy, Johannesburg (South Africa)). 8 Jun 1972. 23p. Dep. NTIS (U. S. Sales Only).

The anodic dissolution of uranium dioxide is shown to occur as a two-electron process with a current efficiency of 100% in both acidic perchlorate and alkaline carbonate solutions. The effects, on the anodic dissolution process, of pH, temperature, and the various anions known to be present in commercial leaching solutions, were studied by the use of stationary potentiostatic measurements. The effects observed are interpreted in terms of the nature and properties of both the uranium dioxide surface and the primary products of oxidation. (auth)

53036 (ORNL–4794, pp 81-3) SPECTROPHOTOMETRIC STUDIES OF SOLUTIONS OF LANTHANIDES AND ACTINIDES. Aug 1972.

In Chemical Technology Division annual progress report for period ending March 31, 1972.

Research progress is reported on: studies of plutonium(IV) polymer, spectral studies of the actinides, and protonic wave functions and spectra. (D.H.M.)

53037 (RFP–1455) TEMPERATURE MEASUREMENT AND CONTROL IN THE BOMB REDUCTION OF PLUTONIUM TETRAFLUORIDE. Long, Jack L.; Brown, James C.; Auge, Robert G. (Dow Chemical Co., Denver, Colo. Rocky Flats Div.). 11 Sep 1972. Contract AT(29-1)-1106. 7p. Dep. NTIS.

A technique was developed for estimating the minimum temperatures attained in small and large scale bomb reductions of plutonium tetrafluoride with calcium metal. The temperatures in both the small (50 gram) scale and large (1.8 kg) scale exceeded 1900°C. The addition of calcium fluoride slag from previous reductions lowered the temperature to less than 1536°C. Slag addition to 2.5 kg reductions resulted in practically no splattering of the molten reaction products and in increased reduction yields. (auth)

53038 (RFP–1889) CONVERSION OF PLUTONIUM OXIDE TO PLUTONIUM TETRAFLUORIDE WITH FLUORINE IN A FLUID BED REACTOR. PART I. DEVELOPMENT STUDIES. Standifer, Richard L.; Robinson, Herbert N.; Sheets, James R.; Wing, Ralph O. (Dow Chemical Co., Denver, Colo. Rocky Flats Div.). 23 Aug 1972. Contract AT(29-1)-1106. 11p. Dep. NTIS.

The use of gaseous fluorine (F_2) to convert purified plutonium oxide (PuO_2) to plutonium tetrafluoride (PuF_4) in a fluidized bed reactor was investigated for possible process application. Through a series of 500-gram to 1000-gram batch fluid bed runs, a set of conditions and techniques was determined, which yielded PuF_4

suitable for the requirements of the Rocky Flats plutonium recovery process. The conversion of PuO_2 to PuF_4 in the recovery process is currently accomplished with anhydrous hydrogen fluoride (HF), using a rotary tube reactor. Extensive tests are planned to fully evaluate the fluid bed-fluorine process as a potential replacement for the current hydrofluorination process. (auth)

53039 (RFP–1890) CONVERSION OF PLUTONIUM OXIDE TO PLUTONIUM TETRAFLUORIDE WITH FLUORINE IN A FLUID BED REACTOR. PART II. DEMONSTRATIONS RUNS: A COMPARISON OF THE FLUORINE PROCESS WITH THE HYDROFLUORINATION PROCESS. Standifer, Richard L.; Wing, Ralph O.; Sheets, James R.; Robinson, Herbert N.; Meyer, F. Graham; Wolf, Jerry R.; Ramsey, William H. (Dow Chemical Co., Denver, Colo. Rocky Flats Div.). 29 Aug 1972. Contract AT(29-1)-1106. 21p. Dep. NTIS.

A series of 82 1-kg-batch pilot plant runs was made to demonstrate the potential of a process using fluorine and a fluid-bed reactor to convert plutonium oxide (PuO_2) to plutonium tetrafluoride (PuF_4). A comparison of this process with the rotary hydrofluorination process, currently used to generate PuF_4 in the Rocky Flats plutonium recovery plant, indicated that replacement of the existing process would result in a number of significant improvements. Properly designed, a fluid bed-fluorine system should reduce the radiation exposure rate presently experienced by the hydrofluorination process operators by a factor of 10. This reduction in exposure would result from the smaller inventory of PuF_4 and the relative ease of remote operation of the fluid bed-fluorine process. Use of the fluorine process would eliminate the generation of approximately 10,000 gallons/month caustic waste solution containing an average of approximately 170 grams plutonium. This waste stream, with the contained plutonium, must be processed for water removal, and ultimately, shipped off-site for burial. The fluorine process should reduce the quantity of plutonium recycled by: reducing the quantity of impure PuF_4 and improving the yield of plutonium metal in the calcium reduction operation. Approximately 95% of the recycle from these sources should be eliminated. Based on an average recovery rate of 400-kg plutonium metal per month and a recycle processing cost of \$1,000-per-kilogram plutonium recycled, cost calculations show a potential savings of approximately \$1.25 million/year by replacing the present hydrofluorinators with a fluid bed-fluorine system. The demonstration runs indicate that because of reduced corrosion and the use of multiple small reactors, dependability and maintenance requirements appear more favorable with the fluid-bed fluorine process. No significant disadvantages were apparent during this series of demonstration runs. (auth)

53040 (SZS–129) APPLICATION OF ORGANIC FLOCCULANTS TO THE DECONTAMINATION OF RADIOACTIVELY CONTAMINATED WATERS BY COAGULATION. Vostrcil, J. (Staatliche Zentrale fuer Strahlenschutz, Berlin (East Germany)). Apr 1972. 60p. (In German). Dep. NTIS (U. S. Sales Only).

The effect of organic flocculants on water decontamination both by ferric chloride coagulation and by a two-stage lime-soda softening with subsequent ferric chloride coagulation. The use of optimum amounts of organic flocculants for improving the removal of turbidity, better sedimentation, and separation of flocs formed during coagulation was investigated. The effect of organic flocculants was studied both by means of jar tests and with a model of floc blanket clarifier. Optimum amounts of organic flocculants for given processes reduce primarily final turbidity of the treated water and by this method improves the removal of those radionuclides that are present in water in colloidal form or that were incorporated into the formed flocs. The amounts of organic flocculants must be optimum because an excess of organic flocculants may impair the process of decontamination. In removing ^{144}Ce and ^{106}Ru from water by ferric chloride coagulation a similar relationship was found between the modified CAMP number and decontamination factor and/or decontamination efficiency as between CAMP number and residual iron and/or final turbidity in the treated water. (auth)

53041 (UJV–2867-M,A) ABSOLUTE ACTIVITY IN IRRADIATED FUEL MATERIAL BY THE METHOD OF "GAMMA SCANNING". Klima, Jaroslav; Kyncl, Jan; Macku, Ales; Vins, Vaclav; Pour, Frantisek; Havel, Jaroslav (Ceskoslovenska Akademie Ved, Rez. Ustav Jaderneho Vyzkumu). Dec 1971. 21p. (In Czech). Dep. NTIS (U. S. Sales Only).

A self-absorption correction for gamma scanning of UO_2 pellets is described. The linear absorption coefficient for gamma radiation was measured for the energy of 0.662 MeV (Cs) in pellets of sintered UO_2 in the range of 74 to 96% of the theoretical density of the pellets. The gamma scanning system in hot cells at the Nuclear Research Institute in Řež is described. (auth)

53042 BENZOATO COMPLEXES OF URANYL. III. INFRARED SPECTRUM AND STRUCTURE OF DIOXOBISBENZOATODIAQUOURANYL(VI), $[UO_2(C_6H_5COO)_2(H_2O)_2]$. Rojas Lopez, R. M.; Arenas Rosado, J.; Bermudez Polonio, J. (Instituto de Quimica Inorganica, Madrid). An. Quim.; 68: 223-8(1972). (In Spanish).

The infrared spectra of the compounds $[UO_2(C_6H_5COO)_2\ (H_2O)_2]$ and $[UO_2(C_6H_5COO)_2]$ were studied in the spectral region of 4000 to 200 cm^{-1}. The previously proposed structure of the uranyl benzoate was confirmed and on the basis of the spectral data, a structure with hexacoordinated UO_2^{++} is proposed for the former compound. (auth)

53043 FLUORO COMPLEXES OF HEXAVALENT URANIUM. IV. COMPLEXES OF THE SERIES $[UO_2F_3]^-$ AND $[(UO_2)_2F_5]^-$. Chakravorti, M. C.; Bandyopadhyay, N. (Indian Inst. of Tech., Kharagpur). J. Inorg. Nucl. Chem.; 34: No. 9, 2867-74(Sep 1972).

Thermogravimetric studies were made of various salts of the ion $[UO_2F_3]^-$ with organic basic cations. By the pyrolysis of the complexes of the salts with α-picoline, quinoline, 2,2′-dipyridyl (indexed as bipyridine), and anthranilic acid, compounds of the type $BH[(UO_2)_2F_5]$ were isolated. Similar salts with dimethylaniline, cis- and trans- $[CO(NH_3)_4F_2]^+$ and also the quinoline compound were obtained by direct precipitation of uranyl fluoride with the organic bases or with salts containing the complex cations in dilute HF medium. The conductivities and the solubilities of the salts and also of the salts belonging to the series $[UO_2F_3]^-$ were determined. A free acid formulated as $H[UO_2F_3] \cdot H_2O$ was isolated by reacting uranium trioxide with aqueous HF. It was characterized by conductivity and pH measurement of dilute solutions, potentiometric titration with alkali, determination of dissociation constant, thermogravimetric analysis, and by a comparison of these results with those of $UO_2F_2 \cdot 2H_2O$. (auth)

53044 MECHANISMS OF INORGANIC REACTIONS. PART I. THE KINETICS AND MECHANISM OF THE OXIDATION–REDUCTION REACTION OF URANIUM(IV)–CHLORINE(III) IN THE PRESENCE OF EXCESS PHENOL IN AQUEOUS ACID SOLUTION. PART II. THE TRANS EFFECT IN THE SUBSTITUTION REACTIONS OF IODOAQUOTETRAAMMINECHROMIUM(III). Buchacek, Robert Joseph. Iowa City, Iowa; Univ. of Iowa (1972). 105p. University Microfilms Order No. 72-17,543.

Thesis.

The oxidation-reduction reaction of uranium(IV)-chlorine(III) was studied in the presence of 0.1 M phenol. The addition of phenol to the reaction mixture effectively removes the side reactions of the intermediate Cl_2O_2 product. Under these conditions the stoichiometry of the reaction is represented by U(IV) + Cl(III) + phenol → U(VI) + H^+ + chlorophenols. The results of an oxygen-18 tracer analysis suggest that the principal pathway involves a two-electron oxygen atom transfer from chlorine(III) to uranium(IV). An increase in the concentrations of both chlorine(III) and hydrogen ion retard the rate of the reaction. (Diss. Abstr. Int., B)

53045 CRYSTALLOGRAPHIC STUDY OF TETRAVALENT $M(IV)(PO_3)_4$ COMPOUNDS (M(IV) = Ce, U, AND Th). Masse, Rene; Grenier, Jean-Claude (CNRS, Grenoble, France). Bull. Soc. Fr. Miner. Crist.; 95: No. 1, 136-42(Jan 1972). (In French).

The chemical preparation of orthorhombic $Ce(PO_3)_4$ crystals, orthorhombic and triclinic $U(PO_3)_4$ crystals, and orthorhombic, triclinic, and quadratic $Th(PO_3)_4$ crystals is described. The Weissenberg method was used to determine the crystallographic parameters of the various lattices. The powder diagrams of these phosphates are presented. (France)

53046 LATTICE DYNAMICS OF M_2XY_6 HEXABROMOMETALLATES: Cs_2UBr_6. Chodos, Steven L. (Univ. of California, Los Angeles). J. Chem. Phys.; 57: No. 7, 2712-14(1 Oct 1972).

A seven parameter model based on a modified Urey—Bradley potential with long range Coulomb terms was used to describe the lattice dynamics of M_2XY_6 compounds. Optical data were used to evaluate the force constants for the case of Cs_2UBr_6. The model is to be used as a starting point for a comprehensive calculation of the vibronic structure of Cs_2UBr_6. (auth)

53047 STABLE URANIUM(IV) ALKYL AND ARYL COMPLEXES. Marks, Tobin J.; Seyam, Afif M. (Northwestern Univ., Evanston, Ill.). J. Amer. Chem. Soc.; 94: No. 18, 6545-6(6 Sep 1972).

The synthesis of a series of compounds $(h^5-C_5H_5)_3$ UR (where R = CH_3, n-C_4H_9, allyl, neopentyl, C_6F_5, and i-C_3H_7) is reported. NMR data are presented for the compounds. The molecules all possess considerable thermal stability. All compounds reacted instantly with methanol producing as the major product $(C_5H_5)_3$ $UOCH_3$. No reaction was observed when it was attempted to bring about nucleophilic addition of $(C_5H_5)_3UCH_3$ to acetone. (D.H.M.)

53048 LIQUID AND SOLID Th–OH–NO_3–H_2O SYSTEMS. INFRARED AND LIGHT SCATTERING INVESTIGATIONS. Deptula, Andrzej (Inst. of Nuclear Research, Warsaw). Nukleonika; 17: No. 1-2, 47-58(1972).

Infrared investigations indicate that in solutions of Th–OH–NO_3–H_2O systems a weak interaction of the type $Th^{4+}-(H_2O)_x-NO_3^-$ takes place (independent of the NO_3 : Th molar ratio). In the following solid compounds of this system $Th(NO_3)_4 \cdot 4H_2O$ (I), $Th_2(OH)_2(NO_3)_6(H_2O)_8$ (II), $Th(OH)_2(NO_3)_2(H_2O)_3$ (III), and in thoria gels the nitrates are coordinated as a bidentate nitrate groups ($Th \leftleftarrows O_2NO$). In compounds (I) and (II), the strength of every coordination bond Th ← O–N is different, but in (III) as well as in thoria gels the Th ← O–N bonds are of equal strength. The outer oxygen atoms of the nitrate groups are engaged in different hydrogen bonds. On the basis of light scattering measurements it was found that thoria sols are formed in solutions of molar ratios $NO_3 : Th < 2:1$. The smaller the NO_3 : Th molar ratio and older the sols the bigger the molecular weight of the sol and larger the grain size of the corresponding gel. Dissymmetry values and depolarization factors of the scattered light indicate that particles of the investigated thoria sols are spherical and isotropic. (auth)

53049 PROCESS FOR PREPARING ALPHA AMMONIUM URANOUS PENTAFLUORIDE. Selman, Murray; Wamser, Christian A.; Wilkalis, John E. (to Allied Chemical Corp.). U. S. Patent 3,681,035. 1 Aug 1972. Filed 1 Oct 1969.

NH_4UF_5 was prepared in alpha crystalline form by adding to an aqueous acidic solution of a uranyl salt containing cupric ions, chloride ions and ammonium ions, hydrogen fluoride and hydroxylamine. The hydroxylamine was added in amounts and time of addition so as to maintain a concentration of at least about 0.07 mol of hydroxylamine per liter of solution until the major portion of the uranium in the uranyl salt was converted to NH_4UF_5. (Official Gazette)

53050 PREPARATION OF AQUEOUS SOLUTIONS OF THORIA SOLS FOR LIGHT SCATTERING MEASUREMENTS. Deptula, Andrzej (Inst. of Nuclear Research, Warsaw). Nukleonika; 17: No. 3-4, 197-8(1972).

It was shown that deionized water can be used to prepare solutions for light scattering measurements. The procedure is as follows: 1) preparation of concentrated solutions using deionized water (e.g., 2.15 M thoria sol with molar ratio $NO_3 : Th = 0.5 : 1$); 2) filtration of this solution through G-5 Jena sintered glass under pressure (~0.5 atm) of nitrogen; 3) preparation of basic solutions by dilution of the concentrated solutions with deionized water (e.g., 2.23 cm^3 of thoria sol was diluted to 100 cm^3 in order to obtain a concentration of 0.011 g/cm^3); and 4) preparation of solutions of various concentrations for light scattering measurements directly in the cell, e.g., to 40 cm^3 of deionized water contained in the cell different volumes from 0.03 to 1.8 cm^3 of the basic solution (see point 3) were added. The observed dissymmetry in the concentration range 0.834 to 47.929×10^{-5} gTh/cm^3 varied from 0.8 to 1.23. The molecular weight was found to be 2,540,000. (auth)

53051 KINETICS AND MECHANISM OF THE OXIDATION–REDUCTION REACTION BETWEEN URANIUM(IV) AND CHLORINE(III) IN THE PRESENCE OF PHENOL IN AQUEOUS ACID SOLUTION. Buchacek, Robert; Gordon, Gilbert (Univ. of Iowa, Iowa City). Inorg. Chem.; 11: No. 9, 2154-60(Sep 1972).

The oxidation–reduction reaction between uranium(IV) and chlorine(III) was studied in the presence of 0.1 M phenol. The addition of phenol to the reaction mixture effectively removes the side reactions of the chlorine-containing intermediates. Under these conditions the stoichiometry of the reaction becomes $U(IV) + Cl(III) + \text{phenol} \rightarrow U(VI) + H^+ + \text{chlorophenols}$. The results of an ^{18}O tracer experiment suggest that the principal pathway involves a two-electron oxygen atom transfer from the oxidant to the reductant. An increase in the concentrations of both chlorine (III) and hydrogen ion retards the rate of the reaction. The data are consistent with the rate expression $-d[U(IV)]/dt = k_1[U(IV)][Cl(III)]/\{1 + K_2[HClO_2]\}\{1 + K_3[H^+]\}$. At 25°C, $k_1 = 291.3 \pm 4.2\ M^{-1}\ sec^{-1}$, $K_2 = 4.13 \pm 0.25\ M^{-1}$, and $K_3 = 20.8 \pm 3.2\ M^{-1}$. Mechanistically, the rate law is interpreted in terms of a hydrogen ion dependent two-electron transfer reaction and the formation of a nonproductive intermediate. (auth)

53052 SYNTHESIS OF NEW COMPOUNDS LABELED WITH TRITIUM AND ^{14}C FOR BIOLOGICAL INVESTIGATIONS. I. COMPOUND ROM-203:N,N'-BIS(3-PHENOXYHYDROXYPROPYL)-ETHYLENEDIAMINE.2HCl. Ozdowska, Zofia; Marjankowska, Barbara (Instytut Farmaceutyczny, Warsaw). Nukleonika; 17: No. 3-4, 163-8(1972). (In Polish).

In a deuteration reaction the positions of protons that undergo to isotope exchange with deuterated and tritiated water were designed. The compound ROM-203 was labeled with tritium and carbon-14. (auth)

53053 APPLICATION OF THE MENDELEEV PERIODIC LAW TO ELEMENTS HAVING Z VALUES LYING BETWEEN 104 AND 107. Haissinsky, M. (Institut du Radium, Paris). J. Chim. Phys.; 69: No. 5, 845-50(May 1972). (In French).

It is assumed that the close analogies that exist between the following couples: Zr and Hf, Nb and Ta, Mo and W, and Tc and Re (32 electron difference) should also exist for the following couples: Hf–104, Ta–105, W–106, Re–107 (32 electron difference). This hypothesis enables approximate values to be obtained by extrapolation for the ionic and atomic radii, the ionization potential, and the electronegativities of the four elements immediately preceding the filling-up of the 5f shell. Using these values together with data concerning the physico-chemical behavior of the homologues, it is demonstrated that the essential chemical features of the four elements can be predicted. (France)

53054 FORMATION OF COMPLEXES OF UCl_4 WITH α- OR β-CARBOXYLIC ACIDS AND α-QUINOLINECARBOXYLIC ACID IN POLAR SOLUTIONS. Rakhimov, Kh. R.; Khamraev, T. A.; Muftakhov, A. G. (Tashkent State Univ.). Uzb. Khim. Zh.; No. 2, 29-32(1972). (In Russian).

Complex formation of UCl_4 with representative monopyridine carboxylic acids (picolinic and nicotinic acids) and α-quinolinecarboxylic acid was studied in water and alcohol solutions by means of a spectrophotometer. Compounds with the following compositions were detected: 1 :1 and 1 :2 (U^{+4} : α-picolinic acid) in water or C_2H_5OH, but only 1 : 1 in CH_3OH; 1 : 1 and 1 :2 (U^{+4} : β-nicotinic acid) in C_2H_5OH; and 1 :2 (U^{4+} : α-quinolinecarboxylic acid) in C_2H_5OH. (K.S.W.)

53055 COMPUTER ANALYSIS OF SPECTRA BY DECONVOLUTION. Szoke, J. (Central Research Inst. for Physics, Budapest). Chem. Phys. Lett.; 15: No. 3, 404-7(15 Aug 1972).

An iterative deconvolution procedure was applied in order to eliminate instrument distortions from a spectrum and to determine the number and the approximate parameters of spectrum components that can be used as input parameters for a least squares fit procedure. The spectrum of ammonium uranyl carbonate is used as one example. (auth)

Radioactive Waste Treatment

Refer also to abstract 52915.

53056 (AREAEE–129) RADIOCHEMICAL STUDIES OF ^{125}I. PART I. PRODUCTION AND SEPARATION. Allam, S. (Atomic Energy Establishment, Cairo (Egypt). Nuclear Chemistry Dept.). 1971. 32p. Dep. NTIS (U. S. Sales Only).

The preparation and purification of the ^{125}I are reported. The production of the isotope was achieved by using 83% enriched ^{125}Te as a target material. Irradiation experiments were carried out at the 60 inch cyclotron of the Argonne National Laboratories. The isotope was separated by distillation, and chemically purified from the target material, which was recovered for further irradiations. The specific activity yield obtained was 4.65 mCi/g for a proton flux of 1 W/h and no traces of contaminating ^{126}I were detected three weeks after irradiation. Different counting techniques were investigated and the results indicated that 50% efficiency was achieved by gamma scintillation well-type detectors, and 15% efficiency by liquid scintillation methods. Activity levels of ^{125}I as small as 1×10^{-3} microcurie may be determined with an absolute accuracy of ±1%. (auth)

53057 (BNWL-tr–75) MELTING OF RADIOACTIVE SUBSTANCES IN GLASS OR CERAMIC SUBSTANCES. THIRD COMMUNICATION: SUITABILITY STUDY OF VULCANITES OF DOMESTIC ORIGIN. Sachse, G.; Rosenberger, H. Translated for Battelle Pacific Northwest Labs., Richland, Wash., from Kernenergie; 11: No. 1, 15-23(1968). 20p. Dep. NTIS.

The characteristics of basalts, phonolites, trap tuff, and pitchstones for use in radioactive waste disposal are evaluated. Results show that Barenstein basalt, Kaltenstein phonolite, and Hammer–Unterwiesenthal phonolite are considered good to excellent. (D.H.M.)

53058 (CONF-720823–10) LONG-TERM EFFECTS ON RADIOIODINE TRAPPING BY CHARCOAL. Davis, R. J.; Ackley, R. D. (Oak Ridge National Lab., Tenn.). 1972. 15p. Dep. NTIS.

From twelfth air cleaning conference; Oak Ridge, TN. (28 Aug 1972).

A program of tests is underway to determine the $CH_3{}^{131}I$ efficiencies of some commercial impregnated charcoals as a function of time exposed to reactor off-gas. A TEDA-impregnated charcoal retained a high $CH_3{}^{131}I$ trapping efficiency (>90%) during six months service whereas an iodized charcoal retained that efficiency for only about one month. The $CH_3{}^{131}I$ trapping efficiency test was performed at 90% relative humidity with a loading of about 0.4 mg I as CH_3I/cm^3 of bed. This test loading is about ten times larger than the maximum total iodine loading estimated to be possible in ORNL off-gas systems and additional tests are underway to determine whether the trapping efficiencies for a more realistic loading will be maintained for a longer service period. A second, more urgent problem is related to the slow release of iodine from charcoal beds. The ORNL need is to provide a method of predicting, from a short-term, in-place test result, the fraction of iodine that would be retained over a period of several weeks under accident and post-accident conditions. The results of some long-term (28 day) iodine retention tests are presented and compared with previous results (from ORNL and elsewhere). The releases are larger than acceptable under some conditions. The release depends on at least four environmental parameters: the prevailing relative humidity, the service history, organic contamination in the air, and ionizing radiation. Additional tests are in progress to demonstrate the magnitude of the first three of these parameters. It is anticipated that the results of the planned tests, along with those from the Savannah River Laboratory program pertaining to the effects of radiation, will provide an outline of the magnitude of possible iodine releases from adsorbers under ORNL usage. (auth)

53059 (CONF-720823-12) DECONTAMINATION OF HTGR REPROCESSING OFF-GASES. Whatley, M. E.; Glass, R. W.; Haas, P. A.; Meservey, A. B.; Notz, K. J. (Oak Ridge National Lab., Tenn.). 1972. 22p. Dep. NTIS.

From twelfth air cleaning conference; Oak Ridge, TN. (28 Aug 1972).

Off-gas from the reprocessing of HTGR fuel elements contains large amounts of CO_2 produced by the burning of fuel elements that contain about ten times as much graphite as heavy metals. The relatively high temperature of the burning process (~800°C) releases virtually all of the volatile fission products, and troublesome amounts of some that are normally solid. Filters remove particulate solids and sorption methods are used for I_2 and ^3H_2O, but no existing technology was found to remove and concentrate the Kr. The high concentration of CO_2 in the filtered gas stream (~90%) CO_2, 10% light gases, 10 to 20 ppM Kr), and the similarity of CO_2 behavior to that of Kr preclude the use of commonly employed processes such as membrane permeation, sorption on charcoal or molecular sieves, and physical absorption by a third component. The removal of CO_2 before such an operation appears feasible, but undesirable. A process involving Kr absorption in liquid CO_2 (KALC), which exploits the fact that Kr is more soluble in liquid CO_2 than is O_2, N_2, or CO, appears to be a natural solution to this particular problem. The solubility of Kr in liquid CO_2 was experimentally determined by an in situ radioactive counting method using ^{85}Kr. Kr (a total content of about 100 ppM) and CO_2 were contained in a sealed stainless steel tube, brought to equilibrium by rocking in a constant temperature bath, and counted with the tube in a vertical position to measure the radioactivity in each phase. Data were obtained at various temperatures over almost the entire CO_2 liquid range. Engineering calculations, based on literature values for the solubility of O_2, N_2, and CO and the measured values for Kr, on a KALC system that employs a fractionator and a stripper as well as an absorber indicate that a decontamination factor for Kr of 1000 can be achieved and that the Kr can be concentrated such that it comprises several percent of the removal stream. The Rare Gas Removal Pilot Plant at the ORGDP was used to explore the feasibility of operating a KALC system. In addition to demonstrating that feasibility, the initial pilot campaign provided encouragement that the KALC process will be a good way to decontaminate the HTGR reprocessing off-gases. (auth)

53060 (CONF-720823-14) ESTIMATE OF THE PROCESS DECONTAMINATION FACTORS REQUIRED TO MEET FEDERAL EFFLUENT REGULATIONS FOR THE BURNING OF HTGR FUEL ELEMENTS. Snider, J. W.; Leuze, R. E. (Oak Ridge National Lab., Tenn.). 1972. 26p. Dep. NTIS.

From 12th air cleaning conference; Oak Ridge, TN. (28 Aug 1972).

Calculations were made of the various quantities of air required to dilute 139 isotopes, present at two reprocessing times, in HTGR fuel elements to meet existing federal effluent regulations. One isotope (^{238}Pu) represents 79% of the total, calculated isotopic potential hazard from the burning of HTGR fuel elements. The largest calculated decontamination factor required was 640,000 for ^{238}Pu. (auth)

53061 (DP-MS-72-14) EFFECT OF INTENSE GAMMA RADIATION ON RADIOIODINE RETENTION BY ACTIVATED CARBON. Evans, A. G. (Du Pont de Nemours (E. I.) and Co., Aiken, S. C. Savannah River Lab.). 1972. Contract AT(07-2)-1. 14p. (CONF-720823-8). Dep. NTIS.

From 12th air cleaning conference; Oak Ridge, TN. (28 Aug 1972).

Most nuclear reactor installations have activated carbon beds to confine radioactive halogens following a reactor accident. The intense radiation field resulting from adsorption of radiohalogens on these carbon beds can convert elemental halides to organic halides. The rates of formation and desorption of organic iodides are functions of radiation field intensity, relative humidity of the purge gas stream, type and service history of the carbon, and particle size distribution of the carbon. The principal formation mechanisms are probably free radical reactions; the necessary reaction components for these reactions are water, iodine, carbon, and an intense radiation field. Desorption rates from several types of carbon and inorganic-base iodine adsorbers under various conditions are presented. Impregnated adsorbers (carbon and inorganic) retain iodine better under gamma radiation than unimpregnated carbons. New triethylenediamine-impregnated carbons have the best overall retention characteristics of the materials tested to date. Service aging characteristics are being determined. The type of carbon and method of impregnation may significantly affect iodine retention, particularly at higher temperatures (up to 180°C). (auth)

53062 (LA-DC-72-920) SIZE CHARACTERISTICS OF PLUTONIUM AEROSOLS. Ettinger, Harry J.; Elder, John C.; Gonzales, Manuel (Los Alamos Scientific Lab., N. Mex.). [nd]. 15p. (CONF-720823-13). Dep. NTIS.

From 12th air cleaning conference; Oak Ridge, TN. (28 Aug 1972).

A program is in progress to measure size characteristics and activity concentrations (source term) of plutonium aerosols generated by typical operations handling significant quantities of plutonium. This will provide a basis for generating similar aerosols in the laboratory to study the effectiveness of multiple stages of HEPA filtration. Initial data shows Pu concentrations ranging up to 16.5×10^6 dpm/m^3, with the following aerodynamic size characteristics: aerodynamic activity median diameter (aamd) = .52 to 5.5 μm and geometric standard deviation (σ_g) = 1.5 to 6.60. (auth)

53063 (ORNL-4794, pp 33-5) WASTE TREATMENT AND DISPOSAL. Aug 1972.

In Chemical Technology Division annual progress report for period ending March 31, 1972.

Research progress is reported on: radioactive waste repository, thermal stability of alpha wastes, isotope migration in crushed salt, engineering economic and safety evaluations, and combustion of plutonium-bearing solid wastes. (D.H.M.)

53064 (ORNL-tr-2621) SEPARATION OF FISSION PRODUCT RARE GASES FROM COMBUSTION WASTE GASES FROM HIGH TEMPERATURE FUEL ELEMENTS BY SCRUBBING WITH LIQUID CARBON DIOXIDE. Laser, M.; Beaujean, H. (Kernforschungsanlage, Juelich (West Germany). Institut fuer Chemische Technologie). Translated by R. Gregg Mansfield (Oak Ridge National Lab., Tenn.), from German report. 14p. (CONF-710966-1). Dep. NTIS.

From Meeting of the Society of German Chemists; Karlsruhe, Germany (13 Sep 1971).

The solubility of krypton in liquid CO_2 was studied, and the data used for developing a process for the absorption of rare gas fission products from combustion off-gases. The off-gas is compressed, passed through a heat exchanger into a packed column where it is scrubbed countercurrently with liquid CO_2. The decontaminated gas can be discharged through a reducing valve, and the liquid CO_2 containing Kr fractionated. The purified CO_2 is withdrawn from the sump of the fractionating column and returned to the head of the absorber column. The design of the installation is given by means of McCabe—Thiele diagrams. (J.G.B.)

53065 ESTIMATION OF THE COST OF PROCESSING LIQUID RADIOACTIVE WASTES. Pavlov-Verevkin, B. S.; Krasnaya, M. F. At. Energ. (USSR); 32: No. 6, 463-4(Jun 1972). (In Russian).

On the basis of data from several waste-water deactivation stations, the dependence of the cost of processing on station capacity and level of deactivation technology is determined. It is shown that the logarithm of the required cost of processing is linearly dependent on the logarithm of the station capacity. Depending on the level of technology there will be corresponding deviations from this theoretical cost. The obtained relationship is suitable for preliminary estimation of the cost of processing for a given station capacity and makes it possible to compare the economic efficiencies of water-purifying stations of various capacities. (auth)

Radioisotope Production

Refer also to abstract 53337.

53066 (ORNL–4794, pp 36-44) TRANSURANIUM-ELEMENT PROCESSING. Aug 1972.

In Chemical Technology Division annual progress report for period ending March 31, 1972.

ACTINIDE HYDRIDES—preparation and characterization of, p.41
ACTINIDE HYDROXIDES—crystal structure of, electron microscopic, electron diffraction, and x-ray diffraction studies of, p.42–3
ACTINIDE OXIDES—crystal structure of, electron diffraction study of, p.42
ACTINIDES—complexes of trivalent, research on sulfate and thiocyanate, pp.39–41
—preparation by vapor deposition, p.42
AMERICIUM HALIDES—preparation of divalent, p.42
CALIFORNIUM-252—calibration of neutron source of, with fast neutron detector, p.38
—fabrication of neutron sources of, p.38
CURIUM-244—preparation of high purity, by reduction of curium oxide, p.41
GAMMA SOURCES—preparation for Moessbauer studies, pp.38–9
LANTHANUM HYDRIDES—preparation and characterization of, p.41
TRANSURANIUM ELEMENTS—phase diagrams of sesquioxides of, p.42
—processing of, research on
—purification of TRU product, pp.37–8
TRANSURANIUM PROCESSING PLANT—operation of, pp.36–7
(D.H.M.)

53067 (ORNL–4794, pp 88-90) SURFACE AND INTERFACE PROPERTIES IN HETEROGENEOUS SYSTEMS. Aug 1972.

In Chemical Technology Division annual progress report for period ending March 31, 1972.

Research progress is reported on: isotope enrichment by (n,γ) reactions in molecular sieves, oxidation of colloidal urania, and theoretical model of colloidal interaction. (D.H.M.)

53068 ATTEMPTS OF REACTOR LOOP USE FOR ^{125}I PRODUCTION. Kulesza, Albin; Lada, Witold; Michalik, Jacek (Instytut Badan Jadrowych, Swierk, Poland). Nukleonika; 16: No. 11-12, 565-71(1971). (In Polish).

Attempts at production of ^{125}I by natural xenon activation in a reactor gas loop are described. Active xenon removal by liquid nitrogen cooling in a pressure vessel is described. The ^{125}I was extracted from the liquid by distillation. The yield of the reactor gas loop method is considered. The radiation purity of the product amounted to more than 99%. (auth)

53069 EXTRACTION OF ^{32}P FROM NEUTRON-IRRADIATED SULFUR DISSOLVED IN HOT TOLUENE. Domondon, D. B.; Ocon, F. T.; Valdezco, J. L. (Philippine Atomic Research Center, Diliman). Philipp. Nucl. J.; 2: No. 2, 197-203(1970).

The method (Method I) currently in use at PARC for routine processing of ^{32}P and two alternative methods (Method II and Method III) of extracting ^{32}P from neutron-irradiated sulfur dissolved in hot toluene are described. Method I is liquid-liquid extraction using pure water as extractant. Two consecutive extractions give about 75% of the total ^{32}P content. Method II consists in refluxing the hot toluene solution with powdered magnesia, after which the spent toluene solution is removed from the extraction flask. The magnesia is washed successively with fresh toluene, alcohol and water, then dissolved with HCl. The extract contains 90% or better of the initial ^{32}P content. In Method III, hot toluene is made to trickle over irradiated sulfur placed on top of a column of magnesia. The sulfur is dissolved and the ^{32}P quantitatively retained on the magnesia. The magnesia is washed and dissolved as in Method II. A yield of 95% or better is obtained. The ^{32}P extracts from the different methods are purified in the same way. After filtration, the extract is passed through a cation exchanger to remove cationic impurities, treated with H_2O_2 to destroy organic impurities, then the ^{32}P is taken up in pyrogen-free, distilled H_2O. (auth)

53070 CARRIER-FREE ^{131}I FROM TELLURIC ACID. Montesa, Elizabeth F. (Philippine Atomic Research Center, Quezon City). Philipp. Nucl. J.; 2: No. 2, 205-10(1970).

Carrier-free ^{131}I, suitable for medical use, was prepared by the wet distillation of telluric acid. Telluric acid in aluminum cans was irradiated intermittently in the Philippine Research Reactor (PRR-1) up to a maximum of 250 hours. After dissolution of the irradiated telluric acid in sulfuric acid, hydrogen peroxide was added and ^{131}I was distilled into a dilute solution of sodium hydroxide. Chromatographic examination of the product showed it to be primarily iodide (99 to 99.5%) with negligible amounts of periodate and iodate; half-life determinations gave an average value of 8.07 days and gamma spectrometry using a 256 channel analyzer exhibited the peaks of ^{131}I only. (auth)

53071 PREPARATION OF ADHERENT ^{241}Am ALPHA SOURCES BY ELECTRODEPOSITION. Iwinska, Hanna (Instytut Badan Jadrowych, Swirk, Poland). Nukleonika; 17: No. 1-2, 69-73(1972). (In Polish).

The method of preparation of thin layer α sources by electrodeposition from 0.1M H_2SO_4 solution is described. The conditions of electrolysis were: pH = 3.7, time–110 min. The maximal activity obtained on platinum cathode was about 100 μCi/cm^2. After ignition adherent coatings were obtained. (auth)

53072 REMOVAL OF MATERIALS FROM ION EXCHANGE RESINS. Dietrich, Lee A.; Dikeman, John C.; Johnson, Kenneth R. (to United States Atomic Energy Commission). U. S. Patent 3,669,631. 13 Jun 1972. Filed 8 Jan 1970.

A process is described for recovering radioisotopes from spent ion exchange resins that comprises mixing a spent ion exchange resin with an acidic solution containing a catalyst and hydrogen peroxide, heating the mixture to initiate an exothermic reaction, and maintaining the mixture at the reaction temperature until the reaction is complete with the resin entrapped materials dissolved. (auth)

53073 RECOVERY OF ^{238}Pu IN THE MILLI LABORATORY. Koch, G.; Ochsenfeld, W. (Kernforschungszentrum, Karlsruhe, Ger.). KFK-Nachr.; 3: No. 1, 9-11(1972). (In German).

Within the framework of the Plutonium-238 Program, which is part of the Actinide Project, NpO_2 (10%) iron cermet pellets in Zircaloy capsules were irradiated in the BR-2. After the cooling period, these pellets were transferred to the MILLI laboratory for chemical reprocessing and plutonium recovery. As the facility was originally designed for reprocessing SNR fuel elements, there is no ion exchange equipment within the heavily shielded part of the laboratory. Thus an extraction procedure had to be developed that uses tributyl phosphate (TBP), as is usually done in nuclear fuel reprocessing. The experience gained in the reprocessing of the first test charge by the newly developed procedure is described. (GF)

53074 EFFECT OF THE CHEMICAL PREPARATION OF ^{45}Ca ON THE NONPROTEIN BOUND SERUM FRACTION. Giuliano, C. (Institut National de la Sante et de la Recherche Medicale, Paris). Pathol.-Biol.; 29: No. 3-4, 205-11(Feb 1972). (In French).

The fraction of nonprotein bound calcium was measured simultaneously for stable ^{40}Ca and radioactive ^{45}Ca using the ultracentrifuge method. The amount of ^{45}Ca present varied with the method of preparation. Neutron activation of $^{44}CaCO_3$ led to the simultaneous production of ^{46}Sc and ^{45}Ca. These elements could be separated either by complexometry or by fractional chemical precipitation, the first method resulting in a higher rate of production for nonprotein bound ^{45}Ca than nonprotein bound ^{40}Ca. Some of the ^{45}Ca may be already complexed with an organic molecule in the ^{45}Ca mother source. In this case, possible modifications in the degree of metabolization of the ^{45}Ca tracer must be taken into consideration. (France)

53075 APPARATUS FOR PRODUCING GASEOUS FISSION PRODUCTS, PARTICULARLY ^{133}Xe. U. S. Patent 3,680,284. 1 Aug 1972.

A method and an apparatus are described for the commercial production of gaseous fission products without contamination by foreign gases. For ^{133}Xe production, a U compound of low melting point (such as prepared by dissolving UO_2 in molten sodium pyrosulfate) is irradiated by neutrons in an evacuated steel container. After irradiation, the target is melted, the container pierced, and the released gases led to a carbon trap. Then the trap is heated to release the rare gases, while retaining the iodine. ^{37}Ar may also be produced from the ^{40}Ca(n,α) reaction using NaF–CaF_2 or NaCl–$CaCl_2$, or tritium from the ^{6}Li(n,α) reaction using LiCl–NaCl or LiCl–$CaCl_2$. (D.L.C.)

53076 EXTRACTION OF IRON, COBALT, AND MANGANESE FROM HYDROCHLORIC ACID WITH QUATERNARY AMINE ALIQUAT-336. Aly, H. F.; El-Garhy, M.; El-Reefy, S. Microchem. J.; 17: No. 4, 431-5(Aug 1972).

The extraction of iron, cobalt, and manganese by Aliquat-336 from HCl media was investigated. Dependence on both HCl and amine concentration was studied. The separation factors between iron and both cobalt and manganese were determined and optimum conditions for separation are given. Two procedures for separation of carrier-free ^{59}Fe from irradiated cobalt target and ^{54}Mn from irradiated iron target are given. The products obtained were more than 99% radiochemically pure. (auth)

Reactor Fuel Reprocessing

Refer also to abstract 52977.

53077 (CONF-720823–9) EFFECT OF EXTENDED EXPOSURE TO SIMULATED LMFBR FUEL REPROCESSING OFF-GAS ON RADIOIODINE TRAPPING PERFORMANCE OF SORBENTS. Ackley, R. D.; Davis, R. J. (Oak Ridge National Lab., Tenn.). 1972. 15p. Dep. NTIS.

From twelfth air cleaning conference; Oak Ridge, TN. (28 Aug 1972).

For LMFBR fuel reprocessing plants, a required radioiodine retention factor of ~10^8 is projected. Also projected is a cumulative retention factor of ~10^6 for iodine fixation achieved upstream of the filter-adsorber assembly used for final off-gas treatment. Thus, this assembly will need to provide a decontamination factor (DF) of ~10^2, but considerable reserve capability is desired. Certain silver-containing sorbents in a 2-in. depth at 100°C and/or 200°C have, in short-term laboratory tests, exhibited DF's of >10^3 for iodine as methyl iodide or elemental iodine under conditions including 3 vol % water vapor and iodine loadings estimated equivalent to that for at least one year of operation. Present objectives are to obtain information on the effective service life of such sorbents and to ascertain the desirability of locating a catalytic oxidation bed upstream of the sorbents to minimize poisoning by organics and to convert organic iodides to I_2. Accordingly, a laboratory facility for exposing sorbents to simulated fuel reprocessing off-gas is being operated. The main air stream is humidified to around 85% saturation (referred to room temperature). Elemental iodine (60-day ^{125}I-labeled), dodecane, and nitric oxide are continuously injected at their anticipated concentrations. One group of sorbents is exposed to untreated off-gas while another group is exposed to off-gas that has traversed a Hopcalite bed at 350°C. Methyl iodide (12.3-hr ^{130}I-labeled) is injected periodically to furnish short-term results, whereas long-term cumulative results are obtained with the I_2. Sorbents investigated include three varieties of silver zeolite (designated AgX with the percent Ag^+ for Na^+ exchange denoted), GX135 (silver salt-treated alumina-silica), and a type of iodized charcoal. Sorbent depths are 2 in. Excellent performance (indicated I_2 and CH_3I DF's ≥10^3) was observed for the following test situations: 26% AgX, $^1/_{16}$ in. pellets, at 200°C, both with and without Hopcalite upstream, 196 days exposure; 99% AgX, $^1/_{16}$ in. pellets, 100°C, both with and without Hopcalite, 105 days; GX135 (8 × 16 mesh, U.S.), 200°C, with Hopcalite, 196 days; and GX135, 100°C, without Hopcalite, 119 days. (Data are not yet available for GX135, 100°C, with Hopcalite). Performances observed for other test situations ranged from poor to good. The importance of sorbent particle size was demonstrated by the less favorable performance of 88% AgX, $^1/_8$ in. pellets, 100 and 200°C, relative to that for the 26% AgX, $^1/_{16}$ in. pellets (200°C). The use of Hopcalite was highly beneficial in trapping iodine injected as CH_3I; in trapping iodine injected as I_2, its use was beneficial for 26% AgX, 99% AgX, and GX135 and deleterious for 88% AgX ($^1/_8$ in. pellets) and iodized charcoal (the latter at 66°C). This investigation is being continued. (auth)

53078 (CONF-720823–11) DETERMINATION OF THE RADIOACTIVE NUCLIDES PRESENT IN THE OFF-GAS STREAM GENERATED BY THE HEAD-END STEPS IN REPROCESSING HTGR TYPE FUELS. Lowrie, R. S.; Fitzgerald, C. L.; Vaughen, V. C. A. (Oak Ridge National Lab., Tenn.). 1972. 15p. Dep. NTIS.

From twelfth air cleaning conference; Oak Ridge, TN. (28 Aug 1972).

Results of studies to determine the behavior of radioactive nuclides in gaseous waste streams generated during the reprocessing of spent High Temperature Gas-Cooled Reactor (HTGR) fuel are presented. The fuel is in the form of coated particles of uranium and thorium, bonded into fuel sticks, and inserted into holes in large hexagonal graphite blocks. Spent fuel is reprocessed to recover the bred ^{233}U and the unburned ^{235}U. Studies were performed on a small scale in a hot-cell using a generalized head-end reprocessing flowsheet. The fuel specimens were crushed, burned to remove as much graphite as possible, and the burner residue separated into appropriate size fractions. Those fractions containing TRISO-coated particles were then ground to break the SiC coating and burned a second time. Residues from each fraction were leached with acid Thorex reagent. The off-gas from each step was collected and analyzed. Burning BISO-coated $(U-Th)O_2$ particles released the bulk of the ^{85}Kr (97 to 98%) and the tritium (98 to 99%); the remainder was released during the leaching step. The initial burning of the mixed TRISO-coated ThC_2 and TRISO-coated UC_2 fuel released ~7.4% of the ^{85}Kr. Subsequent grind-burn steps released an additional 7.4% of the ^{85}Kr from the ThC_2 particles and 84.5% from the UC_2 particles. Tests were completed on a fuel specimen containing TRISO-coated fertile ThC_2 particles and TRISO-coated fissile UC_2 particles. The initial burn released 20% of the tritium and less than 1% of the ^{85}Kr. Most of the tritium and ^{85}Kr in the fertile particles was released during the grinding step, the remainder in the burning and leaching steps. Grinding the fissile particle released most of the ^{85}Kr; the subsequent burning and leaching steps released the tritium and remaining ^{85}Kr. About 3.5% of the gross gamma activity present in the fuel stick was carried over by the off-gas streams during the burning tests. Although the primary sintered metal filters collected most of this activity, ~1% of the amount carried-over passed through the filter. Most (98%) of the tritium and ^{85}Kr present in spent HTGR fuel will be released during the grind-burn step in the head-end operations, although the amounts released during grinding or burning will depend on the fuel particle being processed. Further, small amounts of fission products do pass the primary sintered metal filter and may have to be removed by other means. (auth)

53079 (EUR–4812) EXTRACTION OF PLUTONIUM FROM HEAVY WATER FUELS BY THE SALTEX PROCESS. Heylen, P. R. (Centre d'Etude de l'Energie Nucleaire, Mol (Belgium)); Wurm, J. G.; Avogadro, A. (European Atomic Energy Community). 1972. 45p. (In French). Dep. NTIS (U. S. Sales Only).

A process known as the Saltex process was designed to extract plutonium from irradiated natural uranium fuel elements of the UO_2 (PuO_2)/Zircaloy type. It is essentially a head-end process based on pyrochemical reactions in molten salts for the recovery of a plutonium concentrate by precipitation and filtration. These operations are carried out in compact plants situated, in principle, in the same place as a group of power reactors. The uraniferous waste is treated and conditioned in such a way as to obtain insoluble material that can easily be stored permanently on the spot. The description of the flowsheet ends with a material balance sheet of products consumed and waste to be stored. (auth)

53080 (ORNL–4794) CHEMICAL TECHNOLOGY DIVISION ANNUAL PROGRESS REPORT FOR PERIOD ENDING MARCH 31, 1972. (Oak Ridge National Lab., Tenn.). Aug 1972. Contract W-7405-eng-26. 121p. Dep. NTIS.

Research is reported on: molten salt reactor processing; development of aqueous processes for LMFBR fuels; development of methods for reprocessing HTGR fuels; waste treatment and disposal; transuranium element processing; development of the thorium fuel cycle; preparation of $^{233}UO_2$ for light water breeder reactors; separations chemistry research; chemical applications of nuclear explosives; biochemical technology; spectrophotometric studies of solutions of lanthanides and actinides; preparation and properties of actinide oxides; surface and interface properties in heterogeneous systems; chemical engineering research; reactor evaluation studies; and miscellaneous programs. Separate abstracts were prepared for 15 of the 16 sections. Biochemical technology, not covered separately, includes macromolecular separations, high resolution analytical systems, water pollution studies, and miniaturized fast analyzer. (D.H.M.)

For abstracts of individual sections see: 52986, 53036, 53063, 53066, 53067, 53081–53085, 53128, 53552–53554, and 55197.

53081 (ORNL–4794, pp 1-14) MOLTEN-SALT REACTOR PROCESSING. Aug 1972.

In Chemical Technology Division annual progress report for period ending March 31, 1972.

BISMUTH—solvent properties of liquid, for rare earths and thorium, pp.4–5
EXTRACTION APPARATUS—interface detector for, salt–metal, p.12
MOLTEN SALT BREEDER REACTOR—fuel reprocessing for, design and construction of molybdenum reductive extraction equipment for, pp.11–12
  —fuel reprocessing for, research progress on
PROTACTINIUM—precipitation as oxide from molten salts, pp.5–6
RARE EARTH ALLOYS AND SYSTEMS—rare earths–Th, solubility in liquid bismuth, pp.4–5
RARE EARTHS—separation from MSBR fuel salt by metal transfer process, pp.7–8
  —separation from MSBR fuel salt by metal transfer process, contactor studies for, pp.8–9
REACTOR FUELS—reprocessing of MSBR, research progress on
  —reprocessing of MSBR, chemistry of fuel reconstitution in, p.6
  —reprocessing of molten salt, axial dispersion in simulated continuous fluorinator for, pp.9–10
  —reprocessing of molten salt, development of frozen-wall continuous fluorinator for, pp.10–11
URANIUM—distribution between liquid bismuth and MSBR fuel salt, pp.6–7

—separation from molten fluoride salts by oxide precipitation, p.12–14
URANIUM FLUORIDES UF_6—reactions with uranium tetrafluoride in molten beryllium fluoride–lithium fluoride–thorium fluoride, p.6 (D.H.M.)

53082 (ORNL–4794, pp 15-25) DEVELOPMENT OF AQUEOUS PROCESSES FOR LMFBR FUELS. Aug 1972.

In Chemical Technology Division annual progress report for period ending March 31, 1972.

FISSION PRODUCTS—separation of volatile, in reprocessing of LMFBR fuels by voloxidation, pp.17–20
IODINE—separation of fission product, from off-gases in reprocessing of LMFBR fuel, pp.21–2
LIQUID METAL FAST BREEDER REACTOR—fuel reprocessing for, development of aqueous methods for
—fuels for, radiation properties and shielding requirements of, pp.22–3
RADIOCHEMICAL PROCESSING PLANTS—effluent control from, pp.24–5
REACTOR FUELS—thermal conductivity of sheared prototype LMFBR, p.16
—radiation effects on dissolution characteristics of LMFBR, pp.20–1
SHIELDED CONTAINERS—development for shipping irradiated LMFBR fuel, pp.15–6
TRITIUM—separation from off-gases in reprocessing of LMFBR fuel, pp.21–2 (D.H.M.)

53083 (ORNL–4794, pp 26-32) DEVELOPMENT OF METHODS FOR REPROCESSING HTGR FUELS. Aug 1972.

In Chemical Technology Division annual progress report for period ending March 31, 1972.

Research progress is reported on: head-end reprocessing studies with unirradiated fuel, head-end reprocessing studies with irradiated fuel, engineering studies of burner off-gas decontamination, and laboratory studies of burner off-gas decontamination. (D.H.M.)

53084 (ORNL–4794, pp 54-62) SEPARATIONS CHEMISTRY RESEARCH. Aug 1972.

In Chemical Technology Division annual progress report for period ending March 31, 1972.

Research is reported on: new separation agents, plutonium purification with amines, recovery of uranium from commercial phosphoric acid, extraction of lithium from salt solutions, high resolution rare earth separations, and distribution equilibria and mechanisms in uranium extraction by primary amine from sulfuric acid solutions. (D.H.M.)

53085 (ORNL–4794, pp 91-5) CHEMICAL ENGINEERING RESEARCH. Aug 1972.

In Chemical Technology Division annual progress report for period ending March 31, 1972.

Research progress is reported on: thorium anion exchange with very small resin particles, multicomponent mass transfer in electrolyte systems, mass transfer of water from sol droplets, production of sol-gel microspheres of small uniform size, chemical engineering research studies related to MSR processing, and recovery of tritium from blankets of controlled thermonuclear reactors. (D.H.M.)

53086 METHOD FOR REPROCESSING SPENT MOLTEN SALT REACTOR FUELS. McNeese, Leonard E.; Ferguson, Don E. (to United States Atomic Energy Commission). U. S. Patent 3,672,846. 27 Jun 1972. Filed 21 Apr 1970.

A method for reprocessing spent molten metallic fluoride salt mixtures suitable as molten salt breeder reactor fuels is provided wherein uranium, protactinium and certain rare earths are removed from the spent salt mixture prior to recycle of the purified salt mixture back to the reactor. A major fraction of the uranium contained in the spent salt mixture is removed by fluorination with the uranium hexafluoride being reconstituted into the purified salt for return to the reactor. The remaining uranium and protactinium are removed in a protactinium isolation unit by reductive extraction into a molten bismuth solution containing lithium, thorium, and ^{233}Pa as metal reductants. The extracted uranium is carried out of the unit by the metal solution while the protactinium is held-up within the unit in the bismuth phase. The rare earths are then reductively extracted from the uranium and protactinium-free spent salt mixture in a rare earth removal unit into a molten bismuth solution containing lithium and thorium as metal reductants. The rare earths are then back extracted from the bismuth phase into an acceptor salt selected from lithium chloride, lithium bromide and their mixture. Hydrogen fluoride oxidizers are provided for removal of extracted materials, including fission products which form non-volatile fluorides during fluorination, metal corrosion products, and $^{231}PaF_4$, from the bismuth in order to regenerate the bismuth solution. Provision is also made for the separate recovery from the acceptor salt of divalent and trivalent rare earths. (auth)

53087 MILLI, A FACILITY FOR THE CHEMICAL REPROCESSING OF IRRADIATED SUBSTANCES. Leichsenring, C. H. (Kernforschungszentrum, Karlsruhe, Ger.). KFK-Nachr.; 3: No. 1, 6-9(1972). (In German).

MILLI is a facility established for chemical reprocessing of irradiated fuels and is now used for the extraction of uranium, plutonium, and other actinides, such as americium and curium. For this purpose, new extraction processes had to be developed. The name MILLI stems from the nominal throughput of the installation which is one milliton, i.e., 1 kg of irradiated uranium-plutonium fuel per day. Its mode of operation is outlined by describing the reprocessing of breeder fuels by a modified Purex process. The special requirements that had to be met by an appropriate shielding and by a criticality-proof design of the overall facility is described. This is followed by a short outline of the analytical process control, of waste gas, and solvent cleaning. (GF)

53088 CHEMICAL PROCESS ENGINEERING. FLUORIDE PROCESS AS AN ADVANTAGEOUS PROCESS IN FUEL REPROCESSING. 7. CHEMICAL PROCESSES IN THE DEVELOPMENT OF NUCLEAR TECHNOLOGY. Lanius, E. H. VDI (Ver. Deut. Ing.) Nachr.; 26: No. 14, 14(1972). (In German).

The advantages of a process for the enrichment of deuterium, which circumvents the corrosion problems that arise in the $HDS + H_2O \rightarrow H_2S + HDO$ method due to the high aggressiveness of the hydrogen sulfide are described. The technique discussed is the ammonia process, which makes use of countercurrent isotope exchange between hydrogen and ammonia, ($HD + NH_3 \rightarrow H_2 + NH_2D$). This reaction needs the presence of a catalyst (dissolved potassium amide). The fuel reprocessing techniques used so far are based on selective countercurrent extraction of Pu and U from aqueous solutions into an organic phase. Further improvements of the fluorine technique will very likely lead to the fluoride process being preferred to aqueous reprocessing methods. (GF)

ENGINEERING

Energy Conversion

Refer also to abstracts 53117, 53335, 53337, and 53338.

53089 (AD–737380) DESCRIPTION OF HIGH-PRESSURE ELECTROFLUIDDYNAMIC (EFD) FACILITY. Final Scientific Report. Willke, Theodore L.; Fretter, Ernest F. (Aerospace Research Labs., Wright-Patterson AFB, Ohio). Nov 1971. 59p. (ARL–71-260). NTIS.

A facility is described which simulates EFD generator operation using high pressure air as the working fluid. The humidity, temperature, mass flow, and pressure of the air can be controlled and monitored in two nearly identical air systems. The working fluid is supplied to one of three high pressure list stands enclosing experimental EFD conversion channels. Excitation voltage of up to 150 kV and generate voltages up to 2000 kV are supplied. Types and specifications of various types of instruments are described as well as the types of experiments performed. (auth) (NTIS)

53090 (BNL–16889) METAL HYDRIDES FOR ENERGY STORAGE. Wiswall, R. H. Jr.; Reilly, J. J. (Brookhaven National Lab., Upton, N. Y.). 1972. 22p. (CONF-720925–6). Dep. NTIS.

From seventh intersociety energy conversion engineering conference; San Diego, CA. (25 Sep 1972).

The use of metal hydrides as hydrogen reservoirs facilitates the storage and subdivision of central-station power for automotive and other purposes. Hydrides with a wide range of properties have been synthesized and studied, and several appear to have promise for specific storage applications. Results are reported on the effect of alloy constituents on hydride stability; on the formation of hydrides by metals reacting with gas mixtures such as those produced by the steam reforming of hydrocarbons; and on the feasibility of integrated systems of hydride reservoir plus engine or fuel cell. (auth)

53091 (IPP-IV–36) PERFORMANCE OF MHD GENERATORS AND THE THERMAL EFFICIENCY OF CLOSED CYCLE MHD POWER PLANTS. Salvat, M. (Max-Planck-Institut fuer Plasmaphysik, Garching (West Germany)). Apr 1972. 22p. (In German). Dep. NTIS (U. S. Sales Only).

The thermal efficiency of a nuclear power plant incorporating a gas-cooled high-temperature reactor, a MHD-generator, a heat exchanger and compressors depends, among other things, on the polytropic efficiency of the MHD generator. Since the local polytropic efficiency is reduced by heat and friction losses, realistic cycle efficiency computations must take into account the variation of the local polytropic efficiency along the length of the MHD channel. It has been pointed out that for this type of power plant a Ne-Cs mixture seems to be more advantageous than a He-Cs mixture. Results of computations pertaining to the power output of a MHD generator and to the thermal efficiency of the cycle operating with Ne-Cs as working medium are presented. It is shown that for stagnation (reactor) pressure and temperature values of 30 atm and 2000°K (or 40 atm and 2150°K, respectively), the thermal efficiency is about 50%. (auth)

53092 (MMM–3691-5(Rev.1)) SNAP-21 PROGRAM, PHASE II. DEEP SEA RADIOISOTOPE-FUELED THERMOELECTRIC GENERATOR POWER SUPPLY SYSTEM. PRELIMINARY DESIGN DESCRIPTION 10-WATT SYSTEM. Wharam, J. (Minnesota Mining and Mfg. Co., St. Paul. Electrical Products Group). Feb 1967. Contract AT(30-1)-3691. 96p. Dep. NTIS.

SNAP-21 is a ^{90}Sr-fueled thermoelectric generator 10-W power system for providing electric power for use under the surface of the sea. The preliminary design, design and safety requirements, and a detailed description of the development and testing of all components of the system are presented. (L.C.L.)

53093 (NASA-TM-X–2440, pp 13-25) SPACE NUCLEAR POWER SYSTEMS. Carpenter, R. T. (Space Nuclear Systems Office, Washington, D. C.). Jan 1972.

From Symposium on natural and manmade radiation in space; Las Vegas, Nev. (1 Mar 1971).

Space nuclear power systems have been, are being, and will be developed for use in those particular spacecraft applications for which nuclear power systems offer unique advantages over solar and/or chemical space power systems. Many of these advantages are discussed relative to the past and future applications of nuclear power systems in the space program. Both isotopic and reactor heated space electrical power units are described in an attempt to illustrate their operating characteristics, spacecraft integration aspects, and factory-to-end of mission operational considerations. Much experience has been gained with nuclear space power sources which have been flown. This experience is being used to guide current developments to make those units more attractive for operational use. The status of technology developments in nuclear power systems is presented. Some projections of these technologies are made to form a basis for the applications of space nuclear power systems to be expected over the next 10 to 15 years. (auth)

53094 (NASA-TM-X–2440, pp 26-33) NUCLEAR APPLICATIONS IN MANNED SPACE STATION. Brooksbank, W. A. Jr.; Sieren, G. J. (Marshall Space Flight Center, Huntsville, Ala.). Jan 1972.

From Symposium on natural and manmade radiation in space; Las Vegas, Nev. (1 Mar 1971).

Current and future NASA Space Station studies will place a great deal of emphasis on economical systems which can start small and grow as the station itself grows. Space station electrical power systems based on nuclear sources will have to be increasingly adaptable to the lower power ranges to be competitive with other systems, while at the same time exploiting their inherent growth capability. Power growth capabilities as high as three of four-to-one will be required to meet the needs of a space station which is initially manned with a small crew and grows incrementally to a large station capable of accommodating a very complex experiment program. The zirconium hydride reactor, coupled to a thermoelectric or Brayton conversion system, and the ^{238}Pu isotope/Brayton system are considered to be the viable nuclear candidates for the modular space station electrical power system. The basic integration aspects of these nuclear electrical power systems, including unique requirements imposed by the buildup and incremental utilization considerations of the modular station, are reviewed. Also treated are the various programmatic aspects of nuclear power system design and selection. (auth)

53095 (NASA-TM-X–2440, pp 844-9) DESIGN CONSIDERATIONS FOR COMBINED RADIATION EFFECTS FACILITIES FOR TWELVE-YEAR OUTER PLANET SPACECRAFT VOYAGES. Miller, Charles G. (California Inst. of Tech., Pasadena). Jan 1972.

From Symposium on natural and manmade radiation in space; Las Vegas, Nev. (1 Mar 1971).

The design considerations influencing the choice and utility of environmental simulation methods and facilities are described, insofar as they relate to the new requirements imposed on outer planet spacecraft because of radiation environments to be expected. Possible means for duplicating the radioisotope thermoelectric generator radiation environment, and for duplicating the effects of trapped radiation belt environment are described, together with an assessment of radiation levels to be expected in the vicinity of an environmental testing chamber when in use. (auth)

53096 (UCRL–51221) ENERGY: USES, SOURCES, ISSUES. Austin, A. L.; Rubin, B.; Werth, G. C. (California Univ., Livermore. Lawrence Livermore Lab.). 30 May 1972. 129p. Dep. NTIS.

Data on current and predicted future energy uses, costs, and sources are compiled as a reference for studies of the complex problems involved in providing the US with abundant supplies of low cost energy while minimizing the environmental effects of energy production and use. The data are presented in graphs or tables with the data sources itemized. (L.C.L.)

53097 POWER GENERATION OPTIONS FOR THE EIGHTIES AND NINETIES. Kent, M. F. Pub. Util. Fortn.; 90: No. 4, 17-23(17 Aug 1972).

An evaluation of power generation from sources such as fusion, solar energy, geothermal energy, magnetohydrodynamic reactions, fuel cells, breeder reactors, desulfurized coal, and hydrogen is presented. Generation options for the 1980-to-1990 period are discussed along with power needs in the U. S. during the period 1980 to 2000. (J.R.D.)

53098 TWENTY-TWENTY VISION: A VIEW OF THE FUTURE. Faust, George R. (Gilbert Associates, Inc., Washington, D. C.). Pub. Util. Fortn.; 90: No. 4, 24-32(17 Aug 1972).

The state of present technology related to gas and electric utilities is examined and the chances of using advanced technology in dealing with the problems associated with utility depreciation accrual rates are evaluated. Discussions are included on gas industry, coal gasification research, atomic energy, magnetohydrodynamics, fuel cells, and underground transmission lines. (J.R.D.)

53099 DETERMINATION OF THE MAGNETIC FIELD EXTENSION PROFILE FOR REDUCING THE END LOSSES IN THE MHD GENERATOR CHANNEL. Bajaria, Hansraj J. Houghton, Mich.; Michigan Technological Univ. (1972). 98p. University Microfilms Order No. 72-21,633.

Thesis.

A constant area rectangular channel was studied. The end power loss due to the leaking currents was computed on the basis of Ohm's law and with an empirical estimation of the leakage currents. The accuracy of this circuit-theory approach to estimate the end losses was verified over the wide range of parameters (aspect ratio, loading factor) with the well known solution based on the conformed mapping method. The equation of actual power developed was used as the key expression for the parameter studies (including aspect ratio, loading factor, magnetic field, etc.). The Laplace equation was shown to be the governing equation for the electric potential and current density distribution. Two main assumptions made were: velocity was constant across the channel and induced magnetic field effects were negligible due to magnetic Reynolds number being much smaller than unity or by the use of the backstraps. To solve the equation a numerical finite difference equation method was applied. Through Gauss–Seidel iteration procedure, the distribution profiles of the end current density with proper boundary conditions were obtained for different values of K in the equation $B = B_0e^{-Ky}$. The current density profiles so obtained were compared to find the value of K corresponding to the optimum end loss compensation. The same procedure was repeated for different load factors varying from 0.2 to 1.0. Magnetohydrodynamic losses were discussed to show qualitatively the effects of overcompensation and incomplete compensation. It also showed the overcompensation could not mean the useful conversion of energy into electrical power as claimed by Sutton et al. Experimental results which have used the constant extension and exponential extension were cited to support the analysis. For the practical laboratory application of the present analysis, various shimming methods were suggested to modify the profile curve of the natural-decayed magnetic field to obtain the desired optimum shape. It was concluded that (i) the end power loss expression was quite adequate for the design and construction of the electro-mechanical set-up for a modern MHD power generator, and (ii) there was a definite optimum value of K corresponding to each loading factor which gave more complete end loss compensation; the value of K lower than the optimum value resulted in overcompensation, whereas higher values resulted in incomplete compensation. (Diss. Abstr. Int., B)

53100 ENERGY CRISIS: THE ISSUES AND A PROPOSED RESPONSE. McCloskey, Michael. Environ. Aff.; 1: No. 3, 587-605(Nov 1971).

The environmentalists' views, as opposed to industrialists' views, of the energy crisis are presented. Environmentalists contend that: the crisis lies in the need to halt excessive pressures for increased consumption; the present rate of energy growth is unrealistic, environmentally damaging, and artificially induced; and there are reasonable ways to bring this rate of energy growth under control. Arguments and data to support each of these contentions are discussed. (L.C.L.)

53101 LEGAL SOLUTION TO THE ELECTRIC POWER CRISIS: CONTROLLING DEMAND THROUGH REGULATION OF ADVERTISING, PROMOTION, AND RATE STRUCTURE. Permar, David H. Environ. Aff.; 1: No. 3, 670-93(Nov 1971).

Electric power generation and use in the U.S. is discussed with respect to the factors which contribute to growth in demand; economic incentives which stimulate the building of more new power plants; failure of regulatory controls; effects of advertising and promotional activities; rate structure of utilities; and suggested legal steps which could be taken to limit the growth of electric power generation. (L.C.L.)

53102 TOTAL ENERGY: POWER (NUCLEAR) AND DISTRICT HEATING. Aler, B. (Aktiebolaget Atomenergi, Studsvik, Sweden). Phil. Trans. Roy. Soc. London, Ser. A; 272: No. 1229, 627-37(27 Jul 1972).

An assessment is made of the possibilities of meeting the total future energy requirement of urban areas in Sweden by nuclear energy and comparisons are made with requirements in Great Britain. It is considered that nuclear power will supply a large proportion of the Swedish energy requirements by the 1980's provided either by combined nuclear heat and power plants located close to the major cities or by hot-water heated by bleed-off steam from large condensing nuclear plants in the neighborhood. Most of the electricity will be produced by nuclear power in the 1980's and its share will successively increase during the following decades. (UK)

53103 NON CONVENTIONAL TWO PHASE CYCLES IN AUTOTRACTION. Maizza, Vito (Univ., Bari, Italy). Termotecnica (Milan); 26: No. 2, 71-83(Feb 1972). (In Italian).

In view of a possible use of steam propulsion in autotraction, some of the techniques used to solve aero-space problems are reviewed and it is shown how autotraction may benefit by them. The problems related to the choice of the parameters of the operative cycles are pointed out and discussed. It is shown that pressure and temperature values within a narrow range and not too low are the most satisfactory for autotraction. Some working fluids, allowing high efficiency of operative cycles and exhibiting fast vaporization necessary for autotraction, are considered and their thermodynamic characteristics are discussed. The efficiencies of cycles using the above working fluids have been calculated and the results graphically presented. The latter are discussed with particular reference to condensation pressure and temperatures. It is then shown that there is a range in which pressures and temperatures should be kept to attain an advantageous combination of weight, size, plant and operating cost. Finally, the effect of the chosen parameters on the design of the various components in an automotive power plant is discussed. (auth)

53104 EXPERIMENTAL STUDY OF THE RELAXATION PHENOMENA IN NON-EQUILIBRIUM MHD GENERATOR DUCT. Ikegami, Tetsuo; Yoshikawa, Kiyoshi; Morimoto, Kenji; Numano, Masahiro; Michiyoshi, Itaru (Kyoto Univ.). J. Nucl. Sci. Technol. (Tokyo); 9: No. 8, 439-44(Aug 1972).

The non-equilibrium electrical conductivity and the relaxation of electron density in seeded plasma for MHD power generators were studied experimentally. The experiments were performed with use made of potassium seeded argon plasma (A + 0.14% K) at 1,800° ~ 2,000°K, flowing in a rectangular duct at constant velocity (about 240 m/sec) under atmospheric pressure. The dependence of the electrical conductivity on the electric current density was found to agree well with theoretical prediction based on the two-temperature model, if a value of 40 was chosen for the collision loss parameter. The effect of the radiative energy loss of potassium atoms was not significant in the present experiments. Furthermore, it was found that the relaxation of the electron density can be well expressed by the recombination coefficient for the electronic three-body recombination processes, and that the relaxation time is about 4×10^{-4} sec for the present experimental conditions. (auth)

53105 EFFECT OF HETEROGENEITY AND HALL CURRENT ON THE MHD POWER GENERATOR. Rudraiah, N.; Narasimha Murthy, S.; Chandrasekhara, B. C. (Univ. of Visvesvaraya, Bangalore, India). Jap. J. Appl. Phys.; 11: No. 9, 1372-9(Sep 1972).

The aim of the present investigation is to consider the influence of Hall effect on the performance of a liquid metal generator using a heterogeneous conducting fluid. The results show that the combined effect of Hall current and heterogeneity increases the electrical efficiency as well as output power of the generator for a given aspect ratio. (auth)

53106 PRESSURE DROP OF LIQUID MERCURY MHD POWER GENERATORS. Michiyoshi, Itaru; Nakura, Saburo (Kyoto Univ.). J. Nucl. Sci. Technol. (Tokyo); 9: No. 8, 490-6(Aug 1972).

Results of experimental studies of performance characteristics of both constant-area (34 × 7 × 295 mm) and diverging-area (23 × 7 to 43 × 7 × 295 mm) MHD power generators with liquid mercury as working fluid, with particular reference to the pressure drop created in the inlet and outlet ducts as well as inside the generator channel, are presented. Discussions are presented on the following aspects. In respect of the constant-area channel, pressure drop in laminar and turbulent flow inside the channel, transition Reynolds number for given Hartmann number, pressure drop in the inlet duct and eddy current created near the end of electrode, output electrical power. For diverging channel, applied magnetic field intensity required for zero pressure drop inside the channel, pressure distribution inside the channel, output electrical power in the case of zero pressure drop. The experimental conditions were as follows: $Re < 10^5$ and $Ha < 60$. (auth)

53107 ENERGIE IN DER KRAFTWERKSTECHNIK. LEISTUNGSREAKTOREN, DAMPFKRAFTWERKE, GASTURBINEN, WAERME-KRAFT-KOPPLUNG. (Energy in Power Plant Engineering. Power Reactors, Steam Power Plants, Gas Turbines, Heat, and Power). Kriese, S. Essen; Vulkan-Verl. Dr. Classen (1971). 176p.

A fundamental explanation of the term energy which represents the maximum of a given energy that can be used in thermal processes is followed by a section where this model is applied to some of the well-known thermodynamic processes. The efficiency of the energy conversion in power reactors and in a power unit is determined and explained within this framework. Moreover, the way of setting up energy and energy flow sheets is outlined, illustrated by one example each. (GF)

53108 PROCESS FOR GENERATING ELECTRICAL ENERGY. Pozwolski, Alexandre Edgar. French Patent 2,093,020. 28 Jan 1972. Filed 25 May 1970. (In French).

A magnetohydrodynamic (MHD) electrical energy generator is described. This generator extends the direct conversion principle to exceptionally low temperatures (for this type of generator). A considerable specific power is obtained. Gas at high pressure is used as the working fluid (water vapor or methanol near or above its critical pressure). This gas is given a high electrical conductivity by dissolving at least one of the following strong electrolytes in it: KOH, KI, NH_4I, CH_3OK. (France)

Facilities and Equipment

Refer also to abstracts 53695 and 54461.

53109 (DP-MS-72-37) ^{252}Cf NEUTRON ACTIVATION FACILITY AT THE SAVANNAH RIVER LABORATORY. Peterson, S. F. (Du Pont de Nemours (E. I.) and Co., Aiken, S. C. Savannah River Lab.). 15 Aug 1972. Contract AT(07-2)-1. 6p. (CONF-720902-3). Dep. NTIS.

From National topical meeting on the applications of ^{252}Cf; Austin, TX. (11 Sep 1972).

A neutron irradiation facility has been established to develop new analytical methods and for the support of research programs. A major component of this facility is a ^{252}Cf source which provides both fission spectrum and thermal neutrons. (auth)

53110 (ORNL-TM-3841) VTE-X MODEL TEST AND COMPUTER CALCULATION OF ROW BY ROW PERFORMANCE AND COMPARISON WITH MEASURED DATA. Van Winkle, R. (Oak Ridge National Lab., Tenn.). Aug 1972. Contract W-7405-eng-26. 42p. (CONF-710555-1). Dep. NTIS.

From VTE-X symposium; Washington, D. C. (26 May 1971).

Comparisons are made between the observed performance of the VTE-X tube bundles during Oct. 1970 to Feb. 1971 and predictions based on model tests and general literature information. A summary is given of steam-side friction factors for enhanced VTE bundles and good agreement gained with VTE-X data. Tests of a $\frac{1}{6}$-scale flow model of the VTE-X bundle showed good velocity distribution outside the tubes when the side gaps were at their design value, but recirculation was observed at twice design value. VTE-X heat transfer data from individual clusters are related to process conditions and to the presence of noncondensables. (auth)

53111 (RDT-E-1-13-T(8-72)) VALVE, ISOLATION, BUTTERFLY TYPE. (Division of Reactor Development and Technology (AEC), Washington, D. C.). Aug 1972. 11p. RSO.

A standard prescribing requirements for butterfly-type isolation values for nuclear and associated applications is presented. This standard supersedes RTD E1- 13T dated December 1970. (J.R.D.)

53112 (RDT-F-8-6-T(8-72)) HOISTING AND RIGGING OF CRITICAL COMPONENTS AND RELATED EQUIPMENT. (Division of Reactor Development and Technology (AEC), Washington, D. C.). Aug 1972. 30p. RSO.

A standard prescribing requirements for hoisting and rigging of critical components and related equipment for nuclear and associated applications is presented. (J.R.D.)

53113 (Y-DA-4541(Rev.1)) PRACTICAL DESIGN CONSIDERATIONS FOR THE APPLICATION OF GAS BEARINGS TO MACHINING PROCESSES. Steger, P. J. (Union Carbide Corp., Oak Ridge, Tenn. Y-12 Plant). 1972. Contract W-7405-eng-26. 14p. (CONF-720918-1). Dep. NTIS.

From thirteenth international machine tool design and research conference; Birmingham, England (18 Sep 1972).

Application of gas bearings to the machining process can provide important advantages in performance and operational reliability. It is important in the design to consider the practical aspects of fabrication, assembly, and maintenance if these advantages are to be fully realized. Externally pressurized gas-bearing-supported machine tool and gaging machine components were developed and applied to machining processes. Implicit in the designs was the selection of easily fabricated geometries, stable structural systems, and a material compatibility which enhanced the bearing reliability. Bearing runouts of from 5 to 25 μ in., part load capacities of from 1,000 to 7,000 lb, and inherent stiffnesses of 50 lb/μ in. have been readily obtainable. Operating experience indicates that gas bearings, using the design and fabrication techniques and procedures discussed, are both practical and economically feasible for production machine tools under moderate operating conditions. (auth)

53114 CALCULATION OF THE DYNAMIC BEHAVIOR OF HEAT EXCHANGERS IN GAS TURBINES. Bammert, K.; Klaeukens, H. Forsch. Ingenieurw.; 38: No. 1, 1-8(1972). (In German).

The dynamic behavior of the heat exchangers plays a major part in the control of nuclear-heated gas turbines of the enclosed type. Two methods have been developed which offer the possibility of performing the corresponding calculations with a digital computer. Programs have been elaborated for each method, with the first yielding a high degree of accuracy, requiring sufficiently small intervals, whereas the second program offers the advantage of a shorter computing time due to larger intervals for those cases where the degree of accuracy is not of prime importance. (INIS)

53115 MEASUREMENTS ON A FUEL-SALT INTERFACE IN THE ANNULAR WELL SPACE DURING THE PRODUCTION OF A CAVITY BY SALT DISSOLUTION. Donat, G.; Tellier, C. (Gaz de France, Paris). Rev. Inst. Fr. Petrole Ann. Combust. Liquides; 26: No. 12, 1203-11(Dec 1971). (In French).

The exploitation of two underground pressurized natural gas reservoirs created at Tersanne (Drome) has begun. These reservoirs are in the form of two cavities having volumes of 100,000 and 130,000 m^3, the gas being stored at a depth of 1,400 m and at a pressure of 220 bars. Each cavity was formed by vertical leaching from a cemented tube constructed between the top of the salt layer and the surface. An annular volume around this tube was filled with a substance, which did not react with the salt (fuel). In this way the dissolution in the upper part of the cavity was controlled. These results were obtained by successive leaching operations, each operation corresponding to the dissolution of a given depth of the exposed area. The depth of the fuel-salt interface was found using γ ray detection techniques after having injected a quantity of ^{82}Br-labeled water into the outer annular volume. (France)

53116 PLUGGING TEMPERATURE INDICATORS (28 Dec 1970) (Engineering Materials). (Richland Operations Office (AEC), Wash.). (CAPE-2251).

5 drawings.

A stacked foil filter and an orifice plate plugging device are temperature indicators which determine the temperature of liquid-metal systems, where plugging of the system is likely to occur from precipitation of the impurities in the liquid metal. In operating the indicators, the liquid metal is cooled below the saturation temperature of the impurities, where nucleation and precipitation of the impurities in the filter or orifice plate occur, producing a decrease in the flow rates through the device. The temperature at which the flow loss occurs is referred to as the plugging temperature (P.T.). The indicators, when used in the single-cycle mode, give a P.T. lower than the actual P.T. because impurities dissolved in the liquid metal become supersaturated before precipitation occurs. When the indicators operate in the oscillatory mode, P.T. values agree more closely with the true saturation temperature. When operated in this mode, the reproducibility is ±10% in the P.T. range of 300° to 400°F. The indicators were evaluated over bulk sodium temperatures of 400° to 1500°F and a P.T. of 300° to 450°F. These devices indicate gross impurities and they are not necessarily specific for a single impurity. The P.T. determinations below a saturation of 300°F are difficult and time consuming, requiring several hours for determination. The stacked foil filter indicator consists of a series of stacked discs. Sodium enters the indicator and flows down an outer annulus. Flowing sodium separates at the filter end of the indicator: one flow path is through the filter and the flow return is through another annulus which serves as a bypass flow. Bypass and filter flow rates are recorded on two strip recorders. The temperature of the filter is recorded on the same strip chart recorder as the filter flow rate. In the other indicator, Na enters the indicator through a center tube and loses heat to the Na flowing up the outside annulus. A thermowell and a thermocouple monitor the temperature of the orifice plate. Flow rate and orifice temperature are recorded on a strip chart with a dual pen recorder. (For details see TID-4100 Suppl.72). (F.S.)

53117 FORMATION OF FOG AND GLAZED FROST DUE TO COOLING-TOWER OPERATION. Bach, H. (Deutscher Wetterdienst-Wetteramt, Essen). Tech. Mitt.; 65: No. 5, 230-6(1972). (In German).

The topics reviewed are operational data on evaporation and drift loss in wet cooling; atmospheric exchange processes within the tower region; absorption capacity of the environmental air; meteorological conditions; changes of the microclimate; definition of the radius of action; and suitable arrangement and construction of cooling towers. (GF)

53118 CONSTRUCTION AND CALIBRATION OF A STANDARD THERMAL NEUTRON FLUX FACILITY. Ryves, T. B. (National Physical Lab., Teddington, Eng.). J. Inst. Nucl. Eng.; 13: No. 3, 74-7(1972).

A thermal neutron flux density standard in excess of 10^7n cm^{-2}s^{-1} was produced with high stability and a very small flux gradient at the irradiation position. The standard thermal neutron flux was produced from sources of fast neutrons consisting of beryllium targets bombarded by a 3-MeV deuteron beam from the Van de Graaff accelerator, moderated in a large graphite block. The standard thermal neutron flux density was measured by activation of bare and cadmium covered thin gold foils. Activation was interpreted by means of the Westcott (1958) method using renormalized expressions for the epithermal flux density to fit the assumed epithermal spectrum. The 2200 ms^{-1} activation neutron capture cross section of about 30 other isotopes were measured relative to gold in the facility. Most accurately measured were ^{23}Na, ^{27}Al, ^{37}Cl and ^{51}V with random plus systematic errors of 1 to 2%. The main experimental difficulty was in determining the absolute foil activities. Where possible β/γ coincidence counting was used. (UK)

Heat Transfer and Fluid Flow

Refer also to abstracts 53110, 53114, 55174, 55179, 55180, 55188, and 55449.

53119 (AREAEE–122) THERMAL EQUILIBRIUM OF A BUBBLE NEAR A HEATED SOLID SURFACE AND ASSOCIATED FLOW PATTERN. Gaddis, E. S. (Atomic Energy Establishment, Cairo (Egypt). Reactors Dept.). 1971. 33p. Dep. NTIS (U. S. Sales Only).

A model is presented that yields the conditions under which thermal equilibrium of a vapor bubble near a heated solid surface can be attained. In the model, liquid motion induced by the evaporation and condensation at the bubble surface as well as variation of surface tension with variation of temperature of the interface were considered. Numerical results are presented as well as a typical distribution of the stream lines of the associated liquid flow pattern. (auth)

53120 (CEA-R–4318) INTERDIFFUSION, IN THE REGION OF CONTINUUM FLOW, OF BINARY GASEOUS MIXTURES INSIDE INHOMOGENEOUS POROUS MEDIA. APPLICATION TO THE EVALUATION OF THE TRANSPORT COEFFICIENTS BY MEANS OF DEVAUX EFFECT. Breton, Jean-Paul (Commissariat a l'Energie Atomique, Saclay (France). Centre d'Etudes Nucleaires). Jun 1972. 33p. (In French). Dep. NTIS (U. S. Sales Only).

The general transport equations for binary mixtures are applied to the problem of interdiffusion in porous media. The fluxes of the two gases are first calculated as functions of the characteristics of the gases and of the porous medium. Then this derivation is generalized to the case of inhomogeneous media. Finally, an interesting example is studied, namely the Devaux effect, from which one can evaluate simultaneously the diffusive and convective resistances of the porous medium. (auth)

53121 (CONF-710959–, Paper 7) ACTIVATED MATERIAL TEST LOOP. 4p.

From Meeting on fission and corrosion product behaviour in primary systems of LMFBR's; Bensberg, Germany (20 Sep 1971).

A sodium mass transfer test loop is described in which activated material is used as a part of specimen in studies of activation to clarify mass transfer phenomenon and to observe behavior of corrosion product and activated Na in liquid Na and to obtain data for design, operation, and maintenance of FBR. So far three cold test runs covering 500 hours, 500 hours, and 1,000 hours were conducted. An initial 1,000 hour hot test run is scheduled for August. (auth)

53122 PHOTOGRAPHIC STUDY OF TWO-PHASE HIGHLY DISPERSED FLOWS. Cumo, Maurizio; Ferrari, Giuseppe; Farello, Giovanni Elvio (CNEN-CSN, Rome). Termotecnica (Milan); 25: No. 9, 450-8(Sep 1971).

A post-burnout two-phase flow of a highly dispersed mixture of Freon-12 (reduced pressure 0.3) was analyzed by mean of high-speed (40,000 ph.p.s.) cinematography. The Freon was electrically heated in a section of a loop and then, moved downward from the heating section, into a sight section through which high-speed films were taken. The photograms were analyzed taking into account such droplet population characteristics as droplet dimensional distribution, droplet velocity, and trajectories. The main conclusions were: there is photographic evidence of a thermodynamic disequilibrium up to the calculated qualities of 200% in post burnout two phase flows; the droplet mean dia decreases with increasing heat flux (the test section was uniformly heated by Joule effect) and the vapor mass velocity; the droplet velocity is independent of droplet dia and is almost the same for all droplets (theoretical equations of droplet entrainment were confirmed); the droplet velocity transversal profiles are very close to those theoretically deduced for the vapor (the local slip ratios are very close to 1); and droplet trajectories (graphically deduced from the photograms and plotted) are straight and parallel to the flow. Many diagrams of droplet dimensional distribution versus mass velocity, versus quality and versus heat flux were plotted; the investigation involved more than 10,000 droplets. As the flowrate and the heat flux increase the dimensional distribution curves tend to move toward the smallest diameters. (auth)

53123 OBSERVATION ON THE CISE CRITERION FOR THE EXTENSION OF THE CRITICAL HEAT FLUX TUBE CORRELATION TO THE ROD BUNDLE GEOMETRY. Gaudiosi, Gaetano (CNEN–CSN, Rome). Termotecnica (Milan); 26: No. 2, 89-104(Feb 1972).

The CISE criterion for the extension of the Critical Heat Flux (CHF) tube correlations to the rod bundle geometry is presented. Some additional refinements are suggested. The criterion was applied to the CISE and Becker CHF tube correlations. The proposed subchannel CISE and Becker correlations have been preliminarily compared to the former mixed flow correlations, to some Hambo and Cobra thermohydraulic subchannel code results, and to some experimental data for a uniform heat flux distribution. The two last proposed rod bundle correlations show correct trends and results. However, a more complete comparison is needed to check their accuracy. (auth)

53124 SOME BASIC EXPERIMENTAL METHODS OF WET-STEAM FLOW INVESTIGATION. Stastny, Miroslav; Falout, Frantisek; Tajc, Ladislav; Zeleny, Josef; Plzen, N. P. Energetika; 22: No. 6, 249-55(Jun 1972). (In Czech).

Basic experimental apparatus and measuring methods for the investigation of the two-phase steam–water flow in which the prevailing steam component and the liquid phase in the form of water drops, which is a typical case at some power-generating plants, especially at the light-water reactor turbines, are discussed. The experimental investigation of the wet-steam flow was made on experimental as well as on full-scale turbines and in the two-phase tunnels. Some types of pressure probes serve to measure the parameters of the steam component of the two-phase flow in the turbines and an optical probe for water-film investigations are mentioned. The determination of the mean moisture content from the balance and the visual observation of the liquid-phase motions belong to the basic measuring methods to be used in the two-phase tunnels. The use of the method based on the temperature-difference measurements between the liquid and the steam can be made when detecting the presence of the water drops in the reheated steam. The investigation of the water drops dispersed more coarsely is to be made using the impact method. (auth)

Materials Testing

Refer also to abstracts 53599, 55221, and 55222.

53125 EDDY CURRENT TESTING OF STAINLESS STEEL FUEL JACKET CLADDING TUBING. Ito, Hideyuki; Uetake, Ichizo (National Research Inst. for Metals, Tokyo). Hihakai Kensa; 21: No. 6, 344-54(Jun 1972). (In Japanese).

Eddy current testing of 316 stainless steel tubing using an instrument with single coil and precise impedance bridge is described. Bridge output signals are separated by a filter into a signal which indicates defects; the other gives information about metallurgical and dimensional variations. Testing and coil impedance measurements are carried out over frequency range 300 kHz to 1.25 MHz. Optimum condition for defect detection, test frequency, bridge balancing, filter frequency, and testing speed was determined experimentally. From the results obtained by micrographic examination of the parts where the defect indications appeared, it proved that the instrument successively detects a small defect (25μ in depth, inner surface defect). The effects of defect distribution on the signal and noise due to the ferromagnetic precipitate appearing in several tubes after heat treatment are described. (auth)

53126 DETECTION OF FAULTS IN METALLIC WELDS USING ULTRASOUNDS. Saglio, Robert (to Commissariat a l'Energie Atomique). French Patent 2,093,406. 28 Jan 1972. Filed 12 Jun 1970. (In French).

A method of examining welds using ultrasound is presented. The method involves measuring the time between the incident echo and the corresponding return echo (in the case of a defect). The measurements are effected by the positioning of the sensors relative to the part examined. With respect to the incident transverse waves, each sensor is displaced along a rectilinear path inclined at an angle β to the interface. β is a constant depending on the value of the angle of incidence α of the transverse waves, the velocity of the longitudinal waves in water, and the velocity of the transverse waves in the part examined (steel, Al, etc). If longitudinal waves are used to examine the material (delta technique), then β is also a function of the longitudinal velocity of the waves in the material. (France)

Nuclear Explosions

Refer also to abstracts 53115, 53137, 53303, and 53316.

53127 (CEA-R-4288) TEMPERATURE DISTRIBUTION AFTER AN UNDERGROUND NUCLEAR EXPLOSION IN A GRANITE TERRAIN. Lavollee, Philippe (Commissariat a l'Energie Atomique, Bruyeres-le-Chatel (France). Centre d'Etudes). Jul 1972. 38p. (In French). Dep. NTIS (U. S. Sales Only).

The phenomenology of an underground nuclear explosion enabled the volume of rock containing the calorific energy, just after the explosion, to be defined. Analysis of heat transfer by conduction from the hot zones crosschecked with experiments performed in a granite mass, allowed analytical experiments for the heat transfer to be established. Comparison of the experimental results from various different media permitted the effects of the physicochemical composition of the terrain on the heat transfer to be established. (France)

53128 (ORNL-4794, pp 63-4) CHEMICAL APPLICATIONS OF NUCLEAR EXPLOSIVES. Aug 1972.

In Chemical Technology Division annual progress report for period ending March 31, 1972.

Research is reported on: studies of the behavior of radionuclides in natural gas storage reservoirs and the disposal of tritiated water solutions that are generated in gas stimulation and gas storage applications. (D.H.M.)

53129 (UCRL-Trans-10616-2) MECHANICAL EFFECTS BEYOND THE CLOSE-IN ZONE OF AN UNDERGROUND NUCLEAR EXPLOSION IN GRANITE. Michaud, L. Translated for Univ. of California Lawrence Livermore Lab., from report IAEA-PL-388/8. 14p. Dep. NTIS.

During French nuclear experiments in a granite massif at Hoggar, the movements of the medium were recorded by mechanical detectors measuring displacements, velocities and accelerations. The results are fairly well grouped and the principles established experimentally for the widely differing explosion energies and distances from ground zero agree well with similarity relationships having the following form: movement = $K(W^{1/3}/R)^n$, with a dispersion not exceeding 50%. In addition, a number of observations were made on structures and materials exposed to such movements. Several hundred photographs were taken before and after the explosions in horizontal galleries oriented toward ground zero and also on the surface of the massif. The results make it possible to calculate limiting distances for damage for each type of material and mode of attachment. For example, for a perpendicular wall of light concrete blocks, the limiting distance for moderate damage (very obvious cracks) is found to be 700 $m/kt^{1/3}$. A study correlating ground movements and the extent of the damage shows the displacement velocity of ground movement at the point of interest to be the most reliable criterion of the observed effect. For the above example, the radial displacement velocity is 18 cm/sec. Further data have been collected on various kinds of materials, metal containers, electronic equipment, electric motors, etc. The results enable us to predict the probable damage from a nuclear explosion and to make recommendations to minimize such damage. (auth)

53130 (UCRL-Trans-10616-4) EFFECTS OF AN UNDERGROUND NUCLEAR EXPLOSION ON THE SURROUNDING ROCK. CONTENT OF THE CAVITY AND CHIMNEY, AND OF THE ZONES OF CRUSHING AND FRACTURING. Derlich, S. Translated for Univ. of California Lawrence Livermore Lab., from report IAEA-PL-388-10. 24p. Dep. NTIS.

French nuclear experiments in a granite massif have produced cavities and associated chimneys due to rock collapse. The cavities are surrounded by concentric zones of crushed and fractured rock. Transformations of the rock medium have been studied by means of boreholes which pass near the detonation point or are drilled to various parts of the cavity or chimney. The lower half of the cavity is roughly hemispherical. The chimney geometry is affected by the geologic nature of the rock medium and by the extent to which it is already fractured. The shape of the cavity-chimney complex resembles an ellipsoid of revolution whose major axis is 4.5 times, and the minor axis 2.8 times, the cavity radius. The contents consist of debris and resolidified molten rock. The crushed zone consists of coherent rock of chalk-like appearance with porosity of 14% and permeability of the order of 10 millidarcy, and the fractured zone of fragmented rock of increasing size as one moves away from the detonation point. The relationship between the explosion yield W (in kilotons) and the cavity radius R (in meters) is in good agreement with the theoretical laws based on physical phenomena. The relationship does not always correspond to the formulas proposed elsewhere for other rock media, or even for granite. The differences can be explained in terms of parameters such as the pressure of vaporized products, constants derived from the equations of state, the dimensions of the explosive chamber, and the rock stresses. (auth)

53131 (UCRL-Trans-10616-5) MECHANICAL EFFECTS IN THE CLOSE-IN ZONE OF AN UNDERGROUND NUCLEAR EXPLOSION IN GRANITE. Michaud, L.; Maury, J. Translated for Univ. of California Lawrence Livermore Lab., from report IAEA-PL-388/11. 16p. Dep. NTIS.

During the French underground nuclear tests at Hoggar a large number of measurements and observations were carried out in the close-in zone, to determine in particular the time of arrival of the shock wave and the characteristics of the cavity formed by the explosion. Calculation programs were developed in order to predict and interpret the various results. Code S in particular, is a Lagrangian one-dimensional program giving a numerical stimulation of the shock wave propagation. In addition to the calculation of the shock parameters, it provides a means of evaluating the following effects: vaporization and melting due to shock, crushing and brittle or plastic rupture of the material, opening and closing of radial and tangential fractures, elastoplastic and elastic deformations of a solid, and the initial profile of the energy liberated by the shock in the form of heat. Applied to the case of granite, code S supplemented by the adiabatic elasticity and the characteristic quantities of the medium as determined in the laboratory enabled us to describe all the characteristic phenomena in the close-in zone. Calculated and experimental arrival times of the shock wave were compared, and good agreement was obtained up to pressures of several megabars. Detectors located up to a few decimeters from the wall enabled us to follow the evolution of the shock wave during the first few microseconds of its travel. Calculations also show that the dimensions of the final cavity are a function not only of the explosion yield and the local lithostatic pressure but also of shear strength of the rock and the dimensions of the explosion chamber. (auth)

53132 (UCRL-Trans-10617-2) RADIOLOGICAL RISKS RELATIVE TO THE DISTRIBUTION OF CONTAMINATED GAS. Combet, M.; Gerard, R. Translated for Univ. of California Lawrence Livermore Lab., from report 103/SPS. 15p. Dep. NTIS.

The average and maximum radiation doses likely to reach consumers who, for all their usual requirements, use natural gas that has been stored in a cavity created by a nuclear explosion are given. The incidences of contamination with ^{85}K and tritium for gas used commercially, industrially, and in agriculture were studied in detail. The results indicate that the doses involved are 5000 times less than the limits admissible for the population. (T.D.)

53133 (USGS-474-155) EXPLOSION-INDUCED FRACTURES OF SELECTED ANNOUNCED UNDERGROUND NUCLEAR TESTS, YUCCA FLAT, NEVADA TEST SITE, NEVADA, JANUARY 1971-DECEMBER 1971. Steele, Susan G.; Snyder, R. P. (Geological Survey, Denver, Colo.). Aug 1972. 31p. (NTS-237). Dep. NTIS.

During 1971, personnel of the U.S. Geological Survey mapped the surface effects produced by eight announced underground nuclear tests conducted in Areas 2, 3, and 9 in Yucca Flat, Nevada Test Site. Faults on which previous explosion-induced movement had been noted were reactivated by some tests. Some tests produced neither surface fractures nor collapse features. (auth)

53134 BACKGROUND INFORMATION FOR THE DEVELOPMENT OF A RADIATION STANDARD FOR TRITIUM IN NUCLEAR-STIMULATED NATURAL GAS. Moghissi, A. A.; Patzer, R. G.; McNelis, D. N.; Carter, M. W. (Western Environmental Research, Lab., Las Vegas, Nev.). pp 228-35 of Radiation Protection Standards: Quo Vadis. Vol. I. Howell, Wallace P. (ed.). Richland, Wash.; Health Physics Society (1972).

From 6th annual topical symposium on radiation protection standards: quo vadis; Richland, Wash. (2 Nov 1971).

The development of a radiation standard for tritium in natural gas requires the knowledge of the relationship between the tritium concentration in the gas and the annual dose received by the people resulting from the usage of the gas. Although this relationship can be calculated, the uncertainties associated with the input parameters are so large that the results could have a range of 10^3 or higher. Consequently, laboratory experiments were carried out to better estimate this ratio. In the first set of experiments, the transfer of tritium from natural gas into food cooked under realistic conditions was determined. In a second set of experiments, the contribution of heating with tritiated gas in an area with limited ventilation, to the tritium body burden was experimentally determined. Under the selected experimental condition it was found that a natural gas concentration of 1 nCi/1 (STP) would result in tritium concentration in body water of 14 nCi/1. (auth)

Protective Structures and Equipment

53135 (ORNL-TM-3485(Vol.1)) ACTIVE AND PASSIVE DEFENSE INTERACTION STUDIES. VOLUME I. SUMMARY, MODELS, AND CALCULATIONS. Haaland, Carsten M.; Wigner, Eugene P.; Wilson, John V. (Oak Ridge National Lab., Tenn.). Dec 1971. 232p. Dep. NTIS.

The shortness of the time of flight of submarine launched missiles renders both quick access to shelters and delay of the attack by missile defense important. In order to evaluate the relative effectiveness of the two types of protection—quick access shelters and missile defense—three models were investigated. The first of these is concerned with individual cities or territories (called "islands") which are within the range of a single missile defense installation. The second and third models are concerned with the interaction of the defenses of the islands of the entire nation. The second one assumes, as does the first, that the attacker knows whether or not his missile reached its target before committing a second missile to the same target. This "shoot-look-shoot" assumption is surely not valid if the defense adopts a probabilistic tactic whereby some targets are defended and others are not and if reasonable civil defense is available so that the vulnerability of people decreases as a result of the movement to shelter. Hence, the last model considered discards the shoot-look-shoot assumption and deals in particular with the idea of the probabilistic defense. However, the study is not complete in this regard. Calculations are made for the first two models with parametric attack levels and defense budgets, with three types of shelter postures, including shelters obtained by slanting techniques in new construction towards blast resistance, and also special-purpose shelters. Costs of current safeguard components are assumed for active defense and no leakage is assumed. The results show that combinations of ABM and shelters are usually more effective in reducing fatalities than either ABM or shelters alone. (auth)

53136 RADIATION PROTECTION SHIELDING. Bonet-Maury, Paul; Audouin, Maurice. French Patent 2,070,548. 10 Sep 1971. Filed 9 Dec 1969. (In French).

This inexpensive radiation protection shielding consists of an assembly of juxtaposed railway lines, the longitudinal axes being parallel. The spaces between the rails are filled with a dense material, e.g., ferrous-type material. The cores of the rails are mutually parallel and perpendicular to the plane of the assembly. The rails are arranged so that the heads of adjacent rails interlock with the cores of intermediate adjacent rails. (France)

Safety Engineering

Refer also to abstract 55445.

53137 (JAB-99-96) INVESTIGATION OF GROUND MOTION–DAMAGE RELATIONSHIPS FOR RESIDENTIAL BUILDINGS IN GLENDALE, CALIFORNIA: SAN FERNANDO EARTHQUAKE, FEBRUARY 1971. Farhoomand, I.; Scholl, R. E. (Blume (John A.) and Associates Research Div., San Francisco, Calif.). Aug 1972. Contract AT(26-1)-99. 35p. Dep. NTIS.

The investigation of the relationship between the observed damage to the residential buildings in two selected control areas within Glendale, California, and the ground motion resulting from the San Fernando earthquake is presented. The procedures used in performing the structure inventory and the damage survey are described. The ground motion characterization, structure idealization, and damage description used to derive the ground motion–damage relationships are also given. Results of the investigation are ground motion–damage relationships for overall building damage as well as for building components. One of the more significant conclusions is that interior walls and chimneys are more susceptible to damage than other building components. (auth)

Vacuum Engineering

Refer also to abstracts 53318 and 54085.

53138 INTERNATIONAL COLLOQUIUM ON THE APPLICATION OF VACUUM TECHNIQUES TO THE SEMICONDUCTOR INDUSTRY, ELECTRONIC, AND MICROELECTRONIC COMPONENTS. AVISEM 71. Conference Held at Versailles, France, September 13, 1971. Paris; Societe Francaise des Ingenieurs et Techniciens du Vide (1971). 467p. (In French and English). (CONF-710932).

Of sixty-six papers presented, a separate abstract was prepared for four. An abstract of one paper previously appeared in NSA as 26: 4213. (TSS)

For abstracts of individual papers see: 52902, 52937, 53139, and 54976.

53139 DEVELOPMENT OF A ULTRAHIGH VACUUM EVAPORATION UNIT USING A LIQUID He CRYOPUMP WITH A HIGH PUMPING SPEED. Thibault, J. J. (L'Air Liquide, Sassenage, France); Boissin, J. C.; Richardt, A. pp 40-7 of International Colloquium on the Application of Vacuum Techniques to the Semiconductor Industry, Electronic, and Microelectronic Components. Paris; Societe Francaise des Ingenieurs et Techniciens du Vide (1971). (In French).

From third international symposium on the application of vacuum techniques in semiconductor industry, electronic components, and microelectronics; Versailles, France (13 Sep 1971). See CONF-710932.

A unit is presented for the in-vacuo deposition of thin films. It has the following characteristics: rapid operation; an uncontaminated ultrahigh vacuum (5×10^{-9} torr); a high pumping rate ensuring a small pressure rise during evaporation (1.5×10^{-8} torr for a Nb deposit). (France)

53140 VAKUUMTECHNIK. GRUNDLAGEN UND ANWENDUNGEN. (Vacuum Techniques. Principles and Applications). Pupp, Wolfgang. Thiemig-Taschenbuecher, Band 43. Munich; Verlag Karl Thiemig (1972). 4011p. DM 28,-.

The fundamentals of vacuum techniques including vacuum physics, measurement of vacuum, and use of the mass spectrometer as a device for measuring partial pressure and transport of gases are presented. Special emphasis is placed on ultrahigh vacuum technology. Also discussed are the design and operation of vacuum installations, advantages and disadvantages of various structural materials, criteria for the spatial arrangement and coordination of pumps and monitoring devices, and the control and safety aspects in automated facilities. Amplifiers, television tubes, photomultipliers, x-ray tubes, and electron microscopes for special applications such as in nuclear physics installations and space simulation are discussed. With respect to industrial applications, the drying of chemical products is discussed as well as freeze drying, impregnation of electrical cables, distillation, high vacuum metallurgy, and the production of thin layers through cathode evaporation. (H.B.G.)

53141 IMPROVEMENTS TO ION PUMPS. (to Societe RIBER, SA). French Patent 2,097,288. 3 Mar 1972. Filed 1 Jul 1970. (In French).

An ion pump is described which consists of at least one cathode and anode inside a casing. The cathode is retained by a sliding device. The removal of the cathode from this casing (or its introduction) is effected by sliding it in this device. This pump enables pressures of less than 10^{-12} torr to be obtained. (France)

ENVIRONMENTAL AND EARTH SCIENCES

Minerals and Ores

53142 (AREAEE-138) MINERALOGY AND SOME TRACE ELEMENTS GEOCHEMISTRY OF SAMPLES FROM SOUTHWEST ASWAN RADIOACTIVE SYENITE ROCK WESTERN DESERT. Sayyah, T. A.; Mahdy, M. A. (Atomic Energy Establishment, Cairo (Egypt). Geology and Raw Materials Dept.). 1972. 22p. Dep. NTIS (U. S. Sales Only).

Mineralogical, as well as some trace elements geochemical studies, were carried out on some samples from southwest Aswan radioactive syenite rock. The presence of thorite–thorogummite radioactive mineral suite as well as the rare earth mineral bastnaesite were reported for the first time in this radioactive syenite rock occurrence. Zircon, rutile and its polymorph brookite, anatase, and the Nb-rich variety are present as heavy accessory minerals. Geochemically, these rocks are characterized by high Th, Zr, Nb, Y, and Ti contents. The iron is present mainly in an oxidized state which may be due to hydrothermal alteration that might accompany the radioactive mineralization. (auth)

53143 (GJO-936-1) GEOLOGY AND ALTERATION ASSOCIATED WITH WYOMING URANIUM DEPOSITS. Files, Frederic Grant (California Univ., Berkeley). 1972. 132p. Dep. NTIS.
Thesis.

Results are reported of a study aimed at establishing the physical and chemical factors responsible for roll formation and migration of uranium ore bodies at the Crooks Gap, Gas Hills, and Shirley Basin deposits in Wyoming. (D.H.M.)

53144 (GJO-936-2) TREND OREBODIES OF THE SECTION 27 MINE, AMBROSIA LAKE URANIUM DISTRICT, NEW MEXICO. Kendall, Ernest Whitney (California Univ., Berkeley). 1972. 178p. Dep. NTIS.
Thesis.

The sandstone-uranium deposits at the southern edge of the San Juan Basin near Grants, New Mex. were studied. The work concentrated on the trend ore in an attempt to better understand the physical and chemical conditions responsible for ore formation. The trend ore consists of flattened, elongated, ellipsoidal masses of Westwater Canyon sandstone whose pore space has been filled with ore phases. The individual ore pods are roughly concordant with bedding and are clustered in narrow belts called ore trends. The ore consists principally of pyrite, calcite, and a submicroscopic mixture of humic material and the uranium silicate, coffinite. Vanadium and selenium phases and jordisite were also found. It is concluded that the trend ore was probably formed by slowly moving ground water in early Cretaceous time, and that the ore bodies represent a slowly migrating reaction zone in which phases are destroyed by oxidation and dissolution at the southern edge and reprecipitated at the northern edge of the ore trend. (L.C.L.)

53145 STRUCTURAL STUDIES ON THE URANIUM DEPOSIT OF THE FAY MINE, ELDORADO, NORTHWEST SASKATCHEWAN. Morton, R. D.; Sassano, G. P. (Univ. of Alberta, Edmonton). Can. J. Earth Sci.; 9: No. 7, 803-23(Jul 1972).

The Fay Mine uranium deposit is composed of veins parallel to the foliation of the paragneisses and paraschists of the Fay Mine Complex, which in turn overlies the Donaldson Lake Gneiss and Foot Bay Gneiss, within the Tazin Group of the Beaverlodge District, northern Saskatchewan. A computer oriented study of 5500 strike-dip measurements of planar features within the Fay Mine reveals that the lowest member of the metamorphic sequence, the Foot Bay Gneiss, is unique in that it exhibits Kenoran (?) structures associated with F1, NW-SE or N-S trending folds. Subsequent to the Kenoran (?) folding, an Aphebian (?) sequence of sediments and volcanics, now represented by the Donaldson Lake Gneiss and the Fay Mine Complex, was deposited. NE-SW trending, Hudsonian, F2 folds then developed and extensive cataclasis was effected. The F2 structures also affected the uppermost, taphrogeosynclinal Martin Formation sediments and volcanics. The major faults of the district are thought to have been initiated either as F2-shear joints or F2-tension fractures and have undergone multiple movement over a long period of time. The pitchblende ± quartz ± carbonates ± hematite ± chlorite veins, classified as "mobilized stratabound deposits", occur parallel to S2 foliation planes in the crests, troughs, or limbs of F2 folds, wherever minimal plunge is observed. Such deposits may have been generated during regional metamorphism by mobilization of uranium-rich fractions from the originally uraniferous Aphebian precursors of the Fay Mine Complex. Later movement of such major structures as the St. Louis Fault has apparently caused only local deformation and brecciation of the uraniferous veins and has caused no more than limited recrystallization. (auth) (Canada)

53146 URANIUM CONTENT OF THE UPPER JURASSIC BLACK BITUMINOUS ARGILLITES OF THE WEST SIBERIAN PLATE. Pluman, I. I. (Novosibirsk Geological Bureau, USSR). Geochem. Int. (Engl. Transl.); 8: No. 6, 845-51(1971).
Translated from Geokhimiya; No. 11, 1362-8(1971).

The upper Jurassic black bituminous argillites of the West Siberian plate are regionally enriched in uranium (up to 70 ppM U). The argillites have high organic carbon content (up to 10% and more) and are also enriched in molybdenum, vanadium, and zinc. (auth)

53147 URANIUM AND THORIUM IN THE ALKALI OLIVINE BASALT SERIES. Gladkikh, V. S.; Lebedev-Zinov'yev, A. A. (Inst. of Mineralogy, Geochemistry, and Crystal Chemistry of Rare Elements, Moscow). Geochem. Int. (Engl. Transl.); 8: No. 6, 813-20(1971).
Translated from Geokhimiya; No. 11, 1315-23(1971).

Distribution of uranium and thorium has been determined in 158 samples of lavas belonging to the alkali olivine basalt series (of the Maymecha–Kotuy and Kuznetsk–Alatau provinces and the graben zone of the southern part of the Russian platform). The concentrations of the radioactive elements in the lavas of the same petrochemical type are similar. The highest uranium and thorium concentrations are found in the differentiates of the alkali olivine basalt magma with the highest sodium and potassium contents. (auth)

53148 CONQUISTA MINES WIDE-RANGING SOUTH TEXAS URANIUM DEPOSITS. Eng. Mining J.; 173: No. 8, 74-7(Aug 1972).

The equipment and methods used to find, mine, and process uranium ore from deposits near Falls City, Tex. are described. The Conquista Project, which includes these activities is designed to produce 1.5 M lb/y of U_3O_8. The program for monitoring liquid and solid wastes from the extraction plant operations is mentioned. (L.C.L.)

Radioactive Effluents

Refer also to abstracts 53192, 55220, 55285, 55293, 55301, 55331, 55337, and 55338.

53149 (RLO-2227-T-12-26) ^{65}Zn SPECIFIC ACTIVITIES FROM OREGON AND WASHINGTON (U.S.A.) CONTINENTAL SHELF SEDIMENTS AND BENTHIC INVERTEBRATE FAUNA. Carey, A. G. Jr.; Cutshall, N. (Oregon State Univ., Corvallis (USA). School of Oceanography). 1972. Contract AT(45-1)-2227. 16p. Dep. NTIS.

The relationships between the benthic fauna and sediments on the continental shelf of Oregon and Washington were investigated by determining specific activities of ^{65}Zn, a radionuclide present in the Northeast Pacific Ocean. Zinc-65, induced by neutron activation in Columbia River water used to cool plutonium production reactors at Richland, Washington, was carried down the river and into the marine environment. Sediment from the Columbia River moves northward. Zinc-65 specific activities in sediment and benthic invertebrates decrease northward with distance from the river and westward with both distance and depth. Many organisms to the south of the river mouth and westward with depth have higher ^{65}Zn specific activities than the sediments in, or on, which they live. Other sources of ^{65}Zn via the food web are suspected as the cause for the differential in specific activity between the sediment and benthic fauna. Long-term declines in ^{65}Zn specific activities were noted. A wide range of ecological and systematic forms are included. (auth)

Radioactivity Transport and Monitoring

Refer also to abstract 53459.

53150 (ANL-7860(Pt.3)) RADIOLOGICAL PHYSICS DIVISION ANNUAL REPORT. Environmental Research, January–December 1971. Rowland, R. E.; Gustafson, P. F. (Argonne National Lab., Ill.). [nd]. Contract W-31-109-eng-38. 320p. Dep. NTIS.

Major divisions included are: terrestrial ecology, aquatic ecology, bioenvironmental studies, and atmospheric physics. Separate abstracts were prepared for fifteen of the thirty-seven sections. (D.H.M.)

For abstracts of individual sections see: 52914, 53151, 53152, 53162–53164, 53169, and 53182–53189.

53151 (ANL–7860(Pt.3), pp 46-50) TRITIATED WATER RECOVERY SYSTEM. Stewart, M. L.; Kline, J. R.; Jordan, C. F. [nd].

In Radiological Physics Division annual report, January–December 1971.

Equipment used in extracting and collecting tritiated water is described. The technique is based on well-known freeze-drying methods. The primary features of this system are: simplicity of the glassware, ease of operation, the large number of samples which can be processed simultaneously, range of sample sizes, and cost of the equipment. (auth)

53152 (ANL–7860(Pt.3), pp 230-49) PLUME RISE DETERMINATION BY THE TABULATION PREDICTION TECHNIQUE. Moses, Harry; Kraimer, Martin R. [nd].

In Radiological Physics Division annual report, January–December 1971.

Six hundred and fifteen plume rise measurements from 26 different stacks obtained during 10 research programs conducted in 5 different countries have been collected and used to construct the Tabulation Prediction Technique tables for determining plume rise. This technique is rather easy to use, but both statistical and meteorological skills are required to construct the prediction tables. Since results obtained appear to be as good or superior to those obtained with any of the formulas appearing in the literature, the operational simplicity of the present method recommends its use for routine plume rise estimates required in engineering problems. (auth)

53153 (DPSPU–72-30-1) ENVIRONMENTAL MONITORING IN THE VICINITY OF THE SAVANNAH RIVER PLANT. Annual Report, 1971. (Du Pont de Nemours (E. I.) and Co., Aiken, S. C. Savannah River Plant). 1972. 21p. Dep. NTIS.

A continuous monitoring program has been maintained since 1951 (before plant startup) to determine the concentrations of radioactive materials in a 1200-square mile area outside the Savannah River Plant. Included are parts of Aiken, Barnwell, and Allendale counties in South Carolina; and Richmond, Burke, and Screven counties in Georgia. Although very small amounts of gaseous and liquid radioactive materials are discharged to the environment, environmental levels continue to be far below levels considered significant from a public health viewpoint. The quantity of radioactivity released by SRP to its environs during 1971 is, for the most part, too small to be distinguished from natural background radiation and fallout from worldwide nuclear weapons tests. Particulate beta activity detectable in air is due entirely to global fallout. This concentration in air at the plant perimeter and 25 miles away represents 0.2% of the Concentration Guide (defined in the Applicable Standards section which follows). Tritium oxide in air at the plant perimeter is greater than in air at more distant locations. The average concentration at the plant perimeter, only 0.1% of the Concentration Guide, is the largest percentage of any air Concentration Guide for plant-released radionuclides. Tritium, cesium-137, strontium-89, and strontium-90 are the only radionuclides of plant origin detectable in river water. None of these had an average concentration that exceeded 0.2% of the Concentration Guide in river water sampled 8 miles downstream from the plant. Radioactive materials in river fish also continue to be very low. Various water-quality analyses of river water samples surveyed by SRP indicate that Savannah River water is not adversely affected by SRP operations. This is substantiated by surveys of the health of the Savannah River biota by the Academy of Natural Sciences of Philadelphia (Appendix C). (auth)

53154 (INIS-mf–160, pp 22-52) MICROMETEOROLOGICAL STUDIES FOR AIR POLLUTION CONTROL IN ATOMIC ENERGY. Shirvaikar, V. V. (Bhabha Atomic Research Centre, Bombay (India)). 1971. (CONF-700847–5). INIS.

From Seminar on pollution and human environment; New Delhi, India (26 Aug 1970).

The measures adopted for control and prevention of air pollution, during the design stage of reactors and power plants in India, are outlined. The safety philosophy was adopted to ensure that under normal operating conditions, the maximum dose to any individual member of the public does not exceed 500 mr/year and that under accident conditions the dose is below 25 r. These values are well below the limits prescribed by ICRP for safety limits. Micro-meteorological studies have been carried out at the four nuclear power plant sites, viz., Trombay, Tarapur, Rajasthan, and Kalpakkam, with the aim of studying the diffusion potential of atmosphere at different seasons of the year and also to determine the worst meteorological conditions obtainable at a site. Specific devices used for proper strategy to be applied for studies at such sites, which are uneven and near large water bodies, have been described. Smoke photography technique has been used for diffusion studies. The data collected have been used for determining the height of stacks and for calculating the required containment factors for various exclusion distances for power reactors. (auth) (INIS)

53155 (MLM–1946) BIBLIOGRAPHY ON HANDLING, CONTROL, AND MONITORING OF TRITIUM (DECEMBER 1968–JANUARY 1972). Hannahs, B. J.; Kershner, C. J. (Mound Lab., Miamisburg, Ohio). 5 Sep 1972. Contract AT(33-1)-Gen-53. 44p. Dep. NTIS.

This annotated bibliography was prepared for the purpose of providing a collected source of information on recent literature available on subjects relating to the control, monitoring, and handling of tritium. Particular emphasis was placed on literature that relates to the tritium handling and control needs of the Division of Military Applications/United States Atomic Energy Commission. The period covered in the preparation of this bibliography was from 1968 to January 31, 1972, and includes both journal and report literature. Keyword and author indexes are provided for general applicability of this document and a subject grouping format was followed in arranging the references so as to increase its utility for those interested in tritium effluent control and waste management. (auth)

53156 (SZS–128) RESULTS OF FALLOUT MONITORING IN THE GERMAN DEMOCRATIC REPUBLIC 1970. Kunert, J.; Schulze-Wollgast, U.; Zindler, H.; Gegusch, H. (Staatliche Zentrale fuer Strahlenschutz, Berlin (East Germany)). Feb 1972 47p. (In German). Dep. NTIS (U. S. Sales Only).

The results of monitoring of air, precipitation, fallout, water, soil, plants and foodstuffs are presented. The gross beta activity deposited on the territory of the GDR was higher than in the preceding year. This increase was caused by the influx of fresh fission products. However, an increase of the cumulative amount of ^{90}Sr and ^{137}Cs in fallout could not be detected unequivocally. In most of the other environmental samples surveyed no changes could be observed in comparison to 1969, with the exception of plants which showed an increase of excessive beta activity, ^{90}Sr and ^{137}Cs as a result of the higher deposition on the soil surface during the corresponding growing seasons. (auth)

53157 RADIATION AND HEALTH. McLean, A. S.; Morley, F.; Peirson, D. H.; (and others). London; Royal Society for the Promotion of Health (1971). 80p.

The subject is dealt with under the following sections: atomic energy — benefits and precautions (1. the public attitude, 2. maximum permissible levels, 3. the role of the public health authority); radiation levels in relation to nuclear power (1. nuclear power and radioactive wastes, 2. waste management objectives, 3. disposal methods, 4. legal controls); radiation levels — air (1. natural radioactivity, 2. artificial radioactivity, 3. radiological hazard); radiation in water I (1. natural alpha-activity, 2. artificial alpha-activity, 3. natural beta-activity, 4. artificial beta-activity, 5. contribution of activity by water); radiation in water II (1. natural radioactivity, 2. surveillance of sources, 3. levels of radioactivity in drinking water, 4. fallout); significance of dietary contamination with radioactive substances (1. radioactivity in foodstuffs, 2. the critical nuclides, 3. relative significance of the critical nuclides in different circumstances). (UK)

Atmosphere

Refer also to abstracts 53227 and 53511.

53158 (FOA–4-4502-A-1) INVESTIGATION OF AIRBORNE RADIOACTIVE MATERIAL ORIGINATING FROM AN UNDERGROUND NUCLEAR EXPLOSION IN USSR THE 23 OF MARCH 1971. Eriksen, Bjoern (Forsvarets Forskningsanstalt, Stockholm (Sweden)). Jul 1972. 18p. (In Swedish). Dep. NTIS (U. S. Sales Only).

Short-lived radioactive substances, primarily ^{140}Ba were discovered in samples from ground-level air in different parts of Sweden during the latter part of March and early May 1971. The activity composition and cloud calculations in combination with seismological observations indicated that the most probable explanation to this radioactivity was a leakage from an underground nuclear explosion west of the Ural mountains on the 23rd of March 1971. The results of gamma-spectrometric measurements performed on samples of ground-level air during the period, as well as calculations of the amount and composition of the extra radioactivity are described. (Sweden)

53159 (UUIM–26) NATURAL β-ACTIVITY IN THE AIR NEAR THE GROUND. Parts B–E. Israelsson, S.; Knudsen, E.; Ungethuem, E. (Uppsala Univ. (Sweden). Inst. of Meteorology). 1972. 46p. Dep. NTIS (U. S. Sales Only).

Studies were made on the natural β-activity in the air near the ground at Marsta Observatory (59°55′N, 17°35′E Gr). Four separate parts (B–E) are included. In part B the influence of wind upon the natural β-activity is discussed. Part C deals with the influence of the precipitation upon the natural β-activity. In part D the vertical distribution of the natural β-activity is described. In Part E analysis of the natural β-activity variations with time is made. (auth) (Sweden)

53160 (UUIM-27) NATURAL α-ACTIVITY IN THE AIR NEAR THE GROUND. Israelsson, S.; Knudsen, E.; Ungethuem, E. (Uppsala Univ. (Sweden). Inst. of Meteorology). 1972. 34p. Dep. NTIS (U. S. Sales Only).

The results of part of a program for investigating the radioactivity in the air near the ground and its connection with atmospheric electricity are reported. Studies have been made of the meteorological influence upon the natural α-activity concentration in the air near the ground. The method of measuring α-activity concentration is presented along with a few preliminary results from measurements made in the summer of 1970. The variation with time of the natural α-activity concentration was also studied. (auth)

53161 RADIOACTIVE FALLOUT IN NORWAY. Hvinden, T. (Forsvarets Forskningsinstitutt, Kjeller, Norway). Sivilt Beredskap; 14: No. 3, 24-6(1971). (In Norwegian).

Radioactive fallout in the period 1956 to 1970 in Norway was analyzed. A series of diagrams show the concentration in air and precipitation at Kjeller (near Oslo) as a function of time, the geographic distribution of fallout and of ^{131}I, ^{137}Cs, and ^{90}Sr in milk from 10 places in Norway averaged over the whole period, and ^{137}Cs concentrations in the meat from sheep, cattle and reindeer as a function of time. The text comments and explains these diagrams. The State Council for Radiation Hygiene has published estimates of the radiation effects on the population as a result of radioactive fallout concluding that while fallout can have caused some cases of cancer, leukemia and genetic damage, the estimated number of cases is less than 5 percent of the naturally occurring cases and cannot be statistically corroborated. (Norway)

Soil

53162 (ANL-7860(Pt.3), pp 1-13) DISTRIBUTION OF ^{137}Cs IN SOILS AND VEGETATION ON THE ISLAND OF PUERTO RICO. Kline, J. R.; Colon, J. A.; Brar, S. S. [nd].

In Radiological Physics Division annual report, January-December 1971.

Soils and vegetation of Puerto Rico were collected along five north-south transects of the island and analyzed for ^{137}Cs content. The results showed an apparent gradient of this nuclide with high amounts in the eastern samples and low amounts in the western samples. Activity in samples was strongly related to rainfall patterns on the island; however, high mountain forests were much more highly contaminated than could be accounted for on the basis of rainfall deposition alone. This was attributed to the properties of vegetation itself, rather than alteration of deposition patterns. The vegetation is suggested to have high aerosol interception efficiency and low turnover rates, which could combine to produce the observed concentrations. Data from soil samples suggest that the island has intercepted a minimum of 535 curies of ^{137}Cs from past nuclear weapons tests. (auth)

53163 (ANL-7860(Pt.3), pp 32-7) INDEPENDENT TEST OF THE ARGONNE MODEL FOR TRITIUM MOVEMENT IN SOIL. Jordan, C. F.; Stewart, M. L.; Kline, J. R. [nd].

In Radiological Physics Division annual report, January-December 1971.

An independent test of the Argonne model for tritium movement in soil was carried out during the summer of 1971. There was good agreement between the predicted and observed downward movement of the tritium peak, the predicted and observed peak broadening, and the predicted and observed peak immobilization. Observed and predicted concentrations of tritium (HTO) differed by about one percent of the tritium (HTO) entering the soil per unit surface area. This difference probably is caused by tritium exchange with clay-bound hydroxyl groups. (auth)

Water

Refer also to abstract 53535.

53164 (ANL-7860(Pt.3), pp 64-76) STUDIES OF RECENT SEDIMENTATION IN GREEN BAY. Edgington, D. N.; Thommes, M. M.; Callender, E. [nd].

In Radiological Physics Division annual report, January-December 1971.

Results are reported of the determination of trace elements in sediments and core samples from the Green Bay. Data on the distribution of U, Th, Zn, Fe, La, Co, Cd, Cu, As, and Hg with depth in cores from Green Bay are given. (D.H.M.)

53165 (RLO-2225-T-25-6) COLUMBIA RIVER EFFECTS IN THE NORTHEAST PACIFIC: PHYSICAL STUDIES. Progress Report, June 1971-June 1972. Barnes, Clifford A.; Smith, J. Dungan (comps.) (Washington Univ., Seattle. Dept. of Oceanography). 20 Jul 1972. Contract AT(45-1)-2225, TA 25. 12p. Dep. NTIS.

During the past year efforts continued in the physical oceanography studies started in 1961 for determining the properties, distributions and movements of Columbia River water and its transported materials in the northeast Pacific Ocean. Based on the general background circulation as established in earlier studies the work stressed making, in detail, direct current measurements using vertical arrays of 6 or 7 meters each at two locations concurrently on the Washington shelf, one some 20 km off the coast at 77 m, and the other 50 km off near the shelf edge at 130 to 160 m. Despite an increased and improved stock of current meters and supporting equipment and techniques the desired continuous recordings of currents at the two type locations throughout the year are still lacking. To avoid breaks in continuity this would require double sets of equipment for each location, one to be deployed as the other was retrieved. A third array is needed to establish and interpret the horizontal field. A quite coherent picture of the current structure in the vertical was found but the variations laterally are so complex that details of this picture will evolve slowly. Knowledge of the general area mass and current structure at selected periods has been strengthened northward to the Strait of Juan de Fuca and seaward of the Washington shelf. Analysis of the observations made the past year, still continuing, and further analysis made of previous information both substantiate and add needed detail to the picture of coastal circulation and sediment transport that was developed earlier. Work in the immediate future as in the past year should continue to emphasize the circulation on the Washington shelf on a relatively fine scale in both space and time, relate the variations to the forcing functions and establish such local anomalies as may occur from the Columbia River mouth north to the Strait of Juan de Fuca. (auth)

53166 (RLO-2227-T-12-28) EFFECTS OF OCEAN WATER ON THE SOLUBLE-SUSPENDED DISTRIBUTION OF COLUMBIA RIVER RADIONUCLIDES. Evans, D. W.; Cutshall, N. H. (Oregon State Univ., Corvallis (USA). School of Oceanography). [nd]. Contract AT(45-1)-2227. 30p. Dep. NTIS.

The relationship of dissolved concentrations of Hanford radionuclides with salinity in the Columbia River estuary was interpreted in terms of the exchange of the radionuclides between dissolved and suspended particulate phases. Both ^{65}Zn and ^{54}Mn carried by the Columbia River were partially desorbed from suspended particulate matter upon mixing with ocean water in the estuary. Experiments in which ocean water was added to Columbia River water and to suspended particulate matter collected on filters confirmed the partial desorption of ^{65}Zn and ^{54}Mn from the particulate phase. The percentage of ^{65}Zn and ^{54}Mn desorbed varied with experimental approach but desorption of ^{65}Zn seemed to lie in the range 15 to 45% and ^{54}Mn in the range 30 to 60%. None of the experiments revealed any effect of salinity upon the soluble-suspended particle distribution of ^{51}Cr, ^{124}Sb, or ^{46}Sc. Dissolved concentrations of these nuclides varied inversely with salinity. There was no evidence that any of the radionuclides studied were removed from solution by flocculation, precipitation, or adsorption as a result of mixing with ocean water. Ocean water contact partially removed ^{54}Mn but not ^{65}Zn, ^{46}Sc, or ^{60}Co from Columbia River bottom sediments transferred to the marine environment. The inability of ocean water to desorb ^{65}Zn from bottom sediment contrasts with its action with suspended particulate ^{65}Zn. (auth)

53167 RADIOISOTOPE PARTITION BETWEEN SEA WATER AND SEDIMENTS. Kuznetsov, Yu. V.; Shchebetkovskii, V. N. Geochem. Int. (Engl. Transl.); 8: No. 6, 891-6(1971).

Translated from Geokhimiya; No. 12, 1466-72(1971).

Determinations of the absorption of ^{137}Cs, ^{144}Ce, and ^{234}Th by deep-water red clay and for iceberg, foraminiferal, and diatom oozes are reported. Geochemical concepts are used to explain the sorption series. It is shown that the isotopes are distributed in different ways. (auth)

53168 ISOTOPE HYDROLOGY IN LATIN AMERICA. Payne, Bryan R. Int. At. Energy Agency Bull.; 14: No. 3, 17-20(1972).

Current uses of radioisotopes in hydrological research in Latin America are discussed. The most common uses are in studies of sediment transport and pollution and in projects for the development of groundwater in arid areas. Radioisotope tracer studies of sediment transport have been used in connection with the maintenance of navigable channels and harbors, location of cooling water intakes and sewage outlets, and the location of sand dredging sites for building purposes. Ground water tracer studies have been used to define the source, location, and flow of water supplies in all the Latin American countries where water supply problems are acute. (L.C.L.)

Ecosystems and Food Cycles

Refer also to abstracts 53134, 53506, 53520, 53522, 53527, 53530, 53532, and 53539.

53169 (ANL–7860(Pt.3), pp 141-50) RADIONUCLIDES IN LAKE MICHIGAN FISH. Nelson, D. M.; Romberg, G. P.; Prepejchal, W. [nd].
In Radiological Physics Division annual report, January–December 1971.

Fish samples were collected from Lake Michigan during 1970 and 1971 and analyzed for γ-ray emitting radionuclides. The Point Beach site had no history of radioactivity release prior to 1971 and measurements did not show an increase in radioactivity of organisms near the discharge point due to the section's small releases. The Big Rock site, however, has been exposed to routine releases for about 10 years. Many of the Big Rock fish contained measurable amounts of ^{65}Zn, ^{60}Co, ^{134}Cs, as well as ^{137}Cs, and ^{40}K. A table listing the contribution of Big Rock fish toward the maximum permissible ingestion of radionuclides is presented. (D.H.M.)

53170 (ORO–4066-5) INVESTIGATION OF THE UNUSUAL BEHAVIOR OF ^{137}Cs AND OTHER RADIONUCLIDES IN THE FLORIDA ENVIRONMENT. Progress Report, September 1, 1971–August 31, 1972. Gamble, J. F.; Ewel, K. C.; Lugo, A. E. (Florida Univ., Gainesville. Inst. of Food and Agricultural Sciences). 1972. Contract AT(40-1)-4066. 55p. Dep. NTIS.

The research study of ^{137}Cs activity and its role in the Florida environment are reported for the June 1971 to June 1972 period. Environmental levels of ^{137}Cs are summarized for rainfall, throughfall, stem flow, and ground water. Rainfall inputs are the same as ground water levels of activity (0.20 pCi/l). Stem flow averaged 3.65 pCi/l. A Bahama seawater sample had an activity of 7.0 pCi/l. Groundwater activity levels were the same in Fort Pierce as in Gainesville. Dairies 10 miles apart on similar soil and groundwater showed 76 pCi/l and no detection, respectively. Activity in an orange sample was found to be primarily in the rind. The juice showed 37 pCi/l and rinds 834 pCi/k. All of the mushroom samples collected in the hardwood ecosystem at Gainesville were mycorrhizal. Activity ranged from 450 to 47,000 pCi/k. Caterpillars grazing hickory leaves doubled the activity level of the resulting frass but did not accumulate ^{137}Cs burdens. Energy and matter results are presented for the major compartments in the hardwood ecosystem. A preliminary analog model has been simulated for the hardwood system and is included. (auth)

53171 (SRO–708-1) DISTRIBUTION AND CYCLING OF RADIOACTIVE ISOTOPES RELEASED INTO THE SAVANNAH RIVER SWAMP FOREST: ENVIRONMENTAL IMPLICATIONS. Progress Report, November 1, 1971–August 1, 1972. (Savannah River Ecology Lab., Aiken, S. C.). 1972. 44p. Dep. NTIS.

The distribution and cycling of radioisotopes released into the Savannah River swamp forest are being studied by reviewing literature on the subject, sampling the soil and vegetation of the area, measuring the ^{137}Cs content of these samples, and finally, determining the body burden of ^{137}Cs in biological specimens. Progress in each of these areas is reported. Data are presented on the animal, amphibian, bird, dragonfly, fish, plant, and reptile species of the area and the ^{137}Cs content or distribution in soils, plants, sagittaria roots, cotton rats, and snakes. (L.C.L.)

53172 DETERMINATION OF THE VARIATION OF RADIOACTIVE CONTAMINATION IN THE ENVIRONMENT BASED ON THE CONTAMINATION OF FOODSTUFFS. Kovacs, J. (Fovarosi Elelmiszerellenorzo es Vegyvizsgalo Intezet, Budapest). Izotoptechnika; 15: No. 2, 85-96(Feb 1972). (In Hungarian).

As a result of measurements in the last decade, no areas with significant food contamination were found. (auth)

Radiometric Techniques

Refer also to abstracts 52943 and 54670.

53173 (INP–793) DIFFERENTIAL INTERPRETATION OF GAMMA-RAY LOGS. II. CASE OF THE DYNAMIC GAMMA-RAY CURVE. Czubek, Jan Andrzej (Institute of Nuclear Physics, Krakow (Poland)). Mar 1972. 50p. Dep. NTIS (U. S. Sales Only).

The problem of digital interpretation of natural gamma-ray logs is presented for the case when the gamma-ray curve is measured in a continuous manner (logging speed ν) using a rate-meter with a time constant τ. The direct result of measurement, J(z), along the borehole axis z is related to the specific radioactivity distribution, q(z), being investigated by the equation: $J(z) + \nu\tau \cdot [dJ(z)/dz] = K \cdot \int_{-\infty}^{+\infty} \varphi_s(z - x) \cdot q(x) \cdot dx$ where K is the calibration constant and the kernel $\varphi_s(z - x)$ is given by the theory of gamma-ray logging. The solution of this equation is given in the form of a rapidly convergent series $q(z_0) = \Sigma\, J(z_j) \cdot d_j(p)$, where $p = 2,3,\ldots$ and $j = -p$ and where the coefficients $d_j(p)$ are given in the analytical form taking into account the borehole radius R, the length L of the detector, the thickness Δh of a hypothetical elementary layer, the effective gamma-ray absorption coefficient μ of rocks, the logging speed ν, and the rate-meter time constant τ. All numerical data needed for the calculation of the $d_j(p)$ coefficients are included. Examples of the gamma-ray log interpretation are presented. A method of transformation of the dynamic logging curve onto the static one is also given. (auth)

53174 BOREHOLE ACTIVATION ANALYSIS BY DELAYED AND CAPTURE GAMMA RAYS USING A ^{252}Cf NEUTRON SOURCE. Moxham, R. M.; Senftle, Frank E.; Boynton, G. R. (Geological Survey, Washington, D. C.). Econ. Geol.; 67: No. 5, 579-91 (Aug 1972).

Results of theoretical analysis and experimental comparison of the radiative capture and delayed gamma-ray activation techniques indicate the latter to be more efficient for the detection of copper, whereas the radiative capture method is preferable for nickel. A conservative lower detection limit for both copper and nickel is ~0.5%. Borehole spectra by both techniques were made in a copper- and nickel-bearing gabbro, utilizing a Ge(Li) propane-cooled detector. Al, Mn, Na, Mg, Cu, and V were readily activated and detected by the delayed method. H, Fe, Si, and Ni were not usually present in the delayed spectra but they responded well in the capture mode. It is shown that the borehole sonde can be configured to permit simultaneous delayed and capture spectra, permitting detection of all of these elements. Results of simulated borehole experiments indicate that, in the delayed gamma-ray mode, an infinite sample is achieved when the ore layer has vertical thickness of ~20 cm and a horizontal distance of ~10 cm into the wallrock. The depth resolution is thus relatively good but horizontal penetration through the wallrock is limited. (auth)

53175 RADIOTRACER ADSORPTION STUDY ON BAGUIO SOILS. Pablo, Benjamin B. (Philippine Atomic Energy Commission, Manila). Philipp. Nucl. J.; 2: No. 2, 211-14(1970).

Cationic tracers used in seepage tracing have been found to suffer great losses from adsorption. This investigation of the adsorptive properties of different soils near Baguio City was carried out to find a most suitable radiotracer. Chelation of these cations or conversion to complexes and addition of carrier improved the performance of these tracers. Sodium iodide (^{131}I) and potassium cobalticyanide (^{60}Co) were found to be the least adsorbed. (auth)

53176 XENON ISOTOPES IN TELLUROBISMUTHITE, BOLIDEN, SWEDEN. Srinivasan, B.; Alexander, E. C.; Manual, O. K. (Univ. of Missouri, Rolla). J. Inorg. Nucl. Chem.; 34: No. 8, 2381-96(Aug 1972).

The isotopic composition of xenon is reported in four different samples of tellurobismuthite, Boliden, Sweden, of varying tellurium content. It is observed that excess ^{128}Xe, ^{130}Xe, and ^{131}Xe, vary proportionately to the tellurium content of the sample. From the excess ^{130}Xe measurement, the half-life for double beta decay of ^{130}Te is calculated to be 2.51×10^{21} yr. From the observed excess of ^{128}Xe in the most tellurium rich sample, the half-life for the double beta decay of ^{128}Te is estimated to be greater than 2.7×10^{23} yr. It is shown that solar neutrino induced reactions on ^{128}Te and ^{130}Te do not contribute significantly to the observed excesses of ^{128}Xe and ^{130}Xe. The isotopic composition of xenon in a pyrite sample from the Boliden mine and in two samples of the cesium-rich mineral, pollucite, is used to examine previous hypotheses for the origin of excess ^{129}Xe and ^{131}Xe in tellurium ores. It is shown that these two xenon isotopes are produced in situ by nuclear reactions on tellurium. (auth)

53177 PROGRESS IN TL DATING AT RISOE. Mejdahl, V. (Danish Atomic Energy Commission, Risoe). Archaeometry; 14: No. 2, 245-56(Aug 1972).

The thermoluminescent dating technique employed at Risoe is outlined. The intensity of beta and gamma radiation was determined by means of the TL phosphors $CaSO_4$: Mn and $CaSO_4$: Dy, and the determination of accumulated exposure was based on quartz and feldspar inclusions with a size of 0.3 to 0.5 mm. Results are presented of a dating program comprising sherds, bricks, burned stones, and burned clay (from kilns) from seventeen excavation sites. The age of the sites ranged from 1600 AD to 4000 BC. (auth)

53178 ISOTOPIC COMPOSITION OF BIOGENIC SILICA. Labeyrie, Laurent (Centre National de la Recherche Scientifique, Gif-sur-Yvette, France). Compt. Rend., Ser. D; 274: No. 11, 1605-8(13 Mar 1972). (In French).

The elimination of organic matter and water from biogenic silica is necessary if the isotopic composition is to be measured.

The $^{18}O/^{16}O$ ratio obtained in this way is characteristic of the depositing conditions. The enrichment between this biogenic silica and water is about 3.87% at 10°C and varies slightly with temperature (about 0.03% for 1°C). (France)

53179 CORAL GROWTH RATES USING ^{228}Ra AND ^{210}Pb. Moore, Willard S. (Naval Oceanographic Office, Washington, D. C.); Krishnaswami, S. Earth Planet. Sci. Lett.; 15: No. 2, 187-90(Jun 1972).

Two radiometric methods are described to measure coral growth rates. The ^{228}radium method follows the theoretical model and is applicable to measurements of the last 30 years of growth. The ^{210}lead method is not ideal but may be used to document major changes in coral growth during the past 100 years. (auth)

53180 OXYGEN ISOTOPIC RATIOS OF SOME EVAPORITES FROM PRECAMBRIAN TO RECENT AGES. Sakai, H. (Okayama Univ., Tottori, Japan). Earth Planet. Sci. Lett.; 15: No. 2, 201-5(Jun 1972).

The $\delta\ ^{18}O$ values of eighteen marine evaporites of Precambrian to Recent ages were found to vary from +8 to 25‰ relative to SMOW, while the $\delta\ ^{34}S$ values previously measured by Thode and Monster vary from +10 to +38‰ relative to meteoritic sulfur. The results strongly suggest that the $\delta\ ^{18}O$ value of ocean sulfate varied with geologic age with a minimum at the Permian age. (auth)

53181 DATING ERROR. Wagner, G. A.; Reimer, M. (Univ. of Pennsylvania, Philadelphia). Nature (London); 237: No. 5349, 57(5 May 1972).

Some comments are offered on the communication by Nishimura on "Fission Track Dating of Archaeological Materials from Japan" (Nature, 230: 242(1971)) (NSA 25: 32078), and some errors are pointed out. A reply by Nishimura is included. (UK)

Thermal Effluents

Refer also to abstracts 53117, 53150, 55285, 55301, 55326, 55331, 55337, and 55338.

53182 (ANL–7860(Pt.3), pp 101-2) ECOLOGICAL STUDIES AT POINT BEACH NUCLEAR POWER STATION AND BIG ROCK POINT NUCLEAR POWER STATION: INTRODUCTION. Spigarelli, S. A. [nd].

In Radiological Physics Division annual report, January–December 1971.

Thermal studies at Point Beach consisted of: (1) thermal plume mapping and physical measurements related to plume dynamics; (2) chemical analyses of inshore waters affected by the thermal discharge; and (3) studies of the various aquatic communities to detect and quantify the potential effects of waste heat. A detailed map of the sampling stations is presented. Information regarding the locations and depths of each station relative to the Point Beach discharge is given. (auth)

53183 (ANL–7860(Pt.3), pp 103-8) MEASUREMENT OF MAJOR NUTRIENTS AND WATER QUALITY PARAMETERS AT POINT BEACH: 1971. Weschler, Mary Charles; Spigarelli, S. A.; Edgington, D. N. [nd].

In Radiological Physics Division annual report, January–December 1971.

The possible effects of the thermal discharge from a nuclear power plant on the aquatic environment were studied by conducting sampling program in the vicinity of the reactor operated by the Wisconsin Electric Company at Point Beach, Wisconsin. The parameters measured were pH, specific conductance, dissolved oxygen, total alkalinity, nitrate, nitrite, silicate (reported as silicon), and soluble orthophosphate. No major differences or trends were apparent for the values from various stations during any month. The only major trend that was apparent from the data was the seasonal (monthly) variation in the primary nutrients. (D.H.M.)

53184 (ANL–7860(Pt.3), pp 109-17) EFFECTS OF A THERMAL DISCHARGE ON THE INSHORE BIOLOGICAL COMMUNITIES OF LAKE MICHIGAN. Spigarelli, S. A.; Prepejchal, W. [nd].

In Radiological Physics Division annual report, January–December 1971.

The plankton, periphyton, and benthos communities of inshore waters were studied near the Point Beach Nuclear Power Station during 1971 to determine the biological effects of once-through cooling. In general, the observed biological effects of the thermal discharge were extremely localized and beyond the measurable plume boundaries were not statistically different from ambient conditions. (D.H.M.)

53185 (ANL–7860(Pt.3), pp 118-20) OBSERVATIONS OF FISH AT POINT BEACH NUCLEAR PLANT. Romberg, G. P.; Prepejchal, W. [nd].

In Radiological Physics Division annual report, January–December 1971.

A correlation was made of the discharge temperature and the type and quantity of fish collected at Point Beach Nuclear Power Plant for the period May through October 1971. (D.H.M.)

53186 (ANL–7860(Pt.3), pp 121-30) ACOUSTIC LOCATION TECHNIQUES TO STUDY THE DISTRIBUTION OF FISH IN THE VICINITY OF A THERMAL PLUME. Romberg, G. P.; Spigarelli, S. A. [nd].

In Radiological Physics Division annual report, January–December 1971.

The acoustic fish locating system was used to investigate the distribution of fish relative to a thermal plume. Fish observed during the day series of transects were primarily in schools that were concentrated in water warmer than 13°C and greater than 14 feet deep. Individual fish during the day and night series were more numerous in shallower water, but there appeared to be no preference for a temperature region. In neither series were fish observed in water warmer than 14.9°C, indicating that the near-field plume was not attractive to the inshore fish at this particular time. Many fish, however, are known to frequent the discharge channel in much warmer water. (D.H.M.)

53187 (ANL–7860(Pt.3), pp 131-40) AVERAGE TEMPERATURE MEASUREMENTS IN THE AQUATIC ENVIRONMENT USING THERMOLUMINESCENT DOSIMETERS. Oltman, B. G.; Eckerman, K. F.; Edgington, D. N.; Pohlman, T. [nd].

In Radiological Physics Division annual report, January–December 1971.

It is suggested that the temperature-induced fading of a thermoluminescent dosimeter can provide an economical method for monitoring thermal plumes. This technique could provide an estimate of the environmental temperature averaged over extended time periods. The wide range in the properties of various thermoluminescent materials indicates that the technique could be adapted to the various needs of ecologists. The precision of $CaSO_4$: Mn-Teflon dosimeters can be defined by 3 to 4% standard deviation. However, the precision may be considerably improved by precalibration to better than 2% standard deviation. The unit price for this type of dosimeter is about sixty cents. Therefore, it is possible to obtain several individual average temperature measurements at one site for low cost and with high precision. The thermograph, on the other hand, is a completely portable instrument that will produce a permanent record of temperature versus time with a relatively high degree of precision (±1°F). The types of thermographs available range in cost from 300 to 1500 dollars each and may restrict the number of sites that can be simultaneously observed. (auth)

53188 (ANL–7860(Pt.3), pp 250-69) ATMOSPHERIC CONSEQUENCES OF THERMAL DISCHARGES FROM POWER GENERATING STATIONS. Carson, James E. [nd].

In Radiological Physics Division annual report, January–December 1971.

Concern for the biological and ecological effects of heated water has resulted in legal actions that will prevent power companies from dumping the waste heat from the majority of their new generating units into rivers and lakes. Many nuclear- and fossil-fueled plants now under construction, and even some now on-line, are being required to change from once-through cooling systems to other methods, such as wet cooling towers, cooling ponds and spray canals, despite higher costs and lower thermal efficiencies. Yet, these alternate cooling procedures are not without their own environmental problems. The primary weather change due to once-through cooling on a large water body is a local increase in fogginess at the plant outfall. But the relative probability of significant local meteorological effects is much higher with alternate procedures, since these reduce the area of heat and moisture transfer. It is, therefore, concluded that, from a meteorological point of view, the least undesirable way to dispose of waste heat is by using once-through cooling on large water bodies. (auth)

53189 (ANL–7860(Pt.3), pp 270-98) SURFACE ENERGY BUDGET MEASUREMENTS OVER LAKE MICHIGAN. Frenzen, Paul; Hart, R. L.; Langs, R. K. [nd].

In Radiological Physics Division annual report, January–December 1971.

Consecutive hourly thermal energy budgets for the lake–atmosphere system are presented here in the form of smooth curves through the hourly averages. The observations provide an extensive body of quantitative information on the natural, vertical heat exchange over Lake Michigan, information which should be taken into account in the consideration of thermal pollution problems affecting the Great Lakes. In particular, variations of the undisturbed, natural heat exchange observed to occur in response to changing weather conditions, time of day, and season give useful insight into the thermal dynamics of cooling ponds, as well as the day-to-day energy balance of the lake observed. Further, the data suggest similar meteorologically-dependent behavior on the part of the heat lost directly to the atmosphere from thermal plumes discharged in open waters. (auth)

53190 (ORNL-EIS-72-28) THERMAL EFFECTS ON AQUATIC ORGANISMS: ANNOTATED BIBLIOGRAPHY OF 1971 LITERATURE. Coutant, C. C.; Huber, E. E.; Pfuderer, H. A. (Oak Ridge National Lab., Tenn.). Sep 1972. Contract W-7405-eng-26. 162p. Dep. NTIS.

A bibliography on thermal effects on aquatic organisms is presented which includes 404 items published in 1971 and arranged in specified subject categories. Indexes on authors, keywords, and taxonomic names and a permuted index on titles are provided. (L.C.L.)

53191 PATIENT EARTH. Harte, John; Socolow, Robert H. New York; Holt, Rinehart, and Winston, Inc. (1971). 377p.

Environmental problems in contemporary American society, experiences in the 1930's Dust Bowl, the story of the Maya civilization, and essays on water, energy, and radiation are included. Separate abstracts were prepared for 3 papers. (M.C.G.)

For abstracts of individual papers see: 53192, 53193, and 53396.

53192 NUCLEAR POWER ON CAYUGA LAKE. Eipper, Alfred W. pp 112-31 of Patient Earth. /Harte, John. New York; Holt, Rinehart, and Winston, Inc. (1971).

Generation of electricity by steam electric stations is reviewed and Cayuga Lake is described. The utility company plan was to obtain 45°F cooling water from a depth of about 100 ft, warm it 20 to 25°F in the nuclear plant's condensers, and return it to the surface waters at a rate of 1100 ft^3/sec year-round. The effects of heated effluents and of radioisotopes released from the plant were studied. Public response to the studies is described along with the utility's response, and legislators' response. (M.C.G.)

53193 ENERGY. Harte, John; Socolow, Robert H. pp 276-94 of Patient Earth. /Harte, John. New York; Holt, Rinehart, and Winston, Inc. (1971).

Solar energy and the earth's heat balance, energy in the biosphere, magnitude of energy consumption, and impact on the environment are discussed. (M.C.G.)

53194 COPING WITH HEATED WASTE WATER DISCHARGES FROM STEAM-ELECTRIC POWER PLANTS. Cairns, John Jr. (Virginia Polytechnic Inst. and State Univ., Blacksburg). Bioscience; 22: No. 7, 411-19; 423(Jul 1972).

Some of the questions of our time are whether all ecological alteration is necessarily bad; whether or not ecological damage is a necessary consequence of technological progress; and whether it is possible to put man or nature "first." Waste heat added to the environment is of special interest, and it will be necessary to decide how much waste heat from steam-electric power plants may be placed in the environment without seriously degrading it. Predictions on the quantity of waste heat to be released to the environment, effects of power plant thermal effluents on aquatic ecosystems, methods other than surface water-discharge which may be used for dissipating or beneficially using waste heat, and the design and operating costs of modern cooling towers are discussed. It is concluded that we must accept the common goals of both environmental protection and energy production, and that biologists interested in environmental problems should devote their major efforts to predicting and judging the regional environmental effects, both adverse and beneficial, of waste heat discharge from power plants. (L.C.L.)

INSTRUMENTATION

Radiation Detection Instruments

Refer also to abstract 53187.

General Detectors and Monitors

Refer also to abstracts 53041 and 54078.

53195 (AD–737993) PROBLEM H01-32 AIRBORNE RADIAC. Progress Report, January 1–June 30, 1971. Peters, C. W.; Cook, D. C. (Naval Research Lab., Washington, D. C.). Jan 1972. 16p. (NRL-MR–2391). NTIS.

The results of computer calculations of the response of the scintillation spectrometer Airborne Radiac detector are summarized. The calculations were made as a function of altitude from 2,000 to 8,000 feet and for barometric pressures from 50 to 76 cm of Hg. Analytical equations for converting the detector response to dose rate at ground level are presented. The final status of the Airborne Radiac is reviewed. A Flyable Breadboard is complete and ready for flight testing. Other models are partially completed and are available as spare equipment or for measurements that may be required for future advanced development. (auth) (GRA)

53196 (COO–323-28) PROGRESS REPORT FOR PERIOD JUNE 1, 1971 TO MAY 31, 1972. (Illinois Benedictine Coll., Lisle (USA). Physical Sciences Lab.). 30 May 1972. Contract AT(11-1)-323. 26p. Dep. NTIS.

ARGON SYSTEMS—Ar–Hg, ionization of gaseous
BETA PARTICLES—effects on water vapor, energy for ion pair formation from
PLASTICS—preparation of air-equivalent, for ionization chambers
RADIATION DETECTORS, IONIZATION CHAMBER—development for environmental radiation
—development of small 0.5-cc air-equivalent, muscle-equivalent, and magnesium
VIBRATING REED ELECTROMETERS—improvement of Shonka
WATER VAPOR—radioinduced ionization of undeuterated and deuterated, energy for ion pair formation in beta (D.L.C.)

53197 (EGG–1183-2277) LINEARITY, TIME DOMAIN REFLECTOMETER, AND FOURIER ANALYSIS STUDIES OF AN EVACUATED COMPTON DETECTOR. Artuso, J.; Stevens, J. (EG and G, Inc., Goleta, Calif.). Sep 1971. Contract AT(29-1)-1183. 72p. (S–544-R). Dep. NTIS.

For California Univ., Livermore. Lawrence Livermore Lab.

The experimental procedure used to measure the dependence of the L-125A detector's relative sensitivity on the width of incident gamma pulses is described. When exposed to bremsstrahlung pulses whose widths were changed from 1 nsec to 4 μsec, the detector was found to be linear to within ±6%. The value of the time domain reflectometry (TDR) technique for improving the time response of the L-125A detector was established by comparing its results with those obtained by measuring the frequency response of the detector using a 50-psec bremsstrahlung pulse. These studies show that properly interpreted TDR techniques can give information that can be applied to the design of detectors with a higher frequency response than that of the L-125A detector. The peak linear output current of the L-125A detector was also measured and results are presented on the influence of excitation amplitude on detector linearity. (auth)

53198 (FRNC-TH–189) EXPERIMENTAL AND THEORETICAL STUDY OF GAS AMPLIFICATION IN A LOW PRESSURE CYLINDRICAL PROPORTIONAL COUNTER. Cukier, Michel (Paris Univ., Orsay (France)). 1971. 69p. (In French). Dep. NTIS (U. S. Sales Only).

Thesis.

Methods of calculating the gas amplification in a low pressure cylindrical proportional counter are reviewed. It is shown that these methods do not account for the experimental results when the E/p (electric field to pressure) ratio exceeds 10^3 V/cm torr. A theoretical study of the form of the signal delivered by this type of counter was performed. From this study, the variation of the gas amplification was deduced as a function of the pressure and voltage for E/p values up to 10^5 V/cm torr. A theoretical electron avalanche model was developed for the calculations. It is shown that this model is satisfactory when the avalanche is produced in methane. The optimal conditions for the operation of the counter corresponding to various experimental situations can be predicted. (France)

53199 (LBL–585) HIGH RELIABILITY ENVIRONMENTAL RADIATION MONITORING AND EVALUATING SYSTEM. Stephens, L. D.; Dakin, H. S. (California Univ., Berkeley. Lawrence Berkeley Lab.). Jan 1972. Contract W-7405-eng-48. 25p. (CONF-720328–2). Dep. NTIS.

From sixth international congress on new trends in radiation protection; Bordeaux, France (27 Mar 1972).

Centralized monitoring and recording of accelerator-produced radiation fields at points within the Lawrence Berkeley Laboratory site is done by a telemetry system, which began operation in 1964. Using standard telephone lines, the system collects data simultaneously from all points, giving both the rate and the time-integrated intensity of radiation at each point. At the collection stations conventional counting equipment is used in conjunction with a simple device which converts scaler decade output signals into a form which is transmitted over telephone lines. This directly activates electromechanical event-recorder movements and impulse counters. Transmission of signals from two consecutive decades of a single scaler at a remote station over a single telephone line makes it possible to record a wide range of radiation intensities, extending over several orders of magnitude. For special applications apart from the regular operation of the system, telephone lines transmit 5-μs pulse signals and small count-rate metering currents with noise interference practically eliminated by means of ground isolation and common-mode rejection techniques. A computer program (PLOT DOG) is then used as a means of evaluating the environmental radiation. It provides a printout and bar graph plot of the daily or hourly radiation dose for each monitoring station. The data from each of these stations can be intercompared to provide information as to causes of significant increases of the machine-produced radiation or the effect of new shielding situations on the overall stray radiation patterns. (11 figures) (auth)

53200 (LBL–707(Summ.)) NEUTRON RADIOGRAPHY WITH A MULTIWIRE PROPORTIONAL CHAMBER: PERFORMANCE AND PROJECTIONS. Kaplan, Selig; Valentine, Kenneth; Kaufman, Leon; Perez-Mendez, Victor (California Univ., Berkeley. Lawrence Berkeley Lab.). Feb 1972. Contract W-7405-eng-48. 3p. (CONF-720607–26). Dep. NTIS.

From eighteenth annual American Nuclear Society conference; Las Vegas, NV. (18 Jun 1972).

A multiwire proportional chamber with delay-line readout can be employed for electronic neutron-radiographic imaging in a sensitive, highly selective, moderate-resolution system where low-intensity thresholds and high information yield per unit neutron dose are important considerations. The basic system is equivalent to an N × N array of 1- to 2-mm^2 neutron-sensitive proportional chambers. Independent of chamber size, signal detection and position location require only a single integrated detector and three amplifiers. One amplifier provides a prompt signal indicating an ionizing event anywhere in the chamber, and the other two each receive signals from delay lines which are capacitively coupled to each wire of one of two orthogonal grids that serve as cathode or anode planes of the proportional chamber. The two analog timing signals are then processed for display or storage. Neutron sensitivity is achieved by coating the inside surfaces of the chamber windows with neutron-to-charged-particle converting material. The performance of a small natural-boron-lined, prototype chamber, 3 × 4-cm sensitive area, was tested for thermal-neutron imaging. With 2-mm wire spacing and a single neutron converting surface 0.5% detection efficiency and 2-mm 10 to 90% resolution of a Cd knife edge or a Lucite step were achieved. Efficiency characteristics for neutrons of various energies are given. (1 figure) (R.W.R.)

53201 (NASA-TM-X-2440, pp 142-8) REAL-TIME SPECTRUM-TO-DOSE CONVERSION SYSTEM. Farmer, B. J.; Johnson, J. H.; Bagwell, R. G. (Advanced Technology Center, Inc., Dallas). Jan 1972.

From Symposium on natural and manmade radiation in space; Las Vegas, Nev. (1 Mar 1971).

A system has been developed which will permit the determination of dose in real time or near real time directly from the pulse-height output of a radiation spectrometer. The technique has been demonstrated in the laboratory using the output of a NaI(Tl) anticoincidence gamma-ray spectrometer and a beta-gamma spectrometer which was flown on Gemini XII and also in space with the electron-proton spectrometer on the Radiation and Meteoroid Satellite. The technique involves the use of the resolution matrix of a spectrometer, the radiation energy-to-dose conversion function, and the geometrical factors, although the order of matrix operations is reversed. The usual method requires that a complete pulse-height spectrum (which is reasonably accurate statistically) be accumulated. The instrument resolution is then removed from this distribution giving the true radiation energy spectrum. This step requires the use of an inverted instrument resolution matrix or a more accurate but more time-consuming iterative process. A geometric function and the radiation energy-to-dose function must then be applied to obtain dose. This requires the use of a significant remote or on-board computer and unnecessary and time-consuming computer operations if only the dose is required. The new technique yields a result which is mathematically identical to the standard method while requiring no matrix manipulations or resolution matrix storage in the remote computer. It utilizes only a single function for each type dose required (e.g., physical dose, biological dose) and each geometric factor involved (e.g., surface dose at a specific location inside a space vehicle). The dose functions are generated using the same resolution functions, geometric factors, and dose curves that would be used in the standard technique; however, the matrix manipulations are made only once for each function instead of each time a new pulse-height spectrum is obtained. Also, the dose may be calculated and accumulated while the data are being received, since it is not necessary to have a complete instrument spectrum before making a calculation. (auth)

53202 (NASA-TM-X-2440, pp 723-8) HIGH-RESOLUTION SEMICONDUCTOR DETECTOR FOR APPLICATIONS IN SPACE. Alexander, Peter; Shulman, Herman (Teledyne Isotopes, Westwood, N. J.). Jan 1972.

From Symposium on natural and manmade radiation in space; Las Vegas, Nev. (1 Mar 1971).

Nuclear radiation detectors with volumes of ~1 cm^3 have been fabricated from single crystals of germanium-silicon alloy containing as much as 20 weight percent germanium. The properties of these detectors are discussed. Tests reveal that the gamma ray photoelectric peak efficiency of an alloy detector with only 12 weight percent germanium is ~4 times that of a silicon detector of equal volume. The alloy detector will operate with excellent energy resolution at –75°C. Operation at room temperature appears to be a good possibility. Storage for long periods at room temperature does not seem to adversely affect these devices. The results of preliminary radiation damage experiments suggest that the alloy detectors possess a radiation damage resistance far greater than that of silicon. (auth)

53203 (NASA-TM-X-2440, pp 874-83) EVALUATION OF TWO POSSIBLE FURTHER DEVELOPMENTS OF THE UK IN-FLIGHT RADIATION WARNING METER FOR SSTs. Wilson, I. J.; Eustace, R. C. (Atomic Weapons Research Establishment, Aldermaston, Eng.). Jan 1972.

From Symposium on natural and manmade radiation in space; Las Vegas, Nev. (1 Mar 1971).

Various radiation measurements have been made to investigate 2 possible further developments of the present hybrid ionization and neutron detection system of the Dose-Equivalent Ratemeter commissioned for the SST Concorde, namely (i) A reduction of the mass of the moderator from that of the Anderson-Braun neutron-remmeter assembly, and (ii) the inclusion of a response to the nucleon flux responsible for the tissue-star component of the total dose-equivalent rate by means of a high atomic number material as a nucleon-neutron converter within the moderator. Radiation situations at SST cruising altitudes (~20 km) due to solar proton flares were simulated approximately both in the stratosphere and on the ground. Actual stratospheric situations due to galactic cosmic radiation with a limited range of quality factor values (2 to 4) were encountered during slow ascents by balloons to 36 km from Aire-sur-Adour (France). Synthetic situations obtained from high and low energy accelerator radiations were used to obtain radiation distributions having a larger range of quality factor values (1½ to 9) than experienced in the stratosphere. The measurements made in these simulations related to the directly ionizing, neutron and tissue-star components of dose-equivalent rate. The stratospheric and high energy accelerator experiments taken together with results from both radioactive and machine neutron sources indicated 2 conclusions. Firstly that, due to the restricted range of neutron spectra encountered in the stratosphere, a significant and welcome reduction of the mass of the moderator by 4 kgm could be made, provided the moderator is clad with cadmium or some other slow neutron absorber. Secondly, that to achieve a tissue-star response with a lead insert would result in a net increase in moderator-assembly weight of 5½ kgm. Hence the lead insert proposal was abandoned, while the potential moderator reduction is being exploited. A reduced moderator geometry compatible with the existing electronics package was derived; its oversensitivity with respect to the Anderson-Braun neutron remmeter was determined for a number of fast neutron energies. Two different methods of correcting the oversensitivity—a slow neutron absorber within the moderator and a reduced sensitivity boron trifluoride counter—were tested. As a result, a new—reduced weight—version of the In-Flight Radiation Warning Meter for SSTs can now be designed in detail. (auth)

53204 (RDT-C–15-11-T(8-72)) BF_3 GAMMA TOLERANT NEUTRON DETECTOR TUBES. (Division of Reactor Development and Technology (AEC), Washington, D. C.). Aug 1972. 19p. RSO.

This tentative standard describes the requirements for a high-gamma-tolerant, BF_3-filled proportional counter for use in neutron detection systems requiring operation in gamma flux environments to 10^3 R/h. Specifically, this detector will be used to detect thermal neutrons in a neutron monitoring system, and will be installed in the vicinity of primary sodium piping system. This standard applied only to the detector. Required performance characteristics are given in detail, and the tests to assure this performance are described. Six test report certificates are included in the appendix. (1 table) (R.W.R.)

53205 (TID–26132) HEALTH PHYSICS MANUAL. (Oak Ridge Associated Universities, Inc., Tenn. (USA). Special Training Div.). 1971. 213p. Dep. NTIS.

Some general information of interest to the health physicist is presented first. This is followed by instructions for 31 laboratory exercises. (R.W.R.)

53206 THIN POLYPROPYLENE WINDOW PROPORTIONAL COUNTERS FOR THE OBSERVATION OF COSMIC SOFT X-RAYS. Kato, Takako; Kohno, Tsuyoshi; Nagase, Fumiaki; (and others) (Nagoya Univ.). Jap. J. Appl. Phys.; 11: No. 9, 1351-6(Sep. 1972).

Thin polypropylene window proportional counters are being developed for rocket observations of cosmic soft x-rays. Film thicknesses down to half a micron have been obtained, and practically all wavelengths shorter than 100 Å have become observable. This technique is also applicable to the detection of electrons above a few keV whose existence at rocket altitudes has been recently discovered. The preparation of thin polypropylene film, its application to proportional counters, and the associated gas control systems are described. An electrostatic shutter which discriminates between soft x-rays and low energy electrons is tested, and its function in the ambient plasma is also discussed. (auth)

53207 BINOMIAL DISTRIBUTION AND GAUSSIAN DISTRIBUTION IN NUCLEAR RADIATION MEASURING. Andresen, E. G. (Technische Fachhochschule, Berlin). Kerntechnik; 14: No. 5, 226-31(May 1972). (In German and English).

Fundamental statistical methods for evaluating counting results in radiation measurements are reviewed. Topics include the binomial distribution, safety systems in 2-out-of-3 logic, the Gaussian distribution, use of probability coordinates, and statistical uncertainty of pulse counts. (W.H.K.)

53208 TEILCHEN-DETEKTOREN. (Particle Detectors). Allkofer, Otto Claus. Thiemig-Taschenbuecher, Band 41. Munich; Verlag Karl Thiemig KG (1971). 251p. DM 19,80.

Topics include the interaction of radiation and particles with matter, ionization chambers, proportional counters, Geiger–Mueller counters, spark chambers, scintillation detectors, semiconductor detectors, Cherenkov counters, neon flash tubes, counter hodoscopes, cloud chambers, bubble chambers, nuclear emulsions, plastic detectors, other detectors, and counting fluctuations. (W.H.K.)

53209 CHERENKOV COUNTING OF BETA-EMITTING RADIONUCLIDES. Santoso, Daniel. College Park, Md.; Univ. of Maryland (1972). 167p. University Microfilms Order No. 72-21,131. Thesis.

A theoretical and experimental study was made on the role of a number of parameters in Cherenkov counting of beta emitters in commercially available liquid scintillation systems. A modified form of the Frank and Tamm equation was used to evaluate the amount of light produced by the beta particles in the medium. The photon yield improves with increasing refractive index and decreases with increasing density. The index of refraction also determines the value of the Cherenkov threshold and thereby determines the fraction of beta particles capable of generating photons via the Cherenkov effect. This fraction was computed from the Fermi distribution and the value of the threshold energy. The influence exerted by refractive index and density are more readily observed with low energy than with high energy beta particles. The experiments were conducted using a Nuclear Chicago Liquid Scintillation Counter which was interfaced with a Nuclear Data Multichannel Analyzer. The original photomultipliers were replaced by phototubes having a quartz window enabling detection of ultraviolet as well as visible light. Pre- and main amplifiers with provisions for pulse shaping were installed in place of the original amplifier circuits. Above five ml the solvent volume was found to have little, if any, effect upon the count rate. There exists a modest variation in counting efficiency from solvent to solvent. An unusually high detection efficiency was observed with benzene and toluene. As a result of experiments showing the presence of a small hump in the spectra when the latter two solvents were used, which disappeared upon addition of a few μl of $CHCl_3$, it was postulated that the high detection efficiency was due to radioluminescence occurring in addition to the Cherenkov effect. Investigations of the channel ratio method revealed that appropriate window widths can be selected to enable the use of a linear interpolation method for quenching correction. The quench curves obtained are linear, except in the region of very low detection efficiencies. The continuous distribution of the beta spectrum makes the Cherenkov method far from ideal for the separate quantitative assay of two or more nuclides in a mixture. However, results of experiments with $^{24}Na + ^{42}K$ and $^{32}P + ^{36}Cl$ showed that a precision of less than ten percent can be achieved in many cases. The greater the difference in energy between the two isotopes, the better the precision attainable. (Diss. Abstr. Int., B)

53210 DIAPHRAGM-LESS RADIOACTIVE RADIATION COUNTER. Kawashima, Nobuki (to Tokyo Univ.). U. S. Patent 3,678,274. 18 Jul 1972. Priority date 29 Oct 1969, Japan.

A radioactive radiation counter is provided with a counter chamber having a diaphragm-less open window, and two collecting electrodes are disposed in said chamber and separated from each other. A gas to be ionized is injected in a pulse into the chamber intermittently to create a gas cloud for a short duration in the space where the electrodes are disposed, and a voltage pulse is applied across the electrodes during the presence of said gas cloud between the electrodes to operate the counter in order to measure the radiation coming into the chamber during the voltage being applied to the electrodes. Because of the absence of a diaphragm in the ray entrance window of the counter chamber, the absorption of radiation energy in a diaphragm is avoided and thereby it is possible to measure radiations of energy less than 1 keV. (auth)

53211 SOLVENT COMPOSITION FOR LIQUID SCINTILLATION COUNTING. Webb, Richard V. (to Eastman Kodak Co.). U. S. Patent 3,677,964. 18 Jul 1972. Filed 31 Dec 1970.

A solvent composition is proposed for dissolving samples for liquid scintillation counting consisting essentially of (a) a solvent suitable for use in liquid scintillation counting, (b) at least one quaternary ammonium base selected from the group of the formula:

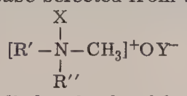

$$[R'-\overset{\displaystyle X}{\underset{\displaystyle R''}{N}}-CH_3]^+OY^-$$

wherein R′ and R″ are alkyl radicals of from 4 to 18 carbon atoms, X is selected from the group consisting of methyl and benzyl radicals, and Y is selected from the group consisting of hydrogen and lower alkyl radicals, the predominant class of quaternary ammonium consisting of the group wherein R′ and R″ contain from 4 to 14 carbon atoms, (c) methanol, and (d) an alcohol selected from the group consisting of t-pentyl alcohol and 2-methoxy ethanol. The quaternary ammonium base preferably is didodecyldimethylammonium hydroxide or methoxide, and is present in at least 0.25 molar concentration. The solvent advantageously is toluene, benzene, xylene, or dioxane, and is present in 60–70% by volume. The t-pentyl alcohol or 2-methoxy ethanol preferably are present in 4–10% by volume. (auth)

53212 GEIGER-MUELLER COUNTER DESIGNED TO MEASURE REPRODUCIBLY ACTIVITIES RETAINED ON RESIN COLUMNS. Heurtebise, M.; Lubkowitz, J. A. (Instituto Venezolano de Investigaciones Cientificas, Caracas). Anal. Chem.; 44: No. 11, 1918-21(Sep 1972).

A G–M counter was designed which consists of two anodes that are contained within one cylindrical counter. The detector efficiency for 2-MeV β particles was estimated by using an ^{128}I source and found to be good. (4 figures, 1 table) (R.W.R.)

53213 PERFORMANCES OF A PROPORTIONAL CHAMBER WITH INTERMEDIATE HIGH VOLTAGE PLANES. Aebischer, D. (Univ., Geneva); Hess, R.; Marcoli, R.; (and others). Helv. Phys. Acta; 45: 57-60(1972).

Results of work to increase the signal amplitude on the wires of multiwire proportional chambers are presented; the goal was to reduce the large amount of expensive electronics ordinarily needed. The region of electron multiplication around the wires can be enlarged by introducing two intermediate high-voltage planes. The signal amplitude obtained is shown as a function of voltage and gas mixture, and global efficiency is plotted against voltage. Time tion was found to be 9 ns. (4 figures) (R.W.R.)

53214 GAMMA CAMERA IN MALIGNANT DISEASE. THE GAMMA CAMERA. McCready, V. R. (Inst. of Cancer Research, Sutton, Eng.). Proc. Roy. Soc. Med.; 65: No. 8, 703-5(Aug 1972).

The diagnostic use of the gamma camera in conjunction with scintillation scanning is briefly reviewed under the following headings: dynamic studies throughout the body; thyroid; liver; pancreas; spleen; kidneys; and skeleton. (UK)

53215 DIGITAL STEREOSCINTIGRAPHIC EXPERIMENTS WITH A GAMMA-CAMERA. Larsson, E. Ingemar (Univ. of Lund, Sweden). Acta Radiol., Ther., Phys., Biol.; 11: No. 2, 135-44(Apr 1972).

A simple and cheap method for stereoscintigraphy using conventional gamma-camera equipment and digital storage-facilities is described. Some experimental results are presented and discussed. (auth)

53216 PORTABLE TRITIUM PROPORTIONAL COUNTER (3 Apr 1972) (Engineering Materials). (California Univ., Livermore. Lawrence Radiation Lab.). (CAPE-2204).
41 drawings.

A γ-compensated tritium proportional counter indicates and records the count rate corresponding directly to the T air concentration (either as HTO or ^3H) even if the area background changes up to 5 mR/hr in a uniform radiation field. The counter is a large-area, thin-window gas-flow counting system which measures 5 μCi/m^3 of tritium oxide in the presence of 3 mR/hr of a uniform γ-radiation field. To provide γ-background discrimination, two detectors are used: (1) the "tritium" detector which detects all radiation and (2) the "background" detector which has an infinitely thick window for tritium but detects all other radiation. Subtracting the analog output of (2) from the analog output of (1) gives a dc voltage proportional to the T count rate. (41 drawings) (For details see TID-4100 Suppl. 70) (see also 23: 50122 and 26: 9311) (F.S.)

53217 RANDOM DRIVER (5 May 1972) (Engineering Materials). (Los Alamos Scientific Lab., N. Mex.). (CAPE-2240).
23 drawings.

A random source interrogation system is described. The system consists of a compact, nondestructive assay instrument used principally to determine the ^{235}U content of containers up to 5 gallon capacity. An Am–Li random neutron source (of strength ~5×10^5 n/s) is used to induce fissions in the ^{235}U present in the sample. Induced fissions are observed by coincidence counting the time-correlated fission neutrons with two fast plastic scintillation detectors. By requiring the detection of neutrons in both detectors within a time interval of ~50 nsec, it is possible to distinguish the time-correlated induced fission neutrons from the randomly produced source neutrons. The "Random Driver" has been used to assay ^{235}U in a wide variety of matrix materials: U_3O_8, UO_3, UNH, and UF_4, and in various sample configurations. The sensitivity for ^{235}U detection depends strongly on sample size: ~5 g ^{235}U for two-liter samples and ~25 g ^{235}U for 5 gal containers. The assay time depends on the amount of ^{235}U in the sample and the assay precision desired. An assay time of ~100 sec is required to obtain a 10 g standard deviation on 200 g of ^{235}U in a two-liter bottle. Samples containing up to ~10 kg ^{235}U have been assayed with nearly linear calibration curves. It should be possible to assay fertile isotopes, such as ^{238}U, with this instrument by using both a subthreshold Am–Li source and a superthreshold (>1 MeV) random source, such as AmB or AmF. This "two-spectrum" interrogation technique will enable the Random Driver to assay both ^{235}U and ^{238}U content. (23 drawings) (For details see TID-4100 Suppl. 72) (F.S.)

53218 DOSE RATE RECORDING MONITOR (27 Dec 1971) (Engineering Materials). (New York Operations Office (AEC), N. Y. Health and Safety Lab.). (CAPE-2257). 40 drawings.

This monitor, with a sensitivity of ~10^{-4} A/μR/hr and an unusual degree of stability, measures the natural, or normal environmental levels of γ radiation. An internal impulse-driver strip-chart recorder provides information in a form suitable for permanent storage of incident radiation levels for subsequent analysis. A stainless-steel-walled 10-in. dia spherical ionization chamber is filled with ultra-pure Ar to a pressure of 20 atmospheres. A MOSFET electrometer provides current amplification to a level compatible with the recorder. The system operates for over two weeks on its internal batteries or it may be powered from an ac powered supply. The unit is packaged in two water-proof housings. One contains the ionization chamber and the electrometer and the other section has the battery supply, controls, strip-chart recorder, and an automatic circuit for checking the electrometer. (40 drawings) (F.S.)

53219 HIGH-RATE DIRECT-COUPLED PREAMPLIFIER (Feb 1972) (Engineering Materials). (California Univ., Livermore. Lawrence Radiation Lab.). (CAPE-2208).
15 drawings.

This preamplifier is used with high-energy Ge-detector systems for fast counting of high-energy γ events. Good resolution is possible with recycling and data can be obtained with and without pile-up rejection for count rates up to 150,000 counts/sec. Resolution without pile-up rejection for ^{60}Co is 2.50 keV fwhm at 75,000 counts/sec (1.5 μsec shaping). The preamplifier does not require pole-zero compensation. After single differentation, the pulses return precisely to the baseline. The charge-sensitive loop uses a cooled FET input stage. (15 drawings) (For details see TID-4100 Suppl. 70) (see also 26: 6835) (F.S.)

53220 COMPUTER-CONTROLLED IN-LINE MONITORING SYSTEM (18 Nov 1971) (Engineering Materials). (Savannah River Operations Office (AEC), Aiken, S. C.). (CAPE-2237).
5 drawings.

The computer-controlled in-line system collects data from detectors, which are monitoring a chemical process stream containing radionuclides, to compute control parameters from the data, and to supply information and instructions to production operators. Three types of detectors monitor the process stream: a high-resolution Ge(Li) detector produces a gamma spectrum from which specific radionuclides can be identified, a BF$_3$ neutron detector measures gross neutron activity, and a NaI γ detector coupled to a single-channel pulse-height analyzer measures the high-energy gross γ activity. (For details see TID-4100 Suppl. 71) (F.S.)

53221 PROPORTIONAL COUNTERS FOR THE LOCALISATION OF IONISING RADIATION. Hough, J.; Drever, R. W. P. (Glasgow Univ.). Nucl. Instrum. Methods; 103: No. 2, 365-72 (1972).

Gas proportional counters which can be used for the localization of ionizing radiation in one or two dimensions are described. The technique of charge division on a resistive electrode is used to obtain position information, this electrode being the anode in the linear detector. In two dimensions the counter signal is obtained in a new way, from two induction grids placed between the anode and the cathode, each grid providing position information in one direction. Application of the two-dimensional counter for x-ray imaging is illustrated. These counters combine ease of readout with good spatial resolution; in the one-dimensional detector the standard deviation of position measurements can be 0.04% of the sensitive length. (9 figures) (auth)

53222 MAGNETO-, SPARKO-, AND THERMOSTRICTIVE PHENOMENA IN THIN WIRES. Bichara, M. R. E.; Jauch, K. M. (Univ., Geneva). Nucl. Instrum. Methods; 103: No. 2, 385-7 (1972). (In French).

As part of the work on a novel spark chamber technique, an effort was made to elucidate the nature of "sparkostriction" (shock waves produced in wires due to sparks) by using a high-power pulsed and focused laser beam to produce similar signals on the same wires. However, it was found that the signals due to sparks are linearly proportional to the input power, whereas those due to the laser are proportional to the square root of the input power; the latter result is supported on theoretical grounds. (4 figures) (auth)

53223 NEUTRON IRRADIATION MONITOR FOR USE WITH Ge(Li) DETECTORS. Wilenzick, R. M. (Univ. of Texas, Houston). Nucl. Instrum. Methods; 103: No. 2, 429-30(1972).

A fission-track dosimeter is suggested as a method of monitoring the integrated fast neutron flux incident on a Ge(Li) detector in order to prevent overexposure and subsequent radiation damage. (auth)

53224 ION-CHAMBER DEVICE AS ELECTRONIC SWITCH IN HIGH RADIATION FIELD. Chakraborty, P. P.; Sahasrabudhe, S. G.; Samant, R. K. (Bhabha Atomic Research Centre, Bombay). Nucl. Instrum. Methods; 103: No. 2, 411-14(1972).

The design of an ionization chamber which makes use of the change in ionization current to record and control irradiation times of samples in a pneumatic transport system installed in a reactor is described. (4 figures) (auth)

53225 METHOD FOR RAPID COMPARISON OF ANGULAR DISTRIBUTION ATTENUATION COEFFICIENTS FOR DETECTORS OF ARBITRARY GEOMETRY. Avignone III, F. T. (Univ. of South Carolina, Columbia). Nucl. Instrum. Methods; 103: No. 2, 225-8(1972).

A very simple method for comparing a well-known angular correlation or distribution attenuation coefficient, Q_2, of one geometry to that of a detector geometry which is not known was developed. The method consists of generating an artificial angular distribution of γ rays by placing the radioactive source on the axis of a cylindrical absorber which has a circular inside surface and an outside surface shaped so as to transmit γ rays with a relative probability given by $W(\theta) = 1 + A_2P_2(\cos\theta)$. The observed directional distributions are found to be very close to $W(\theta)$ given above. The method was tested for both NaI(Tl) and Ge(Li) detectors in several counting geometries. (3 figures) (auth)

53226 MORE ACCURATE DETERMINATION OF THE ATMOSPHERIC CONCENTRATIONS OF RADON DAUGHTERS BY AN α-SPECTROMETRIC EXTRAPOLATION METHOD. Goumnerova, L.; Minev, L. (Sofia Univ.). Nucl. Instrum. Methods; 103: No. 2, 253-6(1972).

RaA and RaC were recorded separately with a Si(Au) surface barrier detector. Their decay curves were plotted, and the values of their activity on the filter at the end of the accumulation were found by extrapolation. (3 figures) (auth)

53227 MEASUREMENTS OF THORON IN THE ATMOSPHERE. Shimo, Michikuni; Ikebe, Yukimasa; Kawano, Minoru (Nagoya Univ., Japan). Nippon Genshiryoku Gakkaishi; 14: No. 8, 415-21(Aug 1972). (In Japanese).

A study was made on a method for calibrating the ionization current to be determined when measuring thoron concentration with an ionization chamber. The ionization current generated by the thoron exhausted from RdTh solution would appear to be controlled mainly by the bubbling velocity in the bottle, and the reciprocal of the current is a linear function of the reciprocal of the velocity. The ionization current was calculated from thoron concentration by taking the following three conditions into consideration: loss of ions by columnar recombination, loss of range by the chamber wall, and the condition of the air flow through the chamber. The calibrated and measured values coincided well with each other. Thoron concentrations in the atmosphere were measured on the university campus in Nov. 1968, and the concentration was found to be $0.3 \sim 0.6 \times 10^{-16}$ Ci/cm^3 at 1 m above the ground surface. (7 figures) (auth)

53228 FIRST STAGE OF AN ASSEMBLY OF PROGRAMS FOR THE COMPUTERIZED PROCESSING OF DIGITAL SCINTIGRAPHIC DATA. Portmann, M.-C.; Legras, B.; Legras, J.; Martin, J. (Univ., Nancy). J. Biol. Med. Nucl.; 7: No. 27, 22-30(1972). (In French).

The general characteristics of a package of programs for the processing of clinical scintigraphic data are described. Various curve- and surface-smoothing techniques are used in conjunction with statistical analysis methods according to the problems studied. In certain other cases a single averaging technique is used to produce smoothed lines, determinations of the activities of several zones being sufficient for the purpose required. Such techniques have been tested with simulated scintigraphs or models, and are beginning to find applications in medicine. (France)

Radiation Dosimeters

Refer also to abstracts 52979, 53397, 53420, 54895, 54922, and 55457.

53229 (COO-1105-172) FAST NEUTRON RADIATION DAMAGE EFFECTS IN CRYSTALLINE ANTHRACENE AND EVALUATION AS A DOSIMETRIC TECHNIQUE. Moran, P. R. (Wisconsin Univ., Madison. Dept. of Physics). 1971. 6p. (CONF-710714-2). Dep. NTIS.

From Workshop on personnel neutron dosimetry; New York, N. Y. (8 Jul 1971).

Preliminary results of a study on the fast neutron radiation damage effects on the optical properties of metastable excitons in anthracene are presented. The relative annihilation blue fluorescence total yield under steady state red light excitation and the delayed fluorescence decay curve after pulsed red light illumination were measured. The fading and stability properties were found to be excellent. It is concluded that the damage effects in anthracene offer some potential for selected dosimetric applications. (W.H.K.)

53230 (NASA-TM-X-2440, pp 138-41) HEAVY-ION PASSIVE DOSIMETRY WITH SILVER HALIDE SINGLE CRYSTALS. Childs, Charles B. (Univ. of North Carolina, Chapel Hill); Parnell, Thomas A. Jan 1972.

From Symposium on natural and manmade radiation in space; Las Vegas, Nev. (1 Mar 1971).

A method of detecting radiation damage tracks due to heavy particles in large single crystals of the silver halides is described. The tracks, when made visible with simple electrical apparatus, appear similar to tracks in emulsions. The properties of the crystals, the technique of printing out the tracks, and evidence concerning the threshold energy for registering particles indicate that this method may find application in heavy ion dosimetry. The method has been found to be sensitive to stopping He nuclei and relativistic M group cosmic rays. Some impurities strongly influence the "decoration" or printout of the tracks, and the effects of these impurities are discussed. (auth)

53231 (NASA-TM-X-2440, pp 149-56) HIGH-Z-PARTICLE APOLLO ASTRONAUT DOSIMETRY WITH PLASTICS. Benton, E. V.; Henke, R. P. (Univ. of San Francisco). Jan 1972.

From Symposium on natural and manmade radiation in space; Las Vegas, Nev. (1 Mar 1971).

On Apollo missions, the individual astronaut's high Z particle exposure is measured by means of Lexan polycarbonate plastic. These layers form one component of the passive dosimetry packets worn in the constant wear garment. They serve as threshold type, high Z, charged particle track detectors, recording only the very highly ionizing particles such as E < 6 MeV/amu ^{12}C, E < 45 MeV/amu ^{28}Si, E < 250 MeV/amu ^{56}Fe, etc. The detectors yield information on the particles' charge, energy, and direction of travel. These data, in turn, are used to obtain the track fluence, the stopping particle density as an integral Z distribution, and the particles' integral LET spectrum. Some of the data gathered on Apollo missions 8-13 are presented. (auth)

53232 (NASA-TM-X-2440, pp 435-7) METHODS AND APPROACHES TO DOSIMETRY. Rossi, Harald H. (Columbia Univ., New York). Jan 1972.

From Symposium on natural and manmade radiation in space; Las Vegas, Nev. (1 Mar 1971).

The development of a dosimetric system capable of determining energy depositions in tissue regions that are smaller than a few 100 nanometers is projected. These objectives are met by evaluation of the data produced by a macro-subsystem and a micro-subsystem. Both systems are in essence multiple ionization chambers that are normally operated in a gated pulse mode. The macro-system yields absorbed radiation dose as a function of location in a phantom of the human trunk when it operates in the dose mode; it registers only those sections as a signal in which the primary particle or any of its secondaries have passed, in the pulse mode. The function of the micro-system is to provide detailed information of the track structure by determining lateral energy spread due to delta ray formation or other secondary particle production. (GRA)

53233 (NASA-TM-X-2440, pp 466-70) SELECTION AND USE OF TLDs FOR HIGH-PRECISION NERVA SHIELDING MEASUREMENTS. Woodsum, H. C. (Westinghouse Electric Corp., Large, Pa.). Jan 1972.

From Symposium on natural and manmade radiation in space; Las Vegas, Nev. (1 Mar 1971).

An experimental evaluation of Thermoluminescent Dosimeters (TLDs) was performed in order to select high precision dosimeters for a study whose purpose is to measure gamma streaming through the coolant passages of a simulated flight type internal NERVA reactor shield. The criteria for selection of the dosimeters was that they should be reproducible within +2% and some must have spatial resolution within +1.5 mm. The experimental procedure was to expose batches of 50 to 100 CaF_2 and LiF chip, mini, and micro TLDs to ^{60}Co radiation by mounting these dosimeters on a rotating wheel (to minimize positional differences). ^{60}Co radiation was used since it approximates the average energy of the gammas entering the shield. The 30 Ci source was placed ~150 cm from an aluminum wheel 51.1 cm dia. by 0.079 cm thick on which dosimeters were taped. All TLDs had been annealed for 1 hour at 400°C followed by 17 hours at 80°C prior to exposure. Reading of the TLD exposures was performed on a digital readout system. All dosimeter data were processed by the TLDEVAL code which calculates the mean standard deviation variance for each dosimeter and fractional standard deviation of the mean. Based on this study, the CaF_2 chip TLDs are the most reproducible dosimeters with reproducibility generally within a few percent, but none of the TLDs tested met the reproducibility criterion of ±2%. The microdosimeters were the least reproducible to the point of not being usable for measurements below several hundred rads. The dosimeters tested are linear with dose over the range of 1 to 180 rads within ±10% and fading of dosimeters after exposure was found to be negligible within the accuracy of the measurements. The non-reproducibility of ^{7}LiF mini TLDs is not presently understood, but may be due to a combination of the following: lack of sensitivity (compared to comparable CaF_2 dosimeters), non-radiation-induced thermoluminescence, or radiation damage from previous reactor irradiations. These effects are currently under further investigation. (auth)

53234 (NASA-TM-X-2440, pp 609-13) PORTABLE ABSORBED-DOSE MEASURING INSTRUMENT WITH GAMMA DISCRIMINATION. Quam, W. M.; Wilde, W. O. (EG and G, Inc., Santa Barbara, Calif.). Jan 1972.

From Symposium on natural and manmade radiation in space; Las Vegas, Nev. (1 Mar 1971).

The characteristics of an electronic instrument for measuring the radiation dose absorbed by tissues are presented. The detector is a sphere of tissue-equivalent plastic with a single wire located on a diameter of the sphere. The electronic circuits and method of operation of the detector are described. Advantages are the small size and easy portability plus ability to selectively measure neutron and gamma plus neutron events. (auth) (GRA)

53235 (NASA-TM-X-2440, pp 944-56) ADVANCED-DOSIMETRY SYSTEMS FOR THE SPACE TRANSPORT AND SPACE STATION. Wailly, Louis F. (Air Force Academy, Colorado Springs, Colo.); Schneider, Marion F.; Clark, Benton C. Jan 1972.

From Symposium on natural and manmade radiation in space; Las Vegas, Nev. (1 Mar 1971).

Instrumentation to measure the operationally significant high energy radiations encountered in future manned spaceflight is of fundamental importance in ensuring astronaut safety, system survivability, and ultimate mission success. Advanced dosimetry systems concepts that will provide automated and instantaneous measurement of dose and particle spectra are described. Proposed are systems to measure dose rate from cosmic radiation background to >3600 rads/hour. Charged particle spectrometers, both internal and external to the spacecraft, to determine the mixed field energy spectra and particle fluxes for both real time on-board and ground based computer evaluation of the radiation hazard are described. New and advanced automated passive dosimetry systems consisting of thermoluminescent dosimeters and activation techniques are proposed for recording the dose levels for twelve or more crew members. This system will allow automatic on-board readout and data storage of the accumulated dose and can be transmitted to ground after readout or data records recovered with each crew rotation. (auth)

53236 (NASA-TM-X-2440, pp 958-73) EXPERIMENTAL ACTIVE- AND PASSIVE-DOSIMETRY SYSTEMS FOR THE NASA SKYLAB PROGRAM. Schneider, Marion F.; Janni, Joseph F.; Ainsworth, Glenn C. (Air Force Weapons Lab., Kirtland AFB, N. Mex.). Jan 1972.

From Symposium on natural and manmade radiation in space; Las Vegas, Nev. (1 Mar 1971).

Active and passive dosimetry instrumentation to measure absorbed dose, charged particle spectra, and linear energy transfer spectra inside the command module and orbital workshop on the NASA Skylab Program in 1972 has been developed and tested. The active dosimetry system consists of one integral unit employing both a tissue equivalent ionization chamber and silicon solid state detectors. The instrument measures dose rates from 0.2 millirad/hour to 25 rads/hour, linear energy transfer spectra from 2.8 to 42.4 keV/micron, and the proton and alpha particle energy spectra from 0.5 to 75 MeV. The active dosimeter is equipped with a portable radiation sensor for use in astronaut on-body and spacecraft shielding surveys during passage of the Skylab through significant space radiations. Data are transmitted in real time or are recorded by an on-board spacecraft tape recorder for rapid evaluation of the radiation levels. The passive dosimetry systems consist of twelve (12) hard-mounted assemblies, each containing a variety of passive radiation sensors which are recoverable at the end of the mission for analysis. The passive dosimeters consist of calcium and lithium fluoride thermoluminescent dosimeters, special discharge ionization chambers, activation foils, Ilford G.5 and K.2 nuclear emulsions and plastic heavy particle track dosimeters. The passive dosimeters record the total mission dose from 5 millirads to 5000 rads and the linear energy transfer spectra from 0.20 to >85 keV/micron. (auth)

53237 (RD/B/N-2369) USE OF Ge(Li) DETECTORS IN HIGH DOSE RATE GAMMA SPECTROMETRY. Woollam, P. B.; Jones, L. T. (Central Electricity Generating Board, Berkeley (England). Berkeley Nuclear Labs.). Jul 1972. 10p. Dep. NTIS (U. S. Sales Only).

The use of a Ge(Li) detector system for measuring spectra in high dose rates is discussed. Results are presented of measurements at dose rates up to 2.5 rad h^{-1} with a typical radium spectrum taken at 1.2 rad h^{-1}. (auth)

53238 AN INTRAUTERINE DOSIMETER. Parker, H. M.; Endres, G. W. R.; Wheeler, R. G. (Battelle-Northwest, Richland, Wash.). Health Phys.; 23: No. 3, 389-90(Sep 1972).

In order to measure the long term integrated radiation dose delivered to a nonsurgically implanted dosemeter the possibility of incorporating a thermoluminescent dosimeter (TLD) into the structure of an intrauterine contraception device (IUD) was investigated. Care must be taken to ensure isolation of the thermoluminescent materials from body fluids. The relative sensitivities and fading properties of LiF, CaF_2 : Mn and CaF_2 : Dy are considered. The acceptable replacement cycle, the size and weight of the proposed dosemeters, readout facilities, and encapsulation are discussed. The preliminary results suggest that the use of LiF to measure dose at uterine depth appears feasible and a satisfactory sensitivity and accuracy for determining dose accumulated up to 1 year is obtainable. (UK)

53239 COMPARISON OF FILM BADGES AND THERMOLUMINESCENT DOSIMETERS. Crosby, E. H. (Guthrie Clinic, Sayre, Pa.). Health Phys.; 23: No. 3, 371-5(Sep 1972).

Ten individuals in 3 hospitals wore film badges and TLD monitors side by side on a monthly cycle for a period of 1 yr. Comparison of the exposures reported by both systems shows many inconsistencies, with one very noticeable trend. For those individuals working exclusively in diagnostic radiology, as opposed to radiotherapy or nuclear medicine, the agreement was generally poor. There were 15 instances out of a total of 120 where the exposure reported for the film badge was at least 10 times that reported for the TLD badge. All of these substantial discrepancies were for individuals working in diagnostic radiology. In view of the minimal energy dependence of lithium fluoride it is the author's opinion that the TLD reported exposures are nearer correct. Although both the film badge services involved have earned the National Sanitation Foundation seal of approval, there appears to be room for improvement in their interpretation of exposures to diagnostic x-rays. (auth) (UK)

53240 NATURAL FLUORITE IN THE DOSIMETRY OF THE MIXED FIELD OF GAMMA RAYS AND THERMAL NEUTRONS. Mishev, I. T.; Radicheva, M. A.; Levi, S. M. (Inst. of Physics, Sofia). Health Phys.; 23: No. 3, 367-9(Sep 1972).

The dependence of gamma sensitivity V_γ and of the sensitivity to thermal neutrons V_n of a homogeneous mixture of natural fluorite and LiF on the percentage content of ^{6}Li is investigated. It is found that at 10% ^{6}Li content in the mixture, $V_\gamma \approx 1/3\, V_\gamma o$ and $V_n \approx 40\, V_\gamma$, where $V_\gamma o$ is the gamma sensitivity of pure natural fluorite. (auth) (UK)

53241 DOSIMETRY SYSTEM FOR MEASURING INSTANTANEOUS DOSE AND LINEAR ENERGY TRANSFER SPECTRUM OF SPACE RADIATIONS. Schneider, Marion F.; Breen, Edward L. (to Secretary of the Air Force). U. S. Patent 3,678,275. 18 Jul 1972. Filed 15 Apr 1971.

A space radiation dosimetry system utilizing a portable tissue-equivalent ionization chamber mountable in a housing containing associated electronics and a linear energy transfer (LET) spectrometer with associated electronics is described. The LET spectrometer utilizes a telescope pair of solid state detectors in combination with amplifiers, a discretionary number of discriminator channels, logic circuits and counters to measure the linear energy transfer spectrum of high energy ionizing radiations. (auth)

53242 RADIOPHOTOLUMINESCENCE DOSIMETER WITH LOW γ-ENERGY DEPENDENCE. Kaes, H. H. (Fa. Ernst Leitz, Wetzlar, Ger.). Atomkernenergie; 20: No. 1, 75-8(1972). (In German).

The dosimetric properties of newly developed silver-activated radiophotoluminescence glasses on a fluoride base were investigated. With a suitable cation composition RPL glasses up to 75 Mol% fluoride content could be produced. Compared with a metaphosphate glass of the same activator concentration and cation composition, the fluoride glass possesses a comparable predose, higher sensitivity, lower γ-energy dependence, and slower fading. For sufficiently low silver concentration the dose reading is independent of the γ energy. The composition is free of toxic substances and stable against humidity. By consideration of all aspects, RPL dosimeters of fluoride base seem to be especially qualified for the use in integrating personnel dosimetry. (6 figures, 1 table) (auth)

53243 AUTOMATIC PRODUCTION OF ISODOSE CURVES. Kalnaes, Ole; Munk, Jens (Odense Sygehus, Denmark). Acta Radiol., Ther., Phys., Biol.; 11: No. 1, 90-6(Feb 1972).

The measuring equipment, the principles and the computer program for the automatic production of isodose curves for treatment planning at a 6-MeV linac are described. The measurements are carried out in a water phantom with an ionization chamber. This method necessitates measurements only of square fields and the computer plotted curves may be used directly in treatment planning. The accuracy obtainable is discussed. (auth)

53244 CONCEPTS W AND G USED IN RADIATION DOSIMETRY. COMMENTS ON CURRENT DEFINITIONS. Carlsson, Carl A. (Linkoepings Hoegskola, Sweden). Acta Radiol., Ther., Phys., Biol.; 11: No. 1, 106-12(Feb 1972).

The ICRU-definition of W, the average energy expended in a gas per ion pair formed, is applicable only when the charged particles are completely stopped by the gas or under charged particle equilibrium conditions. By changing the definition from $W = E/N$, where E stands for initial kinetic energy to $W = E_D/N$, where E_D means energy imparted, W can be used even when charged particle equilibrium does not exist, as in the case of cavity ionization dosimetry. A further advantage of the proposed definition is that W is closer related to the inverse of the quantity G used in radiation chemistry, where $G = M/E_D$ is defined as the average number, M, of changed molecules of one type per unit absorbed energy. Fundamental differences between W and G^{-1} are discussed. (auth)

53245 DOSIMETRIC PROPERTIES OF SOME THERMOLUMINESCENT SUBSTANCES. Szymczyk, Wieslawa; Polak, Bogumil; Byrski, Edward (Inst. of Oncology, Krakow). Nukleonika; 17: No. 3-4, 233-40(1972).

Lithium fluoride activated with Mg and Ti from two different batches and calcium fluoride activated with Mn were studied. The factors investigated were: Tl response vs dose, Tl response vs effective photon energy, and fading effect due to light exposure. (auth)

53246 HUMAN ENGINEERING STANDARDS FOR HEALTH PHYSICS INSTRUMENTATION. Erickson, G. L. (Douglas United Nuclear, Inc., Richland, Wash.). pp 257-70 of Radiation Protection Standards: Quo Vadis. Vol. II. Howell, Wallace P. (ed.). Richland, Wash.; Health Physics Society (1972).

From 6th annual topical symposium on radiation protection standards: quo vadis; Richland, Wash. (2 Nov 1971).

The pressing need for developing improved health physics instrumentation over the past 25 years has been greatly assisted by technological advances in instrument components. However, while measurement capability has improved significantly, the human engineering elements have not. Health physicists have complained loudly that instruments are bulky, too sensitive to environmental influences, hard to decontaminate and do not operate effectively under the adverse conditions they sometimes are subjected to. The instrument-developer, on-the-other-hand, responds, sometimes quietly, what do you want? If the questions and answers are properly pursued, the needed elements of human engineering emerge and are built into the instrument. If not, partly useful instruments may remain in service or be discarded while people "get along" with the "old stuff." This paper identifies some of the human engineering elements, points out how they are applied in radioactive environments and suggests that human engineering standards be developed. (4 figures) (auth)

53247 CRITIQUE OF STANDARD TESTING METHODS FOR PERSONNEL DOSIMETRIC DEVICES. Piltingsrud, H. V.; Love, P. E. (Radiological Health Lab., Wright-Patterson AFB, Ohio). pp 271-81 of Radiation Protection Standards: Quo Vadis. Vol. II. Howell, Wallace P. (ed.). Richland, Wash.; Health Physics Society (1972).

From 6th annual topical symposium on radiation protection standards: quo vadis; Richland, Wash. (2 Nov 1971).

Commonly recommended procedures for evaluating ionizing radiation responses of personnel radiation dosimetric devices or systems are usually centered around measuring responses of the devices with the incident radiation beam oriented to some favored surface of the dosimetric device. Included in this presentation are comments concerning the utility of this approach to dosimeter testing based on experience of the authors in evaluating angular and energy responses of several personnel dosimetric devices including several types of pocket ion chamber dosimeters, a film badge dosimeter system, thermoluminescent dosimeter (TLD) badge systems, and a neutron TLD badge system. (5 figures) (auth)

53248 MANUFACTURER'S VIEWS ON INSTRUMENT STANDARDS. Bellian, Joseph G. (Victoreen Instrument Div., Cleveland). pp 282-5 of Radiation Protection Standards: Quo Vadis. Vol. II. /Howell, Wallace P. (ed.). Richland, Wash.; Health Physics Society (1972).

From 6th annual topical symposium on radiation protection standards: quo vadis; Richland, Wash. (2 Nov 1971).

Instrument standards are needed by both manufacturers and users. There are definite advantages and some disadvantages to the user and manufacturer. Action should be taken to insure that standards do not create unnecessary problems. Proper procedures in developing standards and accurate methods of writing standards must be derived. In addition, realistic limits should be placed on organization with the authority to write standards. A proliferation of standards by several organizations will definitely reduce the effectiveness of all standards. In conclusion, what standards would the instrument manufacturers like to see written, if any? (auth)

53249 THERMOLUMINESCENT DOSIMETER (15 Sep 1961) (Engineering Materials). (Savannah River Operations Office (AEC), Aiken, S. C.). (CAPE-2239).

1 drawing.

A thermoluminescent (TL) dosimeter using two ^{7}LiF chips which monitors penetrating and nonpenetrating components of personnel radiation exposures is described. TL dosimeters are more accurate, less energy dependent, have a wider range of sensitivity and are simpler to use than film dosimeters. The TL badge consists of a pressed fiberboard insert embedded with two ^{7}Li chips, a folded paper (5.6 mg/cm^2), and a badge cover. The badge cover is the same as that used with film because the fiberboard and film packet are the same size. The folded paper holds the ^{7}Li chips in the two $3/16$-in. dia recesses in the fiberboard and protects the chips from sunlight and contamination. One TLD chip is in the center of an open window and the other is behind an Al shield (460 mg/cm^2) on the badge cover. These positions give a means of differentiating between skin exposures and penetrating beta and gamma radiation. Extruded ^{6}LiF chips are used because they are insensitive to neutrons. A separate dosimeter is used for neutrons. (For details see TID-4100 Suppl. 72) (see also 26: 1288) (F.S.)

53250 MICROCALORIMETER (Jun 1971) (Engineering Materials). (New York Operation Office (AEC), N. Y.). (CAPE-2209).

3 drawings.

The tissue-equivalent absorbed-dose microcalorimeter is a primary standard for evaluating dosimeter-system's response to fast neutrons. It has a high degree of compactness and durability for transportation of the equipment to sources of $-\pi$ meson and ion beams of adequate intensity for calorimetric dosimetry. The microcalorimeter incorporates both active and passive thermal shields and is constructed of Shonka A-150 tissue-equivalent conducting plastic. (3 drawings) (For details see TID-4100 Suppl. 70) (see also 25: 55208) (F.S.)

Nuclear Spectroscopic Instrumentation

53251 (AREAEE-137) FAST NEUTRON SCINTILLATION SPECTROMETER WITH DOUBLE COMPENSATION CIRCUIT FOR GAMMA-RAY DISCRIMINATION. Megahid, R.; El-Razek, M. Abd; Makarious, A. S.; Kolevatoff, J.; Hamouda, I. (Atomic Energy Establishment, Cairo (Egypt). Reactor and Neutron Physics Dept.). 1972. 58p. Dep. NTIS (U. S. Sales Only).

The present work is concerned with the application of a single stilbene crystal spectrometer for measuring neutron spectra within the energy range of 0.5 to 15 MeV. The principles of operation of scintillation counters and their characteristics are briefly described. Consideration is given to the electronic method which is used for separating between voltage pulses resulted from the interaction of various particles of different ionization density with the scintillator. The method employed to transform the pulse spectrum into a neutron energy spectrum is discussed. A check-up on the correctness of the results obtained with the spectrometer is made by measuring continuous energy distributions of neutrons from the Pu–Be source and the UA–RR–1 reactor neutrons that passed through carbon, iron and water filters of different thickness. (auth)

53252 (CONF-720901-(Bks.1 and 2), pp 524-40) CRITICAL COMPARISON AND EVALUATION OF NEUTRON SPECTRUM UNFOLDING CODES: THE NEED TO KNOW. Meyer, W.; Mutone, G. A. (Kansas State Univ., Manhattan). 1972.

From Meeting on new developments in reactor physics and shielding calculations; Kiamesha Lake, NY. (12 Sep 1972).

With most on-line fast neutron spectrometry systems it is not possible to measure directly the energy spectrum of neutrons incident on the detector. The experimental data must be analyzed or "unfolded" to obtain the spectrum. To accomplish this special analysis, numerous analytical unfolding techniques and computer codes have been developed and applied. Unfortunately only very limited efforts have been made to compare and evaluate critically the many unfolding procedures, either in terms of the validity of the basic analytic procedures used or the value of the results obtained. Such a comparison and evaluation of the accuracy and the validity of error estimates of the various procedures are of utmost importance because if the experimental results of a neutron reflection or transmission experiment are to be used to infer nuclear cross sections values or if the measured data are to be used to evaluate a transport model, the accuracy of the experimental results must be known. (auth)

53253 (FRNC-TH-237) STUDY OF A CALIBRATION UNIT FOR γ-RAY SPECTROSCOPY. ANALYSIS OF PROBLEMS INVOLVED IN THE MEASUREMENT OF γ RAY ENERGIES BETWEEN 0 AND 10 MeV. Lapierre, Alain (Bordeaux Univ. (France)). 1972. 90p. (In French). Dep. NTIS (U.S. Sales Only).

Thesis.

The various problems involved in the calibration of a γ spectrometer in the energy range between 0 and 10 MeV are studied. The basic principles of the least square method are briefly developed. Possible applications of the method to a standard obtained from an (n,γ) radiative capture of thermal neutrons are envisaged. Above 2.5 MeV the best solution is shown to be a cubic. Below 2.5 MeV it is better not to use the whole curve and to use a truncated spectrum in view of obtaining a more valid equation of conversion. The device used for the acquisition of the standard spectra from an Am–Be neutron source is studied. The determination of the position of each standard peak is shown to be one of the most important problems in the least square method for calibration. (France)

53254 (NASA-TM-X-2440, pp 614-17) COMPTON SCATTER ATTENUATION GAMMA-RAY SPECTROMETER. Austin, W. E. (General Electric Co., Philadelphia). Jan 1972.

From Symposium on natural and manmade radiation in space; Las Vegas, Nev. (1 Mar 1971).

A Compton scatter attenuation gamma ray spectrometer conceptual design is discussed for performing gamma spectral measurements in monodirectional gamma fields from 10^2R hr^{-1} to 10^6R hr^{-1}. Selectable Compton targets are used to scatter gamma photons onto an otherwise heavily shielded detector with changeable scattering efficiencies such that the count rate is maintained between 500 and 10^4 sec^{-1}. Use of two sum-Compton coincident detectors, one for energies up to 1.5 MeV and the other for 600 keV to 10 MeV, will allow good peak to tail pulse height ratios to be obtained over the entire spectrum and reduces the neutron recoil background rate. (auth)

53255 (NASA-TM-X-2440, pp 714-22) IDENTIFICATION AND CONTROL OF SPACECRAFT RADIATION SOURCES OF INTERFERENCE TO X-RAY AND GAMMA-RAY EXPERIMENTS. Metzger, Albert E. (California Inst. of Tech., Pasadena); Trombka, Jacob I. Jan 1972.

From Symposium on natural and manmade radiation in space; Las Vegas, Nev. (1 Mar 1971).

Apollo 15 and 16 will carry instruments for the purpose of measuring x-ray and gamma ray fluxes from the lunar surface and in cis-lunar space. The intensity levels expected are low over most of the energy range of interest, requiring that background contributions be minimized. The radiation sources on Apollo have been determined and their interference with these instruments evaluated. The results have been used as a basis for dealing with this problem and for recommendations applicable to future manned and unmanned missions. (auth)

53256 (NASA-TM-X-2440, pp 744-6) Ge(Li) DATA REDUCTION USING SMALL COMPUTERS. McDermott, W. E. (McClellam AFB, Sacramento, Calif.). Jan 1972.

From Symposium on natural and manmade radiation in space; Las Vegas, Nev. (1 Mar 1971).

The use of a PDP 8/I computer for Ge(Li) spectra analysis for analyzing mixtures of radioisotopes is briefly described. The computer is interfaced to the analyzer memory in which the data are stored. A flow chart of a typical peak location and analysis program is shown. (W.H.K.)

53257 (RT/FI-(72)14) AUTOMATIC PEAK IDENTIFICATION IN THE ANALYSIS OF GAMMA-RAY SPECTRA OBTAINED WITH Ge(Li) DETECTORS. Giannini, M.; Oliva, P. R.; Ramorino, M. C. (Comitato Nazionale per l'Energia Nucleare, Rome (Italy)). 14 Apr 1972. 79p. Dep. NTIS (U. S. Sales Only).

A computer code for full automatic analysis of γ-ray spectra obtained with Ge(Li) detectors is described. The significant peaks in the spectrum are detected by observing the behavior of the second derivative function after random variations in count rate have been minimized by the application of a smoothing filter function. Particular care is taken in the recognition of weak or adjacent peaks, even in the presence of high statistical fluctuations. This is achieved by means of a new check procedure working during the fit routine. The possibility of trying a new fit every time some spurious peak prevents a good fit from being reached is also introduced; it results in a considerable improvement in the elimination of pseudopeaks. Applications to experimental and simulated spectra are shown. (16 figures, 8 tables) (auth)

53258 (SC-DR-720630) PASSIVE CALORIMETER FOR PULSED ELECTRON BEAM ENERGY MEASUREMENT. Heckman, R. C.; Stephens, H. P.; Donaldson, A. B. (Sandia Labs., Albuquerque, N. Mex.). Sep 1972. 27p. Dep. NTIS.

A passive calorimeter for diagnostics of high energy pulsed electron beams is described. It consists of a thin rectangular sheet which is irradiated by the electron beam in a central region. The generated heat diffuses outwardly to the ends so that each position experiences a temperature maximum. Thin strips of materials which melt at various temperatures are coated on the surface to provide a record of the temperature maxima of the calorimeters. The corresponding heat diffusion problem is analyzed and used with the experimental results to calculate the initial temperature of the irradiated region, and thus the dose. The calorimeter absorbs only a small fraction of the beam energy and is therefore useful for making dose measurements simultaneously with experiments. (auth)

53259 MAGNETIC-PRISM β SPECTROMETERS. Peregud, B. P. (Ioffe Inst. of Physics and Tech., Leningrad). Sov. Phys.-Tech. Phys. (Engl. Transl.); 17: No. 3, 365-84(Sep 1972).

Translated from Zh. Tekh. Fiz.; 42: No. 3, 457-83(Mar 1972).

The theory of the magnetic-prism β spectrometer is reviewed, including the electron-optical scheme, ray paths in the paraxial approximation, dispersion, and relative aperture. The resolution and aberrations of electron-optical devices are discussed; these include adjustment errors, lens aberrations, and aberrations of the magnetic prism. Methods for designing electron-optical devices, such as magnetic lenses and magnetic prisms, are described; and the spectroscopic properties of the instruments are summarized. (15 figures, 2 tables, 52 references) (R.W.R.)

53260 SYSTEM FOR TIME OF 50 m FLIGHT ANALYSIS AND CHARACTERISTICS OF SHORT PULSE BEAM. Kawamura, Nobuaki (Tohoku Univ., Sendai); Saito, Hajime; Tsubota, Hiroaki; Mutsuro, Naoshi. Kakuriken Kenkyu Hokoku; 4: No. 1, 48-52 (Sep 1971). (In Japanese).

A neutron detection system was installed at a distance of 50 m in a time-of-flight system of 125 m. An absorption spectrum of photoneutrons from ^{12}C was taken for the purpose of calibration. Large time-dependent background was found on low-channel side. The source of the background was found to be gamma-rays scattered by a lead target. The attenuation of the gamma-rays by absorbers was small. It is difficult to measure neutrons above 10 MeV with the present experimental arrangement. Troubles were found in a pulse beam system. Multiple short beams occurred for one trigger cycle; and so-called grass, spill other than the main short pulses, was seen. Improvement of the system was performed, and the troubles were reduced. Temporary shielding will be set around the flight tube in the near future. (Japan)

53261 SPENT FUEL MONITOR (28 Sep 1970) (Engineering Materials). (Battelle-Northwest, Richland, Wash. Pacific Northwest Lab.). (CAPE-2238).

3 drawings.

A system consisting of a low-resolution NaI detector with a stabilizer and five single-channel analyzers provides sufficient data to determine the age of the spent fuel (time in days since the irradiated fuel was discharged from a reactor). Count data from the single-channel analyzers are processed manually to determine the age of the fuel. The manual process involves taking the ratio of specific scaler data and determining the age of the fuel which corresponds to the measured ratio from a graph. (3 drawings) (For details see TID-4100 Suppl. 72) (see also 25: 39734 and 26: 2266) (F.S.)

53262 REFERENCE PULSER (23 Jun 1971) (Engineering Materials). (California Univ., Livermore. Lawrence Radiation Lab.). (CAPE-2210).

21 drawings.

A transistorized pulser which features a highly-stable dual-transistor pulse generation network is described. The temperature stability of the pulser output is $\leq \pm 5$ ppM/°C from 10 to 50°C. Long term stability is approximately ±.02 channels/day. The pulser is used to improve the performance and reliability of the bio-medical γ-ray spectrometers which use high-resolution Ge(Li) detectors. The spectrometers analyze γ-emitting samples originating from biological research and environmental sampling programs. The pulser provides high-stability output pulses which, when applied to the spectrometer preamplifier, produce two-reference peaks necessary for spectrum stabilization. (21 drawings) (For details see TID-4100 Suppl. 70) (see also 26: 9354) (F.S.)

53263 TWO DECADES OF RESEARCH ON RADIOACTIVITY. THE IMPACT OF ADVANCES IN INSTRUMENTATION. Hamilton, J. H. (Vanderbilt Univ., Nashville); Manthuruthil, J. C.; Rasmussen, J. O. Nucl. Instrum. Methods; 103: No. 2, 277-90(1972).

A review is made of the impact that sophisticated new instrumentation and detectors are having on the quantity and quality of data acquired from radioactivity studies. Such studies are providing much new information to test details of current nuclear models and offer challenges to further theoretical development. The new frontiers, in-beam and on-line spectroscopy, open up many areas for research. (9 figures, 50 references) (auth)

53264 COMPACT ELECTRON SPECTROMETER FOR IN-BEAM MEASUREMENTS OF INTERNAL CONVERSION COEFFICIENTS. Cambi, A.; Fazzini, T. F.; Giannatiempo, A.; Maurenzig, P. R. (Univ., Florence). Nucl. Instrum. Methods; 103: No. 2, 331-5(1972).

A compact magnetic spectrometer for measuring electron conversion coefficients is described. A very efficient method to subtract the activation background, based on a pulsed beam-coincidence technique, is also presented and discussed. The chosen angle of detection for the electrons avoids the ambiguities present in previous methods and allows straightforward assignments of transition multipolarities in a number of specified cases. (3 figures) (auth)

53265 THIN FILM OF ORGANIC FLUORESCENT MATERIALS FOR SIMPLE DETECTION OF ALPHA RAYS. Koike, Y.; Handa, M.; Yamamoto, K. (Tokyo Metropolitan Isotope Research Center). Nucl. Instrum. Methods; 103: No. 2, 249-52(1972).

Vacuum-deposited and sprayed thin films of organic fluorescent materials are useful as detectors for simple detection of alpha particles. Films of 1,12-benzperylene and sodium salicylate showed excellent pulse height properties for alpha rays at room temperature in air. The films of fluorescent solutes used in the liquid scintillation counting also showed excellent pulse height properties. The full widths at half maximum of the films for alpha spectra are between 8 and 35% and of the same order as that of thin plastic scintillator used as a standard scintillator. The films of these materials are insensitive to high-energy beta and gamma rays because the thickness of these films is too thin to detect these rays. (3 figures, 1 table) (auth)

High Energy Physics Instrumentation

53266 (BNL-17020) PORCUPINE. Kirk, T. W. (Brookhaven National Lab., Upton, N. Y.). [nd]. 18p. Dep. NTIS.

A new 4π counter for detecting reaction products from high-multiplicity reactions involving perhaps 20 or more final-state particles is described. It consists of about 47,000 proportional wire counters with their active volumes aligned so that the multiplying wire electrodes all point at the interaction region (hence the name). Each counter thereby becomes its own charged-particle detector, and the large total number of elements insures (at least to first order) that each reaction product will trigger a unique detector. One thus gets a complete spatial picture of each event with no further analysis or reconstruction necessary. No information is known about the individual charged-particle momenta or the neutral-particle multiplicities, however, the Porcupine should be combined with some sort of segmented calorimeter like the Impactometer. The economic justification for this detector is discussed. The geometry of the detector array, as well as electronics and mechanical details, is also described. (5 figures) (R.W.R.)

53267 (BNL-17064) FOR THE MEASUREMENT OF MULTIPLICITIES: THE "MULTIMETER". Nygren, David R. (Brookhaven National Lab., Upton, N. Y.). [nd]. 8p. Dep. NTIS.

A 4π counter for interactions with high multiplicities is described. The basic idea of the multimeter is to use multiwire proportional chambers (MWPC's) in an x−y configuration and to record not only which wires are hit, but also to measure where along the wire the signal is generated. The electronics required in the fabrication of such a detector is discussed in some detail. If gammas and other neutrals are of interest, converters and other MWPC's can be conveniently added. (1 figure) (R.W.R.)

53268 (BNL-17066) CONCEPTUAL DESIGN OF A HYBRID DETECTOR FOR ELECTRON PHYSICS AT ISABELLE AND PEP: SOLENOID + QUANTAMETER + HADROMETER (CALORIMETER). Stevenson, M. L. (Brookhaven National Lab., Upton, N. Y.). 31 Jul 1972. 17p. Dep. NTIS.

An electron detector for colliding e−p beams at ISABELLE and PEP is described. The size, field strength, and measurement accuracy of the superconducting solenoid are discussed. The design and performance of the complementing quantameter are then described. Reasons for adding a hadrometer to the above combination are considered. (10 figures) (R.W.R.)

53269 (BNL-17070) PROGRAM FOR DEVELOPMENT OF A LIQUID ARGON CALORIMETER. Willis, William J. (Brookhaven National Lab., Upton, N. Y.). 21 Jul 1972. 4p. Dep. NTIS.

A specific program is outlined for the evaluation of liquid argon as a scintillator and the development of large total absorption counters based on its use. (auth)

53270 (BNL-17071) CALORIMETERS FOR ISABELLE. Willis, William J. (Brookhaven National Lab., Upton, N. Y.). 21 Jul 1972. 14p. Dep. NTIS.

A review is given of the available types of total absorption counters for hadrons. The design and operating features are described, with emphasis on the factors which limit energy resolution. (auth)

53271 (JINR-P13-6522) SYSTEM OF WIRE SPARK CHAMBERS WITH FERRITE CORE MEMORY. Azhgirei, L. S.; Asanov, V. V.; Budkin, L. V.; Bychkov, V. A.; Kuznetsov, A. S.; Stoletov, G. D.; Filozov, A. F. (Joint Inst. for Nuclear Research, Dubna (USSR)). 1972. 18p. (In Russian). Dep. NTIS (U. S. Sales Only).

A system of wire spark chambers with ferrite core memory is described. The data are presented on the chamber construction and on the mode of information readout. The efficiency and memory time of the chambers with various gas filling are studied.

It is shown that, under certain conditions, the accuracy of the detection of charged particle coordinates reaches ≈ ±$\frac{1}{4}$ from the distance between the wires. (auth)

52272 (JINR–P13-6541) ON POSSIBLE MEASURING HIGH-ENERGY ELECTRON ENERGY BY IONIZATION DETECTORS OF TOTAL ABSORPTION ON THE BASIS OF CONDENSED XENON. **Kulikov, Yu. V.; Ryabtsov, V. D.; Silaev, E. A. (Joint Inst. for Nuclear Research, Dubna (USSR). Lab. of High Energy). 1972. 14p. (In Russian). Dep. NTIS (U. S. Sales Only).**

The problems concerning the fabrication of a total-absorption ionization electron-pulsed detector for measuring electron and high-energy gamma-quanta energies on the basis of condensed xenon are considered. (5 figures) (auth)

52273 (LA–4968) BIFILAR HELICAL MULTIWIRE PROPORTIONAL CHAMBER FOR POSITION SENSITIVE DETECTION OF MINIMUM IONIZING PARTICLES. Lee, D. M.; Sobottka, S. E.; Thiessen, H. A. (Los Alamos Scientific Lab., N. Mex.). Aug 1972. Contract W-7405-eng-36. 11p. Dep. NTIS.

A new type of multiwire proportional chamber with a helical cathode for delay-line readout was developed and studied in detail. It gives cathode delay-line pulses nearly as large as the anode pulses; hence, it is well-suited for minimum ionizing particles. Measurements on such a chamber yielded spatial resolution better than 0.33 mm fwhm for ^{90}Sr β particles, a resolving time less than 30 ns, and maximum counting rate greater than 2 MHz. The most probable pulse height induced on the delay line by minimum ionizing particles in this chamber is approximately 8 mV. (15 figures) (auth)

52274 (RHEL/R–241) TRACK DETECTION PROGRAM FOR A HOUGH POWELL DEVICE. Hallowell, P. J. (Rutherford High Energy Lab., Chilton (England)). May 1972. 15p. Dep. NTIS (U. S. Sales Only). UK 20 pence.

A track detection program, designed to reduce data from the HPD installations at Rutherford High Energy Laboratory for analysis of bubble chamber photographs is described. The method employs a stringing technique to produce precision master points for input to the R.H.E.L. Geometry Program. (auth)

52275 (RPP/H–101) COMPACT EHT POWER SUPPLY FOR USE WITH HIGH PULSE RATE SPARK CHAMBERS. Connolly, J. F.; Gilby, A. S. (Rutherford High Energy Lab., Chilton (England)). Jun 1972. 21p. Dep. NTIS (U. S. Sales Only).

High pulse rate spark chambers require EHT power supplies capable of charging up the capacitive load of the pulser units employed in such systems. Typical values for this capacitive load are in the range 10 to 50 nF which for pulse rates of 10 per second and above results in a high current demand from the EHT supply. A compact EHT capacitor charging unit, developed at the Rutherford High Energy Laboratory for use in such applications, is described. (auth)

52276 IZMERENIE RADIATSII V KOSMOSE. (Measurement of Radiation in Space). Gal'perin, Yu. I.; Gorn, L. S.; Khazanov, B. I. Moscow; Atomizdat (1972). 344p.

Fundamental problems in the measurement of ionizing radiation in space near the earth and the detection of fluxes of electrons, neutrons, heavy charged particles up to 1 GeV and electromagnetic radiation are examined. Some block diagrams and circuitry of measuring equipment are discussed. (446 references) (K.S.W.)

52277 TRANSITION COUNTER. Wang, C. L.; Dell, G. F. Jr.; Uto, H.; Yuan, Luke C. L. (Brookhaven National Lab., Upton, N. Y.). Phys. Rev. Lett.; 29: No. 12, 814-17(18 Sep 1972).

A new type of counter based on the transition radiation from ultrarelativistic charged particles is reported. The efficiency of the "transition counter" depends almost linearly on the Lorentz factor of the particle in the energy region covered and is over 80% for 2-GeV electrons. Particles heavier than electrons in a 2-GeV unseparated beam are effectively rejected. A possible application of the counter at multihundred-GeV accelerators is discussed. (auth)

52278 ULTRA-LINEAR 16-BIT DIGITAL-TO-ANALOG CONVERTER (13 Feb 1970) (Engineering Materials). Chicago Operation Office (AEC), Ill. Reactor Engineering Div.). (CAPE–2192).
29 drawings.

The 16-bit binary digital-to-analog converter is used for the deflection yokes of the Dolly CRT flying-spot scanning system in order to provide a high-resolution raster from which measurements are made digitally. The digital input is converted directly to binary-weighted currents. For each bit there is a constant current source and a current switch. The current sources are weighted according to their digital-bit value and current switches deliver the current either to one half of the yoke or the other half. Voltage across the current-determining resistor of each current source is identical and constant. The resistors are of sufficient accuracy that no trimming is necessary. In this method of conversion, binary-weighted constant current sources are switched into a summing junction, the yoke of the CRT. A conversion linearity of 0.00025% and a stability of 0.0004%/hr were measured for a full scale current of one ampere. For long-term linearity, good thermal stability, and minimal maintenance, the converter requires little or no adjustment. (29 drawings) (For details see TID-4100 Suppl. 70) (see also 24: 7687) (F.S.)

52279 ANNIHILATION SPECTROMETER FOR INVESTIGATION OF HEAVY MESON SPECTRA. Alspector, J. (Rutgers—The State Univ., New Brunswick, N. J.); Cohen, K.; Harrison, C.; (and others). Nucl. Instrum. Methods; 103: No. 2, 239-43(1972).

The "Rutgers Annihilation Spectrometer" (RAS) measures cross sections for antiproton annihilations as a function of the $\bar{p}p$ mass, final-state multiplicities, and degree of nonperipheralism, with a resolution of ±5 MeV and typical statistics of 10^6 events per mass bin 5 MeV wide. The nonannihilation events are suppressed by anticoincidence with the events in which charged particles are emitted within the forward cones defined by the lab polar angles 2½°, 5°, 10°, and 20° (4 "degrees of nonperipheralism"); in this way single-meson exchange mechanisms, which are nonresonant and highly peripheral, are eliminated. Measurements are done at 7 incident momenta simultaneously. Scintillation counters are the only detectors used. On-line data acquisition is accomplished by a hard-wired electronic processor ("MEGAHPOL") capable of sorting data on 100,000 incident antiprotons per second. (7 figures) (auth)

52280 VERSATILE, HIGH-RESOLUTION PARTICLE IDENTIFIER: THEORY. Greiner, D. E. (Univ. of California, Berkeley). Nucl. Instrum. Methods; 103: No. 2, 291-308(1972).

A method of measurement and analysis is presented which makes maximum use of the dependence of energy loss dE/dx upon range to identify isotopically particles which stop in an identifier consisting of several thick solid state detectors. Theoretical identification efficiency, mass resolution, charge resolution, and energy resolution are determined. (22 figures) (auth)

52281 HELIUM-RECOIL SPECTROMETER. Dahlgren, S. (CERN, Geneva); Herz, A. J.; Kullander, S.; (and others). Nucl. Instrum. Methods; 103: No. 2, 309-23(1972).

The instrument described is intended for the detection and measurement of α particles from coherent interactions of high-energy particles with ^{4}He nuclei. It allows the determination of the magnitude and the direction of the momenta of the helium recoils from interactions in a pressurized gas target. The measurements are carried out with spark chambers and scintillation counters. Recoils emitted at angles greater than 65° with respect to the beam direction are accepted, and the range of azimuth angles covered is 294°. (16 figures) (auth)

52282 MUON IDENTIFICATION USING MULTIWIRE PROPORTIONAL CHAMBERS. Harris, F. A. (Univ. of Hawaii, Honolulu); Parker, S. I.; Peterson, V. Z.; Yount, D. E.; Stevenson, M. L. Nucl. Instrum. Methods; 103: No. 2, 345-55(1972).

Test data are summarized for a muon identifier consisting of iron absorber plates followed by multiwire proportional chambers. Because of the penetrating secondaries that result from hadronic interactions, conventional muon identifiers lacking spatial resolution require many collision lengths to attenuate the hadron flux and thus separate incident hadrons from muons. By using multiwire proportional chambers, hadronic interactions can be detected well before the subsequent hadron cascades have been fully absorbed. This permits a substantial reduction in absorber thickness, and is important in applications in which the muons originate in a large volume or in which they are to be identified over a large area or large solid angle. A typical result from these tests is that at 3 GeV/c a single multiwire proportional chamber, following only 50 cm of iron, can reject pions with 96 ± 1% efficiency while accepting 96% of the incident muons. An important advantage of this technique is that the performance is expected to be rather independent of energy above a few GeV. (9 figures, 2 tables) (auth)

52283 GENERAL PROPERTIES OF THE CURRENT-LIMITED SPARK CHAMBER. Stubbs, R. J.; Breare, J. M. (Univ. of Durham, Eng.). Nucl. Instrum. Methods; 103: No. 2, 389-93(1972).

The operating characteristics of sealed, current-limited spark chambers filled with 98% neon, 2% helium were studied and found to be similar to those of the more conventional chambers in many respects. However, some properties of the chambers show anomalous effects, which are suggested as being due to an internal electric field caused by the discharges. (5 figures, 1 table) (auth)

52284 2π STERADIAN MAGNETIC SPECTROMETER. McReynolds, J. F.; Newton, D.; Wenzel, W. A. (Univ. of California, Berkeley). Nucl. Instrum. Methods; 103: No. 2, 397-403 (1972).

The magnetic properties of a 2π-steradian spectrometer used in the study of K^+ decays at rest are described. Charged particles emitted from the axis of a cylindrically symmetric field are focused back to the axis after one nearly circular orbit. The field was shaped to give small spherical aberration and a relatively small overall chromatic aberration for momenta in a ten percent momentum range. Other possible experiments are described. (5 figures) (auth)

52285 CORRECTION OF LIGHT ATTENUATION IN LARGE SHOWER COUNTERS. Lakin, W. L.; Petraske, E. W.; Toner, W. T. (Stanford Univ., Calif.). Nucl. Instrum. Methods; 103: No. 2, 431-3(1972).

A simple procedure, based on elementary shower theory, was devised to compensate for attenuation losses over the surface of large sandwich-type shower counters. It uses tapered lead sheets in place of the usual flat plates, and is capable of compensating for attenuation of as much as a factor of two. (2 figures, 1 table) (auth)

Radiometric Instruments

52286 (N-71-37956) DESIGN OF A RADIOACTIVE NON-CONTACT ENCODER. Barnett, M. B. (National Aeronautics and Space Administration, Greenbelt, Md. Goddard Space Flight Center). Aug 1971. 20p. (NASA-TM-X-65715; X-721-71-349). NTIS.

A non-contact encoder device for the detection of radioactive sources is described. The device consists of: (1) encoder assembly; (2) radioactive source of Am-241 and (3) a semiconductor silicon diode detector. The theory of operations, performance, advantages, disadvantages, and applications are discussed. (STAR)

52287 EVALUATION OF A CROSS SECTION IONIZATION DETECTOR SUITABLE FOR MINE AIR ANALYSIS. Pursall, B. R.; Dugar, A. C. (Univ. of Sheffield, Eng.). J. Phys., E (London); 5: No. 9, 862-8(Sep 1972).

Detection of the permanent gases in mine air using the cross section ionization detection system is described. A dual chamber ionization cross section detector, with a tritium source, was designed and the results of analysis compared with the results obtained from an argon detector, with a ^{90}Sr source, in its cross section mode of operation. The performance characteristics of both the detectors suggest that the ionization cross section method is precise and reliable and capable of detecting a minute quantity of the test gas in the parts per million range or less. The performance characteristics were compared with those of other reported designs, but using carbon dioxide as the test gas instead of propane. The performance was measured by the exponential decay method of calibration and the construction of a dilution chamber containing a magnetically driven stirrer is described. It is suggested that a series of parallel column method of a balanced pair cross section detector system would reduce the random noise level and improve its performance characteristics still further. (auth)

52288 RADIOIZOTOPNYE RELE. IZDANIE ETOROE, PERERABOTANNOE I DOPOLNENNOE. (Radioisotopic Relays. Second Edition, Revised and Expanded). Vasil'ev, A. G.; Klempner, K. S. Moscow; Izdatel'stvo Mashinostroenie (1971). 176p.

Relays which utilize nuclear radiation sources are discussed, intensimetric and electrical aspects are examined. Considerable attention is given to reliability criteria for operating relays. Fundamental parameters of radioisotopic relays, their experimental determination, and the engineering design of relays are discussed. (104 references) (K.S.W.)

Radiation Effects on Instrument Components, Instruments, and Electronic Systems

Refer also to abstracts 53223, 53307—53309, 53338, and 53927.

52289 (NASA-TM-X-2440, pp 481-6) HARDENING ELECTRONIC DEVICES AGAINST VERY-HIGH-TOTAL-DOSE RADIATION ENVIRONMENTS. Buchanan, B.; Shedd, W.; Roosild, S.; Dolan, R. (Air Force Cambridge Research Labs., Bedford, Mass.). Jan 1972.

From Symposium on natural and manmade radiation in space; Las Vegas, Nev. (1 Mar 1971).

The possibilities and limitations of hardening silicon semiconductor devices to the high neutron and gamma radiation levels (greater than 10^{16} neutrons/cm^2 (1 MeV eq.) and greater than 10^8 rads (Si)) required for the NERVA nuclear engine development are discussed. A comparison is made of the high dose neutron and gamma hardening potential of bipolar, metal insulator semiconductor (MIS), and junction field effect transistors (JFET). Experimental data are presented on device degradation for the high neutron and gamma doses. Previous data and comparisons indicate that the JFET is much more immune to the combined neutron displacement and gamma ionizing effects than other transistor types. Presently, hardened JFET's degrade about 50% at 10^{16} neutrons/cm^2. Theoretically they can be improved, but the resulting hardened JFET's have low breakdown voltages (less than 20 volts). Experimental evidence (5 volt threshold shift at 10^8 rads) is also presented, which indicates that p channel MOS devices, made by Hughes Aircraft may be able to meet the requirements. Electrical characteristics compromises caused by device hardening and the ability to satisfy requirements on a practical reliable basis are discussed. (auth)

52290 (NASA-TM-X-2440, pp 577-83) SOLAR CELL RADIATION RESPONSE NEAR THE INTERFACE OF DIFFERENT-ATOMIC-NUMBER MATERIALS. Burke, E. A.; Cappelli, J. R.; Lowe, L. F.; Wall, J. A. (Air Force Cambridge Research Labs., Bedford, Mass.). Jan 1972.

From Symposium on natural and manmade radiation in space; Las Vegas, Nev. (1 Mar 1971).

The response of Co-60 irradiated N/P silicon solar cells was measured as a function of the atomic number of the medium adjacent to the cell and the direction of the gamma ray beam. The interpositioning of various thicknesses of aluminum between the adjacent material and the cell had the effect of moving the cell to various locations in an approximate monatomic numbered medium. Using this technique the solar cell response was determined at various distances from the interface for gold and beryllium. The results were compared with predictions based upon ionization chamber measurements of dose perturbations in aluminum and found to agree within five percent. Ionization chamber data were then used to estimate the influence of various base contact materials. The directional effect is most noticeable for gold contacts leading to a response when the beam enters the cell face which is 40% greater than for the opposite direction. The situation is reversed for beryllium which produces a response which is 17% greater when the beam enters through the base than for the reversed direction. (auth)

52291 (NASA-TM-X-2440, pp 708-13) RESPONSE OF A 300-μ SILICON DETECTOR TO MONOENERGETIC NEUTRONS DETERMINED BY THE USE OF THE MONTE CARLO TECHNIQUE. Taherzadeh, M.; Anno, G. (California Inst. of Tech., Pasadena). Jan 1972.

From Symposium on natural and manmade radiation in space; Las Vegas, Nev. (1 Mar 1971).

The response of a 300 μ thick silicon detector to an incident monoenergetic neutron beam is evaluated by the Monte Carlo method for the cases of both a shielded and a bare detector. The result of the Monte Carlo calculation, using elastic, inelastic and absorption reactions indicates that the response of the silicon detector to neutrons is basically due to the elastic scattering. In addition, the gamma rays generated in the shield of the detector will result in a response which is 3 or 4 orders of magnitude smaller than response to incident photons. The response of a bare silicon detector is calculated for neutron energies up to 6 MeV and bias energies from 50 to 250 keV. It is found that the maximum response for a 300 μ thick silicon detector is less than 4×10^{-3} c/n within this selected neutron and bias energy range. When the pulse height defect is introduced in the calculation, the results at low energy are reduced. The study was undertaken to evaluate the effects of radiation from radioisotope thermoelectric generators on detectors in space vehicles. (auth)

52292 (NASA-TM-X-2440, pp 729-34) RADIATION EFFECTS ON SCIENCE INSTRUMENTS IN GRAND TOUR-TYPE MISSIONS. Parker, Richard H. (California Inst. of Tech., Pasadena). Jan 1972.

From Symposium on natural and manmade radiation in space; Las Vegas, Nev. (1 Mar 1971).

The extent of the radiation effects problem is delineated, along with the status of protective designs for 15 representative science instruments. Designs for protecting science instruments from radiation damage are discussed for the various instruments to be employed in the Grand Tour type missions. A literature search effort has been undertaken to collect science instrument components damage/interference effects data on the various sensitive components such as Si detectors, vidicon tubes, etc. A small experimental effort is underway to provide verification of the radiation effects predictions. The various experimenters whose instruments are used as models have made available some of their own radiation effects experience for this study. (auth)

52293 (NASA-TM-X-2440, pp 735-43) RADIATION NOISE IN A HIGH-SENSITIVITY STAR SENSOR. Parkinson, J. B.; Gordon, E. (Aerojet ElectroSystems Co., Azusa, Calif.). Jan 1972.

From Symposium on natural and manmade radiation in space; Las Vegas, Nev. (1 Mar 1971).

An extremely accurate attitude determination has been developed by Aerojet Electro Systems Company for space applications. This system uses a high sensitivity star sensor in which the photomultiplier tube is subject to noise generated by space radiations. The space radiation induced noise arises from trapped electrons, solar protons and other ionizing radiations, as well as from dim star background. The individual noise components have been successfully simulated for pre-flight evaluation of the star sensor performance. The steady trapped electron and the intermittent solar proton environments for a high altitude orbit are related to solar activity. The solar activity and hence the electron and proton environments are predicted through the end of the twentieth century. The available data for the response of the phototube to proton, electron, gamma ray, and bremsstrahlung radiations are reviewed and new experimental data are presented. Prompt and delayed pulses from the faceplate/photocathode and contributions from the dynodes are isolated, and pulse height distributions are given for each. The predicted electron and proton environments are then combined with phototube response. The average noise due to the relatively steady electron environment is of the order of 10^4 pulses per second compared with 2×10^5 pulses per second for the signal from a single 4.6 magnitude star. For a typical worst solar proton event, the noise will be 10^5 to 10^6 pulses per second, which is comparable to the signal from a nominal 4.6 magnitude star. This noise will typically last about one day. The model for the dim star background averages 3×10^4 pulses per second but varies widely. A simulation was developed which represents the characteristics of the effect of radiations on the star sensor, including the non-stationarity of the backgrounds. (auth)

52294 (NASA-TM-X-2440, pp 866-72) PROGRAM AT JPL TO INVESTIGATE THE NUCLEAR INTERACTION OF RTGs WITH SCIENTIFIC INSTRUMENTS ON DEEP SPACE PROBES. Truscello, Vincent (California Inst. of Tech., Pasadena). Jan 1972.

From Symposium on natural and manmade radiation in space; Las Vegas, Nev. (1 Mar 1971).

A major concern in the integration of a radioisotope thermoelectric generator (RTG) with a spacecraft designed to explore the outer planets is the effect of the emitted radiation on the normal operation of scientific instruments. The program presently being conducted at the Jet Propulsion Laboratory to evaluate these effects is discussed. The problem is being approached in both an analytical and experimental manner. The necessary techniques and tools have been developed to allow accurate calculation of the neutron and gamma spectrum emanating from the RTG. The specific sources of radiation have been identified and quantified. Monte Carlo techniques are then employed to perform the nuclear transport calculations. The results of these studies are presented. An extensive experimental program has been initiated to measure the response of a number of scientific components to the nuclear radiation. Such devices as Geiger-Muller tubes, solid-state detectors, and electron multipliers have been identified as being most probable for use on these missions and extremely sensitive to gamma radiation. Experiments on these devices are being conducted in the JPL radiation laboratory. The capabilities of this laboratory are discussed as well as the results of some of the experiments. The technique used to measure the response of instruments is to irradiate them with monoenergetic radiation sources. The energy range of interest is between 275 and 2800 keV. Approximately seven isotopes have been selected which provide emissions in this range. Analytical techniques have been developed which fold the measured energy response of the instrument with the calculated energy spectrum emitted by the RTG. Shielding studies are then performed to determine the thickness of shield required to reduce the spurious count level of the instrument to an acceptable level. The final design must be qualified by irradiating the instrument with the polyenergetic spectrum emitted by the ^{238}Pu fuel capsule. Since actual fuel capsules are not generally available and since the spectrum from a generator will change with time due to aging of the fuel (spectrum actually becomes harder and more intense due to buildup of the daughter products of the impurity ^{236}Pu) it becomes more practical to use simulated sources. (auth)

Miscellaneous Instruments and Components

Refer also to abstracts 52957, 53421, 53648, 54971, 54972, 54975, 55122, and 55448.

52295 (AREAEE-132) TRANSISTORIZED PULSE GENERATOR FOR TESTING NUCLEAR COUNTING EQUIPMENT. Hanna, Nabil N. (Atomic Energy Establishment, Cairo (Egypt). Engineering and Scientific Instruments Dept.). 1972. 21p. Dep. NTIS (U. S. Sales Only).

A multirange pulse generator for supplying positive and negative rectangular output pulses of adjustable amplitude over the range 0 to 10 V is described. The repetition rate is continuously adjustable from 10 Hz to 100 kHz in 4 ranges. Pulse duration is variable from 1 μsec to 10 msec in 4 ranges with rise and fall times of less than 40 nsec. The output impedance is 50 ohms and the generator can be operated at duty cycles of up to 0.8. The generator can be triggered from the positive slope of external synchronizing signals whose frequency may range from D.C. to 500 kHz to deliver delayed rectangular pulses of the desired height and duration. The minimum triggering level can be adjusted in the range 0 to 10 V. The delay is continuously variable from 0 to 10 msec in 4 ranges. The generator is fully transistorized and of simple design. The relatively high stability of pulse parameters makes it particularly useful for testing nuclear counting equipment. (auth)

52296 (CEA-N-1539) STUDY AND DEVELOPMENT OF TWO HIGH PERFORMANCE SPECTROMETER MAGNETS. de Sereville, Bernard; Ohayon, Maurice; Penicaud, Jean-Pierre; Turck, Bernard (Commissariat a l'Energie Atomique, Saclay (France). Centre d'Etudes Nucleaires). Jun 1972. 71p. (In French). Dep. NTIS (U. S. Sales Only).

Two high-performance spectrometer magnets (window frame type) were constructed. Detailed analysis of the possible causes of error in the measurement of the magnetic field was used to determine the precision with which the equipment had to be constructed and the accuracy with which the measurements had to be made. The two-dimensional program MARE-C was used to investigate the magnetic field and to determine its effect on the coil structure. The study of the fringing magnetic field was performed with the same program, a similar aperture magnet being used. The radius of the magnetic fringing field was determined with an accuracy better than 1%. The forces acting on the coils and the important aspects concerning their construction are presented. The principal experimental results are given. (France)

52297 (CEA-N-1549) CAMAC SYSTEM: PRACTICAL INFORMATION FOR A COMPUTERIZED TREATMENT. Gallice, Pierre; Robin, Georges (Commissariat a l'Energie Atomique, Saclay (France). Centre d'Etudes Nucleaires). May 1972. 20p. (In French). Dep. NTIS (U. S. Sales Only).

The CAMAC system is an international system, defined by the Comite ESONE (EURATOM), which can be used in conjunction with several types of computers. The interconnection system between the digital nuclear physics equipment and a computer is described. Complementary information is given on the adapting of a particular language to the system with the normal programming envisaged. (France)

52298 (COO-3058-9) ECONOMICAL SCALER DRIVER. Krycuk, G.; Tatarczuk, J. R. (Rensselaer Polytechnic Inst., Troy, N. Y. Dept. of Nuclear Science). 1972. Contract AT-(11-1)-3058. 6p. Dep. NTIS.

A scaler driver is described which permits the driving of slow scalers and slow nuclear modules with fast nuclear pulses of the order of 10 nanoseconds FWHM. The output of the device is a 4.25 volt square pulse when terminated in 50 ohms and is variable in width from 100 to 800 nsec. Since the output is transformer coupled positive or negative pulses may be obtained. The device is constructed of three integrated circuits including (1) a Motorola MC1545L pulse amplifier, (2) a TI SN74121 multivibrator, and (3) a TI SN75450 driver. (W.H.K.)

52299 (COO-3058-10) GATEABLE DELAY-GATE GENERATOR. Tatarczuk, J. R. (Rensselaer Polytechnic Inst., Troy, N. Y. Dept. of Nuclear Science). 1972. Contract AT(11-1)-3058. 4p. Dep. NTIS.

A delay-gate generator for gating of scalers and other instruments and for timing synchronization of slow coincidence pulses is described. The unit consists of five integrated circuits which are diagramed. (W.H.K.)

52300 (EUR-4797) CALIBRATION METHODS OF VACUUM TECHNIQUE. Eschbach, H. L. (European Atomic Energy

Community, Geel (Belgium). Central Nuclear Measurements Bureau). 1972. 34p. (In German). Dep. NTIS (U. S. Sales Only).

The calibration of vacuum gauges and their recalibration have in recent years become more and more important. On one hand, the evaluation of scientific experiments at low pressures very often depends on a precise knowledge of the actual gas density (sorption, diffusion, heterogeneous catalysis). On the other hand, precise pressure measurements are of equal importance for many industrial applications of vacuum technique (determination of pumping speed, conductance, outgassing rates). For some years national and international organizations (PNEUROP, ISO) have been collaborating to establish general rules and regulations to ensure unambiguous and reliable pressure measurements. These difficult investigations have led in some cases to internationally acknowledged norms; in others, only preliminary proposals are available. A short introduction into the problems of precise (absolute) physical measurements is given first; the special difficulties encountered in the absolute measurement of gas densities are then discussed. The efforts to arrive at primary standards for all pressure regions are mentioned. Calibration methods for secondary standards are of special importance for many practical applications. Advantages and disadvantages of methods developed to this end are discussed. (10 figures, 2 tables) (auth)

52301 (EUR-4807) MANUFACTURING SPECIFICATION FOR HIGH TEMPERATURE THERMOCOUPLES FOR USE IN NUCLEAR IRRADIATION EXPERIMENTS. Mason, F. (European Atomic Energy Community, Petten (Netherlands). Joint Nuclear Research Center). 1972. 42p. Dep. NTIS (U. S. Sales Only). EUR B. Fr. 50.-.

This specification details the requirements for materials of construction, methods of manufacture, test procedures, certification, and packing, together with acceptable standards of ancillary processes, which are to be employed in the production of high-temperature mineral-insulated thermocouple units for irradiation experiments. (8 figures, 10 tables) (auth)

52302 (EUR-5100) CAMAC: A MODULAR INSTRUMENTATION SYSTEM FOR DATA HANDLING. SPECIFICATION OF AMPLITUDE ANALOGUE SIGNALS. (European Atomic Energy Community, Ispra (Italy). Joint Nuclear Research Center). 1972. 10p. Dep. NTIS (U. S. Sales Only). EUR B. Fr. 25.-.

Amplitude analog signals which are recommended for use by CAMAC compatible units are specified. (W.H.K.)

52303 (LA-4999) PROBE VELOCITY TRANSDUCER. Starkovich, V. S.; Todd, B. E.; Stephani, E. L.; Hawkins, E. V. (Los Alamos Scientific Lab., N. Mex.). Sep 1972. Contract W-7405-eng-36. 6p. Dep. NTIS.

A simple velocity transducer for determining x-ray-produced blowoff impulse is described. The device does not require active calibration, and can operate over a wide dynamic range in severe nuclear radiation environments. (6 figures, 3 tables) (auth)

52304 (LIB/Trans-431) EXAMINATION OF BURNOUT DETECTORS BY DIFFERENTIAL CIRCUIT METHODS. Kitayama, Yoshifumi; Namba, Shyunji; Kuniyasu, Yoshihito. Translated for Australian Atomic Energy Commission, Lucas Heights from Nippon Genshiryoku Gakkaishi; 14: No. 4, 9-13(1972). 8p. Dep. NTIS (U. S. Sales Only).

An abstract of this article taken from the original appeared as NSA 26: 33538 (1972). (Australia)

52305 (LMEC-72-4) TRANSIT TIME FLOWMETER: SIX-INCH-DIAMETER WATER AND SODIUM TESTING SUMMARY. De Muri, R. J. (Atomics International, Canoga Park, Calif. Liquid Metal Engineering Center). 15 Aug 1972. Contract AT(04-3)-700. 84p. Dep. NTIS.

An evaluation of the feasibility of using the Transit Time Flowmeter as a precise measurement system for volumetric flow in large circular ducts is presented. The development test program was conducted by Atomics International. The 6-in.-diameter Transit Time Flowmeter was tested in water and liquid sodium systems, following previous work on a smaller 2-in.-diameter device. Operation at elevated temperatures in sodium was satisfactory with the test data indicating an observed bias in measured flow of from 1% low to 5% high and a maximum error of from ±4% to ±9% in water and ±9% to ±15% in sodium. Based on the results of this test program, it is anticipated that a precalibrated device of this size could be built to measure flow velocity to a maximum error of ±3%. (auth)

52306 (RFP-1902) TIME DOMAIN REFLECTOMETRY FOR LIQUID LEVEL MEASUREMENT. Lehmkuhl, George D. (Dow Chemical Co., Denver, Colo. Rocky Flats Div.). 21 Aug 1972. Contract AT(29-1)-1106. 7p. Dep. NTIS.

The time domain reflectometry technique was used to measure liquid levels in a tank. Remote readings of liquid level were easily obtained. The state of the art allows direct readout of volume, level, or pulse travel time through use of proper calibration techniques and a computer—calculator. Calibration and readout using the same fluid allowed level measurement of ±0.3 cm. When solutions of different ionic strengths were used for calibration and readout, the errors in liquid level measurement varied from ±1 cm to ±4 cm. The magnitude of the error depended on the difference in ionic strength and on the trigger voltages used in the electronic instrumentation. (6 figures) (auth)

52307 (SC-DC-721159) RADIATION TOLERANT GATED VIDEO AMPLIFIER. Gray, R. M.; Petty, T. D. (Sandia Labs., Albuquerque, N. Mex.). [nd]. 10p. (CONF-721011-1). Dep. NTIS.

From Government microcircuit applications conference; San Diego, CA. (10 Oct 1972).

The circuit described is a radiation tolerant, gated, differential video amplifier. The amplifier is an all PNP design realized in monolithic integrated circuit form, featuring dielectric isolation, thin film resistors, and gold beam leads. (6 figures) (auth)

52308 (SC-DC-721161) UNIVERSAL DIGITAL INTEGRATED CIRCUIT. Gray, R. M.; Skogmo, D. G. (Sandia Labs., Albuquerque, N. Mex.). [nd]. 13p. (CONF-721011-2). Dep. NTIS.

From Government microcircuit applications conference; San Diego, CA. (10 Oct 1972).

The Universal Digital Integrated Circuit (UDIC) is a radiation-tolerant, beam-leaded design capable of forming with appropriate external pin interconnections any one of four digital circuits. (9 figures, 1 table) (auth)

52309 (SC-DC-721162) DIAMOND: A NEW APPROACH TO MICROELECTRONIC CIRCUIT DESIGN (DIELECTRICALLY ISOLATED ARRAYS OF MONOLITHIC DEVICES). Williams, J. D.; Skogmo, D. G. (Sandia Labs., Albuquerque, N. Mex.). 1970. 11p. (CONF-721011-3). Dep. NTIS.

From Government microcircuit applications conference; San Diego, CA. (10 Oct 1972).

DIAMOND is an approach to microelectronic circuit design which reduces many of the problems associated with the design and procurement of radiation-tolerant integrated circuits. Building block standardization is achieved while allowing special-purpose circuits, when required. (5 figures, 1 table) (auth)

52310 (SC-DC-721302) RETARDING FIELD-CYLINDRICAL MIRROR ANALYZER. Gerlach, Robert L. (Sandia Labs., Albuquerque, N. Mex.). 1971. 15p. (CONF-721003-1). Dep. NTIS.

From nineteenth national vacuum symposium; Chicago, IL. (2 Oct 1972).

An electron energy analyzer system incorporating a two-stage spherical retarding field-cylindrical mirror analyzer as well as high-current, coaxial and glancing incidence electron guns is described. The retarding field and cylindrical mirror analyzers act as high-pass and band-pass energy filters, respectively. The resulting two-stage device has the advantages of both types of analyzers: low shot noise, high transmission, adjustable energy resolution, nearly constant energy resolution and transmission as a function of band-pass energy, and relative insensitivity to sample positioning. The glancing incidence electron gun is mounted directly on the front of the analyzer and is bore sighted onto the sample; the need for deflection electrodes is thereby avoided. Design and performance of this system are examined. (5 figures) (auth)

52311 (UCRL-51130(Vol.8)) FINAL REPORT ON THE DEVELOPMENT OF THE GEOGRAPHICAL POSITION LOCATOR (GPL). VOLUME 8. TECHNICAL SUPPORT. Aley, R. E.; Schiff, A. (California Univ., Livermore. Lawrence Livermore Lab.). 19 Oct 1971. Contract W-7405-eng-48. 56p. Dep. NTIS.

The Geographical Position Locator "A" (GPL-A) system, consisting of a commercial aviation inertial navigation unit and a small external computer, was installed in an instrumented van so that the mathematical error-reduction techniques developed for the GPL system could be tested under realistic conditions. This volume of the GPL final report gives technical descriptions of the equipment assembled for this testing and discusses the various programs that were written for such functions as controlling the inertial platform, calculating position and velocity information, error reduction, motion sensing, and data logging. (38 figures, 9 tables) (auth)

52312 NETWORK FOR ACQUIRING AND REMOTE HANDLING OF DATA USING A SMALL COMPUTER. Le Sourne, M.; Girod, J. J. (CEN, Grenoble, France). Rev. Fr. Automat. Inform. Rech. Oper.; 6: No. B-1, 75-91(Jan 1972). (In French).

A description is given of the transmission network installed at the CEN Grenoble which provides a rapid connection between experimenters and a data processing computer (IBM 360-50) located a few kilometers away at the computer center. The connection is made using a collecting computer (CII 90—10) and a central make-and-break unit which controls the whole network. The transmission line consists of two coaxial cables distributed in the various buildings. The experimenters connect to these cables by an intermediate terminal. The following devices can be hooked up: multichannel analyzers, block memories, other small computers, and type uniters with paper tape readers and punches. The users have access to processing programs, and catalogs stored on the IBM 360 disks, which can be readily connected to a teletyping machine. The connection is two directional and the results of calculations effected at the center are quickly reviewed by the user. The transmission rate is 750 Kbauds with a useful information transmission rate of 10^5 bits/second. (France)

52313 SAFETY DEVICE FOR REMOVING TRITIUM GAS FROM A GAS STREAM. Benson, Royal H.; Bodre, Robert J. (to Monsanto Co.). U. S. Patent 3,679,366. 25 Jul 1972. Filed 9 Jan 1970.

A safety device for removing tritium gas from flowing fluid streams is described. It is comprised of a means to convert the tritium in the stream to a labile-tritium-containing compound and a trapping means connected to the conversion means such that the fluid stream, upon exiting from the conversion means, flows through the trapping means; the trapping means comprises a means to prevent the escape of the labile-tritium-containing compound to atmosphere. In a specific embodiment, the invention is a safety device for use in combination with gas chromatographic detectors of the electron-capture type, which employ a tritiated material as a source of beta radiation. In these devices the converter means is connected to the outlet of the detector and the trapping means, which in the preferred embodiment takes the form of a tritium-exchange means, is connected to the outlet of the converter means such that the tritium in the labile-tritium-containing compound is exchanged with labile hydrogen in the tritium-exchange means. (2 figures) (auth)

52314 CARRIER TRANSPORT AND STORAGE EFFECTS IN Au ION IMPLANTED SiO_2 STRUCTURES. Chen, L. I.; Pickar, K. A.; Sze, S. M. (Bell Telephone Labs., Murray Hill, N. J.). Solid-State Electron.; 15: No. 9, 979-86(Sep 1972).

To investigate the possibility of fabricating a multilayer gate IGFET using an ion-implanted floating electrode, an MOS structure was made using thermally grown SiO_2 layers into which 100-keV Au^+ ions were implanted. The effects of ion dose (10^{12} to 10^{14} cm^{-2}) oxide thickness (500 to 1000 Å) and postimplantation annealing treatment on the capacitance—voltage and current—voltage characteristics were studied. A significant flatband voltage shift is observed for ion doses larger than 10^{13} cm^{-2}. Most of the interface states created by the implantation damage anneal at 400°C ($N_{ss} \sim 10^{10}$ cm^{-2} for oxide thickness 750 Å). The carrier transport mechanism of the implanted SiO_2 layer is converted from Fowler—Nordheim tunneling conduction to Frenkel—Poole bulk conduction with a trapping energy level 1.2 eV below the oxide conduction band. From these mechanisms the flatband voltage shift due to electrons trapped at assumed localized Au charge storage centers is predicted. This reversible shift is experimentally confirmed by C—V measurements. The time required for a 1-V flatband shift is about 10^{-3} sec when a field of 10^7 V/cm is applied. Thus the resulting MOS structure behaves similarly to a floating gate or multilayer device with obvious simplifications in the processing. It is believed that improvements in reducing the charging time and the writing voltage may be realized by the use of thinner oxides in conjunction with lower implantation energies. (auth)

52315 POTENTIAL MEASUREMENT AND STABILIZATION OF AN ISOLATED TARGET USING ELECTRON BEAMS. Kudirka, P. E.; Crawford, C. K. (Massachusetts Inst. of Tech., Cambridge). Solid-State Electron.; 15: No. 9, 987-92(Sep 1972).

The construction of very large arrays of electronic components on a single semiconductor chip implies a need for new methods of component testing. The presently used contact pads take up too much space. The method proposed uses primary electron beams to excite low-energy secondary electrons which are used to sense surface potentials. The primary electrons are to be allowed to strike only very small diameter metallic contact areas on the interior of a chip, in an environment where surface electric fields are carefully controlled (i.e., no exposed insulator surfaces). Data are presented for a preprototype system using a mockup target and a single large-diameter electron beam. Two operating modes, potential stabilization (corresponding to voltage signal input) and potential measurement (corresponding to voltage signal output), were demonstrated. Accuracies better than 100 mV were observed for both modes using a 5 kV, 10^{-6} A, primary beam. If the method could be extended to multiple small-diameter beams, it could be used to simultaneously inject several voltage signals while measuring output signals from extremely small microcircuits. (auth)

52316 VTAB, PASSIVE IMPULSE GAGE (31 Mar 1972) (Engineering Materials). (California Univ., Livermore. Lawrence Radiation Lab.). (CAPE—2254).
30 drawings.

This passive impulse gage for impulse measurements in a nuclear environment is unaffected by ground motion of 30 to 50 g and using design tradeoffs can be made to extend this level to 1000 g or more, depending on the sample and impulse levels to be measured. A single gage can be designed so that its measuring range is 15 to 20 times its threshold value. The configuration of the gage is a cantilever beam with a sample attached to the free end. The fixed end bends over a curved angle of known radius which serves to define the maximum strain in the beam so that the ultimate strain is not exceeded and plastic bending occurs over some distance rather than at a point. By increasing the width of the beam linearly, starting at the fixed end, the calibration curve of impulse versus angle of bend is nearly linear rather than parabolic as in most passive impulse gages. This gage is relatively inexpensive, for applications in a hostile radiation environment. The gage is relatively insensitive to extraneous shock. An associated computer code, VTAB, calculates design parameters and predicts gage response (30 drawings) (For details see TID-4100 Suppl. 72) (see also 26: 22917) (F.S.)

52317 PASSIVE CRACK-DETECTING SYSTEM (2 Apr 1971) (Engineering Materials). (California Univ., Livermore. Lawrence Radiation Lab.). CAPE—2191).
18 drawings.

This passive-recoverable system determines when a crack occurs in a part which is exposed to neutron radiation. During the first 100 msec after a crack occurs, the part is subject to large thermal stresses and g loading. The assembly can get as warm as 200°F after exposure. This system includes a conductive strip, neutron switch, inertia or g switch, batteries, and tapers. Cracks of ½ mil or larger are detected. Assemblies withstand tests in high g environment as well as at 300°C with no interruption of conductivity (more than 30 kΩ resistance). (18 drawings) (For details see TID-4100 Suppl. 70) (F.S.)

52318 VACUUM LOCK FOR THERMAL-IONIZATION-SOURCE MASS SPECTROMETER (14 Oct 1971) (Engineering Materials). (New Brunswick Lab. (AEC), N. J.). (CAPE—2193).
15 drawings.

A vacuum lock for use on a 12 in. radius multiple-filament-source mass spectrometer reduces sample change time by reducing the volume which must be evacuated to a minimum to allow sample insertion into the vacuum system without disturbing the vacuum significantly. The lock consists of a sample insertion bar, which is supported by "O"-rings fitted into the wall of an evacuation cylinder, and a two inch gate valve located between the source housing and the evacuation cylinder to isolate the source region when a sample is changed. Sample analysis times have been reduced by 50%, from 1 hr to 30 min. Two additional advantages of the lock are: the accelerating voltage (14 kV) no longer has to be turned off during the sample change, and therefore requires no re-stabilization time; the operating pressure of 10^{-6} torr in the source region is lower than that of 2×10^{-6} torr when the vacuum lock is not used. (15 drawings) (For details see TID-4100 Suppl. 70) (see also 25: 39411) (F.S.)

52319 CRYSTAL MOUNT FOR THREE- OR FOUR-CIRCLE X-RAY OR NEUTRON DIFFRACTOMETERS (10 Jul 1972) (Engineering Materials). (Oak Ridge National Lab., Tenn.). (CAPE—2244). 3 drawings.

A crystal mount can be used in place of a goniometer on three- or four-circle x-ray and neutron diffractometers. Such a crystal mount consists of a base and an inexpensive insert for the base. The base provides two of the motions needed to center the specimen and is left on the diffractometer. The crystal is mounted on the insert which also provides the third positioning motion. A key on the insert insures replacement of the insert without change of orientation of the crystal. During the course of crystal structure investigation, it may be necessary to remove the single crystal from the diffractometer several times. The crystal mount prohibits the loss of the knowledge of specimen orientation, saves tieing up the goniometer head, is less expensive, more stable with less bulk, and is less likely to collide with the beam tunnels used on x-ray diffractometers. (3 drawings) (For details see TID-4100 Suppl. 72) (F.S.)

52320 SHAPER WITH UNIVERSAL LOGIC OF OPERATION. Basiladze, S. G. (Joint Inst. for Nuclear Research, Dubna, USSR). Nucl. Instrum. Methods; 103: No. 2, 357-9(1972).

A pulse shaper is described which has a proper dead time of 9 ns and which makes possible pulse counting up to 100 MHz, independent of the nominal duration of the output pulse (smoothly controlled within 5 to 20 ns). The nominal sensitivity of the shaper is 100 mV, and the range of its control is 50 to 350 mV. Electronic control of the duration of the output pulse and the threshold is provided. (4 figures, 1 table) (auth)

52321 DESIGN AND DEVELOPMENT OF A RANDOM PULSE SAMPLER. Khan, M. S.; Vallee, R. L. (Atomic Energy Centre, Dacca, Bangladesh). Nucl. Instrum. Methods; 103: No. 2, 361-4 (1972).

In nuclear experiments it is often required to design an instrument capable of detecting pulses from among a train of random pulses produced by nuclear reactions. An asynchronous random pulse sampler is developed to sample out the first pulse in amplitude and width from among the trains of random pulses. The pulse that arrives immediately after the command "a = 1" is given is considered as the first pulse. Now if, during the transition (0 → 1) of "a" a pulse is already present, then the second pulse must be considered as the first pulse, which must be sampled out. All the first pulses must be sampled entirely in amplitude and width even if the gate "a" closes before the sampling of a first pulse is complete. (7 figures) (auth)

52322 GONIOMETER FOR IMPLANTATION AND CHANNELLING EXPERIMENTS. Pegoraro, A.; Quirci, G. (Joint Nuclear Research Center, Ispra, Italy). Nucl. Instrum. Methods; 103: No. 2, 417-20(1972).

A two-axis goniometer is described, together with facilities for heating or cooling the sample for implantation and channeling experiments. A direct visual control allows an accuracy of 0.05° on both axes, independent of the forward or reverse rotation. (4 figures) (auth)

52323 OPTIMUM CHOPPING. Pearce, J. B. (Univ. of Colorado, Boulder). Nucl. Instrum. Methods; 103: No. 2, 435-6 (1972).

The optimum value of the open aperture fraction for a chopper is derived. The penalty for use of a nonoptimum value is assessed. (2 figures) (auth)

52324 AUTOMATIC DATA ACQUISITION AND REGISTRATION FROM MASS SPECTROMETER. Hoffman, Zbigniew; Kulka, Zbigniew; Sawicki, Aleksander (Inst. of Nuclear Research, Swierk, Poland). Nukleonika; 17: No. 3-4, 217-25(1972).

The instrument serves to digitize voltages representing ion intensity of the mass spectrometer and to print them in digital form together with the time value corresponding to the position of registered peak. The data are printed during the measurement by means of a teleprinter. At the end of the experiment the sum of all registered peak values is printed. A general description of the logic system and electronics used in the instrument is given. (9 figures) (auth)

ISOTOPE AND RADIATION SOURCE TECHNOLOGY

52325 (BNL–50335) BIBLIOGRAPHY OF TECHNICAL PUBLICATIONS AND REPORTS OF THE RADIATION DIVISION, BROOKHAVEN NATIONAL LABORATORY, JULY 1968–JUNE 1971 INCLUSIVE. Kopp, L. E.; Metz, D. J. (Brookhaven National Lab., Upton, N. Y.). Jan 1972. 4p. Dep. NTIS.

A listing of technical publications and reports issued by the BNL Radiation Division from July 1968 through June 1971 is given. References to literature on radiation engineering, process and material development, atmospheric diagnostics, and basic and exploratory research are included. (T.D.)

Isotope Separation (Industrial)

Refer also to abstracts 52975, 52977, 53067, and 53088.

52326 (AREAEE–131) EMPIRICAL EXPRESSIONS FOR THE THERMAL DIFFUSION COLUMN SHAPE FACTORS IN THE EXTREME CYLINDRICAL CASE. Youssef, A.; Saad, S. M.; Hanna, M. M. (Atomic Energy Establishment, Cairo (Egypt). Nuclear Physics Dept.). 1971. 19p. Dep. NTIS (U. S. Sales Only).

Empirical expressions are introduced for the thermal diffusion column shape factors. They were chosen to be simple analytical functions of the ratio of hot-wall to cold-wall temperatures (θ) and the ratio of the cold-wall to hot-wall radii (R) which satisfy certain boundary conditions. These empirical relations are found to reproduce the tabulated values of the shape factors with a sufficient degree of accuracy. They will help to calculate the shape factors for all possible values of θ and R, and for molecules governed by an arbitrary inverse-power potential instead of the interpolation process which has to be applied in conjunction with the tables provided in order to obtain the shape factors corresponding to any particular case. (auth)

52327 (JEN–244) ISOTOPIC SEPARATION BY CENTRIFUGATION. ROTATING PLASMA. Perello, M.; Vigon, M. A. (Junta de Energia Nuclear, Madrid (Spain). Division de Fisica). 1972. 45p. (In Spanish). Dep. NTIS (U. S. Sales Only).

The motion of a gas simultaneously submitted to an electric discharge and a magnetic field was studied in order to analyze the possibility of producing isotope separation by rotation of a plasma. Some experimental results obtained under different discharge conditions are given. Differences of pressure up to 15 mm between both electrodes was attained. No definite conclusion on separation factors could be reached because of the low reproducibility of results, probably due to the short duration of the discharge with a new chamber designed to support stronger thermal shocks more reliable data can be expected. (auth)

52328 URANIUM ENRICHMENT. Benzler, Hartwig. Euro-Spectra; 10: No. 3, 66-72(Sep 1971).

Uranium enrichment by gaseous diffusion, gas centrifugation, and nozzle separation processes are reviewed. Principles of operation, separating capacity, energy consumption, capital expenditures and development potential for each process are discussed. (T.D.)

52329 METHODS OF CALCULATION ON A STEP CASCADE FOR ENRICHING URANIUM. Yamashita, Shizuo (Sumitomo Atomic Energy Industries, Ltd., Tokyo). J. Nucl. Sci. Technol. (Tokyo); 9: No. 8, 480-9(Aug 1972).

A method of calculation is proposed for finding the exact total flow rate of the entering stream fed to the separator in a step cascade in steady state and without losses. The method can be applied without approximation even to step cascades constituted of separators with large values of separation factor. A method of approximation is also presented for application to the case of infinitesimal separator. The reflux in each step can be chosen such that the total flow rate of the entering stream fed to the separator in the step cascade is minimized. The effect on the total flow rate of the entering stream in the step cascade brought by such factors as the mole fraction of production, the number of steps, and the separation factor are revealed from the results of calculation using these methods. The optimization of the stripping section is found to be important for the design of plants producing low-enriched uranium required for nuclear power generation. (auth)

Isotopic Power Sources

Refer also to abstracts 53094, 53551, and 54921.

52330 (BNWL–1308-10) PACIFIC NORTHWEST LABORATORY, ISOTOPE DEVELOPMENT PROGRAMS QUARTERLY REPORT: FEBRUARY–APRIL 1972. Jarrett, J. H. (comp.) (Battelle Pacific Northwest Labs., Richland, Wash.). May 1972. Contract AT(45-1)-1830. 40p. Dep. NTIS.

Research progress is reported on low cost Cs and Sr sources, and development of uses for fission products such as Rh, Pd, Ru, and Tc. Research on neutron radiography using ^{252}Cf is also reported along with results of work on advanced source development, circulatory support systems, and nuclear techniques for seabed mineral exploration. (J.R.D.)

52331 (CEA-CONF–2026) SAFETY ASPECTS OF SEALED ^{238}Pu SOURCES USED IN PACEMAKERS. Boucher, Rene; Barthelemy, Pierre; Milet, Claude (Commissariat a l'Energie Atomique, Fontenay-aux-Roses (France). Centre d'Etudes Nucleaires). 1972. 26p. (In French). (CONF-720519–3). Dep. NTIS (U. S. Sales Only).

From 2nd international symposium on power from radioisotopes; Madrid, Spain (29 May 1972).

A very refined canning was developed, which ensures the complete confinement of the radioisotope. The various safety aspects studied involve: specifications concerning radioactive materials in special form; recommendations formulated by the Study Group on Isotopic Batteries of the ENEA; complementary studies necessary for the manufacture of the sources. The sealed capsules developed are very safe. (France)

52332 (MLM–1150) PREPARATION OF ^{238}Pu METAL. Lonadier, F. D.; Griffo, J. S. (Mound Lab., Miamisburg, Ohio). 12 Oct 1962. Contract AT-33-1-Gen-53. 19p. Dep. NTIS.

The chemical procedures and the processing equipment to prepare plutonium-238 metal for SNAP heat sources are described. Plutonium nitrate is precipitated as the oxalate, the oxalate is converted to the fluoride, and the fluoride is reduced to the metal. Techniques to store and cast the metal are also described. (auth)

52333 (MLM–1213) STUDIES OF ^{238}Pu FUEL FORMS AND THEIR CONTAINMENT. Powers, J. A. (Mound Lab., Miamisburg, Ohio). 8 May 1964. Contract AT-33-1-Gen-53. 10p. Dep. NTIS.

Declassified 2 Nov 1971.

Several forms of the plutonium-238 isotope are being considered for use as radioisotopic heat sources. Compatibility studies of the fuel forms with container materials for various applications are also being carried on. Of the forms studied, plutonium metal is the least desirable for high-temperature applications. The stability, ease of handling, and high melting point of plutonium dioxide make it the first choice among the alternate fuel forms. (auth)

52334 (MLM–1228) ^{210}Po ISOTOPIC FUELS. Kershner, C. J.; Lonadier, F. D. (Mound Lab., Miamisburg, Ohio). 18 May 1964. Contract AT-33-1-Gen-53. 13p. Dep. NTIS.

Declassified 2 Nov 1971.

The physical, chemical, and radiochemical properties of polonium-210 were studied. The properties of polonium-210 are reviewed, and it is shown that the isotope has many properties that make it attractive as an isotopic fuel for SNAP programs. Information concerning various fuel forms and container materials are presented. (auth)

52335 (NASA-TM-X–2440, pp 850-2) DESIGN OF A SOURCE TO SIMULATE THE GAMMA-RAY SPECTRUM EMITTED BY A RADIOISOTOPE THERMOELECTRIC GENERATOR. Reier, Melvin (California Inst. of Tech., Pasadena). Jan 1972.

From Symposium on natural and manmade radiation in space; Las Vegas, Nev. (1 Mar 1971).

A simulated source was designed to duplicate the gamma spectrum of a uniform cylindrical 2200-W PuO_2 radioisotope thermoelectric generator (RTG) containing 81% ^{238}Pu and 1.2 ppm ^{236}Pu. Gamma rays from the decay of ^{238}Pu, ^{241}Am, ^{239}Pu, and the $^{18}O(\alpha,n)^{21}Ne$ reaction were cataloged in broad energy groups. ^{236}Pu, which decays ultimately to ^{228}Th, was treated separately, since an exact duplicate can be made by using ^{228}Th. The selection of sources involves a compromise between half-life, cost, and gamma energy. ^{133}Ba($T_{1/2}$ = 7.2y), ^{137}Cs($T_{1/2}$ = 30y), and ^{60}Co($T_{1/2}$ = 5.2y), which provide gamma rays to cover the spectrum from about 350 keV to 1.3 MeV were chosen. Two 46 and one 22 mCi ^{228}Th sources provide simulation at various times in the life of the fuel capsule up to 18 years, which covers the time span of an outer planet mission. The emission from the ^{228}Th represents the overwhelming contribution of the gamma spectrum after the first few years. Therefore, the small changes in the intensity of the rest of the spectrum represent a minor perturbation on the entire spectrum. The sources, in the form of 13-inch long rods, are placed in a concentric hole in a cylinder of depleted uranium which provides shielding equivalent to the self shielding of the fuel capsule. The thickness of the ^{238}U cylinder (0.55 cm) was determined by Monte Carlo calculations to insure that the spectrum emerging from the simulated source closely matched that of the fuel capsule. (auth)

53336 (NASA-TM-X-2440, pp 853-8) SOME NEUTRON AND GAMMA RADIATION CHARACTERISTICS OF PLUTONIUM CERMET FUEL FOR ISOTOPIC POWER SOURCES. Neff, R. A.; Anderson, M. E.; Campbell, A. R.; Haas, F. X. (Mound Lab., Miamisburg, Ohio). Jan 1972.

From Symposium on natural and manmade radiation in space; Las Vegas, Nev. (1 Mar 1971).

Gamma and neutron measurements on various types of plutonium sources are presented in order to show the effects of ^{17}O, ^{18}O, ^{19}F, ^{236}Pu, age of the fuel, and size of the source on the gamma and neutron spectra. Analysis of the radiation measurements showed that fluorine is the main contributor to the neutron yields from present plutonium—molybdenum cermet fuel while both fluorine and ^{238}Pu daughters contribute significantly to the gamma intensities. (auth)

53337 (NASA-TM-X-2440, pp 859-61) RADIATION FROM ^{238}Pu USED IN SPACE APPLICATIONS. Keenan, T. K. (Los Alamos Scientific Lab., N. Mex.); Vallee, R. E.; Powers, J. A. Jan 1972.

From Symposium on natural and manmade radiation in space; Las Vegas, Nev. (1 Mar 1971).

Plutonium-238 is an alpha emitter with an 87 year half-life that is produced by neutron irradiation of neptunium-237 in a reactor. Plutonium-238 has been used in all applications of space electric power using isotopes as the energy source. These applications include the SNAP-3, 9, 19, and 27 units. The SNAP-3 and SNAP-9 units were used in Navy TRANSIT satellites while the SNAP-19 was used for auxiliary power aboard a NASA NIMBUS and the SNAP-27 provided all the power for the ALSEP package left on the moon's surface by the Apollo 12 and planned subsequent Apollo landings. The principal mode of the nuclear decay of plutonium-238 is by alpha particle emission at a rate of 17 curies per gram. Gamma radiation also present in the nuclear fuel arises primarily from the nuclear de-excitation of daughter nuclei as a result of the alpha decay of plutonium-238 and reactor produced impurities. The gamma radiation associated with the alpha decay of plutonium-238 ranges in energy from 0.044 to 1.085 MeV. Thallium-208, a subsequent decay product of the reactor produced impurity, plutonium-236, emits 0.583 and 2.6-MeV gamma rays at a significant rate if the initial plutonium-236 content is of the order of one part per million of total plutonium. Plutonium-238 has a spontaneous fission half-life of 4.8×10^{10} years. Neutrons associated with this spontaneous fission are emitted at a rate of 2.8×10^3 neutrons per second per gram. Since the space fuel form of plutonium-238 is the oxide pressed into a cermet with molybdenum, a contribution to the neutron emission rate arises from (α,n) reactions with ^{17}O and ^{18}O, which occur in natural oxygen and contribute approximately 2×10^4 neutrons per second per gram of plutonium-238. This contribution can be controlled by ^{16}O enrichment in the fuel. Other (α,n) reactions with low atomic number impurities (principally fluorine) bring the total neutron emission rate from the plutonia molybdenum cermet to near 3×10^4 neutrons per second per gram of plutonium-238. This contribution can, also, be reduced by proper fuel production techniques. (auth)

53338 (NASA-TM-X-2440, pp 862-5) NUCLEAR RADIATION ENVIRONMENT ANALYSIS FOR THERMOELECTRIC OUTER PLANET SPACECRAFT. Davis, H. S. (California Inst. of Tech., Pasadena); Koprowski, E. F. Jan 1972.

From Symposium on natural and manmade radiation in space; Las Vegas, Nev. (1 Mar 1971).

The radioisotope thermoelectric generator (RTG) nuclear radiation environment analysis of a recent design of the Thermoelectric Outer Planet Spacecraft (TOPS) is presented. The neutron and gamma transport calculations were performed using Monte Carlo methods and a three-dimensional geometric model of the spacecraft. The results were compared with similar calculations performed for an earlier design. (auth)

Radiation Sources

Refer also to abstracts 53109, 53157, 53722, and 54936.

53339 (KFK-1568) INFLUENCE OF DIFFERENT DESIGNS AND MATERIALS ON THE WEAR OF PISTON RING AND PISTON RING GROOVE IN A 6-CYLINDER DIESEL ENGINE. Kaiser, Wilfried (Kernforschungszentrum, Karlsruhe (West Germany). Laboratorium fuer Isotopentechnik). Feb 1972. 104p. (In German). Dep. NTIS (U. S. Sales Only).

Thesis. Submitted to Karlsruhe Univ. (West Germany).

The wear behavior of different piston ring and piston ring groove designs and of different groove materials in an air-cooled 6-cylinder diesel engine was investigated by means of a radioactive tracer technique. The test parts are activated by neutrons in a thermal reactor and by deuterons and α-particles in a cyclotron. Thus, up to three wear components can be determined simultaneously. Furthermore, the activation by deuterons and α-particles enables the separate measuring of the wear of the upper and lower sides of piston rings and piston grooves. Besides the influence of the lubricant oil temperature the influence of speed and load on the wear was investigated. The results show a very different wear behavior of the plain compression and keystone-rings, of the sides in armored and nonarmored piston grooves, and of the upper and lower sides of piston rings and piston ring grooves. (auth)

53340 PRODUCTION AND TESTING OF HOMOGENEOUS STERILIZATION DOSE DURING RADIOSTERILIZATION. Stenger, V.; Horvath, Zs. (MTA Isotop Intezete, Budapest). Izotoptechnika; 15: No. 3-4, 199-205(1972). (In Hungarian).

The dose distribution in the gamma facility of the Isotopes Institute was determined. A quick and economical dosimetric method for routine dose testing in irradiation boxes is described. (auth)

53341 RADIOTHERAPEUTIC METHOD IN THE TREATMENT OF SKIN CANCER. Scott, R. Kaye (Royal Melbourne Hospital). pp 307-21 of Melanoma and Skin Cancer. /McCarthy, W. H. (ed.). Sydney; Australian Cancer Society (1972). (CONF-720321-2).

From International cancer conference; Sydney, Australia (13 Mar 1972).

Radiotherapeutic equipment is described and the particular advantages of each unit of apparatus for the treatment of skin cancer are discussed. Beta rays are available from radioactive Sr plates of small areas. The effective radiation depth is 2 mm, so lesions of small size (keratoses, dyskeratoses, etc.) are treatable. X-ray therapy machines vary from the Be window unit working at low voltage and short focal skin distance to the superficial and deep x-ray therapy machines to the linear accelerator. Increased applied voltage gives increased beam penetration and increase of focal skin distance increases relative depth dose. The principles governing the prescription of radiation treatment are described and related to depth dose distributions. Uses of radium and radon are briefly described. (Australia)

Industrial Uses

Refer also to abstracts 53346, 53347, 53381, and 53459.

53342 (AED-C-5-11) BIBLIOGRAPHIES IN NUCLEAR SCIENCE AND TECHNOLOGY. SECTION 5. RADIATION EFFECTS ON FOOD. Beising, Kurt (comp.) (Zentralstelle fuer Atomkernenergie-Dokumentation, Leopoldshafen (West Germany)). Jul 1972. 127p. (In English and German). Dep. NTIS (U. S. Sales Only).

References (512) are given to conferences, dissertations, reports, journals, and books published from 1959 through 1969 on the effects of radiation on food, including radiosterilization and radiopreservation. (P.C.H.)

53343 BUILT-IN RADIOTRACER (^{24}Na) FOR MEASURING CATALYST CIRCULATION RATES. Domondon, D. B.; Berbano, M. C. (Philippine Atomic Research Center, Diliman). Philipp. Nucl. J.; 2: No. 2, 231-2(1970).

A radioactive tracer technique using ^{24}Na was adapted for measuring catalyst circulation rates in catalytic cracking units and proved useful in readily providing accurate and reliable data on this critical process variable in petroleum refining. The tracer method and results obtained are described. (L.C.L.)

53344 INFLUENCE OF γ IRRADIATION ON THE CONTENT OF NICOTINIC ACID OF WHEAT, WHEAT-FLOUR, AND WHEAT-BREAD. Washuettl, J. (Technishce Hochschule, Vienna). Ernaehr. Umsch.; 18: No. 3, 95-8(1971). (In German).

Gamma radiation can be applied for pest control purposes in cereals and bakery-goods. Experiments have been made with doses of 50 and 500 Krad on wheat grains, wheat-flour and wheat-bread whose nicotinic-acid-PP-contents have been determined through acid decomposition and, with regard to bread, by means of new methods first published in this paper, i.e., by enzymatic decomposition, as well as by means of a digestion experiment in vitro. After application of the germination-inhibiting dose of 500 Krad, wheat grains showed an unaltered content of nicotinic acid, whereas wheat-flour showed a decrease, and wheat-bread an increase in vitamin content. In directly irradiated bread the vitamin content was higher than in unirradiated controls, but in bread made from irradiated wheat a loss of vitamins has been found. Considerable differences have been found for the relative values measured for acid decomposition, enzymatic decomposition, and for the digestion experiment. (GF)

LIFE SCIENCES

Radiation Effects on Biochemicals (External Source)

Refer also to abstracts 53021, 53342, and 53381.

53345 (NASA-TM-X-2440, pp 222-8) REVIEW: SOME BIOCHEMICAL EFFECTS OF HIGH LET RADIATIONS. Wiley, Albert L. Jr. (Univ. of Wisconsin, Madison). Jan 1972.
From Symposium on natural and manmade radiation in space; Las Vegas, Nev. (1 Mar 1971).

The natural environment of outer space may theoretically produce a significant exposure of high LET radiation to the space traveler. The use of nuclear reactor power systems may increase this exposure. Since biological endpoints of radiation damage are inevitably due to biochemical changes, it becomes of interest to consider the effect of high LET radiations at the biochemical level. There are qualitative and quantitative differences in the biological damage observed after exposure to high LET radiation (such as heavy ions, protons, neutrons and π^- mesons) as compared to that caused by low LET radiations (such as electrons, x-rays, and gamma rays). This review is concerned with these differences, which are ultimately reflected at the biochemical, cellular, and even whole animal levels. In general, high LET radiations seem to produce biochemical damage that is more severe and possibly less reparable. Experimental data for these effects will be presented in terms of biochemical RBE's with consideration of both early and late manifestations. (auth)

53346 CHARACTERIZATION OF THE RED PIGMENTS PRODUCED FROM FERRIMYOGLOBIN BY IONIZING RADIATION. Giddings, George G.; Markakis, P. (Michigan State Univ., East Lansing). J. Food Sci.; 37: No. 3, 361-4(1972).

It can now be unequivocally stated that there are in fact two red myoglobin derivatives produced by gamma irradiation of ferrimyoglobin solutions under the conditions usually employed in such work. When solutions are anoxic prior to irradiation, a reductive oxygenation to oxymyoglobin takes place (as suggested by earlier work), and in oxygen-containing solutions ferrylmyoglobin is generated. This is consistent with observations that when beefsteaks having an oxidized (brown) surface color are vacuum packaged and irradiated with a pasteurizing dose of ionizing radiation, a purple surface color develops indicative of a reduction of surface ferrimyoglobin. Upon exposure to the atmosphere this radiation-reduced surface pigment oxygenates, becoming bright red, whereas prior to anoxic irradiation the color was brown. Unlike oxygen-containing ferrimyoglobin solutions, however, we have not observed ferrylmyoglobin development of the surface of brown-appearing beefsteaks exposed to irradiation in the presence of oxygen. This may be because catalase activity in the meat tissue removes H_2O_2 as fast as it is produced. The same results were obtained with human hemoglobin as are reported for bovine myoglobin. (auth)

53347 NEWER TRENDS IN PRODUCTION OF CITRUS FRUITS. Penner, H. (Bundesforschungsanstalt fuer Lebensmittelfrischhaltung, Karlsruhe, Ger.). Ind. Obst- Gemueseverwert.; 55: 436-8(1970). (In German).

A report is given on the actual status of citrus production in Israel, on harvesting methods, pest control, packaging, commerce, and transport. Further, the results of experiments on radiation sterilization of food, especially citrus fruits, are discussed. There is no health hazard to be expected due to consumption of irradiated fruits, but certain changes in metabolism of orange skin were observed e.g. increased respiration, activation of enzyme systems, enhanced ethylene formation, and an increase of phenol content. The optical changes of orange skin resulting from this diminish the sales value of fruits. Because of this, the radiation sterilization of oranges seems not to be promising. Nevertheless the scientific investigations on this field are continued. (GF)

53348 MOLECULAR STRUCTURE OF DNA REPLICATION AND RADIATION DAMAGE OF DNA. Okazaki, Reiji (Nagoya Univ., Japan). Igaku No Ayumi; 80: No. 5, 232-43(Jan 1971). (In Japanese).

Studies with intention of clarifying replication, transcription, and their modulation of DNA in bacteria and bacteriophage were carried out from the viewpoint of molecular biology. Semiconservative replication, model of discontinuous replication, nascent short DNA pieces, DNA chain growth, thymidine and thymidine pulse, discontinuous replication and Kornberg DNA polymerase, discontinuous replication in vitro, and symmetry of discontinuous replication were subsequently discussed laying stress on the experiment of the author. The following statements were made as a result of the study: DNA replication occurred by a discontinuous mechanism (short segment synthesis and "gap filling") followed by "joining"; there seems to exist common causes between replication at replication point and biological repair of radiation disturbance of DNA; and replication areas within DNA molecules were assumed to have higher sensitivity to radiation. (Japan)

53349 DOUBLE-STRAND SCISSIONS IN DNA OF GAMMA-IRRADIATED MICROCOCCUS RADIODURANS AND THEIR REPAIR DURING POSTIRRADIATION INCUBATION. Kitayama, Shigeru; Matsuyama, Akira (Inst. of Physical and Chemical Research, Saitama, Japan). Agr. Biol. Chem. (Tokyo); 35: No. 5, 644-52(May 1971).

Strand scissions in DNA of Micrococcus radiodurans after in vivo irradiation with ^{60}Co gamma rays were investigated by sedimentation analysis using neutral sucrose gradients. Double-strand scission in DNA was estimated to occur at the rate of one double cut per 800 eV. This rate is in good agreement with the value reported for mammalian cells. The rejoining of these double-strand scissions was observed during the repair process of the postirradiation incubation and the mean rejoining time, i.e., the time reducing the remaining fraction of the double-strand scission to 0.37, was found to be 52 min. This rejoining repair was inhibited by adding chloramphenicol, tetracycline, or actinomycin D to the postirradiation incubation medium. It is suggested that the high resistance character of M. radiodurans to gamma rays may be due to the efficient capacity of this rejoining repair. (auth)

53350 MECHANISM OF DNA REPAIR AND RECOMBINATION. Sekiguchi, Mutsuo (Kyushu Univ., Fukuoka). Igaku No Ayumi; 80: No. 5, 244-51(Jan 1972). (In Japanese).

A review of the result of experiments carried out to elucidate the mechanism of DNA repair and recombination, especially the enzymic mechanism of elimination-repair, is presented. Results reported from other laboratories are also reviewed and the present state of research and future problems are described. Mention is made of the enzymes taking part in the repair of DNA, uv-sensitive mutants of T_4 phage, endonuclease specific to DNA irradiated with ultraviolet rays, two steps of incision and excision of nucleotides, including a dimer from uv-irradiated DNA, and the mechanisms of elimination-repair and recombination-repair of DNA from Escherichia coli. (Japan)

53351 ENZYMES FOR REPAIR FOR DNA DAMAGES. Okubo, Shunzo (Osaka Univ.). Taisha; 8: No. 8, 568-75(Aug 1971). (In Japanese).

Repair mechanism for DNA damage is closely related with replication, recombination, and mutation, and the mechanism is explained by enzymes acting on the repair of DNA damages. The role of DNA polymerase in the extract of Escherichia coli in the in vitro repair of DNA is described, centered on the report of Korberg, de Lucia, and Cairns. Reaction mechanism is shown for DNA ligase, which is considered to bind the nicked DNA chain. Some past experiments are given to show that DNA ligase takes part in the replication, recombination, and repair of DNA. (Japan)

53352 X-RAY DAMAGE TO DNA AND LOSS OF BIOLOGICAL FUNCTION: EFFECT OF SENSITIZING AGENTS. Emmerson, Peter T. (Univ. of Newcastle upon Tyne, Eng.). Advan. Radiat. Chem.; 3: 209-70(1972).

A review is presented of the effects of the following sensitizing agents on x-radioinduced damage in DNA: oxygen, N-ethylmaleimide, nitric oxide, and N-oxyl radicals. A discussion is also presented of adduct formation and interference with repair processes as mechanisms of the sensitizing effect. (191 references) (H.L.W.)

Radiation Effects on Cells (External Source)

Refer also to abstracts 53021, 53024, and 53505.

53353 (UR-3490-194) EFFECTS OF ULTRAVIOLET RADIATION ON MAMMALIAN CELLS: JU56 WALLABY CELL LINE. Fu, Ying-Kai (Rochester Univ., N. Y. Dept. of Radiation Biology and Biophysics). 1972. 37p. Dep. NTIS.
Thesis.

An aneuploid marsupial epitheleoid cell line, JU56, derived from the black-tailed wallaby (Protemnodon bicolor), was used for investigating the effects of ultraviolet (uv) light. The cells were grown in monolayer cultures, thereby presenting a more uniform cross section to and permitting the ready penetration of the incident uv light. By means of autoradiography following addition of

^{3}H-thymidine to the media the average generation time was determined to be 17.5 to 18 hrs, which included: 10.5 to 11 hrs for S (DNA synthesis), 2 to 3 hrs for G_2 (post-synthesis interphase), and 4 to 5 hrs for G_1 (pre-synthesis interphase) plus M (mitosis). Severe cellular damage was induced by the uv radiation, resulting in cell death, sterility, delay in DNA synthesis and mitosis, and chromosome aberrations. The various kinds of damage depended upon the intensity of the uv dose. (C.H.)

53354 ESTABLISHMENT OF LINE OF CULTURED OF HEPATOMA CELLS (CULB TC) OF THE RAT AND THE ANALYSIS OF THE EFFECTS OF GAMMA RAYS. Sakka, Masatoshi (Tohoku Univ., Sendai); Katsuta, Hajime; Takaoka, Toshiko. Nippon Igaku Hoshasen Gakkai Zasshi; 31: No. 5, 550-4(Aug 1971). (In Japanese).

Cinemicrograms of four NQO-induced hepatoma cells of the rat, Culb TC, were recorded every 2 min for 130 hr before and after 600 R of a single gamma irradiation. Each cell was followed up and cellular events were indicated in a pedigree. In control pedigrees, mean of the first generation time was 1810 min with a variance of 620^2 min for a sample size of 68. The second and the third generation time were 1992 and 2272 min, respectively, with variance of 588^2 and 964^2. After a single 600 R exposure, about half of the total cell death occurred in the first post-irradiation generation and a quarter in interphase and the residual quarter took place in the second post-irradiation generation. It seems very probable that cell death takes place quite at random in each generation, because mean and variance of cell death was 2700 and 1156^2 min in interphase, 2132 and 1644^2 min in the first post-irradiation generation, and 1730 and 1702^2-min in the second post-irradiation generation. Cellular events were given in tables and their biological characteristics were tested statistically. Differences in the behaviour of the population in usual kinetic analysis and in pedigree studies were discussed. (auth)

53355 BIOLOGICAL DOSIMETERS. I. STUDIES ON THE CHROMOSOMAL ABERRATIONS IN HUMAN LYMPHOCYTES IRRADIATED IN VITRO. Ziemba-Zak, Bogumila; Bocian, Ewa; Kloczewiak, Marek; Kopec, Maria (Instytut Badan Jadrowych, Warsaw). Nukleonika; 16: No. 11-12, 621-31(1971). (In Polish).

The relationship was studied between x-ray dose and yield of chromosomal aberrations (dicentrics, rings, acentric fragments, and minutes) in human lymphocytes in vitro. Frequency of the aberrations was described using two types of regression function: power function $y = ax^{\beta} + c$ and second order polynom $y = a_1x + a_2x^2 + c$. The results are better described by the polynom $y = a_1x + a_2x^2 + c$. No statistically significant differences were found between the yield of chromosomal aberrations in cultures of human lymphocytes that were stimulated with phytohaemagglutinin after or before irradiation. (auth)

53356 EFFECTS OF UV-LIGHT AND X-RAYS ON MURINE LYMPHOMA CELLS L5178Y-S IN VITRO. Beer, Janusz Z.; Walicka, Malgorzata (Inst. of Nuclear Research, Warsaw). Nukleonika; 16: No. 11-12, 573-81(1971).

For L5178Y-S cells irradiated with various doses of uv light, survival was determined by growth kinetics observations and by cloning. The dose-survival relationship is exponential and mean lethal dose is about 85 erg mm^{-2}. Observations of the growth of cell cultures irradiated with doses ranging from 16 to 535 erg mm^{-2} were carried for a period of time corresponding to 140 cell generations. The growth was compared of cultures irradiated with 160 and 535 erg mm^{-2} of uv, and with 100 and 300 rads of x rays. In both cases, irradiation caused transitory retardation of the growth of cell populations. It was noticed that the cells lethally damaged by uv disintegrate much more rapidly than those lethally damaged by x rays. All cultures irradiated with uv light after the period of growth retardation grew more rapidly than controls. This phenomenon was not observed after irradiation with x rays. (auth)

53357 RADIATION DAMAGE AND ITS REPAIR. Takebe, Hiraku (Osaka Univ.). Taisha; 8: No. 8, 561-7(Aug 1971). (In Japanese).

A review is made on the repair mechanism of DNA damage, especially by ultraviolet (uv) rays which is known to produce a thymine dimer, a biological effect of uv rays. Past reports on the elucidation of the repair of uv-damaged DNA at the molecular level are reviewed, together with the Elkind—Sutton type recovery of cultured cells damaged by ionizing radiation. The repair mechanism is not limited to radiation damage such as by uv and x rays but is common to damages by various kinds of action source. Effect of radiation is not only lethal but also mutational, and the same repair process works for higher animals and microorganisms alike. (Japan)

53358 THERMALLY ENHANCED RADIOSENSITIVITY OF CULTURED CHINESE HAMSTER CELLS. Ben-Hur, E. (Brookhaven National Lab., Upton, N. Y.); Bronk, B. V.; Elkind, M. M. Nature (London) New Biol.; 238: No. 85, 209-11(16 Aug 1972).

Experiments are described to investigate enhancement of radiation induced lethality of Chinese hamster cells by elevation of temperature at low dose rate. The cells, suspended in DUM 20, were irradiated with 250 kvp x rays, filtered with 0.25 mm Cu and 1.0 mm Al, with a dose rate of 3.3 rad/min, in plastic tubes immersed in water. After irradiation, the cells were diluted and plated for colony formation. Survival curves from cells irradiated at 0, 34, 37, 39, 40, 41, and 42°C are given. It is suggested that the thermally enhanced radiosensitivity that these results indicate is due, at least in part, to inhibition of repair of sublethal damage. (UK)

53359 ANALYSIS OF CHROMOSOMAL SENSITIVITY OF HPK1 CELLS FROM THE MARSUPIAL POTOROUS TRIDACTYLUS TO X RAYS AND TO HELIOTRINE. Bick, Y. A. E. (Univ. of Tasmania, Sandy Bay, Australia); Brown, J. K. Cytobios, 5: No. 19, 189-200(1972).

The relative sensitivity of the individual chromosomes in the diploid cell line HPK1 from the male Potorous tridactylus was analyzed after x irradiation and after heliotrine treatments. In heliotrine experiments, the X chromosome showed a significantly greater sensitivity than the rest of the chromosomes. This was due largely to the sensitivity of the heterochromatic region on the long arm of X. With x rays, up to 8% of the damage occurred in the heterochromatic regions, whereas with heliotrine up to 36% of the total breaks were localized in all heterochromatin. A detailed analysis of chromosomal damage by heliotrine is also given, the results of which suggest that this pyrrolizidine alkaloid inflicts most of its damage during the period of DNA synthesis. For x irradiation, differences in sensitivity were found not only between chromosomes, but the sensitivity of some of the chromosomal elements varied with the stage of the cell cycle during which the x-ray dose was delivered. However, the variation in sensitivity was not simply related to the stage of chromosomal replication. (auth)

53360 METABOLISM OF RICKETTSIA TYPHI AND RICKETTSIA AKARI IN IRRADIATED L CELLS. Weiss, E.; Newman, L. W.; Grays, R.; Green, A. E. (Naval Medical Research Inst., Bethesda, Md.). Infec. Immunity; 6: No. 1, 50-7 (Jul 1972).

L cells that had been exposed to 3,000 R of ^{60}Co γ radiation the previous day were used to study the growth and metabolism of Rickettsia typhi and R. akari. Viable (unirradiated) L cells were used to study the effect of rickettsial infection on host-cell metabolism. Monolayers were infected with a rickettsial multiplicity of 1.2 and given Eagle's minimal essential medium containing 25 mM N-2-hydroxyethylpiperazine-N′-2′-ethanesulfonic acid buffer and 10% calf serum. At various intervals, cycloheximide (2 μg/ml) was added to one set of cultures, to inhibit eukaryotic protein and deoxyribonucleic acid (DNA) metabolism; phosphate-buffered saline (PBS) was added to another set. After 1 hr, the cultures received a mixture of 15 ^{14}C-labeled amino acids or adenine-8-^{14}C. The cultures were harvested 16 hr later and were tested for incorporation of labeled carbon into the fraction precipitated by cold trichloroacetic acid. Viable cells were exposed to thymidine-2-^{14}C for 2-hr periods. Infectivity of R. typhi increased to a peak of 150 to 400 hemolytic units/culture on day 4; the titer remained approximately the same on days 5 and 6, and declined rapidly on day 7. Total amino acid incorporation was about the same in infected and uninfected cultures up to day 6, but metabolic activity was reduced to a negligible level on day 7 in infected cells. Cycloheximide-resistant activity was higher in the infected cultures, with a peak equivalent to one-half the total activity at day 4 to 5. Total as well as cycloheximide-resistant adenine incorporation was higher in the infected cells between days 3 and 5 after infection, with a peak at day 3 to 4. Somewhat similar results were obtained with R. akari, except that the cycle of infection and of cycloheximide-resistant activity proceeded and was completed more rapidly. ^{14}C-DNA of both rickettsiae was isolated from infected cultures that had received labeled adenine. With labeled thymidine, which was not incorporated by the rickettsiae, it was shown that R. typhi and R. akari differ considerably in their effects on the host cell. R. typhi elicited moderate inhibition, whereas R. akari infection led to a complete inhibition of thymidine incorporation by the third day, at the time of highest rickettsial activity. It is concluded that rickettsiae have the necessary enzymes for protein and nucleic acid synthesis, but, thus far, these enzymes have been activated or induced only in an intracellular environment. (auth)

53361 MUTATIONAL ASSAY SYSTEM USING THE THYMIDINE KINASE LOCUS IN MOUSE LYMPHOMA CELLS. Clive, D.; Flamm, W. G.; Machesko, M. R.; Bernheim, N. J. (National Inst.

of Environmental Health Sciences, Research Triangle Park, N. C.). Mutat. Res.; 16: No. 1, 77-87(Sep 1972).

A mutational assay system utilizing the thymidine kinase (TK) locus in L5178 Y mouse lymphoma cells is described. The TK locus is believed to be diploid and the three expected phenotypes—denoted as TK$^{+/+}$, TK$^{+/-}$, and TK$^{-/-}$—have been isolated and characterized. The TK$^{+/+}$ and TK$^{+/-}$ phenotypes are sensitive to 5-bromodeoxyuridine (BUdR) and resistant to THMG (thymidine + hypoxanthine + methotrexate + glycine) while the TK$^{-/-}$ phenotype is BUdR-resistant and THMG-sensitive. In addition, the thymidine kinase activities of the TK$^{+/+}$, TK$^{+/-}$, and TK$^{-/-}$ clonal lines are, respectively, 61, 27, and 0 $\mu\mu$moles of thymidine phosphorylated per 10^6 cells per min of incubation. And finally, using BUdR or THMG selection medium, the spontaneous TK$^{+/-}$ → TK$^{-/-}$ and TK$^{-/-}$ → TK$^{+/-}$ mutation rates are $1.2 \cdot 10^{-7}$ and $6.4 \cdot 10^{-9}$ mutations per locus per generation, respectively. In BUdR selection medium concentrations of up to $0.8 \cdot 10^5$ BUdR-sensitive cells per ml can be plated with no effect on the recovery of BUdR-resistant cells; at least $1 \cdot 10^5$ THMG-sensitive cells can be plated in THMG selection medium without affecting the recovery of THMG-resistant cells. Background mutant frequencies can be kept at or below $2 \cdot 10^{-7}$ in TK$^{+/-}$ cultures. Stimulation of the TK$^{+/-}$ → TK$^{-/-}$ forward mutation rate was effected with x irradiation, ethyl methanesulfonate (EMS), and hycanthone methanesulfonate. By comparing the observed induced mutation rates with the spontaneous TK$^{+/-}$ → TK$^{-/-}$ mutation rate an estimate can be made of the relative mutagenicities of various treatments. Thus, for example, 600 R x irradiation stimulated the mutation rate 2500-fold over the spontaneous rate, while 2-hr exposures to 10^{-2} M EMS or 10^{-4} M hycanthone methanesulfonate gave corresponding stimulations of 17000-fold and 450-fold, respectively. (auth)

53362 MUTAGENESIS IN CULTURED MAMMALIAN CELLS. II. INDUCTION OF GENE MUTATIONS IN CHINESE HAMSTER CELLS. Shapiro, N. I.; Khalizev, A. E.; Luss, E. V.; (and others) (Inst. of Atomic Energy, Moscow). Mutat. Res.; 16: No. 1, 89-101(Sep 1972).

Mutations controlling the resistance to 6-mercaptopurine (6-M) and the ability to multiply in a medium with a low concentration of glucose (glucose-independent mutants) were induced in cultured Chinese hamster cells by N-nitrosomethylurea (NMU), 5-bromodeoxyuridine (BUdR), uv, and x rays. The chemical agents were found to be very active in induction of mutations to 6-M resistance (NMU and BUdR) and mutations of glucose independence (NMU). These agents increase the yield of mutations as compared to the spontaneous mutation rate by about two orders of magnitude. The induced rate of 6-M-resistant mutations by x rays was $2.0 \cdot 10^{-7}$ per viable cell per roentgen. BUdR approximately equally increases the cell's sensitivity to both inactivating and mutagenic action of x rays. The maximum induction of mutations to 6-M resistance by uv was observed at 100 erg/mm^2. This dose leads to a 16-fold increase of the mutation frequency as compared to the spontaneous rate. Further increase of the uv dose up to 200 erg/mm^2 resulted in a lower yield of mutations per dose unit. The highest yield of mutations to 6-M resistance induced by NMU, BUdR, and x rays was observed if cells were plated in selective medium several generations after the mutagenic treatment. The maximum yield of mutations to 6-M resistance induced by uv and of glucose-independence induced by NMU was recorded if cells were transferred to selective media immediately after treatment. The kinetics of expression of mutations and the decline of their number observed after prolonged incubation of treated cells in nonselective conditions are discussed. (auth)

53363 PHENOTYPIC PROPERTIES OF A LARGE-CELL, RADIATION-RESISTANT STRAIN OF ESCHERICHIA COLI. Kvetkas, M. J.; Krisch, R. E.; Zelle, M. R. (Argonne National Lab., Ill.). Can. J. Microbiol.; 18: No. 9, 1417-25(Sep 1972).

Mean cell volumes, total amount of deoxyribonucleic acid (DNA), number of nuclear bodies, and x-ray responses were determined for exponential cultures of Escherichia coli P6, a large-cell radiation-resistant mutant strain, and for E. coli 82/r, the parent strain of P6, growing in three different media at varying growth rates. Combined results comparing cultures in the same growth medium indicated that exponentially growing P6 cells are 2.5 ± 0.2 times larger, contain 3.6 ± 0.3 times more DNA, and 1.8 ± 0.1 times more nuclear bodies than comparable 82/r cells. Individual P6 nuclear bodies contained 2.01 ± 0.13 times as much DNA as 82/r nuclear bodies in comparable cultures, suggesting that each P6 nuclear body may contain two complete 82/r genomes. All P6 cultures gave sigmoidal x-ray survival curves with extrapolation numbers averaging 2.0 and with limiting slopes smaller in absolute value than the slopes of the exponential survival curves obtained for 82/r cultures. P6 cells appeared to be no more efficient than 82/r cells in enzymatic dark repair of x-ray or uv damage, suggesting that the greater x-ray resistance of P6 cells may be associated with the doubled DNA content of each P6 nuclear body. (auth)

Radiation Effects on Microorganisms (External Source)

Refer also to abstracts 53024, 53342, 53347–53351, 53357, and 53505.

53364 (N–72–20063) INDUCTION OF LYSOGENIC BACTERIA IN THE SPACE ENVIRONMENT. Mattoni, R. H. T.; Keller, E. C. Jr.; Ebersold, W. T.; Eiserling, F. A.; Romig, W. R. (California Univ., Berkeley). 1971. 16p. NTIS.

The Biosatellite 2 experiment using the lysogenic bacterium Salmonella typhimurium was designed to test the hypotheses that weightlessness, both with and without gamma irradiation, would affect bacterial cell growth or induction of bacterial prophage. The bacterial data were analyzed by three methods: analysis of variance, t tests between flight and earth control data (where t is the percentage difference between experiment and control sets), and graphic presentation. The data on bacterial growth led to rejection of the hypotheses; space flight produced both increased density of Salmonella typhimurium when grown in liquid medium and interaction to give greater resistance to gamma irradiation at levels between 265 and 1648 R total dose (17 and 103 R per average cell generation). Tests of other variables eliminated all but weightlessness in accounting for the difference. On the basis of the t tests there was no difference in the free phage per bacterium produced under conditions of control and those of flight. The induced bacteriophage per viable bacterium showed significant differences between flight and control at two radiation levels (265 and 645 R). The flight set had consistently lower yields at all levels of radiation. (STAR)

53365 (N–72–20065) RADIATION EXPOSURES DURING THE BIOSATELLITE 2 FLIGHT. Hewitt, John E. (National Aeronautics and Space Administration, Moffett Field, Calif. Ames Research Center). 1971. 14p. NTIS.

Seven of the experiments flown on Biosatellite 2 were designed to determine the combined effects of γ radiation and weightlessness on mortality and mutagenesis in a variety of living systems (insects, microorganisms, and plants) exposed to an onboard source of radiation. Several months after the flight, a series of ground tests was initiated to determine whether the observed effects of interaction were due to vibration and acceleration associated with the flight, rather than to weightlessness. The results of dosimetry measurements indicate that it is unlikely that any difference found to occur between the biologic response of the same experiment in the flight and earth control capsules can be attributed to radiation exposure differences. No unusual results are due to the presence in the capsules of a large component of low energy radiation produced by multiple scattering. (STAR)

53366 (ORO–3347-8) PHYSIOLOGICAL STUDIES ON CLOSTRIDIUM BOTULINUM, TYPE F. Final Report. Walls, Nancy W. (Georgia Inst. of Tech., Atlanta. Engineering Experiment Station). 30 Jun 1971. Contract AT(40-1)-3347. 111p. Dep. NTIS.

A series of experiments was performed to investigate the effects on growth and toxin production, compared to unirradiated controls, of exposure of spores of a proteolytic and a nonproteolytic strain of Clostridium botulinum, type F to sublethal doses (0.1 and 0.2 Mrad) of γ irradiation. This included studies on the ability of these strains of C. botulinum, type F, isolated from natural sources, to grow and produce toxin at a low temperature (10°C). (C.H.)

53367 (SC-RR-720516) FINAL REPORT OF PLANETARY QUARANTINE ACTIVITIES. (Sandia Labs., Albuquerque, N. Mex.). Aug 1972. Contract AT(29-2)-1816. 100p. Dep. NTIS.

This report summarizes the activities of the Planetary Quarantine Department at Sandia Laboratories during the period April 1965 through June 1972. Included are the rationale, the methods and the results of modeling and experimentation used in dry heat, uv radiation, thermoradiation, and chemical sterilization studies and data on the uv sterilization of bacterial spores. A list of publications describing these activities and closely related research is included. (C.H.)

53368 INFLUENCE OF LINEAR ENERGY TRANSFER ON THE RADIORESISTANCE OF BUDDING HAPLOID YEAST CELLS. Raju, M. R.; Gnanapurani, M.; Stackler, B.; (and others) (Univ. of California, Berkeley). Radiat. Res.; 51: No. 2, 310-17(Aug 1972).

The radioresistant component of haploid yeast cells (SC-7) was established by previous investigators to be due to budding cells, and cells with small buds are known to be undergoing DNA synthesis. The response of budding cells of haploid strain SC-7 (Saccharomyces cerevisiae) as a function of LET was studied in this investigation by use of heavy ions (in the LET$_\infty$ range 420 to 17,000 MeV g^{-1}cm^2) from the Berkeley heavy-ion linear accelerator. The maximum sensitivity for budding cells occurs at approximately the same LET_∞ (1300 to 1500 MeV $g^{-1}cm^2$) as that for nonbudding cells. The radiosensitivity as a function of LET, of budding haploid yeasts relative to nonbudding cells, is found to be remarkably similar to that of S-phase Chinese hamster cells in culture relative to cells not undergoing DNA synthesis. (auth)

53369 POST-IRRADIATION EVALUATION OF PATHOGENS AND INDICATOR BACTERIA. Tiwari, N. P.; Maxcy, R. B. (Univ. of Nebraska, Lincoln). Contract AT(11-1)-2038. J. Food Sci.; 37: No. 3, 485-7(1972).

The post-irradiation behavior of selected pathogenic and indicator bacteria of public health significance was studied. Stationary cultures of Escherichia coli, Streptococcus faecalis, Staphylococcus aureus, and selected species of Salmonella were exposed to ^{60}Co γ radiation and subsequently handled according to the desired observations. The following conclusions were drawn on the basis of the results obtained: substerilizing doses of radiation kill some bacteria and injure others; survival and recovery are influenced by post-exposure storage time, storage temperature, culture medium, and the radiation dose; irradiation reduced significantly the infectivity of S. typhimurium. (E.R.B.)

53370 PYRIMIDINE DIMERS AS PRE-MUTATIONAL LESIONS IN ESCHERICHIA COLI WP2 Hcr^-. Mennigmann, H.-D. (Johann Wolfgang Goethe-Univ., Frankfurt am Main). Mol. Gen. Genet.; 117: No. 2, 167-86(1972).

Mutation to prototrophy in Escherichia coli WP2 Hcr^- induced by far-uv radiation (F-UV) in an intermediate dose range follows dose-squared kinetics. In a comparable dose range with near-uv radiation in the presence of acetophenone (N-UV + Acph), mutation induction follows kinetics that are linearly related to dose. The difference in response to the two types of irradiation is a more general one in that it is the same for true revertants, for suppressor mutants, and for several markers. Double-irradiation experiments together with treatment by photoreactivating light (PR) after the first irradiation (i.e., F-UV → PR → F-UV; N-UV + Acph → PR → N-UV + Acph; N-UV + Acph → F-UV; N-UV + Acph → PR → F-UV) seem to indicate the following: a) the dose-squared kinetics for F-UV are due to the necessary co-operation of at least two types of pre-mutational lesions, only one of which is photoreversible; b) N-UV + Acph also produces these photoreversible lesions in addition to such photoreversible ones that do not require the co-operation of other types; the production of the former is not indicated by the appearance of visible mutants because the non-photoreversible type, whose co-operation is required to give rise to such mutants, is not produced. (auth)

53371 RELATION BETWEEN REPAIR MECHANISMS AND INDUCED MITOTIC RECOMBINATION AFTER UV IRRADIATION, IN THE YEAST SCHIZOSACCHAROMYCES POMBE. EFFECTS OF CAFFEINE. Fabre, F. (Institut du Radium-Biologie, Orsay, France). Mol. Gen. Genet.; 117: No. 2, 153-66(1972).

Two different pathways, A and 1, are known to control the repair of uv lesions in the yeast Schizosaccharomyces pombe. The relation between the uv-induced intergenic mitotic crossing over (MCO) and the repair of prelethal lesions controlled by these pathways was studied in the following strains: $UVS1_{,1}/UVS1_{,1}$, where pathway A acts; UVSA/UVSA where pathway 1 acts; UVS^+/UVS^+ (wild type); and UVS1A/UVS1A (double mutant). The analysis of the survival and MCO induction curves, and the comparison, as a function of the dose and as a function of survival, of the MCO induction curves corresponding to the different strains, show that the repair pathway 1 controls a mechanism involving recombination, and that the repair pathway A controls a mechanism that removes prerecombinational lesions. Studies were done with $UVS1_{,1}/UVS1_{,1}$ cells in different physiological conditions affecting the repair efficiency of prelethal lesions (irradiation during the logarithmic growth phase, liquid holding). In all cases, the more efficient the repair of prelethal lesions is, the smaller is the recombination inducibility. This is expected if pathway A controls an excision repair mechanism. The effect of the repair inhibitor, caffeine, was studied. It inhibits only the repair of uv prelethal lesions controlled by pathway 1. The involvement of recombination in the repair of uv lesions in UVS^+/UVS^+ and UVSA/UVSA cells is also shown by the fact that the sensitization to the lethal effect of uv by caffeine in these strains is correlated with a decrease in uv MCO inducibility. Caffeine has no effect either on the uv survival, or on the MCO inducibility in $UVS1_{,1}/UVS1_{,1}$ cells. It is concluded that it inhibits the recombinational repair pathway and not the excision repair pathway. The MCO induction observed in UVS1/UVS1 and UVS1A/UVS1A cells could be due to the presence of a second recombinational pathway, not sensitive to caffeine. At least a fraction of the prerecombinational lesions would not be prelethal, and they are repairable by the excision repair mechanism. (auth)

53372 EFFECTS OF IONIZING RADIATION ON THE CAPACITY OF ESCHERICHIA COLI TO SUPPORT BACTERIOPHAGE T4 GROWTH. Marsden, Howard; Ginoza, William; Pollard, Ernest C. (Pennsylvania State Univ., University Park). J. Virol.; 9: No. 6, 1004-16(Jun 1972).

The loss in capacity of irradiated bacteria to support the growth of T4 phage was studied for two strains, Escherichia coli B and E. coli B_{s-1}. Following a dose of 25 krads, the capacity is quite rapidly lost during postirradiation incubation so that after two hr of such incubation at 37 C only 12% remains in strain B and 3% in strain B_{s-1}. Evidence that capacity is lost in an all-or-none fashion was provided by two types of experiments: a single-burst analysis of those cells that survived to give a burst; and an analysis of the regulation of an early phage enzyme. Several processes were examined to try to determine the cause of the loss in capacity. These were the ability of the irradiated and postirradiation incubated cells to respire, to allow phage adsorption and injection of phage deoxyribonucleic acid, to support the transcription and translation of an early gene, and to support replication of phage deoxyribonucleic acid. Of these processes, transcription and translation appeared to be the most closely associated with the capacity loss, although respiration was reduced to 50% after 2 hr. (auth)

53373 ULTRAVIOLET-INDUCED CROSSLINKS IN THE DEOXYRIBONUCLEIC ACID OF SINGLE-STRANDED DEOXYRIBONUCLEIC ACID VIRUSES AS A PROBE OF DEOXYRIBONUCLEIC ACID PACKAGING. Francke, Bertold; Ray, Dan. S. (Univ. of California, Los Angeles). J. Virol.; 9: No. 6, 1027-32 (Jun 1972).

Deoxyribonucleic acid (DNA) from ultraviolet (uv)-irradiated ϕX174 sediments in alkali at rates up to 1.7 times that of unirradiated ϕX174 DNA and is observed as a condensed, cross-linked structure when examined in the electron microscope by the formamide spreading technique. This structure appears to result from multipole cross-links induced in the tightly coiled DNA contained within the spherical ϕX174 capsid. In contrast, the DNA extracted after uv irradiation of the filamentous bacteriophage M13 is not strikingly altered in its sedimentation properties and appears by electron microscopy to be rod-shaped as a result of side-to-side association of the circular DNA. The differences in these uv-induced structures reflect the differences in the packaging of the single-stranded DNA in the two virions. (auth)

53374 USE OF MUTAGENIC AGENTS FOR BREEDING OF EREMOTHECIUM ASHBYII, THE PRODUCER OF RIBOFLAVIN. Stepanov, A. I.; Zhdanov, V. G. (Inst. of Genetics of Microorganisms, Moscow). Genetika; 8: No. 6, 86-91(Jun 1972). (In Russian).

A comparative study of the effect of three mutagens (uv-light, diethyl sulphate, and nitrosoguanidine) on the producer of riboflavin in Eremothecium ashbyii revealed no advantage of either of these mutagenic factors over the other two with respect to the induction of plus-variants. At each stage of selection stable mutants exceeding the initial strain in their riboflavin-producing activity were induced by uv-light and nitrosoguanidine. (auth)

53375 INDUCTION AND REPAIR OF GENE CONVERSION IN UV-SENSITIVE MUTANTS OF YEAST. Mori, Shigeyuki; Nakai, Sayaka (National Inst. of Radiological Sciences, Chiba, Japan). Mol. Gen. Genet.; 117: No. 3, 187-96(1972).

Photoreactivation effect on uv-induced allelic recombination was examined using various combinations of leu 1 alleles in uv-sensitive and wild type diploid yeast, Saccharomyces cerevisiae. The frequencies of uv-induced heteroallelic reversion in uv-sensitive strains, presumably lacking dark-repair, are strikingly enhanced compared to those in wild type at the same doses under dark condition. However, these enhanced frequencies of reversion are diminished by photoreactivation almost to the level of those in wild type. The induced frequencies of homoallelic reversion (mutation) of relevant alleles are apparently lower than those of heteroallelic reversion. Phenotypic analysis for linked gene leu 1 on uv-induced heteroallelic revertants has shown that most of the revertants are of the nonreciprocal type recombination (mitotic gene conversion). These results would indicate that most of the dark-repairable damage leading to mitotic gene conversion after uv light is due to pyrimidine dimers. (auth)

53376 INVESTIGATION INTO THE RADIOBIOLOGICAL CONSEQUENCES OF K-SHELL IONIZATIONS OF PHOSPHOROUS ATOMS USING SOFT X RAYS. Clark III, Benton Clyde. New York; Columbia Univ. (1969). 164p. University Microfilms Order No. 72-15,565.

Thesis.

When an x-ray photon ionizes a phosphorus atom in the K-shell, the resulting electron rearrangement ("vacancy cascade") leaves, in general, a residual phosphorus ion of charge +4 due to the emission of three Auger electrons following the ejection of the photoelectron. If such an event occurs to a phosphorus atom located in a biologically important molecule like deoxyribonucleic acid (DNA), observable consequences may follow since an unusually large amount of ionization and excitation energy is deposited in a very localized region. In the present work, endospores of the bacteria B. subtilis were irradiated with very soft x rays of different energies. The energies used were selected to be above, in some cases, the K edge energy of the phosphorus atom and below, in other cases, this energy. For the latter condition, K-shell ionizations are energetically impossible. An apparatus was developed for investigating this problem by producing high intensity x-ray beams at constant potentials between 1 and 6 kV and currents up to 500 ma. Spores of B. subtilis were produced by growth of vegetative cells on suitable media. The spores were harvested, washed, and stored in cold, distilled water. Aliquots of known concentrations were pipetted onto membrane filters and allowed to dry for at least three days. The filters were irradiated to predetermined exposure levels, both in air and in a high-humidity nitrogen atmosphere. Colony-forming-ability of the irradiated spores was tested by incubating the membrane filters on MR-VP medium. The slopes of the radiation survival curves thus determined were found to be the same, within experimental uncertainty, for x rays of all energies tested provided survival was plotted against the dose delivered to the sporal nuclear body. Although the irradiation apparatus and biological system were carefully selected to detect vacancy cascade damage, no experimental evidence for damage of this type was discerned. The sensitivity of the experiment places a minimum limit of 37 vacancy cascades, on the average, required to inactivate the sporal genome. (Diss. Abstr. Int., B)

53377 LOSS OF PATHOGENICITY BY RADIORESISTANT STAPHYLOCOCCI. Samoilenko. I. I.; Rusakova, E. V.; Pershina. Z. G. (Inst. of Epidemiology and Microbiology, Moscow). Byull. Eksp. Biol. Med.; 73: No. 5, 87-9(May 1972). (In Russian).

Under the effect of repeated irradiation with ^{60}Co gamma-rays, it was possible to obtain radioresistant variants of pathogenic Staphylococci cultures. Radioresistant cultures lost such signs of Staphylococcus pathogenicity as production of plasmocoagulase, DNA-ase, alpha- and delta-hemolysins, dermonecrotic and lethal activity, and capacity to be typed with bacteriophages. There were found no changes in the nucleotide DNA composition of radioresistant variants in comparison with the initial cultures. (auth)

53378 RAPID METHOD FOR COMPLEMENTATION TESTING OF ULTRAVIOLET-SENSITIVE (UVS) MUTANTS OF STREPTOMYCES COELICOLOR. Harold, Richard J.; Hopwood, David A. (John Innes Inst., Norwick, Eng.). Mutat. Res.; 16: No. 1, 27-31(Sep 1972).

Seventy-one uvs mutations were isolated and tested for complementation with mutations representing the known closely linked uvs A, C, and D loci by a rapid replicating technique involving "ultra-fertile" crosses. Most of the mutations were successfully classified by this technique. Of the 71 mutations, 23 were assigned to uvsA, 15 to uvsC, and 28 to uvsD. Four strains may have carried mutations in more than one of the three loci, or conceivably polar mutations. The remaining mutation occurred outside the uvsA, C, D cluster. (auth)

53379 INFLUENCE OF AMINO ACID STARVATION ON THE UV REVERSIBILITY OF THE STRAINS OF ESCHERICHIA COLI B/r THY$^-$ TRP$^-$ HCR$^+$ AND ESCHERICHIA COLI B/r THY$^-$ TRP$^-$ HCR$^-$. Slamenova, D. (Inst. of Experimental Oncology, Bratislava). Folia Microbiol. (Prague); 17: No. 4, 274-80 (1972).

The fraction of induced trp$^+$ reversions in the strains of Escherichia coli B/r thy$^-$ trp$^-$ Hcr$^+$ and Escherichia coli B/r thy$^-$ trp$^-$ Hcr$^-$ was studied in the course of starvation for an essential amino acid (tryptophan). UV light as a mutagenic factor was used. It was found that there is a decrease in the proportion of induced trp$^+$ reversions in the strain of Hcr$^+$ type during starvation. Such a decrease was however observed only with that fraction of trp$^+$ reversions that is expressed in selective plates where several divisions of irradiated cells are caused. The proportion of trp$^+$ reversions expressed on minimal plates does not change during starvation. With the strain of Hcr$^-$ type the proportion of induced trp$^+$ mutations remains unaltered irrespective of the nature of the selective plates. (auth)

53380 SPECIFIC EFFECTS OF MUTAGENS ON ASPERGILLUS NIGER PRODUCING CITRIC ACID. Das, Arati; Nandi, P. (Univ. of Calcutta). Folia Microbiol. (Prague); 17: No. 4, 248-50(1972).

Aspergillus niger C was treated with uv and gamma irradiation (^{60}Co), nitrogen mustard, and colchicine. Mutagenic treatments resulted in substrains with either increased or decreased citric acid production, while some were unchanged in this respect. Low-yielding strains predominated in all experiments. Analysis of the superior substrains showed gamma irradiation to be most effective in producing the greatest number of superior mutants. (auth)

Radiation Effects on Plants (External Source)

Refer also to abstracts 53365 and 53459.

53381 (CNEA-309) EFFECT OF GAMMA RADIATION ON AN ARGENTINE VARIETY OF WHEAT. Pahissa Campa, J.; Herscovich de Pahissa, M. H.; Gabarain, R. V. A.; Tramontini, C. (Comision Nacional de Energia Atomica, Buenos Aires (Argentina)). 1972. 14p. (In Spanish). Dep. NTIS (U. S. Sales Only).

A dose of γ radiation ranging from 15 to 20 krads is normally used for the disinfestation of insect pests in stored grain. Results are reported from a study on the effects of γ radiation on nutritional and organoleptic characteristics of flour produced from irradiated grain. Wheat (an Argentine variety) was exposed to doses ranging from 10 to 2000 krad and data are presented on the effects of the various doses on the weight, moisture content, ash content, and ability to germinate when used as seed. Data are included on the effects of the various doses on the content of moisture, protein, ash, and dry and wet gluten in flour produced from the wheat and on the bread-making characteristics of the flour. The analytical values were found to vary with the radiation dose and marked differences, will respect to the control, were noted in the texture, odor, color, and flavor of bread made with flour from wheat exposed to the higher doses. (C.H.)

53382 (N-72-20054) RADIOBIOLOGIC STUDIES OF TRADESCANTIA PLANTS ORBITED IN BIOSATELLITE 2. Sparrow, Arnold H.; Schairer, Lloyd A.; Marimuthu, Kodumudi M. (Brookhaven National Lab., Upton, N. Y.). 1971. 24p. NTIS.

The Biosatellite 2 Tradescantia experiment was designed to determine the effect of weightlessness and other spacecraft environmental conditions on spontaneous and radiation-induced somatic mutation rates and on selected cytologic changes. Data obtained from γ irradiated and nonirradiated plants flown in Biosatellite 2 were compared with data from nonflight irradiated and nonirradiated plants maintained under conditions similar to those of the flight material. (STAR)

53383 RADIOSENSITIVITY OF SOME CORN VARIETIES. Diaconu, P. An. Inst. Cercet. Pentru Cereale Plante Teh.-Fundulea, Ser. C; 36: 183-91(1968). (In Rumanian).

The radiosensitivity of the ICAR 54, Dobrogean, and Românesc de Studina home varieties, and of the A 19 (home), A 73, and W 32 (U.S.A.) lines was investigated during 1964 to 1967. Radiosensitivity was established by number of emerged plants, by plants having reached maturity, by plants attacked by smut, and by thermal yield. It was found that radiosensitivity differs according to variety and line and according to the investigated character, and this proves that the factors conditioning these characters differ with respect to radiosensitivity. A higher radiosensitivity is found in the Dobrogean variety and in the W 32 line. The A 19 home line is radioresistant. It was found that irradiations favor smut attack and allow thus the discarding of radiosensitive biotypes. (auth)

53384 GENETIC CHANGES INDUCED BY SPACE FLIGHT FACTORS IN THE BARLEY SEEDS TAKEN INTO SPACE ON BOARD THE SPACESHIPS SOYUZ-5 AND SOYUZ-9. Nuzhdin, N. I.; Dozortseva, R. L. (Inst. of Biological Physics, Moscow). Zh. Obshch. Biol.; 33: No. 3, 336-46(1972). (In Russian).

Dry seeds of barley were taken into space on board the spaceships Sojuz-5 and Sojuz-9. On board the ship Sojuz-5 the seeds were in the state of natural rest (the embryonal cells were at G_0 stage). The experiment included two series: untreated seeds were used in Series I; in Series II the seeds were irradiated with ^{137}Cs γ before the flight (15 kR, 620 R/min). Space flight was found to induce chromosomal aberrations. The damage induced by a combined effect of space flight factor (SFF) and γ manifested itself in the two following ways, depending on the physiological state of the cells: The additive effect of the two above factors took place, the seeds having germinated immediately on transition of the embryonal cells from the G_0 stage to the G_1 stage. If the seeds were kept in the open air and subsequently germinated an interaction of the two above effects was observed and the effect of SFF augmented after irradiation. On board the Sojuz-9 the seeds of the abovementioned species were in a state of induced rest (the embryonal cells were at G_1 stage). One half of non-irradiated seeds taken into space were soaked in the water and the solutions of two radioprotectors. One half of the seeds, both radioprotector-treated and untreated, were irradiated with γ ^{137}Cs (15 kR, 610 R/min). A cytological study of the mitoses in meristemic cells in rootlet terminals revealed that SFF in non-irradiated seeds induced about 3% of aberrant cells. After irradiation the effect of SFF increased over two-fold. Although the radioprotectors ensured the seeds against the γ-induced damage, they failed to protect the seeds from the SFF-induced damage either in irradiated or non-irradiated seed cells which is inconsistent with the previously obtained data. (auth)

53385 GAMMA STIMULATION OF MAIZE. Caldera, P. G. (Gammatom S.p.a., Gaunzate, Italy). Stimulation Newslett.; No. 2, 5-10(1971).

Maize seeds were irradiated with 100 to 1,200 rads of γ rays before seeding. At the harvest, the number of plants and the weight of maize-cobs and grains were noted and the water content determined. A comparison of grain weight per g of plant revealed an increase as against the control. A statistical evaluation of results is given. (GF)

53386 EFFECT OF γ-IRRADIATION OF SEED ON PROPERTIES OF SUGAR BEET. Mantovani, G.; Fasulo, M. P.; Mancini, F.; (and others). (Univ., Ferrara, Italy). Zucker; 25: No. 4; 113-16(1972). (In German)

Diploid seeds of two different varieties of sugar beet were irradiated with doses of γ-rays from 250 up to 50,000 rads. For two years the effect of different doses of irradiation on the agricultural properties of beets grown from these seed was tested and compared with that of beets grown from seed without preceding irradiation. High doses of irradiation (50,000 rads) caused a marked decrease in the agricultural properties of the beet, while in general no significant differences were obtained after medium and low doses of irradiation. Only in some cases a clear tendency toward improving particular properties of the beet could be found after irradiation with some doses. The results of analogous investigations published in literature are discussed. (GF)

53387 EFFECT OF SEED IRRADIATION WITH ^{60}Co ON SOME PHYSIOLOGICAL PROCESSES AND THE CROP QUALITY IN BEAN PLANTS. Silli, Elena. Lucr. Stiint., Inst. Agron., Bucuresti, Ser. A; 13: 377-83(1970). (In Rumanian).

By irradiating bean seeds with different doses of gamma radiations, physiological modifications occur in plants which are reflected in the crop quality. The small doses of the gamma radiations (500 R and 1000 R) have a stimulative action upon the photosynthesis process and upon the accumulation of dry matter and the higher doses (2,000 R and 6,000 R) have a hindering action. As regards the transpiration intensity, all doses used have determined its decrease. The positive effect of the small doses and the negative one of the high doses is ascertained also as far as the starch and protein contents of the grains is concerned. (auth)

53388 ALTERATIONS OF SUGAR BEETS BY γ-IRRADIATION OF THE SEED. Fasulo, M. P.; Mantovani, G.; Dall'Olio, G.; Berti, M.; Pancaldi, G. (Univ., Ferrara, Italy). Zucker; 25: No. 8, 247-56(1972). (In German).

Experiments were carried out concerning the influence of varying doses of γ irradiation (250 to 50,000 rads) on seed of two diploid sugar beet varieties, one of the high-yielding and the other of the high-quality type. In these investigations the effects on morphology of plants grown in pots as well as in the field, on histological structure of roots in the primary and secondary stage of development, as well as influences on the process of germination were observed. High doses of irradiation (50,000 rads) caused definite damages. Lower doses produced diverse effects difficult to describe. (auth)

53389 STIMULATION OF EMERGENCE BY X-IRRADIATION IN SUGAR BEETS OF DIFFERENT GRADES OF PLOIDY. Pannonhalmi, K. (Noevenynemesitesi es Noevenytermesztesi Kutato Intezet, Sopronhorpacs, Hungary). Stimulation Newslett.; No. 1, 21-2(1970).

Sugar beet seeds of three varieties were irradiated with 5 to 40 kR of x rays at a dose rate of 1,489 R/min. The seeds were stored in desiccators for 100 hrs and subsequently sown. Emergence was noticed daily, with a stimulation being found at different doses. On the 14th day the plants were harvested and the fresh and dry weight determined. A stimulation was recorded which reached a maximum at exactly that dose stimulating emergence for two varieties. (GF)

53390 EFFECT OF IRRADIATION ON VARIABILITY IN OKRA (ABELMOSCHUS ESCULENTUS (L) MOENCH.). Nandpuri, K. S.; Sandhu, K. S.; Randhawa, K. S. (Punjab Agricultural Univ., Ludhiana, India). J. Res. (Ludhiana); 8: No. 2, 183-8 (1971).

Studies on the effect of gamma rays (^{60}Co) on germination, growth, fruit quality, and yield of okra were conducted. Inbred pure seeds of Pusa Sawani var. were irradiated with gamma rays and dosages including the control were 0 Kr, 30 Kr, 40 Kr, 50 Kr, and 60 Kr. The gamma rays retarded the rate of germination and the percentage of germination also tended to decrease with the increase in the dose. Various treatments of gamma rays significantly increased variation for the ht. of plants, either for dwarfness or tallness, for the number of days taken for flowering and for yield in X_1 generation. Plants treated with 30 Kr gamma rays attained significantly more ht. and produced increased yields. One bushy type mutant was observed in the progeny of a plant treated with 60 Kr. Some mutants which were early, late and high-yielders were also spotted out from the progenies of irradiated material in X_2 generation. (Indian Sci. Abstr.)

53391 EFFECT OF LOW DOSES OF X-RAYS ON RADISH AND CARROT. Desai, B. M.; Gaur, B. K. (Bhabha Atomic Research Centre, Bombay). Stimulation Newslett.; No. 2, 27-30(1971).

Seeds of radishes and carrots were irradiated with 100 to 5,000 R of x rays at a dose rate of 100 R/min. The seeds were sown four hrs after irradiation and cultivated in the normal way. After the harvest, the fresh weight of roots and shoots and the length and volume of root were determined. A stimulation of growth was more obvious in roots than in shoots but significant only at 5,000 R. (GF)

53392 WAYS OF FORMATION OF GENETIC HETEROGENEITY AND SOME PROBLEMS OF HETEROSIS SELECTION IN CROSS-POLLINATING AND SELF-POLLINATING PLANTS. I. EFFECT OF BALANCED HETEROZYGOSITY ON THE FREQUENCY OF CHROMOSOME ABERRATIONS IN RYE. Molchan, I. M. (Moscow Agricultural Academy). Genetika; 8: No. 6, 5-12(Jun 1972). (In Russian).

Self-pollination, as compared with free cross-pollination, was shown to increase considerably radiosensitivity and the frequency of chromosome aberrations in rootlets, and to decrease the mitotic activity and germination capacity of self-pollinated rye seeds. (auth)

53393 MUTAGENIC EFFECT OF UV- AND GAMMA-RAYS ON ANTIBIOTIC PRODUCTION OF ASPERGILLUS CHEVALIERI. Nanda, G.; Chandra, A. L.; Nandi, P. (Bose Inst., Calcutta). Curr. Sci. (India); 41: No. 17, 644-5(5 Sep 1972).

Spore suspensions of Aspergillus chevalieri were gamma and uv-irradiated, transferred to agar plates, and biochemical and morphological mutants determined. Increased antibiotic production was observed in several mutants and two were selected for further study. A comparison of the antibiotic activity of the two mutants with that of the parent strain showed that the growth of several species of bacteria was considerably more inhibited by the mutants than by the parent strain. It was also found that the mutants differed in their antibacterial spectra and in the nature of the antibiotics as evidenced by paper chromatography. (H.L.W.)

53394 BIOLOGICAL EFFECTIVENESS OF THE PRIMARY REACTIONS OF THERMAL NEUTRONS. 2. CONTRIBUTION TO THE EFFECTIVENESS OF THE ^{14}N(n,p)^{14}C-CAPTURE REACTION AND ITS COMPONENTS. Knoop, H.-U. (Kernforschungsanlage, Juelich, Ger.). Radiat. Bot.; 12: No. 3, 191-5(Jul 1972). (In German).

Nitrogen-15 fed cells of the unicellular green alga Chlorella pyrenoidosa were suspended in a Polymin-solution of variable concentration and exposed to thermal neutrons. Polymin-SN is a polyelectrolyte, $(CN_2CN_2NH)_n$, of high nitrogen content and low osmotic pressure. From the ^{14}N(n,p)^{14}C-capture reactions of the solution, only the 0.582 MeV-protons are able to pass through the algae, thus giving the possibility to study their biological effectiveness without contribution of the simultaneously produced 0.043 MeV-^{14}C-recoil nuclei. Colony-forming ability of the algae and rate of unusual (mutated) colonies were chosen as criteria for radiation damage. Referred to their dose the external protons proved half as effective as the complete ^{14}N-reaction. The ^{14}C-recoil nuclei with only 7.1% of the dose generated by the ^{14}N-reaction thus showed an extremely high efficiency exceeding that of the protons by a factor of 24.3 ± 14.8 and 16.4 ± 7.2 concerning the reduction of colony-forming ability and the increase of mutation rate respectively. The results supported the hypothesis that both effects were caused by damaged DNA. (auth)

53395 INVESTIGATIONS ON THE CONTENT OF FREE AND BOUND TRYPTOPHAN IN WHEAT AFTER γ IRRADIATION. Washuettl, J. (Technische Hochschule, Vienna). Ernaehr. Umsch.; 18: No. 3, 98-100(1971). (In German).

The effect of gamma radiation, applied for pest control purposes, on the tryptophan content of wheat has been investigated for two different doses. At a dose of 50 Krad, no tryptophan-decreasing effect could be found in wheat and shredded wheat, whereas a dose of 500 Krad resulted in a considerable loss of this amino acid. Furthermore, it has been possible for the first time to reveal the catabolism of the tryptophan bound to a protein. (GF)

Radiation Effects on Animals (External Source)

Refer also to abstracts 53021, 53024, 53505, and 54870.

53396 RADIATION. Harte, John; Socolow, Robert H.; Ginocchio, Joseph N. pp 295-320 of Patient Earth. /Harte, John. New York: Holt, Rinehart, and Winston, Inc. (1971).

Radiation and how it interacts with matter, the biological effects of radiation, and natural and man-made sources of radiation are discussed. Some of the government standards for radiation protection are considered. (M.C.G.)

Man

Refer also to abstracts 53507, 54876, 54877, 54880, 54882, 54883, 54888, 54896, 54897, 54900, 54901, 54906, 54909, 54913, 54914, 54922, 54951, 55454, and 55456.

53397 (FOA-4-4500-A-3) BIOLOGICAL DOSIMETRY FOR APPLICATION ON THE CIVILIAN POPULATION AFTER A NUCLEAR EXPLOSION. **Rydberg, Bjoern (Forsvarets Forskningsanstalt, Stockholm (Sweden)). Jun 1972. 22p. (In Swedish).** Dep. NTIS (U. S. Sales Only).

Possibilities to use biological dosimetry on the civil population after a nuclear weapon explosion are examined. Biological dosimetry is based on chromosomal aberrations in leukocytes. The cultivation and preparation of blood samples are described. Estimations of the number of cells that have to be examined are done. (KK) (Sweden)

53398 (LA-4874, pp 79-83) BIOMEDICAL PROGRAM. Kligerman, Morton M. (Yale Univ., New Haven, Conn.). Mar 1972.

From fifth LAMPF users meeting; Los Alamos, NM (8 Nov 1971).

Research programs in biomedicine at the Los Alamos Meson Physics Facility are discussed. Consideration is given to the following factors that affect the probability of curing cancer patients: size of tumor; number of cells in the tumor; differential ability of cells to recover from sublethal damage; the oxygen effect; immune responses of the host; and volume of tissue in the tumor. The importance of testing pion beams as a means of cancer treatment is emphasized. (H.L.W.)

53399 (NASA-TM-X-2440, pp 229-32) EFFECTS OF X-RAY IRRADIATION ON HUMAN SPERMATOGENESIS. Thorslund, T. W.; Paulsen, C. A. (Univ. of Washington, Seattle). Jan 1972.

From Symposium on natural and manmade radiation in space; Las Vegas, Nev. (1 Mar 1971).

Direct cell kill and inhibition of mitosis have been suggested as mechanisms to explain the occurrence of absolute sterility following the irradiation of the testes. In order to obtain information on the existence and dose dependency of the mechanisms for man, a controlled study was initiated in 1963. A total of 209 normal adult non-Catholic inmate volunteers at the Washington State Penitentiary in Walla Walla participated in the experiment. Sixty-four of the men received a single midorgan dose to both of their testes ranging from 7.5 to 400 R. The remaining men served as various control groups. Testicular function was evaluated primarily on the basis of weekly seminal fluid examinations where the response or end-point was taken to be azoospermia or complete sterility. In order to obtain direct information on testicular morphological changes, periodic unilateral testicular biopsies were also performed on a number of individuals in both the exposed and non-exposed groups. It was deduced from the resulting length of the pre-sterile period and sterile period data that both cell kill and mitosis halting mechanisms were operating. Estimates of ED_{50} of 75 R and 27 R for cell kill and mitosis halting, respectively, were obtained. The maximum observed sterile period was 501 days with eventual recovery observed in each individual where the follow-up was complete. Thus man appears to be highly radiosensitive in regard to temporary sterility but quite radioresistant in regard to permanent sterility. (auth)

53400 (NASA-TM-X-2440, pp 233-7) MULTIFACTORIAL ANALYSIS OF HUMAN BLOOD CELL RESPONSES TO CLINICAL TOTAL-BODY IRRADIATION. Yuhas, John M.; Stokes, T. R.; Lushbaugh, C. C. (Oak Ridge National Lab., Tenn. Oak Ridge Associated Universities, Tenn.). Jan 1972.

From Symposium on natural and manmade radiation in space; Las Vegas, Nev. (1 Mar 1971).

Multiple regression analysis techniques are used to study the effects of therapeutic radiation exposure, number of fractions, and time on such quantal responses as tumor control and skin injury. The potential of these methods for the analysis of human blood cell responses is demonstrated and estimates are given of the effects of total amount of exposure and time of protraction in determining the minimum white blood cell concentration observed after exposure of patients from four disease groups. (auth)

53401 (NASA-TM-X-2440, pp 238-48) PULMONARY-IMPEDANCE POWER SPECTRAL ANALYSIS: A FACILE MEANS OF DETECTING RADIATION-INDUCED GASTROINTESTINAL DISTRESS AND PERFORMANCE DECREMENT IN MAN. Ricks, Robert C. (Oak Ridge Associated Universities, Tenn.); Lushbaugh, C. C.; McDow, Earl; Frome, Edward. Jan 1972.

From Symposium on natural and manmade radiation in space; Las Vegas, Nev. (1 Mar 1971).

Changes in respiratory variance revealed by power spectral analysis of the pulmonary impedance pneumogram can be used to detect and measure stresses directly or indirectly affecting human respiratory function. When gastrointestinal distress occurred during a series of five whole-body exposures of 30 R at a rate of 1.5 R/min, it was accompanied by typical shifts in pulmonary impedance power spectra. These changes did not occur after protracted exposure of 250 R (30 R daily) at 1.5 R/hr that failed to cause radiation sickness. This system for quantitating respiratory effort can also be used to detect alterations in one's ability to perform under controlled exercise conditions. Performance decrement due to various stresses is difficult to quantitate because of a lack of objectivity in most tests and bias due to different levels of motivation. In our tests, the end point of increased respiratory variance and the method of measuring it is too obtuse for the test subject to recognize and falsify. Increased fatigability has been reported after whole-body irradiation but little is known about doses required and the time for its occurrence. Using pulmonary impedance power spectral analysis we found while observing four irradiated patients that increased fatigability could occur during prolonged fractionated exposures to 10 R daily and after completion of continuous exposures to 30 R/day for 5 days. The performance decrement detected by this means occurred at lower total doses than previously reported for radiation-induced fatigue and at lower exposure rates than those that cause gastrointestinal distress. (auth)

53402 (NASA-TM-X-2440, pp 398-415) PREDICTED LEVELS OF HUMAN RADIATION TOLERANCE EXTRAPOLATED FROM CLINICAL STUDIES OF RADIATION EFFECTS. Lushbaugh, C. C. (Oak Ridge Associated Univ., Tenn.). Jan 1972.

From Symposium on natural and manmade radiation in space; Las Vegas, Nev. (1 Mar 1971).

Results of clinical studies of radiation effects on man are used to evaluate space radiation hazards encountered during manned space travel. Considered are effects of photons as well as of mixed fission neutrons and gamma irradiations in establishing body radiosensitivity and tolerance levels. Upper and lower dose-response-time relations for acute radiation syndromes in patients indicate that man is more than sufficiently radioresistant to make the risks of an early radiation effect during one short space mission intangibly small in relation to the other nonradiation risks involved. (auth)

53403 (NASA-TM-X-2440, pp 416-22) HUMAN VISUAL RESPONSE TO NUCLEAR-PARTICLE EXPOSURES. Tobias, C. A.; Budinger, T. F.; Lyman, J. T. (Univ. of California, Berkeley). Jan 1972.

From Symposium on natural and manmade radiation in space; Las Vegas, Nev. (1 Mar 1971).

Experiments with accelerated helium ions were performed in an effort to localize the site of initial radiation interactions in the eye that lead to light flash observations by astronauts during spaceflight. The character and efficiency of helium ion induction of visual sensations depended on the state of dark adaptation of the retina; also, the same events were seen with different efficiencies and details when particle flux density changed. It was concluded that fast particles cause interactions in the retina, particularly in the receptor layer, and thus give rise to the sensations of light flashes, streaks, and supernovae. (auth)

53404 (NASA-TM-X-2440, pp 424-34) USE OF QUALITY FACTORS AND FLUENCE TO DOSE-RATE CONVERSION IN HUMAN RADIATION EXPOSURES. Sondhaus, C. A. (Univ. of California, Irvine). Jan 1972.

From Symposium on natural and manmade radiation in space; Las Vegas, Nev. (1 Mar 1971).

It has not yet been possible to use biological data with the same degree of precision with which one can obtain or estimate physical radiation data. Certainly, a QF, even properly used, is by no means the only modifying factor that one must apply to a flux-to-dose conversion; the distribution factor and the time factor are there to contend with, and the area factor as well. But above all, one must at least consider the possibility of treating a total exposure not simply on the basis of a collection of separate organs wired together, each with its own sensitivity, but by applying a separate organ approach only very judiciously as a part of the characterization of a total body exposure. It would seem that the most reasonable way one can use the human data that exists is to apply it as far as possible to the human animal as a whole. The particular dosimetric problems of the space environment have been a stimulus to such efforts, but the results can clearly be useful in terrestrial human affairs. (auth)

53405 (NASA-TM-X-2440, pp 767-72) DIRECT STIMULATION OF THE RETINA BY THE METHOD OF VIRTUAL QUANTA FOR HEAVY COSMIC-RAY NUCLEI. McNulty, P. J. (Clarkson Coll. of Tech., Potsdam, N. Y. Air Force Cambridge Research Labs., Bedford, Mass.); Madey, Richard. Jan 1972.

From Symposium on natural and manmade radiation in space; Las Vegas, Nev. (1 Mar 1971).

The method of virtual-quanta is based on the fact that the electromagnetic field of a fast charged particle approaches the field of a plane wave as the particle speed approaches the speed of light. The electromagnetic field of a particle that passes through the retina appears to a rod in the retina as an electromagnetic pulse in time. The quantization of the components of the Fourier frequency spectrum of this pulse of electromagnetic radiation yields the virtual quanta. This method assumes that the virtual-quanta interact with the retina in the same way as ordinary photons. We have calculated the contribution to the frequency of visual sensations induced in the dark-adapted eye by the virtual-photon field associated with the heavy-nuclei that exist in the region of space beyond the geomagnetic field. In order to determine the probability that the virtual-photon field induces a light-flash, we utilize only the portion of the virtual-photon spectrum that corresponds to the known frequency dependence of the sensitivity of human rods to visible light. The results of our calculation can be expressed as a curve of the mean frequency of light-flashes induced by the absorption of at least R virtual-photons versus the threshold number R. The contribution to the light-flash frequency from the virtual-photon field of heavy cosmic-ray nuclei is smaller than that from Cherenkov photons. We have used the flux and energy spectra of galactic cosmic-ray nuclei helium to iron measured by Comstock, Fan, and Simpson. (auth)

53406 (NASA-TM-X-2440, pp 974-80) DOSIMETRY FOR RADIOBIOLOGICAL STUDIES OF THE HUMAN HEMATOPOIETIC SYSTEM. Beck, W. L.; Stokes, T. R.; Lushbaugh, C. C. (Oak Ridge Associated Universities, Tenn.). Jan 1972.

From Symposium on natural and manmade radiation in space; Las Vegas, Nev. (1 Mar 1971).

The three total-body irradiation facilities at Oak Ridge Associated Universities are described. The methods used to determine the γ dose to human bone marrow in these facilities are described including the use of an Alderson Rando phantom and the use of extruded lithium fluoride dosimeters in the phantom. The method used for calculating the bone marrow dose is discussed. The average dose in rads/100 R in the various marrow compartments is given for each of the irradiation facilities. (E.R.B.)

53407 (NASA-TM-X-2440, pp 1002-6) OBSERVATIONS OF COSMIC-RAY-INDUCED PHOSPHENES ON APOLLO 14. Chapman, P. K. (Manned Spacecraft Center, Houston, Tex.); Pinsky, L. S.; Benson, R. E.; Budinger, T. F. Jan 1972.

From Symposium on natural and manmade radiation in space; Las Vegas, Nev. (1 Mar 1971).

The observations of cosmic-ray phosphenes on Apollo 14 were very simple, required no equipment, and were carried out on a time-available basis. They provided the first quantitative data on the statistics of this phenomenon, but by far the most significant result was the discovery that it is not necessary to be dark-adapted to see flashes. This is strong evidence that some, and probably most, of the flashes are produced by mechanisms other than Cherenkov radiation. It is probable that many of the flashes are due to direct ionizing interactions in the retina. This conclusion is supported by experiments of Tobias and his associates, in which flashes were observed by subjects exposed to low-energy neutron beams. Neutrons, being uncharged, of course cannot produce Cherenkov radiation directly, and the beams employed were energetically incapable of producing charged spallation products of sufficient velocity. (auth)

53408 (NASA-TM-X-2440, pp 1007-15) HEAVY-PARTICLE HAZARD: WHAT PHYSICAL DATA ARE NEEDED? Curtis, S. B. (Univ. of California, Berkeley); Wilkinson, M. C. Jan 1972.

From Symposium on natural and manmade radiation in space; Las Vegas, Nev. (1 Mar 1971).

Several areas are mentioned where physical data are needed in order to evaluate adequately the potential hazard of high-energy heavy ions in the galactic cosmic radiation to long manned missions outside our magnetosphere. The first, more data on the lower energy portion of the differential energy spectrum of the iron group, can be obtained in appropriately instrumented satellites during the next period of solar inactivity 1975 to 1977. The other two areas, nuclear interaction parameters in tissue and aluminum and the structure of the energy deposition along the trajectory of the tracks, appear to require an accelerator that accelerates ions of the iron group up to at least 300 to 500 MeV/nucleon. This information, along with the necessary biological information concerning the extent of damage and functional impairment to various critical organs, is necessary before we can confidently send manned expeditions to explore the near planets or establish bases for extended exploration of the moon. (auth)

53409 (STI/PUB-295(Vol.4)) ATLAS OF RADIATION DOSE DISTRIBUTIONS. VOLUME IV. BRACHYTHERAPY ISODOSE CHARTS SEALED RADIUM SOURCES. Stovall, Marilyn; Lanzl, L. H.; Moos, W. S. (International Atomic Energy Agency, Vienna (Austria)). 1972. 142p. IAEA $20.00.

This volume of the Atlas of Radiation Dose Distributions is devoted to brachytherapy isodose charts for sealed ^{226}Ra sources used for therapy. Part I comprises the main text, bibliography, a list of suppliers of sources and accessory equipment. Part II includes 192 isodose charts of the γ dose distribution. (C.H.)

53410 RADIATION PROTECTION PROSTHESES FOR EDENTULOUS PATIENTS. Aramany, Mohamed A.; Drane, Joe B. (Univ. of Pittsburgh. M. D. Anderson Hospital and Tumor Inst., Houston, Tex.). J. Prosth. Dent.; 27: No. 3, 292-6(Mar 1972).

A simplified technique for the construction of radiation protection prostheses for edentulous patients is described. A direct wax pattern is formed on a cold-curing acrylic resin base. A direct method for applying radiation shield material in the stent is incorporated in the procedure. (auth)

53411 CLINICAL ASPECTS OF RADIATION INJURY SIMULATION AND RECUPERATION. Gus'kova, A. K. (Inst. of Industrial Hygiene and Occupational Diseases, Moscow). Med. Radiol.; 17: No. 8, 7-15(Aug 1972). (In Russian).

Difficulties arising in simulating radiation injuries and recovery in man are analyzed. The author's personal clinical experience and literature sources served as a background for recommendations as to the choice of the most suitable classification of clinical forms, significant dosimetric parameters, and a rational simplification of the intricate pathological process, bringing it to the level of a critical structure or function allowing one to quantificate the lesion and post-radiation recovery. Mention is made of peculiarities particular to the solution of these problems with special reference to systems and organs presenting different anatomo-functional organization. (auth)

53412 MORTALITY EXPERIENCE OF THE COMMUNITY AND OF THE FLUORSPAR MINING EMPLOYEES AT ST. LAWRENCE, NEWFOUNDLAND. de Villiers, A. J.; Windish, J. P.; Brent, F. de N.; (and others). Occup. Health Rev.; 22: 1-15(1971).

Data are summarized from an epidemiological survey of mortality at St. Lawrence, Newfoundland, a community where approximately 2,000 men had been employed in fluorspar mining for various periods of time. Surveys conducted during 1959 showed high concentrations of radon and radon daughter products in the mine air, although there was no known source of any uranium ore. The installation of additional mechanical ventilation in 1962 resulted in concentrations of airborne radioactivity below the safety level. The relationship between occupational factors and causes of death was studied using mortality data for the years 1933 to 1968, during which 250 deaths occurred for miners. Data are tabulated on the number of malignant neoplasms of all sites, and those involving the trachea, bronchus, and lungs; tuberculosis of the respiratory system; other respiratory system diseases; and accidents. One-hundred and fifty-five deaths occurred among individuals who had accumulated more than 1,000 underground working hours, of which 78 (50.3%) were due to lung conditions, including 52 cases (33.5%) of lung cancer, 11 cases (7.1%) of malignant diseases of the buccal cavity and gastrointestinal tract, and 20 cases (12.9%) of tuberculosis death. A review of the lung cancer deaths showed the average age at death to be 48.9 years, with the average age at first exposure being 21 years, or a latent period between first exposure to radon and death of 21.7 years. (C.H.)

53413 MEDICAL USES OF IONIZING RADIATION AND RADIOISOTOPES. REPORT OF A JOINT IAEA/WHO EXPERT COMMITTEE. World Health Organ., Tech. Rep. Ser.; No. 492, 1-56 (1972).

The medical uses of radiation have gradually expanded and three separate disciplines have emerged: radiodiagnosis, radiotherapy and nuclear medicine. A Joint IAEA/WHO Expert Committee examined the benefits that can be derived from the medical uses of radiation and radioisotopes, and the means of obtaining the best results. The use of diagnostic radiology has increased dramatically in the highly developed countries, where over half the population is likely to receive an x ray diagnostic examination each year. The Committee considered the possibilities of improving existing services and the number and type of examinations for which facilities should be made available. The equipment and supplies needed by departments of diagnostic radiology and the training of personnel are also discussed. Radiotherapy has now become one of the most important methods of treating cancer, taking its place alongside surgery as a method for both curative and palliative treatment. The Committee considered the organization of radiotherapy departments, with particular reference to the accommodation, equipment, and staff required. During the last 10 years there has been a rapid increase in the applications of unsealed radioactive materials for diagnostic and therapeutic purposes, and nuclear medicine has now become an established branch of radiation medicine. A brief account is given of the types of procedure now available, the types of establishment in which these procedures can appropriately be carried out, and the facilities required. Attention is paid to objectives and priorities in the development of nuclear medicine services. A number of conclusions are presented and recommendations for improvements are included. (C.H.)

53414 LATE EFFECTS OF ATOMIC RADIATION. Shiomi, T. Bild Wiss.; 9: No. 5, 466-75(1972). (In German).

For many years, experts have held the view that the fission products of the fallout and the residual radiation resulting from the explosion of the atomic bombs over Japan have not produced any biological effect. This view has now been overthrown by an investigation on inhabitants of Nagasaki. Three test groups were examined for chromosomal aberrations, and it was found that persons subjected to residual radiation showed a significantly higher percentage of chromosomal aberrations than a control group that had not been exposed to radiation. According to the author, the radiation exposure caused by the explosion of the atomic bomb over Nagasaki is to be regarded as a special case within the framework of a generally increasing contamination of the environment by artificially induced radiation. (GF)

53415 THERMOLUMINESCENT DOSIMETRY IN PATIENTS TREATED WITH HIGH-ENERGY ELECTRONS. Van Dam, J. (Academisch Ziekenhuis St. Rafaeel, Louvain, Belgium). J. Belge Radiol.; 55: No. 2, 293-6(1972). (In Dutch).

Thermoluminescent dosimetry was used as a daily check of the reproducibility of the ratio of the dose delivered to the dose asked by the doctor for patients irradiated with electrons of high energy. A special study was devoted to cases where the curvature of the skin surface rendered difficult correct and reproducible positioning of the patient. From one therapeutic session to another the differences between the ratios of the dose delivered to the dose asked can be of the order of 10%. (auth)

53416 DOSIMETRY IN RADIODIAGNOSIS. Van Elegem, P. (Univ. Libre, Brussels); Brunfaut, C.; Lejeune, S. J. Belge Radiol.; 55: No. 2, 271-83(1972). (In French).

The doses absorbed by the patient for various classical tests in diagnostic radiography were measured in a tissue equivalent phantom. These measurements were compared with those given in the literature and a method for predetermination of absorbed doses is suggested. The paper ends with a recall of means to be used to reduce the dose at the patient level, all necessary information for the diagnosis being kept. (auth)

53417 PEDIATRIC RADIOLOGY AND IRRADIATION. Claus, D.; Gillet, R.; Wambersie, A. (Univ., Louvain, Belgium). J. Belge Radiol.; 55: No. 2, 163-9(1972). (In French).

Protection in pediatric radiology presents a particular problem as the child is especially sensitive to x rays and is in fact very often unnecessarily overexposed. A correct adjustment of the apparatus and of the test techniques is indispensable. On the basis of a few measurements, a tentative estimate of the doses received by the child during radiological tests was made, as well as of the way the irradiation varies according to the utilized technique. (auth)

53418 OSTEORADIONECROSIS OF THE MANDIBLE. Rankow, Robin M.; Weissman, Bruce (Columbia Presbyterian Medical Center, New York). Ann. Otol., Rhinol., Laryngol.; 80: No. 4, 603-11(Aug 1971).

The usual accepted incidence of osteoradionecrosis of the mandible after radiotherapy for a head and neck cancer is 5 to 10%. The trend to higher doses of irradiation with megavoltage and hyperbaric oxygenation techniques is providing a greater cure rate, but increases severe complications such as osteoradionecrosis. Surgical treatment is indicated after one year of intractable pain or bone exposure unresponsive to vigorous medical therapy. Orocutaneous fistulization is a more immediate cause for surgery. The technical advantages of intraoral hemimandibulectomy are emphasized. (auth)

53419 COMBINED RADIATION INJURIES. Messerschmidt, O. Strahlenschutz Forsch. Prax.; 11: 78-90(1971). (In German).

Combined radiation injuries and traumatic injuries are discussed, especially with respect to the Russian literature. The healing of traumatic skin injuries following whole-body irradiation is considered and early and complete closure of the wounds is recommended. Also the combination of irradiation and gunshot wounds is considered. Prognosis and type of treatment depend on the time interval between irradiation and infliction of the wound; surgical treatment of abdominal injuries yields much poorer results in irradiated animals. Best results are obtained when surgery is performed during the latent period, after subsiding of the initial reaction. The combination of radiation with thermal burns is considered, and the effects of irradiation on the results of skin transplantation and on the healing of bone fractures are reviewed. (H.B.G.)

53420 CHROMOSOME ANOMALIES FOR BIOLOGICAL DOSIMETRY. Fritz-Niggli, H. Strahlenschutz Forsch. Prax.; 11: 36-47(1971). (In German).

The feasibility of using chromosome aberrations in human lymphocytes as a biological dosimeter is reviewed. It is concluded that doses of about 10 rem can be detected. Only for high doses delivered in a short time, a clear dose-effect relationship can be established. Chromosome analysis may be of value in installations with high accident risks. In any case, chromosome analysis should be performed on every person before employment in such installations. Disadvantages of chromosome analysis are the facts that the method is time-consuming and that aberrations can also be produced by chemicals and viruses. (H.B.G.)

53421 IMAGE INTENSIFIERS AND FLUOROSCOPY STABILIZERS. Airth, G. R. (Southmead Hospital, Bristol, Eng.). Brit. J. Radiol.; 45: No. 536, 627(Aug 1972).

The problems of achieving a constant and adequate input x ray dose rate to an image intensifier when fluoroscopy stabilization is in use during diagnostic radiography are briefly considered. Patient hazards are considered as the intensifier ages and the stabilizer needs more current. It is pointed out that a maximum number of patients should be examined using one image intensifier, because of its relatively short working life. The need for frequent checks on currents and dose rates is also emphasized. (UK)

53422 DOSIMETRY IN INTERSTITIAL THERAPY ^{192}Ir WIRES (PARIS TECHNIQUE): APPLICATIONS IN ONE PLANE. Wambersie, A. (Institut du Cancer, Louvain, Belgium); Dutreix, A.; Pierquin, B.; Dardenne, J. C. J. Belge Radiol.; 55: No. 2, 197-206(1972). (In French).

The results of a previsional dosimetric study in interstitial therapy are presented. They concern applications in one plane of rectilinear, parallel, equidistant ^{192}Ir wires ("Paris technique"). Dose distribution in orthogonal planes was computed systematically for different arrangements of the wires (number, length, separation). From these results, the dimensions of the target volumes that can be treated by an application of 1, 2, . . . 5 coplanar wires are determined. For this aim, four rules for the applications are defined and discussed. Diagrams are proposed for the evaluation of the numbers of wires to be used as a function of the dimensions of the volume to be treated. Then, other diagrams allow to evaluate the separation between the wires and the reference dose to be chosen. Two examples are discussed. (auth)

53423 CLINICAL CONTRIBUTION TO THE UNDERSTANDING OF RADIATION-INDUCED SIALOADENITIS. Jucker, C. (Univ., Pavia, Italy). Radiaz. Alta Energ.; 11: No. 1, 21-38(Jan 1972). (In Italian).

A description of two cases of inflammation of the salivary glands caused by therapeutic irradiation is presented. The following aspects of this quite infrequent complication are described: chemical aspects; sialographic reports; the element which, in laboratory analyses, provide evidence of sialoadenitis due to massive irradiation, namely hyperamylasaemia; and the anatomic-histological substratum. (auth)

53424 RADIATED DOSE TO SKIN OF FINGERS DURING INJECTION OF RADIOACTIVE SUBSTANCES. Takaku, Yuji (Fukushima Medical Coll., Japan); Kida, Toshiyuki. Rinsho Hoshasen; 16: No. 10, 814-16(Oct 1971). (In Japanese).

With the development of nuclear medicine, the frequency of radioisotope application has greatly increased, and exposure of the operators' fingers at injection has become a problem. The exposure of the operator due to routine operations was determined. Gold-198, ^{131}I, ^{203}Hg, and ^{59}Fe, which are often used for clinical examination, were applied as radioactive substances. Doses of 10 μCi of ^{59}Fe and 100 μCi of the other substances were placed into either 1 ml or 2.5 ml plastic syringes. Oil clay models of the fingers were made, and the conditions of the exposure were determined with a thermoluminescent dosemeter for counts on skin, and Toshiba fluorescence glass dosemeter for counts on bone. As the result, the exposure decreased conspicuously with increasing distance from the radioisotope filled part of the syringes. The maximum dose limit permitted by law is 20 rem for 3 months. Frequencies corresponding to the limit for each isotope are shown. The larger syringe showed less exposure. The exposure depended on γ-ray energy rather than β-ray energy, and higher exposures were obtained by higher energies. (Japan)

53425 TWO AUTOPSY CASES OF RADIATION MYELOPATHY. CONSIDERATION ABOUT THE PATHOGENESIS. Okeda, Riki (Tokyo Medical and Dental Univ.). Shinkei Kenkyu No Shinpo; 15: No. 3, 619-39(Aug 1971). (In Japanese).

Two autopsy cases of radiation myelopathy are reported. Case 1 was a 51 year old man with carcinoma of the larynx, to which a tumor dose of 7100 R/65 days by Tele-therapy (^{60}Co) was administered from the bilateral sides of the neck. Each field size was 8 × 10 cm. Thus, from the 2nd to 7th cervical vertebrae were involved in the direct beam. Case 2 was a 38 year old man with carcinoma of the epipharynx with metastasis to the bilateral submaxillary lymph nodes. To these lymph nodes, a tumor dose of 5986 R/48 days by Tele-therapy (^{60}Co) was administered in the same way as in case 1. In the direct beam, this time, from the 2nd to 5th cervical vertebrae were involved. Localization of lesions in the spinal cord of these two cases corresponded to the area exposed to the direct beam of ^{60}Co, namely, in case 1 from the 5th to 7th cervical segments and in case 2 from the 3rd to 4th cervical segments. In neither case was tumor invasion in and around the spinal cord, deformation of vertebrae, or vascular anomaly in the arachnoidea found. The spacial dispositions of the parenchymal lesions were closely related with the pathological changes of vessels, from capillaries to veins. It was not possible to determine if these vascular changes were secondary to the parenchymal alterations. Similarity of these parenchymal and vascular changes with Foix-Alajouanine's disease is discussed in the paper. As for the cause of these changes, increase of intramedullary venous pressure, which is mainly due to disturbance of venous return by venous lesions in the arachnoida and arterio-venous shunt developed or newly formed secondary to decrease of capillary beds, is considered. (Japan)

53426 EVALUATION OF EXPOSURE DOSES TO PERSONNEL AT HIGH-POWER BETA RADIATION INSTALLATIONS. Korenkov, I. P.; Mamin, E. B.; Chistov, E. D. At. Energ. (USSR); 32: No. 5, 434-5(May 1972). (In Russian).

Personnel at high-level beta installations are subjected to mixed β-γ radiations, the γ component being comprised of bremsstrahlung and accompanying radiations. An analysis of the B, γ, and $\beta + \gamma$ doses received by five different parts of the body was tabulated for assembly–disassembly workers and for operating personnel. A comparison of these data with corresponding phantom measurements showed that the worker constantly changes his orientation relative to the radiation sources, with the hands and pelvis, in particular, receiving smaller doses than those of the phantom. (K.S.W.)

53427 CHROMOSOME ABERRATIONS FOLLOWING REPEATED GASTRIC ROENTGEN EXAMINATIONS. Hajdu, Imre. Orv. Hetil.; 112: No. 31, 1834-8(1 Aug 1971). (In Hungarian).

In order to examine the known radiation injury of chromosomes after repeated exposure to x radiation, the chromosomes in leukocytes of 50 patients in the reproductive age group subjected to diagnostic x radiation because of sickness of the digestive tract were examined for aberrations. Each of the patients, aged 23 to 41 years, experienced at least 3 diagnostic radiographic examinations, but were not subjected to any therapeutic x-ray treatment. The man:woman ratio of the group was 27:23. During the 10-minute long fluoroscopic radiographic examination of the stomach the stomach wall is exposed to a dose of about 100 to 150 R; the gonad dose was estimated at 500 mR. In every case 50 dividing cells in the peripheral blood were examined in order to determine the occurrence of mitotic cells with chromosome anomalies. In 38.8% of the 36 cases for which the examination were completed, dicentric chromosomes, considered the most sensitive indicators of radiation injury, were observed. No chromosome anomalies were detected in the control group. In view of the potential danger of stomach x-ray examinations for the populations, it is recommended to limit them strictly; not only radiologists but clinicians requesting such examinations should be advised of this genetic risk. (TTT)

53428 STUDIES OF CHROMOSOME ABERRATIONS IN PERIPHERAL BLOOD OF ROENTGENOLOGISTS. Slowikowska, Maria G.; Grzymala, Wieslaw (State Inst. of Hygiene, Warsaw). Nukleonika; 17: No. 3-4, 241-8(1972). (In Polish).

Cytogenetic analyses were performed on peripheral leukocytes from 13 roentgenologists and 10 controls. On the basis of the results it was concluded that there was a difference between the exposed persons and the controls in occurrence of aneuploid and polyploid cells. The frequency of chromatid breaks and the rate of chromosome aberration per metaphase were clearly greater in the exposed than in the control group. (auth)

53429 RADIATION MYELOPATHY, WITH SPECIAL REFERENCE TO ITS ETIOLOGY. Ishida, Yoichi (Gunma Univ., Maebashi, Japan). Igaku No Ayumi; 80: No. 9, 555-63(Feb 1972). (In Japanese).

The etiology of radiation myelopathy is discussed in relation to the theory of circulatory necrosis, that of antigen-antibody reactions, and the cell reproductive death theory. Radiation myelopathy is a myelopathy occurring following radiotherapy of cancer when the spinal cord is included in the field of radiation and is a delayed radionecrosis of mature nervous tissues in the spinal cord. The histological picture of lesions in the spinal cord nerve cells, blood vessels, and collagen cells during radionecrosis development are described. (Japan)

53430 CLINICAL TRIALS OF RADIOSENSITIZERS AND FRACTIONATION. Revesz, L. (Karolinska Institutet, Stockholm); Scott, O. C. A. Brit. J. Radiol.; 45: No. 536, 626(Aug 1972).

The dangers of assuming that sensitization is independent of radiation dose are briefly mentioned in relation to clinical trials of Synkavit and to dose fractionation. Examples are given from experiments with O_2 or TAN. It is pointed out that it is not known whether hypoxic or anoxic foci in tumors are the greater concern in radiotherapy. Hypoxic cells have a large D_0, but are capable of recovery. On the other hand, the hypoxic cells may be eliminated as a result of reoxygenation, fully anoxic cells not being so accessible. If anoxic cells were to persist during a fractionated treatment, later giving rise to local recurrence, they might not respond to known sensitizers if combined with small fractions. (UK)

53431 RADIOBIOLOGY FORUM ON RADIOLOGICAL PROTECTION AND THE SKIN. SPECIAL REPORT No. 6. PROTECTION AGAINST IONIZING RADIATIONS. Vennart, J.; Cryer, M. A. (Medical Research Council, Harwell, Eng.). Brit. J. Radiol.; 45: No. 536, 610-20(Aug 1972).

A brief report is made of the forum under the following headings: microanatomy and thickness of the skin; radiation dose and minimal reactions in chronically irradiated skin; clinical effects of radiation; radiation induced tumors, including human experience; radiological protection of workers; and cells at risk, dose limits, and critical area. (UK)

53432 RADIATION, IMMUNITY, AND CANCER. Lancet; 2: No. 7770, 217-18(29 Jul 1972).

The effects of radiotherapy in terms of the effects on the immunological system are briefly discussed in general terms. It is pointed out that current predictions are that most human tumor cells will prove to have specific antigens on their surface. The following examples of immunological disturbance are given: analysis of the survivors of Hiroshima and Nagasaki indicated that lymphoma tended to be induced at the relatively high radiation doses affecting the body's immunity; and irradiation for therapy of mammary cancer produces a lymphopenia, reflecting a fall in the formation of lymphocytes. It is pointed out that this would diminish cell-mediated hypersensitivity reactions and the humoral antibody response to thymus-dependent antigens. (UK)

53433 TOXIC ERUPTIONS COMBINED WITH RADIATION THERAPY OF MALIGNANT TUMORS. Moriya, Hiroshi; Kaneko; Itsuo; Matsushima, Hideno; Yamada, Teruyo (Toho Univ., Tokyo). Toho Igakkai Zasshi; 18: No. 6, 925-8(Dec 1971). (In Japanese).

Three cases of skin eruptions occurring during radiation therapy of malignant tumors were reported. The cutaneous reactions developed at various periods after irradiation. Case No. 1 was a 55-year-old female with uterine cervical carcinoma, who was treated with telecobalt irradiation (^{60}Co). Spatial doses of 300 R were delivered to the 15 × 15 cm^2 field of the frontal and lateral pelvic walls alternately every day. After 9 days, mild macular eruptions occurred with a fever. Case No. 2 was a male 66 years of age with lung cancer combined with gynecomastism, who was treated with total doses of 6000 R telecobalt irradiation (^{60}Co) for 45 days. Seven days after the radiation therapy, macular eruptions accompanied with a high fever were observed. Case No. 3 was a 25-year-old female with adenocarcinoma, to whom total doses of 6000 R telecobalt irradiation were given during the treatment period totaling 45 days with intervals. Eight weeks after the therapy, mild eruptions were observed. It was considered that these reactions were caused by therapeutic irradiation. The toxic eruptions disappeared eventually, 2 to 3 months later by stopping irradiation. (Japan)

53434 DOSE TO PATIENTS FROM ROENTGENOGRAPHY. Antoku, S.; Russell, W. J.; Milton, R. C.; (and others) (Atomic Bomb Casualty Commission, Hiroshima). Health Phys.; 23: No. 3, 291-9(Sep 1972).

The roentgenological examinations reported by A-bomb survivors and their comparisons participating in the ABCC-JNIH Adult Health Study were confirmed in surveys of Hiroshima and Nagasaki hospitals and clinics. Technical exposure factors provided during the latter were used in phantom dosimetry, duplicating the examinations received by the subjects. Bone marrow integral, gonadal, and skin doses so obtained were compared with those of other investigators, and were applied to population data to estimate the magnitude of cumulated dose from medical x-ray examinations in comparison to that from the Hiroshima and Nagasaki A-bombs. (auth)

53435 EVALUATION OF EPIDEMIOLOGIC STUDIES OF LEUKEMIA AND OTHER MALIGNANCIES AFTER DIAGNOSTIC X RADIATION. Stewart, Alice; Davis, A. K.; Silverman, Charlotte (Food and Drug Administration, Rockville, Md.). pp 117-26 of Radiation Protection Standards: Quo Vadis. Vol. I. Howell, Wallace P. (ed.). Richland, Wash.; Health Physics Society (1972).

From 6th annual topical symposium on radiation protection standards: quo vadis; Richland, Wash. (2 Nov 1971).

Ninety percent of the excess radiation exposure of the population is due to diagnostic procedures and, consequently, possible biological effects of this low-level exposure are of great significance. A controversy has developed as to whether such exposures produce measurable changes in the incidence not only of leukemia but also of other malignancies. Since Stewart's original survey of all malignancies in children showed that prenatal radiation was correlated with malignant disease, this problem has been examined by several investigators. Such studies require large numbers of children, as leukemias and other malignancies are relatively rare and the dose of the few hundred millirem is unlikely to produce a large increase in the basic rate. Certain investigators have reported a correlation between diagnostic radiation exposure and an increase in malignancy, but others have been unable to substantiate this. A critical review of the past and current work in this field is presented, and an attempt is made to interpret the different findings of the several investigators. (auth)

53436 COMMENTS ON NUMERICAL VALUES FOR RADIATION EXPOSURE LIMITS. Baietti, Albert L. (International Chemical and Nuclear Corp., Irvine, Calif.). pp 452-7 of Radiation Protection Standards: Quo Vadis. Vol. II. Howell, Wallace P. (ed.). Richland, Wash.; Health Physics Society (1972).

From 6th annual topical symposium on radiation protection standards: quo vadis; Richland, Wash. (2 Nov 1971).

Personal observations are made on the use and application of numerical values for radiation exposure limits as specified by regulatory agencies. Examples are given of possible criteria that might more meaningfully reflect the relationship between radiation protection criteria and guides used or needed by operational health physicists. Particular emphasis is given to radiation exposure records and their meaning. It is suggested that present day practice may be encouraging the use of overly precise numerical values for radiation exposure measurements. (auth)

53437 IONIZING RADIATIONS AND MALFORMATIONS OF THE BRAIN. Murakami, Ujihiro (Nagoya Univ., Japan). Shinkei Kenkyu No Shinpo; 16: No. 2, 330-6(Apr 1972). (In Japanese).

Pathological effects of prenatal ionizing radiations on the developing brain and postnatal manifestations are divided into two types: the one caused by misuse of radiation treatment and the other caused by exposure to the atomic bomb, during various stages of gestation. Results of the experimental irradiation of pregnant animals during preimplantation period and stage of organogenesis, and at various stages of embryonic and fetal development, are discussed citing reference sources. The following conditions were observed frequently in animal experiments as pathological effects: stunted growth, hydrocephaly, microcephaly, microphthalmus, anencephaly, and brain stem and bone marrow anomalies. Malformations, especially those of the central nervous system, and pigmentary degeneration of the retina, cataracts, and urogenital and skeletal anomalies in children following therapeutic application of radium and x-rays during pregnancy are discussed with reference to the literature, and pathological effects of the atomic bomb explosion are reviewed. (Japan)

53438 SURGICAL TREATMENT FOR LOCAL RADIATION INJURIES FOLLOWING RADIOTHERAPY. Yasuna, Osamu; Nakamura, Kinichi; Sano, Hiroshi; Matsushita, Masamitsu; Yamazaki, Makoto (Shinshu Univ., Japan). Nippon Saigai Igakkai Kaishi; 19: No. 8, 367-72(Aug 1971). (In Japanese).

Nineteen cases of local radiation injury were examined. In patients with carcinoma of the esophagus, esophageal perforation and esophagotracheal fistula occurred during radiation therapy in which relatively small dosages of irradiation were given for a period of 2 weeks to 1 month. Esophageal perforation tended to occur during the early stage of irradiation administered for sarcoma of the stomach. The radiation injury of the small intestine tended to occur a few months or even a few years after the therapy program was completed. Chronic radiation injuries became gradually worse and tended to advance into stenosis or intestinal obstruction. Ulcer and perforation sometimes occurred from radiation injury of the blood vessels. One year after radiation therapy for uterine cancer and cancer of the rectum, fistula tended to occur either in the digestive tract or in the urinary passage. Radiation ulcers in the skin, caused by pathological changes in blood vessels as a result of mammary carcinoma therapy, tended to cause hemorrhage. Such a condition can not be cured easily. Therefore the careful observation and treatment after therapy should be continued. Use of thoracoepigastric tubes was recommended for healing the area affected by ulcer. Excessive radiation therapy should be avoided, by conducting regular biopsies to examine pathological changes. (Japan)

53439 RADIATION INDUCED HEART FAILURE. 1. ELECTROCARDIOGRAPHY FINDING. Sato, S. (Aichi Cancer Center, Nagoya, Japan); Tomita, Kazuo; Kitagawa, Toshio. Nippon Igaku Hoshasen Gakkai Zasshi; 31: No. 7, 859-64(Oct 1971). (In Japanese).

When massive doses are administered to the tumorous lesion homogeneously in the treatment field with high energy radiation, radiation damage to the heart, which is involved in the same treatment field incidentally, should be taken into consideration. In 115 cases with carcinoma of the esophagus, the heart and lungs were studied. Twenty-six cases were treated with a telecobalt unit and 89 cases underwent 6 MV x-ray treatment. They were treated with the opposing-field technique antero-posteriorly. The estimated dose to the heart was 4000 to 7000 rads in 6 to 8 weeks with the ^{60}Co unit, and 5000 to 7000 rads in 6 to 8 weeks with the 6 MV x-ray unit. Electrocardiograms (ECG) were taken during and after completion of the treatment course in conjunction with clinical observations. Appearance rate and variety of the abnormal findings of the ECG were analyzed. The following results were observed. Abnormal findings on the ECG appeared in 60% of all cases. They were found mostly at the period of the time between one and two months after completion of the treatment. Sixty percent of these improved into the normal limit in two months without any treatment. These changes were thought to be the result of acute or subacute reversible radiation reactions in the heart and they did not show any definite clinical symptoms. Irreversible changes in the remaining cases were indicative of real heart failure for clinical purposes. Not enough information was available to continue this study because the follow up of many cases in this series was not more than one year because of their progressed tumor lesions. Dose dependency in the abnormal ECG appearance was not clearly indicated. (auth)

53440 EXTRACORPOREAL IRRADIATION OF THE BLOOD. EFFECT OF VARYING TRANSIT DOSE ON THE DEGREE AND THE RATE OF DEVELOPMENT OF LYMPHOPENIA. Weeke, Eva (Rigshospitalet, Copenhagen). Acta Med. Scand.; 191: No. 5, 455-62(May 1972).

The main data of three types of equipments for extracorporeal irradiation of blood (ECIB) are presented. Results from irradiation of 80 patients are given. The average duration of ECIB was 103 hr. The mean transit dose was 295 rads and the mean total dose 42,850 rads. The lymphocyte concentration was reduced from 1,350 ± 526 before to 335 ± 122 after ECIB. The rate of development of lymphopenia was slower for patients having received significantly lower transit doses, but reduction of the lymphocyte concentration was the same for all patients. There was no correlation between flow rate, calculated as the number of patients' blood volumes irradiated per hour, and the rate of development of lymphopenia. For the patients who were not transplanted immediately, the lymphocyte concentration was followed for the next 12 months. It was shown that a prolonged lymphocyte reduction is obtained after ECIB with high transit doses. (Sweden)

53441 DNA, RNA, AND ULTRASTRUCTURAL ASPECTS OF HUMAN EPIDERMIS IN CHRONIC REACTIONS OF THE SKIN AFTER ROENTGEN IRRADIATION. Squassabia, A.; Maestro, A.; Donati, L.; Casolo, F. (Univ., Pavia, Italy). Med. Nucl.-Radiobiol. Lat.; 12: No. 3-4, 221-36(1969). (In Italian).

The ultrastructural aspects and the contents of DNA and RNA in two series of human epidermis samples taken from skin having both chronic radioatrophic and radiodermatitis aspects were studied. An increase of DNA in chronic radiodermatitis was observed. In radioatrophic skin, DNA was slightly reduced. On the electron microscope, the epidermis alterations of radioatrophic skin were prevalently observed in the nucleus. As to skin with radiodermatitis, cytoplasmatic lesions were prevalently observed. (auth)

53442 CARCINOGENESIS IN THE SURVIVORS EXPOSED TO A-BOMB IRRADIATION IN THEIR YOUTH, 1950 TO 1969. Jablon, Seymour; Tachikawa, Kiyoshi (Atomic Bomb Casualty Commission, Hirsohima). Hiroshima Igaku; 24: No. 11, 1115-19(Nov 1971). (In Japanese).

The occurrence rate of malignant neoplasms was investigated in 20,609 subjects (15,584 with irradiation; 5,025 without direct irradiation) who were under 10 yrs old and lived in Nagasaki city when the atomic bomb was dropped. Among survivors who had 100 R of irradiation at the time of bombing, there were none who had been diagnosed as having malignant neoplasms (except leukemia) before 1958. Among 1,109 survivors (at the time of Jan. 1955) who either had more than 100 R or had an unknown dosage of A-Bomb irradiation, eight died of leukemia (estimating death rate: 0.42) and eight died of other malignant neoplasms (estimating death rate: 1.1) by 1969. This statistical rate was significantly high. Furthermore, there occurred five cases of carcinoma of the thyroid (estimating occurrence rate: 2.2) and six cases of other malignant neoplasms (estimating occurrence rate: 1.3). (Japan)

53443 EXPOSURE OF RADIOLOGISTS DURING SPECIAL PROCEDURES. Riley, Richard C.; Birks, John W.; Palacios, Enrique; Templeton, Arch W. (Univ. of Kansas, Kansas City). Radiology; 104: No. 3, 679-83(Sep 1972).

During special procedures, radiologists may receive substantial radiation exposure, especially to the unprotected lens of the eye: 92% of a radiologist's exposure at arteriography is due to radiography at the time of contrast medium injection. The mean lens exposure per exam is 5.8 mR for cerebral and 27.1 mR for abdominal arteriograms. Unshielded by the lead apron, a front-collar film badge overestimates lens exposure by 20% for cerebral and underestimates by 20% for abdominal arteriograms. Since most exposure occurs during contrast medium injection, manual injection should be avoided whenever possible. (auth)

53444 RETINAL AND OPTIC NERVE COMPLICATIONS IN A HIGH DOSE IRRADIATION TECHNIQUE OF ETHMOID SINUS AND NASAL CAVITY. Shukovsky, Leonard J.; Fletcher, Gilbert H. (Univ. of Texas, Houston). Radiology; 104: No. 3, 629-34(Sep 1972).

Thirty patients with tumor of the ethmoid sinus and nasal cavity were treated with megavoltage irradiation. High doses were delivered to the tumor and adjacent retina and optic nerve. Eighty-seven per cent of the squamous cell carcinomas were locally controlled and 67% of the patients were alive and free of disease at four years or more. The clinical and funduscopic changes associated with radiation injury of the retina and optic nerve include macular and retinal degeneration, optic nerve atrophy, central artery thromboisis, and blindness. Damage to the retina and optic nerve is correlated with a time-dose response curve. (auth)

53445 CHROMOSOME ABERRATIONS INDUCED IN HUMAN BONE-MARROW CELLS BY THERAPEUTICAL LOCAL γ IRRADIATION: TIME AND DOSE RELATIONSHIPS. Pyatkin, E. K.; Alexsandrov, N. N.; Vorobev, A. I.; Petrova, S. A.; Suskov, I. I. (Inst. of Biophysics, Moscow). Mutat. Res.; 16: No. 1, 103-9 (Sep 1972).

Bone-marrow cell chromosome aberrations were studied in 14 unirradiated control patients with malignant tumors and 132 comparable patients after a single localized exposure to ^{60}Co γ irradiation. In control patients, the chromosome break frequency was 0.01 per cell and aberrant cell frequency was 1.1%. In 79 patients, the dependence of chromosome aberrations on the time interval after irradiation following a dose of 250 rad was studied. The highest frequency of aberrant cells was observed 18 and 21 hr after a single irradiation (about 65%). It was shown that the number of chromosome aberrations in cells entering mitosis soon after irradiation (apparently the G_2 cells) was much greater (438.1 aberrations per 100 cells) than that in cells entering mitosis in other periods. A sharp decrease in the number of aberrant cells and aberrations was observed 72 and 96 hr after irradiation, and especially at 120 and 168 hr. In 67 patients, the relation between dose and chromosome aberration yield was studied. It was shown that the yield of chromosomally aberrant cells increases linearly with dose, according to the equation $Y = 6.385 + 0.195 \cdot D$. (auth)

53446 NEUROPATHOLOGIC EFFECTS OF PROTON-BEAM IRRADIATION IN MAN. II. EVALUATION AFTER PITUITARY IRRADIATION. Nielsen, S. L.; Kjellberg, R. N.; Asbury, A. K.; Koehler, A. M. (Massachusetts General Hospital, Boston). Acta Neuropathol.; 21: No. 1, 76-82(1972).

Neuropathological material from eight patients hypophysectomized by proton-beam irradiation was studied. In no instance was radiation damage to the brain clinically evident. However, in the brains of five of these patients, small radionecrotic lesions were found in the medial temporal lobes and hypothalamus, and the extent of pituitary necrosis was documented. Possible pathogenic factors in the development of lesions in these areas of the brain are briefly discussed. (auth)

Vertebrates

Refer also to abstracts 53512 and 54871.

53447 (CONF-720822-2) RADIATION-INDUCED HEMOPOIETIC LESIONS IN FISH. Cosgrove, G. E.; Blaylock, B. G.; Ulrikson, G. U. (Oak Ridge National Lab., Tenn.); Cohan, P. C. (Cooperative Science Education Center, Inc., Oak Ridge, Tenn.). [nd]. 23p. Dep. NTIS.

From Symposium on fish pathology; Washington, D. C. (7 Aug 1972).

Radioinduced changes in hematopoietic tissues of some 13 species of native and aquarium reared fish were studied following acute or chronic exposure to various doses and dose rates of γ radiation. Acute irradiation induced hemopoietic damage to a greater extent than did chronic or fractionated dose irradiation, even when massive doses were accumulated. A bibliography on hematopoiesis in fish is included. (C.H.)

53448 (COO-1332-78) EFFECTS OF RADIATION ON THE BEHAVIOR OF ANIMALS: A REVIEW OF THE LITERATURE. Appendix to 1972 Progress Report. Preston, J. L. (Minnesota Univ., Minneapolis). 1972. Contract AT(11-1)-1332. 66p. Dep. NTIS.

A review of the literature on effects of radiation on the behavior of animals is presented. The following aspects of behavior were investigated: detection, arousal, and activity changes; orientation; feeding; emotionality; social behavior; reproductive behavior; learning and performance; discrimination learning; maze learning; distractibility; avoidance conditioning; prenatal irradiation effects; aging effects; and genetic effects. (approximately 400 references) (H.L.W.)

53449 (COO-3017-4) RENAL TUMORS IN PARABIOSED IRRADIATED RATS. Warren, Shields; Brown, Clark E.; Porter, Marilyn W. (New England Deaconess Hospital, Boston, Mass. Cancer Research Inst.). [nd]. Contract AT(11-1)-3017. 19p. (CONF-720530-5). Dep. NTIS.

From 20th annual meeting of the Radiation Research Society; Portland, OR. (14 May 1972).

Ninety-five (7.6%) irradiated partners of 1244 parabiosed rats receiving 1000 R of whole-body irradiation developed renal tumors, 10.3% of the males and 5.2% of the females. The commonest types of renal tumors were renal cell carcinomas, adenomas and transitional cell carcinomas. As with irradiation carcinogenesis in general, renal tumors in irradiated rats appear earlier and with greater frequency than spontaneous tumors in nonirradiated rats. The nonneoplastic renal tubular epithelium of the irradiated tumor-bearing kidneys contained fewer mitoses than the renal tubular epithelium of their nonirradiated partners. (auth)

53450 (LA-4874, pp 126-44) SWINE SKIN CHANGES PRODUCED BY DIFFERENT RADIATIONS. Archambeau, John O. (Nassau County Medical Center, East Meadow, N. Y. (USA)). Mar 1972.

From fifth LAMPF users meeting; Los Alamos, NM. (8 Nov 1971).

Studies were conducted on quantification of gross and histologic skin changes produced by increasing absorbed dose increments of different radiations and different time-dose schedules. Cell kinetics of the irradiated epidermal cell population were identified and quantified. The evolution, time course, and dose dependence of the reactions produced by absorbed doses of x rays, thermal neutrons, fission neutrons, the ^{10}B(n,α)^{7}Li reaction, and multiple exposures to x ray were quantified. Variations in the epidermal population and other histological and cytologic changes of the epidermis and dermis were quantified following single absorbed doses of x ray and the ^{10}B(n,α)^{7}Li reactions. Basal cell x ray dose-survival estimates were made. A model of the skin response was developed for making comparisons with the observed results. (H.L.W.)

53451 (NASA-TM-X-2440, pp 622-32) FACTORS MODIFYING THE RESPONSE OF LARGE ANIMALS TO LOW-INTENSITY RADIATION EXPOSURE. Page, Norbert P. (National Cancer Inst., Bethesda, Md.); Still, Edwin T. Jan 1972.

From Symposium on natural and manmade radiation in space; Las Vegas, Nev. (1 Mar 1971).

In assessing the biological response to space radiation, two of the most important modifying factors are dose protraction and dose distribution to the body. Studies are reported in which sheep and swine were used to compare the hematology and lethality response resulting from radiation exposure encountered in a variety of forms, including acute (high dose-rate), chronic (low dose-rate), combinations of acute and chronic, and whether received as a continuous or as fractionated exposure. While sheep and swine are basically similar in response to acute radiation, their sensitivity to chronic irradiation is markedly different. Sheep remain relatively sensitive as the radiation exposure is protracted while swine are more resistant and capable of surviving extremely large doses of chronic irradiation. This response to chronic irradiation correlated well with changes in radiosensitivity and recovery following an acute, sublethal exposure. Swine recover remarkably fast and develop a large and persistent radioresistance. The change in radiosensitivity of sheep after either acute or chronic sublethal exposure is basically the same, consisting of a triphasic pattern of an initial slow recovery, transient radioresistance and regression into a long-lasting period of relative radiosensitivity. The overall effect of receiving both acute and chronic exposures within a short period of time may depend upon the sequence of the exposures. In addition to protraction, spatial or body distribution is a significant factor in the response of large animals to radiation exposure. (auth)

53452 (NASA-TM-X-2440, pp 633-40) EFFECT OF CONTINUOUS GAMMA-RAY EXPOSURE ON PERFORMANCE OF LEARNED TASKS AND EFFECT OF SUBSEQUENT FRACTIONATED EXPOSURES ON BLOOD-FORMING TISSUE. Spalding, J. F.; Holland, L. M.; Prine, J. R.; Farrer, D. N.; Braun, R. G. (Los Alamos Scientific Lab., N. Mex.). Jan 1972.

From Symposium on natural and manmade radiation in space; Las Vegas, Nev. (1 Mar 1971).

Sixteen Macaca mulatta monkeys trained to perform continuous and discrete-avoidance and fixed-ratio tasks with visual and auditory cues were performance-tested before, during, and after 10-day gamma-ray exposures totaling 0, 500, 750, and 1000 rads. Approximately 14 months after the performance-test exposures, surviving animals were exposed to 100-rad gamma-ray fractions at 56-day intervals to observe injury and recovery patterns of blood-forming tissues. The fixed-ratio, food-reward task performance showed a transient decline in all dose groups within 24 hrs of the start of gamma-ray exposure, followed by recovery to normal food-consumption levels within 48 to 72 hrs. Avoidance tasks were performed successfully by all groups during the 10-day exposure, but reaction times of the two higher dose-rate groups in which animals received 3 and 4 rads per hour or total doses of 750 and 1000 rads, respectively, were somewhat slower. Performance of reward and avoidance tasks was equal to control levels 60 days after termination of gamma-ray exposures, showing no residual neurological injury reflected as a decrement in motivation to perform learned tasks. Peripheral blood characteristics showed dose-dependent injury to blood-forming tissue. Radiation-induced injury in higher dose groups reached critical levels, resulting in death of three subjects. During a 60-day recovery period, peripheral blood elements returned to control levels. During the fractionated gamma-ray exposure regime, initiated 414 days after the performance-test exposures, bone-marrow suppression was observed after each 100-rad exposure. Recovery to pre-exposure levels was observed in all groups during each 56-day recovery period between exposures. All animals in each of the four pre-test dose groups were vigorous, active, and aggressive after fifteen 100-rad fractions, and the bone marrow of each group was sufficiently resilient to maintain animals in a clinically healthy condition. (auth)

53453 (NASA-TM-X-2440, pp 641) RELATIVE BIOLOGICAL EFFECTIVENESS OF FAST NEUTRONS COMPARED WITH X RAYS: PRENATAL MORTALITY IN THE MOUSE. Friedberg, W. (Federal Aviation Administration, Oklahoma City, Okla); Hanneman, G. D.; Faulkner, D. N.; Darden, E. B. Jan 1972.

From Symposium on natural and manmade radiation in space; Las Vegas, Nev. (1 Mar 1971).

The effects of fast neutrons on mouse zygotes were investigated. Virgin female mice were mated and then exposed to fast neutrons or x rays while the zygotes were still in the pronuclear stage. Sixteen days after irradiation, the mice were killed and the uteri dissected. The number of dead embryos, live embryos, and gross anomalies was recorded. The relative biological effectiveness of fast neutrons, in comparison to x rays, for inducing prenatal mortality in mice was determined. (E.R.B.)

53454 (NASA-TM-X-2440, pp 642-6) PROTON IRRADIATION OF STEM CELLS: RADIATION DAMAGE AND CHEMICAL RADIOPROTECTION. Riley, Richard C.; Montour, James L.; Gurney, Clifford W. (Univ. of Kansas, Kansas City. Medical Coll. of Virginia, Richmond). Jan 1972.

From Symposium on natural and manmade radiation in space; Las Vegas, Nev. (1 Mar 1971).

Although many systems for studying radiobiological effects of high energy protons are available, much work has utilized whole mammals as the test system. Cellular level studies in mammals have included characterization of hematopoietic sequelae of total body exposure. In this study the effects of high energy protons on erythropoietic stem cells (erythropoietin responsive cells) and radioprotection by chemical agents have been measured. The facilities of the NASA Space Radiation Effects Laboratory, Newport News, Virginia, were used. Carworth Farms CF-1 mice were exposed (five in tandem) to a parallel beam of 600 MeV protons. The fluence distribution was determined by ^{11}C foil counting. The fluence, when converted to dose, was referenced to the synchrocyclotron beam monitors that were then used to administer radiation exposures. Mice were given graded doses to 300 rads to determine the dose-response curve. Other mice received saline, AET, or 5-hydroxytryptamine 10 to 15 min before irradiation. All mice received six units human urinary erythropoietin on day 2 following exposure, 0.5 μCi ^{59}Fe on day 4, and were killed on day 7. Percent iron incorporation was then determined as a measure of the fraction of stem cells remaining. Preliminary experiments, carried out as described, show a dose-response curve similar to that obtained with 250 kV x rays indicating an RBE of approximately one. Chemical radioprotection can be shown under these conditions for both AET and 5-HT with doses well below the LD_{50} dose. Under the conditions of these experiments AET and 5-HT are equally effective and a dose reduction factor of 2.5 is obtained. The specification of radiation tolerance doses for manned space missions requires quantitative information from sub-lethal doses. These experiments indicate that the stem cell system can be further utilized to obtain such information. (auth)

53455 (NASA-TM-X-2440, pp 647-51) RADIATION CARCINOGENESIS AND ACUTE RADIATION MORTALITY IN THE RAT AS PRODUCED BY 2.2-GeV PROTONS. Shellabarger, C. J.; Straub, R. F.; Jesseph, J. E.; Montour, J. L. (Univ. of Michigan, Ann Arbor. Brookhaven National Lab., Upton, N. Y.). Jan 1972.

From Symposium on natural and manmade radiation in space; Las Vegas, Nev. (1 Mar 1971).

The Brookhaven National Laboratory Cosmotron was used to produce 2.2 GeV protons for whole-body exposure of young, female Sprague-Dawley rats. A single exposure of 42-day old rats to 92 rads of protons produced a mammary neoplastic response over a 365-day period that was qualitatively and quantitatively similar to the response produced by 158 rads of ^{60}Co gamma rays. When the two types of radiation exposures were combined they appeared to produce an additive mammary neoplastic response. Because of the qualitative similarity of the mammary neoplastic response to the two types of radiation and because the two types of radiation appeared to be additive, it was suggested that 2.2 GeV protons act by a mode of action that is similar to that of low LET radiation. Acute radiation mortality produced by a single exposure of 42-day old rats to protons was qualitatively similar in terms of mean survival time to mortality produced by ^{60}Co gamma rays. It was suggested that 2.2 GeV protons act to produce acute radiation mortality in a fashion similar to that of low LET radiation. The administration of a radioprotective drug, AET, to 36-day old rats produced a small decrease in radiation mortality and a small increase in mean survival time when the drug was given before exposure to 2.2 GeV protons. This result was taken to mean that 2.2 GeV protons act at least in part as low LET radiation. Although exact RBE values could not be determined for acute mortality and carcinogenesis in the young rat, approximate values appear to be 1.4 and 1.5. (auth)

53456 (NASA-TM-X-2440, pp 652-8) RESPONSE OF MOUSE EPIDERMAL CELLS TO SINGLE DOSES OF HEAVY PARTICLES. Leith, J. T.; Schilling, W. A.; Welch, G. P. (Univ. of California, Berkeley). Jan 1972.

From Symposium on natural and manmade radiation in space; Las Vegas, Nev. (1 Mar 1971).

The survival of mouse epidermal cells to heavy-particles was studied in vivo by the Withers clone technique. Experiments with accelerated helium, lithium, and carbon ions were performed. The survival curve for the helium ion irradiations used a modified Bragg curve method with a maximum tissue penetration of 465 microns, and indicated that the dose needed to reduce the original cell number to 1 surviving cell/cm^2 was 1525 rads with a D_0 of 95 rads. The LET at the basal cell layer was 28.6 keV/micron. Preliminary experiments with lithium and carbon used treatment doses of 1250 rads with LET's at the surface of the skin of 56 and 193 keV/micron, respectively. Penetration depths in skin were 350 and 530 microns for the carbon and lithium ions whose Bragg curves were unmodified. Results indicate a maximum RBE for skin of about 2 using the skin cloning technique. An attempt has been made to relate the epidermal cell survival curve to mortality of the whole animal for helium ions. (auth)

53457 (NASA-TM-X-2440, pp 659-64) LYMPHATIC INVOLUTION AND EARLY MORTALITY IN THE YOUNG CHICKEN PRODUCED BY 2.2-GeV PROTONS. Montour, James L.; Shellabarger, Claire J. (Virginia Commonwealth

Univ., Richmond. Univ. of Michigan, Ann Arbor. Brookhaven National Lab., Upton, N. Y.). Jan 1972.

From Symposium on natural and manmade radiation in space; Las Vegas, Nev. (1 Mar 1971).

Young single-comb white Leghorn cockerels were subjected to single acute doses of either 2.2 GeV protons or 250 kVp x rays. Since young chickens exposed in the lethal range die within 48 hrs of exposure, an hourly tabulation of deaths was recorded for this length of time after exposure. Animals that were exposed to sublethal doses were killed five days after exposure and their major lymphatic organs (thymus, bursa, and spleen) removed and weighed. In the lethal range, animals exposed to 2.2 GeV protons died sooner than those receiving similar doses of x rays, but total mortality was similar in each case at similar dose levels. The 48 hr LD$_{50}$ was determined to be 710 rad. Measured five days after exposure, 50% depression (ED$_{50}$) for lymphatic organs occurred as follows: thymus, 350 rad; bursa 500 rad; spleen 450 rad. In all cases, RBE values were not different from unity. The total dose from protons of this energy is comprised of a low LET portion due to dE/dx energy loss and a high LET portion due to nuclear interactions. RBE values considerably below unity would be predicted on the basis of dE/dx energy loss alone. It is suggested then, that the RBE of that portion of the dose contributed by nuclear interactions is very high. If high LET interactions account for only 5% of the total dose, then these interactions could have an RBE great as 7. (auth)

53458 (NASA-TM-X-2440, pp 665-71) EVALUATION OF THE HAZARD FROM EXPOSURE TO ELECTRON IRRADIATION SIMULATING THAT IN THE SYNCHRONOUS ORBIT. Lippincott, Stuart W.; Foelsche, Trutz; Montour, James; Bender, Roger; Wilson, John (Virginia Commonwealth Univ., Richmond. Langley Research Center, Hampton, Va. The Citadel, Charleston, S. C.). Jan 1972.

From Symposium on natural and manmade radiation in space; Las Vegas, Nev. (1 Mar 1971).

The electron spectrum predicted for the synchronous orbit was simulated to determine the effects that might occur to astroscientists exposed to such irradiation while on a prolonged space station mission in that region. Miniature swine were exposed to monoenergetic and spectral-fractionated irradiations with 0.5 to 2.1 MeV electrons. Clinical and pathological alterations observed in biopsies were correlated with depth-dose pattern and length of post-irradiation period up to one year. With monoenergetic electrons, the lowest dose causing a recognizable lesion was 1450 rad and with increasing dose lesions appeared earlier and were more severe. At the highest dose given, 2650 rad, ulceration extending into the dermis was present by twenty-one days and required about four months for complete healing. Spectral-fractionated irradiations, in which the total dose range was essentially comparable to that of the monoenergetic series, resulted in very minimal outer dermis edema at 1790 rad and at no dose employed did necrosis of epidermis or ulceration into dermis occur. (auth)

53459 (NP-19403) APPLICATION OF ATOMIC ENERGY IN AGRICULTURE. Annual Report, 1971. (Instituut voor Toepassing van Atoomenergie in de Landbouw, Wageningen (Netherlands)). 1972. 153p. Dep. NTIS (U. S. Sales Only).

The research was carried out at the Association's Institute in Wageningen and at other institutes in Belgium, Germany, Italy, and the Netherlands. Results of the following scientific studies are reported: applications and methodology in mutation breeding; chemical, physical, and ontogenetic factors in radiation genetics; related genetic studies; related in vitro studies; radiation preservation of food; radiation genetics of insect pests; uptake of specific elements by plants; movement of specific elements and water in soils; and related physical studies. Practical applications, courses, and services are also discussed. (H.L.W.)

53460 (SZS-132) STATE AND TENDENCIES OF CHEMICAL PROTECTION AGAINST IONIZING RADIATION. A Literature Survey 1970/71. Fischer, H.; Siegel, G.; Haehn, J.; Tapp, E.; Scheefeld, E. (Staatliche Zentrale fuer Strahlenschutz, Berlin (East Germany)). Jun 1972. 52p. (In German). Dep. NTIS (U. S. Sales Only).

Summaries are presented of 309 papers published in 1970 and 1971 on chemical protection against radiation. Protection studies in vitro and in vivo, the biochemical and pharmacological effects of radioprotective agents, and the trends in this field of research are described. (auth)

53461 (UCB-34-P-82-13) ELECTROPHYSIOLOGICAL AND BIOCHEMICAL STUDIES OF THE EFFECTS OF RADIATION ON BRAIN ACTIVITY AND DEVELOPMENT. Progress Report, August 1971-31 July 1972. Timiras, Paola S. (California Univ., Berkeley). 1 Aug 1972. Contract AT(04-3)-34. 41p. Dep. NTIS.

Previous studies demonstrated that the enzymes of acetylcholine metabolism are affected by neonatal x radiation. These alterations depend upon the stage of development of the CNS structure at the time of irradiation as well as the applied dose. Extended studies in rats showed that the increase observed in AChE and ChAc activity are accompanied by changes in ACh content. The activity of other enzymes was also investigated in order to clarify whether the enzymes of acetylcholine were affected specifically or whether other enzymes, similar in their distribution and localization in the CNS, were also affected. Efforts to assess the mode of action by which neonatal x radiation alters cholinergic neurotransmission pointed to two possible mechanisms: imbalances between cholinergic and noncholinergic neurons, and/or the malformation of their synaptic arborization. Studies of the effects of x radiation on the adult rat CNS also indicated changes in acetylcholine content of the cerebral hemispheres; however, the effects are the reverse of those observed in the developing organism and are not accompanied by changes in the enzymes associated with ACh synthesis or hydrolysis. In the rat, as in other mammals, each brain area showed a characteristic maturational pattern, evidenced also with respect to the development of the cholinergic system. (C.H.)

53462 (UR-3490-183) SEQUENTIAL PATHOPHYSIOLOGY OF IONIZING RADIATION ON THE BEAGLE THYROID GLAND. Lu, Shin-tsu; Michaelson, Sol M.; Quinlan, William J. (Rochester Univ., N. Y. Dept. of Radiation Biology and Biophysics). 1971. 60p. Dep. NTIS.

Response of the thyroid gland to external ionizing radiation exposure may manifest itself in a temporal manner, functionally, by transient increased activity, and progressive hypothyroidism and pathologically, by degeneration, hyperplasia, and carcinogenesis. Although such derangements have been characterized in animals and man, the pathogenesis and mechanism of the reaction have not been elucidated. Using the dog as an experimental model, evidence has been obtained which indicates vascular alteration may initiate and amplify the visible and functional thyroid derangement. Increase in circulating TSH appears to be secondary to the glandular damage and TSH also appears to be the promoting factor not only in progressive changes and its self-perpetuation, but also in the sequence of events leading to permanent hyperplasia or carcinogenesis. The post-irradiation latency for induction of thyroid neoplasia in the dog (4 to 10 years), man (9 to 14 years), and the rat (1 to 2 years) shows a linear relationship with basal metabolic rate. Although this relationship may be fortuitous, it may be indicative of a fundamental factor related to tissue metabolism and thyroid cell turnover rate. (auth)

53463 SODIUM TURNOVER IN IRRADIATION HYPERTENSION. Ermel, A. E. (Univ., Louvain, Belgium). Clin. Sci.; 43: No. 2, 219-32(Aug 1972).

Changes in sodium turnover in experimental hypertension were studied by tracer kinetic methods after injection of the long-lived radioisotope ^{22}Na. In rats treated with renal irradiation, the prehypertensive latent period is characterized by a modified distribution of body sodium that can be interpreted as a transfer from peripheral stores to a more centrally located pool. Before the development of hypertension, the rapidly exchangeable sodium increased by 14%. The rise in blood pressure to a hypertensive level is associated with a decrease in the fractional excretion rate of sodium. During the established phase of hypertension, serial determinations of exchangeable sodium indicate rapidly fluctuating shifts of body sodium, the significance of which remains unknown. (auth)

53464 ACUTE EFFECTS OF IONIZING RADIATION ON ANTIBODY-PRODUCING CELLS (PFC) IN MOUSE SPLEEN DURING PRIMARY AND SECONDARY RESPONSES TO SHEEP ERYTHROCYTES (SRC). Harris, G.; Sljivic, V. (St. Mary's Hospital Medical School, London). Immunology; 23: No. 2, 147-58(Aug 1972).

The acute effects of various doses of whole-body x radiation over a dose range 0 to 1000 R on the splenic antibody-producing cells (PFC) of mice responding to primary and secondary immunization with sheep red cells (SRC) were studied. The results showed that suppression of plaque-forming capacity occurred 2 hr after varying doses of x rays and was very severe by 6 hr. No differences in sensitivity were seen at any stage of primary or secondary response examined. This acute depressive effect showed that the maintenance of splenic PFC was highly sensitive to radiation and was associated with a severely reduced uptake of ^{3}H-thymidine into the spleen at the same time after irradiation. Since previous studies [Harris and Pelc, Immunology, 19, 865 (1970)] have shown that incorporation of ^{3}H-thymidine occurred in non-dividing cells in mouse spleen, it was concluded that this turnover of DNA was important for the development of the capacity of cells to produce specific antibodies and that the acute depressive effects of x radiation on splenic PFC were primarily due to inhibition of this process. (auth)

53465 BALNEOTHERAPY EFFECTS ON MICE IRRADIATED WITH MIXED FAST NEUTRONS AND GAMMA RAYS. Arima, Masashi (Kyushu Univ., Beppu, Japan). Onken Kiyo; 23: No. 1, 57-78(Mar 1971). (In Japanese).

Six groups of mice were irradiated with the mixed irradiation composed of 200 rads fast neutrons and 300 R γ rays simulating the radiation produced by atomic bomb explosion. Each group of animals thus irradiated was subjected to daily thermal bathing in one of the following types of spring water for 20 successive days — Umijigoku (NaCl containing acidic water), Yanagi (simple thermal), Genbaku-center spring (simple thermal), modified thermal (added with sulphur and cobalt), and tap water bathing. One group served as a non-treated control. Recovery from body weight loss was fast in the Umijigoku group, and recovery of circulating erythrocyte count was fast in the thermal bathing groups. The Genbaku-center and modified thermal groups did not show any decrease in hemoglobin content, while in the other groups, hemoglobin content decreased markedly. Recovery from circulating leukocyte decrease in the modified thermal and Genbaku-center bathing groups was remarkable. Histologic examination of spleens showed accelerated recovery from change caused by the irradiation in the modified, Yanagi, and Genbaku-center bathing groups. These results seem to show that bathing in thermal springs is beneficial for promoting recovery from the radiation disturbance caused by the mixed irradiation of fast neutrons and gamma rays. Of the springs examined, the Genbaku-center thermal and modified simple thermal gave the best result in general. (Japan)

53466 RADIOSENSITIVITY OF CIRCULATING HEMOPOIETIC STEM CELLS (CFU). Duplan, J. F.; Mazurek, C. (Institut du Radium, Paris). Compt. Rend. Soc. Biol.; 165: No. 7-8, 1542-5 (1971). (In French).

Certain hemopoietic stem cells (CFU) possess the ability to provide microscopically visible spleen nodules when transplanted intravenously into isogeneic mice having received a 100% lethal dose of x rays. This technique demonstrates that the radiosensitivity of the cells varies with the organs from which they originate: fetal liver, bone marrow, or spleen. It is also noticed that the cell strains of the peripheral blood are significantly more radiosensitive than those of the hemopoietic organs. (France)

53467 ULTRASTRUCTURE CHANGES IN THE ADENOHYPOPHYSIS OF RODENTS AFTER TOTAL OR SEGMENTARY IRRADIATION WITH RADIOCOBALT. Theret, C. G.; Lavedan, Jacques; Lalegerie, Pierre; Comlan, Guy. Compt. Rend. Soc. Biol.; 165: No. 7-8, 1546-9(1971). (In French).

The cell sensitivity to radiolesions was observed in relation to the trophine of the gland studied. Positive PAS cells are more sensitive than negative PAS cells above all in the gonadotropes even when the gonads are protected or at rest. This sensitivity exists also for the thyreotropes. The ultrastructural mechanisms explaining the lesions and the distribution of endocrine cells in the adenohypophysis are the same as those explaining the physiological or pathological excitation of hormone secretion. (France)

53468 FUNCTION OF THE RETICULOENDOTHELIAL SYSTEM IN WHOLE-BODY IRRADIATED MICE. Schildt, B. E.; Eriksson, K.-H. (Foersvarets Forskningsanstalt, Stockholm). Acta Radiol., Ther., Phys., Biol.; 11: No. 1, 48-58(Feb 1972).

The influence of whole-body roentgen irradiation on the function of the reticuloendothelial system was investigated in mice by determining the phagocytic index for and tissue localization of ^{51}Cr-labeled xenogenic erythrocytes injected intravenously. Exposure to LD_{10} reduced the phagocytic capacity significantly within 7 days, while the same effect was evident as early as 1 day after LD_{50}. Sublethal exposure ($0.5 \times LD_{50}$) failed to affect phagocytosis to any degree. Possible explanations for the impaired capacity after irradiation are discussed. (auth)

53469 EFFECTS OF HIGH INTENSITY PULSED X-RAY (LINEAR ACCELERATOR) OR GAMMA-RAY IRRADIATION UPON TUMORIGENESIS AND IMMUNOCOMPETENCE IN MICE. Imamura, Nobutaka; Nakano, Mimako; Takizawa, Shoichi; Yokoro, Kenjiro (Hiroshima Univ.). Hiroshima Igaku; 24: No. 11, 1074-84(Nov 1971). (In Japanese).

Whole-body irradiation was carried out by Linac 25 MV x-ray with 670 to 850 rads on female ICR/JCL mice of 10 weeks. Within 360 days after irradiation, the mean rate of occurrence of leukemia was 30.3%, and increased to 39.3% by irradiation of ^{60}Co gamma ray with 750 to 950 rads. Female ICR/JCL mice of 3 months were sensitized with sheep erythrocytes before and after irradiation by Linac x-ray with 730 rads. Numbers of plaque forming cells (PFC) in the spleen were measured on the 4th day after irradiation. The number of PFC in the immune group after irradiation was decreased more than that in the group before irradiation. Female ICR/JCL mice of 3 months were irradiated by whole-body irradiation with 100 through 500 rads of Linac x-ray and ^{60}Co gamma-ray. One day after irradiation, these mice were sensitized with sheep erythrocytes and the number of PFC in the spleen was measured on the 4th day. Up to a dose of 200 rads, no change was observed, but above 200 rads the number of PFC decreased abruptly for both Linac x-ray and ^{60}Co gamma-ray exposures. The same type of change was observed in the values of plasma hemolysin and of hemagglutinin. There were no particular differences in tumorigenesis and immunocompetence between irradiations by linear accelerator and by ^{60}Co gamma-ray, except that there existed some possibility of RBE on hematopoietic reactions and immune responses by high intensity pulsed x-ray (Linear accelerator). (Japan)

53470 CHROMOSOMAL AND HISTOLOGICAL CHANGES IN EMBRYOS EXPOSED TO 14.1 MeV FAST NEUTRONS. Shimada, Katsunobu (Hiroshima Univ.). Med. J. Hiroshima Univ., 19: No. 3-4, 59-81(Apr 1971). (In Japanese).

Chromosomes of rat embryo were examined by the direct method, and serial sections were observed histologically. After a short time of mitotic arrest following irradiation, unstable types of aberrations increased, and then decreased gradually with time. At 72 hrs after irradiation, unstable types disappeared. On the other hand, stable types of aberrations appeared 4 hrs after irradiation, and continued until 120 hrs, although the incidence was low. Aneuploid cells, especially hypodiploid cells, increased shortly after irradiation, and then gradually decreased to the control level. Polyploid cells appeared during the period of 48 to 120 hrs after irradiation, though the incidence was low. Abnormal chromosomes showed type specificity, i.e., most frequently in the telocentric type, less frequently in the sub-telocentric, and rarely in the meta-centric. Cell damages were remarkable during 3 to 4 hrs after irradiation, followed by the repair process of the embryonic structures during the periods of 6 to 12 hrs following irradiation. At 24 hrs after irradiation, degeneration products disappeared from the surroundings of the embryo, and mitoses became remarkable. However, retardation and abnormal differentiation were observed in the embryo. From the radiobiological viewpoints, embryonic responses to the radiation were different among dermal tissues. Mesoderm and cylindrical cell-lined entoderm were relatively tolerant to the fast neutrons. These results suggested that direct cell damage and repair errors might be involved in teratogenesis. (Japan)

53471 MALFORMATION OF DIGITS IN MOUSE FOETUS CAUSED BY GAMMA-RAY IRRADIATION DURING PREGNANCY. Ueka, Keiko; Yoshizawa, Yasuo (Tokyo Univ.). Nippon Igaku Hoshasen Gakkai Zasshi; 30: No. 11, 107-15(Feb 1971). (In Japanese).

The development of digital malformations and their usefulness as biological indicators of radiation effects were studied. The experimental animals used were the ddY strain of mice, 70 days old. After keeping for a week, the esterus mice were kept with males in cages overnight and the next morning those found with vaginal plugs were considered to be in day zero of pregnancy. The pregnant mice were exposed to the gamma ray of cesium-137. The pregnant mice were irradiated with 200 R of γ rays (dose rate, 3.3 R/min) at different stages of gestation between 8 and 13 days after fertilization. The mice were irradiated at the six different dose-rates of 1.0, 3.3, 6.7, 20, 40, and 100 R/min (total exposure dose, 200 R) on the 11th day of pregnancy. The mice were irradiated with the six different doses of 75, 100, 150, 200, 250, and 300 R on the 11th day of pregnancy. On the 18th day of pregnancy, the fetuses were removed from sacrificed mothers, and were observed for digital malformations (Ectrodactylism, Brachydactylism, Polydactylism, and Syndactylism) and body weight. The critical period for the digital malformations was found on the 11th day of pregnancy. The dose-effects relationship of the digital abnormal development showed that the threshold dose existed between 75 and 100 R, and the appearance rate of the malformations reached about 100% at the dose of 250 R. An inverse correlation was found between digital abnormality and fetus weight. In fetuses irradiated at lower doses and dose rates, malformations appeared in two forelimbs, and at higher doses and dose rates they appeared in all digits. The malformations of only hindlimbs, one digit or three digits, were rare. The dose-rate dependencies were found both in the abnormality and body weight. (auth)

53472 DOSE RATE DEPENDENCE IN THE GOITROGEN STIMULATED MOUSE THYROID. A COMPARATIVE INVESTIGATION OF THE EFFECTS OF ROENTGEN, ^{131}I, AND ^{132}I IRRADIATION. Walinder, G.; Jonsson, C.-J.; Sjoeden, A.-M. (Foersvarets Forskningsanstalt, Stockholm). Acta Radiol., Ther., Phys., Biol.; 11: No. 1, 24-36(Feb 1972).

The doses of radiation necessary to inhibit goitrogen stimulated thyroid growth in the CBA mouse are much lower after roentgen exposure than those needed to produce the same effects after ^{131}I administrations. Similar differences in the "effectiveness" of the two types of radiation have been observed in several different animals as well as in man. A comparison of the dose-effect relationships after irradiation of the mouse thyroid with roentgen rays, ^{131}I, and ^{132}I has shown that the difference in the "effectiveness" of the three types of radiation largely consists of a dose rate effect. Inhomogeneities in the distribution of the ^{131}I-dose, and effects on the perithyroidal tissue produced by external irradiation, are of little significance in this connection. (auth)

53473 BIOLOGICAL DOSIMETRY USING BONE MARROW SAMPLES. Segreto, Camilo; Ludwig, Frederic (Univ. of California, Irvine). Compt. Rend., Ser. D; 274: No. 18, 2610-12 (3 May 1972). (In French).

A positive correlation exists between the erythrocyte/nucleated cell ratio and the radiation dose absorbed by the bone marrow of animals subjected to whole-body irradiation. The ratio (contrary to the absolute number of erythrocytes or the number of nucleated bone marrow cells) can be determined from medulla (samples having unknown and variable volumes). This biological dosimetry method was applied to experiments with laboratory mice. (France)

53474 IDENTIFICATION OF THE CELL POPULATION RESPONDING TO DNP-GL IN LETHALLY IRRADIATED STRAIN 13 CHIMERIC GUINEA PIGS RECONSTITUTED WITH STRAIN 13 BONE MARROW AND (2 x 13) F_1 LYMPH NODE AND SPLEEN CELLS. Ellam, Leonard; Green, Ira; Benacerraf, Baruj (National Institutes of Health, Bethesda, Md.). Cell. Immunol.; 1: 445-54(Oct 1970).

The ability of guinea pigs to make an immune response to synthetic polypeptides (DNP-GL) was successfully transferred to lethally irradiated, nonresponder strain-13 guinea pigs protected with syngeneic bone marrow and immunologically reconstituted with lymph node and spleen cells. An analysis of the origin of the lymphoid cells involved in anti-DNP antibody production and antigen-mediated stimulation of lymph node cells in vitro was performed in the chimeric animals. It was found that both functions depended entirely on the presence of the donor cells. (auth)

53475 PROTECTIVE EFFECT OF CYSTEAMINE AT FRACTIONATED IRRADIATION. 3. HISTOPATHOLOGIC DIAGNOSES AT DEATH. Nelson, A.; Jaerplid, B.; Nilsson, A.; Roennbaeck, C.; Eriksson, K.-H. Acta Radiol., Suppl.; No. 310, 181-99(1971).

Groups of mice were exposed to repeated doses of 80 R and 160 R at various time intervals with a view to studying the protective effect of cysteamine against late effects from sublethal doses of irradiation. The accumulated doses were selected to fall definitely in the range between sublethal and supralethal doses. Half the number of animals in each group were given cysteamine before each irradiation. The histopathological diagnoses at death were investigated among those surviving the acute effects, i.e., 30 days after last irradiation. It was concluded that cysteamine had a protective effect only against radiation induced unclassified leukemias. The effect on other specific late effects was equivocal. (auth)

53476 GASTRULATION IN MOUSE EMBRYOS IN COURSE OF RADIATION INJURY. Rudnicki, Tadeusz; Kochmanska, Anna (Zaklad Radiobiologii Instytutu Nauk Fizjologicznych, Poznan, Poland). Nukleonika; 17: No. 3-4, 249-58(1972). (In Polish).

Early mouse embryos were irradiated with 200 rads of x rays just as gastrulation was started. At 2, 12, 24, 36, and 48 hr after irradiation, the mitotic activity in cells of germ layers and cell death following radiation injury, as well as the influence of these alterations at the cellular level on the process of gastrulation and neural tube formation was studied. It was found that both cell death and depression of mitotic activity occurred, but embryos were able to compensate these injuries in a short time. The only consequence of these alterations, morphologically evident, was the retardation of embryo development for about 12 hr as compared with normals. It follows from these studies that morphological criteria in estimation of mechanisms of fundamental radiobiological effect in early mouse embryo (i.e., its death) are not useful. (auth)

53477 INTERACTION OF EMBRYONIC CHICKEN SPLEEN CELLS AND ADULT ALLOGENEIC LEUCOCYTES. Killby, Virginia A. A.; Lafferty, K. J.; Ryan, Madeleine A. (Australian National Univ., Canberra). Aust. J. Exp. Biol. Med. Sci.; 50: No. 3, 309-21(Jun 1972).

Leucocytes from inbred AA chickens produced pocks when inoculated onto the chorioallantoic membrane of non-inbred embryos (direct pock formation), but produced very few or no pocks on the chorioallantoic membrane of syngeneic embryos. Pock formation was observed when AA leucocytes were mixed with non-inbred embryonic spleen cells before being assayed on the chorioallantoic membrane of recipient embryos that were unresponsive to either cell population alone (indirect pock formation). Indirect pock formation was found to be more γ radioresistant than direct pock formation and doses of Mitomycin-C that inhibited direct pock formation by AA leucocytes did not inhibit the capacity of these cells to induce indirect pocks. Indirect pock formation was inhibited when non-inbred embryonic spleen cells were treated with Mitomycin-C prior to mixing with AA leucocytes. It is suggested that indirect pock formation does not result from the stimulation of adult leucocytes by antigen presented on the surface of allogeneic embryonic cells. Rather, this response is a manifestation of the direct stimulation of embryonic spleen cells by adult allogeneic leucocytes. (auth)

53478 DIURNAL RHYTHM OF NEUROSECRETORY ACTIVITY IN NORMAL AND X-RAY IRRADIATED MICE. Lach, H.; Srebro, Z. (Teacher Training Coll., Krakow). Acta Biol. Acad. Sci. Hung.; 23: No. 1, 1-9(1972).

The nuclear diameter of neurosecretory cells and the amount of neurosecretory material (NSM) were measured in the hypothalamo-neurohypophysial neurosecretory system of adult male albino mice at different hours of the day. The amount of NSM was estimated cytophotometrically. It was highest at 6 p.m. both in the neurosecretory centres and in the posterior lobe. The lowest values occurred at noon in the hypothalamic nuclei and at midnight in the posterior lobe. X irradiation considerably changed this rhythm: a decrease was observed in the supraoptic and paraventricular nuclei 13 hrs postexposure. The posterior lobe, on the contrary, showed at that time increased amounts of NSM as compared with the control. The difference between the irradiated and control animals was statistically significant as well as the maximal intragroup differences (maxima vs. minima). Neurosecretory cell nuclear diameter showed a distinct diurnal variation. Significant differences were observed between normal and irradiated animals. (auth)

53479 ROLE OF THE THYMUS IN THE POSTRADIATIONAL RESTORATION OF THE BONE MARROW IN RATS. Fedotova, M. I.; Belousova, O. I. Byull, Eksp. Biol. Med.; 73: No. 4, 101-5(Apr 1972). (In Russian).

Experiments were carried out on 470 Wistar rats subjected to the operation of true or fake thymectomy. A study was made (by quantitative methods) of bone marrow restoration following irradiation with γ rays of ^{60}Co in doses of 400 and 700 R. Restoration of bone marrow cells proved to be delayed (in comparison with control) in thymectomized rats. The number of lymphoid cells was reduced at the period from the 10th to the 15th day, and of myeloid cells—at later periods. A conclusion was drawn that migration of thymocytes into the bone marrow occurred during the postradiation period. An association of the mentioned phenomenon with the subsequent restoration of myelopoiesis is supposed. (auth)

53480 ANIMAL EXPERIMENTAL EXAMINATIONS ON THE EFFECT OF IONIZING RADIATION ON THE MAXILLARY BONE WITH METALLIC BRIDGES. Beetke, E.; Bienengraeber, V.; Hafke, P.; Kittner, K.-H. (Univ., Rostock, Ger.). Radiobiol.-Radiother.; 13: No. 3, 367-74(1972). (In German).

For the further elucidation of the influence of metallic bridges on the surrounding tissue in γ irradiation, experimental examinations were performed with five dogs. The radiation reactions in the environment of teeth surrounded by lead are compared with reactions with undressed teeth and with those teeth having the lead ring covered by a plastic cap. The results of these examinations are given. (auth)

53481 OBSERVATIONS ON THE COMBINED RADIOPROTECTIVE EFFECT OF PANTOTHENIC ACID AND AMINOETHYLISOTHIURONIUM. Szegszardy, T.; Gazdagh, I.; Szorady, I. (Medizinische Univ., Szeged). Radiobiol.-Radiother.; 13: No. 3, 375-8 (1972). (In German).

Together with pantothenic acid, the radioprotective effect of AET in mice in the case of a whole-body irradiation of 800 R can be greatly increased. This is manifested by the survival percentage of the animals, in the prolonged survival, and in a decrease of the postirradiation loss of weight. (auth)

53482 VARIATIONS OF THE ^{75}Se-SELENOMETHIONINE ERYTHROCYTIC INCORPORATION INDUCED IN THE RAT BY PAN-IRRADIATION. Martinenghi, C.; Bergonzi, M.; Limido, G. (Univ., Milan). Med. Nucl.-Radiobiol. Lat.; 12: No. 3-4, 153-71(1969). (In Italian).

The study of the variations of the ^{75}Se-selenomethionine erythrocytic incorporation induced in the rat following γ pan-irradiation with different doses showed a linear correlation between the logarithmic exposition and the maximum value of the erythrocytic radioactivity concentration, expressed as a ratio with the maximum value observed in the nonirradiated control animals. The analysis of the curve showing the variations of the radioisotope erythrocytic incorporation as a function of time shows that such a curve may be analytically expressed, with good approximation, by a monoexponential function. (auth)

53483 STUDY AS A FUNCTION OF TIME AND DOSE OF THE NUMERICAL VARIATIONS OF THE LEUCOCYTES CIRCU-

LATING IN A TOTALLY IRRADIATED RAT. Martinenghi, C.; Bergonzi, M.; Fidanza, M. A.; (and others) (Univ., Milan). Med. Nucl.-Radiobiol. Lat.; 12: No. 3-4, 245-66(1969). (In Italian).

One hundred and sixty two Norwegian white rats were whole-body γ-irradiated and divided into nine groups on the basis of exposure times. The time variation of the total leucocythemia, lymphocythemia, and neutrophilous granulocythemia was studied numerically, extending the study to 32 days after irradiation for the surviving animals. A correlation was observed between exposure and biological effects, by studying the behavior of the circulating leucocytes and especially by examining separately the granulocytic and lymphocytic curves. In particular, a quantitative measure was given to the correlation between lymphocytic damage and exposure, at least within the experimental dosage range. (auth)

53484 RELATIVE BIOLOGICAL EFFECTIVENESS OF ^{252}Cf ON ACUTE MAMMALIAN LETHALITY. Dean, Frederick K.; Bushong, Stewart C.; Prasad, Naresh; Briney, Sharon (Baylor Univ., Houston, Tex.). Radiology; 104: No. 3, 699-703(Sep 1972).

The relative biological effectiveness (RBE) of ^{252}Cf was compared with radium on the basis of lethality over a 30-day period. Mice were irradiated with ^{252}Cf, radium, and ^{60}Co. Probit analysis of the number of deaths showed an $LD_{50/30}$ of 537 rads for ^{252}Cf, 1,286 rads for 240 mg radium, 1,609 rads for 120 mg radium, and 663 rads following high-dose ^{60}Co. The RBE estimate for ^{252}Cf compared to radium over a comparable time interval is 3.01. These findings are consistent with other recently reported RBE values. The ^{60}Co values were not compared due to differences in dose distribution and dose-rate. (auth)

53485 INCIDENCE OF DELAYED MORTALITY (SECONDARY DISEASE) IN ALLOGENEIC RADIATION CHIMERAS RECEIVING BONE MARROW FROM AGED MICE. Chen, Michael G.; Price, Gerald B.; Makinodan, T. (Oak Ridge National Lab., Tenn.). Exp. Hematol.; 22: No. 1, 68-9(Mar 1972).

The effect of aging on a cell-mediated immune function; namely, the ability of bone marrow from aged donor mice to cause secondary disease and death in young, lethally irradiated, allogeneic recipient mice was studied. The influence of the thymus on the potential effector cells in the bone marrow was also examined. Studies were made using, (C57BL/Cum (H-2^b) × C3H/Anf Cum (H-2^k) mice (hereafter $BC3F_1$) of both sexes as bone marrow donors. Old mice were 25 months or more in age; young mice were 3 to 6 months old. Recipient mice were (BALB/c MI(H-2^d) × DBA/2 MI (H-2^d) hybrids (hereafter $CD2F_1$), 2 to 5 months old, of both sexes. These recipients were given 850 R whole-body x irradiation and injected with $5-7.5 \times 10^6$ ($BC3F_1$) bone marrow cells within 3 hr of irradiation. In one series of experiments, $BC3F_1$ donors received 400 R whole-body radiation 22 days before sacrifice and collection of bone marrow for transplantation. Thymectomies were performed on groups of old and young $BC3F_1$ donors and $CD2F_1$ recipients at two months of age. Daily tabulation of deaths in each group of recipient mice was made, excluding the few animals dying during the first two weeks. Postmortem examination was performed on a random sample of mice dying with each group, and survivors were tested for erythrocyte chimerism. These results are compatible with existence of a large, long-lived stable population of cells, reactive in initiating delayed mortality, which does not diminish appreciably with senescence. (C.H.)

53486 SEROTONIN UPTAKE BY PLATELETS IN ACUTE RADIATION SICKNESS. Dorofeev, V. M.; Nestaiko, G. V. (Inst. of Medical Radiology, Obninsk, USSR). Byull. Eksp. Biol. Med.; 73· No. 5, 58-60(May 1972). (In Russian).

It was shown on 35 Chinchilla rabbits irradiated at a dose of 600 R (gamma-rays of ^{60}Co, dose rate = 140 R/min), that the capacity of blood platelets for serotonin uptake proved to diminish at the height of the acute radiation sickness. The authors consider that disturbance of this platelet function can serve as one of the causes of serotoninopenia in the blood in acute radiation sickness. (auth)

53487 EFFECTS OF GAMMA RADIATION ON THE SHARK BRAIN. Olsson, Yngve; Carsten, Arland L.; Klatzo, Igor (National Inst. of Health, Bethesda, Md.). Acta Neuropathol.; 21: No. 1, 1-10(1972).

A comparison was made between the effects of gamma radiation on the elasmobranch and the mammalian brain. Thirty-seven nurse sharks (Ginglymostoma cirratum) received a single exposure, in a range of 1,000 to 30,000 rads, to the brain. The animals remained seemingly unaffected in their behavior and at their sacrifice, between one day and 28 months after irradiation, no histological changes could be detected with the exception of one shark (exposed to 30,000 and sacrificed after 12 months) which showed two small necrotic lesions in the tegmentum. No detectable difference in amount and distribution of glycogen in the brain could be demonstrated between irradiated and non-irradiated sharks. Also, the irradiated sharks showed no changes of the blood-brain barrier to protein tracer. Rats irradiated with 25,000 to 30,000 rads to the brain from the same source died shortly after exposure or showed extensive necrotic lesions in the brain. There was also an intense accumulation of glycogen mostly in the astrocytes and a widespread disturbance of the blood-brain barrier to Evans Blue-albumin tracer. (auth)

53488 EFFECT OF SMALL X-RAY DOSES ON THE MOTOR ACTIVITY OF RATS IRRADIATED DURING THEIR EMBRYONIC DEVELOPMENT. Baev, Il.; Paskalev, Z.; Benova, D.; Banceva, E. Rentgenol. Radiol.; 10: No. 3, 194-9(1971). (In Russian).

The motor activity of 2 month-old rats exposed on the 14th day of their embryonic development to 5, 10, 15 or 25 R of x-rays was studied. The quantitative and qualitative characteristics of the movements induced by a sound stimulant served as an index of the motor activity. In the group of animals exposed to 5 and 10 R the motor reactions were reduced, whereas in animals exposed to 15 and 25 R the mean value of these same reactions was significantly increased as compared with control animals. (Abstr. Bulg. Sci. Med. Lit.)

53489 POSTIRRADIATION SYNTHESIS AND DEGRADATION OF DNA IN VARIOUS TISSUES OF RATS. Kang, Man Sik. Tongmul Hakhoe Ji; 14: No. 4, 199-204(1971).

The effect of 400 R total-body x-irradiation on the rate of deoxycytidine-2-^{14}C (CdR-2-^{14}C) incorporation into DNA and on the degradation of DNA has been studied in the liver, spleen and thymus of the rat. The postirradiation period can be divided into a radiation reaction period followed by a regeneration period. During the period of radiation reaction, which consists of days 1 − 2, markedly decreased CdR-2-^{14}C incorporation into DNA of each organ is observed. The rate of incorporation of labeled precursor in the thymus shows the most profound decrease. The change in the amount of DNA as percent of normal exhibits a similar pattern in all organs, but the rate of decrease is larger in the spleen and thymus compared to that in the liver. The period of regeneration as judged by the incorporation experiment appears on day 4 to 5. The second phase is highlighted by a markedly increased rate of CdR-2-^{14}C incorporation and by a slow and continued increase in the amount of DNA in all organs. The regeneration occurs faster in the liver and spleen than in the thymus which is the most radiosensitive of all. The findings of the present experiments are strongly suggestive of the fact that the radiation-induced loss of spleen and thymus DNA as well as the radiation induced inhibition in the CdR incorporation into DNA of the thymus are the important factors in the elevated levels of CdR in the urine and plasma. (Korean Sci. Abstr.)

53490 EFFECT OF CORTISONE ON SERUM PROTEIN OF GAMMA-IRRADIATED MICE. Cho, You Joung; Choi, Kook Hun; Ham, Sang Yul. Tongmul Hakhoe Ji; 14: No. 3, 119-24(1971). (In Korean).

Male mice of strain SM were given 128 rads of single whole-body gamma irradiation of ^{60}Co, 14 to 16 minutes following a subcutaneous injection of physiological saline or cortisone acetate (1 mg/day, for 4 days preirradiation). The serum protein patterns and the level of the total serum proteins were determined at various time intervals after exposure. Total body gamma-irradiation caused a rise in the level of the total serum protein at 1 day and in the level of the serum albumin-globulin ratio at 5 days in both cortisone acetate-treated and control groups. Cortisone acetate delayed the total serum protein rise at 5, 10, and 20 days after exposure. Cortisone acetate delayed the A/G ratio rise at 1, 5, and 10 days after exposure. It may be inferred that cortisone greatly reduces the sensitivity of mice to gamma-irradiation on the blood protein, provided that cortisone is given before the exposure. (Korean Sci. Abstr.)

53491 ACTIVITY CHANGES IN LOCALLY IRRADIATED RAT LIVER L-ARGININE AMIDINOHYDROLASE (EC 3, 5, 3, 1) FOLLOWING IRRADIATION AT DOSES OF 2000 R, 4000 R, AND 8000 R. Bathori, Edit. Kiserl. Orvostud.; 24: No. 3, 289-92 (Jun 1972).

Studies with male Wistar rats are described. The results are analyzed statistically, using the Student-t test. Observations were carried out for 21 days following irradiation. Significant activity changes were found only following irradiation with large total doses. In the case of lower doses (2000 to 4000 R), there was only a temporary (few days) activity increase after irradiation. The activity of the L-arginine amidinohydrolase does not indicate the damages to the liver that may have been caused by irradiation. (JPRS)

53492 ORIGIN OF ALVEOLAR MACROPHAGES IN MOUSE RADIATION CHIMERAS. Godleski, John J.; Brain, Joseph D.

(Harvard Univ., Boston). J. Exp. Med.; 136: No. 3, 630-43 (1 Sep 1972).

This investigation attempted to determine whether the primary source of alveolar macrophages is pulmonary or hematopoietic. An antigenic marker was used to identify cells of hematopoietic origin. Mouse chimeras were produced by irradiating C57B6/AF$_1$ mice (900 R) and then injecting them intravenously with B10D2/AF$_1$ bone marrow. The donor animal has an antigenic specificity on the H-2 locus, not shared by the recipient. Alveolar macrophages were obtained by repeated lung washings with physiologic saline at 37°C. Cytotoxic tests were done on bone marrow and alveolar macrophages using anti-31 mouse antibody, absorbed rabbit serum as complement, and trypan blue exclusion as a test for viability. Animals were studied at 7, 14, 21, 28, and 35–50 days and 4, 5, 8, and 11 months after irradiation and bone marrow replacement. By 21 days after irradiation, 90% of the animals had greater than 80% replacement of marrow with donor tissue; and white blood cell and alveolar macrophage counts approached normal. At this time and at later intervals the per cent of donor cells in the lung free cell population was not significantly different from the per cent of donor cells in the bone marrow. Similarly, after aerosol particulate exposure, the percentage of marrow cells and alveolar macrophages of donor origin were not significantly different. This immunologic approach suggests that alveolar macrophages in radiation chimeras are entirely of hematopoietic origin. (auth)

53493 RESPIRATION AND STRUCTURAL CHANGES OF MITOCHONDRIA OF INTESTINAL EPITHELIAL CELLS IN THE COURSE OF AMINO ACID ABSORPTION IN IRRADIATED ANIMALS. Strelina, A. V.; Batyuto, T. D.; Manina, A. A. (Central Research Roentgeno-Radiological Inst. of Experimental Medicine, Leningrad). Byull. Eksp. Biol. Med.; 73: No. 5, 60-3(May 1972). (In Russian).

Stimulation of respiration and ultrastructural transformations of mitochondria in the epithelial cells of the jejunum in absorption of amino acids (a mixture of alanine and glycine) were shown in experiments on intact rats. Amino acid absorption was accompanied by diminished oxygen utilization and a reduction of ultrastructure reaction within 30 min after whole-body x-ray irradiation in a dose of 600 rad. The results obtained are discussed from the aspect of the effect of radiation on the systems of reproduction of energy and energy-dependent functions. (auth)

53494 EFFECT OF X-RAY IRRADIATION ON REGENERATION OF THE THYROID GLAND IN RATS WITHOUT TUMORS AND AFTER INOCULATION OF SARCOMA-45. Prizhivoit, I. F.; Matyushkova, R. M. (Research Inst. of Oncology and Radiology, Frunze, USSR). Byull. Eksp. Biol. Med.; 73: No. 5, 96-8(May 1972). (In Russian).

Three fourths of the thyroid gland was resected in 240 rats, and its condition was studied postoperatively. The first group of rats served as control; the second group was totally irradiated in a dose of 360 R 24 hrs before the operation; sarcoma-45 was inoculated eight days before the operation to rats of the third group; in difference from the third group, tumor-bearers of the fourth group were subjected to irradiation 24 hrs before the operation. Comparison of the results in these four groups has shown that irradiation of animals without any tumor inhibited the regenerative growth of thyroid epithelium 3.8 times; the presence of a tumor, 7 times; and irradiation of tumor-bearers, only 1.6 times. Consequently, irradiation of tumor-bearers eliminated the inhibition of regenerative processes in the thyroid gland caused by the tumor, and the presence of the tumor reduced the effect of irradiation. (auth)

53495 COURSE OF THE POST-IRRADIATION SYNDROME AFTER IRRADIATION WITH LETHAL DOSES IN NEWBORN CONVENTIONAL, GERM-FREE AND ESCHERICHIA COLI-MONOASSOCIATED PIGLETS. Miler, I.; Mandel, L.; Moravek, F.; Kruml, J.; Klepalova, J. (Inst. of Microbiology, Prague). Folia Microbiol. (Prague); 17: No. 4, 291-9(1972).

The influence of whole-body irradiation with lethal doses of ionizing radiation (^{60}Co) was studied in conventional, germ-free, and Escherichia coli-monoassociated newborn piglets. The dose 1,200 R produced an acute intestinal death (i.e. within 3 to 4 days) in conventional animals, whereas survival was three times as long in their germ-free counterparts. Artificial colonization of the intestinal tract of germ-free piglets with non-pathogenic strain of Escherichia coli, prior to irradiation with the same dose, produced the conventionalization of these animals and reduction in the survival time almost to the level of conventional animals. In conventional animals, profound focal regressive changes of the epithelium accompanying the denudation of intestinal villi were found already on the 2nd to 3rd day after irradiation with 1,200 R. On the other hand, the intestinal epithelium of germ-free piglets, irradiated with 1,200 R, was found to be intact on the 7th to 9th day of post-irradiation, and the first signs of damage started to occur around the 9th to 10th days. The morphological characteristics of the intestinal mucous membrane of Escherichia coli-monoassociated piglets were comparable to those of conventional, irradiated piglets. The role of the presence of the microbial factor for the turnover and radiosensitivity-resistance of enterocytes, and for the survival-death rate of animals irradiated with doses producing the post-irradiation gastrointestinal syndrome, is discussed. (auth)

53496 LEUKEMOGENIC EFFECT OF RADIOSTRONTIUM (^{90}Sr) IN MICE, A COMPARATIVE STUDY OF LEUKEMOGENICITY OF ^{90}Sr AND X-RAYS. 2. TRANSMISSIBILITY OF THE INDUCED LEUKEMIAS, ALKALINE PHOSPHATASE ACTIVITY AND CYTOGENETIC CHANGES OF LEUKEMIC CELLS. Ito, Takaaki (Hiroshima Univ.). Nippon Ketsueki Gakkai Zasshi; 33: No. 4, 432-48(Aug 1971). (In Japanese).

Studies were made on the transmissibility of leukemias, the alkaline phosphatase activity, and chromosome changes of the leukemic cells, which were induced by intraperitoneal administration of ^{90}Sr or fractionated whole-body x irradiation. Cell-free extracts prepared from leukemias induced either by ^{90}Sr or x rays were inoculated into newborn ICR/JCL, ddN/JCL, or RFM/U strains of mice. Of eight cases of ^{90}Sr-induced leukemia, five were transmitted in recipient mice with a latency period of 73 to 547 days, though the leukemogenic potency of extracts was rather low (9.1 to 33.3%). Of four cases of the x-ray-induced leukemia, three were transmitted in ICR/JCL and ddN/JCL mice with a latency period of 240 to 465 days; the leukemogenic potency of these extracts was also low (9.1 to 23.1%). Serial cell-free transmissions were also achieved in two cases of leukemia originally induced by ^{90}Sr. These results strongly suggest that virus may participate in induction of leukemia by ^{90}Sr as it does in leukemia induction by x rays. Alkaline phosphatase (AP) activity of leukemic cells was histochemically determined. AP activity in ^{90}Sr-induced leukemias elevated remarkably, whereas it varied from negative to moderately positive in x-ray-induced cases. Although a few cases showed high AP activity, most cases showed negative or low activity in cell-free passaged leukemias which were originally induced by ^{90}Sr. In the majority of leukemias induced by ^{90}Sr or x-rays, abnormalities in chromosome number such as aneuploidy, polyploidy and pseudo-polyploidy were frequently observed. In 2 cases, one induced by ^{90}Sr and the other by x-rays, respectively, structural abnormalities such as metacentric, minute or giant chromosome were observed in majority of cells, suggesting the proliferation of leukemic stem cell with the marker chromosome. The chromosome abnormalities were relatively infrequent in cell-free passaged leukemias, which were originally induced by ^{90}Sr. (Japan)

Invertebrates

Refer also to abstract 53365.

53497 (COO-1748-12) TOTAL RADIATION-INDUCED GENETIC DAMAGE IN ENTIRE GENOMES OF DROSOPHILA MELANOGASTER. Progress Report, November 1, 1971–October 31, 1972. Valencia, Ruby M. Allen (Wisconsin Univ., Madison). [nd]. Contract AT(11-1)-1748. 30p. Dep. NTIS.

Mature spermatozoa of Drosophila melanogaster were treated with acute doses of 4000 R or 2000 R, x rays. The frequency of damaged genomes among those recovered and studied was 63.2% for 4000 R and 54.8% for 2000 R, but the rate of damage induction among treated sperm was 89.3% for 4000 R and 73% for 2000 R. The rate of heritable damage induction among treated sperm was 10.7% for 4000 R and 27.6% for 2000 R. In addition, the damage transmitted was qualitatively different at the two doses. (C.H.)

53498 (PRNC-156) FASCIOLA HEPATICA PROGRAM IN PUERTO RICO. Progress Summary Report, December 1971. Chiriboga, Jorge; de Leon, Delfin; Ritchie, Lawrence S. (Puerto Rico Nuclear Center, Mayaguez). 1972. Contract AT(40-1)-1833. 61p. (In English and Spanish). Dep. NTIS.

Progress is reported on the following research projects: life cycle studies on Fasciola hepatica using the snails, Lymnaea cubensis and L. columella, as vectors and rats and mice as final hosts; studies on vaccination of cattle using irradiated metacercariae; liverfluke infestation of cattle in relation to economic losses in the livestock industry; studies on growth, reproduction, and life span of Lymnaea cubensis; methods for mass production of F. hepatica miracidia; immunogenic effects on rats of triple vaccination with 2500 R gamma-irradiated F. hepatica metacercariae; immunogenic responses of cattle to oral vaccination with gamma-irradiated metacercariae; cryptobiosis of snail vectors of F. hepatica in the tropics and its epidemiological importance; and comparative studies on susceptibility of L. cubensis and L. columella to F. hepatica infection. (H.L.W.)

53499 RADIOSENSITIVITY OF THE OVOCYTES IN SITOTROGA CEREALELLA OLIV. Dryanovska, O. A.; Glavanakova, S. I. Compt. Rend. Acad. Bulg. Sci.; 25: No. 2, 253-4(1972).

The γ-radiosensitivity of the late prophase and the early metaphase of meiosis in the oocytes of the grain moth (Sitotroga cerealella) was studied. Irradiated females were mated with normal males and the number of eggs hatching during the first 24 hrs, corresponding to irradiation at early metaphase, and during the second 24 hrs, corresponding to irradiation at late prophase, was determined. Results indicated that oocytes in the early metaphase of meiosis were more sensitive to γ irradiation than those in late prophase. (E.R.B.)

53500 ACTION OF SMALL DOSE OF RADIATIONS UPON THE MANIFESTATION OF BAR GENE IN DROSOPHILA MELANOGASTER MEIG. Precup, O.; Pora, E. A. Stud. Cercet. Biol., Ser. Zool.; 23: No. 5, 465-77(1971). (In Rumanian).

Homozygote Bar mutants of Drosophila melanogaster were used to investigate the effect of a 900 mR dose of radiation upon the manifestation of Bar gene. The irradiation was made in the gametic or pregametic cell stage and the larval stage. It was noticed the above mentioned dose of radiation acted in a metabolic-stimulatory way, demonstrated by the increase of the mean number of omatidia by Bar mutants of both sexes. (Rom. Sci. Abstr.)

53501 CHROMOSOMAL INTERCHANGE IN MATURE OOCYTES OF DROSOPHILA. Parker, D. R.; Busby, Nancy (Univ. of California, Riverside). Mutat. Res.; 16: No. 1, 49-58(Sep 1972).

Detachments of a reversed acrocentric compound-X chromosome (C(I)RA) resulting from interchange with a doubly-marked Y chromosome (y^+Yy^+) were induced by irradiating mature, stage-14 oocytes in 5-day-old, adult virgin females of Drosophila melanogaster. The period of egg laying after irradiation was limited to 12 hr to prevent inclusion in the sample of eggs that were irradiated in immature stages. It was confirmed that some rearrangements must be completed prior to the completion of division I, since chromosomes that regularly assort apart at division I—C(I)RA and y^+Yy^+—have been able to interchange parts to permit the recovery of half-translocations. Further evidence is afforded by the higher recovery of proximal (capped) than of distal (captured) X's, from which can be inferred nonrandom segregation of heteromorphic dyads. The absence of fractionation effects in mature oocytes was accounted for in previous publications by postulating delayed repair, but the delay cannot extend beyond the initiation of chromosome movement in division I of meiosis. Our data, however, do not exclude the possibility that some interchanges might be completed postmeiotically, but neither do they suggest it. It is argued that the kinds of data that were derived from mature Drosophila oocytes are not yet adequate to form a basis for choosing between breakage-first and exchange models of interchange. The significance of these findings in relation to the kinds of aberrations that can be recovered from irradiated mature oocytes is briefly discussed. (auth)

53502 EFFECTS OF TREATING DROSOPHILA FEMALES WITH ACTINOMYCIN-D ON THE YIELDS OF DOMINANT LETHALS, TRANSLOCATIONS, AND RECESSIVE LETHALS RECOVERED FROM X-IRRADIATED SPERMATOZOA. Proust, Jacqueline P.; Sankaranarayanan, K.; Sobels, F. H. (Univ. of Leiden). Mutat. Res.; 16: No. 1, 65-76(Sep 1972).

Drosophila females were injected with actinomycin-D. After a day they were mated (for 24 hr only) to males that were exposed to 2000 or 2500 R x irradiation, so that only mature spermatozoa were sampled. The radiation-induced frequencies of dominant lethals, II–III translocations, and recessive sex-linked lethals in the paternal genome were determined. When compared to the appropriate controls, it is found that such treatment of the females with actinomycin leads to an increase of the frequency of dominant lethals and to a decrease of those of translocations and recessive lethals. Characteristic is the delayed expression of the actinomycin effect, in that the modification of translocation and recessive lethal frequencies is most pronounced in oocyte stages utilized 4 to 6 days after injection. The present findings are interpreted to mean that actinomycin acts by partially inhibiting the restitution of chromosome breaks, thereby increasing the frequency of dominant lethals, and decreasing that of translocations and recessive lethals. This implies that maternal repair processes acting at the stage of pronucleus formation are required for the repair (restitution) or misrepair (reunion giving rise to translocations) of chromosome breaks induced in mature spermatozoa. (auth)

53503 EXPERIMENTAL VERIFICATION OF EFFECTIVENESS OF RADIATION VACCINE AGAINST CATTLE DICTYOCAULOSIS. Pokorna, J. (Bioveta, Ivanovice na Hane, Czech.). Veterinarstvi; 22: No. 1, 16-19(1972). (In Czech).

The results are presented of experiments carried out in 1971 with active immunization of cattle against dictyocaulosis by irradiated vaccine. The vaccine was prepared from the larval suspension of stage III Dictyocaulus viviparus by x-irradiation. The double administration of the irradiated vaccine to the experimental animals resulted in a highly significant protection of the immunized animals against subsequent massive invasion by non-irradiated larvae. The similar dose of larvae administered to the control group resulted in grave dictyocaulosis. The evaluation of the effect of the vaccine was based on clinical investigations of the health conditions of the animals, the excretion of larvae in the faeces, and on the pathological and anatomical findings yielded by autopsy. The results pertaining to the experimental and control animals showed statistically significant differences. (INIS)

53504 EFFECT OF γ RADIATION ON THE RESISTANCE AND LONGEVITY OF TWO ONISCOIDEAS SPECIES: PORCELLIO DILATATUS AND CHAETOPHILOSCIA SICULA AND THEIR MUTANTS. Bonnet, Louis; Dalens, Henri (Univ., Toulouse). Compt. Rend., Ser. D; 274: No. 20, 2794-7(15 May 1972). (In French).

Marked differences occur between the radiation resistance of Porcellio dilatatus and Chaetophiloscia sicula, the species being represented by their wild phenotypes and certain mutant phenotypes. Great similarity is however observed between phenotypes belonging to the same species. (France)

Radionuclide Effects (Internal Source)

Refer also to abstracts 53021, 53024, and 53396.

53505 CELLULAR LESIONS INDUCED BY EXTERNAL AND INTERNAL RADIATION SOURCES. Goutier, R. (CEN, Mol, Belgium). J. Belge Radiol.; 55: No. 2, 253-62(1972). (In French).

Chain breaks in DNA seem to be at the origin of the short term lethal effect of ionizing radiation from external source, as well as of the lethal effect of an incorporated radionuclide. The RBE of β-rays of incorporated ^{3}H for lethal effect is close to one, since, for that particular effect, x rays and ^{3}H-β-rays both act by ionization, provided the dose of β-rays calculated be the dose received by DNA. Therefore, the maximal efficiency of a radionuclide is provided by carrier molecules which, such as thymidine, are specifically incorporated into DNA; any incorporation in another site of the cell results in a decreased killing efficiency of ^{3}H. In the mutagenic effect of ^{3}H and in the lethal as well as mutagenic effects of ^{14}C and ^{32}P, transmutation seems to play an important role not only by producing DNA chain breaks but also by producing changes in base pairing (point mutation). Lastly, DNA repair processes, well known after uv or x irradiation, also seem to occur during the action of an incorporated radionuclide. (auth)

Man

Refer also to abstracts 53419, 53511, and 53542.

53506 (ORNL-tr-2629) AGE-DEPENDENT INGESTION DOSE FACTORS g_G AND $g_{G'}$ OF ^{131}I. Bayer, A. (Kernforschungszentrum, Karlsruhe (West Germany). Institut fuer Neutronenphysik und Reaktortechnik). Translated for Oak Ridge National Lab., Tenn., from report KFK-1582. 38p. Dep. NTIS.

An age-dependent curve for fallout ^{131}I ingestion by children was obtained, based on the iodine concentration in milk. The extended ingestion dose, based on the iodine concentration in air and the milk-air-transport factor was determined. The extended ingestion dose was compared with the inhalation dose. A proposed maximum thyroid dose of 90 mrem/yr for children, based on the maximum iodine concentration in air of $3.6 \cdot 10^{-14}$ C/m^3, is proposed. (C.H.)

53507 COMBINED FRACTIONATED ISOTOPIC AND EXTERNAL IRRADIATION OF THE LIVER IN HODGKIN'S DISEASE. A STUDY OF 21 PATIENTS. Kraut, Joseph W.; Kaplan, Henry S.; Bagshaw, Malcolm A. (Santa Clara Valley Medical Center, San Jose, Calif.). Cancer; 30: No. 1, 39-46(Jul 1972).

Of 21 Hodgkin's disease patients with laparotomy-documented splenic and/or hepatic involvement (Stages III$_S$ and IV$_H$) treated with total lymphoid and combined external and internal (^{198}Au) whole liver irradiation, nine patients remain disease-free for 17 to 34 months. All but two of the relapses occurred in patients previously treated to local fields only. One death is directly attributable to the isotope. Another death at 34 months was due to intercurrent disease. About half of the combined whole liver dose of 2,500 rads is delivered by external megavoltage x-ray therapy and half by radioactive colloidal gold (^{198}Au). The usual isotopic dose is 25 to 30 mCi administered intravenously at a maximum rate of 10 mCi every 2 weeks. Tumoricidal doses can thus be delivered to the critical periportal areas within the liver, whereas dose to the central vein region of the lobule remains within the normal liver tissue tolerance level, thus avoiding the immediate reaction of radiation hepatitis and the remote development of cirrhosis. Thrombocytopenia, the most serious complication, may be prevented or lessened by adjusting the fractionated and total dose of the isotope. (auth)

53508 RELATIONS BETWEEN THE INHALED POTENTIAL α-ENERGY OF ^{222}Rn- AND ^{220}Rn-DAUGHTERS AND THE ABSORBED α-ENERGY IN THE BRONCHIAL AND PULMONARY REGION. Jacobi, W. (Hahn-Meitner-Institut fuer Kernforschung GmbH, Berlin). Health Phys.; 23: No. 1, 3-11(Jul 1972).

On the basis of the new ICRP-lung model the ratio of the absorbed α-energy or integral α-dose in the bronchial and pulmonary region to the inhaled potential α-energy was estimated as functions of the aerosol concentration, the ventilation rate, and the wall-deposition rate in the working area. With increasing aerosol concentration and decreasing ventilation rate this ratio decreases in the bronchial region but increases in the pulmonary region. The possible variation of bronchial and pulmonary dose per WLM inhaled is also discussed with respect to the maximum permissible annual intake of Rn- and Tn-daughters. (auth)

53509 DOSIMETRY IN THE USE OF COLLOIDAL ISOTOPES. Fleay, R. F. (Royal Perth Hospital, Australia). Australas. Radiol.; 15: No. 4, 388-90(Nov 1971).

Measurements have shown detectable levels of radioactivity in the urine and high levels of radioactivity in the pleural fluid of patients many days after injection of phosphorus-32 and gold-198 colloids used for treatment of malignant pleural effusion. These findings led to a review of the procedure at present in use in the hospital and an estimation of the radiation doses. (auth)

53510 COMPARISON OF TECHNIQUES FOR CALCULATING DOSES TO THE WHOLE BODY AND TO THE LUNGS FROM RADIOACTIVE NOBLE GASES. Russell, John L.; Galpin, Floyd L. (Environmental Protection Agency, Rockville, Md.). pp 286-308 of Radiation Protection Standards: Quo Vadis. Vol. II. Howell, Wallace P. (ed.). Richland, Wash.; Health Physics Society (1972).

From 6th annual topical symposium on radiation protection standards: quo vadis; Richland, Wash. (2 Nov 1971).

An issue that is frequently discussed in connection with dose projections of the radioactive noble gases krypton and xenon is the degree of conservatism built into the recommended maximum permissible concentrations through simplifying assumptions. The ICRP recommendation requires summation of the effective energy per disintegration and no differentiation is made relative to β and γ contributions. Thus, the energies of the β particles are included as contributors to the whole body dose, regardless of the fact that most of the energy is delivered to the skin. The methodology recently developed by the Medical Internal Radiation Dose Committee is used to estimate whole body and lung doses for the γ component of the radioactive gases constituting the plume of a boiling water nuclear power reactor (BWR) for three exposure pathways: gas dissolved in body tissues; immersion in an infinite cloud of gas; and gas in the lung. Estimated doses for β particles are calculated for the same pathways. The summations of the γ and β whole body doses in a MPCa cloud range between 3% and 60% of 500 mrad per year for the noble gases with established decay schemes. The contribution of gases in the lung and dissolved in body tissues to the whole body dose is a small fraction of this. The projected dose for a BWR plume at a weighted MPC with 30 minutes decay is 322 mrad per year, or approximately 65% of the 500 mrad per year recommended Radiation Protection Guide. (auth)

Animals

Refer also to abstracts 53459, 53472, and 53496.

53511 (TID-26142) RISKS AND EMERGENCY RADIATION DOSES FROM PLUTONIUM DIOXIDE EXPOSURES. Gavankar, Harsharaj Ganesh (California Univ., Berkeley). Jun 1972. 99p. Dep. NTIS.

Thesis.

Principal route of entry of plutonium dioxide into the human body is via inhalation of the plutonium-bearing aerosols released from a fast reactor accident. In order to estimate radiation doses, therefore, consideration of the aerosol transport characteristics is necessary along with understanding of the physiology and anatomy of the human respiratory tract, its particle deposition, clearance and translocation processes and their influence on the ultimate fate of inhaled PuO_2. Based on a review of the available long-term experimental data on animals involving inhalation of $^{239}PuO_2$, and the limited ^{239}Pu data in man, the critical organs chosen for dose calculation are: lung, liver, and bone. Although the lymph nodes are an important deposition site for PuO_2 translocated from the lung, no life-shortening attributable to tumors or other lymphatic tissue damage has been demonstrated in experimental animals. On the basis of calculated doses and the extrapolated tumor risk probabilities, per microcurie of initial deposition of $^{239}PuO_2$ in the deep lung, and per microcurie of fifty-year accumulated deposition in the liver and bone, the following $^{239}PuO_2$ dose guidelines are considered to be risk-equivalent to 25 rem whole body exposure: fifty-year accumulated doses to lung, liver, and bone of 10, 25 and 75 rem respectively are separately risk-equivalent to cancer risks believed to be associated with 25 rem whole body exposure; on a total risk basis (tumors for lung + liver + bone), the same reference risk would occur with 0.019 microcurie of inhaled $^{239}PuO_2$ for a typical 0.5μ AMAD aerosol; the resulting 50-year accumulated doses to the lung, liver, and bone of a 20-year old adult will be 7.0 rem, 7.7 rem, and 3.0 rem respectively. Until substantial operating experience is gained on sodium-cooled plutonium dioxide-fueled reactors and until the current low-level dog inhalation experiments initiated in 1970 are completed (about 10 to 15 years from now), this approach may form a rational basis for siting and safety of liquid metal fast breeder reactors. (82 references) (auth)

53512 LEUKEMOGENIC EFFECT OF RADIOSTRONTIUM (^{90}Sr) IN MICE, A COMPARATIVE STUDY OF LEUKEMOGENICITY OF ^{90}Sr AND X RAYS. 1. INCIDENCE AND CHARACTERISTICS OF ^{90}Sr-INDUCED AND X-RAY-INDUCED LEUKEMIAS. Ito, Takaaki (Hiroshima Univ.). Nippon Ketsueki Gakkai Zasshi; 33: No. 4, 415-31(Aug 1970). (In Japanese).

The leukemogenicity of radiostrontium (^{90}Sr) was studied in comparison with that of fractionated whole-body x irradiation in female ICR/JCL mice. A single intraperitoneal administration of ^{90}Sr (1.0 μCi/gm) produced leukemia in 61.8% of the mice, mostly with a latency period of 110 to 240 days. The ^{90}Sr-induced leukemias originated in the peripheral lymph nodes but not in the thymus, although the major radiation injury is restricted to the bone marrow cells. Cytologically, these leukemias were lymphoblastic, reticulum cell, or stem cell type. The occurrence of the leukemia was not affected by thymectomy. The fractionated whole-body x irradiation of 680 R induced leukemia in 77.3% of mice, in which the majority of cases were of thymic origin and cytologically lymphoblastic. Thymectomy was effective in reducing the incidence. Only one case of leukemia (3.0%) occurred among untreated control mice up to 600 days after birth. As to the mechanism of leukemogenesis by both agents, it is postulated that whole-body x irradiation produces leukemic progenitor cells not only in the thymus but also in the bone marrow or spleen and these cells migrate into injured thymus where they proliferate, while ^{90}Sr produces similar progenitor cells in the bone marrow by the internal emission of beta rays and they migrate into peripheral lymphoid tissues but not into intact thymus. Furthermore, x-ray induced leukemic progenitor cells, that are not yet specified for any particular cell type, might be endowed with the capability of lymphoid differentiation in the thymus by an as yet unknown thymic factor. On the other hand, most of the ^{90}Sr-induced leukemic cells that settled in the peripheral lymphoid tissue without passing through the thymic environment might remain as primitive undifferentiated cell type (stem cell or reticulum cell). (auth)

53513 QUANTITATIVE EFFECTS OF ^{131}I ON DIFFERENT TISSUE COMPONENTS IN FOETAL AND GOITROGEN CHALLENGED MOUSE THYROIDS. Walinder, G. (Foersvarets Forskningsanstalt, Stockholm). Acta Radiol., Ther., Phys., Biol.; 11: No. 1, 1-23(Feb 1972).

The effects of radiation on cell number and on the relative amount of tissue components in the thyroid gland were investigated morphometrically in immature mice and in adult, goitrogen-challenged CBA mice at different times after the injection of ^{131}I. Cell survival was examined by measuring residual tritium activity in the glands of mice injected with tritium-labelled thymidine before the administration of radioiodine. The radiation-induced growth arrest of the thyroid tissue appeared to be due mainly to mitotic death of the cells. (auth)

53514 CHANGES OF THE CELLULAR DIVISION AND DNA SYNTHESIS IN GLANDS OF THE GASTRIC FLOOR OF RATS UNDER THE EFFECT OF RADIUM EMANATION. Zaporozhchenko, I. G. (Inst. of Medical Genetics, Moscow). Byull. Eksp. Biol. Med.; 73: No. 4, 95-8(Apr 1972). (In Russian).

Circadian changes of the mitotic index in rat glands of the gastric floor have a high level at 7 a.m. to 4 p.m. and at 8 p.m. The circadian rhythm of the index of labeled nuclei is characterized by the highest levels at 10 a.m. to 2 p.m. and at 10 p.m. In peroral administration of radon water of diverse concentration, alpha-radiation influences the circadian changes of the mitotic index and the index of labeled nuclei in the glands of rat gastric floor. The degree of changes in the proliferation and level of DNA synthesis depends on the concentration of radon in the water. (auth)

53515 RADIATION DOSE AND RADIOPROTECTIVE EFFECT IN THE EXAMINATION OF THE THYROID GLAND OF BIRDS. Robiller, F.; Unverricht, A. (Friedrich-Schiller-Univ., Jena, Ger.). Radiobiol.-Radiother.; 13: No. 3, 393-6(1972). (In German).

After parenteral injection, the accumulation of ^{131}I was measured over the thyroid gland of different kinds of birds (budgerigar, serin) of both sexes. The radiation dose was determined by Loewinger's method. Despite an organ dose of 12,000 rad, functional or morphological changes of the thyroid gland and a limitation of the generative power could not be observed. (auth)

53516 HEMATOLOGIC CHANGES AND CHANGES IN THE BLOOD PROTEINS IN EXPERIMENTS ON WHITE RATS FOLLOWING INTRATRACHEAL ADMINISTRATION OF RADIOCERIUM. Hecko, I.; Trnovec, T.; Grunt, J.; Kortus, J. (Research Inst. of Hygiene, Bratislava). Bratislav. Lek. Listy; 56: No. 4, 465-72 (Oct 1971). (In Czech).

Several hematologic values, the protein content of blood plasma as well as the elements of this content were ascertained on the 32nd and the 64th days following the placing of ^{144}Ce (of a 3.9 activity of μC on the animal) into the trachea of 5 or 8 experimental white rats. With equally large control groups, altogether 26 rats have been examined. The differences between the experimental and the control groups of rats have been confirmed as statistically significant using five hematologic values (in two on the 32nd day and in three on the 64th day of the experiment): once in the number of leukocytes, twice in the hematocrit value and twice in the indices calculated always from two values of the red blood picture (mean hemoglobin corpuscular concentration and mean corpuscular hemoglobin). The differences between the experimental and the control groups of rats as regards the protein content of the blood plasma (ascertained refractometrically) and in the elements of this content (ascertained by electrophoresis on paper) have not been confirmed as statistically significant. (auth)

53517 INFLUENCE OF RADIOACTIVE PHOSPHORUS (^{32}P) ON THE CHICK EMBRYO DEVELOPMENT, HATCHABILITY, AND CHICK GROWTH. Lee, K. W. Korean J. Anim. Sci.; 13: No. 2, 116-25(1971).

Radioactive phosphorus (^{32}P) in single doses up to 40 μC was injected into the egg yolk during the 5th to 15th incubation day. Embryo development, hatchability and chick growth rate up to 150 days old were observed. A single dose of 5 to 40 μC of ^{32}P on the 5th to 15th incubation day resulted in the significantly retarded development of the 18 day-old chick embryo as the ^{32}P dosage increased. A significant negative correlation between the ^{32}P dosage on the 12th incubation day and hatchability ($r = -0.946$) and a linear regression of hatchability loss to ^{32}P dosage ($Y = 0.372X + 17.06$) were obtained. The chick growth rate up to 150 days old was decreased significantly as the ^{32}P dosage on the 12th incubation day increased. (Korean Sci. Abstr.)

Microorganisms

53518 SPECIFIC ENRICHMENT OF MUTANTS OF ESCHERICHIA COLI WITH AN ALTERED ACYL CoA SYNTHETASE BY TRITIUM SUICIDE. Hill, F. F.; Angelmaier, Doris (Univ., Cologne). Mol. Gen. Genet.; 117: No. 2, 143-52(1972).

In a rich growth medium, tritium-labeled oleate is incorporated preferentially into the lipid fraction of Escherichia coli K 12. The incorporation of the radioactive oleate after a temperature shift kills the majority of the cells during subsequent storage. Most of the surviving cells can no longer grow with oleate as the sole carbon source at 40°C or 30°C, though some exhibit a thermosensitive behavior, and are able to grow at 30°C but not at 40°C. It will be shown that mutants of the first group lack the enzyme acyl CoA synthetase, and that this enzyme is thermolabile in mutants of the second group. In addition, one further mutant was isolated that possessed a normal acyl CoA synthetase but was unable to degrade or incorporate oleic acid. (auth)

Nuclide Kinetics and Toxicology

Refer also to abstracts 53021, 53024, 53149, and 53396.

53519 ANALYSIS OF KINETIC CURVES. APPLICATION OF DATA PROCESSING. Uchikawa, Toru; Fukuda, Nobuo (National Inst. of Radiological Sciences, Chiba, Japan). Sogo Rinsho; 20: No. 8, 1793-9(Aug 1971). (In Japanese).

A brief review is made of kinetic analysis with reference to the results of the analysis of in vivo radioisotope metabolism conducted by the authors. Brownell's symbols are used in accordance with the ICRU recommendation. The parameters of kinetics obtained from the radioactivity-time curves of whole-body, blood, and urine include: turnover rate and turnover time; initial distribution volume; rate of exit from the space of fast initial mixing; fraction of irreversible removal and fraction of re-entry into circulation; and mean transit time. The transfer rate is obtained from the formulation of compartment models exemplified by a mammillary or parallel model, catenary or series model, or the combination of the former two models, i.e., cateno-mammillary model and mammillocatenary model. The effectiveness of this kinetic analysis is conditioned mainly by the kind and quality of data and the proper choice of model. The choice of a model most pertinent to a particular biological system is extremely difficult. Besides only certain kinds of isotopes can be used for this method. Further studies on methodology and the standardization of terminology, that of the Japanese in particular, are expected. (Japan)

Man

Refer also to abstracts 53074 and 53413.

53520 (CEA-N-1535) ^{90}Sr LEVELS IN HUMAN BONES COLLECTED IN 1970. Jeanmaire, Lucien; Patti, Francois (Commissariat a l'Energie Atomique, Fontenay-aux-Roses (France). Centre d'Etudes Nucleaires). May 1972. 25p. (In French). Dep. NTIS (U. S. Sales Only).

The level of ^{90}Sr and stable Sr in human bones collected in the Paris area in 1970 is presented. The general tendency observed is a slight decrease in the level of contamination for all age groups, except that of newborn babies. (France)

53521 POLLUTION TRANSFER TO MAN. PART 2. DYNAMIC STUDY OF THE BEHAVIOR AND TRANSFER OF RADIOACTIVE POLLUTION. Bresson; Bittel; Coulon; (and others) (CEN, Fontenay-aux-Roses, France). Nuisances Environ.; No. 7, 33-9(Jan 1972). (In French).

In order to protect the population from the adverse effects of radiation, it is important to know the relation between the effects (dose delivered) and the cause (level of radioisotopes introduced into the environment). This relation depends upon the mechanism controlling the transport of the radioisotopes and transfer to man, and thus upon the parameters characteristic of this transfer. The way in which the radioisotope is introduced into the environment and removed from different media is examined as well as its behavior in the different media. An inventory of the relevant parameters (mechanical, physical, physicochemical, biological) is presented. The vegetable and animal media, food products, and the materials used by man are studied. (France)

53522 POLLUTION TRANSFER TO MAN. PART 1. DYNAMIC STUDY OF BEHAVIOR AND TRANSFER OF RADIOACTIVE POLLUTION. Bresson; Bittel; Coulon; (and others) (CEN, Fontenay-aux-Roses, France). Nuisances Environ.; No. 6, 33-40(Dec 1971). (In French).

A quantitative inventory of the various characteristics and parameters capable of modifying the transfer to man of radioactive pollutants is presented. An improved protection system is sought. The behavior of a radioactive pollutant in the environment is examined dynamically, i.e. in addition to examining the phenomena intervening in the different media, (atmosphere, soil, water) the characteristics of inter-medium transfer are examined. (France)

53523 DOSE ACTION LEVELS FOR ACCIDENTAL RADIATION EXPOSURE OF THE GENERAL PUBLIC. Voilleque, Paul G. (Health Services Lab., Idaho Falls, Idaho). pp 183-204 of Radiation Protection Standards: Quo Vadis. Vol. I. Howell, Wallace P. (ed.). Richland, Wash.; Health Physics Society (1972).

From 6th annual topical symposium on radiation protection standards: quo vadis; Richland, Wash. (2 Nov 1971).

The problems of establishing criteria for limiting radiation exposure of members of the general public in the unlikely event of a radiological emergency are discussed. The dose limitation criteria, termed Action Levels in ICRP Publication 9, can serve as the foundation for making decisions based on environmental measurements taken during the evaluation of an accidental release of radioactivity from a nuclear facility to its environs. (auth)

53524 AMOUNT AND FORM OF RADIOACTIVITY IN HUMAN MILK AFTER LUNG SCANNING, RENOGRAPHY, AND PLACENTAL LOCALIZATION BY ^{131}I LABELED TRACERS. Karjalainen, P.; Penttilae, I. M.; Pystynen, P. (Kuopio Central Hospital, Finland). Acta Obstet. Gynecol. Scand.; 50: No. 4, 357-61(1971).

The secretion of radioisotope into mothers' milk was studied after the administration of carriers labelled with ^{131}I. The radiopharmaceuticals used were 300 μCi macroaggregated human serum albumin (MAA) (for lung scanning), 25 μCi ortho-iodohippuric acid

(OIH) (for renography), and 10 μCi human serum albumin (HSA) (for placental localization). In the MAA series (7 patients), the maximum radioactivity secreted into milk in the 24 hr following injection was 0.7%, and the mean activity 0.14% of the injected dose. The corresponding figures of the OIH series (25 patients) were 2.4 and 0.32%. In both cases activity was at its maximum during the first 24 hr after injection. In the HSA series (8 patients), the maximum radioactivity secreted into the milk during 24 hr after injection was 0.22% of the injected dose. After the administration of OIH and apparently also of MAA, the radioactivity secreted in 24 hrs increases if the excreted volume of milk increases. The ^{131}I secreted in the milk was not bound to the radiopharmaceutical originally administered, but was mainly in the form of free isotope. The breast feeding of babies whose mothers had undergone lung scanning, renography, or placental localization was discussed. It was proposed that milk should be discarded for a minimum of 7 days following lung scanning and a minimum of 2 days following renography, provided the examinations were carried out by means of the radiopharmaceuticals and doses used by the present authors. (auth)

53525 ^{226}Ra IN POLISH DIET AND FOODSTUFFS. Pietrzak-Flis, Zofia (Central Lab. for Radiological Protection, Warsaw). Nukleonika; 17: No. 3-4, 227-31(1972).

Contents of ^{226}Ra and calcium were determined in diet, some foodstuffs, and urine, collected in the Kowary Valley, and in some foodstuffs and urine collected in the Warsaw region. The content of ^{226}Ra in diet in the Kowary Valley was about 0.58 ± 0.04 pCi/day, the contribution from water being about 0.30 pCi/day. The mean ^{226}Ra content in foodstuffs from the Kowary Valley was about three times higher than that in foodstuffs from the Warsaw region. The ^{226}Ra content in urine collected in Kowary was about two times higher than that in urine collected in Warsaw. (auth)

Animals

Refer also to abstract 53515.

53526 (BNWL-tr-71) MECHANISMS OF HEPATIC UPTAKE OF HEPATOTROPIC RADIONUCLIDES. Trnovec, Tomas; Plaskova, Anna. Translated for Battelle Pacific Northwest Labs., Richland, Wash., from Prac. Lek.; 23: No. 5, 175-81(1971). 20p. Dep. NTIS.

A survey concerning the mechanism of the uptake of radionuclides in the liver is presented. The mechanism of hepatic uptake of polymerizable radionuclides depends markedly on the physicochemical condition in which they exist in the blood. Both principal types of liver cells, i.e. parenchymal and Kupffer cells, take part during uptake of the radionuclides of rare earths and transuranium elements into the liver. Emphasis is placed on the uptake of ^{239}Pu and ^{241}Am by the liver of mammals. Further investigation of the mechanism of hepatic uptake of polymerizable radionuclides must begin with the latest discoveries concerning the morphology and physiology of the liver tissue. Such discoveries, from a point of view of association between these radionuclides and plasma proteins are, for example, findings concerning the metabolism of isologous proteins in the liver cells. (auth)

53527 (FOA-4-4503-A-3) TRANSFER OF SIMULATED FALLOUT-PARTICLES FROM PASTURE TO GRAZING DAIRY CATTLE. I. INTRODUCTORY EXPERIMENTS WITH WET DEPOSITED 100 TO 200 μm PARTICLES. Auraldsson, Hans-Ake; Ekman, Lars; Eriksson, Ake; Greitz, Ulf (Forsvarets Forskningsanstalt, Stockholm (Sweden)). Jul 1972. 18p. Dep. NTIS (U. S. Sales Only).

When estimating internal radiation risks in a local fallout area knowledge of the transport of fallout particles from pasture to grazing cows is essential. The present report deals with the design of grazing experiments in order to test their suitability to determine simulant fallout particle transport to cows. The principle of the experiments was that labeled (^{140}La) silica sand particles 100 to 200 μm in diameter were deposited in a water suspension on pasture where cows were kept grazing. The fraction of the deposition ingested by the animals was assessed by assay of the radioactivity content in feces. It was found that the differently designed experiments gave similar results. About twenty percent of the wet deposited particles were consumed by the grazing cows. For further studies of the transport of close-in particulate fallout simulant one type of experiment was found to be the most suitable. It gives information on the fraction of particles consumed by the grazing cows during the first two days after deposition when the retention of particles on the grass is high. (auth)

53528 (LF-tr-71) PULMONARY LAVAGE, THERAPY OF PULMONARY CONTAMINATIONS. Kunzle-Lutz, M.; Metivier, H.; Nolibe, D.; Simon-Vermot, A.; Gimbert, J. L.; Jockey, P. Translated by A. A. Horvath (Lovelace Foundation for Medical Education and Research, Albuquerque, N. Mex.), from Poumon Coeur; 26: 1029-38(1970). 10p. Dep. NTIS.

An abstract of this article was prepared from the original language publication and appears in NSA Vol. 26 as number 9528. (C.H.)

53529 (NASA-TM-X-2440, pp 982-8) HAIR RADIOACTIVITY AS A MEASURE OF EXPOSURE TO RADIOISOTOPES. Strain, W. H.; Pories, W. J.; Fratianne, R. B.; Flynn, A. (Cleveland Metropolitan General Hospital. Case Western Reserve Univ., Cleveland). Jan 1972.

From Symposium on natural and manmade radiation in space; Las Vegas, Nev. (1 Mar 1971).

Measurement of hair radioactivity appears to be a suitable method for monitoring systemic exposure to radioisotopes and certain types of manmade radiation. This concept has developed from a suggestion we made in 1963 that the strontium-90 content of hair affords a nondestructive method of estimating the body burden of this radionuclide. Since many radioisotopes accumulate in hair, this tropism was investigated by comparing the radioactivity of shaved with plucked hair collected from rats at various time intervals up to 24 hrs. after intravenous injection of about 5 μCi of the ecologically important radioisotopes, iodine-131, manganese-54, strontium-85, and zinc-65. The plucked hair includes the hair follicles where important biochemical transformations are taking place. The data indicate a slight surge of each radioisotope into the hair immediately after injection, a variation of content of each radionuclide in the hair, and a greater accumulation of radioactivity in plucked than in shaved hair. These results have application not only to hair as a measure of exposure to radioisotopes, but also to tissue damage and repair at the hair follicle. (auth)

53530 (TID-3915(Suppl.1)) RUSSIAN RADIOECOLOGY: A BIBLIOGRAPHY OF SOVIET PUBLICATIONS WITH CITATIONS OF ENGLISH TRANSLATIONS AND ABSTRACTS. Klement, Alfred W. Jr. (Division of Radiological and Environmental Protection (AEC), Washington, D. C.); Schultz, Vincent (Washington State Univ., Pullman. Dept. of Zoology). Sep 1972. 70p. Dep. NTIS.

A list is presented of 646 annotated references to Soviet publications in the field of radioecology. English translations of all titles are included and citations to available English abstracts and translations are given. Publications that discuss the distribution, effects, and utilization of radioisotopes in animals and plants in freshwater, marine, and terrestrial environments; ecological techniques employing radioisotopes; and laboratory studies having applications in ecology are included. (C.H.)

53531 (UCRL-Trans-1477) EXPERIMENTAL STUDY OF DECONTAMINATION OF THE SKELETON AFTER INHALATION OF AMERICIUM NITRATE. Nenot, J. C.; Morin, M.; Lafuma, J. Translated by Howard G. Parker (Univ. of California, Lawrence Berkeley Lab.), from Health Phys.; 21: 395-400(1971). 11p. Dep. NTIS.

An abstract of this article was prepared from the original language publication and appeared in NSA Vol. 25 as number 49092. (C.H.)

53532 RADIATSIONNAYA I KHIMICHESKAYA EKOLOGIYA GIDROBIONTOV. (Radiation and Chemical Ecology of Hydrobionts). Polikarpov, G. G. (ed.). Kiev; Izdatel'stvo Naukova Dumka (1972). 120p.

Eleven papers by different authors are included. The first part, the Physical Chemistry of Radionuclide Uptake by Sea Organisms, is particularly concerned with the transport of ^{65}Zn in sea water, its uptake by animals and plants, and the mathematics of radionuclide exchange between sea organisms and their environment. The second part, A Search for a Biochemical Storage Point for Radionuclides in Hydrobionts, includes eight papers on alginic acid, hydrolysis of some alginates, and the relation of alginic acid to uptake of ^{90}Sr by animals and plants and possible mechanisms for the fixation of radionuclides in connection with alginic acid. (K.S.W.)

53533 CHANGES IN THE DISTRIBUTION OF ^{137}Cs IN RABBITS DURING PERITONEAL DIALYSIS. Dziuk, Eugeniusz (Osrodek Ochrony Radiologicznej i Radiobiologii, Warsaw). Nukleonika; 16: No. 11-12, 583-9(1971). (In Polish).

The investigation on 30 rabbits (in three groups) contaminated intravenously with ^{137}Cs was carried out. In two groups, 15 min after the contamination, peritoneal dialysis was started; continuous and intermittent method being used. While dealing with the dialysis of animals, the speedier removing of ^{137}Cs from blood than took place in a control group was noticed. After 120 min, the animals were killed and the samples of tissue were taken. The content of ^{137}Cs in skeletal muscles, myocardium, and liver hasn't differed among individual groups. But changes in the distribution of ^{137}Cs in the kidneys were noticed. The removal of ^{137}Cs with urine and with dialyzing fluid was also estimated. (auth)

53534 LONG-TERM RETENTION OF RADIOBARIUM AND RADIOSTRONTIUM IN RABBITS. Liniecki, Julian; Karniewicz, Wieslawa (Inst. of Occupational Medicine, Lodz, Poland). Nukleonika; 16: No. 11-12, 591-604(1971).

Whole-body retention of single doses of ^{90}Sr and ^{133}Ba was followed for about 1000 days in rabbits. The data were fitted to a series of exponentials and a modified power function $R_t = A(\epsilon + t)^{-b}$. When the latter function was used, a poor fit was obtained at times beyond about 300 days after injection of the nuclides; when excretion became much slower than predicted by the parameters of the initial power function. This slowly eliminated fraction of alkaline earth traces had a mean residence time in the skeleton of several thousand days. From comparison of whole body retention and plasma clearance data for Sr and Ba it follows that a long-term preferential residence, due to the positive discrimination in the initial uptake of Ba(Ra) against Sr(Ca) into the skeleton, operates in this species. (auth)

53535 BALANCES OF ^{137}Cs, STABLE CESIUM, AND POTASSIUM OF BLUEGILL (LEPOMIS MACROCHIRUS RAF.) AND OTHER FISH IN WHITE OAK LAKE. Kolehmainen, S. E. (Oak Ridge National Lab., Tenn.). Health Phys.; 23: No. 3, 301-15 (Sep 1972).

Concentrations of ^{137}Cs, stable cesium, and potassium, and the intake and elimination rates of these nuclides were determined in bluegill and six other species of fish inhabiting a small radioactively contaminated lake in Oak Ridge, Tennessee during the period from June 1967 to January 1969. Cesium-137 concentrations increased by a factor of four in bluegills from 1 to 70 g, but the concentration of stable cesium decreased slightly with increasing fish size. In all species, the concentrations of ^{137}Cs cycled seasonally with a minimum in summer and a maximum in winter. Radiocesium concentration was highest in species feeding on food from which a high percentage of ^{137}Cs was absorbed. The concentration of stable cesium cycled similar to that of ^{137}Cs. Concentrations of potassium decreased somewhat with increasing fish size, but did not fluctuate seasonally. There were only small differences in the concentration of potassium in different species. The specific activities of ^{137}Cs in fish were in the same ranges as the specific activity of ^{137}Cs in water. In bluegill, the absorbed ^{137}Cs was eliminated by a two-component exponential process. Potassium was eliminated at a single exponential rate, 0.019/day at 15°C in bluegill. The absorption of potassium was almost complete for all types of food. Intake rates of ^{137}Cs, stable cesium, and potassium in bluegill were calculated on the basis of seasonal changes in body burden and elimination rates of these nuclides. (auth)

53536 RELATIVE NONHOMOGENEITIES OF RADIATION DOSE TO THE RESPIRATORY TRACT FROM INHALED RADIONUCLIDES. Barnes, J. E.; Hulbert, A. J.; Osborn, L. A. (Lovelace Foundation for Medical Education and Research, Albuquerque, N. Mex.). pp 96-116 of Radiation Protection Standards: Quo Vadis Vol. I. Howell, Wallace P. (ed.). Richland, Wash.; Health Physics Society (1972).

From 6th annual topical symposium on radiation protection standards: quo vadis; Richland, Wash. (2 Nov 1971).

Knowledge of the distribution of inhaled radionuclides along the respiratory tract is essential to evaluating the resultant radiation dose and potential biological effect. To obtain such information, Beagle dogs were exposed to a variety of aerosols in several different forms, sacrificed, frozen and sectioned. Autoradiographs of sections through upper respiratory tract show the accumulation of material in the turbinates and the nasopharynx. Autoradiographs of thoracic sections were analyzed with a scanning microdensitometer. Computer techniques were used to yield isodose contour mappings of the radiation dose distribution. The homogeneity of the lung dose from inhaled ^{90}Sr fused clay, a pure beta-emitter, is described. A nonhomogeneous accumulation of inhaled radionuclides in a striated pattern near the costal surface of the lung was also studied. This was observed autoradiographically and apparently results from the influence of the ribs during respiration. The phenomenon was observed in dogs sacrificed from within 10 minutes to as late as 768 days after exposure to a relatively insoluble aerosol. It was also observed in the lungs of a Rhesus monkey after inhalation. Gross biological lesions on the costal lung surface were observed which correlate with the striated pattern of activity accumulation. A subpleural accumulation of carbon particles in a similar striated pattern has been reported in human lungs at autopsy. The significance of these phenomena to lung burden measurements and hazard evaluation is discussed. (auth)

53537 STIMULATION OF RENAL ORGANIC BASE TRANSPORT BY URANYL NITRATE. Hirsch, G. H. (Health Protection Branch Research Labs., Ottawa). Can. J. Physiol. Pharmacol.; 50: No. 6, 533-9(Jun 1972).

Administration of 6 mg/kg uranyl nitrate to adult male rats resulted in a significant enhancement of N-methylnicotinamide (NMN) uptake by renal cortical slices when measured 24 or 48 hr after injection. The accumulation of another organic base, tetraethylammonium (TEA), by renal cortical slices was also significantly increased by uranyl nitrate treatment, but transport of the organic acid p-aminohippurate (PAH) was not altered in these experiments. The kidney weight to body weight ratio was increased in treated rats. Accumulation of NMN by renal cortical slices was significantly enhanced within 8 hr after administration of 6 mg/kg uranyl nitrate. NMN uptake was also significantly enhanced 24 and 48 hr after administration of 0.5 or 1.0 mg/kg uranyl nitrate to rats. The nephrotoxicity produced by uranyl nitrate was not directly related to its induction of organic base transport. The data support the hypothesis that the organic base transport system can be selectively induced by appropriate stimuli. Treatment of rats with potassium chloride did not enhance NMN uptake by renal cortical slices. (auth)

53538 STUDIES ON ARSENIC METABOLISM. 1. A STUDY ON THE DIFFERENCES IN ANIMALS IN ^{74}As UPTAKE. Tsutsumi, Shoji (Tokyo Dental Coll.). Nippon Shonika Gakkai Zasshi; 75: No. 9, 897-906(Sep 1971). (In Japanese).

Oral administration of ^{74}As was given to rabbits, rats, and mice to study its incorporation into various tissues of the animals and the subsequent fate in the course of time. In rabbits, radioactive concentration reached highest levels in 2 hrs in all tissues except hair. The liver obtained the highest concentration. The concentration per 1 mg of tissue was in the decreasing order of lung, liver, kidney, spleen, and brain. Hair was slightly higher in concentration than were muscle, skin, nail, femur, mandibula, molars, and incisors which were all low. Excretion of the radioactive substance was rapid. The concentration per 1 ml of blood was also low. In rats, the highest value was obtained in 2 to 6 hrs after administration. The concentration by organ was highest in the liver. Radioactive pool on the 24th day was in the decreasing order of lung, liver, spleen, heart, and kidney and extremely small in femur, mandibula, incisor, molar, and brain. Greatest uptake per 100 mg of tissue was observed in the spleen, followed by kidney, lung, liver, heart, femur, incisor, mandibula, molar, and skin in contrast to extremely small amounts in hair, muscle, and brain. The disappearance of the radioactive element was generally slow. Blood concentration per 1 ml was fairly high, the disappearance of radioactivity being also slow. In mice, uptake reached highest levels in 2 to 6 hrs in most organs. Nails ranked top in concentration per 100 mg of tissue. More than 1% of the radioactivity remained in nail, molar, and hair even after 5 days. Radioactivity disappeared in the order of spleen, incisors, mandibulas, muscle, femur, heart, lung, brain, kidney, and liver. Blood concentration per 0.1 ml was lower than rats and the disappearance of radioactivity from blood was also rapid. More ^{74}As was detected in the digestive tract of mice compared with rats until 6 hrs after administration, but was remarkably reduced in 24 hrs to levels lower than in rats. Almost no change was observed after 5 days. In rats, the concentration in urine was slightly higher than in feces. (Japan)

Plants

53539 (SRO-641-4) RADIOACTIVE TRACER STUDIES OF SOIL AND LITTER ARTHROPOD. Progress Report, November 1, 1971–October 31, 1972. (Georgia Univ., Athens. Dept. of Entomology). 1 Aug 1972. Contract AT(38-1)-641. 32p. Dep. NTIS.

The movement of potassium and calcium in the arthropod food web of a forest floor was quantified, using ^{134}Cs and ^{85}Sr as tracers for K and Ca. Four models were developed, a summer and an annual model for each element. On an annual basis, Oribatid mites (Cryptostigmata) were found to be the most important saprovore for elemental movement from decomposing litter. Cryptostigmata were second in importance to millipedes when summer seasons were considered alone. Evaluation of a recent model for retention and assimilation of radioactive tracers demonstrated the value of dual tagging with nonassimilated ^{51}Cr. The usual two-component model describing retention was shown to yield estimates of assimilation as a rate function, provided good measurements were obtained for the gut clearance rate. Measurements of fallout ^{137}Cs in plant species from granitic outcrops in Georgia confirm the values reported in 1965. (auth)

53540 INFLUENCE OF CLINOPTILOLITE ON ^{90}Sr AND ^{137}Cs UPTAKES BY PLANTS. Nishita, H.; Haug, R. M. (Univ. of California, Los Angeles). Soil Sci.; 114: No. 2, 149-57(Aug 1972).

An experiment was conducted to determine the effect of clinoptilolite on the ^{90}Sr and ^{137}Cs contents of bean and barley plants grown in soils contaminated at the surface (experiment I). An experiment was also conducted to determine the release of ^{90}Sr and ^{137}Cs to clover plants upon continuous and prolonged cropping of a contaminated soil with and without clinoptilolite treatment (experiment II). In experiment I, clinoptilolite was found to decrease the average ^{90}Sr contents of plants. The percentage reduction of ^{90}Sr contents of the different parts of the bean plants ranged from 48 to 70, 54 to 77, and 44 to 77% in the leaves, stems, and fruits, respectively, depending on the amount of clinoptilolite application and the kind of soil. The percentage reduction of ^{90}Sr in barley plants under various treatments ranged from 57 to 77 and 57 to 79 for the leaves and stems and the heads, respectively. In experiment II, eight harvests of clover were obtained. The application of Ca-treated clinoptilolite was effective in reducing ^{90}Sr contents of the plants grown in the mineral soil used, but it had no effect in the organic soil. Depending on the harvest time, the average ^{90}Sr contents of the plants grown in the treated mineral soil were 59 to 69% less than that of the control plants. Clinoptilolite was effective in maintaining the reduced ^{90}Sr contents of the plants throughout the experimental period. The ^{137}Cs contents of the plants were not changed appreciably by the application of clinoptilolite. (auth)

New Tracer Techniques

Refer also to abstracts 53214, 53413, 53539, 55058, and 55457.

53541 (TID-26128) MEDICAL RADIOISOTOPES MANUAL. (Oak Ridge Associated Universities, Inc., Tenn. (USA). Special Training Div.). 1971. 220p. Dep. NTIS.

This manual was prepared for use in a training course on the uses of radioisosopes in medicine. Twenty-four experiments cover the characteristics of β and γ radiations, radiation safety principles and monitoring instruments, radiation counting instruments and techniques, radioisotope scanning, in vitro diagnostic tests, and related subjects. Pertinent information on radiation safety rules, a classification of radioisotopes, sources of materials, and a list of reference books is included. (C.H.)

53542 VISUALIZATION OF ARTERIAL AND ARTERIAL GRAFT PATENCY BY INTRAVENOUS RADIONUCLIDE ANGIOGRAPHY. Meindok, H. (Toronto Western Hospital). Can. Med. Ass. J.; 106: No. 11, 1180-2(10 Jun 1972).

A method of visualizing patency of arteries and arterial grafts by means of intravenous ^{99m}Tc-pertechnetate using a Nuclear Chicago Pho/Gamma HP camera is described. Gamma camera polaroid pictures showing normal arteries in the upper and lower limbs as well as partial and complete occlusion of arteries and the state of arterial bypass grafts in pre- and postoperative patients are compared with conventional arteriograms. The advantages and limitations of this method are discussed. Intravenous radionuclide arterioradiography exposes the patient to 0.14 rads of whole-body radiation and 1.3 rads to the colon per 10 mc injection of ^{99m}Tc-pertechnetate. (Canada)

53543 DETERMINATION OF THE SYSTOLIC VOLUME BY EXTERNAL COUNTING. A MODEL FOR CALIBRATING THE CURVES. Zwirn, P.; Sebaoun, E.; Franceschi, A.; Fondarai, J. (Univ., Marseille). Ann. Phys. Biol. Med.; 6: No. 2, 79-86 (1972). (In French).

The recording of the variations in the volume of blood flow in the heart using ^{131}I and external counting techniques enabled curves representing the evolution of the cardiac volume to be obtained during the heart cycle. Experiments were performed on a model in order to develop a calibration method. In this way, it was possible to determine the parameters for calibrating the volume variation curves. However, when in vivo measurements are considered (in which all the conditions can not be controlled), the accuracy obtained is diminished. This case corresponds to the in situ heart, the volume variation being affected by the radioactivity of the surrounding tissues. (France)

53544 READING, AUTOMATIC TREATMENT, AND VISUAL DISPLAY OF RADIOACTIVITY SPECTRA RECORDED ON PUNCHED TAPE; APPLICATION TO THE STUDY OF THE METABOLISM OF TWO IN-VIVO RADIOISOTOPES. Soussaline, F.; Parmentier, C.; Bazin, J. P. (Institut Gustave Roussy, Villejuif, France). Ann. Phys. Biol. Med.; 6: No. 2, 53-68 (1972). (In French).

A completely automatic method for analyzing radioactivity spectra is described. The method facilitates the checking of the supporting data tapes, their computer treatment, and their visual display using a digital plotter. The method is applied to the analysis of the spectra of an ^{59}Fr/^{51}Cr mixture recorded by external counting during a double labeling test. The spectral shift correction technique utilized involves the fitting of these spectra by an orthogonal polynominal sum. This method, which is accurate and sufficiently fast to be used as a routine technique, eliminates all errors due to the detector, nonlinearities of the analyzer, or electronic instabilities. The spectral subtraction realized in this way enables the examination period to be shortened when ^{51}Cr is injected into the body. The scattered γ ray spectrum of the ^{59}Fe presents little distortion. (France)

MATERIALS

Ceramics and Cermets

Refer also to abstracts 52893, 53039, 53067, 53317, 53601—53603, 53617, 53620, 53632, 53651, 53704, 55022, 55027, 55031, 55032, 55035, 55189, and 55190.

53545 (ANL–7945) DEFORMATION AND FRACTURE OF UO_2–20 WT PERCENT PuO_2. Roberts, J. T. A.; Wrona, B. J. (Argonne National Lab., Ill.). Jun 1972. Contract W-31-109-eng-38. 39p. Dep. NTIS.

The four-point bend strength of UO_2–20 wt % PuO_2 was measured as a function of temperature and strain rate. The brittle-fracture stress was limited by fabrication flaws and/or impurities and was therefore relatively insensitive to changes in microstructure. The brittle-to-ductile transition temperature T_C increased with a reduction in porosity and an increase in applied strain rate. Above T_C, specimens generally exhibited extensive ductility, and a steady-state flow stress was maintained throughout the test. Based on the equivalence of steady-state flow and creep, T_C was described in terms of the brittle-fracture stress and the compressive creep strength. This allowed us to examine the sensitivity of T_C to fission rate and strain rate over a wide range, and it introduced an additional condition for fuel cracking into the LIFE-II code cracking subroutine. Thus, for cracking to occur now, at any instant in time, any of the principal stresses must exceed the fracture stress, and the zone-boundary temperature must be below T_C. The implications of the modified cracking model are discussed, and a typical predicted fuel history in-reactor is described. (auth)

53546 (AREAEE–134) PREPARATION OF SINTERABLE URANIUM DIOXIDE. Haroun, N. A.; Aly, M. M. E.; El-Adham, K. A. (Atomic Energy Establishment, Cairo (Egypt). Dept. of Metallurgy). 1972. 28p. Dep. NTIS (U. S. Sales Only).

Factors affecting the preparation of sinterable uranium dioxide powders have been extensively and critically reviewed. Experimental work on the reduction of ammonium polyuranate (APU) to UO_2, stabilization by cooling in different media, storage behavior, characterization, and sinterability of the resulting oxides is described. Results indicated that the more stable the powders the higher the reduction temperature. However the deterioration of powder activity and sinterability for the higher temperature preparations led to the choice of an optimum temperature of reduction. Of the cooling media investigated: ethyl alcohol-laden nitrogen (and nitrogen) were more effective than argon and hydrogen in stabilizing the powders. Differential thermal analysis was found most suitable for characterizing the powders. (69 references). (auth)

53547 (AREAEE–135) DENSIFICATION OF URANIUM DIOXIDE: A LITERATURE REVIEW. Haroun, N. A. (Atomic Energy Establishment, Cairo (Egypt). Dept. of Metallurgy). 1972. 27p. Dep. NTIS (U. S. Sales Only).

Factors affecting the densification of UO_2 are extensively reviewed. It was concluded that low-temperature sintering of nonstoichiometric oxides in neutral atmospheres is most promising. Variables discussed include, process variables, physical and physicochemical variables, and chemical variables. (101 references). (auth)

53548 (AREAEE–139) FACTORS AFFECTING THE REDUCTION OF URANIUM TRIOXIDE POWDERS. El-Shanshoury, I. A.; Bishay, A. F. (Atomic Energy Establishment, Cairo (Egypt). Dept. of Metallurgy). 1972. 22p. Dep. NTIS (U. S. Sales Only).

The reduction of uranium trioxide powders was investigated using ammonia gas as a reducing atmosphere. The effect of flow rate and particle size was also studied for ammonia and hydrogen reductions. Hydrogen reduction was found to be more effective than that of ammonia. This is attributed to the cracking of ammonia into the reactor during the reduction process. Fine particles reduced much faster than coarse ones. A linear relation between the average particle size of the trioxide powders and the time to reach a certain reduction value is presented for hydrogen reduction. The importance of surface area in the reduction of powders was shown by the presence of surface area concentration in the kinetic rate equation applied in this investigation. (auth)

53549 (EUR–4765, pp 343-63) NON-CONGRUENT VAPORIZATION STAGE OF LANTHANUM OXIDE ON FIRST HEATING TO HIGH TEMPERATURE. Trevisan, G.; Depaus, R. (CCR-Euratom, Petten, Netherlands).

From 2nd conference on mass spectrometry; Ispra, Italy (1 Sep 1971).

Results of isothermal vapor pressure measurements on La_2O_3 carried out using a high temperature mass spectrometer are reported. It was found that the increase of vaporization rate during the first heating period is the result of CO overloss; the increased vaporization rate is proportional to the initial hydroxide content of the sample. (J.R.D.)

53550 (IS-T–540) HIGH TEMPERATURE OXIDATION OF GADOLINIUM AND DYSPROSIUM UNDER CONTROLLED OXYGEN PARTIAL PRESSURE. Basler, D. B. (Ames Lab., Iowa). Aug 1972. Contract W-7405-eng-82. 77p. Dep. NTIS.

Thesis.

The oxidation of gadolinium and dysprosium was studied under controlled oxygen partial pressures in the temperature range 727 to 1327°C. The oxygen partial pressure range was $10^{-0.3}$ to $10^{-14.5}$ atm. Weight gain as a function of time was measured through the use of a thermobalance. From the plots of rational scaling rate constant versus ln P_{02}, it may be inferred that Gd_2O_3 exhibits p-type semiconductivity at oxygen pressures above $10^{-9.4}$ atm in the temperature range 727 to 1177°C and that Dy_2O_3 exhibits p-type semiconductivity at oxygen pressures above $10^{-11.3}$ atm in the temperature range 727 to 1327°C. Utilizing the Wagner parabolic oxidation theory in the semiconducting range, self-diffusion coefficients of oxygen in Gd_2O_3 and Dy_2O_3 were found. The results are described by the relations $D = 1.149 \times 10^{-7} \exp(-40,269/RT)$ cm^2/s for Gd_2O_3 (727 to 1177°C), and $D = 2.831 \times 10^{-8} \exp(-21,393/RT)$ cm^2/s for Dy_2O_3 (727 to 1327°C). (auth)

53551 (MDC G–3153) PLUTONIA/CURIA COMPATIBILITY TESTING. Quarterly Report No. 15, April–June 1972. Watrous, J. D. (McDonnell Douglas Astronautics Co., Richland, Wash. Donald W. Douglas Labs.). Jul 1972. Contract AT(45-1)-2138. 41p. Dep. NTIS.

Compatibility tests with plutonia-238 in refractory metal capsules have shown that Mo–46 Re is the best container material in exposures at 1800°C for 15,000 to 18,000 hours. Rhenium is also adequate but results in greater transport of plutonia within the container. Compatibility tests of plutonia–molybdenum cermets (PMC) and plutonia–thoria–molybdenum cermets (SSC) in double layer refractory containers at 1500, 1800, and 2000°C resulted in complex interactions. The SSC fuel form was equivalent to the PMC fuel form in helium release, degraded more structurally, but indicated less aggressive attack on the container materials. TZM and Mo–46 Re appeared to provide the best structural containment at 1500 and 1800°C. T-111 appeared inadequate in all tests conducted at these temperatures. Plutonia and PMC fuel aging specimens with curium-242 additions to accelerate helium generation will complete exposure and be examined during the next quarter. Systems oriented tests are being prepared for the Multi-Hundred Watt Thermoelectric Generator Program with exposure to commence during the next quarter and initial results before the end of the calender year. (auth)

53552 (ORNL–4794, pp 45-51) DEVELOPMENT OF THE THORIUM FUEL CYCLE. Aug 1972.

In Chemical Technology Division annual progress report for period ending March 31, 1972.

Research progress is reported on: sol-gel process development for preparation of microspheres, engineering demonstration of the preparation of UO_2 microspheres, process development for the preparation of microspheres using ion exchange resins, preparation of test materials, and ^{233}U storage, purification, and distribution. (D.H.M.)

53553 (ORNL–4794, pp 52-3) PREPARATION OF $^{233}UO_2$ FOR LIGHT-WATER BREEDER REACTORS. Aug 1972.

In Chemical Technology Division annual progress report for period ending March 31, 1972.

Research progress is reported on: process development and flowsheets, design and installation of equipment for the UO_2 conversion line, and plant safety. (D.H.M.)

53554 (ORNL–4794, pp 84-7) PREPARATION AND PROPERTIES OF ACTINIDE OXIDES. Aug 1972.

In Chemical Technology Division annual progress report for period ending March 31, 1972.

Research progress is reported on: oxidation–reduction studies of uranium–plutonium oxides, development of the UO_2–PuO_2 sol-gel process, thoria desintering studies, and preparation of carbides and carbonitrides. (D.H.M.)

53555 (RD/B/N–2214) EXAMINATION OF IRRADIATED UO_2 HTR FUEL PARTICLES. PART I. EXPERIMENTAL TECHNIQUES. Bathe, J. E.; Simpson, K. A. (Central Electricity Generating Board, Berkeley (England). Berkeley Nuclear Labs.). Jun 1972. 17p. Dep. NTIS (U. S. Sales Only).

The experimental techniques used for the preparation and examination of irradiated UO_2 HTR fuel particles by x-radiography, metallography, scanning electron microscopy, and electron probe microanalysis are described. The studies are designed to provide detailed information on a limited number of fuel particles. (auth)

53556 (SC-CR–723158) STRUCTURAL AND THERMODYNAMIC PROPERTIES OF THE Sc–H SYSTEM. Lundin, Charles E. (Denver Research Inst., Colo.). [nd]. 17p. Dep. NTIS.

The Sc–H system was investigated by metallographic, x-ray diffraction, and Sievert's techniques to define the structural and thermodynamic properties. Phase boundaries were delineated and the saturated phases identified by metallographic and x-ray diffraction analysis. These data were correlated with values deduced from the pressure-temperature-composition relationships as determined by Sievert's technique. The gas-solid equilibria were studied in the temperature range of 450 to 750°C, the pressure range of 5×10^{-5} to 760 torr, and a composition range of from 0 to 66-⅔ atomic percent hydrogen. The dissociation pressure equation was obtained by a least squares analysis and found to be: $\log_{10} p\ (\text{torr}) = (-10{,}300 \pm 300/T) + 10.17 \pm 0.09$. The calculated heat of reaction of the dihydride phase from the saturated solid solution is $\Delta H = -47.1 \pm 1.4$ kcal/mole and the entropy of reaction is $\Delta S = -33.4 \pm 0.4$ cal/mole degree. (auth)

53557 (SC-DC–721080) DYNAMIC FRACTURE BEHAVIOR OF BORSIC–Al COMPOSITES. Hoover, W. R.; Allred, R. E. (Sandia Labs., Albuquerque, N. Mex.). 1972. 16p. (CONF-720709–1). Dep. NTIS.

From International conference on dynamic crack propagation; Bethlehem, PA. (9 Jul 1972).

The impact behavior of unidirectional Borsic–Al composites has been studied using an instrumented Charpy system. In order to experimentally determine the most appropriate impact failure criterion for these composites, dynamic load-deflection traces were obtained under plane strain conditions. Specimens with crack length to width ratios (a/W) from 0.15 to 0.65 and crack root radii from 0.002 in. to 0.036 in. were utilized. Results indicated that the dynamic fracture toughness was independent of crack length over an a/W range of from about 0.20 to 0.50 while other fracture criteria such as the dynamic fracture stress, the strain to fracture, and the energy absorbed per unit area of fracture surface varied continuously with crack length. Results also indicated that over the range of root radii studied, the dynamic fracture toughness was independent of crack acuity. Consequently, the dynamic fracture toughness appears to be an appropriate impact failure criterion for Borsic–Al composites and has been used to study the effects of fiber-matrix bond strength and Borsic volume fraction. In addition, the dynamic behavior of these materials has been compared with their behavior during slow bend tests. (auth)

53558 (UCRL–51244) LITERATURE SURVEY OF METALLIC TERNARY AND QUATERNARY HYDRIDES. Newkirk, Herbert W. (California Univ., Livermore. Lawrence Livermore Lab.). 28 Jun 1972. Contract W-7405-Eng-48. 22p. Dep. NTIS.

The unclassified literature was reviewed to find reported metallic ternary and quaternary hydride compounds of the type $MM'H_x$; M′ is a transition element, and M is a transition element, a member of the rare earth series or a member of the actinide series. A summary is presented of some of their most important properties. (auth)

53559 EFFECTS OF IMPURITIES ON THE MIGRATION OF LENTICULAR PORES IN UO_2. Oldfield, William (Materials Research and Computer Simulation, Westerfield, Ohio); Markworth, Alan J. Scr. Met.; 6: No. 8, 757-62(Aug 1972).

Results of studies are presented on the effects of artificially implanted impurities on the behavior of pores in unirradiated UO_2 subjected to a temperature gradient. It was found that the rates of nuclear fuel restructuring related to pore migration can be reduced by suitable impurities added to the fuel during fabrication. (J.R.D.)

53560 STUDY OF THE FORMATION OF TUNGSTEN CARBIDE IN THE FIELD–ION MICROSCOPE. Richman, M. H. (Brown Univ., Providence, R. I.). pp 453-76 of Applications of Field–Ion Microscopy in Physical Metallurgy and Corrosion. /Hochman, R. F. (ed.). Atlanta; Georgia Inst. of Tech. (1969).

From Conference on applications of field–ion microscopy in physical metallurgy and corrosion; Atlanta, GA. (15 May 1968). See CONF-680570.

Equipment and methods used in experiments conducted to carburize tungsten, in field-ion microscopes are described. Results of experiments are analyzed and used as the basis for concluding that detailed studies can be made of compound formation, interfaces between compounds and solid solutions, and diffusion by use of a combination of in situ compound formation and electron diffraction and microscopic techniques. (J.R.D.)

53561 FORMATION OF A PHASE Nb_xO_2 ($0.8 \le x \le 1.0$) UNDER SHOCK COMPRESSION OF NIOBIUM PENTOXIDE. Adadurov, G. A.; Breusov, O. N.; Dremin, A. N.; (and others) (Inst. of Chemical Physics, Chernogolovka, USSR). Dokl. Akad. Nauk SSSR; 202: No. 4, 864-7(1 Feb 1972). (In Russian).

When Nb_2O_5 was subjected to compression shock waves of the order of 1.5 Mbar, x-ray studies of the product indicated that it was not one of the previously known polymorphic modifications of Nb_2O_5, but a variable composition Nb_xO_2. Conditions of the experiment could be altered so as to produce a practically continuous transition with respect to composition from a Nb_2O_5 structure to NbO_2. Using containers of different materials, high pulse pressures, high pressure gradients, and high residual temperatures, led to a wide range of results. Reaction of the Nb_2O_5 with the container material was apparently a factor. (K.S.W.)

53562 METHOD OF MAKING A NUCLEAR REACTOR FUEL ELEMET OF URANIUM MONONITRIDE IN A REFRACTORY METAL MATRIX. Kizer, Donald E.; Smith, Roy A.; Speidel, Edward O. (to United States Atomic Energy Commission). U. S. Patent 3,662,042. 9 May 1972. Filed 25 Sep 1970.

A high-temperature dimensionally stable nuclear reactor fuel element of uranium mononitride in a refractory metal matrix having evenly distributed porosity is prepared by cold pressing a mixture of a powdered refractory metal and powdered U_2N_3, forming a body which is then densified by heating under pressure to prevent complete decomposition of the U_2N_3. The densified body is then heated to decompose the U_2N_3 to UN, leaving evenly distributed porosity throughout the element. (Official Gazette)

53563 OXIDATION OF UO_2 FUEL PELLETS DURING HYDROGEN SINTERING. Bannister, M. J.; Buykx, W. J. (Australian Atomic Energy Commission Research Establishment, Lucas Heights). J. Aust. Ceram. Soc.; 8: No. 2, 27-32(Aug 1972).

Surface cracking occurred in UO_2 fuel pellets sintered to high density in a hydrogen atmosphere pusher furnace with counter-current gas flow. The presence of a two-phase microstructure close to the surface of these pellets suggested that the cracking was caused by surface oxidation, resulting from the oxygen impurity in the inlet hydrogen. X-ray diffraction of the pellet surface after the removal of progressive layers confirmed that oxidation had occurred, as major amounts of one of the tetragonal U_3O_7 oxides were found close to the surface. Experiments were performed to establish whether surface oxidation could cause cracking, to determine the oxidation temperature required, and to discover whether oxygen could be retained in the sintering furnace to temperatures high enough to cause cracking. It was concluded that surface cracking was probably caused by surface oxidation above 900°C, the retention of oxygen in the gas stream at these temperatures being dependent on the geometry of the furnace, the flow rate of the gases and the catalytic activity of the internal furnace surfaces. (auth)

53564 EPITAXIAL GROWTH OF TANTALUM CARBIDE. Naiki, Toshio; Ninomiya, Masayuki; Ihara, Masayoshi (Kyoto Technical Univ.). Jap. J. Appl. Phys.; 11: No. 8, 1106-12(Aug 1972).

Films of tantalum carbide (TaC) known as a material with high melting point (3877°C) are formed on substrates by electron beam evaporation technique. The substrates are CaF_2, MgO, and NaCl single crystals cleaved in air. The range of substrate temperature is from 25°C to 1030°C. Pressures in the evaporation chamber are about 10^{-6} torr during the deposition. Rates of deposition are about 25 Å per second. Thicknesses of the deposits are less than 500 Å. These films were investigated by transmission electron diffraction and electron microscopy. Diffraction patterns of TaC films deposited on CaF_2 (111) and NaCl (100) surface are (111) and (100) spots with Debye-rings, respectively. Perfect epitaxial growth was observed for the TaC film deposited on the MgO (100) surface. The orientation relations were TaC(100)//MgO(100) and TaC[001]//MgO[011] at substrate temperatures above 390°C, and below this temperature Debye-rings were observed. (auth)

53565 HETEROGENEOUS NUCLEATION OF FISSION GAS BUBBLES AND GAS MIGRATION IN URANIUM DIOXIDE. Whapham, A. D. (Atomic Energy Research Establishment, Harwell, Eng.). Phil. Mag.; 26: No. 2, 399-407(Aug 1972).

The number and size of fission gas bubbles precipitated in irradiated uranium dioxide are calculated from a theory based on a balance between nucleation of bubbles at vacancy clusters produced by fission fragments and the agglomeration of bubbles by random motion. The distribution of bubble sizes is determined by gas atom capture, bubble agglomeration and irradiation re-solution. Irradiation re-solution exceeds gas atom capture for large bubbles and causes the larger bubbles formed by agglomeration to shrink. The effect of the precipitated gas bubbles on gas-migration is considered, and it is shown that the bubble diffusion coefficient is likely to be larger than the trap-release diffusion coefficient. The predictions are compared with other theories of bubble nucleation, and with experimental observation. (auth)

53566 PROCEDURE FOR FABRICATION OF SPHERICAL OXIDIC FUEL AND BREEDER PARTICLES. Hackstein, Karl; Venet, Pierre; Pirk, Hans (to Brown, Boveri Krupp Reaktorbau GmbH. Kernforschungsanlage). German Patent 1,542,344. 18 Jun 1970. Filed 2 Apr 1966. (In German).

The procedure for fabrication of spheroid oxide fuel and breeder particles is characterized by a fine-milling process through which the surface properties of the oxide powder are changed in such a way that subsequently, without any additives, it can be granulated into spherical particles and, at higher temperatures, it can be sintered into dense particles. The fine-milling occurs in either air or steam beam mills (so-called micronizers or jetomizers). Preferably, milling is conducted to a grain-size smaller than 1 micron. The milling and granulation processes are conducted continuously. The granulate is continuously sintered to dense spherical particles at temperatures from 1600 to 1700°C. (H.B.G.)

53567 PREPARATION OF TRANSPARENT EuO FILMS BY OXIDATION OF Eu FILMS. Kawabe, Ushio; Tarutani, Yoshinobu; Kudo, Mitsuhiro (Hitachi, Ltd., Tokyo). Jap. J. Appl. Phys.; 11: No. 8, 1215(Aug 1972).

Films of EuO were prepared by oxidation of Eu films after vacuum deposition of bulk Eu, and effects of oxidizing and annealing temperatures upon the room temperature optical absorption band were studied. Oxidized films showed a characteristic x-ray diffraction pattern, which was identified essentially as that of bulk EuO with the NaCl-type structure. The lattice constants of the films were between 5.14 and 5.15 Å. The films were also unstable after oxidation. However, annealed films were stable even in air and colored blue. (P.C.H.)

53568 ANODE EROSION WITH ALLOYS OF CARBIDES OF TRANSITION METALS WITH IRON, COBALT, AND NICKEL. Samsonov, G. V.; Verkhoturov, A. D.; Petrova, E. M. Fiz. Khim. Obrab. Mater.; No. 1, 140-4(1972). (In Russian).

Carbides of group IV–V metals of the periodic system when alloyed with Fe, Co, and Ni showed sharply reduced erosion tendencies in comparison with pure carbides, and the transfer coefficient was raised from 6 or 7 to 70 to 80%. The carbides tested were chiefly TiC, ZrC, and HfC, and in the systems of metal-carbide investigated, the erosion resistance decreased in the order: MeC–Ni, MeC–Co, and MeC–Fe. (K.S.W.)

53569 MATERIALS REVIEW FOR '72. National SAMPE Symposium and Exhibition, Los Angeles, California, April 11–13, 1972. SAMPE Volume 17. Azusa, Calif.; Society of Aerospace Material and Process Engineers (1972). 312p. (CONF-720437).

Thirty-one articles are included; a separate abstract was prepared for each of seven. The remaining 24 articles contain information on: improved tap laying machine; effects of microstructural variations on K_{1c} in 2024-T851 plate; plywrapping—a low cost fabrication method for composite structures; fabrication of advanced composites; continuous filament reinforced thermoplastics; Type A graphite fiber—high performance—low cost; fabrication and properties of AVCO 3D C/C cylinder materials; development and evaluation of MOD 3 C/C composites; bulk effect of particulate fillers in epoxy resin compositions; NR-150 polyimide binders; addition-type polyimides from solutions of monomeric reactants; flexural strength of pyco-bond pan precursor carbon fiber substrates; C–C composite material; autoclavable resins; applications of polymer technology; novel low-cost thermoplastic material; orthopedic applications of biocarbon implants; emerging requirements for aerospace materials in transportation industry; aerospace materials technology in consumer appliances; graphite/epoxy composites; advanced organic fibers for L-1011 interior structures; and composite vane fabrication development for gas turbine application. (P.C.H.)

For abstracts of individual papers see: 53570–53575 and 53716.

53570 COCURING ADVANCED COMPOSITE MATERIALS. Casale, R. (Air Force Materials Lab., Wright Patterson AFB, Ohio); Stansbarger, D. L. pp IA.1.1-35 of Materials Review for '72. Azusa, Calif.; Society of Aerospace Material and Process Engineers (1972).

From seventeenth National SAMPE symposium and exhibit; Los Angeles, CA. (11 Apr 1972). See CONF-720437.

While the feasibility of cocuring operations has been shown, additional studies were required to demonstrate the validity and reproducibility of this technique, as well as show a reduction in the production cost of advanced composite structures, prior to implementation into a production atmosphere. The results of an Air Force funded study on the investigation and optimization of cocuring techniques for primary aircraft components are presented. Included are test data on the effects of dimpling on the physical and mechanical properties of both graphite and boron reinforced composite systems using various honeycomb cell sizes, laminate thicknesses, fiber orientations, and cure pressures. Test data are also presented on mechanical and dimensional properties of cocured graphite-to-graphite, graphite-to-boron, and boron-to-boron composite panels. Fabrication of boron and graphite cocured subscale assemblies to define shape limitation is presented and discussed. Primary graphite and boron component (horizontal stabilizer spar-splice and horizontal stabilizer root end assemblies) fabrication utilizing cocuring techniques are reviewed and discussed. Production cost analysis to demonstrate high cost centers and/or cost saving in tooling, manufacturing, and cure time by the utilization of cocuring operations in lieu of conventional manufacturing methods is presented with a projected view as to production cost for typical aircraft structures. (auth)

53571 CHEMICAL VAPOR DEPOSITION OF BORON ON A CARBON MONOFILAMENT SUBSTRATE. DeBolt, H. E. (Avco Corp., Lowell, Mass.); Krukonis, V. J.; Neff, R. M.; Wawner, F. E. pp IIB.2.1-10 of Materials Review for '72. Azusa, Calif.; Society of Aerospace Material and Process Engineers (1972).

From seventeenth National SAMPE symposium and exhibit; Los Angeles, CA. (11 Apr 1972). See CONF-720437.

A boron filament elongates as the boron layer is vapor deposited, and the elongation increases with increasing radius of boron, reaching about 2% for 2 mil radial growth. This elongation can exceed the ultimate strain of the carbon monofilament and can result in substrate fracture which simultaneously damages the boron layer. The mismatch in boron-substrate elongation limited for a long period the development of boron on carbon as a viable material. Deposition of a layer of pyrolytic graphite (PG) on the carbon monofilament before deposition of boron was found to eliminate fracture, and the damage to the boron was thereby avoided; the breakthrough in circumventing the boron-carbon strain mismatch placed carbon substrate in a potentially competitive position with boron on tungsten. Deposition of 4 mil boron on a 1.3 mil carbon monofilament yielded a product with a specific modulus higher than that of 4 mil boron on 0.5 mil tungsten by 4%. Tensile strength averages in the 400-500 Ksi range are common, and frequently tests at the 600 Ksi level are achieved, indicating that strengths at least as good as those obtained with boron-on-tungsten are realizable. The use of PG-coated carbon as a substrate results in higher production speeds and combined with a potential savings in substrate cost, there is expected to result an overall cost reduction of the boron filament product. (auth)

53572 BORON NITRIDE COATED BORON FIBERS. Camahort, Jose L. (Avco Corp., Lowell, Mass.). pp IIIB.2.1-7 of Materials Review for '72. Azusa, Calif.; Society of Aerospace Material and Process Engineers (1972).

From seventeenth National SAMPE symposium and exhibit; Los Angeles, CA. (11 Apr 1972). See CONF-720437.

A method for surface nitriding boron fibers is described. The process involves initially forming a liquid boron oxide coating on the fiber by heating the boron fiber at approximately 1300°F in air and then converting the liquid oxide coating to a solid, continuous boron nitride coating by heating the fiber at approximately 1875°F in an ammonia-nitrogen atmosphere. The resulting boron nitride coated boron fiber shows great potential as a reinforcement for metal matrix composites. (auth)

53573 APPLICATION OF ADVANCED METAL-MATRIX COMPOSITES TO AIRCRAFT STRUCTURES. Maikish, C. R.; Wennhold, W. F.; Weisinger, M. D. (General Dynamics, San Diego, Calif.). pp VA.2.1-4 of Materials Review for '72. Azusa, Calif.; Society of Aerospace Material and Process Engineers (1972).

From seventeenth National SAMPE symposium and exhibit; Los Angeles, CA. (11 Apr 1972). See CONF-720437.

A program was conducted to expand the range of usefulness of metal-matrix composite materials as applied to primary aircraft structure. Previous work with metal-matrix composites has shown the potential for significant weight savings and indicated the need for improvements in several areas. The principal task accomplished during this program was the design, analysis, and fabrication of an aircraft bulkhead using boron/aluminum as the primary structural material. In support of the task, subcomponent test specimens were built and tested. Other supporting tasks included increasing the shear and transverse strength of the matrix by heat treatment, and the investigation of matrix materials other than aluminum. (auth)

53574 RESIN BONDED BORON–ALUMINUM COMPOSITES. Novak, R. C.; Pike, R. A.; Prewo, K. M.; Kreider, K. G. (United Aircraft Research Labs., East Hartford, Conn.). pp VA.5.1-6 of Materials Review for '72. Azusa, Calif.; Society of Aerospace Material and Process Engineers (1972).

From seventeenth National SAMPE symposium and exhibit; Los Angeles, CA. (11 Apr 1972). See CONF-720437.

A new composite material is described which combines the excellent properties of metal matrix composites with the ease of fabrication of resin composites. The material consists of thin preconsolidated monolayer tapes of boron-aluminum which are coated with a resin adhesive, then bonded together. The process for fabricating the monolayer tape is discussed along with techniques for cleaning and coating it with resin. Composites have been prepared using several resins as adhesives. The techniques used to fabricate these composites are described, and the results of mechanical tests on several of the materials are presented. (auth)

53575 BLADE DEVELOPMENT IN THE ADVANCED COMPOSITE ENGINE (ACE) PROGRAM. Stargardter, Hans (Pratt and Whitney Aircraft, East Hartford, Conn.). pp VB.5.1-13 of Materials Review for '72. Azusa, Calif.; Society of Aerospace Material and Process Engineers (1972).

From seventeenth National SAMPE symposium and exhibit; Los Angeles, CA. (11 Apr 1972). See CONF-720437.

Composite fan blades were developed for high temperature applications under the Advanced Composite Engine (ACE) Contract. Stage One blades were made of boron-polyimide for 500°F and Stage Three blades were made of BORSIC-aluminum for 600°F. (auth)

53576 EFFECT OF COMMINUTION ON THE SINTERABILITY OF ALUMINA AND TUNGSTEN CARBIDE POWDERS. Pryde, R. B. (Univ. of Surrey, Eng.); Sarkar, B. K.; Towner, J. M.; Waldron, M. B. pp 4.1-8 of Proceedings of the 7th Plansee Seminar on Powder Metallurgy of High Temperature Materials. Vol. I. /Benesvosky, F. (ed.). Reutte/Tyrol, Austria; Metallwerk Plansee (1971).

From seventh Plansee seminar on powder metallurgy of high temperature materials; Reutte/Tyrol, Austria (21 Jun 1971). See CONF-710602-(Vol.1).

The effects of ball milling and ball milling and annealing on the microstrains, crystallite size, and particle size in alumina and tungsten carbide were measured using x-rays, electron microscopy, and BET measurements. The effects of contamination were also evaluated. Thus, tungsten carbide gave very different sintering characteristics when milled in air and in argon; these differences were attributed to the oxygen absorbed during milling reacting to give gaseous carbon monoxide and W_2C at the sintering temperature. Milling was found to improve the sinterability of alumina as measured by densification and of tungsten carbide as measured by cold crushing strength. This improved sinterability was found to be due to the microstrain introduced into the powders during milling, the improvement occurring at temperatures where the majority of the strain was being removed. (auth)

53577 GROWTH AND HARDNESS OF SPHERICAL AGGLOMERATES FROM POWDERS OF HIGH MELTING POINT MATERIALS. Claussen, N.; Petzow, G. (Max-Planck Institut fuer Metallforschung, Stuttgart). pp 6.1-14 of Proceedings of the 7th Plansee Seminar on Powder Metallurgy of High Temperature Materials. Vol. I. /Benesvosky, F. (ed.). Reutte/Tyrol, Austria; Metallwerk Plansee (1971). (In German).

From seventh Plansee seminar on powder metallurgy of high temperature materials; Reutte/Tyrol, Austria (21 Jun 1971). See CONF-710602-(Vol.1).

A procedure is described for the production of spheres from powders in a wobbling rotating container. Preconditions for growth of the spheres are appropriate germinal agglomerates and a certain particle size depending on the binding additive. Growth proceeds in four distinct steps which are influenced by various process parameters. The most important parameters are angle of inclination of the container, humidity of air, rate of rotation, and amount of material. An angle of 40° yields best mixing and narrowest spectrum of diameters. High humidity leads to rapid growth and great firmness. Several hitherto unknown effects are discussed, such as diameter, distribution, and tetraeder formation during agglomeration. The procedure was tested on various oxides such as Al_2O_3, MoO_3, and WO_3 as well as on WC, alloys, and tungsten metal powders. Results are discussed with respect to technical application. (H.B.G.)

53578 HOT ISOSTATIC PRESSING: A NEW METHOD FOR PRODUCTION OF HARD METALS AND ALLOY STEELS. Johansson, Rune (ASEA, Vaesteras, Sweden). pp 8.1-12 of Proceedings of the 7th Plansee Seminar on Powder Metallurgy of High Temperature Materials. Vol. I. /Benesvosky, F. (ed.). Reutte/Tyrol, Austria; Metallwerk Plansee (1971). (In German).

From seventh Plansee seminar on powder metallurgy of high temperature materials; Reutte/Tyrol, Austria (21 Jun 1971). See CONF-710602-(Vol.1).

Hot isostatic pressing is now, after many years of research, ready for production as processes are developed and hot isostatic production presses for high pressure and high temperature and with large dimensions and short cycle-times are available. The manufacture of tungsten carbides and high-speed tool steels by means of hot isostatic pressing are described. Tungsten carbide is a dense material but there remains, nevertheless, always a number of pinholes that influence the tensile strength of the material to a high degree. A reduction of the pinhole volume of 10^2 to 10^3 times has been measured. The conventional-made high-speed tool steel shows a very great tendency to segregations and irregular coarse-grained structure. By manufacturing high-speed tool steel out of powder, a material with a very fine structure is achieved. The carbide grain size is very small. Further segregations in the material are eliminated. Increase in life of 390% has been observed with drills made by hot isostatic pressed high-speed tool steel. (auth)

53579 INFLUENCE OF NICKEL ADDITION ON THE REDUCTION OF WO_3 WITH HYDROGEN AND ON THE SINTERING OF THE THUS PRODUCED TUNGSTEN POWDERS. Lambiev, D. K.; Gospodinov, G. A.; Pangarova, B. H. (NITI-Metal Ceramics, Sofia. Higher Inst. of Chemical Tech., Sofia). pp 15.1-19 of Proceedings of the 7th Plansee Seminar on Powder Metallurgy of High Temperature Materials. Vol. I. /Benesvosky, F. (ed.). Reutte/Tyrol, Austria; Metallwerk Plansee (1971). (In French).

From seventh Plansee seminar on powder metallurgy of high temperature materials; Reutte/Tyrol, Austria (21 Jun 1971). See CONF-710602-(Vol.1).

Studies were made on the effects of nickel additions from 0.06 to 4% and of reduction temperatures from 750 to 1050°C on the physical properties of produced tungsten powders. The addition of nickel led to larger surface and smaller size of the mosaic blocks. Increased reduction temperature had the opposite effect. Sintering of these powders was examined at 1300°C. The sintered bodies had improved physicomechanical properties in comparison to pure tungsten powder. (H.B.G.)

53580 EQUILIBRIA AND KINETICS OF DEGASSING IN THE SYSTEMS Mo–N, W–N, AND Re–N. Fromm, E.; Jehn, H. (Max-Planck-Institut fuer Metallforschung, Stuttgart). pp 26.1-15 of Proceedings of the 7th Plansee Seminar on Powder Metallurgy of High Temperature Materials. Vol. I. /Benesvosky, F. (ed.). Reutte/Tyrol, Austria; Metallwerk Plansee (1971). (In German).

From seventh Plansee seminar on powder metallurgy of high temperature materials; Reutte/Tyrol, Austria (21 Jun 1971). See CONF-710602-(Vol.1).

The nitrogen solubility was determined in the systems Mo–N, W–N, and Re–N as a function of pressure and temperature (15 to 600 torr N_2, 1600 to 3000°C). In all three systems the solubility was very low (0.5 to 100 ppM N) and decreased in the order molybdenum, tungsten, rhenium. With increasing temperature the isobaric solubility rose and Sieverts law was obeyed. Thermodynamic data of the solution of nitrogen in these metals were calculated and the terminal solubility of nitrogen in molybdenum has been estimated. Furthermore, the kinetics of the degassing of nitrogen containing molybdenum and tungsten was investigated. In the first period of the degassing process the rate was determined by the transition of nitrogen from the solute into the adsorbed state. After longer annealing periods, the nitrogen diffusion in the metal became the rate determining step and the rate constants could be used for the evaluation of the diffusion coefficient of nitrogen in molybdenum, tungsten, and rhenium (1200 to 2200°C). In order to demonstrate the difference between the nitrogen systems of group Va and group VIa metals, the results of these investigations were compared with corresponding data for the other refractory metals, vanadium, tantalum, niobium, and chromium. (auth)

53581 NASA RESEARCH ON REFRACTORY COMPOUNDS. Gangler, James J. (National Aeronautics and Space Administration, Washington, D. C.). pp 48.1-36 of Proceedings of the 7th Plansee Seminar on Powder Metallurgy of High Temperature Materials. Vol. II. /Benesvosky, F. (ed.). Reutte/Tyrol, Austria; Metallwerk Plansee (1971).

From seventh Plansee seminar on powder metallurgy of high temperature materials; Reutte/Tyrol, Austria (21 Jun 1971). See CONF-710602-(Vol.2).

The behavior and properties of the refractory carbides, nitrides, and borides are being investigated by NASA as part of its research aimed at developing superior heat resistant materials for aerospace applications. Fundamental studies are being conducted on the electronic and defect structures of the carbides. The results indicate that there is promise for improving the strength and ductility of these materials. The nature of the bonding in carbides and nitrides is also being studied by determining their vaporization and decomposition characteristics. Studies of the zirconium—carbon—oxygen system showed that zirconium oxycarbides of different compositions and lattice parameters can be formed between 1500 and 1900°C and are stable below 1500°C. More applied studies showed that hot working generally improves the microstructure and therefore the strength of TiC and NbC. Sintering studies on UN indicated that very high densities can be achieved. Hot pressing of cermets of HfN and HfC produced good mechanical properties for high temperature bearing applications. Attempts to improve the impact resistance of boride composites by the addition of a nickel or carbon yarn were not overly successful. The present technology of the refractory compounds suggests that they will be used in aerospace applications in the near future. (auth)

53582 STUDY OF THE OBTAINING CONDITIONS AND THERMOEMISSION CHARACTERISTICS OF BORIDES OF THE RARE-EARTH METALS. Meerson, G. A.; Manelis, R. M.; Nurmukhamedov, V. Kh.; Mamedov, F. G. pp 52.1-15 of Proceedings of the 7th Plansee Seminar on Powder Metallurgy of High Temperature Materials. Vol. II. /Benesvosky, F. (ed.). Reutte/Tyrol, Austria; Metallwerk Plansee (1971).

From seventh Plansee seminar on powder metallurgy of high temperature materials; Reutte/Tyrol, Austria (21 Jun 1971). See CONF-710602-(Vol.2).

Studies were made on conditions for preparing La, Y, and Gd borides and their emissive and physical properties. The results showed that borides of stoichiometric composition can be obtained by the vacuum-thermic reduction of oxides with boron at 5% boron excess in the initial charge, in order to compensate for volatilization, and at a definite optimal porosity (53 to 55%) of the initial briquettes. It was found that the electron emission properties of the borides improved as the boron: metal ratio decreased. LaB_4 had the best emission properties. Conditions for obtaining and sintering double borides, $La(Ba)B_6$, as well as their properties were also studied. It was proved that up to 40 molecular percent solid solutions of LaB_6-BaB_6 retained the metallic character of conductivity, had a smaller electron work function, and higher density of emission current than LaB_6. (P.C.H.)

53583 SILICON DIFFUSION IN THE Me_5Si_3 PHASES OF THE METALS NIOBIUM, TANTALUM, MOLYBDENUM, AND TUNGSTEN. Fitzer, E.; Schmidt, F. K. (Univ., Karlsruhe, Ger.). pp 53.1-14 of Proceedings of the 7th Plansee Seminar on Powder Metallurgy of High Temperature Materials. Vol. II. /Benesvosky, F. (ed.). Reutte/Tyrol, Austria; Metallwerk Plansee (1971). (In German).

From seventh Plansee seminar on powder metallurgy of high temperature materials; Reutte/Tyrol, Austria (21 Jun 1971). See CONF-710602-(Vol.2).

Technical significance of the Me_5Si_3 phase formation, silicon transport in the Me_5Si_3 phases of various high-melting metals, calculation of diffusion coefficients for silicon diffusion in the Mo_5Si_3 and Nb_5Si_3 phases, and other influences on the growth rate of Me_5Si_3 phases are discussed. Among the four metals studied, a distinct difference in the rate of silicon transport prevailed. Silicon transport in the Mo_5Si_3 phase surpassed that in the other metals. The Ta_5Si_3 phase showed the lowest rate of silicon transport. Transport rates in Nb_5Si_3 and W_5Si_3 were similar and crossed each other in the temperature range of 1200°C. (H.B.G.)

53584 PROCEEDINGS OF 7th PLANSEE SEMINAR ON POWDER METALLURGY OF HIGH TEMPERATURE MATERIALS, REUTTE/TYROL, AUSTRIA, JUNE 21–25, 1971. VOLUME III. Benesvosky, F. (ed.). Reutte/Tyrol, Austria; Metallwerk Plansee (1971). 167p. (In several languages). (CONF-710602-(Vol.3)).

Seven articles are included: separate abstracts were prepared for six. The remaining article on vacuum atomization was not in scope for NSA. (P.C.H.)

For abstracts of individual papers see: 53585–53589 and 53678.

53585 OXIDATION BEHAVIOR OF $Mo + ZrO_2$ CERMETS. Heitzinger, F. (Metallwerk Plansee AG, Reutte, France). pp 1-8 of Proceedings of the 7th Plansee Seminar on Powder Metallurgy of High Temperature Materials. Vol. III. /Benesvosky, F. (ed.). Reutte/Tyrol, Austria; Metallwerk Plansee (1971). (In German).

From 7th Plansee seminar on powder metallurgy of high temperature materials; Reutte/Tyrol, Austria (21 Jun 1971). See CONF-710602-(Vol.3).

Below the MoO_3 melting point, zirconium oxide addition significantly increased the oxidation rate of molybdenum. Above the MoO_3 melting point, the total oxidation characteristics of molybdenum were changed and the linear oxidation course was altered to a parabolic ΔG-time relationship. Only in the range from 1100 to 1200°C, the so-called range of catastrophic oxidation, the linear oxidation course of molybdenum recurred. Nevertheless, the oxidation rate was about 10 times lower than that of pure molybdenum in the same temperature range. The oxidation behavior of Mo + ZrO_2-cermets can be expressed in the simplified statement that below the MoO_3 melting point, oxidation rate of molybdenum is significantly enhanced through addition of ZrO_2 while, above the MoO_3 melting point, it is significantly decreased through ZrO_2 addition. (tr-auth)

53586 PRODUCTION OF FORMED BODIES FROM HIGH-MELTING COMPOUNDS ACCORDING TO THE CASTING PROCEDURE FOR THERMOPLASTIC MASSES. Samsonov, G. V.; Slepzov, V. M.; Trunov, G. V. (Inst. of Problems in Material Studies, Kiev). pp 12.1-13 of Proceedings of the 7th Plansee Seminar on Powder Metallurgy of High Temperature Materials. Vol. III. /Benesvosky, F. (ed.). Reutte/Tyrol, Austria; Metallwerk Plansee (1971). (In German).

From 7th Plansee seminar on powder metallurgy of high temperature materials; Reutte/Tyrol, Austria (21 Jun 1971). See CONF-710602-(Vol.3).

Principal feasibility was demonstrated for the casting of thermoplastic masses to form products from high-melting compounds and hard materials. The influence of shape and grain of powder particles was studied with respect to viscosity as well as to optimal ratio of liquid to solid phases. Advantages of using spherical powders were demonstrated. It was found that, to obtain high density casting products, the use of polydispersed powders containing 40 to 50% gross grains was necessary. Removal of the liquid phase and sintering of the raw product were examined. It was demonstrated that the procedure yields products of high quality with perfect configuration, independent of their complexity. (tr-auth)

53587 ACTIVATION MECHANISM OF SINTERING. Accary, A. (Univ., Clermont-Ferrand, France). pp 14.1-16 of Proceedings of the 7th Plansee Seminar on Powder Metallurgy of High Temperature Materials. Vol. III. /Benesvosky, F. (ed.). Reutte/Tyrol, Austria; Metallwerk Plansee (1971). (In French).

From 7th Plansee seminar on powder metallurgy of high temperature materials; Reutte/Tyrol, Austria (21 Jun 1971). See CONF-710602-(Vol.3).

The relative meaning of activated sintering is defined, and examples of such processes involving activation either by chemical means or physical ones are reviewed. The most probable mechanisms are discussed and classified into three main groups: increase of the diffusion velocity; improvement of the morphology of the compact before and during sintering; and annihilation of negative activation factors that might impair the sinterability of the powder used. (P.C.H.)

53588 THERMODYNAMICS OF LIQUID SOLUTIONS Mo–O AND Mo–C. Kozina, L. N.; Revyakin, A. V.; Samarin, A. M. (Inst. of Metallurgy, Moscow). pp 32.1-20 of Proceedings of the 7th Plansee Seminar on Powder Metallurgy of High Temperature Materials. Vol. III. /Benesvosky, F. (ed.). Reutte/Tyrol, Austria; Metallwerk Plansee (1971).

From 7th Plansee seminar on powder metallurgy of high temperature materials; Reutte/Tyrol, Austria (21 Jun 1971). See CONF-710602-(Vol.3).

A thermodynamic analysis was made of the deoxidation of molten Mo. Methods are described for calculating the oxygen concentration in the metal. Mass transfer processes were examined for determining the oxygen concentration in the gas phase at the metal surface. The reaction between Mo and CO was investigated by the same method. The determination of the thermodynamic functions of the solution of oxygen in molten Mo made it possible to carry out certain thermodynamic calculations connected with the removal of oxygen from Mo during vacuum fusion. The results showed that oxygen is removed from a binary solution mainly in the atomic state. (P.C.H.)

53589 EFFECTS OF ALLOYING ON STRUCTURAL STABILITY AND COHESION BETWEEN PHASES IN METAL–OXIDE COMPOSITES. Navara, Erik; Easterling, Kenneth; Fischmeister, Hellmut (Chalmers Univ. of Tech., Goteborg). pp 43.1-13 of Proceedings of the 7th Plansee Seminar on Powder Metallurgy of High Temperature Materials. Vol. III. /Benesvosky, F. (ed.). Reutte/Tyrol, Austria; Metallwerk Plansee (1971).

From 7th Plansee seminar on powder metallurgy of high temperature materials; Reutte/Tyrol, Austria (21 Jun 1971). See CONF-710602–(Vol.3).

Studies were made on the cohesion between the matrix and the strengthening phase of a composite, and also the effects of structural stability on the strengthening mechanism. The main concern was the effect of minor alloying additions on particle stability and particle-matrix cohesion. The matrices studied were Ni, Fe, and Fe—40 Ni, each with various minor alloying additions. The results showed that contact angle measurements probably allow a more precise assessment of the work of adhesion than mechanical measurements of the type used. Solute additions to the matrix had a great effect on structural stability, i.e., on the resistance to particle coarsening. Detrimental effects arose when the solute, in partitioning to the oxide, reduced the thermodynamic stability of the particle phase (Al_2O_3). However, improvements in service life by a factor of 1.6 in austenitic Fe-base alloys, and by a factor of 3.4 in Ni-based alloys were indicated by the best observed rate constants in the materials studied. It was concluded that it is possible to improve the ductility of particle strengthened materials considerably by suitable interface-active solutes. (P.C.H.)

53590 POWDER METALLURGY OF HIGH-TEMPERATURE MATERIALS. Kieffer, R. (Technische Hochschule, Vienna). pp 1.1-16 of Proceedings of the 7th Plansee Seminar on Powder Metallurgy of High Temperature Materials. Vol. IV. /Benesvosky, F. (ed.). Reutte/Tyrol, Austria; Metallwerk Plansee (1971). (In German).

From 7th Plansee seminar on powder metallurgy of high temperature materials; Reutte/Tyrol, Austria (21 Jun 1971). See CONF-710602–(Vol.4).

A survey of the powder metallurgy for heat-resistant materials is presented. Melting points and combination possibilities for various groups of raw materials are discussed. Next the progress from iron through platinum and osmium to tungsten is reviewed. A section is devoted to the utilization of heat-resistant materials and powder metals in the space program. Also discussed is the application of sintered high-temperature material to tools, ovens, and plasma nozzles. Studies performed by the Vienna research circle comprise HfC-containing heat-resistant metals; the carbidothermal production of high-melting alloys; development of high-temperature—high-pressure autoclaves and study of nitrogen-containing systems; coating of hard metals with nitrides and carbonitrides; hard metals with carbonitride bases; sintered tool steels; the new hectoboride (M_1B_{70}-100); and cermets. (44 references). (H.B.G.)

53591 COLDSTREAM PROCESS. Walraedt, Jean; Mathy, Pierre (Floridienne, SA, Brussels). pp 2.1-12 of Proceedings of the 7th Plansee Seminar on Powder Metallurgy of High Temperature Materials. Vol. IV. /Benesvosky, F. (ed.). Reutte/Tyrol, Austria; Metallwerk Plansee (1971).

From 7th Plansee seminar on powder metallurgy of high temperature materials; Reutte/Tyrol, Austria (21 Jun 1971). See CONF-710602–(Vol.4).

The production of powders in the Coldstream process is based on impacting the particles at high velocities against a fixed target. The raw material is fed into the blast generator and pressurized to the desired blasting pressure. From there it is metered, mainly by gravity, into the main air stream. It is accelerated through a venturi towards the blast chamber. The materials hit and break against the target in the blast chamber. At the same time, cooling takes place through adiabatic air expansion. Advantages of the process are listed, and the results of reprocessing sintered tungsten carbide scrap into powder are described. (P.C.H.)

53592 TECHNOLOGY OF CERMETS. Nazare, S.; Ondracek, G.; Thuemmler, F. (Institut fuer Material- und Festkoerperforschung, Karlsruhe, Ger.). pp 44.1-32 of Proceedings of the 7th Plansee Seminar on Powder Metallurgy of High Temperature Materials. Vol. IV. /Benesvosky, F. (ed.). Reutte/Tyrol, Austria; Metallwerk Plansee (1971). (In German).

From 7th Plansee seminar on powder metallurgy of high temperature materials; Reutte/Tyrol, Austria (21 Jun 1971). See CONF-710602–(Vol.4).

The literature on cermets is reviewed. Powder characteristics, combinations, compaction, pressing, sintering, and fabrication are discussed. As a special example, the technology of plate-shaped fuel elements for nuclear reactors is outlined. A flow scheme is given for the production of plate-shaped fuel elements and for the pressing of rod-shaped dispersion fuel elements. 88 references are included. (H.B.G.)

53593 INFLUENCE OF ELECTRON CONFIGURATION ON THE ABSORPTION BEHAVIOR OF MIXED CRYSTALS OF HARD MATERIALS. Goretzki, H.; Scheuermann, W. (Max-Planck Institut fuer Metallforschung, Stuttgart). pp 50.1-13 of Proceedings of the 7th Plansee Seminar on Powder Metallurgy of High Temperature Materials. Vol. IV. /Benesvosky, F. (ed.). Reutte/Tyrol, Austria; Metallwerk Plansee (1971). (In German).

From 7th Plansee seminar on powder metallurgy of high temperature materials; Reutte/Tyrol, Austria (21 Jun 1971). See CONF-710602–(Vol.4).

Absorption studies on carbides, nitrides, and oxides of the 4a and 5a transition metals showed that the non-metallic component exerts a significant influence on absorption. Carbides and nitrides showed the greatest difference in energetic conditions of their surface layers. Carbides showed an unequivocal relationship between concentration of free charges and adhesion energy. Without exception, nitrides poorly absorbed molten metals. Complete absorption of the binding phase on carbides required high charge concentrations in the lattice. The unfavorable absorption properties of the 4a metal carbides can be improved through mixed crystal formation with carbides of the 5th and 6th subgroups. It is advisable to produce only a thin surface layer with high charge concentration. This principle is largely used in hard metals on the TiC basis with admixtures to the binding phase. (H.B.G.)

53594 ADDITION EFFECTS OF SILICIDES OF SEVERAL TRANSITION METALS BELONGING TO GROUPS IV THROUGH VI ON THE SINTERING AND OXIDATION RESISTANCE AT HIGH TEMPERATURE OF DIBORIDES OF TITANIUM AND ZIRCONIUM. Pastor, H.; Meyer, R. (Ugine-Carbone, Grenoble, France). pp 51.1-19 of Proceedings of the 7th Plansee Seminar on Powder Metallurgy of High Temperature Materials. Vol. IV. /Benesvosky, F. (ed.). Reutte/Tyrol, Austria; Metallwerk Plansee (1971). (In French).

From 7th Plansee seminar on powder metallurgy of high temperature materials; Reutte/Tyrol, Austria (21 Jun 1971). See CONF-710602–(Vol.4).

Experiments on 18 pseudo-binary systems $(Ti,Zr)B_2$-M_xSi_y showed the difficulties and the complexity of sintering these compounds. From a structural standpoint, the couple boron—silicon displayed more or less pronounced interactions, especially the formation of a solid solution $(Ti,Zr)B_2$-MSi_x with a cubic phase (Ti,Zr)B which probably was ternary. Certain combinations of the systems TiB_2-TiSi_2, $TiB_2-Ti_5Si_3$, ZrB_2-ZrSi_2, $ZrB_2-Zr_5Si_3$, ZrB_2-MoSi_2, and especially TiB_2-CrSi_2, as well as ZrB_2-CrSi_2 were particularly interesting because of their sintering tendency, their micrographic picture, and their high resistance to heat oxidation. (H.B.G.)

53595 NONISOTHERMAL TECHNIQUES FOR STUDYING INITIAL-STAGE SINTERING. Woolfrey, J. L.; Bannister, M. J. (Australian Atomic Energy Commission Research Establishment, Lucas Heights). J. Amer. Ceram. Soc.; 55: No. 8, 390-4(Aug 1972).

Nonisothermal techniques for analyzing initial-stage sintering are reviewed. It is shown that in principle they permit the determination of all the sintering parameters (rate law, activation energy, and diffusion coefficients) normally obtained from isothermal experiments. Comparison with results from isothermal experiments performed on the same materials (UO_2 and ThO_2 gel) demonstrates the validity and accuracy of the nonisothermal techniques. (auth)

53596 POLYMORPHIC MODIFICATIONS OF Pm_2O_3. Chikalla, T. D.; McNeilly, C. E.; Roberts, F. P. J. Amer. Ceram. Soc.; 55: No. 8, 428-9(Aug 1972).

Basic physical and chemical properties of Pm_2O_3 are tabulated and described. Discussions and data are included on cubic → monoclinic transformations, phase transformation temperatures, and melting point. (J.R.D.)

53597 EFFECT OF GREEN DENSITY ON THE INITIAL-STAGE SINTERING KINETICS OF UO_2. Woolfrey, J. L. (Australian Atomic Energy Commission Research Establishment, Lucas Heights). J. Amer. Ceram. Soc.; 55: No. 8, 383-9(Aug 1972).

The kinetics of the initial-stage sintering of a UO_2 powder in H_2 were investigated over the range 600 to 1200°C by dilatometry. Decreasing green density below $\approx 40\%$ of theoretical leads to progressively reduced rates of sintering. Initiation of the effect is related to a critical value of the ratio of pore size to particle size at which pores become stabilized and inhibit local shrinkage. Green density did not affect the sintering law or the apparent activation energy for sintering. A constant apparent activation energy for sintering of 86 ± 8 kcal/mol was found, indicating that diffusion of the same species is rate-controlling over this temperature range. Above 900°C, the rate-controlling mechanism is consistent with grain-boundary diffusion of the uranium ions. (auth)

53598 DIFFUSION IN THE SYSTEM K_2O–SrO–SiO_2. IV. MOBILITY MODEL, ELECTROSTATIC EFFECTS, AND MULTICOMPONENT DIFFUSION. Varshneya, A. K.; Cooper, A. R. (Case Western Reserve Univ., Cleveland). J. Amer. Ceram. Soc.; 55: No. 8, 418-21(Aug 1972).

Experimentally determined coefficients to describe multicomponent diffusion in the system $K_2O-SrO-SiO_2$ are compared with predictions of a simple model assuming ideal solution behavior. The agreement is satisfactory overall. On the basis of this model, it is suggested that the differences in mobilities of various ions cause deviations from the condition $\Sigma Z_i j_i = 0$ (Z = valence, j = flux) of no space-charge buildup. Although these deviations are small, e.g., after diffusion for 1 s, (charge flux)/(ionic flux) $\leq 10^{-7}$, the electric field caused by this deviation from electrical neutrality influences the diffusion kinetics markedly. (auth)

53599 TECHNIQUE FOR THE VISUALIZATION OF HEAVY METALS IN FUEL ELEMENTS FOR HIGH TEMPEATURE REACTORS. Leischner, E. (NUKEM GmbH, Wolfgang, Ger.); Stockhausen, J. Kerntechnik; 14: No. 7, 316-17(Jul 1972). (In German and English).

A roentgenographic technique, well known in medical diagnostic practice, which offers the possibility of demonstrating nondestructively the fuel distribution in fuel elements for high-temperature reactors is described. (auth)

Metals and Alloys

Refer also to abstracts 53584 and 53729.

53600 (WASH–1181–72) METALLURGY AND MATERIALS PROGRAMS, FISCAL YEAR 1972. (Division of Physical Research (AEC), Washington, D. C.). Jul 1972. 86p. Dep. NTIS.

A compilation and index of USAEC's programs is presented as an aid to research coordination and in selection of new programs. Information is included in sections on projects at laboratories and universities, funding levels, and an index. (P.C.H.)

53601 PROCEEDINGS OF 7th PLANSEE SEMINAR ON POWDER METALLURGY OF HIGH TEMPERATURE MATERIALS, REUTTE/TYROL, AUSTRIA, JUNE 21–25, 1971. VOLUME I. Benesvosky, F. (ed.). Reutte/Tyrol, Austria; Metallwerk Plansee (1971). 214p. (In several languages). (CONF-710602–(Vol.1)).

Nineteen articles are included; separate abstracts were prepared for 18. One article on internal nitriding of Mo–Hf alloys was previously included in NSA as 25: 40020. (P.C.H.)

For abstracts of individual papers see: 53576–53580, 53613, 53617–53624, and 53670–53673.

53602 PROCEEDINGS OF 7th PLANSEE SEMINAR ON POWDER METALLURGY OF HIGH TEMPERATURE MATERIALS, REUTTE/TYROL, AUSTRIA, JUNE 21–25, 1971. VOLUME II. Benesvosky, F. (ed.). Reutte/Tyrol, Austria; Metallwerk Plansee (1971). 197p. (In several languages). (CONF-710602–(Vol.2)).

Sixteen articles are included; separate abstracts were prepared for 12. The remaining four articles contain information on: microstructural studies of a synthetic material prepared by powder metallurgy; effects of small Mg additions on high-temperature properties of Ni–2.5 vol/% Al_2O_3; studies on silicide systems using differential thermal analysis; and synthesis of refractory compounds of transition metals by molten metal dissolution. (P.C.H.)

For abstracts of individual papers see: 53581–53583, 53625–53629, and 53674–53677.

53603 PROCEEDINGS OF 7th PLANSEE SEMINAR ON POWDER METALLURGY OF HIGH TEMPERATURE MATERIALS, REUTTE/TYROL, AUSTRIA, JUNE 21–25, 1971. VOLUME IV. Benesvosky, F. (ed.). Reutte/Tyrol, Austria; Metallwerk Plansee (1971). 326p. (In several languages). (CONF-710602–(Vol.4)).

Eighteen articles are included; separate abstracts were prepared for 14. The remaining four articles contain information on: powder metallurgy versus melting and casting of high temperature alloys, tool steels, and specialty alloys; processing of stellites to fully dense forms; creep properties of dispersion strengthened Ag–Ga oxide alloys; and pressure sintering of refractory metal germanides. (P.C.H.)

For abstracts of individual papers see: 53590–53594, 53630–53632, and 53679–53684.

Corrosion and Erosion

Refer also to abstracts 52895, 53121, 55165–55169, 55172, and 55173.

53604 (BNWL-CC–449) CORROSIVITY OF THORIA DISSOLVENT SOLUTIONS. Maness, Roy F. (Battelle-Northwest, Richland, Wash. Pacific Northwest Lab.). 18 Jan 1966. Contract AT(45-1)-1830. 10p. Dep. NTIS.

The dissolution of thoria requires a fluoride-catalyzed nitric acid solution which is quite corrosive to most materials of construction. Aluminum nitrate is usually added to the dissolvent to reduce the hydrofluoric acid activity and thus the corrosivity of the system. As dissolution of thoria proceeds, Th(IV) forms a complex with fluoride ion which further reduces the corrosivity of the system. Corrosion tests of 304L stainless steel, Corronel 230, and HAPO-20 alloy were made in proposed thoria dissolvent solutions. The primary variables were nitric and hydrofluoric acid concentration, the presence of oxidants in the dissolvent and the metallurgical condition of the test specimens. Observed corrosion rates are presented. (auth)

53605 (DP-Report–522) BASIC STUDIES ON THE GROWTH OF CARBON DEPOSITION FROM CARBON MONOXIDE ON A METAL CATALYST. Project DRAGON. Third Annual Report, March 1, 1966–February 28, 1967. Warzee, M. (Atomic Energy Establishment, Winfrith (England)). Mar 1968. 82p. (THTR–56). Dep. NTIS (U. S. Sales Only).

The behavior of commercial steels in reactor coolant gases was studied. It was found that at 550°C, no protective layers were formed on mild steels nor on low alloy steels, whatever the superficial structure of the steel and the composition of the reactant gas mixture. Ferritic steels with chromium concentration above 8% were covered with partially or fully protective oxides, under the experimental conditions. A full protection under all experimental conditions has been achieved with a 12% Cr annealed ferritic steel. AISI 304 austenitic steel was covered by a protective oxide layer only after having been superficially strained. In the annealed state, the formed oxide was not protective and showed the same characteristics as that formed at 600°C, under the same conditions. At 600°C, austenitic alloys AISI 304, 321, 316 and Incoloy 800 became covered by a protective oxide layer after preliminary superficial straining. In the annealed state, such films appeared only on Incoloy 800 and then only if the gas mixture was not very oxidizing: 500 μ atm H_2, 500 μ atm CO, 5 μ atm H_2O, and 5 μ atm CO. This alloy subjected to mixture no. 1 (500 μ atm H_2, 500 μ atm CO, 50 μ atm H_2O, 50 μ atm CO_2) and still more the three other austenitic alloys, exposed to the two types of mixtures were involved in complex oxidation phenomena leading to the formation of unprotective layers and to a heterogeneity of the alloy at the grain boundaries. It could be shown that the condition, necessary and sufficient to ensure that the formed oxides were protective, is that the selective oxidation of Cr and Mn occurs outside the alloy. This implies that the diffusion rates of Cr and Mn in the alloy were far above the penetration rate of the anions into the alloy. If this condition is not met, internal selective oxidation of the elements constituting the alloy occurs, giving rise to partially oxidized and nonprotective superficial zones. The problem of the choice of the alloy convenient to heat exchangers must not be considered only from the point of view of the carbon deposit. The outlined results showed that compatibility of the chosen steel with the gas phase must also be examined taking corrosion resistance into account. It appears that the content of impurities in helium of a high temperature reactor is such that the gas mixture will be oxidizing. Under such circumstances, it appears that carbon deposition is unlikely but some difficulties might be encountered with respect to corrosion resistance of some types of materials. The heterogeneities at the grains boundaries, observed with austenitic steels undergoing internal selective oxidation are likely to alter the behavior, under stress, of the material. Long duration tests in gas mixtures corresponding to the probable composition in the reactor would be necessary in order to investigate the penetration rate, of internal oxidation zones. These tests should be carried out under stress conditions in order to investigate the risks of intergranular cracks. (auth)

53606 (MLM–1355) HYDROGEN IN STEEL. Chaney, K. F. (Mound Lab., Miamisburg, Ohio). 1 Jun 1966. Contract AT-33-1-Gen-53. 18p. Dep. NTIS.

Declassified 22 Oct 1971.

A survey of the literature was made to determine the effect of hydrogen in steel. The mechanism by which the hydrogen is introduced into the steel, the permeation of hydrogen in steel, and the various deleterious effects that it may have are discussed. (auth)

53607 (RFP–1891) CORROSION AND STRESS-CORROSION CRACKING OF PAINTED U–4.2 WT. PERCENT Nb. Macki, James M.; Kochen, Robert L. (Dow Chemical Co., Denver, Colo. Rocky Flats Div.). 7 Aug 1972. Contract AT(29-1)-1106. 11p. Dep. NTIS.

Salt spray (fog) and stress-corrosion cracking (SCC) tests were conducted on painted U-4.2 wt % Nb alloy specimens. The paint coating consisted of an epoxy primer with a polyurethane cover coat. The primer and cover coat were applied by spraying. The test results showed that the alloy was protected, but not completely, from corrosion in the 3.5 wt % NaCl salt fog environment. The C-ring SCC tests showed that the paint system would not effectively protect the substrate metal from SCC in an aqueous chloride environment because the C-rings failed at flaws in the paint coating. (auth)

53608 (RFP-1904) STRESS-CORROSION CRACKING OF UNDERAGED AND OVERAGED U-2.3 WT PERCENT Nb IN AN AQUEOUS CHLORIDE ENVIRONMENT. Macki, James M.; Kochen, Robert L. (Dow Chemical Co., Golden, Colo. Rocky Flats Div.). 4 Aug 1972. Contract AT(29-1)-1106. 6p. Dep. NTIS.

The stress-corrosion cracking (SCC) behaviors of the U-2.3 wt % Nb alloy aged 24 hours at 230°C (underaged) and 24 hours at 430°C (overaged) have been studied. The SCC test utilized smooth, dead-weight loaded, static tensile specimens which were exposed to oxygen-saturated water containing 50 ppM chloride ions. The tests showed that the underaged material was more susceptible to SCC than the overaged material. SCC in the underaged material appeared to proceed by a transgranular fracture mode. The overaged material might not fracture by a SCC mode; but rather, it might fracture by a mechanical mode after corrosion has reduced the cross-sectional areas of the specimens. (auth)

53609 (RT/ING-(72)7) EXPERIMENTAL RESULTS OF SEVERAL TESTS OF FRETTING CORROSION OF METALLIC MATERIAL. Lupoli, P. (Comitato Nazionale per l'Energia Nucleare, Rome (Italy)). 30 Mar 1972. 54p. (In Italian). Dep. NTIS (U. S. Sales Only).

Fretting corrosion at ambient temperature has been investigated for copper/steel couples in water, and for Zircaloy-2/Zircaloy-2, Zircaloy-2/steel, and inconel/Zircaloy-2 couples in water, air, and nitrogen. Fretting corrosion tests were carried out mainly with laboratory equipment, by which the influence of some experimental parameters, such as environment, temperature, slip and frequency of vibrations, specific load, material, and geometry of samples, may be investigated. (auth)

53610 STUDY OF STRESS CORROSION CRACKING OF U-10 PERCENT Mo WIRES: OBSERVATIONS WITH THE FIELD EMISSION MICROSCOPE. Hoenig, Stuart A.; Sulsona, Herman (Univ. of Arizona, Tucson). pp 477-97 of Applications of Field-Ion Microscopy in Physical Metallurgy and Corrosion. /Hochman, R. F. (ed.). Atlanta; Georgia Inst. of Tech. (1969).

From Conference on applications of field-ion microscopy in physical metallurgy and corrosion; Atlanta, GA. (15 May 1968). See CONF-680570.

Aspects of stress corrosion cracking (SCC) such as cracking mode, agents responsible, and protection techniques are discussed. Results of investigations show that stress corrosion cracking of U-10% Mo can be intergranular, transgranular, or both depending upon the specific ambient atmosphere during the stress cycle. Heat treatment can improve the alloy by impeding the motion of dislocations. But this method of generating resistance to SCC is limited because of manufacturing problems. A dry nitrogen environment, during the stress cycle, is protective in the sense that no specimens showed signs of SCC after 1000 stress cycles from zero to 36,000 psi. (J.R.D.)

53611 COMPARISON OF THE OXIDATION PROCESS IN STRONTIUM AND CERIUM BY ULTRAVIOLET PHOTOELECTRON SPECTROSCOPY. Helms, C. R.; Spicer, W. E. (Stanford Electronics Labs., Calif.). Appl. Phys. Lett.; 21: No. 5, 237-9(1 Sep 1972).

The ultraviolet photoemission technique was applied to the study of the oxidation of strontium and cerium. It was found that the photoemission measurement provides a method to determine the oxide growth rate perpendicular to the surface, the composition of the surface, and the stable oxide phases formed during the oxidation process. (auth)

53612 COR-TEN STEEL. PROPERTIES AND USES. Mater. Tech.; No. 4, 97-101(Apr 1972). (In French).

A carbon steel, COR-TEN, was developed which combines excellent corrosion resistance properties with the good mechanical characteristics of carbon steels. The adhesion of paint to this steel, its high temperature characteristics (elastic limit, creep limit when hot, oxidation properties when hot) and resistance to abrasion were studied. It is easy to work and to weld. The principal originality of COR-TEN is its ability to be used without any coatings in rural, urban or industrial environments. It does, however, require painting in marine environments. Some applications of this steel are given, e.g., rolling stock, civil engineering applications, equipment for thermoelectric or thermonuclear power plants (Na heat exchangers for Rapsodie, and sodium cooling sheaths). (France)

53613 OXIDATION PROTECTION OF TANTALUM AND TANTALUM ALLOYS UP TO 1500°C. Fitzer, E.; Schlichting, J. (Univ., Karlsruhe, Ger.). pp 25.1-20 of Proceedings of the 7th Plansee Seminar on Powder Metallurgy of High Temperature Materials. Vol. I. /Benesvosky, F. (ed.). Reutte/Tyrol, Austria; Metallwerk Plansee (1971). (In German).

From 7th Plansee seminar on powder metallurgy of high temperature materials; Reutte/Tyrol, Austria (21 Jun 1971). See CONF-710602-(Vol.1).

A basic research program was conducted on diffusion in silicides and on the oxidation mechanism of silicides. Based on the results, a coating system for tantalum was developed. In stress tests, one millimeter thick plates of pure tantalum with 200 μ coating withstood 1000 hours without destruction of the samples. Thus far, tests at 1200°C were conducted only up to 2500 hours and tests in the critical deep temperature range of oxidation around 800°C were not completed to destruction. The results justified the expectation that the protective action of coating might be much higher than reported in the literature. (H.B.G.)

53614 ASPECTS CONCERNING THE CORROSION BEHAVIOR OF ZIRCONIUM AND ZIRCONIUM ALLOYS IN WATER AT HIGH TEMPERATURE. Popescu, Elena; Lazarescu, Adriana; Mandru, Galina. Rev. Coroz.; 2: No. 2, 79-85(1972). (In Rumanian).

The general aspects of the corrosion of zirconium and its alloys, at high temperature, in water, are discussed. The influence of internal and external factors on corrosion has been examined. The action of impurities such as hydrogen, nitrogen, oxygen and carbon which diminish the chemical, mechanical and corrosive properties of the metals is pointed out. Temperature, thermic cycling and vibrations particularly influence the corrosion resistance of the metals. (auth)

Preparation and Fabrication

Refer also to abstracts 53037, 53139, 53577-53579, 53587, and 53595.

53615 (SC-DC-722284) FUNDAMENTALS OF ION PLATING. Mattox, D. M. (Sandia Labs., Albuquerque, N. Mex.). 1972. 26p. (CONF-721003-3). Dep. NTIS.

From nineteenth national vacuum symposium; Chicago, IL. (2 Oct 1972).

The term ion plating is applied to atomistic film deposition processes in which the substrate is subjected to a flux of high-energy ions sufficient to cause appreciable sputtering before and during interface formation. The fundamental concepts of ion plating are reviewed along with a discussion of problems peculiar to this deposition process. Several representative applications are described. From the standpoint of adhesion, the principal benefits obtained from ion plating are (1) ability to sputter clean the surface and maintain it ''clean'' until the film begins to form; (2) provide a high-energy flux to the substrate surface giving a high surface temperature without necessitating bulk heating, thus enhancing diffusion, chemical reaction, etc.; and (3) alter the surface and interfacial structure by introducing high defect concentration, physically mixing the film and substrate material, and influencing the nucleation and growth of the depositing film. Another effect found in the ion plating process is the very great ''throwing power'' of the depositing film material. It is shown that ion plating is particularly effective in obtaining good adhesion in some systems where conventional deposition techniques give poor results. (auth)

53616 STRENGTHENING OF TUNGSTEN BY POWDER METALLURGICAL INTERNAL OXIDATION. Blickensderfer, Robert; Copeland, Mark I.; O'Brien, William L. (Bureau of Mines, Albany, Oreg.). Int. J. Powder Met.; 8: No. 3, 145-55(Jul 1972).

Tungsten alloys with excellent tensile strength and stress-rupture properties at 1,650°C and 1,920 C were prepared from powder blends of tungsten and W_2Zr or ZrN. The strengthening was attributed to solid solution strengthening by zirconium and to submicron particles of ZrO_2. (auth)

53617 PROBLEMS IN POWDER MIXING. Hausner, Henry H. (Polytechnic Inst. of Brooklyn). pp 5.1-21 of Proceedings of the 7th Plansee Seminar on Powder Metallurgy of High Temperature Materials. Vol. I. /Benesvosky, F. (ed.). Reutte/Tyrol, Austria; Metallwerk Plansee (1971).

From 7th Plansee seminar on powder metallurgy of high temperature materials; Reutte/Tyrol, Austria (21 Jun 1971). See CONF-710602-(Vol.1).

Attempts were made to establish a general point of view that could be helpful in a better understanding of the mixing process and to establish optimum conditions for mixing various powders of different materials, particle sizes, shapes, and amounts. The friction conditions in a powder mass were studied and analyzed, and friction behavior was correlated with the behavior of the powder in the mixer. Examples are given that clearly indicate that the friction conditions during the mixing play an important role in the mixing process. (P.C.H.)

53618 SIMPLE HOT ISOSTAT FOR BERYLLIUM. Lowe, J. N.; Knight, R. A. pp 9.1-4 of Proceedings of the 7th Plansee Seminar on Powder Metallurgy of High Temperature Materials. Vol. I. /Benesvosky, F. (ed.). Reutte/Tyrol, Austria; Metallwerk Plansee (1971).

From 7th Plansee seminar on powder metallurgy of high temperature materials; Reutte/Tyrol, Austria (21 Jun 1971). See CONF-710602–(Vol.1).

A simple and economic hot isostatic pressing technique was developed for the manufacture of Be thin wall tubes. Basically, powder is vibrated into an annulus formed between a graphite outer die and an inner steel membrane. This assembly is HF heated under vacuum and at the sintering temperature, the membrane is pressurized by high-pressure gas (up to 2000 psi) and expanded to consolidate the powder against the die wall. The method is simple, safe to operate, and is easily accommodated within existing equipment with the minimum of modifications. (auth)

53619 POSSIBILITIES OF EXPLOSIVE COMPACTION OF POWDERS, ESPECIALLY THOSE OF TUNGSTEN, WITH THE DIRECT PROCEDURE. Schmidt, D.; Bock-Nussbaum, Fr.; Pruemmer, R.; Balzerowiak, H. P. pp 11.1-7 of Proceedings of the 7th Plansee Seminar on Powder Metallurgy of High Temperature Materials. Vol. I. /Benesvosky, F. (ed.). Reutte/Tyrol, Austria; Metallwerk Plansee (1971). (In German).

From 7th Plansee seminar on powder metallurgy of high temperature materials; Reutte/Tyrol, Austria (21 Jun 1971). See CONF-710602–(Vol.1).

Following a short survey of the possibility of explosive powder compaction, experimental compaction studies on tungsten powder are described. Results showed that compaction of cylindrical samples can be achieved to a final density of about 95% of the theoretical value. The significant parameters are reported for explosive compaction of tungsten powder, such as type and amount of explosives. (tr-auth)

53620 MATERIAL TRANSPORT BY DISLOCATION MOTION IN SINTERING. Morgan, C. S. (Oak Ridge National Lab., Tenn.). pp 13.1-10 of Proceedings of the 7th Plansee Seminar on Powder Metallurgy of High Temperature Materials. Vol. I. /Benesvosky, F. (ed.). Reutte/Tyrol, Austria; Metallwerk Plansee (1971).

From 7th Plansee seminar on powder metallurgy of high temperature materials; Reutte/Tyrol, Austria (21 Jun 1971). See CONF-710602–(Vol.1).

Some aspects of sintering mechanisms in refractory materials are considered. Densification kinetics occurring as the temperature of the sintering compact is being increased were not compatible with a diffusion-controlled process. A possible alternative mechanism compatible with the densification kinetics is dislocation slip. Dislocations created during short high-temperature excursions were observed by electron transmission microscopy in partially sintered compacts of MgO and tungsten. The dislocations appeared to contribute to the material transport process and support the probable importance of dislocation slip in sintering of fine particle powders. (auth)

53621 KINETICS AND MECHANISM OF MOLYBDENUM POWDER SINTERING. Uskokovic, D.; Zivkovic, M.; Zivanovic, B.; Ristic, M. M. (Boris Kidric Inst. of Nuclear Science, Belgrade. Univ., Nis, Yugoslavia). pp 16.1-9 of Proceedings of the 7th Plansee Seminar on Powder Metallurgy of High Temperature Materials. Vol. I. /Benesvosky, F. (ed.). Reutte/Tyrol, Austria; Metallwerk Plansee (1971).

From 7th Plansee seminar on powder metallurgy of high temperature materials; Reutte/Tyrol, Austria (21 Jun 1971). See CONF-710602–(Vol.1).

The effects of heating rate from 5 to 50°C/min, on the shrinkage kinetics of disperse molybdenum powder in the temperature range from 1200 to 1450°C were investigated. In the same temperature interval, the shrinkage was also studied by isothermal and steplike heating techniques. On the basis of the experimental data, it was found that kinetic equations for isothermal conditions which include some diffusion mechanism as the responsible mechanism for mass transfer are not applicable in the case of real powder sintering, in the whole temperature and time interval under consideration. On the contrary, it was found that effective diffusion coefficient computed from isothermal shrinkage data is the function both, of sintering temperature and soaking time. (auth)

53622 RECENT DEVELOPMENT IN CVD TUNGSTEN AND MOLYBDENUM. Shroff, A. M.; Delval, G. (Thomson-CSF, Corbeville, France). pp 18.1-15 of Proceedings of the 7th Plansee Seminar on Powder Metallurgy of High Temperature Materials. Vol. I. /Benesvosky, F. (ed.). Reutte/Tyrol, Austria; Metallwerk Plansee (1971).

From 7th Plansee seminar on powder metallurgy of high temperature materials; Reutte/Tyrol, Austria (21 Jun 1971). See CONF-710602–(Vol.1).

Chemical vapor deposition (CVD) of W and Mo by the hydrogen reduction of its fluoride or chloride composite was investigated as a potential fabrication method to supplement or even replace the present metal working methods. From the results it was found that no bubbles were obtained if the deposit was done at the ratio H_2/WF_6 varying from 3 to 6 which means moderate total flow low pressure below 20 torr and relatively high temperature above 700°C. The fluorine content could not be correlated with the presence of bubbles in the deposit, but it seemed that very low fluorine content led to thermal instability of the deposit. The vacuum work function was of the order of 4.7 eV. Surface treatment improved this value by 0.1 eV. The emitters for longtime operation should be realized at a ratio H_2/WF_6 equal to 3, a pressure around 10 torr, and a minimum temperature of 700°C. The working model based on the fact that the adsorbed molecules of impurity change the work function of the substrate and influence the preferential crystal orientation seemed to be a promising one. (P.C.H.)

53623 DEFORMATION AND RECRYSTALLIZATION BEHAVIOR OF SINTERED TANTALUM AND TANTALUM FORMED BY ELECTRON BOMBARDMENT. Alheritiere, E.; Moisan, J.; Molinier, R. (Departement des Recherches et Produits Avances, Argenteuil, France). pp 24.1-12 of Proceedings of the 7th Plansee Seminar on Powder Metallurgy of High Temperature Materials. Vol. I. /Benesvosky, F. (ed.). Reutte/Tyrol, Austria; Metallwerk Plansee (1971). (In French).

From 7th Plansee seminar on powder metallurgy of high temperature materials; Reutte/Tyrol, Austria (21 Jun 1971). See CONF-710602–(Vol.1).

Two procedures to produce tantalum were utilized: first, sintering, and second, fusion through electron bombardment. Cast metal is deformed in a very heterogeneous manner; the gross grains in the cast grow differently according to their orientation. During tempering at 1000 to 1100°C, weakly grown grains restore themselves without recrystallization. The zones with strong growth recrystallize normally. Sintered metal behaves differently: deformation texture is more homogeneous, the recrystallization proceeds more regularly and is finer. (H.B.G.)

53624 SOLID STATE REACTIONS DURING THE POWDER METALLURGICAL PRODUCTION AND FABRICATION OF THE MOLYBDENUM ALLOY TZM. Eck, R. (Metallwerk Plansee AG, Reutte/Tyrol, Austria). pp 31.1-10 of Proceedings of the 7th Plansee Seminar on Powder Metallurgy of High Temperature Materials. Vol. I. /Benesvosky, F. (ed.). Reutte/Tyrol, Austria; Metallwerk Plansee (1971). (In German).

From 7th Plansee seminar on powder metallurgy of high temperature materials; Reutte/Tyrol, Austria (21 Jun 1971). See CONF-710602–(Vol.1).

With special consideration to the sintering process the production of sintered bodies is described for the molybdenum alloy TZM containing 0.5% Ti, 0.07% Zr, and 0.01 to 0.05% C. Reactions of the powdered oxygen and the sinter gas moisture with the alloy elements are discussed. Carbon addition acts during the deoxidation as well as during carbide formation. The sintered TZM can be fabricated with high oxygen content; whereas pure molybdenum fails at much lower oxygen concentrations. Examples are given for the growth and recrystallization behavior of forged TZM and TZM plates in comparison with pure molybdenum. (H.B.G.)

53625 STUDY OF DIFFUSION WELDING OF MOLYBDENUM. Gardes, G.; Jacquin, B.; de la Bastie, J. pp 33.1-10 of Proceedings of the 7th Plansee Seminar on Powder Metallurgy of High Temperature Materials. Vol. II. /Benesvosky, F. (ed.). Reutte/Tyrol, Austria; Metallwerk Plansee (1971). (In French).

From 7th Plansee seminar on powder metallurgy of high temperature materials; Reutte/Tyrol, Austria (21 Jun 1971). See CONF-710602–(Vol.II).

The effects of parameters of time, pressure, and tempering have not been explored entirely thus far. Nevertheless, it appears possible to obtain, with sintered molybdenum, a diffusion weld that possesses a mechanical resistance which is equivalent to the basic material. The quality of the weld essentially depends on smoothness of the contact surface (a deviation of 2 microns is important) and on favorable structure. The latter point is the particular object of this study. (tr-auth)

53626 PRODUCTION OF A Ni–ThO_2 ALLOY WITH A DISPERSED PHASE STARTING FROM ORGANOMETALLIC COM-

POUNDS. Marty, Michel; Walder, Andre; Hivert, Andre (Office National d'Etudes et de Recherches Aerospatiales, Chatillon, France). pp 37.1-12 of Proceedings of the 7th Plansee Seminar on Powder Metallurgy of High Temperature Materials. Vol. II. /Benesvosky, F. (ed.). Reutte/Tyrol, Austria; Metallwerk Plansee (1971). (In French).

From 7th Plansee seminar on powder metallurgy of high temperature materials; Reutte/Tyrol, Austria (21 Jun 1971). See CONF-710602--(Vol.2).

The Onera method for the production of a Ni$-$ThO$_2$ alloy avoids the principal difficulties inherent in wet methods. First of all, the choice of thorium as a component yields a fine dispersion of thorium during high-temperature treatment. Second, the use of poly-(methylmethacrylate) as stabilizer of the suspension avoids, among other factors, difficulties associated with the elimination of the solvent. The diverse operations involved in the procedure as well as the various parameters entering each step permit an understanding of the relatively slow development of these particular types of alloys of which Ni$-$ThO$_2$ is one of the first examples. (tr-auth)

53627 PRODUCTION OF Ni--Cr--ThO$_2$ ALLOYS BY MEANS OF CHROMIUM DIFFUSION THROUGH HALOGEN CARRIER IN A NiThO$_2$ GRAIN. Marty, Michel; Walder, Andre; Galmiche, Philippe; Hivert, Andre (Office National d'Etudes et de Recherches Aerospatiales, Chatillon, France). pp 38.1-11 of Proceedings of the 7th Plansee Seminar on Powder Metallurgy of High Temperature Materials. Vol. II. /Benesvosky, F. (ed.). Reutte/Tyrol, Austria; Metallwerk Plansee (1971). (In French).

From 7th Plansee seminar on powder metallurgy of high temperature materials; Reutte/Tyrol, Austria (21 Jun 1971). See CONF-710602--(Vol.2).

Since their appearance on the market, Ni$-$Th, and especially Ni$-$Cr$-$Th, have elicited great interest because of their remarkable mechanical properties at high temperatures. Among materials possessing similar thermomechanical properties, they are the only ones that can be laminated. Although not possessing great practical interest because of oxidizibility, Ni$-$Th has the merit of being first in a new series of alloys for high temperatures and has contributed to better understanding of certain mechanisms of reinforcement. In sharp contrast, Ni$-$Cr$-$Th is suitable for practical application. In the USA, for example, it is used in elements of space rockets, reaching maximal temperatures of about 1200°C. The work performed under Onera, as is presented, proposes an original technique for production of this type of material. Chromium incorporation through an intermediary gaseous halogen phase into the elementary grains of Ni$-$Th permits the production of a homogeneous Ni$-$Cr$-$Th alloy without non-diffused chromium inclusions and very small content of chromium oxide. Study of the various parameters, entering into the thermomechanical treatment, permits the definition of laminating conditions which confer to the material a lifetime of 100 h at 1050°C under 5 hectobars. (tr-auth)

53628 ELECTRIC DISCHARGE-TYPE ACTIVATED PRESSURE SINTERING AND BONDING OF A SUPERALLOY COMPOSITE STRUCTURE. Goetzel, C. G. (Lockheed Palo Alto Research Lab., Calif.). pp 40.1-9 of Proceedings of the 7th Plansee Seminar on Powder Metallurgy of High Temperature Materials. Vol. II. /Benesvosky, F. (ed.). Reutte/Tyrol, Austria; Metallwerk Plansee (1971).

From 7th Plansee seminar on powder metallurgy of high temperature materials; Reutte/Tyrol, Austria (21 Jun 1971). See CONF-710602--(Vol.2).

Electric discharge-type activated hot pressing, known as spark sintering, has been successfully employed in the commercial production of beryllium parts for aerospace applications. The process has also been used experimentally for the consolidation of titanium alloy and superalloy powders into forging preforms. Composite structures combining powder and wrought-metal shapes appear to be one of the most interesting applications of the process. The inherently short combined consolidation and bonding cycles tend to reduce adverse reactions or degradation at the interfaces of disparate metals. In composites of the same material but of different state, the process parameters can be adjusted to produce fully dense powder sections joined solidly to sheet or plate by metallurgical bond zones while grain size and distortions are controlled. This type of structure should be of considerable interest in view of the substantial materials and labor savings that may be realized. Process parameters were optimized for several types of Inconel 718 superalloy powders. The degree of consolidation and bond integrity between the powder section and the wrought-metal base was observed metallographically, as was the effect of a subsequent diffusion treatment. A special shear test was used to measure the strength of the bond zone. (auth)

53629 SIMPLE METHOD OF PRECISE ALIGNMENT AND UNIFORM DISTRIBUTION OF REINFORCING FIBERS IN A METAL MATRIX. Berghezan, A. (Union Carbide European Research Associated, Brussels). pp 45.1-17 of Proceedings of the 7th Plansee Seminar on Powder Metallurgy of High Temperature Materials. Vol. II. /Benesvosky, F. (ed.). Reutte/Tyrol, Austria; Metallwerk Plansee (1971).

From 7th Plansee seminar on powder metallurgy of high temperature materials; Reutte/Tyrol, Austria (21 Jun 1971). See CONF-710602--(Vol.2).

A simple method of incorporation of reinforcing fibers in a metal matrix has been developed and tested. It permits both a precise alignment and a perfect uniform distribution of the fibers in a metal matrix. The method is described in two variants and examples of composite materials prepared upon each variant are given. The method appears very versatile as it allows the incorporation of any kind of fibers such as rigid or flexible metallic fibers and ceramic or carbon filaments, etc., in a metal matrix. Additionally, it allows the incorporation of any volume fraction of fibers and is particularly suitable for the incorporation of high volume fractions. Materials have been prepared in different shapes such as heavy bars or in a sheet form. (auth)

53630 ROLLING IN VACUUM. Krupin, A. V. (Inst. of Steel and Alloy, Moscow). pp 19.1-24 of Proceedings of the 7th Plansee Seminar on Powder Metallurgy of High Temperature Materials. Vol. IV. /Benesvosky, F. (ed.). Reutte/Tyrol, Austria; Metallwerk Plansee (1971). (In German).

From 7th Plansee seminar on powder metallurgy of high temperature materials; Reutte/Tyrol, Austria (21 Jun 1971). See CONF-710602--(Vol.4).

The international status of the rolling of hard metals and their alloys is surveyed. Especially discussed are reactions between gases and metals during their high-temperature fabrication under vacuum; the effects of rolling in vacuum on fine structure and properties of metals, alloys, and bimetals; and influence of fabrication in vacuum on conditions and parameters of the rolling process. (52 references). (H.B.G.)

53631 HIGH DENSITY P/M COMPONENTS FOR ELEVATED TEMPERATURE APPLICATIONS. Reichman, S. H.; Smythe, J. W. pp 35.1-13 of Proceedings of the 7th Plansee Seminar on Powder Metallurgy of High Temperature Materials. Vol. IV. /Benesvosky, F. (ed.). Reutte/Tyrol, Austria; Metallwerk Plansee (1971).

From 7th Plansee seminar on powder metallurgy of high temperature materials; Reutte/Tyrol, Austria (21 Jun 1971). See CONF-710602--(Vol.4).

The Federal$-$Mogul Corporation, Metal Powder Division approach to superalloy powder-metallurgy is given. The process whereby molten metal is inert gas-atomized to low interstitial content powders and subsequently densified by extrusion is shown relative to other consolidation methods. Superior intermediate temperature mechanical properties to 1400°F are given for the P/M nickel-based superalloys and comparisons drawn to cast/wrought counterparts. The principal properties discussed are tensile and stress rupture for the alloys IN-100, U-700, Waspaloy, and Rene 95. Examples of conventional forging and superplastic forging are given, and mechanical properties of material forged by each method are given. The superiority of the P/M alloys is evident in both forming methods. An experimental thermomechanical process is discussed in which coarse grained and single crystal structures are produced in the U-700 alloy. Material so processed showed enhanced mechanical properties (including 1800°F stress rupture lives). A series of low carbon P/M based alloys is explained, which permits rapid grain growth for good 1800°F stress rupture properties. The potential of these alloys is shown for a total process of superplastic forming, heat treating to large grain structures, and carburizing the resultant grain boundaries for stability. (auth)

53632 ELECTRONIC MECHANISM OF THE BASIC TECHNOLOGICAL PROCESSES IN THE POWDER METALLURGY OF HIGH TEMPERATURE MATERIALS. Samsonov, G. V.; Upadhyaya, G. S. (Inst. of Materials Science, Kiev. Univ. of Roorkee, India). pp 49.1-22 of Proceedings of the 7th Plansee Seminar on Powder Metallurgy of High Temperature Materials. Vol. IV. /Benesvosky, F. (ed.). Reutte/Tyrol, Austria; Metallwerk Plansee (1971).

From 7th Plansee seminar on powder metallurgy of high temperature materials; Reutte/Tyrol, Austria (21 Jun 1971). See CONF-710602--(Vol.4).

Progress in the field of basic powder metallurgical processes has so far been based mainly on physical or physicochemical concepts. An attempt has been made to review the complete picture on the basis of the stable electronic configuration model of the condensed state. Metal powder production by the reduction method can be visualized as a donation of electrons from the reducing agent to the metal ions; the reduction rate naturally depends on the electron donor capacity. During pressing of metal powders, apart from macroscopic and microscopic changes, there is sufficient scope for electronic exchange between the excited atoms and this suggests a very great similarity between the processes of pressing and sintering. Numerous attempts at theoretical interpretations of the sintering mechanism viz., chemical reactions at the surface and boundaries of particles, surface and volume diffusion, and thermally activated dislocation processes have achieved some success, but only in the interpretation of phenomena typical for individual sintering stages. However, the present model presents the different sintering stages in a coherent picture. Various examples have been adduced from the field of powder metallurgy of the refractory metals and their compounds in order to justify the unified approach of the electronic configuration model. (auth)

53633 OUTLOOK FOR THE ON-SITE WELDING OF THICK METAL SHEETS. Roudier, R.; Bachelay, J.; Thome, P. (CEN de Saclay, Gif-sur-Yvette, France). Soudage Tech. Connexes; 26: No. 5, 196-209(May 1972). (In French).

Electron welding may be used to weld large structures, portable welding equipment being used. Structures such as the large diameter skirtings, the tubular plates of exchangers, the lid of the dissolver, and the Phenix valve tank can be handled in this way. Systematic research on the state of the surfaces of the parts to be joined and the chamfered edges, the gaps between these parts, and the welding position confirmed that this technique is compatible with ordinary workshop facilities. The welding can be effected rapidly and for any position of the parts. The weld penetrates very deeply into these parts. The technique has thus widespread applications. (France)

Properties, Structure, and Phase Studies

Refer also to abstracts 52956, 53033, 53116, 53125, 53551, 53589, 53590, 55023, 55036, 55040, 55052, and 55178.

53634 (CONF-720806-3) EFFECTS OF STRAIN GRADIENTS ON THE GROSS STRAIN CRACK TOLERANCE OF A 533-B STEEL. Randall, P. N. (TRW Systems, Redondo Beach, Calif.); Merkle, J. G. (Oak Ridge National Lab., Tenn.). 1972. Subcontract 3134. 28p. Dep. NTIS.

From sixth national symposium on fracture mechanics; Philadelphia, Pa. (28 Aug 1972).

To satisfy the need for a measure of fracture toughness at stress levels above yield, a quantity called gross strain crack tolerance has been proposed. It is the total elastic-plus-plastic strain measured at maximum load in a laboratory test of a specimen containing a surface crack, and is of course a function of crack size and temperature. The object has been to develop the test to produce results that can be used to estimate the tolerance of material in full-scale hardware for strain in the presence of a crack. Previous work utilized precracked tensile specimens of A 533-B steel to study the effects of specimen geometry and crack size as a function of temperature. Now, the effects of strain gradients have been studied by loading the specimen in bending or by placing the crack in the bottom of a groove. Analysis of the displacement measurements showed that proper characterization of all the strain gradients tested required consideration of the strain values at two locations. The first, defined as the gross strain crack tolerance (GSCT), was located in the net section normal to the crack plane at mid-crack depth, the approximate location along the crack border where fracture originated. The second strain value was the gross strain on the back face in the gross section above and below the crack. At temperatures within the transition region, GSCT increased in direct proportion to the degree of tensile strain on the back face of the gross section. Tests in bending, which put the neutral axis between the crack tip and the back face, produced the lowest value of GSCT, while those in which the crack propagated into regions of increasing strain yielded the highest GSCT. These effects were attributed to the influence of back face strain on the development of the plastic zone and consequent relief of constraint. (auth)

53635 (EURFNR-998) INFLUENCE OF THERMOMECHANICAL TREATMENTS ON THE CREEP RUPTURE AND CREEP BEHAVIOR OF X10 NiCrMoTiB 1515 STEEL. Schirra, M. (Kernforschungszentrum, Karlsruhe (West Germany). Institut fuer Material und Festkoerperforschung). Translation of report KFK-1535. 53p. Dep. NTIS.

Work Performed under United States-Euratom Fast Reactor Exchange Program.

In order to study the influence of different thermomechanical treatments on the creep behavior and time-to-rupture of stainless steel X10 NiCrMoTiB 1515 (DIN 1.4970) samples of seven different pretreatments were investigated. The reason for this investigation was the fact that the yield point of austenitic steels at high temperatures (600 to 800°C) is in the range 12 to 15 kp/mm^2. With respect to the requirements for fuel-clad there exists the necessity to increase the strength, particularly the yield point by way of proper treatment. Specimens made from the same heat of a Sandvik steel (12R72HV) were investigated after solution treatment in the temperature range 550 to 800°C and after thermomechanical treatments at 650, 700, and 750°C. Among the pretreatments employed were coldwork and annealing 15 and 30% respectively, at temperatures between 700 to 850°C. It was found that 15% coldwork improved the time-to-rupture most for times $>10^4$ hours and temperatures between 650 and 700°C. The ductility decreased for specimens which were only solution treated with increasing time to rupture, while on the other hand it was time independent for samples which underwent a mechanical or thermomechanical treatment. The important creep-data for designing fuel-element-cladding are given for all thermomechanical pretreatments for a wide range of stresses. The metallographic investigations gave insight into crack formation, fracture, and changes in the grain structure. (auth)

53636 (IS-T-554) DIFFUSION IN DILUTE BISMUTH-MERCURY AND LEAD-MERCURY SYSTEMS. Smith, D. L. (Ames Lab., Iowa). Aug 1972. Contract W-7405-eng-82. 65p. Dep. NTIS.

Thesis.

Diffusion coefficients for dilute liquid solutions of lead in mercury and bismuth in mercury at 25°C were determined. A capillary-reservoir experimental technique was used in which the capillary composition profile was periodically monitored. The composition was determined from voltage drops, converted to resistivities. Resistivity-composition relations for the two systems were determined experimentally. Diffusivities calculated for both the lead and bismuth systems were found to follow the same composition dependency. A second-degree polynomial was determined which describes the composition dependence of diffusivity for dilute bismuth and lead amalgams, $D(\times 10^{-5}\ \mathrm{cm^2/sec}) = 4.170 - 814.2n + 52181n^2$ for $0.002 \leq n \leq 0.008$, where n is the atom fraction solute. (auth)

53637 (LBL-101) I. LATTICE HEAT CAPACITIES OF ALLOYS AT LOW TEMPERATURES; InPb, AuCd, Mg_3Sb_2. II. EFFECT OF ORDERING ON LATTICE HEAT CAPACITY; $AuCu_3$. Yoon, Hong Il (California Univ., Berkeley. Lawrence Berkeley Lab.). Aug 1971. Contract W-7405-eng-48. 74p. Dep. NTIS.

Thesis.

Heat capacities of three alloys were measured by isothermal calorimetry from 20 to 298°K. The alloys were InPb, endothermically formed from the elements, the moderately exothermic AuCd, and the highly exothermic Mg_3Sb_2. Deviations from Kopp's law of additivity of C_p were rather small, except for a small anomaly of undetermined origin at 240 to 300°K for InPb, and a decided negative deviation (~5%) above 200°K for Mg_3Sb_2. Heat capacities of the $AuCu_3$ alloy in both the ordered and disordered states have been measured between 20 and 298°K by isothermal calorimetry. Combining the heat capacity data for $AuCu_3$ from this study with existing high temperature thermodynamic data, S_0°, disordered, the configurational entropy, was found to be 0.987 eu, which is somewhat lower than the theoretical value for complete disorder, 1.117 eu. The difference may be explained in terms of short-range order, the existence of which is confirmed by heat of formation measurements with tin solution calorimetry. (T.D.)

53638 (ORNL-4781) BEHAVIOR OF WELDED JOINTS IN STAINLESS AND ALLOY STEELS AT ELEVATED TEMPERATURES. Gilliland, R. G. (Oak Ridge National Lab., Tenn.). Aug 1972. Contract W-7405-eng-26. 62p. Dep. NTIS.

An extensive survey was conducted of the available literature concerning the mechanical properties of weldments in Types 304 and 316 stainless steel and in 2¼ Cr-1 Mo low-alloy steel. The temperature range of interest was 900 to 1300°F. Data on weldments in these materials were found to be sparse, especially for the case of 304 stainless steel. This situation was especially true, for all materials, in the case of cyclic data (fatigue, etc.). Comparisons of weld-metal/base-metal properties and property variations between filler metals are presented. These data are evaluated with regard to service and fabrication application and experience, and the effect of service-oriented microstructural changes on component integrity is discussed. Finally, recommendations are presented as to additional data and investigations needed to more fully understand the behavior of welded joints in stainless and alloy steels at elevated temperatures. (auth)

53639 (ORO-3262-25) DEFORMATION PROCESSES IN HEXAGONAL METALS. Progress Report, December 1, 1971-

November 30, 1972. Garde, A. M.; Reed-Hill, R. E. (Florida Univ., Gainesville). 1972. Contract AT(40-1)-3262. 35p. Dep. NTIS.

Five papers in preparation and nearing completion are discussed. These show that lowering the impurity level of zirconium from about 2000 ppM (commercial purity) to about 200 ppM strongly affects a number of its mechanical properties. First, the very low twinning rate of commercial purity zirconium (longitudinal specimens) at 77°K is markedly increased. This changes the stress-strain curve shape from nearly parabolic to approximately linear with a corresponding increase in tensile elongation by a factor of three to four. Several stages of deformation were observed in the high-purity zirconium stress-strain curve that can be related to changes in the twinning pattern that occur in certain strain intervals. Increasing the purity also markedly lowered the temperature and rate dependence of the flow stress of zirconium below about 600°K. This tended to produce a deformation behavior similar to that observed in pure face-centered cubic metals. The high-purity zirconium data have also allowed the magnitudes of the dynamic strain aging phenomena in zirconium to be estimated. This evaluation shows that in general dynamic strain aging is much weaker in zirconium than it is in titanium. Other work accomplished last year has demonstrated that prestraining titanium at 77°K so as to nucleate twins has beneficial effects on the room temperature mechanical properties. A study to test the validity of the Cottrell–Stokes Law in titanium and zirconium has also been made. (auth)

53640 (RDT-M-2-2-T(8-72)) STAINLESS AND LOW ALLOY STEEL FORGINGS (ASME SA-182 WITH ADDITIONAL REQUIREMENTS). (Division of Reactor Development and Technology (AEC), Washington, D. C.). Aug 1972. 11p. RSO.

A standard prescribing requirements for stainless and low-alloy forgings (ASME SA-182 with additional requirements) for nuclear and associated applications is presented. This standard supersedes RDT M 2-2T dated January 1972. (J.R.D.)

53641 (SC-DR-720471) MECHANICAL PROPERTIES AND STRESS RELAXATION OF BERYLLIUM–COPPER ALLOY 25. Nordstrom, T. V.; Rohde, R. W. (Sandia Labs., Albuquerque, N. Mex.). Aug 1972. 21p. Dep. NTIS.

The mechanical properties of Beryllium–Copper Alloy 25 were investigated. In particular, the proportional limit, yield strength, and ductility were measured from –320 to 300°F for AT and HT strength levels. All three properties varied inversely with temperature. Short term stress relaxation was studied for various strains and temperatures using AT and HT conditions. Fractional relaxation was found to increase with increasing strain. There was no apparent temperature dependence of relaxation. Preliminary relaxation results from long term bend tests are presented. The results thus far agree with extrapolation of the short term testing. Other areas investigated were the effects of deformation after aging on hardness and hardening during relaxation. The results are discussed with respect to safe design criteria for the alloy. (auth)

53642 (STU–70-419/U-350(Pt.1,2)) CHANGE OF STRUCTURE AND MECHANICAL PROPERTIES IN STAINLESS STEEL BY IRRADIATION. PART 1,2. THE INTERRELATIONSHIP OF THE CREEP AND STRESS RELAXATION PHENOMENA. Gott, K.; Lagneborg, R.; Modeer, B. (Aktiebolaget Atomenergi, Studsvik (Sweden)). Sep 1971. 20p. (AE-MF-232).

Creep and stress relaxation tests were performed on a 20 Cr–35 Ni austenitic stainless steel at 700°C. The results were evaluated using the recovery-creep model of Lagneborg and also the steady-state creep power law. Both models were also applied in a slightly modified form to the relaxation results. Good agreement was found between the experimental results and the recovery-creep model. (auth) (Sweden)

53643 INFLUENCE OF INTERSTITIAL NITROGEN ON THE ASYMMETRY OF THE YIELD STRESS OF TANTALUM. Lachenmann, R.; Schultz, H. (Max-Planck-Institut fuer Metallforschung, Stuttgart. Univ., Stuttgart). Scr. Met.; 6: No. 8, 731-6(Aug 1972).

Properties of high-purity and N-doped Ta single crystals were investigated. It was concluded that an asymmetry in yield stress in pure Ta is associated with lattice characteristics. The asymmetry of yield stress is continuously reduced by adding impurity interstitials such as N. (J.R.D.)

53644 NOTE ON THE NATURE OF MASSIVE TRANSFORMATION INTERFACES. Perepezko, J. H.; Massalski, T. B. (Carnegie-Mellon Univ., Pittsburgh). Scr. Met.; 6: No. 8, 743-52(Aug 1972).

Features of the transformation interface of massive transformations in metal systems are discussed. It is noted that in many cases a single-phase massive transformation product forms in a two-phase field. In these cases effective solute partitioning is prevented because of kinetic considerations. A concept of liquid-like structure at massive reaction interfaces is offered in explanation of observed and implied features of such reactions. (J.R.D.)

53645 INFLUENCE OF THE SURFACE ORIENTATION ON YIELD IN Mo SINGLE CRYSTALS. Vesely, D. (Oxford Univ.). Scr. Met.; 6: No. 8, 753-6(Aug 1972).

Results of investigations are presented and discussed which show that slip systems in Mo single crystals are related to the surface effect. It is concluded that surface orientation influences the choice of slip systems and may affect yielding in Mo single crystals at low temperatures. (J.R.D.)

53646 HEAT TREATMENT, MICROSTRUCTURE, AND MECHANICAL PROPERTIES OF HEAVY GAGE STEELS FOR NUCLEAR REACTOR PRESSURE VESSELS. 1. HEAT TREATMENT, MICROSTRUCTURE, AND MECHANICAL PROPERTIES OF Mn–Mo–Ni STEEL PLATE. Miyano, Katao; Shimazaki, Masahide; Hasegawa, Akio (Japan Steel Works, Ltd., Hokkaido). Nippon Seiko Giho; No. 29, 11-19(May 1971). (In Japanese).

The effect of prolonged post-weld heat treatment on the microstructure and mechanical properties is one of the most important subjects not only for the fabrication of nuclear reactor vessels but also for various types of high pressure vessels. The fundamental studies for the effects of quenching, tempering, and prolonged post-weld heat treatment on mechanical properties were carried out for the heavy gage steel plates of Mn–Mo–Ni. The change of mechanical properties caused by prolonged post-weld heat treatment was found to be mainly due to grain growth of ferrite and cohesion of carbide in grain boundary and the formation of molybdenum carbide. (auth) (Japan)

53647 APPLICATIONS OF FIELD–ION MICROSCOPY IN PHYSICAL METALLURGY AND CORROSION. Conference Held at Atlanta, Georgia, May 15–17, 1968. Hochman, R. F.; Mueller, E. W.; Ralph, B. (eds.). Atlanta; Georgia Institute of Technology (1969). 503p. (CONF-680570).

A total of twenty-two papers was presented at the conference. A separate abstract was prepared for each of thirteen papers. Nine papers were not in scope for NSA. (J.R.D.)

For abstracts of individual papers see: 53560, 53610, 53648–53657, and 53704.

53648 ATOM PROBE FIM. Mueller, Erwin W. (Pennsylvania State Univ., University Park). pp 59-65 of Applications of Field–Ion Microscopy in Physical Metallurgy and Corrosion. /Hochman, R. F. (ed.). Atlanta; Georgia Inst. of Tech. (1969).

From Conference on applications of field–ion microscopy in physical metallurgy and corrosion; Atlanta, GA. (15 May 1968). See CONF-680570.

A field ion microscope designed for use in imaging individual atoms is described. The instrument has been used only for testing and calibrating. It is noted that the instrument should be useful in absorption and corrosion studies and in metallography for determining the nature of interstitial segregations, lattice imperfections, and short-range order in alloys. (J.R.D.)

53649 ANALYSIS OF DISLOCATIONS AND STACKING FAULTS BY FIM. Hren, J. J. (Univ. of Florida, Gainesville). pp 87-129 of Applications of Field–Ion Microscopy in Physical Metallurgy and Corrosion. /Hochman, R. F. (ed.). Atlanta; Georgia Inst. of Tech. (1969).

From Conference on applications of field–ion microscopy in physical metallurgy and corrosion; Atlanta, GA. (15 May 1968). See CONF-680570.

Methods for quantitative interpretation of field ion microscopic images from crystal dislocations are described. Discussions are also included on dissociated dislocations and their associated stacking faults. Information is presented on computer simulation of field-ion images of defects, analysis of dislocations in cubic metals, crystal structure of hcp metals, and partial dislocations and stacking faults. (J.R.D.)

53650 STUDIES OF GRAIN BOUNDARIES IN METALS WITH THE FIELD–ION MICROSCOPE. Ranganathan, S. (Banaras Hindu Univ., India). pp 131-54 of Applications of Field–Ion Microscopy in Physical Metallurgy and Corrosion. /Hochman, R. F. (ed.). Atlanta; Georgia Inst. of Tech. (1969).

From Conference on applications of field–ion microscopy in physical metallurgy and corrosion; Atlanta, GA. (15 May 1968). See CONF-680570.

Developments in methods for field-ion microscopic studies are reviewed. Information is included on analysis of grain boundaries, methods for studies of low-angle boundaries, methods for studies of twin boundaries, methods for studies of high angle boundaries, and structures in segregations near grain boundaries. (J.R.D.)

53651 LATTICE DEFORMATION BY MECHANICAL AND ELECTRICAL CONTACTS. Nishikawa, Osamu; Mueller, Erwin W. (Pennsylvania State Univ., University Park). pp 155-76 of Applications of Field-Ion Microscopy in Physical Metallurgy and Corrosion. /Hochman, R. F. (ed.). Atlanta; Georgia Inst. of Tech. (1969).

From Conference on applications of field-ion microscopy in physical metallurgy and corrosion; Atlanta, GA. (15 May 1968). See CONF-680570.

A review is presented of early and recent developments in field-ion microscopic investigations of mechanical and electric contacts. These methods appear to offer promise of yielding new insight into surface topography and processes occurring in the bulk immediately underneath the contact surface. Information is included on contact procedures and results of contacts with hard metals, contacts with soft materials, and contacts with glass. (J.R.D.)

53652 FIELD ION MICROSCOPY OF DILUTE ALLOYS. Machlin, E. S. (Columbia Univ., New York). pp 177-97 of Applications of Field-Ion Microscopy in Physical Metallurgy and Corrosion. /Hochman, R. F. (ed.). Atlanta; Georgia Inst. of Tech. (1969).

From Conference on applications of field-ion microscopy in physical metallurgy and corrosion; Atlanta, GA. (15 May 1968). See CONF-680570.

The state of knowledge concerning the application of field ion microscopy in the study of dilute solid solutions is summarized. The main results obtained from such studies are the interaction energy between solute atoms as a function of their distance of separation and a knowledge of the "molecularity" of the clusters formed by different solute atoms in solid solution. This application of field ion microscopy is in its infancy and has promise of a long and useful life. (auth)

53653 STUDY OF TWO-PHASE SYSTEMS BY FIELD-ION MICROSCOPY. Bayuzick, R. J.; Goodrich, R. S. (Vanderbilt Univ., Nashville). pp 199-229 of Applications of Field-Ion Microscopy in Physical Metallurgy and Corrosion. /Hochman, R. F. (ed.). Atlanta; Georgia Inst. of Tech. (1969).

From Conference on applications of field-ion microscopy in physical metallurgy and corrosion; Atlanta, GA. (15 May 1968). See CONF-680570.

Methods are described for study of crystal phases between which both crystal structure and composition are variable. Developments related to two-phase studies are reviewed and applications of field-ion microscopy to studies of interfaces, nucleation, and growth are described. Applications of field-ion microscopy to studies of dispersion strengthening in two-phase systems are also discussed along with applications in yield strength studies and work hardening studies. (J.R.D.)

53654 STUDY OF ORDERED ALLOYS BY FIELD-ION MICROSCOPY. LeFevre, B. G. (Georgia Inst. of Tech., Atlanta); Newman, R. W. pp 243-69 of Applications of Field-Ion Microscopy in Physical Metallurgy and Corrosion. /Hochman, R. F. (ed.). Atlanta; Georgia Inst. of Tech. (1969).

From Conference on applications of field-ion microscopy in physical metallurgy and corrosion; Atlanta, GA. (15 May 1968). See CONF-680570.

A survey of phenomena associated with atomic order in alloys is presented. Aspects of atomic order which are suited to analysis by field ion microscopy are discussed. A review of the common ordered structures is included along with information on the microstructure of ordered alloys, and image characteristics of domain boundaries. (J.R.D.)

53655 INTERPRETATION OF ALLOY IMAGES. Southworth, H. N.; Ralph, B. (Univ. of Cambridge, Eng.). pp 291-327 of Applications of Field-Ion Microscopy in Physical Metallurgy and Corrosion. /Hochman, R. F. (ed.). Atlanta; Georgia Inst. of Tech. (1969).

From Conference on applications of field-ion microscopy in physical metallurgy and corrosion; Atlanta, GA. (15 May 1968). See CONF-680570.

A unified theory of solid solution imaging is presented. Discussions and analyses supporting the theory are presented in sections on the image from ordered equiatomic PtCo, distinguishing between the atomic species, models for superlattices, the effects of temperature on Pt_3Co, and models for selective ionization. (J.R.D.)

53656 INTERACTION OF SINGLE ATOMS WITH ATOMICALLY DEFINED SURFACES. Plummer, E. W. (National Bureau of Standards, Washington, D. C.). pp 371-89 of Applications of Field-Ion Microscopy in Physical Metallurgy and Corrosion. /Hochman, R. F. (ed.). Atlanta; Georgia Inst. of Tech. (1969).

From Conference on applications of field-ion microscopy in physical metallurgy and corrosion; Atlanta, GA. (15 May 1968). See CONF-680570.

Experiments are described which exemplify the unique types of surface studies possible by the use of field-ion microscopy. A discussion is also included of experiments conducted to measure the surface binding energy of atomic species on W. These examples are used to demonstrate the importance of surface characterization on an atomic scale and the fundamental role that field-ion microscopy has in advanced experiments on metal surfaces. (J.R.D.)

53657 GAS-METAL INTERACTIONS: FIELD ION AND EMISSION MICROSCOPY. Grenga, Helen E.; Hochman, Robert F. (Georgia Inst. of Tech., Atlanta). pp 391-411 of Applications of Field-Ion Microscopy in Physical Metallurgy and Corrosion. /Hochman, R. F. (ed.). Atlanta; Georgia Inst. of Tech. (1969).

From Conference on applications of field-ion microscopy in physical metallurgy and corrosion; Atlanta, GA. (15 May 1968). See CONF-680570.

Field ion microscopy results on gas-metal interactions are reviewed. Results of field ion microscopic studies on material couples for which the mechanical strength is affected by the environment are also presented. Information is included on effects of environment on mechanical strength, hydrogen embrittlement, studies of gas-metal interactions, and field-ion microscopy of Ti and ordered Ti_3Al. (J.R.D.)

53658 INFLUENCE OF HOLD-TIME AND TEMPERATURE ON THE LOW-CYCLE FATIGUE OF INCOLOY 800. Jaske, C. E. (American Society of Mechanical Engineers, New York); Mindlin, H.; Perrin, J. S. J. Eng. Ind.; 94: No. 3, 930-4(Aug 1972).

A study has been conducted to determine the low-cycle fatigue behavior of solution-annealed Incoloy 800 bars at temperatures from 800 to 1400°F. The experimental work included evaluation of specimens under both continuous, completely reversed strain cycling and under strain cycling with hold time periods at the strain limits. At 1000, 1200, and 1400°F, it was found that 10-min hold-times at the tensile strain limit during every cycle significantly reduced the cyclic fatigue life compared with continuous cycling. However, there was little reduction in cyclic fatigue life when 10-min hold-times were introduced at the compressive strain limits or at both the tensile and compressive limits. The ratio of hold-time cyclic fatigue life to no-hold-time cyclic fatigue life decreased as the length of hold time increased (at constant total strain range) and as the magnitude of strain range decreased (at constant hold-time length). (auth)

53659 ORDERING TRANSFORMATION IN Ni_2V. Tanner, L. E. (Kennecott Copper Corp., Lexington, Mass.). Acta Met.; 20: No. 10, 1197-1227(Oct 1972).

The transformation to long-range order in stoichiometric Ni_2V was studied in detail over a wide range of subcritical temperatures. The alloy was subjected to both continuous cooling and isothermal aging treatments and specimens were examined by electron and light optical microscopy and x-ray diffraction techniques. The observations indicate that in the range $920°C > T > 750°C$ the transformation proceeds by means of homogeneous nucleation and growth throughout each disordered grain and heterogeneous nucleation and growth along grain boundaries. At $T \le 750°C$ homogeneous nucleation appears to be superseded by a continuous transition to LRO. However, heterogeneous nucleation and growth cannot be suppressed during cooling and so this process is also operative at the low temperatures. (auth)

53660 FRACTURE TOUGHNESS TESTING AT CRYOGENIC TEMPERATURES. Symposium Presented at the Seventy-Third Annual Meeting, Toronto, Ontario, Canada, June 21-26, 1970. ASTM Special Technical Publication 496. Philadelphia; American Society for Testing and Materials (1971). 86p. $5.00. (ASTM-STP-496; CONF-700670).

Four articles are included; a separate abstract was prepared for one. The remaining three articles contain information on: plane strain fracture toughness of Al alloys at room and subzero temperatures; influence of specimen design in plane strain fracture toughness testing, and fracture of thin sections containing through and part-through cracks. (P.C.H.)

For an abstract of an individual paper see: 53661.

53661 PLANE STRAIN FRACTURE TOUGHNESS OF SOME CRYOGENIC MATERIALS AT ROOM AND SUBZERO TEMPERATURES. Vishnevsky, C.; Steigerwald, E. A. (TRW Inc., Cleveland). ASTM (Amer. Soc. Test. Mater.) Spec. Tech. Publ.; No. 496, 3-26(1971).

From Fracture toughness testing at cryogenic temperatures symposium; Toronto, Ontario (21 Jun 1970). See ASTM-STP-496; CONF-700670.

An investigation was conducted to measure the plane strain fracture toughness, K_{Ic}, of eight potential cryogenic service alloys at 75, −100, and −321°F. The test materials included 7039-

T61 and 2021-T81 aluminum alloys, Ti−6Al−4V STA in both alpha + beta and beta processed conditions, and the following steels: ASTM A553-A, PH 13-8Mo (H 1150-M), HP 9-4-20, and 18 Ni (200 grade) maraging. Results include both fracture toughness and tensile data as a function of test temperature for each alloy, together with overall comparisons in terms of the plane strain crack size factor $(K_{Ic}/\sigma_{ys})^2$, versus yield strength and yield strength to density ratio. In cases where valid K_{Ic} data could not be generated, the appropriate aspects of the ASTM Tentative Method of Test for Plane Strain Fracture Toughness of Metallic Materials (E 399−70T) are discussed. (auth)

53662 EFFECT OF QUENCHSINTERING ON THE GRAIN-STRUCTURE OF SINTERED METALS. Häusner, H. H. (Polytechnic Inst., Brooklyn). Int. J. Powder Met.; 8: No. 3, 159-61(Jul 1972).

Results of a study of the effect of quench sintering (interruption of the sintering cycle by rapid cooling and subsequent continuation of the sintering process) on the grain structure of tungsten show that specimens compacted at 2500 psi have more grains (small grains) than those compacted at 50,000 psi. Specimens quenched after 2 hours presintering time and then sintered for an additional 16 hours have approximately 40 to 50% more grain than specimens quenched after 16 hours presintering and then sintered for an additional 2 hours. The earlier interruption of the sintered cycle results in finer grains. The final densities of the specimens depend on compacting pressure, but not on the type sintering cycle. Possible causes for these effects of quench sintering on grain structure are proposed. (D.H.M.)

53663 THERMODYNAMIC PROPERTIES OF ZIRCONIUM–CADMIUM AND CERTAIN OTHER SOLID SOLUTIONS. Frye, J. H. Jr.; Betterton, J. O. Jr.; Easton, D. S. (Oak Ridge National Lab., Tenn.). Acta Met.; 20: No. 10, 1183-95(Oct 1972).

The phase diagram was determined up to a concentration of 20 at.% Cd, and lattice parameters were measured for the hexagonal phase. The vapor pressure of cadmium in equilibrium with the solid solution was measured for both the hexagonal and cubic phases as a function of temperature and concentration. These data are considered together with earlier data on the Zr−Ag, Zr−In, Zr−Sn and Zr−Sb primary substitutional solid solutions. Empirical relations are found between the hexagonal (c/a) ratio, the temperature of the transformation from cubic to hexagonal zirconium and the electronic specific heat coefficient on the one hand and the concentration of principal quantum number 5 electrons on the other. These simple relations suggest the possibility that the principal quantum number 5 electrons are entering a rigid conduction band in zirconium. In order to investigate this possibility, the partial molal energy of cadmium in zirconium was calculated from the vapor pressure measurements. It was concluded that the rigid band model is a bad approximation and points out that this is in accord with recent quantum mechanical calculations. Furthermore, the effect of cadmium on the transformation temperature of zirconium is the resultant of two opposite and nearly balanced effects — an absolute zero energy effect which tends to stabilize the cubic form and an entropy effect which tends to stabilize the hexagonal form. Finally, it is shown that, for most of the solutions considered here, the energy of a Wigner−Seitz polyhedron is independent of concentration within experimental error. (auth)

53664 MUTUAL INTERACTIONS OF THORIUM, LANTHANIDES, AND BISMUTH IN Th−Ln−Bi SOLUTIONS: EVIDENCE FOR THE FORMATION OF $ThLnBi_y$ COMPOUNDS. Smith, F. J. (Oak Ridge National Lab., Tenn.). J. Less-Common Metals; 29: 73-9(1972).

The mutual solubilities of thorium, and lanthanum, neodymium, or europium in bismuth solution have been determined over the temperature range 350 to 700°C. Thorium and each lanthanide (Ln), dissolved in liquid bismuth, were found to interact to produce a solid compound with the apparent composition $ThLnBi_y$. The variation of the mole fraction solubility products with temperature can be expressed as $\log K_{sp} = \log(N_{Th}N_{Ln}) = 2.410 - 6480/T(K)$ for $ThLaBi_y$ and $\log K_{sp} = 3.233 - 7285/T(K)$ for $ThNdBi_y$. The standard free energies of formation for $ThLaBi_y$ and $ThNdBi_y$ were estimated to be about (−114.8 + 0.0208T) and (−99.8 + 0.0207T) kcal/mole, respectively. The solubility of europium in bismuth was determined over the temperature range 350 − 550°C. The data can be represented by the expression: $\log S_{Eu}$ (wt %) = 4.4823 − 2973/T(K). (auth)

53665 NUMERICAL CALCULATION OF THE REDISTRIBUTION OF AN INTERSTITIAL SOLUTE IN A THERMAL GRADIENT. Marino, G. P. (Bettis Atomic Power Lab., West Mifflin, Pa.). Nucl. Sci. Eng.; 49: No. 1, 93-8(Sep 1972).

An analytical method is described for calculation of the concentration profile of an interstitial solute of finite solubility in an alloy under a given thermal gradient. The method requires that the diffusion coefficient, the terminal solid solubility, and the heat of transport of the solute be known. The work is applied to the experimental conditions of Sawatzky and of Markowitz for hydrogen in Zircaloy. The agreement between the predicted profiles and the experimentally determined profiles is quite good for total concentrations less than ~1000 ppM. For concentrations greater than this, some deviation is seen but the overall agreement is still considered good within the accuracy of the assumptions employed. The principles embodied in the analysis are easily generalized to include multidimensional thermal and concentration gradients. (auth)

53666 ULTRA-FAST SOLUTE DIFFUSION IN α-Ti AND α-Zr. Hood, G. M.; Schultz, R. J. (Atomic Energy of Canada Ltd., Chalk River, Ont.). Phil. Mag.; 26: No. 2, 329-36(Aug 1972).

Diffusion of ^{63}Ni in polycrystalline α-Ti and of ^{59}Fe, ^{60}Co, and ^{63}Ni in α−Zr was measured. In α−Zr, single crystals were used for studies of Ni and Co diffusion, while the experiments on Fe diffusion were done on polycrystalline specimens. All the solutes studied exhibited extremely fast diffusion compared to self-diffusion in the host metals. It is suggested that these solutes diffuse by an interstitial mechanism and that very fast solute diffusion in the bcc forms of Ti and Zr may be predominantly of an interstitial nature. (auth)

53667 INTERCONNECTING PHENOMENA OF ULTRAPLASTICITY OF ALLOYS AND THEIR CHEMICAL AND PHASE COMPOSITION. Tikhonov, A. S. Fiz. Khim. Obrab. Mater.; No. 1, 159-61(1972). (In Russian).

The mechanical properties of a Ni−33% Mo alloy were investigated during tension experiments over the temperature range 800 to 1,200°C. The phenomenon of ultraplasticity was detected in deformation of the alloy at 900 to 1,100°C, corresponding to the two-phase region Ni + δ in the phase composition diagram Ni−Mo. For the preservation of "micro-structural" factors, the phenomena of ultraplasticity may predominate over such important considerations as the temperature factor of plastic deformation. (tr-auth)

53668 INVESTIGATION OF THE SURFACE OF TUNGSTEN SINGLE CRYSTALS FOLLOWING ELECTRO-EROSIVE TREATMENT. Zolotykh, B. N.; Marchuk, A. I.; Sen'kina, M. S. Fiz. Khim. Obrab. Mater.; No. 1, 145-50(1972). (In Russian).

Results of experimental investigations of the electro-erosive action on single crystals of W are presented. The effects of electric pulses and of the crystallographic orientation of the crystal face of W on the magnitude of the erosion and the character of the disintegration of the surface layers were studied. Brittle shattering of the single crystals along the sliding surfaces may play a decisive role in electro-erosive treatment, equally with evaporation and melting. (tr-auth)

53669 EFFECT OF CHROMIUM AND ZIRCONIUM ON THE DUCTILITY OF COPPER. Chervyakova, V. V. Tr. Inst. Yadern. Fiz., Akad. Nauk Kaz. SSR; 12: 3-6(1971). (In Russian).

The mechanical properties of cast and deformed samples of chromium and chromium−zirconium bronzes were investigated at two elongation rates: 1 and 4 mm/min. The ductility of copper at moderate temperatures increased when alloyed with Cr and Zr. The ductility of Cu and its Cr- and Zr- alloys was measured as a function of temperature up to about 900°C. An increase in the tensile strength limits of these alloys at 300 to 500°C was observed, which was associated with aging. (K.S.W.)

53670 DEFORMATION TEXTURES OF B.C.C. METALS (TUNGSTEN). Rieck, G. D. (Univ. of Tech., Eindhoven, Netherlands). pp 20.1-9 of Proceedings of the 7th Plansee Seminar on Powder Metallurgy of High Temperature Materials. Vol. I. /Benesvosky, F. (ed.). Reutte/Tyrol, Austria; Metallwerk Plansee (1971).

From 7th Plansee seminar on powder metallurgy of high temperature materials; Reutte/Tyrol, Austria (21 Jun 1971). See CONF-710602--(Vol.1).

The experimental details of texture resulting from swaging and drawing of bcc metals (tungsten) are discussed. A consistent picture of the drawing texture of polycrystalline W seems to be available now. This may be the base for future models on deformation mechanism. (auth)

53671 THERMODYNAMIC DESCRIPTION OF THE METAL-RICH REGION IN THE SYSTEM NIOBIUM–MOLYBDENUM–NITROGEN. Hoerz, G.; Steinheil, E. (Max-Planck-Institut fuer Metallforschung, Stuttgart). pp 27.1-18 of Proceedings of the 7th Plansee Seminar on Powder Metallurgy of High Temperature Materials. Vol. I. /Benesvosky, F. (ed.). Reutte/Tyrol, Austria; Metallwerk Plansee (1971). (In German).

From 7th Plansee seminar on powder metallurgy of high temperature materials; Reutte/Tyrol, Austria (21 Jun 1971). See CONF-710602-(Vol.1).

In the system Nb−Mo−N for the range of the ternary α-Nb−Mo−N solid solution, the equilibrium nitrogen concentration as a function of pressure (10^{-4} to 5×10^2 torr), temperature (1600 to 2400°C), and Mo-concentration (0 to 100 at.%) has been measured as well as the solubility limit of nitrogen in the α solid solution as a function of temperature (1600 to 2100°C) and Mo-concentration (0 to 80 at.%). In addition the kinetics of the dissolution of nitrogen in the α solid solution were determined. The studies were carried out using a gravimetric method and thin disc shaped specimens which were heated by induction. The results showed that the equilibrium nitrogen concentration in the α solid solution obeys the Sieverts $\sqrt{p}$ law and decreases by 3 to 5 orders of magnitude, when the Mo concentration is increased from 0 to 100 at.% at constant pressure and temperature. The enthalpy of solution of nitrogen increased between 0 and 100 at.% Mo from −46,0 kcal/½ mole N_2 (exothermic reaction) to +19,9 kcal/½ mole N_2 (endothermic reaction) and was 0 at about 80 at.% Mo. The saturation concentration of nitrogen in the α solid solution decreased between 0 and 80 at.% Mo by 1 to 2 orders of magnitude, depending on temperature, while the corresponding equilibrium nitrogen pressure increased by many orders of magnitude. The β-nitride in equilibrium with the saturated α solid solution had the hexagonal structure of the subnitride Nb_2N up to Mo concentrations of at least 30 at.%. The initial rate of nitrogen dissolution decreased by about 2 orders of magnitude between 0 and 100 at.% Mo. In the system Nb−N the rate determining step was dissociation and chemisorption. A thermodynamic description of the metal rich region of the system Nb−Mo−N is given using activity coefficients and interaction coefficients. (auth)

53672 ARC-CAST MOLYBDENUM-BASE TZM ALLOY PROPERTIES AND APPLICATIONS. Briggs, J. Z.; Barr, R. Q. (Climax Molybdenum Co., New York). pp 29.1-39 of Proceedings of the 7th Plansee Seminar on Powder Metallurgy of High Temperature Materials. Vol. I. /Benesvosky, F. (ed.). Reutte/Tyrol, Austria; Metallwerk Plansee (1971).

From 7th Plansee seminar on powder metallurgy of high temperature materials; Reutte/Tyrol, Austria (21 Jun 1971). See CONF-710602-(Vol.1).

During the past 12 years that vacuum-melted TZM has been commercial, considerable information has been developed on its properties. Basically, its physical properties, corrosion resistance, and oxidation resistance are similar to those of unalloyed molybdenum. TZM's advantages over unalloyed molybdenum are its higher recrystallization temperature, which permits retention of work hardening to higher temperatures, and its superior toughness. A major advance over the past 12 years has been improvements in processing and fabricating. It is now feasible to make almost any type of part from TZM, often with conventional equipment, although special care and sometimes preheating are required. TZM was originally developed for the aerospace field in applications where high, hot strength was thought to be necessary. More recently, however, its interesting combination of properties, particularly high thermal conductivity, high stiffness, low thermal expansion, high, hot hardness, and excellent resistance to many molten metals has led to a much broader field of use, including die-casting dies and cores, hot-working dies, mandrels, heating elements, and boats. The future looks bright for TZM as more design engineers become acquainted with its properties and realize that its performance far outweighs its cost in many applications. (167 references). (auth)

53673 PROPERTIES OF A 1300 kg P/M TZM BILLET. Clare, L. P.; Smith, J. S.; Kegel, A. J.; Koss, R. L. (GTE Sylvania Inc., Towanda, Pa.). pp 30.1-19 of Proceedings of the 7th Plansee Seminar on Powder Metallurgy of High Temperature Materials. Vol. I. /Benesvosky, F. (ed.). Reutte/Tyrol, Austria; Metallwerk Plansee (1971).

From 7th Plansee seminar on powder metallurgy of high temperature materials; Reutte/Tyrol, Austria (21 Jun 1971). See CONF-710602-(Vol.1).

Problems associated with the forging of P/M TZM billets are reviewed. The chemical composition, physical properties, and microstructure of an unworked P/M TZM forging billet, 41 cm in diameter by 101 cm long, weighing 1300 kg, are described. (auth)

53674 INFLUENCE OF OXYGEN, CARBON, AND BORON ON THE SINTERING AND STRESS RUPTURE PROPERTIES OF SINTERED NICKEL-BASE SUPERALLOYS. Soler-Gomez, A. J. R.; Todd, A. G. (General Electric Co. Ltd., Wembley, Eng.). pp 36.1-18 of Proceedings of the 7th Plansee Seminar on Powder Metallurgy of High Temperature Materials. Vol. II. /Benesvosky, F. (ed.). Reutte/Tyrol, Austria; Metallwerk Plansee (1971).

From 7th Plansee seminar on powder metallurgy of high temperature materials; Reutte/Tyrol, Austria (21 Jun 1971). See CONF-710602-(Vol.2).

The liquid phase sintering behavior of two nickel base superalloys was investigated using powders with a range of oxygen contents. The influence of carbon and boron on the progress of sintering was determined by examination of shrinkage characteristics and pressure variation in the sintering furnace. The stress-rupture behavior of the various sintered materials was determined and related to composition and sintering characteristics. The results indicated that both boron and carbon counteract the effects of oxygen and aid sintering. The stress-rupture life of both alloys tended to a maximum at particular carbon, boron, and oxygen levels. (auth)

53675 STRUCTURE AND PROPERTIES OF DISPERSION STRENGTHENED COBALT ALLOYS. Drapier, J. M.; Coutsouradis, D.; Habraken, L. (CRM, Liege). pp 39.1-16 of Proceedings of the 7th Plansee Seminar on Powder Metallurgy of High Temperature Materials. Vol. II. /Benesvosky, F. (ed.). Reutte/Tyrol, Austria; Metallwerk Plansee (1971).

From 7th Plansee seminar on powder metallurgy of high temperature materials; Reutte/Tyrol, Austria (21 Jun 1971). See CONF-710602-(Vol.2).

Studies were made on the microstructures and properties of various experimental dispersion hardened alloys in the as-received and in the heat-treated conditions. The alloys included $Co-2ThO_2-0.2\ Zr$, $Co-4\ ThO_2$, $Co-10\ Ni-2\ ThO_2-0.2\ Zr$, and $Co-20\ Ni-18\ Cr-2$ and 4 ThO_2. The techniques used on the microstructural study were mainly light microscopy, transmission electron microscopy on thin foils, x-ray diffraction, and electron microprobe analysis. The effects of variables relative to composition, structure, and processing on the strengthening mechanisms in dispersion-strengthened materials are discussed on the basis of the experimental results and also in terms of data in the literature pertaining to the mechanical strength of related materials. (auth)

53676 STABILITY AND HEAT CORROSION OF ALUMINUM COVERING ON ALLOY INCO 713 C AND ON ALLOYS OF COBALT. Davin, A.; Coutsouradis, D.; Habraken, L. (Univ., Liege). pp 40.1-19 of Proceedings of the 7th Plansee Seminar on Powder Metallurgy of High Temperature Materials. Vol. I. /Benesvosky, F. (ed.). Reutte/Tyrol, Austria; Metallwerk Plansee (1971). (In French).

From 7th Plansee seminar on powder metallurgy of high temperature materials; Reutte/Tyrol, Austria (21 Jun 1971). See CONF-710602-(Vol.2).

Structure as well as stability of aluminum claddings were studied at various temperatures. Results showed that, with Inconel 713, the cladding consisted of two zones. One layer constituted NiAl, the second one was a diffusion zone displaying the phases NiAl and Ni_3Al between which were dispersed particles of Mo_2C, NbC, and Ni−Cr−Mo. In the case of cobalt alloys, the diffusion zone appeared uniform and no precipitations could be observed under the light microscope. Resistance to heat corrosion was studied in combustion gases that were contaminated with sulfur and alkalines. Results showed that an aluminum cladding lengthened the lifetime of Inconel 713 by a factor of about 2 and that of cobalt alloys by a factor of 10 in the temperature range from 800 to 950°C. Ta and Ti additions favorably influenced the chemical stability of the cladding in cobalt alloys. Tungsten caused flaking of the cladding. (H.B.G.)

53677 DIFFUSION MEASUREMENTS IN THE SYSTEMS Pd−V AND Pd−Ti AS WELL AS METAL−CERAMIC SYSTEMS BY MEANS OF A MICROPROBE. Lamparter, Peter; Steeb, Siegfried; Gukelberger, Armin (Max-Planck Inst. for Metal Research, Stuttgart). pp 41.1-28 of Proceedings of the 7th Plansee Seminar on Powder Metallurgy of High Temperature Materials. Vol. II. /Benesvosky, F. (ed.). Reutte/Tyrol, Austria; Metallwerk Plansee (1971).

From 7th Plansee seminar on powder metallurgy of high temperature materials; Reutte/Tyrol, Austria (21 Jun 1971). See CONF-710602-(Vol.2).

In the Pd−V system, solid solutions of V in Pd, Pd_3V, and Pd_2V were observed. The measurement of partial diffusion coefficients is described, and data are tabulated. The existing phase diagram for the system was confirmed. During the annealing of Pd−Ti diffusion couples between 600 and 1000°C, three phases, namely $TiPd_3$, $TiPd_2$, and Ti_2Pd_3 were formed. One other phase whose composition ranged from TiPd to Ti_4Pd_3 was also observed. These results were not in agreement with the existing phase diagram for the system. The largest part of the diffusion layer at temperatures above 700°C was formed by the β phase. The validity of the Arrhenius' law for the temperature dependency of the chemical diffusion coefficient of the β phase was demonstrated. The partial diffusion coefficients were evaluated from the shift of markers versus the Matano plane at 800 and 900°C. Data on the diffusion of Ti, V, Nb, and Ta in AlN, Si_3N_4, and TiO are tabulated. (P.C.H.)

53678 HIGH-TEMPERATURE CREEP BEHAVIOR OF A TUNGSTEN–3 PERCENT RHENIUM ALLOY WITH THORIUM OXIDE DISPERSION HARDENING OF VARIOUS PARTICLE SHAPES. **Wirth, G.** pp 23.1-32 of Proceedings of the 7th Plansee Seminar on Powder Metallurgy of High Temperature Materials. Vol. III. /Benesvosky, F. (ed.). Reutte/Tyrol, Austria; Metallwerk Plansee (1971). (In German).

From 7th Plansee seminar on powder metallurgy of high temperature materials; Reutte/Tyrol, Austria (21 Jun 1971). See CONF-710602–(Vol.3).

Creep and time behavior were studied on a $W-3Re-2ThO_2$ alloy in plate and rod shapes under vacuum in the temperature range from 1800 to 2200°C. Despite finer distribution of the ThO_2 particles in plates, the two types of intermediate products showed the same rate of secondary creep in the entire temperature range studied. Up to 2200°C, time resistance of plates was superior to that of rods. At this temperature, a transformation of the elongated ThO_2 particles took place which was accelerated through creep. By means of electromicroscopic examinations and determinations of the activation energy of creep, grain boundary sliding was found to be the process determining creep rate. This concept also explained behavior of the two intermediate products with respect to creep rate and time resistance. Means for improvement of heat resistance are outlined. (tr–auth)

53679 PREPARATION AND PROPERTIES OF W–Ni–Mo ALLOYS. **Barta, J.; Gorni, J.; Kimmel, G.** pp 1-12 of Proceedings of the 7th Plansee Seminar on Powder Metallurgy of High Temperature Materials. Vol. IV. /Benesvosky, F. (ed.). Reutte/Tyrol, Austria; Metallwerk Plansee (1971).

From 7th Plansee seminar on powder metallurgy of high temperature materials; Reutte/Tyrol, Austria (21 Jun 1971). See CONF-710602–(Vol.4).

Studies were made on the preparation, phase distribution and composition, and mechanical properties of W-base–Ni–Mo alloys. The results showed that improvement of the mechanical properties of the alloys should be obtained if the macro-pores formed during sintering can be avoided and a thermal treatment given after sintering. It is suggested that the potential advantages of these alloys compared to the known heavy metals would be higher hardness and better corrosion resistance than those containing Fe. (P.C.H.)

53680 NEW DEVELOPMENTS IN THE PREPARATION OF COMPOSITE POWDERS. **Kunda, W.** pp 1-13 of Proceedings of the 7th Plansee Seminar on Powder Metallurgy of High Temperature Materials. Vol. IV. /Benesvosky, F. (ed.). Reutte/Tyrol, Austria; Metallwerk Plansee (1971).

From 7th Plansee seminar on powder metallurgy of high temperature materials; Reutte/Tyrol, Austria (21 Jun 1971). See CONF-710602–(Vol.4).

Composite powders were prepared by the deposition of metals from aqueous solution onto various core materials by gaseous hydrogen at elevated temperature and pressure. The results showed that this technique can be applied for coating of many metals, metalloids, metal alloys, non-metallic elements, refractory materials, and plastics. Nickel is a very suitable material for coating, however, under proper conditions, other metals such as cobalt, molybdenum, copper, and silver alone or in combinations of two or more metals, can also be applied for coating. The physical properties and chemical compositions of some of the composite powders prepared are listed. Areas for the application of composite powders are enumerated. (auth)

53681 METALLOGRAPHY OF CAST TUNGSTEN. **Savitskii, E. M.; Povarova, K. B.** (Inst. of Metallurgy, Moscow). pp 1-17 of Proceedings of the 7th Plansee Seminar on Powder Metallurgy of High Temperature Materials. Vol. IV. /Benesvosky, F. (ed.). Reutte/Tyrol, Austria; Metallwerk Plansee (1971).

From 7th Plansee seminar on powder metallurgy of high temperature materials; Reutte/Tyrol, Austria (21 Jun 1971). See CONF-710602–(Vol.4).

Studies were made on the effects of non-metal (mainly C) inclusions on different grades of cast tungsten. The results showed that alloying and a higher rate of cooling during crystallization affected the fine structure of W, making for the formation of the polygonal structure, i.e., for an increase in the density of dislocation in the metal, and especially in the proportion of screw dislocations. This in turn enhanced the effort exerted at spreading a crack in the case of a cleavage, thereby enhancing the resistance of the material to fracture by cleavage. (P.C.H.)

53682 INFLUENCE OF CARBON AND OXYGEN ON THE BRITTLENESS OF MOLYBDENUM. **Touboul, J. P.; Minel, L.; Langeron, J. P.** pp 1-18 of Proceedings of the 7th Plansee Seminar on Powder Metallurgy of High Temperature Materials. Vol. IV. /Benesvosky, F. (ed.). Reutte/Tyrol, Austria; Metallwerk Plansee (1971). (In French).

From seventh Plansee seminar on powder metallurgy of high temperature materials; Reutte/Tyrol, Austria (21 Jun 1971). See CONF-710602–(Vol.4).

Studies showed that it is possible to remove carbon from molybdenum by tempering at high temperature and under reduced oxygen pressure. Reaction kinetics is controlled by carbon diffusion in the metal. At high temperature, carbon and oxygen are present in a solid solution and lead to absorption layers on external surfaces and on internal grain surfaces. These layers can be recognized as surface striations. Carbon, dissolved in molybdenum at high temperature, precipitates during cooling predominantly on surfaces. The precipitate MO_2C appears as needles which are oriented in the dense crystallographic direction. At low temperatures, carbon precipitation on the external surface is less important than that on grain boundaries. Here, some precipitates can be detected at concentrations as low as 10^{-6}. (H.B.G)

53683 CREEP BEHAVIOR OF FINE WIRES OF POWDER-METALLURGICAL PURE, DOPED, AND THORIATED TUNGSTEN. **Moon, D. M.; Stickler, R.** (Westinghouse Research Labs., Pittsburgh). pp 21.1-13 of Proceedings of the 7th Plansee Seminar on Powder Metallurgy of High Temperature Materials. Vol. IV. /Benesvosky, F. (ed.). Reutte/Tyrol, Austria; Metallwerk Plansee (1971).

From 7th Plansee seminar on powder metallurgy of high temperature materials; Reutte/Tyrol, Austria (21 Jun 1971). See CONF-710602–(Vol.4).

A technique to evaluate the high-temperature creep behavior of fine wires has been developed and applied to determine the creep properties of wires of pure, doped, and thoriated tungsten. The obtained data differ in some cases considerably from the creep data reported for large specimens of the same materials. The differences are explained by the fact that in recrystallized fine wires numerous grain boundaries traverse the entire specimen diameter, facilitating grain boundary sliding without the necessity of grain deformation such as required during creep deformation of large specimens. Fine dispersions of small bubbles in doped tungsten and of fine particles in the thoriated tungsten, which affect the recrystallized grain morphology and the retained dislocation substructure, were found to alter characteristically the creep behavior. (auth)

53684 ELECTRIC AND THERMAL CONDUCTIVITY, ELASTIC PROPERTIES, AND BENDING RESISTANCE OF POROUS TUNGSTEN OVER THE ENTIRE RANGE OF POROSITY. **Francois, D.** (CEA, Montrouge, France); **Terraz, C.; Meyer, R.; Pastor, H.** pp 22.1-14 of Proceedings of the 7th Plansee Seminar on Powder Metallurgy of High Temperature Materials. Vol. IV. /Benesvosky, F. (ed.). Reutte/Tyrol, Austria; Metallwerk Plansee (1971). (In French).

From seventh Plansee seminar on powder metallurgy of high temperature materials; Reutte/Tyrol, Austria (21 Jun 1971). See CONF-710602–(Vol. 4).

At a given porosity, variations in properties of tungsten powders are caused by texture and size of the different pores. Therefore, the degree of sintering is not the same. Even under identical sintering conditions, particle size of the powder differs. A mathematical equation for the degree of sintering is given. The various properties as affected by porosity are discussed. (H.B.G.)

53685 CLEAVAGE IN Ti–8Al–1Mo–1V CAUSED BY HYDROGEN GAS. **Meyn, D. A.** (Naval Research Lab., Washington, D. C. Met. Trans.; 3: No. 8, 2302-5(Aug 1972).

Studies were made on the hydrogen-embrittlement mechanisms proposed to explain cleavage in Ti–8Al–1Mo–1V caused by H gas. The results showed that crack propagation by gaseous H in Ti–8Al–1Mo–1V does not occur by the same mechanism as stress corrosion cracking, sustained load cracking, or low amplitude fatigue. Thus, either H is not directly causative in these latter cracking modes, or it somehow gives rise to different effects when supplied by other means to the crack tip than as a gas at the surface. (P.C.H.)

53686 NEW METASTABLE PHASE IN RAPIDLY SOLIDIFIED Al–Zr ALLOYS. **Ohashi, T.; Ichikawa, R.** (Nagoya Inst. of Tech., Japan). Met. Trans.; 3: No. 8, 2300-2(Aug 1972).

Studies were made on the crystal structure of the metastable Al_3Zr phase formed by rapid solidification of the molten Al–3 ~ 6 wt % Zr alloys. The results showed that the crystal structure was the same as that of the metastable precipitate from the supersaturated solid solutions that were obtained by rapid solidification of the molten Al–1 ~ 1.1 wt% Zr alloys. (P.C.H.)

53687 TRANSVERSE TENSILE PROPERTIES OF BORON FIBER REINFORCED ALUMINUM MATRIX COMPOSITES. Prewo, K. M.; Kreider, K. G. (United Aircraft Research Labs., East Hartford, Conn.). Met. Trans.; 3: No. 8, 2201-11(Aug 1972).

The transverse tensile properties of boron fiber reinforced aluminum have been determined as a function of fabrication parameters, matrix alloy and fiber types, fiber content, specimen geometry, and thermal environment. Matrix alloys investigated include 2024, 6061, 5052, 5056, 2219, 1100, and Al – 7 pct Si. The fibers investigated include 4.0 mil boron, 4.2 mil BORSIC, R.F. boron, 5.6 mil boron, 5.7 mil BORSIC, and 4.0 mil silicon carbide. It was found that the composite transverse tensile performance is a function of all of these variables and that transverse strengths of up to 45,000 psi can be achieved by the choice of the proper combination of matrix, fiber type, and fabrication procedures. (auth)

53688 EFFECT OF OXYGEN ON TANTALUM—SODIUM COMPATIBILITY. Klueh, R. L. (Oak Ridge National Lab., Tenn.). Met. Trans.; 3: No. 8, 2145-50(Aug 1972).

The effects of oxygen in both phases on the compatibility of tantalum with sodium were investigated at 600°C by exposing tantalum specimens to liquid sodium in static capsules. Increasing the initial oxygen concentration of the sodium from 50 to 12,000 ppM led to increased dissolution of the tantalum in the sodium; oxygen migrated from the sodium to the tantalum. As the initial oxygen concentration of the sodium increased, the accompanying tantalum specimens first gained and then lost weight. It was concluded that the addition of oxygen to sodium results in the formation of a loosely adhering ternary oxide scale on the tantalum surface. The increased dissolution of tantalum and the weight change behavior of the tantalum specimens when the initial oxygen concentration of the sodium is increased indicated that the nonadherent ternary oxide flakes off in progressively greater amounts as its thickness increases. When the concentration of oxygen in tantalum before test exceeded 200 ppM, sodium penetrated the tantalum. Penetration, as in other refractory metal-oxygen-alkali metal systems previously investigated, proceeded with the formation of a ternary oxide by a wedging mechanism. At low oxygen concentrations attack occurred along grain boundaries, and as the oxygen concentration of the tantalum was increased, the number of grain boundaries attacked and the depth of attack increased. Still higher oxygen concentrations induced transgranular attack. (auth)

53689 EXPLORATORY INVESTIGATION OF Y, La, AND Hf COATINGS FOR NITRIDATION PROTECTION OF CHROMIUM ALLOYS. Stephens, Joseph R. (Lewis Research Center, Cleveland). Met. Trans.; 3: No. 8, 2075-86(Aug 1972).

Chromium alloys were coated with Y, La, and Hf, either singly or in combination, by pack cementation. Based on ductile-brittle transition temperature, a complex Cr + Y + La coating offered the most potential for protecting chromium alloys from nitrogen embrittlement. For example, the transition temperature for a chromium + 0.17 wt % Y substrate coated with this complex Cr + Y + La coating was 450°K after isothermal exposure in air at 1420°K for 200 h, compared to a transition temperature of 840°K for the similarly exposed uncoated substrate. Simple yttrium coatings were more attractive as coatings for chromium alloys than simple lanthanum and hafnium coatings. (auth)

53690 CYCLIC CREEP-RUPTURE BEHAVIOR OF THREE HIGH-TEMPERATURE ALLOYS. Halford, G. R. (Lewis Research Center, Cleveland). Met. Trans.; 3: No. 8, 2247-56 (Aug 1972).

Some important characteristics of the cyclic creep-rupture curves have been studied for the titanium alloy 6Al – 2Sn – 4Zr – 2Mo at 900 and 1100°F, the cobalt-base alloy L-605 (Haynes 25 alloy) at 1180°F, and for two hardness levels of 316 stainless steel at 1300°F. Such curves have been used successfully in a previous investigation for the evaluation and prediction of strain-cycling life at elevated temperatures within the creep range. The cyclic creep-rupture curve relates tensile stress and tensile time-to-rupture for strain-limited cyclic loading and has been found to be independent of the total strain range and the level of compressive stress employed in the cyclic creep-rupture tests. The cyclic creep-rupture curve was always found to be above and to the right of the conventional (constant load) monotonic creep-rupture curve by factors ranging from 2 to 10 in time-to-rupture. This factor tends to be greatest when the creep ductility is large. Cyclic creep acceleration was observed in every cyclic creep-rupture test conducted. The phenomenon was most pronounced at the highest stress levels and when the tensile and compressive stresses were completely reversed. In general, creep rates were found to be lower in compression than in tension for equal true stresses. The differences, however, were strongly material dependent. (auth)

53691 LOW STRAIN TENSILE BEHAVIOR OF U–7.5 WT. PCT Nb–2.5 WT. PCT Zr. Albright, C. (Sandia Labs., Albuquerque, N. M.); Stein, C. Met. Trans.; 3: No. 8, 2217-23(Aug 1972).

The stress-strain response of polycrystalline, γ-quenched U – 7.5 wt % Nb – 2.5 wt % Zr alloy was studied as a function of strain rate and compared to equilibrium stress-strain tests performed by allowing the strain to reach a maximum value at incrementally increasing stresses. Equilibrium stress-strain tests were also performed on prestressed samples. Sheet tensile specimens were held at various states of strain in an x-ray diffractometer to determine crystal structural changes during deformation. Prestressed tensile bars were sectioned and examined metallographically and with the x-ray diffractometer. Two linear regions were observed in the equilibrium stress-strain tests: a low stress region with a slope of 5.3 to 5.5 × 10^6 psi, and a region above 40,000 psi with a slope of 3.3 × 10^6 psi. Finite strain rates tended to increase both slopes. The diffractometer experiments yielded plots of lattice parameter vs strain which showed a shift from a bcc structure of the γ_S phase, to a bct structure of the γ_0 phase between 1 and 3% deformation. It is postulated that this is a thermoelastic martensite transformation. A semiempirical equation was developed which describes the equilibrium stress-strain behavior of this alloy in terms of a stress induced phase transformation. (auth)

53692 INTERNAL FRICTION PEAKS DUE TO NITROGEN IN Nb-Zr ALLOYS. Heulin, B.; Geschier, R.; Vercaemer, C. (Ecole Nationale Superieure de Chimie, Strasbourg). Mem. Sci. Rev. Met.; 69: No. 4, 309-14(Apr 1972). (In French).

The internal friction spectra of Nb – Zr – N alloys were determined as a function of the nitrogen contents for two zirconium concentrations: 2.0 and 3.8 at.%. Analysis of these spectra revealed the existence of two principal peaks at temperatures much higher than the temperature corresponding to the Snoek peak of nitrogen in pure niobium. The interpretation of these results suggests that one of these peaks results from the interaction between nitrogen atoms and zirconium atoms and the other from interactions between nitrogen atoms and the zirconium doublets. (France)

53693 CRYSTAL ORIENTATION AND THE HARDNESS OF ZIRCONIUM. Sayar, A.; Lehr, M. P. (CNRS, Vitry-sur-Seine, France). Metaux (Corros.-Ind.); 47: No. 560, 121-42(Apr 1972). (In French).

Large α Zr crystals were examined and the nature and orientation of their faces investigated. The Vickers hardness with a 300 g load varied between 85 and 150 kg/mm^2 and the Vickers microhardness with an 80 g load varied between 100 and 180 kg/mm^2. The Vickers hardness increases as the crystallographic faces approach the (0001) planes. It is shown how this hardness anisotropy is related to the relaxation of the mechanical stresses due to the plastic deformation of the metal around the deformation produced by the tool. Slip and twinning deformation mechanisms compete with one another. (France)

Radiation Effects

Refer also to abstracts 53317, 54972, 54989, 54990, 55008, 55010, 55011, 55189, and 55190.

53694 (JAERI-Memo–3936) STUDIES OF FISSION PRODUCT RELEASE IN TLG-1 IN-PILE GAS LOOP. 3. MEASUREMENT OF SHORT-LIVED GASEOUS FISSION PRODUCTS. Kitahara, T.; Shirai, E.; Kaieda, K.; Toyoshima, N.; Kumagai, K.; Yamada, T.; Gotoh, H.; Yagi, H. (Japan Atomic Energy Research Inst., Tokyo). Feb 1970. (In Japanese). NTIS (U. S. Sales Only).

Fission-product release from a sheet of U – Al foil has been studied using an in-pile gas loop, TLG-1 (JRR-2). Gamma-ray spectra of released fission products were measured with Ge(Li) detectors located at the inlet piping of the gas-purification system. Over 30 full-energy peaks were detected in the energy range of 0 ~ 1.8 MeV, including short-lived gaseous fission products: ^{89}Kr (0.220, 0.586 and 1.533 MeV), ^{90}Kr (0.125, 0.245, 0.540, 1.125, 1.542 and 1.778 MeV), ^{137}Xe (0.456 MeV), ^{138}Xe (0.260 and 0.436 MeV) and ^{139}Xe (0.177, 0.220 and 0.297 MeV). The fractional fission-gas release (the ratio of released activity/produced activity) was obtained for the various isotopes,and was found to be independent of the respective decay constants, indicating that fission gas release from the specimen was mainly due to direct recoil. (auth)

53695 (NASA-TM-X–2440, pp 570-6) DESIGN CONSIDERATIONS AND TEST FACILITIES FOR ACCELERATED RADIATION EFFECTS TESTING. Price, William E.; Miller, Charles G.; Parker, Richard H. (California Inst. of Tech., Pasadena). Jan 1972.

From Symposium on natural and manmade radiation in space; Las Vegas, Nev. (1 Mar 1971).

Test design parameters for accelerated dose rate radiation effects tests for spacecraft parts and subsystems used in long-term missions (years) are detailed. A facility for use in long-term accelerated and unaccelerated testing is described. (auth)

53696 (NASA-TM-X-2440, pp 595-602) IRRADIATION EFFECTS STUDIES OF NERVA MATERIALS. DeMastry, J. A.; Merrick, T. P. (Westinghouse Astronuclear Lab., Large, Pa.). Jan 1972.

From Symposium on natural and manmade radiation in space; Las Vegas, Nev. (1 Mar 1971).

Several materials, beryllium, CuB, BATH (Al-24 v/o TiH$_2$–6 v/o B$_4$C) and A-286, were irradiated at cryogenic temperatures to neutron fluences between 10^{17} and 10^{19} n/cm^2 ($E > 1.0$ MeV). Tensile properties were determined over a temperature range to evaluate the effects of irradiation on the material properties. The expected radiation damage typical of other materials was observed, a general increase in strength and decrease in ductility. The effects at LN$_2$ temperature (140°R) were more pronounced since radioinduced defects were not annealed out at 140°R. Decreases in both strength and ductility of beryllium were noted at 140°R. Mechanical strength was generally recovered at temperatures as low as 406°R for 10 minute anneals. Thermal conductivity in beryllium was decreased by almost a factor of six at 1×10^{19} n/cm^2 ($E > 1$ MeV). Both Cu 12 v/o B and Cu 24 v/o B exhibited increases in strength and decreases in elongation due to irradiation. BATH showed an increase in mechanical strength after irradiation and testing at 140°R. The A-286 alloy underwent decreased ultimate strength and increased yield strength under the conditions studied. These were no significant changes in elongation at the temperatures studied. Comparison of test data from different reactors and the statistical techniques employed in this program are also reviewed. (auth)

53697 (NASA-TM-X-2440, pp 603-8) EFFECT OF CRYOGENIC IRRADIATION ON NERVA STRUCTURAL ALLOYS. Dixon, C. E.; Davidson, M. J.; Funk, C. W. (General Dynamics, Fort Worth, Tex.). Jan 1972.

From Symposium on natural and manmade radiation in space; Las Vegas, Nev. (1 Mar 1971).

Several alloys (Hastelloy X, AISI 347, A-286 bolts, Inconel 718, Al 7039-T63, and Ti–5Al–2.5Sn ELI) were irradiated in liquid nitrogen (140°R) to neutron fluences between 10^{17} and 10^{19} nvt ($E > 1.0$ MeV). After irradiation, tensile properties were obtained in liquid nitrogen without permitting any warmup except for some specimens which were annealed at 540°R. The usual trend of radiation damage typical for materials irradiated at and above room temperature was observed, e.g., increase in strength and decrease in ductility. However, the damage at 140°R was greater because this temperature prevented the annealing of radioinduced defects which occur above 140°R. The results showed that the threshold for measurable mechanical property damage in these materials at 140°R was between 10^{16} and 10^{17} nvt ($E > 1.0$ MeV). Room temperature annealing of tensile properties was performed prior to testing some of the alloys. Al 7039-T63 recovered about half the damage incurred at the highest exposure while the other alloys recovered a smaller amount. Previous similar studies of Al 2219 showed almost complete recovery after annealing at room temperature. Aluminum components in the NERVA engine will be at temperatures above 140°R during its coast periods. Additional postradiation annealing studies are required to establish design properties after thermal cycling to various temperatures. (auth)

53698 (NRL-7446) EFFECT OF NEUTRON IRRADIATION ON FATIGUE CRACK PROPAGATION IN TYPES 304 AND 316 STAINLESS STEELS AT HIGH TEMPERATURE. Shahinian, P.; Watson, H. E.; Smith, H. H. (Naval Research Lab., Washington, D. C.). 8 May 1972. Contract AT(49-5)-2110. 18p.

The resistance of pre- and postirradiation AISI Types 304 and 316 stainless steels to fatigue crack propagation was determined at 800 and 1100°F (427 and 593°C) using the fracture mechanics approach. The effects of irradiation on the fatigue resistance of these steels were dependent upon test temperature and irradiation conditions. In general, irradiation degraded the fatigue resistance at 1100°F (593°C), but at 800°F (427°C) enhancement was also observed. In both steels irradiated in a thermal reactor to a neutron fluence of 1.8×10^{21} n/cm^2 for neutron energies >0.1 MeV, fatigue crack growth rates at 800°F (427°C) were lower than in the unirradiated steels for a given stress intensity factor range ΔK. However, at 1100°F (593°C) the effect was reversed and crack growth rates were higher in the irradiated steels. Irradiation in a fast reactor to a fluence of $\approx 1.2 \times 10^{22}$ n/cm$^2 > 0.1$ MeV caused fatigue crack growth rates at 800°F (427°C) to increase at low values of ΔK and decrease at high values of ΔK. At 1100°F (593°C) the crack growth rates in the irradiated steel were either the same as, or higher than, the unirradiated steel. The influence of irradiation on fatigue lives generally reflected the effects observed on crack growth rate. (auth)

53699 (RT/FI–(72)10) RADIATION DAMAGE IN SINTERED ALUMINA: AN E.P.R. STUDY. Galli, A. (Comitato Nazionale per l'Energia Nucleare, Rome (Italy)). 24 Mar 1972. 49p. Dep. NTIS (U. S. Sales Only).

The effects of γ and reactor irradiations on sintered alumina, as revealed by EPR spectra, were studied. The absorption lines can be divided into groups to be identified with as many paramagnetic centers. Further support was found for the different action of the neutrons and of the γ's. Saturation effects with doses are pointed out. The nature of the centers was analyzed in the light of results obtained in studies on α-Al$_2$O$_3$ monocrystals. Some particular interpretation is suggested, concerning the structure of the spectral lines and related inferences even in the field of optical absorption spectroscopy. Other possible effects are also mentioned. (auth)

53700 (SC-T–722540) X-RAY STUDY OF MOLYBDENUM AND NICKEL IRRADIATED WITH HELIUM IONS. Bykov, V. M.; Zdorovtseva, G. G.; Troyan, V. A.; Khaimovich, V. S. Translated for Sandia Labs., Albuquerque, N. Mex., from Ukr. Fiz. Zh. (Ukr. Ed.); 15: No. 1, 135-8(1970). 6p. Dep. NTIS.

Studies were made on the changes in the x-ray diffraction picture of polycrystalline molybdenum and nickel specimens caused by ion bombardment with 60-keV He$^+$ ions. The study revealed splitting of the Debye lines with reflection angles close to 90°, which may be associated with tetragonal distortion of the crystal lattice. This change in the form of the elementary cell may be due to ordering of the helium atoms in the metal lattice. On annealing these changes decreased, disappearing completely at a temperature of 400°C. (auth)

53701 (STU–70–419/U–350(Pt.1.1)) CHANGE OF STRUCTURE AND MECHANICAL PROPERTIES IN STAINLESS STEEL BY IRRADIATION. PART 1.1. METALLOGRAPHIC STUDY OF NEUTRON IRRADIATED AND UNIRRADIATED 12R72HV AFTER TENSILE TESTING. Lindhagen, P.; Westin, R.; Hellstrand, E. (Aktiebolaget Atomenergi, Studsvik (Sweden)). May 1971. 26p. (In Swedish). (AE-MF–204).

A metallographic study of neutron irradiated, as well as unirradiated, 12R72HV steel after tensile testing is described. Before testing, the steel has been resolving annealed at 1150°C as well as cold-worked to 15% and annealed at 830°C. It was shown that neutron irradiation lowers the ductility by tensile testing in the temperature range 500 to 800°C. Helium bubbles formed by plastic deformation prevented dislocation movements. It was established that there is only a slight grain deformation before crack. Comparison has been made with earlier observations after heat treatment at 1100°. The lowering of ductility according to irradiation is less in these earlier observations. This can be explained with smaller grain size, more favorable titanium carbide structure, and bigger helium bubbles. (Sweden)

53702 (TID–26150) DIFFUSIONAL GROWTH OF VOIDS INDUCED BY IRRADIATION AND STRESS. Wolfer, W. G. (Westinghouse Electric Corp., Madison, Pa. Advanced Reactor Div.). Dec 1971. Contract AT(11-1)-3045. 30p. Dep. NTIS.

An expression was derived for the growth rate of a spherical void in a metal subjected to irradiation and a triaxial stress system. The flow of vacancies and interstitials to the void was found to be affected by the stress field in two distinct ways. First, the diffusion coefficients for point defect migration were altered by the local hydrostatic stress. Second, and most important, the point defect concentrations in the vicinity of the void were changed. Although both mechanisms apply to interstitials and vacancies as well, only the vacancy flow to the void was considerably perturbed by the stresses. Thus, tensile stresses led to an enhanced void growth rate. It was found that this effect may substantially influence the radioinduced swelling in metals. (auth)

53703 EFFECT OF CREEP TEST TEMPERATURE ON CREEP RUPTURE PROPERTIES OF ALPHA-RAY IRRADIATED AISI 316 STAINLESS STEEL. Furuta, Teruo; Ogawa, Yutaka; Nagasaki, Ryukichi (Japan Atomic Energy Research Inst., Tokai). Tetsu To Hagane; 58: No. 8, 1117-25(Jul 1972). (In Japanese).

Since it is known that helium bubbles deteriorate the mechanical properties of stainless steel used as fuel cladding in fast-breeding reactors, the effect of helium was studied. Thin plate specimens of Type 316 stainless steel with helium content of 7.5×10^{-6} atom fraction that had been injected by α-ray irradiation from a cyclotron were creep-rupture tested at 550, 650 and 750°C. The presence of helium caused large reductions in rupture life and elongation as test temperature increased. The loss of ductility was shown to be constant at one test temperature. By observing fracture surfaces with optical and scanning electron microscope, the difference between the specimen with or without containing helium was clear, and it was shown that the embrittling effect of helium resulted from its tendency to concentrate at grain boundaries, leading to intergranular cracking. (auth) (Japan)

53704 APPLICATION OF FIELD–ION MICROSCOPY IN STUDIES OF POINT DEFECTS AND RADIATION DAMAGE. Ralph, B.; Hudson, J. A. (Cambridge Univ., Eng.). pp 67-85 of Applications of Field–Ion Microscopy in Physical Metallurgy and Corrosion. /Hochman, R. F. (ed.). Atlanta; Georgia Inst. of Tech. (1969).

From Conference on applications of field–ion microscopy in physical metallurgy and corrosion; Atlanta, GA. (15 May 1968). See CONF-680570.

An account of the application of field-ion microscopy to the investigation of point defects and their clusters induced by irradiation is presented. A detailed examination of current ideas concerning the expected contrast from defects is given together with possible difficulties associated with the introduction of artefact defects which tend to demote the statistical significance of the results. Developments in technique are summarized together with a discussion of recent studies. (J.R.D.)

53705 YIELD STRESS RADIATION DAMAGE FUNCTION OF IRON. Odette, G. R.; Ziebold, T. O. (Massachusetts Inst. of Tech., Cambridge). Nucl. Sci. Eng.; 49: No. 1, 72-81(Sep 1972).

An experiment was performed to measure the energy-dependent damage function for the neutron irradiation induced increase in the lower yield strength of iron. Small tensile test specimens were exposed at low temperatures (<100°C) to 10^{17} to 10^{18} n/cm^2 (E > 1 MeV) in seven reactor spectra while a high degree of consistency among all other variables known to be significant was maintained. The neutron flux spectra in all locations were measured using the multiple foil activation technique and the SAND-II code for the data analysis. The mechanical property and flux spectral data were then analyzed using SAND-II to unfold the damage functions. Estimates of errors induced in the solution by the iterative unfolding procedure were made considering possible contributions from both the lack of mathematical solution uniqueness and data error propagation. (auth)

53706 EFFECT OF ELECTRON RADIATION ON THE MECHANICAL PROPERTIES OF Fe–Cr AND Fe–Mo ALLOYS. Bystrov, L. N.; Zhukova, L. P.; Platov, Yu. M. Fiz. Khim. Obrab. Mater.; No. 1, 19-22(1972). (In Russian).

The mechanical properties of Fe-15 or 20% Cr, and Fe-5% Mo were studied after exposure to 2.3 MeV electrons over the temperature interval 20 to 200°C, and in a dose of from 1 to 4.5 × 10^{18} cm^{-2}. Irradiation of the Fe-Cr alloys caused a decrease in the tensile strength, an increase in the yield point, and a drop in the relative elongation to rupture. These effects are associated with a deposit of the σ-phase as a result of intensified radiation-diffusion. Irradiation of Fe-Mo lead to analogous changes in its mechanical properties as a result of the appearance of an ϵ-phase. (tr-auth)

53707 DOSE DEPENDENCE OF SWELLING IN IRRADIATED METALS. Fisher, S. B.; Williams, K. R. (Central Electricity Generating Board, Berkeley, Eng.). Radiat. Eff.; 14: No. 3-4, 165-70(Jun 1972).

The dose and dose rate dependences of swelling were determined theoretically for metals under different types of irradiation. The simple theory assumes that it is the preferential absorption of interstitials by climbing dislocations that is directly responsible for the swelling. In particular, the different dose dependences observed under ion, electron, and neutron irradiation are explained in terms of the dislocation configurations operative in each case. (auth)

53708 HIGH FLUX IRRADIATIONS IN THE HVEM. Fisher, S. B. (Central Electricity Generating Board, Berkeley, Eng.). Radiat. Eff.; 14: No. 3-4, 171-4(Jun 1972).

The Hitachi HU-1000 and AEI EM7 high-voltage microscopes were used for high-flux (~10^{-2} d/a) irradiation experiments on the Nimonic alloy PE16. The advantages and problems associated with the use of the HVEM at this flux level are discussed in detail and a comparison between the two machines in respect of this type of study is made. (auth)

53709 THERMAL RELEASE OF HELIUM INJECTED INTO NICKEL, STAINLESS STEELS, AND NIMONIC PE16. Whitmell, D. S.; Nelson, R. S. (Atomic Energy Research Establishment, Harwell, Eng.). Radiat. Eff.; 14: No. 3-4, 249-55(Jun 1972).

The release of helium from nickel, 316 and 18/8 stainless steels, and Nimonic PE 16 foils uniformly filled with helium to concentrations of the order of 10^{-5} atom/atom was measured during linear-rise anneals and compared with the release from nickel foils implanted with low-energy helium ions. Annealing peaks were observed and attributed to radiation damage annealing, helium diffusion to form gas bubble nuclei, and gas release by bubble migration. The fraction of helium released was found to be concentration dependent and to be much smaller from stainless steels than from nickel. This was attributed to increased trapping. The activation energy for diffusion of helium in nickel was found to be 2.50 eV. In nickel annealed at 600°C all of the helium was incorporated in bubbles, which were predicted to be approximately 20 Å diameter. It was concluded that voids formed by ion bombardment to high doses at elevated temperatures in helium-filled foils were nucleated on these bubbles. (auth)

53710 EFFECT OF RESIDUAL ELEMENTS ON RADIATION STRENGTHENING IN IRON ALLOYS, PRESSURE VESSEL STEELS, AND WELDS. Smidt, F. A. Jr.; Watson, H. E. (Naval Research Lab., Washington, D. C.). Met. Trans.; 3: No. 8, 2065-73 (Aug 1972).

Embrittlement of pressure vessel steels and welds during irradiation at service temperatures around 290°C is known to be related to the presence of residual elements such as copper but the mechanism of embrittlement has not been clear. Pressure vessel steels and welds with high and low copper content and binary iron alloys with 0.3 at. % of Cu, V, Ni, and P and 0.1 at. % C were irradiated to fluences of 2.5 × 10^{19} and 4.5 × 10^{20} n/cm^2 <1 MeV and compression tested to determine the radiation strengthening. Alloys containing copper had more rapid and greater radiation strengthening. It was concluded that the embrittlement is due to this radiation strengthening which in turn results from a higher density of defect aggregates. Vacancy trapping by the copper atoms which modifies the kinetics of defect aggregate nucleation was found to be the most likely cause for the differences in microstructure. (auth)

53711 RECRYSTALLIZATION OF α PARTICLE IRRADIATED TUNGSTEN. Stepper, Heinz-J. (Westinghouse Lamp Divisions, Bloomfield, N. J.). Met. Trans.; 3: No. 8, 2293-4(Aug 1972).

Heavily deformed, pure powder metallurgy W ribbons were irradiated with high-energy α particles in order to investigate whether bubbles introduced by this method would affect the recrystallized grain size and the recrystallization temperature. The results showed that helium bubbles precipitate in a narrow band after postirradiation annealing of α particle irradiated W ribbons. As a consequence, recrystallization was retarded and the recrystallization temperature of the band containing helium bubbles was increased from 1300°C to approximately 2100°C. The precipitation of helium bubbles gave rise to a recrystallized grain structure, very much like that in doped W, with the long dimension of the grains oriented parallel to the working direction. (P.C.H.)

53712 STUDY OF POINT DEFECT INDUCED IN Al BY QUENCH HARDENING AND ELECTRON BOMBARDMENT. Brugiere, R.; Lucasson, P. (Univ., Paris). Mem. Sci. Rev. Met.; 69: No. 4, 277-84(Apr 1972). (In French).

Zone refined Al was quenched from temperatures between 260 and 370 to −196°C, subjected to irradiation at −160°C with 1.6 MeV electrons, or subjected to quenching and subsequently irradiated. The curve representing the increase in resistivity as a function of the incident electron flux presents a plateau for samples quenched from a high temperature and subsequently irradiated. In addition, a correlation is observed between this anomaly in the curve and the production of defects as a function of the electron flux and shape of the annealing isochrones. These phenomena are interpreted in terms of the interaction between point defects and impurities and are discussed for the different models for stage III of the recovery in electrical resistivity of the irradiated metal. (France)

Other Materials

Refer also to abstracts 53061, 53090, 53317, 53569, 53570, 53651, 54049, and 54991.

53713 (CEA-CONF-1894) IN PILE RADIATION DAMAGE IN GRAPHITE. CORRELATION BETWEEN TEMPERATURE AND FLUX DENSITY IN THE RANGE OF HIGH TEMPERATURE. Genthon, J. P.; Micaud, G. (Commissariat a l'Energie Atomique, Saclay (France). Centre d'Etudes Nucleaires). 1972. 3p. (In French). (CONF-720609-4). Dep. NTIS (U. S. Sales Only).

From International carbon conference; Baden-Baden, Germany (26 Jun 1972).

A series of in pile irradiation experiments with graphite confirm and define a model; this model is defined by a displacement zone structure of elementary defects induced by one neutron collision. It was concluded that monovacancies were not present but the existence (possibly among others) of a defect of activation energy Q = 4 eV (which may be a divacancy) was confirmed. This value Q = 4 eV is suggested for the classic adjustment of equivalent temperature in the interval 600 to 1400°C. (auth)

53714 (NAA-SR-8533) STABILITY OF A LIGHT METAL HYDRIDE. Vetrano, J. B. (Atomics International, Canoga Park, Calif.). 1 Aug 1963. Contract AT-11-1-Gen-8. 25p. Dep. NTIS.

Declassified 25 Oct 1971.

The potential weight saving that could be made by using a certain light metal hydride as a neutron shield in a nuclear space-power system stimulated an investigation of its thermal stability. After an induction period, the compound was found to decompose irreversibly. The induction period was sufficiently short, and the decomposition sufficiently rapid, at 250°C, to make the material unsuitable for the intended application. The kinetics of the decomposition fit a second order autocatalytic rate expression. An x-ray diffraction analysis, a displacement density analysis, and a petrographic analysis were performed on the starting material. (auth)

53715 (NASA-TM-X-2440, pp 476-80) THERMODYNAMIC AND TRANSPORT PROPERTIES OF FROZEN AND REACTING pH_2–oH_2 MIXTURES. Carter, H. G.; Bullock, R. E. (General Dynamics Corp., Fort Worth, Tex.). Jan 1972.

From Symposium on natural and manmade radiation in space; Las Vegas, Nev. (1 Mar 1971).

Application of experimental state data and spectroscopic term values shows that the thermodynamic and transport properties of reacting parahydrogen-orthohydrogen (pH_2-oH_2) mixtures are considerably different than those of chemically frozen pH_2 at temperatures below 300°R. Such differences will be significant from the standpoint of nuclear rocket design if it turns out that para- to orthohydrogen conversion can be catalyzed by radiation in the cold dense phase. Calculated H-S data also showed that radioinduced pH_2-oH_2 equilibration at constant enthalpy can produce a temperature drop of at least 28°R, corresponding to an ideal shaft work loss of 15% or more for a turbine operating downstream from the point of conversion. Aside from differences in thermodynamic and transport properties, frozen pH_2-oH_2 mixtures may differ from pure pH_2 on a purely hydrodynamical basis. (auth)

53716 POLYMERIZATION OF ADHESIVES UTILIZING HIGH-ENERGY RADIATION. Allen, James D. (North American Rockwell Corp., Tulsa, Okla.). pp IB.2.1-14 of Materials Review for '72. Azusa, Calif.; Society of Aerospace Material and Process Engineers (1972).

From seventeenth National SAMPE symposium and exhibit; Los Angeles, CA. (11 Apr 1972). See CONF-720437.

The results from a research and development investigation into the use of penetrating high-energy radiation for the rapid ambient temperature curing of adhesives are described. Utilization of cobalt-60 gamma rays and accelerated electrons, electron beams, to cure specially formulated radiation sensitive adhesive materials is described. Lap-shear adhesive strengths obtained on 2024T3 aluminum using cobalt-60 gamma rays and accelerated electrons for cure are reported. Variables such as the exposure, or dosage, required for cure are discussed as well as the room and elevated temperature adhesive strengths obtainable via radiation curing. Also described is the fabrication of flat aluminum sandwich panels using cobalt-60 and/or accelerated electrons to cure the adhesive layers. Methods of panel preparation, exposure times, and exposure rates are given. Flat panel production rates possible with the electron beams are discussed. Mechanical properties of some of the bonded aluminum sandwich panels, i.e., flatwise tensile and climbing drum peel have been determined and are reported. (auth)

53717 INTERPRETATION OF RADIATION EFFECTS ON MECHANICAL PROPERTIES OF CARBON FIBERS BASED ON A SHEATH AND CORE MODEL OF FIBER STRUCTURE. Bullock, R. E. (General Dynamics, Fort Worth, Tex.). J. Mater. Sci.; 7: No. 8, 964-7(Aug 1972).

Fast neutron irradiation in air has a considerable effect on the strength of HTS (high strength) carbon fiber and on the modulus for both HTS and HMS (high modulus) fibers, but very little effect on the strength of HMS fiber. The properties that are affected behave similarly, first rising with neutron fluence and then decreasing. Irradiations were also carried out in liquid nitrogen. An interpretation of the effects (and an explanation for the differences between HTS and HMS fibers) is proposed, based on a previously suggested "sheath" and "core" structure for the fiber. (UK)

53718 CHEMICAL REACTION RATE UNDER THE INFLUENCE OF A HIGH-ENERGY ELECTRON BEAM. Smiyan, O. D. Fiz. Khim. Obrab. Mater.; No. 1, 163(1972). (In Russian).

The catalytic effect of a high-energy electron beam on certain chemical reactions is discussed, e.g., the time of formation of CH^+ from C + H as a function of the energy of the bombarding electrons (from 30 to 45 keV). At 45 keV the formation of CH is practically instantaneous. (K.S.W.)

53719 ALKALINE HALIDES IN THE CARRIER DISTILLATION PROCESS IN U_3O_8 MATRIX. THERMOCHEMICAL REACTIONS HYPOTHESIS IN THE EVAPORATION MECHANISM. Boniforti, R.; Ciancia, A.; Di Giorgio, G. (Comitato Nazionale per l'Energia Nucleare, Casaccia, Italy). Spectrochim. Acta, Part B; 27: No. 7, 309-21(Jul 1972).

The action mechanism of the alkaline halides in the carrier distillation process was studied. From the temperature data in the anodic charge it was concluded that the alkaline carriers were melted, and a solvent action of the carrier salt on the oxide impurities contained in the U_3O_8 matrix was postulated. The possibility of some thermochemical reactions in the anodic cup was evaluated; the reaction products, formed during arcing, were identified by x-ray diffraction analysis. The x-ray diffraction data and the thermodynamic calculations generally are in rather good agreement. (auth)

53720 STUDY ON THE EFFECTS OF RADIATION ON THE MOLDING OF POLYMERS. Kimura, Hiroshi; Yamaguchi, Takuzi; Imachi, Masaki (Fukui Univ., Japan). Fukui Daigaku Kogakubu Kenkyu Hokoku; 19: No. 1, 45-51(Mar 1971).

An empirical study is presented of the effects of a ^{60}Co gamma radiation on molding of polyethylene with respect to cross-linking, where different irradiation conditions are employed. Results obtained were: (1) the elongation of molded materials decreases and becomes brittle with an increase of the quantity of radioactivity; (2) a rapid change of fluidity and molding can be found between 1×10^7 R and 5×10^7 R; (3) the quantity of radioactivity has a relatively slight effect on strength; (4) with an increase in the irradiation temperature, fluidity and molding decrease; (5) the effects of high-temperature irradiation is, if in water, much greater; and (6) it is possible to mold F.R.T.P.'s from the irradiated polyethylene that have great strength. (auth) (Japan)

53721 MELTING POINT DIAGRAMS FOR THE $LiCl-UCl_3-UCl_4$ SYSTEM. Desyatnik, V. N.; Kurbatov, N. N.; Raspopin, S. P.; Trifonov, I. I. At. Energ. (USSR); 32: No. 6, 479-80(Jun 1972). (In Russian).

The melting point behavior of the binary and ternary systems containing LiCl, UCl_3, and UCl_4 was studied. Two eutectics in the $LiCl-UCl_4$ system were detected at 31 and 44 mole% UCl_4 as well as the congruently-melting compound $2LiCl \cdot UCl_4$. A solid solution UCl_4-UCl_3, and eutectics corresponding to LiCl–40 mole% UCl_4–10 mole% UCl_3 and LiCl–19 mole% UCl_4–13 mole% UCl_3 were found. (K.S.W.)

53722 PROGRESS IN APPLICATION OF RADIATION TO THE CHEMICAL INDUSTRY. APPLICATION TO NEW COMPOSITE MATERIALS. Machi, Sueo (Japan Atomic Energy Research Inst., Takasaki). Sekiyu To Sekiyu Kagaku; 15: No. 8, 73-8(Jul 1971). (In Japanese).

The application of radiation to concrete-polymer composite materials, wood-plastic composite materials, glass fiber-reinforced plastics, and metal-plastic composite materials is reviewed. When composite materials are produced from several materials by reactions in a matrix after addition of reactive substances to the known matrix substances, radioactive processes are useful for such purposes as suppression of evaporation loss of low molecular weight substances and of strain that takes place at high temperatures, induction of uniform reactions in solid materials when γ rays are used, elimination of processes for addition and removal of catalysts, and attainment of high production rates by induction of reactions with electron accelerators in case of thin composite materials. Explanations are given on the change of various properties of composite materials by the irradiation. (Japan)

NUCLEAR MATERIALS AND WASTE MANAGEMENT

Accountability and Safeguards

Refer also to abstract 53306.

53723 DEVELOPMENT OF ON-LINE AUTOMATIC WEIGHING AND RECORDING SYSTEM FOR NUCLEAR FUEL MATERIAL. Kakimoto, Jiro (Furukawa Electric Co. Ltd., Tokyo). FAPIG (Tokyo): No. 63, 166-8(Nov 1971). (In Japanese).

A reliable automatic weighing and recording system was developed to control nuclear fuel material by weighing it in processing facilities. Inspection by official organizations required that the reliability of controlled data at main points of process lines is supported by physical measurements. The system was applied to the stack assembling process in a UO_2 pellet processing facility because this process gave the last chance to directly weigh the UO_2 quantity in the pellet processing line. The system consists of a continuous pellet transfer mechanism, a device for measuring length and weight, an operational and controlling means, and a recorder. Continuous operation was tested by circulating test pellets for about 250 h. A check of accuracy was carried out with standard sample every 50 h, and sufficient reliability was obtained to three significant digits. (Japan)

Disposal and Storage

Refer also to abstracts 53063, 53157, and 53261.

53724 (ORNL-TM-3815) PROPERTIES OF DRY CRUSHED SALT AND RELATED CONSOLIDATED MEDIA WITH EMPHASIS ON THEIR GAS TRANSPORT CHARACTERISTICS. Evans III, R. B.; Rutherford, J. L.; Truitt, J. (Oak Ridge National Lab., Tenn.). Sep 1972. Contract W-7405-eng-26. 123p. Dep. NTIS.

The gas-flow properties in dry and moist crushed salt beds were characterized. This study is related to the burial of packages of solidified radioactive waste, which generate heat, in salt mines using crushed salt as a back-fill material. Brine in bedded salt moves toward hot regions, releases water vapor, aids in waste package deterioration (possibly followed by activity release), and alters the back-fill properties. The first task was to determine whether dry back-fill would inhibit the flow of gases and aerosols of the type that might be released from a defective package. Experimental results, coupled with other considerations, indicate that unconsolidated salt does not constitute an effective barrier to gas-borne contaminants, even if their transport were diffusion controlled. No consideration was given to the filtering properties of the back-fill, however, and this may significantly inhibit aerosol transport. Next, the work was extended to the water vapor-air system using salt beds of fixed composition. Two experiments involved imposition of time-constant temperature profiles on the beds. Flow mechanisms were varied, but the results were identical with the exception of the time required to form a weak seal or bridge. The bridge resided at a position (temperature) determined by the source potential. Retention of 5g $H_2O(1)/in.^2$ bed cross section signals bridge formation. During moisture accumulation, brine-water reflux causes localized bridge formation through evaporative porosity reduction, and sacrificial void formation above the bridge. When temperatures were increased with time, the entire moisture region was forced up the bed, leaving dried out bridges and voids behind. The interval of dry consolidation was markedly increased. Effects of compressive forces, present in mines, were not included. Only in situ mine experiments will reveal true back-fill behavior. (auth)

53725 (ORNL-TM-3903) IMPLICATIONS OF THE AMERICAN SALT CORPORATION'S UNDERGROUND WORKINGS ON THE PROPOSED FEDERAL WASTE REPOSITORY AT LYONS, KANSAS. Lomenick, T. F. (Oak Ridge National Lab., Tenn.). Aug 1972. Contract W-7405-eng-26. 36p. Dep. NTIS.

A study of excavations in the rock salt deposit in the vicinity of Lyons, Kansas, where a site, which includes the abandoned Carey Salt Mine, has been considered for the location of a proposed Federal Repository for radioactive wastes. The effects of the nearby American Salt Corporation's workings on the development of this site were determined, with no insurmountable problems being observed. These excavations were considered to be an asset to the project, since they provide a nearby repository for the several million tons of unsalable salt that would be generated as a result of mining activities associated with the proposed repository. (T.D.)

53726 CREATION OF A COMMUNITY SYSTEM OF RADIOACTIVE WASTE DUMPS. Grison, Gaston. Euro-Spectra; 10: No. 3, 91-4(Sep 1971).

Forecasts of solid radioactive waste accumulations in Europe through the year 2000 are made. The importance of developing community storage sites for these wastes is discussed. These sites could be better supervised at a lower cost and would be in safer locations than would be possible if they were in individual countries. In some instances the distance that wastes would have to be transported would be shorter. In addition, some countries might not have suitable sites for waste repositories. (T.D.)

Handling Equipment and Procedures

Refer also to abstract 53735.

53727 (ANL/HFEF-1) CONCEPTUAL DESIGN FOR THE HANDLING AND REMOTE DISASSEMBLY OF THE FUEL ELEMENT FAILURE PROPAGATION LOOP AT THE HFEF. Hagmann, D. B.; Chilenskas, A. A. (Argonne National Lab., Ill. Argonne National Lab., Idaho Falls, Idaho). May 1972. Contract W-31-109-eng-38. 117p. Dep. NTIS.

The Hot Fuel Examination Facility (HFEF) was assigned the remote disassembly and examination of the Fuel Element Failure Propagation (FEFP) loops. These loops, containing bundles of fast-reactor fuel elements, will be irradiated in the Engineering Test Reactor to obtain information on failure propagation in this type of fuel. A detailed preliminary plan and procedure have been developed by the HFEF staff for handling, disassembling, and examining the irradiated loops. The concepts developed meet the functional criteria established by the FEFP Project in the System Design Description. The disassembly and examination will be performed in the HFEF/N main cell, which is large enough to accommodate a loop in the vertical position. The equipment to be added to HFEF/N for the handling of the FEFP loop will include a loop-insertion cell, support structures for the loop and test train, a tube heater, several cutting machines, and many disassembly and examination fixtures. (auth)

53728 (JAERI-Memo-4009) POST-IRRADIATION EXAMINATION FACILITY FOR Pu-FUELS. (Japan Atomic Energy Research Inst., Tokyo). May 1970. (In Japanese). NTIS (U. S. Sales Only).

The first post-irradiation examination facility of Japan, designed for metallurgical examination of plutonium bearing fuels, has been constructed in a hot laboratory. This cell is located in the extension line of the metallurgical testing cells for uranium fuels. It consists of γ shielding of 150 mm thick lead and a stainless steel alpha containment box which is of sturdy construction. A pair of master-slave manipulators with double-sleeve alpha sealing and a ball-socket manipulator are installed over the alpha box and on the front respectively. Radioactive specimens and other items are loaded into the alpha-box through the pass-in port, where radiation-resistant neoprene rings are fitted on the inner surface. An aluminum can is fixed tightly in it to maintain the airtightness of the alpha box. Main in-cell equipment consists of a NaK capsule opener, a diamond wheel cutting machine, an optical microscope, two mechanical polishers and a length-measurement apparatus. Each of the in-cell items is of comparatively simple construction for facilitating decontamination. Radioactive wastes originating within the alpha box are removed after being sealed in a p.v.c. bag through the pass-out port. Electrodes of a high-frequency heat-sealing apparatus and p.v.c. bag-isolating device are placed under the pass-out port. The operating philosophy and shielding do not permit the penetrating radiation dose rate to exceed 2 mR/h at the outer surface of cell wall. Under these conditions, irradiated nuclear fuels up to a level of 500 Ci are safely handled. Unnecessary flammable materials are excluded from the cell to keep the risk of fire to a minimum. Reaction of alcohol with NaK is carried out in a nitrogen atmosphere while the air intake is closed with a damper. Decontamination of in-cell equipment for repair or maintenance is performed in a separate glove box. (auth)

53729 (LA-DC-72-230) SAMPLE PREPARATION AND EQUIPMENT PROBLEMS ASSOCIATED WITH RE-CYCLED, PURIFIED ATMOSPHERES. Bender, John H. (Los Alamos Scientific Lab., N. Mex.). [nd]. 5p. (CONF-720911-1). Dep. NTIS.

From International Metallographic Society meeting; Denver, CO. (21 Sep 1972).

Sample preparation for metallography in hot cells equipped with a system to remove water and oxygen from re-cycled argon requires extreme care in the choice of lubricants and cleansing solvents. This care is necessary to prevent chemical reactions with the purification "bed" that produce by-products which attack the plumbing of the system. Etching solutions are also incompatible with purification systems but minimal amounts and quick disposal prevent serious attack. Polishers and grinders equipped with carbon brushes require changing to resin-bonded graphite/molybdenum disulfide brushes and ultrasonic cleaners have shown the need for high quality components in the generator circuitry. (auth)

53730 (NASA-TM-X-2440, pp 277-9) TELEOPERATORS FOR REMOTE OPERATIONS IN SPACE. Little, L. E.; DiLorenzo, F. L. (Aerojet Nuclear Systems Co., Sacramento, Calif.). Jan 1972.

From Symposium on natural and manmade radiation in space; Las Vegas, Nev. (1 Mar 1971).

The primary objective of the remote nuclear teleoperator study program was to define in detail a program plan which would provide a qualified operational space teleoperator system by about 1980. The concept and philosophy presented provides a product considered to be an advanced teleoperator when compared to today's state-of-the-art. Previous studies have shown that an operational space teleoperator could be developed in two to three years, but such a teleoperator would contain today's technology and be considerably restricted in its capabilities. The teleoperator concept was formulated to meet NERVA requirements. This concept is considered preliminary, permitting flexibility during the development period and the time at which the total integrated space program is being defined. Considerable effort can be expended in the areas of subsystem development (e.g., actuators, sensors, communications, and controls) assuring a program of developed basic subsystems prior to final concept selection. The areas of propulsion, attitude control, and logistics can follow. The conclusions reached are discussed. (auth)

53731 (NASA-TM-X-2440, pp 280-90) TELEOPERATOR SYSTEMS FOR MANNED SPACE MISSIONS. Interian, Alfred. Jan 1972.

From Symposium on natural and manmade radiation in space; Las Vegas, Nev. (1 Mar 1971).

Space teleoperator system applications in the Space Station/Space Shuttle Program, which is where the most immediate need exists and the potential return is greatest, are discussed. (P.C.H.)

53732 (WCAP-1615) SHOCK LOADING ANALYSIS OF CORE SUBASSEMBLY: APDA CORE. Schramm, R.; Widmer, T. F. (Westinghouse Electric Corp., Pittsburgh, Pa. Atomic Power Dept.). Aug 1960. 26p. Dep. NTIS.

Values of bending stress and deflections are presented which are based on the maximum acceleration recorded in the shipping container drop tests, i.e., 24 G's. The sub-assembly wrapper tube, under impact, deflects 0.307 in. at the center and is subjected to 34,560 psi bending stress in the outer fibers. The fuel pins in an 11-grid core assembly are deflected a maximum of 0.006 in. with respect to the support grids. This deflection is a composite of pin deflection and grid tab deflection. The maximum bending stress in the pins is 2828 psi. Under impact, the support grid tabs are deflected 0.0033 in. for an 11-grid type "A" assembly. Data on deflections for other grid arrangements are included. The impact load on the most critical grid structural parts is 6% of the allowable load before buckling and develops 2310 psi stress at this cross-section. (auth)

53733 (WCAP-2999) CRITICALITY CONTROL PARAMETERS AND SUPPORTING CALCULATIONS FOR URANIUM BEARING NUCLEAR FUEL AT LOW ENRICHMENT. Lacey, P. G. (Westinghouse Electric Corp., Pittsburgh, Pa. Atomic Power Div.). Oct 1966. 88p.

Criticality control parameters applicable for safe handling of uranium bearing fuel in the form of powders, pellets, and rods for U-235 enrichments of 6.0 w/o or less are presented. Major emphasis is given to the oxide fuel form typical of that to be processed in the Westinghouse Core Manufacturing facility. Experimental data are used to validate the calculational procedures for critical systems, and the basis for presenting the safe parameters is discussed. (auth)

53734 MANIPULATORS: A SURVEY. Newman, N.; Tait, K. E. (Univ. of New South Wales, Kensington, Australia). Elec. Eng. Trans., Inst. Eng., Aust.; EE-8: No. 1, 1-8(Apr 1972).

An outline of some applications of manipulators is given together with an appreciation of developments in the areas of augmentative, facilitative, hostile environment, prosthetic and orthotic manipulators. Indications are given of possible extensions for the use of manipulators when technology permits the production of more versatile economic devices. (auth)

Transportation

53735 (ORO-651(Rev.3)) URANIUM HEXAFLUORIDE: HANDLING PROCEDURES AND CONTAINER CRITERIA. (Oak Ridge Operations Office (AEC), Tenn.). Aug 1972. 75p. Dep. NTIS.

Revised handling procedures and container design and utilization criteria are presented for transactions involving the receipt or shipment of UF_6 by AEC. Topics covered are UF_6 weighing, sampling, cylinder emptying and filling, and cylinder inspection, cleaning, testing, and repair. Analytical and shipping procedures are discussed in general terms. Standard cylinder information, UF_6 properties, and safety considerations are presented as appendixes. (T.D.)

53736 (SC-DR-720597) SPECIAL TESTS FOR PLUTONIUM SHIPPING CONTAINERS 6M, SP5795, AND L-10. Stravasnik, L. F. (Sandia Labs., Albuquerque, N. Mex.). Sep 1972. 72p. Dep. NTIS.

The results of three extra-severe environments imposed on three plutonium shipping containers are summarized. (auth)

53737 STEEL-BANDED WOODEN SHIPPING CONTAINERS (29 Feb 1972) (Engineering Materials). (National Lead Co. of Ohio, Cincinnati). (CAPE-2259).

10 drawings.

A steel-banded wooden shipping container is described. The container has been approved by the AEC and the Department of Transportation for Fissile Class III shipments of uranium metal billets, ingots, and fuel cores, slightly enriched in ^{235}U. Two general types of wooden containers are used; boxes with lids, which are used primarily for fuel cores and pallets with covers used for billets and ingots. There is no chemical, galvanic, or other reaction between the U metal and wood but when pieces with a machined surface are shipped an Al foil liner is used to protect the surface. The containers are shipped in a closed, exclusive use trailer or railcar with a tamper-proof seal attached. (For details see TID-4100 Suppl. 72). (F.S.)

PARTICLE ACCELERATORS

Design, Development, and Operation

Refer also to abstract 53755.

53738 (FOA-4-4490-A-3) GAMMA RADIATION DOSE RATE IN THE SURROUNDINGS OF THE ELECTRON ACCELERATOR FX-45 AT URSVIK. Lefvert, Tomas; Persson, Marjorie (Forsvarets Forskningsanstalt, Stockholm (Sweden)). Apr 1972. 13p. (In Swedish). Dep. NTIS (U. S. Sales Only).

In order to investigate the possibilities of running the electron accelerator FX-45 at Ursvik with increased current, the gamma radiation dose rate in the surroundings of the accelerator has been calculated using a Monte-Carlo method. (Sweden)

53739 (LA-4874, pp 16-20) STATUS OF LAMPF. Rosen, Louis (Los Alamos Scientific Lab., N. Mex.). Mar 1972.

From fifth LAMPF users meeting; Los Alamos, NM. (8 Nov 1971).

Topics include the importance of LAMPF in the national and international scientific enterprise; construction progress on buildings, site, and services; accelerator construction status; R&D budgets and their implications; and user participation. (W.H.K.)

53740 (LA-4874, pp 21-33) WILL MEDIUM ENERGY PHYSICS FLY OR DIE? Kolstad, George A. (Division of Research (AEC), Washington, D. C.). Mar 1972.

From fifth LAMPF users meeting; Los Alamos, NM. (8 Nov 1971).

The cultural, economic and social, and educational or structural reasons for the support of medium energy physics research are discussed. Also, medium energy physics research history and funding are discussed. Sources of funding including government-wide funding levels and AEC funding are outlined. (W.H.K.)

53741 (NP-19416) ANNUAL REPORT, 1971. Brearley, N. (ed.) (TRI-Univ. Meson Facility, Vancouver (British Columbia)). May 1972. 58p. Dep. NTIS (U. S. Sales Only).

The cyclotron erection; construction; cyclotron design and engineering; safety, shielding, and activation; central region cyclotron model, project management and scheduling; and the experimental program are discussed. Also, reports from users groups, organizations and committees, conferences, reports and publications, staff, and a financial statement are given. (W.H.K.)

53742 STRAHLENSCHUTZ AN HOCHENERGIEBESCHLEUNIGERN. (Radiation Protection at High-Energy Accelerators). Freytag, Eberhard. Karlsruhe, Ger.; G. Braun (1972). 127p.

Topics include high-energy acceleration, interactions of particles with matter, interactions of photons with matter, hadron cascades, electron-photon cascade, dose and dose equivalents, survey instruments for radiation protection at high-energy accelerators, shielding, activation, radiation damage in accelerator materials, dead-man's-handle, and space travel. (W.H.K.)

53743 EFFECT OF THE MAGNETIC FIELD ON A CLOSED-ELECTRON-DRIFT ACCELERATOR. Morozov, A. I.; Esipchuk, Yu. V.; Kapulkin, A. M.; Nevrovskii, V. A.; Smirnov, V. A. Sov. Phys.-Tech. Phys. (Engl. Transl.); 17: No. 3, 482-7(Sep 1972).

Translated from Zh. Tekh. Fiz.; 42: No. 3, 612-19(Mar 1972).

Measurements were made to elucidate the effect of the magnetic field configuration in the coaxial channel on the volt-amp characteristics and variation of the potential in the system. It was found that the discharge condition in the accelerator and the nature of the oscillations in the potential depend on the variation in the radial component of the magnetic field along the channel. In a magnetic field with a negative gradient, a strong azimuthal wave $m = 1$ is excited, and the electron current through the system increases several times. (6 figures) (R.W.R.)

53744 FIELD DISTRIBUTION, POWER LOSSES, AND PARAMETER OPTIMIZATION OF HELICAL ACCELERATOR STRUCTURES. Klein, H.; Merz, N.; Siart, O. (Univ., Frankfurt am Main). Particle Accel.; 3: No. 4, 235-44(Aug 1972).

A method for the parameter optimization of a helix accelerator providing minimum total power losses is given. Approximate calculations of surface charge and current distribution on helical waveguides and their application to the problem of power losses and maximum field strengths are reported. Perturbation measurements of axial and surface fields in helix resonators were made and compared with theoretical results. (10 figures, 2 tables) (auth)

53745 CERN PROTON SYNCHROTRON PROJECT (40 METERS UNDERGROUND). Anthoine, Roger (CERN, Geneva). Rev. Fr. Elec.; 45: No. 236, 43-7(1972). (In French).

The underground proton synchrotron envisaged by CERN, and due to be completed in 8 years time, is presented. The essential elements of the accelerator are described: the quasi-circular ring, which forms the vacuum enclosure in which the particles are accelerated, the accelerating equipment, the electromagnet which guides the particles in the evacuated enclosure, the cooling system, the computerized control system, and the experimental areas. (France)

Auxiliaries and Components

Refer also to abstract 53258.

53746 (RISO-M-1518) IMPROVING THE MATCH BETWEEN THE MICROWAVE SOURCE AND THE MICROWAVE TRANSMISSION SYSTEM AT THE RISOE 10 MeV ELECTRON LINEAR ACCELERATOR. Fenger, Joergen; Hansen, Johnny (Danish Atomic Energy Commission, Risoe. Research Establishment). Jul 1972. 31p. Dep. NTIS (U. S. Sales Only).

To achieve tolerable load conditions for the high-power microwave source at the 10 MeV linear accelerator, comprehensive measurements of various parameters in the accelerator tubes and the waveguide system were carried out. Based on the measurements a modification of the parameter-defining linac components has improved the present performance and caused a higher overall efficiency. (auth)

53747 (SC-DR-720447) FEASIBILITY OF USING THE FARADAY EFFECT TO MEASURE CURRENTS IN THE ELECTRON BEAM ENVIRONMENT. McArthur, David A. (Sandia Labs., Albuquerque, N. Mex.). Aug 1972. 42p. Dep. NTIS.

Optical analogues of the integrating $\partial B/\partial t$ probe and the integrating Rogowski coil have been successfully developed for use in the environment of the intense relativistic electron beam. Under normal operating conditions these optical current monitors do not require an almost-closed electrostatic shield, and no signal cables are connected to the machine; therefore, this type of current monitor should be free from much of the noise and ringing which is seen on some current monitors used with electron beam machines. The experimental techniques used, comparison between the signals from the optical monitor and an integrating Rogowski coil, comparison between theory and experiment for the optical monitor sensitivity, and elimination of some spurious effects which were observed are described. The response time of the present optical system is limited by the photomultiplier to $\tau = 5$ nsec, but this can probably be decreased to $\tau \lesssim 1$ nsec, by using a better photomultiplier. (auth)

53748 SURFACE CONDITION OF NIOBIUM FOR SUPERCONDUCTING RF CAVITIES. Strongin, M. (Brookhaven National Lab., Upton, N. Y.); Farrell, H. H.; Halama, H. J.; (and others). Particle Accel.; 3: No. 4, 209-23(Aug 1972).

In recent years superconducting rf cavities with extremely small losses have become important for linear electron accelerators and rf beam separators. Niobium appears to be the most favorable metal for these devices; however, the rf field at which "breakdown" to the normal state occurs is much lower than expected, and it is probable that this effect is related to the surface condition of the niobium. Previous work in this area is reviewed, and additional measurements are presented. Low-energy electron diffraction measurements of surface oxides were made, and Auger spectroscopy was used to study the amount of surface impurities. The Auger results show that, upon cooling niobium from high-temperature treatments, significant amounts of oxygen migrate to the surface. A simple calculation was made for how surface impurities can influence the value of the "breakdown" fields, and some ways of protecting the niobium surface with high-T_c superconductors are also discussed. (9 figures, 6 tables) (auth)

53749 DESIGN OF THE CYCLOTRON MAGNET FOR TRIUMF. Kiesners, U. (Dilworth, Secord, Meagher, and Associates, Ltd., Toronto). Eng. J. (Montreal); 55: No. 6, 18-24(Jun 1972).

The TRIUMF H^- Cyclotron will produce intense beams of mesons and protons having a maximum energy of 500 MeV at maximum beam current 100 μA. To do this requires a very large magnet, consisting of six spiral sectors, whose combined size will be approximately 850 inches diameter and the total weight of over 4,000 tons. The magnet profile was determined from twentieth-scale-model studies. The mechanical design involved investigations of material availability, effect of chemical composition and micro structure on magnetic properties, limitations of Canadian manufacturing capabilities, transportation and handling capacities. Alternative concepts were compared and evaluated on performance, cost, and overall cyclotron arrangement. Davie Shipbuilding was awarded the construction contract from five Canadian bidders. Three-inch plates were supplied by STELCO; and heavier plates, by Lukens Steel Co. The cost of material, construction, and shop assembly was over $3,000,000. (auth)

53750 TESTS ON SUPERCONDUCTING HELIX RESONATORS. Benaroya, R.; Jaffey, A. H.; Johnson, K.; (and others) (Argonne National Lab., Ill.). Appl. Phys. Lett.; 21: No. 5, 235-6(1 Sep 1972).

A niobium helix-resonator cavity close to the frequency suitable for a heavy-ion accelerator was subject to an 8-week test, including 323 h at full power (axial electric field $E_{ax} > 2.5$ MV/m). The cavity, with an anodically deposited protective film of Nb_2O_5, had a high Q and supported high fields without deterioration over the whole period during which it was subject to a moderate internally generated x-ray dose. Properties were found to be stable against considerable thermal cycling and exposure to air. Measurement of emitted x-ray maximum energy allowed an independent corroboration of the field measurement calibration. (auth)

Ion Sources, Injection, and Extraction

Refer also to abstract 54976.

53751 (BNL-tr-498) POWER SUPPLY SYSTEM FOR THE PREINJECTOR OF THE I-100 LINEAR ACCELERATOR. Mal'tsev, I. G. (Gosudarstvennyi Komitet po Ispol'zovaniyu Atomnoi Energii SSSR, Serpukhov. Institut Fiziki Vysokikh Energii). Translated by S. J. Amoretty (Brookhaven National Lab., Upton, N. Y.), from report IFVE-71-83. 11p. Dep. NTIS.

The semiconductor power supply system for a duoplasmatron-type ion source with pulsed admission of gas, which works in conjunction with the preinjector of the I-100 linac, is described. (W.H.K.)

53752 (FRNC-CONF-54) PRODUCTION OF Ca AND Ge IONS IN A PIG SOURCE. Malard, M.; Steinegger, A. (Paris Univ., Orsay (France). Institut de Physique Nucleaire). 1972. 5p. (In French). (CONF-720120-11). Dep. NTIS (U. S. Sales Only).

From Conference on the sources of multicharged ions; Paris, France (28 Jan 1972).

A PIG hot-cathode source equipped with an oven and utilizing solid elements (Ca, Ge, Zn) was studied. The dependence of the production of multiply charged gas ions on the temperature of the arc chamber was examined. The gas selected for the test was Kr, and the 8^+ charged ion was studied. The results obtained are briefly listed. (France)

53753 (FRNC-CONF-56) HEAVY ION SOURCE WITH A CONFINED ELECTRON BEAM. Arianer, J.; Baixas, J.; Baron, E.; Liebe, A.; Serafini, A.; Ton-That, T. (Paris Univ., Orsay (France). Institut de Physique Nucleaire). 1972. 6p. (In French). (CONF-720120-7). Dep. NTIS (U. S. Sales Only).

From Conference on the sources of multicharged ions; Paris, France (29 Jan 1972).

The construction of a source of the EBIS type (the SILFEC source) is in progress; the experimental unit is described. A program was developed for computing the ion and electron trajectories. Experiments for optimizing the various parameters of the source (electron guns, cathode) are described. (France)

53754 (JINR-E9-6538) PROTON BEAM EXTRACTION FROM THE 10-GeV DUBNA SYNCHROPHASOTRON BY EXCITING THE RESONANCE $Q_R = 2/3$ (FURTHER ANALYTICAL CONSIDERATIONS). Conte, Mario (Joint Inst. for Nuclear Research, Dubna (USSR). Lab. of High Energy). 1972. 16p. Dep. NTIS (U. S. Sales Only).

The proposed scheme of ejection from the 10 GeV Dubna SPT via $2/3$ nonlinear resonance is further investigated, mainly by analytical considerations. Checks between these results and others obtained by computer are presented. A method for minimizing the emittance of the extracted beam is suggested. (auth)

53755 (LBL-644) HEAVY ION ACCELERATION AT THE BERKELEY 88-INCH CYCLOTRON. Clark, D. J.; Steyaert, J.; Bowen, J.; Carneiro, A.; Morris, D. (California Univ., Berkeley. Lawrence Berkeley Lab.). Jun 1972. Contract W-7405-eng-48. 8p. (CONF-720717-6). Dep. NTIS.

From sixth international cyclotron conference; Vancouver, B. C. (18 Jul 1972).

A new internal heavy-ion source of the Penning type has been in operation at the Berkeley 88-Inch Cyclotron for 10 months. Beams of lithium, carbon, nitrogen, oxygen, neon, and iron have been accelerated and used in experiments in the energy range 4 to 18 MeV/nucleon. External beam intensities are 1 to 10 μA of most carbon, nitrogen, and oxygen beams. Many experiments have used the new high-resolution reaction product magnetic spectrometer and resistive wire focal plane detector. (6 figures, 1 table) (auth)

53756 (LBL-654) CYCLOTRON INJECTION SYSTEMS. Clark, D. J. (California Univ., Berkeley. Lawrence Berkeley Lab.). Jun 1972. Contract W-7405-eng-48. 12p. (CONF-720717-5). Dep. NTIS.

From sixth international cyclotron conference; Vancouver, B. C. (18 Jul 1972).

A review is given of the various methods which have been used for injecting beams into cyclotrons from external ion sources. The methods of injection include neutral beam, radial ion, and axial ion systems. The performance of presently operating systems is tabulated. Larger separated sector machines now under construction or proposed will use radial ion systems. (32 references) (auth)

53757 SELF-CONSISTENT STATIONARY STATE OF A RELATIVISTIC ELECTRON BEAM IN A DRIFT SPACE. Voronin. V. S.; Zozulya, Yu. T.; Lebedev, A. N. (Lebedev Inst. of Physics, Moscow). Sov. Phys.-Tech. Phys. (Engl. Transl.); 17: No. 3, 432-6(Sep 1972).

Translated from Zh. Tekh. Fiz.; 42: No. 3, 546-52(Mar 1972).

The stationary motion of a relativistic electron beam in the self-consistent potential field is investigated. The theoretical importance of a two-dimensional field geometry at the entrance to the drift space is demonstrated for large currents. A stationary state is obtained for a magnetized beam of arbitrary intensity in a semi-infinite tube. In this state, the equilibrium distribution of the current over the cross section is highly inhomogeneous. (auth)

53758 INFLUENCE OF INJECTION CONDITIONS ON THE TRANSVERSE INSTABILITY OF THE BEAM IN A LINEAR ACCELERATOR. Kramskoi, G. D.; Zykov, A. I.; Grishaev, I. A.; Fursov, G. L. (Physical-Technical Inst., Kharkov). Sov. Phys.-Tech. Phys. (Engl. Transl.); 17: No. 3, 437-40 (Sep 1972).

Translated from Zh. Tekh. Fiz.; 42: No. 3, 553-7(Mar 1972).

The influence of the diameter of the beam injected into an accelerating waveguide is investigated, and the influence of its displacement relative to the waveguide axis on the development of a transverse instability is examined. (auth)

Ion Optics and Field Calculations

Refer also to abstract 53770.

53759 FIELD DISTRIBUTION IN SUPERCONDUCTING LENSES WITHOUT FERROMAGNETIC MATERIALS. Dietrich, I.; Koller, A.; Lefranc, G. (Siemens AG, Munich). Optik; 35: No. 4, 468-78(Jun 1972). (In German).

The field distribution in a superconducting shielding lens and a ring lens is calculated numerically assuming a Kim-Anderson current distribution in the superconductor. The course of field on the optical axis is compared with the experiment. The measured and the calculated values agree well. Characteristic lens data are reported for certain measured field curves. (auth)

53760 EMITTANCE MEASUREMENTS AND DESIGN OF AN ION BEAM TRANSPORTING SYSTEM. Bakewicz, Edmund; Rogalska, Zofia (Inst. of Nuclear Physics, Krakow). Nukleonika; 117: No. 3-4, 145-56(1972).

The properties of the alpha-particle beam extracted from the Cracow cyclotron U-120, at an energy of 25 MeV and with a total beam current of 10 μA, were determined. A beam transport system, serving the five experimental positions, was designed. (6 figures) (auth)

53761 FREQUENCY SHIFT OF AXIAL OSCILLATIONS UNDER THE EFFECT OF THE BEAM SPACE CHARGE. Glazov, A. A.; Dzhelepov, V. P.; Dmitrievskii, V. P.; (and others) (Joint

Inst. of Nuclear Research, Dubna, USSR). Particle Accel.; 3: No. 4, 231-4(Aug 1972).

Experimental studies of the frequency shift of incoherent axial oscillations under the effect of the beam space charge in the electron model of the circular cyclotron are described. The results of the studies are in satisfactory agreement with the existing presentation on the mechanism of this shift. (3 figures) (auth)

53762 ACCELERATION OF POLARIZED PROTONS IN SATURNE. Faure, J.; Hilaire, A.; Vienet, R. (CEN, Saclay, France). Particle Accel.; 3: No. 4, 225-30(Aug 1972). (In French).

The possibility of preserving the polarization of protons in Saturne during the acceleration process is demonstrated. The main resonances are crossed when the spin frequency precession is equal to the frequency of the magnet field error as seen by the particles. The way to overcome the difficulty consists in a complete adiabatic reversal of the polarization for each resonance crossing. (4 figures) (auth)

53763 PART I. NONLINEAR BETATRON OSCILLATIONS. PART II. PARTICLE MOTION IN MUON g-2 EXPERIMENT. Lysenko, Walter Paul. New Haven; Yale Univ. (1972). 177p. University Microfilms Order No. 72-22,397.

Thesis.

PART I: Single particle motion in two dimensions for a nearly linear, nearly periodic system is studied by considering a set of perturbed Hill's equations. A transformation of variables is effected which permits the application of the Krylov–Bogoliubov averaging method. It is shown how this asymptotic perturbation technique can be used to all orders in the perturbation parameter for the nearly periodic resonance situation. The remainder of the work is a specialization to the case of a single resonance in the first approximation. The fourth-order system of equations is reduced to a second order system which describes the amplitude behavior for either the sum or the corresponding difference resonance. By making an approximation consistent with small relative variations in the amplitudes, explicit solutions are obtained for the betatron amplitudes as functions of the independent variable. Four cases are studied in which the operating point is fixed, moves parallel to a resonance line, crosses a resonance line, or passes close by a resonance line.

PART II: The orbit and spin motion in a muon g-2 experiment is studied. The aim is to determine the errors involved in the 10–20 ppm experiment proposed by V. W. Hughes to be run at LAMPF. This experiment involves a 1 m superconducting storage ring for $p = 600$ MeV/c muons. Weak magnetic focussing is used and electric quadrupoles electrodes maintain the precession frequency independent of radius. By studying the uncertainties in the various corrections to the precession motion, it is shown that a magnetic field decreasing linearly with the radius is desirable. An estimate of the particle losses by betatron resonances is made with the conclusion again that a linearly varying field of high accuracy is essential. In order to obtain a complete error analysis, other aspects of the experiment such as muon storage rates are also considered. (Diss. Abstr. Int., B)

53764 CHANGE IN BEAM SPOT SIZE DUE TO SECOND-ORDER EFFECTS IN A FIRST-ORDER ACHROMATIC BEAM TRANSPORT SYSTEM. Lobb, D. E. (Univ. of Victoria, B. C.). Nucl. Instrum. Methods; 103: No. 2, 271-5(1972).

A method is presented for determining which second-order terms have the greatest effect on a particle trajectory and which trajectories are so affected. A method is presented for calculating the maximum value of a position coordinate when second-order chromatic effects are present in a first-order achromatic system. (1 figure, 1 table) (auth)

Storage Rings

Refer also to abstracts 54181, 54182, 54200, and 54284.

53765 (BNL–16816) MAGNET FAULT PROTECTION: ISABELLE. Cottingham, J. G. (Brookhaven National Lab., Upton, N. Y.). 22 Dec 1971. 5p. Dep. NTIS.

An external power diode or a series of such diodes connected across the magnet leads to a dewar system will prevent the energy stored in the total magnet system of ISABELLE from feeding energy into a magnet that has failed. But it cannot remove energy from within the dewar containing the fault. Conditions immediately following a failure are discussed. The magnet terminal voltage reaches 700 V; this can be reduced, however, by connecting a shunt resistor across each magnet. The undesirable side effects of this resistor can be removed by inserting a series diode. (2 figures) (R.W.R.)

53766 (BNL–16818) ISABELLE FOR VERY LOW ENERGY $\bar{p}p$ EXPERIMENTS: WHIPLASH. Kalogeropoulos, T. (Brookhaven National Lab., Upton, N. Y.). 12 Nov 1971. 9p. Dep. NTIS.

The desirability of doing experiments with antinucleons at low energies (~15 MeV cms energy) and associated problems are discussed. It it suggested that experiments involving $\bar{p}p$ collisions between beams running in the same direction have significant advantages over those involving a stationary target. The kinematics of such experiments are considered, and some flux estimates are given. The possibility for obtaining a 200-GeV protonium beam is mentioned. (R.W.R.)

53767 (BNL–16830) SOME SPECULATIONS ON COLLIDING BEAMS OF 200 GeV PROTONS AND 15 GeV ELECTRON–200 GeV PROTONS. Yang, Chen Ning (Brookhaven National Lab., Upton, N. Y.). 31 Jan 1972. 5p. Dep. NTIS.

Although the ISR and NAL machines might produce results at variance with all elementary particle models yet proposed, it is more likely that they will verify the limiting behavior of high-energy collisions. Colliding beam proton–proton machines are needed to investigate slow dependences of theoretical formulations on incoming energy. Colliding beam electron–proton machines have the advantage that the electromagnetic interaction is known, but they can not substitute for a p–p machine. Colliding beam proton–antiproton machines are probably not needed, however, due to the similarity of pp and $p\bar{p}$ interactions. (R.W.R.)

53768 (BNL–16980) COIL CONFIGURATIONS IN SUPERCONDUCTING QUADRUPOLES. Parzen, G.; Jellett, K. (Brookhaven National Lab., Upton, N. Y.). 23 Jun 1972. 9p. Dep. NTIS.

The limitations on the good field aperture of superconducting quadrupoles due to approximating the $\cos 2\theta$ current distribution by using a finite number of ribbon-shaped conductors arranged in blocks are investigated. Results are presented for three ribbon configurations having 2 and 3 blocks per octant, for which the lower undesired multipoles are eliminated by slight azimuthal displacement of the block. For the ISABELLE storage rings, 2 blocks per octant may be sufficient. Results are presented for the good field aperture limit due to the choice of the number of blocks per octant. (4 figures, 1 table). (auth)

53769 (BNL–16996) DETERMINATION OF LUMINOSITY USING THE INTERSECTION OF A HIGH β WITH A LOW β SECTION. Palmer, R. B. (Brookhaven National Lab., Upton, N. Y.). 29 Jun 1972. 3p. Dep. NTIS.

If the luminosity of any special region is known, as well as the rate for any arbitrary reaction measured in that region, then the luminosity at any other region can be established by a measurement of that same rate. There is proposed, therefore, a special crossing whose luminosity is low but whose characteristics make an exact determination of luminosity relatively easy. Specifically, the proposal calls for the intersection of two beams, one with low β and the other with high β, at a finite crossing angle. For reasonable assumptions, a luminosity of 6.5×10^{30} is found; while not great, this is acceptable for the determination of total cross section and elastic scattering at medium angles. It is concluded that errors in current measurement could be made negligible and that the method could give luminosities to the order of 0.3% accuracy. (1 figure) (R.W.R.)

53770 (BNL–17016) BETATRON FREQUENCY SHIFTS DUE TO IMAGE FIELDS. Gluckstern, Robert L. (Brookhaven National Lab., Upton, N. Y.). 30 Jun 1972. 7p. Dep. NTIS.

The variation of betatron frequency across a beam due to image fields is calculated for both circular and plane-parallel beam pipes. An approximate interpolated expression is then constructed which agrees with both limits and with the result for a slightly elliptical pipe. The effect appears to be more serious for the ISR than for the design parameters of the ISA. (auth)

53771 (BNL–17019) LUMINOSITY MEASUREMENTS FOR COLLIDING BEAMS. Marx, Jay N. (Brookhaven National Lab., Upton, N. Y.). 1972. 14p. Dep. NTIS.

Many experiments with colliding beam facilities require rather precise measurements of the luminosity; indeed, such a measurement may be the limiting factor for a given experiment. These experiments are of two general types, those that measure absolute reaction rates and those that require relative luminosity measurements in order to normalize a series of runs. Two approaches to the problem of measurement of beam luminosity are considered: measurements of an interaction channel whose absolute cross section can be calculated in a believable way and measurements of the beam characteristics. The following methods for making the measurement luminosity are considered: measurement of the Coulomb region in pp collisions; Coulomb dissociation of $\Delta(1236)$; electron pair production in pp collisions; the van der Meer method; diffuse beam method; attenuation method for relative luminosity measurements; and luminosity measurement for collinear regions. (R.W.R.)

53772 (BNL–17021) SCHEME FOR ABSOLUTE CALIBRATION OF ISABELLE LUMINOSITY. Gobbi, B.; Rosen, J. L. (Brookhaven National Lab., Upton, N. Y.). [nd]. 9p. Dep. NTIS.

To effect the calibration one would like a simple reaction channel, easily identifiable, with reasonable rate and one which can be reliably predicted on the basis of precise measurement at lower energies. The interaction $p + p \rightarrow p + \Delta^+(1236)$ is proposed for this task. An accuracy of 1% seems achievable. Monte Carlo calculations of the energy and angular distributions of the nucleon and pion produced by the decay of the Coulomb-excited Δ^+ are shown. A feasible detection scheme is described. (3 figures) (R.W.R.)

53773 (BNL–17051) MOMENTUM MATCHING IN ISA LONG INSERTIONS. Garren, A.; Helm, R.; Month, M. (Brookhaven National Lab., Upton, N. Y.). 14 Jul 1972. 5p. Dep. NTIS.

In the long insertion options of the ISABELLE lattice, the momentum dispersion functions are designed to be zero. Quadrupoles and bending magnets at the ends of the insertions are used for this purpose. However, this momentum matching is destroyed within the insertion if focusing and bending of the beam for experimental purposes become coupled. The momentum mismatch due to this coupling is described, and some undesirable consequences are pointed out. The present ISABELLE options manifest this mismatch, and a modification that would solve the problem is proposed. Finally, some numerical results are given using the computer program SYNCH. (2 figures) (auth)

53774 (BNL–17056) MAGNET TOLERANCES IN ISABELLE AND NONLINEAR RESONANCES. Parzen, G. (Brookhaven National Lab., Upton, N. Y.). 26 Jul 1972. 3p. Dep. NTIS.

There is reason to believe that the nonlinear imperfection resonances, which are driven by random errors in the magnetic field, are likely to be considerably stronger in ISABELLE than they are in the ISR. This would require that ISABELLE have a set of magnetic correction elements to control the harmonics which excite the relevant nonlinear imperfection resonances. (1 figure) (auth)

53775 (BNL–17057) APPLICATION OF ISABELLE IN WHIPLASH MODE TO PRODUCE POLARIZED PROTON OR MONOENERGETIC NEUTRON BEAMS. Goldberg, M.; Moneti, G. C. (Brookhaven National Lab., Upton, N. Y.). 17 Jul 1972. 8p. Dep. NTIS.

The production of beams of polarized protons and monoenergetic neutrons by accelerating protons in ISABELLE in the Whiplash mode is discussed, and it is concluded that neither is possible with the design beam intensity because of the very small luminosity that is a characteristic of the Whiplash mode. The high magnification of the longitudinal component of the center-of-mass momentum of the final particles, another characteristic feature of the Whiplash mode, is also discussed; no useful applications are envisioned, however, because of the low luminosity levels. (4 figures, 3 tables) (R.W.R.)

53776 (BNL–17063) COULOMB INDUCED DEUTERON BREAK-UP OF ISABELLE. Gobbi, B.; Rosen, J. (Brookhaven National Lab., Upton, N. Y.). 2 Aug 1972. 1p. Dep. NTIS.

In connection with the possibility of a deuteron beam option for ISABELLE, it is important to know the cross section for deuteron breakup induced by the Coulomb field interaction. By use of the Weizsaecker–Williams formula this was calculated to be 0.3 mb; although fairly large, this value does not preclude any of the proposals presently being advanced. (R.W.R.)

53777 (BNL–17067) LUMINOSITY CONSIDERATIONS FOR COLLIDING ELECTRON AND PROTON BEAMS. Courant, E. D. (Brookhaven National Lab., Upton, N. Y.). 25 Jul 1972. 9p. Dep. NTIS.

The maximum obtainable luminosities for electron–proton colliding beam systems are estimated, subject to the constraints that the power radiated by electron synchrotron radiation is fixed (this limits a combination of electron energy and current) and the detuning (beam–beam interaction) of electrons by protons and vice versa must be kept below a certain limit. It is seen that high luminosity can be obtained either with a weakly bunched or unbunched proton beam and many electron bunches or with a single proton bunch and a single electron bunch, both very short. In the many-bunch mode the optimum luminosity is obtained at lower electron energy than in the single-bunch mode. (auth)

53778 (BNL–17068) DOES ISABELLE NEED UNEQUAL ENERGY RINGS? Lee, Y. Y. (Brookhaven National Lab., Upton, N. Y.). 22 Jun 1972. 2p. Dep. NTIS.

A few examples of reasons why there should be separately functioning storage accelerators are listed. (auth)

53779 (BNL–17142) LARGE APERTURE SPECTROMETER MAGNET FOR THE ISA AND THE POSSIBLE USE OF VISUAL DETECTORS. French, H.; Roe, B. P.; Gelfand, N.; Strand, R. C.; Weilhammer, P. (Brookhaven National Lab., Upton, N. Y.). 1972. 5p. Dep. NTIS.

It is proposed that a large aperture spectrometer magnet be designed as an integral part of the ISA machine to be pulsed with the machine. The design luminosity thus can be optimized in a configuration including the large magnet. Preliminary options concerning magnet types are given and it is argued that as a first survey it is likely to be used with visual detectors. At the ISA, as at lower energies, the strong forces will dominate the $p + p$ interaction. The typical $p + p$ event will be characterized by high track multiplicity and the small transverse momenta of the particles. It is felt that the understanding of these events will be essential if one is to achieve an explanation of the strong interaction. It is therefore considered important that the ISA be provided with a device which enables one to observe and analyze these events. (auth)

53780 (BNL–17152) EFFECT OF LOW-SYMMETRY MATCHED INSERTIONS. Month, M. (Brookhaven National Lab., Upton, N. Y.). 29 Dec 1971. 11p. Dep. NTIS.

The effects of low-periodicity insertions are considered. The insertions are assumed to have the basic properties suitable for particle experiments in storage rings. They are also assumed to be matched to the main lattice cells with respect to both betatron and momentum dispersion variables at a specific tune and momentum. For a momentum error, however, the tune is shifted and the matching is broken. This mismatching introduces instabilities at tunes directly related to the periodicity of the insertions, N. Gradient instabilities occur at all values of the tune given by $\nu \sim (N/2) \times$ integer, while dipole resonances occur at $\nu \sim N \times$ integer. Expressions characterizing these instabilities are derived. Specifically, for gradient instabilities, the growth in the β function and the available momentum aperture near the resonances are estimated. The use of sextupoles as correction devices, for reducing the β growth and opening the momentum aperture, is discussed. An idealized lattice with two-fold symmetry is treated as an example. (1 figure) (auth)

53781 (BNL–17153) VACUUM CHAMBER EDDY CURRENTS. Bittner, J. W. (Brookhaven National Lab., Upton, N. Y.). 24 Feb 1972. 6p. Dep. NTIS.

In order to reduce the power losses due to the beam-induced rf currents in the vacuum chamber of ISABELLE, it seems necessary to furnish the chamber with some kind of copper wall. Since the resistivity of this copper at 4.5°K will be about 100 times lower than that normally encountered at room temperature, it is worthwhile to estimate the effects of eddy currents induced by the slowly rising magnetic fields during the acceleration phase of the magnet cycle. It is found that, in the dipole case, the power dissipated by eddy currents approaches the losses due to beam-induced currents. This dissipation lasts, however, only during the 120 seconds rise time, and exists only in that fraction of the vacuum chamber passing through dipole magnets. It might, however, be a very valid reason to reduce the thickness of the copper wall. (1 figure) (R.W.R.)

53782 (CERN–72–14) INTERSECTING STORAGE RINGS. Lectures Given in the Academic Training Programme of CERN, 1971–1972. Keil, E. (European Organization for Nuclear Research, Geneva (Switzerland)). 21 Jul 1972. 53p. Dep. NTIS (U. S. Sales Only).

Topics include: why colliding beams?, why storage rings?, how to fill storage rings?, how is stacking in synchrotron phase space done?, does one need a good vacuum?, magnet system, rf system, beam transfer, and vacuum. The expected ISR performance is discussed; and space charge Q-shift including calculation of the linear space charge Q-shift, measurement of incoherent Q-shifts, and measurement of coherent Q-shifts is considered. Also, coherent instabilities, experimental data on beam lifetime, experimental data on beam size, and possible theoretical explanations of beam lifetime and beam growth are discussed. (W.H.K.)

Experimental Facilities

Refer also to abstract 54467.

53783 (DNPL/P-131) HIGH INTENSITY MUON BEAM DESIGN FOR CERN II. Aitken, T. W.; Clifft, R. W.; Gabathuler, E. (Daresbury Nuclear Physics Lab. (England)). Jul 1972. 15p. Dep. NTIS (U. S. Sales Only).

Results are presented of detailed investigations into the design of a muon beam-line incorporating a strong focusing decay channel. The principal objectives of the beam-line design are (i) to accept as many as possible of the pions produced at a primary target within a particular momentum band, (ii) to contain the pions and their subsequent decay muons within a decay channel, (iii) to remove all remaining pions at the end of the channel, (iv) to focus as many of the muons as possible on to an experimental target, and (v) to minimize the beam halo. A 1 km beam-line was developed capable of handling particles of momentum $\lesssim$300 GeV/c. Some performance figures are given. (auth)

53784 (LA-4874) PROCEEDINGS OF THE FIFTH LAMPF USERS MEETING HELD AT THE LOS ALAMOS SCIENTIFIC LABORATORY, LOS ALAMOS, N.M., NOVEMBER 8-9, 1971. Agnew, Lewis E.; Howard, Hillard H.; Miller, Billie F. (comps.) (Los Alamos Scientific Lab., N. Mex.). Mar 1972. Contract W-7405-eng-36. 168p. (CONF-711138). Dep. NTIS.

Separate abstracts were prepared for the 19 papers presented. (W.H.K.)

For abstracts of individual papers see: 53398, 53450, 53739, 53740, 53785–53796, 54195, 54876, and 54877.

53785 (LA-4874, pp 45-7) STATUS REPORT ON LAMPF RESEARCH PROPOSALS. Rosen, Louis (Los Alamos Scientific Lab., N. Mex.). Mar 1972.

From fifth LAMPF users meeting; Los Alamos, NM. (8 Nov 1971).

The members of the LAMPF Program Advisory Committee, Biomedical Applications Subcommittee, and Nuclear Chemistry Subcommittee are listed. The research proposals are tabulated according to the LAMPF channel, and action taken on the proposals including beam time assignments are tabulated according to the channel. (W.H.K.)

53786 (LA-4874, pp 48-50) LOW ENERGY PION CHANNEL. Burman, Robert L. (Los Alamos Scientific Lab., N. Mex.). Mar 1972.

From fifth LAMPF users meeting; Los Alamos, NM. (8 Nov 1971).

The proposed Low-Energy Pion Channel, designed to provide $\pi^{\pm}$ beams for the energy region from low energies (approximately 20 MeV) through the resonance region (approximately 300 MeV), is briefly described; and experiments proposed for the low energy pion channel are outlined. (W.H.K.)

53787 (LA-4874, pp 51-4) ENERGETIC PION CHANNEL AND SPECTROMETER (EPICS). Thiessen, H. A. (Los Alamos Scientific Lab., N. Mex.). Mar 1972.

From fifth LAMPF users meeting; Los Alamos, NM. (8 Nov 1971).

The optical design and experimental layout for the LAMPF Energetic Pion Channel and Spectrometer (EPICS) are briefly described, and the status of the project is outlined. Nine experiments approved for beam time at the EPICS facility are listed. (W.H.K.)

53788 (LA-4874, pp 55-8) PION AND PARTICLE PHYSICS (P^3). Macek, Robert J. (Los Alamos Scientific Lab., N. Mex.). Mar 1972.

From fifth LAMPF users meeting; Los Alamos, NM. (8 Nov 1971).

The status of the LAMPF Pion and Particle Physics (P^3) channel is outlined. Topics include status of the hardware, a brief summary of channel parameters including revised fluxes, the work of P^3 users last summer, and a summary of P^3 research proposals. (W.H.K.)

53789 (LA-4874, pp 59-62) STOPPED MUON CHANNEL. Thompson, Patrick A. (Los Alamos Scientific Lab., N. Mex.). Mar 1972.

From fifth LAMPF users meeting; Los Alamos, NM. (8 Nov 1971).

The status of the LAMPF stopped muon channel is summarized, and the estimated stopping rates for the muon channel and the estimated properties of the muon test beam are tabulated. (W.H.K.)

53790 (LA-4874, pp 63-6) NUCLEON PHYSICS LABORATORY (NPL). Hwang, Chester F. (Los Alamos Scientific Lab., N. Mex.). Mar 1972.

From fifth LAMPF users meeting; Los Alamos, NM. (8 Nov 1971).

The status of the LAMPF Nucleon Physics Laboratory is described including development of the polarized proton ion source, the polarized proton and deuterium target, low-energy operation, and micropulse operation. Proposals for experiments are briefly discussed. (W.H.K.)

53791 (LA-4874, pp 67-71) HIGH RESOLUTION PROTON SPECTROMETER (HRS). Spencer, James E. (Los Alamos Scientific Lab., N. Mex.). Mar 1972.

From fifth LAMPF users meeting; Los Alamos, NM. (8 Nov 1971).

The design and development status of the LAMPF High Resolution Proton Spectrometer is outlined. The beam optics and detector electronics are briefly discussed. (W.H.K.)

53792 (LA-4874, pp 72-7) NUCLEAR CHEMISTRY FACILITIES. Dropesky, Bruce J. (Los Alamos Scientific Lab., N. Mex.). Mar 1972.

From fifth LAMPF users meeting; Los Alamos, NM. (8 Nov 1971).

The LAMPF Nuclear Chemistry Laboratory, the hot cells of the Merrimac Service Area, the pneumatic rabbit system, and the proposed nuclear chemistry targeting stations are briefly described. A list of the initial set of nuclear chemistry experiments is given. (W.H.K.)

53793 (LA-4874, pp 78) BIOMEDICAL APPLICATIONS: BEAM LINE AND FACILITY. Hutson, Richard L. (Los Alamos Scientific Lab., N. Mex.). Mar 1972.

From fifth LAMPF users meeting; Los Alamos, NM. (8 Nov 1971).

The personnel structure involved in the LAMPF Pion Radiobiology and Radiotherapy Program is outlined, and the status of the Biomedical Pion Channel is briefly described. (W.H.K.)

53794 (LA-4874, pp 84-5) NEUTRINO FACILITY. Burman, Robert L. (Los Alamos Scientific Lab., N. Mex.). Mar 1972.

From fifth LAMPF users meeting; Los Alamos, NM. (8 Nov 1971).

A neutrino facility which fits directly behind the main proton line beam dump without modification of the dump is described. Essentially all of the neutrinos result from the $\pi^+ \to \mu^+ + \nu_\mu$ decays and $\mu^+ \to e^+ + \nu_e + \overline{\nu}_\mu$ decays. The spectra of these neutrinos is shown graphically. The mean energy in 35 MeV and the maximum energy is 53 MeV. The flux is expected to be about 3×10^7 ν/sec cm^2 of each type of neutrino. Initial proposals for experiments are listed. (W.H.K.)

53795 (LA-4874, pp 86-9) COMPUTING FACILITIES. Butler, Harold S. (Los Alamos Scientific Lab., N. Mex.). Mar 1972.

From fifth LAMPF users meeting; Los Alamos, NM. (8 Nov 1971).

The status of the experimental data acquisition system at LAMPF is reviewed. Data reduction will be handled through the Central Computing Facility (CCF) which now has an inventory of two CDC-7600's and three CDC-6600's. CAMAC will be used as the standard for interfacing the experimental apparatus to each computer. The main beam lines of the accelerator may be controlled from CCF. (W.H.K.)

53796 (LA-4874, pp 92-8) PROMOTION OF THE ACADEMIC USES OF LAMPF. McDaniel, Paul W. (Division of Research (AEC), Washington, D. C.). Mar 1972.

From fifth LAMPF users meeting; Los Alamos, NM. (8 Nov 1971).

Attitudes and approaches that need to be established among the scientists at LAMPF in order to establish an understanding by the American public of the fundamental research program at LAMPF are suggested. (W.H.K.)

53797 (LA-DC-72-881) PION BEAMS AT LAMPF. Burman, R. L. (Los Alamos Scientific Lab., N. Mex.). [nd]. 17p. (CONF-710948-2). Dep. NTIS.

From International seminar on pion–nucleus interactions; Strasbourg, France (Sep 1971).

The three secondary pion channels at the Clinton P. Anderson Meson Physics Facility are described. The low-energy pion channel is designed to provide π^+ beams for the energy region from low energies (approximately 20 MeV) through the resonance region (approximately 300 MeV). Design features of the channel include good momentum resolution for nuclear structure experiments, a small (achromatic) spot for stopped pion experiments and total-absorption counter experiments, and high-intensity beams at moderate resolution. EPICS is designed to have good energy resolution (<50 keV) and good angular resolution (<10 mrad), as well as a pion energy range and beam intensity sufficient to measure cross sections from low energies to above the (3,3) pion–nucleon resonance with adequate count rate. The complete system consists of a high-intensity, high resolution pion beam channel, a particle separator for reducing backgrounds, and two spectrometers. The channel produces a dispersed beam, in which the momentum of each particle is correlated with its position. The P^3 channel is a very flexible, general-purpose pion line capable of transmitting the highest-energy pions that the linac can produce. Additional characteristics are moderate resolution, high intensity, and the flexibility for matching to a wide range of experiment requirements. (11 figures) (R.W.R.)

53798 THEORY OF $\pi/2$-MODE BIPERIODIC DEFLECTORS. Bauer, W.; Hahn, H. (Univ., Karlsruhe, Ger.). Particle Accel.; 3: No. 4, 193-207(Aug 1972).

The extension of the rigorous theory of uniform-periodic iris-loaded deflectors to standing-wave $\pi/2$-mode biperiodic cavities is presented. The particular approach used restricts the solution to the $\pi/2$-mode, but it is possible to find the changes in outer diameter necessary to enforce confluence as required for maximum stability. Interaction impedance and shunt impedance are also computed, and good agreement with the few published results is found. (7 figures) (auth)

53799 PHYSICAL MEASUREMENTS INCLUDING DEPTH DOSE DATA AND ISODOSE CURVES FOR 8 MV ROENTGEN RAYS. Agarwal, S. K.; Scheele, R. V.; Wakley, J. (Univ. of Virginia, Charlottesville). Acta Radiol., Ther., Phys., Biol.; 11: No. 1, 97-105(Feb 1972).

The Arco Mevatron-7 linear accelerator at the University of Virginia, designed to operate at 1 MeV intervals between 3 and 10 MeV, is being used for roentgen rays produced by electron energies of 6 and 8 MeV. The electron energy, roentgen ray flatness, and absorbed dose are determined daily before the commencement of treatments. The energy is measured by extrapolating the electron range in aluminum. Central axis depth doses were measured in water for square fields from 16 to 625 cm^2, employing a remote control moving probe mechanism. The same mechanism was used to determine isodose curves. The results compared favorably with the existing data at this energy. (auth)

53800 MONOCHROMATIC METHOD FOR MEASURING THE 665 MeV MEAN PROTON ENERGY BY USING VAVILOV–CHERENKOV RADIATION. Zrelov, V. P.; Musin, M. A.; Pavlovic, P.; Sulek, P.; Janik, R. (Joint Inst. for Nuclear Research, Dubna, USSR). Nucl. Instrum. Methods; 103: No. 2, 261-9(1972).

The monochromatic method for measuring the proton energy by using the Vavilov–Cherenkov radiation and interference filters with $\lambda \approx 6000$ Å and a passband $\lambda = 100$ Å is described. The results of testing this method with a 665-MeV proton beam extracted from the synchrocyclotron of the Joint Institute for Nuclear Research in Dubna are presented. A measurement accuracy of ±0.02% was achieved which exceeds the accuracy of the best previously known methods by a factor of 5. (10 figures, 4 tables) (auth)

53801 SEPARATED HIGH-ENERGY ELECTRON BEAMS USING SYNCHROTRON RADIATION. Farley, F. J. M. (CERN, Geneva); Picasso, E.; Bracci, L. Nucl. Instrum. Methods; 103: No. 2, 325-9(1972).

Electrons with kinetic energy in the 100 GeV range may be separated from other particles by using their energy loss due to synchrotron radiation in a high-field magnet. The associated fluctuations in energy and angle are shown to be small enough for the method to be useful. Detailed design formulas are presented for several magnet configurations. (auth)

53802 ION BEAM MONITOR FOR NANOAMPERE CURRENTS. Hollis, M. J. (Chalk River Nuclear Labs., Ont.). Nucl. Instrum. Methods; 103: No. 2, 337-9(1972).

The ion beam current monitor can be used for continuous monitoring of MeV ion currents of 0.1 to 10 nA. It is particularly suited to ion channelling and similar experiments. (4 figures) (auth)

53803 TARGET CHAMBER FOR CHARGED PARTICLE INDUCED X-RAY FLUORESCENCE STUDIES. Feldl, E. J. (Kansas State Univ., Manhattan); Umbarger, C. J. Nucl. Instrum. Methods; 103: No. 2, 341-3(1972).

A target chamber is described which combines extremely low acquisition cost with precision adjustment and exchange of as many as 26 targets without breaking chamber vacuum. The chamber was designed for particle-induced x-ray fluorescence studies and allows great detection efficiency due to its small target–detector distance. To expand its usefulness, the chamber can also hold one solid state surface barrier detector at 90° with respect to the beam. This feature allows charge-particle studies as well as particle–gamma ray coincidence measurements. (3 figures) (auth)

53804 COMMENTS ON INTENSITY ESTIMATION FOR A NEUTRON BEAM FOR BIOLOGICAL AND MEDICAL APPLICATIONS. Watson, J. W. (Univ. of Manitoba, Winnipeg). Nucl. Instrum. Methods; 103: No. 2, 421(1972).

Recently published estimations of neutron spectra from the thick target Be(d,n) reaction for biological and medical use are compared with existing data. The estimated and experimental spectra are in reasonable qualitative agreement. (1 figure) (auth)

PHYSICS (ASTROPHYSICS AND COSMOLOGY)

Refer also to abstract 54870.

Cosmic Radiation

Refer also to abstracts 53276, 54185, 54313, 54878, 54888, 54889, and 54964.

53805 (N–71–30295) DETERMINATION OF HEAVY NUCLEI CHARGES. Semikoz, V. B. Translated from report Pr–13. 9p. (NASA-TT-F–13743). NTIS.

The number of delta electrons formed by $N = Z/(137\ \beta)$, where Z is the charge, and β is the velocity of the nucleus, is calculated. Good agreement was observed with the Born formula (at $\eta < 0.3$) and with the Rutherford formula (at $\eta > 1.5$), which give the same results in extreme cases ($\eta \ll 1$ and $\eta \gg 1$, respectively). If the parameter η is ~ 1, then it is necessary to use the exact Mott formula for differential cross sections whose numerical integration is carried out with allowances for kinematic scattering of the nucleus by target electrons. In this case, the introduced correction to charge, Z_{15}, determined in the first Born approximation, is very large, especially for the heavy nuclei of the SH group. (auth) (STAR)

53806 (NASA-TM-X–2440, pp 209–14) CHEMICAL COMPOSITION AND ENERGY CONTENT OF THE ENERGETIC COSMIC RADIATION. Waddington, C. J. (Univ of Minnesota, Minneapolis). Jan 1972.

From Symposium on natural and manmade radiation in space; Las Vegas, Nev. (1 Mar 1971).

A brief survey is made of the present knowledge of the composition and energy spectra of the primary cosmic radiation. The total energy carried by all forms of cosmic radiation that have appreciable penetrability into matter is evaluated. This information, when combined with a knowledge of the rate at which the different components deposit energy in traversing matter, would permit calculations of the dose from exposure to the primary cosmic radiation. It is concluded that the overall radiation effects are rather small but local damage can be of much greater significance. (auth)

53807 (NASA-TM-X–2440, pp 908–13) EXPERIMENTAL DETERMINATION OF COSMIC-RAY CHARGED-PARTICLE INTENSITY PROFILES IN THE ATMOSPHERE. Lowder, W. M.; Raft, P. D.; Beck, H. L. (Atomic Energy Commission, New York). Jan 1972.

From Symposium on natural and manmade radiation in space; Las Vegas, Nev. (1 Mar 1971).

Absolute cosmic-ray free-air ionization and charged-particle fluxes and dose rates throughout the atmosphere were measured on a series of balloon flights that commenced in 1968. Argon-filled ionization chambers equipped with solid-state electrometers, with different gas pressures and steel-wall thicknesses, and a pair of aluminum-wall GM counters have provided the basic data, which are supplemented by measurements with air-filled and tissue-equivalent ionization chambers and a scintillation spectrometer. Detailed laboratory experiments, together with analyses of the theoretical aspects of the detector responses to cosmic radiation, indicate that these profiles can be determined to an overall accuracy of ±5%. Data from various balloon flights at 53°N and 42°N geomagnetic latitude provide ionization profiles consistent with earlier results in the lower atmosphere, but 20% lower than comparable data obtained by the California Institute of Technology. No explanation has yet been found for this discrepancy, although a quantitatively similar one was previously noted by the University of Minnesota group. The results indicate a total charged-particle free-air ionization (dose rate) at 53°N latitude of 6.3 I (9.5 μrad/hr), 114 I (170 μrad/hr), and 290 I (436 μrad/hr) at 10,000, 35,000, and 65,000 ft, respectively. These data are approximately minimum values for the 11-year solar-activity cycle. The ionization and flux data are compared with the analytical calculations of O'Brien, with generally satisfactory agreement. (auth)

53808 (ORNL-tr–2620) BUILDUP OF COSMIC ISOTOPES IN IRON METEORITES. Barashenkov, V. S.; Sobolevskii, N. M.; Toneev, V. D. (Joint Inst. for Nuclear Research, Dubna (USSR)). Translated for Oak Ridge National Lab., Tenn., from report JINR–P2–6225. 9p. Dep. NTIS.

The formation rates of cosmogenic isotopes ^{22}Na, ^{36}Cl, ^{40}K, and ^{49}V in iron meteorites were calculated using the Monte-Carlo method. The question about variations of the cosmic-ray intensities is discussed. Preatmospheric radius of the Arus–Yardymlinsky meteorite is estimated. The results were compared with those obtained by other authors. (auth)

53809 EQUILIBRIUM ENERGY SPECTRUM FOR THE GALACTIC COSMIC ELECTRONS. Suh, Paul K. (Grumman Aerospace Corp., Bethpage, N. Y.). Astron. Astrophys.; 20: No. 3, 375–82 (Sep 1972).

A perturbational analysis of the cosmic electron diffusion equation is developed. In the high-energy domain, cosmic electron diffusion parallel to the galactic disk slab appears not to affect significantly the determination of the equilibrium electron energy spectrum. Diffusion across the galactic disk slab in the high-energy domain is examined in detail. An active cosmic electron leakage at the disk–halo boundaries, coupled with diffusion across the disk slab, sensitiviely affects the cosmic electron spectral behavior up to a considerably high-energy domain. In the high-energy domain, the closed-disk model appears to prevail. In the low-energy domain, the leakage-time may become comparatively long, thus leading to the possible validity of a quasi-open-disk model. (auth)

53810 ISOTOPIC COMPOSITIONS OF RARE GASES IN THE CARBONACEOUS CHONDRITES MOKOIA AND ALLENDE. Manuel, O. K.; Wright, R. J.; Miller, D. K.; Kuroda, P. K. (Univ. of Arkansas, Fayetteville). Geochim. Cosomchim. Acta; 36: No. 9, 961–83(Sep 1972).

The isotopic compositions were measured mass spectrometrically for neon, argon, krypton, and xenon released from the carbonaceous chondrites Mokoia and Allende in stepwise heating experiments. The isotopic compositions of rare gases released from the meteorites at different temperatures varied quite considerably. The observed minimum and maximum values were, for example, as follows: ^{20}Ne/^{22}Ne = 2.10 (Allende 800°C) and 12.95 (Mokoia 400°C); ^{36}Ar/^{38}Ar = 4.20 (Allende 1600°C) and 6.05 (Allende 800°C); ^{84}Kr/^{86}Kr = 3.140 (Allende 1000°C) and 3.306 (Mokoia 600°C); ^{134}Xe/^{136}Xe = 1.019 (Allende 800°C) and 1.192 (Allende 1400°C). A marked enrichment of ^{129}Xe due to the decay of extinct nuclide ^{129}I was observed in both meteorites. The variations of the isotopic ratios are partly caused by the presence of cosmic-ray spallation and neutron-capture products. In addition, however, a marked trend of mass-dependent variation of the isotopic ratios was observed. The rare gas isotopes released from the meteorites appear to be systematically mass-fractionated relative to the relative abundances of the average carbonaceous chondrite (AVCC). It seems that this phenomenon can be best explained by assuming that there exist reservoirs of two isotopically distinct gases in the meteorites and mixtures of these gases are being released at each temperature fraction. The two different gases being considered here are most likely the so-called solar and planetary rare gases, whose isotopic compositions are quite different. (auth)

53811 CHARACTERISTICS OF COSMIC RAY DIURNAL VARIATION FROM DEEP RIVER NEUTRON AND MESON DATA AND TEMPERATURE EFFECTS. Agrawal, S. P.; Ananth, A. G.; Rao, U. R. (Physical Research Lab., Ahmedabad, India). Can. J. Phys.; 50: No. 12, 1323–31(15 Jun 1972).

From an extensive analysis of Deep River meson data for over 5 years, new temperature coefficients were derived for correcting the meson data. It is shown that meson data corrected using new coefficients yield values of diurnal and semidiurnal anisotropy consistent with those obtained from neutron monitors. Using the temperature-corrected meson and neutron data, the upper cutoff rigidity beyond which the diurnal variation ceases is shown to vary with solar cycle showing a minimum of about 35 GV during the Quiet Solar Year of 1965, and a maximum of ≈ 125 GV during 1968–1969. (auth)

53812 THREE-DIMENSIONAL COSMIC-RAY ANISOTROPY IN INTERPLANETARY SPACE. III. ORIGIN OF COSMIC RAY SOLAR SEMI-DIURNAL VARIATION. Nagashima, Kazuo; Ueno, Hirosachi; Fujimoto, Kazuhiko; Fujii, Zenjiro; Kondo, Ichiro (Nagoya Univ., Japan). Rep. Ionosphere Space Res. Jap.; 26: No. 1-2, 1-30(1972).

Annual modulation of cosmic-ray daily variation, observed by ion-chambers at Cheltenham and Christchurch, was studied in order to determine the anisotropy responsible for the solar semi-diurnal variation of cosmic rays. Two hypotheses have been proposed for the explanation of the anisotropy. One is called the density-gradient hypothesis that assumes the existence of cosmic-ray density gradient in the direction perpendicular to the ecliptic plane as a result of diffusion processes. The other is called the pitch-angle distribution hypothesis that assumes a specific form of cosmic-ray pitch-angle distribution against the interplanetary magnetic line of force as a result of a particle's spiral motion along the direction. Although cosmic-ray space distributions, predicted from these hypotheses, are different from one another, they each produce semidiurnal variation similar to the other's. Therefore, they cannot be discriminated from each other by observing simply the semidiurnal variation. In order to determine the origin of the semidiurnal variation, it is required to observe a special diurnal variation, characterizing these anisotropies. Different from the usual diurnal variation, the special variation shows a strange behavior that, in spite of its finite daily amplitude, its yearly average becomes very small or zero as a result of its annual modulation due to the Earth's revolution around the Sun. Because of this nature, it is necessary to observe the annual modulations of the special diurnal variation for the determination of the origin. The present analysis of the annual modulation will give some decisive evidence that will lend support to the pitch-angle distribution hypothesis. (auth)

53813 THREE-DIMENSIONAL COSMIC RAY ANISOTROPY IN INTERPLANETARY SPACE. IV. ORIGIN OF SOLAR SEMIDIURNAL VARIATION. Nagashima, Kazuo; Fujimoto, Kazuhiko; Fujii, Zenjiro; Ueno, Hirosachi; Kondo, Ichiro (Nagoya Univ., Japan). Rep. Ionosphere Space Res. Jap.; 26: No. 1-2, 31-68 (1972).

Origin of solar semidiurnal variation of cosmic-ray intensity is studied on the basis of the analytical method developed in Parts I and II, that utilizes the annual modulation of daily variation due to the Earth's revolution around the Sun. Data used for the analysis are those of multi-directional large area cosmic-ray telescope at Mt. Norikura, which can be made insensitive to the atmospheric effects by taking differences among intensities of different directions. Similar to the conclusion in Part III, the result of the present analysis gives positive support to the pitch-angle distribution hypothesis and eliminates the possibility of density gradient hypothesis for the explanation of solar semidiurnal variation. The space distribution obtained is of $\sin^2 \chi$-type, its reference axis of anisotropy being in the direction of interplanetary magnetic line of force, where χ is the angle between the reference axis and the cosmic-ray incident direction. The rigidity spectrum is of power-exponential type with its maximum at about $P_M = 60-100$ GV. (auth)

53814 12th INTERNATIONAL CONFERENCE ON COSMIC RAYS, HOBART, AUSTRALIA, AUGUST 16–25, 1971. VOLUME 1. Hobart, Australia; International Union of Pure and Applied Physics (1971). 436p. (CONF-710807–(Vol.1)).

One hundred and twenty papers dealing with origin and galactic phenomena including energetic primary protons and other nuclei, electrons, x rays, and gamma rays, as well as relevant information from radio astronomy and other branches of astrophysics are included. Of these, 53 papers are in abstract form only. The remaining 67 are given separate abstracts. (Australia)

For abstracts of individual papers see: 53815–53869, 53917–53926, 53992, and 54000.

53815 INTERACTION OF COSMIC RAYS WITH INTERSTELLAR MATTER AND POSSIBLE EXCITATION OF X-RAY LINES. Verma, Satya Dev (Louisiana State Univ., Baton Rouge). pp 31-6 of 12th International Conference on Cosmic Rays, Hobart, Australia. Vol. 1. Hobart, Australia; International Union of Pure and Applied Physics (1971).

From 12th international conference on cosmic rays; Hobart, Australia (16 Aug 1971). See CONF-710807–(Vol.1).

There are unexplained excess intensities in the 0.25- to 1-keV energy interval of the diffuse cosmic x-ray spectrum. It is suggested that these may be due to characteristic x-ray line spectra from interstellar matter. These spectra may be excited by the interaction of energetic charged cosmic-ray particles with interstellar matter. Since the cross sections for such interactions are known only up to 40 MeV, the intensities of the x-ray lines can be estimated to within an order of magnitude only. It is suggested that the observation of cosmic x-ray lines may serve as a powerful tool for studying interstellar matter. Information about interstellar matter is difficult to obtain by other methods. (auth) (Australia)

53816 OBSERVATION OF COSMIC GAMMA RADIATION ABOVE 10 MeV. Kinzer, R. L.; Seeman, N.; Share, G. H. (Naval Research Lab., Washington, D. C.). pp 51-5 of 12th International Conference on Cosmic Rays, Hobart, Australia. Vol. 1. Hobart, Australia; International Union of Pure and Applied Physics (1971).

From 12th international conference on cosmic rays; Hobart, Australia (16 Aug 1971). See CONF-710807–(Vol.1).

A search for gamma radiation above 20 MeV from the vicinity of the Crab Nebula was performed with an emulsion spark-chamber telescope capable of an angular resolution of $\leq 2\frac{1}{2}°$. Upper limits at the 95% confidence level are deduced for the total emission from the Crab and for the emission from the galactic plane in the direction of the anticenter. These limits are 2×10^{-4} γ/cm^2-sec for the Crab and 4×10^{-4} γ/cm^2-sec-rad for the plane. A linear extrapolation of the recorded gamma-ray flux vs. atmospheric depth allows one to set an upper limit of 4×10^{-3} γ/cm^2-sec-sr on the flux of extraterrestrial diffuse radiation above 10 MeV. Information was also obtained on the spectrum of secondary gamma rays near the top of the atmosphere. Preliminary results are consistent with a photon spectrum calculated by Beuermann (1971) which is dominated by bremsstrahlung below ~70 MeV and by π^0-decay above. (auth) (Australia)

53817 0.511 MeV GAMMA RAYS MEASURED WITH THE Ge(Li) DETECTOR AT THE BALLOON ALTITUDE. Nakagawa, S.; Tsukuda, M.; Okudaira, K.; (and others) (Rikkyo Univ., Tokyo). pp 77-83 of 12th International Conference on Cosmic Rays, Hobart, Australia. Vol. 1. Hobart, Australia; International Union of Pure and Applied Physics (1971).

From 12th international conference on cosmic rays; Hobart, Australia (16 Aug 1971). See CONF-710807–(Vol.1).

The 0.511-MeV gamma rays produced by the annihilation process of the positron and the negatron in the atmosphere were observed with the balloon-borne phoswich scintillation counters and high resolution Ge(Li) detector from 1967 to 1970. Balloon observations were carried out three times at the geomagnetic latitude $\lambda = 26°$N or 27.5°N, and results of the 0.511-MeV gamma-ray observations were consistent. The intensity of the 0.511-MeV gamma rays was 18.5 ± 4.7 photons $\cdot$ cm^{-2} $\cdot$ sec^{-1} at the atmospheric depth 7 g cm^{-2} and the production rate in a 1 cm^2 column of the atmosphere was 36.2 photons cm^{-1} sec^{-1}, which was in good agreement with the estimated value based on the cascade shower theory and energy balance of cosmic rays. The intensity and the production rate of the 0.511-MeV gamma rays in the atmosphere were compared with ones observed by other investigators. (auth) (Australia)

53818 COSMIC FLUX OF LOW ENERGY GAMMA RAYS. Damle, S. V.; Daniel, R. R.; Joseph, George; Lavakare, P. J. (Tata Inst. of Fundamental Research, Bombay). pp 84-9 of 12th International Conference on Cosmic Rays, Hobart, Australia. Vol. 1. Hobart, Australia; International Union of Pure and Applied Physics (1971).

From 12th international conference on cosmic rays; Hobart, Australia (16 Aug 1971). See CONF-710807–(Vol.1).

Measurements were made on the cosmic gamma rays of energy between 0.25 and 4.2 MeV from a balloon experiment made near the geomagnetic equator using a collimated 3" × 3" NaI(Tl) crystal assembly. The depth-intensity curves were used to obtain the contribution due to the cosmic gamma rays in this energy interval. An unfolding of the counting rates was performed to obtain the energy spectrum of the diffuse cosmic gamma rays. It appears that a spectrum of the type $E^{-1.5}$ fitted to the data beyond 200 keV will be consistent with other data available to this energy range. Upper limits on low energy gamma-ray fluxes from Sco X-1 and the Galactic centre region are also reported. (auth) (Australia)

53819 FLUX OF GALACTIC HIGH-ENERGY GAMMA RAYS. Clark, G. W. (Massachusetts Inst. of Tech., Cambridge); Garmire, G. P.; Kraushaar, W. L. pp 91-6 of 12th International Conference on Cosmic Rays, Hobart, Australia. Vol. 1. Hobart, Australia; International Union of Pure and Applied Physics (1971).

From 12th international conference on cosmic rays; Hobart, Australia (16 Aug 1971). See CONF-710807–(Vol.1).

A recalibration of the OSO-3 high-energy gamma-ray detector provided the following galactic gamma-ray fluxes; F_γ(anticenter) = $(3^{+1}_{-1.2}) \times 10^{-5}$ photons/cm^2 sec radian and F_γ(center) = $(1.2^{+.4}_{-.5}) \times 10^{-4}$ photons/cm^2 sec radian for energies above 100 MeV. Possible sources of error are discussed. Several galactic models to explain the observations are presented. (auth) (Australia)

53820 COSMIC GAMMA RAYS FROM SUPRATHERMAL PROTON BREMSSTRAHLUNG. Jones, Frank C. (Goddard Space Flight Center, Greenbelt, Md.). pp 97-101 of 12th International Conference on Cosmic Rays, Hobart, Australia. Vol. 1. Hobart, Australia; International Union of Pure and Applied Physics (1971).

From 12th international conference on cosmic rays; Hobart, Australia (16 Aug 1971). See CONF-710807–(Vol.1).

The radiation cross section for relativistic suprathermal proton bremsstrahlung was calculated using the Weizsaecker–Williams method. Curves representing the radiation spectra for protons of various energies are shown and an approximate expression for the spectrum, valid for photon energies greater than a few MeV, is given. This approximate spectrum is of the form such that the general analysis may be applied. This analysis shows that an inverse power-law spectrum of protons will produce, via the suprathermal proton bremsstrahlung process, an inverse power-law spectrum of gamma rays that is one power steeper than that of the protons. This makes it quite unlikely, contrary to a previously published report, that this process can contribute significantly to cosmic gamma rays. (auth) (Australia)

53821 PRIMARY ELECTRON OBSERVATIONS ($3 \leq E \leq 15$ GeV) RECORDED ON THE ESRO II SATELLITE. Marsden, P. L.; Jakeways, R.; Calder, I. R. (Univ. of Leeds, Eng.). pp 110-15 of 12th International Conference on Cosmic Rays, Hobart, Australia. Vol. 1. Hobart, Australia; International Union of Pure and Applied Physics (1971).

From 12th international conference on cosmic rays; Hobart, Australia (16 Aug. 1971). See CONF-710807-(Vol.1).

Previously reported preliminary observations from the Leeds Univ., electron experiment on the ESRO II satellite were re-examined and together with new data and calibrations were used to redetermine the primary electron spectrum for energies between 3 and 15 GeV. In addition, results on the modulation of the electron flux in the same energy range are presented. (auth) (Australia)

53822 FLUX AND ENERGY SPECTRUM OF COSMIC RAY ELECTRONS BETWEEN 10 AND 1000 GeV. Meyer, Peter; Mueller, Dietrich (Univ. of Chicago). pp 117-21 of 12th International Conference on Cosmic Rays, Hobart, Australia. Vol. 1. Hobart, Australia; International Union of Pure and Applied Physics (1971).

From 12th international conference on cosmic rays; Hobart, Australia (16 Aug 1971). See CONF-710807-(Vol.1).

A balloon borne counter-detector with a geometry factor of 0.1 m^2 ster was exposed for a total of 64 hours under about 4.6 g/cm^2 of residual atmosphere above Palestine, Texas, in 1970. The experimental technique and the method of data analysis are described, and preliminary results of this investigation, based on about 45% of the total amount of available data, are presented. The resulting electron flux is slightly lower than that previously reported and can, over the entire energy range, be represented by a power law with spectral index of about -2.8. (auth) (Australia)

53823 PRIMARY COSMIC RAY ELECTRON SPECTRUM FROM 10 GeV TO ABOUT 200 GeV. Silverberg, R. F.; Ormes, J. F.; Balasubrahmanyan, V. K.; Ryan, M. J. (Goddard Space Flight Center, Greenbelt, Md.). pp 122-7 of 12th International Conference on Cosmic Rays, Hobart, Australia. Vol. 1. Hobart, Australia; International Union of Pure and Applied Physics (1971).

From 12th international conference on cosmic rays; Hobart, Australia (16 Aug 1971). See CONF-710807-(Vol.1).

An ionization spectrometer consisting of 10.8 radiation lengths of tungsten and 35 radiation lengths of iron was used to determine the energy spectrum of cosmic-ray electrons above 10 GeV. The spectrometer was calibrated with electrons from 5.4 to 18 GeV at the Stanford Linear Accelerator and then flown at an altitude of 6 $gm\text{-}cm^{-2}$ for 16 hours. Separation of electron initiated events from proton events was achieved by utilizing starting point distributions, the shower development in tungsten, and the energy deposited in the large thickness of iron absorber. The exponent of the differential energy spectrum of the electrons was -3.1 ± 0.2 while the exponent of the background was consistent with the proton exponent of $-2.7 \pm .2$. (auth) (Australia)

53824 METHOD FOR DETERMINING THE MEAN ATOMIC MASS OF THE ELEMENTS IN THE PRIMARY COSMIC RADIATION THROUGHOUT THE LATITUDE SENSITIVE PART OF THE SPECTRUM. Lund, N.; Lundgaard Rasmussen, Ib; Peters, B. (Danish Space Research Inst., Lyngby). pp 130-7 of 12th International Conference on Cosmic Rays, Hobart, Australia. Vol. 1. Hobart, Australia; International Union of Pure and Applied Physics (1971).

From 12th international conference on cosmic rays; Hobart, Australia (16 Aug 1971). See CONF-710807-(Vol.1).

It is possible to obtain accurate results on the relative charge to mass ratios for the elements in the primary cosmic radiation with the help of the Earth's magnetic field, in the form of a set of ratios between any two elements i and j

$$\frac{\left\langle \left(\frac{Z_i}{A_i}\right)^{\gamma_j} \right\rangle^{\gamma_j/\gamma_i}}{\left\langle \left(\frac{Z_j}{A_j}\right) \right\rangle} = \frac{1}{C_{\rho q}K}\,\frac{R_\rho}{R_q}$$

The quantities which must be measured during an experiment are the local power exponents γ_i and γ_j and the flux ratio of the two elements both observed at equal rigidity cut-off (R_ρ) and at equal pulse height threshold (R_q). An accuracy of 5% for the γ's and about 0.5% for R_ρ and R_q is sufficient to obtain the relative masses to about 0.1 neutron mass for all elements up to silicon, and 0.2 neutron masses for iron. $C_{\rho q}$ is a calculated correction arising from the limited velocity resolution (and the nonuniformity) of the counters. K, which is very close to unity, is the residual uncertainty introduced by the unknown structure of the penumbra of the geomagnetic cut-offs. If the spectra of the two elements are found to be alike ($\gamma_i = \gamma_j$) then $K = 1$ and the structure of the penumbra does not enter the result at all. (auth) (Australia)

53825 UPPER LIMIT ON THE FLUX OF PRIMARY COSMIC RAY ANTI-ALPHA PARTICLES FROM 0.3 TO 3 GeV/NUCLEON. Evenson, Paul; Meyer, Peter (Univ. of Chicago). pp 138-43 of 12th International Conference on Cosmic Rays, Hobart, Australia. Vol. 1. Hobart, Australia; International Union of Pure and Applied Physics (1971).

From 12th international conference on cosmic rays; Hobart, Australia (16 Aug 1971). See CONF-710807-(Vol.1).

A preliminaty analysis of approximately 1200 alpha particle events gathered on three high-altitude balloon flights in summer 1970 at Ft. Churchill, Canada, was made using scintillation counters to measure time of flight and energy loss for each event and photographs of a series of spark chambers to record the deflection of each particle in the field of a permanent magnet. No anti-particles were identified. This implies an upper limit of 0.24% (at the 95% confidence level) on the flux of anti-alpha particles in the energy interval 0.3 to 3 GeV/nucleon. (auth) (Australia)

53826 MEASUREMENT OF THE PRIMARY COSMIC RAY NUCLEAR RIGIDITY SPECTRA FOR INDIVIDUAL ELEMENTS OF CHARGE $Z \geq 2$. Buffington, A.; Smith, L. H.; Smoot, G.; Wahlig, M. A.; Alvarez, L. W. (Univ. of California, Berkeley). pp 147-54 of 12th International Conference on Cosmic Rays, Hobart, Australia. Vol. 1. Hobart, Australia; International Union of Pure and Applied Physics (1971).

From 12th international conference on cosmic rays; Hobart, Australia (16 Aug 1971). See CONF-710807-(Vol.1).

A superconducting magnetic spectrometer was flown to about 5 gm/cm^2 residual atmosphere on September 18, 1970, and May 7, 1971, by a balloon. 12,500 events with charge 3 and greater were rigidity analyzed on the two balloon flights. The trigger criteria were changed for a short while on each flight so that 12,000 helium nuclei could be momentum analyzed. (auth) (Australia)

53827 MEASUREMENT OF THE LOW ENERGY HELIUM ISOTOPES IN THE PRIMARY COSMIC RAYS. Tamai, E.; Narita, N.; Sakai, T. (Nihon Univ., Chiba, Japan). pp 156-61 of 12th International Conference on Cosmic Rays, Hobart, Australia. Vol. 1. Hobart, Australia; International Union of Pure and Applied Physics (1971).

From 12th international conference on cosmic rays; Hobart, Australia (16 Aug 1971). See CONF-710807-(Vol.1).

The isotopic composition of low-energy He nuclei in primary cosmic radiation was analyzed, using a nuclear emulsion stack. The abundance ratio of ^{3}He nuclei to total He nuclei at the top of the atmosphere was determined to be 11.8%, in the kinetic energy interval of 100 to 260 MeV/n. From this ratio, a mean path length traversed by low-energy cosmic rays from their source to the earth is estimated. (auth) (Australia)

53828 PRODUCTION OF ^{2}H AND ^{3}He NUCLEI IN COSMIC RAYS AND PROPAGATION OF PROTONS AND HELIUM NUCLEI THROUGH INTERSTELLAR SPACE. Biswas, S.; Ramadurai, S. (Tata Inst. of Fundamental Research, Bombay). pp 162-7 of 12th International Conference on Cosmic Rays, Hobart, Australia. Vol. 1. Hobart, Australia; International Union of Pure and Applied Physics (1971).

From 12th international conference on cosmic rays; Hobart, Australia (16 Aug 1971). See CONF-710807-(Vol.1).

Final results of detailed calculations on the intensity and energy spectra of ^{2}H and ^{3}He nuclei in cosmic rays are presented. Calculations take into account (a) energy dependent cross sections of thirteen nuclear reactions involving cosmic-ray protons and alpha particles with interstellar hydrogen and helium nuclei; (b) angular distribution and kinematics of these reactions; (c) ionization loss of primary and secondary nuclei; and (d) elastic collisions of protons and helium nuclei. It was assumed that the source spectra are a power law in rigidity, and Fermi spectrum. The following models for the distribution of path lengths were examined: (i) slab, (ii) gaussian, and (iii) exponential. The results of the calculations and comparisons with available experimental data on $^2H/^4He$ and $^3He/(^3He + ^4He)$ ratios showed that a gaussian distribution of path lengths with mean amount of interstellar matter of 6.5 g cm^{-2} explained both these ratios and their energy dependence in the range 30 to 1000 MeV/n. An exponential distribution of path lengths with uniform distribution of sources is not in agreement with observations. (auth) (Australia)

53829 COSMIC RAY PROTON AND HELIUM SPECTRA ABOVE 50 GeV. Ryan, M. J.; Balasubrahmanyan, V. K.; Ormes, J. F. (Goddard Space Flight Center, Greenbelt, Md.). pp 173-7 of 12th International Conference on Cosmic Rays, Hobart, Australia. Vol. 1. Hobart, Australia; International Union of Pure and Applied Physics (1971).

From 12th international conference on cosmic rays; Hobart, Australia (16 Aug 1971). See CONF-710807-(Vol.1).

The primary cosmic-ray proton and He spectra from 50 to 2000 GeV were measured by an ionization spectrometer flown on a balloon at an altitude of 6 gm cm^{-2} for 16 hours. The geometrical factor of the instrument was 300 cm^2 sterad and more than 5,000 events were observed. At low energies, the energies of individual events can be determined to within ±30%. At higher energies, the cascade is not fully contained within the four mean free path thick spectrometer and the problems of estimating the energies of these events are discussed. The proton spectrum continues with constant exponent = -2.7 ± 0.1 up to energies greater than 1,000 GeV. This spectrum is in agreement with the results of Pinkau et al. (1969) at the low energies. However, there is no evidence for the spectral break at about 1,000 GeV. (auth) (Australia)

53830 CHARGE COMPOSITION OF GALACTIC COSMIC RADIATION. Ormes, J. F.; Balasubrahmanyan, V. K.; Ryan, M. J. (Goddard Space Flight Center, Greenbelt, Md.). pp 178-83 of 12th International Conference on Cosmic Rays, Hobart, Australia. Vol. 1. Hobart, Australia; International Union of Pure and Applied Physics (1971).

From 12th international conference on cosmic rays; Hobart, Australia (16 Aug 1971). See CONF-710807-(Vol.1).

Experimental results from the balloon borne ionization spectrometer flown in November 1970 enabled the extension of the measurement of the energy spectra of cosmic rays to 10^{12} eV. The exposure factor for this flight was 1825 m^2-sr-sec and approximately 10,000 nuclei with $Z \geq 3$ were observed. For nuclei with $Z \sim 6$, charges could be resolved to ±0.2 units. The technique used for the measurement of energies of complex nuclei using an ionization spectrometer is reported. Differential spectra of individual nuclei from lithium to oxygen and groups of nuclei with Z = 10 to 14, 15 to 19, 20 to 23, and 24 to 30 were measured. The differential spectra of these nuclear species for the energy range 2×10^{10} eV to 10^{12} eV could be described in a power-law representation with an exponent -2.6. The results indicate that the composition of galactic cosmic rays remains similar to that observed at lower energies. These results from direct measurements, provide evidence for the processes of source acceleration, and interstellar propagation remaining essentially energy independent up to 10^{12} eV. (auth) (Australia)

53831 NUCLEAR-ELECTROMAGNETIC CASCADES FROM ALPHA PARTICLES INCIDENT ON AN IRON ABSORBER. Jones, W. V. (Louisiana State Univ., Baton Rouge). pp 184-9 of 12th International Conference on Cosmic Rays, Hobart, Australia. Vol. 1. Hobart, Australia; International Union of Pure and Applied Physics (1971).

From 12th international conference on cosmic rays; Hobart, Australia (16 Aug 1971). See CONF-710807-(Vol.1).

Mean values and fluctuations of the nuclear-electromagnetic cascade development resulting from alpha particles incident on an iron absorber were determined for the primary energy range 10 to 300 GeV/N. This was accomplished by using a three-dimensional Monte Carlo simulation of the cascade process. The model used was first adjusted until it gave predictions for a small ionization spectrometer which agreed with measurements obtained by exposing the same spectrometer to 10, 20.5, and 28 GeV/c protons at an accelerator. The calculations were then modified to apply to high-energy alpha particles. The results show that measurements of the energies of alpha particles incident on an iron spectrometer with six interaction lengths total depth can be made with accuracies ranging from ~5% at 300 GeV/N to ~16% at 10 GeV/N. (auth) (Australia)

53832 NUCLEAR-ELECTROMAGNETIC CASCADE FROM NUCLEI WITH $Z \geq 3$. Jones, W. V. (Louisiana State Univ., Baton Rouge). pp 190-5 of 12th International Conference on Cosmic Rays, Hobart, Australia. Vol. 1. Hobart, Australia; International Union of Pure and Applied Physics (1971).

From 12th international conference on cosmic rays; Hobart, Australia (16 Aug 1971). See CONF-710807-(Vol.1).

A Monte Carlo simulation method was developed for studying nuclear-electromagnetic cascades initiated by high-energy nuclei with $Z \geq 3$ incident on heavy absorbers. The calculations are based on a cascade model which was first adjusted until it agreed with measurements made with protons at an accelerator. Modifications of the model used for protons include the incorporation of the probabilities for fragmentation of heavy nuclei into lighter nuclei, alpha particles, and nucleons. Mean values and fluctuations of the equivalent numbers of particles in the cascades at various depths in an iron absorber are presented for protons, carbon, and iron nuclei over the 30- to 300-GeV/N energy range. (auth) (Australia)

53833 NEW OBSERVATIONS AND CALCULATIONS OF PRIMARY Be/B IN THE COSMIC RAYS. O'Dell, F. W.; Shapiro, M. M.; Silberberg, R.; Tsao, C. H. (Naval Research Lab., Washington, D. C.). pp 197-202 of 12th International Conference on Cosmic Rays, Hobart, Australia. Vol. 1. Hobart, Australia; International Union of Pure and Applied Physics (1971).

From 12th international conference on cosmic rays; Hobart, Australia (16 Aug 1971). See CONF-710807-(Vol.1).

The fate of ^{10}Be in cosmic rays depends upon cosmic-ray lifetime, and determines the arriving ratio Be/B. In a Texas balloon flight, an emulsion detector stack was exposed. Data yielded a Be/B ratio of 0.37 ± 0.05 at the top of the atmosphere. This compared with a value 0.37 ± 0.07 from previous, comparable emulsion experiments, and with 0.40 ± 0.03 obtained with a counter telescope. Combining all three values (rigidity threshold ~4.5 GV) gave a Be/B ratio of 0.39 ± 0.03. New, calculated estimates of Be/B were, respectively, 0.42 ± 0.06 and 0.29 ± 0.05 for survival and decay of the ^{10}Be. The observations were more compatible with substantial survival of the ^{10}Be, and the confinement time of cosmic-ray nuclei is probably less than 50 million years—possibly much less. (auth) (Australia)

53834 RIGIDITY SPECTRUM OF $Z \geq 3$ NUCLEI FROM 5 GeV TO OVER 300 GeV. Golden, R. L. (Manned Spacecraft Center, Houston, Tex.); Adams, J. H.; Boykin, W. R.; (and others). pp 203-5 of 12th International Conference on Cosmic Rays, Hobart, Australia. Vol. 1. Hobart, Australia; International Union of Pure and Applied Physics (1971).

From 12th international conference on cosmic rays; Hobart, Australia (16 Aug 1971). See CONF-710807-(Vol.1).

A 46 cm^2-sr geometry factor superconducting magnet emulsion spectrometer with resolution exceeding 300 GV was flown for 8 hours at Palestine, Texas, on August 22, 1969. The data gathered on $Z \geq 3$ nuclei indicated a differential rigidity spectrum of the form $\rho^{-2.5\pm.1}$ for rigidities of 8 to 300 GV. Spectral structure in the region 5 to 8 GV was not consistent with geomagnetic cutoff calculations. The data were also divided into L, M, and H charge groups. Spectra for the different groups were mutually consistent. No antinuclei were observed. Preliminary results from 13 hours of flight in Parana, Argentina, are presented. (auth) (Australia)

53835 ENERGY DEPENDENCE OF THE ABUNDANCES OF GALACTIC He, L, AND M NUCLEI FROM SATELLITE MEASUREMENTS. Garcia-Munoz, M.; Mason, G. M.; Simpson, J. A. (Univ. of Chicago). pp 209-14 of 12th International Conference on Cosmic Rays, Hobart, Australia. Vol. 1. Hobart, Australia; International Union of Pure and Applied Physics (1971).

From 12th international conference on cosmic rays; Hobart, Australia (16 Aug 1971). See CONF-710807-(Vol.1).

The differential energy spectra of He and the L and M nuclei were measured from 10 to 1000 MeV per nucleon with cosmic-ray telescopes on board the IMP-4 and IMP-5 satellites in 1967–1970. The ratios He/M and L/M derived from these spectra were found to be nearly energy independent within errors of ~15%, and equal to ~15 and ~0.25, respectively. It was found that a steady state model with an exponential distribution of path lengths and a 6 ± 1 g/cm^2 leakage mean free path can produce the observed high-energy L nuclei. However, as found in earlier observations, the observed ratios for He/M and L/M depart from the calculated ratios below ~100 MeV/N. This discrepancy with the equilibrium model is discussed in terms of additional mechanisms operative at low energies, including adiabatic deceleration in the solar system. The parameters derived from the above observations were used to discuss (1) the calculated versus the observed energy dependence of the ratios C/O and N/O, and (2) the question of whether N nuclei are required in the source composition in order to reproduce the observed N/O = 0.32 ± 0.05 at high energy. (auth) (Australia)

53836 ABUNDANCES OF THE GALACTIC NUCLEI H THROUGH THE Fe GROUP FROM SATELLITE MEASUREMENTS. Cartwright, B. G.; Garcia-Munoz, M.; Simpson, J. A. (Univ. of Chicago). pp 215-20 of 12th International Conference on Cosmic Rays, Hobart, Australia. Vol. 1. Hobart, Australia; International Union of Pure and Applied Physics (1971).

From 12th international conference on cosmic rays; Hobart, Australia (16 Aug 1971). See CONF-710807-(Vol.1).

The University of Chicago instruments on the IMP-4 and IMP-5 satellites were designed to measure simultaneously with a single instrument the relative abundances of nuclei over the range $Z = 1$ to $Z = 26$ in the energy range ~20 to 300 MeV/N with individual charge resolution for all nuclei except Mn and the Fe group of nuclei. In addition, the relative abundances for the nuclei $Z < 10$ were measured on IMP-5 to >1000 MeV/N. The measurements confirm earlier satellite results showing that the relative abundances are energy independent to within ±20%. The determination of the odd-Z abundances between oxygen and silicon and between silicon and the iron group of nuclei makes it possible to draw conclusions regarding the charge composition of the source regions for the cosmic rays after taking account of their production in interstellar propagation. Calculations for a wide range of propagation models were made for the abundances of these two charge regions. For example, it is shown that the abundances of sodium, aluminum, and phosphorus are enriched significantly in the source relative to solar system abundances, whereas fluorine is not required in the source. (auth) (Australia)

53837 REVISED SOURCE COMPOSITION OF COSMIC RAYS FROM HYDROGEN TO NICKEL. Shapiro, M. M.; Silberberg, R.; Tsao, C. H. (Naval Research Lab., Washington, D. C.). pp 221-7 of 12th International Conference on Cosmic Rays, Hobart, Australia. Vol. 1. Hobart, Australia; International Union of Pure and Applied Physics (1971).

From twelfth international conference on cosmic rays; Hobart, Australia (16 Aug 1971). See CONF-710807-(Vol.1).

The primordial cosmic-ray composition was recalculated incorporating improvements in observed abundances, and in measured as well as computed cross sections. Semi-empirical relations that fit a wide range of measured cross sections permit more reliable estimates of many important unmeasured reaction rates. Feeding these into the diffusion equations yielded a path-length distribution function $e^{-0.23x}$ ($x > 1$ g/m^2), and a revised set of abundances at the source. Values are now given for H, He, and Ni, while Cr has been deleted (it is now <1% of carbon). Mg, Si, Ar, and Ca are somewhat enhanced. Trace elements at the source include: S, 4 ± 2; Ar and Ca, each 2 ± 2; Na, Al, and Ni, each 1 ± 1. The ratio R of primordial cosmic-ray to solar system abundances is plotted versus atomic number Z, and extended to include the results of Fowler et al and Price et al on the ultra-heavy nuclei. Although this graph displays a general increase of R with Z, there are appreciable departures from the monotonic trend. (auth) (Australia)

53838 CHEMICAL COMPOSITION OF COSMIC RAYS WITH Z = 3 TO 30 AT HIGH AND LOW ENERGIES. Webber, W. R.; Damle, S. V.; Kish, J. M. (Univ. of New Hampshire, Durham). pp 229-34 of 12th International Conference on Cosmic Rays, Hobart, Australia. Vol. 1. Hobart, Australia; International Union of Pure and Applied Physics (1971).

From twelfth international conference on cosmic rays; Hobart, Australia (16 Aug 1971). See CONF-710807-(Vol.1).

The chemical composition of cosmic rays with $Z \geq 2$ was measured over an energy range from ~100 MeV/N to >2 BeV/N using 2 new large-area counter telescopes. A detailed charge spectrum is obtained at both high and low energies. Composition data was extrapolated to the cosmic ray sources using various types of interstellar path length distributions. (auth) (Australia)

53839 STUDY OF THE CHARGE SPECTRUM OF COSMIC-RAY NUCLEI. Choi, K. A.; Kim, C. O. (Korea Univ., Seoul). pp 235-40 of 12th International Conference on Cosmic Rays, Hobart, Australia. Vol. 1. Hobart, Australia; International Union of Pure and Applied Physics (1971).

From twelfth international conference on cosmic rays; Hobart, Australia (16 Aug 1971). See CONF-710807-(Vol.1).

Ninety-two cosmic-ray primaries, found in the 22-liter emulsion stack, flown for 13 hours at an altitude of 116,000 feet in Texas, were analyzed to determine their charges. Energies (GeV/N) were estimated from the angular distributions of nuclei fragments, and their charges from the method of delta-ray counting. Because of the size and the considerable duration of the flight time of the Texas stack, it was expected to obtain some flux of the primary cosmic rays of high energies. (auth) (Australia)

53840 CHEMICAL COMPOSITION OF HEAVY COSMIC RAY NUCLEI ABOVE 5 GeV. Casse, M. (CEA, Saclay, France); Koch, L.; Lund, N.; (and others). pp 241-5 of 12th International Conference on Cosmic Rays, Hobart, Australia. Vol. 1. Hobart, Australia; International Union of Pure and Applied Physics (1971).

From twelfth international conference on cosmic rays; Hobart, Australia (16 Aug 1971). See CONF-710807-(Vol.1).

Using improved instrumentation similar to that described at the 1970 COSPAR meeting, new results were obtained on the abundance ratio of elements between atomic numbers 4 and 30. (auth) (Australia)

53841 CHEMICAL COMPOSITION OF LOW ENERGY L AND M NUCLEI IN THE PRIMARY COSMIC RADIATION. Tamai, E.; Narita, N.; Sakai, T.; Ogura, K. (Nihon Univ., Chiba, Japan). pp 246-51 of 12th International Conference on Cosmic Rays, Hobart, Australia. Vol. 1. Hobart, Australia; International Union of Pure and Applied Physics (1971).

From twelfth international conference on cosmic rays; Hobart, Australia (16 Aug 1971). See CONF-710807-(Vol.1).

In balloon experiments flown at Fort Churchill during solar minimum, nuclear emulsion stacks were used to study the chemical composition and energy spectra of L and M nuclei in the primary cosmic rays above the atmosphere in the energy interval from 90 to 300 MeV/N. The results show a flux ratio for L to M nuclei of 0.44 in the 107 to 250 MeV/N region. The elemental structures of L and M nuclei are also reported. (auth) (Australia)

53842 CHARGE AND ENERGY SPECTRA OF HEAVY COSMIC RAY NUCLEI. Freier, Phyllis S.; Long, C. E.; Cleghorn, T. F.; Waddington, C. J. (Univ. of Minnesota, Minneapolis). pp 252-7 of 12th International Conference on Cosmic Rays, Hobart, Australia. Vol. 1. Hobart, Australia; International Union of Pure and Applied Physics (1971).

From twelfth international conference on cosmic rays; Hobart, Australia (16 Aug 1971). See CONF-710807-(Vol.1).

A photodensitometer technique was used to measure the charge spectrum of low-energy cosmic ray nuclei heavier than sulphur. This spectrum is mainly characterized by iron and calcium nuclei, with appreciably lesser abundances of other elements. The energy spectrum of $Z \geq 20$ nuclei observed in 1968 was compared with that obtained previously in 1964. This comparison, together with a determination of the energy spectrum of helium nuclei in 1968, allows one to conclude that there is no significant charge dependence of the solar modulation. (auth) (Australia)

53843 OBSERVATION OF VH AND VVH COSMIC RAYS WITH AN IONIZATION–CHERENKOV DETECTOR SYSTEM. Binns, W. R. (McDonnell Douglas Research Labs., St. Louis); Fernandez, J. I.; Israel, M. H.; Klarmann, J.; Mewaldt, R. A. pp 260-5 of 12th International Conference on Cosmic Rays, Hobart, Australia. Vol. 1. Hobart, Australia; International Union of Pure and Applied Physics (1971).

From twelfth international conference on cosmic rays; Hobart, Australia (16 Aug 1971). See CONF-710807-(Vol.1).

A detector system including parallel-plate pulse ionization chambers and a Lucite Cherenkov counter, having geometry factor 0.92 m^2 ster, was operated during a series of balloon flights near 4.5 g/cm^2 atmospheric depth at geomagnetic cutoffs near 4.5 GV and 1.6 GV. Charge spectra and flux ratios are presented. The VH results are consistent with a cosmic-ray source having $J(21 \leq Z \leq 24) = 0$, and $J(20)/J(26) = .12 \pm .06$. The VVH results are consistent with the dominant mode of nucleosynthesis for these nuclei being rapid neutron capture (r-process). (auth) (Australia)

53844 COMMENTS ON THE OBSERVATION OF TRANSURANIC NUCLEI IN THE PRIMARY COSMIC RADIATION. Blanford, G. E. Jr.; Friedlander, M. W.; Klarmann, J.; (and others) (Washington Univ., St. Louis). pp 269-72 of 12th International Conference on Cosmic Rays, Hobart, Australia. Vol. 1. Hobart, Australia; International Union of Pure and Applied Physics (1971).

From twelfth international conference on cosmic rays; Hobart, Australia (16 Aug 1971). See CONF-710807-(Vol.1).

The results of preliminary measurements on the track of a primary cosmic-ray particle, in emulsions and plastics, indicated a possible charge of $Z = 113$. Further measurements and calibration showed that this particle was not relativistic within the detectors, and the best charge estimate was $Z = 76 \pm 4$. During a total of five balloon flights, an exposure of about 10^7 m^2.ster.s. was accumulated, with no particles being detected in the charge range $Z > 96$. Combining this with the data reported by other workers allows estimates to be made of the flux of such particles and their abundance relative to iron nuclei. (auth) (Australia)

53845 CALCULATIONS OF CROSS SECTIONS AND THEIR APPLICATION TO COSMIC-RAY PHYSICS. Silberberg, R.;

Tsao, C. H. (Naval Research Lab., Washington, D. C.). pp 273-7 of 12th International Conference on Cosmic Rays, Hobart, Australia. Vol. 1. Hobart, Australia; International Union of Pure and Applied Physics (1971).

From twelfth international conference on cosmic rays; Hobart, Australia (16 Aug 1971). See CONF-710807—(Vol.1).

A knowledge of partial cross sections of nucleon—nucleus interactions is essential for the determination of (a) the primordial composition of cosmic rays on leaving the source regions, (b) the mean path length in interstellar matter, and (c) the galactic confinement time of cosmic rays. Only a few of the essential cross sections have been measured; most must be calculated by semi-empirical methods or Monte Carlo techniques. Experimental cross sections for products from proton interactions with various nuclei have been tabulated and used to formulate new empirical cross section relations. The relations are applicable to all products having a mass number $A \geq 6$, and for targets ranging from lithium to uranium. For targets with atomic number $Z \leq 30$, the relations are applicable at energies $E \geq 100$ MeV. For $6 \leq Z \leq 16$, the products with $Z \geq 6$, the standard deviation of the calculated cross sections (from the measured values) is about 20% at energies above 1 GeV, and increases to about 30% at 150 MeV; for products with $Z < 6$, it is about 30%. (auth) (Australia)

53846 STUDY OF THE SIDEREAL ANISOTROPY OF COSMIC RAYS WITH MUON TELESCOPES UNDERGROUND. Ahluwalia, H. S. (Univ. of New Mexico, Albuquerque). pp 279-83 of 12th International Conference on Cosmic Rays, Hobart, Australia. Vol. 1. Hobart, Australia; International Union of Pure and Applied Physics (1971).

From twelfth international conference on cosmic rays; Hobart, Australia (16 Aug 1971). See CONF-710807—(Vol.1).

The observations on the sidereal diurnal variation of the medium energy (~100 GeV) cosmic rays reported in the literature over a period of more than three decades are reviewed. These observations have been obtained with muon detectors located on the surface of the earth as well as underground. The observations seem to favor a power-law type of variational spectrum with a negative exponent of: 0.35 ± 0.28. There is considerable uncertainty as to whether there is an upper-bound on the spectrum. (auth) (Australia)

53847 INTERPRETATION OF SIDEREAL COSMIC RAY ANISOTROPIES. Swinson, Derek B. (Univ. of New Mexico, Albuquerque). pp 284-9 of 12th International Conference on Cosmic Rays, Hobart, Australia. Vol. 1. Hobart, Australia; International Union of Pure and Applied Physics (1971).

From twelfth international conference on cosmic rays; Hobart, Australia (16 Aug 1971). See CONF-710807—(Vol.1).

Data from giant muon telescopes at different depths underground in the northern and southern hemispheres are presented for the period 1965-1970, analyzed in sidereal time. It is observed that the phases of the sidereal anisotropies are strongly dependent on the direction of the interplanetary magnetic field, and an upper cut-off to the anisotropy appears to be indicated. Evidence for a two cycle per year modulation of the sidereal anisotropy is also presented, and its interpretation is discussed. It is concluded that no information of any astrophysical significance can be obtained about the direction of any galactic cosmic-ray anisotropy from cosmic rays of rigidity less than about 100 GV. (auth) (Australia)

53848 COMPONENTS OF THE SIDEREAL ANISOTROPY. Jacklyn, R. M. (Dept. of Supply, Melbourne); Cooke, D. J. pp 290-5 of 12th International Conference on Cosmic Rays, Hobart, Australia. Vol. 1. Hobart, Australia; International Union of Pure and Applied Physics (1971).

From twelfth international conference on cosmic rays; Hobart, Australia (16 Aug 1971). See CONF-710807—(Vol.1).

A method of estimating directions and energy ranges of components of the sidereal anisotropy is described. From a trial analysis using data from a prototype high-zenith-angle telescope at Mawson and the vertical underground telescopes at Hobart, there is evidence that: (a) The two-way sidereal component is of sufficiently high mean energy to allow the analysis to discriminate against an energy range appropriate to interplanetary modulation. (b) The uni-directional component is of relatively low mean energy and of variable amplitude. There may have been a reversal of the right ascension, from the value ~0600 (1958-65) to ~1800 (1968-69). (auth) (Australia)

53849 SPURIOUS SIDEREAL ANISOTROPY ARISING FROM ANNUAL MODULATION OF SOLAR DIURNAL VARIATION OF COSMIC RADIATION. Kondo, I.; Ueno, H.; Nagashima, K. (Nagoya Univ., Japan). pp 296-301 of 12th International Conference on Cosmic Rays, Hobart, Australia. Vol. 1. Hobart, Australia; International Union of Pure and Applied Physics (1971).

From twelfth international conference on cosmic rays; Hobart, Australia (16 Aug 1971). See CONF-710807—(Vol.1).

So far the absence of the anti-sidereal time variation has been regarded as a measure for the existence of true sidereal anisotropy of cosmic-ray intensity. This criterion, however, is found not to be effective in the following situation. When a solar anisotropy with constant magnitude and direction relative to the Sun—Earth line is present throughout the year, the daily variation observed at the Earth is modulated by the revolution of the Earth around the Sun. Such an annual modulation produces the anti-sidereal time variation comparable to the sidereal, except one special case. If, however, the anisotropy is subjected to random fluctuation around its mean value according to the variation of interplanetary space condition, the anti-sidereal time variation becomes quite small in comparison with the sidereal. Such a spurious sidereal anisotropy is characterized by its eigenphase whose value is 6 or 18 hr for the diurnal, and 0 or 6 hr for the semi-diurnal components. (auth) (Australia)

53850 SIDEREAL AND SOLAR ANISOTROPY OF HIGH-ENERGY COSMIC RAYS OBSERVED BY AN AIR CHERENKOV TELESCOPE. Sekido, Y.; Nagashima, K.; Kondo, I.; Sakakibara, S. (Nagoya Univ., Japan). pp 302-7 of 12th International Conference on Cosmic Rays, Hobart, Australia. Vol. 1. Hobart, Australia; International Union of Pure and Applied Physics (1971).

From twelfth international conference on cosmic rays; Hobart, Australia (16 Aug 1971). See CONF-710807—(Vol.1).

Observation of high-energy (~200 GeV) cosmic rays was continued from February 1968 to 1971, using the air Cherenkov telescope at Nagoya (35°N). Two declination bands ($\delta = 0°$ and 20°S) in the celestial sphere were scanned. The sidereal anisotropy observed at $\delta = 0°$ showed a predominant second harmonic, which is the characteristic feature of the bi-directional type proposed by Jacklyn. By these observations, this type was established as the unique empirical model of the sidereal anisotropy, and the distribution of intensities against the angle from the axis of the anisotropy was obtained from the observations ($\delta = 30°$N, 0° and 20°S). The diurnal and semi-diurnal harmonics of the solar anisotropy obtained from these observations were similar to those of other underground observations of the same energy region. (auth) (Australia)

53851 GALACTIC MAGNETIC FIELD AND ANISOTROPY OF COSMIC RAYS ABOVE 10^{17} eV. Karakula, S. (Univ. of Durham, Eng.); Osborne, J. L.; Roberts, E.; Tkaczyk, W. pp 310-15 of 12th International Conference on Cosmic Rays, Hobart, Australia. Vol. 1. Hobart, Australia; International Union of Pure and Applied Physics (1971).

From twelfth international conference on cosmic rays; Hobart, Australia (16 Aug 1971). See CONF-710807—(Vol.1).

The detailed form of the anisotropy of ultrahigh-energy cosmic rays of galactic origin for given magnetic fields and source distribution is predicted from proton trajectories. Data on the arrival directions of EAS are then compared with the predicted distributions, and, assuming that metagalactic cosmic rays are isotropic, upper limits are given for the fraction of cosmic rays of galactic origin. (auth) (Australia)

53852 ARRIVAL DIRECTIONS OF LARGE AIR SHOWERS OF PRIMARY ENERGY > 10^{17} eV. Lapikens, J.; Martin, R.; Reid, R. J. O.; (and others) (Univ. of Leeds, Eng.). pp 316-20 of 12th International Conference on Cosmic Rays, Hobart, Australia. Vol. 1. Hobart, Australia; International Union of Pure and Applied Physics (1971).

From twelfth international conference on cosmic rays; Hobart, Australia (16 Aug 1971). See CONF-710807—(Vol.1).

The analysis of 53,733 showers detected in the period July 1966—July 1970 is now complete and is presented; new limits on the magnitude of possible anisotropies are established. More significant aspects of the present work are that, as a result of the enlarged Stage II array, and also because of improvements in the techniques of analysis of EAS, it is now possible to search for anisotropies in relatively narrow intervals of primary energy over the range 10^{17} to 10^{19} eV. Osborne and Wolfendale (private communication), in a preliminary study of the expected anisotropies for proton primaries originating in the spiral arms of the Galaxy, have used the galactic model and magnetic field configuration given by Thielheim and Langhoff (1968). They find that while the phase of the principal maximum is relatively independent of primary energy, the magnitude and detailed form of the predicted anisotropy is very energy sensitive from about 3.10^{17} eV to 5.10^{18} eV. (Australia)

53853 FLARE STAR PRODUCTION OF ENERGETIC CHARGED PARTICLES. Edwards, P. J.; McQueen, M. (Univ. of Otago, Dunedin, N. Z.). pp 323-8 of 12th International Conference on Cosmic Rays, Hobart, Australia. Vol. 1. Hobart, Australia; International Union of Pure and Applied Physics (1971).

From twelfth international conference on cosmic rays; Hobart, Australia (16 Aug 1971). See CONF-710807—(Vol.1).

Recent observations of solar and stellar flares are used in a reexamination of the proposal due to Unsöld (1957) that flare stars may make a substantial contribution to the galactic cosmic radiation. Flares in young convective stars of spectral type later than KO are considered. Observations of the x-ray brightness of the galactic disc indicate a negligible cosmic-ray contribution if the energetic charged particle output relative to the x-ray output is the same in stellar flares as in solar flares. (auth) (Australia)

53854 PARTICLE ACCELERATION BY WHITE DWARFS AND THE CHARGE SPECTRUM OF THE NUCLEAR COMPONENT OF COSMIC RAYS. Cowsik, R. (Univ. of California, Berkeley). pp 329-33 of 12th International Conference on Cosmic Rays, Hobart, Australia. Vol. 1. Hobart, Australia; International Union of Pure and Applied Physics (1971).

From twelfth international conference on cosmic rays; Hobart, Australia (16 Aug 1971). See CONF-710807—(Vol.1).

Using "pulsar mechanisms" for cosmic-ray acceleration an estimate of the rate of injection of cosmic rays by white dwarfs into the galactic volume was made showing that this is an adequate source for the observed cosmic rays. Simple models for the preferential acceleration of heavy nuclei are outlined and it is shown that a reasonable agreement with the observed charge spectrum can be achieved. The advantages and the weaknesses of the white-dwarf model for the acceleration of cosmic rays are indicated. (auth) (Australia)

53855 COSMIC RAY ELECTRONS AND THE GAMMA-RAY BACKGROUND. Cowsik, R. (Univ. of California, Berkeley). pp 334-9 of 12th International Conference on Cosmic Rays, Hobart, Australia. Vol. 1. Hobart, Australia; International Union of Pure and Applied Physics (1971).

From twelfth international conference on cosmic rays; Hobart, Australia (16 Aug 1971). See CONF-710807—(Vol.1).

The cosmic-ray electron spectrum is well measured in the solar neighborhood in the energy interval ~few MeV to ~few 100 GeV. The spectrum of positrons is not well known but reasonable measurements exist up to ~10 GeV. The measured spectra have been distorted by modulation by the outward flowing solar wind but there are many reasonably reliable ways for correcting these effects. Corrected spectra which represent the nature of the spectra in the interstellar space are shown. The positron flux is believed to have arisen in the decay of mesons produced in the nuclear interaction of the protons, α-particles, and other heavier nuclei in the cosmic rays. The difference between the total electron flux and the estimated flux of secondary origin gives the spectrum of the negatrons accelerated by the sources. This spectrum at injection has a slope of ~2.7 at high energies and below a few GeV falls considerably short of the intensity predicted by $\sim E^{-2.7}$. Below $\sim\frac{1}{2}$ GeV the spectrum rolls over and one may even have a positive exponent. (auth) (Australia)

53856 POSSIBILITY OF ENERGETIC COSMIC RAYS ARRIVING FROM THE CRAB NEBULA. Osborne, J. L.; Roberts, E. (Univ. of Durham, Eng.). pp 340-3 of 12th International Conference on Cosmic Rays, Hobart, Australia. Vol. 1. Hobart, Australia; International Union of Pure and Applied Physics (1971).

From twelfth international conference on cosmic rays; Hobart, Australia (16 Aug 1971). See CONF-710807—(Vol.1).

Of the particles originating in the Crab supernova explosion only those whose trajectories have a length greater by 0.28 kpc than the straight line distance to the Crab will be arriving at the Earth at the present time. For a specific model of the galactic magnetic field the trajectories of protons from the Crab were calculated and it was concluded that those arriving now have energy 6.6 10^{17} eV. The absence of any observed point source sets an upper limit to the number of protons emitted with this energy of 10^{19} eV^{-1}. (auth) (Australia)

53857 ACCELERATION AND PROPAGATION OF HIGH Z COSMIC RAYS IN A PULSAR ENVIRONMENT. Balasubrahmanyan, V. K.; Ormes, J. F.; Ryan, M. J. (Goddard Space Flight Center, Greenbelt, Md.). pp 344-8 of 12th International Conference on Cosmic Rays, Hobart, Australia. Vol. 1. Hobart, Australia; International Union of Pure and Applied Physics (1971).

From twelfth international conference on cosmic rays; Hobart, Australia (16 Aug 1971). See CONF-710807—(Vol.1).

The survival of high Z nuclei in the x-ray photon field of a pulsar is investigated. For heavy nuclei with energies $\geq$100 GeV/N, 100 keV x-ray photons have sufficient energy to cause photodisintegration with cross sections of $\approx 10^{-25}$ cm^2. Using the observed properties of the Crab pulsar, extrapolation back to epochs when the pulsar was more active indicates that the photon field is sufficiently dense to prevent the acceleration of heavy nuclei in the region surrounding the pulsar. On this model, the upper limit on the energy of the escaping nuclei varies with time. The models for cosmic-ray acceleration in supernova explosions or by pulsars themselves will be related to experimental observations. (auth) (Australia)

53858 PULSARS AND THE COSMIC RAY SPECTRUM. Rengarajan, T. N. (Tata Inst. of Fundamental Research, Bombay). pp 350-3 of 12th International Conference on Cosmic Rays, Hobart, Australia. Vol. 1. Hobart, Australia; International Union of Pure and Applied Physics (1971).

From twelfth international conference on cosmic rays; Hobart, Australia (16 Aug 1971). See CONF-710807—(Vol.1).

Since the discovery of pulsars and their identification with rotating neutron stars, it has been recognized that these objects have sufficient energies available to contribute effectively to the observed cosmic rays. It has been shown that it is possible to accelerate particles to very high energies in the low-frequency electromagnetic field of obliquely rotating magnetic neutron stars. Some aspects of source requirements, energy spectrum, and composition of cosmic rays are investigated under the assumption that pulsars are the dominant sources of cosmic rays. The pulsar acceleration model of Ostriker and Gunn (1969), in which the relevant parameters are fixed by taking the Crab pulsar as a typical one, is used. (auth) (Australia)

53859 EXTRAGALACTIC COSMIC RAYS. Brecher, K.; Burbidge, G. (Univ. of California, San Diego, La Jolla). pp 362-6 of 12th International Conference on Cosmic Rays, Hobart, Australia. Vol. 1. Hobart, Australia; International Union of Pure and Applied Physics (1971).

From 12th international conference on cosmic rays; Hobart, Australia (16 Aug 1971). See CONF-710807-(Vol.1).

Difficulties with the galactic origin and confinement of all of the locally observed cosmic-ray heavies, electrons, and protons ($E_p \leq 10^{17}$ eV) are briefly presented. Evidence is presented for the existence of cosmic rays filling regions of 1 Mpc extent, and their possible sources are considered. CR propagation out of, and between galaxies is examined assuming various properties of any ambient medium. A CR model is presented involving contributions from our Galaxy, the Virgo Supercluster, and the entire Universe. (auth) (Australia)

53860 RADIONUCLIDE PRODUCTION BY COSMIC RAYS IN LUNAR ROCKS. Ito, K. (Rikkyo Univ., Tokyo); Yamamoto, H.; Okazoe, H. pp 372-6 of 12th International Conference on Cosmic Rays, Hobart, Australia. Vol. 1. Hobart, Australia; International Union of Pure and Applied Physics (1971).

From twelfth international conference on cosmic rays; Hobart, Australia (16 Aug 1971). See CONF-710807—(Vol.1).

Measurements of the concentration of long-lived radionuclides in lunar rocks are of great use for studying the secular variations of solar and galactic cosmic rays. The depth variations of specific activities of such species as 7.4×10^5 yr ^{26}Al, 1.9×10^6 yr ^{53}Mn, and 2.5×10^6 yr ^{10}Be are rated. If lunar rocks have been at rest and no erosion had occurred over a long period of time, it would be suggested that galactic cosmic-ray intensity of 10^{6-7} years ago was about twice to three times as large as that now observed. (auth) (Australia)

53861 COSMIC RAY PROPAGATION AND SOURCE DISTRIBUTION. Lingenfelter, R. E. (Univ. of California, Los Angeles); Ramaty, R. pp 377-82 of 12th International Conference on Cosmic Rays, Hobart, Australia. Vol. 1. Hobart, Australia; International Union of Pure and Applied Physics (1971).

From twelfth international conference on cosmic rays; Hobart, Australia (16 Aug 1971). See CONF-710807—(Vol.1).

The effects of the source distribution and propagation on the cosmic-ray composition and anisotropy were investigated using a statistical discrete source distribution for primary cosmic-ray sources in the galactic disk and a continuous and time independent distribution for secondary particles. For cosmic-ray propagation by 3-dimensional diffusion in a confinement volume with absorbing boundaries the observed fragmentation product abundances and anisotropy were found to require a mean free path <0.1 pc; while with reflecting boundaries, the fragmentation depended principally on the escape probability at the boundary and was almost independent of the mean free path. For compound diffusion, the fragmentation and anisotropy required a characteristic length in the 3-dimensional random magnetic field of ~ 30 pc, a mean free path for 1-dimensional diffusion along field lines <30 pc, and the escape time from the confinement volume of about 2×10^7 years. (auth) (Australia)

53862 EFFECT OF IONISATION LOSS ON THE ENERGY SPECTRA OF COSMIC RAY NUCLEI UNDERGOING FERMI ACCELERATION. Ramadurai, S. (Tata Inst. of Fundamental Research, Bombay). pp 384-9 of 12th International Conference on Cosmic Rays, Hobart, Australia. Vol. 1. Hobart, Australia; International Union of Pure and Applied Physics (1971).

From twelfth international conference on cosmic rays; Hobart, Australia (16 Aug 1971). See CONF-710807-(Vol.1).

New analytical expressions are derived taking into account the velocity dependence of the rate of energy gain in the Fermi acceleration process which was neglected earlier. The resulting spectra indicate the pile up of nuclei near their critical energy for acceleration. The shapes of the energy spectra after acceleration are different, for various types of nuclei, the higher the charge the steeper being the spectra. This result differs quantitatively from the earlier result. The critical energies of acceleration of the same nuclei for the same acceleration parameters are higher than the ones derived earlier. (auth) (Australia)

53863 SCATTERING OF HIGHER ENERGY COSMIC RAYS. Melrose, D. B. (Australian National Univ., Canberra). pp 390-4 of 12th International Conference on Cosmic Rays, Hobart, Australia. Vol. 1. Hobart, Australia; International Union of Pure and Applied Physics (1971).

From twelfth international conference on cosmic rays; Hobart, Australia (16 Aug 1971). See CONF-710807-(Vol.1).

Pitch-angle scattering of cosmic rays by hydromagnetic waves generated by the cosmic rays themselves is ineffective for $E \gtrsim 10^{11}$ eV. Scattering and the associated parallel diffusion due to waves already present is discussed with particular reference to a model for confinement and escape. The required spectrum is derived and the presence of the required waves is discussed. (auth) (Australia)

53864 EFFECT OF GALACTIC MAGNETIC FIELD LINE WANDERING ON COSMIC-RAY PARAMETERS. Jones, Frank C. (Goddard Space Flight Center, Greenbelt, Md.). pp 396-400 of 12th International Conference on Cosmic Rays, Hobart, Australia. Vol. 1. Hobart, Australia; International Union of Pure and Applied Physics (1971).

From twelfth international conference on cosmic rays; Hobart, Australia (16 Aug 1971). See CONF-710807-(Vol.1).

The local configuration of the galactic magnetic field is an important factor in determining local cosmic-ray parameters such as density, mean age, and streaming velocity. According to the theory of Jokipii and Parker the flux tube that confines the cosmic rays seen at Earth undergoes a random wandering about the average field direction. It continues this wandering until it reaches a distance sufficiently far from the central plane of the Galaxy such that the bubble blowing instability occurs and it thus comes to an end as a container of cosmic rays. In a previous paper a probability density for the end points of the flux tube passing through the Earth was calculated employing the theory of Gaussian processes. This result is used to calculate the probability densities of the cosmic-ray parameters based on a smoothed out source, one dimensional diffusion model. It is seen that these parameters have a very wide range of fluctuation but that even when the mean age is confined to a narrow range the mean and most probable value of the streaming velocity is zero. From this it is argued that a very small observed value for the cosmic-ray anisotropy requires no special explanation any more than would any other value compatible with the probability distribution. (auth)

53865 MECHANISM FOR CONFINEMENT OF COSMIC RAYS IN THE GALAXY. Jokipii, J. R. (California Inst. of Tech., Pasadena). pp 401-6 of 12th International Conference on Cosmic Rays, Hobart, Australia. Vol. 1. Hobart, Australia; International Union of Pure and Applied Physics (1971).

From 12th international conference on cosmic rays; Hobart, Australia (16 Aug 1971). See CONF-710807-(Vol.1).

Various mechanisms for confinement of cosmic rays in the Galaxy are discussed. The simple diffusion model faces difficulties because the small scattering mean-free-paths required imply a very high rate of Fermi acceleration. Diffusive confinement by self-excited waves does not have this problem but has others. It is concluded that present evidence argues against diffusive confinement of cosmic rays and in favor of confinement mechanisms, such as the "leaky box," which rely on the overall topology of the galactic magnetic field or on processes taking place at the boundary of the confinement region. (auth) (Australia)

53866 SOME COSMIC EFFECTS OF THE FINITE REST-MASS OF THE WAVE QUANTUM. Cole, Keith D. (La Trobe Univ., Bundoora, Australia). pp 408-13 of 12th International Conference on Cosmic Rays, Hobart, Australia. Vol. 1. Hobart, Australia; International Union of Pure and Applied Physics (1971).

From twelfth international conference on cosmic rays; Hobart, Australia (16 Aug 1971). See CONF-710807-(Vol.1).

A quantum of wave energy in a medium can be considered to be a particle in a vacuum with rest-mass determined by the dispersion relationship of waves in the medium, the de Broglie relationships, and the theory of special relativity. In a simple plasma the rest-mass of radio frequency photons is $h\,\nu_p/c^2$ where ν_p is the plasma frequency. Treating the photon in a plasma as a particle in vacuum the dynamical equations are solved for the case of a plasma surrounding a massive celestial object. A new component of the bending radio-wave trajectories in a gravitational field is found. This is distinct from Einstein's bending of light rays. For a star like the Sun the bending is $\nu_p/4(\nu-\nu_p)$ times that for light in vacuo. In more massive objects like pulsars the bending is enormous and must be evaluated numerically. An expression for the gravitational redshift, which reduces in the proper conditions to the well-known Einstein formula, is found. It is shown that a prerequisite for photon-photon interaction is that the phase velocity should exceed c. (auth) (Australia)

53867 SUPERHEAVY ELEMENTS IN COSMIC RAYS. Peaslee, D. C. (Australian National Univ., Canberra). pp 419-22 of 12th International Conference on Cosmic Rays, Hobart, Australia. Vol. 1. Hobart, Australia; International Union of Pure and Applied Physics (1971).

From twelfth international conference on cosmic rays; Hobart, Australia (16 Aug 1971). See CONF-710807-(Vol.1).

Two facts suggest the same mean age, $t_{SH} \sim 10^5$ yrs, for superheavy cosmic-ray primaries: the cosmic-ray abundance of elements with $Z > 83$, and the upper limit of observed charge number, $Z \approx 96$. These features also suggest that the generating r-processes are efficient enough to produce the island of stability at $Z \simeq 114$, if it exists. (auth) (Australia)

53868 THEORY OF NARROW-ANGLE COSMIC RAY ANISOTROPIES. Barrowes, S. C. (Univ. of Utah, Salt Lake City). pp 423-8 of 12th International Conference on Cosmic Rays, Hobart, Australia. Vol. 1. Hobart, Australia; International Union of Pure and Applied Physics (1971).

From twelfth international conference on cosmic rays; Hobart, Australia (16 Aug 1971). See CONF-710807-(Vol.1).

A theory of cosmic-ray anisotropies is described, based upon a fairly smooth galactic magnetic field and rotating magnetic neutron stars or white dwarfs as cosmic-ray sources. If there are few small-scale irregularities in the galactic magnetic field, so that scattering of cosmic rays is unimportant for distances within 10,000 l y, then during sunspot minima a narrow-angle anisotropy should probably be observable at low energies ($E \leq 10^{12}$ eV). Such anisotropies were observed during the last two sunspot minima in 1952-56 and 1964. On the basis of theory and previous experience, an anisotropy may be anticipated in 1973-75 if adequate experiments are being done to observe it. (auth) (Australia)

53869 EXPLANATION OF THE BREAK IN THE PRIMARY SPECTRUM. Barrowes, S. (Univ. of Utah, Salt Lake City). pp 429-31 of 12th International Conference on Cosmic Rays, Hobart, Australia. Vol. 1. Hobart, Australia; International Union of Pure and Applied Physics (1971).

From twelfth international conference on cosmic rays; Hobart, Australia (16 Aug 1971). See CONF-710807-(Vol.1).

The acceleration of cosmic rays in pulsars should be capable of producing cosmic rays of energy up to 10^{21} eV. These will be absorbed in the envelope of the supernova however, unless sufficient time is allowed for the shell to become thin. For a typical pulsar, the roughly calculated energy cutoff is 3×10^{16} eV. Unknown factors might well bring this number down, thus explaining the break in the primary cosmic-ray spectrum at 3×10^{15} eV without reference to any sharp energy dependence for leakage of cosmic rays from the Galaxy. (auth) (Australia)

53870 CHANGE IN THE ELEVEN-YEAR MODULATION AT THE TIME OF THE JUNE 8, 1969, FORBUSH DECREASE. Lockwood, John A.; Lezniak, Jerry A.; Webber, William R. (Univ. of New Hampshire, Durham). J. Geophys. Res.; 77: No. 25, 4839-44(1 Sep 1972).

The functional form of the modulation for the 11-year variation changed abruptly after the Forbush decrease of June 8, 1969. This change in the 11-year modulation suggests that this Forbush decrease was an integral part of the 11-year variation. Some details of the change as observed by neutron monitors and by spacecraft at low energies are discussed. (auth)

Stars

Refer also to abstracts 53853, 53854, 53940, 53986, 54404, and 54663.

53871 PULSATING VARIABLES IN THE PLEIADES CLUSTER. Breger, Michel (State Univ. of New York, Stony Brook). Astrophys. J.; 176: No. 2, 367-71(1 Sep 1972).

Thirty-one B and A stars in the Pleiades cluster were tested for short-period variability. Five δ Scuti stars and one Be Shell variable were detected. The pulsation periods under 1 hour for the stars on the zero-age main sequence are predicted by the period–density relation. The period of 34 minutes for TR 51 is the shortest known so far for Cepheid-like pulsation. The new variables extend the hot border of the instability strip to spectral type A2 on the zero-age main sequence. (auth)

53872 MAIN-SEQUENCE PULSATION IN OPEN CLUSTERS. Breger, Michel. (State Univ. of New York, Stony Brook). Astrophys. J.; 176: No. 2, 373-80(1 Sep 1972).

Studies of short-period pulsation in open clusters show that pulsation occurs in clusters of all ages provided stars are present in the instability strip (A2 V – F0 V). This includes pre–main-sequence stars. The value of the pulsation constant Q is similar in the clusters studied, i.e., $\langle Q \rangle = 0.026$ days. This points toward pulsation in the first overtone. About 30% of the main-sequence cluster stars inside the instability strip show detectable variability Hyades-type stars may show a particularly high incidence of pulsation, possibly connected to a high helium abundance. Statistically extremely significant correlations between slow rotation, metallicity, and pulsational stability are established for different clusters. The observed relations can be explained by a diffusion hypothesis: (i) Slowly rotating A dwarfs usually possess extreme stability in some subsurface zones which causes element segregation. This leads to metallicism as well as increased pulsational stability because of the low helium content in the critical He II ionization zone. (ii) Low rotation, however, is not a sufficient condition to cause metallicism. Some examples are given. These slow rotators may, and often do, pulsate. (iii) Dwarfs with rotational velocities greater than ~100 km s^{-1} may pulsate and do not become Am stars. These stars, however, are so close to stability that less than 50% have detectable variability. (auth)

53873 CONSISTENT MODEL OF THE PLANETARY NEBULA NGC 7662. Kirkpatrick, Ronald C. (Texas A and M Univ., College Station). Astrophys. J.; 176: No. 2, 381-93 (1 Sep 1972).

A numerical model of NGC 7662 was computed which very closely matches the observations. It was found that in order to obtain a model which is consistent with all of the observed line strengths and line ratios, one must take into account not only the double-shell structure but also the contribution of condensations in the nebula and the departure of the central-star flux distribution from that of a black-body. The distance, mass, and reddening correction derived by coupling this model with the Hβ and radio flux measurements should be fairly reliable. Also, the abundances deduced for helium, oxygen, neon, and argon should be reasonably well determined. (auth)

53874 RELAXATION OSCILLATIONS IN THE ENVELOPES OF LUMINOUS RED GIANTS. Smith, Richard L.; Rose, William K. (Massachusetts Inst. of Tech., Cambridge). Astrophys. J.; 176: No. 2, 395-403(1 Sep 1972).

The envelopes of luminous red-giant stars have thermal timescales that are nearly as short as their dynamical timescales. The expansion of such an envelope is readily reversed and a collapse phase initiated as a result of large radiative losses. Numerical hydrodynamic calculations are described which indicate that high radiation-pressure gradients at the base of the envelope, resulting from thermal instability in the core, are capable of driving envelope relaxation oscillations. Instability to nonadiabatic pulsations may provide yet another mechanism for driving envelope oscillations, but this mechanism has not been fully investigated. Relaxation oscillations in the envelope are found to produce strong shock waves that appear capable of causing rapid mass loss in sufficiently luminous red giants. The calculations suggest that planetary nebulae may result from the final phase of mass loss on the red-giant branch. (auth)

53875 INTERSTELLAR LINES IN THE ULTRAVIOLET SPECTRUM OF ZETA OPHIUCHI. Smith, Andrew M. (Goddard Space Flight Center, Greenbelt, Md.). Astrophys. J.; 176: No. 2, 405-23(1 Sep 1972).

Interstellar lines arising in C^0, C^+, O^0, Si^+, and S^+ observed in the ultraviolet spectrum of ζ Oph by rocket spectrographic techniques were analyzed. The main results were that within a factor of 10 the abundances of C^+, O^0, and Si^+ outside the H II region surrounding ζ Oph relative to the hydrogen abundance were equal to solar values. The lines in C^0 and S^+ implied that the interstellar matter is distributed among several clouds as indicated by high-resolution visible spectra. The $^2P^0_{3/2}$ (0.0079 eV) fine-structure level of the ground-state configuration in C^+ was strongly populated, the abundance ratio of the $^2P^0_{3/2}$ level to the $^2P^0_{1/2}$ ground level being 1.5. It is suggested that the excited C^+ ions are inside the Strömgren sphere where proton densities equal to or greater than 220 cm^{-3} can collisionally excite the ions at sufficient rates. Stellar absorption lines of C IV (1548.2, 1550.8 Å) and Nv (1238.8, 1242.8 Å) were seen shifted to lower wavelengths, indicating stellar mass loss. The stellar material will be stopped in the H II region by Coulomb forces, and it is suggested that most of the C^+ ions in the $^2P^0_{3/2}$ level comes from this source. (auth)

53876 MAGNETIC-FIELD VARIATIONS IN 78 VIRGINIS, BETA CORONAE BOREALIS, AND 73 DRACONIS. Wolff, Sidney C.; Bonsack, Walter K. (Univ. of Hawaii, Honolulu). Astrophys. J.; 176: No. 2, 425-32(1 Sep 1972).

Photographic observations of the Zeeman effect in stellar spectra were made with new equipment at the Mauna Kea Observatory. Measurements of the effective longitudinal field H_e were obtained for 78 Vir, β CrB, and 73 Dra. Comparison of the values obtained for 78 Vir and β CrB with the measurements made by Preston at Lick Observatory established the absence of any significant systematic difference between the two observatories. The results do not support the suggestion of long-term systematic changes in the cycles of magnetic variation of β CrB and 73 Dra, which were marginally indicated by previous investigations. (auth)

53877 PERIODIC VARIABILITY OF THE PECULIAR A STAR HD 111133. Wolff, Sidney C.; Wolff, Richard J. (Univ. of Hawaii, Honolulu). Astrophys. J.; 176: No. 2, 433-8(1 Sep 1972).

The period of the peculiar A star HD 111133 is 16.31 days. Maximum light coincides in phase with minimum longitudinal magnetic field. The strengths of the lines of the iron-peak elements vary and are greatest at maximum light. This star belongs to that subgroup of Ap stars in which the magnetic and rotation axes are nearly aligned. (auth)

53878 TRANSFER OF RESONANCE-LINE RADIATION IN DIFFERENTIALLY EXPANDING ATMOSPHERES. I. GENERAL CONSIDERATIONS AND MONTE CARLO CALCULATIONS. Caroff, Lawrence J.; Noerdlinger, Peter D.; Scargle, Jeffrey D. (Ames Research Center, Moffett Field, Calif.). Astrophys. J.; 176: No. 2, 439-61(1 Sep 1972).

A Monte Carlo method is given for analyzing the transfer of resonance radiation in a rapidly and differentially expanding nebula. Coherence in the frame of the atom is shown to lead to interesting modifications of the emergent radiation field, as compared with the other more usual assumptions of coherence or redistribution in the fluid frame. Results are presented in tabular form suitable for further use. Sample line profiles produced by pure scattering out of the continuum are generated, and it is shown that an arbitrarily high peak can be obtained. This conclusion is independent of the coherence assumption used. The distribution of the number of scatterings is found in all cases. An analytic solution is presented for the case of coherence in the fluid frame. (auth)

53879 TRANSFER OF RESONANCE-LINE RADIATION IN DIFFERENTIALLY EXPANDING ATMOSPHERES. II. ANALYTIC SOLUTION FOR THE CASE OF COHERENCE IN THE FRAME OF THE FLUID. Noerdlinger, Peter D. (Ames Research Center, Moffett Field, Calif.); Scargle, Jeffrey D. Astrophys. J.; 176: No. 2, 463-78(1 Sep 1972).

An exact solution is obtained for the problem of line transfer by resonant scattering (assumed coherent in the fluid frame) in a differentially expanding atmosphere. The probabilistic method developed is a generalization of the method of addition of layers plus a decomposition of the radiation field into partial radiation fields due to those photons that scatter exactly n times before escaping ($n = 0, 1, 2, 3, \ldots$). Generalization to finite destruction probability per scattering is immediate, allowing treatment of nonresonance lines such as Lβ. Some results of interest for the theory of expanding stellar atmospheres are presented graphically. (auth)

53880 SYNTHESIS OF COMPOSITE SPECTRA: A STUDY OF FOUR GLOBULAR CLUSTERS OF THE GALAXY, FIVE GLOBULAR CLUSTERS OF M31, AND THE NUCLEUS OF NGC 205. Christensen, Clark G. Pasadena, Calif.; California Inst. of

Tech. (1972). 221p. University Microfilms Order No. 72-22,546.

Thesis.

A spectral synthesis technique similar to that of Spinrad and Taylor (1971) was applied to the integrated light of globular clusters M5, M13, M15, and M92 of the Galaxy; H12, H55, H140, B282, and MIV of M31; and to the nucleus of the elliptical galaxy NGC 205. The derived stellar contents of the four local clusters were compared with color–magnitude diagrams and luminosity functions based on studies of individual stars within these systems. Results agree. The technique yields information on both the metal content of clusters and their horizontal-branch colors and thus is useful for extracting the two parameters which apparently describe galactic globular clusters. Principal results of the study of the six extragalactic systems are listed. (TSS) (Diss. Abstr. Int., B)

53881 STUDY OF THE UNIDENTIFIED INTERSTELLAR DIFFUSE FEATURES. Wu, Chi-Chao. Madison, Wis.; Univ. of Wisconsin (1972). 56p. University Microfilms Order No. 72-19,017.

Thesis.

The interstellar diffuse lines λλ5780, 5797 were observed in 66 stars using the Washburn Observatory echelle spectrograph coupled with an image tube. At a resolution of 0.17Å, the profiles of these diffuse lines are asymmetric and steeper to the blue. There is also a broad, shallow feature shortward of λ5780. Equivalent widths of λλ5780, 5797 were measured from tracings which had a resolution of 0.26Å. The unlikelihood and/or difficulties of the following models for diffuse interstellar features are also discussed: (1) molecular processes, (2) shifted and broadened resonance lines of atomic and molecular impurities in solids. (3) F-centers in alkali halides, and (4) plasma oscillations in solids. (TSS) (Diss. Abstr. Int., B)

53882 STUDY OF TWENTY-ONE SHARP-LINED NON-VARIABLE COOL PECULIAR A STARS. Adelman, Saul Joseph. Pasadena, Calif.; California Inst. of Tech. (1972). 371p. University Microfilms Order No. 72-22,597.

Thesis.

Elemental abundance analyses were performed for twenty-one cool Ap stars, also known as SrCrEu stars, which are not known to be spectrum variables and whose projected rotational velocity is not greater than 10 km/sec. Zeeman and thermal Doppler broadening are the basic line intensification mechanisms considered. Effective temperatures estimated initially from UBV photoelectric data were modified by requiring that the iron abundances derived from both neutral and singly-ionized lines be equal. Log g was assumed to be 4.0. In addition, two normal stars were included for comparison. (TSS) (Diss. Abstr. Int., B)

53883 MEMBERSHIP IN THE EXTREMELY YOUNG OPEN CLUSTER NGC 6530 (M8). van Altena, W. F. (Univ. of Chicago); Jones, B. F. Astron. Astrophys.; 20: No. 3, 425-36(Sep 1972).

Relative proper motions for 363 stars in the vicinity of the extremely young open cluster NGC 6530 (M8) were determined from plates taken with the Yerkes Observatory 40-inch refractor. Based on these relative proper motions, which had an average mean error of ±0.0006″/yr, probabilities of membership were determined with the result that of the 363 stars measured there were 76 expected members. The average reddening was found to be 0.35 mag with little scatter. Adopting the ratio of total to selective absorption to be 3.0, a corrected distance modulus of 11.25 mag or a distance of 1780 pc was found. An age for the cluster of 2×10^6 yr was determined based on the theoretical gravitational contraction isochrones of Iben, although the observations were perhaps fit slightly better by the ^{3}He main sequence of Ulrich. The two yellow stars suggested as possible giant members of the cluster by Walker, as well as the five brightest red stars found by Blanco and Grant, had zero probabilities of membership. Five probable nonmembers were suspected of being variable in light. Of the six Hα emission line stars found by Herbig, three were probable members. The two bright O stars, HD 164794 and HD 165052, had negligible relative proper motions. From an analysis of their proper motion errors, a minimum expansion age of 0.6×10^6 yr was derived, in agreement with the gravitational contraction age of 2×10^6 yr for the cluster. Herschel 36, the exciting star for the "hour glass" nebula, is possibly a cluster member. (auth)

53884 VARIABLE STARS OF SMALL AMPLITUDE I: SUPERGIANTS AND OB STARS. Maeder, A.; Rufener, F. (Observatoire, Geneva). Astron. Astrophys.; 20: No. 3, 437-43(Sep 1972).

The light variability of various kinds of stars is discussed, by means of 5000 measurements of color-indices made for 660 stars. These stars were observed in the Geneva Observatory photometric system; they were not measured for this purpose and they belong to various programs. The Am stars were found to be nonvariable in agreement with Breger's results (1970). The Ap stars were variable in agreement with Preston's results (1971). All the red giants of type K5 III and later may be suspected of variability. The case of supergiants and OB stars is considered. For the supergiants of type B3–G8, it was found that: (1) All the Ia supergiants are variable in light with an amplitude in color index of about 0.02 to 0.04 in.; for the Ib supergiants, a large fraction, if not all, also showed variability. (2) An amplitude–luminosity relation exists in the sense of the largest amplitudes for the brightest stars. (3) Some arguments are given which suggest that, besides the mass loss, at least a part of these variations may be due to an oscillatory mechanism. For the OB stars, it was found that: (1) A large fraction of OB stars show photometric variations. (2) A very striking concentration of stars with large dispersion of their color indices (amplitude $\sim 0.4^m$) appears for very high T_{eff} and luminosity. (3) These stars occur in an area of the HR diagram, where there exist much theoretical and uv or visible spectroscopic evidence of mass loss. (auth)

53885 EFFECTS OF SEMICONVECTION ON THE HORIZONTAL-BRANCH. Sweigart, A. V.; Demarque, P. (Yale Univ. Observatory, New Haven). Astron. Astrophys.; 20: No. 3, 445-53 (Sep 1972).

The effects of semiconvection on the horizontal-branch evolution of a 0.60 $M_\odot$ Population II star with the envelope composition parameters $X = 0.732$ and $Z = 0.001$ are investigated. Following an initial phase of convective-core overshooting the models form a semiconvective zone which at its maximum extent results in the depletion of helium out to a mass value of 0.25 $M_\odot$. A comparison between sequences computed with and without a treatment of semiconvection indicates that the neglect of semiconvection will (a) reduce the length of the horizontal-branch track by a factor of 1.8 and (b) decrease the horizontal-branch lifetime by a factor of 1.9. A number of additional horizontal-branch sequences including a treatment of semiconvection are presented over the mass range from 0.51 to 0.65 $M_\odot$. These sequences suggest that a mass spread on the order of 0.05 $M_\odot$ would be sufficient to produce a dispersion of 0.30 in log T_{eff} over the log T_{eff} interval from roughly 3.70–4.15. (auth)

53886 CONDITIONS FOR HOMOGENEOUS STELLAR MODELS TO HAVE ONLY REAL SECULAR EIGENVALUES. Gabriel, M.; Noels, A. (Univ., Liege). Astron. Astrophys.; 20: No. 3, 455-9 (Sep 1972).

The conditions to have only real eigenvalues in the secular spectrum of homogeneous stars are discussed numerically. Results suggest that they are identical to those for the existence of a nearly homologous solution as an eigensolution. When one deviates enough from these conditions, complex eigenvalues are generally present except when very special conditions on the opacity and energy generation laws are fulfilled. (auth)

53887 ULTRAVIOLET ABSORPTION LINES IN THE SPECTRUM OF VEGA. Gurzadyan, G. A.; Ohanesyan, J. B. (BAO, Erevan). Astron. Astrophys.; 20: No. 3, 321-4(Sep 1972).

Ultraviolet spectrograms of Vega, covering the wavelength 2000 to 3800 Å, are presented. More than ten ultraviolet absorption lines and bands were detected and identified. The strongest line was the resonance doublet of ionized magnesium—2802.7 Mg II and 2795.5 Mg II, with an equivalent width of 3 Å. All the other absorption lines or bands (blended lines) are produced by metals, mainly neutral and ionized iron and nickel. Using the results of other space observations of three stars—γ Cas (B 0.5), Canopus (F 0) and Sun (G 1)—a markedly distinctive dependence between the equivalent width of the doublet 2800 Å Mg II and the spectra class of the star was established. This relationship can be used, in particular, to make an accurate spectral classification of stars. (auth)

53888 QUANTITATIVE ANALYSIS OF γ CAPRICORNI. Selvelli, P. L. (Astronomical Observatory, Trieste, Italy). Astron. Astrophys.; 20: No. 3, 325-32 (Sep 1972).

A quantitative analysis of the transition star γ Cap was made in order to investigate the reasons of the disagreement among its chemical-physical parameters derived by previous researches. The analysis by the differential curve of growth method relative to 30 L Mi and 63 Tau, which have about the same θ_{eff} and log g, indicated that γ Cap has characteristics common to the Am stars: deficiencies of calcium and scandium and overabundances by factors around 10^2 of heavy elements and rare earths. The values of the microturbulence range between 3.1 and 6.4 km/s. A strong systematic difference arises from the comparison between the values of the equivalent widths found in this work and in the previous analysis. Moreover the curves of growth of γ Cap in the blue and red spectral regions (from spectrograms taken at different epochs) give abundance differences for Ti, Cr, Ni, Y, beyond the order of the experimental errors. This fact suggests that γ Cap is spectrum variable in spite of the similarity that γ Cap presents with the Am star groups. (auth)

53889 INFRARED PHOTOMETRY OF NORTHERN WOLF–RAYET STARS. Allen, D. A. (Carnegie Inst., Washington, D. C.); Swings, J. P.; Harvey, P. M. Astron. Astrophys.; 20: No. 3, 333-6(Sep 1972).

Observations of Wolf–Rayet stars were made at 1.6 and 2.2 μ. The $[2.2\ \mu]-[1.6\ \mu]$ colors were found to be systematically greater in WC than in WN stars. (auth)

53890 EQUIVALENT WIDTH OF INTERSTELLAR MOLECULAR LINES. II. CO, SiO, CS, H_2, AND HD IN THE INTERSTELLAR SPECTRUM OF ζ PERSEI. Krishna, Swamy, K. S.; Tarafdar, S. P. (Tata Inst. of Fundamental Research Bombay). Astron. Astrophys.; 20: No. 3, 341-5(Sep 1972).

Analysis of the measured equivalent widths of the Lyman band of H_2 by Carruthers for the star ζ Per, gives $n(H_2) \approx 10^{21}$ cm^{-2}. It appears that the density of H_2 is larger than that of H in the direction of ζ Per. Calculation of the equivalent widths of the lines of the bands (C–X) of H_2 and (B–X) and (C–X) of CO and HD reveal that they may be observable shortward of 1150 Å. (auth)

53891 EXTENDED HORIZONTAL BRANCH LOCI. Caloi, Vittoria (Laboratorio de Astrofisica Spaziale, Frascati, Italy). Astron. Astrophys.; 20: No. 3, 357-60(Sep 1972).

Models for extremely blue horizontal branch type stars are presented. An interpretation of B subdwarfs in the halo is attempted in terms of these models. The importance of reliable determinations of the luminosities of these objects for indications about the original He-content is stressed. (auth)

53892 ABUNDANCES OF NOBLE GASES IN EXTREME POPULATION I MATTER AND THE SUN. Scholz, M. (Univ., Heidelberg). Astron. Astrophys.; 20: No. 3, 465-7(Sep 1972).

Recent abundance determinations in extreme Population I matter on the one hand and the Sun on the other indicate that helium has about the same abundance but neon and argon are enhanced in young objects. (auth)

53893 STELLAR ENERGY-LOSS RATES IN A CONVERGENT THEORY OF WEAK AND ELECTROMAGNETIC INTERACTIONS. Dicus, Duane A. (Univ. of Rochestester, N. Y.). Phys. Rev., D; 6: No. 4, 941-9(15 Aug 1972).

The stellar energy-loss rates due to the production of neutrino pairs are calculated in Weinberg's theory of electromagnetic and weak interactions. The ratio of the total rate calculated here to the rate calculated in the ordinary theory of weak interactions is $10^{0+0.03}_{0-0.30}$, where the uncertainty comes entirely from the lack of knowledge of the W-meson mass. The ratio of the experimental rate to the rate calculated in the ordinary theory is $10^{0\pm2}$. Thus Weinberg's theory gives numbers well within the experimental limits for all values of the W mass. (auth)

53894 STABILITY OF NONRADIAL VIBRATIONAL MODES OF RELATIVISTIC NEUTRON STARS. Cazzola, P. (Univ., Ferrara, Italy); Lucaroni, L. Phys. Rev., D; 6: No. 4, 950-6 (15 Aug 1972).

An analytical connection is established between the amplitudes of gravitational waves scattered by a relativistic neutron star and its nonradial vibrational modes. The procedure is similar to the one followed by Jost and other authors who recognized that the bound-state Schroedinger wave functions in potential theory are analytically connected with the S function for the scattering. In the case of potential theory, the S function for the scattering is analytic in the wave number k, except for singular points or branch lines. The resonant and antiresonant states are represented by poles of S in the lower half Gauss k plane. The bound states, on the other hand, correspond to poles on the positive imaginary axis. Similarly, in the case of a neutron star the amplitudes of gravitational waves scattered by the star are shown, in the present paper, to be analytic in the wave circular frequency ω. The stable and unstable vibrational modes of the neutron star give rise to resonances in the scattering of gravitational waves described by poles of scattering amplitude lying, respectively, in the upper and lower half Gauss ω plane. In particular, a result is obtained (similar to Levinson's theorem for potential scattering) which relates the unstable modes to scattering phase shifts. (auth)

53895 OBSERVATIONS OF RAPID BLUE VARIABLES. VII. EX HYDRAE. Warner, Brian (Univ. of Texas, Austin). Mon. Notic. Roy. Astron. Soc.; 158: No. 4, 425-30(1972).

Photometric observations of EX Hya with time resolutions of 2 and 5 s are reported. EX Hya is very active on time scales of 10 to 100 s. A comparison with WZ Sge is made. It is suggested that the x-ray source 2ASE 1253-28 may be identified with EX Hya. (auth)

53896 STRUCTURE AND EVOLUTION OF HELIUM STARS. Dinger, Ann St. Clair (Northwestern Univ., Evanston, Ill.). Mon. Notic. Roy. Astron. Soc.; 158: No. 4, 383-403(1972).

Numerical models of helium stars were constructed in an effort to fit the models to the observed extreme-helium stars, i.e., those which have equivalent spectral types of O7 to B5, absolute magnitudes brighter than −1.6, and weak or missing hydrogen lines. Main-sequence models of 1, 2, 4, and 8 $M_\odot$ were computed for $Y = 0.98$, $Z = 0.02$. The effect of the inclusion of the $^{14}N(\alpha,\gamma)^{18}F(e^{+}\nu)^{18}O$ reaction was investigated. It is shown that the addition of 10^{-3} of hydrogen by mass had a negligible effect on these models. One-solar-mass models with 2, 6, 14, 30, and 58% additional carbon were also computed. Carbon enrichment increased the luminosity, effective temperature and central temperature of the model and decreased the central density. A four-solar-mass model with $Z = 0.60$ (0.02 solar metals and 0.58 additional carbon) was also computed. The four-solar-mass $Z = 0.02$ and $Z = 0.60$ models were evolved until carbon ignited in their cores under nondegenerate conditions. The evolution of the one-solar-mass, $Z = 0.60$ model was followed to the white dwarf state. Computations of the evolution of the one-solar-mass, $Z = 0.02$ model were stopped when the mass of the helium-exhausted core was 0.767 $M_\odot$. This model crossed the main sequence for hydrogen-burning in the region of the observed helium stars and evolved towards the red giant region of the H–R diagram. (auth)

53897 ABSORPTION SPECTRA OF TYPE II SUPERNOVAE. Patchett, Bruce; Branch, David (Royal Greenwich Observatory, Hailsham, Eng.). Mon. Notic. Roy. Astron. Soc.; 158: No. 4, 375-82(1972).

On the basis of wavelength coincidence and comparison of observed and synthetic spectra, intensity minima in Type II supernova spectra are attributed to blueshifted absorption lines of hydrogen and Fe II. (auth)

53898 STELLAR COMPOSITIONS FROM NARROW-BAND PHOTOMETRY. III. IRON ABUNDANCES IN A FURTHER 120 EVOLVED STARS. Williams, P. M. (Cambridge Univ., Eng.). Mon. Notic. Roy. Astron. Soc.; 158: No. 4, 361-73 (1972).

Using narrow-band indices observed with the Cambridge spectrophotometer and analyzed using synthetic spectra computed from model atmospheres, the iron abundances of a further 120 evolved stars were determined. The results compare well with those from high-dispersion spectroscopic analyses. A number of super-metal-rich stars were isolated, including three high-velocity stars lying below the M67 subgiant branch in the H–R diagram. (auth)

53899 V_{553} CENTAURI. A TYPE II CEPHEID WITH AN OVERABUNDANCE OF CARBON. Evans, T. Lloyd (Radcliffe Observatory, Pretoria); Wisse, P. N. J.; Wisse, M. Mon. Notic. Roy. Astron. Soc.; 159: No. 1, 67-78(1972).

The Cepheid V553 Centauri (P = 2.06d) has strong C_2, CH, and CN bands in its spectrum. These show a pronounced variation with phase, being strongest at minimum light. Their presence implies a considerable overabundance of carbon in the star's atmosphere. The radial velocity curve shows a phase lag similar to that of other Cepheids. The radial velocity is −6km s^{-1}. The light and color curves show the characteristic features of a globular cluster Cepheid of this period. RT TrA (P = 1.95d), for which fragmentary data are available, is very similar. V553 Cen and RT TrA probably belong to the disk rather than the halo population. Theory predicts an excess of carbon in the atmospheres of some of the longer period Type II Cepheids. The possibility that V553 and RT TrA are related to the Cepheids found in dwarf spheroidal galaxies, which are confined to short periods, is discussed. (auth)

53900 NON-LTE ANALYSIS OF THE O-TYPE SUBDWARF, HD 49798. Dufton, P. L. (Observatories, Cambridge, Eng.). Mon. Notic. Roy. Astron. Soc.; 159: No. 1, 79-93(1972).

Equivalent width and line profile data are presented for the O-type subdwarf, HD 49798. These observations cannot be explained on the assumption of LTE. Comparison with the results of non-LTE calculations produces the atmospheric parameters $T_{eff} = 45000 \pm 5000$°K (from the Balmer discontinuity) and $\log a = 4.3 \pm 0.3$ (from the Hγ profile). The ionized helium line wings are considerably stronger than the non-LTE calculations predicted with "normal" abundances and this is interpreted as evidence of a helium overabundance by a factor of five. An approximately solar mass is deduced for the primary using the absolute magnitude, M_V, of -0.2 ± 1.0m found from the interstellar calcium K line strength. The star is a spectroscopic binary. Assuming the rotation of the primary to be synchronous with the orbital motion, (a) the primary is not at present filling its Roche lobe, and (b) the invisible secondary is the more massive component. (auth)

53901 OBSERVATIONS OF RAPID BLUE VARIABLES. 8. THE COMPANION TO MIRA. Warner, Brian (Univ. of Texas, Austin). Mon. Notic. Roy. Astron. Soc.; 159: No. 1, 95-100 (1972).

Ultraviolet photoelectric photometry with 2 s time resolution of Mira near minimum is reported. The light variations observed are attributed to o Cet B. It is shown that there are slow (~15 min) variations, superimposed on which are rare, short-lived flares. The luminosity of o Cet B is attributed to accretion heating, arising from mass loss from o Cet A, the slow variations being caused by inhomogeneities in the infalling material. The flares are probably intrinsic to o Cet B. (auth)

53902 OBSERVATIONS OF RAPID BLUE VARIABLES. 9. AM CVn (HZ29). Warner, Brian; Robinson, Edward L. (Univ. of Texas, Austin). Mon. Notic. Roy. Astron. Soc.; 159: No. 1, 101-11(1972).

Photometric observations with 1- and 3-s time resolution demonstrate the existence of rapid flickering in AM CVn. Mean light curves confirm the existence of a double-humped light curve with a period near 18 min. Using current data, and previously published observations by Ostriker and Hesser (Astrophys. J. (Letters), 153, L151, 1968) and Krzeminski (Acta Astr., 21, 133, 1971) a mean period of 1051.0505 s is derived, but it is shown that there is some phase jitter about this period. Periodogram analyses show the existence of long-lived coherent periodicities in the range 115 to 120 s. A binary star model is suggested for AM CVn, with an orbital period of 18 min. It is proposed that AM CVn represents a late stage of evolution of a cataclysmic variable star, in which all hydrogen has been removed from the system. (auth)

53903 STELLAR EVOLUTION TOWARD THE MAIN SEQUENCE. Bodenheimer, P. (Univ. of California, Santa Cruz). Rep. Progr. Phys.; 35: No. 1, 1-54(1972).

A review is presented of the evolution of stars during the period that starts just after formation in interstellar clouds and ends at the point of stabilization on the main sequence where nuclear reactions begin to provide the entire energy supply. During this pre-main-sequence phase the star shines at the expense of its gravitational potential energy. At the earlier stages this energy is released rapidly as the star experiences hydrodynamic collapse; later on the star contracts slowly through a series of states of quasihydrostatic equilibrium. The initial-boundary-value problem that must be solved to obtain the structure of a star as a function of time is discussed. The equations have been solved numerically for a wide range of stellar masses. The character of these solutions is described, with particular attention given to the effect upon the results of the assumed initial conditions. The theoretical results are subject to a number of observational tests. The observations which are discussed include (i) the properties of T Tauri stars, (ii) the color-magnitude diagrams of young clusters, (iii) the abundances of the rare light nuclei, particularly lithium, and (iv) the properties of the "infrared" stars. The observations of a number of objects which have been identified as protostars are reviewed. Inclusion of the effects of rotation in calculations of pre-main-sequence evolution presents a difficult numerical problem, and relevant observational material is very scarce. Some recent progress has been made; in particular, numerical work has strengthened the hypothesis that close binary systems are formed by fission of a rapidly rotating single star. Rotation must be of dominant importance during the earliest phases of evolution just after star formation. Future work on this problem is essential to an understanding of the formation of the solar system. (auth)

53904 R CORONAE BOREALIS VARIABLES IN THE LARGE MAGELLANIC CLOUD. Feast, M. W. (Radcliffe Observatory, Pretoria). Mon. Notic. Roy. Astron. Soc.; 158: No. 3, 11P-13P(1972).

Spectra were obtained of three RCB stars in the LMC. W Men ($M_v = -5.1$) and HV 12842 ($M_v \sim -4$) have weak C_2 absorption bands (maximum depression of the continuum ~11% in the 4737 Å sequence). This C_2 strength is similar to that in the galactic F type RCB stars, R CrB and RY Sgr. HV 5637 ($M_v = -4.0$) has very strong C_2 bands (maximum continuum depression ~72% in 4737 Å sequence). Such strong C_2 bands are characteristic of R type RCB stars like S Aps. Evidently both F and R type RCB stars are high luminosity objects. (auth)

53905 SPECTROSCOPIC AND PHOTOMETRIC STUDY OF THE PULSATING R CORONAE BOREALIS TYPE VARIABLE, RY SAGITTARII. Alexander, J. B.; Andrews, P. J.; Catchpole, R. M.; (and others) (Royal Observatory, Cape Town). Mon. Notic. Roy. Astron. Soc.; 158: No. 3, 305-60(1972).

Results are given of an intensive study of RY Sgr during the period 1967 to 1970. The rapid decline in brightness at the beginning of this period and the gradual rise to maximum light are covered. 382 emission lines (mostly identified) were found during the initial decline as was a continuum attributed to the electron attachment spectrum of CN. The development with time of this emission line chromospheric spectrum indicates both a lowering of the excitation and decrease in the effects of self-absorption. The chromosphere decays on a time scale of ~22 days. The initial decrease in photospheric radiation has a time scale of ~5 days or less. The absence of [Fe II] emission suggests that the density in the emitting region is greater than $\sim 10^{14}$ atoms cm^{-3} in the early stages of the decline if collisional excitation is dominant. During the decline displaced shell lines of Ca II (-200 km s^{-1}) were present. On the rise to light maximum and at maximum, the light and color curves show smooth variations ($V = 0.5m$, $(B-V) = 0.3m$, $(U-B) = 0.5m$) with a period of 38.6 days. A similar periodicity is present in the radial velocities (amplitude ~30 km s^{-1}) and it is concluded that RY Sgr is a pulsating variable (as originally suggested by Jacchia) as well as an RCB star. At some epochs on the rising branch the spectrum is normal (i.e., as at maximum) but the star is faint and red. This together with the infrared observations of Lee and Feast strongly supports the hypothesis of extinction by a circumstellar dust shell. Values of $A_V/E_{B-V} = 4.3$ and $E_{U-B}/E_{B-V} = 1.3$ are found for the shell. Abnormal spectra and colors follow a drop in light on the rising branch. They are apparently due to the filling in of the photospheric absorption lines by chromospheric emission. The primary cause of this phase seems to be a decrease in photospheric light, possibly due to the formation of a fresh dust shell near the photosphere. Displaced shell absorption lines (Ca II and Na I) are present at this stage. The pulsations of RY Sgr are broadly consistent with recent work by Trimble on the pulsation of helium stars. (auth)

53906 BLACK HOLES AND THE SECOND LAW. Bekenstein, J. D. (Joseph Henry Labs., Princeton, N. J.). Lett. Nuovo Cim.; 4: No. 15, 737-40(12 Aug 1972).

Black-hole physics seems to provide at least two ways in which the second law of thermodynamics may be transcended or violated. The second law is formulated in a form suitable for black-hole physics which resolved the transcendence problem. It is also indicated why Geroch's gedanken experiment does not, in fact, violate the second law. (W.D.M.)

53907 DETECTION OF NEUTRON STARS. Apparao, K. M. V. (Tata Inst. of Fundamental Research, Bombay). Lett. Nuovo Cim.; 4: No. 15, 809-10(12 Aug 1972).

Neutron stars when formed have surface temperatures in excess of 10^7°K, but generally cool down to about 10^6°K in about a million years. These stars are expected to emit x radiation and it is suggested that the x rays from the neutron stars in the nearest pulsars CP 0950, CP 1133, PSR 1929, and CP 0808 can be detected. The flux from CP 0950 may have already been detected, if it can be identified with the x-ray source Leo XR-1. (W.D.M.)

53908 INTERNAL STRUCTURE OF NEUTRON STARS. Arponen, Jouko (Univ. of Helsinki). Nucl. Phys.; A191: No. 2, 257-82(1972).

The equation of state and the structure and composition of neutron star matter are investigated in the density region 3.1×10^{11} to 2×10^{15} g/cm^3. Below the density 3.1×10^{11} g/cm^3 the matter is a solid consisting of neutron-rich nuclei in a degenerate electron gas. At 3.1×10^{11} g/cm^3 neutrons start to drip out of the nuclei; as the density increases, the lattice spacing continuously decreases while the geometrical size of the nuclei only slightly increases, until at about 15×10^{13} g/cm^3 the nuclei disappear by coalescing into a homogeneous liquid in an almost continuous phase transition. The maximum proton number per nucleus is 40, which is obtained between the densities 1 to 2.5×10^{13} g/cm^3; after that the proton number decreases until at the solid-to-liquid phase boundary it is about 20. In the liquid-core region, muons appear at the density 20.5×10^{13} g/cm^3. The calculations use the differential Thomas–Fermi theory in connection with a new model for the nuclear matter energy. The model is based on the parametrization of the Brueckner G-matrix in conjunction with a few empirical requirements concerning the saturation of the symmetric nuclear matter. It is shown that very small modifications in the details of the nuclear matter energy may lead to considerable differences in the resulting neutron star structure; for example the density of matter at the solid-to-liquid phase boundary is found to be very sensitive to such details. One of the main reasons for this is that the stability of the liquid against clustering into separate nuclei depends mainly on the second derivatives of the nuclear matter energy with respect to neutron and proton densities; for these second derivatives there exist no very reliable theoretical or phenomenological predictions so far. To check that the Thomas–Fermi theory together with the model for the nuclear matter energy works satisfactorily, a test calculation is made about finite nuclei of difference sizes between A = 16 and 400. (auth)

Quasi-Stellar, Radio, and X-Ray Sources

Refer also to abstracts 53818, 53857, and 54144.

53909 PARAMETRIC DOWN-CONVERSION IN ASTROPHYSICAL MASERS. Goldreich, Peter; Kwan, John Y. (California Inst. of Tech., Pasadena). Astrophys. J.; 176: No. 2, 345-51 (1 Sep 1972).

The mechanism of parametric down-conversion proposed by Litvak cannot explain the observed preference for circular polarization in OH maser emission because the nonlinear interaction between oppositely circularly polarized microwaves is too weak. (auth)

53910 FINE STRUCTURE IN H II REGIONS: SYNTHESIS OBSERVATIONS AT 11 AND 3.7 CENTIMETERS. Balick, Bruce (Cornell Univ., Ithaca, N. Y.). Astrophys. J.; 176: No. 2, 353-65(1 Sep 1972).

Interferometric synthesis observations of the H II regions DR 21, W51 components G49.5−0.4 and G49.3−0.3, W33, NGC2264 (southern component), NGC 2175, and IC 410 are reported. The sources were observed at frequencies of 2695 and 8085 MHz; the resulting synthesized beam diameters were ~10″ and 3″, respectively. Fine structure with scale sizes of $10^{-1.5}$ pc were observed in some sources, whereas intermediate (~$10^{-0.5}$ pc) or no structure was observed in others. Typical emission measures of $10^{7.5}$ pc cm^{-6} and electron temperatures of 10^4 °K were found for the fine structure. Thus densities of $10^{4.5}$ cm^{-3} and masses of $10^{-1.5}$ $M_\odot$ are implied. The relationship between the structure and the parent H II region is discussed. (auth)

53911 INTERPRETATION OF ROTATION MEASURES OF RADIO SOURCES. II. Mitton, Simon; Reinhardt, Michael (Inst. of Theoretical Astronomy, Cambridge, Eng.). Astron. Astrophys.; 20: No. 3, 337-40(Sep 1972).

The systematic behavior of the rotation measures of radio galaxies, quasars, and unidentified sources is discussed. The contribution of a galactic magnetic field directed along the local spiral arm and the dependence on galactic latitude are investigated for different classes of object. Radio galaxies have significantly larger rotation measures than quasars. This is to be expected, as the intrinsic source contributions are a function of redshift because of the wavelength dependent definition of the rotation measure. A redshift dependence of the rotation measures of quasars, after subtraction of the regular galactic contribution, is indicated. The data are compatible with the assumption that the intrinsic rotation measures of quasars on the average do not differ from those of radio galaxies, and that they are independent of redshift. At present the rotation measures of the unidentified sources do not give any strong clues as to their nature. (auth)

53912 STUDY OF GALACTIC SUPERNOVA REMNANTS. II. SUPERNOVA RATE, GALACTIC RADIO EMISSION AND PULSARS. Ilovaisky, Sergio A.; Lequeux, James (CEN, Saclay, France). Astron. Astrophys.; 20: No. 3, 347-56(Sep 1972).

Using the radio luminosity function at 1 GHz for galactic supernova remnants (SNR) derived in a previous article (Paper I) together with independent age estimates for six SNR, a mean interval between supernova outbursts in the Galaxy of 50 yr was obtained. The total number of discrete remnants in the Galaxy is presented as a function of the linear diameter, D. Upper and lower limits are given by two possible cases, Case A; adiabatic expansion for $D > 4$ pc, and Case B: adiabatic expansion for $4 < D < 30$ pc followed by isothermal expansion for $D > 30$ pc. Lower and upper limits corresponding to Cases A and B respectively for the maximum diameter, D_M, and age, t_M, that a discrete remnant may have, and the total number of objects in the Galaxy, $N(<D_M)$ are given. It was found that $110 < D_M < 380$ pc, $1.0 \times 10^6 < t_M < 6.0 \times 10^6$, and $2.0 \times 10^4 < N(<D_M) < 1.2 \times 10^5$ SNR. The surface density of supernova remnants is compared to that of radio pulsars, using objects in the same age range and allowing for the two selection effects found to be present in the pulsar sample (age-limiting and flux-limiting effects). It was found that the surface density of pulsars, within a factor of two, is equal to that of SNR. This, plus the fact that the z-distributions of the two types of objects are quite similar, shows that it is possible that most supernova explosions have given birth to pulsars. A new model is presented for the nonthermal galactic radio emission, based on the 150 MHz sky map of Landecker and Wielebinski (1970). This model features a two-disk structure with a radial extent of 8 to 10 kpc. The disks have full thicknesses of 500 and 2000 pc. The outer disk contributes 65% of the total emission and has an emissivity of 100 K kpc^{-1} at 150 MHz, about half that of the inner disk. The total integrated radio power at 1 GHz due to discrete, old SNR is compared to the output of the two-disk structure, for Cases A and B as well as a complementary case, where the radio emission ceases not at D_M but rather at 50 pc. In none of these cases does the total effective SNR output account for more than one-tenth of the total nonthermal galactic luminosity. However, it is possible that old SNR account for part of the non-thermal emissivity close to the galactic plane. (auth)

53913 OPTICAL POSITIONS OF RADIOSOURCES. Veron, M. P. (Observatoire Haute Provence, France). Astron. Astrophys.; 20: No. 3, 471-3(Sep 1972).

Optical positions of quasars and radiogalaxies were measured with an accuracy better than one arc second. The method of Schlesinger (1926) and usually for reference, stars from the AGK3 catalog, were used for this. (auth)

53914 STUDY OF THE LUNAR OCCULTATIONS OF ELEVEN RADIO SOURCES. Lyne, A. G. (Univ. of Manchester, Eng.). Mon. Notic. Roy. Astron. Soc.; 158: No. 4, 431-62(1972).

Observations of the lunar occultations of 11 radio sources were made at Jodrell Bank, using an interferometer to surmount some technical difficulties. Accurate positions and brightness distributions for these sources are given. Some of the observations were made at several frequencies, allowing a study of the variations of spectral index within the sources. In particular, 3C2, 3C245, and 3C279 are quasars which bear a striking resemblance to 3C273. For 3C2, the data suggest an identification of the radio jet with an optical one. (auth)

53915 INTERSTELLAR SCINTILLATION PATTERN OF PSR + 54. Galt, J. A.; Lyne, A. G. (Dominion Radio Astrophysical Observatory, Penticton, B. C.). Mon. Notic. Roy. Astron. Soc.; 158: No. 3, 281-90(1972).

The pulsar PSR 0329 + 54 was observed at 408 MHz simultaneously for an entire day at Jodrell Bank and Penticton. The separation of these stations is sufficient to permit detection of motions of the diffraction pattern produced by irregularities in the interstellar medium. The observations suggest that the scintillation pattern is stable. If this is the case, the results indicate a decorrelation length of 77,000 km and a velocity of 360 km s^{-1} at position angle 295° referred to the local standard of rest. This velocity is high compared to most motions in the Galaxy but it is consistent with velocity estimates made on the basis of single telescope observations. The motion can be attributed to either the interstellar plasma or the pulsar itself. Although this experiment does not distinguish between these two possibilities, it may indicate the existence of high pulsar velocities required by certain theories of pulsar formation. (auth)

53916 FASTER-THAN-LIGHT SYNCHROTRON RADIATION IN A VACUUM. Eidman, V. Ya. (Scientific-Research Radiophysics Inst., Gorky, USSR). Izv. Vyssh. Ucheb. Zaved., Radiofiz.; 15: No. 4, 634-5(1972). (In Russian).

After the discovery of pulsars attention was turned to the possibilities of the radiation source moving at a velocity close to that of light, with the attendant difficulty of large amounts of matter with this characteristic. The author examines here still another possibility—that of producing radiation equivalent to the faster-than light radiation in a vacuum, a situation free of such a difficulty. (K.S.W.)

53917 TIME VARIATION OF X-RAY SPECTRUM AND OPTICAL LUMINOSITY OF SCO X-1. Rao, U. R. (Physical Research Lab., Ahmedabad, India); Chitnis, E. V.; Jayanthi, U. B.; (and others). pp 2-6 of 12th International Conference on Cosmic Rays, Hobart, Australia. Vol. 1. Hobart, Australia; International Union of Pure and Applied Physics (1971).

From twelfth international conference on cosmic rays; Hobart, Australia (16 Aug 1971). See CONF-710807-(Vol.1).

Simultaneous, optical and x-ray observations from Sco X-1, conducted with rocket-borne instrumentation both from the Thumba Equatorial Rocket Launching Station, India, and the Kagoshima Space Centre, Japan, during the period April–August 1969 are presented and compared with similar results obtained from Lawrence Radiation Laboratory Group. X-ray observations reported were performed over the spectral range 2 to 20 keV. The interrelationships of various parameters such as temperature, density, and size which characterize the properties of the isothermal cloud postulated for Sco X-1 x-ray source and the correlation of these physical parameters with the optical luminosity were investigated. The results conclusively show that the Scorpio x-ray source is completely characterized by its temperature. As the temperature increases, its source size decreases with a corresponding increase in the density and a decrease in the optical luminosity. The order of magnitude calculations indicates that Sco X-1 is characterized by a temperature of about 10^7 to 10^8°K, a density of about 10^{16} to 10^{17} cm^{-3} and radius of about 10^8 to 10^9 cm respectively and is consistent with the source being a white dwarf. (auth) (Australia)

53918 X-RAY AND OPTICAL OBSERVATIONS OF SCO X-1 AND OBSERVATIONS OF THE X-RAY BACKGROUND. Garmire, G. P. (California Inst. of Tech., Pasadena); Moore, W.; Stevens, J. C.; Kristian, J.; Lanning, H. pp 7-12 of 12th International Conference on Cosmic Rays, Hobart, Australia. Vol. 1. Hobart, Australia; International Union of Pure and Applied Physics (1971).

From 12th international conference on cosmic rays; Hobart, Australia (16 Aug 1971). See CONF-710807-(Vol.1).

Optical and x-ray observations using a novel x-ray detector configuration were made of Sco X-1 on June 27, 1970 and August 28, 1970. Two spectra were obtained on the 200-inch Hale Telescope during and following the June 27 flight. The results show only a change in x-ray temperature from $T_6 = 63^{+2}_{-3}$ to $T_6 = 58 \pm 3$ for an optical change from $m_B = 12.35$ to $m_B = 13.0$, respectively. No line at 6 keV was observed in the x-ray background to a one standard derivation level of 0.03 ph/(cm^2 sec sr) contrary to several current observations. (auth) (Australia)

53919 SPECTRAL AND PULSED X-RAY EMISSION FROM THE CRAB NEBULA. Tuohy, I. R. (Univ. of Adelaide); Harries, J. R.; Luyendyk, A. P. J.; Broderick, A. J.; Fenton, K. B. pp 13-18 of 12th International Conference on Cosmic Rays, Hobart, Australia. Vol. 1. Hobart, Australia; International Union of Pure and Applied Physics (1971).

From twelfth international conference on cosmic rays; Hobart, Australia (16 Aug 1971). See CONF-710807—(Vol.1).

The Crab Nebula was observed during an unstabilized Skylark rocket flight from Woomera, South Australia on July 10, 1970. The instrumentation included two wall-less proportional counters which were calibrated continuously throughout the flight. The Crab Nebula x-ray spectrum between 2.3 and 9.9 keV was found to be: $(dN/dE) = (0.50 \pm 0.04)\ (E/5)^{-2.04 \pm .09}$ photons/cm^2-sec-keV. Pulsed emission from NP 0532 was also detected. In addition to the two main peaks, the possibility of a third peak is discussed. (auth) (Australia)

53920 INTENSITY AND ENERGY SPECTRA OF SEVERAL X-RAY SOURCES IN THE 20- TO 150-keV ENERGY BAND. Agarwal, P. C.; Biswas, S.; Gokhale, G. S.; (and others) (Tata Inst. of Fundamental Research, Bombay). pp 20-5 of 12th International Conference on Cosmic Rays, Hobart, Australia. Vol. 1. Hobart, Australia; International Union of Pure and Applied Physics (1971).

From 12th international conference on cosmic rays; Hobart, Australia (16 Aug 1971). See CONF-710807—(Vol.1).

Using oriented x-ray telescopes the region of the sky R.A. 13 hrs to 22 hrs and δ – 20° to +50° was scanned in five balloon flights carried out from Hyderabad since April 1968. The combined data reveals the presence of two high galactic latitude regions of hard x-ray emission, one in Virgo and the other close to the Coma cluster. The spectral characteristics of all the sources seen in the 20 to 150 keV range are presented. (auth) (Australia)

53921 SHORT PERIOD VARIATIONS IN THE INTENSITY AND ENERGY SPECTRUM OF CYG X-1. Agarwal, P. C.; Gokhale, G. S.; Iyengar, V. S.; (and others) (Tata Inst. of Fundamental Research, Bombay). pp 26-9 of 12th International Conference on Cosmic Rays, Hobart, Australia. Vol. 1. Hobart, Australia; International Union of Pure and Applied Physics (1971).

From twelfth international conference on cosmic rays; Hobart, Australia (16 Aug 1971). See CONF-710807—(Vol.1).

A balloon flight was carried out from Hyderabad on April 5, 1971 using an oriented x-ray telescope to study short-period variations and possible pulsations in the x-ray intensity of Cyg X-1. The telescope was programmed to point alternately due north and 45° east of north. The total effective time of exposure on Cyg X-1 was about 3 hours. During this period the results show that the intensity of x-rays in the energy range 20 to 150 keV varies rapidly over periods of a few minutes by a factor of 2 to 3. The spectral analysis of the data shows that besides the intensity the spectrum also varies. The data was subjected to a fast folding analysis to examine whether any periodic components were present at high energies in the x-ray emission from Cyg X-1. There was no indication of a pulsating component with an intensity higher than 10% of the total emission. (auth) (Australia)

53922 SEARCH FOR PULSED GAMMA RAYS FROM THE CRAB. Kinzer, R. L.; Seeman, N.; Share, G. H. (Naval Research Lab., Washington, D. C.). pp 45-50 of 12th International Conference on Cosmic Rays, Hobart, Australia. Vol. 1. Hobart, Australia; International Union of Pure and Applied Physics (1971).

From twelfth international conference on cosmic rays; Hobart, Australia (16 Aug 1971). See CONF-710807—(Vol.1).

A telescope incorporating a stack of nuclear emulsions as a converter, a wide-gap spark chamber, and other particle detectors was flown in a search for gamma radiation from the Crab Pulsar. Preliminary results obtained from spark chamber photographs have given some evidence for emission of pulsed photons >10 MeV. An attempt to confirm this observation by locating the γ-ray interactions in the emulsion was made. This analysis reduces the angular uncertainty to $\leq 2\frac{1}{2}$° but also raises the telescope's effective energy threshold. Of 29 γ-ray events located to date which were coincident in time with optical pulsations, only 1 originated $<2\frac{1}{2}$° from the Crab. This is consistent with the number expected from background and places an upper limit of 1×10^{-4} γ/cm^2-sec to the pulsed flux above 20 MeV. The lack of confirmation suggests that the earlier result was due primarily to photons below the 20 MeV effective threshold set by the emulsion analysis, or was a statistical fluctuation. (auth) (Australia)

53923 INVESTIGATION OF GAMMA RADIATION FROM THE CRAB PULSAR. Kettenring, G.; Mayer-Hasselwander, H. A.; Pfeffermann, E.; (and others) (Max-Planck-Institut fuer Physik und Astrophysik, Munich). pp 57-62 of 12th International Conference on Cosmic Rays, Hobart, Australia. Vol. 1. Hobart, Australia; International Union of Pure and Applied Physics (1971).

From twelfth international conference on cosmic rays; Hobart, Australia (16 Aug 1971). See CONF-710807—(Vol.1).

The Crab pulsar was investigated with a gamma-ray astronomy spark chamber balloon experiment. The results of one of several successful flights indicate an upper limit of the pulsed gamma-ray spectrum above ~20 MeV that is lower than values reported previously, but still lies a factor of three above the extrapolation from lower energies into the region above 20 MeV. (auth) (Australia)

53924 NEW POINT GAMMA RAY SOURCE LIBRA γ-1: EVIDENCE FOR TIME VARIATION. Frye, G. M. Jr. (Case Western Reserve Univ., Cleveland); Albats, P. A.; Zych, A. D.; (and others). pp 70-5 of 12th International Conference on Cosmic Rays, Hobart, Australia. Vol. 1. Hobart, Australia; International Union of Pure and Applied Physics (1971).

From twelfth international conference on cosmic rays; Hobart, Australia (16 Aug 1971). See CONF-710807—(Vol.1).

The first possible discrete source of gamma radiation, Sgr γ-1, was reported in 1969 by combining the results of two balloon flights made two weeks apart at latitude 33°S in south eastern Australia. An additional two sources Gγ 2 + 3 and Gγ 341 + 1 were reported by the same teams in 1971 following the combined analyses of these two flights plus a third flight at latitude 23°S made 9 months later in north eastern Australia. Only the region having greater than 50% of the maximum effective exposure for the combined three flights was considered in this analysis and all three sources showed some excess radiation during each flight. An analysis was made of the third flight over a region of sky having an exposure exceeding 50% of the maximum exposure and this indicated the presence of another possible discrete source named tentatively Libra γ-1. The region was also covered by the second flight but no excess gamma radiation from the same region was evident on that flight. (Australia)

53925 RADIATION MECHANISM FOR PULSARS. Lerche, I. (Univ. of Chicago). pp 354-8 of 12th International Conference on Cosmic Rays, Hobart, Australia. Vol. 1. Hobart, Australia; International Union of Pure and Applied Physics (1971).

From twelfth international conference on cosmic rays; Hobart, Australia (16 Aug 1971). See CONF-710807—(Vol.1).

An oscillating interface between a rotating, radiating magnetic dipole and an external plasma is the source of pulsar radiation produced over a broad band of high frequencies (10^8 to 10^{18} cHz/s). The efficiency of the mechanism is so high that the oscillation energy goes mainly into radiation in each cycle of the oscillation. The mechanism automatically accounts for (i) pulse structure, (ii) polarization, (iii) power spectral dependence of pulsar radiation. A recent application of the basic mechanism to extragalactic radio sources by Rees (1970) indicates that it is of wider astrophysical import than just as a mechanism to account for the observed properties of pulsars. (auth) (Australia)

53926 TRANSFER EFFECTS ON LINES AND CONTINUUM IN OPTICALLY THICK X-RAY SOURCES. Felten, J. E. (Univ. of Arizona, Tucson); Rees, M. J. pp 415-18 of 12th International Conference on Cosmic Rays, Hobart, Australia. Vol. 1. Hobart, Australia; International Union of Pure and Applied Physics (1971).

From twelfth international conference on cosmic rays; Hobart, Australia (16 Aug 1971). See CONF-710807-(Vol.1).

The thermal spectrum emergent from a hot plasma cloud may be altered substantially by transfer effects if the cloud is not optically thin. If an isothermal cloud in Sco X-1 has electron-scattering optical thickness $\tau_{es} \gg 1$, the radiation density is sufficient to alter the ionization equilibrium. Compton-scattered wings of prominent x-ray lines will be suppressed by a factor ~10 for $\tau_{es} \gtrsim 10$. Line cores arise in the surface layer and will be less affected. Resonance scattering as well as Compton scattering affects the line profiles. The emergent free–free continuum is also changed by Compton scatterings. Rayleigh–Jeans at low ν shows a characteristic transition region with $I(\nu) \overset{\sim}{\propto} \nu$ if $\tau_{es} \gtrsim 10$ and the cloud is homogeneous. For Sco X-1 this may lie near 1.5 μ. It might appear at other frequencies in other objects with large τ_{es}. The x-ray continuum in $h\nu > kT$ will approach an equilibrium (Bose–Einstein) shape $\nu^3 \exp(-h\nu/kT)$ if $\tau_{es} \gtrsim (m_e c^2/3kT)^{½}$. This affects temperature estimates. For larger τ_{es} this thermalization may extend down to the optical band. (auth) (Australia)

Solar Phenomena

Refer also to abstracts 54048, 54390, 54508, 54955, and 54956.

53927 (NASA-TM-X-2440, pp 193-208) SOLAR-FLARE PARTICLE RADIATION. Lanzerotti, L. J. (Bell Telephone Labs., Inc., Murray Hill, N. J.). Jan 1972.

From Symposium on natural and manmade radiation in space; Las Vegas, Nev. (1 Mar 1971).

The characteristics of the solar particles accelerated by solar flares and subsequently observed near the orbit of the earth are studied. Considered are solar particle intensity–time profiles, the composition and spectra of solar flare events, and the propagation of solar particles in interplanetary space. The effects of solar particles at the earth, riometer observations of polar cap cosmic noise absorption events, and the production of solar cell damage at synchronous altitudes by solar protons are also discussed. 94 references, 19 figures. (auth) (STAR)

53928 (NASA-TM-X-2440, pp 329-35) SIGNIFICANT SOLAR-PROTON EVENTS IN THE 20TH SOLAR CYCLE FOR THE PERIOD OCTOBER 1964 TO MARCH 1970. Atwell, W. (Lockheed Electronics Co., Houston, Tex.). Jan 1972.

From Symposium on natural and manmade radiation in space; Las Vegas, Nev. (1 Mar 1971).

Solar-proton data are presented from observations by the IMP 2, 3, F and G satellites. The NASA Solar Particle Alert Network (SPAN) solar optical- and radio-frequency data for the period May 1967 to March 1970 are associated with the proton events observed by the IMP F and G satellites; however, missing data are supplemented with data recorded at other international observatories. From a radiation-hazard standpoint, NASA is concerned with solar-proton events of the order of 10^8 proton/cm^2. Radiation dose data are presented for some of the large proton events that have occurred thus far in the 20th solar cycle and are compared with some of the large proton events of the 19th solar cycle. Finally, the results of a simple parametric correlation study are presented for both the 19th and 20th solar cycles. 7 tables. (auth)

53929 (NASA-TM-X-2440, pp 336-44) TIME BEHAVIOR OF SOLAR-FLARE PARTICLES TO 5 AU. Haffner, J. W. (North American Rockwell Corp., Downey, Calif.). Jan 1972.

From Symposium on natural and manmade radiation in space; Las Vegas, Nev. (1 Mar 1971).

A simple model of solar flare radiation event particle transport is developed to permit the calculation of fluxes and related quantities as a function of distance from the sun (R). This model assumes the particles spiral around the solar magnetic field lines with a constant pitch angle. The particle angular distributions and onset plus arrival times as functions of energy at 1 AU agree with observations if the pitch angle distribution peaks near 90°. As a consequence, the time-dependence factor is essentially proportional to $R^{-1.7}$, (R in AU), and the event flux is proportional to R^{-2}. (auth)

53930 (NASA-TM-X-2440, pp 345-55) SOLAR COSMIC-RAY HAZARD TO INTERPLANETARY AND EARTH-ORBITAL SPACE TRAVEL. Yucker, W. R. (McDonnell Douglas Astronautics Co., Huntington Beach, Calif.). Jan 1972.

From Symposium on natural and manmade radiation in space; Las Vegas, Nev. (1 Mar 1971).

A statistical treatment is given of the radiation hazard to astronauts due to solar cosmic-ray protons. While several similar studies have been conducted in the past, objections to the use of this approach to determining shielding requirements have been raised due to the limited number of solar proton events for which data are available. More recent data are incorporated into the present analysis, including events from 1956 to 1969, in order to improve the accuracy of the predicted mission fluence and dose. The effects of the finite data sample are discussed. Also, an attempt is made to present a unified and consistent view of the solar cosmic ray proton hazard and to justify the application of a statistical approach for mission planning. Mission fluence and dose versus shield thickness data are presented for mission lengths up to 3 years during periods of maximum and minimum solar activity; these correspond to various levels of confidence that the predicted hazard will not be exceeded. 16 figures, 23 references. (auth)

53931 (NASA-TM-X-2440, pp 356-61) SHORT-TERM PREDICTION OF E ≥ 10-MeV PROTON FLUXES FROM SOLAR FLARES. Kuck, George A. (Air Force Weapons Lab., Kirtland AFB, N. Mex.). Jan 1972.

From Symposium on natural and manmade radiation in space; Las Vegas, Nev. (1 Mar 1971).

One problem is the prediction of ionospheric effects related to energetic proton emissions from the sun. The intensity and duration of these charged particle emissions are related to the optical, radio, and x-ray emissions from the solar flares. Radio and x-ray data give an important indication of proton production. Cm radio bursts with a high flux density and a slope reflecting greater flux values at higher frequencies are often proton productive. Examination of the data summaries has shown that the meter classification of flares as type II or type IV, even though qualitative, should be used in conjunction with the cm radio criteria. The peak intensity of the proton flux E ≥ 10 MeV correlates better with the integrated 1 to 8 Å x-ray bursts than with the integrated cm radio bursts, peak cm radio flux, or peak x-ray flux. Free-free transition theory was used to relate the x-ray flux. Free-free transition theory was used to relate the x-ray intensities recorded by different satellites with the peak proton fluxes observed at the earth. Both the anisotropic and isotropic diffusion theories could be used to extrapolate proton fluxes for E ≥ 10 MeV for over 50% of the particle events. The isotropic diffusion theory uses a diffusion coefficient: $D = Mr^{\beta}$. It was found that M and β tended to be functions of flare position on the solar disk. A measurement of the interplanetary flux in near-earth space gives a good indication of the polar cap fluxes. It was found that the 30-MHz absorption over the poles during a PCA is proportional to the square root of the integral proton flux E ≥ 11 MeV in interplanetary space: $J = KA^2$, with $K = 8 \pm 2$ and J in protons/cm^2-sec-ster. (auth)

53932 SOLAR-FLARE-PARTICLE PROPAGATION: COMPARISON OF A NEW ANALYTIC SOLUTION WITH SPACECRAFT MEASUREMENTS. Lupton, John Edward. Pasadena, Calif.; California Inst. of Tech. (1972). 197p. University Microfilms Order No. 72-22,555.

Thesis.

A new analytic solution has been obtained to the complete Fokker–Planck equation for solar-flare particle propagation including the effects of convection, energy-change, corotation, and diffusion with κ_r = constant and $\kappa_\theta \propto r^2$. It is assumed that the particles are injected impulsively at a single point in space, and that a boundary exists beyond which the particles are free to escape. Several solar-flare particle events have been observed with the Caltech Solar and Galactic Cosmic Ray Experiment aboard OGO-6. Detailed comparisons of the predictions of the new solution with these observations of 1- to 70-MeV protons show that the model adequately describes both the rise and decay times, indicating that κ_r = constant is a better description of conditions inside 1 AU than is $\kappa_r \propto r$. With an outer boundary at 2.7 AU, a solar-wind velocity of 400 km/sec, and a radial diffusion coefficient $\kappa_r \approx 2\text{–}8 \times 10^{20}$ cm^2/sec, the model gives reasonable fits to the time-profile of 1- to 10-MeV protons from “classical” flare-associated events. It is not necessary to invoke a scatter-free region near the Sun in order to reproduce the fast rise times observed for directly-connected events. The new solution also yields a time-evolution for the vector anisotropy which agrees well with previously reported observations. In addition, the new solution predicts that, during the decay phase, a typical convex spectral feature initially at energy T_0 will move to lower energies at an exponential rate given by $T_{KINK} = T_0 \exp(-t/\tau_{KINK})$. Assuming adiabatic deceleration and a boundary at 2.7 AU, the solution yields $\tau_{KINK} \approx 100$h, which is faster than the measured $\sim$200h time constant and slower than the adiabatic rate of $\sim$78h at 1 AU. Two possible explanations are that the boundary is at $\sim$5 AU or that some other energy-change process is operative. (Diss. Abstr. Int., B)

53933 VIDEOMAGNETOGRAPH STUDY OF DIFFUSION OF SOLAR MAGNETIC FIELDS IN WEAK-PLAGE REGIONS. Smithson, Robert Carroll. Pasadena, Calif.; California Inst. of Tech. (1972). 223p. University Microfilms Order No. 72-22,615.

Thesis.

A new instrument for use in astronomical research has been developed. This is the differential video photometer, a device for detecting differences in light intensity between two television pictures. With a suitable source of video, the device is capable of detecting intensity differences of the order of one part in one thousand. It should be useful in many applications, such as colorimetry, polarimetry, motion detection, and doppler shift measurements. It has been used thus far primarily as a videomagnetograph which measures the line-of-sight component of the solar magnetic field in the photosphere. Sensitivity to magnetic field strength is on the order of 5 to 10 gauss. A study has been made of the characteristics of magnetic flux diffusion in weak plage regions. Points of enhanced magnetic field have been found to exist which have lifetimes of about 3 to 4 days, and which move in a random walk with a step time short compared to 24 hours. The random walk of these points considered as discrete entities is not, however, responsible for much of the flux diffusion in the weak plage regions. The R.M.S. displacement of the points is about 7800 km in 24 hours. A second form of flux transport has been found in which in a period of a few hours a previously stable point will become unstable, and either shoot out a tongue of flux, or begin to move as a unit. This process can move flux over distances of the order of 10,000 km at apparent velocities of 1 to 2 km/sec. This process may be responsible for most of the flux transport in weak plage regions. (Diss. Abstr. Int., B)

53934 STUDIES OF TYPE III BURSTS AND REFRACTION IN THE SOLAR CORONA AT HECTOMETER WAVELENGTHS. Howard, Edward Glenn. Washington, D. C.; Georgetown Univ. (1972). 181p. University Microfilms Order No. 72-22,772.

Thesis.

A ray tracing program was developed and applied to a coronal model in order to study the visibility of Type III radio bursts seen from the Earth. The model includes an enhanced conical shaped streamer in the solar corona in which emission takes place. It is possible to vary emission bandwidth, enhancement of the streamer over the ambient corona, opening angle of the streamer, and the lateral or off-axis width of the emission region. Using this model, one can construct curves of radiation intensity as seen at Earth as a function of the heliocentric longitude of the source. These curves are termed I(L) curves, for intensity as a function of longitude. Both refraction due to the radial gradient of the solar electron density and refraction due to the transverse gradient due to the streamer enhancement electron density are included in the radiation plots. The plots show an isotropically radiating point source at locations both on and off the streamer axis. By combining point sources to form a distributed source it is possible to produce a wide range of radiation intensity I(L) curves. (TSS) (Diss. Abstr. Int., B)

53935 POSITION MEASUREMENTS OF SOLAR CONTINUUM AND TYPE-III BURST SOURCES AT DECAMETER WAVELENGTHS. Fitzenreiter, Richard Julius. Washington, D. C.; Catholic Univ. of America (1972). 173p. University Microfilms Order No. 72-22,688.

Thesis.

The position of a source of continuum in the active solar corona is analyzed as a function of frequency and aspect angle in order to explain the emission mechanism of stationary continuum. A plasma radiation source in the corona is characterized by a variation of position with frequency corresponding to the plasma level distribution in the source region. The other possible source mechanism, gyro-synchrotron radiation, is characterized by a localized source, i.e., radiation at all frequencies originating from the same position in the corona. Positions of sources of stationary continuum and Type III bursts occurring simultaneously during an 11-day period of solar activity in July, 1970, are determined using data in the range 20 to 60 MHz from the Clark Lake sweep frequency two mile baseline grating interferometer. With Type III bursts as the reference, relative positions of continuum and Type III bursts show that the continuum originates from the critical plasma levels over a wide range of frequencies corresponding to the range of coronal levels extending from 1.7 to 2.3 solar radii from the center of the Sun. This is clear evidence that the observed stationary continuum source radiates by the plasma radiation mechanism. The emission cone of a plasma radiation source is very narrow, but yet the source is observed over a wide range of aspect angles, implying the existence of density gradients in the source region. Using ray tracing, a model is determined for the density enhancement and gradients which allow the radiation to escape and be observed at the measured positions as a function of aspect angle. The resulting model is consistent with other radio and optical observations of active region streamers. (Diss. Abstr. Int., B)

53936 NEW SOLAR FLUCTUATION. Dicke, R. H. (Princeton Univ., N. J.). Astrophys. J.; 176: No. 2, 479-86(1 Sep 1972).

The fluctuation in the solar-oblateness signal during 1966 has been found to be strongly autocorrelated with a 25.3-day lag. The autocovariance functions show that the disturbed regions of the Sun occur in the vicinity of ±45° latitude for which the synodic rotation period is ~29.5 days. The 25-day correlation peak is positive as expected, but there is no indication of the equally strong 13-day negative half-rotation peak that would also be expected. It is concluded that the 25-day correlation may be due to density fluctuations occurring near the top of the radiative zone. (auth)

53937 CURRENT LIMITATION IN SOLAR FLARES. Smith, Dean F.; Priest, E. R. (National Center for Atmospheric Research, Boulder, Colo.). Astrophys. J.; 176: No. 2, 487-95 (1 Sep 1972).

It is shown that the ion-sound current instability will be the relevant mechanism of current dissipation in most instances in the fully ionized part of the solar atmosphere (upper chromosphere and corona). Since this instability has the same initial threshold as the Alfvén—Carlqvist instability, but a considerably lower threshold once the instability has started toward saturation, the Alfvén—Carlqvist instability will not occur. The linear and nonlinear stages of the ion-sound current instability are examined and a turbulent resistivity is given for the saturated state which is in agreement with laboratory experiments. This turbulent resistivity is applied to the Alfvén—Carlqvist model of a cylindrical current filament, and it is shown that enough energy could not be dissipated sufficiently fast for a solar flare. This turbulent resistivity is also applied to the "hard" phase of Syrovatsky's dynamic dissipation model, and it is shown that Syrovatsky's electromagnetic instability for instantaneous current-sheet interruption cannot occur. The possibility that the ion-sound turbulence can systematically accelerate a select group of particles is investigated. It is concluded that heating rather than acceleration will result. It is suggested that a small electric field acting over large distances is a potentially much more efficient accelerating mechanism. (auth)

53938 F AND K COMPONENTS OF THE SOLAR CORONA. Calbert, Roosevelt; Beard, David B. (Univ. of Kansas, Lawrence). Astrophys. J.; 176: No. 2, 497-509(1 Sep 1972).

By taking advantage of the different spatial dependencies of electrons and dust in the solar system, a reliable method was developed of separating the K component from the F component in measurements of the total solar coronal light as a function of elongation angle. By assuming a sum of inverse power of distance terms for electron density and using the same observational data, dust and electron density separation was obtained in good agreement with others who have used polarization and spectroscopic methods for the separation. An exponential dependence on the inverse of the distance consonant with contemporary cornal theory was also assumed and a very good fit to previous determinations of electron density was obtained. The F component was found to be nearly absent in long-wavelength (2.2 μ) measurements of the solar corona—an indication that diffraction is absent and that the minimum dust size is 0.2 μ. The minute F component present has an albedo of about 0.3. It was indicated that the minimum approach to the Sun of the dust particles is 10 solar radii, in agreement with theoretical calculations. As a result, compelling evidence was found that the F component is very much less at small elongations than believed previously. (auth)

53939 PROPERTIES OF A CORONAL HOLE DERIVED FROM EXTREME-ULTRAVIOLET OBSERVATIONS. Munro, Richard H.; Withbroe, George L. (Harvard Coll. Observatory, Cambridge, Mass.). Astrophys. J.; 176: No. 2, 511-20(1 Sep 1972).

A coronal "hole" is characterized by significant deficiency in the intensity of coronal emission lines, yet there is little change in lines and continua formed below 800,000°K except for the He I and He II emission features. Comparison of the hole with the normal quiet Sun indicates that the electron pressure is reduced by a factor of 3, the coronal temperature is lower by 600,000°K, and the temperature gradient in the chromospheric—coronal transition layer is less steep by an order of magnitude. The apparent insensitivity of the lines formed in the transition layer to the physical conditions of the hole implies that the conductive flux from the corona is proportional to the square of the electron pressure. (auth)

53940 RAYLEIGH–TAYLOR INSTABILITY IN A COMPOSITE MEDIUM. Bhatia, P. K. (Univ. of Jodhpur, India). Cosmic Electrodyn.; 3: No. 2, 124-8(Jul 1972).

The effects of collisions with neutral atoms were studied on the dynamic stability of a composite medium in the presence of a uniform vertical magnetic field. The case of one-dimensional density gradient in the fluid medium was studied. An explicit solution was obtained by making use of a variational principle which is shown to characterize the problem. It was found that the stability criterion is the same as in the absence of collisions. The collisions, however, have a stabilizing influence. (auth)

53941 NONLINEAR MAGNETOSONIC WAVES IN A PLASMA WITH A FINITE CONDUCTIVITY. Sakai, Jun-ichi (Nagoya Univ., Japan). Cosmic Electrodyn.; 3: No. 2, 260-70(Jul 1972).

Nonlinear magnetosonic waves in a turbulent plasma, characterized by an effective electrical conductivity σ_{eff} due to microinstabilities, are governed by the Burgers type equation, which has a shock-like stationary solution. It is shown that initial magnetic pulses of gaussian and solitary wave forms first decay due to dissipation, and subsequently form a shock front whose steepness is determined by the opposing effects of nonlinearity and dissipation. This process is thought to be important in connection with shock formation in space plasmas. (auth)

53942 SOLAR-WIND HEATING. Barnes, Aaron (Ames Research Center, Moffett Field, Calif.); Brandt, John C.; Hartle, R. E.; Wolff, Charles L. Cosmic Electrodyn.; 3: No. 2, 254-9 (Jul 1972).

A number of workers (Barnes et al., 1971; Cuperman and Harten 1971; Wolff, et al., 1971) have developed detailed models aimed at understanding energy transport in the solar wind. The differences in objectives, physical assumptions, and results among these models are analyzed. (W.D.M.)

53943 THEORETICAL TREATMENT OF LUNAR PARTICLE SHADOWS. McGuire , Robert E. (Univ. of California, Berkeley). Cosmic Electrodyn.; 3: No. 2, 208-39(Jul 1972).

The interaction of particles having nonzero gyroradii with a spherical absorber such as the Moon is theoretically treated. The Moon is assumed to have no effect on ambient magnetic or electric fields, and collective interactions of the particles are ignored. Properties of particle shadows are investigated in a uniform magnetic field and also in the presence of a uniform particle drift normal to this field (as might be produced by a uniform electric field transverse to the magnetic field). Shadow properties are calculated for particles in specified narrow energy and pitch angle intervals. Numerous results are derived for the specific case of a detector in a low lunar orbit as well as some results on the structure of particle shadows as a general function of spatial position. (auth)

53944 MEAN DEPTH OF LINE FORMATION IN A MAGNETIC FIELD. Staude, Juergen (Zentralinstitut fuer Solar-Terrestrische Physik, Potsdam, Ger.). Solar Phys.; 24: No. 2, 255-61 (Jun 1972).

Probability interpretation of radiative transfer is used to calculate the contribution of different layers of the solar atmosphere to the emergent intensity. Generally the mean depths of line formation increase with increasing intensity; this is valid also for arbitrarily polarized constituents of a line formed in a magnetic field. (auth)

53945 SOLAR SEEING AND THE SPATIAL PROPERTIES OF THE FIVE-MINUTE OSCILLATIONS. Thomas, John H. (Univ. of Rochester, N. Y.). Solar Phys.; 24: No. 2, 262-73 (Jun 1972).

A numerical simulation of observations of the spatial properties of the five-minute oscillations is carried out, assuming the oscillations are internal gravity waves excited by granular convection according to the theory of Thomas et al. (1971). The simulation includes the effects of seeing and finite aperture. The details of the simulation are chosen to model the observational method of Frazier (1968a, b). The results show that the peak in the observed power spectrum of the oscillations can occur at a wavelength considerably longer than the true wavelength of the oscillations. In particular, the peak in Frazier's observed power spectra at wavelength $\lambda \approx 5000$ km is consistent with the considerably shorter true wavelength $\lambda \approx 1500$ km predicted by the gravity wave theory. (auth)

53946 VELOCITY OSCILLATIONS IN THE SOLAR ATMOSPHERE. Bhattacharyya, J. C. (Indian Inst. of Astrophysics, Kodaikanal). Solar Phys.; 24: No. 2, 274-87(Jun 1972).

From a series of long duration continuous Doppler records of selected spectral lines, characteristics of solar velocity oscillations were studied. Statistical distribution of the durations of the bursts of oscillations was estimated. From the nature of distortion of the waveforms of the oscillation, the presence of disturbing impulses was speculated. Constancy and homogeneity of the oscillations were examined from detailed spectral density plots. Duration indices for the oscillations at different heights in the solar atmosphere were derived by estimating mean spectral densities of characteristic oscillation amplitudes during several individual bursts and comparing them with corresponding spectral densities from long records. The variation among experimental results is explained as due to the limitations of the power spectral analysis method on short records. (auth)

53947 MAGNETIC FIELDS AND HELIUM-D_3 SPECTROHELIOGRAMS. Chapman, G. A. (Aerospace Corp., El Segundo, Calif.). Solar Phys.; 24: No. 2, 288-300(Jun 1972).

Spectroheliograms, having a resolution approaching 2″, were obtained which show He$-D_3$ in absorption against the disk. The He$-D_3$ features were compared with the distribution of magnetic fields and with Hα structures. The brightest regions in Hα usually show the strongest D_3 absorption. Most Hα dark filaments show some D_3 absorption, but the degree of correlation varies from filament to filament. The correlation between $B_{||}$ and He$-D_3$ absorption is rather poor and the He features are much more diffuse than the photospheric magnetic field. (auth)

53948 CHARACTERISTICS OF THE Ca II K-LINE PROFILES IN THE QUIET SUN. Liu, Sou-yang; Smith, Elske v.P. (Univ. of Maryland, College Park). Solar Phys.; 24: No. 2, 301-9(Jun 1972).

Feature-to-feature identification is made on simultaneous Ca II K-line spectrograms (SG) and K_{2v} spectroheliograms (SHG). The line profiles in plages and in the network boundary nearly always have double-peaked reversal in the core, while those inside the cells present all possibilities: double-peaked, single-peaked on violet side, single-peaked on red side, and unreversed absorption. Statistics of the profiles in the quiet chromosphere show that 50% are K_{232} double-peaked, 20% are K_{2v} single-peaked, 10% are K_{2r} single-peaked, and 20% show only incipient reversal or even totally lack any reversal. Attention is directed to the nontrivial contribution of these absorption profiles which are formed in "dark regions" shown on SHG's. The physical conditions inferred from different kinds of profiles are briefly discussed. (auth)

53949 IONIZED HELIUM IN PROMINENCES AND IN THE CHROMOSPHERE. Hirayama, Tadashi (Sacramento Peak Observatory, Sunspot, N. Mex.). Solar Phys.; 24: No. 2, 310-23 (Jun 1972).

Quiescent Prominences: It is found that HE II 4686 is emitted in the same cold region of $\lesssim$10,000 K as hydrogen, metal, and neutral helium emission lines. This conclusion is based on the finding that the observed width of λ4686 is the same as the calculated width of λ4686. The calculated width is derived from the observed widths of hydrogen and metallic lines. The large intensity of He II 4686 in $\lesssim$10,000 K can be explained by the ionization of He II due to the uv radiation below 228 Å that comes from the corona and the transition region. Loop Prominences: The very broad width (30 to 50 km s^{-1}) of λ4686 for two post-flare loop prominences shows that the He II line is emitted in hot regions different from regions of hydrogen and metal emission. From the widths of the Balmer lines and many metallic lines the kinetic temperature for one loop is found to be 16,000 K in one part and 7600 K in another part. The electron densities are $10^{12.0}$ cm^{-3} and less than $10^{11.0}$ cm^{-3} respectively. Chromosphere: The intensity of λ4686 in the chromosphere can be interpreted in terms of a temperature of $\lesssim$10,000 K with the ionization due to uv radiation. But, since observations of the width of λ4686 are not available, a definitive conclusion for the chromosphere cannot be reached. (auth)

53950 METHOD TO CALCULATE ELECTRIC CURRENTS IN QUIESCENT PROMINENCES. Anzer, Ulrich (Max-Planck-Institut fuer Physik und Astrophysik, Munich). Solar Phys.; 24: No. 2, 324-35(Jun 1972).

A 2-dimensional model of the magnetic field associated with quiescent prominences is presented. The coronal field is assumed to be current-free, currents are only allowed in the photosphere and inside the prominence. The prominence is taken to be infinitely thin. For this model a method is given to calculate the field configuration from the observed normal component of the field both in the photosphere and the prominence. The normal field components are inferred from disc observations and Hα limb observations. The sheet currents inside the prominence are calculated and the resulting Lorentz force is compared with the gravitational force. Within the range of uncertainty in the total hydrogen density of quiescent prominences it is possible to give models where the gravity is balanced by the Lorentz force. (auth)

53951 INTERPRETATION OF THE π-COMPONENT SPLITTING IN SUNSPOT SPECTRA. Obridko, V. N.; Demkina, L. B. (Inst. of Terrestrial Magnetism, Ionosphere, and Radio-wave Propagation, Moscow). Solar Phys.; 24: No. 2, 336-41 (Jun 1972).

It is shown that in order to explain the observed splitting of the π-component in the sunspot umbra spectrum by the hypothesis of the coexistence in sunspots of weak- and strong-field regions with opposite polarities, one has to admit the additional assumption that in the weak-field regions the Doppler halfwidth ($\Delta\lambda_D$) and the ratio between line opacity and continuum opacity (η_0) are both less than those in the strong-field regions. (auth)

53952 C_2 LINES IN SUNSPOT SPECTRA. Woehl, Hubertus (Univ., Sternwarte, Goettingen, Ger.). Solar Phys.; 24: No. 2, 342-53(Jun 1972).

The questionable existence of C_2 absorption lines in spectra of sunspots was checked. In two umbral spectra of large single sunspots evidence for the presence of lines of the (0,0) band and of the (0,1) band was found. (auth)

53953 C_2 IN SUNSPOTS. Harvey, J. W. (Kitt Peak National Observatory, Tucson, Ariz.). Solar Phys.; 24: No. 2, 354-5(Jun 1972).

The existence of C_2 lines in the spectrum of sunspot umbras has been questioned by Branch (1969) and Schadee (1970), while Wöhl (1971, 1972) found positive evidence for their presence. Since molecular equilibrium calculations (e.g., Tsuji, 1964) show that C_2 should be extremely weak in sunspot umbras, a resolution of these conflicting results is important. Results are presented which show that C_2 lines are strengthened in the penumbra relative to the photosphere and are much weaker in the umbra in agreement with the predictions of molecular equilibrium calculations. (W.D.M.)

53954 Z DEPENDENCE OF THE LEVEL INTERVALS IN $2s^2 2p^2$, $2s^2 2p^3$, AND $2s^2 2p^4$. Edlen, Bengt (Univ. of Lund, Sweden). Solar Phys.; 24: No. 2, 356-67(Jun 1972).

Values of the level intervals in the ground configurations $2s^2\ 2p^2$, $2s^2\ 2p^3$, and $2s^2\ 2p^4$ have been critically compiled from laboratory observations and from observations of nebular and coronal forbidden transitions. The data are represented within experimental errors by means of semi-empirical extrapolation formulae which contain from 3 to 5 adjusted parameters. The results provide means for checking laboratory and astrophysical identifications and measurements. Tables of "best" level values are given for the configurations concerned. (auth)

53955 ATLAS OF MAGNETIC FIELDS IN THE SOLAR CORONA. Newkirk, Gordon Jr. (High Altitude Observatory, Boulder, Colo.); Trotter, Dorothy E.; Altschuler, Martin D.; Howard, Robert. Solar Phys.; 24: No. 2, 370-2(Jun 1972).

An atlas is described which provides maps of the coronal (current-free) magnetic field from August 1959 to June 1970. The Atlas contains some 11,000 maps depicting magnetic field lines from 1.0 to 3.0 $R_\odot$ from the solar center, at 10° intervals of longitude. (W.D.M.)

53956 HYDRODYNAMIC STUDY OF THE LARGE CORONAL STREAMER OBSERVED DURING THE ECLIPSE OF MARCH 7, 1970. Koutchmy, S. (Institut d'Astrophysique de Paris, France). Solar Phys.; 24: No. 2, 373-84(Jun 1972). (In French).

Photometry of the large coronal streamer located on the N–E limb of the Sun observed on March 7, 1970 in Mexico was performed using compensated plates in unpolarized light as well as in tangentially and radially polarized light. The measured polarizations locate the streamer in space using a generally used method. The density distribution in the core of the streamer and for $r > 1.5\ R_\odot$ is given as well as the half-widths of the density distribution perpendicular to the axis of the streamer. Densities n(r) in the $1(R_\odot) < r < 1.5(R_\odot)$ region were obtained assuming hydrostatic equilibrium (4) for $1.5 < r < 2$. The axial values of n(r) are given which agree with those of other models. The values of parameters for the model given are tabulated. The variation of the expansion velocity was derived from the hydrodynamical continuity equation. This velocity becomes supersonic [$\nu > 150$(km s^{-1})] above the height of minimum cross section of the streamer, $r = 3.5\ (R_\odot)$. This result was verified by a simple calculation based on the observed curvature of the streamer's "stalk." The velocity corresponding to the garden hose effect considered had a lower value equal to 60 (km s^{-1}). The radial distribution of the expansion velocity is shown. The model allows one to extrapolate in order to obtain the value of $\nu(r)$ at the Sun's surface. This value, $\nu \approx 0.07$ (km s^{-1}) can be compared with the value of the differential rotation velocity of the "foot" of the streamer. The values of the corpuscular flux of the streamer were calculated [$F = 2.4 \times 10^{34}$(e s^{-1})] and agreed with the value of the flux corresponding to the density enhancements of the solar "wind", measured in situ. This shows the importance of large streamers for the coronal expansion processes. (auth)

53957 CORONAGRAPHIC OBSERVATIONS OF AN ENHANCED CORONAL REGION. II. TEMPERATURE AND DENSITY STRUCTURE THROUGH THE ENHANCED REGION. Fisher, Richard R. (Univ. of Hawaii, Honolulu). Solar Phys.; 24: No. 2, 385-94(Jun 1972).

Ratios of emission line intensities were used to calculate the variation of temperature and the variation of electron density as a function of ion class for differing paths through a coronal enhancement. The data indicated (a) a peak mean electron density of 2.3×10^9 cm^{-3}, (b) a temperature maximum greater than 2.3×10^6 K, and (c) the noncoincidence of the peak temperature and peak mean electron density. The latter demonstrates the invalidity of the assumption of symmetric models for coronal enhancements. The abundance of Ni was found to be equal to 0.045 that of Fe from the line ratio I(λ 6702)/I(λ 7059) and a density model based on the variation of the ratio I(λ 8024)/I(λ 6702). (auth)

53958 PHOTOGRAPHS OF THE SUN IN THE XUV REGION. Burger, M.; Dijkstra, J. H. (Astronomical Inst., Utrecht). Solar Phys.; 24: No. 2, 395-404(Jun 1972).

X-ray photographs obtained with a zone plate camera on October 3, 1967 in the wavelength band 49.5 to 52.5 Å were investigated photometrically. The most intense x-ray emission corresponded with active regions in Hα and Ca II. About one quarter of the total solar flux was emitted by the three brightest x-ray sources (A, E and J). X-ray emission from quiet regions was also observed. Limb brightening was found, also at the poles, which indicated a higher electron density at the poles than during solar minimum. The brightest x-ray regions had a very small core of the order of 20″. No relation to magnetic field strengths of sunspots was found. However, a correlation with active prominences cannot be ruled out. X-ray source A was related either to prominence activity or to flare activity. One x-ray region (J) was probably related to flare activity. Assuming an electron temperature of 3 to 5×10^6 K for coronal active regions an emission measure of a few times 10^{49} cm^{-3} was derived, which yielded an electron density of a few times 10^{10} cm^{-3}. (auth)

53959 OBSERVATIONS AND COMMENTS FOR THE SOLAR EVENT OF OCTOBER 24, 1969. Covington, Arthur E. (National Research Council of Canada, Ottawa). Solar Phys.; 24: No. 2, 405-10(Jun 1972).

Observations of the flare of October 24, 1969 by Zirin et al. (1971) Solar Phys. 19, 463, are given with accompanying graphs of XUV emissions from satellites and four microwave radio emissions from Sagamore Hill Observatory. This event provides an excellent example of the development of two types of radio spectra within the same center and similar profiles for the hard x-ray burst and the 8800 MHz radio profile. The examination of the 2700 MHz burst from the Dominion Radio Astrophysical Observatory provides a clarification of the radio profile and shows the existence of a long enduring burst not previously considered. This event parallels a similar variation of intensity in the soft x-ray burst. (auth)

53960 MEASUREMENT OF THE ELECTRON TEMPERATURE OF SMALL 3-CM RADIO BURSTS. Foukal, Peter (Carnegie Institution of Washington, D. C.). Solar Phys.; 24: No. 2, 411-13(Jun 1972).

An attempt was made to correlate low-amplitude radio bursts at 3 cm with transient features on Hα films. (W.D.M.)

53961 THICK-TARGET PROCESSES AND WHITE-LIGHT FLARES. Hudson, H. S. (Univ. of California, San Diego, La Jolla). Solar Phys.; 24: No. 2, 414-28(Jun 1972).

Observations indicate that fast electrons in solar flares, which cause the hard x-ray burst and the impulsive microwave burst, lose energy predominantly by collisional processes. This requires a thick-target theory of the emission, for which the electron spectrum inferred from the x-ray spectrum becomes 1.5 powers steeper than in the usual thin-target theory. The low-energy end of this spectrum contains enough energy above about 5 keV to supply the white-light continuum emission occasionally observed in major flares. The penetration of the nonthermal electrons creates long-lived excess ionization which enhances the free–free and free–bound continuum in the heated medium. The emission will occur high above the photosphere at small optical depth in the visible continuum. Thus its spectrum will extend into the infrared and ultraviolet. (auth)

53962 NEW MEASUREMENTS OF THE POLARIZATION OF X-RAY SOLAR FLARES. Tindo, I. P.; Ivanov, V. D.; Mandel'stam, S. L.; Shuryghin, A. I. (Lebedev Inst. of Physics, Moscow). Solar Phys.; 24: No. 2, 429-33(Jun 1972).

Measurements of three x-ray flares in October/November 1970 aboard the Intercosmos 4 satellite confirm the existence of polarization in the initial phase of the x-ray bursts. The polarization can be observed for a few up to ten minutes, and an increase in polarization is observed during secondary maxima of the bursts as well. (auth)

53963 SOLAR SOFT X RAYS AND SOLAR ACTIVITY. II. OBSERVATIONAL ASSESSMENT OF THE ROLE OF THE TYPE III ACCELERATION MECHANISM IN ESTABLISHMENT OF THE SOFT X-RAY SOURCE VOLUME. Teske, Richard G. (Univ. of Michigan, Ann Arbor); Thomas, Roger J. Solar Phys.; 24: No. 2, 434-43(Jun 1972).

Peak fluxes of flare-associated 8- to 12-Å x-ray bursts occur at or near the time of the maximum energy content of the soft x-ray source volume. The amplitudes of flare-associated bursts may thus be used as a measure of the energy deposited in the source volume by nonthermal electrons and other processes. In the mean, the soft x-ray burst amplitude is apparently independent of the occurrence of a Type III event. This is interpreted to indicate that electrons accelerated by the Type III process do not directly participate in establishing the soft x-ray source volume. (auth)

53964 DYNAMIC THEORY OF TYPE-III SOLAR RADIO BURSTS. Zaitsev, V. V.; Mityakov, N. A.; Rapoport, V. O. (Inst. of Radiophysical Research, Gorky, USSR). Solar Phys.; 24: No. 2, 444-56(Jun 1972).

Numerous experimental data indicate that Type III solar radio bursts are generated by the streams of fast electrons in the corona. The process of the electron acceleration in the flare region is, in general, of the character of a short time local explosion. As a result, a spatially limited stream with inhomogeneous front and back is formed in the corona. It is shown that such a spatial structure of fast electrons radically changes the dynamics of the stream instability development. In particular, for example, despite strong quasilinear relaxation, in this case the electron stream can generate plasma waves in the corona for a long time due to faster electrons escaping out of the front of the stream. The extension of the stream in the outer corona where the collisions are negligible is of similar character. The maximum of the energy density in the packet of excited plasma waves travels in the corona with constant mean velocity which is defined by the fast-electron energy at the moment of their formation in the flare region. Therefore, in spite of the considerable influence of quasilinear effects on the stream motion, the velocity of Type III sources found in terms of the drift velocity remains unchanged. This creates the illusion of stream stabilization. The energy dissipation of plasma waves for the low-frequency Type III bursts is fully determined by Landau damping in the tail of the stream. Because of this, the temperature estimates of the outer corona from time profiles of Type III bursts are incorrect. The theoretical curves of the time variation of radiation at different frequencies agree well with the experimental data in the hectometer wave range under the assumption that the electromagnetic wave generation takes place at the second harmonic of the plasma frequency. In this case it is necessary to decrease the electron density in the solar corona at distances of about 5 to 30 $R_\odot$ 4 times as compared with the densities previously derived from Type III data. (auth)

53965 TIME BEHAVIOUR OF THE CONTINUA DURING THE INITIAL STAGE OF TYPE-IV BURSTS. Boehme, A. (Zentralinstitut fuer Solar-Terrestrische Physik, Potsdam, Ger.). Solar Phys.; 24: No. 2, 457-74(Jun 1972).

The existence of a group of broad-band continua during the initial stage of some Type IV bursts can be shown which are polarized in the extraordinary sense. Unfortunately interferometric records were available only for one of these continua. In this case no movement of the radiation source could be stated during the whole of its lifetime. It can be shown that the time behavior of the broad-band continua is clearly different from that of the moving Type IV bursts recorded directly by interferometers. Therefore, it must be concluded that both types of continua originate from different physical processes at the Sun, though both are caused by synchrotron radiation. (auth)

53966 CHANGE OF SOLAR-FLARE PROTON-TO-ALPHA RATIOS DURING AN ENERGETIC STORM PARTICLE EVENT. Scholer, M.; Hovestadt, D.; Hausler, B. (Max-Planck-Institut fuer Physik und Astrophysik, Munich). Solar Phys.; 24: No. 2, 475-82(Jun 1972).

Observations of the temporal behavior of energetic storm protons and alpha particles are presented for the event associated with the sudden storm commencement observed on Earth on March 8, 1970. The data were obtained on board the low-altitude polar orbiting satellite GRS-A/AZUR by means of two particle telescopes. Large changes in the proton to alpha ratios for particles of equal energy and for particles of equal energy per nucleon were observed, whereas no significant changes in the equal energy per charge ratio were observed. Electric fields, Fermi acceleration, and cyclotron resonance are discussed as possible modulation mechanisms. (auth)

53967 SEARCH FOR NEUTRONS OF SOLAR ORIGIN USING BALLOON-BORNE DETECTORS: 1967–69. Eyles, C. J.; Linney, A. D.; Rochester, G. K. (Imperial Coll. of Science and Tech., London). Solar Phys.; 24: No. 2, 483-97(Jun 1972).

A series of telescopes having approximately a 30° half opening angle and responding to neutrons in the energy range 50 to 350 MeV has been flown to the top of the atmosphere on balloons released from an equatorial launching site at Kampala, Uganda, between 1967 and 1969. The aim of the experiment was to attempt to detect solar neutrons during periods of enhanced solar activity. No neutrons of solar origin were detected, but an upper limit of the order of 30 neutrons m^{-2} s^{-1} at the Earth has been placed on the continuous solar neutron flux in the above energy range, and a limit of four photons m^{-2} s^{-1} has also been placed on the corresponding γ-ray flux above 80 MeV. Limits have likewise been placed on the total emission from various flares. For a 1B flare the values were 23×10^4 neutrons m^{-2} and 6×10^4 photons m^{-2}. (auth)

53968 RELATIVISTIC ELECTRONS ASSOCIATED WITH SOLAR FLARES. Sakurai, Kunitomo (Goddard Space Flight Center, Greenbelt, Md.). Planet. Space Sci.; 20: No. 8, 1229-34(Aug 1972).

Solar flares that produce relativistic electrons generally occur within sunspot groups that are active in the emission of meter type-I noise storms. It is suggested that relativistic electrons in solar flares are accelerated from the keV-energy electrons responsible for the type-I noise storms. The relationship between flare developments and the ejection of keV electrons is briefly considered. (auth)

53969 DENSITY DEPENDENT IONIZATION BALANCE OF CARBON, OXYGEN, AND NEON IN THE SOLAR ATMOSPHERE. Summers, Hugh P. (Univ. of Bristol, Eng.). Mon. Notic. Roy. Astron. Soc.; 158: No. 3, 255-75(1972).

Density dependent ionization equilibria for carbon, oxygen, and neon ions in the optically thin solar atmosphere are calculated. All relevant processes are included and the results are expected to be accurate to ~40%. Except for the neutral and first ionized ions in each case, the results are applicable to the ionization equilibrium in any thermal plasma where the ionization is maintained by the free electrons. Fractional ion abundances on incorporating a chromosphere and corona model are also presented. (auth)

53970 COMPARISON OF SOLAR-FLARE ENERGY ESTIMATES MADE BY ANALYTICAL AND NUMERICAL TECHNIQUES. Dryer, Murray (National Oceanic and Atmospheric Administration, Boulder, Colo.). J. Geophys. Res.; 77: No. 25, 4851-4(1 Sep 1972).

The mechanical energy release of several solar flares is estimated by analytical and numerical methods. Analytical estimates, made originally by M. Dryer and D. L. Jones (1968) using similarity blast-wave theory, are corrected and compared with those based upon numerical studies of A. J. Hundhausen and R. A. Gentry (1969). Complete agreement is found in a limited study of three events in the original investigation, which assumed that the shock waves observed at 1 AU were blast waves. As a result of this study, it is suggested that the July 7, 1966 (0026 UT), solar flare may, instead, have produced a piston-driven shock wave. Some of the relative advantages and disadvantages of the similarity and numerical techniques (limited to the blast case only) are discussed. (auth)

Galaxies

Refer also to abstracts 53815 and 53880.

53971 APERTURE SYNTHESIS OBSERVATIONS OF NEUTRAL HYDROGEN IN THREE GALAXIES. Shostak, Gerson

Seth. Pasadena, Calif.; California Inst. of Tech. (1972). 233p. University Microfilms Order No. 72-22,613.

Thesis.

Aperture synthesis techniques were used to study the three galaxies NGC2403 (Scd), NGC4236 (SBdm), and IC10 (Irr) in the 21-cm line of neutral hydrogen and off-line continuum. Spatial resolution was 2 minutes of arc; velocity resolution was 21 km-s^{-1} The data yield information on the distribution of the HI, and its associated velocity field. Hydrogen extent of the objects agreed well with their optical size, and evidenced a lumpy structure. HI peaks occur away from the nuclei for NGC2403 and NGC4236, and are suggestive of a ring structure for the former galaxy. The hydrogen distribution of IC10 is similar in appearance to that of the Small Magellanic Cloud. In all objects HI peaks show good positional agreement with major HII regions. Velocity fields were derived for all objects, and rotation curves obtained for NGC2403 and NGC4236. These curves evidenced differential rotation but did not include Keplerian tails, implying that the mass distributions are considerably extended and the total masses poorly determined. The velocity field of IC10 suggests rotation. Noncircular motions of ~10 km-s^{-1} were seen in NGC2403, and these agreed well with the streaming motions predicted by the density-wave theory of spiral structure. A comparison of NGC2403 with the late-type spirals M33 and M101 revealed a progressive deepening of the central HI depression with increasing mass. Rotation curves for these three galaxies are similar, and consequently all are expected to have mass-to-light ratios which increase rapidly with radius. All have similar maximum HI surface densities (~10^{21} atoms-cm^{-2}) and observed fractional hydrogen masses (~9%). (Diss. Abstr. Int., B)

53972 GROSS PROPERTIES OF FIVE Scd GALAXIES AS DETERMINED FROM 21-CENTIMETER OBSERVATIONS. Rogstad, D. H.; Shostak, G. S. (California Inst. of Tech., Pasadena). Astrophys. J.; 176: No. 2, 315-21(1 Sep 1972).

Neutral-hydrogen studies of the five Scd galaxies M33, NGC 2403, IC 342, M101, and NGC 6946 revealed substantial similarities in their hydrogen distributions and rotation curves. It was found that ~80% of the observable H I lies within the boundary defined by the Holmberg diameter for each galaxy. The ratio of the H I mass to the total mass contained within this same boundary had a mean value of ~0.11. The central H I surface density was also nearly constant within the Scd classification. It was found that all the H I global properties and ratios are nearly constant or scale approximately with Holmberg radius or total mass. An observed correlation of maximal rotation velocity with Holmberg radius allowed characterization of the total mass with only one parameter. Because of the very flat rotation curves observed for these Scd galaxies, total masses extrapolated to infinite radius are not known. Surface mass—luminosity ratios must reach values of ~20 at the Holmberg radius. (auth)

53973 GALACTIC ORIGIN FOR THE SOFT X-RAY BACKGROUND. Gorenstein, Paul; Tucker, Wallace H. (American Science and Engineering, Cambridge, Mass.). Astrophys. J.; 176: No. 2, 333-44(1 Sep 1972).

The results of a new observation of the soft x-ray background in the Virgo region with high angular resolution are reported. Using results from this and previous observations, the following observational features for the background were derived: (a) the intrinsic emission spectrum of the background is quite soft, for an exponential spectrum $KT \leq 0.1$ keV, (b) the ratio of the pole to plane flux decreases with energy below 0.28 keV, and (c) the diffuse flux in the Virgo region has a granularity of ~14% in regions of 4.5 square degrees. No evidence was found which supports the hypothesis of an extragalactic component for any substantial portion of the background. Assuming that the diffuse flux arises entirely from a galactic distribution of point sources, features indicating that the scale height of the distribution is ~800 pc, the number density is ~10^{-2} (pc)$^{-3}$, and the effective temperature and luminosity of individual sources are ~10^{6} °K and 3×10^{30} ergs s^{-1}, respectively, were derived. These requirements might be satisfied by radiation from a hot plasma produced by accretion onto disk and/or intermediate Population II stars in close binary systems. (auth)

53974 NEW METHOD FOR ESTIMATING THE HUBBLE CONSTANT. van den Bergh, Sidney (Univ. of Toronto, Richmond Hill). Astron. Astrophys.; 20: No. 3, 469-70(Sep 1972).

Radio observations of galactic supernova remnants indicate that the mean interval between supernova outbursts in the Galaxy is 50 ± 25 y. Comparison of this value with Tammann's determination of the frequency of supernovae in distant spirals yields $H = 95 \pm 36$ km s^{-1} Mpc^{-1}. (auth)

53975 ORIGIN AND FORM OF THE GALACTIC MAGNETIC FIELD. II. THE PRIMORDIAL-FIELD MODEL. Piddington, J. H. (National Standards Lab., Sydney). Cosmic Electrodyn.; 3: No. 2, 129-46(Jul 1972).

A primordial field (10^{-9} to 10^{-8} G) is required to account for the magnetic fields of galaxies. Making random angles with the galactic rotational vectors it may thus account for the different galactic forms and degrees of central activity. In spiral galaxies the two vectors are oblique, leading to moderate activity and spiral structure. The oblique rotator model of the galactic disk field and halo explains the radio continuum emission and the fact that the disk field and cosmic rays are gravitationally contained even in regions of low gas density. Further observational evidence includes metagalactic Faraday rotation, intergalactic "bridges", and the magnetic field system of the Magellanic clouds. Two questionable assumptions made two decades ago have persisted: that because there is no dust between the spiral arms of M31 there can be no gas, and that the H I gas concentrations seen in our Galaxy are parts of spiral arms. These assumptions have led to the rejection of hydromagnetic theories of spiral arms and the wide acceptance of the Lin—Shu density wave theory. It is shown that the first assumption is incorrect and the second probably incorrect so that the wave theory has no observational support and a magnetic model is not excluded. A hydromagnetic theory of twin spiral arms is based on gas motions mainly perpendicular to the disk caused by a field whose tilt varies sinusoidally with rotation. Star formation is controlled by gas streaming obliquely along field lines in the manner described by Parker. The modes of formation of gas rings and bars are also discussed. (auth)

53976 AGE AND STRUCTURE OF II ZWICKY 40. Jaffe, W. J. (Sterrewacht te Leiden). Astron. Astrophys.; 20: No. 3, 461-4(Sep 1972).

The dwarf galaxy II Zw 40 was detected at 1415 Mhz continuum with the WSRT. The measured flux density, combined with previous H I measurements, indicates a diameter of about 1 kpc. The kinetic energy of the galaxy seems primarily nonrotational, and the system is probably less than 10^{7} years old. (auth)

53977 QUADRATIC PROGRAMMING APPLIED TO THE PROBLEM OF GALAXY POPULATION SYNTHESIS. Faber, S. M. (Harvard Univ., Cambridge, Mass.). Astron. Astrophys.; 20: No. 3, 361-74(Sep 1972).

The technique of quadratic programming as applied to the problem of galaxy population synthesis is described. The method offers significant advantages over the trial-and-error approach usually employed. This technique is applied to 38-color data on the nuclei of M 31, M 32, and M 81 and to integrated 10-color photometry for elliptical galaxies. The results indicate that estimates of mean line strengths in external galaxies by means of population synthesis are well determined. Ages based on the main-sequence turnoff point are uncertain by a factor of two. The method is not sensitive to the number of stars on the main sequence between K 0 V and M 7 V. Consequently the slope of the luminosity function below turnoff cannot be determined. The mass-to-light ratio of the computed population for M 31 is uncertain by a factor of 4. The corresponding factors for M 32 and M 81 are 50 and 16 respectively. Models for elliptical galaxies suggest that the mean metal abundance of the stellar population increases with increasing galaxy luminosity. (auth)

53978 GALACTIC EVOLUTION: PROGRAM AND INITIAL RESULTS. Tinsley, Beatrice M. (Univ. of Texas, Dallas). Astron. Astrophys.; 20: No. 3, 383-96(Sep 1972).

A program is described for studying the evolution of galaxies. Some initial results are presented, suggesting future applications of the program. In the models, stars are formed from interstellar gas, and the evolution of each star is followed from the main sequence to death. Semi-empirical tracks based on old open clusters and old-disk moving groups are used for the later stages of low-mass stars. Properties of the models that can be calculated at times from 1 to 11×10^{9} years (in discrete time steps of 10^{9} yr) are: the detailed stellar population at 566 points of the H—R diagram; the mass of gas and its helium and metal content; the bolometric magnitude; integrated broad-band colors and magnitudes on Johnson's 8-color system; the mass to light ratio; the uv flux at 1700 Å; integrated intermediate-band colors on McClure and van den Bergh's system; narrow-band colors on Wood's system; and narrow-band scanner colors and indices on Spinrad and Taylor's system. The models studied are homogeneous and contain solar-composition stars only. Metal-poor and super-metal-rich stars can be added (as integrated globular clusters and SMR K giants) to a computed population before its photometric properties are found. Stellar birthrates used include a variety of initial luminosity functions and functions of time or gas mass. These functions provide a set of models with which to survey the potentialities of the method. Future studies will use birthrate functions based on theories of star formation in various types of galaxies. Models discussed were not planned to match any galaxy precisely, but the types of birthrate required for various typical galactic populations, and their overall evolution, are clearly indicated. Some results of interest are: (1) Models evolve redwards along the observed galactic 2-color relation, so UBV colors cannot tell if a galaxy contains only, or just predominantly, young stars. (2) The observed far ultraviolet flux could arise from young main sequence stars, in galaxies with a finite present birthrate. (3) Super metal-rich stars are probably formed in elliptical galaxies and the central regions of spirals. (4) The infrared light of galaxies is predicted to be dominated by late giants, even in systems with a high mass-to-light ratio, (5) The Spinrad—Taylor indices are far the most sensitive of the properties studied to the distribution of stellar temperatures, luminosities, and abundances in a population. Use of broad-band colors alone can be seriously misleading. (auth)

53979 ANGULAR DISTRIBUTION OF INTERSTELLAR ATOMIC HYDROGEN. Daltabuit, E.; Meyer, S. (Univ. of Wisconsin, Madison). Astron. Astrophys.; 20: No. 3, 415-24(Sep 1972).

A summary of recent values of the columnar density of galactic atomic hydrogen appearing in the literature is presented in the form of plots of N_H vs · l^{II} for every 5° in galactic longitude. (auth)

53980 GALAXY FORMATION IN ANISOTROPIC COSMOLOGIES. Perko, T. E.; Matzner, R. A.; Shepley, L. C. (Univ. of Texas, Austin). Phys. Rev., D; 6: No. 4, 969-83(15 Aug 1972).

The growth rates of perturbations of the generic dust-filled Bianchi type-I cosmology (which exhibits anisotropy but not rotation) are analyzed. Anisotropy induces coupling between gravitational wave and density modes and can enhance the power-law rate of growth of the density perturbations. A maximum growth rate for pregalaxy perturbations is $t^{4/3}$ (where t is cosmic time), so that no conclusive solution to the galaxy formation problem is found. The detailed structure of the flow of energy between gravitational wave and density modes and of the growth of rotational modes (decoupled from other perturbations) is presented. A detailed discussion is also given of the gauge-invariance properties of these perturbations. (auth)

53981 GALACTIC ASTRONOMY. VOLUME 1. Proceedings of the Summer Institute for Astronomy and Astrophysics, Held at Stony Brook, New York, Summer 1968. Chiu, Hong-yee; Muriel, Amador (eds.). New York; Gordon and Breach, Science Publishers, Inc. (1970). 340p.

Separate abstracts were prepared for the six chapters. (W.D.M.)

For abstracts of individual chapters see: 53982—53987.

53982 BASIC PROBLEMS ON THE STRUCTURE AND DYNAMICS OF OUR GALAXY. Bok, Bart J. (Univ. of Arizona, Tucson). pp 1 of Galactic Astronomy. Vol. 1. /Chiu, Hong-yee (ed.). New York; Gordon and Breach, Science Publishers, Inc. (1970).

Topics covered include: recent history and outline of the Galaxy; basic data (spectral classification, photometry, photography, proper motions, parallaxes, and radial velocities); moving clusters; calibration problems; kinematics of stellar motions (galactic rotation, solar motion, ellipsoidal distributions of peculiar motions, asymmetry of stellar motions, and Bottlinger's diagram); Lindblad's epicyclic orbits; principles of galactic dynamics; dynamics of star clusters. (W.D.M.)

53983 SPIRAL STRUCTURE OF GALAXIES. Oort, J. H. (Univ., Leiden). pp 121-45 of Galactic Astronomy. Vol. 1. /Chiu, Hong-yee (ed.). New York; Gordon and Breach, Science Publishers, Inc. (1970).

Lectures included in this section were spiral structure of the Galaxy as determined from 21-cm line observations, central region, observations of high-velocity clouds, and origin of the high-velocity clouds. (W.D.M.)

53984 GALACTIC RADIO EMISSION IN THE 21-CM LINE AND THE CONTINUUM. Westerhout, G. (Univ. of Maryland, College Park). pp 147-90 of Galactic Astronomy. Vol. 1. /Chiu, Hong-yee (ed.). New York; Gordon and Breach, Science Publishers, Inc. (1970).

Topics covered include historical introduction to radio astronomy, fundamentals of 21-cm line emission, galactic rotation from 21-cm line emission, large-scale distribution of hydrogen, clouds and small-scale structure, hydrogen distribution in Galaxy and solar neighborhood, and the galactic continuum. (W.D.M.)

53985 SELECTED TOPICS ON THE PHYSICS OF THE INTERSTELLAR MEDIUM. Muench, G. (California Inst. of Tech., Pasadena). pp 191-243 of Galactic Astronomy. Vol. 1. /Chiu, Hong-yee (ed.). New York; Gordon and Breach, Science Publishers, Inc. (1970).

Interstellar absorption (optical lines) is considered in terms of modern observing techniques, optical interstellar spectrum, ultraviolet spectrum, structural model for interstellar medium, kinematics of clouds, interpretation of line intensities, mean motions and densities of Na I and Ca II, internal velocity dispersion of clouds, ionization equilibrium, interstellar abundances, spectrum of ζ Oph, rocket uv spectrum, high-velocity clouds, high-galactic-latitude clouds, and the galactic corona. Problems related to the structure of planetary and galactic nebulae are treated including ionization stratification, spectra of emission nebulae, nebular absorption lines, and internal motions in emission nebulae. (W.D.M.)

53986 CEPHEID VARIABLES IN LARGE AND SMALL MAGELLANIC CLOUDS. Payne-Gaposchkin, Cecilia (Smithsonian Institution, Washington, D. C.). pp 245-329 of Galactic Astronomy. Vol. 1. /Chiu, Hong-yee (ed.). New York; Gordon and Breach, Science Publishers, Inc. (1970).

Five lectures are presented on Cepheid variables in the Magellanic clouds and in the Milky Way. The significance of Cepheid studies is discussed. (W.D.M.)

53987 IRREGULAR SPIRAL STRUCTURE: CAUSES AND EFFECTS. Rickard, J. (Univ. of Maryland, College Park). pp 331-4 of Galactic Astronomy. Vol. 1. /Chiu, Hong-yee (ed.). New York; Gordon and Breach, Science Publishers, Inc. (1970).

The problems caused by large-scale deviations from regular spiral structure in the Galaxy are discussed using the Cas—Per arm as an example. The possibility of super supernovae in spiral arms is considered. (W.D.M.)

53988 X-RAY EMISSION FROM INTERGALACTIC GAS IN THE NEIGHBOURHOOD OF GALAXIES. Hunt, R.; Sciama, D. W. (Oxford Univ.). Nature (London); 238: No. 5363, 320-3(11Aug 1972).

It is suggested that massive galaxies may have x-ray coronas associated with accretion of hot intergalactic gas. X-ray observations of Virgo A fit this hypothesis. Andromeda may also have an observable x-ray corona. (auth)

53989 RECENT WORK ON INTERSTELLAR GRAINS. Wickramasinghe, N. C. (Cambridge Univ., Eng.); Nandy, K. Rep. Progr. Phys.; 35: No. 2, 157-234(1972).

Observational data accumulated over the past decade have considerably narrowed down the choice of proposals for grain models. Mixtures of particles composed of refractory species such as graphite, silicates, quartz, and iron appear likely. Such particles may form in a wide range of astronomical situations, for example, cool stars, protostars, and supernovae explosions. Dust grains are responsible for infrared radiation in galactic sources, and also play an important role in the synthesis of interstellar molecules. (auth)

53990 EMISSION-LINE SPECTRUM OF CYGNUS A. Mitton, Simon; Mitton, Jacqueline (Cambridge Univ., Eng.). Mon. Notic. Roy. Astron. Soc.; 158: No. 3, 245-54(1972).

Spectra of Cygnus A taken at the Hale Observatories were analyzed. A line list of the nebular emission is presented. The results can be accounted for by a two-component model of the nucleus in which condensations at $T_e = 10^4$°K produce most of the emission lines; these condensations are embedded in a tenuous plasma at $T_e \approx 10^6$°K. A continuing source of excitation probably exists in the optical nucleus of this radio galaxy. (auth)

53991 NEW REDSHIFTS OF RADIO GALAXIES. Tritton, K. P. (Royal Greenwich Observatory, Hailsham, Eng.). Mon. Notic. Roy. Astron. Soc.; 158: No. 3, 277-80(1972).

Redshifts were obtained for 20 radio galaxies, including 0620-52, a new identification. (auth)

53992 DYNAMICAL MODELS OF THE GALAXY AND ITS GAMMA RAY EMISSION. Cowsik, R.; Hutcheon, I. D. (Univ. of California, Berkeley). pp 102-7 of 12th International Conference on Cosmic Rays, Hobart, Australia. Vol. 1. Hobart, Australia; International Union of Pure and Applied Physics (1971).

From twelfth international conference on cosmic rays; Hobart, Australia (16 Aug 1971). See CONF-710807—(Vol.1).

The intensity and angular distribution of gamma rays of $E > 100$ MeV emitted by the galactic disc is explained. The model is based on the spatial distribution of stars required to explain the dynamical properties of the Galaxy. The gamma rays are postulated to arise from the Compton scattering of starlight by cosmic-ray electrons. This calculation also supports the idea that the cosmic-ray density in the Galaxy is reasonably uniform. The implications of this result are briefly discussed. (auth) (Australia)

Cosmology

Refer also to abstracts 53974 and 54396.

53993 (INIS-mf-252) THE NUCLEUS. Annual Review of the Science Foundation for Physics and the School of Physics Within the University of Sydney. (Sydney Univ. (Australia)). Jan 1972. 84p. INIS.

Various activities of the Science Foundation for the year 1971 are reviewed. Brief summaries are made of projects being undertaken by the theoretical physics, nuclear research, computer science, plasma physics, astronomy, and astrophysics departments at Sydney University. (Australia)

53994 STATISTICAL STUDIES OF THE EVOLUTION OF EXTRA-GALACTIC RADIO SOURCES. I. QUASARS. Schmidt, Maarten (California Inst. of Tech., Pasadena). Astrophys. J.; 176: No. 2, 273-87(1 Sep 1972).

Radio source counts attributable to quasars were derived on the assumption that their redshifts are cosmological. Evolution effects seen in the statistics of both optically selected quasars and identified quasi-stellar radio sources are consistent with density evolution or appropriately optical luminosity-dependent density evolution. Two alternative laws for density evolution, $\rho = 10^{5\tau}$ and $\rho = (1 + z)^6$, were adopted. Statistics of high-redshift quasars suggest that the density cannot increase beyond redshift 2.5. An earlier result that the radio luminosity function depends on optical luminosity such that the ratio R has a universal distribution function was adopted. An attempt was made to determine this function and then derive quasar source counts, redshift–flux density tables, and a magnitude–flux density table. The predicted quasar source counts are quite similar for the two alternative density laws. A comparison with general counts of extragalactic radio sources at 408 MHz shows that quasars contribute between 20 and 30%, with little dependence on flux density. (auth)

53995 STATISTICAL STUDIES OF THE EVOLUTION OF EXTRA-GALACTIC RADIO SOURCES. II. RADIO GALAXIES. Schmidt, Maarten (California Inst. of Tech., Pasadena). Astrophys. J.; 176: No. 2, 289-301(1 Sep 1972).

Radio source counts attributable to radio galaxies and ordinary galaxies were derived. There was little direct evidence that radio galaxies show evolution. However, general radio source counts freed from the contributions of quasars and ordinary galaxies showed that radio galaxies must be subject to evolution. Since 5% of the giant elliptical galaxies are radio galaxies, a limit of a factor of 20 was imposed on the overall density increase of the latter with redshift. Neither this type of restricted density evolution nor luminosity evolution can explain the radio source counts attributed to radio galaxies. Two alternative luminosity-dependent density laws, $\rho = 10^{c\tau}$ and $\rho = (1 + z)^k$, with exponents c and k smoothly increasing with radio luminosity are presented, that are compatible with the source counts. Extensive use was made of tables of redshift versus flux density that allow insight in the effect of luminosity function, density law, redshift cutoff, etc., on the source counts. (auth)

53996 STATISTICAL STUDIES OF THE EVOLUTION OF EXTRAGALACTIC RADIO SOURCES. III. INTERPRETATION OF SOURCE COUNTS AND DISCUSSION. Schmidt, Maarten (California Inst. of Tech., Pasadena). Astrophys. J.; 176: No. 2, 303-14(1 Sep 1972).

Radio source counts predicted on the basis of evolution models for quasars, radio galaxies, and ordinary galaxies are compared to observed total source counts at various radio frequencies. The observed increase with frequency of the fraction of sources with flat spectra is approximately reproduced in the evolution models. The predicted background temperature is slightly less than the observed value. Optical and radio luminosity functions are presented for quasars and radio galaxies. They depend strongly on the assumed type of density evolution law. At a redshift of 2.5 the space density of quasars appears to be of the same order as that of giant elliptical galaxies, the parent objects of radio galaxies. This may explain why the space density of quasars does not seem to increase beyond redshift 2.5. It is shown that certain arguments based on general source counts against the need for evolution or against the large distances of the sources are not supported by detailed evolution models. Finally the many uncertainties in the evolution models are emphasized; some of which can be resolved eventually by extensive optical and radio studies at low flux levels. (auth)

53997 PERTURBATIONS IN AN EXPANDING UNIVERSE OF FREE PARTICLES. Stewart, John M. (Inst. of Theoretical Astronomy, Cambridge, Eng.). Astrophys. J.; 176: No. 2, 323-32(1 Sep 1972).

In the canonical big-bang cosmology, one of the major energy sources in the temperature range $10^{10} > T > 10^5$ °K would be collision-free neutrinos. These might be expected to interact with gravitational radiation—including density perturbations, vorticity perturbations, and gravitational waves—in a radically different way from the usual cosmological models filled with collision-dominated radiation. The Jeans swindle, Newtonian cosmology, and relativistic cosmology are discussed using a kinetic-theory approach, and the same qualitative results are found in all three cases. Although perturbations on a scale larger than the horizon can grow, smaller ones are quickly dissipated. The mechanism is similar to Landau damping, and could not have appeared in the conventional hydrodynamic calculations. The effect may raise serious problems for theories of galaxy formation. (auth)

53998 SCALAR–TENSOR COSMOLOGY AND THE CLASSICAL TESTS. Luke, S. K.; Szamosi, G. (Univ. of Windsor, Ont.). Astron. Astrophys.; 20: No. 3, 397-405(Sep 1972).

The scalar–tensor field equations for the matter Universe are solved numerically by a self-consistent method. The rate of change of the scalar field at the present epoch is limited to $3.0 \times 10^{-11} > \phi_0^{-1} (d\phi/dt)_0 > 8.0 \times 10^{-13}$ year^{-1} by recent observation and the present calculation respectively. The three classical tests of cosmology are calculated for a range of the parameters ρ_0 and $(d\phi/dt)_0$. Comparing observational data with theory suggests that the absolute visual magnitude of the first rank galaxy is −22, the cosmic density is of the order 10^{-30} g cm^{-3}, and the average linear diameter of the galaxies is 4.3 kpc. No definite conclusion about world models can be drawn from the presently available data. If the redshifts of the quasi-stellar objects are cosmological, it is not possible to construct a Brans–Dicke model to fit the redshift–magnitude data without luminosity evolution. (auth)

53999 EXACT EXPRESSIONS FOR THE PROPERTIES OF THE ZERO-PRESSURE FRIEDMANN MODELS. Edwards, Dilwyn (Thames Polytechnic, London). Mon. Notic. Roy. Astron. Soc.; 159: No. 1, 51-66(1972).

Exact expressions in terms of Jacobian Elliptic Functions are obtained for the properties of the expanding singular cosmological models of the Friedmann kind, assuming zero pressure and a general cosmological constant. (auth)

54000 COMMENT ON INVERSE COMPTON MODELS FOR THE ISOTROPIC X-RAY BACKGROUND. Cowsik, R.; Kobetich, E. J. (Univ. of California, Berkeley). pp 38-43 of 12th International Conference on Cosmic Rays, Hobart, Australia. Vol. 1. Hobart, Australia; International Union of Pure and Applied Physics (1971).

From twelfth international conference on cosmic rays; Hobart, Australia (16 Aug 1971). See CONF-710807-(Vol.1).

An exact calculation of the spectrum of the isotropic background x radiation was made assuming that it arises through the Compton scattering of the universal microwave photons by the relativistic electrons leaking out of the Galaxies. The elegant fit to the experimental data obtained by earlier authors who made many approximations in their calculations disappears in the exact treatment presented here. It is felt that the "Inverse Compton" models for the origin of background x rays are therefore not yet adequate to explain all the spectral features in detail. (auth) (Australia)

Planetary Phenomena

54001 (NASA-TM-X-2440, pp 556-60) JUPITER RADIATION-BELT ENGINEERING MODEL. Divine, Neil (California Inst. of Tech., Pasadena). Jan 1972.

From Symposium on natural and manmade radiation in space; Las Vegas, Nev. (1 Mar 1971).

On the basis of earth observations of the hf and uhf radio emission generated near Jupiter, the presence of energetic charged particles trapped in the planet's dipole magnetic field was inferred. For electrons, energies of the order of 10 MeV and peak fluxes of the order of 10^7 cm^{-2} s^{-1} can be derived from the data for equatorial regions about two planetary radii from the dipole. Energetic protons and lower-energy electrons and protons are also expected, but the limited data require that their fluxes be based on theory or earth analogy. Because descriptions available in the literature suggest large associated uncertainties, both nominal and limiting models for the charged-particle populations of Jupiter's belts are derived. These new engineering models describe electron and proton fluxes and their distributions in energy and position in forms suitable as space vehicle design criteria. (auth)

54002 (NASA-TM-X-2440, pp 781-4) JUPITER RADIATION TEST LEVELS AND THEIR EXPECTED IMPACT ON AN ENCOUNTER MISSION. Barengoltz, J. B. (California Inst. of Tech., Pasadena.). Jan 1972.

From Symposium on natural and manmade radiation in space; Las Vegas, Nev. (1 Mar 1971).

Upper limit electron and proton fluences for a Thermoelectric Outer Planet Spacecraft (TOPS) mission in a near-Jupiter environment, for use as radiation design restraints, are extracted from the JPL engineering model of the Jovian trapped-radiation belts. Considerations of radiation effects in semiconductor devices are employed to construct simplified radiation test levels based on the design restraints. Corresponding levels, based on the nominal belt models, are found to be one to three orders of magnitude smaller. In terms of expected radiation-induced degradation in semiconductor devices, an encounter with an environment as severe as the design restraints would require hardening the system in order to guarantee high reliability. On the other hand, the nominal levels would only necessitate care in the selection of components and the avoidance of certain discrete semiconductor piece-parts. (auth)

54003 STATISTICAL MECHANICS OF LIGHT ELEMENTS AT HIGH PRESSURE. II. HYDROGEN AND HELIUM ALLOYS. Hubbard, W. B. (Univ. of Texas, Austin). Astrophys. J.; 176: No. 2, 525-31(1 Sep 1972).

A Monte Carlo method described in a previous paper is used to evaluate various thermodynamic quantities for hydrogen—helium mixtures at temperatures and pressures characteristic of the Jovian interior. The additive-volume law for chemical mixtures appears to be an excellent approximation. However, the Debye equation of state for the temperature dependence of the pressure is rather crude and tends to overestimate the pressure for a given temperature and density. (auth)

54004 ELECTRODYNAMIC EFFECTS OF JUPITER'S SATELLITE Io. Piddington, J. H. (CSIRO, Sydney). Cosmic Electrodyn.; 3: No. 2, 240-53(Jul 1972).

The motion of Jupiter's satellite Io in the magnetosphere creates a disturbance which provides the decametric radio emission. Recent measurements tend to confirm a disturbance model in which a magnetic force tube is partially frozen into Io and so moves through the ionosphere almost as a solid in a fluid. Ambipolar drift deposits ions and electrons in the equatorward boundary layers of Io's force tube in the ionosphere; a density of 10^7 electrons cm^{-3} seems possible. The propagation time of the hydromagnetic disturbance from Io to the ionosphere and back is found to be about one third the previous estimate. This greatly reduces the required electrical conductivity of Io. The deformation of the force tube and the power transmitted are revised because of the effects of Hall current. The new disturbance model provides the radio emissions by plasma oscillations from a dense sheet of ions and electrons on the surface of Io's force tube in the lower ionosphere. It also suggests that Jupiter's Van Allen belts are powered by the Io disturbance, and that a Jupiter space probe should be directed at Io's force tube. (auth)

54005 FORMATION OF PLANETS FROM A SOLAR NEBULA. Lyttleton, R. A. (California Inst. of Tech., Pasadena). Mon. Notic. Roy. Astron. Soc.; 158: No. 4, 463-83 (1972).

The development of planets within a solar nebula of both gas and dust is shown to occur in two main stages. First, in a time comparable with the orbital period at any distance the dust comes to move with Keplerian motion in a thin plane disc. This is an essential prerequisite since the volume—density in such a disc is amply sufficient for the self-gravitation of condensations to overcome the differential action of the Sun. By such means small solid planets can form independently of the gaseous component of the nebula. Second, the range-of-influence of a planet (of mass m moving at distance R) out to which its gravitation dominates over that of the Sun is $(m/3M)^{1/3}R$. At any stage material within this distance can be captured, and the growth of bodies to mass of lunar order requires about 10^4 yr. It seems probable that many small bodies would begin to form separately, and then themselves combine any collisions to yield larger bodies fewer in number. The vorticity associated with the motion of the disc round the Sun will reappear as angular momentum of the bodies and give them initial rotation periods of about 4 to 5 hr, but collisions would tend to give the later larger masses longer periods of rotation. The energy of infall to the surface would be sufficient to melt the material for bodies as large as the Moon, but it would arrive only at an equatorial band because of the thinness of the dust-disc, and flow of molten material polarwards would produce a condition highly conducive to cooling. If larger masses than of lunar order result mainly from collisions, it seems probable that initially only all-solid planets would be formed. The great outer planets must also start their growth within the dust-disc as small solid bodies and thereafter they would continue growth by capture of gaseous material from the nebula. Only for Jupiter is capture of gas in accordance with thermal accretion likely to have occurred, since only for it could the accretion radius ever exceed the range of gravitational influence. (auth)

54006 LIMITS TO ENERGETIC PROTON FLUXES TRAPPED IN JUPITER'S MAGNETOPSHERE. Mihalov, J. D. (Ames Research Center, Moffett Field, Calif.). Planet. Space Sci.; 20: No. 8, 1345-7(Aug 1972).

Fluxes of energetic electrons (E ~ 10 MeV) trapped in Jupiter's magnetic field were inferred from measurements at Earth of the decimetric synchrotron radio noise flux. Energetic trapped protons should be expected at Jupiter in association with energetic electrons, analogous to the case at Earth. Upper limit energies for trapped protons at Jupiter are given. Using these values for peak proton energies, it can be deduced that it is not possible to obtain direct information about Jupiter's energetic trapped proton fluxes from radio noise observations at Earth. A test for energetic protons is applied to a recently developed trapped proton model. Limits to trapped proton fluxes based on the model are presented. (auth)

54007 D/H RATIO IN JUPITER'S ATMOSPHERE. Reeves, H. (CEN de Saclay, Gif-sur-Yvette, France); Bottinga, Y. Nature (London); 238: No. 5363, 326-7(11 Aug 1972).

Deuterium has recently been detected in the methane component of the Jovian atmosphere, and theoretical estimation of the D/H ratio is made with the help of recent work by Geiss and Reeves, (Astron. Astrophys. 18: 127 (1972)). (auth)

54008 ELECTRON-IMPACT EXCITATION CROSS SECTIONS AND ENERGY DEGRADATION IN CO. Sawada, T.; Sellin, D. L.; Green, A. E. S. (Univ. of Florida, Gainesville). J. Geophys. Res.; 77: No. 25, 4819-28(1 Sep 1972).

A comprehensive set of electron-impact cross sections was determined for carbon monoxide mainly on the basis of recently accumulated data on electron impact spectra, the Born approximation at high energies, and simple rules developed earlier to take into account low-energy effects. The calculation of the complete energy degradation of electrons incident on CO is carried out with these input cross sections, and the efficiencies associated with possible loss channels are presented. (41 references) (auth)

54009 ELECTRON ENERGY DEPOSITION IN CO$_2$. Sawada, T.; Strickland, D. J.; Green, A. E. S. (Univ. of Florida, Gainesville). J. Geophys. Res.; 77: No. 25, 4812-18(1 Sep 1972).

Semi-empirical cross sections of Strickland and Green (1969) are compared with and supplemented by more recent data. The composite set is used in the energy degradation calculation of electrons with emphasis on energies below 100 eV. Good agreements are obtained with accepted values of the loss function and the average electron volts per ion pair at high energies. Efficiencies associated with various loss channels are obtained. The relationship with the recent Mariner uv data is discussed. (25 references) (auth)

PHYSICS (ATMOSPHERIC)

Refer also to abstract 54870.

54010 52nd ANNUAL MEETING OF THE AMERICAN GEOPHYSICAL UNION, WASHINGTON, D. C., APRIL 12–16, 1971. EOS, Trans. Amer. Geophys. Union; 52: No. 4, 122-392(Apr 1971). (CONF-710408–(Absts.)).

Abstracts of ~1070 papers given at the meeting are presented. Sessions were devoted to geodesy; geomagnetism and paleomagnetism; hydrology; meteorology; oceanography; planetology; seismology; aeronomy, cosmic rays, magnetospheric physics, and solar and interplanetary physics; tectonophysics; volcanology; geochemistry; and petrology. An article on environmental crises is presented and news from the U. S. National Committee for the International Hydrological Decade is included. (J.C.W.)

Auroral and Ionospheric Phenomena

Refer also to abstract 54056.

54011 (ONERA-Publ.–137) FLOW OF A COLLISIONLESS PLASMA AROUND A CYLINDER IN VIEW OF APPLICATIONS TO IONOSPHERIC PROBES. **Fournier, Gerard (Office National d'Etudes et de Recherches Aerospatiales, Chatillon-sous-Bagneux (France)). 1971. 81p. (In French). Dep. NTIS (U. S. Sales Only).**

An iterative numerical method (analogue network, computerized treatment of trajectories) is proposed for the steady-state case in the absence of a magnetic field. There are considerably less constraints on the choice of parameters in this method than in those previously used. A very important aspect is the possibility of removing the Maxwell–Boltzmann equilibrium distribution restriction for the electrons. In this way, it is demonstrated that, at potentials slightly in excess of the plasma potential, the sheath structure no longer exists. In the wake, special phenomena take place that involve a potential sink, and a two-beam structure. The probe currents are examined. The complete characteristics are established, together with the evolution of the electrostatic drag. These results are compared with experimental results obtained in the ionosphere, and in simulation experiments. The investigation demonstrates that the ion current decreases between the plasma potential and the beam stagnation potential. It also demonstrates that probes in hypersonic flight, whose diameters are too long (with respect to the Debye length) cannot be used to measure the electron temperature. (France)

54012 (SC-RR–720543) ROCKET-BORNE AURORAL OPTICAL MEASUREMENTS. Tisone, G. C.; Woods, R. O.; Hoffman, J. M. (Sandia Labs., Albuquerque, N. Mex.). Aug 1972. 62p. Dep. NTIS.

The optical results from rocket-borne auroral experiments are presented. Measurement of the Hβ intensities indicate that there was no appreciable precipitation of protons for the flight on March 19, 1971, while data for the flight on March 27, 1971, indicate that there may have been localized precipitation of protons. Data are presented for the overhead brightness and volume emission rates for N_2 (3371 A), N_2^+ (3914 A), and O (5577 A). Comparisons between observed volume emission rate for 3914 A and a calculated volume emission rate using two different forms of the differential electron spectrum have been made. The O (5577 A) data have been compared to various proposed excitation mechanisms. Because of the uncertainty in atomic oxygen densities, direct electron excitation of the O(^{1}S) state cannot be ruled out as the main mechanism above 110 km. Comparison between the experimental data and excitation due to dissociative recombination is also discussed. An estimate of the magnitude of the cross section for excitation due to dissociative excitation has been made assuming that this is the main mechanism for excitation of the O(^{1}S) state. (auth)

54013 AURORAL PHOTOMETRIC OBSERVATIONS AT GEOMAGNETICALLY CONJUGATE POINTS. Spitz, A. L. (Arctic Inst. of North America, Washington, D. C.); Watson, M. D. Planet. Space Sci.; 20: No. 8, 1337-43(Aug 1972).

Identical auroral photometers were operated at the conjugate pair, Great Whale River and Quebec–Byrd Station, Antarctica, during the austral winter of 1966. Using a small field centered on the geographic zenith, correlation studies of auroral intensity at 5577 Å show a decrease in the level of conjugacy with increasing planetary magnetic index, K_p. (auth)

54014 SPECTROSCOPIC STUDIES OF THE ARC OF MARCH 8-9, 1970. Hernandez, G. (National Oceanic and Atmospheric Administration, Boulder, Colo.). Planet. Space Sci.; 20: No. 8, 1309-21(Aug 1972).

Optical measurements of the emissions from O(^{1}D), O(^{1}S), and N(^{2}D) states during the arc event of March 8 to 9, 1970, are reported. Neutral kinetic temperatures derived from (O I) 6300-Å emission line profiles indicate a slight, near 100°K, heating of the atmosphere within the arc region. (N I) 5200-Å radiation from within the arc with an emission rate of about 0.2 R was measured, and from this measurement an estimate of N(^{4}S) concentration of 2.5×10^7 cm^{-3}, at 240 km, was obtained. Calculated peak height emissions as well as experimental measurements, for (O I) 6300 Å, showed the arc to be about 500 km for most of the observations decaying at the end of the observations to about 400 km. The (O I) 6300-Å height of peak emission was found to be strongly correlated with the peak electron concentration, and weakly with height of maximum electron concentration. (O I) 5577-Å emission associated with the arc was observed, in agreement with the previously proposed electron thermal-conduction mechanism, and apparently as well as with the soft-electron precipitation mechanism, for the excitation of optical emissions leading to arcs. (auth)

54015 REFRACTIVE INDEX AND ATTENUATION SURFACES IN THE VICINITY OF THE CROSS–OVER LEVEL. **Jones, D. (ESTEC, Noordwijk, Netherlands). Planet. Space Sci.; 20: No. 8, 1173-84(Aug 1972).**

Below the proton gyrofrequency, both polarization reversal and coupling are of paramount importance in any discussion involving ion-cyclotron whistlers and related phenomena. In the absence of collisions the critical coupling angle θ_c is zero but, when collisions are included, θ_c takes a value between zero and $\pi/2$. It is therefore of interest, particularly for ray tracing at these frequencies, to investigate the refractive index and attenuation surfaces. These are found to be deformed near the crossover level for angles between zero and θ_c, and could possibly lead to focussing of the waves. (auth)

54016 CORRELATION BETWEEN THE ELECTRON CONCENTRATION OF E REGION WITH HEIGHT OF SUN. **Alimov, O. Byull. Inst. Astrofiz., Akad. Nauk Tadzh. SSR; No. 59, 28-30(1971). (In Russian).**

Results of calculations of the electron concentration of the E region N_mE in summer–winter, 1964, and a correlation between N_mE and (cos z)^n for the latitude of Duschanbe are given. It is established that the index n has a value 0.50 ± 0.02 for summer and 0.48 ± 0.03 for winter. (tr-auth)

54017 RESULTS OF INVESTIGATIONS OF E REGION OF IONOSPHERE OVER DUSHANBE IN 1964. **Alimov, O. Byull. Inst. Astrofiz., Akad. Nauk Tadzh. SSR; No. 59, 31-3(1971). (In Russian).**

The conditions of the E region of the ionosphere over Dushanbe in 1964 were analyzed. Results and conclusions of the experimental investigations on the E-region critical frequency are included. (tr-auth)

54018 ATMOSPHERIC-WAVE-INDUCED INSTABILITY IN THE E REGION. **Beer, Thomas Ivan. London, Ont.; Univ. of Western Ontario (1971). National Library of Canada, Ottawa. Thesis.**

It is shown that ionospheric E-region gradient instabilities induced by westward propagating internal atmospheric gravity waves in the presence of westward directed electric fields would explain the observed velocities and heights of nighttime sporadic E. The relationship between the thickness and horizontal extent of the low blanketing frequency sporadic E formed by this mechanism is plotted for various heights in the E region. It is also pointed out that the drift motion of the ionization due to the perpendicular electric and magnetic fields can inhibit the formation of wind-shear sporadic-E layers. The first quantitative assessment of the spatial resonance mechanism predicted by Whitehead (1971) is made, and it is shown that it is very unlikely to play any significant ionospheric role. In the course of this analysis, a number of D-region results come to light and it is shown that in the D region all irregularities will tend to move with the ion drift velocity. (Diss. Abstr. Int., B)

54019 HISTORY OF THE USE OF BALLOONS IN SCIENTIFIC EXPERIMENTS. Pfotzer, G. (Max-Planck-Institut fuer Aeronomie, Lindau, Ger.). Space Sci. Rev.; 13: No. 2, 199-242(Jun 1972).

Balloons have been used for nearly 190 years in scientific experiments and the first astronauts went aloft on Nov. 21, 1783, maintaining a straw fire to ascend or descend at will. After a discussion of the early hot-air balloons, the first experiment of Charles and the Robert brothers with a hydrogen-filled balloon is followed, including the history of flights with animals and man. In the early 1800's, environmental conditions, height-dependent magnetic-field variations, and other meteorological parameters were investigated. In the later half of 1800, balloon astronomy began with an observation by Sivel and Croce–Spinelli at an altitude of 6000 m. In the period from 1912 to 1932, the agent that maintains the conductivity of the air was investigated and cosmic-radiation knowledge and instrumentation were advanced. Stratospheric measurements began in 1932 and, until 1947, manned flights remained below 23,000 m with an air mass overhead of 40 g/cm^2, whereas the sounding balloons, at altitudes of more than 30,000 m with less than 10 g/cm^2 air overhead were reached. Plastics became available in 1947 suitable for the construction of big balloons with a very light-weight skin that also met the requirements to withstand stresses exerted by heavy payloads. (97 references) (J.C.W.)

54020 CONJUGATE FEATURES OF MAGNETOSPHERIC ELECTRON DYNAMICS OBSERVED AT BALLOON ALTITUDES. Barcus, J. R. (Univ. of Denver). Space Sci. Rev.; 13: No. 2, 295-312(Jun 1972).

Analysis of recent observations (from balloons, spacecraft, and surface observatories) demonstrate regional, shell, and nearpoint conjugacy at L ~ 7 during precipitative events that were characterized by local acceleration as well as release of gradient-drifted electrons injected during substorms. A number of new features of magnetospheric dynamics relating to substorm development and sudden-commencement effects, have been brought to light which, though poorly understood at present, may prove of considerable importance and are worthy of further investigation. During the initial period of instability in substorm evolution, preceding the slower magnetotail convective injection, precipitation of waves of electrons in rapid polewards motion exhibit L-shell conjugacy near midnight. Transient, large-scale expansions of the magnetospheric electron population accompanied by temporally imbedded substorms display large scale regional conjugacy and are simultaneously observed as similarly transient dropouts at balloon altitudes. Precipitation from gradient-drifting electrons in the dayside magnetosphere exhibits near-point conjugacy, at least down to the order of 50 km and quite probably less. Similarly tight conjugacy applies to the release of electrons showing a specific local response to sudden commencements. Analysis of the approach to and attainment of spectral equilibrium in the precipitation observed from drifting electrons may provide information about either, or both, the source spectrum at injection and the process of local release. The specific precipitation effect sometimes observed at the time of an sc remains a rather puzzling feature, although it seems clear now that the acceleration and/or release process responsible is of a highly local nature and works selectively at small pitch angles well within the magnetospheric boundary. Coupling of the interplanetary shock with the magnetosphere must be an important aspect, but the details are not clear as yet. On at least one occasion, a large part (perhaps all) of the magnetospheric electron population varied in a nearly synchronous manner in response to solar-wind-induced distortions during the variable compressive phase of a sudden-commencement geomagnetic storm. In the ongoing effort to identify and understand acceleration and release mechanisms involved in magnetospheric dynamics, balloon-borne experiments will continue to be useful, providing essential information presently unattainable by other means. (auth)

54021 POLARIZATION PROPERTIES OF Pc 1 MICROPULSATIONS AT LOW LATITUDES. Summers, W. R. (Univ. of Newcastle, Australia); Fraser, B. J. Planet. Space Sci.; 20: No. 8, 1323-35(Aug 1972).

Polarization studies of hydromagnetic-emission-type Pc-1 micropulsation events in the plane of the Earth's surface were undertaken using a three station network in South–East Australia. Using selected data over a three-year period, a consistent polarization pattern was observed from the three stations. This is discussed in terms of temporal variations in the ellipse major axis direction, ellipticity, and direction of rotation of the perturbation vector. Interpretation of these results in terms of ionospheric waveguide propagation is also considered. (auth)

54022 ELECTRON ENERGY TRANSFER RATES IN THE IONOSPHERE. Stubbe, P.; Varnum, W. S. (Max-Planck-Institut fuer Aeronomie, Lindau, Ger.). Planet. Space Sci.; 20: No. 8, 1121-6(Aug 1972).

In upper-atmospheric physics the energy transfer rates from electron to neutral gases, especially through inelastic collisions, are important and frequently needed quantities. The rates for vibrational excitation of O_2 and N_2 and for electronic excitation of O to the ^1D state were calculated and fitted to analytic expressions as an aid to the researcher and a necessity for atmospheric and ionospheric modeling by computer. The other important transfer rates were summarized for quick reference. (auth)

54023 POSITIVE GEOMAGNETIC BAYS IN EVENING HIGH LATITUDES AND THEIR POSSIBLE CONNECTION WITH PARTIAL RING CURRENT. Kamide, Yohsuke; Fukushima, Naoshi (Tokyo Univ.). Rep. Ionosphere Space Res. Jap.; 26: No. 1-2, 79-101(1972).

Space-time characteristics of polar magnetic substorms in the evening hours are investigated with the aid of a dense network of geomagnetic observatories in Europe. The positive bays in the evening high latitudes are not necessarily always the return current of an intense westward electrojet extended along the auroral oval, although it is true that a strongly concentrated eastward electrojet does often appear at the maximum phase of substorm. The H increase from the pre-bay level at conjugate stations shows approximately the same magnitude. The features of the eastward electrojet are: (1) the current center is situated at the auroral zone (not on the auroral oval), and it shifts equatorward during the developing stage of substorm, (2) the positive bay region drifts westward, and (3) the appearance of eastward electrojet is accompanied by an enhancement in the partial ring current, proton aurora, and CNA. Since the growth and decay of the eastward electrojet is so closely connected with those of a partial ring current in the magnetosphere centering the evening region, it is conjectured that the positive bay in high latitudes appears when the ionospheric conductivity is increased by the impinging protons from the partial ring current in the magnetosphere. The positive bay in high latitudes is revealed by the concentration along the auroral-zone ionosphere of electric currents, which are connected with field-aligned currents from the partial ring current. (auth)

54024 PHOTOCHEMISTRY OF THE AIRGLOW CONTINUUM. Sternberg, J. R. (Oxford Univ.). Mon. Notic. Roy. Astron. Soc.; 159: No. 1, 21-9(1972).

Recent observations of the airglow continuum and related phenomena are discussed in an effort to identify the photochemical processes responsible for the emission. After an exhaustive examination it is suggested that most of the continuum is due to collision-induced transitions of the O_2 molecule from bound states close to the dissociation limit,

$$O_2^*(^1\Sigma_g^+) \rightarrow O_2^*(^3\Sigma_g^-) + h\nu \ (5000 \text{ to } 9000 \text{ Å})$$
$$O_2^*(^1\Delta_g) \rightarrow O_2^*(^3\Sigma_g^-) + h\nu \ (7000 \text{ Å to } 2.2\ \mu)$$

with estimated emission rates of 1 and 150 kR, respectively. Present ideas about the mechanism of recombination of atoms cannot explain the existence of this emission and need revising. There is also a continuum from the reaction $NO + O \rightarrow NO_2 + h\nu$ (4000 to 5500 Å) with an emission rate of about 200 R that can vary independently from that of the O_2 continuum. (auth)

54025 OBSERVATIONS OF THE AIRGLOW CONTINUUM. Sternberg, J. R.; Ingham, M. F. (Oxford Univ.). Mon. Notic. Roy. Astron. Soc.; 159: No. 1, 1-20(1972).

A program of observations of the night-sky continuum over the range 4100 to 8200 Å is described. In reducing the results careful consideration was given to the brightness and spectral distribution of the zodiacal light and integrated starlight, which are then subtracted from the total continuum to obtain the airglow. As well as confirming the existence of an airglow continuum, the results show evidence of discrete structure at certain wavelengths and a large increase in brightness in the near infrared. A preliminary study of the temporal variations of the continuum was also made. (auth)

54026 ION ADMIXTURE DISTRIBUTION IN THE IONOSPHERIC F REGION. Zhmur, L. E. (Gorky State Univ., USSR). Izv. Vyssh. Ucheb. Zaved., Radiofiz.; 15: No. 4, 490-6(1972). (In Russian).

A one-dimensional nonisothermal diffusion in the ionospheric F region is considered for the stationary case. The analysis is made for two sorts of positive ions taking into account the ionization and recombination, as well as the influence of the force of gravity. A system of two related equations was obtained for electron and ion densities. A reduction is made to the case of admixture ions, determining the dissociative recombination. The criteria are given for this case. When they are satisfied, the distribution found coincides with that obtained by Mange without allowance for photochemical processes. (tr-auth)

54027 THEORY OF INSTABILITY IN THE IONOSPHERIC CURRENT JET. Kotik, D. S. (Gorky State Univ., USSR). Izv. Vyssh. Ucheb. Zaved., Radiofiz.; 15: No. 4, 497-503 (1972). (In Russian).

The generation of potential waves by a transverse current in the ionospheric electrojet region is considered. A numerical method is used to solve the dispersion equation for the cases of weak current and small increments. The region of the lower hybrid resonance is analytically investigated. The dispersion curves and the dependence of the increments on the wave number and the ionospheric plasma parameters have been found. (tr-auth)

54028 SIMULTANEOUS MEASUREMENTS OF THE ELECTRON DENSITY AND THE COLLISION FREQUENCY IN IONOSPHERIC D REGION BY THE METHOD OF PARTIAL REFLECTION. Benediktov, E. A.; Grishkevich, L. V.; Ivanov, V. A. Izv. Vyssh. Ucheb. Zaved., Radiofiz.; 15: No. 5, 694-702(1972). (In Russian).

The electron density N in the ionospheric D region may be found by the correlation coefficient of amplitudes of ordinary and extraordinary radio-wave components backscattered by D-region inhomogeneities. Using the simultaneous measurement of the difference in the normal-wave differential absorption, the number of electron collisions with the neutral molecules ν_m may be found. A method of estimating N and ν_m is described. The preliminary measurement results of ν_m during two sudden ionospheric disturbances at the frequency 5.75 MHz are given. (tr-auth)

54029 POWER-LAW WAVENUMBER SPECTRUM DEDUCED FROM IONOSPHERIC SCINTILLATION OBSERVATIONS. Rufenach, Clifford L. (National Oceanic and Atmospheric Administration, Boulder, Colo.). J. Geophys. Res.; 77: No. 25, 4761-72 (1 Sep 1972).

Ionospheric scintillation observations near Boulder, Colorado, from the radio source Cygnus A were spectral analyzed at 26 MHz. The scintillation spectral features are used to calculate the diffraction effects and hence deduce the F-region irregularity wavenumber spectrum for sizes from about 4 to 0.6 km. The wavenumber spectrum on many occasions follows a power-law variation $P_N(\kappa_x) \propto \kappa_x^{-\beta_H+1}$, where β_H typically varies from 3 to 4. An example based on the Gaussian spectrum shows that the extrapolation to radio frequencies much higher than 26 MHz will not explain the observed equatorial and auroral scintillations. Abrupt changes in electron density are required to support the higher-wavenumber spectral densities that cause these higher-frequency scintillations. These abrupt density changes can be represented by a power-law wavenumber spectrum. The scintillation-deduced power-law variation agrees with in-situ density spectra measurements from the Ogo-6 satellite. Several production mechanisms that follow a power-law variation are discussed. The measurement of the wavenumber spectrum will help explain the mechanism that produces small-scale irregularities. (40 references) (auth)

54030 EXTREME-ULTRAVIOLET EMISSIONS FROM AN AURORA. Paresce, Francesco; Lampton, Michael; Holberg, Jay (Univ. of California, Berkeley). J. Geophys. Res.; 77: No. 25, 4773-81(1 Sep 1972).

Two ultraviolet photometers were flown on a Javelin sounding rocket launched from Fort Churchill, Canada, on February 18, 1970, into a weak auroral breakup. The photometers covered the wavelength bands 300 to 1000 A and 1050 to 1500 A and observed the aurora while the rocket was above the emitting regions. The observed radiations were found to originate from the visible and x-ray auroral forms recorded by ground-based all-sky cameras and on-board gas proportional x-ray counters. The intensities in the 1050- to 1500-A band were compatible with previous experimental data and available theoretical intensity calculations. The determination of the emitted intensities in the 300- to 1000-A band was hampered by the uncertainties about the wavelength of the radiations being observed, but, if electron excitation of the molecular nitrogen bands at approximately 900 A is assumed to be the dominant mechanism, intensities of up to 150 kR were recorded. Alternate mechanisms considered involved an additional source of radiation in the 650- to 750-A range. In this case, the observed signals corresponded to approximately 20 to 40 kR of 900-A radiation. Evidence that, on one occasion, radiation from an auroral feature exhibited a temporal pulsation at a frequency of ≃10 Hz is presented. This event was correlated with a simultaneous hardening of the particle energy spectrum. (auth)

54031 THEORETICAL CALCULATIONS OF THE F-REGION TROPICAL ULTRAVIOLET AIRGLOW INTENSITY. Anderson, D. N. (Univ. of Colorado, Boulder). J. Geophys. Res.; 77: No. 25 4782-9(1 Sep 1972).

Far ultraviolet airglow emissions at 1304 and 1356 A from atomic oxygen have been observed to exist in two bands or arcs 12 to 15° north and south of the magnetic equator, the height-integrated intensity of the emissions maximizing between 2100 and 2200 LT during equinox. Two of the mechanisms thought to be responsible for producing the excited states of atomic oxygen are neutralization ($O^+ + O^- \rightarrow O^* + O$) and radiative recombination ($O^+ + e \rightarrow O^* + h\nu$). To investigate the contribution made by each process, the daily variation of the column emission rate from 20°N to 20°S dip latitude in the ionospheric F region is theoretically calculated by numerically solving the time-dependent electron continuity equation, taking into account the effects of production, loss, ambipolar diffusion, vertical E × B drift, and neutral winds. The geomagnetic field is approximated by a centered, tilted dipole, and the effects of east—west drift have been neglected. Since the electron density's latitudinal distribution is strongly dependent on vertical E × B drift, the generated airglow intensity is also drift dependent, but in a different way for each generating mechanism. Results are presented, and the differences are investigated for two electric-field models assuming solar-cycle maximum and minimum. Of the two mechanisms, radiative recombination produces results that are in better agreement with the observations, although the calculated emission rates are still lower than the observed values. (28 references) (auth)

54032 D-REGION MEASUREMENTS WITH THE DIFFERENTIAL-ABSORPTION, DIFFERENTIAL-PHASE PARTIAL-REFLECTION EXPERIMENTS. Belrose, J. S. (Communications Research Centre, Ottawa); Burke, M. J.; Coyne, T. N. R.; Reed, J. E. J. Geophys. Res.; 77: No. 25, 4829-38(1 Sep 1972).

Measurements of the differential phase of partial reflections over a limited height range (60 to 75 km) have been made simultaneously with the differential amplitude measurements normally made at Ottawa (45°N, 76°W) on a frequency of 2.66 MHz. The addition of the differential-phase data provides a means of measuring the collision frequency in the lower D region that is independent of differential-amplitude measurements in the region where differential absorption is negligible. The two types of measurement have been found to be in satisfactory agreement. Furthermore, the simultaneous measurement of differential phase and amplitude provides a means of investigating the nature of the irregularities causing the partial reflections. It is concluded that these are predominantly irregularities in the electron density in the region. (auth)

54033 ELECTRON DEPOSITION IN WATER VAPOR, WITH ATMOSPHERIC APPLICATIONS. Olivero, J. J.; Stagat, R. W.; Green, A. E. S. (Univ. of Florida, Gainesville). (Contract AT(40-1)-3798. J. Geophys. Res.; 77: No. 25, 4797-4811(1 Sep 1972).

The consequences of electron impact on water vapor in terms of the microscopic details of excitation, dissociation, and ionization and combinations of these processes were examined. Basic electron-impact cross-section data are assembled in many forms and are incorporated into semi-analytic functions suitable for analysis with digital computers. Energy deposition in water vapor is discussed and the energy-loss function is presented, along with the "electron volts per ion pair" and the efficiencies of energy loss in various processes. Several applications of electron and water-vapor interactions in the atmospheric sciences such as H_2O comets, aurora and airglow, and lightning are considered. In general it is found that, except in the case of lightning, other processes are more likely sources of H*, O*, and OH* emissions. (47 references) (auth)

54034 OCCURRENCE OF Pc 4, 5 MICROPULSATION ACTIVITY AT THE POLAR CUSP. Rostoker, Gordon; Samson, John C.; Higuchi, Y. (Univ. of Alberta, Edmonton). J. Geophys. Res.; 77: No. 25, 4700-6(1 Sep 1972).

Data from a line of magnetometers stretching along a corrected geomagnetic meridian ~302°E through western Canada are used to study the latitude-dependent characteristics of Pc-4 and Pc-5 micropulsation activity. Though most of this activity follows a well-defined frequency—latitude dependence, a broadband class of Pc-4 and Pc-5 activity is found to occur at very high latitudes ($\Lambda > 75°$) during the daytime hours. It is suggested that this high-latitude magnetic activity is generated in the daytime polar cusp and that the observation of this activity from ground-based stations can be used to determine the latitude of the dayside polar cusp. Three possible mechanisms for the generation of the Pc-4 and Pc-5 activity in the polar cusp are the Alfvén-wave instability, the drift-wave instability, and the Kelvin—Helmholtz instability. (46 references) (auth)

54035 INVESTIGATION OF INTERACTION BETWEEN Pc 1 AND 2 AND Pc 5 MICROPULSATIONS AT THE SYNCHRONOUS ORBIT DURING MAGNETIC STORMS. Barfield, J. N.; McPherron, R. L. (Univ. of California, Los Angeles). J. Geophys. Res.; 77: No. 25, 4707-19(1 Sep 1972).

Coincident Pc-5 and Pc-1 and Pc-2 micropulsations were observed at the synchronous equatorial satellite ATS 1 during the main phase of 11 geomagnetic storms that occurred in 1967. The Pc-1 and Pc-2 oscillations were quasi sinusoidal, with periods of 5 to 20 sec and amplitudes of 1 to 2 γ. Their average polarization was transverse to the ambient magnetic field. The oscillations were elliptical and rotation was to the left in relation to the main field. The observed characteristics suggest that the Pc-1 and Pc-2 activity was due to ion-cyclotron resonance of Alfvén waves with energetic protons. It is shown that, in the afternoon sector of the ATS 1 orbit, several mechanisms exist that could cause the ion-cyclotron resonance to occur with particles of ring-current energy, producing waves of the observed frequency. (22 references) (auth)

54036 STATISTICAL CHARACTERISTICS OF STORM-ASSOCIATED Pc 5 MICROPULSATIONS OBSERVED AT THE SYNCHRONOUS EQUATORIAL ORBIT. Barfield, J. N.; McPherron, R. L. (Univ. of California, Los Angeles). J. Geophys. Res.; 77: No. 25, 4720-33(1 Sep 1972).

The results of a statistical study of storm-associated Pc-5 magnetic oscillations observed at the synchronous equatorial satellite ATS 1 during 1967 are presented. The observed oscillations had a mean frequency of 0.005 Hz and a mean amplitude of 10 γ; the typical event lasted approximately one hour. The oscillations were highly elliptical, with a mean ellipticity of <0.1, and the preferred direction of the major axis of polarization lay within 19° of the geomagnetic meridian plane. Dynamic spectral analysis showed that the wave events were quite stable in the spectral characteristics; that is, the auto spectra, ellipticity, orientation, et cetera, did not change significantly during the course of the individual events. Examination of the occurrence distribution clearly showed that the observed Pc-5 oscillations were associated with the main-phase minimum and were confined to the afternoon sector. A study of ground magnetograms for the times of interest showed that for 85% of the events the onset of the waves was clearly correlated with the expansion phase of magnetospheric substorms. The results of this study strongly support the earlier suggestion (Barfield, et al., 1972) that the storm-time oscillations are generated by an instability of the enhanced storm-time partial ring current and its associated hot ($\beta \gtrsim 1$) plasma. 39 references. (auth)

54037 SPATIAL AND TEMPORAL VARIATIONS OF THE THERMAL PLASMA BETWEEN 3000 AND 5700 KILOMETERS AT L = 2 TO 4. Bewersdorff, A. B. (Regis Coll., Weston, Mass.); Sagalyn, R. C. J. Geophys. Res.; 77: No. 25, 4734-45(1 Sep 1972).

The spatial and temporal variations of the thermal plasma between L = 2 and L = 4 over the altitude range 3000 to 5700 km have been studied. The data were obtained from two spherical electrostatic analyzers flown on the polar orbiting satellite OV 3-1 between April 1966 and February 1967. During magnetically quiet periods the ionization density is characteristically found to decrease monotonically with increasing L. Between L = 2 and L = 3 a dependence of the average electron density on longitude is found, with the maximum between April and August occurring at 150°E and the minimum at 300°E. At L < 4, major charge-density irregularities are found on 30% of the orbits at times of quiet to moderate magnetic activity, sometimes consisting of over an order of magnitude changes in density in less than 0.1 L. Comparison of density profiles obtained on the same day at different longitudes shows the irregularities to be of limited longitudinal extent. It is suggested that the depletions result from inward shifts of sectors of the plasmapause to lower L shells by E × B drifts. Large-amplitude, small-scale irregularities extending over tens of kilometers are often superimposed on the major density gradients and appear to be the result of plasma instabilities. 24 references. (auth)

54038 VHF POWER SPECTRA OF THE RADAR AURORA. Balsley, B. B. (National Oceanic and Atmospheric Administration, Boulder, Colo.); Ecklund, W. L. J. Geophys. Res.; 77: No. 25, 4746-60(1 Sep 1972).

Power spectra of vhf radar auroral echoes were obtained near Anchorage, Alaska, during October 15–23, 1970. These spectra were obtained concurrently with standard range-time-intensity (RTI) film strips of the echoing region using the same radar system. In this paper, these spectra and the RTI film strips are examined and are compared with previously defined radar auroral classifications. The results indicate that there are at least two, and possibly three, separate types of spectra that correspond to identifiable echo configurations on the RTI film strips. Identification of the two-stream instability as an irregularity-producing mechanism for one of these spectral types is possible but not definitive. Another type of spectrum is similar to the type-II spectra seen in the equatorial electrojet. The third spectral type bears no similarity to any results obtained at the equator. (34 references) (auth)

54039 POSSIBLE CONNECTION BETWEEN A BARIUM CLOUD AND ELECTRON INTENSITY FLUCTUATIONS OBSERVED ON A ROCKET FLIGHT AT KIRUNA. Koehn, D.; Page, D. E. (European Space Research and Tech. Centre, Noordwijk, Netherlands). J. Geophys. Res.; 77: No. 25, 4888-90(1 Sep 1972).

A Skylark rocket was launched from Kiruna on Feb. 14, 1970 when a moderate magnetic disturbance was in progress and an auroral E layer of a few megahertz could be observed. The payload contained an electric double-probe experiment, a Langmuir probe, a plasma-wake detector, and a barium-cloud experiment for measurement of electric fields in the auroral ionosphere. A simple Geiger counter system was aboard to determine the integrated electron precipitation at energies above 15 keV. Details of the Geiger counter experiment are given. The rocket reached an apogee of 208 km, and the mean electron intensity was of the order of 5×10^3 el/cm^2 sec ster for a height above 150 km. A sudden increase by a factor of 2 started at 167 sec flight time and a less significant enhancement started at 230 sec flight time. Both events occurred immediately after the release of the barium clouds of the rocket payload. Other phenomena occurred in relation to the other payloads and the barium-cloud releases. An investigation continues dealing with the observations. (J.C.W.)

54040 AVERAGE BEHAVIOR OF MIDLATITUDE F-REGION PARAMETERS N_T/N_{max} AND τ DURING GEOMAGNETIC STORMS. Mendillo, Michael (Boston Univ.); Papagiannis, Michael D.; Klobuchar, John A. J. Geophys. Res.; 77: No. 25, 4891-5(1 Sep 1972).

A general description of the average F-region behavior during geomagnetic storms is summarized from data on twenty-eight storms observed from Dec. 1, 1967 to Nov. 8, 1969. The ionospheric total electron content N_T data were examined from a midlatitude station and average patterns were presented for disturbances measured from the monthly median behavior. The parameters peak density N_{max} and slab thickness $\tau \equiv N_T/N_{max}$ were examined during the same storms and average patterns were determined. The study attacks the question, "In what way does geomagnetic activity contribute to the spread in the monthly distribution of F-region parameters at midlatitudes?" (J.C.W.)

54041 COMMENTS ON LUNAR VARIATIONS IN THE PERUVIAN ELECTROJET. Geller, Marvin A. (Univ. of Illinois, Urbana). J. Geophys. Res.; 77: No. 25, 4896-8(1 Sep 1972).

An analysis was made of L_2(H), the lunar semidiurnal variation in the horizontal geomagnetic field at Huancayo, and L_2(v), the lunar daily variation in the E-region electron drift at Jicamarca by Tarpley and Balsley (J. Geophys. Res., 77: 1951(1972)). Two of the conclusions drawn by Tarpley and Balsley are discussed. A concluding fact by Tarpley and Balsley states, "there is a pronounced seasonal variation in both L_2(H) and L_2(v), the maximums and minimums occurring in January–February and July–August, respectively. The cause of this variation is unknown." Geller states the variation should more properly be called annual, and he presents a strong case to explain this annual variation in the phase and magnitude of L_2(H) and L_2(v) in a consistent manner. Another concluding fact of Tarpley and Balsley states, "L_2(v) is stronger in the daytime by at least 50%. A solar time modulation of the lunar atmospheric tide provides the simplest explanation of this effect." Geller suggests that this is not a likely explanation for the day-night variation in L_2(v) and explains that a more likely explanation could come from the nighttime decrease in the ratio $(\sigma_2 \cos I)/(\sigma_0 \sin^2 I + \sigma_1 \cos^2 I)$ from work by Tarpley and Balsley, 1972, but that possibly no variation in magnitude of the Sq drift velocity exists. Geller suggests that solar modulation of lunar effects might be easier to explain than solar modulation of solar effects. (J.C.W.)

54042 ALTITUDE DISTRIBUTION OF THE $O_2(^1\Delta)$ NIGHTGLOW EMISSION. Evans, W. F. J. (Univ. of Saskatchewan, Saskatoon); Llewellyn, E. J.; Jones, A. Vallance. J. Geophys. Res.; 77: No. 25, 4899-4901(1 Sep 1972).

Measurements were made of the 1.27-μ emission during the day and twilight, and the altitude distributions of $O_2(^1\Delta)$ were reported. On Feb. 8, 1972, a Black Brant 3A rocket was launched from Fort Churchill to an apogee of 122 km to measure emission in the 1.3-, 1.6-, and 1.8-μ spectral regions in addition to the 1.27-μ spectral region. This is the first report of the nightglow profile of the altitude distribution made 11 hours after sunset. Integrated intensity distributions were differentiated to obtain the volume emission rate as a function of altitude on upleg and downleg measurements. Mechanisms most likely for the production of $O_2(^1\Delta)$ and rate constants required to coincide with other data are discussed. (J.C.W.)

54043 POLAR AURORAS. Faelthammar, Carl-Gunne (Kungliga Tekniska Hoegskolan, Stockholm). Recherche (Paris); 3: No. 24, 537-45(Jun 1972). (In French).

The extremely varied aspects presented by the polar auroras are described. The parts played by the magnetosphere and the solar wind in their creation are discussed. The phenomena intervening are not very well understood; the study of the primary particles responsible for the auroras has applications in plasma physics. (France)

Effects of Nuclear Detonations

54044 (NASA-TM-X-2440, pp 178-92) ARTIFICIAL PERTURBATIONS OF THE RADIATION BELTS. Cladis, John B. (Lockheed Palo Alto Research Lab., Palo Alto, Calif.). Jan 1972.

From Symposium on natural and manmade radiation in space; Las Vegas, Nev. (1 Mar 1971).

A review is given of the properties of the radiation belts produced by high-altitude nuclear detonations. The low-yield, Argus devices, 1, 2, and 3, and the Soviet test of 1 November 1962 injected intense electron fluxes in narrow L-shell intervals, with peaks at $L = 1.72$, 2.11, 2.17, and 1.77, respectively. The energy spectra of the electrons were indistinguishable from the equilibrium fission beta spectrum, and the fluxes initially decayed at rates approximately proportional to $(\text{time})^{-1.1}$. Across L shells the electrons diffused very slowly ($\Delta[\text{full width of peak at half maximum}]^2/\Delta[\text{time}] \approx 10^{-4}$ $[\text{earth radii}]^2/\text{day}$) The high-yield devices, Starfish and the Soviet tests of 22 October and 28 October 1962, injected electrons over wide ranges of L—extending from L values near the burst locations ($L \approx 1.14$ for Starfish, $L \approx 1.8$ for the Soviet tests) to $L \approx 6$. At L values near the lower boundary, the electron spectra were similar to the equilibrium fission beta spectrum; but the spectra appeared to be softer at the higher L values. The decay rates at $L \lesssim 1.25$ were in agreement with predictions based on atmospheric scattering theory; but at $L > 1.25$ the decay rates were higher, indicating the predominance of electromagnetic interactions. In addition to injecting energetic electrons a high-altitude detonation may also cause previously trapped particles to be redistributed. Evidence for the occurrence of such a redistribution is presented and mechanisms which may have caused the redistribution are discussed. 33 references, 12 figures. (auth)

Particle Kinetics and Trapping

Refer also to abstracts 54023, 54868, and 54952.

54045 (NASA-TM-X-2440, pp 530-8) LOW-ENERGY PARTICLE RADIATION ENVIRONMENT AT SYNCHRONOUS ALTITUDE. Shelley, E. G.; Lew, S. K. (Lockheed Palo Alto Research Lab., Palo Alto, Calif.). Jan 1972.

From Symposium on natural and manmade radiation in space; Las Vegas, Nev. (1 Mar 1971).

Low-energy charged particles in the space environment are known to be important contributors to the degradation of thermal control surfaces on satellites and may affect thin films such as cover materials used in connection with large flexible solar arrays. These particle-induced degradation effects are of particular importance in planned future satellite projects with projected lifetimes up to ten years. Early measurements in the vicinity of synchronous altitude showed that intense and highly variable fluxes of protons and electrons with energies between one and 50 keV populate this region of space. The ATS-5 satellite, launched into synchronous orbit in August 1969, was the first synchronous satellite to include instrumentation for the investigation of the plasma properties of these low-energy charged particles. The Lockheed Palo Alto Research experiment on ATS-5 measured electron and proton fluxes in the energy range from approximately one-half to several hundred keV with primary emphasis on the region below 50 keV which contains most of the plasma energy. A statistical analysis of the data, sampled over the period from September 1969 through December 1969, shows systematic variations in the average low-energy particle radiation environment at synchronous altitude with local time and magnetic activity (K_p). The existence of a systematic variation with K_p suggests the possibility of estimating the environment under various conditions of magnetic activity from the present data. 16 figures. (auth)

54046 (NASA-TM-X-2440, pp 539-47) NATURAL VARIATIONS IN THE GEOMAGNETICALLY TRAPPED ELECTRON POPULATION. Vampola, A. L. (Aerospace Corp., El Segundo, Calif.). Jan 1972.

From Symposium on natural and manmade radiation in space; Las Vegas, Nev. (1 Mar 1971).

Temporal variations in the trapped natural-electron flux intensities and energy spectra are discussed and demonstrated using recent satellite data. These data are intended to acquaint the space systems engineer with the types of natural variations that may be encountered during a mission and to augment the models of the electron environment currently being used in space system design and orbit selection (Vette et al.) For systems or subsystems that are particularly sensitive to radiation and that respond to changes in the environment on a short time scale, these models by themselves may be inadequate for proper subsystem design or interpretation of on-orbit data. Some of the temporal variations demonstrated, which are not widely known, include: addition of very energetic electrons ($E \geq 5$ MeV) to the outer zone during moderate magnetic storms; addition of energetic electrons ($E > 1$ MeV) to the inner zone during major magnetic storms; inversions in the outer-zone electron energy spectrum during the decay phase of a storm injection event; and occasional formation of multiple maxima (≥ 4) in the flux vs altitude profile of moderately energetic electrons ($E \leq 1$ MeV). 14 figures. (auth)

54047 (NASA-TM-X-2440, pp 548-55) TRAPPING OF TRANSURANIUM ELEMENTS BY THE EARTH'S MAGNETIC FIELD. Bloom, Justin L.; Eastlund, Bernard J. (Atomic Energy Commission, Washington, D. C.). Jan 1972.

From Symposium on natural and manmade radiation in space; Las Vegas, Nev. (1 Mar 1971).

The search for a transuranium element component of cosmic radiation has been carried out in high-altitude balloon experiments by Price, Fleischer, Walker, and Fowler. It is shown that the trapping of high-Z elements on orbits in the Earth's magnetic field may lead to a sufficient enhancement of the intensity of particle flux to make it possible to detect these elements by satellite experiments. Calculations are presented that predict the behavior of trapped particles as a function of the predicted flux and energy distribution of high-Z elements incident on the Earth's magnetic field. Techniques are suggested for the detection of such particles. In addition, the possibility of production of transuranium elements in the recently discovered pulsars is discussed. (auth)

54048 (NASA-TM-X-2440, pp 561-8) SUMMARY OF THE OV1-19 SATELLITE DOSE, DEPTH DOSE, AND LINEAR ENERGY TRANSFER SPECTRAL MEASUREMENTS. Cervini, John T. Jan 1972.

From Symposium on natural and manmade radiation in space; Las Vegas, Nev. (1 Mar 1971).

Measurements were made in the inner Van Allen radiation belt by tissue-equivalent ionization chambers (TEICs) and cellular absorbed dose linear energy transfer spectrometer on the OV1-19 satellite. Results of data reduction are presented for the solar flare events in April, Nov., and Dec. 1969. The TEIC data show that a considerable dose rate can be expected even behind shielding whose cutoff energy is ≥ 70 MeV. Protons of high energy (>60 MeV) are the dominant hazard to man in space. The geomagnetic field screens out the solar flare protons in the nonpolar regions, but not if the flare rigidity is great enough. 14 figures. (D.L.C.)

54049 (NASA-TM-X-2440, pp 748-55) RADIATION PROBLEMS ASSOCIATED WITH SKYLAB. Braly, John E.; Heaton, Thomas R. (Martin Marietta Corp., Baltimore). Jan 1972.

From Symposium on natural and manmade radiation in space; Las Vegas, Nev. (1 Mar 1971).

Skylab, an experimental space station, will orbit the earth during 1972–73. Sixty experiments will be carried out during its flight, 26 of which use some type of photographic film. In its circular orbit of 235 n mi, inclined 50°, it passes through the Van Allen belt several times a day. Radiation tests were conducted on the various types of Skylab film to establish the total radiation dosages compatible with an acceptable level of film fogging, and on the S190 borosilicate window to establish radiation limits for an acceptable darkening level. The results verified that most of the films would be unusable when returned to earth, and that the borosilicate window would be darkened beyond allowable limit, unless additional protection was provided. The operational solutions to these problems involve protecting the film with five film vaults and protecting the window with a radiation shield. The largest vault is made of aluminum and weighs over 2000 lb (its thickest compartment wall is 3.4 in.). The window radiation shield is a light honeycomb structure which is swung away for limited astronaut viewing or when the S190 experiment is in operation. Although the shield is lightweight, it is heavy enough to stop the large number of low-energy electrons making up a major part of the external environment and which are potentially damaging to the window. The paper contains a brief description of the Skylab mission and some of the associated experiments. The radiation environment which the spacecraft will encounter is discussed. The results of the radiation test programs on Skylab photographic film and on borosilicate glass are presented. Operational solutions to the two problems of excessive film fog and loss of transmittance through the glass are described. (auth)

54050 NONLINEAR THEORY OF MONOCHROMATIC CIRCULARLY POLARIZED VLF AND ULF WAVES IN THE MAGNETOSPHERE. Bud'ko, N. I. (Inst. of Terrestrial Magnetism, Ionosphere and Radio-wave Propagation, Moscow); Karpman, V. I.;

Pokhotelov, O. A. Cosmic Electrodyn.; 3: No. 2, 147-64(Jul 1972).

The interaction of resonant particles with a monochromatic circularly polarized wave propagating along the magnetic field in a homogeneous plasma is investigated. It is shown that the damping (or growth) rate of the wave vanishes after a time of order of the characteristic oscillation period of resonant particles. Propagation of monochromatic waves in an unstable plasma is accompanied by the generation of two side bands, which have frequency shifts relatively to the main wave of the order of the oscillation frequency of resonant particles. Theoretical results are compared with known experimental data concerning monochromatic vlf (monochromatic whistler) and ulf (Pc-1 micropulsation waves). (auth)

54051 PHYSICAL MECHANISM OF THE MAGNETOSPHERIC SUBSTORM DEVELOPMENT. Kropotkin, A. P. (Moscow State Univ.). Planet. Space Sci.; 20: No. 8, 1245-57(Aug 1972).

A phenomenological model of the plasma flow at the inner edge of the magnetotail plasma sheet is proposed. Convective transfer and spatial diffusion of plasma across geomagnetic-field lines together with particle precipitation into the ionosphere (caused by pitch-angle scattering) are taken into account. Two types of steady-state solutions are obtained; they represent conditions for the substorm growth and expansion phases, respectively. The earthward flow of the plasma is retarded, and a convective instability of the flow occurs at the inner boundary of the plasma sheet. This may be a cause of transformation of one-flow mode into the other. The model predicts a fast transit from the growth phase to the expansion phase. (auth)

54052 RESONANT INTERACTION OF AN ELECTROSTATIC WAVE WITH ELECTRONS IN A CURRENT SHEET. Gjoeen, Einer (Univ., Bergen). Planet. Space Sci.; 20: No. 8, 1205-12(Aug 1972).

A one-dimensional model of a current-sheet with a static electric potential is considered. Free electrons and protons move in opposite directions under the influence of the potential and a solution is sought for the potential in a bounded region in space (over the sheet width). The general solution is found to be plasma oscillations. Then, introducing a short-wavelength monochromatic wave as a perturbation, it is shown by the method of stationary phase that electrons in resonance give a growth (damping) rate similar to the Landau formula. There is the possibility, however, that the wave can both grow and damp in different regions when traversing the sheet as it will sample electrons from various parts of the zero-order distribution function. (auth)

54053 GEOMAGNETIC DISTURBANCES IN THE POLAR CAP. S_q^p AND DP-2. Kawasaki, K.; Akasofu, S.-I. (Univ. of Alaska, College). Planet. Space Sci.; 20: No. 8, 1163-72(Aug 1972).

It is shown that the daily magnetic variation in the polar cap on moderately disturbed days is essentially identical to that of extremely quiet days, but significantly enhanced. On the basis of an extensive analysis of magnetic and auroral records, it is shown that the particular type of magnetic variation identified as the DP-2 mode is not a new and distinct variation, but is one of the manifestations of magnetospheric substorms. (auth)

54054 EQUILIBRIUM POTENTIAL OF A MAGNETOSPHERIC SATELLITE IN AN ECLIPSE SITUATION. Knott, K. (ESTEC, Noordwijk, Netherlands). Planet. Space Sci.; 20: No. 8, 1137-46(Aug 1972).

The order of magnitude of the equilibrium potential of a surface exposed to the particle environment outside the magnetospheric plasmasphere is calculated. This is done under the assumption that no solar irradiation reaches the surface, thus no photoemission becomes effective. It is shown that for a given surface material the equilibrium potential depends strongly on the energy distribution of the particle environment. In some cases secondary electron emission helps to avoid high negative equilibrium potentials. It can be concluded that materials with high secondary electron yields such as BeCu and SiO_2 have the most useful properties to the extent that highly negative surface charges are avoided in nearly all particle environments that are encountered inside the magnetosphere. (auth)

54055 SUDDEN IMPULSES IN THE GEOMAGNETOTAIL AND THE VICINITY. Patel, V. L. (Univ. of Denver). Planet. Space Sci.; 20: No. 8, 1127-36(Aug 1972).

Explorer-33 magnetic-field observations were analyzed to study the propagation of sudden impulses in the geomagnetic tail and the magnetosheath. Average speed of propagation in these regions is 760 km per sec with a range of 550 to 1230 km per sec. Most of the si's have propagation speed that is close to that of the shock wave observed in this region. Positive si is shown to have a positive change in the tail or magnetosheath and a negative si has a similar negative change. Nine out of thirteen correlated si's have their origin in the solar-wind continuities, while four si's have possible origin in the perturbations of tail or magnetosheath field. It is found that the si propagation is not confined to the tail region but it has correlated effects in the magnetosheath also. The propagation region studied is in 2000 to 0200 local time sector. (auth)

54056 INTERACTION OF A STEADY PLASMA FLOW WITH A DIPOLE MAGNETIC FIELD IN THE PRESENCE OF A RADIAL ELECTRIC FIELD. Kono, Migiwa (Sagami Inst. of Tech., Kanazawa, Japan); Kawashima, Nobuki; Kubo, Haruya. Rep. Ionosphere Space Res. Jap.; 26: No. 1-2, 102-5(1972).

The general layout of an experimental device is shown that simulates the Earth's environmental space. The interactions between the flow of charged particles and the geomagnetic field result in various phenomena such as the formation of the magnetosphere, collision-free shock waves and the plasmapause, and the excitation of aurora. In the experiment, a steady-state plasma is produced in a TP-D device (Takayama, 1966). A plasma diffuses out from the discharge chamber into the experimental region through a small aperture at the center of the anode along a guiding magnetic field. Directions are given for the experiment to simulate the geophysical situation and the relationship between the results and geophysical phenomena such as the plasmapause formation are being studied. (J.C.W.)

54057 SPATIAL DISTRIBUTION OF ENERGETIC PLASMA-SHEET ELECTRONS. Walker, Raymond J.; Farley, Thomas A. (Univ. of California, Los Angeles). J. Geophys. Res.; 77: No. 25, 4650-60(1 Sep 1972).

The spatial distribution of energetic plasma sheet electrons ($E \geq 50$ keV) out to a radial distance of 24 R_E using data from the University of California at Los Angeles electron spectrometer and fluxgate magnetometer experiments on Ogo 5 is presented. A comparison of distributions in geocentric solar magnetospheric coordinates (GSM) prepared with and without the use of a neutral-sheet model indicates that the use of such a model facilitates organization of plasma-sheet data. The distribution in the Y_{GSM}-ZN plane, where ZN is the distance above or below the neutral sheet in the Z_{GSM} direction, for limited values of X_{GSM} shows a tendency for the energetic electrons to concentrate near the neutral sheet. However, no characteristic behavior is seen in electron fluxes during individual neutral sheet crossings. The percentage of flux occurrence above a given flux threshold falls off rapidly with distance from the neutral sheet. Contours of constant percentage of occurrence diverge slightly from the neutral sheet at local times away from midnight. This effect decreases with increasing flux threshold. Contours in the X_{GSM}-Y_{GSM} plane for a limited range in ZN are extended toward dawn, and thus a limited dawn—dusk asymmetry is indicated. This effect is limited to the extent that percentages of occurrence comparable to those on the dawnside are found in the region about midnight. The degree of asymmetry increases as the flux threshold is increased. The contours in the X_{GSM}-ZN plane converge toward the neutral sheet with increasing distance in the antisolar direction ($-X_{GSM}$). A comparison of this result with the results from Imp 1 indicates that X_{GSM} is preferable to the radial distance R for organizing tail data. (auth)

54058 DIAMAGNETIC EFFECT OF THE PLASMA SHEET NEAR 60 R_e. Meng, C.-I. (Univ. of California, Berkeley); Mihalov, J. D. J. Geophys. Res.; 77: No. 25, 4661-9(1 Sep 1972).

The two-dimensional (YZ plane) spatial distribution of magnetic field magnitudes in the geomagnetic tail at the lunar distance is given in both the solar magnetospheric and the neutral-sheet coordinate systems by using 3 years of data from the Ames magnetometer on Explorer 35. The effect of changes in geomagnetic activity is also presented. In the magnetotail near 60 R_E a broad region in which the magnetic field intensity is relatively weak in comparison with that in the other region of the tail is located adjacent to the solar magnetospheric equatorial plane and the calculated neutral sheet. This depression of the field due to the diamagnetic effect of the plasma sheet is more evident during times of minimum geomagnetic activity ($Kp \leq 1+$). Plasma energy densities of 200 to 300 eV/cm^3 in the plasma sheet are inferred by interpreting the field magnitude decrease as the effect of plasma diamagnetism. (33 references) (auth)

54059 BALANCE OF STRESSES IN THE PLASMA SHEET. Rich, F. J. (Rice Univ., Houston, Tex.); Vasyliunas, V. M.; Wolf, R. A. J. Geophys. Res.; 77: No. 25, 4670-6(1 Sep 1972).

The stress resulting from magnetic tension on the neutral sheet must, in a steady state, be balanced by any one or a combination of (1) a pressure gradient in the direction along the axis of the tail, (2) a similar gradient of plasma flow kinetic energy, and (3) the tension resulting from a pressure anisotropy, with $P_{||} > P_{\perp}$ within the plasma sheet. Stress balance in the first two cases requires that the ratios h/L_x and B_z/B_x be of the same order of magnitude, where h is the half-thickness of the neutral sheet, L_x is the length scale for variations along the axis of the tail, and B_z and B_x are the magnetic field components in the plasma sheet just outside the neutral sheet. The values usually quoted for these quantities do not satisfy this requirement: h is too small and/or B_z is too large. The second case requires, in addition, that the plasma flow speed within the neutral sheet be of the order of or larger than the Alfvén speed outside the neutral sheet. Stress balance in the third case requires that just outside the neutral sheet the plasma pressure obey the marginal firehose stability condition $P_{||} - P_{\perp} = B^2/\mu_0$. (29 references) (auth)

54060 ONSET OF MAGNETOSPHERIC SUBSTORMS. Tsurutani, B. (Univ. of California, Berkeley); Bogott, F. J. Geophys. Res.; 77: No. 25, 4677-81(1 Sep 1972).

An examination of the onset of magnetospheric substorms is made by using ATS-5 energetic particles, conjugate balloon x rays and electric fields, all-sky camera photographs, and auroral-zone magnetograms. It is shown that plasma injection to ATS distances, conjugate 1- to 10-keV auroral particle precipitation, energetic >40-keV electron precipitation, and enhancements of westward magnetospheric electric-field component all occur with the start of slowly developing negative magnetic bays. No trapped or precipitating energetic-particle features are seen at ATS 5 when later sharp negative magnetic-bay onsets occur at Churchill or Great Whale River. (auth)

54061 COORDINATED OBSERVATIONS OF THE MAGNETOSPHERE: THE DEVELOPMENT OF A SUBSTORM. Mende, S. B. (Lockheed Palo Alto Research Lab., Calif.); Sharp, R. D.; Shelley, E. G.; Haerendel, G.; Hones, E. W. J. Geophys. Res.; 77: No. 25, 4682-99(1 Sep 1972).

Coordinated observations of a substorm are reported by using data from all-sky camera (ASCA) stations near the northern conjugate of the ATS 5 geostationary satellite, plasma and magnetic-field experiments on the ATS 5 satellite, Vela 5B at 18 R_E in the magnetotail, the Heos 1 interplanetary probe, and ground-based magnetograms. The substorm event occurred after a very quiet day and was preceded by a development period during which the interplanetary field turned southward and the plasma energy density increased near the Earth (6.6 R_E) on the nightside. This period was also evidenced by a depression of the midlatitude H component of the geomagnetic field at the Earth's surface. The auroral breakup was preceded by the appearance of quiet arcs, the leveling off of the plasma energy density increase at ATS, and the disappearance of the tail plasma at 18 R_E. The onset of the expansive phase was evidenced by brightening and subsequent breakup of the auroral arcs, the development of a westward-traveling surge, an increase in the fluxes of energetic electrons, and the increase of the magnetic field at ATS 5. The ground-based magnetograms show the sudden intensification of the westward electrojet and the appearance of field-aligned currents. (40 references) (auth)

54062 POLAR-CAP ELECTRIC FIELD DISTRIBUTIONS RELATED TO THE INTERPLANETARY MAGNETIC FIELD DIRECTION. Heppner, J. P. (Goddard Space Flight Center, Greenbelt, Md.). J. Geophys. Res.; 77: No. 25, 4877-87(1 Sep 1972).

Measurements were made previously of the electric field during a 13-day period (June 10—22, 1969) when the satellite orbital plane was centered on the 1800—0600 LT meridian. It was shown that, at auroral-belt latitudes in both hemispheres, the electric field is consistently directed poleward in the midevening sector and equatorward in the midmorning sector, whereas the field at higher (polar cap) latitudes is consistently directed from dawn toward dusk, independent of magnetic disturbances, interplanetary-field directions, and other parameters expected to have some relationship to the electric-field pattern. Different characteristic distributions of the polar-cap field reappeared on different days and at a variety of UT throughout the 13 days. An attempt was made to classify the distributions in terms of signatures that could be compared with other geophysical parameters. The distribution of fields within auroral-belt (i.e., sunward convection) regions is ignored, and only the spatial distribution of the dawn—dusk polar-cap field is considered. The northern hemisphere signatures are applied only to passes crossing the noon-midnight meridian between $\Lambda = 75°$ on the nightside and $\Lambda = 85°$ on the dayside. For the southern polar cap, noon—midnight meridian crossings extend from about $\Lambda = 70°$ on the dayside to $\Lambda = 85°$ on the nightside. Classifications for southern and northern polar-cap traverses were made. Correlations between the azimuthal direction of the interplanetary magnetic field and the most simple polar-cap signatures were immediately obvious. (J.C.W.)

54063 ELECTRIC FIELD INDUCED BY A SLOWLY DECAYING RING CURRENT. Wang, C. S.; Kim, J. S. (State Univ. of New York, Albany). J. Geophys. Res.; 77: No. 25, 4867-9(1 Sep 1972).

Magnetic inflation and particle distribution of magnetospheric plasma assure the existence of the ring current. Induction effects of a slowly decaying ring current and model calculations were made to estimate the magnitude of the induced electric field through the equation $\nabla \times E = -\partial B/\partial t$. Calculations are also presented for an electric field induced at the equator by different ring currents having decay time constants of 6, 8, 10, 20, and 40 hours. The ring current is assumed to be at a fixed distance of 4.6 R_E from the Earth. It is known that a continuous slow shift of the location of the ring current occurs, introducing a new electric field. The magnitude of the electric field is evaluated mathematically. (J.C.W.)

54064 SELF-CONSISTENT DESCRIPTION OF THE MAGNETOTAIL CURRENT SYSTEM. Bird, M. K.; Beard, D. B. (Univ. of Kansas, Lawrence). J. Geophys. Res.; 77: No. 25, 4864-6(1 Sep 1972).

The plasma-pressure distribution and magnetic-field configuration of the quiet geomagnetic tail were examined. Electric fields arising from incidence of the solar wind on the magnetospheric field $E = -v/c \times B$ cause a drift of plasma but do not contribute to the current. The structure of the magnetic field and the plasma within and surrounding the plasma sheet of the magnetotail were determined by solving the differential equation for the field, which is obtained by equating the current from Ampere's law to the current obtained from first-order adiabatic drift theory, composed of gradient drift, curvature drift, and magnetization currents. When the plasma distribution and the magnetic field are known, the individual contributions to the total current from the effects of magnetization, curvature drift, and gradient drift may be determined. The solution given shows that 80 to 90% of the current supporting the magnetotail field was due to particle-drift current. Total magnetization current was <20% of the net current per unit length of tail and the remainder entirely due to the drift of magnetosheath solar-wind particles entering and drifting across the equatorial plane primarily because of the curvature of the magnetocylinder field lines within the cavity. (J.C.W.)

54065 DAILY VARIATION OF ELECTRON AND PROTON GEOMAGNETIC CUTOFFS CALCULATED FOR FORT CHURCHILL, CANADA. Smart, D. F.; Shea, M. A. (Air Force Cambridge Research Labs., Bedford, Mass.). J. Geophys. Res.; 77: No. 25, 4595-4601(1 Sep 1972).

The trajectory-tracing process has been used, with an improved mathematical model of the magnetosphere containing magnetic fields of both internal and external origin, to calculate cutoff rigidities for electrons and protons incident at Fort Churchill, Canada. These calculations, made for the vertical direction and at zenith angles of 60°E and 60°W at each hour of the day, give cutoff values of approximately 150 MV during the daytime and less than 20 MV at night. These values are in qualitative agreement with measurements obtained by balloon experiments. (auth)

Solar Wind and Cosmic Ray Interactions

Refer also to abstracts 53968, 54164, 54177, and 54313.

54066 (NASA-TM-X-2440, pp 922-5) NEUTRON SPECTRAL MEASUREMENTS IN THE UPPER ATMOSPHERE. Zobel, W.; Love, T. A.; Delorenzo, J. T.; McNew, C. O. (Oak Ridge National Lab., Tenn.). Jan 1972.

From Symposium on natural and manmade radiation in space; Las Vegas, Nev. (1 Mar 1971).

An experiment to measure neutrons in the upper atmosphere was performed on a balloon flight from Palestine, Texas, at an altitude of about 32 km. The experimental arrangement is discussed briefly, and results of a preliminary analysis of the data for neutrons in the energy range 3 to 30 MeV are given. (auth)

54067 (NASA-TM-X-2440, pp 926-41) PHYSICAL THEORY OF ONE-DIMENSIONAL GALACTIC COSMIC-RAY PROPAGATION IN THE ATMOSPHERE. O'Brien, Keran (Atomic Energy Commission, New York). Jan 1972.

From Symposium on natural and manmade radiation in space; Las Vegas, Nev. (1 Mar 1971).

An essentially analytical theory of atmospheric cosmic-ray propagation is developed on the basis of a phenomenological model of hadron–nucleus collisions. This model correctly predicts the sea-level cosmic-ray nucleon, pion, and muon spectra, the cosmic-ray ionization profile in the atmosphere, and neutron flux and density profiles in the atmosphere. It is concluded that the large-scale properties of atmospheric cosmic rays can be accurately predicted on the basis of a purely nucleonic cascade as a result of which all secondaries are mediated by pion production. Implications for energy independence of cross sections, the recent 70-GeV results from Serpukhov, and nucleonic relaxation rates in the atmosphere are discussed. 16 figures, 55 references. (auth)

54068 PIONEER 7 OBSERVATIONS OF THE AUGUST 29, 1966, INTERPLANETARY SHOCK-WAVE ENSEMBLE. Dryer, Murray (Space Environment Lab., Boulder, Colo.); Smith, Zdenka K.; Endrud, Glenn H.; Wolfe, John H. Cosmic Electrodyn.; 3: No. 2, 184-207(Jul 1972).

An interplanetary shock wave—possibly due to an importance 2N flare in McMath region 8461 at N23 E22 at 1805 UT on August 26, 1966—was observed by IMP 3, Explorer 33, Explorer 34, and (possibly) Vela 3, at approximately 1315 UT (SSC) on August 29, 1966. The same shock wave, with undiminished velocity, was observed by two plasma instruments and a magnetometer aboard Pioneer 7 when it was about 275 Earth radii downstream of the Earth. Observation of the important plasma parameters of the shocked solar wind for many hours after the shock's passage provided an opportunity to search for a double-shock structure. A time-dependent similarity theory, which incorporates both the effect of the magnetic field and finite electrical conductivity, was used as a guide in this search. The "piston" could not be identified; for example, if present, it was not characterized by an enriched alpha/proton abundance or by peaks in the magnitudes of the proton density or magnetic field as suggested by the theory. A reverse shock was identified within 12 min of its predicted arrival time. Thus, this forward–reverse shock ensemble may be among the first so identified since the speculations of Sonett, Colburn, Schubert, and Cummings. The theoretical energy in the entire disturbance is in excellent agreement with the value determined experimentally, although a detailed comparison of plasma and field parameters between the theory and observations was not successful. A partial explanation for the lack of a detailed comparison (described, at best, as fair) is the neglect in the theory of additional transport properties (thermal conduction and viscosity). A supplemental explanation may be the possibility that the double-shock ensemble was no longer propagating at 1 AU as assumed in the theory, but, instead, had taken on some properties of a blast wave. (auth)

54069 MAGNETOSPHERIC ACCESS OF SOLAR PARTICLES AND THE CONFIGURATION OF THE DISTANT GEOMAGNETIC FIELD. Evans, Lawrence Curtis. Pasadena, Calif.; California Inst. of Tech. (1972). 281p. University Microfilms Order No. 72-22,601.

Thesis.

The access of 1.2- to 40-MeV protons and 0.4- to 1.0-MeV electrons from interplanetary space to the polar-cap regions was investigated with an experiment on board a low-altitude, polar-orbiting satellite (OGO 4). A total of 333 quiet-time observations of the electron polar-cap boundary gave a mapping of the boundary between open and closed geomagnetic-field lines that was an order of magnitude more comprehensive than previously available. Persistent features (north/south asymmetries) in the polar-cap proton flux, which are established as normal during solar proton events, are shown to be associated with different flux levels on open geomagnetic-field lines than on closed field lines. The pole in which these persistent features are observed is strongly correlated to the sector structure of the interplanetary magnetic field and uncorrelated to the north/south component of this field. The features were observed in the north (south) pole during a negative (positive) sector 91% of the time, while the solar field had a southward component only 54% of the time. In addition, changes in the north/south component have no observable effect on the persistent features. Observations of events associated with co-rotating regions of enhanced proton flux in interplanetary space are used to establish the characteristics of the 1.2- to 40-MeV proton access windows: the access window for low polar latitudes is near the Earth, that for one high polar latitude region is ~250 $R_{\oplus}$ behind the Earth, while that for the other high polar latitude region is ~1750 $R_{\oplus}$ behind the Earth. All of the access windows are of approximately the same extent (~120 $R_{\oplus}$). Results are compared to the particle-access predictions of the distant geomagnetic tail configurations proposed by Michel and Dessler, Dungey, and Frank. The data are consistent with neither the model of Michel and Dessler nor that of Dungey. The role played by interplanetary anisotropies in the observation of persistent polar-cap features is discussed. Special emphasis is given to the problem of nonadiabatic particle entry through regions where the magnetic field is changing direction. The degree to which such particle entry can be assumed to be nearly adiabatic is related to the particle rigidity, the angle through which the field turns, and the rate at which the field changes direction; this relationship is established for the case of polar-cap observations. (TSS) (Diss. Abstr. Int., B)

54070 ANALYSIS OF THREE-STATION INTERPLANETARY SCINTILLATION. Armstrong, J. W.; Coles, W. A. (Univ. of California, San Diego, La Jolla). J. Geophys. Res.; 77: No. 25, 4602-10(1 Sep 1972).

Statistical models used in the analysis of drifting random patterns are discussed. A new method of estimating the drift velocity with minimal a priori assumptions is presented. It is shown that all the models that allow for pattern rearrangement, including the new method, can be highly sensitive to systematic errors. These techniques are applied to recent observations of interplanetary scintillation in the ecliptic plane. A comparison is made with mean proton velocities measured by satellite, and a clear correspondence between high velocity features is found. 26 references. (auth)

54071 POLAR-CAP MEASUREMENTS OF SOLAR-FLARE PROTONS WITH ENERGIES DOWN TO 12.4 keV. Mizera, P. F.; Fennell, J. F.; Blake, J. B. (Aerospace Corp., Los Angeles). J. Geophys. Res.; 77: No. 25, 4845-50(1 Sep 1972).

Solar protons with energies down to 12.4 keV were measured over the polar caps by instruments aboard the OV 1–17 satellite. The observations were made following the March 21, 1969, solar-particle event. The polar-cap differential fluxes measured by OV 1-17 and Injun 5 from 0.012 to 1.1 MeV are well represented by a single power law. Over a 22-hour period the spectral index changed from 1.7 to 1.9. Temporal and spatial comparisons were made with data from the Explorer-35 and Injun-5 spacecraft. Good agreement is found at energies (>300 keV) where a comparison can be made. (auth)

54072 SOLAR-WIND AND INTERPLANETARY ELECTRON MEASUREMENTS ON THE APOLLO 15 SUBSATELLITE. Anderson, K. A. (Univ. of California, Berkeley); Chase, L. M.; Lin, R. P.; McCoy, J. E.; McGuire, R. E. J. Geophys. Res.; 77: No. 25, 4611-26(1 Sep 1972).

Measurements of high-energy solar-wind electrons have been made from a low orbit around the Moon. Solar-wind electrons can be identified up to energies of ~3000 eV, at which an electron population of entirely different characteristics becomes dominant. The solar-wind cavity on the Moon's antisolar side shows evidence of being filled by plasma coming from the downstream direction. When the direction of the interplanetary field corresponds to solar ecliptic azimuth angles of about 90°, a partial solar-wind cavity extends across most of the eastern sunlitside of the Moon within ~20° of the noon meridian. There are localized increases in the ~500-eV electron flux over much of the sunlit hemisphere. These increases are highly persistent and stable in their location over a $2\frac{1}{2}$-day period and hence are not due to intrinsic variations in the solar wind. They are usually associated with disturbances in the magnetic field. These increases are interpreted to be the result of an interaction between the solar wind and the Moon that deflects some of the solar-wind flow and results in limb shocks. (auth)

54073 MAGNETOHYDRODYNAMIC THEORY FOR THE INTERACTION OF AN INTERPLANETARY DOUBLE-SHOCK ENSEMBLE WITH THE EARTH'S BOW SHOCK. Shen, Wen-wu (Univ. of Colorado, Boulder); Dryer, Murray. J. Geophys. Res.; 77: No. 25, 4627-44(1 Sep 1972).

The interactions between interplanetary shocks and the Earth's bow shock are formulated first on a gas-dynamic basis. The problem is repeated on a magnetohydrodynamic (MHD) basis for the special case of perpendicular shocks. In particular, an interplanetary double-shock ensemble (composed of forward and reverse shocks) is allowed to interact with the Earth's bow shock. It is found that the collision of a forward shock with the bow shock creates two shocks and a contact surface; the symbolism $S_{\rightarrow}S_{\leftarrow} \rightarrow S_{\leftarrow}CS_{\rightarrow}$ is used to represent this particular interaction. The collision of a reverse shock with the bow shock, hitherto not discussed, yields a shock, contact surface, and rarefaction wave: $S_{\leftarrow}S_{\leftarrow} \rightarrow S_{\leftarrow}CR_{\rightarrow}$. The results of the interactions are discussed on the basis of several representative computations. An order-of-magnitude increase of thermal pressure is the major consequence of the "shock-on-shock" interaction. The effect of the magnetic field is minor; for example, the bow-shock velocity after impact of a forward shock is only ~10% less than the velocity computed on the basis of ordinary gas dynamics. Interaction dynamics are applied, in the case of the geomagnetic storm's sudden commencement, to the characteristic time and energy of the instantaneous compression. Several magnetic-storm sudden-commencement events (including the March 8, 1970, event) are discussed on the basis of spacecraft plasma observations and magnetogram records on the Earth. Comparison of available diagnostics with the theory suggests the physical plausibility of the present fluid-dynamic study. (34 references) (auth)

54074 SIMULTANEOUS SOLAR-WIND PLASMA AND MAGNETIC-FIELD MEASUREMENTS IN THE EXPECTED REGION OF THE EXTENDED GEOMAGNETIC TAIL. Intriligator, D. S. (California Inst. of Tech., Pasadena); Wolfe, J. H.; McKibbin, D. D. J. Geophys. Res.; 77: No. 25, 4645-9(1 Sep 1972).

A comparison is made of simultaneous plasma and magnetic-field measurements obtained by Pioneer 7 in the expected region of the geomagnetic tail at ~1000 R_E. The results indicate that, unlike the data for the near-Earth ($\leq 80\ R_E$) geomagnetic tail, the data for the plasma and magnetic field have no unique signature of tail-associated phenomena. Furthermore, there are differences between the two types of data concerning the tentative identification of tail-associated phenomena for a number of intervals. The physical implications of these differences may be associated with anomalous transport properties that introduce turbulence in the form of mass diffusion and diamagnetic behavior adjacent to plasma eddies. As a result, the magnetopause, as it is recognized close to Earth, loses its identity at far distances ($>80\ R_E$) and combines in a turbulent and hence ill-defined way with the geomagnetic tail. Thus there would be no reason to expect a consistent tail identification on a one-to-one basis with plasma and magnetic-field observations, the criterion presently used close to Earth (i.e., $<80\ R_E$). (auth)

54075 UPPER LIMIT OF THE TORQUE OF THE SOLAR WIND ON THE EARTH. Hirshberg, J. (Ames Research Center, Moffett Field, Calif.). J. Geophys. Res.; 77: No. 25, 4855-7(1 Sep 1972).

An analysis previously presented by Coleman (J. Geophys. Res., 71: 3800(1971)) depended on the assumption that the magnetospheric boundary was held fixed, but no physical mechanism was suggested to prevent the boundary-layer plasma from rotating. It is now shown that there is not enough matter in the solar wind to inhibit the rotation of the boundary-layer might be the cause of some tend to rotate with the Earth, and the possible maximum torque is less than 10^{21} dyne cm and unobservable at 10 R_E. Coleman had suggested torque exerted on the Earth by the solar wind from the coupling between the Earth's ionosphere and the solar-wind plasma in the magnetospheric boundary-layer might be the cause of some of the slower changes in the length of day. The upper limit of the torque is calculated and found to be 3 to 4 orders of magnitude too small to be responsible for the slowing of the Earth's rotation. (J.C.W.)

54076 MAGNETIC-FIELD STRUCTURE IN FLARE-ASSOCIATED SOLAR-WIND DISTURBANCES. Schatten, Kenneth H.; Schatten, Judith E. (Goddard Space Flight Center, Greenbelt, Md.). J. Geophys. Res.; 77: No. 25, 4858-63(1 Sep 1972).

Conclusions were drawn about proposed solar-wind disturbance models by examining the interplanetary magnetic field. Piddington (1958) proposed that material could be ejected from solar flares to form a semipermanent magnetic feature in interplanetary space. Gold (1959) proposed a magnetic tongue or bottle as the field structure being ejected by these active regions. The interplanetary-field increase that might be associated with the additional outburst of a Gold bottle was described. A Gold bottle could also have a shock and/or compressed ambient field region in front of it. Later Gold (1962) proposed a model where field-line reconnection occurred, closing magnetic loops being ejected by the flare. Thus, the looped field lines attached to the active region would tie off in interplanetary space, and any radial field increase observed would be short-lived. Coleman et al. (1960) used measurements showing a null in the interplanetary magnetic field that might fit Gold's model. Parker considered both a blast-wave model and drive-disturbance model. Data from fifteen solar-wind disturbances (1965 to 1967) associated with solar flares and available interplanetary field data were used. (J.C.W.)

PHYSICS (ATOMIC AND MOLECULAR)

Atomic, Electron, Ion, and Molecular Beams and Their Reactions

Refer also to abstracts 52936, 53322, 54105, and 54467.

54077 (CEA-CONF-2048) MEASUREMENT OF THE ABUNDANCE OF A $^{14}N^{7+}$ ION BEAM. Geller, R. (Commissariat a l'Energie Atomique, Grenoble (France). Centre d'Etudes Nucleaires). 1972. 6p. (In French). (CONF-720120-3). Dep. NTIS (U. S. Sales Only).

From Conference on the sources of multicharged ions; Paris, France (28 Jan 1972).

The $^{2}H^{+}$ ion abundance is minimized by establishing a vacuum limit of 10^{-8} torr. A time-of-flight method is used to separate the $^{14}N^{7+}$ ions from the other nitrogen ions, after having accelerated the ions by very short pulses. Obstacles inside the flight tube minimize the diffusion plasma. The abundance can be measured only for beams with an extraction intensity lower than 10 μA. The detection system consists in a secondary emission target associated with a scintillator and a photomultiplier. The fast electronics (time constants < 30 ns) includes a linear gate variable in time with a 100 ns time duration. (France)

54078 (CEA-CONF-2050) X-RAY SPECTROMETRY BETWEEN 5A AND 20A. APPLICATION TO THE MULTIPLY-CHARGED ION EXPERIMENT. Jacquot, C. (Commissariat a l'Energie Atomique, Grenoble (France). Centre d'Etudes Nucleaires). 14 Mar 1972. 5p. (In French). (CONF-720120-5). Dep. NTIS (U. S. Sales Only).

From Conference on the sources of multicharged ions; Paris, France (28 Jan 1972).

The principle for the most suitable x-ray-spectrometry unit, a compromise between high sensitivity and good spectral resolution, in the 500-eV to 10-keV energy range (1A to 20A) is discussed. This spectral range was selected for use in proving the existence of stripped ions in the stripped-ion experiment at the electron cyclotron resonance and determining the abundance ratio for the stripped nitrogen ions. (France)

54079 (FRNC-CONF-53) RESEARCH PROGRAM OF THE PARTICLE SOURCE GROUP IN THE FIELD OF MULTICHARGED IONS. Gautherin, G.; Lejeune, C. (Paris Univ., Orsay (France)). 1972. 18p. (In French). (CONF-720120-10). Dep. NTIS (U. S. Sales Only).

From Conference on the sources of multicharged ions; Paris, France (28 Jan 1972).

The possibilities of discharges with magnetic and geometric compression (duoplasmatron) were studied. Various structures were envisaged (duopigatron, triplamatron, hot-cathode magnetron) with regard to obtaining a multicharged-ion source with the following specifications: continuous pulsed operation, weak energy dispersion and emittance, easy utilization (volume, power, complexity, vacuum). (France)

54080 (FRNC-CONF-55) SOURCES WITH CONFINED ELECTRON BEAMS (REVIEW). Baron, Eric (Paris Univ., Orsay (France). Institut de Physique Nucleaire). 1972. 17p. (In French). (CONF-720120-8). Dep. NTIS (U. S. Sales Only).

From Conference on the sources of multicharged ions; Paris, France (28 Jan 1972).

The various types of ion sources with confined electron beams are surveyed, the toroidal HIPAC system being excluded: the Redhead device, the Dubna source, and the MEBIS source. The difficulties involved in these sources are emphasized, and their performances are discussed. (France)

54081 (FRNC-CONF-57) PRELIMINARY STUDIES ON A MODIFIED VERSION OF THE EBIS SOURCE. Septier, A.; Brebec, J. M.; Ambourg, Y. (Paris Univ., Orsay (France)). 1972. 9p. (In French). (CONF-720120-12). Dep. NTIS (U. S. Sales Only).

From Conference on the sources of multicharged ions; Paris, France (28 Jan 1972).

The principle of the MEBIS source is presented. This source should offer the following performance: a working pressure higher than that of the EBIS source, a reduction in the electric power supply, a continuous operation. The electric power used for the focusing system should be reduced and a longitudinal ion trapping should be obtained by replacing the homogeneous focusing magnetic field by a system with alternate magnets. (France)

54082 (FRNC-CONF-58) PROJECT FOR THE SPECTROSCOPIC STUDY OF A PIG ION SOURCE. Dufay, M. (Paris Univ., Orsay (France). Institut de Physique Nucleaire). 1972. 2p. (In French). (CONF-720120-9). Dep. NTIS (U. S. Sales Only).

From Conference on the sources of multicharged ions; Paris, France (28 Jan 1972).

In a first stage a bulk statistical study is envisaged followed by a spatial resolution study. In a second stage, a dynamical study of the processes involved in the plasma formation and evolution is envisaged. (France)

54083 SCATTERING OF LOW-ENERGY RARE-GAS IONS FROM TUNGSTEN. Krauss, Roland Henry. Charlottesville, Va.; Univ. of Virginia (1972). 71p. University Microfilms Order No. 72-22,636.

Thesis.

Angular and energy distributions of He^{+}, Ne^{+}, and Ar^{+} ions scattered from a clean polycrystalline tungsten surface with incident energies ranging from 150 to 1000 eV were measured. Scattering angles ranged from 45 to 100 degrees for He^{+} scattering and from 30 to 100 degrees for Ne^{+} and Ar^{+} scattering. The energy distributions of ions scattered from a clean target surface are almost entirely typical of single collisions of the incident ions with effectively free tungsten atoms. Results are reported as the number of ions scattered per second within the solid angle of the detector vs. the scattering angle and also as the ratio of measured ion scattering cross section for scattering from a single layer of surface atoms to cross sections for single collisions with surface atoms obtained using a Bohr potential model. The ratio of measured ion scattering cross section to calculated cross section is always less than .07. (Diss. Abstr. Int., B)

54084 ION EMISSION FROM ELECTRON-BOMBARDED SOLIDS AND MASS-SPECTROMETER APPLICATIONS. Tsigel'man, G. E. (Special Design Bureau for Analytic Instrument Construction, Leningrad). Sov. Phys.-Tech. Phys. (Engl. Transl.); 17: No. 3, 525-7(Sep 1972).

Translated from Zh. Tekh. Fiz.; 42: No. 3, 667-9(Mar 1972).

Experimental measurements of the ion and neutral components in vapor emitted from bombarded solids (Ni, Al_2O_3, and NaCl) by a high-energy electron beam are described. Mass-spectrometer applications are considered. (auth)

54085 SURFACE AND VACUUM PHYSICS INDEX. VOLUME 7, No. 6, 1972. Bibliography, Author Index, Subject Index in Alphabetical Order, Cumulative Subject Index in Logical Order. Leopoldshafen, Ger.; Zentralstelle fuer Atomkernenergie-Dokumentation (1972). 74p.

This listing contains 269 references on various aspects of surface and vacuum physics. (M.O.W.)

54086 ION FOCUSING OF AN ELECTRON BEAM IN A TRANSVERSE GAS FLOW. Bliokh, P. V.; Glutsyuk, A. M.; Nazarenko, O. K.; Pats'ora, S. K. Radio Eng. Electron. Phys. (USSR) (Engl. Transl.); 16: No. 11, 1930-5(Nov 1971).

Translated from Radiotekh. Elektron.; 16: No. 11, 2183-9 (Nov 1971).

A theoretical analysis is presented of ion focusing of an electron beam under transverse gas flow conditions. For the experimental work, relative motion was created by moving the electron beam in a stationary gas. It is shown that the defocusing action of the space charge is observed at lateral electron beam velocities ≥ 1 km/sec. Experiments were performed with an electron beam 14 m long; the beam power was 0.4 to 3 kW for accelerating voltages of 20 to 60 kV. The residual gases were air, argon, and helium; the vacuum was 10^{-3} to 10^{-6} mm Hg. (auth)

54087 DETERMINATION OF ATOM-SURFACE PROPERTIES FOR Ne-LiF BY SCATTERING STUDIES. McClure, J. Doyle (Boeing Scientific Research Labs., Seattle). J. Chem. Phys.; 57: No. 7, 2823-9(1 Oct 1972).

The preceding paper (J. Chem. Phys., 57: 2810(1972)) contains a quantitative comparison of calculated and experimental intensity distributions for atomic beams of Ne scattered from the (001) LiF surface. Those results imply self-consistency of both the scattering model and the semiempirical atom-surface potential derived from the study, since a large number of observables are predicted on the basis of a semiempirical potential determined by appropriate choice of three disposable parameters. A systematic trials study used both to determine these potential parameters from a limited part of the experimental data and to assess the significance of uncertain values of other parameters associated with the scattering model is reported here. The trials study clarifies mechanisms associated with scattering phenomenology and permits one to identify characteristic features of the colorful intensity structure (surface rainbows) with specific physical parameters that influence the atom–surface interaction. The use of scattering theory to extract atom–surface properties from experimental observables is dependent on the latter relationship. (auth)

54088 HIGH-RESOLUTION CALCULATIONS ON ATOM–SURFACE SCATTERING: METHOD AND COMPARISON WITH EXPERIMENT FOR Ne–LiF. McClure, J. Doyle (Boeing Scientific Research Labs., Seattle). J. Chem. Phys.; 57: No. 7, 2810-22(1 Oct 1972).

Calculated scattering distributions for Ne on (001) LiF are compared with corresponding experimental distributions. For calculational purposes, the surface is effectively modeled by a monolayer of 3D harmonic oscillators representing F^- ions. The atom–surface potential at close range is assumed to arise from two-body dispersion–exchange interactions, which are represented by superposed Lennard–Jones (12, 6) model potentials. The foregoing potential is shown to be large with respect to that due to induced-dipole interaction. The long-range van der Waal's potential, for which the strength is independently specified, is taken to be one-dimensional in nature. The classical trajectory method combined with Monte Carlo distribution of surface impact coordinates and thermal states of gas surface atoms is used to determine angular distributions of scattered beam intensity. Physical concepts underlying an efficient calculational algorithm required for high-resolution scattering calculations are described. For a variety of incident beam conditions, including variation of beam "temperature," angle of incidence, and azimuth of the plane of incidence, calculated angular positions of dominant intensity peaks in the scattered beam typically agree with experimental determinations to within 3 to 5°. Predictions of high-intensity "ridge" structure, which is quite different in form for the ⟨010⟩ and the ⟨110⟩ planes of incidence, are confirmed by experimental studies undertaken elsewhere. Calculated values of absolute scattering probability in the plane of incidence typically agree with prior experimental determinations to within 10 to 15%. Statistical fluctuations in the calculated intensities (~5 to 10% of the calculated value) preclude a rigorous determination of whether or not the model reproduces all observed substructure on the high-intensity ridges. The parameters defining the semiempirical Ne–LiF potential used in the present study correspond to a heat of adsorption of ~0.016 eV and to a two-body range parameter of 3.9 Å. Means for determination of the potential parameters from a small part of the available experimental data and means for assessing the accuracy of these values are reported in a companion paper. (auth)

54089 MODEL FOR THE REPULSIVE ELASTIC SCATTERING OF ATOMS BY SOLID SURFACES. Goodman, Frank O. (Univ. of Waterloo, Ont.); Liu, William S.; Cabrera, Nicolas. J. Chem. Phys.; 57: No. 7, 2698-2702(1 Oct 1972).

A model is developed, enabling the intensities of diffracted beams to be calculated in closed form, starting from a pairwise (Yukawa-type) interaction law between a gas atom and a solid atom. The treatment is more satisfying than most previous treatments, which calculate the diffracted intensities as functions of empirical parameters describing the overall gas–solid interaction, without reference to the microscopic (pairwise) interaction. The model is illustrated by an application of the He–LiF system. (auth)

Atomic and Molecular Properties

Refer also to abstracts 53803, 54111, 54134, 54145, and 54375.

54090 OBSERVABILITY OF THE H_3^+ FUNDAMENTAL SPECTRUM. Patch, R. W. (Lewis Research Center, Cleveland). J. Chem. Phys.; 57: No. 6, 2594-5(15 Sep 1972).

Two studies of the possibility of observing the dipole-allowed fundamental transition in H_3^+ in an infrared absorption experiment are reported briefly. The first study was based on a box model for the fundamental band, which is a reasonable approximation if the spectral lines overlap. The second study was based on the assumption that the H_3^+ fundamental has discrete lines rather than the overlapping lines assumed in the box model. It is concluded that the H_3^+ spectrum would be difficult to observe in the laboratory, but there is a good possibility that it could be observed in high-resolution measurements of the spectra of stars or planets if infrared absorption by the Earth's atmosphere were eliminated. (A.G.W.)

54091 PHOTOIONIZATION OF EXCITED H_2 MOLECULES. Cohn, Arthur (Air Force Cambridge Research Labs., Bedford, Mass.). J. Chem. Phys.; 57: No. 6, 2456-8(15 Sep 1972).

The photoionization cross sections of the singly excited H_2 states are calculated. The Coulomb approximation method utilizing the Temkin–Vasavada electron–H_2^+ scattering phase shifts is used. Cross sections of ~1 to 2 × 10^{-17} cm^2 are found for all states at threshold, the same range as found for H (n = 2) atoms. (auth)

54092 PERTURBATION CALCULATION OF THE NUCLEAR SPIN–SPIN COUPLING CONSTANT IN HD BASED ON THE BARE-NUCLEUS POTENTIAL. Schulman, Jerome M.; Kaufman, D. Neal (Polytechnic Inst. of Brooklyn). J. Chem. Phys.; 57: No. 6, 2328-32(15 Sep 1972).

Perturbation calculations of the Fermi contact part of the electron-coupled nuclear spin–spin coupling constant (J) in the HD molecule were performed in the bare-nucleus potential. A very large Gaussian basis was employed, and, in addition, the effect on J of varying the HD internuclear separation was considered. The term zeroth order in correlation, J_0, is in good agreement with an independent basis set study as is the geometric approximate to the coupled Hartree–Fock value. The J_0 and J_1 values reported here differ significantly from those reported in a recent bare-nucleus perturbation study using numerical H_2^+ orbitals. A refined value of previous Hartree perturbative results based on this larger atomic basis set is given. (auth)

54093 ONE DIMENSIONAL HYDROGEN ATOM WITH A REPULSIVE CORE. Care, C. M. (Univ. of Sheffield, Eng.). J. Phys., C (London); 5: No. 14, 1799-1805(24 Jul 1972).

The problem of an electron moving in a one-dimensional Coulomb potential $e^2/|x|$ is of interest in connection with the energy levels of the hydrogen atom in a strong magnetic field. It is shown that the ground-state energy of the one-dimensional hydrogen atom is profoundly changed if a repulsive core is included in the Coulomb potential. The sensitivity of the ground-state energy to this repulsive potential is investigated, and it is found that if the core is sufficiently "hard" the ground-state energy is very nearly the first Balmer energy. The results appear to be relevant to the Yafet–Keyes–Adams (J. Phys. Chem. Solids, 1: 137 (1956)) theory of a hydrogen atom in a strong magnetic field and suggests that this theory may need modification. (auth)

54094 LIGHT-INTENSITY DEPENDENCE OF THE MULTI-PHOTON IONIZATION PROBABILITY IN THE RESONANCE CASE. Bakos, J.; Kiss, A.; Szabo, L.; Tendler, M. (Central Research Inst. for Physics, Bupadest). Phys. Lett.; 41A: No. 2, 163-4 (11 Sep 1972).

The general intensity dependence of the five-photon ionization probability of triplet metastable helium was measured. (auth)

54095 OPTICAL 4d → 4f TRANSITION AND THE BINDING ENERGY OF THE 4d LEVEL IN La AND Ce. Suzuki, S; Nagakura, I.; Ishii, T.; Satoh, T.; Sagawa, T. (Tohoku Univ., Sendai). Phys. Lett.; 41A: No. 2, 95-6(11 Sep 1972).

The comparison between the optical absorption spectra due to the 4d → 4f transition and the photoemission lines due to 4d electrons in lanthanum and cerium shows that a simple-band theoretical interpretation cannot be applied to the 4d → 4f transition. (auth)

Positronium, Muonium, and Mesic Atoms and Molecules

Refer also to abstracts 54119, 54568, and 55064.

54096 PRODUCTION OF MUONIUM IN A VACUUM BY DIFFUSION FROM A HOT METAL FOIL. Kendall, Kenneth Robert. Tucson, Ariz.; Univ. of Arizona (1972). 79p. University Microfilms Order No. 72-21,437.

Thesis.

The first observation of muonium produced in a vacuum is reported. A special very-low-momentum muon channel is described. The muon production technique yields a 100% polarized beam. The muons were stopped in a 0.001″ metal foil. When the foil is heated, muonium is produced by muons diffusing to the foil surface and evaporating into an evacuated chamber. Production rates for the metals Pt, W, Mo, and Ta were measured. Approximately 10% of the stopping beam can be made to form muonium by this method. The application of this technique to search for muonium–antimuonium conversion is discussed. By taking advantage of the similarity between muons and hydrogen in solids this technique may be used as a probe for studying gas–solid chemistry on a microsecond time scale. (Diss. Abstr. Int., B)

54097 DOPPLER BROADENING OF POSITRON ANNIHILATION PHOTONS IN SILVER HALIDE CRYSTALS FOLLOWING HIGH-ENERGY IMPLANTATIONS OF C^{5+}, N^{5+}, O^{6+}, AND S^{6+}. Leber, R. Eric; Lambrecht, Richard M. (Brookhaven National

Lab., Upton, N. Y.). J. Chem. Phys.; 57: No. 6, 2273-6(15 Sep 1972).

The Doppler broadening of positron annihilation photons detected by a Ge(Li) detector was employed to probe the interactions of positrons in high purity AgCl and AgBr (95%) + AgCl sheet crystals that had been exposed to 10^{11} to 10^{13} ions cm^{-2} of implanted $^{12}C^{5+}$, $^{14}N^{5+}$, $^{16}O^{6+}$, or $^{32}S^{6+}$. The narrowing of the Doppler broadened spectrum varied with the implanted ion, the concentration of the dopant, and the composition of the halide crystals. The decrease in linewidth is attributed to the electronic environment of the defects and an increased probability of annihilation of near-thermal positrons with conduction electrons relative to annihilation with core electrons. (auth)

54098 ELECTRIC MULTIPOLE TRANSITIONS IN MESIC ATOMS. Savushkin, L. N. Vestn. Leningrad. Univ., No. 22, Fiz., Khim.; No. 4, 146-7(Nov 1971). (In Russian).

The corrections to the long-wavelength approximation in the example of x radiation from heavy muonic atoms were estimated. The transitions of electric type are considered, with the relativistic hydrogen-like wave functions being used for the calculations. In the case of muonic ^{208}Pb the corrections to the long-wavelength approximation appear to be essential. (auth)

54099 DEPOLARIZATION OF NEGATIVE MUONS IN WATER AND AQUEOUS SOLUTIONS. Dzhuraev, A. A.; Evseev, V. S.; Obukhov, Yu. V.; Roganov, V. S. (Joint Inst. for Nuclear Research, Dubna, USSR). Zh. Eksp. Teor. Fiz.; 62: No. 6, 2210-20(Jun 1972). (In Russian).

The dependence of negative-muon depolarization on temperature and hydrogen peroxide concentration is measured in various aqueous solutions located in longitudinal or transverse magnetic fields. It is shown that the experimental data are not inconsistent with the familiar concepts regarding the behavior of free radicals in aqueous solutions. The residual polarization in a water solution of hydrogen peroxide is found to be 1.8 times higher than that in pure water. This is interpreted as being the result of chemical interaction between mesic nitrogen and hydrogen peroxide molecules leading to the formation of diamagnetic compounds. It is shown that the degree of depolarization does not depend on the magnetic field strength. According to the depolarization model in which mesic-nitrogen chemical reactions are taken into account, this signifies that the mesoatom enters the chemical reactions during a time $t \approx 10^{-11}$ s at T = 300°K; the paramagnetic products of these primary reactions involving mesic-nitrogen then participate in secondary reactions during a time $t_1 \lesssim 10^{-7}$ s. The rate constants of the reactions leading to the formation of diamagnetic products can be obtained by treating the concentration and temperature dependences of depolarization in an aqueous solution of hydrogen peroxide in accordance with the model assuming chemical reactions between the mesoatom and H_2O_2 molecules. The order of magnitude of the constant $k \approx 3 \times 10^{-11}\ s^{-1} \cdot cm^3$ is the same as that of the constant for reactions between free H and OH radicals in water. The temperature dependences of residual depolarization in water and a water solution of hydrogen peroxide are the same and consistent with the concept that the mesic-nitrogen reactions are chemical reactions limited by diffusion. (auth)

54100 INTENSITY OF ORTHO-POSITRONIUM COMPONENT IN LIQUID AND SOLID AMIDES. Ito, Yasuo; Tabata, Yoneho (Tokyo Univ.). Chem. Phys. Lett.; 15: No. 4, 584-5(1 Sep 1972).

Lifetime measurements of positrons in polar media were made. It was suggested from the experiments that positrons are captured in liquid or amorphous media, owing to the strong dipolar electric field of polar groups that are free from surrounding molecules. (auth)

Collision Phenomena

Refer also to abstracts 54008, 54033, 54279, and 54280.

54101 (EUR-CEA-FC--630) LARGE-ANGLE SCATTERING OF NEUTRAL PARTICLES IN THE 40 TO 100 keV RANGE. Eliot, M. (Commissariat a l'Energie Atomique, Fontenay-aux-Roses (France). Centre d'Etudes Nucleaires). Feb 1972. 101p. (In French). Dep. NTIS (U. S. Sales Only).

Thesis. Submitted to Paris Univ., Orsay (France).

The angular distributions of elastically scattered neutral particles (atoms) were measured for different projectile—target systems for energies in the 40- to 100-keV range. The experimental angular-distribution curves are compared with the theoretical differential-cross-section curves. This comparison demonstrates that for the light systems studied the Po = No/N ratio remains constant and independent of the energy of the incident particle. The results are consistent with those obtained for ion—atom collisions. In contrast, heavy systems present angular distributions decaying more rapidly than the theoretical curves. Information on the importance of ionization phenomena in relation to the angle and energy can be derived from these distributions. The close association between the form of the angular distributions and the distance of closest approach in relation to the scattering angle was also demonstrated. The differential cross sections, distances of closest approach, and the impact parameters were determined as a function of the b/a parameter for angles between 2° and 175° (center of mass system). These calculations were made using the Thomas—Fermi potential in the Firsov approximation. (France)

54102 (EUR-CEA-FC--644) ENERGY SPECTRA OF THE DISSOCIATION PRODUCTS OF CH_n^+ IONS ($1 <= n <= 5$) WITH A MOLECULAR NITROGEN TARGET. Julienne, A. (Commissariat a l'Energie Atomique, Fontenay-aux-Roses (France). Centre d'Etudes Nucleaires). May 1972. 65p. (In French). Dep. NTIS (U. S. Sales Only).

Thesis. Submitted to Paris Univ., Orsay (France).

The various collisional dissociation reactions of CH_n^+ ions were studied with respect to production of H^0 neutral particles. The important role of the vibrations in molecular-ion predissociation is demonstrated, and the most probable electronic states of CH^+ ions before collision are determined from the various lifetimes of the competing processes. The correlations between certain states of CH_3, CH_3^+, and their dissociation products are studied. The experimental conditions, the measuring method, and the cms transformation of the energy spectra are briefly described. The spectra from CH^+ and CH_n^+ dissociation ($2 <= n <= 5$) are studied in detail. (France)

54103 (FRNC-CONF--51) PROCESSES OF FORMATION OF MULTIPLY CHARGED IONS BY ELECTRON IMPACT. Abouaf, R. (Paris Univ., Orsay (France)). 1972. 21p. (In French). (CONF-720120--6). Dep. NTIS (U. S. Sales Only).

From Conference on the sources of multicharged ions; Paris, France (28 Jan 1972).

The various processes involved in atom ionization by electrons with an energy between 0 and a few keV are surveyed: the direct process involving the ejection of one or many electrons from the outer shells, and the processes associated with preionization with the ejection of an electron from an inner shell. The radiative and nonradiative (Auger) reorganization processes are considered for Ne, Kr, and W; the shake-off process is also envisaged. The cross sections obtained for Ca^{2+}, Sr^{2+}, Al^{2+}, Al^{3+}, In^{7+}, and In^{8+} are given. (France)

54104 K-SHELL IONIZATION CROSS SECTIONS FOR 2.04-MeV ELECTRONS. Scholz, W. (State Univ. of New York, Albany); Li-Scholz, Angela; Colle, R.; Preiss, I. L. Phys. Rev. Lett.; 29: No. 12, 761-4(18 Sep 1972).

K-shell ionization cross sections were measured at 2.04-MeV incident electron energy for 32 elements from V (Z = 23) to Bi (Z = 83). Measured cross sections drop from a value of 353 b at V to 9.9 at Bi. The general trend of the Z dependence of the cross sections is in agreement with theoretical predictions of Kolbenstvedt. However, variations in cross sections by as much as 30% from one element to the next are not accounted for by the theory. (auth)

54105 STRIPPING IN COLLISIONS BETWEEN HYDROGEN MOLECULES. Peterson, Robert Keith. Houston, Tex.; (Univ. of Houston (1971). 92p. University Microfilms Order No. 72-22,361.

Thesis.

The cross sections for the production of fast molecular ions in collisions of H_2 on H_2 and D_2 on D_2 were measured at lab kinetic energies between 50 and 500 eV. The cross section for the H_2 reaction ranges from 2.2×10^{-17} cm^2 at 500 eV to 5.0×10^{-18} cm^2 at 50 eV. The D_2 cross section varies from 1.7×10^{-17} to 3.8×10^{-18} cm^2 in the same energy range. The angular dependence of the reaction products was found to be highly peaked in the forward direction so that for the geometry used, practically all fast ions left the collision chamber for energies above 100 eV. The angular loss was found to be within reasonable limits at the lowest energies. The total stripping cross sections for H_2 and D_2, when plotted vs. incident velocity, are found to approach the same values at the highest velocities. The two cross sections diverge toward lower velocities as they approach their respective cutoffs where each process becomes energetically impossible. These cross sections have been found to fit a theoretical model based on ideas first presented by Demkov and Komarov (Sov. Phys. JETP, 23: 189(1966)). in which ionization is presumed to take place via a series of pseudocrossings of the initial state into the continuum of the adiabatic states of the collision complex. For the interaction of two hydrogen molecules, the internuclear separation of each molecule is assumed fixed and the adiabatic states are defined in terms of the distance between the two molecular centers (R). Best agreement between the observed cross sections and those predicted from the model is obtained by assuming the transition region to be centered around R = .43 A, 16.5 eV above the energy of the ground state at large R. For the purpose of monitoring the neutral beam intensity, the secondary-electron emission coefficients (γ) were measured for H_2 and D_2 impinging on a brass surface. The γ values were found to vary from .77 and .65 at 500 eV to .045 and .020 at 50 eV for H_2 and D_2, respectively. (auth) (Diss. Abstr. Int., B)

54106 DISTORTED-WAVE THEORY AND ITS APPLICATION TO THE EXCITATION OF THE ^1p STATES OF HELIUM AND MERCURY. Madison, Don Harvey. Tallahasse, Fla.; Florida State Univ. (1972). 188p. University Microfilms Order No. 72-21,319.

Thesis.

Theoretical results are given for the application of the distorted-wave approximation to the excitation of atoms by electron impact. The antisymmetrized atomic wave functions are assumed to be L−S coupled initially and arbitrarily coupled finally. Expressions for the differential cross section and spin polarization of the emitted electrons are given for unpolarized electron beams incident upon unpolarized atoms. These results are applied to the excitation of the 1s2p $^1p_1$ state of helium and the excitation of the 6s6p $^1P_1$ state of mercury. For the case of helium, differential and integral cross sections are given for incident-electron energies between 26.5 and 300 eV. The distorted-wave results are compared with experimental work and previous theoretical work. It is found that the distorted-wave calculations are superior to the previous theoretical calculations in fitting the absolute magnitude and angular distribution of the experimental data. Almost complete agreement with experiment is obtained for the higher energies. For the case of mercury, differential cross sections and spin polarizations of the emitted electrons are given for incident-electron energies between 25 and 180 eV. The distorted-wave calculations are compared with unnormalized experimental data and with the plane-wave Born approximation. It is found that the distorted-wave results give good agreement with the experimental spin polarizations and with the shape of the experimental differential cross sections. Again almost complete agreement with experiment is obtained for the higher energies. For both atoms, it is found that the differential cross sections given by the Born approximation fail by several orders of magnitude at large angles. (Diss. Abstr. Int., B)

54107 WKB APPROXIMATION IN TIME-DEPENDENT SCATTERING THEORY, INCLUDING REARRANGEMENT PROCESSES. Eu, Byung Chan (McGill Univ., Montreal). J. Chem. Phys.; 57: No. 6, 2531-7(15 Sep 1972).

The classical correspondence of the S matrix for scattering processes is examined with a view to obtaining the classical approximation and also to clarifying the nature of the approximations required for the classical formula. In this discussion the Schroedinger equation in the momentum representation is employed instead of the usual coordinate representation in order to provide a more direct route to the classical limit of the S matrix. The S matrix thus obtained essentially corresponds to the WKB approximation, and, with a further approximation, leads to Miller's expression except for a multiplicative factor and an additional phase which are in general not equal to 1 and 0, respectively. The classical limit is also discussed in terms of the Wigner−Moyal phase space distribution function, and, when the classical limit of this function is taken, an additional factor and phase appear in the S matrix. (auth)

54108 STUDY OF ELECTRON EXCITATION CROSS SECTIONS OF THE HELIUM ATOM AND NITROGEN MOLECULE. Chung, Sunggi. Norman, Okla.; Univ. of Oklahoma (1972). 185p. University Microfilms Order No. 72-22,438.

Thesis.

The formalism of the close-coupling method is used to study the indirect coupling effects on cross sections for electron-induced excitation of atoms via intermediate states. It is found that the indirect coupling potentials are as important as or even more important than the direct coupling potential in the case of excitation to dipole-forbidden states, whereas they are not too important in the case of excitation to dipole-allowed states. A detailed examination is presented as to the important intermediate states that must be considered given the initial and final states of excitation. The sensitivity of the computed cross sections to the accuracy of the wave functions used in the computation is also presented. Excitation cross sections of the nitrogen molecule were also studied. Application of Gaussian-type orbitals to the computation of excitation cross sections of electronic states of the nitrogen molecule reduces the computational complexity to the level of the corresponding atomic case. The excitation cross sections of twelve electronic states of the nitrogen molecule are presented. The Born approximation was used throughout; however, the exchange effects were included by means of Ochkur's and Rudge's modifications of the Born−Oppenheimer approximation. Four different sets of wave functions are used to determine how the computed cross sections depend on the accuracy of the wave functions employed in computation, including the one with Gaussian-type basis functions calculated here. (TSS) (Diss. Abstr. Int., B)

54109 TIME-OF-FLIGHT ANALYSIS OF NEUTRAL PRODUCTS FROM INELASTIC ION−MOLECULE COLLISIONS. Conrads, R. J.; Pomerance, W.; Moran, T. F. (Georgia Inst. of Tech., Atlanta). J. Chem. Phys.; 57: No. 6, 2648-71(15 Sep 1972).

Cross sections for inelastic charge-transfer reactions producing neutral excited atoms were measured for the interactions of 500- to 1500-eV He^+ ions with He. Time-of-flight methods coupled with post acceleration techniques were used to separate neutral from charged products of ion−molecule reaction. The position of inelastic peaks appearing in the neutral product energy loss spectra is consistent with the excitation of colliding particles to known spectroscopic excitation potentials with the relative importance of inelastic scattering decreasing as the reactant ion kinetic energy is lowered. (auth)

54110 COLLISIONS OF FAST ELECTRONS WITH HELIUM. 2. IDENTITIES SATISFIED BY THE SECOND BORN SCATTERING AMPLITUDE. Woollings, M. J. (Royal Holloway Coll., Englefield Green, Eng.). J. Phys., B (London); 5: No. 8, L164-6 (Aug 1972).

It is shown that the second Born scattering amplitude satisfies relationships analogous to the optical theorem and the dispersion relation of Gerjuoy and Krall (Phys. Rev., 119: 705(1960)). (auth)

54111 SUPERHEAVY ELECTRONIC MOLECULES. Rafelski, J.; Mueller, B.; Greiner, W. (Univ., Frankfurt am Main). Lett. Nuovo Cim.; 4: No. 11, 469-74(15 Jul 1972).

The possibility that the two nuclei involved in heavy-ion collisions may approach so closely that even the inner electrons belong to both nuclei is considered. The effective potential for the resulting superheavy molecule is defined and calculated. The calculations are based on two assumptions: that the movement of the nuclei is adiabatic compared to that of the electrons and that the inner shells are filled with electrons. It is concluded that the formation of intermediate superheavy electronic molecules will lead to deviations from the standard Rutherford scattering and will show up particularly in the angular distribution. (A.G.W.)

54112 ELECTRON EMISSION IN NEGATIVE ION AND ATOM COLLISIONS IN THE SUDDEN-SWITCHING APPROXIMATION. Bronfin, F. B.; Ermolaev, A. M. Vestn. Leningrad. Univ., No. 22, Fiz., Khim.; No. 4, 29-34(Nov 1971). (In Russian).

A nonstationary quantum problem in which the bound state of a quantum system first approaches and then for a certain time merges with the continuous energy spectrum because of the variation of an external parameter was considered. The above conditions may occur during the collisions between negative ions and atoms. The energy distribution of the emitted particles (electrons) was obtained and the probability of the emission was determined. (auth)

54113 DETERMINATION OF ABSOLUTE DIFFERENTIAL CROSS SECTIONS FOR THE $1^1S \rightarrow 4^1D$ TRANSITION OF THE HELIUM ATOM. Peresse, J.; Pochat, A.; Gelebart, F. (Faculte des Sciences, Brest, France). Phys. Lett.; 41A: No. 2, 135-6 (11 Sep 1972). (In French).

Absolute differential cross sections are determined by measuring delayed coincidences between inelastically scattered electrons and the subsequent decay photons. Preliminary results are given for the $1^1S \rightarrow 4^1D$ transition of helium. (auth)

54114 ISOTOPE DEPENDENCE OF K-SHELL IONIZATION CROSS SECTIONS BY ^{20}Ne AND ^{22}Ne BOMBARDMENTS. Takasaki, M.; Shima, K.; Terashima, Y.; Sakai, S. (Kyoto Univ.). Phys. Lett.; 41A: No. 2, 181-2(11 Sep 1972).

Ionization cross sections of Mg and Al K shells were measured by bombarding with 0.7- to 7.4-MeV ^{20}Ne and ^{22}Ne isotopes. No isotope dependence was observed within experimental error; this agrees with a theory based on Coulomb deflection. (auth)

54115 CHARGE STATE ALTERATION PROCESSES IN COLLISIONS OF HYDROGEN ATOMS WITH HYDROGEN MOLECULES. Afrosimov, V. V.; Leiko, G. A.; Mamaev, Yu. A.; Panov, M. N.; Fedorenko, N. V. (Ioffe Inst. of Physics and Tech., Leningrad). Zh. Eksp. Teor. Fiz.; 62: No. 6, 2049-59 (Jun 1972). (In Russian).

The cross sections for all elementary processes of charge-state changes in $H-H_2$ interactions are measured by simultaneous mass analysis of the atomic particles produced in a single H^0-H_2

collision and recording by the coincidence technique. The energy of the impinging fast hydrogen atoms T_0 was varied between 5 and 50 keV. It is found that the main contribution to slow H_2^+ and H^+ ion formation is by ionization processes, i.e., by processes in which one or two electrons are removed from the target molecule and the charge state of the fast particle (H) remains unchanged. It is found that for ionization and electron capture by the H atom the electron-state populations of the target molecule ($1s\sigma_g$, $2p\sigma_u$, electron-excited state of the H_2^+ ion, and the state formed by two protons $H^+ + H^+$) are practically the same. On the other hand for ionization of molecules with simultaneous stripping of the impinging atom H the population of the upper states ($2p\sigma_u$ and $H^+ + H^+$) is higher. It is found that an appreciable role in dissociation processes of the target molecule is played by direct transfer of kinetic energy to nuclei by the incident particle. This effect is most important in elementary ionization processes involving dissociation in the case of H^+-H_2 and for stripping with ionization and dissociation for $H-H_2$. (auth)

54116 ELECTRON CAPTURE FROM HYDROGEN NEGATIVE IONS BY FAST PROTONS. Janev, R. K. (Inst. of Physics, Belgrade); Salin, A. Fizika (Zagreb); 4: No. 3, 165-72(Jul 1972).

A generalization of the continuum distorted-wave method of Cheshire is made for electron capture in proton—negative-ion collisions. The attractive Coulomb interaction of the partners in the initial state is fully taken into account in this method. For reasons of simplicity of derivations, the generalization is given on the $p + H^-$ system. The cross section for this reaction is calculated in the continuum distorted-wave-Born approximation. (auth)

54117 INELASTIC e–H AND e–He COLLISIONS IN THE ADIABATIC APPROXIMATION. Burnashev, M. A.; Janev, R. K.; Ob'edkov, V. D. (Leningrad State Univ.). Fizika (Zagreb); 4: No. 3, 157-63(Jul 1972).

Using a diagonalized form of the interaction matrix in the electron—atom scattering problem (adiabatic representation), some excitation and spin-change processes are calculated in e—H and e—He collisions. The configuration mixing of the diabatic states, allowing for the correlation effects in the system, is shown to be a significant factor in determining the near-threshold behavior of the inelastic cross section. The calculations demonstrate the superiority of the adiabatic representation with respect to the Born method even in the first order of the theory. The results are compared with more elaborate calculations in the Vainshtein and close-coupling methods as well as with the experimental data. (auth)

54118 EXCITATION IN HEAVY-PARTICLE COLLISIONS. Thomas, E. W. Wiley-Interscience Series in Atomic and Molecular Collisional Processes. New York; John Wiley and Sons, Inc. (1972). 449p. $22.50.

All available data, published between 1945 and Jan. 1, 1970, on the formation of specific excited states of atomic and molecular systems as a result of collisions between atoms, ions, and molecules are tabulated and critically evaluated. Areas included are (1) processes of direct excitation, (2) simultaneous removal of one or more electrons and excitation of an electron that remains bound, (3) transfer of an electron from one of the collision systems into the excited state of the other, and (4) dissociation of molecules giving rise to excited atomic and molecular fragments. Criteria that must be fulfilled in order for an experiment to be considered a valid and accurate measurement are formulated, and experimental techniques are examined in relation to these criteria. The compilation includes a complete bibliography of all work discussed (362 references), an appendix listing data published after Jan. 1, 1970 (89 additional references), a summary index to collisional excitation mechanisms, and tables reproducing the most highly reliable data. (A.G.W.)

54119 MEASUREMENT OF TOTAL CROSS SECTIONS FOR LOW ENERGY POSITRON-HELIUM COLLISIONS. Canter, K. F.; Coleman, P. G.; Griffith, T. C.; Heyland, G. R. (University Coll., London). J. Phys., B (London); 5: No. 8, L167-9(Aug 1972).

An efficient method for the conversion of the high-energy positrons emitted by ^{22}Na into slow positrons of energy about 1 eV was developed using the backscattering of positrons from a gold surface coated with magnesium oxide powder. These positrons were used for the measurement of the total cross section for positron—helium collisions at energies between 2 and 20 eV. A preliminary value for the positron—argon cross section at 8 eV is also given. (auth)

54120 SOME ENERGY CURVES OF ArH^+ AND THEIR USE IN THE STUDY OF THE SCATTERING OF H^+ BY Ar. Sidis, V. (Centre de Mechanique Ondulatoire Appliquee, Paris). J. Phys., B (London; 5: No. 8, 1517-28(Aug 1972).

Calculations on the ground state and some excited states of ArH^+ in the LCAO—STO—MO—SCF approximation are reported. The ground-state interaction potential is then used to study the elastic scattering of protons by argon atoms at low and moderate energies. Partial-wave calculations involving the JWKB evaluation of the phase shifts are compared to the available experimental results and subsequently used to improve the well depth obtained in the ab initio calculation. The values U = 4.3 eV and R_e = 1.34 Å are thus found. Qualitative discussions of the approximate excited states lead to the conclusions that the excitation of the argon target, at moderate energies, can take place only via the charge-exchange channel. This charge-exchange channel is itself coupled to the ground state at internuclear distances $1.70\ \text{Å} \lesssim R_x \lesssim 1.85$ Å. A tentative explanation of the preferential excitation of Ar^* ($3p^5\ 3d$) is given. (auth)

54121 ELECTRON LOSS IN ATOM-MOLECULE COLLISIONS. Mathur, K. C.; Tripathi, A. N.; Joshi, S. K. (Univ. of Roorkee, India). J. Phys., B (London); 5: No. 8, 1529-32(Aug 1972).

The cross sections for the electron loss from hydrogen atoms colliding with molecular targets H_2, N_2, and O_2 are calculated using the free collision model of Dmitriev and Nikolaev (Sov. Phys. JEPT, 17: 447(1963)). The molecules are treated under the separated-atom approximation, and the phase difference between the electrons scattered from the two atoms of the molecule is considered. The vibrational motion of the molecule is also accounted for. The results are compared with other calculations and experimental data. (auth)

54122 DIFFERENTIAL MEASUREMENTS ON ION-ATOM COLLISIONS IN THE ENERGY RANGE 500 TO 3000 eV. 4. H^+-NOBLE GAS ATOM COLLISIONS. Abignoli, M.; Barat, M.; Baudon, J.; Fayeton, J.; Houver, J. C. (Centre National de la Recherche Scientifique, Orsay, France). J. Phys., B (London): 5: No. 8, 1533-53(Aug 1972).

Collisions between H^+ and rare gas atoms (He, Ne, Ar, Kr, Xe) were studied in the energy range $0.5 \leq E_0$ (lab) ≤ 3 keV and in the angular range $0.5° \leq \theta \leq 10°$. Differential cross sections were measured for the main collision processes: elastic collision, charge exchange, simple excitation of the atom, and excitation of the atom to autoionizing levels. In most of the cases, the elastic cross sections are in rather good agreement with theoretical semiclassical, or semiquantal, cross sections calculated from ab initio potentials. As the atomic number of the target atom is increased, the charge-exchange probability becomes larger and shows a stronger angular dependence. These features are explained by considering the energy diagrams of the molecular systems, in which the "exchanged" state potential curves become closer to the ground state curve as heavier atoms are taken; in the case of Xe, a pseudocrossing of the two curves occurs and Stueckelberg's interferences are observed in the charge-exchange probability. The excitation process evolves in the same way as the charge exchange, but its threshold in τ is slightly larger. As no excited state (dissociating into H^+ plus the excited atom) interacts with the ground state, the excitation is considered as a two-step process, taking place via charge exchange. The excitation of the target atom to autoionizing levels is qualitatively explained, in the MO model framework, by the promotion of two p electrons and can be considered also as occurring via charge exchange. (auth)

54123 COLLISIONAL IONIZATION OF HELIUM BY SLOW ELECTRONS. Ehrhardt, H.; Hesselbacher, K. H.; Jung, K.; Willmann, K. (Univ. Trier-Kaiserslauter, Ger.). J. Phys., B (London); 5: No. 8, 1559-71(Aug 1972).

For single ionization of helium by electron impact the energies and scattering angles of the scattered and ejected electrons were measured in a coincidence experiment at primary energies E_0 between 30 and 80 eV. Two types of collision are found, those in which the momentum transfer to the ion produced is small (binary encounter) and those in which the momentum transfer is large (recoil encounter). The maximum in the measured coincidence rate due to collisions of the binary-encounter type is located in the forward direction. Its angular position varies with the collision parameters, whereas its angular half width is approximately 60° for all data obtained. The recoil collisions cause a maximum of the coincidence cross section at about 160° with a half width larger than 90°. The relative intensity of the binary-encounter and the recoil peaks as well as the total number of ionizing transitions depends strongly on the energies and angles of the two outgoing electrons. Binary peak and recoil peak do not have a common symmetry axis, probably because of the interaction between the two ionization electrons. (auth)

54124 COVENIENT DETERMINATION OF RESONANCE STATES IN ATOMIC COLLISIONS. Truhlar, Donald G. (Univ.

of Minnesota, Minneapolis). Chem. Phys. Lett.; 15: No. 4, 483-5(1 Sep 1972).

A new method, using the finite-difference boundary-value method, is proposed for finding the wave functions and energies of shape-resonance states in atomic collisions. A numerical illustration is presented for the $l = 50$ states of OH ($X^2\Pi$). (auth)

54125 TEST OF MASSEY'S METHOD FOR CALCULATING THE STATIC POTENTIAL FOR ELECTRON SCATTERING BY N_2. Truhlar, Donald G. (Univ. of Minnesota, Minneapolis). Chem. Phys. Lett.; 15: No. 4, 486-9(1 Sep 1972).

The method of linear combination of scaled atomic charge distributions, as invented by Massey, is tested for electron scattering by the nitrogen molecule. (auth)

54126 NEAR-RESONANT VIBRATION–ROTATION ENERGY TRANSFER IN ATOM–DIATOM COLLISIONS: $Ar-OH(A^2\Sigma^+)$. Smith, Wesley D.; Pack, Russell T. (Brigham Young Univ., Provo, Utah). Chem. Phys. Lett.; 15: No. 4, 500-4(1 Sep 1972).

Cross sections and rate constants for the inelastic collision, $OH(A^2\Sigma^+, \nu = 1, j = 15) + Ar \rightarrow OH(A^2\Sigma^+, \nu = 0, j = 20) + Ar$, were calculated in the infinite-order sudden (IOS) and distorted-wave (DW) approximations. The results agree well with experiment. (auth)

54127 THEORETICAL DESCRIPTION OF AN ASYMMETRIC, NONRESONANT CHARGE-TRANSFER PROCESS, $Li + Na^+ \rightleftharpoons Li^+ + Na$: THE TWO-STATE APPROXIMATION. Melius, Carl F.; Goddard III, William A. (California Inst. of Tech., Pasadena). Chem. Phys. Lett.; 15: No. 4, 524-9(1 Sep 1972).

The charge-transfer process for the collision $Li + Na^+ \rightleftharpoons Li^+ + Na$ was studied theoretically by a two-state impact-parameter approach using molecular wave function. By including the Born–Oppenheimer breakdown term $\langle\psi_1|\partial/\partial R|\psi_2\rangle$ as the coupling term between states, total charge-transfer cross sections in good agreement with experimental results are obtained. (auth)

54128 DETERMINATION OF OPTICAL SUMS FROM THE SMALL-ANGLE ELECTRON-IMPACT SPECTRA OF ARGON. Wellenstein, H. F.; Bonham, R. A. (Indiana Univ., Bloomington). Chem. Phys. Lett.; 15: No. 4, 530-5(1 Sep 1972).

A method for obtaining optical sums directly from high-energy (25-keV) electron-impact spectra in the forward direction is suggested. The electron energy-loss spectrum of argon at an energy resolution of ±600 meV was obtained for energy losses from zero to 50 eV and 200 to 300 eV at an energy resolution of 5 eV averaged over an angular range of $\pm 5 \times 10^{-4}$ radians. The data were corrected for finite detector size, gas and electron beam spatial distributions to obtain an estimate of the zero-angle scattering spectrum. A hydrogenic contribution was assumed for the 3p, 3s continuum for energy loss greater than 50 eV and for the 2p continuum for energy loss greater than 280 eV. Various moments of the spectrum were computed and related to optical sums by use of the measured experimental moments of the energy distribution of the incident beam and the scale factor needed to place the data on an absolute scale. The scale factor was obtained by use of the Thomas–Reiche–Kuhn sum rule. The results are in excellent agreement with previous estimates of the various sum rules and the present approach shows promise for providing useful data for a large number of atomic and molecular targets. (auth)

54129 THEORY OF SEMICLASSICAL TRANSITION PROBABILITIES FOR INELASTIC AND REACTIVE COLLISIONS. IV. CLASSICALLY-INACCESSIBLE TRANSITIONS CALCULATED BY INTEGRATION ALONG COMPLEX-VALUED TRAJECTORIES. Stine, J.; Marcus, R. A. (Univ. of Illinois, Urbana). Chem. Phys. Lett.; 15: No. 4, 536-44(1 Sep 1972).

Semiclassical S-matrix elements S_{mn} were calculated by numerical integration along complex-valued trajectories, by avoiding (simply) previously reported trajectory divergences. Now, one can numerically calculate even $|S_{mn}| \approx 10^{-11}$ for the Secrest–Johnson system (their lowest $|S_{mn}|^2$), instead of only $|S_{mn}|^2 > 10^{-3}$. Agreement is excellent. (auth)

54130 MEASUREMENTS OF ABSOLUTE INTEGRAL TOTAL CROSS SECTIONS OF $He-H_2$ AND THE INTERACTION POTENTIAL. Gengenbach, R.; Hahn, Ch. (Univ., Bonn). Chem. Phys. Lett.; 15: No. 4, 604-8(1 Sep 1972).

The integral total collision cross section for $He-H_2$ was measured with an absolute accuracy of ±1% to ±4% between 0.14 meV and 2.9 eV. The data have been fitted by a spherical symmetric multiparameter Morse-spline-dispersion potential, which agrees well with results of ab initio calculations at short distances. The long range attraction can be described by the theoretical van der Waals constant C_8, if the dipole–quadrupole interaction $-C_8R^{-8}$ with $C_8 = 41$ au is taken into account. The potential has one bound state for every possible isotopic combination. (auth)

54131 VIBRATIONAL EXCITATION OF A DIATOMIC MORSE OSCILLATOR BY IMPULSIVE COLLISION WITH AN ATOM. Eckelt, P.; Korsch, H. J. (Univ., Muenster, Ger.). Chem. Phys. Lett.; 15: No. 4, 586-9(1 Sep 1972).

The vibrational excitation of a diatomic Morse oscillator by collinear collision with a third atom is treated in the quantum-mechanical impulse approximation. A closed analytic expression for the transition probabilities $P_{n'n}$ is derived. Change in $P_{n'n}$ as a function of the kinetic energy and of the energy transfer if one passes over from a harmonic to a Morse oscillator is discussed. Some numerical results are given for the O_2^+-He system. (auth)

54132 INFLUENCE OF ATTRACTIVE FORCES ON THE QUANTUM-MECHANICAL TRANSITION PROBABILITIES FOR ATOM–DIATOMIC OSCILLATOR COLLISIONS. Roberts, R. E. (Indiana Univ., Bloomington); Diestler, D. J. J. Chem. Phys.; 57: No. 7, 2998-3002(1 Oct 1972).

Numerically exact quantum-mechanical transition probabilities for the collinear collision between an atom and a diatomic oscillator interacting via a strongly attractive Morse potential are compared with those obtained in various simple perturbation approximations. It is concluded that many of the improved perturbation approximations that work well for purely repulsive interactions are also quantitatively accurate for Morse interactions having deeply attractive wells. A simple distorted-wave correction factor, derived, for example, via second-order perturbation theory, yields quite accurate transition probabilities, even for very small reduced collision energies ($E_{coll}/D = 0.05$) where attractive forces dominate in determining the dynamics of the collision. Furthermore, when the perturbation limit is no longer applicable, the so-called exponential approximation provides a viable method for calculating both direct and multiquantum transition probabilities. (auth)

54133 QUANTUM MECHANICAL STUDIES OF THE VIBRATIONAL EXCITATION OF H_2 BY Li^+. White, R. Allen; Hayes, Edward F. (Rice Univ., Houston). J. Chem. Phys.; 57: No. 7, 2985-93(1 Oct 1972).

The quantum mechanical equations of motion for the vibrational excitation of an harmonic are solved via the set of coupled Volterra equations describing that motion. Numerical techniques that allow accurate inclusion of closed channels are developed. The equations are solved for an ab initio interaction potential and for a model potential. The ab initio interaction potential gives results in poor agreement with experiments. A comparison with the results of a two-parameter model potential, which can give results close to the experimental results, provides some insight into features of the surface which are important for vibrational excitation. (auth)

54134 TRANSLATIONAL ABSORPTION OF HeH. Ulrich, Bruce T. (Univ. of Texas, Austin); Ford, Lewis; Browne, J. C. J. Chem. Phys.; 57: No. 7, 2906-10(1 Oct 1972).

Calculation of the translational absorption spectrum of a system of a helium atom and a ground-state hydrogen atom is reported. Values of calculated potential curves for the ground state of the molecular system HeH and the dipole moment of the ground molecular state of HeH as a function of internuclear separation are also given. The behavior of the dipole moment is of particular interest as it passes through zero at about $R = 7a_0$. This change of sign follows from and correlates with the known long-range behavior of the dipole moment of this system. (auth)

54135 DISSOCIATIVE ATTACHMENT OF THERMAL ELECTRONS TO N_2O AND SUBSEQUENT ELECTRON DETACHMENT. Warman, J. M.; Fessenden, Richard W.; Bakale, G. (Carnegie-Mellon Univ., Pittsburgh). J. Chem. Phys.; 57: No. 7, 2702-11 (1 Oct 1972).

The attachment of electrons to nitrous oxide was studied, following pulse ionization, by a microwave conductivity technique. For pure N_2O, and N_2O diluted with N_2, extrapolation of the experimentally observed attachment rate constant to zero pressure gives an upper limit of 1×10^{-15} cm^3 $molecule^{-1} \cdot s^{-1}$ for the rate constant for two-body attachment at 298°K. When C_2H_6 or C_3H_8 is used as diluent a higher two-body rate constant of 6×10^{-15} cm^3 $molecule^{-1} \cdot s^{-1}$ is found, which is believed to represent the rate constant of the dissociative attachment reaction $e^- + N_2O \rightarrow N_2 + O^-$. The much lower value for pure N_2O or N_2O-N_2 mixtures is explained by the regeneration of electrons, via the reactions $O^- + N_2O \rightarrow NO + NO^-$ and $NO^- + N_2O \rightarrow NO + N_2O + e^-$, which largely nullifies the primary attachment step. The presence of a hydrocarbon prevents electron regeneration by irreversibly reacting with O^- and allows observation of the uncomplicated rate constant for dissociative attachment. The rate constant for dissociative attachment increases markedly with increasing temperature and in the range studied, 278 to 355°K, has an activation energy of 0.42 ± 0.04 eV. Confirming evidence for the proposed mechanism is obtained from the effect, on the attachment rate constant, of H_2 added to $C_2H_6-N_2O$ mixtures. The H_2 reacts with O^- by the associative detachment reaction $O^- + H_2 \rightarrow H_2O + e^-$ to nullify the primary attachment step and to reduce the rate constant by an appropriate amount. In the steady-state radiolysis of N_2O, the yields of the products N_2 and NO are found to increase markedly with decreasing pressure below 50 torr. These increases in yields may be quantitatively related to the chain reaction resulting from dissociative attachment followed by electron regeneration. (auth)

54136 DEPENDENCE OF REACTIVITY ON INTERNAL TRANSLATIONAL ENERGY IN K + SF_6, CCl_4, AND $SnCl_4$. Sloane, Thompson M.; Tang, S. Y.; Ross, John (Massachusetts Inst. of Tech., Cambridge). J. Chem. Phys.; 57: No. 7, 2745-55(1 Oct 1972).

The dependences of the nonreactive scattering of potassium atoms at thermal energies from SF_6, CCl_4, and $SnCl_4$ on internal energy of the molecules and initial relative kinetic energy are studied as a function of scattering angle. A collimated, velocity-selected beam of potassium atoms is crossed at right angles with a molecular beam whose source temperature is varied over the range of 300 to 580°K. The angular dependence of the nonreactive cross sections is analyzed with an optical model of chemical reactions to obtain information about potential parameters in an assumed form of two-body interaction, the threshold conditions for reaction, the probability of reaction as a function of the distance of closest approach and internal energy, as well as an estimate of the total reaction cross section. The threshold conditions, energy, and distance in the reaction K + SF_6 are independent of the initial relative kinetic energy at both low and high SF_6 temperatures; the threshold distance increases by about 6% from $T(SF_6) =$ 300°K to 580°K. The variation of the nonreactive scattering with the SF_6 beam source temperature, or SF_6 internal excitation, can best be explained by a model in which only the stretching vibrational modes of SF_6 are assumed to have an effect on the reactivity with K. The calculated differential cross sections based on this model fit very well to the measured results over the experimental ranges of SF_6 temperature and of initial relative kinetic energy (2.05 to 5.18 kcal/mole). The effect of internal energy in CCl_4 on its reactivity with K is similar to that of SF_6 but smaller. The effect in $SnCl_4$ is very small and uncertain; the interpretation is complicated by the lack of knowledge about the interaction potential. (auth)

54137 REACTIONS BETWEEN HYDROCARBON IONS CH_n^+ AND GASEOUS TARGETS, IN THE 40 TO 140 keV ENERGY RANGE. Roussel, M. (CEN, Fontenay-aux-Roses, France). J. Phys. (Paris); No. 4, 321-9(Apr 1972). (In French).

Some products of collisions between CH_n^+ ($0 <= n <= 4$) ions in the 40- to 140-keV energy range and gaseous targets (H_2, N_2, He, Ne, Ar) were studied. The cross sections for the following reactions were measured: charge exchange of C^+ ions, dissociation of CH_n^+ ions through reactions like $CH_n^+ \rightarrow CH_{n-p}^+$, and production of hydrogen atoms in coincidence with hydrocarbon ions through reactions like $CH_n^+ \rightarrow CH_{n-p}^+ + H + \ldots$. (France)

54138 COLLISIONS OF FAST ELECTRONS WITH HELIUM. I. VARIOUS FORMS OF THE SECOND BORN APPROXIMATION. Woollings, M. J.; McDowell, M. R. C. (Royal Holloway Coll., London). J. Phys., B (London); 5: No. 7, 1320-31(Jul 1972).

Various forms of the second Born approximation are applied to electron collisions with helium in the energy range 200 to 500 eV. In each case all intermediate states up to 3^1P are included explicitly, and a closure approximation is used for higher states, the energy parameter being chosen to fit the total cross section and dispersion relation values for Re f(0) and Im f(0). Calculations are carried out with and without V^4 terms and in a 1,1 Padé approximation, for the 1^1S, 2^1S, and 2^1P transitions. Results are compared with experiment and with results of other calculations. The present results cast doubt upon the practice of normalizing experiment to the first Born approximation at intermediate energies. (auth)

54139 ION-ATOM SCATTERING AND INTERATOMIC POTENTIALS FOR IONS OF NOBLE METALS AND PERIOD II ELEMENTS INCIDENT ON NEON AND ARGON WITH ENERGIES IN THE RANGE 8 TO 25 keV. Foster, C.; Wilson, I. H.; Thompson, M. W. (Univ. of Sussex, Brighton, Eng.). J. Phys., B (London); 5: No. 7, 1332-42(Jul 1972).

Information about the potential energy of interaction was obtained for the ions, Na^+, Mg^+, Al^+, P^+, Cl^+, Cu^+, Ag^+, Au^+, Ni^+, and Zr^+, on the inert gases Ar and Ne. The scattering of an ion beam in the energy range 8 to 25 keV by passage through a gas was used to measure incomplete total cross sections against energy curves, from which the parameters K and S in an assumed form for the potential $V(r) = K/r^s$ were determined. Theoretical potentials were compared with those obtained experimentally, and for the range of separation 1.1 Å to 1.6 Å a Moliere-type screened Coulomb potential was found to give good agreement, whereas the Thomas–Fermi potential of Firsov gave poor agreement. The variation of the potential with Z_1 was noted and thought to be a product of detailed atomic structure in a way not predicted by any statistically determined potential. (auth)

54140 INELASTIC PROCESSES IN He^+-He COLLISIONS. Barat, M.; Dhuicq, D.; Francois, R.; (and others) (Paris Univ., Orsay, France). J. Phys., B (London): 5: No. 7, 1343-50(Jul 1972).

Measurements are reported of the differential cross sections for excitation of inelastic processes in He^+-He collisions for the range of incident ion energy from 1 to 3 keV. The use of an improved energy analyzer permits the detection of a number of inelastic channels, hitherto unresolved. In particular, the excitation of He in the (1s2p) $^{1,3}P$ state is well separated from other channels; the reactions for the formation of $He^+(2p)$ and He^{2+} are studied for the first time. The results, which are given for scattering angles θ up to 8° in the laboratory system, confirm that for $E \gtrsim$ 4 keV deg, excitation occurs mainly via rotational coupling between the $^2\Sigma_u$ and $^2\pi_u$ states and between the $^2\Sigma_g$, $^2\pi_g$, and $^2\Delta_g$ states of the He_2^+ quasimolecule. As for the measurements of direct ionization, the oscillatory structure observed in the energy distribution of the ejected electrons for a given E is interpreted by a crossing mechanism between the $^2\Sigma_g$ state of He_2^+ and the $^2\Sigma_g$ continuum state of the system ($He_2^{2+} + e$). (auth)

54141 IONIZATION PROCESSES IN SLOW COLLISIONS OF HEAVY PARTICLES. I. He AND He^+ ON Ne, Ar, Kr, AND Xe. Gerber, G.; Morgenstern, R.; Niehaus, A. (Univ., Freiburg i. B.). J. Phys., B (London); 5: No. 7, 1396-1411(Jul 1972).

Apparatus for the investigation of ionizing collisions of heavy particles by electron spectroscopy is described. Collisions of He^+ and He on Ne, Ar, Kr, and Xe are studied in the kinetic-energy range from 100 to 5000 eV by measurement of energy spectra and angular distributions of the ejected electrons. As in collisions at higher energies, the spectra are composed of discrete peaks arising from autoionizations of the separated particles and a continuous part. This latter part is much more pronounced for collisions with He^+. A mechanism for the production of the continuous part is proposed, which explains this fact. The angular distributions of electrons of discrete energies (peaks) are found to be nonisotropic in some cases and dependent on the collision energy. In one case the distribution is asymmetric with respect to $\theta = \pi/2$ (angle measured from beam direction). (auth)

54142 ELASTIC SCATTERING OF 5 TO 90 eV NEUTRAL GOLD ATOMS BY ARGON. Foster, C.; Wilson, I. H.; Thompson, M. W. (Univ. of Sussex, Brighton, Eng.). J. Phys., B (London); 5: No. 7, L140-2(Jul 1972).

The velocity dependence of the total elastic cross section for 5- to 90-eV gold neutrals on Ar was measured. Information about the interaction potential was obtained, which shows evidence of a Lennard-Jones type of behavior. A similarity of the Cs–Ar case is noted. (auth)

Atomic Theory

Refer also to abstracts 54374, 54382, and 55077.

54143 OPTIMIZATION OF THE TRANSFERABILITY OF ATOMIC HARTREE-FOCK VALENCE-SHELL ORBITALS. Adams, William H. (Rutgers–The State Univ., New Brunswick, N. J.). J. Chem. Phys.; 57: No. 6, 2340-3(15 Sep 1972).

Two procedures by which atomic valence-shell orbitals may be transferred between atoms were studied numerically. The one procedure optimizes the overlap between transferred and true orbitals, and the second optimizes the electronic energy calculated with the transferred orbitals. The two procedures give significantly different results. Both improve on the results obtained in a previous study. (auth)

54144 ATOMS IN INTENSE MAGNETIC FIELDS AND AN ATTRACTIVE ALTERNATIVE TO THE THOMAS–FERMI MODEL OF ATOMS. Mueller, Ronald Otto. New York; New York Univ. (1972). 126p. University Microfilms Order No. 72-21,526.

Thesis.

The enormous magnetic fields ($B \sim 10^{12}$ gauss) that presumably exist on pulsars can greatly change the structure of atoms. The motion of all electrons in the plane perpendicular to the magnetic field is assumed fixed by the magnetic field (adiabatic approximation). The response of the electrons to the Coulomb attraction is essentially restricted to a one-dimensional motion parallel to the field. Two regimes of field strength are distinguished. For $Z^{4/3} \ll 10^{-9}B \ll 10Z^3$ gauss a variationally formulated "one-dimensional" Thomas–Fermi-like model is valid for heavy atoms. The dimensions of the atom are greatly reduced and the total ground-state binding energies greatly increased from the no-B field situation. Surprisingly, the overall electronic number density, n(r), retains spherical symmetry (even though the number density of each electron is strongly asymmetrical). The choice $n(r) \alpha ZR^{-3} \sigma - 1/4 \exp(-\sigma)$, $\sigma = r^2/R^2$, gives $E \cong -150 (B/10^{12})^{2/5} Z^{9/5}$ eV for neutral atoms. For $B \gg 10^{10}Z^3$ gauss a crude variational calculation for the energy (applicable for heavy atoms) indicates that the electronic number density is strongly elongated along the field direction and gives for the ground-state binding energy $E \simeq -13.6N(Z - N/3)^2 \ln^2(2B/10^{10})$ eV (nuclear charge Z, N electrons). The binding and ionization energies of a few very light atoms and ions of astrophysical interest (He, H^-) are also presented. The Thomas–Fermi-like method is extended to "crushed" atoms (that is, atoms restricted to volumes much less than their normal volumes by the pressure of neighboring atoms) in the outermost layers of the pulsar crust. The resulting pressure–density equation of state changes the thickness of these layers (with $\rho \lessapprox 10^4$g cm^{-3}) from the no-B field situation and, further results in a much higher value for the density that marks the surface of the star. These results may be of interest for calculations of opacity coefficients and other properties associated with the outer reaches of the pulsar. In a separate consideration, a simple atomic model, which physically is far more realistic than the normal Thomas–Fermi model (B = O), is developed. In particular, it improves upon the description of regions close to and far away from the nucleus (regions where there is a breakdown of the assumptions of the Thomas–Fermi method). Furthermore, it applies equally to atoms of small as well as large atomic number as opposed to the Thomas–Fermi method, which is a statistical model. Placing the electrons in hydrogen-like states with different nuclear charge (always maintaining orthogonality of the set of single particle states) chosen to satisfy the Pauli principle, a variational upper bound for the energy is obtained, which is more accurate than Thomas–Fermi. Moreover, calculations reduce to simple algebra and can be improved by the inclusion of more variational parameters (the different nuclear charges serve as variational parameters). The resulting charge density and effective Coulomb potential are analytic and when used in the calculation of other atomic properties yield the usual "Thomas–Fermi scaling laws." Some aspects of shell structure are also inculded; for example, the model gives reasonable estimates of the ionization energy of the last electron. (Diss. Abstr. Int., B)

54145 INTEGRAL-EQUATION APPROACH TO BOUND-STATE ATOMIC SYSTEMS: PRELIMINARY STUDIES OF HELIUM AND HYDROGEN. Cooper, W. Grant; Kouri, Donald J. (Univ. of Houston, Tex.). J. Chem. Phys.; 57: No. 6, 2487-97(15 Sep 1972).

The Sams–Kouri method for noniteratively solving integral equations is used to solve the integral form of Schrödinger's equation for He such that the Hartree–Fock approximation is avoided and the inclusion of nuclear motion is straightforward. An exact formalism is presented, which requires the solution to coupled integral equations, and the method for generalizing to many-electron atoms is indicated. Calculations are reported for a single integral equation approximation to He, which illustrates the essential features of the method. The energy value obtained is approximately 85% of the total binding energy. Calculations for the H atom are given so comparisons with an exactly soluble atomic problem can be made, and the energy values for the ground and first three excited states are in excellent agreement with the exact values. Excited-state calculations are found to be no more difficult than those for the ground state. (auth)

54146 PROBABILISTIC INTERPRETATION OF CLUSTER FUNCTION SERIES DEVELOPMENT OF MANY-ELECTRON WAVE FUNCTIONS. Hertia, D. I.; Ivanov, Al. (Inst. of Physical Chemistry, Bucharest). J. Chem. Phys.; 57: No. 6, 2581-5 (15 Sep 1972).

A probabilistic treatment of the polyfermionic systems is made. The idea of localizability of the particles on bounded sets in the X-configuration space of the system is used. The decomposition of this space into a union of bounded sets permits a natural decomposition of the wave function into a cluster function series. A physical interpretation of this type of expansion and the establishment of a definition for the correlation phenomenon independently of a Hartree–Fock or other particular model are discussed. (auth)

54147 RELATIVISTIC CORRECTIONS IN HEAVY ATOMS. Braun, M. A.; Sibirkina, T. N. Vestn. Leningrad. Univ., No. 22, Fiz., Khim.; No. 4, 13-22(Nov 1971). (In Russian).

A method has been proposed for the construction of the Hamiltonian that describes the interacting atomic electrons for $Z\alpha \sim 1$. The method uses the Furry representation. The two- and three-body interaction potentials are found up to order α^2. The expression for the electron energy shift due to the three-body potentials is obtained. A simplified calculation of the relativistic corrections for the K electrons is discussed, which neglects their relativistic and exchange interactions with other electrons. (auth)

54148 MANY-PARTICLE CORRELATION FOR MANY-ELECTRON SYSTEMS IN DIFFERENT ORDERS OF PERTURBATION THEORY. Zashikhin, M. N. Vestn. Leningrad. Univ., No. 22, Fiz., Khim.; No. 4, 23-8(Nov 1971). (In Russian).

Many-particle equations, which generalize the two-particle equations of Fock–Veselov, and Petrashen, were studied. The cluster expansion for the energy of a many-electron system is obtained in any order of the perturbation theory. (auth)

54149 Z-EXPANSION COEFFICIENTS AND THE NUMBER OF ELECTRONS. Synder, R. (Queen's Univ., Belfast). J. Phys., B (London); 5: No. 8, L147-50(Aug 1972).

It is shown that in a closed-shell atom with a large number of electrons, N, the zero- and first-order Z-expansion coefficients are given approximately by $E_0(N) \simeq -\beta N^{1/3} + {}^1/_2 - {}^1/_{18} \beta\, {}^2N^{-1/3}$ and by $E_1(N) \simeq {}^1/_2 \beta N^{1/3}$, where $\beta = ({}^3/_2)^{1/3}$. (auth)

54150 PROPERTIES AND USES OF NATURAL ORBITALS. Davidson, Ernest R. (Univ. of Washington, Seattle). Rev. Mod. Phys.; 44: No. 3, 451-64(Jul 1872).

Natural orbitals are a particularly efficient choice of single-particle states for use in construction of electronic wave functions. This review discusses the general properties of the natural orbitals. Natural orbitals are compared to Hartree–Fock orbitals and relative merits are presented. Methods of determining and using natural orbitals in construction of electronic wave functions are presented. (94 references) (auth)

54151 ATOMIC STRUCTURE OSCILLATION EFFECTS. Kirzhnits, D. A.; Shpatakovskaya, G. V. (Lebedev Inst. of Physics, Moscow). Zh. Eksp. Teor. Fiz.; 62: No. 6, 2082-96 (Jun 1972). (In Russian).

An expression for the oscillation corrections to the Thomas–Fermi model is obtained within the framework of the quasi-classical approximation. The expression permits one to describe averaged characteristics of the physical system as well as irregularities related to the shell structure. Spatial oscillations of the electron density of a heavy atom can be described with an accuracy of about 5%. (auth)

54152 TWO PERTURBATIONS IN THE PRESENCE OF DEGENERACY. Chisholm, C. D. H.; Lodge, K. B. (Univ. of Sheffield, Eng.). Chem. Phys. Lett.; 15: No. 4, 571-4(1 Sep 1972).

The second-order energy in Rayleigh–Schrödinger single perturbation theory for a degenerate level with two perturbations is written in "double perturbation" form. The difficulties in formal double perturbation theory are avoided. (auth)

54153 ASYMPTOTIC BEHAVIOR OF ATOMIC-BOUND-STATE WAVE FUNCTIONS. Ahlrichs, Reinhart (Univ., Karlsruhe, Ger.). Chem. Phys. Lett.; 15: No. 4, 609-12(1 Sep 1972).

An upper bound is derived for $\|r_i^\mu \varphi\|$, $\mu = 1,2,\ldots$, where φ denotes an atomic bound-state eigenfunction and r_i is the distance of the ith electron from the nucleus. It is then shown that φ vanishes exponentially if any of the r_i approaches infinity. (auth)

54154 MANY-ELECTRON WAVE FUNCTIONS EXPANDED IN SPIN-ADAPTED ANTISYMMETRIZED PRODUCTS, AND THEIR EXPECTATION VALUES. Salmon, William I.; Ruedenberg, Klaus (Iowa State Univ, Ames). J. Chem. Phys.; 57: No. 7, 2776-86(1 Oct 1972).

Unrestricted configuration-interaction wave functions are constructed according to certain conventions that simplify the calculation of expectation values when S is a good quantum number. General wave functions are expressed in terms of antisymmetric space-spin functions that are eigenstates of S^2 and S_z, and form a complete orthonormal set. The building blocks, called "spin-adapted antisymmetrized products" or SAAP's, are designed to take advantage of double occupancy. It is shown that SAAP's, when constructed from orthonormal space orbitals, can be handled in multiconfigurational calculations more easily than Slater determinants. Simple formulas are derived for matrix elements of observable operators expressible in terms of one- and two-electron integrals. (auth)

54155 IMPLEMENTING THE SAAP FORMALISM. I. SERBER-TYPE SPIN EIGENFUNCTIONS BY DIRECT DIAGONALIZATION. Salmon, W. I.; Ruedenberg, K.; Cheung, L. M. (Iowa State Univ., Ames). J. Chem. Phys.; 57: No. 7, 2787-90(1 Oct 1972).

A method is given for generating Serber-type spin eigenfunctions for use in expansions of general electronic wave functions in terms of spin-adapted antisymmetrized products (SAAP's). The procedure is efficient and avoids the large storage requirements of spin-coupling schemes using Wigner coefficients. Running times of computer programs are given. (auth)

54156 IMPLEMENTING THE SAAP FORMALISM. II. SIMULTANEOUS EIGENFUNCTIONS OF L^2 AND S^2 BY DIRECT DIAGONALIZATION. Salmon, W. I.; Ruedenberg, Klaus (Iowa State Univ., Ames). J. Chem. Phys.; 57: No. 7, 2791-3(1 Oct 1972).

A procedure is described for generating simultaneous atomic eigenfunctions of S^2, S_z, L^2, and L_z as linear combinations of spin-adapted antisymmetrized products of atomic orbitals. The resulting functions are of the Serber type, i.e., they also are eigenfunctions of all geminal pair–spin operators. Flow diagrams for computer programs are given and running times are quoted. (auth)

54157 COMPLEX AND UNRESTRICTED HARTREE–FOCK WAVE FUNCTIONS. Ostlund, Neil S. (Univ. of Arkansas, Fayetteville). J. Chem. Phys.; 57: No. 7, 2994-7(1 Oct 1972).

The general conditions under which real, restricted Hartree–Fock wave functions become unstable with respect to variation of the orbitals are derived. It is shown that complex solutions to the Hartree–Fock equations are associated with a singlet instability in the usual real restricted solution. A comment is made concerning the complex wave functions found by Harris and Pohl for hydrogen halides at short internuclear distances. (auth)

PHYSICS (ELECTROFLUID AND MAGNETOFLUID)

54158 MAGNETOHYDRODYNAMIC FLOW NEAR A TIME-VARYING ACCELERATED PLATE. Mohapatra, Priti (Utkal Univ., Bhubaneswar, India). Indian J. Phys.; 45: No. 9, 421-31(Sep 1971).

The flow of an electrically conducting incompressible viscous liquid due to the time-varying motion of an infinite flat plate is studied in the presence of a uniform magnetic field. The magnetic lines of force are taken to be fixed relative to the fluid. General expressions of the velocity and skin friction are obtained when the plate moves with the velocity $e^{at}t^n$. Several particular cases are studied, and the results are compared with the aid of some graphs and tables. (auth)

54159 REFLECTION OF A HYDROMAGNETIC SHOCK WAVE FROM A BOUNDARY SHOCK. Verma, B. G.; Prasad, Baleshwar (Univ. of Gorakhpur, India). Indian J. Phys.; 45: No. 10, 439-42(Oct 1971).

After consideration of the earlier works on boundary shock waves in a gas, under viscous stress and magnetic pressure, the Hugoniot relation is used and a linear relationship is obtained between reflected velocity, magnetic field, and viscous compressive stress. (auth)

54160 THEORETICAL STUDY OF THE ELECTROMAGNETIC COUPLING (IN THE FORCED OSCILLATION REGION) OF TWO ONE-DIMENSIONAL LAMINAR FLOWS OF A VISCOUS ELECTRICALLY CONDUCTING LIQUID IN THE PRESENCE OF A UNIFORM TRANSVERSE ELECTROMAGNETIC FIELD. Dorlhac, Francois (College Scientifique Universitaire, Avignon, France). Compt. Rend., Ser. A; 274: No. 22, 1586-9 (29 May 1972). (In French).

The electromagnetic coupling (in the forced oscillation region) of two one-dimensional flows was studied. The two hydraulically independent flows are in perfect electrical contact at infinity in a direction perpendicular to the flow and to the magnetic field. Phase shift curves and curves representing the variations in the coefficient of performance are presented as functions of the pulsation and the magnetic field. (France)

54161 THEORETICAL STUDY OF THE FLOW OF AN ELECTRICALLY CONDUCTING VISCOUS LIQUID, AGITATED BY AN OSCILLATING PLANE, IN A MAGNETIC INDUCTION FIELD. Poirier, Yves (Centre Universitaire, Saint-Denis, France). Compt. Rend., Ser. A; 274: No. 21, 1514-16(24 May 1972). (In French).

A theoretical study of the viscous flow of an electrically conducting liquid between a fixed plane and an oscillating parallel plane is presented. A uniform magnetic induction is assumed to be applied in a direction normal to the planes limiting the flow. Curves illustrating the variations in the amplitude of the mean velocity of the liquid and its phase shift with respect to the motion of the oscillating plane are presented. (France)

PHYSICS (HIGH-ENERGY)

Particle Interactions and Properties (Experimental)

54162 (ISS–71/31) SEMINAR AT THE PHYSICS LABORATORY DURING THE PERIOD JULY–DECEMBER 1970. (Istituto Superiore di Sanita, Rome (Italy). Laboratori di Fisica). 10 Nov 1971. 22p. (In Italian and English). Dep. NTIS (U. S. Sales Only).

This report presents a synopsis of the lectures held at the Physics Laboratory of the Istituto Superiore di Sanita during the period July–December 1970. (auth)

54163 (NP–19421) HIGH ENERGY MEASUREMENTS OF TOTAL CROSS SECTIONS ON PROTON, DETECTING VERY LOW ENERGY NEUTRONS. Note No. 370. D'Angelo, S.; Monacelli, P.; Sebastiani, F. (Rome Univ. (Italy). Istituto di Fisica. Istituto Nazionale di Fisica Nucleare, Rome (Italy)). 7 Apr 1972. 4p. Dep. NTIS (U. S. Sales Only).

It is pointed out that the total cross sections for particle interactions with protons at high energies and momentum transfers may be measured using a deuterium target and detecting very low energy spectator neutrons. (J.F.P.)

54164 SEARCH FOR $^1/_3$e AND $^2/_3$e CHARGED QUARKS IN THE COSMIC RADIATION AT 2750-m ATTITUDE. Cox, A. J.; Beauchamp, W. T.; Bowen, T.; Kalbach, R. M. (Univ. of Arizona, Tucson). Phys. Rev., D; 6: No. 5, 1203-11(1 Sep 1972).

A scintillation counter telescope consisting of eight liquid scintillation counters and four wide-gap spark chambers was used to search for particles with electric charge $^1/_3$e and $^2/_3$e in cosmic rays at 2750 m above sea level. No such particles were detected during the 1500-h experimental run, establishing upper limits on the vertical fluxes of 8.3×10^{-11} cm^{-2} sec^{-1} sr^{-1} and 9.6×10^{-11} cm^{-2} sec^{-1} sr^{-1} for charge $^1/_3$e and $^2/_3$e, respectively. Estimates of the corresponding sea-level fluxes are made for comparison with previous results. (auth)

54165 SEARCH FOR QUARKS AT THE 70 GeV ACCELERATOR. Zaitsev, A. M.; Landsberg, L. G. (Inst. of High Energy Physics, Moscow). Yadern. Fiz.; 15: No. 6, 1184-98(Jun 1972). (In Russian).

An analysis and comparison of the results of various experiments on search for quarks, made at the accelerators and in cosmic rays are presented. The model of phase volumes and the phenomenological model, that takes into account the basic peculiarities of heavy particle production in strong interactions were used in calculating the quark spectrum. It is shown that the previous IHEP results are of higher sensitivity for the wide mass range $M_Q = 2 \div 7$ GeV/c^2. (auth)

Electromagnetic

Refer also to abstract 53279.

54166 (CALT–68–322) NEW EVIDENCE ON THE PHOTOEXCITATION OF I = $^1/_2$ NUCLEON ISOBARS. Heusch, C. A.; McNeely, W. A.; Winstein, B. D.; Yellin, S. J. (California Inst. of Tech., Pasadena). Aug 1971. 14p. (CONF-710816–24). Dep. NTIS.

From International symposium on electron and photon interactions at high energies; Ithaca, N. Y. (23 Aug 1971).

The reaction $\gamma + N \rightarrow N^*, N^* \rightarrow N + \eta^0$ is studied. The transition amplitudes and cross sections for $\gamma + p$ and $\gamma + n$ interactions at threshold to 1.1 GeV are found. (J.F.P.)

54167 (COO–3069–71) POLARIZATION OF THE RECOIL PROTON IN THE REACTIONS $\gamma p \rightarrow \pi^0 p$ AND $\gamma p \rightarrow \gamma p$. Technical Report No. 92. Deutsch, M.; Golub, L.; Kijewski, P.; Potter, D.; Quinn, D.; Rutherfoord, J. (Massachusetts Inst. of Tech., Cambridge. Lab. for Nuclear Science). 1972. Contract AT(11-1)-3069. 40p. (DSR–77907-D). Dep. NTIS.

The polarization of the recoil proton in the reaction $\gamma + p \rightarrow \pi^0 p$ was measured. The range $t = -.2$ (GeV/c)^2 to $t = -.65$ (GeV/c)^2 with a bremsstrahlung beam that extends from 3 to 7 GeV. Showers from the π^0 decay are detected with a lead converter, scintillation counter hodoscope, and lead glass counter. Protons are detected by means of counters and wire spark chambers. A sandwich of 10 carbon plates and wire chambers serves as an analyzer. There were 8800 π^0 events selected from a sample of $1.2 \cdot 10^6$ triggers. The polarization is 0 at $t = -.2$ (GeV/c)^2 and decreases to -1 at $t = -.45$ (GeV/c)^2. Since the target asymmetry is expected to be about the same as the recoil proton polarization, the results can be compared with a target asymmetry measurement done at Daresbury. Also the polarization of the proton was examined in the reaction $\gamma + p \rightarrow \gamma + p$ over the same t range. With a total of 3200 events the average polarization is found to be $12 \pm .06$. (auth)

54168 (DESY–72/38) SEPARATION OF σ_1 AND σ_t AT $q^2 \sim 1$ (GeV/c)^2 IN THE RESONANCE REGION. Alder, J. C.; Brasse, F. W.; Chazelas, E.; (and others) (Deutsches Elektronen-Synchrotron, Hamburg (West Germany)). Jul 1972. 12p. Dep. NTIS (U. S. Sales Only).

Some new values of $R = \sigma_1/\sigma_t$ taken in the resonance region from inelastic e-p-scattering at DESY are reported. Cross sections were measured at $\theta = 57°$ and $\theta = 15$ to $17°$ at $q^2 = 1$ GeV^2. R was calculated at masses $1495 \leq W \leq 1715$ MeV. It was found that the contribution of σ_1 to the total cross section is small, below 20%. The errors are less than $\Delta R = 16\%$. (auth)

54169 (JINR–E1-6647) e – d SCATTERING AND NEUTRON FORM FACTORS. Bilen'kaya, S. I.; Kazarinov, Yu. M.; Lapidus, L. I. (Joint Inst. for Nuclear Research, Dubna (USSR). Lab. of Nuclear Problems). 1972. 8p. Dep. NTIS (U. S. Sales Only).

All the available data on the elastic e–d cross section in the squared momentum transfer range $0.3\ F^{-2} \leq q^2 \leq 34.1\ F^{-2}$ were analyzed. It is shown that a statistically satisfactory fit to all data is impossible without renormalization. The neutron magnetic form factor is in agreement with the scaling law. The systematic errors in normalization of experimental data do not allow one to draw definite conclusions on the value of the neutron electric form factor. (auth)

54170 (LAL–1255) ANALYSIS OF FORM FACTORS IN $K^+ \rightarrow \pi^0 \mu^+ \nu$ AND $K^+ \rightarrow \pi^0 e^+ \nu$ DECAYS. Le Dong (Paris Univ., Orsay (France). Faculte des Sciences). Dec 1971. 194p. (In French). Dep. NTIS (U.S. Sales Only).

Thesis.

In the framework of the X2 program carried out with the heavy liquid bubble chamber of CERN, the following semilepton three-body decays were studied: $K^+ \rightarrow \pi^0 + \mu^+ + \nu\ K_{\mu 3}$ and $K^+ \rightarrow \pi^0 + e^+ + \nu\ K_{e3}$. The interaction may be described in terms of 2 factors having the following forms: $f_+ (q^2)$ and $f_- (q^2)$. The ratio xi = f_-/f_+ was determined using the two following methods: measurement of the $K^+_{\mu 3}/K^+_{e3}$ branching ratio; analysis of the population density of the Dalitz diagram of the $K^+_{\mu 3}$ decay. The methods used are described. These results are compared with results obtained using other methods. The results are discussed in view of various theoretical predictions. (France)

54171 (LNF–72/31) ANALYSIS OF THE REACTION $\gamma + n \rightarrow p + \pi^-$ IN THE FIRST AND SECOND RESONANCE REGION. Carbonara, F.; Gialanella, G.; Lodi-Rizzini, E.; (and others) (Comitato Nazionale per l'Energia Nucleare, Frascati (Italy). Laboratori Nazionali di Frascati). 5 Apr 1972. 33p. Dep. NTIS (U.S. Sales Only).

The results of an experimental investigation of the reaction $\gamma + n \rightarrow p + \pi^-$ up to 1 GeV with a deuterium bubble chamber at the Frascati Electron Synchrotron are reported. The experimental procedure is briefly described, and the problem of the use of the deuteron as a target is considered in detail. Total and differential cross sections, derived by using the spectator model, are presented. The results are discussed with respect to possible T violation and isotensor current contribution, a phenomenological fit to the differential cross sections, and photoproduction of the P_{11} (1470) resonance. (17 figures, 6 tables, 31 references) (R.W.R.)

54172 (NP-19415) PHOTOPRODUCTION OF π^+-MESONS ON POLARIZED PROTONS AT PHOTON ENERGIES BETWEEN 0.5 AND 2.2 GeV. Althoff, K. H.; Feller, P.; Herr, H.; Hoffmann, W.; Kadansky, V.; Menze, D.; Opara, U.; Schittko, F. J.; Schulz, W.; Schwille, W. J. (Bonn Univ. (West Germany). Physikalisches Institut). Aug 1972. 15p. (PIB-1-181). Dep. NTIS (U. S. Sales Only).

The target asymmetry $T = (\sigma\uparrow - \sigma\downarrow)/(\sigma\uparrow + \sigma\downarrow)$ for the reaction $\gamma p \rightarrow \pi^+ n$ was measured at the Bonn 2.5-GeV electron synchrotron for a pion CM angle of 40° and γ-energies between 0.5 and 2.2 GeV. Butanol was used as target material. About 35% of the protons could be polarized using the dynamic polarization method in a continuous flow cryostat operating at 1°K and 25 kG. The π^+-mesons were detected in a magnetic spectrometer system. A considerable structure of the asymmetry was observed. (auth)

54173 (RPP/H–97) LEPTON HADRON INTERACTIONS. Toner, W. T. (Rutherford High Energy Lab., Chilton (England)). Aug 1972. 52p. Dep. NTIS (U. S. Sales Only).

It is stated that all recent data on lepton hadron scattering at high energy are inelastic electron scattering data. A review is presented of data from experiments in which only the scattered electron is detected (the so-called single-arm experiments); and from experiments in which one or more of the hadrons produced in the interactions are detected in coincidence with the scattered electrons (the coincidence experiments). The subjects covered are single-arm kinematics; determination of R (where $R = \sigma_L/\sigma_T$, σ_L and σ_T being cross sections for the absorption of longitudinal and transverse virtual photons); scaling at high q^2, sum rules in the Bjorken limit; scaling at low q^2; scattering from deuterons; scattering from complex nuclei; kinematics and general features of coincidence measurements; single π^+ electroproduction; miscellaneous two-body reactions ($\pi\Delta$ channels, $K\Lambda$ and $K\Sigma$, backwards mesons); diffractive electroproduction of vector mesons. (U.K.)

54174 (RPP/H–99) MEASUREMENT OF THE Ξ HYPERON LIFETIMES AND α PARAMETERS. Mayeur, C.; Van Binst, P.; Wilquet, G.; (and others) (Rutherford High Energy Lab., Chilton (England)). 1972. 23p. Dep. NTIS (U.S. Sales Only).

In an experiment using a heavy liquid bubble chamber the the Ξ hyperon lifetimes and α parameters were measured to be $\tau_{\Xi}^{0} = (3.04 \pm {}^{0.26}_{0.23}) \times 10^{-10}$ sec, $\tau_{\Xi^-} = (1.73 \pm {}^{0.08}_{0.07}) \times 10^{-10}$ sec, $\alpha_{\Xi}^{0} = -0.84 \pm 0.27$ and $\alpha_{\Xi^-} = -0.42 \pm 0.11$. These values agree with measurements which employed different techniques and are consistent with the predictions of the $\Delta I = \frac{1}{2}$ rule. (auth)

54175 (SLAC–143) STUDY OF NON-STRANGE BOSON RESONANCES PRODUCED BY QUASI-MONOCHROMATIC PHOTON BEAMS OF ENERGIES BETWEEN 4.3 AND 7.5 GeV IN A HYDROGEN BUBBLE CHAMBER. Menke, Michael M. (Stanford Linear Accelerator Center, Calif.). Dec 1971. Contract AT(04-3)-515. 186p. Dep. NTIS.

The photoproduction of resonances was studied in three exposures of a hydrogen bubble chamber to positron annihilation radiation of 4.3, 5.25 and 7.5 GeV nominal energies. The general analysis procedure and results on the three-prong event topology are presented. The highly constrained reaction $\gamma p \rightarrow p\pi^+\pi^-$ was studied over the energy range 2 to 8 GeV, and the reactions $\gamma p \rightarrow p\pi^+\pi^-\pi^0$ and $\gamma p \rightarrow \pi^+\pi^+\pi^-n$ were studied at the annihilation energies. Cross sections are given. Using various models to parameterize ρ^0 photoproduction in $\gamma p \rightarrow p\pi^+\pi^-$, the mean t-slope found is 7.0 ± 0.4 GeV^{-2}, while the ρ^0 forward cross section decreases from about 130 μb/GeV^2 at 3.3 GeV to about 100 μb/GeV^2 at 7.5 GeV. The cross section for $\gamma p \rightarrow \omega p$ is decomposed into an OPE and a diffractive part, which is found to be 1.5 ± 0.3 μb. $(d\sigma(\rho)/dt)/(d\sigma(\omega)/dt)|_{t=0}$ is then 9.4 ± 2.3 at 7.5 GeV. In comparing $d\sigma/dt$ for vector meson production with that of Compton scattering via VDM for photon energies above 4 GeV, it is found that for $\gamma_\rho^2/4\pi = 0.32 \pm 0.03$ there is good agreement at all s and t. This same value of $\gamma_\rho^2/4\pi$ relates the forward ρ^0 cross sections to $\sigma_T(\gamma p)$ at all our energies. A search for $\rho' \rightarrow 2\pi$ finds, at the 90% confidence level, $\rho_{\rho'}(1250) < 0.3$ μb and $\sigma_{\rho'}(1650) < 0.1$ μb per 100 MeV width. Inelastic peripheral ρ^0 production is seen in both the proton and the neutron channels, but with present statistics specific nucleon isobars cannot be associated with it. The quasi-two body reactions $\gamma p \rightarrow \pi^-\Delta^{++}$, $\rho^-\Delta^{++}$, and $A_2^+ n$ are observed, with cross sections decreasing with photon energy like E_γ^{-a}. For the first two $a = 1.74 \pm 0.16$ and 0.6 ± 0.2 respectively, indicating that they are unlikely to have the same production mechanism. It follows that if the reaction $\gamma p \rightarrow \rho^-\Delta^{++}$ is due to an OPE process, the required rho radiative decay width (~0.5 MeV) is much in excess of the value predicted by SU(3). (auth)

54176 (SLAC-PUB–1043) e^+e^- ANNIHILATION TO HADRONS. Ritson, D. M. (Stanford Linear Accelerator Center, Calif.). May 1972. 27p. (CONF-720409–14). Dep. NTIS.

From third international conference on experimental meson spectroscopy; Philadelphia, PA. (28 Apr 1972).

The discussion of $e^+ + e^-$ annihilation to hadrons covers the information at higher energy which is available and which is expected in the next few years: The total cross sections for hadron production, SU(3) ratios for two-body final states, SU(6) quark model predictions for quasi-two-body particle production, multiplicities and transverse momentum distributions, the production and observation of new resonances, and γ–γ processes. (J.F.P.)

54177 SEARCH FOR $\frac{4}{3}$e CHARGED DIQUARKS IN THE COSMIC RADIATION AT 2750-m ALTITUDE. Beauchamp, W. T.; Bowen, T.; Cox, A. J.; Kalbach, R. M. (Univ. of Arizona, Tucson). Phys. Rev., D; 6: No. 5, 1211-17(1 Sep 1972).

A large-area 3.35-m^2 scintillation-counter telescope consisting of eight scintillation counters and four wide-gap spark chambers was arranged to detect single particles with charges $\pm\frac{4}{3}$ e which might be present in the cosmic radiation at 2750 m above sea level. The upper limit for the vertical flux of such particles is found to be 4.1×10^{-10} cm^{-2} sr^{-1} sec^{-1}. Estimates of the corresponding sea-level flux are made for comparison with previous results. (auth)

54178 MEASUREMENTS OF INCLUSIVE HADRON MOMENTUM DISTRIBUTIONS IN DEEP INELASTIC ELECTROPRODUCTION. Alder, J. C.; Brasse, F. W.; Chazelas, E.; (and others) (DESY, Hamburg). Nucl. Phys.; B46: No. 2, 415-28(1972).

In the deep inelastic region of electron scattering the distribution of hadrons in the direction of the virtual photon was investigated. At $q^2 = 1.16$ GeV^2 and W = 2.63 GeV coincidence measurements between the scattered electron and proton, $\pi^\pm$ and $K^\pm$ were made. Momentum and missing mass distributions are presented. They are compared with other electroproduction measurements, with photoproduction, and with hadronic reactions. (auth)

54179 PHOTOPRODUCTION OF π^- FROM DEUTERIUM AT LABORATORY ENERGIES 600 TO 1250 MeV AND C. M. π PRODUCTION ANGLES 6 TO 160°. Walden, Patrick Lorne. Pasadena, Calif.; California Inst. of Tech. (1972). 237 p. University Microfilms Order No. 72-22,563.

Thesis.

The differential cross sections for reaction $\gamma + n \rightarrow \pi^- + p$ were measured for laboratory photon energies between 600 and 1250 MeV, using a liquid deuterium target. The measurements were made using a magnetic spectrometer and a recoil counter in which π's and p's were detected in various combinations. Measurements of the π^- counting rate, the π^-/π^+ counting rate ratio, and the π^-, p coincidence counting rate were used to calculate three independent values for the π^- photoproduction cross section. The cross sections from the latter two measurements were less sensitive to deuterium effects and were averaged to form the set of final data. The most notable feature of the data is the absence of an enhancement near the $F_{15}(1688)$ resonance. This feature was predicted from quark model calculations. The $D_{13}(1520)$ resonance appears to be excited by a helicity $\frac{3}{2}$ amplitude as was the case in π^+ photoproduction. (Diss. Abstr. Int., B)

54180 PROTON COMPTON EFFECT IN THE REGION OF THE Δ(1236)-RESONANCE. Genzel, H.; Jung, M.; Rausch, K. R.; Wedemeyer, R.; Weyer, H. J. (Univ., Bonn). Lett. Nuovo Cim.; 4: No. 14, 695-8(5 Aug 1972).

A new measurement of differential cross sections for elastic photon–proton scattering in the region of the first πN resonance is reported. The numerical values are tabulated. The excitation curves illustrate a resonance-like behavior as it is known from π photoproduction. At all angles the cross-section maximum appears at about 320 MeV. The partial width $\Gamma_{\gamma\gamma}$ of the Δ resonance is found to be in good agreement with results from pion photoproduction. (L.B.S.)

Weak

54181 (BNL–16977) FORWARD MUONS AND MUON PAIRS AT ISABELLE. Smith, A. J. S.; Strovink, Mark (Brookhaven National Lab., Upton, N. Y.). 16 Jun 1972. 8p. Dep. NTIS.

Some of the processes possibly giving rise to muons and muon pairs produced at ISABELLE along the beam directions are mentioned, and the problems associated with their detection are considered. To be specific, attention is focussed on muons which intersect the spectrometer. At one end of the 20 m "west" straight section, five magnetized iron toroids of 4 m diameter and 1 m thickness are distributed along the beam. Detectors in the 0.5 m interstices measure both position and angle of the muon trajectory. Nearly the full azimuthal range is accepted between polar angles of 50 and 400 mrad. Additional details appear in section C below. From a scheduling viewpoint, there are several attractive features. First, the forward muon spectrometer is physically compatible with a 90° lepton detector of the type described by Lederman. In addition, successful operation of the 90° spectrometer will require suppression of forward hadrons produced by beam-gas interactions near the ends of the straight sections. The necessary shielding at one end is provided by these iron toroids. It is emphasized that magnetic field containment within the iron toroids effectively removes the possibility of interference with synchrotron tuning. (auth)

54182 (BNL–17092) WEAK INTERACTIONS AT ISABELLE '72. Lederman, L. M. (Brookhaven National Lab., Upton, N. Y.). 18 Jul 1972. 14p. Dep. NTIS.

A weak interaction experiment is proposed; $p + p \rightarrow \mu^+ + \nu_u +$ anything which will work at maximum luminosity proposed for ISABELLE. The above reaction, in which only the muon is measured, is shown to have remarkably good resolution in Q^2, the mass-squared of the outgoing lepton pair. Neutral weak currents may interfere with electromagnetic currents in the reaction p + p → $\mu^+ + \mu^-$ + anything. (auth)

54183 (CEA-N-1553) EXPERIMENTAL STUDY OF THE $K^+ \rightarrow \pi^+\pi^-e\nu$ DECAY: DETERMINATION OF THE $\pi\pi$ PHASE SHIFT BY THE PAIS-TREIMAN METHOD. Basile, Pierre (Commissariat a l'Energie Atomique, Saclay (France). Centre d'Etudes Nucleaires). May 1972. 144p. (In French). Dep. NTIS (U. S. Sales Only).

640 events observed in a $K^+ \rightarrow \pi^+\pi^-e^+\nu$ spark chamber experiment were analyzed, and the pion-pion phase difference was measured for dipion masses lower than 420 MeV. The method used was a Pais-Treiman method where the phase difference is determined without any interference of the other decay parameters. The formalism is extended to the case where the detection efficiency must be taken into account. The tests effected confirmed the possibility of using the method in the phase difference determination. The results obtained (phase difference = 25 deg ± 12 deg) are discussed and compared with theoretical predictions and other experimental data. (France)

54184 (LBL-4) NEUTRINO MASS LIMITS FROM THE $K_L^0 \rightarrow \pi^{\pm}l^{\pm}\nu$ DECAY SPECTRA. Johnson, Rolland P.; Clark, Alan R.; Elioff, T.; Frisch, H. J.; Shen, G.; Kerth, Leroy T.; Wenzel, W. A. (California Univ., Berkeley. Lawrence Berkeley Lab.). .2 Aug 1971. Contract W-7405-eng-48. 13p. (CONF-710810-6). Dep. NTIS.

From Meeting on particles and fields; Rochester, N. Y. (30 Aug 1971).

A double magnetic spectrometer at the Bevatron was used to study the low neutrino energy ends of the $K_L^0 \rightarrow \pi\mu\nu$ ($K_{\mu 3}$) and $K_L^0 \rightarrow \pi e\nu$ (K_{e3}) decay spectra. The resolution of the apparatus and absolute invariant mass calibration were determined from $K_L^0 \rightarrow \pi^+\pi^-$ events accumulated with the K_{l3} events. A partial analysis yields neutrino mass upper limits (90% C.L.) of 1.0 MeV for the muon neutrino and 1.1 MeV for the electron neutrino. (auth)

54185 (NEIC-RR-47) COSMIC ν. Kuchowicz, B. (Nuclear Energy Information Center, Warsaw (Poland)). 1972. 129p. Dep. NTIS (U.S. Sales Only).

A review is presented of all the major developments in cosmic neutrino research from 1965 to the early part of 1972. Solar neutrinos, the universal Fermi interaction and stellar evolution, extrasolar sources of neutrino radiation, cosmological neutrinos, neutrinos from cosmic radiation, and theoretical developments are covered. (J.F.P.)

54186 K^+ DECAY IN FLIGHT. Chiang, I-h. (Univ. of Rochester, N. Y.); Rosen, J. L.; Shapiro, S.; (and others). Phys. Rev., D; 6: No. 5, 1254-65(1 Sep 1972). COO-881-331.

From a sample of 10^5 K^+ decays in flight the following branching ratios were obtained: $K_{\mu 2}$ = (63.24 ± 0.44)%, $K_{\pi 2}$ = (21.18 ± 0.28)%, $\tau(K^+ \rightarrow \pi^+\pi^+\pi^-)$ = (5.56 ± 0.20%, $\tau'(K^+ \rightarrow \pi^+\pi^0\pi^0)$ = (1.84 ± 0.06)%, $K_{\mu 3}$ = (3.33 ± 0.16)%, and K_{e3} = (4.86 ± 0.10)%. The phase-space distributions for three-body semileptonic modes were studied in detail from a second sample of 10^5 decays. For 4017 $K^+ \rightarrow \pi^0e^+\nu$ events, $\lambda_+ = 0.029 \pm 0.011$. Limits on scalar and tensor form factors of $|f_s/f_+| < 0.13$ and $|f_T/f_+| < 0.75$ (90% confidence) were obtained. For $K^+ \rightarrow \pi^0\mu^+\nu$ a parametrized fit to 3900 events assuming $\lambda_+ = \lambda_- = +0.030$ gave $\xi = -0.09 \pm 0.28$. (auth)

54187 MEASURING OF THE BRANCHING RATIO $\Gamma(K_L \rightarrow 3\pi^0)/\Gamma(K_L \rightarrow \pi^+\pi^-\pi^0)$. Barmin, V V.; Barylov, V. G.; Davidenko, G V.; (and others) (Inst. of Theoretical and Experimental Physics, Moscow). Yadern. Fiz.; 15: No. 6, 1152-3(Jun 1972). (In Russian).

The branching ratio $\Gamma(K_L \rightarrow 3\pi^0)/\Gamma(K_L \rightarrow \pi^+\pi^-\pi^0) = 1.65 \pm 0.07$ was measured with the help of the ITEP 180 liter xenon bubble chamber. (auth)

54188 CP AND THE THREE PION DECAY OF THE K^0. Mallary, Michael Leigh. Pasadena, Calif.; California Inst. of Tech. (1972). 177p. University Microfilms Order No. 72-22,556.

Thesis.

The time distribution of the decays of an initially pure K^0 beam into $\pi^+\pi^-\pi^0$ was analyzed to determine the complex parameter W (also known as η^{+-0} and (x + iy)). The K^0 beam was produced in a brass target by the interactions of a 2.85 GeV/c π^- beam which was generated on an internal target in the Lawrence Radiation Laboratory (LRL) Bevatron. The counters and hodoscopes in the apparatus selected for events with a neutral (K^0) produced in the brass target, two charged secondaries passing through a magnet spectrometer and a γ-ray shower in a shower hodoscope. From the 275 K apparatus triggers, 148 $K \rightarrow \pi^+\pi^-\pi^0$ events were isolated. The presence of a γ-ray shower in the optical shower chambers and a two-prong vee in the optical spark chambers were devices used to isolate the events. The backgrounds were further reduced by reconstructing the momenta of the two charged secondaries and applying kinematic constraints. The best fit to the final sample of 148 events distributed between .3 and 7.0 K_S lifetimes gives: ReW = -.05 ±.17 and ImW = $+.39^{+.35}_{-.37}$. This result is consistent with both CPT invariance (ReW = 0) and CP invariance (W = 0). Backgrounds are estimated to be less than 10% and systematic effects have also been estimated to be negligible. An analysis of the present data on CP violation in this decay mode and other K^0 decay modes has estimated the phase of ϵ to be 45.3 ± 2.3 degrees. This result is consistent with the super weak theories of CP violation which predicts the phase of ϵ to be 43^0. This estimate is in turn used to predict the phase of η^{00} to be 48.0 ± 7.9 degrees. This is a substantial improvement on presently available measurements. The largest error in this analysis comes from the present limits on W from the world average of recent experiments. The $K \rightarrow \pi\mu\nu$ mode produces the next largest error. Therefore further experimentation in these modes would be useful. (Diss. Abstr. Int., B)

54189 MEASUREMENT OF THE MUON ENERGY IN THE DECAY $\pi^+ \rightarrow \mu^+ + \nu$. Shrum, Edgar Vaughan. Charlottesville, Va.; Univ. of Virginia (1972). 84p. University Microfilms Order No. 72-22,639.

Thesis.

The muon energy following positive pion decay from rest is measured with a Ge(Li) detector using sixteen electronic sampling systems to obtain the shape of the pion decay pulse. The muon energy determined from this experiment is 4.1207 ± 0.0036 MeV. This can be used to set an upper limit on the muon neutrino mass of 1.15 MeV/c^2, at a confidence level of 90%. Assuming the neutrino mass to be exactly zero, the positive pion mass can be calculated. This gives a positive pion mass of 139.576 ± 0.025 MeV/c^2. The negative pion mass can be compared with this as a check on charge independence. $M_\pi-/M_\pi-$ = 1.00001 ± 0.0002 is found. Making no assumptions on the neutrino mass gives a value for the positive pion mass of $M_\pi-$ = 139.644 ± 0.134 MeV/c^2, and $M_\pi-/M+$ = 0.99952 ± .00097. (Diss. Abstr. Int., B)

54190 STUDY OF THE PROPERTIES OF THREE-PRONG DECAYS OF K^- MESONS IN FLIGHT IN A HYDROGEN BUBBLE CHAMBER. Lucas, Peter Wayne. New Haven; Yale Univ. (1972). 243p. University Microfilms Order No. 72-22,396.

Thesis.

Properties of the decays τ, $K_{\pi 2}$, K_{e3}, $K_{\mu 3}$, and τ' were studied through observation of three prong decays of K^- mesons in flight in the BNL 30'' hydrogen bubble chamber. The decays with one charged prong have been detected through the observation of Dalitz decays of π°'s. The estimated numbers of events are combined to yield branching ratios which are consistent with those for K^+. The slopes of the Dalitz plots for the τ and τ' decay modes were measured. The τ results are consistent with a bubble chamber experiment of comparable statistics measuring the same quantity and inconsistent with a high statistics spectrometer measurement. The τ' result is consistent with measurements of this quantity for K^+ decays. (Diss. Abstr. Int., B)

Strong (Baryon-induced)

Refer also to abstracts 53766, 54467, 54503, and 54512.

54191 (BNL-17065) MEASUREMENT OF THE PROTON-PROTON TOTAL CROSS SECTION BY BEAM ATTENUATION. Marx, Jay N.; Sandweiss, Jack (Brookhaven National Lab., Upton, N. Y.). 2 Aug 1972. 8p. Dep. NTIS.

A method for the measurement of the total rate of beam interactions in colliding proton beams is proposed. This technique, which directly measures a modulated beam attenuation far from the interaction region, can be combined with an independent luminosity determination to yield the proton-proton total cross section to better than 1%. (auth)

54192 (BNL-17141) CHARGED PARTICLE MULTIPLICITY AND ANGULAR CORRELATION MEASUREMENTS IN pp AND γp COLLISIONS. Arnold, R.; Finocchiaro, G.; Grannis, P.; Kirz, J.; Quigg, C.; Carroll, A. S. (Brookhaven National Lab., Upton, N.Y.). 1972. 29p. Dep. NTIS.

A proposed experiment to measure charged particle multiplicity and angular correlations in p + p and γ + p interactions is discussed. The experimental and theoretical motivation for the study, a possible experimental setup using multiwire proportional chambers or wide-gap spark chambers, background, and requirements on the ISA are covered. (J.F.P.)

54193 (JINR-E1-6613) DIFFERENTIAL CROSS SECTIONS OF THE ELASTIC p-p SCATTERING IN THE ENERGY RANGE OF 8 TO 70 GeV. Beznogikh, G. G.; Buyak, A.; Kirillova, L. F.; (and others) (Joint Inst. for Nuclear Research, Dubna (USSR). Lab. of High Energy). 1972. 26p. Dep. NTIS (U. S. Sales Only).

The tables of the absolute differential cross sections of the elastic p-p scattering are presented together with the values of the slope parameter B = (d/dt) [ln(dσ/dt)], and the real part parameter a = [ReA(0)]/[ImA(0)] (A(0) is the amplitude of the elastic p-p scattering at t = 0). The cross section data were obtained at Serpukhov accelerator over 8 to 70 GeV in the t – range of 0.0007–0.12 $(\mathrm{GeV/c})^2$. (auth)

54194 (JINR–E1-6615) DIFFERENTIAL CROSS SECTIONS OF THE ELASTIC p-d SCATTERING IN THE ENERGY RANGE OF 10 TO 70 GeV. Beznogikh, G. G.; Buyak, A.; Kirillova, L. F.; (and others) (Joint Inst. for Nuclear Research, Dubna (USSR). Lab. of High Energy). 1972. 17p. Dep. NTIS (U. S. Sales Only).

The tables of the absolute differential cross sections of the elastic p-d scattering are presented. The cross section data were obtained at Serpukhov accelerator over 10 to 70 GeV in the t-range of 0.002 to 0.2 GeV^2/c^2. The elastic p-d scattering amplitude was parametrized as: $A(t) = (d\sigma/dt)^{1/2}_{0pT}\ (i + a) \cdot \exp\,[1/2\ (Bt + Ct^2)]$. The values a = [ReA(0)]/[ImA(0)], B and C are presented in these tables also. (auth)

54195 (LA–4874, pp 36-44) OVERVIEW OF THE LAMPF RESEARCH PROGRAM. Feshbach, Herman (Massachusetts Inst. of Tech., Cambridge). Mar 1972.

From fifth LAMPF users meeting; Los Alamos, NM. (8 Nov 1971).

A review of research proposals at LAMPF is given. Types of strong interactions (hadrons), weak interactions (muons), and the weak interaction itself (neutrino physics) are outlined. (W.H.K.)

54196 VELOCITY DISTRIBUTION OF SECONDARY π MESONS FROM 22.6-GeV/c PROTON–NUCLEUS INTERACTIONS IN EMULSION. Roy, T.; Daftari, I. K. (Jadavpur Univ., Calcutta). Phys. Rev., D; 6: No. 5, 1217-19(1 Sep 1972).

Emulsion plates exposed to a 24-GeV proton beam are scanned. A velocity distribution of the secondary π mesons produced in such nuclear interactions is obtained. A Gaussian-type function is observed to simulate the experimental data and the usual phenomena of isotropy in the center-of-mass frame. The results indicate that the assumption of the constant velocity for all the secondary particles is only an approximation to the real world. (auth)

54197 INVESTIGATION OF ELASTIC pd-SCATTERING IN THE DIFFRACTION CONE REGION IN THE ENERGY RANGE 10 TO 70 GeV. Bartenev, V. D.; Beznogikh, G. G.; Buyak, A.; (and others) (Joint Inst. for Nuclear Research, Dubna, USSR). Yadern. Fiz.; 15: No. 6, 1174-80(Jun 1972). (In Russian).

The results on measuring the slope parameter of the diffraction cone b and the ratio a of the real part of the amplitude to the imaginary one in elastic pd scattering at momentum transfer $|t| < 0.2\ (\mathrm{GeV/c})^2$ are presented. It was found, that b increases, a changes from –0.29 ± 0.05 up to –0.14 ± 0.05 with the proton energy increase from 10 up to 70 GeV. The experiment was carried out at the IHEP accelerator. (auth)

54198 COMPARISON OF PION MOMENTUM DISTRIBUTIONS IN 19 GeV/c pp COLLISIONS WITH AND WITHOUT STRANGE-PARTICLE PRODUCTION. Marquit, E. (Univ. of Copenhagen). Nucl. Phys.; B46: No. 2, 568-72(1972).

A comparison is made of the inclusive π^- momentum spectra for pp interactions at 19 GeV/c with V^0 and without V^0 (or any other strange-particle signal). It is found that the spectra for interactions with a V^0 and charged-particle multiplicity n are rather similar to the spectra for interactions without a V^0 and multiplicity n + 2. (auth)

54199 ANALYSIS OF $K\bar{K}$ AND $K\bar{K}\pi$ RESONANCES PRODUCED IN $\bar{p}p$ ANNIHILATIONS AT 1.2 GeV/c. Duboc, J. (Univ., Paris); Goldberg, M.; Makowski, B.; (and others). Nucl. Phys.; B46: No. 2, 429-48(1972).

The analysis of 18,900 V^0 events is presented, with reference to the production of $K\bar{K}$ and $K\bar{K}\pi$ resonances in the three-, four-, five- and six-body final states. It is established that there is a threshold structure in the $(K\bar{K})_{I=1}$ state which comes entirely from the decay of $K\bar{K}\pi$ resonances, the D^0 and E^0. The S* and E^0 are definitely observed. The isospin of the D^0 is confirmed to be 0, $J_{D^0} \geq 1$ and, under the assumption $L_{D\omega} = 0$, $J_D^{PC} = 1^{2+}$. The F_1 is observed in the final state $F_1\eta^0$ and the analysis of this channel leads to the conclusion that $J_{F_1}^{PC} = 1^{\pm}$ or 2^-. In the five-body final state there is some appearance of two-peaks in the D^0 mass region, but with the present statistics there is no clear evidence for this effect. The cross sections for single and associated resonance production are given. (auth)

Strong (Meson-induced)

Refer also to abstracts 54232 and 54317.

54200 (BNL–17069) SOME THOUGHTS ABOUT PION–PROTON INTERACTION EXPERIMENTS AT ISABELLE. Lee, Y. Y. (Brookhaven National Lab., Upton, N. Y.). 27 Jul 1972. 6p. Dep. NTIS.

A possibility of doing pion-proton colliding beam experiments at ISABELLE is investigated. The rate is low and ~40 events/hour, however, it is found that events to background ratio is very favorable. (auth)

54201 (CERN/HERA–72-1) COMPILATION OF CROSS SECTIONS. I. π^- AND π^+ INDUCED REACTIONS. Bracci, E.; Droulez, J. P.; Flaminio, E.; Hansen, J. D.; Morrison, D. R. O. (European Organization for Nuclear Research, Geneva (Switzerland)). 11 May 1972. 183p. Dep. NTIS (U.S. Sales Only).

A compilation of cross sections for reactions produced by negative and positive pions on targets of protons, neutrons, and deuterons is presented. This is an updated version of CERN/HERA 70-5 and 70-7, and contains 40% more data than the earlier publications. Graphs of the variation of cross section with incident laboratory momentum are plotted. Values of the rate of decrease of cross section with incident momentum are given. (105 figures, 8 tables) (auth)

54202 (COO–1195-238) REACTION $K^+n \to K^+\pi^-p$ AT 3.8 GeV/c. Marshall, Don Allen (Illinois Univ., Urbana). Oct 1972. Contract AT(11-1)-1195. 192p. Dep. NTIS.

Thesis.

The ANL 30-inch bubble chamber was exposed to a separated K^+ beam at 3.8 GeV/c. The 300,000 pictures were scanned for 3- and 4-prong events. After measuring all of the 4-prong events with a stopping track and 61% of the 3-prong events, 4919 events were reconstructed which kinematically fit the reaction $K^+d \to K^+\pi^-pp$; this cross section was found to be 1.78 ± 0.10 mb. The reaction is dominated by the quasi-two-body interaction $K^+n \to K^{*0}(890)p$; this cross section was found to be 0.80 ± 0.07 mb. Results of an analysis of the spin density matrix elements indicate 0^- exchange is dominant. The reaction $K^+n \to K^{*0}(1420)p$ was examined for the effect reported by Firestone et al. The effect was confirmed, but the interpretation of the effect at 3.8 GeV/c as a broad S-wave resonance is clouded by a possible interpretation involving a secondary scattering between the spectator proton and the decay products of the K*(1420). (auth)

54203 (COO–1428-308) S-WAVE STRUCTURE IN THE Kπ SYSTEM. Cords, D.; Carmony, D. D.; Garfinkel, A. F.; Loeffler, F. J.; Rangan, L. K.; (Purdue Univ., Lafayette, Ind.).; Lander, R. L.; Pellett, D. E.; Yager, P. M. (California Univ., Davis); Meiere, F. T.; Yen, W. L. (Indiana-Purdue Univ., Indianapolis). 1972. 13p. Dep. NTIS.

The Kπ spectrum (4827 events) of the reaction $K^+n \to K^+\pi^-p$ at 9 GeV/c was analyzed and independent of any particular assumption of the production mechanism the existence of a broad S-wave enhancement was found. Since its phase with respect to the K*(890) P-wave is correctly given by a relativistic Breit–Wigner amplitude, this enhancement was interpreted as a resonance of mass 1.305 ± .030 $\mathrm{GeV/c}^2$ and width 0.330 ± .060 GeV. (auth)

54204 (COO–1428-310) PROPOSAL FOR AN ADDITIONAL EXPOSURE OF 9 GeV/c K^+ MESONS IN THE 80" D_2 FILLED CHAMBER. Carmony, D. Duane (Purdue Univ., Lafayette, Ind. Dept. of Physics). 1972. 11p. Dep. NTIS.

An additional 600,000 pictures of K^+ interactions in the 80" deuterium filled chamber are requested. Details of $K_N^*(1760)$ and $K_N^*(2200)$ production and decay will be studied and the various decay modes compared with the SU(3) predictions. (auth)

54205 (COO–1428-311) EVIDENCE FOR A NEUTRAL MESON NEAR 1033 MeV. Garfinkel, A. F. (Purdue Univ., Lafayette, Ind.); Hoffman, E. W. (Argonne National Lab., Ill.); Jacobel, R. W.; Cheshire, D. L.; Lamb, R. C.; Peterson, F. C. (Iowa State Univ. of Science and Technology, Ames). 1972. 12p. Dep. NTIS.

In a scintillation counter experiment studying the reaction $\pi^-p \to M^0n$ at 2.4 GeV/c, evidence was obtained for a neutral meson denoted $M^0(1033)$ with a mass of 1032.6 ± 2.3 MeV and a width of $16.2 \pm^{4.8}_{1.5}$ MeV. (auth)

54206 (COO–2009-36) INDIANA UNIVERSITY SPARK CHAMBER GROUP TECHNICAL PROGRESS REPORT, DECEMBER 1, 1971–NOVEMBER 30, 1972. Ankenbrandt, C. M.; Brabson, B. B.; Crittenden, R. R.; Heinz, R. M.; Neal, H. A. (Indiana Univ., Bloomington). [nd]. Contract AT(11-1)-2009. 10p. Dep. NTIS.

Research on the A_2 resonance and strong interactions using spark chambers is summarized. (J.F.P.)

54207 (COO–3064-3) REACTION $\pi^-p \to p\pi^+\pi^-\pi^-\pi^0$ AT 20 GeV/c. Sisterson, L. K.; Harrison, W. C.; Heyda, D.; Johnson, W. H. Jr.; Kim, J. K.; Law, M. E.; Mueller, J. E.; Salzberg,

B. M. (Harvard Univ., Cambridge, Mass. Lyman Lab. of Physics). 1972. 48p. Dep. NTIS.

Data from the reaction $\pi^- p \rightarrow p\pi^+\pi^-\pi^-\pi^0$ at 20 GeV/c are studied in detail. The cross sections for the production of ρ, η^0 and ω^0 mesons, and $\Delta(1236)$ isobars are estimated. The channels $p\eta^0\pi^-$ and $p\omega^0\pi^-$ are compared with a double Regge pole model calculation and the cross section for the contribution from individual diagrams calculated. The data are divided by the method of longitudinal phase space and each category examined in detail. A search is made for possible production of $\rho^-(1700)$, A_1^0 and A_2^0 and upper limits placed on their cross sections. (auth)

54208 (COO—3065-16) π^- INTERACTIONS IN DEUTERIUM AT 7 GeV/c. Katz, W. (Rochester Univ., N. Y. Dept. of Physics and Astronomy). 1971. Contract AT(11-1)-3065. 150p. (UR—387). Dep. NTIS.

Results are presented from a study of π^- deuterium interactions at an incident beam momentum of 7 GeV/c. The experiment to be described was performed at the 80-inch deuterium-filled bubble chamber at the Brookhaven National Laboratory AGS. The size of the exposure is such as to yield ~7 events per μb of cross section. The reactions to be discussed are the following: (1) $\pi^- d \rightarrow pp\pi^-\pi^-$, (2) $\pi^- d \rightarrow pp\pi^-\pi^-\pi^0$, (3) $\pi^- d \rightarrow pp\pi^-\pi^- + N\pi^0$, $N > 1$, (4) $\pi^- d \rightarrow pp\pi^+\pi^-\pi^-\pi^-$, (5) $\pi^- d \rightarrow pp\pi^+\pi^-\pi^-\pi^-\pi^0$, and (6) $\pi^- d \rightarrow pp\pi^+\pi^-\pi^-\pi^- + N\pi^0$, $N > 1$. Stimulated by recent symmetry arguments a search was conducted for multipion resonances having two units of electric charge. No significant evidence was found for these exotic states in reactions (1), (2), (4) and (5); the upper limit for the production of such resonances in these reactions is ~5 μb. The s-wave and d-wave $\pi\pi$ scattering phase shifts were determined using a simple extrapolation procedure for the events from reaction (1). The deduced d-wave phase shift has the same sign as the s-wave phase shift. The value for the I = 2 s-wave phase shift at the mass of the K meson is $-11.0 \pm 2.5°$. In order to examine the validity of spectator model (i.e., the hypothesis that in high energy experiments the deuteron can be treated as a source of essentially free neutrons and protons) the cross section for the $\Delta^0\rho^-$ channel in reaction (2) was compared with the $\Delta^{++}\rho^0$ cross section in the charge symmetric reaction $\pi^+ p \rightarrow \Delta^{++}\rho^0$ at the same incident beam momentum. Assuming isotopic spin invariance, the ratio of these cross sections is $^2/_9$; the observed ratio is found to be consistent with this prediction. This result suggests the validity of the spectator model. (auth)

54209 (JINR—P1-6414) RECONSTRUCTION OF DIFFERENTIAL CROSS SECTION OF THE REACTION $\pi^- p \rightarrow \pi^0(\eta)n$ IN THE SMALL TRANSFERRED MOMENTA REGION. Khvastunov, M. S. (Joint Inst. for Nuclear Research, Dubna (USSR). Lab. of High Energy). 1972. 8p. (In Russian). Dep. NTIS (U.S. Sales Only).

A method is discussed for reconstruction of the emission angle of the $\pi^0(\eta)$ meson in the reaction $\pi^- p \rightarrow \pi^0(\eta)n$ over the opening angle of photons from the $\pi^0(\eta)$ meson decay and over the energy of this meson. It is shown that with this method precision measurements of the direction and the momenta of the incident π^- meson and of the opening angle of photons from the $\pi^0(\eta)$ meson decay are needed in order to guarantee an acceptable accuracy in t square of the transferred 4-momentum which is determined through the $\pi^0(\eta)$ meson emission angle. Carrying out of these conditions gives an error in t (for the method discussed) several times smaller than that for the direct method when reconstruction of the $\pi^0(\eta)$ meson flight direction is made over the emission angles of photons from the $\pi^0(\eta)$ meson decay and over the energies of these photons measured with an available accuracy. The advantages of the method discussed over the direct one are especially appreciable in the region of small t ($t \simeq 0.001$ (GeV/c)^2). (2 tables) (auth)

54210 (NP-19419) MEASUREMENT AND ANALYSIS OF THE CROSS SECTION FOR THE REACTION $K^- p \rightarrow \bar{K}^0 n$ AT MEDIUM ENERGY. Bricman, Claude (Paris Univ., Orsay France)). 1972. 167p. (In French). Dep. NTIS (U. S. Sales Only).

A measurement of the partial cross section for the reaction $K^- p \rightarrow \bar{K}^0 n$ between 1 and 3 GeV/c is described. Although the measurement is simple from the point of view of technique, the effect of interactions of n and $\bar{K}^0$ in the final state in the counters is not easy to evaluate. The method used to take account of these interactions is discussed. Study of the variation with momentum of the cross section for $K^- p \rightarrow \bar{K}^0 n$ permitted confirming the existence and defining the parameters of the most important resonances between 1.9 and 2.3 GeV: $\Sigma(1910)$, $^5/_2{}^+$; $\Sigma(2030)$, $^7/_2{}^+$; $\Lambda(2100)$, $^7/_2{}^-$; and $\Lambda(2350)$, $^9/_2{}^+$. It is shown that the principal resonances (of high spin) can be identified with recurrences of stable particles (Λ and Σ) or of well-known resonances ($\Lambda(1520)$, $^3/_2{}^\pm$ and $\Sigma(1385)$, $^3/_2{}^+$). The resonances can also be classified by the SU(3) scheme. All the principal resonances were placed in the singlets, octets, or decuplets; one can expect that high-spin resonances to be found at higher energies will be placed with equal facility in the multiplets. The situation is more confusing for the case of resonances not found on the principal trajectories; the majority cannot be classified, and the strange partners of a great number of resonances found during πN analyses have not yet been found. (32 figures, 11 tables, 96 references) (R.W.R.)

54211 (RPP/H—95) MEASUREMENTS OF K^+p ELASTIC DIFFERENTIAL CROSS-SECTIONS FOR KAON MOMENTA BETWEEN 0.9 AND 1.9 GeV/c. Charles, B. J.; Cowan, I. M.; Edwards, T. R. M.; (and others) (Rutherford High Energy Lab., Chilton (England)). 1972. 27p. Dep. NTIS (U. S. Sales Only).

The results of K^+p differential and total elastic cross-section measurements at seventeen values of the kaon laboratory momentum between 0.9 and 1.9 GeV/c are presented. The data come from an experiment carried out at the Rutherford High Energy Laboratory, using the 7-GeV proton synchrotron Nimrod. An enriched K^+ secondary beam was focussed at a liquid hydrogen target, and arrays of acoustic spark chambers and scintillation counters detected the incident and scattered particles. (auth) (UK)

54212 (TID—26138) HIGH ENERGY COUNTER GROUP PROGRESS REPORT, JANUARY 1, 1971—DECEMBER 31, 1971. (State Univ. of New York, Stony Brook). 1971. Contract AT-(11-1)-3472. 34p. Dep. NTIS.

The activities of the High Energy Counter Group can be divided into three parts: analysis of data on past experiments, experimentation at the CERN Intersecting Storage Rings, and preparation for future experiments. Results of the experiments discussed either are being prepared for publication or have already appeared. (R.W.R.)

54213 PION—NUCLEON TOTAL CROSS SECTIONS FROM 0.4 TO 0.90 GeV/c. Davidson, D.; Bowen, T.; Caldwell, P. K.; (and others) (Univ. of Arizona, Tucson). Phys. Rev., D; 6: No. 5, 1199-1202(1 Sep 1972).

The total cross sections of $\pi^\pm$ on protons in the momentum interval from 0.40 to 0.90 GeV/c were measured with high relative precision. In this interval the statistical error varies between 10 and 20 μb. No new structure is observed. (auth)

54214 PARAMETRIZATION OF THE NONEVASIVE EXCHANGE PROCESSES AND BACKGROUND CONTRIBUTIONS IN THE REACTION $\pi^- p \rightarrow n\pi^+\pi^-$ AT 2.77 GeV/c. Jacobs, L. D. (CEN de Saclay, Gif-sur-Yvette, France). Phys. Rev., D; 6: No. 5, 1291-1302(1 Sep 1972).

An analysis of 20,000 events from the reaction $\pi^- p \rightarrow n\pi^+\pi^-$ at 2.77 GeV/c is performed according to a parametrization given by Froggatt and Morgan. With reasonable assumptions as to the form of the s-wave $\pi\pi$ amplitude, the low-t behavior of the mean moments and differential cross section was reproduced after obtaining best values for the parameters $\Gamma_i^{s,p}$ in a maximum-likelihood fit. The method may be termed nonevasive. Some discussion is presented on the validity of evasive extrapolation. (auth)

54215 REACTIONS $K^- p \rightarrow \Lambda\pi^0$ AND $K^- p \rightarrow \bar{K}^0 n$ IN THE CENTER-OF-MASS ENERGY RANGE 1700 to 2100 MeV. Van Horn, A. J.; Ely, R. P.; Louie, J. (Univ. of California, Berkeley). Phys. Rev., D; 6: No. 5, 1275-90(1 Sep 1972).

Cross sections, angular distributions, and polarizations are presented for the reactions $K^- p \rightarrow \Lambda\pi^0$ and $K^- p \rightarrow \bar{K}^0 n$ for 19 incident beam momenta in the c.m. energy range 1709—2106 MeV. Legendre-polynomial expansion coefficients to seventh order are also given for the data. The experimental procedures and results from two exposures in the Lawrence Berkeley Laboratory 25-in. hydrogen bubble chamber are discussed. (auth)

54216 FURTHER ASPECTS OF THE REACTION $\pi^- p \rightarrow \pi^-\pi^+ n$ AT 8 GeV/c. Takahashi, K. (Tohoku Univ., Sendai, Japan); Sato, T.; Kitagaki, T.; (and others). Phys. Rev., D; 6: No. 5, 1266-75(1 Sep 1972).

A sample of 3567 events of the reaction $\pi^- p \rightarrow \pi^-\pi^+ n$ was obtained from the measurement of about 50,600 two-prong events in an exposure of the Brookhaven National Laboratory 80-in. hydrogen bubble chamber to an 8-GeV/c π^- beam. The production and decay angular distributions for the ρ^0 were studied comparing with the predictions of the absorptive one-pion-exchange and vector-dominance models. The production and decay angular distributions of the f^0 were also analyzed and compared with the prediction of the gauge-invariance model. A study of the $\pi^+\pi^-$ mass distribution suggests an enhancement at ~2100 MeV. (auth)

54217 TWO-BODY STRANGE-PARTICLE FINAL STATES IN $\pi^- p$ INTERACTIONS AT 4.5 AND 6 GeV/c. Crennell, David J.; Gordon, Howard A.; Lai, Kwan-wu; Scarr, J. Michael (Brookhaven National Lab., N. Y.). Phys. Rev., D; 6: No. 5, 1220-54 (1 Sep 1972).

Results on the following π^-p reactions involving a hyperon are studied at 4.5 and 6.0 GeV/c from a high-statistics bubble-chamber experiment. (1) $\pi^-p \rightarrow (\Lambda, \Sigma^0)K^0$: Differential cross sections and hyperon polarizations are presented. Comparison with the line-reversed reactions $\overline{K}N \rightarrow (\Lambda, \Sigma^0)\pi$ indicates the failure of the predictions of $K^*(890)$ and $K^*(1420)$ exchange degeneracy. Effective trajectories for these two reactions are compared. Shrinkage is observed in $\overline{K}N \rightarrow \Lambda\pi$ and not in $\pi^-p \rightarrow \Lambda K^0$. (2) $\pi^-p \rightarrow (\Lambda, \Sigma^0) K^*(890)^0$: Differential cross sections, hyperon polarizations, and $K^*(890)^0$ density-matrix elements are determined. $\Lambda K^*(890)^0$ decay correlations are found to impose strong constraints on the scattering amplitudes. The data indicate that both natural- and unnatural-parity exchanges contribute large, but opposite, Λ polarizations. This behavior cannot be explained by a simple exchange model utilizing K and the exchange-degenerate $K^*(890)$ and $K^*(1420)$ only. Additional trajectories or absorption effects are required to obtain the observed Λ-polarization effects. Comparison of $\Lambda K^*(890)^0$ and $\Sigma^0 K^*(890)^0$ indicates the greater importance of unnatural-parity exchange in the former reaction. No evidence is observed for deviations from isospin predictions in $\Lambda K^*(890)^0$ production where $K^*(890)^0 \rightarrow K^+\pi^-$ and $K_S^0\pi^0$. (3) $\pi^-p \rightarrow \Lambda K^*(1420)^0$ and $\Lambda K^*(1300)^0$: $K^*(1420)^0$ density-matrix elements satisfying positivity constraints are determined allowing for s-wave interference effects. Evidence of the existence of a narrow $K^*(1300)^0 \rightarrow K\pi\pi$ with a dominant $K^+\rho^-$ decay mode is observed in the 4.5- and 6-GeV/c data. (4) $\Sigma(1385)$, $\Lambda(1405)$, $\Lambda(1520)$ production: Differential cross sections for the quasi-two-body reactions $\pi^-p \rightarrow Y^0K^0$, where Y^0 is $\Lambda(1405)$, $\Lambda(1520)$, or $\Sigma(1385)^0$, are presented and found to have a very similar flat slope in the forward direction. Data for forward K^+ scattering in the reaction $\pi^-p \rightarrow \Sigma(1385)^-K^+$ are presented and discussed. It is argued that this forward peak cannot be explained by kinematic reflection or an s-channel effect and therefore must be due to either two-particle exchange or a single exotic exchange in the t channel. (auth)

54218 PRODUCTION OF PROTON–ANTIPROTON AND CHARGED K MESON PAIRS IN 7 GeV/c π^+d INTERACTIONS. Diamond, Ronald Norman. Madison, Wis.; Univ. of Wisconsin (1972). 224p. University Microfilms Order No. 72-18,975. Thesis.

The production of proton–antiproton and K^+K^- pairs in π^+d interactions at 7 GeV/c incident π^+ beam momentum is studied. The data consist of a 650,000 picture exposure of the Argonne 30″ deuterium filled bubble chamber. Three and four prong topologies were scanned for, measured, and fitted. Candidate $p\text{-}\bar{p}$ and K^+K^- pair events were rescanned and their ionizations measured on a vidicon device. A calculation based on only the measured quantities corroborated the fits for the four constant events. Cross sections are obtained for the final states $p_s pK^+K^-$, $p_s pp\bar{p}$, $p_s NK^+K^-\pi$, and $p_s Np\bar{p}\pi$. The reactions studied here appear to be peripheral in nature and comparison is made between the slope of the momentum transfer distribution for the four constraint events and for the $p_s p\pi^+\pi^-$ final state. Resonance production appears to be more important for K^+K^- final states than for $p\bar{p}$. Indications of the $S^*(1070)$, $f^0(1260)$, $A_2^0(1310)$, $K_sK_s(1440)$, $f'(1514)$, $g(1660)$, and $\rho(1710)$ are seen in the K^+K^- mass spectrum. In the $p\bar{p}$ mass spectrum by contrast there is only a single small enhancement near 2.02 GeV/c^2. The threshold enhancement in the K^+K^- mass spectrum is well fitted by Breit–Wigner resonances, though statistics are not sufficient to rule out the complex scattering length interpretation. The $f^0 \rightarrow K^+K^-$ and $A_2^0 \rightarrow K^+K^-$ cross sections and branching ratios are obtained. In this K^+K^- mass region the angular distributions show strong S wave, as well as possible S and D wave interference effects. Possible $f^0\text{-}A_2^0$ interference was investigated. The D wave appears to be sizable up to a K^+K^- mass of 1.6 GeV/c^2. The $p_s Np\bar{p}\pi$ final state mass spectra are well described by phase space. In the $p_s NK^+K^-\pi$, the $\Delta(1238)$ is the most prominent resonance produced and virtually no $K^*(890)$ is seen, an observation similar to what is observed in the final state $\pi^-pK_sK_s$ for 7 GeV/c π^-p interactions. (Diss. Abstr. Int., B)

54219 PARTIAL WAVE ANALYSIS OF THE $\pi\pi$ SPECTRUM TO 1.5 GeV/c^2: A STUDY OF THE REACTION $\pi^+d \rightarrow p_s p\, \pi^+\pi^-$ AT 13 GeV/c. Barton, Henry Ruwe Jr. Lafayette, Ind.; Purdue Univ. (1972). 143p. University Microfilms Order No. 72-21,156. Thesis.

The $\pi\pi$ spectrum from the reaction $\pi^-d \rightarrow p_s p\, \pi^+\pi^-$ has been studied in an 8.8 event/μb exposure at 13 GeV/c incident π^+ momentum. The production cross sections for ρ and f mesons decaying into $\pi^+\pi^-$ were measured to be 108 ± 11 μb and 59.8 ± 6.0 μb respectively. A maximum likelihood fit to the dipion decay distributions was made to determine the density matrix as a function of dipion mass and momentum transfer. The decay angular distribution was divided into partial waves by assuming the mass dependence of the factorized dipion production amplitude. The isotropic background in the $\pi\pi$ spectrum was found to be large for all dipion masses to 1.5 GeV/c^2. From this, one may conclude that the I = 0 S-wave phase shift is approximately 90 degrees throughout this mass interval. In the range $0.005 < |t| < 0.36$ (GeV/c)^2 covered with adequate statistics by this experiment, the fraction of isotropic background in the $\pi\pi$ spectrum increased with larger momentum transfer. When these data were compared to photoproduction data at 16 GeV/c, a violation was observed for one of the predictions based on vector meson dominance. When the comparison was made using the separated P-wave of this experiment, the disagreement with vector meson dominance extended over the entire range $0.005 < |t| < 0.36$ (GeV/c)^2. The data were used to test a model which attempts to give the t dependence of the density matrix elements in terms of three constants. When the values of the three constants were determined at different values of momentum transfer, sizable fluctuations of the three parameters were found. Disagreement between the model and the experimental density matrix elements was noted. The questionable separation of S-wave and P-wave given by the model was discussed. (Diss. Abstr. Int., B)

54220 INVESTIGATION OF THE REACTIONS $\pi^-p \rightarrow n\pi^+\pi^- + (1,2,3,4,5)\pi^0$ AT GeV/c. Budagov, Y. A.; Valkar, Sh.; Vinogradov, V. B; (and others). (Joint Inst. for Nuclear Research, Dubna, USSR). Yadern. Fiz.; 15: No. 6, 1165-73 (Jun 1972). (In Russian).

The experimental study of the process $\pi^-p \rightarrow n\pi^+\pi^-$ + "neutral particles" at 5 GeV/c with the help of the JINR one meter propane bubble chamber is reported. Partial cross sections for the reactions $\pi^-p \rightarrow n\pi^+\pi^- + (1,2,3,4,5)\pi^0$, angular and momentum distributions of the secondary particles in the c.m.s. were obtained. The production of resonant states was investigated. These results are compared with the predictions of various theoretical models. (auth)

54221 SCALING IN $p\pi^- \rightarrow pX^-$ AND AN ESTIMATE OF THE TRIPLE-POMERANCHUKON COUPLING. Paige, Frank E.; Wang, Ling-lie (Brookhaven National Lab., Upton, N. Y.). Nucl. Phys.; B46: No. 2, 477-82(1972).

It is shown that the CERN-IHEP data on $p\pi^- \rightarrow pX^-$ at 25 and 40 GeV/c exhibit scaling in s′/s. An estimate is given of the triple-Pomeranchukon coupling and the possibility of its measurement at NAL is discussed. (auth)

54222 CENTRAL EMISSION OF PIONS AND SEARCH FOR A SYMMETRY SYSTEM. (Aachen-Berlin-Bonn-CERN-Cracow-Heidelberg-London-Vienna-Warsaw Collaboration). Nucl. Phys.; B46: No. 2, 371-80(1972).

Results are presented on the production of pions having the same direction as the incident particles, but opposite charge, in reactions of π^+p at 8 and 16 GeV/c, π^-p at 16 GeV/c and K^-p at 10 GeV/c. The $d\sigma/dp_L^*$ distributions in the region $|p_L^*| < 0.75$ GeV/c are of the form $\exp(-A|p_L^*|)$, with unequal values of A in the forward and backward directions. A study is made of this asymmetry as a function of the mass and energy of the incoming particle. (auth)

54223 PRELIMINARY STUDY OF $\pi^+\pi^-$ SCATTERING IN THE REACTION $\pi^+p \rightarrow (\pi^+\pi^-)\Delta^{++}$ AT 13 GeV/c. Gaidos, J. A.; McIlwain, R. L.; Thompson, G.; Willmann, R. B. (Purdue Univ., Lafayette, Ind.). Nucl. Phys.; B46: No. 2, 449-59(1972).

A phase shift analysis of $\pi^+\pi^-$ scattering in the mass range 0.6 to 1.4 GeV confirms the rapid rise of the I = 0 s-wave through the $K\overline{K}$ threshold. (auth)

54224 π^-p FORWARD ELASTIC SCATTERING NEAR 1 GeV/c. Abillon, J. M.; Borg, A.; Crozon, M.; (and others) (College de France, Paris). Nucl. Phys.; B46: No. 2, 630-6(1972).

The differential cross section of the reaction $\pi^-p \rightarrow \pi^-p$ was measured in the range $0.92 \leq \cos\theta_{cm} \leq 0.99$ at 15 momenta between 0.875 and 1.580 GeV/c. The results reported complete the available data; previous measurements of this reaction do not extend beyond $\cos\theta_{cm} = 0.90$. The experimental results are compared with dispersion relation predictions. A comparison of the results for B, the slope of the differential cross section, with earlier results shows many discrepancies. (auth)

54225 RESONANCE PRODUCTION IN THE REACTIONS $K^-p \rightarrow p\overline{K}^0\pi^+\pi^-\pi^-$ AND $K^-p \rightarrow p\overline{K}^0\pi^+\pi^-\pi^-\pi^0$ AT 10 GeV/c. (Aachen-Berlin-CERN-London-Vienna Collaboration). Nucl. Phys.; B46: No. 2, 356-70(1972).

An analysis is presented of resonance production in the reactions $K^-p \rightarrow p\overline{K}^0\pi^+\pi^-\pi^-$ and $K^-p \rightarrow p\overline{K}^0\pi^+\pi^-\pi^-\pi^0$ at 10 GeV/c, performed by a maximum likelihood method. In neither process is any significant nonresonant background found. The former reaction is dominated by $K^{*-}(890)$, $\Delta^{2+}(1236)$ and ρ^0 production and the latter by K^{*-}, Δ^{2+} and ω^0. In the second reaction there is no evidence for any ρ^0 production. Two-body intermediate states appear to be negligible, but the three-body states $K^{*-}\rho^0p$ and

$K^{*-}\Delta^{2+}\pi^-$ definitely contribute. A detailed analysis has been performed of the simultaneous resonance production in $K^-p \rightarrow \Delta^{2+}K^{*-}\pi^-$ and the predictions of a Veneziano model calculation for this quasi-three-body final state are found to be in good agreement with the experimental results. (auth)

54226 LPS ANALYSIS OF THE REACTIONS $K^+p \rightarrow K^+\pi^+\pi^-p$ AND $K^+p \rightarrow K^0\pi^+\pi^0p$. De Wolf, E.; Goldschmidt-Clermont, Y.; Grard, F.; Verbeure, F. (CERN–Brussels Collaboration, Geneva). Nucl. Phys.; B46: No. 2, 333-55(1972).

Results are presented on the reactions $K^+p \rightarrow K^+\pi^-\pi^+p$ and $K^+p \rightarrow K^0\pi^0\pi^+p$ studied with the method of the longitudinal phase space. The analysis is based on data at 7 incoming K^+ momenta, ranging from 5 to 12.7 GeV/c. The energy dependence of partial cross sections in various regions of the LPS is discussed. Evidence is presented for the dominance of diffractive processes in particular regions of the phase space and for the hypothesis of factorization. (auth)

54227 PRODUCTION PROPERTIES OF A_1^+ IN π^+p INTERACTIONS AT 5.45 GeV/c. Bloodworth, I. J.; Jackson, W. C.; Prentice, J. D.; Yoon, T. S. (Univ. of Toronto). Nucl. Phys.; B46: No. 2, 402-14(1972).

The production of the peripheral 3π mass enhancement in the A_1 region is described. The differential cross section and its variation with 3π mass is studied and the spin density matrix elements are given for the t-channel and s-channel helicity frames. As observed in π^-p interactions t channel but not s channel helicity is conserved. A Deck type double Regge trajectory exchange amplitude gives good fits to the experimental distributions. Its use is supported by the equality of ρ_{00} for the A_1 and ρ_{00} for the ρ in the t-channel, as noted by Donohue. (auth)

54228 Q REGION OF THE $K^+\pi^+\pi^-$ SPECTRUM FROM K^+ MESON INTERACTIONS IN DEUTERIUM AT 9 GeV/c. Holland, Richard Frederick. Lafayette, Ind.; Purdue Univ. (1972). 135p. University Microfilms Order No. 72-22,303.

Thesis.

The results of a study of the Q region of the $K^+\pi^+\pi^-$ spectrum produced by a 9 GeV/c K^+ meson beam targeted on a deuterium filled bubble chamber are contained in this report. The data, which was obtained from a 360,000 exposure run at the Brookhaven National Laboratory, was processed and analyzed at Purdue University. An analysis of the $K^+\pi^+\pi^-$ spectrum indicates that the Q is a diffractively produced enhancement which may contain two isospin one-half resonances. The two resonances are possibly mixed states of K*'s belonging to two separate SU(3) nonets. A spin-parity analysis of the region indicates that the two resonances are consistent with $J^P = 1^+$, although $J^P = 2^-$ cannot be completely ruled out. The decay modes of the Q are primarily $K^*_{890}\pi^+$ (70 percent) and $K\rho$ (30 percent). There is very little, if any, three body decay. (Diss. Abstr. Int., B)

54229 SOME FINAL STATES WITH A Λ IN K^-n INTERACTIONS AT 4.9 GeV/c. Korpi, John Leonard Cleveland; Case Western Reserve Univ. (1972). 93p. University Microfilms Order No. 72-18,702.

Thesis.

The results of a 5.43 μb/event exposure of the deuterium-filled Brookhaven National Laboratory 80-inch bubble chamber are reported. In particular K^-n reactions with a Λ hyperon and a single charged particle in the final state are considered. Total and differential cross sections are presented for the final states $\Lambda\pi^-$, $\Sigma^0\pi^-$, $\Lambda\pi^-\pi^0$, $\Lambda\pi^-$MM, $\Lambda\pi^-\eta$ and $\Lambda\pi^- - K^0\overline{K}^0$. Resonance production cross sections and decay parameters are given for the multiparticle final states. The reaction $K^-n \rightarrow \Lambda\pi^-\pi^0$ is compared with the predictions of the generalized Veneziano model of Petersson and Törnqvist. (Diss. Abstr. Int., B)

54230 PSEUDOSCALAR-MESON-NUCLEON SCATTERING AND REGGE CUTS; AND AN EXPERIMENTAL STUDY OF THE $K_L^0 \rightarrow K_S^0$ REGENERATION AMPLITUDE IN COPPER. Roth, Timothy Stephan. Pittsburgh; Carnegie-Mellon Univ. (1972). 146p. University Microfilms Order No. 72-21,602.

Thesis.

A simultaneous fit to the data on the four charge exchange reactions ($\pi^-p \rightarrow \pi^0n$, $K^-p \rightarrow \overline{K}^0n$, $K^+n \rightarrow K^0p$ and $\pi^-p \rightarrow \eta n$) is made using a Regge pole model modified by the inclusion of the lowest order Regge cuts produced by means of the impact parameter representation. A measurement of the $K_L^0 \rightarrow K_S^0$ regeneration amplitude in copper is performed using a two arm wire spark chamber magnetic spectrometer in a neutral beam at the Argonne National Laboratory ZGS. There are several kaon nucleon resonance states in the beam momentum range 500–1500 MeV/c covered by the experiment, and their effect on the regeneration amplitude is demonstrated. (Diss. Abstr. Int., B)

54231 INELASTIC K^+p REACTIONS AT INCIDENT MOMENTA FROM 1.27 GeV/c TO 2.17 GeV/c. Loken, Stewart Christian. Pasadena, Calif.; California Inst. of Tech. (1972). 113p. University Microfilms Order No. 72-22,608.

Thesis.

A number of recent experiments have suggested the possibility of a highly inelastic resonance in K^+p scattering. To study the inelastic K^+p reactions, a 400 K exposure was taken at the L.R.L. 25-inch bubble chamber. The data are spread over seven K^+ momenta between 1.37 and 2.17 GeV c. Cross sections were measured for the reaction $K^+p \rightarrow pK^\circ\pi^+$ which is dominated by the quasi-two body channels $K\Delta$ and K^*N. Both these channels are strongly peripheral, as at other momenta. The decay of the Δ is in good agreement with the predictions of the rho-proton analogy of Stodolsky and Sakurai. The data on the K^*p channel show evidence of both pseudo scalar and vector exchange. Cross sections for the final state $pK^+\pi^+\pi^-$ show a strong contribution from the quasi-two body channel $K^*\Delta$. This reaction is also very peripheral even at threshold. The decay angular distributions indicate the reaction is dominated as at higher momenta by a pion exchange mechanism. The data are also in good agreement with the quark model predictions of Bialas and Zalewski for the K^* and Δ decay. (Diss. Abstr. Int. B)

54232 APPARATUS FOR SPIN-ROTATION MEASUREMENTS IN PION–PROTON SCATTERING AT HIGH ENERGIES. Autones, P.; Brisson, J. C.; Boucherie, A.; (and others) (CEN, Saclay, France). Nucl. Instrum. Methods; 103: No. 2, 211-23(1972).

Measurements of spin-rotation parameters allow a complete determination of the pion–nucleon scattering amplitudes when the differential cross section and the polarization normal to the scattering plane are known. This requires the scattering of pions by a proton target that is polarized along a direction in the scattering plane and analysis of the polarization of the recoil protons in a carbon plate polarimeter. Scintillation counter hodoscopes associated with fast logic allow the spark chambers of the polarimeter to be triggered mainly on elastic scatterings by the free protons in the target. (auth)

Particle Interactions and Properties (Theoretical)

Refer also to abstract 54698.

54233 (LA-DC-72-848) NEUTRINO–DEUTERON INTERACTION CROSS SECTIONS AT LAMPF ENERGIES. Brolley, John E. (Los Alamos Scientific Lab., N. Mex.); Huffman, Arthur H. (California Inst. of Tech., Pasadena). [nd]. 4p. (CONF-720819–4). Dep. NTIS.

From International conference on few particle problems in nuclear interactions; Los Angeles, CA. (28 Aug 1972).

The cross section for the process $\nu + d \rightarrow 2p + e^-$ for neutrino energies in the neighborhood of 50 MeV was calculated using proton and deuteron wave functions fitted to recent data and a recently determined value of the coupling constant. Meson exchange corrections were included. The results are compared with previous data. (J.W.R.)

General

Refer also to abstract 54385.

54234 (BNL–50342) WHAT IS AN ELEMENTARY PARTICLE? Peierls, Ronald F. (Brookhaven National Lab., Upton, N. Y.). 9 Apr 1972. Contract AT(30-1)-16. 10p. Dep. NTIS.

The search for the ultimate constituents of matter has been going on since before the time of Democritus. The investigation of the internal structure of protons and neutrons using high energy accelerators leads to some conceptual difficulties. If protons are bombarded by protons many "fragments" are produced, but these cannot be readily understood as constituents of the proton. When high energy electrons are scattered by the electrical distribution of the proton, the proton acts as if composed of independently acting point charges, but such a description does not describe other aspects of the proton's behavior. The large number of different short-lived particles which have been observed in the past two decades can all be understood as different combinations of three fundamental "quarks," but the dynamics of their interactions does not seem to make sense. An attempt is made to present the current point of view of the physicist in considering this ancient question. (auth)

54235 (COO–264-611) NEW FORM FACTORS IN THE DUAL RESONANCE MODEL. Willemsen, Jorge F. (Chicago Univ., Ill. Enrico Fermi Inst. Chicago Univ., Ill. Dept. of Physics). Jul 1972. Contract AT(11-1)-264. 15p. Dep. NTIS.

A new set of fields, satisfying a Mobius invariant equation, is used in a dual model of vector currents. The elastic form factor exhibits power-law fall off, but the inelastic νW_2 structure function does not scale. (auth)

54236 (COO–1428–303) ANNUAL PROGRESS REPORT, TASK B, JUNE 1, 1971–MAY 31, 1972. (Purdue Univ., Lafayette, Ind. Dept. of Physics). [nd]. Contract AT(11-1)-1428. 27p. Dep. NTIS.

Theoretical research on particle interactions is summarized. A list of publications is included. (J.F.P.)

54237 (ITF–72-48-E) UNITARY RENORMALIZATION, POSITIVITY, AND SELFADJOINTNESS OF THE HAMILTONIAN FOR A LEE MODEL OF THE TYPE Y_{3+1}. Zolotaryuk, A. V. (Akademiya Nauk Ukrainskoi SSR, Kiev. Institut Teoreticheskoi Fiziki). 1972. 21p. Dep. NTIS (U.S. Sales Only).

The Lee model in four space–time dimensions is renormalized by unitary transformation. A strongly convergent sequence of unitary operators is defined which transform a sequence of cutoff Hamiltonians to a sequence of operators converging strongly on a dense set of states. The semiboundedness from below in each sector and selfadjointness of the renormalized Hamiltonian are proved. (auth)

54238 (LYCEN–7211) AN ELEMENTARY PARTICLE TREATMENT OF NUCLEAR CURRENTS. Delorme, Jean (Lyon Univ. (France). Institut de Physique Nucleaire). Feb 1972. 103p. (In French). Dep. NTIS (U. S. Sales Only).

Thesis.

The construction in the Rarita and Schwinger formalism of a vectorial function based under the transformation of the proper homogeneous Lorentz group is presented. The consequences of discrete P and T transformations are thus envisaged. Operations involving the SU(2) group and charge conjugation that enable the currents to be classified using the Weinberg and Cabibbo terminology, are considered. The constraints imposed by the C. V. C. and P. C. A. C. hypotheses on the form factors are defined. It is then shown how this formalism is transformed into the multipolar formalism of Galindo and Pascual. Comparisons can be made with classical methods using the impulse approximation and charge exchange corrections (when necessary). In this way, the nonrelativistic contents of the various form factors are studied. After attempting to define the present day limits of elementary particle treatment methods, examples of the applications of such methods are given: treatment of small currents of the second class, muon capture reactions, and the radiative capture of pions in the ^{6}Li → ^{6}He transition. (France)

54239 SOME GENERAL PROPERTIES OF REPRESENTATIONS OF LOCAL CURRENTS. Divakaran, P. P. (Tata Inst. of Fundamental Research, Bombay). Ann. Phys. (N. Y.); 72: No. 2, 512-23(Aug 1972).

Some properties of representations of local current operators are studied. The currents are assumed to be conserved and to have charge densities transforming like the regular representation of any internal symmetry group G containing the isospin SU$_2$. The representation space is the "physical" Hilbert space, having a positive definite metric and carrying time-like positive-energy representations of the Poincaré group. The main results are that, in every irreducible representation space, arbitrarily large irreducible representations of G must occur, and the mass spectrum is unbounded and continuous from some point onwards if it is not strictly degenerate. These results have strong implications for current algebra saturation schemes, both at finite and infinite momentum. (auth)

54240 HIGH ENERGY PHYSICS INDEX. VOLUME 10, No. 14, 1972. Leopoldshafen, Ger.; Zentralstelle fuer Atomkernenergie-Dokumentation (1972). 82p.

54241 HIGH ENERGY PHYSICS INDEX. VOLUME 10, No. 15, 1972. Leopoldshafen, Ger.; Zentralstelle fuer Atomkernenergie-Dokumentation (1972). 88p.

54242 HIGH ENERGY PHYSICS INDEX. VOLUME 10, NO. 16, 1972. Leopoldshafen, Ger.; Zentralstelle fuer Atomkernenergie-Dokumentation (1972). 78p.

Electromagnetic

Refer also to abstracts 53776, 53893, and 54176.

54243 (DESY–72/30) k^2-DEPENDENCE OF THE TRANSVERSE PION ELECTROPRODUCTION CROSS SECTION IN A GENERALIZED BORN TERM MODEL. Gutbrod, F.; Kramer, G. (Deutsches Elektronen-Synchrotron, Hamburg (West Germany)). Jun 1972. 22p. Dep. NTIS (U. S. Sales Only).

Data on π^+ electroproduction off protons are analyzed in a generalized Born term model, where the off-shell nucleon form factor $F_1(k^2)$ is allowed to differ from its on-shell value. The longitudinal–transverse interference cross section is sensitive to the ratio of the nucleon form factor to the pion form factor, and the data require this ratio to be larger than one. The resulting transverse cross section, integrated over a small t interval, follows the slow decrease of the total inelastic cross section as a function of the photon mass squared. (6 figures, 4 tables) (auth)

54244 (DESY–72/36) POLARIZATION EFFECTS IN DEEP INELASTIC LEPTON–NUCLEON SCATTERING. Walsh, T. F. (Hamburg Univ. (West Germany). Institut fuer Theoretische Physik (II)); Zerwas, P. (Deutsches Elektronen-Synchrotron, Hamburg (West Germany)). Apr 1972. 36p. Dep. NTIS (U. S. Sales Only).

An introduction is given to questions related to polarization experiments in deep inelastic lepton–nucleon scattering. After discussing the kinematics a summary is presented of the results from different models which have been proposed as descriptions of spin effects in the Bjorken scaling region. Longitudinal and perpendicular asymmetries at various incident lepton energies and scattering angles are estimated in order to show how to distinguish between models which give nearly identical results for spin averaged cross sections. (auth)

54245 (IS-T–531) THEORETICAL TREATMENT OF THE SCHWARZ–HORA EFFECT. Hadley, George Ronald (Ames Lab., Iowa). Aug 1972. Contract W-7405-eng-82. 56p. Dep. NTIS.

Thesis.

In the Schwarz–Hora effect, an electron beam passing through a crystal is modulated by laser light and then reproduces the light when it strikes a nonluminescent target. The theory for the modulation process is developed for incident plane wave electrons using the Born approximation to second order. A wave packet treatment of the incident electrons is also included to study interparticle phasing. Finally, light production at a nonresonant target is discussed classically and quantum mechanically, and an upper limit for the amount of light emitted at the laser frequency is calculated using a semiclassical model. (auth)

54246 (JINR–P2-6636) AUTOMODEL ASYMPTOTIC OF THE SPECTRAL FUNCTIONS OF VIRTUAL COMPTON EFFECT. Matveev, V. A. (Joint Inst. for Nuclear Research, Dubna (USSR). Lab. of Theoretical Physics). 1972. 37p. (In Russian). Dep. NTIS (U. S. Sales Only).

Strict mathematical grounds are given for the consistency of the hypothesis about automodel asymptotic behavior of the spectral functions of the virtual Compton effect in the range of high energy and large momenta of a photon. The relation between the automodel asymptotic and the behavior of the electromagnetic current commutator in the vicinity of the light cone is studied. (auth)

54247 (NP–19417) PION ELECTROPRODUCTION AT THRESHOLD. Note No. 268. Benfatto, G.; Nicolo, F.; Rossi, G. C. (Rome Univ. (Italy). Istituto di Fisica). 29 Mar 1972. 32p. Dep. NTIS (U. S. Sales Only).

A method to calculate the axial nucleon form factor, g_A, and the electromagnetic pion from factor, F_π, at threshold is discussed. The theoretical ingredients are gange invariance, low energy theorems and t-fixed dispersion relations. Also the errors involved in the unavoidable approximations are discussed. (auth)

54248 (ORO–3992-106) S MATRIX ELEMENTS IN THE PRESENCE OF STANDING WAVE STATES, THE BJORKEN LIMIT, AND SHADOW-QUARKS. Nelson, C. A. (Louisiana State Univ., Baton Rouge. Dept. of Physics and Astronomy. Texas Univ., Austin. Center for Particle Theory). Aug 1972. Contract AT(40-1)-3992. 51p. (CPT–160). Dep. NTIS.

When a scattering reaction occurs, it is usually assumed that the complete set of collision states is entirely composed of traveling waves, hence any constituent, in principle, is observable. Should, however, either quarks regulator photons or lepton satellites be standing wave states, i.e. only shadow states, one would not expect to have observed them. The new terms which modify the usual dispersion relations and Low equation are discussed, and it is argued that present two-body experiments do not provide strong tests for their presence. In the Bjorken limit these piecewise analytic terms vanish. Yet, in a shadow indefinite-metric theory, the logarithmic terms breaking this limit are still absent. The triangle anomalies, therefore, should only be taken seriously in low-energy reactions. A stronger constraint on the presence of shadow states can be provided by verification of the Callen–Gross sum rule. By means of a simple version of the Kuti–Weisskopf model, containing valence quarks and quark-antiquark pairs, it is demonstrated explicitly how quarks can be shadow states. In formal scattering theory with shadow states, the correct formal solutions for the exact asymptotic states, both physical and shadow, are obtained. (auth)

54249 INVESTIGATION OF LINEAR POLARIZATION OF SYNCHROTRON RADIATION. Nikitin, M. M. (Tomsk Polytechnic Inst., USSR). Izv. Vyssh. Ucheb. Zaved., Fiz.; No. 12, 133-5(1970). (In Russian).

The linear polarization of synchrotron radiation from 300- to 1200-MeV electrons was studied for the vertical angular distribution of intensities. The calculated results are given. (J.F.P.)

54250 BREMSSTRAHLUNG OF SOFT PHOTONS IN REACTION $p + p \rightarrow \pi^+ + d + \gamma$. Shekhter, L. Sh. (Saratov State Univ., USSR). Izv. Vyssh. Ucheb. Zaved., Fiz.; No. 12, 29-32(1970). (In Russian).

An amplitude was found for soft-photon bremsstrahlung in the process $p + p \rightarrow \pi^+ + d + \gamma$. This amplitude is expressed in terms of $p + p \rightarrow \pi^+ + d$ scattering amplitudes. (J.F.P.)

54251 CHIRAL SYMMETRY AND STRUCTURE OF THE NUCLEON. Chapline, George F. Jr. Phys. Rev., D; 6: No. 5, 1324-8(1 Sep 1972).

Starting from the nonlinear σ model it is shown that for large momentum transfer the proton charge form factor is approximately equal to $(1 + Q^2/Q_0^2)^{-2}$, where the constant Q_0 is related by a simple transcendental equation to the pion–nucleon coupling constant f and to a constant f_π related to the charged-pion decay rate. Using the experimental values of f and f_π $Q_0 = 800$ MeV is obtained. The charge radius of the proton is calculated to be 0.85 F. Further, it is shown that the "hard core" radius for nucleon–nucleon interactions should be approximately equal to $(2/Q_0) = 0.5$ F. An interpretation of the most prominent pion–nucleon resonances is also offered. (auth)

54252 LOW-ENERGY THEOREM FOR $\gamma\gamma \rightarrow 3\pi$ AND THE REACTION $\gamma + Z \rightarrow 3\pi + Z$. Smith, J.; Stanko, N. (State Univ. of New York, Stony Brook). Phys. Rev., D; 6: No. 5, 1332-9 (1 Sep 1972).

Recently a low-energy theorem was proposed by Adler, Lee, Treiman, and Zee and by Terent'ev for the reaction $2\gamma \rightarrow 3\pi$. This theorem is supposed to be valid at an unphysical point in the production amplitude. One possible way to test its reliability is to measure the reaction $e^+e^- \rightarrow e^+e^- + 3\pi$ which unfortunately has a very small cross section. In this paper another reaction is investigated which may allow a more satisfactory check of the low-energy theorem, namely, the photoproduction of three pions off a target nucleus. Cross sections, angular and energy distributions, and invariant-mass plots are given for several beam energies assuming a lead target. The η-meson background is also examined. (auth)

54253 TEST OF THE ALGEBRA OF BILOCAL OPERATORS. Iliopoulos, J. (Laboratoire de Physique Theorique et Hautes Energies, Orsay, France); Paschos, E. A. Phys. Rev., D; 6: No. 5, 1340-6(1 Sep 1972).

It is shown that the electroproduction of massive muon pairs provides a test of the algebra of bilocal operators. The cross section for the contribution of the Compton term is derived and estimates of the background terms are indicated. As expected, numerical estimates indicate that the cross sections are fairly small. (auth)

54254 EVALUATION OF THE J = 0 FIXED POLE IN NEUTRON COMPTON SCATTERING. Dominguez, C. A.; Gunion, J. F.; Suaya, R. (Stanford Univ., Calif.). Phys. Rev., D; 6: No. 5, 1404-11(1 Sep 1972).

The recent deuteron Compton data are used to evaluate the J = 0 fixed pole in neutron Compton scattering. This calculation includes the effects of both Glauber and Fermi-motion corrections in the extraction of the free-neutron cross section from the deuteron data. The result is consistent with the Born answer, zero. As a by-product, it is shown that the f: A_2 ratio in Compton scattering is much larger than previously expected. (auth)

54255 COMPTON SCATTERING. I. SPECTRAL FORMS FOR THE INVARIANT AMPLITUDES TO ORDER e^4. Milton, Kimball A.; Tsai, Wu-yang; DeRaad, Lester L. Jr. (Univ. of California, Los Angeles). Phys. Rev., D; 6: No. 5, 1411-27 (1 Sep 1972).

The six invariant amplitudes for Compton scattering are explicitly calculated to order e^4. Gauge-invariant amplitudes which are free of kinematic singularities and zeros are derived in double-spectral form. They are calculated in the framework of Schwinger's source theory which makes crucial use of causality and space-time extrapolation. The accompanying single-spectral forms (contact terms) are determined by analysis of forward scattering. The resulting amplitudes contain all the information necessary to calculate radiative corrections to polarized electron–photon scattering experiments. (auth)

54256 COMPTON SCATTERING. II. DIFFERENTIAL CROSS SECTIONS AND LEFT–RIGHT ASYMMETRY. Tsai, Wu-yang; DeRaad, Lester L. Jr.; Milton, Kimball A. (Univ. of California, Los Angeles). Phys. Rev., D; 6: No. 5, 1428-38(1 Sep 1972).

The differential cross sections for polarized electron–photon scattering are calculated to order e^6 and the unpolarized result of Brown and Feynman is rederived. The left-right asymmetry is calculated for a polarized target electron in agreement with Miller and Wilcox. This leaves the disagreement between theory and experiment unresolved. These results are obtained by using the six invariant amplitudes in spectral form, which were calculated in the preceding communication. (auth)

54257 DEEP-INELASTIC CONTRIBUTION TO BARYON ELECTROMAGNETIC MASS DIFFERENCES. Katsumori, Hiroshi (Chubu Inst. of Tech., Nagoya, Japan). Phys. Rev., D; 6: No. 5, 1438-44(1 Sep 1972).

Unsubtracted dispersion relations for $t_1(q^2,\nu)$ and $t_2(q^2,\nu)$ are proposed even in the case of the $\Delta I = 1$ mass difference, with the requirement of the absence of divergences worse than logarithmic ones. By the use of the experimental data on the inelastic nucleon structure functions, the possibility is shown that the deep-inelastic effect leads to the correct sign of the observed n–p mass difference. In consideration of the experimental fact that the ratio of structure functions, $W_{2,n}/W_{2,p}$, in the range where the greater part of the contribution to the relevant integral results is not far away from the threshold value as $\omega/2M \rightarrow 1$ predicted by Bloom and Gilman, the deep-inelastic part of the n–p mass difference is effectively written in the form of the magnetic-moment-type self-energy. It is also shown that if this is similarly applicable to other baryons, and if the SU(3) magnetic-moment relations hold, the correct signs and right orders of magnitude of the mass differences $\Sigma^- - \Sigma^+$, $\Xi^- - \Xi^0$, as well as $\frac{1}{2}(\Sigma^+ + \Sigma^-) - \Sigma^0$, are reproduced by the theory with no adjustable parameter except an input of the observed n–p mass difference. (auth)

54258 COMMENT ON THE POSSIBLE RELATION BETWEEN PROMINENT RESONANCES AND LIMITING SCALING DATA IN INELASTIC ELECTROPRODUCTION ON NUCLEONS. Pestieau, Jean (Instituto Politecnico Nacional, Mexico City). Phys. Rev., D; 6: No. 5, 1449-50(1 Sep 1972).

A recent parametrization of a relation between prominent resonances and limiting scaling data in inelastic electroproduction on nucleons is shown to be incompatible with experiment, unless the electromagnetic current has an isotensor component. (auth)

54259 $\eta \rightarrow 3\pi$ DECAYS IN A MODEL SATISFYING ANALYTICITY, CROSSING SYMMETRY, AND APPROXIMATE UNITARITY. Picciotto, Charles; Smith, Donald (Univ. of Victoria, B.C.). Phys. Rev., D; 6: No. 5, 1450-2(1 Sep 1972).

Recently developed solutions to Moffat's model for meson–meson scattering are applied to the decays $\eta \rightarrow 3\pi$ and $K \rightarrow 3\pi$. Very good fits to the data are obtained. (auth)

54260 ROLE OF NEUTRAL VECTOR MESONS IN THE PHOTOFORMATION OF LEPTON PAIRS BY NUCLEI. Kerimov, B. K.; Ablakulov, Kh. A.; Sadykhov, F. S. (Moscow State Univ.). Izv. Akad. Nauk SSSR, Ser. Fiz.; 36: No. 1, 194-7(Jan 1972). (In Russian).

An expression for the differential cross section of photoproduction of $e^+ - e^-$ pairs at a point nucleus with spin $\frac{1}{2}$ was obtained from a model of vector dominance. The expression corresponded to two Compton diagrams. The participation of neutral vector mesons (ρ^0, ω, and φ) leads to the appearance of a peak in the angular dependence of the cross section of the process. (tr-auth)

54261 DISPERSION RELATIONS AND DATA FOR THE REACTION $\gamma n \rightleftharpoons p\pi^-$ IN THE 33-RESONANCE REGION. Aznauryan, I. G.; Zaslavskii, A. N. (Inst. of Physics, Erevan). Yadern. Fiz.; 15: No. 6, 1261-5(Jun 1972). (In Russian).

It is shown that there is a difference between prediction of dispersion relations and experiment for the isovector part of photoproduction amplitude. This difference cannot be canceled by introduction of isotensor electromagnetic current. For the analyzed isotopic combination the result practically does not depend upon possible uncertainties in the solution of dispersion relations. (auth)

54262 e^+e^--PAIR ANNIHILATION AND DEEP INELASTIC ep-SCATTERING IN PERTURBATION THEORY. Gribov, V. N.; Lipatov, L. N. (Inst. of Nuclear Physics, Leningrad). Yadern. Fiz.; 15: No. 6, 1218-37(Jun 1972). (In Russian).

The connection between e^+e^- annihilation into hadrons and deep inelastic ep scattering in pseudoscalar theory and vector theory with conserving current was considered. It is shown, that in the both theories there is simple relation between structural functions $W(\omega, \xi)$ and $W^a(\omega, \xi)$, that describe ep scattering and e^+e^- annihilation, if antiproton is selected in the final state. This relation is: $W^a(\omega, \xi) = -(1/\omega) \cdot W(1/\omega, \xi)$, where ω – the Bjorken variable, ξ – some function of q^2, that is expressed in logarithmic approximation $g^2 \ln q^2 \sim 1$, $g^2 \ll 1$ as an integral by the invariant charge. Similar relation for $\widetilde{W}(\omega, \xi)$ and $\widetilde{W}^a(\omega, \xi)$ describing electron-meson scattering and annihilation with a selected meson in final state, appears to be valid only for large $q^2(\xi \gg 1)$. As for analytic connection of $W(\omega,\xi)$ and $W^a(\omega, \xi)$ (assumed by Drell et al.) is absent in vector theory. The functions $W^a(\omega, \xi)$ and $\widetilde{W}^a(\omega, \xi)$ obtained in logarithmic approximation, satisfy simple sum rules. (auth)

54263 PRODUCTION OF MUONIC PAIRS IN μp-COLLISIONS. Kobrinskii, M. N.; Tikhonin, F. F. (Inst. of High Energy Physics, Moscow). Yadern. Fiz.; 15: No. 6, 1238-42(Jun 1972). (In Russian).

The process of electroproduction of lepton pairs is considered. The matrix element squared was calculated. The masses of all the particles and the target recoil was taken into account. The numeric results deal with the muonic trident process on proton. At the initial energy 30 GeV an angular distribution of the final muons, the mass spectrum of a muonic pair with different charges, and the total cross-section of the process were obtained. The problem of the contribution to the cross section of different types of the diagrams was considered, and in this it was revealed that the process is fully determined by the "space-like" diagrams (a–d) only. (auth)

54264 RADIATION FROM A CHARGE IN THE FIELD OF TWO PLANE WAVES. Khalilov, V. R. (Moscow State Univ.). Izv. Vyssh. Ucheb. Zaved., Fiz.; No. 3, 76-9(1972). (In Russian).

The problem of radiation from a relativistic charge in a field of two plane electromagnetic waves was examined, where the propagation of both waves was in the same direction. The total intensity and the spectral-angular distribution of the polarized radiation were found. Several special cases were also investigated. (tr-auth)

54265 STRUCTURE OF OBSERVABLE AMPLITUDES FOR PHOTON-SOFT-PION INTERACTION. Terent'ev, M. V. (Inst. of Theoretical and Experimental Physics, Moscow). Yadern. Fiz.; 15: No. 6, 1199-1217(Jun 1972). (In Russian).

The processes $\gamma\gamma \rightarrow \pi\pi$, $\gamma\pi \rightarrow \pi\pi$, $\gamma\gamma \rightarrow 3\pi$ with "soft" pions are considered. It has been exhibited, that the amplitude of the process $\gamma\gamma \rightarrow \pi\pi$ is defined with pole diagrams, if γ-quanta are real; and if they are extremely virtual it is expressed via spectral-functions of the vector and axial currents. $\gamma\pi \rightarrow \pi\pi$ amplitude is expressed via "f" constant of π^0-meson decay. This relation is the main result; it is fulfilled in case the anomalous condition for divergences of neutral axial current is valid. The amplitude of the process $\gamma\gamma \rightarrow 3\pi$ is expressed through $\gamma\pi \rightarrow \pi\pi$ and $\pi^0 \rightarrow 2\gamma$ amplitudes. Possible experimental tests of the relations obtained are discussed. (auth)

54266 PAIR PRODUCTION IN ELECTROMAGNETIC FIELD (CASE OF ARBITRARY SPIN). Marinov, M. S.; Popov, V. S. (Inst. of Theoretical and Experimental Physics, Moscow). Yadern. Fiz.; 15: No. 6, 1271-85(Jun 1972). (In Russian).

Quasiclassical method of "imaginary time" is generalized for the case of a spin particle. The production probability of pairs in strong electromagnetic field for particles with an arbitrary spin and magnetic moment is calculated. (auth)

54267 p–p BREMSSTRAHLUNG CALCULATIONS AND RELATIVISTIC SPIN CORRECTIONS. Liou, M. K.; Sobel, M. I. (Brooklyn Coll.). Ann. Phys. (N. Y.); 72: No. 2, 323-52 (Aug 1972).

The Hamiltonian for p–p bremsstrahlung, including relativistic corrections to the Pauli–Schrodinger equation, is discussed in detail. The cross section for this process is derived, and calculations, based on the Hamada–Johnston potential with and without relativistic corrections, are presented. When the relativistic spin correction is neglected, the results, here found by calculating the amplitude in the c.m. frame, are quite different from results found previously by using the lab frame; however, when the relativistic correction is included, then the lab and c.m. calculations are in agreement with each other, and also with experimental data. The correction is small in the c.m. frame and large at higher energies in the lab frame. Comparisons between theory and experiment are made at various energies, and for cases of unequal proton polar angles, and noncoplanar scattering. (16 figures) (auth)

54268 π^0 ELECTROPRODUCTION AT THE FIRST RESONANCE AT MOMENTUM TRANSFERS $q^2 = 0.6$, 1.0, AND 1.56 GeV^2. Alder, J. C. (DESY, Hamburg); Brasse, F. W.; Chazelas, E.; (and others). Nucl. Phys.; B46: No. 2, 573-92(1972).

Recent measurements on the electroproduction of π^0 mesons in the region of the first pion nucleon resonance at four momentum transfers of $q^2 = 0.6$ and $q^2 = 1$ GeV^2 are extended to $q^2 = 1.56$ GeV^2. All the results are discussed in terms of angular coefficients and multipole amplitudes. Assuming that the angular distributions are dominated by the magnetic dipole M_{1+}, the square of the magnetic dipole amplitude and its interference terms with the multipoles E_{0+}, S_{0+}, E_{1+}, S_{1+} and M_{1-} are determined. The results are compared with theoretical models. The dependence of $|M_{1+}|^2$ on the invariant mass W at different q^2 is discussed by comparison with a standard Breit Wigner formula. (auth)

54269 TWO-PHOTON EXCHANGE EFFECTS IN DEEP INELASTIC ELECTROPRODUCTION. Kingsley, R. L. (Univ. of Cambridge, Eng.). Nucl. Phys.; B46: No. 2, 615-29(1972).

The order of magnitude of expected contributions to deep inelastic electron-proton scattering which are of higher order in the fine structure constant than those usually considered is examined in a spin $^1/_2$ parton model. They are found to be probably negligible in their contribution to the inelastic electron-proton scattering cross section. (auth)

54270 PROPERTIES OF THE PION EXCHANGE CONTRIBUTION TO TWO AND QUASI TWO BODY REACTIONS. Gotsman, E.; Maor, U. (Tel-Aviv Univ., Israel). Nucl. Phys.; B46: No. 2, 525-37(1972).

The structure of the t-channel unnatural parity exchange contribution to two and quasi two body reactions is examined. A method in which the absorbed pion exchange contribution is strongly suppressed for $-t \geq 0.2$ GeV^2 is discussed. A hybrid model is presented which enables us to concurrently provide a consistent description of reactions in which the pion exchange plays an important role. This is achieved without recourse to additional parameters. (auth)

54271 CONTRIBUTION TO THE SIXTH-ORDER ELECTRON AND MUON ANOMALIES. Billi, D. (Univ., Bologna); Caffo, M.; Remiddi, E. Lett. Nuovo Cim.; 4: No. 14, 657-60(5 Aug 1972).

The sixth-order contribution to the electron and muon anomalous gyromagnetic ratios a_e, a_u, was evaluated analytically from simple Feynman graphs. (L.B.S.)

54272 PION–MUON MODEL AND LINEAR MASS RELATIONS. Tangherlini, F. R. (Coll. of the Holy Cross, Worcester, Mass.). Lett. Nuovo Cim.; 4: No. 14, 671-7(5 Aug 1972).

Some further development of the pion–muon model presented recently is given as well as some mass regularities that were suggested by this model. The results are summarized by the following rule: There exist very precise, linear, rational mass relations, even for particles that belong to different multiplets, inclusive of leptons. These relations are found to hold with accuracies ranging from 230 to 20 ppm. (L.B.S.)

54273 INFORMATION ON THE PION FORM FACTORS FROM THE ABSENCE OF ZEROS. Raszillier, I. (Inst. of Physics, Bucharest). Lett. Nuovo Cim.; 4: No. 14, 690-2(5 Aug 1972).

Information on the pion electromagnetic form factor was previously derived from analyticity, normalization, and bounds given on its modulus by $e^+e^- \rightarrow \pi^+\pi^-$ data. The additional information brought by the hypothesis is that the pion form factor has no zeros inside its analyticity domains. (L.B.S.)

54274 PHOTON STABILITY. Hare, M. G. (Univ. of Saskatchewan, Regina). Lett. Nuovo Cim.; 4: No. 14, 693-4(5 Aug 1972).

The possibility of a photon with a rest mass decaying into a neutrino-antineutrino pair is examined. An expression is derived for the lifetime that varies as the inverse square of the photon rest mass, thus showing that a massless photon would be completely stable. It also shows that the higher the photon energy the longer the lifetime, hence the odds of detecting the decay of a photon in the electric-wave region of frequency of 1 Hz are insignificant. (L.B.S.)

54275 GENERAL APPROACH TO SCALING IN ELECTRO-INCLUSIVE REACTIONS. Bardakci, K.; Pak, N. K. (Univ. of California, Berkeley). Lett. Nuovo Cim.; 4: No. 14, 719-24 (5 Aug 1972).

A simple unified approach to off-mass shell photon processes, based on the well-known Regge picture of strong interactions, is reviewed. The analysis is extended to the electro-inclusive process. The various kinematic limits suggested by the Regge analysis are studied. The asymptotic form of the average pion multiplicity is then determined. It is found that the multiplicity goes like log ν both in the Regge (Q^2 = fixed, $\nu \rightarrow \infty$) and in the scaling (ω = fixed, $\nu \rightarrow \infty$) limits. (L.B.S.)

54276 APPLICATION OF MOFFAT'S MODEL TO $\eta \rightarrow 3\pi$ AND $K \rightarrow 3\pi$ DECAYS. Smith, Donald; Picciotto, Charles. (Univ. of Victoria, B. C.). Can. J. Phys.; 50: No. 12, 1346-9 (15 Jun 1972).

Moffat's model for meson–meson scattering, satisfying the Mandelstam representation, crossing symmetry, and Regge behavior, is applied to $\eta \rightarrow 3\pi$ and $K \rightarrow 3\pi$ decays. It is found that agreement with the data is excellent when the model is used with Lovelace's trajectory, but not as good with Moffat's trajectory. The model is also applied to the process $pn \rightarrow 3\pi$, and fair agreement is found in the low energy region; however, since the model is unitary only at low energies, no strong conclusions can be reached in this case. (auth)

54277 WEAK AND ELECTROMAGNETIC PROCESSES. Mikaelian, Karnig O. Stony Brook, N. Y.; State Univ. of New York (1972). 90p. University Microfilms Order No. 72-22,862. Thesis.

In Part I the production of single W bosons in electron-positron colliding beams, via the reaction $e^+ + e^- \rightarrow W^- + e^+ \nu_e$, is considered. The total cross section and angular and energy distributions of the positron and the W boson produced in the above reaction are computed. The calculation of the total cross section includes all four lowest order Feynman diagrams contributing to this process. The analysis is limited to center of mass energies $E < 2M_W$ (M_W = boson mass). In this range it is found that the contribution of two of the diagrams is negligible, but the presence of a pole in one of these diagrams invalidates all previous calculations of the total cross section for $E > 2M_W$. Total cross sections are given for three values of the boson's anomalous magnetic moment. A rather flat energy distribution of outgoing positrons and a slight peak in the high energy region of the boson energy distribution are found. The angular distribution of positrons has a very sharp forward peak (defined as the direction of the initial positrons), while the bosons are distributed mostly in the backward direction. A short discussion of the process $e^+ + e^- \rightarrow W^- + \mu^+ + \nu_\mu$ is also included. Part II is devoted to the study of radiative corrections to the general process $A \rightarrow Be^+e^-$ where A is a hadron and B is either a hadron or a photon. The radiative corrections to the $\pi^0 \rightarrow \gamma e^+e^-$ decay are first calculated over the whole range of the Dalitz plot, with no restrictions on the radiative photon energy. The corrections are found to be negative and large in magnitude in the region of large invariant mass of the Dalitz pair, and small but positive for small values of the same quantity. The total correction to the decay rate, defined by $\Gamma^{rad}(\pi^0 \rightarrow \gamma e^+e^-)/\Gamma(\pi^0 \rightarrow \gamma\gamma)$ is positive and agrees with the results of previous calculations. Consideration is then given to the general process $A \rightarrow Be^+e^-$ and an analytic formula is derived for the radiative corrections to the invariant mass spectrum of the Dalitz pair. Considering the decay of a neutral pseudoscalar particle, all the integrations indicated in this formula are performed. Finally, the results are applied to the decay $\eta \rightarrow \gamma e^+e^-$. (Diss. Abstr. Int., B)

54278 THEORY OF COMPTON SCATTERING BY A CHARGED DIRAC PARTICLE WHICH POSSESSES INTRINSIC DIPOLE MOMENTS. Kukanov, A. B.; Kuang, Tkhai (Moscow State Univ.). Izv. Vyssh. Ucheb. Zaved., Fiz.; No. 1, 113-15(1972). (In Russian).

An electric dipole moment may exist for an elementary particle only if the law regarding parity conservation is violated. For the purposes of the development a Dirac particle, an electric charge, an intrinsic magnetic dipole moment, and, in addition, an electric dipole moment are assumed. The effective differential cross section of Compton scattering was calculated for a particle initially at rest. (K.S.W.)

54279 COMPTON SCATTERING BY K-SHELL ELECTRONS. I. NONRELATIVISTIC THEORY WITH RETARDATION. Gavrila, Mihai (Univ. of Colorado, Boulder). Phys. Rev., A; 6: No. 4, 1348-59(Oct 1972).

An exact analytic calculation is presented for the cross section of the nonrelativistic Compton-type inelastic scattering of photons by electrons bound in the ground state of a hydrogen-like atom. The matrix element of the process was taken to be of the Kramers–Heisenberg–Waller form. It was integrated by the Coulomb–Green's-function method, developed previously by the author in connection with Rayleigh scattering. This is based on replacing the sum over intermediate states by the Green's function which is expressed in terms of the integral representation in momentum space given by Schwinger. The final continuum-state wave function was also described by an integral representation. Thus the evaluation of the matrix element requires the carrying out of momentum-space integrations, followed by two contour integrations. Its final form was expressed in terms of hypergeometric functions of four variables of Lauricella's type F_D. At small photon energies, where the dipole approximation is valid, the result simplifies considerably. The low-energy end of the scattered-photon spectrum is considered in detail in connection with the infrared divergence problem. The shape of the spectrum is discussed and a comparison with previous results is given. (auth)

54280 COMPTON SCATTERING BY K-SHELL ELECTRONS. II. NONRELATIVISTIC DIPOLE APPROXIMATION. Gavrila, Mihai (Univ. of Colorado, Boulder). Phys. Rev., A; 6: No. 4, 1360-7(Oct 1972).

The dipole approximation of the nonrelativistic cross section for Compton scattering by electrons bound in the ground state of a hydrogenlike atom, obtained by the present author, is computed and discussed. In this approximation the cross-section differential with respect to the angles and energy of the scattered photon is proportional to $C_1 + C_2 \cos^2\theta$, where θ is the scattering angle of the photon. The coefficients C_1, C_2 are combinations of Appell functions F_1, depending on the atomic number Z and the energies of the initial and final photons κ_1, κ_2 by means of the dimensionless variables $k_i = \kappa_i/Z^2R$, $i = 1, 2$, where R is the rydberg. In order to compute the Appell functions, these were first continued analytically and expressed in terms of other hypergeometric functions of two variables, which under our circumstances admit convergent series expansions. These were then summed numerically. The incident photon energies considered lie in the interval $1.05 \leq k_1 \leq 20$. For each value k_1 the coefficients C_1 and C_2 were computed for a number of values of k_2 ($0 \leq k_2 \leq k_1 - 1$). Special attention was given to the end points $k_2 = 0$ and $k_2 = k_1$. C_1 and C_2 turn out to be monotonically decreasing functions of k_2 presenting the infrared-divergent behavior $1/k_2$ for $k_2 \rightarrow 0$. The limitations of the result due to retardation corrections are considered. (auth)

54281 ANGULAR DISTRIBUTIONS IN THE ANNIHILATION OF AN ELECTRON–POSITRON PAIR. Kheifets, S. A.; Khoze, V. A. (Inst. of Physics, Erevan. Inst. of Nuclear Physics, Novosibirsk, USSR). Dokl. Akad. Nauk SSSR; 203: No. 2, 320-2 (11 Mar 1972). (In Russian).

Some general properties of angular distributions during two-particle annihilation of an electron-positron pair were considered. It was expedient to examine the case of polarized particles, since during prolonged motion in a magnetic field the electrons and positrons may be polarized as a result of radiation. The approach used is quite well known, but it is stressed that the basic properties of angular distributions have a completely simple origin and may be obtained without detailed computation in each separate case. (K.S.W.)

54282 QUARK MASS AND STRUCTURE FUNCTIONS FOR ELECTRON SCATTERING. Okumura, Yoshitaka (Kyoto Univ.). Progr. Theor. Phys. (Kyoto); 48: No. 1, 331-2(Jul 1972).

Deep inelastic electron scattering off a hadron is considered in the quark-parton model. The bare quark mass is estimated using the Cottingham formula and it is conjectured that mF_2 is universal for all hadrons except for the unitary spin factor. (L.B.S.)

54283 PHOTO-NEUTRAL VECTOR MESON COUPLINGS IN THE RELATIVISTIC EXTENDED QUARK MODEL. Kobayashi, Tsunehiro (Tokyo Univ. of Education). Progr. Theor. Phys. (Kyoto); 48: No. 1, 335-7(Jul 1972).

The infinite numbers of coupling constants of photo-vector meson transitions are determined in the quark model with relativistically extended internal structure. It is also shown that the photo-vector meson couplings for high mass mesons are quite large and that the existence of high mass vector mesons can be tested by the storage-ring experiments. (L.B.S.)

Weak

Refer also to abstracts 54181, 54185, 54365, and 54366.

54284 (BNL–16978) WEAK INTERACTIONS AT ISABELLE. Berman, S. M. (Brookhaven National Lab., Upton, N. Y.). 27 Jun 1972. 16p. Dep. NTIS.

The Fermi theory of weak interactions is tested in a study of the reaction $p + p \rightarrow e^+(e^-) + \nu$ + anything. The cross sections are estimated in the parton model using a point Fermi interaction between leptons and partons. Intermediate boson effects on the distributions and cross sections are included. It is found that the studied process leads to quite measurable counting rates if the luminosity is of the order of 10^{23} cm^{-2} sec^{-1} and hence could be one of the most significant investigations carried out at ISABELLE. (J.F.P.)

54285 (DESY–72/32) QUARK MODEL PREDICTIONS FOR WEAK PRODUCTION OF PSEUDOSCALAR MESONS. Koepp, G., Rein, D.; Zerwas, P. (Deutsches Elektronen-Synchrotron, Hamburg (West Germany)). Jun 1972. 13p. Dep. NTIS (U. S. Sales Only).

By applying the quark model to weak production of pseudoscalar mesons, the absence of some reactions is predicted by requiring only nonexotic t-channel exchanges. Further, relationships between several production cross sections based on the additivity assumption of the quark model are derived. (1 figure, 2 tables) (auth)

54286 (DNPL/P–130) OCTET DOMINANCE IN NON-LEPTONIC DECAYS. Riazuddin (Daresbury Nuclear Physics Lab. (England)). Jul 1972. 19p. Dep. NTIS (U. S. Sales Only).

The question of Octet enhancement for the non-leptonic decays is studied within the framework of a current-algebra approach. By writing an unsubtracted dispersion relation for the matrix elements $\langle B_k|H_w|B_j\rangle$ and $\langle M_k|H_w|M_j\rangle$ (B denoting a $\frac{1}{2}^+$ baryon and M a 0^- meson) in the momentum transfer-squared variable t and using the assumption of threshold dominance, namely that two pseudoscalar meson states dominate the absorptive parts of the above matrix elements and that in the chiral limit the meson–baryon and meson–meson scattering amplitudes which enter in the absorptive parts are exactly given by current algebra low-energy theorems, it is shown that the above matrix elements are octet enhanced without assuming the octet transformation property for H_w. Further it is shown that the d'/f' ratio for the octet-enhanced matrix elements $\langle B_k|H_w|B_j\rangle$ satisfies the relation $(d'/f') = (3/10)\,[3(f/d)_A^2 - 1/(f/d)_A]$, where $(f/d)_A$ denotes the f/d ratio of the axial vector current baryon couplings. The implications of this result for the s- and p-wave hyperon non-leptonic decays are discussed. (auth)

54287 (LBL–766) PART I: APPLICATIONS OF THE SCHWARZ INEQUALITY TO WEAK AND ELECTROMAGNETIC PROCESSES. PART II: S-CHANNEL HELICITY CONSERVATION IN ELASTIC PROCESSES. Langacker, Paul (California Univ., Berkeley. Lawrence Berkeley Lab.). 16 Mar 1972. Contract W-7405-eng-48. 76p. Dep. NTIS.

Thesis.

A class of inequalities is derived for certain weighted integrals of the spectral functions of the vector currents. The inequalities involve the low-energy p-wave meson-meson cross sections and slopes of the form factors that describe the matrix element of a vector current between single-particle pseudoscalar meson states. One set of applications involves the pion electromagnetic form factor. A lower bound on the hadronic contribution to the muon magnetic moment is estimated in terms of the pion electromagnetic charge radius r_π. The bound is twice as large as the ρ-dominance value if $r_\pi = 0.86$ F, as indicated by old data, but no useful result is obtained if one uses the value of r_π obtained in a new experiment. The inequalities can also be used to test various predictions concerning the asymptotic behavior of the e^+e^- annihilation cross section. A slowly decreasing behavior is favored over a rapidly decreasing one like $\sigma^{e^+e^-}(t) = ct^{-3}$, but more accurate data are needed to draw a definite conclusion. Another class of inequalities relates the slope parameter λ_+ of K_{13} decays to the spectral function of the isovector electromagnetic current. Weinberg's first spectral function sum rule is used. It is shown that a large value for λ_+ (e.g., $\lambda_+ = 0.045$) is not compatible with ρ saturation of the isovector spectral function. Since the principal tests of the sum rule have relied on the additional assumption that such resonance saturations are possible, some doubt is cast on the validity, or at least on the previous applications, of the sum rule. Implications for the Weinberg mass relations, c-number Schwinger terms, and the e^+e^- annihilation cross section are discussed. The unitarity equation for elastic partial wave amplitudes is considered. Defining helicity total flip elastic amplitudes as those in which both helicities change sign, it is observed that the unitarity equation strongly suggests that the imaginary part of the helicity total flip partial wave amplitude is much smaller than that of the nonflip amplitude at high energies. Appealing to a plausibility argument, the ratio of helicity total flip to nonflip partial wave amplitudes is estimated to be $(1/s)^{1/2}$ or smaller. The implications of this result for the full amplitude, the possibility of extending the result to other amplitudes if factorization is true, and the implications for Regge theory are discussed. (auth)

54288 (RPP/T–26) MUON–PROTON SCATTERING AND THE EFFECT OF NEUTRAL CURRENTS IN THE SCALING REGION. Love, A.; Nanopoulos, D. V.; Ross, G. G. (Rutherford High Energy Lab., Chilton (England)). 1972. 17p. Dep. NTIS (U. S. Sales Only).

The problem of testing weak interaction models with the next generation of accelerators is discussed, and it is concluded that muon–proton scattering must be considered. The cross sections for both polarized and unpolarized targets are obtained in the scaling region. The feasibility of detecting neutral weak currents is examined and optimum kinematical conditions to do this are found. Finally, ways to isolate the neutral weak current are suggested. (auth)

54289 WEAK κ-DOMINANCE MODEL AND BOUNDS ON K_{13} DECAY PARAMETERS. Shih, I-fu; Okubo, S. (Univ. of Rochester, N. Y.). Phys. Rev., D; 6: No. 5, 1393-1403(1 Sep 1972).

The previously found bounds on the K_{13} form factors were improved without assuming the validity of unsubtracted dispersion relations for two-point functions and without assuming specific SW(3)-symmetry-breaking Hamiltonians. For this generality, it is necessary to assume a weak form of κ dominance for the two-point function (but not for the three-point functions). Under this assumption the two-point function may still have a nonzero and sizable contribution from the high-energy region. The derived bounds still give results inconsistent with the present experiments if the soft-pion theorem is used as input information. (auth)

54290 POSSIBLE INFLUENCE OF POLARIZED PROPERTIES OF LEPTONS ON THE FORM OF PHOTON AND ELECTRON SPECTRA WHICH ARISE FROM INELASTIC NEUTRINO–MUON SCATTERING. Romanov, Yu. I. Izv. Akad. Nauk SSSR, Ser. Fiz.; 36: No. 1, 208-11(Jan 1972). (In Russian).

The process of inelastic neutrino-muon scattering accompanied by bremsstrahlung is discussed within the framework of the four-component theory of the neutrino. The form of the photon and electron spectra was determined not only by the electromagnetic nature of the reaction, but was dependent on the components of a weak interaction. The participation of only left-polarized electrons and μ-mesons in the reaction was predicted. (tr-auth)

54291 SEARCH FOR A NEUTRAL VECTOR MESON IN K_L-DECAYS. Barmin, V. V.; Davidenko, G. V.; Demidov, V. S.; (and others). (Inst. of Theoretical and Experimental Physics, Moscow). Yadern. Fiz.; 15: No. 6, 1149-51(Jun 1972). (In Russian).

An attempt was made to check experimentally the Alles and Pati hypothesis on existence of a neutral vector meson in K_L decays. The upper limits for the decay probabilities were found to be $\Gamma\{K_L \rightarrow \chi^0 + \gamma(\chi^0 \rightarrow \pi^0 + \gamma)\}/\Gamma(K_L) < 1.85 \cdot 10^{-4}$ and $\Gamma(K_L \rightarrow e^+ + e^- + \gamma)/\Gamma(K_L) < 2.7 \cdot 10^{-5}$, at 90% confidence level. It has been exhibited, that the decay $K_L \rightarrow \chi^0 + \gamma$ is at least 50 times smaller, than it is predicted by theory. (auth)

54292 WEAK RADIATIVE DECAYS OF HYPERONS IN THE POLE MODEL. Yakimiw, E. (Laboratoire de Physique Theorique et Hautes Energies, Orsay, France); Jakimiw, G. Can. J. Phys.; 50: No. 12, 1300-6(15 Jun 1972).

It is found that the pole model which includes the decuplet pole contributions in the weak radiative decays of hyperons fails to give the correct sign of the $\Sigma^+ \rightarrow p\gamma$ asymmetry parameters α, although the magnitude of the decay rate and of α is consistent with the present experimental data. This conclusion holds in the Rarita–Schwinger formalism. Earlier calculations are incorrect due mainly to an error in the spin-$\frac{3}{2}$ propagator used in the theory, and inconsistencies in the SU(3) phase convention. (auth)

54293 NONMESIC DECAYS OF HYPERNUCLEI ^{4}H AND ^{4}He IN A MODEL OF THE DIRECT TRANSITION OF THE Λ-HYPERON INTO A NEUTRON. Potashev, A. G.; Nikiforov, B. P.; Filimonov, V. A. (Tomsk Polytechnical Inst., USSR). Izv. Vyssh. Ucheb. Zaved., Fiz.; No. 1, 86-94(1972). (In Russian).

The decay probabilities of hypernuclei $^4H_\Lambda$ and $^4He_\Lambda$ were calculated for all possible nonmeson channels: $^4H_\Lambda \rightarrow$ tn,d2n,p3n and $^4He_\Lambda \rightarrow {}^3$Hen,tp, dd, dpn, 2p2n. Mutual interaction in the final state between decay products was neglected, but Pauli's principle was completely allowed for in the same ultimate particles. The predominant decay channels are three- and four-particle in nature. The results were compared with experimental data. (tr-auth)

54294 THEORY OF LEPTONS. Katayama, Yasuhisa; Kobayashi, Nobuo (Kyoto Univ.). Progr. Theor. Phys. (Kyoto); 48: No. 1, 247-60(Jul 1972).

A unified theory describing four leptons, i.e., muon, electron and two neutrinos together is presented. Leptons are represented by a single fundamental field: Without any interaction the field satisfies a fourth-order differential wave equation. When the influence of the electromagnetic field is taken into account, the appearance of reactive terms in the equation makes it possible to decompose the fundamental field into two Dirac fields (electron's and muon's) and a residual field. Though the residual field interacts with the electromagnetic field in a way similar to the separated two Dirac fields, the corresponding phenomena are shown to be ineffective owing to the mechanism analogous to Bleuler and Gupta's in quantum electrodynamics, provided the right (or left) handed component of the residual field is assumed not to exist: The proposed nonlocal weak interaction of the fundamental field leads to the coupling, on the mass shell, of the charge exchange current-current type. The current of approximate V–A with small T-mixture type gives the neutrino a small mass, which causes the separation of one neutrino field from the other. From these investigations, the following problems are suggested: (i) The existence of two kinds of neutral lepton fields with nearly zero mass would be understood in connection with their appearance through the two-component parts in nature. (ii) There would be a possible description of one pair of lepton (for instance, muon and massive neutrino) by means of the indefinite metric in Hilbert space, which is suggested by the existence of two kinds of lepton number conservation. (iii) In connection with the occurrence of lepton weak interaction, at least one of the masses of neutrinos, should be finite (non-zero), but less than the electron mass. (auth)

54295 $K_s \rightarrow 2\gamma$ DECAY. Kohara, Yoji (Tokyo Univ.). Progr. Theor. Phys. (Kyoto; 48: No. 1, 261-6(Jul 1972).

The $K_s \rightarrow 2\gamma$ decay rate is evaluated on the basis of dispersion relations and unitarity in the approximation of retaining the two-pion intermediate states. The numerical result of the branching ratio $\Gamma(K_s \rightarrow 2\gamma)/\Gamma(K_s \rightarrow \pi^+\pi^-)$ is given by 3.1×10^{-6}. (auth)

54296 POSSIBLE TESTS OF LEPTON NUMBER ASSIGNMENTS. Yokoo, Yoshimatsu (Osaka Univ.). Progr. Theor. Phys. (Kyoto); 48: No. 1, 353-5(Jul 1972).

The following scheme for assignment of lepton number is considered: a single lepton number is introduced, the signs of which are opposite for e^- and μ^-. It is proposed that a test of this scheme is provided by observing the strangeness-changing decay processes (1) $\Sigma^- \rightarrow p + \mu^- + e^-$, (2) $\Xi^- \rightarrow \Sigma^+ + \mu^- + e^-$, and (3) $K^\pm \rightarrow \pi^\pm + \mu^\pm + e^\pm$. It is pointed out that these elementary processes could give unambiguous information about the current $\mu^\pm \longleftrightarrow e^\pm$. (L.B.S.)

54297 NOTE ON THE URBARYON MODELS. Hayashi, Takemi; Karino, Tutomu; Kurokawa, Hidekazu (Hiroshima Univ.). Progr. Theor. Phys. (Kyoto): 48: No. 1, 359-60(Jul 1972).

An experimental clue is given for discriminating between the new Nagoya model and the Hiroshima model for the structure of urbaryons. Considering the interactions (1) $\nu_e + N \rightarrow \nu_e + N'$ and (2) $\nu_\mu + N \rightarrow \nu_\mu + N'$, it is pointed out that the cross sections for the reactions (1) and (2) are equal in the new Nagoya model, but in the Hiroshima model the cross section for the reaction (1) is much larger than that for the reaction (2) unless an extraordinarily larger constant than the usual one is used. This is suggested as a crucial test for choosing the urbaryon model. (L.B.S.)

Strong (General)

Refer also to abstracts 54388 and 54724.

54298 (BNL-16997) PHYSICS WITH ISABELLE. Quigg, C. (Brookhaven National Lab., Upton, N. Y.). [nd]. 18p. Dep. NTIS.

Some of the ways in which more information about the constitution and interactions of hadrons may be elucidated by means of strong- and electromagnetic-interaction experiments at ISABELLE energies are considered. Reactions leading to many-particle final states in both p + p and e + p collisions are discussed, with some emphasis on experiments well-suited to storage rings. Results on single-particle inclusive cross sections from the ISR are presented, and some speculations on deep e + p interactions in the Bjorken limit are discussed. (7 figures) (R.W.R.)

54299 (ITF-72-49-P) APPLICATIONS OF THE STATISTICAL MECHANICS METHODS IN A DUAL MODEL. Demchenko, G. P.; Kukhtin, V. V.; Struminskii, B. V. (Akademiya Nauk Ukrainskoi SSR, Kiev. Institut Teoreticheskoi Fiziki). 1972. 8p. (In Russian). Dep. NTIS (U. S. Sales Only).

The distribution function for resonance spins and the dependence on mass of the elastic widths of resonances are obtained by statistical mechanics methods by using the factorization of three dual amplitudes with a finite number of oscillators. (auth)

54300 (ITF-72-53-E) STATISTICAL VIEW ON RESONANCE WIDTHS AND MULTIPLICITY IN DUAL MODELS. Gorenstein, M. I.; Makarov, V. I.; Miranskii, V. A.; Shelest, V. P.; Zinov'ev, G. M. (Akademiya Nauk Ukrainskoi SSR, Kiev. Institut Teoreticheskoi Fiziki). 1972. 8p. Dep. NTIS (U. S. Sales Only).

A statistical approach to dual resonance models (DRM) is developed. Total and partial resonance widths, as well as the multiplicity of π-meson production, are calculated within the framework of such an approach. (auth)

54301 (ITF-72-55-P) TWO-PARTICLE DISTRIBUTIONS IN DUAL RESONANCE MODEL. Demchenko, G. P.; Kukhtin, V. V.; Struminskii, B. V. (Akademiya Nauk Ukrainskoi SSR, Kiev. Institut Teoreticheskoi Fiziki). 1972. 24p. (In Russian). Dep. NTIS (U. S. Sales Only).

Two-particle inclusive reactions are considered on the basis of the dual resonance model. A formula for the inclusive reaction cross section is obtained. Limiting expressions for the cross section in the case of simple, double and triple Regge limits are treated; the way the correlation function is obtained is discussed. All the calculations are carried out in the physical region. The results derived support the Feynman–Yang hypothesis for the existence of the secondary-particle limiting distributions. (7 figures) (auth)

54302 (LBL-1007) PHENOMENOLOGY OF INCLUSIVE REACTIONS. Cahn, Robert N. (California Univ., Berkeley. Lawrence Berkeley Lab.). 18 Jul 1972. Contract W-7405-eng-48. 162p. Dep. NTIS.

Thesis.

Inclusive reactions are examined in the context of the Mueller formalism, which exploits the connection of the inclusive cross section with the six-point amplitude and Regge behavior. Some previous results of the model are reviewed. Internal symmetries together with the Mueller picture are used to produce a large number of testable predictions. The fundamental symmetries of the strong interactions yield predictions which test the validity of the basic assumptions of the model. SU(3) gives predictions which are expected to be violated, and thus furnish extensive information about symmetry breaking. Angular distributions yield information about behavior in the central rapidity region, if the transverse momentum distribution is known. The dual resonance model provides predictions for fragmentation and pionization, but the results are based on a naive model and do not agree with the data. Inclusive photon distributions are examined in detail. They provide information mainly about the inclusive π^0 distribution. In the low-transverse momentum region, bremsstrahlung is significant and can provide a measure of the charged multiplicity. The photon distribution arising from π^0 decays in the central region obeys an equality relating the spectrum at zero transverse momentum to the integral of the spectrum over all transverse momenta. A variety of experimental data are reviewed and compared with the preceding predictions and prescriptions. (auth)

54303 (RPP/T-25) DIFFRACTIVE MODELS IN NON-DIFFRACTIVE REGIONS. Lam, C. S. (Rutherford High Energy Lab., Chilton (England)). 1972. 9p. Dep. NTIS (U. S. Sales Only).

Within the spirit of fragmentation models, various quantities may be calculated only when behaviours in the non-diffractive regions are known. These include the dispersion of multiplicity distributions, the rate of approach to asymptotic limits, etc. A priori very little can be said about the non-diffractive region in fragmentation models. However, if it is made a condition that the invariant pion spectrum in pp inclusive collisions is to be flat in the central region, then information about the non-diffractive regions may be obtained. In particular, in the diffractive excitation model, this requires the n^{-2} law to be valid almost right up to the kinematical boundary, in a way which is specified. (auth)

54304 EXOTIC FRAGMENTING STATES IN INCLUSIVE REACTIONS. Capps, Richard H. (Purdue Univ., Lafayette, Ind.). Phys. Rev., D; 6: No. 5, 1314-17(1 Sep 1972).

The general inclusive process $a + b \rightarrow c + X$ is considered in the b fragmentation region. It is proved that if the fragmenting state $(b\bar{c})$ is exotic, the presence or absence of energy-dependent terms in the invariant cross section f cannot depend on whether or not $(ab\bar{c})$ is exotic. If f is a smooth function of the kinematic variables, there must be a nonzero but limited region of the variables, in which the energy-dependent terms for exotic $(b\bar{c})$ are small compared to their average size when $(b\bar{c})$ is not exotic. In this region, present experimental evidence is in agreement with the hypothesis that the energy-dependent terms are small when $(ab\bar{c})$ is exotic. (auth)

54305 COMMENT ON A LIMITING TEMPERATURE IN HADRON PHYSICS. Tuan, S. F. (Univ. of Hawaii, Honolulu). Contract AT(04-3)-511. Phys. Rev., D; 6: No. 5,1445-9(1 Sep 1972).

It has been pointed out by Yang that if hadron physics were indeed governed by a limiting temperature $T_0 \sim 160$ MeV, then such a far-reaching conclusion would constitute no less than the establishment of a fourth law of thermodynamics. Here brief but critical comments are made on the basis for the limiting-temperature concept with particular emphasis on its implications for the production of massive exotic hadron states. (auth)

54306 QUASI-EIKONAL APPROXIMATION. Ter-Martirosyan, K. A. (Inst. of Theoretical and Experimental Physics, Moscow). JETP Lett. (USSR) (Eng. Transl.); 15: No. 12, 519-23(20 Jun 1972).

Translated from Zh. Eksp. Teor. Fiz., Pis'ma Red.; 15: No. 12, 734-8(20 Jun 1972).

A simple approximation for the scattering amplitude is proposed. This approximation is quite exact at high energies. Account is taken of the contributions of the Regge poles and all rescatterings. A good description of all the known experimental data of various strong interactions was found. (J.F.P.)

54307 DUAL-AMPLITUDE ANALYSIS OF TWO-PARTICLE PRODUCTIONS. II. Jen, Chian-li; Kang, Kyungsik; Shen, Pu; Tan, Chung-I (Brown Univ., Providence). Ann. Phys. (N. Y.); 72: No. 2, 548-83(Aug 1972). (COO-3130-TA-256).

The two-particle distribution function for the process $a + b \rightarrow x_1 + x_2$ + anything at high energy is analyzed by using the dual-resonance model. The distribution functions for all the kinematic regions are explicitly shown to have the expected variable dependence. In the uncorrelated-pionization and the double-fragmentation (this includes the ditriple Regge limit) regions, the distribution functions are factorized into the product of the corresponding single-particle distributions. To obtain the factorization requires nontrivial treatment of the singularities and the kinematic relations. The correlation effects in the pionization region are studied in detail. The transition from the correlated pionization to the uncorrelated pionization regions reveals that the correlation length in the relative rapidity y is of the order 1. For fixed y, the two-particle distribution exhibits the gross exponential cut-off behavior $f^{12} \sim \exp[-4(p_1^{\perp 2} + p_2^{\perp 2} + 2p_1^{\perp}p_2^{\perp} \cos\beta)]$, where β depends on y and the relative azimuthal angle between the two transverse momenta. (5 figures) (auth)

54308 MARKOFFIAN MODEL FOR HADRONS. Majernik, V. (Inst. of Physics, Bratislava). Nucl. Phys.; B46: No. 2, 483-96 (1972).

The hadron is considered as a system consisting of other bound hadrons, the configuration state of which changes with the time. Its time development is described as a Markov process by Kolmogorov's equations. The stationary solution of Kolmogorov's equations for the Markoffian hadronic system makes it possible to calculate certain physical parameters for stable hadrons. The calculation of the magnetic moments of the proton and neutron in this model yields values which are in good agreement with the experimental data. (auth)

54309 DUAL MODELS WITH SL(2,C) SYMMETRY. Brink, L.; Kihlberg, A. (CERN, Geneva). Nucl. Phys.; B46: No. 2, 505-24 (1972).

Making use of homogeneous space techniques, a class of dual models is constructed, which is a generalization of the Virasoro—Shapiro type of model. The integrand in the integral representation for the N-point function depends not only on the modulus of the distances between two-dimensional Koba—Nielsen variables, but also on the corresponding phases. This is in fact the most general SL(2,C) invariant amplitude that can be constructed using complex integration variables. The extra phase factors in the integrand provide a possible means of avoiding tachyons both as external particles and as intermediate states in the amplitude. When factorized in a simple-minded fashion the intercepts are fixed to be integers. Although the external particles can be chosen not to be tachyons, such states appear as intermediate states. Within this factorization it can be shown that there are gauge conditions for the amplitude that can provide a ghostkilling mechanism. (auth)

54310 GENERALIZED NONLINEAR LEE MODEL AND INFINITY SUPPRESSION DUE TO NONLINEARITY. Calogero, F. (Univ., Rome. Istituto Nazionale di Fisica Nucleare, Rome); Degasperis, A. Lett. Nuovo Cim.; 4: No. 14, 661-70(5 Aug 1972).

The generalized nonlinear Lee model is examined, starting from the finite and well-defined version of the theory when the high-energy cut-off is present, and then analyzing the effect on the physical quantities as the cut-off tends to infinity. Consideration is limited to the simpler nontrivial sector of the Hilbert space of the model (V-ΘN sector). Both the cases with nonrelativistic and with relativistic kinematics (for the Θ-boson) are considered. It is shown that in the former case, the ordinary Lee model requires (infinite) mass renormalization but no (infinite) charge renormalization, the nonlinear structure of the generalized model can compensate the divergence, so as to yield finally, in the limit of point-like interaction, finite results for all quantities of physical interest. (L.B.S.)

54311 PARTON MODEL: ELASTIC AND INELASTIC FORM FACTORS OF HADRONS. Senju, Hirofumi; Kakuto, Akira (Nagoya Univ., Japan). Progr. Theor. Phys. (Kyoto): 48: No. 1, 272-80(Jul 1972).

On the basis of the idea that hadrons consist of more fundamental particles whose transverse momenta are sharply cut off at $k_\perp$ in the hadron, three physical regions are classified. In particular a new condition is added to the Drell-Levy-Yan conditions for the validity of the parton model. Based on the above analysis, explicit forms of the electromagnetic form factors of all mesons and baryons are given and moreover it is shown that $\nu W_{2n} = \nu W_{2p}$ in the region where the parton model holds, at least in regard to the data available at present. (auth)

54312 INCLUSIVE REACTION IN THE MULTIPERIPHERAL MODEL. II. TWO-PARTICLE CORRELATIONS IN THE PIONIZATION REGION. Sakai, Sunao (Tokyo Univ. of Education). Progr. Theor. Phys. (Kyoto); 48: No. 1, 329-30(Jul 1972).

The two-particle distribution function for the inclusive reaction $a + b \rightarrow c_1 + c_2$ + anything is calculated in the multiperipheral model and a few characteristic features of the model are extracted. (L.B.S.)

54313 CUT-OFF PROBLEM IN THE INTEGRAL SPECTRUM OF ULTRAHIGH ENERGY COSMIC RAYS AND URBARYONS. Terasaki-Okada, Kunihiko (Hiroshima Univ.). Progr. Theor. Phys. (Kyoto); 48: No. 1, 349-50(Jul 1972).

The cut-off problem in the integral spectrum of ultrahigh energy cosmic rays is discussed under the assumption that cosmic urbaryons with ultrahigh energies will lose their energies dominantly by hadronic interactions with the thermal radiation which bring emission of hadrons. A rough estimate is made for the cross section for photo-pion production on urbaryons under assumed values for the mass and strength of the hadronic interaction of urbaryons. The result suggests that a steepening or a cut-off in the spectra of primary cosmic rays will occur at energies of order 10^{21} eV. (L.B.S.)

54314 MODEL OF MULTIPLE PRODUCTION BASED ON THE INTUITIVE PICTURE OF HADRONS. Sasaki, Tateaki (Tokyo Univ.). Progr. Theor. Phys. (Kyoto); 48: No. 1, 98-209(Jul 1972).

A new model of multiple production developed from the optical model is proposed and is examined in the energy region about 50 ~ 1200 GeV. Numerical calculations are made by treating it as a potential problem and by making use of Glauber's high energy approximation. The result is not unreasonable. In particular the longitudinal momentum distribution does not show the scaling behavior above ~1000 GeV. (auth)

Strong (Baryon No. = 0)

Refer also to abstract 54219.

54315 (JINR-E2-6525) ANALYSIS OF THE Kπ-INTERACTION IN THE ENERGY REGION UP TO 1 GeV. Isaev, P. S.; Khleskov, V. I. (Joint Inst. for Nuclear Research, Dubna (USSR). Lab of Theoretical Physics). 1972. 22p. Dep. NTIS (U. S. Sales Only).

An analysis of the Kπ interaction in the energy region up to 1 GeV was performed by using dispersion relations for S and P waves. A set of $\delta_0^{1/2}$, $\delta_0^{3/2}$, and $\delta_1^{1/2}$ phase shifts satisfying simultaneously the dispersion relations is found. Resonance behavior is predicted for the $\delta_0^{1/2}$ phase shift in the energy region $M(K\pi) \approx$ 1.1 GeV. (auth)

54316 (RPP/T—24) UNCORRELATED JET MODEL PREDICTIONS FOR THE MULTIPLICITY DISTRIBUTION OF π^- MESONS PRODUCED IN HIGH ENERGY ANNIHILATIONS $p\bar{p} \rightarrow$ PIONS. de Groot, E. H.; Zalewski, K. (Rutherford High Energy Lab., Chilton (England)). 1972. 13p. Dep. NTIS (U. S. Sales Only).

The uncorrelated jet model is used to obtain a grand partition function for the pions produced in the process $p\bar{p} \rightarrow$ pions. The grand partition function is evaluated asymptotically for large energies. It is used to relate the correlation parameter $f_2 = \langle n_-^2\rangle - \langle n_-\rangle^2 - \langle n_-\rangle$ to the average multiplicity of negative pions $\langle n_-\rangle$. The results are consistent with the presently available experimental data, though data at higher energies are necessary to draw physically interesting conclusions. (auth)

54317 (RPP/T-27) QUESTIONS IN ππ SCATTERING AND RELATED PROCESSES. Morgan, D. (Rutherford High Energy Lab., Chilton (England)). 1972. 106p. Dep. NTIS (U. S. Sales Only).

Current activity in the field of ππ scattering and related processes is described. The material includes survey of scattering, experiment and theory, questions; extracting information from dipion production data; inferences from analyticity, crossing and unitarity; inelastic channels and related processes. It is not a comprehensive review of ππ scattering. Several important contributions appeared after the material was originally prepared and allusions to them were inserted. Reference is made to the existence, in the literature, of a number of reviews from different aspects. (auth)

54318 THREE-MESON RESONANCES IN A RELATIVISTIC FADDEEV-TYPE APPROACH. Mennessier, G. (Laboratoire de Physique Theorique et Hautes Energies, Orsay, France); Pasquier, J.-Y.; Pasquier, R. Phys. Rev., D; 6: No. 5, 1351-72(1 Sep 1972).

Three-body resonances are studied within the framework of a relativistic version of the Faddeev equations, in which the input two-body amplitudes are assumed to be separable. A first discussion concerns the simplest $\pi\pi\pi$ and $K\bar{K}\pi$ systems in which only the ρ(765 MeV) or the K*(890 MeV) resonance is taken into account. Compared to preceding works on a similar subject, more flexible parametrizations are used, allowing a larger class of two-body interactions to be considered and a better understanding of the influence of the main parameters involved in the model. A more satisfactory agreement with experiment is also found in the three-pion case and this for more realistic two-body amplitudes. The success is less convincing for the $K\bar{K}\pi$ case, but this might be due to the neglect of the two-body $K\bar{K}$ interaction. Finally the study of the $K\pi\pi$ case gives an insight into the constructive and destructive interference effects which can be observed when more than one two-body resonance is taken into account. In the Appendix some comments are made about the properties one can reasonably require for the input separable two-body amplitudes owing to potential theory or its relativistic generalizations. (auth)

54319 I = 0 $\pi\pi$ s WAVE AND BROKEN SCALE INVARIANCE. Pennington, M. R. (Univ. of California, Berkeley). Phys. Rev., D; 6: No. 5, 1458-60(1 Sep 1972).

Renner and Staunton have shown that an I = 0 $\pi\pi$ s wave with only an ϵ resonance cannot satisfy the low-energy theorems of broken scale invariance. Recent experimental results indicate that this partial-wave amplitude also has a strongly inelastic S*(980) resonance. It is shown that if contributions from this resonance are included in the calculation of Renner and Staunton the low-energy theorems can be satisfied and suggest that the dimension of the operator which breaks both scale and chiral invariance is one. Although this result is not completely conclusive, because of the approximations used, this calculation does illustrate once again that the breaking of scale invariance cannot be ascribed to the ϵ resonance alone. (auth)

54320 ANNIHILATION OF $\bar{N}N \rightarrow 3\pi$ IN DUAL MODELS. Bugrii, A. I.; Enkovskii, L. L.; Kobylinskii, N. A. (Inst. of Theoretical Physics, Kiev). Yadern. Fiz.; 15: No. 6, 1266-70 (Jun 1972). (In Russian).

The reaction $\bar{p}n \rightarrow \pi^+\pi^-\pi^-$ is studied for momentum of the incident antiproton 1,2 GeV in the framework of the Veneziano model with satellites and a dual amplitude with Mandelstam analyticity. The theoretical predictions are compared with experimental data. (auth)

54321 DYNAMIC CHIRAL SYMMETRY AND CANCELLATION OF DIVERGENCES IN MASS DIFFERENCES OF THE MEMBERS OF A_1-, ρ-, π-MESONIC ISOMULTIPLETS. Kaganovich, A. B. (Chita State Pedagogical Inst., USSR). Yadern. Fiz.; 15: No. 6, 1251-60(Jun 1972). (In Russian).

With the method of "hard pions" it was exhibited, that in cancellation logarithmic divergences in the sum of electromagnetic and weak interaction contributions to the mass differences of the members of ρ-, A_1- and π-mesonic isomultiplets the following requirements are necessary: (1) the second Weinberg sum rule in one-particle approximation; (2) equality to zero of an anomalous magnetic moment of A_1 meson; (3) the relation, that gives the mass value of intermediate boson $M_W \approx 55$ GeV. (auth)

54322 LADDER APPROXIMATION FOR THE VERTEX FUNCTION OF NONRENORMALIZABLE $\omega\rho\pi$-INTERACTION. Epifanov, Yu. N.; Filippov, A. T. (Joint Inst. for Nuclear Research, Dubna, USSR). Yadern. Fiz.; 15: No. 6, 1286-93(Jun 1972). (In Russian).

A previously proposed method to solve ladder equation for a vertex function in nonrenormalizable theories of VPP-interactions is applied to PVV-interactions, at the same time it is generalized for the case, when 4-momenta of all the particles differ from zero. Using as an example $\omega\rho\pi$-interaction, which is very important for applications, it is shown how one may obtain the expansion of the vertex function into a power series in g and ln g (modified perturbation theory). There are calculated terms $\sim g^2$ and $\sim g^2 \ln g^2$ which are compared with the estimation, obtained by cutting off a triangular diagram at the "unitary limit." Possible application of the result obtained is discussed. (auth)

54323 $\omega-\varphi$ MIXING AND PHOTON INTERACTIONS FROM AN EXTENSION OF ODORICO'S BOOTSTRAP. Capps, Richard H. (Purdue Univ., Lafayette, Ind.). Phys. Rev. Lett.; 29: No. 12, 820-3(18 Sep 1972).

The bootstrap condition applied by Odorico to the scattering of pseudoscalar mesons is extended to processes involving vector mesons and photons. The $\omega-\varphi$ mixing angle is predicted to be the quark-model value. A photon interacting as a U-spin scalar is one of a small number of solutions. (auth)

Strong (Baryon No. = 1)

Refer also to abstract 54221.

54324 (COO-1428-309) PION-NUCLEON CHARGE EXCHANGE SCATTERING IN A NEW REGGE POLE-CUT MODEL. Garfinkel, A. F. (Purdue Univ., Lafayette, Ind.); Vasavada, Kashyap V. (Indiana-Purdue Univ., Indianapolis). 1972. 11p. Dep. NTIS.

A fit was obtained to most of the available data on pion-nucleon charge exchange scattering using a new Regge pole-cut model. This shows quantitatively the importance of the double Regge cuts, as opposed to the Regge–Pomeron cuts. (auth)

54325 (COO-3533-2) PION AND K MESON PRODUCTION IN THE MULTIPERIPHERAL MODEL. Amann, R. F. (Syracuse Univ., N. Y. Dept. of Physics). Jun 1972. 24p. (SU-4205-2). Dep. NTIS.

A simple multiperipheral model that utilizes only three parameters, two coupling constants and an exponential damping for each momentum transfer, is developed and applied to the calculation of inclusive distributions. The pion rapidity and p^2 distributions are successfully predicted, as are the energy dependences of strange particle production cross sections. The development of inclusive distributions with increasing energy and possible improvements to the model are discussed. (4 figures, 2 tables) (auth)

54326 (DESY-72/40) LIMITING DISTRIBUTIONS FOR INCLUSIVE CHARGED PION PRODUCTION AT VERY HIGH ENERGY. Meyer, H.; Struczinski, W. (Deutsches Elektronen-Synchrotron, Hamburg (West Germany)). Jul 1972. 8p. Dep. NTIS (U. S. Sales Only).

A conjecture is given, of how limiting distributions are approached in the target fragmentation region and in the central region, for inclusive charged pion production. (auth)

54327 (JINR-E2-6596) MULTIPLE CHARGED PARTICLE PRODUCTION IN π^-p AND π^-n INTERACTIONS AT p = 40 GeV/c. Grishin, V. G.; Jancso, G.; Kuleshov, S. P.; Matveev, V. A.; Sisakyan, A. N. (Joint Inst. for Nuclear Research, Dubna (USSR)). 1972. 11p. Dep. NTIS (U. S. Sales Only).

A model is suggested for a common description of multiple charged particle production in π^-p and π^-n interactions. Comparison of the model with experimental data at pc = 40 GeV gives good agreement. The value for an average number of produced $\pi^+\pi^-$ meson pairs (a = 1.81 ± 0.02) as well as the coefficient of the nucleon charge exchange (β = 0.36 ± 0.04) are determined. The identity of the distribution of events over the charged secondary particles, e.g., for π^+p and π^-p; pp and $p\bar{p}$ collisions, is predicted. (auth)

54328 (LBL-544) PARTIAL WAVE ANALYSIS OF THE REACTION $\pi N \rightarrow N\pi\pi$ IN THE CMS ENERGY RANGE 1.6 GeV TO 2.0 GeV. Herndon, David J. (California Univ., Berkeley. Lawrence Berkeley Lab.). 30 May 1972. Contract W-7405-eng-48. 95p. Dep. NTIS.

Thesis.

The results of an energy-independent partial-wave analysis of the single-pion production reactions at nine center of mass energies from 1.6 to 2.0 GeV are presented. This maximum likelihood analysis was based upon the isobar model. The results of a preliminary K-matrix analysis are used to remove the overall phase ambiguity at each of the energies. The Argand plots confirm the S11(2100) and P13(1850) resonances and show no evidence for the P31(1900) in the channels. There are indications of the existence of the D13(1700), badly needed by the quark model, and for a new P11 resonance around 2100 MeV. (auth)

54329 (NYO-3533-265) INTERFERENCE TERMS IN THE MULTIPERIPHERAL MODEL. Amann, R. F.; Shah, Prakash M. (Syracuse Univ., N. Y. Dept. of Physics). May 1972. 11p. (SU-4205-265). Dep. NTIS.

The customary assumption of the neglect of interference or crossed graph terms is investigated within a simple multiperipheral model and found to be completely unjustified. The inclusion of these terms, in a multi-Regge model, allows the correct prediction of the ratio of Kp to πp cross sections and of the energy dependences of inelastic cross sections and pion multiplicities. A natural explanation is provided for dramatic structures observed in correlation functions. (auth)

54330 DESCRIPTION FOR THE REACTIONS a + b → c + d + e. Cashmore, R. J. (Stanford Univ., Calif.); Hey, A. J. G. Phys. Rev., D; 6: No. 5, 1303-13(1 Sep 1972).

A formalism for describing the reactions a + b → c + d + e is presented in detail and the experiments necessary for the reconstruction of the transition amplitude described. Experiments involving polarized targets are discussed carefully and a partial-wave analysis is made which is particularly suitable for application at low c.m. energies. It is shown that in order to resolve parity ambiguities it is necessary to observe the final particle polarizations. (auth)

54331 BACKWARD-SCATTERING EXTRAPOLATIONS AND BARYON COUPLINGS. Roy, D. P.; Roberts, R. G.; Phillips,

R. J. N.; Miettinen, H. I. (Rutherford High Energy Lab., Chilton, Eng.). Phys. Rev., D; 6: No. 5, 1317-21(1 Sep 1972).

Extrapolation of an asymptotic cross section to a baryon pole cannot uniquely determine the coupling constant. The only asymptotic quantities capable of doing this are the R and A parameters. The notorious discrepancy between extrapolation of $d\sigma(\pi^-p)/du$ and the known Δ width is shown to be purely illusory. (auth)

54332 PHENOMENOLOGY OF THE TRIPLE-REGGE REGION. Ellis, S. D.; Sanda, A. I. (National Accelerator Lab., Batavia, Ill.). Phys. Rev., D; 6: No. 5, 1347-50(1 Sep 1972).

A two-term triple-Regge formula, which follows from a simple theoretical picture of the single-particle inclusive cross section, is presented and studied. A comparison is made with recent data for $pp \rightarrow p$ + anything, and $p\pi^- \rightarrow p$ + anything. The description of the data offered by this simple form is found to be remarkably good over a large region of phase space. (auth)

54333 BARYONIC INTERACTIONS IN AN EFFECTIVE-LAGRANGIAN MODEL. Bhargava, Ashok Kumar (Indian Inst. of Tech., Kanpur). Phys. Rev., D; 6: No. 5, 1453-5 (1 Sep 1972).

An effective Lagrangian for the study of strong interactions of $\frac{1}{2}^+$ baryons with spin-one and spin-zero mesons is constructed. Expressions for masses, coupling constants, and weak decay constants for the leptonic decays of baryons are obtained. Predictions of the model are compared with the experimental data. (auth)

54334 POSSIBLE STUDY OF BOUND $\bar{p}n$ STATES IN EXPERIMENTS ON THE ANNIHILATION OF $\bar{p}$ ON d. Bogdanova, L. N.; Dal'karov, O. D.; Shapiro, I. S. (Inst. of Theoretical and Experimental Physics, Moscow). JETP Lett. (USSR) (Eng. Transl.); 15: No. 12, 531-3(20 Jun 1972).

Translated from Zh. Eksp. Teor. Fiz., Pis'ma Red.; 15: No. 12, 748-51(20 Jun 1972).

The theoretically expected form of the momentum spectrum of the recoil protons in the reaction $\bar{p} + d \rightarrow p$ + anything is studied for different energies. The analysis shows that a study of the spectra for different recoil-proton spectra emission angles makes it possible to determine experimentally the nonzero orbital momenta of the bound states of $\bar{p}$ and n. (J.F.P.)

54335 REACTIONS OF SINGLE Σ- AND Λ-HYPERON PRODUCTION. Nikolaev, N. N. (Inst. of Theoretical and Experimental Physics, Moscow). Yadern. Fiz.; 15: No. 6, 1243-50 (Jun 1972). (In Russian).

Single Σ- and Λ-hyperon production in reactions $\pi N \rightarrow \pi\Sigma(\Lambda)$ near the reaction threshold is discussed. Cross sections and polarization phenomena are predicted using PCAC. (auth)

54336 NEW REGGE ABSORPTION MODEL. Thews, R. L. (Univ. of Arizona, Tucson); Goldstein, Gary R.; Owens III, Joseph F. Nucl. Phys.; B46: No. 2, 557-67(1972).

The weak-cut Regge absorption model is generalized to allow for unequal absorption of the rotating ($e^{-i\pi\alpha}$) and non-rotating (1) parts of the Regge-pole exchange amplitude. Some justification for this procedure is given in terms of duality and peripheral resonance dominance. Fits to data for πN charge-exchange cross section and polarization and cross sections for the line-reversed hypercharge-exchange reactions $\bar{K}N \rightarrow \pi\Sigma$ and $\pi N \rightarrow K\Sigma$ are obtained. (auth)

54337 TESTING OF ANALYTICITY OF THE πN FORWARD SCATTERING AMPLITUDE AND THE DETERMINATION OF THE πN COUPLING CONSTANT. Pazman, A. (Inst. for Measurement Theory, Bratislava); Pisut, J.; Presnajder, P.; Lichard, P. Nucl. Phys.; B46: No. 2, 637-43(1972).

A new method is proposed for the testing of analyticity. Instead of using dispersion relations with traditional uncertainties in estimating the errors of the principal value integrals a suitably defined set of moments is used. As an example the pion-nucleon CEX forward amplitude is discussed. The results indicate that the errors of the phase shift analysis used should probably be increased by a factor of two. Taking this into account the pion-nucleon coupling constant is calculated by analytic extrapolation and $f^2 = 0.0835 \pm 0.0040$ is found. (auth)

54338 POSSIBLE CORRELATIONS AMONG BARYON TRAJECTORIES. Ida, M. (Kyoto Univ.). Lett. Nuovo Cim.; 4: No. 14, 707-10(5 Aug 1972).

Some regularities exhibited by baryon resonances of small spin are pointed out and the possibility that they have non-degenerate parity partners is discussed. The existence of first-daughter trajectories which are not parallel to partners is suggested. The exchange degenerate patterns of baryon trajectories are studied by considering the backward scattering of pseudoscalar-meson octets off baryon octets. (L.B.S.)

54339 LOW-ENERGY πN SCATTERING IN A CURRENT ALGEBRA MODEL WITH PHYSICAL PIONS. Radutskii, G. M.; Tabachenko, A. N. (Tomsk Polytechnical Inst., USSR). Izv. Vyssh. Ucheb. Zaved., Fiz.; No. 1, 63-71(1972). (In Russian).

In models of current algebra with physical pions scattering and the energy dependence of S- and P-phase πN scattering were calculated. The results agreed with experimental data at low energies. (tr-auth).

54340 INEQUALITIES WITH πN POLARIZATION. Sakmar, I. A. (Univ. of Western Ontario, London). Progr. Theor. Phys. (Kyoto); 48: No. 1, 235-46(Jul 1972).

πN polarization is investigated as a function of the relative magnitude and relative phase of the spin-non-flip and spin-flip amplitudes. Inequalities for the magnitude and phase in terms of the polarization are obtained and physical implications are discussed. From Schwartz's inequality relations involving the polarization in integrated forms are obtained. (auth)

54341 COMMUTATION OF AXIAL CHARGES WITH AXIAL DIVERGENCES. Kaushal, V. (Panjab Univ., Chandigarh, India). Progr. Theor. Phys. (Kyoto) 48: No. 1, 357-9(Jul 1972).

The baryon decuplet contribution to the sum rules obtained using the commutator between axial charge and axial divergence and by taking the matrix elements between two sets of baryon states (Σ^+,Σ^+) and (Σ^0,Σ^0) are calculated, and it is shown that the contribution is not small. Another commutator is considered in which the right-hand side is the sum of two different components of the scalar density octet, and it is found that in general sensible results are not obtained in the saturation approximation. (L.B.S.)

54342 SYSTEMATIC STRUCTURE IN HADRONIC TWO-BODY SCATTERING AND RESONANCE CORRELATION. III. HADRON REACTIONS AND URBARYON REARRANGEMENT. Ghoroku, Kazuo (Kyushu Univ., Fukuoka); Imachi, Masahiro; Otsuki, Shoichiro; Toyoda, Fumihiko. Progr. Theor. Phys. (Kyoto); 48: No. 1, 210-30(Jul 1972).

Elastic and inelastic two-body (πN, KN, $\bar{K}N$, NN, and $\bar{N}N$) scattering is investigated by using the following amplitude corresponding to the pattern of the urbaryon rearrangement diagram: the H-type (s-t dual) amplitude $f^H_{\Delta\lambda} \sim iJ_{\Delta\lambda}(b_0\sqrt{-t}) - J_{\Delta\lambda+1}(b_0\sqrt{-t})$ and the X-type (t-u dual) amplitude $f^X_{\Delta\lambda} \sim -\{J^2_{\Delta\lambda}(b_0\sqrt{-t}) + J^2_{\Delta\lambda+1}(b_0\sqrt{-t})\}^{1/2}$ where Δλ denotes the helicity change. These forms come from the effective resonance, or the resonance correlation subject to generalized Ogawa's rule of a constant impact parameter b_0. Two degrees of freedom of the counting scheme of the urbaryon rearrangement diagram in the framework of SU(3) symmetry are combined with the helicity change in the way suggested from a duality interpretation of the urbaryon rearrangement diagram. This counting scheme together with the above forms of the amplitude of the Bessel type offers a satisfactory over-all agreement with experiment in a forward region $-t \lesssim 2$ GeV². The value of b_0 is found to be 4.5/GeV for meson-baryon scattering and 5.5/GeV for NN and $\bar{N}N$ scattering. (auth)

Strong (Baryon No. ≥ 2)

Refer also to abstracts 54520 and 54532.

54343 (DESY-72/35) ANOMALOUS DIMENSIONS IN p-p ELASTIC SCATTERING? Theis, W. R. (Deutsches Elektronen-Synchrotron, Hamburg (West Germany)). Jul 1972. 11p. Dep. NTIS (U. S. Sales Only).

The concept of anomalous dimensions is used to connect high energy, large angle elastic p-p scattering with the high momentum behavior of the proton electromagnetic form factor consistent with the existing data. (auth)

54344 (ITF-72-10-P) SOLUTIONS OF THE SKORNYAKOV-TER-MARTIROSYAN EQUATIONS FOR THREE NUCLEONS WITH CUT-OFF AT LARGE MOMENTA. Kharchenko, V. F. (Akademiya Nauk Ukrainskoi SSR, Kiev. Institut Teoreticheskoi Fiziki). 1972. 11p. (In Russian). Dep. NTIS (U. S. Sales Only).

The consistency of three-nucleon low-energy parameters in the doublet spin state is investigated on the basis of the Skornyakov-Ter-Martirosyan equations with cutoff at large momenta. The deuteron binding energy and the singlet n-p scattering length are used as two-nucleon parameters. The cut-off parameter introduced is determined by fitting the triton binding energy. The calculations in this way give a value for the doublet n-d scattering length in agreement with the experimental results obtained by Hurst and Alcock and by Dilig, Koester, and Nistler. (2 figures) (auth)

54345 (JINR-P4-6505) FACTORIZATION OF THE PAIR POTENTIAL BY THE BATEMAN MODIFIED METHOD IN THE TWO- AND THREE-BODY PROBLEM. Belyaev, V. B.; Zubarev, A. L.; Irgaziev, B. F. (Joint Inst. for Nuclear Research Dubna (USSR). Lab. of Theoretical Physics). 1972. 13p. (In Russian). Dep. NTIS (U. S. Sales Only).

The factorization of the Fourier-image of the pair short-range potential v(k,k′) by the expression $\tilde{\tilde{v}}^N(k,k') = \Sigma_{i,j}(d^{-1})_{ij} v(k,s_i)v(k',s_j)$, where one of the fixed parameters s_i is replaced by the value equal to the energy of considered two-particle system is suggested. Such a replacement improves considerably the behavior of the approximated phases of the nucleon-nucleon scattering and turns out to be especially useful when solving the Faddeev equations. (auth)

54346 (RPP/T–28) SIMPLE EXPLANATION OF CORRELATION DATA IN INCLUSIVE pp INTERACTIONS AT HIGH ENERGY. Fialkowski, K. (Rutherford High Energy Lab., Chilton (England)). 1972. 10p. Dep. NTIS (U. S. Sales Only).

The existing integral and differential data for two-particle correlations between negative pions produced in high energy pp collisions are discussed. They are shown to be explained in a simple way by adopting the Feynman–Wilson two-component picture. The diffractive part of the distribution, which appears to be small, is evaluated from experimental data. For the nondiffractive interaction the conservation laws are assumed to play the dominant role in correlation effects. (auth)

54347 (UM–P–72–6) ANALYSIS OF BREAKUP SCATTERING IN A DEUTERIUM TARGET. APPLICATION TO ANTIPROTON–DEUTERON BREAKUP SCATTERING. MacDowell, C. E.; Opta, Geoffrey I. (Melbourne Univ., Parkville (Australia). School of Physics). 1972. 31p. Dep. NTIS (U. S. Sales Only).

The problems of extracting low momentum transfer cross sections for the "elastic" scattering of a projectile particle by the "neutron" in a deuterium target are discussed for the case in which the deuteron breaks up. The difficulties in the analysis of deuterium events due to the Fermi motion are discussed. Further, the influence of the final-state neutron-proton interaction is presented in detail. Application is made to the reaction $\bar{p}d \rightarrow \bar{p}pn$. (auth)

54348 DAMPED PSEUDOSCALAR- AND VECTOR-MESON MODEL FOR NUCLEON–NUCLEON SCATTERING. Bock, Charles W.; Haracz, Richard D. (Drexel Univ., Philadelphia). Phys. Rev., D; 6: No. 5, 1373–8(1 Sep 1972).

Recently, a pseudoscalar–vector-meson (PV) model for elastic nucleon–nucleon scattering was presented by Barker and Haracz in which phase parameters are defined by a perturbative method which is similar to the geometric unitarization scheme used in other models. These phase parameters are dominated by the two-pion-exchange (TPE) contribution for the low values of L, and TPE is unreasonably large for the phases associated with the S state. In order to suppress this large contribution, relativistic Heitler damping or K-matrix unitarization is applied to the PV model. It is found that the low-partial-wave phase parameters ${}^1K_0^S$, ${}^3\theta_1^S$, ${}^3\theta_1^D$, and ρ_1 are drastically reduced and made much more reasonable by damping. Moreover, the P- and D-state phase shifts are reduced by as much as 20% at the higher scattering energies. The resulting damped phase parameters are in good agreement with the phenomenological values for $L \geq 2$ and energies up to 200 MeV, excluding ${}^3\theta_1^D$. Coupling constants more consistent with experiment are used contrasting with our previous usage. It is also found that the presence of a strongly coupled scalar ϵ resonance does not improve this model. (auth)

54349 BOSE DISTRIBUTION AND SCALING LAW. Hoang, T. F. (Argonne National Lab., Ill.). Phys. Rev., D; 6: No. 5, 1328–32(1 Sep 1972).

Properties of a two-parameter Bose-type distribution were investigated using data on π and K mesons of inclusive p-p collisions from 12 to 30 GeV/c. It is found that the temperature T is characteristic of the particle emission: $T_\pi > T_K$, and T for π^- is about 5 MeV higher than that of π^+. The scaling behavior is found to hold for both π and K for incident lab momentum above 20 GeV/c. (auth)

54350 DAMPED THEORY OF NUCLEON–NUCLEON SCATTERING. Bock, Charles Walter. Philadelphia; Drexel Univ. (1972). 129p. University Microfilms Order No. 72-21,419. Thesis.

An accurate determination of the effects of radiation damping on the nucleon–nucleon scattering amplitudes and phase parameters is established by solving exactly Gupta's covariant field-theoretic generalization of the Heitler integral equation. This is accomplished by using a partial wave projection technique developed by Jacob and Wick. Equations relating the damped and undamped scattering amplitudes are obtained, and their respective relations to the phase parameters are discussed. Explicit damped phase shifts are obtained for the one- plus two-pion-exchange (OPE + TPE) and pseudoscalar vector meson (PV) models of the nucleon–nucleon interaction. A comparison of the damped and undamped phase shifts shows that damping effects are significant for L < 3, and improve the theoretical phase shifts when compared to the Yale phenomenological values. (Diss. Abstr. Int., B)

54351 SHELL-MODEL ANALYSIS OF Λ BINDING ENERGIES FOR THE p-SHELL HYPERNUCLEI. II. NUMERICAL FITTING, INTERPRETATION, AND HYPERNUCLEAR PREDICTIONS. Gal, A. (Hebrew Univ., Jerusalem); Soper, J. M.; Dalitz, R. H. Ann. Phys. (N. Y.); 72: No. 2, 445–88(Aug 1972).

A phenomenological analysis of the Λ binding energies known for the p-shell hypernuclei is given in terms of their representation by the shell-model configuration $[(1s)_N^4(1p)_N^{A-5}(1s)_\Lambda]$, by using the formalism set up in Part I. The ΛN interactions are described quite generally by five free parameters, and the inclusion of ΛNN interactions with the forms arising through the double-OPE mechanism requires five further parameters. Various constraints motivated by theoretical arguments concerning the nature of ΛN and ΛNN interactions are imposed on these parameters, and best fits are then obtained for them by following a minimization procedure. A good and economical fit to these data is obtained for a parameter set in good accord with theoretical notions about these interactions (although the fit otherwise most attractive does require ΛN spin–orbit forces with sign opposite those known for the NN system). On the basis of these fits to the B_Λ data, a discussion is given of the energy-level spectra for the p-shell hypernuclei, of isomeric states for ${}_\Lambda^7He^*$ and ${}_\Lambda^7Li^*$, and of the resulting predictions for the properties of the Λ hypernuclei corresponding to core nuclei assigned to the $p_{1/2}$ shell. (4 figures, 9 tables) (auth)

54352 RECOIL AND FRESNEL CORRECTIONS TO SCATTERING BY THE DEUTERON. Faeldt, Goeran (SIN, Zurich). Nucl. Phys.; B46: No. 2, 460–6(1972).

It is shown how both recoil and Fresnel corrections can be obtained from a careful treatment of the double scattering term in the Watson multiple-scattering series. (auth)

54353 COMMENTS ON ARNOLD AND BARNETT'S SHIELDING-CUT MECHANISM. II. Fujisaki, Haruo (Rikkyo Univ., Tokyo). Progr. Theor. Phys. (Kyoto); 48: No. 1, 231–4(Jul 1972).

Brief comments are given at extremely high energies on the fixed-pole Pomeron with two Arnold and Barnett's shielding branch-cuts, i.e., $\overline{\alpha}_C(t)$ of $\overline{\alpha}_C(4m_\pi^2) = 1$ and $\widetilde{\alpha}_C(t)$ of $\widehat{\alpha}_C(4m_K^2) = 1$. Assuming that the Pomeronia has already been attained at the CERN-ISR energy ranges, it is also argued in the case of proton-proton collision that asymptotic values of the total cross section and the slope parameter of the diffraction peak are 59.9 mb and 14.6 GeV^{-2}, respectively. (auth)

54354 SCALING OF INTERACTION RADIUS AND POLARIZATION. Otsuki, Shoichiro (Kyushu Univ., Fukuoka). Progr. Theor. Phys. (Kyoto); 48: No. 1, 347–8(Jul 1972).

New evidence for the hypothesis of interaction radius scaling is obtained by analyzing precise polarization data on elastic pp, K^+p, $\bar{p}p$, and K^-p scattering between 6 and 14 GeV/c. (L.B.S.)

Particle Invariance Principles and Symmetries

General

54355 (ITF–72–33–E) WIGNER–ECKART THEOREM FOR NONUNITARY REPRESENTATIONS OF SEMI-SIMPLE LIE GROUPS. CONTINUUM CASE. Klimyk, A. U. (Akademiya Nauk Ukrainskoi SSR, Kiev. Institut Teoreticheskoi Fiziki). 1972. 17p. Dep. NTIS (U. S. Sales Only).

An analog of the Wigner–Eckart theorem is proved for the tensor operators with transform according to the finite-dimensional representation of a semi-simple group when the Hilbert space is decomposed into the direct integral of representations spaces of the group under consideration. The question is considered concerning the application of the theorem proved for the construction of invariant wave equations and representations of the Lie group. As a result, the relativistic invariant wave equations which are absent in the Gelfand–Yaglom classification of such equations are obtained. (auth)

54356 ONE PARTICLE SINGULARITIES AND PHYSICAL SYMMETRIES. Fabricius, K. (Univ. of Bielefeld, Ger.). Nucl. Phys.; B46: No. 2, 467–76(1972).

It is shown that a physical symmetry is completely determined by the one-particle singularities of current matrix elements. (auth)

54357 ASYMPTOTICALLY FLAT SPACE–TIMES AND ELEMENTARY PARTICLES. McCarthy, Patrick J. (Univ. of British Columbia, Vancouver). Phys. Rev. Lett.; 29: No. 12, 817–19 (18 Sep 1972).

It is suggested that elementary particles should be defined as irreducible unitary representations of the group of asymptotically flat space-times in general relativity. The implications of such a definition are described in physical terms. In particular, it is pointed out that this definition (unlike the corresponding "flat space–time" definition) explains the observed discreteness of elementary-particle spins. The possibility of using the definition to explain "internal" symmetries is discussed. (auth)

54358 RESULT BY R. KADISON AND J. RINGROSE. Bulinskii, A. V. (Moscow Physical-Technical Inst.). Teor. Mat. Fiz.; 12: No. 2, 197-203(Aug 1972). (In Russian).
For compact Lie groups of automorphisms of a C*-algebra continuity in the norm topology implies covariance of representations of the algebra. (auth)

54359 LORENTZ-COVARIANT BILINEAR FORMS. Oksak, A. I. Teor. Mat. Fiz.; 12: No. 2, 179-96(Aug 1972). (In Russian).
Convariant bilinear forms and covariant operators over spaces transforming under infinite-dimensional and, more generally, elementary representations of the connected Lorentz group are described in the manifestly covariant formalism. (auth)

54360 STATISTICAL MODEL WHICH ALLOWS FOR THE CONSERVATION OF P-, C-, AND G-PARITY. Gridneva, S. A.; Kosmachev, O. S.; Rus'kin, V. I. Izv. Akad. Nauk Kaz. SSR, Ser. Fiz.-Mat.; No. 4, 29-34(Jul-Aug 1971). (In Russian).
A new variant of a statistical model is presented, which considers the laws of conservation of P-, G-, and C-parity. (tr-auth)

Applications (Electromagnetic and Weak)

Refer also to abstract 54188.

54361 (COO–1195-242) COMPARISON OF CP VIOLATION IN THE DECAYS $K^0 \rightarrow \pi^+\pi^-$ AND $\overline{K}^0 \rightarrow \pi^+\pi^-$. Raither, Siegbert Wilhelm (Illinois Univ., Urbana). Oct 1972. Contract AT(11-1)-1195. 96p. Dep. NTIS.
Thesis.
The time dependence of the decay rates $K^0 \rightarrow \pi^+\pi^-$ and $\overline{K}^0 \rightarrow \pi^+\pi^-$ was measured in order to test the validity of current formulations of CP violations. An enriched kaon beam at Argonne National Laboratory was used to produce K^0 ($\overline{K}^0$) by charge exchange of 850 MeV/c K^+ (K^-) on complex nuclei. Magnetostrictive wire spark chambers and scintillation counters were used to measure the $\pi^+\pi^-$ rates in the interval from four to twelve K^0_S lifetimes. The time distributions of these decay rates agree with those expected from prevalent theories of CP violation. (auth)

54362 (COO–1195-244) TIME DECAY DISTRIBUTIONS OF $\overline{K}^0$ AND K^0 TO $\pi^+\pi^-$: A CP TEST. Frank, James Sidney (Illinois Univ., Urbana). Oct 1972. 96p. Dep. NTIS.
Thesis.
A direct comparison of the time decay distributions of $\overline{K}^0$ and K^0 to $\pi^+\pi^-$ was made at the Argonne National Laboratory Zero Gradient Synchrotron. The neutral kaons were produced by charge exchange of 850-MeV/c charged kaons on a carbon target. Their subsequent decays were tracked with magnetostrictive wire spark chambers in the range from 4 to 12 K_S lifetimes. No magnetic analysis was required in order to analyze the kinematics of each event. A 3.5 standard deviation effect was found for direct evidence of CP violation. This is independent of any theoretical decay formalism. Also good agreement was found with the usual formalism of CP violation in the $\pi^+\pi^-$ decay mode of the neutral kaon system. This is the first time that CP violation was observed in $\overline{K}^0$ decay. (auth)

54363 (IS-T–536) CONTRIBUTIONS OF TIME-REVERSAL NONINVARIANT TERMS IN ELECTRON–NUCLEUS ELASTIC SCATTERING. Krase, Loren Dell (Ames Lab., Iowa). Aug 1972. Contract W-7405-eng-82. 83p. Dep. NTIS.
Thesis.
The possibility of using elastic scattering of electrons from nuclei having spin one or greater to search for T noninvariant effects in electromagnetic processes was investigated. In the one photon exchange approximation of the elastic scattering process, terms which are invariant under P and PCT but noninvariant under T may be explicitly included in the nuclear current for the interaction of these nuclei. The transformation properties of the various terms which may contribute to the current were developed and discussed within a manifestly covariant framework. The current was then specialized to a noncovariant form in the Breit (or brick-wall) frame of the nucleus where the physical form factors of the nuclear current were easily identified. This noncovariant form was then used to determine tests which could be used to search for T noninvariant effects. Two restrictions were placed on the types of experimental tests which could be made: since the polarization tensors of large rank can be produced only with a large momentum transfer, or emission or absorption of radiation of large multipolarity, the polarization tensors were taken to be, at most, second rank; to ensure that the results would be as statistically accurate as possible, the measurable quantities were taken to be the cross sections and the electron beam polarizations. Within these restrictions, at least two types of tests are possible. If the nuclear target is completely described by a vector polarization only, with a component normal to the scattering plane, the cross section for the scattering of unpolarized electrons has an asymmetry if the electromagnetic interaction is noninvariant under T. If the nuclear target is completely described by a second rank tensor only, with components in the scattering plane, an initially unpolarized electron beam has a polarization after the scattering if the electromagnetic interaction is noninvariant under T. These tests, however, are not completely unambiguous. The polarization tensors of other rank may give a contribution which is not zero even when the electromagnetic interaction is invariant under T. In addition, the higher order processes may give a nonzero contribution even when the interaction is T invariant, as is demonstrated for the test involving the asymmetry in the cross section. (auth)

54364 (NYO–3533-264) UNIFIED WEAK-ELECTROMAGNETIC GAUGE SCHEMES BASED ON THE THREE DIMENSIONAL UNITARY GROUP. Schechter, J.; Ueda, Y. (Syracuse Univ., N. Y. Dept. of Physics). May 1972. 20p. (SU–4205-264). Dep. NTIS.
SU(3) × U(1) and chiral SU(3) × SU(3) × U(1) × U(1) models for the weak and electromagnetic interactions of leptons and hadrons are proposed. The usual quark model for hadrons as well as the usual Cabibbo rotation scheme is assumed. Symmetry breaking effects due to inequalities in the masses of the gauge bosons are considered. By making a simple choice of the gauge boson masses based on the U-spin subgroup of SU(3), the undesired $|\Delta S| = 2$ weak nonleptonic transitions can be completely eliminated and the undesired $|\Delta S| = 1$ neutral current semi-leptonic transitions drastically suppressed. These models can reproduce the ordinary phenomenological weak interaction but are sufficiently flexible to give the possibility of interesting new effects for neutral leptonic and semi-leptonic processes, as well as to allow the possibility of an overall arbitrariness in normalization for the effective nonleptonic interaction. Another consequence of the present scheme is the existence of very heavy leptons. A brief discussion of including the strong interactions in a grand unification is also presented. (auth)

54365 WEAK RADIATIVE DECAYS OF K MESONS. Moshe, M.; Singer, P. (Technion-Israel Inst. of Tech., Haifa, Israel). Phys. Rev., D; 6: No. 5, 1379-92(1 Sep 1972).
The possibility of a unified description for several weak radiative decays of K mesons is being investigated. In particular, those processes are considered in which the decay mechanism can be related to the strong (or electromagnetic) PVV vertex, namely $K^+ \rightarrow e^+\nu\gamma$, $K^0_2 \rightarrow \pi^+\pi^-\gamma$, and $K^+ \rightarrow \pi^+\gamma\gamma$, in addition to the process $K^0_2 \rightarrow \gamma\gamma$, which was treated before. Vector gauge fields with current mixing and octet breaking in the PVV vertex are used, as indicated from a phenomenological Lagrangian model fitting the data on strong and radiative meson decays. For the weak nonleptonic interaction two alternatives were considered, the current-current "simplest" Hamiltonian suggested recently in connection with $K^0_2 \rightarrow \gamma\gamma$ decay, as well as the current-current octet Hamiltonian in the form introduced by Sakurai, both satisfying the $\Delta S = 1$, $\Delta I = \frac{1}{2}$ rule. The experimental upper limit on $K^+ \rightarrow e^+\nu\gamma$ imposes limits on a free parameter of the theory related to the SU(3) symmetry breaking in the PVV vertex. Within these limits the width for $K^0_2 \rightarrow \pi^+\pi^-\gamma$ is calculated, which differs considerably from the SU(3)-symmetric value and is predicted to be close to the present experimental upper limit. In the calculation of $K^+ \rightarrow \pi^+\gamma\gamma$ a new class of diagrams is considered which appear because of the use of vector gauge fields in the Lagrangian. These diagrams involving four-leg vertices are shown to give the dominant contribution to the decay. The calculated rate and spectrum differ from those of previous calculations. (auth)

54366 TIME REVERSAL FOR UNSTABLE PARTICLES. Schulman, L. S. (Indiana Univ., Bloomington). Ann. Phys. (N. Y.); 72: No. 2, 489-96(Aug 1972).
The time reversal operator (T) for unstable particles is defined such that the fact of decay of the particle is not mistaken for a dynamical violation of T in the decay. This definition is not valid where the medium in which the decay takes place may have its own intrinsic T violation. Based on this limitation, some effort is made to restrict the conclusions drawn from apparent T violation in K-meson decay. (1 figure) (auth)

54367 CP-VIOLATING GAUGE INTERACTIONS. Isham, C. J. (Imperial Coll. of Science and Tech., London); Salam, A.; Stratdhee, J. Lett. Nuovo Cim.; 4: No. 14, 678-80(5 Aug 1972).
An attempt is made to derive an Okubo-like Lagrangian using the gauge principle, which yields (a) vector-type interactions, (b) universality, and (c) restrictions on the possible interaction types. The natural violation of C or (CP) which arises from gauging kinetic-energy vs. surface terms is demonstrated. (L.B.S.)

54368 RELATIVISTIC EQUATION FOR BARYONS OF A 45-DIMENSIONAL REPRESENTATION OF SCHWINGER GROUPS W(3). PART 2. Masleev, N. N. Izv. Akad. Nauk Kaz. SSR, Ser. Fiz.-Mat.; No. 4, 12-19(Jul-Aug 1971). (In Russian).

Electromagnetic interactions of baryons $\frac{1}{2}^+$ were investigated on the basis of the results obtained in Part 1. The representations of Schwinger relativistic groups, relative to the baryons investigated, were examined. Combining two reducible representations of groups SU(3) × SL(4), good values for the magnetic moments may be obtained, which do not contradict Fermi statistics, by using integral charges for the fundamental fields. (tr-auth)

54369 LOWER BOUND FOR CP-NONCONSERVATION IN THE $K_{L,S}{}^0$ DECAY INTO $\mu^+\mu^-$. Shirafuji, Tadahiko (Chiba Univ., Japan). Progr. Theor. Phys. (Kyoto); 48: No. 1, 337-9(Jul 1972).

The inequality $[\text{Rate } (K_L^0 \to \mu^+\mu^-)]^{1/2} < (\text{Re}\,\epsilon)\ [\text{Rate } (K_S^0 \to \mu^+\mu^-)]^{1/2}$ was obtained by Christ and Lee on the assumptions that (1) the absorptive part of the $K_L^0 \to 2\gamma$ decay amplitude is zero, (ii) the absorptive part of the $K_L^0 \to \mu^+\mu^-$ decay amplitude is due only to the on-mass-shell 2γ intermediate state, and (iii) both CPT-invariance and quantum electrodynamics are valid, but CP conservation is not, and using the experimental upper bound on the branching ratio. Several consequences from this inequality are discussed: contradiction with super weak theory; and the lower bound for CP nonconservation. (L.B.S.)

Applications (Strong)

Refer also to abstract 54309.

54370 (NP-19418) REPRESENTATION OF SU(3) x SU(3) CHIRAL ALGEBRA FOR BARYONS. Note No. 369. Buccella, F.; Nicolo, F.; Pugliese, A. (Rome Univ. (Italy). Istituto di Fisica). 6 Apr 1972. 17p. Dep. NTIS (U. S Sales Only).

A mixing operator U(Z′) for baryons, which transforms the SU(6) axial charges in a more realistic set satisfying at the same time the equations: $(\sigma_5^\alpha, \sigma_5^\beta) = i\, f^{\alpha\beta\gamma}\sigma^\gamma$ and $[\sigma_5^+, (\sigma_5^+, m^2)] = 0$, is presented. The (56 ⊕ 70, any L) SU(6) ⊗ 0(3) representations are considered to obtain a consistent result. The octet chiral wave function comes out in good agreement with experimental data and the coupling constants between the (56, L = 0) and any other representation with arbitrary L correspond exactly in a dual sense to the exchange in the t-channel of a tensor nonet and a vector octet with the couplings proposed by Cabibbo, Horwitz and Ne'eman. The explicit form of the m^2 operator is given. (auth)

54371 CHIRAL TENSORS AND THE AXIAL CHARGE. Vasholz, David P. (Univ. of Florida, Gainesville). Phys. Rev., D; 6: No. 5, 1322-4(1 Sep 1972).

Tensors which transform according to the (1,8) representation of SU(3) ⊗ SU(3) and whose commutators with axial charges are to good approximation saturated by octet and decuplet intermediate states are investigated. The mere existence of such operators is sufficient to impose a constraint between g_s and g_a, the symmetric and antisymmetric axial-charge-baryon-octet couplings. When this constraint is plotted in the $g_s - g_a$ plane, the resulting graph passes remarkably close to the experimental point. Using the experimental value of g_A as an input, the constraint predicts an axial-charge D/F ratio of 2.12 ± 0.03. (auth)

54372 RELATIVISTIC EQUATION FOR BARYONS OF A 45-DIMENSIONAL REPRESENTATION OF SCHWINGER GROUPS W(3). PART I. Masleev, N. N. Izv. Akad. Nauk Kaz. SSR, Ser. Fiz.-Mat.; No. 4, 5-12(Jul-Aug 1971). (In Russian).

It was proposed that baryons, corresponding to a 45-dimensional representation of Schwinger groups, consist of four particles, three of which are fermions with a spin of $\frac{1}{2}$, and one a boson with a spin of one. An interaction matrix of a special type was introduced into the equation of the four particles, and during the transition to a limit, wherein the masses of the composite baryons tend to approach infinity, an equation was obtained, which after transition to suitable variables and some additional conversions, was brought to a form which was applicable to a relativistic-invariant description of baryons in the free state and in the presence of a weak electromagnetic field. (tr-auth)

Field Theories

General

Refer also to abstract 55070.

54373 (ITF-72-35-P) ON THE EXTERNAL INVARIANT EQUATIONS OF ELECTROMAGNETIC FIELD. Zaitsev, G. A.; Solunin, A. M. (Akademiya Nauk Ukrainskoi SSR, Kiev. Institut Teoreticheskoi Fiziki). 1972. 21p. (In Russian). Dep. NTIS (U. S. Sales Only).

The invariant properties of Maxwell equations are considered in the presence of electric and magnetic charges with respect to a group of external transformations. The variational principle is formulated and consequences of the external invariance of field equations are derived. (auth)

54374 SYMMETRY OF THE COULOMB FIELD AND ITS APPLICATIONS. Kulkarni, Ramesh G. Stillwater, Okla.; Oklahoma State Univ. (1971). 188p. University Microfilms Order No. 72-21,916.

Thesis.

The study of the symmetries of non-relativistic, relativistic, and approximate relativistic Coulomb problem is of value both in atomic and particle physics. The invariance and noninvariance group structure and associated generators would give a deep interpretation of the energy level spectra and certain selection rules in the multipole transitions. The structure of the basis functions for the irreducible representations in the complex spaces of the Fock–Bargmann type give a clear picture of the role played by the symmetry. The study of the Stark effect has received a renewed experimental interest. The experimental accuracies have improved by few orders of magnitude making it necessary to have a correct theoretical calculation of the Stark shifts. It is also interesting to study the effect of symmetry on the Coulomb field on the Stark shift calculations. The study shows that the symmetry of the Coulomb field explains vanishing of certain radial integrals involving multipole operators. It can also be used to evaluate some radial integrals in problems like Coulomb excitation. The symmetry shows that the parabolic and spherical wave functions of the nonrelativistic Coulomb field are connected through the Clebsch–Gordan theorem. The parabolic and spherical wave functions were obtained in Fock–Bargmann space and relation between them was established. The momentum space wave functions of the symmetric Hamiltonian were also discussed. The first order Stark shifts are calculated using Dirac wave functions, Pauli wave functions and relativistic symmetric wave functions. The shifts calculated on the basis of symmetric Hamiltonian are linear and spin dependent. For low values of electric field the experimental Stark shifts are quadratic and the discrepancy between the calculated first order shifts and the experimental values is large. For intermediate values of electric fields the shifts are linear. The agreement between theory and experiment is better. (Diss. Abstr. Int., B)

Quantum Field Theory

Refer also to abstract 54413.

54375 (COO-1811-3) MEASUREMENT OF THE LAMB-SHIFT IN A HYDROGEN-LIKE ATOM OF NUCLEAR CHARGE Z ≥ 3. Final Report. Fan, C. Y. (Arizona Univ., Tucson). 1972. Contract AT(11-1)-1811. 4p. Dep. NTIS.

The Lamb shift in $^{16}O^{7+}$ was measured in order to uncover some fundamental defect in quantum electrodynamics. The averaged Lamb shift calculated from the measured decay constants is 2215.6 ± 7.5 GHz. (J.F.P.)

54376 (ITF-72-15-E) EQUATIONS FOR THE S-MATRIX ELEMENT IN $g(:\phi^4:)_2$ THEORY. Ivanov, S. S. (Akademiya Nauk Ukrainskoi SSR, Kiev. Institut Teoreticheskoi Fiziki). 1972. 14p. Dep. NTIS (U. S. Sales Only).

The equations for the S-matrix elements for the $g(:\phi^4:)_2$ theory in the Euclidean domain are considered. The existence theorem for the space-time cutoff equation is proved. It is shown that the perturbation series is asymptotic for an exact solution. (auth)

54377 (ITF-72-54-P) DISPERSION SUM RULES AND THE JOST–LEHMAN–DYSON REPRESENTATION IN AXIOMATIC QUANTUM THEORY. Zinov'ev, G. M.; Miranskii, V. A.; Shelest, V. P. (Akademiya Nauk Ukrainskoi SSR, Kiev. Institut Teoreticheskoi Fiziki). 1972. 19p. (In Russian). Dep. NTIS (U. S. Sales Only).

The spectral Jost–Lehman–Dyson representation is used to determine the structure of dispersion sum rules and Ward identities in axiomatic quantum theory. (auth)

54378 (ITF-72-62-E) WIGHTMAN AXIOMS FOR THE CONCENTRATABLE FIELD AND RECONSTRUCTION THEOREM. I. GLOBAL PROPERTIES OF THE FIELD. Lomsadze, Yu. M.; Krivskii, I. Yu.; Shuba, I. M. (Akademiya Nauk Ukrainskoi SSR, Kiev. Institut Teoreticheskoi Fiziki). 1972. 27p. Dep. NTIS (U. S. Sales Only).

The first steps are made in constructing the Wightman axiomatic approach for the so-called concentratable field $\hat{\varphi}(f)$. The concentratability of the additive functional $\hat{\varphi}(f)$ means that it belongs to one of maximum functional class concentratable, in rigorously defined sense, in any Borel set $\Delta \subseteq R_x^4$. Some general axioms and axioms about global properties of this field are formulated. Some algebraic constructions are given. (auth)

54379 COMPOSITENESS AND VANISHING OF RENORMALIZATION CONSTANTS. Passi, J. N. (Joint Inst. for Nuclear Research, Dubna, USSR). Nucl. Phys.; B46: No. 2, 497-504 (1972).

It is demonstrated within the framework of a model field theory that the vanishing of wavefunction and vertex-function renormalization constants is not a sufficient condition to make an elementary particle equivalent to a three particle bound state. It is noticed that the Jin—MacDowell cancellation for the three particle bound state does not hold good. (auth)

54380 VARIATIONAL PADE SOLUTION OF THE BETHE–SALPETER EQUATION. Alabiso, C.; Butera, P.; Prosperi, G. M. (Univ., Milan). Nucl. Phys.; B46: No. 2, 593-614(1972).

A variational Padé approximant technique for the calculation of the bound states, resonances and phase shifts is applied to the Bethe—Salpeter equation describing the interaction of two scalar particles in the ladder approximation. The main result is that the technique retains the very simple features and the fast convergence properties learned from a previous study of the potential scattering case. (auth)

54381 FEYNMAN RULES FOR MASSIVE GAUGE FIELDS WITH DUAL DIAGRAM TOPOLOGY. Gervais, J. L.; Neveu, A. (Laboratoire de Physique Theorique et Hautes Energy, Orsay, France). Nucl. Phys.; B46: No. 2, 381-401(1972).

The relationship of dual models with renormalizable theories of massive Yang—Mills fields of the type recently proposed by 't Hooft is studied through the zero slope. The field theoretic meaning of the twisting operator and the topology of dual models are clarified; these features result from the choice of a special non-Hermitian gauge condition in the underlying field theory. The local gauge invariance of that theory is the exact reflection of the first set of "gauge identities" appearing in the dual theory. In the non-Hermitian gauge, some renormalizable massive vector meson theories are both manifestly renormalizable, and this leads to a spectacular simplification of the Feynman rules. (auth)

54382 GENERALIZED FIELD THEORY AND FORM FACTORS OF NUCLEONS AND ATOMS. Riewe, Frederick Eugene. Gainesville, Fla.; Univ. of Florida (1971). 258p. University Microfilms Order No. 72-21,096.

Thesis.

Fields which obey equations containing derivatives of higher-than-usual order are the subject of generalized field theory. The use of such generalized fields results in a nonlocal theory which eliminates many of the infinities and divergences from quantum field theory. However, the theory is often considered to be unacceptable because of its many problems of physical interpretation. It is the purpose of the present investigation to develop a consistent interpretation of generalized field theory in terms of the internal structure of particles and then to apply the theory to realistic problems in nuclear and atomic physics. After briefly tracing the history of generalized field theory, the mathematical basis of the theory is developed in a classical context. The formalism is applied to the simple case of a classical point particle characterized by a Lagrangian which is a function of both velocity and acceleration. The theory leads directly to a description of a classical spinning particle. By placing the theory in canonical form and quantizing the Hamiltonian, one obtains a wave equation which, like the Dirac equation, is first order in time and manifestly covariant. Next, higher-derivative field equations are considered. The generalized quantum field theory is formulated in an indefinite metric space and applied to higher-derivative boson fields. These equations are physically interpreted as being the equations of a field exhibiting nonlocal interactions characterized by form factors. The form factor interpretation is shown to be mathematically consistent as well as to provide form factors which realistically describe known particles. The problem of determining the fundamental nuclear force is then discussed. The use of generalized fields is shown to be equivalent to the introduction of nucleon form factors, with the result that the two-nucleon potential is nonsingular. A generalized one-boson-exchange potential model is presented which accurately describes the nuclear force in terms only of known mesons. A second model is given in which charge independence is not assumed. Besides providing improved agreement with experimental data, the model indicates the extent of charge independence in the nuclear force. A third model of the two-nucleon force is presented which can be shown to accurately predict properties of finite nuclei. The use of generalized field theory as a mathematically equivalent substitute for the usual formalism used to describe atomic interactions is shown to have the practical consequence of characterizing atomic potentials by means of the same functions used in the nuclear-force problem, so that the same computational methods can be applied. In turn, the study of atomic processes provides a physical interpretation of infinite-order field equations in terms of charge-cloud polarization. The simplest form factor which includes charge-cloud polarization effects is shown to give a quantitative description of the electromagnetic structure of the proton. Thus the form factor interpretation of generalized field theory is satisfactory for field equations of both finite and infinite order. (Diss. Abstr. Int., B)

54383 N. N. BOGOLIUBOV'S TRANSFORMATION IN THE STRONG COUPLING THEORY. III. Solodovnikova, E. P.; Tavkhelidze, A. N.; Khrustalev, O. A. (Joint Inst. for Nuclear Research, Dubna, USSR). Teor. Mat. Fiz.; 12: No. 2, 164-78 (Aug 1972). (In Russian).

Translation invariant systems with strong couplings are considered. Application of N. N. Bogoliubov's transformation makes it possible to take explicitly into account the conservation laws, to construct the perturbation series with respect to a small parameter and to calculate the stationary states in the first approximation. The equidistant spectrum of the mass squared is obtained for the case of interaction of classical relativistic particles with an external field. (auth)

54384 PRODUCTION OF BOSON PAIRS BY STATIC FIELD. Arbusov, B. A.; Rochev, V. E. Teor. Mat. Fiz.; 12: No. 2, 204-8(Aug 1972). (In Russian).

Production of pairs of scalar particles by a square-well potential with smooth sides is considered. It is shown that the probability of the pair production in the threshold region includes an exponentially small factor depending on the degree of the "smoothness" of the potential well. (auth)

54385 TWO-DIMENSIONAL CLASSICALLY SOLVABLE MODEL WITH NONTRIVIAL SCATTERING. Pogrebkov, A. K. (Mathematics Inst., Moscow). Teor. Mat. Fiz.; 12: No. 2, 209-13(Aug 1972). (In Russian).

The model $(:j^{\mu} j_{\mu} \varphi:)_2$ describing the interaction of the massive scalar field φ with the massless spinor field is studied. It is shown that this model is explicitly solvable in the classical case and leads to nontrivial mutual transitions of the boson and fermion particles in the quantum case. (auth)

54386 HAMILTONIAN DEFINED AS A GRAPH LIMIT IN A SIMPLE SYSTEM WITH AN INFINITE RENORMALIZATION. Aoki, Masakazu; Mugibayashi, Nobumichi (Kagawa Univ., Takamatsu, Japan). Progr. Theor. Phys. (Kyoto); 48: No. 1, 281-9(Jul 1972).

The Hamiltonian of the neutral scalar field in interaction with a fixed source, when the infinite renormalization of vacuum energy is necessary, is defined by the graph limit of approximate Hamiltonians. Remarks are made on the asymptotic fields in this case. (auth)

54387 SPONTANEOUS BREAKDOWN OF SYMMETRY AND THE GAUGE INVARIANCE IN A RELATIVISTIC FIELD THEORY. Aurilia, Antonio (Univ. of Alberta, Edmonton) Takahashi, Yasushi; Umezawa, Hiroomi. Progr. Theor. Phys. (Kyoto); 48: No. 1, 290-315(Jul 1972).

The Nambu-Jona-Lasinio model in which the helicity current is coupled with a massless chiral gauge field, is discussed in the pair approximation. The model is invariant under the constant as well as local gauge transformations. The excitation spectrum of physical states is investigated in this model, under the requirement that the chiral gauge invariance is maintained at every stage. Symmetry breaking solutions are found in a noncovariant form. Contrary to previous assertions, massless fields are still present in the theory. Thus, the physical fields are a massive vector field, a massless vector field and a phase field. It is shown that the gauge transformations are carried by the phase field and the massless vector field, respectively. (auth)

54388 REMARKS ON SCHERK'S PAPER ENTITLED ZERO-SLOPE LIMIT OF THE DUAL RESONANCE MODEL. Nakanishi, Noboru (Kyoto Univ.). Progr. Theor. Phys. (Kyoto); 48: No. 1, 355-6(Jul 1972).

The following observation was recently made by Scherk: In the zero-slope limit, the dual resonance model reduces to the ϕ^3 theory. It is pointed out that Scherk's proof of this proposition is incorrect except for the case of 4-point tree graphs, but it is proved that his conclusion is true at least for all tree graphs. (T.B.S.)

Gravitation and General Relativity

Refer also to abstracts 53894 and 54162.

54389 (ITF-71-85-P) ABOUT THE INFINITESIMAL TRANSFORMATIONS CONSERVING THE TEST-BODY TRAJECTORIES IN GENERAL RELATIVITY. Aminova, A. V. (Akademiya Nauk Ukrainskoi SSR, Kiev. Institut Teoreticheskoi Fiziki). 1971. 21p. (In Russian). Dep. NTIS (U. S. Sales Only).

Group methods in general relativity are developed. Groups of projective motions, i.e., the groups of infinitesimal transformations, conserving the geodesic (the path of trial bodies) are discussed. A further step in defining the gravitational field in a unique manner by the test-body trajectories, this task is closely linked with important problems of modelling the field of gravitation and building fundamental mechanical and field laws of conservation in general relativity. The projective group properties of free and homogeneous fields of gravitation described by Einstein spaces are explored. The spaces V_4 that allow two independent constant vector fields among which the spaces of maximal projective mobility (variable curvature) are contained are also investigated. (auth)

54390 (ITF–71-130-P) ON THE MODELING OF GRAVITATIONAL FIELDS. **Petrov, A. Z.** (Akademiya Nauk Ukrainskoi SSR, Kiev. Institut Teoreticheskoi Fiziki). 1971. 16p. (In Russian). Dep. NTIS (U. S. Sales Only).

The modeling of gravitational field is discussed within the framework of Einstein's theory. The modeling is defined as a mapping in which the geodesic lines (paths of test bodies) of the original transform into a family of the curves given by the equations of the test-body motion in a model. Different ways of modeling are indicated: Complete, selective, approximate-selective ones. The theory is applied for the solar gravitational field. (auth)

54391 (ITF–71-132-P) ON THE GEOMETRY OF RELATIVISTIC SPACE OF PARTICLE STATES. **Schtrobel, Hans** (Akademiya Nauk Ukrainskoi SSR, Kiev. Institut Teoreticheskoi Fiziki). 1971. 23p. (In Russian). Dep. NTIS (U. S. Sales Only).

The relativistic μ space (state space) of a free particle in a gravitational field is taken as a tangent bundle (fiber space) over the space–time V_4 and investigated as a special Riemannian space V_8 with the methods of Ricci calculus. The use of unholonomic coordinates is the most important remedy to make clear the symmetries of V_8, to define tensors in V_8 and relate them to tensors of V_4, and to prove theorems on vector fields and conservation, e.g., the relativistic Liouville theorem for point-sets on two 6-dimensional relativistic analogs of classical phase space. (1 figure). (auth)

54392 (ITF–72-3-P) RELATIONS BETWEEN THE COSMOLOGICAL AND QUANTUM CONSTANTS. **Stanyukovich, K. P.** (Akademiya Nauk Ukrainskoi SSR, Kiev. Institut Teoreticheskoi Fiziki). 1972. 10p. (In Russian). Dep. NTIS (U. S. Sales Only).

The relations between cosmological and quantum constants are discussed. In particular, it is shown that, given three experimentally measured values G, c, and h, different in dimensions, as well as a scalar curvature R changing in time, it is possible to define all the remaining functions of fundamental values in terms of these four basic parameters. (auth)

54393 (ITF–72-5-P) ON THE SPATIAL LOCALIZABILITY OF ENERGY–MOMENTUM TENSOR OF GRAVITATIONAL FIELD. **Kiriya, V. S.; Kereselidze, A. B.; Vepkhvadze, G. T.; Lezhava, O. I.** (Akademiya Nauk Ukrainskoi SSR, Kiev. Institut Teoreticheskoi Fiziki). 1972. 10p. (In Russian). Dep. NTIS (U. S. Sales Only).

Some properties of the energy-momentum tensor of gravitational field including the second derivatives of metric tensor are considered. Some of these properties are investigated by considering an example of Kötler's solution. (auth)

54394 (ITF–72-20-P) RIESSNER–NORDSTROEM PROBLEM IN PRESENCE OF SCALAR FIELD. **Bronnikov, K. A.** (Akademiya Nauk Ukrainskoi SSR, Kiev. Institut Teoreticheskoi Fiziki). 1972. 13p. (In Russian). Dep. NTIS (U. S. Sales Only).

An exact static central-symmetric solution of the set of equations for the Einstein gravitational field, massless scalar field, and electromagnetic field is obtained and investigated. The scalar field Lagrangian density is chosen in the conformally invariant form $L_s = \phi^{*,\alpha}\phi_{,\alpha} - (R/6)\ \phi^*\phi$, where R is scalar curvature. This solution is compared with that of a similar problem with the usual scalar field Lagrangian density $L_s = \phi^{*,\alpha}\ \phi_{,\alpha}$. (auth)

54395 (ITF–72-21-P) SCALAR-TENSOR THEORY OF GRAVITATION. **Zaitsev, N. A.; Kolesnikov, S. M.; Radynov, A. G.** (Akademiya Nauk Ukrainskoi SSR, Kiev. Institut Teoreticheskoi Fiziki). 1972. 37p. (In Russian). Dep. NTIS (U. S. Sales Only).

A new variant of the scalar-tensor theory of gravitation is proposed. The static field of a charged source is obtained. The first term of the expansion of this solution in inverse power series of the radius shows that the inclusion of an electric charge can both increase and decrease the mass of a neutral source. The solution obtained is compared with the observable effects of a geodesic motion of a test particle in the field of a central body. (auth)

54396 (ITF–72-41-P) COSMOLOGICAL MODELS OF A SCALAR-TENSOR THEORY OF GRAVITATION. **Bronnikov, K. A.; Yakimov, V. E.** (Akademiya Nauk Ukrainskoi SSR, Kiev. Institut Teoreticheskoi Fiziki). 1972. 14p. (In Russian). Dep. NTIS (U. S. Sales Only).

Isotropic cosmological models in Zaitsev–Kolesnikov scalar-tensor theory of gravitation are considered. A number of qualitative conclusions is formulated, including conditions for a model to be singularity-free. For the case of massless scalar field exact solutions are obtained in the presence of dustlike matter and radiation. Among these solutions a class of models which may be used to describe the observable universe, is found. Some of these models are singularity-free. (auth)

54397 (ITF–72-46-P) TWO-SYMMETRIC AND TWO-RECURRENT FIELDS OF GRAVITATION. **Kaigorodov, V. R.** (Akademiya Nauk Ukrainskoi SSR, Kiev. Institut Teoreticheskoi Fiziki). 1972. 21p. (In Russian). Dep. NTIS (U. S. Sales Only).

Two-symmetric and two-recurrent fields are investigated in detail by a single algebraic method which makes it possible to determine all classes of the relativistic spaces mentioned and to prove that the Lichnerowicz and Potter theorems proved for the spaces with a positively definite metric no longer hold in general relativity unless the space-times are conformally flat, and their scalar curvature is equal to zero. (auth)

54398 (ITF–72-52-P) TWO-BODY PROBLEM IN THE THEORY OF DIRECT GRAVITATIONAL INTERACTION. I. **Zhdanov, V. I.; Piragas, K. A.** (Akademiya Nauk Ukrainskoi SSR, Kiev. Institut Teoreticheskoi Fiziki). 1972. 21p. (In Russian). Dep. NTIS (U. S. Sales Only).

The problem of two gravitating bodies is considered within the framework of Fokker formalism. The existence and uniqueness theorem for a solution of the equations of motion which arise from the vanishing of the first variation of Fokker action is proved under certain conditions. (auth)

54399 (ITF–72-58-P) ON A TWO-BODY PROBLEM IN THE THEORY OF DIRECT GRAVITATIONAL INTERACTION. **Zhdanov, V. I.; Piragas, K. A.** (Akademiya Nauk Ukrainskoi SSR, Kiev. Institut Teoreticheskoi Fiziki). 1972. 24p. (In Russian). Dep. NTIS (U. S. Sales Only).

The two-body motion in a circular orbit in the theory of direct gravitational interaction. The problem of stability of such motion is the focus of the attention. It is shown that at small rates the formations of the binary star type are unstable. (auth)

54400 (ITF–72-59-P) RELATIVISTIC GRAVITATIONAL EFFECT ON INFLUENCE OF EARTH ROTATION ON MECHANICAL VIBRATIONS. **Shirokov, M. F.; Ivashchenko, A. V.** (Akademiya Nauk Ukrainskoi SSR, Kiev. Institut Teoreticheskoi Fiziki). 1972. 12p. (In Russian). Dep. NTIS (U. S. Sales Only).

The general equations for small deviations ξ^i of the world line of a particle with one-dimensional elastic coupling from its equilibrium position in the earth laboratory on the equator are deduced. It is shown that the squares of frequency ω_θ and ω_ϕ vibrations of a particle in the planes of meridian and latitude differs from one another by the square of the earth rotation frequency u^3, with the correction of Einstein's theory of gravity by a magnitude $A(u^3)^2$ (m/R). (2 figures) (auth)

54401 (ITF–72-60-P) EFFECTS OF EINSTEIN'S THEORY OF GRAVITY AT THE TWO-PARTICLE VIBRATIONS IN SCHWARZCHILD'S FIELD. **Ivashchenko, A. V.** (Akademiya Nauk Ukrainskoi SSR, Kiev. Institut Teoreticheskoi Fiziki). 1972. 6p. (In Russian). Dep. NTIS (U. S. Sales Only).

The transition from the Schwarzchild coordinate system in the central symmetrical gravitational field to that of the local pseudo-decart connected with the observer moving in a geodetic or nongeodetic circle is determined. For a system consisting of 2 particles elastically coupled and moving in close geodesics in this field, the expression for the squares of vibration frequencies in various directions is obtained; it is equal to zero in the Newtonian case and different from zero in general relativity. This relation can be experimentally verified. (auth)

54402 LIE GROUPS AND THE THEORY OF GRAVITATION. **Ketsaris, A. A.** (Moscow Energy Inst.). Izv. Vyssh. Ucheb. Zaved., Fiz.; No. 12, 40-7(1970). (In Russian).

From length and time standards in the theory of gravitation, a generalized space with distortion and curvature determined by the fundamental group was constructed. Field variables coincide with coefficients ϵ_μ^i the infinitesimal group operator. It is shown that the structural equations of the group depend on the transformation properties of the object to which they are applied. The simplest equations which satisfy ϵ_μ^i are given. (tr-auth)

54403 TESTING GENERAL RELATIVITY: PROGRESS, PROBLEMS, AND PROSPECTS. **Shapiro, I. I.** (Massachusetts

Inst. of Tech., Cambridge). Gen. Relativity Gravitation; 3: No. 2, 135-48(Jun 1972).

Results from radar and radio gravity experiments are given for retardation of radar signals, deflection of radio waves, relativistic perihelion advance of Mercury, and time variation of the gravitational constant. The first three are expressed as fractions of the corresponding effects predicted by general relativity. In terms of the Eddington—Robertson parameters, the first two are approximately equal to $(1 + \gamma)/2$ and the third to $(2 + 2\gamma - \beta)/3$. The third depends on the assumption that the solar gravitational quadrupole moment vanishes; its effects cannot be separated usefully from those of general relativity with the present data set. The uncertainties are as given by the individual experimenters; in some cases they represent formal standard errors, in others an allowance for possible systematic errors is included. (auth)

54404 POTENTIALS OF THE TYPE a_n/r^n, $n > 1$, IN COLLAPSING SYSTEMS OF GENERAL RELATIVITY THEORY. Berezin, V. A.; Markov, M. A. (Levedev Inst. of Physics, Moscow). Teor. Mat. Fiz.; 12: No. 2, 153-63(Aug 1972). (In Russian).

The nonlinear generalization of the Maxwell equations is constructed which leads to the static repulsive potentials of the type under consideration. The corresponding analog of the Nordström—Reissner metrics is constructed. In the framework of the classical (nonquantum) physics it is shown that the forces under consideration (a_n/r^{n+1}, $n > 1$) in general relativity theory do not lead to divergences of the self energy of their source. It is shown that in the case when the collapsing system goes beyond the gravitational radius ("the black hole"), the classical forces a_n/r^{n+1}, $n > 1$, as well as electrostatic and gravitational ones do not vanish in the external space. This result is contrary to the result by Hartle which was obtained for the pair neutrino forces ($\sim r^{-5}$). (auth)

54405 POTENTIAL IN THE CANONICAL FORMALISM OF GRAVITY. Kimura, Toshiei; Toiya, Takehiro (Hiroshima Univ.). Progr. Theor. Phys. (Kyoto); 48: No. 1, 316-28(Jul 1972).

An attempt is made to derive the gravitational potential from the canonical formalism viewpoint of the gravitational field coupled with matter. The two-body potential in an arbitrary coordinate frame (i.e., gauge) is obtained by solving constraint equations. It is shown, by making a transformation of the time coordinate, that the potential coincides with Hiida's obtained with the aid of the "diagrammatic" quantization. A simple equation to get the static potential to any order is presented. Explicit forms of the static potential are given up to the five-body potential. From the form of potential it is immediately seen that there exists a relation between two-body and many-body static potentials. (auth)

54406 GRAVITATIONAL WAVES OF THIRD AND HIGHER ORDER. Tokuoka, Tatsuo (Kyoto Univ.). Progr. Theor. Phys. (Kyoto): 48: No. 1, 333-4(Jul 1972).

The gravitational waves of third and higher order are discussed briefly for tensor and scalar-tensor fields according to analytic methods adopted by Tokuoka. The following conclusions are given: The gravitational waves of third and higher order for tensor and scalar-tensor fields have the identical propagation conditions with those of the second order, and they are classified into three types, transverse, longitudinal, and shear. The transverse wave is real and has speed c, while the longitudinal and shear waves are imaginary. (L.B.S.)

Scattering Theory

Refer also to abstracts 54345, 54711, 54737, and 55068.

54407 (BNL—16752) SCATTERING THEORY FOR ELLIPTIC DIFFERENTIAL OPERATORS IN UNBOUNDED DOMAINS. Goldstein, Charles I. (Wisconsin Univ., Madison. Mathematics Research Center). 10 Feb 1972. Contract DA-31-124-ARO-D-462. 60p. Dep. NTIS.

A new method is developed for meromorphically continuing the S-matrix and distorted waves associated with a general class of elliptic partial differential operators and for relating the poles to "resonant states". The method is applied to nonselfadjoint second-order perturbations of the Laplacian acting in wedge-like regions contained in R^N. The main analytic tools employed are the limiting absorption principle and the Schwarz reflection principle. (auth)

54408 (ITF—72-14-E) ON STABILITY OF THE SYSTEMS WITH SINGULAR POTENTIALS. Simenog, I. V. (Akademiya Nauk Ukrainskoi SSR, Kiev. Institut Teoreticheskoi Fiziki). 1972. 6p. Dep. NTIS (U. S. Sales Only).

It is shown for the systems with singular attractive potentials, that the concept of independent particles in the sense of Hartree is exactly realized in the asymptotic limit $N \to \infty$. (auth)

54409 (ITF—72-37-P) ANALYTIC REGULARIZATION DEPENDING ON THE PARAMETER. Kovalenko, V. F. (Akademiya Nauk Ukrainskoi SSR, Kiev. Institut Teoreticheskoi Fiziki). 1972. 20p. (In Russian). Dep. NTIS (U. S. Sales Only).

It is shown that logarithmic terms arising under the scale transformations of renormalized Feynman amplitudes are an additive finite regularization. Analytic regularization depending on the parameter which is an analog of subtraction point in the Bogolubov R-operation is defined. (auth)

54410 (ITF—72-38-P) BEHAVIOUR OF THE RENORMALIZED FEYNMAN AMPLITUDES UNDER SCALE TRANSFORMATIONS. Kovalenko, V. F. (Akademiya Nauk Ukrainskoi SSR, Kiev. Institut Teoreticheskoi Fiziki). 1972. 22p. (In Russian). Dep. NTIS (U. S. Sales Only).

The behavior of analytically renormalized Feynman amplitudes under scale transformations in a scalar field theory with $\lambda L^4(x)$ interaction and $m^2 \neq 0$ is studied. It is shown that under the scale transformations of renormalized Feynman amplitudes, the logarithmic terms arise as a result of regularization. The results obtained make it possible to define large-momentum behavior of an arbitrary renormalized Feynman amplitude and to investigate the violation of homogeneity of Feynman amplitudes by regularization at $m^2 \to 0$. (auth)

54411 (ITF—72-39-P) VIOLATION OF THE HOMOGENEITY OF THE FEYNMAN AMPLITUDES OF SELF-ENERGY GRAPHS UNDER REGULARIZATION. Kovalenko, V. F. (Akademiya Nauk Ukrainskoi SSR, Kiev. Institut Teoreticheskoi Fiziki). 1972. 11p. (In Russian). Dep. NTIS (U. S. Sales Only).

It is shown that analytic regularization violates the homogeneity of Feynman amplitudes of self-energy graphs in a zero-mass scalar field theory with $\lambda\phi^4(\varkappa)$ interaction. Analysis of the logarithmic terms breaking homogeneity leads one to conclude that with $m^2 = 0$, the renormalized Feynman amplitudes of self-energy graphs are homogeneous functions under combined scale transformations of the parameter of analytic regularization and momenta. (auth)

54412 (ITF—72-63-E) DAMA AND REGGE ASYMPTOTIC BEHAVIOUR. Bugrii, A. I.; Enkovskii, L. L.; Kobylinskii, N. A.; Shelest, V. P. (Akademiya Nauk Ukrainskoi SSR, Kiev. Institut Teoreticheskoi Fiziki). 1972. 16p. Dep. NTIS (U. S. Sales Only).

The high-energy behavior of a dual amplitude with Mandelstam analyticity (DAMA) is investigated. A detailed analysis of this dependence of the asymptotic behavior of DAMA on the position of the boundary of the spectral function and on the asymptotic form of the Regge trajectory is given. It is proved that the amplitude does have Regge asymptotic behavior for arbitrary momentum transfers if the trajectories increase more slowly than S. (3 figures) (auth)

54413 (JINR—P2-6586) PROOF OF UNITARITY OF THE S-MATRIX IN NON-LOCAL QUANTUM FIELD THEORY. Alebastrov, V. A.; Efimov, G. V. (Joint Inst. for Nuclear Research, Dubna (USSR). Lab. of Theoretical Physics). 1972. 17p. (In Russian). Dep. NTIS (U. S. Sales Only).

In nonlocal quantum field theory the unitarity of the S-matrix is proved in each order of perturbation theory for polynomial Lagrangians. (auth)

54414 UNITARITY AND THE INHOMOGENEOUS EQUATIONS METHOD FOR IDENTICAL PARTICLE SCATTERING. Levin, F. S. (Brown Univ., Providence). Ann. Phys. (N. Y.); 72: No. 2, 497-511(Aug 1972).

A K-matrix solution to the coupled, inhomogeneous equations describing the scattering of a particle by a system of identical particles is developed. It is shown that K is a sum of two terms, one arising from the homogeneous solution and one from the particular integral. The former is a direct contribution, i.e., with no exchange, while the latter is a pure exchange contribution. Thus, as in the previously studied case of the T matrix arising from this system of equations, the direct and exchange portions of K are additive, and can be computed separately. A unitary S matrix is obtained from K in the usual way: $S = (1 + iK)(1 - iK)^{-1}$. The problem of how to calculate K when an apparent two-channel problem is actually a two-particle problem with the channels referring to the identical particle labels is also solved. (auth)

54415 DIFFRACTION SCATTERING OF CHARGED PARTICLES. Frahn, W. E. (Univ. of Capetown, S. Afr.). Ann. Phys. (N. Y.); 72: No. 2, 524-47(Aug 1972).

It is shown that, contrary to popular belief, diffraction scattering in nuclear and particle physics is not always of Fraunhofer type. By establishing a simple physical connection between scattering in a Coulomb field and Fresnel diffraction, it is shown that diffractive collisions of heavy charged particles are predominantly of Fresnel type. Quantitative criteria for Fraunhofer and Fresnel scattering are derived which lead to a classification of all scattering processes by means of a "diffraction diagram." This enables specific prediction to be made about the gross structure of angular distributions for any experimental conditions. (10 figures) (auth)

54416 S-MATRIX APPROACH TO GLAUBER THEORY. Osborn, T. A. (Brooklyn Coll., New York). Nucl. Phys.; B46: No. 2, 538-46(1972).

An S-matrix approach to Glauber theory based on an eikonal-Hamiltonian formalism is presented. The variant of Glauber's multiple diffraction theory obtained here is rigorously unitary. The construction of the approximate composite scattering amplitudes requires only two-body phase shift data. (auth)

54417 FOUR-FERMION SCATTERING AMPLITUDE FREE FROM KINEMATICAL SINGULARITIES. Gogolitsin, Yu. L.; Prokhorov, L. V. (Leningrad State Univ.). Lett. Nuovo Cim.; 4: No. 14, 715-18(5 Aug 1972).

An attempt is made to find the general four-fermion scattering amplitude using CPT and relativistic invariance only. Identities are found which allow the possibility for choosing the set of invariant amplitudes free from kinematic singularities. (L.B.S.)

54418 UNITARITY CONSTRAINTS ON HELICITY AMPLITUDES. Hodgkinson, D. P. (Cavendish Lab., Cambridge, Eng.). Lett. Nuovo Cim.; 4: No. 14, 731-5(5 Aug 1972).

It is shown that bounds analogous to those derived by Singh and Roy (Phys. Rev. D, 2: 2638(1970)) exist for a suitably chosen amplitude, which is the sum of all amplitudes with no helicity-flip. New unitary restrictions on helicity-flip amplitudes are also discussed. (L.B.S.)

54419 HELICITY-CONSERVING AND HELICITY-NONCONSERVING POMERON-EXCHANGE AMPLITUDES IN THE DUAL ABSORPTIVE MODEL. Avni, Y. (Stanford Univ., Calif.). Lett. Nuovo Cim.; 4: No. 14, 725-30(5 Aug 1972).

It is shown that the present dual absorptive model has no predictive power with respect to the presence of zeros in t in pomeron-exchange diffractive amplitudes. Thus it is concluded that the correct description of the t-dependence of the diffractive amplitudes in meson-baryon reactions should not be considered as a success of the model, and the possible existence of a zero in the diffractive amplitudes of $pp \rightarrow pp$ should not be considered as a failure of the model. It is suggested that the strong predictive power of the dual absorptive model for nondiffractive amplitudes may serve as a very useful tool in deciding whether the possible helicity nonconservation in $\gamma p \rightarrow \rho^0 p$ is a property of diffractive amplitudes. (L.B.S.)

54420 NEW DERIVATION OF THE OFF-SHELL DUAL-RESONANCE AMPLITUDES. Tataru-Mihai, P. I. (Univ., Cluj). Lett. Nuovo Cim.; 4: No. 14, 711-14(5 Aug 1972).

A new attempt to derive an off-shell dual-resonance amplitude is presented. As a basic property the invariance of the integrand of the dual-resonance amplitude under Moebius transformations is considered. (L.B.S.)

54421 APPLICATION OF THE NEWTON–KANTOROVICH METHOD TO THE CHEW–LOW N/D EQUATIONS. I. Taira, Konno; Nelipa, N. F. (Moscow State Univ.). Teor. Mat. Fiz.; 12: No. 2, 214-22(Aug 1972). (In Russian).

By means of the Newton–Kantorovich method the sequence of iterations of the Chew–Low equations put in the N/D form is obtained taking into account the Castilljeho–Dalitz–Dyson poles. The convergence conditions of this sequence of iterations are found. The estimation of the coupling constant is performed. (auth)

54422 GENERALIZATION OF SEMILOCAL DUALITY. Ball, J. S.; Pinsky, Stephen (Univ. of Utah, Salt Lake City). Phys. Rev., D; 6: No. 5, 1456-7(1 Sep 1972).

Semilocal duality is applied to the process $a + b + c \rightarrow a + b + c$, in the double-Regge region. Using the Mueller formalism, this leads to a formula for elastic and quasielastic two-body scattering at large momentum transfers previously proposed by the authors. (auth)

54423 POSSIBLE BEHAVIOR OF REGGE TRAJECTORIES IN VENEZIANO-LIKE REPRESENTATIONS. Kobayashi, Masanori (Kyoto Univ.). Progr. Theor. Phys. (Kyoto); 48: No. 1, 267-71(Jul 1972).

Canonical product representations for scattering amplitudes which possess meromorphy in s and t as well as Regge behaviour are investigated in terms of entire functions of order ρ. The representation found turns out to be of order either $\rho = 1$ or $\rho = 0$. The case of $\rho = 1$ corresponds to the Veneziano representation and the case of $\rho = 0$ to the Coon representation which has logarithmic trajectories and polynomial residues of order n in s(t) at the n-th pole in t(s). (auth)

PHYSICS (LOW-TEMPERATURE)

Superfluidity

54424 HIGH-FREQUENCY HYDRODYNAMICS NEAR THE λ POINT. Khalatnikov, I. M.; Pokrovskii, V. L.; Semiz, D. M. (Landau Inst. for Theoretical Physics, Moscow). J. Low Temp. Phys.; 6: No. 3-4, 305-21(Feb 1972).

Dynamic phenomena are treated in a weakly interacting Bose gas model. It is considered that particles with momenta higher than the coupling constant g are free and distributed on energies according to Bose—Einstein statistics. In the critical regions all momenta are divided into two regions: an ideal-gas region $p \ll g$, and a small fluctuation region $p \lesssim g$. From the microscopic theory, the hydrodynamic wave equation is derived analogous to the combination of the Navier—Stokes and mass conservation law equations. The mechanocaloric effect is also considered. In the evaluation of the fluctuations—free particles coupling, the usual microscopic technique in the many-body problem was used. (M.H.R.)

54425 ROTON-LIMITED MOBILITY OF IONS IN SUPERFLUID ^{4}He. Barrera, Ruben, Baym, Gordon (Univ. of Illinois, Urbana). Phys. Rev., A; 6: No. 4, 1558-66(Oct 1972).

The roton-limited mobility of ions in superfluid ^{4}He are calculated for temperatures below ~1.7°K. Taking, as a first approximation, a constant ion-roton transition-matrix element, which is treated as an adjustable parameter, good agreement is found with experiment for both positive and negative ions. This model calculation indicates that the most mobile of the recently discovered exotic negative carriers is a very light ion. (auth)

54426 STUDY OF THE SPECIFIC HEAT OF A ^{3}He–^{4}He MIXTURE NEAR ITS GAS–LIQUID CRITICAL POINT. Brown, G. Raymond; Meyer, Horst (Duke Univ., Durham, N. C.). Phys. Rev., A; 6: No. 4, 1578-87(Oct 1972).

Measurements are presented of the specific heat C_{vx} of a mixture of ^{3}He and ^{4}He with a nominal concentration of ^{3}He, $X_3 = 0.80$. Data were taken with a flat calorimeter cell in the vicinity of the gas—liquid critical point of the mixture, which is characterized (at a given X_3) by its density ρ_c and temperature T_c. The data consist of nine isochores within the approximate density range $0.52 < \rho/\rho_c < 1.20$ and in the temperature range $-0.1 \leq t \leq 0.1$, where $t = (T - T_c)/T_c$. Data were taken to within 0.4 mK of the transition temperature on all but one of the isochores. It was found that the behavior of the specific heat in the mixture for a given reduced density ρ/ρ_c is in general very similar to that seen in pure ^{3}He. In particular, the behavior of C_{vx} along the critical isochore is the same as that for pure ^{3}He in the range $10^{-4} \leq t \leq 10^{-2}$. There the apparent weak divergence is characterized by an exponent $\alpha \approx 0.1$. From thermodynamic considerations of the upper bound of C_{vx} along a line of singularities in mixtures, the apparent weak divergence observed does not, however, represent the asymptotic behavior. This question is discussed in the light of the paper by Griffiths and Wheeler and of new calculations by Leung and Griffiths for a binary fluid. The thermal-equilibrium times in the two-phase region were found to be much longer than the pure ^{3}He fluid, and these are briefly discussed. The thermal diffusivity in this region is found to have a maximum at a density approximately 20% lower than ρ_c, in rough correspondence to the density of the temperature extremum of the two-phase-region boundary. (auth)

54427 APPLICATION OF THE EQUATION-OF-MOTION METHOD TO THE SPECTRUM OF SUPERFLUID HELIUM. II. Enz, Charles P. (IBM Zurich Research Lab.). Phys. Rev., A; 6: No. 4, 1605-13(Oct 1972).

On the basis of the formalism developed in a previous paper, several features of the two-branch excitation spectrum observed by Cowley and Woods are discussed. In the long-wavelength limit a T^4 dependence of the sound velocity is derived, which is in agreement with a T^3 law for the specific heat. Furthermore, a simple derivation of the Pitavskii singularity at the end point $q_c \cong 3.55$ Å^{-1} of the phonon—roton spectrum is presented, and it is argued that, above q_c, the excitations are essentially decoupled from the condensate. Finally, the author gives convincing arguments that the diffuse second branch of Cowley and Woods should converge, for $q \rightarrow 0$, near twice the roton gap where, however, it should disappear in neutron scattering but show up in Raman scattering, in accordance with experiments by Greytak et al. (auth)

54428 APPLICATION OF THE EQUATION-OF-MOTION METHOD TO THE SPECTRUM OF SUPERFLUID HELIUM. I. Enz, Charles P. (IBM Zurich Research Lab.). Phys. Rev., A; 6: No. 4, 1596-1605(Oct 1972).

The two three-body correlation terms occurring in the equation of motion for the density response function are expressed in terms of three-point vertex functions. By neglecting retardation effects in the latter, this leads to frequency-dependent effective kinetic and potential energies $K_{eff}(\vec{q},\omega)$ and $V_{eff}(\vec{q},\omega)$. K_{eff} is expressed by the one-particle correlation functions and V_{eff} by the density correlation function. K_{eff} and V_{eff} determine the density response function $\chi(\vec{q},\omega)$, the poles of which define the phonon—roton spectrum ω_q. In addition, an eigenvalue equation is derived which is shown to have two distinct eigenvalues. While the first is again ω_q, the second is identified with the diffuse second branch recently found by Cowley and Woods. It is shown that in the limit $q \rightarrow \infty$ the two eigenvalues both merge into the free-particle spectrum. The limit $q \rightarrow 0$ of the two eigenvalues as well as the endpoint singularity of the phonon—roton branch are discussed in a second paper. (auth)

54429 THEORY OF THE ROTON LIFETIME IN SUPERFLUID HELIUM. Solana, J. (Univ. of Virginia, Charlottesville); Celli, V.; Ruvalds, J.; Tuettoe, I.; Zawadowski, A. Phys. Rev., A; 6: No. 4, 1665-76(Oct 1972).

The theory of the roton lifetime is extended to include two-roton resonances in the final-state interaction. When resonances are taken into account, the final density of states ρ_2 exhibits a complicated energy dependence and bears little resemblance to the noninteracting roton density $\rho_2^{(0)}$used in the Landau—Khalatnikov theory. Using a point-interaction model for the roton coupling and including only direct roton—roton scattering, a single-roton linewidth is obtained that is consistent with the upper bound given by other authors; then a linewidth is obtained for the two-roton resonance that is smaller than the experimental value. In contrast to previous work, roton hydridization is included in the lifetime theory. The effect of hybridization is twofold: (a) The final density of states ρ_2 is markedly altered, and (b) the hybridization opens new scattering channels involving a single quasiparticle in the final state. Although the net effect of mechanism (a) on the roton lifetime seems to be small, the additional scattering (b) gives a non-negligible contribution. Furthermore, the importance of self-consistency and roton scattering in nonzero angular momentum channels is discussed. The theory predicts an unusual pressure dependence for the roton linewidth which may be checked experimentally. It is concluded that further experiments, such as light and neutron scattering, are needed to resolve the strength of the various contributions to the linewidth and thereby provide a truly quantitative analysis of the roton lifetime. (auth)

54430 SCINTILLATION OF LIQUIDS ^{3}He, ^{4}He, AND ^{3}He–^{4}He SOLUTIONS. Roberts, Huey Allen. Charlottesville, Va.; Univ. of Virginia (1972). 104p. University Microfilms Order No. 72-22,638.

Thesis.

An investigation was made of the alpha-particle-induced scintillation intensity of liquids He II and ^{3}He—^{4}He solutions between 2.15°K at the vapor pressure and of pure ^{3}He between 4.2°K and 0.3°K at pressures ranging from the vapor pressure to a pressure of 8 atmospheres. It has been found that about 30% of the total luminescence from He II and ^{3}He—^{4}He solutions above 1.2°K derives from radiative destruction of metastable states. The pulse-height intensity decreases 16% between 1.8°K and 0.7°K. Between 1.8°K and 1.2°K the drop in pulse height is 9% whereas the total intensity is constant in this region, thus, indicating delayed photon emissions. A model based on a temperature-dependent radiative destruction rate for metastable states is proposed to account for the temperature variations in pulse height of He II and ^{3}He—^{4}He solutions. The pulse height data for ^{3}He—^{4}He solutions suggests that ^{3}He atoms condense onto metastable structures in the vicinity of the alpha track. Variations in ^{3}He scintillations with temperature and pressure are discussed in terms of a pressure- and temperature-dependent radiative recombination of ions. (Diss. Abstr. Int., B)

54431 NEW FEATURES OF He II FILM FLOW TRANSFER. Esel'son, B. N.; Ivanov, V. G.; Shcherbachenko, R. I. (Physical-Technical Inst. of Low Temperature, Kharkov). JETP Lett. (USSR) (Engl. Transl.); 15: No. 10, 435-7(20 May 1972).

Translated from Zh. Eksp. Teor. Fiz.; Pis'ma Red.; 15: No. 10, 616-18(20 May 1972).

Unusual He II flow phenomena were observed for Plexiglas ampoules in glass vessels. For outflow (He level higher in the ampoule than in vessel), the transfer rate does not stop at zero level difference ($\Delta H = 0$) but continues until the ampoule is completely emptied. Preparation of the Plexiglas affected this phenomenon. For inflow into the ampoule, no transfer occurred at all for large H. Gradual lowering of the ampoule led to onset of inflow at several mm, but the inflow did not continue until $\Delta H = 0$, but stopped suddenly at values of ΔH far from zero. These phenomena were not observed for ordinary glass ampoules. Several possible causes are suggested, including electrification of the Plexiglas. (D.L.C.)

54432 THERMODYNAMIC STABILITY OF A NON-IDEAL BOSE–EINSTEIN GAS. Semenchenko, V. K.; Soldatov, E. D. (Moscow State Univ.). Russ. J. Phys. Chem. (Engl. Transl.); 46: No. 1, 131-2(Jan 1972).

Translated from Zh. Fiz. Khim.; 46: No. 1, 221-2(Jan 1972).

The calculations and analysis of the thermodynamic stability of a nonideal Bose–Einstein gas (taking into account the repulsion forces between bosons on the basis of the first approximation of the perturbation theory) shows that, in terms of this approximation, the gas may reach a state with limiting stability. (auth)

54433 OSMOTIC PRESSURE WAVES IN SOLUTIONS OF ^{3}He IN SUPERFLUID ^{4}He. Ghozlan, A. (Univ. Paris, Orsay, France). J. Phys. (Paris); 33: No. 4, 415-22(Apr 1972). (In French).

A simple thermodynamic relation between the second sound velocity in ^{3}He–^{4}He mixtures and the osmotic and fountain pressures was established. The second sound in helium mixtures is interpreted as a wave corresponding to the osmotic pressure of the normal fluid with respect to the superfluid component. This relation and the expression given by Varoquaux for the osmotic pressure were used to determine the second sound velocity at any temperature. The values obtained are in agreement with the experimental results. (France)

54434 EVALUATION OF THE ENERGY FLUX BETWEEN TWO SUPERFLUID He BATHS SEPARATED BY A THIN METALLIC FOIL. Seiden, Joseph (Univ. Paris, Orsay, France). Compt. Rend., Ser. B; 274: No. 22, 1191-4(29 May 1972). (In French).

The energy of the flux crossing a thin metallic foil separating two superfluid He baths having temperatures of T and T + ΔT was calculated previously by applying a phonon transport equation to the foil. The existence of phonons and electrons in the foil at different local temperatures (T_p and T_e) was neglected. A calculation is presented in which the existence of phonons and electrons is treated in a perfectly coherent manner, and a better agreement between theory and experiment subsequently obtained. (France)

Superconductivity

Refer also to abstracts 53759 and 55047.

54435 (ITF-72-56-E) SOME EXACTLY SOLVABLE MODEL PROBLEM WITH POSITIVE INTERACTION. Bogolyubov, N. N. Jr.; Shumovskii, A. S. (Akademiya Nauk Ukrainskoi SSR, Kiev. Institut Teoreticheskoi Fiziki). 1972. 11p. Dep. NTIS (U. S. Sales Only).

The mathematically exact method is presented for constructing an asymptotic expression for free energy of general quasi-spin model with pair positive interaction. (auth)

54436 (NP-19425) INFLUENCE OF DIMENSIONALITY ON BOSE CONDENSATION AND MACROSCOPIC COHERENCE IN SUPERCONDUCTORS. Note No. 365. Lucano, G.; Pace, S.; Romani, G. L. (Rome Univ. (Italy). Istituto di Fisica). 23 Mar 1972. 6p. Dep. NTIS (U. S. Sales Only).

A numerical evaluation of the Bose condensation temperature for superconductors of restricted dimensionality is given and dimensionality's influence on the appearance of a specific macroscopic coherence effect, i.e., flux quantization, is discussed. (M.H.R.)

54437 ULTRASONIC EVIDENCE AGAINST MULTIPLE ENERGY GAPS IN SUPERCONDUCTING NIOBIUM. Almond, D. P.; Lea, M. J.; Dobbs, E. R. (Univ. of Lancaster, Eng.). Phys. Rev. Lett.; 29: No. 12, 764-7(18 Sep 1972).

The attenuation of longitudinal ultrasound along the [100] direction in Nb, resistivity ratio $R_{300}/R_0 = 5200$, was measured with precision at low temperatures. The total attenuation in the normal state can be accurately deduced by a BCS calculation, with a single gap $2\Delta(0) = (3.52 \pm 0.02)kT_c$, from the measured superconducting attenuation. No experimental evidence was found for the existence of either a smaller or a larger gap. (auth)

54438 STUDY OF SUPERCONDUCTIVITY IN FAST FROZEN (SPLAT-COOLED) INDIUM–GALLIUM ALLOYS (INCLUDING A CRITICAL ANALYSIS OF THE AC SUSCEPTIBILITY FOR STUDYING NORMAL PROPERTIES OF METALS). Carroll, Paul Joseph. Washington, D. C.; Georgetown Univ. (1972). 225p. University Microfilms Order No. 72-22,769.

Thesis.

The superconducting properties of seven fast frozen (77 K) In–Ga samples of varying indium concentration (0 to 10% by weight) were studied using ac susceptibility, dc magnetization and specific heat capacity methods. Several models of superconductivity for the In–Ga system were analyzed using the superconductivity data. The resistive component behavior of In–Ga and pure single-crystal gallium samples in ac magnetic fields was also studied. The temperature, T_p, at which the peak occurs was calculated for resistively isotropic and anisotropic materials. The variation of T_p with frequency was measured in single-crystal gallium samples. Measurements of $T_p(\omega)$ for a single-crystal gallium sample show that $\ln \rho_{peak} \sim \ln \omega_{peak}$ for both measured $T_p(\omega)$ and $T_p(\omega)$ calculated using the anisotropic model. This proportionality relation between $\ln \rho(T)$ of gallium reported in the literature and $\ln \omega_{peak}$, both measured and calculated, suggests that the temperature variation of the resistivity of a material may be calculated within constant from measurements of T_p as a function of frequency. (TSS) (Diss. Abstr. Int., B)

54439 LOW-FREQUENCY ACOUSTIC INTERACTIONS IN SUPERCONDUCTORS. Goodrich, Gary Wayne. Stillwater, Okla.; Oklahoma State Univ. (1971). 123p. University Microfilms Order No. 72-21,872.

Thesis.

This investigation involved the use of acoustical measurement techniques to observe the superconducting-to-normal-state transition in Type-I (Ta,Sn) and Type-II (Nb,V) superconductors. Parameters such as the modulus of elasticity, the attenuation coefficients, and magnetization were used to study the superconducting transition. The low-frequency acoustic interaction with a magnetic field for metals in the normal state was developed theoretically and found to be in very good agreement with the experimental results for the longitudinal mode. The torsional mode lacks a theoretical explanation, since the proposed theories yield results two orders of magnitude too small compared to the experimental results for the modulus and one order of magnitude too small for the acoustic loss factor. The changes in torsional modulus do follow a quadratic dependence on magnetic field like the longitudinal mode. An unusual effect was found in the normal-state anisotropic elasticity of both the longitudinal and torsional modes. The observation of lobes along the primary slip planes for the (111) oriented crystals seems to indicate that dislocations are the primary mechanism responsible for the anisotropy. In the superconducting state data, the dislocation effect was observed via a magnetic fluctuation in the acoustic attenuation above H_{c2}. The acoustic parameters were shown to be indicative of the characteristic features of superconductors by their comparison with magnetization data which was taken simultaneously with the elastic data. The total change in longitudinal modulus across the transition was related to the electronic-mean-free-path-dependent coherence length. The changes in modulus across the superconducting mixed state were shown to be dependent on the normal volume fraction of material for both types of modes, while the attenuation was not dependent on this. This pointed out the difference between the harmonic and anharmonic components of elasticity, and it indicated the value of these simultaneous measurements. (TSS) (Diss. Abstr. Int., B)

54440 ANISOTROPY OF SURFACE SUPERCONDUCTIVITY OF LEAD SINGLE CRYSTALS. Krasnopolin, I. Ya.; Rup, Raj; Khaikin, M. S. (Inst. of Physics Problems, Moscow). JETP Lett. (USSR) (Engl. Transl.); 15: No. 9, 365-8(5 May 1972).

Translated from Zh. Eksp. Teor. Fiz., Pis'ma Red.; 15: No. 9, 516-20(5 May 1972).

Measurements are reported of the surface resistance of lead single crystals in which superconductivity has been destroyed by a magnetic field. The anisotropy of the field H_{c3} was investigated in detail in the (011) plane, and the results are shown. The temperature dependence is shown of $H_{c3}(t)/\sqrt{2}\,H_c(t) = C(t)\,\kappa(t)$, normalized to its values at t = 1, for three rational directions in the (011) plane. (M.H.R.)

54441 ENTROPY OF VORTICES IN SUPERCONDUCTORS. de Lange, Owen Leon Potsdam, N. Y.; Clarkson Coll. of Tech. (1972). 149p. University Microfilms Order No. 72-21,593.

Thesis.

The research reported here is concerned with the transport (S_d) and incremental (S_l) entropy of vortices in superconductors, and with a comparison of the thermal gradient and Lorentz forces on a vortex in a type-II superconductor. A brief introduction and review are presented. The experimental method used to measure the transport entropy and the results of the experiments on Nb_{80}–^{20}Mo are given. The results indicate that, at low reduced temperatures and low fields, the transport entropy exceeds the incremental entropy of vortices. A simple model for the low-field transport and incremental entropy, which seems capable of explaining this observation, is given. The theory for S_d and S_i is compared with all available experimental results, and the following conclusions are reached: (i) in a relatively pure type-I and a pure-II superconductor the thermal gradient contribution to S_d is absent, and the core contribution is in good agreement with experiment; (ii) in the dirty type-II superconductors the thermal gradient contribution is present, and agreement with experiment is satisfactory at low reduced temperature, but not near T_c, where the S_d calculated for an isolated vortex is too large. An explanation is suggested in a chapter where the effects of vortex interaction are discussed. The field dependence of S_i at low fields is treated using the London model, and the results are compared with experiment. The model is further checked by calculating the relative change in energy gap with field, at low fields, from the experimental field dependence of S_d and S_i. The results from S_d and S_i agree to within experimental error. It is pointed out that the slope of the incremental entropy at the upper critical field, $(\partial S_i/\partial B)B_{c2}$ provides a sensitive test of the microscopic theory: the third-order term, $\phi_m(T) = -(^1/_6)(\partial^3\Delta G_{mn}/\partial B^3)B_{c2}$, in the Gibbs free energy is related to $(\partial S_i/\partial B)B_{c2}$ and compared with experiment. Measurements of the Lorentz force and the thermal gradient force on a vortex in a bulk type-II superconductor ($^{80}Nb-^{20}Mo$) are presented. The two forces are found to be quite different in magnitude. The field and temperature dependence of the forces indicates that interaction with the surface is the dominant mechanism of vortex pinning is this sample. Consideration of this mechanism suggests an explanation for the inequality of the two forces. At intermediate reduced temperatures the penetration depth and transport entropy vary only slightly in the sample when a fairly small temperature gradient is applied. Near T_c the Lorentz force exceeds the thermal gradient force by an order of magnitude, and a qualitative explanation is proposed, based on the change in penetration depth and transport entropy at the cold surface (where the flux driven by a thermal gradient is exiting) relative to their values at the center of the sample. (Diss. Abstr. Int., B)

54442 ROLE OF PARAMAGNETIC IMPURITIES IN THE BARRIER REGION FOR SUPERCONDUCTING TUNNELLING. Gupta, H. M.; Upadhyaya, U. N. (Univ., Udaipur, India). J. Phys., C (London); 5: No. 14, 1806-16(24 Jul 1972).

A microscopic theory for the tunnelling current through a superconductor/insulator/superconductor junction containing a pair of paramagnetic impurities is developed. A general interaction between the impurity spins is considered and the tunnelling current is calculated by considering both the elastic and inelastic scattering of conduction electrons with the impurity pair. It is found that the single particle tunnelling current exhibits discontinuities as a function of the bias voltage. The positions of discontinuities occur at voltages which depend on the energy gap and the strength of the impurity—impurity interaction. (auth)

54443 EXCITATIONS IN THE QUANTUM CONDENSATED FERMION GAS. Lueders, Gerhart (Univ., Goettingen, Ger.). Z. Phys.; 253: No. 5, 391-403(1972).

The excitations (both collective and quasi pair states) connected with quantum condensation of a fermion gas are examined. These gapless excitations do not only turn up for finite-range interaction but also for Coulomb interaction, i.e., as electronic excitations in a superconductor. (auth)

54444 SUPERCONDUCTIVITY IN THE Mg—Cd SYSTEM: EXTRAPOLATED T_c FOR PURE MAGNESIUM. Mota, A. C. (Univ. of California, San Diego, La Jolla); Brewster, P.; Wang, R. Phys. Lett.; 41A: No. 2, 99-101(11 Sep 1972).

Measurements of superconducting transition temperatures for the system Mg—Cd are reported. An extrapolation from the data on Mg-rich alloys gives a value of T_c = 0.5 m°K for pure magnesium. (auth)

54445 INFLUENCE OF FERMI-SURFACE TOPOLOGY CHANGE UNDER PRESSURE ON TWO-BAND SUPERCONDUCTORS PROPERTIES. Palistrant, M. E.; Kolpagiu, M. K. (Inst. of Applied Physics, Kishinev, USSR). Phys. Lett.; 41A: No. 2, 123-4(11 Sep 1972).

An investigation is made of the influence of Fermi-surface topology change under pressure on the superconducting transition temperature T_c and on energy gaps at zero temperature $\gamma_n(0)$ of a two-band superconductor. Two extrema in the pressure derivate of T_c and $\gamma_n(0)$ are predicted. (auth)

54446 GAP PARAMETER OUTSIDE THE CORE OF AN ISOLATED FLUX LINE FOR $T \geq 0.7\ T_c$. Brandt, E. H. (Institut fuer Physik, Stuttgart). Phys. Lett.; 41A: No. 2, 127-8(11 Sep 1972).

The gap parameter of an isolated flux line is shown to increase monotonically for large distances from the vortex core and to never exceed the BCS value $\Delta_0(T)$. (auth)

54447 DEPENDENCE OF VARIATION OF THE DISLOCATION ELECTRON SLOWING DOWN FORCE IN A SUPERCONDUCTING TRANSITION ON STRESS, TEMPERATURE, AND VELOCITY. Fomenko, V. S. (Physical-Technical Inst. of Low Temperatures, Kharkov). Zh. Eksp. Teor. Fiz.; 62: No. 6, 2190-8(Jun 1972). (In Russian).

The effect of stress, temperature, and deforming rate on variation of the deforming stress $\Delta\sigma$ arising on transition of a sample from the superconducting to normal state under conditions of uniform deforming rate is studied. The samples studied were Pb (99.9995% and 99.97%), In (99.999%) and the alloy Pb—13 at. % In. Purity of the metal was found to affect the dependence of $\Delta\sigma$ on stress and temperature. The dependence $\Delta\sigma(\sigma)$ was different for the alloy and pure metals. A dependence of $\Delta\sigma$ on the deforming rate was observed at 1.65°K. It is shown that a comparison of the experimental results with present day theoretical concepts regarding the change of the interaction mechanism between conductivity electrons and dislocations during superconducting transitions does not permit one to give preference to any of them. (auth)

54448 STRUCTURE OF THE MIXED STATE NEAR THE BOUNDARY OF A SEMI-INFINITE SUPERCONDUCTOR OF THE SECOND KIND. Ternovskii, F. F.; Shekhata, L. N. (Moscow State Univ.). Zh. Eksp. Teor. Fiz.; 62: No. 6, 2297-2310(Jun 1972). (In Russian).

The equilibrium equations for vortex lines are solved for a number of particular cases by taking into account interaction of the lines with the boundary of an ideal Type-II superconductor. It is shown that, for a certain position with respect to the boundary, the vortex-line lattice is almost not deformed. The maximum and minimum values of the external field, for which a mixed state with a prescribed induction value can still exist, are determined. (auth)

54449 SUPERCONDUCTIVITY IN SEMICONDUCTORS. Shneerson, V. L. (Inst. of Theoretical Physics, Moscow). Zh. Eksp. Teor. Fiz.; 62: No. 6, 2311-17(Jun 1972). (In Russian).

A model of a polar degenerate semiconductor with a low-lying branch of transverse optical oscillations is considered. For impurity concentrations sufficient for obtaining a high-density carrier gas, the semiconductor at sufficiently low temperatures goes over to the superconducting state. The interaction between electrons and phonons of the low-lying branch, which is specifically strong with respect to the parameter ϵ_0, is responsible for the superconductivity. (auth)

54450 SPECIFIC HEAT OF GRANULAR ALUMINUM FILMS. Greene, R. L. (Stanford Univ., Calif.); King, C. N.; Zubeck, R. B.; Hauser, J. J. Phys. Rev., B; 6: No. 9, 3297-3305(1 Nov 1972).

The specific heat of granular $Al-Al_2O_3$ films with $T_c \cong 2$°K was measured between 1.3 and 8°K. The results show that the enhancement of T_c is a bulk effect. Within experimental accuracy the electron density of states at the Fermi surface is the same as that of pure Al. The lattice heat capacity is increased in the granular films such that the measured Θ_D is 28% less than that of pure Al. This result indicates that the phonon density of states is greatly enhanced at low frequencies and seems to confirm the tunneling data of Klein and Leger. The experimental methods used to measure the small (~0.5 erg/°K) heat capacity of the films are discussed. The thermal conductivity of Au—7 at. % Cu wire and the heat capacity of silicon (~50 mg) were also measured to test the capability and accuracy of the experimental techniques. (auth)

54451 THERMAL CONDUCTIVITY IN DIRTY TRANSITION-METAL SUPERCONDUCTORS NEAR THE UPPER CRITICAL FIELD. Chow, W. S. (Univ. of Cincinnati). Phys. Rev., B; 6: No. 9, 3315-21(1 Nov 1972).

The two-band model is used to explain the thermal conductivity in dirty type-II transition-metal superconductors, such as niobium and vanadium, immediately below the upper critical field $H_{c2}(T)$. It is shown that because of the existence of interband impurity scattering, characterized by the interband-impurity-scattering relaxation time τ_{ds}, and with τ_{ds}^{-1} acting as a pair-breaking parameter, the d-band thermal conductivity immediately below the upper critical field $K_d^{(s)}$ is given by the following relation: $K_d^{(s)} = K_d^{(n)} - (1/2e)\{(H_{c2} - H)/[2\kappa_2^2(t) - 1]\beta_A\}\rho\ L(t)$, where $K_d^{(n)}$ is the thermal conductivity of the d band in the normal state and $\rho = \epsilon_{d0}/4\pi T = 2eD_d H_{c2}/4\pi T$. It is noted that L(t) as a function of temperature $t = T/T_c$ is smaller when the transition-metal superconductor is dirtier. This relation is in qualitative agreement with the experimental findings of Lowell and Sousa. (auth)

54452 STATISTICAL MECHANICS OF ONE-DIMENSIONAL GINZBURG—LANDAU FIELDS. Scalapino, D. J. (Univ. of California, Santa Barbara); Sears, M.; Ferrell, R. A. Phys. Rev., B; 6: No. 9, 3409-16(1 Nov 1972).

The statistical mechanics of one-dimensional Ginzburg–Landau fields for real, complex, and phase-only fields were studied. Results for the specific heat, the order-parameter–order-parameter, and energy-density–energy-density correlation functions, are presented. Formally, these solutions are of interest because they describe the behavior of systems which are nearly ordered but do not undergo sharp phase transitions. Physically, the real-field results may have application in some organic chain systems, while the complex field and phase-only fields are associated with superconducting strips and linear arrays of coupled weak links, respectively. (auth)

54453 SPEED OF MAGNETIC-FLUX PENETRATION INTO ELECTRICAL CONDUCTORS. Stevens, D. E.; Huebener, R. P. (Argonne National Lab., Ill.). Phys. Rev., B; 6: No. 9, 3547 (1 Nov 1972).

The pickup voltage is calculated for a flat coil sandwiched between the two halves of an infinite cylinder placed in an external periodic magnetic field. The relation between the relaxation time for flux penetration and the frequency for the maximum in pickup voltage is discussed. (auth)

54454 INVESTIGATION OF DENSITIES OF THE ELECTRON STATES FOR TWO-BAND SUPERCONDUCTOR WITH NONMAGNETIC IMPURITIES. Botoshan, N. I.; Moskalenko, V. A.; Ursu, A. M. (Inst. of Applied Physics, Moscow). Teor. Mat. Fiz.; 12: No. 2, 264-82(Aug 1972). (In Russian).

Densities of electron states $n_n(\omega)$ and the functions $\bar{n}_n(\omega)$, $m_n(\omega)$, and $\bar{m}_n(\omega)$ (similar to them) of a two-band superconductor with low as well as high concentrations of nonmagnetic impurities are calculated. The calculations are performed in the whole frequency region $\omega \geq \Omega_g$, Ω_g being the energy gap of the single-particle spectrum of the two-band superconductor. It is shown that the quantities n_1 and n_2, in the case of low concentrations of the impurity, display sharp maxima near corresponding energy gaps γ_1 and γ_2 of a pure two-band superconductor. Far from these values ($\omega = \gamma_n$) the low concentration of impurity only slightly modifies the expressions of the densities predicted by the BCS–Bogolyubov theory for pure two-band superconductor. In the case of the high concentration of nonmagnetic impurity, the functions n_n, $\bar{n}_n$, etc., of both bands are hardly distinct from each other and the densities of states display the common maximum at the frequency $\Omega_m = (\Gamma_1 N_1 + \Gamma_2 N_2)/(N_1 + N_2)$. In this limiting case the energy gap Ω_g is slightly less than Ω_m. The values of densities $n_n(\omega)$ obtained in the different frequency regions are joined together at the boundaries of these regions. (auth)

54455 EXPERIMENTAL EVIDENCE FOR THE JOSEPHSON EFFECT IN TIN FILMS. Romagnan, Jean-Pierre (Univ., Nice); Gilabert, Alain; Guyon, Etienne. Compt. Rend., Ser. B; 274: No. 25, 1343-6(19 Jun 1972). (In French).

Experimental results establishing the existence of both dc and ac Josephson effects with thin superconducting tin films are presented. These results are interpreted, making the assumption that the tin film is composed of superconducting grains coupled together by Josephson tunnel barriers or by weak bonds. (France)

54456 EXPERIMENTAL STUDY OF THE SURFACE RESISTANCE ANISOTROPY OF TYPE-II SUPERCONDUCTORS IN THE VICINITY OF H_{c3}. Baixeras, J.; Bodin, C. (Laboratoire Central des Industries Electriques, Fontenay-aux-Roses, France). J Phys. (Paris); 33: No. 4, 407-13(Apr 1972). (In French).

The variation of the surface resistance R(H) was studied as a function of the magnetic field H for various samples of Pb–x%In, H being parallel to the sample surface and parallel or perpendicular to j_ω (electric current of the electromagnetic wave). In the latter case, fluctuations of the order parameter are excited and the slope of R(H) is smaller than in the first case. A quantitative disagreement exists between the experimental value of A_3 = (delta R/delta H) (perpendicular)/(delta R/delta H) (parallel) and the theoretical values obtained by Maki–Fischer and Thompson. Nevertheless, a significant variation of A_3 with the temperature was observed. (France)

54457 EFFECT OF THE METAL–DIELECTRIC PHASE TRANSITION ON THE SUPERCONDUCTING TRANSITION TEMPERATURE. Kopaev, Yu. V.; Timerov, R. Kh. (Inst. of Physics, Moscow). Zh. Eksp. Teor. Fiz.; 63: No. 1, 290-307 (Jul 1972). (In Russian).

A model of a metal with narrow allowed bands is investigated. Instability of the phonon system occurs in certain structures. This instability arises at higher temperatures than that in the electron system. A consequence is that crystal structure distortions of the period-doubling type arise and this leads to the metal–dielectric transition. The conditions which the electron spectrum parameters must satisfy in order that the crystal structure change simultaneously with the formation of dielectric and superconducting gaps on the Fermi surface are determined. It is found that the superconducting transition temperature may considerably exceed the respective temperature in the absence of a dielectric transformation. This is due to the high density of states near the edge of the dielectric-phase allowed bands. The main alterations in the phonon spectrum caused by the structure distortions consist in the appearance of an optical oscillation branch, which is separated from the acoustic branch by a gap. (auth)

54458 NONPERTURBATIONAL CALCULATION OF CRITICAL ANOMALIES OF SUPERCONDUCTORS IN EXTERNAL FIELDS. Koyanagi, Masao (Kyushu Univ., Fukuoka). Progr. Theor. Phys. (Kyoto); 48: No. 1, 1-18(Jul 1972).

It is shown that the application of the Kadanoff–Baym method to the Dyson equation for the fluctuation propagator allows a calculation of the dependence of critical anomalies, which come from the Aslamazov–Larkin process, on the amplitude and the frequency of the external field nonperturbationally. Calculations are presented of the excess Hall conductivity, the enhanced diamagnetism, etc. The contribution to the excess Hall conductivity from the Maki process is also calculated in the static case. (auth)

54459 STRUCTURE OF COOPER PAIRS IN SUPERCONDUCTORS. Wada, Yasushi (Tokyo Univ.). Progr. Theor. Phys. (Kyoto); 48: No. 1, 19-30(Jul 1972).

In the generalized random-phase approximation, introduced by Anderson and applied to the theory of superconductivity, existence of a collective excitation with vanishing excitation energy and momentum was known. It is shown to correspond to the creation of a Cooper pair. The creation operator satisfies a nonlinear operator equation which does not depend on the magnitude of order parameter. It is, therefore, independent of dynamics, that is, of the strength of the pairing interactions. Nevertheless it has the assumed matrix elements between a given state in an N-particle system and the corresponding state in the N + 2 particle system. Discussions are confined to the BCS superconductor at absolute zero temperature. (auth)

54460 SUPERCONDUCTIVITY. Firth, I. M. M and B Monographs. London; Mills and Boon (1972). 71p.

The following subjects are covered: basic properties (behaviour in magnetic fields, behaviour of type-I materials, behaviour of type-II materials, the mixed state); microscopic theory (the occurrence of superconductivity); enhancement of superconductivity; superconducting materials used in technology (superconducting cables); uses of superconductivity (large magnets, sensitive superconducting instruments, Josephson effect and devices). (UK)

Equipment and Devices

Refer also to abstracts 53750 and 54460.

54461 (BNL–50325) UNDERGROUND POWER TRANSMISSION BY SUPERCONDUCTING CABLE. Forsyth, E. B. (ed.) (Brookhaven National Lab., Upton, N. Y.). Mar 1972. 78p. Dep. NTIS.

Introductory materials in the fields of electric power and superconductivity are presented. Forecasts for the next 30 years are used to predict required cable characteristics and helium demand. Current research in underground cable design is reviewed including work on superconductivity in this country and abroad. BNL measurements of losses in niobium–tin at power frequencies are presented. Two conceptual superconducting flexible cables are presented. Some of the implications of using high-current cables are discussed, with particular regard to electrical characteristics, reliability, economics, cryogenic equipment design, and operation under abnormal conditions. The use of superconducting cables in dc transmission schemes is discussed, and conclusions are presented. (M.H.R.)

54462 (LNF–72/27) NUMERICAL CALCULATION OF THE ZERO BIAS CONDUCTIVITY FOR A SUPERCONDUCTING TUNNEL JUNCTION IN THE PRESENCE OF DEPAIRING. II. VOLTAGE APPLIED TO THE JUNCTION. Baker, K.; Paterno, G. (Comitato Nazionale per l'Energia Nucleare, Frascati (Italy). Laboratori Nazionali di Frascati). 25 Mar 1972. 13p. Dep. NTIS (U. S. Sales Only).

A numerical calculation is presented of the differential conductance σ for a metal-insulator-superconductor tunnel junction in the presence of depairing. The calculation was made for different values of temperature and of Z (pair breaking parameter), when there is a voltage applied to the junction. The Fortran program used is presented. A table of values of σ computed by this program is given. Also included are graphs of σ as a function of voltage V_1^1 for three values of Δ_0/KT and three values of Z. (Δ_0 is the energy gap in the absence of depairing). (M.H.R.)

54463 (ORNL-TM–3886) TECHNIQUE FOR OBSERVING MAGNET NORMALCIES. Efferson, K. R. (Oak Ridge National Lab., Tenn.). Jun 1972. Contract W-7405-eng-26. 7p. (CONF-720513–9). Dep. NTIS.

From Applied superconductivity meeting; Annapolis, MD, (1 May 1972).

A continuous fast responding linear liquid level indicator made possible the measurement of fluctuations of the surface of a liquid helium bath. Careful monitoring of the liquid helium surface was found to be useful in the IMP magnet system. The liquid surface was found to be a good indicator of heating effects, both large (coil transition) and small (flux penetration). (M.H.R.)

54464 (ORNL-TM–3921) STATE-OF-THE-ART OF SUPERCONDUCTING MAGNETS. Lubell, M. S. (Oak Ridge National Lab., Tenn.). Sep 1972. Contract W-7405-eng-26. 63p. Dep. NTIS.

A survey of the most recent developments in superconducting magnet materials is presented, and complete data on the upper critical field and transition temperature for the NbTi alloy system are given. The overall critical current density of compound conductors is shown for both low and high field commercial superconductors. A tabulation is given of high field and large bore solenoids, comparing design and test data. Comparative data are also given for some nonsolenoidal coils, and details are listed for the systems under construction or design. A criterion is derived for the stable current density attainable in extremely large magnet systems such as those envisioned for fusion reactors: j ∝ (stored energy)$^{-1/6}$. The review concludes with summaries concerning the structural materials useful in large magnets and the effects of radiation on superconducting magnets. (auth)

54465 HEAT TRANSFER TO BOILING HELIUM FROM ALUMINIUM SURFACES. Jergel, M. (Electrotechnical Inst., Bratislava); Stevenson, R. Cryogenics; 12: No. 4, 312-3(Aug 1972).

Data for heat transfer in an open pool of liquid helium at 1 atm for Al 59, 99.99% purity, compared with those for OFHC copper obtained from previous work, are presented. A marked dependence on surface orientation is shown. Since the electrical properties of OFHC copper at liquid helium temperature are comparable with those of Al 59, it is shown that from the point of view of stability of superconductors, it is more attractive to use super pure aluminium Al 69, 99.9999% purity. (UK)

54466 250 kG COMPLEX SOLENOID. Komar, E. G. (Scientific Research Inst., Leningrad). Nucl. Instrum. Methods; 103: No. 2, 235-8(1972).

The D. V. Efremov Scientific Research Institute of Electrophysical Apparatus manufactured a solenoid with the following magnetic field characteristics—the diameter is 25 mm, the length is 25 mm, the inhomogeneity is less than 2%, and the magnetic field strength in the operating region center is 250 kG. The interior of the solenoid winding is made of bronze cooled by water, the external part is made of a superconductor. The performance is continuous. (5 figures, 1 table) (auth)

PHYSICS (NUCLEAR)

Refer also to abstract 52893.

54467 (ORO–2972-204) RESEARCH IN NUCLEAR PHYSICS. Progress Report, December 1, 1970–November 30, 1971. (Texas Univ., Austin. Center for Nuclear Studies). 1971. Contract AT(40-1)-2972. 174p. Dep. NTIS.

ALUMINUM—oxygen ion reactions at 7.5 to 40 MeV, cross sections for K x-ray production in, (E)
CALCIUM—oxygen ion reactions at 7.5 to 40 MeV, cross sections for K x-ray production in, (E)
CERIUM-142—deuteron reactions (d,p) at 9 to 13 MeV, proton spectra from, (E)
COPPER—oxygen ion reactions at 7.5 to 40 MeV, cross sections for K x-ray production, (E)
DEUTERONS—interactions p + d at 800 MeV, calculation of relative neutron and pion yields in, (T)
ERBIUM-168—proton inelastic scattering at 15 MeV, proton spectra from, (E)
IRON—oxygen ion reactions at 30 MeV, Kα x-ray spectra from, (E)
KRYPTON-86—proton elastic and inelastic scattering at 4.8 to 10.1 MeV, excitation fractions for, (E)
KRYPTON-87—energy levels of, calculation of wave functions and binding energies using weak coupling model, (T)
MAGNESIUM—oxygen ion reactions at 21 MeV, Kα x-ray spectra from, (E)
MAGNESIUM-24—proton elastic and inelastic scattering at 9.7 MeV, polarization in, (E)
MOLYBDENUM-92—proton elastic scattering at 11.2 to 12.4 MeV, excitation functions for, (E)
NEON-20—deuteron reactions (d,α) at 3.5 to 8 MeV, excitation functions for, (E)
NEUTRON SPECTROMETERS—development for pulsed-beam time-of-flight studies
PROTONS—interactions p + d at 800 MeV, calculation of relative neutron and pion yields in, (T)
RUBIDIUM-87—energy levels from krypton-86 proton resonances, widths and weak coupling coefficients for isobaric analog, (E)
SILICON—oxygen ion reactions at 30 MeV, Kα x-ray spectra from, (E)
SILVER-109—deuteron reactions (d,p) at 10 MeV, proton spectra from, (E)
SODIUM-22—energy levels from resonances in neon-20 (d,α) reactions, (E)
VAN DE GRAAFF ACCELERATORS—experimental facilities for EN tandem, pulsed-beam neutron time-of-flight
X-RAY SPECTROMETERS—development of high-resolution Bragg–Soller
XENON-137—energy levels of, calculating using core coupling, (T)
ZIRCONIUM-92—proton reactions (p,α) at 28 MeV, DWBA calculation of form factors for, (T)
ZIRCONIUM-94—proton elastic scattering at 11.2 to 12.4 MeV, excitation functions for, (E)

Neutron Interactions with Matter

Refer also to abstracts 54656, 54937–54940, and 55424.

54468 (ANCR–1042) AUTOMATED CROSS SECTION ANALYSIS PROGRAM (ACSAP). Marshall, N. H.; Codding, J. W.; Simpson, O. D.; Smith, J. R.; Young, R. C. (Aerojet Nuclear Co., Idaho Falls, Idaho). Jul 1972. Contract AT(10-1)-1375. 145p. Dep. NTIS.

The Automated Cross Section Analysis Program (ACSAP) has been developed to assist in the evaluation of neutron cross section data in the resonance region. Experimental data may be compared by means of a wide selection of representations. Single level or multilevel resonance parameters may be fitted to the data by an iterative adjustment routine. Total, fission, capture, or scattering data may be fitted. The fitted curves can be printed or plotted for comparison with the data using Doppler and resolution broadening appropriate to the particular experiment. ACSAP allows each user to "program" his problem to suit his particular needs. This programmability gives ASCAP a versatility that makes it a powerful tool in cross section evaluation. ASCAP is written almost entirely in FORTRAN; however it does contain some subroutines written in IBM 360 assembly language. These are discussed in the text. ASCAP was developed using the FORTRAN H compiler with optimization level 2. This was done on an IBM 360/75 computer using 240K bytes of core and IBM 2314 disc storage. ASCAP is available through the Argonne Code Center. (auth)

54469 (ANCR–1071) CALCULATED REACTIVITY OF VINS. Brugger, R. M.; Wheeler, F. J. (Aerojet Nuclear Co., Idaho Falls, Idaho). Jun 1972. Contract AT(10-1)-1375. 18p. Dep. NTIS.

The Very Intense Neutron Source (VINS) is one proposal for an oscillated reactivity neutron booster to provide intense thermal neutron bursts for use in neutron beam research. Three-dimensional steady state neutron transport calculations have been performed for a module of the system using the Monte Carlo codes RAFFLE and KENO. These calculations have aided in the design of the system by: (1) providing an estimate of the critical mass of a module loaded with one of three fuels, i.e., ^{233}U, ^{235}U, and ^{239}Pu; (2) determining the reactivity response of the module as it passes under a fixed beryllium reflector and thus allowing a design of the reflector geometry such that a near optimum shape of reactivity oscillation is obtained; and (3) yielding an estimate of life time, component reactivity worths, leakage currents and other parameters required in the design of the system. Verification of the cross sections and codes used in the study was obtained by comparison of results from the two independent Monte Carlo codes and comparison with two critical experiments in the literature. Although these calculations are preliminary in nature they have further demonstrated the feasibility of the system and laid the groundwork for further design refinements and critical experiments necessary for further development of the system. (auth)

54470 (AREAEE–133) EXIT TUBE EFFECT UPON THE MEASURED SPACE–ENERGY NEUTRON SPECTRA. Hussein, A.; Kawi, A. Abdel; Naguib, K.; Zakharkin, I.; Hamouda, I. (Atomic Energy Establishment, Cairo (Egypt). Reactor and Neutron Physics Dept.). 1972. 26p. Dep. NTIS (U. S. Sales Only).

Perturbation effect of the exit tube is considered upon the neutron flux directed towards the flat boundary of the medium with a "black" body. On the basis of some simplifying assumptions expressions are obtained for neutron flux perturbation near the exit tube bottom. A particular case of a cadmium plate immersed in water is investigated. Comparison is made between calculations and experiment to show satisfactory agreement. Results are presented of calculating a directed neutron flux for a concrete exit tube used in the experiments on neutron flux measurements near a cadmium plate immersed in water. (auth)

54471 (CISE-R–252) RAS: A SYNTHESIS PROGRAM FOR THE CALCULATION OF 2-GROUP NEUTRON FLUX IN r-θ. Brusa, L.; Giorcelli, M.; Sciocchi, G. (Centro Informazioni Studi Esperienze, Milan (Italy)). Feb 1968. 95p. (In Italian). Dep. NTIS (U.S. Sales Only).

A code was developed which resolves the two-group neutron diffusion equations in r, θ geometry with variation synthesis of Galerkin synthesis methods. The theory of these methods and of the numerical method are developed and the acceleration of the iterative process is given. The code developed is written entirely in FORTRAN IV. Some representative examples of the use and limitations of the RAS code relative to non-localized and localized small perturbations and to large perturbations are presented. (J.S.R.)

54472 (CONF-720901–(Bks.1 and 2), pp 143-61) ADVANCES IN NEUTRON CONTINUOUS SLOWING-DOWN THEORY. Stacey, Weston M. Jr. (Argonne National Lab., Ill.). 1972.

From Meeting on new developments in reactor physics and shielding calculations; Kiamesha Lake, NY. (12 Sep 1972).

The basic equation which describes neutron slowing down contains integral terms which represent the contributions due to neutrons which have scattered from other energies. Evaluation of these scattering integrals is cumbersome and time consuming, in general. This has led to the development of approximations which allow these integrals to be evaluated by simple recursion relations or which allow the integral equation to be replaced by a more tractable differential equation. Early work on this problem was concerned with elastic moderation by heavy mass nuclei in which neutrons lost only a small increment of their energy in each collision, giving rise to the concept of "continuous slowing down." This paper begins with a review of the early theory of continuous slowing-down approximations. This is followed by a discussion of more recent extensions and modifications of the theory. Problems associated with the treatment of resonances and anisotropy are discussed, and extensions to include inelastic scattering are reviewed. (auth)

54473 (CONF-720901–(Bks.1 and 2), pp 335-48) MECHANISM OF FAST NEUTRON TRANSPORT IN IRON. Goldstein, H.; Oblow, E.; Preeg, W.; Ching, J.; Troubetzkoy, E.; Lidofsky, L. J. (Columbia Univ., New York). 1972.

From Meeting on new developments in reactor physics and shielding calculations; Kiamesha Lake, NY. (12 Sep 1972).

The behavior of the total and partial cross sections of iron is reviewed, especially as they affect the transport of fast neutrons. It is pointed out that the non-elastic cross sections make iron a very efficient moderator at high energies. Analysis of deep penetration in reflected layers emphasizes the role of minima in the total cross section acting as effective distributed sources which provide for deep penetration. In small bare systems, the high leakage acts as an effective absorption which confines the effect of cross section structure to local penetrations only. The importance of knowing the energy distribution of secondary neutrons from non-elastic processes is underlined. (auth)

54474 (CONF-720901–(Bks.1 and 2), pp 409-17) SENSITIVITY OF CALCULATED PULSED SPHERE SPECTRA AND NEUTRON AGE TO CARBON CROSS SECTIONS. Weisbin, C. R.; Seamon, R. E.; Harris, D. R.; Stewart, L.; LaBauve, R. J.; Turner, G. D. (Los Alamos Scientific Lab., N. Mex.). 1972.

From Meeting on new developments in reactor physics and shielding calculations; Kiamesha Lake, NY. (12 Sep 1972).

In order to evaluate the adequacy of the present ENDF/B-III carbon data file (MAT1165) a series of Monte Carlo calculations were performed for both fission and monoenergetic sources. The results for neutron age and higher spatial moments are compared with other available experimental and theoretical values. The present computations were made with the ETOPL processor and the MCN Monte Carlo code. All measurements give consistently higher values for age than the calculations reported here. The precise value of the fission age is clearly sensitive to the total cross section in the keV region and below. There are no measurements or recent calculations published using ENDF/B-III data for the 14 MeV age in carbon with which to compare the present result. The value is markedly dependent upon the representation of the secondary energy distribution from the (n,n′3α) reaction, and, to a lesser extent, to the description of inelastic angular distributions. To further investigate the suitability of MAT1165 for transport calculations involving finite media, the LLL 2.9 mfp pulsed sphere experiment was calculated. All of the detail observed in the experiment is faithfully reproduced, however the calculations still lie significantly below the experimental curve. The effect of inelastic anisotropy can be clearly observed. (auth)

54475 (CONF-720901–(Bks.1 and 2), pp 1048-60) TEDIUM: IDEALIZED NEUTRON DATA FOR TESTING LIBRARY PROCESSING CODES. Raymund, Mahlon (Westinghouse Electric Corp., Pittsburgh). 1972.

From Meeting on new developments in reactor physics and shielding calculations; Kiamesha Lake, NY. (12 Sep 1972).

Nine "ETO" computer codes, generally employed as processors of ENDF/B data, were tested with a set of idealized materials called "TEDIUM." Selected tabulations of numerical results show that the ENDF/B data are well interpreted with most differences due to computer strategy features in the ETO codes. Even in the resolved resonance calculations where difficulties are greatest, agreement is usually within 2%. Consequently, reactor calculations from ENDF/B data should proceed with more confidence. Future intercomparisons of ETO results, using real ENDF/B data, are desirable. (auth)

54476 (CONF-720901–(Bks.1 and 2), pp 1063-74) FAST NEUTRON DATA, DIAGNOSIS AND PROGNOSIS. Smith, A. B. (Argonne National Lab., Ill.). 1972.

From Meeting on new developments in reactor physics and shielding calculations; Kiamesha Lake, NY. (12 Sep 1972).

The decks are not quite awash but nuclear data is settling. In itself this is of little note. However, for you whose livelihood depends upon the application of the fission process and for the future of nuclear energy it is a concern, for, without this foundation both are lost. Herein an attempt is made to diagnose the status and to estimate the prognosis of nuclear data, specifically fast neutron data. The objective is an overview indicating strengths and weaknesses in the context of fission reactor applications. The remarks are blatantly subjective with the emphasis upon experiment within a rational physical framework. (auth)

54477 (CONF-720901–(Bks.1 and 2), pp 1115-26) TEMPERATURE-DEPENDENT TRANSMISSION AND SELF-INDICATION MEASUREMENTS UPON DEPLETED U IN THE UNRESOLVED REGION. Byoun, T. Y. (Rensselaer Polytechnic Inst., Troy, N. Y.); Block, R. C.; Semler, T. 1972.

From Meeting on new developments in reactor physics and shielding calculations; Kiamesha Lake, NY. (12 Sep 1972).

Neutron transmission and self-indication ratio measurements have been carried out at the RPI LINAC on depleted U up to 100 keV in order to investigate the temperature dependence of resonance self-shielding. These measurements were performed at three sample temperatures (77°K, 295°K, and 973°K) and with sample thicknesses ranging from 0.0076 to 0.0621 atom/barn. Both stochastic sampling and analytical methods have been used to interpret these data. Average resonance parameters have been obtained and temperature dependence as well as sample thickness dependence of the data have been extensively studied. (auth)

54478 (CONF-720901–(Bks.1 and 2), pp 1127-51) BASIS OF CURRENT EVALUATED DATA FILES. Drake, M. K. (Brookhaven National Lab., Upton, N. Y.). 1972.

From Meeting on new developments in reactor physics and shielding calculations; Kiamesha Lake, NY. (12 Sep 1972).

The ENDF/B III library is described and the varying degrees of reliability represented by the different parts of the library are discussed. Some selected material from the data files are illustrated and discussed in detail. (J.W.R.)

54479 (CONF-720901–(Bks.1 and 2), pp 1152-65) FAST NEUTRON DOPPLER EFFECT. Till, C. E. (Argonne National Lab., Ill.). 1972.

From Meeting on new developments in reactor physics and shielding calculations; Kiamesha Lake, NY. (12 Sep 1972).

In this paper the Doppler effects in fast neutron spectra for the elements and isotopes measured to the present time are compiled. The status of fissile Doppler effect measurements and analytical comparisons is summarized. Finally, the Doppler effect of major practical importance, that of ^{238}U, is examined in some detail: ^{238}U Doppler effect calculations using various versions of ENDF/B data, including Version-III, are compared against measurement. The effects of both assembly and sample heterogeneity are given. Calculations of the effect on the ^{238}U Doppler effect of major changes in reactor composition (plutonium isotopic composition, sodium-voiding, presence of B_4C or B_4C plus BeO) are compared against measurement. (auth)

54480 (CONF-720901–(Bks.1 and 2), pp 1166-82) SOME RECENT DEVELOPMENTS IN RESONANCE AND DOPPLER THEORY. Hwang, Richard N. (Argonne National Lab., Ill.). 1972.

From Meeting on new developments in reactor physics and shielding calculations; Kiamesha Lake, NY. (12 Sep 1972).

This paper summarizes some recent development in resonance and Doppler theory. The first part describes the newly developed methods for treating the self-shielded cross sections in both the resolved and the unresolved energy regions. The second part describes some recent studies on the statistical treatment of the unresolved resonances. The topics discussed are the characteristics of the in-sequence overlap effect, the problems associated with the estimation of the statistical uncertainties of the calculated Doppler effect, the influence of the subthreshold structures on the Doppler effect calculations, and theory and application of the multilevel formalism. (auth)

54481 (EUR–4839) JN-METD2: A FORTRAN-IV PROGRAMME FOR SOLVING NEUTRON TRANSPORT PROBLEMS WITH ISOTROPIC SCATTERING IN MULTILAYER SLABS BY THE j_N METHOD. Asaoka, T.; Caglioti Bonanni, E. (European Atomic Energy Community, Ispra (Italy). Joint Nuclear Research Center). 1972. 57p. Dep. NTIS (U.S. Sales Only). EUR B. Fr. 85.-.

The mathematical formulas of the j_N method for the description of neutron transport in a multilayer slab system are summarized within the context of a multigroup model under the assumption that the scattering of neutrons is spherically symmetric in the laboratory system. A Fortran-IV computer program JN-METD2 is described in detail for the use of accurately solving the transport problem according to these formulas. The computer code calculates the eigenvalue of the integral transport equation, the effective multiplication factor or the asymptotic decay constant of neutrons, as well as the eigenfunction, the space, angle and energy dependent flux distribution. In addition, it evaluates the first three time moments of the time-dependent flux resulting from a delta function boundary source with space, angle and energy variables. (auth)

54482 (INR-P–1405) EFFECT OF SINGULARITIES ON APPROXIMATION IN S_N METHODS. Arkuszewski, Jacek; Kulikowska, Teresa; Mika, Janusz (Institute of Nuclear Research, Warsaw (Poland)). 1972. 25p. Dep. NTIS (U. S. Sales Only).

The discrete ordinate transport equation in two-dimensional rectangular geometry is analyzed. The exact solution is shown to exhibit singularities at the so called singular characteristic even for arbitrarily smooth cross section, source and external boundary conditions. The Box Explicit Method is proposed and used to investigate numerically the effect of the singular characteristic. (auth)

54483 (JAERI-M-4652) ANALYSIS OF PULSED NEUTRON EXPERIMENTS ON BARE FAST MULTIPLYING SYSTEM BY STORRER-STIEVENART'S THEORY. Hiraoka, Toru; Moriguchi, Kinichi; Nakano, Masafumi; Iijima, Tsutomu; Nakamura, Tomoo (Japan Atomic Energy Research Inst., Tokyo). Dec 1971. 15p. NTIS (U. S. Sales Only).

The theory by Storrer and Stievenart on the pulsed neutron experiment on fast multiplying systems has been applied by Code GS-1 to the pulsed neutron experiments on natural uranium systems and twenty percent-enriched uranium bare cores. It predicts well the time behavior of neutrons for the wide range of reactivity from the nearly critical state to the far subcritical state. (auth) (Japan)

54484 (KFK-1519) INFLUENCE OF TEMPERATURE ON THE AVERAGE NEUTRON TRANSMISSION OF GOLD IN THE UNRESOLVED RESONANCE REGION. Schneider, Eugen (Kernforschungszentrum, Karlsruhe (West Germany). Institut fuer Angewandte Kernphysik). Feb 1972. 75p. (In German). Dep. NTIS (U. S. Sales Only).

Thesis. Submitted to Technische Hochschule, Karlsruhe (West Germany).

The influence of the temperature on the average neutron transmission of gold was studied both theoretically and experimentally at room temperature and at 800°C. For heavy nuclei individual resonances can no longer be resolved in the energy-range of 10 to 60 keV considered here. One measures averages over many resonances. To calculate those averages "artificial" resonance cross sections have to be generated by Monte-Carlo methods. The average parameters such as level-width and level-spacing are known from the resolved resonance region. The experimental transmission could only roughly be described by the resonance parameters given in the literature. Contrary to the calculations the measurements show pronounced fluctuations in the transmission. By varying the average widths and spacings we tried to fit the experimental transmissions at room temperature and at 800°C. A further measurement with good resolution showed that strong fluctuations occur in the total cross section at energies where no appropriate resonance parameters could be found. The structure near 24 keV was studied in detail and could be fitted by two broad resonances, which cannot be understood in the compound nucleus picture. (auth)

54485 (ORNL-TM-3768) INVESTIGATION OF THE ADEQUACY OF NITROGEN CROSS-SECTION SETS: COMPARISON OF NEUTRON AND SECONDARY GAMMA-RAY TRANSPORT CALCULATIONS WITH INTEGRAL EXPERIMENTS. Straker, E. A. (Oak Ridge National Lab., Tenn.). Aug 1972. Contract W-7405-eng-26. 66p. Dep. NTIS.

Two sets of cross sections for neutron interactions and secondary gamma-ray production in nitrogen, one recently evaluated by P. G. Young and D. G. Foster and another assembled in 1968 by the author, have been tested in transport calculations corresponding to integral experiments. The experiments are Operation HENRE, during which measurements were made of the neutron and gamma-ray doses produced in the atmosphere by an accelerator emitting approximately 14-MeV neutrons, and two experiments in which liquid-nitrogen-filled dewars were pulsed with approximately 14-MeV neutrons. One of the nitrogen-dewar experiments, performed at Gulf Radiation Technology, yielded the energy spectra of fast and intermediate energy neutrons and secondary gamma rays within the nitrogen, and the other, performed at Lawrence Livermore Laboratory, gave time-dependent count rates due to neutrons leaking from the nitrogen. The comparisons of the calculated and measured results showed that for Operation HENRE both cross-section sets were adequate for calculating the neutron doses but that only the old set correctly predicted the gamma-ray doses, the new set giving results that are 30 to 50% lower than the data. Conversely, the comparisons for the GRT nitrogen-dewar experiment showed that the new set gives gamma-ray spectral data that are in reasonable agreement with the data, whereas the old set overpredicts by as much as a factor of 2. For both nitrogen-dewar experiments, the new cross sections give better predictions of the neutron spectra and time-dependent neutron count rates than the old cross sections. Additional calculations with both sets of cross sections for an infinite-air medium show that the two sets give identical neutron and secondary gamma-ray doses for a fission source; they also give very similar neutron doses for a 12.2- to 15-MeV neutron source, but the secondary gamma-ray doses are in disagreement, those obtained with the newer set being 30 to 50% lower. "Sensitivity" calculations indicate that for high-energy neutron sources most of the secondary gamma rays are produced by neutrons having energies greater than 10 MeV, and the greatest difference between the two cross-section sets is their gamma-ray production probabilities at high neutron energies. On the basis of the various comparisons, it appears that the new neutron cross sections give better predictions of neutron quantities, but that a choice between the gamma-ray production cross sections is not obvious since each set agrees with one of the two gamma-ray experiments. (auth)

54486 (RISO-M-1526) BENCHMARK CALCULATIONS ON HOMOGENEOUS SPHERES. Neltrup, H. (Danish Atomic Energy Commission, Risoe. Research Establishment). Aug 1972. 12p. Dep. NTIS (U. S. Sales Only).

Results from calculations at Risø based on the 1968 UKNDL data library on ^{235}U- and ^{239}Pu-containing homogeneous spheres are compared with experimental results and calculations based on ENDF/B. Strong resemblance between the results of the two different calculations is found. Satisfactory agreement with experiments is found for the ^{235}U-containing spheres, whereas outspoken concentration dependent disagreement is found for the ^{239}Pu-containing spheres. (auth)

54487 (RT/FI-(71)37) EXPERIMENTAL MEASUREMENT OF NEUTRON GROUPS FROM PHONONS IN ZINC AT VARIOUS TEMPERATURES. De Giorgi, G.; Rizzi, G. (Comitato Nazionale per l'Energia Nucleare, Rome (Italy)). 6 Dec 1971. 25p. (In Italian). Dep. NTIS (U. S. Sales Only).

Measurements of thermal neutrons groups inelastically scattered from phonons in Zn monocrystal have been performed at Ispra-1 reactor at the aim to study the effects on phonon lines of the interatomic potential anharmonicity. The "Q-constant" method has been used to analyze the Σ_4 optic, the Σ_4 acoustic and the Σ_1 acoustic branches in the (Ol$\bar{1}$O) direction in the basal plane. The instruments used as well as the criteria of choosing the experimental conditions regarding resolution and focusing effects and the computing program utilized are here described. (auth)

54488 (RT/FI-(72)1)) TRUD: AN ANISOTROPIC DIFFUSION CODE FOR XY GEOMETRY. Daneri, A.; Michelini, M.; Toselli, G. (Comitato Nazionale per l'Energia Nucleare, Rome (Italy)). 24 Jan 1972. 273p. Dep. NTIS (U. S. Sales Only).

TRUD is an anisotropic diffusion code for neutron multigroup problems in x-y geometry, written in FORTRAN IV for the IBM 360/75. This code computes the anisotropic diffusion coefficients D_k ($k = x, y, z$) along the three spatial directions by the anisotropic diffusion theory and resolves the multigroup anisotropic diffusion equations. (auth)

54489 (ZJE-124) APPROXIMATION OF RESONANCE SELF-SHIELDING COEFFICIENTS. Vlachovsky, K. (Skoda Works, Pilsen (Czechoslovakia). Nuclear Power Construction Dept.). 1972. 90p. Dep. NTIS (U. S. Sales Only).

This paper gives instructions for interpolation among the resonance self-shielding coefficients published by Abagyan and others: "Group Constants for Nuclear Reactor Calculation", ATOMIZDAT, Moscow 1964. A set of interpolation formulas dependent on two parameters A, B has been worked out. Here we give the formulas as well as the tables of coefficients A, B together with the maximum relative error of the interpolation. (auth)

54490 DETECTION OF ULTRA-COLD NEUTRONS BY THE ACTIVATION OF MANGANESE. Robson, J. M.; Winfield, D. (McGill Univ., Montreal). Phys. Lett.; 40B: No. 5, 537-8 (7 Aug 1972).

The activation of manganese foils was used to detect ultracold neutrons and to measure their attenuation in helium and air. (auth)

54491 CALCULATION OF NUCLEAR REACTION RATES IN A HOMOGENEOUS SPHERE NEGLECTING ELASTIC SCATTERING. Kapyshev, V. K.; Sakharov, V. I. At. Energ. (USSR); 32: No. 6, 477-8(Jun 1972). (In Russian).

In describing nuclear-physical processes, caused by high-energy neutrons (several MeV), elastic scattering may be neglected in some cases. The possibility of disregarding elastic scattering during the calculation of nuclear reaction rates in a homogeneous sphere is investigated, where a monoenergetic neutron flux from a point source is located at the center of the sphere. As an example, a point source (14.1 MeV) was assumed at the center of a sphere of boron carbide, with the result that experimental and calculated values showed satisfactory agreement. (K.S.W.)

54492 ELEMENTARY SOLUTIONS OF THE NEUTRON TRANSPORT EQUATION TAKING INTO ACCOUNT ANISOTROPIC

SCATTERING. Sultanov, N. V. At. Energ. (USSR); 32: No. 6, 457-62(Jun 1972). (In Russian).

A complete system of plane elementary solutions of the one-velocity Boltzman equation having azimuthal asymmetry has been obtained. It is assumed that the scattering function can be expanded into a finite series of Legendre polynomials. A simultaneous consideration of the azimuthal dependence of the elementary solutions and anisotropic scattering has been undertaken for the first time in this work. Furthermore, the transcendental characteristic equations have been derived and the number of roots of these equations estimated. The orthogonality and completeness of the obtained system of elementary solutions are proved. Several cells were calculated in accordance with the modified code "PRAKTINETS." (auth)

54493 STUDY OF COLD NEUTRON SPECTRA EMERGING FROM SOURCES OF LIQUID HYDROGEN AND DEUTERIUM AND A MONTE CARLO METHOD FOR OPTIMISATION. Carter, P.; Jones, D. M. (Atomic Energy Research Establishment, Harwell, Eng.). J. Nucl. Energy; 26: No. 5, 237-49(May 1972).

Measurements of the moderating efficiency of cold neutron sources (with simple transmission geometry) containing liquid hydrogen, liquid deuterium and mixtures of the two are described. A Monte Carlo method of calculating the cold neutron outputs was devised and calculations based on the theoretical cross sections of Young and Koppel satisfactorily reproduced the experimental spectrum shapes, optimum depths of moderator and cold neutron outputs. This method is quite adequate for optimising the design of future cold sources (±20%). It was found that the calculated deuterium cross sections must be modified for wavelengths beyond 5 Å so that the total cross sections correspond to the measured values of Seiffert (adjusted to the operating temperature). (UK)

Nuclear Properties and Reactions, A ≤ 5

Refer also to abstracts 54602, 54656, and 54715.

54494 (COO-3001-15) MAGNETIC MOMENTS OF ^{3}H AND ^{3}He IN THE QUARK MODEL. Ichimura, M.; Hyuga, H.; Brown, G. E. (State Univ. of New York, Stony Brook. Dept. of Physics). 1972. Contract AT(11-1)-3001. 36p. Dep. NTIS.

The magnetic moments of ^{3}H and ^{3}He were investigated by treating the nucleons N and nucleon resonance states N*(1236 MeV) on the same footing. The quark model is used to determine potentials and magnetic moment operators operating on states consisting of N and/or N*. It is found that strong cancellations take place between effects from wave function renormalization and cross terms between N and N* states. Hence, even a sizable N* component does not shift the magnetic moments of ^{3}H and ^{3}He much from their Schmidt values. Further the two-N* state in trinucleon system as well as the one-N* state were taken into account. The two body exchange magnetic moments coming from the so-called Born term, including the contributions from the transition between the S state and the D state, the S state and the one-N* state and the S state and the two-N* state were also evaluated. They are all additive with the same sign. The calculated values of the isoscalar and the isovector parts are $\mu^s_{cal} = 0.42 \sim 0.43$ and $\mu^v_{cal} = 2.61 \sim 2.67$, which are close to the experimental values $\mu^s_{exp} = 0.426$ and $\mu^v_{exp} = 2.553$. Corrections to the β-decay amplitude are discussed briefly. (auth)

54495 (EUR-4765, pp 435-55) PRECISE ATOMIC MASS MEASUREMENT AT OSAKA UNIVERSITY. Ogata, K. (Osaka Univ.).

From second conference on mass spectrometry; Ispra, Italy (1 Sep 1971).

A brief historical survey of atomic mass measurements is presented. Some recent work at Osaka University is surveyed. Some very precise results for H, D, and ^{35,37}Cl are discussed. (J.W.R.)

54496 (ITF-72-24-P) ON TWO-PARTICLE ELECTRODESINTEGRATION OF THE ^{3}He. Kozlovskii, I. V.; Tartskovskii, V. K.; Fursa, A. D. (Akademiya Nauk Ukrainskoi SSR). 1972. 20p. (In Russian). Dep. NTIS (U. S. Sales Only).

General formulas for the two-particle electrodisintegration cross section of ^{3}He in terms of the matrix elements of radial wave functions of the ^{3}He and proton-deuteron systems are obtained. Calculations were performed using the Gaussian wave function for the ground state of ^{3}He and the final-state wave function included the interaction between the resulting proton and deuteron. It is shown that in many cases the ^{3}He electrodisintegration cross section depends essentially on the final-state interaction. (auth)

54497 (LA-DC-72-876) ACCURATE DEUTERON-DEUTERON ELASTIC SCATTERING CROSS SECTIONS. Jarmie, Nelson; Jett, J. H. (Los Alamos Scientific Lab., N. Mex.). [nd]. 4p. (CONF-720819-5). Dep. NTIS.

From International conference on few particle problems in nuclear interactions; Los Angeles, CA. (28 Aug 1972).

Differential cross sections for deuteron-deuteron elastic scattering were made at 12.305 MeV with relative errors of 0.5% and a scale error of about 0.4%. The measurements were made at 2.5° intervals from 10 to 50° in the laboratory system. The results are compared with previous data. (J.W.R.)

54498 (LA-DC-72-904) PRELIMINARY MEASUREMENTS OF POLARIZATION TRANSFER IN ^{4}He($\vec{d}$, $\vec{d}$)^{4}He ELASTIC SCATTERING. Salzman, G. C.; Ohlsen, Gerald G.; Mitchell, C. K.; Grueebler, W.; Simon, W. G. (Los Alamos Scientific Lab., N. Mex.). [nd]. 4p. (CONF-720819-8). Dep. NTIS.

From International conference on few particle problems in nuclear interactions; Los Angeles, CA. (28 Aug 1972).

Polarization transfer measurements for polarized deuteron elastic scattering by ^{4}He were made. Data were taken at a laboratory deuteron angle of 30° and at deuteron energies of 4.8, 6.3, 7.7, and 8.6 MeV. The measurements are adequate to allow an unambiguous determination of the scattering matrix. (J.W.R.)

54499 (LA-DC-72-905) VECTOR TO TENSOR POLARIZATION TRANSFER IN PROTON-DEUTERON ELASTIC SCATTERING. Ohlsen, Gerald G.; Mitchell, C. K.; Salzman, G. C. (Los Alamos Scientific Lab., N. Mex.). [nd]. 4p. (CONF-720819-7). Dep. NTIS.

From International conference on few particle problems in nuclear interactions; Los Angeles, CA. (28 Aug 1972).

Analyzing power, polarization functions, and vector to tensor polarization coefficients for proton elastic scattering by deuterium were measured at proton energies of 3.6 to 9.1 MeV. (J.W.R.)

54500 (LA-DC-72-906) ANALYZING POWERS IN THE ^{3}He($\vec{d}$,p)^{4}He REACTION AT ENERGIES LESS THAN 1.0 MeV. Simon, W. G.; Mitchell, C. K.; Ohlsen, Gerald G. (Los Alamos Scientific Lab., N. Mex.). [nd]. 4p. (CONF-720819-9). Dep. NTIS.

From International conference on few particle problems in nuclear interactions; Los Angeles, CA. (28 Aug 1972).

Analyzing tensors were measured for the ^{3}He($\vec{d}$,p) reaction for deuteron energies between 366 and 1090 keV. The results are compared with other data. Some conclusions regarding the contribution of partial waves higher than s waves are drawn. (J.W.R.)

54501 (ORNL-TM-3910) COMPARISON OF (n_{th},γ) YIELDS FROM THE CURRENT ENDF/B-III DATA WITH PUBLISHED DATA. Ford III, W. E. (Oak Ridge National Lab., Tenn.). Aug. 1972. Contract W-7405-eng-26. 29p. (ENDF-172). Dep. NTIS.

As a first check of the ENDF/B-III photon production data available as of June 1972, the number of photons per thermal-neutron capture was calculated for 50 keV gamma-ray bins and compared with published data. This comparison was done for ^{1}H(MAT 1148), ^{9}Be(1154), ^{14}N(1133), ^{16}O(1134), ^{23}Na(1156), ^{27}Al(1135), Si(1151), Cl(1149), K(1150), Ca(1152), Fe(1180), and Pb(1136). (auth)

54502 (SC-RR-720513) THICK TARGET YIELD CALCULATIONS FOR STRONG NEUTRON-PRODUCING REACTIONS IN THE ENERGY RANGE 30 keV TO 1.5 MeV. Wilson, W. D.; Crawford, J. C. (Sandia Labs., Albuquerque, N. Mex.). Aug 1972. 28p. Dep. NTIS.

A combination of the Lindhard, Scharff, and Schiott (LSS) theory and a modified Bethe theory is used to calculate electronic stopping power. These results, combined with available reaction cross section data, are used to calculate thick target neutron yields from various neutron reactions in an ion accelerator. The reactions considered are ^{2}H(d,n)^{3}He, ^{2}H(t,n)^{4}He, ^{3}H(d,n)^{4}He, ^{6}Li(d,n)^{7}Be, ^{7}Li(d,n)^{8}Be, ^{9}Be(d,n)^{10}B chosen because of their large reaction cross sections in the energy range 30 keV to 1.5 MeV. Sample calculations are presented and compared to available experimental results and previous calculations over a more limited energy range. (auth)

54503 (UCRL-74069) NUCLEON-NUCLEON SCATTERING LENGTHS FROM INCOMPLETE NUCLEON-DEUTERON BREAK-UP EXPERIMENTS. Davis, J. C.; Anderson, J. D.; Grimes, S. M.; Wong, C. (California Univ., Livermore. Lawrence Livermore Lab.). 16 Aug 1972. 4p. (CONF-720819-2). Dep. NTIS.

From International conference on few particle problems in nuclear interactions; Los Angeles, CA. (28 Aug 1972).

Time-of-flight techniques were used to measure neutron spectra from the D(p,n)2p reaction at nine proton energies between 16 and 26 MeV. The impulse approximation was used to extract the p-p scattering length from the data. The same formalism was then applied to the D(n,p)2n reaction to obtain information on the n-n scattering length. (J.W.R.)

54504 TRINUCLEON PROPERTIES WITH RIIHIMAKI POTENTIAL. Nunberg, P. (Comitato Nazionale per l'Energia Nucleare, Rome); Prosperi, D.; Pace, E. Phys. Lett.; 40B: No. 5, 529-32(7 Aug 1972).

The binding energy and D-state probability of ^{3}H and the charge radii of ^{3}H and ^{3}He are computed using a realistic nucleon–nucleon potential which features a very soft (local plus separable) core. (auth)

54505 D(p,2p)n REACTION AT 51.8 MeV. Sanada, J. (Tokyo Univ. of Education); Seki, S.; Oryu, S. Phys. Lett.; 40B: No. 5, 546-8(7 Aug 1972).

The results of the deuteron breakup by protons, measured in coplanar symmetric geometry at forward angles, were compared with calculations based on the three-body Faddeev formalism and other theories. (auth)

54506 MESON-EXCHANGE CURRENTS AND ^{3}H, ^{3}He MAGNETIC MOMENTS. Harper, E. P. (Purdue Univ., Lafayette, Ind.); Kim, Y. E.; Tubis, A.; Rho, M. Phys. Lett.; 40B: No. 5, 533-6(7 Aug 1972).

It is shown that the discrepancies between the experimental ^{3}H, ^{3}He magnetic moments and single-particle values are very nearly accounted for by two-nucleon one-pion-exchange contributions. About two-thirds of the discrepancy in the isovector magnetic moment is given by trinucleon S–D matrix elements. (auth)

54507 CENTER OF MASS SPURIOSITY EFFECTS ON THE CHARGE FORM FACTOR IN MANY-BODY THEORIES. Gareev, F. A. (Joint Inst. for Nuclear Research, Dubna, USSR); Palumbo, F. Phys. Lett.; 40B: No. 6, 621-4(21 Aug 1972).

The effect of c.m. spuriosity on the charge form factor of the nuclei ^{4}He and ^{16}O is studied by assuming Saxon–Woods wave functions as selfconsistent wave functions. It is found that this effect is quite large at high momentum transfer. (auth)

54508 ARE THE SOLAR-NEUTRINO EXPERIMENTS SUGGESTIVE OF THE EXISTENCE OF A RESONANCE IN THE ^{3}He + ^{3}He SYSTEM? Fetisov, V. N. (Lebedev Inst. of Physics; Moscow); Kopysov, Yu. S. Phys. Lett.; 40B: No. 6, 602-4(21 Aug 1972).

The possibility of the existence of a resonance in the ^{3}He + ^{3}He system, which may be important for explaining the solar-neutrino experiments, is discussed. (auth)

54509 EXACT CALCULATIONS OF N–d POLARIZATION. Doleschall, P. (Central Research Inst. for Physics, Budapest); Aarons, J. C.; Sloan, I. H. Phys. Lett.; 40B: No. 6, 605-6(21 Aug 1972).

The recent N–d polarization calculations of Doleschall and of Aarons and Sloan are compared (after performing the former calculation at 10.85 MeV), and are found to agree well. The theoretical calculations, however, are in complete conflict with the experimental results. (R.W.R.)

54510 POSSIBLE INTERPRETATION OF THE DIFFERENCE BETWEEN THE d(p,2p)n AND d(p,pn)p CROSS SECTIONS. Mithra, B.; Laverriere, R. (Univ. Claude Bernard, Villeurbanne, France). Phys. Lett.; 41B: No. 1, 11-12(4 Sep 1972).

It is shown that the cross-section difference between the reactions d(p,2p)n and d(p,pn)p for small momentum transfer can be interpreted by means of a polar graph if the same pole value is not taken for the two reactions; this possibility is by the theory. (auth)

54511 RESCATTERING EFFECTS IN THE ^{2}H(p,2p)n AND ^{2}H(p,pn)n REACTIONS INDUCED BY 20- TO 60-MeV PROTONS. Durand, J. L.; Arvieux, J.; Fiore, A.; Perrin, C.; Durand, M. (Institut des Sciences Nucleaires, Grenoble, France). Phys. Rev., C; 6: No. 2, 393-403(Aug 1972).

The (p,p) and (n,p) quasifree scatterings have been studied in the same experiment. The data are compared with single-scattering models and with calculations of the rescattering series up to the third order. Single-scattering calculations give the shape of the spectra, but there is a discrepancy between calculated and experimental absolute values of the cross sections. Calculations of the rescattering effect do not converge below 20 MeV but reproduce both the magnitude and the shape of the quasifree peak above 40 MeV. (auth)

54512 ELASTIC SCATTERING OF 600-MeV PROTONS FROM H, D, ^{3}He, AND ^{4}He). Boschitz, E. T. (Lewis Research Center, Cleveland); Roberts, W. K.; Vincent, J. S.; (and others). Phys. Rev., C; 6: No. 2, 457-66(Aug 1972).

The elastic scattering of 600-MeV protons from light nuclei has been studied at the National Aeronautics Space Administration Space Radiation Effects Laboratory (SREL) synchrocyclotron. Differential cross sections have been obtained for the scattering of protons from hydrogen, deuterium, helium-3, and helium-4. Polarization was measured for deuterium and ^{4}He nuclei. The p-p cross-section data are in excellent agreement with the predictions from the Livermore phase shifts. Small-angle p-D, p-^{3}He elastic scattering data are compared with calculations based on the multiple-scattering theories of Watson and Glauber. (auth)

54513 ANALYSIS OF PHASE SHIFTS OF p–d ELASTIC SCATTERING AT 2.0, 2.7, 3.3, AND 3.8 MeV. Schmelzbach, P.-A.; Saratz, G.; Grueebler, W.; (and others) (Eidgenoessisches Technische Hochschule, Zurich). Helv. Phys. Acta; 45: 52-4(1972). (In French).

The formalism used for the phase-shift analysis takes account of non-degeneracy in J and the coupling due to nonconservation of the orbital angular momentum and the spin. Partial waves up to L = 4 are considered; however, the phase shifts of F and G waves are not separated in J. The introduction of coupling is not necessary for the adjustment of the cross sections, the polarization of the protons, or iT_{11}. It is indispensable, on the other hand, for the correct reproduction of the tensor analyzing powers, in particular for T_{21}. With the exception of the doublets ^{2}P and ^{2}D, the phase shifts obtained differ little from those found previously. The most important coupling is observed between the $^2S_{1/2}$ and $^4D_{1/2}$ states and between the $^4P_{1/2}$ and $^2P_{1/2}$ states. (2 figures) (R.W.R.)

54514 ^{4}He–^{4}He INTERACTION POTENTIAL FROM LOW ENERGY TOTAL CROSS SECTION MEASUREMENTS. Bennewitz, H. G.; Busse, H.; Dohmann, H. D.; Oates, D. E.; Schrader, W. (Univ., Bonn). Z. Phys.; 253: No. 5, 435-57(1972).

Total relative and absolute cross sections for ^{4}He–^{4}He were measured between 110 and 1100 m/s velocity of the primary beam at scattering chamber temperatures of 5.0 and 77°K. The measurements were sensitive to the low-energy repulsive and the attractive part of the potential. The resulting potential is able to describe scattering measurements of other authors; it is also in very good agreement with ab initio calculations of Bertoncini and Wahl. (auth)

54515 TWO SEARCHES FOR AN EXCITED STATE OF ^{3}He. Frisbee, P. E.; Pugh, H. G. (Univ. of Maryland, College Park). Nucl. Phys.; A191: No. 3, 658-62(1972).

The ^{3}He(α,α')^{3}He* reaction was studied at 115 MeV, and the ^{4}He(p,d)^{3}He* reaction was studied at 65 MeV. The ^{3}He continuum spectra show no evidence for production of an excited state of ^{3}He at 20.4 MeV. (2 figures, 2 tables) (auth)

54516 FOUR-NUCLEON STUDIES. I. REDETERMINATION OF THE NEUTRON POLARIZATION FOR THE ^{2}H(d,$\vec{n}$)^{3}He REACTION FROM 6 TO 14 MeV. Spalek, G.; Hardekopf, R. A.; Taylor, J. Jr.; Stammach, Th.; Walter, R. L. (Duke Univ., Durham, N. C. Triangle Universities Nuclear Lab., Durham, N. C.). Nucl. Phys.; A191: No. 3, 449-59(1972).

An accurate redetermination of the angular distribution for the polarization of the neutrons produced in the ^{2}H(d,$\vec{n}$)^{3}He reaction was obtained for deuteron energies of 6, 8, 10, 12, and 14 MeV. The differential polarization P_1 $(\theta)\sigma(\theta)$ was fitted at each energy by using two and three terms in an associated Legendre function expansion. Data at 18 MeV from another report were also fitted, and only at this energy was the third term required. The present data are consistent with earlier data below 10 MeV, but at 12 and 14 MeV P_1 (45° cm) is about 50% higher than the previous measurements. (3 figures, 3 tables) (auth)

54517 FOUR-NUCLEON STUDIES. III. MEASUREMENT OF THE ^{2}H(d,$\vec{p}$)^{3}H POLARIZATION VIA THE ^{3}H($\vec{p}$,d)^{2}H REACTION AND COMPARISON TO POLARIZATION IN ^{2}H(d,$\vec{n}$)^{3}He. Hardekopf, R. A. (Duke Univ., Durham, N. C. Triangle Universities Nuclear Lab., Durham, N. C.); Lisowski, P. W.; Rhea, T. C.; Walter, R. L.; Clegg, T. B. Nucl. Phys.; A191: No. 3, 468-80 (1972).

Accurate angular distributions of the analyzing power in the ^{3}H($\vec{p}$,d)^{2}H reaction were measured at eight energies from 6.7 to 14.7 MeV. By reciprocity, these analyzing powers are the same as the proton polarizations of the ^{2}H(d,$\vec{p}$)^{3}H reaction from 2.0 to 14.0 MeV. The products P_1 $(\theta)\sigma(\theta)$ were fitted with a series of even-order associated Legendre functions, and two terms in the series were found to be sufficient to describe the reaction up to 14 MeV. Comparisons are made with the polarizations from the mirror reaction ^{2}H(d,$\vec{n}$)^{3}He, and good agreement is found when the reactions are compared at the same exit-channel energies. The implications of this are discussed in the light of other recent comparisons which suggest that differences in these mirror reactions may be a violation of charge symmetry of nuclear forces. (5 figures, 2 tables) (auth)

54518 FOUR-NUCLEON STUDIES. IV. ANALYZING POWERS IN THE ELASTIC SCATTERING OF PROTONS FROM TRIT-

IUM. Hardekopf, R. A. (Duke Univ., Durham, N. C. Triangle Universities Nuclear Lab., Durham, N. C.); Lisowski, P. W.; Rhea, T. C.; Walter, R. L.; Clegg, T. B. Nucl. Phys.; A191: No. 3, 481-8(1972).

Analyzing powers with statistical uncertainties of approximately 0.005 were measured for $^3H(\vec{p},p)^3H$ elastic scattering by using a proton beam from a polarized-ion source. Angular distributions with about twenty points for angles from 25 to 160° were obtained for E_p = 9.4, 10.7, 12.0, 13.4 and 14.7 MeV. Partial distributions for the range from 110 to 160° were obtained for E_p = 6.7, 7.4, and 8.0 MeV. The data were parametrized in terms of complex phase shifts. (3 figures) (auth)

54519 MEASUREMENT OF ISOTOPIC RATIOS OF HELIUM. Boulloud, J. P.; Michel, S.; Tauveron, P. (CEA-DAM, Montrouge, France). J. Mass Spectrom. Ion Phys.; 9: No. 4, 375-85(Sep 1972). (In French).

Isotopic ratios of the order of 10^{-6} of various samples of helium were determined using a double focusing mass spectrometer. To obtain an accurate count of $^3He^+$ ions, reproducible results may be obtained from the separate collection of the counts of the two isotopes and by combining the results. The reproducibility attained with atmospheric helium gave a spread of less than 0.6%. Possible applications of this technique are discussed. (auth)

54520 n + d BREAK-UP REACTION WITH SEPARABLE POTENTIALS. Ebenhoeh, Wolfgang (Max-Planck-Institut fuer Kernphysik, Heidelberg). Nucl. Phys.; A191: No. 1, 97-117 (1972).

A new technique to calculate the n + d break-up cross sections with separable potentials is presented. Similar calculations were made earlier by Cahill and Sloan (Nucl. Phys., A165: (1971)). Some results of the calculations for many kinematically complete n + d and p + d break-up experiments are given. The agreement is very good. An easily maneuverable computer program exists for the matrix elements. (auth)

54521 POLARIZATION AND CROSS SECTION OF p + ^{3}H ELASTIC SCATTERING AT 19 AND 30 MeV. Darves-Blanc, R.; Nguyen Van Sen; Arvieux, J.; (and others) (Institut des Sciences Nucleaires, Grenoble, France). Nucl. Phys.; A191: No. 2, 353-60(1972). (In French).

With a polarized proton beam, the differential cross section and the proton analyzing power of the p + ^{3}H elastic scattering at 19 and 30 MeV have been measured and compared to the p + ^{3}He data. The proton analyzing power of the latter scattering has also been measured at 30 MeV to supplement the existing data. Real phase shifts from a preliminary analysis are deduced for both of the scatterings. (auth)

54522 ^{2}H(p,2p)n REACTION AT 115 MeV FOR HIGH MOMENTUM TRANSFERS AND THE OFF-ENERGY-SHELL NUCLEON–NUCLEON INTERACTION. Morlet, M.; Frascaria, R.; Marty, N.; Willis, A. (Institut de Physique Nucleaire, Orsay, France). Nucl. Phys.; A191: No. 2, 385-98(1972).

The ^{2}H(p,2p)n cross sections have been measured for kinematical conditions where the energy in the exit channel is nearly equally shared between the three particles. When interpreted in terms of the nucleon-nucleon interaction, this condition leads to significant off-shell terms. A comparison is made with theoretical values computed for different nucleon–nucleon potentials which appear to show important differences. (auth)

Nuclear Properties and Reactions, $6 \leq A \leq 19$

Refer also to abstracts 53804, 54238, 54351, 54501, 54502, 54507, 54508, 54602, 54683, 54713, 54714, 54716, 54745, and 54747.

54523 (CONF-720901–(Bks.1 and 2), pp 325-34) SECONDARY GAMMA-RAY-PRODUCTION CROSS SECTIONS OF SEVERAL MATERIALS. Morgan, G. L.; Dickens, J. K.; Love, T. A.; Perey, F. G. (Oak Ridge National Lab., Tenn.). 1972.

From Meeting on new developments in reactor physics and shielding calculations; Kiamesha Lake, NY. (12 Sep 1972).

Absolute gamma-ray-production cross sections have been measured as a function of both incident neutron and emitted gamma-ray energy for tantalum, iron, silicon, and carbon. The data include gamma-ray energies between 0.7 and 10.6 MeV for incident neutron energies up to 20 MeV. Measurements were made at angles of 90° and 125° for tantalum and carbon and at 125° for iron and silicon. Detailed tables of cross sections have been transmitted to the National Neutron Cross Section Center. (auth)

54524 (COO-2171-14) HOW GOOD IS THE HARTREE-FOCK APPROXIMATION FOR ^{16}O? Parikh, J. C. (Rochester Univ., N. Y. Dept. of Physics and Astronomy. Physical Research Lab., Ahmedabad (India)); Svenne, J. P. (Manitoba Univ., Winnipeg. Dept. of Physics). 1971. Contract AT(11-1)-2171. 13p. (UR-406). Dep. NTIS.

Hartree–Fock intrinsic states in ^{16}O are examined to find out the extent to which they are good approximations to the exact eigenstates of the system. For this purpose the notion of width of a state is introduced. In terms of the width it is found that by itself the Hartree–Fock approximation is not good in ^{16}O, however it does provide a suitable basis to discuss the structure of the low-lying states. The calculation of the 0^+ levels confirms earlier suggestions made regarding the nature of these levels and is also in agreement with exact calculations done in a small basis space. (auth)

54525 (FRNC-TH–191) MEASUREMENT OF THE DEPOLARIZATION PARAMETER, D, IN THE ELASTIC SCATTERING OF PROTONS BY ^{9}Be, ^{10}B, AND ^{27}Al. Schnabel, Peter (Paris Univ., Orsay (France)). 1971. 68p. (In French). Dep. NTIS (U. S. Sales Only).

Thesis.

In order to establish the existence of a possible dependence on the spin of the nucleus, the scattering of polarized protons by targets having nuclei of nonzero spin (^{27}Al, ^{9}Be, ^{10}B) was studied. Measurement of the depolarization parameter, D, enabled the percentage of scattering with spin flip in the elastic scattering of protons to be determined. The following percentages were determined: 1.8 ± 1.1 for ^{27}Al, 3.0 ± 0.8 for ^{9}Be, and 3.7 ± 0.6 for ^{10}B. By attributing the spin-flip effect to the action of a spin-spin force, the parameters of the corresponding potential in the framework of the optical model can be determined. This was done for ^{27}Al and ^{9}Be. The results obtained indicate a possible dependence of the potential on 1/A. (France)

54526 (ITF–72-25-P) ON THE QUASI-ELASTIC ELECTRON SCATTERING ON THE ^{12}C NUCLEI. Fursa, A. D.; Tartakovskii, V. K.; Kozlovskii, I. V. (Akademiya Nauk Ukrainskoi SSR). 1972. 15p. (In Russian). Dep. NTIS (U. S. Sales Only).

Inelastic fast-electron scattering on ^{42}C when only a scattered electron is experimentally fixed is considered. The spectral distributions of two-particle correlation functions for ^{42}C have been calculated to express the cross section of the process. The oscillator shell model without spin-orbit interaction is used for the description of ^{42}C. A method weakening the dependence of the electron spectra obtained on some assumptions of the nuclear model has been used in calculations to obtain a satisfactory agreement with experimental data. (auth)

54527 (LYCEN–7219) (d,^{6}Li) REACTIONS WITH LIGHT NUCLEI AT 28 MeV. Bedjidian, M.; Chevallier, M.; Grossiord, J. Y.; Guichard, A.; Gusakow, M.; Pizzi, J. R.; Ruhla, C. (Lyon Univ. (France). Institut de Physique Nucleaire). [nd]. 12p. (In French). Dep. NTIS (U. S. Sales Only).

The (d,^{6}Li) reactions with ^{12}C, ^{16}O, ^{19}F and ^{40}Ca were studied at 28 MeV. The angular distributions were obtained between 4 deg and 70 deg (cms) for the ground states and two excited-state transitions. A DWBA analysis was made assuming the transfer of an alpha particle in the zero range approximation. Relative spectroscopic factors were compared to Yoshida's calculations. (France)

54528 (NASA-TM-X–2440, pp 523-6) ACCELERATOR MEASUREMENT OF THE ENERGY SPECTRA OF NEUTRONS EMITTED IN THE INTERACTION OF 3-GeV PROTONS WITH SEVERAL ELEMENTS. Nalesnik, W. J.; Devlin, T. J.; Merker, M.; Shen, B. S. P. (Univ. of Pennsylvania, Philadelphia). Jan 1972.

From Symposium on natural and manmade radiation in space; Las Vegas, Nev. (1 Mar 1971).

The shapes of the energy spectra of neutrons between 20 and 400 MeV emitted at 20, 34, and 90° in the bombardment of C (1.8 g cm^{-2}), Al (1.7 g cm^{-2}), Co (4.4 g cm^{-2}), and Pt (81.5 g cm^{-2}) targets by 3-GeV protons were measured by time-of-flight techniques. (auth)

54529 (RPP/NS–8) RATIO OF PION–NUCLEUS REACTION CROSS-SECTIONS AND THE NEUTRON DENSITY DISTRIBUTION FOR LEAD. Allardyce, B. W.; Batty, C. J.; Baugh, D. J.; (and others) (Rutherford High Energy Lab., Chilton (England)). 1972. 10p. Dep. NTIS (U. S. Sales Only).

The ratio of the reaction cross-sections for π^- and π^+-mesons was measured for a series of nuclei over the momentum range from 0.71 to 2.0 GeV/c. An analysis of the results for C and Pb is presented and compared with the predictions of a variety of nuclear models. (auth) (UK)

54530 ANALYSIS OF 20 GeV PROTON–NUCLEI SCATTERING. Sood, P. M. (Panjab Univ., Chandigarh, India); Tuli, S. K. Nucl. Phys.; A187: No. 1, 153-60(1972).

The semi-empirical model for the elastic and quasi-elastic scattering of nucleons by nuclei in the GeV region, proposed by Steenberg, has been applied for the analysis of data for the scattering of ≈20 GeV protons from the light nuclei ^{9}Be and ^{12}C and the medium weight nucleus ^{27}Al. The agreement between the model and the scattering data has been found to be fairly reasonable. Also, in the case of light nuclei, the best-fit parameter x concerning the ratio of the real and imaginary parts of the proton-nucleus scattering amplitude agrees well with the ratio γ between the real and imaginary parts of the p-nucleon forward-scattering amplitude at this energy. (auth)

54531 GIANT DIPOLE RESONANCE IN ^{16}O OBSERVED WITH THE POLARIZED PROTON CAPTURE REACTION. Hanna, S. S.; Glavish, H. F.; Diener, E. M.; (and others) (Stanford Univ., Calif.). Phys. Lett.; 40B: No. 6, 631-4(21 Aug 1972).

The giant E1 resonance of ^{16}O was studied with the polarized proton capture reaction $^{15}N(\vec{p},\gamma_0)^{16}O$. The asymmetry produced in the angular distribution by the proton polarization was large and remarkably constant over the structure of the giant resonance. Combined with unpolarized measurements, the polarized results provide additional information on the configuration of the giant E1 resonance in ^{16}O. (auth)

54532 HIGH-ENERGY LIMIT FOR THE α–d AND τ–t FORM FACTORS IN THE ^{6}Li NUCLEUS AND THE PROBLEM OF EXPERIMENTAL INVESTIGATION OF THE NODES OF THE CORRESPONDING WAVE FUNCTIONS. Kurdyumov, I. V.; Neudatchin, V. G.; Yu. F.; Korennoy, V. P. (Inst. of Nuclear Physics, Moscow). Phys. Lett.; 40B: No. 6, 607-10(21 Aug 1972).

The cluster-model form factors α–d and τ–t of the ^{6}Li nucleus were calculated in analytical form. The optical-potential description of the corresponding scattering phases is given. The Young scheme [42] involves only even τ–t phases; and the Young scheme [33], only odd ones. (auth)

54533 CONTRIBUTION OF RECTANGULAR GRAPHS IN THE REACTION $^{14}N(^{3}He,p)^{16}O^*$ (E* = 8.88 MeV). Allard, J. F.; Amiel, M. (Institut d'Etudes Nucleaires, Algiers). Phys. Lett.; 41B: No. 1, 29-30(4 Sep 1972).

Possible evidence of the manifestation of rectangular graphs is presented in the reaction $^{14}N(^{3}He,p_5)^{16}O^*$ (E* = 8.88 MeV) in a region where such mechanisms were not expected. (auth)

54534 $^{16}O + ^{12}C$ QUASIMOLECULAR STATES. Nagorcka, B. N.; Newton, J. O. (Australian National Univ., Canberra). Phys. Lett.; 41B: No. 1, 34-8(4 Sep 1972).

Resonances in the total reaction yield of the $^{16}O + ^{12}C$ reaction cannot be explained in terms of statistical fluctuations and, as for the $^{12}C + ^{12}C$ reaction, could be quasi-molecular in nature. These resonances were interpreted as single-particle resonances in a complex optical potential well, good qualitative agreement with the data was obtained. (auth)

54535 PIONIC PROTON STRIPPING AND π^- PRODUCTION. Rohlin, J. (Inst. of Physics, Goeteborg); Gabathuler, K.; Tanner, N. W.; Cox, C. R.; Domingo, J. J. Phys. Lett.; 40B: No. 5, 539-42(7 Aug 1972).

Evidence was obtained for the reaction $^{9}Be(p,\pi^-)^{10}C$, by using 600-MeV protons and a magnetic spectrometer at 0° for the pions. This reaction is forbidden in the "pionic proton stripping" description of the mirror reaction $^{9}Be(p,\pi^+)^{10}Be$. The cross section for π^- production is approximately 100 times smaller than that for π^+ production. (auth)

54536 RADIATIVE KAON CAPTURE BY NUCLEI. Korenman, G. Ya.; Popov, V. P. (Inst. of Nuclear Physics, Moscow). Phys. Lett.; 40B: No. 6, 628-30(21 Aug 1972).

The process of the radiative kaon capture by nuclei is considered. The total yields of γ quanta corresponding to the production of different hyperons are calculated. (auth)

54537 NEGATIVE MUON CAPTURE IN CARBON LEADING TO SPECIFIC FINAL STATES. Miller, G. H.; Eckhause, M.; Kane, F. R.; Martin, P.; Welsh, R. E. (Coll. of William and Mary, Williamsburg, Va.). Phys. Lett.; 41B: No. 1, 50-2(4 Sep 1972).

The yields of γ rays from specific final nuclear states excited following negative muon capture in ^{12}C were measured. By using the values for the capture rates to excited states in ^{12}B and the result of an earlier experiment for the total capture to all bound states in ^{12}B, the direct capture rate to the ground state of ^{12}B is found to be $\lambda(^{12}B_{gr}) = (6.0 \pm 0.4) \times 10^{3}\ s^{-1}$. This value is in agreement with theoretical predictions, but the theoretical and experimental uncertainties permit extraction of only a rather imprecise value for the weak-magnetism coupling constant in the muon-capture Hamiltonian. (auth)

54538 OFF-SHELL EFFECTS IN THE ^{18}O AND ^{18}F SHELL-MODEL SPECTRA. Pradhan, H. C.; Sauer, Pu.; Vary, J. P. (Massachusetts Inst. of Tech., Cambridge). Phys. Rev., C; 6: No. 2, 407-14(Aug 1972).

The two-particle shell-model spectra of ^{18}O and ^{18}F are studied using effective interactions obtained from phase-shift-equivalent nucleon–nucleon potentials. The spectra depend significantly on the off-shell behavior of the potentials. (auth)

54539 ISOSPIN-FORBIDDEN AND ALLOWED $^{12}C(d,\alpha)^{10}B$ CROSS SECTIONS. Smith, H. Vernon Jr. (Univ. of Wisconsin, Madison). Phys. Rev., C; 6: No. 2, 441-52(Aug 1972).

Extensive new data on the isospin-forbidden reaction $^{12}C(d,\alpha_2)^{10}B$ (1.74) for 7.19 MeV ≤ E_d ≤ 13.99 MeV is reported. Also extensive data for the isospin-allowed reactions $^{12}C(d,\alpha_{0,1,3,})^{10}B$ is reported. All channels exhibit resonant behavior indicative of compound-nucleus formation. No evidence for appreciable direct or semidirect contribution to the α_2 cross sections was found. A partial-wave expansion of the α_2 data fixes J^π for a number of (isospin-mixed) ^{14}N compound-nuclear levels. The data do not support either Noble's proposed ^{6}Li mechanism or Weller's modification to Noble's proposal. (auth)

54540 ASYMMETRIC PROTON YIELDS FROM THE SEQUENTIAL REACTION $^{6}Li(^{3}He,\alpha p)^{4}He$. Thompson, D. T.; Tripard, G. E. (Washington State Univ., Pullman). Phys. Rev., C; 6: No. 2, 452-6(Aug 1972).

Measurements have been made of the asymmetric proton yields about the ^{5}Li recoil direction using the sequential reaction $^{6}Li(^{3}He,\alpha p)^{4}He$ for both the ground and first excited states of ^{5}Li at a beam energy of 1.54 MeV. Measurements were made out of the reaction plane, and the results are in qualitative agreement with the predictions of a model proposed by Reimann, Martin, and Vogt. Distorted-wave Born-approximation stripping theory may also be capable of explaining the asymmetric results. (auth)

54541 SEMILEPTONIC WEAK INTERACTIONS WITH ^{12}C. O'Connell, J. S. (National Bureau of Standards, Washington, D. C.); Donnelly, T. W.; Walecka, J. D. Phys. Rev., C; 6: No. 3, 719-33(Sep 1972).

A unified analysis of semileptonic weak and electromagnetic interactions in nuclei is applied to the A = 12 system. The particle–hole model is used to describe the nuclear dynamics of ^{12}B, ^{12}C, and ^{12}N. Neutrino reaction cross sections are presented for comparison with future experiments. (9 figures, 3 tables) (auth)

54542 CORE-EXCITED 5^+ STATE IN ^{14}N. Noe, J. W.; Balamuth, D. P.; Zurmuehle, R. W. (Univ. of Pennsylvania, Philadelphia). Phys. Rev., C; 6: No. 3, 780-3(Sep 1972).

The proton and γ-ray decay of the T = 0 level at $E_x = 10.81$ MeV in ^{14}N was studied with the reactions $^{12}C(^{3}He,p)^{14}N(p')^{13}C_{g.s.}$ and $^{12}C(^{3}He,p\gamma)^{14}N$ at an incident ^{3}He energy of 14 MeV. The state was populated in an axially symmetric geometry in which the outgoing reaction protons were detected at 0° to the incident beam direction at the focus of a magnetic spectrometer. Analysis of the decay proton and γ-ray angular correlations leads to an assignment of $J^\pi = 5^+$ to the 10.81-MeV state. The γ-ray decay goes entirely to the $J^\pi = 3^+$, T = 0 state at $E_x = 6.44$ MeV; the fractional γ-ray branch of the 10.81-MeV state was measured as $\Gamma_\gamma/\Gamma_{total} = (4.1 \pm 0.8)\%$. (3 figures) (auth)

54543 SPECTROSCOPIC FACTORS FROM THE REACTIONS $^{12}C(d,n)^{13}N$ AND $^{12}C(d,p)^{13}C$ USING THE WBP MODEL. Pearson, C. A. (Univ. of Alabama, Birmingham); Covan, J. M.; Zissermann, D.; (and others). Nucl. Phys.; A191: No. 1, 1-18(1972).

Weakly bound projectile model calculations have been made for the reactions $^{12}C(d,p)^{13}C$ (ground state and 3.09 MeV state) and $^{12}C(d,n)^{13}N$ (ground state) to extract spectroscopic factors. Optical-potential parameters for the calculations have been obtained by fitting nucleon-nucleus elastic scattering from ^{12}C between 4 MeV and 20 MeV. The spectroscopic factors extracted are independent of the deuteron energy and overlap those from nuclear structure calculations. Uncertainties in these spectroscopic factors arising from ambiguities in the optical parameters are found to be $\lesssim 20\%$. (auth)

54544 ADIABATIC AND ANGULAR-MOMENTUM DEPENDENT POTENTIAL FOR ^{16}O–^{16}O SCATTERING. Perez, J. D. (Univ. of California, San Diego, La Jolla). Contracts AT(11-1)-GEN-10; AT(04-3)-113. Nucl. Phys.; A191: No. 1, 19-28(1972).

The statistical model of Brueckner et al. is used to calculate adiabatic potentials for elastic ^{16}O–^{16}O scattering. A rotational-energy term is added to the energy functional in order to include angular-momentum effects in the potential. This also allows consideration of the energy and density of yrast levels in ^{32}S. (auth)

54545 CONTINUUM SHELL MODEL CALCULATION FOR THE ^{15}N GIANT DIPOLE RESONANCE. Barrett, R. F. (Univ., Frankfurt am Main); Fraser, R. F.; Delsanto, P. P. Phys. Lett.; 40B: No. 3, 326-8(10 Jul 1972).

Results of a continuum shell-model calculation of the ^{15}N total photo-absorption cross section and (γ,p_0) cross section are presented and discussed. (auth)

54546 CROSS-SECTION FOR EJECTION OF DEUTERONS FROM ^{6}Li BY ELECTRONS. Jeremie, H. (Univ. of Montreal). Phys. Lett.; 40B: No. 3, 311-13(10 Jul 1972).

The cross section for ejection of deuterons from ^{6}Li is estimated in Born-approximation neglecting electric-quadrupole and magnetic scattering. The s- and p-state of ^{6}Li are described by simple and perturbed harmonic-oscillator wave functions respectively. Absorption is accounted for through a modified eikonal approximation and the results are normalized to elastic electron-deuteron scattering. (auth)

54547 DETERMINATION OF THE NEUTRON RADII OF SOME NUCLEI BY THE STUDY OF ALPHA ELASTIC SCATTERING AT 166 MeV. Brissaud, I.; Le Bornec, Y.; Tatischeff, B.; (nand others) (Institut de Physique Nucleaire, Orsay, France). Nucl. Phys.; A191: No. 1, 145-65(1972). (In French).

The angular distributions for 166 MeV α-particle elastic scattering have been measured and are presented. The differential cross sections obtained are analyzed with optical potentials whose real parts are derived from the convolution of nuclear-matter distributions with an effective α-nucleon interaction. This interaction is defined both from an analysis of α-scattering from N = Z light nuclei and from heavy nuclei whose matter distributions are supposedly well known. The imaginary parts of the optical potentials are either taken to be proportional to the real parts or to have a Woods–Saxon form. Using parameters for nuclear charge distributions derived from elastic electron scattering, radii of neutron matter distributions with errors varying between ±0.09 fm and ±0.16 fm are extracted for the following nuclei: ^{12}C, ^{24}Mg, ^{28}Si, ^{32}S, ^{40,44,48}Ca, ^{48}Ti, ^{56}Fe, ^{59}Co, ^{58,60,62}Ni, ^{68}Zn, ^{88}Sr, ^{89}Y, ^{90,94}Zr, ^{92}Mo, ^{116,118,120,124}Sn, ^{140}Ce and ^{208}Pb. The assumptions made in the present analysis and the resulting uncertainties are presented. Charge and neutron radii are compared in isotope and isotone families and to radii determinations from other sources. In particular, our results agree with those derived from proton-scattering analyses and with Hartree–Fock calculations but are not always in accord with the results obtained from Coulomb energy difference methods. (auth)

54548 STUDY OF THE REACTIONS ^{19}F(d,α), ^{19}F(d,p) AT E_d = 3 MeV AND EXCITED STATES OF ^{20}F. Laribi, S.; Beaumevieille, H.; Bendjaballah, N.; (and others) (Institut d'Etudes Nucleaires, Algiers). Nucl. Phys.; A191: No. 2, 368-84(1972). (In French).

The levels of ^{20}F below an excitation energy of 4.08 MeV have been studied by the ^{19}F(d,p)^{20}F reaction at E_d = 3 MeV with a differentially pumped gas target; absolute differential cross sections have been measured for 15 proton groups. A DWBA analysis indicates an $l_n = 0$ transfer for the 3.49, 3.53 and 4.08 MeV states and an $l_n = 2$ transfer for the 0.66, 2.04, 2.19, 2.97 and 3.59 MeV states. Spectroscopic factors for these levels have been obtained. The other angular distributions have been analyzed in terms of Hauser-Feshbach theory. A spin J = 4 is tentatively assigned to the 0.82 MeV state. (auth)

54549 ODD-PARITY THREE-PARTICLE, ONE-HOLE STRUCTURE IN ^{18}F VIA THE REACTION ^{15}N(^{6}Li,t)^{18}F. Lindgren, R. A.; Gutbrod, H. H.; Fulbright, H. W.; Markham, R. G. (Univ. of Rochester, N. Y.). Phys. Rev. Lett.; 29: No. 12, 798-801(18 Sep 1972).

Strong preferential excitation of the odd-parity levels in ^{18}F and sharply forward-peaked angular distributions were observed in the reaction ^{15}N(^{6}Li,t)^{18}F. These results imply that the reaction mechanism contains a direct component and that the odd-parity levels have large $(p)^{-1}(sd)^3$ configurations. (auth)

Nuclear Properties and Reactions, $20 \leq A \leq 38$

Refer also to abstracts 54495, 54501, 54523, 54525, 54528, 54530, 54547, 54609, 54713, 54745, 54747, and 54960.

54550 (COO–535-671) RESOLUTION OF THE ^{20}Na BETA DECAY ANOMALY. Ingalls, Paul D. (Colorado Univ., Boulder. Dept. of Physics and Astrophysics). [nd]. 8p. Dep. NTIS.

An apparent hindrance of the superallowed Fermi decay ^{20}Na(β^+)^{20}Ne (10.277 MeV, T = 1) is explained. This anomaly is removed by estimates showing that the process ^{24}Mg(p,2n)^{23}Al(β^+)^{23}Mg (0.0) (of indistinguishable half-life and end point energy) interfered with previous measurements of ^{24}Mg(p,αn)^{20}Na(β^+)^{20}Ne (1.633 MeV). (auth)

54551 (COO–535-673) (p,t) AND (p,^{3}He) REACTIONS ON ^{27}Al AT E_p = 27 MeV. Graetzer, R.; Kraushaar, J. J.; Shephard, J. R. (Colorado Univ., Boulder. Dept. of Physics and Astrophysics). [nd]. 33p. Dep. NTIS.

Levels in ^{25}Al and ^{25}Mg were populated via the (p,t) and (p,^{3}He) reactions with 27-MeV protons on an ^{27}Al target. Angular distributions of emitted tritons and ^{3}He were measured simultaneously with a detector telescope. Zero-range DWBA calculations with simple shell model configurations for the two transferred nucleons provided satisfactory fits for several of the observed diffraction patterns. A sharp rise in cross section at forward angles was a good indication of the presence of L = 0 transfer even though transitions occurred with a mixture of L values. Compound nucleus calculations reproduced the smooth angular distribution shapes observed for higher excited levels but predicted cross sections consistently larger than those observed. For the first $\frac{1}{2}^+$ levels neither DWBA, compound nucleus, nor a direct two-step (p,d)(d,t) calculation were able to give a satisfactory description of the data. (auth)

54552 (FRNC-TH–227) STUDY OF THE ^{29}P NUCLEUS, DETERMINATION OF THE ANGULAR MOMENTA AND THE ELEMENTS OF THE GAMMA TRANSITION MATRIX. Byrski, Thaddee (Strasbourg Univ. (France)). 1971. 87p. (In French). Dep. NTIS (U. S. Sales Only).

Thesis.

The ^{28}Si(p,γ) radiative capture reaction was used to study the first ten excited states of ^{29}P. The γ ray angular distributions and $\gamma-\gamma$ angular correlations were measured with a Ge–Li detector and a multicounter goniometer having seven NaI(Tl) detectors respectively. Doppler shift attenuation was used to determine the mean lives of the levels. The results obtained for incident protons with energies corresponding to eight resonances in the ^{28}Si(p,γ) reaction are given, these resonances occurring at 1649, 1383, 2981, 2287, 2634, 2880, 724, and 370 keV. The excitation energies, angular momenta, mean lives, level parities, branching ratios, and transition mixing coefficients were determined. The results obtained are discussed in terms of the shell model and the unified collective model. (France)

54553 SHELL-MODEL AND PROJECTED HARTREE–FOCK CALCULATIONS FOR ^{24}Mg, ^{28}Si, AND ^{32}S. Whitehead, R. R.; Watt, A. (Univ. of Glasgow). Phys. Lett.; 41B: No. 1, 7-10 (4 Sep 1972).

Shell-model and projected Hartree–Fock calculations of the spectra of ^{24}Mg, ^{28}Si, and ^{32}S are compared. The shell-model calculations were done in the untruncated $(sd)^n$ basis. The results show an increasing discrepancy between the two models from ^{24}Mg to ^{32}S. In particular, odd-J states in ^{28}Si found in the shell-model calculation are absent in the Hartree–Fock spectrum. (auth)

54554 EVIDENCE OF FURTHER ROTATIONAL STRUCTURE IN ^{26}Al. Price, H. G.; James, A. N.; Nolan, P. J. (and others) (Univ. of Liverpool). Phys. Rev., C; 6: No. 2, 494-7(Aug 1972).

A unique spin assignment of J = 4 is obtained for the level at 2068.7 keV in ^{26}Al which previously had a spin assignment of J = 3. The level was populated with the reaction ^{26}Mg(p,n)^{26}Al at a proton energy of 7.4 MeV and the angular distribution of the ground-state γ ray determined. The excitation energy and the E2 strengths indicate that this level and the level at 3404 keV with J = 5 are members of a K = 3 rotational band based on the 3^+ level at 417 keV. This proposed band, based on the parallel coupling configuration of a particle in Nilsson orbit 5 ($\Omega = \frac{5}{2}$) with a particle in orbit 9 ($\Omega = \frac{1}{2}$), is evidence of further rotational structure in ^{26}Al. (auth)

54555 YIELDS OF GAMMA RAYS EMITTED FOLLOWING CAPTURE OF NEGATIVE MUONS BY ^{28}Si AND ^{24}Mg. Miller, G. H.; Eckhause, M.; Martin, P.; Welsh, R. E. (Coll. of William and Mary, Williamsburg, Va.). Phys. Rev., C; 6: No. 2, 487-93 (Aug 1972).

The yields of specific final states excited in the capture of negative muons by ^{24}Mg and ^{28}Si were measured. The yields are compared with the cross sections for excitation of the analog states by 180° electron scattering and with the relative populations of levels produced by the decay of the giant-dipole-resonance states. (auth)

54556 POSSIBLE STATISTICAL-MODEL EXPLANATION FOR THE ^{26}Mg(p,t)^{24}Mg REACTION AT E_p = 26 MeV. Kemper, K. W.; Obst, A. W. (Florida State Univ., Tallahassee). Phys. Rev., C; 6: No. 2, 672-4(Aug 1972).

A simplified Hauser–Feshbach treatment of angular distributions of the ^{26}Mg(p,t)^{24}Mg reaction populating levels in ^{24}Mg up to 7.59-MeV excitation energy yields good agreement with the data for several of the states above the 1.37-MeV 2^+ level. In particular, it is not necessary to invoke a direct two-step process to explain the magnitude and shape of the 3^+ level at 5.22 MeV excitation as suggested by Shepard, Kraushaar, and Baer. (auth)

54557 ELASTIC AND INELASTIC SCATTERING OF 12 MeV POLARIZED DEUTERONS BY ^{24}Mg. Brown, R. C.; Griffith, J. A. R.; Karban, O.; Roman, S.; Singh, J. (Univ. of Birmingham, Eng.). Nucl. Phys.; A191: No. 3, 663-72(1972).

The vector analyzing power was measured for 12.1-MeV deuterons scattered by ^{24}Mg. Angular distributions are presented for the ground and 1.37-MeV (2^+) states. The elastic scattering data could not be reproduced satisfactorily by spherical optical-model calculations. Both the DWBA and coupled-channels formalisms yielded an acceptable description of the inelastic scattering data for an average deuteron optical-model potential. Coupled-channels predictions of the elastic scattering vector analyzing power revealed strong dependence on the mode of excitation and the deformation parameter, while an addition of spin–orbit coupling had little effect on the calculated results. (4 figures, 1 table) (auth)

54558 ENHANCEMENT OF DIRECT PROCESSES IN HEAVY-ION REACTIONS AT HIGH ANGULAR MOMENTA. Puehlhofer, F.; Diamond, R. M. (Univ. of California, Berkeley). Nucl. Phys.; A191: No. 3, 561-76(1972).

Direct processes in reactions induced by ^{20}Ne on ^{27}Al were studied at incident energies from 4 to 10 MeV/nucleon by using in-beam γ-ray spectroscopy. In addition to products from compound-nucleus reactions, several nuclei between A = 18 and 28 were identified, and it is shown that most of them are produced in direct reactions. The excitation functions for direct reactions reveal a threshold at about 100 MeV beam energy, above which the cross sections increase by an order of magnitude. A similar increase was also found in measurements with an ^{16}O beam of 6 to 10 MeV/nucleon on the same target. This behavior is explained as a consequence of the restriction of fusion processes due to the limitation on the angular momentum of the compound nucleus and a corresponding increase of the number of partial waves available for direct reactions. (6 figures, 2 tables) (auth)

54559 STUDY OF THE LOW-LYING STATES IN ^{22}Mg. Rolfs, C. (Univ., Freiburg i. B. Univ. of Toronto); Kraemer, R.; Riess, F.; Kuhlmann, E. Nucl. Phys.; A191: No. 1, 209-24(1972).

New states have been found in ^{22}Mg at $E_x = 5006 \pm 2$, 5317 ± 5 and 5837 ± 5 keV with spins of J = ($\leqq$4), (1, 2, 3) and ($\geqq$2), respectively, in coincidence and angular correlation studies of the reaction $^{20}\mathrm{Ne}(^3\mathrm{He},n\gamma)^{22}\mathrm{Mg}$ at $E(^3\mathrm{He}) = 4.3-11.5$ MeV. For the known states below $E_x = 6.3$ MeV the following information has been obtained: E_x(keV) $\{J^\pi\}$ = 1247 (2^+), 3308 (4), 4402 (2), 5037 (1, 2), 5290 (2, 3, 4), 5464 (2, 3, 4), 5714 (1, 2) and 6928 ($\leqq$6). Branching and mixing ratios are reported. The mean-life of the 1247 keV state has been determined to be 1.0 ps with the use of the Doppler-shift attenuation method. (auth)

54560 STUDY OF ^{38}Ar LEVELS FORMED IN THE REACTION $^{34}\mathrm{S}(\alpha,\gamma)^{38}\mathrm{Ar}$. Chevallier, A.; Bozek, E.; Chevallier, J.; Pape, A.; Armbruster, R. (Centre de Recherches Nucleaires, Strasbourg). Nucl. Phys.; A191: No. 1, 201-8(1972). (In French).

Eighteen resonances were observed in the reaction $^{34}\mathrm{S}(\alpha,\gamma)^{38}\mathrm{Ar}$, in the range $E_\alpha = 3.6-4.8$ MeV. Spins and parities have been determined by angular distribution and correlation measurements. The measured transition strengths and branching ratios are discussed. (auth)

54561 ANGULAR CORRELATION STUDIES FOR α-PARTICLE EXCITATION OF THE 1.78 MeV 2^+ STATE IN ^{28}Si. Ahlfeld, C. E.; Assousa, G. E.; Lasalle, R. A.; (and others) (Florida State Univ., Tallahassee). Nucl. Phys.; A191: No. 1, 137-44(1972).

The $\alpha-\gamma$ in-plane angular correlations of the reaction $^{28}\mathrm{Si}(\alpha,\alpha_1\gamma)^{28}\mathrm{Si}$ have been measured at 10, 12, 14 and 18 MeV. Correlations were obtained for c.m. scattering angles from 20° to 170° in 3° steps. Extracted angular-correlation parameters show a strong energy dependence, with a more rapid variation of the correlation pattern as a function of scattering angle with bombarding energy increase. Detailed coupled-channels analyses of the 18 MeV data with coupling of the first three excited states to the ground state of ^{28}Si were performed and a prolate deformation $\beta_R = 0.3$ was deduced. (auth)

54562 ROTATIONAL BANDS OF ^{20}Ne. Vogt, E. (Oxford Univ.). Phys. Lett.; 40B: No. 3, 345-8(10 Jul 1972).

Using alpha-particle reduced-widths to distinguish alpha-cluster states from shell model states it is suggested that the lowest lying 8^+ level of ^{20}Ne belongs to the (8p−4h) rather than to the (4p) ground state band. Many new levels and level properties are predicted. (auth)

54563 ANGULAR DISTRIBUTION OF PHOTONEUTRONS FROM Al, Ti, Cu, Mo, W, Pb. Kovalev, V. P.; Kharin, V. P.; Gordeev, V. V.; Isaev, V. I. At. Energ. (USSR); 32: No. 6, 496-7(Jun 1972). (In Russian).

The angular distribution of photoneutrons was measured for the targets Al, Ti, Cu, Mo, W, and Pb, irradiating the latter with monoenergetic electrons with energies of 12 to 23 MeV. Threshold nuclear reactions of the types (n,p) or (n,α) were used as detectors with effective thresholds of 2.7, 4.5, and 8.1 MeV, respectively. The results are tabulated for angles ranging from 30 to 150°. (K.S.W.)

54564 POLARIZATION OF THE EMITTED NEUTRON IN MUON CAPTURE. Devanathan, V. (Univ. of Madras); Parthasarathy, R.; Ramachandran, G. Ann. Phys. (N. Y.); 72: No. 2, 428-44(Aug 1972).

The polarization of the emitted neutrons resulting from the capture of muons by complex nuclei is investigated, and it is pointed out that this study provides valuable information which is difficult to obtain from any other source. The effective muon-capture interaction Hamiltonian of Fujii and Primakoff is used as a starting point, and the sum and average over lepton spins are performed. The resulting nuclear matrix elements are evaluated and expressed in terms of density matrix ρ defined in the spin space of the emitted neutron. Then the longitudinal polarization of the emitted neutron is given by $\mathrm{Tr}(\sigma \cdot \hat{n}\rho)/\mathrm{Tr}\,\rho$, where $\hat{n}$ is the unit vector denoting the direction of emitted neutron. The expression for polarization involves the neutrino direction; and since a neutrino is not observed, an integration over its direction is performed. Numerical results are presented for ^{40}Ca, ^{32}S, and ^{28}Si. (18 figures, 34 references) (auth)

54565 INELASTIC SCATTERING CALCULATIONS WITH PROJECTED HARTREE-FOCK WAVE FUNCTIONS. II. COUPLED-CHANNEL TREATMENT. Ascuitto, Robert J. (Yale Univ., New Haven); Braley, Richard C.; Ford, William F. Nucl. Phys.; A192: No. 1, 97-124(1972).

A microscopic coupled-channel study of inelastic proton scattering from ^{20}Ne and ^{24}Mg is presented. At least the 0^+, 2^+, and 4^+ members of the ground state rotational band of each nucleus are included explicitly in the coupled equations, using nuclear wave functions obtained by projecting states of good angular momentum from deformed Hartree–Fock intrinsic states. The scattering results are compared with the distorted-wave Born approximation (DWBA) and experiment; truncation of the nuclear model space is also investigated. The results obtained with this microscopic model confirm conclusions drawn earlier based on the macroscopic model; in particular, the shapes and deformations predicted by the macroscopic model are well reproduced by the projected Hartree–Fock model, which is based purely on energy considerations. However, it is found that the magnitudes of cross sections to the higher levels are considerably smaller than experiment. A collective-model calculation, using optical potentials inferred from the intrinsic HF distributions, yields much better results. This suggests that microscopic descriptions of inelastic scattering are quite sensitive to details of the nucleon-nucleon interaction, which does not explicitly enter into the macroscopic description. (auth)

Nuclear Properties and Reactions, $39 \leq A \leq 58$

Refer also to abstracts 54501, 54523, 54527, 54528, 54547, 54563, 54564, 54587, 54591, 54592, 54602, 54609, 54630, 54683, 54713, 54745, and 54960.

54566 (CONF-720901-(Bks.1 and 2), pp 1075-86) keV NEUTRON TOTAL CROSS SECTION MEASUREMENTS AT ORELA. Harvey, J. A. (Oak Ridge National Lab., Tenn.). 1972.

From Meeting on new developments in reactor physics and shielding calculations; Kiamesha Lake, NY. (12 Sep 1972).

Neutron total cross sections are measured at ORELA using samples as small as a few square millimeters, flight paths from 18 to 200 meters, with energy resolutions ($\Delta E/E$) from 1/300 for measurements below ~10 keV to ~1/2500 up to 200 keV and $\sqrt{E(\text{in MeV})}/1000$ above 1 MeV. A new efficient neutron detector using NE 110 has been developed for keV measurements whose efficiency is ~30% for 10 keV neutrons rising to 90% for 50 keV neutrons. Transmission measurements using iron-filtered neutron beams have been made upon thick samples of iron 4″, 6″, 12″ and 20″ to obtain accurate values of the cross-section minima. Enriched ^{54}Fe and ^{57}Fe samples have been measured to determine their contributions to the windows in natural iron. (auth)

54567 (INR-1407) CROSS SECTIONS FOR THE PROTON INDUCED REACTIONS ON THE ^{43}Ca, ^{44}Ca, AND ^{48}Ca ISOTOPES

IN THE PROTONS ENERGY RANGE 1 TO 2 MeV. Grochulski, Witold; Marcinkowski, Andrzej; Wilhelmi, Zdzislaw (Institute of Nuclear Research, Warsaw (Poland)). 1972. 16p. Dep. NTIS (U. S. Sales Only).

Proton-induced reaction cross sections on calcium isotopes ^{42}Ca, ^{43}Ca and ^{48}Ca, as well as the isomeric cross-section ratios in the reaction ^{43}Ca(p,γ)^{44}Sc, measured by the activation method, in the proton energy range 1−2 MeV, are given. (auth)

54568 (LBL--776) KAONIC ATOM TRANSITION COUPLED TO NUCLEAR LEVEL. Godfrey, Gary L.; Wiegand, Clyde E. (California Univ., Berkeley. Lawrence Berkeley Lab.). Jun 1972. Contract W-7405-eng-48. 9p. Dep. NTIS.

A possible resonance coupling has been found between the first excited state of ^{55}Mn nuclei and transitions from Bohr orbits n = 9 to n = 6 in kaonic Mn atoms. (auth)

54569 (ORNL--4798) GAMMA-RAY PRODUCTION DUE TO NEUTRON INTERACTIONS WITH IRON FOR INCIDENT NEUTRON ENERGIES BETWEEN 0.8 AND 20 MeV: TABULATED DIFFERENTIAL CROSS SECTIONS. Dickens, J. K.; Morgan, G. L.; Perey, F. G. (Oak Ridge National Lab., Tenn.). Aug 1972. Contract W-7405-eng-26. 67p. Dep. NTIS.

Numerical values of differential cross sections for gamma rays produced by neutron reactions with iron have been obtained for neutron energies between 0.8 and 20 MeV. The data are primarily for $\theta_\gamma = 125°$ with supporting data at $\theta_\gamma = 35$, 75 and 90°. These data consist of (a) discrete-line values of $d\sigma/d\omega$ for 45 observed transitions due to neutron interactions with natural iron; and (b) neutron gamma-ray production group cross section values of $d^2\sigma/d\omega\ dE$ for $0.7 \geq E_\gamma \leq 10.5$ MeV, with gamma-ray group sizes ranging from 20 keV for $E_\gamma \leq 1$ MeV to 160 keV for $E_\gamma \leq 9$ MeV. The $d\sigma/d\omega$ values were obtained for $4.85 \leq E_n \leq 9.0$ MeV using a Ge(Li) spectrometer. Additional discrete-line $d\sigma/d\omega$ values for $4.85 \leq E_n \leq 6.45$ MeV at $\theta_\gamma = 125°$ have been tabulated for 66 observed transitions due to neutron interactions with an iron sample enriched in the isotope ^{54}Fe. The $d^2\sigma/d\omega\ dE$ values were obtained for $0.8 \leq E_n \leq 20$ MeV using a NaI spectrometer. (auth)

54570 SHELL-MODEL STUDY OF ^{56}Ni, ^{58}Ni, ^{54}Fe, AND ^{56}Fe. Oberlechner, G.; Richert, J. (Centre de Recherches Nucleaires, Strasbourg). Nucl. Phys.; A191: No. 3, 577-95(1972).

Shell-model calculations of ^{56}Ni, ^{58}Ni, ^{54}Fe and ^{56}Fe are presented. States are assumed to belong to configurations involving no excitation and two-particle excitations from the $1f_{7/2}$ shell. A limited number of core-excited states corresponding to four-particle excitations are also taken into account in the cases of ^{56}Ni and ^{58}Ni. The effective two-body interaction in the (1f,2p) shell is deduced from a nonlocal potential which reproduces the nucleon-nucleon scattering data. Calculated energy spectra and transition rates are not in good agreement with experiment. This is certainly related to the truncation of the basis. Some improvements are obtained when single-particle energy spacings are allowed to vary. (auth)

54571 OPTICAL-MODEL ANALYSIS OF ELASTIC SCATTERING OF 53.4 MeV HELIONS FROM ^{56}Fe. Marchese, C. J. (King's Coll., London); Griffiths, R. J.; Clarke, N. M.; (and others). Nucl. Phys.; A191: No. 3, 627-40(1972).

Elastic helion scattering from ^{56}Fe at 53.4 MeV was measured over the angular range 12° to 150°. Using the regular optical model, real-potential ambiguities, the shape of the imaginary term and the need for a spin-orbit term were explored. Coupled-channels (SCA) calculations based on the ground state and principal 2^+ and 3^- states indicate that such coupling effects are not as dominant as the inclusion of a spin-orbit potential in the regular optical model. Previously reported helion scattering from ^{59}Co and ^{60}Ni at 50.1 MeV has been included in an average parameter analysis to generalize the improvements in the helion optical-model parameterization in this energy region. (auth)

54572 ELASTIC SCATTERING OF VECTOR POLARIZED DEUTERONS FROM ^{48}Ti, ^{49}Ti, ^{50}Ti, ^{51}V, ^{52}Cr. Heil, G.; Klier, G.; Wilsch, H. (Univ., Erlangen, Ger.). Nucl. Phys.; A191: No. 3, 489-96(1972).

The elastic scattering of vector polarized deuterons with a mid-target energy of $E_d = 11.9$ MeV from ^{48}Ti, ^{49}Ti, ^{50}Ti, ^{51}V and ^{52}Cr was measured and analyzed in terms of a standard optical potential containing a spin-orbit term. The analysis showed that all nuclei under investigation have very similar parameters. The depth, range and diffuseness of the Thomas-type spin-orbit potential tended to be small, typical values being $V_{s.o.} = 5.06$ MeV, $r_{s.o.} = 0.70$ fm, $a_{s.o.} = 0.40$ fm (^{50}Ti). A comparison of the results for target nuclei with spin (^{49}Ti, ^{51}V) to those for the neighboring spin-zero nuclei yielded no hint for a target spin-dependent interaction. (auth)

54573 $(1f\ )^2_{7/2}$ MULTIPLET IN ^{42}Ca. Ellegaard, C. (Univ. of Copenhagen); Lien, J. R.; Nathan, O.; (and others). Phys. Lett.; 40B: No. 6, 641-4(21 Aug 1972).

The states of ^{42}Ca below 3.2 MeV excitation were studied by the ^{41}Ca(d,p)^{42}Ca reaction at 12 MeV bombarding energy. The experimental spectroscopic factors are compared to predictions based on Gerace and Green's coexistence model. (auth)

54574 g-FACTOR OF THE $3/2^-$ 153-keV STATE IN ^{49}V. Vingiani, G. B. (Univ., Padua. INFN, Padua); Rossi-Alvarez, C.; Buscemi, A.; Brandolini, F.; Cervellera, F. Phys. Lett.; 40B: No. 6, 638-40(21 Aug 1972).

The g factor of the $3/2^-$ state at 153 keV in ^{49}V was measured with the ^{48}Ti(p,γ)^{49}V reaction and the differential spin-precession method. The g value and the remeasured mean life are $g = +1.58 \pm 0.08$ and $\tau = 28.7 \pm 0.5$ ns. The result is compared with some theoretical predictions. (auth)

54575 LIFETIME OF THE 3.74-MeV (3^-) STATE OF ^{40}Ca. Tape, J. W. (Rutgers--The State Univ., New Brunswick, N. J.); Benczer-Koller, N.; Hensler, R.; MacDonald, J. R. Phys. Lett.; 40B: No. 6, 635-7(21 Aug 1972).

The mean life of the 3.74-MeV (3^-) excited state of ^{40}Ca was directly measured by a particle−gamma delayed coincidence technique. A mean life $\tau = 59 \pm 5$ ps was obtained, corresponding to a transition strength $B(E3) = 31 \pm 3$ W.u. (auth)

54576 CALCULATION OF THE STATES IN ^{53}Fe. Shikata, Y. (Aoyama Gakuin Univ, Tokyo). Phys. Lett.; 40B: No. 6, 611-2 (21 Aug 1972).

The states in ^{53}Fe are calculated in an extended space which includes a few 1p−4h states. Calculated energy levels and spectroscopic factors qualitatively agree with experiment. (auth)

54577 GROUND STATE OF ^{40}Ca. Hubbard, L. B. (Oak Ridge National Lab., Tenn. Furman Univ., Greenville, S. C.); McGrory, J. B.; Jolly, H. P. Phys. Rev., C; 6: No. 2, 532-6 (Aug 1972).

The ground-state wave function for ^{40}Ca has been calculated on the basis of 176 configurations containing all $2\hbar\omega$ excitations in addition to the doubly-closed-shell configuration. The ground state is found to be in the closed-shell configuration about 70% of the time. The rest of the intensity is highly fractionated over many of the basis configurations. The ground state is found to lie about 10 MeV lower in energy than the pure closed-shell configuration. (auth)

54578 INVESTIGATIONS OF SPIN ASSIGNMENTS IN ^{41}Ca, ^{53}Cr, AND ^{55}Fe. McIntyre, L. C.; Donahue, D. J. (Univ. of Arizona, Tucson). Phys. Rev., C; 6: No. 2, 568-71(Aug 1972).

The angular correlations of γ rays from (d,pγ) reactions with 3-MeV deuterons to states in ^{41}Ca, ^{53}Cr, and ^{55}Fe have been measured utilizing a collinear geometry and a Ge(Li) γ-ray detector. This study was undertaken in an attempt to resolve conflicts in spin assignments between vector-analyzing-power measurements and other measurements. Results indicate $J = 1/2$ for the 3618-keV level in ^{53}Cr and the 3788-keV level in ^{55}Fe in agreement with the vector-analyzing-power measurements. The conflict is not resolved in the case of the 3614-keV level in ^{41}Ca. There is a strong possibility that there are two unresolved levels in this region, one with $J = 1/2$ and the other with $J = 3/2$. (auth)

54579 REACTION-MECHANISM STUDY IN THE 1f--2p SHELL OF (^{16}O,^{12}C) FOUR-NUCLEON-TRANSFER REACTION. Bonche, P. (Cen, Saclay, France); Giraud, B.; Cunsolo, A.; (and others). Phys. Rev., C; 6: No. 2, 577-86(Aug 1972).

The (^{16}O,^{12}C) four-nucleon-transfer reaction has been performed on a ^{54}Fe target using the 46-MeV ^{16}O beam of the FN tandem Van de Graaff at Saclay. The study of the reaction ^{54}Fe(^{16}O,^{12}C)^{58}Ni shows that the four-nucleon transfer occurs via a direct surface reaction, well described by the quasielastic process formalism due to Frahn and Venter, which is based on the diffractional model. The transfer-reaction cross sections are peaked at the grazing angle where the elastic scattering begins to deviate from the pure Rutherford law. A distorted-wave Born-approximation investigation of nuclear properties of levels reached by (^{16}O,^{12}C) four-nucleon transfer has been performed using the SETILL code based on the generator-coordinate framework. The Q-value dependence of the cross section, as well as the configuration mixing effects, has been estimated. The cases of other 1f−2p-shell nuclei have been also investigated. (auth)

54580 ENERGY DEPENDENCE OF THE ^{3}He OPTICAL POTENTIAL. Marchese, C. J.; Clarke, N. M.; Griffiths, R. J. (King's Coll., London). Phys. Rev. Lett.; 29: No. 10, 660-2(4 Sep 1972).

A multi-data-set optical-model search code was used to produce a set of mean geometry parameters for ^{3}He nuclei incident on medium-weight nuclei. The energy dependence of the volume integrals of the real and imaginary potentials was obtained for this geometry. (auth)

54581 MAGNETIC MOMENT OF THE 1.409-MeV 2^+ STATE OF ^{54}Fe. Hubler, G. K. (Rutgers-The State Univ., New Brunswick, N. J.); Kugel, H. W.; Murnick, D. E. Phys. Rev. Lett.; 29: No. 10, 662-5(4 Sep 1972).

The g factor of the first excited 2^+ state of ^{54}Fe was measured to be $g = 1.43 \pm 0.28$. The $0 \rightarrow 2 \rightarrow 0$ (^{16}O,γ) angular correlation through the 1.4-ps mean-life state was precessed using the transient magnetic field effective in iron on Coulomb-excited and recoiled ^{54}Fe. This result is in agreement with a quite pure $(f_{7/2})^{-2}$ shell-model configuration for the state. (auth)

54582 INELASTIC PROTON SCATTERING FROM ^{48}Ca. Maggiore, Carl Jerome. East Lansing, Mich.; Michigan State Univ. (1972). 224p. University Microfilms Order No. 72-22,252.

Thesis.

Inelastic proton scattering from the nucleus ^{48}Ca has been performed at 25.11, 29.83, 35.00, and 40.21 MeV, using the proton beam from the MSU sector-focused cyclotron. Cross sections were taken every five degrees from 13° to 100° with Ge(Li) counters. The over-all resolution obtained was less than 30 keV at all energies. The elastic scattering from ^{48}Ca was compared with the elastic scattering from ^{40}Ca using the optical model. It was found that the relative distributions are in agreement with the predictions of the $A^{1/3}$ law. The inelastic scattering revealed several previously unreported excited states in ^{48}Ca. Angular momentum transfers for most of the states were obtained by comparison of the shapes of the angular distributions to those of known L. Where possible, spin assignments are inferred on the basis of this and other data. The experimental angular distributions are compared with calculated distributions using the collective model distorted wave Born approximation. The nuclear deformations obtained are used to calculate the vibrational model parameters and the reduced transition probabilities. The results are compared with previous inelastic alpha scattering experiments and inelastic electron scattering results. The energy dependence of the results and the sensitivity of the deformations to the optical model parameters were studied. (Diss. Abstr. Int., B)

54583 STUDY OF EVEN CALCIUM AND NICKEL ISOTOPES WITH SELF-CONSISTENT APPROXIMATIONS. Chandra, Harish; Rustgi, M. L. (State Univ. of New York, Buffalo). Phys. Rev., C; 6: No. 3, 907-14(Sep 1972).

Self-consistent Hartree–Fock, Hartree–Fock–Bogolyubov (HFB), and spherical BCS calculations for even calcium and nickel isotopes are carried out through the use of the central Yukawa interaction and renormalized matrix elements for the Hamada–Johnston and Tabakin potentials. The existence of spherical ^{40}Ca and ^{56}Ni cores is assumed, and the calcium and nickel isotopes are treated within the framework of single-closed-shell structure. It is found that for a given isotope and interaction the HFB and spherical BCS approximations always correspond to the same actual minimum energy solution. This feature is observed for all the isotopes and interactions considered, although the quasiparticle energies and the occupation numbers are found to differ. For Ca isotopes and the BCS results are also compared with the shell-model calculations of McGrory, Wildenthal, and Halbert, and are found to approximate the ground-state properties of all the even isotopes rather well. (2 figures, 2 tables) (auth)

54584 TWO-NUCLEON PICK-UP FROM SPIN-½ TARGETS. I. ^{57}Fe. Peterson, R. J.; Rudolph, H. (Univ. of Colorado, Boulder.). Nucl. Phys.; A191: No. 1, 47-64(1972).

Differential cross sections were measured for the (p,t) and (p,τ) reactions on ^{57}Fe at a proton energy of 27 MeV, and for the (d,α) reaction at 16.0 MeV. Several spin-parity assignments for ^{55}Fe and ^{55}Mn are suggested, and comparisons to DWBA calculations allow the identification of those states with a strong two-hole parentage. Attempts to find simple relations between these results and the yields from two-nucleon pick-up reactions on nearby doubly even targets were not successful. (auth)

54585 RESONANCE ACTIVATION INTEGRALS OF SOME NUCLIDES OF INTEREST IN NEUTRON ACTIVATION ANALYSIS. Steinnes, E. (Institutt for Atomenergi, Kjeller, Norway). J. Inorg. Nucl. Chem.; 34: No. 9, 2699-2703(Sep 1972).

The following previously-unreported resonance activation integrals I_0 were determined: ^{46}Ca, 0.32 ± 0.12b; ^{84}Sr, 10.6 ± 1.1b; ^{130}Ba, 270 ± 70b; ^{152}Gd, 3000 ± 300b; ^{158}Gd, 84 ± 20b. In addition, I_0 values for 21 nuclides were redetermined. The determinations were based on cadmium ratio measurements and on known values for the thermal neutron activation cross-sections. Small samples of ^{197}Au ($\sigma_0 = 98.8$b, $I_0 = 1550$b) were used as flux monitors. The thermal neutron activation cross-section for ^{152}Gd was found to be 1100 ± 100b. (auth) (UK)

54586 (^{6}Li,d) ON ^{58}Ni AND ^{64}Ni. Gutbrod, Hans H.; Markham, Roger G. (Univ. of Rochester, N. Y.). Phys. Rev. Lett.; 29: No. 12, 808-11(18 Sep 1972).

The (^{6}Li,d) reaction was performed on ^{58}Ni and ^{64}Ni at 38 MeV. For ^{58}Ni, angular distributions were obtained and compared with distorted-wave Born-approximation calculations. One spectrum was taken for ^{64}Ni. A reduction in cross section is observed and compared with the results of (^{16}O, ^{12}C), (p,t), and (^{3}He,n) experiments. (auth)

Nuclear Properties and Reactions, $59 \leq A \leq 89$

Refer also to abstracts 54547, 54563, 54580, 54585, 54586, 54609, 54630, 54656, 54667, and 54881.

54587 (FRNC-TH-240) EXPERIMENTAL STUDY OF EXCITED STATES OF ^{58}Ni, ^{60}Ni, ^{62}Ni, AND ^{64}Ni. Beuzit, Pierre (Paris Univ., Orsay (France)). 1971. 114p. (In French). Dep. NTIS (U. S. Sales Only).

Thesis.

The structure of even Ni nuclei was studied by the following experiments: (p,p$'\gamma$) experiments with ^{58}Ni, ^{60}Ni, ^{62}Ni and ^{64}Ni nuclei; (p,p$'$) and (d,p) experiments with ^{62}Ni and ^{64}Ni nuclei. Twelve MeV proton and deuteron beams were used. The γ de-excitation scheme together with the associated branching ratios was established for the levels. The spins and parities were determined. Considerable analogy exists between the excited states of the different isotopes studied. The energies, wave functions, and transition probabilities of the levels of the quasi-particle model were calculated in the framework of the RPA approximation using the codes developed by the theoreticians at Saclay. These calculations, which are confirmed by the results of the ^{59}Co(^{3}He, dγ) reaction, demonstrate the important role played by the core protons in the collective level configurations and the considerable participation of the proton–neutron interaction. This fact suggests the coexistence of pair configurations and more complex 2, 4, and 6 quasi-particle configurations in these nuclei. (France)

54588 CONSISTENT COUPLED-CHANNEL BORN APPROXIMATION ANALYSIS OF ^{88}Sr(d,np)^{88}Sr AND ^{88}Sr(d,p)^{89}Sr. Hoffmann, G. W.; Coker, W. R.; Zaidi, S. A. A.; Elliott, D. O. Jr. (Univ. of Texas, Austin). Phys. Lett.; 41B: No. 1, 47-9(4 Sep 1972).

Differential and total cross sections for ^{83}Sr(d,n$\widetilde{p}$)^{88}Sr were obtained and compared with the results of coupled-channel Born approximation calculations, which also are in agreement with earlier data for ^{88}Sr(d,p)^{89}Sr($d_{5/2}$ g.s.) excitation functions at 170°. (auth)

54589 ISOMER RATIOS IN (n,γ) REACTIONS AT 25 keV. Rao, A. Lakshmana; Rama, Rao J. (Andhra Univ., Waltair, India). Phys. Rev., C; 6: No. 2, 572-7(Aug 1972).

Isomeric cross-section ratios are measured for eight (n,γ) reactions on the target nuclei ^{74}Ge, ^{79}Br, ^{80}Se, ^{85}Rb, ^{103}Rh, ^{121}Sb, ^{151}Eu, and ^{164}Dy at an incident neutron energy of 25 ± 5 keV. These ratios are theoretically calculated using two models, viz., (1) the Huizenga–Vandenbosch model and (2) the γ-ray cascade model of Ponitz. A comparison of the experimental and theoretical ratios shows that the experimental values agree better with the predictions of the Ponitz model than with those of the Huizenga–Vandenbosch model. It is also observed that, on the basis of Ponitz model, the amounts of quadrupole admixtures required to reproduce experimental isomer ratios are in the range 1–25%. The present estimates of the quadrupole admixtures are in line with previous observations made at thermal energies. (auth)

54590 ELASTIC AND INELASTIC WIDTHS OF ANALOGUE STATES IN ^{65}Cu. Ramavataram, K.; Yang, C. S.; Mercier, G. F.; (and others) (Univ. Laval, Quebec). Nucl. Phys.; A191: No. 1, 88-96(1972).

Elastic and inelastic excitation of IAR were studied using protons of 3 to 5 MeV energy incident on ^{64}Ni. The spins of some of the analog states as well as their elastic and inelastic widths are obtained from the experimental results. Spectroscopic factors were deduced from the resonance parameters and calculated single-particle widths and are compared with the shell-model predictions. (auth)

54591 NUCLEAR REACTIONS OF NICKEL WITH PROTONS UP TO 56 MeV. Tanaka, S.; Furukawa, M.; Chiba, M. (Tokyo Univ.). J. Inorg. Nucl. Chem.; 34: No. 8, 2419-26(Aug 1972).

Excitation functions were measured for a number of nuclear reactions of nickel isotopes with 5 to 56 MeV protons. The following peak cross sections were determined: ^{58}Ni-(p,pn)-260 mb, (p,p2n)-21 mb, (p,2p)-540 mb, (p,2pn)-350 mb, (p,α)-40 mb, (p,2p2n)-63 mb, (p,αpn)-38 mb; ^{60}Ni-(p,n)-320 mb, (p,2pn)-180 mb, (p,2p2n)-200 mb, (p,αn)-72 mb, (p,α2n)-14 mb; ^{61}Ni-(p,n)-480 mb; ^{62}Ni-(p,n)-480 mb, ^{64}Ni(p,n)-670 mb. Cross sections for the following reactions were determined up to $E_p = 56$ MeV: ^{58}Ni-(p,

αp2n), (p,α2pn); ^{60}Ni-(p,p3n), (p,α), (p,2p3n), (p,α2pn); ^{61}Ni-(p,α). Measurements were also made for the cross sections of ^{60}Co formation from natural nickel. (auth)

54592 ^{57}Fe(t,p)^{59}Fe AND ^{58}Fe(d,p)^{59}Fe REACTIONS. McLean, K. C.; Dalgliesh, S. M.; Ipson, S. S.; Brown, G. (Univ. of Bradford, Eng.). Nucl. Phys.; A191: No. 2, 417-37(1972).

The level structure of ^{59}Fe has been investigated using the (d,p) and (t,p) reactions at incident energies of 10 MeV and 12 MeV respectively. Unambiguous spin assignments are made for many levels from a comparison of the angular-momentum transfer of the two reactions. It is shown that the experimental data provide strong support for the existence in ^{59}Fe of a rotational band structure. (auth)

54593 GAMMA TRANSITIONS IN ^{60}Ni FOLLOWING THE β^+ DECAY OF ^{60}Co. II. van Patter, D. M. (Franklin Inst., Swarthmore, Pa.); Rauch, F. Nucl. Phys.; A191: No. 2, 245-56(1972).

Gamma-ray spectra following the decay of ^{60}Cu have been reexamined on the basis of recent new information concerning the properties of ^{60}Ni levels. Additional direct β^+ branches to the 3871.4(2$^+$), 3925.6(3$^+$) and 4535.9 keV states of ^{60}Ni have been identified with log ft values of 6.9, 6.4 and 6.1 respectively. Log ft values have been revised for some previously established branches, and limits for direct population of several other energetically available states are presented. It is noted that the 3194.1 keV 1_1^+ and 3735.5 keV 1_2^+ states prefer to decay much more strongly to the 0_2^+ rather than the 0_1^+ state, while the 4020.4 keV 1_3^+ state shows no such preference. (auth)

54594 ANGULAR CORRELATIONS OF γ-RAYS FROM COULOMB EXCITED ^{63,65}Cu. Robinson, R. L.; Grabowski, Z. W. (Oak Ridge National Lab., Tenn.). Nucl. Phys.; A191: No. 2, 225-32(1972).

The multipole admixtures of the transitions between the lowlying $7/2^-$ and $5/2^-$ states of ^{63,65}Cu have been obtained from angular distributions and γ-γ angular correlations. The states were excited via Coulomb excitation effected with α-particles. The admixture δ for the 365.3 keV γ-ray in ^{63}Cu is -0.105 ± 0.025. For the 366.7 keV γ-ray in ^{65}Cu it is -0.16 ± 0.06. Values extracted for the B(E2) and B(M1) transition rates with these admixtures are: $(2.8^{+1.6}_{-1.2}) \times 10^{-50}e^2 \cdot cm^4$ and 0.24 ± 0.04 (eh/2Mc)^2 for the 365 keV γ-ray and $9.2^{+8.8}_{-6.0}$ and 0.34 ± 0.08 for the 367 keV γ-ray. (auth)

54595 HALF-LIFE OF ^{80g}Br. Collins, K. E.; Collins, C. H.; Kapauan, P. A.; (and others) (Philippine Atomic Research Center, Quezon City). J. Inorg. Nucl. Chem.; 34: No. 9, 2971-3(Sep 1972).

The half-life of ^{80g}Br was redetermined using samples purified by utilizing the chemical effects of the ^{80m}Br(I.T.)^{80g}Br transformation to minimize contamination. In one procedure the nuclear transformation was used to prepare organically-combined ^{80g}Br from an inorganic parent containing ^{80g}Br, with the half-life being directly related to the decay of the organically-combined ^{80g}Br, while in the second procedure, the half-life was determined from the grow-in of ^{80g}Br as a consequence of the ^{80m}Br(I.T.)^{80g}Br transformation in an ^{80m}Br-labeled organic parent, CBr$_4$, freed of nearly all of the previous ^{80g}Br. Values of 17.68 ± 0.02 min, and 17.7 ± 0.2 min were obtained, respectively. (auth) (UK)

Nuclear Properties and Reactions, 90 ≤ A ≤ 149

Refer also to abstracts 54547, 54563, 54585, 54589, 54643, 54657, 54667, and 55060.

54596 (CEA-R-4286) EXCITED LEVELS OF EVEN-A ISOTOPES (RUTHENIUM AND PALLADIUM). Pinston, Jean-Alain (Commissariat a l'Energie Atomique, Grenoble (France). Centre d'Etudes Nucleaires). May 1972. 117p. (In French). Dep. NTIS (U. S. Sales Only).

Thesis. Submitted to Universite Scientifique et Medicale de Grenoble, France.

Nuclear spectroscopy has been used to investigate β decay excited levels in the following nuclei: ^{102} and ^{104}Ru and ^{108} and ^{110}Pd. β and γ spectra, coincidences measurements, levels schemes with spins and parity are given for each of the following decays: ^{102}Tc (two isomers) → ^{102}Ru; ^{104}Tc → ^{104}Ru; ^{108}Rh (two isomers) → ^{108}Pd and ^{110}Rh (two isomers) → ^{110}Pd. These nuclei have been obtained by (n,p) reaction or ^{235}U(n,f). Two new isomeric states (6 min and 28 s half-life) have been evidenced in ^{108}Rh and ^{110}Rh respectively. The first excited levels of the even-even nuclei are represented in terms of DAVYDOV collective models. A new theoretical attempt is described: the DAVYDOV model is connected to the "variable inertia moment" model. This model, a pure phenomenological picture, can be reproduced by introducing a special β-vibration potential energy into the DAVYDOV model. (auth)

54597 (CONF-720901-(Bks.1 and 2), pp 1107-14) IRON-FILTERED NEUTRON BEAMS: A NEW APPROACH TO PRECISION TIME-OF-FLIGHT CROSS SECTION MEASUREMENTS. Block, R. C.; Kaushal, N. N.; Hockenbury, R. W. (Rensselaer Polytechnic Inst., Troy, N. Y.). 1972.

From Meeting on new developments in reactor physics and shielding calculations; Kiamesha Lake, NY. (12 Sep 1972).

By placing thick iron filters in a white-source time-of-flight neutron beam, it is possible to obtain a low-background transmitted beam of bands of neutrons with energies corresponding to the cross section minima in the filter. Capture cross section measurements were carried out upon In, Ta, Au, and ^{238}U near the 24.3 keV energy band, and the integrated capture cross sections are determined to be in the ratio $\tilde{\sigma}(\mathrm{In}) : \tilde{\sigma}(\mathrm{Ta}) : \tilde{\sigma}(\mathrm{Au}) : \tilde{\sigma}(^{238}\mathrm{U}) = (0.88) : (0.96) : (0.67) : (0.47)$. This technique is intrinsically capable of an accuracy in the cross section of 2 to 3 percent. (auth)

54598 (FRNC-TH-242) STUDY OF THE DIPOLAR GIANT RESONANCE BY MEASURING PHOTONEUTRON CROSS SECTIONS. Carlos, Pierre (Paris Univ., Orsay (France)). 1972. 245p. (In French). Dep. NTIS (U. S. Sales Only).

Thesis.

The dipolar giant resonance was studied for intermediate-mass nuclei and heavy nuclei, by measuring the photonuclear cross sections sigma (γ,xn) (x = 1,2,3,4). The theoretical results, obtained for photonuclear reactions, which are valid for all nuclear models are examined. The basic calculations relating to the collective models of the giant resonance are presented. The results obtained are discussed for the following nuclei: Sn, ^{127}I, Ba, ^{139}La, Ce, ^{141}Pr, Sm, ^{159}Tb, ^{165}Ho, Er, Lu, Ta and ^{197}Au and on the Nd isotopes with the masses 142, 143, 144, 145, 146, 148, 150. The theory of the particle-hole model of the giant resonance is presented. The results obtained for ^{208}Pb, Rb, Sr, ^{89}Y, ^{90}Zr and ^{93}Nb are given and discussed; emphasis is put on the isobaric splitting of the dipolar states. The results relating to the various dipolar sum rules are briefly illustrated. (France)

54599 (IAE-2116) NEUTRON RESONANCES ^{112}Cd. Shchepkin, Yu. G.; Muradyan, G. V.; Adamchuk, Yu. V. (Institut Atomnoi Energii, Moscow (USSR)). 1971. 24p. (In Russian). Dep. NTIS (U. S. Sales Only).

The neutron resonances of ^{112}Cd were investigated: Spins were assigned to 23 levels out of 29 observed levels. Values of S_0 and S_1 are strength functions determined after allowing for the probability of identification: $S_0 = (0.72^{+0.40}_{-0.23}) \times 10^{-4}$, and $S_1 = (3.9^{+3.9}_{-1.7}) \times 10^{-4}$. For 12 strong levels values of the radiation width $\Gamma\gamma$ were found with an accuracy of ~15%. The average value of $\Gamma\gamma = 80 \pm 4$ MeV was compared with calculated results from various models. (tr-auth)

54600 (INS-J-130) QUASI-BANDS IN EVEN-EVEN NUCLEI. Sakai, Mitsuo (Tokyo Univ. (Japan). Inst. for Nuclear Study). 15 Sep 1971. 41p. NTIS (U. S. Sales Only).

The quasi-band theory of nuclear structure is presented. The general aspect of the quasi-band structure is illustrated schematically. The author and his collaborators studied experimentally nuclei in which the quasi-band structure was seen. The study revealed that there was some band-like structure in so-called soft transitional regions. Extensive experimentation was performed at Institute for Nuclear Study, University of Tokyo, with in-beam spectroscopy. Proton beams accelerated up to 40 MeV were used to produce ^{126}Xe, ^{124}Xe, ^{132}Ba, ^{130}Ba, ^{136}Ce and ^{138}Nd. Emitted gamma-rays were observed with a Ge(Li) detector. Properties of the levels from which the gamma-rays were emitted were assigned from excitation curves. Properties of the quasi-gamma band were discussed in terms of B(E2) values, which were compared with theoretical predictions by Davydov and Filipov. The location of quasi γ_3 state was discussed in connection with the model of Davydov and Chaban. Log-ft values from parent nuclei to quasi-beta (β_0) and quasi-gamma (γ_2) states were investigated, and the results supported the band structure in the soft and transitional nuclei. The author said that the quasi-band concept is useful. (Japan)

54601 (IS-T-534) STUDY OF ELECTRON EMISSIONS OF SOME MASS SEPARATED FISSION PRODUCT ACTIVITIES. Adams, James Paul (Ames Lab., Iowa). Aug 1972. Contract W-7405-eng-82. 100p. Dep. NTIS.

Thesis.

The beta decay energies for seven short-lived radioactive nuclei produced at the TRISTAN experimental facility were measured using a plastic scintillator and a Ge(Li) detector in a beta-gamma arrangement. The beta decay energies were compared with previous measurements and systematics predictions and were used to predict the beta decay energies for 5 additional nuclei by means of systematics. The beta decay energies were also compared with 2 currently accepted mass formulas. In addition, an internal conversion electron measurement was made for the decay of 16-sec ^{140}Xe. Probable multipolarities for 18 gamma transitions in ^{140}Cs were determined and, on the basis of these multipolarities and the calculated log ft values for the beta fed levels in the decay scheme of ^{140}Cs, the spins and parities for 15 levels in this decay scheme are proposed. (auth)

54602 (JAERI-M-4666) BIBLIOGRAPHY FOR THERMAL NEUTRON SCATTERING. Supplement 1. (Japanese Nuclear Data Committee). Dec 1971. 17p. NTIS (U. S. Sales Only).

This is the supplement to the Third Edition of the Bibliography for Thermal Neutron Scattering (JAERI 4043). It contains 150 articles collected from June to October in 1971. These articles are needed for the evaluations of the thermal neutron scattering cross sections. (auth) (Japan)

54603 (JINR-P6-6511) STUDY OF THE ^{149}Tb DECAY. Vylov, Ts.; Gromov, K. Ya.; Gromova, I. I.; Iskhakov, G. I.; Kuznetsov, V. V.; Kuznetsova, M. Ya.; Lebedev, N. A.; Fominykh, M. I. (Joint Inst. for Nuclear Research, Dubna (USSR). Lab. of Nuclear Problems). 1972. 27p. (In Russian). Dep. NTIS (U. S. Sales Only).

Gamma-ray spectra and those of conversion electrons and $\gamma\gamma$-coincidences at the decay of ^{149}Tb are studied. For a number of transitions in ^{149}Gd nucleus the internal conversion coefficients are determined as well as the number of positrons in the ^{149}Tb decay. The positron intensity is (4.0 ± 0.2)% per decay of ^{149}Tb. The branching ratio for ^{149}Tb is determined from the γ-ray intensity of the daughter isotopes ^{149}Gd and ^{145}Eu. It is found to be (0.20 ± .02). The decay scheme $^{149}\text{Tb} \rightarrow {}^{149}\text{Gd}$ is suggested. (auth)

54604 (JINR-P6-6519) EXCITED QUASI-PROTON STATES IN MAGIC ^{141}Pr NUCLEUS. Buttsev, V. S.; Gromov, K. Ya.; Kalinnikov, V. G. (Joint Inst. for Nuclear Research, Dubna (USSR). Lab. of Nuclear Problems). 1972. 22p. (In Russian). Dep. NTIS (U. S. Sales Only).

The spectra of γ- and x-rays, γ-γ-coincidences, conversion electrons and positrons in the decay ^{141}Nd (2.42 ± 0.09 h) were thoroughly studied. Three new γ-transitions were found out. The energies of γ-transitions from the excited states of ^{141}Pr were more accurately determined. The multipolarities of 1126-91 keV – M1 + E2, 1147-30 keV – E2, 1292-64 – E2, 1298-60 – E2 transitions are determined. New levels of 1434-7 ($3/2^+$), 1456-1 keV ($5/2^+$) are introduced. Quantum characteristics are determined for the levels of the magic nucleus ^{141}Pr. The obtained experimental data are compared with the theoretical calculations, performed within the semimicroscopic models. (auth)

54605 (KFK-1602) DETERMINATION OF THE DISTRIBUTION OF THE CHARGE AND THE MAGNETIC DIPOLE MOMENT IN ^{93}Nb FROM THE MUONIC X-RAY SPECTRUM. Povel, H. P. (Kernforschungszentrum, Karlsruhe (West Germany). Institut fuer Experimentelle Kernphysik). May 1972. 177p. (In German). Dep. NTIS (U. S. Sales Only).

Thesis. Submitted to Technische Hochschule, Karlsruhe (West Germany).

The muonic x-ray spectrum of ^{93}Nb has been measured with high resolution Ge(Li)-detectors. The following transitions have been observed: 2p–1s, 3d–2p, 3p–2s, 3s–2p and 2s–2p. The observation of the transitions from and to the 2s-level is important, because this level is next to the 1s-level most sensitive to the electromagnetic properties of the nucleus. From the measured energies and the hyperfine splitting (hfs) of the transitions the space distribution of the nuclear charge and the magnetic dipole moment have been determined. (auth)

54606 (ORNL-TM-3913) ELASTIC AND INELASTIC SCATTERING OF 12-MeV PROTONS FROM ^{92}Mo, ^{94}Mo, ^{96}Mo, AND ^{100}Mo: TABULATED DIFFERENTIAL CROSS SECTIONS. Dickens, J. K.; Eichler, E.; Silva, R. J.; Williams, I. R. (Oak Ridge National Lab., Tenn.). Sep 1972. Contract W-7405-eng-26. 23p. Dep. NTIS.

Numerical values of differential cross sections for elastic and inelastic scattering of 12.0-MeV protons from ^{92}Mo, ^{94}Mo, ^{96}Mo, and ^{100}Mo are reported in tabular form. Cross sections were determined at 5° intervals between laboratory angles of 20 and 165° Inelastic scattering data are reported for 23 excited states of ^{92}Mo, 14 excited states of ^{94}Mo, 2 excited states of ^{96}Mo, and 6 excited states of ^{100}Mo. (auth)

54607 (RD/B/M-2356) AN ORDERED TABLE OF GAMMA RADIATION EMITTED BY FISSION PRODUCTS. Tobias, A. (Central Electricity Generating Board, Berkeley (England). Berkeley Nuclear Labs.). Jun 1972. 180p. Dep. NTIS (U. S. Sales Only).

A set of data for the fission products of ^{235}U, ^{238}U, ^{239}Pu and ^{241}Pu is presented. In this compilation the energy of the gamma radiation emitted by each isotope is given, together with the number of photons per 100 disintegrations and the isotope half-life. The mass chains covered are 72-161 and 166 and the energies of the gamma radiation are given as accurately as they have been determined and are presented in increasing energy order. Almost 7,000 gamma lines are given. (auth)

54608 (UCRL-Trans-1473) EXPERIMENTS ON SEARCH FOR PROTON DECAY FROM THE GROUND STATE. Bogdanov, D. D.; Bochin, V. P.; Karnaukhov, V. A.; Petrov, L. A. (Joint Inst. for Nuclear Research, Dubna (USSR)). Translated by A. Habberton (Univ. of California Lawrence Berkeley Lab.), from report JINR-P6-6313. 25p. Dep. NTIS.

The neutron-deficient products from the reactions, induced by the accelerated ions of ^{32}S and ^{35}Cl in the targets of ^{96}Ru, ^{102}Pd, ^{106}Cd, ^{112}Sn, were studied. Using two techniques it is established that in bombarding ^{96}Ru by ^{32}S ions a proton emitter is produced having energy of 0.83 ± 0.05 MeV and half-life of about 1 sec. It is assumed that this group of protons appears in the decay of a light isotope of praseodymium (or lanthanum) from the ground state. (auth)

54609 COULOMB FLUX CORRECTIONS AND TOTAL CROSS SECTIONS FOR PION–NUCLEUS INTERACTIONS IN THE Δ-RESONANCE REGION. Faeldt, G. (Univ. of Lund, Sweden); Pilkuhn, H. Phys. Lett.; 40B: No. 6, 613-15(21 Aug 1972).

A relativistic generalization of the Blair model is shown to give large flux corrections (up to 20%) to pion–nucleus cross sections in the Δ-resonance region. Total cross sections for heavy nuclei are calculated and used in the evaluation of these corrections. The formulas also apply to incident high-energy protons. (auth)

54610 CONFIGURATION MIXING IN ^{90}Zr AND THE LIFETIME OF THE EXCITED 0^+ STATE. Courtney, W. J.; Fortune, H. T. (Univ. of Pennsylvania, Philadelphia). Phys. Lett.; 41B: No. 1, 4-6(4 Sep 1972).

Inclusion of $p_{1/2}$ core excitation in ^{90}Zr removes the previous factor-of-6 discrepancy between measured and calculated lifetime for decay of the first excited 0^+ state. (auth)

54611 INHIBITED TRANSITIONS AND ISOMERIC STATES IN THE N = 50 ISOTONES. Gloeckner, D. H. (Argonne National Lab., Ill. Univ. of Chicago); MacFarlane, M. H.; Lawson, R. D.; Serduke, F. J. D. Phys. Lett.; 40B: No. 6, 597-601(21 Aug 1972).

Measured E2 transition rates in the N = 50 isotones (^{90}Zr–^{94}Ru) are satisfactorily reproduced by a shell model with proton configurations $(p_{1/2}g_{9/2})^n$. The inhibited $8^+ \rightarrow 6^+$ E2 transition in ^{94}Ru and its connection with seniority mixing is discussed. Isomeric $17/2^-$ states are predicted in ^{91}Nb and ^{93}Tc. (auth)

54612 LEVEL STRUCTURE OF ^{93}Mo AND THE FAILURE OF j-DETERMINATION BY SPECTROSCOPIC FACTOR RATIOS NEAR CLOSED SHELLS. Ball, J. B. (Oak Ridge National Lab., Tenn.). Phys. Lett.; 41B: No. 1, 55-8(4 Sep 1972).

The ^{95}Mo(p,t)^{93}Mo reaction is used to establish the 1.69-MeV level in ^{93}Mo as $5/2^+$ rather than $3/2^+$, as assigned in recent (d,p) and (d,t) studies. An explanation for this failure of j-value determination by comparison of spectroscopic factor ratios is presented. (auth)

54613 LEVELS OF ^{90}Nb EXCITED VIA THE ^{90}Zr(p,nγ) REACTION. Yoshida, Y. (Tokyo Inst. of Tech.); Ogawa, M.; Hattori, T.; (and others). Nucl. Phys.; A187: No. 1, 161-76(1972).

The excitation functions of the ^{90}Zr(p,nγ) reaction have been measured with a Ge(Li) detector to investigate the low-lying levels of ^{90}Nb and their γ-decay. The incident proton energy was varied from 6.90 to 9.50 MeV in steps of 100 keV. Thirty-four levels in ^{90}Nb which include those of the predominant $[(1g_{9/2})_\pi(1g_{9/2})_\nu^{-1}]J^\pi = 2^+ - 8^+$ and $[(2p_{1/2})_\pi(1g_{9/2})_\nu^{-1}]\ J^\pi = 4^-, 5^-$ configurations have been confirmed. A level with a predominant $[(1g_{9/2})_\pi(1g_{9/2})_\nu^{-1}]_{1+}$ configuration is also suggested. The decay scheme of ^{90}Mo has been revised. (auth)

54614 SPECTROSCOPY OF ^{101}Mo BY SUB-COULOMB STRIPPING. Sievers, W. L.; Close, D. A.; Umbarger, C. J.; Bearse, R. C.; Prosser, F. W. Jr. (Univ. of Kanas, Lawrence). Phys. Rev., C; 6: No. 3, 1001-8(Sep 1972).

Sub-Coulomb stripping was employed to study ^{101}Mo with 3.75-MeV deuterons. Proton groups assigned to states in ^{101}Mo at excitation energies of 0, 57, 239, 290, 349, 480, 540, 561, 812, 851, and 898 keV were observed. The states at 349, 561, and 851 keV have not been reported previously. The ground state and the excited state at 349 keV were shown to be $1/2^+$ states with spectroscopic factors of 0.42 and 0.16. Tentative assignments of $l_n = 2$ were made for the states at 57, 239, 290, and 480 keV. If these states have a $3/2^+$ nature, the spectroscopic factors are 0.25, 0.09, 0.12, and 0.11, respectively. The sums of the spectroscopic factors for l = 0 and l = 2 transitions are shown to be consistent with previous results from stripping and pickup reactions on neighboring nuclei. (6 figures, 4 tables) (auth)

54615 COLLECTIVE EFFECTS SHOWN BY THE (p,t) REACTION ON THE CLOSED-SHELL NUCLEUS, ^{141}Pr. Goles, R. W.; Warner, R. A.; McHarris, Wm. C. (Michigan State Univ., East Lansing). Phys. Rev., C; 6: No. 2, 587-90(Aug 1972).

The reaction ^{141}Pr(p,t)^{139}Pr at 40 MeV strongly populates collective states in the residual nucleus. The shapes of the angular distributions, taken at 5° intervals between 15 and 65°, show the inadequacies even of finite-range, two-nucleon-pickup distorted-wave Born-approximation calculations and the need for inclusion of higher-order effects. (auth)

54616 STUDY OF SOME PROPERTIES OF TIN ISOTOPES THROUGH HIGH-ENERGY ALPHA-PARTICLE SCATTERING. Brissaud, I. (Institut de Physique Nucleaire, Orsay, France); Tatischeff, B.; Bimbot, L.; (and others). Phys. Rev. C; 6: No. 2, 595-606(Aug 1972).

Angular distributions of 166-MeV α particles scattered from the Sn isotopes 116, 118, 120, and 124 have been measured. An analysis of the elastic scattering data was performed using an optical potential calculated from an effective interaction between the α particle and a nuclear-matter distribution. The variation of nuclear sizes among the isotopes is considered. Assuming charge densities derived from the results of elastic electron scattering and/or mesonic atom data, values of neutron-matter radii for the tin isotopes are deduced which agree well with theoretical values. An analysis of the inelastic α-particle scattering to the first 2^+ and 3^- levels for each isotope was effected using the optical potentials calculated from the elastic scattering, the distorted-wave Born-approximation, and quasiparticle wave functions for the excited states. Electromagnetic transition rates and form factors for electron scattering were calculated with the same wave functions, and a comparison of the calculations to the experimental results provides information about the proton and neutron configurations in these isotopes. (auth)

54617 DOUBLE K-SHELL IONIZATION IN THE DECAY OF ^{131}Cs AND ^{165}Er. Nagy, H. J.; Schupp, G.; Hurst, R. R. (Univ. of Missouri, Columbia). Phys. Rev., C; 6: No. 2, 607-12(Aug 1972).

Double ionization of the K shell has been studied in the electron capture decays of ^{131}Cs and ^{165}Er by recording coincidences between K x rays emitted when the double vacancies are filled. A Si(Li) x-ray detector was used in conjunction with a NaI(Tl) detector for these measurements. The results obtained for P_{KK}, the probability per K capture that a double K-shell vacancy is formed, were $(1.33 \pm 0.33) \times 10^{-5}$ for ^{131}Cs and $(6.7 \pm 3.9) \times 10^{-6}$ for ^{165}Er. Both of these values are a factor of 2 smaller than previous measurements and, within the experimental uncertainties, are in agreement with predictions based on the relativistic theory of Intemann. (auth)

54618 ^{142}Ce(d,p) AND ^{142}Ce(d,t) REACTIONS AND ISOBARIC ANALOG RESONANCES IN ^{142}Ce(p,p$_0$) AND ^{142}Ce(p,p$_1$). Lessard, L.; Gales, S.; Foster, J. L. Jr. (Univ. of Montreal). Phys. Rev., C; 6: No. 2, 517-31(Aug 1972).

The reactions ^{142}Ce(d,p) and ^{142}Ce(d,t) at an incident deuteron energy of 12.6 MeV have been investigated with an energy resolution of about 16 keV, and excitation functions for the reactions ^{142}Ce(p,p$_0$) and ^{142}Ce(p,p$_1$) have been measured from 9.5- to 12-MeV incident proton energies. The analysis of the analog resonances observed in the excitation functions is compared with the results of the ^{142}Ce(d,p) experiment. (auth)

54619 LEVEL SCHEME OF ^{144}Sm DETERMINED BY THE (γ,γ') REACTION. Arad, B. (Soreq Nuclear Research Center, Yavne, Israel. Bar-Ilan Univ., Ramat Gan, Israel); Ben-David, G.; Schlesinger, Y.; Hass, M. Phys. Rev., C; 6: No. 2, 670-2(Aug 1972).

The 8.998-MeV resonance level excited by the (γ,γ') reaction, which was previously assigned to ^{150}Sm, is shown to belong to ^{144}Sm. The level scheme of ^{144}Sm is given and the reevaluated level parameters of the 8.998-MeV resonance are presented. (auth)

54620 STRUCTURE OF THE LOW-LYING STATES OF THE ODD-A In ISOTOPES. Sen, S. (Saha Inst. of Nuclear Physics, Calcutta). Nucl. Phys.; A191: No. 1, 29-46(1972).

The level schemes and electromagnetic properties of odd-A In isotopes from A = 113 to A = 117 are calculated in a semi-microscopic model which couples the proton-hole motion to the quadrupole and octupole vibrations of the core. The calculated results are compared with recent experimental findings. The addition of octupole vibration is necessary to explain the properties of the negative-parity states. It is found that this coupling scheme is not adequate to explain in detail the observed properties of the positive-parity states. Calculation is also done by mixing the hole-core coupled states with the states forming a $K = \frac{1}{2}^+$ rotational band; good agreement with experimental data is obtained. (auth)

54621 PHASE AND SHAPE OF THE FORM FACTOR FOR INELASTIC ^{3}He SCATTERING. Baker, F. T. (Rutgers–The State Univ., New Brunswick, N. J.); Kruse, T. H.; Williams, M. E.; Matthews, J. L.; Savin, W. Phys. Lett.; 40B: No. 3, 355-6(10 Jul 1972).

Interference between nuclear and Coulomb excitation of the 0.56 MeV 2^+ state of ^{114}Cd by ^{3}He particles with energies near the Coulomb barrier has been observed. The results indicate that the collective model describes the data well and that the form factor for inelastic ^{3}He scattering is therefore largely imaginary. (auth)

54622 LIFETIME OF THE FIRST EXCITED STATE IN ^{96}Zr. Burch, D.; Russo, P.; Swanson, H.; Adelberger, E. G. (Univ. of Washington, Seattle). Phys. Lett.; 40B: No. 3, 357-9(10 Jul 1972).

The reaction ^{96}Zr(p,p'e) was used to measure the lifetime of the 0_2^+(1.59 MeV) state in ^{96}Zr through the observation of delayed coincidences between a pulsed proton beam and the E0 internal conversion electrons. The half-life is 3.80 ± 1.5 ns. This value is compared to a simple shell model calculation. (auth)

54623 MULTIPLE COULOMB INTERFERENCE EFFECTS ON THE QUADRUPOLE MOMENT OF ^{114}Cd. Larsen, R. D.; Thomson, J. A.; Kerr, R. G.; Scharenberg, R. P.; Lutz, W. R. (Purdue Univ., Lafayette, Ind.). Phys. Lett.; 40B: No. 3, 360-2(10 Jul 1972).

The sign of the multiple Coulomb interference term in ^{114}Cd was determined to be positive by comparing low and high excitation probability experiments. With this sign the quadrupole moment of the first 2^+ state was found to be $Q(2^+) = -0.35 \pm 0.07$ b. (auth)

54624 MOESSBAUER OBSERVATION OF THE MAGNETIC MOMENT OF THE 89-keV EXCITED STATE OF ^{119}Sn. Gumprecht, D. F. (Helsinki Univ. of Tech., Otaniemi, Finland); Katila, T. E.; Moberg, L. C.; Lipas, P. O. Phys. Lett.; 40A: No. 4, 297-8(31 Jul 1972).

The magnetic moment of the 89-keV excited state of ^{119}Sn was determined from Mössbauer measurements made below 100 mK. The value obtained was $-1.40 \pm 0.08\ \mu_N$. Its deviation from the Schmidt value $-1.91\ \mu_N$ is consistent with systematics and nuclear theory estimates. (auth)

54625 RELATIVE ISOTOPE SHIFT (112–114)/(110–112) IN THE λ = 4416 A LINE OF CADMIUM. Gerstenkorn, S.; Helbert, J. M.; Lecordier, R. (CNRS, Orsay, France. Faculte des Sciences, Rouen). Phys. Lett.; 40A: No. 3, 229-30(17 Jul 1972). (In French).

The relative isotope shift $\Delta(112-114)/\Delta(110-112)$ in the spectral line λ = 4416 Å ($d^{10}p\ ^2P_{3/2} - d^9\ s^2\ ^2D_{5/2}$) was investigated and found to be 0.87 ± 0.02. The decrease of the isotope shifts between A = 110 and A = 116 is compared to the decrease of the quantities $EA^{1/3}$ where E is the binding energy per nucleon. (auth)

54626 CUMULATIVE YIELD OF 83-SEC ^{136}I FROM THERMAL-NEUTRON INDUCED FISSION OF ^{235}U. Wahl, A. C.; Denig, R. (Washington Univ., St. Louis). J. Inorg. Nucl. Chem.; 34: No. 8, 2413-18(Aug 1972).

The cumulative yield of 83-sec ^{136}I from thermal-neutron induced fission of ^{235}U was redetermined to be 4.3 ± 0.4% if formed independently or 3.4 ± 0.4% if formed by beta decay of 21-sec ^{136}Te. The median value of 3.9 ± 0.8% is recommended since the mode of formation is not known. Allowing for an appreciable yield of the 44-sec ^{136}I isomer, as observed by Lundán, the fractional independent yield of ^{136}Xe is 0.24 ± 0.18, which is within the estimated "normal" range of 0.17 ± 0.07. Thus, there is no longer evidence for yield enhancement of ^{136}Xe$_{82}$ associated with closure of the 82-neutron shell. (auth)

54627 ISOMER RATIOS OF ^{95}Nb FORMED IN THE FISSION OF ^{209}Bi. Rao, C. L.; Saha, G. B.; Yaffe, L. (McGill Univ., Montreal). J. Inorg. Nucl. Chem.; 34: No. 8, 2397-2403(Aug 1972).

Analysis of the isomer ratios of the symmetric fission product, ^{95}Nb, formed in the fission of ^{209}Bi reported by Hagebo (J. Inorg. Nucl. Chem. 27, 927(1965)), in the energy range of 55 to 157 MeV, was made according to the energy-dependent calculation of Saha and Yaffe (J. Inorg. Nucl. Chem. 31, 1891(1969)). Values of angular momentum $8\hbar$ at 55 MeV to $15\hbar$ at 157 MeV were found. These values agree with those calculated from isomer ratios in the heavy-mass region in the fission of heavier elements. (auth)

54628 ISOMER YIELD RATIOS OF ^{115m}Cd AND ^{115g}Cd. Rao, S. A. (Univ. of Arkansas, Fayetteville). J. Inorg. Nucl. Chem.; 34: No. 8, 2405-11(Aug 1972).

The cumulative isomer yield ratios σ_m/σ_g of the ^{115}Cd isomers were measured for the reactions ^{116}Cd(n,2n), ^{118}Sn(n,α), ^{232}Th(n,f), and ^{238}U(n,f) by 14.8 MeV neutrons. The ratios of the 43 day ^{115m}Cd($^{11}/_{2}{}^{-}$) yield to the 2.3 day ^{115g}Cd($^{1}/_{2}{}^{+}$) yield are 0.71 ± 0.06, 1.48 ± 0.20, 0.088 ± 0.015, and 0.12 ± 0.02 for the respective reactions. The most probable excitation energies of the compound nuclei, in the formation of ^{115}Cd isomers from various reactions, were calculated. From the knowledge of the threshold energies for these reactions, it is suggested that there is a relation between cumulative isomer yield ratios and excitation energies above the threshold. (auth)

54629 PHOTONEUTRON CROSS SECTIONS OF ^{139}La AND ^{141}Pr. Deague, T. K.; Stewart, R. J. J. (Univ. of Melbourne, Parkville, Australia). Nucl. Phys.; A191: No. 2, 305-20(1972).

The cross sections for photoneutron production in ^{139}La and ^{141}Pr have been measured from threshold to 24 MeV and 22 MeV respectively by direct neutron detection. A modified Penfold-Leiss method, with an analysis bin optimized at all energies, was used to unfold these cross sections from bremsstrahlung yield data. The results are compared with predictions of the dynamic collective model and a recent collective-correlations calculation. Most of the apparent contradictions between recent measurements of the ^{141}Pr (γ,n) cross section from threshold to 17 MeV can be resolved through (i) a more efficacious choice of bremsstrahlung yield-curve analysis technique, and (ii) a consideration of comparative experimental resolutions and uncertainties. (auth)

54630 COULOMB EXCITATION OF NUCLEI BY HEAVY POLARIZED PARTICLES. Davydov, A. V.; Narodetskii, I. M. (Inst. of Theoretical and Experimental Physics, Moscow). JETP Lett. (USSR) (Eng. Transl.); 15: No. 12, 525-8(20 Jun 1972).

Translated from Zh. Eksp. Teor. Fiz., Pis'ma Red.; 15: No. 12, 741-5(20 Jun 1972).

Existing methods for determining the magnetic moments of short-lived nuclear states are feasible only for states with lifetimes longer than $\sim 10^{-11}$ s. Another method for determining the magnetic moment (m.m.), based on Coulomb excitation of nuclei by polarized particles, is described. A charged-particle magnetic field greatly exceeding that of laboratory fields is used, and the entire process occurs during the time of flight of the particle past the nucleus; hence, it is independent of the lifetime of the nucleus in the excited state. The difference $\sigma\uparrow - \sigma\downarrow$, where $\sigma\uparrow(\sigma\downarrow)$ is the cross section for the Coulomb excitation for a spin directed parallel (antiparallel) to the normal to the reaction plane, is determined by the m.m. of the excited state. By measuring this difference (or the left–right asymmetry in scattering) the m.m. of the excited state can be determined experimentally. The appropriate theory underlying the method is developed, and results are given for ^{7}Li and ^{148}Sm and ^{17}O on ^{64}Zn. (1 figure, 1 table) (R.W.R.)

Nuclear Properties and Reactions, $150 \leq A \leq 189$

Refer also to abstracts 54523, 54563, 54585, 54589, 54597, 54598, 54617, 54630, 54656, 54672, 54881, and 54960.

54631 (BNL-tr-490) CORRELATION OF THE PARTIAL RADIATION WIDTHS IN THE REACTION ^{163}Dy(n,γ)^{164}Dy. Danelyan, L. S.; Demidov, A. M.; Krupin, S. V.; Sotnikov, S. K.; Zarandi, A.; Kardon, B.; Szabo, L.; Seres, Z. Translated by S. J. Amoretty (Brookhaven National Lab., Upton, N. Y.), from Zh. Eksp. Teor. Fiz.; 62: No. 2, 425-9(1972). 8p. Dep. NTIS.

The γ ray spectra in the ^{163}Dy(n,γ)^{164}Dy reaction were investigated with a Ge(Li) spectrometer. A number of phenomena of a nonstatistical nature are observed: correlations between the reduced radiative and neutron widths and between various partial radiative widths. The absolute mean reduced partial width is greater than any of those predicted by the various models or based on the experimental data for other nuclei. The degree of freedom of the partial width distribution for transitions to the ground rotational and γ vibrational bands is ν = 2 ± 0.5. (auth)

54632 (COO-3255-2) DECAY OF ^{161}Er TO LEVELS IN ^{161}Ho. Wood, J. L.; Brenner, D. S. (Clark Univ., Worcester, Mass. (USA). Jeppson Lab. of Chemistry). 8 Jul 1971. 50p. Dep. NTIS.

The gamma-ray spectrum of the decay chain ^{161}Er → ^{161}Ho → ^{161}Dy has been studied with Ge(Li) detectors. Results of γ-ray singles and coincidence experiments are reported and a decay scheme for ^{161}Er → ^{161}Ho is proposed. Asymptotic quantum-number assignments are made for several new energy levels in ^{161}Ho and the results are compared to predictions of the unified model. No evidence was found for the population of three-quasiparticle states in ^{161}Ho. Deexcitation of the $^{3}/_{2}{}^{-}$ $\{^{7}/_{2}{}^{-}[523],2^{+}\}$ γ-vibrational state and Coriolis coupling in the $^{1}/_{2}{}^{+}[411]$ rotational band are discussed. (auth)

54633 (COO-3255-3) LEVELS IN ^{186}Os AS POPULATED BY THE DECAY OF ^{186}Ir. Hofstetter, K. J. (Texas Agricultural and Mechanical Univ., College Station. Kentucky Univ., Lexington. Dept. of Chemistry); Sugihara, T. T. (Texas Agricultural and Mechanical Univ., College Station); Brenner, D. S. (Clark Univ., Worcester, Mass. (USA). Jeppson Lab. of Chemistry). 1971. 48p. Dep. NTIS.

The excited level scheme of ^{186}Os as populated by the decay of 15.8-h ^{186}Ir has been studied by Ge(Li) detectors in singles and coincidence spectrometers. The coincidence data confirm essentially all of the previously known intraband and interband transitions assigned to the ground-state band (to the 6^{+} level), the γ-band (to the 7^{+} level) and to the J = 4, 5, and 6 members of a two-phonon K = 4 band. Coincidence data also establish levels at 1194.45 (4^{+}), 1461.09 (4^{+}), 1480.3 (4^{+}), 1628.3 (5^{-}), 1775.8 (6^{+}), 1812.5 (5^{+}), 1875.40 (4^{+}), 2056.38 (5^{+}), 2081.21 (4^{+}), 2377.3 (6^{+}), and 2771.7 (4^{+}) keV. The J$^{\pi}$ assignments are based on multipolarities determined from internal conversion coefficients. Additional levels based on energy sums are tentatively proposed at 1582.3, 2661.2, 3041.3, 3151.7, 3268.8 and 3413.6 keV. An analysis of the interband transition intensities between members of the γ-band and members of the ground-state band indicates that the first-order band-mixing model fits the data. The mixing parameter z_γ is found to have the value 0.087 ± 0.004 for ^{186}Os. The 15.8-h ^{186}Ir state is believed to be a 6^{+} state with the Nilsson configuration $\pi^{11}/_{2}{}^{-}[505] + \nu^{1}/_{2}{}^{-}[510]$. (auth)

54634 (JINR-E6-6479) g-FACTOR OF THE 108 keV EXCITED STATE IN ^{151}Gd. Afanas'ev, V. P.; Fuya, Kh.; Gromov, K. Ya.; Gromova, I. I.; Ion-Mikhai, R.; Khalikulov, A. B.; Monchka, D.; Morozov, V. A.; Muminov, T. M.; Zhuk, V. (Joint Inst. for Nuclear Research, Dubna (USSR). Lab. of Nuclear Problems). 1972. 12p. Dep. NTIS (U. S. Sales Only).

Measurements of the integral perturbed angular correlation (IPAC) were made using magnetic hyperfine interactions. The ^{151,155}Tb radioactive nuclei were embedded in iron foil by the use of an isotope separator. The measurements of the g-factor of the 108 keV state in ^{151}Gd have yielded a value of $(-0.54^{+0.07}_{-0.10})$. (auth)

54635 (JINR-P4-6509) ONE-NUCLEON TRANSFER REACTIONS TO QUASI-INTERSECTING LEVELS 1/2^{+} (660) AND 1/2^{+} (400), 3/2^{+} (651) AND 3/2^{+} (402). Gareev, F. A.; Bazhat, M.; Vibike, Kh. I.; Shul'ts, G. (Joint Inst. for Nuclear Research, Dubna (USSR). Theoretical Physics). 1972. 20p. (In Russian). Dep. NTIS (U. S. Sales Only).

Based on the coupled channel method, the (d,t) reactions on ^{160}Gd and ^{164}Dy nuclei are considered taking account of Δ N = ± 2 mixing of states $^{1}/_{2}{}^{+}[660]$ and $^{1}/_{2}{}^{+}[400]$, $^{3}/_{2}{}^{+}[651]$ and $^{3}/_{2}{}^{+}[402]$. The results show that this method allows one to give a satisfactory description of the transfer reaction cross sections to these states. When including the Coriolis interaction between the states, where stripping takes place, the cross sections change by 30%. (auth)

54636 SINGLE-NEUTRON-TRANSFER-REACTION STUDIES OF ^{176}Hf AND ^{180}Hf. Zaitz, J. I.; Sheline, R. K. (Florida State Univ., Tallahassee). Phys. Rev., C; 6: No. 2, 506-17(Aug 1972).

The strongly deformed even-even nuclei ^{176}Hf and ^{180}Hf have been studied using the reactions ^{177}Hf(d,t)^{176}Hf and ^{179}Hf(d,p)^{180}Hf. These reactions were performed at 12- and 14-MeV incident energy on the Florida State University super FN tandem Van de Graaff accelerator with the outgoing particles analyzed by means of a Browne–Buechner-type broad-range magnetic spectrograph. 25 states associated with two-quasiparticle rotational bands have been identified or tentatively identified in these nuclei; included are the intrinsic band heads $6^{+}[514\downarrow + 512\uparrow]$, $3^{+}[514\downarrow - 521\downarrow]$, $4^{+}[514\downarrow + 521\downarrow]$, and $6^{+}[514\downarrow + 523\downarrow]$ in ^{176}Hf and the intrinsic band heads $4^{-}[624\uparrow - 510\uparrow]$, $5^{-}624\uparrow + 510\uparrow]$, $6^{-}[624\uparrow + 512\downarrow]$, and $8^{-}[624\uparrow + 503\uparrow]$ in ^{180}Hf. Coriolis-mixing calculations have been an important factor in making the state assignments. (auth)

54637 NUCLEAR LEVELS IN ^{188}Re. Shera, E. B. (Los Alamos Scientific Lab., N. Mex.); Gruber, U.; Maier, B. P. K.; (and others). Phys. Rev., C; 6: No. 2, 537-67(Aug 1972).

Nuclear levels in ^{188}Re have been investigated using the following experimental techniques: measurement of neutron-capture γ-ray transitions with energies between 4.8 and 6.0 MeV using a Ge(Li) pair spectrometer; study of (d,p) spectra using 12-MeV deuterons and a broad-range magnetic spectrograph; measurement of (n,γ) spectra between 45 and 830 keV with a bent-crystal spectrometer; coincidence studies of the (n,γ) radiation using two Ge(Li) detectors, including a study of short-lived isomeric states using delayed-coincidence techniques; and observation of the γ rays following β decay of ^{188}W using a Ge(Li) detector. A nuclear level scheme for ^{188}Re has been constructed by combining the results of the above measurements with published data. Information, including spin and parity assignments, is presented on 36 low-lying levels.

The lifetimes of five excited states are reported. The Nilsson model has been used to interpret the level structure. Assignments are proposed which involve 15 separate rotational bands. Proposed Nilsson configurations, band-head energies, and band-head lifetimes (if known) are: $1^-[402\uparrow - 512\downarrow]$, 0.0 keV; $3^-[402\uparrow + 510\uparrow]$, 169.4 keV, $6^-[402\uparrow + 503\uparrow]$, 172.1 keV, 19 min; $4^-[402\uparrow + 512\downarrow]$, 182.7 keV, 18 nsec; $2^-[402\uparrow - 505\downarrow]$, 205.3 keV, 3.2 nsec; $0^+[514\uparrow - 505\downarrow]$, 207.9 keV, 3.2 nsec; $3^+[514\uparrow - 512\downarrow]$, 230.9 keV, 21 nsec; $2^-[402\uparrow - 510\uparrow]$, 256.9 keV; $1^-[402\uparrow + 503\uparrow]$, 290.7 keV; $4^-[402\uparrow + 501\uparrow]$, 325.9 keV; $5^+[514\uparrow + 510\uparrow]$, 360.9 keV, 5.2 nsec; $3^+[402\uparrow - 615\uparrow]$, 439.7 keV; $1^+[514\uparrow - 503\uparrow]$, 482.2 keV; $1^-[402\uparrow - 501\uparrow]$, 556.8 keV. A $K^\pi = 1^-$ band, believed to be predominantly a $|K - 2|$ γ-vibrational band, is observed at 582.2 keV. The measured (d,p) reaction cross sections are compared with theoretical calculations based on these assignments. The β-decay measurements have revealed a previously unknown β branch from the ^{188}W ground state to a $I^\pi = 0^+$ level at 207.9 keV. This $0^+ \to 0^+$ transition (logft = 9.9) is discussed in terms of isobaric analog state mixing. Results of a calculation which uses a parametrized residual neutron–proton interaction to predict the parallel-antiparallel splitting energies and K = 0 even-odd shifts in ^{186}Re and ^{188}Re are presented and compared with experiment. (auth)

54638 STATIC QUADRUPOLE MOMENTS OF THE FIRST 2^+ STATES OF THE EVEN–EVEN OSMIUM NUCLEI. Lane, S. A.; Saladin, J. X. (Univ. of Pittsburgh). Phys. Rev., C; 6: No. 2, 613-18(Aug 1972).

Measurements of the total thick-target yields of γ rays deexciting the first 2^+ excited states of ^{192,190,188,186,184}Os following Coulomb excitation by helium, oxygen, and sulfur ions have been made. These measurements were compared with theoretically calculated yields in order to extract linear combinations of the static electric quadrupole moments of the 2^+ states. The results were compared with the measurements of Pryor and Saladin of the absolute moments of ^{192,190,188}Os in order to obtain the best combined values for these three isotopes, as well as absolute values for ^{186,184}Os. These values are -0.50 ± 0.20, -0.95 ± 0.19, -1.32 ± 0.43, -1.47 ± 0.54, and -2.4 ± 1.1, respectively. For the isotopes ^{192,190,188,186}Os the $B(E2, 0^+ \to 2^+)$ values determined in the experiment agree with published values to within 10%. The $B(E2, 0^+ \to 2^+)$ value of ^{184}Os was previously unknown and was determined to be 3.20 ± 0.62 e^2b^2. The results are also compared with the model calculations of Kumar and Baranger and found to be in good agreement. (auth)

54639 DECAY OF ^{162}Yb. Chu, Y. Y. (Brookhaven National Lab., Upton, N. Y.). Phys. Rev., C; 6: No. 2, 628-30(Aug 1972).

The decay of ^{162}Yb was studied with samples produced by irradiating ^{164}Er with 52-MeV ^{3}He ions. Mass separation of the irradiated samples provided isotopically pure ^{162}Yb samples for half-life and γ-ray spectra measurements. Three γ rays (44-, 118-, and 162-keV in energy) as well as the Tm K x rays were observed and the half-life of ^{162}Yb was determined to be 18.87 ± 0.19 min. The latter two γ rays were found only in coincidence with Tm K x rays but not with each other. From the growth and decay of the 102-keV γ ray of ^{162}Tm in these same samples, the abundances of the three γ rays and the Tm $K\alpha_1$ x ray were determined. (auth)

54640 EFFECT OF CHANGES IN EQUILIBRIUM DEFORMATIONS OF THE EXCITED STATES OF ODD-A DEFORMED NUCLEI ON THEIR ENERGY AND STRUCTURE. Arsen'ev, D. A.; Fedotov, S. I.; Pashkevich, V. V.; Solov'ev, V. G. (Joint Inst. for Nuclear Research, Dubna, USSR). Phys. Lett.; 40B: No. 3, 305-6 (10 Jul 1972).

In the present note the results of calculations of the equilibrium deformations of the excited states of odd-A nuclei in the region $153 \leq A \leq 177$ are reported. For the states with $\beta_e \neq \beta_0$ the energy and the structure are calculated with the account of the quasiparticle-phonon interaction. (auth)

54641 $0^+ \to 0^+$ β TRANSITION OF ^{188}W. Shera, E. B. (Los Alamos Scientific Lab., N. Mex.); Ikeda, A.; Sheline, R. K. Phys. Lett.; 40B: No. 3, 349-51(10 Jul 1972).

A β-transition with a log ft value of 9.9 has been observed between the ^{188}W 0^+ ground state and a 0^+ state at 207.9 keV in ^{188}Re. This highly forbidden Fermi transition can be quantitatively interpreted in terms of the mixing of the isobaric analog state of the ^{188}W ground state into the $^{188}\mathrm{Re}\{\pi\, {}^9\!/_2^-[514\uparrow] - \nu\, {}^9\!/_2^-[505\downarrow]\}0^+$ state. (auth)

54642 MEASUREMENT OF LIFETIMES IN ^{152}Sm, ^{154}Gd, AND ^{156}Gd BY DOPPLER-SHIFT RECOIL-DISTANCE TECHNIQUES. Rud, N. (Queen's Univ., Kingston, Ont.); Ewan, G. T.; Christy, A.; (and others). Nucl. Phys.; A191: No. 3, 545-60(1972).

The following lifetimes (in ps) were measured for the states in ^{152}Sm: 4_g: 82.8 ± 1.2, 6_g: 14.6 ± 0.4, 8_g: 4.3 ± 0.65, 0_β: 8.92 ± 0.55; in ^{154}Gd: 4_g: 66.3 ± 2.2, 6_g: 11.2 ± 0.6, 0_β: 5.7 ± 0.9; and in ^{156}Gd: 4_g: 163 ± 7 and 6_g: 20.5 ± 1.75. The Doppler-shift recoil-distance method was used in which the states were populated by Coulomb excitation using 100-MeV ^{35}Cl ions. Gamma rays were detected in coincidence with back-scattered ^{35}Cl ions. The results for the 0_β lifetimes are discussed in terms of the monopole matrix elements between the ground state and β-vibrational bands. Deviations from rotational behavior in the ground-state-band transition probabilities are found to be consistent with the simple band-mixing picture. (12 figures, 5 tables) (auth)

54643 NUCLEAR SPECTROSCOPY OF NEUTRON-DEFICIENT La, Dy, AND Er ACTIVITIES. Harmatz, B.; Handley, T. H. (Oak Ridge National Lab., Tenn.). Nucl. Phys.; A191: No. 3, 497-524(1972).

A large accumulation of conversion-electron data made it feasible to study the properties of nuclear levels in the rare earth region of neutron numbers 88 to 94. The first experimental level scheme for ^{153}Tb (N = 88) is constructed; 84 transitions originate from 21 states excited below 1 MeV. The conversion spectrum of ^{155}Tb is augmented from 40 to 120 transitions below 1.1 MeV energy. Multipole orders are deduced for 55 of the 96 transitions placed between 28 levels in ^{155}Tb. Rotational parameters and γ-ray branching ratios are evaluated for ^{155}Tb. Levels in the 0.5 to 1 MeV region are interpreted as β and γ vibrations of the ${}^3\!/_2^+[411]$ state and a single-particle ${}^1\!/_2^+[411]$ band. Data on ^{158}Ho consists of 41 transitions, of which 30 are new, and almost all of the transition intensity is accounted for in the level spectrum. Neutron orbital ${}^3\!/_2^-[521]$ is found to be common to each of four low-lying intrinsic configurations in doubly odd ^{158}Ho. The order of odd-proton orbitals coupled to ${}^3\!/_2^-[521]$ corresponds to that of single-particle states observed in neighboring ^{159}Ho. Eighty conversion-electron transitions were observed below 1 MeV in ^{161}Ho, a six-fold increase over preceding studies. By using photon intensities from independent research, multipole orders are deduced for most of the transitions de-exciting 18 nuclear levels in ^{161}Ho. More evidence is presented on decay spectra of ^{131,132m}La, including transition multipolarity assignments. (auth)

54644 MULTIPOLE MIXING RATIOS OF γ-TRANSITIONS IN ^{185}Re. Behar, M.; Grabowski, Z. W.; Steffen, R. M. (Purdue Univ., Lafayette, Ind.). Nucl. Phys.; A191: No. 2, 361-7(1972).

Gamma-gamma directional correlation experiments were performed on four cascades in ^{185}Re populated from the electron capture decay of ^{185}Os (94 d). Two Ge(Li) detectors in a coincidence arrangement were used in this measurement. The directional correlation coefficients for the 173 keV–593 keV γ-γ cascade together with previously determined conversion coefficients give a unique spin ${}^1\!/_2^+$ assignment for the 879 keV level. The E2/M1 mixing ratios for the 125 keV, 163 keV and 718 keV transitions are $\delta(125) = 0.186 \pm 0.019$, $\delta(163) = 0^{+0.06}_{-0.024}$ and $\delta(718) = -2.23 \pm 0.06$, respectively. (auth)

54645 COLLECTIVE AND HIGHER-ORDER EFFECTS SHOWN BY THE (p,t) REACTION ON THE DEFORMED NUCLEUS ^{159}Tb. Goles, R. W.; Warner, R. A.; McHarris, Wm. C. (Michigan State Univ., East Lansing). Phys. Rev. Lett.; 29: No. 12, 802-5(18 Sep 1972).

The reaction ^{159}Tb(p,t)^{157}Tb at 30 MeV strongly populates collective states in the residual nucleus. Angular distributions of β and γ vibrational and ground-state rotational band members are presented and compared with distorted-wave Born-approximation predictions. Evidence supporting the importance of indirect multiple-step processes accompanying (p,t) reaction is also included. The (p,t) reaction is shown to be a powerful spectroscopic tool for populating higher-lying rotational band members in odd-mass deformed nuclei. (auth)

54646 OBSERVATION OF TEMPERATURE SPIKES FOLLOWING COULOMB EXCITATION. Hardy, K. A. (Johns Hopkins Univ., Baltimore); Walker, J. C.; Shnidman, R. Phys. Rev. Lett.; 29: No. 10, 622-5(4 Sep 1972).

Short-lived temperature spikes were observed following Coulomb excitation in rare earth oxides. The thermal aftereffects were detected by observing the Moessbauer effect in the decay of Coulomb excited states of ^{165}Ho, ^{175}Lu, and ^{167}Er. The results are in reasonable agreement with a simple model based on heat-flow theory. (auth)

Nuclear Properties and Reactions, $190 \leq A \leq 219$

Refer also to abstracts 54501, 54528, 54529, 54547, 54563, 54597, 54598, 54602, 54609, 54627, 54628, 54630, and 54638.

54647 $4^+ \to 0^+$ CROSS-OVER TRANSITION IN ^{204}Pb. Signorini, C.; Morinaga, H. (Technische Univ., Munich). Phys. Lett.; 40B: No. 5, 549-50(7 Aug 1972).

A $4^+ \rightarrow 0^+$ cross-over γ-ray decay in ^{204}Pb was detected. The branching ratio of this transition to the $4^+ \rightarrow 2^+ \rightarrow 0^+$ cascade was measured to be (0.012 ± 0.002)%. (auth)

54648 SPECTRAL SHAPE AND NUCLEAR MATRIX ELEMENTS IN THE β-DECAY OF ^{206}Tl. Wiesner, W. (Univ., Heidelberg); Flothmann, D.; Gils, H. J.; Loehken, R.; Rebel, H. Nucl. Phys.; A191: No. 1, 166-76(1972).

The spectral shape, endpoint energy and half-life of the β-decay of ^{206}Tl were measured. The β-particles were analyzed in a 4π Si(Li) sandwich spectrometer. The sources used were isotopically separated and therefore extremely thin. The measured spectrum was corrected for the escape of bremsstrahlung. The extracted shape factor shows only small deviations from the statistical form, the endpoint energy of the decay is 1527 ± 4 keV, its half-life 4.27 ± 0.05 min. The nuclear matrix elements of this $0^- \rightarrow 0^+$ decay have been calculated from single-particle wave functions. The resulting theoretical spectral form describes the experimental data very well, whereas the total transition probability is underestimated theoretically by a factor of 7. (auth)

54649 INVESTIGATION OF SOME LOW-LYING STATES IN ^{208}Pb BY INELASTIC ELECTRON SCATTERING. Friedrich, J. (Univ., Mainz). Nucl. Phys.; A191: No. 1, 118-36(1972).

Differential cross sections for inelastic electron scattering from ^{208}Pb have been measured in the momentum-transfer range from 0.48 fm^{-1} to 1.54 fm^{-1}. The cross sections for the excitation of the 3^- level at 2.6 MeV cannot be reproduced with a modified liquid-drop model using a two-or three-parameter Fermi distribution, but are instead consistent with a phenomenological distribution which consists of two Gaussian functions multiplied with r^{L-1}. The value obtained for the reduced transition probability B(0.624 ± 0.04 b^3) is somewhat different from that determined in earlier electron scattering experiments. The cross sections for the excitation of the two 5^- levels at 3.2 and 3.7 MeV exhibit a striking difference in that the ratios of the cross section in the two first diffraction maxima are different by a factor of 2.5. The cross sections for the excitation of the level at 3.2 MeV can be reproduced with the modified liquid-drop model using a three-parameter Fermi distribution. The value for B is determined to be 0.053 ± 0.014 b^5. The excitation of the level at 3.7 MeV cannot be described by this model. There are strong indications that the transition charge here consists of two regions with opposite sign. (auth)

54650 EFFECTS OF ^{208}Pb CORE VIBRATIONS ON SHELL-MODEL CALCULATIONS FOR ^{211}At AND ^{211}Pb. Ewart, G. M.; Gerace, W. J.; Walker, James F. (Univ. of Massachusetts, Amherst). Nucl. Phys.; A191: No. 3, 596-608(1972).

The low-lying states of ^{211}Pb and ^{211}At are described as three $j = {}^9\!/_2$ particles coupled to each other and to a ^{208}Pb core. The core states are restricted to zero- or one-quadrupole-phonon excitations. All model parameters are determined uniquely from the available experimental data on nuclei having A = 208, 209, 210. The resulting wave functions and energy levels are given. Reduced transition probabilities for E2 transitions between the states of ^{211}At are calculated and compared with experiment. Good agreement is achieved. (2 figures, 5 tables) (auth)

54651 IN-BEAM α SPECTROSCOPY OF N = 128 ISOTONES. LIFETIMES OF ^{216}Ra AND A NEW ISOTOPE ^{217}Ac. Nomura, T.; Hiruta, K.; Inamura, T.; Odera, M. (Inst. of Physical and Chemical Research, Saitama, Japan). Phys. Lett.; 40B: No. 5, 543-5 (7 Aug 1972).

By means of the pulsed-beam technique a new isotope, ^{217}Ac, was found to decay with E_α = 9.65 ± 0.02 MeV and $\tau_{1/2}$ = 0.10 ± 0.01 μs. The half-life of ^{216}Ra was determined to be 0.18 ± 0.03 μs. (auth)

Nuclear Properties and Reactions, A ≥ 220

Refer also to abstracts 53803, 54602, 54607, 54626, 54630, and 54960.

54652 (ANCR-1069) GAMMA RAYS EMITTED BY THE FISSIONABLE NUCLIDES AND ASSOCIATED ISOTOPES. Cline, J. E.; Gehrke, R. J.; McIsaac, L. D. (Aerojet Nuclear Co., Idaho Falls, Idaho). Jul 1972. Contract AT(10-1)-1375. 51p. Dep. NTIS.

Supplement to IN-1448.

New data on gamma-ray energies and intensities emitted in the decay of the nuclides ^{226}Ra, ^{227}Ac, ^{238}U, ^{240}Pu, and ^{241}Pu are presented in this supplement to IN-1448. For sake of completeness, data presented in the previous report are also given in the tables here. (auth)

54653 (CONF-720901-(Bks.1 and 2), pp 81-96) ENERGY-DEPENDENT CROSS SECTIONS IN THE THERMAL REGION. Leonard, B. R. Jr. (Battelle-Northwest, Richland, Wash.). 1972.

From Meeting on new developments in reactor physics and shielding calculations; Kiamesha Lake, NY. (12 Sep 1972).

The interpretation of neutron cross-section data in the thermal neutron energy region is complicated by many physical effects which are unique or intensified in this energy region. The problem which causes the greatest uncertainty in the interpretation of thermal cross sections is the inherent lack of information about the exact nature of the negative-energy resonances. This problem is most severe in the interpretation of fission and scattering cross sections because the limited number of exit channels require that amplitudes, rather than cross sections, be considered. Lack of attention to these coherent effects can lead to severe biases in the derived shapes and values. Simple continuum models of the negative-energy resonances can be used to derive expectation values of their contribution to the thermal cross sections and the uncertainty of that contribution can also be estimated. These considerations have been applied to the interpretation of cross section data for several heavy nuclei. The results of these considerations give estimates of the uncertainties in shapes and values which can be expected in the interpretations of the cross sections. In specific cases these considerations are of value in determining better estimates of the assignments of negative-energy levels and aid in selecting the most probable values from discrepant measurements. They also indicate that further accurate measurements of coherent scattering amplitudes for the fissile nuclei could lead to improved understanding of their cross sections. (auth)

54654 (CONF-720901-(Bks.1 and 2), pp 97-107) PREDICTING PRODUCTION RATES OF HEAVY ACTINIDES. Graves, W. E.; Benjamin, R. W. (Savannah River Lab., Aiken, S. C.). 1972.

From Meeting on new developments in reactor physics and shielding calculations; Kiamesha Lake, NY. (12 Sep 1972).

The prediction of reactor production and depletion rates for the heavy actinides is discussed. Some recent irradiation studies are briefly presented. An improved theoretical framework for making predictions is described. The current status of differential cross section data is surveyed. (J.W.R.)

54655 (CONF-720901-(Bks.1 and 2), pp 687-99) MEASUREMENTS OF DELAYED FISSION NEUTRON SPECTRA OF ^{235}U, ^{238}U, AND ^{239}Pu WITH PROTON RECOIL PROPORTIONAL COUNTERS. Fieg, G. (Kernforschungszentrum, Karlsruhe, Ger.). 1972.

From Meeting on new developments in reactor physics and shielding calculations; Kiamesha Lake, NY. (12 Sep 1972).

The delayed fission neutron spectra of U-235, U-238 and Pu-239 were measured for different time intervals after fission with proton recoil proportional counters. For these measurements, the spectra of the various time groups were determined. 14 MeV neutrons and, for U-235, also thermal neutrons were used to induce fission. Where published experimental group spectra were available, comparisons with these results were made. (auth)

54656 (COO-3058-21) LINEAR ACCELERATOR PROJECT PROGRESS REPORT, APRIL 1, 1972-JUNE 30, 1972. Gaerttner, Erwin R. (Rensselaer Polytechnic Inst., Troy, N. Y.). [nd]. Contract AT(11-1)-3058. 77p. Dep. NTIS.

GOLD-197—neutron capture near 24.3 keV, pulse height spectra and relative cross section for, (E)
HELIUM—neutron total cross section at 0.7 to 30 MeV, (E)
INDIUM—neutron capture near 24.3 keV, pulse height spectra and relative cross section for, (E)
IRON—neutron total cross section at 22 to 25 keV, R-matrix fit to
LITHIUM-6—neutron total cross section at 0.7 to 30 MeV, (E)
SODIUM—neutron emission time in assembly of
TANTALUM-181—neutron capture near 24.3 keV, pulse height spectra and relative cross section for, (E)
URANIUM—neutron transmission and self-indication measurements in depleted
URANIUM-238—neutron capture near 24.3 keV, pulse height spectra and relative cross section for, (E) (L.T.W.)

54657 (FEI-292) MEASUREMENTS OF NEUTRON CROSS SECTIONS OF RADIATION CAPTURE AND FISSION FOR SOME HEAVY NUCLEI BY THE METHOD OF TIME OF RETARDATION IN LEAD. Chelnokov, V. B.; Tolstikov, V. A.; Stavisskii, Yu. Ya.; Bergman, A. A.; Samsonov, A. E. (Gosudarstvennyi Komitet po Ispol'zovaniyu Atomnoi Energii SSSR, Obninsk. Fiziko-Energeticheskii Institut). 1971. 29p. (In Russian). Dep. NTIS (U. S. Sales Only).

A survey was made of cross section measurements of fissions of the nuclei ^{235}U and ^{239}Pu, the cross sections of radiation capture of neutrons by the nuclei ^{107,109}Ag, ^{197}Au, ^{232}Th and ^{238}U and of the parameter α(E) for ^{239}Pu. These measurements had been made with a spectrometer on the moderation time in lead, with the special features of the method in view: absolute standardization of cross sections, energy resolution, and evaluation of the effect of resonance self-shielding. Comparisons of the data with those of other workers are made. (69 references) (auth)

54658 (JINR-P7-6523) NUCLEAR REACTIONS INDUCED BY XENON IONS AND EXPERIMENTS ON SUPERHEAVY ELEMENT SYNTHESIS. Flerov, G. N.; Oganesyan, Yu. Ts. (Joint Inst. for Nuclear Research, Dubna (USSR). Lab. of Nuclear Reactions). 1972. 28p. (In Russian). Dep. NTIS (U. S. Sales Only).

A short review of experimental studies of the mechanism of complex nucleus interactions with the xenon ions is presented. The technique is described and the results of the first experiments on superheavy element synthesis are presented. The set up and the results of the fast experiments on the synthesis of superheavy elements are presented. (auth)

54659 (JINR-P15-6518) AVERAGE PROMPT NEUTRON NUMBER FOR SPONTANEOUS FISSION OF ^{256}Fm. Dakovskii, M.; Lazarev, Yu. A.; Oganesyan, Yu. Ts. (Joint Inst. for Nuclear Research, Dubna (USSR). Lab. of Nuclear Reactions). 1972. 9p. (In Russian). Dep. NTIS (U. S. Sales Only).

The result of measurement of average prompt neutron number for spontaneous fission of ^{256}Fm is given: $\bar{\nu} = 3.73 \pm 0.18$ relative to $\bar{\nu}$ (^{244}Cm) = 2.69 ± 0.02. ^{256}Fm ($T_{1/2}$ = 2.6 hours) was synthesized using the inner beam of the U-300 cyclotron of the Laboratory of Nuclear Reactions (JINR). (auth)

54660 (RLO-2225-T-17-4) MEASUREMENT OF DELAYED NEUTRON ENERGY SPECTRA. Final Report. Woodruff, Gene L. (Washington Univ., Seattle. Dept. of Nuclear Engineering). Jul 1972. Contract AT(45-1)-2225. 12p. Dep. NTIS.

The equipment and techniques developed for the measurement of delayed neutron energy spectra are described. Some results for the thermal neutron fission of ^{235}U are reported. (J.W.R.)

54661 MOESSBAUER EFFECT IN ^{239}Pu. Gal, J. (Nuclear Research Center, Negev, Israel); Hadari, Z.; Bauminger, E. R.; Ofer, S. Phys. Lett.; 41B: No. 1, 53-4(4 Sep 1972).

The recoilless resonance absorption of the 57.3-keV γ-ray of ^{239}Pu was observed. The half-life of the 57.3-keV level was found to be 101 ± 5 ps. (auth)

54662 RADIATIVE CAPTURE OF ENERGETIC NEUTRONS BY ^{208}Pb. Bergqvist, I.; Drake, D. M.; McDaniels, D. K. (Los Alamos Scientific Lab., N. Mex.). Nucl. Phys.; A191: No. 3, 641-57(1972).

The radiative capture cross section of neutrons with energies covering the range 6.2 to 14.7 MeV has been measured for the ^{208}Pb(n,γ)^{209}Pb reaction. Gamma-ray spectra were recorded with a NaI(Tl) anti-Compton spectrometer. A time-of-flight technique was used to reject undesirable background. Absolute cross sections were determined for γ-ray transitions to the $g_{9/2}$ ground state, the $i_{11/2}$ state at 0.78 MeV, the doublet of $j_{15/2}$ and $d_{5/2}$ states near 1.5 MeV, and the close pair of $g_{7/2}$ and $d_{3/2}$ states at about 2.5 MeV in ^{209}Pb. All cross sections show a resonance behavior in accordance with the prediction of semi-direct capture theory as the neutron energy spans the giant-dipole resonance. The measured cross sections are a factor of 2−3 higher than the predicted values. (auth)

54663 TERMINATION OF THE R-PROCESS AND THE SYNTHESIS OF SUPERHEAVY ELEMENTS. Boleu, R. (Univ. of Lund, Sweden); Nilsson, S. G.; Sheline, R. K.; Takahashi, K. Phys. Lett.; 40B: No. 5, 517-21(7 Aug 1972).

Predictions for spontaneous and neutron-induced fission, alpha decay, and beta decay were made on the basis of potential-energy surfaces for Z ≥ 90 nuclei on the neutron-rich side of the beta-stability line. In spite of their considerable quantitive uncertainties, these predictions appear to negate the possibility of superheavy element synthesis via a one- or two-step r process from supernovae. In addition, artificial superheavy element synthesis by two consecutive exploding nuclear devices appears improbable from these results. Neutron-induced fission seems to be even more decisive than spontaneous fission for the early termination of the r process. (auth)

54664 IDENTIFICATION OF A ROTATIONAL BAND IN THE ^{240}Pu FISSION ISOMER. Specht, H. J. (Univ., Munich); Weber, J.; Konecny, E.; Heunemann, D. Phys. Lett.; 41B: No. 1, 43-6 (4 Sep 1972).

Conversion electrons were measured preceding spontaneous fission of the 4-ns ^{240}Pu fission isomer. The more intense lines found are interpreted as components of three E2 transitions within a K = 0^+ rotational band. The large difference between the corresponding rotational constant $\hbar^2/2\theta$ = 3.33 keV and that of the ^{240}Pu ground-state band (7.16 keV) strongly supports the hypothesis of shape isomerism. (auth)

54665 EXCITATION FUNCTION FOR THE ^{235}U(α,3n)^{236}Pu REACTION. Bethune, G. R.; Britt, H. C.; Erkkila, B. H. (Los Alamos Scientific Lab., N. Mex.). Phys. Rev., C; 6: No. 3, 1087-90(Sep 1972).

Cross sections were measured for the ^{235}U(α,3n)^{236}Pu, ^{235}U(α,t)^{236}Np, and ^{235}U(α,f) reactions at several α-particle bombarding energies between 24.5 and 28.0 MeV. (5 figures, 1 table) (auth)

54666 CALCULATIONS OF SPALLATION-FISSION COMPETITION IN THE REACTIONS OF PROTONS WITH HEAVY ELEMENTS AT ENERGIES ≤ 3 GeV. Hahn, R. L.; Bertini, H. W. (Oak Ridge National Lab., Tenn.). Phys. Rev., C; 6: No. 2, 660-9(Aug 1972).

The intranuclear-cascade codes recently discussed by Bertini were modified to include fission-spallation competition in the heavy elements during the evaporation phase of the reaction, and use an empirical, energy-independent relation for (Γ_n/Γ_f). Calculations of the reactions of protons with ^{238}U at several energies from 0.15 to 3.0 GeV, and with ^{235}U and ^{232}Th at 0.7 GeV, have been done to illustrate the results that are obtainable with these codes. The calculations do not allow any adjustment of parameters. However, the range of applicability of the calculations, especially their extension to nuclei (with $Z \lesssim 91$) that are not very fissionable, was investigated by means of the parameter Z_f, below which fission was taken to be relatively unimportant. A Z_f value of 91 was found to give results that agreed best with experimental data. In general, comparison with a large collection of experimental spallation yields, total fission cross sections, and particle multiplicities indicated that the calculations are able to reproduce the trends, and often the details, exhibited by the data. In the case of neutron multiplicities, only the calculations without fission effects agreed with the data, indicating that it is the energy available for evaporation, and not the fission competition, that influences neutron emission. (auth)

54667 INDEPENDENT YIELDS OF KRYPTON AND XENON ISOTOPES IN THERMAL-NEUTRON FISSION OF ^{235}U. OBSERVATION OF AN ODD-EVEN EFFECT IN THE ELEMENT YIELD DISTRIBUTION. Ehrenberg, B.; Amiel, S. (Soreq Nuclear Research Centre, Yavne, Israel). Phys. Rev., C; 6: No. 2, 618-28 (Aug 1972).

The fractional and independent fission yields of krypton isotopes (masses 87 to 94) and xenon isotopes (masses 137−143) produced in thermal-neutron fission of ^{235}U were measured using a mass separator operating in an on-line mode with a fission source exposed to time-controlled neutron fluxes. The noble-gas isotopes were collected simultaneously at given times and each mass was measured separately. The distribution of the isotopic yields of each element was found to be Gaussian, in general agreement with Wahl's estimates. The total independent yields of krypton and xenon, as well as their complementary elements, barium and strontium, were found to indicate an odd-even effect in the element yield distribution. Even-Z elements are formed in higher yields than their odd-Z neighbors (20−50% higher); the even-Z yields are also higher than Wahl's "normal" element yields (~12% higher for Kr and Ba and ~40% for Xe and Sr). Half-life values of 20 nuclides produced in the decay of krypton and xenon isotopes were measured as well. (auth)

54668 EFFECTIVE NEUTRON ABSORPTION CROSS SECTIONS FOR ^{252}Cf AND ^{253}Cf IN THE CENTRAL CHANNEL OF THE SM-2 REACTOR. Anufriev, V. A.; Gavrilov, V. D.; Zamyatnin, Yu. S.; Ivanenko, V. V.; Yakovlev, G. N. At. Energ. (USSR); 32: No. 6, 493-4(Jun 1972). (In Russian).

Two targets containing ^{252}Cf with admixtures of lighter Cf isotopes (~20%) were irradiated in the central channel of the CM-2 reactor for the purpose of determining the effective neutron absorption cross section. The burn-out cross section of ^{252}Cf was 72 ± 18 barns. The effective cross section for neutron absorption for ^{253}Cf was 6,260 ± 1,800 barns; its radiative capture cross section was about 10 barns. (K.S.W.)

54669 BLOCKING EFFECT IN URANIUM FISSION WITH 14-MeV NEUTRONS. Noelpp, U.; Abegg, R.; Schacher, J.; Wagner, R. (Univ., Basel). Helv. Phys. Acta; 45: 55-6 (1972). (In German).

A method for determining the lifetime of the compound nucleus in the (n,2nf) reaction is described. A UO_2 single crystal is oriented by proton blocking. Fission fragments are detected with glass detectors, and the tracks are etched and photographed. The lifetime of the compound nucleus can be determined from a pair of such photographs, taken for different angles between the incoming neutrons and the emitted fragments. (3 figures) (R.W.R.)

54670 SEARCH FOR TRACKS OF SPONTANEOUS FISSION FRAGMENTS FROM THE HEAVIER TRANSURANIUM ELEMENTS IN NATURALLY-OCCURRING MINERALS. Otgonsuren, O.; Perelygin, V. P.; Tret'yakova, S. P.; Vinogradov, Yu. A. At. Energ. (USSR); 32: No. 4, 344-7(Apr 1972). (In Russian).

Naturally occurring minerals and glasses characterized by various hydrothermal histories, such as pegmatite beds, quartz veins, and sulfide occurrences, were examined for the track density and length which would result from fission fragments by spontaneous fission of unstable nuclei. Such fission tracks in cavities on a quartz surface, for example, occurred in a density of 10^4 to 10^5 tracks/cm^2. The distribution of track length in quartz produced by spontaneous fission agreed well with that produced by induced (^{235}U + thermal neutrons) fission. (K.S.W.)

54671 SEARCH FOR (t,p) TRANSITIONS TO EXCITED 0^+ STATES IN THE ACTINIDE REGION. Casten, R. F. (Los Alamos Scientific Lab., N. Mex.); Flynn, E. R.; Garrett, J. D.; (and others). Phys. Lett.; 40B: No. 3, 333-7(10 Jul 1972).

The (t,p) reactions from ^{230,232}Th and ^{234,236,238}U were studied at 15–20 MeV bombarding energy. The known excited 0^+ states in ^{232}Th, ^{236,238}U were not observed nor was any excited 0^+ strength located in ^{234}Th or ^{234}U. The previously reported strong L = 0 (p,t) transitions in this region as well as the weak L = 0 (t,p) strengths reported here constitute a strong indication of the existence of quadrupole pairing correlations in deformed superfluid nuclei. (auth)

54672 PRODUCTION OF ACTINIDES AND THE SEARCH FOR SUPER-HEAVY ELEMENTS USING SECONDARY REACTIONS INDUCED BY GeV PROTONS. Unik, J. P.; Horwitz, E. P.; Wolf, K. L.; (and others) (Argonne National Lab., Ill.). Nucl. Phys.; A191: No. 2, 233-44(1972).

A search for actinide and super-heavy elements produced by means of secondary reactions during the irradiation of tungsten and uranium targets with 12 and 28 GeV protons has been made. Yields for production of many actinide isotopes in uranium targets are given up to and including ^{248}Cf. Upper limits have also been established for spontaneous fission activities which could be attributed to the decay of possible super-heavy elements produced by means of secondary reactions. (auth)

54673 DECAY OF ^{227}Th FROM $\alpha-\gamma$ COINCIDENCE AND DIRECTIONAL CORRELATION STUDIES. Hesselink, W. H. A.; Wapstra, A. H.; Kromme, J. G. (and others) (Univ. of Tech., Delft, Netherlands). Nucl. Phys.; A191: No. 2, 294-304(1972).

Using ^{227}Th sources obtained by evaporation of the activity onto Al foils, α-γ coincidences and α-γ directional correlations have been measured employing Ge(Li) and silicon surface-barrier detectors. A decoupling experiment using a superconductive magnet of 1.5 Tesla has been carried out to investigate the attenuation of the α-γ directional correlations due to extranuclear effects. Of the about 100 γ-rays observed (20 of them for the first time), all but 6 have been placed in a decay scheme. The directional correlation data have led to several new spin assignments and to the confirmation of earlier tentative assignments. The relative α-particle intensities and the α-γ directional correlation results show that the L = 2 intensities in the favored α-decay to the different levels of the $3/2^+$ [631] band are uncommonly weak, indicating a limitation to the applicability of the Nilsson model at low excitation energy. (auth)

54674 EMISSION OF THE ^{5}He IN THE SPONTANEOUS FISSION OF ^{252}Cf. Cheifetz, E. (Weizmann Inst. of Science, Rehovot, Israel); Eylon, B.; Fraenkel, E. Gavron, A. Phys. Rev. Lett.; 29: No. 12, 805-8(18 Sep 1972).

The emission of ^{5}He($T_{1/2} = 8 \times 10^{-22}$ s for decay into α + n) in spontaneous fission of ^{252}Cf is established from a correlation measurement involving the direction and the kinetic energies of the neutrons and the long-range α particles. Approximately 11% of these α's are products of ^{5}He breakup. The initial energy of the fragments and of the ^{5}He at scission are calculated from the properties of the ^{5}He decay. They are 31 ± 11 and 3.2 ± 0.9 MeV, respectively. (auth)

Nuclear Theory

Refer also to abstracts 54238, 54382, 54600, 55061, 55063, and 55077.

54675 (BNL-17029) RADIATIVE DECAY OF NEUTRON-RESONANT STATES. Chrien, R. E. (Brookhaven National Lab., Upton, N. Y.). 1972. 30p. (CONF-720701-2). Dep. NTIS.

From Conference on nuclear structure studies with neutrons; Budapest, Hungary (29 Jul 1972).

Ways in which neutrons are employed to investigate the radiative decay of highly-excited nuclear states are discussed. Neutron capture γ-rays are useful for spin and parity assignments for such states, as well as providing some insight into the capture reaction mechanism. Recent capture γ-ray experiments and threshold photoneutron studies bear on the distribution of radiative strength with excitation energy. Intermediate structure in photon strength functions leads to an interpretation in which doorway states play an important role. Recent experiments relative to these topics are described. (auth)

54676 (CONF-720901-(Bks.1 and 2), pp 1087-1106) FISSION CROSS SECTIONS AND THE FISSION PROCESS. Michaudon, Andre (CEN de Saclay, Gif-sur-Yvette, France). 1972.

From Meeting on new developments in reactor physics and shielding calculations; Kiamesha Lake, NY. (12 Sep 1972).

The Strutinsky prescription for fission barrier calculations is discussed. This new method for more accurate calculations of the fission barriers, taking into account the effect of shells at all deformations, has provided a better understanding of the fission process. Puzzling experimental results, such as fission isomers and intermediate structure, that remained previously unexplained with conventional models, could then be interpreted in terms of double-humped barrier shapes. This is quite important for the understanding and for the predictions of the fission cross sections. Near threshold, vibrational fission resonances can appear; below threshold, intermediate structure can exist and influence the fission cross section for thermal neutrons; the intermediate structure effect can also be present, though weaker, in the fission cross section of fissile nuclei. (auth)

54677 (CONF-720701-3) OPTICAL MODEL. Satchler, G. R.; Perey, F. G. (Oak Ridge National Lab., Tenn.). [nd]. 56p. Dep. NTIS.

From International conference on nuclear structure study with neutrons; Budapest, Hungary (31 Jul 1972).

Recent applications of the optical model (the local version, except in one case) to various measurements involving neutrons are reviewed. (W.D.M.)

54678 (COO-535-672) REMARKS ON ABSORPTIVE POTENTIALS AND HEAVY ION ELASTIC SCATTERING. Rickertsen, L. D. (Colorado Univ., Boulder. Nuclear Physics Lab.). [nd]. 10p. Dep. NTIS.

The nature of the gross structure in the optical model analysis of heavy ion elastic scattering is investigated. Further, the success of the double-resonance effect in reproducing intermediate structure is studied. (auth)

54679 (COO-3001-17) MAGNETIC MOMENTS OF ODD MASS NUCLEI WITH SIMPLE CONFIGURATIONS. Arima, Akito; Huang-Lin, Lih Jen (State Univ. of New York, Stony Brook. Dept. of Physics). 1972. 13p. Dep. NTIS.

Results of calculations for magnetic moments of odd A nuclei using simple shell model configurations are presented. The effects of core polarization and the mesonic current were accounted for First order perturbation theory was used to estimate the deviation due to core polarization. It was found that while in sum cases the sum of the two corrections is desirable, the two mechanisms strongly cancel in the magnetic moments of $j = l + 1/2$. Also some recently measured magnetic moments in the A = 208 region are not explained if the mesonic correction is taken into account. (J.W.R.)

54680 (COO-3071-7) SIMPLIFIED MICROSCOPIC MODEL OF THE CORIOLIS ANTI-PAIRING TRANSITION. Vallieres, Michel; Klein, Abraham; Dreizler, R. M. (Pennsylvania Univ., Philadelphia. Dept. of Physics). 12 Jun 1972. Contract AT(11-1)-3071. 16p. Dep. NTIS.

The pairing plus quadrupole–quadrupole interaction is studied for a single j level by a sum rule method ("current algebra") in the regime where the "nucleus" is deformed. The ground state rotational band is shown to undergo the Coriolis anti-pairing transition. (auth)

54681 (COO-3071-9) ALGEBRAIC APPROACH TO THE THEORY OF COLLECTIVE MOTION: SPHERICAL TO DEFORMED TRANSITION IN THE SINGLE-j SHELL. Vallieres, Michel; Klein, Abraham; Dreizler, R. M. (Pennsylvania Univ., Philadelphia. Dept. of Physics). 20 Jul 1972. 55p. Dep. NTIS.

The program of the algebraic approach to nuclear collective motion is summarized. In essence, it should permit an accurate solution of the many-body problem within a subspace of the many particle space if the conditions defining collective motion are present. The formulation, containing both dynamical and kinematical aspects, leads to coupled non-linear algebraic equations for the matrix elements between collective states of fermion pair operators. An explicit set of equations is given for the problem of N (even) particles confirmed to a single-j-shell and described by the conventional pairing plus quadrupole–quadrupole interaction Hamiltonian. This formulation is designed to be nearly exact in the pairing dominant (seniority) limit and to be accurate enough (based on plausibility arguments) to describe the transition from spherical to deformed shape. That this is so is verified for configurations—the largest being $j^N = (21/2)^6$—for which exact solutions are available. The present method can be viewed as an angular momentum conserving alternative to the description of the transition based on the Hartree–Bogoliubov-BCS method. Qualitative and detailed comparisons of the two methods are carried out. In particular, it is shown from approximate analytic results that the two theories predict the transition to occur for almost identical values of the parameters. Overall agreement with exact results is much better for the algebraic method, however, confirming its status as an approximate method of variation after projection. (auth)

54682 (COO–3071-10) CONCEPT OF TRANSITION OPERATOR BOSON AND ITS APPLICATION TO AN EXACTLY SOLUBLE MODEL. Dreizler, R. M.; Klein, Abraham (Pennsylvania Univ., Philadelphia. Dept. of Physics). 5 Jul 1972. 34p. Dep. NTIS.

In phenomenological descriptions of nuclear vibrations a close connection is implied or expressed between the most collective transition operator and the harmonic oscillator (boson) variables which are introduced to describe the collective motion. With the help of a widely used example—the monopole vibration model of Meshkov, Lipkin, and Glick—it is shown how this relationship suggests, for the microscopic case, a new and flexible class of boson representations. As shown, these are capable of yielding accurate descriptions of the system, not only in the extremes of weak and strong coupling, but also in the usually more inaccessible intermediate regions as well. (6 figures, 3 tables) (auth)

54683 (FRNC-TH–180) REALISTIC NONLOCAL FORCES AND THEIR IMPORTANCE IN UNDERSTANDING THE MICROSCOPIC PROPERTIES OF NUCLEAR MATTER AND NUCLEI. Hammann, T. F. (Strasbourg Univ. (France)). 1970. 120p. (In French).

Thesis.

A realistic potential which is separable and nonlocal and takes into consideration phase shifts in the S, P and D waves up to 400 MeV is presented. The discrepancies between the calculated and the experimental phase shift curves are of the same order of magnitude as the experimental errors. This potential is without short-range singularity and sufficiently uniform to ensure an adequate convergence in the perturbation series. The potential gives a binding energy of −15.5 MeV (1st-order approximation) per particle at the saturation density (1.45 fm^{-1}), which is in agreement with experiment. When a second-order approximation is used, the agreement disappears, a considerably larger binding energy being obtained which is of the same order of magnitude as that obtained using the G reaction matrix. This potential enables the negative-parity spectra of ^4He to be explained. The ^{18}O, ^{19}O, and ^{20}O levels calculated in the framework of classical shell model with this potential and the reaction matrix deduced from the Hartree–Fock potential compare quite well with experiment, except in the case of ^{20}O, where the model used is less accurate. The spectra of nuclei in the A = 50 region were studied. In the case of ^{50}Sc, it is shown that the inclusion of the most probable 1 particle–hole configurations is equivalent to the 3 particle–1 hole perturbation correction. (France)

54684 (IAE–2115) STUDY OF SOME PROPERTIES OF STRUTINSKII'S "METHOD OF SHELL CORRECTION." Pik-Pichak, G. A.; Grechukhin, D. P. (Institut Atomnoi Energii, Moscow (USSR)). 1971. 36p. (In Russian). Dep. NTIS (U.S. Sales Only).

Various properties of the "shell correction method" were investigated on the basis of S. G. Nilsson's model (1955). A shell correction proved to be very sensitive to a scheme of single-particle states. If a "realistic" scheme of levels arises from Nilsson's scheme through a shift of one of several levels, then the shell correction method ceases to be applicable. Averaging the nuclear masses, as is done for the determination of parameters for the drop model, and averaging according to single-particle states in the shell correction method, both lead to means which differ by 3 to 4 MeV. (tr-auth)

54685 (INP–795) INTERMEDIATE COUPLING APPROACH IN THE UNIFIED MODEL OF THE ^{39}K NUCLEUS. Wiktor, S. (Institute of Nuclear Physics, Krakow (Poland)). Mar 1972. 16p. Dep. NTIS (U. S. Sales Only).

The low energy levels of the ^{39}K nucleus are examined in the framework of the intermediate coupling model in which the $(d_{3/2})^{-1}$ proton hole is assumed to couple to the 2^+, 3^- and 5^- core states of the doubly magic ^{40}Ca nucleus. Comments concerning the parameters are made. In particular the coupling strength parameters are related to the dynamical deformation parameters obtained in coupled channels analysis of the inelastic scattering processes. (auth)

54686 (INR–1406) FRACTIONAL PARENTAGE COEFFICIENTS FOR j = $^{11}/_2$ ORBITAL. Kerek, A.; Kownacki, Jan (Institute of Nuclear Research, Warsaw (Poland)). 1972. 6p. Dep. NTIS (U.S. Sales Only).

The normalized sets of the fractional parentage coefficients $[j^2(J_1)jJ\{|j^3\ VJ]$ for $(j = {}^{11}/_2)^3$ configuration in j–j coupling are calculated. (auth)

54687 (ISS–71/29) INVESTIGATION OF SHORT-RANGE CORRELATIONS IN NUCLEI BY MEANS OF HIGH ENERGY ELECTRON SCATTERING. Ciofi Degli Atti, C. (Istituto Superiore di Sanita, Rome (Italy). Laboratori di Fisica). 8 Oct 1971. 19p. (CONF-710911–15). Dep. NTIS (U. S. Sales Only).

From fourth international conference on high energy physics and nuclear structure; Dubna, USSR (7 Sep 1971).

The present status of the study of short-range correlations in nuclei by means of high energy electron scattering is briefly reviewed. Particular attention is devoted to the recently discussed problem of the effects of Brueckner and Jastrow correlations on the charge form factor of light nuclei. (auth)

54688 (ITF–71-77-P) PRESENT-DAY PROBLEMS OF THE THEORY OF NUCLEAR FORCES. Babikov, V. V.; Pak Ben Gir (Akademiya Nauk Ukrainskoi SSR, Kiev. Institut Teoreticheskoi Fiziki). 1971. 17p. (In Russian). Dep. NTIS (U. S. Sales Only).

Brief discussion is presented on the following present-day problems of the theory of nuclear forces: the relativistic description of the two-nucleon interaction, the coupling of channels, and many-particle effects. (auth)

54689 (ITF–72-12-P) VIBRATIONS OF A FERMI-FLUID DROP AND THE GIANT RESONANCE IN INTERMEDIATE AND HEAVY NUCLEI. Akhiezeri, I. A.; Barts, B. I.; Lazurik-El'tsufin, V. T. (Akademiya Nauk Ukrainskoi SSR, Kiev. Institut Teoreticheskoi Fiziki). 1972. 14p. (In Russian). Dep. NTIS (U. S. Sales Only).

The giant resonance in nuclear reactions with the participation of intermediate and heavy nuclei is considered in the model of a Fermi-fluid drop. Both the purely nuclear and electric interactions of nucleons are taken into account. This model enables one to describe the experimentally observed position of a giant dipole resonance in photonuclear reactions in a great number of particles. In particular, it is possible to account for the slower decrease in resonance energy with increasing A than that according to the law $A^{-1/3}$ for a fluid. A number of experimental points do not fit the curve corresponding to the excitations of dipole vibrations, but come near the estimated curves corresponding to l = 0 and l = 2. It should be of great interest, therefore, to experimentally determine the multipolarity appropriate levels. (auth)

54690 (ITF–72-57-P) HIGH-ENERGY APPROXIMATION AND THE GENERALIZED HUYGEN'S PRINCIPLE. Sitenko, A. G.; Peresypkin, V. V. (Akademiya Nauk Ukrainskoi SSR, Kiev. Institut Teoreticheskoi Fiziki). 1972. 14p. (In Russian). Dep. NTIS (U. S. Sales Only).

The solution of the Lippman–Schwinger equation was investigated within the framework of high-energy approximation. It is proved that the solution of the Lippman–Schwinger equation in the high-energy approximation satisfies the generalized Huygen's principle used in the diffraction theory nuclear processes. The diffraction emission is considered in the interaction of charged hadrons one with another and the nuclei. (auth)

54691 (JINR–P2-6539) ON THE CALCULATION OF ABSORPTION IN NEUTRAL PION COHERENT PHOTOPRODUCTION ON NUCLEI. Pak, A. S.; Tarasov, A. V. (Joint Inst. for Nuclear Research, Dubna (USSR). Lab. of Nuclear Problems). 1972. 8p. (In Russian). Dep. NTIS (U. S. Sales Only).

The more accurate calculation of the absorption in process of neutral pion coherent photoproduction on nuclei is shown to allow the removal of the discrepancy between the upper boundary of the module square of the spin independent part of the amplitude of the $\gamma N \rightarrow \pi^0 N$ process and the value of this quantity obtained from the experimental data analysis according to theoretical formulas. (auth)

54692 (JINR–P4-6543) FOR A BASING OF A CRANKING-MODEL. Dzholos, R. V.; Kartavenko, V. G. (Joint Inst. for Nuclear Research, Dubna (USSR). Lab. of Theoretical Physics). 1972. 15p. (In Russian). Dep. NTIS (U. S. Sales Only).

The dynamic variables, which are parameters of a symmetry group of a Hamiltonian of a fermion system, have been selected using a finite boson representation of fermion operators and

Bogolubov's transformation in a theory of a strong coupling. The obtained Hamiltonian is handy for describing nuclear rotational motion both when an average field is axial symmetric and when it's not. In the case of an axial symmetry this Hamiltonian is equal to a cranking-model Hamiltonian. (auth)

54693 (LA-DC-72-954) NUCLEAR WAVE FUNCTIONS FROM PARTICLE TRANSFER DATA. Kisslinger, Leonard S. (Carnegie-Mellon Univ., Pittsburgh, Pa. Los Alamos Scientific Lab., N. Mex.). [nd]. 11p. (CONF-720819-6). Dep. NTIS.

From International conference on few particle problems in nuclear interactions; Los Angeles, CA. (28 Aug 1972).

The extraction of information on the particle structure of nuclei from particle transfer reactions is discussed. An approach which uses improved representations of the scattering amplitude in order to include cut corrections is described. The application of the method to low energy nuclear physics for the calculation of spectroscopic factors and its extension to high energy to determine high momentum components of nuclear wave functions is illustrated. (J.W.R.)

54694 (LBL-972) COMMON FEATURES AND DIFFERENCES BETWEEN FISSION AND HEAVY ION PHYSICS. Swiatecki, W. J. (California Univ., Berkeley. Lawrence Berkeley Lab.). Jun 1972. Contract W-7405-eng-48. 14p. (CONF-720634-1). Dep. NTIS.

From first topical European nuclear physics conference; Aix-en-Provence, France (26 Jun 1972).

The macroscopic approach to fission and fusion physics is formulated. A minimum set of three degrees of freedom is described qualitatively. The gross features of the potential energy in this configuration space are discussed. The problem of nuclear viscosity is mentioned and comparisons with liquid ^{3}He are made. Some effects of large angular momenta are described. (auth)

54695 (LYCEN-7213) DWBA ANALYSIS OF SUB-COULOMB MULTI-TRANSFER REACTIONS. El Baz, E.; Meyer, J.; Nahabetian, R.; Pigeon, J. (Lyon Univ. (France). Institut de Physique Nucleaire). Feb 1972. 19p. Dep. NTIS (U. S. Sales Only).

The DWBA analysis of the heavy-ion-induced transfer reaction is usually made by approximating the recoil effect. Its validity is based on the fact that the mass of the transferred particle is small compared to the mass of the cores. A method allowing an exact treatment is proposed, and the only change comes from the radial integral which becomes a two-fold integral while the geometrical part is easily expressed in a graphical manner. (France)

54696 (ORNL-TM-3951) DEFORMED RENORMALIZED BRUECKNER-HARTREE-FOCK APPROXIMATION AND ITS APPLICATION TO ^{12}C. Becker, Richard L.; Braley, R. C.; Ford, W. F.; Patterson, M. R. (Oak Ridge National Lab., Tenn.). Sep 1972. Contract W-7405-eng-26. 12p. Dep. NTIS.

The renormalized Brueckner-Hartree-Fock theory is generalized to permit calculation of deformed intrinsic states with realistic nuclear forces. In ^{12}C the Hamada-Johnston interaction gives nearly large enough deformations and good binding, size, and intrinsic separation energies. Angular momentum projection from the oblate state yields moments, B(EL)'s, and electron scattering form factors with big enhancements over rigid rotor values, and substantiates that the 14.1 MeV, 4^{+} state is rotational without requiring such a large intrinsic hexadecapole moment. (auth)

54697 (ORO-4317-7) SENSITIVITY OF LOW-ENERGY 3-BODY PROPERTIES TO THE OFF-SHELL 2-BODY t-MATRIX. Technical Report No. 72-121. Lavine, J. P.; Mukhopadhyay, S. K.; Stephenson, G. J. Jr. (Maryland Univ., College Park. Dept. of Physics and Astronomy). 1972. 18p. Dep. NTIS.

Direct modifications are made to the off-shell two-body t-matrices which are used as input to the Faddeev-Lovelace equations for the three-body bound state and for scattering below breakup. The t-matrices are modified when either momentum argument exceeds a particular value, in a manner consistent with off-shell unitarity. In this way, it is possible to test the dependence of these three-body properties on different regions of the off-shell momenta. A strong sensitivity for both momenta less than 2 f^{-1}; weak, potential dependent sensitivity when either argument is between 2 and 5 f^{-1}, and essentially no dependence if either argument exceeds 5 f^{-1} was found. (auth)

54698 (ORO-4317-8) GEL'FAND-LEVITAN-UNITARY-TRANSFORM FORMALISM FOR DIRECT EXTENSION OF THE TWO-NUCLEON T MATRIX OFF THE ENERGY SHELL. Technical Report No. 73-001. Picker, H. S.; Lavine, J. P (Maryland Univ., College Park. Dept. of Physics and Astronomy). 1972. 28p. Dep. NTIS.

The unitary-transform method of Coester et al. is modified, for uncoupled partial waves in which there are no bound states, so that empirical phase shifts rather than a potential fitted to them may be used as the basic input. This is accomplished by invoking the Gel'fand-Levitan inverse scattering formalism to generate a complete orthonormal set of scattering wave functions from the phase shifts. The result is a convenient formal framework for analyzing the uncertainties in the off-energy-shell behavior of the two-nucleon interaction. Variations in the off-energy-shell T matrix arising from changes in the phase shifts, as well as those due to different short-range nonlocalities, may be studied directly using the method presented here. (auth)

54699 (ORO-4317-11) (p,2p) REACTIONS WITH DIVERS POTENTIALS. Technical Report No. 73-002. Stephenson, G. J. Jr.; Redish, Edward F.; Lerner, Gerald M.; Haftel, M. I. (Maryland Univ., College Park. Dept. of Physics and Astronomy). 1972. 20p. Dep. NTIS.

The p-p cross sections relevant to a factorized impulse approximation treatment of (p,2p) reactions from 150 MeV to 350 MeV were calculated. Several on-shell prescriptions were used and compared with the half-off-shell prescription suggested by the Faddeev-Watson multiple scattering series. Four phenomenological potentials, Hamada-Johnston, Bryan-Scott III, Reid Hard Core, and Reid Soft Core, were investigated as well as three potentials which are phase-shift equivalent to the Reid Soft Core potential. Significant differences were found between the various prescriptions for all of the potentials. A wide range was also observed in the predictions of the various phenomenological potentials for each prescription. However, the ratio of the half-shell cross section to the on-shell cross section is remarkably insensitive to the choice of potential, especially where the half shell prescription is needed. This suggests a simple method for extrapolating from the elastic scattering data to the appropriate half-shell cross section. (auth)

54700 (RT/FI-(72)6) FAST NEUTRON RADIATIVE CAPTURE CROSS SECTIONS OF STABLE NUCLEI WITH $29 \leq Z \leq 79$. Benzi, V.; D'Orazi, R.; Reffo, G.; Vaccari, M. (Comitato Nazionale per l'Energie Nucleare, Rome (Italy)). 22 Feb 1972. 335p. Dep. NTIS (U.S. Sales Only).

The results of a semi-empirical estimate of fast neutron radiative capture cross sections of all stable nuclei with $29 \leq Z \leq 79$ in the energy range 1 keV to 10 MeV are given in this report. The calculations were carried out on the basis of the Hauser-Feshbach-Margolis statistical model; direct and collective capture and (n,2γ) process were also taken into account by means of simplified models. (auth)

54701 (RT/FI-(72)7) MARE: A FORTRAN IV CODE FOR COMPOUND NUCLEUS REACTION CALCULATIONS IN THE CONTINUUM. Reffo, G.; Vaccari, M. (Comitato Nazionale per l'Energia Nucleare, Rome (Italy)). 20 Mar 1972. 53p. Dep. NTIS (U. S. Sales Only).

The physical model and the FORTRAN IV program for compound nucleus reaction calculations in the continuum are described in this report. The adopted model takes into account up to three particle emissions and γ rays deexcitation is considered as a process competing with the evaporation of particles (neutrons, protons, alpha particles). (auth)

54702 RELATIONS AMONG MAGNETIC MOMENTS AND M1 RATES IN SINGLE-CLOSED-SHELL NUCLEI. Nomura, M. (Tokyo Univ.). Phys. Lett.; 40B: No. 5, 522-4(7 Aug 1972).

Under the assumption that the effective magnetic moment operator is expressed in terms of one- and two-body operators which are not explicitly specified, relations among magnetic moments and M1 rates in single-closed-shell nuclei are studied. (auth)

54703 MOESSBAUER TRANSMISSION AND SCATTERING FOR ARBITRARY POLARIZATIONS. Chrisman, B. L. (Univ. of Illinois, Urbana). Nucl. Phys.; A186: No. 2, 264-72(1972).

Polarization effects in Mössbauer experiments are discussed using an S-matrix and density-matrix formalism. Equations are derived for both Mössbauer transmission and scattering. The generality of the formalism is demonstrated by extending the discussion to include interference between Mössbauer and electronic scattering. (auth)

54704 NUCLEAR DENSITIES IN A MODEL WELL OF ARBITRARY SHAPE. Bonche, P. (CEN, Saclay, Gif-sur-Yvette, France). Nucl. Phys.; A191: No. 3, 609-26(1972).

A method of calculation of the nuclear densities of deformed heavy nuclei is proposed. The density is expressed in terms of the Green function which is replaced by its multiple reflection expansion. The contribution to the density of the first terms of this expansion is given. The method is tested in the case of an infinite spherical square well for which the exact calculation is elementary. The agreement gives confidence in the proposed approximation for the densities of deformed heavy nuclei. (auth)

54705 INCOMING WAVE BOUNDARY CONDITION FOR ELASTIC SCATTERING OF HEAVY PARTICLES AT INCIDENT ENERGIES NEAR THE COUPLOMB BARRIER. Eisen, Y.; Vager, Z. (Weizmann Inst. of Science, Rehovot, Israel). Nucl. Phys.; A187: No. 1, 219-24(1972).

An incoming wave boundary condition (IWB) approach is used to calculate differential cross sections for ^{16}O + Ca and α + Pb elastic scattering, at incident energies near the Coulomb barrier. A comparison is made to optical model (OM) calculations and it is shown that the present method is competitive with the OM method in the energy region mentioned above. (auth)

54706 DWBA TREATMENT OF CLUSTER TRANSFER REACTIONS. Kubo, K.-I. (Tokyo Univ.); Hirata, M. Nucl. Phys.; A187: No. 1, 186-204(1972).

The cluster transfer reaction (^{6}Li,d), (^{7}Li,t), (^{3}He,^{7}Be) etc., are investigated in the framework of DWBA with a finite-range interaction. It is proposed how to determine the available wave functions of Li and Be, and the effective interaction that causes the transfer reaction. An additional approximation is discussed to simplify the numerical calculation. The validity of DWBA is tested by a comparison of the results of numerical calculations of the processes (^{6}Li,d) and (^{7}Li,t) with experiment. (auth)

54707 KNOCK-ON MECHANISM FOR (n,α) REACTIONS INDUCED BY FAST NEUTRONS ON THE DEFORMED DOUBLY EVEN NUCLEI. Kozlowski, M.; Glowacka, L.; Jaskola, M.; (and others) (Univ., Warsaw Inst. of Nuclear Research, Warsaw). Nucl. Phys.; A187: No. 1, 177-85(1972).

A method for the calculation of the energy distribution of α-particles from the (n,α) reaction on deformed doubly even nuclei is developed. The Feynman triangular diagram is used for the calculation. The resulting energy distributions for the 14-MeV (n,α) reactions in ^{160}Dy, ^{162}Dy, ^{164}Dy, ^{166}Er and ^{168}Er are compared with the experimental data. The agreement suggests the dominance of the knock-on mechanism in the investigated reactions. (auth)

54708 FINITE-RANGE DWBA ANALYSES OF THE ^{16}O(^{7}Li,t) ^{20}Ne AND ^{15}N(^{7}Li,t)^{19}F REACTIONS. Kubo, K.-I. (Tokyo Univ.). Nucl. Phys.; A187: No. 1, 205-18(1972).

The reactions ^{16}O(^{7}Li,t)^{20}Ne and ^{15}N(^{7}Li,t)^{19}F at $E_{^7Li}$ = 15 MeV, are analyzed theoretically by the DWBA method with a finite-range interaction. On basis of the weak coupling model for the nuclear structure, the differential cross sections are calculated, and the validity of this model is tested by comparing with experimental data. The spectroscopic factors for 4p-0h states are extracted. (auth)

54709 LIMITATION ON THE USE OF IMPULSE APPROXIMATION IN NUCLEAR β-DECAY. Armstrong, L. Jr.; Kim, C. W. (Johns Hopkins Univ., Baltimore). Phys. Lett.; 41B: No. 1, 39-42(4 Sep 1972).

Nuclear β-decay processes are considered using two techniques: the usual impulse approximation and the elementary-particles treatment. Both methods of calculation are shown to lead to essentially equivalent numerical results for allowed transitions ($\Delta J^{P_iP_f}$ = $0^+,1^+$) and for forbidden transitions of the types $\Delta J^{P_iP_f} = 1^-$ and possibly $2^+,3^-,\ldots$. For forbidden transitions of the types, $\Delta J^{P_iP_f}$ = $0^-,2^-,3^+,\ldots$, the two methods may lead to inequivalent results. This discrepancy may be due to neglect of meson-exchange effects in the impulse approximation. (auth)

54710 EXTENSION OF THE VARIABLE MOMENT OF INERTIA MODEL TO ODD–EVEN NUCLEI. Volkov, A. B. (McMaster Univ., Hamilton, Ont.). Phys. Lett.; 41B: No. 1, 1-3(4 Sep 1972).

The variable-moment-of-inertia model is shown to be applicable to odd–even nuclei when Coriolis-coupling effects are small. Under appropriate circumstances the odd–even moments of inertia should be nearly equal to those of an adjoining even–even nucleus. (auth)

54711 FORWARD DISPERSION RELATIONS AND LOW-ENERGY ELASTIC SCATTERING OF CHARGED PARTICLES FROM NUCLEI. Viollier, R. D.; Plattner, G. R.; Trautmann, D.; Alder, K. (Univ., Basel). Phys. Lett.; 40B: No. 6, 625-7(21 Aug 1972).

A forward dispersion relation for charged-particle scattering from nuclei is deduced. Inclusion of the Coulomb interaction leads to a simple modification of the formalism for uncharged projectiles. The modified forward dispersion relation is applied to p–α scattering below 50 MeV. (auth)

54712 PHENOMENOLOGICAL DESCRIPTION OF THE NUCLEAR ROTATIONAL STATES. Stockmann, M. I.; Zelevinsky, V. G. (Inst. of Nuclear Physics, Novosibirsk, USSR). Phys. Lett.; 41B: No. 1, 19-22(4 Sep 1972).

General properties of a class of phenomenological models generalizing the VMI model are considered, as well as their applicability to the numerical description of the ground-state bands and possible relation to the microscopic theory. (auth)

54713 ELECTROMAGNETIC CORRECTIONS OF ORDER $Z\alpha^2$ AND $Z^2\alpha^3$ TO FERMI β-DECAYS. Jaus, W. (Univ., Zurich). Phys. Lett.; 40B: No. 6, 616-21(21 Aug 1972).

Electromagnetic corrections of order $Z\alpha^2$ and $Z^2\alpha^3$ to pure Fermi decays are discussed and used to calculate the effective ft values of seven $0^+ \rightarrow 0^+$ β transitions. These fall into two groups which differ by about 1.5%. (auth)

54714 DAMPING OF HOLE STATES IN THE GIANT DIPOLE RESONANCE. Kabachnik, N. M.; Sagina, I. P. (Inst. of Nuclear Physics, Moscow). Phys. Lett.; 41B: No. 1, 31-3(4 Sep 1972).

Widths of hole states can be naturally included in the particle–hole calculation scheme if the factorization method is employed. (auth)

54715 APPLICATION OF THE METHOD OF MOMENTS TO THREE-BODY SCATTERING. Harms, E. (Fairfield Univ., Conn.). Phys. Lett.; 41B: No. 1, 26-8(4 Sep 1972).

The method of moments is investigated as a possible iterative method of solution of the Faddeev equations. The method is shown to converge rapidly to the three-body wave function for the case of zero-energy neutrons scattering off deuterium. It is suggested that the method should be appropriate for the treatment of three-body break-up with separable or local potentials. (auth)

54716 TRIANGLE GRAPHS AND ISOSPIN VIOLATION IN 3-PARTICLE FINAL-STATE REACTIONS. Beam, J. E.; Valkovic, V. (Rice Univ., Houston, Tex.). Phys. Lett.; 41B: No. 1, 13-15 (4 Sep 1972).

The rescattering process for a 3-particle final-state reaction represented by a triangle diagram should lead to isospin violation. This effect is due to the possibility of kinematically selecting one triangle-graph rescattering process in favor of its charge conjugate. (auth)

54717 INTERMEDIATE-STATE, SINGLE-PARTICLE ENERGIES IN MANY-FERMION ENERGY CALCULATIONS. Baker, George A. Jr. (Brookhaven National Lab., Upton, N. Y. Cornell Univ., Ithaca, N. Y.); Gammel, John L. Phys. Rev., C; 6: No. 2, 403-7(Aug 1972).

It is shown that the naive solution of the two-hole-line-approximation equations for the many-fermion ground-state energy leads to physically incorrect results. As poles cross the integration contour, residue corrections must be appended to the equations. Unfortunately, the corrected equations do not appear to be solvable for nuclear-type potentials. (auth)

54718 APPROACH TO THE NUCLEAR MANY-BODY PROBLEM BY VARIATIONALLY DETERMINED TRANSFORMATION. II. Mann, A. (Hebrew Univ., Jerusalem. Indiana Univ., Bloomington); Unna, I.; Gross, R. Phys. Rev., C; 6: No. 2, 415-25(Aug 1972).

A generalization of the Hartree–Fock (HF) method incorporating two-body correlations is presented. The correlations are introduced by means of a unitary operator e^{iF}, where F is a Hermitian one- and two-body operator to be determined by the variational principle. Assuming that the matrix elements of F are small so that powers of F higher than the second may be neglected, a set of linear equations determining F is obtained. The relation between the method and methods used to treat singular interactions is discussed. The method is applied to two recently suggested models and is compared with the HF method, second-order perturbation theory, and with the random-phase approximation. It is found that the method yields very good results within the range of validity of the approximations, which seems to call forth applications to more realistic problems. Possible applications to the study of collective phenomena in nuclei are indicated. (auth)

54719 IRROTATIONAL OR ROTATIONAL FLOW MOTION IN DEFORMED NUCLEI. Gupta, Raj K. (International Centre for Theoretical Physics, Trieste, Italy). Phys. Rev., C; 6: No. 2, 426-35(Aug 1972).

The "governor model" of Trainor and the author, based on the assumptions of a rotational flow motion and the existence of a rotationally invariant core in nuclei, is completely reformulated in terms of the better-known deformation parameter β_0. It is shown that this model results in an expression for the ground-state moment of inertia which, in agreement with the empirical study of Mariscotti et al. (the variable-moment-of-inertia model), gives a linear dependence on the deformation parameter ($g^{(0)} \propto \beta_0$). The hydrodynamical model, based on the irrotational flow motion and using the condition $g^{(0)} \propto \beta_0^2$, is also reformulated to include all the higher-order corrections to the J(J + 1) law. Both the models are then applied to all the even–even nuclei in the mass regions 152 ≤ A ≤ 188 and A ≥ 224, and the results are compared with experiment. The discussion is restricted to the ground-state rotational bands only. In addition to the rotational-state energies and the ground-state moment of inertia, other nuclear properties, such as the variation of the moment of inertia and the quadrupole moment with the angular momentum, are also investigated. (auth)

54720 UNCERTAINTY IN THE NEUTRON-STRENGTH-FUNCTION EVALUATION FOR A SMALL NUMBER OF MEASURED RESONANCES. Liou, H. I.; Rainwater, J. (Columbia Univ., New York). Phys. Rev., C; 6: No. 2, 435-41(Aug 1972).

When neutron reduced widths, Γ_n^0, are evaluated for N adjacent "single-population" resonances for an isotope, it is customary to express the fractional uncertainty in the s strength function, S_0, as $\pm(2.27/N)^{1/2}$ or $\pm(2/N)^{1/2}$. It is assumed that the Γ_n^0 follow a Porter-Thomas (P.T.) single-channel distribution with a common $\langle\Gamma_n^0\rangle$ for the interval, with no correlation between the different Γ_n^0. If the spacing distribution follows the Wigner formula for nearest neighbor spacings, but with no correlations, the $(2.27/N)^{1/2}$ fractional uncertainty applies for large N. For spacings following a statistical "orthogonal ensemble" (O.E.) behavior, the fractional uncertainty in $\langle D\rangle$ is $\approx N^{-1}$, so the fractional uncertainty in S_0 is $\approx(2/N)^{1/2}$ for large N. Experimentalists need easy to use rules for smaller N. Monte Carlo methods were used with a P. T. form for $\overline{\Gamma}_n^0$, and O.E. for spacings to establish the upper- and lower-bound values for S_0, divided by $\overline{S}_0 \equiv \overline{\Gamma}_n^0/\overline{D}$ (the ratio of the measured averages of Γ_n^0 and D). The method of confidence intervals was used. A "best choice" ratio is suggested for true S_0 to measured $\overline{S}_0$, all for a range of small N. The results should also apply for "single populations" of p levels. The behaviors for Γ_n^0 and D were also studied separately. (auth)

54721 NEUTRON–PROTON INTERACTION IN MIRROR NUCLEI. Jaenecke, Joachim (Max-Planck-Institut fuer Kernphysik, Heidelberg). Phys. Rev., C; 6: No. 2, 467-8(Aug 1972).

Approximate values for the residual neutron-proton interaction in mirror nuclei are derived from binding energy data. The comparison shows no indications for significant symmetry-breaking charge-dependent nuclear effects. (auth)

54722 ELASTIC PION–NUCLEUS SCATTERING FOR STUDIES OF THE NUCLEAR SURFACE. Kisslinger, L. S. (Carnegie-Mellon Univ., Pittsburgh); Burman, R. L.; Koch, J. H.; Sternheim, M. M. Phys. Rev., C; 6: No. 2, 469-75 (Aug 1972).

The use of elastic $\pi^{\pm}$-nucleus scattering to explore the relative neutron-proton distributions in nuclei is studied theoretically. The large difference between π^+-N and π^--N interactions in the nuclear surface leads to substantial effects. Neutron-radius determinations to 0.1 F appears feasible. (auth)

54723 ALPHA-CLUSTER STRUCTURE OF LIGHT SELF-CONJUGATE 4n NUCLEI IN THEIR GROUND STATES. Basu, M. K. (University Coll. of Science, Calcutta). Phys. Rev., C; 6: No. 2, 476-81(Aug 1972).

From phenomenological considerations, a mass formula is derived to calculate the interaction energy among the last two neutrons and last two protons in a nucleus. This interaction energy is the intra-α-cluster energy of the last α cluster in the nucleus. Then from a proper analysis of these intra-α-cluster energies, a separation of the intra- and inter-α-cluster energies out of the total binding energy of the nucleus is made. Clear ideas about the sizes of the α clusters relative to the size of the free α particle and also about the degree of α clustering in each α nucleus are obtained. Positive evidence supporting the additive nature of the α–α-cluster interaction is found. Finally, the intra-α-cluster interaction energies are compared with the nn-, pp-, and np-interaction energies in the same even–even self-conjugate nuclei in order to explore the similarities between the nature of two-body and four-body interactions. (auth)

54724 PION–NUCLEON POTENTIALS FOR USE IN LOW-ENERGY NUCLEAR PHYSICS. Desgrolard, P.; Hammann, T. F. (Institut d'Etudes Nucleaires, Algiers). Phys. Rev., C; 6: No. 2, 482-6(Aug 1972).

One- and two-term nonlocal separable potentials are determined to fit all partial S-, P-, and D-wave experimental phase shifts up to the first energy resonance at about $E_\pi = 180$ MeV (lab). The theoretical and experimental phase shifts, scattering lengths, and volumes are in good agreement. The practical use of this potential in nuclear physics calculations is simplified by the choice of simple form factors and of identical ranges in all S, P, and D relative states. (auth)

54725 ISOMER RATIOS FROM LOW PRIMARY EXCITATION OF RESIDUAL NUCLEI. Watson, J. W. (Knolls Atomic Power Lab., Schenectady, N. Y.); Medicus, H. A.; Turner, R. E. Phys. Rev., C; 6: No. 2, 497-505(Aug 1972).

A calculational procedure based on the Huizenga–Vandenbosch formalism for the determination of isomer ratios has been developed which is applicable also at low primary excitation energies of the residual nuclei, in contrast to earlier methods. This has been accomplished by introducing level densities which are based on the shell-model level calculations of Hillman and Grover rather than a level-density formula. Furthermore, the assumption that all the neutrons are emitted with the average energy 2T (where T is the nuclear temperature) has been replaced by a more realistic neutron spectrum. In order to test this procedure, the isomer ratio of ^{87}Y from the photonuclear reaction ^{89}Y(γ,2n), which has its reaction threshold at 20.8 MeV, was measured for bremsstrahlung of end-point energies 23, 25.6, 28.6, and 50 MeV. The results of the method are in much better agreement with the experiment than the original Huizenga–Vandenbosch approach. The analysis indicates that a relatively large fraction of the product nuclei is formed directly in the ground state and that quadrupole transitions are an important decay mode near the threshold. (auth)

54726 SUPERHEAVY HARTREE–FOCK CALCULATIONS. Saunier, G.; Rouben, B. (Univ. of Montreal). Phys. Rev., C; 6: No. 2, 591-5(Aug 1972).

The superheavy region is explored using a recent two-body interaction which yields, in the Hartree–Fock framework, very good radii and good binding energies for known spherical nuclei, and also a well-ordered occupied ^{208}Pb spectrum near the Fermi surface. A strong shell effect is found for elements 114^{298}_{184} and 120^{304}_{184} and a less pronounced one for 114^{310}_{196}, 114^{342}_{228}, 120^{316}_{196}, and 120^{348}_{228}. Their spectra do not lead to allowed β transitions, and for α decay, 114^{298}_{184} is favored over all others except 114^{342}_{228}. However, the former exhibits a greater binding energy per particle and is closer to the β-stability line predicted by the semiempirical formula. (auth)

54727 NONELASTIC INTERACTIONS OF NUCLEONS AND π MESONS WITH COMPLEX NUCLEI AT ENERGIES BELOW 3 GeV. Bertini, Hugo W. (Oak Ridge National Lab., Tenn.). Phys. Rev., C; 6: No. 2, 631-59(Aug 1972).

Nonelastic interactions corresponding to continuum-state transitions are calculated using the intranuclear-cascade evaporation approach. Spallation yields, energy- and angle-dependent spectra, particle multiplicities, and nonelastic cross sections are calculated for incident nucleons and π mesons with energies below 3 GeV on complex nuclei. Comparisons with experimental data are made and, in general, the agreement is good. Discrepancies in these comparisons are discussed with respect to the deficiencies in the model. (auth)

54728 CORRELATIONS WITHOUT TEARS. Jackson, A. D. (Univ. of Copenhagen); Lande, A. Nucl. Phys.; A191: No. 1, 177-200(1972).

Correlated wave functions and effective operators are obtained using unitary separable approximations to the two-body reaction matrix. These techniques are shown to be both convenient and numerically reliable for purposes of nuclear structure calculations. (auth)

54729 COMPARISON OF SEVERAL CONTINUUM SHELL-MODEL APPROXIMATION SCHEMES. Romo, W. J. (Carleton Univ., Ottawa). Nucl. Phys.; A191: No. 1, 65-87(1972).

A study is made of several schemes designed to give approximate solutions to continuum shell-model problems. The methods studied were all based on a finite-rank approximation to the Lippmann–Schwinger equation. Comparisons are made of both the mathematical basis of the approximation schemes and the accuracies of the methods when applied to a solvable model problem. (auth)

54730 INFLUENCE OF THE CHEMICAL ENVIRONMENT ON α-DECAY. Rubinson, W.; Perlman, M. L. (Brookhaven National Lab., Upton, N.Y.). Phys. Lett.; 40B: No. 3, 352-4(10 Jul 1972).

The effect of a change in the chemical environment of an α-emitter on its decay constant λ, computed on the model of a spatially constant electron density in the region of the Coulomb barrier, is $\delta\lambda/\lambda \approx 10^{-8}$. It is pointed out that on the model used by Alder et al. $\delta\lambda$ is necessarily zero, so their result $\delta\lambda/\lambda \approx 10^{-3}$ is wrong. (auth)

54731 IMPORTANCE OF THE QUADRUPOLE PAIRING FIELD IN THE $J^\pi = 0^+$ VIBRATIONS OF SHAPE DEFORMED NUCLEI. Bes, D. R. (Comision de Energia Atomica, Buenos Aires. Los Alamos Scientific Lab., N. Mex.); Broglia, R. A.; Nilsson, B. Phys. Lett.; 40B: No. 3, 338-44(10 Jul 1972)

The monopole and quadrupole pairing residual interactions acting simultaneously on a system of particles which move in a set of Nilsson single-particle levels and which display a nonuniform distribution of positive and negative quadrupole moments around the Fermi surface give rise to BCS state dependent gaps, which can produce effects which are similar to those appearing when there is an energy gap in the single-particle spectrum. The competition between monopole and quadrupole pairing correlations allows for the existence of $J^{\pi} = 0^{+}$ pairing vibrations which carry large (p,t) cross sections and weak (t,p) cross sections or vice versa. This model is used in the analysis of the observed two-nucleon transfer data on the U-isotopes. (auth)

54732 OCTUPOLE DEFORMATIONS IN THE NUCLEI BEYOND ^{208}Pb. Moeller, P.; Nilsson, S. G.; Sheline, R. K. (Lund Inst. of Tech., Sweden). Phys. Lett.; 40B: No. 3, 329-32(10 Jul 1972).

Calculations of the quadrupole (ϵ_2)—octupole ($\epsilon_3(\epsilon_5)$) potential energy surface for nuclei beyond ^{208}Pb indicates the presence of a very low lying secondary minimum in the oblate octupole region of deformation for certain nuclei. The well-known low-lying K = 0^- bands in the Ra—Th region are interpreted as associated with this secondary minimum. (auth)

54733 DESCRIPTION OF THE BAND STRUCTURE AT HIGH ANGULAR MOMENTA IN ROTATING NUCLEI. Krumlinde, J. (Lund Inst. of Tech., Sweden); Szymanski, Z. Phys. Lett.; 40B: No. 3, 314-18(10 Jul 1972).

A simple solvable model of particles coupled to a rotor is introduced. A qualitative description of the band structure in rotating nuclei in the region above the phase transition is given. (auth)

54734 SPURIOUS CENTER-OF-MASS EFFECT IN THE LOCAL DENSITY APPROXIMATION. Zofka, J. (Inst. of Nuclear Physics, Rez, Czech.). Phys. Lett.; 40B: No. 3, 319-22(10 Jul 1972).

An additional spurious center-of-mass effect is caused by using the local density approximation for the density dependent effective interactions. The approximate correction term is suggested and its contribution for the light even-even nuclei is calculated. This contribution is found to be of about +9 MeV and its slight tendency to increase the size and to decrease the deformation of the nucleus is noted. (auth)

54735 EQUATIONS FOR LINKED CLUSTERS AND THE ENERGY VARIATIONAL PRINCIPLE. Kuemmel, H.; Luehrmann, K. H. (Univ., Bochum, Ger.). Nucl. Phys.; A191: No. 3, 525-34(1972).

Explicit equations for linked cluster amplitudes, S_n, for arbitrary n are derived. They are applied to the energy variational principle. The insight gained thereby into the general structure leads to three conclusions: for hard-core potentials an approximate energy variational principle (neglecting in the energy expectation value all cluster functions S_n with $n > N < A$ and nothing else) cannot be formulated; approximations can be made, however, in the equations after performing the variation of the exact expectation value; these approximations lead to renormalized Brueckner—Hartree—Fock theory only if one ignores cancellations due to the existence of four-body cluster equations. (11 figures) (auth)

54736 SEMI-CLASSICAL DESCRIPTION OF ELASTIC AND INELASTIC HEAVY-ION SCATTERING ABOVE THE COULOMB BARRIER. Broglia, R. A.; Landowne, S.; Winther, A. (Univ. of Copenhagen). Phys. Lett.; 40B: No. 3, 293-9(10 Jul 1972).

The coupled-channel semiclassical description of direct reactions between heavy ions is generalized to bombarding energies where nuclear forces begin to play a significant role. The tails of the real and imaginary ion-ion potentials are estimated from the nucleon optical potential. These estimates are used in the analysis of recent elastic and inelastic scattering data. (auth)

54737 SOFT PHOTONS IN POTENTIAL SCATTERING. Nyman, E. M. (Abo Akademi, Finland). Phys. Lett.; 40B: No. 3, 323-5(10 Jul 1972).

An improved soft-photon theorem for non-relativistic bremsstrahlung is given: the elastic-scattering amplitude enters the final formula through functions of the scattering angle at the initial and final energies; the power-series expansion in scattering angle is avoided. (auth)

54738 ATOMIC NUCLEUS. Reid, J. M. Harmondsworth, Eng.; Penguin Books Ltd., (1972). 269p. Pounds 2.35.

The subject is considered in chapters entitled: radioactive decay laws, radioactivity (α decay), radioactivity (β decay), nuclear mass, nuclear shell model, nuclear moments, nuclear moments (experimental measurements), the collective model, excited states of nuclei, and nuclear fission. Appendices give: the ground-state properties of stable nuclei, the passage of charged particles through matter, the interaction of γ rays with matter, general atomic and nuclear constants, a list of the elements in order of charge number and in alphabetical order. (UK)

54739 MASS NUMBER DEPENDENCE OF NEUTRON AND PROTON RESIDUAL INTERACTION. Momoki, Goroh; Sasaki, Kiyoshi (Nihon Univ., Funabashi, Japan). Nihon Daigaku Seisan Kogakubu Hokoku; 4: No. 2, 147-50(Sep 1971).

The properties of the effective neutron and proton interaction are studied. The odd-odd nuclei of the closed shell ± one neutron and one proton are treated. Using the finite range central force with the spin independent and dependent ones, the depth and mixture parameters of the potential are determined. (auth)

54740 BETA-PROTSESSY. FUNKTSII DLYA ANALIZA BETA-SPEKTROV I ELEKTRONNOGO ZAKHVATA. (Beta-Processes. Functions for Analyzing Beta-Spectra and Electron Capture). Dzhelepov, B. S.; Zyryanova, L. N.; Suslov, Yu. P. Leningrad; Izdatel'stvo Nauka Leningradskoe Otdelenie (1972). 374p.

Tables of numerical values of functions useful in the analysis and treatment of experimental data on β decay and capture of orbital electrons are presented. The self-consistent potential of Hartree-Fock-Slater was used in describing the field of atomic electrons in the computation of the functions. The charge distribution in the nucleus was assumed to be homogeneous with respect to the volume of a sphere whose radius was $R = 1.2\ A^{1/3}$. Beta spectra, electron capture from the K-, L-, M-, and $N_{I,\,II}$• subshells of an atom, and branching coefficients K/β^{+} and ϵ/β^{+} are tabulated. Tables of accessory data for treatment of beta spectra and the calculation of electron capture are included in an appendix. (K.S.W.)

54741 BOSON EXPANSIONS AND HARTREE—BOGOLYUBOV THEORY. Marshalek, E. R.; Holzwarth, G. (Technische Univ., Munich). Nucl. Phys.; A191: No. 2, 438-48(1972).

If the boson operators in boson expansions of the Hamiltonian are suitably replaced by c-numbers regarded as variational parameters, solutions of the Hartree-Bogoliubov or Hartree-Fock-Bogoliubov equations are obtained. The c-number replacement in the boson equations of motion yields solutions of the corresponding time-dependent self-consistent field equations. (auth)

54742 NUMERICAL INVESTIGATIONS WITHIN THE SEMI-CLASSICAL TRANSFER THEORY. Alder, K.; Morf, R.; Pauli, M.; Trautmann, D. (Inst. of Theoretical Physics, Basel). Nucl. Phys.; A191: No. 2, 399-416(1972).

A short review of the semiclassical transfer theory for neutron- and proton-transfer reactions is presented, which should serve as a guide for planning experiments. The transfer function $B_{\lambda}(\partial,\rho,\xi,\delta)$ and $H_{\lambda}(\rho,\xi,\delta)$ describing the kinematics of the transfer reactions are tabulated in the form of contour plots. Furthermore, an estimate of the other quantities which occur in the cross-section formula is given. (auth)

54743 COULOMB BREAK-UP OF THE DEUTERON. Baur, G. (Max-Planck-Institut fuer Kernphysik, Heidelberg); Trautmann, D. Nucl. Phys.; A191: No. 2, 321-31(1972).

A DWBA treatment of the break-up of a deuteron in the Coulomb field of a nucleus is given. A Hulthén wave function is used for the deuteron. There are no free parameters in the theory; therefore, a measurement of this process would give a test of the accuracy of the DWBA. The integral over the continuum wave functions can be reduced to a bremsstrahlung integral given by Sommerfeld and Nordsiek. Numerical calculations for various deuteron energies and targets Z have been performed in order to understand the main features of the process. Coincidence cross sections, cross sections integrated over proton or neutron angles and finally total cross sections are given, along with a discussion of the results. (auth)

54744 RELATIVISTIC NUCLEAR MATTER CALCULATIONS AND THE DEFICIENCY OF ONE-BOSON EXCHANGE POTENTIALS. Lee, Tsung-shung H.; Tabakin, Frank (Univ. of Pittsburgh). Nucl. Phys.; A191: No. 2, 332-52(1972).

Nuclear matter properties are calculated using the Schierholz and Thompson-Gersten-Green relativistic potentials. The Brueckner equations for nuclear matter are modified to incorporate corresponding relativistic kinematics. It is found that both relativistic and non-relativistic one-boson exchange potentials yield overbinding and collapse of nuclear matter. By comparing the relativistic results and earlier non-relativistic results, it is shown that the main deficiency of OBE models is not the use of a non-relativistic limit but is rather the lack of a strong intermediate- and short-range tensor force. The proper treatment of 2π exchange might yield the requisite strong tensor force. (auth)

54745 LIGHT NUCLEI SYSTEMATICS IN THE UNRESTRICTED HARTREE—FOCK APPROXIMATION. Lee, H. C.; Cusson, R. Y. (Chalk River Nuclear Labs., Ont.). Ann. Phys. (N. Y.); 72: No. 2, 353-427(Aug 1972).

Extensive unrestricted Hartree—Fock (HF) calculations are performed for 57 light nuclei in the region $4 \leq A \leq 41$, $N - Z = 0, \pm 1$.

An expansion basis consisting of the first 5 major shells plus the $0h_{11/2}$ subshell of the j−j coupled spherical harmonic oscillator model is used, so that 82 proton and 82 neutron states are considered. The semirealistic N−N interaction No. 2 of Saunier and Pearson is used and seen to be a reasonable energy- and density-independent approximation to the required reaction matrix. All quantum numbers of the Hamiltonian are violated in the single-particle (sp) orbits, except parity and isospin projection τ_z. Time-reversal violation in the sp orbits is shown to be an important effect in odd and odd−odd nuclei and accounts for most of the odd−even pairing energy differences, although no pairing correlations are considered explicitly. No projection from the intrinsic states is performed, but its probable effects are discussed. The Coulomb two-body interaction is included, and its matrix elements are computed exactly by using Talmi integrals. The kinetic energy of the center-of-mass (c.m.) is removed from H before the HF iterations and rms radii are computed with respect to the c.m. so that spurious c.m. effects are minimized. Nilsson-model wave functions are used as initial trial wave functions, and shown to be good approximations for the HF wave functions. Reasonable-to-good agreement with experiment is obtained for the systematics of binding energies, separation energies, rms radii, electric quadrupole moments, and Coulomb energies. Alpha clustering is observed in the density distribution. New quantitative predictions are made for proton−neutron rms radii differences and isospin mixing coefficients, and compared with other calculations. It is concluded that a systematic quantitative account of the ground-state properties of the light nuclei can be given from a knowledge of the N−N interaction and nuclear matter properties alone. (33 figures, 8 tables, 104 references) (auth)

54746 NON-LOCAL POTENTIAL FOR SINGLE-PARTICLE PROPERTIES OF NUCLEI. Janiszewski, J.; McCarthy, I. E. (Flinders Univ. of South Australia, Bedford Park). Nucl. Phys.; A192: No. 1, 85-96(1972).

A real nonlocal potential is developed which describes single-particle properties of nuclei as a function of A and Z. It is useful as a first approximation for nuclear physics applications requiring simple computation of sets of single-particle wave functions. The fits to single-particle energy levels of spherical nuclei and charge distributions are comparable in quality with those obtained by recent Hartree−Fock calculations. Neutron density distributions parallel closely those of the Hartree−Fock calculation. (auth)

54747 EFFECTIVE NEUTRON−PROTON INTERACTION IN DEFORMED DOUBLY ODD NUCLEI. Nakagawa, Kimiko; Obinato, Toshio; Sasaki, Kiyoshi (Nihon Univ., Japan). Nucl. Phys.; A191: No. 3, 535-44(1972).

Properties of the effective neutron−proton interaction in deformed light nuclei, such as ^{18,20}F, ^{22,24}Na, ^{26,28}Al, ^{30,32}P, and ^{34}Cl, are studied using experimental data on the energy difference between the two rotational band heads and the mutual interaction energy between the neutron and proton in each nucleus by using a symmetric core rotational model. The results show that the systematics of the experimental data can be explained by the simple model. The value of the effective-force range parameter obtained is fairly short compared with the range which is usually employed in the spherical shell-model calculation. In connection with these results, the effects of the force range and force mixture on the nuclear deformation are discussed. (2 figures, 5 tables) (auth)

PHYSICS (PLASMA AND THERMONUCLEAR)

54748 TECHNOLOGY INDEX FOR PLASMAPHYSICS RESEARCH AND FUSION REACTORS. VOLUME 6, No. 7, 1972. Bibliography, Author Index, Subject Index, Appendix. Leopoldshafen, Ger.; Zentralstelle fuer Atomkernenergie-Dokumentation (1972). 45p.

This listing contains 226 references on various aspects of the title subjects. (M.O.W.)

Confinement and Heating

54749 (AEC-tr-7330) GENERAL PRINCIPLE OF CURRENT HEATING PROCESSES OF PLASMA IN PULSED z-DISCHARGES. Dubovoi, L. V. (Scientific Research Inst. of Electro-Physical Apparatus, Leningrad (USSR)). Translation of report NP-18947. 7p. Dep. NTIS.

It is shown that in plasma heating processes in pulsed z-discharges, the gas-kinetic pressure nT of particles is related to the discharge current field B_ϕ by the general law $nT \simeq \beta_\phi(B_\phi^2/8\pi)$ (where $\beta_\phi = \text{const} \sim 1$) for most present-day experiments. Conclusions from this relation and generality of its character are discussed. (auth)

54750 (CONF-720705-2) MEASUREMENT OF EFFECTIVE COLLISION FREQUENCY IN RF HEATING THROUGH PARAMETRIC INSTABILITIES. Chu, T. K.; Hendel, H. W. (Princeton Univ., N. J. Plasma Physics Lab.). [nd]. Contracts AT(11-1)-7073; F30602-72-C-0053. 10p. Dep. NTIS.

From first topical conference on rf plasma heating; Lubbock, TX. (6 Jul 1972).

Enhanced absorption of an em wave near ω_{pe} was observed, coincident with the onset of parametric decay instability, in a Q-device plasma. The effective collision frequency $\nu_{eff} \simeq \nu_{ei}(E/E_{cr})^2$. (auth)

54751 (CONF-720705-3) PARAMETRIC INSTABILITY AND ITS INDUCED HEATING. Chu, T. K. (Princeton Univ., N. J. Plasma Physics Lab.). [nd]. Contracts AT(11-1)-3073; F30602-72-C-0053. 15p. Dep. NTIS.

From first topical conference on rf plasma heating; Lubbock TX. (6 Jul 1972).

Laboratory experiments having high-frequency excitation electric fields near ω_{pe} are reviewed. Effects of the inhomogeneity of plasmas are discussed, and the potential use of parametric instability in plasma heating is assessed. (auth)

54752 (CONF-720804-4) WAVE GENERATION AND HEATING NEAR THE ION CYCLOTRON FREQUENCY IN THE ST TOKAMAK. Hooke, W. M.; Hosea, J. C. (Princeton Univ., N. J. Plasma Physics Lab.). [nd]. Contract AT(11-1)-3073. 4p. Dep. NTIS.

From fifth European conference on controlled fusion and plasma physics; Grenoble, France (21 Aug 1972).

A test coil is presently being used to determine the feasibility of employing waves to further heat the ions of the tokamak plasma. Initial results for wave loading of the coil and ion heating are very encouraging. (auth)

54753 (CONF-720804-5) PSEUDOCLASSICAL AND ANOMALOUS CONTAINMENT IN FM-1. Okabayashi, M.; Schmidt, J.; Sinnis, J.; Yoshikawa, S. (Princeton Univ., N. J. Plasma Physics Lab.). [nd]. Contract AT(11-1)-3073. 4p. Dep. NTIS.

From fifth European conference on controlled fusion and plasma physics; Grenoble, France (21 Aug 1972).

Particle confinement times well in excess of one second are observed on FM-1. Below about 1 eV the confinement time scales as $T_e^m(m \sim 3/4)$, while above 1 eV the confinement time scales as $T_e^n(n \sim -1)$. (auth)

54754 (LA-5019) LOW-DENSITY LIMIT OF THE THETA PINCH. Kaufmann, Michael (Los Alamos Scientific Lab., N. Mex.). Aug 1972. Contract W-7405-eng-36. 9p. Dep. NTIS.

The scaling of the onset of sheath broadening in θ-pinch implosions is derived on the basis of a number of assumptions. The most realistic is that the instability threshold is that of the electron-cyclotron-drift instability and that the electrons are heated by resistive or diffusive field mixing during the implosion. This scaling is used to order various existing high-voltage θ-pinch experiments and to predict the conditions for excessive broadening of the sheath in future θ pinches and other shock-heating experiments. (auth)

54755 EFFECT OF PLASMA FLOW ON TOROIDAL CONFINEMENT. Green, B. J. (Max-Planck-Institut fuer Plasmaphysik, Garching, Ger.). Nucl. Fusion; 12: No. 4, 475-83(Jul 1972).

An attempt is made to review recent developments in the study of laminar plasma flow and its effect on toroidal plasma confinement. The topic is presently the object of active research, so that this summary will serve rather as a progress report of development. Discussion will almost exclusively concern the collision-dominated plasma case, as this has received most attention. The different approaches to the problem are classified and presented in such a way as to indicate the status of results which have been achieved, and to highlight the outstanding problems. (auth)

54756 PLASMA CONTAINMENT IN HYBRID FIELDS OF MIRROR WITH QUADRUPOLE AND QUADRUPOLE-CUSP. Morimoto, Shigeyuki (Nagoya Univ., Japan). J. Phys. Soc. Jap.; 33: No. 3, 761-8(Sep 1972).

Containment of gun-produced plasma in stabilized mirror fields is studied: Quadrupole and quadrupole-cusp fields are produced by two and four inner conductors, respectively. The plasma parameters are $n = 10^9$ to 10^{10} cm^{-3}, $T_e = 1$ to 5 eV, T_i (in the mirror quadrupole) $\gtrsim 10$ eV. Flute instability observed in the mirror field is eliminated by superposing the quadrupole field Superposition of the quadrupole-cusp field does not suppress the instability satisfactorily, but when a wall is provided near the stabilizing winding, as in the usual min-B mirror machine, the plasma is well stabilized. These phenomena are explained by the stability $\int(1/B)dl$ with suitable integral limits. The mirror quadrupole field whose lines of force do not contact with the chamber wall has a good stability integral and is promising as a mirror configuration. (auth)

54757 ATOMIC AND CLUSTER INJECTION INTO D-T MIRROR FUSION POWER SYSTEMS. Hiskes, J. R. (Univ. of California, Livermore). Nucl. Fusion; 12: No. 4, 423-32(Jul 1972).

The problem of the penetration of a neutral atomic beam and a cluster ion beam into a fusion plasma is reviewed. The short penetration length of an atomic beam, coupled with certain geometric dependences of the magnet coil costs, implies an optimum injection energy for a D-T mirror fusion power system in the range 200 to 300 keV. The penetration length for a cluster beam is inferred from available data. For certain charge and mass distributions of the cluster fragments, a substantial improvement of beam penetration is possible, allowing for injection as low as 100 keV per deuteron. Additional fragment-charge and mass-distribution data will be necessary, however, to clarify the role of cluster injection. (auth)

54758 MICROWAVE PLASMA HEATING IN TUMAN-2. Golant, V. E.; Kaganskii, M. G.; Pakhomov, L. P.; Podushnikova, K. A.; Shakhovets, K. G. (Ioffe Inst. of Physics and Tech., Leningrad). Sov. Phys.-Tech. Phys. (Engl. Transl.); 17: No. 3, 488-94(Sep 1972).

Translated from Zh. Tekh. Fiz.; 42: No. 3, 620-8(Mar 1972).

Experiments on microwave plasma heating were carried out at frequencies in the upper-hybrid range. At plasma densities (1 to 3) × 10^{12} cm^{-3}, f = 9 GHz, and P = 80 kW, the efficiency of microwave energy injection, as given by the change in plasma parameters, is several tens of percent. At plasma densities (1 to 2) × 10^{13} cm^{-3} and f = 34 GHz, the efficiency falls to 5 to 10%. Since the wavelength is considerably smaller than the chamber dimensions, the change of efficiency with frequency is possibly due to the effect of an opaque region. (auth)

54759 ASYMPTOTIC PARTICLE DISTRIBUTION FUNCTION IN CYCLOTRON HEATING. Polovin, R. V. (Physical-Technical Inst., Kharkov). Sov. Phys.-Tech. Phys. (Engl. Transl.); 17: No. 3, 416-17(Sep 1972).

Translated from Zh. Tekh. Fiz.; 42: No. 3, 526-7(Mar 1972).

Cyclotron heating in a magnetic trap is investigated. The magnetic field is assumed to be constant and homogeneous, while the electric field is assumed to be spatially homogeneous and rotating with the cyclotron frequency. It is shown that the asymptotic form of the energy distribution function of the particles is an exponential that contains a negative radical. (auth)

54760 MAGNETIC-FIELD-ENHANCED HEATING OF PLASMAS WITH CO_2 LASERS. Cohn, Daniel R.; Lax, Benjamin (Massachusetts Inst. of Tech., Cambridge). Appl. Phys. Lett.; 21: No. 5, 217-20(1 Sep 1972).

The effect of high magnetic fields upon the heating rate of CO_2-laser-produced plasmas was calculated. It is found that the inhibition of thermal losses in the presence of high magnetic fields should substantially enhance the effectiveness of the CO_2 laser as a means of creating hot plasmas. Electron and ion temperatures are computed for plasmas produced with 10^{10}-W CO_2 lasers. (auth)

54761 HIGHER HARMONICS AND TRANSPORT COEFFICIENTS OF PLASMAS IN CIRCULARY POLARIZED MAGNETIC FIELDS AND ADDITIONAL ELECTROMAGNETIC FIELDS. Kirsten, T.; Vojta, G. (Karl-Marx-Univ., Leipzig). Beitr. Plasmaphys.; 12: No. 2, 123-47(1972).

With the methods of kinetic theory on the basis of the Boltzmann and Fokker–Planck kinetic equations, the behavior of a Lorentz plasma in a circularly polarized (rotating) magnetic field (rotation frequency ω), an alternating electric field (frequency ω'), and additional constant electromagnetic fields is investigated. By means of a generalized Fourier expansion it is shown that the above fields create in the plasma currents of the frequencies 0, ω', $\omega - \omega'$, ω, $\omega + \omega'$, $2\omega - \omega'$, 2ω, and $2\omega + \omega'$. Transport coefficients are calculated explicitly and the validity of Onsager reciprocity relations and that of Kronig–Kramers relations is discussed. The special case of the electric field induced by the rotating magnetic field is treated separately. Finally, problems of plasma containment are discussed. (auth)

54762 INFLUENCE OF DIFFERENT TYPES OF OSCILLATIONS ON ION HEATING IN PLASMA–BEAM DISCHARGES. Kovpik, O. F.; Kornilov, E. A.; Krivoruchko, S. M.; Moiseev, S. S.; Fainberg, Ya. B. (Physical-Technical Inst., Kiev). JETP Lett. (USSR) (Engl. Transl.); 15: No. 9, 355-7(5 May 1972).

Translated from Zh. Eksp. Teor. Fiz., Pis'ma Red.; 15: No. 9, 501-4(5 May 1972).

Experimental results are presented that confirm the predominant energy absorption by plasma ions in the region of the lower hybrid resonance $\omega^2 \approx \omega_i \omega_e / [1 + \omega_e^2 (\omega_0^2)]$ in comparison with heating by oscillations with $\omega \lesssim \omega_i$. The maximum contribution to the energy absorption by the ions is made by oscillations near the ion-cyclotron frequency ~0.072 MHz and the lower hybrid resonance ~20 MHz. Results show that it is most effective to heat ions by oscillations that cause little transverse diffusion and thermal conductivity. (D.L.C.)

54763 BEHAVIOR OF LARGE-CURRENT ELECTRON BEAM IN A DENSE GAS. Rudakov, L. I.; Smirnov, V. P.; Spektor, A. M. JETP Lett. (USSR) (Engl. Transl.); 15: No. 9, 382-5(5 May 1972).

Translated from Zh. Eksp. Teor. Fiz., Pis'ma Red.; 15: No. 9, 540-4(5 May 1972).

An electron beam traverses in air a distance which is larger than the mean free path of an electron, before it spreads apart. This effect was investigated in air and He at pressures from 10^{-2} torr to 1.6 atm. 660-keV electrons were used, and the glow curves agree with calorimetric measurements. In air at 1 atm, the beam breaks up at ~12 cm. The penetration length L in air decreases with pressure from 20 cm at 0.4 atm to 10 cm at 1.6 atm. L could not be measured in He as it exceeded the drift chamber. This effect is connected with the appearance of a beam instability in a strongly dissipative medium. The dispersive equation has an instable solution that leads to bunching of the beam and its consequent deceleration. L should lie between $\gamma[(n/n')(\Delta\nu/\nu)]$ and $\gamma[(n/n')(\nu/\nu_e)]$. Estimates of L and its pressure dependence agree with experiment. The use of this effect for collective heating of a superdense plasma is suggested. (D.L.C.)

54764 ONE POSSIBLE USE OF THE IR LASERS FOR HIGH-TEMPERATURE HEATING OF A SUPERDENSE PLASMA. Bunkin, F. V.; Pashenin, P. P.; Prokhorov, A. M. (Lebedev Inst. of Physics, Moscow). JETP Lett. (USSR) (Engl. Transl.); 15: No. 9, 394-7(5 May 1972).

Translated from Zh. Eksp. Teor. Fiz., Pis'ma Red.; 15: No. 9, 556-9(5 May 1972).

One possible way of solving the problem of feeding the radiation energy into the superdense plasma produced in laser experiments, is discussed. When a strong magnetic field H_0 is applied to the plasma, wave propagation in a quasi-longitudinal direction is possible if $(\omega_H/\omega) \cos \phi > 1$. For effective excitation of the wave, it is necessary to have small angles ϕ_0 and large gradients of the electron density at the point $\omega_p > \omega$. These conditions are satisfied if the width $\Delta Z = (N_e/N_e^1)_{\omega_p \simeq \omega} \ll 3 \times 10^{-5} \phi_0^{-2}$ cm. For a pulse duration of 10^{-9} sec, $\phi_0 < 2 \times 10^{-2}$ rad. For $H_0 \approx 10^7$ G, the target cross-section area can be ~10^{-4} cm^2. The minimum laser energy is estimated to be 3×10^3 J. (D.L.C.)

54765 THEORY OF STOCHASTIC HEATING OF PARTICLES IN A TURBULENT PLASMA. Kingsep, A. S. (Inst. of Atomic Energy, Moscow). Zh. Eksp. Teor. Fiz.; 62: No. 6, 2179-82 (Jun 1972). (In Russian).

It is pointed out that, in order to solve the problem of turbulent heating of a plasma, the evolution of the particle distribution function in the matrix elements of the wave nonlinear interaction should be taken into account. It is demonstrated that an ion distribution that decreases with increasing velocity ν according to a power law becomes established as heating occurs. It is found that stochastic heating of ions cannot be described by a self-similar solution. (auth)

54766 INVESTIGATION OF HEATING OF A PLASMA ION COMPONENT BY A COLLISIONLESS SHOCK WAVE. Alinovskii, N. I.; Altyntsev, A. T.; Koshilev, N. A. (Inst. of Nuclear Physics, Novosibirsk, USSR). Zh. Eksp. Teor. Fiz.; 62: No. 6, 2121-8 (Jun 1972). (In Russian).

The energy spectra of ions in a plasma heated by a collisionless shock wave are obtained by the technique of passive corpuscular diagnostics. Under conditions when an aperiodic shock front with resistive dissipation is formed in the plasma, ion heating is manifest in the appearance of a small group of ions (~10%) with a mean energy of the order of the electron temperature. The remaining ions are cold. The results are in agreement with a theoretical model which explains the origin of this particle group as being due to Landau linear damping of ion acoustic oscillations excited in a shock wave by resonance ions located at the tail of the distribution function. The main energy content of the plasma is determined by the electron component. Under conditions of overturning of the shock wave front predominant heating of the ion component of the plasma is observed, the ion distribution function being close to the isotropic Maxwellian distribution. (auth)

54767 COLLISIONLESS HEATING OF PLASMA IONS BY AN ION BEAM. Kirichenko, G. S.; Khmaruk, V. G. (Inst. of Nuclear Research, Kiev). Zh. Eksp. Teor. Fiz.; 63: No. 1, 107-11(Jul 1972). (In Russian).

The possibility of employing an ion beam for collisionless heating of plasma ions is investigated. It is shown that the ion temperature can be raised to the electron temperature by excitation of intense low-frequency oscillations by an ion beam in a plasma–beam discharge. (tr-auth)

Diagnostics

Refer also to abstracts 53684 and 54056.

54768 (AEC-tr-7329) MEASUREMENT OF PLASMA PARAMETERS IN STRONG HF DISCHARGE. Dubovoi, L. V.; Ivanov, B. A.; Chernobrovin, V. I. (Scientific Research Inst. of Electro-Physical Apparatus, Leningrad (USSR)). Translation of report NP-18946. 8p. Dep. NTIS.

An attempt is made to use a corpuscular diagnostic method for defining the local characteristics of skinned hf discharge. Plasma density and thermal skin-layer thickness obtained coincide with calculated estimates and measurement data by independent methods. The results of measurements of the ion distribution function in turbulent discharges are presented. (auth)

54769 MEASUREMENT OF THE ELECTRON DENSITY DISTRIBUTION IN PLASMAS FROM THE BENDING OF A GAS LASER BEAM. Potter, I. C.; Falconer, I. S.; Smith, W. I. B. (Univ. of Sydney). J. Phys., E (London); 5: No. 9, 910-14 (Sep 1972).

The electron density distribution in an axisymmetric plasma may be determined by measuring the deviation of a gas-laser beam on passing through the plasma. If the beam is inclined at a small angle to the axis of the plasma the bending is closely proportional to the difference between the axially averaged electron density at the radius at which the beam enters the plasma, and at the radius at which it leaves the plasma. Experimental results demonstrating the validity of this method, and the advantage and limitations of beam bending as a diagnostic tool, are discussed. (auth)

54770 CIRCUIT FOR DIRECT REGISTRATION OF ELECTRON DENSITIES MEASURED INTERFEROMETRICALLY. Funk, L. W.; Camm, D. M.; Curzon, F. L. (British Columbia Univ., Vancouver). J. Phys., E (London); 5: No. 9, 941-3(Sep 1972).

Electron densities are commonly measured by determining the plasma refractive index with an interferometer. The circuit described permits the electron density to be recorded directly as a function of time. For the 6328-Å line of a He–Ne laser, the device has a sensitivity of 3.56×10^{18} electrons cm^{-2} V^{-1} and a resolving time of the order of 40 ns. (auth)

54771 ANALYTICAL AND EXPERIMENTAL INVESTIGATIONS OF THE TRANSIENT PROPERTIES OF DENSE ALUMINIUM PLASMAS. Willis, Harold Wayne. Stillwater, Okla.; Oklahoma State Univ. (1971). 248p. University Microfilms Order No. 72-22,014.

Thesis.

The scope of this work includes the theoretical study of the laser impact and expanding sphere plasma computer models and the experimental study of the laser impact and vacuum spark plasmas with the quadrupole mass filter and the electrostatic lens system. A number of experimental curves were obtained which contribute information on the ionic species of aluminum atoms, the presence of metastable atoms and the ultraviolet light that is emitted by the vacuum breakdown of a spark gap. These measurements, which were taken with the quadrupole mass filter and an electrostatic lens, appear to establish that migration of the spark at the anode occurs during the breakdown. Several curves of the velocity distribution are presented for aluminum ions: Al^{+1} through Al^{+5}. The general conclusion from this study is that the analytical studies, based on the assumption of local thermodynamic equilibrium, have a good basis for application, for the escaping ions approximate a Maxwell—Boltzmann distribution, but the analytical equations are not exact. The computer model for the laser impact plasma was completely formulated in collaboration with L. J. Peery, and a one and one-half hour production run was obtained. Data from the run are included. A new, improved program for the analytical model of an expanding plasma sphere was formulated. The computer program and initial results are presented. (TSS) (Diss. Abstr. Int., B)

54772 DETERMINATION OF THE MAGNETIC FIELDS IN A PLASMA ON BASIS OF THE HYDROGEN SPECTRAL LINE CONTOURS. Demura, A. V.; Lisitsa, V. S. (Inst. of Atomic Energy, Moscow). Zh. Eksp. Teor. Fiz.; 62: No. 6, 2161-9(Jun 1972). (In Russian).

An approximate analytic solution is obtained for the problem pertaining to deformation of the Holtsmark contour of the hydrogen spectral line by an external magnetic field B. The solution yields the difference contour derived by subtraction of two contours corresponding to polarization along and across the magnetic field. A method for determining the magnitude and direction of B by means of the difference contour expressed in terms of three universal functions related to the Holtsmark function is considered. Numerical results for components of the L_α and L_β lines are presented. The possibility of determining the exact analytic solution for a complete line contour is discussed. (auth)

54773 USE OF HIGH-SPEED SPECTROGRAPHY FOR DIAGNOSTICS OF AN EROSIVE PULSED PLASMA ACCELERATOR. El'yashevich, M. A.; Avramenko, V. B.; Bakanovich, G. I.; Min'ko L. Ya. Zh. Prikl. Spektrosk.; 16: No. 3, 422-5(Mar 1972). (In Russian).

Individual frame photographs of spectra were tested for quantitative spectroscopic studies of an erosive pulsed, plasma accelerator. By broadening the spectral lines and the brightness of the continuous spectrum, a spatial distribution of the concentration of charged particles was obtained in discrete moments of time with respect to the photographic frames of the spectra of the transverse cross section of the plasma jet. Particle concentration measurements on a time base showed that the integrated value of the concentration with respect to time was too low in comparison with the maximum values. (tr-auth)

Kinetics (General)

54774 (AEC-tr-7323) PLASMA BREMSSTRAHLUNG FROM RELATIVISTIC PARTICLES IN A TURBULENT PLASMA. Tsytovich, V. N. (Akademiya Nauk SSSR, Moscow. Institut Fiziki). Translation of report NP-18759. 19p. Dep. NTIS.

The existence of two mechanisms of radiation of relativistic particles in turbulent plasma is demonstrated: (1) Previously examined process of induced and spontaneous radiation during Compton scatter on nonresonance turbulent vibrations of plasma; (2) new effect—bremsstrahlung during scatter on resonant turbulent vibrations. The spectral composition and angular distribution of the radiation, particle energy losses due to plasma-bremsstrahlung are analyzed. The effect of low-multiple scatter (Landau—Pomeranchuk effect) on radiation processes is investigated. The strength of plasma-bremsstrahlung depends little on particle mass and is great in particular for ions. The effect of turbulent expansion of Cherenkov resonance, examined earlier, is interpreted as being the result of multiple scatter of particles on resonance plasma pulsations. (auth)

54775 (AEC-tr-7326) CIRCUITS FOR STUDYING THE INTERACTION OF HIGH-FREQUENCY FIELDS WITH A PLASMA IN LINEAR DEVICES. Savchenko, I. S.; Yampol'skii, I. R. (Gosudarstvennyi Komitet po Ispol'zovaniyu Atomnoi Energii SSSR, Sukhumi. Fiziko-Tekhnicheskii Institut). Translation of report NP-18895. 18p. Dep. NTIS.

Diagram solutions of circuits forming high-frequency electromagnetic fields in experimental plasma devices with cylindrical discharge chambers are described. Circuits producing transverse rotating fields with various numbers of poles ($p = 0,1,2$) are considered. The circuits consist of eight rods located uniformly around the generatrix of a cylinder and connected in various ways with circuit condensers in an artificial retention line closed into a ring or in the form of individual magnetically connected circuits. The proposed circuits can be excited from a four-phase voltage source that ensures high symmetry of the field. The circuits can be excited simultaneously at two frequencies. Each frequency corresponds to different values of p. The properties are discussed and computational formulas for determining the basic parameters and some information on the practical achievement of the circuits are given. (auth)

54776 (AEC-tr-7332) RATIO OF LONGITUDINAL AND TRANSVERSE DIFFUSION COEFFICIENTS IN ARGON SHF DISCHARGE PLASMA. Budnikov, V. N.; Novik, K. M.; Obukhov, A. A. (Akademiya Nauk SSSR, Leningrad. Fiziko-Tekhnicheskii Institut). Translation of report NP-18916. 5p. Dep. NTIS.

The results are presented of determination of the ratio of longitudinal and transverse diffusion coefficients in argon plasma, obtained on the basis of analysis of the longitudinal concentration distribution of charged particles outside the active zone of shf discharge. The experimental conditions were: longitudinal magnetic field about 3,000 Oe, discharge cylinder length 70 cm, diameter 2.5 cm, charged-particle concentration 10^{12} to 10^{10} cm^{-3}, $T_0 \sim 2$ to 10 eV. It was found in the pressure range 3×10^{-2} to 3×10^{-3} mm Hg that the ratio $D_{||}/D_\perp$ is constant, equal to 25. (auth)

54777 (BMBW-FBK-72-8) EXPERIMENTAL INVESTIGATION OF THE CONTINUOUS EMISSION OF SHOCK HEATED KRYPTON AND XENON. Weber, W. (Technische Universitaet, Hanover (West Germany). Institut fuer Plasmaphysik). Jul 1972. 110p. (In German). Dep. NTIS (U. S. Sales Only).

The emission coefficients for continuum radiation of shock-heated krypton and xenon plasmas were measured photographically in the wavelength region from 4000 to 6000 Å and the ξ factors for Kr I and Xe I were determined. The plasma temperature and electron density needed for the calculation of the ξ factors were calculated from the velocity of the shock wave with the Rankine—Hugoniot equations. The results are compared with measurements and theoretical calculations of other authors. (auth)

54778 (CEA-CONF-2047) IONIZATION PROCESSES IN HOT PLASMAS. Bliman, S. (Commissariat a l'Energie Atomique, Grenoble (France). Centre d'Etudes Nucleaires). 15 Mar 1972. 6p. (In French). (CONF-720120-2). Dep. NTIS (U. S. Sales Only).

From Conference on the sources of multicharged ions; Paris, France (28 Jan 1972).

The various types of collisions leading to multiply charged ions are considered. Step-by-step ionization and shake-off ionization in hot plasmas are envisaged. (France)

54779 (NP-19393) PHYSICS DISCIPLINE. Annual Progress Report, 1971. (Flinders Univ. of South Australia, Bedford Park. School of Physical Sciences). Dec 1971. 66p. Dep. NTIS (U. S. Sales Only).

Research being conducted in the fields of discharge and plasma physics and atomic scattering, and theoretical studies in nuclear and many-body physics are outlined. Plasma studies include normal ionizing, gas dynamic and collisional studies of shock waves; wave propagation; and interaction between high frequency fields and plasmas (including anomalous skin effects). Other topics are gaseous breakdown and electron transport phenomena and atomic collision processes (electron—atom) including excitation of Ne and Ar; magnetohydrodynamics; statistical mechanics and many body theory; and computational physics. Theoretical nuclear physics is centered on the three-body problem. Studies include pion—deuteron production, d(p,2p)n—impulse approximation and distorted wave theory with s-wave t-matrix; Coulomb contribution to the t-matrix; extensions of the Faddeev equation; off-shell effects in the bound state; and a unitary pole expansion for the coupled-channel case. (Australia)

54780 (NP-19414) WILLS PLASMA PHYSICS DEPARTMENT TWENTY-THIRD SIX-MONTHLY PROGRESS REPORT, 1st JANUARY-30th JUNE 1972. (Sydney Univ. (Australia). School of Physics). 1972. 8p. (PR-23). Dep. NTIS (U. S. Sales Only).

Progress in the following topics is summarized: plasma sources; hydromagnetic ionizing fronts; plasma decay; rotating plasmas; cyclotron harmonic waves; hydromagnetic waves; laser diagnostics; and far-infrared. (Australia)

54781 ENERGY-TRANSFER EFFICIENCY OF A MAGNETIC-IMPLOSION SYSTEM. Timonin, A. M. (Scientific-Research Inst. of Electrophysical Apparatus, Leningrad). Sov. Phys.-Tech. Phys. (Engl. Transl.); 17: No. 2, 344-5(Aug 1972).

Translated from Zh. Tekh. Fiz.; 42: No. 2, 433-5(Feb 1972).

The efficiency with which energy is converted into the energy of a magnetic field in a magnetic-implosion system is found as a function of the flux compression and the field amplification. If the flux compression is limited, an extremely strong initial compression field is required for high efficiency. (auth)

54782 INTERACTION BETWEEN A PLASMA AND ELECTRON BEAM MODULATED BY LOW-FREQUENCY OSCILLATIONS. Berezina, G. P.; Fainberg, Ya. B.; Berezin, A. K.; Zeidlits, V. P. (Physical-Technical Inst., Kharkov). Zh. Eksp. Teor. Fiz.; 62: No. 6, 2115-20(Jun 1972). (In Russian).

The possibility of regulating the low-frequency oscillation spectra in a plasma–beam discharge by means of external low frequency modulation of the electron beam is studied. The high efficiency of this modulation technique is demonstrated. Low-frequency oscillations can be introduced into the beam–plasma system by deep modulation of the beam. When the modulation frequency is the same as that of the proper low-frequency plasma oscillations, the latter are excited in a resonant manner and suppression occurs of those oscillations (including drift oscillations) whose frequencies differ from the modulation frequency; moreover, the degree of turbulency of the oscillations in the low-frequency region decreases. (auth)

54783 NONSTATIONARY SOLENOIDAL REGULAR FLUXES OF LIKE-CHARGE PARTICLES. Ogorodnikov, S. N. Izv. Vyssh. Ucheb. Zaved., Radiofiz.; 15: No. 5, 792-4(1972). (In Russian).

Previous authors have investigated a two-dimensional nonstationary, nonrelativistic solenoidal regular flux of similar charged particles in the absence of a magnetic field, or in a magnetic field perpendicular to the plane of motion. This paper is concerned with an analogous flux in a completely random magnetic field. (K.S.W.)

Kinetics (Experimental)

54784 (IPP-1/125) DEVELOPMENT AND PROPERTIES OF THE HALO IN PINCH PLASMAS. Freund, Juergen (Max-Planck-Institut fuer Plasmaphysik, Garching (West Germany)). Feb 1972. 94p. (In German). Dep. NTIS (U. S. Sales Only).

In pinch discharges a second plasma region outside the central plasma column has been observed, which is called halo in some of the literature. This surrounding plasma was investigated in the experiments with the 5.4-m-long compression coil in the ISAR I linear theta pinch because there it appears highly pronounced. The development of the discharge was observed side-on (stereoscopic) with image converters and a streak camera. It appears possible to resolve the space–time behavior of the plasma, especially in the dynamic phase of the discharge, by using high-speed color reversal film (streak camera). Furthermore, the smear pictures show that after 6 to 8 μsec the halo region is frozen into the external magnetic field, i.e., from this time the halo is characterized by a high electric conductivity. The boundary layer of the halo follows a magnetic flux tube. The parameters of the halo, such as electron density, atomic temperature, and ion temperature were determined spectroscopically as a function of time and location from the broadening of the deuterium Balmer lines. (auth)

54785 PASSAGE OF HIGH-POWER LASER RADIATION THROUGN AN OPTICALLY DENSE PLASMA. Burakov, V. S.; Haumenkov, P. A.; Ivanov, V. P.; Kolosovskii, G. A. Zh. Prikl. Spektrosk.; 16: No. 2, 239-42(Feb 1972). (In Russian).

The transmission of ruby laser radiation (density 10^6 to 5×10^8 watt/cm^2) with a duration of 3×10^{-8} sec through a quasi-stationary plasma was studied. The plasma was contained in an electrical discharge in a capillary and had a temperature of about 4 eV. Nonlinear phenomena were observed during the passage of the laser radiation through the plasma, with an increase in the absorptive properties of the latter. (tr-auth)

54786 DIRECT MEASUREMENT OF DIFFUSION COOLING IN AN AFTERGLOW PLASMA. Boulmer, J.; Sol, C.; Gauthier, J. C. (Univ. Paris, Orsay, France). Phys. Lett.; 41A: No. 1, 83-4(28 Aug 1972).

Measurements of the electron temperature lowering by diffusion cooling in xenon afterglow plasmas are reported. They are in good agreement with available semi-quantitative theories. (auth)

54787 STIMULATED EMISSION EVOKED BY PUMPING WITH A PULSED ELECTRON BEAM PRODUCED IN A LINEAR DISCHARGE. Averin, V. G.; Karchevskii, A. I.; Yurkin, G. V. (Inst. of Atomic Energy, Moscow). Zh. Eksp. Teor. Fiz.; 63: No. 1, 85-91(Jul 1972). (In Russian).

It is demonstrated experimentally that on collective interaction between a powerful pulsed electron beam (~100 MW) produced in a large-current linear discharge and a preformed argon plasma with $n_0 = (3-5) \cdot 10^{13}$ cm^{-3}, argon–ion stimulated emission arises. The generation occurs in the visible (Ar II, λ4764 Å, λ4880 Å) and ultraviolet (Ar III, λ3511 Å, λ3638 Å) spectral ranges. The generation power for the Ar II transition is ~1 kW. (tr-auth)

Kinetics (Theoretical)

54788 (EUR-CEA-FC-642) COLLISIONAL-RADIATIVE VOLUME RECOMBINATION AND IONIZATION COEFFICIENTS FOR He^+–He^{2+}–e PLASMAS. Drawin, H. W.; Emard, F. (Commissariat a l'Energie Atomique, Fontenay-aux-Roses (France). Centre d'Etudes Nucleaires). Mar 1972. 29p. Dep. NTIS (U. S. Sales Only).

Coefficients are calculated for the collisional–radiative recombination of doubly ionized He atoms with electrons, and the collisional–radiative ionization of singly ionized He atoms into doubly ionized He atoms by electronic collisions and radiative absorption. Up to one hundred coupled equations are solved, which correspond to a level scheme in which levels having principal quantum numbers less or equal to 100 are considered. The numerical results are presented in the form of curves corresponding to a large number of parameters representing very different experimental situations. The values obtained are compared with experimental values determined by Mosburg and Gippius et al. All the numerical values obtained for the collisional–radiative coefficients are presented in tabular form. (France)

54789 (ITF-71-96-P) INTRODUCTION TO PHYSICAL KINETICS. Akhiezer, A. I.; Peletminskii, S. V. (Akademiya Nauk Ukrainskoi SSR, Kiev. Institut Teoreticheskoi Fiziki). 1971. 34p. (In Russian). Dep. NTIS (U. S. Sales Only).

Methods for obtaining the kinetic equations for classical systems are reviewed. These methods are based on the principle of spatial weakening of correlations and the idea first advanced by N. N. Bogolyubov about a multistage character of evolution of many-particle dyanmic systems. A chain of equations is established for many-particle distribution functions, on the basis of which the integral equations for these functions are derived. The solution of these equations by perturbation methods in the limiting cases of weak interaction, low density, and small plasma parameter makes it possible to obtain kinetic equations for one-particle distribution functions in various physically interesting cases. (auth)

54790 (JPRS-56713) SECOND HARMONIC GENERATION IN NONUNIFORM LASER-PRODUCED PLASMA. Vinogradov, A. V.; Pustovalov, V. V. (Akademiya Nauk SSSR, Moscow. Fizicheskii Institut). Translation of Russian Preprint No. 63. 17p. NTIS.

Coherent second harmonic emission with electromagnetic waves striking a layer of nonuniform plasma whose density exceeds the critical is examined. The temperature of the plasma is assumed to be high enough so that Coulomb collisions are negligible and the structure of the electromagnetic field near the critical point on the basic frequency is governed by the thermal motion of electrons. The above-stated conditions are satisfied in laser plasma with electron temperature $\kappa T_e \gtrsim 1$ keV and characteristic nonuniformity of 10^{-2} to 10^{-3} cm. In this case the conversion ratio of the laser emission to the second harmonic at optimal angles of incidence may reach 1% at a power of ~10^{13} watt/cm^2. (auth)

54791 RESONANT DIFFUSION IN THE PRESENCE OF STRONG PLASMA TURBULENCE. Birmingham, T. J. (Goddard Space Flight Center, Greenbelt, Md.). Phys. Fluids; 15: No. 10, 1778-85(Oct 1972).

The diffusion equation which describes the evolution of the average one-particle distribution function for an ensemble of strongly turbulent plasmas is derived. The diffusion tensor is a time integral of the autocorrelation tensor of the fluctuations as observed by particles moving along statistically distributed orbits. These orbits contain the effects of fluctuations and thus differ from those encountered in weak turbulence theory. Two statistical orbit effects quadratic in the strength of the fluctuations affect the magnitude of the diffusion: (a) modification of the ensemble average orbits by the fluctuations, and (b) statistical dispersion in particle orbits about the average. The plasma trajectory equations are used to relate each to the diffusion tensor itself when the turbulence is electrostatic. The diffusion tensor is explicitly evaluated for a strongly turbulent unmagnetized plasma. (auth)

54792 RESONANT SCATTERING OF TRAPPED PARTICLES BY TOROIDAL PLASMA MODES. Coppi, B. (Massachusetts

Inst. of Tech., Cambridge); Minardi, E.; Schram, D. C. Lett. Nuovo Cim.; 4: No. 15, 789-93(12 Aug 1972).

Collective modes capable of causing resonant scattering of trapped ions are found to be excited, under realistic conditions on the ion temperature and density gradients, in two-dimensional plasma confinement configurations. In addition, a significant asymptotic limit exists in which the influence of the excited modes on the trapped-particle orbits can be evaluated analytically. The toroidal magnetic field is represented by $B_\zeta = B_0[1 + (r/R_0) \cos\theta]^{-1}$, where r labels the magnetic surface and θ and ζ the poloidal and toroidal angles, respectively. (M.O.W.)

54793 INTERACTION OF A MULTILOOP ELECTRON STREAM WITH A PLASMA. Kotsarenko, N. Ya.; Senkevich, E. L.; Fedorchenko, A. M. (Kiev State Univ.). Sov. Phys.-Tech. Phys. (Engl. Transl.)· 17: No. 3, 402-4(Sep 1972).

Translated from Zh. Tekh. Fiz.; 42: No. 3, 508-10(Mar 1972).

The dispersion equation for a multiloop electron stream interacting with slow waves in a cold magnetized plasma is derived and analyzed. It is shown that instabilities occur in this system as a result of both the anomalous and normal Doppler effects. The instabilities are strongest at the lower harmonics of the cyclotron frequency and for wavelengths of the order of the electron Larmor radius. (auth)

54794 INJECTION OF A DENSE ELECTRON BEAM INTO A PLASMA. Rosinskii, S. E.; Rukhlin, V. G. (Inst. of Space Research, Moscow). Sov. Phys.-Tech. Phys. (Engl. Transl.); 17: No. 3, 405-12(Sep 1972).

Translated from Zh. Tekh. Fiz.; 42: No. 3, 511-21(Mar 1972).

The steady-state motion of an electron beam along a magnetic field after injection is discussed. It is shown that a dense beam propagating in a rarefied plasma assumes the shape of a highly corrugated cylinder; the depth of the corrugations is considerably greater than the initial radius of the beam, and the spacing between corrugations is of the order of the distance traversed by the electrons in a cyclotron period. The basic macroscopic parameters characterizing the beam motion are determined. The effect of the polarization properties of the background plasma on a dense beam is investigated. (auth)

54795 INTERACTION OF FINITE PERTURBATIONS IN A BEAM-PLASMA SYSTEM. Matsiborko, N. G.; Onishchenko, I. N.; Fainberg, Ya. B.; Shapiro, V. D.; Shevchenko, V. I. (Physical-Technical Inst., Kharkov). Sov. Phys.-Tech. Phys. (Engl. Transl.); 17· No. 3, 413-15(Sep 1972).

Translated from Zh. Tekh. Fiz.; 42: No. 3, 522-5(Mar 1972).

Equations describing the nonlinear interaction of waves excited in a system consisting of a plasma and a "cold" electron beam are derived and solved numerically. (auth)

54796 ABOUT THE ELECTRONIC SHIFTS OF THE STARK BROADENED LYMAN-α LINES. Caby-Eyraud, M.; Nguyen-Hoe (Univ., Paris). J. Phys., B (London); 5: No. 8, L153-6(Aug 1972).

Shift and asymmetry of broadened hydrogen lines in plasmas are investigated. All contributing multipoles and interactions between states with different principal quantum numbers (quenching effect) are included in the atom-perturber potential V(t). Numerical results are given for Ly_α line in the impact limit. Especially, for $T = 5 \times 10^4$°K, the shift arising from quenching effect is eight times greater than that arising from quadrupole and monopole. (auth)

54797 KINETIC EQUATIONS. Liboff, Richard L.; Rostoker, Norman (eds.). New York; Gordon and Breach, Science Publishers, Inc. (1971). 356p. $19.50.

A collection of 24 papers and 1 abstract are given that deal with the following aspects of kinetic theory: (1) axiomatics, (2) quantum and relativistic, (3) properties and solutions, and (4) waves and fluctuations. Several of the papers deal directly with kinetic equations for plasmas. (M.O.W.)

54798 INDUCED COMPTON EFFECT IN A PLASMA. Babuel-Peyrissac, J. P. (CEA, Villeneuve-Saint-Georges, France). Phys. Lett.; 41A: No. 2, 143-4(11 Sep 1972).

It is shown that the induced Compton effect explains the generation of a Stokes line in a recent experiment of plasma irradiation by the light of a laser. (auth)

54799 KINETIC PROCESSES IN A LASER PLASMA. Afanas'ev, Yu. V.; Belenov, E. M.; Krokhin, O. N.; Poluektov, I. A. (Inst. of Physics, Moscow). Zh. Eksp. Teor. Fiz.; 63: No. 1, 121-30(Jul 1972). (In Russian).

Kinetic processes in a high-temperature ($T_e \geq 1$ keV) laser plasma are investigated theoretically. The condition of a strong field for which the plasma state is not equilibrium is derived. The kinetic equation for the plasma electron distribution function is investigated under strong field conditions. The electron distribution function in a multicharge plasma ($z \gg 1$) is calculated analytically, and expressions are obtained for its parameters (temperature, ionization multiplicity, proper emission spectra) as functions of intensity and duration of the laser pulse. (tr-auth)

Production

Refer also to abstract 54830.

54800 (AEC-tr-7350) ACCUMULATION OF RESIDUAL GAS IONIZATION PLASMA IN AN ELECTROMAGNETIC TRAP. Pankrat'ev, Yu. I.; Nozrachev, M. G.; Lavrent'ev, O. A.; Safronov, B. G.; Naboka, V. A.; Ponomarenko, E. F. Translated from At. Energ. (USSR); 32: No. 2, 131-6(1972). 14p. Dep. NTIS.

An abstract of this paper, prepared from the original language, appeared as NSA 26: 22008. (M.O.W.)

54801 (CEA-CONF-2049) ANALYSIS OF THE MULTICHARGED HEAVY IONS PRODUCED BY LASER IMPACT ON A METALLIC TARGET. APPLICATION TO THE CONSTRUCTION OF A SOURCE. Perez, A. (Commissariat a l'Energie Atomique, Limeil-Brevannes (France). Centre d'Etudes). 1972. 11p. (In French). (CONF-720120-4). Dep. NTIS (U. S. Sales Only).

From Conference on the sources of multicharged ions; Paris, France (28 Jan 1972).

The spectral characteristics of the plasma created by laser impact on a heavy target were determined. The characteristics of the ion emission (directivity, dependence on the wavelength) were also studied. Tentative extraction and acceleration experiments were also performed. (France)

54802 ION ENERGIES IN A LASER-PRODUCED PLASMA. Bykovskii, Yu. A.; Degtyarev, V. G.; Degtyarenko, N. N.; (and others) (Moscow Engineering-Physics Inst.). Sov. Phys.-Tech. Phys. (Engl. Transl.); 17: No. 3, 517-20(Sep 1972).

Translated from Zh. Tekh. Fiz.; 42: No. 3, 658-61(Mar 1972).

The maximum energy E_{max} of the ions in a laser-produced plasma was measured as a function of the radiation flux density over the range $q \sim 10^8 - 10^{11}$ W/cm^2. A dependence of E_{max} on the ion mass was found. The function $E_{max} = f(q)$ is relatively weak in the range 10^8 to 10^9 W/cm^2. The integrated spectrum is found from the energy distribution of ions with different charge multiplicities. (auth)

54803 SELF-IGNITING PULSED OPTICAL DISCHARGE IN AN EROSIVE LASER PLASMA. Goncharov, V. K.; Poparev, A. N.; Min'ko, L. Ya. (Inst. of Physics, Minsk). Zh. Eksp. Teor. Fiz.; 62: No. 6, 2111-14(Jun 1972). (In Russian).

A pulsed optical discharge at atmospheric pressure was obtained for the first time at the focus of a lens with a radiation flux of 10^7 to 10^8 W/cm^2, the discharge being ignited by an erosive plasma produced by the laser radiation incident on absorbing materials. The burning peculiarities of the self-igniting pulsed optical discharge were studied. The electron density is estimated to be $\sim 2 \times 10^{17}$ cm^{-3} and excitation temperature ~22,000°K on the basis of spectroscopic investigations of the discharge plasma. (auth)

54804 NANOSECOND AND PICOSECOND LASER-PRODUCED CD_2 PLASMAS. Olsen, J. N.; Jones, E. D.; Gobeli, G. W. (Sandia Labs., Albuquerque, N. Mex.). J. Appl. Phys.; 43: No. 10, 3991-9(Oct 1972).

A preliminary comparison is made of plasmas created by irradiation of CD_2 slab targets by single high-energy Nd^{3+} glass laser pulses of 3.5-nsec (35 J max) and 3 to 10-psec (10 J max) duration. For the nanosecond irradiation one finds electron temperatures of 350 to 400 eV and appreciable C^{5+} ions at 20-keV expansion energy. Ion expansion energies for a picosecond pulse are about one-third those for a nanosecond irradiation of comparable energy. Up to 50% of the incident pulse energy may be accounted for in plasma expansion in either case. In each case, the specularly reflected energy back into the input f/5.0 lens is small: 0.4% and 0.8% for the nanosecond and picosecond times, respectively. Detailed ion analysis shows the target composition to be $CD_{2-x}H_x$, where $0.2 < x < 0.9$ with traces of oxygen also observable. (auth)

Stability

54805 (CONF-720705-4) OBSERVATION OF A PARAMETRIC INSTABILITY NEAR THE LOWER HYBRID FREQUENCY. Hooke, W. M.; Bernabei, S. (Princeton Univ., N. J. Plasma Physics Lab.). [nd]. Contract AT(11-1)-3073. 8p. Dep. NTIS.

From 1st topical conference on rf plasma heating; Lubbock, TX. (6 Jul 1972).

A parametric instability was observed at frequencies close to and somewhat above the lower hybrid resonance frequency. The threshold for this decay occurs when the rf electron drift velocity is of the order of the ion sound speed. (auth)

54806 (CONF-720804-6) TOROIDAL EFFECTS ON MHD STABILITY IN TOKAMAKS. Weimer, K. E.; Johnson, J. L.; Greene, J. M.; Frieman, E. A. (Princeton Univ., N. J. Plasma Physics Lab.). [nd]. Contract AT(11-1)-3073. 4p. Dep. NTIS.

From 5th European conference on controlled fusion and plasma physics; Grenoble, France (21 Aug 1972).

Toroidal effects on MHD flute, ballooning, and kink modes are examined in an expansion in the inverse aspect ratio a/R, and stability criteria are found. (auth)

54807 (COO-3497-2) ANNUAL PROGRESS REPORT. Simon, Albert (Rochester Univ., N. Y.). 15 Sep 1972. Contract AT(11-1)-3497. 9p. Dep. NTIS.

A mirror-flute instability analysis was carried through in both the quasi-linear and nonlinear limits in slab and cylindrical geometry. Explosive instability occurs only if one includes "non-constant" gravity in the equations of motion. The analysis for collisional drift instability was carried through in both quasi-linear and nonlinear limits in slab geometry for constant electron temperature. Brief summaries of the above work are given. (M.O.W.)

54808 (LRP-51/72) TRANSVERSE DYNAMIC STABILIZATION OF A THETA PINCH. Lister, G. G.; Troyon, F. S.; Weibel, E. S. (Centre de Recherches en Physique des Plasmas, Lausanne (Switzerland)). Jun 1972. 33p. Dep. NTIS (U. S. Sales Only).

The stability of a straight plasma column confined by a static axial magnetic field and a small oscillating transverse magnetic field is discussed. Growth rates for the most important parametric instabilities are obtained. The influence of damping in providing a stabilizing mechanism against these instabilities is discussed, and a set of stability criteria are obtained using a viscous fluid model for the plasma. The possibility of suppressing the fastest growing instability by "wobbling" the frequency of the applied field is also discussed. An order-of-magnitude calculation for dynamic stabilization of a toroidal plasma is presented. (auth)

54809 (NP-19406) EXCITATION BY VERY HIGH FREQUENCY WAVE PUMPING OF PARAMETRIC INSTABILITIES IN A MAGNETOACTIVE PLASMA. Andreev, H. E.; Batanov, G. M.; SarkSyan, K. A. (Akademiya Nauk SSSR, Moscow. Fizicheskii Institut). 1972. 17p. (In Russian). Dep. NTIS (U. S. Sales Only).

Nonthermal radiation from magnetoactive plasma was experimentally investigated while the plasma was interacting with a vhf wave, the frequency ω_0 of which was greater than the electron Langmuir frequency ω_L but less than the electron cyclotron frequency. Radiation at a displaced frequency, relative to ω_0, was detected in the direction of smaller frequencies on the order of ion-acoustic vibrations. A dependence of plasma density on radiation intensity at the second harmonic of the vhf pumping wave was investigated. The relation of the observed radiation to the development of a parametric instability was discussed. (tr-auth)

54810 LINEAR THEORY OF CURRENT-DRIVEN PLASMA INSTABILITIES. Sizonenko, V. L.; Stepanov, K. N. (Physical-Technical Inst., Kharkov). Sov. Phys.-Tech. Phys. (Engl. Transl.); 17: No. 3, 385-8(Sep 1972).

Translated from Zh. Tekh. Fiz.; 42: No. 3, 484-9(Mar 1972).

If the electrons move with respect to the ions with a velocity appreciably greater than the electron thermal velocity, oscillations can be excited in which resonant electrons and ions participate. The growth rates are of the same order as those for coherent excitation of MHD instabilities. (auth)

54811 NONLINEAR ELECTRON-CYCLOTRON DRIFT INSTABILITY. Biskamp, D.; Chodure, R. (Max-Planck-Institut fuer Plasmaphysik, Garching, Ger.). Nucl. Fusion; 12: No. 4, 485-7 (Jul 1972).

A simple model was used to investigate the dependence of the growth rate of the electron-cyclotron drift instability on parameters such as drift velocity over thermal velocity, and the magnetic field strength given by the ratio Ω_e/ω_{pe}. The results are compared to one-dimensional calculations. (M.O.W.)

54812 DISSIPATIVE INSTABILITY DUE TO SUPERSONIC MOTION OF IONS WITH RESPECT TO NEUTRALS. Stakhanov, I. P. Sov. Phys.-Tech. Phys. (Engl. Transl.); 17: No. 3, 396-401(Sep 1972).

Translated from Zh. Tekh. Fiz.; 42: No. 3, 500-7(Mar 1972).

A dissipative instability in a weakly ionized plasma due to collisions with neutrals is analyzed; hydrodynamic supersonic flow with friction between charged and neutral components in a plasma is also analyzed. If the plasma velocity, with respect to the neutrals, exceeds the ion-acoustic velocity, an instability develops. In the initial stage the growth rate is proportional to the frequency of ion-neutral collisions; the instability disappears in the absence of such collisions. The change in the character of the large-scale flow due to the instability is evaluated in the quasi-linear approximation. (auth)

54813 MAGNETOHYDRODYNAMIC AND TEARING INSTABILITIES IN A TOKAMAK. Amano, Tsuneo (Osaka Univ.); Wakatani, Masahiro; Watanabe, Masami. J. Phys. Soc. Jap.; 33: No. 3, 782-8(Sep 1972).

The stability of a current-carrying plasma in a strong longitudinal magnetic field, such as in Tokamak-type devices, against the MHD and tearing instability is investigated. The growth rates of the MHD instability are computed numerically as eigenvalues of the equation of motion for several current distributions. The influence of the position of the conducting shell on the stability is also investigated. (auth)

54814 DETERMINATION OF THE MAGNETIC FIELD B IN VACUUM FOR GENERAL TWO-DIMENSIONAL MHD EQUILIBRIA. Kerner, W.; Pfirsch, D.; Tasso, H. (Max-Planck-Institut fuer Plasmaphysik, Garching, Ger.). Nucl. Fusion; 12: No. 4, 433-5 (Jul 1972).

For general two-dimensional MHD-equilibria it is possible, by using complex functions, to obtain the solution of the vacuum magnetic field which fits the boundary conditions at the plasma surface. The solution allows a distinction between the geometry-governed and the plasma-magnetic-field-governed singularities and stagnation points. Several examples, particularly the elliptic-plasma-boundary case, are discussed. (auth)

54815 PLASMA EQUILIBRIUM IN CONFIGURATIONS WITH A HELICAL MAGNETIC AXIS WITH ALLOWANCE FOR TOROIDALITY. Aleksin, V. F.; Shishkin, A. A. (Physical-Technical Inst., Kharkov). Nucl. Fusion; 12: No. 4, 437-43(Jul 1972).

Plasma equilibrium is studied in Vintotrons toroidal traps with a spatial magnetic axis established by various combinations of magnetic fields from helical conductors. The displacement of the vacuum magnetic axis is determined in the presence of a plasma as a function of the relationship between the curvature of the helical magnetic axis, the curvature of the torus, and a parameter characterizing the ellipticity of the vacuum magnetic surfaces. The limiting equilibrium values of $\beta = 8\pi P_0/B_0^2$ are determined from the displacement of the magnetic axis. Characteristic equilibrium values of β are compared for Vintotrons and stellarators. The possible effects of resonance phenomena that can occur in a toroidal Vintotron in the presence of a plasma are also discussed. (auth)

54816 LONG-WAVE INSTABILITY CAUSED BY INHOMOGENEOUS ION BEAMS IN A DENSE MAGNETIZED PLASMA. Goncharov, A. A.; Pashitskii, E. A. (Inst. of Physics, Kiev). Sov. Phys.-Tech. Phys. (Engl. Transl.); 17: No. 3, 418-23 (Sep 1972).

Translated from Zh. Tekh. Fiz.; 42: No. 3, 528-35(Mar 1972).

A longwave surface-wave instability is investigated in a system of spatially inhomogeneous ion beams moving along the magnetic field in a dense plasma. In the frequency range $\omega_{Hi} \ll \omega \ll \omega_{He}$ and the velocity range $c_s \ll V_0 \ll V_e$ a density inhomogeneity $n_0(x)$ or a velocity inhomogeneity $V_0(x)$ can cause a gradient-driven instability. (auth)

54817 ELECTROSTATIC INSTABILITY OF A HOT-ELECTRON PLASMA IN A HIGH-FREQUENCY FIELD. Klopovskii, K. S. Sov. Phys.-Tech. Phys. (Engl. Transl.); 17: No. 3, 441-7(Sep 1972).

Translated from Zh. Tekh. Fiz.; 42: No. 3, 558-67(Mar 1972).

Intermittent microscopic instabilities are frequently observed in experiments on the heating of an electron plasma by a high-frequency field. A theoretical discussion of this instability is given on the basis of a model incorporating the features of the experimental situation. An electron plasma is assumed to have a cold component and a hot component. The cold component is uniformly distributed throughout the volume of a cylindrical resonator and has a density greater than that of the hot component. The hot electrons are trapped in the high-frequency field excited in the resonator and perform anharmonic oscillations about the minimum of U_{hf}, where U_{hf} is the effective potential associated with the hf field. Under these conditions the interaction of the cold electrons with the trapped hot electrons can lead to the development of an electrostatic instability in the cold plasma. The instability is similar to the negative mass instability. The instability appears at the cyclotron frequency and the plasma frequency. (auth)

54818 TRANSVERSE INSTABILITY OF HOT-ELECTRON PLASMA IN A CYLINDRICAL RESONATOR. Klopovskii, K. S. Sov. Phys.-Tech. Phys. (Engl. Transl.): 17: No. 3, 448-55 (Sep 1972).

Translated from Zh. Tekh. Fiz.; 42: No. 3, 568-77(Mar 1972).

The microinstabilities associated with the heating of an electron plasma by a high-frequency field in a cylindrical resonator are studied. The resonator is assumed to contain a low-density hot electron plasma confined by the hf field. Under certain conditions, transverse instabilities can occur at frequencies $1\Omega + n\omega_0$ (Ω is the Larmor frequency and ω_0 the axial bounce frequency of the electrons). The strongest instabilities are the E mode ($H_z = 0$), in the direction $k_\perp^2/k_\parallel^2 > 1^2\Omega^2/n^2\omega_0^2 \gg 1$. The instability is similar to the negative-mass instability. The influence of the electron energy distribution on the instability is analyzed. (auth)

54819 INSTABILITY CONTROL IN A BEAM—PLASMA SYSTEM. Udovichenko, Yu. K.; Leont'ev, N. I.; Timoshenko, A. P. Sov. Phys.-Tech. Phys. (Engl. Transl.); 17: No. 3, 477-81(Sep 1972).

Translated from Zh. Tekh. Fiz.; 42: No. 3, 605-11(Mar 1972).

The excitation of low-frequency (ion-acoustic, relaxation) and high-frequency oscillations in a beam—plasma system was studied experimentally. Excitation is controlled by varying the potential of an electrode inserted into the plasma. The instabilities can be controlled by applying relatively low positive potentials to the electrode. (auth)

54820 SYNCHROTRON INSTABILITY FOR PLASMA WAVES. Goreva, T. A.; Suvorov, E. V. (Gorky Radiophysical Research Inst., USSR). Zh. Eksp. Teor. Fiz.; 62: No. 6, 2147-55(Jun 1972). (In Russian).

The conditions of existence in a magnetoactive plasma of longitudinal waves with a phase velocity close to that of light are obtained. The increments of such waves during synchrotron instability due to the presence of isotropically distributed relativistic particles are determined and investigated. It is shown that the increments of the longitudinal waves considerably exceed those of the transverse wave instability appearing for the same parameters of the medium. (auth)

54821 NONLINEAR STABILIZATION OF BEAM INSTABILITY. Demchenko, V. V.; El-Siragy, N. M. (Atomic Energy Establishment, Cairo). Phys. Lett.; 41A: No. 2, 132-4(11 Sep 1972).

If a high-frequency field affects the dielectric properties of the plasma, it can be shown that this results in a dependence of the frequency of natural plasma oscillations on the field amplitude. So, the beam and the excited waves get out of resonance, the instability weakens and sometimes may totally vanish. (auth)

54822 INSTABILITY OF SPATIALLY SEPARATED PLASMA BEAMS. III. Bogdanov, E. P.; Orlov, L. K.; Romanov, Yu. A. (Gorky State Univ., USSR). Izv. Vyssh. Ucheb. Zaved., Radiofiz.; 15: No. 4, 521-7(1972). (In Russian).

The two-stream instability of spatially separated plasma beams of finite thickness is examined in a quasi-hydrodynamic approximation. It is shown that, if the beams have finite thickness, the instability region is limited both by small and large drift velocities. A minimum drift velocity at which the instability occurs may be smaller than the corresponding value in semi-bounded beams. The maximum of the increment of amplified waves decreases with decreasing layer thickness. The influence of the dielectric sublayer between the beams on the instability is studied. (tr-auth)

54823 DYNAMIC STABILIZER FOR PLASMA INSTABILITIES TO IMPROVE PLASMA CONFINEMENT AND TO INCREASE PLASMA DENSITY. Hendel, Hans W.; Tsu-kai, Chu; Simonen, Thomas C. (to United States Atomic Energy Commission). U. S. Patent 3,668,066. 6 Jun 1972. Filed 18 Feb 1970.

Method and apparatus are described for dynamic stabilization of plasma instabilities for improving plasma confinement and for increasing plasma density independent of the phase of the instabilities. The method comprises confining the plasma column between ionizing plates which supply energetic particles to the plasma in a direction parallel to the axis of the plasma column and interacting the plasma in a predetermined direction with externally supplied radio-frequency fields having a selectively variable power level amplitude and a sufficiently high frequency range. (auth)

Thermonuclear Processes

Refer also to abstract 53085.

54824 (AEC-tr-7334) EXPERIMENTAL DETERMINATION OF THE BASIC CHARACTERISTICS OF SPACE-PERIODIC MAGNETIC CONFIGURATIONS. Loktionov, Yu. M.; Sebko, V. P.; Tyupa, V. I. (Akademiya Nauk Ukrainskoi SSR, Kharkov. Fiziko-Tekhnicheskii Institut). Translation of report KHFTI-70/49. 11p. Dep. NTIS.

The specific features of magnetic configurations with the spatial magnetic axis of the "vintotron," "vintotors" and "asymmetrical stellarator" types often do not permit the use of the method employed for systems with a plane magnetic axis ("stellarator," "torsatron") for investigating the magnetic fields by means of electron beams. A certain modification of such a method, however, described in this work, makes it possible to investigate experimentally several important characteristics of configurations exhibiting a helical magnetic axis. Experimentally investigated herein are the structures of magnetic surfaces, position of spatial magnetic axes, angles of rotational transformation and shear in the single-pass "vintotron" and double-pass "vintotors," which are used herein as examples. (auth)

54825 (CLM-R-116) USE OF LIQUID LITHIUM AS COOLANT IN A TOROIDAL FUSION REACTOR. PART II. STRESS LIMITATIONS. Hancox, R.; Booth, J. A. (United Kingdom Atomic Energy Authority, Abingdon (England). Culham Lab.). Nov 1971. 10p. Dep. NTIS (U. S. Sales Only). UK 50 pence.

The pressure gradient induced in liquid lithium as it is pumped across a magnetic field was calculated in Part I of this report. The stress in the walls of the lithium ducts due to this pressure is shown to limit the wall loading in a toroidal reactor, and this limitation is seen to be more severe than the need to restrict the pumping power. A stress criterion is developed and then applied to both a low-power prototype reactor and a large commercial reactor. It is shown that, although the use of the lithium for cooling the nuclear blanket is possible in the former, it leads to an economically unattractive power density in the commercial reactor. (auth)

54826 (CONF-720901—(Bks.1 and 2), pp 559-73) NEUTRON AND GAMMA PHYSICS PROBLEMS IN FUSION REACTORS. Maynard, C. W.; Abdou, M. A. (Univ. of Wisconsin, Madison). 1972.

From Meeting on new developments in reactor physics and shielding calculations; Kiamesha Lake, NY. (12 Sep 1972).

The discussions and results presented here apply to a fusion reactor classified as a D—T fueled low-β toroidal system. However, most of the paper will apply almost equally well to other systems. A low-β toroidal reactor will confine the plasma in a torus surrounded by a coolant and lithium bearing region called the blanket and followed by a shield. The magnet coils are outside this and will be superconducting to achieve the large fields required. Various fueling and exhaust ports breach the blanket and shield and coolant passages must pass between magnet windings. Neutron absorptions in lithium provide the tritium production for fuel breeding. The results of importance for reactor design fall into the following categories. The helium, proton, and atom displacement production rates are important in evaluating radiation damage problems. The (n,2n) reaction rates as well as the ^{6}Li and ^{7}Li tritium production rates influence the tritium breeding ratio. The energy deposition rate by the neutrons and the resulting gammas provide the basic input for heat removal studies. Activation of structural and other materials is important for decay heat and hazards studies; and leakage from the shield determines the heat load to the refrigeration system for the superconducting magnets. (M.O.W.)

54827 (IPP-4/97) LITHIUM AND FLIBE AS COOLANTS FOR FUSION REACTOR BLANKETS. Daenner, W. (Max-Planck-Institut fuer Plasmaphysik, Garching (West Germany)). Jun 1972. 22p. (In German). Dep. NTIS (U. S. Sales Only).

Lithium and flibe which were both proposed as coolants for thermonuclear reactor blankets are different not only in view of their neutronic behavior but also in view of their thermohydraulic properties. The thermal properties of both coolants are summarized and compared with those of sodium. The heat-transport properties appear superior to those of sodium. The influence of strong magnetic fields on the flow conditions and the heat transfer characteristics are pointed out. Pumping losses and pumping power prove to be of mainly hydrodynamic nature in the case of flibe, whereas they are essentially determined by MHD-pressure losses in the case of lithium and sodium. The differences of temperature and pressure-drop characteristics in a cooling channel are discussed for the case of coupling it to a steam thermal power cycle. (auth)

54828 (LA-DC-72-896) SURVEY OF SCYLLAC EXPERIMENTS. Burnett, S. C.; Ellis, W. R.; Gribble, R. F.; (and others)

(Los Alamos Scientific Lab., N. Mex.). [nd]. 12p. (CONF-720804-7). Dep. NTIS.

From 5th European conference on controlled fusion and plasma physics; Grenoble, France (21 Aug 1972).

"Scyllac" research is currently divided among three major experimental efforts: (a) the 5-meter 120° toroidal sector, (b) a 5-meter linear theta pinch with strong end mirrors, and (c) a feedback stabilization experiment on Scylla IV-3. In the sector the toroidal force and outward plasma drift are compensated by a combination of $l = 1$ helical fields and $l = 0$ bumpy fields. A period of equilibrium on the toroidal axis is followed by sideward motion of the plasma column, predominantly in the plane of the torus, that could either be an imbalance between the $l = 1,0$ and toroidal forces or a long-wavelength $m = 1$ instability. Containment times up to 11 μsec, comparable to times for plasma end loss, have been observed. Without mirrors the linear device produces a 2- to 3-keV plasma that shows a "wobble" of up to 1.5-cm amplitude, but otherwise remains centered more than 35 μsec (~3 e-folding times for end loss). With simultaneously applied mirror fields of 2.5 mirror ratio, the plasma column shows evidence of an $m = 1$ instability that carries it to the wall at some point along its length early in time. However, the column re-forms and the neutron yield is larger than without mirrors for the entire plasma lifetime. In the feedback experiment, $l = 0$ windings are driven by a power amplifier from a signal generated by plasma displacement as determined by an optical sensor. Initial results confirm feasibility of the feedback concept. (auth)

54829 (ORNL-TM-3953) SUMMARY OF ENGINEERING DESIGN OF MAGNET SYSTEMS FROM INTERNATIONAL WORKING SESSION ON FUSION REACTOR TECHNOLOGY. Lubell, M. S. (Oak Ridge National Lab., Tenn.). Sep 1972. Contract W-7405-eng-26. 51p. Dep. NTIS.

The emerging importance of superconducting magnet systems not only for fusion reactors but also for fusion research was clearly indicated by the great number of papers presented at this session. There were twenty-four talks, including two state-of-the-art reviews, and thus this summary will attempt to provide a general overall impression of the session without reviewing each contribution in depth. An appendix follows listing the topics and speakers in order of presentation and a short abstract which most of the participants provided for their contribution. Many subjects were discussed and various problems mentioned. The major problems raised and still to be investigated for very large-scale systems are: (1) superconducting material cost, particularly for high fields, (2) large-bore high-field magnets, (3) superconducting instabilities in magnets not completely stabilized, (4) structural problems associated with static and dynamic force containment, (5) switches for inductive energy-storage devices and also persistent switches for superconducting magnets, (6) protection of superconducting magnet systems, including dewars, and structural members against a sudden quench, and (7) refrigeration and field-erected vacuum systems. (auth)

54830 FUSION BY LASER-DRIVEN FLAME PROPAGATION IN SOLID DT TARGETS. Bobin, J. L.; Colombant, D.; Tonon, G. (Centre d'Etudes de Limeil, Villeneuve-Saint-Georges, France). Nucl. Fusion; 12: No. 4, 445-52(Jul 1972).

When a laser light flux ϕ impinges on a solid target, a radiation wave propagates that transforms the material into a hot plasma. The structure of the hot parts is known to show an overdense hot stationary deflagration structure followed by a nearly isothermal rarefaction. The temperature T of the hot plasma varies as $(\phi/n_{ec})^{1/3}$, n_{ec} being the cutoff density. Then the ratio of the energy of the thermonuclear reaction products to the sum of the radiated energy plus the (kinetic + thermal) energy in the plasma is readily calculated for DT as a function of the duration of the interaction. For a 30% efficiency of the energy-conversion cycle, typical figures for a positive energy balance are $\phi = 5 \times 10^{14}$ W/cm^2 (T = 10^8°K), $\tau = 10^{-7}$ s for Nd glass, and $\phi = 5 \times 10^{12}$ W/cm^2 (T = 10^8°K), $\tau = 10^{-5}$ s for CO_2 laser. For both cases, the required laser energy density is a few 10^7 joules/cm^2. In the latter case, a megagauss confining field could be successfully used to maintain a one-dimensional flame-propagation geometry. (auth)

54831 THERMONUCLEAR HOT SPOT. Somon, J. P. (EURATOM-CNEN, Frascati, Italy). Nucl. Fusion; 12: No. 4, 461-74 (Jul 1972).

The expansion of a spherical hot-spot within an infinite D—T medium is examined and the production of thermonuclear energy is calculated through the numerical solution of the plasma-fluid equations in a number of cases. Two kinds of hot-spots are considered in which the ions are initially either hot (ionic H-S) or cold (electronic H-S). The conditions for a positive energy balance and the ignition of a thermonuclear reaction wave are derived. At solid-state density a pulsed fusion reactor requires an energy of 10^3 to 10^4 MJ. Extensions are made to plane and cylindrical H-S and the expansion of a spherical H-S in vacuum. The thermonuclear output is not improved by progressive H-S heating or a decrease in thermal conductivity in a transverse magnetic field. (auth)

54832 INFLUENCE OF TOROIDALITY ON A MAGNETIC CONFIGURATION WITH A HELICAL MAGNETIC AXIS. Aleksin, V. F.; Nemov, V. V.; Shishkin, A. A. (Physical-Technical Inst., Kharkov). Nucl. Fusion; 12: No. 4, 411-17(Jul 1972).

The changes that occur in a configuration with a helical magnetic axis upon bending to form a torus are investigated. Such a magnetic configuration can be created by various combinations of magnetic fields produced by helical conductors. In the calculations it is assumed that the pitch of the helical winding and the radius of the circular axis of the torus are significantly greater than the minor radius of the torus. This means that $\delta = b/R \ll 1$ and $\epsilon = lb/R \ll 1$, where b and R are, respectively, the minor and major radii of the torus and l is the number of turns of the helical conductor around the torus. Toroidality is regarded as a perturbation superposed on the configuration with a helical magnetic axis. The conditions under which the helical magnetic axis breaks down are considered. The distance to which the resulting magnetic axes move away from the magnetic axis of the unperturbed configuration is indicated approximately. (auth)

54833 CONDITIONS FOR QUASI-STEADY DEVELOPMENT OF SELF-SUSTAINING NUCLEAR REACTIONS. Kolesnichenko, Ya. I. (Inst. of Nuclear Research, Kiev). Nucl. Fusion; 12: No. 4, 419-22(Jul 1972).

The conditions in which quasi-steady operation of a thermonuclear reactor is possible are investigated. The examination is based on the equation for the energy balance of a deuterium—tritium plasma layer in which thermonuclear reactions are occurring. It is assumed that the principal energy losses from the system are due to thermal conductivity of the plasma and to bremsstrahlung. It is shown that quasi-steady operation of a thermonuclear reactor requires certain limitations on the transverse plasma dimension L. When this dimension exceeds a critical value L_{max} there will occur self-acceleration of the thermonuclear reactions and self-heating of the plasma, which in the initial stage are similar to a thermal explosion. If $L < L_{min}$, the energy lost from the system will exceed the energy released in it and the thermonuclear reaction will be extinguished. The quantities L_{max} and L_{min} are determined by the transverse transport coefficients of the plasma and by the boundary conditions. The temperature distributions in the plasma layer are found. The stability of these distributions is studied. It is concluded that steady states are unstable in systems with a low boundary temperature. (auth)

54834 MEGAGAUSS PHYSICS. Latal, Heimo G. (Univ., Graz). Acta Phys. Austr.; 34: No. 1-2, 65-82(1971). (In German).

The production of megagauss magnetic fields is reviewed. The various methods with their limitations are discussed, especially the implosion method. In addition to flux compression using explosions as triggers, an interesting variation—electromagnetic compression—is also presented. Findings in megagauss fields are analyzed with respect to such effects as Zeeman's, Faraday's and conductivity. Also discussed are special application of megagauss fields for the study of high-energy quantum-electrodynamic effects. (34 references) (H.B.G.)

54835 POLYGONAL ASTRON REACTOR FOR PRODUCING CONTROLLED FUSION REACTIONS. Christofilos, Nicholas C. (to United States Atomic Energy Commission). U. S. Patent 3,668,067. 6 Jun 1972. Filed 16 Oct 1969.

An Astron reactor is described that includes a plurality of linear magnetic field regions joined by intervening curved magnetic fields and arranged in a polygonal configuration. Energetic charged particles are introduced and trapped in the linear sections to form cylindrical sheaths, i.e., E layers, of charged particles rotating about the axis of each section with the magnetic field thereof interacting with the linear magnetic regions to produce a closed system of magnetic-field lines defining a containment zone for charged particles. Fuel materials introduced into the field are ionized and heated to form a high-temperature plasma trapped in the said zone. The ratio of the lengths of the linear and curved-field regions is regulated to offset Bohm diffusion losses. A high molecular weight initiator plasma may also be introduced to heat the fuel to fusion temperatures. (auth)

Wave Phenomena

Refer also to abstract 54792.

54836 (AEC-tr-7331) GENERATION OF FAST ELECTRONS THROUGH INTERACTION OF SHF WAVE WITH COLLISIONLESS PLASMA. Bariyaov, V. I.; Gekker, I. R.; Sizukhin, O. V.; Khachaturan, Z. G. (Akademiya Nauk SSSR, Moscow. Fizicheskii Institut). Translation of report NP-18958. 7p. Dep. NTIS.

An investigation was carried out in order to determine whether or not fast electrons are generated during observation of anomalous absorption of shf waves in collisionless plasma. The plasma flow is produced by a spark injector (hydrogen—carbon plasma). (auth)

54837 . (AEC-tr-7333) EXCITATION OF ELECTROMAGNETIC WAVES IN A PLASMA BY A RELATIVISTIC ELECTRON BEAM. PART I. LONGITUDINAL WAVES. Rukhadze, A. A.; Bogdankevich, L. S.; Dolzhenko, O. V. (Akademiya Nauk SSSR, Moscow. Institut Fiziki). Translation of report NP-18982. 21p. Dep. NTIS.

A metal waveguide of radius R is filled with a plasma through which a relativistic electron beam with radius $r < R$ passes. The hydrodynamic equations are given for a collision-free, cold plasma contained by an external longitudinal magnetic field B which is greater than the beam current field. On linearizing this set of equations for small deviations from a stationary equilibrium state, a partial differential equation is obtained for the perturbed field potential. The conditions for beam instability and cyclotron instability are explored over a rather narrow range of high-frequency plasma oscillations for the case of $r = R$. The conditions for long- and short-wave oscillations are also given at $r < R$. A discussion is presented on the production of radiation in the region of wavelengths $l = 10^{-1}$ to 3 cm on interaction of a 1-MeV electron beam with a plasma having a particle density of 10^{10} to 10^{12} particles/cm^3. (TTT)

54838 (AEC-tr-7335) ON THE THEORY OF TRANSFORMATION OF SURFACE WAVES INTO LONGITUDINAL OSCILLATIONS IN THE SURFACE LAYER OF A PLASMA WAVEGUIDE. Demchenko, V. V.; Dolgopolov, V. V.; Omel'chenko, A. Ya. (Akademiya Nauk Ukrainskoi SSR, Kharkov. Fiziko-Tekhnicheskii Institut). Translation of report KHFTI-70-55. 12p. Dep. NTIS.

It is shown that surface waves caused by perturbation in a homogeneous plasma cylinder during the interval of time determined by the width of the narrow transition region from plasma to vacuum, are converted to longitudinal oscillations concentrated in the plasma—vacuum transition layer and propagating along the plasma density gradient (radially). (auth)

54839 (AEC-tr-7336) EFFECT OF HIGH-FREQUENCY POTENTIAL ON PROPAGATION OF FAST WAVES ALONG A MAGNETOACTIVE PLASMA LAYER. Demchenko, V. V.; Dolgopolov, V. V.; Omel'chenko, A. Ya. (Akademiya Nauk Ukrainskoi SSR, Kharkov. Fiziko-Tekhnicheskii Institut). Translation of report KHFTI-70-57. 9p. Dep. NTIS.

The effect of electromagnetic wave field pressure on the propagation of fast waves along a plane-parallel layer of magnetoactive plasma is investigated. Expressions are derived for the fields and dispersion equations are derived in limiting cases when the high-frequency potential is low or great compared with the plasma temperature. The dispersion equations differ substantially from the dispersion equations of linear theory. Plasma density distribution through layer thickness is determined. It is shown that high-frequency potential may assure penetration of the electromagnetic field into plasma, which in linear approximation does not penetrate into the plasma due to the skin effect. (auth)

54840 (AEC-tr-7337) ON THE EFFECT OF WAVE FIELD PRESSURE ON LONGITUDINAL OSCILLATIONS IN A PLASMA. Dolgopolov, V. V. (Akademiya Nauk Ukrainskoi SSR, Kharkov. Fiziko-Tekhnicheskii Institut). Translation of report KHFTI-70-58. 4p. Dep. NTIS.

The effect of hf wave potential (electromagnetic wave field pressure) on Langmuir monochromatic oscillations in plasma is investigated. It is shown that the pattern of field oscillations, constructed with consideration of the high-frequency potential, differs substantially from that of oscillations in linear approximation even in the case when gas-kinetic pressure of the plasma is substantially higher than the electromagnetic field pressure. In particular, localized monochromatic standing waves are found to be possible. (auth)

54841 (AEC-tr-7338) CONDITIONS FOR WAVE TRANSFORMATION IN A PLASMA WITH A NONMONOTONIC LONGITUDINAL DISTRIBUTION. Arkhipenko, V. I.; Budnikov, V. N.; Obukhov, A. A. (Akademiya Nauk SSSR, Leningrad. Fiziko-Tekhnicheskii Institut). Translation of report NP-18913. 15p. Dep. NTIS.

The results of experimental studies and analysis of conditions for wave transformation in a plasma with a nonmonotonic longitudinal distribution are described. The plasma was formed in a homogeneous magnetic field at magnetic fields greater than the electron-cyclotron field $H > H_c = mc\omega/e$ under the action of superhigh-frequency power in the 10-cm wavelength range. The experimental conditions were: the working gas was argon at pressure of 10^{-1} to 10^{-3} mm Hg, the magnetic field was up to 3000 Oe, $n = 10^{11}$ to 10^{12} cm^{-3}, and $T_e = 2$ to 10 eV. (auth)

54842 (AEC-tr-7339) STUDY OF THE LOCALIZATION OF THE WAVE TRANSFORMATION REGION IN A SUPERHIGH-FREQUENCY DISCHARGE PLASMA. Arkhipenko, V. I.; Budnikov, V. N.; Obukhov, A. A. (Akademiya Nauk SSSR, Leningrad. Fiziko-Tekhnicheskii Institut). Translation of report NP-18912. 10p. Dep. NTIS.

The position of the wave transformation region in a plasma formed under the action of superhigh-frequency power of the 10-cm range was investigated. Experiments were carried out under magnetic fields smaller and greater than the electron cyclotron field, which corresponds to the high-frequency and middle regions of wave transformation in a plasma. The plasma was produced in a quartz cylinder 70 cm in length and 2.5 cm in diameter placed in a rectangular waveguide of the 10-cm range at argon pressures of 10^{-1} to 10^{-3} mm Hg. The position of the transformation region was determined with the aid of small local perturbations of the magnetic field leading to collapse of the discharge. The longitudinal distribution of light radiation was also measured. The characteristics of the position of the transformation regions and the longitudinal distribution are discussed on the basis of the conclusions of the theory of wave transformation in a plasma with a two-dimensional inhomogeneity. (auth)

54843 (AREAEE-124) PENETRATION OF TRAVELLING HIGH-FREQUENCY ELECTROMAGNETIC FIELD INTO A "NON-TRANSPARENT" PLASMA. Demchenko, V. V.; Hussein, A. M. (Atomic Energy Establishment, Cairo (Egypt). Dept. of Accelerators and Plasma Physics Research). 1971. 20p. Dep. NTIS (U.S. Sales Only).

The effect of the averaged force of a high-frequency field on the propagation of electromagnetic waves by external harmonic currents is investigated in bounded plasma configurations. The account of high-frequency pressure is shown to result in the following: the plasma which was "non-transparent" for waves in a linear approximation (with no account of high-frequency pressure) becomes "transparent" or, in the nonlinear approximation, the waves can penetrate into the plasma if the field is skinned in the linear approximation. (auth)

54844 (AREAEE-125) THEORY OF PARAMETRIC EXCITATION OF OSCILLATIONS IN AN INHOMOGENEOUS PLASMA. Demchenko, V. V.; El-Naggar, I. A. (Atomic Energy Establishment, Cairo (Egypt). Dept. of Accelerators and Plasma Physics Research). 1971. 23p. Dep. NTIS (U. S. Sales Only).

Nonlinear effects that affect longitudinal oscillations of inhomogeneous plasma in the vicinity of plasma (hybrid) resonance points are investigated. The account of nonlinear terms due to plasma inhomogeneity in the equations of motion is shown to lead to the possibility of parametric buildup of oscillations at the subharmonic (harmonic) of the applied-field frequency. (auth)

54845 (CONF-720804-3) OBSERVATION OF NON-LINEAR EFFECTS NEAR THE LOWER HYBRID RESONANCE FREQUENCY. Hooke, W. M.; Bernabei, S. (Princeton Univ., N. J. Plasma Physics Lab.). [nd]. Contract AT(30-1)-1238. 4p. Dep. NTIS.

From 5th European conference on controlled fusion and plasma physics; Grenoble, France (21 Aug 1972).

Waves near the lower hybrid resonance frequency are electrostatically generated with plates just outside a cylindrical plasma column. These waves penetrate radially and, above a threshold power, are observed to undergo a parametric decay into two lower-frequency waves. (auth)

54846 (EUR-CEA-FC-639) THEORETICAL AND EXPERIMENTAL STUDIES OF ELECTRON PLASMA WAVE ECHOES. Guillemot, Michel (Commissariat a l'Energie Atomique, Fontenay-aux-Roses (France). Centre d'Etudes Nucleaires). Apr 1972. 220p. (In French). Dep. NTIS (U. S. Sales Only).

Thesis. Submitted to Univ., of Paris, France.

Electron plasma wave echoes are studied theoretically using a trajectory method. In this way, the disymmetric role played by the two parent waves producing the echo and saturation effects occurring when the amplitude of the second wave increases, are established. A deformation in the echo profile with variations in the second wave amplitude is predicted from the radial density profile and finite radial geometry considerations. Velocity space diffusion due to small-angle collisions produces a strong damping effect. Experimental results that are in good agreement with theoretical predictions enable the emitted-wave amplitude to be established and lead to an order-of-magnitude estimation of the turbulent fields producing the diffusion. (France)

54847 DIFFRACTION OF AN ELECTROMAGNETIC WAVE AT A MAGNETOACTIVE PLASMA CYLINDER. Klavdiev, V. V. Radio Eng. Electron. Phys. (USSR) (Engl. Transl.); 16: No. 11, 1824-30(Nov 1971).

Translated from Radiotekh. Elektron.; 16: No. 11, 2048-55 (Nov 1971).

Using the energy method, i.e., from the work done by the field on the plasma particles, the absorption cross section of an ordinary electromagnetic wave is obtained for the normal incidence of the wave on a magnetized plasma cylinder for the model of mirror reflection of the particles at the plasma boundary. (auth)

54848 SCATTERING OF ELECTROMAGNETIC WAVES DUE TO ELECTRON CHARGE FLUCTUATIONS IN A FLAT WAVEGUIDE WITH A MAGNETOACTIVE PLASMA. Troitskii, S. V.; Yakimenko, I. P. Radio Eng. Electron. Phys. (USSR) (Engl. Transl.) 16: No. 11, 1968-70(Nov 1971).

Translated from Radiotekh. Elektron.; 16: No. 11, 2222-3 (Nov 1971).

A derivation is given for the noncoherent scattering cross section in a plane waveguide with a magnetoactive plasma for an arbitrary external magnetic field. (M.O.W.)

54849 LOW-FREQUENCY OSCILLATIONS IN THE WEAKLY IONIZED PLASMA OF A HIGH-FREQUENCY DISCHARGE IN A MAGNETIC FIELD. Shvilkin, B. N.; Blinova, T. L.; Postnikov, S. A. Radio Eng. Electron. Phys. (USSR) (Engl. Transl.); 16: No. 11, 1970-3(Nov 1971).

Translated from Radiotekh. Elektron.; 16: No. 11, 2224-5 (Nov 1971).

Tests were conducted in cylindrical glass tubes 100-cm long and with inside diameters of 2.5, 2.8, and 3.2 cm. A discharge was excited by means of a hf oscillator with a power of 400 W and a frequency of 6.6 MHz. Measurements showed that a buildup of drift oscillations occurs in the hf discharge at low pressures when the collision frequency of ions with neutral atoms is less than or of the order of the oscillation frequency. A description of the oscillations is given. (M.O.W.)

54850 METHOD FOR NONLINEAR PLASMA WAVE KINETICS. Tanaka, Takayasu (Kyoto Univ.). J. Phys. Soc. Jap.; 33: No. 3, 769-81(Sep 1972).

A new method is presented to investigate the nonlinear wave kinetics in a plasma. While most previous theories assume that the wave amplitudes and other average quantities vary very little within the duration time τ of the wave–wave interaction, the present theory is valid under much less restrictive condition that their variation is small in the oscillation periods of the waves under consideration. The method consists in a systematic use of the interaction representation; the unique point of the present method lies in the introduction of many time variables in order to describe phenomena with many physical quantities in a simple manner. The method is applied to the investigation of quasi-linear and weakly turbulent evolution of the system. Several new features, including the amplitude oscillation discussed in a previous report, are derived for the case where the characteristic time scale of the wave amplitude is short compared with τ. (auth)

54851 AUTOMODULATION OF ION OSCILLATION MODES IN PLASMA. Shimizu, Katsuya; Ichikawa, Yoshi H. (Nihon Univ., Tokyo). J. Phys. Soc. Jap.; 33: No. 3, 789-92(Sep 1972).

Automodulation of ion oscillation mode is investigated by applying the reductive perturbation theory to the fluid equation of a plasma composed of cold ions and isothermal electrons. It is shown that an oscillatory solution of the Korteweg–de Vries equation in the small-wave-number region satisfies a small-wave-number limit of the nonlinear Schroedinger-type equation obtained in the finite-wave-number region. (auth)

54852 SLIGHTLY OBLIQUE SHOCK WAVES IN A COLLISIONLESS MAGNETIZED PLASMA. Abe, Kanji (Tokyo Inst. of Tech.). J. Phys. Soc. Jap.; 33: No. 3, 793-6(Sep 1972).

Numerical computations for collisionless shock waves are carried out by using a simple model that retains the primitive but essential features of hot plasma. It is supposed that the direction of propagation of the wave is parallel or slightly oblique to the magnetic field ahead of the wave. For the case of low temperature and exactly parallel propagation, a train of solitary waves exists, and each of the solitary waves has a shape essentially identical with that of the solitary wave described by Saffman. The train of solitary waves, however, abruptly changes into a shock wave, when the direction of propagation becomes slightly oblique to the magnetic field. When the temperature is relatively high, only shock waves are found to exist for the case of exactly parallel as well as slightly oblique propagation. (auth)

54853 NONLINEAR SPACE-CHARGE WAVES IN A PLASMA SHEATH. Rutkevich, B. N.; Pashchenko, A. V.; Fedorchenko, V. D.; Muratov, V. I. (Physical-Technical Inst., Kharkov). Sov. Phys.-Tech. Phys. (Engl. Transl.) 17: No. 3, 391-5(Sep 1972).

Translated from Zh. Tekh. Fiz.; 42: No. 3, 493-9(Mar 1972).

In a thin plasma sheath, the field associated with the space-charge wave is essentially independent of the transverse coordinate and is proportional to the density oscillations. It is shown that simple waves and solitons can propagate in this sheath. Analysis of the oscillations in a beam–plasma system reveals a nonlinear limitation of the two-stream instability. (auth)

54854 STABILITY OF A MONOCHROMATIC WAVE AGAINST INDUCED SCATTERING. Bliokh, Yu. P. (Physical-Technical Inst., Kharkov). Sov. Phys.-Tech. Phys. (Engl. Transl.); 17: No. 3, 389-90(Sep 1972).

Translated from Zh. Tekh. Fiz.; 42: No. 3, 490-2(Mar 1972).

The stability of a monochromatic longitudinal wave in a plasma is considered in two limiting cases: in the absence of an external magnetic field and in a strong field. The linear damping of the primary wave is small since its phase velocity satisfies $V_{ph} \gg V_{th}$, where V_{th} is the thermal velocity of the plasma particles. The principal mechanism leading to instability of the plasma wave is induced scattering. This is due to the resonant interaction of plasma particles with the beats that arise when the primary wave and the test wave with nearly equal frequencies ω_0 and ω interact. Beats with the difference frequency $\delta\omega = \omega - \omega_0$ have a phase velocity in the region of the thermal velocities. The instability of the test wave leads to transfer of energy to the long-wavelength part of the spectrum. The analysis considers the stability of a monochromatic wave at amplitudes $e\varphi_0/mV^2_{ph} \gg V_{th}/V_{ph}$. (M.O.W.)

54855 TURBULENCE IN ELECTROSTATIC COLLISIONLESS SHOCK WAVES. Means, Robert William. Los Angeles; Univ. of California (1972). 90p. University Microfilms Order No. 72-22,171.

Thesis.

Ion-acoustic wave turbulence in collisionless electrostatic shock waves was observed and studied in a low-density unmagnetized dc discharge plasma produced in a DP machine. Shock waves were observed with amplitudes $0.05 \leq e\phi/T_e \leq 0.8$. Electron-to-ion-temperature ratios available were $5 \leq T_e/T_i \leq 50$. At low-temperature ratios ions were reflected from the shock wave and were measured by an electrostatic energy analyzer. If sufficient ions were reflected by the shock front, the plasma ahead of the front became unstable to the counterstreaming ions and turbulence developed in that region. The growth rates and spectra of the turbulence were measured, and qualitative agreement was found with a linear ion beam plasma theory. The three-dimensional character of the interaction of the beam with the plasma was very important. The turbulent waves must travel at angles to the reflected beam in order for their phase velocity to be resonant with the beam velocity. The density of reflected ions was also controlled at high-temperature ratios by the addition of small amounts of helium in an argon plasma. The light helium ions were the principal reflected component. Test waves were propagated ahead of the shock wave in order to measure growth rates as the reflected beam interacted with the test wave. The interaction of the reflected ion beam with the turbulence was studied by creating a steady-state ion beam in the plasma. The resulting decay of the beam was compared to a quasi-linear theory of a small resonant ion beam. Agreement between experiment and theory was found. The resultant shock wave model is an extension of the Moiseev–Sagdeev laminar model to include warm ions and the three-dimensional turbulence that results from the counterstreaming ion beam. (Diss. Abstr. Int., B)

54856 GENERATION OF BLAST WAVES IN A PLASMA BY A PULSED ELECTRIC DISCHARGE. Podol'skii, V. N.; Chutov, Yu. I. (Kiev State Univ.). Sov. Phys.-Tech. Phys. (Engl. Transl.); 17: No. 3, 502-4(Sep 1972).

Translated from Zh. Tekh. Fiz.; 42: No. 3, 638-41(Mar 1972).

Experiments were carried out in a glass electric shock tube (EST) with ϕ = 1.6 cm; a moving interface is produced between argon, which fills the EST initially (0.74 mm Hg), and a mixture of argon and hydrogen; the interface moves at 2.2 × 10^4 cm/sec. The argon–hydrogen mixture is formed as a result of admission of hydrogen into the tube through a pulsed valve. In the expansion region of the EST a fixed plasma is produced by exponential discharge of a condenser. The temporal behavior of the argon and hydrogen lines is obtained from measurements at different points on the axis of the EST for different experimental conditions. The results show that the emission front formed in the plasma is a blast wave. (auth)

54857 LINEAR AND ALFVEN WAVES IN INCOMPRESSIBLE BEAM-PLASMA SYSTEMS. Verheest, Frank (Univ., Ghent). Int. J. Electron.; 33: No. 2, 201-7(Aug 1972).

The propagation of waves in incompressible beam–plasma systems is investigated on the basis of linear fluid equations. The pressure is assumed scalar and the incompressibility condition is chosen to illustrate a class of nonbarotropic plasmas. The dispersion law for these linear waves is derived, and is generally discussed. The case of oblique propagation differs appreciably from results obtained for barotropic plasmas, mainly because compressional longitudinal waves are absent. Alfvén waves in beam–plasma systems are then defined as low-frequency waves, with wave and drift frequencies small compared to gyrofrequencies. The Alfvén approximation of the dispersion law shows that the wave frequency at fixed wave-number is lower than if no streaming were applied. (auth)

54858 SOUND PROPAGATION IN IONIZED GASES AND ELECTRO ACOUSTIC EFFECT. Bhatnagar, V. P.; Bhatnagar, D. P.; Saxena, A. P. (Coll. of Engineering, Delhi). Int. J. Electron.; 33: No. 2, 193-200(Aug 1972).

Using hydrodynamical methods, the propagation of pressure waves in a nonisothermal fully ionized gas was considered for a situation where collision between various particles cannot be ignored and the following pressure equation was obtained: $(\partial^4 p/\partial t^4) + \nu_{ei}(\partial^3 p/\partial t^3) - (V_e^2 + V_1^2)(\partial^2/\partial t^2)\nabla^2 p + \omega_e^2(\partial^2 p/\partial t^2) - \nu_{ei} V_1^2(\partial/\partial t)\nabla^2 p - \omega_e^2 V_1^2 \nabla^2 p + V_i^2 V_e^2 \nabla^4 p = 0$ where V_i^2, V_e^2, and V_1^2 represent respectively $(\gamma k T_i/m_i)$, $(\gamma k T_e/m_e)$, and $[\gamma k(T_i + T_e)/m_i]$ and other symbols have their usual meaning. This gives the following dispersion relation for a sinusoidal sound wave $V_1^2 V_e^2 k^4 - [V_e^2 \omega^2 - (\omega_e^2 - i\nu_{ie}\omega) V_1^2]k^2 + [\omega^4 - (\omega_e^2 - i\nu_{ei}\omega)\omega^2] = 0$. The phase velocity of propagation and attenuation of the sound waves were discussed in the low frequency and high frequency region and it was shown that low frequency sound waves travel with a velocity V_1, while high frequency sound waves are carried by ions and electrons with velocities V_i and V_e respectively. Because of the difference in the masses of the ions and electrons, an electrostatic field of the same frequency as that of the sound is created during the propagation of sound waves. This field is given by: $E_0 = (e/\epsilon) \cdot (1/\gamma k T_e) \cdot (V/\omega)[(V_1^2/V^2) - 1]P_0$ and it is appreciable only at high frequencies where $V < V_1$. (auth)

54859 APPARENT CONSTANT-WAVELENGTH OSCILLATIONS IN A BOUNDED PLASMA. Keen, B. E.; Alcock, M. W.; Fletcher, W. H. W. (United Kingdom Atomic Energy Authority, Abingdon, Eng.). Phys. Lett.; 41A: No. 2, 183-4(11 Sep 1972).

Constant-wavelength propagated oscillations are apparently observed in a bounded neon plasma column, in which a large-amplitude self-excited ion-sound instability is found to co-exist. A possible theoretical explanation is included. (auth)

54860 INFLUENCE OF COLLISIONS ON PLASMA-WAVE PROPAGATION NEAR ELECTRON GYROFREQUENCY HARMONICS. Krupina, A. E. (Scientific-Research Radiophysics Inst., Gorky, USSR). Izv. Vyssh. Ucheb. Zaved., Radiofiz.; 15: No. 4, 517-20(1972). (In Russian).

The transverse plasma-wave propagation in a magnetoactive plasma is considered near the electron gyrofrequency harmonics under the assumption that the wavelength is smaller than the gyroradius of an electron. In addition to relativistic effects, the collisions of electrons with other particles are taken into account. The dispersion equation derived is analyzed for particular cases of weak and strong collisions, as well as for the dependence on the resonance-frequency detuning. (tr-auth)

54861 VOLUME AND SURFACE WAVE TRANSFORMATION IN PLASMA SYSTEMS. Tolmachev, M. M.; Tseitlin, M. B. (Inst. of Radio Engineering and Electronics, Moscow). Izv. Vyssh. Ucheb. Zaved., Radiofiz.; 15: No. 4, 635-7(1972). (In Russian).

The transformation of a slow volume wave at the surface (and conversely) in a plasma cylinder with a spirally conducting surface was investigated. A continuous plasma concentration change was assumed in the direction of propagation. (K.S.W.)

54862 WAVE INTERACTIONS IN ANISOTROPIC PLASMA. Lolodze, Ts. D.; Khirseli, E. M. (Inst. of Physics, Tbilisi, USSR). Izv. Vyssh. Ucheb. Zaved., Radiofiz.; 15: No. 5, 647-51 (1972).

The processes of nonlinear interactions of high-frequency plasma waves with magnetohydrodynamic wave radiation in anisotropic plasma are considered. The particular cases of the helicon decay interactions with an acoustic wave in the partially ionized plasma and quasi-longitudinal waves with a magnetoacoustic wave in the fully ionized plasma are investigated. For the processes studied the increments of the wave increases are obtained, and the threshold values of the energy of the interacting waves are estimated. (tr-auth)

54863 NONLINEAR WAVE INTERACTIONS IN A CYLINDRICAL COLUMN OF MAGNETO-ACTIVE PLASMA. Kormilets, V. M.; Yakimenko, I. P. (Kharkov Inst. of Radio-Electronics). Izv. Vyssh. Ucheb. Zaved., Radiofiz.; 15: No. 5, 652-9(1972). (In Russian).

The coordinate presentation of the nonlinear current occurring at the interaction of a set of electromagnetic waves in a plasma cylinder placed in the constant magnetic field H_0 $(0, 0, h_0)$ (cold plasma approximation) is obtained in the hydrodynamic approximation. The re-radiated field induced by this current is found on the basis of the reciprocity theorem for the gyrotropic medium. The results obtained are connected with the results of previous papers on the nonlinear interaction at wave propagation and scattering in the cold isotropic cylinder. The particular case of the nonlinear interaction of two electromagnetic fields occurring inside the infinitely long cylinder of the discharged plasma at the normal incidence of two plane waves with p-polarization is considered. (tr-auth)

54864 EXTRAORDINARY ELECTROMAGNETIC WAVE ABSORPTION IN THE LINEAR PLASMA LAYER IN THE HYBRID RESONANCE REGION. Omel'chenko, A. Ya.; Panchenko, V. I.; Stepanov, K. N. Izv. Vyssh. Ucheb. Zaved., Radiofiz.; 15: No. 5, 660-4(1972). (In Russian).

The results are given for numerical calculations of the field distribution and the absorption coefficient at the normal incidence of the extraordinary wave on the linear plasma layer regarding the effect of the field "swelling" in the hybrid resonance region. (tr-auth)

54865 REFLECTION OF ELECTROMAGNETIC WAVES AT THE OBLIQUE INCIDENCE ON THE MOVING FRONT OF IONIZATION. Semenova, V. I. Izv. Vyssh. Ucheb. Zaved., Radiofiz.; 15: No. 5, 665-74(1972). (In Russian).

The oblique incidence of monochromatic TE and TM waves on the sharp plasma boundary formed by the ionization source moving with a constant velocity is considered. Formulas on the reflection and transmission factors are obtained and investigated. The peculiarity of TE waves is the excitation in plasma outside the front of the longitudinal oscillations at any frequency of the incident transverse wave. (tr-auth)

54866 EQUATION OF STATE OF A NONIDEAL CESIUM PLASMA. Lomakin, B. N.; Fortov, V. E. (Moscow Physical-Technical Inst.). Zh. Eksp. Teor. Fiz.; 63: No. 1, 92-103(Jul 1972). (In Russian).

Experimental results are presented of a shock-wave investigation of the equation of state of a nonideal cesium plasma on a heated shock tube. The equation of state in the caloric form $H = H(P, V)$ can be determined by measuring the velocity of the shock discontinuity front and the plasma density; the equation is employed for plotting the isentropes and for calculation of the shock-compressed plasma temperatures. The results are compared with existing theories of plasma nonideality. The problem of phase transitions in a nonideal cesium plasma is discussed. (auth)

54867 KINETIC THEORY OF PARAMETRIC EXCITATION OF SURFACE WAVES IN SEMI-FINITE PLASMA. Aliev, Yu. M.; Gradov, O. M.; Kirii, A. Yu. (Inst. of Physics, Moscow). Zh. Eksp. Teor. Fiz.; 63: No. 1, 112-20(Jul 1972). (In Russian).

A theory of parametric excitation of quasi-static surface waves by a weak high-frequency electric field in a semi-finite plasma is developed. The case is considered when the external high-frequency field intensity vector is parallel to the plasma boundary, the field frequency is close to the proper frequency of the high-frequency quasi-static surface oscillations, and reflection of particles from the boundary of the plasma is specular. A dispersion equation is derived that describes plasma instability with respect to surface wave buildup. Threshold values of the external field strength above which such instabilities arise are found and the oscillation increments in the near-threshold region are calculated. (tr-auth)

54868 NONLINEAR EVOLUTION OF A QUASI-MONOCHROMATIC PACKET OF HELICAL WAVES IN A PLASMA. Istomin, Ya. N.; Karpman, V. I. (Inst. of Terrestrial Magnetism, Ionosphere, and Radio-Wave Propagation, Moscow). Zh. Eksp. Teor. Fiz.; 63: No. 1, 131-42(Jul 1972). (In Russian).

Effects due to nonlinear interaction between resonant particles and quasi-monochromatic wave packets of circularly polarized waves propagating in a plasma along a magnetic field are considered. It is shown that the finiteness of the packet results in some new interesting phenomena that are not manifest in a constant-amplitude wave, viz. steepening of the packet fronts in a stable plasma and its compression, expansion of the packet in an unstable plasma, periodic amplitude modulation of a packet with a sufficiently steep leading front. The results are compared with experiments on the propagation of monochromatic whistlers in a magnetosphere. (tr-auth)

54869 DAMPING OF LONG-WAVE PLASMA OSCILLATIONS. Kapitonov, V. S.; Popov, V. N. (Mathematics Inst., Moscow). Zh. Eksp. Teor. Fiz.; 63: No. 1, 143-9(Jul 1972). (In Russian).

Formulas that are exact in the long-wave limit, are derived for plasma oscillations damping due to collisions between charged particles. In a one-component plasma with a homogeneous compensating background the damping is $\sim k^2$ for $k \to 0$, whereas in a two-component plasma with particles of unequal masses it is constant for $k \to 0$. The integrals defining the damping are calculated explicitly for the one and two-component models in the limiting cases of a hot and cold Boltzmann plasma. (tr-auth)

PHYSICS (RADIATION AND SHIELDING)

54870 (NASA-TM-X-2440) PROCEEDINGS OF THE NATIONAL SYMPOSIUM ON NATURAL AND MANMADE RADIATION IN SPACE HELD AT LAS VEGAS, NEVADA, MARCH 1-5, 1971. Warman, E. A. (ed.) (Aerojet Nuclear Systems Co., Sacramento, Calif.). Jan 1972. 1020p. (CONF-710304). NTIS $10.00.

A separate abstract was prepared for each of 119 of 132 papers. Thirteen papers previously appeared in NSA; see NSA 25: 22777, 24154, 24155, 26178, 28784, 30630, 30631, 31640, 31671, 33390, 36250, 38173, and 57133. (L.M.T.)

For abstracts of individual papers see: 52985, 53093—53095, 53201—53203, 53230—53236, 53254—53256, 53289—53294, 53335—53338, 53345, 53399—53408, 53451—53458, 53529, 53695—53697, 53715, 53730, 53731, 53806, 53807, 53927—53931, 54001, 54002, 54044—54049, 54066, 54067, 54528, 54878—54889, 54945—54964, 55359—55373, and 55406.

Radiation Physics

Refer also to abstracts 53196, 53244, 53410, 53714, 54008, 54009, 54033, 54430, 54937—54939, 54963, and 55016.

54871 (CEA-CONF-1976) EVALUATION OF THE COMPONENTS OF THE ABSORBED DOSE IN THE INTERIOR OF ORGANISMS EXPOSED TO NEUTRONS. Dousset, M.; Ricourt, A.; Lemaire, G. (Commissariat a l'Energie Atomique, Fontenay-aux-Roses (France). Centre d'Etudes Nucleaires). [1971]. 24p. (In French). (CONF-711204-2). Dep. NTIS (U. S. Sales Only).

From Meeting on radiobiological applications of neutron irradiation; Vienna, Austria (6 Dec 1971).

The absorbed dose due to heavy charged particles and the absorbed dose due to secondary γ radiation were studied in cylinders whose dimensions were close to that of the rat, the rabbit, and the human for different energy spectrum of neutrons and for a large beam (large with respect to the animal irradiated). The base calculation for monoenergetic neutrons was applied to complex spectra. The results are shown graphically. The maximum of the dose due to secondary γ radiations in the rat varies in absolute value significantly with the spectrum. For the rabbit, the dimensions are sufficiently large so that the depth doses vary little in absolute value with the spectrum. For the human organism, the importance of the secondary radiations was confirmed. Experimental verification of the theoretical values obtained is in progress; the preliminary comparisons are encouraging. (J.S.R.)

54872 (CONF-720901-(Bks.1 and 2), pp 499-511) DOMINO: A GENERAL PURPOSE DISCRETE ORDINATES TO MONTE CARLO COUPLING CODE FOR RADIATION TRANSPORT. Burgart, C. E.; Emmett, M. B.; Hoffman, T. J. 1972.

From Meeting on new developments in reactor physics and shielding calculations; Kiamesha Lake, NY. (12 Sep 1972).

The ability to perform two-dimensional discrete ordinates calculations and couple the results with three-dimensional Monte Carlo calculations makes many calculations practical which would be quite difficult using the Monte Carlo method for the entire calculation. A method of coupling two-dimensional discrete ordinates calculations with Monte Carlo calculations of arbitrary geometric complexity is incorporated in the DOMINO code and associated routines. The coupling may take place on either a disk or cylindrical surface, thus the discrete ordinates calculation is limited to r—z geometry. The calculations may be coupled in either a forward mode, adjoint mode or as a forward-adjoint integration over the surface. The coupling may be performed either exactly or with approximations depending on the boundary conditions and configurations for both calculations. (auth)

54873 (EUR-4787) MICRODOSIMETRIC INVESTIGATIONS INTO THE ENERGY TRANSFER OF FAST NEUTRONS TO SOFT TISSUE. Oldenburg, U. (European Atomic Energy Community, Ispra (Italy). Joint Nuclear Research Center). 1972. 138p. (In German). Dep. NTIS (U. S. Sales Only).

Single-event spectra of fast neutrons were measured and calculated for spherical tissue-equivalent volumes of cellular and subcellular size (6.5 μm and 1.0 μm). The experimental spectra were measured with a 2" Rossi counter. To provide the radiation fast neutrons were used of 0.62 MeV, 1.02 MeV, 2.01 MeV, 3.45 MeV, 4.44 MeV and 5.85 MeV, produced by a 3-MV Van De Graaff Generator and with thin targets. For the calculations a Monte Carlo program was written in Fortran IV, with which it was possible to simulate the experimental conditions on an IBM 360/65. The experimental and calculated spectra show good agreement above 5 keV/μm. For smaller event magnitudes, however, the corresponding experimental and theoretical spectra are entirely different. This difference must be attributed to the fact that the contamination of the neutron ray with gamma quanta and the neutron scatter in the collimator were not taken into account in the Monte Carlo calculation. The following investigations were also carried out using the Monte Carlo calculation: differences between energy absorption spectra and ionization spectra; proportion of charged secondary particles (p, d, t, α, C, N and O) in the single-event spectra; and breakdown of single-event spectra into crossers, insiders, stoppers, starters, and delta particles. (auth)

54874 (EUR-CEA-FC-647) HEATING OF VERY SMALL SOLID GRAINS BY ELECTRON AND ION BOMBARDMENT. Geller, R. (Commissariat a l'Energie Atomique, Fontenay-aux-Roses (France). Centre d'Etudes Nucleaires). May 1972. 23p. (In French). Dep. NTIS (U. S. Sales Only).

The bombardment of small agglomerates of matter with electrons and ions has various applications. An attempt was made to demonstrate qualitatively that the heating effect varies with the size of the agglomerate. It is assumed that the heating is due to collisions and absorption of secondary electrons and photons created in the matter by the incident particles. The mean free path, Λ, of the secondary particles is evaluated for the various collision processes by assuming that the solid target can be treated as a gas having a density of 4×10^{22} cm^{-3}. (The cross section data available for such gases are utilized.) The different Λ values are related to the different agglomerate diameters, ϕ. It is postulated that if $\Lambda > \phi$, the collision can not produce a heating effect. (France)

54875 (JINR-P1-6552) VAVILOV-CHERENKOV "NEEDLE" RADIATION IN ROCHELLE SALT CRYSTAL. Zrelov, V. P.; Pavlovich, P.; Shulek, P. (Joint Inst. for Nuclear Research, Dubna (USSR). Lab. of Nuclear Problems). 1972. 27p. (In Russian). Dep. NTIS (U. S. Sales Only).

By using 660-MeV protons and the photomethod the basic properties of the Vavilov—Cherenkov radiation were investigated in a biaxial crystal of Rochelle salt (RSC) having a polydomain structure. All the basic radiation properties predicted theoretically were confirmed. It was shown that the azimuthal radiation distribution with a definite polarization in the plate of the z-cut was of a peculiar "needle" character. (auth)

54876 (LA-4874, pp 145-52) DOSE COMPUTATIONS AND TREATMENT PLANNING IN PION THERAPY. Hendee, William R. (Colorado Univ., Denver. Medical Center). Mar 1972.

From fifth LAMPF users meeting; Los Alamos, NM. (8 Nov 1971).

The following subjects are discussed in a general manner: dose determination, tissue-equivalent materials for pions, reference dose, surface contour problem, the use of ultrasound, and use of computers for optimizing the treatment plan. (M.H.R.)

54877 (LA-4874, pp 153-61) RADIATION TREATMENT PLANNING USING PI MESONS. Lanzl, Lawrence H. (Argonne Cancer Research Hospital, Chicago, Ill. Chicago Univ., Ill. Dept. of Radiology). Mar 1972.

From fifth LAMPF users meeting; Los Alamos, NM. (8 Nov 1971).

The dosimetry systems for the conventionally used photons and electrons are reviewed briefly for guidance in the unexplored field of pion-treatment planning. It is suggested that a combination of the two photon dosimetry systems be considered for use in pion therapy. Methods for generating isodose distributions are discussed. The compensating filter is discussed. Principles have been worked out for accounting for inhomogeneities in two-dimensional isodose curves. The possible use of bolus material in combination with a wedge filter in treatment planning is suggested. (M.H.R.)

54878 (NASA-TM-X-2440, pp 104-7) GALACTIC COSMIC-RAY HEAVY PRIMARY SECONDARY DOSES. Wilkinson, M. C. (Boeing Co., Seattle); Curtis, S. B. Jan 1972.

From Symposium on natural and manmade radiation in space; Las Vegas, Nev. (1 Mar 1971).

Results are presented of a calculation which estimates the heavy primary secondary doses from cosmic-ray-interaction data. The incident galactic cosmic-ray heavy primary spectrum is represented as the sum of helium, nitrogen (M group), magnesium (light heavy), and iron (very heavy) components. The incident iron nuclei are allowed to fragment into lesser Z secondaries, which are assumed to travel in the same direction and start with the same energy per nucleon as the interacting primary. The total emergent particle energy spectra and dose are then presented for the galactic heavy primary spectrum incident on aluminum and tissue slabs. The importance of the fragmentation parameters assumed is also evaluated. The total dose from the heavy primaries and their secondaries is found to be reduced by only a factor of two in 20 g/cm^2 of shielding. (auth)

54879 (NASA-TM-X-2440, pp 157-61) FLUCTUATIONS IN ENERGY LOSS AND THEIR IMPLICATIONS FOR DOSIMETRY AND RADIOBIOLOGY. Baily, Norman A.; Steigerwalt, John E. (Univ. of California, San Diego, La Jolla). Jan 1972.

From Symposium on natural and manmade radiation in space; Las Vegas, Nev. (1 Mar 1971).

A discussion is presented of the physics of energy deposition, with emphasis on their application to effects in biological systems. It is shown that energy deposition in small biological volumes has widely separated most-probable and average energy losses. Distribution functions are given for most probable and average energy losses of various charged particles in 1 micron of tissue. The validity of the concept of R.B.E. is questioned. It is concluded that a theory incorporating the probability for events of a given size in the volume of interest is needed for radiobiology and microdosimetry. (D.L.C.)

54880 (NASA-TM-X-2440, pp 364-7) MODULAR APPROACH FOR ASSESSING THE EFFECT OF RADIATION ENVIRONMENTS ON MAN IN OPERATIONAL SYSTEMS: RADIOBIOLOGICAL VULNERABILITY OF MAN DURING TASK PERFORMANCE. Ewing, Dean E. (Air Force Weapons Lab., Kirtland AFB, N. Mex.). Jan 1972.

From Symposium on natural and manmade radiation in space; Las Vegas, Nev. (1 Mar 1971).

The feasibility of the model was proved and the practicality was assessed. It was applied to one operational system to date and the information obtained was submitted to systems analysts and mission planners for the assessment of man's vulnerability and impact on systems survivability. In addition, the model was developed so that the radiobiological data can be input to a sophisticated man—machine interface model to properly relate the radiobiological stress with other mission stresses including the effects of a degraded system. (auth)

54881 (NASA-TM-X-2440, pp 520-2) NEUTRONS PRODUCED BY KNOWN ENERGIES OF IONS ABUNDANT IN SPACE. Wadman, William W. (Univ of California, Irvine). Jan 1972.

From Symposium on natural and manmade radiation in space; Las Vegas, Nev. (1 Mar 1971).

Ions of helium, boron, carbon, nitrogen, and oxygen were accelerated to 10.4 MeV/nucleon and directed onto copper or tantalum targets. The secondary neutron production was determined. From literature data on neutron production data for protons, deuterons, and alpha particles of various energies on various target materials, the neutron yield is a square function of the energy of the projectile ion. From the experimental data, neutron yields were extrapolated into the energy peak region of 300 MeV per nucleon for light ions in space. Beyond that energy, the ion energy spectrum falls off as $\sim E^{-2}$, producing a constancy in the neutron dose per ion beyond 300 MeV/nucleon. Such an extrapolation does not account for changes in the neutron spectra, modifications in the angular distribution in the higher energy model, or strange effects unique to very high energies per nucleon that are not now understood. (TSS)

54882 (NASA-TM-X-2440, pp 757-66) FREQUENCY OF LIGHT FLASHES INDUCED BY CHERENKOV RADIATION FROM HEAVY COSMIC-RAY NUCLEI. Madey, Richard; McNulty, P. J. (Clarkson Coll. of Tech., Potsdam, N. Y.). Jan 1972.

From Symposium on natural and manmade radiation in space; Las Vegas, Nev. (1 Mar 1971).

Astronauts on Apollo missions 11 through 14 have reported seeing light flashes at a typical rate of about one per minute. The expected frequency of light flashes induced in the dark-adapted eye by Cherenkov radiation from cosmic heavy nuclei was calculated. In order to induce a visual sensation, at least two Cherenkov photons must be absorbed in coincidence by the rhodopsin molecules in a small area of the retina served by a single optic nerve fiber. The fact that the photons must be coincident on a small cluster of rods restricts the path length of the heavy nuclei for the production of relevant Cherenkov photons to a thin layer of the nervous tissue of the retina just ahead of the rods. The expected frequency of light flashes depends on the threshold number of photons that must be absorbed in a rod cluster. It is known that individual threshold values in the dark-adapted eye can vary by a factor of five even among young normal human subjects. The result of the calculation can be presented as a curve of the mean frequency of light flashes versus the threshold number of absorbed photons. The results are not sensitive to variations in the path length from 5 to 15 grams per square centimeter of water-equivalent before the nucleus reaches the retina. The calculations are based on the fluxes and energy spectra of galactic cosmic-ray nuclei helium to iron measured at a time of minimum solar modulation. The expected light-flash frequencies induced by Cherenkov radiation are consistent with the frequencies reported by the astronauts on Apollo missions 11 through 14. (auth)

54883 (NASA-TM-X-2440, pp 773-80) INFLUENCE OF A DETAILED MODEL OF MAN ON PROTON DEPTH/DOSE CALCULATIONS. Kase, Paul G. (Martin-Marietta Corp., Lakewood, Colo.). Jan 1972.

From Symposium on natural and manmade radiation in space; Las Vegas, Nev. (1 Mar 1971).

The U. S. Air Force and NASA have jointly sponsored the development of a detailed radiation shielding model of man. This model will be used to plan manned space missions in which especially sensitive human tissues could be subjected to excessive radiation. The model has two configurations—standing and seated. More than 2500 individual elemental volumes are used to depict the external conformation, skeleton, and principal organs. The model is briefly described and several examples of its application to mission planning are given. (auth)

54884 (NASA-TM-X-2440, pp 786-91) MONTE CARLO PHOTOCURRENT/PHOTOMISSION COMPUTER PROGRAM. Chadsey, W. L.; Ragona, C. (General Electric Co., Philadelphia). Jan 1972.

From Symposium on natural and manmade radiation in space; Las Vegas, Nev. (1 Mar 1971).

A Monte Carlo computer program (POEM) was developed for the computation of photocurrents and photoemission in gamma (x-ray)-irradiated materials. The program was used for application to the computation of radiation-induced surface currents on space vehicles and the computation of radiation-induced space-charge environments (IEMP) within space vehicles. The program was successfully correlated with published experimental data. (auth)

54885 (NASA-TM-X-2440, pp 792-800) PHOTON-INDUCED SECONDARY ELECTRON EMISSION. Spencer, R. B. (TRW Systems Group, Redondo Beach, Calif.); Smith, C. B.; McGrath, E. J. Jan 1972.

From Symposium on natural and manmade radiation in space; Las Vegas, Nev. (1 Mar 1971).

Results of numerical models for predicting photon-induced secondary electron emission are presented for copper. These results are compared with recent experimental measurements made at UCLA using a ^{60}Co gamma-ray source. (auth)

54886 (NASA-TM-X-2440, pp 801-15) ELECTRON AND BREMSSTRAHLUNG PENETRATION AND DOSE CALCULATION. Watts, John W. Jr.; Burrell, Martin O. (Marshall Space Flight Center, Huntsville, Ala.). Jan 1972.

From Symposium on natural and manmade radiation in space; Las Vegas, Nev. (1 Mar 1971).

Various techniques for the calculation of electron and bremsstrahlung dose deposition are described. New energy deposition, transmission, and reflection coefficients for electrons incident on plane slabs for angles of 0, 30, 60, 75, and 89.9° and energies of 0.5, 1.0, 2.0, 3.0, 4.0, 5.0, 6.0, and 10.0 MeV are presented, and methods for their use in electron dose calculations are developed. A method for electron dose calculations using the "straight-ahead" approximation is also developed, and the various methods are compared and found to be in good agreement. Accurate and approximate methods of calculating bremsstrahlung dose are derived and compared. The approximation is found to give good order of magnitude estimate of dose where the electron spectrum falls off exponentially with energy. The primary weakness of both calculations is the approximation of the bremsstrahlung source angular distribution; the actual distribution is not easily determined. 24 figures. (auth)

54887 (NASA-TM-X-2440, pp 821-31) APPLICATION OF THE PHASE-SPACE-TIME EVOLUTION METHOD TO ELECTRON SHIELDING. Cordaro, Matthew C. (Long Island Lighting Co., Hicksville, N. Y.); Zucker, Martin S. Jan 1972.

From Symposium on natural and manmade radiation in space; Las Vegas, Nev. (1 Mar 1971).

A computer technique for treating the motion of charged and neutral particles and called the phase-space-time-evolution (PSTE) method was developed. This technique employs the computer bookkeeping capacity to keep track of the time development of a phase space distribution of particles. This method was applied to a study of the penetration of electrons. A 1-MeV beam of electrons normally incident on a semi-infinite slab of aluminum was used. Results of the calculation were compared with Monte Carlo calculations and experimental results. Time-dependent PSTE electron penetration results for the same problem are presented. 13 figures. (auth) (STAR)

54888 (NASA-TM-X-2440, pp 894-901) RADIATION MEASUREMENTS AND DOSES AT SST ALTITUDES. Foelsche, Trutz (Langley Research Center, Hampton, Va.). Jan 1972.
From Symposium on natural and manmade radiation in space; Las Vegas, Nev. (1 Mar 1971).

A brief survey of experimental and theoretical results of biologically important radiation components and dose equivalents due to galactic and solar cosmic rays in the high atmosphere, especially at SST altitudes, is presented. The dose equivalent rate for the flight personnel flying 500 hours per year in cruise altitudes of 60,000−65,000 feet (18−19.5 km) in high magnetic latitudes turned out to be about 0.75 to 1.0 rem per year averaged over the solar cycle, or about 15 to 20 percent of the maximum permissible dose rate for radiation workers as established by ICRP for peacetime operations (5 rem per year). The gross of passengers, who do not encounter major solar events, would be exposed only to the low level galactic cosmic rays. Such exposure would amount to some mrem per North-Atlantic trip and is therefore negligible. Very rarely, groups of passengers, who happen to be passing through the impact zone of a rare giant solar event such as that of February 23, 1956, would be exposed to 0.45 rem, provided the airplane descends to subsonic altitudes at the beginning of the event and continues its flight at the lower altitudes. This exposure, 0.45 rem, is 90 percent of the permissible limit for individuals of the general population (0.5 rem per single year). At cruise altitude, the maximum permissible limit would have been surpassed. The suggested evasion measure of descending to lower altitudes is therefore sufficient to avoid overexposure of passengers in such rare cases. 22 references. (auth)

54889 (NASA-TM-X-2440, pp 902-7) DOSE AND LINEAR ENERGY TRANSFER SPECTRAL MEASUREMENTS FOR THE SUPERSONIC TRANSPORT PROGRAM. Philbrick, Richard B. (Air Force Weapons Lab., Kirtland AFB, N. Mex.). Jan 1972.
From Symposium on natural and manmade radiation in space; Las Vegas, Nev. (1 Mar 1971).

Radiation monitoring systems are being flown on board aircraft provided by the Air Weather Service. The purpose of the package, called the High Altitude Radiation Instrumentation System (HARIS), is to measure the radiation hazard to Supersonic Transport passengers from solar and galactic cosmic rays. The HARIS includes a gaseous linear-energy-transfer spectrometer, a tissue-equivalent ionization chamber, and a Geiger−Mueller tube. The HARIS is flown on RB-57F aircraft at 60,000 feet from Eielson Air Force Base, Alaska. During solar-active periods, crews of the 58th Weather Reconnaissance Squadron are on alert to launch the aircraft during solar flares. Data from the HARIS are reduced to give rad and rem dose rates measured by the package during the flights. Results presented include ambient data obtained on background flights, altitude comparison data, and solar flare data. (auth)

54890 (ORNL-TM-3816) RADIATION TRANSPORT CODES FOR POTENTIAL APPLICATIONS RELATED TO RADIOBIOLOGY AND RADIOTHERAPY USING PROTONS, NEUTRONS, AND NEGATIVELY CHARGED PIONS. Armstrong, T. W. (Oak Ridge National Lab., Tenn.). Aug 1972. 27p. Dep. NTIS.

In connection with long-term programs in space-vehicle, accelerator, and reactor shielding, the Oak Ridge National Laboratory has developed rather sophisticated calculational methods for determining the transport in matter of protons, neutrons, pions, muons, electrons, and photons. This work has resulted in several Monte Carlo radiation-transport computer codes which are quite general with respect to allowable source-particle descriptions, geometries, material compositions, etc. Recently, a limited study has been directed toward applying some of these computer codes to predict quantities of interest in the fields of radiotherapy and radiobiology, such as depth-dose patterns, and toward assessing the accuracy of the codes for applications in these fields. Here, the calculational methods are described and comparisons of calculated and experimental results are presented for dose distributions produced by protons, neutrons, and negatively charged pions. Comparisons of calculated and experimental cell-survival probabilities are also presented. (auth)

54891 (SLAC-153) CONCEPTS OF RADIATION DOSIMETRY. Kase, Kenneth R.; Nelson, Walter R. (Stanford Linear Accelerator Center, Calif.). Jun 1972. Contract AT(04-3)-515. 214p. Dep. NTIS.

The basic information required to understand the principles of photon and charged-particle dose measurement is discussed, from basic particle interactions to cavity chamber theory. The extension of dosimetry principles to the high-energy situation is emphasized. The following topics are covered: the interaction of electromagnetic radiation with matter, charged-particle interactions, energy distribution in matter, dose calculations, and measurement of radiation dose−cavity-chamber theory. (53 references) (M.H.R.)

54892 EXPERIMENTALLY MEASURED DOSE ALBEDOS OF INTERMEDIATE ENERGY BREMSSTRAHLUNG. Crites, Thomas R. (Sandia Corp., Albuquerque, N. Mex.). Nucl. Sci. Eng.; 49: No. 1, 103-6(Sep 1972).

The backscatter of normally incident bremsstrahlung spectra photons from semi-infinite materials was investigated experimentally. The bremsstrahlung sources were broad-beam radiation from a 2.0-MeV radiographic Van de Graaff and high-intensity flash x-ray devices of 3.5-, 7.0-, and 10.5-MeV peak energy. The scattering media were concrete, iron, and lead. Four backscattering angles (120, 130, 140, and 150°) were studied. The scattered radiation was measured by means of thermoluminescent dosimeters (LiF) located in collimated shields. The experiments were designed for shielding studies, and the results are presented in a form primarily for use in health protection shielding calculations. (2 figures, 1 table) (auth)

54893 FAST-NEUTRON THERAPY TREATMENT PLANNING. McGinley, Patton Hopkins. Atlanta; Georgia Inst. of Tech. (1971). 153p. University Microfilms Order No. 72-5053. Thesis.

A clinical trial is being conducted at Hammersmith Hospital, London, using fast neutrons with an average energy of 7.65 MeV and future trials, in which 14 MeV-neutrons will be employed, are being considered. Dose distributions for use in neutron radiotherapy were experimentally determined. Tissue-equivalent ionization chambers were utilized in conjunction with thermoluminescent dosimeters to establish the neutron and γ-ray doses deposited in tissue irradiated by beams of 14-MeV neutrons. Dose distributions in homogeneous and heterogeneous phantoms containing lung and bone components were determined at a source-to-skin distance of 125 cm. From these measurements it was concluded that the dose distributions due to 14-MeV neutrons have properties that make them suitable for use in radiotherapy. However, improved collimation and shielding systems will be required in order to reduce the whole-body dose received by a patient undergoing neutron therapy. An examination of the dose distributions revealed that the percent depth dose at points within the volume of tissue irradiated could be predicted by means of an empirical equation. Based on these measurements, only a slight change in the soft-tissue dose distribution was produced by bone. On the other hand, an increased dose was found for points in and behind the lungs as compared to the dose that would be obtained in a homogeneous phantom. A discussion of the sources of error in the experimental measurements is included as well as suggestions for future work related to 14-MeV neutron therapy. (Diss. Abstr. Int., B)

54894 ENERGY SPECTRUM OF ELECTRONS IN WATER IRRADIATED WITH 10- TO 20- MeV ELECTRON BEAMS. Weiss, Herbert; Epp. Edward R.; Heslin, Jane (Sloan-Kettering Inst. for Cancer Research, New York). Radiat. Res.; 51: No. 2, 211-28(Aug 1972).

The spectrum of the fluence of slowed-down electrons in a water medium irradiated by an external beam of electrons from a betatron was measured. The measurements were made at a number of depths in the medium and for a number of incident electron energies. The approach used was to set an evacuated probe at the point of interest for a number of angular increments. Electrons traveling down the probe within an angle of $\theta \pm 0.6°$ were then detected by a plastic scintillator. The measured spectra were corrected for coincidences and resolution distortion by means of a response function matrix. The fluence spectra were converted to distributions in LET. (auth)

54895 MICRODOSIMETRY OF 250 kVp AND 65 kVp X RAYS, ^{60}Co GAMMA RAYS, AND TRITIUM BETA PARTICLES. Ellett, W. H.; Braby, L. A. (Twinbrook Research Lab., Rockville, Md. Battelle-Northwest Lab., Richland, Wash.). Radiat. Res.; 51: No. 2, 229-43(Aug 1972).

Energy deposition from single events occurring in spherical sites ranging in diameter from about 50 to 550 μg cm^{-2} was studied by means of a grid-walled proportional counter. Single- and multiple-event spectra from medium- and low-energy bremsstrahlung are compared to those produced by ^{60}Co gamma rays and tritium beta rays. From these spectra the dose-mean specific energy from single events and the number of events per rad exceeding a given event size are calculated for sites of various diameter. The relevancy of these data to the Kellerer−Rossi theory of dual radiation action is discussed and, for each of the radiations studied, an estimate is made of the dose range in which the biological effects vary linearly or as the square of the dose. (auth)

54896 DOSE ACROSS A PLANE BONE–TISSUE INTERFACE. Kulkarni, R. N.; Sundararaman, V.; Prasad, M. A. (Directorate of Radiation Protection, Trombay, India). Radiat. Res.; 51: No. 1, 1-9(Jul 1972).

The contribution of photoelectrons to the dose across a plane bone/tissue interface due to x irradiation is calculated using the moments method for the following three angular distributions of photoelectrons: the distribution calculated according to the nonrelativistic Heitler formula; forward; and isotropic. The dose depends to a large extent upon the type of angular distribution assumed. Further, the earlier approximation that the electrons travel in straight lines is also found to introduce a certain amount of error. On the basis of the investigations the total dose across a plane bone/tissue interface has been arrived at by using the Heitler distribution of photoelectrons and by adding to this dose the contribution of Compton electrons which is nearly the same in bone and tissue. (auth)

54897 DISTRIBUTION OF DEEP DOSES NEAR IMPLANTED BETA AND MIXED BETA–GAMMA EMITTERS. Dubinin, I.; Huvar, A. (UJEP, Brno). Cesk. Radiol.; 25: No. 6, 249-51(Nov 1971). (In Czech).

The mathematical method for the assessment of the distribution of deep doses near implanted beta and mixed beta and gamma emitters is described, and the possibility of calculating linear absorption coefficients for both types of radiation is discussed. (auth)

54898 MONTE CARLO INVESTIGATIONS OF CATASTROPHIC COLLISIONS WITH CHARACTERISTICS OF SCATTERED ELECTRON RADIATION TAKEN INTO ACCOUNT. Baranov, V. F.; Arutyunov, V. V.; Zrazhun, A. G.; Smirnov, V. V. This paper was summarized in At. Energ. (USSR); 31: No. 1, 51-2(Jul 1971) as paper No. 506/6062. (In Russian). Full copy of this paper is held by TIC.

An algorithm for Monte Carlo calculations of the energy and angular distributions of electron radiation scattered on a barrier and on a semi-infinite medium as it impinges on the surface of absorber, with the radiation arriving in the form of a broad beam of monoenergetic electrons, is presented. The calculations take catastrophic collisions of electrons leading to the formation of secondary delta electrons into account, as well as the contribution of the delta electrons to the energy distributions and angular distribution of the scattered electron radiation. The energy of the primary electrons ranged from 0.2 to 5 MeV. Aluminum and a tissue-equivalent medium were used as the absorber. The results of the calculations were compared with available experimental data on the transmission coefficients of the electrons and the angular distributions of the scattered electron radiation. The comparison revealed that the calculated characteristics of the scattered electron radiation are in closer agreement with the experimental results, over a wide range of energies, than calculations based on the continuous slowing-down model are. (TSS)

54899 NOTE ON THE LARGE-DEPTH DECREASE OF RANGE AND DAMAGE PROFILES. Winterbon, K. B. (Atomic Energy of Canada Ltd., Chalk River, Ont.). Radiat. Eff.; 15: No. 1-2, 73-5(Jul 1972).

The large-depth decrease of heavy-ion path-length, projected range, and deposited-energy distributions is calculated, assuming power-cross-section nuclear stopping, and estimated in the general case. The rate of decrease can be exponential at sufficiently low incident ion energies and becomes gaussian at high energies. (auth)

54900 COMPUTERIZED DOSIMETRY OF ^{60}Co OPHTHALMIC APPLICATORS. Chan, Bun; Rotman, Marvin; Randall, Gerald J. (New York Medical Coll. Memorial Hospital, New York). Radiology; 103: No. 3, 705-7(Jun 1972).

Theoretical dose distributions of ^{60}Co ophthalmic applicators were calculated with the aid of a computer and the results were compared with experimental measurements obtained by thermoluminescent dosimetry and film emulsions in phantoms. The Sievert line-source method was partially corrected for oblique filtration; however, a more precise dose description should include a program which completely corrects for oblique absorption in the ophthalmic applicator. (auth)

54901 CORRECTION OF ISODOSE-DIAGRAMS FOR ^{60}Co AND 35 MeV ELECTRONS AT PENETRATION OF LUNG TISSUE. Nordberg, U.-B. (Univ. of Lund, Sweden). Acta Radiol., Ther., Phys., Biol.; 11: No. 2, 113-28(Apr 1972).

A simple method for the construction of individual isodose curves in lung tissue for ^{60}Co and 35-MeV electrons is described. The validity of the method was experimentally verified. A mean volume weight for normal lung tissue was determined for 13 patients. (auth)

54902 LOCAL DOSE FROM NEUTRON-PRODUCED-RECOIL IONS IN THE REGION OF A THERAPEUTIC ^{252}Cf NEEDLE. Jones, T. D.; Auxier, J. A. (Oak Ridge National Lab., Tenn.). Radiology; 104: No. 1, 187-9(Jul 1972).

An attempt is made to provide data accurate enough to permit treatment of neoplasms which may show a significant change in radiosensitivity due to a 10% variation in radiation dose. A Monte Carlo neutron transport code was used to compute distributions of dose from neutron-produced-recoil ions about a 20-mm ^{252}Cf needle implanted in soft-tissue media. The results were normalized to free space kerma, and these normalized results were averaged in order to obtain values for a mean tissue medium. Coefficients of variation ranged from 1 to 3.5% for this mean tissue. (auth)

54903 PERTURBATION OF ISODOSE DISTRIBUTIONS ADJACENT TO CAVITIES IN TISSUE-EQUIVALENT MEDIA DURING IRRADIATION BY 10 TO 35 MeV ELECTRONS. Starchman, Dale E.; Chao, Jen-hung (IIT Research Inst., Chicago. Mercy Hosptial, Chicago). Radiology; 104: No. 1, 177-86 (Jul 1972).

Quantitative determination of the effect of cavities on the dose measured by an ionization chamber at a suitable point behind the cavity has shown that the percentage of dose increase varies markedly as a function of the build-up layer, the diameter and thickness of the cavity, and the electron energy. A study of dose distribution showed that cylindrical cavities similar in size to those encountered in the head and neck may result in a localized dose of up to 160% of that measured at the depth of maximum dose within a homogeneous tissue-equivalent medium. (auth)

54904 BROAD-BEAM ATTENUATION IN LEAD FOR X RAYS FROM 50 TO 300 kVp. Kelley, John P.; Trout, E. Dale (Oregon State Univ., Corvallis). Radiology; 104: No. 1, 171-5(Jul 1972).

Broad-beam attenuation data were obtained under conditions updated to present filtrations using uniform geometry and measuring techniques. The results were in remarkably good agreement with those in NCRP reports, when it is considered that the NCRP data were taken from several papers published over a period of about thirty years. (auth)

54905 SCATTERED RADIATION FROM A TISSUE-EQUIVALENT PHANTOM FOR X RAYS FROM 50 TO 300 kVp. Trout, E. Dale; Kelley, John P. (Oregon State Univ., Corvallis). Radiology; 104: No. 1, 161-9(Jul 1972).

Data were taken showing the ratio of scatter-to-incident exposure over a kilovoltage range of 50 to 150 kVp for radiographic conditions wherein the field was centered on the scatterer and wherein the field is at the edge of the scatterer, using a phantom that has a shape similar to that of the trunk of the human body. Similar data were taken for conditions used in therapy for the voltage range of 50 to 300 kVp. The data presented here will be useful to those setting up recommended methods for calculating secondary protective barriers. (auth)

54906 DOSE TABLES FOR ^{252}Cf IMPLANTS. Bloch, Peter; Krishnaswamy, V.; Hale, John (Univ. of Pennsylvania, Philadelphia). Amer. J. Roentgenol., Radium Ther. Nucl. Med.; 115: No. 4, 822-33(Aug 1972

The neutron and gamma dose rate was calculated for ^{252}Cf planar and multiplanar cuboid implants for the Paterson–Parker source distribution system and for the Quimby source distribution system. A modified distribution system for planar implants is described that produces a dose uniformity of ±10 per cent in the target area. This system uses the uniform source distribution of the classical Quimby system with the following modifications: the length of the implant is longer than the length of the treatment area; and the sources at the edge of the implant are left in place longer than the inner sources of the implant. (auth)

54907 EFFECT OF THE MEDIUM ON RADIATION EMISSION BY RELATIVISTIC ELECTRONS. Arutyunyan, F. R.; Nazaryan, A. A.; Frangyan, A. A. (Inst. of Physical Research, Erevan). Zh. Eksp. Teor. Fiz.; 62: No. 6, 2044-8(Jun 1972). (In Russian).

The experimental data on radiation emission by 0.25- to 3.7-GeV electrons in periodic lamellar media and single layers are compared with various theories. It is shown that the experimental data are in good agreement with the theory of resonance emission if account is made for the effect of multiple electron scattering in the lamellar medium. (auth)

54908 THEORETICAL CALCULATION OF SPACE DISTRIBUTION OF DOSE FIELD OF ^{60}Co γ IRRADIATION UNDER A LATTICE. Barkova, A. M.; Kholin, V. V. (Leningrad Inst. for the Advancement of Medicine). Med. Radiol.; 16: No. 11, 64-70 (Nov 1971). (In Russian).

Calculations were made of the depth of dose of ^{60}Co γ radiation under covered and uncovered sections of a protective lattice. Limits were evaluated, beginning with the point where shadow effects become important. A projection method was developed for the quantitative estimation of shadow effects at different depths in tissue. A table is presented which shows the percentage of deep dose under lattices of various types. (tr-auth)

54909 CALCULATION OF INTEGRAL ABSORBED DOSE IN ELECTRON THERAPY OF TUMORS. Khvan, G. V. (Kazakh Scientific-Research Inst. for Oncology and Radiology, USSR). Med. Radiol.; 16: No. 11, 70-3(Nov 1971). (In Russian).

Proceeding from measurements and analysis of known isodose patterns for betatrons with a formed electron flux of 10 to 35 MeV energy, a simple method of calculation of an integral absorbed dose is suggested. In the formula a quadratic relationship for description of the distribution of the specific ionization by depth is used. For transition from the specific ionization to the absorbed dose, the known transition coefficients for primary electrons and mean coefficients for secondary electrons are used. (auth)

54910 INTEGRAL ABSORBED DOSES: EXAMPLES. Bercy, A. (Univ., Liege). J. Belge Radiol.; 54: No. 4, 516-22(1971). (In French).

By means of diagrams and a simple formula, the integral doses absorbed in the known means of radiography (X rays and γ rays) are calculated. The possibility of calculating the integral dosage absorbed during interstitial radium therapy is also demonstrated. A few examples are given in proof of the utility of calculating the integral dose absorbed, also in radioprotection. (auth)

54911 DISTRIBUTION OF QUALITATIVE COMPOSITION AND ABSORBED DOSES OF X-IRRADIATION IN USING THE SCREENS. Nguyen Van Thien; Zaboronskii, A. A.; Krongauz, A. N.; Titov, A. A. (Moscow Scientific-Research Rentgeno-Radiological Inst.). Med. Radiol.; 16: No. 11, 56-9(Nov 1971). (In Russian).

To study the distribution of the effective energies and of absorbed doses of x irradiation acting in the irradiated medium under screen filters, two miniature semiconductor detectors were used. Experimental data of the values of effective energies and of distribution of absorbed doses at various depths of a tissue-equivalent phantom were obtained. (auth)

54912 DOSIMETRY OF ^{87m}Sr. Beck, Robert N. (Argonne Cancer Research Hospital, Chicago). J. Nucl. Med.; 13: No. 9, 705(Sep 1972).

The radiation dose from ^{87m}Sr was calculated using the formulas from Johns and Cunningham (The Physics of Radiology, 1969, pp 570-573). The bone dose was found to be 14.8 mrad/100 μ Ci. The calculation of Meckelnburg (J. Nucl. Med., 5: 929-35(1964)) which uses a similar formula was found to be in error by a factor of 10. (M.H.R.)

Radiation Protection Standards

Refer also to abstracts 53247, 53248, and 53331.

54913 RADIATION PROTECTION GUIDES AND CONSTRAINTS FOR SPACE-MISSION AND VEHICLE-DESIGN STUDIES INVOLVING NUCLEAR SYSTEMS. Report of the Radiobiological Advisory Panel of the Committee on Space Medicine, Space Science Board, National Academy of Sciences—National Research Council. Washington, D. C.; National Academy of Sciences (1970). 81p. $0.25. Space Science Board, Washington, D. C.

The results are presented of an attempt to formulate tentative radiation protection guides to be used as criteria in mission-planning and vehicle-design studies for manned space operations contemplated during the next 10 to 20 years. The bases for deliberations are contained in four appendices: A, in which radiation design criteria are suggested; B, which describes the reusable nuclear rocket program, the proposed missions for reusable systems, and suggested radiation design criteria; C, which includes a publication on a 25-kWe reactor—thermoelectric power system for manned orbiting space stations; and D, NASA document MSC-00183 entitled "Radiation Environment for the 1975—1985 Space Station Program," which predicts radiation exposure rates as a function of uniform cylinder wall thickness (g/cm^2 of aluminum) for a 270-nautical-mile, 55°-inclined orbit, 200-nautical-mile polar orbit, and an equatorial earth-synchronous orbit. (M.H.R.)

54914 RADIATION PROTECTION STANDARDS: QUO VADIS. VOLUME I. Proceedings of the Sixth Annual Health Physics Society Topical Symposium, Richland, Washington, November 2—5, 1971. Howell, Wallace P.; Corley, John P. (comps.). Richland, Wash.; Health Physics Society (1972). 263p. (CONF-711119-(Vol.1)).

A separate abstract was prepared for each of 11 of a total of 13 papers. Two of the remaining papers appeared previously in NSA; see NSA 26: 9556 and 12512. (M.O.W.)

For abstracts of individual papers see: 53134, 53435, 53523, 53536, and 54915—54921.

54915 ROLE OF THE NCRP IN THE DEVELOPMENT OF RADIATION PROTECTION STANDARDS. Taylor, Lauriston S. (National Council on Radiation Protection and Measurements, Washington, D. C.). pp 16-32 of Radiation Protection Standards: Quo Vadis. Vol. I. Howell, Wallace P. (ed.). Richland, Wash.; Health Physics Society (1972).

From 6th annual topical symposium on radiation protection standards: quo vadis; Richland, Wash. (2 Nov 1971).

The National Council on Radiation Protection and Measurements has, for over 40 years, played a key role in the development of radiation protection standards in the U.S. and, in fact, internationally. It dedicated itself to the safer use of radiation for many years before the subject became a popular and political problem. At the same time it feels that proper and productive uses of radiation must not be needlessly curtailed even if some slight risk is involved—virtually nothing is without some element of risk. The NCRP does not regard itself as a "standards setting" body in the strict sense; it develops "recommendations" on protection standards and practices, expecting these to be utilized or modified to meet special needs. Input to its recommendations are primarily scientific or technical, but other considerations enter as needed. Council membership and operating procedures are designed to maximize the diversity of knowledge and organizational affiliations and minimize the possibility of any group, small or large, dominating its policies and recommendations. Council recommendations represent its best judgment based on information up to the sign-off date of a report; it does not necessarily wait for that new data that is just around the corner. It does not attempt to fully document its statements nor does it present its reports as treatises. Its recommendations are those of the Council members, to every one of whom every report is submitted for approval before release. It is anticipated that the NCRP will broaden its radiation protection activities during the foreseeable future. (auth)

54916 AMERICAN NATIONAL STANDARDS INSTITUTE AND NUCLEAR STANDARDS. Fleckenstein, D. C. (General Electric Co., Schenectady, N. Y.). pp 33-49 of Radiation Protection Standards: Quo Vadis. Vol. I. Howell, Wallace P. (ed.). Richland, Wash.; Health Physics Society (1972).

From 6th annual topical symposium on radiation protection standards: quo vadis; Richland, Wash. (2 Nov 1971).

The history and organization of the American National Standards Institute (ANSI) is summarized. Procedures for the development of American National Standards are described. Nuclear standards activities in general, and radiation protection standards programs in particular, are used as examples of ANSI operations and will provide the current status of these efforts. ANSI affiliation with the International Organization for Standardization (ISO) is reported. ISO technical committees of interest are described. Some ANSI future plans and programs in the nuclear standards area are given. (auth)

54917 DESCRIPTION OF THE AMERICAN NUCLEAR SOCIETY'S INFORMATION CENTER ON NUCLEAR STANDARDS (ICONS) RADIATION PROTECTION STANDARDS: QUO VADIS. Voigt, Keith L.; DuTemple, Octave J.; Brown, Roberta S. (American Nuclear Society, Hinsdale, Ill.). pp 50-9 of Radiation Protection Standards: Quo Vadis. Vol. I. Howell, Wallace P. (ed.). Richland, Wash.; Health Physics Society (1972).

From 6th annual topical symposium on radiation protection standards: quo vadis; Richland, Wash. (2 Nov 1971).

The American Nuclear Society recently organized an Information Center on Nuclear Standards (ICON). The reasons for its establishment, its purpose, goals and services are described in detail. Considerable background information concerning the concept of Information Analysis Centers (IAC), their organization and usefulness is discussed. A step-by-step description of the mechanics for setting up an IAC is given. Sources of data, input, storage, retrieval, analysis of data and output of ICONS' information are identified. The purpose and role of the Technical Advisor is explained along with the relationship of ICONS to other standards writing organizations. A new IAC dimension was added with the establishment of ICONS. In addition to providing the traditional services of an IAC, ICONS will periodically take on assignments of a special nature. For example, a thorough examination of the possibility of organizing a nuclear industry-sponsored standards and codes enforcing agency similar to the air- and marine-industry will be made. ICONS, through its Technical Advisors, will take on the task of evaluating, analyzing, and describing why a nuclear industry-sponsored standards and codes enforcing agency is needed, if indeed it is needed; suggest how such an organization could be organized and supported; who could direct this agency; what its purpose and functions should be; and, other considerations important to the development of a preliminary working model. A discussion of the marketing plan for ICONS is included. (auth)

54918 ROLE OF THE HEALTH PHYSICS SOCIETY IN THE DEVELOPMENT OF RADIATION PROTECTION STANDARDS. Vallario, E. J. (Health Physics Society Standards Committee, Washington, D. C.). pp 60-9 of Radiation Protection Standards: Quo Vadis. Vol. I. Howell, Wallace P. (ed.). Richland, Wash.; Health Physics Society (1972).

From 6th annual topical symposium on radiation protection standards: quo vadis; Richland, Wash. (2 Nov 1971).

The Health Physics Society Standards Committee (HPSSC) is a permanent committee of nine Society members assigned to represent the Society to the Board of Directors on matters concerned with standardization of practices in radiation protection. Its multiphased role is to advise the officers and members of the Society on new developments in the field of standardization, examine the need for new standards, establish expert working groups under the HPSSC to develop priority standards and maintain liaison with other standard making organizations to accomplish these objectives effectively. An ancillary function is to provide the Board of Directors technical assistance to establish a Society position on major issues involving new radiation protection standards. (auth)

54919 RECENT ACTIVITES IN THE DEVELOPMENT OF SURFACE CONTAMINATION STANDARDS. Gallagher III, F. E.; Evraets, J. C.; Tschaeche, A. N.; Willis, C. A. (Health Physics Society, Richland, Wash.). pp 206-15 of Radiation Protection Standards: Quo Vadis. Vol. I. Howell, Wallace P. (ed.). Richland, Wash.; Health Physics Society (1972).

From 6th annual topical symposium on radiation protection standards: quo vadis; Richland, Wash. (2 Nov 1971).

The Standards Committee of the Southern California Chapter, Health Physics Society, has prepared a "Position Paper on Surface Contamination Standards for Radioactive Materials." It was written to discuss the need for these standards and to establish the basic criteria for their development, because of the widespread disagreement among health physicists concerning many of the important details. The paper was reviewed by the Health Physics Society Standards Committee in November, 1970, and a revised version, dated January 15, 1971, has been accepted. As a result of this activity, the Health Physics Society Standards Committee has recently established a subcommittee to write surface contamination standards, using the position paper's criteria as background material. A summary of the paper's final version is presented here. (auth)

54920 SUMMARY OF RADIOACTIVE SURFACE CONTAMINATION GUIDES. Schmidt, Gail D. (Bureau of Radiological Health, Rockville, Md.). pp 216-27 of Radiation Protection Standards: Quo Vadis. Vol. I. Howell, Wallace P. (ed.). Richland, Wash.; Health Physics Society (1972).

From 6th annual topical symposium on radiation protection standards: quo vadis; Richland, Wash. (2 Nov 1971).

Results of investigations of guides used for the control of radioactive surface contamination are presented. The study includes: (1) a summary of the guides used by over 40 nuclear facilities in 1965 or recommended in the literature, (2) the guides adopted by U. S. Regulatory agencies, (3) the contamination level associated with MPC (air) based upon resuspension factors, and (4) contamination levels from operational experiences that have been associated with internal body burdens. The investigations indicate that most U.S. nuclear facilities use a conservatively low contamination guide that has apparently been most effective in limiting internal exposure. The data from resuspension studies and operational experience tends to support the values recommended by Dunster (Health Physics, 8: 353-6, (1962). Recently adopted or suggested contamination studies continue to exhibit considerable diversity of opinion. Suggested radioactive contamination guides that represent a compromise are presented along with the admonition that, as a territory standard, they be applied with professional judgment. (3 tables, 19 references) (auth)

54921 SAFETY CRITERIA FOR NUCLEAR POWER IN SPACE. Willis, C. A. (McDonnell Douglas Astronautics Co., Huntington Beach, Calif.). pp 236-56 of Radiation Protection Standards: Quo Vadis. Vol. I. Howell, Wallace P. (ed.). Richland, Wash.; Health Physics Society (1972).

From 6th annual topical symposium on radiation protection standards: quo vadis; Richland, Wash. (2 Nov 1971).

The appropriateness of nuclear power for space application has long been recognized. There have been numerous applications, including Apollo, but the full potential has not been realized. The uncertainty about safety requirements is one of the limiting factors. There are no established criteria for the acceptable risk associated with space nuclear power. It follows that there is no concrete basis for assuring program management that a system will be acceptably safe, no matter how good it may be. Conversely, there is no firm justification for safety requirements because the resulting system may or may not be approved with or without the precautionary measure. A study of the safety criteria problem is reported which compares the various standards which have been met and the criteria which have been suggested. It is concluded that general criteria can be developed and should be the object of concentrated effort. (3 figures, 68 references). (auth)

54922 RADIATION PROTECTION STANDARDS: QUO VADIS. VOLUME II. Proceedings of the Sixth Annual Health Physics Society Topical Symposium, Richland, Washington, November 2–5, 1971. Howell, Wallace P.; Corley, John P. (comps.). Richland, Wash.; Health Physics Society (1972). 244p. (CONF-711119–(Vol.2)).

A separate abstract was prepared for each of 17 of the total of 20 articles. Three articles appeared previously in NSA; see NSA 26: 8575, 9541, and 11453. (M.O.W.)

For abstracts of individual papers see: 53246—53248, 53436, 53510, and 54923—54934.

54923 APPLICATION OF RADIATION EXPOSURE STANDARDS IN THE AEC CONTRACTOR PROGRAM. Ross, Donald M. (Atomic Energy Commission, Washington, D. C.). pp 309-15 of Radiation Protection Standards: Quo Vadis. Vol. II. Howell, Wallace P. (ed.). Richland, Wash.; Health Physics Society (1972).

From 6th annual topical symposium on radiation protection standards: quo vadis; Richland, Wash. (2 Nov 1971).

The AEC radiation protection guides applicable to contractor operations are embodied in AEC Manual Chapter 0524. The basic guides have been derived from the recommendations of the Federal Radiation Council (FRC) whose functional responsibilities have recently been incorporated into those of the newly established Environmental Protection Agency (EPA). In those areas that remained uncovered by the FRC, the AEC follows the recommendations of the National Council on Radiation Protection and Measurements (NCRP) and the International Commission on Radiological Protection (ICRP). (auth)

54924 AEC REGULATORY PROGRAM. Gamertsfelder, Carl C. (Atomic Energy Commission, Washington, D. C.). pp 316-21 of Radiation Protection Standards: Quo Vadis. Vol. II. Howell, Wallace P. (ed.). Richland, Wash.; Health Physics Society (1972).

From 6th annual topical symposium on radiation protection standards: quo vadis; Richland, Wash. (2 Nov 1971).

The Commission's regulation entitled "Standards for Protection Against Radiation," (10 CFR Part 20) establishes standards for external radiation exposure and permissible concentrations in air and water which are based on the recommendations of the NCRP, ICRP, and the FRC. There are also implementing provisions and procedures to assure that every reasonable effort is made to maintain radiation exposures as far below the specified limits as practicable. Other parts of the regulations provide the framework for dealing with byproduct, source and special nuclear materials, and certain nuclear facilities. In these parts, the basic standards are applied in more detail through the requirement for specific licenses which are issued after thorough review of the facilities and the procedures to be used. Control over other activities, of a more routine nature or of more limited scope, are provided by general licenses. In some certain cases, usually related to a specific product or class of products, for which it can be shown that individuals are not likely to be exposed to more than a few percent of the dose limits, the use of the products may be exempted from regulatory control. The Commission recently revised its regulations for the licensing of nuclear power reactors to include requirements for keeping radioactive effluents as low as practicable and is in the process of defining numerical guidance on what can be considered to be as low as practicable. (auth)

54925 APPLICATIONS OF RADIATION PROTECTION RECOMMENDATIONS IN THE DEVELOPMENT OF FEDERAL RADIATION STANDARDS FOR ELECTRONIC PRODUCTS. Snow, Donald L.; Little, Marshall S.; Snavely, David R. (Bureau of Radiological Health, Rockville, Md.). pp 322-43 of Radiation Protection Standards: Quo Vadis. Vol. II. Howell, Wallace P. (ed.). Richland, Wash.; Health Physics Society (1972).

From 6th annual topical symposium on radiation protection standards: quo vadis; Richland, Wash. (2 Nov 1971).

Experiences are reviewed in applying radiation protection recommendations of voluntary standards-setting organizations in the development of regulations to control radiation emissions from electronic products. The impact of voluntary standards on regulatory standards is discussed from such standpoints as: (1) enforceability aspects of standards, (2) needs for documenting the development of the regulatory standards, and (3) conversion of radiation exposure criteria to radiation emission criteria for specific electronic products. The responsibility of a regulatory agency to establish safety factors for emission criteria, based on reasonableness and technical feasibility considerations, is discussed. Also considered are those difficulties which develop when (1) no prior consideration has been given by voluntary standards groups to a problem area, or (2) there is no available information on the technical or scientific bases for recommendations from national or international groups. Factors which may cause a regulatory agency to deviate in whole or part from an accepted national or international recommendation are reviewed to develop further understanding as to where improvements may be possible at every level of the standards development process. (auth)

54926 OCCUPATIONAL SAFETY AND HEALTH ACT OF 1970. Beeston, Richard (Occupational Safety and Health Administration, Seattle). pp 344-51 of Radiation Protection Standards: Quo Vadis. Vol. II. Howell, Wallace P. (ed.). Richland, Wash.; Health Physics Society (1972).

From 6th annual topical symposium on radiation protection standards: quo vadis; Richland, Wash. (2 Nov 1971).

The Williams—Steiger Act is without question the most far-reaching piece of legislation in this field ever enacted. It has reached a new level in thinking about occupational safety and health. The purpose, coverage, responsibility of employees and employers are highlighted. In addition, the enforcement aspects of this Act are discussed along with the Occupational Safety and Health Standards and the particular application of the Radiation Protection Standards in the field of occupational health. (auth)

54927 EPA ROLE IN RADIATION PROTECTION. Palmiter, C. C. (Environmental Protection Agency, Rockville, Md.). pp 352-6 of Radiation Protection Standards: Quo Vadis. Vol. II. Howell, Wallace P. (ed.). Richland, Wash.; Health Physics Society (1972).

From 6th annual topical symposium on radiation protection standards: quo vadis; Richland, Wash. (2 Nov 1971).

The President's Reorganization Plan No. 3 transferred to the Environmental Protection Agency, all the functions of the former Federal Radiation Council to provide Guidance to Federal agencies and from the Atomic Energy Commission the responsibility for setting generally applicable environmental standards. As a result of this transfer, the EPA is now responsible for completing the general review of the guidance issued by the FRC in 1960. It recently issued guidance which limits the exposure of underground uranium miners to the short-lived progeny of radon-222 to 4 WLM per year. It also solicited comments from other Federal agencies regarding the adoption by the Federal Government of all or part of the new recommendations made in NCRP Report No. 39. (auth)

54928 STANDARDS AND STATE REGULATORY CONTROL PROGRAMS. Moen, Arnold J. (Washington State Div. of Health, Olympia). pp 357-61 of Radiation Protection Standards: Quo Vadis. Vol. II. Howell, Wallace P. (ed.). Richland, Wash.; Health Physics Society (1972).

From 6th annual topical symposium on radiation protection standards: quo vadis; Richland, Wash. (2 Nov 1971).

The evolution of regulatory control programs from standards through custom, tradition, and fear is discussed. Problems of establishing regulations to meet the standards and to control major sources of exposure not covered by standards are explored. Establishment of uniformity among states' regulations to avoid unnecessary limitation of interstate activities complicate regulations. These complications make regulations difficult to understand or interpret when locally applied. Enforcement of state regulations is hampered by lack of inherent pressures of custom or tradition. Familiarity through use of radiation, development of bad habits, and lack of knowledge or concern are discussed as deterrents to compliance. Practical problems of establishing motivation to comply through enforcement of regulations are discussed. Lack of involvement of users and states in the standard setting procedures creates problems in establishing regulations and in enforcement of compliance. (auth)

54929 WHY BENEFIT-RISK ANALYSIS? Cohen, Jerry J. (Univ. of California, Livermore). pp 362-5 of Radiation Protection Standards: Quo Vadis. Vol. II. Howell, Wallace P. (ed.). Richland, Wash.; Health Physics Society (1972).

From sixth annual topical symposium on radiation protection standards: quo vadis; Richland, Wash. (2 Nov 1971).

A brief discussion is given on the risk of radiation as compared to the benefit of radiation. Low doses are discussed in particular. (M.O.W.)

54930 WHOSE BENEFIT? WHOSE RISK? WHOSE BALANCE? Grendon, Alexander (Univ. of California, Berkeley). pp 377-85 of Radiation Protection Standards: Quo Vadis. Vol. II. Howell, Wallace P. (ed.). Richland, Wash.; Health Physics Society (1972).

From sixth annual topical symposium on radiation protection standards: quo vadis; Richland, Wash. (2 Nov 1971).

Benefits and risks are generally viewed too narrowly in discussions of radiation standards. This paper tries to expand the perspective, showing some benefits and risks in applications of nuclear energy and radiation that are often overlooked and identifying the population segments affected by them. Because of the wide range of these benefits and risks and of the subpopulations involved, it becomes virtually impossible to compare overall benefits and risks in setting limits of total population exposure; only in particular cases, or for limited classes, is such an effort potentially useful. In those cases, social and political factors need to be weighed along with the technical considerations; for the technical complexity requires delegation of responsibility for that task by the public to specially qualified judges rather than direct voting by an uninformed electorate—a system that is a logical extension of our form of representative democracy. (auth)

54931 BENEFIT–RISK RATIOS: SOME ECCENTRIC VIEWS. Sagan, Leonard A. (Palo Alto Clinic, Calif.). pp 386–400 of Radiation Protection Standards: Quo Vadis. Vol. II. Howell, Wallace P. (ed.). Richland, Wash.; Health Physics Society (1972).

From 6th annual topical symposium on radiation protection standards: quo vadis; Richland, Wash. (2 Nov 1971).

The strategy that ICRP has adopted for control of public exposure to radiation is to assume that effects of radiation may occur, even at very low doses. Therefore, any industrially produced radiation exposure, such as from nuclear power plants, should be justified in terms of a cost-benefit calculation. Unfortunately, they do not provide guidelines for such calculations. Nor in traditional economics is there a theoretical background for estimating and charging costs for human effects produced by releases to the environment. The author proposes that an emissions tax for pollutants, including radioactivity, be established, and that this tax be based on a linear extrapolation from high dose effects and on a standard dollar value of man. Market mechanisms then would operate to control and allocate emissions among industrial users in a more efficient and equitable manner than could be achieved through arbitrary regulatory mechanisms. (auth)

54932 RISKS OF BENEFIT–RISK ANALYSIS. Connolly, T. J. (Stanford Univ., Calif.). pp 401-9 of Radiation Protection Standards: Quo Vadis. Vol. II. Howell, Wallace P. (ed.). Richland, Wash.; Health Physics Society (1972).

From 6th annual topical symposium on radiation protection standards: quo vadis; Richland, Wash. (2 Nov 1971).

The various efforts to date to develop a benefit—risk methodology share a common vision of a goal the achievement of which will enable persons to weigh an evaluation of benefits against an evaluation of all forms of costs of a given innovation and decide whether the balance favors proceeding with the innovation or not. Risks comprise that portion of costs which are borne by individuals in the form of discomfort, ill health, injury or death. The authors confess to some skepticism regarding the extent to which benefit—risk analysis can usefully be developed. It is the theme of this paper that any valid methodology that may be developed should satisfy certain criteria that can be defined at this time. These criteria are discussed. Some assumptions common to benefit—risk analysis are questioned in the light of various social—psychological studies. (auth)

54933 INDUSTRY'S UNDERSTANDING OF THE RADIATION CONTROVERSY. Olds, Fredric C. (Power Engineering Magazine, Barrington, Ill.). pp 444-51 of Radiation Protection Standards: Quo Vadis. Vol. II. Howell, Wallace P. (ed.). Richland, Wash.; Health Physics Society (1972).

From 6th annual topical symposium on radiation protection standards: quo vadis; Richland, Wash. (2 Nov 1971).

Critics of nuclear power in the United States have had great success in spite of minimum financial resources. One finds in Europe that now they are turning sentiment against nuclear power there—often with arguments and people imported from the U. S. How can the critics have this success on a shoestring if they have been discredited as the industry claims? Some important answers were found by looking at the principles of communication which the nuclear industry uses well in a market-competitive situation, but which it uses poorly in an adversary situation where it has to debate a fervent, sometimes fanatical opposition. Errors in communications tactics were illustrated by examples. Basic principles of adversary communications, as they apply to the nuclear power situation, were discussed. Commonly, the industry's strategy in the struggle for the public repute it wants has been superficial. (auth)

54934 USE AND ABUSE OF STANDARDS. Tschaeche, A. N. (General Electric Co., San Jose, Calif.). pp 458-64 of Radiation Protection Standards: Quo Vadis. Vol. II. Howell, Wallace P. (ed.). Richland, Wash.; Health Physics Society (1972).

From 6th annual topical symposium on radiation protection standards: quo vadis; Richland, Wash. (2 Nov 1971).

The growing need for formulating standards is discussed with respect to freeing the plant and laboratory health physicist for more creative and productive work on unique problems. Various types of documents, e.g., material specifications, testing methods, standard terminology, and safety rules are used to illustrate the important differences between standards as rules and standards as guides or models. The abuse of standards, e.g., improper application and blind incorporation in regulations, is illustrated. A method of applying standards to the solution of particular radiation measurement and protection problems is proposed toward stimulating the production of effective standards. (auth)

54935 EXPOSURE RATE. Buchan, R. C. T. (Plymouth General Hospital, Eng.). Brit. J. Radiol.; 45: No. 536, 628 (Aug 1972).

Concern is expressed that in connection with specifications for x-ray tube output, the term exposure rate is defined as the quotient of exposure by electrical charge. It is pointed out that the ICRU defines exposure rate as the quotient of Δx by Δt, where Δx is the increment in exposure in time Δt. This is expressed in units such as mR/sec, mR/min, mR/hr, rather than R/mA/min or mR/mA/sec. (UK)

Radiation Source Calibration and Standardization

54936 DETERMINATION OF THICKNESS OF γ-SOURCES AND ABSORBERS FROM THE DEFORMATION OF THE HARD PART OF THE ENERGY SPECTRUM. Vorob'ev, V. A.; Fridman, Sh. D. This paper was summarized in At. Energ. (USSR); 30: No. 4, 385(Apr 1971) as paper No. 480/5877. (In Russian).

Full copy of this paper is held by TIC.

A method is described for determining the thickness of remote γ sources and absorbers by taking account of the deformation of the hard part of the energy spectrum of the γ radiation from distributed sources. This deformation is measured by a quantity ξ defined as the ratio of the intensity of the primary γ radiation J_0 of energy E_0 to the differential intensity of the hard scattered γ radiation J_0 as $E \rightarrow E_0$, i.e., $\xi = J_0^S/J_0^S$. Relations are presented that associate the function ξ with the thickness of an inactive absorber, and in the absence of an absorber, with the thickness of the radiation source for a plane isotropic source, a uniform half-space, and a uniform layer. Graphs of $\xi(\mu x, \theta)$ were computed for a vertical collimated detector with a half-angle aperture $\theta \rightarrow 0^0$, and also for θ equal to 30, 60, and 90° for a range of thicknesses $0.1 \leq \mu x \leq 5.0$. The method is very sensitive. (auth)

Shielding Calculations and Theory

Refer also to abstracts 53138, 53930, 54892, 54913, 55140–55144, 55360, 55364, 55365, 55368, 55371–55373, 55382, 55383, and 55424.

54937 (CONF-720901–(Bks.1 and 2), pp 349-84) INTEGRAL EXPERIMENTS AND PHILOSOPHY OF BENCHMARK CALCULATIONS. Straker, E. A. 1972.

From Meeting on new developments in reactor physics and shielding calculations; Kiamesha Lake, NY. (12 Sep 1972).

After surveying the benchmark problem and needs, the author points out the apparent renewed interest in standards, benchmarks, etc. Much of the need arises because, at present, radiation transport calculations for complex shielding problems use very large computer codes requiring large data bases, with inherent problems in accuracy of results. From 1967 to present, there was only one addition to the Shielding Benchmark Problem book; during this period there have been numerous measurements and calculations that can be considered candidates. After presenting in one table the characteristics of benchmarks two other tables are used to summarize, respectively, integral experiments and reference calculations that might be considered as benchmarks. The author concludes that, because of the scope of the job, efforts at maintaining "benchmark books" will undoubtedly fall short of the goal. He feels, however, that perhaps it is not too important whether the results are labeled "benchmark" or not; it is probably sufficient to make readily available information about a large number of different types of problems that have received careful consideration. (94 references) (L.M.T.)

54938 (CONF-720901–(Bks.1 and 2), pp 385-96) DEVELOPMENTS IN INTEGRAL SHIELDING EXPERIMENTS INVOLVING FAST-NEUTRON TRANSPORT. Harris, L. Jr. (Gulf Radiation Tech., San Diego, Calif.). 1972.

From Meeting on new developments in reactor physics and shielding calculations; Kiamesha Lake, NY. (12 Sep 1972).

The evolution of integral shielding experiments involving fast-neutron transport is reviewed briefly and recent developments in third generation experiments are described. (M.H.R.)

54939 (CONF-720901–(Bks.1 and 2), pp 397-408) CARBON SHIELDING BENCHMARK PROBLEM AND OTHER NEUTRON TRANSPORT CALCULATIONS IN CARBON. Goldstein, H.; Soran, P. D.; Weisbin, C. R. (Columbia Univ., New York). 1972.

From Meeting on new developments in reactor physics and shielding calculations; Kiamesha Lake, NY. (12 Sep 1972).

Moments method and S_N calculations are presented for the scalar neutron fluxes in Shielding Benchmark Problem 1.0— an isotropic, fission-like source in a carbon medium. It is found that deep penetration of neutrons in carbon is governed by cross section phenomena that do not affect the penetration at such small distances as are involved in the Benchmark problem. It is, therefore, not yet clear how well existing transport methods can calculate deep penetrations in carbon. Flux-ages-to-indium-resonance energy are calculated for a fission source and a number of monoenergetic sources. Differences between the values given here and those presented elsewhere are correlated with differences in the microscopic cross-section sets used. (auth)

54940 (CONF-720901–(Bks.1 and 2), pp 512-23) SENSITIVITY ANALYSIS: A GENERAL APPROACH ILLUSTRATED FOR A Na–Fe SYSTEM. Bartine, D. E.; Oblow, E.; Mynatt, F. R. (Oak Ridge National Lab., Tenn.). 1972.

From Meeting on new developments in reactor physics and shielding calculations; Kiamesha Lake, NY. (12 Sep 1972).

A general approach to sensitivity studies is introduced using a quantitative definition of cross-section sensitivity. The definition offered is intended to be both practical and physically meaningful. Its advantages in comparison with other approaches is discussed and its use in analysis is illustrated for a sodium–iron transport problem. Results of the analysis include a discussion of the role of important total cross-section minima in deep penetration in sodium and iron and the importance of certain energy ranges and partial cross sections for the sodium-iron system. The predictive aspect of the approach is demonstrated in comparisons of rigorous and predicted results for small cross-section perturbations and in conclusions about the order of Legendre expansion of the scattering kernel. (auth)

54941 (CONF-720901–(Bks.1 and 2), pp 541-58) SHIELDING APPLICATION OF PERTURBATION THEORY TO DETERMINE CHANGES IN NEUTRON AND GAMMA DOSES DUE TO CHANGES IN SHIELD LAYERS. Fieno, Daniel (Lewis Research Center, Cleveland). 1972.

From Meeting on new developments in reactor physics and shielding calculations; Kiamesha Lake, NY. (12 Sep 1972).

Perturbation theory for fixed sources was applied to radiation shielding problems to determine changes in neutron and gamma-ray doses due to changes in various shield layers. For a given source and detector position the perturbation method enables dose derivatives due to all layer changes to be determined from one forward and one inhomogeneous adjoint calculation. The direct approach requires two forward calculations for the derivative due to a single layer change. Hence, the perturbation method for obtaining dose derivatives permits an appreciable savings in computation for a multilayered shield. For an illustrative problem, a comparison was made of the fractional change in the dose per unit change in the thickness of each shield layer as calculated by perturbation theory and by successive direct calculations; excellent agreement was obtained between the two methods. (auth)

54942 (CONF-720901–(Bks.1 and 2), pp 574-6) EFFECTIVE MULTIPLE-CONSTRAINT SHIELD OPTIMIZATION TECHNIQUE. Billings, M. P. (McDonnell Douglas Astronautics Co., West Huntington Beach, Calif.). 1972.

From Meeting on new developments in reactor physics and shielding calculations; Kiamesha Lake, NY. (12 Sep 1972).

A general technique developed at McDonnell Douglas Astronautics Company and applied to a variety of shield optimization problems has proven extremely effective in essentially all important aspects; realistically representing system variables (no restriction in geometric modeling is required), simply accommodating any number of (inequality) constraints, accurately representing the dependence of radiation levels and shield mass on the variables, providing computational efficiency, and achieving the optimal result for a given problem. (auth)

54943 (CONF-720901–6) SENSITIVITY ANALYSIS: A GENERAL APPROACH ILLUSTRATED FOR A Na–Fe SYSTEM. Bartine, D. E.; Oblow, E.; Mynatt, F. R. (Oak Ridge National Lab., Tenn.). 1972. 14p. Dep. NTIS.

From Meeting on new developments in reactor physics and shielding calculations; Kiamesha Lake, NY. (12 Sep 1972).

A general approach to sensitivity studies is introduced using a quantitative definition of cross-section sensitivity. The definition offered is intended to be both practical and physically meaningful. Its advantages in comparison with other approaches are discussed, and its use in analysis is illustrated for a sodium/iron transport problem. Results of the analysis include a discussion of the role of important total cross-section minima in deep penetration in sodium and iron and the importance of certain energy ranges and partial cross sections for the sodium/iron system. The predictive aspect of the approach is demonstrated in comparisons of rigorous and predicted results for small cross-section perturbations and in conclusions about the order of Legendre expansion of the scattering kernel. (auth)

54944 (NAA-SR-Memo–8597) ANALYSIS OF THE STF NEUTRON TRANSMISSION MEASUREMENTS (INITIAL MEASUREMENTS). Engle, W. W. (Atomics International, Canoga Park, Calif.). 5 Jun 1963. Contract AT(11-1)-Gen-8. 9p. Dep. NTIS.

The data from the experimental neutron flux measurements in LiH performed at the Shield Test Facility was used as input data for SMAC II. The results of several sets of experimental data are presented. (auth)

54945 (NASA-TM-X–2440, pp 40-7) IMPACT OF RADIATION DOSE ON NUCLEAR SHUTTLE CONFIGURATION. Goetz, C. A.; Billings, M. P. (McDonnell Douglas Astronautics Co., West Huntington Beach, Calif.). Jan 1972.

From Symposium on natural and manmade radiation in space; Las Vegas, Nev. (1 Mar 1971).

The impact of nuclear radiation (from the NERVA propulsion system) on the selection of a reference configuration for each of two classes of the Reusable Nuclear Shuttle (RNS) is assessed. One class was characterized by a single propellant tank, the shape of whose bottom was found to have a pronounced effect on crew radiation levels and associated shield weight requirements. A trade study of shield weight versus structural weight indicated that the minimum-weight configuration for this class had a tank bottom in the shape of a frustum of a 10°-half-angle cone. A hybrid version of this configuration was found to affect crew radiation levels in substantially the same manner. The other class of RNS consisted of a propulsion module and eight propellant modules. Radiation analyses of various module arrangements led to a design configuration with no external shield requirements. (auth)

54946 (NASA-TM-X–2440, pp 48-56) EFFECTS OF RADIATION ENVIRONMENT ON REUSABLE NUCLEAR SHUTTLE SYSTEM. Lane, A. G. (North American Rockwell, Downey, Calif.). Jan 1972.

From Symposium on natural and manmade radiation in space; Las Vegas, Nev. (1 Mar 1971).

Since radiation protection for a manned nuclear rocket represents the most significant design constraint, major emphasis has been placed upon parametric tradeoff analyses of a wide spectrum of alternate tank configurations to minimize both primary and secondary, direct and scattered radiation sources emanating from the NERVA (nuclear engine for rocket vehicle application). The analytical approach utilizing point kernel techniques is described and detailed data are presented on the magnitude of neutron/gamma doses for different locations. Dose rates are presented for both engine firing and post-shutdown periods. Conical aft bulkhead geometries employing a range of included half cone angles from 5 to 15 degrees and end cap radii from 25 to 125 inches were evaluated. Single-tank configurations utilizing smaller cone angles and end cap radii were found to minimize integral radiation levels, hence, stage shielding-weight penalties for shuttle missions. This is due to the greater payload separation distance, reduction of the effective energy disposition and scattering centers in the aft end of the tank, and greater depth of the liquid hydrogen propellant for radiation attenuation at any given time during the draining cycle for a fixed tank propellant capacity. Hybrid configurations employing an upper tank with a reduced cone angle and end cap radius results in low integral payload doses primarily due to the increased separation distance caused by the elongation of the larger capacity upper tank. A preliminary radiation damage assessment is discussed of possible reusable nuclear shuttle (RNS) materials, components, and subsystems, and the possible effects of the radiation environment on various phases of RNS mission operations, i.e., maintenance, rendezvous, docking, and engine disposal. (auth)

54947 (NASA-TM-X–2440, pp 58-64) RADIATION ANALYSIS OF VARIOUS VEHICLE AND PAYLOAD CONFIGURATIONS FOR THE REUSABLE NUCLEAR SHUTTLE. Preeg, W. E. (Aerojet Nuclear Systems Co., Sacramento). Jan 1972.

From Symposium on natural and manmade radiation in space; Las Vegas, Nev. (1 Mar 1971).

Radiation analyses were performed and shielding weight requirements were estimated for various candidate vehicle and payload configurations for use with the Reusable Nuclear Shuttle. The analyses included both Point Kernel and Monte Carlo approaches. The effects on reduced shield weight were determined for propellant tanks with pointed conical tank bottoms and for one case of a cluster of small (15 ft diameter) tanks. This latter case, however, had an arrangement which had no center tank in the upper tier of tanks. This effect negated most of the gain of going to the smaller tanks. A range of shield weights is presented for various light and heavy manned payload configurations when used in conjunction with a single liquid hydrogen propellant tank, 33 ft in diameter with a 15° conical tank bottom. (auth)

54948 (NASA-TM-X–2440, pp 78-83) PRELIMINARY SHIELD DESIGN FOR A SNAP-8 POWER SYSTEM. Karp, I. M.; Soffer, L.; Clark, M. R. (Lewis Research Center, Cleveland, Ohio). Jan 1972.

From Symposium on natural and manmade radiation in space; Las Vegas, Nev. (1 Mar 1971).

A preliminary shield design for a nuclear power system utilizing a SNAP-8 reactor for space base application is presented. A representative space base configuration was selected to set the geometry constraints imposed on the design. The base utilizes two independent power packages each with a reactor operating at 600 kwt and each producing about 50 kwe. The crew compartment is located about 200 feet from each reactor and is large enough in extent to intercept a total shadow angle of 60° measured about the center line of each reactor. Reactor dose constraints for the shield design were: (1) the dose to the crew over a 6 month mission was set at 150 mrem/day, (2) the dose along the side of either power system was set at 30 mrem/hr at a distance of 200 feet, based on considerations of exposure during repair to one power system while the other is operating, and (3) the dose constraint elsewhere around the reactor was set at 5 rem/hr at a distance of 200 feet. Personnel are not expected to be in this region during operation of the power systems except possibly for very brief periods during approach and departure from the base. The shield design presented incorporates the results of calculations and some preliminary engineering considerations. The weight of the idealized layered lithium hydride and depleted uranium shield layout used as the calculational model was about 35,000 pounds whereas the preliminary engineering layout of the shield which includes structure, canning materials, clearance gaps between layers, etc. weighed about 41,000 pounds. (auth)

54949 (NASA-TM-X–2440, pp 92-7) SPACE-REACTOR SHIELDING FABRICATION. Welch, Frank H. (Atomics International, Canoga Park, Calif.). Jan 1972.

From Symposium on natural and manmade radiation in space; Las Vegas, Nev. (1 Mar 1971).

A new facility has been constructed at the Atomics International Nuclear Field Laboratory for the fabrication of space reactor neutron shielding by a melting and casting process utilizing lithium hydride. This facility is equipped to handle lithium hydride not only under the exacting conditions dictated by the nature of the reactive, moisture sensitive material, but also under the stringent requirements of the nuclear shielding engineer for high purity, maximum density, good structural integrity, etc. This facility is capable of producing lithium hydride neutron shields up to 8 feet in diameter weighing 10,000 lbs. In addition, the facility contains a 1650 cubic feet nitrogen atmosphere, glove-ported room capable of handling these massive shields during a destructive examination to determine the internal characteristics of the shield after thermal and vibrational tests simulating operation conditions. The first neutron shield fabricated in this new facility was a large, pancake shape 86 inches in diameter, containing about 1700 pounds of lithium hydride. This shield, fabricated by the unique melting and casting process, is the largest lithium hydride shield ever built. (auth)

54950 (NASA-TM-X-2440, pp 98-102) NUCLEAR REACTOR DESCRIPTIONS FOR SPACE POWER SYSTEMS ANALYSIS. McCauley, E. W.; Brown, N. J. (Univ. of California, Livermore). Jan 1972.

From Symposium on natural and manmade radiation in space; Las Vegas, Nev. (1 Mar 1971).

For the small, high-performance reactors required for space electric applications, adequate neutronic analysis is of crucial importance, but in terms of computational time consumed, nuclear calculations probably yield the least amount of detail for mission analysis study. It has been found possible, after generation of only a few designs of a reactor family in elaborate thermomechanical and nuclear detail to use simple curve-fitting techniques to assure desired neutronic performance while still performing the thermomechanical analysis in explicit detail. The resulting speedup in computation time by three orders of magnitude permits a broad detailed examination of constraints by the mission analyst. (auth)

54951 (NASA-TM-X-2440, pp 108-16) METHODS OF SPACE RADIATION-DOSE ANALYSIS WITH APPLICATIONS TO MANNED SPACE SYSTEMS. Langley, R. W.; Billings, M. P. (McDonnell Douglas Astronautics Co., Huntington Beach, Calif.). Jan 1972.

From Symposium on natural and manmade radiation in space; Las Vegas, Nev. (1 Mar 1971).

The full potential of state-of-the-art space radiation dose analysis for manned missions has not been exploited. Point doses have been overemphasized, and the critical dose to the bone marrow has been only crudely approximated, despite the existence of detailed man models and computer codes for dose integration in complex geometries. The method presented makes it practical to account for the geometrical detail of the astronaut (which typically provides as much protection to the internal organs as does the vehicle) as well as the vehicle. This paper discusses the major assumptions involved and presents the concept of applying the results of detailed proton dose analysis to the real-time interpretation of on-board dosimetric measurements. (auth)

54952 (NASA-TM-X-2440, pp 170-7) GEOMAGNETICALLY TRAPPED RADIATION ENVIRONMENT: A RADIOLOGICAL POINT OF VIEW. Holly, F. Eugene (Air Force Weapons Lab., Kirtland AFB, N. Mex.). Jan 1972.

From Symposium on natural and manmade radiation in space; Las Vegas, Nev. (1 Mar 1971).

The regions of naturally occurring, geomagnetically trapped radiation (Van Allen Belts) are briefly reviewed in terms of physical parameters such as particle types, fluxes, spectra, and spatial distributions. The major emphasis is, however, placed upon a description of this environment in terms of the radiobiologically relevant parameters of absorbed dose and dose rate and a discussion of the radiological implications in terms of the possible impact on space vehicle design and mission planning. These descriptions are based both upon direct measurement and calculation using the more fundamental parameters of particulate energy and flux. Comparison of such calculations with measurements emphasizes that, depending upon the location in space, that calculational techniques are extremely dependent upon detailed knowledge of either the energy spectrum or material (shielding) distribution about the dose point, or both. 35 references. (auth)

54953 (NASA-TM-X-2440, pp 215-19) APOLLO MISSION EXPERIENCE. Schaefer, Herman J. (Naval Aerospace Medical Research Lab., Pensacola, Fla.). Jan 1972.

From Symposium on natural and manmade radiation in space; Las Vegas, Nev. (1 Mar 1971).

Dosimetric implications for manned space flight are evaluated by analyzing the radiation field behind the heavy shielding of a manned space vehicle on a near-earth orbital mission and how it compares with actual exposure levels recorded on Apollo missions. Emphasis shifts from flux densities and energy spectra to incident radiation and absorbed doses and dose equivalents as they are recorded within the ship at locations close to crew members. (auth) (STAR)

54954 (NASA-TM-X-2440, pp 251-6) INFLUENCE OF RADIATION SHELDING ON REUSABLE NUCLEAR SHUTTLE DESIGN. Littman, T. M.; Garcia, D. (North American Rockwell, Downey, Calif.). Jan 1972.

From Symposium on natural and manmade radiation in space; Las Vegas, Nev. (1 Mar 1971).

The nuclear rocket's unique energy source affords unusually high performance while requiring special protection for manned flights. If maximum capability is to be achieved without compromising development or operating costs, stage designs must employ efficient methods for minimizing radiation shield requirement. With this objective, alternate Reusable Nuclear Shuttle (RNS) configurations were synthesized and evaluated. Particular attention was given to design factors which reduced tank exposure to direct and scattered radiation, increased payload—engine separation, and improved self-shielding by the LH_2 propellant. The most attractive RNS concept in terms of cost effectiveness (unit payload delivery cost) consists of a single conical aft bulkhead tank with a high fineness ratio (eight-degree half cone-angle with a 25-inch cap radius). Launch is accomplished by the INT-21 with the tank positioned in the inverted attitude. The NERVA engine is delivered to orbit separately where final stage assembly and checkout are accomplished. This approach is consistent with NERVA definition criteria and required operating procedures to support an economically viable nuclear shuttle transportation program in the post-1980 period. (auth)

54955 (NASA-TM-X-2440, pp 310-23) RISK OF SOLAR PROTON EVENTS TO SPACE MISSIONS. Burrell, Martin O. (Marshall Space Flight Center, Huntsville, Ala.). Jan 1972.

From Symposium on natural and manmade radiation in space; Las Vegas, Nev. (1 Mar 1971).

The total dose in rads-tissue from solar protons was tabulated for weekly time intervals, and the number of weeks which gave a dose above 25 rads behind 10 g/cm^2 of aluminum for the active 6 years of the 19th cycle were called dangerous or large-event weeks. The number of such event weeks was found to be only 3 weeks for the past 20 years. Even though the chance for smaller events is examined, it was found that for any reasonable high confidence level (95%), the smaller events could be ignored. Consequently, the total particle flux for the 19th cycle was divided by a factor of 3 and determined a single large event week. Using this spectrum, the tissue dose in rads is calculated at the center of an aluminum spherical shell. To correct for geometric effects and self shielding, this dose may be reduced by a factor of about 3. To predict the probability of an event occurring, the Poisson distribution was the most logical choice. The confidence one can use in employing the Poisson process and arriving at confidence levels for the experimental value of the mean is investigated. Several examples are given for different mission lengths, and comparisons are made to other authors' results. An extension of the Poisson process is made to incorporate the concept of small-sample theory and arrive at the expected distribution function which answers the following question: if x_0 events are observed in time t_0, what is the probability of seeing x events in any observation time t? (10 tables, 9 figures) (auth)

54956 (NASA-TM-X-2440, pp 324-8) PROBABLE SOLAR-FLARE DOSES ENCOUNTERED ON AN INTERPLANETARY MISSION AS CALCULATED BY THE MCFLARE CODE. Lahti, Gerald P.; Karp, Irving M. (Lewis Research Center, Cleveland). Jan 1972.

From Symposium on natural and manmade radiation in space; Las Vegas, Nev. (1 Mar 1971).

The computer program, MCFLARE, uses Monte Carlo methods to simulate solar flare occurrences during an interplanetary space voyage. The total biological dose inside a shielded crew compartment due to the flares encountered during the voyage is determined. The computer program evaluates the doses obtained on a large number of trips having identical trajectories. From these results, a dose D_p having a probability p of not being exceeded during the voyage can be determined as a function of p for any shield material configuration. The user of the code selects any number of solar flares considered to be representative of the ones that will occur during future solar active periods (these flares are generally selected from the flares that occurred during the last solar active period 1956 to 1962). The flares are assumed to occur during these periods. The dose at a distance of 1 AU from the Sun from each of these flares behind any shield configuration investigated is input to the MCFLARE code. The code accounts for the dependence of the dose received from a flare on the distance from the Sun according to a $(1/r)^\alpha$ variation, where r is the distance from the Sun and the exponent α can be assigned. From trajectory parameters, which are input to the computer program, the distance from the Sun as a function of time during the trip is calculated. To illustrate the use of the code, a trip to Mars and return is calculated, and estimated doses behind several thicknesses of aluminum shield and water shield are presented. (auth)

54957 (NASA-TM-X-2440, pp 368-74) OPTIMAL SHIELD MASS DISTRIBUTION FOR SPACE RADIATION PROTECTION. Billings, M. P. (McDonnell Douglas Astronautics Co., Huntington Beach, Calif.). Jan 1972.

From Symposium on natural and manmade radiation in space; Las Vegas, Nev. (1 Mar 1971).

Computational methods were developed and successfully used for determining the optimum distribution of space radiation shielding on geometrically complex space vehicles. These methods have been incorporated in the computer program SWORD which uses the full capability of state-of-the-art methods for dose evaluation in complex geometry, and iteratively calculates the optimum distribution of (minimum) shield mass satisfying multiple acute and protracted dose constraints associated with each of several body organs. The technique used to accommodate multiple constraints eliminates the awkward discontinuities associated with the formulation of inequality constraints and produces a result meeting mathematical tests for optimality. (auth)

54958 (NASA-TM-X-2440, pp 375-82) DEVELOPMENT AND VERIFICATION OF DESIGN METHODS FOR DUCTS IN A SPACE NUCLEAR SHIELD. Cerbone, R. J.; Selph, W. E.; Read, P. A. (Gulf Radiation Tech., San Diego, Calif.). Jan 1972.

From Symposium on natural and manmade radiation in space; Las Vegas, Nev. (1 Mar 1971).

A practical method for computing the effectiveness of a space nuclear shield perforated by small tubing and cavities was developed and tested. Analysis of ducts and voids in a shield cannot be performed using the two-dimensional transport methods that are presently the most efficient means of analyzing reactor and shield problems. A three-dimensional Monte Carlo analysis is too costly to consider in tradeoff studies. The approach to the problem is to use solutions of a two-dimensional transport code and to evaluate perturbations of that solution using last-flight estimates and other kernel integration techniques. In general, perturbations are viewed as a change in the source strength of scattered radiation and a change in attenuation properties of the region, and the effect of these changes is evaluated by performing last-flight estimates and point kernel integrations. This method was implemented in a new computer program called DUCT. Calculations performed with the DUCT code were compared to experiments conducted at the Gulf Radiation Technology Linac facility. The shield studies involved measurements on a lithium hydride assembly with a sodium-filled duct and a NERVA-BATH shield mockup. Comparison was also made with the MORSE Monte Carlo code. Overall agreement between measurements, DUCT, and MORSE is better than 10 percent. (auth)

54959 (NASA-TM-X-2440, pp 387-91) SIMPLE CODE FOR USE IN SHIELDING AND RADIATION-DOSAGE ANALYSES. Wan, C. C. (Hughes Aircraft Co., Los Angeles). Jan 1972.

From Symposium on natural and manmade radiation in space; Las Vegas, Nev. (1 Mar 1971).

A simple code for use in analyses of gamma radiation effects in laminated materials is described. Simple and good geometry is assumed so that all multiple collision and scattering events are excluded from consideration. Buildup factors may be applied to the results of this simplified analysis, when available, to arrive at improved estimates of energy deposition and attenuated intensity for actual materials. The code proper is capable of handling laminates up to six layers. However, for laminates of more than six layers, the same code may be used to incorporate two additional layers at a time, making use of punch-tape outputs from previous computation on all preceding layers. The spectrum of attenuated radiation may be obtained as both printed output and punch tape output as desired. This code is written in "Extended Basic" language, compatible with the GE 265 Time Sharing system. (auth)

54960 (NASA-TM-X-2440, pp 500-11) MEASUREMENTS OF GAMMA-RAY PRODUCTION CROSS SECTIONS FOR SHIELDING MATERIALS OF SPACE NUCLEAR SYSTEMS. Orphan, V. J.; John, Joseph; Hoot, C. G. (Gulf Radiation Tech., San Diego, Calif.). Jan 1972.

From Symposium on natural and manmade radiation in space; Las Vegas, Nev. (1 Mar 1971).

Measurements of secondary gamma-ray production from neutron interactions were made over the entire energy range (thermal to 16 MeV) of interest in shielding applications. A LINAC-pulsed neutron source having a continuous distribution of neutron energies is used in conjunction with high-resolution Ge(Li) gamma-ray spectrometers and the time-of-flight technique. The two-parameter data (gamma-ray energy vs neutron energy) are obtained using a computer-controlled data acquisition system. Two facilities are used in the measurements: A 16-meter facility is used to measure gamma rays from resonant capture of neutrons up to 100 keV. Gamma production cross sections from (n,xy) reactions are measured up to 16 MeV using a 50-meter facility. The epithermal capture gamma-ray yields for both resolved gamma-ray lines and continuum were measured from thermal energies to 100 keV for natural tungsten and ^{238}U, two important candidate shield materials in SNAP reactor systems. Data are presented to illustrate the variation of epithermal capture gamma-ray yields with neutron energy. In the resolved resonance region, the total observed radiated energy was within ±15% of the known binding energy. The gamma-ray production cross sections from (n,xy) reactions were measured for Fe and Al from the threshold energies for inelastic scattering to ~16 MeV. Typical Fe and Al cross sections obtained with high-neutron energy resolution (~1% at 1 MeV) and averaged over broad neutron-energy groups are presented and compared with previous cross-section determinations made using monoenergetic neutron sources. (auth)

54961 (NASA-TM-X-2440, pp 527-8) CALCULATION OF NEUTRON-CAPTURE GAMMA-RAY YIELDS FOR SPACE-SHIELDING APPLICATIONS. Yost, K. J. (Purdue Univ., Lafayette, Ind.). Jan 1972.

From Symposium on natural and manmade radiation in space; Las Vegas, Nev. (1 Mar 1971).

The application of nuclear models to the calculation of neutron-capture and inelastic-scattering gamma yields is discussed. The gamma-ray cascade model describes the cascade process in terms of parameters which either: (1) embody statistical assumptions regarding electric and magnetic multipole transition strengths, level densities, and spin and parity distributions or (2) are fixed by experiment such as measured energies, spin and parity values, and transition probabilities for low-lying states. (auth) (STAR)

54962 (NASA-TM-X-2440, pp 697-705) SHIELD-WEIGHT OPTIMIZATION USING MONTE CARLO TRANSPORT CALCULATIONS. Jordan, Thomas M. (A.R.T. Research Corp., Los Angeles); Wohl, Millard L. Jan 1972.

From Symposium on natural and manmade radiation in space; Las Vegas, Nev. (1 Mar 1971).

An outline is given of the theory used in FASTER-III, a Monte Carlo computer program for the transport of neutrons and gamma rays in complex geometries. The code has the additional capability of calculating the minimum-weight-layered unit shield configuration that will meet a specified dose rate constraint. It includes the treatment of geometric regions bounded by quadratic and quadric surfaces with multiple radiation sources that have a specified space, angle, and energy dependence. The program calculates, using importance sampling, the resulting number and energy fluxes at specified point, surface, and volume detectors. Results are presented for sample problems involving primary neutron and both primary and secondary photon transport in a spherical reactor-shield configuration. These results include the optimization of the shield configuration. (auth)

54963 (NASA-TM-X-2440, pp 832-41) PARAMETRIC FIT TO ELECTRON-TRANSPORT PROPERTIES. Lonergan, J. A.; Shreve, D. C. (Science Applications, Inc., La Jolla, Calif.). Jan 1972.

From Symposium on natural and manmade radiation in space; Las Vegas, Nev. (1 Mar 1971).

Empirical formulations of electron transport properties are presented. Experimental data acquired by several groups over the past few years were gathered and organized. Parametric fits were made to these data so that the following properties of electron transport can be represented by simple functions of atomic number and energy: transmitted electron number, transmitted electron spectra, range, backscatter coefficient, angular distribution, energy deposition, bremsstrahlung intensity and energy spectra, bremsstrahlung angular distribution, and photon attenuation. Though most of the data used to derive the parametric formulas were measured in experiments, some uses were made of results generated using well-developed Monte Carlo techniques. The formulas cover the energy ranges of interest in space-shielding problems (0.1 to 10.0 MeV). These formulas were developed so they could be included in an engineering handbook addressed at the problems of electron radiation in space and its effects. The intent is to provide a simple means of calculating the radiation expected aboard a spacecraft, both on its external surface and behind arbitrary amounts of effective shielding. To satisfy the requirement that the formulas be simple, mathematical rigor based on physical interaction was replaced by convenient fits to thick target data. The formulas are as accurate as these data in most cases and can be easily evaluated without a computer. Procedures for using these formulas in practical situations are suggested. 7 figures. (auth)

54964 (NASA-TM-X-2440, pp 914-21) GAMMA-RAY SHIELDING MEASUREMENTS MADE AT ALTITUDES GREATER THAN 115,000 FEET USING LARGE Ge(Li) DETECTORS. Chapman, G. T. (Oak Ridge National Lab., Tenn.); Cumby, R. P.; Gibbons, J. H.; Macklin, R. L.; Parker, H. W. Jan 1972.

From Symposium on natural and manmade radiation in space; Las Vegas, Nev. (1 Mar 1971).

A series of balloon-flight experiments at altitudes greater than 115,000 feet were conducted to gain information relative to the use of composite shields (passive and/or active) for shielding large-volume, lithium-drifted, germanium (Ge(Li)) detectors used in gamma-ray spectrometers at these altitudes. The measurements were made in the gamma-ray energy region 60 keV to 2 MeV and clearly illustrate the necessity of using a dense gamma-ray shield protected by an active charged-particle shield for effective shielding of these detectors in the primary cosmic-ray environment. Data showing the pulse-height spectra of the environmental gamma radiation as measured at 5.3 and 3.8 g/cm^2 residual atmosphere with an unshielded diode detector is also presented. (auth)

54965 (ORNL-TM-3871(Rev.)) SDT5. STAINLESS-STEEL BROOMSTICK EXPERIMENT: AN EXPERIMENTAL CHECK OF NEUTRON TOTAL CROSS SECTIONS. Maerker, R. E. (Oak Ridge National Lab., Tenn.). Sep 1972. Contract W-7405-eng-26. 25p. (ENDF-170(Rev.)). Dep. NTIS.

The experimental and calculational details for a CSEWG integral data testing shielding experiment are presented. The experiment was designed to test a given set of neutron total cross sections for a type-310 stainless steel in the range 1.2 to 11 MeV. Separation of neutron- and gamma-induced pulses was made by a modified Forte circuit. The unfolding of the pulse-height distributions was accomplished using the FERDoR code. (M.H.R.)

54966 SPATIAL, ANGULAR, AND ENERGY DISTRIBUTION OF FAST NEUTRONS BEHIND TRIPLE LAYER BARRIERS. Elagin, V. B.; Pekarskii, G. Sh. At. Energ. (USSR); 33: No. 1, 590-1(Jul 1972). (In Russian).

The spatial, energy and angular distributions of fast neutrons from a unidirectional, point source beyond a composite three-layer system of Fe/plastic/Fe and W/Al_2O_3/W were studied as functions of the thickness of the separate layers entering into the composite. The Monte Carlo method was employed with a computer in calculations for 2.5- and 14-MeV neutrons and neutrons from a Po—Be source. (K.S.W.)

54967 CREW RADIATION DOSE FROM A HIGH-IMPULSE GAS-CORE NUCLEAR ROCKET PLUME. Masser, Charles C. (Lewis Research Center, Cleveland). J. Spacecraft Rockets; 9: No. 8, 597-601(Aug 1972).

Analytical calculations are performed to determine the radiation dose rate and total dose to the crew of a gas-core nuclear rocket from the fission fragments located throughout the plume volume. The mission chosen is a manned courier trip to the planet Mars. Four round trip times were picked in which the system was optimized so the initial vehicle mass in Earth orbit was minimized for each trip time. They are 80, 100, 150, and 200 days. For the most probable fission-fragment retention time in the reactor of 100 sec, the unshielded radiation dose to a crew located 100 m from the nozzle exit varies from 170 Rem for the 80-day round trip to 38 Rem for the 200 day round trip. For the 80-day round trip the crew must be protected from the radiation dose. Five centimeters of lead shielding would reduce the radiation dose by two orders of magnitude, thereby protecting the crew. (auth)

PHYSICS (SOLID-STATE)

Radiation Effects

Refer also to abstracts 52985, 53229, 53314, and 54874.

54968 (AD-737312) RESEARCH ON THE PHYSICS OF TRANSIENT RADIATION EFFECTS. Final Report, February 2, 1968–October 31, 1971. Azarewicz, Joseph L.; Berger, Robert A.; Cesena, Rodolfo A.; Colwell, Joseph F.; Denson, Raymond (Gulf Radiation Technology, San Diego, Calif.). Feb 1972. Contract DAAG39-68-C-0060. 140p. (GULF-RT-A-10870; HDI-60-3). NTIS.

CHERENKOV RADIATION—use to measure transient free carrier absorption in insulators, feasibility of
ELECTRONS—effects on silicon, (E/T)
—effects on gallium arsenide, (E)
—effects on electric conductivity of naphthalene, (E/T)
GALLIUM ARSENIDES—radiation damage in, electron, (E)
GAMMA RADIATION—effects on electric properties of polystyrene capacitors with metal electrodes, (E)
NAPHTHALENE—radioinduced electric conductivity of, electron, (E/T)
NEUTRONS—effects on silicon, (E/T)
SILICON—radiation damage in, neutron and electron, (E/T)
STYRENE POLYMERS—radioinduced carriers in capacitors of, γ, (E)

54969 (AECL-4130) COMPUTER PROGRAM TO CALCULATE DAMAGE DISTRIBUTIONS IN ION-BOMBARDED TARGETS. **Caillibot, P. F.; Hunt, C. E. L. (Atomic Energy of Canada Ltd., Chalk River (Ontario). Chalk River Nuclear Labs.). May 1972. 52p. Dep. NTIS (U. S. Sales Only). AECL $1.50.**

Simulation of fission damage by means of ion bombardment eliminates induced radioactivity and reduces experimental time by several orders of magnitude. However, the conditions under which such bombardments are to be done must be carefully determined. The mathematical model developed by Lindhard et al., based on a Thomas–Fermi potential between the atoms, was used. The required calculations are time-consuming; therefore, a computer program, IONR, was written. It calculates the damage profile produced in a target by any projectile. For a range of energies it will calculate the relative bombardment times to approximate a homogeneous damage profile up to the maximum penetration depth. Results are produced both as graphs and tables. An example is presented for argon bombardment of zirconium. (auth)

54970 (CEA-CONF-1890) COMPUTER SIMULATION IN RADIATION DAMAGE STUDIES. Torrens, Ian M. (Commissariat a l'Energie Atomique, Saclay (France). Centre d'Etudes Nucleaires). 1972. 32p. (CONF-720423-4). Dep. NTIS (U. S. Sales Only).

From first European conference on computational physics; Geneva, Switzerland (10 Apr 1972).

The application of atomistic computer simulation to problems involving radiation damage and lattice defects in crystalline solids is discussed. The different topics include static defect configurational simulations, molecular dynamics of thermal motion, low-energy atomic collision events, high-energy atomic displacement cascades, and the thermal annealing of concentrations of defects in a lattice region. The methods described are criticized from the point of view of the assumed physical models, and their capabilities and limitations are indicated. Emphasis is on techniques used rather than on results obtained. (auth)

54971 (CEA-R-4313) ELECTROLUMINESCENT DIODES FORMATION IN ION IMPLANTED ZINC TELLURIDE. **Marine, Jean (Commissariat a l'Energie Atomique, Grenoble (France). Centre d'Etudes Nucleaires). Jun 1972. 101p. (In French). Dep. NTIS (U. S. Sales Only).**
Thesis.

Radiative-recombination mechanisms and minority-carrier injection devices are reviewed, and ion implantation is presented as a doping method in order to achieve electroluminescent diodes in a nonstoichiometric material such as ZnTe. The implanted layer is mainly characterized by: the secondary ion-emission microanalyzer to determine the profile of implanted impurities; the hot probe to determine the conductivity type; the photoluminescence to bring out the levels due to impurities; and the sheet-resistivity measurements. All these measurements show that it is possible to get an n-type layer in a boron- or chlorine-implanted ZnTe. For the diodes achieved, current–voltage characteristic and junction capacitance in reverse-bias measurements show that they were p–i–n type. Two assumptions are suggested to explain the presence of an intrinsic layer between the implanted region (n-type) and the substrate (p-type). Finally, the electroluminescence of these diodes showed that the presence of oxygen gives a red light emission at 6750 Å and, when the material is oxygen-free, the light emission is green at 5580 Å with a quantum efficiency of 0.6% at 300°K. (auth)

54972 (COO-2119-2) EXPERIMENTS IN HIGH-VOLTAGE ELECTRON MICROSCOPY. Progress Report, October 31, 1972–July 31, 1973. Mitchell, T. E.; Das, G.; Kenik, E.; Sklad, P. (Case Western Reserve Univ., Cleveland, Ohio. Div. of Metallurgy and Materials Science). 1 Aug 1972. Contract AT(11-1)-2119. 23p. Dep. NTIS.

Experiments using high-voltage electron microscopy are described that take advantage of the high-resolution selected-area diffraction (SAD) and in-situ electron-radiation-damage capabilities. SAD experiments show that the error distance is 30 times better at 650 kV than at 100 kV; the error distance increases in proportion to the cube of the Bragg angle as expected and is better than 1000 Å for Bragg plane spacings greater than 0.5 Å. Electron-irradiation damage was observed in copper, stainless steel, nickel, vanadium, graphite, and quartz as a function of time and temperature. In Cu, stainless steel, and Ni, faulted interstitial loops are formed that grow, unfault, and then either glide out of the foil or form a dislocation network with other prismatic loops. Void formation was observed in Cu and stainless steel after long doses at high temperatures, using a prior low-temperature irradiation. Radiation-induced carbide precipitation also occurs in stainless steel. In quartz black spot defects are formed, after which the irradiated area becomes amorphous. (auth)

54973 (FRNC-TH-210) PRODUCTION OF HIGH DEFECT CONCENTRATIONS IN ALKALI HALIDES BY ELECTRON BOMBARDMENT. **Herrmann, Friedrich (Lyon Univ. (France)). 1971. 80p. (In French). Dep. NTIS (U. S. Sales Only).**
Thesis.

High-defect densities were produced (10^{19} centers/cm^3) by irradiating alkali-metal halide crystals (KCl, KBr, KI, NaCl, and LiF) with electron beams (10 to 50 keV). Optical absorption measurements were used to determine the color-center density. The growth curve represents the variation in the color-center concentration (or optical density) as a function of the radiation dose (or irradiation time). The value of the exponent in the expression linking the electron path to the primary electron energy was determined. It is shown that it is possible to relate the local increase in concentration to an increase in optical density for a nonuniformly colored crystal. The changes in the absorption bands (F, M, and V) in various substances at different temperatures were compared. The growth rate for F centers decreases uniformly during irradiation. A model was developed explaining this decay; this model can be simulated by computer. Some experiments carried out with LiF enabled an upper limit to be established for the threshold energy for the displacement of a cation (1.64 eV). (France)

54974 (LYCEN-7228) CHANNELING OF LIGHT IONS OF 0.5 TO 2 MeV THROUGH A FEW-HUNDRED ANGSTROM-THICK GOLD CRYSTALS. Poizat, J. C.; Remillieux, J. (Lyon Univ. (France). Institut de Physique Nucleaire). May 1972. 37p. (In French). Dep. NTIS (U. S. Sales Only).

A technique to obtain a few hundred-Å-thick self-supporting gold crystals is described. These crystals were used to perform three channeling experiments with 0.5- to 2-MeV light ions: The wide-angle scattering probability as a function of the distance from the crystal surface was studied for an incident beam of particles in the planar and axial directions. The influence of channeling on the light emission from crystal-excited atomic beams was investigated. A strong channeling effect was found on the probability of transmission of a molecular beam of H_2^+ ions through a thin crystal. (France)

54975 (RT/EL-(72)2) MEASURE OF THE PHOTOVOLTAIC EFFECT IN SILICON DIODES OBTAINED THROUGH IMPLANTATION OF IONS. Russo, M.; Sano, A.; Testa, M. (Comitato Nazionale per l'Energia Nucleare, Rome (Italy)). 22 Feb 1972. 77p. (In Italian). Dep. NTIS (U. S. Sales Only).

Results of a study on the photovoltaic effect in Si diodes obtained by the ion implantation technique are reported. The aim of the work was to weigh the possibility of measurement, on the basis of this effect, of some parameters such as the junction depth, minority-carrier diffusion length, etc. Results show that it is possible to measure the diffusion length of minority carriers in the bulk, by means of the near-infrared spectral response. To obtain the other parameters, it is necessary to utilize also different kinds of measurements. This study also showed that, in the bulk, in proximity of the junction, there was a damage not attributable to the implantation technique. (auth)

54976 ION IMPLANTATION FACILITY AT ORSAY. Chaumont, J.; Baran-Marzak, M.; Camplan, J.; Meunier, R.; Sarrouy, J. L. (CNRS, Orsay, France). pp 105-11 of International Colloquium on the Application of Vacuum Techniques to the Semiconductor Industry, Electronic, and Microelectronic Components. Paris; Societe Francaise des Ingenieurs et Techniciens du Vide (1971).

From third international symposium on the application of vacuum techniques in semiconductor industry, electronic components, and microelectronics; Versailles, France (13 Sep 1971). See CONF-710932.

The various parts of the ion implantation facility at Orsay are described. Emphasis is given to the ion source and the beam extraction system. Preliminary results obtained for ion implantation are given. (France)

54977 EXPERIMENTAL ARRANGEMENT FOR INVESTIGATION OF SINGLE CRYSTALS BY MEANS OF FAST IONS. Haan, G.; Flagmeyer, R.; Geist, V.; Mende, A.; Lehmann, D. (Karl Marx Univ., Leipzig). Exp. Tech. Phys.; 20: No. 1, 67-80(1972). (In German).

A detailed description is given of a measuring equipment for channeling and blocking experiments with a brief introduction to these effects. The main part of the work is concerned with the description and the physical reasons of special elements such as collimator, beam current measurement, crystal mounting, cooling device, and so on. Results are given of first experimental tests with a tungsten single crystal. (auth)

54978 PHONON SCATTERING BY VANADIUM IONS IN Al_2O_3. de Goer, A. M.; Devismes, N. (CEN, Grenoble, France). J. Phys. Chem. Solids; 33: No. 9, 1785-93(Sep 1972).

Thermal conductivity measurements were made between 1.3 and 150°K on several vanadium-doped Al_2O_3 single crystals, in their as-received state and after γ irradiation. One Ti-doped sample was also measured. The results are well explained by ascribing the resonant phonon scattering observed to transitions between low-lying energy levels of V^{4+} and Ti^{3+} ions. A good fit of the curves was obtained using Callaway's (1959) method. Resonant scattering is described by an additional phonon relaxation time of the form: $[\tau_2^{-1} = D_1(\omega^4/(\omega^2 - \omega_1^2)^2) + (D_2/D_1)\ (\omega^4/(\omega^2 - \omega_2^2)^2]$ where $\hbar\omega_1 = \delta_1$ and $\hbar\omega_2 = \delta_2$ are known, and D_2/D_1 is kept constant for all V-doped specimens. From these quantitative analysis and coupled EPR measurements, it was possible to estimate that only 1% of the total vanadium content was in the V^{4+} valence state in all as-received samples. Hence the great sensitivity of low-temperature thermal conductivity to the presence of ions subjected to a dynamic Jahn–Teller effect is confirmed in the case of these Kramers d^1 ions. (auth)

54979 OBSERVATION OF DISLOCATION LOOPS IN GADOLINIUM THIN SINGLE CRYSTAL. Srivastva, M. M.; Srivastava, O. N. (Banaras Hindu Univ., India). Jap. J. Appl. Phys.; 11: No. 9, 1237-8(Sep 1972).

Dislocation loops were found to form in hcp Gd thin single-crystal films in an electron microscope. Tiny dot-like features developed, turning into dislocation loops which were often hexagonal-shaped. Stacking fault tetrahedra were also observed. These loops and tetrahedra are due to the aggregation of point defects produced by the bombardment. (D.L.C.)

54980 INTERSTITIAL HALOGEN CENTERS IN X-IRRADIATED CsBr. Chowdari, B. V. R.; Itoh, N. (Nagoya Univ., Japan). J. Phys. Chem. Solids; 33: No. 9, 1773-83(Sep 1972).

Interstitial halogen centers in CsBr produced by x-irradiation at 4.2 and 77°K were studied and assignments of several absorption bands associated with these centers were made. The most prominent bands formed by x irradiation at 4.2°K were the F and H bands. Besides the known two σ-polarized absorption bands associated with the H center, another weakly π-polarized band at 1062 nm was found. The next prominent bands formed at 4.2°K were the α and I bands whose peak positions are at 205 and 236 nm, respectively. X-irradiation at 4.2°K also caused an absorption band at 324 nm due to H^1 center. It is shown that the height of H^1 band is proportional to the square of the height of the H band, suggesting that the centers associated with the H^1 band are di-H-centers. Optical and thermal bleaching of the H bands causes the increase in H^1 band. The study of the thermal annealing properties of H^1 band suggests the composite nature of the band. After the H bands were thermally bleached, three absorption bands at 425, 502 and 1060 nm were found to grow whose source might be the interstitial atom associated with an impurity. X-irradiation at 77°K produced the F and V_4 centers, the latter of which has an absorption band at 276 nm. The V_4 center has ⟨100⟩ orientation. The formation and thermal bleaching properties of the H^1 and V_4 bands are compared. (auth)

54981 FAST-NEUTRON-COMPENSATED n-GERMANIUM AS A MODEL OF AMORPHOUS SEMICONDUCTORS. Gadzhiev, A. R.; Ryvkin, S. M.; Shlimak, I. S. (Ioffe Inst. of Physics, and Tech., Leningrad). JETP Lett. (USSR) (Engl. Transl.); 15: No. 10, 428-31(20 May 1972).

Translated from Zh. Eksp. Teor. Fiz.; Pis'ma Red.; 15: No. 10, 605-8(20 May 1972).

A model of an amorphous semiconductor can be produced by producing a random distribution of point defects. This was investigated by irradiating As-doped n-type Ge with fast neutrons, which produce spherical disordered regions of p-type character. The spatial variation of the potential is discussed, and it is shown that the conductivity mechanism should be tunneling over states closer and closer to the Fermi level. Experimental results confirm expectations: the conductivity decreased and acquired an activation character with irradiation dose, Mott's law is satisfied, and the current-voltage characteristic has a S-shape with a considerable negative differential resistance section. (D.L.C.)

54982 TUNNEL ASSISTED HOPPING IN NEUTRON IRRADIATED GALLIUM ARSENIDE. Coates, R.; Mitchell, E. W. J. (Univ. of Reading, Eng.). J. Phys., C (London); 5: No. 10, L113-18(25 May 1972).

The resistivity against dose curve in neutron-irradiated gallium arsenide shows an anomaly. At doses in excess of 10^{17} n cm^{-2} the resistivity decreases with dose. The temperature dependence of resistivity indicates that the mechanism of conduction at high doses is tunnel-assisted hopping. Since the structural studies reveal that even at the highest dose the material remains substantially crystalline, the tunnel-assisted hopping is considered to occur via defect energy levels. (auth)

54983 COMPARISON OF DEFECT CENTRES FORMED IN OXIDES BY EXPLOSIVE SHOCKING AND HIGH-ENERGY RADIATION. Nelson, R. L. (Atomic Energy Research Establishment, Harwell, Eng.); Hartley, D. B. J. Chem. Soc., Dalton Trans.; No. 15, 1596-1603(1972).

ESR and reflectance spectroscopic techniques were used to compare point defects present in MgO, ZnO, and SiO_2 both after explosive shocking and after irradiation with high-energy γ rays, electrons, and neutrons. A high correlation of shocking with irradiation exists in MgO, none in SiO_2, and ZnO occupies an intermediate position. In MgO, explosive shocking induced ionization with trapping of electrons at existing defects and produced vacancy defects (F^+ and F_2^+) by displacement of lattice ions. In SiO_2 none of these effects were present but there is evidence of contamination with carbon as a result of the explosion. This significant difference in behavior to shocking is reflected in the different physical properties of these oxides, but could also be brought about by a suitable choice of explosion conditions. (auth)

54984 LOCALIZED VIBRATIONAL MODES IN GALLIUM ARSENIDE CONTAINING SILICON AND BORON. Thompson, F.; Newman, R. C. (Univ. of Reading, Eng.). J. Phys., C (London); 5: No. 15, 1999-2010(7 Aug 1972).

A comparison was made between the infrared local-mode absorption spectra of boat-grown and pulled crystals of GaAs : Si. The samples were compensated either by electron or neutron irradiation or by copper diffusion. Boron is present in the pulled material and previously unreported lines are assigned as follows: $^{11}B(Ga)$ (517.0 cm^{-1}), $^{10}B(Ga)$ (540.2 cm^{-1}), B(Ga)–Si(As) pairs (349.0, 570.9, 596.0, 661.0, and 684.8 cm^{-1}). Two further lines at 762.7 and 796.0 cm^{-1} may be due to interstitial boron atoms produced by the irradiations. It is thought that other lines may be due to the center B(Ga)–Si(As)–Si(Ga). (auth)

54985 DIFFUSION OF POINT DEFECTS TO THE FOIL SURFACE DURING IRRADIATION DAMAGE EXPERIMENTS IN THE HIGH VOLTAGE ELECTRON MICROSCOPE. Foreman, A. J. E. (Atomic Energy Research Establishment, Harwell, Eng.). Radiat. Eff.; 14: No. 3-4, 175-9(Jun 1972).

The high-voltage electron microscope can be used to simultaneously produce and observe irradiation damage structures in thin foils of many materials, including in particular the formation of voidage at elevated temperatures. In such experiments some of the vacancies and interstitial atoms produced in the damage process will be lost by diffusion to the foil surface, so that the results may not be characteristic of the bulk material if the foil is too thin. The steady-state point defect concentrations built up in a thin foil were computed as a function of the foil thickness, defect production rate, and vacancy jump frequency, taking into account the effect of the mutual recombination of vacancies and interstitial atoms. The coupled diffusion equations for the point defect concentrations were solved numerically for a thin foil, assuming the foil surfaces to be perfect sinks for the point defects, and the results for any material expressed in terms of a single dimensionless parameter. The computations show that for a foil containing few internal sinks, which is the most demanding case, defect concentrations typical of the bulk material can be achieved within an appreciable fraction of a 0.5-μm thick foil, for temperatures up to about one-half the absolute melting temperature. The loss of point defects to the foil surface is shown to be further reduced when the foil contains a high density of internal sinks (e.g. dislocations, voids, precipitate particles) and there is an additional improvement at very high temperatures due to the effect of thermal vacancies. (auth)

54986 COMPUTER CALCULATIONS OF SHEET RESISTANCE OF n- AND p-TYPE IMPLANTATIONS IN SILICON. Smith, B. J.; Stephen, J. (Atomic Energy Research Establishment, Harwell, Eng.). Radiat. Eff.; 14: No. 3-4, 181-4(Jun 1972).

Computer calculations of sheet resistance of ion-implanted layers are described. For Gaussian doping profiles, the sheet resistance depends on the surface concentration and electrical conductivity of the implanted impurity and the standard deviation in the projected ion range. Universal curves were produced from which the sheet resistance of any implanted silicon layer could be derived, provided these parameters were known, and assuming that all the implanted atoms contribute to the electrical conductivity. (auth)

54987 LOCATION OF DIFFUSION-DOPED GOLD ATOMS IN SILICON BY MEANS OF CHANNELING. Iue, N.; Matsunami, N.; Morita, K.; (and others) (Nagoya Univ., Japan). Radiat. Eff.; 14: No. 3-4, 191-3(Jun 1972).

The lattice location of gold atoms diffused into silicon is determined using the channeling of He$^+$ ions. It is shown that the gold atoms that accumulate at the back surface are located at the hexagonal interstitial sites. (UK)

54988 DECHANNELING OF HEAVY CHARGED PARTICLES IN DIAMOND LATTICES. Morita, K. (Nagoya Univ., Japan). Radiat. Eff.; 14: No. 3-4, 195-202(Jun 1972).

Dechanneling rates of 1.5-MeV protons, deuterons, and helium ions in the (100) axial and (110) planar channels were obtained by analyzing their backscattering energy spectra for the aligned and random directions. The experimental dechanneling rates in the axial channels, inclusive of those in Si, GaP, NaCl, KCl, and KBr single crystals, followed a universal expression for the dechanneling derived using the diffusion model according to Lindhard's theory. Comparing with the theory, the contribution of the electronic collisions to the dechanneling was separated from the contribution of the nuclear collisions. The experimental value of the electronic contribution agreed well with the theoretical value. The experimental value of the nuclear contribution was smaller than the theoretical value by a factor of about 3. The discrepancy between the experimental and the theoretical value of the nuclear contribution is discussed. (auth)

54989 ELECTRICAL RESISTIVITY INCREASE RATES IN Fe–C AND Fe–N SOLID SOLUTIONS DURING NEUTRON IRRADIATION AT 4.5 K. Wagenblast, H.; Schwerer, F. C.; Horak, J. A. (United States Steel Corp., Monroeville, Pa.). Radiat. Eff.; 14: No. 3-4, 203-13(Jun 1972).

A series of α-iron specimens containing carbon and nitrogen in interstitial solid solution were irradiated simultaneously at 4.5°K with fast neutrons to a fluence of 4.7×10^{17} n/cm^2 with $E > 0.1$ MeV. In-situ electrical resistivity measurements during irradiation showed that the apparent damage rates were dependent on the C or N concentration. In particular, the value of the initial resistivity increment per unit flux (δ), passed through a minimum value at 0.1 at. % N and became larger than the value for pure iron above 0.14 at. % N. The results can be explained qualitatively as interstitial impurity-induced differences in production rates and dispersion of defects or semi-quantitatively as defect-induced deviations from Matthiessen's rule. (auth)

54990 ELECTRON RADIATION DAMAGE NEAR THE THRESHOLD ENERGY IN ALUMINIUM. Wolfenden, A. (Oak Ridge National Lab., Tenn.). Radiat. Eff.; 14: No. 3-4, 225-9(Jun 1972).

Foils of high-purity aluminum, both with and without preinjection of about 10 at. ppM helium, were electron-irradiated in the electron microscope operating at voltages in the range 150 to 200 keV. In the helium-doped aluminum, electron damage in the form of black spots was produced at 150 keV after about 90 min irradiation time. They showed contrast effects characteristic of dislocation loops. No such spotlike damage was observed at 150 keV in the uninjected aluminum for bombardment times over 4 hr. Damage was observed in both pre-injected and uninjected specimens at 175 and 200 keV. Possible mechanisms for subthreshold damage are examined to see which account for the electron damage observed below the accepted threshold of about 170 keV for aluminum. (auth)

54991 PROPERTIES OF PROTON-IRRADIATED DIAMOND. Ananthanarayanan, K. P.; Borer, W. J.; Plendl, H. S.; Gielisse, P. J. (Univ. of Rhode Island, Kingston). Radiat. Eff.; 14: No. 3-4, 245-8(Jun 1972).

Properties of type I diamond were investigated before and after irradiation with 17.0- and 18.3-MeV protons. The optical absorption edge is essentially unchanged. The infrared absorption spectrum shows a strong additional peak at 6.92 μm. A Raman line shift of 4 cm^{-1} indicates an increase of 0.0032 Å in the lattice constant. (auth)

54992 INFLUENCE OF ELECTRON IRRADIATION ON CdS THIN FILMS. Spinulescu, I.; Baltateanu, N. (Univ., Bucharest). Radiat. Eff.; 14: No. 3-4, 257-9(Jun 1972).

The effect of 3-MeV electrons on the crystallographic orientation of cadmium sulfide thin films is studied using electron diffraction. (UK)

54993 FLUX EFFECTS ON DAMAGE IN GaAs AS MEASURED BY THE CHANNELLING OF ^{85}Kr. Grant, W. A.; Baruah, J. N. (Univ. of Salford, Eng.). Radiat. Eff.; 14: No. 3-4, 261-2 (Jun 1972).

The ranges of ions implanted into semiconductors has been extensively studied but little attention has been paid to the dose rate used during the implantation. The influence of dose rate of damage to gallium arsenide single crystals using ^{84}Kr and ^{85}Kr ions is studied. It is concluded that the degree of damage is dependent on the dose rate, the dose dependence of damage will influence the distribution profile of implanted ions, and the dechanneling of heavy ions can be used as a measure of damage. (UK)

54994 PRECIPITATION OF PHOSPHOROUS IN ION IMPLANTED SILICON. Seshan, K.; Washburn, J. Radiat. Eff.; 14: No. 3-4, 267-70(Jun 1972).

Electron microscope observations on phosphorous-ion-implanted ρ-silicon after annealing at 800°C are reported. Heating for ½ hour after implantation of 2×10^{14} ions/cm^2 at 20°C was found to produce dislocation loops and rod-like defects similar to those observed in boron-implanted silicon. It was concluded that the rod-shaped defects were associated with phosphorous precipitation. (auth)

54995 NATURE OF ROD-LIKE DEFECTS OBSERVED IN BORON IRRADIATED SILICON. Madden, P. K.; Davidson, S. M. (Oxford Univ.). Radiat. Eff.; 14 No. 3-4, 271-3(Jun 1972).

The rod-like defects appearing in silicon irradiated with 40-keV B$^+$ ions were studied by electron microscopy. It is suggested that the rods can best be explained on a model of an elongated faulted dislocation loop, extrinsic in character with an α/k (100) Burgers vector. (UK)

54996 OPTICAL ABSORPTION BANDS OF COLOR CENTERS IN IRRADIATED ANTHRACENE SINGLE CRYSTALS AT LOW TEMPERATURES. Matsuyama, Tomochika; Yamaoka, Hitoshi; Okamura, Seizo (Kyoto Univ., Osaka). Radiat. Eff.; 14: No. 3-4, 275-6(Jun 1972).

Anthracene single crystals were irradiated at 77°K by ^{60}Co gamma rays and the optical absorption spectrum measured. The effect of warming to 399°K on the absorption spectrum is shown. (UK)

54997 SIMILARITIES OF THE IONIZATION EFFECTS AND ANNEALING IN P-TYPE AND CONVERTED N-TYPE Ge IRRADIATED WITH ELECTRONS AT 85^{0}K. Kraitchinskii, A.; Rzewuski, H.; Suski, J.; Werner, Z. (Inst. of Nuclear Research, Warsaw). Radiat. Eff.; 14: No. 3-4, 277-8(Jun 1972).

The annealing behavior of p-type Ge and n-type Ge converted into p-type by electron irradiation is studied. It is concluded that as both types of Ge show the same trapping effects and annealing behavior, the behavior of irradiated Ge can be attributed to some intrinsic type of defect. (UK)

54998 EFFECTS OF GAMMA RADIATION ON PHOTOCURRENT-VOLTAGE CHARACTERISTICS OF CdS FILMS. Kao, K. C.; Sadhu, A. (Univ. of Manitoba, Winnipeg, Can.). Radiat. Eff.; 14: No. 3-4, 279-80(Jun 1972).

Cadmium sulfide films were irradiated with gamma rays from a ^{60}Co source while illuminated with sodium light. The threshold field for the onset of high-field photocurrent saturation increased and the saturation current decreased with increasing radiation dose. It was also found that for a given dose and applied voltage the change in the photocurrent due to irradiation for CdS films was much greater than for CdS crystals. (UK)

54999 TEMPERATURE DEPENDENCE OF VIBRONIC SPECTRA IN IRRADIATED SILICON. Hare, A. P. G.; Davies, G.; Collins, A. T. (King's Coll., London). J. Phys., C (London); 5: No. 11, 1265-76(12 Jun 1972).

Crucible-grown and high-purity floating-zone silicon specimens were irradiated at room temperature with γ rays. High-resolution cathodoluminescence spectra of the vibronic bands with zero-phonon lines at 0.717, 0.724, 0.790, 0.795, 0.898, and 0.969 eV are given. The widths and energies of these lines, and the intensities of the 0.790, 0.795, and 0.969-eV lines relative to the total intensities of their associated bands, are given in the temperature range 25 to 75°K. These data are discussed in terms of the theory of linear and quadratic electron–phonon coupling in the adiabatic approximation, using Debye spectra of coupled phonons and, for the 0.790, 0.795 and 0.969-eV lines, densities of coupled phonons derived from the emission band shapes. The theory gives a self-consistency between the spectral band shapes and the widths and energies of the zero-phonon lines, but does not satisfactorily fit the temperature dependence of the intensities of the zero-phonon lines. It is not known whether the failure of the theory is due to a Jahn–Teller effect (no absorption at the centers has been detected) or to the coupling by the electron–phonon interaction of electronic states whose energies are not greatly separated compared with the phonon energies involved. (auth)

55000 LIFETIMES OF FAST RECOMBINATION LUMINESCENCE TRANSITIONS IN ALKALI HALIDES. Blair, I. M.; Pooley, D.; Smith, D. (Atomic Energy Research Establishment, Harwell, Eng.). J. Phys., C (London); 5: No. 12, 1537-52(26 Jun 1972).

Measurements were made of the lifetimes of the fast recombination luminescence transitions in alkali metal halides. The luminescence was excited by 2-MeV proton pulses about 2 ns wide and the lifetimes measured by the technique of single photon counting. All alkali metal halides in which fast luminescence occurs were studied at 5 and 77°K. The lifetimes of the major components lie in the range 1 to 4 ns, and in many cases a second component with a lifetime of about 10 to 20 ns is evident. The temperature dependence of luminescence in NaCl, KBr, and KI was measured and compared with the behavior of the slow luminescence in these crystals. A new model for the electronic structure of the excited states involved in recombination luminescence is proposed and compared with the model based on the inert gas molecule. (auth)

55001 VIBRATIONAL AND ELECTRONIC PROPERTIES OF $Co(CN)_6{}^{3-}$ DOPED IN ALKALI HALIDES. Jain, S. C.; Warrier, A. V. R. (Solid State Physics Lab., Delhi). J. Phys., C (London); 5: No. 12, 1511-18(26 Jun 1972).

The ir spectra of solution-grown crystals of NaCl and KCl doped with $Co(CN)_6^{3-}$ show a multiplet in the Γ_6 stretch frequency region of CN^-. Apparently, the multiplet consists of four components in NaCl and three in KCl. However, a detailed examination of the results shows that the multiplet consists of several components due to different site symmetries in which $Co(CN)_6^{3-}$ is present in the crystal. The most probable symmetries are D_{2h} and D_s. On x irradiation the multiplet characteristic of $Co(CN)_6^{3-}$ decreases in intensity and a new multiplet characteristic of $Co(CN)_6^{4-}$ and a single line characteristic of $Co(CN)_6^{5-}$ appear on the low-energy side. On heating the crystals, irreversible changes in the spectra occur. The spectra consist of many lines, but only the line corresponding to NCO^- could be identified. The electronic spectra of the impurity show seven bands in the wavelength region 600 to 200 nm as compared with only three bands observed in the solution in this region. The bands are interpreted as being due to transitions of the split components of crystal field levels in O_h symmetry. Both peak positions and intensities are consistent with the assignment. (auth)

55002 ANALYSIS OF THE EFFECTS OF ELECTRON DAMAGE ON THE BOUND-TO-BOUND EMISSION INTENSITY OF CADMIUM SULPHIDE. Radford, C. J.; Hagston, W. E.; Bryant, F. J. (Univ. of Hull, Eng.). J. Phys., C (London); 5: No. 12, 1526-36(26 Jun 1972).

Observation of the changes produced in donor–acceptor pair cathodoluminescence emission intensities of as-grown, cadmium-fired, and sulfur-fired cadmium sulfide samples by electron radiation damage allows an estimate to be made of the initial donor concentration present and of the fraction of pairs excited. This analysis also shows that an increase in the donor or acceptor concentration need not necessarily result in an enhancement of the donor–acceptor pair luminescence emission intensity and, under certain circumstances, could lead to a reduction in emission intensity. The observations provide confirmation of this effect. (auth)

55003 SURFACE AND DEPTH DISTRIBUTION DAMAGE OF IONS IN SILICON AS SEEN WITH AN ELECTRON MICROSCOPE. Bertolotti, M.; Sette, D.; Stagni, L.; Vitali, G. (Univ., Rome). Radiat. Eff.; 15: No. 1-2, 31-5(Jul 1972).

The localized damage around ion tracks at the surface of an implanted semiconductor is studied by electron microscopy. It is shown that it is possible to see not only the produced damage but also to follow the depth distribution of the damage under the implanted semiconductor surface. (UK)

55004 PROTON AND FAST NEUTRON DAMAGE STUDIES IN Si AND Ge USING CHANNELING. Marcus, Gail H. (Massachusetts Inst. of Tech., Cambridge); Olson, N. Thomas; Ryan, Jean L. Radiat. Eff.; 15: No. 1-2, 51-6(Jul 1972).

The orientation dependence of the backscattering yield (channeling) of 1.0-MeV protons was used to investigate fast-neutron-induced lattice damage in silicon and germanium single crystals. The measurements were made at room temperature and for protons incident in (110) crystal directions. The reactor irradiations were made, using a fast neutron flux $\phi = 3.3 \times 10^{13}$ n/cm^2-sec (>0.1 MeV) at 60°C, to total exposures (ϕt) between 2.1×10^{17} and 3.4×10^{19} n/cm^2. The per cent of lattice atoms displaced was not linear with neutron exposure. The displacements rose rapidly with exposure initially, then assumed a very slow rise having a dependence on neutron exposure of $(\phi t)^{0.1}$. This appears to be some modification of an exponential saturation mechanism. It agrees qualitatively with a thermal annealing mechanism, which predicts a flux-dependent (i.e., rate of defect introduction dependent) saturation value occurring even for room-temperature irradiations. (auth)

55005 CORRELATED RECOVERY KINETICS. Peak, D.; Brosious, P.; Lee, Y. H.; (and others) (State Univ. of New York, Albany). Radiat. Eff.; 15: No. 1-2, 61-72(Jul 1972).

Diffusion-controlled correlated recovery kinetics are compared for the continuum and discrete lattice treatments. Specific results are given for the simple cubic, face-centered cubic, body-centered cubic, and diamond lattices. It is concluded that samples with anisotropic damage distributions created by irradiation in different crystallographic directions will not exhibit substantial differences in their correlated recovery, but it is argued that for small capture volumes and for the treatment of the early recovery times, the discrete treatment is required. (auth)

55006 NEW EPR SPECTRA IN NEUTRON-IRRADIATED SILICON. Lee, Y. H.; Kim, Y. M.; Corbett, J. W. (State Univ. of New York, Albany). Radiat. Eff.; 15: No. 1-2, 77-84(Jul 1972).

Six new EPR spectra reported are apparently due to intrinsic defects created in the neutron irradiation and, in some cases, annealing of silicon. In addition, a spectrum similar to, but distinct from, that due to the vacancy–phosphorus center is reported. Some tentative defect models are discussed to emphasize the features of the spectra, but more detailed studies are required to establish the identity of the defects giving rise to these spectra. (auth)

55007 THEORY OF FLUX PEAKING EFFECT IN CHANNELING. Kumakhov, M. A. (Moscow State Univ.). Radiat. Eff.; 15: No. 1-2, 85-99(Jul 1972).

The redistribution of the axial- and planar-channeled ion flux was examined. General formulae describing the flux peaking effect were obtained and the main factors on which the effect depends were examined. Backscattering experiments were also analyzed. (auth)

55008 INFLUENCE OF THE INCIDENCE ANGLE ON IRON AND COPPER SURFACE MICROTOPOGRAPHY INDUCED BY ION BOMBARDMENT. Teodorescu, I. A.; Vasiliu, F. (Institutul de Fizica, Atomica, Bucharest). Radiat. Eff.; 15: No. 1-2, 101-13(Jul 1972).

The influence of argon-ion bombardment on iron and copper surface microtropography was studied. Thermal etching revealed a regular microtopography with different oriented grain structure. The surface microrelief is characterized by pyramidal growths at the points where the dislocations intersect the iron surface or by terraced microstructures, depending on the crystallographic orientation on the copper surface. A simple model is introduced for the estimation of the bombardment time necessary for complete erosion of the pyramids on the iron surface. (auth)

55009 ELECTRONIC STOPPING MEASUREMENTS OF CHARGED-PARTICLES IN RADIOPHOTOLUMINESCENT GLASS. Arnold, G. W.; Vook, F. L. (Sandia Labs., Albuquerque, N. Mex.). Radiat. Eff.; 14: No. 3-4, 157-63(Jun 1972).

Measurements were made of the radiophotoluminescence generated in silver-activated phosphate glass by the electronic energy losses of 200- to 400-keV ions (H^+, He^+, O^+) incident on the glass. Measurements of luminescence growth as a function of energy into electronic processes per unit volume showed a departure from linearity above ~10^{18} keV/cm^3. For lower deposition values, detailed measurements of the integral depth distribution of luminescence intensity were made as material was removed by vibratory polishing. The measured depth distributions compared favorably to the integral depth distributions of electronic energy losses predicted by LSS theory (He^+ and O^+) and to experimental values of thin film losses (H^+). These comparisons indicated that the luminescent centers were formed in the glass close to (≤10^3 Å) the point of the initial deposition of electronic energy. (auth)

55010 RECOVERY OF ELECTRON-IRRADIATED PLATINUM. 1. STAGE 1 ANNEALING. Dibbert, H. J.; Sonnenberg, K.; Schilling, W.; Dedek, U. (Kernforschungsanlage, Juelich, Ger.). Radiat. Eff.; 15: No. 1-2, 115-27(Jul 1972).

By means of electrical resistivity measurements, the recovery in stage I of electron-irradiated Pt was studied. The effects of irradiation dose, electron energy, radiation doping, and doping with dilute concentrations of Au atoms on the annealing structure were investigated. The recovery in substages I_A, I_B, and I_C was not influenced by irradiation dose and doping agents, in agreement with the model of close Frenkel-pair recombination in these stages. Substage I_E was strongly and substage I_D was moderately modified by variation of radiation dose and the addition of doping agents. This and the equal values of the activation energies confirmed the model of correlated and uncorrelated recovery of free migrating interstitials in these stages. (auth)

55011 RECOVERY OF ELECTRON-IRRADIATED PLATINUM. PART 2. COMPARISON OF STAGE 1 ANNEALING WITH THEORIES FOR 3- AND 1-DIMENSIONAL MIGRATION OF INTERSTITIALS. Sonnenberg, K.; Schilling, W.; Dibbert, H. J.; Mika, K.; Schoeder, K. (Kernforschungsanlage, Juelich, Ger.). Radiat. Eff.; 15: No. 1-2, 129-41(Jul 1972).

The experimental data for the time and dose and energy dependence of the recovery in substage I_D and I_E of electron-irradiated Pt were compared critically with the results of full diffusional treatments of the correlated plus uncorrelated recovery of interstitial—vacancy pairs. Excellent agreement was obtained if in the theoretical treatment three-dimensional migration of interstitials was assumed. In contrast to this, the assumption of one-dimensional interstitial migration (off-line crowdion model) led to serious disagreements with the observed dose dependence of stage I_E. In addition, the strong dependence of the recovery structure in substage I_D and I_E on the energy of the bombarding electrons predicted by the crowdion model was not observed experimentally. (auth)

55012 DESTRUCTION OF A SOLID BY SUPERDENSE EXCITATION OF ITS ELECTRONIC SUBSYSTEM. Vaisburg, D. I.; Balychev, I. N. (Tomsk Polytechnic Inst., USSR). JETP Lett. (USSR) (Engl. Transl.); 15: No. 9, 380-2(5 May 1972).

Translated from Zh. Eksp. Teor. Fiz., Pis'ma Red.; 15: No. 9, 537-40(5 May 1972).

Various solids were irradiated by an intense electron pulse so that the average excitation energy density reached $W \sim 10^{20}$ to 10^{22} ev/cm^3. Destruction of the solid (rupture of ionic and covalent thin-plate samples, Lichtenberg figures in thick samples, and swelling or erosion of plastic solids) resulted if the energy density absorbed exceeded W_{des} (= 15×10^{20} eV/cm^3 for Ge and 1.1 to 3×10^{20} eV/cm^3 for alkali metal halides). It was determined that the electric charge, thermal gradient, and defects cannot account for the observed effects, which are probably due to the contracting of the electrons and holes into Frankel condensations with equilibrium density 10^{21} to 10^{22} cm^{-3} and W exceeding the binding energy. (D.L.C.)

55013 CHARGE STATE OF DEFECTS IN GERMANIUM CONVERTED INTO p-TYPE BY 1 MeV ELECTRONS. Werner, Zbigniew; Rzewuski, Henryk; Suski, Jan. (Inst. of Nuclear Research, Swierk, Poland). Nukleonika; 17: No. 1-2, 1-9(1972).

The concentration and Hall mobility changes in the reversible isochronal annealing process observed between 100 and 140°K in germanium converted into p-type by 1-MeV electron irradiation at 140°K were measured. It was found that the charge state of minority carrier traps created by 1-MeV electrons oscillates between 0 and +1 for traps populated and ionized, respectively. (auth)

55014 DETERMINATION OF IMPLANTATION PROFILES IN SOLIDS BY SECONDARY-ION MASS SPECTROMETRY. Maul, J.; Schulz, F.; Wittmaack, K. (Gesellschaft fuer Strahlen- und Umweltforschung mbH, Nuremberg). Phys. Lett.; 41A: No. 2, 177-8(11 Sep 1972).

Secondary ion mass spectrometry was applied to a determination of the profile of 22-keV boron ions implanted in amorphous silicon. A Gaussian range distribution is observed with a projected range of 840 Å and a standard deviation of 340 Å. (auth)

55015 THERMALLY STIMULATED CURRENTS AND THERMOLUMINESCENCE OF PARAMAGNETIC CENTERS IN HEXAGONAL BORON NITRIDE. Katzir, A. (Soreq Nuclear Research Centre, Yavne, Israel); Suss, J. T.; Halperin, A. Phys. Lett.; 41A: No. 2, 117-18(11 Sep 1972).

Isochronal annealing of paramagnetic centers in BN showed a correlation between EPR, thermally stimulated currents, and thermoluminescence measurements. It was found that the one- and three-boron centers give rise to two types of traps with activation energies of (0.6 ± 0.1) eV and (1.0 ± 01) eV, respectively. (auth)

55016 EFFECTIVE CROSS SECTIONS OF PROTON AND ALPHA PARTICLE TRACKS IN IONIC CRYSTALS. Vaisburd, D. I.; Vorob'ev, A. A.; Melikyan, L. A. This paper was summarized in At. Energ. (USSR); 30: No. 6, 538(Jun 1971) as paper No. 502/5971. (In Russian).

Full copy of this paper is held by TIC.

Effective transverse sizes of proton (1 to 6 MeV) and alpha-particle (4 to 25 MeV) tracks in NaCl monocrystals were determined from the transformation kinetics of electron color centers. The F_2-center concentration follows the law $n = N[1 - \exp(-\Omega\nu)]$, where N is the saturation level of regenerated centers, Ω is effective track volume, and ν is instantaneous track concentration. The width of the radial distribution of energy transfer per unit volume is 4.5×10^{19} eV/cm^3. The radius of a proton track is 74 ± 5 Å, while an alpha-particle track is 155 ± 15 Å. (D.L.C.)

55017 INVESTIGATION OF STATIC ELECTRON IRRADIATION EFFECTS IN BULK Si AND THIN Si FILMS AT ENERGIES FAR BELOW THRESHOLD. Norris, C. B. (Sandia Labs., Albuquerque, N. Mex.). J. Appl. Phys.; 43: No. 10, 4060-7(Oct 1972).

A study was made of the defect production in Si at electron-irradiation energies far below the theoretically predicted 170-keV bulk-damage threshold. In contrast to published results, the experiments show no permanent resistance changes in bulk samples at fluences as high as 2×10^{18} 20-keV e/cm^2 (78°K). Furthermore, fundamental damage studies using EPR techniques and optical spectroscopy confirm that fewer than 10^{-4} to 10^{-5} atomic displacements occur per 20-keV electron. These results disagree with previous studies of irradiation-induced resistance changes in bulk samples and epitaxial films from which it was indirectly determined that subthreshold atomic displacements appear following ionization of a Si K-shell electron. However, large resistance decreases do occur in p-type Si/spinel films at fluences $\gtrsim 10^{15}$ 20-keV e/cm^2 (300°K) that appear similar to anomalous results in the literature. But the energy and fluence dependences of the resistance change in the experiments are correctly predicted by theory for an irradiation-induced charge accumulation layer localized within <500 Å of the irradiated Si surface. The results do not indicate the presence of a bulk-damage mechanism. The K-shell hypothesis is clearly ruled out since the resistance effect remains at energies well below the K-shell ionization potential. A corresponding irradiation effect in n-type Si/spinel films is not found, which is consistent with the fact that nearly all the previously reported subthreshold irradiation effects have appeared in p-type Si. Results clarify some puzzling aspects of previously reported low-energy electron irradiation effects in Si and also indicate that the unambiguous determination of defect introduction or existing defect modification by subthreshold irradiation of semiconductors requires fundamental techniques that can be rendered immune to surface phenomena. (auth)

55018 THEORETICAL MODEL FOR X-RAY EMISSION AND ABSORPTION, BOND BREAKING, AND POINT-DEFECT PRODUCTION IN SiO_2. Ruffa, A. R. (Naval Research Lab., Washington, D. C.). J. Appl. Phys.; 43: No. 10, 4263-5(Oct 1972).

An analysis of the effects of radiation damage in SiO_2 is made within the framework of the valence-bond approximation. According to this model, the less energetic and intense satellite in the oxygen K_α emission spectrum results from the breaking of an Si—O bond. The calculated energy separation and intensity ratio of the two lines agree favorably with experiment. The model further indicates that the end result of the radiative processes is the production of transient paramagnetic point defects in the pure material and permanent defects in the impure material. In this sense, this model goes a step further than the usual molecular orbital or band pictures in that it provides a different description of the ionized and un-ionized states. Some implications of these conclusions are discussed in detail. (auth)

55019 X-RAY TOPOGRAPHIC DETERMINATION OF THE ABSENCE OF LATERAL STRAINS IN ION-IMPLANTED SILICON.

Tu, K. N.; Chaudhari, P.; Lal, K.; Crowder, B. L.; Tan, S. I. (IBM Watson Research Center, Yorktown Heights, N. Y.). J. Appl. Phys.; 43: No. 10, 4262-3(Oct 1972).

The lattice-to-amorphous transformation of Si caused by implantation of silicon ions results in volumetric expansion. The expansion is primarily in a direction normal to the substrate surface. This is inferred from x-ray topographic analysis where no evidence of plastic flow in the region bounding the implanted volume was detected. By measuring the unidirectional expansion, the average density of the amorphous Si layer is found to be 3.8 to 5.6% smaller than that of crystalline Si. (auth)

55020 X-RAY AND DIELECTRIC STUDIES OF IRRADIATED PEROVSKITE TYPE COMPOUNDS. Solovev, S. P.; Kuzmin, I. I.; Zakurkin, V. V.; Dudarev, V. Ya. J. Phys. (Paris); 33: No. 4, 443-5(Apr 1972).

Polycrystalline samples of $BaTiO_3$, $SrTiO_3$, $PbTiO_3$, $NaNbO_3$, and $PbZrO_3$ were irradiated with fast electrons and gamma radiation from ^{60}Co. Identical reversible changes in their dielectric constants were observed. Fast-neutron in-pile irradiation (up to integrated fluxes of 10^{20} cm^{-2}) of $PbTiO_3$ resulted in crystal structure transformations into an amorphous state, followed by the formation of a $\beta-PbO_2$ phase. The variation of the lattice parameters are similar to those of $BaTiO_3$ and $PbZrO_3$. (France)

Physical Properties

Refer also to abstracts 52937 and 53564.

55021 MAGNETORESISTANCE OF NEODYMIUM METAL. Nagasawa, H. (Tokyo Univ. of Education). Phys. Lett.; 41A: No. 1, 39-40(28 Aug 1972).

The transverse and longitudinal magnetoresistance on the polycrystalline dhcp Nd was measured at 1.38, 4.2, 13.96, and 20.4°K with applied fields up to 20 kOe. (auth)

55022 HIGH-TEMPERATURE VACUUM EVAPORATION OF ZIRCONIUM CARBIDE + TUNGSTEN COMPOUNDS FROM AN OPEN SURFACE AND THROUGH A TUNGSTEN COATING. Nikol'skaya, T. A.; Vil'k, Yu. N. Sov. Phys.-Tech. Phys. (Engl. Transl.); 17: No. 2, 341-3(Aug 1972).

Translated from Zh. Tekh. Fiz.; 42: No. 2, 429-32(Feb 1972).

The evaporation of ZrC + W compounds (ZrC + 10 wt % W and ZrC + 30 wt % W) from an open surface into a vacuum, and the evaporation of ZrC + 30% W with a tungsten coating at 2600 to 2970°K are investigated. The addition of tungsten reduces the ZrC evaporation by 50%; a tungsten coating reduces it by a further factor of 4 to 4.5. The protection provided by the coating is reduced by keeping the specimen at the same temperature, and this effect increases with increasing temperature. (auth)

55023 ADSORPTION AND DISSOCIATION OF CO ON TUNGSTEN SURFACE STUDIED BY FIELD-EMISSION MICROSCOPY. Senzaki, Kiyoshi; Kawasaki, Koji (Electrotechnical Lab., Tokyo). Jap. J. Appl. Phys.; 11: No. 9, 1363-71(Sep 1972).

The adsorption and desorption of CO for tungsten were studied by a field-emission microscope with a steady-state or pulsed field to make clear the location dependency of binding states of CO adsorbed on tungsten surface, i.e., one weakly held α state and three more strongly held β states which are distinguished by flash desorption measurements. CO in the α state is found on all the planes of tungsten, whereas the β states depend on the surface structure. From observations above 600°C, there seems to be some possibility of dissociation of CO on hot tungsten. (auth)

55024 PHOTOELECTRON SPECTROSCOPIC MEASUREMENTS OF CORE LEVEL BINDING ENERGIES OF YTTRIUM, LANTHANUM, AND CERIUM. Nagakura, Ichiro; Ishii, Takehiko; Sagawa, Takasi (Tohoku Univ., Sendai). J. Phys. Soc. Jap.; 33: No. 3, 754-60(Sep 1972).

X-ray photoelectron spectra were measured on in-situ evaporated films of yttrium, lanthanum, and cerium by the use of an electron-energy analyzer of the parallel-plate-electrode type. The binding energies of electronic core levels were determined. Results are compared with the values cited in typical x-ray atomic energy tables. The binding energies of the $M_4(3d_{3/2})$ and $M_5(3d_{5/2})$ levels of lanthanum and cerium as well as the $N_2(4p_{1/2})$ and $N_3(4p_{3/2})$ levels of lanthanum are all found to be split into two components. Possible origins of the splitting are discussed, although no definite conclusion is drawn. (auth)

55025 PROPERTIES AND INTERACTIONS OF LANTHANIDES: INTERACTIONS WITH EXTERNAL FIELDS. Saxena, K. M. S.; Fraga, S. (Univ. of Alberta, Edmonton). Can. J. Phys.; 50: No. 12, 1411-4(15 Jun 1972).

The values of the diamagnetic susceptibilities and nuclear magnetic shielding constants, calculated from numerical Hartree–Fock functions, are reported for the neutral atoms and the first three positive ions of the lanthanides. (auth)

55026 NEW MAGNETOELASTIC INTERACTION. Liu, S. H. (Univ. of Copenhagen). Phys. Rev. Lett.; 29: No. 12, 793-5(18 Sep 1972).

A mechanism is proposed for the mixing of acoustic magnons and optic phonons propagating along the c axis in terbium observed at 79°K. The interaction involves an intermediate state in which an electron–hole pair is excited virtually by the phonon and subsequently recombines into a magnon. This interaction becomes possible when the spin–orbit coupling is taken into account, and it also explains the mixing of optic magnons and acoustic phonons as seen in terbium at 200°K and dysprosium at 4.7°K. (auth)

55027 INVESTIGATION OF THE THERMAL CONDUCTIVITY, ELECTRICAL RESISTIVITY, AND THERMOELECTRIC POWER OF THORIUM NITRIDE–URANIUM NITRIDE ALLOYS. Weaver, Samuel Cavin. Knoxville, Tenn.; Univ. of Tennessee (1972). 217p. University Microfilms Order No. 72-21,368.

Thesis.

Measurements were made on ThN, (Th–2% U)N, (Th–5% U)N, and UN. Results indicated that ThN behaves very nearly as a pure metal in its transport properties. Thermal conductivities (λ) were high, electrical resistivities (ρ) were low, and thermoelectric power (S) measurements were nearly zero. UN, which is antiferromagnetic below 50°K and has a lower λ, a much higher ρ, and a large positive S. The λ of ThN is much higher than nuclear fuels being considered for LMFBR. At reactor operating temperatures, λ for ThN is approximately 20 times that of UO_2. Even when alloyed with UN, ThN retained a λ greater than any other ceramic fuel being considered. Calculations show the fuel potential of ThN alloyed with UN or PuN as fuels in proposed reactor concepts. The ρ measurements showed ThN and the (Th–U)N alloys to have a linear dependence with temperature above about 100°K. Below 100°K, the slope changed to near zero at 0°K. Small additions of UN to ThN of 2 and 5% caused a very large increase in ρ. This probably resulted because the antiferromagnetic UN exhibits a large ρ. In addition to changing the residual resistivity at 4.2°K, $d\rho/dT$ was reduced by alloying. The S of ThN is very small. However, alloying with UN, which has a large value for S, caused a significant change in the S of (Th–U)N alloys. The data treatment permitted a separation of λ into a lattice conductivity, λ_L, and an electronic contribution to the thermal conductivity, λ_e, and both contributions were significant over the temperature range studied. The separation allowed a prediction of λ at temperatures greatly exceeding the range of actual experimental measurements. The Lorentz function was calculated and found to be very near the Sommerfeld value at temperatures of 300°K and above. In order to make high-quality samples, a zone-melting technique was developed that converted the metal directly into the nitride at a state ~100 times as fast as conventional techniques. The fabricated samples were nearly 100% dense with very large grains of ~0.3 cm dia. (TSS) (Diss. Abstr. Int., B)

55028 1971 DIGESTS OF THE INTERMAG CONFERENCE, DENVER, COLORADO, APRIL 13–16, 1971. 71 C 12-MAG. New York; Institute of Electrical and Electronics Engineers, Inc. (1971). 187p. $4.00. (CONF-710446).

The 214 papers were presented in 33 sessions dealing with: ferrites, domain devices and techniques, magneto-optics, charge transfer devices and magnetic bubbles, recording media and techniques, cobalt rare earth magnets, instruments, video recording, bubble materials, memory devices and systems, electromechanical devices, storage hierarchies, magnetic recording theory, low-coercivity materials, permanent magnets, ferroresonant regulators and power conditioning, bulk storage, garnets, hard materials, recording heads, magnetization processes, plated-wire memory, microwave materials and resonance, and microwave integrated circuits. (D.L.C.)

55029 PARAMAGNETIC RELAXATION INITIATED BY FLUX JUMPING. Griffiths, D. J. (Oregon State Univ., Corvallis). Phys. Lett.; 41A: No. 1, 21-2(28 Aug 1972).

Controlled flux jumping of type-II superconductors was used to produce nonequilibrium spin distributions in Ce^{3+} 1 at.%: CaF_2. The subsequent return to thermal equilibrium was examined by monitoring the magnetic-optical Faraday effect of the cerium ions. (auth)

55030 MAGNETIC SUSCEPTIBILITIES OF NONSTOCHIOMETRIC CERIUM OXIDES. Ariya, S. M.; Balashova, E. P. Vestn. Leningrad. Univ., No. 22, Fiz., Khim.; No. 4, 151-2(Nov 1971). (In Russian).

Magnetic susceptibilities of some nonstoichiometric cerium oxides were measured. Magnetic moments calculated for a Ce(III) atom approach the value of $\mu = \sqrt{J(J + 1)} = 2.56$ μ_B. (auth)

55031 VIBRATIONAL SPECTRA AND STRUCTURES OF RARE EARTH OXIDES IN THE A MODIFICATION. Denning, J. H.; Ross, S. D. (Chelsea Coll. of Science and Tech., London). J. Phys., C (London); 5: No. 11, 1123-33(12 Jun 1972).

Crystallographic studies of La_2O_3 and the oxides isostructural with it failed to decide between the noncentrosymmetric space group D_3^2(P321) and the centrosymmetric space group D_{3d}^3($P\bar{3}m$ 1) for their structure. The infrared and Raman spectra of La_2O_3 and Nd_2O_3 were obtained, and the absence of coincidences between the spectra unequivocally favors the centrosymmetric space group. The vibrational spectra were analyzed using the Wilson FG matrix method and force constants for metal—oxygen and oxygen—oxygen interactions derived, assuming a quadratic central force field. (auth)

55032 SPECTROSCOPY OF RARE EARTH OXIDE SYSTEMS. I. FAR INFRARED SPECTRA OF THE RARE EARTH SESQUIOXIDES, CERIUM DIOXIDE, AND NONSTOICHIOMETRIC PRASEODYMIUM AND TERBIUM OXIDES. Bloor, D.; Dean, J. R. (Queen Mary Coll., London). J. Phys., C (London); 5: No. 11, 1237-52(12 Jun 1972).

The far-infrared spectra of the rare earth sesquioxides, cerium dioxide, and nonstoichiometric praseodymium and terbium oxides were observed over the range 10 to 250 cm^{-1} at liquid helium temperatures. Absorptions due to the excitation of phonons and low-lying electronic states of the rare earth ions occur in this region. The long-wavelength phonons in the sesquioxides involve motions of the rare-earth ions in an effectively rigid oxygen lattice. To a first approximation, the absorptions can be described using the rare-earth-ion site symmetries. This, together with observations of the linewidths and frequencies in mixed crystals, suggests that these phonons have the character of a local resonant mode. Strong interactions between these phonons and the electronic excitations of the rare-earth ions were observed. In general, the observed electronic energies agree with those obtained by less direct methods; however, in a few cases significant differences were found. The spectra of the other oxides indicate the presence of complex or mixed phases. (auth)

55033 MAGNETIC STRUCTURE OF $HoAu_2$. Atoji, Masao. (Argonne National Lab., Ill.). J. Chem. Phys.; 57: No. 6, 2402-6(15 Sep 1972).

Neutron-powder diffraction measurements reveal that $HoAu_2$ (the tetragonal body-centered CaC_2-type structure) becomes an antiferromagnet below $T_N(\alpha)$ = 9.2°K with the onset of an incommensurate moment alignment (α) having a transverse wave modulation. The α magnetization wave with the wavelength, 6.373 Å = 1.229 a, propagates along the a axis and is polarized approximately in the direction of the b axis, all in the face-centered lattice description. At $T_N(\beta)$ = 7.8°K, a commensurate transverse magnetization wave (β) starts to grow. The β wave with the wavelength equal to the a spacing propagates along the a or b axis and is polarized in the direction of the c axis. The composite configuration of the α and β transverse waves may be described as an antiferromagnetic triangular-fan structure. In cooling, the α wave amplitude reaches rapidly to a maximum value of 6.7 μ_B at 6.3°K, then decreases monotonically, and diminishes near 0°K. The β wave moment follows the Brillouin curve and approaches 6.4 μ_B at 0°K. The composite ordered moment rises to a maximum value of 7.8 μ_B at around 5.5°K and declines toward 6.4 μ_B at 0°K. These moment values which are considerably smaller than 10 μ_B of the free Ho^{3+} ion indicate a strong crystal field effect. The phenomenon that the maximum composite moment occurs near the midpoint of the ordered phase is due likely to a strongly anisotropic, competing interaction between the RKKY exchange coupling and the crystal field effect. (auth)

55034 MAGNETIC STRUCTURE OF $ErAu_2$. Atoji, Masao (Argonne National Lab., Ill.). J. Chem. Phys.; 57: No. 6, 2407-9(15 Sep 1972).

The magnetic properties of $ErAu_2$ having the tetragonal body-centered CaC_2-type structure were investigated at temperatures between 297 and 1.8°K by neutron diffraction experiments on powdered specimens. The onset of an incommensurate, transverse wave moment alignment (the α structure) occurs at 6.7°K. The α magnetization wave propagates along the a axis and is polarized in the b direction, all in the face-centered description. The α wavelength is 6.443 Å = 1.248 a and is temperature independent. At 4.0°K, a commensurate antiferromagnetic moment wave (the β structure) appears with the propagation direction parallel to the a axis. The β wavelength is equal to the a spacing. As regards the β moment components, the x || a component is slightly larger than the y || b component and the z || c component is undetectably small. The composite configuration of the α and β waves delineates a distorted-fan modulation. In cooling, the α amplitude develops to 6.7 μ_B at 4°K, then decreases to 5.9 μ_B near 3°K, and retains 5.9 μ_B at 3 > T > 0°K. The β wave moments approximate the Brillouin magnetization with the extrapolated moments of 3.2 and 2.7 μ_B at 0°K for the x and y components, respectively. The maximum composite moment is 9.2 μ_B at 0°K, while the ordered moment of the free Er^{3+} ions is 9.0 μ_B. (auth)

55035 MAGNETIC AND CRYSTAL STRUCTURES OF ErC_2 AT 297 -2°K. Atoji, Masao (Argonne National Lab., Ill.). J. Chem. Phys.; 57: No. 6, 2410-13(15 Sep 1972).

Neutron-powder diffraction measurements show that the tetragonal body-centered ErC_2 becomes antiferromagnetic below 19 ± 2°K. The moment alignment is governed by several narrowly dispersed, incommensurate transverse magnetization waves. The major modulation waves propagate along the a axis and are polarized in the b axis direction. The magnetization wavelengths are 5.78, 5.4, 6.7, and 7.1 Å, and the amplitudes are respectively 6.55, 2.2, 2.1, and 1.6 μ_B at 4.2°K. The ferromagnetic alignment in the plane perpendicular to a is slightly altered by several long-periodicity modulations propagating along the b and c axes. A commensurate, antiferromagnetic wave also participates in the moment alignment below 10 ± 3°K. The commensurate wave is represented by setting the wavelength equal to the a spacing in the incommensurate wave mode. The commensurate moment is 2.5 μ_B at 4.2°K. The root-mean-square value of all the moment amplitudes is 7.8 μ_B at 4.2°K and increases to 7.9 μ_B at 2°K. These features are likely caused by a strong perturbation between the RKKY coupling and the crystal-field effect. The proposed structure is by no means unique, although an exhaustive search for other probable models was fruitless. The crystal structure is characterized by the C—C bonding distance of 1.288 ± 0.006 Å and the Er—C distances of 2.403 ± 0.003 and 2.640 ± 0.001 Å. These distances are indicative of a large 5d—$\pi_0$2p contribution in the conduction-band wavefunction. (auth)

55036 ESR STUDY OF THE PYROLYSIS OF HYDROGEN ON TUNGSTEN. Cochran, Edward L.; Bowers, Vernon A.; Adrian, Frank J. (Johns Hopkins Univ., Silver Spring, Md.). J. Chem. Phys.; 57: No. 6, 2384-8(15 Sep 1972).

Electron spin resonance (ESR) techniques were adapted to the study of the atomization of hydrogen occurring on the surface of heated filaments. The method involves heating an axial metal filament in a circular cavity to temperatures of 1000 to 2000°K and measuring the steady-state atom concentration produced in the gas. Heating is accomplished by dc current pulsed at 6000 pulses/sec with a 15% duty cycle. Under these conditions, the sample space is free a relatively high proportion of the time from current-induced field inhomogeneities. The sensitivity and spectral line shapes observed compare favorably with those observed in control experiments in the same cavity in the absence of the heated filament. The atomization of hydrogen on tungsten filaments can be conveniently studied by ESR at hydrogen pressures between 0.1 and 100 torr; thus, this method complements previously developed techniques that are most useful at lower pressures (10^{-6} to 10^{-2} torr). The observed pressure and temperature dependences of the H atom concentration are interpreted in terms of a mechanism involving the production of hydrogen atoms on the filament, their diffusion into the gas, and recombination on the cavity wall. The surface reaction appears to be complex, changing character at an H_2 pressure somewhere around 0.5 torr. Extrapolation of the ESR data to very low H_2 pressures yields results consistent with previous low pressure studies. At higher H_2 pressures the rate of H atom production decreases due to surface saturation effects. (auth)

55037 INHOMOGENEOUS MAGNETIC SYSTEMS. Neumann, L. (Siemens AG, Erlangen, Ger.). Z. Phys.; 253: No. 5, 404-14(1972). (In German).

Within the molecular-field approximation the Gibbs free energy G is calculated for a system with inhomogeneous distribution of magnetic particles. Some properties of such a system derivable from G are compared with magnetic and calorimetric measurements on $Ce_{1-x}Gd_xRu_2$ alloys. (auth)

55038 ATOMIC POSITIONS IN THORIUM SILICATE: AN X-RAY-DIFFRACTION STUDY. Sinha, Devendra Prasad (Patna Univ., India); Prasad, Rameshwar. Indian J. Phys.; 45: No. 9, 435-7(Sep 1971).

The structural study of thorite (thorium silicate) was extended to the powder method using the Hull—Davey chart. The best agreement of observed and calculated intensities was obtained for the tetragonal system. The space group was found to be D_{4h}^{19}—$I4_{1/amd}$. The bond distances are: Th—4O, 2.51 Å; Th—4O, 2.45 Å; and Si—4O, 1.56 Å. (D.L.C.)

55039 STABILITY OF A TRANSVERSE-WAVE MAGNETIC STRUCTURE AT 1.3 K. Gignoux, D.; Lemaire, R.; Paccard, D. (Laboratoire de Magnetisme, Grenoble, France). Phys. Lett.; 41A: No. 2, 187-8(11 Sep 1972).

Some $TbN_{1-x}Cu_x$ exhibit sinusoidal wave magnetic structures between 1.3°K and T_N. When the crystal-field splitting is preponderant, the ordered moment can be induced by exchange field which explains the stability of these structures down to 0°K. (auth)

55040 INFLUENCE OF PLASTIC DEFORMATION AND RECRYSTALLIZATION UPON PERMEABILITY ANOMALIES IN GADOLINIUM METAL. Milstein, Frederick; Zyvoloski, George (Univ. of California, Santa Barbara). J. Appl. Phys.; 43: No. 10, 4217-25(Oct 1972).

Polycrystalline gadolinium metal was plastically deformed by a cold-rolling technique and measurements were subsequently made of the weak-field ac relative permeability as a function of temperature. The Gd was then subjected to a recrystallization anneal, and the magnetic measurements were repeated as a function of temperature. Results observed are (i) in the annealed state, the permeability passes through an anomalous "hump" in the neighborhood of the Curie temperature; this anomaly is absent in the plastically deformed state, (ii) in a range of temperatures below the Curie temperature, the relative permeability in the work-hardened state is greater than that in the annealed state, and (iii) at a lower temperature (about 240°K), the relative permeability in the annealed state undergoes a further, sharp increase which is much greater than that which occurs at the Curie point; this lower temperature increase in relative permeability is largely suppressed in the work-hardened state. The experimental results are discussed in terms of the influence of the cold-rolling process upon magnetocrystalline anisotropy and in terms of the relative importance of domain rotation and domain-wall movement in the plastically deformed and in the annealed state. (auth)

55041 LIGHT SCATTERING IN SOLIDS. Proceedings of the Second International Conference, Paris, July 19—23, 1971. Balkanski, M. (ed.). Portland, Oreg.; International Scholarly Book Services, Inc. (1971). 529p. $45.00. (CONF-710720).

Approximately 120 papers and abstracts were presented on problems concerning the light scattering by elementary excitations in solids. Subjects covered include: resonant Raman effects, electronic excitations, magnetic excitations, stimulated light scattering, polaritons, phonons, phase transitions, and Brillouin and Rayleigh scattering. Separate abstracts were prepared for two of the papers. Subject and author indexes are included. (D.L.C.)

For abstracts of individual papers see: 55042 and 55043.

55042 BOUND STATE IN EuO. Thorpe, M. F. (Yale Univ., New Haven). pp 161-4 of Light Scattering in Solids. /Balkanski, M. (ed.). Portland, Oreg.; International Scholarly Book Services, Inc. (1971).

From International conference on light scattering from fluids; Paris, France (15 Jul 1971). See CONF-710720.

Techniques for finding the two-magnon states in ferromagnets are used to show that an optically active bound state exists in an fcc Heisenberg ferromagnet with nearest-neighbor exchange. The repulsive interaction between magnons with equal and opposite momentum near the zone boundary does not lead to a bound state in most lattices. However, the magnon dispersion in an fcc lattice is such that there is a logarithmic divergence in the density of states at the largest single magnon energy, which causes a bound state to be split off above the band. These ideas are applied to EuO, which has a transition temperature of 69.3°K and therefore a two-magnon band stretching from 0 to 109 cm^{-1}, if the exchange is entirely nearest neighbor. The bound state is predicted to be above the band by only 0.05 cm^{-1} because of the large spin of the Eu^{2+} ion. Experimentally, one should be able to see a rather sharp peak at the top of the two-magnon band due to the smoothed out logarithmic singularity. (auth)

55043 RAMAN SCATTERING IN THE SEMICONDUCTING AND METALLIC PHASES OF VO$_2$. Chase, L. L.; Srivastava, Ramakant (Indiana Univ., Bloomington). pp 380-4 of Light Scattering in Solids. /Balkanski, M. (ed.). Portland, Oreg.; International Scholarly Book Services, Inc. (1971).

From International conference on light scattering from fluids; Paris, France (15 Jul 1971). See CONF-710720.

The Raman scattering spectrum of VO$_2$ single crystals is studied above and below the semiconducting-to-metal transition at 68°C. In the monoclinic semiconducting phase, only sharp phonon structure is observed in contrast with the isomorphic material, TiO$_2$, which also has broad, intense multiphonon bands. No unusual temperature dependence is observed in the positions or intensities of these lines. In the metallic phase only heavily damped features are observed, a result which clearly distinguishes VO$_2$ from the corundum-structure sesquioxides which exhibit insulator—metal transitions. A reasonable interpretation for the one resolved scattering peak in the metallic phase suggests that the rutile-structure A$_{1g}$ mode softens by about 15% of its value in the semiconducting phase. The implications of this result in understanding both the mechanism for the phase transition and the electron—phonon interactions in the metallic phase are discussed. (auth)

55044 DOPPLER-SHIFTED CYCLOTRON RESONANCE IN CADMIUM. Konstantinov, O. V.; Skobov, V. G.; Lavrova, V. V.; Fisher, L. M.; Yudin, V. A. (Physical-Technical Inst., Moscow). Zh. Eksp. Teor. Fiz.; 63: No. 1, 224-41(Jul 1972). (In Russian).

The Doppler-shifted cyclotron resonance in cadmium in a magnetic field $H \| [0001]$ is studied theoretically and experimentally in the radio-frequency region. The resonance is due to carriers with extreme shifts during the cyclotron period. Dispersion of the dielectric permeability related to the resonance leads to the appearance of weakly damped waves—dopplerons. It is found that beside dopplerons, due to lens electrons, there exist hole dopplerons related to orbits near the central cross section of the monster. Excitation of this type of doppleron in cadmium plates leads to surface-resistance oscillations with amplitudes that appear in weaker magnetic fields than do oscillations of the electron doppleron. The regions of existence of both types of dopplerons are bounded from the weak magnetic field side. The effect of the shape of the Fermi surface on the doppleron spectrum and position of the boundary fields is studied. The shape of the electron lens is determined by comparing the theoretical and experimental results. The value of the derivative of the monster cross section area with respect to momentum derived from oscillation period measurements is in agreement with the monster model employed. (tr-auth)

55045 MAGNETIZATION, VELOCITY OF SOUND, AND SPECIFIC HEAT OF Sc$_3$In. Testardi, L. R.; Holmes, L. M.; Reed, W. A.; Hsu, F. S. L. (Bell Telephone Labs., Murray Hill, N. J.). Phys. Rev., B; 6: No. 9, 3365-70(1 Nov 1972).

The magnetization at 1.5 and 4.2°K and the velocity of sound in zero field of Sc$_3$In from 1.5 to 300°K and in applied fields at 1.5 and 4.2°K are reported. The magnetic behavior exhibits essentially no coercive field, remanence, or hysteresis. A thermodynamic formula is obtained relating the field dependence of the velocity of sound with magnetostriction and magnetic susceptibility. A qualitatively successful comparison is made using the results and the magnetostriction data of Fawcett and Meincke. Specific-heat data at zero field and 1.3 kOe are reported and are related thermodynamically to the magnetization data. (auth)

55046 MAGNETIC SUSCEPTIBILITY OF RHENIUM TRIOXIDE. Greiner, John D.; Shanks, Howard R. (Ames Lab., Iowa). J. Solid State Chem.; 5: No. 2, 262-5(Sep 1972).

Magnetic susceptibility measurements were made on ReO$_3$ as a function of temperature between 77 and 300°K. The results of the measurements show that ReO$_3$ has a temperature-independent paramagnetism of 0.086×10^{-6} emu/g. A separation of the individual contributions to the measured susceptibility is made and the resultant values are compared with data on cubic sodium tungsten bronzes. The agreement indicates strong similarities between the properties of ReO$_3$ and Na$_x$WO$_3$ as x approaches 1. (auth)

55047 LOW-TEMPERATURE HEAT CAPACITY OF LaRu$_2$, CeRu$_2$, AND CeRu$_{2-x}$Pt$_x$. Joseph, R. R.; Gschneidner, K. A. Jr.; Koshimaki, D. C. (Ames Lab., Iowa). Phys. Rev., B; 6: No. 9, 3286-96(1 Nov 1972).

The heat capacity of two samples of CeRu$_2$ and one sample each of CeRu$_{1.9}$Pt$_{0.1}$, CeRu$_{1.8}$Pt$_{0.2}$, and LaRu$_2$ were measured from 1.3 to 9°K (to 20°K for LaRu$_2$). All samples are superconducting, have high γ values (10 to 14 mJ/g atom °K^2), and moderately low Debye temperatures (144—158°K). None of these materials behaves as a BCS-type superconductor. All of these materials exhibit a departure from the normal T^3 behavior at a temperature $\frac{1}{3}$ to $\frac{1}{2}$ of that which might be expected from the Debye theory. The departure is unusual in that the Debye temperature increases with increasing temperature, while other Laves-phase compounds that were recently examined show the opposite and more normal (?) behavior. These different behaviors are explained on the basis of the structural nature of the Laves phase. (auth)

55048 s—d EXCHANGE MODEL OF WEAK FERROMAGNETISM WITH AN APPLICATION TO MnB$_2$. Robinson, J. M.; Erdoes, Paul (Florida State Univ., Tallahassee). Phys. Rev., B; 6: No. 9, 3337-43(1 Nov 1972).

A crystalline solid is considered with two types of exchange interactions: a direct exchange coupling of localized spins and s—d or s—f exchange between localized spins and conduction electrons. The model developed is a generalization of the theory proposed by Kasaya and Hihara to explain the weak ferromagnetism of MnB$_2$. In contrast to the latter theory, the finite spatial extension of the d or f wave functions and the distortion of the electronic energy bands induced in the ordered state by the s—d or s—f interactions are taken into account and significantly affect the criteria for weak ferromagnetism. Comparisons are made to the Zener and Rudermann—Kittel—Kasuya—Yosida theories, which are limiting cases of the theory presented. In particular, the nonlinear response of the conduction electrons to the exchange field is demonstrated, with important implications for first-order magnetic phase transitions. (auth)

55049 CRITICAL DIVERGENCE OF THE THERMAL RESISTIVITY AT THE NEEL POINT OF EUROPIUM. Sze, N. H.; Meaden, G. T. (Univ. of Dalhousie, Hailfax, Nova Scotia). J. Phys., F (London)· 2: No. 4, 693-8(Jul 1972).

The appearance of a λ-shaped peak in the temperature coefficient of the thermal resistivity of europium at its magnetic critical point provides the first experimental evidence for the critical divergence of this transport property in a metallic element. In discussing the results, comparison is made with critical divergences observed for the magnetic heat capacity and the temperature coefficient of the electrical resistivity. (auth)

55050 MAGNETIC TRANSITIONS IN THE RARE EARTH INTERMETALLIC COMPOUNDS R_3Ni AND R_3Co. Primavesi, G. J.; Taylor, K. N. R. (Univ. of Durham, Eng.). J. Phys., F (London); 2: No. 4, 761-70(Jul 1972).

Measurements were made of the magnetic properties of rare earth—transition metal compounds having the Fe_3C structure. Results obtained using a pulsed-field magnetometer are appreciably different from those observed previously in static fields by other workers. It is difficult to decide from these results what type of magnetic order is present in several of the compounds. It is clear, however, that in some cases the observed magnetization is time-dependent. (auth)

55051 PHASE TRANSITION IN SAMARIUM. Bulatov, A. S.; Finkel, V. A. (Physical-Technical Inst., Kiev). Zh. Eksp. Teor. Fiz.; 63: No. 1, 213-16(Jul 1972). (In Russian).

The crystal structure of samarium at 77 to 300°K is studied by the low-temperature x-ray-diffraction technique. It is shown that at T ~ 106°K there is a phase transition of the second kind that is apparently related to the paramagnetism—antiferromagnetism transformation. The discontinuous changes of the linear expansion coefficients at 106°K are pronouncedly anisotropic: $\Delta\alpha_\perp < 0$, $\Delta\alpha_{||} > 0$. With decrease of the temperature below 106°K, the period a of the nine-layer hexagonal compact lattice is found to increase. (tr-auth)

55052 THEORY OF THE VOID LATTICE IN MOLYBDENUM. Tewary, V. K.; Bullough, R. (Atomic Energy Research Establishment, Harwell, Eng.). J. Phys., F (London); 2: No. 4, L69-72(Jul 1972).

A model is proposed for the study of various physical properties associated with the void lattices as recently observed in several metals. The model gives the correct value for the equilibrium void lattice spacing in molybdenum and also explains the stability of the void lattice. (auth)

55053 DIRECT FITTING OF SPIN WAVE ENERGIES TO INTERATOMIC EXCHANGE PARAMETERS IN THE FERROMAGNETIC RARE EARTH METALS. Stevens, W. N. R. (Univ. of Manitoba, Winnipeg). J. Phys., F (London)· 2: No. 4, 797-805(Jul 1972).

The description of wave vector dependence of spin wave energy in the ferromagnetic rare-earth metals in terms of interatomic Heisenberg-exchange parameters is considered. Limitations on the exchange coupling information given by the forms of published inelastic-neutron-scattering measurements are demonstrated. The results of a maximum possible analysis of available data for terbium at 90°K are given. The problem of choosing a set of points in reciprocal space for measurement of spin wave energies to obtain a complete description of the exchange coupling (within the Heisenberg model) to the maximum precision is discussed. In general a broad distribution of points through the volume of the zone is desirable. It is found that the intrasublattice coupling can be fully determined to quite a good precision from a relatively small number of measurements but the intersublattice coupling is not as easily determined. (auth)

55054 CRYSTAL FIELD EFFECT ON THE DIRECTION OF MAGNETIC MOMENTS OF RARE EARTH IONS WITH LOW SYMMETRY SITES ($C2-C_s$). Rossat-Mignod, J.; Tcheou, F. (CEN, Grenoble, France). J. Phys. (Paris); 33: No. 4, 423-8(Apr 1972). (In French)

It is possible to determine the direction of the magnetic moment in rare-earth compounds of low symmetry sites, using a crystal-field calculation in the point-charge model. This method was applied to Tb_2O_3 and different rare-earth perovskites. The results are in good agreement with experimental results. (France)

Moessbauer Effects and NMR

Refer also to abstracts 54646 and 54661.

55055 (IS-T-529) MOESSBAUER EFFECT STUDY OF ^{57}Fe IN TRANSITION METAL BORIDES. DeYoung, Donald Bouwman (Ames Lab., Iowa). Aug 1972. Contract W-7405-eng-82. 97p. Dep. NTIS.

Thesis.

The phase characteristics and nuclear hyperfine properties of sixty different transition-metal borides were studied by Moessbauer effect spectroscopy. The prepared mixed iron—transition metal boride phases include MB_2, M_3B_4, MB, M_3B_2, and M_2B types. Transmission experiments with powders were completed in the range 4.2 to 1000°K; additional scattering and 18-kOe applied-field data was collected at 300°K. Measured nuclear hyperfine parameters are discussed in terms of atomic bonding, charge transfer, and spontaneous magnetism in the borides. Isomer-shift data for all phases indicate an electron transfer from boron to the metal 3d band. The effective magnetic field of ferromagnetic monoborides is proportional to the magnetization, and also reveals a possible charge transfer from B to M. Quadrupole coupling results show a strong ionic contribution to the electric field gradient at the ^{57}Fe nucleus in monoborides. A region of ferromagnetism below 173°K was found in ternary $M_2M'B_2$ borides, where M is Mo or W and M' is a 3d transition metal. Moessbauer-effect studies of FeB reveal two distinct modifications, including a defect α phase. (auth)

55056 INTENSITY OF THE QUADRUPOLE STRUCTURE IN THE ^{51}V NMR IN TRANSITION-METAL ALLOYS. Nakajima, H.; Komori, N.; Mori, N. (Hokkaido Univ., Sapporo, Japan). Phys. Lett.; 41A: No. 1, 89-90(28 Aug 1972).

The intensity variation of the quadrupole satellite of the ^{51}V magnetic resonance was studied relative to alloying concentrations in σ-phase V—Co alloys. The nearest-neighbor atoms play the most important role in this fine structure. (auth)

55057 CHARGED STATE OF ^{57}Fe ATOMS FOLLOWING THE DECAY OF ^{57}Co IN SOLID XENON. Micklitz, H.; Barrett, P. H. (Univ. of California, Santa Barbara). Phys. Rev. Lett.; 28: No. 24, 1547-50(12 Jun 1972).

Moessbauer studies with ^{57}Fe atoms following the decay of ^{57}Co in solid Xe find these atoms in two states: the stable Fe $3d^64s^2$ state and an unstable Fe^+ $3d^7$ state. The isomer-shift analysis yields $\Delta R/R = -(8.7 \pm 0.3) \times 10^{-4}$ for the 14.4-keV γ transition in ^{57}Fe. Information is obtained about the charge-transfer mechanism and recombination time of Fe ions in solid xenon. (auth)

55058 STUDY OF BIOLOGICAL MACROMOLECULES USING PERTURBED ANGULAR CORRELATIONS OF GAMMA RADIATION. Meares, Claude F.; Westmoreland, David G. (Stanford Univ., Calif.). Cold Spring Harbor Symp. Quant. Biol.; 36: 511-16(1972).

Preliminary results indicate the potential usefulness of the perturbed angular correlation technique for studies of the motional properties of labeled macromolecules and for in vivo experiments at concentrations of $^{111}In^{3+}$ as low as 10^{-12} M. Exploitation of these advantages is currently hindered by the lack of chemical selectivity of $^{111}In^{3+}$. Applications of this method will be greatly broadened by the development of a labeling reagent which incorporates a strong complexing agent and a reactive group, such as a sulfhydryl reagent. With this reagent, it should be possible to attach indium to interesting regions of biological macromolecules. A program for the synthesis of such a label is currently in progress. (auth)

55059 NMR INVESTIGATIONS ON Y- AND La-DILUTED GdZn. Eckrich, K. (Technische Hochschule, Darmstadt, Ger.); Dormann, E.; Pppelt, A.; Buschow, K. H. J. Phys. Lett.; 41A: No. 1, 23-4(28 Aug 1972).

Gd, La, and Zn zero-field resonances are observed in ferromagnetically ordered $Gd_{1-x}La_xZn$ and $Gd_{1-x}Y_xZn$. Zn satellite lines allow the determination of the contribution of the nearest Gd neighbor shell to the Zn hyperfine field. (auth)

55060 ANGULAR CORRELATION OF A GAMMA CASCADE 329 TO 487 keV IN ^{140}Ce. Georgieva, M. K.; Misheva, M. A.; Tumbev, G. Kh. (Inst. of Physics, Sofia). Compt. Rend. Acad. Bulg. Sci.; 25: No. 2, 181-3(1972). (In Russian).

The cascade gamma transition from 329 to 487 keV in ^{140}Ce is convenient for investigating magnetic fields in various media by the method of perturbed gamma angular correlations. An unsaturated solution of $La(NO_3)_3$ was irradiated with thermal neutrons to produce a source which could be studied with sufficiently high accuracy for parameters of the unperturbed angular correlation of this cascade. (K.S.W.)

55061 MOESSBAUER EXPERIMENTS ON THE LIFETIME OF EXCITED NUCLEI. Kamenov, P. S. (Univ., Sofia). Compt. Rend. Acad. Bulg. Sci.; 25: No. 2, 185-8(1972).

New Moessbauer experiments on the detailed study of the lifetime of excited nuclei in the region of the resonance curve are suggested. The experiments will determine whether the formula of Messiah is the correct one: $\Delta t = (2h/\Gamma_0)\ (\Gamma_0^2/4(E - E_0)^2 + \Gamma_0^2)$. (D.L.C.)

55062 FEASIBILITY OF A γ LASER BASED ON RADIOACTIVE CRYSTALS. Khokhlov, R. V. (Moscow State Univ.). JETP Lett. (USSR) (Engl. Transl.); 15: No. 9, 414-16(5 May 1972). Translated from Zh. Eksp. Teor. Fiz., Pis'ma Red.; 15: No. 9, 580-3(5 May 1972).

The possibility of a γ laser based on Moessbauer radiation is considered. It is shown that, in principle, it is possible to produce a γ laser using long-lived nuclear isomers. (D.L.C.)

55063 THEORY OF THE NUCLEAR QUADRUPOLE INTERACTION IN TERMS OF IRREDUCIBLE TENSORS. Hollingworth, R. W.; Hacobian, S. (Univ. of Sydney). Aust. J. Chem.; 25: No. 4, 683-93(Apr 1972).

Using irreducible tensors throughout, the theory of the interaction of a quadrupolar nucleus surrounded by electrons is presented. The theory is applied both to pure and Zeeman nqr spectra. The relation between the spectroscopic and intrinsic quadrupole moments is derived. (auth)

55064 POSITRON LIFETIMES AND PHASE TRANSITIONS IN SOLIDS. Singh, K. P.; Singru, R. M.; Rao, C. N. R. (Indian Inst. of Tech., Kanpur). J. Phys., C (London); 5: No. 10, 1067-71(25 May 1972).

Lifetimes of positrons annihilating in NH_4Cl and in nitrate glasses were measured as a function of temperature. The observed temperature dependence of τ_2 and I_2 indicates that the I_2 is significantly affected by changes in molar volume accompanying the phase transitions in these solids. I_2 varies in the same direction as the molar volume thus underlining the role of free volume in the positron annihilation process in condensed media. (auth)

Theory

55065 (UCRL-Trans-10643) LONGITUDINAL AND TRANSVERSE EXCITONS IN SEMICONDUCTORS. Denisov, M. M.; Makarov, V. P. (Akademiya Nauk SSSR, Moscow. Fizicheskii Institut). Translated for Univ. of California, Lawrence Livermore Lab. from Preprint No. 78. 15p. Dep. NTIS.

Formulae for the energy of longitudinal excitons in semiconductor crystals with arbitrarily complex band structure are derived from purely microscopic and from phenomenological considerations. The results coincide, as they should. These results are compiled with those of other theoretical studies and with existing experimental data. (auth)

55066 POSITRON CORRELATION ENERGY IN METALS. Bergersen, B.; Carbotte, J. P. (McMaster Univ., Hamilton, Ont.). Can. J. Phys.; 50: No. 12, 1332-6(15 Jun 1972).

The positron correlation energy in an electron gas is calculated in the metallic density region using the random phase dielectric constant. It is found that the positron–plasmon interaction is much more important for the correlation energy than for the annihilation rate, and that the plasmon contribution to the energy is actually larger than the particle–hole contribution. Calculations using the Singwi et al. dielectric constant give essentially the same results as the RPA. It is argued that the ladder approximation need not represent an improvement over linear response theory when computing the correlation energy. (auth)

PHYSICS (THEORETICAL)

Refer also to abstracts 54392, 54408, 54682, and 54797.

55067 (ITF-72-9-E) ON THE SOLUTIONS OF BOGOLYUBOV KINETIC EQUATIONS. QUANTUM STATISTICS. **Petrina, D. Ya. (Akademiya Nauk Ukrainskoi SSR, Kiev. Institut Teoreticheskoi Fiziki). 1972. 24p. Dep. NTIS (U. S. Sales Only).**

The Bogolyubov kinetic equations for quantum statistics are investigated. A method due to Bogolyubov is used to investigate the solutions of kinetic equations in the Banach space composed of a sequence of trace-class operators in the state space. The procedure makes it possible to construct the solutions of kinetic equations in a finite volume by using the physically meaningful initial data. The weak, or smoothed, solutions are constructed in the space of bounded operators. (auth)

55068 (ITF-72-31-P) ASYMPTOTICALLY EXACT SOLUTIONS FOR THE SYSTEMS WITH SINGULAR POTENTIALS. Simenog, I. V. (Akademiya Nauk Ukrainskoi SSR, Kiev. Institut Teoreticheskoi Fiziki). 1972. 22p. (In Russian). Dep. NTIS (U. S. Sales Only).

It is shown that for the quantum-mechanical systems with singular attractive potentials, the Hartree approximation is realized in an asymptotically exact way in the limit of a great number of particles N. The Hartree one-particle solutions are also asymptotically exact for the systems with a bounded monotone potential of interactions. (auth)

55069 (ITF-72-36-E) PRODUCT FORMULA FOR SEMIGROUPS AND ITS APPLICATION TO THE SCHROEDINGER EQUATION WITH SINGULAR POTENTIALS. Semenov, Yu. A. (Akademiya Nauk Ukrainskoi SSR, Kiev. Institut Teoreticheskoi Fiziki). 1972. 22p. Dep. NTIS (U. S. Sales Only).

The class of potentials for which the solution of the Schroedinger equation is representable as the Feynman integrals over a trajectory are investigated. It is proved that in the attractive case all the potentials allowed by the principal postulates of quantum mechanics are such that if a total Hamiltonian of the system is defined by the bilinear form method, then the Feynman integral over a trajectory converges to the propagation. (auth)

55070 (ITF-72-45-P) RELATIONS BETWEEN THE MOMENT FUNCTIONALS OF MEASURES ABSOLUTELY CONTINUOUS WITH RESPECT TO THE GAUSSIAN MEASURE AND THE SOLVABILITY OF SCHWINGER EQUATIONS FOR THE GREEN FUNCTIONS OF A EUCLIDEAN FIELD THEORY. Gonchar, N. S. (Akademiya Nauk Ukrainskoi SSR, Kiev. Institut Teoreticheskoi Fiziki). 1972. 35p. (In Russian). Dep. NTIS (U. S. Sales Only).

The solvability of Schwinger equations for the Green's functions of a Euclidean field theory is investigated for any nonlinear self-interaction bounded from below. First, the "cut off" equations in which all the values are mathematically meaningful are investigated. In this case the representation in terms of a functional integral in some probability measure is obtained for a solution. The vector S_α, which is the solution, belongs to a space $\overline{S}$. Then a "cut off" theory with essentially nonlinear bounded Lagrangians of interaction is investigated. It is shown that in this case the limiting Green's functions coincide with the free Green's functions. (auth)

55071 (LA-4868) DERIVATION OF THE BOLTZMANN DISTRIBUTION LAW WITH ILLUSTRATIONS FROM A HARD-SPHERE MODEL COMPUTER PROGRAM. **Conant, Donald R. (Los Alamos Scientific Lab., N. Mex.). Jun 1972. Contract W-7405-eng-36. 16p. Dep. NTIS.**

The Boltzmann distribution law is derived, and examples illustrating differences among the assumptions of Boltzmann, Bose–Einstein, and Fermi–Dirac statistics are given. The range of applicability of the assumptions and the distortions of molecular systems caused by this limited range are discussed. Results from a hard-sphere model calculated by computer are used to illustrate the distortions and the rather good agreement with the Boltzmann prediction for energies near the average molecular energy even for systems containing only a few molecules. (auth)

55072 APPLICATION OF ORTHOGONAL AND UNITARY GROUP METHODS TO THE N-BODY PROBLEM. Louck, James D. (Los Alamos Scientific Lab., N. Mex.); Galbraith, Harold W. Rev. Mod. Phys.; 44: No. 3, 540-601(Jul 1972).

Methods for constructing states of good total orbital angular momenta of N identical, free, structureless particles through the use of the orthogonal and unitary groups are developed. The first part reviews the existing literature, particularly for the three-particle problem. New results include the discrete symmetry properties of the SU(3) states vectors of the three-particle problem. The general N-particle problem is approached through the use of the subgroup property O (n) ⊂ U (n). An imbedding of O (n) in U (n) is given which greatly simplifies the study of the O (n) subgroup of U (n). Particular applications of this imbedding are: (1) an explicit constructive procedure for obtaining all the single-valued irreducible representations of O (n), and (2) an explicit constructive procedure for obtaining all N-particle states of good angular momenta up through the degree four solid harmonics. (auth)

55073 ASPECTS OF TIME-DEPENDENT PERTURBATION THEORY. Langhoff, P. W. (Harvard Univ., Cambridge, Mass. Indiana Univ., Bloomington); Epstein, S. T.; Karplus, M. Rev. Mod. Phys.; 44: No. 3, 602-43(Jul 1972).

The Dirac variation-of-constants method has long provided a basis for perturbative solution of the time-dependent Schrödinger equation. In spite of its widespread utilization, certain aspects of the method have been discussed only superficially and remain somewhat obscure. The present review attempts to clarify some of these points, particularly those related to secular and normalization terms. Secular terms arise from an overall time-dependent phase in the wave function, while normalization terms preserve the norm of the wave function. A proper treatment of the secular terms is essential in the presence of a physically significant level shift that can produce secular divergences in the time-dependent perturbation functions. The normalization terms are always important, although the formulation of a simple method for including them is of greatest utility in applications requiring higher-order perturbation theory (e.g., nonlinear optical phenomena), where difficulties have arisen in previous treatments. Although the Dirac perturbation technique includes the correct secular and normalization terms when properly executed, it is convenient to reinterpret the perturbation problem so that the secular and normalization terms can be factored from the wave function to all orders. It is shown that an appropriate overall multiplicative, time-dependent normalization and phase factor can be obtained, and that it is simply the amplitude for finding the system in the unperturbed eigenstate at any time t. The regular part of the wave function remaining after this factorization provides a complete description of the physical properties of the system of interest and determines the overall normalization and phase as well. Most important, the regular function and its perturbation expansion satisfy equations which are more convenient for computational applications than are the customary Dirac equations, and, in contrast to the latter, they reduce directly to the familiar time-independent perturbation equations in the static limit. To illustrate the general development, the model problem of a linearly perturbed harmonic oscillator and the static, harmonic, and electromagnetic perturbations of arbitrary quantum-mechanical systems are treated explicitly. In the case of an adiabatically applied static perturbation, the familiar adiabatic theorem is recovered with the overall phase factor giving the perturbed eigenvalue, while in the case of an harmonic perturbation, the overall phase factor obtained includes the system level shift appropriate for a quasiperiodic state. For an electromagnetic perturbation, compact expressions are obtained for various nonlinear optical susceptibilities in forms suitable for computations. Time-dependent Hartree–Fock approximations are treated explicitly to demonstrate that difficulties can arise when normalization and secular terms are not extracted prior to application of the perturbation formalism. Connection is also made with other methods which can be employed to eliminate secular and normalization terms from the wave function; these include a projection procedure and multiple-time-scales perturbation theory. The elimination of secular divergences from the perturbation functions is shown to be important for the construction of a valid Fourier transform. Secular and normalization terms also arise in connection with variational principles for the time-dependent Schrödinger equation. By employing the Frenkel variational principle and an ansatz for the total wave function that explicitly isolates the secular and normalization terms, a computationally convenient variational functional is obtained. This form of the Frenkel principle provides a bound to the system level shift induced by an oscillatory perturbation and is equivalent to the Ritz variational principle in the static limit. Explicit expressions for the variational functional in the Hartree–Fock approximations are derived in forms suitable for computational applications to the interactions of radiation and matter. (auth)

55074 APPROXIMATE METHODS FOR SOLVING SCHROEDINGER EQUATIONS WITH A SINGULAR POTENTIAL. Gogokhiya, V. Sh.; Filippov, A. T. (Joint Inst. for Nuclear Research, Dubna, USSR). Yadern. Fiz.; 15: No. 6, 1294-1306(Jun 1972). (In Russian).

The theory of renormalizing the Schroedinger equations with a singular (at r → 0) potential is briefly reported. It is shown, that singular potentials are quite naturally divided into renormalizable and nonrenormalizable ones, in this the structure of the series of usual perturbation theory (with cutoff at small distances) is similar to the corresponding one in renormalizable and nonrenormalizable field theories. Approximate methods for Schroedinger equations with the singular potential $g_0V(r)$, that allow to find the wave function and scattering amplitude in the form of a series in $g_0^{\nu}(\ln g_0)_{\nu}^{n}$, where n_{ν} is an integer and ν, in a general case, is a noninteger (a modified series of perturbation theory), are suggested. (auth)

55075 EXCITATION OF A TWO-LEVEL SYSTEM DAMPED BY THE INTERACTION WITH BOSONS. III. TRANSVERSE SUSCEPTIBILITY. Loos, J. (Inst. of Solid State Physics, Prague). Czech. J. Phys.; 22: No. 7, 583-8(1972).

The method developed in the preceding paper is used to determine the mean transverse spin components of a magnetic two-level system. Likewise as previously, the excitation by the monochromatic elliptically polarized hf field and the damping by the interaction with certain boson field is considered. No assumption is made concerning the strength of the hf field and therefore, this solution is valid in the saturation region too. The comparison with the solution of the macroscopic equations of motion is made. (auth)

55076 EXCITATION OF A TWO-LEVEL SYSTEM DAMPED BY THE INTERACTION WITH BOSONS. II. STATIONARY POPULATIONS. Loos, J. (Inst. of Solid State Physics, Prague). Czech. J. Phys.; 22: No. 6, 523-9(1972).

A two-level system excited by a monochromatic h.f. field and damped by an interaction with certain boson field is considered. The aim is to derive the steady-state level populations. The behavior of the system considered between two boson transitions is described by the quantum mechanical solution found in the preceding paper. The stationary populations are deduced by averaging the corresponding quantum mechanical probabilities with respect to the initial conditions. (auth)

55077 SPIN-DEPENDENT OPERATORS IN THE OCCUPATION-BRANCHING NUMBER REPRESENTATION. Gouyet, J. F. (Ecole Polytechnique, Paris). J. Math. Phys. (N. Y.); 13: No. 5, 745-51(May 1972).

In two preceding papers, a general method was given of building up open-shell wavefunctions which are eigenfunctions of the spin operators S^2. This method leads to a second quantization type formalism, where degenerate multiplets are described in what we call the occupation-branching number representation. In Paper II, equivalent monoelectronic and bielectronic operators were defined and a diagrammatic technique was developed. In the present paper, the equivalent spin-dependent operators in the occupation-branching number representation are built up, in the cases of monoelectronic and bielectronic operators. The spin—orbit and the spin—spin coupling are the most important operators of this kind. The associated diagrammatic representation is given. (auth)

55078 CONTINUED-FRACTION METHOD FOR PERTURBATION THEORY. Scofield, D. F. (Aerospace Research Labs., Wright-Patterson AFB, Ohio). Phys. Rev. Lett.; 29: No. 12, 811-14(18 Sep 1972).

A direct operational approach to the solution of the Schrödinger equation has led to an iterative nonperturbative method for its solution. The method, when applied to the Mathieu equation and the anharmonic-oscillator equation, is superior to the perturbation-iteration method and to Rayleigh-Schrödinger perturbation theory both in terms of rate of convergence and range of coupling constant allowed. (auth)

55079 ANALYTIC EXTRAPOLATION FROM BOUNDARY AND INTERIOR POINTS. Nenciu, G. (Inst. of Atomic Physics, Bucharest). Lett. Nuovo Cim.; 4: No. 14, 681-4(5 Aug 1972).

The problem of the analytic extrapolation from boundary and interior points is considered in the framework of the functional-integration approach initiated by Cutkosky. (L.B.S.)

55080 NOTE ON FEYNMAN'S PATH INTEGRALS. Goovaerts, M. J.; Devreese, J. T. (Univ., Antwerp). Physica; 60: No. 1, 97-13(Jul 1972).

Path integrals are introduced using the properties of integral equations of the Fredholm type. This framework seems well adapted for studying the equivalence between the path-integral formalism and other formulations of quantum mechanics, and for examining the relation between path integrals and expansions like the Born series. The study of these integral equations shows how a density matrix is related to a Stieltjes integral. In principle our study reduces the problem of calculating a path integral to a problem of traditional analysis. A series expansion of a transform of the path integral which was introduced recently is shown to satisfy Schroedinger's equation and to be also related to a Liouville-type iteration of an integral equation. The problem of oscillatory integrals in Feynman's formalism is also discussed. (auth)

REACTOR TECHNOLOGY

Power Reactor Development

Refer also to abstracts 53107 and 53191–53193.

55081 (AECL–4162) AECL ANNUAL REPORT, 1971–1972. (Atomic Energy of Canada Ltd., Chalk River (Ontario)). 48p. Dep. NTIS (U. S. Sales Only).

The activities of the Atomic Energy of Canada Limited for the year ending March 31, 1972, are summarized. Highlights of developments in nuclear power, radiation and radioisotopes, heavy water production, and research are included. (H.D.R.)

55082 (EIR–215) MOLTEN CHLORIDES FAST BREEDER REACTOR PROBLEMS AND POSSIBILITIES. Taube, M.; Ligou, J. (Eidgenoessisches Institut fuer Reaktorforschung, Wuerenlingen (Switzerland)). Jun 1972. 75p. Dep. NTIS (U. S. Sales Only).

A fast breeder reactor of 2000 MW(t) output using molten chlorides as fuel and coolant is discussed. Some of the most significant characteristics are: the fuel contains only $PuCl_3/NaCl$; the coolant is $UCl_3/NaCl$ and also forms the fertile material along with the blanket, again $UCl_3/NaCl$; and the fuel circulates through the core by forced convection. The thermal stability of the reactor is very good. Power excursions of fuel temperature transients are quickly damped by the phenomena of fuel expansion pushing part of the fissile material out of the critical zone. The balance of fission products including free chlorine seems to be stabilized when some of the semi-noble metals (Ru, Rh, Pd and some Mo) are present in the elementary form. Corrosion effects form the most difficult problem. Thermodynamic studies suggest the use of molybdenum alloys as structural materials. Separation of the fuel component from the fertile component UCl_3 helps to overcome some of the corrosion problems. A reprocessing system based on a salt-metal-transport process seems to be attractive from the point of view of the economics of the plant as a whole. The possibility of using a dissociating gas as a secondary working agent in the turbine for example Al_2Cl_6 and N_2O_4 is discussed. (auth)

55083 (EURFNR–1001) FAST REACTOR PROGRAMME. Fourth Quarter 1971 Progress Report. Hoekstra, E. K. (comp.) (Reactor Centrum Nederland, Petten). Mar 1972. 78p. (RCN–168). Dep. NTIS (U. S. Sales Only).

Work performed under United States–Euratom Fast Reactor Exchange Program.

The RCN programme comprises reactor physics, fuel irradiations, advanced fuels, radiation damage in canning materials, analysis of impurities in sodium, aerosol research and heat transfer and hydraulics. (9 references) (auth)

55084 (INIS-mf–212) ATOM 71. Progress Report, April 1, 1970–March 31, 1971. (United Kingdom Atomic Energy Authority, London (England)). 1971. 23p. INIS.

The nuclear power program undertaken by the UKAEA during 1970–71 is surveyed. The exploitation of the Authority's accumulated expertise and resources for the benefit of industry outside the nuclear power field by means of applied nuclear projects and also non-nuclear applications is presented. The aims of the fusion research program are considered. (U.K.)

55085 NEW ENERGY TECHNOLOGY: SOME FACTS AND ASSESSMENTS. Hottell, H. C.; Howard, J. B. Cambridge, Mass.; Massachusetts Institute of Technology Press (1971). 373p. $2.95.

Past, present, and future US energy production is summarized. Background for assessment of new energy technology is given. Fossil fuel-to-fuel conversion, nuclear power, central station power from fossil fuel, utilization related energy problems, and special energy conversion systems of secondary importance are discussed. (M.C.G.)

55086 OPTIONS IN POWER GENERATION AND TRANSMISSION. Baron, S. Pub. Util. Fortn.; 90: No. 2, 22-31(20 Jul 1972).

Possible alternatives in power generation and transmission available around 1980 and 1990 are discussed and generating costs compared with those for 1970. Topics covered include: fossil fuel costs and air pollution control, thermal effects, fresh-water sources, seawater sources, dry towers, offshore sites, extra-high voltage with hydro or mine-mouth generation, fast-breeder reactors, high-temperature gas turbines, magnetohydrodynamics, fuel cells, and aesthetics. (M.C.G.)

55087 BRITAIN'S NUCLEAR OPTIONS. Kenward, Michael. New Sci.; 55: No. 809, 332-5(17 Aug 1972).

The economic and technical difficulties encountered by designers and engineers in the various programs for production of power with AGR, HTGR, LWR, SGHWR, and LMFBR are reviewed. Britains experience and possible future use of the various systems are discussed. The growth in electricity demand and methods whereby the CEGB could meet it are presented. (UK)

55088 OUTLOOK FOR NUCLEAR POWER GENERATION. Catchpole, S. (Central Electricity Generating Board, London). Chem. Ind. (London)· No. 15, 592-7(5 Aug 1972).

Some of the most important factors determining the growth of nuclear power in the UK are discussed under the following headings: estimates of demand and plant requirements; future availability of competing fuels; availability of nuclear plant and future reactor choice. Uncertainties and conflicting requirements are emphasized. (UK)

55089 NUCLEAR POWER IN JAPAN. Greenhalgh, G. H. London: British Nuclear Forum (1971). 50p.

A report is presented based on a visit to Japan, May 19 to June 3, 1971, and on published information. The subject is covered in sections: the structure of the nuclear industry in Japan (the electrical utilities; the manufacturing industry; government organizations; Japan Atomic Industrial Forum; finance; the public; collaboration with overseas companies in U.S.A., France, Germany, and U.K.); reactor systems in Japan (light water reactors; the gas cooled reactor; the advanced thermal reactor; fast reactors; nuclear ships); the fuel cycle; Japanese nuclear power program. (UK)

55090 CONCEPTION ON NUCLEAR ENERGY TILL 2000 A.D. Data Compiled. Tokyo; Japan Atomic Industrial Forum, Inc. (1971). vp. (In Japanese).

Separate abstracts were prepared for each of 4 papers presented. (M.C.G.)

For abstracts of individual papers see: 55091–55094.

55091 FUTURE VIEW OF ECONOMIC SOCIETY AND ELECTRIC POWER DEMAND. pp 1-18 of Conception on Nuclear Energy Till 2000 A.D. Tokyo; Japan Atomic Industrial Forum, Inc. (1971). (In Japanese).

Adjustment and renovation in the 1970s, de-industrialization in the 1980s, and higher internationalization in the 1990s are predicted. The growth rate will slow under the action of restricting factors in the 1980s and the growth rate will slow to 4 to 5% in the 1990s. Features of the industrial structure in each period are predicted. Expansion of petroleum demand will continue but the demand structure will change due to pollution countermeasures. The development of nuclear energy is predicted as necessary for production of electricity. In the 2000s, the total energy demand converted to petroleum is predicted as 1800 million kl, and its composition will be 56% for industries, 15% for transport, 25% for people's livelihood, and 4% for other. Electricity consumption for one home will be 8000 kWh in the 1980s and 15000 kWh in the 1990s. Total electric power demand will be 2400 billion kWh in 2000s. Its composition will be 26% for lighting, 14.2% for service, 57.4% for industries, and 2.4% for electric vehicles. (Japan)

55092 EXAMINATION OF SCALE OF DEVELOPMENT FOR NUCLEAR POWER GENERATION. pp 21-48 of Conception on Nuclear Energy Till 2000 A.D. Tokyo; Japan Atomic Industrial Forum, Inc. (1971). (In Japanese).

To meet power demand, power generation facilities of nine electric power companies will be 169 million kW in 1980, 286 million kW in 1990, and 440 million kW in 2000. In Japan, most of the primary energy resources depend on oversea countries. Therefore more emphasis may be placed on nuclear power generation in Japan. Maximum effort must be exerted to reduce the sulfur content of oil and this affects fuel cost adversely. On the other hand, the cost of nuclear fuel may be lowered by improvement of fuel design, expansion of fuel cycle industries, and effect of mass production. The fuel cost for 1 million kW LWRs is estimated as 0.56 to 0.68 yen/kWh. Most economically usable hydraulic power has been developed already, and only pumping-up power plants will be developed in the future. Lands suitable for the location of nuclear power plants were surveyed in 1967, and most of them are in northern Japan. Construction cost and power generation cost of the nuclear power plants were estimated and compared with those of thermal power plants. The scale of development of nuclear power generation will be 27, 110, and 220 million kW in 1980, 1990, and 2000, respectively, in view of economy. These values are equivalent to 16, 39, and 50% of the total power generation in each year. (Japan)

55093 DATA FOR CALCULATING VALUES ON NUCLEAR FUEL CYCLES. pp 51-75 of Conception on Nuclear Energy Till 2000 A.D. Tokyo; Japan Atomic Industrial Forum, Inc. (1971). (In Japanese).

It was assumed that the scale of nuclear power generation will be 27 million kW in 1980, 110 million kW in 1990, and 220 million kW in 2000. Types of reactors examined were PWRs, BWRs, AGRs, ATRs, HTGRs, and FBRs. Basic combination pattern of the reactors is LWRs + FBRs and LWRs + ATRs + FBRs. Unit capacity will be 1.5 million kW for LWRs and 1 million kW for ATRs and FBRs. The ATRs will start operation from 1981 and the FBRs from 1986. SIRIUS-NIP-A, FULAM-4 and -5, MITIEN, and NURAN-3 codes were employed for the calculations, and the results were compared and examined. The required amount of U_3O_8 is 8000 to 9000 ST in 1980, 16000 to 21000 ST in 1990, and 15000 to 20000 ST in 2000 according to the proportion of employment of the ATRs. The required amount of enrichment is 4000 to 5000 MT SWU in 1980, 8000 to 14000 MT in 1990, and 9000 to 15000 MT in 2000. The required amount of forming and fabrication is 1200 to 1400 MT U in 1980, 3200 to 4500 MT in 1990, and 3300 to 4900 MT in 2000. The amount of reprocessing is 500 MT U in 1980, 2000 to 3300 MT in 1990, and 3500 to 5100 MT in 2000. The amount of fissionable plutonium is 7 MT in 1980, –3 to 50 MT in 1990, and –180 to 65 MT in 2000. Finally, the required amount of heavy water is 0 MT in 1980, 0 to 1500 MT in 1990, and 0 to 200 MT in 2000. (Japan)

55094 FUTURE VIEW OF INDUSTRIES SUPPLIED WITH ATOMIC ENERGY. pp 79-111 of Conception on Nuclear Energy Till 2000 A.D. Tokyo; Japan Atomic Industrial Forum, Inc. (1971). (In Japanese).

The nuclear energy supply industry supplies equipments, material, fuel, and service proper to nuclear energy in various fields of peaceful uses, such as nuclear power generation, nuclear ships, multipurpose utilization of reactors, and use of radioisotopes and radiation. Investment, turnover, number of employees, and results of introduction of foreign techniques show slow but steady development of the industry. In 1969, the investment was 1,103 million yen, the turnover was 71,475 million yen, and 8,264 engineers, researchers, clerks, and workers were employed. In Japan, engineering for nuclear plants is carried out by the plant makers, and the proportion of domestically produced machinery and equipments increases gradually. Domestic production of uranium fuel was 29,706 kg U in 1971. Major export of machinery for nuclear power generation was 4 pressure vessels, 2 containment vessels, 1 set of turbine and generator, and 5 sets of LP section and LP rotor of turbine. Development of the nuclear power generation in the world was surveyed for the purpose of examining export prospects. Expected domestic demand for reactors will be 11 million kW in 1990 and 16 million kW in 2000, and that for turbines and generators will be 16 million kW in 1990, and 25 million kW in 2000. Annual production capacity for nuclear fuel in 1980, 1990, and 2000 is estimated for LWR and FBR plants and for LWR, ATR, and FBR plants. (Japan)

55095 TENDENCIES IN THE DEVELOPMENT OF FAST BREEDER REACTORS. Haefele, W. (Kernforschungszentrum, Karlsruhe, Ger.). Atomwirt. Atomtech.; 17: No. 7, 378-84 (Jul 1972). (In German).

The German-Benelux project SNR 300, together with the corresponding British and French projects, can be considered as part of a dynamic European fast breeder development. The French and British projects, however, will become operational several years earlier than SNR 300. As an advantage, the initial design of the SNR already took into account all aspects for development of future commercial breeder power plants. Further coordinated development should be centered around extensive irradiation experiments for optimizing burnup, need for a special large test reactor, safety experiments, and efforts to achieve initially low fabrication costs for plutonium fuel elements. (tr-auth)

55096 PROTOTYPE NUCLEAR POWER PLANT SNR 300. Brandstetter, A.; Guthmann, E. (INTERATOM, Bensberg, Ger.). Atomwirt. Atomtech.; 17: No. 7, 368-71(Jul 1972). (In German).

The SNR 300 is described with respect to system groups of the installation such as reactor, fuel element handling and storage, sodium heat exchanger, support systems, steam power system, and electrotechnical installations. Also described are the total layout and the buildings. The reactor building consists of the internal and external containment with rectangular floor plan. The primary system is designed according to the loop concept in which tubings connect the separately placed reactor vessel, pumps, and heat exchanger. The concept permits more freedom with respect to layout of the plant and placement of shielding. In addition, the components are more easily accessible and the prototype permits easier extrapolation to large-scale unit. (tr-auth)

55097 ORGANIZATION AND ECONOMIC SIGNIFICANCE OF BREEDER DEVELOPMENT. Scheuten, G. H. (Schnell-Brueter-Kernkraftwerksgesellschaft mbH, Essen). Atomwirt. Atomtech.; 17: No. 7, 366-8(Jul 1972). (In German).

The SNR 300, representing a joint German–Benelux project, is only an introductory step toward development of commercial fast breeders, which must be coordinated internationally to an even higher degree. Only when economic competitiveness is achieved will breeders exert their great advantages with respect to fuel supply, high efficiency, and decreased environmental hazards. Expenses for breeder development appear justified as a solution to future energy problems. Discussed are preparatory work and present status of the SNR 300 project, enlargement of international cooperation, and economic significance of fast breeder development. (H.B.G.)

55098 PROJECT SNR: GOVERNMENTAL SUPPORT AND INTERNATIONAL COOPERATION. Daeunert, U.; Schmidt-Kuester, W. J. (Bundesministerium fuer Bildung und Wissenschaft, Bonn). Atomwirt. Atomtech.; 17: No. 7, 363-6(Jul 1972). (In German).

Development of fast breeders belongs to the large-scale projects which transcend not only the capabilities of private industry but also of single nations. Therefore, in the BRD, the development is undertaken with governmental support as an international project together with the Benelux countries. In the spring of 1972, the first decisive phase of the project SNR 300 was concluded with government agreements, a letter of intent, and the designation of an upper price limit. Projected is construction of a 280 MW(e) prototype nuclear power plant with a sodium-cooled fast breeder reactor (SNR 300) at Kalkar on the lower Rhine River. (H.B.G.)

Physics and Core Engineering

Refer also to abstract 55398.

55099 (AD–738874) SOLUTION OF A NUCLEAR-REACTOR PARAMETER-IDENTIFICATION PROBLEM. Canepa, Oscar Eduardo Brain (Naval Postgraduate School, Monterey, Calif.). Jun 1971. 87p. NTIS.

Thesis.

A continuous identification of parameters is performed on a simulated fast breeder nuclear reactor system using hybrid computation and applying techniques of statistical regression analysis and exponentially-mapped-past functions. Output states which are not directly measurable are estimated by use of a Kalman filter. The method developed in this study is applied to a numerical example which demonstrates that unknown parameters can be identified within 3% of their actual value, with signal noise ratios as low as 10 : 1 in the measured states. The example also demonstrates that convergence occurs in a reasonably short time. (auth)

55100 (BARC/I–148) PHYSICS DESIGN OF HEAVY WATER MODERATED REACTORS. Srinivasan, K. R. (Bhabha Atomic Research Centre, Bombay (India)). 1971. 215p. INIS.

A collection of lectures given at a course arranged at the Bhabha Atomic Research Centre, Bombay, for theoretical physicists to familiarize them with physics aspects and design characteristics of heavy water moderated reactors is presented. The conventional method using the four factor formula is discussed for calculating lattice parameters and long term reactivity change. Some aspects of fuel management are covered. The reactor theory underlying the calculational methods is described in detail. (INIS)

55101 (CISE-R–203) EXPERIMENTAL INVESTIGATIONS ON U–D_2O LATTICES. Accinni, F.; Mangialajo, M.; Taddei, F. (Centro Informazioni Studi Esperienze, Milan (Italy)); Ciuffolotti, L. (Societa Ricerche Impianti Nucleari, Saluggia (Italy)). Dec 1967. 53p. (In Italian). INIS.

Experimental investigations on D_2O-moderated natural uranium fueled lattices have been carried out. The experimental parameters δ^{28}, ρ^{28}, ICR, intracell neutron density distribution and spectral indices were determined. The results are presented with some comments on the precision and the interpretation of measurements. (INIS)

55102 (CISE-R–239) PRELIMINARY REPORT ON THE MEASUREMENT OF CELL PARAMETERS IN THE RB-1 REACTOR. Accinni, F.; Mangialajo, M. (Centro Informazioni Studi Esperienze, Milan (Italy)); Baccolini, A.; Casali, F.; Corberi, A.; Zappellini, G. (Comitato Nazionale per l'Energia Nucleare, Bologna (Italy). Centro di Calcolo); Ciuffolotti, L. (Societa Ricerche

Impianti Nucleari, Saluggia (Italy)). Jan 1968. 56p. (In Italian). INIS.

Experiments carried out in RB-1 Reactor of Montecuccolino (Bologna) in the framework of CIRENE Program, for UO_2/D_2O lattices are described. The work done in preparation for these experiments is also illustrated. (INIS)

55103 (CISE-R-242) MOICANO-1 CODE FOR REACTIVITY AND TWO-GROUP FLUX CALCULATION OF A FOG-COOLED REACTOR, TAKING INTO ACCOUNT THE TRUE COOLANT DISTRIBUTION AND THE EQUILIBRIUM XENON POISONING. Bruschi, C.; Foresti, G.; Pierini, G.; Rubbia, S. (Centro Informazioni Studi Esperienze, Milan (Italy)). Nov 1967. 19p. INIS.

The Moicano-1 code is described, which provides a rapid tool for survey calculation of CIRENE-type reactors, once material composition and geometrical configuration have been given. The basic features of the core are: a two-group energy treatment of neutron flux, which is spatially used in the approximate mono-separable form; a simplified calculation of the coupling between thermal power and coolant density, which is strongly dependent on the axial coordinate along the power channel; the power level fixed by limiting the power in any point of the reactor core, which has never exceeded a fixed value (given as an input to the code). The FORTRAN IV version of the code exhibits a running time of about 4 minutes on the IBM-7040 computer. (INIS)

55104 (CISE-R-246) TERMO: DIGITAL CODE TO EVALUATE THE STEADY STATE PARAMETERS OF A CIRENE TYPE REACTOR. Goldaniga, G.; Grassi, G. P.; Muscettola, M.; Pedrocchi, F. (Centro Informazioni Studi Esperienze, Milan (Italy)). Oct 1967. 65p. (In Italian). INIS.

The digital program TERMO is presented which has been set up to compute the stationary thermohydraulic parameters of a CIRENE-type reactor, as depending on preassigned geometry, power distribution, feedwater, enthalpy and plant pressure. (INIS)

55105 (CISE-R-258) NEUTRON MEASUREMENTS AT ZERO POWER ON A CIRENE FUEL ELEMENT IN THE ESSOR REACTOR. Accinni, F.; Mangialajo, M.; Morandi, G.; Morselli, M. (Centro Informazioni Studi Esperienze, Milan (Italy)). Dec 1967. 13p. (In Italian). INIS.

Results on neutron physics measurements performed at zero power on a CIRENE fuel element in the ESSOR reactor—Ispra Center—are reported. These experiments were carried out, in the framework of CART plant achievement, in order to obtain an experimental examination of the flux situation to which the CIRENE element will be exposed during the irradiation program for which the CART plant was built. (INIS)

55106 (CISE-R-283) BUCKLING MEASUREMENTS IN ECO WITH FEW CIRENE FUEL ELEMENTS. Accinni, F.; Mangialajo, M.; Taddei, F. (Centro Informazioni Studi Esperienze, Milan (Italy)); Casini, G.; Hettinger, H.; Hohmann, H.; Paillon, M.; Toselli, F. (European Atomic Energy Community, Ispra (Italy). Joint Nuclear Research Center). Oct 1968. 21p. INIS.

Buckling measurements for UO_2/D_2O lattice configurations considered in the framework of the CIRENE project have been performed in the ECO reactor at Ispra. The experimental results and their analysis with homogeneous and heterogeneous (source-sink) methods are presented. (INIS)

55107 (CONF-720901-(Bks.1 and 2), pp 3-22) PHYSICS OF PWR REACTORS. Hellens, R. L. (Combustion Engineering, Inc., Windsor, Conn.). 1972.

From Meeting on new developments in reactor physics and shielding calculations; Kiamesha Lake, NY. (12 Sep 1972).

The physics of pressurized water reactors is reviewed. The main emphasis is placed on some observations drawn from core design and plant follow experience. The degree of success in explaining reactor physics data taken from four operating reactors that have had active measurement programs is discussed. 15 references. (auth)

55108 (CONF-720901-(Bks.1 and 2), pp 23-32) PHYSICS OF GAS COOLED REACTORS. Dahlberg, Richard C. (Gulf General Atomic Co., San Diego, Calif.). 1972.

From Meeting on new developments in reactor physics and shielding calculations; Kiamesha Lake, NY. (12 Sep 1972).

The temperature coefficient of the HTGR is composed of a strong negative Doppler coefficient and a positive moderator coefficient, the net effect being about -10×10^{-5}/°C at room temperature and -2×10^{-5}/°C at operating temperature. The positive moderator coefficient is a result of the absence of significant density coefficients and the nuclear characteristics of ^{233}U. In addition, selected fission products, principally ^{135}Xe, contribute positive components to the temperature coefficient. Current estimates of the value of the temperature coefficient in the HTGR are presented along with recent experimental data pertinent to the subject. 11 references. (auth)

55109 (CONF-720901-(Bks.1 and 2), pp 33-54) PHYSICS OF HIGH TEMPERATURE REACTORS AT THE COMMISSARIAT A L'ENERGIE ATOMIQUE. Laponche, B. (CEN, Saclay, France); Morier, F. 1972.

From Meeting on new developments in reactor physics and shielding calculations; Kiamesha Lake, NY. (12 Sep 1972).

The experimental program on High Temperature Reactor Physics achieved at the Commissariat à l'Energie Atomique is presented. The main studies are based on the low enriched uranium cycle and the tubular interacting fuel element. A first phase, already completed, deals with buckling, k_∞, and reaction rate measurements, in MARIUS, at room temperature: buckling was measured by flux mapping and progressive replacement on a 3.5% enriched UO_2 particulate fuel lattice; k_∞ was measured by the null reactivity method (PCTR technique) on a 1% enriched UO_2 particulate fuel lattice; spectrum indices and relative conversion ratio were also measured in both lattices. Data analysis was performed using the APOLLO code, as part of a general comparison between calculation and experiment covering a variety of uranium fuel types and the three main moderators. The conclusions of this study are also given. A second phase of experimentation (1973) deals with temperature coefficient measurement in CESAR (from 20 to 450°C) on the same lattice and oscillation measurement of UO_2-PuO_2 particulate samples. A third phase, part of a tri-partitate program (UKAEA-DRAGON Project-CEA) is based on irradiated fuel studies: chemical and isotopic analysis of fuels irradiated in the DRAGON Reactor and oscillation of irradiated samples. In cooperation with KFA Jülich, a critical experiment took place in CESAR in 1972. Fluxes, reaction rates and control rod worth were measured at room temperature in a central zone of the reactor, loaded with balls (3.5% enriched UO_2 particulate fuel). 16 references. (auth)

55110 (CONF-720901-(Bks.1 and 2), pp 55-67) SOME PROBLEMS IN THE PHYSICS OF HIGH TEMPERATURE REACTORS. Tyror, J. G.; Askew, J. R.; Johnstone, I. (Atomic Energy Establishment, Winfrith, Eng.). 1972.

From Meeting on new developments in reactor physics and shielding calculations; Kiamesha Lake, NY. (12 Sep 1972).

To meet the accuracies required for design calculations on HTR systems, rather detailed theoretical models have been developed and validated by comparison with the results of an extensive program of specially designed experiments. The general philosophy is illustrated for 2 problem areas: resonance capture in granular fuel and within-block power distribution. While some problems still remain in the areas so far studied, the confirmation of the reactivity time predictions at high irradiation is identified as the most significant outstanding question. 14 references. (auth)

55111 (CONF-720901-(Bks.1 and 2), pp 68-80) METHODS FOR THREE-DIMENSIONAL FUEL MANAGEMENT STUDIES ON HIGH TEMPERATURE REACTORS. Askew, J. R.; Anderson, D. W.; Pearson, K. G. (Atomic Energy Establishment, Winfrith, Eng.). 1972.

From Meeting on new developments in reactor physics and shielding calculations; Kiamesha Lake, NY. (12 Sep 1972).

Methods for studying fuel management in high temperature reactors have been developed in the U.K. by extending techniques already applied to the earlier AGR systems. The more severe modelling problems of the new system have demanded innovations to retain the desired accuracy, and improved coarse mesh finite difference algorithms, spectrum models for data condensation to few groups and novel iterative strategies for solving for control rod positions are described. Together they give a rapid 3-dimensional power solution of acceptable accuracy. (auth)

55112 (CONF-720901-(Bks.1 and 2), pp 114-40) PHYSICS OF BWR's. Crowther, R. L. 1972.

From Meeting on new developments in reactor physics and shielding calculations; Kiamesha Lake, NY. (12 Sep 1972).

The status of the physics of BWR's is summarized with emphasis on new developments and information gained from operating power reactors. 18 references. (auth)

55113 (CONF-720901-(Bks.1 and 2), pp 211-28) STUDIES OF METHODS FOR FAST NEUTRON MULTIGROUP CROSS SECTION GENERATION AND THEIR EFFECT UPON THE NEUTRONICS PROPERTIES OF LMFBR CRITICAL ASSEMBLIES. Stacey, W. M. Jr.; Henryson II, H.; Zolotar, B. A.; Hwang, R. N.; Toppel, B. J.; Stenberg, C. G.; Pennington, E. M. (Argonne National Lab., Ill.). 1972.

From Meeting on new developments in reactor physics and shielding calculations; Kiamesha Lake, NY. (12 Sep 1972).

The sensitivity of the integral neutronics properties of several

LMFBR critical assemblies to multigroup cross section generation methods is investigated with particular emphasis upon comparison of newly developed and routinely used methods. These studies include resonance algorithms, use of an intermediate group library, the effect of spatial nonuniformity, use of consistent B_1 or inconsistent P_1 formulations, and the use of different fine-group structures in the averaging of ultrafine group constants. 12 references. (auth)

55114 (CONF-720901-(Bks.1 and 2), pp 724-38) GE NUCLEAR DESIGN AND BENCHMARK CRITICAL EXPERIMENT PLAN FOR THE LMFBR DEMONSTRATION PLANT. Bailey, H. S.; Stewart, S. L. (General Electric Co., Sunnyvale, Calif.). 1972.

From Meeting on new developments in reactor physics and shielding calculations; Kiamesha Lake, NY. (12 Sep 1972).

The background planning related to the General Electric LMFBR Demonstration Plant design that provides the basis for the configuration and experiments planned for ZPPR-3 is presented. The specified experimental configurations and plans are summarized and some details of the experimental plan for each of the phases are presented. (auth)

55115 (CONF-720901-(Bks.1 and 2), pp 771-88) REVIEW OF FBR PHYSICS. Avery, R. (Argonne National Lab., Ill.). 1972.

From Meeting on new developments in reactor physics and shielding calculations; Kiamesha Lake, NY. (12 Sep 1972).

A qualitative review is made of FBR physics in which primary focus is put on the physics problems facing the fast reactor designer with particular emphasis on current outstanding problems. Some of the problems considered include the central worth discrepancy, Doppler and sodium coefficients, control rod effects, and long term effects related to the fuel cycle. Also discussed is the role and status of the critical experiment program in supplying a base of integral data on large dilute plutonium systems as well as providing specific information on the above items and others. The role and status of differential cross section knowledge is discussed relative to fast reactor needs with emphasis being given to the significant uncertainties that still exist in some of the primary fissile and fertile isotope cross sections. The status of some of the major code development activities in the areas of cross section processing, neutron diffusion, and space-dependent kinetics is discussed relative to fast reactor design needs. (auth)

55116 (CONF-720901-(Bks.1 and 2), pp 789-808) DEMONSTRATION REACTOR BENCHMARK PROGRAM. Davey, W. G. 1972.

From Meeting on new developments in reactor physics and shielding calculations; Kiamesha Lake, NY. (12 Sep 1972).

The critical studies comprising the benchmark program for the Liquid Metal Fast Breeder Reactor demonstration plant are described. The configurations examined and measurements performed on the Zero Power Plutonium Reactor and the ZPR-6 assemblies are discussed. (H.D.R.)

55117 (CONF-720901-(Bks.1 and 2), pp 809-21) SPATIALLY DEPENDENT BENCHMARK PARAMETERS IN THE INITIAL DEMONSTRATION PLANT CRITICAL ASSEMBLY. Amundson, P. I.; Davey, W. G.; Palmer, R. G.; (and others). 1972.

From Meeting on new developments in reactor physics and shielding calculations; Kiamesha Lake, NY. (12 Sep 1972).

The features of the Zero Power Plutonium Reactor Assembly 2 are described. The use of this assembly in benchmark measurements of Liquid Metal Fast Breeder Reactor physics parameters is discussed. (H.D.R.)

55118 (CONF-720901-(Bks.1 and 2), pp 822-38) REACTOR PHYSICS AND FAST POWER BREEDERS: MASURCA CORE R-Z PROGRAM. Barre, J. Y.; Boyer, J.; Mougniot, J. C.; Sicard, B. 1972.

From Meeting on new developments in reactor physics and shielding calculations; Kiamesha Lake, NY. (12 Sep 1972).

The directions of the current CEA program of fast reactor physics are described, focusing on the MASURCA fast critical facility studies. These experiments concern mainly relative variation versus enrichment of characteristics of lattices fuelled either with plutonium (cores Z) or uranium (cores R) with the same diluent. The major results obtained for asymptotic mode neutron balance parameters (material buckling and spectral indices) and for engineering parameters (power distributions, blankets and control rods) are compared with an analysis made using CADARACHE reference data. Conclusions drawn from this analysis are then applied to the main PHENIX predicted parameters. 9 references. (auth)

55119 (CONF-720901-(Bks.1 and 2), pp 888-904) EXPERIMENTAL STUDY OF BURN-UP IN FAST BREEDER REACTORS. Bouchard, J. (CEN, Fontenay-aux-Roses, France); Chavardes, D.; Darrouzet, M.; Gourdon, J.; Robin, M. 1972.

From Meeting on new developments in reactor physics and shielding calculations; Kiamesha Lake, NY. (12 Sep 1972).

Fuel burnup studies using the RAPSODIE reactor are described. These studies include: (1) Determination of burnup. (2) Changes in the core composition, or more precisely in the fuel composition in the part of the core where the neutron distribution is in equilibrium. (3) Changes in the breeding blanket composition. (H.D.R.)

55120 (CONF-720901-(Bks.1 and 2), pp 905-27) EBR-II IRRADIATION PHYSICS. Meneghetti, D.; Loewenstein, W. B. (Argonne National Lab., Ill.). 1972.

From Meeting on new developments in reactor physics and shielding calculations; Kiamesha Lake, NY. (12 Sep 1972).

The use of EBR-II as a fast fuel irradiation facility illustrates its versatility for physics measurements. Its potentials are unique relative to those of the zero-power criticals especially in those areas where at-power conditions are important. For example, power reactivity components, gamma deposition, deep penetration of neutrons and gammas, feedback components, burnup, fission-product productions, and interaction problems of neutronics, gamma, coolant flow, and heat transfer. 35 references. (auth)

55121 (CONF-720901-(Bks.1 and 2), pp 928-39) SIGNIFICANCE OF INTEGRAL PARAMETERS IN THE DESIGN AND PERFORMANCE OF FAST BREEDER REACTORS. Greebler, P.; Hutchins, B. A. 1972.

From Meeting on new developments in reactor physics and shielding calculations; Kiamesha Lake, NY. (12 Sep 1972).

The use of integral parameters from critical experiments in support of fast reactor design and operation is discussed. The incentives for additional integral experiments is examined. (H.D.R.)

55122 (CONF-720901-(Bks.1 and 2), pp 959-72) PROTON-RECOIL PROPORTIONAL COUNTER SPECTROMETRY FOR REACTOR SPECTRUM MEASUREMENTS. Verbinski, V. V.; Young, J. C.; Neill, J. M.; Gionvannini, R.; Houston, D. H. (Gulf Radiation Tech., San Diego, Calif.). 1972.

From Meeting on new developments in reactor physics and shielding calculations; Kiamesha Lake, NY. (12 Sep 1972).

The factors that limit the accuracy of a proton-recoil proportional counter in measuring neutron spectra in reactors are discussed in light of detector response measurements and associated calibrations, reactor spectrum measurements with two different counter geometries, unscrambling experience with several different approaches, and comparisons with calculations and time-of-flight measurements. A critical analysis of proton-recoil spectrometry is attempted in that the approximations and omissions of each method are pointed out and improvements in both method and counter design suggested. 16 references. (auth)

55123 (CONF-720901-(Bks.1 and 2), pp 986-1005) SEFOR: VERIFICATION OF THE DOPPLER TRANSIENT SHUTDOWN CAPABILITY OF LMFBR's. Freeman, D. D.; Greebler, P.; Noble, L. D.; Pflasterer, G. R. (General Electric Co., Sunnyvale, Calif.). 1972.

From Meeting on new developments in reactor physics and shielding calculations; Kiamesha Lake, NY. (12 Sep 1972).

The SEFOR experimental program was undertaken to demonstrate and to measure the Doppler reactivity feedback in neutron spectra and at fuel temperatures and crystalline states representative of an operating LMFBR. Tests involving both static power reactivity measurements and rapid super-prompt-critical reactivity insertion from power (up to 1.3$ in 0.1 sec.) gave good agreement for the Doppler constant (Tdk/dT) in each of two cores. The first core contained six volume per cent BeO and gave a Doppler constant, Tdk/dT of -.0081. In the second core, in which the BeO was replaced by stainless steel to harden the neutron spectrum, a Doppler constant, Tdk/dT, of -.0060 was obtained. The overall experimental uncertainty on Tdk/dT is estimated to be ±10%, exclusive of uncertainties in delayed neutron parameters. Normalization of Doppler calculations to the SEFOR results can provide significant reductions in the uncertainty in transient power and energy calculations of interest in LMFBR accident analysis. A major achievement of the SEFOR experimental program was the successful completion of the super prompt transient tests. They give convincing confirmation of the soundness of the Doppler theory being applied to LMFBR's and demonstrate the inherent safety and stability of this type of reactor. In addition, the good agreement between pre-experiment analysis and experimental results points up the predictable transient neutronics behavior of oxide fueled LMFBR's. 11 references. (auth)

55124 (CONF-720901--(Bks.1 and 2), pp 1016-32) PULSED-ACTIVATION TECHNIQUES FOR THE MEASUREMENT OF DOPPLER EFFECTS. Foell, W. K.; Russell, G. J.; Lucoff, D. M.; Bhattacharyya, S. K. (Univ. of Wisconsin, Madison). 1972.

From Meeting on new developments in reactor physics and shielding calculations; Kiamesha Lake, NY. (12 Sep 1972).

The pulsed activation Doppler (PAD) technique offers an experimental approach appropriate for the measurement of Doppler effects at high temperatures. The experimental methods, data handling techniques, and methods of interpretation presented gave satisfactory results when applied to uranium metal and UO_2 pellets at low and medium energy depositions, but appear to require some improvements for very high energy depositions. Specifically, it is necessary to determine the relative thermal flux depression more accurately in pellets of high enrichment. A feasibility study was carried out for the extension of the PAD technique to fast spectra. SEFOR was used as the model spectra for this study. The SEFOR transient time-shape function was used in computer calculations to obtain the time-dependent energy deposition and the resulting time-dependent temperature rise for PAD samples. At these temperatures and at each time step, self-shielded cross sections were calculated and then integrated with the fluence to yield a Doppler ratio. The results indicate that high effective temperatures could be achieved in PAD measurements with pellets having enrichments slightly higher than nominal LMFBR values. 17 references. (auth)

55125 (CONF-720901--(Bks.1 and 2), pp 1033-47) BENCHMARK TESTING OF NUCLEAR DATA FOR FAST REACTORS. Alter, Harry (Atomics International, Canoga Park, Calif.). 1972.

From Meeting on new developments in reactor physics and shielding calculations; Kiamesha Lake, NY. (12 Sep 1972).

Integral parameters for a series of fast reactor benchmark assemblies, covering a wide range of energy spectra, were calculated with the reference cross section set ENDF/B-3. Multigroup constants relative to each assembly were generated and used in S_n transport and/or diffusion theory calculations to obtain the parameters. The calculated parameters include k_{eff}, spectral indices (activation ratios), and central reactivity worths. Results of the several calculations indicate a significant improvement in the cross section data of the version 3 reference set over that contained in ENDF/B-2. (auth)

55126 (KFK-1577) ANISOTROPIC DIFFUSION IN GAS COOLED FAST BREEDER REACTOR. Eisemann, E. (Kernforschungszentrum, Karlsruhe (West Germany). Institut fuer Neutronenphysik und Reaktortechnik). Mar 1972. 146p. (In German). Dep. NTIS (U. S. Sales Only).

The calculation of anisotropic diffusion effects (streaming effects) in gas cooled fast reactor lattices is presented. For this purpose, expressions have been derived for the components of a homogenized direction dependent cell diffusion coefficient. This was done in a multi-group formalism taking into account the anisotropy of the elastic scattering cross sections up to the first moment. Expressions for the components of the direction dependent diffusion coefficient have been developed which can be evaluated numerically. To demonstrate the influence of this diffusion coefficient calculations have been performed to determine the effective multiplication factor and the criticality change due to coolant variations for certain reactor concepts. 33 references. (auth)

55127 (KFK-1579) REST: PROGRAM FOR CALCULATION OF FISSION PRODUCT ACTIVITY AND DECAY CONSTANT AFTER VARIABLE REACTOR HISTORY IN TWO COUPLED SYSTEMS WITH RESPECT TO FISSION PRODUCT EMISSION. Waibel, E. (Kernforschungszentrum, Karlsruhe (West Germany). Institut fuer Reaktorentwicklung). Apr 1972. 38p. (In German). Dep. NTIS (U. S. Sales Only).

The FORTRAN programs REST 1, REST 2, and REST 3 were developed for the calculation of the fission product decay heat source within a nuclear reactor. REST 3 considers a distribution of the heat source by calculating fission product escape out of the fuel, as might be expected by accidental overheating of the core. The time dependency of the heat source within and outside the fuel is shown. A description and a user's guide for the programs is given. A BWR was used as a model for the calculations. 12 references. (auth)

55128 INSTALLATION FOR OBSERVING THE POSITION OF A STRUCTURE INSIDE A NUCLEAR REACTOR. Debergh, Philippe; Lagrange, Maurice (to Commissariat a l'Energie Atomique). French Patent 2,091,902. 21 Jan 1972. Filed 10 Apr 1970. (In French).

An installation for positioning the core-supporting structure of a reactor (e.g. sodium-cooled fast reactor) is presented. The installation consists of a closed tube containing an appropriately illuminated sighting system at one of its ends and a window at the other end. This tube, which is supported by the structure to be positioned, is elastically held in a fixed outer sheathing; an observation tube penetrates the sheathing from the other side; this tube is provided with a mirror system and a viewing telescope at its upper end. Any vertical displacement of the supporting structure is transmitted to the closed tube and any lateral displacement shifts the position of the tube in the sheathing. Both types of displacement can be observed through the telescope system. (France)

55129 FAST BREEDER REACTOR. Spenke, H. (to Siemens AG). German Patent 1,614,404. 17 Feb 1972. (In German).

A description is given of a technical way to decrease the coolant void coefficient by an appropriate design of the reactor core of steam-cooled or liquid-metal-cooled fast breeder reactors. The amount of fissionable fuel is decreasing within the cylindrically shaped reactor core in radial direction, as related to the axis of symmetry of the core. This decrease may be realized either steadily or in several stages. (GF)

55130 LIGHT-WATER BREEDER REACTOR. Beaudoin, Benoit R.; Cohen, Joseph D.; Jones, David H.; Marier, Lester J. Jr.; Raab, Harry F. (to United States Atomic Energy Commission). U. S. Patent 3,671,392. 20 Jun 1972. Filed 15 Mar 1971.

Described is a light-water-moderated and -cooled nuclear breeder reactor of the seed—blanket type characterized by core modules comprising loosely packed blanket zones enriched with fissile fuel and axial zoning in the seed and blanket regions within each core module. Reactivity control over lifetime is achieved by axial displacement of movable seed zones without the use of poison rods in the embodiment illustrated. The seed is further characterized by a hydrogen-to-uranium-233 atom ratio in the range 10 to 200 and a uranium-233-to-thorium-232 atom ratio ranging from 0.012 to 0.200. The seed occupies from 10 to 35 percent of the core volume in the form of one or more individual islands or annuli. (Official Gazette)

55131 REACTOR WITH SPHERICAL FUEL ELEMENTS. Ritz, H. L. (to Kernforschungszentrum). German Patent 1,302,274. 10 Feb 1972. (In German).

A description is given of configurations of spherical fuel elements, arranged in regular and uniform packings in such a manner that they will form an approximately spherical core. The purpose of this arrangement is to improve the coolant circulation in order to optimize the heat transfer and to obtain a nearly uniform temperature at all fuel elements. (GF)

Control and Instrumentation

55132 (ANL/EBR-63) DATA-PROCESSING SYSTEM FOR INSTRUMENT MAINTENANCE AND CALIBRATION AT EBR-II. Moriarty, K. J.; Ringquist, J. M. (Argonne National Lab., Ill. Argonne National Lab., Idaho Falls, Idaho). Jun 1972. Contract W-31-109-eng-38. 51p. Dep. NTIS.

Early in the operation of EBR-II, it was recognized that a computer program was required for the periodic calibration and maintenance of the more than 1600 instruments in service. Computer Program No. I, set up in 1964, evolved into Computer Program No. II by addition of updated scheduling, history cards, and a new computer to execute the program. Computer Program II, combined with the required procedures, has been operative for about one year. The operation of Computer Program II is described. (auth)

55133 (CISE-R-268) EXPERIMENTAL RESULTS ON THE OPERATION OF THE REACTIVITY FAST CONTROL SYSTEM OF THE CIRENE REACTOR. Marcandalli, R.; Possa, G. (Centro Informazioni Studi Esperienze, Milan (Italy)). May 1968. 43p. (In Italian). INIS.

The reactivity fast control system of the CIRENE reactor is envisioned to be accomplished by fluid rods: reactivity is varied through changes of a two-phase mixture of gas and poisoned light water flowing in separate tubes in the core. An out-of-pile experimental loop has been built at CISE for the hydraulic and dynamic tests. The results of the first complete set of measurements are presented and found to be in agreement with theoretical predictions. Minor modifications to the system are suggested. The hydraulic and dynamic performances match design specifications. (INIS)

55134 (CONF-720901--(Bks.1 and 2), pp 579-98) BORON AND TANTALUM CONTROL ROD STUDIES AND ABSOLUTE GAMMA RAY ABSORBED DOSES IN A LMFBR CRITICAL. Carpenter, S. G.; Simons, G. G.; Olson, A. P.; Goin, R. W.; Plummer, J. P. 1972.

From Meeting on new developments in reactor physics and shielding calculations; Kiamesha Lake, NY. (12 Sep 1972).

A set of measurements was taken on a typical LMFBR mockup (ZPPR Core 2) which provides data against which the components of control rod calculations can be compared for both B and Ta. The small sample control materials are in disagreement with the calculations in about the same amount as the fuel materials. The mockup rods calculations are actually closer to the measurement, which may indicate additional problems. The axial and radial distributions are well calculated. These distributions are not strong functions of rod size or poison material. The interactions between two rods separated by a typical distance are not large and are poorly calculated with diffusion theory. Absorbed gamma radiation dose distributions were measured with ^{7}LiF thermoluminescent dosimeters throughout Core 2. Deviations between calculation and experiment were found to exceed ±10% only at the outer limits of the reactor, where the absolute dose had fallen at least 2 orders of magnitude. For the central mockup control rod cases, the gamma radiation dose in B_4C and Ta was well calculated. 9 references. (auth)

55135 (DUN-SA-169) REDUCING THE EFFECT OF GROUNDS ON CRITICAL REACTOR CONTROL CIRCUITS. Neumayer, E. C. (Douglas United Nuclear, Inc., Richland, Wash.). 29 Jul 1971. 18p. Dep. NTIS.

The sensitivity of the ground detector may be increased as can the input resistance by increasing the resistance of the series resistors and selecting the proper meter sensitivity for them. Provisions for external annunciation and alarm may be utilized by using a meter-relay movement with adjustable alarm contacts. While the discussion deals with dc circuits, the principles can be applied to ac circuits also. (auth)

55136 (DUN-SA-186) APPLICATION OF COMPUTERS TO CONTROL AND MONITORING OF NUCLEAR REACTORS. Worster, L. D. (Douglas United Nuclear, Inc., Richland, Wash.). [nd]. 10p. Dep. NTIS.

A multi-channel system designed to satisfy the IEEE 279 Criteria For Nuclear Power Plant Protective Systems demonstrates how minicomputers dedicated to specific functions can satisfy the failure criteria and provide multiple data processing and control functions. The comprehensive data analysis capability of computers provides potential for power system performance improvement and cost reduction through application of computers in control and monitoring systems. (auth)

55137 (JAERI-Memo-3893) FLUX DISTRIBUTION MEASUREMENT NEAR STRONG ABSORBER USING VISTA METHOD. Takeuchi, Eiji; Takeda, Renzo; Fukumura, Nobuo; Sakata, Hajime (Japan Atomic Energy Research Inst., Tokyo). Feb 1970. (In Japanese). NTIS (U. S. Sales Only).

Calculations on a cruciform control rod have been made as a part of the JP-II final design studies. Experiments were carried out using VISTA method. This method is an experimental physics technique, and by enlarging the system dimension, makes the phenomena easy to be observed. In the VISTA-SHE experiments, a boral absorber slab is substituted for the cruciformed control rod. The space dependency of the flux distribution, fine flux profile very near the absorber and the energy dependency of the neutron spectra were measured. Mn, Au, In and depleted uranium foils were activated with and without Cd cover. (auth)

55138 (ORNL-TM-729(Pt.2B)) MSRE DESIGN AND OPERATIONS REPORT. PART IIB. NUCLEAR AND PROCESS INSTRUMENTATION. Moore, R. L. (Oak Ridge National Lab., Tenn.). Sep 1972. Contract W-7405-eng-26. 439p. Dep. NTIS.

A detailed design is presented for the MSRE control systems, operating instrumentation, safety instrumentation, and circuitry. Included are layouts and schematic diagrams. (J.M.J.)

Containment Systems, Waste Processing, and Radiation Protection

Refer also to abstract 53061.

55139 (ANL-7911(Suppl.1)) COMPARISON OF A TWO-DIMENSIONAL HYDRODYNAMICS CODE (REXCO) TO EXCURSION EXPERIMENTS FOR FAST REACTOR CONTAINMENT. Ash, J. E.; Chang, Y. W.; Julke, R. T. (Argonne National Lab., Ill.). Jul 1972. Contract W-31-109-eng-38. 18p. Dep. NTIS.

The Reactor Excursion Containment Code System (REXCO) is a tool that was developed to predict the effects of excursions originating at the core upon the components and on the containment system of Liquid Metal Fast Breeder Reactors. The codes include hydrodynamic and inelastic material behavior depending on the magnitude of the excursion treated. The physical phenomena computed by the codes involve the shock wave, the sodium momentum, and the early stages of the gas bubble. Experimental excursion data are compared with REXCO computations, with emphasis upon the deformations produced by the pressure loads. The results of these comparisons verify the capability of the REXCO Code System to predict the response of containment structures and of the primary system components to the excursion pressure waves. Computations of the deformation of the containment vessel wall caused by pressure loads generated by high-explosive charges are compared with the experiments. The computation of deformations in the upper vessel region resulting from coolant slug impact is verified by comparison with the SL-1 accident data. 11 references. (auth)

55140 (CONF-720901-(Bks.1 and 2), pp 295-315) MEASUREMENT AND EVALUATION OF CROSS SECTIONS. Orphan, V. J. (Gulf Radiation Tech., San Diego, Calif.). 1972.

From Meeting on new developments in reactor physics and shielding calculations; Kiamesha Lake, NY. (12 Sep 1972).

The following types of neutron interaction cross sections which are important in reactor shielding are discussed: total, scattering (particularly angular distributions), capture and the photon energy spectra from nonelastic reactions. Examples are discussed for each of these cross-section types which typify the progress made in the development of new cross-section measurement techniques. Also, a few examples are given of advances made in the theoretical methods used in evaluations to predict the cross sections in the absence of experimental data. 40 references. (auth)

55141 (CONF-720901-(Bks.1 and 2), pp 316-24) DEVELOPMENT OF ENDF/B SHIELDING DATA PROCESSING CODES, AND INTEGRAL TESTS. LaBauve, R. J.; Seamon, R. E.; Weisbin, C. R.; Harris, D. R.; Muir, D. W. (Los Alamos Scientific Lab., N. Mex.). 1972.

From Meeting on new developments in reactor physics and shielding calculations; Kiamesha Lake, NY. (12 Sep 1972).

The national Evaluated Nuclear Data File (ENDF/B) now contains twelve materials important for shielding applications; these evaluations include data for neutron-induced photon production. During fiscal year 1973, photon production data for at least ten more important materials will become available, and six new photon production evaluations will be undertaken. Existing processing codes are being extended and improved, and new codes are being written to fully exploit the extensive data included in the ENDF/B. A comprehensive data testing program under the direction of the Cross Section Evaluation Working Group (CSEWG) is under way to uncover data deficiencies and suggest areas for improvement. Thus the ENDF/B is rapidly becoming the principal and most up-to-date source of data for shielding calculations. 29 references. (auth)

55142 (CONF-720901-(Bks.1 and 2), pp 418-30) ORNL SODIUM BENCHMARK EXPERIMENT. Maerker, R. E.; Muckenthaler, F. J.; Clifford, C. E. (Oak Ridge National Lab., Tenn.). 1972.

From Meeting on new developments in reactor physics and shielding calculations; Kiamesha Lake, NY. (12 Sep 1972).

The description of an experiment performed at the Tower Shielding Facility is presented which serves as a benchmark for deep neutron penetration through up to 15 ft of sodium. Results of calculations of the experiment are also described, using the MORSE multigroup Monte Carlo code and a preliminary version of the ENDF/B-III cross-section set for sodium. Comparison of the calculations with experiment indicate that the total neutron leakage above thermal energies penetrating 15 ft of sodium can be calculated to within 30% and neutrons penetrating up to 10 ft of sodium to within 10%. 12 references. (auth)

55143 (CONF-720901-(Bks.1 and 2), pp 459-70) DIFFUSION THEORY ANALYSES FOR FAST REACTOR SHIELD DESIGN. Boulette, E. T.; Marr, D. R. (Hanford Engineering Development Lab., Richland, Wash.). 1972.

From Meeting on new developments in reactor physics and shielding calculations; Kiamesha Lake, NY. (12 Sep 1972).

Comparisons of diffusion theory analyses with transport theory results indicate that diffusion theory adequately calculates integral quantities upon which fast reactor shield design criteria are based. Multi-dimensional analyses of fast reactor shield experiments support this conclusion and also demonstrate that the neutron cross section library may be adequately represented in fewer than 50 energy groups. 20 references. (auth)

55144 (CONF-720901-(Bks.1 and 2), pp 480-98) FAST REACTOR SHIELDING METHODS DEVELOPMENT. Mynatt, F. R.; Gritzner, M. L. (Oak Ridge National Lab., Tenn.). 1972.

From Meeting on new developments in reactor physics and shielding calculations; Kiamesha Lake, NY. (12 Sep 1972).

The elements of a shielding program based on a fundamental approach are discussed with a brief evaluation of the status of the technology. A procedure is presented for utilizing the best features of Monte Carlo, discrete ordinates, and diffusion theory in coupled calculations providing good accuracy at minimum expense. As an example, results are presented from a four-step coupled two-dimensional discrete ordinates calculation for determination of the neutron and secondary gamma-ray dose rates in the FTR head compartment. An assessment of computational methods development plans is presented. 39 references. (auth)

55145 (GEAP-13822-1) LMFBR SHIELDING DESIGN EXPERIMENTS AND METHODS EVALUATION. First Quarterly Progress Report, January–March 1972. (General Electric Co., Sunnyvale, Calif. Breeder Reactor Dept.). Apr 1972. Contract AT(04-3)-189. 26p. Dep. NTIS.

Both experimental and analytical work on axial and radial shields are being conducted, with the experimental part being performed at the ORNL Tower Shielding Facility. Activities and technical progress for the period January through March 1972 are reported. The major topics include program definition and scheduling, test assembly design and fabrication, analytical studies, and quality assurance. (auth)

55146 COLLECTION OF RADIOACTIVE IODINE BY FILTERING SYSTEM. Murata, T. (Hitachi Ltd., Tokyo). Kuki Seijo; 8: No. 7, 49-53(Mar 1971). (In Japanese).

Filtering system consisting of a charcoal filter to collect gaseous radioactive iodine and air filters to collect radioactive iodine particles is provided in emergency off-gas system of reactors. The air filters usually include a prefilter and a high efficiency air filter, and sometimes include further silver-plated copper mesh to reduce temperature rise of the charcoal filter due to decay heat of the radioactive iodine and demister. The iodine collection performance of the filtering system as a whole is described on the basis of test results in foreign countries and those obtained by experimentation. It became evident that iodine introduced into the filtering system is mostly collected by the air filters installed in front of the charcoal filter. This indicates that most of the iodine in the passing gas exists in the form of particles. There is a fairly large deviation in individual filter efficiency, reasons for which are: existence of organic iodine, possible change of its concentration, and incompleteness of the sampling system to measure efficiency. The high efficiency filter has good collection efficiency of the iodine at low temperature, for instance 60% at 25°C compared with about 5% at and above 70°C. This is mainly because of formation of waterdrops at the lower temperature, which helps the iodine collection with the high efficiency air filter. This is ascertained also by the fact that when the relative humidity is not less than 80%, the filter efficiency reaches 60%. Thus, the integrated filtering system efficiency for collecting the radioactive iodine is over 99%, and the filtering system seems to be sufficiently effective. (Japan)

Coolant System

Refer also to abstract 53305.

55147 (AI-AEC-Memo-12736) HNPF RETIREMENT: DISPOSITION OF SODIUM. Boardman, T. J.; Paulett, T. A. (Atomics International, Canoga Park, Calif.). 30 Sep 1968. Contract AT(04-3)-701. 137p. Dep. NTIS.

A detailed description is given of the planning, procedures, and actual removal of the sodium from the dismantled Hallam Power Reactor. The dismantling, draining, decontamination, and disposition of piping, pumps, tanks, and other components are discussed. Procedures for heating, cleaning, and pumping of the sodium are included. 10 references. (J.M.J.)

55148 (CISE-R-270) STEADY STATE AND TRANSIENT MEASUREMENTS ON A SCALED-DOWN MODEL OF A POWER CHANNEL OF THE CIRENE REACTOR PROTOTYPE. Peterlongo, G.; Possa, G. (Centro Informazioni Studi Esperienze, Milan (Italy)); Valli, G. (Comitato Nazionale per l'Energia Nucleare, Rome (Italy)). Jun 1968. 41p. (In Italian). INIS.

A scaled down model (1 : 14) of a single power channel of the CIRENE prototype reactor, including a partial simulation of the steam drum, steam pipes and turbine, has been built and tested. A number of steady states of the system have been investigated, with the main purpose of defining stable paths for the start-up procedure. Measurements have been performed also for the study of coolant pressure dynamics with the following transient inputs: step variation of the heat input to the power channel, step variation of the stem position of the turbine valve, sinusoidal variation of the input of heat to the power channel. (INIS)

55149 (CONF-710548) SPECIALISTS' MEETING ON SODIUM-WATER REACTIONS SPONSORED BY THE INTERNATIONAL ATOMIC ENERGY AGENCY, INTERNATIONAL WORKING GROUP ON FAST REACTORS, 18–21 MAY 1971, MELEKESS, USSR. Summary Report and Papers. (International Atomic Energy Agency, Vienna (Austria)). Jul 1972. 263p. Dep. NTIS.

Twelve papers were presented and are abstracted separately. (J.M.J.)

For abstracts of individual papers see: 55150–55161.

55150 (CONF-710548–, pp 1-16) PRESENTATION MADE TO MEETING OF SODIUM-WATER REACTION SPECIALISTS. Lions, N.; Lacroix, A.; Schwab, B.; Lafon, A.; Trimouille, C. (Atomic Energy Commission, Cadarache, France). Jul 1972.

From Specialists' meeting on sodium–water reactions; Melekess, USSR (18 May 1971).

Tests on the Phenix Reactor steam generator confirmed the possibility of limiting the consequences of large-scale sodium–water reactions to insignificant damage to the steam generator. Rupture of one tube does not necessarily rupture adjacent tubes. Calculational methods were verified experimentally, so that simulation studies can be made with confidence. The safety of the Phenix steam generator was established. (J.M.J.)

55151 (CONF-710548–, pp 17-38) LARGE LEAK TESTS IN A MODEL OF A STRAIGHT-TUBE STEAM GENERATOR. Dumm, K. (INTERATOM, Bensberg, Ger.). Jul 1972.

From Specialists' meeting on sodium–water reactions; Melekess, USSR (18 May 1971).

The text of the paper is not given. Captions for slides are presented, followed by the slides, which contain schematics of the equipment tested, comparative data between the test model and the SNR design equipment, test parameters, and curves of measured results. (J.M.J.)

55152 (CONF-710548–, pp 39-56) EXPERIMENTAL STUDY OF THE INTERACTION OF WATER WITH SODIUM DURING SMALL LEAKS OF WATER INTO SODIUM. Andreev, P. A.; Borishanskii, V. M.; Zhokhov, K. A.; Belen'kii, M. Ya. Jul 1972.

From Specialists' meeting on sodium–water reactions; Melekess, USSR (18 May 1971).

The results of an experimental study of processes arising from a small leakage of water into sodium are presented. At low flow rates of liquid metal coolant (up to 1.5 m/sec) increased temperatures and pressures were observed in the region of the leak; the actual values depended on the magnitude of the leak. At small leak rates (10–100 g/hr) no increase in temperature or pressure was detected. Besides an increase in the temperature and pressure of the sodium coolant, the interaction of sodium with water gave rise to an environment which was corrosive towards the steam-generator pipework. The present work studies the possibility of corrosion damage to pipes in the case of an extremely small leakage of water into sodium (15–100 g/hr). The effects on the corrosion rate, of the magnitude of the leak, the location of the pipework relative to microcracks and the nature of the pipe material, were noted. 5 references. (auth)

55153 (CONF-710548–, pp 57-104) STUDY OF Na AND H_2O INTERACTION IN A ONE-MEGAWATT MODULAR STEAM GENERATOR. Kul'pin, B. V.; Mazanov, A. S.; Masnyi, V. F.; Gavrilin, A. I. (Scientific Research Inst. of Atomic Reactors, Melekess, USSR). Jul 1972.

From Specialists' meeting on sodium–water reactions; Melekess, USSR (18 May 1971).

An experimental study of a modular sodium–water steam generator of Czechoslovak design is described. A description of the test stand, data on the thermal balance of the steam generator in different regimes, and the design of a device to produce microleaks of water into sodium to simulate dissolution of the tube bundle of the steam generator and an emergency system for determining the time of the appearance of the leak and preventing breakdown of the steam generator are presented. Results of metallographic analysis of the tube bundle material in the breakdown zone and at a distance from it are presented. 7 references. (auth)

55154 (CONF-710548–, pp 105-28) METHODS OF INDICATION, OPERATION OF A STEAM GENERATOR AND SECONDARY CIRCUIT IN THE CASE OF SLIGHT LEAKAGE OF WATER INTO SODIUM. Kozlov, F. A. Jul 1972.

From Specialists' meeting on sodium–water reactions; Melekess, USSR (18 May 1971).

A study of the problems associated with the ingress of water to sodium through boiler leakage is presented. Expressions are adduced for the solubilities of hydrogen, oxygen, products of the interaction of water and sodium, and sodium hydroxide in sodium; the rate constants have been determined for the reactions of sodium with hydrogen and with sodium hydroxide over the temperature range 300–450°C; the results of corrosion tests of a Cr–Mo steel in the vicinity of the leak are presented; the development of a system for monitoring the leakage of water into sodium is described together with preliminary experimental results of an acoustic method for detecting a leak; problems of purifying sodium from its reaction products with water are discussed. 5 references. (auth)

55155 (CONF-710548–, pp 129-54) OUTLINE OF PNC'S ACTIVITIES IN THE FIELD OF SODIUM-WATER REACTION. Hori, Masao; Sato, Minoru; Nei, Hiromichi; Tanaka, Toshikazu; Hishida, Makoto Jul 1972.

From Specialists' meeting on sodium–water reactions; Melekess, USSR (18 May 1971).

The Japanese sodium–water reaction project (SWAT), carried out to develop safe, reliable steam generators for the Monju fast breeder reactor, is described. The test equipment and the computer codes used are listed. Tests carried out are described. Schematic diagrams of equipment and test parameters are presented. 12 references. (J.M.J.)

55156 (CONF-710548–, pp 155-70) DETECTION OF SMALL-LEAK SODIUM-WATER REACTION IN THE PROTOTYPE LMFBR STEAM GENERATOR BY IN-SODIUM TYPE HYDROGEN DETECTOR. Ikemoto, Ichiro; Hori, Masao. Jul 1972.

From Specialists' meeting on sodium–water reactions; Melekess, USSR (18 May 1971).

The large-leak sodium–water reaction accident in steam generator may occur following the "wastage" of tubes because of a small leak. The possibility of the accident propagation and the required sensitivity of an in-sodium hydrogen detector are examined in the case of the prototype LMFBR steam generator. The hydrogen detector is found out to be highly effective for the detection of very small leaks (5×10^{-3} lb/sec), and the required sensitivity here is less than 0.1 ppm hydrogen concentration. In the very severe case, however, development of detectors which have no delay time, such as an acoustic detector, will be required. (auth)

55157 (CONF-710548–, pp 171-86) ANALYSES OF THE SODIUM-WATER REACTION PRESSURE AND ITS PROPAGATION IN THE SODIUM SYSTEM. Sakano, Kosuke; Tanaka, Yoshihisa; Mochizuki, Hirozi (Kawasaki Heavy Industries, Ltd., Tokyo). Jul 1972.

From Specialists' meeting on sodium–water reactions; Melekess, USSR (18 May 1971).

One dimensional sodium–water reaction code SOWACS that assumes sodium and water to be compressible in order to calculate the propagation of pressure wave was developed and tested. The initial peak pressure calculated at the reaction point was different from the experimental one. In order to improve the accuracy of the calculation of the peak pressure at the reaction point, it will be better to change the model of sodium flow at the beginning of the reaction to the spherical model. Comparing with the pressure (126 ata) at the faulted evaporator, the pressure at the adjacent components and piping becomes lower during it propagates in the secondary sodium system, for example 47 ata at the adjacent evaporators, 25 ata at the super heaters and reheaters and 18 ata at the piping. (auth)

55158 (CONF-710548–, pp 187-205) SOME NOTES ON SODIUM/WATER REACTION WORK. Bray, J. A. (Dounreay Experimental Reactor Establishment, Thurso, Scotland). Jul 1972.

From Specialists' meeting on sodium–water reactions; Melekess, USSR (18 May 1971).

The Super–NOAH rig, for studying large scale sodium–water reactions, is described. Parameters of the experiments are given. Reaction products, which settled to the bottom of the reaction vessel, are described. The design for the Prototype Fast Reactor heat exchanger is presented schematically. (J.M.J.)

55159 (CONF-710548–, pp 206-12) REQUIREMENTS FOR STEAM GENERATOR DESIGN AND SYSTEMS TO ENSURE SAFETY IN THE CASE OF FAILURES IN THE TUBES OF HEAT EXCHANGE SURFACES. Titov, V. F.; Bogdanovich, P. N.; Poplavskii, V. M.; Bagdasarov, Yu. E. Jul 1972.

From Specialists' meeting on sodium–water reactions; Melekess, USSR (18 May 1971).

Experience indicates that the proposed designs ensure the necessary degree of control and safety for sodium steam generators on failure of the heat exchange tubes. However, the safety systems adopted for the designs in question do not eliminate the need for further investigation and development work to improve the reliability in service of sodium steam generators. (auth)

55160 (CONF-710548–, pp 213-20) STATUS OF THE SODIUM-WATER REACTION STUDIES IN ITALY. Jul 1972.

From Specialists' meeting on sodium–water reactions; Melekess, USSR (18 May 1971).

The sodium–water reaction study program in Italy is described very briefly. Historical information is mentioned, and future plans are considered. (J.M.J.)

55161 (CONF-710548–, pp 221-42) ANALYTICAL AND EXPERIMENTAL STUDY OF A REACTING WATER-SODIUM FLOW. Kul'pin, B. V.; Mazanov, A. S. (Scientific Research Inst. of Atomic Reactors, Melekess, USSR). Jul 1972.

From Specialists' meeting on sodium–water reactions; Melekess, USSR (18 May 1971).

The rates of breakdown of 1Kh18N9T austenitic steel in the zone of interaction between sodium and water at small leaks were studied. The results of a determination of the weight loss of a target of this field in the interaction zone are presented and curves showing the burn-through time of the targets as a function of the sodium temperature from 350 through 600°C and the distance from the point of the leak are given. Also given are the results of a study of the temperature field of targets located in the reaction zone and the results of a determination of the burn-through time as a function of the thickness of the target. 5 references. (auth)

55162 (CONF-710959–, Paper 2) OBSERVATIONS ON THE BEHAVIOR OF RADIOACTIVE PRODUCTS ON RAPSODIE. De Fremont, R. (CEN, Cadarache, France). 12p.

From Meeting on fission and corrosion product behaviour in primary systems of LMFBR's; Bensberg, Germany (20 Sep 1971).

During an extensive shutdown for modification, after 3 years of operation, all accessible parts of the primary cooling system of the Rapsodie Reactor were inspected. One failed fuel pin was found, permitting direct contact between the fuel material and the liquid sodium coolant. Measurements of ^{137}Cs levels are given. Radioactivity levels were measured throughout the primary coolant loop. (J.M.J.)

55163 (CONF-710959–, Paper 3) DECONTAMINATION EXPERIENCE ON RAPSODIE. De Fremont, R. (CEN, Cadarache, France). 2p.

From Meeting on fission and corrosion product behaviour in primary systems of LMFBR's; Bensberg, Germany (20 Sep 1971).

Decontamination of the Rapsodie primary coolant loop and pumps is described. Decontamination factors for the primary radionuclides are given. (J.M.J.)

55164 (CONF-710959–, Paper 8) RADIOACTIVE MATERIAL TRANSPORT IN FLOWING SODIUM SYSTEMS. Brehm, W. F.; Koehmstedt, P. L.; Kovacevich, E. A.; Shannon, D. W. (Battelle-Northwest Labs., Richland, Wash.). 17p.

From Meeting on fission and corrosion product behaviour in primary systems of LMFBR's; Bensberg, Germany (20 Sep 1971).

The transport of activated corrosion products in liquid sodium was studied. It was found that fluid boundary-layer resistance to deposition of species exists for many isotopes; deposited activity can either release from the deposition site and migrate through the loop, or diffuse into the base metal; and deposited crud activity can create reactor maintenance problems. The release, transport, and deposition is not yet fully understood. 12 references. (J.M.J.)

55165 (CONF-710959–, Paper 9) CORROSION AND DEPOSITION OF IRRADIATED STAINLESS STEEL IN SODIUM. Brehm, W. F.; Kovacevich, E. A.; Shannon, D. W. (Battelle-Northwest Labs., Richland, Wash.). 21p.

From Meeting on fission and corrosion product behaviour in primary systems of LMFBR's; Bensberg, Germany (20 Sep 1971).

Studies were made of the corrosion in flowing liquid sodium of 300 series stainless steels. At 1200°F, 25 ft per sec sodium velocity, and 10 ppM oxygen in the sodium, the rate of metal loss was 0.0013 cm per year, an acceptable rate. The problem of radioisotopes included in the corrosion products is considered. The radioisotopes involved are identified. 8 references. (J.M.J.)

55166 (CONF-710959–, Paper 10) FISSION AND CORROSION PRODUCT BEHAVIOUR IN PRIMARY SYSTEMS OF LMFBR's: A BRIEF REVIEW OF CURRENT STATUS OF WORK BEING CARRIED OUT IN UK. Thorley, A. 11p.

From Meeting on fission and corrosion product behaviour in primary systems of LMFBR's; Bensberg, Germany (20 Sep 1971).

Techniques were developed to study the behavior of radioactive materials in sodium systems. Studies are being made in the Dounreay Fast Reactor and in out-of-pile loops. The release, transport, and deposition of corrosion products in flowing sodium are studied using tracer techniques. Mass transport of materials in sodium at various temperatures, velocities, and impurity levels was studied. The effect of imposed stresses on cladding materials in a corrosive, carburizing environment was examined. The effects of corrosion and deposition on the performance of a sodium loop was considered. 10 references. (J.M.J.)

55167 (CONF-710959--, Paper 11) BEHAVIOUR OF RADIOACTIVE IMPURITIES IN DFR PRIMARY LIQUID METAL COOLANT. Davies, R. A.; Drummond, J. L. (Dounreay Experimental Reactor Establishment, Scotland). 22p.

From Meeting on fission and corrosion product behaviour in primary systems of LMFBR's; Bensberg, Germany (20 Sep 1971).

The main oxide-forming fission products are present as a suspension of fine insoluble particles in the NaK which tend to deposit on metal surfaces. This suspension also contains fissile material formed by corrosion of uranium metal and disintegration of experimental oxide fuel from failed pins. It is difficult to obtain representative samples of NaK for fission product and fissile material analysis. There is no evidence in DFR that cesium is deposited on either the pipework or in the cold trap. The major part of the activity on components discharged from DFR can be removed by a water wash. 4 references. (auth)

55168 (CONF-710959--, Paper 12) CORROSION MASS TRANSFER IN PRIMARY SYSTEMS OF LMFBR'S. Menken, H. G. (INTERATOM, Bensberg, Ger.). 27p.

From Meeting on fission and corrosion product behaviour in primary systems of LMFBR's; Bensberg, Germany (20 Sep 1971).

Estimates of corrosion problems in the SNR were made based on corrosion loop studies. The SNR mockup corrosion loop is described. A corrosion and deposition model was formulated. Results calculated from the model were compared with those obtained experimentally. (J.M.J.)

55169 (CONF-710959--, Paper 13) SURVEY ABOUT CALCULATION METHODS FOR THE ACTIVITY INVENTORY IN THE PRIMARY SYSTEM OF SNR. Merkel, A. (INTERATOM, Bensberg, Ger.). 8p.

From Meeting on fission and corrosion product behaviour in primary systems of LMFBR's; Bensberg, Germany (20 Sep 1971).

The sources of activity release to the coolant are summarized. Boundary conditions for the fission product release during normal operation are given and used for the design of the SNR power plant. For abnormal reactor operation of the SNR, that is for accident conditions, among the various improbable malfunctions, the activity release is only discussed for the hypothetical design basis accident which is taken for the laying out of the primary system. (auth)

55170 (CONF-710959--, Paper 14) ANALYTICAL DETERMINATION OF IMPURITIES IN SODIUM OF LMFBR. Schillings, K. L. (INTERATOM, Bensberg, Ger.). 13p.

From Meeting on fission and corrosion product behaviour in primary systems of LMFBR's; Bensberg, Germany (20 Sep 1971).

The status of analysis of trace impurities in sodium at INTERATOM is given. The analytical methods for the most important elements were reviewed. The results obtained by the vacuum distillation and its following procedures indicate the excellent precision of less than ±1 ppM under the conditions that the impurities are within 10 ppM. This accuracy is valid for the elements C, O, Cl, H, and some metals. New studies for determining the radioactive trace impurities were discussed. (auth)

55171 (CONF-710959--, Paper 15) IMPURITIES IN COVER GAS SYSTEMS: SOME ASPECTS OF THEIR EFFECTS ON THE DESIGN OF LMFBR's. Webster, J. M. 7p.

From Meeting on fission and corrosion product behaviour in primary systems of LMFBR's; Bensberg, Germany (20 Sep 1971).

Sodium present as vapor and aerosols need to be considered as an impurity of fast reactor cover gas systems. Effective processes are required for its removal in order that recycled cover gas can be used as a purge for mechanisms and penetrations susceptible to sodium deposition or as a preliminary stage in a cover gas fission product removal plant, should this be required. Although the liquid metal coolant will act as a getter for the reactive constituents of air and moisture which could be introduced into the system during in flask and maintenance operations, problems due to deposition could arise. The build up of nitrogen could result in metallurgical features and measures may be required for removal from the cover gas. Cover gas activity caused by reactor operation with defective fuel in the core is expected to arise mainly from the fission gases. (auth)

55172 (CONF-710959--, Paper 16) BRIEF OUTLINE OF RADIATION AND REPAIR ENGINEERING PROGRAM PLAN. Brehm, W. F. (Hanford Engineering Development Lab., Richland, Wash.). 8p.

From Meeting on fission and corrosion product behaviour in primary systems of LMFBR's; Bensberg, Germany (20 Sep 1971).

The possibility of unfavorably high radiation levels in the FFTF heat transport system maintenance cells, arising from deposited corrosion product radionuclides, has been identified. The Radiation and Repair Engineering Program has been set up to find methods of reducing or coping with the radioactivity burden. The specific factors that contribute to the radiation levels, and the feasibility of reducing or accommodating each one are described graphically. A brief outline of overall program objectives is given. (auth)

55173 (CONF-710959--, Paper 17) CORROSION AND DEPOSITION BEHAVIOUR OF STEEL MATERIAL IN SODIUM SYSTEMS. Thorley, A. 11p.

From Meeting on fission and corrosion product behaviour in primary systems of LMFBR's; Bensberg, Germany (20 Sep 1971).

The corrosion and deposition of ferrous materials in simple liquid sodium loops were studied. Mass transport of materials in sodium at various temperatures, flow velocities, and impurity levels were considered. The effect of imposed stresses on cladding materials under corrosive and carburizing conditions was measured. The pattern of corrosion and deposition of corrosion products at various points in a non-isothermal sodium loop was studied. (J.M.J.)

55174 (EURFNR-986) PRESSURE DROP FOR ISOTHERMAL, INCOMPRESSIBLE TURBULENT FLOW IN ROD BUNDLES WITH HEXAGONALLY ARRANGED RODS. Rehme, K. (Kernforschungszentrum, Karlsruhe (West Germany). Institut fuer Neutronenphysik und Reaktortechnik). Translation of report KFK-1427. 45p. Dep. NTIS.

Work Performed under United States-Euratom Fast Reactor Exchange Program.

Systematic investigations were carried out on the pressure drop for an incompressible, isothermal, fully developed turbulent flow in rod bundles with hexagonal arrangement of rods. The results of measurements of the pressure drop over a range of Reynolds numbers $\text{Re} = 6 \times 10^2 \div 2 \times 10^5$ in test sections are reported. The rods with rod distance ratios of $P/D = 1.025 \div 2.324$ were surrounded by hexagonal channels. The number of rods was 7, 19, 37, and 61 respectively. On the basis of a critical survey of data from the literature and of the new measured results it was possible to give a generally valid statement about the pressure drop in rod bundles which is in contrast to numerous experimental and theoretical results by other authors. The pressure drop coefficient quickly rises from approximately 60% of the circular tube value for closely packed rods ($P/D = 1.0$) to the value for circular tubes for $P/D \approx 1.08$. For even higher rod distance ratios, the pressure drop coefficients rise but a little to about 10% above the values for circular tubes at $P/D = 2.0$. The number of rods in the rod bundle has no measurable effect on the pressure drop coefficient. 59 references. (auth)

55175 (GEAP-10207-26) REACTOR PRIMARY COOLANT SYSTEM RUPTURE STUDY. Progress Report No. 26, October 1971-March 1972. (General Electric Co., San Jose, Calif. Atomic Power Equipment Dept.). Apr 1972. Contract AT(04-3)-189. 77p. Dep. NTIS.

Testing was completed on a series of three 550°F, stainless-steel, butt-weld specimens and on the first cyclic pressure plus cyclic bending, stainless steel elbow specimen. Fatigue specimen notch root strains have been calculated with an elastic-plastic finite element computer program. Peak strains during cyclic loading have been measured with miniature strain gages. The Dresden 1 test loop has accumulated over 3900 hours of operation at test conditions (510°F, 1040 psig). A total of 81 of the 149 fatigue specimens being cyclically loaded in the loop have failed: 36 of 71 Type-304 stainless steel specimens, 15 of 28 Type-304L stainless steel specimens, 3 of 23 Inconel-600 specimens, and all of the 27 carbon steel specimens. (auth)

55176 (KFK-1548) PHENOMENOLOGICAL INVESTIGATION OF THE FLOW DISTRIBUTION BEHIND LOCAL COOLANT CHEMICAL BLOCKAGE IN ROD BUNDLES. Basmer, P.; Kirsch, D.; Schultheiss, G. F. (Kernforschungszentrum, Karlsruhe (West Germany). Institut fuer Reaktorentwicklung). Jan 1972. 32p. (In German). Dep. NTIS (U. S. Sales Only).

A hexagonal SNR-subassembly has been bisected between two corners. Closing this part by a plexiglas plate, it was possible to observe the flow behavior. Experiments have been performed with water and air bubbles as flow indicators. In all experiments, a coherent region of 41% of the flow area was completely or partially blocked. For different positions of the blockage, the influence of the spacer grid, the pin bundle, and the wall structure of the plexiglas upon the wake downstream of the blockage have been investigated for two Reynolds numbers. A reduced fluid flow rate within the blocked region has been arranged by drilling narrow holes through the blockage. It is concluded that the dimensions of the wake are practically independent from the Reynolds number within the investigated range. Even in a pin bundle, a distinct recirculation flow develops in the wake. A flow within the blocked region of about 15% of the whole flow rate destroys the recirculation zone in the wake behind the blockage. (auth)

55177 (ORNL-TM-3344) EXPERIENCE WITH SODIUM FLUOROBORATE CIRCULATION IN AN MSRE-SCALE FACILITY. Smith, A. N. (Oak Ridge National Lab., Tenn.). Sep 1972. Contract W-7405-eng-26. 132p. Dep. NTIS.

A eutectic mixture of sodium fluoroborate and sodium fluoride was circulated isothermally at a rate of about 800 gpm for 11,567 hr in a 4-in.-IPS Inconel test loop as part of the program to evaluate the fluoroborate salt for use as a secondary coolant for the Molten-Salt Breeder Reactor. Except for brief periods at 900, 1150, and 1275°F, the bulk salt temperature was controlled at 1025°F. The objective of the experiment was to obtain general experience in the handling and circulation of the fluoroborate salts, with emphasis on the pumping characteristics and on the design and operation of the gas system as it related to handling BF_3 and controlling the salt composition. The test results indicated that water test data may be used to predict the performance of molten-salt pumps with the fluoroborate salt, that reliable performance may be obtained from systems handling BF_3 gas if precautions are taken to exclude water and water-related impurities, that control of the salt composition should not be a problem, and that the thermal conductivity of the gas phase above the salt surface may be used as an indicator for monitoring the salt composition. Preliminary tests were made to examine the feasibility of protecting reactor heat transfer surfaces by preferential deposition of corrosion products in a cold trap. Further work is recommended in this area. The test work indicated that flow restrictions in the off-gas line can be eliminated by pretreatment of the salt to remove volatile impurities and by the use of a hot-mist trap and a cold filter in the off-gas line at the pump bowl outlet. 13 references. (auth)

55178 (RD/B/N-2364) IGNITION OF LIQUID METAL: PEROXIDE MIXTURES. Newman, R. N.; Smith, C. A. (Central Electricity Generating Board, Berkeley (England). Berkeley Nuclear Labs.). Jun 1972. 6p. Dep. NTIS (U. S. Sales Only).

Mixtures of sodium metal and sodium peroxide were ignited both in air and under inert atmospheres. The burning rate and spectra from the flash were recorded. The relevance of this type of reaction in relation to hazards involved in the use of liquid sodium and NaK in civil fast reactors is discussed. (auth)

55179 (TID-25887) BOILING CRISIS AND CRITICAL HEAT FLUX. Tong, L. S. (Westinghouse Electric Corp., Pittsburgh, Pa.). 1972. Contract AT(11-1)-2189. 89p. Dep. NTIS.

The ratio of the predicted critical heat flux (CHF) to the reactor heat flux is used as an index of the power capability of water reactors. Numerous boiling heat-transfer and two-phase-flow studies over the past 15 years have put emphasis on exploring the boiling-crisis mechanisms and on perfecting the CHF predictions. Unfortunately, the problem is more complicated than was thought. Thus far no overall analytical solution has been obtained, and the design equations for CHF predictions are empirical. In this review various types of boiling crisis are categorized according to four major flow patterns: pool boiling, bubbly flow, and normal flow across a cylinder. The physical mechanisms of these boiling crises are described. Experimental observations are summarized and used for verifying various analyses. The missing links in the analyses are identified, and future work is recommended. 123 references. (auth)

55180 EXPERIMENTS ON THE FLOW PAST SPHERES AT VERY HIGH REYNOLDS NUMBERS. Achenbach, E. (Kernforschungsanlage, Juelich, Ger.). J. Fluid Mech.; 54: No. 3, 565-75(8 Aug 1972).

In the Nuclear Research Laboratories at Juelich a gas-cooled high temperature reactor working with spherical fuel elements is being developed. The spheres, which have a diameter of 0.06 m, are transported pneumatically through tubes (diameter $d_t = 0.065$ m) under the conditions of the primary cooling gas, i.e., helium at 40 bars and 250°C. Because of the high pressure of the system large Reynolds numbers are to be expected. It was supposed that, during the transporting process, flow around the sphere could reach the critical state, which is characterized by a low drag coefficient and unsteady flow conditions. Work is reported concerning the flow past spheres in the Reynolds number range 5×10^4 Re 6×10^6. Results are reported for the case of a smooth surface. The total drag, the local static pressure and the local skin friction distribution were measured at a turbulence level of about 0.45%. The present results are compared with other available data as far as possible. Information is obtained from the local flow parameters on the positions of boundary-layer transition from laminar to turbulent flow and of boundary-layer separation. Finally the dependence of friction forces on Reynolds number is pointed out. (auth)

55181 WHAT RESEARCHERS LEARNED ABOUT VALVE PERFORMANCE IN REACTOR HEAT TRANSPORT SYSTEMS. Can. Contr. Instrum.; 11: No. 4, 29-31(Apr 1972).

The economics of Canada's reactor operations place stringent demands on valve performance. Low leakage, dependability and maintainability are of key importance. Most commercial types have weaknesses in one area or the other and a test program at AECL identified problem areas. The work has uncovered new technology which is now being applied to existing reactor valve problems. (auth)

55182 STUDY AND TESTS OF SMALL COMPONENTS OF SECONDARY CIRCUITS OF FAST Na COOLED REACTORS. Beaufrere, J.; de Montardy, A.; Nedelec, J. (Electricite de France, Ecuelles). Energ. Nucl. (Paris); 14: No. 1, 17-28 (1972). (In French).

In fast Na cooled reactors, it is necessary to interpose an intermediate Na circuit between the Na circuit cooling the core and the water vapor circuit feeding the turbine. The construction of the auxiliary equipment of the circuit is indicated: valves and taps, safety membranes, and sealed joints. (France)

Fuels and Fuel Elements

Refer also to abstract 53553.

55183 (ANCR-1038) EVALUATION OF FILAMENT-TYPE ELECTRIC HEATER ROD AS EMPLOYED IN SINGLE-LOOP SEMISCALE TO SIMULATE UO_2 FUEL RODS. Ewers, D.; Larson, J. R. (Aerojet Nuclear Co., Idaho Falls, Idaho). May 1972. Contract AT(10-1)-1375. 40p. Dep. NTIS.

This analysis compares the thermal response, during the blowdown phase of a loss-of-coolant accident, of the electrically heated filament-type heater rods used in the single-loop semiscale system with the thermal response of uranium dioxide fuel rods typically used in a light-water reactor. The analysis was conducted to determine how well the heater rod would simulate a UO_2 fuel rod, to optimize the method of power control to the heaters in the single-loop semiscale test series, and to guide future design of heater rods to be used in later test series. The analysis was accomplished using the HEAT-1 computer code. The results of this analysis indicate that comparable surface temperatures and surface heat fluxes for the two types of rods are very difficult to obtain, primarily because of the greater amount of heat stored in the uranium dioxide fuel rod. Maintaining the initial steady state power generation rate during the transient appears to be the best method for simulating the UO_2 fuel rod thermal response in the early, transient portion of an LOCA. 5 references. (auth)

55184 (ANL/EBR-57) XENON-TAGGING OF EBR-II DRIVER FUEL. EBR-II Project. Madson, A. A.; Laug, M. T. (Argonne National Lab., Ill. Argonne National Lab., Idaho Falls, Idaho). Feb 1972. Contract W-31-109-Eng-38. 24p. Dep. NTIS.

Twenty partially bonded EBR-II driver-fuel elements for an experiment were xenon-tagged with an evacuate-cryogenic transfer method. The xenon was frozen into the element plenum by immersing, in liquid argon, the sodium-loaded jacket complete with the fuel pin. More than 3 cm^3 (STP) of xenon were transferred in order to deliberately increase the plenum pressure so that release of tag upon cladding failure would be ensured. The equipment and procedures used are described, and the method is evaluated. 5 references. (auth)

55185 (CONF-710959-, Paper 1) TEMPETE TEST: IN PILE EXPERIMENT ON THE TRANSFER OF FISSION GASES. De Fremont R. (CEN, Cadarache, France). 5p.

From Meeting on fission and corrosion product behaviour in primary systems of LMFBR's; Bensberg, Germany (20 Sep 1971).

The feasibility of using rare gas tracers to locate failed fuel elements in Rapsodie and Phenix reactors was demonstrated. The transport of rare gases in a reactor core under real reactor operating conditions was studied. (J.M.J.)

55186 (EURFNR–985) TREATMENT OF THE MECHANICAL AND THERMAL BEHAVIOR OF FUEL RODS IN SATURN 1. Kaempf, H.; Elbel, H.; Depisch, F. (Kernforschungszentrum, Karlsruhe (West Germany). Institut fuer Material und Festkoerperforschung). Translation of report KFK–1477. 48p. Dep. NTIS.

Work Performed under United States–Euratom Fast Reactor Exchange Program.

In SATURN 1 the time history of a fuel pin concerning the radial distributions of temperature, stress, porosity and geometry changes is calculated. The operating fuel pin conditions such as linear rod power, outside temperature of the cladding and outside pressure are time dependent input data, so steady state and cyclic conditions are taken into account. The following material phenomena essential for the mechanical and thermal behavior are interconnected in SATURN 1: creep of fuel and clad, swelling of fuel and clad, thermal expansion, crack formation, fission gas release, porosity migration, and heat transfer fuel-clad. Three thermal-mechanical states are distinguished: a) fuel and clad in mechanical interaction, b) freestanding fuel and clad stressed by gas and coolant pressure, and c) freestanding stressed clad in contact or not in contact with cracked fuel assumed to be free of stresses. Three fuel zones are distinguished especially with view to different mechanical behavior. To demonstrate the manifold possibilities of SATURN 1 several illustrative applications are given. (6 references) (auth)

55187 (EURFNR–989) IN-PILE COMPATIBILITY OF OXIDE FUEL. Goetzmann, Odo (Kernforschungszentrum, Karlsruhe (West Germany). Institut fuer Material und Festkoerperforschung). 26 Jan 1972. 14p. Dep. NTIS.

Work performed under United States–Euratom Fast Reactor Exchange Program.

Radiation effects in reactor fuel elements during burnup, affecting the compatibility of the fuel material with the stainless steel cladding, are considered. While these materials are initially compatible, the formation of fission products, plus the liberation of oxygen from the oxide fuel materials, can become critical factors in the compatibility. In particular, tellurium and cesium have proven to be critical. The effects of temperature are considered. (J.M.J.)

55188 (EURFNR–1020) FRICTION FACTORS OF A CLUSTER OF 19 ROUGH RODS. Savatteri, C. (Kernforschungszentrum, Karlsruhe (West Germany). Institut fuer Neutronenphysik und Reaktortechnik). Apr 1972. 24p. (EUR–4728; KFK–1588). Dep. NTIS (U. S. Sales Only).

Work performed under United States–Euratom Fast Reactor Exchange Program.

On the basis of the laws applicable to velocity distribution on smooth and roughened surfaces, as obtained for simple geometries (circular tubes, annular gap), a method is indicated which allows the calculation of friction coefficients and flow distribution in artificially roughened rod bundles. Using this method of calculation, the results of measurements found for a rod bundle of 19 roughened rods in hexagonal arrangement and with a smooth channel wall yielded a parameter $R(h^+)$ which is in good agreement with values applicable to simpler geometries. (15 references) (auth)

55189 (GEAP–10028-39) SODIUM-COOLED REACTORS FAST CERAMIC REACTOR DEVELOPMENT PROGRAM. Thirty-Ninth Quarterly Report, May–July 1971. (General Electric Co., Sunnyvale, Calif. Breeder Reactor Dept.). Aug 1971. Contract AT(04-3)-189. 99p. Dep. NTIS.

EXPERIMENTAL BREEDER REACTOR-2 — fuel irradiation testing in, status of mixed oxide
FAST CERAMIC REACTOR — fuel elements for, development during May to July 1971
— core for, design and kinetics analysis of
— safety of, transient overpower and coolant flow loss effects on
INCOLOY 800 — radiation effects on swelling and mechanical properties of, fast neutron, (E)
LIQUID METAL FAST BREEDER REACTOR — fuel elements for, development of stainless steel clad plutonium oxide (PuO_2) – uranium oxide (UO_2)
NEUTRONS, FAST — effects on Incoloy 800 and stainless steels Type 316, Type 321, and Type 347
PLUTONIUM OXIDES, PuO_2 — $PuO_2 - UO_2$, radiation effects testing of fuels of
— $PuO_2 - UO_2$, properties of fuels of, mechanical, physical, and thermal, (E)
REACTOR FUEL ELEMENTS — performance of defected mixed plutonium oxide (PuO_2) – uranium oxide (UO_2) fast, in flowing liquid sodium
— cladding for mixed plutonium oxide (PuO_2) – uranium oxide (UO_2) fast, development and testing of stainless steel
— radiation effects testing of mixed plutonium oxide (PuO_2) – uranium oxide (UO_2) fast
STAINLESS STEEL — radiation effects on swelling and mechanical properties of Type 316, Type 321, and Type 347, fast neutron, (E)
URANIUM OXIDES, UO_2 — $PuO_2 - UO_2$, radiation effects testing of fuels of
— $PuO_2 - UO_2$, properties of fuels of, mechanical, physical, and thermal, (E) (J.M.J.)

55190 (GEAP–10028-42) SODIUM-COOLED REACTORS FAST CERAMIC REACTOR DEVELOPMENT PROGRAM. Forty-Second Quarterly Report, February–April 1972. (General Electric Co., Sunnyvale, Calif. Breeder Reactor Dept.). May 1972. Contract AT(04-3)-189. 123p. Dep. NTIS.

FAST CERAMIC REACTOR — fuel elements for, development during February to April 1972
— core for, design and kinetics analysis of
— safety of, transient overpower and coolant flow loss effects on
— safety of, development of models for analysis of
FAST FLUX TEST FACILITY — fuel element assemblies for, design of grid spaced driver
NEUTRONS, FAST — radiation effects on stainless steels Type 304, Type 316, Type 321, and Type 321-H
REACTOR FUEL ELEMENTS — performance of defected mixed plutonium oxide (PuO_2) – uranium oxide (UO_2) fast, in flowing liquid sodium
— fission products in, migration of cesium and tellurium
— radiation effects testing of mixed plutonium oxide (PuO_2) – uranium oxide (UO_2) fast
— cladding for mixed plutonium oxide (PuO_2) – uranium oxide (UO_2) fast, development and testing of stainless steel
STAINLESS STEEL — radiation effects on swelling and mechanical properties of Type 304, Type 316, Type 321 and Type 321-H (J.M.J.)

55191 (ORNL-TM–3656) FINAL SYSTEMS DESIGN DESCRIPTION OF THE FAILED FUEL MOCKUP (FFM) OF THE LIQUID-METAL FAST BREEDER REACTOR. Grindell, A. G.; MacPherson, R. E. (comps.) (Oak Ridge National Lab., Tenn.). Sep 1972. Contract W-7405-eng-26. 187p. Dep. NTIS.

The Failed Fuel Mockup (FFM) is an electrically heated, air-cooled sodium test facility in which a wide variety of out-of-pile testing can be performed with electric cartridge heaters that simulate the fuel pins in a portion of a liquid-metal fast breeder reactor (LMFBR) fuel assembly. In experiments carried out in the FFM, the behavior of the simulated partial subassembly under blockage and other test conditions of LMFBR interest can be studied, and information on thermal and hydraulic characteristics of various subassembly configurations may be obtained. The test section, which contains the electric heaters, is designed for 100 psi at 1300°F. The FFM can supply 442 kW of power to the test section, which consists initially of 19 electric cartridge heaters. The test section is conveniently removable from the facility to change the type or location of the flow blockage and also the configuration of the test section or instrumentation. The variable-speed sodium pump is capable of supplying up to 100 gpm of sodium to the test section and simultaneously as much as 200 gpm to the test section bypass line. An electronic data acquisition system is used to record pertinent test measurements on magnetic tape for computer processing. The facility is equipped with automatic equipment to permit unattended operation. The final design description of the several systems that make up the FFM is presented: the sodium circulation, cooling, and purifications systems; the test section; the electrical power system; the inert-gas system, and the unattended operation system. (auth)

55192 (ORNL-TM–3761) PRELIMINARY COOLANT TEMPERATURE OSCILLATION MEASUREMENTS AT THE FUEL-FAILURE MOCKUP. Fry, D. N.; Kerlin, T. W. (Oak Ridge National Lab., Tenn.). Aug 1972. Contract W-7405-eng-26. 23p. Dep. NTIS.

A feasibility study was conducted at the Fuel-Failure Mockup to determine if fluctuations in coolant temperature can be used to study flow and heat transfer mechanisms in a simulated Liquid-Metal Fast Breeder Reactor (LMFBR) fuel rod assembly. Thermocouple signals were cross correlated to obtain the gain and phase lag between thermocouple locations. The results of gain and phase measurements between wire-wrap thermocouples in bundle

1A show that the effect of wire wraps on the crossflow is experimentally observable. Also, these results, obtained at a frequency of 2 Hz, suggest that the crossflow might be proportional to the 0.8 power of the bulk flow. (auth)

Auxiliary Systems and Engineered Safeguards

55193 (BAW–10016) ANALYSIS OF ANTICIPATED TRANSIENTS WITHOUT TRIP. Scott, J. F.; Galan, V. J.; Cartin, L. R.; Heidenbrand, W. R.; Penland, J. R. (Babcock and Wilcox Co., Lynchburg, Va. (USA). Nuclear Power Generation Div.). Sep 1972. 98p.

A study was conducted to determine the consequences of anticipated transients without trip and to evaluate the probability of occurrence for these transients. The study was performed on a typical 177-fuel assembly plant at a rated power of 2772 MW(t). It is concluded that there is no significant potential for system damage due to anticipated transients without trip. (13 references) (auth)

55194 CONVEYING TUBE FOR THE PNEUMATIC TRANSFER OF SPHERICAL ELEMENTS. Mauersberger, R.; Faber, R.; Rausch, W.; (and others) (to Hochtemperatur-Reaktorbau GmbH). German Patent 2,060,673. (In German).

The tube is characterized in that it has at least three longitudinally running internal ribs which will prevent contact of the spherical fuel elements with the tube wall itself. The number, height, and arrangement of the ribs have been calculated so that even spheres with smaller diameters will not touch the wall of the tube. (GF)

Operation and Economics

Refer also to abstract 55376.

55195 (AECL–4254) CANADA'S NUCLEAR POWER PROGRAM IN CONTEXT WITH THAT OF THE WORLD. Mooradian, A. J. (Atomic Energy of Canada Ltd., Chalk River (Ontario). Chalk River Nuclear Labs.). Jun 1972. 10p. Dep. NTIS (U. S. Sales Only). AECL $0.50.

Canadian nuclear capacity is based on the CANDU concept, which is a unique product of the Canadian Nuclear Power Program. With the success of the Pickering Generating Station and promising results from boiling light-water and organically cooled reactors, the future of the Canadian concept as a highly competitive reactor system is assured. (auth)

55196 (CISE-R–241) MOBIDIC: A CODE FOR A SIMPLIFIED EVALUATION OF SOME CONTINUOUS AXIAL REFUELLING SCHEMES. Bruschi, C.; Foresti, G.; Pierini, G. (Centro Informazioni Studi Esperienze, Milan (Italy)). Oct 1967. 27p. INIS.

A method is described for a simplified evaluation of three continuous schemes of axial refueling: one-directional, counter-directional and bi-directional refueling. The starting point is the axial one-group diffusion equation, where radial leakage is simulated by a constant buckling. The code needs a table of one-group constants versus irradiation and reflector properties, to be given as input data; it has to be noticed that the only variation with position in the lattice cell proprieties is the one associated with irradiation (e.g., no effects due to coolant density profile are included). The discharge burnup of the fuel and the axial flux distribution are obtained by solving an integral equation iteratively until the core height is matched. The code MOBIDIC, written for the IBM 7040 computer, displays a running time of about 5 sec for the three cycles. (INIS)

55197 (ORNL–4794, pp 96-7) REACTOR EVALUATION STUDIES. Aug 1972.

In Chemical Technology Division annual progress report for period ending March 31, 1972.

Research is reported on: probabilistic simulation of power systems, power systems integration model, and fuel cycle cost code. (D.H.M.)

55198 (ORNL-TM–2496(Rev.2)(Suppl.3)) NUCLEAR REACTOR CORE ANALYSIS CODE: CITATION. Revision 2, Supplement 3. Fowler, T. B.; Vondy, D. R. (Oak Ridge National Lab., Tenn.). Jul 1972. 28p. Dep. NTIS.

Replacement pages are presented for the CITATION code report. The changes and additions reflect additional development of the code since the issue of Supplement 2. (H.D.R.)

Safety and Siting

Refer also to abstract 55375.

55199 (AEC-tr–7319) SOME PROBLEMS OF STUDYING EMERGENCIES IN A NUCLEAR POWER PLANT WITH PRESSURIZED WATER REACTOR. Kuznetsov, V. D. Translated from Kernenergie, 14: 188-90(1971). 6p. Dep. NTIS.

Some problems of analyzing the loss of coolant accident conditions in pressurized water power reactors are described. Inaccuracies caused by excessive simplification of the models in analysis of loss of coolant accidents are discussed. 5 references. (auth)

55200 (COO–2152-4) INVESTIGATION OF PRESSURE DROPS AND HEAT TRANSFER COEFFICIENTS FOR LOSS OF COOLANT EVALUATIONS. Quarterly Progress Report [for] Period Ending June 30, 1972. (Cincinnati Univ., Ohio. Dept. of Chemical and Nuclear Engineering). 1972. Contract AT(11-1)-2152. 11p. Dep. NTIS.

Progress in three areas of water cooled reactor loss of coolant accident evaluations is reported, including: transient pressure drop investigation; two-phase pressure drop and flow pattern study; and transition boiling and reflooding heat transfer tests. (H.D.R.)

55201 (DUN-SA–168) DEVELOPMENT AND IMPLEMENTATION OF EQUIPMENT MAINTENANCE STANDARDS FOR NUCLEAR REACTORS. Clement, T. M. (Douglas United Nuclear, Inc., Richland, Wash.). 13 May 1971. 8p. Dep. NTIS.

A formal system of maintenance standards is necessary to provide the nuclear power industry with factual, quantitative risk evaluations that will guide us in developing simpler and more reliable energy systems. These facts will also help dispel many of the allegations concerning the safety and environmental effects of nuclear power plants. (auth)

55202 (IRS-F–10) REPORT OF RESEARCH ORDERED BY THE FEDERAL MINISTRY FOR CONSTRUCTION AND RESEARCH IN THE FIELD OF REACTOR SAFETY. Quarterly Progress Report, January 1–March 31, 1972. (Technischer Ueberwachungs-Verein e. V., Cologne (West Germany). Institut fuer Reaktorsicherheit). 90p. (In German). Dep. NTIS (U. S. Sales Only).

Short administrative summaries of the various projects related to reactor safety in the Federal Republic of Germany are presented. Project accountability information is included. (J.M.J.)

55203 (JAERI-M–4473) ANALYSIS OF PRESSURE WAVE PROPAGATION IN PIPE RUPTURE ACCIDENTS OF LIGHT-WATER COOLED REACTORS BY USE OF THE BURST CODE. I. WAVE PROPAGATION THROUGH A SINGLE-PHASE FLUID. Shinoda, Wataru; Imaoka, T.; Kawabe, R.; Ishikawa, Michio (Japan Atomic Energy Research Inst., Tokyo). Jun 1971. 106p. (In Japanese). NTIS (U. S. Sales Only).

The pressure wave propagations in various types of flow systems have been studied by using the computational program BURST to obtain information on the applicability and operational techniques of the program. A range of flow systems is covered: a simple cylinder, a pipe with variable flow area (an adapter), an open end, and a simulated boiling water reactor with a flow restrictor in the main steam line. The system is assumed to be filled with single-phase fluid, subcooled water or superheated steam. From this analysis the following was revealed: (1) the calculated results agree well with theoretical predictions for the systems with simple geometries, thus confirming the mathematical model of the program. (2) The shape of the transmitted pressure wave may be distorted while traveling through an adapter with a length comparable with or greater than that of the wave front. (3) The steam flow rate could be limited by the critical phenomenon within the flow restrictor. (auth)

55204 (JAERI-M–4535) STUDY ON THE WORKS OF ENGINEERING REACTOR-SAFETY. Shimamune, Hiroji; Ishikawa, Michio; Sako, Kiyoshi; Shiba, Masayoshi; Tomii, Kakuzo (Japan Atomic Energy Research Inst., Tokyo). Aug 1971. 41p. (In Japanese). NTIS (U. S. Sales Only).

To carry out reactor-safety research works effectively, accident phenomena must be understood systematically in a realistic manner. For this purpose, trees which indicate the sequences of phenomena are made for important credible accidents. Studies are made on the accident trees to have the state of art in safety research experiments and safety analysis codes. Based on these results, the NSRR program being planned in JAERI is re-studied as part of the safety research works. (auth)

55205 (JAERI-Memo–4041) AN EXPERIMENTAL FACILITY TO SIMULATE THE LOSS-OF-COOLANT ACCIDENT OF LIGHT-WATER REACTORS. PART 5. Ikutame, Ken; Ishiguro, Misako (Japan Atomic Energy Research Inst., Tokyo). 1970. 76p. (In Japanese and English). Dep. NTIS (U. S. Sales Only).

Data sheets were assembled to present some of the details of the instrumentation used at the experimental installation built to simulate accidents arising from the loss of reactor coolant. The experimental equipment is described; the 36 tables and figures cover the detection system, auxiliary devices, flow diagrams and charts and operational characteristics. The detection transducer, primary amplifiers, d-c amplifiers used for matching, integrating digital voltmeters, electromagnetic oscilloscope, desk-top recorder and synchroscope, wave-shape generator, automatic voltage regulator, digital data coder, and analog data coder are described more closely, outlining also the operation of thermocouples with the differential amplifier, the quartz pressure transducer, resistance line pressure transducer and the dynamic resistance line strain gage. The off-line equipment mentioned includes the DATAC-2000 and FACOM-230/60 used for electronic data processing. (TTT)

55206 (KFK-1580) CALCULATION OF THE TIME DEPENDENT FISSION PRODUCT HEAT SOURCE STRENGTH IN TWO COUPLED SYSTEMS WITH CONSIDERATION OF FISSION PRODUCT ESCAPE. Henzel, N.; Simon-Weidner, J.; Waibel, E. (Kernforschungszentrum, Karlsruhe (West Germany). Institut fuer Reaktorentwicklung). Apr 1972. 188p. (In German). Dep. NTIS (U. S. Sales Only).

The fission product heat source within the oxide fuel of a LWR after a MCA with malfunction of the ECC system is investigated. The calculation of the time dependent heat source includes both radioactive decay and individual escape of fission products which is related to temperature and therefore the structure or the physical state of the fuel. A theoretical investigation of fission product escape coefficients for the elements Se to Eu is described. Results of a literature search on the experimental investigation of fission products escape coefficients are tabulated. An escape model including the necessary escape coefficients is presented. BWR Brunsbüttel and PWR BASF Mitte are used as an example to calculate fission product inventory and decay heat source without and with fission product escape after 1000 days of full power and shutdown. Given are the single nuclides, the chemical elements and the totals. Escaped fission products are released into a second system (outside the fuel), and their decay and increase is calculated separately. The model gives a maximum reduction of the heat source within the fuel by escape of fission products up to 50% of the momentary value. This maximum reduction occurs shortly after fuel melting. Special consideration was given to the time dependent contribution of the single chemical elements (total of the nuclides with the same atomic number) to the heat source. It was found that after more than 6 min after the assumed accident (cladding failure will occur at this time) only Nb, I, La and, after 2 days, Pr will contribute more than 10% to the total decay heat source. The results of the calculations are interpreted and recommendations are given for an experimental program aimed at the investigation of the fission product escape model where it is important to the rest-heat source problem. (auth)

55207 (ORNL-TM-3900) ORNL NUCLEAR SAFETY RESEARCH AND DEVELOPMENT PROGRAM BIMONTHLY REPORT FOR MAY-JUNE 1972. Cottrell, Wm. B. (Oak Ridge National Lab., Tenn.). Sep 1972. Contract W-7405-eng-26. 144p. Dep. NTIS.

The accomplishments during the months of May and June in the research and development program are summarized. Much of this work is in general support of water-cooled power reactor technology, including LOFT and industry programs, and reflects current safety problems, such as blow-down heat transfer studies. Several projects are also conducted in support of the high-temperature gas-cooled reactor (HTGR) and the liquid-metal fast breeder reactor (LMFBR) programs. Other major projects include experimental investigations of the attachment of nozzles to shells and the implementation of joint AEC-PVRC programs on heavy-section steel technology and nuclear piping, pumps, and valves. Seismic considerations of particular significance in nuclear plant design are evaluated in the seismic program. Several of the above projects are also directly related to another major undertaking, the AEC's standards program, which entails development of engineering safeguards and the establishment of codes and standards for government-owned or -sponsored reactor facilities. The recent activities of NSIC and the Nuclear Safety journal in behalf of the nuclear community are also discussed. Of particular interest in both of these activities is the recent emphasis on environmental effects. (auth)

55208 (RDT-F-9-1-T(8-72)) REQUIREMENTS FOR NUCLEAR COMPONENTS AT ELEVATED TEMPERATURES (SUPPLEMENT TO ASME ELEVATED TEMPERATURE CODE CASE 1331). (Division of Reactor Development and Technology (AEC), Washington, D. C.). Aug 1972. 36p. RSO.

Supplementary information is presented concerning standards for high temperature requirements of Class 1 components for nuclear reactors. (D.C.C.)

55209 (RISO-M-1500) RELY 4: A MONTE CARLO COMPUTER PROGRAM FOR SYSTEM RELIABILITY ANALYSIS. Kongsoe, H. E. (Danish Atomic Energy Commission, Risoe. Research Establishment). 6 Jun 1972. 78p. Dep. NTIS (U. S. Sales Only).

A computer program for calculation of reliability and availability of systems is described. The program is written in B6700 ALGOL. The program can be used for reliability analysis of both mechanical, electric and electronic systems, also systems containing standby units. The description consists of a summary, block diagrams and complete listings of the four versions of the program in addition to examples of input and output. There are four versions of the program with different distribution functions for the times to failure and repair times. Two of the versions use variance reduction—importance sampling—and the others, direct simulation. The basic theories and concepts are outlined. 9 references. (auth)

55210 RADIATION SAFETY OF NUCLEAR POWER PLANTS. Melichar, Zdenek; Hladky, Eduard. Jad. Energ.; 18: No. 7, 217-24(Jul 1972). (In Czech).

The problems of radiation safety in connection with atomic electric power stations were examined. For the proposed development of Czech nuclear energy a general program of research and development was developed. The necessity of a complex approach to a solution of radiation safety of nuclear power plants is emphasized, and basic fields of application of the results are demonstrated. (tr-auth)

55211 NUCLEAR POWER STATIONS. THE DIFFERENT TYPES OF REACTOR. THE PRINCIPAL TYPES OF ACCIDENT WHICH CAN OCCUR DURING OPERATION. Teste du Bailler, A. (Electricite de France, Saint-Denis). Bull. Inform. A.T.E.N. (Ass. Tech. Energ. Nucl.); No. 91, 13-17(Sep 1971). (In French).

Reactors are classified in terms of the nature of the fuel-moderator system. The laws concerning the compatibility of the two materials are physical (neutronic-thermal), physicochemical (corrosion), and technological or economic (costs-supplies). The existing different types of reactor are reviewed: CGR, AGR, HTR, HWR, PWR, BWR (light water) and fast reactors. A classification of accidents (or serious incidents) according to their causes is proposed: power excursions, accidents involving fuel, and accidents affecting the structures. (France)

Steam and Power Conversion System

55212 (CONF-720925-2) URBAN UTILIZATION OF EXTRACTED HEAT AND WASTE HEAT FROM CENTRAL STATION POWER PLANTS. Beall, Sam E. Jr.; Miller, Arthur J. (Oak Ridge National Lab., Tenn.). [nd]. 20p. Dep. NTIS.

From seventh intersociety energy conversion engineering conference; San Diego, CA. (25 Sep 1972).

An analysis is presented of the feasibility of providing thermal energy as well as electricity to urban areas from central station steam-electric power plants. Consideration is given to the use of thermal energy for applications such as industrial processes, building space heating, air conditioning, sewage treatment, agriculture, and aquaculture. The analysis shows that the use of dual-purpose plants significantly reduces the consumption of fuel and lessens the environmental impact of providing energy as compared to conventional systems. Areas of multifamily dwellings and other multistoried buildings could be served in new cities, or renewed old cities, at costs comparable to those incurred with more conventional separate systems. However, it would require more planning of facilities and coordination of diverse organizations than we normally employ. The costs and dislocations associated with retrofitting existing cities would cause each city to be a separate case. (9 references) (auth)

Commercial Power Reactors

55213 (FIND-50390(8-72)) FIND: WATTS BAR NUCLEAR PLANT, UNITS 1 AND 2. Smith, James G. (ed.) (Technical Information Center (AEC), Oak Ridge, Tenn.). 31 Aug 1972. 18p. (FIND-50391(8-72)). Dep. NTIS.

An index to microfiche issuances of safety analysis reports is provided. Subject citations are to specific frames on the microfiche. (J.M.J.)

55214 (WASH-1208(9-72)) STATUS OF CENTRAL STATION NUCLEAR POWER REACTORS SIGNIFICANT MILESTONES.

(Division of Reactor Development and Technology (AEC), Washington, D. C.). 1 Sep 1972. 9p. Dep. NTIS.

A table listing all constructed, contracted, and planned nuclear power plants in the U.S. is presented. Included in the table are the names and location of the reactors, electric output, type of reactor, steam system suppliers and architect–engineers, and pertinent dates. (J.M.J.)

55215 GANGES OF THE DESERT: RAJASTAN ATOMIC POWER PROJECT. Gupta, Veerendrakumar (Rajastan Atomic Power Project, Kota, India). Vaigyanik; 3: No. 1, 5-7; 21(Mar 1971). (In Hindi).

The Rajastan Atomic Power Plant will be put into operation at Rawatbhata about 40 miles from Kota in Rajasthan. It will have two Candu-type 200-MW reactors, using heavy water as moderator and coolant. The main reactor dome is a 4 ft thick concrete wall and can stand a pressure of 6 lb/in^2 inside the dome. The major reactor equipment such as calandria, dump tank, shield tank, coolant channel assemblies, and auxiliary reactor equipment such as the fueling machine carriage, dousing water tank, etc., will be housed inside the dome. The turbogenerator set and instrumentation and control equipment will be installed in a separate building. Gaseous radioactive wastes will be disposed of through a 300 ft. high stack. Every precaution was taken to reduce accidents to an absolute minimum. (INIS)

55216 SPEEDY ADVANCE OF CONSTRUCTION IN ATUCHA. Gerwin, R. Deut. Forschungsdienst, Sonderber. Kernenerg.; 15: No. 15, 77-8(1970). (In German).

A report is given about the status of construction work on the Atucha reactor followed by a preview of future work. The shell construction by 1970 and operational tests are due to begin in mid 1972. (INIS)

Control and Instrumentation

55217 (BAW-10047(Rev.1)) STUDY OF DISCONTINUITIES IN CONTROL ROD DRIVE MOTOR TUBE EXTENSIONS. Johnson, T. O.; Ayres, P. S.; Echelbarger, G. J.; Lawrie, W. E. (Babcock and Wilcox Co., Lynchburg, Va. (USA). Nuclear Power Generation Div.). Aug 1972. 77p.

Some control rod drive motor tube extensions have exhibited variations in wall thickness and discontinuities on the inner surface of the tube. An extensive investigation of these conditions is discussed. A program for resolving the findings is described. (auth)

55218 (EURFNR–976) CLADDING CONTROL ON NUCLEAR REACTOR FUEL ELEMENTS. Jacobi, S.; Tradowsky, K. (Kernforschungszentrum, Karlsruhe (West Germany). Labor fuer Elektronik und Messtechnik). Translation of report KFK–1452. 11p. Dep. NTIS.

Work performed under United States–Euratom Fast Reactor Exchange Program.

The problem of release of fission products and of fuel material into the coolant is discussed. The operation of failed fuel element detection devices is explained. For water-cooled reactors, the method of precipitation of solid fission products is described. In sodium-cooled reactors, the relative low activity of the fission products must be discriminated from the very high activity of the sodium. This is possible by measuring the delayed neutron emission of some fission products. (12 references) (auth)

55219 (RDT-C-7-18-T(8-72)) THERMOWELL SYSTEMS FOR LIQUID METAL SERVICE. (Division of Reactor Development and Technology (AEC), Washington, D. C.). Aug 1972. 22p. RSO.

This standard covers design and fabrication requirements for thermowell systems for installation in piping or vessels in liquid metal systems. These thermowell systems include a thermocouple or a resistance temperature detector (RTD), a thermowell, tip, extension tube, and connection head. (auth)

Containment Systems, Waste Processing, and Radiation Protection

55220 (BNL–16965) REACTOR EFFLUENTS: AS LOW AS PRACTICABLE OR AS LOW AS REASONABLE. Hull, Andrew P. (Brookhaven National Lab., Upton, N. Y.). 1972. 25p. (CONF-720614–1). Dep. NTIS.

From 17th annual meeting of the Health Physics Society; Las Vegas, NV. (12 Jun 1972).

Recent amendments proposed by the U.S. Atomic Energy Commission to 10CFR50, set forth numerical guides to keep radioactivity in light-water-cooled nuclear power reactors as low as practicable. These are intended to restrict the exposures of nearby persons to 1% or less of the current limits to individuals in the general public. For the most part the amendments contain ''across the board'' concentration limits, primarily based on their technical practicability. These are radiologically questionable, insofar as they are not related to a projected dose to an individual with reference to specific nuclides, and they are not detectable by straightforward environmental sampling and analysis techniques. The proposed 1% limits in radiation exposures from power reactor effluents are lacking in scientific warrant insofar as the calculated risk related to current reactor effluents is insignificant, relative to other sources of exposure and other kinds of environmental hazards. If adopted, they would occasion a projected expenditure of from $\$3 \times 10^4$ to $\$1 \times 10^6$ per man-rem saved, which is shown to be excessive on several cost-benefit comparisons. Design guides for reactor effluent releases based on 10% of current standards would appear adequate to achieve the AEC's intent. To remove public misunderstanding of the possible total population exposure from the operation of nuclear reactors, a population dose limit of 0.017 rem/year to be specifically apportioned to such operation and related activities is also proposed. (auth)

55221 (NP–19338(Vol.1)) IN-SERVICE INSPECTION PROGRAM FOR NUCLEAR REACTOR VESSELS. [VOLUME] I. Biannual Progress Report No. 6, March 1, 1971–September 1, 1971. (Southwest Research Inst., San Antonio, Tex.). 7 Jan 1972. 159p.

Technical Report to Steering Committee, EEI Project RP 79, Edison Electric Institute/Tennessee Valley Authority.

Progress is reported on the development of methods for in-service inspection of power reactor pressure vessels. Electric utility experience with pressure boundary inspection regarding service condition, defect detection capability, defect size, and defect orientation is reviewed. A facility for the evaluation of a nondestructive test method is described. An acoustic emission system for continuous monitoring for defects is evaluated. (J.M.J.)

55222 (NP–19338(Vol.2)) IN-SERVICE INSPECTION PROGRAM FOR NUCLEAR REACTOR VESSELS. [VOLUME] 2. Biannual Progress Report No. 6, March 1, 1971–September 1, 1971. (Southwest Research Inst., San Antonio, Tex.). 7 Jan 1972. 202p.

Technical Report to Steering Committee, EEI Project RP 79, Edison Electric Institute/Tennessee Valley Authority.

Progress is reported on the development of methods for in-service inspection of power reactor pressure vessels. Areas covered in Vol. 2, a continuation of Vol. 1 (abstracted separately) include improvement in reliability and reproducibility of conventional ultrasonic systems, and investigation of ultrasonic halography for visualization of flaws in thick-walled pressure vessels. (auth)

55223 (WCAP–7870) NEUTRON SHIELDING PADS. Kraus, S. (Westinghouse Electric Corp., Pittsburgh, Pa. Nuclear Energy Systems Div.). May 1972. 44p.

As part of the continuing effort to simplify the core support structure and save construction and assembly time, a design study was conducted to investigate the possibility of replacing the thermal shield with locally positioned plate members, called neutron shielding pads. The plot of the circumferential fluence distribution on the vessel, which is very localized, indicated that this was a practical approach. The design study described in this report established the feasibility of replacing the thermal shield with a series of plate members of equivalent thickness attached to the core barrel by pins and bolts. Both analytical and experimental methods were utilized to determine design adequacy. (auth)

55224 LAYOUT AND FABRICATION OF STEEL REACTOR PRESSURE VESSELS. Bonka, H. Aachen; Technische Hochschule (1971). 25p. (In German).

Thesis.

A brief survey is given of the layout of pressure vessel for 1,200-MW(e) LWRs, selection of materials, permissible strains, wall thickness, and welding methods for the fabrication process. (GF)

Coolant System

55225 (BAW–10050) EVALUATION OF OCONEE REACTOR COMPONENT FAILURE. (Babcock and Wilcox Co., Lynchburg, Va. (USA). Nuclear Power Generation Div.). Sep 1972. 41p.

An investigation was conducted to evaluate the failure of certain Oconee 1 reactor components during hot functional tests in early 1972. (auth)

55226 (CONF-710959–, Paper 4) CLEANUP SYSTEM FOR PRIMARY COVER GAS OF LMFBR. Barulli, L.; Bruzzi, L.; Cicognani, G. (CNEN, Bologna). 15p.

From Meeting on fission and corrosion product behaviour in primary systems of LMFBR's; Bensberg, Germany (20 Sep 1971).

The technical feasibility of a Clean-up System for the cover gas primary system of a LMFBR model similar to FERMI Fast Breeder Reactor is shown. From an economic stand point this type of clean up system is feasible because its estimated cost is only about 1% of the total plant cost. (auth)

55227 (EURFNR–1000) RESULTS OF HEAT TRANSFER AND PRESSURE LOSS MEASUREMENTS WITH HELIUM ON A SIXTEEN-TUBE BUNDLE. Marek, J.; Maulbach, K. (Kernforschungszentrum, Karlsruhe (West Germany). Institut fuer Neutronenphysik und Reaktortechnik). Translation of report KFK–1549. 43p. Dep. NTIS.

Work Performed under United States–Euratom Fast Reactor Exchange Program.

Measurements of pressure drop and heat transfer of helium at a pressure of 43 atm flowing through a bundle of 16 tubes in a square arrangement are reported. The tubes were heated directly by dc; the heating power was between 110 and 295 kW corresponding to a power of 40–105 W/cm at the heating tube. The tubes were smooth and arranged in a smooth square channel at a distance ratio of p/d = 1.283. The Reynolds numbers ranged between $1.5 \cdot 10^4$ and $1.4 \cdot 10^5$. Wall temperatures up to 550°C have been measured. The isothermal friction coefficients of the entire bundle, including the channel wall, were determined to be about 2% higher than that of the circular tube. The Nusselt numbers for the central channel are slightly smaller than the comparable values of circular tubes. (14 references) (auth)

55228 (JAERI-Memo–4016) RESULTS OF CYCLIC PRESSURE LOADING TEST DUE TO JPDR PRESSURE VESSEL MODEL NO. 2. **Fujimura, Tadato; Miyazono, Shohachiro; Ueda, Shuzo; Namatame, Hiroshi; Sakamoto, Fumio; Kadaira, Tsuneo; Shibata, Katsuyuki; Oba, Toshihito; Suzuki, Komei (Japan Atomic Energy Research Inst., Tokyo). May 1970. (In Japanese). NTIS (U. S. Sales Only).**

The test program on JPDR pressure vessel model 2 was performed to investigate propagation through base metal for the case where the cladding cracks occur at the location of highest stress in the vessel, that is the nozzles for forced circulation. Strain distribution was measured around nozzles without and with artificial notches. After static strain measurements, the model was loaded by cyclic pressure and investigated for fatigue crack propagation from artificial notch tips. (auth)

Fuels and Fuel Elements

55229 (EURFNR–975) CRITERIA FOR DIFFERENTIATING FUEL AND PLENUM FAULTS ON REACTOR FUEL ELEMENTS WITH VIBROCOMPACTED FUEL. Golly, W.; Jacobi, S. (Kernforschungszentrum, Karlsruhe (West Germany). Labor fuer Elektronik und Messtechnik). Translation of report KFK–1348. 44p. Dep. NTIS.

Work performed under United States–Euratom Fast Reactor Exchange Program.

For research with failed fuel elements the HSD-Loop was installed at the FR 2. The operation with two pins of the HDR-type is described. The pins were failed in the fuel region and at the plenum resp. Criteria are specified to discriminate these two types of defect by means of a precipitator. (10 references) (auth)

Auxiliary Systems and Engineered Safeguards

55230 INCIDENT OF OCTOBER 17, 1969 WITH SAINT-LAURENT-1. POLLUTION OF THE REACTOR AND THE MODIFICATION OF THE FEDAL SYSTEM. Grauvogel, M. A.; Le Noc, J. F. (Electricite de France, Saint-Laurent-des-Eaux). Bull. Inform. A.T.E.N. (Ass. Tech. Energ. Nucl.); No. 92, 23-38 (Nov 1971). (In French).

The essential problems which arose with the FEDAL system when the Saint-Laurent-1 reactor was restarted after the incident of October 17, 1969 are examined. The effect of the contaminating uranium dusts on the failed element detection system (FEDAL) are discussed. The various tests, analyses, and experimental measurements performed in order to estimate the quantity of uranium dispersed inside the core are presented. The modifications introduced into the FEDAL system (addition of an individualized FEDAL system to the existing system) and the new programming and data processing systems are described. The results obtained since the restart of the reactor and the subsequent operational difficulties are reviewed. (France)

Operation and Economics

55231 (DOCKET-50003–124) INDIAN POINT STATION, UNIT 1. Malfunction of Main Steam Stop Valve. (Consolidated Edison Co. of New York, Inc., New York). 6 Sep 1972. 4p. Dep. NTIS.

55232 (DOCKET-50003–125) INDIAN POINT STATION, UNIT 1. Reiteration of Request for Six-Month Test of High Pressure Boron Injection Pumps. (Consolidated Edison Co. of New York, Inc., New York). 14 Sep 1972. 3p. Dep. NTIS.

55233 (DOCKET-50016–170) ENRICO FERMI ATOMIC POWER PLANT, UNIT 1. Report for June 1972. (Power Reactor Development Co., Detroit, Mich.). Jun 1972. 14p. (PRDC-EF–106). Dep. NTIS.

55234 (DOCKET-50029–199) YANKEE NUCLEAR POWER STATION. Modification of Approved Change 97 Accomplished August 30, 1972. (Yankee Atomic Electric Co., Westboro, Mass.). 31 Aug 1972. 2p. Dep. NTIS.

The turbine trip requirements related to the revised trip level for low flow conditions in the cooling system are described. (D.C.C.)

55235 (DOCKET-50029–201) YANKEE NUCLEAR POWER STATION. March 1972 Inservice Examination of Yankee Rowe Atomic Power Plant. (Southwest Research Inst., San Antonio, Tex.). Jun 1972. 311p. Dep. NTIS.

For Yankee Atomic Electric Co., Westboro, Mass.

55236 (DOCKET-50029–202) YANKEE NUCLEAR POWER STATION. Control Rod Drop Times Measured on September 9, 1972. (Yankee Atomic Electric Co., Westboro, Mass.). 11 Sep 1972. 1p. Dep. NTIS.

55237 (DOCKET-50155–123) BIG ROCK POINT NUCLEAR PLANT. Apparent Deficiency in Off-Gas Holdup Line. (Consumers Power Co., Jackson, Mich.). 1 Sep 1972. 3p. Dep. NTIS.

55238 (DOCKET-50171–106) PEACH BOTTOM ATOMIC POWER STATION, UNIT 1. Semiannual Operations Report 66, January 1, 1972–June 30, 1972. (Philadelphia Electric Co., Pa.). 6 Sep 1972. 60p. Dep. NTIS.

55239 (DOCKET-50206–167) SAN ONOFRE NUCLEAR GENERATING STATION, UNIT 1. Unit Trip and Subsequent Activation of Safety Injection Equipment. (Southern California Edison Co., Rosemead, Calif.). 31 Aug 1972. 4p. Dep. NTIS.

55240 (DOCKET-50213–157) HADDAM NECK PLANT, UNIT 1. Operational Environmental Radiation Monitoring Program, January 1, 1972–June 30, 1972. (Interex Corp., Waltham, Mass. (USA)). 31 Aug 1972. 30p. Dep. NTIS.

For Connecticut Yankee Atomic Power Co., Haddam.

55241 (DOCKET-50213–158) HADDAM NECK PLANT, UNIT 1. Containment Testing June 1970–June 1972. (Connecticut Yankee Atomic Power Co., Haddam). 8 Sep 1972. 32p. Dep. NTIS.

55242 (DOCKET-50219–213) OYSTER CREEK NUCLEAR POWER PLANT, UNIT 1. Report of Operations, Semiannual Report 6, January 1, 1972–June 30, 1972. (Jersey Central Power and Light Co., Morristown, N. J.). 31 Aug 1972. 67p. Dep. NTIS.

55243 (DOCKET-50237–257) DRESDEN NUCLEAR POWER STATION, UNITS 2 AND 3. Two EHC Oil Low Pressure Scram Switches Setpoints Drifted Beyond Established Limits. (Commonwealth Edison Co., Chicago, Ill.). 23 Aug 1972. 2p. (DOCKET-50249–154). Dep. NTIS.

55244 (DOCKET-50237–258) DRESDEN NUCLEAR POWER STATION, UNIT 2. Low Flow on "B" Steam Line. (Commonwealth Edison Co., Chicago, Ill.). 7 Sep 1972. 2p. Dep. NTIS.

55245 (DOCKET-50244–118) ROBERT EMMETT GINNA NUCLEAR POWER PLANT, UNIT 1. Monthly Report of Activity Measurements. (Rochester Gas and Electric Corp., N. Y.). 6 Sep 1972. 2p. Dep. NTIS.

55246 (DOCKET-50245–158) MILLSTONE POINT NUCLEAR POWER STATION, UNIT 1. Environmental Radiation Survey Program, Semiannual Report, January 1, 1972–June 30, 1972. (Interex Corp., Waltham, Mass. (USA)). 31 Aug 1972. 45p. Dep. NTIS.

For Millstone Point Co., Hartford, Conn.

55247 (DOCKET-50249–155) DRESDEN NUCLEAR POWER STATION, UNIT 3. Two Incidents. (Directorate of Licensing (AEC), Washington, D. C.). 11 Sep 1972. 1p. Dep. NTIS.

An incorrect set point for electrohydraulic control low oil pressure scram switches is described. The malfunction of a turbine control valve to indicate a half scram when fast closed is discussed. (D.C.C.)

55248 (DOCKET-50250-92) TURKEY POINT PLANT, UNITS 3 AND 4. Abnormal Occurrence No. 3-72-5. (Florida Power and Light Co.). 1 Sep 1972. 2p. (DOCKET-50251-76). Dep. NTIS.

Information is presented concerning the failure of the valve stem packing on the gate valve in the suction line from the residual heat removal system to the cooling system. (D.C.C.)

55249 (DOCKET-50250-94) TURKEY POINT PLANT, UNITS 3 AND 4. Three Unusual Events, August 12 and August 21, 1972. (Florida Power and Light Co.). 8 Sep 1972. 2p. (DOCKET-50251-77). Dep. NTIS.

The unplanned simultaneous actuation of the safety injection systems for Units 3 and 4 is described during the scheduled actuation of the Unit 4 system. The packing failure for the 3A charging pump is discussed. The failure of the emergency diesel generator to produce a required test output is described. (D.C.C.)

55250 (DOCKET-50254-117) QUAD-CITIES STATION, UNIT 1. Valves in the "RCIC" System Failed to Operate on September 3, 1972. (Commonwealth Edison Co., Cordova, Ill.). 4 Sep 1972. 1p. Dep. NTIS.

55251 (DOCKET-50255-99) PALISADES PLANT. Four Control Rods Failed to Drop on Routine Test. (Consumers Power Co., Jackson, Mich.). 8 Sep 1972. 3p. Dep. NTIS.

55252 (DOCKET-50261-109) H. B. ROBINSON UNIT 2. Malfunction of Part Length Rod Control System. (Carolina Power and Light Co., Raleigh, N. C.). 11 Sep 1972. 1p. Dep. NTIS.

55253 (DOCKET-50263-149) MONTICELLO NUCLEAR GENERATING PLANT, UNIT 1. Six Month Operating Report No. 3, January 1, 1972-June 30, 1972. (Northern States Power Co., Minneapolis, Minn.). 1972. 132p. Dep. NTIS.

55254 (DOCKET-50265-115) QUAD-CITIES STATION, UNIT 2. Seven Valves Failed to Test Properly on Routine Inspection. (Commonwealth Edison Co., Cordova, Ill.). 6 Sep 1972. 3p. Dep. NTIS.

The failure of seven suppression chamber to drywell vacuum breaker valves to operate during a routine inspection test is described. Corrective actions are discussed. (D.C.C.)

55255 (DOCKET-50271-100) VERMONT YANKEE NUCLEAR POWER STATION. Offsite Environmental Radiological Monitoring Report, January 1, 1972-June 30, 1972. (Vermont Yankee Nuclear Power Corp., Rutland). 6 Sep 1972. 13p. Dep. NTIS.

55256 (DOCKET-50271-101) VERMONT YANKEE NUCLEAR POWER STATION. Facility Operating License DPR-28, Amendment 2 (Temporary Operating License). (Directorate of Licensing (AEC), Washington, D. C.). 8 Sep 1972. 12p. Dep. NTIS.

55257 (DOCKET-50280-83) SURRY POWER STATION, UNIT 2. Returned to Service on September 3, 1972. (Virginia Electric and Power Co., Richmond). 5 Sep 1972. 2p. Dep. NTIS.

55258 (DOCKET-50282-74) PRAIRIE ISLAND NUCLEAR GENERATING PLANT, UNIT 1. Interim Report on Deficient Motor Operated Valve Torque Switches. (Northern States Power Co., Minneapolis, Minn.). 30 Jun 1972. 2p. Dep. NTIS.

55259 (DOCKET-50333-53) JAMES A. FITZPATRICK NUCLEAR POWER PLANT. Amended and Substituted Application for Licenses, Amendment 12. (Power Authority of the State of New York). 6 Sep 1972. 109p. Dep. NTIS.

Financial data on the owners of the James A. Fitzpatrick Power Reactor are presented. The 1971 Annual Reports for the Power Authority of the State of New York and the Niagara Mohawk Power Corporation are included. (D.C.C.)

55260 (DOCKET-50382-36) WATERFORD STEAM ELECTRIC STATION, UNIT 3. Preliminary Safety Analysis Report, Amendment 22. (Louisiana Power and Light Co., New Orleans). 28 Aug 1972. 100p. Dep. NTIS.

Financial data on the owners of the Waterford Power Reactor Unit 3 are presented. The 1970 and 1971 Annual Reports for the Louisiana Power and Light Company are included. (D.C.C.)

55261 (DOCKET-50397-27) HANFORD NO. 2 NUCLEAR POWER PLANT. Preliminary Safety Analysis Report, Amendment 13. (Washington Public Power Supply System, Richland). 14 Sep 1972. 5p. Dep. NTIS.

Revised information is presented concerning construction costs for the Hanford Power Reactor Unit 2. (D.C.C.)

55262 (DOCKET-50400-23) SHEARON HARRIS NUCLEAR POWER PLANT, UNITS 1, 2, 3, AND 4. License Application, Amendment 14. (Carolina Power and Light Co., Raleigh, N. C.). 31 Aug 1972. 62p. (DOCKET-50401-23; DOCKET-50402-23; DOCKET-50403-23). Dep. NTIS.

Financial data on the owners of the Shearon Harris Power Reactor Units 1, 2, 3, and 4 are presented. The 1971 Annual Report for the Carolina Power and Light Company is included. (D.C.C.)

55263 (DOCKET-50404-24) NORTH ANNA POWER STATION, UNITS 3 AND 4. License Application, Amendment 9. (Virginia Electric and Power Co., Richmond). 13 Sep 1972. 78p. (DOCKET-50405-24). Dep. NTIS.

Financial data on the owners of the North Anna Power Reactor Units 3 and 4 are presented. The 1971 Annual Report of the Virginia Electric and Power Company is included. (D.C.C.)

55264 (JAERI-Memo-4083) NUCLEAR FUEL BALANCE CALCULATION AT JPDR. Ezure, H.; (and others) (Japan Atomic Energy Research Inst., Tokyo). Jul 1970. (In Japanese). NTIS (U. S. Sales Only).

The material balance of the nuclear fuel of JPDR is calculated during the operation time from the initial start-up to JPDR-I operation end using a three-dimensional boiling water reactor simulator code FLARE and a newly coded three-dimensional burn-up code TERA. An outline of the calculations is presented. (auth)

55265 (ORNL-TM-3743) ORCOST: A COMPUTER CODE FOR SUMMARY CAPITAL COST ESTIMATES OF STEAM-ELECTRIC POWER PLANTS. USER'S MANUAL. Fuller, L. C.; Sweet, C. A.; Bowers, H. I. (Oak Ridge National Lab., Tenn.). Sep 1972. Contract W-7405-eng-26. 83p. Dep. NTIS.

ORCOST is a digital computer program for estimating direct and indirect capital costs of nuclear and fossil-fueled steam-electric power plants. The costs are calculated using base cost models which are included in the program for each of the following types of plants: PWR, BWR, HTGR, coal, gas, and oil. The code follows the guidelines of AEC Report NUS-531. The computer output includes a summary of input data and the calculated costs. (4 references) (auth)

55266 (RD/B/N-2261) RELP VERSION C: A REACTOR ECONOMICS LINEAR PROGRAM FOR THE IBM 360/85 COMPUTER. Draper, J. M.; Jones, P. (Central Electricity Generating Board, Berkeley (England). Berkeley Nuclear Labs.). Jun 1972. 31p. Dep. NTIS (U. S. Sales Only).

A users' guide is provided to the computer code RELIP which uses a linear programming technique to calculate the optimum mix of station types in a nuclear generating system in order to minimize the total system cost. The code was written to study, for example, the consequences of design changes of the fuel rating or burn-up on the fabrication, reprocessing, separative work and ore requirements of the system. Details of the input requirements are given together with an outline of the costing calculations and a sample run. (auth)

55267 (WASH-1139(Rev.1)) GROWTH OF NUCLEAR POWER, 1972-1985. (Office of Planning and Analysis (AEC), Washington, D. C.). Dec 1971. 18p. Dep. GPO $0.30.

An updated forecast of nuclear power growth in the United States and the rest of the free world is presented principally for use in AEC production planning. This forecast updates information provided in WASH-1139, the AEC's 1970 forecast, and reflects current consideration of domestic and foreign nuclear power growth, foreign enrichment capabilities in the future and the timing of the application of plutonium recycle technology. The nuclear generating capacities in this forecast have been translated into demands for uranium feed and separative work by use of the known and expected characteristics of nuclear reactors. (auth)

55268 GENTILLY GEARS FOR FULL NUCLEAR POWER. Mod. Power Eng.; 66: No. 5, 66-7(May 1972).

The prototype CANDU (natural-uranium fuelled, heavy-water moderated) reactor at Gentilly, Quebec, is the first of its kind to be cooled by boiling light water. The Gentilly reactor was built by Hydro-Quebec, who will eventually buy it from Atomic Energy of Canada Limited. During the commissioning period following criticality in November 1970, there was trouble with tilting of the axis of neutron flux, necessitating restriction of power to 50% of the maximum 250 MW, and care in the use of enriched booster fuel rods. In the spring of 1972, power was at 75% of capacity, before increase to full power in the summer. During a shutdown in May 1971, repairs were done to the coolant system, and in

February 1972, shutdown-initiating devices for protection against "tilt" were installed. A dual digital computer system is used for acquisition, display, and logging of data, and for controlling power, steam-drum levels, moderator level, and the fueling machine. (Canada)

55269 WYLFA NUCLEAR POWER STATION. Nucl. Eng. Int.; 17: No. 193, 479-80(Jun 1972).

The successful operation of Wylfa Nuclear Station during the first 18 months is briefly outlined. Notable achievements were high stability of control of the boilers, exceptional fuel performance, and success of the more compact on-line computer control system. The extreme dryness of the gas circuit is especially significant in relation to the maximum temperature imposed as a result of CO_2 corrosion problems in earlier reactors, and there is reasonable expectation that eventually the full design power of 1100 MW(e) will be achieved. (UK)

55270 SPECIAL PROJECTS TEAM AT OLDBURY. Elec. Times; 161: No. 25, 43-4(22 Jun 1972).

Examples are given of the work performed by the special project team formed to modify and develop the nuclear station at Oldbury, to give improved availability. Factors contributing to the original low availability and the steps taken that caused an improvement from 61 to 86% between 1968 and 1971 are discussed. (UK)

Safety and Siting

Refer also to abstracts 53182—53185 and 53511.

55271 (BAW–10034(Suppl.1)) MULTINODE ANALYSIS OF B AND W'S 2568-MWt NUCLEAR PLANTS DURING LOSS-OF-COOLANT ACCIDENT. Parks, C. E.; Dunn, B. M.; Jones, R. C. (Babcock and Wilcox Co., Lynchburg, Va. (USA). Nuclear Power Generation Div.). Aug 1972. 23p.

A guillotine break of the line connecting the core flooding tank to the reactor vessel between the vessel's nozzle and the first check valve is analyzed at power levels of 2568 and 2772 MW(t). All conditions of the AEC Interim Acceptance Criteria are met. (auth)

55272 (BAW–10048(Suppl.1)) MULTINODE ANALYSIS OF B AND W'S 145-FUEL ASSEMBLY NUCLEAR PLANTS DURING LOSS-OF-COOLANT ACCIDENT. Parks, C. E.; Allen, R. J.; Schermer, W. J. (Babcock and Wilcox Co., Lynchburg, Va. (USA). Nuclear Power Generation Div.). Aug 1972. 19p.

An analysis of the double-ended break of the pipe that connects a core flood tank to the reactor vessel at a point between the reactor vessel core flooding line nozzle and the first upstream check valve in the flooding line is presented. 4 references. (auth)

55273 (DOCKET-1151–58) ELK RIVER REACTOR. Sixth Report on Status of Deactivated Reactor. (United Power Association, Elk River, Minn. (USA)). 30 Aug 1972. Contract AT-(11-1)-651. 8p. Dep. NTIS.

55274 (DOCKET-50010–117) DRESDEN NUCLEAR POWER STATION, UNITS 1, 2, AND 3. QUAD-CITIES STATION, UNITS 1 AND 2. ZION STATION NUCLEAR POWER PLANT, UNITS 1 AND 2. Valve Wall Thickness. (Directorate of Regulatory Operations (AEC), Glen Ellyn, Ill. Region III). 13 Sep 1972. 7p. (DOCKET-50237–259; DOCKET-50249–156; DOCKET-50254–121; DOCKET-50265–116; DOCKET-50295–62; DOCKET-50304–62). Dep. NTIS.

55275 (DOCKET-50029–200) YANKEE NUCLEAR POWER STATION. Flooding of Critical Equipment. (Directorate of Licensing (AEC), Washington, D. C.). 8 Aug 1972. 4p. Dep. NTIS.

The possible flooding of engineered safeguard equipment due to failure of the circulating water system is analyzed. (D.C.C.)

55276 (DOCKET-50146–111) SAXTON NUCLEAR EXPERIMENTAL REACTOR PROJECT. License DPR-4, Amendment 8. (Directorate of Licensing (AEC), Washington, D. C.). 15 Aug 1972. 30p. Dep. NTIS.

Approved technical specifications related to a reduction in surveillance and staffing for the decommissioning of the Saxton Power Reactor are presented. (D.C.C.)

55277 (DOCKET-50155–124) BIG ROCK POINT NUCLEAR PLANT. Equipment Failure, July 29, 1972. (Consumers Power Co., Jackson, Mich.). 13 Sep 1972. 1p. Dep. NTIS.

The failure of both neutron monitoring startup channels of the Big Rock Point Power Reactor is reported. (H.D.R.)

55278 (DOCKET-50155–125) BIG ROCK POINT NUCLEAR PLANT. PALISADES PLANT. Valve Wall Thickness. (Directorate of Regulatory Operations (AEC), Glen Ellyn, Ill. Region III). 13 Sep 1972. 6p. (DOCKET-50255–100). Dep. NTIS.

55279 (DOCKET-50245–159) MILLSTONE POINT NUCLEAR POWER STATION, UNIT 1. Application for Conversion from Provisional Operating License to Full-Term Operating License. (Millstone Point Co., Hartford, Conn.). 1 Sep 1972. 327p. Dep. NTIS.

55280 (DOCKET-50245–160) MILLSTONE POINT NUCLEAR POWER STATION, UNIT 1. Abnormal Occurrences Nos. 72-21 and 72-22. (Millstone Point Co., Hartford, Conn.). 11 Sep 1972. 3p. Dep. NTIS.

The occurrence of a reactor coolant leakage rate into the primary containment in excess of the allowable rate and of abnormal reactor coolant chemistry limits are reported for the Millstone Point Power Reactor, Unit 1. (H.D.R.)

55281 (DOCKET-50247–81) INDIAN POINT NUCLEAR GENERATING UNIT 2. Order Extending Construction Completion Date to January 2, 1973. (Directorate of Licensing (AEC), Washington, D. C.). 18 Sep 1972. 2p. Dep. NTIS.

55282 (DOCKET-50250–93) TURKEY POINT PLANT, UNIT 3. Technical Specifications, Change 1. (Directorate of Licensing (AEC), Washington, D. C.). 6 Sep 1972. 2p. Dep. NTIS.

Revised technical specifications are presented concerning a reduction in the power tilt limits. (D.C.C.)

55283 (DOCKET-50254–118) QUAD-CITIES STATION, UNITS 1 AND 2. Technical Specifications, Outstanding Items. (Commonwealth Edison Co., Chicago, Ill.). 31 Aug 1972. 5p. (DOCKET-50265–112). Dep. NTIS.

Requested information is presented concerning technical specifications. (D.C.C.)

55284 (DOCKET-50254–119) QUAD-CITIES STATION, UNITS 1 AND 2. Answers to AEC Questions Regarding Condensate Pump Room Flooding. (Commonwealth Edison Co., Chicago, Ill.). 1 Sep 1972. 9p. (DOCKET-50265–113). Dep. NTIS.

55285 (DOCKET-50254–120) QUAD-CITIES STATION, UNITS 1 AND 2. Final Environmental Statement. (Directorate of Licensing (AEC), Washington, D. C.). Sep 1972. 351p. (DOCKET-50265–114). Dep. NTIS.

Information concerning chemical, radioactive, and thermal discharges from the reactors is presented. The effects of reactor operations on the environment are analyzed. Ecological, hydrological, and meteorological data on the reactor site are included. Cost-benefit analysis for reactor operations is presented. (D.C.C.)

55286 (DOCKET-50261–106) H. B. ROBINSON UNIT 2. Final Facility Description and Safety Analysis Report, Volume 3. (Carolina Power and Light Co., Raleigh, N. C.). 26 Nov 1968. 731p. Dep. NTIS.

Information is presented on the H. B. Robinson Power Reactor Unit 2 under the following broad topics: electrical systems; auxiliary and emergency systems; steam and power conversion systems; radioactive waste systems; radiation protection systems; operations; initial tests; and safety analysis. (D.C.C.)

55287 (DOCKET-50261–108) H. B. ROBINSON UNIT 2. Technical Specifications, Change. (Carolina Power and Light Co., Raleigh, N. C.). 8 Sep 1972. 2p. Dep. NTIS.

Revised technical specifications are presented concerning performance requirements of the emergency core cooling system. (D.C.C.)

55288 (DOCKET-50263–150) MONTICELLO NUCLEAR GENERATING PLANT, UNIT 1. Valve Wall Thickness. (Directorate of Regulatory Operations (AEC), Glen Ellyn, Ill. Region III). 13 Sep 1972. 7p. Dep. NTIS.

55289 (DOCKET-50266–79) POINT BEACH NUCLEAR PLANT, UNITS 1 AND 2. Elimination of Hot Leg Injection Emergency Core Cooling System. (Wisconsin Electric Power Co., Milwaukee). 5 Sep 1972. 2p. (DOCKET-50301–70). Dep. NTIS.

55290 (DOCKET-50266–80) POINT BEACH NUCLEAR PLANT, UNITS 1 AND 2. Valve Wall Thickness. (Directorate of Regulatory Operations (AEC), Glen Ellyn, Ill. Region III). 13 Sep 1972. 7p. (DOCKET-50301–71). Dep. NTIS.

55291 (DOCKET-50272–35) SALEM NUCLEAR GENERATING STATION, UNITS 1 AND 2. Final Safety Analysis Report, Amendment 14. (Public Service Electric and Gas Co., Newark, N. J.). 6 Sep 1972. 415p. (DOCKET-50311–35). Dep. NTIS.

Requested and revised data are presented concerning the quality assurance program; the site; containment systems; engineered safeguards; auxiliary and emergency systems; power conversion system; radioactive waste disposal; radiation protection; and safety analysis. (D.C.C.)

55292 (DOCKET-50277–56) PEACH BOTTOM ATOMIC POWER STATION, UNITS 2 AND 3. Study of Possible Expansion Bellows Failure. (Philadelphia Electric Co., Pa.). 1 Sep 1972. 2p. (DOCKET-50278–56). Dep. NTIS.

55293 (DOCKET-50277–57) PEACH BOTTOM ATOMIC POWER STATION, UNITS 2 AND 3. Final Safety Analysis Report, Amendment 20. (Philadelphia Electric Co., Pa.). 12 Sep 1972. 35p. (DOCKET-50278–57). Dep. NTIS.

Requested and revised data are presented concerning containment atmosphere following loss of coolant accident; radioactive effluents; vibration testing of cooling system components; and emergency core cooling system performance evaluation. (D.C.C.)

55294 (DOCKET-50278–58) PEACH BOTTOM ATOMIC POWER STATION, UNIT 3. Interim Report of Damage to Reactor Pressure Vessel Top Fuel Guide. (Philadelphia Electric Co., Pa.). 16 Aug 1972. 3p. Dep. NTIS.

55295 (DOCKET-50280–82) SURRY POWER STATION, UNIT 1. Technical Specifications, Changes. (Virginia Electric and Power Co., Richmond). 30 Aug 1972. 4p. Dep. NTIS.

Revised technical specifications are presented concerning personnel organization, and site temperature monitoring requirements. (D.C.C.)

55296 (DOCKET-50280–84) SURRY POWER STATION, UNIT 1. Inspection to Examine the Malfunction of the Decay Heat Release System. (Directorate of Regulatory Operations (AEC), Atlanta, Ga. (USA). Region II). 12 Sep 1972. 63p. Dep. NTIS.

55297 (DOCKET-50280–85) SURRY POWER STATION, UNIT 1. Operating Incident of July 27, 1972. (Virginia Electric and Power Co., Richmond). 16 Aug 1972. 32p. Dep. NTIS.

On July 27, 1972, the steam vent system of Surry Power Reactor, Unit 1 malfunctioned resulting in the deaths of two Virginia Electric and Power Company employees. The employees were burned when a sudden opening of the decay heat release valve caused the decay heat release pipe to disengage from the vent sleeve and release steam into the safeguards building. The incident and subsequent events are described in detail. There was no release of radioactivity and the reactor was at all times in a safe condition. (H.D.R.)

55298 (DOCKET-50282–72) PRAIRIE ISLAND NUCLEAR GENERATING PLANT, UNITS 1 AND 2. Valve Wall Thicknesses. (Directorate of Regulatory Operations (AEC), Glen Ellyn, Ill. Region III). 5 Sep 1972. 6p. (DOCKET-50306–69). Dep. NTIS.

55299 (DOCKET-50282–73) PRAIRIE ISLAND NUCLEAR GENERATING PLANT, UNITS 1 AND 2. Final Safety Analysis Report, Amendment 22. (Northern States Power Co., Minneapolis, Minn.). 8 Sep 1972. 438p. (DOCKET-50306–70). Dep. NTIS.

Rinsed and additional data are presented concerning operation aspects, reactor site, cooling system, containment system, engineered safeguards, instrumentation, electrical systems, auxiliary systems, power conversion system, radioactive waste disposal system, testing program, and safety analysis. (D.C.C.)

55300 (DOCKET-50285–70) FORT CALHOUN STATION, UNIT 1. Clarification of Environmental Protection of Containment Prestressing Tendons. (Directorate of Regulatory Operations (AEC), Denver, Colo. Region IV). 11 Jul 1972. 5p. Dep. NTIS.

55301 (DOCKET-50285–71) FORT CALHOUN STATION, UNIT 1. Final Environmental Statement. (Directorate of Licensing (AEC), Washington, D. C.). Aug 1972. 272p. Dep. NTIS.

Information concerning chemical, radioactive, and thermal discharges from the reactor is presented. The effects of reactor operations on the environment are analyzed. Ecological, hydrological, and meteorological data on the reactor site are included. Cost-benefit analysis for reactor operation is presented. (D.C.C.)

55302 (DOCKET-50285–72) FORT CALHOUN STATION, UNIT 1. Report of a Minor Variance from the Final Safety Analysis Report. (Directorate of Regulatory Operations (AEC), Denver, Colo. Region IV). 12 Sep 1972. 4p. Dep. NTIS.

Additional information is presented concerning the specifications of welds in the primary pressure boundary piping. (D.C.C.)

55303 (DOCKET-50289–66) THREE MILE ISLAND NUCLEAR STATION, UNIT 1. Final Safety Analysis Report, Amendment 28. (Metropolitan Edison Co., Reading, Pa.). 31 Aug 1972. 27p. Dep. NTIS.

Requested and revised data are presented concerning site meteorology; engineered safeguards; instrumentation; auxiliary systems; radioactive waste disposal system; personnel; operations; and testing program. (D.C.C.)

55304 (DOCKET-50293–88) PILGRIM NUCLEAR POWER STATION. Evaluation of Facilities and Systems. (Directorate of Licensing (AEC), Washington, D. C.). 1 Sep 1972. 4p. Dep. NTIS.

The possibility of Class 1 equipment being flooded by the failure of the circulating water system or the fire protection system is analyzed. (D.C.C.)

55305 (DOCKET-50293–90) PILGRIM NUCLEAR POWER STATION. Issuance of Facility Operating License DPR-35, Amendment 1. (Directorate of Licensing (AEC), Washington, D. C.). 15 Sep 1972. 257p. Dep. NTIS.

55306 (DOCKET-50295–61) ZION STATION NUCLEAR POWER PLANT, UNITS 1 AND 2. Final Safety Analysis Report, Amendment 22. (Commonwealth Edison Co., Chicago, Ill.). 10 Aug 1972. 454p. (DOCKET-50304–61). Dep. NTIS.

Requested and revised data are presented concerning radioactive effluents; containment system; engineered safeguards; emergency core cooling system; post criticality testing; quality assurance program; personnel organization; operation procedures; safety aspects of aircraft impact; instrumentation; and electrical systems. The emergency plan for the Zion Power Reactor Units 1 and 2 is included. (D.C.C.)

55307 (DOCKET-50298–50) COOPER NUCLEAR STATION. Susceptibility of Engineered Safety Systems to Failure as a Result of Flooding. (Nebraska Public Power District, Columbus). 8 Sep 1972. 3p. Dep. NTIS.

55308 (DOCKET-50302–52) CRYSTAL RIVER NUCLEAR GENERATING PLANT, UNIT 3. Antitrust Review. (Florida Power Corp., St. Petersburg). 1 Sep 1972. 2p. Dep. NTIS.

55309 (DOCKET-50305–48) KEWAUNEE NUCLEAR POWER PLANT. Final Safety Analysis Report, Amendment 21. (Wisconsin Public Service Corp., Green Bay). 31 Aug 1972. 113p. Dep. NTIS.

Revised information is presented concerning containment system; engineered safeguards; instrumentation; protection systems; electrical systems; radioactive waste disposal systems; and safety analysis. (D.C.C.)

55310 (DOCKET-50305–49) KEWAUNEE NUCLEAR POWER PLANT. Valve Wall Thickness. (Directorate of Regulatory Operations (AEC), Glen Ellyn, Ill. Region III). 13 Sep 1972. 8p. Dep. NTIS.

55311 (DOCKET-50305–51) KEWAUNEE NUCLEAR POWER PLANT. Final Safety Analysis Report, Amendment 21, Errata Sheets. (Wisconsin Public Service Corp., Green Bay). 11 Sep 1972. 9p. Dep. NTIS.

55312 (DOCKET-50309–68) MAINE YANKEE ATOMIC POWER STATION. Worst Case LOCA Reanalyzed. (Maine Yankee Atomic Power Co., Westboro, Mass.). 12 Sep 1972. 1p. Dep. NTIS.

55313 (DOCKET-50309–69) MAINE YANKEE ATOMIC POWER STATION. Issuance of Facility Operating License DPR-36. (Directorate of Licensing (AEC), Washington, D. C.). 15 Sep 1972. 190p. Dep. NTIS.

55314 (DOCKET-50312–50) RANCHO SECO NUCLEAR GENERATING STATION, UNIT 1. Steps Taken to Correct the Item Brought to Attention in Letter Dated July 26, 1972. (Directorate of Regulatory Operations (AEC), Berkeley, Calif. (USA). Region V). 8 Sep 1972. 2p. Dep. NTIS.

Requested information is presented concerning quality assurance procedures for the installation of electrical cables. (D.C.C.)

55315 (DOCKET-50312–51) RANCHO SECO NUCLEAR GENERATING STATION, UNIT 1. Final Safety Analysis Report and License Application, Amendment 15. (Sacramento Municipal Utility District, Calif.). 11 Sep 1972. 359p. Dep. NTIS.

Requested and revised data are presented concerning the quality assurance program, cooling system, containment system, engineered safeguards, instrumentation, auxiliary systems, power conversion system, radioactive waste disposal system, testing programs, and safety analysis. Financial data on the owners of the reactor are included. The 1971 Annual Report for the Sacramento Municipal Utility District is presented. (D.C.C.)

55316 (DOCKET-50312–52) RANCHO SECO NUCLEAR GENERATING STATION, UNIT 1. Final Report on Minor Imperfections Found in Pipe Welds. (Sacramento Municipal Utility District, Calif.). 31 Aug 1972. 68p. Dep. NTIS.

55317 (DOCKET-50313-50) ARKANSAS NUCLEAR ONE, UNIT 1. Final Safety Analysis Report, Amendment 29. (Arkansas Power and Light Co., Little Rock). 8 Sep 1972. 165p. Dep. NTIS.

Financial data on the owners of the Arkansas Nuclear One Power Reactor are presented. The 1971 Annual Reports for the Arkansas Power and Light Company and the Middle South Utilities Incorporated are included. Revised data on the reactor are also presented concerning personnel, cooling system, and site meteorology. (D.C.C.)

55318 (DOCKET-50315-74) DONALD C. COOK NUCLEAR PLANT, UNITS 1 AND 2. Safety Evaluation. (Indiana and Michigan Power Co., New York). 14 Jan 1969. 152p. (DOCKET-50316-74). Dep. NTIS.

55319 (DOCKET-50315-75) DONALD C. COOK NUCLEAR PLANT, UNITS 1 AND 2. Valve Wall Thickness. (Directorate of Regulatory Operations (AEC), Glen Ellyn, Ill. Region III). 13 Sep 1972. 9p. (DOCKET-50316-75). Dep. NTIS.

55320 (DOCKET-50315-76) DONALD C. COOK NUCLEAR PLANT, UNITS 1 AND 2. Provisional Construction Permits Nos. CPPR-60 and CPPR-61. (Division of Reactor Licensing (AEC), Washington, D. C.). 25 Mar 1969. 6p. (DOCKET-50316-76). Dep. NTIS.

55321 (DOCKET-50315-77) DONALD C. COOK NUCLEAR PLANT, UNITS 1 AND 2. Tornado and Missile Considerations for the Spent Fuel Pit. (American Electric Power Service Corp., New York). Jun 1969. 60p. (DOCKET-50316-77). Dep. NTIS.

55322 (DOCKET-50315-78) DONALD C. COOK NUCLEAR PLANT, UNITS 1 AND 2. Design Changes. (American Electric Power Service Corp., New York). 10 Jun 1969. 6p. (DOCKET-50316-78). Dep. NTIS.

Design changes are described for the steam generator isolation valve, the emergency core cooling system, and the containment spray system. An increase in the average temperature for the reactor coolant is discussed. (D.C.C.)

55323 (DOCKET-50315-79) DONALD C. COOK NUCLEAR PLANT, UNITS 1 AND 2. Initial Decision. (Atomic Energy Commission, Washington, D. C. Atomic Safety and Licensing Board). 21 Mar 1969. 10p. (DOCKET-50316-79). Dep. NTIS.

Authorization for issuance of provisional construction permits for the Donald C. Cook Power Reactor Units 1 and 2 is presented. (D.C.C.)

55324 (DOCKET-50315-80) DONALD C. COOK NUCLEAR PLANT, UNITS 1 AND 2. Ice Condenser Containment Independent Analysis Program. (Division of Reactor Licensing (AEC), Washington, D. C.). 26 Jan 1972. 4p. (DOCKET-50316-80). Dep. NTIS.

55325 (DOCKET-50315-81) DONALD C. COOK NUCLEAR POWER PLANT, UNITS 1 AND 2. Benton Harbor Power Plant Limnological Studies. Part IX. The Biological Survey of July 10, 1970. (Michigan Univ., Ann Arbor. Great Lakes Research Div.). Mar 1972. 74p. (DOCKET-50316-81). Dep. NTIS.

For American Electric Power Service Corp., New York and Indiana and Michigan Electric Co., New York.

55326 (DOCKET-50315-82) DONALD C. COOK NUCLEAR POWER PLANT, UNITS 1 AND 2. Final Safety Analysis Report, Amendment 28. (American Electric Power Service Corp., New York). 23 Aug 1972. 11p. (DOCKET-50316-82). Dep. NTIS.

The environmental monitoring programs for chemical and thermal discharges from the reactors are described. (D.C.C.)

55327 (DOCKET-50317-58) CALVERT CLIFFS NUCLEAR POWER PLANT, UNITS 1 AND 2. Final Safety Analysis Report, Amendment 25. (Baltimore Gas and Electric Co., Md.). 1 Sep 1972. 57p. (DOCKET-50318-58). Dep. NTIS.

Revised and additional data are presented on the following topics: transmission lines; environmental radiation monitoring program; lightning protection for the containment structure; site emergency plan; and reliability testing of the main steam isolation valve actuation system. (D.C.C.)

55328 (DOCKET-50321-49) EDWIN I. HATCH NUCLEAR PLANT, UNIT 1. Pump and Valve Committee Report, Main Steam Isolation Valves, July 26, 1972. (Directorate of Regulatory Operations (AEC), Atlanta, GA. (USA). Region II). 7 Sep 1972. 156p. Dep. NTIS.

55329 (DOCKET-50324-43) BRUNSWICK STEAM ELECTRIC PLANT, UNITS 1 AND 2. Conclusion That BSEP Does Not Have a Flooding Problem. (Carolina Power and Light Co., Raleigh, N. C.). 1 Sep 1972. 1p. (DOCKET-50325-44). Dep. NTIS.

Due to the plant arrangement of the engineered safeguard equipment it is concluded that a failure of the circulating water system would not result in flooding of the equipment. (D.C.C.)

55330 (DOCKET-50331-52) DUANE ARNOLD ENERGY CENTER. Valve Wall Thicknesses. (Directorate of Regulatory Operations (AEC), Glen Ellyn, Ill. Region III). 5 Sep 1972. 3p. Dep. NTIS.

55331 (DOCKET-50335-33) HUTCHINSON ISLAND PLANT, UNIT 1. Draft Environmental Statement. (Directorate of Licensing (AEC), Washington, D. C.). Sep 1972. 171p. Dep. NTIS.

Information concerning chemical, radioactive, and thermal discharges from the reactor is presented. The effects of reactor operations on the environment are analyzed. Geological, ecological, and meteorological data on the reactor site are included. Cost-benefit analysis for reactor operation is presented. (D.C.C)

55332 (DOCKET-50338-51) NORTH ANNA POWER STATION, UNITS 1, 2, 3, AND 4. Environmental Considerations, Additional Information. (Virginia Electric Power Co., Richmond). 11 Sep 1972. 52p. (DOCKET-50339-48; DOCKET-50404-23; DOCKET-50405-23). Dep. NTIS.

Requested additional information is presented concerning transmission lines. (D.C.C.)

55333 (DOCKET-50341-45) ENRICO FERMI ATOMIC POWER PLANT, UNIT 2. Valve Wall Thicknesses. (Directorate of Regulatory Operations (AEC), Glen Ellyn, Ill. Region III). 13 Sep 1972. 7p. Dep. NTIS.

55334 (DOCKET-50344-31) TROJAN NUCLEAR PLANT. Inspection of August 7-11, 1972. (Directorate of Regulatory Operations (AEC), Berkeley, Calif. (USA). Region V). 7 Sep 1972. 4p. Dep. NTIS.

55335 (DOCKET-50352-28) LIMERICK GENERATING STATION, UNITS 1 AND 2. Applicant's Environmental Report, Construction Permit Stage (Revised), Supplement 2. (Philadelphia Electric Co., Pa.). 18 Sep 1972. 19p. (DOCKET-50353-28). Dep. NTIS.

55336 (DOCKET-50354-28) NEWBOLD ISLAND NUCLEAR GENERATING STATION, UNITS 1 AND 2. Population Estimates and Projections for Newbold Island Region. (Public Service Electric and Gas Co., Newark, N. J.). 18 Aug 1972. 165p. (DOCKET-50355-27). Dep. NTIS.

55337 (DOCKET-50358-41) WILLIAM H. ZIMMER NUCLEAR POWER STATION, UNIT 1. Final Environmental Statement. (Directorate of Licensing (AEC), Washington, D. C.). 9 Sep 1972. 196p. Dep. NTIS.

Information concerning chemical, radioactive, and thermal discharges from the reactor is presented. The effects of reactor operations on the environment are analyzed. Ecological, geological, hydrological, and meteorological data on the reactor site are included. Cost-benefit analysis for reactor operations is presented. (D.C.C.)

55338 (DOCKET-50361-27) SAN ONOFRE NUCLEAR GENERATING STATION, UNITS 2 AND 3. Environmental Report, Amendment 1, Supplement. (Southern California Edison Co., Rosemead, Calif.). 5 Sep 1972. 503p. (DOCKET-50362-26). Dep. NTIS.

Information concerning radioactive and thermal discharges from the reactors is presented. The effects of reactor operations on the environment are analyzed. Site meteorology and radiation monitoring program are discussed. Requested data on cost-benefit analysis for reactor operations are included. (D.C.C.)

55339 (DOCKET-50363-37) FORKED RIVER NUCLEAR GENERATING STATION, UNIT 1. Preliminary Safety Analysis Report, Amendment 22. (Jersey Central Power and Light Co., Morristown, N. J.). 8 Sep 1972. 64p. Dep. NTIS.

The preliminary safety analysis report for the Forked River Nuclear Generating Station, Unit 1 is amended by the submission of revised figures. (H.D.R.)

55340 (DOCKET-50367-31) BAILLY GENERATING STATION, NUCLEAR I. Valve Wall Thicknesses. (Directorate of Regulatory Operations (AEC), Glen Ellyn, Ill. Region III). 5 Sep 1972. 2p. Dep. NTIS.

55341 (DOCKET-50373-27) LA SALLE COUNTY STATION, UNITS 1 AND 2. Valve Wall Thicknesses. (Directorate of Regulatory Operations (AEC), Glen Ellyn, Ill. Region III). 5 Sep 1972. 3p. (DOCKET-50374-26). Dep. NTIS.

55342 (DOCKET-50390-23) WATTS BAR NUCLEAR PLANT, UNITS 1 AND 2. Preliminary Safety Analysis Report, Amendment 15. (Tennessee Valley Authority, Chattanooga). 22 Aug 1972. 47p. (DOCKET-50391–23). Dep. NTIS.

The preliminary safety analysis report for the Watts Bar Power Reactor, Units 1 and 2 is amended by the submission of revised and additional information. (H.D.R.)

55343 (DOCKET-50390–24) WATTS BAR NUCLEAR PLANT, UNITS 1 AND 2. Preliminary Safety Analysis Report, Amendment 16. (Tennessee Valley Authority, Chattanooga). 12 Sep 1972. 7p. (DOCKET-50391–24). Dep. NTIS.

The preliminary safety analysis report for the Watts Bar Power Reactor, Units 1 and 2 is amended by the submission of revised information. (H.D.R.)

55344 (DOCKET-50395–28) VIRGIL C. SUMMER NUCLEAR STATION, UNIT 1. Preliminary Safety Analysis Report, Amendment 16. (South Carolina Electric and Gas Co., Columbia). 12 Sep 1972. 223p. Dep. NTIS.

Revised and additional data are presented concerning reactor site, structures, engineered safeguards, containment system, auxiliary systems, power conversion system, and instrumentation. (D.C.C.)

55345 (DOCKET-50397–28) HANFORD NO. 2 NUCLEAR POWER PLANT. Preliminary Safety Analysis Report, Amendment 12. (Washington Public Power Supply System, Richland). 31 Aug 1972. 103p. Dep. NTIS.

Requested and revised data are presented concerning the site; cooling system; containment system; electrical system; auxiliary systems; and structures. (D.C.C.)

55346 (DOCKET-50397–32) HANFORD NO. 2 NUCLEAR POWER PLANT. Preliminary Safety Analysis Report, Amendment 12. (Washington Public Power Supply System, Richland). 31 Aug 1972. 103p. Dep. NTIS.

Requested and revised data are presented concerning auxiliary systems, reactor site, cooling system, containment system, electrical systems, power conversion system, and mechanical structures. (D.C.C.)

55347 (DOCKET-50398–18) MENDOCINO POWER PLANT, UNITS 1 AND 2. Preliminary Safety Analysis Report, Amendment 11. (Pacific Gas and Electric Co., San Francisco, Calif.). 1 Sep 1972. 137p. (DOCKET-50399–18). Dep. NTIS.

Requested and revised information is presented concerning the containment system; radioactive waste disposal; fire protection system; auxiliary systems; Class 1 structures; engineered safeguards; instrumentation; valves; support structures; piping systems; pumps; and power conversion system. (D.C.C.)

55348 (DOCKET-50398–19) MENDOCINO POWER PLANT, UNITS 1 AND 2. Environmental Report, Supplement, Volume 3. (Pacific Gas and Electric Co., San Francisco, Calif.). 11 Sep 1972. 347p. (DOCKET-50399–19). Dep. NTIS.

The environmental aspects of transmission line construction are described for the Mendocino Power Reactor, Units 1 and 2. (H.D.R.)

55349 (DOCKET-50404–22) NORTH ANNA POWER STATION, UNITS 3 AND 4. Preliminary Safety Analysis Report, Amendment 8. (Virginia Electric and Power Co., Richmond). 2 Sep 1972. 55p. (DOCKET-50405–22). Dep. NTIS.

Revised and additional data are presented on the following topics: earthquake stress limits for Class 1 equipment; mechanical properties of stainless steel pipes; quality assurance program; accident analysis; service water reservoir; and containment depressurization system. (D.C.C.)

55350 (DOCKET-50409–13) LA CROSSE BOILING WATER REACTOR. Valve Wall Thickness. (Directorate of Regulatory Operations (AEC), Glen Ellyn, Ill. Region III). 13 Sep 1972. 7p. Dep. NTIS.

55351 (DOCKET-50410–10) NINE MILE POINT NUCLEAR STATION, UNIT 2. Environmental Report, Supplement 1. (Niagara Mohawk Power Corp., Syracuse, N. Y.). 28 Aug 1972. 128p. Dep. NTIS.

Additional information is presented concerning alternate sites and power transmission lines. (D.C.C.)

55352 (INIS-mf–205) FORSMARK'S NUCLEAR POWER STATION. The Distribution of Cooling Water in Oeregrundsgrepen. Report on Experiments with Models, April–June 1971. (Swedish State Power Board, Alvkarleby. Hydraulic Lab.). Jul 1971. 198p. (In Swedish). INIS.

Model experiments are described for finding the most suitable performance and location of the paths of cooling water at the planned nuclear power station at Forsmark in Sweden. The purpose was to obtain a solution which permitted building of an extensible plant with the smallest possible temperature increase in the surroundings. Fifty-five experiments were performed in scale 1 : 350 (horizontal) and 1 : 50 (vertical). (INIS)

55353 (NEDO–10527) ROD DROP ACCIDENT ANALYSIS FOR LARGE BOILING WATER REACTORS. Paone, C. J.; Stirn, R. C.; Woolley, J. A. (General Electric Co., San Jose, Calif. Atomic Power Equipment Dept.). Mar 1972. 74p. (72-NED–18).

The analysis of super-prompt critical nuclear excursions in large water-moderated reactors is described. The technical analysis tools used in studying hypothetical nuclear transients are described herein, without considering the probability of such an occurrence. The rod drop accident has been reanalyzed generically using the improved methods, and the results of these analyses are presented. In addition, detailed sensitivity studies have been performed to evaluate the effects of initial reactor conditions, control rod worth, rod drop velocity, and scram insertion rate on the resultant peak fuel enthalpy. 38 references. (auth)

55354 RADIOPROTECTION DURING THE INTERVENTIONS AT SAINT-LAURENT-DES-EAUX. Grand, J.; Hurtiger, J. (Electricite de France, Saint-Laurent-des-Eaux). Bull. Inform. A.T.E.N. (Ass. Tech. Energ. Nucl.): No. 91, 38-53(Sep 1971). (In French).

The careful preparation of interventions and the development of an efficient radioprotection system enabled repairs to be successfully carried out on the Saint-Laurent-des-Eaux 1 reactor after the accident of 17 October 1969, without injury to the participating personnel. The work involved the localization of U debris, its recovery, and the trapping of inaccessible pieces. The operation was accomplished by establishing two large work yards in which the work was carried out over a period of several months: one on the upper plug of the reactor, and the other inside the reactor vessel. The measures taken to adapt the workers to the radioactive environment (the training of the workers, and their special equipment) are discussed. The toxicity and contamination risks run by the personnel involved in the intervention are considered. (France)

55355 U.S. REACTOR LICENSING RECENT DEVELOPMENTS. Nucl. Eng. Int.; 17: No. 193, 468-71(Jun 1972).

Legislative changes and proposals resulting from the growing opposition to nuclear energy on environmental grounds are described. These include suitable amendments to the Atomic Energy Act concerning interim licensing for plant operation; major changes in structure of AEC regulating functions and staff; new guidelines for release of radioactivity; and a program for improvement of water quality. The effect of NEPA, the National Environmental Policy Act of 1969, is discussed and future changes including proposed alterations for safety and reliability reports are considered. (UK)

Propulsion and Auxiliary Power Reactors

Refer also to abstracts 53093, 53094, 53233, 54921, 54945–54950, 54954, and 54962.

55356 (CONF-720901–(Bks.1 and 2), pp 471-9) CNSG: NUCLEAR SHIP OXYGEN ACTIVATION CALCULATIONAL METHOD WITH EXPERIMENTAL COMPARISON. Anderson, F. N. (Babcock and Wilcox, Lynchburg, Va.). 1972.

From Meeting on new developments in reactor physics and shielding calculations; Kiamesha Lake, NY. (12 Sep 1972).

The Consolidated Nuclear Steam Generator (CNSG) reactor is being considered for maritime application. In this design the compactness of the reactor system permits the steam generator to be located inside the pressure vessel. Consequently, the secondary coolant is exposed to a high-energy neutron flux field which activates the oxygen. This creates a radiation exposure hazard to personnel since the transit time of the activated secondary coolant outside the biological shield is small relative to the half-life of the activated oxygen. A method is outlined for calculating the oxygen activation and the dose rate associated with the decay gamma rays. This method was used to analyze the oxygen activation in the German Nuclear ship OTTO HAHN, which utilizes an earlier version of the CNSG design. Calculated and estimated dose rates are 0.003 and 0.01 mR/h, respectively. 15 references. (auth)

55357 (DOCKET-50238–92) N. S. SAVANNAH. Action Taken with Respect to Noncompliance Items of March 1972 Inspection. (Directorate of Regulatory Operations (AEC), Washington, D. C.). 1 Sep 1972. 3p. Dep. NTIS.

55358 (N–72–18051) BLEED-CYCLE PROPELLANT PUMPING IN A GAS-CORE NUCLEAR ROCKET ENGINE SYSTEM. Kascak, Albert F.; Easley, Annie J. (National Aeronautics and Space Administration, Cleveland, Ohio. Lewis Research Center). Mar 1972. 76p. (NASA-TM-X–2517; E–6639). NTIS.

The performance of ideal and real staged primary propellant pumps and bleed-powered turbines was calculated for gas-core nuclear rocket engines over a range of operating pressures from 500 to 5000 atm. This study showed that for a required engine operating pressure of 1000 atm the pump work was about 0.8 hp/(lb/sec), the specific impulse penalty resulting from the turbine propellant bleed flow as about 10 percent; and the heat required to preheat the propellant was about 7.8 MN/(lb/sec). For a specific impulse above 2400 sec, there is an excess of energy available in the moderator due to the gamma and neutron heating that occurs there. Possible alternative pumping cycles are the Rankine or Brayton cycles. (auth) (STAR)

55359 (NASA-TM-X–2440, pp 2-12) SPACE NUCLEAR PROPULSION SYSTEMS AND APPLICATIONS. Schwenk, Francis C. (Space Nuclear Systems Office, Washington, D. C.). Jan 1972.

From Symposium on natural and manmade radiation in space; Las Vegas, Nev. (1 Mar 1971).

The basic principles of the operation of a nuclear rocket engine are reviewed along with a summary of the early history. In addition, the technology status in the nuclear rocket program for development of the flight-rated NERVA engine is described, and applications for this 75,000-pound-thrust engine and the results of nuclear stage studies are presented. Advanced research and supporting technology activities in the nuclear rocket program are also summarized. (auth)

55360 (NASA-TM-X–2440, pp 84-91) SNAP-8 POST-SHUTDOWN GAMMA-RADIATION APPROXIMATIONS. Byrn, N. R. (Teledyne Brown Eng., Huntsville, Ala); Smith, H. T.; Manning, H. S. Jan 1972.

From Symposium on natural and manmade radiation in space; Las Vegas, Nev. (1 Mar 1971).

An evaluation was made of an approximate method for calculating the dose rate resulting from fission product gamma radiation after reactor shutdown. Safety analyses for advanced nuclear missions in space have used this technique for determining radiologically safe operations. This method assumes that the dose rate, $D_1(r,t)$, received from a shutdown reactor is directly proportional to the residual gamma power level at that time. To check the validity of this "power ratio" assumption, energy-dependent detector responses were calculated for normalized sources in the Perkins and King energy group structure for a SNAP 8 power system on a NASA space station. Gamma decay rates were then calculated by using an expanded, updated list of isotopic decay data, and from these, actual detector responses $D_2(r,t)$ were found for the SNAP 8 system. The two detector responses, D_1 and D_2, were then compared at several times after shutdown and at detector positions around the space station. An error of several thousand percent was found for many detectors at times greater than one year; it was also found that an increase in material attenuation produced an increase in error and that energy-dependent detector response, such as dose rates, showed greater discrepancy between D_1 and D_2 than did the energy flux. It was concluded that these discrepancies were caused by a decrease in the proportion of high-energy gammas released at longer shutdown times. This softening of the decay gamma spectrum with time caused an increased attenuation of decay gamma energy; invalidating the power ratio assumption. Because of the complexity of the space station geometry, these conclusions were checked and verified by a point source in infinite water calculation. The results indicate that energy-dependent calculations must be made to determine decay gamma dose rates for actual reactor configurations. A simplified method for making these calculations has been devised. (auth)

55361 (NASA-TM-X–2440, pp 257-63) RADIATION ENVIRONMENT FOR RENDEZVOUS AND DOCKING WITH NUCLEAR ROCKETS. Rogers, D. R.; Warman, E. A.; Lindsey, B. A. (Aerojet Nuclear Systems Co., Sacramento, Calif.). Jan 1972.

From Symposium on natural and manmade radiation in space; Las Vegas, Nev. (1 Mar 1971).

Planning for operations such as rendezvous and docking of a vehicle powered by a nuclear rocket engine with a space station requires consideration of the radiation environment produced by the engine in addition to the natural space radiation environment. Radiation environment data for the NERVA engine are provided which may be utilized in estimating radiation exposures associated with various space maneuvers. Spatial distributions of neutron and gamma tissue kerma rates produced during full thrust operation of the engine are presented. The corresponding biological dose rates will be due predominantly to neutron contributions except within the region in space which is shadowed by the liquid hydrogen propellant. Forward of the vehicle, dose rates will depend on the characteristics of the propellant module and payload as well as those of the engine and will vary during a mission as propellant is consumed. Final rendezvous with an orbiting space station would be achieved subsequent to full thrust operation during a period of 10 or more hours duration in which impulse is delivered by the propellant used for removal of decay heat. Consequently, post operation radiation levels are of prime importance in estimating space station exposures. Maps of gamma kerma rates around the engine are provided for decay times of 4 and 24 hours after a representative firing. Typical decay curves illustrating the dependence of post operation kerma rates on decay time and operating history are included. Examples of the kerma distributions around the engine which result from integration over specific exposure periods are shown. (auth)

55362 (NASA-TM-X–2440, pp 264-9) RADIATION EXPOSURE TO THE ORBITING LUNAR STATION AND LUNAR SURFACE RELATED TO REUSABLE NUCLEAR SHUTTLE OPERATIONS. Hutchinson, Paul I. (Lockheed Missiles and Space Co., Sunnyvale, Calif.). Jan 1972.

From Symposium on natural and manmade radiation in space; Las Vegas, Nev. (1 Mar 1971).

The radiation environment created by the Reusable Nuclear Vehicle (RNS) in performing its normal mission functions while in the lunar vicinity and the impact of that environment on the Orbiting Lunar Station (OLS) and/or the lunar surface are examined. Trajectory data, representative of nominal lunar arrival and departure maneuvers, reflecting the unique operating characteristics of the nuclear engine, provide the basic geometry model for the evaluation of the radiation exposures. Other factors included in the evaluation are the operating source term (neutron and gamma radiation), shutdown source term (fission point gamma radiation), view angle (shielding effects of stage and engine hardware), separation distance, exposure interval, time after shutdown, and prior reactor operating history. To permit recovery of the impulse available from the coolant flow required by the high decay heat rates at reactor shutdown, the main engine LOI burn is terminated with the RNS in elliptical orbit and the coolant impulse used to circularize the orbit and complete OLS rendezvous. This circularization maneuver may take up to 40 hours or more, depending on the percent of cooldown impulse recovery planned. Radiation exposures at the OLS were evaluated for two conditions: (1) final orbit insertion 10 km ahead of the OLS, and (2) 10 km behind the OLS assuming a 90-percent cooldown impulse recovery about 12 hours of cooling. Radiation exposures to the OLS during the lunar orbit departure burn (TEI) were evaluated for RNS startup 10 km behind the OLS and 10 km and 20 nm ahead of the OLS. Exposures received at the OLS for these cases are higher than for the LOI burn, since the reactor operation occurs much closer to the OLS, indicating greater initial separations will normally be desirable. Lunar surface exposures from the operating reactor were evaluated for both the arrival and departure burns and while there is little probability that manned bases would lie along the paths in which measurable exposures would be recorded, the analyses do indicate the need to consider this possibility in planning such operations. Conclusions supported by the analyses and recommended operational constraints for the RNS are presented. (auth)

55363 (NASA-TM-X–2440, pp 270-6) INTEGRAL DOSE DURING CONSTANT-VELOCITY MOTION NEAR A SPACE POWER REACTOR. Manning, H. S. (Marshall Space Flight Center, Huntsville, Ala.). Jan 1972.

From Symposium on natural and manmade radiation in space; Las Vegas, Nev. (1 Mar 1971).

The dose rate in a rotationally-symmetric radiation field near a space power reactor is assumed to be inversely proportional to separation distance squared and directly proportional either to a constant or a constant times the sine-cubed of a polar angle. Constant velocity motion (constant speed and direction) is examined in both cases in both two- and three-dimensional geometries. The two-dimensional geometry occurs when the line of motion and the field axis of symmetry are co-planar. The dose integral in the sine-cubed region may be integrated directly, but a more useful form is obtained after a change of variable. A coordinate system rotation greatly simplifies the results. The three-dimensional problem is integrated after a change of variable. Finally, tables of normalized functions are presented and discussed. (auth)

55364 (NASA-TM-X–2440, pp 292-8) NUCLEAR RADIATION PROBLEMS, UNMANNED THERMIONIC REACTOR ION PROPULSION SPACECRAFT. Mondt, J. F.; Sawyer, C. D.; Nakashima, A. (California Inst. of Tech., Pasadena). Jan 1972.

From Symposium on natural and manmade radiation in space; Las Vegas, Nev. (1 Mar 1971).

A nuclear thermionic reactor as the electric power source for an electric propulsion spacecraft introduces a nuclear radiation environment. The radiation environment affects the spacecraft configuration, the use and location of electrical insulators and the science experiments. The spacecraft is conceptually configured to minimize the nuclear shield weight by (1) a large length to diameter spacecraft, (2) eliminating piping penetrations through the shield, and (3) using the mercury propellant as gamma shield. The alumina material is damaged by the high nuclear radiation environment in the reactor. For the more ambitious (250 kW(e) 30 to 40,000 hour) electric propulsion missions it is desirable to locate the alumina insulator outside the reflector or develop a more radiation resistant insulator. The net spacecraft nuclear environment is being investigated to determine if there is a problem. It appears some experiments may require local radiation shielding. (auth)

55365 (NASA-TM-X-2440, pp 299-306) THERMIONIC REACTOR POWER SYSTEM: EFFECTS OF RADIATION ON INTEGRATION WITH MANNED SPACE STATION. Gietzen, A. J.; Heath, C. A.; Perry, L. W. (Gulf General Atomic Co., San Diego, Calif.). Jan 1972.

From Symposium on natural and manmade radiation in space; Las Vegas, Nev. (1 Mar 1971).

The application of a thermionic reactor power system to the modular space station is described. The nominal net power is 40 kW(e), with the power system designed to be applicable over the power range from 25 to 60 kW(e). The power system is designed to be launched by the space shuttle. The lifetime goal is 5 years. Radiation protection is provided by LiH neutron shielding and W gamma shielding in a shaped 4π configuration, i.e., the reactor is shielded on all sides but not to equal extent. Isodose contours are presented for the region around the modular space station. Levels and spectral distribution of radiation are given for later evaluation of effects on space station experiments. Parametric data on the effects of separation distance on power system mass are presented. An alternate concept in which a reactor system is connected to the Space Station by a tether at a distance of 1 to 2.5 miles is discussed. The effect upon power system performance and shielding requirements of the tethered concept are presented. (auth)

55366 (NASA-TM-X-2440, pp 392-6) CARPET PLOT DATA FORMAT. O'Byrne, Joseph M. (Univ. of Massachusetts, Amherst). Jan 1972.

From Symposium on natural and manmade radiation in space; Las Vegas, Nev. (1 Mar 1971).

Analysis and interpretation of data is the crucial phase of the decision making process. The interplay between variables must be considered as to their relative significance upon the final result, and sometimes time-sensitive decisions must be made when actual events deviate from predicted information, such as Apollo 13. As the number of variables increases past say four, the traditional method of cross-plotting tends to break down, and digital/analog results cannot present a sharply defined method of analysis. A graphical system named "carpet plot," (since it covers anything), is suggested in which an unlimited number of complicated relationships of variables can be evaluated. (auth)

55367 (NASA-TM-X-2440, pp 440-8) EXTERNAL GAMMA RADIATION ENVIRONMENT FROM THE KIWI, PHOEBUS, AND PEWEE REACTORS. Malenfant, Richard E. (Los Alamos Scientific Lab., N. Mex.). Jan 1972.

From Symposium on natural and manmade radiation in space; Las Vegas, Nev. (1 Mar 1971).

Ground tests of high-powered propulsion-prototype reactors have provided several opportunities to observe the external radiation environment. Although the data may not be directly applicable to the evaluation of radiation levels for flight systems, they do provide an extensive set of results for comparison with calculations on systems similar to those which may be flown. In addition, the experience with reactor radiation fields covering square miles is considered unique. Reactor tests have been conducted in free air (the Kiwi B4D and B4E reactors) and inside of open well shields (the Phoebus 1-B, Phoebus 2-A, and Pewee 1 reactors). Measurements were taken over distances ranging from contact with the pressure vessel out to greater than 5000 feet both during operation and after shutdown. Separate assessments of the effects of direct beam, scatter, capture, and activation were attempted. Some measurements characteristic of each of the systems named will be presented and compared with results of calculations. (auth)

55368 (NASA-TM-X-2440, pp 449-59) APPLICATION OF TRANSPORT TECHNIQUES TO THE ANALYSIS OF NERVA SHADOW SHIELDS. Capo, M. A.; Anderson, S. L. (Westinghouse Electric Corp., Large, Pa.). Jan 1972.

From Symposium on natural and manmade radiation in space; Las Vegas, Nev. (1 Mar 1971).

To design a minimum weight shield internal to the NERVA Nuclear Subsystem, the capabilities and limitations of the analytical techniques must be clearly understood. To further this understanding, an in-depth study was performed in which both one and two dimensional discrete ordinate techniques were applied to the analysis of several shadow shield experiments. These experiments were performed on the PAX reactor which was modified to simulate the R-1 reactor, an upgraded version of the NRX nuclear rocket technology series of reactors tested at Nevada during the past six years. Two significantly different shield mockups were analyzed. In one experiment, the internal shield material called BATH (a composite mixture of boron carbide, aluminum and titanium hydride) was mocked up by alternating thin sheets of titanium, Boral, aluminum and polyethylene. In another experiment a borated steel-liquid hydrogen shield was mocked up by alternating layers of borated steel and polyethylene. The two-dimensional discrete ordinates code, DOT-11W, was employed to calculate 16 group (11 fast and 5 thermal) neutron fluxes internal to the shield mockups. These fluxes were processed by the NAGS code to obtain photon sources throughout the assembly. Photon flux distributions were obtained by employing these sources in fixed source, thirteen group, DOT calculations. An S_8 angular quadrature was employed. Approximately 8000 mesh cells were utilized to describe the two-dimensional geometry. One-dimensional analysis was accomplished by means of the ANISN code. Briefly, this technique employed 29 (16 neutron and 13 photon) energy groups simultaneously in one problem with the photon source generation process treated as a downscattering interaction from one of the neutron groups to one of the photon groups. Two approximations to account for transverse leakage were investigated: (1) the addition of a DB^2 correction to the energy-dependent absorption cross section, and, (2) a "void" streaming correction for geometrical regions containing no material. (auth)

55369 (NASA-TM-X-2440, pp 460-5) RADIATION HEATING IN SELECTED NERVA ENGINE COMPONENTS. Courtney, J. C.; Hertelendy, N. A.; Lindsey, B. A. (Aerojet Nuclear Systems Co., Sacramento, Calif.). Jan 1972.

From Symposium on natural and manmade radiation in space; Las Vegas, Nev. (1 Mar 1971).

The role of heating from nuclear radiation in design of the NERVA engine is treated. Generally, radiation heating is more restrictive in design than material degradation considerations. Some components are subjected to very high gamma heating rates in excess of 0.5 Btu/in^3-sec in steel in the primary nozzle or 0.25 Btu/in^3-sec in aluminum in the pressure vessel. These components must be cooled by a fraction of the liquid hydrogen propellant before it is passed through the core, heated, and expanded out the nozzle as a gas. Other components that are subjected to lower heating rates such as the thrust structure and the disk shield are designed so that they would not require liquid hydrogen cooling. Typical gamma and neutron heating rates, resulting temperatures, and their design consequences are covered. The calculational techniques used in the nuclear and thermal analyses of the NERVA engine are briefly treated. (auth)

55370 (NASA-TM-X-2440, pp 471-5) RADIATION HARDENING OF COMPONENTS AND SYSTEMS FOR NUCLEAR ROCKET VEHICLE APPLICATIONS. Greenhow, William A.; Cheever, Paul R. (Convair Aerospace Div., Fort Worth, Tex.). Jan 1972.

From Symposium on natural and manmade radiation in space; Las Vegas, Nev. (1 Mar 1971).

The results of the analysis of the S-II and S-IVB components, although incomplete, indicate that many Saturn V components and subsystems, e.g., pumps, valves, etc., can be radiation hardened to meet nuclear rocket vehicle (NRV) requirements by material substitution and minor design modifications. Results of these analyses include: (1) recommended radiation tolerance limits for over 100 material applications, (2) design data which describes the components of each system which can be employed on the NRV and the modifications necessary to radiation harden other components, (3) presentation of radiation hardening examples of systems which will provide guidance to component designers, and (4) designing radiation effects tests to supply data for selecting materials with confidence. (auth)

55371 (NASA-TM-X-2440, pp 681-6) DISCRETE ORDINATES—MONTE CARLO COUPLING: A COMPARISON OF TECHNIQUES IN NERVA RADIATION ANALYSIS. Lindstrom, D. G.; Normand, E.; Wilcox, A. D. (Aerojet Nuclear Systems Co., Sacramento, Calif.). Jan 1972.

From Symposium on natural and manmade radiation in space; Las Vegas, Nev. (1 Mar 1971).

In the radiation analysis of the NERVA Nuclear Rocket System, two-dimensional discrete ordinates calculations are sufficient to provide detail in the pressure vessel and reactor assembly. Other parts of the system, however, require three-dimensional Monte Carlo analyses. To use these two methods in a single analysis, a means of coupling was developed whereby the results of a discrete ordinates calculation can be used to produce source data for a Monte Carlo calculation. Several techniques for producing source detail were investigated. Results of calculations on the NERVA system are compared and limitations and advantages of the coupling techniques discussed. (auth)

55372 (NASA-TM-X-2440, pp 692-6) APPLICATION OF MORSE TO RADIATION ANALYSIS OF NUCLEAR FLIGHT PROPULSION MODULES. Woolson, W. A. (Aerojet Nuclear Systems Co., Sacramento, Calif.). Jan 1972.

From Symposium on natural and manmade radiation in space; Las Vegas, Nev. (1 Mar 1971).

Several modifications and additions were made to the multigroup Monte Carlo code MORSE to implement its use in a computational procedure for performing radiation analyses of NERVA Nuclear Flight Propulsion Modules. These changes include the incorporation of a new general geometry module; the inclusion of an expectation tracklength estimator; and the option to obtain source information from two dimensional Discrete Ordinates calculations. Computations comparing MORSE and a point cross section Monte Carlo code, COHORT, were made in which a coupled Discrete Ordinates/Monte Carlo procedure was used to calculate the gamma dose rate at tank top locations of a typical propulsion module. The dose rates obtained from the MORSE computation agreed with the dose rates obtained from the COHORT computation to within the limits of the statistical accuracy of the calculations. (auth)

55373 (NASA-TM-X-2440, pp 1016-20) VENTING OF FISSION PRODUCTS AND SHIELDING IN THERMIONIC NUCLEAR REACTOR SYSTEMS. Salmi, E. W. (Los Alamos Scientific Lab., N. Mex.). Jan 1972.

From Symposium on natural and manmade radiation in space; Las Vegas, Nev. (1 Mar 1971).

Most thermionic reactors are designed to allow the fission gases to escape out of the emitter. There exist several design variations to allow the gas to escape from the reactor core. The final disposition of the gas has several interesting problems. If the gas is put into a chamber, its volume is too large to be contained in the shield. Fortunately the fission gases do not pose a radiation problem at 100 ft. Because of the long half-life the fission gases could prevent any close approach to the reactor after it has been shut down. The fission gases could instead be stored in an absorption trap. An absorption trap is usually assumed to require very low temperatures, however, experimental data indicate that reservoirs at several hundred degrees C can be useful. Another scheme is to simply allow the fission gases to escape. Again, because of the low activity of the fission products, this method should pose no radiation hazards. (auth)

55374 (PREAS-4041-R-4) FRONT ISLAND SHIELD THERMAL DISPLACEMENTS. Tajirian, G. (Allstates Design and Development Co., Inc., Trenton, N. J. (USA)). 16 Mar 1961. Contract AT(11-1)-171. 51p. Dep. NTIS.

For General Electric Co., Cincinnati, Ohio. Aircraft Nuclear Propulsion Dept.

Process Heat and Desalination Reactors

55375 (INIS-mf-172) METROPOLITAN SITING OF NUCLEAR HEATING PLANTS. Beranek, J. (Ceskoslovenska Komise pro Atomovou Energii, Prague). 1970. (CONF-690565-1). INIS.

From Nuclear heating symposium; Tatranska Lomnica, Czechoslovakia (13 May 1969).

Acceptable hazards are discussed to individuals and population around nuclear heating plants constructed inside urban areas, arising from fission products released into the environment during normal operation or in the event of accident. The maximum permissible doses to the thyroid and to the whole body are in Czechoslovakia set at 100 Rems and 25 Rads, respectively. A new limiting factor is discussed concerning the population living in the neighborhood of the projected heating plants in Prague and in Brno—the integral population dose. The question of technical safeguards is dealt with in detail. A combination of all possible types of technical safeguards is required to prevent or minimize damage to safety barriers (emergency cooling system) and to prevent or minimize the release of fission products (various types of containment, containment spray system, filtering system, stack height). Examples of safeguard systems are discussed in relation to the requirements for safety of nuclear power or heating plants sited within conurbations. (INIS)

55376 (INIS-mf-172, pp 7-13) DISTRICT HEATING IN CZECHOSLOVAKIA AND POSSIBILITY OF USING NUCLEAR POWER REACTORS FOR THIS PURPOSE. Vlach, J. (Vyzkumny Ustav Energeticky, Prague (Czechoslovakia)). 1970. (CONF-690565-8). INIS.

From Nuclear heating symposium; Tatranska Lomnica; Czechoslovakia (13 May 1969).

The problems of centralized and decentralized heating in Czechoslovakia are briefly outlined and considerations are presented leading to the orientation to nuclear heating and power plants. To calculate the full heat supply, the overall heat output is divided in nuclear base load and peak load parts. Peak load plants use fossil fuels and also serve as a stand-by. The ratio of nuclear heat to the total output, in addition to fuel prices, depends mainly on duration of the peak load heat demand τ and on the type of the turbine used. For $\tau \geq 5{,}000$ hrs/yr, back-pressure turbines are suitable; smaller τ require condensing bleeder turbines. A distribution of the load among several nuclear reactors may be considered for large plants with high τ. This makes it possible to site nuclear heating and power plants at shorter distances from each other and thus to reduce the cost of the heat distribution system. Further development depends heavily on the cost of nuclear equipment. (INIS)

55377 PROCESS HEAT FROM HIGH TEMPERATURE REACTORS. Bode, K. H.; Schloesser, J. BCC-Nach.; 53: No. 9-10, 259-66(1971). (In German).

A review on the energy market in the Federal Republic of Germany and its estimated further development is followed by a description of various processes for the conversion of fossil raw materials by means of heat from high temperature reactors and the subsequent utilization of these conversion products in some branches of the basic industry. Outlines are given of special reactor engineering problems that have to be solved as they are vital for the utilization of nuclear process heat. (INIS)

Research and Test Reactors

Refer also to abstracts 53224, 55116—55118, 55134, 55144, and 55437.

55378 (AI-AEC-12951) VIM-1: A NON-MULTIGROUP MONTE CARLO CODE FOR ANALYSIS OF FAST CRITICAL ASSEMBLIES. Levitt, L. B.; Lewis, R. C. (Atomics International, Canoga Park, Calif.). 15 May 1970. Contract AT(04-3)-701. 90p. Dep. NTIS.

VIM-1 is the first of a series of Monte Carlo codes designed for analysis of fast critical experiments and fast reactor design. It has been expressly prepared for the analysis of fast critical assemblies of the plate-drawer type. It is written in Fortran, for use on either CDC or IBM computers of the 6600 or 360-75 and up class. Special versions for handling bare and reflected spheres and reflected cylinders are also available, primarily for performing comparisons of heterogeneous and homogeneous calculations. The library uses point cross-section data, rather than multi-group constants. Angular data is in the form of cumulative distribution functions, at energies tailored to the needs of each isotope. Computation times range from three minutes to one hour on the CDC 6600 (depending on the size and spectrum of the assembly) to obtain probable statistical errors in the eigenvalue of less than 0.5%, thus providing a powerful tool for reactor design and experimental analysis at a reasonable cost. 6 references. (auth)

55379 (ANCR-1085) ETR POWER: VARIATION ANALYSIS. Burdick, E. E.; Liebenthal, J. L. (Aerojet Nuclear Co., Idaho Falls, Idaho). Aug 1972. Contract AT(10-1)-1375. 62p. Dep. NTIS.

Between June and December 1971, small (nominally ±0.5% amplitude), intermittent power variations of unknown origin were witnessed at the Engineering Test Reactor. The results of the investigative program carried out to determine the cause of the variations are reported. Included in the report are diagnostics, inspections, and analyses. 11 references. (auth)

55380 (CEA-N-1211) T424 FACILITY FOR DISPLACING FUEL UNDER IRRADIATION. Descamps, Jean-Marie (Commissariat a l'Energie Atomique, Saclay (France). Centre d'Etudes Nucleaires). Jul 1972. 18p. (In French). Dep. NTIS (U. S. Sales Only).

The T424 facility was designed for experimental fuel irradiations in swimming-pool reactors. The amount of nuclear power released in the fuel is either manually controlled or servo-controlled by an experimental parameter. OSIRIS currently uses three facilities of this nature. (auth)

55381 (CONF-710959--, Paper 6) SODIUM INPILE LOOP. Inagaki, H. 5p.

From Meeting on fission and corrosion product behaviour in primary systems of LMFBR's; Bensberg, Germany (20 Sep 1971).

An inpile liquid sodium loop, for use in the JPR-2 Reactor at JAERI, is described. Results of inpile and out-of-pile performance testing are summarized. (J.M.J.)

55382 (CONF-720901--(Bks.1 and 2), pp 431-41) FFTF PIPE CHASE STREAMING EXPERIMENT. McGregor, B. J.; Muckenthaler, F. J. (Oak Ridge National Lab., Tenn.). 1972.

From Meeting on new developments in reactor physics and shielding calculations; Kiamesha Lake, NY. (12 Sep 1972).

The FFTF reactor design includes sodium inlet and outlet pipes which penetrate the 4-ft-thick reactor cavity wall at a height of approximately 19 ft above the top of the core. Most neutrons enter these pipe chases at a slant angle and streaming subsequent to scattering in the chase contributes an important source of neutrons to the heat exchanger vaults. Streaming of neutrons can take place along the sodium in the pipes as well as along the clearance gaps and along the low-density insulation surrounding the pipes. Experiments were designed to validate analytical methods which will be used to predict the flux levels in the heat exchanger vault and piping. The experimental calculation reported was a steel-lined concrete pipe chase and sodium-filled pipe mockup placed in a collimated neutron beam at an angle of 60 deg. (auth)

55383 (CONF-720901--(Bks.1 and 2), pp 445-58) STATUS OF THE FTR SHIELDING DESIGN ANALYSIS AND METHODS. Rathbun, J. L.; Fox, P. F. (Westinghouse Electric Corp., Madison, Pa.). 1972.

From Meeting on new developments in reactor physics and shielding calculations; Kiamesha Lake, NY. (12 Sep 1972).

A summary is presented of the calculation methods and the relationship to the actual shielding design of the Fast Test Reactor (FTR). Particularly difficult shielding analysis areas are described. These areas are the reactor head bulk penetration and streaming problems, the reactor cavity source problem and streaming into adjacent pipeways and main heat transport cells. The methods of resolution of these problem areas are presented. (auth)

55384 (CONF-720901--(Bks.1 and 2), pp 613-22) USE OF CFRMF INTEGRAL DATA IN CROSS SECTION EVALUATIONS. Harker, Y. D.; Turk, E. H. (Aerojet Nuclear Co., Idaho Falls, Idaho). 1972.

From Meeting on new developments in reactor physics and shielding calculations; Kiamesha Lake, NY. (12 Sep 1972).

The Coupled Fast Reactivity Measurement Facility (CRFMF) is being used in evaluating neutron cross section data files for the neutron energy range from 1 keV to 1 MeV. The main materials being studied are fission product isotopes where little or no differential data are available. Two methods of measurement are used, capture measurements and reactivity measurements. The results are combined with semi-empirical model calculations to produce evaluated files of differential cross section values. The evaluation methods described are expected to reduce overall uncertainties in fission product cross sections from 40% to less than 10%. This reduction would result in significant reductions in the uncertainties of the important parameters of a Liquid Metal Fast Breeder Reactor and the final overall uncertainties would fall within the acceptable limits as established in literature. 10 references. (auth)

55385 (CONF-720901--(Bks.1 and 2), pp 623-35) EVALUATION AND INTERPRETATION OF INTEGRAL EXPERIMENTS IN FAST CRITICALS. Kiefhaber, Edgar (Kernforschungszentrum, Karlsruhe, Ger.). 1972.

From Meeting on new developments in reactor physics and shielding calculations; Kiamesha Lake, NY. (12 Sep 1972).

Clean integral experiments are examined because they are of general interest and use compared to the rather limited applicability of mock-up experiments. The different approaches to using the information obtained from integral experiments are indicated. The activities at Karlsruhe to improve the nuclear data and methods of calculation are described, with special emphasis on some of the more recent results. First, the improvements in the group constant sets are considered; this is followed by studies of more specific problems, such as the influence of the energy dependence of the fission neutron spectrum, or the difficulties encountered in calculating the reactivity coefficients of reactor materials. 21 references. (auth)

55386 (CONF-720901--(Bks.1 and 2), pp 636-44) MONTE CARLO CALCULATIONS FOR THE CRITICAL EXPERIMENT OF THE GERMAN INCORE THERMIONIC REACTOR. Schmidt, F. A. R.; Bernnat, W.; Dagbjartsson, S. (Institut fuer Kernenergetik, Stuttgart). 1972.

From Meeting on new developments in reactor physics and shielding calculations; Kiamesha Lake, NY. (12 Sep 1972).

A critical facility for the German Incore Thermionic Reactor (ITR) was established at the Jülich Nuclear Research Center. Various measurements were performed at this facility. Partly they have to be analyzed by Monte Carlo. This is done using the multigroup Monte Carlo Code MORSE-K. A short description of this code is given. Among the tasks which had to be solved were the investigation of various cross section libraries, the discussion of geometrical details necessary to describe the facility in calculations and the determination of reactivity worths of different materials at different positions in the reactor. The principal approaches to solve these problems are described. First results are given and discussed. (auth)

55387 (CONF-720901--(Bks.1 and 2), pp 645-59) EXPERIMENTAL RESULTS FROM TWO Pu-FUELED FAST CRITICAL ASSEMBLIES. Boehme, R.; Fischer, E. A.; Mc Grath, P. E.; Scholtyssek, W. (Kernforschungszentrum, Karlsruhe, Ger.). 1972.

From Meeting on new developments in reactor physics and shielding calculations; Kiamesha Lake, NY. (12 Sep 1972).

Two Pu-fueled fast critical assemblies of different enrichment were studied in the Karlsruhe Fast Critical Facility SNEAK to test cross section data and calculational methods. The measurements suitable for this purpose are central reaction rates and reactivity worths. In addition, measurement of the core material buckling, which characterizes the core material independent of its geometry and surroundings, was also included. The measurement procedures employed are described in some detail. The evaluation of these measurements was done with the most recent cross section sets and computer codes available at Karlsruhe. A portion of the experiments were also calculated with a cross section set based on ENDF/B data. 8 references. (auth)

55388 (CONF-720901--(Bks.1 and 2), pp 660-86) IMPACT OF THE NEW LASL DELAYED NEUTRON DATA ON FTR DESIGN. Ramchandran, S.; Birney, K. R. (Westinghouse Advanced Reactors Div., Madison, Pa.). 1972.

From Meeting on new developments in reactor physics and shielding calculations; Kiamesha Lake, NY. (12 Sep 1972).

Three different sets of delayed neutron parameters were used for evaluating β_{eff} and the Ihs to %Δk/k conversion factor in FTR and its criticals. The impact of using different delayed neutron data in the analysis of critical experiments and FTR design is discussed. The new delayed neutron parameters have particular significance in determining the ^{10}B poison loading in FTR control rods resulting in a potential improvement in the lifetime characteristics of the poison assemblies. 18 references. (auth)

55389 (CONF-720901--(Bks. 1 and 2), pp 700-12) MEASUREMENT OF β_{eff} IN Pu-FUELED FAST CRITICAL ASSEMBLIES. Boehme, R.; Fisher, E. A.; McGrath, P. E. (Kernforschungszentrum, Karlsruhe, Ger.).

From Meeting on new developments in reactor physics and shielding calculations; Kiamesha Lake, NY. (12 Sep 1972).

The effective delayed neutron fraction, β_{eff}, and the normalization integral were measured in two mixed-oxide fueled fast critical assemblies, using the apparent reactivity of a ^{252}Cf-source, and traverses of reaction rates. In addition, ratios of β_{eff} values of different isotopes were measured by studying effect of the transport of delayed neutron precursors with a pile oscillator. The evaluation of these measurements was done with the most recent cross section sets available at Karlsruhe. The experiments give larger β_{eff} values than those calculated with Keepin's data, and indicate that the difference is mainly due to β of ^{239}Pu and, to a lesser extent, to β of ^{238}U. 9 references. (auth)

55390 (CONF-720901--(Bks.1 and 2), pp 739-67) ANALYSIS OF SODIUM-VOID EXPERIMENTS IN THE FTR ENGINEERING MOCKUP CRITICAL ASSEMBLY. Travelli, A.; Beitel, J. C. (Argonne National Lab., Ill.). 1972.

From Meeting on new developments in reactor physics and shielding calculations; Kiamesha Lake, NY. (12 Sep 1972).

A series of sodium-void experiments in the engineering mockup critical assembly of the FTR (FTR-EMC) is analyzed. The computational model is based on X-Y diffusion perturbation theory with ENDF/B-I data. The analytical procedure yields results in excellent agreement with the experiments and provides a demonstrated tool for the prediction of other sodium-void effects. In addition, the results indicate that the gross heterogeneities of the FTR core, including control rods, sodium channels and test loops, exert an overwhelming influence on the spatial distribution of the sodium-void coefficient throughout the FTR core. 13 references. (auth)

55391 (CONF-720901–(Bks.1 and 2), pp 839-87) FTR NEUTRONICS: STATUS, PROBLEMS, AND DEVELOPMENT PROGRAMS. Hofmann, P. L. (Hanford Engineering Development Lab., Richland, Wash.). 1972.

From Meeting on new developments in reactor physics and shielding calculations; Kiamesha Lake, NY. (12 Sep 1972).

The nuclear design features of the FTR and the more significant nuclear problem areas are discussed. A description of the nuclear development programs is given and their impact on FFTF design decisions is assessed. Finally, a brief discussion of the plans for nuclear startup and for the Irradiation Test Program is presented. 93 references. (auth)

55392 (CONF-720901–(Bks.1 and 2), pp 973-85) SODIUM VOID STUDIES AND RELATED HETEROGENEITY EFFECTS IN ZPPR-2, THE BENCHMARK DEMONSTRATION ASSEMBLY. Palmer, R. G.; Davey, W. G.; Collins, P. J.; Amundson, P. I.; Kaiser, R. E.; Beck, C. L. 1972.

From Meeting on new developments in reactor physics and shielding calculations; Kiamesha Lake, NY. (12 Sep 1972).

Sodium reactivity experiments in the ZPPR-2 critical assembly are described. The problems in relating the measurements to a large power reactor are discussed from the aspect of differences in heterogeneity in the cores. (H.D.R.)

55393 (CONF-720901–(Bks.1 and 2), pp 1006-15) EFFECT OF CORE CONFIGURATION ON ^{238}U DOPPLER MEASUREMENTS IN ZPPR ASSEMBLY 2. Kaiser, R. E.; Gasidlo, J. M. 1972.

From Meeting on new developments in reactor physics and shielding calculations; Kiamesha Lake, NY. (12 Sep 1972).

From the data on the sodium-void comparisons and the heterogeneity comparisons on natural UO_2 samples in ZPPR-2, it would appear that the effects of both can be calculated reasonably well, and that the heterogeneity effect is small. The Doppler reactivities, however, are calculated with two to three times the accuracy of the gross sample worths and the ^{238}U small-sample measurements. There are at least two possible factors to explain this phenomenon; (1) the discrepancy in the gross worth calculation is due to a non-resonance component of the cross-section, (2) the hot-cold interaction between the sample and the surrounding core leads to a slight distortion of the measurements. 8 references. (auth)

55394 (CONF-720901–3) FFTF PIPE CHASE STREAMING EXPERIMENT. McGregor, B. J.; Muckenthaler, F. J. (Oak Ridge National Lab., Tenn.). 1972. 12p. Dep. NTIS.

From Meeting on new developments in reactor physics and shielding calculations; Kiamesha Lake, NY. (12 Sep 1972).

The present FFTF reactor design includes sodium inlet and outlet pipes which penetrate the 4-ft-thick reactor cavity wall at a height of approximately 19 ft above the top of the core. Most neutrons enter these pipe chases at a slant angle and streaming subsequent to scattering in the chase contributes an important source of neutrons to the heat exchanger vaults. Streaming of neutrons can take place along the sodium in the pipes as well as along the clearance gaps and along the low-density insulation surrounding the pipes. Experiments were designed to validate analytical methods which will be used to predict the flux levels in the heat exchanger vault and piping. The experimental calculation reported on was a steel-lined concrete pipe chase and sodium-filled pipe mockup placed in a collimated neutron beam at an angle of 60 deg. (auth)

55395 (CONF-720901–12) SUMMARY OF ANALYSES OF PLATE VS. PIN MEASUREMENTS EMPHASIZING REACTIVITY AND SODIUM VOID EFFECTS. Pitterle, T. A.; Paik, N. C. (Westinghouse Electric Corp., Madison, Pa. Advanced Reactors Div.). 1972. Contract AT(11-1)-3045. 31p. Dep. NTIS.

From Meeting on new developments in reactor physics and shielding calculations; Kiamesha Lake, NY. (12 Sep 1972).

Analyses of measurements performed in pin and plate environments of nearly identical composition in critical assemblies ZPPR-2 and ZPR-6-7 are presented. Plate environment of critical assemblies introduces heterogeneity effects which differ significantly from that of an LMFBR which is comprised of fuel pins typically about $^1/_4$ inch in diameter. Consequently, the recent pin versus plate measurements are an important contribution to removing uncertainties in the extrapolation from plate critical measurements and analyses to the LMFBR pin environment. (13 references) (auth)

55396 (EURFNR–1014) CALCULATION OF HETEROGENEOUS FLUXES, REACTION RATES, AND REACTIVITY WORTHS IN THE PLATE STRUCTURE OF ZERO POWER FAST CRITICAL ASSEMBLIES. McGrath, P. E.; Fischer, E. A. (Kernforschungszentrum, Karlsruhe (West Germany). Institut fuer Angewandte Reaktorphysik). Mar 1972. 64p. (KFK–1557). Dep. NTIS (U. S. Sales Only).

Work performed under United States–Euratom Fast Reactor Exchange Program.

The methods utilized in the computer program KAPER (Karlsruhe Perturbation Evaluation Routine) are presented. The program is a multigroup cell code for the calculation of cross sections, fluxes, reaction rates, and small-sample reactivity worths in the plate geometry of zero power critical assemblies. The methods in the program are based on integral transport theory in the collision probability formulation. The resonance self-shielding of the cross sections in the multiregion cells is calculated with a formulation based on the f-factor concept. The program has the unique feature of treating local perturbations in the normal unit cell in which the local properties of the cell have been changed as a result of the experiments. Small-sample reactivity worths are found with perturbation theory in which the perturbed flux in the sample and environment is used. Application of the program in the analysis of measurements performed in the zero power critical facility SNEAK at Karlsruhe is described. The measurements include reaction rates and small-sample reactivity worths. (17 references). (auth)

55397 (EURFNR–1016) KFKINR-SET OF GROUP CONSTANTS; NUCLEAR DATA BASIS AND FIRST RESULTS OF ITS APPLICATION TO THE RECALCULATION OF FAST ZERO-POWER REACTORS. Kiefhaber, E. (comp.) (Kernforschungszentrum, Karlsruhe (West Germany). Institut fuer Neutronenphysik und Reaktortechnik). Mar 1972. 81p. (KFK–1572). Dep. NTIS (U. S. Sales Only).

Work performed under United States–Euratom Fast Reactor Exchange Program.

The preparation of the MOXTOT-set in 1969 was a first step in the desired direction of improving the group constants used for nuclear calculations of fast reactors. Using this data-set, it was possible to predict the criticality of all zero-power reactor-assemblies studied as test cases at that time within an uncertainty limit of ±2% Further improvements superseding the MOXTOT-set have been necessary in order to reduce the uncertainty range for the criticality prediction and to improve the prediction of other important quantities besides criticality, e.g., reaction rates which are important for the breeding properties of fast power reactors. For the test of the improved set of group constants, named KFKINR-set, the same critical assemblies which were taken for the test of the preceding MOXTOT-set are used. The important changes in the group constants with respect to the MOXTOT-set, which was used as starting point, concern mainly the heavy isotopes which are important for fast breeder reactors, especially Pu239, U238, U235, and Pu240. For the determination of the group constants for the elastic downscattering we have used as the weighting spectrum the collision density of a typical sodium cooled fast reactor, namely that of the SNR. The complete nuclear data basis of the improved group constants is described. First results for the recalculation of fast critical assemblies are presented. Some essential characteristics of the new set of group constants and the results obtained by its first test applications are summarized. (69 references) (auth)

55398 (EURFNR–1029) PHYSICS INVESTIGATIONS OF SODIUM COOLED FAST REACTORS SNEAK-ASSEMBLIES 6A/6B. Jourdan, G.; Plum, F.; Reichel, H. (Kernforschungszentrum, Karlsruhe (West Germany)). Jun 1972. 99p. (KFK–1612). Dep. NTIS (U. S. Sales Only).

Work performed under United States–Euratom Fast Reactor Exchange Program.

SNEAK Assembly 6 was aimed at measuring physics parameters of a fast sodium cooled breeder core having a number of features typical for the prototype SNR. Whereas in SNEAK-Assembly 2 /1/ particular attention was given to a close simulation of the radial geometry, in SNEAK-Assembly 6 the axial behavior of the prototype SNR was simulated and studied. SNEAK-Assembly 6 had three modifications SNEAK-6A, SNEAK-6B and SNEAK-6D. SNEAK-6A has three zones, an inner Pu-zone with SNEAK material, a buffer zone composed of MASURCA rod material and the outer uranium zone. SNEAK-6B had the same zones without the buffer zone; in both assemblies some identical experiments were performed for studying the influence of the buffer zone. SNEAK-6D was a core with an inner Pu-zone with MASURCA material, a buffer zone, and a uranium driver zone. In this case, the buffer zone was composed of SNEAK-material. The influence of the material geometry on some experiments was studied by comparing the results of these experiments in SNEAK-6A and 6D. The experimental results were compared to detailed calculations. (19 references) (auth)

55399 (IKF–27) EXPOSURE OF PERSONS AFTER WATER LOSS IN THE TANK OF THE FRF2 REACTOR. Wensel, A. (Frankfurt Univ. (West Germany). Institut fuer Kernphysik). Apr 1972. 19p. (In German). Dep. NTIS (U. S. Sales Only).

Water level in the FRF2 tank as a function of time after damage to a primary coolant pipe is calculated. The core is bared after 25 sec. Dose rate on the surface of the upper shield plug (50 cm Fe) 25 sec after shutdown is 40 m Rem/h. If the shield plug is not in place exposure of persons is possible by backscattering at the reactor hall ceiling. Calculations using the Chilton–Huddleston formula for exposure albedo indicate that the dose rate at a lateral distance of 1 m from the tank is 2.5 Rem/h. Results of measurements of exposure albedo using a ^{60}Co source agree with calculated data. 6 references. (auth)

55400 (JAERI-M–4630) OPERATION REPORT ON THE LOW TEMPERATURE FISSIOCHEMICAL LOOP (JTFL). I. TEST OPERATIONS DURING THE PERIOD OF APRIL 1969 TO MARCH 1970. Sato, Shoichi; Moriyama, Noboru; Danno, Akibumi; Sukegawa, Tomohide; Oshima, K. (Japan Atomic Energy Research Inst., Tokyo). Nov 1971. 17p. (In Japanese). NTIS (U. S. Sales Only).

The Low Temperature Fissiochemical Loop (LTFL) has been operated seven times for out-pile and in-pile tests, during F.Y. 1969–1970. Operational characteristics of the loop were measured, evaluated and compared with the design calculations, including pressure loss and temperature distribution along the helium coolant piping, performance of the instruments, and thermal effects of reactor radiation on the capsule and in-pile plug of the loop. It was found that the loop can be operated with sufficient safety for the irradiation of chemical reaction systems in the presence of fissionable materials as designed. (auth)

55401 (JAERI-Memo–3891) CRITICAL EXPERIMENTS ON FCA I-6. Nakano, Masafumi; Hiraoka, Toru; Nakamura, Tomoo (Japan Atomic Energy Research Inst., Tokyo). Jan 1970. (In Japanese). NTIS (U. S. Sales Only).

Critical experiments were carried out on a 20% enriched uranium metal core with a graphite reflector of 25 cm thickness named FCA I-6. This core was built as one of the assemblies at which a series of pulsed neutron experiments was performed to study the kinetics of two-region fast systems. The critical mass of the assembly is 78 ± 1 kg of ^{235}U. This value is about 10% less than that of FCA I-1, a 20% EU core with 30 cm natural uranium metal blanket. The values of fission ratios at the core center show little discrepancy to those of a 20% EU bare system, FCA I-5. The neutron spectrum at the center of the 20% EU core is almost independent of the kind of reflectors. From the results of the reaction rate traverse by the detectors of different energy response, it became clear that the neutron spectrum in the reflector was quite different from that in the core. However, only a small variation in the neutron spectrum is observed in the central zone of each region. (Japan)

55402 (JAERI-Memo–4002) CONSTRUCTION OF THE JRR-1. (Japan Atomic Energy Research Inst., Tokyo). 1 May 1970. (In Japanese). NTIS (U. S. Sales Only).

JRR-1 was the first reactor to be constructed in Japan; it went critical on Aug. 27, 1957. The reactor was made by Atomics International in the United States. The procedure leading to the completion of JRR-1, including the construction works performed, is described. (auth)

55403 (JAERI-Memo–4004) SEMI-EXPERIMENTAL MEASUREMENT OF EFFECTIVE DELAYED NEUTRON FRACTION OF A FAST REACTOR SYSTEM BY APPLICATION OF PULSED NEUTRON TECHNIQUE. Hiraoka, Toru; Nakano, Masafumi; Konishi, Toshio (Japan Atomic Energy Research Inst., Tokyo). Apr 1970. (In Japanese). NTIS (U. S. Sales Only).

The effective delayed neutron fraction of FCA I-5 was measured by applying the pulsed neutron technique and the eigenvalue calculation checked by the critical experiments. The reactivity change due to the distribution of small voids in the core was measured. The distribution of small voids causes the change of the leakage characteristics. The reactivity change was estimated in the unit of $\Delta K/K$ by eigenvalue calculations. From the ratio between them, it is possible to compute the β_{eff} directly. The effective delayed neutron fraction of FCA I-5 thus obtained is $(7.09 \pm 0.12) \times 10^{-3}$. (auth)

55404 (JAERI-Memo–4052) SUMMARY OF THE JRR-2 IN-CORE IRRADIATION FACILITY AND IRRADIATION EXPERIENCES. (Japan Atomic Energy Research Inst., Tokyo). 31 May 1970. (In Japanese). NTIS (U. S. Sales Only).

A summary of the JRR-2 in-core irradiation facility and irradiation experiences for the past years is presented. The JRR-2 core consists of 22 MTR type fuel (^{235}U content 195 gr/element) and 2 cylindrical fuel elements (^{235}U content 120 gr/assembly). Dimensions of in-core irradiation capsule are 34 mm dia. × about 700 mm long. The capsule is inserted into center hole in cylindrical fuel element. (auth)

55405 (JAPFNR–43) PRELIMINARY CONCEPTUAL DESIGN OF JOYO MK-II IRRADIATION APPARATUS. (Tokyo Shibaura Electric Co. Ltd., Kawasaki, Kanagawa Prefecture (Japan)). Translation of report PNC-N-141-72-1-13. 12p. Dep. NTIS (U. S. Sales Only).

For Power Reactor and Nuclear Fuel Development Corp., Tokyo (Japan).

PNC has a plan to set up the irradiation facilities in the experimental fast reactor JOYO around 1978 as one of the important programs of JOYO MK-II Project. The preliminary conceptual design is described. (auth)

55406 (NASA-TM-X–2440, pp 618-19) SPACE RADIATION STUDIES AT THE WHITE SANDS MISSILE RANGE FAST BURST REACTOR. De La Paz, A. (Army Missile Test and Evaluation, White Sands Missile Range, N. Mex.). Jan 1972.

From Symposium on natural and manmade radiation in space; Las Vegas, Nev. (1 Mar 1971).

The operation of the White Sands Missile Range Fast Burst Reactor is discussed. Space radiation studies in radiobiology, dosimetry, and transient radiation effects on electronic systems and components are described. Proposed modifications to increase the capability of the facility are discussed. (auth)

55407 (ORNL-TM–3769) STUDY OF REACTIVITY BALANCE DURING STARTUP OF THE HFIR. Allen, J. W.; Sides, W. H. Jr. (Oak Ridge National Lab., Tenn.). Aug 1972. Contract W-7405-eng-26. 16p. Dep. NTIS.

The reactivity balance during startup in the High Flux Isotope Reactor calculated by a mathematical model on a CDC 1700 online computer was studied. The balance was improved by postulating a new reactivity term due to a power coefficient (temperature feedback) and one due to the burn-out of a target poison, ^{135}Xe. (auth)

55408 (ORNL-TM–3949) BULK SHIELDING FACILITY QUARTERLY REPORT, APRIL, MAY, AND JUNE OF 1972. Tabor, W. H.; Hurt III, S. S.; Lance, E. D. (Oak Ridge National Lab., Tenn.). Sep 1972. Contract W-7405-eng-26. 23p. Dep. NTIS.

The BSR operated at an average power level of 1879 kW for 38.9% of the time during April, May, and June. Water-quality control in both the reactor primary and secondary cooling systems was satisfactory. There were no unscheduled shutdowns during the quarter. The BSR was operated at low and variable power during this quarter for 51.6 hrs to provide training for nuclear engineering students. The PCA was operated 11 days during this quarter. (auth)

55409 (RD/B/N–2272) ZERO ENERGY REACTOR FACILITY AT B.N.L., 1972. Clarke, R. W.; Heaven, S. H.; Staniland, R. J.; Walsh, M. (Central Electricity Generating Board, Berkeley (England). Berkeley Nuclear Labs.). May 1972. 26p. (BNLSC–63). Dep. NTIS (U. S. Sales Only).

A zero energy reactor facility at the Berkeley Nuclear Laboratories is capable of accommodating a graphite moderated reactor, fueled with low enrichment uranium (<7% ^{235}U) in the form of the Mk. I, Mk. II or Mk. III G.C.R. concept. Provision is also available for handling low enrichment plutonium bearing ceramic fuel. The first Mk. III type reactor constructed in the facility is described in detail, including the automatic and administrative controls which, while preserving normal safety procedures, were planned to meet the flexibility of core design required for a variety of experiments. Improvements made to make the facility suitable for the new program were: a greatly extended control system; the ability to handle plutonium bearing ceramic fuels; changes in control logic for more flexibility; and improve ergonomic design of the control room layout. (auth)

55410 HIGH FLUX FRANCO–GERMAN REACTOR. CIVIL ENGINEERING AND CONFINEMENT OF THE REACTOR BUILDING. Levet, R. (CEN de Saclay, Gif-sur-Yvette, France). Bull. Inform. Sci. Tech. (Paris); No. 165, 77-85(Dec 1971). (In French).

The civil engineering aspects of the plant are dependent upon the characteristics of site, which were determined by meteorology, soil structure investigations, hydrology and seismology. The HFR building is designed to house the reactor and its installations, to provide a containment in relation to the exterior, and to provide an internal containment affording the appropriate degree of protection at the different levels, and for the different uses of the reactor. Calculations indicate that the inner concrete envelope is capable of supporting an internal pressure overload in excess of that which would be produced by the maximum accident (120mbar). The gas leak rate towards the outside is considerably reduced by the double concentric envelope within which fresh air is maintained at a pressure in excess of that likely to be produced in the inner envelope in the case of an accident, the rapid shutting off of the valves isolating the ventilation system. The waste evacuated by the chimney, after crossing the filters and vacuum traps, varies with the radioactivity of confined air. Internally, the places subjected to tritium contamination risks are isolated by pressure differences such that these areas are protected from any contamination arising in the operation area. (France)

55411 HIGH FLUX FRANCO–GERMAN REACTOR. SAFETY ASPECTS. Bureau du Colombier, J. (CEN de Saclay, Gif-sur-Yvette, France); Reutler, H. Bull. Inform. Sci. Tech. (Paris); No. 165, 87-93(Dec 1971). (In French).

A classical material, whose characteristics under similar conditions were known, was chosen for the construction of the reactor. In the transition region, the power evacuation from the core of the reactor is assured with a minimum margin of 1.25 (1.5 in operation) in relation to the flow redistribution phenomenon in the fuel element cooling channel. The primary circuit and the associated equipment are designed so that under no circumstances can the reflector be emptied and the core left exposed. The double confinement avoids any possible contact between the air and the deuterium of the cold source in the case of the failure of one of the walls. A double enclosure with an interspace containing He under pressure prevents any contact between the water and graphite of the hot source. The swimming pool walls are capable of undergoing a plastic deformation sufficient to absorb most of the mechanical energy generated during a major accident. The reactor confinement vessel also has a double envelope (concrete inner protection wall, stainless steel outer wall, an excess pressure maintained in the space between the walls). (France)

55412 HIGH FLUX FRANCO–GERMAN REACTOR. PRESENTATION OF THE REACTOR AND ITS PRINCIPAL CHARACTERISTICS. Chatoux, J. (CEN de Grenoble, France). Bull. Inform. Sci. Tech. (Paris); No. 165, 9-26(Dec 1971). (In French).

The importance of neutron experiments is recalled and their possible applications are reviewed. A survey of the performance required from a high flux reactor acting as a neutron source is presented together with the principal characteristics. (France)

55413 SIGNALING SYSTEM FOR PNEUMATIC INSTALLATIONS IN NUCLEAR REACTORS. Dieck, Enoui Leopold (to Kernforschungsanlage). U. S. Patent 3,681,194. 1 Aug 1972. Priority date 9 Mar 1968, Germany.

A pneumatic-tube installation for positioning a sample in the flux of a reactor is provided with a metallic tube extending from a stop for the sample. An electro-acoustical transducer, preferably a microphone, is disposed along the tube at a location outside the reactor core to detect the sound wave transmitted along the tube upon engagement of the sample with the stop. The output of the transducer is applied through a variable-threshold (amplitude comparator) trigger circuit (Schmitt trigger) to a switching device whose output, in turn, can initiate a timing cycle. An optical detector ahead of the microphone is connected through an AND-gate designed to enable the switching device so that the system responds only at the sound of impact with the stop. (Official Gazette)

55414 HIGH FLUX FRANCO–GERMAN REACTOR. THE COLD NEUTRON SOURCE OF THE HIGH FLUX REACTOR. Ageron, P. (Institut Max von Laue–Paul Langevin, Grenoble, France); Astruc, J. M.; Geipel, H.; Verdier, J. Bull. Inform. Sci. Tech. (Paris); No. 166: 17-22(Jan 1972). (In French).

The reasons why a liquid deuterium source was chosen as a very low energy neutron source are analyzed. A description of the main elements of this cold source is then given: dueterium circuit containing 8 kg D_2 (4 kg of which are liquefied); helium refrigerator having a power of 10 kW between 18.6 and 24.5K; control panels. The working principle of the cold source, which has a very simple design ensuring maximum reliability, is examined. (France)

55415 HIGH FLUX FRANCO–GERMAN REACTOR. COOLING CIRCUITS AND DETRITIATION INSTALLATION. Chazalon, M.; Lecuyer, Y. (CEN de Saclay, Gif-sur-Yvette, France). Bull. Inform. Sci. Tech. (Paris); No. 165, 57-66(Dec 1971). (In French).

The principle of the cooling circuits is as follows: a primary circuit which is completely contained in a containment vessel transfers power directly, using classical exchangers, to a secondary circuit. The primary circuit contains heavy water for the core circuits, and demineralized water for the swimming pool and channel circuits. The secondary circuit is an open circuit using water pumped from and evacuated back into the Drac River. A complete diagram is given for these circuits. The utilization of the different parts of the cycle is discussed: the power region, the stopping region, and the natural convection region. The different equipment is also described: exchanger pumps, isolating valves, taps, tubing and materials. The detritiating installation purifies the heavy water. It is capable of eliminating 160 liters of light water/year from water having a hydrogen molar content of 0.004. A tritium diminution of 2.78 for the heavy water is assured, thus enabling an equilibrium activity of 3Ci/liter instead of 80 Ci/liter (without detritiation) to be obtained. A production of 6.87 Nml/h is obtained with a 0.99 ratio. The equipment consists of two principal parts, operating a catalytic exchange and a fractional distillation respectively. (France)

Reactor Components, Fuels, and Accessories

Refer also to abstracts 53204, 53555, 53559, 53562, 53563, 53565, 53566, and 53605.

55416 (BNWL–1522-5) AEC REACTOR DEVELOPMENT AND TECHNOLOGY PROGRAMS. Technical Activities Report, October–December 1971; January–March 1972. (Battelle Pacific Northwest Labs., Richland, Wash.). May 1972. Contract AT(45-1)-1830. 66p. Dep. NTIS.

The high temperature Lattice Test Reactor, successfully operated for 4 years in support of high-temperature gas-cooled and molten-salt breeder reactor development, has been defueled and is now in standby status. The reactivity effect of 25 μ PuO_2 particles relative to homogenous fuel, has been calculated. Radiolytic measurements in H_2O and CO were made. A fuel heat-transfer model was developed for inclusion in the COBRA-3B computer program. It was shown that in multi-rod bundles, velocity profile, intensity, and scale were nearly independent of Reynolds number over the range 50,000 to 200,000. Results and analyses are presented on measurements of critical parameters in PuO_2–polystyrene lattices. Correlations of experimental critical data for high burnup Pu solutions were made. ENDF/B cross section data have been checked against integral experiments for a number of fast critical assemblies. (36 references) (J.M.J.)

55417 (CONF-710959) SPECIALISTS' MEETING ON "FISSION AND CORROSION PRODUCT BEHAVIOUR IN PRIMARY SYSTEMS OF LMFBR'S SEPTEMBER 20–22, 1971, BENSBERG/FRG. Summary Report. (International Atomic Energy Agency, Vienna (Austria)). 1971. 232p.

Eighteen papers were presented at the conference. A separate abstract was prepared for each of seventeen papers. It is suggested that cesium is the major contributor to long-term activity. This does not appear to deposit in quantity, but more studies are required to substantiate its behavior and whether it can be cold trapped. There is a lack of information in the release fraction and behavior of iodine and tellurium. (J.M.J.)

For abstracts of individual papers see: 52895, 53121, 55162–55173, 55185, 55226, and 55381.

55418 (GEAP–13788) BEHAVE-2: OXIDE FUEL PERFORMANCE CODE IN TWO SPATIAL DIMENSIONS AND TIME. Oldberg, S. Jr. (General Electric Co., Sunnyvale, Calif. Breeder Reactor Dept.). Feb 1972. Contract AT(04-3)-189. 84p. Dep. NTIS.

BEHAVE-2 is a FORTRAN 4 computer program written for the GE-635 computer. The program calculates the position in space of cladding, fuel, and voidage in an operating oxide fuel pin with unfailed cladding. Axial symmetry is assumed throughout the program. Also calculated are stress, strain, displacement, and temperature fields. Influential processes simulated include cracking of fuel, dilatation of fuel and cladding due to irradiation effects and thermal expansion, fuel densification by stress and diffusion controlled processes, axial slippage or locking at the fuel-cladding interface, and axial flow of fuel. 49 references. (auth)

55419 REACTOR FUEL ELEMENT. Rolf-Woltje (to Gessellschaft fuer Kernenergieverwertung). German Patent 1,464,645. 27 Apr 1972. (In German).

The special feature of this fuel element with high negative fuel temperature coefficient of the reactivity, containing a solid fuel and a solid moderator in one casing, is a thermal insulating layer which separates fuel and moderator from the casing. The thermal insulating layer may be a slit, the moderator may be a metal hydride, moderator and fuel may be contained in a homogeneous internal region either as a mixture or as a chemical compound. (GF)

Reactor Physics and Core Engineering

Refer also to abstract 54469.

Physics

Refer also to abstracts 54480 and 55416.

55420 (AREAEE-141) PIBIMUG: A CODE FOR MULTI-GROUP SLOWING DOWN SPECTRUM CALCULATION IN THE P-1 AND B-1 APPROXIMATIONS FOR THE IBM-1130. El-Cherif, A. I.; Gaafer, M. A.; Nassar, S. F. (Atomic Energy Establishment, Cairo (Egypt). Reactor and Neutron Physics Dept.). 1972. 20p. Dep. NTIS (U. S. Sales Only).

PIBIMUG is a multigroup code for hydrogenous moderated reactors based on P-1 and B-1 approximations. The code is written in a FORTRAN II language suited for the IBM-1130 to provide a powerful nuclear design computing tool equivalent to IBM-704 computer program MUFT-4 and PHILCO-2000 computer program MUFT-5. 4 references. (auth)

55421 (BNWL-CC-2274) USER'S MANUAL FOR DASQHE. Traver, T. M. (Battelle-Northwest, Richland, Wash. Pacific Northwest Lab.). 15 Sep 1969. 12p. Dep. NTIS.

An improved technique has been developed to calculate the Dancoff correction for an infinite array of circular rods in square or hexagonal lattices. This technique is coded in a FORTRAN-IV and is called DASQHE. This method has been adopted for use in the thermal reactor analytical physics work. The DASQHE code was modified and coded in FORTRAN-V for use on the UNIVAC-1108 computer. 4 references. (auth)

55422 (CISE-R-243) ANALYTICAL SOLUTION OF THE TWO-SEPARABLE VARIATIONAL SYNTHESIS APPROACH FOR THE TWO-GROUP DIFFUSION r,z EQUATIONS. Bruschi, C.; Pierini, G. (Centro Informazioni Studi Esperienze, Milan (Italy)). Feb 1969. 81p. INIS.

A code is presented which synthesizes the two-dimensional two-group flux of a cylindrical reactor out of one-dimensional solutions of the diffusion equation. The two-separable approximation $\Phi_k(r,z) = u_k^{(1)}(r)\ v_k^{(1)}(z) + u_k^{(2)}(r)v_k^{(2)}(z)$ (k = 1.2) is made where $u_k^{(n)}(r)$'s are trial functions and the $v_k^{(n)}(z)$'s are weight functions. The latter ones are obtained by solving an equivalent four-group diffusion problem in the axial direction with a block-diagonal diffusion matrix. The criticality eigenvalue is that obtained from a run of the MONOS code which is fully included in the new code. The one-dimensional solutions of the two-group (radial and axial) and of the four-group (axial) diffusion problems are obtained by an analytical method. (INIS)

55423 (CISE-R-273) ITERATIVE SOLUTION OF HETEROGENEOUS EQUATIONS IN A FINITE CYLINDRICAL SYSTEM. METHOD OF HARMONICS. Bruschi, C.; Pedretti, F. (Centro Informazioni Studi Esperienze, Milan (Italy)). Sep 1968. 23p. (In Italian). INIS.

A possible approach to the solution of heterogeneous equations in a finite cylindrical system with axial dependence is presented. These equations consider a description in three groups (fast-resonance-thermal) of slowing down and account for absorptions in the epithermal group in addition to fission and thermal absorptions. Moreover the migration properties of the system are properly accounted for through a suitable scheme which interprets the heterogeneous parameters. The method of solution is that of harmonics for the treatment of the z axis. The equations can easily be extended to a multigroup scheme because of their recurrent nature. A possible iterative scheme for the solution of these equations on a digital computer is presented. (INIS)

55424 (CONF-720901-(Bks.1 and 2)) NATIONAL TOPICAL MEETING ON NEW DEVELOPMENTS IN REACTOR PHYSICS AND SHIELDING, SEPT. 12-15, 1972, KIAMESHA LAKE, NY. (American Nuclear Society (USA). Northeastern New York Section). 1972. 1207p. Dep. NTIS $15.00.

Included are 78 papers on calculation and measurement methods for use in reactor shielding and physics analyses. A separate abstract was prepared for each paper. (H.D.R.)

For abstracts of individual papers see: 53252, 54472—54480, 54523, 54566, 54597, 54653—54655, 54676, 54826, 54872, 54937—54942, 55107—55125, 55134, 55140—55144, 55356, 55382—55393, and 55425—55439.

55425 (CONF-720901-(Bks.1 and 2), pp 108-13) EFFECT OF PARTICLE SIZE ON RESONANCE CAPTURE. Goldstein, Rubin (Combustion Engineering, Inc., Windsor, Conn.). 1972.

From Meeting on new developments in reactor physics and shielding calculations; Kiamesha Lake, NY. (12 Sep 1972).

The effect that particle size has on the reactivity of a system depends mainly on the size of the particles, the volume fraction of the absorber and the dilution of the lattice. With some restrictions, the resonance integral decreases approximately linearly with increasing particle size. An analytic expression is used that permits a rapid calculation of the effect of particle size on resonance absorption. The mathematical formulation for particularized resonance integrals gives results which are in excellent agreement with experiments performed on gold particles. For the plutonium-fuel compositions and lattice dilutions considered, resonance integrals decreased by more than 10% and the overall reactivity of ESADA criticals decreased by as much as 0.4% for 25 micron particles. (auth)

55426 (CONF-720901-(Bks.1 and 2), pp 162-7) DEVELOPMENTS IN VARIATIONAL THEORY AND PERTURBATION METHODS. Lewins, Jeffery (University Coll., London). 1972.

From Meeting on new developments in reactor physics and shielding calculations; Kiamesha Lake, NY. (12 Sep 1972).

The present usage of variational and perturbation methods in reactor physics is surveyed. (auth)

55427 (CONF-720901-(Bks.1 and 2), pp 168-78) ADVANCES AND CURRENT PROBLEMS IN REACTOR KINETICS. Ott, Karl O. (Purdue Univ., Lafayette, Ind.). 1972.

From Meeting on new developments in reactor physics and shielding calculations; Kiamesha Lake, NY. (12 Sep 1972).

Advances and current problems in fast reactor dynamics are surveyed. The general problems are reviewed first in order to provide a framework for the discussion of the recent advances. Further, some results of methodological interest are presented and discussed. 16 references. (auth)

55428 (CONF-720901-(Bks.1 and 2), pp 179-94) GREEN'S FUNCTION COUPLING METHOD FOR TIME-DEPENDENT NEUTRON SLOWING DOWN IN HEAVY MEDIA. Conn, Robert; Sawan, Mohamed (Univ. of Wisconsin, Madison). 1972.

From Meeting on new developments in reactor physics and shielding calculations; Kiamesha Lake, NY. (12 Sep 1972).

A new approach based upon the coupling together via Green's functions of distinctly different calculational methods for different time-energy regimes was developed to calculate the time-dependent neutron flux slowing down in a pulsed, heavy medium. In the approach, different methods are used to solve the slowing down problem in the energy ranges where the chosen method is both advantageous and valid. The slowing down energy range (typically, 14 MeV to thermal when the standard D(t,n) He reaction is used as source) is divided into three different energy regimes where the slowing down mechanisms are distinctly different. The problem in each regime is solved differently and a Green's function approach is used to couple the solutions together. 20 references. (auth)

55429 (CONF-720901-(Bks.1 and 2), pp 195-206) MANY-RESONANCE APPROXIMATION FOR THE NEUTRON ENERGY SPECTRUM. Segev, M. 1972.

From Meeting on new developments in reactor physics and shielding calculations; Kiamesha Lake, NY. (12 Sep 1972).

A study of the effect of a resonance ensemble on the reactor neutron spectrum, based on the properties of the ensemble as a whole, is summarized. The sections present: (a) a qualitative argument for the approximation, (b) the basic formulas, (c) conditions for negligible oscillations in the collision density, (d) a series solution for ν, where exp $(-\nu)$ is the relative change in the collision density per unit lethargy, (e) the generalization of the formulas for slowly varying average resonance parameters, (f) numerical tests of the approximation. (auth)

55430 (CONF-720901-(Bks.1 and 2), pp 207-10) PREDETERMINING STATISTICAL ERRORS IN MONTE CARLO TRANSPORT CALCULATIONS. Amster, Harvey J. (Univ. of California, Berkeley). 1972.

From Meeting on new developments in reactor physics and shielding calculations; Kiamesha Lake, NY. (12 Sep 1972).

The use of ordinary adjoint transport codes to provide statistical error estimates of problems to be run on contemplated Monte Carlo codes is discussed. This would allow the accuracy of a Monte Carlo calculation to be estimated before a code is developed. (H.D.R.)

55431 (CONF-720901-(Bks.1 and 2), pp 229-39) ZERO VARIANCE ESTIMATOR FOR REACTOR CRITICALITY. Kalos, M. H. (New York Univ., N. Y.). 1972.

From Meeting on new developments in reactor physics and shielding calculations; Kiamesha Lake, NY. (12 Sep 1972).

A scheme is proposed for biasing in the Monte Carlo solution of reactor criticality problems. Under ideal conditions which require knowledge and correct use of an "adjoint fission neutron distribution" it leads to zero variance estimates of the reactor eigenvalue and other quantities. Also discussed are practical ways of obtaining and representing numerical information about this adjoint function. Of particular interest is the fact that estimates of the needed information for biassing can be obtained as a by-product in the course of an ordinary or biassed calculation. As the biassing is improved, the efficiency with which such estimates are made can be made arbitrarily high. Numerical results from the Monte Carlo solution of a simplified problem are presented to support the anticipation that computing time can be significantly reduced even when perfect biassing is not used. (auth)

55432 (CONF-720901--(Bks.1 and 2), pp 240-51) DETERMINATION OF OPTIMAL K-INFINITY MISMATCH CURVES VIA MODERN CONTROL THEORY. Terney, William B.; Wade, David C. (Knolls Atomic Power Lab., Schenectady, N. Y.). 1972.

From Meeting on new developments in reactor physics and shielding calculations; Kiamesha Lake, NY. (12 Sep 1972).

The problem of determining the burnup dependence of k_∞ in the loading zones of a reactor core so as to yield the best reactor performance throughout life is treated as an optimal control problem. An iterative solution scheme based on a gradient approach is derived for solving the resulting two point boundary value equations. Results from sample calculations on realistic design models demonstrate the validity and usefulness of the approach. (auth)

55433 (CONF-720901--(Bks.1 and 2), pp 253-65) SIMULTANEOUS LINE OVER-RELAXATION (SLOR) IN HEXAGONAL LATTICE. Honeck, H. C.; Stewart, J. W. (Savannah River Lab., Aiken, S. C.). 1972.

From Meeting on new developments in reactor physics and shielding calculations; Kiamesha Lake, NY. (12 Sep 1972).

A Simultaneous Line Over-Relaxation (SLOR) method was developed for the solution of the one-group difference form of the neutron diffusion equation in regular hexagonal lattices. This method was successfully implemented as a part of a hex-z geometry, multigroup diffusion theory module in the Generalized Reactor Analysis Sub-System (GRASS) of JOSHUA. The theory and equations for this SLOR method and some results are presented. (auth)

55434 (CONF-720901--(Bks.1 and 2), pp 266-74) OPTIMUM ANGULAR SEGMENTATIONS IN NEUTRON TRANSPORT ANALYSIS. Harms, A. A.; Garland, W. J. (McMaster Univ., Hamilton, Ont.). 1972.

From Meeting on new developments in reactor physics and shielding calculations; Kiamesha Lake, NY. (12 Sep 1972).

The problem of specifying optimum angular segmentations in neutron transport analysis is considered. A new directional-group representation using partial-range Legendre polynomials is introduced for this purpose. It is found that this solution formalism can be used to specify angular segmentations which minimize the error of certain neutron transport parameters for a given order of approximation. 9 references. (auth)

55435 (CONF-720901--(Bks.1 and 2), pp 275-92) IMPROVED S_N INNER ITERATION CONVERGENCE CRITERION. Atkinson, Gerald L. (Pentagon, Washington, D. C.); Kerr, William; Dunderstadt, James J. 1972.

From Meeting on new developments in reactor physics and shielding calculations; Kiamesha Lake, NY. (12 Sep 1972).

The angular flux form of the S_N equations in plane geometry is formulated within a mathematical framework which allows an insight into the mechanics of the convergence process. The infinity-norm of the S_N iteration matrix is explicitly calculated for a problem with a homogeneous isotropically scattering medium. This event allows the calculation of an improved convergence criterion compared to the conventional criterion. This new criterion, along with the demonstrated convergence properties of the S_N algorithm, guarantees that the fractional iterative error is arbitrarily small. (auth)

55436 (CONF-720901--(Bks.1 and 2), pp 599-612) USE OF DATA FROM FAST ASSEMBLIES FOR ADJUSTMENTS OF NEUTRON DATA. Haeggblom, H. (Aktiebolaget Atomenergi, Studsvik, Sweden). 1972.

From Meeting on new developments in reactor physics and shielding calculations; Kiamesha Lake, NY. (12 Sep 1972).

A series of calculations was made for obtaining adjusted neutron data by a simultaneous consideration of a large number of integral data from fast reactors. In the first stage, sensitivities of k_{eff} and reaction rate ratios to changes in neutron data were calculated. The second stage consisted of a least-squares fit of calculated integral data to experimental results. The errors in the integral data and in the energy-dependent data were assumed to follow Gaussian distributions. Correlation factors were introduced between a number of energy-dependent data. The calculations were based upon 57 integral data from 31 different assemblies and give corrections for 31 neutron data divided into 6 energy groups. The Swedish neutron data library was used as the starting point, but comparisons were made between the most important data in this library and ENDF/B-II and UKNDL. The results included standard errors of the adjusted energy-dependent data, the remaining discrepancy between measured and calculated integral quantities, and the corresponding standard errors. The adjusted neutron data were compared with adjusted data obtained in Winfrith, UK. In most cases, a satisfactory agreement between the results from both laboratories was established. The most interesting result was that the adjusted fission cross section in ^{235}U and the capture cross section in ^{238}U were significantly lower than the data in ENDF/B-II over the most important part of the energy region for fast reactors. 9 references. (auth)

55437 (CONF-720901--(Bks.1 and 2), pp 713-23) VERIFICATION OF A NEW METHOD FOR CALCULATING AND MEASURING GENERATION TIME IN A SUBCRITICAL FAST REACTOR. Buhl, A. R. (Oak Ridge National Lab., Tenn.); Robinson, J. C. 1972.

From Meeting on new developments in reactor physics and shielding calculations; Kiamesha Lake, NY. (12 Sep 1972).

A new method is discussed for calculating and measuring the generation time (Λ) in a subcritical fast reactor using a recently developed transfer and scattering kinetics scheme (TASK). The method is an extrapolation of a four-node fluctuations theory in which the generation time in a thermal reactor was shown to be equal to the slope of the tangent of the phase angle from the power spectra between a high-energy-sensitive and low-energy-sensitive detector. The TASK method directly computes the prompt die-away time constant and the Λ based on the tangent method. To substantiate TASK calculations, Λ was compared with the experimental value at critical and computed Λ using the standard lambda (λ) mode and omega (ω) mode definitions for critical and for three subcritical states of the Fast Test Reactor. 10 references. (auth)

55438 (CONF-720901--(Bks.1 and 2), pp 943-58) REVIEW OF FAST NEUTRON SPECTRUM MEASUREMENTS. Preskitt, C. A. (Gulf Radiation Tech., San Diego, Calif.); Malaviya, B. K.; Bennett, E. F. 1972.

From Meeting on new developments in reactor physics and shielding calculations; Kiamesha Lake, NY. (12 Sep 1972).

Rapid advancement has taken place in the experimental technology for determining fast neutron spectra. In reactor systems, the most important techniques are neutron time-of-flight and proton-recoil proportional chambers. For certain shielding applications, other integral spectrometers are important. A wealth of experimental data is available, and most of this has been analyzed in varying degrees by the laboratories responsible for the measurements. However, the full value of the available data will only be realized when it has been widely distributed, and is analyzed using current cross sections by a larger number of groups, especially those involved in reactor design. 34 references. (auth)

55439 (CONF-720901--(Bks.1 and 2), pp 1183-91) GROUP CONSTANT GENERATION FOR THE RESOLVED RESONANCE REGION. Ruehle, R.; Emendoerfer, D.; Gulden, W.; Lutz, D. (Univ., Stuttgart). 1972.

From Meeting on new developments in reactor physics and shielding calculations; Kiamesha Lake, NY. (12 Sep 1972).

In order to check different methods for group cross section generation in the resolved resonance region, the computer code RESAB was developed. RESAB solves the slowing down Boltzmann equation in micro energy-group representation by exact first flight collision probabilities for multiregion cells with white cell boundaries. The input cross sections for RESAB are calculated as functions of energy and temperature from ENDF/B II resonance parameters and smooth data from ENDRES. Based on the same ENDF/B II cross section set, group constants were evaluated with the generally available multigroup cross section code GGC-4 in the case of a PWR pin cell. The results of RESAB- and GGC-4- calculations are discussed from a physical point of view. (auth)

55440 (INIS-mf--195) MULTIGROUP NEUTRON TRANSPORT THEORY IN PLANE GEOMETRY. Clancy, B. E. (Wollongong Univ. Coll. (Australia)). Oct 1970. 178p. NTIS. Thesis.

The multigroup form of the transport equation describing the steady state population of neutrons in a plane geometry is studied. The existing techniques of finding numerical solutions to the transport equation in the discrete ordinate approximation are considered in relation to the deep penetration problem of reactor shielding theory. Some of the computational difficulties are examined and a major one found to be the excessive time used in iterating the equation over a large number of mesh points. A review is given of Chandrasekhar's reflection function method for finding solutions to an astrophysical problem equivalent to the one group form of the deep penetration problem in finite and semi-infinite homogeneous media. After generalizing the method it is shown how accurate solutions may be obtained for realistic multigroup problems in semi-infinite media without the need for spatial iterations. For many deep penetration problems in finite heterogeneous slabs only certain integrals of the angular neutron fluxes emerging from the slabs are of interest. A variational principle is devised with the aid of which solutions to appropriately chosen semi-infinite medium problems can be used to calculate directly approximations to any integral of these emerging angular fluxes. From the results obtained with a computer program embodying these methods it is found that the significant savings in computing time can be achieved when a number of survey calculations need to be performed. Some possible applications of the reflection function method to other problems in neutron transport theory are examined briefly. (auth) (INIS)

55441 (LA-DC-72-660) REACTOR POWER TRANSIENT STUDIES. Stratton, W. R.; Engle, L. B.; Peterson, D. M. (Los Alamos Scientific Lab., N. Mex.). 2 Jun 1972. 14p. (CONF-721006-1). Dep. NTIS.

From International conference on engineering of fast reactors for safe and reliable operation; Karlsruhe, Germany (9 Oct 1972).

The Pajarito Dynamics (PAD) code is described in general terms. Its use for reactor power transient calculations, especially its ability of describing not only total fission energy release, but also a measure of the conversion of thermal energy to explosive energy during the power transient, is evaluated. (J.M.J.)

55442 (RT/FI-(72)11) REACTOR NEUTRON NOISE ANALYSIS: STATE OF THE ART, 1971. Pacilio, N. (Comitato Nazionale per l'Energia Nucleare, Rome (Italy)). 21 Mar 1972. 33p. Dep. NTIS (U. S. Sales Only).

A short presentation is given of reactor-noise time-analysis techniques. Instead of the traditional exposition of theoretical, computational and experimental problems implied in this nuclear reactor physics branch, a documentary approach is tried. The subject is treated according to the following perspectives: (1) what is noise?'', (2) prehistory of reactor-noise analysis, (3) an example of general theory, (4) some considerations on time-analysis methods, (5) recent advancements, (6) present and future directions, and (7) reactor-noise in power systems. (auth)

55443 (RT/FI-(72)13) 259 REFERENCES IN REACTOR NOISE TIME ANALYSIS. Pacilio, N. (Comitato Nazionale per l'Energia Nucleare, Rome (Italy)). 7 Apr 1972. 96p. Dep. NTIS (U. S. Sales Only).

An extensive reference list is given of reports, articles and books covering the matter of reactor-noise analysis in the time-domain. The comprehensive bibliography is divided into six main sections, which are entitled: monographies, surveys and general introductions; stochastic and kinetic theory; correlation analysis among neutron detection pulses; analysis of the moments of neutron distribution; analysis of the probability of a neutron detection; and correlation analysis among the signs of the power level fluctuations. Two minor sections are dedicated to gamma noise and information theory. The list is assembled according to two other criteria. First, a chronological year-after-year disposition of the various works is presented; second, an alphabetical list of authors is given and the scientific production is summarized for each of them. (auth)

55444 (TRG-2189) SPECTRA OF ENERGY RELEASED BY THERMAL NEUTRON CAPTURE. Sidebotham, E. W. (United Kingdom Atomic Energy Authority, Risley (England). Reactor Group). 1972. 8p. INIS.

Neutron capture gamma spectra are required to determine the true heat generation in reactors and its distribution over the core materials. It was observed that experimentally determined spectra although accurately determined in fine detail rarely equate to the binding energy because of a continuum of energies in the middle range. A method was devised to allocate the gamma energy spectra, corrected to the binding energy, to certain kernel energies which are of importance in determining the heating distribution in reactor core materials. Tables of thermal neutron capture gamma and radioactive decay energy spectra cover elements, compounds, alloys and fission product groups more frequently present in reactor cores. (auth) (INIS)

55445 (Y-KC-96) RELIABILITY OF CRITICALITY SAFETY CALCULATIONS USING THE NEW CODES CSC AND KENO. Crume, E. C. Jr. (Union Carbide Corp., Oak Ridge, Tenn. Y-12 Plant). 21 Apr 1967. Contract W-7405-eng-26. 14p. Dep. NTIS.

The present state of the reliability of criticality safety calculations using the two Monte Carlo codes CSC and KENO is discussed. It is concluded that reliable system criticality calculations can be made for systems of a number of compositions of general interest in criticality safety in which the only fissile isotope is ^{235}U at high enrichment. 15 references. (auth)

55446 CONSISTENT APPROACH OF HETEROGENEOUS THEORY LEADING TO A DIPOLAR FORMULATION. I. FORMULATION. Berna, Ph. (SERMA, Gif-sur-Yvette, France). J. Nucl. Energy; 26: No. 6, 303-17(Jun 1972).

Starting from a theorem established in transport theory, a new dipolar heterogeneous formulation was developed where channels were characterized by parameters depending on the environment only through cross-sections. The formulas for these parameters could be calculated in less than 0.3 sec (by channel type) on an IBM 360/91. The FODITH code based on this formulation gave an acceptable value for the experimental reactivity of a reactor having 3 narrow zones of different scattering properties (deviation lower than 200 pcm). The code therefore gave results in better agreement with the experiment than other codes based on diffusion or source-sink theory. The new formulation appears as the extension of the ABH method initially developed for cell calculations to heterogeneous reactor calculations. (auth)

55447 CONSISTENT APPROACH OF HETEROGENEOUS THEORY LEADING TO A DIPOLAR FORMULATION. II. CALCULATION OF HETEROGENEOUS PARAMETERS. Berna, Ph. (SERMA. Gif-sur-Yvette, France). J. Nucl. Energy; 26: No. 6, 319-31(Jun 1972).

The detailed calculation of the polar and dipolar parameters used in a new consistent formulation for heterogeneous theory is presented. For the sake of simplicity it is assumed that the channel contains only two concentric media, a central fuel rod and an annular cavity, and that collisions are isotopic. (auth)

55448 IMPROVED COMPUTER METHOD FOR POLARITY CROSS CORRELATION. Cohn, C. E. (Argonne National Lab., Ill.). Nucl. Instrum. Methods; 103: No. 2, 257-9(1972).

An improved computer method for polarity-correlation noise analysis yields increased throughput and provides for monitoring of discriminator bias. (1 figure) (auth)

Core Thermal Hydraulics

55449 (KFK-1503) LAMINAR FLOW IN ROD BUNDLES. Rehme, K. (Kernforschungszentrum, Karlsruhe (West Germany). Institut fuer Neutronenphysik und Reaktortechnik). Sep 1971. 5p. INIS.

Values for the geometrical parameter, K, in the expression lambda × Fe = K (pressure-drop law) were calculated for incompressible, isothermal, perfect laminar flow along hexagonal and square bundles of rods enclosed in hexagonal and square conduits respectively. The pressure drop in bundles consisting of a large number of rods can be calculated with the aid of K values obtained for the subchannels by numerical integration of the Navier–Stokes equation. Investigations covered a large range of rod spacings and wall separations. The result obtained are compared with data given in the literature. On the basis of the results, the pressure drop for flow in rod bundles can be calculated sufficiently accurately in all likely cases. (INIS)

GENERAL

Law

55450 (CEA-CONF-2005) USE OF PL/1 AS INTERROGATION LANGUAGE OF A DECK OF CARDS. Schauer, G. (Commissariat a l'Energie Atomique, Grenoble (France). Centre d'Etudes Nucleaires). 19 Apr 1971. 9p. (In French). (CONF-710549-1). Dep. NTIS (U. S. Sales Only).

From 12th European conference on leading; Brussels, Belgium (11 May 1971).

55451 (LA-DC-72-626) IMAGE RESTORATION BY CONSTRAINED LEAST-SQUARES ESTIMATION. Hunt, B. R. (Los Alamos Scientific Lab., N. Mex.). 1972. 8p. (CONF-720813-1). Dep. NTIS.

From Symposium on computer image processing; Columbia, MO. (24 Aug 1972).

55452 (NP-19407) ANNUAL REPORT, 1971-72. (Department of Atomic Energy, Bombay (India)). 192p. Dep. NTIS (U. S. Sales Only).

AGRICULTURE—research in India, 1971–1972
BIOCHEMISTRY—research in India, 1971–1972
BIOLOGY—research in India, 1971–1972
CHEMICAL ENGINEERING—research in India, 1971–1972
CHEMISTRY—research in India, 1971–1972
COMPUTERS—research in India, 1971–1972
DESALTING—research in India, 1971–1972
MEDICINE—research in India, 1971–1972
METALLURGY—research in India, 1971–1972
NUCLEAR POWER—development in India 1971–1972
PHYSICS—research in India, 1971–1972
PROSPECTING—developments in India, for nuclear materials
RADIATION PROTECTION—research in India, 1971–1972
RADIOCHEMISTRY—research in India, 1971–1972
RADIOISOTOPES—research in India, 1971–1972
REACTOR FUELS—reprocessing in India, 1971–1972
REACTORS—development in India, 1971–1972
SPACE—research in India, 1971–1972 (W.H.K.)

55453 (NP-19410) FIFTEENTH ANNUAL REPORT, 1971. (Atomic Energy Board, Pretoria (South Africa)). 64p. Dep. NTIS (U. S. Sales Only).

INSTRUMENTS—development and research in South Africa, 1971
NUCLEAR PHYSICS—research in South Africa, 1971
NUCLEAR POWER—development and research in South Africa, 1971
RADIOISOTOPES—development and research in South Africa, 1971
REACTORS—development and research in South Africa, 1971
REACTORS, RESEARCH—operation of SAFARI-I, 1971
URANIUM—separation from ores in South Africa
URANIUM RESERVES—estimates in South Africa (W.H.K.)

55454 (NP-19412) RADIATION HEALTH AND SAFETY. Annual Report for the Year Ended 31st December 1971. (New South Wales Univ., Kensington (Australia)). 17p. Dep. NTIS (U. S. Sales Only).

Aspects of radiation health and safety under the auspices of the radiation protection officer are reviewed for the year 1971. These include personnel monitoring, disposal of radioactive waste, radiation incidents, radiation insurance, purchase and transfer of radioactive sources, investigations and reports on school projects and research on electrostatic collection of particular fission products and their contribution to a scintillation detector signal. (Australia)

55455 (OSU-CISRC-TR-72-8) PATTERN RECOGNITION BY RETINA-LIKE DEVICES. Weiman, Carl F. R.; Rothstein, Jerome (Ohio State Univ., Columbus. Computer and Information Science Research Center). Jul 1972. 154p.

55456 (SZS-136) 10 YEARS NATIONAL CENTER FOR RADIATION PROTECTION OF THE GERMAN DEMOCRATIC REPUBLIC. (Staatliche Zentrale fuer Strahlenschutz, Berlin (East Germany)). Aug 1972. 72p. (In German). Dep. NTIS (U. S. Sales Only).

The organization, technical and personnel conditions established in the GDR to fulfill the medical tasks in radiation protection are described. These include precautions and protective measures at the level of the individual user, as well as on a national scale, i.e., in the Division of Radiation Protection Medicine of the National Center for Radiation Protection. The necessity of close cooperation between the medical supervisors of radiation workers and the specialized clinical diagnostic installation of the Division of Radiation Protection Medicine is shown. The described system of medical supervision of persons working with radiation seems to be an appropriate countermeasure against all imaginable hazards caused by ionizing radiation to man. (G.F.)

55457 (TID-26141) APPLICATIONS OF COMPUTERS AND DIGITAL TECHNIQUES IN CLINICAL AND INVESTIGATIVE NUCLEAR MEDICINE. Erickson, Jon Jay (Vanderbilt Univ., Nashville, Tenn.). May 1972. 311p. Dep. NTIS.

Thesis.

An integrated hardware/software system for computer collection and analysis of scintillation camera radionuclide imaging data in a clinical and research oriented nuclear medicine laboratory is described. (auth)

55458 STATE OF ENFORCEMENT OF RADIATION INJURY PREVENTION LAW IN 1970. Genshiryoku Iinkai Geppo; 16: No. 10, 12-18(Oct 1971). (In Japanese).

Recently, the use of radioisotopes and radiation generating equipment has increased steadily and has become diversified in private businesses, medical treatment, research, and education. Accordingly, enforcement of the law concerning prevention of radiation injuries due to the use of radioisotopes and other radiation sources is very important. In March 1971, the number of business establishments using radiation was 2,091, an increase of 256 over the previous year. This is due to a rapid increase in the use of gas chromatography equipment and sulfur analyzers for pollution prevention measures. The establishments include 39.2% private businesses, 29.5% medical institutions, 20.4% research institutions, 7.6% educational facilities, and 3.3% others. Expansion in the private businesses is especially conspicuous. The establishments are distributed all over Japan, but ⅓ of them concentrate in Tokyo, Kanagawa, and Osaka. The number of the establishments for sale was 77, and that for waste disposal was six, in March 1971. The utilization of radioisotopes and other radiation sources will increase more and more hereafter, especially in the private businesses. It is predicted that radiation equipment such as thickness gauges, level gauges, and sulfur analyzers will be employed on a full scale for the purpose of production control, product control, and labor saving. The number of qualified chief radiation technicians was 8,156 in March 1971, distributed mainly in large enterprises and research institutions. Since April 1958, spot inspection was carried out in 3,690 cases according to the law. 2,887 applications and notifications were received in 1970 concerning radiation injury prevention. (Japan)

55459 REVISION OF THE LAWS AND REGULATIONS CONCERNING INDEMNITY FOR DAMAGE DUE TO ATOMIC ENERGY AND ATTENDANT REVISION OF ATOMIC ENERGY INSURANCE. Hokaku, Nobuyoshi (Nippon Fire and Marine Insurance Co. Ltd., Tokyo). FAPIG (Tokyo); No. 63, 169-72(Nov 1971).

The system of indemnity for damage due to atomic energy in Japan consists of two laws, the law concerning the indemnity for damage due to atomic energy and the law concerning compensation contract in the indemnity for damage due to atomic energy. Since the establishment of this system in 1961, more than nine years have elapsed. Conspicuous development has been achieved in the field of atomic energy during that period, and various problems to be examined arose on the content and administration of this system. Also, international treaties were adopted in order to unify the indemnity system. The Japanese government established a special committee for the examination of the indemnity system for damage due to atomic energy in 1969, and the examination was carried out. As a result, a revision of the laws was enforced in Oct. 1971. The gist of the idemnity system lies in faultless responsibility of and concentration of the responsibility on atomic energy enterprises, compulsion of indemnity measures for the damage, and aid by the government. Main items of the revision are limitation of right demanding compensation of the atomic energy enterprises, raise of indemnity amount for the damage, treatment at the time of nuclear fuel transportation between atomic energy enterprises, and treatment of nuclear ships. Revision of atomic energy insurances was minimized because of a small revision of the laws. It was enforced on Oct. 1, 1971. The revised insurances are indemnity responsibility insurance in atomic energy facilities, indemnity responsibility insurance in atomic energy transportation, and atomic energy property insurance. A newly established insurance is indemnity responsibility insurance for damage of nuclear ship operators. (Japan)

Miscellaneous

55460 (ACRH-1000-349) TRAINING OF MEDICAL PHYSICISTS: SOME EXISTING TRAINING SCHEMES. Lanzl, Lawrence H. (Argonne Cancer Research Hospital, Chicago, Ill.). [nd]. 3p. (CONF-720435-4). Dep. NTIS.
From Seminar on training and education in medical physics; Kiel, Germany (10 Apr 1972).

55461 (ACRH-1000-350) MEDICAL PHYSICS IN THE UNITED STATES. Lanzl, Lawrence H. (Argonne Cancer Research Hospital, Chicago, Ill.). [nd]. 10p. (CONF-720435-5). Dep. NTIS.
From Seminar on training and education in medical physics; Kiel, Germany (10 Apr 1972).

55462 (AECL-3957) PLANT ASSOCIATIONS IN THE WHITESHELL NUCLEAR RESEARCH ESTABLISHMENT CONTROLLED AREA. Dugle, Janet R. (Atomic Energy of Canada Ltd., Pinawa (Manitoba). Whiteshell Nuclear Research Establishment). Apr 1972. 77p. Dep. NTIS (U. S. Sales Only). AECL $2.00.

55463 (AECL-4208) SURFACE FLATNESS MEASUREMENT BY BROAD SOURCE INTERFERENCE: RELATED TO MECHANICAL FACE SEALS. Metcalfe, R. (Atomic Energy of Canada Ltd., Chalk River (Ontario). Chalk River Nuclear Labs.). May 1972. 20p. Dep. NTIS (U. S. Sales Only). AECL $0.50.

55464 (AERE-R-6601) PARALLEL ORGANISATION OF CAMAC PROCESSES. Lewis, A. (Atomic Energy Research Establishment, Harwell (England)). Jan 1971. 11p. Dep. NTIS (U. S. Sales Only). UK 13 pence.

55465 (AERE-R-6623) TECHNIQUE FOR HANDLING DATA BUFFERS IN REAL-TIME ON-LINE COMPUTER SYSTEMS. Lewis, A. (Atomic Energy Research Establishment, Harwell (England)). Dec 1970. 6p. Dep. NTIS (U. S. Sales Only). UK 1s. 9d.

55466 (ANL-7858) MODELING THE VISUAL PATHWAY FOR INTERACTIVE DIAGNOSIS OF VISUAL FIELDS. Goldbogen, Geof; Shelman, C. B. (Argonne National Lab., Ill.). Aug 1972. Contract W-31-109-Eng-38. 74p. Dep. NTIS.

55467 (ANL/ES-15) TRANSPORTATION AIR POLLUTANT EMISSIONS HANDBOOK. Wolsko, T. D.; Matthies, M. T.; Wendell, R. E. (Argonne National Lab., Ill.). Jul 1972. Contract W-31-109-eng-38. 187p. Dep. NTIS.

55468 (AREAEE-136) SEMICLASSICAL THEORY OF ELECTROMAGNETIC FIELD INTERACTION WITH A MANY-LEVEL MOLECULAR SYSTEM. Demchenko, V. V.; El-Siragy, N. M.; Hussein, A. M. (Atomic Energy Establishment, Cairo (Egypt). Dept. of Accelerators and Plasma Physics Research). 1972. 38p. Dep. NTIS (U. S. Sales Only).

55469 (BDX-613-382(Rev.)) FABRICATION OF MULTILAYER PRINTED WIRING BOARDS. Wilson, M. L. (Bendix Corp., Kansas City, Mo.). Sep 1972. Contract AT(29-1)-613. 68p. Dep. NTIS.

55470 (BDX-613-518(Rev.)) PROCESSING EVALUATION OF MAGNETIC PRODUCTS. Final Report. Moyle, W. F. (Bendix Corp., Kansas City, Mo.). Sep 1972. Contract AT(29-1)-613. 81p. Dep. NTIS.

55471 (BLG-461) INDEX OF S.C.K./C.E.N. PAPERS ISSUED IN 1970. (Centre d'Etude de l'Energie Nucleaire, Mol (Belgium)). [nd]. 52p. (In several languages). Dep. NTIS (U. S. Sales Only).

55472 (BMBW-FBK-72-9) STEROID GLUCURONYLTRANSFERASES. Rao, G. S.; Rao, M. L.; Breuer, H. (Bonn Univ. (West Germany). Institut fuer Klinische Biochemie). Jul 1972. 69p. (In German). Dep. NTIS (U. S. Sales Only).

55473 (BNL-16609) CONCRETE-POLYMER COMPOSITE MATERIALS DEVELOPMENT. Steinberg, Meyer (Brookhaven National Lab., Upton, N. Y.). Feb 1972. 18p. CONF-720832-3). Dep. NTIS.
From 3rd inter-American conference on materials technology; Rio de Janeiro, Brazil (14 Aug 1972).

55474 (BNL-17004) INTESTINAL BARRIER TO BACTERIAL INVASION. Hess, M. W.; Cottier, H.; Sordat, B. (Bern Univ. (Switzerland). Pathologisches Institut); Joel, D. D.; Chanana, A. D. (Brookhaven National Lab., Upton, N. Y.). 1972. 6p. (CONF-720645-1). Dep. NTIS.
From Conference on a re-examination of non-specific factors influencing host resistance; Bern, Switzerland (19 Jun 1972).

55475 (BNL-17110) CERTAIN INVARIANCE AND CONVERGENCE PROPERTIES OF THE PADE APPROXIMANT. Baker, George A. Jr. (Cornell Univ., Ithaca, N. Y. (USA). Baker Lab. of Chemistry. Brookhaven National Lab., Upton, N. Y.). 1972. 13p. (CONF-720626-2). Dep. NTIS.
From International conference on Pade approximants, continued fraction and related topics; Boulder, CO. (22 Jun 1972).

55476 (BNL-17115) PROGRAM IRT. Cullen, Dermott E. (Brookhaven National Lab., Upton, N. Y.). Jul 1972. 74p. Dep. NTIS.

55477 (BNL-50345) CALCIUM HOMEOSTASIS: THE HARD FACTS ABOUT SOFT BONES. Cohn, Stanton H. (Brookhaven National Lab., Upton, N. Y.). 15 Mar 1972. Contract AT(30-1)-16. 15p. Dep. NTIS.

55478 (BNWL-1605) CLIMATOGRAPHY OF THE HANFORD AREA. Stone, W. A.; Jenne, D. E.; Thorp, J. M. (Battelle Pacific Northwest Labs., Richland, Wash.). Jun 1972. Contract AT(45-1)-1830. 269p. Dep. NTIS.

55479 (BNWL-SA-4385) TECHNIQUES FOR THE CHARACTERIZATION OF SUSPENDED SEDIMENT AND SELECTED APPLICATIONS FOR THE ACQUIRED DATA. Routson, R. C.; Wildung, R. E. (Battelle-Northwest, Richland, Wash. Pacific Northwest Lab.). 1972. 18p. (CONF-720825-1). Dep. NTIS.
From fifth Summer meeting of Highway Research Board; Madison, WI. (2 Aug 1972).

55480 (BNWL-tr-72) CARBON ACTIVITY AND SOLUBILITY IN A STAINLESS CHROMIUM-NICKEL STEEL WITH ABOUT 18 PERCENT Cr AND 9 PERCENT Ni. Tuma, Hanus; Groebner, Pavel; Loebl, Karel. Translated for Battelle Pacific Northwest Labs., Richland, Wash., from Arch. Eisenhuettenw.; 40: No. 9, 727-31(1969). 14p. Dep. NTIS.

55481 (BNWL-tr-73) CARBON ACTIVITY AND SOLUBILITY IN AUSTENITIC CHROMIUM-NICKEL STEELS WITH ABOUT 18 PERCENT Cr. Tuma, Hanus; Vyklicky, Miloslav; Loebl, Karel. Translated for Battelle Pacific Northwest Labs., Richland, Wash., from Arch. Eisenhuettenw.; 41: No. 10, 98-3(1970). 14p. Dep. NTIS.

55482 (CEA-CONF-2000) APPLICATIONS OF THE SWEEPING MICROSCOPE TO SEMICONDUCTORS. Bresse, J. F. (Commissariat a l'Energie Atomique, Grenoble (France). Centre d'Etudes Nucleaires). Jun 1971. 3p. (In French). (CONF-710730-1). Dep. NTIS (U. S. Sales Only).
From Conference on microprobe of the National Association on Research Technique; Strasbourg, France (3 Jul 1971).

55483 (CONF-720642-1) QUALITY IMPROVEMENT IN PLANTAINS BY SELECTION. Cuevas-Ruiz, Jose; Koo, Francis K. S. (Puerto Rico Nuclear Center, Mayaguez). 1971. 7p. Dep. NTIS.
From tenth annual meeting of the Caribbean Food Crops Society; Mayaguez, Puerto Rico (11 Jun 1972).

55484 (CONF-720925-3) TECHNOLOGY AND ECONOMICS OF UTILITY TUNNELS AND COMMON TRENCHING. Boegly, W. J. Jr.; Griffith, W. L. (Oak Ridge National Lab., Tenn.). [nd]. 18p. Dep. NTIS.
From seventh intersociety energy conversion engineering conference; San Diego, CA. (25 Sep 1972).

55485 (COO-908-37) PHOTOTAXIS IN EUGLENA: BIOCHEMICAL ASPECTS. Tollin, Gordon (Arizona Univ., Tucson. Dept. of Chemistry). [nd]. Contract AT(11-1)-908. 37p. Dep. NTIS.

55486 (COO-1400-41) RESOLVING THE ENIGMA OF MULTIPLE MUTANT SECTORS IN STAMEN HAIRS OF TRADESCANTIA. Mericle, L. W.; Mericle, R. P. (Michigan State Univ., East Lansing). 1972. 13p. Dep. NTIS.

55487 (COO-1437-8) STUDY OF MATHEMATICAL MODELS OF MUTATION AND SELECTION IN MULTI-LOCUS SYSTEMS. Annual Progress Report, December 1, 1971-November 30, 1972. Lewontin, R. C.; Slatkin, Montgomery (Chicago Univ., Ill. (USA). Dept. of Theoretical Biology). 1972. Contract AT(11-1)-1437. 6p. Dep. NTIS.

55488 (COO-1469-208) COMPUTER SYSTEMS RESEARCH. Annual Report, September 1, 1971-August 31, 1972. (Illinois Univ., Urbana. Dept. of Computer Science). 31 Aug 1972. 84p. Dep. NTIS.

55489 (COO–1469-210) PERSPECTIVE TRANSFORMER FOR THE STEREOMATRIX 3-D DISPLAY SYSTEM. Verma, Shiv Prakash (Illinois Univ., Urbana. Dept. of Computer Science). Oct 1972. Contract AT(11-1)-1469. 77p. (UIUCDCS-R–72-532). Dep. NTIS.

55490 (COO–1495-17) CALCIUM AND STRONTIUM TRANSPORT TO PLANT ROOTS. Elgawhary, S. M.; Malzer, G. L.; Barber, S. A. (Purdue Univ., Lafayette, Ind. Dept. of Agronomy). 1972. Contract AT(11-1)-1495. 32p. Dep. NTIS.

55491 (COO–1562-17) CANAVANINE DEATH AND THE MECHANISM OF DNA REPLICATION IN E. COLI. Progress Report, August 1, 1971–August 1, 1972. Rogers, Palmer (Minnesota Univ., Minneapolis. Dept. of Microbiology). Aug 1972. Contract AT(11-1)-1562. 5p. Dep. NTIS.

55492 (COO–1585-22) RESEARCH ON ATMOSPHERIC DIFFUSION AND TURBULENCE. Final Report. Kao, S. K. (Utah Univ., Salt Lake City. Dept. of Meteorology). Jul 1972. Contract AT(11-1)-1585. 142p. Dep. NTIS.

55493 (COO–1599-58) METABOLISM OF DISSOLVED AND PARTICULATE DETRITAL CARBON IN A TEMPERATE HARDWATER LAKE. Wetzel, Robert G.; Rich, P. H.; Miller, M. C.; Allen, H. L. (Michigan State Univ., Hickory Corners. W. K. Kellogg Biological Station). [nd]. Contract AT(11-1)-1599. 106p. (CONF-720546–1). Dep. NTIS.

From Symposium on detritus and its ecological role in aquatic ecosystems; Pallanza, Italy (May 1972).

55494 (COO–1599-63) INTERACTION OF YELLOW ORGANIC ACIDS WITH CALCIUM CARBONATE IN FRESHWATER. Otsuki, Akira; Wetzel, Robert G. (Michigan State Univ., Hickory Corners. W. K. Kellogg Biological Station). 1972. Contract AT(11-1)-1599. 8p. Dep. NTIS.

55495 (COO–1627-22) PHOTO-INITIATED PROCESSES IN VISION. Technical Progress Report for the Period November 15, 1971–November 14, 1972. Guzzo, Anthony V. (Wyoming Univ., Laramie. Dept. of Chemistry). [nd]. Contract AT(11-1)-1627. 4p. Dep. NTIS.

55496 (COO–1627-23) PHOTO INITIATED PROCESSES IN VISION. Three Year Report for the Period November 15, 1969–November 14, 1972. Guzzo, Anthony V. (Wyoming Univ., Laramie. Dept. of Chemistry). [nd]. Contract AT(11-1)-1627. 22p. Dep. NTIS.

55497 (COO–1630-29) METABOLISM OF THE RARE EARTHS FOLLOWING INHALATION: PATHOLOGIC AND BIOCHEMICAL RESPONSE IN THE LUNG AND OTHER ORGANS. Final Report for Period to September 15, 1972. Berke, Harry L. (Wayne State Univ., Detroit, Mich.). 1972. Contract AT(11-1)-1630. 21p. Dep. NTIS.

55498 (COO–1668-46) MECHANISMS OF CALCIUM TRANSPORT IN SMALL INTESTINE. Overall Review of the Contract, January 1, 1970–September 1, 1972. DeLuca, H. F. (Wisconsin Univ., Madison). 1972. Contract AT(11-1)-1668. 24p. Dep. NTIS.

55499 (COO–2003-17) NUTRIENT ENRICHMENT AND EUTROPHICATION OF LAKE MICHIGAN. Progress Report for the Period November 1, 1968–July 31, 1972. Schelske, Claire L. (Michigan Univ., Ann Arbor. Great Lakes Research Div.). Jul 1972. Contract AT(11-1)-2003. 26p. Dep. NTIS.

55500 (COO–2048-7) BASIS FOR DESIGN ON ALLOWABLE PLASTIC STRAIN. Spretnak, Joseph W.; Tilton, Earl M. (Ohio State Univ., Columbus). 1971. 35p. (CONF-710903–32). Dep. NTIS.

From first international conference on structural mechanics in reactor technology; Berlin, Germany (20 Sep 1971).

55501 (COO–2118-35) ANALYSIS OF TEXTURE. McCormick, B. H.; Jayaramamurthy, S. N. (Illinois Univ., Urbana. Dept. of Computer Science). Jul 1972. Contract AT(11-1)-2118. 91p. (UIUCDCS-R–72-531). Dep. NTIS.

55502 (COO–2126-7) [STUDY OF VIBRATIONAL EXCITATIONS IN AMORPHOUS AND CRYSTALLINE SOLIDS]. Technical Progress Report, December 1, 1971–August 30, 1972. (Chicago Univ., Ill.). [nd]. Contract AT(11-1)-2126. 5p. Dep. NTIS.

55503 (COO–2208-1) STUDY TO DETERMINE THE SIZE AND SHAPE OF THE AVAILABLE SPACE IN THE INTRATHORACIC AND INTRAABDOMINAL CAVITY FOR A TOTALLY IMPLANTABLE CARDIAC PROSTHESIS. Interim Progress Report, February 15–May 1, 1972. (Cleveland Clinic Foundation, Ohio (USA). Dept. of Artificial Organs). 1972. Contract AT(11-1)-2208. 34p. Dep. NTIS.

55504 (COO–2223-1) SPIN LABELED MEMBRANES. Progress Report, November 1, 1971–August 8, 1972. Keith, Alec D. (Pennsylvania State Univ., University Park. Dept. of Biophysics). [nd]. 11p. Dep. NTIS.

55505 (COO–3012-21) IMMUNOCHEMICAL STUDIES WITH THE CARCINOEMBRYONIC ANTIGEN. Reif, Arnold E.; Robinson, Cynthia M.; Naeim, Faramarz; de la Maza, Luis M. (Tufts Univ., Boston, Mass. Dept. of Surgery. Boston City Hospital, Mass. (USA). Mallory Inst. of Pathology). [nd]. Contract AT(11-1)-3012. 15p. (CONF-720208–3). Dep. NTIS.

From second conference on embryonic and fetal antigens in cancer; Oak Ridge, TN. (14 Feb 1972).

55506 (COO–3120-2) EFFECT OF SPATIAL COHERENCE ON THE PHOTOELECTRIC COUNTING STATISTICS OF GAUSSIAN LIGHT. Technical Report No. 13. Cantrell, C D ; Fields, , John R. (Princeton Univ., N. J. Joseph Henry Labs.). 3 Apr 1972. Contract AT(11-1)-3120. 90p. Dep. NTIS.

55507 (COO–3150-6) THERMAL RESISTIVITY AND THERMAL MAGNETORESISTIVITY OF POTASSIUM. Newrock, R. S.; Maxfield, B. W. (Cornell Univ., Ithaca, N. Y. Lab. of Atomic and Solid State Physics). Jul 1972. 12p. Dep. NTIS.

55508 (COO–3151-4) FAR INFRARED SURFACE RESISTANCE OF Cu:Fe; DYNAMICS OF A KONDO SYSTEM. Braendli, G.; Derbenwick, S. R.; Murata, K. K.; Sievers, A. J.; Wilkins, J. W. (Cornell Univ., Ithaca, N. Y. Lab. of Atomic and Solid State Physics). Jul 1972. 13p. Dep. NTIS.

55509 (COO–3151-5) HYDROSTATIC PRESSURE STUDY OF THE AFMR IN $FeCl_2$. Johnson, K. C.; Sievers, A. J. (Cornell Univ., Ithaca, N. Y. Lab. of Atomic and Solid State Physics). Jul 1972. 13p. Dep. NTIS.

55510 (COO–3151-6) EXPERIMENTAL EVIDENCE FOR EXCHANGE POLARIZATION IN SUPEREXCHANGE INTERACTIONS. Johnson, K. C.; Sievers, A. J. (Cornell Univ., Ithaca, N. Y. Lab. of Atomic and Solid State Physics). Jul 1972. 9p. Dep. NTIS.

55511 (COO–3151-8) RESONANT SCATTERING. Pohl, R. O. (Cornell Univ., Ithaca, N. Y. Dept. of Physics). [nd]. Contract AT(11-1)-3151. 3p. Dep. NTIS.

55512 (COO–3151-139) PHONON GENERATION IN $KCl{:}Li^+$ AND $KCl{:}OH^-$ WITH PULSED ELECTRIC FIELDS. Goubau, W. M. (Cornell Univ., Ithaca, N. Y. Lab. of Atomic and Solid State Physics). 28 Jun 1972. Contract AT(11-1)-3151. 25p. Dep. NTIS.

55513 (COO–3158-10) COMMENTS ON THE RANGE OF APPLICABILITY OF THE GRAIN BOUNDARY (SECONDARY) DISLOCATION MODEL TO HIGH ANGLE GRAIN BOUNDARIES. Balluffi, R. W.; Tan, T. Y. (Cornell Univ., Ithaca, N. Y. Dept. of Materials Science and Engineering). 1972. Contract AT-(11-1)-3158. 9p. Dep. NTIS.

55514 (COO–3158-11) CALCULATION OF CORRELATION EFFECTS FOR GRAIN-BOUNDARY AND DISLOCATION-PIPE SELF-DIFFUSION. Robinson, J. T.; Peterson, N. L. (Cornell Univ., Ithaca, N. Y. Materials Science Center). Jul 1972. 18p. Dep. NTIS.

55515 (COO–3161-3) APPROXIMATE PHONON FREQUENCY DISTRIBUTIONS FOR FCC LENNARD–JONES HARMONIC CRYSTALS. Pollock, E. L. (Cornell Univ., Ithaca, N. Y. Lab. of Atomic and Solid State Physics). May 1972. 34p. Dep. NTIS.

55516 (COO–3161-4) PAIR POTENTIAL IN LIQUIDS FROM THE EXACT BORN-GREEN EQUATION: I. MODEL TESTING. Wang, Shein-shion (Guelph Univ. (Ontario). Dept. of Physics); Krumhansl, J. A. (Cornell Univ., Ithaca, N. Y. Lab. of Atomic and Solid State Physics). Jun 1972. 21p. Dep. NTIS.

55517 (COO–3162-12) MEASURING THE DELAYED FLUORESCENCE OF CHLOROPHYLL IN VIVO. Clayton, Roderick K. (Cornell Univ., Ithaca, N. Y.). [nd]. 8p. Dep. NTIS.

55518 (COO–3173-10) INFLUENCE OF IODINE INTAKE UPON KINETICS OF IODINE METABOLISM IN THE DOG. Progress Report, November 1, 1971–October 31, 1972. (Cornell Univ., New York. Medical Coll.). 1972. Contract AT(30-1)-4048. 51p. Dep. NTIS.

55519 (COO-3242-4) DETERMINATIONS OF ELEMENTARY REACTION RATE CONSTANTS FOR THE REACTION OF HYDROGEN ATOMS WITH VARIOUS SUBSTRATE MOLECULES IN THE GAS PHASE. Annual Progress Report, 1971–72. Michael, Joe V. (Carnegie-Mellon Univ., Pittsburgh, Pa. Dept. of Chemistry). 1 Sep 1972. Contract AT(11-1)-3242. 95p. Dep. NTIS.

55520 (COO-3254-6) TROPHIC DYNAMICS AND NICHES OF SALT MARSH FORAMINIFERA. Lee, John J.; Muller, William A. (City Coll., New York). [nd]. 23p. (CONF-720922-2). Dep. NTIS.

From seventeenth international congress of zoology; Monaco (24 Sep 1972).

55521 (COO-3277-14) ACTION SPECTRUM FOR PHOTOINHIBITION OF MECHANICALLY STIMULABLE BIOLUMINESCENCE IN THE MARINE DINOFLAGELLATES GONYAULAX CATENELLA, G. ACTENELLA, AND G. TAMARENSIS. Esaias, Wayne E.; Curl, Herbert C. Jr. (Oregon State Univ., Corvallis (USA). School of Oceanography); Seliger, Howard H. (Johns Hopkins Univ., Baltimore, Md.). Aug 1972. 18p. Dep. NTIS.

55522 (COO-3390-2) GROWTH CHARACTERISTICS OF TINTINNIDA IN CONTINUOUS CULTURE. Gold, Kenneth (New York Aquarium, Brooklyn. Osborn Labs. of Marine Sciences). [nd]. 13p. (CONF-720922-1). Dep. NTIS.

From seventeenth international congress of zoology; Monaco (24 Sep 1972).

55523 (COO-3544-1) COVALENTLY BONDED COMPOUNDS OF THE LIGHT ELEMENTS. Final Report for the Period November 1, 1968–October 31, 1970. Urry, Grant (Tufts Univ., Medford, Mass. Dept. of Chemistry). [nd]. Contract AT(11-1)-3544. 25p. Dep. NTIS.

55524 (DP-1295) ANALYSIS OF HYDROGEN EXPLOSION HAZARDS. Porter, J. B. (Du Pont de Nemours (E. I.) and Co., Aiken, S. C. Savannah River Lab.). Jul 1972. Contract AT(07-2)-1. 39p. Dep. NTIS.

55525 (EUR-4871) POSSIBLE FUNCTION FOR RNA TO DNA INVERTED TRANSCRIPTION IN ANTIBODY BIOSYNTHESIS AND IRREVERSIBLE DIFFERENTIATION. Forti, G. (European Atomic Energy Community, Ispra (Italy). Joint Nuclear Research Center). 1972. 10p. Dep. NTIS (U. S. Sales Only). EUR B. Fr. 25.-.

55526 (IPP-IV-31) INVESTIGATIONS ON THE SPECTRUM OF A PULSED DISCHARGE-INITIATED HF-LASER. Pummer, H. (Max-Planck-Institut fuer Plasmaphysik, Garching (West Germany)). Jan 1972. 50p. (In German). Dep. NTIS (U. S. Sales Only).

55527 (IPP-IV-38) INVESTIGATION OF HYDROGEN FLUORIDE CHEMICAL LASERS. DETERMINATION OF SOME FLUORINE ATOM REACTION RATES. Wanner, J. (Max-Planck-Institut fuer Plasmaphysik, Garching (West Germany)). Jun 1972. 82p. (In German). Dep. NTIS (U. S. Sales Only).

55528 (IS-2838) EDGEWISE GROWTH KINETICS OF WIDMANSTAETTEN PRECIPITATES. Simonen, E. P.; Trivedi, R. K. (Ames Lab., Iowa). Aug 1972. Contract W-7405-eng-82. 174p. Dep. NTIS.

55529 (IS-T-526) NUCLEAR QUADRUPOLE RESONANCE STUDY OF HEAVY TRANSITION METAL HALIDE COMPOUNDS WITH BRIDGING HALOGEN ATOMS. Edwards, Paul Alan (Ames Lab., Iowa). Aug 1972. Contract W-7405-eng-82. 90p. Dep. NTIS.

Thesis.

55530 (ISS-71/22) APPLICATION OF KLEINSCHMIDT'S TECHNIQUE TO THE STUDY OF THE STRUCTURE OF DNA IN SOLUTIONS. Notargiacomo, S. (Istituto Superiore di Sanita, Rome (Italy). Laboratori di Fisica). 6 Sep 1971. 14p. (In Italian). Dep. NTIS (U. S. Sales Only).

55531 (ITF-71-95-P) ON THE TWO-PARTICLE LIGHT ABSORPTION BY A SOLID α-OXYGEN CRYSTAL. Loktev, V. M.; Petrov, E. G. (Akademiya Nauk Ukrainskoi SSR, Kiev. Institut Teoreticheskoi Fiziki). 1972. 48p. (In Russian). Dep. NTIS (U.S. Sales Only).

55532 (ITF-72-2-P) ASYMPTOTIC BEHAVIOUR OF THE PAIR-CORRELATION FUNCTION OF THE NORMAL FERMI-SYSTEMS. Yukhnovskii, I. R.; Petrashko, R. N. (Akademiya Nauk Ukrainskoi SSR, Kiev. Institut Teoreticheskoi Fiziki). 1972. 37p. (In Russian). Dep. NTIS (U. S. Sales Only).

55533 (ITF-72-16-E) ELECTRON ENERGY SPECTRUM OF A CRYSTAL CONDUCTOR IN A MAGNETIC FIELD. Belokolos, E. D. (Akademiya Nauk Ukrainskoi SSR, Kiev. Institut Teoreticheskoi Fiziki). 1972. 14p. Dep. NTIS (U. S. Sales Only).

55534 (ITF-72-27-P) VIBRONIC ABSORPTION SPECTRUM OF MOLECULAR DIMERS. Semenets, T. I. (Akademiya Nauk Ukrainskoi SSR, Kiev. Institut Teoreticheskoi Fiziki). 1972. 16p. (In Russian). Dep. NTIS (U. S. Sales Only).

55535 (ITF-72-29-P) ON THE KINETICS OF THE WEAKLY INHOMOGENEOUS STATES IN THE "FLUID-GAS" TYPE SYSTEM. Prikhod'ko, V. I. (Akademiya Nauk Ukrainskoi SSR, Kiev. Institut Teoreticheskoi Fiziki). 1972. 19p. (In Russian). Dep. NTIS (U. S. Sales Only).

The related hydrodynamic and kinetic equations taking into account both the self-consistent field effects and the effects resulting from the collisions of the particles of "gas with those of fluid" are obtained for an inhomogeneous system of the type "fluid-gas". These effects are expressed in terms of the exact correlation functions of the "gas–fluid" interaction kernel. The consideration of the kinetics of inhomogeneous states in the given system is based on some limiting ergodic relations for the density matrix. These relations reflect, in a natural way, the fact that in the evolution process of a macroscopic system, the description of its state is simplified; as a result, the possibility arises to give a macroscopic description of the system in terms of a small number of variables. (auth)

55536 (ITF-72-32-P) THEORY OF BETHE AND DAVYDOV MAGNETIC SPLITTINGS IN A CUBIC ANTIFERRODIELECTRIC. Petrov, E. G.; Kharkyanen, V. N. (Akademiya Nauk Ukrainskoi SSR, Kiev. Institut Teoreticheskoi Fiziki). 1972. 68p. (In Russian). Dep. NTIS (U. S. Sales Only).

55537 (ITF-72-40-P) FEATURES OF OPTICAL SPECTRA, CAUSED BY THE SURFACE OF A CRYSTAL. Davydov, A. S.; Myasnikov, E. N. (Akademiya Nauk Ukrainskoi SSR, Kiev. Institut Teoreticheskoi Fiziki). 1972. 14p. (In Russian). Dep. NTIS (U. S. Sales Only).

55538 (ITF-72-50-P) THEORY OF POLYMORPHOUS TRANSFORMATIONS IN THE IONIC CRYSTALS WITH TRIPARTICLE INTERACTIONS. Bazarov, I. P.; Kotenok, V. V. (Akademiya Nauk Ukrainskoi SSR, Kiev. Institut Teoreticheskoi Fiziki). 1972. 29p. (In Russian). Dep. NTIS (U. S. Sales Only).

55539 (ITF-72-67-P) LIGHT DISPERSION IN THE ABSORPTION REGION BY IMPURITY CENTRES. Fishchuk, I. I.; Oleksin, D. I.; Nguen Kkhak N'yap (Akademiya Nauk Ukrainskoi SSR, Kiev. Institut Teoreticheskoi Fiziki). 1972. 20p. (In Russian). Dep. NTIS (U. S. Sales Only).

55540 (JINR-P2-6532) ON THE TROUTON–NOBLE EXPERIMENT. Strel'tsov, V. N. (Joint Inst. for Nuclear Research, Dubna (USSR). Lab. of High Energy). 1972. 7p. (In Russian). Dep. NTIS (U. S. Sales Only).

55541 (KFK-1526) UNIVERSAL TIME ADMINISTRATION IN A REAL TIME SYSTEM. Hilse, D. (Kernforschungszentrum, Karlsruhe (West Germany). Institut fuer Datenverarbeitung in der Technik). Mar 1972. 17p. (In German). Dep. NTIS (U. S. Sales Only).

55542 (KFK-1601) INTERPOLATION OF GERMANIUM THERMOMETER CHARACTERISTICS. Buschmann, J.; Decker, W. (Kernforschungszentrum, Karlsruhe (West Germany). Zyklotron-Laboratorium). May 1972. 19p. Dep. NTIS (U. S. Sales Only).

55543 (KFKI-72-32) SLIP: A SYMMETRICAL SUBROUTINE DEVELOPED FOR THE CDC 3300 AND ICL 1905 COMPUTERS. Gergely, Krammer; Istvanne, Lovas (Magyar Tudomanyos Akademia Kozponti Fizikai Kutato Intezete, Budapest). 1972. 55p. (In Hungarian). Dep. NTIS (U. S. Sales Only).

55544 (KFKI-72-41) MEASUREMENT OF MODE-LOCKED ULTRASHORT LASER PULSES BY DIFFERENT ORDER PHOTOELECTRIC EFFECTS. Farkas, Gy.; Horvath, Z. Gy.; Kertesz, I. (Magyar Tudomanyos Akademia Kozponti Fizikai Kutato Intezete, Budapest). 1972. 11p. Dep. NTIS (U. S. Sales Only).

55545 (LA-4925) ANALYSES FOR RESIDUAL EXPLOSIVES IN DRAINAGE DITCH SOIL AT SUMP EFFLUENT OUTLETS. Baytos, John F. (Los Alamos Scientific Lab., N. Mex.). Aug 1972. Contract W-7405-eng-36. 7p. Dep. NTIS.

55546 (LA-4973) METRICS IN BIOLOGY, AN INTRODUCTION. Beyer, W. A.; Stein, M. L.; Ulam, S. M.; Smith, Temple

(Los Alamos Scientific Lab., N. Mex.). Aug 1972. Contract W-7405-eng-36. 6p. Dep. NTIS.
The use of metrics in biology is discussed. Attention is given to metrics in pattern recognition, taxonomy, and especially molecular taxonomy. Various ways of constructing metrics between sequences for use in molecular taxonomy are discussed. (auth)

55547 (LA-DC-72-141) SPECIFICATION OF PROGRAM FLOW IN MADCAP VI. Morris, James B. Jr.; Wells, Mark B. (Los Alamos Scientific Lab., N. Mex.). 1971. 32p. (CONF-720829-1). Dep. NTIS.
From ACM annual conference; Boston, MA. (14 Aug 1972).

55548 (LA-DC-72-243) TRILOGY ON ERRORS IN THE HISTORY OF COMPUTING. Metropolis, N.; Worlton, J. (Los Alamos Scientific Lab., N. Mex.). 7 Mar 1972. 30p. (CONF-721013-1). Dep. NTIS.
From USA-Japan computer conference; Tokyo, Japan (3 Oct 1972).

55549 (LA-DC-72-331) TWO-DIMENSIONAL PROGRAMMING LANGUAGES. Wells, Mark B. (Los Alamos Scientific Lab., N. Mex.). 1971. 19p. (CONF-721007-4). Dep. NTIS.
From Symposium on two-dimensional man-machine communication; Los Alamos, NM. (5 Oct 1972).

55550 (LA-DC-72-410) META-LANGUAGE FOR DESCRIBING KEYBOARD-BASED TWO-DIMENSIONAL LANGUAGES. Morris, James B. (Los Alamos Scientific Lab., N. Mex.). [nd]. 14p. (CONF-721007-3). Dep. NTIS.
From Symposium on two-dimensional man-machine communication; Los Alamos, NM. (5 Oct 1972).

55551 (LA-DC-72-411) TERMINAL CONTROL LANGUAGE FOR THE MADCAP PROGRAMMING LANGUAGE. Devaney, M. A. J.; Hudgins, H. J. (Los Alamos Scientific Lab., N. Mex.). 1971. 10p. (CONF-721007-1). Dep. NTIS.
From Symposium on two-dimensional man-machine communication; Los Alamos, NM. (5 Oct 1972).

55552 (LA-DC-72-632) EXPERIENCE IN HANDLING, TRANSPORT AND STORAGE OF LIQUID HYDROGEN: THE RECYCLABLE FUEL. Bartlit, J. R.; Edeskuty, F. J.; Williamson, K. D. Jr. (Los Alamos Scientific Lab., N. Mex.). 1971. 13p. (CONF-720925-1). Dep. NTIS.
From seventh intersociety energy conversion engineering conference; San Diego, CA. (25 Sep 1972).

55553 (LA-DC-72-783) ANALYZED BINARY COMPUTING. Metropolis, N. (Los Alamos Scientific Lab., N. Mex.). [nd]. 4p. (CONF-720916-2). Dep. NTIS.
From Computer Society conference digest; San Francisco, CA. (12 Sep 1972).

55554 (LA-DC-72-855) CRYOGENIC INSTRUMENTATION AT AND ABOVE LIQUID HYDROGEN TEMPERATURE: PRESENT AND FUTURE. Keller, W. E. (Los Alamos Scientific Lab., N. Mex.). [nd]. 23p. (CONF-720803-6). Dep. NTIS.
From Cryogenic engineering conference; Boulder, CO. (9 Aug 1972).

55555 (LA-DC-72-872) GENERALIZATIONS OF PADE APPROXIMANTS. Fleischer, J. (Los Alamos Scientific Lab., N. Mex.). [nd]. 11p. (CONF-720612-2). Dep. NTIS.
From Conference on Pade approximants; Canterbury, England (25 Jun 1972).

55556 (LA-DC-72-873) NONLINEAR PADE APPROXIMANTS FOR LEGENDRE SERIES. Fleischer, J. (Los Alamos Scientific Lab., N. Mex.). [nd]. 5p. (CONF-720612-3). Dep. NTIS.
From Conference on Pade approximants; Canterbury, England (25 Jun 1972).

55557 (LA-DC-72-879) REVIEW OF TWO RECENT GENERALIZATIONS OF THE PADE APPROXIMANT. Gammel, J. L. (Los Alamos Scientific Lab., N. Mex.). [nd]. 7p. (CONF-720612-4). Dep. NTIS.
From Conference on Pade approximants; Canterbury, England (25 Jun 1972).

55558 (LA-DC-72-880) EFFECT OF RANDOM ERRORS (NOISE) IN THE TERMS OF A POWER SERIES ON THE CONVERGENCE OF THE PADE APPROXIMANTS. Gammel, J. L. (Los Alamos Scientific Lab., N. Mex.). [nd]. 4p. (CONF-720612-5). Dep. NTIS.
From Conference on Pade approximants; Canterbury, England (25 Jun 1972).

55559 (LA-DC-72-903) PHASE TRANSITIONS AND CRYSTAL STRUCTURES OF DEUTERIUM. Schuch, A. F.; Yarnell, J. L.; Mills, R. L. (Los Alamos Scientific Lab., N. Mex.). [nd]. 12p. (CONF-720814-2). Dep. NTIS.
From ninth general assembly and international congress of crystallography; Kyoto, Japan (26 Aug 1972).

55560 (LA-tr-72-16) MINERAL CHEMISTRY. AN ALKALINE BORIDE: THE HEXABORIDE NaB_6. Hagenmuller, Paul; Naslain, Roger. Translated by Rose Mary Boicourt (Los Alamos Scientific Lab., N. Mex.), from Compt. Rend.; 257: 1294-6(1963). 4p. Dep. NTIS.

55561 (LBL-383) PHOTOSYNTHETIC CARBON METABOLISM. Bassham, James A. (California Univ., Berkeley. Lawrence Berkeley Lab.). Apr 1971. Contract W-7405-eng-48. 26p. (CONF-710436-2). Dep. NTIS.
From Symposium on energy for the future; Washington, D. C. (26 Apr 1971).

55562 (LBL-416) NOBLE-GAS CHEMISTRY AND ITS SIGNIFICANCE. Bartlett, Neil (California Univ., Berkeley. Lawrence Berkeley Lab.). Nov 1971. Contract W-7405-eng-48. 18p. Dep. NTIS.

55563 (LBL-515) PROGRAM AUGAT. Kopf, John O. (California Univ., Berkeley. Lawrence Berkeley Lab.). Dec 1971. Contract W-7405-eng-48. 22p. Dep. NTIS.

55564 (LBL-876) POLYCRYSTALLINE SPINEL FROM POWDERS PREPARED BY FREEZE DRYING TECHNIQUE. Tao, Chi-Shine Cliff (California Univ., Berkeley. Lawrence Berkeley Lab.). Jun 1972. Contract W-7405-eng-48. 70p. Dep. NTIS.
Thesis.

55565 (LF-tr-72) SOME FINDINGS ON PULMONARY SURFACTANT BY BIOCHEMICAL STUDY. Fujiwara, Tetusro. Translated by Yoshio Kobayashi (Lovelace Foundation for Medical Education and Research, Albuquerque, N. Mex.), from Nippon Ishikai Zasshi; 66: 1-15(1971). 35p. Dep. NTIS.

55566 (LYCEN-7232) RESTATEMENT OF A FABRICATION TECHNIQUE BY EPITAXY OF THIN MONOCRYSTALLINE GOLD FILMS USED AS BEARING SAMPLES IN CANALIZATION TESTS. Kirsch, Robert (Lyon Univ. (France). Institut de Physique Nucleaire). Jul 1972. 31p. (In French). Dep. NTIS (U. S. Sales Only).

55567 (MLM-1847) INTRODUCTION TO ANALYSIS OF COVARIANCE AND ANALCOV, A COMPUTER PROGRAM FOR COVARIANCE ANALYSIS. Grandillo, A. D. (Mound Lab., Miamisburg, Ohio). 20 Oct 1971. Contract AT-33-1-Gen-53. 56p. Dep. NTIS.

55568 (NIM-1430) USE OF THE EKCO MINERAL ANALYSER FOR THE DETERMINATION OF COPPER AND ZINC IN THE PRESENCE OF IRON. Domel, Gisela (National Inst. for Metallurgy, Johannesburg (South Africa)). 27 Jun 1972. 26p. Dep. NTIS (U. S. Sales Only).

55569 (NP-19404) LIST OF REPORT PUBLICATIONS. (Australian Atomic Energy Commission Research Establishment, Lucas Heights). Apr 1972. 188p. Dep. NTIS (U. S. Sales Only).

55570 (NP-19408) ANNUAL REPORT, 1971. (Commissariat a l'Energie Atomique, Paris (France)). 183p. (In French). Dep. NTIS (U. S. Sales Only).

55571 (NRC-TT-1557) EXPERIMENTAL STUDY OF THE ULTIMATE STRENGTH OF COMPOSITE BEAMS SUBJECTED TO ALTERNATE LOADING OF POSITIVE AND NEGATIVE BENDING. Makino, H.; Hirosawa, M.; Tabata, S.; Takada, T.; Maki, J. Translated by Seishi Arao (National Research Council of Canada, Ottawa), from Proc. Jap. Soc. Architect. Eng., Spec. Publ.; 42: No. 10, 478(1967). 5p. Dep. NTIS (U. S. Sales Only).

55572 (NYO-3823-12) MOESSBAUER EFFECT MEASUREMENTS ON ^{57}Fe IN A NICKEL HOST NEAR THE CURIE POINT. Benski, H. Claudio (Brandeis Univ., Waltham, Mass. Dept. of Physics). Oct 1971. Contract AT(30-1)-3823. 92p. Dep. NTIS.
Thesis.

55573 (ORNL-NSF-EP-23) REGIONAL MODELING ABSTRACTS. VOLUME III. Meyers, Charles R. Jr. (Oak Ridge National Lab., Tenn.). Jun 1972. Contract W-7405-eng-26. 331p. (ORNL-EIS-72-24). Dep. NTIS.

55574 (ORNL-TIP/TIRC-72-4) MAMMALIAN TOXICITY OF PURPURIN, QUINIZARIN, QUINALIZARIN, DIPHENYLTHIOCARBAZONE, AND 1,5-DIPHENYL-3-THIOCARBOHYDRAZIDE. Miller, Kathy (Toxicology Information Response Center, Oak Ridge, Tenn.). Aug 1972. 9p. Dep. NTIS.

55575 (ORNL-TIP/TIRC-72-10) TOXICITY OF POTASSIUM IODATE. Warren, Helen S. (Toxicology Information Response Center, Oak Ridge, Tenn.). Aug 1972. 2p. Dep. NTIS.

55576 (ORNL-TIP/TIRC-72-13) MATERIAL FOR USE BY PARENTS OF HANDICAPPED CHILDREN. Gerstner, Helga (Toxicology Information Response Center, Oak Ridge, Tenn.). Aug 1972. 33p. Dep. NTIS.

55577 (ORNL-TIP/TIRC-72-45) EFFECTS OF SODIUM NITRITE ON THE HEMOPOIETIC AND VASCULAR SYSTEM OF THE MAMMAL. Gerstner, Helga (Toxicology Information Response Center, Oak Ridge, Tenn.). Aug 1972. 4p. Dep. NTIS.

55578 (ORNL-TIP/TIRC-72-49) ANIMAL TOXICITY OF COUMAPHOS AND CONTAMINANTS. Gerrard, Martha (Toxicology Information Response Center, Oak Ridge, Tenn.). Sep 1972. 6p. Dep. NTIS.

55579 (ORNL-TIP/TIRC-72-52) DIETHYLPYROCARBONATE TOXICOLOGY AND PHARMACOLOGY. Holland, Florence (Toxicology Information Response Center, Oak Ridge, Tenn.). Aug 1972. 4p. Dep. NTIS.

55580 (ORNL-TIP/TIRC-72-53) MAXIMUM SAFE LEVELS OF FLUORINE FOR MAN AND ANIMALS. Gerrard, Martha (Toxicology Information Response Center, Oak Ridge, Tenn.). Aug 1972. 3p. Dep. NTIS.

55581 (ORNL-TIP/TIRC-72-54) TOXICITY DATA FOR IMIDO (IMIDATE) ESTERS. Warren, Helen (Toxicology Information Response Center, Oak Ridge, Tenn.). Aug 1972. 3p. Dep. NTIS.

55582 (ORNL-TIP/TIRC-72-59) EFFECT OF PYRAMIDON ON THE HEMOPOIETIC AND VASCULAR SYSTEM OF THE MAMMAL. Gerstner, Helga (Toxicology Information Response Center, Oak Ridge, Tenn.). Sep 1972. 5p. Dep. NTIS.

55583 (ORNL-TIP/TIRC-72-60) CARCINOGENICITY OF METHYL-NITRO-NITROSO-GUANIDINE. Warren, Helen S. (Toxicology Information Response Center, Oak Ridge, Tenn.). Sep 1972. 3p. Dep. NTIS.

55584 (ORNL-TIP/TIRC-72-61) TOXICOLOGY OF ISO-AMYLAMINE AND RELATED AMINES. Warren, Helen S. (Toxicology Information Response Center, Oak Ridge, Tenn.). Sep 1972. 6p. Dep. NTIS.

55585 (ORNL-TIP/TIRC-72-62) TOXICITY ASPECTS OF SILICA OR QUARTZ PARTICLES. Gerstner, Helga (Toxicology Information Response Center, Oak Ridge, Tenn.). Sep 1972. 9p. Dep. NTIS.

55586 (ORNL-TIP/TIRC-72-63) TOXICITY OF ELEMENTAL PHOSPHORUS. Gerstner, Helga (Toxicology Information Response Center, Oak Ridge, Tenn.). Sep 1972. 13p. Dep. NTIS.

55587 (ORNL-TM-3898) SEASONAL ALTERATIONS IN RODENT BLOOD. Dunaway, P. B.; Story, J. D.; Kitchings III, J. T.; Payne, J. A. (Oak Ridge National Lab., Tenn.). Sep 1972. Contract W-7405-eng-26. 93p. Dep. NTIS.

55588 (ORNL-tr-2394) ELEMENTARY MECHANISMS IN HETEROGENEOUS KINETICS. IV. COMPLEX AND PURE RATE SYSTEMS KINETIC LAWS AND INFLUENCE OF PRESSURE IN PURE RATE SYSTEMS. Besson, Jean; Azzopardi, Max; Caillet, Marcel; Sarrazin, Pierre; Soustelle, Michel. Translated for Oak Ridge National Lab., Tenn., from J. Chim. Phys.; 63: No. 7-8, 1049-54(1966). 12p. Dep. NTIS.

55589 (ORNL-tr-2603) STATUS OF MICRO-EMISSION SPECTRAL ANALYSIS WITH SOLID-STATE LASERS. Moenke, Horst. Translated by R. Gregg Mansfield (Oak Ridge National Lab., Tenn.), from Messtechnik; 10: 13-18(1968). 16p. Dep. NTIS.

55590 (ORNL-tr-2613-A) LIMITS OF DETECTION IN LOCALIZED SPECTROCHEMICAL ANALYSIS WITH LASERS. Hagenah, W. D.; Klocke, K.; Laqua, K. Translated for Oak Ridge National Lab., Tenn. from pp 634-5 of 14. International Colloquium of Spectroscopy, Debrecen, Hungary, August 7-12, 1967. 5p. Dep. NTIS.

55591 (ORNL-tr-2636) VIBRATION ANALYSIS OF E. P. DISCHARGE ELECTRODE. Hiramatsu, Tsutomu; Kobori, Yoichi. Translated by H. Kubota (Oak Ridge National Lab., Tenn.), from Hitachi Hyoron; 45: No. 4, 130-6(1963). 30p. Dep. NTIS.

55592 (PEL-220) LIST OF UNCLASSIFIED PEL REPORTS, 1st MARCH 1957-31st DECEMBER 1971. (Atomic Energy Board, Pelindaba, Pretoria (South Africa)). Feb 1972. 13p. Dep. NTIS (U. S. Sales Only).

55593 (RFP-Trans-108) INFLUENCE OF AUSTENITE GRAIN SIZE AND FORGING RATIO ON FERRITE BANDED STRUCTURE. Kusaka, Kunio; Araki, Shotaro; Iwamaru, Masaaki. Translated for Dow Chemical Co., Rocky Flats Div., from J. Jap. Inst. Metals; 34: 957-62(1970). 12p. Dep. NTIS.

55594 (RFP-Trans-110) X-RAY RESIDUAL STRESS ANALYSIS IN HARDENED STEELS. Pruemmer, R. A. (Karlsruhe Univ. (West Germany). Institut fuer Werkstoffkunde I). Translated for Dow Chemical Co., Rocky Flats Div., from a German report. 15p. Dep. NTIS.

55595 (RT/FIMA-(72)1) EULERO PROGRAM. Kranyc, A.; Fedele, V. D. (Comitato Nazionale per l'Energia Nucleare, Rome (Italy)). 11 Feb 1972. 7p. (In Italian). Dep. NTIS (U. S. Sales Only).

55596 (SC-CR-723162) MAGNUS FORCE TESTS FOR SANDIA CORPORATION, 1971-72. Wind-Tunnel Report No. 59. Ragsdale, William C. (Naval Ordnance Lab., White Oak, Md.). Jun 1972. 117p. Dep. NTIS.

55597 (SC-DC-714099) SURFACE PREPARATION FOR ADHESIVE BONDING. Jennings, C. W. (Sandia Labs., Albuquerque, N. Mex.). 1972. 19p. (CONF-720830-1). Dep. NTIS.

From Symposium on adhesion; Dover, NJ. (Aug 1972).

55598 (SC-DC-721020) ROOM TEMPERATURE ELECTRICAL PROPERTIES AND DOPANT PRECIPITATION FOR SiGe THERMOELECTRIC ALLOYS. Nasby, R. D.; Burgess, E. L. (Sandia Labs., Albuquerque, N. Mex.). 1972. 23p. (CONF-720925-5). Dep. NTIS.

From seventh intersociety energy conversion engineering conference; San Diego, CA. (25 Sep 1972).

55599 (SC-DC-721376) PROGRAM OPTIMIZATION. Gasser, Sidney B. (Sandia Labs., Albuquerque, N. Mex.). 12 Jun 1972. 14p. (CONF-721004-1). Dep. NTIS.

From third annual symposium for computing machinery; Gaithersburg, MD. (17 Oct 1972).

55600 (SC-DC-722244(RD)) FLIGHT TEST EVALUATION OF A FLUIDICALLY ACTUATED MONOPROPELLANT HYDRAZINE ROLL CONTROL SYSTEM. Hodapp, A. E. Jr.; Beckmann, R. C. (Sandia Labs., Albuquerque, N. Mex.). 1972. 67p. (CONF-720921-1). Dep. NTIS.

From second atmospheric flight mechanics conference; Moffett Field, GA. (11 Sep 1972).

55601 (SC-DC-722297) AROMATIC POLYIMIDE SYNTACTIC FOAM. Rand, Peter B. (Sandia Labs., Albuquerque, N. Mex.). Jun 1972. 17p. (CONF-720915-2). Dep. NTIS.

From 3rd international cellular plastics conference; Montreal, Canada (26 Sep 1972).

55602 (SC-DC-722298) LONG LIFE, WIDE TEMPERATURE RANGE ORGANIC ELECTROLYTE BATTERY. Levy, Samuel C. (Sandia Labs., Albuquerque, N. Mex.). 1972. 3p. (CONF-721008-1). Dep. NTIS.

From 142nd national fall meeting of the electrochemical society; Miami Beach, FL. (8 Oct 1972).

55603 (SC-DR-70-617) MECHANICAL AND THERMAL EXPANSION PROPERTIES OF A PARTICULATE FILLED POLYMER. Brassell, Gilbert W.; Wischmann, Kenneth B. (Sandia Labs., Albuquerque, N. Mex.). Nov 1971. 28p. Dep. NTIS.

55604 (SC-DR-720303) SIGNIFICANT DIGIT INCOMPLETE GAMMA RATIOS. Amos, D. E.; Daniel, S. L. (Sandia Labs., Albuquerque, N. Mex.). Apr 1972. 21p. Dep. NTIS.

55605 (SC-M-68-808) PLANT EQUIPMENT INVENTORY MANAGEMENT. Hollingsworth, L. E. (Sandia Labs., Albuquerque, N. Mex.). Nov 1968. 42p. Dep. NTIS.

55606 (SC-M-720514) TRASHP: TRANSEMBLER FOR THE HEWLETT-PACKARD MINICOMPUTERS. Petty, S. M. (Sandia Labs., Albuquerque, N. Mex.). Aug 1972. 12p. Dep. NTIS.

55607 (SC-R-722879) USING BASIC AS A REAL TIME EXECUTIVE ON A SMALL SYSTEM. Stiefeld, B. (Sandia Labs., Albuquerque, N. Mex.). [nd]. 4p. Dep. NTIS.

55608 (SC-RR-720286) IMAGEN: A COMPUTER PROGRAM FOR IMAGE ENHANCEMENT AND DISPLAY OF TWO-DIMENSIONAL DATA. Fisk, C. J. (Sandia Labs., Albuquerque, N. Mex.). Jul 1972. 62p. Dep. NTIS.

55609 (SC-TM-710557) MESH-GENERATION CODE AND A CONTOUR-PLOTTING ROUTINE. Lobitz, D. W. (Sandia Labs., Albuquerque, N. Mex.). Feb 1972. 50p. Dep. NTIS.

55610 (SCL-DR-720004) HEATMESH-71: A COMPUTER CODE FOR GENERATING GEOMETRICAL DATA REQUIRED FOR STUDIES OF HEAT TRANSFER IN AXISYMMETRIC STRUCTURES. Gabrielson, V. K. (Sandia Labs., Livermore, Calif.). Sep 1972. Contract AT(29-1)-789. 80p. Dep. NTIS.
Supersedes SCL-DR-67-30.

55611 (SCL-RR-710113) STEADY-STATE RESPONSE OF AN INFINITE PLATE TO AN EXPONENTIAL EDGE LOAD ALONG A FUSING CRACK: A MODEL FOR THE DYNAMIC EDGE FUSION OF TWO SEMI-INFINITE PLATES. Wesenberg, D. L.; Murphy, L. M. (Sandia Labs., Livermore, Calif.). Sep 1972. Contract AT(29-1)-789. 36p. Dep. NTIS.

55612 (SRO-639-12) FLUX OF RADIONUCLIDES THROUGH A SALT MARSH ECOSYSTEM. Progress Report, January 1–December 30, 1972. (Georgia Univ., Athens). 16 Aug 1972. Contract AT(38-1)-639. 15p. Dep. NTIS.

55613 (SU-326-P-17-X-2) STRUCTURE DEPENDENCE OF HIGH TEMPERATURE DEFORMATION OF METALS. Progress Report, March 1, 1970–March 1, 1971. Nix, William D.; Barrett, Craig R. (Stanford Univ., Calif. (USA). Dept. of Materials Science and Engineering). 1 Apr 1971. Contract AT-(04-3)-326. 66p. Dep. NTIS.

55614 (TID-25974) APPROXIMATE STRUCTURE FOR THE ANTIFERROELECTRIC PHASE OF COPPER FORMATE TETRAHYDRATE. Kay, M. I.; Kleinberg, R. (Puerto Rico Nuclear Center, Mayaguez). 1971. 16p. (CONF-720814-3). Dep. NTIS.
From ninth general assembly and international congress of crystallography; Kyoto, Japan (26 Aug 1972).

55615 (TID-26148) PRECIPITATION FROM SUPERSATURATED COPPER–TITANIUM SOLID SOLUTIONS: THE AGING PROCESS AND PRECIPITATION HARDENING IN COPPER–TITANIUM SIDEBAND ALLOYS. Progress Report, 1971–1972. Soffa, William A. (Pittsburgh Univ., Pa. (USA). Dept. of Metallurgical and Materials Engineering). Mar 1972. Contract AT-(11-1)-3434. 21p. Dep. NTIS.

55616 (TID-26149) FREE RADICALS IN BIOLOGICAL ENERGY CONVERSION: EPR STUDIES OF MODEL SYSTEMS. Three Year Review and Technical Progress Report, September 1, 1969–August 31, 1972. Tollin, Gordon (Arizona Univ., Tucson). 1972. Contract AT(11-1)-908. 45p. Dep. NTIS.

55617 (TID-26159) MAGNETIC PROPERTIES OF TRANSITION METALS AND THEIR ALLOYS DETERMINED BY MOESSBAUER MEASUREMENTS WITH ^{61}Ni. Obenshain, Felix E. (Oak Ridge National Lab., Tenn.). [nd]. 2p. Dep. NTIS.

55618 (UCID-16099) ENRP 69-5: DESIGN CRITERIA FOR CONFIDENCE AND RELIABILITY BASED ON SMALL SAMPLES. Robinson, E. Y. (California Univ., Livermore. Lawrence Livermore Lab.). 23 Jun 1969. Contract W-7405-Eng-48. 17p. Dep. NTIS.

55619 (UCID-16100) ENRP 69-8: COMPOSITE STATIC FATIQUE INTERPRETATION OF SOME DATA. Robinson, E. Y. (California Univ., Livermore. Lawrence Livermore Lab.). 18 Aug 1972. Contract W-7405-Eng-48. 38p. Dep. NTIS.

55620 (UCLA-12-871) METABOLISM OF 1-^{14}C PALMITIC ACID IN THE DEVELOPING BRAIN: PERSISTENCE OF RADIOACTIVITY IN THE CARBOXYL CARBON. Dhopeshwarkar, G. A.; Subramanian, Carole; Mead, James F. (California Univ., Los Angeles. Lab. of Nuclear Medicine and Radiation Biology). 1972. Contract AT-04-1-GEN-12. 18p. Dep. NTIS.

55621 (UCLA-12-877) PRODUCTION OF A NERVOUS-SYSTEM-SPECIFIC PROTEIN (14-3-2) BY HUMAN NEUROBLASTOMA CELLS IN CULTURE. Herschman, Harvey R.; Lerner, Michael P. (California Univ., Los Angeles. Lab. of Nuclear Medicine and Radiation Biology). 1972. Contract AT-04-1-GEN-12. 11p. Dep. NTIS.

55622 (UCLA-12-879) EFFECTS OF TEMPERATURE AND FATTY ACID STRUCTURE ON LIPID METABOLISM IN BACILLUS LICHENIFORMIS 9259. Chang, Norman C.; Fulco, Armand J. (California Univ., Los Angeles. School of Medicine). 1972. Contract AT(04-1)-GEN-12. 63p. Dep. NTIS.

55623 (UCLA-34-P-91-48) PHOSPHORESCENCE-MICROWAVE DOUBLE RESONANCE SPECTROSCOPY OF 1,2,4,5 TETRACHLOROBENZENE. Annual Report, September 15, 1971–September 14, 1972, Part 1. Chen, Chuan-Run (California Univ., Los Angeles. Dept. of Chemistry). Apr 1972. Contract AT(04-3)-34. 248p. Dep. NTIS.
Thesis.

55624 (UCRL-51255) USE OF GRATING TO INCREASE RECORDING CAPABILITY OF LASER FAR FIELD CAMERA. Weaver, H. Joseph Jr. (California Univ., Livermore. Lawrence Livermore Lab.). 26 Jul 1972. Contract W-7405-eng-48. 7p. Dep. NTIS.

55625 (UCRL-73334) SEMIMICRO GEL PERMEATION CHROMATOGRAPHIC ANALYSIS OF HMX-CONTAINING EXPLOSIVES. Clarkson, Jack E. (California Univ., Livermore. Lawrence Radiation Lab.). 19 Oct 1971. 15p. (CONF-711117-2). Dep. NTIS.
From second JANNAF Propellant Characterization Working Group meeting; Las Vegas, Nev. (1 Nov 1971).

55626 (UCRL-73610) SPECIMEN STRAIN MEASUREMENT IN THE SPLIT HOPKINSON PRESSURE BAR EXPERIMENT. Sharpe, William N. Jr.; Hoge, Kenneth G. (California Univ., Livermore. Lawrence Livermore Lab.). 18 Jan 1972. 23p. (CONF-721012-1). Dep. NTIS.
For Presentation at fall meeting of the Society of Experimental Stress Analysis; Seattle, WA. (17 Oct 1972).

55627 (UCRL-73772) FIBER STRENGTH OF S-GLASS/EPOXY COMPOSITES UNDER BIAXIAL LOADING. Chiao, T. T.; Commins, A. D. (California Univ., Livermore. Lawrence Livermore Lab.). 4 May 1972. 10p. (CONF-721009-1). Dep. NTIS.
From fourth SAMPE national technical conference; Palo Alto, CA. (17 Oct 1972).

55628 (UCRL-73773) CHARACTERIZATION OF AN EPOXY SYSTEM FOR FILAMENT WINDING. Chiao, T. T.; Althouse, L. P. (California Univ., Livermore. Lawrence Livermore Lab.). 4 May 1972. 8p. (CONF-721009-2). Dep. NTIS.
From fourth SAMPE national technical conference; Palo Alto, CA. (17 Oct 1972).

55629 (UCRL-73921) PNEUMATIC LOGIC CONTROLS FOR AUTOMATIC VACUUM SYSTEMS. Hugenberger, Charles E.; Petrich, Donald E. (California Univ., Livermore. Lawrence Livermore Lab.). 14 Jul 1972. 11p. (CONF-721003-2). Dep. NTIS.
From 19th national vacuum symposium; Chicago, IL. (2 Oct 1972).

55630 (UCRL-73943) BASEBAND DISTORTION EQUALIZATION IN THE TRANSMISSION OF PULSE INFORMATION. Ekstrom, M. P. (California Univ., Livermore. Lawrence Livermore Lab.). 1 Jun 1972. 27p. (CONF-720624-1). Dep. NTIS.
From Conference on precision electromagnetic measurements; Boulder, CO. (26 Jun 1972).

55631 (UCRL-74039) TEST RESULT OF THE GEOGRAPHIC POSITION LOCATOR: A SYSTEM FOR IMPROVING LAND NAVIGATION WITHOUT EXTERNAL AIDS. Salisbury, John D. (California Univ., Livermore. Lawrence Livermore Lab.). 21 Jul 1972. 40p. (CONF-721005-1). Dep. NTIS.
From sixth biennial guidance test symposium; Holloman AFB, NM. (4 Oct 1972).

55632 (UCRL-Trans-1479) VISCOSITY OF Al$_2$O$_3$–SiO$_2$ MELTS. Mishin, B. S.; Nagibin, Yu. A. Translated for Univ. of California, Lawrence Berkeley Lab., from Izv. Vyssh. Ucheb. Zaved., Chern. Met.; 12: No. 7, 8-10(1969). 4p. Dep. NTIS.

55633 (UCRL-Trans-10640) GAS COULOMETRY. Tanaka, Y.; Muto, G. Translated for Univ. of California, Lawrence Livermore Lab., from Nippon Kagaku Zasshi; 88: No. 1, 107-9 (1967). 5p. Dep. NTIS.

55634 (UR-3490-136) PULMONARY ABSORPTION OF TOXIC METALS. Morrow, P. E. (Rochester Univ., N. Y. Dept. of Radiation Biology and Biophysics). 1972. 35p. (CONF-720919-1). Dep. NTIS.
From 17th international congress on occupational health; Buenos Aires, Argentina (11 Sep 1972).

55635 (UR-3490-174) EFFECT OF K^+ AND K^+ GRADIENTS ON ACCUMULATION OF SUGARS BY ISOLATED INTESTINAL EPITHELIAL CELLS. Kimmich, George A.; Randles, Joan (Rochester Univ., N. Y. Dept. of Radiation Biology and Biophysics). 1971. Contract AT(11-1)-3490. 41p. Dep. NTIS.

55636 (UR-3490-177) STUDIES ON THE TRANSPORT OF L-LYSINE BY ISOLATED CHICK INTESTINAL EPITHELIAL CELLS. Barrett, Eugene; Kimmich, George (Rochester Univ., N. Y. Dept. of Radiation Biology and Biophysics). 1972. 44p. Dep. NTIS.

55637 (UR-3490-184) DIRECT DETERMINATION OF TOTAL IONIC FLUORIDE IN BIOLOGICAL FLUIDS. Hall, Larry L.; Smith, Frank A.; De Lopez, Ofelia H.; Gardner, Dwight E. (Rochester Univ., N. Y. Dept. of Radiation Biology and Biophysics). 1970. Contract AT(11-1)-3490. 23p. Dep. NTIS.

55638 (UR-3490-187) REDUCED RED CELL 2,3-DIPHOSPHOGLYCERATE AND ADENOSINE TRIPHOSPHATE, HYPOPHOSPHATEMIA AND INCREASED HEMOGLOBIN-OXYGEN AFFINITY AFTER CARDIAC SURGERY. Young, Jerald A.; Lichtman, Marshall A.; Cohen, Jules (Rochester Univ., N. Y. (USA). Dept. of Medicine). 1972. 21p. Dep. NTIS.

55639 (Y-1841) REAL-TIME ANALYSIS OF THERMAL DIFFUSIVITY DATA FROM A PULSED LASER FACILITY. Davenport, C. M.; Carver, D. W.; Schneider, P. G. (Union Carbide Corp., Oak Ridge, Tenn. Y-12 Plant). 11 Sep 1972. 27p. Dep. NTIS.

55640 (Y-1848) ANALYSIS OF THE EFFECTS OF SELECTED SCHEDULING RULES IN A PARALLEL PROCESSOR SHOP. Gentry, D. H. (Union Carbide Corp., Oak Ridge, Tenn. Y-12 Plant). 25 Aug 1972. Contract W-7405-eng-26. 160p. Dep. NTIS.

55641 EXPERIMENTAL DETERMINATION OF ION DENSITY TRAPPED BY ELECTRON BEAM. Hartnagel, H. L.; Herkmen, I. (Univ. of Newcastle upon Tyne, Eng.). Electron. Lett.; 8: No. 17, 430-1(24 Aug 1972).

A new probing technique was employed to determine the ion density trapped by the potential well of an electron beam as used in microwave tubes, and unexpectedly high values of ionic charge were found on the axis, the strong space-charge fields of which are neutralized by slow secondary electrons. (auth)

55642 SOLID-STATE CONTROLLED-POTENTIAL COULOMETERS (Jul 1969) (Engineering Materials). (New Brunswick Lab. (AEC), N. J.). (CAPE-2194).

4 drawings.

Modified versions of the ORNL Controlled-Potential Coulometers Z-2005 and Q-2564 (See CAPES-785 and -1196) using solid-state parts are described. The solid-state instrument shows smaller size, less power consumption, less heat evolution, and low long-term drift of the current and integrating amplifiers. Short term drift of the control amplifiers and a control potential less than 0.1 mV/day are possible. (4 drawings) (For details see TID-4100 Suppl. 70) (see also 25: 39411) (F.S.)

CORPORATE AUTHOR INDEX

In the Corporate Author Index, technical report literature is indexed to the organization or institution responsible for issuing the report. Headings are given for all report literature and for published literature for which a corporate author approach is especially desirable, e.g., symposium and conference proceedings.

Each entry under a corporate author heading gives the publication title and the *NSA* volume and abstract numbers. Report numbers, where applicable, are given in parentheses at the end of the entry.

Corporate Author Headings Used by the U. S. Atomic Energy Commission in Cataloging Reports, TID-5059 (10th Rev.), is available from the National Technical Information Service (NTIS), U. S. Department of Commerce, Springfield, Virginia 22151, for $3.00 for full size or reproduction copy and $0.95 for microfiche copy.

A

- AEROJET NUCLEAR CO., IDAHO FALLS, IDAHO.
  - Automated Cross Section Analysis Program (ACSAP), 26:54468 (ANCR-1042)
  - Calculated reactivity of VINS, 26:54469 (ANCR-1071)
  - ETR power: variation analysis, 26:55379 (ANCR-1085)
  - Evaluation of filament-type electric heater rod as employed in single-loop semiscale to simulate UO_2 fuel rods, 26:55183 (ANCR-1038)
  - Gamma rays emitted by the fissionable nuclides and associated isotopes, 26:54652 (ANCR-1069)
- AEROJET NUCLEAR SYSTEMS CO., SACRAMENTO, CALIF.
  - Conference on natural and manmade radiation in space held at Las Vegas, Nevada, 3/71, 26:54870 (NASA-TM-X-2440)
- AEROSPACE RESEARCH LABS., WRIGHT-PATTERSON AFB, OHIO.
  - High-pressure electrofluiddynamic facility, 26:53089 (AD-737380)
- AKADEMIYA NAUK SSSR, LENINGRAD. FIZIKO-TEKHNICHESKII INSTITUT.
  - Conditions for wave transformation in a plasma with a nonmonotonic longitudinal distribution, 26:54841 (AEC-tr-7338)
  - Ratio of longitudinal and transverse diffusion coefficients in argon SHF discharge plasma, 25:54776 (AEC-tr-7332)
  - Study of the localization of the wave transformation region in a superhigh-frequency discharge plasma, 26:54842 (AEC-tr-7339)
- AKADEMIYA NAUK SSSR, MOSCOW. FIZICHESKII INSTITUT.
  - Excitation by very high frequency wave pumping of parametric instabilities in a magnetoactive plasma, 26:54809 (NP-19406)
  - Generation of fast electrons through interaction of SHF wave with collisionless plasma, 26:54836 (AEC-tr-7331)
  - Longitudinal and transverse excitons in semiconductors, 26:55065 (UCRL-Trans-10643)
  - Second harmonic generation in nonuniform laser-produced plasma, 26:54790 (JPRS-56713)
- AKADEMIYA NAUK SSSR, MOSCOW. INSTITUT FIZIKI.
  - Excitation of electromagnetic waves in a plasma by a relativistic electron beam. Part I. Longitudinal waves, 26:54837 (AEC-tr-7333)
  - Plasma bremsstrahlung from relativistic particles in a turbulent plasma, 26:54774 (AEC-tr-7323)
- AKADEMIYA NAUK UKRAINSKOI SSR.
  - Quasi-elastic electron scattering on ^{12}C nuclei, 26:54526 (ITF-72-25-P)
  - Two-particle electrodesintegration of ^3He, 26:54496 (ITF-72-24-P)
- AKADEMIYA NAUK UKRAINSKOI SSR, KHARKOV. FIZIKO-TEKHNICHESKII INSTITUT.
  - Effect of high-frequency potential on propagation of fast waves along a magnetoactive plasma layer, 26:54839 (AEC-tr-7336)
  - Experimental determination of the basic characteristics of space-periodic magnetic configurations, 26:54824 (AEC-tr-7334)
  - On the effect of wave field pressure on longitudinal oscillations in a plasma, 26:54840 (AEC-tr-7337)
  - On the theory of transformation of surface waves into longitudinal oscillations in the surface layer of a plasma wave-guide, 26:54838 (AEC-tr-7335)
- AKADEMIYA NAUK UKRAINSKOI SSR, KIEV. INSTITUT TEORETICHESKOI FIZIKI.
  - Analytic regularization depending on the parameter, 26:54409 (ITF-72-37-P)
  - Applications of the statistical mechanics methods in a dual model, 26:54299 (ITF-72-49-P)
  - Asymptotic behavior of pair-correlation function of normal Fermi-systems, 26:55532 (ITF-72-2-P)
  - Asymptotically exact solutions for the systems with singular potentials, 26:55068 (ITF-72-31-P)
  - Behavior of renormalized Feynman amplitudes under scale transformations, 26:54410 (ITF-72-38-P)
  - Cosmological models of a scalar-tensor theory of gravitation, 26:54396 (ITF-72-41-P)
  - DAMA and Regge asymptotic behavior, 26:54412 (ITF-72-63-E)
  - Dispersion sum rules and Jost--Lehman--Dyson representation in axiomatic quantum theory, 25:54377 (ITF-72-54-P)
  - Effects of Einstein's theory of gravity at two-particle vibrations in Schwarzchild's field, 26:54401 (ITF-72-60-P)
  - Electron energy spectrum of a crystal conductor in a magnetic field, 26:55533 (ITF-72-16-E)
  - Equations for the S-matrix element in g(:phi^4:)$_2$ theory, 26:54376 (ITF-72-15-E)
  - External invariant equations of electromagnetic field, 26:54373 (ITF-72-35-P)
  - Features of optical spectra, caused by surface of a crystal, 26:55537 (ITF-72-40-P)
  - Geometry of relativistic space of particle states, 26:54391 (ITF-71-132-P)
  - High-energy approximation and generalized Huygen's principle, 26:54690 (ITF-72-57-P)
  - Infinitesimal transformations conserving test-body trajectories in general relativity, 26:54389 (ITF-71-85-P)
  - Introduction to physical kinetics, 26:54789 (ITF-71-96-P)
  - Kinetics of weakly inhomogeneous states in ''fluid-gas'' type system, 26:55535 (ITF-72-29-P)
  - Light dispersion in the absorption region by impurity centres, 26:55539 (ITF-72-67-P)
  - Modeling of gravitational fields, 26:54390 (ITF-71-130-P)
  - Present-day problems of the theory of nuclear forces, 26:54688 (ITF-71-77-P)
  - Product formula for semigroups and its application to Shroedinger equation with singular potentials, 26:55069 (ITF-72-36-E)
  - Relations between moment functionals of measures absolutely continuous with respect to Gaussian measure and solvability of Schwinger equations for Green functions of Euclidean field theory, 26:55070 (ITF-72-45-P)
  - Relations between the cosmological and quantum constants, 26:54392 (ITF-72-3-P)
  - Relativistic gravitational effect on influence of earth rotation on mechanical vibrations, 26:54400 (ITF-72-59-P)
  - Riessner--Nordstroem problem in presence of scalar field, 26:54394 (ITF-72-20-P)
  - Scalar-tensor theory of gravitation, 26:54395 (ITF-72-21-P)
  - Solutions of Bogolyubov kinetic equations. Quantum statistics, 26:55067 (ITF-72-9-E)
  - Solutions of Skornyakov-Ter-Martirosyan equations for three nucleons with cut-off at large momenta, 26:54344 (ITF-72-10-P)
  - Some exactly solvable model problem with positive interaction, 26:54435 (ITF-72-56-E)
  - Spatial localizability of energy--momentum tensor of gravitational field, 26:54393 (ITF-72-5-P)
  - Stability of systems with singular potentials, 26:54408 (ITF-72-14-E)
  - Statistical view on resonance widths and multiplicity in dual models, 26:54300 (ITF-72-53-E)
  - Theory of Bethe and Davydov magnetic splittings in cubic antiferrodielectric, 26:55536 (ITF-72-32-P)
  - Theory of polymorphous transformations in the ionic crystals with triparticle interactions, 26:55538 (ITF-

- 72-50-P)
  - Two-body problem in theory of direct gravitational interaction, 26:54399 (ITF-72-58-P)
  - Two-body problem in theory of direct gravitational interaction. I, 26:54398 (ITF-72-52-P)
  - Two-particle distributions in dual resonance model, 26:54301 (ITF-72-55-P)
  - Two-particle light absorption by solid α--oxygen crystal, 26:55531 (ITF-71-95-P)
  - Two-symmetric and two-recurrent fields of gravitation, 26:54397 (ITF-72-46-P)
  - Unitary renormalization, positivity, and selfadjointness of the Hamiltonian for a Lee model of the type Y/sub 3+1/, 26:54237 (ITF-72-48-E)
  - Vibrations of Fermi-fluid drop and giant resonance in intermediate and heavy nuclei, 26:54689 (ITF-72-12-P)
  - Vibronic absorption spectrum of molecular dimers, 26:55534 (ITF-72-27-P)
  - Violation of homogeneity of Feynman amplitudes of self-energy graphs under regularization, 26:54411 (ITF-72-39-P)
  - Wightman axioms for concentratable field and reconstruction theorem. I, 26:54378 (ITF-72-62-E)
  - Wigner--Eckart theorem for nonunitary representations of semi-simple Lie groups, 26:54355 (ITF-72-33-E)
- AKTIEBOLAGET ATOMENERGI, STUDSVIK (SWEDEN).
  - Change of structure and mechanical properties in stainless steel by irradiation. Part 1.2. The interrelationship of creep and stress relaxation phenomena, 26:53642 (STU-70-419/U-350(Pt.1.2))
  - Change of structure and mechanical properties in stainless steel by irradiation. Part 1.1. Metallographic study of neutron irradiated and unirradiated 12R72HV after tensile testing, 25:53701 (STU-70-419/U-350(Pt.1.1))
- ALLSTATES DESIGN AND DEVELOPMENT CO., INC., TRENTON, N.J. (USA).
  - Front Island shield thermal displacements, 26:55374 (CERN-HERA-72-1)
- AMERICAN ELECTRIC POWER SERVICE CORP., NEW YORK.
  - Donald C. Cook Nuclear Plant, Units 1 and 2. Design changes, 26:55322 (DOCKET-50315-78)
  - Donald C. Cook Nuclear Plant, Units 1 and 2. Tornado and missile considerations for the spent fuel pit, 26:55321 (DOCKET-50315-77)
  - Donald C. Cook Nuclear Power Plant, Units 1 and 2. Benton Harbor Power Plant limnological studies. Part IX. The biological survey of July 10, 1970, 26:55325 (DOCKET-50315-81)
  - Donald C. Cook Nuclear Power Plant, Units 1 and 2. Final safety analysis report, Amendment 28, 25:55326 (DOCKET-50315-82)
- AMERICAN NUCLEAR SOCIETY (USA). NORTHEASTERN NEW YORK SECTION.
  - National topical meeting on new developments in reactor physics and shielding, Sept. 12--15, 1972, Kiamesha Lake, NY, 26:55424 (CONF-720901-(Bks.1 and 2))
- AMES LAB., IOWA.
  - Contributions of time-reversal noninvariant terms in electron--nucleus elastic scattering, 26:54363 (IS-T-536)
  - Diffusion in dilute bismuth--mercury and lead--mercury systems, 26:53636 (IS-T-554)
  - Edgewise growth kinetics of Widmanstaetten precipitates, 26:55528 (IS-2838)
  - High temperature oxidation of gadolinium and dysprosium under controlled oxygen partial pressure, 26:53550 (IS-T-540)
  - Moessbauer effect study of ^{57}Fe in transition metal borides, 26:55055 (IS-T-529)
  - Nuclear quadrupole resonance study of heavy transition metal halide compounds with bridging halogen atoms, 26:55529 (IS-T-526)
  - Study of electron emissions of some mass separated fission product activities, 26:54601 (IS-T-534)
  - Theoretical treatment of the Schwarz--Hora effect, 26:54245 (IS-T-531)
- ARGONNE CANCER RESEARCH HOSPITAL, CHICAGO, ILL.
  - Medical physics in the United States, 26:55461 (ACRH-1000-350)
  - Radiation treatment planning using pi mesons, 25:54877 (LA-4874, pp 153-61)
  - Training of medical physicists: some existing training schemes, 26:55460 (ACRH-1000-349)
- ARGONNE NATIONAL LAB., IDAHO FALLS, IDAHO.
  - Conceptual design for the handling and remote disassembly of the fuel element failure propagation loop at the HFEF, 26:53727 (ANL/HFEF-1)
  - Data-processing system for instrument maintenance and calibration at EBR-II, 26:55132 (ANL/EBR-63)
  - Xenon-tagging of EBR-II driver fuel. EBR-II Project, 26:55184 (ANL/EBR-57)
- ARGONNE NATIONAL LAB., ILL.
  - Comparison of a two-dimensional hydrodynamics core (REXCO) to excursion experiments for fast reactor containment, 26:55139 (ANL-7911(Suppl.1))
  - Conceptual design for the handling and remote disassembly of the fuel element failure propagation loop at the HFEF, 26:53727 (ANL/HFEF-1)
  - Data-processing system for instrument maintenance and calibration at EBR-II, 26:55132 (ANL/EBR-63)
  - Deformation and fracture of UO$_2$--20 wt percent PuO$_2$, 26:53545 (ANL-7945)
  - Evidence for a neutral meson near 1033 MeV, 26:54205 (COO-1428-311)
  - Modeling the visual pathway for interactive diagnosis of visual fields, 26:55466 (ANL-7858)
  - Radiological Physics Division annual report. Environmental research, January--December 1971, 26:53150 (ANL-7860(Pt.3))
  - Transportation air pollutant emissions handbook, 26:55467 (ANL/ES-15)
  - Xenon-tagging of EBR-II driver fuel. EBR-II Project, 26:55184 (ANL/EBR-57)
- ARIZONA UNIV., TUCSON.
  - Measurement of the Lamb-shift in a hydrogen-like atom of nuclear charge Z greater than or equal to 3. Final report, 26:54375 (COO-1811-3)
  - Prog. rpt. on free radicals in biological energy conversion: EPR studies of model systems, 3 years, 9/1/69--8/31/72, 26:55616 (TID-26149)
- ARIZONA UNIV., TUCSON. DEPT. OF CHEMISTRY.
  - Phototaxis in Euglena: biochemical aspects, 26:55485 (COO-908-37)
- ARKANSAS POWER AND LIGHT CO., LITTLE ROCK.
  - Arkansas Nuclear One, Unit 1. Final safety analysis report, Amendment 29, 26:55317 (DOCKET-50313-50)
- ATOMIC ENERGY BOARD, PELINDABA, PRETORIA (SOUTH AFRICA).
  - List of unclassified PEL reports, 3/1/57--12/31/71, 26:55592 (PEL-220)
- ATOMIC ENERGY BOARD, PRETORIA (SOUTH AFRICA).
  - Fifteenth annual report, 1971, 26:55453 (NP-19410)
- ATOMIC ENERGY COMMISSION, WASHINGTON, D.C. ATOMIC SAFETY AND LICENSING BOARD.
  - Donald C. Cook Nuclear Plant, Units 1 and 2. Initial decision, 26:55323 (DOCKET-50315-79)
- ATOMIC ENERGY ESTABLISHMENT, CAIRO (EGYPT). DEPT. OF ACCELERATORS AND PLASMA PHYSICS RESEARCH.
  - Penetration of travelling high-frequence electromagnetic field into a ''non-transparent'' plasma, 26:54843 (AREAEE-124)
  - Semiclassical theory of electromagnetic field interaction with a many-level molecular system, 26:55468 (AREAEE-136)
  - Theory of parametric excitation of oscillations in an inhomogeneous plasma, 26:54844 (AREAEE-125)
- ATOMIC ENERGY ESTABLISHMENT, CAIRO (EGYPT). DEPT. OF METALLURGY.
  - Densification of uranium dioxide: a literature review, 26:53547 (AREAEE-135)
  - Factors affecting the reduction of uranium trioxide powders, 26:53548 (AREAEE-139)
  - Preparation of sinterable uranium dioxide, 26:53546 (AREAEE-134)
- ATOMIC ENERGY ESTABLISHMENT, CAIRO (EGYPT). ENGINEERING AND SCIENTIFIC INSTRUMENTS DEPT.
  - Transistorized pulse generator for testing nuclear counting equipment, 26:53295 (AREAEE-132)
- ATOMIC ENERGY ESTABLISHMENT, CAIRO (EGYPT). GEOLOGY AND RAW MATERIALS DEPT.
  - Mineralogy and some trace elements geochemistry of samples from southwest Aswan radioactive syenite rock western desert, 26:53142 (AREAEE-138)
- ATOMIC ENERGY ESTABLISHMENT, CAIRO (EGYPT). NUCLEAR CHEMISTRY DEPT.
  - Radiochemical studies of ^{125}I. I, 26:53056 (AREAEE-129)
- ATOMIC ENERGY ESTABLISHMENT, CAIRO (EGYPT). NUCLEAR PHYSICS DEPT.
  - Empirical expressions for the thermal diffusion column shape factors in the extreme cylindrical case, 26:53326 (AREAEE-131)
- ATOMIC ENERGY ESTABLISHMENT, CAIRO (EGYPT). REACTOR AND NEUTRON PHYSICS DEPT.
  - Exit tube effect upon the measured space--energy neutron spectra, 26:54470 (AREAEE-133)
  - Fast neutron scintillation spectrometer with double compensation circuit for gamma-ray discrimination, 26:53251 (AREAEE-137)
  - PIBIMUG: code for multigroup slowing down spectrum calculation in the P-1 and B-1 approximations for the IBM-1130, 26:55420 (AREAEE-141)
- ATOMIC ENERGY ESTABLISHMENT, CAIRO (EGYPT). REACTORS DEPT.
  - Thermal equilibrium of a bubble near a heated solid surface and associated flow pattern, 26:53119 (AREAEE-122)
- ATOMIC ENERGY ESTABLISHMENT, WINFRITH (ENGLAND).
  - Prog. rpt. on growth of carbon deposition from carbon monoxide on a metal catalyst, annual, 3/1/66--2/28/67, 26:53605 (DP-Report-522)
- ATOMIC ENERGY OF CANADA LTD., CHALK RIVER (ONTARIO).
  - AECL annual report, 1971--72, 26:55081 (AECL-4162)
- ATOMIC ENERGY OF CANADA LTD., CHALK RIVER (ONTARIO). CHALK RIVER NUCLEAR LABS.
  - Canada's Nuclear Power Program in context with that of the world, 26:55195 (AECL-4254)
  - Computer program to calculate damage distributions in ion-bombarded targets, 26:54969 (AECL-4130)
  - Surface flatness measurement by broad source interference: related to mechanical face seals, 26:55463 (AECL-4208)

ATOMIC ENERGY OF CANADA LTD., PINAWA (MANITOBA). WHITESHELL NUCLEAR RESEARCH ESTABLISHMENT.
- Plant associations in Whiteshell Nuclear Research Establishment controlled area, 26:55462 (AECL-3957)

ATOMIC ENERGY RESEARCH ESTABLISHMENT, HARWELL (ENGLAND).
- Parallel organization of CAMAC processes, 26:55464 (AERE-R-6601)
- Technique for handling data buffers in real-time on-line computer systems, 26:55465 (AERE-R-6623)

ATOMICS INTERNATIONAL, CANOGA PARK, CALIF.
- Analysis of the STF neutron transmission measurements, 26:54944 (NAA-SR-Memo-8597)
- HNPF retirement: disposition of sodium, 26:55147 (AI-AEC-Memo-12736)
- Stability of a light metal hydride, 26:53714 (NAA-SR-8533)
- VIM-1: a non-multigroup Monte Carlo code for analysis of fast critical assemblies, 26:55378 (AI-AEC-12951)

ATOMICS INTERNATIONAL, CANOGA PARK, CALIF. LIQUID METAL ENGINEERING CENTER.
- Transit Time Flowmeter: six-inch-diameter water and sodium testing summary, 26:53305 (LMEC-72-4)

AUSTRALIAN ATOMIC ENERGY COMMISSION RESEARCH ESTABLISHMENT, LUCAS HEIGHTS.
- List of report publications, 26:55569 (NP-19404)

B

BABCOCK AND WILCOX CO., LYNCHBURG, VA. (USA). NUCLEAR POWER GENERATION DIV.
- Analysis of anticipated transients without trip, 26:55193 (BAW-10016)
- Evaluation of Oconee reactor component failure, 26:55225 (BAW-10050)
- Multinode analysis of B and W's 145-fuel assembly nuclear plants during loss-of-coolant accident, 26:55272 (BAW-10048(Suppl.1))
- Multinode analysis of B and W's 2568-MWt nuclear plants during loss-of-coolant accident, 26:55271 (BAW-10034(Suppl.1))
- Study of discontinuities in control rod drive motor tube extensions, 26:55217 (BAW-10047(Rev.1))

BALTIMORE GAS AND ELECTRIC CO., MD.
- Calvert Cliffs Nuclear Power Plant, Units 1 and 2. Final safety analysis report, Amendment 25, 26:55327 (DOCKET-50317-58)

BATTELLE-NORTHWEST, RICHLAND, WASH. PACIFIC NORTHWEST LAB.
- Corrosivity of thoria dissolvent solutions, 26:53604 (BNWL-CC-449)
- Techniques for the characterization of suspended sediment and selected applications for the acquired data, 26:55479 (BNWL-SA-4385)
- User's manual for DASQHE, 26:55421 (BNWL-CC-2274)

BATTELLE PACIFIC NORTHWEST LABS., RICHLAND, WASH.
- AEC reactor development and technology programs. Technical activities report, October--December 1971; January--March 1972, 26:55416 (BNWL-1522-5)
- Climatography of the Hanford area, 26:55478 (BNWL-1605)
- Pacific Northwest Laboratory, Isotope Development Programs quarterly report: February--April 1972, 26:53330 (BNWL-1308-10)

BENDIX CORP., KANSAS CITY, MO.
- Fabrication of multilayer printed wiring boards, 26:55469 (BDX-613-382(Rev.))
- Processing evaluation of magnetic products. Final report, 26:55470 (BDX-613-518(Rev.))

BERN UNIV. (SWITZERLAND). PATHOLOGISCHES INSTITUT.
- Intestinal barrier to bacterial invasion, 26:55474 (BNL-17004)

BHABHA ATOMIC RESEARCH CENTRE, BOMBAY (INDIA).
- Physics design of heavy water moderated reactors, 26:55100 (BARC/I-148)

BLUME (JOHN A.) AND ASSOCIATES RESEARCH DIV., SAN FRANCISCO, CALIF.
- Investigation of ground motion--damage relationships for residential buildings in Glendale, California: San Fernando earthquake, February 1971, 26:53137 (JAB-99-95)

BONN UNIV. (WEST GERMANY). INSTITUT FUER KLINISCHE BIOCHEMIE.
- Steroid glucuronyltransferases, 26:55472 (BMBW-FBK-72-9)

BONN UNIV. (WEST GERMANY). PHYSIKALISCHES INSTITUT.
- Photoproduction of π^+-mesons on polarized protons at photon energies between 0.5 and 2.2 GeV, 26:54172 (NP-19415)

BORDEAUX UNIV. (FRANCE).
- Calibration unit for γ-ray spectroscopy, 26:53253 (FRNC-TH-237)

BOSTON CITY HOSPITAL, MASS. (USA). MALLORY INST. OF PATHOLOGY.
- Immunochemical studies with the carcinoembryonic antigen, 26:55505 (COO-3012-21)

BRANDEIS UNIV., WALTHAM, MASS. DEPT. OF PHYSICS.
- Moessbauer effect measurements on ^{57}Fe in a nickel host near the Curie point, 26:55572 (NYO-3823-12)

BROOKHAVEN NATIONAL LAB., UPTON, N. Y.
- Application of ISABELLE in Whiplash mode to produce polarized proton or monoenergetic neutron beams, 26:53775 (BNL-17057)
- Betatron frequency shifts due to image fields, 26:53770 (BNL-17016)
- Bibliography of technical publications and reports of the Radiation Division, Brookhaven National Laboratory, July 1968--June 1971 inclusive, 26:53325 (BNL-50335)
- Calcium homeostasis: the hard facts about soft bones, 26:55477 (BNL-50345)
- Calorimeters for ISABELLE, 26:53270 (BNL-17071)
- Certain invariance and convergence properties of the Pade approximant, 26:55475 (BNL-17110)
- Charged particle multiplicity and angular correlation measurements in pp and γp collisions, 26:54192 (BNL-17141)
- Coil configurations in superconducting quadrupoles, 26:53768 (BNL-16980)
- Conceptual design of a hybrid detector for electron physics at ISABELLE and PEP: solenoid + quantameter + hadrometer (calorimeter), 26:53268 (BNL-17066)
- Concrete-polymer composite materials development, 26:55473 (BNL-16609)
- Coulomb induced deuteron break-up of ISABELLE, 26:53776 (BNL-17063)
- Determination of luminosity using the intersection of a high β with a low β section, 26:53769 (BNL-16996)
- Does ISABELLE need unequal energy rings, 26:53778 (BNL-17068)
- Effect of low-symmetry matched insertions, 26:53780 (BNL-17152)
- For the measurement of multiplicities: the ''multimeter'', 26:53267 (BNL-17064)
- Forward muons and muon pairs at ISABELLE, 26:54181 (BNL-16977)
- Intestinal barrier to bacterial invasion, 26:55474 (BNL-17004)
- Isabelle for very low energy anti pp experiments: WHIPLASH, 26:53766 (BNL-16818)
- Large aperture spectrometer magnet for the ISA and the possible use of visual detectors, 26:53779 (BNL-17142)
- Luminosity considerations for colliding electron and proton beams, 26:53777 (BNL-17067)
- Luminosity measurements for colliding beams, 26:53771 (BNL-17019)
- Magnet fault protection: Isabelle, 26:53765 (BNL-16816)
- Magnet tolerances in ISABELLE and nonlinear resonances, 26:53774 (BNL-17056)
- Measurement of the proton--proton total cross section by beam attenuation, 26:54191 (BNL-17065)
- Metal hydrides for energy storage, 26:53090 (BNL-16889)
- Momentum matching in ISA long insertions, 26:53773 (BNL-17051)
- Physics with ISABELLE, 26:54298 (BNL-16997)
- Porcupine, 26:53266 (BNL-17020)
- Program for development of a liquid argon calorimeter, 26:53269 (BNL-17070)
- Program IRT, 26:55476 (BNL-17115)
- Radiative decay of neutron--resonant states, 26:54675 (BNL-17029)
- Radiobiologic studies of Tradescantia plants orbited in Biosatellite 2, 26:53382 (N-72-20054)
- Reactor effluents: as low as practicable or as low as reasonable, 26:55220 (BNL-16965)
- Scheme for absolute calibration of ISABELLE luminosity, 26:53772 (BNL-17021)
- Some speculations on colliding beams of 200 GeV protons and 15 GeV electron--200 protons, 26:53767 (BNL-16830)
- Some thoughts about pion--proton interaction experiments at ISABELLE, 26:54200 (BNL-17069)
- Underground power transmission by superconducting cable, 26:54461 (BNL-50325)
- Vacuum chamber eddy currents, 26:53781 (BNL-17153)
- Weak interactions at ISABELLE, 26:54284 (BNL-16978)
- Weak interactions at ISABELLE '72, 26:54182 (BNL-17092)
- What is an elementary particle, 26:54234 (BNL-50342)

BUREAU OF MINES, BOULDER CITY, NEV. BOULDER CITY METALLURGY RESEARCH LAB.
- Separation of columbium, tantalum, titanium, and zirconium from titanium chlorination residues, 26:52947 (BM-RI-7671)

C

CALIFORNIA INST. OF TECH., PASADENA.
- Neutrino--deuteron interaction cross sections at LAMPF energies, 26:54233 (LA-DC-72-848)
- New evidence on the photoexcitation of $I = {}^1/_2$ nucleon isobars, 26:54166 (CALT-68-322)

CALIFORNIA UNIV., BERKELEY.
- Electrophysiological and biochemical studies of the effects of radiation on brain activity and development. Progress report, August 1971--31 July 1972, 26:53461 (UCB-34-P-82-13)
- Geology and alteration associated with Wyoming uranium deposits, 26:53143 (GJO-936-1)
- Induction of lysogenic bacteria in the space environment, 26:53364 (N-72-20063)
- Risks and emergency radiation doses from plutonium dioxide exposures, 26:53511 (TID-26142)
- Trend orebodies of the Section 27 mine, Ambrosia Lake Uranium District, New Mexico, 26:53144 (GJO-936-2)

CALIFORNIA UNIV., BERKELEY. LAWRENCE BERKELEY LAB.
- Common features and differences between fission and heavy ion physics, 26:54694 (LBL-972)

Cyclotron injection systems, 26:53756 (LBL-654)

Heavy ion acceleration at the Berkeley 88-Inch Cyclotron, 26:53755 (LBL-644)

High reliability environmental radiation monitoring and evaluating system, 26:53199 (LBL-585)

Kaonic atom transition coupled to nuclear level, 26:54568 (LBL-776)

Lattice heat capacities of alloys, 26:53637 (LBL-101)

Neutrino mass limits from the $K/sub\ L/^0 \to \pi^{+-} l^{-+} \nu$ decay spectra, 26:54184 (LBL-4)

Neutron radiography with a multiwire proportional chamber: performance and projections, 26:53200 (LBL-707(Summ.))

Noble-gas chemistry and its significance, 26:55562 (LBL-416)

Part I: applications of the Schwarz inequality to weak and electromagnetic processes. Part II: S-channel helicity conservation in elastic processes, 26:54287 (LBL-766)

Partial wave analysis of the reaction $\pi N \to N\pi\pi$ in the CMS energy range 1.6 GeV to 2.0 GeV, 26:54328 (LBL-544)

Phenomenology of inclusive reactions, 26:54302 (LBL-1007)

Photosynthetic carbon metabolism, 26:55561 (LBL-383)

Polycrystalline spinel from powders prepared by freeze drying technique, 26:55564 (LBL-876)

Program AUGAT, 26:55563 (LBL-515)

CALIFORNIA UNIV., DAVIS.

S-wave structure in the $K\pi$ system, 26:54203 (COO-1428-308)

CALIFORNIA UNIV., LIVERMORE. LAWRENCE LIVERMORE LAB.

Baseband distortion equalization in the transmission of pulse information, 26:55630 (UCRL-73943)

Characterization of an epoxy system for filament winding, 26:55628 (UCRL-73773)

Energy: uses, sources, issues, 26:53096 (UCRL-51221)

ENRP 69-5: design criteria for confidence and reliability based on small samples, 26:55618 (UCID-16099)

ENRP 69-8: composite static fatigue interpretation of some data, 26:55619 (UCID-16100)

Fiber strength of S-glass/epoxy composites under biaxial loading, 26:55627 (UCRL-73772)

Final report on the development of the Geographical Position Locator (GPL). Volume 8. Technical support, 26:53311 (UCRL-51130(Vol.8))

Linearity, time domain reflectometer, and Fourier analysis studies of an evacuated Compton detector, 26:53197 (EGG-1183-2277)

Literature survey of metallic ternary and quaternary hydrides, 26:53558 (UCRL-51244)

Nucleon--nucleon scattering lengths from incomplete nucleon--deuteron breakup experiments, 26:54503 (UCRL-74069)

Pneumatic logic controls for automatic vacuum systems, 26:55629 (UCRL-73921)

Specimen strain measurement in the split Hopkinson pressure bar experiment, 26:55626 (UCRL-73610)

Test result of the geographic position locator: a system for improving land navigation without external aids, 26:55631 (UCRL-74039)

Use of grating to increase recording capability of laser far field camera, 26:55624 (UCRL-51255)

CALIFORNIA UNIV., LIVERMORE. LAWRENCE RADIATION LAB.

Semimicro gel permeation chromatographic analysis of HMX-containing explosives, 26:55625 (UCRL-73334)

CALIFORNIA UNIV., LOS ANGELES. DEPT. OF CHEMISTRY.

Phosphorescence-microwave double resonance spectroscopy of 1,2,4,5 tetrachlorobenzene. Annual report, September 15, 1971--September 14, 1972, Part 1, 26:55623 (UCLA-34-P-91-48)

CALIFORNIA UNIV., LOS ANGELES. LAB. OF NUCLEAR MEDICINE AND RADIATION BIOLOGY.

Metabolism of $1-^{14}C$ palmitic acid in the developing brain: persistence of radioactivity in the carboxyl carbon, 26:55620 (UCLA-12-871)

Production of a nervous-system-specific protein (14-3-2) by human neuroblastoma cells in culture, 26:55621 (UCLA-12-877)

CALIFORNIA UNIV., LOS ANGELES. SCHOOL OF MEDICINE.

Effects of temperature and fatty acid structure on lipid metabolism in Bacillus licheniformis 9259, 26:55622 (UCLA-12-879)

CARNEGIE-MELLON UNIV., PITTSBURGH, PA.

Nuclear wave functions from particle transfer data, 26:54693 (LA-DC-72-954)

CARNEGIE-MELLON UNIV., PITTSBURGH, PA. DEPT. OF CHEMISTRY.

Determinations of elementary reaction rate constants for the reaction of hydrogen atoms with various substrate molecules in the gas phase. Annual progress report, 1971--72, 26:55519 (COO-3242-4)

CAROLINA POWER AND LIGHT CO., RALEIGH, N.C.

Brunswick Steam Electric Plant, Units 1 and 2. Conclusion that BSEP does not have a flooding problem, 26:55329 (DOCKET-50324-43)

H. B. Robinson Unit 2. Final facility description and safety analysis report, Volume 3, 26:55286 (DOCKET-50261-106)

H. B. Robinson Unit 2. Malfunction of part length rod control system, 26:55252 (DOCKET-50261-109)

H. B. Robinson Unit 2. Technical specifications, change, 26:55287 (DOCKET-50261-108)

Shearon Harris Nuclear Power Plant, Units 1, 2, 3, and 4. License application, Amendment 14, 26:55262 (DOCKET-50400-23)

CASE WESTERN RESERVE UNIV., CLEVELAND, OHIO. DIV. OF METALLURGY AND MATERIALS SCIENCE.

Experiments in high-voltage electron microscopy. Progress report, October 31, 1972--July 31, 1973, 26:54972 (COO-2119-2)

CENTRAL ELECTRICITY GENERATING BOARD, BERKELEY (ENGLAND). BERKELEY NUCLEAR LABS.

Examination of irradiated UO_2 HTR fuel particles. Part I. Experimental techniques, 26:53555 (RD/B/N-2214)

Ignition of liquid metal: peroxide mixtures, 26:55178 (RD/B/N-2364)

Ordered table of gamma radiation emitted by fission products, 26:54607 (RD/B/M-2356)

RELP version C: a reactor economics linear program for IBM 360/85 computer, 26:55266 (RD/B/N-2261)

Use of Ge(Li) detectors in high dose rate γ spectrometry, 26:53237 (RD/B/N-2369)

Zero energy reactor facility at B.N.L., 1972, 26:55409 (RD/B/N-2272)

CENTRE DE RECHERCHES EN PHYSIQUE DES PLASMAS, LAUSANNE (SWITZERLAND).

Transverse dynamic stabilization of a theta pinch, 26:54808 (LRP-51/72)

CENTRE D'ETUDE DE L'ENERGIE NUCLEAIRE, MOL (BELGIUM).

Extraction of plutonium from heavy water fuels by the SALTEX process, 26:53079 (EUR-4812)

Index of SCK/CEN papers issued in 1970, 26:55471 (BLG-461)

CENTRE NATIONAL D'ASSISTANCE TECHNIQUE ET DE RECHERCHE APPLIQUEE, ANTWERP (BELGIUM).

Study by differential absorption in infrared of irradiated lipids and polymers, 26:52983 (EUR-4828)

CENTRO INFORMAZIONI STUDI ESPERIENZE, MILAN (ITALY).

Analytical solution of two-separable variational synthesis approach for two-group diffusion r,z equations, 26:55422 (CISE-R-243)

Buckling measurements in ECO with few CIRENE fuel elements, 26:55106 (CISE-R-283)

Experimental investigations on $U--D_2O$ lattices, 26:55101 (CISE-R-203)

Experimental results on operation of reactivity fast control system of CIRENE reactor, 26:55133 (CISE-R-268)

Iterative solution of heterogeneous equations in finite cylindrical system. Method of harmonics, 26:55423 (CISE-R-273)

Measurement of cell parameters in RB-1 reactor, 26:55102 (CISE-R-239)

MOBIDIC: a code for simplified evaluation of some continuous axial refueling schemes, 26:55196 (CISE-R-241)

MOICANO-1 code for reactivity and two-group flux calculation of fog-cooled reactor, taking into account true coolant distribution and equilibrium xenon poisoning, 26:55103 (CISE-R-242)

Neutron measurements at zero power on CIRENE fuel element in ESSOR reactor, 26:55105 (CISE-R-258)

RAS: synthesis program for calculation of 2-group neutron flux in r-theta, 26:54471 (CISE-R-252)

Steady state and transient measurements on scaled-down model of power channel of CIRENE reactor prototype, 26:55148 (CISE-R-270)

TERMO: digital code to evaluate steady state parameters of CIRENE type reactor, 26:55104 (CISE-R-246)

CESKOSLOVENSKA AKADEMIE VED, REZ. USTAV JADERNEHO VYZKUMU.

Absolute activity in irradiated fuel material by method of gamma scanning, 26:53041 (UJV-2867-M,A)

Nondestructive neutron activation analysis of mineral materials. II, 26:52901 (UJV-2851-F,Ch)

CHICAGO UNIV., ILL.

Prog. rpt. on [study of vibrational excitations in amorphous and crystalline solids], 12/1/72--8/30/72, 26:55502 (COO-2126-7)

CHICAGO UNIV., ILL. DEPT. OF PHYSICS.

New form factors in the dual resonance model, 26:54235 (COO-264-611)

CHICAGO UNIV., ILL. DEPT. OF RADIOLOGY.

Radiation treatment planning using pi mesons, 26:54877 (LA-4874, pp 153-61)

CHICAGO UNIV., ILL. (USA). DEPT. OF THEORETICAL BIOLOGY.

Study of mathematical models of mutation and selection in multi-locus systems. Annual progress report, December 1, 1971--November 30, 1972, 26:55487 (COO-1437-8)

CHICAGO UNIV., ILL. ENRICO FERMI INST.

New form factors in the dual resonance model, 26:54235 (COO-264-611)

CINCINNATI UNIV., OHIO. DEPT. OF CHEMICAL AND NUCLEAR ENGINEERING.

Investigation of pressure drops and heat transfer coefficients for loss of coolant evaluations. Quarterly progress report [for] period ending June 30, 1972, 26:55200 (COO-2152-4)

CITY COLL., NEW YORK.

Trophic dynamics and niches of salt marsh foraminifera, 26:55520 (COO-3254-6)

CLARK UNIV., WORCESTER, MASS. (USA). JEPPSON LAB. OF CHEMISTRY.

Decay of ^{161}Er to levels in ^{161}Ho, 26:54632 (COO-3255-2)

- CLEVELAND CLINIC FOUNDATION, OHIO (USA). DEPT. OF ARTIFICIAL ORGANS.
  - Study to determine the size and shape of the available space in the intrathoracic and intraabdominal cavity for a totally implantable cardiac prosthesis. Interim progress report, February 15--May 1, 1972, 26:55503 (COO-2208-1)
- COLORADO UNIV., BOULDER. DEPT. OF PHYSICS AND ASTROPHYSICS.
  - (p,t) and (p,^{3}He) reactions on ^{27}Al at E/sub p/ = 27 MeV, 26:54551 (COO-535-673)
  - Resolution of the ^{20}Na beta decay anomaly, 26:54550 (COO-535-671)
- COLORADO UNIV., BOULDER. NUCLEAR PHYSICS LAB.
  - Remarks on absorptive potentials and heavy ion elastic scattering, 26:54678 (COO-535-672)
- COLORADO UNIV., DENVER. MEDICAL CENTER.
  - Dose computations and treatment planning in pion therapy, 26:54876 (LA-4874, pp 145-52)
- COMISION NACIONAL DE ENERGIA ATOMICA, BUENOS AIRES (ARGENTINA).
  - Effect of gamma radiation on an Argentine variety of wheat, 26:53381 (CNEA-309)
- COMITATO NAZIONALE PER L'ENERGIA NUCLEARE, BOLOGNA (ITALY). CENTRO DI CALCOLO.
  - Measurement of cell parameters in RB-1 reactor, 26:55102 (CISE-R-239)
- COMITATO NAZIONALE PER L'ENERGIA NUCLEARE, FRASCATI (ITALY). LABORATORI NAZIONALI DI FRASCATI.
  - Analysis of reaction $\gamma + n \to p + \pi^-$ in first and second resonance region, 26:54171 (LNF-72/31)
  - Numerical calculation of zero bias conductivity for superconducting tunnel junction in presence of depairing. II, 26:54462 (LNF-72/27)
- COMITATO NAZIONALE PER L'ENERGIA NUCLEARE, ROME (ITALY).
  - 259 references in reactor noise time analysis, 26:55443 (RT/FI-(72)13)
  - Automatic peak identification in analysis of gamma-ray spectra obtained with Ge(Li) detectors, 26:53257 (RT/FI-(72)14)
  - Electron emission from solids by ionic bombardment, 26:52936 (RT/EL-(72)4)
  - EULERO program, 26:55595 (RT/FIMA-(72)1)
  - Experimental measurement of neutron groups from phonons in zinc at various temperatures, 26:54487 (RT/FI-(71)37)
  - Experimental results of several tests of fretting corrosion of metallic material, 26:53609 (RT/ING-(72)7)
  - Fast neutron radiative capture cross sections of stable nuclei with 29 less than or equal to Z less than or equal to 79, 26:54700 (RT/FI-(72)6)
  - MARE: a FORTRAN IV code for compound nucleus reaction calculations in the continuum, 26:54701 (RT/FI-(72)7)
  - Measure of the photovoltaic effect in silicon diodes obtained through implantation of ions, 26:54975 (RT/EL-(72)2)
  - Progress in standardization of analytical methods for materials of nuclear interest. I, 26:52920 (RT/CHI-(72)3)
  - Radiation damage in sintered alumina: an EPR study, 26:53699 (RT/FI-(72)10)
  - Reactor neutron noise analysis: state of the art, 1971, 26:55442 (RT/FI-(72)11)
  - Steady state and transient measurements on scaled-down model of power channel of CIRENE reactor prototype, 26:55148 (CISE-R-270)
  - Thermochemical reactions between alkaline halides and oxide impurities in U_3O_8 matrix, 26:52955 (RT/CHI-(72)4)
  - TRUD: an anisotropic diffusion code for xy geometry, 26:54488 (RT/FI-(72)1)
- COMMISSARIAT A L'ENERGIE ATOMIQUE, BRUYERES-LE-CHATEL (FRANCE). CENTRE D'ETUDES.
  - Manufacture and analysis of single crystals of labeled lithium hydride, 26:52894 (CEA-R-4338)
  - Temperature distribution after an underground nuclear explosion in a granite terrain, 26:53127 (CEA-R-4288)
- COMMISSARIAT A L'ENERGIE ATOMIQUE, FONTENAY-AUX-ROSES (FRANCE). CENTRE D'ETUDES NUCLEAIRES.
  - ^{90}Sr levels in human bones collected in 1970, 25:53520 (CEA-N-1535)
  - Collisional-radiative volume recombination and ionization coefficients for He$^+$--He^{2+}--e plasmas, 26:54788 (EUR-CEA-FC-642)
  - Energy spectra of dissociation products of CH/sub n/$^+$ ions (1 < = n < = 5) with a molecular nitrogen target, 26:54102 (EUR-CEA-FC-644)
  - Evaluation of the components of the absorbed dose in the interior of organisms exposed to neutrons, 26:54871 (CEA-CONF-1976)
  - Heating of very small solid grains by electron and ion bombardment, 26:54874 (EUR-CEA-FC-647)
  - Large-angle scattering of neutral particles in 40 to 100 keV range, 26:54101 (EUR-CEA-FC-630)
  - Safety aspects of sealed ^{238}Pu sources used in pacemakers, 26:53331 (CEA-CONF-2026)
  - Theoretical and experimental studies of electron plasma wave echoes, 26:54846 (EUR-CEA-FC-639)
- COMMISSARIAT A L'ENERGIE ATOMIQUE, GRENOBLE (FRANCE). CENTRE D'ETUDES NUCLEAIRES.
  - Applications of the sweeping microscope to semiconductors, 26:55482 (CEA-CONF-2000)
  - Electroluminescent diodes formation in ion implanted zinc telluride, 26:54971 (CEA-R-4313)
  - Excited levels of even-A isotopes (ruthenium and palladium), 26:54596 (CEA-R-4286)
  - Ionization processes in hot plasmas, 26:54778 (CEA-CONF-2047)
  - Measurement of abundance of ^{14}N^{7+} ion beam, 26:54077 (CEA-CONF-2048)
  - Use of PL/1 as interrogation language of a deck of cards, 26:55450 (CEA-CONF-2005)
  - X-ray spectrometry between 5A and 20A. Application to multiply-charged ion experiment, 26:54078 (CEA-CONF-2050)
- COMMISSARIAT A L'ENERGIE ATOMIQUE, LIMEIL-BREVANNES (FRANCE). CENTRE D'ETUDES.
  - Analysis of multicharged heavy ions produced by laser impact on metallic target, 26:54801 (CEA-CONF-2049)
- COMMISSARIAT A L'ENERGIE ATOMIQUE, PARIS (FRANCE).
  - Annual report, 1971, 26:55570 (NP-19408)
- COMMISSARIAT A L'ENERGIE ATOMIQUE, SACLAY (FRANCE). CENTRE D'ETUDES NUCLEAIRES.
  - CAMAC system: practical information for computerized treatment, 26:53297 (CEA-N-1549)
  - Computer simulation in radiation damage studies, 26:54970 (CEA-CONF-1890)
  - Experimental study of $K^+ \to \pi^+\pi^- e\nu$ decay, 26:54183 (CEA-N-1553)
  - High performance spectrometer magnets, 26:53296 (CEA-N-1539)
  - In pile radiation damage in graphite. Correlation between temperature and flux density in range of high temperature, 26:53713 (CEA-CONF-1894)
  - Interdiffusion, in region of continuum flow, of binary gaseous mixtures inside inhomogeneous porous media. Application to evaluation of transport coefficients by means of Devaux effect, 26:53120 (CEA-R-4318)
  - Photolysis and radiolysis of nitromethane in the liquid phase, 26:52978 (CEA-N-1528)
  - T424 facility for displacing fuel under irradiation, 26:55380 (CEA-N-1211)
- COMMONWEALTH EDISON CO., CHICAGO, ILL.
  - Dresden Nuclear Power Station, Unit 2. Low flow on ''B'' steam line, 26:55244 (DOCKET-50237-258)
  - Dresden Nuclear Power Station, Units 2 and 3. Two EHC oil low pressure scram switches setpoints drifted beyond established limits, 26:55243 (DOCKET-50237-257)
  - Quad-Cities Station, Units 1 and 2. Answers to AEC questions regarding condensate pump room flooding, 26:55284 (DOCKET-50254-119)
  - Quad-Cities Station, Units 1 and 2. Technical specifications, outstanding items, 26:55283 (DOCKET-50254-118)
  - Zion Station Nuclear Power Plant, Units 1 and 2. Final safety analysis report, Amendment 22, 26:55306 (DOCKET-50295-61)
- COMMONWEALTH EDISON CO., CORDOVA, ILL.
  - Quad-Cities Station, Unit 1. Valves in the ''RCIC'' system failed to operate on September 3, 1972, 26:55250 (DOCKET-50254-117)
  - Quad-Cities Station, Unit 2. Seven valves failed to test properly in routine inspection, 26:55254 (DOCKET-50265-115)
- CONNECTICUT YANKEE ATOMIC POWER CO., HADDAM.
  - Haddam Neck Plant, Unit 1. Containment Testing June 1970--June 1972, 26:55241 (DOCKET-50213-158)
  - Haddam Neck Plant, Unit 1. Operational radiation monitoring program, January 1, 1972--June 30, 1972, 26:55240 (DOCKET-50213-157)
- CONSOLIDATED EDISON CO. OF NEW YORK, INC., NEW YORK.
  - Indian Point Station, Unit 1. Malfunction of main steam stop valve, 26:55231 (DOCKET-50003-124)
  - Indian Point Station, Unit 1. Reiteration of request for six-month test of high pressure boron injection pumps, 26:55232 (DOCKET-50003-125)
- CONSUMERS POWER CO., JACKSON, MICH.
  - Big Rock Point Nuclear Plant. Apparent deficiency in off-gas holdup line, 26:55237 (DOCKET-50155-123)
  - Big Rock Point Nuclear Plant. Equipment failure, July 29, 1972, 26:55277 (DOCKET-50155-124)
  - Palisades Plant. Four control rods failed to drop on routine test, 26:55251 (DOCKET-50255-99)
- CONSUMERS PUBLIC POWER DISTRICT, COLUMBUS, NEBR.
  - Cooper Nuclear Station. Susceptibility of engineered safety systems to failure as a result of flooding, 26:55307 (DOCKET-50298-50)
- COOPERATIVE SCIENCE EDUCATION CENTER, INC., OAK RIDGE, TENN. (USA).
  - Radiation-induced hemopoietic lesions in fish, 26:53447 (CONF-720822-2)
- CORNELL UNIV., ITHACA, N. Y.
  - Measuring the delayed fluorescence of chlorophyll in vivo, 26:55517 (COO-3162-12)
- CORNELL UNIV., ITHACA, N.Y. (USA). BAKER LAB. OF CHEMISTRY.
  - Certain invariance and convergence properties of the Pade approximant, 26:55475 (BNL-17110)
- CORNELL UNIV., ITHACA, N. Y. DEPT. OF MATERIALS SCIENCE AND ENGINEERING.
  - Comments on the range of applicability of the grain boundary (secondary) dislocation model to high angle

- grain boundaries, 26:55513 (COO-3158-10)
- CORNELL UNIV., ITHACA, N. Y. DEPT. OF PHYSICS.
  - Resonant scattering, 26:55511 (COO-3151-8)
- CORNELL UNIV., ITHACA, N. Y. LAB. OF ATOMIC AND SOLID STATE PHYSICS.
  - Approximate phonon frequency distributions for FCC Lennard--Jones harmonic crystals, 26:55515 (COO-3161-3)
  - Experimental evidence for exchange polarization in superexchange interactions, 26:55510 (COO-3151-6)
  - Far infrared surface resistance of Cu:Fe; dynamics of a Kondo system, 26:55508 (COO-3151-4)
  - Hydrostatic pressure study of the AFMR in $FeCl_2$, 26:55509 (COO-3151-5)
  - Pair potential in liquids from the exact Born-Green equation: I. Model testing, 26:55516 (COO-3161-4)
  - Phonon generation in $KCl:Li^+$ and $KCl:OH^-$ with pulsed electric fields, 26:55512 (COO-3151-139)
  - Thermal resistivity and thermal magnetoresistivity of potassium, 26:55507 (COO-3150-6)
- CORNELL UNIV., ITHACA, N. Y. MATERIALS SCIENCE CENTER.
  - Calculation of correlation effects for grain-boundary and dislocation-pipe self-diffusion, 26:55514 (COO-3158-11)
- CORNELL UNIV., NEW YORK. MEDICAL COLL.
  - Influence of iodine intake upon kinetics of iodine metabolism in the dog. Progress report, November 1, 1971--October 31, 1972, 26:55518 (COO-3173-10)

D

- DANISH ATOMIC ENERGY COMMISSION, RISOE. RESEARCH ESTABLISHMENT.
  - Benchmark calculations on homogeneous spheres, 26:54486 (RISO-M-1526)
  - Improving match between microwave source and microwave transmission system at Risoe 10 MeV electron linear accelerator, 26:53746 (RISO-M-1518)
  - RELY 4: a Monte Carlo computer program for system reliability analysis, 26:55209 (RISO-M-1500)
- DARESBURY NUCLEAR PHYSICS LAB. (ENGLAND).
  - High intensity muon beam design for CERN II, 26:53783 (DNPL/P-131)
  - Octet dominance in non-leptonic decays, 26:54286 (DNPL/P-130)
- DENVER RESEARCH INST., COLO.
  - Structural and thermodynamic properties of the Sc--H system, 26:53556 (SC-CR-723158)
- DEPARTMENT OF ATOMIC ENERGY, BOMBAY (INDIA).
  - Prog. rpt., annual, 1971--72, 26:55452 (NP-19407)
- DEUTSCHES ELEKTRONEN-SYNCHROTRON, HAMBURG (WEST GERMANY).
  - Anomalous dimensions in p--p elastic scattering, 26:54343 (DESY-72/35)
  - k^2-dependence of transverse pion electroproduction cross section in generalized Born term model, 26:54243 (DESY-72/30)
  - Limiting distributions for inclusive charged pion production at very high energy, 26:54326 (DESY-72/40)
  - Polarization effects in deep inelastic lepton--nucleon scattering, 26:54244 (DESY-72/36)
  - Quark model predictions for weak production of pseudoscalar mesons, 26:54285 (DESY-72/32)
  - Separation of sigma/sub l/ and sigma/sub t/ at q^2 approximately 1 $(GeV/c)^2$ in resonance region, 25:54168 (DESY-72/38)
- DIRECTORATE OF LICENSING (AEC), WASHINGTON, D.C.
  - Dresden Nuclear Power Station, Unit 3. Two incidents, 26:55247 (DOCKET-50249-155)
  - Fort Calhoun Station, Unit 1. Final Environmental statement, 26:55301 (DOCKET-50285-71)
  - Hutchinson Island Plant, Unit 1. Draft environmental statement, 26:55331 (DOCKET-50335-33)
  - Indian Point Nuclear Generating Unit 2. Order extending construction completion date to January 2, 1973, 26:55281 (DOCKET-50247-81)
  - Maine Yankee Atomic Power Station. Issuance of Facility Operating License DPR-36, 26:55313 (DOCKET-50309-69)
  - Pilgrim Nuclear Power Station. Evaluation of facilities and systems, 26:55304 (DOCKET-50293-88)
  - Pilgrim Nuclear Power Station. Issuance of Facility Operating License DPR-35, Amendment 1, 26:55305 (DOCKET-50293-90)
  - Quad-Cities Station, Units 1 and 2. Final environmental statement, 26:55285 (DOCKET-50254-120)
  - Saxton Nuclear Experimental Reactor Project. License DPR-4, Amendment 8, 26:55276 (DOCKET-50146-111)
  - Turkey Point Plant, Unit 3. Technical specifications, change 1, 26:55282 (DOCKET-50250-93)
  - Vermont Yankee Nuclear Power Station. Facility operating license DPR-28, Amendment 2 (temporary operating license), 26:55256 (DOCKET-50271-101)
  - William H. Zimmer Nuclear Power Station, Unit 1. Final environmental statement, 26:55337 (DOCKET-50358-41)
  - Yankee Nuclear Power Station. Flooding of critical equipment, 26:55275 (DOCKET-50029-200)
- DIRECTORATE OF REGULATORY OPERATIONS (AEC), ATLANTA, GA. (USA). REGION II.
  - Edwin I. Hatch Nuclear Plant, Unit 1. Pump and valve committee report, main steam isolation valves, July 26, 1972, 26:55328 (DOCKET-50321-49)
  - Surry Power Station, Unit 1. Inspection to examine the malfunction of the decay heat release system, 26:55296 (DOCKET-50280-84)
- DIRECTORATE OF REGULATORY OPERATIONS (AEC), BERKELEY, CALIF. (USA). REGION V.
  - Rancho Seco Nuclear Generating Station, Unit 1. Steps taken to correct the item brought to attention in letter dated July 26, 1972, 26:55314 (DOCKET-50312-50)
  - Trojan Nuclear Plant. Inspection of August 7--11, 1972, 26:55334 (DOCKET-50344-31)
- DIRECTORATE OF REGULATORY OPERATIONS (AEC), DENVER, COLO. REGION IV.
  - Fort Calhoun Station, Unit 1. Clarification of environmental protection of containment prestressing tendons, 26:55300 (DOCKET-50285-70)
  - Fort Calhoun Station, Unit 1. Report of a minor variance from the final safety analysis report, 26:55302 (DOCKET-50285-72)
- DIRECTORATE OF REGULATORY OPERATIONS (AEC), GLEN ELLYN, ILL. REGION III.
  - Bailly Generating Station, Nuclear I. Valve wall thicknesses, 26:55340 (DOCKET-50367-31)
  - Big Rock Point Nuclear Plant. Palisades Plant. Valve wall thickness, 26:55278 (DOCKET-50155-125)
  - Donald C. Cook Nuclear Plant, Units 1 and 2. Valve wall thickness, 26:55319 (DOCKET-50315-75)
  - Dresden Nuclear Power Station, Units 1, 2, and 3. Quad-Cities Station, Units 1 and 2. Zion Station Nuclear Power Plant, Units 1 and 2. Valve wall thickness, 26:55274 (DOCKET-50010-117)
  - Duane Arnold Energy Center. Valve wall thicknesses, 26:55330 (DOCKET-50331-52)
  - Enrico Fermi Atomic Power Plant, Unit 2. Valve wall thicknesses, 26:55333 (DOCKET-50341-45)
  - Kewaunee Nuclear Power Plant. Valve wall thickness, 26:55310 (DOCKET-50305-49)
  - La Crosse Boiling Water Reactor. Valve wall thickness, 26:55350 (DOCKET-50409-13)
  - La Salle County Station, Units 1 and 2. Valve wall thicknesses, 26:55341 (DOCKET-50373-27)
  - Monticello Nuclear Generating Plant, Unit 1. Valve wall thickness, 26:55288 (DOCKET-50263-150)
  - Point Beach Nuclear Plant, Units 1 and 2. Valve wall thickness, 26:55290 (DOCKET-50266-80)
  - Prairie Island Nuclear Generating Plant, Units 1 and 2. Valve wall thicknesses, 26:55298 (DOCKET-50282-72)
- DIRECTORATE OF REGULATORY OPERATIONS (AEC), WASHINGTON, D.C.
  - N. S. Savannah. Action taken with respect to noncompliance items of March 1972 inspection, 26:55357 (DOCKET-50238-92)
- DIVISION OF PHYSICAL RESEARCH (AEC), WASHINGTON, D.C.
  - Metallurgy and Materials Programs, fiscal year 1972, 26:53600 (WASH-1181-72)
- DIVISION OF RADIOLOGICAL AND ENVIRONMENTAL PROTECTION (AEC), WASHINGTON, D.C.
  - Russian radioecology: a bibliography of Soviet publications with citations of English translations and abstracts, 26:53530 (TID-3915(Suppl.1))
- DIVISION OF REACTOR DEVELOPMENT AND TECHNOLOGY (AEC), WASHINGTON, D. C.
  - BF_3 gamma tolerant neutron detector tubes, 26:53204 (RDT-C-15-11-T(8-72))
  - Hoisting and rigging of critical components and related equipment, 26:53112 (RDT-F-8-6-T(8-72))
  - Requirements for nuclear components at elevated temperatures (supplement to ASME elevated temperature Code Case 1331), 26:55208 (RDT-F-9-1-T(8-72))
  - Stainless and low alloy steel forgings (ASME SA-182 with additional requirements), 26:53640 (RDT-M-2-2-T(8-72))
  - Status of central station nuclear power reactors significant milestones, 26:55214 (WASH-1208(9-72))
  - Thermowell systems for liquid metal service, 26:55219 (RDT-C-7-18-T(8-72))
  - Valve, isolation, butterfly type, 26:53111 (RDT-E-1-13-T(8-72))
- DIVISION OF REACTOR LICENSING (AEC), WASHINGTON, D. C.
  - Donald C. Cook Nuclear Plant, Units 1 and 2. Ice condenser containment independent analysis program, 26:55324 (DOCKET-50315-80)
  - Donald C. Cook Nuclear Plant, Units 1 and 2. Provisional Construction Permits Nos. CPPR-60 and CPPR-61, 26:55320 (DOCKET-50315-76)
- DIVISION OF RESEARCH (AEC), WASHINGTON, D. C.
  - Promotion of the academic uses of LAMPF, 26:53796 (LA-4874, pp 92-8)
  - Will medium energy physics fly or die, 26:53740 (LA-4874, pp 21-33)
- DOUGLAS UNITED NUCLEAR, INC., RICHLAND, WASH.
  - Application of computers to control and monitoring of nuclear reactors, 26:55136 (DUN-SA-186)
  - Development and implementation of equipment maintenance standards for nuclear reactors, 26:55201 (DUN-SA-168)
  - Reducing the effect of grounds on critical reactor control circuits, 26:55135 (DUN-SA-169)
- DOW CHEMICAL CO., DENVER, COLO. ROCKY FLATS DIV.
  - Conversion of plutonium oxide to plutonium tetrafluoride with fluorine in a fluid bed reactor. Part II. Demonstration runs: a comparison of the fluorine process with the hydrofluorination process, 26:53039 (RFP-1890)
  - Conversion of plutonium oxide to plutonium tetrafluoride

with fluorine in a fluid bed reactor. Part I. Development studies, 26:53038 (RFP-1889)

Corrosion and stress-corrosion cracking of painted U--4.2 wt. percent Nb, 26:53607 (RFP-1891)

Temperature measurement and control in the bomb reduction of plutonium tetrafluoride, 26:53037 (RFP-1455)

Thermal and radiation stability of polyvinyl chloride, 26:52992 (RFP-1924)

Time domain reflectometry for liquid level measurement, 26:53306 (RFP-1902)

DOW CHEMICAL CO., GOLDEN, COLO. ROCKY FLATS DIV.

Stress-corrosion cracking of underaged and overaged U--2.3 wt percent Nb in an aqueous chloride environment, 26:53608 (RFP-1904)

DU PONT DE NEMOURS (E.I.) AND CO., AIKEN, S. C. SAVANNAH RIVER LAB.

^{252}Cf neutron activation facility at the Savannah River Laboratory, 26:53109 (DP-MS-72-37)

Analysis of hydrogen explosion hazards, 26:55524 (DP-1295)

Effect of intense gamma radiation on radioiodine retention by activated carbon, 26:53061 (DP-MS-72-14)

E

EG AND G, INC., GOLETA, CALIF.

Linearity, time domain reflectometer, and Fourier analysis studies of an evacuated Compton detector, 26:53197 (EGG-1183-2277)

EIDGENOESSISCHES INSTITUT FUER REAKTORFORSCHUNG, WUERENLINGEN (SWITZERLAND).

Molten chlorides fast breeder reactor problems and possibilities, 26:55082 (EIR-215)

EUROPEAN ATOMIC ENERGY COMMUNITY.

Extraction of plutonium from heavy water fuels by the SALTEX process, 26:53079 (EUR-4812)

EUROPEAN ATOMIC ENERGY COMMUNITY, GEEL (BELGIUM). CENTRAL NUCLEAR MEASUREMENTS BUREAU.

Calibration methods of vacuum technique, 26:53300 (EUR-4797)

EUROPEAN ATOMIC ENERGY COMMUNITY, ISPRA (ITALY). JOINT NUCLEAR RESEARCH CENTER.

Buckling measurements in ECO with few CIRENE fuel elements, 26:55106 (CISE-R-283)

CAMAC: modular instrumentation system for data handling, 26:53302 (EUR-5100)

JN-METD2: Fortran-IV programme for solving neutron transport problems, 26:54481 (EUR-4839)

Microdosimetric investigations into the energy transfer of fast neutrons to soft tissue, 26:54873 (EUR-4787)

Possible function for RNA to DNA inverted transcription in antibody biosynthesis and irreversible differentiation, 26:55525 (EUR-4871)

EUROPEAN ATOMIC ENERGY COMMUNITY, LUXEMBOURG. CENTER FOR INFORMATION AND DOCUMENTATION.

2nd conference on mass spectrometry, Ispra, Italy, 9/71, 26:52893 (EUR-4765)

EUROPEAN ATOMIC ENERGY COMMUNITY, PETTEN (NETHERLANDS). JOINT NUCLEAR RESEARCH CENTER.

Manufacturing specification for high temperature thermocouples for use in nuclear irradiation experiments, 26:53301 (EUR-4807)

EUROPEAN ORGANIZATION FOR NUCLEAR RESEARCH, GENEVA (SWITZERLAND).

Compilation of cross sections. I. π^- and π^+ induced reactions, 26:54201 (CERN/HERA-72-1)

Intersecting storage rings, 26:53782 (CERN-72-14)

F

FLINDERS UNIV. OF SOUTH AUSTRALIA, BEDFORD PARK. SCHOOL OF PHYSICAL SCIENCES.

Prog. rpt. on physics, annual, 1971, 26:54779 (NP-19393)

FLORIDA POWER AND LIGHT CO.

Turkey Point Plant, Unit 3 and 4. Three unusual events, August 12 and August 21, 1972, 26:55249 (DOCKET-50250-94)

Turkey Point Plant, Units 3 and 4. Abnormal Occurrence No. 3-72-5, 26:55248 (DOCKET-50250-92)

FLORIDA POWER CORP., ST. PETERSBURG.

Crystal River Nuclear Generating Plant, Unit 3. Antitrust review, 26:55308 (DOCKET-50302-52)

FLORIDA UNIV., GAINESVILLE.

Deformation processes in hexagonal metals. Progress report, December 1, 1972--November 30, 1972, 26:53639 (ORO-3262-25)

FLORIDA UNIV., GAINESVILLE. INST. OF FOOD AND AGRICULTURAL SCIENCES.

Investigation of the unusual behavior of ^{137}Cs and other radionuclides in the Florida environment. Progress report, September 1, 1971--August 31, 1972, 26:53170 (ORO-4066-5)

FORSVARETS FORSKNINGSANSTALT, STOCKHOLM (SWEDEN).

Biological dosimetry for application on the civilian population after a nuclear explosion, 26:53397 (FOA-4-4500-A-3)

Gamma radiation dose rate in surroundings of electron accelerator FX-45 at Ursvik, 26:53738 (FOA-4-4490-A-3)

Investigation of airborne radioactive material originating from an underground nuclear explosion in USSR 3/23/71, 26:53158 (FOA-4-4502-A-1)

Transfer of simulated fallout-particles from pasture to grazing dairy cattle. I, 26:53527 (FOA-4-4503-A-3)

FRANKFURT UNIV. (WEST GERMANY). INSTITUT FUER KERNPHYSIK.

Exposure of persons after water loss in tank of FRF2 reactor, 26:55399 (IKF-27)

G

GENERAL ELECTRIC CO., CINCINNATI, OHIO. AIRCRAFT NUCLEAR PROPULSION DEPT.

Front Island shield thermal displacements, 26:55374 (CERN-HERA-72-1)

GENERAL ELECTRIC CO., SAN JOSE, CALIF. ATOMIC POWER EQUIPMENT DEPT.

Reactor primary coolant system rupture study. Progress report No. 26, October 1971--March 1972, 26:55175 (GEAP-10207-26)

Rod drop accident analysis for large boiling water reactors, 26:55353 (NEDO-10527)

GENERAL ELECTRIC CO., SUNNYVALE, CALIF. BREEDER REACTOR DEPT.

BEHAVE-2: oxide fuel performance code in two spatial dimensions and time, 26:55418 (GEAP-13788)

LMFBR shielding design experiments and methods evaluation. First quarterly progress report, January--March 1972, 26:55145 (GEAP-13822-1)

Sodium-cooled reactors fast Ceramic Reactor Development Program. Thirty-ninth quarterly report, May--July 1971, 26:55189 (GEAP-10028-39)

Sodium-cooled reactors Fast Ceramic Reactor Development Program. Forty-second quarterly report, February--April 1972, 26:55190 (GEAP-10028-42)

GEOLOGICAL SURVEY, DENVER, COLO.

Explosion-induced fractures of selected announced underground nuclear tests, Yucca Flat, Nevada Test Site, Nevada, January 1971--December 1971, 26:53133 (USGS-474-155)

GEORGIA INST. OF TECH., ATLANTA.

Applications of field--ion microscopy in physical metallurgy and corrosion. Conference held at Atlanta, Georgia, May 15--17, 1968, 26:53647

GEORGIA INST. OF TECH., ATLANTA. ENGINEERING EXPERIMENT STATION.

Physiological studies on Clostridium botulinum, type F. Final report, 26:53366 (ORO-3347-8)

GEORGIA UNIV., ATHENS.

Flux of radionuclides through a salt marsh ecosystem. Progress report, January 1--December 30, 1972, 26:55612 (SRO-639-12)

GEORGIA UNIV., ATHENS. DEPT. OF ENTOMOLOGY.

Radioactive tracer studies of soil and litter arthropod. Progress report, November 1, 1971--October 31, 1972, 26:53539 (SRO-641-4)

GOSUDARSTVENNYI KOMITET PO ISPOL'ZOVANIYU ATOMNOI ENERGII SSSR, OBNINSK. FIZIKO-ENERGETICHESKII INSTITUT.

Measurements of neutron cross sections of radiation capture and fission for some heavy nuclei by the method of time of retardation in lead, 26:54657 (FEI-292)

GOSUDARSTVENNYI KOMITET PO ISPOL'ZOVANIYU ATOMNOI ENERGII SSSR, SERPUKHOV. INSTITUT FIZIKI VYSOKIKH ENERGII.

Power supply system for the preinjector of the I-100 linear accelerator, 26:53751 (BNL-tr-498)

GOSUDARSTVENNYI KOMITET PO ISPOL'ZOVANIYU ATOMNOI ENERGII SSSR, SUKHUMI. FIZIKO-TEKHNICHESKII INSTITUT.

Circuits for studying the interaction of high-frequency fields with a plasma in linear devices, 26:54775 (AEC-tr-7326)

GUELPH UNIV. (ONTARIO). DEPT. OF PHYSICS.

Pair potential in liquids from the exact Born-Green equation: I. Model testing, 26:55516 (COO-3161-4)

GULF RADIATION TECHNOLOGY, SAN DIEGO, CALIF.

Prog. rpt. on physics of transient radiation effects, final, 2/68--10/71, 26:54968 (AD-737312)

H

HAMBURG UNIV. (WEST GERMANY). INSTITUT FUER THEORETISCHE PHYSIK (II).

Polarization effects in deep inelastic lepton--nucleon scattering, 26:54244 (DESY-72/36)

HARVARD UNIV., CAMBRIDGE, MASS. LYMAN LAB. OF PHYSICS.

Reaction $\pi^- p \to p\pi^+\pi^-\pi^-\pi^0$ at 20 GeV/c, 26:54207 (COO-3064-3)

I

ILLINOIS UNIV., URBANA.

Comparison of CP violation in the decays $K^0 \to \pi^+\pi^-$ and anti $K^0 \to \pi^+\pi^-$, 26:54361 (COO-1195-242)

Reaction $K^+n \to K^+\pi^-p$ at 3.8 GeV/c, 26:54202 (COO-1195-238)

Time decay distributions of anti K^0 and K^0 to $\pi^+\pi^-$: a CP test, 26:54362 (COO-1195-244)

ILLINOIS UNIV., URBANA. DEPT. OF COMPUTER SCIENCE.

Analysis of texture, 26:55501 (COO-2118-35)

Computer systems research. Annual report, September 1, 1971--August 31, 1972, 26:55488 (COO-1469-208)

- Perspective transformer for the stereomatrix 3-D display system, 26:55489 (COO-1469-210)

INDIANA AND MICHIGAN ELECTRIC CO., FORT WAYNE, IND.
- Donald C. Cook Nuclear Plant, Units 1 and 2. Safety evaluation, 26:55318 (DOCKET-50315-74)

INDIANA AND MICHIGAN ELECTRIC CO., NEW YORK.
- Donald C. Cook Nuclear Power Plant, Units 1 and 2. Benton Harbor Power Plant limnological studies. Part IX. The biological survey of July 10, 1970, 26:55325 (DOCKET-50315-81)

INDIANA-PURDUE UNIV., INDIANAPOLIS.
- Pion--nucleon charge exchange scattering in a new Regge pole-cut model, 26:54324 (COO-1428-309)
- S-wave structure in the Kπ system, 26:54203 (COO-1428-308)

INDIANA UNIV., BLOOMINGTON.
- Indiana University Spark Chamber Group technical progress report, December 1, 1971--November 30, 1972, 26:54206 (COO-2009-36)

INSTITUT ATOMNOI ENERGII, MOSCOW (USSR).
- Neutron resonances ^{112}Cd, 26:54599 (IAE-2116)
- Properties of Strutinskii's method of shell correction, 26:54684 (IAE-2115)

INSTITUTE OF NUCLEAR PHYSICS, KRAKOW (POLAND).
- Differential interpretation of gamma-ray logs. II, 26:53173 (INP-793)
- Intermediate coupling approach in the unified model of the ^{39}K nucleus, 26:54685 (INP-795)

INSTITUTE OF NUCLEAR RESEARCH, WARSAW (POLAND).
- Cross sections for proton induced reactions on ^{43}Ca, ^{44}Ca, and ^{48}Ca isotopes in protons energy range 1 to 2 MeV, 26:54567 (INR-1407)
- Effect of singularities on approximation in S/sub N/ methods, 26:54482 (INR-P-1405)
- Fractional parentage coefficients for j = 11/2 orbital, 26:54686 (INR-1406)

INSTITUTO DE ENERGIA ATOMICA, SAO PAULO (BRAZIL).
- Preparation of clear uranyl nitrate solution by fractional dissolution of sodium diuranate, 25:52976 (IEA-250)

INSTITUUT VOOR TOEPASSING VAN ATOOMENERGIE IN DE LANDBOUW, WAGENINGEN (NETHERLANDS).
- Prog. rpt. on application of atomic energy in agriculture, annual, 1971, 26:53459 (NP-19403)

INTEREX CORP., WALTHAM, MASS. (USA).
- Haddam Neck Plant, Unit 1. Operational radiation monitoring program, January 1, 1972--June 30, 1972, 26:55240 (DOCKET-50213-157)
- Millstone Point Nuclear Power Station, Unit 1. Environmental radiation survey program, semiannual report, January 1, 1972--June 30, 1972, 26:55246 (DOCKET-50245-158)

INTERNATIONAL ATOMIC ENERGY AGENCY, VIENNA (AUSTRIA).
- Atlas of radiation dose distributions. IV, 26:53409 (STI/PUB-295(Vol.4))
- Specialists' meeting on ''fission and corrosion product behavior in primary systems of LMFBR's,'' September 20--22, 1971, Bensberg/FRG. Summary report, 26:55417 (CONF-710959)
- Specialists' meeting on sodium--water reactions sponsored by the International Atomic Energy Agency, International Working Group on Fast Reactors, 18--21 May 1971, Melekess, USSR. Summary report and papers, 26:55149 (CONF-710548)

IOWA STATE UNIV. OF SCIENCE AND TECHNOLOGY, AMES.
- Evidence for a neutral meson near 1033 MeV, 26:54205 (COO-1428-311)

ISTITUTO NAZIONALE DI FISICA NUCLEARE, ROME (ITALY).
- High energy measurements of total cross sections on proton, detecting very low energy neutrons, 25:54163 (NP-19421)

ISTITUTO SUPERIORE DI SANITA, ROME (ITALY). LABORATORI DI FISICA.
- Application of Kleinschmidt's technique to the study of the structure of DNA in solutions, 26:55530 (ISS-71/22)
- Investigation of short-range correlations in nuclei by means of high energy electron scattering, 26:54687 (ISS-71/29)
- Seminar at the Physics Laboratory during the period July--December 1970, 26:54162 (ISS-71/31)

J

JAPAN ATOMIC ENERGY RESEARCH INST., TOKYO.
- Analysis of pressure wave propagation in pipe rupture accidents of light-water cooled reactors by use of the burst code. I, 26:55203 (JAERI-M-4473)
- Analysis of pulsed neutron experiments on bare fast multiplying system by Storrer--Stievenart's theory, 26:54483 (JAERI-M-4652)
- Application of electrophoresis for burnup determination, 26:52933 (JAERI-Memo-4094)
- Construction of JRR-1, 26:55402 (JAERI-Memo-4002)
- Critical experiments on FCA I-6, 26:55401 (JAERI-Memo-3891)
- Experimental facility to simulate loss-of-coolant accident of light-water reactors. V, 26:55205 (JAERI-Memo-4041)
- Fission product release in TLG-1 in-pile gas loop. III, 26:53694 (JAERI-Memo-3936)
- Flux distribution measurement near strong absorber using VISTA method, 26:55137 (JAERI-Memo-3893)
- Nuclear fuel balance calculation at JPDR, 26:55264 (JAERI-Memo-4083)
- Operation report on low temperature fissiochemical loop (JTFL). I, 26:55400 (JAERI-M-4630)
- Post-irradiation examination facility for Pu-fuels, 26:53728 (JAERI-Memo-4009)
- Results of cyclic pressure loading test due to JPDR pressure vessel model No. 2, 26:55228 (JAERI-Memo-4016)
- Semi-experimental measurement of effective delayed neutron fraction of a fast reactor system by application of pulsed neutron technique, 26:55403 (JAERI-Memo-4004)
- Study on the works of engineering reactor-safety, 26:55204 (JAERI-M-4535)
- Summary of JRR-2 in-core irradiation facility and irradiation experiences, 26:55404 (JAERI-Memo-4052)

JAPAN ATOMIC INDUSTRIAL FORUM, INC., TOKYO.
- Conception on nuclear energy, 26:55090

JAPANESE NUCLEAR DATA COMMITTEE.
- Bibliography for thermal neutron scattering. Supplement 1, 26:54602 (JAERI-M-4666)

JERSEY CENTRAL POWER AND LIGHT CO., MORRISTOWN, N. J.
- Forked River Nuclear Generating Station, Unit 1. Preliminary safety analysis report, Amendment 22, 26:55339 (DOCKET-50363-37)
- Oyster Creek Nuclear Power Plant, Unit 1. Report of operations, semiannual report 6, January 1, 1972--June 30, 1972, 26:55242 (DOCKET-50219-213)

JOHNS HOPKINS UNIV., BALTIMORE, MD.
- Action spectrum for photoinhibition of mechanically stimulable bioluminescence in the marine dinoflagellates gonyaulax catenella, G. actenella, and G. tamarensis, 26:55521 (COO-3277-14)

JOINT INST. FOR NUCLEAR RESEARCH, DUBNA (USSR).
- Buildup of cosmic isotopes in iron meteorites, 26:53808 (ORNL-tr-2620)
- Experiments on search for proton decay from the ground state, 26:54608 (UCRL-Trans-1473)
- Multiple charged particle production in π^-p and π^-n interactions at p = 40 GeV/c, 26:54327 (JINR-E2-6596)
- System of wire spark chambers with ferrite core memory, 26:53271 (JINR-P13-6522)

JOINT INST. FOR NUCLEAR RESEARCH, DUBNA (USSR). LAB. OF HIGH ENERGY.
- Differential cross sections of elastic p-d scattering in energy range of 10 to 70 GeV, 26:54194 (JINR-E1-6615)
- Differential cross sections of elastic p-p scattering in energy range of 8 to 70 GeV, 26:54193 (JINR-E1-6613)
- Possible measuring high-energy electron energy by ionization detectors of total absorption on basis of condensed xenon, 26:53272 (JINR-P13-6541)
- Proton beam extraction from the 10-GeV Dubna synchrophasotron by exciting the resonance Q/sub R/ = $^2/_3$, 26:53754 (JINR-E9-6538)
- Reconstruction of differential cross section of reaction $\pi^-p \to \pi^0$(eta)n in small transferred momenta region, 26:54209 (JINR-P1-6414)
- Trouton--Noble experiment, 26:55540 (JINR-P2-6532)

JOINT INST. FOR NUCLEAR RESEARCH, DUBNA (USSR). LAB. OF NUCLEAR PROBLEMS.
- Calculation of absorption in neutral pion coherent photoproduction on nuclei, 26:54691 (JINR-P2-6539)
- e - d scattering and neutron form factors, 26:54169 (JINR-E1-6647)
- Excited quasi-proton states in magic ^{141}Pr nucleus, 26:54604 (JINR-P6-6519)
- g-factor of 108 keV excited state in ^{151}Gd, 26:54634 (JINR-E6-6479)
- Study of ^{149}Tb decay, 26:54603 (JINR-P6-6511)
- Vavilov--Cherenkov ''needle'' radiation in Rochelle salt crystal, 26:54875 (JINR-P1-6552)

JOINT INST. FOR NUCLEAR RESEARCH, DUBNA (USSR). LAB. OF NUCLEAR REACTIONS.
- Average prompt neutron number for spontaneous fission of ^{256}Fm, 26:54659 (JINR-P15-6518)
- Nuclear reactions induced by xenon ions and experiments on superheavy element synthesis, 26:54658 (JINR-P7-6523)

JOINT INST. FOR NUCLEAR RESEARCH, DUBNA (USSR). LAB. OF THEORETICAL PHYSICS.
- Analysis of Kπ-interaction in energy region up to 1 GeV, 26:54315 (JINR-E2-6525)
- Automodel asymptotic of spectral functions of virtual Compton effect, 26:54246 (JINR-P2-6636)
- Basing of cranking-model, 26:54692 (JINR-P4-6543)
- Factorization of pair potential by Bateman modified method in two- and three-body problem, 26:54345 (JINR-P4-6505)
- One-nucleon transfer reactions to quasi-intersecting levels, 26:54635 (JINR-P4-6509)
- Proof of unitarity of S-matrix in non-local quantum field theory, 26:54413 (JINR-P2-6586)

JUNTA DE ENERGIA NUCLEAR, MADRID (SPAIN). DIVISION DE FISICA.
- Isotopic separation by centrifugation. Rotating plasma, 26:53327 (JEN-244)

K

KANSAS STATE UNIV., MANHATTAN.
- Distribution of tritium in glucose and starch labeled by tritium atom bombardment, 26:53028 (COO-584-50)

KARLSRUHE UNIV. (WEST GERMANY).
- Influence of different designs and materials on the wear of piston ring and piston ring groove in a 6-cylinder diesel engine, 26:53339 (KFK-1568)

KARLSRUHE UNIV., (WEST GERMANY). INSTITUT FUER WERKSTOFFKUNDE I.
- X-ray residual stress analysis in hardened steels, 26:55594 (RFP-Trans-110)

KERNFORSCHUNGSANLAGE, JUELICH (WEST GERMANY). INSTITUT FUER CHEMISCHE TECHNOLOGIE.
- Separation of fission product rare gases from combustion waste gases from high temperature fuel elements by scrubbing with liquid carbon dioxide, 26:53064 (ORNL-tr-2621)

KERNFORSCHUNGSZENTRUM, KARLSRUHE (WEST GERMANY).
- Physics investigations of sodium cooled fast reactors SNEAK-Assemblies 6A/6B, 26:55398 (EURFNR-1029)

KERNFORSCHUNGSZENTRUM, KARLSRUHE (WEST GERMANY). INSTITUT FUER ANGEWANDTE KERNPHYSIK.
- Influence of temperature on the average neutron transmission of gold in the unresolved resonance region, 26:54484 (KFK-1519)

KERNFORSCHUNGSZENTRUM, KARLSRUHE (WEST GERMANY). INSTITUT FUER ANGEWANDTE REAKTORPHYSIK.
- Calculation of heterogeneous fluxes, reaction rates, and reactivity worths in the plate structure of zero power fast critical assemblies, 26:55396 (EURFNR-1014)

KERNFORSCHUNGSZENTRUM, KARLSRUHE (WEST GERMANY). INSTITUT FUER DATENVERARBEITUNG IN DER TECHNIK.
- Universal time administration in a real time system, 26:55541 (KFK-1526)

KERNFORSCHUNGSZENTRUM, KARLSRUHE (WEST GERMANY). INSTITUT FUER EXPERIMENTELLE KERNPHYSIK.
- Determination of distribution of charge and magnetic dipole moment in ^{93}Nb from muonic x-ray spectrum, 26:54605 (KFK-1602)

KERNFORSCHUNGSZENTRUM, KARLSRUHE (WEST GERMANY). INSTITUT FUER MATERIAL UND FESTKOERPERFORSCHUNG.
- In-pile compatibility of oxide fuel, 26:55187 (EURFNR-989)
- Influence of thermomechanical treatments on the creep rupture and creep behavior of X10 NiCrMoTiB 1515 steel, 26:53635 (EURFNR-998)
- Treatment of the mechanical and thermal behavior of fuel rods in SATURN 1, 26:55186 (EURFNR-985)

KERNFORSCHUNGSZENTRUM, KARLSRUHE (WEST GERMANY). INSTITUT FUER NEUTRONENPHYSIK UND REAKTORTECHNIK.
- Age-dependent ingestion dose factors g/sub G/ and g/sub G'/ of ^{131}I, 26:53506 (ORNL-tr-2629)
- Anisotropic diffusion in gas cooled fast breeder reactor, 26:55126 (KFK-1577)
- Friction factors of a cluster of 19 rough rods, 26:55188 (EURFNR-1020)
- KFKINR-set of group constants; nuclear data basis and first results of its application to the recalculation of fast zero-power reactors, 26:55397 (EURFNR-1016)
- Laminar flow in rod bundles, 26:55449 (KFK-1503)
- Pressure drop for isothermal, incompressible turbulent flow in rod bundles with hexagonally arranged rods, 26:55174 (EURFNR-986)
- Results of heat transfer and pressure loss measurements with helium on a sixteen-tube bundle, 26:55227 (EURFNR-1000)

KERNFORSCHUNGSZENTRUM, KARLSRUHE (WEST GERMANY). INSTITUT FUER REAKTORENTWICKLUNG.
- Calculation of the time dependent fission product heat source strength in two coupled systems with consideration of fission product escape, 26:55206 (KFK-1580)
- Phenomenological investigation of the flow distribution behind local coolant chemical blockage in rod bundles, 26:55176 (KFK-1548)
- REST: program for calculation of fission product activity and decay constant after variable reactor history in two coupled systems with respect to fission product emission, 26:55127 (KFK-1579)

KERNFORSCHUNGSZENTRUM, KARLSRUHE (WEST GERMANY). LABOR FUER ELEKTRONIK UND MESSTECHNIK.
- Cladding control on nuclear reactor fuel elements, 26:55218 (EURFNR-976)
- Criteria for differentiating fuel and plenum faults on reactor fuel elements with vibrocompacted fuel, 26:55229 (EURFNR-975)

KERNFORSCHUNGSZENTRUM, KARLSRUHE (WEST GERMANY). LABORATORIUM FUER ISOTOPENTECHNIK.
- Influence of different designs and materials on the wear of piston ring and piston ring groove in a 6-cylinder diesel engine, 26:53339 (KFK-1568)

KERNFORSCHUNGSZENTRUM, KARLSRUHE (WEST GERMANY). ZYKLOTRON-LABORATORIUM.
- Interpolation of germanium thermometer characteristics, 26:55542 (KFK-1601)

L

LOS ALAMOS SCIENTIFIC LAB., N. MEX.
- Accurate deuteron--deuteron elastic scattering cross sections, 26:54497 (LA-DC-72-876)
- Active ^{3}He activation analysis for carbon and oxygen, 26:52899 (LA-DC-72-809)
- Analyses for residual explosives in drainage ditch soil at sump effluent outlets, 26:55545 (LA-4925)
- Analyzed binary computing, 26:55553 (LA-DC-72-783)
- Analyzing powers in the ^{3}He(d Vector,p)^{4}He reaction at energies less than 1.0 MeV, 26:54500 (LA-DC-72-906)
- Bifilar helical multiwire proportional chamber for position sensitive detection of minimum ionizing particles, 26:53273 (LA-4968)
- Biomedical applications: beam line and facility, 26:53793 (LA-4874, pp 78)
- Computing facilities, 26:53795 (LA-4874, pp 86-9)
- Cryogenic instrumentation at and above liquid hydrogen temperature: present and future, 26:55554 (LA-DC-72-855)
- Derivation of the Boltzmann distribution law with illustrations from a hard-sphere model computer program, 26:55071 (LA-4868)
- Effect of random errors in terms of power series on convergence of Pade approximants, 26:55558 (LA-DC-72-880)
- Energetic pion channel and spectrometer (EPICS), 26:53787 (LA-4874, pp 51-4)
- Experience in handling, transport, and storage of liquid hydrogen: the recyclable fuel, 26:55552 (LA-DC-72-632)
- Generalizations of Pade approximants, 26:55555 (LA-DC-72-872)
- High resolution proton spectrometer (HRS), 26:53791 (LA-4874, pp 67-71)
- Image restoration by constrained least-squares estimation, 26:55451 (LA-DC-72-626)
- Low energy pion channel, 26:53786 (LA-4874, pp 48-50)
- Low-density limit of the theta pinch, 26:54754 (LA-5019)
- Meta-language for describing keyboard-based two-dimensional languages, 26:55550 (LA-DC-72-410)
- Metrics in biology, an introduction, 26:55546 (LA-4973)
- Neutrino facility, 26:53794 (LA-4874, pp 84-5)
- Neutrino--deuteron interaction cross sections at LAMPF energies, 26:54233 (LA-DC-72-848)
- Nonlinear Pade approximants for Legendre series, 26:55556 (LA-DC-72-873)
- Nuclear chemistry facilities, 26:53792 (LA-4874, pp 72-7)
- Nuclear wave functions from particle transfer data, 26:54693 (LA-DC-72-954)
- Nucleon Physics Laboratory (NPL), 26:53790 (LA-4874, pp 63-6)
- Phase transitions and crystal structures of deuterium, 26:55559 (LA-DC-72-903)
- Pion and particle physics (P^3), 26:53788 (LA-4874, pp 55-8)
- Pion beams at LAMPF, 26:53797 (LA-DC-72-881)
- Preliminary measurements of polarization transfer in ^{4}He(d Vector,d Vector)^{4}He elastic scattering, 26:54498 (LA-DC-72-904)
- Probe velocity transducer, 26:53303 (LA-4999)
- Proceedings of the fifth LAMPF users meeting held at the Los Alamos Scientific Laboratory, Los Alamos, N.M., November 8-9, 1971, 26:53784 (LA-4874)
- Reactor power transient studies, 26:55441 (LA-DC-72-660)
- Review of two recent generalizations of Pade approximant, 26:55557 (LA-DC-72-879)
- Sample preparation and equipment problems associated with re-cycled, purified atmospheres, 26:53729 (LA-DC-72-230)
- Size characteristics of plutonium aerosols, 26:53062 (LA-DC-72-920)
- Specification of program flow in Madcap VI, 26:55547 (LA-DC-72-141)
- Status of LAMPF, 26:53739 (LA-4874, pp 16-20)
- Status report on LAMPF research proposals, 26:53785 (LA-4874, pp 45-7)
- Stopped muon channel, 26:53789 (LA-4874, pp 59-62)
- Survey of Scyllac experiments, 26:54828 (LA-DC-72-896)
- Terminal control language for the MADCAP programming language, 26:55551 (LA-DC-72-411)
- Trilogy on errors in the history of computing, 26:55548 (LA-DC-72-243)
- Two-dimensional programming languages, 26:55549 (LA-DC-72-331)
- Vector to tensor polarization transfer in proton--deuteron elastic scattering, 26:54499 (LA-DC-72-905)

LOUISIANA POWER AND LIGHT CO., NEW ORLEANS.
- Waterford Steam Electric Station, Unit 3. Preliminary safety analysis report, Amendment 22, 26:55260 (DOCKET-50382-36)

LOUISIANA STATE UNIV., BATON ROUGE. DEPT. OF PHYSICS AND ASTRONOMY.
- S matrix elements in the presence of standing wave states, the Bjorken limit, and shadow-quarks, 26:54248 (ORO-3992-106)

LYON UNIV. (FRANCE).
- Production of high defect concentrations in alkali halides by electron bombardment, 26:54973 (FRNC-TH-210)

LYON UNIV. (FRANCE). INSTITUT DE PHYSIQUE NUCLEAIRE.
- (d,^{6}Li) reactions with light nuclei at 28 MeV, 26:54527 (LYCEN-7219)
- Analysis of thin layers of chalcogenide glasses for Te, As, Ge, and S. Use of nuclear reactions and x rays produced by proton bombardment, 26:52900 (LYCEN-7236)
- Channeling of light ions of 0.5 to 2 MeV through few-hundred Angstrom-thick gold crystals, 26:54974 (LYCEN-7228)
- DWBA analysis of sub-Coulomb multi-transfer reactions, 26:54695 (LYCEN-7213)
- Elementary particle treatment of nuclear currents, 26:54238 (LYCEN-7211)
- Restatement of a fabrication technique by epitaxy of thin monocrystalline gold films used as bearing samples in canalization tests, 26:55566 (LYCEN-7232)

M

MCDONNELL DOUGLAS ASTRONAUTICS CO., RICHLAND, WASH. DONALD W. DOUGLAS LABS.
- Plutonia/curia compatibility testing. Quarterly report No. 15, April--June 1972, 26:53551 (MDC G-3153)

MAGYAR TUDOMANYOS AKADEMIA KOZPONTI FIZIKAI KUTATO INTEZETE, BUDAPEST.
- Measurement of mode-locked ultrashort laser pulses by different order photoelectric effects, 26:55544 (KFKI-72-41)
- SLIP: a symmetrical subroutine developed for CDC 3300 and ICL 1905 computers, 26:55543 (KFKI-72-32)

MAINE YANKEE ATOMIC POWER CO., WESTBORO, MASS.
- Maine Yankee Atomic Power Station. Worst case LOCA reanalyzed, 26:55312 (DOCKET-50309-68)

MANITOBA UNIV., WINNIPEG. DEPT. OF PHYSICS.
- How good is the Hartree--Fock approximation for ^{16}O, 26:54524 (COO-2171-14)

MARYLAND UNIV., COLLEGE PARK. DEPT. OF PHYSICS AND ASTRONOMY.
- (p,2p) reactions with divers potentials. Technical Report No. 73-002, 26:54699 (ORO-4317-11)
- Gel'fand--Levitan-unitary-transform formalism for direct extension of the two-nucleon T matrix off the energy shell. Technical Report No. 73-001, 26:54698 (ORO-4317-8)
- Sensitivity of low-energy 3-body properties to the off-shell 2-body t-matrix. Technical Report No. 72-121, 26:54697 (ORO-4317-7)

MASSACHUSETTS INST. OF TECH., CAMBRIDGE.
- Overview of the LAMPF research program, 26:54195 (LA-4874, pp 36-44)

MASSACHUSETTS INST. OF TECH., CAMBRIDGE. LAB. FOR NUCLEAR SCIENCE.
- Polarization of the recoil proton in the reactions $\gamma p \to \pi^0 p$ and $\gamma p \to \gamma p$, 26:54167 (COO-3069-71)

MAX-PLANCK-INSTITUT FUER PLASMAPHYSIK, GARCHING (WEST GERMANY).
- Development and properties of the halo in pinch plasmas, 26:54784 (IPP-1/125)
- Investigation of hydrogen fluoride chemical lasers, 26:55527 (IPP-IV-38)
- Investigations on spectrum of pulsed discharge-initiated HF-laser, 26:55526 (IPP-IV-31)
- Lithium and flibe as coolants for fusion reactor blankets, 26:54827 (IPP-4/97)
- Performance of MHD generators and thermal efficiency of closed cycle MHD power plants, 26:53091 (IPP-IV-36)

MELBOURNE UNIV., PARKVILLE (AUSTRALIA). SCHOOL OF PHYSICS.
- Analysis of breakup scattering in a deuterium target. Application to antiproton--deuteron breakup scattering, 26:54347 (UM-P-72-6)

MELLON INST., PITTSBURGH, PA.
- Application of nuclear technology to art identification problems. Final report, 26:52898 (COO-3034-2)

MELLON INST. OF SCIENCE, PITTSBURGH, PA. RADIATION RESEARCH LABS.
- Quarterly report, April 1, 1972--June 30, 1972. Fundamental research No. 6041, 26:52993 (RRL-3238-398)

METALLWERK PLANSEE, REUTTE/TYROL (AUSTRIA).
- Conference on powder metallurgy of high temperature materials, Reutte/Tyrol, Austria, 6/71. I, 26:53601
- Conference on powder metallurgy of high temperature materials, Reutte/Tyrol, Austria, 6/71. II, 26:53602
- Conference on powder metallurgy of high temperature materials, Reutte/Tyrol, Austria, 6/71. III, 26:53584
- Conference on powder metallurgy of high temperature materials, Reutte/Tyrol, Austria, 6/71. IV, 26:53603

METROPOLITAN EDISON CO., READING, PA.
- Three Mile Island Nuclear Station, Unit 1. Final safety analysis report, Amendment 28, 26:55303 (DOCKET-50289-66)

MICHIGAN STATE UNIV., EAST LANSING.
- Resolving the enigma of multiple mutant sectors in stamen hairs of Tradescantia, 26:55486 (COO-1400-41)

MICHIGAN STATE UNIV., HICKORY CORNERS. W. K. KELLOGG BIOLOGICAL STATION.
- Interaction of yellow organic acids with calcium carbonate in freshwater, 26:55494 (COO-1599-63)
- Metabolism of dissolved and particulate detrital carbon in a temperate hard-water lake, 26:55493 (COO-1599-58)

MICHIGAN UNIV., ANN ARBOR. GREAT LAKES RESEARCH DIV.
- Donald C. Cook Nuclear Power Plant, Units 1 and 2. Benton Harbor Power Plant limnological studies. Part IX. The biological survey of July 10, 1970, 26:55325 (DOCKET-50315-81)
- Prog. rpt. on nutrient enrichment and eutrophication of Lake Michigan, 11/1/68--7/31/72, 26:55499 (COO-2003-17)

MILLSTONE POINT CO., HARTFORD, CONN.
- Millstone Point Nuclear Power Station, Unit 1. Abnormal Occurrences Nos. 72-21 and 72-22, 26:55280 (DOCKET-50245-160)
- Millstone Point Nuclear Power Station, Unit 1. Application for conversion from provisional operating license to full-term operating license, 26:55279 (DOCKET-50245-159)
- Millstone Point Nuclear Power Station, Unit 1. Environmental radiation survey program, semiannual report, January 1, 1972--June 30, 1972, 26:55246 (DOCKET-50245-158)

MINISTERE DES AFFAIRES ECONOMIQUES, BRUSSELS (BELGIUM).
- Study by differential absorption in infrared of irradiated lipids and polymers, 26:52983 (EUR-4828)

MINNESOTA MINING AND MFG. CO., ST. PAUL. ELECTRICAL PRODUCTS GROUP.
- SNAP-21 program, Phase II. Deep sea radioisotope-fueled thermoelectric generator power supply system. Preliminary design description 10-watt system, 26:53092 (MMM-3691-5(Rev.1))

MINNESOTA UNIV., MINNEAPOLIS.
- Effects of radiation on the behavior of animals: a review of the literature. Appendix to 1972 progress report, 26:53448 (COO-1332-78)

MINNESOTA UNIV., MINNEAPOLIS. DEPT. OF MICROBIOLOGY.
- Prog. rpt. on canavanine death and mechanism of DNA replication in E. coli, 8/1/71--8/1/72, 26:55491 (COO-1562-17)

MOUND LAB., MIAMISBURG, OHIO.
- ^{210}Po isotopic fuels, 26:53334 (MLM-1228)
- Bibliography on handling, control, and monitoring of tritium (December 1968--January 1972), 26:53155 (MLM-1946)
- Hydrogen in steel, 26:53606 (MLM-1355)
- Introduction to analysis of covariance and analcov, a computer program for covariance analysis, 26:55567 (MLM-1847)
- Mound Laboratory chemistry and physics progress report: October--December 1971, 26:52935 (MLM-1888)
- New techniques for relative calibration of tritium sources by bremsstrahlung counting, 26:52934 (MLM-1368)
- Preparation of ^{238}Pu metal, 26:53332 (MLM-1150)
- Studies of ^{238}Pu fuel forms and their containment, 26:53333 (MLM-1213)

N

NASSAU COUNTY MEDICAL CENTER, EAST MEADOW, N.Y. (USA).
- Swine skin changes produced by different radiations, 26:53450 (LA-4874, pp 126-44)

NATIONAL ACADEMY OF SCIENCES - NATIONAL RESEARCH COUNCIL, WASHINGTON, D. C. SPACE SCIENCE BOARD.
- Radiation protection guides and constraints for space-mission and vehicle-design studies involving nuclear systems, 26:54913

NATIONAL AERONAUTICS AND SPACE ADMINISTRATION, CLEVELAND, OHIO. LEWIS RESEARCH CENTER.
- Bleed-cycle propellant pumping in a gas-core nuclear rocket engine system, 26:55358 (N-72-18051)

NATIONAL AERONAUTICS AND SPACE ADMINISTRATION, GREENBELT, MD. GODDARD SPACE FLIGHT CENTER.
- Design of a radioactive noncontact encoder, 26:53286 (N-71-37956)

NATIONAL AERONAUTICS AND SPACE ADMINISTRATION, MOFFETT FIELD, CALIF. AMES RESEARCH CENTER.
- Radiation exposures during the Biosatellite 2 flight, 26:53365 (N-72-20065)

NATIONAL INST. FOR METALLURGY, JOHANNESBURG (SOUTH AFRICA).
- Determination of ruthenium and osmium in the residues resulting from the leaching of mattes, 26:52919 (NIM-1432)
- Potentiostatic study of the anodic dissolution of uranium dioxide in aqueous solutions, 26:53035 (NIM-1448)
- Reaction of sulphide minerals with thiol compounds, 26:52954 (NIM-1439)
- Use of the Ekco Mineral Analyser for the determination of copper and zinc in the presence of iron, 26:55568 (NIM-1430)

NAVAL ORDNANCE LAB., WHITE OAK, MD.
- Magnus force tests for Sandia Corporation, 1971--72. Wind-tunnel report No. 59, 26:55596 (SC-CR-723162)

NAVAL POSTGRADUATE SCHOOL, MONTEREY, CALIF.
- Solution of a nuclear-reactor parameter-identification problem, 26:55099 (AD-738874)

NAVAL RESEARCH LAB., WASHINGTON, D. C.
Effect of neutron irradiation on fatigue crack propagation in Types 304 and 316 stainless steels at high temperatures, 26:53698 (NRL-7446)
Problem H01-32 Airborne Radiac, 26:53195 (AD-737993)
NEW ENGLAND DEACONESS HOSPITAL, BOSTON, MASS. CANCER RESEARCH INST.
Renal tumors in parabiosed irradiated rats, 26:53449 (COO-3017-4)
NEW SOUTH WALES UNIV., KENSINGTON (AUSTRALIA).
Prog. rpt. on radiation health and safety, annual, 12/71, 26:55454 (NP-19412)
NEW YORK AQUARIUM, BROOKLYN. OSBORN LABS. OF MARINE SCIENCES.
Growth characteristics of Tintinnida in continuous culture, 26:55522 (COO-3390-2)
NIAGARA MOHAWK POWER CORP., SYRACUSE, N. Y.
Nine Mile Point Nuclear Station, Unit 2. Environmental report, Supplement 1, 26:55351 (DOCKET-50410-10)
NORTHERN STATES POWER CO., MINNEAPOLIS, MINN.
Monticello Nuclear Generating Plant, Unit 1. Six month operating report No. 3, January 1, 1972--June 30, 1972, 26:55253 (DOCKET-50263-149)
Prairie Island Nuclear Generating Plant, Unit 1. Interim report on deficient motor operated valve torque switches, 26:55258 (DOCKET-50282-74)
Prairie Island Nuclear Generating Plant, Units 1 and 2. Final safety analysis report, Amendment 22, 26:55299 (DOCKET-50282-73)
NUCLEAR ENERGY INFORMATION CENTER, WARSAW (POLAND).
Cosmic ν, 26:54185 (NEIC-RR-47)

O

OAK RIDGE ASSOCIATED UNIVERSITIES, INC., TENN. (USA). SPECIAL TRAINING DIV.
Health physics manual, 26:53205 (TID-26132)
Medical radioisotopes manual, 26:53541 (TID-26128)
OAK RIDGE NATIONAL LAB., TENN.
Active and passive defense interaction studies. Volume I. Summary, models, and calculations, 26:53135 (ORNL-TM-3485(Vol.1))
Analysis of traces at ORNL's new High-Flux Neutron Activation Laboratory, 26:52897 (CONF-721010-3)
Behavior of welded joints in stainless and alloy steels at elevated temperatures, 26:53638 (ORNL-4781)
Bulk shielding facility quarterly report, April, May, and June of 1972, 26:55408 (ORNL-TM-3949)
Chemical Technology Division annual progress report for period ending March 31, 1972, 26:53080 (ORNL-4794)
Comparison of (n/sub th/,γ) yields from the current ENDF/B-III data with published data, 26:54501 (ORNL-TM-3910)
Decontamination of HTGR reprocessing off-gases, 26:53059 (CONF-720823-12)
Deformed renormalized Brueckner--Hartree--Fock approximation and its application to ^{12}C, 26:54696 (ORNL-TM-3951)
Determination of the radioactive nuclides present in the off-gas stream generated by the head-end steps in reprocessing HTGR type fuels, 26:53078 (CONF-720823-11)
Effect of extended exposure to simulated LMFBR fuel reprocessing off-gas on radioiodine trapping performance of sorbents, 26:53077 (CONF-720823-9)
Effects of strain gradients on the gross strain crack tolerance of a 533-B steel, 26:53634 (CONF-720806-3)
Elastic and inelastic scattering of 12-MeV protons from ^{92}Mo, ^{94}Mo, ^{96}Mo, and ^{100}Mo: tabulated differential cross sections, 26:54606 (ORNL-TM-3913)
Estimate of the process decontamination factors required to meet federal effluent regulations for the burning of HTGR fuel elements, 26:53060 (CONF-720823-14)
Experience with sodium fluoroborate circulation in an MSRE-scale facility, 26:55177 (ORNL-TM-3344)
FFTF pipe chase streaming experiment, 26:55394 (CONF-720901-3)
Final systems design description of the failed fuel mockup (FFM) of the liquid-metal fast breeder reactor, 26:55191 (ORNL-TM-3656)
Gamma-ray production due to neutron interactions with iron for incident neutron energies between 0.8 and 20 MeV: tabulated differential cross sections, 26:54569 (ORNL-4798)
Implications of the American Salt Corporation's underground workings on the proposed Federal Waste Repository at Lyons, Kansas, 26:53725 (ORNL-TM-3903)
Investigation of the adequacy of nitrogen cross-section sets: comparison of neutron and secondary gamma-ray transport calculations with integral experiments, 26:54485 (ORNL-TM-3768)
Long-term effects on radioiodine trapping by charcoal, 26:53058 (CONF-720823-10)
Magnetic properties of transition metals and their alloys determined by Moessbauer measurements with ^{61}Ni, 26:55617 (TID-26159)
MSRE design and operations report. Part IIB. Nuclear and process instrumentation, 26:55138 (ORNL-TM-729(Pt.2B))
Nuclear reactor core analysis code: CITATION. Revision 2, Supplement 3, 26:55198 (ORNL-TM-2496(Rev.2)(Suppl.3))
Optical model, 26:54677 (CONF-720701-3)
ORCOST: a computer code for summary capital cost estimates of steam-electric power plants. User's manual, 26:55265 (ORNL-TM-3743)
ORNL nuclear safety research and development program bimonthly report for May--June 1972, 26:55207 (ORNL-TM-3900)
Preliminary coolant temperature oscillation measurements at the fuel-failure mockup, 26:55192 (ORNL-TM-3761)
Properties of dry crushed salt and related consolidated media with emphasis on their gas transport characteristics, 26:53724 (ORNL-TM-3815)
Radiation transport codes for potential applications related to radiobiology and radiotherapy using protons, neutrons, and negatively charged pions, 26:54890 (ORNL-TM-3816)
Radiation-induced hemopoietic lesions in fish, 26:53447 (CONF-720822-2)
Rapid, sensitive method for the determination of the chemical oxygen demand of polluted waters, 26:52915 (CONF-720827-2)
Regional modeling abstracts. III, 26:55573 (ORNL-NSF-EP-23)
Reliability in scientific evidence based on multi-trace forensic NAA, 26:52896 (CONF-720920-2)
SDT5. Stainless-steel broomstick experiment: an experimental check of neutron total cross sections, 26:54965 (ORNL-TM-3871(Rev.))
Seasonal alterations in rodent blood, 26:55587 (ORNL-TM-3898)
Sensitivity analysis: a general approach illustrated for a Na--Fe system, 26:54943 (CONF-720901-6)
State-of-the-art of superconducting magnets, 26:54464 (ORNL-TM-3921)
Study of reactivity balance during startup of the HFIR, 26:55407 (ORNL-TM-3769)
Summary of engineering design of magnet systems from international working session on fusion reactor technology, 26:54829 (ORNL-TM-3953)
Surface interactions of iodine with Fe_3O_4, 26:52953 (CONF-720716-1)
Technique for observing magnet normalcies, 26:54463 (ORNL-TM-3886)
Technology and economics of utility tunnels and common trenching, 26:55484 (CONF-720925-3)
Thermal effects on aquatic organisms: annotated bibliography of 1971 literature, 26:53190 (ORNL-EIS-72-28)
Urban utilization of extracted heat and waste heat from central station power plants, 26:55212 (CONF-720925-2)
VTE-X model test and computer calculation of row by row performance and comparison with measured data, 26:53110 (ORNL-TM-3841)
OAK RIDGE OPERATIONS OFFICE (AEC), TENN.
Uranium hexafluoride: handling procedures and container criteria, 26:53735 (ORO-651(Rev.3))
OFFICE NATIONAL D'ETUDES ET DE RECHERCHES AEROSPATIALES, CHATILLON-SOUS-BAGNEUX (FRANCE).
Flow of a collisionless plasma around a cylinder in view of applications to ionospheric probes, 26:54011 (ONERA-Publ.-137)
OFFICE OF PLANNING AND ANALYSIS (AEC), WASHINGTON, D.C.
Growth of nuclear power, 1972--1985, 26:55267 (WASH-1139(Rev.1))
OHIO STATE UNIV., COLUMBUS.
Basis for design on allowable plastic strain, 26:55500 (COO-2048-7)
OHIO STATE UNIV., COLUMBUS. COMPUTER AND INFORMATION SCIENCE RESEARCH CENTER.
Pattern recognition by retina-like devices, 26:55455 (OSU-CISRC-TR-72-8)
OREGON STATE UNIV., CORVALLIS (USA). SCHOOL OF OCEANOGRAPHY.
^{65}Zn specific activities from Oregon and Washington (U.S.A.) continental shelf sediments and benthic invertebrate fauna, 26:53149 (RLO-2227-T-12-26)
Action spectrum for photoinhibition of mechanically stimulable bioluminescence in the marine dinoflagellates gonyaulax catenella, G. actenella, and G. tamarensis, 26:55521 (COO-3277-14)
Effects of ocean water on the soluble-suspended distribution of Columbia River radionuclides, 26:53166 (RLO-2227-T-12-28)

P

PACIFIC GAS AND ELECTRIC CO., SAN FRANCISCO, CALIF.
Mendocino Power Plant, Units 1 and 2. Environmental report, supplement, Volume 3, 26:55348 (DOCKET-50398-19)
Mendocino Power Plant, Units 1 and 2. Preliminary safety analysis report, Amendment 11, 26:55347 (DOCKET-50398-18)
PARIS UNIV. (FRANCE).
Theoretical and experimental studies of electron plasma wave echoes, 26:54846 (EUR-CEA-FC-639)
PARIS UNIV., ORSAY (FRANCE).
Energy spectra of dissociation products of CH/sub n/$^+$ ions (1 < = n < = 5) with a molecular nitrogen target,

- 26:54102 (EUR-CEA-FC-644)
- Experimental and theoretical study of gas amplification in a low pressure cylindrical proportional counter, 26:53198 (FRNC-TH-189)
- Experimental study of excited states of ^{58}Ni, ^{60}Ni, ^{62}Ni, and ^{64}Ni, 26:54587 (FRNC-TH-240)
- Large-angle scattering of neutral particles in 40 to 100 keV range, 26:54101 (EUR-CEA-FC-630)
- Measurement and analysis of the cross section for the reaction $K^-p \to$ anti K^0n at medium energy, 26:54210 (NP-19419)
- Measurement of depolarization parameter, D, in elastic scattering of protons by ^{9}Be, ^{10}B, and ^{27}Al, 26:54525 (FRNC-TH-191)
- Photolysis and radiolysis of nitromethane in the liquid phase, 26:52978 (CEA-N-1528)
- Preliminary studies on modified version of EBIS source, 26:54081 (FRNC-CONF-57)
- Processes of formation of multiply charged ions by electron impact, 26:54103 (FRNC-CONF-51)
- Research program of the particle source group in the field of multicharged ions, 26:54079 (FRNC-CONF-53)
- Study of the dipolar giant resonance by measuring photoneutron cross sections, 26:54598 (FRNC-TH-242)

PARIS UNIV., ORSAY (FRANCE). FACULTE DES SCIENCES.
- Analysis of form factors in $K^+ \to \pi^0\mu^+\nu$ and $K^+ \to \pi^0e^+\nu$ decays, 26:54170 (LAL-1255)

PARIS UNIV., ORSAY (FRANCE). INSTITUT DE PHYSIQUE NUCLEAIRE.
- Heavy ion source with a confined electron beam, 26:53753 (FRNC-CONF-56)
- Production of Ca and Ge ions in a PIG source, 25:53752 (FRNC-CONF-54)
- Project for the spectroscopic study of a PIG ion source, 26:54082 (FRNC-CONF-58)
- Sources with confined electron beams (review), 26:54080 (FRNC-CONF-55)

PENNSYLVANIA STATE UNIV., UNIVERSITY PARK. DEPT. OF BIOPHYSICS.
- Prog. rpt. on spin-labeled membranes, annual, 11/1/71--8/8/72, 26:55504 (COO-2223-1)

PENNSYLVANIA UNIV., PHILADELPHIA. DEPT. OF PHYSICS.
- Algebraic approach to the theory of collective motion: spherical to deformed transition in the single-j shell, 26:54681 (COO-3071-9)
- Concept of transition operator boson and its application to an exactly soluble model, 26:54682 (COO-3071-10)
- Simplified microscopic model of the Coriolis anti-pairing transition, 26:54680 (COO-3071-7)

PHILADELPHIA ELECTRIC CO., PA.
- Limerick Generating Station, Units 1 and 2. Applicant's environmental report, construction permit stage (revised), Supplement 2, 26:55335 (DOCKET-50352-28)
- Peach Bottom Atomic Power Station, Unit 1. Semiannual operations report 66, January 1, 1972--June 30, 1972, 26:55238 (DOCKET-50171-106)
- Peach Bottom Atomic Power Station, Unit 3. Interim report of damage to Reactor Pressure Vessel Top Fuel Guide, 26:55294 (DOCKET-50278-58)
- Peach Bottom Atomic Power Station, Units 2 and 3. Final safety analysis report, Amendment 20, 26:55293 (DOCKET-50277-57)
- Peach Bottom Atomic Power Station, Units 2 and 3. Study of possible expansion bellows failure, 26:55292 (DOCKET-50277-56)

PHYSICAL RESEARCH LAB., AHMEDABAD (INDIA).
- How good is the Hartree--Fock approximation for ^{16}O, 26:54524 (COO-2171-14)

PITTSBURGH UNIV., PA. (USA). DEPT. OF METALLURGICAL AND MATERIALS ENGINEERING.
- Prog. rpt. on precipitation from supersaturated copper--titanium solid solutions: the aging process and precipitation hardening in copper--titanium sideband alloys, annual, 1971--1972, 26:55615 (TID-26148)

POWER AUTHORITY OF THE STATE OF NEW YORK.
- James A. Fitzpatrick Nuclear Power Plant. Amended and substituted application for licenses, Amendment 12, 26:55259 (DOCKET-50333-53)

POWER REACTOR AND NUCLEAR FUEL DEVELOPMENT CORP., TOKYO (JAPAN).
- Preliminary conceptual design of JOYO MK-II irradiation apparatus, 26:55405 (JAPFNR-43)

POWER REACTOR DEVELOPMENT CO., DETROIT, MICH.
- Enrico Fermi Atomic Power Plant, Unit 1. Report for June 1972, 26:55233 (DOCKET-50016-170)

PRINCETON UNIV., N.J. JOSEPH HENRY LABS.
- Effect of spatial coherence on the photoelectric counting statistics of Gaussian light. Technical report No. 13, 26:55506 (COO-3120-2)

PRINCETON UNIV., N. J. PLASMA PHYSICS LAB.
- Measurement of effective collision frequency in rf heating through parametric instabilities, 26:54750 (CONF-720705-2)
- Observation of a parametric instability near the lower hybrid frequency, 26:54805 (CONF-720705-4)
- Observation of non-linear effects near the lower hybrid resonance frequency, 26:54845 (CONF-720804-3)
- Parametric instability and its induced heating, 25:54751 (CONF-720705-3)
- Pseudoclassical and anomalous containment in FM-1, 26:54753 (CONF-720804-5)
- Toroidal effects on MHD stability in Tokamaks, 26:54806 (CONF-720804-6)
- Wave generation and heating near the ion cyclotron frequency in the ST Tokamak, 26:54752 (CONF-720804-4)

PUBLIC SERVICE ELECTRIC AND GAS CO., NEWARK, N.J.
- Newbold Island Nuclear Generating Station, Units 1 and 2. Population estimates and projections for Newbold Island region, 26:55336 (DOCKET-50354-28)
- Salem Nuclear Generating Station, Units 1 and 2. Final safety analysis report, Amendment 14, 26:55291 (DOCKET-50272-35)

PUERTO RICO NUCLEAR CENTER, MAYAGUEZ.
- Approximate structure for the antiferroelectric phase of copper formate tetrahydrate, 26:55614 (TID-25974)
- Fasciola hepatica program in Puerto Rico. Progress summary report, December 1971, 26:53498 (PRNC-156)
- Quality improvement in plantains by selection, 26:55483 (CONF-720642-1)

PURDUE UNIV., LAFAYETTE, IND.
- Evidence for a neutral meson near 1033 MeV, 26:54205 (COO-1428-311)
- Pion--nucleon charge exchange scattering in a new Regge pole-cut model, 26:54324 (COO-1428-309)
- S-wave structure in the $K\pi$ system, 26:54203 (COO-1428-308)

PURDUE UNIV., LAFAYETTE, IND. DEPT. OF AGRONOMY.
- Calcium and strontium transport to plant roots, 26:55490 (COO-1495-17)

PURDUE UNIV., LAFAYETTE, IND. DEPT. OF PHYSICS.
- Annual progress report, Task B, June 1, 1971--May 31, 1972, 26:54236 (COO-1428-303)
- Proposal for an additional exposure of 9 GeV/c K^+ mesons in the 80'' D_2 filled chamber, 26:54204 (COO-1428-310)

R

REACTOR CENTRUM NEDERLAND, PETTEN.
- Prog. rpt. on fast reactor program, 10--12/71, 26:55083 (EURFNR-1001)

RENSSELAER POLYTECHNIC INST., TROY, N. Y.
- Linear accelerator project progress report, April 1, 1972--June 30, 1972, 26:54656 (COO-3058-21)
- Study of the pulse radiolysis of gases. Final report, 26:52980 (COO-3461-1)

RENSSELAER POLYTECHNIC INST., TROY, N.Y. DEPT. OF NUCLEAR SCIENCE.
- Economical scaler driver, 26:53298 (COO-3058-9)
- Gateable delay-gate generator, 26:53299 (COO-3058-10)

ROCHESTER GAS AND ELECTRIC CORP., N. Y.
- Robert Emmett Ginna Nuclear Power Plant, Unit 1. Monthly report of activity measurements, 26:55245 (DOCKET-50244-118)

ROCHESTER UNIV., N. Y.
- Annual progress report, 26:54807 (COO-3497-2)

ROCHESTER UNIV., N.Y. (USA). DEPT. OF MEDICINE.
- Reduced red cell 2,3-diphosphoglycerate and adenosine triphosphate, hypophosphatemia and increased hemoglobin--oxygen affinity after cardiac surgery, 26:55638 (UR-3490-187)

ROCHESTER UNIV., N. Y. DEPT. OF PHYSICS AND ASTRONOMY.
- How good is the Hartree--Fock approximation for ^{16}O, 26:54524 (COO-2171-14)
- π^- interactions in deuterium at 7 GeV/c, 26:54208 (COO-3065-16)

ROCHESTER UNIV., N. Y. DEPT. OF RADIATION BIOLOGY AND BIOPHYSICS.
- Direct determination of total ionic fluoride in biological fluids, 26:55637 (UR-3490-184)
- Effect of K^+ and K^+ gradients on accumulation of sugars by isolated intestinal epithelial cells, 26:55635 (UR-3490-174)
- Effects of ultraviolet radiation on mammalian cells: JU56 wallaby cell line, 26:53353 (UR-3490-194)
- Pulmonary absorption of toxic metals, 26:55634 (UR-3490-136)
- Quenching of tyrosine and tryptophan fluorescence by H_2O and D_2O, 26:52958 (UR-3490-193)
- Sequential pathophysiology of ionizing radiation on the beagle thyroid gland, 26:53462 (UR-3490-183)
- Studies on the transport of L-lysine by isolated chick intestinal epithelial cells, 26:55636 (UR-3490-177)

ROME UNIV. (ITALY). ISTITUTO DI FISICA.
- High energy measurements of total cross sections on proton, detecting very low energy neutrons, 25:54163 (NP-19421)
- Influence of dimensionality on Bose condensation and macroscopic coherence in superconductors, 26:54436 (NP-19425)
- Pion electroproduction at threshold, 26:54247 (NP-19417)
- Representation of SU(3) x SU(3) chiral algebra for baryons, 26:54370 (NP-19418)

RUMANIAN COMMITTEE FOR NUCLEAR ENERGY, BUCHAREST.
- Environmental monitoring in the vicinity of the Savannah River Plant. Annual report, 1971, 26:53153 (DPSPU-72-30-1)

RUTHERFORD HIGH ENERGY LAB., CHILTON (ENGLAND).
- Compact EHT power supply for use with high pulse rate spark chambers, 26:53275 (RPP/H-101)
- Diffractive models in non-diffractive regions, 26:54303 (RPP/T-25)
- Explanation of correlation data in inclusive pp

interactions at high energy, 26:54346 (RPP/T-28)
- Lepton hadron interactions, 26:54173 (RPP/H-97)
- Measurement of the Ξ hyperon lifetimes and α parameters, 26:54174 (RPP/H-99)
- Measurements of K^+p elastic differential cross-sections for kaon momenta between 0.9 and 1.9 GeV/c, 25:54211 (RPP/H-95)
- Muon--proton scattering and the effect of neutral currents in the scaling region, 26:54288 (RPP/T-26)
- Questions in $\pi\pi$ scattering and related processes, 26:54317 (RPP/T-27)
- Ratio of pion--nucleus reaction cross-sections and the neutron density distribution for lead, 26:54529 (RPP/NS-8)
- Track detection program for a Hough Powell Device, 26:53274 (RHEL/R-241)
- Uncorrelated jet model predictions for the multiplicity distribution of π^- mesons produced in high energy annihilations anti pp → pions, 26:54316 (RPP/T-24)

S

SACRAMENTO MUNICIPAL UTILITY DISTRICT, CALIF.
- Rancho Seco Nuclear Generating Station, Unit 1. Final report on minor imperfections found in pipe welds, 26:55316 (DOCKET-50312-52)
- Rancho Seco Nuclear Generating Station, Unit 1. Final safety analysis report and license application, Amendment 15, 26:55315 (DOCKET-50312-51)

SANDIA CORP., ALBUQUERQUE, N. MEX.
- Magnus force tests for Sandia Corporation, 1971--72. Wind-tunnel report No. 59, 26:55596 (SC-CR-723152)

SANDIA LABS., ALBUQUERQUE, N. MEX.
- Aromatic polyimide syntactic foam, 26:55601 (SC-DC-722297)
- DIAMOND: a new approach to microelectronic circuit design (dielectrically isolated arrays of monolithic devices), 26:53309 (SC-DC-721162)
- Dynamic fracture behavior of Borsic--Al composites, 26:53557 (SC-DC-721080)
- Feasibility of using the Faraday effect to measure currents in the electron beam environment, 26:53747 (SC-DR-720447)
- Final report of planetary quarantine activities, 26:53367 (SC-RR-720516)
- Flight test evaluation of a fluidically actuated monopropellant hydrazine roll control system, 26:55600 (SC-DC-722244(RD))
- Fundamentals of ion plating, 26:53615 (SC-DC-722284)
- IMAGEN: a computer program for image enhancement and display of two-dimensional data, 26:55608 (SC-RR-720286)
- Long life, wide temperature range organic electrolyte battery, 26:55602 (SC-DC-722298)
- Mechanical and thermal expansion properties of a particulate filled polymer, 26:55603 (SC-DR-70-617)
- Mechanical properties and stress relaxation of beryllium--copper alloy 25, 26:53641 (SC-DR-720471)
- Mesh-generation code and a contour-plotting routine, 26:55609 (SC-TM-710557)
- Passive calorimeter for pulsed electron beam energy measurement, 26:53258 (SC-DR-720630)
- Plant equipment inventory management, 26:55605 (SC-M-68-808)
- Program optimization, 26:55599 (SC-DC-721376)
- Radiation tolerant gated video amplifier, 26:53307 (SC-DC-721159)
- Retarding field-cylindrical mirror analyzer, 26:53310 (SC-DC-721302)
- Rocket-borne auroral optical measurements, 26:54012 (SC-RR-720543)
- Room temperature electrical properties and Dopant precipitation for SiGe thermoelectric alloys, 26:55598 (SC-DC-721020)
- Significant digit incomplete gamma ratios, 26:55604 (SC-DR-720303)
- Special tests for plutonium shipping containers 5M, SP5795, and L-10, 26:53736 (SC-DR-720597)
- Surface preparation for adhesive bonding, 26:55597 (SC-DC-714099)
- Thick target yield calculations for strong neutron-producing reactions in the energy range 30 keV to 1.5 MeV, 26:54502 (SC-RR-720513)
- TRASHP: transembler for the Hewlett--Packard minicomputers, 26:55606 (SC-M-720514)
- Universal digital integrated circuit, 26:53308 (SC-DC-721161)
- Using BASIC as a real time executive on a small system, 26:55607 (SC-R-722879)

SANDIA LABS., LIVERMORE, CALIF.
- HEATMESH-71: a computer code for generating geometrical data required for studies of heat transfer in axisymmetric structures, 26:55610 (SCL-DR-720004)
- Steady-state response of an infinite plate to an exponential edge load along a fusing crack: a model for the dynamic edge fusion of two semi-infinite plates, 26:55611 (SCL-RR-710113)

SAVANNAH RIVER ECOLOGY LAB., AIKEN, S. C.
- Distribution and cycling of radioactive isotopes released into the Savannah River swamp forest: environmental implications. Progress report, November 1, 1971--August 1, 1972, 26:53171 (SRO-708-1)

SCIENTIFIC RESEARCH INST. OF ELECTRO-PHYSICAL APPARATUS, LENINGRAD (USSR).
- General principle of current heating processes of plasma in pulsed z-discharges, 26:54749 (AEC-tr-7330)
- Measurement of plasma parameters in strong hf discharge, 26:54768 (AEC-tr-7329)

SKODA WORKS, PILSEN (CZECHOSLOVAKIA). NUCLEAR POWER CONSTRUCTION DEPT.
- Approximation of resonance self-shielding coefficients, 26:54489 (ZJE-124)

SOCIETA RICERCHE IMPIANTI NUCLEARI, SALUGGIA (ITALY).
- Experimental investigations on U--D_2O lattices, 26:55101 (CISE-R-203)
- Measurement of cell parameters in RB-1 reactor, 26:55102 (CISE-R-239)

SOUTH CAROLINA ELECTRIC AND GAS CO., COLUMBIA.
- Virgil C. Summer Nuclear Station, Unit 1. Preliminary safety analysis report, Amendment 16, 26:55344 (DOCKET-50395-28)

SOUTHERN CALIFORNIA EDISON CO., ROSEMEAD, CALIF.
- San Onofre Nuclear Generating Station, Unit 1. Unit trip and subsequent activation of safety injection equipment, 26:55239 (DOCKET-50206-167)
- San Onofre Nuclear Generating Station, Units 2 and 3. Environmental report, Amendment 1, supplement, 26:55338 (DOCKET-50361-27)

SOUTHWEST RESEARCH INST., SAN ANTONIO, TEX.
- In-service inspection program for nuclear reactor vessels. Biannual progress report No. 6, March 1, 1971--September 1, 1971, 26:55222 (NP-19338(Vol.2))
- In-service inspection program for nuclear reactor vessels. [Volume] I. Biannual progress report No. 6, March 1, 1971--September 1, 1972, 26:55221 (NP-19338(Vol.1))
- Yankee Nuclear Power Station. March 1972 inservice examination of Yankee Rowe Atomic Power Plant, 26:55235 (DOCKET-50029-201)

STAATLICHE ZENTRALE FUER STRAHLENSCHUTZ, BERLIN (EAST GERMANY).
- 10 years National Center for Radiation Protection of the GDR, 26:55456 (SZS-136)
- Application of organic flocculants to the decontamination of radioactively contaminated waters by coagulation, 26:53040 (SZS-129)
- Results of fallout monitoring in the German Democratic Republic 1970, 26:53156 (SZS-128)
- State and tendencies of chemical protection against ionizing radiation. A literature survey 1970/71, 26:53460 (SZS-132)

STANFORD LINEAR ACCELERATOR CENTER, CALIF.
- Concepts of radiation dosimetry, 26:54891 (SLAC-153)
- e^+e^- annihilation to hadrons, 26:54176 (SLAC-PUB-1043)
- Study of non-strange boson resonances produced by quasi-monochromatic photon beams of energies between 4.3 and 7.5 GeV in a hydrogen bubble chamber, 26:54175 (SLAC-143)

STANFORD UNIV., CALIF. (USA). DEPT. OF MATERIALS SCIENCE AND ENGINEERING.
- Prog. rpt. on structure dependence of high temperature deformation of metals, 3/1/70--3/1/71, 26:55613 (SU-326-P-17-X-2)

STATE UNIV. OF NEW YORK, STONY BROOK.
- High Energy Counter Group progress report, January 1, 1971--December 31, 1971, 26:54212 (TID-26138)

STATE UNIV. OF NEW YORK, STONY BROOK. DEPT. OF PHYSICS.
- Magnetic moments of ^3H and ^3He in the quark model, 26:54494 (COO-3001-15)
- Magnetic moments of odd mass nuclei with simple configurations, 26:54679 (COO-3001-17)

STRASBOURG UNIV. (FRANCE).
- Realistic nonlocal forces and their importance in understanding the microscopic properties of nuclear matter and nuclei, 26:54683 (FRNC-TH-180)
- Study of ^{29}P nucleus. Determination of angular momenta and elements of gamma transition matrix, 26:54552 (FRNC-TH-227)

SWEDISH STATE POWER BOARD, ALVKARLEBY. HYDRAULIC LAB.
- Forsmark's nuclear power station, 26:55352 (INIS-mf-205)

SYDNEY UNIV. (AUSTRALIA).
- Nucleus: annual review of Science Foundation for Physics and School of Physics within University of Sydney, 26:53993 (INIS-mf-252)

SYDNEY UNIV. (AUSTRALIA). SCHOOL OF PHYSICS.
- Wills Plasma Physics Department twenty-third six-monthly progress report, January 1--June 30, 1972, 26:54780 (NP-19414)

SYRACUSE UNIV., N. Y. DEPT. OF PHYSICS.
- Interference terms in the multiperipheral model, 26:54329 (NYO-3533-265)
- Pion and K meson production in the multiperipheral model, 26:54325 (COO-3533-2)
- Unified weak-electromagnetic gauge schemes based on the three dimensional unitary group, 26:54364 (NYO-3533-264)

T

TECHNICAL INFORMATION CENTER (AEC), OAK RIDGE, TENN.
- FIND: Watts Bar Nuclear Plant, Units 1 and 2, 26:55213

(FIND-50390(8-72))

TECHNISCHE HOCHSCHULE, KARLSRUHE (WEST GERMANY).
- Determination of distribution of charge and magnetic dipole moment in ^{93}Nb from muonic x-ray spectrum, 26:54605 (KFK-1602)
- Influence of temperature on the average neutron transmission of gold in the unresolved resonance region, 26:54484 (KFK-1519)

TECHNISCHE UNIVERSITAET, HANOVER (WEST GERMANY). INSTITUT FUER PLASMAPHYSIK.
- Experimental investigation of the continuous emission of shock heated krypton and xenon, 26:54777 (BMBW-FBK-72-8)

TECHNISCHER UEBERWACHUNGS-VEREIN E. V., COLOGNE (WEST GERMANY). INSTITUT FUER REAKTORSICHERHEIT.
- Report of research ordered by Federal Ministry for construction and research in field of reactor safety, 1--3/72, 26:55202 (IRS-F-10)

TENNESSEE UNIV., KNOXVILLE. DEPT. OF CHEMISTRY.
- Research concerning ionic and free radical reactions in radiation chemistry. Progress report, September 15, 1971--August 15, 1972, 26:52987 (ORO-2968-78)

TENNESSEE VALLEY AUTHORITY, CHATTANOOGA.
- Watts Bar Nuclear Plant, Units 1 and 2. Preliminary safety analysis report, Amendment 16, 26:55343 (DOCKET-50390-24)
- Watts Bar Nuclear Plant, Units 1 and 2. Preliminary safety analysis report, Amendment 15, 26:55342 (DOCKET-50390-23)

TEXAS AGRICULTURAL AND MECHANICAL UNIV., COLLEGE STATION.
- Levels in ^{186}Os as populated by the decay of ^{186}Ir, 26:54633 (COO-3255-3)

TEXAS UNIV., AUSTIN. CENTER FOR NUCLEAR STUDIES.
- Research in nuclear physics. Progress report, December 1, 1970--November 30, 1971, 26:54467 (ORO-2972-204)

TEXAS UNIV., AUSTIN. CENTER FOR PARTICLE THEORY.
- S matrix elements in the presence of standing wave states, the Bjorken limit, and shadow-quarks, 25:54248 (ORO-3992-106)

TOKYO SHIBAURA ELECTRIC CO. LTD., KAWASAKI, KANAGAWA PREFECTURE (JAPAN).
- Preliminary conceptual design of JOYO MK-II irradiation apparatus, 26:55405 (JAPFNR-43)

TOKYO UNIV. (JAPAN). INST. FOR NUCLEAR STUDY.
- Quasi-bands in even--even nuclei, 26:54600 (INSJ-130)

TOXICOLOGY INFORMATION RESPONSE CENTER, OAK RIDGE, TENN.
- Animal toxicity of coumaphos and contaminants, 25:55578 (ORNL-TIP/TIRC-72-49)
- Carcinogenicity of methyl-nitro-nitroso-guanidine, 26:55583 (ORNL-TIP/TIRC-72-60)
- Diethylpyrocarbonate toxicology and pharmacology, 26:55579 (ORNL-TIP/TIRC-72-52)
- Effect of pyramidon on the hemopoietic and vascular system of the mammal, 26:55582 (ORNL-TIP/TIRC-72-59)
- Effects of sodium nitrite on the hemopoietic and vascular system of the mammal, 26:55577 (ORNL-TIP/TIRC-72-45)
- Mammalian toxicity of purpurin, quinizarin, quinalizarin, diphenylthiocarbazone, and 1,5-diphenyl-3-thiocarbohydrazide, 26:55574 (ORNL-TIP/TIRC-72-4)
- Material for use by parents of handicapped children, 26:55576 (ORNL-TIP/TIRC-72-13)
- Maximum safe levels of fluorine for man and animals, 26:55580 (ORNL-TIP/TIRC-72-53)
- Toxicity aspects of silica or quartz particles, 26:55585 (ORNL-TIP/TIRC-72-62)
- Toxicity data for imido (imidate) esters, 26:55581 (ORNL-TIP/TIRC-72-54)
- Toxicity of elemental phosphorus, 26:55586 (ORNL-TIP/TIRC-72-63)
- Toxicity of potassium iodate, 26:55575 (ORNL-TIP/TIRC-72-10)
- Toxicology of isoamylamine and related amines, 25:55584 (ORNL-TIP/TIRC-72-61)

TRI--UNIV. MESON FACILITY, VANCOUVER (BRITISH COLUMBIA).
- Prog. rpt., annual, 1971, 26:53741 (NP-19416)

TRW SYSTEMS, REDONDO BEACH, CALIF.
- Effects of strain gradients on the gross strain crack tolerance of a 533-B steel, 26:53634 (CONF-720806-3)

TUFTS UNIV., BOSTON, MASS. DEPT. OF SURGERY.
- Immunochemical studies with the carcinoembryonic antigen, 26:55505 (COO-3012-21)

TUFTS UNIV., MEDFORD, MASS. DEPT. OF CHEMISTRY.
- Prog. rpt. on covalently bonded compounds of the light elements, final, 11/1/68--10/31/70, 26:55523 (COO-3544-1)

U

UNION CARBIDE CORP., OAK RIDGE, TENN. Y-12 PLANT.
- Analysis of the effects of selected scheduling rules in a parallel processor shop, 26:55640 (Y-1848)
- Practical design considerations for the application of gas bearings to machining processes, 26:53113 (Y-DA-4541(Rev.1))
- Real-time analysis of thermal diffusivity data from a pulsed laser facility, 26:55639 (Y-1841)
- Reliability of criticality safety calculations using the new codes CSC and KENO, 26:55445 (Y-KC-96)

UNITED KINGDOM ATOMIC ENERGY AUTHORITY, ABINGDON (ENGLAND). CULHAM LAB.
- Use of liquid lithium as coolant in toroidal fusion reactor. II, 26:54825 (CLM-R-116)

UNITED KINGDOM ATOMIC ENERGY AUTHORITY, LONDON (ENGLAND).
- Prog. rpt., 4/70--3/71, 26:55084 (INIS-mf-212)

UNITED KINGDOM ATOMIC ENERGY AUTHORITY, RISLEY (ENGLAND). REACTOR GROUP.
- Spectra of energy released by thermal neutron capture, 26:55444 (TRG-2189)

UNITED POWER ASSOCIATION, ELK RIVER, MINN. (USA).
- Elk River Reactor. Sixth report on status of deactivated reactor, 26:55273 (DOCKET-1151-58)

UNITED STATES-EURATOM FAST REACTOR EXCHANGE PROGRAM.
- Calculation of heterogeneous fluxes, reaction rates, and reactivity worths in the plate structure of zero power fast critical assemblies, 26:55396 (EURFNR-1014)
- Cladding control on nuclear reactor fuel elements, 26:55218 (EURFNR-976)
- Criteria for differentiating fuel and plenum faults on reactor fuel elements with vibrocompacted fuel, 26:55229 (EURFNR-975)
- Friction factors of a cluster of 19 rough rods, 26:55188 (EURFNR-1020)
- In-pile compatibility of oxide fuel, 26:55187 (EURFNR-989)
- Influence of thermomechanical treatments on the creep rupture and creep behavior of X10 NiCrMoTiB 1515 steel, 26:53635 (EURFNR-998)
- KFKINR-set of group constants; nuclear data basis and first results of its application to the recalculation of fast zero-power reactors, 26:55397 (EURFNR-1016)
- Physics investigations of sodium cooled fast reactors SNEAK-Assemblies 6A/6B, 26:55398 (EURFNR-1029)
- Pressure drop for isothermal, incompressible turbulent flow in rod bundles with hexagonally arranged rods, 26:55174 (EURFNR-986)
- Prog. rpt. on fast reactor program, 10--12/71, 26:55083 (EURFNR-1001)
- Results of heat transfer and pressure loss measurements with helium on a sixteen-tube bundle, 26:55227 (EURFNR-1000)
- Treatment of the mechanical and thermal behavior of fuel rods in SATURN 1, 26:55186 (EURFNR-985)

UNIVERSITE SCIENTIFIQUE ET MEDICALE DE GRENOBLE (FRANCE).
- Excited levels of even-A isotopes (ruthenium and palladium), 26:54596 (CEA-R-4286)
- Radiation effects on ionic and molecular crystals, 26:52984 (FRNC-TH-262)

UPPSALA UNIV. (SWEDEN). INST. OF METEOROLOGY.
- Natural α-activity in air near ground, 26:53160 (UUIM-27)
- Natural β-activity in air near ground. Parts B--E, 26:53159 (UUIM-26)

UTAH UNIV., SALT LAKE CITY. DEPT. OF METEOROLOGY.
- Research on atmospheric diffusion and turbulence. final report, 26:55492 (COO-1585-22)

V

VANDERBILT UNIV., NASHVILLE, TENN.
- Applications of computers and digital techniques in clinical and investigative nuclear medicine, 26:55457 (TID-26141)

VERMONT YANKEE NUCLEAR POWER CORP., RUTLAND.
- Vermont Yankee Nuclear Power Station. Offsite environmental radiological monitoring report, January 1, 1972--June 30, 1972, 26:55255 (DOCKET-50271-100)

VIRGINIA ELECTRIC AND POWER CO., RICHMOND.
- North Anna Power Station, Units 1, 2, 3, and 4. Environmental considerations, additional information, 26:55332 (DOCKET-50338-51)
- North Anna Power Station, Units 3 and 4. License application, Amendment 9, 26:55263 (DOCKET-50404-24)
- North Anna Power Station, Units 3 and 4. Preliminary safety analysis report, Amendment 8, 26:55349 (DOCKET-50404-22)
- Surry Power Station, Unit 1. Operating incident of July 27, 1972, 26:55297 (DOCKET-50280-85)
- Surry Power Station, Unit 1. Technical specifications, changes, 26:55295 (DOCKET-50280-82)
- Surry Power Station, Unit 2. Returned to service on September 3, 1972, 26:55257 (DOCKET-50280-83)

W

WASHINGTON PUBLIC POWER SUPPLY SYSTEM, RICHLAND.
- Hanford No. 2 Nuclear Power Plant. Preliminary safety analysis report, Amendment 12, 26:55346 (DOCKET-50397-32)
- Hanford No. 2 Nuclear Power Plant. Preliminary safety analysis report, Amendment 13, 26:55261 (DOCKET-50397-27)
- Hanford No. 2 Nuclear Power Plant. Preliminary safety analysis report, Amendment 12, 26:55345 (DOCKET-50397-28)

WASHINGTON STATE UNIV., PULLMAN. DEPT. OF ZOOLOGY.
- Russian radioecology: a bibliography of Soviet publications with citations of English translations and abstracts, 26:53530 (TID-3915(Suppl.1))

WASHINGTON UNIV., SEATTLE. DEPT. OF NUCLEAR ENGINEERING.
Measurement of delayed neutron energy spectra. Final report, 26:54660 (RLO-2225-T-17-4)
WASHINGTON UNIV., SEATTLE. DEPT. OF OCEANOGRAPHY.
Columbia River effects in the Northeast Pacific: physical studies. Progress report, June 1971--June 1972, 26:53165 (RLO-2225-T-25-6)
WAYNE STATE UNIV., DETROIT, MICH.
Metabolism of the rare earths following inhalation: pathologic and biochemical response in the lung and other organs. Final report for period to September 15, 1972, 26:55497 (COO-1630-29)
WESTINGHOUSE ELECTRIC CORP., MADISON, PA. ADVANCED REACTORS DIV.
Diffusional growth of voids induced by irradiation and stress, 26:53702 (TID-26150)
Summary of analyses of plate vs. pin measurements emphasizing reactivity and sodium void effects, 26:55395 (CONF-720901-12)
WESTINGHOUSE ELECTRIC CORP., PITTSBURGH, PA.
Boiling crisis and critical heat flux, 26:55179 (TID-25887)
WESTINGHOUSE ELECTRIC CORP., PITTSBURGH, PA. ATOMIC POWER DEPT.
Shock loading analysis of core subassembly: APDA core, 26:53732 (WCAP-1615)
WESTINGHOUSE ELECTRIC CORP., PITTSBURGH, PA. ATOMIC POWER DIV.
Criticality control parameters and supporting calculations for uranium bearing nuclear fuel at low enrichment, 26:53733 (WCAP-2999)
WESTINGHOUSE ELECTRIC CORP., PITTSBURGH, PA. NUCLEAR ENERGY SYSTEMS DIV.
Neutron shielding pads, 26:55223 (WCAP-7870)
WISCONSIN ELECTRIC POWER CO., MILWAUKEE.
Point Beach Nuclear Plant, Units 1 and 2. Elimination of hot leg injection emergency core cooling system, 26:55289 (DOCKET-50266-79)
WISCONSIN PUBLIC SERVICE CORP., GREEN BAY.
Kewaunee Nuclear Power Plant. Final safety analysis report, Amendment 21, 26:55309 (DOCKET-50305-48)
Kewaunee Nuclear Power Plant. Final safety analysis report, Amendment 21, errata sheets, 26:55311 (DOCKET-50305-51)
WISCONSIN UNIV., MADISON.
Mechanisms of calcium transport in small intestine. Overall review of the contract, January 1, 1970--September 1, 1972, 26:55498 (COO-1668-46)
Total radiation-induced genetic damage in entire genomes of Drosophila melanogaster. Progress report, November 1, 1971--October 31, 1972, 26:53497 (COO-1748-12)
WISCONSIN UNIV., MADISON. DEPT. OF PHYSICS.
Fast neutron radiation damage effects in crystalline anthracene and evaluation as a dosimetric technique, 26:53229 (COO-1105-172)
Some preliminary paramagnetic resonance studies for dosimetry research, 26:52979 (COO-1105-179)
WISCONSIN UNIV., MADISON. MATHEMATICS RESEARCH CENTER.
Scattering theory for elliptic differential operators in unbounded domains, 26:54407 (BNL-16752)
WOLLONGONG UNIV. COLL. (AUSTRALIA).
Multigroup neutron transport theory in plane geometry, 26:55440 (INIS-mf-195)
WYOMING UNIV., LARAMIE. DEPT. OF CHEMISTRY.
Prog. rpt. on photo initiated processes in vision, 11/15/69--11/14/72, 26:55496 (COO-1627-23)
Prog. rpt. on photo-initiated processes in vision, 11/15/71--11/14/72, 26:55495 (COO-1627-22)

Y

YALE UNIV., NEW HAVEN, CONN.
Biomedical program, 26:53398 (LA-4874, pp 79-83)
YALE UNIV., NEW HAVEN, CONN. DEPT. OF MOLECULAR BIOPHYSICS AND BIOCHEMISTRY.
Relation between single-strand DNA mass and sedimentation distance in alkaline sucrose gradients, 26:52981 (COO-3571-3)
YANKEE ATOMIC ELECTRIC CO., WESTBORO, MASS.
Yankee Nuclear Power Station. Control rod drop times measured on September 9, 1972, 26:55236 (DOCKET-50029-202)
Yankee Nuclear Power Station. March 1972 inservice examination of Yankee Rowe Atomic Power Plant, 26:55235 (DOCKET-50029-201)
Yankee Nuclear Power Station. Modification of approved Change 97 accomplished August 30, 1972, 26:55234 (DOCKET-50029-199)

Z

ZENTRALSTELLE FUER ATOMKERNENERGIE-DOKUMENTATION, LEOPOLDSHAFEN (WEST GERMANY).
Bibliographies in Nuclear Science and Technology. Section 5. Radiation effects on food, 26:53342 (AED-C-5-11)
High energy physics index. Vol. 10, No. 16, 1972, 26:54242
High energy physics index, Vol. 10, No. 14, 1972, 26:54240
High energy physics index, Vol. 10, No. 15, 1972, 26:54241
Surface and vacuum physics index. Vol. 7, No. 6, 1972, 26:54085
Technology index for plasma physics research and fusion reactors, Vol. 6, No. 6, 1972, 26:54748

PERSONAL AUTHOR INDEX

Authors' names are indexed in the form appearing in the abstracted publication. Each entry under an author's name gives the publication title and the *NSA* volume and abstract numbers. Report numbers, where applicable, are given in parentheses at the end of the entry.

Because of problems involved in the mechanical preparation of this index, all accent marks are omitted. The following changes in spelling have been introduced to reduce some of the confusion which might result from omitting the accents:

Germanic	ä appears as	ae
Germanic	ö	oe
Germanic	ü	ue
Scandinavian	ϕ	oe

A

- **AACHEN-BERLIN-CERN-LONDON-VIENNA COLLABORATION**, Resonance production in reactions $K^-p \to$ pantiK$^0\pi^+\pi^-\pi^-$ and $K^-p \to$ pantiK$^0\pi^+\pi^-\pi^-\pi^0$ at 10 GeV/c, 26:54225
- **AARONS, J. C.**, Exact calculations of N--d polarization, 26:54509
- **ABDOU, M. A.**, Neutron and gamma physics problems in fusion reactors, 26:54826 (CONF-720901-(Bks.1 and 2), pp 559-73)
- **ABE, Kanji**, Slightly oblique shock waves in a collisionless magnetized plasma, 26:54852
- **ABEGG, R.**, Blocking effect in U fission with 14-MeV neutrons, 26:54669
- **ABIGNOLI, M.**, Differential measurements on ion-atom collisions in energy range 500 to 3000 eV. IV, 26:54122
- **ABILLON, J. M.**, π^-p forward elastic scattering near 1 GeV/c, 26:54224
- **ABLAKULOV, Kh. A.**, Role of neutral vector mesons in the photoformation of lepton pairs by nuclei, 26:54260
- **ABO-TALEB, S. A.**, Microdetermination of metals in organometallic compounds by the oxine method after oxygen flask combustion. I. Cadmium, magnesium, uranium, and zinc, 26:52930
- **ABOUAF, R.**, Processes of formation of multiply charged ions by electron impact, 26:54103 (FRNC-CONF-51)
- **ABRAO, Alcidio**, Preparation of clear uranyl nitrate solution by fractional dissolution of sodium diuranate, 26:52976 (IEA-250)
- **ACCARY, A.**, Activation mechanism of sintering, 26:53587
- **ACCINNI, F.**, Buckling measurements in ECO with few CIRENE fuel elements, 26:55106 (CISE-R-283)
  - Experimental investigations on U--D$_2$O lattices, 26:55101 (CISE-R-203)
  - Measurement of cell parameters in RB-1 reactor, 26:55102 (CISE-R-239)
  - Neutron measurements at zero power on CIRENE fuel element in ESSOR reactor, 26:55105 (CISE-R-258)
- **ACHENBACH, E.**, Experiments on flow past spheres at very high Reynolds numbers, 26:55180
- **ACKLEY, R. D.**, Effect of extended exposure to simulated LMFBR fuel reprocessing off-gas on radioiodine trapping performance of sorbents, 26:53077 (CONF-720823-9)
  - Long-term effects on radioiodine trapping by charcoal, 26:53058 (CONF-720823-10)
- **ADADUROV, G. A.**, Formation of phase Nb/sub x/O$_2$ (0.8 less than or equal to x less than or equal to 1.0) under shock compression of Nb pentoxide, 26:53561
- **ADAMCHUK, Yu. V.**, Neutron resonances ^{112}Cd, 26:54599 (IAE-2116)
- **ADAMS, G. E.**, Radiation chemical mechanisms in radiation biology, 26:53024
- **ADAMS, J. H.**, Rigidity spectrum of Z greater than or equal to 3 nuclei from 5 GeV to over 300 GeV, 26:53834
- **ADAMS, James Paul**, Study of electron emissions of some mass separated fission product activities, 26:54601 (IS-T-534)
- **ADAMS, William H.**, Optimization of the transferability of atomic Hartree--Fock valence-shell orbitals, 26:54143
- **ADELBERGER, E. G.**, Lifetime of the first excited state in ^{96}Zr, 26:54622
- **ADELMAN, Saul Joseph**, Study of twenty-one sharp-lined nonvariable cool peculiar A stars, 26:53882
- **ADRADA, J.**, Radioanalytical purification of protactinium by anion exchange in hydrochloric acid-hydrofluoric acid medium, 26:52903
- **ADRIAN, Frank J.**, ESR study of the pyrolysis of hydrogen on tungsten, 26:55036
- **AEBISCHER, D.**, Performances of a proportional chamber with intermediate high voltage planes, 26:53213
- **AFANAS'EV, V. P.**, g-factor of 108 keV excited state in ^{151}Gd, 26:54634 (JINR-E6-6479)
- **AFANAS'EV, Yu. V.**, Kinetic processes in a laser plasma, 26:54799
- **AFROSIMOV, V. V.**, Charge state alteration processes in collisions of hydrogen atoms with hydrogen molecules, 26:54115
- **AGARWAL, P. C.**, Intensity and energy spectra of several x-ray sources in the 20- to 150-keV energy band, 26:53920
  - Short period variations in intensity and energy spectrum of Cyg X-1, 26:53921
- **AGARWAL, S. K.**, Physical measurements including depth dose data and isodose curves for 8 mv roentgen rays, 26:53799
- **AGERON, P.**, High flux Franco--German reactor, 26:55414
- **AGNEW, Lewis E.**, Proceedings of the fifth LAMPF users meeting held at the Los Alamos Scientific Laboratory, Los Alamos, N.M., November 8-9, 1971, 26:53784 (LA-4874)
- **AGRAWAL, S. P.**, Characteristics of cosmic ray diurnal variation from deep river neutron and meson data and temperature effects, 26:53811
- **AHLFELD, C. E.**, α-particle excitation of 1.78 MeV 2$^+$ state in ^{28}Si, 26:54561
- **AHLRICHS, Reinhart**, Asymptotic behavior of atomic-bound-state wave functions, 26:54153
- **AHLUWALIA, H. S.**, Study of the sidereal anisotropy of cosmic rays with muon telescopes underground, 26:53846
- **AINSWORTH, Glenn C.**, Experimental active- and passive-dosimetry systems for the NASA Skylab program, 26:53236 (NASA-TM-X-2440, pp 958-73)
- **AIRTH, G. R.**, Image intensifiers and fluoroscopy stabilizers, 26:53421
- **AITKEN, T. W.**, High intensity muon beam design for CERN II, 26:53783 (DNPL/P-131)
- **AKASOFU, S.-I.**, Geomagnetic disturbances in the polar cap, 26:54053
- **AKHIEZER, A. I.**, Introduction to physical kinetics, 26:54789 (ITF-71-96-P)
- **AKHIEZERI, I. A.**, Vibrations of Fermi-fluid drop and giant resonance in intermediate and heavy nuclei, 26:54689 (ITF-72-12-P)
- **AKHMEDLI, M. K.**, Spectrophotometric study of the reaction of Nb with Alizarin red, 26:52926
- **ALABISO, C.**, Variational Pade solution of Bethe--Salpeter equation, 26:54380
- **ALBATS, P. A.**, New point gamma ray source Libra γ-1, 26:53924
- **ALBRIGHT, C.**, Low strain tensile behavior of U--7.5 wt. pct Nb--2.5 wt. pct Zr, 26:53691
- **ALCOCK, M. W.**, Apparent constant-wavelength oscillations in a bounded plasma, 26:54859
- **ALDER, J. C.**, Measurements of inclusive hadron momentum distributions in deep inelastic electroproduction, 26:54178
  - π^0 electroproduction at first resonance at momentum transfers $q^2 = 0.6$, 1.0, and 1.56 GeV^2, 26:54268
  - Separation of sigma/sub l/ and sigma/sub t/ at q^2 approximately 1 (GeV/c)^2 in resonance region, 26:54168 (DESY-72/38)
- **ALDER, K.**, Forward dispersion relations and low-energy elastic scattering of charged particles from nuclei, 26:54711
  - Numerical investigations within the semiclassical transfer theory, 26:54742
- **ALEBASTROV, V. A.**, Proof of unitarity of S-matrix in non-local quantum field theory, 26:54413 (JINR-P2-6586)
- **ALEKSIN, V. F.**, Influence of toroidality on a magnetic configuration with a helical magnetic axis, 26:54832
  - Plasma equilibrium in configurations with a helical magnetic axis with allowance for toroidality, 26:54815

ALER, B., Total energy: power (nuclear) and district heating, 26:53102
ALEXANDER, E. C., Xenon isotopes in tellurobismuthite, Boliden, Sweden, 26:53176
ALEXANDER, J. B., Spectroscopic and photometric study of pulsating R Coronae Borealis type variable, RY Sagittarii, 26:53905
ALEXANDER, Peter, High-resolution semiconductor detector for applications in space, 26:53202 (NASA-TM-X-2440, pp 723-8)
ALEXSANDROV, N. N., Chromosome aberrations induced in human bone-marrow cells by therapeutical local γ irradiation: time and dose relationships, 26:53445
ALEY, R. E., Final report on the development of the Geographical Position Locator (GPL). Volume 8. Technical support, 26:53311 (UCRL-51130(Vol.8))
ALHERITIERE, E., Deformation and recrystallization behavior of sintered tantalum and tantalum formed by electron bombardment, 26:53623
ALIEV, Yu. M., Kinetic theory of parametric excitation of surface waves in semi-finite plasma, 26:54867
ALIMOV, O., Correlation between electron concentration of E region with height of Sun, 26:54016
  Results of investigations of E region of ionosphere over Dushanbe in 1964, 26:54017
ALINOVSKII, N. I., Investigation of heating of a plasma ion component by a collisionless shock wave, 26:54766
ALLAM, S., Radiochemical studies of ^{125}I. I, 26:53056 (AREAEE-129)
ALLARD, J. F., Contribution of rectangular graphs in reaction $^{14}N(^{3}He,p_{5})^{16}O^{*}$ (E^{*} = 8.88 MeV), 26:54533
ALLARDYCE, B. W., Ratio of pion--nucleus reaction cross-sections and the neutron density distribution for lead, 26:54529 (RPP/NS-8)
ALLEN, D. A., Infrared photometry of northern Wolf--Rayet stars, 26:53889
ALLEN, H. L., Metabolism of dissolved and particulate detrital carbon in a temperate hard-water lake, 26:55493 (COO-1599-58)
ALLEN, J. W., Study of reactivity balance during startup of the HFIR, 26:55407 (ORNL-TM-3769)
ALLEN, James D., Polymerization of adhesives utilizing high-energy radiation, 26:53716
ALLEN, R. J., Multinode analysis of B and W's 145-fuel assembly nuclear plants during loss-of-coolant accident, 26:55272 (BAW-10048(Suppl.1))
ALLEN, W. C., Molecular g-value, magnetic susceptibility anisotropy, molecular quadrupole moment, and sign of the electric dipole moment in chloroacetylene, 26:52969
ALLKOFER, Otto Claus, Particle detectors, 26:53208
ALLRED, R. E., Dynamic fracture behavior of Borsic--Al composites, 26:53557 (SC-DC-721080)
ALMOND, D. P., Ultrasonic evidence against multiple energy gaps in superconducting niobium, 26:54437
ALSPECTOR, J., Annihilation spectrometer for investigation of heavy meson spectra, 26:53279
ALTER, Harry, Benchmark testing of nuclear data for fast reactors, 26:55125 (CONF-720901-(Bks.1 and 2), pp 1033-47)
ALTHOFF, K. H., Photoproduction of π^{+}-mesons on polarized protons at photon energies between 0.5 and 2.2 GeV, 26:54172 (NP-19415)
ALTHOUSE, L. P., Characterization of an epoxy system for filament winding, 26:55628 (UCRL-73773)
ALTSCHULER, Martin D., Atlas of magnetic fields in the solar corona, 26:53955
ALTYNTSEV, A. T., Investigation of heating of a plasma ion component by a collisionless shock wave, 26:54766
ALVAREZ, L. W., Measurement of the primary cosmic ray nuclear rigidity spectra for individual elements of charge Z greater than or equal to 2, 26:53826
ALY, H. F., Extraction of iron, cobalt, and manganese from hydrochloric acid with quaternary amine Aliquat-336, 26:53076
ALY, M. M. E., Preparation of sinterable uranium dioxide, 26:53546 (AREAEE-134)
AMANN, R. F., Interference terms in the multiperipheral model, 26:54329 (NYO-3533-265)
  Pion and K meson production in the multiperipheral model, 26:54325 (COO-3533-2)
AMANO, Tsuneo, Magnetohydrodynamic and tearing instabilities in a tokamak, 26:54813
AMBOURG, Y., Preliminary studies on modified version of EBIS source, 26:54081 (FRNC-CONF-57)
AMIEL, M., Contribution of rectangular graphs in reaction $^{14}N(^{3}He,p_{5})^{16}O^{*}$ (E^{*} = 8.88 MeV), 26:54533
AMIEL, S., Independent yields of krypton and xenon isotopes in thermal-neutron fission of ^{235}U. Observation of an odd--even effect in the element yield distribution, 26:54667
AMINOVA, A. V., Infinitesimal transformations conserving test-body trajectories in general relativity, 26:54389 (ITF-71-85-P)
AMOS, D. E., Significant digit incomplete gamma ratios, 26:55604 (SC-DR-720303)
AMSTER, Harvey J., Predetermining statistical errors in Monte Carlo transport calculations, 26:55430 (CONF-720901-(Bks.1 and 2), pp 207-10)
AMUNDSON, P. I., Sodium void studies and related heterogeneity effects in ZPPR-2, the Benchmark Demonstration Assembly, 26:55392 (CONF-720901-(Bks.1 and 2), pp 973-85)
  Spatially dependent benchmark parameters in the initial demonstration plant critical assembly, 26:55117 (CONF-720901-(Bks.1 and 2), pp 809-21)
ANANTH, A. G., Characteristics of cosmic ray diurnal variation from deep river neutron and meson data and temperature effects, 26:53811
ANANTHANARAYANAN, K. P., Properties of proton-irradiated diamond, 26:54991
ANDERSON, A., Raman spectra of molecular crystals, 26:52968
ANDERSON, D. N., Theoretical calculations of the F-region tropical ultraviolet airglow intensity, 26:54031
ANDERSON, D. W., Methods for three-dimensional fuel management studies on high temperature reactors, 26:55111 (CONF-720901-(Bks.1 and 2), pp 68-80)
ANDERSON, F. N., CNSG: nuclear ship oxygen activation calculational method with experimental comparison, 26:55356 (CONF-720901-(Bks.1 and 2), pp 471-9)
ANDERSON, J. D., Nucleon--nucleon scattering lengths from incomplete nucleon--deuteron breakup experiments, 26:54503 (UCRL-74069)
ANDERSON, K. A., Solar-wind and interplanetary electron measurements on the Apollo 15 subsatellite, 26:54072
ANDERSON, M. E., Some neutron and gamma radiation characteristics of plutonium cermet fuel for isotopic power sources, 26:53336 (NASA-TM-X-2440, pp 853-8)
ANDERSON, Raymond P., Crosslinked nylon by irradiation of a graft copolymer of nylon with an ethylene/acrylate or modified copolymer, 26:53013
ANDERSON, S. L., Application of transport techniques to the analysis of NERVA shadow shields, 26:55368 (NASA-TM-X-2440, pp 449-59)
ANDREEV, H. E., Excitation by very high frequency wave pumping of parametric instabilities in a magnetoactive plasma, 26:54809 (NP-19406)
ANDREEV, P. A., Experimental study of the interaction of water with sodium during small leaks of water into sodium, 26:55152 (CONF-710548-, pp 39-56)
ANDRESEN, E. G., Binomial distribution and Gaussian distribution in nuclear radiation measuring, 26:53207
ANDREWS, P. J., Spectroscopic and photometric study of pulsating R Coronae Borealis type variable, RY Sagittarii, 26:53905
ANGELMAIER, Doris, Specific enrichment of mutants of Escherichia coli with an altered acyl CoA synthetase by tritium suicide, 26:53518
ANKENBRANDT, C. M., Indiana University Spark Chamber Group technical progress report, December 1, 1971--November 30, 1972, 26:54206 (COO-2009-36)
ANNO, G., Response of a 300-μ silicon detector to monoenergetic neutrons determined by the use of the Monte Carlo technique, 26:53291 (NASA-TM-X-2440, pp 708-13)
ANTHOINE, Roger, CERN proton synchrotron project (40 meters underground), 26:53745
ANTOKU, S., Dose to patients from roentgenography, 26:53434
ANUFRIEV, V. A., Effective neutron absorption cross sections for ^{252}Cf and ^{253}Cf in central channel of SM-2 reactor, 26:54668
ANZER, Ulrich, Method to calculate electric currents in quiescent prominences, 26:53950
AOKI, Masakazu, Hamiltonian defined as a graph limit in a simple system with an infinite renormalization, 26:54386
APPARAO, K. M. V., Detection of neutron stars, 26:53907
ARAD, B., Level scheme of ^{144}Sm determined by the (γ,γ') reaction, 26:54619
ARAKI, Shotaro, Influence of austenite grain size and forging ratio on ferrite banded structure, 26:55593 (RFP-Trans-108)
ARAMANY, Mohamed A., Radiation protection prostheses for edentulous patients, 26:53410
ARBUSOV, B. A., Production of boson pairs by static field, 26:54384
ARCHAMBEAU, John O., Swine skin changes produced by different radiations, 26:53450 (LA-4874, pp 126-44)
ARENAS ROSADO, J., Benzoato complexes of uranyl. III, 26:53042
ARIANER, J., Heavy ion source with a confined electron beam, 26:53753 (FRNC-CONF-56)
ARIMA, Akito, Magnetic moments of odd mass nuclei with simple configurations, 26:54679 (COO-3001-17)
ARIMA, Masashi, Balneotherapy effects on mice irradiated with neutrons and gamma rays, 26:53465
ARIYA, S. M., Magnetic susceptibilities of nonstochiometric cerium oxides, 26:55030
ARKHIPENKO, V. I., Conditions for wave transformation in a plasma with a nonmonotonic longitudinal distribution, 26:54841 (AEC-tr-7338)
  Study of the localization of the wave transformation region in a superhigh-frequency discharge plasma, 26:54842 (AEC-tr-7339)
ARKUSZEWSKI, Jacek, Effect of singularities on approximation in S/sub N/ methods, 26:54482 (INR-P-1405)
ARMBRUSTER, R., ^{38}Ar levels formed in reaction $^{34}S(\alpha,\gamma)^{38}Ar$, 26:54560
ARMSTRONG, J. W., Analysis of three-station interplanetary scintillation, 26:54070

ARMSTRONG, L. Jr., Limitation on use of impulse approximation in nuclear β-decay, 26:54709
ARMSTRONG, T. W., Radiation transport codes for potential applications related to radiobiology and radiotherapy using protons, neutrons, and negatively charged pions, 26:54890 (ORNL-TM-3816)
ARNOLD, G. W., Electronic stopping measurements of charged-particles in radiophotoluminescent glass, 26:55009
ARNOLD, R., Charged particle multiplicity and angular correlation measurements in pp and γp collisions, 26:54192 (BNL-17141)
ARPONEN, Jouko, Internal structure of neutron stars, 26:53908
ARSEN'EV, D. A., Effect of changes in equilibrium deformations of the excited states of odd-A deformed nuclei on their energy and structure, 26:54640
ARTUSO, J., Linearity, time domain reflectometer, and Fourier analysis studies of an evacuated Compton detector, 26:53197 (EGG-1183-2277)
ARUTYUNOV, V. V., Monte Carlo investigations of catastrophic collisions with characteristics of scattered electron radiation taken into account, 26:54898
ARUTYUNYAN, F. R., Effect of the medium on radiation emission by relativistic electrons, 26:54907
ARVIEUX, J., Polarization and cross section of p + ^3H elastic scattering, 26:54521
  Rescattering effects in the $^2H(p,2p)n$ and $^2H(p,pn)n$ reactions induced by 20- to 60-MeV protons, 26:54511
ASANOV, V. V., System of wire spark chambers with ferrite core memory, 26:53271 (JINR-P13-6522)
ASAOKA, T., JN-METD2: Fortran-IV programme for solving neutron transport problems, 26:54481 (EUR-4839)
ASBURY, A. K., Neuropathologic effects of proton-beam irradiation in man. II, 26:53446
ASCUITTO, Robert J., Inelastic scattering calculations with projected Hartree--Fock wave functions. II, 26:54565
ASH, J. E., Comparison of a two-dimensional hydrodynamics core (REXCO) to excursion experiments for fast reactor containment, 26:55139 (ANL-7911(Suppl.1))
ASKEW, J. R., Methods for three-dimensional fuel management studies on high temperature reactors, 26:55111 (CONF-720901-(Bks.1 and 2), pp 68-80)
  Some problems in the physics of high temperature reactors, 26:55110 (CONF-720901-(Bks.1 and 2), pp 55-67)
ASSOUSA, G. E., α-particle excitation of 1.78 MeV 2^+ state in ^{28}Si, 26:54561
ASTRUC, J. M., High flux Franco--German reactor, 26:55414
ATKINSON, Gerald L., Improved S/sub N/ inner iteration convergence criterion, 26:55435 (CONF-720901-(Bks.1 and 2), pp 275-92)
ATOJI, Masao, Magnetic and crystal structures of ErC_2 at 297 -2°K, 26:55035
  Magnetic structure of $ErAu_2$, 26:55034
  Magnetic structure of $HoAu_2$, 26:55033
ATWELL, W., Significant solar-proton events in the 20th solar cycle for the period October 1964 to March 1970, 26:53928 (NASA-TM-X-2440, pp 329-35)
AUDOUIN, Maurice, Radiation protection shielding, 26:53136
AUGE, Robert G., Temperature measurement and control in the bomb reduction of plutonium tetrafluoride, 26:53037 (RFP-1455)
AURALDSSON, Hans-Ake, Transfer of simulated fallout-particles from pasture to grazing dairy cattle. I, 26:53527 (FOA-4-4503-A-3)
AURIC, P., Lifetime variation of ^{64}Cu and the chemical state of (n,γ) recoil copper in α-copper phtalocyanine crystals, 26:53032
AURILIA, Antonio, Spontaneous breakdown of symmetry and the gauge invariance in a relativistic field theory, 26:54387
AUSTIN, A. L., Energy: uses, sources, issues, 26:53096 (UCRL-51221)
AUSTIN, W. E., Compton scatter attenuation gamma-ray spectrometer, 26:53254 (NASA-TM-X-2440, pp 614-17)
AUTONES, P., Apparatus for spin-rotation measurements in pion--proton scattering at high energies, 26:54232
AUXIER, J. A., Local dose from neutron-produced-recoil ions in the region of a therapeutic ^{252}Cf needle, 26:54902
AVERIN, V. G., Stimulated emission evoked by pumping with a pulsed electron beam produced in a linear discharge, 26:54787
AVERY, R., Review of FBR physics, 26:55115 (CONF-720901-(Bks.1 and 2), pp 771-88)
AVIGNONE III, F. T., Rapid comparison of angular distribution attenuation coefficients for detectors of arbitrary geometry, 26:53225
AVNI, Y., Helicity-conserving and helicity-nonconserving pomeron-exchange amplitudes in the dual absorptive model, 26:54419
AVOGADRO, A., Extraction of plutonium from heavy water fuels by the SALTEX process, 26:53079 (EUR-4812)
AVRAMENKO, V. B., Use of high-speed spectrography for diagnostics of an erosive pulsed plasma accelerator, 26:54773
AYRES, P. S., Study of discontinuities in control rod drive motor tube extensions, 26:55217 (BAW-10047(Rev.1))
AZAREWICZ, Joseph L., Prog. rpt. on physics of transient radiation effects, final, 2/68--10/71, 26:54968 (AD-737312)
AZHGIREI, L. S., System of wire spark chambers with ferrite core memory, 26:53271 (JINR-P13-6522)
AZNAURYAN, I. G., Dispersion relations and data for the reaction γn reversible pπ⁻ in the 33-resonance region, 26:54261
AZZOPARDI, Max, Elementary mechanisms in heterogeneous kinetics. IV, 26:55588 (ORNL-tr-2394)

B

BABAEV, A., Determination of bismuth in some minerals by activation analysis, 26:52910
BABIKOV, V. V., Present-day problems of the theory of nuclear forces, 26:54688 (ITF-71-77-P)
BABUEL-PEYRISSAC, J. P., Induced Compton effect in plasma, 26:54798
BACCOLINI, A., Measurement of cell parameters in RB-1 reactor, 26:55102 (CISE-R-239)
BACH, H., Formation of fog and glazed frost due to cooling-tower operation, 26:53117
BACHELAY, J., Outlook for the on-site welding of thick metal sheets, 26:53633
BAEV, Il., Effect of small x-ray doses on the motor activity of rats irradiated during their embryonic development, 26:53488
BAGDASAROV, Yu. E., Requirements for steam generator design and systems to ensure safety in the case of failures in the tubes of heat exchange surfaces, 26:55159 (CONF-710548-, pp 206-12)
BAGSHAW, Malcolm A., Combined fractionated isotopic and external irradiation of the liver in Hodgkin's disease. A study of 21 patients, 26:53507
BAGWELL, R. G., Real-time spectrum-to-dose conversion system, 26:53201 (NASA-TM-X-2440, pp 142-8)
BAIETTI, Albert L., Comments on numerical values for radiation exposure limits, 26:53436
BAILEY, H. S., GE nuclear design and benchmark critical experiment plan for the LMFBR demonstration plant, 26:55114 (CONF-720901-(Bks.1 and 2), pp 724-38)
BAILY, Norman A., Fluctuations in energy loss and their implications for dosimetry and radiobiology, 26:54879 (NASA-TM-X-2440, pp 157-61)
BAIXAS, J., Heavy ion source with a confined electron beam, 26:53753 (FRNC-CONF-56)
BAIXERAS, J., Experimental study of surface resistance anisotropy of Type-II superconductors in vicinity of H/sub c3/, 26:54456
BAJARIA, Hansraj J., Determination of the magnetic field extension profile for reducing the end losses in the MHD generator channel, 26:53099
BAKALE, G., Dissociative attachement of thermal electrons to N_2O and subsequent electron detachment, 26:54135
BAKANOVICH, G. I., Use of high-speed spectrography for diagnostics of an erosive pulsed plasma accelerator, 26:54773
BAKER, F. T., Phase and shape of the form factor for inelastic ^3He scattering, 26:54621
BAKER, George A. Jr., Certain invariance and convergence properties of the Pade approximant, 26:55475 (BNL-17110)
  Intermediate-state, single-particle energies in many-fermion energy calculations, 26:54717
BAKER, K., Numerical calculation of zero bias conductivity for superconducting tunnel junction in presence of depairing. II, 26:54462 (LNF-72/27)
BAKEWICZ, Edmund, Emittance measurements and design of an ion beam transporting system, 26:53760
BAKOS, J., Light-intensity dependence of the multiphoton ionization probability in the resonance case, 26:54094
BALAMUTH, D. P., Core-excited 5^+ state in ^{14}N, 26:54542
BALASHOVA, E. P., Magnetic susceptibilities of nonstochiometric cerium oxides, 26:55030
BALASUBRAHMANYAN, V. K., Acceleration and propagation of high Z cosmic rays in pulsar environment, 26:53857
  Charge composition of galactic cosmic radiation, 26:53830
  Cosmic ray proton and He spectra above 50 GeV, 26:53829
  Primary cosmic ray electron spectrum from 10 GeV to about 200 GeV, 26:53823
BALICK, Bruce, Fine structure in H II regions: synthesis observation at 11 and 3.7 centimeters, 26:53910
BALKANSKI, M., Light scattering in solids. Proceedings of the second international conference, Paris, July 19--23, 1971, 26:55041
BALL, J. B., Level structure of ^{93}Mo and failure of j-determination by spectroscopic factor ratios near closed shells, 26:54612
BALL, J. S., Generalization of semilocal duality, 26:54422
BALLADA, J., Determination of urinary plutonium by radiochemical analysis on ion exchanger filters, 26:52940
BALLUFFI, R. W., Comments on the range of applicability of the grain boundary (secondary) dislocation model to high angle grain boundaries, 26:55513 (COO-3158-10)
BALSLEY, B. B., Vhf power spectra of the radar aurora, 26:54038
BALTATEANU, N., Influence of electron irradiation on CdS thin films, 26:54992
BALYCHEV, I. N., Destruction of a solid by superdense excitation of its electronic subsystem, 26:55012
BALZEROWIAK, H. P., Possibilities of explosive compaction

of powders, especially those of W, with direct procedure, 26:53619
BAMMERT, K., Calculation of the dynamic behavior of heat exchangers in gas turbines, 26:53114
BANCEVA, E., Effect of small x-ray doses on the motor activity of rats irradiated during their embryonic development, 26:53488
BANDYOPADHYAY, N., Fluoro complexes of hexavalent uranium. IV, 26:53043
BANERJEE, Krishnadas, Correction of a formula used in radioassay of /sup 99m/Tc, 26:52946
BANNISTER, M. J., Nonisothermal techniques for studying initial-stage sintering, 26:53595
  Oxidation of UO_2 fuel pellets during hydrogen sintering, 26:53563
BARAN-MARZAK, M., Ion implantation facility at Orsay, 26:54976
BARANOV, V. F., Monte Carlo investigations of catastrophic collisions with characteristics of scattered electron radiation taken into account, 26:54898
BARASHENKOV, V. S., Buildup of cosmic isotopes in iron meteorites, 26:53808 (ORNL-tr-2620)
BARAT, M., Differential measurements on ion-atom collisions in energy range 500 to 3000 eV. IV, 26:54122
  Inelastic processes in He^+--He collisions, 26:54140
BARBER, S. A., Calcium and strontium transport to plant roots, 26:55490 (COO-1495-17)
BARCUS, J. R., Conjugate features of magnetospheric electron dynamics observed at balloon altitudes, 26:54020
BARDAKCI, K., General approach to scaling in electroinclusive reactions, 26:54275
BARENGOLTZ, J. B., Jupiter radiation test levels and their expected impact on an encounter mission, 26:54002 (NASA-TM-X-2440, pp 781-4)
BARFIELD, J. N., Investigation of interaction between Pc 1 and 2 and Pc 5 micropulsations at the synchronous orbit during magnetic storms, 26:54035
  Statistical characteristics of storm-associated Pc 5 micropulsations observed at the synchronous equatorial orbit, 26:54036
BARIYAOV, V. I., Generation of fast electrons through interaction of SHF wave with collisionless plasma, 26:54836 (AEC-tr-7331)
BARKOVA, A. M., Theoretical calculation of space distribution of dose field of ^{60}Co γ irradiation under lattice, 26:54908
BARMIN, V. V., Measuring of branching ratio GAMMA(K/sub L/ $\to 3\pi^0$)/GAMMA(K/sub L/ $\to \pi^+\pi^-\pi^0$), 26:54187
  Search for a neutral vector meson in K/sub L/-decays, 26:54291
BARNES, Aaron, Solar-wind heating, 26:53942
BARNES, Barry K., Active ^3He activation analysis for carbon and oxygen, 26:52899 (LA-DC-72-809)
BARNES, Clifford A., Columbia River effects in the Northeast Pacific: physical studies. Progress report, June 1971--June 1972, 26:53165 (RLO-2225-T-25-6)
BARNES, J. E., Relative nonhomogeneities of radiation dose to the respiratory tract from inhaled radionuclides, 26:53536
BARNETT, M. B., Design of a radioactive noncontact encoder, 26:53286 (N-71-37956)
BARON, E., Heavy ion source with a confined electron beam, 26:53753 (FRNC-CONF-56)
BARON, Eric, Sources with confined electron beams (review), 26:54080 (FRNC-CONF-55)
BARON, S., Options in power generation and transmission, 26:55086
BARR, R. Q., Arc-cast Mo-base TZM alloy properties and applications, 26:53672
BARRE, J. Y., Reactor physics and fast power breeders: MASURCA core R-Z program, 26:55118 (CONF-720901-(Bks.1 and 2), pp 822-38)
BARRERA, Ruben, Roton-limited mobility of ions in superfluid ^4He, 26:54425
BARRETT, Craig R., Prog. rpt. on structure dependence of high temperature deformation of metals, 3/1/70--3/1/71, 26:55613 (SU-326-P-17-X-2)
BARRETT, Eugene, Studies on the transport of L-lysine by isolated chick intestinal epithelial cells, 26:55636 (UR-3490-177)
BARRETT, P. H., Charged state of ^{57}Fe atoms following the decay of ^{57}Co in solid xenon, 26:55057
BARRETT, R. F., Continuum shell model calculation for the ^{15}N giant dipole resonance, 26:54545
BARROWES, S., Explanation of the break in the primary spectrum, 26:53869
BARROWES, S. C., Theory of narrow-angle cosmic ray anisotropies, 26:53868
BARTA, J., Preparation and properties of W--Ni--Mo alloys, 26:53679
BARTENEV, V. D., Investigation of elastic pd-scattering in diffraction cone region in the energy range 10 to 70 GeV, 26:54197
BARTHELEMY, Pierre, Safety aspects of sealed ^{238}Pu sources used in pacemakers, 26:53331 (CEA-CONF-2026)
BARTINE, D. E., Sensitivity analysis: a general approach illustrated for a Na--Fe system, 26:54943 (CONF-720901-6)
  Sensitivity analysis: a general approach illustrated for a Na--Fe system, 26:54940 (CONF-720901-(Bks.1 and 2), pp 512-23)
BARTLETT, Neil, Noble-gas chemistry and its significance, 26:55562 (LBL-416)
BARTLIT, J. R., Experience in handling, transport, and storage of liquid hydrogen: the recyclable fuel, 26:55552 (LA-DC-72-632)
BARTON, Henry Ruwe Jr., Partial wave analysis of the $\pi\pi$ spectrum to 1.5 GeV/c^2: a study of the reaction $\pi^+d \to$ p/sub s/p $\pi^+\pi^-$ at 13 GeV/c, 26:54219
BARTS, B. I., Vibrations of Fermi-fluid drop and giant resonance in intermediate and heavy nuclei, 26:54689 (ITF-72-12-P)
BARUAH, J. N., Flux effects on damage in GaAs as measured by the channelling of ^{85}Kr, 26:54993
BARULLI, L., Cleanup system for primary cover gas of LMFBR, 26:55226 (CONF-710959-, Paper 5)
BARYLOV, V. G., Measuring of branching ratio GAMMA(K/sub L/ $\to 3\pi^0$)/GAMMA(K/sub L/ $\to \pi^+\pi^-\pi^0$), 26:54187
BASILADZE, S. G., Shaper with universal logic of operation, 26:53320
BASILE, Pierre, Experimental study of $K^+ \to \pi^+\pi^-e\nu$ decay, 26:54183 (CEA-N-1553)
BASLER, D. B., High temperature oxidation of gadolinium and dysprosium under controlled oxygen partial pressure, 26:53550 (IS-T-540)
BASMER, P., Phenomenological investigation of the flow distribution behind local coolant chemical blockage in rod bundles, 26:55176 (KFK-1548)
BASSHAM, James A., Photosynthetic carbon metabolism, 26:55561 (LBL-383)
BASU, M. K., Alpha-cluster structure of light self-conjugate 4n nuclei in their ground states, 26:54723
BATANOV, G. M., Excitation by very high frequency wave pumping of parametric instabilities in a magnetoactive plasma, 26:54809 (NP-19406)
BATE, L. C., Reliability in scientific evidence based on multi-trace forensic NAA, 26:52896 (CONF-720920-2)
BATHE, J. E., Examination of irradiated UO_2 HTR fuel particles. Part I. Experimental techniques, 26:53555 (RD/B/N-2214)
BATHORI, Edit, Activity changes in locally irradiated rat liver L-arginine amidinohydrolase (EC 3, 5, 3, 1) following irradiation at doses of 2000 R, 4000 R, and 8000 R, 26:53491
BATTY, C. J., Ratio of pion--nucleus reaction cross-sections and the neutron density distribution for lead, 26:54529 (RPP/NS-8)
BATYUTO, T. D., Respiration and structural changes of mitochondria of intestinal epithelial cells in the course of amino acid absorption in irradiated animals, 26:53493
BAUDON, J., Differential measurements on ion-atom collisions in energy range 500 to 3000 eV. IV, 26:54122
BAUER, W., Theory of π/2-mode biperiodic deflectors, 26:53798
BAUGH, D. J., Ratio of pion--nucleus reaction cross-sections and the neutron density distribution for lead, 26:54529 (RPP/NS-8)
BAUMINGER, E. R., Moessbauer effect in ^{239}Pu, 26:54661
BAUR, G., Coulomb break-up of the deuteron, 26:54743
BAYER, A., Age-dependent ingestion dose factors g/sub G/ and g/sub G'/ of ^{131}I, 26:53506 (ORNL-tr-2629)
BAYM, Gordon, Roton-limited mobility of ions in superfluid ^4He, 26:54425
BAYTOS, John F., Analyses for residual explosives in drainage ditch soil at sump effluent outlets, 26:55545 (LA-4925)
BAYUZICK, R. J., Study of two-phase systems by field--ion microscopy, 26:53653
BAZAROV, I. P., Theory of polymorphous transformations in the ionic crystals with triparticle interactions, 26:55538 (ITF-72-50-P)
BAZHAT, M., One-nucleon transfer reactions to quasi-intersecting levels, 26:54635 (JINR-P4-6509)
BAZIN, J. P., Reading, automatic treatment, and visual display of radioactivity spectra recorded on punched tape, 26:53544
BEALL, Sam E. Jr., Urban utilization of extracted heat and waste heat from central station power plants, 26:55212 (CONF-720925-2)
BEAM, J. E., Triangle graphs and isospin violation in 3-particle final-state reactions, 26:54716
BEARD, D. B., Self-consistent description of the magnetotail current system, 26:54064
BEARD, David B., F and K components of the solar corona, 26:53938
BEARSE, R. C., Spectroscopy of ^{101}Mo by sub-Coulomb stripping, 26:54614
BEAUCHAMP, W. T., Search for $^1/_2$e and $^2/_3$e charged quarks in the cosmic radiation at 2750-m altitude, 26:54164
  Search for $^4/_3$e charged diquarks in the cosmic radiation at 2750-m altitude, 26:54177
BEAUDOIN, Benoit R., Light-water breeder reactor, 26:55130
BEAUFRERE, J., Study and tests of small components of secondary circuits of fast Na cooled reactors, 26:55182
BEAUJEAN, H., Separation of fission product rare gases from combustion waste gases from high temperature fuel elements by scrubbing with liquid carbon dioxide, 26:53064 (ORNL-tr-2621)

BEAUMEVIEILLE, H., Reactions ^{19}F(d,α), ^{19}F(d,p), and excited states of ^{20}F, 26:54548

BECK, C. L., Sodium void studies and related heterogeneity effects in ZPPR-2, the Benchmark Demonstration Assembly, 26:55392 (CONF-720901-(Bks.1 and 2), pp 973-85)

BECK, H. L., Experimental determination of cosmic-ray charged-particle intensity profiles in the atmosphere, 26:53807 (NASA-TM-X-2440, pp 908-13)

BECK, Robert N., Dosimetry of /sup 87m/Sr, 26:54912

BECK, W. L., Dosimetry for radiobiological studies of the human hematopoietic system, 26:53406 (NASA-TM-X-2440, pp 974-80)

BECKER, Richard L., Deformed renormalized Brueckner--Hartree--Fock approximation and its application to ^{12}C, 26:54696 (ORNL-TM-3951)

BECKMANN, R. C., Flight test evaluation of a fluidically actuated monopropellant hydrazine roll control system, 26:55600 (SC-DC-722244(RD))

BEDJIDIAN, M., (d,^{6}Li) reactions with light nuclei at 28 MeV, 26:54527 (LYCEN-7219)

BEER, Janusz Z., Effects of uv-light and x-rays on murine lymphoma, 26:53356

BEER, Thomas Ivan, Atmospheric-wave-induced instability in the E region, 26:54018

BEESTON, Richard, Occupational Safety and Health Act of 1970, 26:54926

BEETKE, E., Animal experimental examinations on the effect of ionizing radiation on the maxillary bone with metallic bridges, 26:53480

BEHAR, M., Multipole mixing ratios of γ-transitions in ^{185}Re, 26:54644

BEISING, Kurt, Bibliographies in Nuclear Science and Technology. Section 5. Radiation effects on food, 26:53342 (AED-C-5-11)

BEITEL, J. C., Analysis of sodium-void experiments in the FTR engineering mockup critical assembly, 26:55390 (CONF-720901-(Bks.1 and 2), pp 739-67)

BEKENSTEIN, J. D., Black holes and the second law, 26:53906

BELEN'KII, M. Ya., Experimental study of the interaction of water with sodium during small leaks of water into sodium, 26:55152 (CONF-710548-, pp 39-56)

BELENOV, E. M., Kinetic processes in a laser plasma, 26:54799

BELLIAN, Joseph G., Manufacturers's views on instrument standards, 26:53248

BELLONI, Jacqueline Dolores Therese, Preparation of anhydrous hydrazine by the radiolysis of liquid ammonia, 26:53001

BELOKOLOS, E. D., Electron energy spectrum of a crystal conductor in a magnetic field, 26:55533 (ITF-72-16-E)

BELOUSOVA, O. I., Role of the thymus in the postradiational restoration of the bone marrow in rats, 26:53479

BELROSE, J. S., D-region measurements with the differential-absorption; differential-phase partial-reflection experiments, 26:54032

BELYAEV, V. B., Factorization of pair potential by Bateman modified method in two- and three-body problem, 26:54345 (JINR-P4-6505)

BENACERRAF, Baruj, Identification of the cell population responding to DNP--GL in lethally irradiated chimeric guinea pigs, 26:53474

BENADA, J., Nondestructive neutron activation analysis of mineral materials. II, 26:52901 (UJV-2851-F,Ch)

BENAROYA, R., Tests on superconducting helix resonators, 26:53750

BENCZER-KOLLER, N., Lifetime of 3.74-MeV (3^-) state of ^{40}Ca, 26:54575

BEN-DAVID, G., Level scheme of ^{144}Sm determined by the (γ,γ') reaction, 26:54619

BENDER, John H., Sample preparation and equipment problems associated with re-cycled, purified atmospheres, 26:53729 (LA-DC-72-230)

BENDER, Roger, Evaluation of the hazard from exposure to electron irradiation simulating that in the synchronous orbit, 26:53458 (NASA-TM-X-2440, pp 665-71)

BENDJABALLAH, N., Reactions ^{19}F(d,α), ^{19}F(d,p), and excited states of ^{20}F, 26:54548

BENEDIKTOV, E. A., Simultaneous measurements of electron density and collision frequency in ionospheric D region, 26:54028

BENESVOSKY, F., Conference on powder metallurgy of high temperature materials, Reutte/Tyrol, Austria, 6/71. I, 26:53601
  Conference on powder metallurgy of high temperature materials, Reutte/Tyrol, Austria, 6/71. II, 26:53602
  Conference on powder metallurgy of high temperature materials, Reutte/Tyrol, Austria, 6/71. III, 26:53584
  Conference on powder metallurgy of high temperature materials, Reutte/Tyrol, Austria, 6/71. IV, 26:53603

BENFATTO, G., Pion electroproduction at threshold, 26:54247 (NP-19417)

BEN-HUR, E., Thermally enhanced radiosensitivity of cultured Chinese hamster cells, 26:53358

BENJAMIN, R. W., Predicting production rates of heavy actinides, 26:54654 (CONF-720901-(Bks.1 and 2), pp 97-107)

BENNETT, E. F., Review of fast neutron spectrum measurements, 26:55438 (CONF-720901-(Bks.1 and 2), pp 943-58)

BENNEWITZ, H. G., ^{4}He--^{4}He interaction potential from low energy total cross section measurements, 26:54514

BENOVA, D., Effect of small x-ray doses on the motor activity of rats irradiated during their embryonic development, 26:53488

BENSKI, H. Claudio, Moessbauer effect measurements on ^{57}Fe in a nickel host near the Curie point, 26:55572 (NYO-3823-12)

BENSON, R. E., Observations of cosmic-ray-induced phosphenes on Apollo 14, 26:53407 (NASA-TM-X-2440, pp 1002-6)

BENSON, Royal H., Safety device for removing tritium gas from a gas stream, 26:53313

BENTON, E. V., High-Z-particle Apollo astronaut dosimetry with plastics, 26:53231 (NASA-TM-X-2440, pp 149-56)

BENTZ, L. L., New techniques for relative calibration of tritium sources by bremsstrahlung counting, 26:52934 (MLM-1368)

BENZI, V., Fast neutron radiative capture cross sections of stable nuclei with 29 less than or equal to Z less than or equal to 79, 26:54700 (RT/FI-(72)6)

BENZLER, Hartwig, Uranium enrichment, 26:53328

BERANEK, J., Metropolitan siting of nuclear heating plants, 26:55375 (INIS-mf-172)

BERBANO, M. C., Built-in radiotracer (^{24}Na) for measuring catalyst circulation rates, 26:53343

BERCY, A., Integral absorbed doses: examples, 26:54910

BEREZIN, A. K., Interaction between a plasma and electron beam modulated by low-frequency oscillations, 26:54782

BEREZIN, V. A., Potentials in collapsing systems of general relativity theory, 26:54404

BEREZINA, G. P., Interaction between a plasma and electron beam modulated by low-frequency oscillations, 26:54782

BERGER, Robert A., Prog. rpt. on physics of transient radiation effects, final, 2/68--10/71, 26:54968 (AD-737312)

BERGERSEN, B., Positron correlation energy in metals, 26:55066

BERGHEZAN, A., Simple method of precise alignment and uniform distribution of reinforcing fibers in a metal matrix, 26:53629

BERGMAN, A. A., Measurements of neutron cross sections of radiation capture and fission for some heavy nuclei by the method of time of retardation in lead, 26:54657 (FEI-292)

BERGONZI, M., Study as a function of time and dose of the numerical variations of the leucocytes circulating in a totally irradiated rat, 26:53483
  Variations of ^{75}Se-selenomethionine erythrocytic incorporation induced in rat by pan-irradiation, 26:53482

BERGOVIST, I., Radiative capture of energetic neutrons by ^{208}Pb, 26:54662

BERKE, Harry L., Metabolism of the rare earths following inhalation: pathologic and biochemical response in the lung and other organs. Final report for period to September 15, 1972, 26:55497 (COO-1630-29)

BERMAN, S. M., Weak interactions at ISABELLE, 26:54284 (BNL-16978)

BERMUDEZ POLONIO, J., Benzoato complexes of uranyl. III, 26:53042

BERNA, Ph., Consistent approach of heterogeneous theory leading to a dipolar formulation. I, 26:55446
  Consistent approach of heterogeneous theory leading to a dipolar formulation. II, 26:55447

BERNABEI, S., Observation of a parametric instability near the lower hybrid frequency, 26:54805 (CONF-720705-4)
  Observation of non-linear effects near the lower hybrid resonance frequency, 26:54845 (CONF-720804-3)

BERNHEIM, N. J., Mutational assay system using the thymidine kinase locus in mouse lymphoma cells, 26:53361

BERNNAT, W., Monte Carlo calculations for the critical experiment of the German incore thermionic reactor, 26:55386 (CONF-720901-(Bks.1 and 2), pp 636-44)

BERTI, M., Alterations of sugar beets by γ-irradiation of the seed, 26:53388

BERTINI, H. W., Calculations of spallation-fission competition in the reactions of protons with heavy elements at energies less than or equal to 3 GeV, 26:54666

BERTINI, Hugo W., Nonelastic interactions of nucleons and π mesons with complex nuclei at energies below 3 GeV, 26:54727

BERTOLOTTI, M., Surface and depth distribution damage of ions in silicon as seen with an electron microscope, 26:55003

BERZINA, V., Amperometric and potentiometric determination of copper and molybdenum in ore concentrates and alloys with 5-bromo-8-mercapto- and 8-mercapto-4-methylquinoline, 26:52924

BES, D. R., Importance of the quadrupole pairing field in the J/sup π/ = 0^+ vibrations of shape deformed nuclei, 26:54731

BESSON, Jean, Elementary mechanisms in heterogeneous kinetics. IV, 26:55588 (ORNL-tr-2394)

BETHUNE, G. R., Excitation function for the ^{235}U(α,3n)^{236}Pu reaction, 26:54665

BETTERTON, J. O. Jr., Thermodynamic properties of zirconium--cadmium and certain other solid solutions, 26:53663

BEUZIT, Pierre, Experimental study of excited states of ^{58}Ni, ^{60}Ni, ^{62}Ni, and ^{64}Ni, 26:54587 (FRNC-TH-240)

BEWERSDORFF, A. B., Spatial and temporal variations of the thermal plasma between 3000 and 5700 kilometers at L = 2 to 4, 26:54037

BEYER, W. A., Metrics in biology, an introduction, 26:55546 (LA-4973)

BEZNOGIKH, G. G., Differential cross sections of elastic p-p scattering in energy range of 8 to 70 GeV, 26:54193 (JINR-E1-6613)

  Differential cross sections of elastic p-d scattering in energy range of 10 to 70 GeV, 26:54194 (JINR-E1-6615)

  Investigation of elastic pd-scattering in diffraction cone region in the energy range 10 to 70 GeV, 26:54197

BHANDARI, D. R., Nuclear fuels and fuel processing, 26:52977

BHARGAVA, Ashok Kumar, Baryonic interactions in an effective-Lagrangian model, 26:54333

BHATIA, P. K., Raleigh--Taylor instability in a composite medium, 26:53940

BHATNAGAR, D. P., Sound propagation in ionized gases and electro acoustic effect, 26:54858

BHATNAGAR, V. P., Sound propagation in ionized gases and electro acoustic effect, 26:54858

BHATTACHARYYA, J. C., Velocity oscillations in the solar atmosphere, 26:53946

BHATTACHARYYA, S. K., Pulsed-activation techniques for the measurement of Doppler effects, 26:55124 (CONF-720901-(Bks.1 and 2), pp 1016-32)

BICHARA, M. R. E., Magneto-, sparko-, and thermostrictive phenomena in thin wires, 26:53222

BICK, Y. A. E., Analysis of chromosomal sensitivity of HPK1 cells from the marsupial Potorous tridactylus to x rays and to heliotrine, 26:53359

BIENENGRAEBER, V., Animal experimental examinations on the effect of ionizing radiation on the maxillary bone with metallic bridges, 26:53480

BILEN'KAYA, S. I., e - d scattering and neutron form factors, 26:54169 (JINR-E1-6647)

BILLI, D., Contribution to the sixth-order electron and muon anomalies, 26:54271

BILLINGS, M. P., Effective multiple-constraint shield optimization technique, 26:54942 (CONF-720901-(Bks.1 and 2), pp 574-6)

  Impact of radiation dose on nuclear shuttle configuration, 26:54945 (NASA-TM-X-2440, pp 40-7)

  Methods of space radiation-dose analysis with applications to manned space systems, 26:54951 (NASA-TM-X-2440, pp 108-16)

  Optimal shield mass distribution for space radiation protection, 26:54957 (NASA-TM-X-2440, pp 368-74)

BIMBOT, L., Study of some properties of tin isotopes through high-energy alpha-particle scattering, 26:54616

BINBREK, O. S., Raman spectra of molecular crystals, 26:52968

BINNS, W. R., Observation of VH and VVH cosmic rays with an ionization--Cherenkov detector system, 26:53843

BIRD, M. K., Self-consistent description of the magnetotail current system, 26:54064

BIRKS, John W., Exposure of radiologists during special procedures, 26:53443

BIRMINGHAM, T. J., Resonant diffusion in the presence of strong plasma turbulence, 26:54791

BIRNEY, K. R., Impact of the new LASL delayed neutron data on FTR design, 26:55388 (CONF-720901-(Bks.1 and 2), pp 660-86)

BISHARA, S. W., Microdetermination of metals in organometallic compounds by the oxine method after oxygen flask combustion. I. Cadmium, magnesium, uranium, and zinc, 26:52930

BISHAY, A. F., Factors affecting the reduction of uranium trioxide powders, 26:53548 (AREAEE-139)

BISKAMP, D., Nonlinear electron-cyclotron drift instability, 26:54811

BISWAS, S., Intensity and energy spectra of several x-ray sources in the 20- to 150-keV energy band, 26:53920

  Production of ^{2}H and ^{3}He nuclei in cosmic rays and propagation of protons and helium nuclei through interstellar space, 26:53828

BITTEL, Pollution transfer to man. I, 26:53522

  Pollution transfer to man. II, 26:53521

BITTNER, J. W., Vacuum chamber eddy currents, 26:53781 (BNL-17153)

BLAIR, I. M., Lifetimes of fast recombination luminescence transitions in alkali halides, 26:55000

BLAKE, J. B., Polar-cap measurements of solar-flare protons with energies down to 12.4 keV, 26:54071

BLANCHARD, B., Analysis using secondary ion emission in semiconductors, 26:52937

BLANFORD, G. E. Jr., Comments on the observation of transuranic nuclei in the primary cosmic radiation, 26:53844

BLAYLOCK, B. G., Radiation-induced hemopoietic lesions in fish, 26:53447 (CONF-720822-2)

BLICKENSDERFER, Robert, Strengthening of tungsten by powder metallurgical internal oxidation, 26:53616

BLIMAN, S., Ionization processes in hot plasmas, 26:54778 (CEA-CONF-2047)

BLINOVA, T. L., Low-frequency oscillations in the weakly ionized plasma of a high-frequency discharge in a magnetic field, 26:54849

BLIOKH, P. V., Ion focusing of an electron beam in a transverse gas flow, 26:54086

BLIOKH, Yu. P., Stability of a monochromatic wave against induced scattering, 26:54854

BLOCH, Peter, Dose tables for ^{252}Cf implants, 26:54906

BLOCK, R. C., Iron-filtered neutron beams: a new approach to precision time-of-flight cross section measurements, 26:54597 (CONF-720901-(Bks.1 and 2), pp 1107-14)

  Temperature-dependent transmission and self-indication measurements upon depleted U in the unresolved region, 26:54477 (CONF-720901-(Bks.1 and 2), pp 1115-26)

BLOODWORTH, I. J., Production properties of A_1^+ in π^+p interactions at 5.45 GeV/c, 26:54227

BLOOM, Justin L., Trapping of transuranium elements by the Earth's magnetic field, 26:54047 (NASA-TM-X-2440, pp 548-55)

BLOOR, D., Spectroscopy of rare earth oxide systems. I, 26:55032

BOARDMAN, T. J., HNPF retirement: disposition of sodium, 26:55147 (AI-AEC-Memo-12736)

BOBIN, J. L., Fusion by laser-driven flame propagation in solid DT targets, 26:54830

BOCHIN, V. P., Experiments on search for proton decay from the ground state, 26:54608 (UCRL-Trans-1473)

BOCIAN, Ewa, Biological dosimeters. I, 26:53355

BOCK, Charles W., Damped pseudoscalar- and vector-meson model for nucleon--nucleon scattering, 26:54348

BOCK, Charles Walter, Damped theory of nucleon--nucleon scattering, 26:54350

BOCK-NUSSBAUM, Fr., Possibilities of explosive compaction of powders, especially those of W, with direct procedure, 26:53619

BODE, K. H., Process heat from high temperature reactors, 26:55377

BODENHEIMER, P., Stellar evolution toward the main sequence, 26:53903

BODIN, C., Experimental study of surface resistance anisotropy of Type-II superconductors in vicinity of H/sub c3/, 26:54456

BODRE, Robert J., Safety device for removing tritium gas from a gas stream, 26:53313

BOEGLY, W. J. Jr., Technology and economics of utility tunnels and common trenching, 26:55484 (CONF-720925-3)

BOEHME, A., Time behavior of the continua during the initial stage of Type-IV bursts, 26:53965

BOEHME, R., Experimental results from two Pu-fueled fast critical assemblies, 26:55387 (CONF-720901-(Bks.1 and 2), pp 645-59)

  Measurement of β/sub eff/ in Pu-fueled fast critical assemblies, 26:55389 (CONF-720901-(Bks.1 and 2), pp 700-12)

BOGDANKEVICH, L. S., Excitation of electromagnetic waves in a plasma by a relativistic electron beam. Part I. Longitudinal waves, 26:54837 (AEC-tr-7333)

BOGDANOV, D. D., Experiments on search for proton decay from the ground state, 26:54608 (UCRL-Trans-1473)

BOGDANOV, E. P., Instability of spatially separated plasma beams. III, 26:54822

BOGDANOVA, L. N., Possible study of bound anti pn states in experiments on the annihilation of anti p on d, 26:54334

BOGDANOVICH, P. N., Requirements for steam generator design and systems to ensure safety in the case of failures in the tubes of heat exchange surfaces, 26:55159 (CONF-710548-, pp 206-12)

BOGOLYUBOV, N. N. Jr., Some exactly solvable model problem with positive interaction, 26:54435 (ITF-72-56-E)

BOGOTT, F., Onset of magnetospheric substorms, 26:54060

BOGUS, Wlodzimierz, Radiation sulfoxidation of n-paraffins. I, 26:53012

BOISSIN, J. C., Development of a ultrahigh vacuum evaporation unit using a liquid He cryopump with a high pumping speed, 26:53139

BOK, Bart J., Basic problems on the structure and dynamics of our Galaxy, 26:53982

BOLEU, R., Termination of the r-process and the synthesis of superheavy elements, 26:54663

BOLTZ, D. F., Spectrophotometric determination of molybdenum and phosphorus by carminic acid method, 26:52931

BONCHE, P., Nuclear densities in a model well of arbitrary shape, 26:54704

  Reaction-mechanism study in the 1f--2p shell of (^{16}O,^{12}C) four-nucleon-transfer reaction, 26:54579

BONET-MAURY, Paul, Radiation protection shielding, 26:53136

BONHAM, R. A., Determination of optical sums from the small-angle electron-impact spectra of argon, 26:54128

BONIFORTI, R., Alkaline halides in carrier distillation process in U_3O_8 matrix, 26:53719

  Thermochemical reactions between alkaline halides and oxide impurities in U_3O_8 matrix, 26:52955 (RT/CHI-(72)4)

BONIN, M. A., ESR studies of aliphatic radical anions and radical-anion pairs in γ-irradiated crystalline solids, 26:52991 (ORO-2968-78, Paper 6)

BONKA, H., Layout and fabrication of steel reactor pressure vessels, 26:55224

BONNET, Louis, Effect of γ radiation on the resistance and longevity of two Oniscoideas species, 26:53504

BONSACK, Walter K., Magnetic-field variations in 78

Virginis, beta Coronae Borealis, and 73 Draconis, 26:53876

BOOTH, J. A., Use of liquid lithium as coolant in toroidal fusion reactor. II, 26:54825 (CLM-R-116)

BORER, W. J., Properties of proton-irradiated diamond, 26:54991

BORG, A., π^-p forward elastic scattering near 1 GeV/c, 26:54224

BORISHANSKII, V. M., Experimental study of the interaction of water with sodium during small leaks of water into sodium, 26:55152 (CONF-710548-, pp 39-56)

BOSCHITZ, E. T., Elastic scattering of 60-MeV protons from H, D, ^{3}He, and ^{4}He, 26:54512

BOTOSHAN, N. I., Investigation of densities of the electron states for two-band superconductor with nonmagnetic impurities, 26:54454

BOTTINGA, Y., D/H ratio in Jupiter's atmosphere, 26:54007

BOUCHARD, J., Experimental study of burn-up in fast breeder reactors, 26:55119 (CONF-720901-(Bks.1 and 2), pp 888-904)

BOUCHER, Rene, Safety aspects of sealed ^{238}Pu sources used in pacemakers, 26:53331 (CEA-CONF-2026)

BOUCHERIE, A., Apparatus for spin-rotation measurements in pion--proton scattering at high energies, 26:54232

BOULETTE, E. T., Diffusion theory analyses for fast reactor shield design, 26:55143 (CONF-720901-(Bks.1 and 2), pp 459-70)

BOULLOUD, J. P., Measurement of isotopic ratios of helium, 26:54519

BOULMER, J., Direct measurement of diffusion cooling in an afterglow plasma, 26:54786

BOWEN, J., Heavy ion acceleration at the Berkeley 88-Inch Cyclotron, 26:53755 (LBL-644)

BOWEN, T., Pion--nucleon total cross sections from 0.4 to 0.90 GeV/c, 26:54213

  Search for $^{1}/_{2}$e and $^{2}/_{3}$e charged quarks in the cosmic radiation at 2750-m altitude, 26:54164

  Search for $^{4}/_{3}$e charged diquarks in the cosmic radiation at 2750-m altitude, 26:54177

BOWERS, H. I., ORCOST: a computer code for summary capital cost estimates of steam-electric power plants. User's manual, 26:55265 (ORNL-TM-3743)

BOWERS, Vernon A., ESR study of the pyrolysis of hydrogen on tungsten, 26:55036

BOYER, J., Reactor physics and fast power breeders: MASURCA core R-Z program, 26:55118 (CONF-720901-(Bks.1 and 2), pp 822-38)

BOYKIN, W. R., Rigidity spectrum of Z greater than or equal to 3 nuclei from 5 GeV to over 300 GeV, 26:53834

BOYNTON, G. R., Borehole activation analysis by delayed and capture gamma rays using a ^{252}Cf neutron source, 26:53174

BOZEK, E., ^{38}Ar levels formed in reaction ^{34}S(α,γ)^{38}Ar, 26:54560

BRABSON, B. B., Indiana University Spark Chamber Group technical progress report, December 1, 1971--November 30, 1972, 26:54206 (COO-2009-36)

BRABY, L. A., Microdosimetry of 250 kVp and 65 kVp x rays, ^{60}Co gamma rays, and tritium beta particles, 26:54895

BRACCI, E., Compilation of cross sections. I. π^- and π^+ induced reactions, 26:54201 (CERN/HERA-72-1)

BRACCI, L., Separated high-energy electron beams using synchrotron radiation, 26:53801

BRAENDLI, G., Far infrared surface resistance of Cu:Fe; dynamics of a Kondo system, 26:55508 (COO-3151-4)

BRAIN, Joseph D., Origin of alveolar macrophages in mouse radiation chimeras, 26:53492

BRALEY, R. C., Deformed renormalized Brueckner--Hartree--Fock approximation and its application to ^{12}C, 26:54696 (ORNL-TM-3951)

BRALEY, Richard C., Inelastic scattering calculations with projected Hartree--Fock wave functions. II, 26:54565

BRALY, John E., Radiation problems associated with Skylab, 26:54049 (NASA-TM-X-2440, pp 748-55)

BRANCH, David, Absorption spectra of Type II supernovae, 26:53897

BRANDOLINI, F., g-factor of 3/2$^-$ 153-keV state in ^{49}V, 26:54574

BRANDSTETTER, A., Prototype nuclear power plant SNR 300, 26:55096

BRANDT, E. H., Gap parameter outside core of isolated flux line for T greater than or equal to 0.7 T/sub c/, 26:54446

BRANDT, John C., Solar-wind heating, 26:53942

BRAR, S. S., Distribution of ^{137}Cs in soils and vegetation on the island of Puerto Rico, 26:53162 (ANL-7860(Pt.3), pp 1-13)

BRASSE, F. W., Measurements of inclusive hadron momentum distributions in deep inelastic electroproduction, 26:54178

  π^0 electroproduction at first resonance at momentum transfers q^2 = 0.6, 1.0, and 1.56 GeV^2, 26:54268

  Separation of sigma/sub l/ and sigma/sub t/ at q^2 approximately 1 (GeV/c)^2 in resonance region, 26:54168 (DESY-72/38)

BRASSELL, Gilbert W., Mechanical and thermal expansion properties of a particulate filled polymer, 26:55603 (SC-DR-70-617)

BRAUN, M. A., Relativistic corrections in heavy atoms, 26:54147

BRAUN, R. G., Effect of continuous gamma-ray exposure on performance of learned tasks and effect of subsequent fractionated exposures on blood-forming tissue, 26:53452 (NASA-TM-X-2440, pp 633-40)

BRAY, J. A., Some notes on sodium/water reaction work, 26:55158 (CONF-710548-, pp 187-205)

BREARE, J. M., General properties of the current-limited spark chamber, 26:53283

BREARLEY, N., Prog. rpt., annual, 1971, 26:53741 (NP-19416)

BREBEC, J. M., Preliminary studies on modified version of EBIS source, 26:54081 (FRNC-CONF-57)

BRECHER, K., Extragalactic cosmic rays, 26:53859

BREEN, Edward L., Dosimetry system for measuring instantaneous dose and linear energy transfer spectrum of space radiations, 26:53241

BREGER, Michel, Main-sequence pulsation in open clusters, 26:53872

  Pulsating variables in the Pleiades cluster, 26:53871

BREHM, W. F., Brief outline of radiation and repair engineering program plan, 26:55172 (CONF-710959-, Paper 16)

  Corrosion and deposition of irradiated stainless steel in sodium, 26:55165 (CONF-710959-, Paper 9)

  Radioactive material transport in flowing sodium systems, 26:55164 (CONF-710959-, Paper 8)

BRENNER, D. S., Decay of ^{161}Er to levels in ^{161}Ho, 26:54632 (COO-3255-2)

  Levels in ^{186}Os as populated by the decay of ^{186}Ir, 26:54633 (COO-3255-3)

BRENT, F. de N., Mortality experience of the community and of the fluorspar mining employees, 26:53412

BRESSE, J. F., Applications of the sweeping microscope to semiconductors, 26:55482 (CEA-CONF-2000)

BRESSON, Pollution transfer to man. I, 26:53522

  Pollution transfer to man. II, 26:53521

BRETON, Jean-Paul, Interdiffusion, in region of continuum flow, of binary gaseous mixtures inside inhomogeneous porous media. Application to evaluation of transport coefficients by means of Devaux effect, 26:53120 (CEA-R-4318)

BREUER, H., Steroid glucuronyltransferases, 26:55472 (BMBW-FBK-72-9)

BREUSOV, O. N., Formation of phase Nb/sub x/O$_2$ (0.8 less than or equal to x less than or equal to 1.0) under shock compression of Nb pentoxide, 26:53561

BREWSTER, P., Superconductivity in Mg--Cd system: extrapolated T/sub c/ for pure magnesium, 26:54444

BRICMAN, Claude, Measurement and analysis of the cross section for the reaction K$^-$p → anti K^{0}n at medium energy, 26:54210 (NP-19419)

BRIGGS, J. Z., Arc-cast Mo-base TZM alloy properties and applications, 26:53672

BRINEY, Sharon, Relative biological effectiveness of ^{252}Cf on acute mammalian lethality, 26:53484

BRINK, L., Dual models with SL(2,C) symmetry, 26:54309

BRISSAUD, I., Determination of neutron radii by alpha elastic scattering, 26:54547

  Study of some properties of tin isotopes through high-energy alpha-particle scattering, 26:54616

BRISSON, J. C., Apparatus for spin-rotation measurements in pion--proton scattering at high energies, 26:54232

BRITT, H. C., Excitation function for the ^{235}U(α,3n)^{236}Pu reaction, 26:54665

BRODERICK, A. J., Spectral and pulsed x-ray emission from the Crab Nebula, 26:53919

BROGLIA, R. A., Importance of the quadrupole pairing field in the J/sup π/ = 0$^+$ vibrations of shape deformed nuclei, 26:54731

  Semi-classical description of elastic and inelastic heavy-ion scattering above the Coulomb barrier, 26:54736

BROLLEY, John E., Neutrino--deuteron interaction cross sections at LAMPF energies, 26:54233 (LA-DC-72-848)

BRON, J., Effect of vibrational anharmonicity on hydrogen--deuterium exchange equilibria involving ammonia molecules, 26:52973

BRONFIN, F. B., Electron emission in negative ion and atom collisions in the sudden-switching approximation, 26:54112

BRONK, B. V., Thermally enhanced radiosensitivity of cultured Chinese hamster cells, 26:53358

BRONNIKOV, K. A., Cosmological models of a scalar-tensor theory of gravitation, 26:54396 (ITF-72-41-P)

  Riessner--Nordstroem problem in presence of scalar field, 26:54394 (ITF-72-20-P)

BROOKSBANK, W. A. Jr., Nuclear applications in manned space station, 26:53094 (NASA-TM-X-2440, pp 26-33)

BROSIOUS, P., Correlated recovery kinetics, 26:55005

BROWN, Clark E., Renal tumors in parabiosed irradiated rats, 26:53449 (COO-3017-4)

BROWN, G., ^{57}Fe(t,p)^{59}Fe and ^{58}Fe(d,p)^{59}Fe reactions, 26:54592

BROWN, G. E., Magnetic moments of ^{3}H and ^{3}He in the quark model, 26:54494 (COO-3001-15)

BROWN, G. Raymond, Study of the specific heat of a ^{3}He--^{4}He mixture near its gas-liquid critical point, 26:54426

BROWN, J. K., Analysis of chromosomal sensitivity of HPK1 cells from the marsupial Potorous tridactylus to x rays and to heliotrine, 26:53359

BROWN, James C., Temperature measurement and control in the bomb reduction of plutonium tetrafluoride, 26:53037 (RFP-1455)

BROWN, N. J., Nuclear reactor descriptions for space power systems analysis, 26:54950 (NASA-TM-X-2440, pp 98-102)
BROWN, R. C., Elastic and inelastic scattering of 12 MeV polarized deuterons by ^{24}Mg, 26:54557
BROWN, Roberta S., Description of the American Nuclear Society's Information Center on Nuclear Standards (ICONS) radiation protection standards: Quo Vadis, 26:54917
BROWNE, J. C., Translational absorption of HeH, 26:54134
BRUGGER, R. M., Calculated reactivity of VINS, 26:54469 (ANCR-1071)
BRUGIERE, R., Study of point defect induced in Al by quench hardening and electron bombardment, 26:53712
BRUNFAUT, C., Dosimetry in radiodiagnosis, 26:53416
BRUSA, L., RAS: synthesis program for calculation of 2-group neutron flux in r-theta, 26:54471 (CISE-R-252)
BRUSCHI, C., Analytical solution of two-separable variational synthesis approach for two-group diffusion r,z equations, 26:55422 (CISE-R-243)
  Iterative solution of heterogeneous equations in finite cylindrical system. Method of harmonics, 26:55423 (CISE-R-273)
  MOBIDIC: a code for simplified evaluation of some continuous axial refueling schemes, 26:55196 (CISE-R-241)
  MOICANO-1 code for reactivity and two-group flux calculation of fog-cooled reactor, taking into account true coolant distribution and equilibrium xenon poisoning, 26:55103 (CISE-R-242)
BRUZZI, L., Cleanup system for primary cover gas of LMFBR, 26:55226 (CONF-710959-, Paper 5)
BRYANT, F. J., Analysis of the effects of electron damage on the bound-to-bound emission intensity of cadmium sulphide, 26:55002
BUCCELLA, F., Representation of SU(3) x SU(3) chiral algebra for baryons, 26:54370 (NP-19418)
BUCHACEK, Robert, Kinetics and mechanism of the oxidation--reduction reaction between uranium(IV) and chlorine(III) in the presence of phenol in aqueous acid solution, 26:53051
BUCHACEK, Robert Joseph, Mechanism of inorganic reactions. Part I. The kinetics and mechanism of the oxidation--reduction reaction of uranium(IV)--chlorine(III) in the presence of excess phenol in aqueous acid solution. Part III. The trans effect in the substitution reactions of iodoaquoteratraamminechromium(III), 26:53044
BUCHAN, R. C. T., Exposure rate, 26:54935
BUCHANAN, B., Hardening electronic devices against very-high-total-dose radiation environments, 26:53289 (NASA-TM-X-2440, pp 481-6)
BUDAGOV, Y. A., Investigation of the reactions $\pi^- p \to n\pi^+\pi^- + (1,2,3,4,5)\pi^0$ at GeV/c, 26:54220
BUDINGER, T. F., Human visual response to nuclear-particle exposures, 26:53403 (NASA-TM-X-2440, pp 416-22)
  Observations of cosmic-ray-induced phosphenes on Apollo 14, 26:53407 (NASA-TM-X-2440, pp 1002-6)
BUDKIN, L. V., System of wire spark chambers with ferrite core memory, 26:53271 (JINR-P13-6522)
BUD'KO, N. I., Nonlinear theory of monochromatic circularly polarized vlf and ulf waves in the magnetosphere, 26:54050
BUDNIKOV, V. N., Conditions for wave transformation in a plasma with a nonmonotonic longitudinal distribution, 26:54841 (AEC-tr-7338)
  Ratio of longitudinal and transverse diffusion coefficients in argon SHF discharge plasma, 26:54776 (AEC-tr-7332)
  Study of the localization of the wave transformation region in a superhigh-frequency discharge plasma, 26:54842 (AEC-tr-7339)
BUFFINGTON, A, Measurement of the primary cosmic ray nuclear rigidity spectra for individual elements of charge Z greater than or equal to 2, 26:53826
BUGRII, A. I., Annihilation of anti NN $\to$ 3π in dual models, 26:54320
  DAMA and Regge asymptotic behavior, 26:54412 (ITF-72-63-E)
BUHL, A. R., Verification of a new method for calculating and measuring generation time in a subcritical fast reactor, 26:55437 (CONF-720901-(Bks.1 and 2), pp 713-23)
BULATOV, A. S., Phase transition in samarium, 26:55051
BULINSKII, A. V., Result by R. Kadison and J. Ringrose, 26:54358
BULLOCK, R. E., Interpretation of radiation effects on mechanical properties of carbon fibers based on a sheath and core model of fiber structure, 26:53717
  Thermodynamic and transport properties of frozen and reacting pH_2--oH_2 mixtures, 26:53715 (NASA-TM-X-2440, pp 476-80)
BULLOUGH, R., Theory of the void lattice in molybdenum, 26:55052
BUNKIN, F. V., Possible use of IR lasers for high-temperature heating of superdense plasma, 26:54764
BURAKOV, V. S., Passage of high-power laser radiation through an optically dense plasma, 26:54785
BURBIDGE, G., Extragalactic cosmic rays, 26:53859
BURCH, D., Lifetime of the first excited state in ^{96}Zr, 26:54622
BURDICK, E. E., ETR power: variation analysis, 26:55379 (ANCR-1085)
BUREAU DU COLOMBIER, J., High flux Franco--German reactor, 26:55411
BURGART, C. E., DOMINO: a general purpose discrete ordinates to Monte Carlo coupling code for radiation transport, 26:54872 (CONF-720901-(Bks.1 and 2), pp 499-511)
BURGER, M., Photographs of the Sun in the XUV region, 26:53958
BURGESS, E. L., Room temperature electrical properties and Dopant precipitation for SiGe thermoelectric alloys, 26:55598 (SC-DC-721020)
BURKE, E. A., Solar cell radiation response near the interface of different-atomic-number materials, 26:53290 (NASA-TM-X-2440, pp 577-83)
BURKE, M. J., D-region measurements with the differential-absorption; differential-phase partial-reflection experiments, 26:54032
BURMAN, R. L., Elastic pion--nucleus scattering for studies of the nuclear surface, 26:54722
  Pion beams at LAMPF, 26:53797 (LA-DC-72-881)
BURMAN, Robert L., Low energy pion channel, 26:53786 (LA-4874, pp 48-50)
  Neutrino facility, 26:53794 (LA-4874, pp 84-5)
BURNASHEV, M. A., Inelastic e--H and e--He collisions in adiabatic approximation, 26:54117
BURNETT, S. C., Survey of Scyllac experiments, 26:54828 (LA-DC-72-896)
BURRELL, Martin O., Electron and bremsstrahlung penetration and dose calculation, 26:54886 (NASA-TM-X-2440, pp 801-15)
  Risk of solar proton events to space missions, 26:54955 (NASA-TM-X-2440, pp 310-23)
BURTON, Milton, Advances in radiation chemistry. Volume 3, 26:53021
BUSBY, Nancy, Chromosomal interchange in mature oocytes of Drosophila, 26:53501
BUSCEMI, A., g-factor of 3/2⁻ 153-keV state in ^{49}V, 26:54574
BUSCHMANN, J., Interpolation of germanium thermometer characteristics, 26:55542 (KFK-1601)
BUSCHOW, K. H. J., NMR investigations on Y- and La-diluted GdZn, 26:55059
BUSHONG, Stewart C., Relative biological effectiveness of ^{252}Cf on acute mammalian lethality, 26:53484
BUSSE, H., ^{4}He--^{4}He interaction potential from low energy total cross section measurements, 26:54514
BUTERA, P., Variational Pade solution of Bethe--Salpeter equation, 26:54380
BUTLER, Harold S., Computing facilities, 26:53795 (LA-4874, pp 86-9)
BUTTSEV, V. S., Excited quasi-proton states in magic ^{141}Pr nucleus, 26:54604 (JINR-P6-6519)
BUYAK, A., Differential cross sections of elastic p-p scattering in energy range of 8 to 70 GeV, 26:54193 (JINR-E1-6613)
  Differential cross sections of elastic p-d scattering in energy range of 10 to 70 GeV, 26:54194 (JINR-E1-6615)
  Investigation of elastic pd-scattering in diffraction cone region in the energy range 10 to 70 GeV, 26:54197
BUYKX, W. J., Oxidation of UO_2 fuel pellets during hydrogen sintering, 26:53563
BYCHKOV, V. A., System of wire spark chambers with ferrite core memory, 26:53271 (JINR-P13-6522)
BYKOV, V. M., X-ray study of molybdenum and nickel irradiated with helium ions, 26:53700 (SC-T-722540)
BYKOVSKII, Yu. A., Ion energies in a laser-produced plasma, 26:54802
BYOUN, T. Y., Temperature-dependent transmission and self-indication measurements upon depleted U in the unresolved region, 26:54477 (CONF-720901-(Bks.1 and 2), pp 1115-26)
BYRN, N. R., SNAP-8 post-shutdown gamma-radiation approximations, 26:55360 (NASA-TM-X-2440, pp 84-91)
BYRSKI, Edward, Dosimetric properties of some thermoluminescent substances, 26:53245
BYRSKI, Thaddee, Study of ^{29}P nucleus. Determination of angular momenta and elements of gamma transition matrix, 26:54552 (FRNC-TH-227)
BYSTROV, L. N., Effect of electron radiation on mechanical properties of Fe--Cr and Fe--Mo alloys, 26:53706

C

CABRERA, Nicolas, Model for the repulsive elastic scattering of atoms by solid surfaces, 26:54089
CABY-EYRAUD, M., About the electronic shifts of Stark broadened Lyman-α lines, 26:54796
CACHARD, A., Analysis of thin alumina films obtained by reactive sputtering, 26:52902
CAFFO, M., Contribution to the sixth-order electron and muon anomalies, 26:54271
CAGLIOTI BONANNI, E., JN-METD2: Fortran-IV programme for solving neutron transport problems, 26:54481 (EUR-4839)
CAHN, Robert N., Phenomenology of inclusive reactions, 26:54302 (LBL-1007)
CAILLET, Marcel, Elementary mechanisms in heterogeneous kinetics. IV, 26:55588 (ORNL-tr-2394)
CAILLIBOT, P. F., Computer program to calculate damage distributions in ion-bombarded targets, 26:54969

(AECL-4130)
CAIRNS, John Jr., Coping with heated waste water discharges from steam--electric power plants, 26:53194
CALBERT, Roosevelt, F and K components of the solar corona, 26:53938
CALDER, I. R., Primary electron observations (3 less than or equal to E less than or equal to 15 GeV) recorded on the ESRO II satellite, 26:53821
CALDERA, P. G., Gamma stimulation of maize, 26:53385
CALDWELL, P. K., Pion--nucleon total cross sections from 0.4 to 0.90 GeV/c, 26:54213
CALLENDER, E., Studies of recent sedimentation in Green Bay, 26:53164 (ANL-7860(Pt.3), pp 64-76)
CALOGERO, F., Generalized nonlinear Lee model and infinity suppression due to nonlinearity, 26:54310
CALOI, Vittoria, Extended horizontal branch loci, 26:53891
CAMAHORT, Jose L., Boron nitride coated boron fibers, 26:53572
CAMBI, A., Compact electron spectrometer for in-beam measurements of internal conversion coefficients, 26:53264
CAMM, D. M., Circuit for direct registration of electron densities measured interferometrically, 26:54770
CAMPBELL, A. R., Some neutron and gamma radiation characteristics of plutonium cermet fuel for isotopic power sources, 26:53336 (NASA-TM-X-2440, pp 853-8)
CAMPION, Alan, Hydrogen atom abstraction by methyl radicals in methanol glasses at 67 to 77°K, 26:52990 (ORO-2968-78, Paper 5)
  Pulse radiolysis study of succinonitrile in the rotator phase, 26:53003
CAMPLAN, J., Ion implantation facility at Orsay, 26:54976
CANEPA, Oscar Eduardo Brain, Solution of a nuclear-reactor parameter-identification problem, 26:55099 (AD-738874)
CANTER, K. F., Measurement of total cross sections for low energy positron-helium collisions, 26:54119
CANTRELL, C. D., Effect of spatial coherence on the photoelectric counting statistics of Gaussian light. Technical report No. 13, 26:55506 (COO-3120-2)
CAPO, M. A., Application of transport techniques to the analysis of NERVA shadow shields, 26:55368 (NASA-TM-X-2440, pp 449-59)
CAPPELLI, J. R., Solar cell radiation response near the interface of different-atomic-number materials, 26:53290 (NASA-TM-X-2440, pp 577-83)
CAPPS, Richard H., Exotic fragmenting states in inclusive reactions, 26:54304
  ω--phi mixing and photon interactions from an extension of Odorico's bootstrap, 26:54323
CARBONARA, F., Analysis of reaction $\gamma + n \to p + \pi^-$ in first and second resonance region, 26:54171 (LNF-72/31)
CARBOTTE, J. P., Positron correlation energy in metals, 26:55066
CARE, C. M., One dimensional hydrogen atom with a repulsive core, 26:54093
CAREY, A. G. Jr., ^{65}Zn specific activities from Oregon and Washington (U.S.A.) continental shelf sediments and benthic invertebrate fauna, 26:53149 (RLO-2227-T-12-26)
CARLOS, Pierre, Study of the dipolar giant resonance by measuring photoneutron cross sections, 26:54598 (FRNC-TH-242)
CARLSSON, Carl A., Concepts W and G used in radiation dosimetry, 26:53244
CARMONY, D. D., S-wave structure in the Kπ system, 26:54203 (COO-1428-308)
CARMONY, D. Duane, Proposal for an additional exposure of 9 GeV/c K$^+$ mesons in the 80'' D$_2$ filled chamber, 26:54204 (COO-1428-310)
CARNEIRO, A., Heavy ion acceleration at the Berkeley 88-Inch Cyclotron, 26:53755 (LBL-644)
CAROFF, Lawrence J., Transfer of resonance-line radiation in differentially expanding atmospheres. I. General considerations and Monte Carlo calculations, 26:53878
CARP, A. E., Decomposition of aldrin by gamma radiation. I. In organic solvents, 26:53014
  Decomposition of aldrin by gamma radiation. II, 26:52997
CARPENTER, R. T., Space nuclear power systems, 26:53093 (NASA-TM-X-2440, pp 13-25)
CARPENTER, S. G., Boron and tantalum control rod studies and absolute gamma ray absorbed doses in a LMFBR critical, 26:55134 (CONF-720901-(Bks.1 and 2), pp 579-98)
CARR, T., Study of the pulse radiolysis of gases. Final report, 26:52980 (COO-3461-1)
CARROLL, A. S., Charged particle multiplicity and angular correlation measurements in pp and γp collisions, 26:54192 (BNL-17141)
CARROLL, Paul Joseph, Study of superconductivity in fast frozen (splat-cooled) indium--gallium alloys (including a critical analysis of the ac susceptibility for studying normal properties of metals), 26:54438
CARRON, Jean-Paul, Study by neutron activation analysis of the distribution of Cs in K minerals of granitic Corsican rocks, 26:52908
CARSON, James E., Atmospheric consequences of thermal discharges from power generating stations, 26:53188 (ANL-7860(Pt.3), pp 250-69)
CARSTEN, Arland L., Effects of gamma radiation on the shark brain, 26:53487
CARTER, H. G., Thermodynamic and transport properties of frozen and reacting pH$_2$--oH$_2$ mixtures, 26:53715 (NASA-TM-X-2440, pp 476-80)
CARTER, M. W., Background information for the development of a radiation standard for tritium in nuclear-stimulated natural gas, 26:53134
CARTER, P., Study of cold neutron spectra emerging from sources of liquid H and deuterium and a Monte Carlo method for optimisation, 26:54493
CARTIN, L. R., Analysis of anticipated transients without trip, 26:55193 (BAW-10016)
CARTWRIGHT, B. G., Abundances of the galactic nuclei H through the Fe group from satellite measurements, 26:53836
CARVER, D. W., Real-time analysis of thermal diffusivity data from a pulsed laser facility, 26:55639 (Y-1841)
CASALE, R., Cocuring advanced composite materials, 26:53570
CASALI, F., Measurement of cell parameters in RB-1 reactor, 26:55102 (CISE-R-239)
CASHMORE, R. J., Description for the reactions $a + b \to c + d + e$, 26:54330
CASINI, G., Buckling measurements in ECO with few CIRENE fuel elements, 26:55106 (CISE-R-283)
CASOLO, F., DNA, RNA, and ultrastructural aspects of human epidermis in chronic reactions of skin after roentgen irradiation, 26:53441
CASSE, M., Chemical composition of heavy cosmic ray nuclei above 5 GeV, 26:53840
CASTAGNOLA, A. M., Progress in standardization of analytical methods for materials of nuclear interest. I, 26:52920 (RT/CHI-(72)3)
CASTEN, R. F., Search for (t,p) transitions to excited 0$^+$ states in the actinide region, 26:54671
CASTLEMAN, B. W., Electron spin resonance and electron nuclear double resonance studies of DL-serine. II. Identification of free radicals produced in the range 153 to 340°K, 26:53004
CASTLEMAN, Bruce Wayne, Electron spin resonance and electron nuclear double resonance of single crystals of DL-serine, 26:52996
CATCHPOLE, R. M., Spectroscopic and photometric study of pulsating R Coronae Borealis type variable, RY Sagittarii, 26:53905
CATCHPOLE, S., Outlook for nuclear power generation, 26:55088
CATONI, F., Electron emission from solids by ionic bombardment, 26:52936 (RT/EL-(72)4)
CAZZOLA, P., Stability of nonradial vibrational modes of relativistic neutron stars, 26:53894
CELLI, V., Theory of the roton lifetime in superfluid helium, 26:54429
CERBONE, R. J., Development and verification of design methods for ducts in a space nuclear shield, 26:54958 (NASA-TM-X-2440, pp 375-82)
CERVELLERA, F., g-factor of 3/2- 153-keV state in ^{49}V, 26:54574
CERVINI, John T., Summary of the OV1-19 satellite dose, depth dose, and linear energy transfer spectral measurements, 26:54048 (NASA-TM-X-2440, pp 561-8)
CESENA, Rodolfo A., Prog. rpt. on physics of transient radiation effects, final, 2/68--10/71, 26:54968 (AD-737312)
CHADSEY, W. L., Monte Carlo photocurrent/photomission computer program, 26:54884 (NASA-TM-X-2440, pp 786-91)
CHAKRABORTY, P. P., Ion-chamber device as electronic switch in high radiation field, 26:53224
CHAKRAVORTI, M. C., Fluoro complexes of hexavalent uranium. IV, 26:53043
CHAN, Bun, Computerized dosimetry of ^{60}Co ophthalmic applicators, 26:54900
CHANANA, A. D., Intestinal barrier to bacterial invasion, 26:55474 (BNL-17004)
CHANDRA, A. L., Mutagenic effect of uv- and gamma-rays on antibiotic production of Aspergillus chevalieri, 26:53393
CHANDRA, Harish, Study of even calcium and nickel isotopes with self-consistent approximations, 26:54583
CHANDRASEKHARA, B. C., Effect of heterogeneity and Hall current on the MHD power generator, 26:53105
CHANEY, K. F., Hydrogen in steel, 26:53606 (MLM-1355)
CHANG, Norman C., Effects of temperature and fatty acid structure on lipid metabolism in Bacillus licheniformis 9259, 26:55622 (UCLA-12-879)
CHANG, Y. W., Comparison of a two-dimensional hydrodynamics core (REXCO) to excursion experiments for fast reactor containment, 26:55139 (ANL-7911(Suppl.1))
CHAN KHIEM TKHAM, Spectrophotometric study of the reaction of Nb with Alizarin red, 26:52926
CHAO, Jen-hung, Perturbation of isodose distributions adjacent to cavities in tissue-equivalent media during irradiation by 10 to 35 MeV electrons, 26:54903
CHAPLINE, George F. Jr., Chiral symmetry and structure of the nucleon, 26:54251
CHAPMAN, G. A., Magnetic fields and helium-D$_3$ spectroheliograms, 26:53947
CHAPMAN, G. T., Gamma-ray shielding measurements made at altitudes greater than 115,000 feet using large Ge(Li) detectors, 26:54964 (NASA-TM-X-2440, pp 914-21)
CHAPMAN, Gretchen S., Kinetics of proton transfer to cyanines. a temperature-jump study, 26:52964
CHAPMAN, P. K., Observations of cosmic-ray-induced

phosphenes on Apollo 14, 26:53407 (NASA-TM-X-2440, pp 1002-6)
CHARBUCINSKI, J., Investigations of equivalence between heavy elements concentrations in rock, 26:52943
CHARLES, B. J., Measurements of K^+p elastic differential cross-sections for kaon momenta between 0.9 and 1.9 GeV/c, 26:54211 (RPP/H-95)
CHARLTON, James L., Observation and calculation of a position dependent deuterium effect on the triplet lifetime of anthracene-d_4, 26:52972
CHASE, L. L., Raman scattering in the semiconducting and metallic phases of VO_2, 26:55043
CHASE, L. M., Solar-wind and interplanetary electron measurements on the Apollo 15 subsatellite, 26:54072
CHATOUX, J., High flux Franco--German reactor, 26:55412
CHAUDHARI, P., X-ray topographic determination of the absence of lateral strains in ion-implanted silicon, 26:55019
CHAUMONT, J., Ion implantation facility at Orsay, 26:54976
CHAVARDES, D., Experimental study of burn-up in fast breeder reactors, 26:55119 (CONF-720901-(Bks.1 and 2), pp 888-904)
CHAZALON, M., High flux Franco--German reactor, 26:55415
CHAZELAS, E., Measurements of inclusive hadron momentum distributions in deep inelastic electroproduction, 26:54178
π^0 electroproduction at first resonance at momentum transfers q^2 = 0.6, 1.0, and 1.56 GeV^2, 26:54268
Separation of sigma/sub l/ and sigma/sub t/ at q^2 approximately 1 $(GeV/c)^2$ in resonance region, 26:54168 (DESY-72/38)
CHEEVER, Paul R., Radiation hardening of components and systems for nuclear rocket vehicle applications, 26:55370 (NASA-TM-X-2440, pp 471-5)
CHEIFETZ, E., Emission of the ^5He in the spontaneous fission of ^{252}Cf, 26:54674
CHELNOKOV, V. B., Measurements of neutron cross sections of radiation capture and fission for some heavy nuclei by the method of time of retardation in lead, 26:54657 (FEI-292)
CHEN, Chuan-Run, Phosphorescence-microwave double resonance spectroscopy of 1,2,4,5 tetrachlorobenzene. Annual report, September 15, 1971--September 14, 1972, Part 1, 26:55623 (UCLA-34-P-91-48)
CHEN, L. I., Carrier transport and storage effects in Au ion implanted SiO_2 structures, 26:53314
CHEN, Michael G., Incidence of delayed mortality (secondary disease) in allogeneic radiation chimeras receiving bone marrow from aged mice, 26:53485
CHERNOBROVIN, V. I., Measurement of plasma parameters in strong hf discharge, 26:54768 (AEC-tr-7329)
CHERVYAKOVA, V. V., Effect of chromium and zirconium on the ductility of copper, 26:53669
CHESHIRE, D. L., Evidence for a neutral meson near 1033 MeV, 26:54205 (COO-1428-311)
CHEUNG, L. M., Implementing the SAAP formalism. I. Serber-type spin eigenfunctions by direct diagonalization, 26:54155
CHEVALLIER, A., ^{38}Ar levels formed in reaction $^{34}S(\alpha,\gamma)^{38}Ar$, 26:54560
CHEVALLIER, J., ^{38}Ar levels formed in reaction $^{34}S(\alpha,\gamma)^{38}Ar$, 26:54560
CHEVALLIER, M., $(d,^6Li)$ reactions with light nuclei at 28 MeV, 26:54527 (LYCEN-7219)
CHIANG, I-h., K^+ decay in flight, 26:54186
CHIAO, T. T., Characterization of an epoxy system for filament winding, 26:55628 (UCRL-73773)
Fiber strength of S-glass/epoxy composites under biaxial loading, 26:55627 (UCRL-73772)
CHIBA, M., Nuclear reactions of Ni with protons up to 56 MeV, 26:54591
CHIKALLA, T. D., Polymorphic modifications of Pm_2O_3, 26:53596
CHILDS, Charles B., Heavy-ion passive dosimetry with silver halide single crystals, 26:53230 (NASA-TM-X-2440, pp 138-41)
CHILENSKAS, A. A., Conceptual design for the handling and remote disassembly of the fuel element failure propagation loop at the HFEF, 26:53727 (ANL/HFEF-1)
CHING, J., Mechanism of fast neutron transport in iron, 26:54473 (CONF-720901-(Bks.1 and 2), pp 335-48)
CHIRIBOGA, Jorge, Fasciola hepatica program in Puerto Rico. Progress summary report, December 1971, 26:53498 (PRNC-156)
CHISHOLM, C. D. H., Two perturbations in the presence of degeneracy, 26:54152
CHISTOV, E. D., Evaluation of exposure doses to personnel at high-power beta radiation installations, 26:53426
CHITNIS, E. V., Time variation of x-ray spectrum and optical luminosity of Sco X-1, 26:53917
CHIU, Hong-yee, Galactic astronomy. Volume 1. Proceedings of the summer Institute for Astronomy and Astrophysics, held at Stony Brook, New York, Summer 1968, 26:53981
CHO, You Joung, Effect of cortisone on serum protein of gamma-irradiated mice, 26:53490
CHODOS, Steven L., Lattice dynamics of M_2XY_6 hexabromometallates: Cs_2UBr_6, 26:53046
CHODURA, R., Nonlinear electron-cyclotron drift instability, 26:54811
CHOI, K. A., Study of the charge spectrum of cosmic-ray nuclei, 26:53839
CHOI, Kook Hun, Effect of cortisone on serum protein of gamma-irradiated mice, 26:53490
CHOW, W. S., Thermal conductivity in dirty transition-metal superconductors near the upper critical field, 26:54451
CHOWDARI, B. V. R., Interstitial halogen centers in x-irradiated CsBr, 26:54980
CHRIEN, R. E., Radiative decay of neutron--resonant states, 26:54675 (BNL-17029)
CHRISMAN, B. L., Moessbauer transmission and scattering for arbitrary polarizations, 26:54703
CHRISTENSEN, Clark G., Synthesis of composite spectra: a study of four globular clusters of the Galaxy, five globular clusters of M31, and the nucleus of NGC 205, 26:53880
CHRISTOFILOS, Nicholas C., Polygonal Astron reactor for producing controlled fusion reactions, 26:54835
CHRISTOPHER, A. J., Technique for the qualitative spectrographic analysis of very small samples, 26:52929
CHRISTY, A., Measurement of lifetimes in ^{152}Sm, ^{154}Gd, and ^{156}Gd, 26:54642
CHU, T. K., Measurement of effective collision frequency in rf heating through parametric instabilities, 26:54750 (CONF-720705-2)
Parametric instability and its induced heating, 26:54751 (CONF-720705-3)
CHU, Y. Y., Decay of ^{162}Yb, 26:54639
CHUN, Sea Yull, Determination by neutron analysis of mercury residues in foodstuffs, 26:52911
Determination of Br, As, Hg, and Se in plants by neutron activation analysis, 26:52907
CHUNG, Sunggi, Study of electron excitation cross sections of the helium atom and nitrogen molecule, 26:54108
CHUNG, Y. J., ESR studies of aliphatic radical anions and radical-anion pairs in γ-irradiated crystalline solids, 26:52991 (ORO-2968-78, Paper 6)
CHUTOV, Yu. I., Generation of blast waves in a plasma by a pulsed electric discharge, 26:54856
CIANCIA, A., Alkaline halides in carrier distillation process in U_3O_8 matrix, 26:53719
Thermochemical reactions between alkaline halides and oxide impurities in U_3O_8 matrix, 26:52955 (RT/CHI-(72)4)
CICOGNANI, G., Cleanup system for primary cover gas of LMFBR, 26:55226 (CONF-710959-, Paper 5)
CIOFI DEGLI ATTI, C., Investigation of short-range correlations in nuclei by means of high energy electron scattering, 26:54687 (ISS-71/29)
CIUFFOLOTTI, L., Experimental investigations on U--D_2O lattices, 26:55101 (CISE-R-203)
Measurement of cell parameters in RB-1 reactor, 26:55102 (CISE-R-239)
CLADIS, John B., Artificial perturbations of the radiation belts, 26:54044 (NASA-TM-X-2440, pp 178-92)
CLANCY, B. E., Multigroup neutron transport theory in plane geometry, 26:55440 (INIS-mf-195)
CLANET, F., Determination of urinary plutonium by radiochemical analysis on ion exchanger filters, 26:52940
CLARE, L. P., Properties of 1300 kg P/M TZM billet, 26:53673
CLARK, Alan R., Neutrino mass limits from the K/sub L/^{0} $\to$ $\pi^{+-}l^{-+}\nu$ decay spectra, 26:54184 (LBL-4)
CLARK, Benton C., Advanced-dosimetry systems for the space transport and space station, 26:53235 (NASA-TM-X-2440, pp 944-56)
CLARK, D. J., Cyclotron injection systems, 26:53756 (LBL-654)
Heavy ion acceleration at the Berkeley 88-Inch Cyclotron, 26:53755 (LBL-644)
CLARK, G. W., Flux of galactic high-energy gamma rays, 26:53819
CLARK, M. R., Preliminary shield design for a SNAP-8 power system, 26:54948 (NASA-TM-X-2440, pp 78-83)
CLARKE, N. M., Energy dependence of the ^3He optical potential, 26:54580
Optical-model analysis of elastic scattering of 53.4 MeV helions from ^{56}Fe, 26:54571
CLARKE, R. W., Zero energy reactor facility at B.N.L., 1972, 26:55409 (RD/B/N-2272)
CLARK III, Benton Clyde, Investigation into the radiobiological consequences of K-shell ionizations of phosphorous atoms using soft x rays, 26:53376
CLARKSON, Jack E., Semimicro gel permeation chromatographic analysis of HMX-containing explosives, 26:55625 (UCRL-73334)
CLAUS, D., Pediatric radiology and irradiation, 26:53417
CLAUSSEN, N., Growth and hardness of spherical agglomerates from powders of high melting point materials, 26:53577
CLAYTON, Roderick K., Measuring the delayed fluorescence of chlorophyll in vivo, 26:55517 (COO-3162-12)
CLEGG, T. B., Four-nucleon studies. III, 26:54517
Four-nucleon studies. IV, 26:54518
CLEGHORN, T. F., Charge and energy spectra of heavy cosmic ray nuclei, 26:53842
CLEMENT, T. M., Development and implementation of equipment maintenance standards for nuclear reactors, 26:55201 (DUN-SA-168)
CLIFFORD, C. E., ORNL sodium benchmark experiment, 26:55142 (CONF-720901-(Bks.1 and 2), pp 418-30)

CLIFFT, R. W., High intensity muon beam design for CERN II, 26:53783 (DNPL/P-131)
CLINE, J. E., Gamma rays emitted by the fissionable nuclides and associated isotopes, 26:54652 (ANCR-1069)
CLIVE, D., Mutational assay system using the thymidine kinase locus in mouse lymphoma cells, 26:53361
CLOSE, D. A., Spectroscopy of ^{101}Mo by sub-Coulomb stripping, 26:54614
COATES, R., Tunnel assisted hopping in neutron irradiated gallium arsenide, 26:54982
COCHRAN, Edward L., ESR study of the pyrolysis of hydrogen on tungsten, 26:55036
CODDING, J. W., Automated Cross Section Analysis Program (ACSAP), 26:54468 (ANCR-1042)
COHAN, P. C., Radiation-induced hemopoietic lesions in fish, 26:53447 (CONF-720822-2)
COHEN, Jerry J., Why benefit--risk analysis, 26:54929
COHEN, Joseph D., Light-water breeder reactor, 26:55130
COHEN, Jules, Reduced red cell 2,3-diphosphoglycerate and adenosine triphosphate, hypophosphatemia and increased hemoglobin--oxygen affinity after cardiac surgery, 26:55638 (UR-3490-187)
COHEN, K., Annihilation spectrometer for investigation of heavy meson spectra, 26:53279
COHN, Arthur, Photoionization of excited H_2 molecules, 26:54091
COHN, C. E., Improved computer method for polarity cross correlation, 26:55448
COHN, Daniel R., Magnetic-field-enhanced heating of plasmas with CO_2 lasers, 26:54760
COHN, Stanton H., Calcium homeostasis: the hard facts about soft bones, 26:55477 (BNL-50345)
COKER, W. R., Consistent coupled-channel Born approximation analysis of ^{88}Sr(d,np) ^{88}Sr and ^{88}Sr(d,p)^{89}Sr, 26:54588
COLE, Keith D., Some cosmic effects of the finite rest-mass of the wave quantum, 26:53866
COLEMAN, P. G., Measurement of total cross sections for low energy positron-helium collisions, 26:54119
COLES, W. A., Analysis of three-station interplanetary scintillation, 26:54070
COLLE, R., K-shell ionization cross sections for 2.04-MeV electrons, 26:54104
COLLINS, A. T., Temperature dependence of vibronic spectra in irradiated silicon, 26:54999
COLLINS, C. H., Half-life of /sup 80g/Br, 26:54595
COLLINS, K. E., Half-life of /sup 80g/Br, 26:54595
COLLINS, P. J., Sodium void studies and related heterogeneity effects in ZPPR-2, the Benchmark Demonstration Assembly, 26:55392 (CONF-720901-(Bks.1 and 2), pp 973-85)
COLOMBANT, D., Fusion by laser-driven flame propagation in solid DT targets, 26:54830
COLON, J. A., Distribution of ^{137}Cs in soils and vegetation on the island of Puerto Rico, 26:53162 (ANL-7860(Pt.3), pp 1-13)
COLWELL, Joseph F., Prog. rpt. on physics of transient radiation effects, final, 2/68--10/71, 26:54968 (AD-737312)
COMBET, M., Radiological risks relative to the distribution of contaminated gas, 26:53132 (UCRL-Trans-10617-2)
COMLAN, Guy, Ultrastructure changes in the adenohypophysis of rodents after total or segmentary irradiation with radiocobalt, 26:53467
COMMINS, A. D., Fiber strength of S-glass/epoxy composites under biaxial loading, 26:55627 (UCRL-73772)
CONANT, Donald R., Derivation of the Boltzmann distribution law with illustrations from a hard-sphere model computer program, 26:55071 (LA-4868)
CONN, Robert, Green's function coupling method for time-dependent neutron slowing down in heavy media, 26:55428 (CONF-720901-(Bks.1 and 2), pp 179-94)
CONNOLLY, J. F., Compact EHT power supply for use with high pulse rate spark chambers, 26:53275 (RPP/H-101)
CONNOLLY, T. J., Risks of benefit--risk analysis, 26:54932
CONRADS, R. J., Time-of-flight analysis of neutral products from inelastic ion--molecule collisions, 26:54109
CONTE, Mario, Proton beam extraction from the 10-GeV Dubna synchrophasotron by exciting the resonance Q/sub R/ = $^2/_3$, 26:53754 (JINR-E9-6538)
COOK, D. C., Problem H01-32 Airborne Radiac, 26:53195 (AD-737993)
COOKE, D. J., Components of the sidereal anisotropy, 26:53848
COOPER, A. R., Diffusion in the system K_2O--SrO--SiO_2. IV. Mobility model, electrostatic effects, and multicomponent diffusion, 26:53598
COOPER, W. Grant, Integral-equation approach to bound-state atomic systems: preliminary studies of helium and hydrogen, 26:54145
COPELAND, Mark I., Strengthening of tungsten by powder metallurgical internal oxidation, 26:53616
COPPI, B., Resonant scattering of trapped particles by toroidal plasma modes, 26:54792
CORBERI, A., Measurement of cell parameters in RB-1 reactor, 26:55102 (CISE-R-239)
CORBETT, J. W., New EPR spectra in neutron-irradiated silicon, 26:55006
CORDARO, Matthew C., Application of the phase--space--time evolution method to electron shielding, 26:54887 (NASA-TM-X-2440, pp 821-31)
CORDS, D., S-wave structure in the $K\pi$ system, 26:54203 (COO-1428-308)
CORLEY, John P., Radiation protection standards: quo vadis. Volume I. Proceedings of the sixth annual health physics society topical symposium, Richland, Washington, November 2--5, 1971, 26:54914
  Radiation protection standards: quo vadis. Volume II. Proceedings of the sixth annual health physics society topical symposium, Richland, Washington, November 2--5, 1971, 26:54922
COSANDEY, M., Ionic chemistry of gaseous cC_6H_{12}, 26:52982 (EUR-4765, pp 11-24)
COSGROVE, G. E., Radiation-induced hemopoietic lesions in fish, 26:53447 (CONF-720822-2)
COTTIER, H., Intestinal barrier to bacterial invasion, 26:55474 (BNL-17004)
COTTINGHAM, J. G., Magnet fault protection: Isabelle, 26:53765 (BNL-16816)
COTTRELL, Wm. B., ORNL nuclear safety research and development program bimonthly report for May--June 1972, 26:55207 (ORNL-TM-3900)
COUCH, D. E., Separation of columbium, tantalum, titanium, and zirconium from titanium chlorination residues, 26:52947 (BM-RI-7671)
COULON, Pollution transfer to man. I, 26:53522
  Pollution transfer to man. II, 26:53521
COURANT, E. D., Luminosity considerations for colliding electron and proton beams, 26:53777 (BNL-17067)
COURTNEY, J. C., Radiation heating in selected NERVA engine components, 26:55369 (NASA-TM-X-2440, pp 460-5)
COURTNEY, W. J., Configuration mixing in ^{90}Zr and lifetime of excited 0^+ states, 26:54610
COUTANT, C. C., Thermal effects on aquatic organisms: annotated bibliography of 1971 literature, 26:53190 (ORNL-EIS-72-28)
COUTSOURADIS, D., Stability and heat corrosion of Al covering on alloy Inco 713 C and on alloys of Co, 26:53676
  Structure and properties of dispersion strengthened cobalt alloys, 26:53675
COVAN, J. M., Spectroscopic factors from reactions ^{12}C(d,n)^{13}N and ^{12}C(d,p)^{13}C using WBP model, 26:54543
COVINGTON, Arthur E., Observations and comments for the solar event of October 24, 1969, 26:53959
COWAN, I. M., Measurements of K^+p elastic differential cross-sections for kaon momenta between 0.9 and 1.9 GeV/c, 26:54211 (RPP/H-95)
COWSIK, R., Comment on inverse Compton models for the isotropic x-ray background, 26:54000
  Cosmic ray electrons and the gamma-ray background, 26:53855
  Dynamical models of the Galaxy and its gamma ray emission, 26:53992
  Particle acceleration by white dwarfs and the charge spectrum of the nuclear component of cosmic rays, 26:53854
COX, A. J., Search for $^1/_2$e and $^2/_3$e charged quarks in the cosmic radiation at 2750-m altitude, 26:54164
  Search for $^4/_3$e charged diquarks in the cosmic radiation at 2750-m altitude, 26:54177
COX, C. R., Pionic proton stripping and π^- production, 26:54535
COYNE, T. N. R., D-region measurements with the differential-absorption; differential-phase partial-reflection experiments, 26:54032
CRAWFORD, C. K., Potential measurement and stabilization of an isolated target using electron beams, 26:53315
CRAWFORD, J. C., Thick target yield calculations for strong neutron-producing reactions in the energy range 30 keV to 1.5 MeV, 26:54502 (SC-RR-720513)
CRENNELL, David J., Two-body strange-particle final states in π^-p interactions at 4.5 and 6 GeV/c, 26:54217
CRICCHIO, A., Application and automation of mass spectrometry in the analysis of irradiated nuclear fuels, 26:52917 (EUR-4765, pp 77-89)
CRITES, Thomas R., Experimentally measured dose albedos of intermediate energy bremsstrahlung, 26:54892
CRITTENDEN, R. R., Indiana University Spark Chamber Group technical progress report, December 1, 1971--November 30, 1972, 26:54206 (COO-2009-36)
CROSBY, E. H., Comparison of film badges and thermoluminescent dosimeters, 26:53239
CROWDER, B. L., X-ray topographic determination of the absence of lateral strains in ion-implanted silicon, 26:55019
CROWTHER, R. L., Physics of BWR's, 26:55112 (CONF-720901-(Bks.1 and 2), pp 114-40)
CROZON, M., π^-p forward elastic scattering near 1 GeV/c, 26:54224
CRUME, E. C. Jr., Reliability of criticality safety calculations using the new codes CSC and KENO, 26:55445 (Y-KC-96)
CRYER, M. A., Radiobiology forum on radiological protection and the skin, 26:53431
CUEVAS-RUIZ, Jose, Quality improvement in plantains by selection, 26:55483 (CONF-720642-1)
CUKIER, Michel, Experimental and theoretical study of gas amplification in a low pressure cylindrical proportional counter, 26:53198 (FRNC-TH-189)
CULLEN, Dermott E., Program IRT, 26:55476 (BNL-17115)
CUMBY, R. P., Gamma-ray shielding measurements made at altitudes greater than 115,000 feet using large Ge(Li)

detectors, 26:54964 (NASA-TM-X-2440, pp 914-21)
CUMO, Maurizio, Photographic study of two-phase highly dispersed flows, 26:53122
CUNSOLO, A., Reaction-mechanism study in the 1f--2p shell of $(^{16}O,^{12}C)$ four-nucleon-transfer reaction, 26:54579
CURL, Herbert C. Jr., Action spectrum for photoinhibition of mechanically stimulable bioluminescence in the marine dinoflagellates gonyaulax catenella, G. acteneila, and G. tamarensis, 26:55521 (COO-3277-14)
CURTIS, M. L., New techniques for relative calibration of tritium sources by bremsstrahlung counting, 26:52934 (MLM-1368)
CURTIS, S. B., Galactic cosmic-ray heavy primary secondary doses, 26:54878 (NASA-TM-X-2440, pp 104-7)
Heavy-particle hazard: what physical data are needed, 26:53408 (NASA-TM-X-2440, pp 1007-15)
CURZON, F. L., Circuit for direct registration of electron densities measured interferometrically, 26:54770
CUSSON, R. Y., Light nuclei systematics in the unrestricted Hartree--Fock approximation, 26:54745
CUTSHALL, N., ^{65}Zn specific activities from Oregon and Washington (U.S.A.) continental shelf sediments and benthic invertebrate fauna, 26:53149 (RLO-2227-T-12-26)
CUTSHALL, N. H., Effects of ocean water on the soluble-suspended distribution of Columbia River radionuclides, 26:53166 (RLO-2227-T-12-28)
CZUBEK, Jan Andrzej, Differential interpretation of gamma-ray logs. II, 26:53173 (INP-793)

D

DAENNER, W., Lithium and flibe as coolants for fusion reactor blankets, 26:54827 (IPP-4/97)
DAEUNERT, U., Project SNR: governmental support and international cooperation, 26:55098
DAFTARI, I. K., Velocity distribution of secondary π mesons from 22.6-GeV/c proton--nucleus interactions in emulsion, 26:54196
DAGBJARTSSON, S., Monte Carlo calculations for the critical experiment of the German incore thermionic reactor, 26:55386 (CONF-720901-(Bks.1 and 2), pp 636-44)
DAHLBERG, Richard C., Physics of gas cooled reactors, 26:55108 (CONF-720901-(Bks.1 and 2), pp 23-32)
DAHLGREN, S., Helium-recoil spectrometer, 26:53281
DAKIN, H. S., High reliability environmental radiation monitoring and evaluating system, 26:53199 (LBL-585)
DAKOVSKII, M., Average prompt neutron number for spontaneous fission of ^{256}Fm, 26:54659 (JINR-P15-6518)
DALENS, Henri, Effect of γ radiation on the resistance and longevity of two Oniscoideas species, 26:53504
DALGLIESH, S. M., $^{57}Fe(t,p)^{59}Fe$ and $^{58}Fe(d,p)^{59}Fe$ reactions, 26:54592
DALITZ, R. H., Shell-model analysis of Λ binding energies for the p-shell hypernuclei. II. Numerical fitting, interpretation, and hypernuclear predictions, 26:54351
DAL'KAROV, O. D., Possible study of bound anti pn states in experiments on the annihilation of anti p on d, 26:54334
DALL'OLIO, G., Alterations of sugar beets by γ-irradiation of the seed, 26:53388
DALTABUIT, E., Angular distribution of interstellar atomic hydrogen, 26:53979
DAMLE, S. V., Chemical composition of cosmic rays with Z = 3 to 30 at high and low energies, 26:53838
Cosmic flux of low energy gamma rays, 26:53818
DANELYAN, L. S., Correlation of the partial radiation widths in the reaction $^{163}Dy(n,\gamma)^{164}Dy$, 26:54631 (BNL-tr-490)
DANERI, A., TRUD: an anisotropic diffusion code for xy geometry, 26:54488 (RT/FI-(72)1)
D'ANGELO, S., High energy measurements of total cross sections on proton, detecting very low energy neutrons, 26:54163 (NP-19421)
DANIEL, R. R., Cosmic flux of low energy gamma rays, 26:53818
DANIEL, S. L., Significant digit incomplete gamma ratios, 26:55604 (SC-DR-720303)
DANNO, Akibumi, Operation report on low temperature fissiochemical loop (JTFL). I, 26:55400 (JAERI-M-4630)
DARDEN, E. B., Relative biological effectiveness of fast neutrons compared with x rays: prenatal mortality in the mouse, 26:53453 (NASA-TM-X-2440, pp 641)
DARDENNE, J. C., Dosimetry in interstitial therapy using ^{192}Ir wires, 26:53422
DARROUZET, M., Experimental study of burn-up in fast breeder reactors, 26:55119 (CONF-720901-(Bks.1 and 2), pp 888-904)
DARVES-BLANC, R., Polarization and cross section of p + ^{3}H elastic scattering, 26:54521
DAS, Arati, Specific effects of mutagens on Aspergillus niger producing citric acid, 26:53380
DAS, G., Experiments in high-voltage electron microscopy. Progress report, October 31, 1972--July 31, 1973, 26:54972 (COO-2119-2)
DAVENPORT, C. M., Real-time analysis of thermal diffusivity data from a pulsed laser facility, 26:55639 (Y-1841)
DAVEY, W. G., Demonstration Reactor Benchmark Program, 26:55116 (CONF-720901-(Bks.1 and 2), pp 789-808)
Sodium void studies and related heterogeneity effects in ZPPR-2, the Benchmark Demonstration Assembly, 26:55392 (CONF-720901-(Bks.1 and 2), pp 973-85)
Spatially dependent benchmark parameters in the initial demonstration plant critical assembly, 26:55117 (CONF-720901-(Bks.1 and 2), pp 809-21)
DAVIDENKO, G. V., Measuring of branching ratio GAMMA(K/sub L/ $\to 3\pi^0$)/GAMMA(K/sub L/ $\to \pi^+\pi^-\pi^0$), 26:54187
Search for a neutral vector meson in K/sub L/-decays, 26:54291
DAVIDSON, D., Pion--nucleon total cross sections from 0.4 to 0.90 GeV/c, 26:54213
DAVIDSON, Ernest R., Properties and uses of natural orbitals, 26:54150
DAVIDSON, M. J., Effect of cryogenic irradiation on NERVA structural alloys, 26:53697 (NASA-TM-X-2440, pp 603-8)
DAVIDSON, S. M., Nature of rod-like defects observed in boron irradiated silicon, 26:54995
DAVIES, G., Temperature dependence of vibronic spectra in irradiated silicon, 26:54999
DAVIES, R. A., Behavior of radioactive impurities in DFR primary liquid metal coolant, 26:55167 (CONF-710959-, Paper 11)
Behaviour of fission and corrosion products in sodium, 26:52895 (CONF-710959-, Paper 18)
DAVIN, A., Stability and heat corrosion of Al covering on alloy Inco 713 C and on alloys of Co, 26:53676
DAVIS, A. K., Evaluation of epidemiologic studies of leukemia and other malignancies after diagnostic x radiation, 26:53435
DAVIS, H. S., Nuclear radiation environment analysis for thermoelectric outer planet spacecraft, 26:53338 (NASA-TM-X-2440, pp 862-5)
DAVIS, J. C., Nucleon--nucleon scattering lengths from incomplete nucleon--deuteron breakup experiments, 26:54503 (UCRL-74069)
DAVIS, R. J., Effect of extended exposure to simulated LMFBR fuel reprocessing off-gas on radioiodine trapping performance of sorbents, 26:53077 (CONF-720823-9)
Long-term effects on radioiodine trapping by charcoal, 26:53058 (CONF-720823-10)
DAVYDOV, A. S., Features of optical spectra, caused by surface of a crystal, 26:55537 (ITF-72-40-P)
DAVYDOV, A. V., Coulomb excitation of nuclei by heavy polarized particles, 26:54630
DEAGUE, T. K., Photoneutron cross sections of ^{139}La and ^{141}Pr, 26:54629
DEAN, Frederick K., Relative biological effectiveness of ^{252}Cf on acute mammalian lethality, 26:53484
DEAN, J. R., Spectroscopy of rare earth oxide systems. I, 26:55032
DEBERGH, Philippe, Installation for observing the position of a structure inside a nuclear reactor, 26:55128
DE BIEVRE, P., High accuracy isotope analysis of the elements, 26:52916 (EUR-4765, pp 41-75)
DEBOLT, H. E., Chemical vapor deposition of boron on a carbon monofilament substrate, 26:53571
DECARREAU, Alain, Determination of vanadium in silicate materials by neutron activation, 26:52909
DECKER, W., Interpolation of germanium thermometer characteristics, 26:55542 (KFK-1601)
DEDEK, U., Recovery of electron-irradiated Pt. I, 26:55010
DE FREMONT, R., Decontamination experience on rapsodie, 26:55163 (CONF-710959-, Paper 3)
Observations on the behavior of radioactive products on rapsodie, 26:55162 (CONF-710959-, Paper 2)
Tempete test: in pile experiment on the transer of fission gases, 26:55185 (CONF-710959-, Paper 1)
DEGASPERIS, A., Generalized nonlinear Lee model and infinity suppression due to nonlinearity, 26:54310
DE GIORGI, G., Experimental measurement of neutron groups from phonons in zinc at various temperatures, 26:54487 (RT/FI-(71)37)
DE GOER, A. M., Phonon scattering by V ions in Al_2O_3, 26:54978
DE GROOT, E. H., Uncorrelated jet model predictions for the multiplicity distribution of π^- mesons produced in high energy annihilations anti pp $\to$ pions, 26:54316 (RPP/T-24)
DEGTYARENKO, N. N., Ion energies in a laser-produced plasma, 26:54802
DEGTYAREV, V. G., Ion energies in a laser-produced plasma, 26:54802
DE LA BASTIE, J., Study of diffusion welding of molybdenum, 26:53625
DE LA MAZA, Luis M., Immunochemical studies with the carcinoembryonic antigen, 26:55505 (COO-3012-21)
DE LANGE, Owen Leon, Entropy of vortices in superconductors, 26:54441
DE LA PAZ, A., Space radiation studies at the White Sands Missile Range Fast Burst Reactor, 26:55406 (NASA-TM-X-2440, pp 618-19)
DE LEON, Delfin, Fasciola hepatica program in Puerto Rico. Progress summary report, December 1971, 26:53498 (PRNC-156)
DELL, G. F. Jr., Transition counter, 26:53277
DE LOPEZ, Ofelia H., Direct determination of total ionic fluoride in biological fluids, 26:55637 (UR-3490-184)
DELORENZO, J. T., Neutron spectral measurements in the upper atmosphere, 26:54066 (NASA-TM-X-2440, pp 922-5)
DELORME, Jean, Elementary particle treatment of nuclear

currents, 26:54238 (LYCEN-7211)
DELSANTO, P. P., Continuum shell model calculation for the ^{15}N giant dipole resonance, 26:54545
DELUCA, H. F., Mechanisms of calcium transport in small intestine. Overall review of the contract, January 1, 1970--September 1, 1972, 26:55498 (COO-1668-46)
DELVAL, G., Recent development in CVD W and Mo, 26:53622
DEMARQUE, P., Effects of semiconvection on the horizontal-branch, 26:53885
DEMASTRY, J. A., Irradiation effects studies of NERVA materials, 26:53696 (NASA-TM-X-2440, pp 595-602)
DEMCHENKO, G. P., Applications of the statistical mechanics methods in a dual model, 26:54299 (ITF-72-49-P)
  Two-particle distributions in dual resonance model, 26:54301 (ITF-72-55-P)
DEMCHENKO, V. V., Effect of high-frequency potential on propagation of fast waves along a magnetoactive plasma layer, 26:54839 (AEC-tr-7336)
  Nonlinear stabilization of beam instability, 26:54821
  On the theory of transformation of surface waves into longitudinal oscillations in the surface layer of a plasma wave-guide, 26:54838 (AEC-tr-7335)
  Penetration of travelling high-frequence electromagnetic field into a ''non-transparent'' plasma, 26:54843 (AREAEE-124)
  Semiclassical theory of electromagnetic field interaction with a many-level molecular system, 26:55468 (AREAEE-136)
  Theory of parametric excitation of oscillations in an inhomogeneous plasma, 26:54844 (AREAEE-125)
DEMIDOV, A. M., Correlation of the partial radiation widths in the reaction ^{163}Dy(n,γ)^{164}Dy, 26:54631 (BNL-tr-490)
DEMIDOV, V. S., Search for a neutral vector meson in K/sub L/-decays, 26:54291
DEMKINA, L. B., Interpretation of π-component splitting in sunspot spectra, 26:53951
DE MONTARDY, A., Study and tests of small components of secondary circuits of fast Na cooled reactors, 26:55182
DEMURA, A. V., Determination of the magnetic fields in a plasma on basis of the hydrogen spectral line contours, 26:54772
DE MURI, R. J., Transit Time Flowmeter: six-inch-diameter water and sodium testing summary, 26:53305 (LMEC-72-4)
DENIG, R., Cumulative yield of 83-sec ^{136}I from thermal-neutron induced fission of ^{235}U, 26:54626
DENISOV, M. M., Longitudinal and transverse excitons in semiconductors, 26:55065 (UCRL-Trans-10643)
DENNING, J. H., Vibrational spectra and structures of rare earth oxides in the a modification, 26:55031
DENSON, Raymond, Prog. rpt. on physics of transient radiation effects, final, 2/68--10/71, 26:54968 (AD-737312)
DEPAUS, R., Non-congruent vaporization stage of lanthanum oxide on first heating to high temperature, 26:53549 (EUR-4765, pp 343-63)
DEPISCH, F., Treatment of the mechanical and thermal behavior of fuel rods in SATURN 1, 26:55186 (EURFNR-985)
DEPTULA, Andrzej, Liquid and solid Th--OH--NO$_3$--H$_2$O systems, 26:53048
  Preparation of aqueous solutions of thoria sols for light scattering measurements, 26:53050
DERAAD, Lester L. Jr., Compton scattering. I. Spectral forms for the invariant amplitudes to order e^4, 26:54255
  Compton scattering. II. Differential cross sections and left--right asymmetry, 26:54256
DERBENWICK, S. R., Far infrared surface resistance of Cu:Fe; dynamics of a Kondo system, 26:55508 (COO-3151-4)
DERLICH, S., Effects of an underground nuclear explosion on the surrounding rock. Content of the cavity and chimney, and of the zones of crushing and fracturing, 26:53130 (UCRL-Trans-10616-4)
DESAI, B. M., Effect of low doses of x-rays on radish and carrot, 26:53391
DESCAMPS, Jean-Marie, T424 facility for displacing fuel under irradiation, 26:55380 (CEA-N-1211)
DESCHREIDER, A. R., Study by differential absorption in infrared of irradiated lipids and polymers, 25:52983 (EUR-4828)
DE SEREVILLE, Bernard, High performance spectrometer magnets, 26:53296 (CEA-N-1539)
DESGROLARD, P., Pion--nucleon potentials for use in low-energy nuclear physics, 26:54724
DE SOETE, D., Neutron activation analysis, 26:52912
DESYATNIK, V. N., Melting point diagrams for LiCl--UCl$_3$--UCl$_4$ system, 26:53721
DEUTSCH, M., Polarization of the recoil proton in the reactions $\gamma p \rightarrow \pi^0 p$ and $\gamma p \rightarrow \gamma p$, 26:54167 (COO-3069-71)
DEVANATHAN, V., Polarization of the emitted neutron in muon capture, 26:54564
DEVANEY, M. A. J., Terminal control language for the MADCAP programming language, 26:55551 (LA-DC-72-411)
DE VILLIERS, A. J., Mortality experience of the community and of the fluorspar mining employees, 26:53412
DEVISMES, N., Phonon scattering by V ions in Al$_2$O$_3$, 26:54978
DEVLIN, T. J., Accelerator measurement of the energy spectra of neutrons emitted in the interaction of 3-GeV protons with several elements, 26:54528 (NASA-TM-X-2440, pp 523-6)
DEVREESE, J. T., Note on Feynman's path integrals, 26:55080
DE WOLF, E., LPS analysis of reactions $K^+p \rightarrow K^+\pi^+\pi^-p$ and $K^+p \rightarrow K^0\pi^+\pi^0p$, 26:54226
DEYOUNG, Donald Bouwman, Moessbauer effect study of ^{57}Fe in transition metal borides, 26:55055 (IS-T-529)
DHOPESHWARKAR, G. A., Metabolism of 1-^{14}C palmitic acid in the developing brain: persistence of radioactivity in the carboxyl carbon, 26:55620 (UCLA-12-871)
DHUICQ, D., Inelastic processes in He$^+$--He collisions, 26:54140
DIACONU, P., Radiosensitivity of some corn varieties, 26:53383
DIAINE, C., Analysis of thin alumina films obtained by reactive sputtering, 26:52902
DIAMOND, R. M., Enhancement of direct processes in heavy-ion reactions at high angular momenta, 26:54558
DIAMOND, Ronald Norman, Production of proton--antiproton and charged K meson pairs in 7 GeV/c π^+d interactions, 26:54218
DIBBERT, H. J., Recovery of electron-irradiated Pt. I, 26:55010
  Recovery of electron-irradiated. II, 26:55011
DICKE, R. H., New solar fluctuation, 26:53936
DICKENS, J. K., Elastic and inelastic scattering of 12-MeV protons from ^{92}Mo, ^{94}Mo, ^{96}Mo, and ^{100}Mo: tabulated differential cross sections, 26:54606 (ORNL-TM-3913)
  Gamma-ray production due to neutron interactions with iron for incident neutron energies between 0.8 and 20 MeV: tabulated differential cross sections, 26:54569 (ORNL-4798)
  Secondary gamma-ray-production cross sections of several materials, 26:54523 (CONF-720901-(Bks.1 and 2), pp 325-34)
DICUS, Duane A., Stellar energy-loss rates in a convergent theory of weak and electromagnetic interactions, 26:53893
DIECK, Enoui Leopold, Signaling system for pneumatic installations in nuclear reactors, 26:55413
DIENER, E. M., Giant dipole resonance in ^{16}O observed with polarized proton capture reaction, 26:54531
DIESTLER, D. J., Influence of attractive forces on the quantum-mechanical transition probabilities for atom--diatomic oscillator collisions, 26:54132
DIETRICH, I., Field distribution in superconducting lenses without ferromagnetic materials, 26:53759
DIETRICH, Lee A., Removal of materials from ion exchange resins, 26:53072
DI GIORGIO, G., Alkaline halides in carrier distillation process in U$_3$O$_8$ matrix, 26:53719
  Thermochemical reactions between alkaline halides and oxide impurities in U$_3$O$_8$ matrix, 26:52955 (RT/CHI-(72)4)
DIJKSTRA, J. H., Photographs of the Sun in the XUV region, 26:53958
DIKEMAN, John C., Removal of materials from ion exchange resins, 26:53072
DILORENZO, F. L., Teleoperators for remote operations in space, 26:53730 (NASA-TM-X-2440, pp 277-9)
DIMITROPOULOS, Constantin, Radiation effects on ionic and molecular crystals, 26:52984 (FRNC-TH-262)
DIMITROVA, M., Rapid spectrophotometric determination of Ta in hard-metal alloy mixtures using Nile blue, 26:52925
DINGER, Ann St. Clair, Structure and evolution of helium stars, 26:53896
DIPRIMIO, Joseph, Correction of a formula used in radioassay of /sup 99m/Tc, 26:52946
DIRIAN, Gregoire, Production of hydrogen for deuterium extraction, 26:52975
DIVAKARAN, P. P., Some general properties of representations of local currents, 26:54239
DIVINE, Neil, Jupiter radiation-belt engineering model, 26:54001 (NASA-TM-X-2440, pp 556-60)
DIXON, C. E., Effect of cryogenic irradiation on NERVA structural alloys, 26:53697 (NASA-TM-X-2440, pp 603-8)
DMITRIEV, S. M., ESR study of free radical reactions of γ-irradiated polypropylene with nethyl methacrylate, 26:53019
DMITRIEVSKII, V. P., Frequency shift of axial oscillations under the effect of the beam space charge, 26:53761
DOBBS, E. R., Ultrasonic evidence against multiple energy gaps in superconducting niobium, 26:54437
DOHMANN, H. D., ^{4}He--^{4}He interaction potential from low energy total cross section measurements, 26:54514
DOLAN, R., Hardening electronic devices against very-high-total-dose radiation environments, 26:53289 (NASA-TM-X-2440, pp 481-6)
DOLESCHALL, P., Exact calculations of N--d polarization, 26:54509
DOLGOPOLOV, V. V., Effect of high-frequency potential on propagation of fast waves along a magnetoactive plasma layer, 26:54839 (AEC-tr-7336)
  On the effect of wave field pressure on longitudinal oscillations in a plasma, 26:54840 (AEC-tr-7337)
  On the theory of transformation of surface waves into longitudinal oscillations in the surface layer of a plasma wave-guide, 26:54838 (AEC-tr-7335)
DOLZHENKO, O. V., Excitation of electromagnetic waves in a plasma by a relativistic electron beam. Part I. Longitudinal waves, 26:54837 (AEC-tr-7333)

DOMEL, Gisela, Use of the Ekco Mineral Analyser for the determination of copper and zinc in the presence of iron, 26:55568 (NIM-1430)
DOMINGO, J. J., Pionic proton stripping and π^- production, 26:54535
DOMINGUEZ, C. A., Evaluation of the J = 0 fixed pole in neutron Compton scattering, 26:54254
DOMINGUEZ, G., Radioanalytical purification of protactinium by anion exchange in hydrochloric acid-hydrofluoric acid medium, 26:52903
DOMONDON, D. B., Built-in radiotracer (^{24}Na) for measuring catalyst circulation rates, 26:53343
  Extraction of ^{32}P from neutron-irradiated S dissolved in hot toluene, 26:53069
DONAHUE, D. J., Investigation of spin assignments in ^{41}Ca, ^{53}Cr, and ^{55}Fe, 26:54578
DONALDSON, A. B., Passive calorimeter for pulsed electron beam energy measurement, 26:53258 (SC-DR-720630)
DONAT, G., Measurements on a fuel--salt interface in the annular well space during the production of a cavity by salt dissolution, 26:53115
DONATI, L., DNA, RNA, and ultrastructural aspects of human epidermis in chronic reactions of skin after roentgen irradiation, 26:53441
DONDES, S., Study of the pulse radiolysis of gases. Final report, 26:52980 (COO-3461-1)
DONNELLY, T. W., Semileptonic weak interactions with ^{12}C, 26:54541
D'ORAZI, R., Fast neutron radiative capture cross sections of stable nuclei with 29 less than or equal to Z less than or equal to 79, 26:54700 (RT/FI-(72)6)
DORLHAC, Francois, Theoretical study of electromagnetic coupling of two one-dimensional laminar flows of a viscous electrically conducting liquid, 26:54160
DORMANN, E., NMR investigations on Y- and La-diluted GdZn, 26:55059
DOROFEEV, V. M., Serotonin uptake by platelets in acute radiation sickness, 26:53486
DOUSSET, M., Evaluation of the components of the absorbed dose in the interior of organisms exposed to neutrons, 26:54871 (CEA-CONF-1976)
DOZORTSEVA, R. L., Genetic changes induced by space flight in barley seeds, 26:53384
DRAKE, D. M., Radiative capture of energetic neutrons by ^{208}Pb, 26:54662
DRAKE, M. K., Basis of current evaluated data files, 26:54478 (CONF-720901-(Bks.1 and 2), pp 1127-51)
DRANE, Joe B., Radiation protection prostheses for edentulous patients, 26:53410
DRAPER, J. M., RELP version C: a reactor economics linear program for IBM 360/85 computer, 26:55266 (RD/B/N-2261)
DRAPIER, J. M., Structure and properties of dispersion strengthened cobalt alloys, 26:53675
DRAWIN, H. W., Collisional-radiative volume recombination and ionization coefficients for He$^+$--He^{2+}--e plasmas, 26:54788 (EUR-CEA-FC-642)
DREIZLER, R. M., Algebraic approach to the theory of collective motion: spherical to deformed transition in the single-j shell, 26:54681 (COO-3071-9)
  Concept of transition operator boson and its application to an exactly soluble model, 26:54682 (COO-3071-10)
  Simplified microscopic model of the Coriolis anti-pairing transition, 26:54680 (COO-3071-7)
DREMIN, A. N., Formation of phase Nb/sub x/O$_2$ (0.8 less than or equal to x less than or equal to 1.0) under shock compression of Nb pentoxide, 26:53561
DREVER, R. W. P., Proportional counters for the localisation of ionising radiation, 26:53221
DROPESKY, Bruce J., Nuclear chemistry facilities, 26:53792 (LA-4874, pp 72-7)
DROULEZ, J. P., Compilation of cross sections. I. π^- and π^+ induced reactions, 26:54201 (CERN/HERA-72-1)
DRUMMOND, J. L., Behavior of radioactive impurities in DFR primary liquid metal coolant, 26:55167 (CONF-710959-, Paper 11)
DRYANOVSKA, O. A., Radiosensitivity of ovocytes in Sitotroga cerealella Oliv, 26:53499
DRYER, Murray, Comparison of solar-flare energy estimates made by analytical and numerical techniques, 26:53970
  Magnetohydrodynamic theory for the interaction of an interplanetary double-shock ensemble with the Earth's bow shock, 26:54073
  Pioneer 7 observations of Aug. 29, 1966, interplanetary shock-wave ensemble, 26:54068
DUBININ, I., Distribution of deep doses near implanted beta and mixed beta--gamma emitters, 26:54897
DUBOC, J., Analysis of KantiK and KantiKπ resonances produced in antipp annihilations at 1.2 GeV/c, 26:54199
DUBOVOI, L. V., General principle of current heating processes of plasma in pulsed z-discharges, 26:54749 (AEC-tr-7330)
  Measurement of plasma parameters in strong hf discharge, 26:54768 (AEC-tr-7329)
DUDAREV, V. Ya., X-ray and dielectric studies of irradiated perovskite type compounds, 26:55020
DUDERSTADT, James J., Improved S/sub N/ inner iteration convergence criterion, 26:55435 (CONF-720901-(Bks.1 and 2), pp 275-92)
DUFAY, M., Project for the spectroscopic study of a PIG ion source, 26:54082 (FRNC-CONF-58)
DUFTON, P. L., Non-LTE analysis of O-type subdwarf, HD 49798, 26:53900
DUGAR, A. C., Evaluation of a cross section ionization detector suitable for mine air analysis, 26:53287
DUGLE, Janet R., Plant associations in Whiteshell Nuclear Research Establishment controlled area, 26:55462 (AECL-3957)
DULCIC, A., Radiation abstraction of hydrogen atoms in single crystals of thymine, 26:52999
DUMM, K., Large leak tests in a model of a straight-tube steam generator, 26:55151 (CONF-710548-, pp 17-38)
DUNAWAY, P. B., Seasonal alterations in rodent blood, 26:55587 (ORNL-TM-3898)
DUNN, B. M., Multinode analysis of B and W's 2568-MWt nuclear plants during loss-of-coolant accident, 26:55271 (BAW-10034(Suppl.1))
DUPLAN, J. F., Radiosensitivity of circulating hemopoietic stem cells (CFU), 26:53466
DUPUY, C. H. S., Analysis of thin alumina films obtained by reactive sputtering, 26:52902
DURAND, J. L., Rescattering effects in the ^{2}H(p,2p)n and ^{2}H(p,pn)n reactions induced by 20- to 60-MeV protons, 26:54511
DURAND, M., Rescattering effects in the ^{2}H(p,2p)n and ^{2}H(p,pn)n reactions induced by 20- to 60-MeV protons, 26:54511
DUTEMPLE, Octave J., Description of the American Nuclear Society's Information Center on Nuclear Standards (ICONS) radiation protection standards: Quo Vadis, 26:54917
DUTREIX, A., Dosimetry in interstitial therapy using ^{192}Ir wires, 26:53422
DYER, F. F., Analysis of traces at ORNL's new High-Flux Neutron Activation Laboratory, 26:52897 (CONF-721010-3)
  Reliability in scientific evidence based on multi-trace forensic NAA, 26:52896 (CONF-720920-2)
DYNES, Paul J., Kinetics of proton transfer to cyanines. a temperature-jump study, 26:52964
DZHELEPOV, B. S., Beta processes, 26:54740
DZHELEPOV, V. P., Frequency shift of axial oscillations under the effect of the beam space charge, 26:53761
DZHOLOS, R. V., Basing of cranking-model, 26:54692 (JINR-P4-6543)
DZHURAEV, A. A., Depolarization of negative muons in water and aqueous solutions, 26:54099
DZIUK, Eugeniusz, Changes in the distribution of ^{137}Cs in rabbits during peritoneal dialysis, 26:53533

E

EACHUS, R. S., Possible identification of Pb^{1+} and PbH^{2+}: an electron paramagnetic resonance study, 26:53008
EASLEY, Annie J., Bleed-cycle propellant pumping in a gas-core nuclear rocket engine system, 26:55358 (N-72-18051)
EASTERLING, Kenneth, Effects of alloying on structural stability and cohesion between phases in metal--oxide composites, 26:53589
EASTLUND, Bernard J., Trapping of transuranium elements by the Earth's magnetic field, 26:54047 (NASA-TM-X-2440, pp 548-55)
EASTON, D. S., Thermodynamic properties of zirconium--cadmium and certain other solid solutions, 26:53663
EBENHOEH, Wolfgang, n + d break-up reaction with separable potentials, 26:54520
EBERSOLD, W. T., Induction of lysogenic bacteria in the space environment, 26:53364 (N-72-20063)
ECHELBARGER, G. J., Study of discontinuities in control rod drive motor tube extensions, 26:55217 (BAW-10047(Rev.1))
ECK, R., Solid state reactions during powder metallurgical production and fabrication of Mo alloy TZM, 26:53624
ECKELT, P., Vibrational excitation of diatomic Morse oscillator by impulsive collision with atom, 26:54131
ECKERMAN, K. F., Average temperature measurements in the aquatic environment using thermoluminescent dosimeters, 26:53187 (ANL-7860(Pt.3), pp 131-40)
ECKHAUSE, M., Negative muon capture in carbon leading to specific final states, 26:54537
  Yields of gamma rays emitted following capture of negative muons by ^{28}Si and ^{24}Mg, 26:54555
ECKLUND, W. L., Vhf power spectra of the radar aurora, 26:54038
ECKRICK, K., NMR investigations on Y- and La-diluted GdZn, 26:55059
EDESKUTY, F. J., Experience in handling, transport, and storage of liquid hydrogen: the recyclable fuel, 26:55552 (LA-DC-72-632)
EDGINGTON, D. N., Average temperature measurements in the aquatic environment using thermoluminescent dosimeters, 26:53187 (ANL-7860(Pt.3), pp 131-40)
  Determination of selected trace elements in natural water samples using spark source mass spectroscopy, 26:52914 (ANL-7860(Pt.3), pp 55-63)
  Measurement of major nutrients and water quality parameters at Point Beach: 1971, 26:53183 (ANL-7860(Pt.3), pp 103-8)
  Studies of recent sedimentation in Green Bay, 26:53164 (ANL-7860(Pt.3), pp 64-76)

EDLEN, Bengt, Z dependence of level intervals in $2s^22p^2$,$2s^22p^3$, and $2s^22p^4$, 26:53954
EDWARDS, Dilwyn, Exact expressions for properties of zero-pressure Friedmann models, 26:53999
EDWARDS, P. J., Flare star production of energetic charged particles, 26:53853
EDWARDS, Paul Alan, Nuclear quadrupole resonance study of heavy transition metal halide compounds with bridging halogen atoms, 26:55529 (IS-T-526)
EDWARDS, T. R. M., Measurements of K^+p elastic differential cross-sections for kaon momenta between 0.9 and 1.9 GeV/c, 26:54211 (RPP/H-95)
EFFERSON, K. R., Technique for observing magnet normalcies, 26:54463 (ORNL-TM-3886)
EFIMOV, G. V., Proof of unitarity of S-matrix in non-local quantum field theory, 26:54413 (JINR-P2-6586)
EHRENBERG, B., Independent yields of krypton and xenon isotopes in thermal-neutron fission of ^{235}U. Observation of an odd--even effect in the element yield distribution, 26:54667
EHRHARDT, H., Collisional ionization of helium by slow electrons, 26:54123
EICHLER, E., Elastic and inelastic scattering of 12-MeV protons from ^{92}Mo, ^{94}Mo, ^{96}Mo, and ^{100}Mo: tabulated differential cross sections, 26:54606 (ORNL-TM-3913)
EIDMAN, V. Ya., Faster-than-light synchrotron radiation in a vacuum, 26:53916
EIPPER, Alfred W., Nuclear power on Cayuga Lake, 26:53192
EISEMANN, E., Anisotropic diffusion in gas cooled fast breeder reactor, 26:55126 (KFK-1577)
EISEN, Y., Incoming wave boundary condition for elastic scattering of heavy particles at incident energies near the Coulomb barrier, 26:54705
EISERLING, F. A., Induction of lysogenic bacteria in the space environment, 26:53364 (N-72-20063)
EKMAN, Lars, Transfer of simulated fallout-particles from pasture to grazing dairy cattle. I, 26:53527 (FOA-4-4503-A-3)
EKSTROM, M. P., Baseband distortion equalization in the transmission of pulse information, 26:55630 (UCRL-73943)
EL-ADHAM, K. A., Preparation of sinterable uranium dioxide, 26:53546 (AREAEE-134)
ELAGIN, V. B., Spatial, angular, and energy distribution of fast neutrons behind triple layer barriers, 26:54966
EL BAZ, E., DWBA analysis of sub-Coulomb multi-transfer reactions, 26:54695 (LYCEN-7213)
ELBEL, H., Treatment of the mechanical and thermal behavior of fuel rods in SATURN 1, 26:55186 (EURFNR-985)
EL-CHERIF, A. I., PIBIMUG: code for multigroup slowing down spectrum calculation in the P-1 and B-1 approximations for the IBM-1130, 26:55420 (AREAEE-141)
ELDER, John C., Size characteristics of plutonium aerosols, 26:53062 (LA-DC-72-920)
EL-GARHY, M., Extraction of iron, cobalt, and manganese from hydrochloric acid with quaternary amine Aliquat-336, 26:53076
ELGAWHARY, S. M., Calcium and strontium transport to plant roots, 26:55490 (COO-1495-17)
ELIOFF, T., Neutrino mass limits from the K/sub L/^{0} → $\pi^{+-}l^{-+}\nu$ decay spectra, 26:54184 (LBL-4)
ELIOT, M., Large-angle scattering of neutral particles in 40 to 100 keV range, 26:54101 (EUR-CEA-FC-630)
ELKIND, M. M., Thermally enhanced radiosensitivity of cultured Chinese hamster cells, 26:53358
ELLAM, Leonard, Identification of the cell population responding to DNP--GL in lethally irradiated chimeric guinea pigs, 26:53474
ELLEGAARD, C., (1f/sub 7/2)^2 multiplet in ^{42}Ca, 25:54573
ELLETT, W. H., Microdosimetry of 250 kVp and 65 kVp x rays, ^{60}Co gamma rays, and tritium beta particles, 26:54895
ELLIOTT, D. O. Jr., Consistent coupled-channel Born approximation analysis of ^{88}Sr(d,np) ^{88}Sr and ^{88}Sr(d,p)^{89}Sr, 26:54588
ELLIS, S. D., Phenomenology of the triple-Regge region, 26:54332
ELLIS, W. R., Survey of Scyllac experiments, 26:54828 (LA-DC-72-896)
EL-NAGGAR, I. A., Theory of parametric excitation of oscillations in an inhomogeneous plasma, 26:54844 (AREAEE-125)
EL-RAZEK, M. Abd, Fast neutron scintillation spectrometer with double compensation circuit for gamma-ray discrimination, 26:53251 (AREAEE-137)
EL-REEFY, S., Extraction of iron, cobalt, and manganese from hydrochloric acid with quaternary amine Aliquat-336, 26:53076
EL-SHANSHOURY, I. A., Factors affecting the reduction of uranium trioxide powders, 26:53548 (AREAEE-139)
EL-SIRAGY, N. M., Nonlinear stabilization of beam instability, 26:54821
  Semiclassical theory of electromagnetic field interaction with a many-level molecular system, 26:55468 (AREAEE-136)
ELY, R. P., Reactions $K^-p \to \Lambda\pi^0$ and $K^-p \to$ antiK^0n in the center-of-mass energy range 1700 to 2100 MeV, 26:54215
EL'YASHEVICH, M. A., Use of high-speed spectrography for diagnostics of an erosive pulsed plasma accelerator, 26:54773
ELZIE, Johnny Lee, Neutron activation of silver, cadmium, indium, tin, antimony, tellurium, and iodine: analysis of meteoritic, terrestrial, and lunar materials, 26:52906
EMARD, F., Collisional-radiative volume recombination and ionization coefficients for He$^+$--He^{2+}--e plasmas, 26:54788 (EUR-CEA-FC-642)
EMENDOERFER, D., Group constant generation for the resolved resonance region, 26:55439 (CONF-720901-(Bks.1 and 2), pp 1183-91)
EMMERSON, Peter T., X-ray damage to DNA and loss of biological function: effect of sensitizing agents, 26:53352
EMMETT, M. B., DOMINO: a general purpose discrete ordinates to Monte Carlo coupling code for radiation transport, 26:54872 (CONF-720901-(Bks.1 and 2), pp 499-511)
ENDRES, G. W. R., An intrauterine dosimeter, 26:53238
ENDRUD, Glenn H., Pioneer 7 observations of Aug. 29, 1966, interplanetary shock-wave ensemble, 26:54068
ENGLE, L. B., Reactor power transient studies, 26:55441 (LA-DC-72-660)
ENGLE, W. W., Analysis of the STF neutron transmission measurements, 26:54944 (NAA-SR-Memo-8597)
ENKOVSKII, L. L., Annihilation of anti NN → 3π in dual models, 26:54320
  DAMA and Regge asymptotic behavior, 26:54412 (ITF-72-63-E)
ENZ, Charles P., Application of the equation-of-motion method to the spectrum of superfluid helium. II, 26:54427
  Application of the equation-of-motion method to the spectrum of superfluid helium. I, 26:54428
EPIFANOV, Yu. N., Ladder approximation for the vertex function of nonrenormalizable πrhoπ-interaction, 26:54322
EPP, Edward R., Energy spectrum of electrons in water irradiated with 10- to 20-MeV electron beams, 26:54894
EPSTEIN, S. T., Aspects of time-dependent perturbation theory, 26:55073
ERDOES, Paul, s--d exchange model of weak ferromagnetism with an application to MnB$_2$, 26:55048
EREMENKO, V. Ya., Spectrographic determination of Ni, Co, Ag, V, Sn, Mo, Ti, Al, Bi, Fe, Pb, Mn in natural water in the presence of relatively large amounts of Cu, 26:52927
ERICKSON, G. L., Human engineering standards for health physics instrumentation, 26:53246
ERICKSON, Jon Jay, Applications of computers and digital techniques in clinical and investigative nuclear medicine, 26:55457 (TID-26141)
ERIKSEN, Bjoern, Investigation of airborne radioactive material originating from an underground nuclear explosion in USSR 3/23/71, 26:53158 (FOA-4-4502-A-1)
ERIKSSON, Ake, Transfer of simulated fallout-particles from pasture to grazing dairy cattle. I, 26:53527 (FOA-4-4503-A-3)
ERIKSSON, K.-H., Function of the reticuloendothelial system in whole-body irradiated mice, 26:53468
  Protective effect of cysteamine at fractionated irradiation. III, 26:53475
ERKKILA, B. H., Excitation function for the $^{235}U(\alpha,3n)^{236}Pu$ reaction, 26:54665
ERMEL, A. E., Sodium turnover in irradiation hypertension, 26:53463
ERMOLAEV, A. M., Electron emission in negative ion and atom collisions in the sudden-switching approximation, 26:54112
ESAIAS, Wayne E., Action spectrum for photoinhibition of mechanically stimulable bioluminescence in the marine dinoflagellates gonyaulax catenella, G. actenella, and G. tamarensis, 26:55521 (COO-3277-14)
ESCHBACH, H. L., Calibration methods of vacuum technique, 26:53300 (EUR-4797)
ESEL'SON, B. N., New features of He II film flow transfer, 26:54431
ESIPCHUK, Yu. V., Effect of the magnetic field on a closed-electron-drift accelerator, 26:53743
ETTINGER, Harry J., Size characteristics of plutonium aerosols, 26:53062 (LA-DC-72-920)
EU, Byung Chan, WKB approximation in time-dependent scattering theory, including rearrangement processes, 26:54107
EUSTACE, R. C., Evaluation of two possible further developments of the UK in-flight radiation warning meter for SSTs, 26:53203 (NASA-TM-X-2440, pp 874-83)
EVANS, A. G., Effect of intense gamma radiation on radioiodine retention by activated carbon, 26:53061 (DP-MS-72-14)
EVANS, D. W., Effects of ocean water on the soluble-suspended distribution of Columbia River radionuclides, 26:53166 (RLO-2227-T-12-28)
EVANS, Lawrence Curtis, Magnetospheric access of solar particles and the configuration of the distant geomagnetic field, 26:54069
EVANS, T. Lloyd, V$_{553}$ centauri. A type 2 Cepheid with an overabundance of C, 26:53899
EVANS, W. F. J., Altitude distribution of the O$_2$($^1\Delta$) nightglow emission, 26:54042
EVANS III, R. B., Properties of dry crushed salt and related consolidated media with emphasis on their gas transport characteristics, 26:53724 (ORNL-TM-3815)
EVENSON, Paul, Upper limit on the flux of primary cosmic ray anti-alpha particles from 0.3 to 3 GeV/nucleon,

26:53825
EVRAETS, J. C., Recent activities in the development of surface contamination standards, 26:54919
EVSEEV, V. S., Depolarization of negative muons in water and aqueous solutions, 26:54099
EWAN, G. T., Measurement of lifetimes in ^{152}Sm, ^{154}Gd, and ^{156}Gd, 26:54642
EWART, G. M., Effects of ^{208}Pb core vibrations on shell-model calculations for ^{211}At and ^{211}Pb, 26:54650
EWEL, K. C., Investigation of the unusual behavior of ^{137}Cs and other radionuclides in the Florida environment. Progress report, September 1, 1971--August 31, 1972, 26:53170 (ORO-4066-5)
EWERS, D., Evaluation of filament-type electric heater rod as employed in single-loop semiscale to simulate UO$_2$ fuel rods, 26:55183 (ANCR-1038)
EWING, Dean E., Modular approach for assessing the effect of radiation environments on man in operational systems: radiobiological vulnerability of man during task performance, 26:54880 (NASA-TM-X-2440, pp 364-7)
EYLES, C. J., Search for neutrons of solar origin using balloon-borne detectors: 1967--69, 26:53967
EYLON, B., Emission of the ^{5}He in the spontaneous fission of ^{252}Cf, 26:54674
EZURE, H., Nuclear fuel balance calculation at JPDR, 26:55264 (JAERI-Memo-4083)

F

FABER, R., Conveying tube for the pneumatic transfer of spherical elements, 26:55194
FABER, S. M., Quadratic programming applied to the problem of galaxy population synthesis, 26:53977
FABRE, F., Relation between repair mechanisms and induced mitotic recombination after UV irradiation, in Schizosaccharomyces pombe, 26:53371
FABRICIUS, K., One particle singularities and physical symmetries, 26:54356
FACCHETTI, S., Surface ionization applied to some materials of nuclear interest, 26:53033 (EUR-4765, pp 117-30)
FACCHETTI, Sergio, 2nd conference on mass spectrometry, Ispra, Italy, 9/71, 26:52893 (EUR-4765)
FAELDT, G., Coulomb flux corrections and total cross sections for pion--nucleus interactions in Δ-resonance region, 26:54609
FAELDT, Goeran, Recoil and Fresnel corrections to scattering by deuteron, 26:54352
FAELTHAMMAR, Carl-Gunne, Polar auroras, 26:54043
FAINBERG, Ya. B., Influence of different types of oscillations on ion heating in plasma--beam discharges, 26:54762
  Interaction between a plasma and electron beam modulated by low-frequency oscillations, 26:54782
  Interaction of finite perturbations in a beam--plasma system, 26:54795
FALCONER, I. S., Measurement of the electron density distribution in plasmas from the bending of a gas laser beam, 26:54769
FALOUT, Frantisek, Some basic experimental methods of wet-steam flow investigation, 26:53124
FAN, C. Y., Measurement of the Lamb-shift in a hydrogen-like atom of nuclear charge Z greater than or equal to 3. Final report, 26:54375 (COO-1811-3)
FARELLO, Giovanni Elvio, Photographic study of two-phase highly dispersed flows, 26:53122
FARHATAZIZ, Pulse radiolysis of liquids at high pressures. III. Hydrated-electron reactions not controlled by diffusion, 26:53006
FARHOOMAND, I., Investigation of ground motion--damage relationships for residential buildings in Glendale, California: San Fernando earthquake, February 1971, 26:53137 (JAB-99-96)
FARKAS, Gy., Measurement of mode-locked ultrashort laser pulses by different order photoelectric effects, 26:55544 (KFKI-72-41)
FARLEY, F. J. M., Separated high-energy electron beams using synchrotron radiation, 26:53801
FARLEY, Thomas A., Spatial distribution of energetic plasma-sheet electrons, 26:54057
FARMER, B. J., Real-time spectrum-to-dose conversion system, 26:53201 (NASA-TM-X-2440, pp 142-8)
FARRELL, H. H., Surface condition of niobium for superconducting rf cavities, 26:53748
FARRER, D. N., Effect of continuous gamma-ray exposure on performance of learned tasks and effect of subsequent fractionated exposures on blood-forming tissue, 26:53452 (NASA-TM-X-2440, pp 633-40)
FASULO, M. P., Alterations of sugar beets by γ-irradiation of the seed, 26:53388
  Effect of γ-irradiation of seed on properties of sugar beet, 26:53386
FAULKNER, D. N., Relative biological effectiveness of fast neutrons compared with x rays: prenatal mortality in the mouse, 26:53453 (NASA-TM-X-2440, pp 641)
FAURE, J., Acceleration of polarized protons in Saturne, 26:53762
FAUST, George R., Twenty-twenty vision: a view of the future, 26:53098
FAYETON, J., Differential measurements on ion-atom collisions in energy range 500 to 3000 eV. IV, 26:54122
FAZZINI, T. F., Compact electron spectrometer for in-beam measurements of internal conversion coefficients, 26:53264
FEAST, M. W., R Coronae Borealis variables in Large Magellanic Cloud, 26:53904
FEDELE, V. D., EULERO program, 26:55595 (RT/FIMA-(72)1)
FEDORCHENKO, A. M., Interaction of a multiloop electron stream with a plasma, 26:54793
FEDORCHENKO, V. D., Nonlinear space-charge waves in a plasma sheath, 26:54853
FEDORENKO, N. V., Charge state alteration processes in collisions of hydrogen atoms with hydrogen molecules, 26:54115
FEDOTOV, S. I., Effect of changes in equilibrium deformations of the excited states of odd-A deformed nuclei on their energy and structure, 26:54640
FEDOTOVA, M. I., Role of the thymus in the postradiational restoration of the bone marrow in rats, 26:53479
FELDL, E. J., Target chamber for charged particle induced x-ray fluorescence studies, 26:53803
FELDMAN, Isaac, Quenching of tyrosine and tryptophan fluorescence by H$_2$O and D$_2$O, 26:52958 (UR-3490-193)
FELLER, P., Photoproduction of π^+-mesons on polarized protons at photon energies between 0.5 and 2.2 GeV, 26:54172 (NP-19415)
FELTEN, J. E., Transfer effects on lines and continuum in optically thick x-ray sources, 26:53926
FENGER, Joergen, Improving match between microwave source and microwave transmission system at Risoe 10 MeV electron linear accelerator, 26:53746 (RISO-M-1518)
FENNELL, J. F., Polar-cap measurements of solar-flare protons with energies down to 12.4 keV, 26:54071
FENTON, K. B., Spectral and pulsed x-ray emission from the Crab Nebula, 26:53919
FERGUSON, Don E., Method for reprocessing spent molten salt reactor fuels, 26:53086
FERNANDEZ, J. I., Observation of VH and VVH cosmic rays with an ionization--Cherenkov detector system, 26:53843
FERRARI, Giuseppe, Photographic study of two-phase highly dispersed flows, 26:53122
FERRELL, R. A., Statistical mechanics of one-dimensional Ginzburg--Landau fields, 26:54452
FESHBACH, Herman, Overview of the LAMPF research program, 26:54195 (LA-4874, pp 36-44)
FESSENDEN, Richard W., Dissociative attachement of thermal electrons to N$_2$O and subsequent electron detachment, 26:54135
FETISOV, V. N., Are solar-neutrino experiments suggestive of existence of resonance in ^{3}He + ^{3}He system, 26:54508
FIALKOWSKI, K., Explanation of correlation data in inclusive pp interactions at high energy, 26:54346 (RPP/T-28)
FIDANZA, M. A., Study as a function of time and dose of the numerical variations of the leucocytes circulating in a totally irradiated rat, 26:53483
FIEG, G., Measurements of delayed fission neutron spectra of ^{235}U, ^{238}U, and ^{239}Pu with proton recoil proportional counters, 26:54655 (CONF-720901-(Bks.1 and 2), pp 687-99)
FIELDS, John R., Effect of spatial coherence on the photoelectric counting statistics of Gaussian light. Technical report No. 13, 26:55506 (COO-3120-2)
FIENO, Daniel, Shielding application of perturbation theory to determine changes in neutron and gamma doses due to changes in shield layers, 26:54941 (CONF-720901-(Bks.1 and 2), pp 541-58)
FILES, Frederic Grant, Geology and alteration associated with Wyoming uranium deposits, 26:53143 (GJO-936-1)
FILIMONOV, V. A., Nonmesic decays of hypernuclei ^{4}H and ^{4}He in a model of direct transition of the Λ-hyperon into a neutron, 26:54293
FILIPPOV, A. T., Approximate methods for solving Schroedinger equations with a singular potential, 26:55074
  Ladder approximation for the vertex function of nonrenormalizable ωrhoπ-interaction, 26:54322
FILOZOV, A. F., System of wire spark chambers with ferrite core memory, 26:53271 (JINR-P13-6522)
FINKEL, V. A., Phase transition in samarium, 26:55051
FINOCCHIARO, G., Charged particle multiplicity and angular correlation measurements in pp and γp collisions, 26:54192 (BNL-17141)
FIORE, A., Rescattering effects in the ^{2}H(p,2p)n and ^{2}H(p,pn)n reactions induced by 20- to 60-MeV protons, 26:54511
FIRTH, I. M., Superconductivity, 26:54460
FISCHER, E. A., Calculation of heterogeneous fluxes, reaction rates, and reactivity worths in the plate structure of zero power fast critical assemblies, 26:55396 (EURFNR-1014)
  Experimental results from two Pu-fueled fast critical assemblies, 26:55387 (CONF-720901-(Bks.1 and 2), pp 645-59)
  Measurement of β/sub eff/ in Pu-fueled fast critical assemblies, 26:55389 (CONF-720901-(Bks.1 and 2), pp 700-12)
FISCHER, Gad, Variable trap problem in isotopic mixed crystals of s-triazine, 26:52963
FISCHER, H., State and tendencies of chemical protection

against ionizing radiation. A literature survey 1970/71, 26:53460 (SZS-132)

FISCHMEISTER, Hellmut, Effects of alloying on structural stability and cohesion between phases in metal--oxide composites, 26:53589

FISHCHUK, I. I., Light dispersion in the absorption region by impurity centres, 26:55539 (ITF-72-67-P)

FISHER, L. M., Doppler-shifted cyclotron resonance in cadmium, 26:55044

FISHER, Richard R., Coronagraphic observations of an enhanced coronal region. II, 26:53957

FISHER, S. B., Dose dependence of swelling in irradiated metals, 26:53707

High flux irradiations in HVEM, 26:53708

FISK, C. J., IMAGEN: a computer program for image enhancement and display of two-dimensional data, 26:55608 (SC-RR-720286)

FITZENREITER, Richard Julius, Position measurements of solar continuum and Type-III burst sources at decameter wavelengths, 26:53935

FITZER, E., Oxidation protection of Ta and Ta alloys up to 1500°C, 26:53613

Silicon diffusion in Me_5Si_3 phases of metals Nb, Ta, Mo, and W, 26:53583

FITZGERALD, C. L., Determination of the radioactive nuclides present in the off-gas stream generated by the head-end steps in reprocessing HTGR type fuels, 26:53078 (CONF-720823-11)

FITZSIMMONS, W. A., Some preliminary paramagnetic resonance studies for dosimetry research, 26:52979 (COO-1105-179)

FLAGMEYER, R., Experimental arrangement for investigation of single crystals by means of fast ions, 26:54977

FLAMINIO, E., Compilation of cross sections. I. π^- and π^+ induced reactions, 26:54201 (CERN/HERA-72-1)

FLAMM, W. G., Mutational assay system using the thymidine kinase locus in mouse lymphoma cells, 26:53361

FLEAY, R. F., Dosimetry in the use of colloidal isotopes, 26:53509

FLECKENSTEIN, D. C., American National Standards Institute and nuclear standards, 26:54916

FLEISCHER, J., Generalizations of Pade approximants, 26:55555 (LA-DC-72-872)

Nonlinear Pade approximants for Legendre series, 26:55556 (LA-DC-72-873)

FLEROV, G. N., Nuclear reactions induced by xenon ions and experiments on superheavy element synthesis, 26:54658 (JINR-P7-6523)

FLETCHER, Gilbert H., Retinal and optic nerve complications in a high dose irradiation technique of ethmoid sinus and nasal cavity, 26:53444

FLETCHER, W. H. W., Apparent constant-wavelength oscillations in a bounded plasma, 26:54859

FLOTHMANN, D., β-decay of ^{206}Tl, 26:54648

FLYGARE, W. H., Molecular g-value, magnetic susceptibility anisotropy, molecular quadrupole moment, and sign of the electric dipole moment in chloroacetylene, 26:52969

FLYNN, A., Hair radioactivity as a measure of exposure to radioisotopes, 26:53529 (NASA-TM-X-2440, pp 982-8)

FLYNN, E. R., Search for (t,p) transitions to excited 0^+ states in the actinide region; 26:54671

FOELL, W. K., Pulsed-activation techniques for the measurement of Doppler effects, 26:55124 (CONF-720901-(Bks.1 and 2), pp 1016-32)

FOELSCHE, Trutz, Evaluation of the hazard from exposure to electron irradiation simulating that in the synchronous orbit, 26:53458 (NASA-TM-X-2440, pp 665-71)

Radiation measurements and doses at SST altitudes, 26:54888 (NASA-TM-X-2440, pp 894-901)

FOMENKO, V. S., Dependence of variation of dislocation electron slowing down force in a superconducting transition on stress, temperature, and velocity, 26:54447

FOMINYKH, M. I., Study of ^{149}Tb decay, 26:54603 (JINR-P6-6511)

FONDARAI, J., Determination of the systolic volume by external counting, 26:53543

FORD, Lewis, Translational absorption of HeH, 26:54134

FORD, W. F., Deformed renormalized Brueckner--Hartree--Fock approximation and its application to ^{12}C, 26:54696 (ORNL-TM-3951)

FORD, William F., Inelastic scattering calculations with projected Hartree--Fock wave functions. II, 26:54565

FORD III, W. E., Comparison of (n/sub th/,γ) yields from the current ENDF/B-III data with published data, 26:54501 (ORNL-TM-3910)

FOREMAN, A. J. E., Diffusion of point defects to the foil surface during irradiation damage experiments in the high voltage electron microscope, 26:54985

FORESTI, G., MOBIDIC: a code for simplified evaluation of some continuous axial refueling schemes, 26:55196 (CISE-R-241)

MOICANO-1 code for reactivity and two-group flux calculation of fog-cooled reactor, taking into account true coolant distribution and equilibrium xenon poisoning, 26:55103 (CISE-R-242)

FORSYTH, E. B., Underground power transmission by superconducting cable, 26:54461 (BNL-50325)

FORTI, G., Possible function for RNA to DNA inverted transcription in antibody biosynthesis and irreversible differentiation, 26:55525 (EUR-4871)

FORTOV, V. E., Equation of state of a nonideal cesium plasma, 26:54866

FORTUNE, H. T., Configuration mixing in ^{90}Zr and lifetime of excited 0^+ states, 26:54610

FORYS, Mieczyslaw, Hydrogen sulfide radiolysis sensitized by Ar, Kr, Xe, and N, 26:53011

FOSTER, C., Elastic scattering of 5 to 90 eV neutral Au atoms by Ar, 26:54142

Ion--atom scattering and interatomic potentials for ions of noble metals and period II elements incident on Ne and Ar with energies in the range 8 to 25 keV, 26:54139

FOSTER, J. L. Jr., ^{142}Ce(d,p) and ^{142}Ce(d,t) reactions and isobaric analog resonances in ^{142}Ce(p,p_0) and ^{142}Ce(p,p_1), 26:54618

FOUKAL, Peter, Measurement of the electron temperature of small 3-cm radio bursts, 26:53960

FOURNIER, Gerard, Flow of a collisionless plasma around a cylinder in view of applications to ionospheric probes, 26:54011 (ONERA-Publ.-137)

FOWLER, T. B., Nuclear reactor core analysis code: CITATION. Revision 2, Supplement 3, 26:55198 (ORNL-TM-2496(Rev.2)(Suppl.3))

FOX, P. F., Status of the FTR shielding design analysis and methods, 26:55383 (CONF-720901-(Bks.1 and 2), pp 445-58)

FRADIN DE LA RENAUDIERE, Jean Jacques Marie, Preparation of anhydrous hydrazine by the radiolysis of liquid ammonia, 26:53001

FRAENKEL, E., Emission of the ^{5}He in the spontaneous fission of ^{252}Cf, 26:54674

FRAGA, S., Properties and interactions of lanthanides, 26:55025

FRAHN, W. E., Diffraction scattering of charged particles, 26:54415

FRANCA, J. M. Jr., Preparation of clear uranyl nitrate solution by fractional dissolution of sodium diuranate, 26:52976 (IEA-250)

FRANCESCHI, A., Determination of the systolic volume by external counting, 26:53543

FRANCKE, Bertold, Ultraviolet-induced cross-links in the deoxyribonucleic acid of single-stranded deoxyribonucleic acid viruses as a probe of deoxyribonucleic acid packaging, 26:53373

FRANCOIS, D., Electric and thermal conductivity, elastic properties, and bending resistance of porous W over entire range of porosity, 26:53684

FRANCOIS, R., Inelastic processes in He$^+$--He collisions, 26:54140

FRANGYAN, A. A., Effect of the medium on radiation emission by relativistic electrons, 26:54907

FRANK, James Sidney, Time decay distributions of anti K^0 and K^0 to $\pi^+\pi^-$: a CP test, 26:54362 (COO-1195-244)

FRASCARIA, R., ^{2}H(p,2p)n reaction at 155 MeV, 26:54522

FRASER, B. J., Polarization properties of Pc 1 micropulsations at low latitudes, 26:54021

FRASER, R. F., Continuum shell model calculation for the ^{15}N giant dipole resonance, 26:54545

FRATIANNE, R. B., Hair radioactivity as a measure of exposure to radioisotopes, 26:53529 (NASA-TM-X-2440, pp 982-8)

FREEMAN, D. D., SEFOR: verification of the Doppler transient shutdown capability of LMFBR's, 26:55123 (CONF-720901-(Bks.1 and 2), pp 986-1005)

FREIER, Phyllis S., Charge and energy spectra of heavy cosmic ray nuclei, 26:53842

FRENCH, H., Large aperture spectrometer magnet for the ISA and the possible use of visual detectors, 26:53779 (BNL-17142)

FRENZEN, Paul, Surface energy budget measurements over Lake Michigan, 26:53189 (ANL-7860(Pt.3), pp 270-98)

FRETTER, Ernest F., High-pressure electrofluiddynamic facility, 26:53089 (AD-737380)

FREUND, Juergen, Development and properties of the halo in pinch plasmas, 26:54784 (IPP-1/125)

FREYTAG, Eberhard, Radiation protection at high-energy accelerators, 26:53742

FRIDMAN, Sh. D., Determination of thickness of γ-sources and absorbers from deformation of hard part of energy spectrum, 26:54936

FRIEDBERG, W., Relative biological effectiveness of fast neutrons compared with x rays: prenatal mortality in the mouse, 26:53453 (NASA-TM-X-2440, pp 641)

FRIEDLANDER, M. W., Comments on the observation of transuranic nuclei in the primary cosmic radiation, 26:53844

FRIEDRICH, J., Low-lying states in ^{208}Pb, 26:54649

FRIEMAN, E. A., Toroidal effects on MHD stability in Tokamaks, 26:54806 (CONF-720804-6)

FRISBEE, P. E., Two searches for an excited state of ^{3}He, 26:54515

FRISCH, H. J., Neutrino mass limits from the K/sub L/^{0} $\to$ $\pi^{+-}l^{-+}\nu$ decay spectra, 26:54184 (LBL-4)

FRITZ-NIGGLI, H., Chromosome anomalies for biological dosimetry, 26:53420

FROME, Edward, Pulmonary-impedance power spectral analysis: a facile means of detecting radiation-induced gastrointestinal distress and performance decrement in man, 26:53401 (NASA-TM-X-2440, pp 238-48)

FROMM, E., Equilibria and kinetics of degassing in the systems Mo--N, W--N, and Re--N, 26:53580

FRY, D. N., Preliminary coolant temperature oscillation measurements at the fuel-failure mockup, 26:55192 (ORNL-TM-3761)
FRYE, G. M. Jr., New point gamma ray source Libra γ-1, 26:53924
FRYE, J. H. Jr., Thermodynamic properties of zirconium--cadmium and certain other solid solutions, 26:53663
FU, Ying-Kai, Effects of ultraviolet radiation on mammalian cells: JU56 wallaby cell line, 26:53353 (UR-3490-194)
FUJII, Zenjiro, Three-dimensional cosmic ray anisotropy in interplanetary space. IV, 26:53813
  Three-dimensional cosmic-ray anisotropy in interplanetary space. III, 26:53812
FUJIMOTO, Kazuhiko, Three-dimensional cosmic ray anisotropy in interplanetary space. IV, 26:53813
  Three-dimensional cosmic-ray anisotropy in interplanetary space. III, 26:53812
FUJIMURA, Tadato, Results of cyclic pressure loading test due to JPDR pressure vessel model No. 2, 26:55228 (JAERI-Memo-4016)
FUJISAKI, Haruo, Comments on Arnold and Barnett's shielding-cut mechanism. II, 26:54353
FUJIWARA, Tetusro, Some findings on pulmonary surfactant by biochemical study, 26:55565 (LF-tr-72)
FUKUDA, Nobuo, Analysis of kinetic curves, 26:53519
FUKUMURA, Nobuo, Flux distribution measurement near strong absorber using VISTA method, 26:55137 (JAERI-Memo-3893)
FUKUSHIMA, Naoshi, Positive geomagnetic bays in evening high latitudes and their possible connection with partial ring current, 26:54023
FULBRIGHT, H. W., Odd-parity three-particle, one-hole structure in ^{18}F via the reaction ^{15}N(^{6}Li,t)^{18}F, 26:54549
FULCO, Armand J., Effects of temperature and fatty acid structure on lipid metabolism in Bacillus licheniformis 9259, 26:55622 (UCLA-12-879)
FULLER, G. E., Some preliminary paramagnetic resonance studies for dosimetry research, 26:52979 (COO-1105-179)
FULLER, L. C., ORCOST: a computer code for summary capital cost estimates of steam-electric power plants. User's manual, 26:55265 (ORNL-TM-3743)
FUNK, C. W., Effect of cryogenic irradiation on NERVA structural alloys, 26:53697 (NASA-TM-X-2440, pp 603-8)
FUNK, L. W., Circuit for direct registration of electron densities measured interferometrically, 26:54770
FURSA, A. D., Quasi-elastic electron scattering on ^{12}C nuclei, 26:54526 (ITF-72-25-P)
  Two-particle electrodesintegration of ^{3}He, 26:54496 (ITF-72-24-P)
FURSOV, G. L., Influence of injection conditions on the transverse instability of the beam in a linear accelerator, 26:53758
FURUKAWA, M., Nuclear reactions of Ni with protons up to 56 MeV, 26:54591
FURUTA, Teruo, Creep rupture properties of alpha-ray irradiated AISI 316 stainless steel, 26:53703
FUYA, Kh., g-factor of 108 keV excited state in ^{151}Gd, 26:54634 (JINR-E6-6479)

G

GAAFER, M. A., PIBIMUG: code for multigroup slowing down spectrum calculation in the P-1 and B-1 approximations for the IBM-1130, 26:55420 (AREAEE-141)
GABARAIN, R. V. A., Effect of gamma radiation on an Argentine variety of wheat, 26:53381 (CNEA-309)
GABATHULER, E., High intensity muon beam design for CERN II, 26:53783 (DNPL/P-131)
GABATHULER, K., Pionic proton stripping and π^- production, 26:54535
GABRIEL, M., Conditions for homogeneous stellar models to have only real secular eigenvalues, 26:53886
GABRIELSON, V. K., HEATMESH-71: a computer code for generating geometrical data required for studies of heat transfer in axisymmetric structures, 26:55610 (SCL-DR-720004)
GADDIS, E. S., Thermal equilibrium of a bubble near a heated solid surface and associated flow pattern, 26:53119 (AREAEE-122)
GADZHIEV, A. R., Fast-neutron-compensated n-germanium as a model of amorphous semiconductors, 26:54981
GAERTTNER, Erwin R., Linear accelerator project progress report, April 1, 1972--June 30, 1972, 26:54656 (COO-3058-21)
GAIDOS, J. A., Preliminary study of $\pi^+\pi^-$ scattering in reaction $\pi^+p \rightarrow (\pi^+\pi^-)\Delta^{++}$ at 13 GeV/c, 26:54223
GAL, A., Shell-model analysis of Λ binding energies for the p-shell hypernuclei. II. Numerical fitting, interpretation, and hypernuclear predictions, 26:54351
GAL, J., Moessbauer effect in ^{239}Pu, 26:54661
GALAN, V. J., Analysis of anticipated transients without trip, 26:55193 (BAW-10016)
GALBRAITH, Harold W., Application of orthogonal and unitary group methods to the N-body problem, 26:55072
GALES, S., ^{142}Ce(d,p) and ^{142}Ce(d,t) reactions and isobaric analog resonances in ^{142}Ce(p,p_0) and ^{142}Ce(p,p_1), 26:54618
GALIANO, Francis R., Crosslinked nylon by irradiation of a graft copolymer of nylon with an ethylene/acrylate or modified copolymer, 26:53013
GALIBIN, V. A., Quantitative spectral determination of Nb, Ta, Fe, and Mn in minerals of columbite--tantalite group, 26:52932
GALLAGHER III, F. E., Recent activities in the development of surface contamination standards, 26:54919
GALLI, A., Radiation damage in sintered alumina: an EPR study, 26:53699 (RT/FI-(72)10)
GALLICE, Pierre, CAMAC system: practical information for computerized treatment, 26:53297 (CEA-N-1549)
GALMICHE, Philippe, Production of Ni--Cr--ThO_2 alloys by means of chromium diffusion through halogen carrier in $NiThO_2$ grain, 26:53627
GAL'PERIN, Yu. I., Measurement of radiation in space, 26:53276
GALPIN, Floyd L., Comparison of techniques for calculating doses to the whole body and to the lungs from radioactive noble gases, 26:53510
GALT, J. A., Interstellar scintillation pattern of PSR + 54, 26:53915
GAMBAROV, D. G., Spectrophotometric study of the reaction of Nb with Alizarin red, 26:52926
GAMBLE, J. F., Investigation of the unusual behavior of ^{137}Cs and other radionuclides in the Florida environment. Progress report, September 1, 1971--August 31, 1972, 26:53170 (ORO-4066-5)
GAMERTSFELDER, Carl C., AEC regulatory program, 26:54924
GAMMEL, J. L., Effect of random errors in terms of power series on convergence of Pade approximants, 26:55558 (LA-DC-72-880)
  Review of two recent generalizations of Pade approximant, 26:55557 (LA-DC-72-879)
GAMMEL, John L., Intermediate-state, single-particle energies in many-fermion energy calculations, 26:54717
GANGLER, James J., NASA research on refractory compounds, 26:53581
GARCIA, D., Influence of radiation shielding on reusable nuclear shuttle design, 26:54954 (NASA-TM-X-2440, pp 251-6)
GARCIA-MUNOZ, M., Abundances of the galactic nuclei H through the Fe group from satellite measurements, 26:53836
  Energy dependence of the abundances of galactic He, L, and M nuclei from satellite measurements, 26:53835
GARDE, A. M., Deformation processes in hexagonal metals. Progress report, December 1, 1972--November 30, 1972, 26:53639 (ORO-3262-25)
GARDES, G., Study of diffusion welding of molybdenum, 26:53625
GARDNER, Dwight E., Direct determination of total ionic fluoride in biological fluids, 26:55637 (UR-3490-184)
GAREEV, F. A., Center of mass spuriosity effects on charge form factor in many-body theories, 26:54507
  One-nucleon transfer reactions to quasi-intersecting levels, 26:54635 (JINR-P4-6509)
GARFINKEL, A. F., Evidence for a neutral meson near 1033 MeV, 26:54205 (COO-1428-311)
  Pion--nucleon charge exchange scattering in a new Regge pole-cut model, 26:54324 (COO-1428-309)
  S-wave structure in the Kπ system, 26:54203 (COO-1428-308)
GARLAND, W. J., Optimum angular segmentations in neutron transport analysis, 26:55434 (CONF-720901-(Bks.1 and 2), pp 266-74)
GARMIRE, G. P., Flux of galactic high-energy gamma rays, 26:53819
  X-ray and optical observations of Sco X-1 and observations of the x-ray background, 26:53918
GARREN, A., Momentum matching in ISA long insertions, 26:53773 (BNL-17051)
GARRETT, J. D., Search for (t,p) transitions to excited 0$^+$ states in the actinide region, 26:54671
GASIDLO, J. M., Effect of core configuration on ^{238}U Doppler measurements in ZPPR Assembly 2, 26:55393 (CONF-720901-(Bks.1 and 2), pp 1006-15)
GASPAR, P. P., Hydride ion transfer and isotope effects in CD_4--silane ion molecule reactions, 26:52961
GASSER, Sidney B., Program optimization, 26:55599 (SC-DC-721376)
GAUDIOSI, Gaetano, Observation on CISE criterion for extension of critical heat flux tube correlation to rod bundle geometry, 26:53123
GAUR, B. K., Effect of low doses of x-rays on radish and carrot, 26:53391
GAUTHERIN, G., Research program of the particle source group in the field of multicharged ions, 26:54079 (FRNC-CONF-53)
GAUTHIER, J. C., Direct measurement of diffusion cooling in an afterglow plasma, 26:54786
GAVANKAR, Harsharaj Ganesh, Risks and emergency radiation doses from plutonium dioxide exposures, 26:53511 (TID-26142)
GAVRILA, Mihai, Compton scattering by K-shell electrons. I. Nonrelativistic theory with retardation, 26:54279
  Compton scattering by K-shell electrons. II. Nonrelativistic dipole approximation, 26:54280
GAVRILIN, A. I., Study of Na and H_2O interaction in a one-megawatt modular steam generator, 26:55153 (CONF-710548-, pp 57-104)
GAVRILOV, V. D., Effective neutron absorption cross sections for ^{252}Cf and ^{253}Cf in central channel of SM-2

reactor, 26:54668
GAVRON, A., Emission of the ^{5}He in the spontaneous fission of ^{252}Cf, 26:54674
GAWLOWSKI, Janusz, Formation of acetylene and methane in argon and xenon sensitized radiolysis of gaseous ethylene, 26:53000
GAZDAGH, I., Observations on the combined radioprotective effect of pantothenic acid and aminoethylisothiuronium, 26:53481
GEGUSCH, H., Results of fallout monitoring in the German Democratic Republic 1970, 26:53156 (SZS-128)
GEHRKE, R. J., Gamma rays emitted by the fissionable nuclides and associated isotopes, 26:54652 (ANCR-1069)
GEIPEL, H., High flux Franco--German reactor, 26:55414
GEIST, V., Experimental arrangement for investigation of single crystals by means of fast ions, 26:54977
GEKKER, I. R., Generation of fast electrons through interaction of SHF wave with collisionless plasma, 26:54836 (AEC-tr-7331)
GELEBART, F., Determination of absolute differential cross sections for $1^1S \rightarrow 4^1D$ transition of helium atom, 26:54113
GELFAND, N., Large aperture spectrometer magnet for the ISA and the possible use of visual detectors, 26:53779 (BNL-17142)
GELLER, Marvin A., Comments on lunar variations in the Peruvian electrojet, 26:54041
GELLER, R., Heating of very small solid grains by electron and ion bombardment, 26:54874 (EUR-CEA-FC-647)
  Measurement of abundance of $^{14}N^{7+}$ ion beam, 26:54077 (CEA-CONF-2048)
GENGENBACH, R., Measurements of absolute integral total cross sections of He--H_2 and the interaction potential, 26:54130
GENTHON, J. P., In pile radiation damage in graphite. Correlation between temperature and flux density in range of high temperature, 26:53713 (CEA-CONF-1894)
GENTRY, D. H., Analysis of the effects of selected scheduling rules in a parallel processor shop, 26:55640 (Y-1848)
GENZEL, H., Proton Compton effect in the region of the Δ(1236)-resonance, 26:54180
GEORGIEVA, M. K., Angular correlation of a gamma cascade 329 to 487 keV in ^{140}Ce, 26:55060
GERACE, W. J., Effects of ^{208}Pb core vibrations on shell-model calculations for ^{211}At and ^{211}Pb, 26:54650
GERARD, R., Radiological risks relative to the distribution of contaminated gas, 26:53132 (UCRL-Trans-10617-2)
GERBER, G., Ionization processes in slow collisions of heavy particles. I, 26:54141
GERGELY, Krammer, SLIP: a symmetrical subroutine developed for CDC 3300 and ICL 1905 computers, 26:55543 (KFKI-72-32)
GERIN, F., Application and automation of mass spectrometry in the analysis of irradiated nuclear fuels, 26:52917 (EUR-4765, pp 77-89)
GERLACH, Robert L., Retarding field-cylindrical mirror analyzer, 26:53310 (SC-DC-721302)
GERRARD, Martha, Animal toxicity of coumaphos and contaminants, 26:55578 (ORNL-TIP/TIRC-72-49)
  Maximum safe levels of fluorine for man and animals, 26:55580 (ORNL-TIP/TIRC-72-53)
GERSTENKORN, S., Relative isotope shift (112-114)/(110-112) in lambda = 4416 A line of cadmium, 26:54625
GERSTNER, Helga, Effect of pyramidon on the hemopoietic and vascular system of the mammal, 26:55582 (ORNL-TIP/TIRC-72-59)
  Effects of sodium nitrite on the hemopoietic and vascular system of the mammal, 26:55577 (ORNL-TIP/TIRC-72-45)
  Material for use by parents of handicapped children, 26:55576 (ORNL-TIP/TIRC-72-13)
  Toxicity aspects of silica or quartz particles, 26:55585 (ORNL-TIP/TIRC-72-62)
  Toxicity of elemental phosphorus, 26:55586 (ORNL-TIP/TIRC-72-63)
GERVAIS, J. L., Feynman rules for massive gauge fields with dual diagram topology, 26:54381
GERWIN, R., Speedy advance of construction in Atucha, 26:55216
GESCHIER, R., Internal friction peaks due to N in Nb--Zr alloys, 26:53692
GETZ, D., H_3O radical, 26:53026
GHORMLEY, John A., Pulse radiolysis study of succinonitrile in the rotator phase, 26:53003
GHOROKU, Kazuo, Systematic structure in hadronic two-body scattering and resonance correlation. III, 26:54342
GHOZLAN, A., Osmotic pressure waves in solutions of ^{3}He in superfluid ^{4}He, 26:54433
GIALANELLA, G., Analysis of reaction $\gamma + n \rightarrow p + \pi^-$ in first and second resonance region, 26:54171 (LNF-72/31)
GIANNATIEMPO, A., Compact electron spectrometer for in-beam measurements of internal conversion coefficients, 26:53264
GIANNINI, M., Automatic peak identification in analysis of gamma-ray spectra obtained with Ge(Li) detectors, 26:53257 (RT/FI-(72)14)
GIARDINI, A., Ionic chemistry of gaseous cC_6H_{12}, 26:52982 (EUR-4765, pp 11-24)
GIBBONS, J. H., Gamma-ray shielding measurements made at altitudes greater than 115,000 feet using large Ge(Li) detectors, 26:54964 (NASA-TM-X-2440, pp 914-21)
GIBSON, James S., Microwave spectrum and ring-bending vibration of 3-oxetanone, 26:52960
GIDDINGS, George G., Characterization of the red pigments produced from ferrimyoglobin by ionizing radiation, 26:53346
GIELISSE, P. J., Properties of proton-irradiated diamond, 26:54991
GIETZEN, A. J., Thermionic reactor power system: effects of radiation on integration with manned space station, 26:55365 (NASA-TM-X-2440, pp 299-306)
GIGNOUX, D., Stability of transverse-wave magnetic structure at 1.3 K, 26:55039
GIJBELS, R., Neutron activation analysis, 26:52912
GIL, C., Determination of urinary plutonium by radiochemical analysis on ion exchanger filters, 26:52940
GILABERT, Alain, Experimental evidence for the Josephson effect in tin films, 26:54455
GILBY, A. S., Compact EHT power supply for use with high pulse rate spark chambers, 26:53275 (RPP/H-101)
GILLET, R., Pediatric radiology and irradiation, 26:53417
GILLILAND, R. G., Behavior of welded joints in stainless and alloy steels at elevated temperatures, 26:53638 (ORNL-4781)
GILLIS, H. A., Solvation of electrons in 3-methylhexane at 77^{0}K, 26:53007
GILS, H. J., β-decay of ^{206}Tl, 26:54648
GIMBERT, J. L., Pulmonary lavage, therapy of pulmonary contaminations, 26:53528 (LF-tr-71)
GINOCCHIO, Joseph N., Radiation, 26:53396
GINOZA, William, Effects of ionizing radiation on the capacity of Escherichia coli to support bacteriophage T4 growth, 26:53372
GIONVANNINI, R., Proton-recoil proportional counter spectrometry for reactor spectrum measurements, 26:55122 (CONF-720901-(Bks.1 and 2), pp 959-72)
GIORCELLI, M., RAS: synthesis program for calculation of 2-group neutron flux in r-theta, 26:54471 (CISE-R-252)
GIRAUD, B., Reaction-mechanism study in the 1f--2p shell of (^{16}O,^{12}C) four-nucleon-transfer reaction, 26:54579
GIROD, J. J., Network for acquiring and remote handling of data using a small computer, 26:53312
GISLON, R., Electron emission from solids by ionic bombardment, 26:52936 (RT/EL-(72)4)
GIULIANO, C., Effect of chemical preparation of ^{45}Ca on nonprotein bound serum fraction, 26:53074
GJOEEN, Einer, Resonant interaction of an electrostatic wave with electrons in a current sheet, 26:54052
GLADKIKH, V. S., Uranium and thorium in the alkali olivine basalt series, 26:53147
GLASS, R. W., Decontamination of HTGR reprocessing off-gases, 26:53059 (CONF-720823-12)
GLAVANAKOVA, S. I., Radiosensitivity of ovocytes in Sitotroga cerealella Oliv, 26:53499
GLAVISH, H. F., Giant dipole resonance in ^{16}O observed with polarized proton capture reaction, 26:54531
GLAZOV, A. A., Frequency shift of axial oscillations under the effect of the beam space charge, 26:53761
GLOECKNER, D. H., Inhibited transitions and isomeric states in N = 50 isotones, 26:54611
GLOWACKA, L., Knock-on mechanism for (n,α) reactions induced by fast neutrons on the deformed doubly even nuclei, 26:54707
GLUCKSTERN, Robert L., Betatron frequency shifts due to image fields, 26:53770 (BNL-17016)
GLUTSYUK, A. M., Ion focusing of an electron beam in a transverse gas flow, 26:54086
GNANAPURANI, M., Influence of linear energy transfer on the radioresistance of budding haploid yeast cells, 26:53368
GOBBI, B., Coulomb induced deuteron break-up of ISABELLE, 26:53776 (BNL-17063)
  Scheme for absolute calibration of ISABELLE luminosity, 26:53772 (BNL-17021)
GOBELI, G. W., Nanosecond and picosecond laser-produced CD_2 plasmas, 26:54804
GODDARD III, William A., Theoretical description of asymmetric, nonresonant charge-transfer process, $Li + Na^+$ in equilibrium $Li^+ + Na$, 26:54127
GODFREY, Gary L., Kaonic atom transition coupled to nuclear level, 26:54568 (LBL-776)
GODLESKI, John J., Origin of alveolar macrophages in mouse radiation chimeras, 26:53492
GOETZ, C. A., Impact of radiation dose on nuclear shuttle configuration, 26:54945 (NASA-TM-X-2440, pp 40-7)
GOETZEL, C. G., Electric discharge-type activated pressure sintering and bonding of a superalloy composite structure, 26:53628
GOETZMANN, Odo, In-pile compatibility of oxide fuel, 26:55187 (EURFNR-989)
GOGOKHIYA, V. Sh., Approximate methods for solving Schroedinger equations with a singular potential, 26:55074
GOGOLITSIN, Yu. L., Four-fermion scattering amplitude free from kinematical singularities, 26:54417
GOIN, R. W., Boron and tantalum control rod studies and absolute gamma ray absorbed doses in a LMFBR critical, 26:55134 (CONF-720901-(Bks.1 and 2), pp 579-98)
GOKHALE, G. S., Intensity and energy spectra of several x-ray sources in the 20- to 150-keV energy band, 26:53920

Short period variations in intensity and energy spectrum of Cyg X-1, 26:53921

GOLANT, V. E., Microwave plasma heating in Tuman-2, 26:54758

GOLD, Kenneth, Growth characteristics of Tintinnida in continuous culture, 26:55522 (COO-3390-2)

GOLDANIGA, G., TERMO: digital code to evaluate steady state parameters of CIRENE type reactor, 26:55104 (CISE-R-246)

GOLDBERG, M., Analysis of KantiK and KantiKπ resonances produced in antipp annihilations at 1.2 GeV/c, 26:54199

Application of ISABELLE in Whiplash mode to produce polarized proton or monoenergetic neutron beams, 26:53775 (BNL-17057)

GOLDBOGEN, Geof, Modeling the visual pathway for interactive diagnosis of visual fields, 26:55466 (ANL-7858)

GOLDEN, R. L., Rigidity spectrum of Z greater than or equal to 3 nuclei from 5 GeV to over 300 GeV, 26:53834

GOLDREICH, Peter, Parametric down-conversion in astrophysical masers, 26:53909

GOLDSCHMIDT-CLERMONT, Y., LPS analysis of reactions $K^+p \to K^+\pi^+\pi^-p$ and $K^+p \to K^0\pi^+\pi^0p$, 26:54226

GOLDSTEIN, Charles I., Scattering theory for elliptic differential operators in unbounded domains, 26:54407 (BNL-16752)

GOLDSTEIN, Gary R., New Regge absorption model, 25:54336

GOLDSTEIN, H., Carbon shielding benchmark problem and other neutron transport calculations in carbon, 26:54939 (CONF-720901-(Bks.1 and 2), pp 397-408)

Mechanism of fast neutron transport in iron, 26:54473 (CONF-720901-(Bks.1 and 2), pp 335-48)

GOLDSTEIN, Rubin, Effect of particle size on resonance capture, 26:55425 (CONF-720901-(Bks.1 and 2), pp 108-13)

GOLES, R. W., Collective and higher-order effects shown by the (p,t) reaction on the deformed nucleus ^{159}Tb, 26:54645

Collective effects shown by the (p,t) reaction on the closed-shell nucleus, ^{141}Pr, 26:54615

GOLLY, W., Criteria for differentiating fuel and plenum faults on reactor fuel elements with vibrocompacted fuel, 26:55229 (EURFNR-975)

GOLUB, L., Polarization of the recoil proton in the reactions $\gamma p \to \pi^0p$ and $\gamma p \to \gamma p$, 26:54167 (COO-3069-71)

GONCHAR, N. S., Relations between moment functionals of measures absolutely continuous with respect to Gaussian measure and solvability of Schwinger equations for Green functions of Euclidean field theory, 26:55070 (ITF-72-45-P)

GONCHAROV, A. A., Long-wave instability caused by inhomogeneous ion beams in a dense magnetized plasma, 26:54816

GONCHAROV, V. K., Self-igniting pulsed optical discharge in an erosive laser plasma, 26:54803

GONZALES, Manuel, Size characteristics of plutonium aerosols, 26:53062 (LA-DC-72-920)

GOODMAN, Frank O., Model for the repulsive elastic scattering of atoms by solid surfaces, 26:54089

GOODRICH, Gary Wayne, Low-frequency acoustic interactions in superconductors, 26:54439

GOODRICH, R. S., Study of two-phase systems by field--ion microscopy, 26:53653

GOOLD, L. A., Reaction of sulphide minerals with thiol compounds, 26:52954 (NIM-1439)

GOOVAERTS, M. J., Note on Feynman's path integrals, 26:55080

GORDEEV, V. V., Angular distribution of photoneutrons from Al, Ti, Cu, Mo, W, Pb, 26:54563

GORDON, E., Radiation noise in a high-sensitivity star sensor, 26:53293 (NASA-TM-X-2440, pp 735-43)

GORDON, Gilbert, Kinetics and mechanism of the oxidation--reduction reaction between uranium(IV) and chlorine(III) in the presence of phenol in aqueous acid solution, 26:53051

GORDON, Howard A., Two-body strange-particle final states in π^-p interactions at 4.5 and 6 GeV/c, 26:54217

GORENSTEIN, M. I., Statistical view on resonance widths and multiplicity in dual models, 26:54300 (ITF-72-53-E)

GORENSTEIN, Paul, Galactic origin for the soft x-ray background, 26:53973

GORETZKI, H., Influence of electron configuration on the absorption behavior of mixed crystals of hard materials, 26:53593

GOREVA, T. A., Synchrotron instability for plasma waves, 26:54820

GORN, L. S., Measurement of radiation in space, 26:53276

GORNI, J., Preparation and properties of W--Ni--Mo alloys, 26:53679

GOSPODINOV, G. A., Influence of Ni addition on reduction of WO_3 with H on sintering of the thus produced W powders, 26:53579

GOTO, Rensuke, Formation of antibiological substances by radiation-chemical reaction, 26:52998

GOTOH, H., Fission product release in TLG-1 in-pile gas loop. III, 26:53694 (JAERI-Memo-3936)

GOTSMAN, E., Properties of the pion exchange contribution to two and quasi two body reactions, 26:54270

GOTT, K., Change of structure and mechanical properties in stainless steel by irradiation. Part 1.2. The interrelationship of creep and stress relaxation phenomena, 26:53642 (STU-70-419/U-350(Pt.1.2))

GOUBAU, W. M., Phonon generation in KCl:Li$^+$ and KCl:OH- with pulsed electric fields, 26:55512 (COO-3151-139)

GOUMNEROVA, L., Determination of atomospheric concentrations of radon daughters by α-spectrometric extrapolation method, 26:53226

GOURDON, J., Experimental study of burn-up in fast breeder reactors, 26:55119 (CONF-720901-(Bks.1 and 2), pp 888-904)

GOUTIER, R., Cellular lesions induced by radiation sources, 26:53505

GOUYET, J. F., Spin-dependent operators in the occupation-branching number representation, 26:55077

GRABOWSKI, Z. W., Angular correlations of γ-rays from Coulomb excited ^{63} ^{65}Cu, 26:54594

Multipole mixing ratios of γ-transitions in ^{185}Re, 26:54644

GRADOV, O. M., Kinetic theory of parametric excitation of surface waves in semi-finite plasma, 26:54867

GRAETZER, R., (p,t) and (p,^{3}He) reactions on ^{27}Al at E/sub p/ = 27 MeV, 26:54551 (COO-535-673)

GRAND, J., Radioprotection during the interventions at Saint-Laurent-des-Eaux, 26:55354

GRANDILLO, A. D., Introduction to analysis of covariance and analcov, a computer program for covariance analysis, 26:55567 (MLM-1847)

GRANNIS, P., Charged particle multiplicity and angular correlation measurements in pp and γp collisions, 26:54192 (BNL-17141)

GRANT, W. A., Flux effects on damage in GaAs as measured by the channelling of ^{85}Kr, 26:54993

GRARD, F., LPS analysis of reactions $K^+p \to K^+\pi^+\pi^-p$ and $K^+p \to K^0\pi^+\pi^0p$, 26:54226

GRASSI, G. P., TERMO: digital code to evaluate steady state parameters of CIRENE type reactor, 26:55104 (CISE-R-246)

GRAUVOGEL, M. A., Incident of October 17, 1969 with Saint-Laurent-1, 26:55230

GRAVES, W. E., Predicting production rates of heavy actinides, 26:54654 (CONF-720901-(Bks.1 and 2), pp 97-107)

GRAY, R. M., Radiation tolerant gated video amplifier, 26:53307 (SC-DC-721159)

Universal digital integrated circuit, 26:53308 (SC-DC-721161)

GRAYS, R., Metabolism of Rickettsia typhi and Rickettsia akari in irradiated L cells, 26:53360

GRECHUKHIN, D. P., Properties of Strutinskii's method of shell correction, 26:54684 (IAE-2115)

GREEBLER, P., SEFOR: verification of the Doppler transient shutdown capability of LMFBR's, 26:55123 (CONF-720901-(Bks.1 and 2), pp 986-1005)

Significance of integral parameters in the design and performance of fast breeder reactors, 26:55121 (CONF-720901-(Bks.1 and 2), pp 928-39)

GREEN, A. E., Metabolism of Rickettsia typhi and Rickettsia akari in irradiated L cells, 26:53360

GREEN, A. E. S., Electron deposition in water vapor, with atmospheric applications, 26:54033

Electron energy deposition in CO_2, 26:54009

Electron-impact excitation cross sections and energy degradation in CO, 26:54008

GREEN, B. J., Effect of plasma flow on toroidal confinement, 26:54755

GREEN, Ira, Identification of the cell population responding to DNP--GL in lethally irradiated chimeric guinea pigs, 26:53474

GREENE, J. M., Toroidal effects on MHD stability in Tokamaks, 26:54806 (CONF-720804-6)

GREENE, R. L., Specific heat of granular aluminum films, 26:54450

GREENHALGH, G. H., Nuclear power in Japan, 26:55089

GREENHOW, William A., Radiation hardening of components and systems for nuclear rocket vehicle applications, 26:55370 (NASA-TM-X-2440, pp 471-5)

GREINER, D. E., Versatile, high-resolution particle identifier: theory, 26:53280

GREINER, John D., Magnetic susceptibility of rhenium trioxide, 26:55046

GREINER, W., Superheavy electronic molecules, 26:54111

GREITZ, Ulf, Transfer of simulated fallout-particles from pasture to grazing dairy cattle. I, 26:53527 (FOA-4-4503-A-3)

GRENDON, Alexander, Whose benefit. Whose risk. Whose balance, 26:54930

GRENGA, Helen E., Gas--metal interactions: field ion and emission microscopy, 26:53657

GRENIER, Jean-Claude, Crystallographic study of tetravalent $M(IV)(PO_3)_4$ compounds (M(IV) = Ce, U, and Th), 26:53045

GRIBBLE, R. F., Survey of Scyllac experiments, 26:54828 (LA-DC-72-896)

GRIBOV, V. N., e^+e^--pair annihilation and deep inelastic ep-scattering in perturbation theory, 26:54262

GRIDNEVA, S. A., Statistical model which allows for the conservation of P-, C-, and G-parity, 26:54360

GRIFFITH, J. A. R., Elastic and inelastic scattering of 12 MeV polarized deuterons by ^{24}Mg, 26:54557

GRIFFITH, T. C., Measurement of total cross sections for low energy positron-helium collisions, 26:54119

GRIFFITH, W. L., Technology and economics of utility

tunnels and common trenching, 26:55484 (CONF-720925-3)
GRIFFITHS, D. J., Paramagnetic relaxation initiated by flux jumping, 26:55029
GRIFFITHS, R. J., Energy dependence of the ^{3}He optical potential, 26:54580
Optical-model analysis of elastic scattering of 53.4 MeV helions from ^{56}Fe, 26:54571
GRIFFO, J. S., Preparation of ^{238}Pu metal, 26:53332 (MLM-1150)
GRIMES, S. M., Nucleon--nucleon scattering lengths from incomplete nucleon--deuteron breakup experiments, 26:54503 (UCRL-74069)
GRINDELL, A. G., Final systems design description of the failed fuel mockup (FFM) of the liquid-metal fast breeder reactor, 26:55191 (ORNL-TM-3656)
GRISHAEV, I. A., Influence of injection conditions on the transverse instability of the beam in a linear accelerator, 26:53758
GRISHIN, V. G., Multiple charged particle production in π^{-}p and π^{-}n interactions at p = 40 GeV/c, 26:54327 (JINR-E2-6596)
GRISHKEVICH, L. V., Simultaneous measurements of electron density and collision frequency in ionospheric D region, 26:54028
GRISON, Gaston, Creation of a community system of radioactive waste dumps, 26:53726
GRITZNER, M. L., Fast reactor shielding methods development, 26:55144 (CONF-720901-(Bks.1 and 2), pp 480-98)
GROCHULSKI, Witold, Cross sections for proton induced reactions on ^{43}Ca, ^{44}Ca, and ^{48}Ca isotopes in protons energy range 1 to 2 MeV, 26:54567 (INR-1407)
GROEBNER, Pavel, Carbon activity and solubility in a stainless chromium--nickel steel with about 18 percent Cr and 9 percent Ni, 26:55480 (BNWL-tr-72)
GROMOV, K. Ya., Excited quasi-proton states in magic ^{141}Pr nucleus, 26:54604 (JINR-P6-6519)
g-factor of 108 keV excited state in ^{151}Gd, 26:54634 (JINR-E6-6479)
Study of ^{149}Tb decay, 26:54603 (JINR-P6-6511)
GROMOVA, I. I., g-factor of 108 keV excited state in ^{151}Gd, 26:54634 (JINR-E6-6479)
Study of ^{149}Tb decay, 26:54603 (JINR-P6-6511)
GROSS, R., Approach to the nuclear many-body problem by variationally determined transformation. II, 26:54718
GROSSIORD, J. Y., (d,^{6}Li) reactions with light nuclei at 28 MeV, 26:54527 (LYCEN-7219)
GRUBER, U., Nuclear levels in ^{188}Re, 26:54637
GRUEEBLER, W., Phase shifts of p--d elastic scattering at 2.0, 2.7, 3.3, and 3.8 MeV, 26:54513
Preliminary measurements of polarization transfer in ^{4}He(d Vector,d Vector)^{4}He elastic scattering, 26:54498 (LA-DC-72-904)
GRUNT, J., Hematologic changes and changes in the blood proteins in experiments on white rats following intratracheal administration of radiocerium, 26:53516
GRZYMALA, Wieslaw, Studies of chromosome aberrations in peripheral blood of roentgenologists, 26:53428
GSCHNEIDNER, K. A. Jr., Low-temperature heat capacity of LaRu$_{2}$, CeRu$_{2}$, and CeRu/sub 2 -x/Pt/sub x/, 26:55047
GUERIN, Danielle, Manufacture and analysis of single crystals of labeled lithium hydride, 26:52894 (CEA-R-4338)
GUICHARD, A., (d,^{6}Li) reactions with light nuclei at 28 MeV, 26:54527 (LYCEN-7219)
GUIDOTTI, G. R., Progress in standardization of analytical methods for materials of nuclear interest. I, 26:52920 (RT/CHI-(72)3)
GUILLAUMONT, R., Hydrolysis of tetravalent plutonium, 26:53034 (MLM-1964(tr))
GUILLEMOT, Michel, Theoretical and experimental studies of electron plasma wave echoes, 26:54846 (EUR-CEA-FC-639)
GUKELBERGER, Armin, Diffusion measurements in systems Pd-V and Pd--Ti as well as metal--ceramic systems by means of microprobe, 26:53677
GULDEN, W., Group constant generation for the resolved resonance region, 26:55439 (CONF-720901-(Bks.1 and 2), pp 1183-91)
GUMPRECHT, D. F., Moessbauer observation of magnetic moment of 89-keV excited state of ^{119}Sn, 26:54624
GUNION, J. F., Evaluation of the J = 0 fixed pole in neutron Compton scattering, 26:54254
GUPTA, H. M., Role of paramagnetic impurities in the barrier region for superconducting tunnelling, 26:54442
GUPTA, Raj K., Irrotational or rotational flow motion in deformed nuclei, 26:54719
GUPTA, Veerendrakumar, Rajastan Atomic Power Project, 26:55215
GURNEY, Clifford W., Proton irradiation of stem cells: radiation damage and chemical radioprotection, 26:53454 (NASA-TM-X-2440, pp 642-6)
GURZADYAN, G. A., Ultraviolet absorption lines in spectrum of Vega, 26:53887
GUSAKOW, M., (d,^{6}Li) reactions with light nuclei at 28 MeV, 26:54527 (LYCEN-7219)
GUS'KOVA, A. K., Clinical aspects of radiation injury simulation and recuperation, 26:53411
GUSTAFSON, P. F., Radiological Physics Division annual report. Environmental research, January--December 1971, 26:53150 (ANL-7860(Pt.3))
GUTBROD, F., k^{2}-dependence of transverse pion electroproduction cross section in generalized Born term model, 26:54243 (DESY-72/30)
GUTBROD, H. H., Odd-parity three-particle, one-hole structure in ^{18}F via the reaction ^{15}N(^{6}Li,t)^{18}F, 26:54549
GUTBROD, Hans H., (^{6}Li,d) on ^{58}Ni and ^{64}Ni, 26:54586
GUTHMANN, E., Prototype nuclear power plant SNR 300, 26:55096
GUYON, Etienne, Experimental evidence for the Josephson effect in tin films, 26:54455
GUZZO, Anthony V., Prog. rpt. on photo initiated processes in vision, 11/15/69--11/14/72, 26:55496 (COO-1627-23)
Prog. rpt. on photo-initiated processes in vision, 11/15/71--11/14/72, 26:55495 (COO-1627-22)
GYURCSAK, J., Investigations of equivalence between heavy elements concentrations in rock, 26:52943

H

HAALAND, Carsten M., Active and passive defense interaction studies. Volume I. Summary, models, and calculations, 26:53135 (ORNL-TM-3485(Vol.1))
HAAN, G., Experimental arrangement for investigation of single crystals by means of fast ions, 26:54977
HAAS, F. X., Some neutron and gamma radiation characteristics of plutonium cermet fuel for isotopic power sources, 26:53336 (NASA-TM-X-2440, pp 853-8)
HAAS, P. A., Decontamination of HTGR reprocessing off-gases, 26:53059 (CONF-720823-12)
HABRAKEN, L., Stability and heat corrosion of Al covering on alloy Inco 713 C and on alloys of Co, 26:53676
Structure and properties of dispersion strengthened cobalt alloys, 26:53675
HACKSTEIN, Karl, Procedure for fabrication of spherical oxidic fuel and breeder particles, 26:53566
HACOBIAN, S., Theory of the nuclear quadrupole interaction in terms of irreducible tensors, 26:55063
HADARI, Z., Moessbauer effect in ^{239}Pu, 26:54661
HADLEY, George Ronald, Theoretical treatment of the Schwarz--Hora effect, 26:54245 (IS-T-531)
HAEFELE, W., Tendencies in the development of fast breeder reactors, 26:55095
HAEGGBLOM, H., Use of data from fast assemblies for adjustments of neutron data, 26:55436 (CONF-720901-(Bks.1 and 2), pp 599-612)
HAEHN, J., State and tendencies of chemical protection against ionizing radiation. A literature survey 1970/71, 26:53460 (SZS-132)
HAERENDEL, G., Coordinated observations of the magnetosphere: the development of a substorm, 26:54061
HAFFNER, J. W., Time behavior of solar-flare particles to 5 AU, 26:53929 (NASA-TM-X-2440, pp 336-44)
HAFKE, P., Animal experimental examinations on the effect of ionizing radiation on the maxillary bone with metallic bridges, 26:53480
HAFTEL, M. I., (p,2p) reactions with divers potentials. Technical Report No. 73-002, 26:54699 (ORO-4317-11)
HAGEMANN, R., Absolute measurement of the isotopic ratio of a water sample with a very low deuterium content, 26:52913 (AEC-tr-7345)
HAGENAH, W. D., Limits of detection in localized spectrochemical analysis with lasers, 26:55590 (ORNL-tr-2613-A)
HAGENMULLER, Paul, Mineral chemistry. An alkaline boride: the hexaboride NaB$_{6}$, 26:55560 (LA-tr-72-16)
HAGMANN, D. B., Conceptual design for the handling and remote disassembly of the fuel element failure propagation loop at the HFEF, 26:53727 (ANL/HFEF-1)
HAGSTON, W. E., Analysis of the effects of electron damage on the bound-to-bound emission intensity of cadmium sulphide, 26:55002
HAHN, Ch., Measurements of absolute integral total cross sections of He--H$_{2}$ and the interaction potential, 26:54130
HAHN, H., Theory of $\pi/2$-mode biperiodic deflectors, 26:53798
HAHN, R. L., Calculations of spallation-fission competition in the reactions of protons with heavy elements at energies less than or equal to 3 GeV, 26:54666
HAISSINSKY, M., Application of the Mendeleev periodic law to elements having Z values lying between 104 and 107, 26:53053
HAJDU, Imre, Chromosome aberrations following repeated gastric roentgen examinations, 26:53427
HALAMA, H. J., Surface condition of niobium for superconducting rf cavities, 26:53748
HALE, John, Dose tables for ^{252}Cf implants, 26:54906
HALFORD, G. R., Cyclic creep-rupture behavior of three high-temperature alloys, 26:53690
HALL, Larry L., Direct determination of total ionic fluoride in biological fluids, 26:55637 (UR-3490-184)
HALLOWELL, P. J., Track detection program for a Hough Powell Device, 26:53274 (RHEL/R-241)
HALPERIN, A., Thermally stimulated currents and thermoluminescence of paramagnetic centers in hexagonal boron nitride, 26:55015
HAM, Sang Yul, Effect of cortisone on serum protein of gamma-irradiated mice, 26:53490

HAMILTON, J. H., Two decades of research on radioactivity, 26:53263
HAMMANN, T. F., Pion--nucleon potentials for use in low-energy nuclear physics, 26:54724
  Realistic nonlocal forces and their importance in understanding the microscopic properties of nuclear matter and nuclei, 26:54683 (FRNC-TH-180)
HAMOUDA, I., Exit tube effect upon the measured space--energy neutron spectra, 26:54470 (AREAEE-133)
  Fast neutron scintillation spectrometer with double compensation circuit for gamma-ray discrimination, 26:53251 (AREAEE-137)
HANCOX, R., Use of liquid lithium as coolant in toroidal fusion reactor. II, 26:54825 (CLM-R-116)
HANDA, M., Thin film of organic fluorescent materials for simple detection of alpha rays, 26:53265
HANDLEY, T. H., Analysis of traces at ORNL's new High-Flux Neutron Activation Laboratory, 26:52897 (CONF-721010-3)
  Nuclear spectroscopy of neutron-deficient La, Dy, and Er activities, 26:54643
HANNA, M. M., Empirical expressions for the thermal diffusion column shape factors in the extreme cylindrical case, 26:53326 (AREAEE-131)
HANNA, Nabil N., Transistorized pulse generator for testing nuclear counting equipment, 26:53295 (AREAEE-132)
HANNA, S. S., Giant dipole resonance in ^{16}O observed with polarized proton capture reaction, 26:54531
HANNAHS, B. J., Bibliography on handling, control, and monitoring of tritium (December 1968--January 1972), 26:53155 (MLM-1946)
HANNEMAN, G. D., Relative biological effectiveness of fast neutrons compared with x rays: prenatal mortality in the mouse, 26:53453 (NASA-TM-X-2440, pp 641)
HANSEN, Earl M., Pulse radiolysis of liquids at high pressures. III. Hydrated-electron reactions not controlled by diffusion, 26:53006
HANSEN, J. D., Compilation of cross sections. I. π^- and π^+ induced reactions, 26:54201 (CERN/HERA-72-1)
HANSEN, Johnny, Improving match between microwave source and microwave transmission system at Risoe 10 MeV electron linear accelerator, 26:53746 (RISO-M-1518)
HARACZ, Richard D., Damped pseudoscalar- and vector-meson model for nucleon--nucleon scattering, 26:54348
HARDEKOPF, R. A., Four-nucleon studies. I, 26:54516
  Four-nucleon studies. III, 26:54517
  Four-nucleon studies. IV, 26:54518
HARDY, K. A., Observation of temperature spikes following Coulomb excitation, 26:54646
HARE, A. P. G., Temperature dependence of vibronic spectra in irradiated silicon, 26:54999
HARE, M. G., Photon stability, 26:54274
HARKER, Y. D., Use of CFRMF integral data in cross section evaluations, 26:55384 (CONF-720901-(Bks.1 and 2), pp 613-22)
HARMATZ, B., Nuclear spectroscopy of neutron-deficient La, Dy, and Er activities, 26:54643
HARMS, A. A., Optimum angular segmentations in neutron transport analysis, 26:55434 (CONF-720901-(Bks.1 and 2), pp 266-74)
HARMS, E., Application of the method of moments to three-body scattering, 26:54715
HAROLD, Richard J., Rapid method for complementation testing of ultraviolet-sensitive mutants of Streptomyces coelicolor, 26:53378
HAROUN, N. A., Densification of uranium dioxide: a literature review, 26:53547 (AREAEE-135)
  Preparation of sinterable uranium dioxide, 26:53546 (AREAEE-134)
HARPER, E. P., Meson-exchange currents and ^{3}H, ^{3}He magnetic moments, 26:54506
HARRIES, J. R., Spectral and pulsed x-ray emission from the Crab Nebula, 26:53919
HARRIS, D. R., Development of ENDF/B shielding data processing codes, and integral tests, 26:55141 (CONF-720901-(Bks.1 and 2), pp 316-24)
  Sensitivity of calculated pulsed sphere spectra and neutron age to carbon cross sections, 26:54474 (CONF-720901-(Bks.1 and 2), pp 409-17)
HARRIS, David O., Microwave spectrum and ring-bending vibration of 3-oxetanone, 26:52960
HARRIS, F. A., Muon identification using multiwire proportional chambers, 26:53282
HARRIS, G., Acute effects of ionizing radiation on antibody-producing cells (PFC) in mouse spleen during primary and secondary responses to sheep erythrocytes (SRC), 26:53464
HARRIS, L. Jr., Developments in integral shielding experiments involving fast-neutron transport, 26:54938 (CONF-720901-(Bks.1 and 2), pp 385-96)
HARRISON, C., Annihilation spectrometer for investigation of heavy meson spectra, 26:53279
HARRISON, W. C., Reaction $\pi^- p \rightarrow p\pi^+\pi^-\pi^-\pi^0$ at 20 GeV/c, 26:54207 (COO-3064-3)
HART, R. L., Surface energy budget measurements over Lake Michigan, 26:53189 (ANL-7860(Pt.3), pp 270-98)
HARTE, John, Energy, 26:53193
  Patient earth, 26:53191
  Radiation, 26:53396
HARTECK, P., Study of the pulse radiolysis of gases. Final report, 26:52980 (COO-3461-1)
HARTLE, R. E., Solar-wind heating, 26:53942
HARTLEY, D. B., Comparison of defect centres formed in oxides by explosive shocking and high-energy radiation, 26:54983
HARTNAGEL, H. L., Experimental determination of ion density trapped by electron beam, 26:55641
HARVEY, J. A., keV neutron total cross section measurements at ORELA, 26:54566 (CONF-720901-(Bks.1 and 2), pp 1075-86)
HARVEY, J. W., C_2 in sunspots, 26:53953
HARVEY, P. M., Infrared photometry of northern Wolf--Rayet stars, 26:53889
HASEGAWA, Akio, Heat treatment, microstructure, and mechanical properties of heavy gage steels for nuclear reactor pressure vessels. I, 26:53646
HASKELL, R., Study of the pulse radiolysis of gases. Final report, 26:52980 (COO-3461-1)
HASS, M., Level scheme of ^{144}Sm determined by the (γ,γ') reaction, 26:54619
HATTORI, T., Levels of ^{90}Nb excited via the ^{90}Zr$(p,n\gamma)$ reaction, 26:54613
HAUG, R. M., Influence of clinoptilolite on ^{90}Sr and ^{137}Cs uptakes by plants, 26:53540
HAUMENKOV, P. A., Passage of high-power laser radiation through an optically dense plasma, 26:54785
HAUSER, J. J., Specific heat of granular aluminum films, 26:54450
HAUSLER, B., Change of solar-flare proton-to-alpha ratios during an energetic storm particle event, 26:53966
HAUSNER, H. H., Effect of quenchsintering on the grainstructure of sintered metals, 26:53662
HAUSNER, Henry H., Problems in powder mixing, 26:53617
HAVEL, Jaroslav, Absolute activity in irradiated fuel material by method of gamma scanning, 26:53041 (UJV-2867-M,A)
HAWKINS, E. V., Probe velocity transducer, 26:53303 (LA-4999)
HAYASHI, Takemi, Note on the urbaryon models, 26:54297
HAYASHI, Teiji, Application of electrophoresis for burnup determination, 26:52933 (JAERI-Memo-4094)
HAYES, Edward F., Quantum mechanical studies of the vibrational excitation of H_2 by Li$^+$, 26:54133
HEASTIE, R., Raman spectra of orthorhombic and cubic H and deuterium chlorides at temperatures above 80°K, 26:52971
HEATH, C. A., Thermionic reactor power system: effects of radiation on integration with manned space station, 26:55365 (NASA-TM-X-2440, pp 299-306)
HEATON, Thomas R., Radiation problems associated with Skylab, 26:54049 (NASA-TM-X-2440, pp 748-55)
HEAVEN, S. H., Zero energy reactor facility at B.N.L., 1972, 26:55409 (RD/B/N-2272)
HECKMAN, R. C., Passive calorimeter for pulsed electron beam energy measurement, 26:53258 (SC-DR-720630)
HECKO, I., Hematologic changes and changes in the blood proteins in experiments on white rats following intratracheal administration of radiocerium, 26:53516
HEIL, G., Elastic scattering of vector polarized deuterons from ^{48}Ti, ^{49}Ti, ^{50}Ti, ^{51}V, ^{52}Cr, 26:54572
HEINZ, R. M., Indiana University Spark Chamber Group technical progress report, December 1, 1971--November 30, 1972, 26:54206 (COO-2009-36)
HEITZINGER, F., Oxidation behavior of Mo + ZrO_2 cermets, 26:53585
HELBERT, J. M., Relative isotope shift (112-114)/(110-112) in lambda = 4416 A line of cadmium, 26:54625
HELDENBRAND, W. R., Analysis of anticipated transients without trip, 26:55193 (BAW-10016)
HELLENS, R. L., Physics of PWR reactors, 26:55107 (CONF-720901-(Bks.1 and 2), pp 3-22)
HELLSTRAND, E., Change of structure and mechanical properties in stainless steel by irradiation. Part 1.1. Metallographic study of neutron irradiated and unirradiated 12R72HV after tensile testing, 26:53701 (STU-70-419/U-350(Pt.1.1))
HELM, R., Momentum matching in ISA long insertions, 26:53773 (BNL-17051)
HELMS, C. R., Comparison of the oxidation process in strontium and cerium by ultraviolet photoelectron spectroscopy, 26:53611
HENDEE, William R., Dose computations and treatment planning in pion therapy, 26:54876 (LA-4874, pp 145-52)
HENDEL, H. W., Measurement of effective collision frequency in rf heating through parametric instabilities, 26:54750 (CONF-720705-2)
HENDEL, Hans W., Dynamic stabilizer for plasma instabilities to improve plasma confinement and to increase plasma density, 26:54823
HENIS, J. M. S., Hydride ion transfer and isotope effects in CD_4--silane ion molecule reactions, 26:52961
HENKE, R. P., High-Z-particle Apollo astronaut dosimetry with plastics, 26:53231 (NASA-TM-X-2440, pp 149-56)
HENRY, Bryan R., Observation and calculation of a position dependent deuterium effect on the triplet lifetime of anthracene-d_8, 26:52972
HENRY, Maureen L., Correction of a formula used in radioassay of /sup 99m/Tc, 26:52946
HENRYSON II, H., Studies of methods for fast neutron multigroup cross section generation and their effect upon the neutronics properties of LMFBR critical assemblies, 26:55113 (CONF-720901-(Bks.1 and 2), pp

211-28)

HENSLER, R., Lifetime of 3.74-MeV (3-) state of ^{40}Ca, 26:54575

HENTZ, Robert R., Pulse radiolysis of liquids at high pressures. III. Hydrated-electron reactions not controlled by diffusion, 26:53006

HENZEL, N., Calculation of the time dependent fission product heat source strength in two coupled systems with consideration of fission product escape, 26:55206 (KFK-1580)

HEPPNER, J. P., Polar-cap electric field distributions related to the interplanetary magnetic field direction, 26:54062

HERAK, J. N., Radiation abstraction of hydrogen atoms in single crystals of thymine, 26:52999

HERKMEN, I., Experimental determination of ion density trapped by electron beam, 26:55641

HERLEY, P. J., Microscopic observation of x-ray and γ-ray-induced decomposition of ammonium perchlorate crystals, 26:52985 (NASA-TM-X-2440, pp 584-94)

HERNANDEZ, G., Spectroscopic studies of the arc of March 8-9, 1970, 26:54014

HERNDON, David J., Partial wave analysis of the reaction $\pi N \rightarrow N\pi\pi$ in the CMS energy range 1.6 GeV to 2.0 GeV, 26:54328 (LBL-544)

HERR, H., Photoproduction of π^+-mesons on polarized protons at photon energies between 0.5 and 2.2 GeV, 26:54172 (NP-19415)

HERRMANN, Friedrich, Production of high defect concentrations in alkali halides by electron bombardment, 26:54973 (FRNC-TH-210)

HERSCHMAN, Harvey R., Production of a nervous-system-specific protein (14-3-2) by human neuroblastoma cells in culture, 26:55621 (UCLA-12-877)

HERSCOVICH DE PAHISSA, M. H., Effect of gamma radiation on an Argentine variety of wheat, 26:53381 (CNEA-309)

HERTELENDY, N. A., Radiation heating in selected NERVA engine components, 26:55369 (NASA-TM-X-2440, pp 460-5)

HERTIA, D. I., Probabilistic interpretation of cluster function series development of many-electron wave functions, 26:54146

HERZ, A. J., Helium-recoil spectrometer, 26:53281

HESLIN, Jane, Energy spectrum of electrons in water irradiated with 10- to 20-MeV electron beams, 26:54894

HESS, M. W., Intestinal barrier to bacterial invasion, 26:55474 (BNL-17004)

HESS, R., Performances of a proportional chamber with intermediate high voltage planes, 26:53213

HESSELBACHER, K. H., Collisional ionization of helium by slow electrons, 26:54123

HESSELINK, W. H. A., Decay of ^{227}Th from α--γ coincidence and directional correlation studies, 26:54673

HETTINGER, H., Buckling measurements in ECO with few CIRENE fuel elements, 26:55106 (CISE-R-283)

HEULIN, B., Internal friction peaks due to N in Nb--Zr alloys, 26:53692

HEUNEMANN, D., Identification of rotational band in ^{240}Pu fission isomer, 26:54664

HEURTEBISE, M., Geiger-Mueller counter designed to measure reproducibly activities retained on resin columns, 26:53212

HEUSCH, C. A., New evidence on the photoexcitation of I = $^1/_2$ nucleon isobars, 26:54166 (CALT-68-322)

HEWITT, John E., Radiation exposures during the Biosatellite 2 flight, 26:53365 (N-72-20065)

HEY, A. J. G., Description for the reactions a + b → c + d + e, 26:54330

HEYDA, D., Reaction $\pi^-p \rightarrow p\pi^+\pi^-\pi^-\pi^0$ at 20 GeV/c, 26:54207 (COO-3064-3)

HEYLAND, G. R., Measurement of total cross sections for low energy positron-helium collisions, 26:54119

HEYLEN, P. R., Extraction of plutonium from heavy water fuels by the SALTEX process, 26:53079 (EUR-4812)

HIGUCHI, Y., Occurrence of Pc 4, 5 micropulsation activity at the polar cusp, 26:54034

HILAIRE, A., Acceleration of polarized protons in Saturne, 26:53762

HILL, F. F., Specific enrichment of mutants of Escherichia coli with an altered acyl CoA synthetase by tritium suicide, 26:53518

HILLERET, N., Analysis using secondary ion emission in semiconductors, 26:52937

HILSE, D., Universal time administration in a real time system, 26:55541 (KFK-1526)

HIRAMATSU, Tsutomu, Vibration analysis of E. P. discharge electrode, 26:55591 (ORNL-tr-2636)

HIRAOKA, Toru, Analysis of pulsed neutron experiments on bare fast multiplying system by Storrer--Stievenart's theory, 26:54483 (JAERI-M-4652)

  Critical experiments on FCA I-6, 26:55401 (JAERI-Memo-3891)

  Semi-experimental measurement of effective delayed neutron fraction of a fast reactor system by application of pulsed neutron technique, 26:55403 (JAERI-Memo-4004)

HIRATA, M., DWBA treatment of cluster transfer reactions, 26:54706

HIRAYAMA, Tadashi, Ionized helium in prominences and in the chromosphere, 26:53949

HIROSAWA, M., Experimental study of the ultimate strength of composite beams subjected to alternate loading of positive and negative bending, 26:55571 (NRC-TT-1557)

HIRSCH, G. H., Stimulation of renal organic base transport by uranyl nitrate, 26:53537

HIRSHBERG, J., Upper limit of the torque of the solar wind on the Earth, 26:54075

HIRUTA, K., In-beam alpha spectroscopy of N = 128 isotones, 26:54651

HISHIDA, Makoto, Outline of PNC's activities in the field of sodium-water reaction, 26:55155 (CONF-710548-, pp 129-54)

HISKES, J. R., Atomic and cluster injection into D--T mirror fusion power systems, 26:54757

HIVERT, Andre, Production of Ni--Cr--ThO$_2$ alloys by means of chromium diffusion through halogen carrier in NiThO$_2$ grain, 26:53627

  Production of Ni--ThO$_2$ alloy with dispersed phase starting from organometallic compounds, 26:53626

HLADKY, Eduard, Radiation safety of nuclear power plants, 26:55210

HOANG, T. F., Bose distribution and scaling law, 26:54349

HOCHMAN, R. F., Applications of field--ion microscopy in physical metallurgy and corrosion. Conference held at Atlanta, Georgia, May 15--17, 1968, 26:53647

HOCHMAN, Robert F., Gas--metal interactions: field ion and emission microscopy, 26:53657

HOCKENBURY, R. W., Iron-filtered neutron beams: a new approach to precision time-of-flight cross section measurements, 26:54597 (CONF-720901-(Bks.1 and 2), pp 1107-14)

HODAPP, A. E. Jr., Flight test evaluation of a fluidically actuated monopropellant hydrazine roll control system, 26:55600 (SC-DC-722244(RD))

HODGKINSON, D. P., Unitarity constraints on helicity amplitudes, 26:54418

HOEKSTRA, E. K., Prog. rpt. on fast reactor program, 10--12/71, 26:55083 (EURFNR-1001)

HOENIG, Stuart A., Study of stress corrosion cracking of U--10 percent Mo wires, 26:53610

HOERZ, G., Thermodynamic description of the metal-rich region in the system niobium--molybdenum--nitrogen, 26:53671

HOFFMAN, E. W., Evidence for a neutral meson near 1033 MeV, 26:54205 (COO-1428-311)

HOFFMAN, J. M., Rocket-borne auroral optical measurements, 26:54012 (SC-RR-720543)

HOFFMAN, T. J., DOMINO: a general purpose discrete ordinates to Monte Carlo coupling code for radiation transport, 26:54872 (CONF-720901-(Bks.1 and 2), pp 499-511)

HOFFMAN, Zbigniew, Automatic data acquisition and registration from mass spectrometer, 26:53324

HOFFMANN, G. W., Consistent coupled-channel Born approximation analysis of ^{88}Sr(d,np) ^{88}Sr and ^{88}Sr(d,p)^{89}Sr, 26:54588

HOFFMANN, W., Photoproduction of π^+-mesons on polarized protons at photon energies between 0.5 and 2.2 GeV, 26:54172 (NP-19415)

HOFMANN, P. L., FTR neutronics: status, problems, and development programs, 26:55391 (CONF-720901-(Bks.1 and 2), pp 839-87)

HOFSTETTER, K. J., Levels in ^{186}Os as populated by the decay of ^{186}Ir, 26:54633 (COO-3255-3)

HOGE, Kenneth G., Specimen strain measurement in the split Hopkinson pressure bar experiment, 26:55626 (UCRL-73610)

HOHMANN, H., Buckling measurements in ECO with few CIRENE fuel elements, 26:55106 (CISE-R-283)

HOINKIS, E., Surface interactions of iodine with Fe$_3$O$_4$, 26:52953 (CONF-720716-1)

HOKAKU, Nobuyoshi, Revision of the laws and regulations concerning indemnity for damage due to atomic energy and attendant revision of atomic energy insurance, 26:55459

HOLBERG, Jay, Extreme-ultraviolet emissions from an aurora, 26:54030

HOLLAND, Florence, Diethylpyrocarbonate toxicology and pharmacology, 26:55579 (ORNL-TIP/TIRC-72-52)

HOLLAND, L. M., Effect of continuous gamma-ray exposure on performance of learned tasks and effect of subsequent fractionated exposures on blood-forming tissue, 26:53452 (NASA-TM-X-2440, pp 633-40)

HOLLAND, Richard Frederick, Q region of the $K^+\pi^+\pi^-$ spectrum from K^+ meson interactions in deuterium at 9 GeV/c, 26:54228

HOLLINGSWORTH, L. E., Plant equipment inventory management, 26:55605 (SC-M-68-808)

HOLLINGWORTH, R. W., Theory of the nuclear quadrupole interaction in terms of irreducible tensors, 26:55063

HOLLIS, M. J., Ion beam monitor for nanoampere currents, 26:53802

HOLLY, F. Eugene, Geomagnetically trapped radiation environment: a radiological point of view, 26:54952 (NASA-TM-X-2440, pp 170-7)

HOLM, Dale M., Active ^{3}He activation analysis for carbon and oxygen, 26:52899 (LA-DC-72-809)

HOLMES, D. E., ESR study of amino acid and protein-free radicals in solution. IV, 26:52995

HOLMES, L. M., Magnetization, velocity of sound, and specific heat of Sc$_3$In, 26:55045

HOLZWARTH, G., Boson expansions and Hartree--Bogolyubov theory, 26:54741

HONECK, H. C., Simultaneous line over-relaxation (SLOR) in hexagonal lattice, 26:55433 (CONF-720901-(Bks.1 and 2), pp 253-65)

HONES, E. W., Coordinated observations of the magnetosphere: the development of a substorm, 26:54061

HONG, Sun Joo, ESR study of amino acid and protein-free radicals in solution. IV, 26:52995

HOOD, G. M., Ultra-fast solute diffusion in α-Ti and α-Zr, 26:53666

HOOKE, W. M., Observation of a parametric instability near the lower hybrid frequency, 26:54805 (CONF-720705-4)

  Observation of non-linear effects near the lower hybrid resonance frequency, 26:54845 (CONF-720804-3)

  Wave generation and heating near the ion cyclotron frequency in the ST Tokamak, 26:54752 (CONF-720804-4)

HOOT, C. G., Measurements of gamma-ray production cross sections for shielding materials of space nuclear systems, 26:54960 (NASA-TM-X-2440, pp 500-11)

HOOVER, W. R., Dynamic fracture behavior of Borsic--Al composites, 26:53557 (SC-DC-721080)

HOPWOOD, David A., Rapid method for complementation testing of ultraviolet-sensitive mutants of Streptomyces coelicolor, 26:53378

HORAK, J. A., Electrical resistivity increase rates in Fe--C and Fe--N solid solutions during neutron irradiation at 4.5 K, 26:54989

HORI, Masao, Detection of small-leak sodium-water reaction in the prototype LMFBR steam generator by in-sodium type hydrogen detector, 26:55156 (CONF-710548-, pp 155-70)

  Outline of PNC's activities in the field of sodium-water reaction, 26:55155 (CONF-710548-, pp 129-54)

HORRELL, D. R., Thermal and radiation stability of polyvinyl chloride, 26:52992 (RFP-1924)

HORVATH, Z. Gy., Measurement of mode-locked ultrashort laser pulses by different order photoelectric effects, 26:55544 (KFKI-72-41)

HORVATH, Zs., Production and testing of homogeneous sterilization dose during radiosterilization, 26:53340

HORWITZ, E. P., Production of actinides and search for super-heavy elements using secondary reactions induced by GeV protons, 26:54672

HOSEA, J. C., Wave generation and heating near the ion cyclotron frequency in the ST Tokamak, 26:54752 (CONF-720804-4)

HOSTE, J., Neutron activation analysis, 26:52912

HOTTELL, H. C., New energy technology: some facts and assessments, 26:55085

HOUGH, J., Proportional counters for the localisation of ionising radiation, 26:53221

HOUSTON, D. H., Proton-recoil proportional counter spectrometry for reactor spectrum measurements, 26:55122 (CONF-720901-(Bks.1 and 2), pp 959-72)

HOUVER, J. C., Differential measurements on ion-atom collisions in energy range 500 to 3000 eV. IV, 26:54122

HOVESTADT, D., Change of solar-flare proton-to-alpha ratios during an energetic storm particle event, 26:53966

HOWARD, Edward Glenn, Studies of Type III bursts and refraction in the solar corona at hectometer wavelengths, 26:53934

HOWARD, Hilard H., Proceedings of the fifth LAMPF users meeting held at the Los Alamos Scientific Laboratory, Los Alamos, N.M., November 8-9, 1971, 26:53784 (LA-4874)

HOWARD, J. B., New energy technology: some facts and assessments, 26:55085

HOWARD, Robert, Atlas of magnetic fields in the solar corona, 26:53955

HOWELL, Wallace P., Radiation protection standards: quo vadis. Volume I. Proceedings of the sixth annual health physics society topical symposium, Richland, Washington, November 2--5, 1971, 26:54914

  Radiation protection standards: quo vadis. Volume II. Proceedings of the sixth annual health physics society topical symposium, Richland, Washington, November 2--5, 1971, 26:54922

HREN, J. J., Analysis of dislocations and stacking faults by FIM, 26:53649

HSU, F. S. L., Magnetization, velocity of sound, and specific heat of Sc_3In, 26:55045

HUANG-LIN, Lih Jen, Magnetic moments of odd mass nuclei with simple configurations, 26:54679 (COO-3001-17)

HUBBARD, L. B., Ground state of ^{40}Ca, 26:54577

HUBBARD, W. B., Statistical mechanics of light elements at high pressure. II. Hydrogen and helium alloys, 26:54003

HUBER, E. E., Thermal effects on aquatic organisms: annotated bibliography of 1971 literature, 26:53190 (ORNL-EIS-72-28)

HUBLER, G. K., Magnetic moment of the 1.409-MeV 2^+ state of ^{54}Fe, 26:54581

HUDGINS, H. J., Terminal control language for the MADCAP programming language, 26:55551 (LA-DC-72-411)

HUDSON, H. S., Thick-target processes and white-light flares, 26:53961

HUDSON, J. A., Application of field--ion microscopy in studies of point defects and radiation damage, 26:53704

HUEBENER, R. P., Speed of magnetic-flux penetration into electrical conductors, 26:54453

HUFFMAN, Arthur H., Neutrino--deuteron interaction cross sections at LAMPF energies, 26:54233 (LA-DC-72-848)

HUGENBERGER, Charles E., Pneumatic logic controls for automatic vacuum systems, 26:55629 (UCRL-73921)

HULBERT, A. J., Relative nonhomogeneities of radiation dose to the respiratory tract from inhaled radionuclides, 26:53536

HULL, Andrew P., Reactor effluents: as low as practicable or as low as reasonable, 26:55220 (BNL-16965)

HUNT, B. R., Image restoration by constrained least-squares estimation, 26:55451 (LA-DC-72-626)

HUNT, C. E. L., Computer program to calculate damage distributions in ion-bombarded targets, 26:54969 (AECL-4130)

HUNT, R., X-ray emission from intergalactic gas in the neighbourhood of galaxies, 26:53988

HURST, R. R., Double K-shell ionization in the decay of ^{131}Cs and ^{165}Er, 26:54617

HURTIGER, J., Radioprotection during the interventions at Saint-Laurent-des-Eaux, 26:55354

HURT III, S. S., Bulk shielding facility quarterly report, April, May, and June of 1972, 26:55408 (ORNL-TM-3949)

HUSSEIN, A., Exit tube effect upon the measured space--energy neutron spectra, 26:54470 (AREAEE-133)

HUSSEIN, A. M., Penetration of travelling high-frequence electromagnetic field into a ''non-transparent'' plasma, 26:54843 (AREAEE-124)

  Semiclassical theory of electromagnetic field interaction with a many-level molecular system, 26:55468 (AREAEE-136)

HUTCHEON, I. D., Dynamical models of the Galaxy and its gamma ray emission, 26:53992

HUTCHINS, B. A., Significance of integral parameters in the design and performance of fast breeder reactors, 26:55121 (CONF-720901-(Bks.1 and 2), pp 928-39)

HUTCHINS, J. E. C., H_2BH_3 as an intermediate in tetrahydriodoborate hydrolysis, 26:52965

HUTCHINSON, Franklin, Relation between single-strand DNA mass and sedimentation distance in alkaline sucrose gradients, 26:52981 (COO-3571-3)

HUTCHINSON, Paul I., Radiation exposure to the Orbiting Lunar Station and lunar surface related to reusable nuclear shuttle operations, 26:55362 (NASA-TM-X-2440, pp 264-9)

HUTSON, Richard L., Biomedical applications: beam line and facility, 26:53793 (LA-4874, pp 78)

HUVAR, A., Distribution of deep doses near implanted beta and mixed beta--gamma emitters, 26:54897

HVINDEN, T., Radioactive fallout in Norway, 26:53161

HWANG, Chester F., Nucleon Physics Laboratory (NPL), 26:53790 (LA-4874, pp 63-6)

HWANG, R. N., Studies of methods for fast neutron multigroup cross section generation and their effect upon the neutronics properties of LMFBR critical assemblies, 26:55113 (CONF-720901-(Bks.1 and 2), pp 211-28)

HWANG, Richard N., Some recent developments in resonance and Doppler theory, 26:54480 (CONF-720901-(Bks.1 and 2), pp 1166-82)

HYUGA, H., Magnetic moments of ^3H and ^3He in the quark model, 26:54494 (COO-3001-15)

I

ICHIKAWA, R., New metastable phase in rapidly solidified Al--Zr alloys, 26:53686

ICHIKAWA, Yoshi H., Automodulation of ion oscillation modes in plasma, 26:54851

ICHIMURA, M., Magnetic moments of ^3H and ^3He in the quark model, 26:54494 (COO-3001-15)

IDA, M., Possible correlations among baryon trajectories, 26:54338

IHARA, Masayoshi, Epitaxial growth of tantalum carbide, 26:53564

IIJIMA, Tsutomu, Analysis of pulsed neutron experiments on bare fast multiplying system by Storrer--Stievenart's theory, 26:54483 (JAERI-M-4652)

IKEBE, Yukimasa, Measurements of thoron in the atmosphere, 26:53227

IKEDA, A., $0^+ \rightarrow 0^+$ beta transition of ^{188}W, 26:54641

IKEGAMI, Tetsuo, Experimental study of relaxation phenomena in non-equilibrium MHD generator duct, 26:53104

IKEMOTO, Ichiro, Detection of small-leak sodium-water reaction in the prototype LMFBR steam generator by in-sodium type hydrogen detector, 26:55156 (CONF-710548-, pp 155-70)

IKUTAME, Ken, Experimental facility to simulate loss-of-coolant accident of light-water reactors. V, 26:55205 (JAERI-Memo-4041)

ILIOPOULOS, J., Test of the algebra of bilocal operators, 26:54253

ILOVAISKY, Sergio A., Study of galactic supernova remnants. II, 26:53912

IMACHI, Masahiro, Systematic structure in hadronic two-body scattering and resonance correlation. III, 26:54342

IMACHI, Masaki, Study on the effects of radiation on the molding of polymers, 26:53720

IMAMURA, Nobutaka, Effects of high intensity pulsed x-ray (linear accelerator) or gamma-ray irradiation upon tumorigenesis and immunocompetence in mice, 26:53469

IMAOKA, T., Analysis of pressure wave propagation in pipe

rupture accidents of light-water cooled reactors by use of the burst code. I, 26:55203 (JAERI-M-4473)
INAGAKI, H., Sodium inpile loop, 26:55381 (CONF-710959-, Paper 6)
INAMURA, T., In-beam alpha spectroscopy of N = 128 isotones, 26:54651
INCZEDY, J., Use of ion exchangers in analytical chemistry, 26:52948
INGALLS, Paul D., Resolution of the ^{20}Na beta decay anomaly, 26:54550 (COO-535-671)
INGHAM, M. F., Observations of the airglow continuum, 26:54025
INTERIAN, Alfred, Teleoperator systems for manned space missions, 26:53731 (NASA-TM-X-2440, pp 280-90)
INTRILIGATOR, D. S., Simultaneous solar-wind plasma and magnetic-field measurements in the expected region of the extended geomagnetic tail, 26:54074
ION-MIKHAI, R., g-factor of 108 keV excited state in ^{151}Gd, 26:54634 (JINR-E6-6479)
IPSON, S. S., ^{57}Fe(t,p)^{59}Fe and ^{58}Fe(d,p)^{59}Fe reactions, 26:54592
IRGAZIEV, B. F., Factorization of pair potential by Bateman modified method in two- and three-body problem, 26:54345 (JINR-P4-6505)
ISAEV, P. S., Analysis of $K\pi$-interaction in energy region up to 1 GeV, 26:54315 (JINR-E2-6525)
ISAEV, V. I., Angular distribution of photoneutrons from Al, Ti, Cu, Mo, W, Pb, 26:54563
ISHAM, C. J., CP-violating gauge interactions, 26:54367
ISHIDA, Yoichi, Radiation myelopathy etiology, 26:53429
ISHIGURO, Misako, Experimental facility to simulate loss-of-coolant accident of light-water reactors. V, 26:55205 (JAERI-Memo-4041)
ISHII, T., Optical 4d → 4f transition and binding energy of 4d level in La and Ce, 26:54095
ISHII, Takehiko, Photoelectron spectroscopic measurements of core level binding energies of Y, La, and Ce, 26:55024
ISHIKAWA, Michio, Analysis of pressure wave propagation in pipe rupture accidents of light-water cooled reactors by use of the burst code. I, 26:55203 (JAERI-M-4473)
  Study on the works of engineering reactor-safety, 26:55204 (JAERI-M-4535)
ISKHAKOV, G. I., Study of ^{149}Tb decay, 26:54603 (JINR-P6-6511)
ISRAEL, M. H., Observation of VH and VVH cosmic rays with an ionization--Cherenkov detector system, 26:53843
ISRAELSSON, S., Natural α-activity in air near ground, 26:53160 (UUIM-27)
  Natural β-activity in air near ground. Parts B--E, 26:53159 (UUIM-26)
ISTOMIN, Ya. N., Nonlinear evolution of a quasi-monochromatic packet of helical waves in a plasma, 26:54868
ISTVANNE, Lovas, SLIP: a symmetrical subroutine developed for CDC 3300 and ICL 1905 computers, 26:55543 (KFKI-72-32)
ITO, Hideyuki, Eddy current testing of stainless steel fuel jacket cladding tubing, 26:53125
ITO, K., Radionuclide production by cosmic rays in lunar rocks, 26:53860
ITO, Tadaharu, Application of electrophoresis for burnup determination, 26:52933 (JAERI-Memo-4094)
ITO, Takaaki, Leukemogenic effect of radiostrontium. I, 26:53512
  Leukemogenic effect of radiostrontium in mice. II, 26:53496
ITO, Yasuo, Intensity of ortho-positronium component in liquid and solid amides, 26:54100
ITOH, N., Interstitial halogen centers in x-irradiated CsBr, 26:54980
IUE, N., Location of diffusion-doped gold atoms in silicon by means of channeling, 26:54987
IVANENKO, V. V., Effective neutron absorption cross sections for ^{252}Cf and ^{253}Cf in central channel of SM-2 reactor, 26:54668
IVANOV, Al., Probabilistic interpretation of cluster function series development of many-electron wave functions, 26:54146
IVANOV, B. A., Measurement of plasma parameters in strong hf discharge, 26:54768 (AEC-tr-7329)
IVANOV, S. S., Equations for the S-matrix element in g(:phi^4:)$_2$ theory, 26:54376 (ITF-72-15-E)
IVANOV, V. A., Simultaneous measurements of electron density and collision frequency in ionospheric D region, 26:54028
IVANOV, V. D., New measurements of the polarization of x-ray solar flares, 26:53962
IVANOV, V. G., New features of He II film flow transfer, 26:54431
IVANOV, V. P., Passage of high-power laser radiation through an optically dense plasma, 26:54785
IVASHCHENKO, A. V., Effects of Einstein's theory of gravity at two-particle vibrations in Schwarzchild's field, 26:54401 (ITF-72-60-P)
  Relativistic gravitational effect on influence of earth rotation on mechanical vibrations, 26:54400 (ITF-72-59-P)
IVERSEN, M. S., Radiochemical determination of vitamin B_{12}, 26:52938
IWAMARU, Masaaki, Influence of austenite grain size and forging ratio on ferrite banded structure, 26:55593 (RFP-Trans-108)
IWASAKI, Machio, ESR study of an irradiated single crystal of acetylene dicarboxylic acid dihydrate, 26:53005
IWINSKA, Hanna, Preparation of adherent ^{241}Am alpha sources by electrodeposition, 26:53071
IYENGAR, V. S., Short period variations in intensity and energy spectrum of Cyg X-1, 26:53921

J

JABLON, Seymour, Carcinogenesis in the survivors exposed to A-bomb irradiation in their youth, 1950 to 1969, 26:53442
JACKLYN, R. M., Components of the sidereal anisotropy, 26:53848
JACKSON, A. D., Correlations without tears, 26:54728
JACKSON, W. C., Production properties of A_1^+ in π^+p interactions at 5.45 GeV/c, 26:54227
JACOBEL, R. W., Evidence for a neutral meson near 1033 MeV, 26:54205 (COO-1428-311)
JACOBI, S., Cladding control on nuclear reactor fuel elements, 26:55218 (EURFNR-976)
  Criteria for differentiating fuel and plenum faults on reactor fuel elements with vibrocompacted fuel, 26:55229 (EURFNR-975)
JACOBI, W., Relations between inhaled potential α-energy of ^{222}Rn- and ^{220}Rn-daughters and absorbed α-energy in bronchial and pulmonary region, 26:53508
JACOBS, L. D., Parametrization of the nonevasive exchange processes and background contributions in the reaction $\pi^-p \rightarrow n\pi^+\pi^-$ at 2.77 GeV/c, 26:54214
JACQUIN, B., Study of diffusion welding of molybdenum, 26:53625
JACQUOT, C., X-ray spectrometry between 5A and 20A. Application to multiply-charged ion experiment, 26:54078 (CEA-CONF-2050)
JAENECKE, Joachim, Neutron--proton interaction in mirror nuclei, 26:54721
JAERPLID, B., Protective effect of cysteamine at fractionated irradiation. III, 26:53475
JAFFE, W. J., Age and structure of II Zwicky 40, 26:53976
JAFFEY, A. H., Tests on superconducting helix resonators, 26:53750
JAFFREZIC, Henry, Determination of vanadium in silicate materials by neutron activation, 26:52909
JAIN, S. C., Vibrational and electronic properties of $Co(CN)_6{}^{3-}$ doped in alkali halides, 26:55001
JAKEWAYS, R., Primary electron observations (3 less than or equal to E less than or equal to 15 GeV) recorded on the ESRO II satellite, 26:53821
JAKIMIW, G., Weak radiative decays of hyperons in the pole model, 26:54292
JAMES, A. N., Evidence of further rotational structure in ^{26}Al, 26:54554
JANCSO, G., Multiple charged particle production in π^-p and π^-n interactions at p = 40 GeV/c, 26:54327 (JINR-E2-6596)
JANEV, R. K., Electron capture from hydrogen negative ions by fast protons, 26:54116
  Inelastic e--H and e--He collisions in adiabatic approximation, 26:54117
JANIK, R., Monochromatic method for measuring 665 MeV mean proton energy by using Vavilov--Cherenkov radiation, 26:53800
JANISZEWSKI, J., Non-local potential for single-particle properties of nuclei, 26:54746
JANNI, Joseph F., Experimental active- and passive-dosimetry systems for the NASA Skylab program, 26:53236 (NASA-TM-X-2440, pp 958-73)
JANSONS, E., Amperometric and potentiometric determination of copper and molybdenum in ore concentrates and alloys with 5-bromo-8-mercapto- and 8-mercapto-4-methylquinoline, 26:52924
JARMIE, Nelson, Accurate deuteron--deuteron elastic scattering cross sections, 26:54497 (LA-DC-72-876)
JARRETT, J. H., Pacific Northwest Laboratory, Isotope Development Programs quarterly report: February--April 1972, 26:53330 (BNWL-1308-10)
JASKE, C. E., Influence of hold-time and temperature on low-cycle fatigue of Incoloy 800, 26:53658
JASKOLA, M., Knock-on mechanism for (n,α) reactions induced by fast neutrons on the deformed doubly even nuclei, 26:54707
JAUCH, K. M., Magneto-, sparko-, and thermostrictive phenomena in thin wires, 26:53222
JAUS, W., Electromagnetic corrections of order $Z\alpha^2$ and $Z^2\alpha^3$ to Fermi β-decays, 26:54713
JAYANTHI, U. B., Time variation of x-ray spectrum and optical luminosity of Sco X-1, 26:53917
JAYARAMAMURTHY, S. N., Analysis of texture, 26:55501 (COO-2118-35)
JEANMAIRE, Lucien, ^{90}Sr levels in human bones collected in 1970, 26:53520 (CEA-N-1535)
JEHN, H., Equilibria and kinetics of degassing in the systems Mo--N, W--N, and Re--N, 26:53580
JELLETT, K., Coil configurations in superconducting quadrupoles, 26:53768 (BNL-16980)
JEN, Chian-li, Dual-amplitude analysis of two-particle productions. II, 26:54307
JENNE, D. E., Climatography of the Hanford area, 26:55478

(BNWL-1605)
JENNINGS, C. W., Surface preparation for adhesive bonding, 26:55597 (SC-DC-714099)
JEREMIE, H., Cross-section for ejection of deuterons from ^{6}Li by electrons, 26:54546
JERGEL, M., Heat transfer to boiling helium from aluminium surfaces, 26:54465
JESSEPH, J. E., Radiation carcinogenesis and acute radiation mortality in the rat as produced by 2.2-GeV protons, 26:53455 (NASA-TM-X-2440, pp 647-51)
JETT, J. H., Accurate deuteron--deuteron elastic scattering cross sections, 26:54497 (LA-DC-72-876)
JEZIERSKA, Krystyna, Hydrogen sulfide radiolysis sensitized by Ar, Kr, Xe, and N, 26:53011
JOCKEY, P., Pulmonary lavage, therapy of pulmonary contaminations, 26:53528 (LF-tr-71)
JOEL, D. D., Intestinal barrier to bacterial invasion, 26:55474 (BNL-17004)
JOHANSEN, O., Routine determinations of traces of cobalt in soil and plant tissue by instrumental neutron activation analysis, 26:52904
JOHANSSON, Rune, Hot isostatic pressing: a new method for production of hard metals and alloy steels, 26:53578
JOHARI, S. S., Nuclear fuels and fuel processing, 26:52977
JOHN, Joseph, Measurements of gamma-ray production cross sections for shielding materials of space nuclear systems, 26:54960 (NASA-TM-X-2440, pp 500-11)
JOHNSON, J. H., Real-time spectrum-to-dose conversion system, 26:53201 (NASA-TM-X-2440, pp 142-8)
JOHNSON, J. L., Toroidal effects on MHD stability in Tokamaks, 26:54806 (CONF-720804-6)
JOHNSON, K., Tests on superconducting helix resonators, 26:53750
JOHNSON, K. C., Experimental evidence for exchange polarization in superexchange interactions, 26:55510 (COO-3151-6)
  Hydrostatic pressure study of the AFMR in $FeCl_2$, 26:55509 (COO-3151-5)
JOHNSON, Kenneth R., Removal of materials from ion exchange resins, 26:53072
JOHNSON, Rolland P., Neutrino mass limits from the K/sub L/^{0} $\rightarrow$ $\pi^{+-}l^{-+}\nu$ decay spectra, 26:54184 (LBL-4)
JOHNSON, T. O., Study of discontinuities in control rod drive motor tube extensions, 26:55217 (BAW-10047(Rev.1))
JOHNSON, W. H. Jr., Reaction $\pi^-p \rightarrow p\pi^+\pi^-\pi^-\pi^0$ at 20 GeV/c, 26:54207 (COO-3064-3)
JOHNSTONE, I., Some problems in the physics of high temperature reactors, 26:55110 (CONF-720901-(Bks.1 and 2), pp 55-67)
JOKIPII, J. R., Mechanism for confinement of cosmic rays in the Galaxy, 26:53865
JOLLY, H. P., Ground state of ^{40}Ca, 26:54577
JONES, A. Vallance, Altitude distribution of the $O_2(^1\Delta)$ nightglow emission, 26:54042
JONES, B. F., Membership in extremely young open cluster NGC 6530 (M8), 26:53883
JONES, D., Refractive index and attenuation surfaces in the vicinity of the cross--over level, 26:54015
JONES, D. M., Study of cold neutron spectra emerging from sources of liquid H and deuterium and a Monte Carlo method for optimisation, 26:54493
JONES, David H., Light-water breeder reactor, 26:55130
JONES, E. D., Nanosecond and picosecond laser-produced CD_2 plasmas, 26:54804
JONES, Frank C., Cosmic gamma rays from suprathermal proton bremsstrahlung, 26:53820
  Effect of galactic magnetic field line wandering on cosmic-ray parameters, 26:53864
JONES, L. T., Use of Ge(Li) detectors in high dose rate γ spectrometry, 26:53237 (RD/B/N-2369)
JONES, P., RELP version C: a reactor economics linear program for IBM 360/85 computer, 26:55266 (RD/B/N-2261)
JONES, R. C., Multinode analysis of B and W's 2568-MWt nuclear plants during loss-of-coolant accident, 26:55271 (BAW-10034(Suppl.1))
JONES, T. D., Local dose from neutron-produced-recoil ions in the region of a therapeutic ^{252}Cf needle, 26:54902
JONES, W. V., Nuclear-electromagnetic cascades from nuclei with Z greater than or equal to 3, 26:53832
  Nuclear-electromagnetic cascades from alpha particles incident on an iron absorber, 26:53831
JONSSON, C.-J., Dose rate dependence in the goitrogen stimulated mouse thyroid, 26:53472
JORDAN, C. F., Independent test of the Argonne model for tritium movement in soil, 26:53163 (ANL-7860(Pt.3), pp 32-7)
  Tritiated water recovery system, 26:53151 (ANL-7860(Pt.3), pp 46-50)
JORDAN, Thomas M., Shield-weight optimization using Monte Carlo transport calculations, 26:54962 (NASA-TM-X-2440, pp 697-705)
JOSEPH, George, Cosmic flux of low energy gamma rays, 26:53818
JOSEPH, R. R., Low-temperature heat capacity of $LaRu_2$, $CeRu_2$, and CeRu/sub 2 -x/Pt/sub x/, 26:55047
JOSHI, S. K., Electron loss in atom-molecule collisions, 26:54121
JOURDAN, G., Physics investigations of sodium cooled fast reactors SNEAK-Assemblies 6A/6B, 26:55398 (EURFNR-1029)
JUCKER, C., Clinical contribution to the understanding of radiation-induced sialoadenitis, 26:53423
JULIENNE, A., Energy spectra of dissociation products of CH/sub n/$^+$ ions (1 < = n < = 5) with a molecular nitrogen target, 26:54102 (EUR-CEA-FC-644)
JULKE, R. T., Comparison of a two-dimensional hydrodynamics core (REXCO) to excursion experiments for fast reactor containment, 26:55139 (ANL-7911(Suppl.1))
JUNG, K., Collisional ionization of helium by slow electrons, 26:54123
JUNG, M., Proton Compton effect in the region of the $\Delta(1236)$-resonance, 26:54180

K

KABACHNIK, N. M., Damping of hole states in the giant dipole resonance, 26:54714
KABAKCHI, A. M., Effect of various kinds of ionizing radiation on poly(vinyl chloride), 26:53020
KABAKCHI, S. A., Kinetics of the hydrated electron disappearance in concentrated aqueous alkali solutions, 26:53018
KADAIRA, Tsuneo, Results of cyclic pressure loading test due to JPDR pressure vessel model No. 2, 26:55228 (JAERI-Memo-4016)
KADANSKY, V., Photoproduction of π^+-mesons on polarized protons at photon energies between 0.5 and 2.2 GeV, 26:54172 (NP-19415)
KAEMPF, H., Treatment of the mechanical and thermal behavior of fuel rods in SATURN 1, 26:55186 (EURFNR-985)
KAES, H. H., Radiophotoluminescence dosimeter with low γ-energy dependence, 26:53242
KAGANOVICH, A. B., Dynamic chiral symmetry and cancellation of divergences in mass differences of members of A_1-, rho-, π-mesonic isomultiplets, 26:54321
KAGANSKII, M. G., Microwave plasma heating in Tuman-2, 26:54758
KAIEDA, K., Fission product release in TLG-1 in-pile gas loop. III, 26:53694 (JAERI-Memo-3936)
KAIGORODOV, V. R., Two-symmetric and two-recurrent fields of gravitation, 26:54397 (ITF-72-46-P)
KAISER, R. E., Effect of core configuration on ^{238}U Doppler measurements in ZPPR Assembly 2, 26:55393 (CONF-720901-(Bks.1 and 2), pp 1006-15)
  Sodium void studies and related heterogeneity effects in ZPPR-2, the Benchmark Demonstration Assembly, 26:55392 (CONF-720901-(Bks.1 and 2), pp 973-85)
KAISER, Wilfried, Influence of different designs and materials on the wear of piston ring and piston ring groove in a 6-cylinder diesel engine, 26:53339 (KFK-1568)
KAKIMOTO, Jiro, Development of on-line automatic weighing and recording system for nuclear fuel material, 26:53723
KAKUTO, Akira, Parton model: elastic and inelastic form factors of hadrons, 26:54311
KALBACH, R. M., Search for $^1/_2$e and $^2/_3$e charged quarks in the cosmic radiation at 2750-m altitude, 26:54164
  Search for $^4/_3$e charged diquarks in the cosmic radiation at 2750-m altitude, 26:54177
KALINNIKOV, V. G., Excited quasi-proton states in magic ^{141}Pr nucleus, 26:54604 (JINR-P6-6519)
KALNAES, Ole, Automatic production of isodose curves, 26:53243
KALOGEROPOULOS, T., Isabelle for very low energy anti pp experiments: WHIPLASH, 26:53766 (BNL-16818)
KALOS, M. H., Zero variance estimator for reactor criticality, 26:55431 (CONF-720901-(Bks.1 and 2), pp 229-39)
KAMENOV, P. S., Moessbauer experiments on the lifetime of excited nuclei, 26:55061
KAMIDE, Yohsuke, Positive geomagnetic bays in evening high latitudes and their possible connection with partial ring current, 26:54023
KANE, F. R., Negative muon capture in carbon leading to specific final states, 26:54537
KANEKO, Itsuo, Toxic eruptions combined with radiation therapy of malignant tumors, 26:53433
KANG, Kyungsik, Dual-amplitude analysis of two-particle productions. II, 26:54307
KANG, Man Sik, Postirradiation synthesis and degradation of DNA in various tissues of rats, 26:53489
KAO, K. C., Effects of gamma radiation on photocurrent-voltage characteristics of CdS films, 26:54998
KAO, S. K., Research on atmospheric diffusion and turbulence. final report, 26:55492 (COO-1585-22)
KAPAUAN, P. A., Half-life of /sup 80g/Br, 26:54595
KAPITONOV, V. S., Damping of long-wave plasma oscillations, 26:54869
KAPLAN, Henry S., Combined fractionated isotopic and external irradiation of the liver in Hodgkin's disease. A study of 21 patients, 26:53507
KAPLAN, Selig, Neutron radiography with a multiwire proportional chamber: performance and projections, 26:53200 (LBL-707(Summ.))
KAPULKIN, A. M., Effect of the magnetic field on a closed-electron-drift accelerator, 26:53743
KAPYSHEV, V. K., Calculation of nuclear reaction rates in a homogeneous sphere neglecting elastic scattering,

26:54491
KARAKULA, S., Galactic magnetic field and anisotropy of cosmic rays above 10^{17} eV, 26:53851
KARBAN, O., Elastic and inelastic scattering of 12 MeV polarized deuterons by ^{24}Mg, 26:54557
KARCHEVSKII, A. I., Stimulated emission evoked by pumping with a pulsed electron beam produced in a linear discharge, 26:54787
KARDON, B., Correlation of the partial radiation widths in the reaction ^{163}Dy(n,γ)^{164}Dy, 26:54631 (BNL-tr-490)
KARINO, Tutomu, Note on the urbaryon models, 26:54297
KARJALAINEN, P., Amount and form of radioactivity in human milk after lung scanning, renography, and placental localization by ^{131}I labeled tracers, 26:53524
KARNAUKHOV, V. A., Experiments on search for proton decay from the ground state, 26:54608 (UCRL-Trans-1473)
KARNIEWICZ, Wieslawa, Long-term retention of radiobarium and radiostrontium in rabbits, 26:53534
KARP, I. M., Preliminary shield design for a SNAP-8 power system, 26:54948 (NASA-TM-X-2440, pp 78-83)
KARP, Irving M., Probable solar-flare doses encountered on an interplanetary mission as calculated by the MCFLARE code, 26:54956 (NASA-TM-X-2440, pp 324-8)
KARPLUS, M., Aspects of time-dependent perturbation theory, 26:55073
KARPMAN, V. I., Nonlinear evolution of a quasi-monochromatic packet of helical waves in a plasma, 26:54868
  Nonlinear theory of monochromatic circularly polarized vlf and ulf waves in the magnetosphere, 26:54050
KARTAVENKO, V. G., Basing of cranking-model, 26:54692 (JINR-P4-6543)
KASCAK, Albert F., Bleed-cycle propellant pumping in a gas-core nuclear rocket engine system, 26:55358 (N-72-18051)
KASE, Kenneth R., Concepts of radiation dosimetry, 26:54891 (SLAC-153)
KASE, Paul G., Influence of a detailed model of man on proton depth/dose calculations, 26:54883 (NASA-TM-X-2440, pp 773-80)
KATAYAMA, Yasuhisa, Theory of leptons, 26:54294
KATILA, T. E., Moessbauer observation of magnetic moment of 89-keV excited state of ^{119}Sn, 26:54624
KATO, Takako, Thin polypropylene window proportional counters for the observation of cosmic soft x-rays, 26:53206
KATSUMORI, Hiroshi, Deep-inelastic contribution to baryon electromagnetic mass differences, 26:54257
KATSUTA, Hajime, Establishment of line of cultured of hepatoma cells (Culb TC) of the rat and the analysis of effects of gamma rays, 26:53354
KATZ, Sidney, Rapid, sensitive method for the determination of the chemical oxygen demand of polluted waters, 26:52915 (CONF-720827-2)
KATZ, W., π^- interactions in deuterium at 7 GeV/c, 26:54208 (COO-3065-16)
KATZIR, A., Thermally stimulated currents and thermoluminescence of paramagnetic centers in hexagonal boron nitride, 26:55015
KAUFMAN, D. Neal, Perturbation calculation of the nuclear spin--spin coupling constant in HD based on the bare-nucleus potential, 26:54092
KAUFMAN, Leon, Neutron radiography with a multiwire proportional chamber: performance and projections, 26:53200 (LBL-707(Summ.))
KAUFMANN, Michael, Low-density limit of the theta pinch, 26:54754 (LA-5019)
KAUSHAL, N. N., Iron-filtered neutron beams: a new approach to precision time-of-flight cross section measurements, 26:54597 (CONF-720901-(Bks.1 and 2), pp 1107-14)
KAUSHAL, V., Commutation of axial charges with axial divergences, 26:54341
KAWABATA, Keisuke, Shoulder of optical absorption spectrum of the trapped electron in gamma-irradiated crystalline ice, 26:53002
KAWABE, R., Analysis of pressure wave propagation in pipe rupture accidents of light-water cooled reactors by use of the burst code. I, 26:55203 (JAERI-M-4473)
KAWABE, Ushio, Preparation of transparent EuO films by oxidation of Eu films, 26:53567
KAWAMURA, Nobuaki, System for time of 50 m flight analysis and characteristics of short pulse beam, 26:53260
KAWANO, Minoru, Measurements of thoron in the atmosphere, 26:53227
KAWASAKI, K., Geomagnetic disturbances in the polar cap, 26:54053
KAWASAKI, Koji, Adsorption and dissociation of CO on W surface studied by field-emission microscopy, 26:55023
KAWASHIMA, Nobuki, Diaphragm-less radioactive radiation counter, 26:53210
  Interaction of a steady plasma flow with a dipole magnetic field in the presence of a radial electric field, 26:54056
KAWI, A. Abdel, Exit tube effect upon the measured space--energy neutron spectra, 26:54470 (AREAEE-133)
KAY, M. I., Approximate structure for the antiferroelectric phase of copper formate tetrahydrate, 26:55614 (TID-25974)
KAZANJIAN, A. R., Thermal and radiation stability of polyvinyl chloride, 26:52992 (RFP-1924)
KAZARINOV, Yu. M., e - d scattering and neutron form factors, 26:54169 (JINR-E1-6647)
KEBEDE, Eshetu, Kinetics of proton transfer to cyanines. a temperature-jump study, 26:52964
KEEN, B. E., Apparent constant-wavelength oscillations in a bounded plasma, 26:54859
KEENAN, T. K., Radiation from ^{238}Pu used in space applications, 26:53337 (NASA-TM-X-2440, pp 859-61)
KEGEL, A. J., Properties of 1300 kg P/M TZM billet, 26:53673
KEIL, E., Intersecting storage rings, 26:53782 (CERN-72-14)
KEISCH, Bernard, Application of nuclear technology to art identification problems. Final report, 26:52898 (COO-3034-2)
KEITH, Alec D., Prog. rpt. on spin-labeled membranes, annual, 11/1/71--8/8/72, 26:55504 (COO-2223-1)
KELLER, E. C. Jr., Induction of lysogenic bacteria in the space environment, 26:53364 (N-72-20063)
KELLER, W. E., Cryogenic instrumentation at and above liquid hydrogen temperature: present and future, 26:55554 (LA-DC-72-855)
KELLEY, John P., Broad-beam attenuation in lead for x rays from 50 to 300 kVp, 26:54904
  Scattered radiation from a tissue-equivalent phantom for x rays from 50 to 300 kVp, 26:54905
KEMPER, K. W., Possible statistical-model explanation for the ^{26}Mg(p,t)^{24}Mg reaction at E/sub p/ = 26 MeV, 26:54556
KENDALL, Ernest Whitney, Trend orebodies of the Section 27 mine, Ambrosia Lake Uranium District, New Mexico, 26:53144 (GJO-936-2)
KENDALL, Kenneth Robert, Production of muonium in a vacuum by diffusion from a hot metal foil, 26:54096
KENIK, E., Experiments in high-voltage electron microscopy. Progress report, October 31, 1972--July 31, 1973, 26:54972 (COO-2119-2)
KENT, M. F., Power generation options for the eighties and nineties, 26:53097
KENWARD, Michael, Britain's nuclear options, 26:55087
KEPERT, D. L., Early transition metals, 26:52956
KEREK, A., Fractional parentage coefficients for j = 11/2 orbital, 26:54686 (INR-1406)
KERESELIDZE, A. B., Spatial localizability of energy--momentum tensor of gravitational field, 26:54393 (ITF-72-5-P)
KERIMOV, B. K., Role of neutral vector mesons in the photoformation of lepton pairs by nuclei, 26:54260
KERLIN, T. W., Preliminary coolant temperature oscillation measurements at the fuel-failure mockup, 26:55192 (ORNL-TM-3761)
KERNER, W., Determination of magnetic field B in vacuum for general two-dimensional MHD equilibria, 26:54814
KERR, Carolyn M. L., Investigation of the structure of the hydrated electron based on unpaired electron densities calculated by the INDO method, 26:52989 (ORO-2968-78, Paper 4)
KERR, R. G., Multiple Coulomb interference effects on the quadrupole moment of ^{114}Cd, 26:54623
KERR, William, Improved S/sub N/ inner iteration convergence criterion, 26:55435 (CONF-720901-(Bks.1 and 2), pp 275-92)
KERSHNER, C. J., ^{210}Po isotopic fuels, 26:53334 (MLM-1228)
  Bibliography on handling, control, and monitoring of tritium (December 1968--January 1972), 26:53155 (MLM-1946)
KERTESZ, I., Measurement of mode-locked ultrashort laser pulses by different order photoelectric effects, 26:55544 (KFKI-72-41)
KERTH, Leroy T., Neutrino mass limits from the K/sub L/^{0} → π^{+-}l$^{-+}\nu$ decay spectra, 26:54184 (LBL-4)
KETSARIS, A. A., Lie groups and the theory of gravitation, 26:54402
KETTENRING, G., Investigation of gamma radiation from the Crab pulsar, 26:53923
KHACHATURAN, Z. G., Generation of fast electrons through interaction of SHF wave with collisionless plasma, 26:54836 (AEC-tr-7331)
KHAIDAROV, A., Determination of bismuth in some minerals by activation analysis, 26:52910
KHAIKIN, M. S., Anisotropy of surface superconductivity of lead single crystals, 26:54440
KHAIMOVICH, V. S., X-ray study of molybdenum and nickel irradiated with helium ions, 26:53700 (SC-T-722540)
KHALATNIKOV, I. M., High-frequency hydrodynamics near the lambda point, 26:54424
KHALIKULOV, A. B., g-factor of 108 keV excited state in ^{151}Gd, 26:54634 (JINR-E6-6479)
KHALILOV, V. R., Radiation from a charge in the field of two plane waves, 26:54264
KHALIZEV, A. E., Mutagenesis in cultured mammalian cells. II, 26:53362
KHAMRAEV, T. A., Formation of complexes of UCl$_4$ with α- or β-carboxylic acids and α-quinolinecarboxylic acid in polar solutions, 26:53054
KHAN, M. S., Design and development of a random pulse sampler, 26:53321
KHARCHENKO, V. F., Solutions of Skornyakov-Ter-Martirosyan equations for three nucleons with cut-off at large momenta, 26:54344 (ITF-72-10-P)
KHARIN, V. P., Angular distribution of photoneutrons from Al, Ti, Cu, Mo, W, Pb, 26:54563

KHARKYANEN, V. N., Theory of Bethe and Davydov magnetic splittings in cubic antiferrodielectric, 26:55536 (ITF-72-32-P)
KHAZANOV, B. I., Measurement of radiation in space, 26:53276
KHEIFETS, S. A., Angular distributions in the annihilation of an electron--positron pair, 26:54281
KHIRSELI, E. M., Wave interactions in anisotropic plasma, 26:54862
KHLESKOV, V. I., Analysis of Kπ-interaction in energy region up to 1 GeV, 26:54315 (JINR-E2-6525)
KHMARUK, V. G., Collisionless heating of plasma ions by an ion beam, 26:54767
KHOKHLOV, R. V., Feasibility of γ laser based on radioactive crystals, 26:55062
KHOLIN, V. V., Theoretical calculation of space distribution of dose field of ^{60}Co γ irradiation under lattice, 26:54908
KHOZE, V. A., Angular distributions in the annihilation of an electron--positron pair, 26:54281
KHRUSTALEV, O. A., N. N. Bogoliubov's transformation in strong coupling theory. III, 26:54383
KHVAN, G. V., Calculation of integral absorbed dose in electron therapy of tumors, 26:54909
KHVASTUNOV, M. S., Reconstruction of differential cross section of reaction $\pi^-p \to \pi^0$(eta)n in small transferred momenta region, 26:54209 (JINR-P1-6414)
KIDA, Toshiyuki, Radiated dose to skin during injection of radioactive substances, 26:53424
KIEFFER, R., Powder metallurgy of high-temperature materials, 26:53590
KIEFHABER, E., KFKINR-set of group constants; nuclear data basis and first results of its application to the recalculation of fast zero-power reactors, 26:55397 (EURFNR-1016)
KIEFHABER, Edgar, Evaluation and interpretation of integral experiments in fast criticals, 26:55385 (CONF-720901-(Bks.1 and 2), pp 623-35)
KIESNERS, U., Design of the cyclotron magnet for TRIUMF, 26:53749
KIHLBERG, A., Dual models with SL(2,C) symmetry, 26:54309
KIJEWSKI, P., Polarization of the recoil proton in the reactions $\gamma p \to \pi^0 p$ and $\gamma p \to \gamma p$, 26:54167 (COO-3069-71)
KILLBY, Virginia A. A., Interaction of embryonic chicken spleen cells and adult allogeneic leucocytes, 26:53477
KIM, C. O., Study of the charge spectrum of cosmic-ray nuclei, 26:53839
KIM, C. W., Limitation on use of impulse approximation in nuclear β-decay, 26:54709
KIM, J. K., Reaction $\pi^-p \to p\pi^+\pi^-\pi^-\pi^0$ at 20 GeV/c, 26:54207 (COO-3064-3)
KIM, J. S., Electric field induced by a slowly decaying ring current, 26:54063
KIM, Y. E., Meson-exchange currents and ^{3}H, ^{3}He magnetic moments, 26:54506
KIM, Y. M., New EPR spectra in neutron-irradiated silicon, 26:55006
KIMMEL, G., Preparation and properties of W--Ni--Mo alloys, 26:53679
KIMMICH, George, Studies on the transport of L-lysine by isolated chick intestinal epithelial cells, 26:55636 (UR-3490-177)
KIMMICH, George A., Effect of K$^+$ and K$^+$ gradients on accumulation of sugars by isolated intestinal epithelial cells, 26:55635 (UR-3490-174)
KIMURA, Hiroshi, Study on the effects of radiation on the molding of polymers, 26:53720
KIMURA, Toshiei, Potential in the canonical formalism of gravity, 26:54405
KING, C. N., Specific heat of granular aluminum films, 26:54450
KINGSEP, A. S., Theory of stochastic heating of particles in a turbulent plasma, 26:54765
KINGSLEY, R. L., Two-photon exchange effects in deep inelastic electroproduction, 26:54269
KINZER, R. L., Observation of cosmic gamma radiation above 10 MeV, 26:53816
  Search for pulsed gamma rays from the Crab, 26:53922
KIRICHENKO, G. S., Collisionless heating of plasma ions by an ion beam, 26:54767
KIRII, A. Yu., Kinetic theory of parametric excitation of surface waves in semi-finite plasma, 26:54867
KIRILLOVA, L. F., Differential cross sections of elastic p-d scattering in energy range of 10 to 70 GeV, 26:54194 (JINR-E1-6615)
  Differential cross sections of elastic p-p scattering in energy range of 8 to 70 GeV, 26:54193 (JINR-E1-6613)
KIRIYA, V. S., Spatial localizability of energy--momentum tensor of gravitational field, 26:54393 (ITF-72-5-P)
KIRK, T. W., Porcupine, 26:53266 (BNL-17020)
KIRKPATRICK, Ronald C., Consistent model of the planetary nebula ngc 7662, 26:53873
KIRSCH, D., Phenomenological investigation of the flow distribution behind local coolant chemical blockage in rod bundles, 26:55176 (KFK-1548)
KIRSCH, Robert, Restatement of a fabrication technique by epitaxy of thin monocrystalline gold films used as bearing samples in canalization tests, 26:55566 (LYCEN-7232)
KIRSTEN, T., Higher harmonics and transport coefficients of plasmas in circulary polarized magnetic fields and additional electromagnetic fields, 26:54761
KIRZ, J., Charged particle multiplicity and angular correlation measurements in pp and γp collisions, 26:54192 (BNL-17141)
KIRZHNITS, D. A., Atomic structure oscillation effects, 26:54151
KISH, J. M., Chemical composition of cosmic rays with Z = 3 to 30 at high and low energies, 26:53838
KISS, A., Light-intensity dependence of the multiphoton ionization probability in the resonance case, 26:54094
KISSLINGER, L. S., Elastic pion--nucleus scattering for studies of the nuclear surface, 26:54722
KISSLINGER, Leonard S., Nuclear wave functions from particle transfer data, 26:54693 (LA-DC-72-954)
KITAGAKI, T., Further aspects of the reaction $\pi^-p \to \pi^-\pi^+n$ at 8 GeV/c, 26:54216
KITAGAWA, Toshio, Radiation induced heart failure. I, 26:53439
KITAHARA, T., Fission product release in TLG-1 in-pile gas loop. III, 26:53694 (JAERI-Memo-3936)
KITAYAMA, Shigeru, Double-strand scissions in DNA of gamma-irradiated Micrococcus radiodurans and their repair during postirradiation incubation, 26:53349
KITAYAMA, Yoshifumi, Examination of burnout detectors by differential circuit methods, 26:53304 (LIB/Trans-431)
KITCHINGS III, J. T., Seasonal alterations in rodent blood, 26:55587 (ORNL-TM-3898)
KITTNER, K.-H., Animal experimental examinations on the effect of ionizing radiation on the maxillary bone with metallic bridges, 26:53480
KIZER, Donald E., Method of making a nuclear reactor fuel element of uranium mononitride in a refractory metal matrix, 26:53562
KJELLBERG, R. N., Neuropathologic effects of proton-beam irradiation in man. II, 26:53446
KLAEUKENS, H., Calculation of the dynamic behavior of heat exchangers in gas turbines, 26:53114
KLARMANN, J., Comments on the observation of transuranic nuclei in the primary cosmic radiation, 26:53844
  Observation of VH and VVH cosmic rays with an ionization--Cherenkov detector system, 26:53843
KLASSEN, N. V., Solvation of electrons in 3-methylhexane at 77°K, 26:53007
KLATZO, Igor, Effects of gamma radiation on the shark brain, 26:53487
KLAVDIEV, V. V., Diffraction of an electromagnetic wave at a magnetoactive plasma cylinder, 26:54847
KLEIN, Abraham, Algebraic approach to the theory of collective motion: spherical to deformed transition in the single-j shell, 26:54681 (COO-3071-9)
  Concept of transition operator boson and its application to an exactly soluble model, 26:54682 (COO-3071-10)
  Simplified microscopic model of the Coriolis anti-pairing transition, 26:54680 (COO-3071-7)
KLEIN, H., Field distribution, power losses, and parameter optimization of helical accelerator structures, 26:53744
KLEINBERG, R., Approximate structure for the antiferroelectric phase of copper formate tetrahydrate, 26:55614 (TID-25974)
KLEMENT, Alfred W. Jr., Russian radioecology: a bibliography of Soviet publications with citations of English translations and abstracts, 26:53530 (TID-3915(Suppl.1))
KLEMPNER, K. S., Radioisotopic relays, 26:53288
KLEPALOVA, J., Course of the post-irradiation syndrome after irradiation with lethal doses in piglets, 26:53495
KLIER, G., Elastic scattering of vector polarized deuterons from ^{48}Ti, ^{49}Ti, ^{50}Ti, ^{51}V, ^{52}Cr, 26:54572
KLIGERMAN, Morton M., Biomedical program, 26:53398 (LA-4874, pp 79-83)
KLIMA, Jaroslav, Absolute activity in irradiated fuel material by method of gamma scanning, 26:53041 (UJV-2867-M,A)
KLIMYK, A. U., Wigner--Eckart theorem for nonunitary representations of semi-simple Lie groups, 26:54355 (ITF-72-33-E)
KLINE, J. R., Distribution of ^{137}Cs in soils and vegetation on the island of Puerto Rico, 26:53162 (ANL-7860(Pt.3), pp 1-13)
  Independent test of the Argonne model for tritium movement in soil, 26:53163 (ANL-7860(Pt.3), pp 32-7)
  Tritiated water recovery system, 26:53151 (ANL-7860(Pt.3), pp 46-50)
KLINSHPONT, E. R., ESR study of free radical reactions of γ-irradiated polypropylene with methyl methacrylate, 26:53019
KLOBUCHAR, John A., Average behavior of midlatitude F-region parameters N/sub T,/N/sub max,/ and tau during geomagnetic storms, 26:54040
KLOCKE, K., Limits of detection in localized spectrochemical analysis with lasers, 26:55590 (ORNL-tr-2613-A)
KLOCZEWIAK, Marek, Biological dosimeters. I, 26:53355
KLOPOVSKII, K. S., Electrostatic instability of a hot-electron plasma in a high-frequency field, 26:54817
  Transverse instability of hot-electron plasma in a cylindrical resonator, 26:54818
KLOTZ, P., Synergistic effect of tri-n-octylamine on the solvent extraction of cerium(III) by thenoyltrifluoroacetone, 26:52952

KLUEH, R. L., Effect of oxygen on tantalum--sodium compatibility, 26:53688
KNIGHT, R. A., Simple hot isostat for beryllium, 26:53618
KNOOP, H.-U., Biological effectiveness of primary reactions of thermal neutrons. II, 26:53394
KNOTT, K., Equilibrium potential of a magnetospheric satellite in an eclipse situation, 26:54054
KNUDSEN, E., Natural α-activity in air near ground, 26:53160 (UUIM-27)
  Natural β-activity in air near ground. Parts B--E, 26:53159 (UUIM-26)
KOBAYASHI, Masanori, Possible behavior of Regge trajectories in Veneziano-like representatons, 26:54423
KOBAYASHI, Nobuo, Theory of leptons, 26:54294
KOBAYASHI, Tsunehiro, Photo-neutral vector meson couplings in the relativistic extended quark model, 26:54283
KOBETICH, E. J., Comment on inverse Compton models for the isotropic x-ray background, 26:54000
KOBORI, Yoichi, Vibration analysis of E. P. discharge electrode, 26:55591 (ORNL-tr-2636)
KOBRINSKII, M. N., Production of muonic pairs in μp-collisions, 26:54263
KOBYLINSKII, N. A., Annihilation of anti NN → 3π in dual models, 26:54320
  DAMA and Regge asymptotic behavior, 26:54412 (ITF-72-63-E)
KOCH, G., Recovery of ^{238}Pu in the MILLI laboratory, 26:53073
KOCH, J. H., Elastic pion--nucleus scattering for studies of the nuclear surface, 26:54722
KOCH, L., Application and automation of mass spectrometry in the analysis of irradiated nuclear fuels, 26:52917 (EUR-4765, pp 77-89)
  Chemical composition of heavy cosmic ray nuclei above 5 GeV, 26:53840
KOCHEN, Robert L., Corrosion and stress-corrosion cracking of painted U--4.2 wt. percent Nb, 26:53607 (RFP-1891)
  Stress-corrosion cracking of underaged and overaged U--2.3 wt percent Nb in an aqueous chloride environment, 26:53608 (RFP-1904)
KOCHMANSKA, Anna, Gastrulation in mouse embryos in course of radiation injury, 26:53476
KOEHLER, A. M., Neuropathologic effects of proton-beam irradiation in man. II, 26:53446
KOEHMSTEDT, P. L., Radioactive material transport in flowing sodium systems, 26:55164 (CONF-710959-, Paper 8)
KOEHN, D., Possible connection between a barium cloud and electron intensity fluctuations observed on a rocket flight at Kiruna, 26:54039
KOEPP, G., Quark model predictions for weak production of pseudoscalar mesons, 26:54285 (DESY-72/32)
KOHARA, Yoji, K/sub s/ → 2γ decay, 26:54295
KOHNO, Tsuyoshi, Thin polypropylene window proportional counters for the observation of cosmic soft x-rays, 26:53206
KOIKE, Y., Thin film of organic fluorescent materials for simple detection of alpha rays, 26:53265
KOLEHMAINEN, S. E., Balances of ^{137}Cs, stable Cs, and K of bluegill (lepomis macrochirus Raf.) and other fish in White Oak Lake, 26:53535
KOLESNICHENKO, Ya. I., Conditions for quasi-steady development of self-sustaining nuclear reactions, 26:54833
KOLESNIKOV, S. M., Scalar-tensor theory of gravitation, 26:54395 (ITF-72-21-P)
KOLEVATOFF, J., Fast neutron scintillation spectrometer with double compensation circuit for gamma-ray discrimination, 26:53251 (AREAEE-137)
KOLLER, A., Field distribution in superconducting lenses without ferromagnetic materials, 26:53759
KOLOSOVSKII, G. A., Passage of high-power laser radiation througn an optically dense plasma, 26:54785
KOLPAGIU, M. K., Influence of Fermi-surface topology change under pressure on two-band superconductors properties, 26:54445
KOLSTAD, George A., Will medium energy physics fly or die, 26:53740 (LA-4874, pp 21-33)
KOMAR, E. G., 250 kG complex solenoid, 26:54466
KOMORI, N., Quadrupole structure in ^{51}V NMR in transition-metal alloys, 26:55056
KONDO, I., Sidereal and solar anisotropy of high-energy cosmic rays observed by an air Cherenkov telescope, 26:53850
  Spurious sidereal anisotropy arising from annual modulation of solar diurnal variation of cosmic radiation, 26:53849
KONDO, Ichiro, Three-dimensional cosmic ray anisotropy in interplanetary space. IV, 26:53813
  Three-dimensional cosmic-ray anisotropy in interplanetary space. III, 26:53812
KONDO, Takaaki, Ion-exchange behaviour of metals on DEAE-cellulose in methanol--thiocyanate--hydrochloric acid media, 26:52951
KONECNY, E., Identification of rotational band in ^{240}Pu fission isomer, 26:54664
KONGSOE, H. E., RELY 4: a Monte Carlo computer program for system reliability analysis, 26:55209 (RISO-M-1500)
KONISHI, Toshio, Semi-experimental measurement of effective delayed neutron fraction of a fast reactor system by application of pulsed neutron technique, 26:55403 (JAERI-Memo-4004)
KONO, Migiwa, Interaction of a steady plasma flow with a dipole magnetic field in the presence of a radial electric field, 26:54056
KONSTANTINOV, O. V., Doppler-shifted cyclotron resonance in cadmium, 26:55044
KOO, Francis K. S., Quality improvement in plantains by selection, 26:55483 (CONF-720642-1)
KOPAEV, Yu. V., Effect of the metal--dielectric phase transition on the superconducting transition temperature, 26:54457
KOPEC, Maria, Biological dosimeters. I, 26:53355
KOPF, John O., Program AUGAT, 26:55563 (LBL-515)
KOPP, L. E., Bibliography of technical publications and reports of the Radiation Division, Brookhaven National Laboratory, July 1968--June 1971 inclusive, 26:53325 (BNL-50335)
KOPROWSKI, E. F., Nuclear radiation environment analysis for thermoelectric outer planet spacecraft, 26:53338 (NASA-TM-X-2440, pp 862-5)
KOPYSOV, Yu. S., Are solar-neutrino experiments suggestive of existence of resonance in ^{3}He + ^{3}He system, 26:54508
KORENKOV, I. P., Evaluation of exposure doses to personnel at high-power beta radiation installations, 26:53426
KORENMAN, G. Ya., Radiative kaon capture by nuclei, 26:54536
KORENNOY, V. P., High-energy limit for α-d and tau--t form factors in ^{6}Li nucleus, 26:54532
KORMILETS, V. M., Nonlinear wave interactions in a cylindrical column of magneto-active plasma, 26:54863
KORNILOV, E. A., Influence of different types of oscillations on ion heating in plasma--beam discharges, 26:54762
KORPI, John Leonard, Some final states with a Λ in K⁻n interactions at 4.9 GeV/c, 26:54229
KORSCH, H. J., Vibrational excitation of diatomic Morse oscillator by impulsive collision with atom, 26:54131
KORTUS, J., Hematologic changes and changes in the blood proteins in experiments on white rats following intratracheal administration of radiocerium, 26:53516
KOSHILEV, N. A., Investigation of heating of a plasma ion component by a collisionless shock wave, 26:54766
KOSHIMAKI, D. C., Low-temperature heat capacity of LaRu$_2$, CeRu$_2$, and CeRu/sub 2 -x/Pt/sub x/, 26:55047
KOSMACHEV, O. S., Statistical model which allows for the conservation of P-, C-, and G-parity, 26:54360
KOSS, R. L., Properties of 1300 kg P/M TZM billet, 26:53673
KOTENOK, V. V., Theory of polymorphous transformations in the ionic crystals with triparticle interactions, 26:55538 (ITF-72-50-P)
KOTIK, D. S., Theory of instability in the ionospheric current jet, 26:54027
KOTSARENKO, N. Ya., Interaction of a multiloop electron stream with a plasma, 26:54793
KOURI, Donald J., Integral-equation approach to bound-state atomic systems: preliminary studies of helium and hydrogen, 26:54145
KOUTCHMY, S., Hydrodynamic study of large coronal streamer observed during the eclipse of Mar. 7, 1970, 26:53956
KOVACEVICH, E. A., Corrosion and deposition of irradiated stainless steel in sodium, 26:55165 (CONF-710959-, Paper 9)
  Radioactive material transport in flowing sodium systems, 26:55164 (CONF-710959-, Paper 8)
KOVACS, J., Determination of the variation of radioactive contamination in the environment based on the contamination of foodstuffs, 26:53172
KOVALENKO, L. M., Effect of various kinds of ionizing radiation on poly(vinyl chloride), 26:53020
KOVALENKO, V. F., Analytic regularization depending on the parameter, 26:54409 (ITF-72-37-P)
  Behavior of renormalized Feynman amplitudes under scale transformations, 26:54410 (ITF-72-38-P)
  Violation of homogeneity of Feynman amplitudes of self-energy graphs under regularization, 26:54411 (ITF-72-39-P)
KOVALEV, V. P., Angular distribution of photoneutrons from Al, Ti, Cu, Mo, W, Pb, 26:54563
KOVPIK, O. F., Influence of different types of oscillations on ion heating in plasma--beam discharges, 26:54762
KOWALSKI, Antoni, Radiation sulfoxidation of n-paraffins. I, 26:53012
KOWNACKI, Jan, Fractional parentage coefficients for j = 11/2 orbital, 26:54686 (INR-1406)
KOYANAGI, Masao, Nonperturbational calculation of critical anomalies of superconductors in external fields, 26:54458
KOZINA, L. N., Thermodynamics of liquid solutions Mo--O and Mo--C, 26:53588
KOZLOV, F. A., Methods of indication, operation of a steam generator and secondary circuit in the case of slight leakage of water into sodium, 26:55154 (CONF-710548-, pp 105-28)
KOZLOVSKII, I. V., Quasi-elastic electron scattering on ^{12}C nuclei, 26:54526 (ITF-72-25-P)
  Two-particle electrodesintegration of ^{3}He, 26:54496 (ITF-72-24-P)
KOZLOWSKA-MILNER, Ewa, Effect of structure of solid phase on HNO$_3$ radiolysis, 26:53009

KOZLOWSKI, M., Knock-on mechanism for (n,α) reactions induced by fast neutrons on the deformed doubly even nuclei, 26:54707

KRAEMER, R., Low-lying states in ^{22}Mg, 26:54559

KRAIMER, Martin R., Plume rise determination by the tabulation prediction technique, 26:53152 (ANL-7860(Pt.3), pp 230-49)

KRAITCHINSKII, A., Similarities of ionization effects and annealing in P-type and converted N-type Ge irradiated with electrons at 85^{0}K, 26:54997

KRAMER, G., k^2-dependence of transverse pion electroproduction cross section in generalized Born term model, 26:54243 (DESY-72/30)

KRAMSKOI, G. D., Influence of injection conditions on the transverse instability of the beam in a linear accelerator, 26:53758

KRANYC, A., EULERO program, 26:55595 (RT/FIMA-(72)1)

KRASE, Loren Dell, Contributions of time-reversal noninvariant terms in electron--nucleus elastic scattering, 26:54363 (IS-T-536)

KRASNAYA, M. F., Cost of processing liquid radioactive wastes, 26:53065

KRASNOPOLIN, I. Ya., Anisotropy of surface superconductivity of lead single crystals, 26:54440

KRAUS, S., Neutron shielding pads, 26:55223 (WCAP-7870)

KRAUSHAAR, J. J., (p,t) and (p,^{3}He) reactions on ^{27}Al at E/sub p/ = 27 MeV, 26:54551 (COO-535-673)

KRAUSHAAR, W. L., Flux of galactic high-energy gamma rays, 26:53819

KRAUSS, Roland Henry, Scattering of low-energy rare-gas ions from tungsten, 26:54083

KRAUT, Joseph W., Combined fractionated isotopic and external irradiation of the liver in Hodgkin's disease. A study of 21 patients, 26:53507

KREEVOY, M. M., H_2BH_3 as an intermediate in tetrahydriodoborate hydrolysis, 26:52965

KREIDER, K. G., Resin bonded boron--aluminum composites, 26:53574
  Transverse tensile properties of boron fiber reinforced aluminum matrix composites, 26:53687

KRIESE, S., Energy in power plant engineering, 26:53107

KRISCH, R. E., Phenotypic properties of a large-cell, radiation-resistant strain of Escherichia coli, 26:53363

KRISHNASWAMI, S., Coral growth rates using ^{228}Ra and ^{210}Pb, 26:53179

KRISHNA SWAMY, K. S., Equivalent width of interstellar molecular lines. II, 26:53890

KRISHNASWAMY, V., Dose tables for ^{252}Cf implants, 26:54906

KRISTIAN, J., X-ray and optical observations of Sco X-1 and observations of the x-ray background, 26:53918

KRIVORUCHKO, S. M., Influence of different types of oscillations on ion heating in plasma--beam discharges, 26:54762

KRIVSKII, I. Yu., Wightman axioms for concentratable field and reconstruction theorem. I, 26:54378 (ITF-72-62-E)

KROH, Jerzy, Radiothermoluminescence of cyclohexene, 26:53010

KROKHIN, O. N., Kinetic processes in a laser plasma, 26:54799

KROMME, J. G., Decay of ^{227}Th from α--γ coincidence and directional correlation studies, 26:54673

KRONGAUZ, A. N., Distribution of qualitative composition and absorbed doses of x-irradiation in using the screens, 26:54911

KROPOTKIN, A. P., Physical mechanism of the magnetospheric substorm development, 26:54051

KRUEGER, Magdalena M., Determination of ruthenium and osmium in the residues resulting from the leaching of mattes, 26:52919 (NIM-1432)

KRUKONIS, V. J., Chemical vapor deposition of boron on a carbon monofilament substrate, 26:53571

KRUMHANSL, J. A., Pair potential in liquids from the exact Born-Green equation: I. Model testing, 26:55516 (COO-3161-4)

KRUML, J., Course of the post-irradiation syndrome after irradiation with lethal doses in piglets, 26:53495

KRUMLINDE, J., Description of the band structure at high angular momenta in rotating nuclei, 26:54733

KRUPIN, A. V., Rolling in vacuum, 26:53630

KRUPIN, S. V., Correlation of the partial radiation widths in the reaction $^{163}Dy(n,\gamma)^{164}Dy$, 26:54631 (BNL-tr-490)

KRUPINA, A. E., Influence of collisions on plasma-wave propagation near electron gyrofrequency harmonics, 26:54860

KRUSE, T. H., Phase and shape of the form factor for inelastic ^{3}He scattering, 26:54621

KRYCUK, G., Economical scaler driver, 26:53298 (COO-3058-9)

KRZUK, Jerzy, Radiometric method for standard uranium ore samples: comparison with standard thorium ore samples by means of the gamma rays spectroscopy, 26:52941

KUANG, Tkhai, Theory of Compton scattering by a charged dirac particle which possesses intrinsic dipole moments, 26:54278

KUBO, Haruya, Interaction of a steady plasma flow with a dipole magnetic field in the presence of a radial electric field, 26:54056

KUBO, K.-I., DWBA treatment of cluster transfer reactions, 26:54706
  Finite-range DWBA analyses of the $^{16}O(^7Li,t)^{20}Ne$ and $^{15}N(^7Li,t)^{19}F$ reactions, 26:54708

KUCHOWICZ, B., Cosmic ν, 26:54185 (NEIC-RR-47)

KUCK, George A., Short-term prediction of E greater than or equal to 10-MeV proton fluxes from solar flares, 26:53931 (NASA-TM-X-2440, pp 356-61)

KUDIRKA, P. E., Potential measurement and stabilization of an isolated target using electron beams, 26:53315

KUDO, Mitsuhiro, Preparation of transparent EuO films by oxidation of Eu films, 26:53567

KUEMMEL, H., Equations for linked clusters and the energy variational principal, 26:54735

KUGEL, H. W., Magnetic moment of the 1.409-MeV 2^+ state of ^{54}Fe, 26:54581

KUHLMANN, E., Low-lying states in ^{22}Mg, 26:54559

KUKANOV, A. B., Theory of Compton scattering by a charged dirac particle which possesses intrinsic dipole moments, 26:54278

KUKHTIN, V. V., Applications of the statistical mechanics methods in a dual model, 26:54299 (ITF-72-49-P)
  Two-particle distributions in dual resonance model, 26:54301 (ITF-72-55-P)

KULESHOV, S. P., Multiple charged particle production in π^-p and π^-n interactions at p = 40 GeV/c, 26:54327 (JINR-E2-6596)

KULESZA, Albin, Attempts of reactor loop use for ^{125}I production, 26:53068

KULIKOV, Yu. V., Possible measuring high-energy electron energy by ionization detectors of total absorption on basis of condensed xenon, 26:53272 (JINR-P13-6541)

KULIKOWSKA, Teresa, Effect of singularities on approximation in S/sub N/ methods, 26:54482 (INR-P-1405)

KULKA, Zbigniew, Automatic data acquisition and registration from mass spectrometer, 26:53324

KULKARNI, R. N., Dose across a plane bone--tissue interface, 26:54896

KULKARNI, Ramesh G., Symmetry of the coulomb field and its applications, 26:54374

KULLANDER, S., Helium-recoil spectrometer, 26:53281

KUL'PIN, B. V., Analytical and experimental study of a reacting water-sodium flow, 26:55161 (CONF-710548-, pp 221-42)
  Study of Na and H_2O interaction in a one-megawatt modular steam generator, 26:55153 (CONF-710548-, pp 57-104)

KUMAGAI, K., Fission product release in TLG-1 in-pile gas loop. III, 26:53694 (JAERI-Memo-3936)

KUMAKHOV, M. A., Theory of flux peaking effect in channeling, 26:55007

KUNCIR, J., Nondestructive neutron activation analysis of mineral materials. II, 26:52901 (UJV-2851-F,Ch)

KUNDA, W., New developments in the preparation of composite powders, 26:53680

KUNERT, J., Results of fallout monitoring in the German Democratic Republic 1970, 26:53156 (SZS-128)

KUNIYASU, Yoshihito, Examination of burnout detectors by differential circuit methods, 26:53304 (LIB/Trans-431)

KUNZLE-LUTZ, M., Pulmonary lavage, therapy of pulmonary contaminations, 26:53528 (LF-tr-71)

KURBATOV, N. N., Melting point diagrams for $LiCl$--UCl_3--UCl_4 system, 26:53721

KURDYUMOV, I. V., High-energy limit for α-d and tau--t form factors in ^{6}Li nucleus, 26:54532

KURILENKO, A. I., ESR study of free radical reactions of γ-irradiated polypropylene with methyl methacrylate, 26:53019

KURODA, P. K., Isotopic compositions of rare gases in the carbonaceous chondrites mokoia and allende, 26:53810

KURODA, Rokuro, Ion-exchange bebaviour of metals on DEAE-cellulose in methanol--thiocyanate--hydrochloric acid media, 26:52951

KUROKAWA, Hidekazu, Note on the urbaryon models, 26:54297

KUSAKA, Kunio, Influence of austenite grain size and forging ratio on ferrite banded structure, 26:55593 (RFP-Trans-108)

KUZMIN, I. I., X-ray and dielectric studies of irradiated perovskite type compounds, 26:55020

KUZNETSOV, A. S., System of wire spark chambers with ferrite core memory, 26:53271 (JINR-P13-6522)

KUZNETSOV, V. D., Some problems of studying emergencies in a nuclear power plant with pressurized water reactor, 26:55199 (AEC-tr-7319)

KUZNETSOV, V. V., Study of ^{149}Tb decay, 26:54603 (JINR-P6-6511)

KUZNETSOV, Yu. V., Radioisotope partition between sea water and sediments, 26:53167

KUZNETSOVA, M. Ya., Study of ^{149}Tb decay, 26:54603 (JINR-P6-6511)

KVETKAS, M. J., Phenotypic properties of a large-cell, radiation-resistant strain of Escherichia coli, 26:53363

KWAN, John Y., Parametric down-conversion in astrophysical masers, 26:53909

KYNCL, Jan, Absolute activity in irradiated fuel material by method of gamma scanning, 26:53041 (UJV-2867-M,A)

L

LABAUVE, R. J., Development of ENDF/B shielding data processing codes, and integral tests, 26:55141 (CONF-720901-(Bks.1 and 2), pp 316-24)

Sensitivity of calculated pulsed sphere spectra and neutron age to carbon cross sections, 26:54474 (CONF-720901-(Bks.1 and 2), pp 409-17)
LABEYRIE, Laurent, Isotopic composition of biogenic silica, 26:53178
LACEY, P. G., Criticality control parameters and supporting calculations for uranium bearing nuclear fuel at low enrichment, 26:53733 (WCAP-2999)
LACH, H., Diurnal rhythm of neurosecretory activity in normal and x-ray irradiated mice, 26:53478
LACHENMANN, R., Influence of interstitial nitrogen on the asymmetry of the yield stress of tantalum, 26:53643
LACROIX, A., Presentation made to meeting of sodium-water reaction specialists, 26:55150 (CONF-710548-, pp 1-16)
LADA, Witold, Attempts of reactor loop use for ^{125}I production, 26:53068
LAFFERTY, K. J., Interaction of embryonic chicken spleen cells and adult allogeneic leucocytes, 26:53477
LAFON, A., Presentation made to meeting of sodium-water reaction specialists, 26:55150 (CONF-710548-, pp 1-16)
LAFUMA, J., Experimental study of decontamination of the skeleton after inhalation of americium nitrate, 26:53531 (UCRL-Trans-1477)
LAGACHE, Martine, Study by neutron activation analysis of the distribution of Cs in K minerals of granitic Corsican rocks, 26:52908
LAGNEBORG, R., Change of structure and mechanical properties in stainless steel by irradiation. Part 1.2. The interrelationship of creep and stress relaxation phenomena, 26:53642 (STU-70-419/U-350(Pt.1.2))
LAGRANGE, Maurice, Installation for observing the position of a structure inside a nuclear reactor, 26:55128
LAHTI, Gerald P., Probable solar-flare doses encountered on an interplanetary mission as calculated by the MCFLARE code, 26:54956 (NASA-TM-X-2440, pp 324-8)
LAI, Kwan-wu, Two-body strange-particle final states in π^-p interactions at 4.5 and 6 GeV/c, 26:54217
LAKIN, W. L., Correction of light attenuation in large shower counters, 26:53285
LAL, K., X-ray topographic determination of the absence of lateral strains in ion-implanted silicon, 26:55019
LALEGERIE, Pierre, Ultrastructure changes in the adenohypophysis of rodents after total or segmentary irradiation with radiocobalt, 26:53467
LAM, C. S., Diffractive models in non-diffractive regions, 26:54303 (RPP/T-25)
LAMB, R. C., Evidence for a neutral meson near 1033 MeV, 26:54205 (COO-1428-311)
LAMBIEV, D. K., Influence of Ni addition on reduction of WO_3 with H on sintering of the thus produced W powders, 26:53579
LAMBRECHT, Richard M., Doppler broadening of positron annihilation photons in silver halide crystals following high-energy implantations of C^{5+}, N^{5+}, O^{6+}, and S^{6+}, 26:54097
LAMPARTER, Peter, Diffusion measurements in systems Pd-V and Pd--Ti as well as metal--ceramic systems by means of microprobe, 26:53677
LAMPTON, Michael, Extreme-ultraviolet emissions from an aurora, 26:54030
LANCE, E. D., Bulk shielding facility quarterly report, April, May, and June of 1972, 26:55408 (ORNL-TM-3949)
LANDE, A., Correlations without tears, 26:54728
LANDER, R. L., S-wave structure in the $K\pi$ system, 26:54203 (COO-1428-308)
LANDOWNE, S., Semi-classical description of elastic and inelastic heavy-ion scattering above the Coulomb barrier, 26:54736
LANDSBERG, L. G., Search for quarks at the 70 GeV accelerator, 26:54165
LANE, A. G., Effects of radiation environment on reusable nuclear shuttle system, 26:54946 (NASA-TM-X-2440, pp 48-56)
LANE, S. A., Static quadrupole moments of the first 2^+ states of the even--even osmium nuclei, 26:54538
LANGACKER, Paul, Part I: applications of the Schwarz inequality to weak and electromagnetic processes. Part II: S-channel helicity conservation in elastic processes, 26:54287 (LBL-766)
LANGERON, J. P., Influence of carbon and oxygen on the brittleness of molybdenum, 26:53682
LANGHOFF, P. W., Aspects of time-dependent perturbation theory, 26:55073
LANGLEY, R. W., Methods of space radiation-dose analysis with applications to manned space systems, 26:54951 (NASA-TM-X-2440, pp 108-16)
LANGS, R. K., Surface energy budget measurements over Lake Michigan, 26:53189 (ANL-7860(Pt.3), pp 270-98)
LANIUS, E. H., Chemical process engineering. Fluoride process as an advantageous process in fuel reprocessing. VII, 26:53088
LANNING, H., X-ray and optical observations of Sco X-1 and observations of the x-ray background, 26:53918
LANZEROTTI, L. J., Solar-flare particle radiation, 26:53927 (NASA-TM-X-2440, pp 193-208)
LANZL, L. H., Atlas of radiation dose distributions. IV, 26:53409 (STI/PUB-295(Vol.4))
LANZL, Lawrence H., Medical physics in the United States, 26:55461 (ACRH-1000-350)
Radiation treatment planning using pi mesons, 26:54877 (LA-4874, pp 153-61)
Training of medical physicists: some existing training schemes, 26:55460 (ACRH-1000-349)
LAPIDUS, L. I., e - d scattering and neutron form factors, 26:54169 (JINR-E1-6647)
LAPIERRE, Alain, Calibration unit for γ-ray spectroscopy, 26:53253 (FRNC-TH-237)
LAPIKENS, J., Arrival directions of large air showers of primary energy $> 10^{17}$ eV, 26:53852
LAPONCHE, B., Physics of high temperature reactors at the Commissariat a l'Energie Atomique, 26:55109 (CONF-720901-(Bks.1 and 2), pp 33-54)
LAQUA, K., Limits of detection in localized spectrochemical analysis with lasers, 26:55590 (ORNL-tr-2613-A)
LARIBI, S., Reactions $^{19}F(d,\alpha)$, $^{19}F(d,p)$, and excited states of ^{20}F, 26:54548
LARSEN, R. D., Multiple Coulomb interference effects on the quadrupole moment of ^{114}Cd, 26:54623
LARSON, J. R., Evaluation of filament-type electric heater rod as employed in single-loop semiscale to simulate UO_2 fuel rods, 26:55183 (ANCR-1038)
LARSSON, E. Ingemar, Digital stereoscintigraphic experiments with a gamma-camera, 26:53215
LASALLE, R. A., α-particle excitation of 1.78 MeV 2^+ state in ^{28}Si, 26:54561
LASER, M., Separation of fission product rare gases from combustion waste gases from high temperature fuel elements by scrubbing with liquid carbon dioxide, 26:53064 (ORNL-tr-2621)
LATAL, Heimo G., Megagauss physics, 26:54834
LAUG, M. T., Xenon-tagging of EBR-II driver fuel. EBR-II Project, 26:55184 (ANL/EBR-57)
LAVAKARE, P. J., Cosmic flux of low energy gamma rays, 26:53818
LAVEDAN, Jacques, Ultrastructure changes in the adenohypophysis of rodents after total or segmentary irradiation with radiocobalt, 26:53467
LAVERRIERE, R., Possible interpretation of difference between d(p,2p)n and d(p,pn)p cross sections, 26:54510
LAVINE, J. P., Gel'fand--Levitan-unitary-transform formalism for direct extension of the two-nucleon T matrix off the energy shell. Technical Report No. 73-001, 26:54698 (ORO-4317-8)
Sensitivity of low-energy 3-body properties to the off-shell 2-body t-matrix. Technical Report No. 72-121, 26:54697 (ORO-4317-7)
LAVOLLEE, Philippe, Temperature distribution after an underground nuclear explosion in a granite terrain, 26:53127 (CEA-R-4288)
LAVRENT'EV, O. A., Accumulation of residual gas ionization plasma in an electromagnetic trap, 26:54800 (AEC-tr-7350)
LAVRENTOVICH, Ya. I., Effect of various kinds of ionizing radiation on poly(vinyl chloride), 26:53020
LAVROVA, V. V., Doppler-shifted cyclotron resonance in cadmium, 26:55044
LAW, M. E., Reaction $\pi^-p \to p\pi^+\pi^-\pi^-\pi^0$ at 20 GeV/c, 26:54207 (COO-3064-3)
LAWRIE, W. E., Study of discontinuities in control rod drive motor tube extensions, 26:55217 (BAW-10047(Rev.1))
LAWSON, R. D., Inhibited transitions and isomeric states in N = 50 isotones, 26:54611
LAX, Benjamin, Magnetic-field-enhanced heating of plasmas with CO_2 lasers, 26:54760
LAZARESCU, Adriana, Aspects concerning the corrosion behavior of zirconium and zirconium alloys in water at high temperature, 26:53614
LAZAREV, Yu. A., Average prompt neutron number for spontaneous fission of ^{256}Fm, 26:54659 (JINR-P15-6518)
LAZURIK-EL'TSUFIN, V. T., Vibrations of Fermi-fluid drop and giant resonance in intermediate and heavy nuclei, 26:54689 (ITF-72-12-P)
LEA, M. J., Ultrasonic evidence against multiple energy gaps in superconducting niobium, 26:54437
LEACH, R. K., Some preliminary paramagnetic resonance studies for dosimetry research, 26:52979 (COO-1105-179)
LEBEDEV, A. N., Self-consistent stationary state of a relativistic electron beam in a drift space, 26:53757
LEBEDEV, N. A., Study of ^{149}Tb decay, 26:54603 (JINR-P6-6511)
LEBEDEV-ZINOV'YEV, A. A., Uranium and thorium in the alkali olivine basalt series, 26:53147
LEBER, R. Eric, Doppler broadening of positron annihilation photons in silver halide crystals following high-energy implantations of C^{5+}, N^{5+}, O^{6+}, and S^{6+}, 26:54097
LE BORNEC, Y., Determination of neutron radii by alpha elastic scattering, 26:54547
LECORDIER, R., Relative isotope shift (112-114)/(110-112) in lambda = 4416 A line of cadmium, 26:54625
LECUYER, Y., High flux Franco--German reactor, 26:55415
LEDERMAN, L. M., Weak interactions at ISABELLE '72, 26:54182 (BNL-17092)
LE DONG, Analysis of form factors in $K^+ \to \pi^0\mu^+\nu$ and $K^+ \to \pi^0e^+\nu$ decays, 26:54170 (LAL-1255)
LEE, Albert, Spectrophotometric determination of molybdenum and phosphorus by carminic acid method, 26:52931
LEE, D. M., Bifilar helical multiwire proportional chamber for position sensitive detection of minimum ionizing particles, 26:53273 (LA-4968)
LEE, H. C., Light nuclei systematics in the unrestricted

Hartree--Fock approximation, 26:54745
LEE, John J., Trophic dynamics and niches of salt marsh foraminifera, 26:55520 (COO-3254-6)
LEE, K. W., Influence of radioactive phosphorus (^{32}P) on chick embryo development, hatchability, and chick growth, 26:53517
LEE, Tsung-shung H., Relativistic nuclear matter calculations and the deficiency of one-boson exchange potentials, 26:54744
LEE, Y. H., Correlated recovery kinetics, 26:55005
New EPR spectra in neutron-irradiated silicon, 26:55006
LEE, Y. Y., Does ISABELLE need unequal energy rings, 26:53778 (BNL-17068)
Some thoughts about pion--proton interaction experiments at ISABELLE, 26:54200 (BNL-17069)
LEFEVRE, B. G., Study of ordered alloys by field--ion microscopy, 26:53654
LEFEVRE, Hubert, Manufacture and analysis of single crystals of labeled lithium hydride, 26:52894 (CEA-R-4338)
LEFRANC, G., Field distribution in superconducting lenses without ferromagnetic materials, 26:53759
LEFVERT, Tomas, Gamma radiation dose rate in surroundings of electron accelerator FX-45 at Ursvik, 26:53738 (FOA-4-4490-A-3)
LEGER, Daniel, Production of hydrogen for deuterium extraction, 26:52975
LEGRAS, B., First stage of an assembly of programs for the computerized processing of digital scintigraphic data, 26:53228
LEGRAS, J., First stage of an assembly of programs for the computerized processing of digital scintigraphic data, 26:53228
LEHMANN, D., Experimental arrangement for investigation of single crystals by means of fast ions, 26:54977
LEHMKUHL, George D., Time domain reflectometry for liquid level measurement, 26:53306 (RFP-1902)
LEHR, M. P., Crystal orientation and the hardness of zirconium, 26:53693
LEICHSENRING, C. H., MILLI, a facility for the chemical reprocessing of irradiated substances, 26:53087
LEIKO, G. A., Charge state alteration processes in collisions of hydrogen atoms with hydrogen molecules, 26:54115
LEISCHNER, E., Technique for the visualization of heavy metals in fuel elements for high tempeature reactors, 26:53599
LEITH, J. T., Response of mouse epidermal cells to single doses of heavy particles, 26:53456 (NASA-TM-X-2440, pp 652-8)
LEJEUNE, C., Research program of the particle source group in the field of multicharged ions, 26:54079 (FRNC-CONF-53)
LEJEUNE, S., Dosimetry in radiodiagnosis, 26:53416
LEMAIRE, G., Evaluation of the components of the absorbed dose in the interior of organisms exposed to neutrons, 26:54871 (CEA-CONF-1976)
LEMAIRE, R., Stability of transverse-wave magnetic structure at 1.3 K, 26:55039
LE NOC, J. F., Incident of October 17, 1969 with Saint-Laurent-1, 26:55230
LEONARD, B. R. Jr., Energy-dependent cross sections in the thermal region, 26:54653 (CONF-720901-(Bks.1 and 2), pp 81-96)
LEONT'EV, N. I., Instability control in a beam--plasma system, 26:54819
LEQUEUX, James, Study of galactic supernova remnants. II, 26:53912
LERCHE, I., Radiation mechanism for pulsars, 26:53925
LERNER, Gerald M., (p,2p) reactions with divers potentials. Technical Report No. 73-002, 26:54699 (ORO-4317-11)
LERNER, Michael P., Production of a nervous-system-specific protein (14-3-2) by human neuroblastoma cells in culture, 26:55621 (UCLA-12-877)
LE SOURNE, M., Network for acquiring and remote handling of data using a small computer, 26:53312
LESSARD, L., ^{142}Ce(d,p) and ^{142}Ce(d,t) reactions and isobaric analog resonances in ^{142}Ce(p,p$_0$) and ^{142}Ce(p,p$_1$), 26:54618
LEUZE, R. E., Estimate of the process decontamination factors required to meet federal effluent regulations for the burning of HTGR fuel elements, 26:53060 (CONF-720823-14)
LEVET, R., High flux Franco--German reactor, 26:55410
LEVI, S. M., Natural fluorite in the dosimetry of the mixed field of gamma rays and thermal neutrons, 26:53240
LEVIN, David, Relation between single-strand DNA mass and sedimentation distance in alkaline sucrose gradients, 26:52981 (COO-3571-3)
LEVIN, F. S., Unitarity and the inhomogeneous equations method for identical particle scattering, 26:54414
LEVITT, L. B., VIM-1: a non-multigroup Monte Carlo code for analysis of fast critical assemblies, 26:55378 (AI-AEC-12951)
LEVY, P. W., Microscopic observation of x-ray and γ-ray-induced decomposition of ammonium perchlorate crystals, 26:52985 (NASA-TM-X-2440, pp 584-94)
LEVY, Samuel C., Long life, wide temperature range organic electrolyte battery, 26:55602 (SC-DC-722298)
LEW, S. K., Low-energy particle radiation environment at synchronous altitude, 26:54045 (NASA-TM-X-2440, pp 530-8)
LEWINS, Jeffery, Developments in variational theory and perturbation methods, 26:55426 (CONF-720901-(Bks.1 and 2), pp 162-7)
LEWIS, A., Parallel organization of CAMAC processes, 26:55464 (AERE-R-6601)
Technique for handling data buffers in real-time on-line computer systems, 26:55465 (AERE-R-6623)
LEWIS, R. C., VIM-1: a non-multigroup Monte Carlo code for analysis of fast critical assemblies, 26:55378 (AI-AEC-12951)
LEWONTIN, R. C., Study of mathematical models of mutation and selection in multi-locus systems. Annual progress report, December 1, 1971--November 30, 1972, 26:55487 (COO-1437-8)
LEZHAVA, O. I., Spatial localizability of energy--momentum tensor of gravitational field, 26:54393 (ITF-72-5-P)
LEZNIAK, Jerry A., Change in the eleven-year modulation at the time of the June 8, 1969, Forbush decrease, 26:53870
LIANG, T., Distribution of tritium in glucose and starch labeled by tritium atom bombardment, 26:53028 (COO-584-50)
LIBOFF, Richard L., Kinetic equations, 26:54797
LICHARD, P., Testing of analyticity of πN forward scattering amplitude and determination of πN coupling constant, 26:54337
LICHTMAN, Marshall A., Reduced red cell 2,3-diphosphoglycerate and adenosine triphosphate, hypophosphatemia and increased hemoglobin--oxygen affinity after cardiac surgery, 26:55638 (UR-3490-187)
LIDOFSKY, L. J., Mechanism of fast neutron transport in iron, 26:54473 (CONF-720901-(Bks.1 and 2), pp 335-48)
LIEBE, A., Heavy ion source with a confined electron beam, 26:53753 (FRNC-CONF-56)
LIEBENTHAL, J. L., ETR power: variation analysis, 26:55379 (ANCR-1085)
LIEN, J. R., (1f/sub 7/2)^2 multiplet in ^{42}Ca, 26:54573
LIGOU, J., Molten chlorides fast breeder reactor problems and possibilities, 26:55082 (EIR-215)
LIMIDO, G., Variations of ^{75}Se-selenomethionine erythrocytic incorporation induced in rat by pan-irradiation, 26:53482
LIN, R. P., Solar-wind and interplanetary electron measurements on the Apollo 15 subsatellite, 26:54072
LINDGREN, R. A., Odd-parity three-particle, one-hole structure in ^{18}F via the reaction ^{15}N(^{6}Li,t)^{18}F, 26:54549
LINDHAGEN, P., Change of structure and mechanical properties in stainless steel by irradiation. Part 1.1. Metallographic study of neutron irradiated and unirradiated 12R72HV after tensile testing, 26:53701 (STU-70-419/U-350(Pt.1.1))
LINDSEY, B. A., Radiation environment for rendezvous and docking with nuclear rockets, 26:55361 (NASA-TM-X-2440, pp 257-63)
Radiation heating in selected NERVA engine components, 26:55369 (NASA-TM-X-2440, pp 460-5)
LINDSTROM, D. G., Discrete ordinates--Monte Carlo coupling: a comparison of techniques in NERVA radiation analysis, 26:55371 (NASA-TM-X-2440, pp 681-6)
LINGENFELTER, R. E., Cosmic ray propagation and source distribution, 26:53861
LINIECKI, Julian, Long-term retention of radiobarium and radiostrontium in rabbits, 26:53534
LINNEY, A. D., Search for neutrons of solar origin using balloon-borne detectors: 1967--69, 26:53967
LIONS, N., Presentation made to meeting of sodium-water reaction specialists, 26:55150 (CONF-710548-, pp 1-16)
LIOU, H. I., Uncertainty in the neutron-strength-function evaluation for a small number of measured resonances, 26:54720
LIOU, M. K., p--p bremsstrahlung calculations and relativistic spin corrections, 26:54267
LIPAS, P. O., Moessbauer observation of magnetic moment of 89-keV excited state of ^{119}Sn, 26:54624
LIPATOV, L. N., e^+e^--pair annihilation and deep inelastic ep-scattering in perturbation theory, 26:54262
LIPPINCOTT, Stuart W., Evaluation of the hazard from exposure to electron irradiation simulating that in the synchronous orbit, 26:53458 (NASA-TM-X-2440, pp 665-71)
LI-SCHOLZ, Angela, K-shell ionization cross sections for 2.04-MeV electrons, 26:54104
LISITSA, V. S., Determination of the magnetic fields in a plasma on basis of the hydrogen spectral line contours, 26:54772
LISKA, B. J., Decomposition of aldrin by gamma radiation. II, 26:52997
Decomposition of aldrin by gamma radiation. I. In organic solvents, 26:53014
LISOWSKI, P. W., Four-nucleon studies. III, 26:54517
Four-nucleon studies. IV, 26:54518
LISTER, G. G., Transverse dynamic stabilization of a theta pinch, 26:54808 (LRP-51/72)
LITTLE, L. E., Teleoperators for remote operations in space, 26:53730 (NASA-TM-X-2440, pp 277-9)
LITTLE, Marshall S., Applications of radiation protection recommendations in the development of federal radiation standards for electronic products, 26:54925
LITTMAN, T. M., Influence of radiation shielding on reusable nuclear shuttle design, 26:54954 (NASA-TM-X-

2440, pp 251-6)
LITZ, John E., Recovery of rhenium and molybdenum values from solution, 26:52950
LIU, S. H., New magnetoelastic interaction, 26:55026
LIU, Sou-yang, Characteristics of Ca II K-line profiles in quiet Sun, 26:53948
LIU, William S., Model for the repulsive elastic scattering of atoms by solid surfaces, 26:54089
LLEWELLYN, E. J., Altitude distribution of the $O_2(^1\Delta)$ nightglow emission, 26:54042
LOBB, D. E., Change in beam spot size due to second-order effects in a first-order achromatic beam transport system, 26:53764
LOBITZ, D. W., Mesh-generation code and a contour-plotting routine, 26:55609 (SC-TM-710557)
LOCKWOOD, John A., Change in the eleven-year modulation at the time of the June 8, 1969, Forbush decrease, 26:53870
LODGE, K. B., Two perturbations in the presence of degeneracy, 26:54152
LODI-RIZZINI, E., Analysis of reaction $\gamma + n \to p + \pi^-$ in first and second resonance region, 26:54171 (LNF-72/31)
LOEBL, Karel, Carbon activity and solubility in a stainless chromium--nickel steel with about 18 percent Cr and 9 percent Ni, 26:55480 (BNWL-tr-72)
  Carbon activity and solubility in austenitic chromium--nickel steels with about 18 percent Cr, 26:55481 (BNWL-tr-73)
LOEFFLER, F. J., S-wave structure in the $K\pi$ system, 26:54203 (COO-1428-308)
LOEHKEN, R., β-decay of ^{206}Tl, 26:54648
LOEWENSTEIN, W. B., EBR-II irradiation physics, 26:55120 (CONF-720901-(Bks.1 and 2), pp 905-27)
LOKEN, Stewart Christian, Inelastic K^+p reactions at incident momenta from 1.37 GeV/c to 2.17 GeV/c, 26:54231
LOKTEV, V. M., Two-particle light absorption by solid α--oxygen crystal, 26:55531 (ITF-71-95-P)
LOKTIONOV, Yu. M., Experimental determination of the basic characteristics of space-periodic magnetic configurations, 26:54824 (AEC-tr-7334)
LOLODZE, Ts. D., Wave interactions in anisotropic plasma, 26:54862
LOMAKIN, B. N., Equation of state of a nonideal cesium plasma, 26:54866
LOMENICK, T. F., Implications of the American Salt Corporation's underground workings on the proposed Federal Waste Repository at Lyons, Kansas, 26:53725 (ORNL-TM-3903)
LOMSADZE, Yu. M., Wightman axioms for concentratable field and reconstruction theorem. I, 26:54378 (ITF-72-62-E)
LONADIER, F. D., ^{210}Po isotopic fuels, 26:53334 (MLM-1228)
  Preparation of ^{238}Pu metal, 26:53332 (MLM-1150)
LONERGAN, J. A., Parametric fit to electron-transport properties, 26:54963 (NASA-TM-X-2440, pp 832-41)
LONG, C. E., Charge and energy spectra of heavy cosmic ray nuclei, 26:53842
LONG, Jack L., Temperature measurement and control in the bomb reduction of plutonium tetrafluoride, 26:53037 (RFP-1455)
LOOS, J., Excitation of a two-level system damped by the interaction with bosons. III, 26:55075
  Excitation of two-level system damped by interaction with bosons. II, 26:55076
LORENZINI, L., Progress in standardization of analytical methods for materials of nuclear interest. I, 26:52920 (RT/CHI-(72)3)
LOUCK, James D., Application of orthogonal and unitary group methods to the N-body problem, 26:55072
LOUIE, J., Reactions $K^-p \to \Lambda\pi^0$ and $K^-p \to$ antiK^0n in the center-of-mass energy range 1700 to 2100 MeV, 26:54215
LOVE, A., Muon--proton scattering and the effect of neutral currents in the scaling region, 26:54288 (RPP/T-26)
LOVE, P. E., Critique of standard testing methods for personnel dosimetric devices, 26:53247
LOVE, T. A., Neutron spectral measurements in the upper atmosphere, 26:54066 (NASA-TM-X-2440, pp 922-5)
  Secondary gamma-ray-production cross sections of several materials, 26:54523 (CONF-720901-(Bks.1 and 2), pp 325-34)
LOWDER, W. M., Experimental determination of cosmic-ray charged-particle intensity profiles in the atmosphere, 26:53807 (NASA-TM-X-2440, pp 908-13)
LOWE, J. N., Simple hot isostat for beryllium, 26:53618
LOWE, L. F., Solar cell radiation response near the interface of different-atomic-number materials, 26:53290 (NASA-TM-X-2440, pp 577-83)
LOWRIE, R. S., Determination of the radioactive nuclides present in the off-gas stream generated by the head-end steps in reprocessing HTGR type fuels, 26:53078 (CONF-720823-11)
LU, Shin-tsu, Sequential pathophysiology of ionizing radiation on the beagle thyroid gland, 26:53452 (UR-3490-183)
LUBELL, M. S., State-of-the-art of superconducting magnets, 26:54464 (ORNL-TM-3921)
  Summary of engineering design of magnet systems from international working session on fusion reactor technology, 26:54829 (ORNL-TM-3953)
LUBKOWITZ, J. A., Geiger-Mueller counter designed to measure reproducibly activities retained on resin columns, 26:53212
LUCANO, G., Influence of dimensionality on Bose condensation and macroscopic coherence in superconductors, 26:54436 (NP-19425)
LUCARONI, L., Stability of nonradial vibrational modes of relativistic neutron stars, 26:53894
LUCAS, J., Determination of urinary plutonium by radiochemical analysis on ion exchanger filters, 26:52940
LUCAS, Peter Wayne, Study of the properties of three prong decays of K^- mesons in flight in a hydrogen bubble chamber, 26:54190
LUCASSON, P., Study of point defect induced in Al by quench hardening and electron bombardment, 26:53712
LUCOFF, D. M., Pulsed-activation techniques for the measurement of Doppler effects, 26:55124 (CONF-720901-(Bks.1 and 2), pp 1016-32)
LUDWIG, Frederic, Biological dosimetry using bone marrow samples, 26:53473
LUDWIG, Peter K., Short-lived transients, 26:53022
LUECKE, Werner, Atomic absorption determination of alkaline earth metals and refractory oxides in geochemical standards with a nitrous oxide--acetylene flame, 26:52921
LUEDERS, Gerhart, Excitations in the quantum condensated fermion gas, 26:54443
LUEHRMANN, K. H., Equations for linked clusters and the energy variational principal, 26:54735
LUGO, A. E., Investigation of the unusual behavior of ^{137}Cs and other radionuclides in the Florida environment. Progress report, September 1, 1971--August 31, 1972, 26:53170 (ORO-4066-5)
LUKE, S. K., Scalar--tensor cosmology and the classical tests, 26:53998
LUND, N., Chemical composition of heavy cosmic ray nuclei above 5 GeV, 26:53840
  Method for determining the mean atomic mass of the elements in the primary cosmic radiation throughout the latitude sensitive part of the spectrum, 26:53824
LUNDGAARD RASMUSSEN, Ib, Method for determining the mean atomic mass of the elements in the primary cosmic radiation throughout the latitude sensitive part of the spectrum, 26:53824
LUNDIN, Charles E., Structural and thermodynamic properties of the Sc--H system, 26:53556 (SC-CR-723158)
LUPOLI, P., Experimental results of several tests of fretting corrosion of metallic material, 26:53609 (RT/ING-(72)7)
LUPTON, John Edward, Solar-flare-particle propagation: comparison of a new analytic solution with spacecraft measurements, 26:53932
LUSHBAUGH, C. C., Dosimetry for radiobiological studies of the human hematopoietic system, 26:53406 (NASA-TM-X-2440, pp 974-80)
  Multifactorial analysis of human blood cell responses to clinical total-body irradiation, 26:53400 (NASA-TM-X-2440, pp 233-7)
  Predicted levels of human radiation tolerance extrapolated from clinical studies of radiation effects, 26:53402 (NASA-TM-X-2440, pp 398-415)
  Pulmonary-impedance power spectral analysis: a facile means of detecting radiation-induced gastrointestinal distress and performance decrement in man, 26:53401 (NASA-TM-X-2440, pp 238-48)
LUSS, E. V., Mutagenesis in cultured mammalian cells. II, 26:53362
LUTZ, D., Group constant generation for the resolved resonance region, 26:55439 (CONF-720901-(Bks.1 and 2), pp 1183-91)
LUTZ, W. R., Multiple Coulomb interference effects on the quadrupole moment of ^{114}Cd, 26:54623
LUYENDYK, A. P. J., Spectral and pulsed x-ray emission from the Crab Nebula, 26:53919
LYMAN, J. T., Human visual response to nuclear-particle exposures, 26:53403 (NASA-TM-X-2440, pp 416-22)
LYNE, A. G., Interstellar scintillation pattern of PSR + 54, 26:53915
  Study of the lunar occultations of eleven radio sources, 26:53914
LYON, W. S., Reliability in scientific evidence based on multi-trace forensic NAA, 26:52896 (CONF-720920-2)
LYSENKO, Walter Paul, Part I. Nonlinear betatron oscillations. Part II. Particle motion in muon g-2 experiment, 26:53763
LYTTLETON, R. A., Formation of planets from a solar nebula, 26:54005

M

MACDONALD, J. R., Lifetime of 3.74-MeV (3^-) state of ^{40}Ca, 26:54575
MACDOWELL, C. E., Analysis of breakup scattering in a deuterium target. Application to antiproton--deuteron breakup scattering, 26:54347 (UM-P-72-6)
MACEK, Robert J., Pion and particle physics (P^3), 26:53788 (LA-4874, pp 55-8)
MACFARLANE, M. H., Inhibited transitions and isomeric states in N = 50 isotones, 26:54611
MACHESKO, M. R., Mutational assay system using the

thymidine kinase locus in mouse lymphoma cells, 26:53361
MACHI, Sueo, Progress in application of radiation to chemical industry, 26:53722
MACHLIN, E. S., Field ion microscopy of dilute alloys, 26:53652
MACKI, James M., Corrosion and stress-corrosion cracking of painted U--4.2 wt. percent Nb, 26:53607 (RFP-1891)
  Stress-corrosion cracking of underaged and overaged U--2.3 wt percent Nb in an aqueous chloride environment, 26:53608 (RFP-1904)
MACKLIN, R. L., Gamma-ray shielding measurements made at altitudes greater than 115,000 feet using large Ge(Li) detectors, 26:54964 (NASA-TM-X-2440, pp 914-21)
MACKU, Ales, Absolute activity in irradiated fuel material by method of gamma scanning, 26:53041 (UJV-2867-M,A)
MACPHERSON, R. E., Final systems design description of the failed fuel mockup (FFM) of the liquid-metal fast breeder reactor, 26:55191 (ORNL-TM-3656)
MADDEN, P. K., Nature of rod-like defects observed in boron irradiated silicon, 26:54995
MADEY, Richard, Direct stimulation of the retina by the method of virtual quanta for heavy cosmic-ray nuclei, 26:53405 (NASA-TM-X-2440, pp 767-72)
  Frequency of light flashes induced by Cherenkov radiation from heavy cosmic-ray nuclei, 26:54882 (NASA-TM-X-2440, pp 757-66)
MADISON, Don Harvey, Distorted-wave theory and its application to the excitation of the ^{1}p states of helium and mercury, 26:54106
MADSON, A. A., Xenon-tagging of EBR-II driver fuel. EBR-II Project, 26:55184 (ANL/EBR-57)
MAEDER, A., Variable stars of small amplitude I, 26:53884
MAERKER, R. E., ORNL sodium benchmark experiment, 26:55142 (CONF-720901-(Bks.1 and 2), pp 418-30)
  SDT5. Stainless-steel broomstick experiment: an experimental check of neutron total cross sections, 26:54965 (ORNL-TM-3871(Rev.))
MAESTRO, A., DNA, RNA, and ultrastructural aspects of human epidermis in chronic reactions of skin after roentgen irradiation, 26:53441
MAGEE, John L., Advances in radiation chemistry. Volume 3, 26:53021
MAGGIORE, Carl Jerome, Inelastic proton scattering from ^{48}Ca, 26:54582
MAHDY, M. A., Mineralogy and some trace elements geochemistry of samples from southwest Aswan radioactive syenite rock western desert, 26:53142 (AREAEE-138)
MAHENDROO, P. P., Temperature dependence of hyperfine interactions of Eu^{2+} in SrCl$_2$, 26:52970
MAIER, B. P. K., Nuclear levels in ^{188}Re, 26:54637
MAIKISH, C. R., Application of advanced metal-matrix composites to aircraft structures, 26:53573
MAIZZA, Vito, Non conventional two phase cycles in autotraction, 26:53103
MAJERNIK, V., Markoffian model for hadrons, 26:54308
MAKARIOUS, A. S., Fast neutron scintillation spectrometer with double compensation circuit for gamma-ray discrimination, 26:53251 (AREAEE-137)
MAKAROV, V. I., Statistical view on resonance widths and multiplicity in dual models, 26:54300 (ITF-72-53-E)
MAKAROV, V. P., Longitudinal and transverse excitons in semiconductors, 26:55065 (UCRL-Trans-10643)
MAKI, J., Experimental study of the ultimate strength of composite beams subjected to alternate loading of positive and negative bending, 26:55571 (NRC-TT-1557)
MAKINO, H., Experimental study of the ultimate strength of composite beams subjected to alternate loading of positive and negative bending, 26:55571 (NRC-TT-1557)
MAKINODAN, T., Incidence of delayed mortality (secondary disease) in allogeneic radiation chimeras receiving bone marrow from aged mice, 26:53485
MAKOWSKI, B., Analysis of KantiK and KantiK* resonances produced in antipp annihilations at 1.2 GeV/c, 26:54199
MALARD, M., Production of Ca and Ge ions in a PIG source, 26:53752 (FRNC-CONF-54)
MALAVIYA, B. K., Review of fast neutron spectrum measurements, 26:55438 (CONF-720901-(Bks.1 and 2), pp 943-58)
MALCOLME-LAWES, D. J., Effect of scavenger competition on hot atom chemistry. II. Computer simulation, 26:53030
  Effect of scavenger competition on hot atom chemistry. I. Correction to the kinetic theory, 26:53031
MALENFANT, Richard E., External gamma radiation environment from the Kiwi, Phoebus, and Pewee reactors, 26:55367 (NASA-TM-X-2440, pp 440-8)
MALLARY, Michael Leigh, CP and the three pion decay of the K^0, 26:54188
MAL'TSEV, I. G., Power supply system for the preinjector of the I-100 linear accelerator, 26:53751 (BNL-tr-498)
MALZER, G. L., Calcium and strontium transport to plant roots, 26:55490 (COO-1495-17)
MAMAEV, Yu. A., Charge state alteration processes in collisions of hydrogen atoms with hydrogen molecules, 26:54115
MAMEDOV, F. G., Study of the obtaining conditions and thermoemission characteristics of borides of the rare-earth metals, 26:53582
MAMIN, E. B., Evaluation of exposure doses to personnel at high-power beta radiation installations, 26:53426
MANCINI, F., Effect of γ-irradiation of seed on properties of sugar beet, 26:53386
MANDEL, L., Course of the post-irradiation syndrome after irradiation with lethal doses in piglets, 26:53495
MANDEL'STAM, S. L., New measurements of the polarization of x-ray solar flares, 26:53962
MANDRU, Galina, Aspects concerning the corrosion behavior of zirconium and zirconium alloys in water at high temperature, 26:53614
MANELIS, R. M., Study of the obtaining conditions and thermoemission characteristics of borides of the rare-earth metals, 26:53582
MANESS, Roy F., Corrosivity of thoria dissolvent solutions, 26:53604 (BNWL-CC-449)
MANGIALAJO, M., Buckling measurements in ECO with few CIRENE fuel elements, 26:55106 (CISE-R-283)
  Experimental investigations on U--D$_2$O lattices, 26:55101 (CISE-R-203)
  Measurement of cell parameters in RB-1 reactor, 26:55102 (CISE-R-239)
  Neutron measurements at zero power on CIRENE fuel element in ESSOR reactor, 26:55105 (CISE-R-258)
MANINA, A. A., Respiration and structural changes of mitochondria of intestinal epithelial cells in the course of amino acid absorption in irradiated animals, 26:53493
MANN, A., Approach to the nuclear many-body problem by variationally determined transformation. II, 26:54718
MANNING, H. S., Integral dose during constant-velocity motion near a space power reactor, 26:55363 (NASA-TM-X-2440, pp 270-6)
  SNAP-8 post-shutdown gamma-radiation approximations, 26:55360 (NASA-TM-X-2440, pp 84-91)
MANTHURUTHIL, J. C., Two decades of research on radioactivity, 26:53263
MANTOVANI, G., Alterations of sugar beets by γ-irradiation of the seed, 26:53388
  Effect of γ-irradiation of seed on properties of sugar beet, 26:53386
MANUAL, O. K., Xenon isotopes in tellurobismuthite, Boliden, Sweden, 26:53176
MANUEL, O. K., Isotopic compositions of rare gases in the carbonaceous chondrites mokoia and allende, 26:53810
MAOR, U., Properties of the pion exchange contribution to two and quasi two body reactions, 26:54270
MARCANDALLI, R., Experimental results on operation of reactivity fast control system of CIRENE reactor, 26:55133 (CISE-R-268)
MARCHESE, C. J., Energy dependence of the ^{3}He optical potential, 26:54580
  Optical-model analysis of elastic scattering of 53.4 MeV helions from ^{56}Fe, 26:54571
MARCHUK, A. I., Investigation of the surface of tungsten single crystals following electro-erosive treatment, 26:53668
MARCINKOWSKI, Andrzej, Cross sections for proton induced reactions on ^{43}Ca, ^{44}Ca, and ^{48}Ca isotopes in protons energy range 1 to 2 MeV, 26:54567 (INR-1407)
MARCOLI, R., Performances of a proportional chamber with intermediate high voltage planes, 26:53213
MARCUS, Gail H., Proton and fast neutron damage studies in Si and Ge using channeling, 26:55004
MARCUS, R. A., Theory of semiclassical transition probabilities for inelastic and reactive collisions. IV, 26:54129
MAREK, J., Results of heat transfer and pressure loss measurements with helium on a sixteen-tube bundle, 26:55227 (EURFNR-1000)
MARELL, A., Surface ionization applied to some materials of nuclear interest, 26:53033 (EUR-4765, pp 117-30)
MARIER, Lester J. Jr., Light-water breeder reactor, 26:55130
MARIMUTHU, Kodumudi M., Radiobiologic studies of Tradescantia plants orbited in Biosatellite 2, 26:53382 (N-72-20054)
MARINE, Jean, Electroluminescent diodes formation in ion implanted zinc telluride, 26:54971 (CEA-R-4313)
MARINO, G. P., Numerical calculation of the redistribution of an interstitial solute in a thermal gradient, 26:53665
MARINOV, M. S., Pair production in electromagnetic field, 26:54266
MARJANKOWSKA, Barbara, Synthesis of new compounds labeled with tritium and ^{14}C for biological investigations. I, 26:53052
MARKAKIS, P., Characterization of the red pigments produced from ferrimyoglobin by ionizing radiation, 26:53346
MARKHAM, R. G., Odd-parity three-particle, one-hole structure in ^{18}F via the reaction ^{15}N(^{6}Li,t)^{18}F, 26:54549
MARKHAM, Roger G., (^{6}Li,d) on ^{58}Ni and ^{64}Ni, 26:54586
MARKOV, M. A., Potentials in collapsing systems of general relativity theory, 26:54404
MARKS, Tobin J., Stable uranium(IV) alkyl and aryl complexes, 26:53047
MARKWORTH, Alan J., Effects of impurities on migration of lenticular pores in UO$_2$, 26:53559
MARQUIT, E., Comparison of pion momentum distributions in 19 GeV/c pp collisions with and without strange-

particle production, 26:54198
MARR, D. R., Diffusion theory analyses for fast reactor shield design, 26:55143 (CONF-720901-(Bks.1 and 2), pp 459-70)
MARSDEN, Howard, Effects of ionizing radiation on the capacity of Escherichia coli to support bacteriophage T4 growth, 26:53372
MARSDEN, P. L., Primary electron observations (3 less than or equal to E less than or equal to 15 GeV) recorded on the ESRO II satellite, 26:53821
MARSHALEK, E. R., Boson expansions and Hartree--Bogolyubov theory, 26:54741
MARSHALL, Don Allen, Reaction $K^+n \rightarrow K^+\pi^-p$ at 3.8 GeV/c, 26:54202 (COO-1195-238)
MARSHALL, N. H., Automated Cross Section Analysis Program (ACSAP), 26:54468 (ANCR-1042)
MARTIN, J., First stage of an assembly of programs for the computerized processing of digital scintigraphic data, 26:53228
MARTIN, P., Negative muon capture in carbon leading to specific final states, 26:54537
  Yields of gamma rays emitted following capture of negative muons by ^{28}Si and ^{24}Mg, 26:54555
MARTIN, R., Arrival directions of large air showers of primary energy > 10^{17} eV, 26:53852
MARTINENGHI, C., Study as a function of time and dose of the numerical variations of the leucocytes circulating in a totally irradiated rat, 26:53483
  Variations of ^{75}Se-selenomethionine erythrocytic incorporation induced in rat by pan-irradiation, 26:53482
MARTY, Michel, Production of Ni--Cr--ThO_2 alloys by means of chromium diffusion through halogen carrier in $NiThO_2$ grain, 26:53627
  Production of Ni--ThO_2 alloy with dispersed phase starting from organometallic compounds, 26:53626
MARTY, N., $^2H(p,2p)n$ reaction at 155 MeV, 26:54522
MARX, Jay N., Luminosity measurements for colliding beams, 26:53771 (BNL-17019)
  Measurement of the proton--proton total cross section by beam attenuation, 26:54191 (BNL-17065)
MASLEEV, N. N., Relativistic equation for baryons. II, 26:54368
  Relativistic equation for baryons. I, 26:54372
MASNYI, V. F., Study of Na and H_2O interaction in a one-megawatt modular steam generator, 26:55153 (CONF-710548-, pp 57-104)
MASON, F., Manufacturing specification for high temperature thermocouples for use in nuclear irradiation experiments, 26:53301 (EUR-4807)
MASON, G. M., Energy dependence of the abundances of galactic He, L, and M nuclei from satellite measurements, 26:53835
MASSALSKI, T. B., Note on the nature of massive transformation interfaces, 26:53644
MASSE, Rene, Crystallographic study of tetravalent $M(IV)(PO_3)_4$ compounds (M(IV) = Ce, U, and Th), 26:53045
MASSER, Charles C., Crew radiation dose from a high-impulse gas-core nuclear rocket plume, 26:54967
MATHUR, K. C., Electron loss in atom-molecule collisions, 26:54121
MATHY, Pierre, Coldstream process, 26:53591
MATIVIER, H., Hydrolysis of tetravalent plutonium, 26:53034 (MLM-1964(tr))
MATSIBORKO, N. G., Interaction of finite perturbations in a beam--plasma system, 26:54795
MATSUNAMI, N., Location of diffusion-doped gold atoms in silicon by means of channeling, 26:54987
MATSUSHIMA, Hideno, Toxic eruptions combined with radiation therapy of malignant tumors, 26:53433
MATSUSHITA, Masamitsu, Surgical treatment for local radiation injuries following radiotherapy, 26:53438
MATSUYAMA, Akira, Double-strand scissions in DNA of gamma-irradiated Micrococcus radiodurans and their repair during postirradiation incubation, 26:53349
MATSUYAMA, Tomochika, Optical absorption bands of color centers in irradiated anthracene single crystals at low temperatures, 26:54996
MATTHEWS, J. L., Phase and shape of the form factor for inelastic ^3He scattering, 26:54621
MATTHIES, M. T., Transportation air pollutant emissions handbook, 26:55467 (ANL/ES-15)
MATTONI, R. H. T., Induction of lysogenic bacteria in the space environment, 26:53364 (N-72-20063)
MATTOX, D. M., Fundamentals of ion plating, 26:53615 (SC-DC-722284)
MATVEEV, V. A., Automodel asymptotic of spectral functions of virtual Compton effect, 26:54246 (JINR-P2-6636)
  Multiple charged particle production in π^-p and π^-n interactions at p = 40 GeV/c, 26:54327 (JINR-E2-6596)
MATYUSHKOVA, R. M., Effect of x-ray irradiation on regeneration of the thyroid gland in rats without tumors and after inoculation of sarcoma-45, 26:53494
MATZNER, R. A., Galaxy formation in anisotropic cosmologies, 26:53980
MAUERSBERGER, R., Conveying tube for the pneumatic transfer of spherical elements, 26:55194
MAUL, J., Determination of implantation profiles in solids by secondary-ion mass spectrometry, 26:55014
MAULBACH, K., Results of heat transfer and pressure loss measurements with helium on a sixteen-tube bundle, 26:55227 (EURFNR-1000)
MAURENZIG, P. R., Compact electron spectrometer for in-beam measurements of internal conversion coefficients, 26:53264
MAURY, J., Mechanical effects in the close-in zone of an underground nuclear explosion in granite, 26:53131 (UCRL-Trans-10616-5)
MAXCY, R. B., Post-irradiation evaluation of pathogens and indicator bacteria, 26:53369
MAXFIELD, B. W., Thermal resistivity and thermal magnetoresistivity of potassium, 26:55507 (COO-3150-6)
MAYER, J. W., Microanalysis of materials by backscattering spectrometry, 26:52939
MAYER, Walter A., Activation analysis for vanadium in mineral oil, 26:52905
MAYER-HASSELWANDER, H. A., Investigation of gamma radiation from the Crab pulsar, 26:53923
MAYEUR, C., Measurement of the Ξ hyperon lifetimes and α parameters, 26:54174 (RPP/H-99)
MAYNARD, C. W., Neutron and gamma physics problems in fusion reactors, 26:54826 (CONF-720901-(Bks.1 and 2), pp 559-73)
MAZANOV, A. S., Analytical and experimental study of a reacting water-sodium flow, 26:55161 (CONF-710548-, pp 221-42)
  Study of Na and H_2O interaction in a one-megawatt modular steam generator, 26:55153 (CONF-710548-, pp 57-104)
MAZUREK, C., Radiosensitivity of circulating hemopoietic stem cells (CFU), 26:53466
MAZURKIEWICZ, Barbara, Effect of gamma radiation on ion exchange resins. IV, 26:53016
MCALLISTER, John D., Correction of a formula used in radioassay of /sup 99m/Tc, 26:52946
MCARTHUR, David A., Feasibility of using the Faraday effect to measure currents in the electron beam environment, 26:53747 (SC-DR-720447)
MCCARTHY, I. E., Non-local potential for single-particle properties of nuclei, 26:54746
MCCARTHY, Patrick J., Asymptotically flat space--times and elementary particles, 26:54357
MCCAULEY, E. W., Nuclear reactor descriptions for space power systems analysis, 26:54950 (NASA-TM-X-2440, pp 98-102)
MCCLOSKEY, Michael, Energy crisis: the issues and a proposed response, 26:53100
MCCLURE, J. Doyle, Determination of atom--surface properties for Ne--LiF by scattering studies, 26:54087
  High-resolution calculations on atom--surface scattering: method and comparison with experiment for Ne--LiF, 26:54088
MCCORMICK, B. H., Analysis of texture, 26:55501 (COO-2118-35)
MCCOY, J. E., Solar-wind and interplanetary electron measurements on the Apollo 15 subsatellite, 26:54072
MCCREADY, V. R., Gamma camera in malignant disease, 26:53214
MCDANIEL, Paul W., Promotion of the academic uses of LAMPF, 26:53796 (LA-4874, pp 92-8)
MCDANIELS, D. K., Radiative capture of energetic neutrons by ^{208}Pb, 26:54662
MCDERMOTT, W. E., Ge(Li) data reduction using small computers, 26:53256 (NASA-TM-X-2440, pp 744-6)
MCDOW, Earl, Pulmonary-impedance power spectral analysis: a facile means of detecting radiation-induced gastrointestinal distress and performance decrement in man, 26:53401 (NASA-TM-X-2440, pp 238-48)
MCDOWELL, M. R. C., Collisions of fast electrons with He. I, 26:54138
MCGINLEY, Patton Hopkins, Fast-neutron therapy treatment planning, 26:54893
MCGRATH, E. J., Photon-induced secondary electron emission, 26:54885 (NASA-TM-X-2440, pp 792-800)
MCGRATH, P. E., Calculation of heterogeneous fluxes, reaction rates, and reactivity worths in the plate structure of zero power fast critical assemblies, 26:55396 (EURFNR-1014)
  Experimental results from two Pu-fueled fast critical assemblies, 26:55387 (CONF-720901-(Bks.1 and 2), pp 645-59)
  Measurement of β/sub eff/ in Pu-fueled fast critical assemblies, 26:55389 (CONF-720901-(Bks.1 and 2), pp 700-12)
MCGREGOR, B. J., FFTF pipe chase streaming experiment, 26:55394 (CONF-720901-3)
  FFTF pipe chase streaming experiment, 26:55382 (CONF-720901-(Bks.1 and 2), pp 431-41)
MCGRORY, J. B., Ground state of ^{40}Ca, 26:54577
MCGUIRE, R. E., Solar-wind and interplanetary electron measurements on the Apollo 15 subsatellite, 26:54072
MCGUIRE, Robert, Quenching of tyrosine and tryptophan fluorescence by H_2O and D_2O, 26:52958 (UR-3490-193)
MCGUIRE, Robert E., Theoretical treatment of lunar particle shadows, 26:53943
MCHARRIS, Wm. C., Collective and higher-order effects shown by the (p,t) reaction on the deformed nucleus ^{159}Tb, 26:54645
  Collective effects shown by the (p,t) reaction on the closed-shell nucleus, ^{141}Pr, 26:54615
MCILWAIN, R. L., Preliminary study of $\pi^+\pi^-$ scattering in reaction $\pi^+p \rightarrow (\pi^+\pi^-)\Delta^{++}$ at 13 GeV/c, 26:54223
MCINTYRE, L. C., Investigation of spin assignments in ^{41}Ca,

^{53}Cr, and ^{55}Fe, 26:54578
MCISAAC, L. D., Gamma rays emitted by the fissionable nuclides and associated isotopes, 26:54652 (ANCR-1069)
MCKIBBIN, D. D., Simultaneous solar-wind plasma and magnetic-field measurements in the expected region of the extended geomagnetic tail, 26:54074
MCLEAN, A. S., Radiation and health, 26:53157
MCLEAN, K. C., ^{57}Fe(t,p)^{59}Fe and ^{58}Fe(d,p)^{59}Fe reactions, 26:54592
MCNEELY, W. A., New evidence on the photoexcitation of I = $^1/_2$ nucleon isobars, 26:54166 (CALT-68-322)
MCNEESE, Leonard E., Method for reprocessing spent molten salt reactor fuels, 26:53086
MCNEILLY, C. E., Polymorphic modifications of Pm_2O_3, 26:53596
MCNELIS, D. N., Background information for the development of a radiation standard for tritium in nuclear-stimulated natural gas, 26:53134
MCNEW, C. O., Neutron spectral measurements in the upper atmosphere, 26:54066 (NASA-TM-X-2440, pp 922-5)
MCNULTY, P. J., Direct stimulation of the retina by the method of virtual quanta for heavy cosmic-ray nuclei, 26:53405 (NASA-TM-X-2440, pp 767-72)
  Frequency of light flashes induced by Cherenkov radiation from heavy cosmic-ray nuclei, 26:54882 (NASA-TM-X-2440, pp 757-66)
MCPHERRON, R. L., Investigation of interaction between Pc 1 and 2 and Pc 5 micropulsations at the synchronous orbit during magnetic storms, 26:54035
  Statistical characteristics of storm-associated Pc 5 micropulsations observed at the synchronous equatorial orbit, 26:54036
MCQUEEN, M., Flare star production of energetic charged particles, 26:53853
MCREYNOLDS, J. F., 2π steradian magnetic spectrometer, 26:53284
MEAD, James F., Metabolism of 1-^{14}C palmitic acid in the developing brain: persistence of radioactivity in the carboxyl carbon, 26:55620 (UCLA-12-871)
MEADEN, G. T., Critical divergence of thermal resistivity at Neel point of Eu, 26:55049
MEANS, Robert William, Turbulence in electrostatic collisionless shock waves, 26:54855
MEARES, Claude F., Study of biological macromolecules using perturbed angular correlations of gamma radiation, 26:55058
MEDICUS, H. A., Isomer ratios from low primary excitation of residual nuclei, 26:54725
MEERSON, G. A., Study of the obtaining conditions and thermoemission characteristics of borides of the rare-earth metals, 26:53582
MEGAHID, R., Fast neutron scintillation spectrometer with double compensation circuit for gamma-ray discrimination, 26:53251 (AREAEE-137)
MEIERB, F. T., S-wave structure in the Kπ system, 26:54203 (COO-1428-308)
MEINDOK, H., Visualization of arterial and arterial graft patency by intravenous radionuclide angiography, 26:53542
MEINZER, A. L., Potential function for the ring puckering vibration of B_2H_6 and B_2D_6, 26:52966
MEJDAHL, V., Progress in TL dating at Risoe, 26:53177
MEKHTIEV, M. M., Chromatographic separation of In from elements that form periodates of low solubility, and its subsequent determination, 26:52949
MELAMUD, E., H_3O radical, 26:53026
MELICHAR, Zdenek, Radiation safety of nuclear power plants, 26:55210
MELIKYAN, L. A., Effective cross sections of proton and alpha particle tracks in ionic crystals, 26:55016
MELIUS, Carl F., Theoretical description of asymmetric, nonresonant charge-transfer process, Li + Na$^+$ in equilibrium Li$^+$ + Na, 26:54127
MEL'NIKOV, E. A., Spectrographic determination of Ni, Co, Ag, V, Sn, Mo, Ti, Al, Bi, Fe, Pb, Mn in natural water in the presence of relatively large amounts of Cu, 26:52927
MELROSE, D. B., Scattering of higher energy cosmic rays, 26:53863
MENDE, A., Experimental arrangement for investigation of single crystals by means of fast ions, 26:54977
MENDE, G., Use of Knobloch elementary microanalyzer for combustion of analytical samples containing ^{14}C, 26:52944
MENDE, S. B., Coordinated observations of the magnetosphere: the development of a substorm, 26:54061
MENDILLO, Michael, Average behavior of midlatitude F-region parameters N/sub T,/N/sub max,/ and tau during geomagnetic storms, 26:54040
MENEGHETTI, D., EBR-II irradiation physics, 26:55120 (CONF-720901-(Bks.1 and 2), pp 905-27)
MENG, C.-I., Diamagnetic effect of the plasma sheet near 60 R/sub E/, 26:54058
MENKE, Michael M., Study of non-strange boson resonances produced by quasi-monochromatic photon beams of energies between 4.3 and 7.5 GeV in a hydrogen bubble chamber, 26:54175 (SLAC-143)
MENKEN, H. G., Corrosion mass transfer in primary systems of LMFBR's, 26:55168 (CONF-710959-, Paper 12)
MENNESSIER, G., Three-meson resonances in a relativistic Faddeev-type approach, 26:54318
MENNIGMANN, H.-D., Pyrimidine dimers as pre-mutational lesions in Escherichia coli WP2 Hcr$^-$, 26:53370
MENZE, D., Photoproduction of π^+-mesons on polarized protons at photon energies between 0.5 and 2.2 GeV, 26:54172 (NP-19415)
MERCIER, G. F., Elastic and inelastic widths of analogue states in ^{65}Cu, 26:54590
MERICLE, L. W., Resolving the enigma of multiple mutant sectors in stamen hairs of Tradescantia, 26:55486 (COO-1400-41)
MERICLE, R. P., Resolving the enigma of multiple mutant sectors in stamen hairs of Tradescantia, 26:55486 (COO-1400-41)
MERKEL, A., Survey about calculation methods for activity inventory in primary system of SNR, 26:55169 (CONF-710959-, Paper 13)
MERKER, M., Accelerator measurement of the energy spectra of neutrons emitted in the interaction of 3-GeV protons with several elements, 26:54528 (NASA-TM-X-2440, pp 523-6)
MERKLE, J. G., Effects of strain gradients on the gross strain crack tolerance of a 533-B steel, 26:53634 (CONF-720806-3)
MERRICK, T. P., Irradiation effects studies of NERVA materials, 26:53696 (NASA-TM-X-2440, pp 595-602)
MERRILL, Carl C., Separation of columbium, tantalum, titanium, and zirconium from titanium chlorination residues, 26:52947 (BM-RI-7671)
MERZ, N., Field distribution, power losses, and parameter optimization of helical accelerator structures, 26:53744
MESERVEY, A. B., Decontamination of HTGR reprocessing off-gases, 26:53059 (CONF-720823-12)
MESSERSCHMIDT, O., Combined radiation injuries, 26:53419
METCALFE, R., Surface flatness measurement by broad source interference: related to mechanical face seals, 26:55463 (AECL-4208)
METIVIER, H., Pulmonary lavage, therapy of pulmonary contaminations, 26:53528 (LF-tr-71)
METROPOLIS, N., Analyzed binary computing, 26:55553 (LA-DC-72-783)
  Trilogy on errors in the history of computing, 26:55548 (LA-DC-72-243)
METZ, D. J., Bibliography of technical publications and reports of the Radiation Division, Brookhaven National Laboratory, July 1968--June 1971 inclusive, 26:53325 (BNL-50335)
METZGER, Albert E., Identification and control of spacecraft radiation sources of interference to x-ray and gamma-ray experiments, 26:53255 (NASA-TM-X-2440, pp 714-22)
MEUNIER, R., Ion implantation facility at Orsay, 26:54976
MEWALDT, R. A., Observation of VH and VVH cosmic rays with an ionization--Cherenkov detector system, 26:53843
MEYER, F. Graham, Conversion of plutonium oxide to plutonium tetrafluoride with fluorine in a fluid bed reactor. Part II. Demonstration runs: a comparison of the fluorine process with the hydrofluorination process, 26:53039 (RFP-1890)
MEYER, H., Limiting distributions for inclusive charged pion production at very high energy, 26:54326 (DESY-72/40)
MEYER, Horst, Study of the specific heat of a ^{3}He--^{4}He mixture near its gas-liquid critical point, 26:54426
MEYER, J., DWBA analysis of sub-Coulomb multi-transfer reactions, 26:54695 (LYCEN-7213)
MEYER, Peter, Flux and energy spectrum of cosmic ray electrons between 10 and 1000 GeV, 26:53822
  Upper limit on the flux of primary cosmic ray anti-alpha particles from 0.3 to 3 GeV/nucleon, 26:53825
MEYER, R., Electric and thermal conductivity, elastic properties, and bending resistance of porous W over entire range of porosity, 26:53684
  Sintering and oxidation resistance of diborides of Ti and Zr, 26:53594
MEYER, S., Angular distribution of interstellar atomic hydrogen, 26:53979
MEYER, W., Critical comparison and evaluation of neutron spectrum unfolding codes: the need to know, 26:53252 (CONF-720901-(Bks.1 and 2), pp 524-40)
MEYERS, Charles R. Jr., Regional modeling abstracts. III, 26:55573 (ORNL-NSF-EP-23)
MEYN, D. A., Cleavage in Ti--8Al--1Mo--1V caused by hydrogen gas, 26:53685
MICAUD, G., In pile radiation damage in graphite. Correlation between temperature and flux density in range of high temperature, 26:53713 (CEA-CONF-1894)
MICHAEL, Joe V., Determinations of elementary reaction rate constants for the reaction of hydrogen atoms with various substrate molecules in the gas phase. Annual progress report, 1971--72, 26:55519 (COO-3242-4)
MICHAELSON, Sol M., Sequential pathophysiology of ionizing radiation on the beagle thyroid gland, 26:53462 (UR-3490-183)
MICHALIK, Jacek, Attempts of reactor loop use for ^{125}I production, 26:53068
MICHAUD, L., Mechanical effects beyond the close-in zone of an underground nuclear explosion in granite, 26:53129 (UCRL-Trans-10616-2)
  Mechanical effects in the close-in zone of an underground nuclear explosion in granite, 26:53131 (UCRL-Trans-

10616-5)
MICHAUDON, Andre, Fission cross sections and the fission process, 26:54676 (CONF-720901-(Bks.1 and 2), pp 1087-1106)
MICHEL, S., Measurement of isotopic ratios of helium, 26:54519
MICHELINI, M., TRUD: an anisotropic diffusion code for xy geometry, 26:54488 (RT/FI-(72)1)
MICHIYOSHI, Itaru, Experimental study of relaxation phenomena in non-equilibrium MHD generator duct, 26:53104
  Pressure drop of liquid Hg MHD power generators, 26:53106
MICKLITZ, H., Charged state of ^{57}Fe atoms following the decay of ^{57}Co in solid xenon, 26:55057
MIETTINEN, H. I., Backward-scattering extrapolations and baryon couplings, 26:54331
MIHALOV, J. D., Diamagnetic effect of the plasma sheet near 60 R/sub E/, 26:54058
  Limits to energetic proton fluxes trapped in Jupiter's magnetosphere, 26:54006
MIKA, Janusz, Effect of singularities on approximation in S/sub N/ methods, 26:54482 (INR-P-1405)
MIKA, K., Recovery of electron-irradiated. II, 26:55011
MIKAELIAN, Karnig O., Weak and electromagnetic processes, 26:54277
MILER, I., Course of the post-irradiation syndrome after irradiation with lethal doses in piglets, 26:53495
MILET, Claude, Safety aspects of sealed ^{238}Pu sources used in pacemakers, 26:53331 (CEA-CONF-2026)
MILINCHUK, V. K., ESR study of free radical reactions of γ-irradiated polypropylene with methyl methacrylate, 26:53019
MILLER, Arthur J., Urban utilization of extracted heat and waste heat from central station power plants, 26:55212 (CONF-720925-2)
MILLER, Billie F., Proceedings of the fifth LAMPF users meeting held at the Los Alamos Scientific Laboratory, Los Alamos, N.M., November 8-9, 1971, 26:53784 (LA-4874)
MILLER, Charles G., Design considerations and test facilities for accelerated radiation effects testing, 26:53695 (NASA-TM-X-2440, pp 570-6)
  Design considerations for combined radiation effects facilities for twelve-year outer planet spacecraft voyages, 26:53095 (NASA-TM-X-2440, pp 844-9)
MILLER, D. K., Isotopic compositions of rare gases in the carbonaceous chondrites mokoia and allende, 26:53810
MILLER, G. H., Negative muon capture in carbon leading to specific final states, 26:54537
  Yields of gamma rays emitted following capture of negative muons by ^{28}Si and ^{24}Mg, 26:54555
MILLER, Holly H., Application of nuclear technology to art identification problems. Final report, 26:52898 (COO-3034-2)
MILLER, Kathy, Mammalian toxicity of purpurin, quinizarin, quinalizarin, diphenylthiocarbazone, and 1,5-diphenyl-3-thiocarbohydrazide, 26:55574 (ORNL-TIP/TIRC-72-4)
MILLER, M. C., Metabolism of dissolved and particulate detrital carbon in a temperate hard-water lake, 26:55493 (COO-1599-58)
MILLS, R. L., Phase transitions and crystal structures of deuterium, 26:55559 (LA-DC-72-903)
MILSTEIN, Frederick, Influence of plastic deformation and re-crystallization upon permeability anomalies in gadolinium metal, 26:55040
MILTON, Kimball A., Compton scattering. I. Spectral forms for the invariant amplitudes to order e^4, 26:54255
  Compton scattering. II. Differential cross sections and left--right asymmetry, 26:54256
MILTON, R. C., Dose to patients from roentgenography, 26:53434
MINARDI, E., Resonant scattering of trapped particles by toroidal plasma modes, 26:54792
MINDLIN, H., Influence of hold-time and temperature on low-cycle fatigue of Incoloy 800, 26:53658
MINEL, L., Influence of carbon and oxygen on the brittleness of molybdenum, 26:53682
MINEV, L., Determination of atomospheric concentrations of radon daughters by α-spectrometric extrapolation method, 26:53226
MIN'KO, L. Ya., Self-igniting pulsed optical discharge in an erosive laser plasma, 26:54803
  Use of high-speed spectrography for diagnostics of an erosive pulsed plasma accelerator, 26:54773
MIRANSKII, V. A., Dispersion sum rules and Jost--Lehman--Dyson representation in axiomatic quantum theory, 26:54377 (ITF-72-54-P)
  Statistical view on resonance widths and multiplicity in dual models, 26:54300 (ITF-72-53-E)
MISHEV, I. T., Natural fluorite in the dosimetry of the mixed field of gamma rays and thermal neutrons, 26:53240
MISHEVA, M. A., Angular correlation of a gamma cascade 329 to 487 keV in ^{140}Ce, 26:55060
MISHIN, B. S., Viscosity of Al_2O_3--SiO_2 melts, 26:55632 (UCRL-Trans-1479)
MITCHELL, C. K., Analyzing powers in the ^{3}He(d Vector,p)^{4}He reaction at energies less than 1.0 MeV, 26:54500 (LA-DC-72-906)
  Preliminary measurements of polarization transfer in ^{4}He(d Vector,d Vector)^{4}He elastic scattering, 26:54498 (LA-DC-72-904)
  Vector to tensor polarization transfer in proton--deuteron elastic scattering, 26:54499 (LA-DC-72-905)
MITCHELL, E. W. J., Tunnel assisted hopping in neutron irradiated gallium arsenide, 26:54982
MITCHELL, I. V., Microanalysis of materials by backscattering spectrometry, 26:52939
MITCHELL, T. E., Experiments in high-voltage electron microscopy. Progress report, October 31, 1972--July 31, 1973, 26:54972 (COO-2119-2)
MITHRA, B., Possible interpretation of difference between d(p,2p)n and d(p,pn)p cross sections, 26:54510
MITTON, Jacqueline, Emission-line spectrum of Cygnus A, 26:53990
MITTON, Simon, Emission-line spectrum of Cygnus A, 26:53990
  Interpretation of rotation measures of radio sources. II, 26:53911
MITYAKOV, N. A., Dynamic theory of Type-III solar radio bursts, 26:53964
MIYANO, Katao, Heat treatment, microstructure, and mechanical properties of heavy gage steels for nuclear reactor pressure vessels. I, 26:53646
MIYAZONO, Shohachiro, Results of cyclic pressure loading test due to JPDR pressure vessel model No. 2, 26:55228 (JAERI-Memo-4016)
MIZERA, P. F., Polar-cap measurements of solar-flare protons with energies down to 12.4 keV, 26:54071
MOBERG, L. C., Moessbauer observation of magnetic moment of 89-keV excited state of ^{119}Sn, 26:54624
MOCHIZUKI, Hirozi, Analyses of the sodium-water reaction pressure and its propagation in the sodium system, 26:55157 (CONF-710548-, pp 171-86)
MODEER, B., Change of structure and mechanical properties in stainless steel by irradiation. Part 1.2. The interrelationship of creep and stress relaxation phenomena, 26:53642 (STU-70-419/U-350(Pt.1.2))
MOELLER, P., Octupole deformations in the nuclei beyond ^{208}Pb, 26:54732
MOEN, Arnold J., Standards and state regulatory control programs, 26:54928
MOENKE, Horst, Status of micro-emission spectral analysis with solid-state lasers, 26:55589 (ORNL-tr-2603)
MOGHISSI, A. A., Background information for the development of a radiation standard for tritium in nuclear-stimulated natural gas, 26:53134
MOHAPATRA, Priti, Magnetohydrodynamic flow near a time-varying accelerated plate, 26:54158
MOISAN, J., Deformation and recrystallization behavior of sintered tantalum and tantalum formed by electron bombardment, 26:53623
MOISEEV, S. S., Influence of different types of oscillations on ion heating in plasma--beam discharges, 26:54762
MOLCHAN, I. M., Formation of genetic heterogeneity and some problems of heterosis selection in cross-pollinating and self-pollinating plants. I, 26:53392
MOLINIER, R., Deformation and recrystallization behavior of sintered tantalum and tantalum formed by electron bombardment, 26:53623
MOMOKI, Goroh, Mass number dependence of neutron and proton residual interaction, 26:54739
MONACELLI, P., High energy measurements of total cross sections on proton, detecting very low energy neutrons, 26:54163 (NP-19421)
MONCHKA, D., g-factor of 108 keV excited state in ^{151}Gd, 26:54634 (JINR-E6-6479)
MONDT, J. F., Nuclear radiation problems, unmanned thermionic reactor ion propulsion spacecraft, 26:55364 (NASA-TM-X-2440, pp 292-8)
MONETI, G. C., Application of ISABELLE in Whiplash mode to produce polarized proton or monoenergetic neutron beams, 26:53775 (BNL-17057)
MONTESA, Elizabeth F., Carrier-free ^{131}I from telluric acid, 26:53070
MONTH, M., Effect of low-symmetry matched insertions, 26:53780 (BNL-17152)
  Momentum matching in ISA long insertions, 26:53773 (BNL-17051)
MONTOUR, J. L., Radiation carcinogenesis and acute radiation mortality in the rat as produced by 2.2-GeV protons, 26:53455 (NASA-TM-X-2440, pp 647-51)
MONTOUR, James, Evaluation of the hazard from exposure to electron irradiation simulating that in the synchronous orbit, 26:53458 (NASA-TM-X-2440, pp 665-71)
MONTOUR, James L., Lymphatic involution and early mortality in the young chicken produced by 2.2-GeV protons, 26:53457 (NASA-TM-X-2440, pp 659-64)
  Proton irradiation of stem cells: radiation damage and chemical radioprotection, 26:53454 (NASA-TM-X-2440, pp 642-6)
MOON, D. M., Creep behavior of fine wires of powder-metallurgical pure, doped, and thoriated W, 26:53683
MOORADIAN, A. J., Canada's Nuclear Power Program in context with that of the world, 26:55195 (AECL-4254)
MOORE, R. L., MSRE design and operations report. Part IIB. Nuclear and process instrumentation, 26:55138 (ORNL-TM-729(Pt.2B))
MOORE, W., X-ray and optical observations of Sco X-1 and observations of the x-ray background, 26:53918

MOORE, Willard S., Coral growth rates using ^{228}Ra and ^{210}Pb, 26:53179
MOOS, W. S., Atlas of radiation dose distributions. IV, 26:53409 (STI/PUB-295(Vol.4))
MORAN, P. R., Fast neutron radiation damage effects in crystalline anthracene and evaluation as a dosimetric technique, 26:53229 (COO-1105-172)
  Some preliminary paramagnetic resonance studies for dosimetry research, 26:52979 (COO-1105-179)
MORAN, T. F., Time-of-flight analysis of neutral products from inelastic ion--molecule collisions, 26:54109
MORANDI, G., Neutron measurements at zero power on CIRENE fuel element in ESSOR reactor, 26:55105 (CISE-R-258)
MORAVEK, F., Course of the post-irradiation syndrome after irradiation with lethal doses in piglets, 26:53495
MORETTI, Jean-Luc, Labeled iodoquine, 26:53029
MORF, R., Numerical investigations within the semiclassical transfer theory, 26:54742
MORGAN, C. S., Material transport by dislocation motion in sintering, 26:53620
MORGAN, D., Questions in $\pi\pi$ scattering and related processes, 26:54317 (RPP/T-27)
MORGAN, G. L., Gamma-ray production due to neutron interactions with iron for incident neutron energies between 0.8 and 20 MeV: tabulated differential cross sections, 26:54569 (ORNL-4798)
  Secondary gamma-ray-production cross sections of several materials, 26:54523 (CONF-720901-(Bks.1 and 2), pp 325-34)
MORGENSTERN, R., Ionization processes in slow collisions of heavy particles. I, 26:54141
MORI, N., Quadrupole structure in ^{51}V NMR in transition-metal alloys, 26:55056
MORI, Shigeyuki, Induction and repair of gene conversion in UV-sensitive mutants of yeast, 26:53375
MORIARTY, K. J., Data-processing system for instrument maintenance and calibration at EBR-II, 26:55132 (ANL/EBR-63)
MORIER, F., Physics of high temperature reactors at the Commissariat a l'Energie Atomique, 26:55109 (CONF-720901-(Bks.1 and 2), pp 33-54)
MORIGUCHI, Kinichi, Analysis of pulsed neutron experiments on bare fast multiplying system by Storrer--Stievenart's theory, 26:54483 (JAERI-M-4652)
MORIMOTO, Kenji, Experimental study of relaxation phenomena in non-equilibrium MHD generator duct, 26:53104
MORIMOTO, Shigeyuki, Plasma containment in hybrid fields of mirror with quadrupole and quadrupole-cusp, 26:54756
MORIN, M., Experimental study of decontamination of the skeleton after inhalation of americium nitrate, 26:53531 (UCRL-Trans-1477)
MORINAGA, H., $4^{+} \to 0^{+}$ cross-over transition in ^{204}Pb, 26:54647
MORITA, K., Dechanneling of heavy charged particles in diamond lattices, 26:54988
  Location of diffusion-doped gold atoms in silicon by means of channeling, 26:54987
MORIYA, Hiroshi, Toxic eruptions combined with radiation therapy of malignant tumors, 26:53433
MORIYAMA, Noboru, Operation report on low temperature fissiochemical loop (JTFL). I, 26:55400 (JAERI-M-4630)
MORLET, M., ^{2}H(p,2p)n reaction at 155 MeV, 26:54522
MORLEY, F., Radiation and health, 26:53157
MOROZOV, A. I., Effect of the magnetic field on a closed-electron-drift accelerator, 26:53743
MOROZOV, V. A., g-factor of 108 keV excited state in ^{151}Gd, 26:54634 (JINR-E6-6479)
MORRIS, D., Heavy ion acceleration at the Berkeley 88-Inch Cyclotron, 26:53755 (LBL-644)
MORRIS, James B., Meta-language for describing keyboard-based two-dimensional languages, 26:55550 (LA-DC-72-410)
MORRIS, James B. Jr., Specification of program flow in Madcap VI, 26:55547 (LA-DC-72-141)
MORRISON, D. R. O., Compilation of cross sections. I. π^- and π^+ induced reactions, 26:54201 (CERN/HERA-72-1)
MORROW, P. E., Pulmonary absorption of toxic metals, 26:55634 (UR-3490-136)
MORSELLI, M., Neutron measurements at zero power on CIRENE fuel element in ESSOR reactor, 26:55105 (CISE-R-258)
MORTON, R. D., Structural studies on U deposit of Fay Mine, Eldorado, Northwest Saskatchewan, 26:53145
MOSER, H., Distribution of tritium in glucose and starch labeled by tritium atom bombardment, 26:53028 (COO-584-50)
MOSES, Harry, Plume rise determination by the tabulation prediction technique, 26:53152 (ANL-7860(Pt.3), pp 230-49)
MOSHE, M., Weak radiative decays of K mesons, 26:54365
MOSKALENKO, V. A., Investigation of densities of the electron states for two-band superconductor with nonmagnetic impurities, 26:54454
MOTA, A. C., Superconductivity in Mg--Cd system: extrapolated T/sub c/ for pure magnesium, 26:54444
MOUGNIOT, J. C., Reactor physics and fast power breeders: MASURCA core R-Z program, 26:55118 (CONF-720901-(Bks.1 and 2), pp 822-38)
MOULTON, Grace C., Electron spin resonance and electron nuclear double resonance studies of DL-serine. II. Identification of free radicals produced in the range 153 to 340°K, 26:53004
MOXHAM, R. M., Borehole activation analysis by delayed and capture gamma rays using a ^{252}Cf neutron source, 26:53174
MOYLE, W. F., Processing evaluation of magnetic products. Final report, 26:55470 (BDX-613-518(Rev.))
MUCKENTHALER, F. J., FFTF pipe chase streaming experiment, 26:55394 (CONF-720901-3)
  FFTF pipe chase streaming experiment, 26:55382 (CONF-720901-(Bks.1 and 2), pp 431-41)
  ORNL sodium benchmark experiment, 26:55142 (CONF-720901-(Bks.1 and 2), pp 418-30)
MUELLER, B., Superheavy electronic molecules, 26:54111
MUELLER, Dietrich, Flux and energy spectrum of cosmic ray electrons between 10 and 1000 GeV, 26:53822
MUELLER, E. W., Applications of field--ion microscopy in physical metallurgy and corrosion. Conference held at Atlanta, Georgia, May 15--17, 1968, 26:53647
MUELLER, Erwin W., Atom probe FIM, 26:53648
  Lattice deformation by mechanical and electrical contacts, 26:53651
MUELLER, J. E., Reaction $\pi^-p \to p\pi^+\pi^-\pi^-\pi^0$ at 20 GeV/c, 26:54207 (COO-3064-3)
MUELLER, Ronald Otto, Atoms in intense magnetic fields and an attractive alternative to the Thomas--Fermi model of atoms, 26:54144
MUENCH, G., Selected topics on the physics of the interstellar medium, 26:53985
MUFTAKHOV, A. G., Formation of complexes of UCl_4 with α- or β-carboxylic acids and α-quinolinecarboxylic acid in polar solutions, 26:53054
MUGIBAYASHI, Nobumichi, Hamiltonian defined as a graph limit in a simple system with an infinite renormalization, 26:54386
MUIR, D. W., Development of ENDF/B shielding data processing codes, and integral tests, 26:55141 (CONF-720901-(Bks.1 and 2), pp 316-24)
MUKHOPADHYAY, S. K., Sensitivity of low-energy 3-body properties to the off-shell 2-body t-matrix. Technical Report No. 72-121, 26:54697 (ORO-4317-7)
MULLER, William A., Trophic dynamics and niches of salt marsh foraminifera, 26:55520 (COO-3254-6)
MUMINOV, T. M., g-factor of 108 keV excited state in ^{151}Gd, 26:54634 (JINR-E6-6479)
MUNK, Jens, Automatic production of isodose curves, 26:53243
MUNRO, Richard H., Properties of a coronal hole derived from extreme-ultraviolet observations, 26:53939
MURADYAN, G. V., Neutron resonances ^{112}Cd, 26:54599 (IAE-2116)
MURAKAMI, Ujihiro, Ionizing radiations and malformations of the brain, 26:53437
MURATA, K. K., Far infrared surface resistance of Cu:Fe; dynamics of a Kondo system, 26:55508 (COO-3151-4)
MURATA, T., Collection of radioactive iodine by filtering system, 26:55146
MURATOV, V. I., Nonlinear space-charge waves in a plasma sheath, 26:54853
MURIEL, Amador, Galactic astronomy. Volume 1. Proceedings of the summer Institute for Astronomy and Astrophysics, held at Stony Brook, New York, Summer 1968, 26:53981
MURNICK, D. E., Magnetic moment of the 1.409-MeV 2^{+} state of ^{54}Fe, 26:54581
MURPHY, L. M., Steady-state response of an infinite plate to an exponential edge load along a fusing crack: a model for the dynamic edge fusion of two semi-infinite plates, 26:55611 (SCL-RR-710113)
MUSCETTOLA, M., TERMO: digital code to evaluate steady state parameters of CIRENE type reactor, 26:55104 (CISE-R-246)
MUSIN, M. A., Monochromatic method for measuring 665 MeV mean proton energy by using Vavilov--Cherenkov radiation, 26:53800
MUTO, G., Gas coulometry, 26:55633 (UCRL-Trans-10640)
MUTO, Hachizo, ESR study of an irradiated single crystal of acetylene dicarboxylic acid dihydrate, 26:53005
MUTONE, G. A., Critical comparison and evaluation of neutron spectrum unfolding codes: the need to know, 26:53252 (CONF-720901-(Bks.1 and 2), pp 524-40)
MUTSURO, Naoshi, System for time of 50 m flight analysis and characteristics of short pulse beam, 26:53260
MYASNIKOV, E. N., Features of optical spectra, caused by surface of a crystal, 26:55537 (ITF-72-40-P)
MYNATT, F. R., Fast reactor shielding methods development, 26:55144 (CONF-720901-(Bks.1 and 2), pp 480-98)
  Sensitivity analysis: a general approach illustrated for a Na--Fe system, 26:54943 (CONF-720901-6)
  Sensitivity analysis: a general approach illustrated for a Na--Fe system, 26:54940 (CONF-720901-(Bks.1 and 2), pp 512-23)

N

NABOKA, V. A., Accumulation of residual gas ionization plasma in an electromagnetic trap, 26:54800 (AEC-tr-7350)
NAEIM, Faramarz, Immunochemical studies with the carcinoembryonic antigen, 26:55505 (COO-3012-21)
NAGAKURA, I., Optical 4d → 4f transition and binding energy of 4d level in La and Ce, 26:54095

NAGAKURA, Ichiro, Photoelectron spectroscopic measurements of core level binding energies of Y, La, and Ce, 26:55024
NAGASAKI, Ryukichi, Creep rupture properties of alpha-ray irradiated AISI 316 stainless steel, 26:53703
NAGASAWA, H., Magnetoresistance of neodymium metal, 26:55021
NAGASE, Fumiaki, Thin polypropylene window proportional counters for the observation of cosmic soft x-rays, 26:53206
NAGASHIMA, K., Sidereal and solar anisotropy of high-energy cosmic rays observed by an air Cherenkov telescope, 26:53850
  Spurious sidereal anisotropy arising from annual modulation of solar diurnal variation of cosmic radiation, 26:53849
NAGASHIMA, Kazuo, Three-dimensional cosmic ray anisotropy in interplanetary space. IV, 26:53813
  Three-dimensional cosmic-ray anisotropy in interplanetary space. III, 26:53812
NAGIBIN, Yu. A., Viscosity of Al_2O_3--SiO_2 melts, 26:55632 (UCRL-Trans-1479)
NAGORCKA, B. N., ^{16}O + ^{12}C quasimolecular states, 26:54534
NAGUIB, K., Exit tube effect upon the measured space--energy neutron spectra, 26:54470 (AREAEE-133)
NAGY, H. J., Double K-shell ionization in the decay of ^{131}Cs and ^{165}Er, 26:54617
NAHABETIAN, R., DWBA analysis of sub-Coulomb multi-transfer reactions, 26:54695 (LYCEN-7213)
NAIKI, Toshio, Epitaxial growth of tantalum carbide, 26:53564
NAKAGAWA, Kimiko, Effective neutron-proton interaction in deformed doubly odd nuclei, 26:54747
NAKAGAWA, S., 0.511 MeV gamma rays measured with the Ge(Li) detector at balloon altitude, 26:53817
NAKAI, Sayaka, Induction and repair of gene conversion in UV-sensitive mutants of yeast, 26:53375
NAKAJIMA, H., Quadrupole structure in ^{51}V NMR in transition-metal alloys, 26:55056
NAKAMURA, Kinichi, Surgical treatment for local radiation injuries following radiotherapy, 26:53438
NAKAMURA, Tomoo, Analysis of pulsed neutron experiments on bare fast multiplying system by Storrer--Stievenart's theory, 26:54483 (JAERI-M-4652)
  Critical experiments on FCA I-6, 26:55401 (JAERI-Memo-3891)
NAKANISHI, Noboru, Remarks on Scherk's paper entitled zero-slope limit of dual resonance model, 26:54388
NAKANO, Masafumi, Analysis of pulsed neutron experiments on bare fast multiplying system by Storrer--Stievenart's theory, 26:54483 (JAERI-M-4652)
  Critical experiments on FCA I-6, 26:55401 (JAERI-Memo-3891)
  Semi-experimental measurement of effective delayed neutron fraction of a fast reactor system by application of pulsed neutron technique, 26:55403 (JAERI-Memo-4004)
NAKANO, Mimako, Effects of high intensity pulsed x-ray (linear accelerator) or gamma-ray irradiation upon tumorigenesis and immunocompetence in mice, 26:53469
NAKASHIMA, A., Nuclear radiation problems, unmanned thermionic reactor ion propulsion spacecraft, 26:55364 (NASA-TM-X-2440, pp 292-8)
NAKAYAMA, Shiro, Application of electrophoresis for burnup determination, 26:52933 (JAERI-Memo-4094)
NAKURA, Saburo, Pressure drop of liquid Hg MHD power generators, 26:53106
NALESNIK, W. J., Accelerator measurement of the energy spectra of neutrons emitted in the interaction of 3-GeV protons with several elements, 26:54528 (NASA-TM-X-2440, pp 523-6)
NAMATAME, Hiroshi, Results of cyclic pressure loading test due to JPDR pressure vessel model No. 2, 26:55228 (JAERI-Memo-4016)
NAMBA, Shyunji, Examination of burnout detectors by differential circuit methods, 26:53304 (LIB/Trans-431)
NANDA, G., Mutagenic effect of uv- and gamma-rays on antibiotic production of Aspergillus chevalieri, 26:53393
NANDI, P., Mutagenic effect of uv- and gamma-rays on antibiotic production of Aspergillus chevalieri, 26:53393
  Specific effects of mutagens on Aspergillus niger producing citric acid, 26:53380
NANDPURI, K. S., Effect of irradiation on variability in okra, 26:53390
NANDY, K., Recent work on interstellar grains, 26:53989
NANOPOULOS, D. V., Muon--proton scattering and the effect of neutral currents in the scaling region, 26:54288 (RPP/T-26)
NARASIMHA MURTHY, S., Effect of heterogeneity and Hall current on the MHD power generator, 26:53105
NAREBSKA, Anna, Effect of gamma radiation on ion exchange resins. IV, 26:53016
NARITA, N., Chemical composition of low energy L and M nuclei in the primary cosmic radiation, 26:53841
  Measurement of the low energy helium isotopes in the primary cosmic rays, 26:53827
NARODETSKII, I. M., Coulomb excitation of nuclei by heavy polarized particles, 26:54630
NASBY, R. D., Room temperature electrical properties and Dopant precipitation for SiGe thermoelectric alloys, 26:55598 (SC-DC-721020)
NASCUTIU, Tiberiu, Radiometric methods of analysis, 26:52942
NASLAIN, Roger, Mineral chemistry. An alkaline boride: the hexaboride NaB_6, 26:55560 (LA-tr-72-16)
NASSAR, S. F., PIBIMUG: code for multigroup slowing down spectrum calculation in the P-1 and B-1 approximations for the IBM-1130, 26:55420 (AREAEE-141)
NATHAN, O., $(1f/sub 7/2)^2$ multiplet in ^{42}Ca, 26:54573
NAVARA, Erik, Effects of alloying on structural stability and cohesion between phases in metal--oxide composites, 26:53589
NAZARE, S., Technology of cermets, 26:53592
NAZARENKO, O. K., Ion focusing of an electron beam in a transverse gas flow, 26:54086
NAZARYAN, A. A., Effect of the medium on radiation emission by relativistic electrons, 26:54907
NEAL, H. A., Indiana University Spark Chamber Group technical progress report, December 1, 1971--November 30, 1972, 26:54206 (COO-2009-36)
NEDELEC, J., Study and tests of small components of secondary circuits of fast Na cooled reactors, 26:55182
NEEDES, C. R. S., Potentiostatic study of the anodic dissolution of uranium dioxide in aqueous solutions, 26:53035 (NIM-1448)
NEFF, R. A., Some neutron and gamma radiation characteristics of plutonium cermet fuel for isotopic power sources, 26:53336 (NASA-TM-X-2440, pp 853-8)
NEFF, R. M., Chemical vapor deposition of boron on a carbon monofilament substrate, 26:53571
NEI, Hiromichi, Outline of PNC's activities in the field of sodium-water reaction, 26:55155 (CONF-710548-, pp 129-54)
NEILL, J. M., Proton-recoil proportional counter spectrometry for reactor spectrum measurements, 26:55122 (CONF-720901-(Bks.1 and 2), pp 959-72)
NELIPA, N. F., Application of Newton--Kantorovich method to Chew--Low N/D equations. I, 26:54421
NELSON, A., Protective effect of cysteamine at fractionated irradiation. III, 26:53475
NELSON, C. A., S matrix elements in the presence of standing wave states, the Bjorken limit, and shadow-quarks, 26:54248 (ORO-3992-106)
NELSON, D. M., Radionuclides in Lake Michigan fish, 26:53169 (ANL-7860(Pt.3), pp 141-50)
NELSON, R. L., Comparison of defect centres formed in oxides by explosive shocking and high-energy radiation, 26:54983
NELSON, R. S., Thermal release of He injected into Ni, stainless steels, and nimonic PE16, 26:53709
NELSON, Walter R., Concepts of radiation dosimetry, 26:54891 (SLAC-153)
NELTRUP, H., Benchmark calculations on homogeneous spheres, 26:54486 (RISO-M-1526)
NEMOV, V. V., Influence of toroidality on a magnetic configuration with a helical magnetic axis, 26:54832
NENCIU, G., Analytic extrapolation from boundary and interior points, 26:55079
NENOT, J. C., Experimental study of decontamination of the skeleton after inhalation of americium nitrate, 26:53531 (UCRL-Trans-1477)
NESTAIKO, G. V., Serotonin uptake by platelets in acute radiation sickness, 26:53486
NEUDATCHIN, V. G., High-energy limit for α-d and tau--t form factors in ^6Li nucleus, 26:54532
NEUMANN, L., Inhomogeneous magnetic systems, 26:55037
NEUMAYER, E. C., Reducing the effect of grounds on critical reactor control circuits, 26:55135 (DUN-SA-169)
NEVEU, A., Feynman rules for massive gauge fields with dual diagram topology, 26:54381
NEVROVSKII, V. A., Effect of the magnetic field on a closed-electron-drift accelerator, 26:53743
NEWKIRK, Gordon Jr., Atlas of magnetic fields in the solar corona, 26:53955
NEWKIRK, Herbert W., Literature survey of metallic ternary and quaternary hydrides, 26:53558 (UCRL-51244)
NEWMAN, L., Synergistic effect of tri-n-octylamine on the solvent extraction of cerium(III) by thenoyltrifluoroacetone, 26:52952
NEWMAN, L. W., Metabolism of Rickettsia typhi and Rickettsia akari in irradiated L cells, 26:53360
NEWMAN, N., Manipulators: a survey, 26:53734
NEWMAN, R. C., Localized vibrational modes in gallium arsenide containing silicon and boron, 26:54984
NEWMAN, R. N., Ignition of liquid metal: peroxide mixtures, 26:55178 (RD/B/N-2364)
NEWMAN, R. W., Study of ordered alloys by field--ion microscopy, 26:53654
NEWROCK, R. S., Thermal resistivity and thermal magnetoresistivity of potassium, 26:55507 (COO-3150-6)
NEWTON, D., 2π steradian magnetic spectrometer, 26:53284
NEWTON, J. O., ^{16}O + ^{12}C quasimolecular states, 26:54534
NGUEN KKHAK N'YAP, Light dispersion in the absorption region by impurity centres, 26:55539 (ITF-72-57-P)
NGUYEN-HOE, About the electronic shifts of Stark broadened Lyman-α lines, 26:54796
NGUYEN VAN SEN, Polarization and cross section of p + ^3H elastic scattering, 26:54521
NGUYEN VAN THIEN, Distribution of qualitative composition and absorbed doses of x-irradiation in using the

screens, 26:54911
NICOL, M. J., Potentiostatic study of the anodic dissolution of uranium dioxide in aqueous solutions, 26:53035 (NIM-1448)
NICOLET, M.-A., Microanalysis of materials by backscattering spectrometry, 26:52939
NICOLO, F., Pion electroproduction at threshold, 26:54247 (NP-19417)
  Representation of SU(3) x SU(3) chiral algebra for baryons, 26:54370 (NP-19418)
NIEDZIELSKI, Jan, Formation of acetylene and methane in argon and xenon sensitized radiolysis of gaseous ethylene, 26:53000
NIEF, G., Absolute measurement of the isotopic ratio of a water sample with a very low deuterium content, 26:52913 (AEC-tr-7345)
NIEHAUS, A., Ionization processes in slow collisions of heavy particles. I, 26:54141
NIELSEN, S. L., Neuropathologic effects of proton-beam irradiation in man. II, 26:53446
NIKIFOROV, B. P., Nonmesic decays of hypernuclei ^{4}H and ^{4}He in a model of direct transition of the Λ-hyperon into a neutron, 26:54293
NIKITIN, M. M., Investigation of linear polarization of synchrotron radiation, 26:54249
NIKOLAEV, N. N., Reactions of single Σ- and Λ-hyperon production, 26:54335
NIKOL'SKAYA, T. A., High-temperature vacuum evaporation of zirconium carbide + tungsten compounds, 26:55022
NILSSON, A., Protective effect of cysteamine at fractionated irradiation. III, 26:53475
NILSSON, B., Importance of the quadrupole pairing field in the J/sup π/ = 0^{+} vibrations of shape deformed nuclei, 26:54731
NILSSON, S. G., Octupole deformations in the nuclei beyond ^{208}Pb, 26:54732
  Termination of the r-process and the synthesis of superheavy elements, 26:54663
NINOMIYA, Masayuki, Epitaxial growth of tantalum carbide, 26:53564
NISHIKAWA, Osamu, Lattice deformation by mechanical and electrical contacts, 26:53651
NISHITA, H., Influence of clinoptilolite on ^{90}Sr and ^{137}Cs uptakes by plants, 26:53540
NIX, William D., Prog. rpt. on structure dependence of high temperature deformation of metals, 3/1/70--3/1/71, 26:55613 (SU-326-P-17-X-2)
NOBLE, L. D., SEFOR: verification of the Doppler transient shutdown capability of LMFBR's, 26:55123 (CONF-720901-(Bks.1 and 2), pp 986-1005)
NOE, J. W., Core-excited 5^{+} state in ^{14}N, 26:54542
NOELPP, U., Blocking effect in U fission with 14-MeV neutrons, 26:54669
NOELS, A., Conditions for homogeneous stellar models to have only real secular eigenvalues, 26:53886
NOERDLINGER, Peter D., Transfer of resonance-line radiation in differentially expanding atmospheres. I. General considerations and Monte Carlo calculations, 26:53878
  Transfer of resonance-line radiation in differentially expanding atmospheres. II. Analytic solution for the case of coherence in the frame of the fluid, 26:53879
NOLAN, P. J., Evidence of further rotational structure in ^{26}Al, 26:54554
NOLIBE, D., Pulmonary lavage, therapy of pulmonary contaminations, 26:53528 (LF-tr-71)
NOMURA, M., Relations among magnetic moments and M1 rates in single-closed-shell nuclei, 26:54702
NOMURA, T., In-beam alpha spectroscopy of N = 128 isotones, 26:54651
NORDBERG, U.-B., Correction of isodose-diagrams for ^{60}Co and 35 MeV electrons at penetration of lung tissue, 26:54901
NORDIN, P., Distribution of tritium in glucose and starch labeled by tritium atom bombardment, 26:53028 (COO-584-50)
NORDSTROM, T. V., Mechanical properties and stress relaxation of beryllium--copper alloy 25, 26:53641 (SC-DR-720471)
NORMAND, E., Discrete ordinates--Monte Carlo coupling: a comparison of techniques in NERVA radiation analysis, 26:55371 (NASA-TM-X-2440, pp 681-6)
NORRIS, C. B., Investigation of static electron irradiation effects in bulk Si and thin Si films at energies far below threshold, 26:55017
NOTARGIACOMO, S., Application of Kleinschmidt's technique to the study of the structure of DNA in solutions, 26:55530 (ISS-71/22)
NOTZ, K. J., Decontamination of HTGR reprocessing off-gases, 26:53059 (CONF-720823-12)
NOVAK, R. C., Resin bonded boron--aluminum composites, 26:53574
NOVIK, K. M., Ratio of longitudinal and transverse diffusion coefficients in argon SHF discharge plasma, 26:54776 (AEC-tr-7332)
NOZRACHEV, M. G., Accumulation of residual gas ionization plasma in an electromagnetic trap, 26:54800 (AEC-tr-7350)
NUMANO, Masahiro, Experimental study of relaxation phenomena in non-equilibrium MHD generator duct, 26:53104
NUNBERG, P., Trinucleon properties with Riihimaki potential, 26:54504
NURMUKHAMEDOV, V. Kh., Study of the obtaining conditions and thermoemission characteristics of borides of the rare-earth metals, 26:53582
NUZHDIN, N. I., Genetic changes induced by space flight in barley seeds, 26:53384
NYGREN, David R., For the measurement of multiplicities: the ''multimeter'', 26:53267 (BNL-17064)
NYMAN, E. M., Soft photons in potential scattering, 26:54737

O

OATES, D. E., ^{4}He--^{4}He interaction potential from low energy total cross section measurements, 26:54514
OBA, Toshihito, Results of cyclic pressure loading test due to JPDR pressure vessel model No. 2, 26:55228 (JAERI-Memo-4016)
OB'EDKOV, V. D., Inelastic e--H and e--He collisions in adiabatic approximation, 26:54117
OBENSHAIN, Felix E., Magnetic properties of transition metals and their alloys determined by Moessbauer measurements with ^{61}Ni, 26:55617 (TID-26159)
OBERLECHNER, G., Shell-model study of ^{56}Ni, ^{58}Ni, ^{54}Fe, and ^{56}Fe, 26:54570
OBINATO, Toshio, Effective neutron--proton interaction in deformed doubly odd nuclei, 26:54747
OBLOW, E., Mechanism of fast neutron transport in iron, 26:54473 (CONF-720901-(Bks.1 and 2), pp 335-48)
  Sensitivity analysis: a general approach illustrated for a Na--Fe system, 26:54943 (CONF-720901-6)
  Sensitivity analysis: a general approach illustrated for a Na--Fe system, 26:54940 (CONF-720901-(Bks.1 and 2), pp 512-23)
OBRIDKO, V. N., Interpretation of π-component splitting in sunspot spectra, 26:53951
O'BRIEN, Keran, Physical theory of one-dimensional galactic cosmic-ray propagation in the atmosphere, 26:54067 (NASA-TM-X-2440, pp 926-41)
O'BRIEN, William L., Strengthening of tungsten by powder metallurgical internal oxidation, 26:53616
OBST, A. W., Possible statistical-model explanation for the ^{26}Mg(p,t)^{24}Mg reaction at E/sub p/ = 26 MeV, 26:54556
OBUKHOV, A. A., Conditions for wave transformation in a plasma with a nonmonotonic longitudinal distribution, 26:54841 (AEC-tr-7338)
  Ratio of longitudinal and transverse diffusion coefficients in argon SHF discharge plasma, 26:54776 (AEC-tr-7332)
  Study of the localization of the wave transformation region in a superhigh-frequency discharge plasma, 26:54842 (AEC-tr-7339)
OBUKHOV, Yu. V., Depolarization of negative muons in water and aqueous solutions, 26:54099
O'BYRNE, Joseph M., Carpet plot data format, 26:55366 (NASA-TM-X-2440, pp 392-6)
OCHSENFELD, W., Recovery of ^{238}Pu in the MILLI laboratory, 26:53073
OCON, F. T., Extraction of ^{32}P from neutron-irradiated S dissolved in hot toluene, 26:53069
O'CONNELL, J. S., Semileptonic weak interactions with ^{12}C, 26:54541
O'DELL, F. W., New observations and calculations of primary Be/B in the cosmic rays, 26:53833
ODERA, M., In-beam alpha spectroscopy of N = 128 isotones, 26:54651
ODETTE, G. R., Yield stress radiation damage function of iron, 26:53705
OFER, S., Moessbauer effect in ^{239}Pu, 26:54661
OGANESYAN, Yu. Ts., Average prompt neutron number for spontaneous fission of ^{256}Fm, 26:54659 (JINR-P15-6518)
  Nuclear reactions induced by xenon ions and experiments on superheavy element synthesis, 26:54658 (JINR-P7-6523)
OGATA, K., Precise atomic mass measurement at Osaka University, 26:54495 (EUR-4765, pp 435-55)
OGAWA, M., Levels of ^{90}Nb excited via the ^{90}Zr(p,nγ) reaction, 26:54613
OGAWA, Yutaka, Creep rupture properties of alpha-ray irradiated AISI 316 stainless steel, 26:53703
OGORODNIKOV, S. N., Nonstationary solenoidal regular fluxes of like-charge particles, 26:54783
OGUMA, Koichi, Ion-exchange behaviour of metals on DEAE-cellulose in methanol--thiocyanate--hydrochloric acid media, 26:52951
OGURA, K., Chemical composition of low energy L and M nuclei in the primary cosmic radiation, 26:53841
OHANESYAN, J. B., Ultraviolet absorption lines in spectrum of Vega, 26:53887
OHASHI, T., New metastable phase in rapidly solidified Al--Zr alloys, 26:53686
OHAYON, Maurice, High performance spectrometer magnets, 26:53296 (CEA-N-1539)
OHLSEN, Gerald G., Analyzing powers in the ^{3}He(d Vector,p)^{4}He reaction at energies less than 1.0 MeV, 26:54500 (LA-DC-72-906)
  Preliminary measurements of polarization transfer in ^{4}He(d Vector,d Vector)^{4}He elastic scattering, 26:54498 (LA-DC-72-904)
  Vector to tensor polarization transfer in proton--deuteron elastic scattering, 26:54499 (LA-DC-72-905)

OKABAYASHI, M., Pseudoclassical and anomalous containment in FM-1, 26:54753 (CONF-720804-5)

OKABE, Shigeru, Shoulder of optical absorption spectrum of the trapped electron in gamma-irradiated crystalline ice, 26:53002

OKAMURA, Seizo, Optical absorption bands of color centers in irradiated anthracene single crystals at low temperatures, 26:54996

OKAZAKI, Reiji, DNA radiation damage of DNA, 26:53348

OKAZOE, H., Radionuclide production by cosmic rays in lunar rocks, 26:53860

OKEDA, Riki, Two autopsy cases of radiation myelopathy, 26:53425

OKSAK, A. I., Lorentz-covariant bilinear forms, 26:54359

OKUBO, S., Weak K-dominance model and bounds on K/sub 13/decay parameters, 26:54289

OKUBO, Shunzo, Enzymes for repair of DNA damages, 26:53351

OKUDAIRA, K., 0.511 MeV gamma rays measured with the Ge(Li) detector at balloon altitude, 26:53817

OKUMURA, Yoshitaka, Quark mass and structure functions for electron scattering, 26:54282

OLDBERG, S. Jr., BEHAVE-2: oxide fuel performance code in two spatial dimensions and time, 26:55418 (GEAP-13788)

OLDENBURG, U., Microdosimetric investigations into the energy transfer of fast neutrons to soft tissue, 26:54873 (EUR-4787)

OLDFIELD, William, Effects of impurities on migration of lenticular pores in UO$_2$, 26:53559

OLDS, Fredric C., Industry's understanding of the radiation controversy, 26:54933

OLEKSIN, D. I., Light dispersion in the absorption region by impurity centres, 26:55539 (ITF-72-67-P)

OLIVA, P. R., Automatic peak identification in analysis of gamma-ray spectra obtained with Ge(Li) detectors, 26:53257 (RT/FI-(72)14)

OLIVERO, J. J., Electron deposition in water vapor, with atmospheric applications, 26:54033

OLSEN, J. N., Nanosecond and picosecond laser-produced CD$_2$ plasmas, 26:54804

OLSON, A. P., Boron and tantalum control rod studies and absolute gamma ray absorbed doses in a LMFBR critical, 26:55134 (CONF-720901-(Bks.1 and 2), pp 579-98)

OLSON, N. Thomas, Proton and fast neutron damage studies in Si and Ge using channeling, 26:55004

OLSSON, Yngve, Effects of gamma radiation on the shark brain, 26:53487

OLTMAN, B. G., Average temperature measurements in the aquatic environment using thermoluminescent dosimeters, 26:53187 (ANL-7860(Pt.3), pp 131-40)

OMEL'CHENKO, A. Ya., Effect of high-frequency potential on propagation of fast waves along a magnetoactive plasma layer, 26:54839 (AEC-tr-7336)
  Extraordinary electromagnetic wave absorption in the linear plasma layer in the hybrid resonance region, 26:54864
  On the theory of transformation of surface waves into longitudinal oscillations in the surface layer of a plasma wave-guide, 26:54838 (AEC-tr-7335)

ONDRACEK, G., Technology of cermets, 26:53592

ONISHCHENKO, I. N., Interaction of finite perturbations in a beam--plasma system, 26:54795

OORT, J. H., Spiral structure of galaxies, 26:53983

OPARA, U., Photoproduction of π^+-mesons on polarized protons at photon energies between 0.5 and 2.2 GeV, 26:54172 (NP-19415)

OPPELT, A., NMR investigations on Y- and La-diluted GdZn, 26:55059

OPTA, Geoffrey I., Analysis of breakup scattering in a deuterium target. Application to antiproton--deuteron breakup scattering, 26:54347 (UM-P-72-6)

ORLOV, L. K., Instability of spatially separated plasma beams. III, 26:54822

ORMES, J. F., Acceleration and propagation of high Z cosmic rays in pulsar environment, 26:53857
  Charge composition of galactic cosmic radiation, 26:53830
  Cosmic ray proton and He spectra above 50 GeV, 26:53829
  Primary cosmic ray electron spectrum from 10 GeV to about 200 GeV, 26:53823

ORPHAN, V. J., Measurement and evaluation of cross sections, 26:55140 (CONF-720901-(Bks.1 and 2), pp 295-315)
  Measurements of gamma-ray production cross sections for shielding materials of space nuclear systems, 26:54960 (NASA-TM-X-2440, pp 500-11)

ORYU, S., D(p,2p)n reaction at 51.8 MeV, 26:54505

OSBORN, L. A., Relative nonhomogeneities of radiation dose to the respiratory tract from inhaled radionuclides, 26:53536

OSBORN, T. A., S-matrix approach to Glauber theory, 26:54416

OSBORNE, J. L., Galactic magnetic field and anisotropy of cosmic rays above 10^{17} eV, 26:53851
  Possibility of energetic cosmic rays arriving from the Crab Nebula, 26:53856

OSHIMA, K., Operation report on low temperature fissiochemical loop (JTFL). I, 26:55400 (JAERI-M-4630)

OSTLUND, Neil S., Complex and unrestricted Hartree--Fock wave functions, 26:54157

OTGONSUREN, O., Search for tracks of spontaneous fission fragments from the heavier transuranium elements in naturally-occurring minerals, 26:54670

OTSUKI, Akira, Interaction of yellow organic acids with calcium carbonate in freshwater, 26:55494 (COO-1599-63)

OTSUKI, Shoichiro, Scaling of interaction radius and polarization, 26:54354
  Systematic structure in hadronic two-body scattering and resonance correlation. III, 26:54342

OTT, Karl O., Advances and current problems in reactor kinetics, 26:55427 (CONF-720901-(Bks.1 and 2), pp 168-78)

OWENS III, Joseph F., New Regge absorption model, 26:54336

OZDOWSKA, Zofia, Synthesis of new compounds labeled with tritium and ^{14}C for biological investigations. I, 26:53052

P

PABLO, Benjamin B., Radiotracer adsorption study on Baguio soils, 26:53175

PACCARD, D., Stability of transverse-wave magnetic structure at 1.3 K, 26:55039

PACE, E., Trinucleon properties with Riihimaki potential, 26:54504

PACE, S., Influence of dimensionality on Bose condensation and macroscopic coherence in superconductors, 26:54436 (NP-19425)

PACILIO, N., 259 references in reactor noise time analysis, 26:55443 (RT/FI-(72)13)
  Reactor neutron noise analysis: state of the art, 1971, 26:55442 (RT/FI-(72)11)

PACK, Russell T., Near-resonant vibration--rotation energy transfer in atom--diatom collisions: Ar--OH($A^2\Sigma^+$), 26:54126

PAGE, D. E., Possible connection between a barium cloud and electron intensity fluctuations observed on a rocket flight at Kiruna, 26:54039

PAGE, Norbert P., Factors modifying the response of large animals to low-intensity radiation exposure, 26:53451 (NASA-TM-X-2440, pp 622-32)

PAHISSA CAMPA, J., Effect of gamma radiation on an Argentine variety of wheat, 26:53381 (CNEA-309)

PAIGE, Frank E., Scaling in $p\pi^- \to pX^-$ and an estimate of triple-Pomeranchukon coupling, 26:54221

PAIK, N. C., Summary of analyses of plate vs. pin measurements emphasizing reactivity and sodium void effects, 26:55395 (CONF-720901-12)

PAILLON, M., Buckling measurements in ECO with few CIRENE fuel elements, 26:55106 (CISE-R-283)

PAK, A. S., Calculation of absorption in neutral pion coherent photoproduction on nuclei, 26:54691 (JINR-P2-6539)

PAK, N. K., General approach to scaling in electro-inclusive reactions, 26:54275

PAKALNS, P., Direct spectrophotometric determination of boron in aluminium alloys, 26:52928

PAK BEN GIR, Present-day problems of the theory of nuclear forces, 26:54688 (ITF-71-77-P)

PAKHOMOV, L. P., Microwave plasma heating in Tuman-2, 26:54758

PALACIOS, Enrique, Exposure of radiologists during special procedures, 26:53443

PALISTRANT, M. E., Influence of Fermi-surface topology change under pressure on two-band superconductors properties, 26:54445

PALMER, R. B., Determination of luminosity using the intersection of a high β with a low β section, 26:53769 (BNL-16996)

PALMER, R. G., Sodium void studies and related heterogeneity effects in ZPPR-2, the Benchmark Demonstration Assembly, 26:55392 (CONF-720901-(Bks.1 and 2), pp 973-85)
  Spatially dependent benchmark parameters in the initial demonstration plant critical assembly, 26:55117 (CONF-720901-(Bks.1 and 2), pp 809-21)

PALMITER, C. C., EPA role in radiation protection, 26:54927

PALUMBO, F., Center of mass spuriosity effects on charge form factor in many-body theories, 26:54507

PANCALDI, G., Alterations of sugar beets by γ-irradiation of the seed, 26:53388

PANCHENKO, V. I., Extraordinary electromagnetic wave absorption in the linear plasma layer in the hybrid resonance region, 26:54864

PANGAROVA, B. H., Influence of Ni addition on reduction of WO$_3$ with H on sintering of the thus produced W powders, 26:53579

PANKRAT'EV, Yu. I., Accumulation of residual gas ionization plasma in an electromagnetic trap, 26:54800 (AEC-tr-7350)

PANNONHALMI, K., Stimulation by x-irradiation in sugar beets, 26:53389

PANOV, M. N., Charge state alteration processes in collisions of hydrogen atoms with hydrogen molecules, 26:54115

PANTELEEVA, M., Rapid spectrophotometric determination of Ta in hard-metal alloy mixtures using Nile blue, 26:52925

PAONE, C. J., Rod drop accident analysis for large boiling water reactors, 26:55353 (NEDO-10527)

PAPA, C., Electron emission from solids by ionic bombardment, 26:52936 (RT/EL-(72)4)
PAPAGIANNIS, Michael D., Average behavior of midlatitude F-region parameters N/sub T,/N/sub max,/ and tau during geomagnetic storms, 26:54040
PAPE, A., ^{38}Ar levels formed in reaction ^{34}S(α,γ)^{38}Ar, 26:54560
PARESCE, Francesco, Extreme-ultraviolet emissions from an aurora, 26:54030
PARIKH, J. C., How good is the Hartree--Fock approximation for ^{16}O, 26:54524 (COO-2171-14)
PARKER, D. R., Chromosomal interchange in mature oocytes of Drosophila, 26:53501
PARKER, H. M., An intrauterine dosimeter, 26:53238
PARKER, H. W., Gamma-ray shielding measurements made at altitudes greater than 115,000 feet using large Ge(Li) detectors, 26:54964 (NASA-TM-X-2440, pp 914-21)
PARKER, Richard H., Design considerations and test facilities for accelerated radiation effects testing, 26:53695 (NASA-TM-X-2440, pp 570-6)
  Radiation effects on science instruments in Grand Tour-type missions, 26:53292 (NASA-TM-X-2440, pp 729-34)
PARKER, S. I., Muon identification using multiwire proportional chambers, 26:53282
PARKINSON, J. B., Radiation noise in a high-sensitivity star sensor, 26:53293 (NASA-TM-X-2440, pp 735-43)
PARKS, C. E., Multinode analysis of B and W's 145-fuel assembly nuclear plants during loss-of-coolant accident, 26:55272 (BAW-10048(Suppl.1))
  Multinode analysis of B and W's 2568-MWt nuclear plants during loss-of-coolant accident, 26:55271 (BAW-10034(Suppl.1))
PARMENTIER, C., Reading, automatic treatment, and visual display of radioactivity spectra recorded on punched tape, 26:53544
PARNELL, Thomas A., Heavy-ion passive dosimetry with silver halide single crystals, 26:53230 (NASA-TM-X-2440, pp 138-41)
PARTHASARATHY, R., Polarization of the emitted neutron in muon capture, 26:54564
PARZEN, G., Coil configurations in superconducting quadrupoles, 26:53768 (BNL-16980)
  Magnet tolerances in ISABELLE and nonlinear resonances, 26:53774 (BNL-17056)
PASCHOS, E. A., Test of the algebra of bilocal operators, 26:54253
PASHCHENKO, A. V., Nonlinear space-charge waves in a plasma sheath, 26:54853
PASHENIN, P. P., Possible use of IR lasers for high-temperature heating of superdense plasma, 26:54764
PASHITSKII, E. A., Long-wave instability caused by inhomogeneous ion beams in a dense magnetized plasma, 26:54816
PASHKEVICH, V. V., Effect of changes in equilibrium deformations of the excited states of odd-A deformed nuclei on their energy and structure, 26:54640
PASKALEV, Z., Effect of small x-ray doses on the motor activity of rats irradiated during their embryonic development, 26:53488
PASQUIER, J.-Y., Three-meson resonances in a relativistic Faddeev-type approach, 26:54318
PASQUIER, R., Three-meson resonances in a relativistic Faddeev-type approach, 26:54318
PASSI, J. N., Compositeness and vanishing of renormalization constants, 26:54379
PASTOR, H., Electric and thermal conductivity, elastic properties, and bending resistance of porous W over entire range of porosity, 26:53684
  Sintering and oxidation resistance of diborides of Ti and Zr, 26:53594
PATCH, R. W., Observability of the H_3^+ fundamental spectrum, 26:54090
PATCHETT, Bruce, Absorption spectra of Type II supernovae, 26:53897
PATEL, V. L., Sudden impulses in the geomagnetotail and the vicinity, 26:54055
PATERNO, G., Numerical calculation of zero bias conductivity for superconducting tunnel junction in presence of depairing. II, 26:54462 (LNF-72/27)
PATS'ORA, S. K., Ion focusing of an electron beam in a transverse gas flow, 26:54086
PATTERSON, M. R., Deformed renormalized Brueckner--Hartree--Fock approximation and its application to ^{12}C, 26:54696 (ORNL-TM-3951)
PATTI, Francois, ^{90}Sr levels in human bones collected in 1970, 26:53520 (CEA-N-1535)
PATZER, R. G., Background information for the development of a radiation standard for tritium in nuclear-stimulated natural gas, 26:53134
PAULETT, T. A., HNPF retirement: disposition of sodium, 26:55147 (AI-AEC-Memo-12736)
PAULI, M., Numerical investigations within the semiclassical transfer theory, 26:54742
PAULSEN, C. A., Effects of x-ray irradiation on human spermatogenesis, 26:53399 (NASA-TM-X-2440, pp 229-32)
PAULY, Jean, Production of hydrogen for deuterium extraction, 26:52975
PAVLOVIC, P., Monochromatic method for measuring 665 MeV mean proton energy by using Vavilov--Cherenkov radiation, 26:53800
PAVLOVICH, P., Vavilov--Cherenkov ''needle'' radiation in Rochelle salt crystal, 26:54875 (JINR-P1-6552)
PAVLOV-VEREVKIN, B. S., Cost of processing liquid radioactive wastes, 26:53065
PAYNE, Bryan R., Isotope hydrology in Latin America, 26:53168
PAYNE, J. A., Seasonal alterations in rodent blood, 26:55587 (ORNL-TM-3898)
PAYNE-GAPOSCHKIN, Cecilia, Cepheid variables in Large and Small Magellanic Clouds, 26:53986
PAZMAN, A., Testing of analyticity of πN forward scattering amplitude and determination of πN coupling constant, 26:54337
PEAK, D., Correlated recovery kinetics, 26:55005
PEARCE, J. B., Optimum chopping, 26:53323
PEARSON, C. A., Spectroscopic factors from reactions ^{12}C(d,n)^{13}N and ^{12}C(d,p)^{13}C using WBP model, 26:54543
PEARSON, K. G., Methods for three-dimensional fuel management studies on high temperature reactors, 26:55111 (CONF-720901-(Bks.1 and 2), pp 68-80)
PEASLEE, D. C., Superheavy elements in cosmic rays, 26:53867
PEDRETTI, F., Iterative solution of heterogeneous equations in finite cylindrical system. Method of harmonics, 26:55423 (CISE-R-273)
PEDROCCHI, F., TERMO: digital code to evaluate steady state parameters of CIRENE type reactor, 26:55104 (CISE-R-246)
PEGORARO, A., Goniometer for implantation and channelling experiments, 26:53322
PEIERLS, Ronald F., What is an elementary particle, 26:54234 (BNL-50342)
PEIRSON, D. H., Radiation and health, 26:53157
PEISTEINER, E., Determination of uranium in high-alloy steel, 26:52922
PEKARSKII, G. Sh., Spatial, angular, and energy distribution of fast neutrons behind triple layer barriers, 26:54966
PELETMINSKII, S. V., Introduction to physical kinetics, 26:54789 (ITF-71-96-P)
PELLETT, D. E., S-wave structure in the Kπ system, 26:54203 (COO-1428-308)
PENICAUD, Jean-Pierre, High performance spectrometer magnets, 26:53296 (CEA-N-1539)
PENLAND, J. R., Analysis of anticipated transients without trip, 26:55193 (BAW-10016)
PENNER, H., Production of citrus fruits, 26:53347
PENNINGTON, E. M., Studies of methods for fast neutron multigroup cross section generation and their effect upon the neutronics properties of LMFBR critical assemblies, 26:55113 (CONF-720901-(Bks.1 and 2), pp 211-28)
PENNINGTON, M. R., I = 0 $\pi\pi$ s wave and broken scale invariance, 26:54319
PENNINGTON, Sam N., Calorimetric methods of analysis, 26:52923
PENTTILAE, I. M., Amount and form of radioactivity in human milk after lung scanning, renography, and placental localization by ^{131}I labeled tracers, 26:53524
PEREGUD, B. P., Magnetic-prism β spectrometers, 26:53259
PERELLO, M., Isotopic separation by centrifugation. Rotating plasma, 26:53327 (JEN-244)
PERELYGIN, V. P., Search for tracks of spontaneous fission fragments from the heavier transuranium elements in naturally-occurring minerals, 26:54670
PEREPEZKO, J. H., Note on the nature of massive transformation interfaces, 26:53644
PERESSE, J., Determination of absolute differential cross sections for $1^1S \rightarrow 4^1D$ transition of helium atom, 26:54113
PERESYPKIN, V. V., High-energy approximation and generalized Huygen's principle, 26:54690 (ITF-72-57-P)
PEREY, F. G., Gamma-ray production due to neutron interactions with iron for incident neutron energies between 0.8 and 20 MeV: tabulated differential cross sections, 26:54569 (ORNL-4798)
  Optical model, 26:54677 (CONF-720701-3)
  Secondary gamma-ray-production cross sections of several materials, 26:54523 (CONF-720901-(Bks.1 and 2), pp 325-34)
PEREZ, A., Analysis of multicharged heavy ions produced by laser impact on metallic target, 26:54801 (CEA-CONF-2049)
PEREZ, J. D., Adiabatic and angular-momentum dependent potential for ^{16}O--^{16}O scattering, 26:54544
PEREZ-MENDEZ, Victor, Neutron radiography with a multiwire proportional chamber: performance and projections, 26:53200 (LBL-707(Summ.))
PERIE, Jacques, Isotopic migration effects of alkaline ions in sulfuric solutions, 26:52967
PERIE, Michele, Isotopic migration effects of alkaline ions in sulfuric solutions, 26:52967
PERKO, T. E., Galaxy formation in anisotropic cosmologies, 26:53980
PERKOWSKI, Jan, Radiation sulfoxidation of n-paraffins. I, 26:53012
PERLMAN, M. L., Influence of the chemical environment on α-decay, 26:54730
PERMAR, David H., Legal solution to the electric power crisis: controlling demand through regulation of advertising, promotion, and rate structure, 26:53101
PERRIN, C., Rescattering effects in the ^{2}H(p,2p)n and ^{2}H(p,pn)n reactions induced by 20- to 60-MeV protons,

26:54511

PERRIN, J. S., Influence of hold-time and temperature on low-cycle fatigue of Incoloy 800, 26:53658

PERRY, L. W., Thermionic reactor power system: effects of radiation on integration with manned space station, 26:55365 (NASA-TM-X-2440, pp 299-306)

PERSHINA, Z. G., Loss of pathogenicity by radioresistant staphylococci, 26:53377

PERSSON, Marjorie, Gamma radiation dose rate in surroundings of electron accelerator FX-45 at Ursvik, 26:53738 (FOA-4-4490-A-3)

PESTIEAU, Jean, Comment on the possible relation between prominent resonances and limiting scaling data in inelastic electroproduction on nucleons, 26:54258

PETERLONGO, G., Steady state and transient measurements on scaled-down model of power channel of CIRENE reactor prototype, 26:55148 (CISE-R-270)

PETERS, B., Method for determining the mean atomic mass of the elements in the primary cosmic radiation throughout the latitude sensitive part of the spectrum, 26:53824

PETERS, C. W., Problem H01-32 Airborne Radiac, 26:53195 (AD-737993)

PETERSON, D. M., Reactor power transient studies, 26:55441 (LA-DC-72-660)

PETERSON, F. C., Evidence for a neutral meson near 1033 MeV, 26:54205 (COO-1428-311)

PETERSON, N. L., Calculation of correlation effects for grain-boundary and dislocation-pipe self-diffusion, 26:55514 (COO-3158-11)

PETERSON, R. J., Two-nucleon pick-up from spin-$^1/_2$ targets. I, 26:54584

PETERSON, Robert Keith, Stripping in collisions between hydrogen molecules, 26:54105

PETERSON, S. F., ^{252}Cf neutron activation facility at the Savannah River Laboratory, 26:53109 (DP-MS-72-37)

PETERSON, V. Z., Muon identification using multiwire proportional chambers, 26:53282

PETRASHKO, R. N., Asymptotic behavior of pair-correlation function of normal Fermi-systems, 26:55532 (ITF-72-2-P)

PETRASKE, E. W., Correction of light attenuation in large shower counters, 26:53285

PETRICH, Donald E., Pneumatic logic controls for automatic vacuum systems, 26:55629 (UCRL-73921)

PETRINA, D. Ya., Solutions of Bogolyubov kinetic equations. Quantum statistics, 26:55067 (ITF-72-9-E)

PETROV, A. Z., Modeling of gravitational fields, 26:54390 (ITF-71-130-P)

PETROV, E. G., Theory of Bethe and Davydov magnetic splittings in cubic antiferrodielectric, 26:55536 (ITF-72-32-P)

Two-particle light absorption by solid α--oxygen crystal, 26:55531 (ITF-71-95-P)

PETROV, L. A., Experiments on search for proton decay from the ground state, 26:54608 (UCRL-Trans-1473)

PETROVA, E. M., Anode erosion with alloys of carbides of transition metals with Fe, Co, and Ni, 26:53568

PETROVA, S. A., Chromosome aberrations induced in human bone-marrow cells by therapeutical local γ irradiation: time and dose relationships, 26:53445

PETTY, S. M., TRASHP: transembler for the Hewlett--Packard minicomputers, 26:55606 (SC-M-720514)

PETTY, T. D., Radiation tolerant gated video amplifier, 26:53307 (SC-DC-721159)

PETZOW, G., Growth and hardness of spherical agglomerates from powders of high melting point materials, 26:53577

PFEFFERMANN, E., Investigation of gamma radiation from the Crab pulsar, 26:53923

PFIRSCH, D., Determination of magnetic field B in vacuum for general two-dimensional MHD equilibria, 26:54814

PFLASTERER, G. R., SEFOR: verification of the Doppler transient shutdown capability of LMFBR's, 26:55123 (CONF-720901-(Bks.1 and 2), pp 986-1005)

PFOTZER, G., History of the use of balloons in scientific experiments, 26:54019

PFUDERER, H. A., Thermal effects on aquatic organisms: annotated bibliography of 1971 literature, 26:53190 (ORNL-EIS-72-28)

PHILBRICK, Richard B., Dose and linear energy transfer spectral measurements for the supersonic transport program, 26:54889 (NASA-TM-X-2440, pp 902-7)

PHILLIPS, R. J. N., Backward-scattering extrapolations and baryon couplings, 26:54331

PICASSO, E., Separated high-energy electron beams using synchrotron radiation, 26:53801

PICCIOTTO, Charles, Application of Moffat's model to eta → 3π and K → 3π decays, 26:54276

eta → 3π decays in a model satisfying analyticity, crossing symmetry, and approximate unitarity, 26:54259

PICKAR, K. A., Carrier transport and storage effects in Au ion implanted SiO_2 structures, 26:53314

PICKER, H. S., Gel'fand--Levitan-unitary-transform formalism for direct extension of the two-nucleon T matrix off the energy shell. Technical Report No. 73-001, 26:54698 (ORO-4317-8)

PIDDINGTON, J. H., Electrodynamic effects of Jupiter's satellite Io, 26:54004

Origin and form of the Galactic magnetic field. II. The primordial-field model, 26:53975

PIERINI, G., Analytical solution of two-separable variational synthesis approach for two-group diffusion r,z equations, 26:55422 (CISE-R-243)

MOBIDIC: a code for simplified evaluation of some continuous axial refueling schemes, 26:55196 (CISE-R-241)

MOICANO-1 code for reactivity and two-group flux calculation of fog-cooled reactor, taking into account true coolant distribution and equilibrium xenon poisoning, 26:55103 (CISE-R-242)

PIERQUIN, B., Dosimetry in interstitial therapy using ^{192}Ir wires, 26:53422

PIETRZAK-FLIS, Zofia, ^{226}Ra in Polish diet and foodstuffs, 26:53525

PIETTE, L. H., ESR study of amino acid and protein-free radicals in solution. IV, 26:52995

PIGEON, J., DWBA analysis of sub-Coulomb multi-transfer reactions, 26:54695 (LYCEN-7213)

PIGOZZI, G., Progress in standardization of analytical methods for materials of nuclear interest. I, 26:52920 (RT/CHI-(72)3)

PIKE, R. A., Resin bonded boron--aluminum composites, 26:53574

PIK-PICHAK, G. A., Properties of Strutinskii's method of shell correction, 26:54684 (IAE-2115)

PILKUHN, H., Coulomb flux corrections and total cross sections for pion--nucleus interactions in Δ-resonance region, 26:54609

PILTINGSRUD, H. V., Critique of standard testing methods for personnel dosimetric devices, 26:53247

PINSKY, L. S., Observations of cosmic-ray-induced phosphenes on Apollo 14, 26:53407 (NASA-TM-X-2440, pp 1002-6)

PINSKY, Stephen, Generalization of semilocal duality, 26:54422

PINSTON, Jean-Alain, Excited levels of even-A isotopes (ruthenium and palladium), 26:54596 (CEA-R-4286)

PIRAGAS, K. A., Two-body problem in theory of direct gravitational interaction. I, 26:54398 (ITF-72-52-P)

Two-body problem in theory of direct gravitational interaction, 26:54399 (ITF-72-58-P)

PIRK, Hans, Procedure for fabrication of spherical oxidic fuel and breeder particles, 26:53566

PISUT, J., Testing of analyticity of πN forward scattering amplitude and determination of πN coupling constant, 26:54337

PITT, W. Wilson Jr., Rapid, sensitive method for the determination of the chemical oxygen demand of polluted waters, 26:52915 (CONF-720827-2)

PITTERLE, T. A., Summary of analyses of plate vs. pin measurements emphasizing reactivity and sodium void effects, 26:55395 (CONF-720901-12)

PIVOT, J., Analysis of thin alumina films obtained by reactive sputtering, 26:52902

PIZZI, J. R., (d,^{6}Li) reactions with light nuclei at 28 MeV, 26:54527 (LYCEN-7219)

PLASKOVA, Anna, Mechanisms of hepatic uptake of hepatotropic radionuclides, 26:53526 (BNWL-tr-71)

PLATOV, Yu. M., Effect of electron radiation on mechanical properties of Fe--Cr and Fe--Mo alloys, 26:53706

PLATTNER, G. R., Forward dispersion relations and low-energy elastic scattering of charged particles from nuclei, 26:54711

PLENDL, H. S., Properties of proton-irradiated diamond, 26:54991

PLUM, F., Physics investigations of sodium cooled fast reactors SNEAK-Assemblies 6A/6B, 26:55398 (EURFNR-1029)

PLUMAN, I. I., Uranium content of the upper Jurassic black bituminous argillites of the West Siberian plate, 26:53146

PLUMMER, E. W., Interaction of single atoms with atomically defined surfaces, 26:53656

PLUMMER, J. P., Boron and tantalum control rod studies and absolute gamma ray absorbed doses in a LMFBR critical, 26:55134 (CONF-720901-(Bks.1 and 2), pp 579-98)

PLZEN, N. P., Some basic experimental methods of wet-steam flow investigation, 26:53124

POCHAT, A., Determination of absolute differential cross sections for $1^1S \rightarrow 4^1D$ transition of helium atom, 26:54113

PODOL'SKII, V. N., Generation of blast waves in a plasma by a pulsed electric discharge, 26:54856

PODUSHNIKOVA, K. A., Microwave plasma heating in Tuman-2, 26:54758

POGREBKOV, A. K., Two-dimensional classically solvable model with nontrivial scattering, 26:54385

POHL, R. O., Resonant scattering, 26:55511 (COO-3151-8)

POHLMAN, T., Average temperature measurements in the aquatic environment using thermoluminescent dosimeters, 26:53187 (ANL-7860(Pt.3), pp 131-40)

POIRIER, Yves, Theoretical study of flow of an electrically conducting viscous liquid in a magnetic induction field, 26:54161

POIZAT, J. C., Channeling of light ions of 0.5 to 2 MeV through few-hundred Angstrom-thick gold crystals, 26:54974 (LYCEN-7228)

POKHOTELOV, O. A., Nonlinear theory of monochromatic circularly polarized vlf and ulf waves in the magnetosphere, 26:54050

POKORNA, J., Experimental verification of effectiveness of radiation vaccine against cattle dictyocaulosis, 26:53503

POKROVSKII, V. L., High-frequency hydrodynamics near the

lambda point, 26:54424
POLAK, Bogumil, Dosimetric properties of some thermoluminescent substances, 26:53245
POLIKARPOV, G. G., Radiation and chemical ecology of hydrobionts, 26:53532
POLLARD, Ernest C., Effects of ionizing radiation on the capacity of Escherichia coli to support bacteriophage T4 growth, 26:53372
POLLOCK, E. L., Approximate phonon frequency distributions for FCC Lennard--Jones harmonic crystals, 26:55515 (COO-3161-3)
POLOVIN, R. V., Asymptotic particle distribution function in cyclotron heating, 26:54759
POLUEKTOV, I. A., Kinetic processes in a laser plasma, 26:54799
POMERANCE, W., Time-of-flight analysis of neutral products from inelastic ion--molecule collisions, 26:54109
PONOMARENKO, E. F., Accumulation of residual gas ionization plasma in an electromagnetic trap, 26:54800 (AEC-tr-7350)
POOLEY, D., Lifetimes of fast recombination luminescence transitions in alkali halides, 26:55000
POPAREV, A. N., Self-igniting pulsed optical discharge in an erosive laser plasma, 26:54803
POPESCU, Elena, Aspects concerning the corrosion behavior of zirconium and zirconium alloys in water at high temperature, 26:53614
POPLAVSKII, V. M., Requirements for steam generator design and systems to ensure safety in the case of failures in the tubes of heat exchange surfaces, 26:55159 (CONF-710548-, pp 206-12)
POPOV, V. N., Damping of long-wave plasma oscillations, 26:54869
POPOV, V. P., Radiative kaon capture by nuclei, 26:54536
POPOV, V. S., Pair production in electromagnetic field, 26:54266
PORA, E. A., Action of small dose of radiations upon gene in Drosophila, 26:53500
PORIES, W. J., Hair radioactivity as a measure of exposure to radioisotopes, 26:53529 (NASA-TM-X-2440, pp 982-8)
PORTE, Louis, Analysis of thin layers of chalcogenide glasses for Te, As, Ge, and S. Use of nuclear reactions and x rays produced by proton bombardment, 26:52900 (LYCEN-7236)
PORTER, J. B., Analysis of hydrogen explosion hazards, 26:55524 (DP-1295)
PORTER, Marilyn W., Renal tumors in parabiosed irradiated rats, 26:53449 (COO-3017-4)
PORTMANN, M.-C., First stage of an assembly of programs for the computerized processing of digital scintigraphic data, 26:53228
POSSA, G., Experimental results on operation of reactivity fast control system of CIRENE reactor, 26:55133 (CISE-R-268)
  Steady state and transient measurements on scaled-down model of power channel of CIRENE reactor prototype, 26:55148 (CISE-R-270)
POSTNIKOV, S. A., Low-frequency oscillations in the weakly ionized plasma of a high-frequency discharge in a magnetic field, 26:54849
POTASHEV, A. G., Nonmesic decays of hypernuclei ^{4}H and ^{4}He in a model of direct transition of the Λ-hyperon into a neutron, 26:54293
POTTER, D., Polarization of the recoil proton in the reactions $\gamma p \rightarrow \pi^0 p$ and $\gamma p \rightarrow \gamma p$, 26:54167 (COO-3069-71)
POTTER, I. C., Measurement of the electron density distribution in plasmas from the bending of a gas laser beam, 26:54769
POUR, Frantisek, Absolute activity in irradiated fuel material by method of gamma scanning, 26:53041 (UJV-2867-M,A)
POVAROVA, K. B., Metallography of cast tungsten, 26:53681
POVEL, H. P., Determination of distribution of charge and magnetic dipole moment in ^{93}Nb from muonic x-ray spectrum, 26:54605 (KFK-1602)
POWERS, J. A., Radiation from ^{238}Pu used in space applications, 26:53337 (NASA-TM-X-2440, pp 859-61)
  Studies of ^{238}Pu fuel forms and their containment, 26:53333 (MLM-1213)
POZWOLSKI, Alexandre Edgar, Process for generating electrical energy, 26:53108
POZZI, F., Isotopic analysis of uranium as running control of EUREX process, 26:52918 (EUR-4765, pp 91-115)
PRADHAN, H. C., Off-shell effects in the ^{18}O and ^{18}F shell-model spectra, 26:54538
PRASAD, Baleshwar, Reflection of a hydromagnetic shock wave from a boundary shock, 26:54159
PRASAD, M. A., Dose across a plane bone--tissue interface, 26:54896
PRASAD, Naresh, Relative biological effectiveness of ^{252}Cf on acute mammalian lethality, 26:53484
PRASAD, Rameshwar, Atomic positions in thorium silicate: an x-ray-diffraction study, 26:55038
PRECUP, O., Action of small dose of radiations upon gene in Drosophila, 26:53500
PREEG, W., Mechanism of fast neutron transport in iron, 26:54473 (CONF-720901-(Bks.1 and 2), pp 335-48)
PREEG, W. E., Radiation analysis of various vehicle and payload configurations for the reusable nuclear shuttle, 26:54947 (NASA-TM-X-2440, pp 58-64)
PREISS, I. L., K-shell ionization cross sections for 2.04-MeV electrons, 26:54104
PRENTICE, J. D., Production properties of A_1^+ in $\pi^+ p$ interactions at 5.45 GeV/c, 26:54227
PREPEJCHAL, W., Effects of a thermal discharge on the inshore biological communities of Lake Michigan, 26:53184 (ANL-7860(Pt.3), pp 109-17)
  Observations of fish at Point Beach Nuclear Plant, 26:53185 (ANL-7860(Pt.3), pp 118-20)
  Radionuclides in Lake Michigan fish, 26:53169 (ANL-7860(Pt.3), pp 141-50)
PRESKITT, C. A., Review of fast neutron spectrum measurements, 26:55438 (CONF-720901-(Bks.1 and 2), pp 943-58)
PRESNAJDER, P., Testing of analyticity of πN forward scattering amplitude and determination of πN coupling constant, 26:54337
PRESTON, J. L., Effects of radiation on the behavior of animals: a review of the literature. Appendix to 1972 progress report, 26:53448 (COO-1332-78)
PREWO, K. M., Resin bonded boron--aluminum composites, 26:53574
  Transverse tensile properties of boron fiber reinforced aluminum matrix composites, 26:53687
PRICE, Gerald B., Incidence of delayed mortality (secondary disease) in allogeneic radiation chimeras receiving bone marrow from aged mice, 26:53485
PRICE, H. G., Evidence of further rotational structure in ^{26}Al, 26:54554
PRICE, William E., Design considerations and test facilities for accelerated radiation effects testing, 26:53695 (NASA-TM-X-2440, pp 570-6)
PRIEDITE, R., Amperometric and potentiometric determination of copper and molybdenum in ore concentrates and alloys with 5-bromo-8-mercapto- and 8-mercapto-4-methylquinoline, 26:52924
PRIEST, E. R., Current limitation in solar flares, 26:53937
PRIKHOD'KO, V. I., Kinetics of weakly inhomogeneous states in ''fluid-gas'' type system, 26:55535 (ITF-72-29-P)
PRIMAVESI, G. J., Magnetic transitions in rare earth intermetallic compounds R_3Ni and R_3Co, 26:55050
PRINE, J. R., Effect of continuous gamma-ray exposure on performance of learned tasks and effect of subsequent fractionated exposures on blood-forming tissue, 26:53452 (NASA-TM-X-2440, pp 633-40)
PRINGLE, W. C. Jr., Potential function for the ring puckering vibration of B_2H_6 and B_2D_6, 26:52966
PRIZHIVOIT, I. F., Effect of x-ray irradiation on regeneration of the thyroid gland in rats without tumors and after inoculation of sarcoma-45, 26:53494
PROKHOROV, A. M., Possible use of IR lasers for high-temperature heating of superdense plasma, 26:54764
PROKHOROV, L. V., Four-fermion scattering amplitude free from kinematical singularities, 26:54417
PROSPERI, D., Trinucleon properties with Riihimaki potential, 26:54504
PROSPERI, G. M., Variational Pade solution of Bethe--Salpeter equation, 26:54380
PROSSER, F. W. Jr., Spectroscopy of ^{101}Mo by sub-Coulomb stripping, 26:54614
PROUST, Jacqueline P., Effects of treating Drosophila females with Actinomycin-D on the yields of dominant lethals, translocations, and recessive lethals recovered from x-irradiated spermatozoa, 26:53502
PRUEMMER, R., Possibilities of explosive compaction of powders, especially those of W, with direct procedure, 26:53619
PRUEMMER, R. A., X-ray residual stress analysis in hardened steels, 26:55594 (RFP-Trans-110)
PRYDE, R. B., Effect of comminution on the sinterability of alumina and tungsten carbide powders, 26:53576
PUEHLHOFER, F., Enhancement of direct processes in heavy-ion reactions at high angular momenta, 26:54558
PUGH, H. G., Two searches for an excited state of ^{3}He, 26:54515
PUGLIESE, A., Representation of SU(3) x SU(3) chiral algebra for baryons, 26:54370 (NP-19418)
PUMMER, H., Investigations on spectrum of pulsed discharge-initiated HF-laser, 26:55526 (IPP-IV-31)
PUPP, Wolfgang, Vacuum techniques, 26:53140
PURSALL, B. R., Evaluation of a cross section ionization detector suitable for mine air analysis, 26:53287
PUSTOVALOV, V. V., Second harmonic generation in nonuniform laser-produced plasma, 26:54790 (JPRS-56713)
PYATKIN, E. K., Chromosome aberrations induced in human bone-marrow cells by therapeutical local γ irradiation: time and dose relationships, 26:53445
PYSTYNEN, P., Amount and form of radioactivity in human milk after lung scanning, renography, and placental localization by ^{131}I labeled tracers, 26:53524

Q

QUAM, W. M., Portable absorbed-dose measuring instrument with gamma discrimination, 26:53234 (NASA-TM-X-2440, pp 609-13)
QUIGG, C., Charged particle multiplicity and angular correlation measurements in pp and γp collisions, 26:54192 (BNL-17141)
  Physics with ISABELLE, 26:54298 (BNL-16997)
QUINLAN, William J., Sequential pathophysiology of ionizing

radiation on the beagle thyroid gland, 26:53462 (UR-3490-183)

QUINN, D., Polarization of the recoil proton in the reactions $\gamma p \to \pi^0 p$ and $\gamma p \to \gamma p$, 26:54167 (COO-3069-71)

QUIRCI, G., Goniometer for implantation and channelling experiments, 26:53322

QUOIRIN, J. B., Analysis using secondary ion emission in semiconductors, 26:52937

R

RAAB, Harry F., Light-water breeder reactor, 26:55130

RADFORD, C. J., Analysis of the effects of electron damage on the bound-to-bound emission intensity of cadmium sulphide, 26:55002

RADICHEVA, M. A., Natural fluorite in the dosimetry of the mixed field of gamma rays and thermal neutrons, 26:53240

RADUTSKII, G. M., Low-energy πN scattering in a current algebra model with physical pions, 26:54339

RADYNOV, A. G., Scalar-tensor theory of gravitation, 26:54395 (ITF-72-21-P)

RAFELSKI, J., Superheavy electronic molecules, 26:54111

RAFT, P. D., Experimental determination of cosmic-ray charged-particle intensity profiles in the atmosphere, 26:53807 (NASA-TM-X-2440, pp 908-13)

RAGONA, C., Monte Carlo photocurrent/photomission computer program, 26:54884 (NASA-TM-X-2440, pp 786-91)

RAGSDALE, William C., Magnus force tests for Sandia Corporation, 1971--72. Wind-tunnel report No. 59, 26:55596 (SC-CR-723162)

RAINWATER, J., Uncertainty in the neutron-strength-function evaluation for a small number of measured resonances, 26:54720

RAITHER, Siegbert Wilhelm, Comparison of CP violation in the decays $K^0 \to \pi^+\pi^-$ and anti $K^0 \to \pi^+\pi^-$, 26:54361 (COO-1195-242)

RAJU, M. R., Influence of linear energy transfer on the radioresistance of budding haploid yeast cells, 26:53368

RAKHIMOV, Kh. R., Formation of complexes of UCl_4 with α- or β-carboxylic acids and α-quinolinecarboxylic acid in polar solutions, 26:53054

RALPH, B., Application of field--ion microscopy in studies of point defects and radiation damage, 26:53704
  Applications of field--ion microscopy in physical metallurgy and corrosion. Conference held at Atlanta, Georgia, May 15--17, 1968, 26:53647
  Interpretation of alloy images, 26:53655

RAMACHANDRAN, G., Polarization of the emitted neutron in muon capture, 26:54564

RAMADURAI, S., Effect of ionization loss on energy spectra of cosmic ray nuclei undergoing Fermi acceleration, 26:53862
  Production of ^{2}H and ^{3}He nuclei in cosmic rays and propagation of protons and helium nuclei through interstellar space, 26:53828

RAMA RAO, J., Isomer ratios in (n,γ) reactions at 25 keV, 26:54589

RAMATY, R., Cosmic ray propagation and source distribution, 26:53861

RAMAVATARAM, K., Elastic and inelastic widths of analogue states in ^{65}Cu, 26:54590

RAMCHANDRAN, S., Impact of the new LASL delayed neutron data on FTR design, 26:55388 (CONF-720901-(Bks.1 and 2), pp 660-86)

RAMORINO, M. C., Automatic peak identification in analysis of gamma-ray spectra obtained with Ge(Li) detectors, 26:53257 (RT/FI-(72)14)

RAMSEY, William H., Conversion of plutonium oxide to plutonium tetrafluoride with fluorine in a fluid bed reactor. Part II. Demonstration runs: a comparison of the fluorine process with the hydrofluorination process, 26:53039 (RFP-1890)

RAND, Peter B., Aromatic polyimide syntactic foam, 26:55601 (SC-DC-722297)

RANDA, Z., Nondestructive neutron activation analysis of mineral materials. II, 26:52901 (UJV-2851-F,Ch)

RANDALL, Gerald J., Computerized dosimetry of ^{60}Co ophthalmic applicators, 26:54900

RANDALL, P. N., Effects of strain gradients on the gross strain crack tolerance of a 533-B steel, 26:53634 (CONF-720806-3)

RANDHAWA, K. S., Effect of irradiation on variability in okra, 26:53390

RANDLES, Joan, Effect of K^+ and K^+ gradients on accumulation of sugars by isolated intestinal epithelial cells, 26:55635 (UR-3490-174)

RANGAN, L. K., S-wave structure in the $K\pi$ system, 26:54203 (COO-1428-308)

RANGANATHAN, S., Studies of grain boundaries in metals with the field--ion microscope, 26:53650

RANKOW, Robin M., Osteoradionecrosis of the mandible, 26:53418

RAO, A. Lakshmana, Isomer ratios in (n,γ) reactions at 25 keV, 26:54589

RAO, C. L., Isomer ratios of ^{95}Nb formed in fission of ^{209}Bi, 26:54627

RAO, C. N. R., Positron lifetimes and phase transitions in solids, 26:55064

RAO, G. S., Steroid glucuronyltransferases, 26:55472 (BMBW-FBK-72-9)

RAO, K. N., Determination of rate constants for reactions of H, OH, and e/sub aq/$^-$ with indole-3-acetic acid and other plant hormones, 26:53015

RAO, M. L., Steroid glucuronyltransferases, 26:55472 (BMBW-FBK-72-9)

RAO, S. A., Isomer yield ratios of /sup 115m/Cd and /sup 115g/Cd, 26:54628

RAO, U. R., Characteristics of cosmic ray diurnal variation from deep river neutron and meson data and temperature effects, 26:53811
  Time variation of x-ray spectrum and optical luminosity of Sco X-1, 26:53917

RAPOPORT, V. O., Dynamic theory of Type-III solar radio bursts, 26:53964

RASMUSSEN, J. O., Two decades of research on radioactivity, 26:53263

RASPOPIN, S. P., Melting point diagrams for $LiCl$--UCl_3--UCl_4 system, 26:53721

RASZILLIER, I., Information on the pion form factors from the absence of zeros, 26:54273

RATHBUN, J. L., Status of the FTR shielding design analysis and methods, 26:55383 (CONF-720901-(Bks.1 and 2), pp 445-58)

RAUCH, F., Gamma transitions in ^{60}Ni following β^+ decay of ^{60}Co. II, 26:54593

RAUSCH, K. R., Proton Compton effect in the region of the Δ(1236)-resonance, 26:54180

RAUSCH, W., Conveying tube for the pneumatic transfer of spherical elements, 26:55194

RAWLINGS, F. F., Determination of selected trace elements in natural water samples using spark source mass spectroscopy, 26:52914 (ANL-7860(Pt.3), pp 55-63)

RAY, Dan S., Ultraviolet-induced cross-links in the deoxyribonucleic acid of single-stranded deoxyribonucleic acid viruses as a probe of deoxyribonucleic acid packaging, 26:53373

RAYMUND, Mahlon, TEDIUM: idealized neutron data for testing library processing codes, 26:54475 (CONF-720901-(Bks.1 and 2), pp 1048-60)

READ, P. A., Development and verification of design methods for ducts in a space nuclear shield, 26:54958 (NASA-TM-X-2440, pp 375-82)

REBEL, H., β-decay of ^{206}Tl, 26:54648

REDISH, Edward F., (p,2p) reactions with divers potentials. Technical Report No. 73-002, 26:54699 (ORO-4317-11)

REED, J. E., D-region measurements with the differential-absorption; differential-phase partial-reflection experiments, 26:54032

REED, W. A., Magnetization, velocity of sound, and specific heat of Sc_3In, 26:55045

REED-HILL, R. E., Deformation processes in hexagonal metals. Progress report, December 1, 1972--November 30, 1972, 26:53639 (ORO-3262-25)

REES, M. J., Transfer effects on lines and continuum in optically thick x-ray sources, 26:53926

REEVES, H., D/H ratio in Jupiter's atmosphere, 26:54007

REFFO, G., Fast neutron radiative capture cross sections of stable nuclei with 29 less than or equal to Z less than or equal to 79, 26:54700 (RT/FI-(72)6)
  MARE: a FORTRAN IV code for compound nucleus reaction calculations in the continuum, 26:54701 (RT/FI-(72)7)

REHME, K., Laminar flow in rod bundles, 26:55449 (KFK-1503)
  Pressure drop for isothermal, incompressible turbulent flow in rod bundles with hexagonally arranged rods, 26:55174 (EURFNR-986)

REICHEL, H., Physics investigations of sodium cooled fast reactors SNEAK-Assemblies 6A/6B, 26:55398 (EURFNR-1029)

REICHMAN, S. H., High density P/M components for elevated temperature applications, 26:53631

REID, J. M., Atomic nucleus, 26:54738

REID, R. J. O., Arrival directions of large air showers of primary energy > 10^{17} eV, 26:53852

REIER, Melvin, Design of a source to simulate the gamma-ray spectrum emitted by a radioisotope thermoelectric generator, 26:53335 (NASA-TM-X-2440, pp 850-2)

REIF, Arnold E., Immunochemical studies with the carcinoembryonic antigen, 26:55505 (COO-3012-21)

REILLY, J. J., Metal hydrides for energy storage, 26:53090 (BNL-16889)

REIMER, M., Dating error, 26:53181

REIN, D., Quark model predictions for weak production of pseudoscalar mesons, 26:54285 (DESY-72/32)

REINHARDT, Michael, Interpretation of rotation measures of radio sources. II, 26:53911

REMIDDI, E., Contribution to the sixth-order electron and muon anomalies, 26:54271

REMILLIEUX, J., Channeling of light ions of 0.5 to 2 MeV through few-hundred Angstrom-thick gold crystals, 26:54974 (LYCEN-7228)

RENGARAJAN, T. N., Pulsars and the cosmic ray spectrum, 26:53858

REUTER III, F. William, Full-range solution for the measurement of thin-film surface densities with proton-excited x rays, 26:52945

REUTLER, H., High flux Franco--German reactor, 26:55411

REVESZ, L., Clinical trials of radiosensitizers and fractionation, 26:53430

REVYAKIN, A. V., Thermodynamics of liquid solutions Mo--O

and Mo--C, 26:53588
RHEA, T. C., Four-nucleon studies. III, 26:54517
Four-nucleon studies. IV, 26:54518
RHO, M., Meson-exchange currents and ^{3}H, ^{3}He magnetic moments, 26:54506
RIAZUDDIN, Octet dominance in non-leptonic decays, 26:54286 (DNPL/P-130)
RICCI, E., Reliability in scientific evidence based on multi-trace forensic NAA, 26:52896 (CONF-720920-2)
RICCI, Enzo, Analysis of traces at ORNL's new High-Flux Neutron Activation Laboratory, 26:52897 (CONF-721010-3)
RICH, F. J., Balance of stresses in the plasma sheet, 26:54059
RICH, P. H., Metabolism of dissolved and particulate detrital carbon in a temperate hard-water lake, 26:55493 (COO-1599-58)
RICHARDS, J. T., Solvation of electrons in 3-methylhexane at 77°K, 26:53007
RICHARDT, A., Development of a ultrahigh vacuum evaporation unit using a liquid He cryopump with a high pumping speed, 26:53139
RICHERT, J., Shell-model study of ^{56}Ni, ^{58}Ni, ^{54}Fe, and ^{56}Fe, 26:54570
RICHMAN, M. H., Study of the formation of tungsten carbide in the field--ion microscope, 26:53560
RICKARD, J., Irregular spiral structure: causes and effects, 26:53987
RICKERTSEN, L. D., Remarks on absorptive potentials and heavy ion elastic scattering, 26:54678 (COO-535-672)
RICKS, Robert C., Pulmonary-impedance power spectral analysis: a facile means of detecting radiation-induced gastrointestinal distress and performance decrement in man, 26:53401 (NASA-TM-X-2440, pp 238-48)
RICOURT, A., Evaluation of the components of the absorbed dose in the interior of organisms exposed to neutrons, 26:54871 (CEA-CONF-1976)
RIECK, G. D., Deformation textures of bcc metals, 26:53670
RIESS, F., Low-lying states in ^{22}Mg, 26:54559
RIEWE, Frederick Eugene, Generalized field theory and form factors of nucleons and atoms, 26:54382
RILEY, Richard C., Exposure of radiologists during special procedures, 26:53443
Proton irradiation of stem cells: radiation damage and chemical radioprotection, 26:53454 (NASA-TM-X-2440, pp 642-6)
RINGQUIST, J. M., Data-processing system for instrument maintenance and calibration at EBR-II, 26:55132 (ANL/EBR-63)
RISTIC, M. M., Kinetics and mechanism of molybdenum powder sintering, 26:53621
RITCHIE, Lawrence S., Fasciola hepatica program in Puerto Rico. Progress summary report, December 1971, 26:53498 (PRNC-156)
RITSON, D. M., e^+e^- annihilation to hadrons, 26:54176 (SLAC-PUB-1043)
RITZ, H. L., Reactor with spherical fuel elements, 26:55131
RIZZI, G., Experimental measurement of neutron groups from phonons in zinc at various temperatures, 26:54487 (RT/FI-(71)37)
ROBERT, R. V. D., Determination of ruthenium and osmium in the residues resulting from the leaching of mattes, 26:52919 (NIM-1432)
ROBERTS, E., Galactic magnetic field and anisotropy of cosmic rays above 10^{17} eV, 26:53851
Possibility of energetic cosmic rays arriving from the Crab Nebula, 26:53856
ROBERTS, F. P., Polymorphic modifications of Pm_2O_3, 26:53596
ROBERTS, H. C., Possible identification of Pb^{1+} and PbH^{2+}: an electron paramagnetic resonance study, 26:53008
ROBERTS, Huey Allen, Scintillation of liquids ^{3}He, ^{4}He, and ^{3}He--^{4}He solutions, 26:54430
ROBERTS, J. T. A., Deformation and fracture of UO_2--20 wt percent PuO_2, 26:53545 (ANL-7945)
ROBERTS, R. E., Influence of attractive forces on the quantum-mechanical transition probabilities for atom--diatomic oscillator collisions, 26:54132
ROBERTS, R. G., Backward-scattering extrapolations and baryon couplings, 26:54331
ROBERTS, W. K., Elastic scattering of 60-MeV protons from H, D, ^{3}He, and ^{4}He, 26:54512
ROBILLER, F., Radiation dose and radioprotective effect in the examination of the thyroid gland of birds, 26:53515
ROBIN, Georges, CAMAC system: practical information for computerized treatment, 26:53297 (CEA-N-1549)
ROBIN, M., Experimental study of burn-up in fast breeder reactors, 26:55119 (CONF-720901-(Bks.1 and 2), pp 888-904)
ROBINSON, Cynthia M., Immunochemical studies with the carcinoembryonic antigen, 26:55505 (COO-3012-21)
ROBINSON, E. Y., ENRP 69-5: design criteria for confidence and reliability based on small samples, 26:55618 (UCID-16099)
ENRP 69-8: composite static fatigue interpretation of some data, 26:55619 (UCID-16100)
ROBINSON, Edward L., Observations of rapid blue variables. IX, 26:53902
ROBINSON, Herbert N., Conversion of plutonium oxide to plutonium tetrafluoride with fluorine in a fluid bed reactor. Part I. Development studies, 26:53038 (RFP-1889)
Conversion of plutonium oxide to plutonium tetrafluoride with fluorine in a fluid bed reactor. Part II. Demonstration runs: a comparison of the fluorine process with the hydrofluorination process, 26:53039 (RFP-1890)
ROBINSON, J. C., Verification of a new method for calculating and measuring generation time in a subcritical fast reactor, 26:55437 (CONF-720901-(Bks.1 and 2), pp 713-23)
ROBINSON, J. M., s--d exchange model of weak ferromagnetism with an application to MnB_2, 26:55048
ROBINSON, J. T., Calculation of correlation effects for grain-boundary and dislocation-pipe self-diffusion, 26:55514 (COO-3158-11)
ROBINSON, R. L., Angular correlations of γ-rays from Coulomb excited ^{63} ^{65}Cu, 26:54594
ROBSON, J. M., Detection of ultra-cold neutrons by the activation of manganese, 26:54490
ROCHESTER, G. K., Search for neutrons of solar origin using balloon-borne detectors: 1967--69, 26:53967
ROCHEV, V. E., Production of boson pairs by static field, 26:54384
ROE, B. P., Large aperture spectrometer magnet for the ISA and the possible use of visual detectors, 26:53779 (BNL-17142)
ROENNBAECK, C., Protective effect of cysteamine at fractionated irradiation. III, 26:53475
ROGALSKA, Zofia, Emittance measurements and design of an ion beam transporting system, 26:53760
ROGANOV, V. S., Depolarization of negative muons in water and aqueous solutions, 26:54099
ROGER, J. A., Analysis of thin alumina films obtained by reactive sputtering, 26:52902
ROGERS, D. R., Radiation environment for rendezvous and docking with nuclear rockets, 26:55361 (NASA-TM-X-2440, pp 257-63)
ROGERS, Palmer, Prog. rpt. on canavanine death and mechanism of DNA replication in E. coli, 8/1/71--8/1/72, 26:55491 (COO-1562-17)
ROGSTAD, D. H., Gross properties of five Scd galaxies as determined from 21-centimeter observations, 26:53972
ROHDE, R. W., Mechanical properties and stress relaxation of beryllium--copper alloy 25, 26:53641 (SC-DR-720471)
ROHLIN, J., Pionic proton stripping and π^- production, 26:54535
ROJAS LOPEZ, R. M., Benzoato complexes of uranyl. III, 26:53042
ROLFS, C., Low-lying states in ^{22}Mg, 26:54559
ROLF-WOLTJE, Reactor fuel element, 26:55419
ROMAGNAN, Jean-Pierre, Experimental evidence for the Josephson effect in tin films, 26:54455
ROMAN, S., Elastic and inelastic scattering of 12 MeV polarized deuterons by ^{24}Mg, 26:54557
ROMANI, G. L., Influence of dimensionality on Bose condensation and macroscopic coherence in superconductors, 26:54436 (NP-19425)
ROMANOV, Yu. A., Instability of spatially separated plasma beams. III, 26:54822
ROMANOV, Yu. I., Possible influence of polarized properties of leptons on the form of photon and electron spectra which arise from inelastic neutrino--muon scattering, 26:54290
ROMBERG, G. P., Acoustic location techniques to study the distribution of fish in the vicinity of a thermal plume, 26:53186 (ANL-7860(Pt.3), pp 121-30)
Observations of fish at Point Beach Nuclear Plant, 26:53185 (ANL-7860(Pt.3), pp 118-20)
Radionuclides in Lake Michigan fish, 26:53169 (ANL-7860(Pt.3), pp 141-50)
ROMIG, W. R., Induction of lysogenic bacteria in the space environment, 26:53364 (N-72-20063)
ROMO, W. J., Comparison of several continuum shell-model approximation schemes, 26:54729
ROOSILD, S., Hardening electronic devices against very-high-total-dose radiation environments, 26:53289 (NASA-TM-X-2440, pp 481-6)
ROSE, William K., Relaxation oscillations in the envelopes of luminous red giants, 26:53874
ROSEN, J., Coulomb induced deuteron break-up of ISABELLE, 26:53776 (BNL-17063)
ROSEN, J. L., K^+ decay in flight, 26:54186
Scheme for absolute calibration of ISABELLE luminosity, 26:53772 (BNL-17021)
ROSEN, Louis, Status of LAMPF, 26:53739 (LA-4874, pp 16-20)
Status report on LAMPF research proposals, 26:53785 (LA-4874, pp 45-7)
ROSENBERGER, H., Melting of radioactive substances in glass or ceramic substances. Third communication: suitability study of vulcanites of domestic origin, 26:53057 (BNWL-tr-75)
ROSINSKII, S. E., Injection of a dense electron beam into a plasma, 26:54794
ROSS, Donald M., Application of radiation exposure standards in the AEC contractor program, 26:54923
ROSS, G. G., Muon--proton scattering and the effect of neutral currents in the scaling region, 26:54288 (RPP/T-26)
ROSS, John, Dependence of reactivity on internal and

translational energy in K + SF_6, CCl_4, and $SnCl_4$, 26:54136
ROSS, S. D., Vibrational spectra and structures of rare earth oxides in the a modification, 26:55031
ROSSAT-MIGNOD, J., Crystal field effect on the direction of magnetic moments of rare earth ions with low symmetry sites (C2--C/sub s/), 26:55054
ROSSI, G. C., Pion electroproduction at threshold, 26:54247 (NP-19417)
ROSSI, Harald H., Methods and approaches to dosimetry, 26:53232 (NASA-TM-X-2440, pp 435-7)
ROSSI-ALVAREZ, C., g-factor of $3/2^-$ 153-keV state in ^{49}V, 26:54574
ROSTOKER, Gordon, Occurrence of Pc 4, 5 micropulsation activity at the polar cusp, 26:54034
ROSTOKER, Norman, Kinetic equations, 26:54797
ROTH, E., Absolute measurement of the isotopic ratio of a water sample with a very low deuterium content, 26:52913 (AEC-tr-7345)
ROTH, Timothy Stephan, Pseudoscalar-meson--nucleon scattering and Regge cuts; and an experimental study of the K/sub L/^{0} + K/sub S/^{0} regeneration amplitude in copper, 26:54230
ROTHSTEIN, Jerome, Pattern recognition by retina-like devices, 26:55455 (OSU-CISRC-TR-72-8)
ROTMAN, Marvin, Computerized dosimetry of ^{60}Co ophthalmic applicators, 26:54900
ROUBEN, B., Superheavy Hartree--Fock calculations, 26:54726
ROUDIER, R., Outlook for the on-site welding of thick metal sheets, 26:53633
ROUSSEL, M., Reactions between hydrocarbon ions CH/sub n/$^+$ and gaseous targets, in the 40 to 140 keV energy range, 26:54137
ROUTSON, R. C., Techniques for the characterization of suspended sediment and selected applications for the acquired data, 26:55479 (BNWL-SA-4385)
ROWLAND, R. E., Radiological Physics Division annual report. Environmental research, January--December 1971, 26:53150 (ANL-7860(Pt.3))
ROY, D. P., Backward-scattering extrapolations and baryon couplings, 26:54331
ROY, T., Velocity distribution of secondary π mesons from 22.6-GeV/c proton--nucleus interactions in emulsion, 26:54196
RUBBIA, S., MOICANO-1 code for reactivity and two-group flux calculation of fog-cooled reactor, taking into account true coolant distribution and equilibrium xenon poisoning, 26:55103 (CISE-R-242)
RUBIN, B., Energy: uses, sources, issues, 26:53096 (UCRL-51221)
RUBINSON, W., Influence of the chemical environment on α-decay, 26:54730
RUD, N., Measurement of lifetimes in ^{152}Sm, ^{154}Gd, and ^{156}Gd, 26:54642
RUDAKOV, L. I., Behavior of large-current electron beam in a dense gas, 26:54763
RUDNICKI, Tadeusz, Gastrulation in mouse embryos in course of radiation injury, 26:53476
RUDOLPH, H., Two-nucleon pick-up from spin-$^1/_2$ targets. I, 26:54584
RUDRAIAH, N., Effect of heterogeneity and Hall current on the MHD power generator, 26:53105
RUEDENBERG, K., Implementing the SAAP formalism. I. Serber-type spin eigenfunctions by direct diagonalization, 26:54155
RUEDENBERG, Klaus, Implementing the SAAP formalism. II. Simultaneous eigenfunctions of L^2 and S^2 by direct diagonalization, 26:54156
  Many-electron wave functions expanded in spin-adapted antisymmetrized products, and their expectation values, 26:54154
RUEHLE, R., Group constant generation for the resolved resonance region, 26:55439 (CONF-720901-(Bks.1 and 2), pp 1183-91)
RUFENACH, Clifford L., Power-law wavenumber spectrum deduced from ionospheric scintillation observations, 26:54029
RUFENER, F., Variable stars of small amplitude I, 26:53884
RUFFA, A. R., Theoretical model for x-ray emission and absorption, bond breaking, and point-defect production in SiO_2, 26:55018
RUHLA, C., (d,^{6}Li) reactions with light nuclei at 28 MeV, 26:54527 (LYCEN-7219)
RUKHADZE, A. A., Excitation of electromagnetic waves in a plasma by a relativistic electron beam. Part I. Longitudinal waves, 26:54837 (AEC-tr-7333)
RUKHLIN, V. G., Injection of a dense electron beam into a plasma, 26:54794
RUP, Raj, Anisotropy of surface superconductivity of lead single crystals, 26:54440
RUSAKOVA, E. V., Loss of pathogenicity by radioresistant staphylococci, 26:53377
RUS'KIN, V. I., Statistical model which allows for the conservation of P-, C-, and G-parity, 26:54360
RUSSELL, G. J., Pulsed-activation techniques for the measurement of Doppler effects, 26:55124 (CONF-720901-(Bks.1 and 2), pp 1016-32)
RUSSELL, John L., Comparison of techniques for calculating doses to the whole body and to the lungs from radioactive noble gases, 26:53510
RUSSELL, W. J., Dose to patients from roentgenography, 26:53434
RUSSO, M., Measure of the photovoltaic effect in silicon diodes obtained through implantation of ions, 26:54975 (RT/EL-(72)2)
RUSSO, P., Lifetime of the first excited state in ^{96}Zr, 26:54622
RUSTGI, M. L., Study of even calcium and nickel isotopes with self-consistent approximations, 26:54583
RUTHERFOORD, J., Polarization of the recoil proton in the reactions $\gamma p \to \pi^0 p$ and $\gamma p \to \gamma p$, 26:54167 (COO-3069-71)
RUTHERFORD, J. L., Properties of dry crushed salt and related consolidated media with emphasis on their gas transport characteristics, 26:53724 (ORNL-TM-3815)
RUTKEVICH, B. N., Nonlinear space-charge waves in a plasma sheath, 26:54853
RUVALDS, J., Theory of the roton lifetime in superfluid helium, 26:54429
RYABTSOV, V. D., Possible measuring high-energy electron energy by ionization detectors of total absorption on basis of condensed xenon, 26:53272 (JINR-P13-6541)
RYAN, Jean L., Proton and fast neutron damage studies in Si and Ge using channeling, 26:55004
RYAN, M. J., Acceleration and propagation of high Z cosmic rays in pulsar environment, 26:53857
  Charge composition of galactic cosmic radiation, 26:53830
  Cosmic ray proton and He spectra above 50 GeV, 26:53829
  Primary cosmic ray electron spectrum from 10 GeV to about 200 GeV, 26:53823
RYAN, Madeleine A., Interaction of embryonic chicken spleen cells and adult allogeneic leucocytes, 26:53477
RYBICKI, Edward, Radiothermoluminescence of cyclohexene, 26:53010
RYDBERG, Bjoern, Biological dosimetry for application on the civilian population after a nuclear explosion, 26:53397 (FOA-4-4500-A-3)
RYVES, T. B., Construction and calibration of a standard thermal neutron flux facility, 26:53118
RYVKIN, S. M., Fast-neutron-compensated n-germanium as a model of amorphous semiconductors, 26:54981
RZEWUSKI, H., Similarities of ionization effects and annealing in P-type and converted N-type Ge irradiated with electrons at 85°K, 26:54997
RZEWUSKI, Henryk, Charge state of defects in Ge converted into p-type by 1 MeV electrons, 26:55013

S

SAAD, S. M., Empirical expressions for the thermal diffusion column shape factors in the extreme cylindrical case, 26:53326 (AREAEE-131)
SACHSE, G., Melting of radioactive substances in glass or ceramic substances. Third communication: suitability study of vulcanites of domestic origin, 26:53057 (BNWL-tr-75)
SADHU, A., Effects of gamma radiation on photocurrent-voltage characteristics of CdS films, 26:54998
SADYKHOV, F. S., Role of neutral vector mesons in the photoformation of lepton pairs by nuclei, 26:54260
SAFI, Nour, Labeled iodoquine, 26:53029
SAFRONOV, B. G., Accumulation of residual gas ionization plasma in an electromagnetic trap, 26:54800 (AEC-tr-7350)
SAGALYN, R. C., Spatial and temporal variations of the thermal plasma between 3000 and 5700 kilometers at L = 2 to 4, 26:54037
SAGAN, Leonard A., Benefit--risk ratios: some eccentric views, 26:54931
SAGAWA, T., Optical 4d → 4f transition and binding energy of 4d level in La and Ce, 26:54095
SAGAWA, Takasi, Photoelectron spectroscopic measurements of core level binding energies of Y, La, and Ce, 26:55024
SAGINA, I. P., Damping of hole states in the giant dipole resonance, 26:54714
SAGLIO, Robert, Detection of faults in metallic welds using ultrasounds, 26:53126
SAHA, G. B., Isomer ratios of ^{95}Nb formed in fission of ^{209}Bi, 26:54627
SAHASRABUDHE, S. G., Ion-chamber device as electronic switch in high radiation field, 26:53224
SAITO, Hajime, System for time of 50 m flight analysis and characteristics of short pulse beam, 26:53260
SAKAI, H., Oxygen isotopic ratios of some evaporites from Precambrian to recent ages, 26:53180
SAKAI, Jun-ichi, Nonlinear magnetosonic waves in a plasma with a finite conductivity, 26:53941
SAKAI, Mitsuo, Quasi-bands in even--even nuclei, 26:54600 (INSJ-130)
SAKAI, S., Isotope dependence of K-shell ionization cross sections by ^{20}Ne and ^{22}Ne bombardments, 26:54114
SAKAI, Sunao, Inclusive reaction in multiperipheral model. II, 26:54312
SAKAI, T., Chemical composition of low energy L and M nuclei in the primary cosmic radiation, 26:53841
  Measurement of the low energy helium isotopes in the primary cosmic rays, 26:53827
SAKAKIBARA, S., Sidereal and solar anisotropy of high-energy cosmic rays observed by an air Cherenkov telescope, 26:53850
SAKAMOTO, Fumio, Results of cyclic pressure loading test

due to JPDR pressure vessel model No. 2, 26:55228 (JAERI-Memo-4016)
SAKANO, Kosuke, Analyses of the sodium-water reaction pressure and its propagation in the sodium system, 26:55157 (CONF-710548-, pp 171-86)
SAKATA, Hajime, Flux distribution measurement near strong absorber using VISTA method, 26:55137 (JAERI-Memo-3893)
SAKHAROV, V. I., Calculation of nuclear reaction rates in a homogeneous sphere neglecting elastic scattering, 26:54491
SAKKA, Masatoshi, Establishment of line of cultured of hepatoma cells (Culb TC) of the rat and the analysis of effects of gamma rays, 26:53354
SAKLA, A. B., Microdetermination of metals in organometallic compounds by the oxine method after oxygen flask combustion. I. Cadmium, magnesium, uranium, and zinc, 26:52930
SAKMAR, I. A., Inequalities with πN polarization, 26:54340
SAKO, Kiyoshi, Study on the works of engineering reactor-safety, 26:55204 (JAERI-M-4535)
SAKURAI, Kunitomo, Relativistic electrons associated with solar flares, 26:53968
SALADIN, J. X., Static quadrupole moments of the first 2^+ states of the even--even osmium nuclei, 26:54538
SALAM, A., CP-violating gauge interactions, 26:54367
SALIN, A., Electron capture from hydrogen negative ions by fast protons, 26:54116
SALISBURY, John D., Test result of the geographic position locator: a system for improving land navigation without external aids, 26:55631 (UCRL-74039)
SALMI, E. W., Venting of fission products and shielding in thermionic nuclear reactor systems, 26:55373 (NASA-TM-X-2440, pp 1016-20)
SALMON, W. I., Implementing the SAAP formalism. I. Serber-type spin eigenfunctions by direct diagonalization, 26:54155
  Implementing the SAAP formalism. II. Simultaneous eigenfunctions of L^2 and S^2 by direct diagonalization, 26:54156
SALMON, William I., Many-electron wave functions expanded in spin-adapted antisymmetrized products, and their expectation values, 26:54154
SALVAT, M., Performance of MHD generators and thermal efficiency of closed cycle MHD power plants, 26:53091 (IPP-IV-36)
SALZBERG, B. M., Reaction $\pi^- p \to p\pi^+\pi^-\pi^-\pi^0$ at 20 GeV/c, 26:54207 (COO-3064-3)
SALZMAN, G. C., Preliminary measurements of polarization transfer in ^{4}He(d Vector,d Vector)^{4}He elastic scattering, 26:54498 (LA-DC-72-904)
  Vector to tensor polarization transfer in proton--deuteron elastic scattering, 26:54499 (LA-DC-72-905)
SAMANT, R. K., Ion-chamber device as electronic switch in high radiation field, 26:53224
SAMARIN, A. M., Thermodynamics of liquid solutions Mo--O and Mo--C, 26:53588
SAMOILENKO, I. I., Loss of pathogenicity by radioresistant staphylococci, 26:53377
SAMSON, John C., Occurrence of Pc 4, 5 micropulsation activity at the polar cusp, 26:54034
SAMSONOV, A. E., Measurements of neutron cross sections of radiation capture and fission for some heavy nuclei by the method of time of retardation in lead, 26:54657 (FEI-292)
SAMSONOV, G. V., Anode erosion with alloys of carbides of transition metals with Fe, Co, and Ni, 26:53568
  Electronic mechanism of the basic technological processes in the powder metallurgy of high temperature materials, 26:53632
  Production of formed bodies from high-melting compounds according to the casting procedure for thermoplastic masses, 26:53586
SANADA, J., D(p,2p)n reaction at 51.8 MeV, 26:54505
SANDA, A. I., Phenomenology of the triple-Regge region, 26:54332
SANDERS, Wm. Mort, Active ^{3}He activation analysis for carbon and oxygen, 26:52899 (LA-DC-72-809)
SANDHU, K. S., Effect of irradiation on variability in okra, 26:53390
SANDWEISS, Jack, Measurement of the proton--proton total cross section by beam attenuation, 26:54191 (BNL-17065)
SANKARANARAYANAN, K., Effects of treating Drosophila females with Actinomycin-D on the yields of dominant lethals, translocations, and recessive lethals recovered from x-irradiated spermatozoa, 26:53502
SANO, A., Measure of the photovoltaic effect in silicon diodes obtained through implantation of ions, 26:54975 (RT/EL-(72)2)
SANO, Hiroshi, Surgical treatment for local radiation injuries following radiotherapy, 26:53438
SANTOSO, Daniel, Cherenkov counting of beta-emitting radionuclides, 26:53209
SARATZ, G., Phase shifts of p--d elastic scattering at 2.0, 2.7, 3.3, and 3.8 MeV, 26:54513
SARKAR, B. K, Effect of comminution on the sinterability of alumina and tungsten carbide powders, 26:53576
SARKSYAN, K. A., Excitation by very high frequency wave pumping of parametric instabilities in a magnetoactive plasma, 26:54809 (NP-19406)
SARRAZIN, Pierre, Elementary mechanisms in heterogeneous kinetics. IV, 26:55588 (ORNL-tr-2394)
SARROUY, J. L., Ion implantation facility at Orsay, 26:54976
SASAKI, Kiyoshi, Effective neutron--proton interaction in deformed doubly odd nuclei, 26:54747
  Mass number dependence of neutron and proton residual interaction, 26:54739
SASAKI, Tateaki, Model of multiple production based on the intuitive picture of hadrons, 26:54314
SASSANO, G. P., Structural studies on U deposit of Fay Mine, Eldorado, Northwest Saskatchewan, 26:53145
SATCHLER, G. R., Optical model, 26:54677 (CONF-720701-3)
SATO, Minoru, Outline of PNC's activities in the field of sodium-water reaction, 26:55155 (CONF-710548-, pp 129-54)
SATO, S., Radiation induced heart failure. I, 26:53439
SATO, Shoichi, Operation report on low temperature fissiochemical loop (JTFL). I, 26:55400 (JAERI-M-4630)
SATO, T., Further aspects of the reaction $\pi^- p \to \pi^-\pi^+ n$ at 8 GeV/c, 26:54216
SATOH, T., Optical 4d → 4f transition and binding energy of 4d level in La and Ce, 26:54095
SAUER, P. U., Off-shell effects in the ^{18}O and ^{18}F shell-model spectra, 26:54538
SAUNIER, G., Superheavy Hartree--Fock calculations, 26:54726
SAVATTERI, C., Friction factors of a cluster of 19 rough rods, 26:55188 (EURFNR-1020)
SAVCHENKO, I. S., Circuits for studying the interaction of high-frequency fields with a plasma in linear devices, 26:54775 (AEC-tr-7326)
SAVIN, W., Phase and shape of the form factor for inelastic ^{3}He scattering, 26:54621
SAVITSKII, E. M., Metallography of cast tungsten, 26:53681
SAVUSHKIN, L. N., Electric multipole transitions in mesic atoms, 26:54098
SAWADA, T., Electron energy deposition in CO_2, 26:54009
  Electron-impact excitation cross sections and energy degradation in CO, 26:54008
SAWAN, Mohamed, Green's function coupling method for time-dependent neutron slowing down in heavy media, 26:55428 (CONF-720901-(Bks.1 and 2), pp 179-94)
SAWICKI, Aleksander, Automatic data acquisition and registration from mass spectrometer, 26:53324
SAWYER, C. D., Nuclear radiation problems, unmanned thermionic reactor ion propulsion spacecraft, 26:55364 (NASA-TM-X-2440, pp 292-8)
SAXENA, A. P., Sound propagation in ionized gases and electro acoustic effect, 26:54858
SAXENA, K. M. S., Properties and interactions of lanthanides, 26:55025
SAYAR, A., Crystal orientation and the hardness of zirconium, 26:53693
SAYYAH, T. A., Mineralogy and some trace elements geochemistry of samples from southwest Aswan radioactive syenite rock western desert, 26:53142 (AREAEE-138)
SCALAPINO, D. J., Statistical mechanics of one-dimensional Ginzburg--Landau fields, 26:54452
SCARGLE, Jeffrey D., Transfer of resonance-line radiation in differentially expanding atmospheres. I. General considerations and Monte Carlo calculations, 26:53878
  Transfer of resonance-line radiation in differentially expanding atmospheres. II. Analytic solution for the case of coherence in the frame of the fluid, 26:53879
SCARR, J. Michael, Two-body strange-particle final states in $\pi^- p$ interactions at 4.5 and 6 GeV/c, 26:54217
SCHACHER, J., Blocking effect in U fission with 14-MeV neutrons, 26:54669
SCHAEFER, Herman J., Apollo mission experience, 26:54953 (NASA-TM-X-2440, pp 215-19)
SCHAIRER, Lloyd A., Radiobiologic studies of Tradescantia plants orbited in Biosatellite 2, 26:53382 (N-72-20054)
SCHARENBERG, R. P., Multiple Coulomb interference effects on the quadrupole moment of ^{114}Cd, 26:54623
SCHATTEN, Judith E., Magnetic-field structure in flare-associated solar-wind disturbances, 26:54076
SCHATTEN, Kenneth H., Magnetic-field structure in flare-associated solar-wind disturbances, 26:54076
SCHAUER, G., Use of PL/1 as interrogation language of a deck of cards, 26:55450 (CEA-CONF-2005)
SCHECHTER, J., Unified weak-electromagnetic gauge schemes based on the three dimensional unitary group, 26:54364 (NYO-3533-264)
SCHEEFELD, E., State and tendencies of chemical protection against ionizing radiation. A literature survey 1970/71, 26:53460 (SZS-132)
SCHEELE, R. V., Physical measurements including depth dose data and isodose curves for 8 mv roentgen rays, 26:53799
SCHELSKE, Claire L., Prog. rpt. on nutrient enrichment and eutrophication of Lake Michigan, 11/1/68--7/31/72, 26:55499 (COO-2003-17)
SCHERMER, W. J., Multinode analysis of B and W's 145-fuel assembly nuclear plants during loss-of-coolant accident, 26:55272 (BAW-10048(Suppl.1))
SCHEUERMANN, W., Influence of electron configuration on the absorption behavior of mixed crystals of hard materials, 26:53593

SCHEUTEN, G. H., Organization and economic significance of breeder development, 26:55097

SCHIFF, A., Final report on the development of the Geographical Position Locator (GPL). Volume 8. Technical support, 26:53311 (UCRL-51130(Vol.8))

SCHILDT, B. E., Function of the reticuloendothelial system in whole-body irradiated mice, 26:53468

SCHILLING, W., Recovery of electron-irradiated Pt. I, 26:55010

  Recovery of electron-irradiated. II, 26:55011

SCHILLING, W. A., Response of mouse epidermal cells to single doses of heavy particles, 26:53456 (NASA-TM-X-2440, pp 652-8)

SCHILLINGS, K. L., Analytical determination of impurities in sodium of LMFBR, 26:55170 (CONF-710959-, Paper 14)

SCHIRRA, M., Influence of thermomechanical treatments on the creep rupture and creep behavior of X10 NiCrMoTiB 1515 steel, 26:53635 (EURFNR-998)

SCHITTKO, F. J., Photoproduction of π^+-mesons on polarized protons at photon energies between 0.5 and 2.2 GeV, 26:54172 (NP-19415)

SCHLESINGER, Y., Level scheme of ^{144}Sm determined by the (γ,γ') reaction, 26:54619

SCHLICHTING, J., Oxidation protection of Ta and Ta alloys up to 1500°C, 26:53613

SCHLICK, S., H_3O radical, 26:53026

SCHLOESSER, J., Process beat from high temperature reactors, 26:55377

SCHMELZBACH, P.-A., Phase shifts of p--d elastic scattering at 2.0, 2.7, 3.3, and 3.8 MeV, 26:54513

SCHMIDT, D., Possibilities of explosive compaction of powders, especially those of W, with direct procedure, 26:53619

SCHMIDT, F. A. R., Monte Carlo calculations for the critical experiment of the German incore thermionic reactor, 26:55386 (CONF-720901-(Bks.1 and 2), pp 636-44)

SCHMIDT, F. K., Silicon diffusion in Me_5Si_3 phases of metals Nb, Ta, Mo, and W, 26:53583

SCHMIDT, Gail D., Summary of radioactive surface contamination guides, 26:54920

SCHMIDT, J., Pseudoclassical and anomalous containment in FM-1, 26:54753 (CONF-720804-5)

SCHMIDT, Maarten, Statistical studies of the evolution of extra-galactic radio sources. II. Radio galaxies, 26:53995

  Statistical studies of the evolution of extra-galactic radio sources. I. Quasars, 26:53994

  Statistical studies of the evolution of extragalactic radio sources. III. Interpretation of source counts and discussion, 26:53996

SCHMIDT-KUESTER, W. J., Project SNR: governmental support and international cooperation, 26:55098

SCHNABEL, Peter, Measurement of depolarization parameter, D, in elastic scattering of protons by ^{9}Be, ^{10}B, and ^{27}Al, 26:54525 (FRNC-TH-191)

SCHNEIDER, Eugen, Influence of temperature on the average neutron transmission of gold in the unresolved resonance region, 26:54484 (KFK-1519)

SCHNEIDER, Friedemann W., Kinetics of proton transfer to cyanines. a temperature-jump study, 26:52964

SCHNEIDER, Marion F., Advanced-dosimetry systems for the space transport and space station, 26:53235 (NASA-TM-X-2440, pp 944-56)

  Dosimetry system for measuring instantaneous dose and linear energy transfer spectrum of space radiations, 26:53241

  Experimental active- and passive-dosimetry systems for the NASA Skylab program, 26:53236 (NASA-TM-X-2440, pp 958-73)

SCHNEIDER, Mary Elizabeth, Theoretical studies of hydrogen kinetic isotope effects, 26:52959

SCHNEIDER, P. G., Real-time analysis of thermal diffusivity data from a pulsed laser facility, 26:55639 (Y-1841)

SCHOEDER, K., Recovery of electron-irradiated. II, 26:55011

SCHOLER, M., Change of solar-flare proton-to-alpha ratios during an energetic storm particle event, 26:53966

SCHOLL, R. E., Investigation of ground motion--damage relationships for residential buildings in Glendale, California: San Fernando earthquake, February 1971, 26:53137 (JAB-99-96)

SCHOLTYSSEK, W., Experimental results from two Pu-fueled fast critical assemblies, 26:55387 (CONF-720901-(Bks.1 and 2), pp 645-59)

SCHOLZ, M., Abundances of noble gases in extreme population I matter and Sun, 26:53892

SCHOLZ, W., K-shell ionization cross sections for 2.04-MeV electrons, 26:54104

SCHRADER, W., ^{4}He--^{4}He interaction potential from low energy total cross section measurements, 26:54514

SCHRAM, D. C., Resonant scattering of trapped particles by toroidal plasma modes, 26:54792

SCHRAMM, R., Shock loading analysis of core subassembly: APDA core, 26:53732 (WCAP-1615)

SCHTROBEL, Hans, Geometry of relativistic space of particle states, 26:54391 (ITF-71-132-P)

SCHUCH, A. F., Phase transitions and crystal structures of deuterium, 26:55559 (LA-DC-72-903)

SCHULMAN, Jerome M., Perturbation calculation of the nuclear spin--spin coupling constant in HD based on the bare-nucleus potential, 26:54092

SCHULMAN, L. S., Time reversal for unstable particles, 26:54366

SCHULTHEISS, G. F., Phenomenological investigation of the flow distribution behind local coolant chemical blockage in rod bundles, 26:55176 (KFK-1548)

SCHULTZ, H., Influence of interstitial nitrogen on the asymmetry of the yield stress of tantalum, 26:53643

SCHULTZ, R. J., Ultra-fast solute diffusion in α-Ti and α-Zr, 26:53666

SCHULTZ, Vincent, Russian radioecology: a bibliography of Soviet publications with citations of English translations and abstracts, 26:53530 (TID-3915(Suppl.1))

SCHULZ, F., Determination of implantation profiles in solids by secondary-ion mass spectrometry, 26:55014

SCHULZ, W., Photoproduction of π^+-mesons on polarized protons at photon energies between 0.5 and 2.2 GeV, 26:54172 (NP-19415)

SCHULZE-WOLLGAST, U., Results of fallout monitoring in the German Democratic Republic 1970, 26:53156 (SZS-128)

SCHUPP, G., Double K-shell ionization in the decay of ^{131}Cs and ^{165}Er, 26:54617

SCHWAB, B., Presentation made to meeting of sodium-water reaction specialists, 26:55150 (CONF-710548-, pp 1-16)

SCHWENK, Francis C., Space nuclear propulsion systems and applications, 26:55359 (NASA-TM-X-2440, pp 2-12)

SCHWERER, F. C., Electrical resistivity increase rates in Fe--C and Fe--N solid solutions during neutron irradiation at 4.5 K, 26:54989

SCHWILLE, W. J., Photoproduction of π^+-mesons on polarized protons at photon energies between 0.5 and 2.2 GeV, 26:54172 (NP-19415)

SCIAMA, D. W., X-ray emission from intergalactic gas in the neighbourhood of galaxies, 26:53988

SCLOCCHI, G., RAS: synthesis program for calculation of 2-group neutron flux in r-theta, 26:54471 (CISE-R-252)

SCOFIELD, D. F., Continued-fraction method for perturbation theory, 26:55078

SCOTT, J. F., Analysis of anticipated transients without trip, 26:55193 (BAW-10016)

SCOTT, O. C. A., Clinical trials of radiosensitizers and fractionation, 26:53430

SCOTT, R. Kaye, Radiotherapeutic method in the treatment of skin cancer, 26:53341

SEAMON, R. E., Development of ENDF/B shielding data processing codes, and integral tests, 26:55141 (CONF-720901-(Bks.1 and 2), pp 316-24)

  Sensitivity of calculated pulsed sphere spectra and neutron age to carbon cross sections, 26:54474 (CONF-720901-(Bks.1 and 2), pp 409-17)

SEARS, M., Statistical mechanics of one-dimensional Ginzburg--Landau fields, 26:54452

SEBAOUN, E., Determination of the systolic volume by external counting, 26:53543

SEBASTIANI, F., High energy measurements of total cross sections on proton, detecting very low energy neutrons, 26:54163 (NP-19421)

SEBKO, V. P., Experimental determination of the basic characteristics of space-periodic magnetic configurations, 26:54824 (AEC-tr-7334)

SEEMAN, N., Observation of cosmic gamma radiation above 10 MeV, 26:53816

  Search for pulsed gamma rays from the Crab, 26:53922

SEGEV, M., Many-resonance approximation for the neutron energy spectrum, 26:55429 (CONF-720901-(Bks.1 and 2), pp 195-206)

SEGRETO, Camilo, Biological dosimetry using bone marrow samples, 26:53473

SEIDEN, Joseph, Evaluation of the energy flux between two superfluid He baths separated by a thin metallic foil, 26:54434

SEKI, S., D(p,2p)n reaction at 51.8 MeV, 26:54505

SEKIDO, Y., Sidereal and solar anisotropy of high-energy cosmic rays observed by an air Cherenkov telescope, 26:53850

SEKIGUCHI, Mutsuo, Mechanism of DNA repair and recombination, 26:53350

SELIGER, Howard H., Action spectrum for photoinhibition of mechanically stimulable bioluminescence in the marine dinoflagellates gonyaulax catenella, G. actenella, and G. tamarensis, 26:55521 (COO-3277-14)

SELLIN, D. L., Electron-impact excitation cross sections and energy degradation in CO, 26:54008

SELMAN, Murray, Process for preparing alpha ammonium uranous pentafluoride, 26:53049

SELPH, W. E., Development and verification of design methods for ducts in a space nuclear shield, 26:54958 (NASA-TM-X-2440, pp 375-82)

SELVELLI, P. L., Quantitative analysis of γ Capricorni, 26:53888

SEMENCHENKO, V. K., Thermodynamic stability of non-ideal Bose--Einstein gas, 26:54432

SEMENETS, T. I., Vibronic absorption spectrum of molecular dimers, 26:55534 (ITF-72-27-P)

SEMENOV, Yu. A., Product formula for semigroups and its application to Shroedinger equation with singular potentials, 26:55069 (ITF-72-36-E)

SEMENOVA, V. I., Reflection of electromagnetic waves at the oblique incidence on the moving front of ionization, 26:54865

SEMIKOZ, V. B., Determination of heavy nuclei charges,

26:53805 (N-71-30295)
SEMIZ, D. M., High-frequency hydrodynamics near the lambda point, 26:54424
SEMLER, T., Temperature-dependent transmission and self-indication measurements upon depleted U in the unresolved region, 26:54477 (CONF-720901-(Bks.1 and 2), pp 1115-26)
SEN, S., Structure of low-lying states of odd-A In isotopes, 26:54620
SENFTLE, Frank E., Borehole activation analysis by delayed and capture gamma rays using a ^{252}Cf neutron source, 26:53174
SENJU, Hirofumi, Parton model: elastic and inelastic form factors of hadrons, 26:54311
SENKEVICH, E. L., Interaction of a multiloop electron stream with a plasma, 26:54793
SEN'KINA, M. S., Investigation of the surface of tungsten single crystals following electro-erosive treatment, 26:53668
SENZAKI, Kiyoshi, Adsorption and dissociation of CO on W surface studied by field-emission microscopy, 26:55023
SEPTIER, A., Preliminary studies on modified version of EBIS source, 26:54081 (FRNC-CONF-57)
SERAFINI, A., Heavy ion source with a confined electron beam, 26:53753 (FRNC-CONF-56)
SERDUKE, F. J. D., Inhibited transitions and isomeric states in N = 50 isotones, 26:54611
SERES, Z., Correlation of the partial radiation widths in the reaction ^{163}Dy(n,γ)^{164}Dy, 26:54631 (BNL-tr-490)
SESHAN, K., Precipitation of phosphorous in ion implanted silicon, 26:54994
SETTE, D., Surface and depth distribution damage of ions in silicon as seen with an electron microscope, 26:55003
SEYAM, Afif M., Stable uranium(IV) alkyl and aryl complexes, 26:53047
SHAH, Prakash M., Interference terms in the multiperipheral model, 26:54329 (NYO-3533-265)
SHAHINIAN, P., Effect of neutron irradiation on fatigue crack propagation in Types 304 and 316 stainless steels at high temperatures, 26:53698 (NRL-7446)
SHAKHOVETS, K. G., Microwave plasma heating in Tuman-2, 26:54758
SHANKAR, J., Determination of rate constants for reactions of H, OH, and e/sub aq/$^-$ with indole-3-acetic acid and other plant hormones, 26:53015
SHANKS, Howard R., Magnetic susceptibility of rhenium trioxide, 26:55046
SHANNON, D. W., Corrosion and deposition of irradiated stainless steel in sodium, 26:55165 (CONF-710959-, Paper 9)
  Radioactive material transport in flowing sodium systems, 26:55164 (CONF-710959-, Paper 8)
SHAPIRO, I. I., Testing general relativity: progress, problems, and prospects, 26:54403
SHAPIRO, I. S., Possible study of bound anti pn states in experiments on the annihilation of anti p on d, 26:54334
SHAPIRO, M. M., New observations and calculations of primary Be/B in the cosmic rays, 26:53833
  Revised source composition of cosmic rays from hydrogen to nickel, 26:53837
SHAPIRO, N. I., Mutagenesis in cultured mammalian cells. II, 26:53362
SHAPIRO, S., K$^+$ decay in flight, 26:54186
SHAPIRO, V. D., Interaction of finite perturbations in a beam--plasma system, 26:54795
SHARE, G. H., Observation of cosmic gamma radiation above 10 MeV, 26:53816
  Search for pulsed gamma rays from the Crab, 26:53922
SHARP, R. D., Coordinated observations of the magnetosphere: the development of a substorm, 26:54061
SHARPE, William N. Jr., Specimen strain measurement in the split Hopkinson pressure bar experiment, 26:55626 (UCRL-73610)
SHCHEBETKOVSKII, V. N., Radioisotope partition between sea water and sediments, 26:53167
SHCHEPKIN, Yu. G., Neutron resonances ^{112}Cd, 26:54599 (IAE-2116)
SHCHERBACHENKO, R. I., New features of He II film flow transfer, 26:54431
SHEA, M. A., Daily variation of electron and proton geomagnetic cutoffs calculated for Fort Churchill, Canada, 26:54065
SHEDD, W., Hardening electronic devices against very-high-total-dose radiation environments, 26:53289 (NASA-TM-X-2440, pp 481-6)
SHEETS, James R., Conversion of plutonium oxide to plutonium tetrafluoride with fluorine in a fluid bed reactor. Part II. Demonstration runs: a comparison of the fluorine process with the hydrofluorination process, 26:53039 (RFP-1890)
  Conversion of plutonium oxide to plutonium tetrafluoride with fluorine in a fluid bed reactor. Part I. Development studies, 26:53038 (RFP-1889)
SHEKHATA, L. N., Structure of the mixed state near the boundary of a semi-infinite superconductor of the second kind, 26:54448
SHEKHTER, L. Sh., Bremsstrahlung of soft photons in reaction p + p → π^+ + d + γ, 26:54250
SHELEST, V. P., DAMA and Regge asymptotic behavior, 26:54412 (ITF-72-63-E)
  Dispersion sum rules and Jost--Lehman--Dyson representation in axiomatic quantum theory, 26:54377 (ITF-72-54-P)
  Statistical view on resonance widths and multiplicity in dual models, 26:54300 (ITF-72-53-E)
SHELINE, R. K., 0$^+$ → 0$^+$ beta transition of ^{188}W, 26:54641
  Octupole deformations in the nuclei beyond ^{208}Pb, 26:54732
  Single-neutron-transfer-reaction studies of ^{176}Hf and ^{180}Hf, 26:54636
  Termination of the r-process and the synthesis of superheavy elements, 26:54663
SHELLABARGER, C. J., Radiation carcinogenesis and acute radiation mortality in the rat as produced by 2.2-GeV protons, 26:53455 (NASA-TM-X-2440, pp 647-51)
SHELLABARGER, Claire J., Lymphatic involution and early mortality in the young chicken produced by 2.2-GeV protons, 26:53457 (NASA-TM-X-2440, pp 659-64)
SHELLEY, E. G., Coordinated observations of the magnetosphere: the development of a substorm, 26:54061
  Low-energy particle radiation environment at synchronous altitude, 26:54045 (NASA-TM-X-2440, pp 530-8)
SHELMAN, C. B., Modeling the visual pathway for interactive diagnosis of visual fields, 26:55466 (ANL-7858)
SHEN, B. S. P., Accelerator measurement of the energy spectra of neutrons emitted in the interaction of 3-GeV protons with several elements, 26:54528 (NASA-TM-X-2440, pp 523-6)
SHEN, G., Neutrino mass limits from the K/sub L/^{0} → π^{+-}l$^{-+}\nu$ decay spectra, 26:54184 (LBL-4)
SHEN, Pu, Dual-amplitude analysis of two-particle productions. II, 26:54307
SHEN, Wen-wu, Magnetohydrodynamic theory for the interaction of an interplanetary double-shock ensemble with the Earth's bow shock, 26:54073
SHEPARD, J. R., (p,t) and (p,^{3}He) reactions on ^{27}Al at E/sub p/ = 27 MeV, 26:54551 (COO-535-673)
SHEPLEY, L. C., Galaxy formation in anisotropic cosmologies, 26:53980
SHERA, E. B., 0$^+$ → 0$^+$ beta transition of ^{188}W, 26:54641
  Nuclear levels in ^{188}Re, 26:54637
SHETIYA, R. S., Determination of rate constants for reactions of H, OH, and e/sub aq/$^-$ with indole-3-acetic acid and other plant hormones, 26:53015
SHEVCHENKO, V. I., Interaction of finite perturbations in a beam--plasma system, 26:54795
SHIBA, Masayoshi, Study on the works of engineering reactor-safety, 26:55204 (JAERI-M-4535)
SHIBATA, Katsuyuki, Results of cyclic pressure loading test due to JPDR pressure vessel model No. 2, 26:55228 (JAERI-Memo-4016)
SHIH, I-fu, Weak K-dominance model and bounds on K/sub l3/decay parameters, 26:54289
SHIKATA, Y., Calculation of states in ^{53}Fe, 26:54576
SHIMA, K., Isotope dependence of K-shell ionization cross sections by ^{20}Ne and ^{22}Ne bombardments, 26:54114
SHIMADA, Katsunobu, Chromosomal and histological changes in embryos exposed to 14.1 MeV fast neutrons, 26:53470
SHIMAMUNE, Hiroji, Study on the works of engineering reactor-safety, 26:55204 (JAERI-M-4535)
SHIMAZAKI, Masahide, Heat treatment, microstructure, and mechanical properties of heavy gage steels for nuclear reactor pressure vessels. I, 26:53646
SHIMIZU, Harumichi, Peroxidation of polymethylhydrogensiloxane and cellulose by γ-irradiation in air and grafting induced by their decomposition, 26:52994
SHIMIZU, Katsuya, Automodulation of ion oscillation modes in plasma, 26:54851
SHIMO, Michikuni, Measurements of thoron in the atmosphere, 26:53227
SHINODA, Wataru, Analysis of pressure wave propagation in pipe rupture accidents of light-water cooled reactors by use of the burst code. I, 26:55203 (JAERI-M-4473)
SHIOMI, T., Late effects of atomic radiation, 26:53414
SHIRAFUJI, Tadahiko, Lower bound for CP-nonconservation in the K/sub LS/^{0} decay into $\mu^+\mu^-$, 26:54369
SHIRAI, E., Fission product release in TLG-1 in-pile gas loop. III, 26:53694 (JAERI-Memo-3936)
SHIROKOV, M. F., Relativistic gravitational effect on influence of earth rotation on mechanical vibrations, 26:54400 (ITF-72-59-P)
SHIRVAIKAR, V. V., Micrometeorological studies for air pollution control in atomic energy, 26:53154 (INIS-mf-160, pp 22-52)
SHISHKIN, A. A., Influence of toroidality on a magnetic configuration with a helical magnetic axis, 26:54832
  Plasma equilibrium in configurations with a helical magnetic axis with allowance for toroidality, 26:54815
SHLIMAK, I. S., Fast-neutron-compensated n-germanium as a model of amorphous semiconductors, 26:54981
SHNEERSON, V. L., Superconductivity in semiconductors, 26:54449
SHNIDMAN, R., Observation of temperature spikes following Coulomb excitation, 26:54646
SHOSTAK, G. S., Gross properties of five Scd galaxies as determined from 21-centimeter observations, 26:53972
SHOSTAK, Gerson Seth, Aperture synthesis observations of neutral hydrogen in three galaxies, 26:53971
SHPATAKOVSKAYA, G. V., Atomic structure oscillation

effects, 26:54151
SHREVE, D. C., Parametric fit to electron-transport properties, 26:54963 (NASA-TM-X-2440, pp 832-41)
SHROFF, A. M., Recent development in CVD W and Mo, 26:53622
SHRUM, Edgar Vaughan, Measurement of the muon energy in the decay $\pi^+ \to \mu^+ + \nu$, 26:54189
SHUBA, I. M., Wightman axioms for concentratable field and reconstruction theorem. I, 26:54378 (ITF-72-62-E)
SHUBIN, V. N., Kinetics of the hydrated electron disappearance in concentrated aqueous alkali solutions, 26:53018
SHUKOVSKY, Leonard J., Retinal and optic nerve complications in a high dose irradiation technique of ethmoid sinus and nasal cavity, 26:53444
SHULEK, P., Vavilov--Cherenkov ''needle'' radiation in Rochelle salt crystal, 26:54875 (JINR-P1-6552)
SHULMAN, Herman, High-resolution semiconductor detector for applications in space, 26:53202 (NASA-TM-X-2440, pp 723-8)
SHUL'TS, G., One-nucleon transfer reactions to quasi-intersecting levels, 26:54635 (JINR-P4-6509)
SHUMOVSKII, A. S., Some exactly solvable model problem with positive interaction, 26:54435 (ITF-72-56-E)
SHURYGHIN, A. I., New measurements of the polarization of x-ray solar flares, 26:53962
SHVILKIN, B. N., Low-frequency oscillations in the weakly ionized plasma of a high-frequency discharge in a magnetic field, 26:54849
SIART, O., Field distribution, power losses, and parameter optimization of helical accelerator structures, 26:53744
SIBIRKINA, T. N., Relativistic corrections in heavy atoms, 26:54147
SICARD, B., Reactor physics and fast power breeders: MASURCA core R-Z program, 26:55118 (CONF-720901-(Bks.1 and 2), pp 822-38)
SIDEBOTHAM, E. W., Spectra of energy released by thermal neutron capture, 26:55444 (TRG-2189)
SIDES, W. H. Jr., Study of reactivity balance during startup of the HFIR, 26:55407 (ORNL-TM-3769)
SIDIS, V., Some energy curves of ArH^+ and their use in study of scattering of H^+ by Ar, 26:54120
SIEGEL, G., State and tendencies of chemical protection against ionizing radiation. A literature survey 1970/71, 26:53460 (SZS-132)
SIEREN, G. J., Nuclear applications in manned space station, 26:53094 (NASA-TM-X-2440, pp 26-33)
SIEVERS, A. J., Experimental evidence for exchange polarization in superexchange interactions, 26:55510 (COO-3151-6)
  Far infrared surface resistance of Cu:Fe; dynamics of a Kondo system, 26:55508 (COO-3151-4)
  Hydrostatic pressure study of the AFMR in $FeCl_2$, 26:55509 (COO-3151-5)
SIEVERS, W. L., Spectroscopy of ^{101}Mo by sub-Coulomb stripping, 26:54614
SIGNORINI, C., $4^+ \to 0^+$ cross-over transition in ^{204}Pb, 26:54647
SILAEV, E. A., Possible measuring high-energy electron energy by ionization detectors of total absorption on basis of condensed xenon, 26:53272 (JINR-P13-6541)
SILBERBERG, R., Calculations of cross sections and their application to cosmic-ray physics, 26:53845
  New observations and calculations of primary Be/B in the cosmic rays, 26:53833
  Revised source composition of cosmic rays from hydrogen to nickel, 26:53837
SILLI, Elena, Effect of seed irradiation on bean plants, 26:53387
SILVA, R. J., Elastic and inelastic scattering of 12-MeV protons from ^{92}Mo, ^{94}Mo, ^{96}Mo, and ^{100}Mo: tabulated differential cross sections, 26:54606 (ORNL-TM-3913)
SILVER, Brian L., H_3O radical, 26:53026
SILVERBERG, R. F., Primary cosmic ray electron spectrum from 10 GeV to about 200 GeV, 26:53823
SILVERMAN, Charlotte, Evaluation of epidemiologic studies of leukemia and other malignancies after diagnostic x radiation, 26:53435
SIMENOG, I. V., Asymptotically exact solutions for the systems with singular potentials, 26:55068 (ITF-72-31-P)
  Stability of systems with singular potentials, 26:54408 (ITF-72-14-E)
SIMON, Albert, Annual progress report, 26:54807 (COO-3497-2)
SIMON, W. G., Analyzing powers in the ^{3}He(d Vector,p)^{4}He reaction at energies less than 1.0 MeV, 26:54500 (LA-DC-72-906)
  Preliminary measurements of polarization transfer in ^{4}He(d Vector,d Vector)^{4}He elastic scattering, 26:54498 (LA-DC-72-904)
SIMONEN, E. P., Edgewise growth kinetics of Widmanstaetten precipitates, 26:55528 (IS-2838)
SIMONEN, Thomas C., Dynamic stabilizer for plasma instabilities to improve plasma confinement and to increase plasma density, 26:54823
SIMONS, G. G., Boron and tantalum control rod studies and absolute gamma ray absorbed doses in a LMFBR critical, 26:55134 (CONF-720901-(Bks.1 and 2), pp 579-98)
SIMON-VERMOT, A., Pulmonary lavage, therapy of pulmonary contaminations, 26:53528 (LF-tr-71)
SIMON-WEIDNER, J., Calculation of the time dependent fission product heat source strength in two coupled systems with consideration of fission product escape, 26:55206 (KFK-1580)
SIMPSON, J. A., Abundances of the galactic nuclei H through the Fe group from satellite measurements, 26:53836
  Energy dependence of the abundances of galactic He, L, and M nuclei from satellite measurements, 26:53835
SIMPSON, K. A., Examination of irradiated UO_2 HTR fuel particles. Part I. Experimental techniques, 26:53555 (RD/B/N-2214)
SIMPSON, O. D., Automated Cross Section Analysis Program (ACSAP), 26:54468 (ANCR-1042)
SINGER, P., Weak radiative decays of K mesons, 26:54365
SINGH, J., Elastic and inelastic scattering of 12 MeV polarized deuterons by ^{24}Mg, 26:54557
SINGH, K. P., Positron lifetimes and phase transitions in solids, 26:55064
SINGRU, R. M., Positron lifetimes and phase transitions in solids, 26:55064
SINHA, Devendra Prasad, Atomic positions in thorium silicate: an x-ray-diffraction study, 26:55038
SINNIS, J., Pseudoclassical and anomalous containment in FM-1, 26:54753 (CONF-720804-5)
SISAKYAN, A. N., Multiple charged particle production in π^-p and π^-n interactions at p = 40 GeV/c, 26:54327 (JINR-E2-6596)
SISTERSON, L. K., Reaction $\pi^-p \to p\pi^+\pi^-\pi^-\pi^0$ at 20 GeV/c, 26:54207 (COO-3064-3)
SITENKO, A. G., High-energy approximation and generalized Huygen's principle, 26:54690 (ITF-72-57-P)
SIZONENKO, V. L., Linear theory of current-driven plasma instabilities, 26:54810
SIZUKHIN, O. V., Generation of fast electrons through interaction of SHF wave with collisionless plasma, 26:54836 (AEC-tr-7331)
SJOEDEN, A.-M., Dose rate dependence in the goitrogen stimulated mouse thyroid, 26:53472
SKLAD, P., Experiments in high-voltage electron microscopy. Progress report, October 31, 1972--July 31, 1973, 26:54972 (COO-2119-2)
SKOBOV, V. G., Doppler-shifted cyclotron resonance in cadmium, 26:55044
SKOGMO, D. G., DIAMOND: a new approach to microelectronic circuit design (dielectrically isolated arrays of monolithic devices), 26:53309 (SC-DC-721162)
  Universal digital integrated circuit, 26:53308 (SC-DC-721161)
SLAMENOVA, D., Influence of amino acid starvation on the uv reversibility of the strains of E. coli, 26:53379
SLATKIN, Montgomery, Study of mathematical models of mutation and selection in multi-locus systems. Annual progress report, December 1, 1971--November 30, 1972, 26:55487 (COO-1437-8)
SLEPZOV, V. M., Production of formed bodies from high-melting compounds according to the casting procedure for thermoplastic masses, 26:53586
SLJIVIC, V., Acute effects of ionizing radiation on antibody-producing cells (PFC) in mouse spleen during primary and secondary responses to sheep erythrocytes (SRC), 26:53464
SLOAN, I. H., Exact calculations of N--d polarization, 26:54509
SLOANE, Thompson M., Dependence of reactivity on internal and translational energy in K + SF_6, CCl_4, and $SnCl_4$, 26:54136
SLOWIKOWSKA, Maria G., Studies of chromosome aberrations in peripheral blood of roentgenologists, 26:53428
SMART, D. F., Daily variation of electron and proton geomagnetic cutoffs calculated for Fort Churchill, Canada, 26:54065
SMIDT, F. A. Jr., Effect of residual elements on radiation strengthening in iron alloys, pressure vessel steels, and welds, 26:53710
SMIRNOV, V. A., Effect of the magnetic field on a closed-electron-drift accelerator, 26:53743
SMIRNOV, V. P., Behavior of large-current electron beam in a dense gas, 26:54763
SMIRNOV, V. V., Monte Carlo investigations of catastrophic collisions with characteristics of scattered electron radiation taken into account, 26:54898
SMIRNOV, Yu. F., High-energy limit for α-d and tau--t form factors in ^{6}Li nucleus, 26:54532
SMITH, A. B., Fast neutron data, diagnosis and prognosis, 26:54476 (CONF-720901-(Bks.1 and 2), pp 1063-74)
SMITH, A. J. S., Forward muons and muon pairs at ISABELLE, 26:54181 (BNL-16977)
SMITH, A. N., Experience with sodium fluoroborate circulation in an MSRE-scale facility, 26:55177 (ORNL-TM-3344)
SMITH, Andrew M., Interstellar lines in the ultraviolet spectrum of zeta Ophiuchi, 26:53875
SMITH, B. J., Computer calculations of sheet resistance of n- and p-type implantations in silicon, 26:54986
SMITH, C. A., Ignition of liquid metal: peroxide mixtures, 26:55178 (RD/B/N-2364)
SMITH, C. B., Photon-induced secondary electron emission, 26:54885 (NASA-TM-X-2440, pp 792-800)
SMITH, D., Lifetimes of fast recombination luminescence transitions in alkali halides, 26:55000
SMITH, D. L., Diffusion in dilute bismuth--mercury and

lead--mercury systems, 26:53636 (IS-T-554)
SMITH, Dean F., Current limitation in solar flares, 26:53937
SMITH, Donald, Application of Moffat's model to eta $\to 3\pi$ and K $\to 3\pi$ decays, 26:54276
  eta $\to 3\pi$ decays in a model satisfying analyticity, crossing symmetry, and approximate unitarity, 26:54259
SMITH, Elske P., Characteristics of Ca II K-line profiles in quiet Sun, 26:53948
SMITH, F. J., Mutual interactions of Th, lanthanides, and Bi in Th--Ln--Bi solutions, 26:53664
SMITH, Frank A., Direct determination of total ionic fluoride in biological fluids, 26:55637 (UR-3490-184)
SMITH, H. H., Effect of neutron irradiation on fatigue crack propagation in Types 304 and 316 stainless steels at high temperatures, 26:53698 (NRL-7446)
SMITH, H. T., SNAP-8 post-shutdown gamma-radiation approximations, 26:55360 (NASA-TM-X-2440, pp 84-91)
SMITH, H. Vernon Jr., Isospin-forbidden and allowed ^{12}C(d,α)^{10}B cross sections, 26:54539
SMITH, Harold P. Jr., Full-range solution for the measurement of thin-film surface densities with proton-excited x rays, 26:52945
SMITH, J., Low-energy theorem for $\gamma\gamma \to 3\pi$ and the reaction $\gamma + Z \to 3\pi + Z$, 26:54252
SMITH, J. Dungan, Columbia River effects in the Northeast Pacific: physical studies. Progress report, June 1971--June 1972, 26:53165 (RLO-2225-T-25-6)
SMITH, J. R., Automated Cross Section Analysis Program (ACSAP), 26:54468 (ANCR-1042)
SMITH, J. S., Properties of 1300 kg P/M TZM billet, 26:53673
SMITH, James G., FIND: Watts Bar Nuclear Plant, Units 1 and 2, 26:55213 (FIND-50390(8-72))
SMITH, L. H., Measurement of the primary cosmic ray nuclear rigidity spectra for individual elements of charge Z greater than or equal to 2, 26:53826
SMITH, Richard L., Relaxation oscillations in the envelopes of luminous red giants, 26:53874
SMITH, Roy A., Method of making a nuclear reactor fuel element of uranium mononitride in a refractory metal matrix, 26:53562
SMITH, Temple, Metrics in biology, an introduction, 26:55546 (LA-4973)
SMITH, W. I. B., Measurement of the electron density distribution in plasmas from the bending of a gas laser beam, 26:54769
SMITH, Wayne E., Crosslinked nylon by irradiation of a graft copolymer of nylon with an ethylene/acrylate or modified copolymer, 26:53013
SMITH, Wesley D., Near-resonant vibration--rotation energy transfer in atom--diatom collisions: Ar--OH($A^2\Sigma^+$), 26:54126
SMITH, Zdenka K., Pioneer 7 observations of Aug. 29, 1966, interplanetary shock-wave ensemble, 26:54068
SMITHSON, Robert Carroll, Videomagnetograph study of diffusion of solar magnetic fields in weak-plage regions, 26:53933
SMIYAN, O. D., Chemical reaction rate under the influence of a high-energy electron beam, 26:53718
SMOOT, G., Measurement of the primary cosmic ray nuclear rigidity spectra for individual elements of charge Z greater than or equal to 2, 26:53826
SMYTHE, J. W., High density P/M components for elevated temperature applications, 26:53631
SNAVELY, David R., Applications of radiation protection recommendations in the development of federal radiation standards for electronic products, 26:54925
SNIDER, J. W., Estimate of the process decontamination factors required to meet federal effluent regulations for the burning of HTGR fuel elements, 26:53060 (CONF-720823-14)
SNOW, Donald L., Applications of radiation protection recommendations in the development of federal radiation standards for electronic products, 26:54925
SNYDER, R. P., Explosion-induced fractures of selected announced underground nuclear tests, Yucca Flat, Nevada Test Site, Nevada, January 1971--December 1971, 26:53133 (USGS-474-155)
SOBEL, M. I., p--p bremsstrahlung calculations and relativistic spin corrections, 26:54267
SOBELS, F. H., Effects of treating Drosophila females with Actinomycin-D on the yields of dominant lethals, translocations, and recessive lethals recovered from x-irradiated spermatozoa, 26:53502
SOBKOWSKI, Jerzy, Formation of acetylene and methane in argon and xenon sensitized radiolysis of gaseous ethylene, 26:53000
SOBOLEVSKII, N. M., Buildup of cosmic isotopes in iron meteorites, 26:53808 (ORNL-tr-2620)
SOBOTTKA, S. E., Bifilar helical multiwire proportional chamber for position sensitive detection of minimum ionizing particles, 26:53273 (LA-4968)
SOCOLOW, Robert H., Energy, 26:53193
  Patient earth, 26:53191
  Radiation, 26:53396
SOFFA, William A., Prog. rpt. on precipitation from supersaturated copper--titanium solid solutions: the aging process and precipitation hardening in copper--titanium sideband alloys, annual, 1971--1972, 26:55615 (TID-26148)
SOFFER, L., Preliminary shield design for a SNAP-8 power system, 26:54948 (NASA-TM-X-2440, pp 78-83)
SOL, C., Direct measurement of diffusion cooling in an afterglow plasma, 26:54786
SOLANA, J., Theory of the roton lifetime in superfluid helium, 26:54429
SOLDATOV, E. D., Thermodynamic stability of non-ideal Bose--Einstein gas, 26:54432
SOLER-GOMEZ, A. J. R., Influence of O, C, and B on sintering and stress rupture properties of sintered Ni-base superalloys, 26:53674
SOLODOVNIKOVA, E. P., N. N. Bogoliubov's transformation in strong coupling theory. III, 26:54383
SOLOVEV, S. P., X-ray and dielectric studies of irradiated perovskite type compounds, 26:55020
SOLOV'EV, V. G., Effect of changes in equilibrium deformations of the excited states of odd-A deformed nuclei on their energy and structure, 26:54640
SOLUNIN, A. M., External invariant equations of electromagnetic field, 26:54373 (ITF-72-35-P)
SOMON, J. P., Thermonuclear hot spot, 26:54831
SONDHAUS, C. A., Use of quality factors and fluence to dose-rate conversion in human radiation exposures, 26:53404 (NASA-TM-X-2440, pp 424-34)
SONNENBERG, K., Recovery of electron-irradiated Pt. I, 26:55010
  Recovery of electron-irradiated. II, 26:55011
SOOD, P. M., Analysis of 20 GeV proton--nuclei scattering, 26:54530
SOPER, J. M., Shell-model analysis of Λ binding energies for the p-shell hypernuclei. II. Numerical fitting, interpretation, and hypernuclear predictions, 26:54351
SORAN, P. D., Carbon shielding benchmark problem and other neutron transport calculations in carbon, 26:54939 (CONF-720901-(Bks.1 and 2), pp 397-408)
SORDAT, B., Intestinal barrier to bacterial invasion, 26:55474 (BNL-17004)
SOTNIKOV, S. K., Correlation of the partial radiation widths in the reaction ^{163}Dy(n,γ)^{164}Dy, 26:54631 (BNL-tr-490)
SOUSSALINE, F., Reading, automatic treatment, and visual display of radioactivity spectra recorded on punched tape, 26:53544
SOUSTELLE, Michel, Elementary mechanisms in heterogeneous kinetics. IV, 26:55588 (ORNL-tr-2394)
SOUTHWORTH, H. N., Interpretation of alloy images, 26:53655
SPALDING, J. F., Effect of continuous gamma-ray exposure on performance of learned tasks and effect of subsequent fractionated exposures on blood-forming tissue, 26:53452 (NASA-TM-X-2440, pp 633-40)
SPALEK, G., Four-nucleon studies. I, 26:54516
SPARROW, Arnold H., Radiobiologic studies of Tradescantia plants orbited in Biosatellite 2, 26:53382 (N-72-20054)
SPECHT, H. J., Identification of rotational band in ^{240}Pu fission isomer, 26:54664
SPEIDEL, Edward O., Method of making a nuclear reactor fuel element of uranium mononitride in a refractory metal matrix, 26:53562
SPEKTOR, A. M., Behavior of large-current electron beam in a dense gas, 26:54763
SPENCER, James E., High resolution proton spectrometer (HRS), 26:53791 (LA-4874, pp 67-71)
SPENCER, R. B., Photon-induced secondary electron emission, 26:54885 (NASA-TM-X-2440, pp 792-800)
SPENKE, H., Fast breeder reactor, 26:55129
SPICER, W. E., Comparison of the oxidation process in strontium and cerium by ultraviolet photoelectron spectroscopy, 26:53611
SPIGARELLI, S. A., Acoustic location techniques to study the distribution of fish in the vicinity of a thermal plume, 26:53186 (ANL-7860(Pt.3), pp 121-30)
  Ecological studies at Point Beach Nuclear Power Station and Big Rock Point Nuclear Power Station: introduction, 26:53182 (ANL-7860(Pt.3), pp 101-2)
  Effects of a thermal discharge on the inshore biological communities of Lake Michigan, 26:53184 (ANL-7860(Pt.3), pp 109-17)
  Measurement of major nutrients and water quality parameters at Point Beach: 1971, 26:53183 (ANL-7860(Pt.3), pp 103-8)
SPINULESCU, I., Influence of electron irradiation on CdS thin films, 26:54992
SPITZ, A. L., Auroral photometric observations at geomagnetically conjugate points, 26:54013
SPRAGUE, E. D., ESR studies of aliphatic radical anions and radical-anion pairs in γ-irradiated crystalline solids, 26:52991 (ORO-2968-78, Paper 6)
SPRETNAK, Joseph W., Basis for design on allowable plastic strain, 26:55500 (COO-2048-7)
SQUASSABIA, A., DNA, RNA, and ultrastructural aspects of human epidermis in chronic reactions of skin after roentgen irradiation, 26:53441
SREBRO, Z., Diurnal rhythm of neurosecretory activity in normal and x-ray irradiated mice, 26:53478
SRINIVASAN, B., Xenon isotopes in tellurobismuthite, Boliden, Sweden, 26:53176
SRINIVASAN, K. R., Physics design of heavy water moderated reactors, 26:55100 (BARC/I-148)
SRIVASTAVA, O. N., Observation of dislocation loops in gadolinium thin single crystal, 26:54979

SRIVASTAVA, Ramakant, Raman scattering in the semiconducting and metallic phases of VO_2, 26:55043
SRIVASTVA, M. M., Observation of dislocation loops in gadolinium thin single crystal, 26:54979
STACEY, W. M. Jr., Studies of methods for fast neutron multigroup cross section generation and their effect upon the neutronics properties of LMFBR critical assemblies, 26:55113 (CONF-720901-(Bks.1 and 2), pp 211-28)
STACEY, Weston M. Jr., Advances in neutron continuous slowing-down theory, 26:54472 (CONF-720901-(Bks.1 and 2), pp 143-61)
STACKLER, B., Influence of linear energy transfer on the radioresistance of budding haploid yeast cells, 26:53368
STAGAT, R. W., Electron deposition in water vapor, with atmospheric applications, 26:54033
STAGNI, L., Surface and depth distribution damage of ions in silicon as seen with an electron microscope, 26:55003
STAKHANOV, I. P., Dissipative instability due to supersonic motion of ions with respect to neutrals, 26:54812
STAMMBACH, Th., Four-nucleon studies. I, 26:54516
STANDIFER, Richard L., Conversion of plutonium oxide to plutonium tetrafluoride with fluorine in a fluid bed reactor. Part II. Demonstration runs: a comparison of the fluorine process with the hydrofluorination process, 26:53039 (RFP-1890)
Conversion of plutonium oxide to plutonium tetrafluoride with fluorine in a fluid bed reactor. Part I. Development studies, 26:53038 (RFP-1889)
STANILAND, R. J., Zero energy reactor facility at B.N.L., 1972, 26:55409 (RD/B/N-2272)
STANKO, N., Low-energy theorem for $\gamma\gamma \to 3\pi$ and the reaction $\gamma + Z \to 3\pi + Z$, 26:54252
STANSBARGER, D. L., Cocuring advanced composite materials, 26:53570
STANYUKOVICH, K. P., Relations between the cosmological and quantum constants, 26:54392 (ITF-72-3-P)
STARCHMAN, Dale E., Perturbation of isodose distributions adjacent to cavities in tissue-equivalent media during irradiation by 10 to 35 MeV electrons, 26:54903
STARGARDTER, Hans, Blade development in the advanced composite engine (ACE) program, 26:53575
STARKOVICH, V. S., Probe velocity transducer, 26:53303 (LA-4999)
STASTNY, Miroslav, Some basic experimental methods of wet-steam flow investigation, 26:53124
STAUDE, Juergen, Mean depth of line formation in a magnetic field, 26:53944
STAVISSKII, Yu. Ya., Measurements of neutron cross sections of radiation capture and fission for some heavy nuclei by the method of time of retardation in lead, 26:54657 (FEI-292)
STEEB, Siegfried, Diffusion measurements in systems Pd-V and Pd--Ti as well as metal--ceramic systems by means of microprobe, 26:53677
STEELE, Susan G., Explosion-induced fractures of selected announced underground nuclear tests, Yucca Flat, Nevada Test Site, Nevada, January 1971--December 1971, 26:53133 (USGS-474-155)
STEFFEN, R. M., Multipole mixing ratios of γ-transitions in ^{185}Re, 26:54644
STEGER, P. J., Practical design considerations for the application of gas bearings to machining processes, 26:53113 (Y-DA-4541(Rev.1))
STEIGERWALD, E. A., Plane strain fracture toughness of some cryogenic materials at room and subzero temperatures, 26:53661
STEIGERWALT, John E., Fluctuations in energy loss and their implications for dosimetry and radiobiology, 26:54879 (NASA-TM-X-2440, pp 157-61)
STEIN, C., Low strain tensile behavior of U--7.5 wt. pct Nb--2.5 wt. pct Zr, 26:53691
STEIN, M. L., Metrics in biology, an introduction, 26:55546 (LA-4973)
STEINBERG, Meyer, Concrete-polymer composite materials development, 26:55473 (BNL-16609)
STEINEGGER, A., Production of Ca and Ge ions in a PIG source, 26:53752 (FRNC-CONF-54)
STEINHEIL, E., Thermodynamic description of the metal-rich region in the system niobium--molybdenum--nitrogen, 26:53671
STEINNES, E., Resonance activation integrals of some nuclides of interest in neutron activation analysis, 26:54585
Routine determinations of traces of cobalt in soil and plant tissue by instrumental neutron activation analysis, 26:52904
STENBERG, C. G., Studies of methods for fast neutron multigroup cross section generation and their effect upon the neutronics properties of LMFBR critical assemblies, 26:55113 (CONF-720901-(Bks.1 and 2), pp 211-28)
STENGER, V., Production and testing of homogeneous sterilization dose during radiosterilization, 26:53340
STEPANOV, A. I., Use of mutagenic agents for breeding of Eremothecium ashbyii, 26:53374
STEPANOV, K. N., Extraordinary electromagnetic wave absorption in the linear plasma layer in the hybrid resonance region, 26:54864
Linear theory of current-driven plasma instabilities, 26:54810
STEPHANI, E. L., Probe velocity transducer, 26:53303 (LA-4999)
STEPHEN, J., Computer calculations of sheet resistance of n- and p-type implantations in silicon, 26:54986
STEPHENS, H. P., Passive calorimeter for pulsed electron beam energy measurement, 26:53258 (SC-DR-720630)
STEPHENS, Joseph R., Exploratory investigation of Y, La, and Hf coatings for nitridation protection of chromium alloys, 26:53689
STEPHENS, L. D., High reliability environmental radiation monitoring and evaluating system, 26:53199 (LBL-585)
STEPHENSON, G. J. Jr., (p,2p) reactions with divers potentials. Technical Report No. 73-002, 26:54699 (ORO-4317-11)
Sensitivity of low-energy 3-body properties to the off-shell 2-body t-matrix. Technical Report No. 72-121, 26:54697 (ORO-4317-7)
STEPPER, Heinz-J., Recrystallization of α particle irradiated tungsten, 26:53711
STERNBERG, J. R., Observations of the airglow continuum, 26:54025
Photochemistry of the airglow continuum, 26:54024
STERNHEIM, M. M., Elastic pion--nucleus scattering for studies of the nuclear surface, 26:54722
STEVENS, D. E., Speed of magnetic-flux penetration into electrical conductors, 26:54453
STEVENS, J., Linearity, time domain reflectometer, and Fourier analysis studies of an evacuated Compton detector, 26:53197 (EGG-1183-2277)
STEVENS, J. C., X-ray and optical observations of Sco X-1 and observations of the x-ray background, 26:53918
STEVENS, W. N. R., Direct fitting of spin wave energies to interatomic exchange parameters in the ferromagnetic rare earth metals, 26:55053
STEVENSON, M. L., Conceptual design of a hybrid detector for electron physics at ISABELLE and PEP: solenoid + quantameter + hadrometer (calorimeter), 26:53268 (BNL-17066)
Muon identification using multiwire proportional chambers, 26:53282
STEVENSON, R., Heat transfer to boiling helium from aluminium surfaces, 26:54465
STEWART, Alice, Evaluation of epidemiologic studies of leukemia and other malignancies after diagnostic x radiation, 26:53435
STEWART, G. W., Hydride ion transfer and isotope effects in CD_4--silane ion molecule reactions, 26:52961
STEWART, J. W., Simultaneous line over-relaxation (SLOR) in hexagonal lattice, 26:55433 (CONF-720901-(Bks.1 and 2), pp 253-65)
STEWART, John M., Perturbations in an expanding universe of free particles, 26:53997
STEWART, L., Sensitivity of calculated pulsed sphere spectra and neutron age to carbon cross sections, 26:54474 (CONF-720901-(Bks.1 and 2), pp 409-17)
STEWART, M. L., Independent test of the Argonne model for tritium movement in soil, 26:53163 (ANL-7860(Pt.3), pp 32-7)
Tritiated water recovery system, 26:53151 (ANL-7860(Pt.3), pp 46-50)
STEWART, R. J. J., Photoneutron cross sections of ^{139}La and ^{141}Pr, 26:54629
STEWART, S. L., GE nuclear design and benchmark critical experiment plan for the LMFBR demonstration plant, 26:55114 (CONF-720901-(Bks.1 and 2), pp 724-38)
STEYAERT, J., Heavy ion acceleration at the Berkeley 88-Inch Cyclotron, 26:53755 (LBL-644)
STICKLER, R., Creep behavior of fine wires of powder-metallurgical pure, doped, and thoriated W, 26:53683
STIEFELD, B., Using BASIC as a real time executive on a small system, 26:55607 (SC-R-722879)
STILL, Edwin T., Factors modifying the response of large animals to low-intensity radiation exposure, 26:53451 (NASA-TM-X-2440, pp 622-32)
STINE, J., Theory of semiclassical transition probabilities for inelastic and reactive collisions. IV, 26:54129
STIRN, R. C., Rod drop accident analysis for large boiling water reactors, 26:55353 (NEDO-10527)
STOCKHAUSEN, J., Technique for the visualization of heavy metals in fuel elements for high tempeature reactors, 26:53599
STOCKMANN, M. I., Phenomenological description of the nuclear rotational states, 26:54712
STOKES, T. R., Dosimetry for radiobiological studies of the human hematopoietic system, 26:53406 (NASA-TM-X-2440, pp 974-80)
Multifactorial analysis of human blood cell responses to clinical total-body irradiation, 26:53400 (NASA-TM-X-2440, pp 233-7)
STOLETOV, G. D., System of wire spark chambers with ferrite core memory, 26:53271 (JINR-P13-6522)
STONE, W. A., Climatography of the Hanford area, 26:55478 (BNWL-1605)
STORY, J. D., Seasonal alterations in rodent blood, 26:55587 (ORNL-TM-3898)
STOVALL, Marilyn, Atlas of radiation dose distributions. IV, 26:53409 (STI/PUB-295(Vol.4))
STRAIN, W. H., Hair radioactivity as a measure of exposure to radioisotopes, 26:53529 (NASA-TM-X-2440, pp 982-8)
STRAKER, E. A., Integral experiments and philosophy of

benchmark calculations, 26:54937 (CONF-720901-(Bks.1 and 2), pp 349-84)

Investigation of the adequacy of nitrogen cross-section sets: comparison of neutron and secondary gamma-ray transport calculations with integral experiments, 26:54485 (ORNL-TM-3768)

STRAND, R. C., Large aperture spectrometer magnet for the ISA and the possible use of visual detectors, 26:53779 (BNL-17142)

STRATDHEE, J., CP-violating gauge interactions, 26:54367

STRATTON, W. R., Reactor power transient studies, 26:55441 (LA-DC-72-660)

STRAUB, R. F., Radiation carcinogenesis and acute radiation mortality in the rat as produced by 2.2-GeV protons, 26:53455 (NASA-TM-X-2440, pp 647-51)

STRAVASNIK, L. F., Special tests for plutonium shipping containers 6M, SP5795, and L-10, 26:53736 (SC-DR-720597)

STRELINA, A. V., Respiration and structural changes of mitochondria of intestinal epithelial cells in the course of amino acid absorption in irradiated animals, 26:53493

STREL'TSOV, V. N., Trouton--Noble experiment, 26:55540 (JINR-P2-6532)

STRICKLAND, D. J., Electron energy deposition in CO$_2$, 26:54009

STRONGIN, M., Surface condition of niobium for superconducting rf cavities, 26:53748

STROVINK, Mark, Forward muons and muon pairs at ISABELLE, 26:54181 (BNL-16977)

STRUCZINSKI, W., Limiting distributions for inclusive charged pion production at very high energy, 26:54326 (DESY-72/40)

STRUMINSKII, B. V., Applications of the statistical mechanics methods in a dual model, 26:54299 (ITF-72-49-P)

Two-particle distributions in dual resonance model, 26:54301 (ITF-72-55-P)

STUBBE, P., Electron energy transfer rates in the ionosphere, 26:54022

STUBBS, R. J., General properties of the current-limited spark chamber, 26:53283

SU, H. Y., Hot atom reactions in the HBr--Br$_2$, DBr--Br$_2$ systems, 26:52962

SUAYA, R., Evaluation of the J = 0 fixed pole in neutron Compton scattering, 26:54254

SUBRAMANIAN, Carole, Metabolism of 1-^{14}C palmitic acid in the developing brain: persistence of radioactivity in the carboxyl carbon, 26:55620 (UCLA-12-871)

SUGIER, Henryk, Influence of water vapor on γ-radiolysis of crystalline KI, 26:53017

Isotopic exchange between solid silver iodide and iodine in p-cymene solution, 26:52974

SUGIHARA, T. T., Levels in ^{186}Os as populated by the decay of ^{186}Ir, 26:54633 (COO-3255-3)

SUH, Paul K., Equilibrium energy spectrum for the galactic cosmic electrons, 26:53809

SUKEGAWA, Tomohide, Operation report on low temperature fissiochemical loop (JTFL). I, 26:55400 (JAERI-M-4630)

SULEK, P., Monochromatic method for measuring 665 MeV mean proton energy by using Vavilov--Cherenkov radiation, 26:53800

SULSONA, Herman, Study of stress corrosion cracking of U--10 percent Mo wires, 26:53610

SULTANOV, N. V., Elementary solutions of the neutron transport equation, 26:54492

SUMMERS, Hugh P., Density dependent ionization balance of C, O, and Ne in the solar atmosphere, 26:53969

SUMMERS, W. R., Polarization properties of Pc 1 micropulsations at low latitudes, 26:54021

SUNDARARAMAN, V., Dose across a plane bone--tissue interface, 26:54896

SUSKI, J., Similarities of ionization effects and annealing in P-type and converted N-type Ge irradiated with electrons at 85^{0}K, 26:54997

SUSKI, Jan, Charge state of defects in Ge converted into p-type by 1 MeV electrons, 26:55013

SUSKOV, I. I., Chromosome aberrations induced in human bone-marrow cells by therapeutical local γ irradiation: time and dose relationships, 26:53445

SUSLOV, Yu. P., Beta processes, 26:54740

SUSS, J. T., Thermally stimulated currents and thermoluminescence of paramagnetic centers in hexagonal boron nitride, 26:55015

SUVOROV, E. V., Synchrotron instability for plasma waves, 26:54820

SUZUKI, Komei, Results of cyclic pressure loading test due to JPDR pressure vessel model No. 2, 26:55228 (JAERI-Memo-4016)

SUZUKI, S., Optical 4d → 4f transition and binding energy of 4d level in La and Ce, 26:54095

SVENNE, J. P., How good is the Hartree--Fock approximation for ^{16}O, 26:54524 (COO-2171-14)

SWANSON, H., Lifetime of the first excited state in ^{96}Zr, 26:54622

SWEET, C. A., ORCOST: a computer code for summary capital cost estimates of steam-electric power plants. User's manual, 26:55265 (ORNL-TM-3743)

SWEIGART, A. V., Effects of semiconvection on the horizontal-branch, 26:53885

SWIATECKI, W. J., Common features and differences between fission and heavy ion physics, 26:54694 (LBL-972)

SWINGS, J. P., Infrared photometry of northern Wolf--Rayet stars, 26:53889

SWINSON, Derek B., Interpretation of sidereal cosmic ray anisotropies, 26:53847

SYNDER, R., Z-expansion coefficients and the number of electrons, 26:54149

SZABO, L., Correlation of the partial radiation widths in the reaction ^{163}Dy(n,γ)^{164}Dy, 26:54631 (BNL-tr-490)

Light-intensity dependence of the multiphoton ionization probability in the resonance case, 26:54094

SZAMOSI, G., Scalar--tensor cosmology and the classical tests, 26:53998

SZE, N. H., Critical divergence of thermal resistivity at Neel point of Eu, 26:55049

SZE, S. M., Carrier transport and storage effects in Au ion implanted SiO$_2$ structures, 26:53314

SZEGSZARDY, T., Observations on the combined radioprotective effect of pantothenic acid and aminoethylisothiuronium, 26:53481

SZOKE, J., Computer analysis of spectra by deconvolution, 26:53055

SZORADY, I., Observations on the combined radioprotective effect of pantothenic acid and aminoethylisothiuronium, 26:53481

SZYMANSKI, Z., Description of the band structure at high angular momenta in rotating nuclei, 26:54733

SZYMCZYK, Wieslawa, Dosimetric properties of some thermoluminescent substances, 26:53245

T

TABACHENKO, A. N., Low-energy πN scattering in a current algebra model with physical pions, 26:54339

TABAKIN, Frank, Relativistic nuclear matter calculations and the deficiency of one-boson exchange potentials, 26:54744

TABATA, S., Experimental study of the ultimate strength of composite beams subjected to alternate loading of positive and negative bending, 26:55571 (NRC-TT-1557)

TABATA, Yoneho, Intensity of ortho-positronium component in liquid and solid amides, 26:54100

TABOR, W. H., Bulk shielding facility quarterly report, April, May, and June of 1972, 26:55408 (ORNL-TM-3949)

TACHIKAWA, Kiyoshi, Carcinogenesis in the survivors exposed to A-bomb irradiation in their youth, 1950 to 1969, 26:53442

TACHIYA, M., Configuration diagram of the solvated electron, 26:53025

TADDEI, F., Buckling measurements in ECO with few CIRENE fuel elements, 26:55106 (CISE-R-283)

Experimental investigations on U--D$_2$O lattices, 26:55101 (CISE-R-203)

TAHERZADEH, M., Response of a 300-μ silicon detector to monoenergetic neutrons determined by the use of the Monte Carlo technique, 26:53291 (NASA-TM-X-2440, pp 708-13)

TAIRA, Konno, Application of Newton--Kantorovich method to Chew--Low N/D equations. I, 26:54421

TAIT, K. E., Manipulators: a survey, 26:53734

TAJC, Ladislav, Some basic experimental methods of wet-steam flow investigation, 26:53124

TAJIRIAN, G., Front Island shield thermal displacements, 26:55374 (CERN-HERA-72-1)

TAKADA, T., Experimental study of the ultimate strength of composite beams subjected to alternate loading of positive and negative bending, 26:55571 (NRC-TT-1557)

TAKAHASHI, K., Further aspects of the reaction $\pi^-p \to \pi^-\pi^+n$ at 8 GeV/c, 26:54216

Termination of the r-process and the synthesis of superheavy elements, 26:54663

TAKAHASHI, Yasushi, Spontaneous breakdown of symmetry and the gauge invariance in a relativistic field theory, 26:54387

TAKAKU, Yuji, Radiated dose to skin during injection of radioactive substances, 26:53424

TAKAOKA, Toshiko, Establishment of line of cultured of hepatoma cells (Culb TC) of the rat and the analysis of effects of gamma rays, 26:53354

TAKASAKI, M., Isotope dependence of K-shell ionization cross sections by ^{20}Ne and ^{22}Ne bombardments, 26:54114

TAKEBE, Hiraku, Radiation damage and its repair, 26:53357

TAKEDA, K., ESR studies of aliphatic radical anions and radical-anion pairs in γ-irradiated crystalline solids, 26:52991 (ORO-2968-78, Paper 6)

TAKEDA, Renzo, Flux distribution measurement near strong absorber using VISTA method, 26:55137 (JAERI-Memo-3893)

TAKEUCHI, Eiji, Flux distribution measurement near strong absorber using VISTA method, 26:55137 (JAERI-Memo-3893)

TAKIZAWA, Shoichi, Effects of high intensity pulsed x-ray (linear accelerator) or gamma-ray irradiation upon tumorigenesis and immunocompetence in mice, 26:53469

TAMAI, E., Chemical composition of low energy L and M nuclei in the primary cosmic radiation, 26:53841

Measurement of the low energy helium isotopes in the primary cosmic rays, 26:53827

TAMEMASA, Osamu, Formation of antibiological substances by radiation-chemical reaction, 26:52998

TAN, Chung-I, Dual-amplitude analysis of two-particle productions. II, 26:54307
TAN, S. I., X-ray topographic determination of the absence of lateral strains in ion-implanted silicon, 26:55019
TAN, T. Y., Comments on the range of applicability of the grain boundary (secondary) dislocation model to high angle grain boundaries, 26:55513 (COO-3158-10)
TANAKA, S., Nuclear reactions of Ni with protons up to 56 MeV, 26:54591
TANAKA, Takayasu, Method for nonlinear plasma wave kinetics, 26:54850
TANAKA, Toshikazu, Outline of PNC's activities in the field of sodium-water reaction, 26:55155 (CONF-710548-, pp 129-54)
TANAKA, Y., Gas coulometry, 26:55633 (UCRL-Trans-10640)
TANAKA, Yoshihisa, Analyses of the sodium-water reaction pressure and its propagation in the sodium system, 26:55157 (CONF-710548-, pp 171-86)
TANG, S. Y., Dependence of reactivity on internal and translational energy in K + SF$_6$, CCl$_4$, and SnCl$_4$, 26:54136
TANGHERLINI, F. R., Pion--muon model and linear mass relations, 26:54272
TANIGUCHI, Setsuo, Shoulder of optical absorption spectrum of the trapped electron in gamma-irradiated crystalline ice, 26:53002
TANNER, L. E., Ordering transformation in Ni$_2$V, 26:53659
TANNER, N. W., Pionic proton stripping and π^- production, 26:54535
TAO, Chi-Shine Cliff, Polycrystalline spinel from powders prepared by freeze drying technique, 26:55564 (LBL-876)
TAPE, J. W., Lifetime of 3.74-MeV (3$^-$) state of ^{40}Ca, 26:54575
TAPP, E., State and tendencies of chemical protection against ionizing radiation. A literature survey 1970/71, 26:53460 (SZS-132)
TARAFDAR, S. P., Equivalent width of interstellar molecular lines. II, 26:53890
TARASOV, A. V., Calculation of absorption in neutral pion coherent photoproduction on nuclei, 26:54691 (JINR-P2-6539)
TARTAKOVSKII, V. K., Quasi-elastic electron scattering on ^{12}C nuclei, 26:54526 (ITF-72-25-P)
TARTSKOVSKII, V. K., Two-particle electrodesintegration of ^{3}He, 26:54496 (ITF-72-24-P)
TARUTANI, Yoshinobu, Preparation of transparent EuO films by oxidation of Eu films, 26:53567
TASSO, H., Determination of magnetic field B in vacuum for general two-dimensional MHD equilibria, 26:54814
TATARCZUK, J. R., Economical scaler driver, 26:53298 (COO-3058-9)
  Gateable delay-gate generator, 26:53299 (COO-3058-10)
TATARU-MIHAI, P. I., New derivation of the off-shell dual-resonance amplitudes, 26:54420
TATISCHEFF, B., Determination of neutron radii by alpha elastic scattering, 26:54547
  Study of some properties of tin isotopes through high-energy alpha-particle scattering, 26:54616
TAUBE, M., Molten chlorides fast breeder reactor problems and possibilities, 26:55082 (EIR-215)
TAUVERON, P., Measurement of isotopic ratios of helium, 26:54519
TAVKHELIDZE, A. N., N. N. Bogoliubov's transformation in strong coupling theory. III, 26:54383
TAYLOR, J. Jr., Four-nucleon studies. I, 26:54516
TAYLOR, K. N. R., Magnetic transitions in rare earth intermetallic compounds R$_3$Ni and R$_3$Co, 26:55050
TAYLOR, Lauriston S., Role of the NCRP in development of radiation protection standards, 26:54915
TCHEOU, F., Crystal field effect on the direction of magnetic moments of rare earth ions with low symmetry sites (C2--C/sub s/), 26:55054
TELLIER, C., Measurements on a fuel--salt interface in the annular well space during the production of a cavity by salt dissolution, 26:53115
TEMPLETON, Arch W., Exposure of radiologists during special procedures, 26:53443
TENDLER, M., Light-intensity dependence of the multiphoton ionization probability in the resonance case, 26:54094
TEODORESCU, I. A., Influence of the incidence angle on iron and copper surface microtopography induced by ion bombardment, 26:55008
TERASAKI-OKADA, Kunihiko, Cut-off problem in the integral spectrum of ultrahigh energy cosmic rays and urbaryons, 26:54313
TERASHIMA, Y., Isotope dependence of K-shell ionization cross sections by ^{20}Ne and ^{22}Ne bombardments, 26:54114
TERENT'EV, M. V., Structure of observable amplitudes for photon-soft-pion interaction, 26:54265
TER-MARTIROSYAN, K. A., Quasi-eikonal approximation, 26:54306
TERNEY, William B., Determination of optimal k-infinity mismatch curves via modern control theory, 25:55432 (CONF-720901-(Bks.1 and 2), pp 240-51)
TERNOVSKII, F. F., Structure of the mixed state near the boundary of a semi-infinite superconductor of the second kind, 26:54448
TERRAZ, C., Electric and thermal conductivity, elastic properties, and bending resistance of porous W over entire range of porosity, 26:53684
TESKE, Richard G., Solar soft x rays and solar activity. II, 26:53963
TESTA, M., Measure of the photovoltaic effect in silicon diodes obtained through implantation of ions, 26:54975 (RT/EL-(72)2)
TESTARDI, L. R., Magnetization, velocity of sound, and specific heat of Sc$_3$In, 26:55045
TESTE DU BAILLER, A., Nuclear power stations, 26:55211
TEWARY, V. K., Theory of the void lattice in molybdenum, 26:55052
THACKABERRY, Samuel P., Crosslinked nylon by irradiation of a graft copolymer of nylon with an ethylene/acrylate or modified copolymer, 26:53013
THACKER, Louis H., Rapid, sensitive method for the determination of the chemical oxygen demand of polluted waters, 26:52915 (CONF-720827-2)
THEIS, W. R., Anomalous dimensions in p--p elastic scattering, 26:54343 (DESY-72/35)
THERET, C. G., Ultrastructure changes in the adenohypophysis of rodents after total or segmentary irradiation with radiocobalt, 26:53467
THEWS, R. L., New Regge absorption model, 26:54336
THIBAULT, J. J., Development of a ultrahigh vacuum evaporation unit using a liquid He cryopump with a high pumping speed, 26:53139
THIESSEN, H. A., Bifilar helical multiwire proportional chamber for position sensitive detection of minimum ionizing particles, 26:53273 (LA-4968)
  Energetic pion channel and spectrometer (EPICS), 26:53787 (LA-4874, pp 51-4)
THOMAS, E. W., Excitation in heavy-particle collisions, 26:54118
THOMAS, J. K., Solvation of electrons in 3-methylhexane at 77°K, 26:53007
THOMAS, John H., Solar seeing and the spatial properties of the five-minute oscillations, 26:53945
THOMAS, Roger J., Solar soft x rays and solar activity. II, 26:53963
THOME, P., Outlock for the on-site welding of thick metal sheets, 26:53633
THOMMES, M. M., Studies of recent sedimentation in Green Bay, 26:53164 (ANL-7860(Pt.3), pp 64-76)
THOMPSON, D. T., Asymmetric proton yields from the sequential reaction ^{6}Li(^{3}He,αp)^{4}He, 26:54540
THOMPSON, F., Localized vibrational modes in gallium arsenide containing silicon and boron, 26:54984
THOMPSON, G., Preliminary study of $\pi^+\pi^-$ scattering in reaction $\pi^+p \rightarrow (\pi^+\pi^-)\Delta^{++}$ at 13 GeV/c, 26:54223
THOMPSON, M. W., Elastic scattering of 5 to 90 eV neutral Au atoms by Ar, 26:54142
  Ion--atom scattering and interatomic potentials for ions of noble metals and period II elements incident on Ne and Ar with energies in the range 8 to 25 keV, 26:54139
THOMPSON, Patrick A., Stopped muon channel, 26:53789 (LA-4874, pp 59-62)
THOMSON, J. A., Multiple Coulomb interference effects on the quadrupole moment of ^{114}Cd, 26:54623
THORLEY, A., Corrosion and deposition behaviour of steel material in sodium systems, 26:55173 (CONF-710959-, Paper 17)
  Fission and corrosion product behaviour in primary systems of LMFBR's: a brief review of current status of work being carried out in UK, 26:55166 (CONF-710959-, Paper 10)
THORP, J. M., Climatography of the Hanford area, 26:55478 (BNWL-1605)
THORPE, M. F., Bound state in EuO, 26:55042
THORSLUND, T. W., Effects of x-ray irradiation on human spermatogenesis, 26:53399 (NASA-TM-X-2440, pp 229-32)
THUEMMLER, F., Technology of cermets, 26:53592
TIKHONIN, F. F., Production of muonic pairs in μp-collisions, 26:54263
TIKHONOV, A. S., Interconnecting phenomena of ultraplasticity of alloys and their chemical and phase composition, 26:53667
TILK, Stefan, Influence of water vapor on γ-radiolysis of crystalline KI, 26:53017
TILL, C. E., Fast neutron Doppler effect, 26:54479 (CONF-720901-(Bks.1 and 2), pp 1152-65)
TILTON, Earl M., Basis for design on allowable plastic strain, 26:55500 (COO-2048-7)
TIMEROV, R. Kh., Effect of the metal--dielectric phase transition on the superconducting transition temperature, 26:54457
TIMIRAS, Paola S., Electrophysiological and biochemical studies of the effects of radiation on brain activity and development. Progress report, August 1971--31 July 1972, 26:53461 (UCB-34-P-82-13)
TIMONIN, A. M., Energy-transfer efficiency of a magnetic-implosion system, 26:54781
TIMOSHENKO, A. P., Instability control in a beam--plasma system, 26:54819
TINDO, I. P., New measurements of the polarization of x-ray solar flares, 26:53962
TINSLEY, Beatrice M., Galactic evolution: program and initial results, 26:53978
TISONE, G. C., Rocket-borne auroral optical measurements, 26:54012 (SC-RR-720543)
TITOV, A. A., Distribution of qualitative composition and absorbed doses of x-irradiation in using the screens, 26:54911

TITOV, V. F., Requirements for steam generator design and systems to ensure safety in the case of failures in the tubes of heat exchange surfaces, 26:55159 (CONF-710548-, pp 206-12)
TIWARI, N. P., Post-irradiation evaluation of pathogens and indicator bacteria, 26:53369
TKACZYK, W., Galactic magnetic field and anisotropy of cosmic rays above 10^{17} eV, 26:53851
TOBIAS, A., Ordered table of gamma radiation emitted by fission products, 26:54607 (RD/B/M-2356)
TOBIAS, C. A., Human visual response to nuclear-particle exposures, 26:53403 (NASA-TM-X-2440, pp 416-22)
TODD, A. G., Influence of O, C, and B on sintering and stress rupture properties of sintered Ni-base superalloys, 26:53674
TODD, B. E., Probe velocity transducer, 26:53303 (LA-4999)
TOIYA, Takehiro, Potential in the canonical formalism of gravity, 26:54405
TOKUOKA, Tatsuo, Gravitational waves of third and higher order, 26:54406
TOLLIN, Gordon, Phototaxis in Euglena: biochemical aspects, 26:55485 (COO-908-37)
  Prog. rpt. on free radicals in biological energy conversion: EPR studies of model systems, 3 years, 9/1/69--8/31/72, 26:55616 (TID-26149)
TOLMACHEV, M. M., Volume and surface wave transformation in plasma systems, 26:54861
TOLSTIKOV, V. A., Measurements of neutron cross sections of radiation capture and fission for some heavy nuclei by the method of time of retardation in lead, 26:54657 (FEI-292)
TOMII, Kakuzo, Study on the works of engineering reactor-safety, 26:55204 (JAERI-M-4535)
TOMITA, Kazuo, Radiation induced heart failure. I, 26:53439
TONEEV, V. D., Buildup of cosmic isotopes in iron meteorites, 26:53808 (ORNL-tr-2620)
TONER, W. T., Correction of light attenuation in large shower counters, 26:53285
  Lepton hadron interactions, 26:54173 (RPP/H-97)
TONG, L. S., Boiling crisis and critical heat flux, 26:55179 (TID-25887)
TONON, G., Fusion by laser-driven flame propagation in solid DT targets, 26:54830
TON-THAT, T., Heavy ion source with a confined electron beam, 26:53753 (FRNC-CONF-56)
TOPPEL, B. J., Studies of methods for fast neutron multigroup cross section generation and their effect upon the neutronics properties of LMFBR critical assemblies, 26:55113 (CONF-720901-(Bks.1 and 2), pp 211-28)
TORIYAMA, Kazumi, ESR study of an irradiated single crystal of acetylene dicarboxylic acid dihydrate, 26:53005
TORRENS, Ian M., Computer simulation in radiation damage studies, 26:54970 (CEA-CONF-1890)
TOSELLI, F., Buckling measurements in ECO with few CIRENE fuel elements, 26:55106 (CISE-R-283)
TOSELLI, G., TRUD: an anisotropic diffusion code for xy geometry, 26:54488 (RT/FI-(72)1)
TOUBOUL, J. P., Influence of carbon and oxygen on the brittleness of molybdenum, 26:53682
TOWNER, J. M., Effect of comminution on the sinterability of alumina and tungsten carbide powders, 26:53576
TOYODA, Fumihiko, Systematic structure in hadronic two-body scattering and resonance correlation. III, 26:54342
TOYOSHIMA, N., Fission product release in TLG-1 in-pile gas loop. III, 26:53694 (JAERI-Memo-3936)
TRADOWSKY, K., Cladding control on nuclear reactor fuel elements, 26:55218 (EURFNR-976)
TRAMONTINI, C., Effect of gamma radiation on an Argentine variety of wheat, 26:53381 (CNEA-309)
TRAN-DINH-SON, Photolysis and radiolysis of nitromethane in the liquid phase, 26:52978 (CEA-N-1528)
TRAUTMANN, D., Coulomb break-up of the deuteron, 26:54743
  Forward dispersion relations and low-energy elastic scattering of charged particles from nuclei, 26:54711
  Numerical investigations within the semiclassical transfer theory, 26:54742
TRAVELLI, A., Analysis of sodium-void experiments in the FTR engineering mockup critical assembly, 26:55390 (CONF-720901-(Bks.1 and 2), pp 739-67)
TRAVER, T. M., User's manual for DASQHE, 26:55421 (BNWL-CC-2274)
TRET'YAKOVA, S. P., Search for tracks of spontaneous fission fragments from the heavier transuranium elements in naturally-occurring minerals, 26:54670
TREVISAN, G., Non-congruent vaporization stage of lanthanum oxide on first heating to high temperature, 25:53549 (EUR-4765, pp 343-63)
TRIFONOV, I. I., Melting point diagrams for $LiCl$--UCl_3--UCl_4 system, 26:53721
TRIMOUILLE, C., Presentation made to meeting of sodium-water reaction specialists, 26:55150 (CONF-710548-, pp 1-16)
TRINCHERINI, R. P., Isotopic analysis of uranium as running control of EUREX process, 26:52918 (EUR-4765, pp 91-115)
TRIPARD, G. E., Asymmetric proton yields from the sequential reaction $^6Li(^3He,\alpha p)^4He$, 26:54540
TRIPATHI, A. N., Electron loss in atom-molecule collisions, 26:54121
TRITTON, K. P., New redshifts of radio galaxies, 26:53991
TRIVEDI, R. K., Edgewise growth kinetics of Widmanstaetten precipitates, 26:55528 (IS-2838)
TRNOVEC, T., Hematologic changes and changes in the blood proteins in experiments on white rats following intratracheal administration of radiocerium, 26:53516
TRNOVEC, Tomas, Mechanisms of hepatic uptake of hepatotropic radionuclides, 26:53526 (BNWL-tr-71)
TROITSKII, S. V., Scattering of electromagnetic waves due to electron charge fluctuations in a flat waveguide with a magnetoactive plasma, 26:54848
TROMBKA, Jacob I., Identification and control of spacecraft radiation sources of interference to x-ray and gamma-ray experiments, 26:53255 (NASA-TM-X-2440, pp 714-22)
TROTTER, Dorothy E., Atlas of magnetic fields in the solar corona, 26:53955
TROUBETZKOY, E., Mechanism of fast neutron transport in iron, 26:54473 (CONF-720901-(Bks.1 and 2), pp 335-48)
TROUT, E. Dale, Broad-beam attenuation in lead for x rays from 50 to 300 kVp, 26:54904
  Scattered radiation from a tissue-equivalent phantom for x rays from 50 to 300 kVp, 26:54905
TROYAN, V. A., X-ray study of molybdenum and nickel irradiated with helium ions, 26:53700 (SC-T-722540)
TROYON, F. S., Transverse dynamic stabilization of a theta pinch, 26:54808 (LRP-51/72)
TRUHLAR, Donald G., Covenient determination of resonance states in atomic collisions, 26:54124
  Test of Massey's method for calculating static potential for electron scattering by N_2, 26:54125
TRUITT, J., Properties of dry crushed salt and related consolidated media with emphasis on their gas transport characteristics, 26:53724 (ORNL-TM-3815)
TRUNOV, G. V., Production of formed bodies from high-melting compounds according to the casting procedure for thermoplastic masses, 26:53586
TRUSCELLO, Vincent, Program at JPL to investigate the nuclear interaction of RTGs with scientific instruments on deep space probes, 26:53294 (NASA-TM-X-2440, pp 866-72)
TSAI, Wu-yang, Compton scattering. I. Spectral forms for the invariant amplitudes to order e^4, 26:54255
  Compton scattering. II. Differential cross sections and left--right asymmetry, 26:54256
TSAO, C. H., Calculations of cross sections and their application to cosmic-ray physics, 26:53845
  New observations and calculations of primary Be/B in the cosmic rays, 26:53833
  Revised source composition of cosmic rays from hydrogen to nickel, 26:53837
TSCHAECHE, A. N., Recent activities in the development of surface contamination standards, 26:54919
  Use and abuse of standards, 26:54934
TSEITLIN, M. B., Volume and surface wave transformation in plasma systems, 26:54861
TSIGEL'MAN, G. E., Ion emission from electron-bombarded solids and mass-spectrometer applications, 26:54084
TSUBOTA, Hiroaki, System for time of 50 m flight analysis and characteristics of short pulse beam, 26:53260
TSU-KAI, Chu, Dynamic stabilizer for plasma instabilities to improve plasma confinement and to increase plasma density, 26:54823
TSUKUDA, M., 0.511 MeV gamma rays measured with the Ge(Li) detector at balloon altitude, 26:53817
TSURUTANI, B., Onset of magnetospheric substorms, 26:54060
TSUTSUMI, Shoji, Studies on arsenic metabolism. I, 26:53538
TSYINA, N. V., Quantitative spectral determination of Nb, Ta, Fe, and Mn in minerals of columbite--tantalite group, 26:52932
TSYTOVICH, V. N., Plasma bremsstrahlung from relativistic particles in a turbulent plasma, 26:54774 (AEC-tr-7323)
TU, K. N., X-ray topographic determination of the absence of lateral strains in ion-implanted silicon, 26:55019
TUAN, S. F., Comment on a limiting temperature in hadron physics, 26:54305
TUBIS, A., Meson-exchange currents and ^3H, ^3He magnetic moments, 26:54506
TUCKER, Wallace H., Galactic origin for the soft x-ray background, 26:53973
TUETTOE, I., Theory of the roton lifetime in superfluid helium, 26:54429
TULI, S. K., Analysis of 20 GeV proton--nuclei scattering, 26:54530
TUMA, Hanus, Carbon activity and solubility in a stainless chromium--nickel steel with about 18 percent Cr and 9 percent Ni, 26:55480 (BNWL-tr-72)
  Carbon activity and solubility in austenitic chromium--nickel steels with about 18 percent Cr, 26:55481 (BNWL-tr-73)
TUMBEV, G. Kh., Angular correlation of a gamma cascade 329 to 487 keV in ^{140}Ce, 26:55060
TUOHY, I. R., Spectral and pulsed x-ray emission from the Crab Nebula, 26:53919
TURCK, Bernard, High performance spectrometer magnets, 26:53296 (CEA-N-1539)
TURK, E. H., Use of CFRMF integral data in cross section evaluations, 26:55384 (CONF-720901-(Bks.1 and 2), pp 613-22)
TURNER, G. D., Sensitivity of calculated pulsed sphere spectra and neutron age to carbon cross sections,

26:54474 (CONF-720901-(Bks.1 and 2), pp 409-17)
TURNER, R. E., Isomer ratios from low primary excitation of residual nuclei, 26:54725
TYROR, J. G., Some problems in the physics of high temperature reactors, 26:55110 (CONF-720901-(Bks.1 and 2), pp 55-67)
TYUPA, V. I., Experimental determination of the basic characteristics of space-periodic magnetic configurations, 26:54824 (AEC-tr-7334)

U

UCHIKAWA, Toru, Analysis of kinetic curves, 26:53519
UDOVICHENKO, Yu. K., Instability control in a beam--plasma system, 26:54819
UEDA, Shuzo, Results of cyclic pressure loading test due to JPDR pressure vessel model No. 2, 26:55228 (JAERI-Memo-4016)
UEDA, Y., Unified weak-electromagnetic gauge schemes based on the three dimensional unitary group, 26:54364 (NYO-3533-264)
UEKA, Keiko, Malformation of digits in mouse foetus caused by gamma-ray irradiation during pregnancy, 26:53471
UENO, H., Spurious sidereal anisotropy arising from annual modulation of solar diurnal variation of cosmic radiation, 26:53849
UENO, Hirosachi, Three-dimensional cosmic ray anisotropy in interplanetary space. IV, 26:53813
  Three-dimensional cosmic-ray anisotropy in interplanetary space. III, 26:53812
UETAKE, Ichizo, Eddy current testing of stainless steel fuel jacket cladding tubing, 26:53125
ULAM, S. M., Metrics in biology, an introduction, 26:55546 (LA-4973)
ULRICH, Bruce T., Translational absorption of HeH, 26:54134
ULRIKSON, G. U., Radiation-induced hemopoietic lesions in fish, 26:53447 (CONF-720822-2)
UMBARGER, C. J., Spectroscopy of ^{101}Mo by sub-Coulomb stripping, 26:54614
  Target chamber for charged particle induced x-ray fluorescence studies, 26:53803
UMEZAWA, Hiroomi, Spontaneous breakdown of symmetry and the gauge invariance in a relativistic field theory, 26:54387
UNGETHUEM, E., Natural α-activity in air near ground, 26:53160 (UUIM-27)
  Natural β-activity in air near ground. Parts B--E, 26:53159 (UUIM-26)
UNIK, J. P., Production of actinides and search for superheavy elements using secondary reactions induced by GeV protons, 26:54672
UNNA, I., Approach to the nuclear many-body problem by variationally determined transformation. II, 26:54718
UNVERRICHT, A., Radiation dose and radioprotective effect in the examination of the thyroid gland of birds, 26:53515
UPADHYAYA, G. S., Electronic mechanism of the basic technological processes in the powder metallurgy of high temperature materials, 26:53632
UPADHYAYA, U. N., Role of paramagnetic impurities in the barrier region for superconducting tunnelling, 26:54442
URRY, Grant, Prog. rpt. on covalently bonded compounds of the light elements, final, 11/1/68--10/31/70, 26:55523 (COO-3544-1)
URSU, A. M., Investigation of densities of the electron states for two-band superconductor with nonmagnetic impurities, 26:54454
USKOKOVIC, D., Kinetics and mechanism of molybdenum powder sintering, 26:53621
UTLEY, H. B., Temperature dependence of hyperfine interactions of Eu^{2+} in $SrCl_2$, 26:52970
UTO, H., Transition counter, 26:53277

V

VACCARI, M., Fast neutron radiative capture cross sections of stable nuclei with 29 less than or equal to Z less than or equal to 79, 26:54700 (RT/FI-(72)6)
  MARE: a FORTRAN IV code for compound nucleus reaction calculations in the continuum, 26:54701 (RT/FI-(72)7)
VAGER, Z., Incoming wave boundary condition for elastic scattering of heavy particles at incident energies near the Coulomb barrier, 26:54705
VAISBURD, D. I., Destruction of a solid by superdense excitation of its electronic subsystem, 26:55012
  Effective cross sections of proton and alpha particle tracks in ionic crystals, 26:55016
VALDEZCO, J. L., Extraction of ^{32}P from neutron-irradiated S dissolved in hot toluene, 26:53069
VALENCIA, Ruby M. Allen, Total radiation-induced genetic damage in entire genomes of Drosophila melanogaster. Progress report, November 1, 1971--October 31, 1972, 26:53497 (COO-1748-12)
VALENTINE, Kenneth, Neutron radiography with a multiwire proportional chamber: performance and projections, 26:53200 (LBL-707(Summ.))
VALKAR, Sh., Investigation of the reactions $\pi^- p \rightarrow n\pi^+\pi^- + (1,2,3,4,5)\pi^0$ at GeV/c, 26:54220
VALKOVIC, V., Triangle graphs and isospin violation in 3-particle final-state reactions, 26:54716
VALLARIO, E. J., Role of the Health Physics Society in the development of radiation protection standards, 26:54918
VALLEE, R. E., Radiation from ^{238}Pu used in space applications, 26:53337 (NASA-TM-X-2440, pp 859-61)
VALLEE, R. L., Design and development of a random pulse sampler, 26:53321
VALLI, G., Steady state and transient measurements on scaled-down model of power channel of CIRENE reactor prototype, 26:55148 (CISE-R-270)
VALLIERES, Michel, Algebraic approach to the theory of collective motion: spherical to deformed transition in the single-j shell, 26:54681 (COO-3071-9)
  Simplified microscopic model of the Coriolis anti-pairing transition, 26:54680 (COO-3071-7)
VAMPOLA, A. L., Natural variations in the geomagnetically trapped electron population, 26:54046 (NASA-TM-X-2440, pp 539-47)
VAN ALTENA, W. F., Membership in extremely young open cluster NGC 6530 (M8), 26:53883
VAN BINST, P., Measurement of the Ξ hyperon lifetimes and α parameters, 26:54174 (RPP/H-99)
VAN DAM, J., Thermoluminescent dosimetry in patients treated with high-energy electrons, 26:53415
VAN DEN BERGH, Sidney, New method for estimating the Hubble constant, 26:53974
VAN ELEGEM, P., Dosimetry in radiodiagnosis, 26:53416
VAN HORN, A. J., Reactions $K^- p \rightarrow \Lambda\pi^0$ and $K^- p \rightarrow$ anti$K^0 n$ in the center-of-mass energy range 1700 to 2100 MeV, 26:54215
VAN PATTER, D. M., Gamma transitions in ^{60}Ni following β^+ decay of ^{60}Co. II, 26:54593
VAN WINKLE, R., VTE-X model test and computer calculation of row by row performance and comparison with measured data, 26:53110 (ORNL-TM-3841)
VARGAS, J. I., Lifetime variation of ^{64}Cu and the chemical state of (n,γ) recoil copper in α-copper phtalocyanine crystals, 26:53032
VARNUM, W. S., Electron energy transfer rates in the ionosphere, 26:54022
VARSHNEYA, A. K., Diffusion in the system K_2O--SrO--SiO_2. IV. Mobility model, electrostatic effects, and multicomponent diffusion, 26:53598
VARY, J. P., Off-shell effects in the ^{18}O and ^{18}F shell-model spectra, 26:54538
VASAVADA, Kashyap V., Pion--nucleon charge exchange scattering in a new Regge pole-cut model, 26:54324 (COO-1428-309)
VASHOLZ, David P., Chiral tensors and the axial charge, 26:54371
VASIL'EV, A. G., Radioisotopic relays, 26:53288
VASILIU, F., Influence of the incidence angle on iron and copper surface microtopography induced by ion bombardment, 26:55008
VASYLIUNAS, V. M., Balance of stresses in the plasma sheet, 26:54059
VAUGHEN, V. C. A., Determination of the radioactive nuclides present in the off-gas stream generated by the head-end steps in reprocessing HTGR type fuels, 26:53078 (CONF-720823-11)
VENET, Pierre, Procedure for fabrication of spherical oxidic fuel and breeder particles, 26:53566
VENNART, J., Radiobiology forum on radiological protection and the skin, 26:53431
VEPKHVADZE, G. T., Spatial localizability of energy--momentum tensor of gravitational field, 26:54393 (ITF-72-5-P)
VERBEURE, F., LPS analysis of reactions $K^+ p \rightarrow K^+\pi^+\pi^- p$ and $K^+ p \rightarrow K^0\pi^+\pi^0 p$, 26:54226
VERBINSKI, V. V., Proton-recoil proportional counter spectrometry for reactor spectrum measurements, 26:55122 (CONF-720901-(Bks.1 and 2), pp 959-72)
VERCAEMER, C., Internal friction peaks due to N in Nb--Zr alloys, 26:53692
VERDIER, J., High flux Franco--German reactor, 26:55414
VERDIZADE, A. A., Chromatographic separation of In from elements that form periodates of low solubility, and its subsequent determination, 26:52949
VERESHCHINSKII, I. V., Some topics in radiation chemical synthesis of organic compounds, 26:53023
VERHEEST, Frank, Linear and Alfven waves in incompressible beam-plasma systems, 26:54857
VERKHOTUROV, A. D., Anode erosion with alloys of carbides of transition metals with Fe, Co, and Ni, 26:53568
VERMA, B. G., Reflection of a hydromagnetic shock wave from a boundary shock, 26:54159
VERMA, Satya Dev, Interaction of cosmic rays with interstellar matter and possible excitation of x-ray lines, 26:53815
VERMA, Shiv Prakash, Perspective transformer for the stereomatrix 3-D display system, 26:55489 (COO-1469-210)
VERON, M. P., Optical positions of radiosources, 26:53913
VESELY, D., Influence of surface orientation on yield in Mo single crystals, 26:53645
VETRANO, J. B., Stability of a light metal hydride, 26:53714 (NAA-SR-8533)
VIBIKE, Kh. I., One-nucleon transfer reactions to quasi-

intersecting levels, 26:54635 (JINR-P4-6509)
VIENET, R., Acceleration of polarized protons in Saturne, 26:53762
VIGNERON, J. M., Study by differential absorption in infrared of irradiated lipids and polymers, 26:52983 (EUR-4828)
VIGON, M. A., Isotopic separation by centrifugation. Rotating plasma, 26:53327 (JEN-244)
VIL'K, Yu. N., High-temperature vacuum evaporation of zirconium carbide + tungsten compounds, 26:55022
VINCENT, J. S., Elastic scattering of 60-MeV protons from H, D, ^{3}He, and ^{4}He, 26:54512
VINGIANI, G. B., g-factor of 3/2^{-} 153-keV state in ^{49}V, 26:54574
VINOGRADOV, A. V., Second harmonic generation in nonuniform laser-produced plasma, 26:54790 (JPRS-56713)
VINOGRADOV, V. B., Investigation of the reactions $\pi^-p \to n\pi^+\pi^- + (1,2,3,4,5)\pi^0$ at GeV/c, 26:54220
VINOGRADOV, Yu. A., Search for tracks of spontaneous fission fragments from the heavier transuranium elements in naturally-occurring minerals, 26:54670
VINS, Vaclav, Absolute activity in irradiated fuel material by method of gamma scanning, 26:53041 (UJV-2867-M,A)
VIOLLIER, R. D., Forward dispersion relations and low-energy elastic scattering of charged particles from nuclei, 26:54711
VISHNEVSKY, C., Plane strain fracture toughness of some cryogenic materials at room and subzero temperatures, 26:53661
VITALI, G., Surface and depth distribution damage of ions in silicon as seen with an electron microscope, 26:55003
VLACH, J., District heating in Czechoslovakia and possibility of using nuclear power reactors for this purpose, 26:55376 (INIS-mf-172, pp 7-13)
VLACHOVSKY, K., Approximation of resonance self-shielding coefficients, 26:54489 (ZJE-124)
VOBECKY, M., Nondestructive neutron activation analysis of mineral materials. II, 26:52901 (UJV-2851-F,Ch)
VOGT, E., Rotational bands of ^{20}Ne, 26:54562
VOIGT, Keith L., Description of the American Nuclear Society's Information Center on Nuclear Standards (ICONS) radiation protection standards: Quo Vadis, 26:54917
VOILLEQUE, Paul G., Dose action levels for accidental radiation exposure of the general public, 26:53523
VOJTA, G., Higher harmonics and transport coefficients of plasmas in circulary polarized magnetic fields and additional electromagnetic fields, 26:54761
VOLKOV, A. B., Extension of variable moment of inertia model to odd--even nuclei, 26:54710
VONDY, D. R., Nuclear reactor core analysis code: CITATION. Revision 2, Supplement 3, 26:55198 (ORNL-TM-2496(Rev.2)(Suppl.3))
VOOK, F. L., Electronic stopping measurements of charged-particles in radiophotoluminescent glass, 26:55009
VOROB'EV, A. A., Effective cross sections of proton and alpha particle tracks in ionic crystals, 26:55016
VOROBEV, A. I., Chromosome aberrations induced in human bone-marrow cells by therapeutical local γ irradiation: time and dose relationships, 26:53445
VOROB'EV, V. A., Determination of thickness of γ-sources and absorbers from deformation of hard part of energy spectrum, 26:54936
VORONIN, V. S., Self-consistent stationary state of a relativistic electron beam in a drift space, 26:53757
VOSTRCIL, J., Application of organic flocculants to the decontamination of radioactively contaminated waters by coagulation, 26:53040 (SZS-129)
VYKLICKY, Miloslav, Carbon activity and solubility in austenitic chromium--nickel steels with about 18 percent Cr, 26:55481 (BNWL-tr-73)
VYLOV, Ts., Study of ^{149}Tb decay, 26:54603 (JINR-P6-6511)

W

WADA, Yasushi, Structure of Cooper pairs in superconductors, 26:54459
WADDINGTON, C. J., Charge and energy spectra of heavy cosmic ray nuclei, 26:53842
  Chemical composition and energy content of the energetic cosmic radiation, 26:53806 (NASA-TM-X-2440, pp 209-14)
WADE, David C., Determination of optimal k-infinity mismatch curves via modern control theory, 26:55432 (CONF-720901-(Bks.1 and 2), pp 240-51)
WADMAN, William W., Neutrons produced by known energies of ions abundant in space, 26:54881 (NASA-TM-X-2440, pp 520-2)
WAGENBLAST, H., Electrical resistivity increase rates in Fe--C and Fe--N solid solutions during neutron irradiation at 4.5 K, 26:54989
WAGNER, G. A., Dating error, 26:53181
WAGNER, R., Blocking effect in U fission with 14-MeV neutrons, 26:54669
WAHL, A. C., Cumulative yield of 83-sec ^{136}I from thermal-neutron induced fission of ^{235}U, 26:54626
WAHLGREN, M. A., Determination of selected trace elements in natural water samples using spark source mass spectroscopy, 26:52914 (ANL-7860(Pt.3), pp 55-63)
WAHLIG, M. A., Measurement of the primary cosmic ray nuclear rigidity spectra for individual elements of charge Z greater than or equal to 2, 26:53826
WAIBEL, E., Calculation of the time dependent fission product heat source strength in two coupled systems with consideration of fission product escape, 26:55206 (KFK-1580)
  REST: program for calculation of fission product activity and decay constant after variable reactor history in two coupled systems with respect to fission product emission, 26:55127 (KFK-1579)
WAILLY, Louis F., Advanced-dosimetry systems for the space transport and space station, 26:53235 (NASA-TM-X-2440, pp 944-56)
WAKATANI, Masahiro, Magnetohydrodynamic and tearing instabilities in a tokamak, 26:54813
WAKLEY, J., Physical measurements including depth dose data and isodose curves for 8 mv roentgen rays, 26:53799
WALDEN, Patrick Lorne, Photoproduction of π^- from deuterium at laboratory energies 600 to 1250 MeV and cm π production angles 6 to 160°, 26:54179
WALDER, Andre, Production of Ni--Cr--ThO$_2$ alloys by means of chromium diffusion through halogen carrier in NiThO$_2$ grain, 26:53627
  Production of Ni--ThO$_2$ alloy with dispersed phase starting from organometallic compounds, 26:53626
WALDRON, M. B., Effect of comminution on the sinterability of alumina and tungsten carbide powders, 26:53576
WALECKA, J. D., Semileptonic weak interactions with ^{12}C, 26:54541
WALICKA, Malgorzata, Effects of uv-light and x-rays on murine lymphoma, 26:53356
WALINDER, G., Dose rate dependence in the goitrogen stimulated mouse thyroid, 26:53472
  Quantitative effects of ^{131}I on different tissue components in foetal and goitrogen challenged mouse thyroids, 26:53513
WALKER, D. C., Solvation of electrons in 3-methylhexane at 77°K, 26:53007
WALKER, J. C., Observation of temperature spikes following Coulomb excitation, 26:54646
WALKER, James F., Effects of ^{208}Pb core vibrations on shell-model calculations for ^{211}At and ^{211}Pb, 26:54650
WALKER, Raymond J., Spatial distribution of energetic plasma-sheet electrons, 26:54057
WALL, J. A., Solar cell radiation response near the interface of different-atomic-number materials, 26:53290 (NASA-TM-X-2440, pp 577-83)
WALLS, Nancy W., Physiological studies on Clostridium botulinum, type F. Final report, 26:53366 (ORO-3347-8)
WALRAEDT, Jean, Coldstream process, 26:53591
WALSH, M., Zero energy reactor facility at B.N.L., 1972, 26:55409 (RD/B/N-2272)
WALSH, T. F., Polarization effects in deep inelastic lepton--nucleon scattering, 26:54244 (DESY-72/36)
WALTER, R. L., Four-nucleon studies. I, 26:54516
  Four-nucleon studies. III, 26:54517
  Four-nucleon studies. IV, 26:54518
WAMBERSIE, A., Dosimetry in interstitial therapy using ^{192}Ir wires, 26:53422
  Pediatric radiology and irradiation, 26:53417
WAMSER, Christian A., Process for preparing alpha ammonium uranous pentafluoride, 26:53049
WAN, C. C., Simple code for use in shielding and radiation-dosage analyses, 26:54959 (NASA-TM-X-2440, pp 387-91)
WANG, C. L., Transition counter, 26:53277
WANG, C. S., Electric field induced by a slowly decaying ring current, 26:54063
WANG, J. T., ESR studies of aliphatic radical anions and radical-anion pairs in γ-irradiated crystalline solids, 26:52991 (ORO-2968-78, Paper 6)
WANG, Ling-lie, Scaling in $p\pi^- \to pX^-$ and an estimate of triple-Pomeranchukon coupling, 26:54221
WANG, R., Superconductivity in Mg--Cd system: extrapolated T/sub c/ for pure magnesium, 26:54444
WANG, Shein-shion, Pair potential in liquids from the exact Born-Green equation: I. Model testing, 26:55516 (COO-3161-4)
WANNER, J., Investigation of hydrogen fluoride chemical lasers, 26:55527 (IPP-IV-38)
WAPSTRA, A. H., Decay of ^{227}Th from α--γ coincidence and directional correlation studies, 26:54673
WARGON, Jorge A., Electron spin resonance studies of radical trapping in the radiolysis of organic liquids. I. Evidence for the primary formation of the methoxy radical in methanol, 26:52988 (ORO-2968-78, Paper 2)
WARMAN, E. A., Conference on natural and manmade radiation in space held at Las Vegas, Nevada, 3/71, 26:54870 (NASA-TM-X-2440)
  Radiation environment for rendezvous and docking with nuclear rockets, 26:55361 (NASA-TM-X-2440, pp 257-63)
WARMAN, J. M., Dissociative attachement of thermal electrons to N$_2$O and subsequent electron detachment, 26:54135
WARNER, Brian, Observations of rapid blue variables. VII, 26:53895
  Observations of rapid blue variables. VIII, 26:53901
  Observations of rapid blue variables. IX, 26:53902
WARNER, R. A., Collective and higher-order effects shown by the (p,t) reaction on the deformed nucleus ^{159}Tb, 26:54645
  Collective effects shown by the (p,t) reaction on the

closed-shell nucleus, ^{141}Pr, 26:54615
WARREN, Helen, Toxicity data for imido (imidate) esters, 26:55581 (ORNL-TIP/TIRC-72-54)
WARREN, Helen S., Carcinogenicity of methyl-nitro-nitrosoguanidine, 26:55583 (ORNL-TIP/TIRC-72-60)
  Toxicity of potassium iodate, 26:55575 (ORNL-TIP/TIRC-72-10)
  Toxicology of isoamylamine and related amines, 26:55584 (ORNL-TIP/TIRC-72-61)
WARREN, Shields, Renal tumors in parabiosed irradiated rats, 26:53449 (COO-3017-4)
WARRIER, A. V. R., Vibrational and electronic properties of $Co(CN)_6^{3-}$ doped in alkali halides, 26:55001
WARZEE, M., Prog. rpt. on growth of carbon deposition from carbon monoxide on a metal catalyst, annual, 3/1/66--2/28/67, 26:53605 (DP-Report-522)
WASHBURN, J., Precipitation of phosphorous in ion implanted silicon, 26:54994
WASHUETTL, J., Influence of γ irradiation on content of nicotinic acid of wheat, wheat-flour, and wheat-bread, 26:53344
  Investigations on content of free and bound tryptophan in wheat after γ irradiation, 26:53395
WATANABE, Masami, Magnetohydrodynamic and tearing instabilities in a tokamak, 26:54813
WATROUS, J. D., Plutonia/curia compatibility testing. Quarterly report No. 15, April--June 1972, 26:53551 (MDC G-3153)
WATSON, H. E., Effect of neutron irradiation on fatigue crack propagation in Types 304 and 316 stainless steels at high temperatures, 26:53698 (NRL-7446)
  Effect of residual elements on radiation strengthening in iron alloys, pressure vessel steels, and welds, 26:53710
WATSON, J. W., Intensity estimation for neutron beam for biological and medical applications, 26:53804
  Isomer ratios from low primary excitation of residual nuclei, 26:54725
WATSON, M. D., Auroral photometric observations at geomagnetically conjugate points, 26:54013
WATT, A., Shell-model and projected Hartree--Fock calculations for ^{24}Mg, ^{28}Si, and ^{32}S, 26:54553
WATTS, John W. Jr., Electron and bremsstrahlung penetration and dose calculation, 26:54886 (NASA-TM-X-2440, pp 801-15)
WAWNER, F. E., Chemical vapor deposition of boron on a carbon monofilament substrate, 26:53571
WEAVER, H. Joseph Jr., Use of grating to increase recording capability of laser far field camera, 26:55624 (UCRL-51255)
WEAVER, Samuel Cavin, Investigation of the thermal conductivity, electrical resistivity, and thermoelectric power of thorium nitride--uranium nitride alloys, 26:55027
WEBB, Richard V., Solvent composition for liquid scintillation counting, 26:53211
WEBBER, W. R., Chemical composition of cosmic rays with Z = 3 to 30 at high and low energies, 26:53838
WEBBER, William R., Change in the eleven-year modulation at the time of the June 8, 1969, Forbush decrease, 26:53870
WEBER, J., Identification of rotational band in ^{240}Pu fission isomer, 26:54664
WEBER, W., Experimental investigation of the continuous emission of shock heated krypton and xenon, 26:54777 (BMBW-FBK-72-8)
WEBSTER, J. M., Impurities in cover gas systems: some aspects of their effects on design of LMFBR's, 26:55171 (CONF-710959-, Paper 15)
WECH, R. E., Yields of gamma rays emitted following capture of negative muons by ^{28}Si and ^{24}Mg, 26:54555
WEDEMBYER, R., Proton Compton effect in the region of the Δ(1236)-resonance, 26:54180
WEEKE, Eva, Extracorporeal irradiation of the blood, 26:53440
WEIBEL, E. S., Transverse dynamic stabilization of a theta pinch, 26:54808 (LRP-51/72)
WEILHAMMER, P., Large aperture spectrometer magnet for the ISA and the possible use of visual detectors, 26:53779 (BNL-17142)
WEIMAN, Carl F. R., Pattern recognition by retina-like devices, 26:55455 (OSU-CISRC-TR-72-8)
WEIMER, K. E., Toroidal effects on MHD stability in Tokamaks, 26:54806 (CONF-720804-6)
WEISBIN, C. R., Carbon shielding benchmark problem and other neutron transport calculations in carbon, 26:54939 (CONF-720901-(Bks.1 and 2), pp 397-408)
  Development of ENDF/B shielding data processing codes, and integral tests, 26:55141 (CONF-720901-(Bks.1 and 2), pp 316-24)
  Sensitivity of calculated pulsed sphere spectra and neutron age to carbon cross sections, 26:54474 (CONF-720901-(Bks.1 and 2), pp 409-17)
WEISINGER, M. D., Application of advanced metal-matrix composites to aircraft structures, 26:53573
WEISS, E., Metabolism of Rickettsia typhi and Rickettsia akari in irradiated L cells, 26:53360
WEISS, Herbert, Energy spectrum of electrons in water irradiated with 10- to 20-MeV electron beams, 26:54894
WEISSMAN, Bruce, Osteoradionecrosis of the mandible, 26:53418
WELCH, Frank H., Space-reactor shielding fabrication, 26:54949 (NASA-TM-X-2440, pp 92-7)
WELCH, G. P., Response of mouse epidermal cells to single doses of heavy particles, 26:53456 (NASA-TM-X-2440, pp 652-8)
WELLENSTEIN, H. F., Determination of optical sums from the small-angle electron-impact spectra of argon, 26:54128
WELLS, Mark B., Specification of program flow in Madcap VI, 26:55547 (LA-DC-72-141)
  Two-dimensional programming languages, 26:55549 (LA-DC-72-331)
WELSH, R. E., Negative muon capture in carbon leading to specific final states, 26:54537
WENDELL, R. E., Transportation air pollutant emissions handbook, 26:55467 (ANL/ES-15)
WENNHOLD, W. F., Application of advanced metal-matrix composites to aircraft structures, 26:53573
WENSEL, A., Exposure of persons after water loss in tank of FRF2 reactor, 26:55399 (IKF-27)
WENZEL, W. A., 2π steradian magnetic spectrometer, 26:53284
  Neutrino mass limits from the K/sub L/$^0 \to \pi^{+-}l^{-+}\nu$ decay spectra, 26:54184 (LBL-4)
WERNER, Z., Similarities of ionization effects and annealing in P-type and converted N-type Ge irradiated with electrons at 85°K, 26:54997
WERNER, Zbigniew, Charge state of defects in Ge converted into p-type by 1 MeV electrons, 26:55013
WERTH, G. C., Energy: uses, sources, issues, 26:53096 (UCRL-51221)
WESCHLER, Mary Charles, Measurement of major nutrients and water quality parameters at Point Beach: 1971, 26:53183 (ANL-7860(Pt.3), pp 103-8)
WESENBERG, D. L., Steady-state response of an infinite plate to an exponential edge load along a fusing crack: a model for the dynamic edge fusion of two semi-infinite plates, 26:55611 (SCL-RR-710113)
WESTERHOUT, G., Galactic radio emission in the 21-cm line and the continuum, 26:53984
WESTIN, R., Change of structure and mechanical properties in stainless steel by irradiation. Part 1.1. Metallographic study of neutron irradiated and unirradiated 12R72HV after tensile testing, 26:53701 (STU-70-419/U-350(Pt.1.1))
WESTMORELAND, David G., Study of biological macromolecules using perturbed angular correlations of gamma radiation, 26:55058
WETZEL, Robert G., Interaction of yellow organic acids with calcium carbonate in freshwater, 26:55494 (COO-1599-63)
  Metabolism of dissolved and particulate detrital carbon in a temperate hard-water lake, 26:55493 (COO-1599-58)
WEYER, H. J., Proton Compton effect in the region of the Δ(1236)-resonance, 26:54180
WHAPHAM, A. D., Heterogeneous nucleation of fission gas bubbles and gas migration in uranium dioxide, 26:53565
WHARAM, J., SNAP-21 program, Phase II. Deep sea radioisotope-fueled thermoelectric generator power supply system. Preliminary design description 10-watt system, 26:53092 (MMM-3691-5(Rev.1))
WHATLEY, M. E., Decontamination of HTGR reprocessing off-gases, 26:53059 (CONF-720823-12)
WHEELER, F. J., Calculated reactivity of VINS, 26:54469 (ANCR-1071)
WHEELER, R. G., An intrauterine dosimeter, 26:53238
WHITE, John M., Hot atom reactions in the HBr--Br_2, DBr--Br_2 systems, 26:52962
WHITE, R. Allen, Quantum mechanical studies of the vibrational excitation of H_2 by Li^+, 26:54133
WHITEHEAD, R. R., Shell-model and projected Hartree--Fock calculations for ^{24}Mg, ^{28}Si, and ^{32}S, 26:54553
WHITMELL, D. S., Thermal release of He injected into Ni, stainless steels, and nimonic PE16, 26:53709
WICKRAMASINGHE, N. C., Recent work on interstellar grains, 26:53989
WIDMER, T. F., Shock loading analysis of core subassembly: APDA core, 26:53732 (WCAP-1615)
WIEGAND, Clyde E., Kaonic atom transition coupled to nuclear level, 26:54568 (LBL-776)
WIESNER, W., β-decay of ^{206}Tl, 26:54648
WIGNER, Eugene P., Active and passive defense interaction studies. Volume I. Summary, models, and calculations, 26:53135 (ORNL-TM-3485(Vol.1))
WIKTOR, S., Intermediate coupling approach in the unified model of the ^{39}K nucleus, 26:54685 (INP-795)
WILCOX, A. D., Discrete ordinates--Monte Carlo coupling: a comparison of techniques in NERVA radiation analysis, 26:55371 (NASA-TM-X-2440, pp 681-6)
WILDE, W. O., Portable absorbed-dose measuring instrument with gamma discrimination, 26:53234 (NASA-TM-X-2440, pp 609-13)
WILDUNG, R. E., Techniques for the characterization of suspended sediment and selected applications for the acquired data, 26:55479 (BNWL-SA-4385)
WILENZICK, R. M., Neutron irradiation monitor for use with Ge(Li) detectors, 26:53223
WILEY, Albert L. Jr., Review: some biochemical effects of high LET radiations, 26:53345 (NASA-TM-X-2440, pp 222-8)
WILHELMI, M., Application and automation of mass spectrometry in the analysis of irradiated nuclear fuels, 26:52917 (EUR-4765, pp 77-89)

WILHELMI, Zdzislaw, Cross sections for proton induced reactions on ^{43}Ca, ^{44}Ca, and ^{48}Ca isotopes in protons energy range 1 to 2 MeV, 26:54567 (INR-1407)
WILKALIS, John E., Process for preparing alpha ammonium uranous pentafluoride, 26:53049
WILKINS, J. W., Far infrared surface resistance of Cu:Fe; dynamics of a Kondo system, 26:55508 (COO-3151-4)
WILKINSON, M. C., Galactic cosmic-ray heavy primary secondary doses, 26:54878 (NASA-TM-X-2440, pp 104-7)
 Heavy-particle hazard: what physical data are needed, 26:53408 (NASA-TM-X-2440, pp 1007-15)
WILLEMSEN, Jorge F., New form factors in the dual resonance model, 26:54235 (COO-264-611)
WILLIAMS, F., ESR studies of aliphatic radical anions and radical-anion pairs in γ-irradiated crystalline solids, 26:52991 (ORO-2968-78, Paper 6)
WILLIAMS, Ffrancon, Electron spin resonance studies of radical trapping in the radiolysis of organic liquids. I. Evidence for the primary formation of the methoxy radical in methanol, 26:52988 (ORO-2968-78, Paper 2)
 Hydrogen atom abstraction by methyl radicals in methanol glasses at 67 to 77°K, 26:52990 (ORO-2968-78, Paper 5)
 Investigation of the structure of the hydrated electron based on unpaired electron densities calculated by the INDO method, 26:52989 (ORO-2968-78, Paper 4)
 Pulse radiolysis study of succinonitrile in the rotator phase, 26:53003
WILLIAMS, I. R., Elastic and inelastic scattering of 12-MeV protons from ^{92}Mo, ^{94}Mo, ^{96}Mo, and ^{100}Mo: tabulated differential cross sections, 26:54606 (ORNL-TM-3913)
WILLIAMS, J. D., DIAMOND: a new approach to microelectronic circuit design (dielectrically isolated arrays of monolithic devices), 26:53309 (SC-DC-721162)
WILLIAMS, K. R., Dose dependence of swelling in irradiated metals, 26:53707
WILLIAMS, M. E., Phase and shape of the form factor for inelastic ^{3}He scattering, 26:54621
WILLIAMS, P. M., Stellar compositions from narrow-band photometry. III, 26:53898
WILLIAMS, T. Ffrancon, Research concerning ionic and free radical reactions in radiation chemistry. Progress report, September 15, 1971--August 15, 1972, 26:52987 (ORO-2968-78)
WILLIAMSON, K. D. Jr., Experience in handling, transport, and storage of liquid hydrogen: the recyclable fuel, 26:55552 (LA-DC-72-632)
WILLIS, A., ^{2}H(p,2p)n reaction at 155 MeV, 26:54522
WILLIS, C. A., Recent activities in the development of surface contamination standards, 26:54919
 Safety criteria for nuclear power in space, 26:54921
WILLIS, Harold Wayne, Analytical and experimental investigations of the transient properties of dense aluminium plasmas, 26:54771
WILLIS, William J., Calorimeters for ISABELLE, 26:53270 (BNL-17071)
 Program for development of a liquid argon calorimeter, 26:53269 (BNL-17070)
WILLKE, Theodore L., High-pressure electrofluiddynamic facility, 26:53089 (AD-737380)
WILLMANN, K., Collisional ionization of helium by slow electrons, 26:54123
WILLMANN, R. B., Preliminary study of $\pi^+\pi^-$ scattering in reaction $\pi^+p \to (\pi^+\pi^-)\Delta^{++}$ at 13 GeV/c, 26:54223
WILQUET, G., Measurement of the Ξ hyperon lifetimes and α parameters, 26:54174 (RPP/H-99)
WILSCH, H., Elastic scattering of vector polarized deuterons from ^{48}Ti, ^{49}Ti, ^{50}Ti, ^{51}V, ^{52}Cr, 26:54572
WILSON, I. H., Elastic scattering of 5 to 90 eV neutral Au atoms by Ar, 26:54142
 Ion--atom scattering and interatomic potentials for ions of noble metals and period II elements incident on Ne and Ar with energies in the range 8 to 25 keV, 26:54139
WILSON, I. J., Evaluation of two possible further developments of the UK in-flight radiation warning meter for SSTs, 26:53203 (NASA-TM-X-2440, pp 874-83)
WILSON, John, Evaluation of the hazard from exposure to electron irradiation simulating that in the synchronous orbit, 26:53458 (NASA-TM-X-2440, pp 665-71)
WILSON, John V., Active and passive defense interaction studies. Volume I. Summary, models, and calculations, 26:53135 (ORNL-TM-3485(Vol.1))
WILSON, M. L., Fabrication of multilayer printed wiring boards, 26:55469 (BDX-613-382(Rev.))
WILSON, W. D., Thick target yield calculations for strong neutron-producing reactions in the energy range 30 keV to 1.5 MeV, 26:54502 (SC-RR-720513)
WINDISH, J. P., Mortality experience of the community and of the fluorspar mining employees, 26:53412
WINFIELD, D., Detection of ultra-cold neutrons by the activation of manganese, 26:54490
WING, Ralph O., Conversion of plutonium oxide to plutonium tetrafluoride with fluorine in a fluid bed reactor. Part II. Demonstration runs: a comparison of the fluorine process with the hydrofluorination process, 26:53039 (RFP-1890)
 Conversion of plutonium oxide to plutonium tetrafluoride with fluorine in a fluid bed reactor. Part I. Development studies, 26:53038 (RFP-1889)
WINSTEIN, B. D., New evidence on the photoexcitation of I = $^{1}/_{2}$ nucleon isobars, 26:54166 (CALT-68-322)
WINTERBON, K. B., Note on the large-depth decrease of range and damage profiles, 26:54899
WINTHER, A., Semi-classical description of elastic and inelastic heavy-ion scattering above the Coulomb barrier, 26:54736
WIRTH, G., High-temperature creep behavior of a tungsten--3 percent rhenium alloy with thorium oxide dispersion hardening of various particle shapes, 26:53678
WISCHMANN, Kenneth B., Mechanical and thermal expansion properties of a particulate filled polymer, 26:55603 (SC-DR-70-617)
WISSE, M., V$_{553}$ centauri. A type 2 Cepheid with an overabundance of C, 26:53899
WISSE, P. N. J., V$_{553}$ centauri. A type 2 Cepheid with an overabundance of C, 26:53899
WISWALL, R. H. Jr., Metal hydrides for energy storage, 26:53090 (BNL-16889)
WITHBROE, George L., Properties of a coronal hole derived from extreme-ultraviolet observations, 26:53939
WITTMAACK, K., Determination of implantation profiles in solids by secondary-ion mass spectrometry, 26:55014
WOEHL, Hubertus, C$_2$ lines in sunspot spectra, 26:53952
WOHL, Millard L., Shield-weight optimization using Monte Carlo transport calculations, 26:54962 (NASA-TM-X-2440, pp 697-705)
WOLF, Jerry R., Conversion of plutonium oxide to plutonium tetrafluoride with fluorine in a fluid bed reactor. Part II. Demonstration runs: a comparison of the fluorine process with the hydrofluorination process, 26:53039 (RFP-1890)
WOLF, K. L., Production of actinides and search for superheavy elements using secondary reactions induced by GeV protons, 26:54672
WOLF, R. A., Balance of stresses in the plasma sheet, 26:54059
WOLFE, J. H., Simultaneous solar-wind plasma and magnetic-field measurements in the expected region of the extended geomagnetic tail, 26:54074
WOLFE, John H., Pioneer 7 observations of Aug. 29, 1966, interplanetary shock-wave ensemble, 26:54068
WOLFENDEN, A., Electron radiation damage near the threshold energy in aluminium, 26:54990
WOLFER, W. G., Diffusional growth of voids induced by irradiation and stress, 26:53702 (TID-26150)
WOLFF, Charles L., Solar-wind heating, 26:53942
WOLFF, Richard J., Periodic variability of the peculiar A star HD 111133, 26:53877
WOLFF, Sidney C., Magnetic-field variations in 78 Virginis, beta Coronae Borealis, and 73 Draconis, 26:53876
 Periodic variability of the peculiar A star HD 111133, 26:53877
WOLFSBERG, Max, Effect of vibrational anharmonicity on hydrogen--deuterium exchange equilibria involving ammonia molecules, 26:52973
WOLSKO, T. D., Transportation air pollutant emissions handbook, 26:55467 (ANL/ES-15)
WONG, C., Nucleon--nucleon scattering lengths from incomplete nucleon--deuteron breakup experiments, 26:54503 (UCRL-74069)
WOOD, J. L., Decay of ^{161}Er to levels in ^{161}Ho, 26:54632 (COO-3255-2)
WOODRUFF, Gene L., Measurement of delayed neutron energy spectra. Final report, 26:54660 (RLO-2225-T-17-4)
WOODS, R. O., Rocket-borne auroral optical measurements, 26:54012 (SC-RR-720543)
WOODSUM, H. C., Selection and use of TLDs for high-precision NERVA shielding measurements, 26:53233 (NASA-TM-X-2440, pp 466-70)
WOOLFREY, J. L., Effect of green density on the initial-stage sintering kinetics of UO$_2$, 26:53597
 Nonisothermal techniques for studying initial-stage sintering, 26:53595
WOOLLAM, P. B., Use of Ge(Li) detectors in high dose rate γ spectrometry, 26:53237 (RD/B/N-2369)
WOOLLEY, J. A., Rod drop accident analysis for large boiling water reactors, 26:55353 (NEDO-10527)
WOOLLINGS, M. J., Collisions of fast electrons with helium. II, 26:54110
 Collisions of fast electrons with He. I, 26:54138
WOOLSON, W. A., Application of MORSE to radiation analysis of nuclear flight propulsion modules, 26:55372 (NASA-TM-X-2440, pp 692-6)
WORLTON, J., Trilogy on errors in the history of computing, 26:55548 (LA-DC-72-243)
WORSTER, L. D., Application of computers to control and monitoring of nuclear reactors, 26:55136 (DUN-SA-186)
WRIGHT, R. J., Isotopic compositions of rare gases in the carbonaceous chondrites mokoia and allende, 26:53810
WRONA, B. J., Deformation and fracture of UO$_2$--20 wt percent PuO$_2$, 26:53545 (ANL-7945)
WU, Chi-Chao, Study of the unidentified interstellar diffuse features, 26:53881
WURM, J. G., Extraction of plutonium from heavy water fuels by the SALTEX process, 26:53079 (EUR-4812)

Y

YAFFE, L., Isomer ratios of ^{95}Nb formed in fission of ^{209}Bi, 26:54627
YAGER, P. M., S-wave structure in the Kπ system, 26:54203 (COO-1428-308)

YAGI, H., Fission product release in TLG-1 in-pile gas loop. III, 26:53694 (JAERI-Memo-3936)

YAKIMENKO, I. P., Nonlinear wave interactions in a cylindrical column of magneto-active plasma, 26:54863

Scattering of electromagnetic waves due to electron charge fluctuations in a flat waveguide with a magnetoactive plasma, 26:54848

YAKIMIW, E., Weak radiative decays of hyperons in the pole model, 26:54292

YAKIMOV, V. E., Cosmological models of a scalar-tensor theory of gravitation, 26:54396 (ITF-72-41-P)

YAKOVLEV, G. N., Effective neutron absorption cross sections for ^{252}Cf and ^{253}Cf in central channel of SM-2 reactor, 26:54668

YAMADA, T., Fission product release in TLG-1 in-pile gas loop. III, 26:53694 (JAERI-Memo-3936)

YAMADA, Teruyo, Toxic eruptions combined with radiation therapy of malignant tumors, 26:53433

YAMAGUCHI, Takuzi, Study on the effects of radiation on the molding of polymers, 26:53720

YAMAMOTO, H., Radionuclide production by cosmic rays in lunar rocks, 26:53860

YAMAMOTO, K., Thin film of organic fluorescent materials for simple detection of alpha rays, 26:53265

YAMAOKA, Hitoshi, Optical absorption bands of color centers in irradiated anthracene single crystals at low temperatures, 26:54996

YAMASHITA, Shizuo, Methods of calculation on a step cascade for enriching uranium, 26:53329

YAMAZAKI, Makoto, Surgical treatment for local radiation injuries following radiotherapy, 26:53438

YAMPOL'SKII, I. R., Circuits for studying the interaction of high-frequency fields with a plasma in linear devices, 26:54775 (AEC-tr-7326)

YANG, C. S., Elastic and inelastic widths of analogue states in ^{65}Cu, 26:54590

YANG, Chen Ning, Some speculations on colliding beams of 200 GeV protons and 15 GeV electron--200 protons, 26:53767 (BNL-16830)

YARNELL, J. L., Phase transitions and crystal structures of deuterium, 26:55559 (LA-DC-72-903)

YASUNA, Osamu, Surgical treatment for local radiation injuries following radiotherapy, 26:53438

YELLIN, S. J., New evidence on the photoexcitation of $I = {}^{1}/_{2}$ nucleon isobars, 26:54166 (CALT-68-322)

YEN, W. L., S-wave structure in the Kπ system, 26:54203 (COO-1428-308)

YOKOO, Yoshimatsu, Possible tests of lepton number assignments, 26:54296

YOKORO, Kenjiro, Effects of high intensity pulsed x-ray (linear accelerator) or gamma-ray irradiation upon tumorigenesis and immunocompetence in mice, 25:53469

YOON, Hong Il, Lattice heat capacities of alloys, 26:53637 (LBL-101)

YOON, T. S., Production properties of A_1^+ in π^+p interactions at 5.45 GeV/c, 26:54227

YOSHIDA, Y., Levels of ^{90}Nb excited via the ^{90}Zr(p,nγ) reaction, 26:54613

YOSHIKAWA, Kiyoshi, Experimental study of relaxation phenomena in non-equilibrium MHD generator duct, 26:53104

YOSHIKAWA, S., Pseudoclassical and anomalous containment in FM-1, 26:54753 (CONF-720804-5)

YOSHIZAWA, Yasuo, Malformation of digits in mouse foetus caused by gamma-ray irradiation during pregnancy, 26:53471

YOST, K. J., Calculation of neutron-capture gamma-ray yields for space-shielding applications, 26:54961 (NASA-TM-X-2440, pp 527-8)

YOUNG, J. C., Proton-recoil proportional counter spectrometry for reactor spectrum measurements, 26:55122 (CONF-720901-(Bks.1 and 2), pp 959-72)

YOUNG, Jerald A., Reduced red cell 2,3-diphosphoglycerate and adenosine triphosphate, hypophosphatemia and increased hemoglobin--oxygen affinity after cardiac surgery, 26:55638 (UR-3490-187)

YOUNG, R. C., Automated Cross Section Analysis Program (ACSAP), 26:54468 (ANCR-1042)

YOUNT, D. E., Muon identification using multiwire proportional chambers, 26:53282

YOUSSEF, A., Empirical expressions for the thermal diffusion column shape factors in the extreme cylindrical case, 26:53326 (AREAEE-131)

YUAN, Luke C. L., Transition counter, 26:53277

YUCKER, W. R., Solar cosmic-ray hazard to interplanetary and earth-orbital space travel, 26:53930 (NASA-TM-X-2440, pp 345-55)

YUDIN, V. A., Doppler-shifted cyclotron resonance in cadmium, 26:55044

YUHAS, John M., Multifactorial analysis of human blood cell responses to clinical total-body irradiation, 26:53400 (NASA-TM-X-2440, pp 233-7)

YUKHNOVSKII, I. R., Asymptotic behavior of pair-correlation function of normal Fermi-systems, 26:55532 (ITF-72-2-P)

YURKIN, G. V., Stimulated emission evoked by pumping with a pulsed electron beam produced in a linear discharge, 26:54787

Z

ZABORONSKII, A. A., Distribution of qualitative composition and absorbed doses of x-irradiation in using the screens, 26:54911

ZAIDI, S. A. A., Consistent coupled-channel Born approximation analysis of ^{88}Sr(d,np) ^{88}Sr and ^{88}Sr(d,p)^{89}Sr, 26:54588

ZAITSEV, A. M., Search for quarks at the 70 GeV accelerator, 26:54165

ZAITSEV, G. A., External invariant equations of electromagnetic field, 26:54373 (ITF-72-35-P)

ZAITSEV, N. A., Scalar-tensor theory of gravitation, 26:54395 (ITF-72-21-P)

ZAITSEV, V. V., Dynamic theory of Type-III solar radio bursts, 26:53964

ZAITZ, J. I., Single-neutron-transfer-reaction studies of ^{176}Hf and ^{180}Hf, 26:54636

ZAKHARKIN, I., Exit tube effect upon the measured space--energy neutron spectra, 26:54470 (AREAEE-133)

ZAKURKIN, V. V., X-ray and dielectric studies of irradiated perovskite type compounds, 26:55020

ZALEWSKI, K., Uncorrelated jet model predictions for the multiplicity distribution of π^- mesons produced in high energy annihilations anti pp → pions, 26:54316 (RPP/T-24)

ZAMYATNIN, Yu. S., Effective neutron absorption cross sections for ^{252}Cf and ^{253}Cf in central channel of SM-2 reactor, 26:54668

ZAPOROZHCHENKO, I. G., Changes of cellular division and DNA synthesis in glands of gastric floor of rats under effect of Ra emanation, 26:53514

ZAPPELLINI, G., Measurement of cell parameters in RB-1 reactor, 26:55102 (CISE-R-239)

ZARANDI, A., Correlation of the partial radiation widths in the reaction ^{163}Dy(n,γ)^{164}Dy, 26:54631 (BNL-tr-490)

ZASHIKHIN, M. N., Many-particle correlation for many-electron systems in different orders of perturbation theory, 26:54148

ZASLAVSKII, A. N., Dispersion relations and data for the reaction γn reversible pπ^- in the 33-resonance region, 26:54261

ZAWADOWSKI, A., Theory of the roton lifetime in superfluid helium, 26:54429

ZDOROVTSEVA, G. G., X-ray study of molybdenum and nickel irradiated with helium ions, 26:53700 (SC-T-722540)

ZEIDLITS, V. P., Interaction between a plasma and electron beam modulated by low-frequency oscillations, 26:54782

ZELENY, Josef, Some basic experimental methods of wet-steam flow investigation, 26:53124

ZELEVINSKY, V. G., Phenomenological description of the nuclear rotational states, 26:54712

ZELLE, M. R., Phenotypic properties of a large-cell, radiation-resistant strain of Escherichia coli, 26:53363

ZERWAS, P., Polarization effects in deep inelastic lepton--nucleon scattering, 26:54244 (DESY-72/36)

Quark model predictions for weak production of pseudoscalar mesons, 26:54285 (DESY-72/32)

ZHDANOV, V. G., Use of mutagenic agents for breeding of Eremothecium ashbyii, 26:53374

ZHDANOV, V. I., Two-body problem in theory of direct gravitational interaction, 26:54399 (ITF-72-58-P)

Two-body problem in theory of direct gravitational interaction. I, 26:54398 (ITF-72-52-P)

ZHMUR, L. E., Ion admixture distribution in the ionospheric F region, 26:54026

ZHOKHOV, K. A., Experimental study of the interaction of water with sodium during small leaks of water into sodium, 26:55152 (CONF-710548-, pp 39-56)

ZHUK, V., g-factor of 108 keV excited state in ^{151}Gd, 26:54634 (JINR-E6-6479)

ZHUKOVA, L. P., Effect of electron radiation on mechanical properties of Fe--Cr and Fe--Mo alloys, 26:53706

ZIEBOLD, T. O., Yield stress radiation damage function of iron, 26:53705

ZIEMBA-ZAK, Bogumila, Biological dosimeters. I, 26:53355

ZIEMER, P. L., Decomposition of aldrin by gamma radiation. II, 26:52997

Decomposition of aldrin by gamma radiation. I. In organic solvents, 26:53014

ZINDLER, H., Results of fallout monitoring in the German Democratic Republic 1970, 26:53156 (SZS-128)

ZINOV'EV, G. M., Dispersion sum rules and Jost--Lehman--Dyson representation in axiomatic quantum theory, 26:54377 (ITF-72-54-P)

Statistical view on resonance widths and multiplicity in dual models, 26:54300 (ITF-72-53-E)

ZISSERMANN, D., Spectroscopic factors from reactions ^{12}C(d,n)^{13}N and ^{12}C(d,p)^{13}C using WBP model, 26:54543

ZIVANOVIC, B., Kinetics and mechanism of molybdenum powder sintering, 26:53621

ZIVKOVIC, M., Kinetics and mechanism of molybdenum powder sintering, 26:53621

ZOBEL, W., Neutron spectral measurements in the upper atmosphere, 26:54066 (NASA-TM-X-2440, pp 922-5)

ZOCCHI, F., Ionic chemistry of gaseous cC$_6$H$_{12}$, 26:52982 (EUR-4765, pp 11-24)

ZOFKA, J., Spurious center-of-mass effect in the local density approximation, 26:54734

ZOLOTAR, B. A., Studies of methods for fast neutron

multigroup cross section generation and their effect upon the neutronics properties of LMFBR critical assemblies, 26:55113 (CONF-720901-(Bks.1 and 2), pp 211-28)
ZOLOTARYUK, A. V., Unitary renormalization, positivity, and selfadjointness of the Hamiltonian for a Lee model of the type Y/sub 3+1/, 26:54237 (ITF-72-48-E)
ZOLOTYKH, B. N., Investigation of the surface of tungsten single crystals following electro-erosive treatment, 26:53668
ZOZULYA, Yu. T., Self-consistent stationary state of a relativistic electron beam in a drift space, 26:53757
ZRAZHUN, A. G., Monte Carlo investigations of catastrophic collisions with characteristics of scattered electron radiation taken into account, 26:54898
ZRELOV, V. P., Monochromatic method for measuring 665 MeV mean proton energy by using Vavilov--Cherenkov radiation, 26:53800
Vavilov--Cherenkov ''needle'' radiation in Rochelle salt crystal, 26:54875 (JINR-P1-6552)
ZUBAREV, A. L., Factorization of pair potential by Bateman modified method in two- and three-body problem, 26:54345 (JINR-P4-6505)
ZUBECK, R. B., Specific heat of granular aluminum films, 26:54450
ZUCKER, Martin S., Application of the phase--space--time evolution method to electron shielding, 26:54887 (NASA-TM-X-2440, pp 821-31)
ZURMUEHLE, R. W., Core-excited 5^+ state in ^{14}N, 26:54542
ZVEREV, A. B., Effect of various kinds of ionizing radiation on poly(vinyl chloride), 26:53020
ZWIRN, P., Determination of the systolic volume by external counting, 26:53543
ZYCH, A. D., New point gamma ray source Libra γ-1, 26:53924
ZYKOV, A. I., Influence of injection conditions on the transverse instability of the beam in a linear accelerator, 26:53758
ZYRYANOVA, L. N., Beta processes, 26:54740
ZYVOLOSKI, George, Influence of plastic deformation and recrystallization upon permeability anomalies in gadolinium metal, 26:55040

SUBJECT INDEX

Cross references are included in cumulative subject indexes and in *Subject Headings Used by the USAEC Technical Information Center* (USAEC report TID-5001).

The reader is also referred to *Guide to Abstracting and Indexing for Nuclear Science Abstracts* (USAEC report TID-4576).

Most headings in the subject index are the names of specific materials, things, and processes. Each heading is followed by a modifier that describes the properties of, or processes applied to, that heading.

All index entries cite *NSA* volume and abstract numbers; volume number precedes the colon and the abstract number follows it. The designation (R) following the abstract number indicates a progress report; (P) indicates a patent; and (T) indicates a translation. Abstracts for reports other than progress reports carry no letter designation. Report numbers, where applicable, are included in parentheses after the abstract number of the citation. Published literature (journal article or book) can be identified by the absence of a report number.

Ideas presented in the original literature, rather than key words, have been indexed. The indexers have selected what seemed the most probable and logical place to look for typical information. Since it is not always possible to anticipate where a user would look for information, the cumulative indexes include numerous cross references. Consideration of synonymous or closely related terms will prove valuable.

Information is indexed for the greatest use to the greatest number of users. This requires that a topic be indexed to headings that most specifically describe it and not ordinarily to the headings that describe its ultimate use or to the general class headings that include the specific headings. For example, information on boiler design for the Fermi Fast Breeder Reactor would be indexed under the headings BOILERS and FERMI FAST BREEDER REACTOR but not necessarily under the headings REACTORS, FAST or REACTORS, BREEDER.

General or broad headings are reserved for general summaries, reviews, comprehensive reports, and similar literature.

Subject Heading Styles

Generally, the direct form of subject entry is used rather than inverted headings; e.g., AMINO ACIDS rather than ACIDS, AMINO; HELIUM ISOTOPES He-4 rather than HELIUM—ISOTOPES He-4 or HELIUM—He-4 ISOTOPES. Note, however, that in some cases parenthetic modifying terms or inverted headings such as NEUTRONS, FAST, are used where the alphabetical arrangement of a direct entry would cause information to be scattered. In addition, organic compounds are usually entered in the index in the inverted form to facilitate grouping like or related compounds with the parent compounds; e.g., BENZENE, BROMO- rather than BROMOBENZENE.

Alphabetization

Subject headings are alphabetized word by word. Parenthetic qualifiers, numbers, and Greek letters within subject headings are disregarded in alphabetizing unless there are two or more headings that are otherwise identical, in which case the qualifier, numerical progression, or spelled names for the Greek letters determine the order.

Examples:

M-Capture
  see ELECTRON CAPTURE
MAGNESIUM
MAGNESIUM ALLOYS AND SYSTEMS
MESONS
MESONS (π)
MESONS (rho)
1-PENTANOL
2-PENTANOL
URANIUM OXIDES
URANIUM OXIDES UO_2

Modifying Phrases

The modifiers appearing under a subject heading are written specifically to show the relation between the item being indexed and the heading. The modifier therefore contains a maximum of useful information. Although the modifier begins with the word judged to be of greatest use to the greatest number of users, there is still need for the searcher to consider all modifiers under the heading(s) of interest.

Modifiers usually form meaningful phrases when combined with the subject heading. Some are intended to be read following the subject heading, e.g., the entry HYDROGEN—*sorption by charcoal,* should be read *hydrogen sorption by charcoal.* As a result of placing the important word first, however, many modifiers must be rearranged for smooth reading, e.g., FORMALDEHYDE—*yields in radiolysis of ethyl ether, effects of deuterium on,* should be read *effects of deuterium on formaldehyde yields in radiolysis of ethyl ether* and URANIUM—*crystal structure of, effect of cooling rate on allotropic transformations in,* should be read *effect of cooling rate on allotropic transformations in crystal structure of uranium.*

Special characters are added to modifiers in the fields of physics and reactor technology; if the modifier does not establish the experimental or theoretical character of a reference, a symbol (E), (T), or (E/T) is placed immediately after the modifying phrase and before the abstract number.

Physical States and Configurations of Materials

The specific physical state, if other than normal, or the geometric configuration of the material is included in the modifying phrase; e.g., information on liquid metals is indexed under the specific metal with "liquid" in the modifier and carbon crucibles is indexed under CARBON with "crucibles" appropriately placed in the modifier. The information on carbon crucibles is also indexed under CRUCIBLES.

Nomenclature of Inorganic Compounds

Inorganic compounds are indexed to subject headings in the direct form. Cations are listed in the order of increasing valence for polycationic salts of varying valence and in alphabetic order for polycationic salts in which all cations have the same valence; e.g., SODIUM ALUMINUM SILICATES and POTASSIUM SODIUM SULFATES. If more than one anionic species is presented in a compound, the anions are arranged alphabetically, e.g., BERYLLIUM FLUORIDE HYDROXIDES.

Nomenclature of Organic Compounds

Complex organic compounds occur in such variety as to require a systematic nomenclature. Headings for most substituted organic compounds are found in an inverted form following names of the parent compounds. Examples of two such headings are:

```
2,4-HEPTANEDIONE
2,4-HEPTANEDIONE, 1-PHENYL-
```

Headings are included for broad class names of enzymes, e.g., HYDROLASES and TRANSFERASES. Specific enzyme names are to be found in modifiers under these headings. Similarly, broad class names for hormones are included as headings, except in this case the headings are entered in the inverted form as, e.g., HORMONES, ADRENAL and HORMONES, SEX. The more specific names of hormones are to be found in the modifiers under the appropriate broad headings.

For compounds used as drugs, an effort is made to use subject headings that reflect the recommendations of the USAN (United States Adopted Names) compilation or the "New Names" columns of the *Journal of the American Medical Association.* The *Merck Index* has also been used in selecting subject headings for drugs.

Nomenclature of Life Sciences

Except for those in the phylum Tracheophyta, subject headings for plants are common names. For example, ALGAE, FUNGI, SLIME MOLDS, MOSSES, and LIVERWORTS are subject headings. The phylum name TRACHEOPHYTA and several classes and subclasses belonging to it are entered as subject headings. The specific classes entered are PSILOPSIDA, LYCOPSIDA, SPHENOPSIDA, and PTEROPSIDA. The three subclasses FILICINIDAE, GYMNOSPERMIDAE, and ANGIOSPERMIDAE which belong under Pteropsida are also subject headings. Scientific names (genus and species) and common names if known are used in the modifying phrase.

Subject headings for microorganisms are VIRUSES, RICKETTSIA, and BACTERIA. The name of the type or kind of virus or the genus and species names of the organisms should appear in the modifying phrase.

The names of animal phyla are subject headings. The arthropods are also indexed to subject headings for classes INSECTA, CRUSTACEA, ARACHNIDA, DIPLOPODA, and CHILOPODA. The invertebrate chordates are indexed to subject headings UROCHORDATA and CEPHALOCHORDATA. The vertebrates are indexed to headings for the classes AGNATHA, CHONDRICHTHYES, OSTEICHTHYES, AMPHIBIA, REPTILIA, AVES, and MAMMALIA as well as to the general heading VERTEBRATA. Common names are used as subject headings in the class Mammalia.

Subject headings are entered for various classes of commodities, and specific products are identified in the file-word position of the modifier. In the following examples, approved subject headings are capitalized and typical modifier file words are listed in lower case.

Example 1

```
CEREALS
  bread
  flour
  oats
  rice
  rye
  wheat
```

Example 2

```
MEATS
  beef
  fish
  mutton
  pork
  poultry
  seafood
```

Diseases, pathological conditions, and in vitro studies of atypical cells and tissues are indexed under subject headings for the organism affected, under the appropriate anatomical structure of physiological phenomenon affected, and under the appropriate disease heading. Subject headings for diseases (defined as any deviation from the norm) are common names such as ANEMIA, FIBROSIS, INFECTIONS, LEUKEMIA, NEOPLASMS, and RADIATION SICKNESS. Also, the general headings DISEASES and DISEASES, PLANTS are available as subject headings.

Multicomponent Alloys and Other Systems

Multicomponent alloys and systems, except those with well-known trade names, are indexed under a subject heading for each component in the form "element systems" for nonmetals or "element alloys and systems" for metals. The modifier begins with element symbols for each component arranged alphabetically. In addition, if significance is placed on the base metal of the alloy, this is indicated by adding "-base" to the element symbol.

Example: A 1.5C, 12Cr, 0.25V, 0.8Mo, bal Fe alloy is indexed as

```
CARBON SYSTEMS
  C--Cr--Fe-base--Mo--V, ...
CHROMIUM ALLOYS AND SYSTEMS
  C--Cr--Fe-base--Mo--V, ...
IRON ALLOYS AND SYSTEMS
  C--Cr--Fe-base--Mo--V, ...
MOLYBDENUM ALLOYS AND SYSTEMS
  C--Cr--Fe-base--Mo--V, ...
VANADIUM ALLOYS AND SYSTEMS
  C--Cr--Fe-base--Mo--V, ...
```

Well-known alloys, such as ZIRCALOY-2, are indexed under the trade name; cross references from each component of the alloy to the trade name appear in cumulative indexes.

Multicomponent systems in which nonmetallic elements are present in large percentage and which are commonly referred to as systems or mixtures are indexed in a manner similar to alloys.

Example: A tungsten–silicon preparation is indexed as

```
TUNGSTEN ALLOYS AND SYSTEMS
  Si--W, ...
SILICON SYSTEMS
  Si--W, ...
```

Multicompound systems and mixtures of inorganic compounds are indexed under the subject heading for each component compound; the modifiers begin with an alphabetical listing of compound formulas.

Example: A lead titanate–lead zirconate mixture is indexed as

- LEAD TITANATES
  - $PbTiO_3$--$PbZrO_3$
- LEAD ZIRCONATES
  - $PbTiO_3$--$PbZrO_3$

Mixtures of organic compounds are indexed under subject headings for each component of the mixture; the modifiers begin with an alphabetical listing of compound names.

Example:

- ACETIC ACID
  - acetic acid--BF_3, ...
- BORON FLUORIDES
  - acetic acid--BF_3, ...

Example:

- BENZENE, CHLORO-
  - bromophenol--chlorobenzene, ...
- PHENOL, BROMO-
  - bromophenol--chlorobenzene, ...

A mixed system of compounds and elements is indexed by a combined form of the preceding conventions; e.g., a dispersion of copper and alumina would be indexed as

- ALUMINUM OXIDES
  - Al_2O_3--Cu, ...
- COPPER ALLOYS AND SYSTEMS
  - Al_2O_3--Cu, ...

If modifiers for alloys and systems are included with other modifiers under the same subject heading, they are filed last.

Example:

- CARBON SYSTEMS
  - deposition on nuclear fuel particles
  - molecular structure of
  - neutron total cross section for
  - sorptive properties for xenon
  - Young's modulus for
  - Al--C--Cr, superconductivity in
  - B--C, phase studies for
  - C--U--Zr, fabrication and physical properties of

Nomenclature of High Energy Physics

Information on particle-particle events is indexed under subject headings for the specific particles involved. The modifier file word *interactions* is followed by the specific interaction written in symbolic form. Particle nomenclature and symbols follow that of the Particle Data Group published in *Review of Particle Properties* (latest revision). For consistency the incident particle is always written first. The mass (in MeV) of a resonance state is included in parentheses after the symbol to avoid ambiguity. Hyperfragments are indicated in modifiers as in the following examples: Λ-He^5, Σ-H^3, $\Lambda\Lambda$-Be^{10}. The superscript on the right indicates the total number of baryons in the composite system.

Examples:

- MESONS (π^-)
  - interactions $\pi^- + p \rightarrow \Lambda + K^+ + \pi^-$ at 6 GeV/c in hydrogen bubble chamber, $\Lambda K(1700)$ enhancement in, (E)
- BARYONS, RESONANCE (Δ)
  - production of $\Delta^{++}(1236)$ and $\Delta^0(1236)$ from $K^- + p \rightarrow K^- + p + \pi^+ + \pi^-$ interactions at 2.63 and 2.70 GeV/c, (E)
- HYPERNUCLEI
  - binding energy of $\Lambda\Lambda$-He^6, three-body α--Λ--Λ model for

Subject headings are also provided for specific models and theories.

Examples:

- ELEMENTARY PARTICLE MODELS
  - quark, hadron total cross sections in, numerical analysis of
- CURRENT ALGEBRA
  - PCAC hypothesis for A_1 and rho dominance in $\pi \rightarrow e + \nu + \gamma$ decay
- REGGE POLE THEORY
  - predictions for polarization in $K^- + p \rightarrow$ anti $K^0 + n$, $\pi^- + p \rightarrow \pi^0 + n$, and $\pi^- + p \rightarrow$ eta + n interactions at high energies
- SYMMETRY GROUPS
  - SU(2) x SU(4) intermediate-coupling model for nucleon and hyperon isobars

Nomenclature of Reactor Technology

Subject headings for reactors are of three types:

(1) Specific reactors, e.g., ARGONNE RESEARCH REACTOR, SAXTON POWER REACTOR

(2) Reactors having a common physics or engineering characteristic, e.g., REACTORS, FAST; REACTORS, ORGANIC-COOLED; REACTORS, PRESSURIZED-WATER

(3) Reactors having a common purpose, e.g., REACTORS, POWER; REACTORS, RESEARCH

Information on specific reactors, type (1), is indexed under the one specific subject heading. Information on classes or types of reactors, types (2) (characteristics) and (3) (purpose), is indexed under all applicable headings. For example, information on a heavy-water-moderated organic-cooled power reactor is indexed under REACTORS, HEAVY WATER-MODERATED; REACTORS, ORGANIC-COOLED; and REACTORS, POWER.

Subject headings exist for selected reactor components, e.g., REACTOR FUEL ELEMENTS. When applicable, headings for components are indexed even though they may have been included in a modifier under a type (2) or (3) heading. The materials in reactor components are indexed when the information is peculiar to the material.

Modifier file words under reactor headings are of two primary types: one type expresses reactor characteristics, e.g., reactivity; the other, components, e.g., control rod. If no subject heading appears for a reactor component, the heading REACTORS is used, and the component is used as the modifier file word.

A

A-286 (IRON ALLOY)
- radiation effects on tensile properties of bolts of, at cryogenic temperatures for use in NERVA Program, fast neutron, 26:53697 (NASA-TM-X-2440, pp 603-8)
- radiation effects on tensile properties of, at cryogenic temperatures for use in NERVA Program, fast neutron, 26:53696 (NASA-TM-X-2440, pp 595-602)

ACCELERATORS
- book: Radiation Protection at High-Energy Accelerators, 26:53742
- funding for medium energy physics research, outlook for, 26:53740 (LA-4874, pp 21-33)
- power losses in helical, methods of parameter optimization for minimizing, 26:53744
- radiation dose distributions near Ursvik FX-45 electron, Monte Carlo calculations of gamma, 26:53738 (FOA-4-4490-A-3)

ACCELEROMETERS
- design of passive impulse, for underground nuclear explosions, engineering drawings for, 26:53316

ACETAMIDE
- reactions with radiolytic hydrated electrons, kinetics of, 26:53006

ACETAMIDE, 2,2-DICHLORO-N-[2-HYDROXY-1-(HYDROXYMETHYL)ETHYL]-
- radiation effects on antibacterial activity of, and in mixtures with 1-bromo-4-nitrobenzene, nitrobenzene, and p-nitrophenol, γ, 26:52998

ACETIC ACID, [(CARBOXYMETHYLIMINO)BIS(ETHYLENENITRILO)]TETRA-
- effectiveness for removal of americium-241 from rats, 26:53531(T) (UCRL-Trans-1477)

ACETIC ACID, PHENYL-
- radiolysis of aqueous solutions of, rate constants for reaction of hydrogen atoms, hydroxyl radicals, and hydrated electrons in, 26:53015

ACETONE
- oxime, reactions with radiolytic hydrated electrons, kinetics of, 26:53006

ACETONITRILE
- radiolysis of crystals of, ESR studies on, 26:52991 (ORO-2968-78, Paper 6)

ACETYLCHOLINE
- effects on x-radiosensitivity of rat brain, 26:53461(R) (UCB-34-P-82-13)
- metabolism in rats, age dependence of, 26:53461(R) (UCB-34-P-82-13)

ACETYLENE
- yields from argon- and xenon-sensitized radiolysis of gaseous ethylene, 26:53000

ACETYLENEDICARBOXYLIC ACID
- radiolysis of monocrystals of dihydrate, ESR studies on, 26:53005

ACOUSTIC EMISSION TESTING
- use for continuous monitoring for pressure vessel defects, evaluation of, 26:55221 (NP-19338(Vol.1))

ACRYLIC ACID
- polyacrylates--polyethylene, radioinduced crosslinking polymerization of nylon grafted on, 26:53013(P)

ACRYLONITRILE
- radiolysis of crystals of, ESR studies on, 26:52991 (ORO-2968-78, Paper 6)

ACTINIDE HYDRIDES
- preparation and characterization of, p. 41, 26:53066 (ORNL-4794, pp 36-44)

ACTINIDE HYDROXIDES
- crystal structure of, electron microscopic, electron diffraction, and x-ray diffraction studies of, p. 42-3, 26:53066 (ORNL-4794, pp 36-44)

ACTINIDE OXIDES
- crystal structure of, electron diffraction study of, p. 42, 26:53066 (ORNL-4794, pp 36-44)

ACTINIDES
- chemical properties of aqueous solutions of, spectrophotometric studies of, pp. 81-2, 26:53036 (ORNL-4794, pp 81-3)
- complexes of trivalent, research on sulfate and thiocyanate, pp. 39-41, 26:53066 (ORNL-4794, pp 36-44)
- neutron cross sections for heavy, status of reactor, 26:54654 (CONF-720901-(Bks.1 and 2), pp 97-107)
- preparation by vapor deposition, p. 42, 26:53066 (ORNL-4794, pp 36-44)
- production by secondary reactions induced by GeV protons in tungsten and uranium-238, yields for, (E), 26:54672
- production of heavy, survey on prediction of reactor, 26:54654 (CONF-720901-(Bks.1 and 2), pp 97-107)
- properties of ternary hydrides of, literature review on, 26:53558 (UCRL-51244)
- separation from irradiated materials, solvent extraction processes in MILLI laboratory for, 26:53087

ACTINIUM
- separation of protactinium from, by anion exchange, 26:52903

ACTINIUM ISOTOPES Ac-217
- alpha decay of, half-life, Q value, and width for, (E), 26:54651

ACTINIUM ISOTOPES Ac-227
- decay of, γ-ray energies and intensities from, (E), 26:54652 (ANCR-1069)

ACTIVATION ANALYSIS
- book: Neutron Activation Analysis, 26:52912
- laboratory for neutron, at ORNL High Flux Isotope Reactor, features and tests of, 26:52897 (CONF-721010-3)
- methods for art identification, 26:52898 (COO-3034-2)
- methods of, review on, 26:52942
- sensitivity for forensic investigations, 26:52896 (CONF-720920-2)

ADHESIVES
- radioinduced curing of structural, for use in aerospace industry, electron and γ, 26:53716

ADIPONITRILE
- radiolysis of crystals of, ESR studies on, 26:52991 (ORO-2968-78, Paper 6)

AEROSOLS
- distribution of strontium-90 fused clay, in respiratory tract tissues of dogs and monkeys following inhalation, 26:53536

AET
- radioprotective effect on erythropoietic stem cells in mice, proton, 26:53454 (NASA-TM-X-2440, pp 642-6)
- radioprotective effects of, in combination with pantothenic acid on mice, whole-body x, 26:53481

AGE ESTIMATION
- thermoluminescent method for, Risoe development of, 26:53177

AGRICULTURE
- applications of radiation in research in, in Euratom Community, 26:53459(R) (NP-19403)
- heat sources for, feasibility of use of power plant waste heat for, 26:55212 (CONF-720925-2)
- radioactivity monitoring in products of, in Savannah River Area, 1971, 26:53153(R) (DPSPU-72-30-1)
- research in India, 1971--1972, 26:55452(R) (NP-19407)

AIKEN AREA (S.C.)
- radioactivity monitoring in vicinity of, 1971, 26:53153(R) (DPSPU-72-30-1)

AIR
- analysis in mines, electron-capture ionization detector for, 26:53287
- corrosive effects on copper/steel, Inconel/Zircaloy-2, and Zircaloy-2/Zircaloy-2 couples, fretting, 26:53609 (RT/ING-(72)7)
- electron-beam penetration in dense, (E/T), 26:54763
- monitoring of tritium in, gamma compensated flowthrough proportional counter for, 26:53216
- neutron attenuation in, measurement using manganese activation, (E), 26:54490
- neutron transport in, calculation of neutron and γ doses for evaluation of nitrogen neutron cross section sets, 26:54485 (ORNL-TM-3768)

AIRCRAFT
- radiation dose rate measurements at SST altitudes during solar flares, 26:54889 (NASA-TM-X-2440, pp 902-7)
- radiation doses to crew and passengers at SST altitudes from cosmic and solar rays, 26:54888 (NASA-TM-X-2440, pp 894-901)
- radiation monitoring system for SST Concorde, development of hybrid detector, 26:53203 (NASA-TM-X-2440, pp 874-83)

AIRGLOW
- electron energy deposition in water vapor in, (E/T), 26:54033
- intensity at 1304 and 1356 A from atomic oxygen in tropical ionospheric F region, theoretical time-dependent behavior of far uv, 26:54031
- oxygen emission in nightglow, altitude distribution of $O_2(^1\Delta)$ 1.27-μ, (E), 26:54042
- spectral continuum from 4100 to 8200 A, observations of night-sky, 26:54025
- spectral continuum from collision-induced transition of O_2 molecule and from NO + O reaction, (E/T), 26:54024

ALANINE
- radiolysis of frozen aqueous solutions of, ESR study of free radicals from γ, 26:52995

ALDRIN
- radiolysis in lipid solutions, effects of irradiation temperature on γ, 26:52997
- radiolysis of, dissolved in organic solvents, effects of temperature and solvent on γ, 26:53014

ALGAE
- Chlorella pyrenoidosa, radiation effects on reproductive capacity of, effects of energy on external and internal neutron, 26:53394
- Euglena sp., biochemical aspects of phototaxis in, 26:55485 (COO-908-37)

ALIQUAT-336
- solvent properties for cobalt, iron, and manganese, 26:53076

ALKALI METAL HALIDES
- radioinduced destruction of, pulse electron, 26:55012
- reactions with oxide impurities in uranium oxide (U_3O_8) matrix in carrier distillation process, 26:52955 (RT/CHI-(72)4)

ALKALINE EARTH HALIDES
- thermochemical reactions with impurities in uranium oxide matrices during carrier distillation, 26:53719

ALKANES
- radioinduced sulfoxidation of, effects of purity of

  compounds, dose, and pressure on kinetics of, 26:53012

ALLOYS
  crystal structure of dilute, field-ion microscopy studies of, 26:53652
  crystal structure of two-phase, field-ion microscopy studies of, 26:53653
  dislocations and stacking faults in, field-ion microscopy studies of, 26:53649
  fabrication by rolling at high temperature under vacuum, 26:53630
  fracture toughness testing at cryogenic temperatures, conference on, Toronto, Ontario, Canada, June 21 to 26, 1970, 26:53660
  microstructure of ordered, field-ion microscopy studies of, 26:53654
  microstructure of solid-solution, studies of ion microscopy images from, 26:53655
  precipitates in, edgewise growth kinetics of Widmanstaetten, 26:55528 (IS-2838)
  radioinduced point defects in, field-ion microscopy studies of, 26:53704
  strengthening of two-phase, mechanisms of dispersion, 26:53653

ALPHA DECAY
  decay constants for, effect of chemical environment on, (T), 26:54730

ALPHA PARTICLES
  channeling in thin gold crystals, 26:54974 (LYCEN-7228)
  content in environment of Savannah River Plant, 1971, 26:53153(R) (DPSPU-72-30-1)
  detection and measurement from coherent interactions of high-energy particles with helium-4, design and performance of recoil spectrometer for, 26:53281
  detection of, properties of thin films of organic fluorescent materials for, 26:53265
  dose to respiratory tract tissues following inhalation of radon-222 and radon-220 daughter products as aerosols, use of ICRP human lung model for estimation of, 26:53508
  effects on crosslinking and fading in poly(vinyl chloride) containing 1,4-diaminoanthraquinone, 26:53020
  effects on recrystallized grain size and recrystallization temperature of tungsten ribbons, 26:53711
  flux during energetic storm particle event, (E), 26:53966
  interactions $\alpha + d$ at 1 to 200 MeV (cms), optical-potential description of phases for scattering, (T), 26:54532
  interactions in an iron absorber of 10 to 300 GeV/N primary cosmic, (E/T), 26:53831
  propagation of primary cosmic, in interstellar space, (E), 26:53828
  reactions $(\alpha,2n)$ with uranium-238 at 25 MeV, conversion-electron spectra from, (E), 26:54664
  reactions $(\alpha,3n)$, (α,f), and (α,t) with uranium-235 at 24.5 to 28.0 MeV, excitation function for, (E), 26:54665
  reactions (α,γ) with sulfur-34 at 3.6 to 4.8 MeV, γ angular distributions and γ--γ angular correlations for, (E), 26:54560
  scattering by A = 12 to 208 nuclei at 166 MeV, angular distributions for elastic, (E), 26:54547
  scattering by copper-63 and -65 at 5.5 and 7 MeV, γ-γ angular correlations for inelastic, (E), 26:54594
  scattering by erbium-167 at 7 to 10 MeV, with Coulomb excitation, heat-flow analysis of temperature spikes following inelastic, (E/T), 26:54646
  scattering by helium-3 at 115 MeV, cross sections and energy spectra from inelastic, (E), 26:54515
  scattering by holmium-165 at 10 MeV with Coulomb excitation, heat-flow analysis of temperature spikes following inelastic, (E/T), 26:54646
  scattering by lead near the Coulomb barrier, incoming wave boundary condition for elastic, (T), 26:54705
  scattering by silicon-28 at 10, 12, 14, and 18 MeV, α--γ angular correlations from inelastic, (E), 26:54561
  scattering by tin-116, -118, -120, and -124 at 166 MeV, angular distributions for elastic and inelastic, (E), 26:54616
  track size in sodium chloride monocrystals, (E), 26:55016

ALPHA SOURCES
  monitoring of natural, in ground-level atmosphere, meteorological effects on, 26:53160 (UUIM-27)
  preparation of thin-layer americium-241, by electrodeposition from sulfuric acid solutions, 26:53071

ALUMINUM
  analysis for boron by direct spectrophotometry, 26:52928
  cosmic secondary particle dose calculations, heavy galactic, 26:54878 (NASA-TM-X-2440, pp 104-7)
  determination in water samples by spark source mass spectroscopy, 26:52914 (ANL-7860(Pt.3), pp 55-63)
  determination in water, effects of large amounts of copper on spectrographic, 26:52927
  electron and bremsstrahlung dose deposition calculations for shield slab of, comparison of methods for 0.5- to 10-MeV, 26:54886 (NASA-TM-X-2440, pp 801-15)
  electron penetration of semi-infinite slab of, phase-space-time-evolution calculations of 1-MeV, 26:54887 (NASA-TM-X-2440, pp 821-31)
  electron reactions up to 1 keV with, cross sections for formation of Al^{2+} and Al^{3+} in, 26:54103 (FRNC-CONF-51)
  electron scattering by, Monte Carlo study with catastrophic collisions in, 26:54898
  heat transfer from surfaces of pure, to boiling helium, comparison with OFHC copper, 26:54465
  microstructure and stability of coatings of, on chromium-cobalt alloy and Inconel 713C, effects of heat corrosion on, 26:53676
  neon-ion reactions at 0.7 to 4 MeV with, neon isotope effects on cross sections for K-shell ionization in, (E), 26:54114
  neutron reactions at energies up to 16 MeV, cross sections for gamma-ray production in, (E), 26:54960 (NASA-TM-X-2440, pp 500-11)
  oxygen ion reactions at 7.5 to 40 MeV, cross sections for K x-ray production in, (E), 26:54467(R) (ORO-2972-204)
  plasma of, measurements of transient properties of dense, (E/T), 26:54771
  radiation damage in undoped and helium-doped, threshold effect in 150- to 200-keV electron, 26:54990
  radioinduced defects in, relations of quench hardening with electron, 26:53712
  separation from indium by ion exchange chromatography, 26:52949
  thermal capacity of superconducting granular films of, at 1.3 to 8°K, 26:54450

ALUMINUM ALLOYS AND SYSTEMS
  analysis for boron by direct spectrophotometry, 26:52928
  fracture toughness of 2021-T81 and 7039-T61, at room and subzero temperatures, measurement of plane strain, 26:53661
  radiation effects on tensile properties of 7039-T63, at cryogenic temperatures for use in NERVA Program, fast neutron, 26:53697 (NASA-TM-X-2440, pp 603-8)
  tensile properties of boron and Borsic, and silicon carbide fiber-reinforced composites of 1100, 2024, 2219, 5052, 5056, and 6061, transverse, 26:53687
  Al--B, design and fabrication of composites of, for use in aircraft structures, 26:53573
  Al--B, fabrication of resin-bonded composites of, method for, 26:53574
  Al--B, mechanical properties of composites of, for use in aircraft structures, 26:53573
  Al--B, mechanical properties of resin-bonded composites of, 26:53574
  Al--B--SiC, development of aluminum--Borsic composite blades for use in advanced composite engine, 26:53575
  Al--B--SiC, fracture properties of Al--Borsic composites, dynamic, 26:53557 (SC-DC-721080)
  Al--Co--Cr--Mo--Ni-base--Ta--Ti--W, sintering and stress-rupture properties of, effects of boron, carbon, and oxygen additions on, 26:53674
  Al--Co--Cr--Mo--Ni-base--Ti, sintering and stress-rupture properties of, effects of boron, carbon, and oxygen additions on, 26:53674
  Al--Cr--Mo--Nb--Ni-base--Ta--W, production and properties of powder metallurgy components of, for use at high temperatures, 26:53631
  Al--Mo--Sn--Ti-base--Zr, creep rupture of, at 755 and 865°K, cyclic, 26:53690
  Al--Mo--Ti-base--V, crack propagation and embrittlement by gaseous hydrogen, mechanism of, 26:53685
  Al--Ni-base--W--Zr, production and properties of powder metallurgy components of, for use at high temperatures, 26:53631
  Al--Sn--Ti-base, radiation effects on tensile properties of, at cryogenic temperatures for use in NERVA Program, fast neutron, 26:53697 (NASA-TM-X-2440, pp 603-8)
  Al--Ti, reactions of ion-refined surfaces of intermetallic Ti_3Al, with hydrogen and oxygen, field-ion microscopy, studies of, 26:53657
  Al--Ti-base--V, fracture toughness of $\alpha + \beta$ and β processed, at room and subzero temperatures, measurement of plane strain, 26:53661
  Al--U, fission product release from irradiated foils of, mechanisms and measurement of recoil gaseous, 26:53694 (JAERI-Memo-3936)
  Al-base--B_4C--TiH_2, radiation effects on tensile properties of, at cryogenic temperatures for use in NERVA Program, fast neutron, 26:53696 (NASA-TM-X-2440, pp 595-602)
  Al-base--Si, tensile properties of boron, Borsic, and silicon carbide fiber-reinforced composites of, transverse, 26:53687
  Al-base--Zr, crystal structure of intermetallic metastable phase Al_3Zr in molten, produced by rapid solidification, 26:53686

ALUMINUM IONS
  scattering by argon and neon at 8 to 25 keV, total cross sections and interatomic potentials for, (E), 26:54139

ALUMINUM ISOTOPES Al-25
  energy levels from aluminum-27 (p,t) reactions, (E), 26:54551 (COO-535-673)

ALUMINUM ISOTOPES Al-26
  beta and electron-capture decay of, electromagnetic corrections to ft values for, (T), 26:54713
  cosmic-ray production in lunar rocks, (E/T), 26:53860
  energy levels from magnesium-26 (p,n) reactions, rotational-band, (E), 26:54554

ALUMINUM ISOTOPES Al-27
- meson (π) reactions at 100 to 260 MeV, Coulomb flux corrections to total cross sections for, (T), 26:54609
- neon-20 reactions at 85 to 206 MeV, direct-reaction effects in excitation functions and gamma spectra from, (E), 26:54558
- neutron capture by, comparison of ENDF/B III and published data for thermal, 26:54501 (ORNL-TM-3910)
- oxygen-16 reactions at 96 to 165 MeV, direct-reaction effects in excitation functions and gamma spectra from, (E), 26:54558
- photon reactions (γ,n) at 12 to 23 MeV, neutron spectra from, (E), 26:54563
- proton elastic scattering at 15.1 to 22.9 MeV, cross section and depolarization parameter for, (E), 26:54525 (FRNC-TH-191)
- proton reactions (p,t) and (p,He-3) at 27 MeV, angular distributions for, (E), 26:54551 (COO-535-673)
- proton reactions at 3 GeV, time-of-flight measurements of neutron spectra from, (E), 26:54528 (NASA-TM-X-2440, pp 523-6)
- proton scattering at 20 GeV, analysis using Steenberg model, (T), 26:54530

ALUMINUM NITRATES
- $Al(NO_3)_3$--HNO_3--NH_4F, corrosive effects on Corronel 230, HAPO-20 alloy, and Type 304L stainless steel, 26:53604 (BNWL-CC-449)

ALUMINUM NITRIDES
- diffusion of niobium, tantalum, titanium, and vanadium in, 26:53677

ALUMINUM OXIDES
- analysis of thin films of, obtained from reactive sputtering by nuclear reactions and ir spectrophotometry, 26:52902
- fabrication by hot isostatic pressing, 26:53578
- films of, use of proton-excited x rays for thickness measurement on, 26:52945
- growth and hardness of spherical agglomerates of, produced from powders, 26:53577
- ion emission by electron-bombarded, mass-spectral analysis of, 26:54084
- neutron distributions behind $W/Al_2O_3/W$ barriers, spatial, angular, and energy, 26:54966
- phonon resonant scattering in vanadium- and titanium-doped single crystals of, 26:54978
- production of microspheres of, from powders in rotating container, 26:53577
- radiation effects on sintered, ESR spectral studies on γ and in-pile, 26:53699 (RT/FI-(72)10)
- radiation effects on thermal conductivity of vanadium- and titanium-doped single crystals of, γ-, 26:54978
- reactions with alkali metal halides in carrier distillation process for uranium oxide (U_3O_8), 26:52955 (RT/CHI-(72)4)
- sintering of, effects of annealing and ball milling on, 26:53576
- Al_2O_3--Fe, cohesion and structural stability of composites of, effects of chromium, cobalt, manganese, molybdenum, nickel, and titanium additions on, 26:53589
- Al_2O_3--Ni, cohesion and structural stability of composites of, effects of chromium, manganese, and molybdenum additions on, 26:53589
- Al_2O_3--SiO_2, sorptive properties of silver salt-treated, for iodine and methyl iodide, 26:53077 (CONF-720823-9)
- Al_2O_3--SiO_2, viscosity of melts of, 26:55632(T) (UCRL-Trans-1479)

AMERICIUM HYDRIDES
- preparation of divalent, p. 42, 26:53066 (ORNL-4794, pp 36-44)

AMERICIUM ISOTOPES Am-241
- distribution and retention in tissues of rats following inhalation, time dependence of, 26:53531(T) (UCRL-Trans-1477)
- excretion in urine of rats following inhalation, time dependence of, 26:53531(T) (UCRL-Trans-1477)
- preparation of alpha--photon sources of, development of sputtering methods for, 26:53330(R) (BNWL-1308-10)
- preparation of thin-layer α sources of, by electrodeposition from sulfuric acid solutions, 26:53071
- uptake and retention in liver of mammals, mechanisms for, 26:53526(T) (BNWL-tr-71)

AMIDE POLYMERS
- radioinduced crosslinking polymerization of, grafted on polyacrylate--polyethylene system, 26:53013(P)

AMIDES
- positron lifetimes in liquid or solid, effects of dipolar electric fields of amide groups on, (E), 26:54100

AMMETERS
- design of chrono-, for analysis of molten salts, engineering drawings for, 26:52957

AMMONIA
- radiolysis of liquid, preparation of anhydrous hydrazine by electron or γ, 26:53001(P)
- reactions with uranium trioxide powders, factors affecting reduction, 26:53548 (AREAEE-139)

AMMONIUM CHLORIDES
- muon (μ^-) depolarization in aqueous solutions of, effects of chemical reactions, hydrogen peroxide concentration, and temperature on, (E), 26:54099
- positron lifetimes in, measurement of temperature-dependent, (E), 26:55064

AMMONIUM COMPOUNDS, SUBSTITUTED
- tetraethylammonium base, uptake by rat kidneys following injection, effects of uranyl nitrate on, 26:53537

AMMONIUM FLUORIDES
- $Al(NO_3)_3$--HNO_3--NH_4F, corrosive effects on Corronel 230, HAPO-20 alloy, and Type 304L stainless steel, 26:53604 (BNWL-CC-449)

AMMONIUM HYDROXIDES
- muon (μ^-) depolarization in aqueous solutions of, effects of chemical reactions, hydrogen peroxide concentration, and temperature on, (E), 26:54099

AMMONIUM IODIDES
- description of low-temperature, for production of electricity, 26:53108(P)

AMMONIUM PERCHLORATES
- radiolysis of single crystals of, electron microscopic studies of γ and x, 26:52985 (NASA-TM-X-2440, pp 584-94)

AMMONIUM PHOSPHATES
- radiolysis of arsenate-doped, ESR spectra of free radicals from, 26:52979 (COO-1105-179)

AMMONIUM URANIUM FLUORIDES
- preparation of crystals of α-NH_4UF_5 from uranyl compounds, 26:53049(P)

AMMONIUM URANYL CARBONATES
- spectra of, iterative deconvolution method for computer analysis of, 26:53055

AMPLIFIERS
- circuit for gated differential video, design and performance of radiation-hardened, 26:53307 (SC-DC-721159)
- radiation effects on gated differential video, neutron, 26:53307 (SC-DC-721159)

ANALYTICAL CHEMISTRY
- methods for solids, using electron emission by low-energy ion bombardment, 26:52936 (RT/EL-(72)4)

ANGIOSPERMIDAE
- Abelmoschus esculentus (okra), radiation effects on germination, growth, fruit quality, and yield of, following seed exposure, dose dependence of gamma, 26:53390
- Beta sp. (sugar beet), radiation effects on agricultural qualities of, following seed exposure, dose dependence of gamma, 26:53386
- Beta sp. (sugar beet), radiation effects on crop yield, plant morphology, and seed germination of, following seed exposure, dose dependence of gamma, 26:53388
- Beta sp. (sugar beet), radiation effects on, following seed exposure, effects of ploidy on seed germination and weight of, x, 26:53389
- Daucus sp. (carrot), radiation effects on growth and yield of, following exposure of seeds, dose dependence of x, 26:53391
- Hordeum sp. (barley), radiation effects on seeds of, combined effects of space flight environment on genetic, γ, 26:53384
- Hordeum vulgare (barley), radioisotope uptake by, from surface contaminated soils, effects of clinoptilolite on cesium-137 and strontium-90, 26:53540
- Musa paradisiaca (banana), quality improvement by selection, programs in Puerto Rico for, 26:55483 (CONF-720642-1)
- Phaseolus sp. (bean), radiation effects on crop quality and plant photosynthesis and transpiration following seed exposure, dose dependence of gamma, 26:53387
- Phaseolus vulgaris (bean), radioisotope uptake by, from surface contaminated soils, effects of clinoptilolite on cesium-137 and strontium-90, 26:53540
- radiation effects on, combined effects of space flight environment on mutagenesis and survival of, γ, 26:53365 (N-72-20065)
- Raphanus sp. (radish), radiation effects on growth and yield of, following exposure of seeds, dose dependence of x, 26:53391
- Secale sp. (rye), radiation effects on germination and mitotic activity in seeds of, effects of genetic heterogeneity on γ, 26:53392
- Secale sp. (rye), radioinduced chromosome aberrations in root cells of, effects of genetic heterogeneity on frequency of γ, 26:53392
- Tradescantia sp. (spiderwort), multiple mutant sectors in stamen hairs of, 26:55486 (COO-1400-41)
- Tradescantia sp. (spiderwort), radiation effects on, combined effects of space flight environment on cytologic and mutagenic, γ, 26:53382 (N-72-20054)
- Trifolium repens (clover), radioisotope uptake by, from continuously cropped uniformly contaminated soils, effects of clinoptilolite on cesium-137 and strontium-90, 26:53540
- Triticum sp. (wheat), radiation effects on free and bound tryptophan of, dose dependence of gamma, 26:53395
- Zea mays (maize), radiation effects on grain weight and water content of, following seed exposure, dose dependence of gamma, 26:53385
- Zea mays (maize), radiosensitivity of, effects of dose and genotype on thermal neutron, 26:53383

ANILINE, N,N-DIMETHYL-
- complexes with oxyfluorouranate ions, thermogravimetric studies on, 26:53043

ANIMALS
- coumaphos effects on, bibliography on, 26:55578 (ORNL-TIP/TIRC-72-49)
- plutonium-239 uptake and retention in tissues of, following inhalation as oxide aerosols, extrapolation of pathological data to man, 26:53511 (TID-26142)
- radiation effects on behavior of, review of literature on, 26:53448 (COO-1332-78)
- radiation effects on rate of recovery from traumatic injuries, whole-body, 26:53419
- radiation effects on, relevance for prediction of effects on man, 26:53411
- radioisotope uptake and retention in, following release to environment, bibliography on, 26:53530 (TID-3915(Suppl.1))
- radioisotope uptake by marine, from seawater, strontium-90 and zinc-65, 26:53532
- zinc-65 uptake in benthic fauna from Oregon and Washington continental shelf, 26:53149 (RLO-2227-T-12-26)

ANTHRACENE
- radiation damage effects in crystalline, for fast neutron dosimetry, 26:53229 (COO-1105-172)
- radioinduced color centers in single crystals of, absorption spectra of 77°K γ, 26:54996

2-ANTHRACENESULFONIC ACID, 9,10-DIHYDRO-3,4-DIHYDROXY-9,10-DIOXO-
- complexes with niobium, spectrophotometric studies on formation of, 26:52926

ANTHRANILIC ACID
- complexes with oxyfluorouranate ions, thermogravimetric studies on, 26:53043

ANTHRAQUINONE, 1,4-DIAMINO-
- radiation effects on fading of, in poly(vinyl chloride), alpha particle, deuteron, and γ, 26:53020

ANTIBIOTICS
- radiation effects on production of, in Aspergillus, gamma and uv, 26:53393

ANTIBODIES
- synthesis and irreversible differentiation of, RNA to DNA inverted transcription mechanism in, 26:55525 (EUR-4871)

ANTIGENS
- immunochemical studies with carcinoembryonic, 26:55505 (COO-3012-21)

ANTIMONY
- determination in meteoritic and terrestrial materials by neutron activation following separation from other elements, 26:52906
- determination in minerals by neutron activation and γ spectroscopy, nondestructive, 26:52901 (UJV-2851-F,Ch)
- determination in water samples by spark-source mass spectroscopy, 26:52914 (ANL-7860(Pt.3), pp 55-63)
- separation from indium by ion exchange chromatography, 26:52949
- solubility in liquid sodium, tracer studies on, 26:52895 (CONF-710959-, Paper 18)

ANTIMONY ALLOYS AND SYSTEMS
- Mg--Sb, lattice heat capacity of intermetallic Mg_3Sb_2, at 20 to 298°K, 26:53637 (LBL-101)

ANTIMONY ISOTOPES Sb-121
- neutron capture at 25 keV, model analysis of isomeric cross section ratio for, (E/T), 26:54589

ANTIMONY ISOTOPES Sb-124
- distribution in Columbia River, effects of seawater on soluble-suspended, 26:53166 (RLO-2227-T-12-28)

ARCHAEOLOGICAL SPECIMENS
- age of, errors in fission track method for estimation of, 26:53181

ARGON
- abundance in extreme Population I stars and Sun, (T), 26:53892
- abundance in NGC 7662, (E/T), 26:53873
- carbon-ion reactions at 40 to 140 keV with, cross sections for charge exchange in, (E), 26:54137
- effects on radiolysis of gaseous ethylene, 26:53000
- effects on yields from γ radiolysis of gaseous hydrogen sulfide, 26:53011
- electron reactions at 25 keV and small angles with, determination of optical sums from energy-loss spectra from, 26:54128
- gold-atom elastic scattering at 5 to 90 eV by, interatomic potentials and total cross sections for, (E), 26:54142
- helium-atom and -ion reactions at 100 to 5000 eV with, angular and energy distributions of electrons from ionization and autoionization in, (E), 26:54141
- hydrocarbon-ion (CH/sub n/$^+$) reactions at 40 to 140 keV with, cross sections for dissociation and production of hydrogen atoms in, (E), 26:54137
- ion scattering at 8 to 25 keV by, total cross sections and interatomic potentials for, (E), 26:54139
- plasma of, conditions for wave transformation considering nonmonotonic longitudinal distribution, (E/T), 26:54841(T) (AEC-tr-7338)
- plasma of, interaction of pulsed large-current linear-discharge-produced electron beam with, argon-ion stimulated emission from, (E), 26:54787
- plasma of, localization of wave transformation region in shf discharges, (E), 26:54842(T) (AEC-tr-7339)
- plasma of, longitudinal and transverse diffusion coefficients for shf discharges, (E), 26:54776(T) (AEC-tr-7332)
- positron reactions at 8 eV with, total cross sections for, (E), 26:54119
- proton elastic scattering at low and moderate energies by, partial-wave calculations of, 26:54120
- proton reactions at 500 to 3000 eV with, differential cross sections for charge exchange, elastic scattering, excitation to autoionizing levels, and simple excitation in, (E/T), 26:54122
- proton reactions at moderate energies with, excitation by charge-exchange channel in, (T), 26:54120
- reactions with hydroxyl (OH), calculation of cross sections and rate constants for vibration--rotation energy transfer in, using distorted-wave and sudden approximations, 26:54126
- thermal capacity of solid, calculation of, 26:55515 (COO-3161-3)

ARGON HYDRIDES
- potential-energy curves for ground and excited states of ArH^+, LCAO--STO--MO--SCF calculations of, 26:54120

ARGON IONS
- effects on budding haploid yeast cells, sensitivity to lethal, 26:53368
- effects on surface microtopography of iron and copper, 26:55008
- effects on zirconium, calculated damage profiles of, 26:54969 (AECL-4130)
- emission from interaction of pulsed large-current linear-discharge-produced electron beam with argon plasma, stimulated, (E), 26:54787
- scattering by tungsten polycrystalline surfaces at 150 to 1000 eV, angular and energy distributions and cross sections for, (E), 26:54083

ARGON ISOTOPES
- abundance in Mokoia and Allende chondrites, (E), 26:53810

ARGON ISOTOPES Ar-37
- production of, reactor irradiation method and apparatus for, 26:53075(P)

ARGON ISOTOPES Ar-38
- energy levels from sulfur-34 (α,γ) reactions, spin--parity assignments and widths for, (E), 26:54560

ARGON ISOTOPES Ar-41
- content in atmosphere in vicinity of Savannah River Plant, 1971, 26:53153(R) (DPSPU-72-30-1)

ARGON SYSTEMS
- Ar--Hg, ionization of gaseous, 26:53196(R) (COO-323-28)
- Ar--N, radiolysis of, determination of short-lived species from electron pulse, 26:52980(R) (COO-3461-1)

ARGUS OPERATION
- electron belts and effects on Van Allen belts, 26:54044 (NASA-TM-X-2440, pp 178-92)

ARKANSAS NUCLEAR ONE POWER REACTOR
- cooling system for, revised data on, 26:55317 (DOCKET-50313-50)
- owners of, financial data on, 26:55317 (DOCKET-50313-50)
- personnel for, revised data on, 26:55317 (DOCKET-50313-50)
- site for, revised data on meteorology of, 26:55317 (DOCKET-50313-50)

ARSENIC
- determination in environmental samples by neutron activation, 26:52897 (CONF-721010-3)
- determination in thin layers of chalcogenide glasses by proton activation or x-ray fluorescence, 26:52900 (LYCEN-7236)
- determination of trace amounts of, in tobacco by neutron activation, 26:52907
- distribution in cores from Green Bay, relations with depth, 26:53164 (ANL-7860(Pt.3), pp 64-76)
- separation from indium by ion exchange chromatography, 26:52949

ARSENIC ISOTOPES As-74
- distribution and metabolism in tissues of mice, rabbits, and rats following oral administration, time dependence of, 26:53538

ARTERIES
- visualization of normal and occluded, in human limbs, effectiveness of metastable technetium-99-labeled pertechnetate for gamma camera, 26:53542

ARTHROPODA
- nutrient uptake and retention by, in forest floor ecosystem, calcium and potassium, 26:53539(R) (SRO-641-4)

ASTATINE ISOTOPES At-211
- energy levels of, shell-model calculations of wave functions and E2 transition probabilities for low-lying, (T), 26:54650

ASTRON DEVICE
- design of polygonal, with linear field regions, 26:54835(P)

ASTRONAUTS
- proton dose calculations using USAF--NASA model man, 26:54883 (NASA-TM-X-2440, pp 773-80)
- radiation dose and shielding calculations for, methods for, 26:54951 (NASA-TM-X-2440, pp 108-16)
- radiation hazards to, during prolonged space flight, cosmic, 26:53408 (NASA-TM-X-2440, pp 1007-15)
- radioinduced phosphene formation in eyes of, during space flight, cosmic, 26:53407 (NASA-TM-X-2440, pp 1002-6)

ASTRONOMY
- review of 1971 activities at Sydney Univ, 26:53993 (INIS-mf-252)

ASTROPHYSICS
- review of 1971 activities at Sydney Univ, 26:53993 (INIS-mf-252)

ATMOSPHERE
- alpha activity in ground-level, meteorological effects on natural, 26:53160 (UUIM-27)
- balloon flights in, history of use for scientific experiments, 26:54019
- beta activity in, near ground at Marsta Observatory, Sweden, natural, 26:53159 (UUIM-26)
- contamination by transportation vehicles, computer and manual methods for calculation of, 26:55467 (ANL/ES-15)
- cosmic-particle flux and ionization profiles in, balloon measurements of, 26:53807 (NASA-TM-X-2440, pp 908-13)
- cosmic-ray propagation in, theory of galactic, 26:54067 (NASA-TM-X-2440, pp 926-41)
- diffusion and turbulence in, research on, 26:55492 (COO-1585-22)
- gamma-ray shield testing on balloon flights with Ge(Li) detectors, 26:54964 (NASA-TM-X-2440, pp 914-21)
- radioactivity monitoring in Norwegian, 1956 to 1970, 26:53161
- radioactivity monitoring of, in vicinity of Savannah River Plant, 1971, 26:53153(R) (DPSPU-72-30-1)
- radon-220 content in, Nagoya, Japan, Nov. 1968, 26:53227
- thermal effluent effects on meteorological conditions in, 26:53188 (ANL-7860(Pt.3), pp 250-69)

ATMOSPHERIC PRECIPITATION
- radioactivity monitoring in Norwegian, 1956 to 1970, 26:53161

ATOMIC BEAMS
- injection into deuterium--tritium magnetic mirror devices, (T), 26:54757

ATOMIC ENERGY
- industrial requirements of, in Japan, 26:55094
- research activities in France for 1971, 26:55570 (NP-19408)

ATOMIC ENERGY, LEGAL ASPECTS
- legislation regarding nuclear liability in Japan, revision of, 26:55459
- radiation protection legislation in Japan during 1970, enforcement of, 26:55458

ATOMIC MASSES
- measurements of, survey on, 26:54495 (EUR-4765, pp 435-55)

ATOMIC MODELS
- development of realistic, 26:54144
- oscillation corrections to Thomas--Fermi, in quasi-classical approximation, 26:54151

ATOMIC PHYSICS
- bibliography on surface and vacuum physics, 26:54085

ATOMIC STRUCTURE
- calculation for closed-shell many-electron atoms, zero- and first-order Z-expansion coefficients for, 26:54149
- magnetic-field effects on, (T), 26:54144
- pressure effects on, (T), 26:54144
- wave functions in, spin-dependent operators in occupation-branching number representation for open-shell, (T), 26:55077

ATOMS
- electron correlation in, many-particle equations in different orders of perturbation theory for, 26:54148
- electron correlation in, model-independent definition of, 26:54146
- electron density in heavy, spatial oscillations of, (T), 26:54151
- electron interactions in heavy, Hamiltonian and two- and three-body interaction potentials for, (T), 26:54147
- electron interactions in heavy, relativistic corrections for K-, (T), 26:54147
- electron reactions at 2.04 MeV with A = 23 to 83, atomic-number dependence of cross sections for K-shell ionization in, (E), 26:54104
- electron reactions up to few keV with, processes of formation of multicharged ions in, 26:54103 (FRNC-CONF-51)
- electron reactions with, distorted-wave approximation for excitation in, 26:54106
- electron reactions with, role of configuration mixing of diabatic states in excitation in, (T), 26:54117
- energy levels of, symmetries of nonrelativistic, relativistic, and approximate relativistic Coulomb field for first-order Stark shifts for, (T), 26:54374
- energy of degenerate levels of, with two perturbations, double perturbation form for second-order, 26:54152
- energy of many-electron, cluster expansion for, (T), 26:54148
- energy of, calculation using transferred orbitals, 26:54143
- expectation values for, calculation using spin-adapted antisymmetrized products, 26:54154
- form factors in generalized field theory for, 26:54382
- ion reactions with, calculation of ejection probability and energy distribution from negative-, using sudden-switching approximation, 26:54112
- reactions of hot, computer simulation of effect of scavenger competition on, 26:53030
- reactions of hot, effects of scavenger competition in kinetic theory of, 26:53031
- reactions with atoms, ions, and molecules, bibliography and compilation of data on charge exchange, dissociations, excitation, and ionization, in, 26:54118
- reactions with diatomic molecules, effects of attractive Morse potential on quantum mechanical transition probabilities for, (T), 26:54132
- reactions with diatomic Morse oscillators, impulse approximation for vibrational-excitation probabilities in, 26:54131
- reactions with harmonic oscillators, calculation of semiclassical S-matrix elements for transitions in inelastic and reactive, by integration along complex-valued trajectories, 26:54129
- scattering by atoms at 40 to 100 keV, differential cross sections, distances of closest approach, and impact parameters for elastic, (E/T), 26:54101 (EUR-CEA-FC-630)
- scattering by solid surfaces, model for repulsive elastic, based on pairwise interaction potential, 26:54089
- Schroedinger equation for bound states, Sams--Kouri method for noniterative solution to integral form of, 26:54145
- wave functions for many-electron, physical interpretation of cluster expansion of, 26:54146
- wave functions for, asymptotic behavior of bound-state, 26:54153
- wave functions for, direct diagonalization method for generation of Serber-type simultaneous angular-momentum and spin eigenfunctions for use in expansion of, 26:54156
- wave functions for, direct-diagonalization method for generation of Serber-type spin eigenfunctions for use in expansion of, 26:54155
- wave functions for, expansion in terms of spin-adapted antisymmetrized products, 26:54154
- wave functions for, instabilities associated with complex and unrestricted Hartree--Fock, 26:54157
- wave functions for, optimization of transferability of Hartree--Fock valence-shell orbitals, 26:54143
- wave functions for, review of properties and uses of natural spin orbitals in construction of, 26:54150

ATUCHA POWER REACTOR
- construction of, status of, 26:55216

AUGER ELECTRONS
- detection and measurement of, design and performance of retarding field-cylindrical mirror analyzer for, 26:53310 (SC-DC-721302)

AURORAE
- arc event of Mar. 8--9, 1970, spectroscopy of O(^{1}D), O(^{1}S), and N(^{2}D) states during, (E), 26:54014
- creation of polar, relation of magnetosphere and solar wind phenomena with, (E/T), 26:54043
- electron energy deposition in water vapor in, (E/T), 26:54033
- ion origins in, optical measurements of electron and proton precipitations for determination of primary, (E), 26:54012 (SC-RR-720543)
- phenomena of, from simulated steady-flow interaction of charged particles with geomagnetic dipole field, (E), 26:54056
- spectra of radar, auroral-region plasma-instability identification from range-time-intensity film strip and vhf power, (E), 26:54038
- ultraviolet-radiation emission during weak breakup of, sounding-rocket observation on Feb. 18, 1970 of strong extreme, (E), 26:54030

AURORAL ZONE
- geomagnetic conjugacy level decrease with increasing planetary magnetic index K/sub p/ at auroral intensity of 5577 A, (E), 26:54013
- geomagnetic-field pulsations at magnetospheric polar cusp, occurrence of latitude-dependent Pc-4 and Pc-5, (E), 26:54034
- plasma instability identification from study of vhf power spectra of radar aurorae and range-time-intensity film strips, (E), 26:54038

AUSTRALIA
- radiation protection programs in New South Wales during 1971, 26:55454(R) (NP-19412)

AVES
- Gallus sp. (chicken), radiation effects on embryonic development, hatchability, and growth of, phosphorus-32, 26:53517
- Gallus sp. (chicken), radiation effects on immune reactions to adult allogeneic leukocytes in embryos, γ, 26:53477
- Gallus sp. (chicken), radiation effects on survival of young, following acute whole-body exposure, proton, 26:53457 (NASA-TM-X-2440, pp 659-64)
- Gallus sp. (chicken), radioinduced injuries of lymphatic organs in young, following acute sublethal exposure, proton, 26:53457 (NASA-TM-X-2440, pp 659-64)
- radiation effects on morphology and physiology of thyroid gland in, following parenteral injection of iodine-131, β and γ, 26:53515

AVIATION PERSONNEL
- radiobiological vulnerability to weapons during task performance, modular analysis of, 26:54880 (NASA-TM-X-

2440, pp 364-7)

AVR REACTOR
- coolant flow at high Reynolds numbers in, aerodynamics of, 26:55180

B

BACKGROUND RADIATION
- identification and control of Apollo sources of, that interfere with x-ray and gamma experiments, 26:53255 (NASA-TM-X-2440, pp 714-22)

BACTERIA
- Bacillus subtilis, radiation effects on survival and reproduction of spores of, effects of energy level on x, 26:53376
- Clostridium botulinum, radiation effects on growth and toxin production following spore exposure, temperature dependence of sublethal γ, 26:53366(R) (ORO-3347-8)
- Escherichia coli, canavanine death and mechanism of DNA replication in, 26:55491(R) (COO-1562-17)
- Escherichia coli, effects on course of gastrointestinal syndrome in γ-irradiated germ-free newborn swine following artificial colonization, 26:53495
- Escherichia coli, radiation effects on capacity of, to support growth of bacteriophage T4, γ, 26:53372
- Escherichia coli, radiation effects on cell volume and DNA content of parent strain and radioresistant mutant of, x, 26:53363
- Escherichia coli, radioinduced cell killing in, following uptake of tritium-labeled oleate, use for selective enrichment of altered acyl CoA synthetase mutants, β, 26:53518
- Escherichia coli, radioinduced pre-mutational lesions in, comparison of dose-response kinetics and photoreactivation of 254 nm and 313 nm uv, 26:53370
- Escherichia coli, radioinduced reversion mutations in, effects of tryptophan starvation on uv, 26:53379
- intestinal barrier to invasion by, 26:55474 (BNL-17004)
- Micrococcus radiodurans, radioinduced double-strand breaks in DNA of, inhibitory effects of chloramphenicol, dactinomycin, and tetracycline on repair of γ, 26:53349
- radiation effects on DNA in, review of role of enzymes in repair of uv, 26:53351
- radiation effects on DNA replication in, role in molecular repair mechanism, 26:53348
- radioinduced injuries of pathogenic, effects of culture media, dose, and storage temperature on recovery from γ, 26:53369
- radioinduced lesions in DNA in, role of enzymes in repair of uv, 26:53350
- radioinduced lesions in DNA of, role of repair processes in recovery from lethal and mutagenic γ, uv, and x, review of, 26:53357
- radiosterilization of spores of, on space vehicle components, dose response for uv, 26:53367(R) (SC-RR-720516)
- Salmonella typhimurium, radiation effects on growth and prophage induction in, during space flight, combined effects of weightlessness on γ, 26:53364 (N-72-20063)
- Salmonella typhimurium, radiation effects on infectivity of, for chick embryos following exposure of cultures to substerilizing doses, γ, 26:53369
- Staphylococcus sp., radiosensitivity of, relation between loss of pathogenicity and decreased γ, 26:53377

BACTERIOPHAGES
- M13, radiation effects on sedimentation properties of DNA in, in relation to molecular structure, uv, 26:53373
- phiX174, radiation effects on sedimentation properties of DNA in, in relation to molecular structure, uv, 26:53373
- radiation effects on DNA in, review of role of enzymes in repair of uv, 26:53351
- radiation effects on DNA replication in, role in molecular repair mechanism, 26:53348
- radiation effects on induction of, in Salmonella typhimurium during space flight, combined effects of weightlessness on γ, 26:53364 (N-72-20063)
- radioinduced lesions in DNA in, role of enzymes in repair of uv, 26:53350
- radioinduced lesions in DNA of, role of repair processes in recovery from lethal and mutagenic γ, uv, and x, review of, 26:53357
- T4, radiation effects on capacity of Escherichia coli to support growth of, γ, 26:53372

BAILLY POWER REACTOR, UNIT 1
- valves for, verification of wall thickness for nuclear service, 26:55340 (DOCKET-50367-31)

BALLOONS
- use in scientific experiments, history of, 26:54019

BALNEOTHERAPY
- effects of thermal, on recovery of mice following exposure to mixed fast neutron and γ radiation, 26:53465

BARIUM
- content in rock, γ--γ selective method for determination of equivalence between other heavy element and, 26:52943
- determination in geochemical standards by atomic absorption using nitrous oxide--acetylene flame, 26:52921
- determination in water samples by spark-source mass spectroscopy, 26:52914 (ANL-7860(Pt.3), pp 55-63)
- photon reactions (γ,xn) with, model analysis of giant dipole resonance in, (E/T), 26:54598 (FRNC-TH-242)

BARIUM BORIDES
- BaB$_6$--LaB$_6$, preparation, sintering, and thermoemission properties of, 26:53582

BARIUM IONS
- release of clouds of, possible correlation with electron-intensity fluctuations observed on Feb. 14, 1970 in ionosphere, (E), 26:54039

BARIUM ISOTOPES Ba-130
- energy levels of, quasi-band structure in, (E/T), 26:54600 (INSJ-130)
- neutron reactions with, resonance activation integrals for, (E), 26:54585

BARIUM ISOTOPES Ba-131
- energy levels from lanthanum-131 decay, spin--parity assignments for, (E), 26:54643
- energy-level transitions from lanthanum-131 decay, branching ratios and multipolarities for, (E), 26:54643

BARIUM ISOTOPES Ba-132
- energy levels of, quasi-band structure in, (E/T), 26:54600 (INSJ-130)

BARIUM ISOTOPES Ba-133
- design of γ source of, for simulation of spectrum emitted by radioisotope thermoelectric generator, 26:53335 (NASA-TM-X-2440, pp 850-2)
- distribution and retention in rabbits following intravenous injection, kinetics of, 26:53534

BARIUM ISOTOPES Ba-139
- half-life of, (E), 26:54667

BARIUM ISOTOPES Ba-140
- content in Savannah River, 1971, 26:53153(R) (DPSPU-72-30-1)
- monitoring in Sweden from March 23, 1971 USSR underground nuclear explosion, 26:53158 (FOA-4-4502-A-1)

BARIUM ISOTOPES Ba-141
- beta decay endpoint energy of, (E), 26:54601 (IS-T-534)
- half-life of, (E), 26:54667

BARIUM ISOTOPES Ba-142
- half-life of, (E), 26:54667

BARIUM ISOTOPES Ba-143
- beta decay of, prediction of β endpoint energy using Way--Wood diagram, 26:54601 (IS-T-534)

BARIUM ISOTOPES Ba-144
- beta decay of, prediction of β endpoint energy using Way--Wood diagram, 26:54601 (IS-T-534)

BARIUM TITANATES
- radiation effects on dielectric constants and crystal structure of, electron and γ, 26:55020

BARYONS
- coupling to baryons and pseudoscalar mesons, effective-Lagrangian model for, (T), 26:54333
- couplings in chiral SU(3) x SU(3), tensors and axial charges for octet, 26:54371
- decay of, effective Lagrangian model for leptonic, (T), 26:54333
- form factors in parton model, elastic and inelastic, (T), 26:54311
- interactions of, relativistic equation in representation of Schwinger group W(3) for four-particle model of electromagnetic, (T), 26:54368
- interactions of, Schwinger group W(3) for electromagnetic, 26:54368
- interactions with mesons, effective Lagrangian model for, (T), 26:54333
- interactions with mesons, transition amplitudes, cross sections, and partial-wave decompositions for three-particle final state in, 26:54330
- magnetic moments of, Schwinger group W(3) for four-particle model of, (T), 26:54368
- mass of, effective Lagrangian model for, (T), 26:54333
- mixing operator for, representation of SU(3) x SU(3) chiral algebra for, (T), 26:54370 (NP-19418)
- structure of, relativistic equation in representation of Schwinger group W(3) for four-particle model for, 26:54372
- sum rules for octet and decuplet, from commutators of axial charges with axial divergences, (T), 26:54341

BARYONS, RESONANCE
- production in $K^- + n$ interactions at 4.9 GeV/c, cross sections and decay parameters for, (E), 26:54229
- production in $\pi^- + p \to N + 2\pi$ and $\pi^+ + p \to N + 2\pi$ interactions at 1.6 to 2.0 GeV, energy-independent partial-wave analysis of, (T), 26:54328 (LBL-544)
- production of πN, in nonlinear sigma model for nucleon structure, 26:54251
- trajectories of, correlations among, 26:54338

BARYONS, RESONANCE (Δ)
- production of $\Delta(1236)$ in three- and four-prong anti $p + p$ interactions at 7 GeV/c, (E), 26:54218
- production of Δ^0 in $\pi^- + d \to 2p + 2\pi^- + \pi^0$ interactions at 7 GeV/c in deuterium bubble chamber, validity of spectator model for cross sections for, (E), 26:54208 (COO-3065-16)
- production of Δ^{++} in $\gamma + p$ interactions at 2 to 7.5 GeV in hydrogen bubble chamber, cross sections for, (E), 26:54175 (SLAC-143)
- production of $\Delta^{++}(1236)$, $\Delta^0(1236)$, and $\Delta^+(1236)$ in $\pi^- + p$

  $\rightarrow p + \pi^+ + 2\pi^- + \pi^0$ interactions at 20 GeV/c, cross sections for, (E), 26:54207 (COO-3064-3)
BARYONS, RESONANCE (Λ)
  production in $K^- + p \rightarrow$ anti $K^0 + n$ interactions, properties of, (E/T), 26:54210 (NP-19419)
  production of $\Lambda(1405)$ and $\Lambda(1520)$ in $\pi^- + p$ interactions at 4.5 and 6 GeV/c, differential cross sections for, (E), 26:54217
BARYONS, RESONANCE (N)
  production in $\gamma + n \rightarrow n +$ eta and $\gamma + p \rightarrow p +$ eta interactions at threshold to 1.1 GeV, transition amplitudes and cross sections for, (E), 26:54166 (CALT-68-322)
  production of N(1500) and N(1700) in $\pi^- + p \rightarrow p + \pi^+ + 2\pi^- + \pi^0$ interactions at 20 GeV/c, cross sections for, (E), 26:54207 (COO-3064-3)
  production of N(1520) in $\gamma + n \rightarrow \pi^- + p$ interactions at 600 to 1250 MeV, (E), 26:54179
BARYONS, RESONANCE (Σ)
  production in $K^- + p \rightarrow$ anti $K^0 + n$ interactions, properties of, (E/T), 26:54210 (NP-19419)
  production of $\Sigma(1385)$ in $\pi^- + p$ interactions at 4.5 and 6 GeV/c, differential cross sections for, (E), 26:54217
BASALT
  properties for radioactive waste fixation, evaluation of, 26:53057(T) (BNWL-tr-75)
  thorium content of alkali olivine, in USSR, (E), 26:53147
  uranium content of alkali olivine, in USSR, (E), 26:53147
BASTNAESITES
  content in southwest Aswan syenite rock, 26:53142 (AREAEE-138)
BATTERIES
  performance testing of organic electrolyte, at -10 to 60°C, 26:55602 (SC-DC-722298)
BEAM MONITORS
  design and operation of Faraday effect, for relativistic electron beam current measurements, 26:53747 (SC-DR-720447)
  design and performance for MeV ion currents of 0.1 to 10 nA, 26:53802
  design and performance of passive calorimeter, for pulsed electron beam energy measurement, 26:53258 (SC-DR-720630)
BEAM SEPARATORS
  cavity resonators for, surface condition of niobium for superconducting rf, 26:53748
  deflectors for superconducting rf, theory of $\pi/2$-mode biperiodic, 26:53798
  design for producing separated electron beams over 100 GeV by using synchrotron radiation, 26:53801
BEARINGS
  design and fabrication of gas, for production machine tools, 26:53113 (Y-DA-4541(Rev.1))
BEHAVIOR
  radiation effects on learned-task performance, of monkeys following continuous whole-body exposure, effects of dose and dose rate on γ, 26:53452 (NASA-TM-X-2440, pp 633-40)
  radiation effects on stress-related performance, in man following continuous or protracted fractionated whole-body exposure, effectiveness of pulmonary-impedance power spectral analysis for determining γ, 26:53401 (NASA-TM-X-2440, pp 238-48)
  radiation effects on, of animals, review of, 26:53448 (COO-1332-78)
BELGIUM
  applications of radiation in agriculture research in, 26:53459(R) (NP-19403)
BELL STATION POWER REACTOR
  heated effluents from, prediction of effects on Cayuga Lake of, 26:53192
  radioisotope releases from, to Cayuga Lake, evaluation of effects of, 26:53192
BENZENE
  effects on γ-induced thermoluminescence of cyclohexene, 26:53010
BENZENE, 1-BROMO-4-NITRO-
  radiation effects on antibacterial activity of, and in mixtures with 2,2-dichloro-N-[2-hydroxy-1-(hydroxymethyl)ethyl]acetamide, γ, 26:52998
BENZENE, p-DICHLORO-
  radiation effects on crystals of, studies on γ, neutron, and x, 26:52984 (FRNC-TH-262)
BENZENE, NITRO-
  radiation effects on antibacterial activity of, and in mixtures with 2,2-dichloro-N-[2-hydroxy-1-(hydroxymethyl)ethyl]acetamide, γ, 26:52998
BENZENE, TETRACHLORO-
  spectroscopy of, phosphorescence--microwave double resonance, 26:55623(R) (UCLA-34-P-91-48)
BENZYL ALCOHOL
  reactions with radiolytic hydrated electrons, kinetics of, 26:53006
BERYLLIUM
  determination in geochemical standards by atomic absorption using nitrous oxide--acetylene flame, 26:52921
  fabrication of thin wall tubes of, by hot isostatic pressing, 26:53618
  radiation effects on tensile properties of, at cryogenic temperatures for use in NERVA Program, fast neutron, 26:53696 (NASA-TM-X-2440, pp 595-602)
BERYLLIUM ALLOYS AND SYSTEMS
  Be--Cu-base, mechanical properties and stress relaxation of Alloy 25 at -320 to 300°F, 26:53641 (SC-DR-720471)
BERYLLIUM FLUORIDES
  BeF_2--LiF, thermodynamic evaluation for use as fusion reactor coolant, 26:54827 (IPP-4/97)
BERYLLIUM HYDRIDES
  stability at 25 to 250°C, 26:53714 (NAA-SR-8533)
BERYLLIUM ISOTOPES Be-6
  resonance in ^{3}He + ^{3}He system, implications for solar neutrino emission of, (T), 26:54508
BERYLLIUM ISOTOPES Be-7
  content in rainwater and vegetation in vicinity of Savannah River Plant, 1971, 26:53153(R) (DPSPU-72-30-1)
BERYLLIUM ISOTOPES Be-9
  deuteron reactions (d,n) at 30 keV to 1.5 MeV, calculation of thick target yields for, (T), 26:54502 (SC-RR-720513)
  deuteron reactions (d,n) at 50 and 54 MeV, biological implications of neutron spectra from, (E/T), 26:53804
  neutron capture by, comparison of ENDF/B III and published data for thermal, 26:54501 (ORNL-TM-3910)
  proton elastic scattering at 15.1 to 22.9 MeV, cross section and depolarization parameter for, (E), 26:54525 (FRNC-TH-191)
  proton reactions (p,π^-) and (p,π^+) at 600 MeV, cross sections and spectra from, (E), 26:54535
  proton scattering at 20 GeV, analysis using Steenberg model, (T), 26:54530
BERYLLIUM ISOTOPES Be-10
  abundance in primary cosmic radiation, (E), 26:53833
  cosmic-ray production in lunar rocks, (E/T), 26:53860
BETA DECAY
  book: Beta Processes. Functions for Analyzing Beta Spectra and Electron Capture, 26:54740
  corrections of order $Z\alpha^2$ and $Z^2\alpha^3$ to pure Fermi, calculation of electromagnetic, (T), 26:54713
  theory of, limitation on use of impulse approximation in, (T), 26:54709
BETA PARTICLES
  content in environment of Savannah River Plant, 1971, 26:53153(R) (DPSPU-72-30-1)
  detection of, retained on resin columns, design and performance of Geiger--Mueller counter for, 26:53212
  dose distribution in man following administration of colloids of gold-198 or phosphorus-32 for treatment of malignant pleural effusions, time dependence of, 26:53509
  dose distribution in orthogonal plane surrounding iridium-192 wires implanted for interstitial therapy, effects of arrangement, number, and size of implants on, 26:53422
  dose distribution in respiratory tract of dogs and monkeys following inhalation of strontium-90 as fused clay aerosols, 26:53536
  dose to fingers of medical personnel during injection of radioisotopes, phantom studies of, 26:53424
  dose to personnel, comparison of results of actual and phantom measurements of, 26:53426
  dosimetry of tritium, grid-walled proportional counter study of micro-, 26:54895
  dosimetry of, ^{7}LiF thermoluminescent dosimeter for personnel, 26:53249
  effects on cells following incorporation of β-emitting radioisotopes into DNA, comparison of effects of external x-ray exposure with lethal and mutagenic, 26:53505
  effects on DNA following incorporation of β-emitting radioisotopes, repair processes for, 26:53505
  effects on thrombocyte count in man following intravenous injection of colloidal gold-198 for therapy of liver involvement in Hodgkin's disease, relation of dose fractionation and protraction to, 26:53507
  effects on water vapor, energy for ion pair formation from, 26:53196(R) (COO-323-28)
  production in atmosphere by high-altitude nuclear explosions, review, 26:54044 (NASA-TM-X-2440, pp 178-92)
BETA SOURCES
  activity in atmosphere near ground at Marsta Observatory, Sweden, natural, 26:53159 (UUIM-26)
  activity measurements of, in radiator solution, Cherenkov detector for, 26:53209
  dose distribution near implanted β and mixed β/γ emitters, (T), 26:54897
  use in skin cancer therapy, description of equipment for, 26:53341
BETA SPECTROMETERS
  description of compact magnetic, for in-beam measurements of internal conversion coefficients, 26:53264
  theory of magnetic prism, review of, 26:53259
BIBLIOGRAPHIES
  on boiling crisis and critical heat flux, 26:55179 (TID-25887)
  on carcinogenicity of 1-methyl-3-nitro-1 nitrosoguanidine, 26:55583 (ORNL-TIP/TIRC-72-60)
  on chemical radioprotective compounds, 26:53460 (SZS-132)

- on control, handling, and monitoring of tritium, 26:53155 (MLM-1946)
- on coumaphos effects on animals, 26:55578 (ORNL-TIP/TIRC-72-49)
- on excitation in heavy-particle collisions, 26:54118
- on hematopoiesis in fish, 26:53447 (CONF-720822-2)
- on material for use by parents of handicapped children, 26:55576 (ORNL-TIP/TIRC-72-13)
- on maximum safe levels of fluorine for animals and man, 26:55580 (ORNL-TIP/TIRC-72-53)
- on pharmacology and toxicology of diethyl oxydiformate, 26:55579 (ORNL-TIP/TIRC-72-52)
- on plasma physics and fusion reactors, 26:54748
- on pyramidon effect on hematopoietic system of mammals, 26:55582 (ORNL-TIP/TIRC-72-59)
- on radiation effects on food, 26:53342 (AED-C-5-11)
- on radioecology, 26:53530 (TID-3915(Suppl.1))
- on reactor noise analysis, 26:55443 (RT/FI-(72)13)
- on surface and vacuum physics, 26:54085
- on technical publications issued by BNL Radiation Division, July 1968 through June 1971, 26:53325 (BNL-50335)
- on thermal effects on aquatic organisms, 1971 survey, 26:53190 (ORNL-EIS-72-28)
- on thermal neutron scattering, 26:54602 (JAERI-M-4666)
- on toxicity data for imido esters, 26:55581 (ORNL-TIP/TIRC-72-54)
- on toxicity of elemental phosphorus, 26:55586 (ORNL-TIP/TIRC-72-63)
- on toxicity of potassium iodates for animals and man, 26:55575 (ORNL-TIP/TIRC-72-10)
- on toxicity of quartz particles, 26:55585 (ORNL-TIP/TIRC-72-62)
- on toxicology of isopentylamine, 26:55584 (ORNL-TIP/TIRC-72-61)
- on unclassified PEL reports, 26:55592 (PEL-220)
- on USAEC materials and metallurgy research programs for 1972, 26:53600 (WASH-1181-72)
- Regional Modeling Abstracts, Vol. III, 26:55573 (ORNL-NSF-EP-23)

BIG ROCK POINT POWER REACTOR
- neutron monitoring startup channels for, failure of, 26:55277 (DOCKET-50155-124)
- radioactive effluents from, effects on radioisotope content in Lake Michigan fish, 26:53169 (ANL-7860(Pt.3), pp 141-50)
- thermal effluents from, ecological studies on effects of, 26:53182 (ANL-7860(Pt.3), pp 101-2)
- valves for, verification of wall thicknesses for nuclear service, 26:55278 (DOCKET-50155-125)
- waste processing systems for, malfunction of holdup line for off gas, 26:55237 (DOCKET-50155-123)

BIOCHEMISTRY
- research in India, 1971--1972, 26:55452(R) (NP-19407)

BIOLOGICAL MATERIALS
- radiation effects on, 26:53396

BIOLOGICAL MODELS
- description of USAF--NASA Computerized Anatomical Model Man for calculating radiation doses for space missions, 26:54883 (NASA-TM-X-2440, pp 773-80)
- development for multi-parameter analysis of radioisotope kinetics in biological systems, 26:53519
- development for nutrient uptake and retention in forest floor-arthropod ecosystems, 26:53539(R) (SRO-641-4)
- development for radiation effects on epidermal cell kinetics in swine, 26:53450 (LA-4874, pp 126-44)
- development of heart, for measurements of blood volume distribution using iodine-131 scanning, 26:53543

BIOLOGICAL STRESS
- radioinduced, in man following continuous or fractionated dose exposure, effectiveness of pulmonary-impedance power spectral analysis for diagnosis of, 26:53401 (NASA-TM-X-2440, pp 238-48)

BIOLOGICAL SYSTEMS
- energy conversion processes in, at molecular level, EPR studies on, 26:55616(R) (TID-26149)

BIOLOGY
- metric concepts for molecular taxonomy, 26:55545 (LA-4973)
- research in India, 1971--1972, 26:55452(R) (NP-19407)

BIOTITES
- analysis of granitic, for cesium by neutron activation and γ spectrometry, 26:52908

BIPYRIDINE
- complexes with oxyfluorouranate ions, thermogravimetric studies on, 26:53043

BISMUTH
- determination in chalcopyrite and galena by neutron activation and α scintillation counting, 26:52910
- determination in water samples by spark-source mass spectroscopy, 26:52914 (ANL-7860(Pt.3), pp 55-63)
- determination in water, effects of large amounts of copper on spectrographic, 26:52927
- diffusion in mercury at 25°C, 26:53636 (IS-T-554)
- distribution between liquid bismuth--lithium alloys and molten lithium chloride, p. 4, 26:53081 (ORNL-4794, pp 1-14)
- separation from indium by ion exchange chromatography, 26:52949
- solubility in rare earth--thorium solutions, free energies of formation for compounds produced by, 26:53664
- solvent properties of liquid, for rare earths and thorium, pp. 4-5, 26:53081 (ORNL-4794, pp 1-14)
- sorption on diethylaminoethylcellulose in methanol--thiocyanate--hydrochloric acid media, 26:52951

BISMUTH ISOTOPES Bi-209
- fission of, isomer ratios of niobium-95 from, (E), 26:54627

BISMUTH ISOTOPES Bi-214
- content in uranium mine air, α-spectrometric method for determining, 26:53226

BLACK HOLES
- physics of, violation of second law of thermodynamics in, (T), 26:53906
- potentials in general relativity for, nonlinear generalization of Maxwell equations for static repulsive, (T), 26:54404

BLOOD
- alterations in rodent, seasonal, 26:55587 (ORNL-TM-3898)
- analysis for vitamin B_{12} by radiochemical method, 26:52938
- arsenic-74 uptake and retention by, of mice, rabbits, and rats following oral administration, time dependence of, 26:53538
- radiation effects on human, following extracorporeal exposure, effects of dose on count of lymphocytes in, 26:53440
- volume distribution in heart, measurement by iodine-131 scanning, 26:53543

BLOOD CELLS
- radiation effects on, of rats following intratracheal administration of cerium-144, 26:53516

BLOOD PLATELETS
- radiation effects on serotonin uptake by, in rabbits in relation to content during acute radiation syndrome, γ, 26:53486

BOILERS
- design of 1 MW liquid sodium--water steam generator, for leak tests, 26:55153 (CONF-710548-, pp 57-104)
- development of sodium--water steam generator, test programs for, 26:55155 (CONF-710548-, pp 129-54)
- leak testing of straight tube, parameters for large, 26:55151 (CONF-710548-, pp 17-38)
- leakage of water into sodium in steam generator, damage and effects on safety of, 26:55150 (CONF-710548-, pp 1-16)
- leaks in sodium--water steam generators, use of hydrogen detector for detection of small, 26:55156 (CONF-710548-, pp 155-70)
- leaks of water into liquid sodium in 1 MW steam generator, corrosive effects on tube bundles of, 26:55153 (CONF-710548-, pp 57-104)
- leaks of water into sodium in steam generator, effects of reactions from, 26:55154 (CONF-710548-, pp 105-28)
- performance of 1 MW sodium--water steam generator, 26:55153 (CONF-710548-, pp 57-104)
- performance of sodium--water steam generator, 26:55159 (CONF-710548-, pp 206-12)
- safety of sodium--water steam generators, 26:55159 (CONF-710548-, pp 206-12)
- tube failure in austenic steel steam generator, effects of sodium--water reactions on, 26:55161 (CONF-710548-, pp 221-42)

BOILING
- crisis in water cooled reactors, critical review on state of the art on, 26:55179 (TID-25887)
- detection of sodium, acoustic method for, 26:55083(R) (EURFNR-1001)

BONDING
- surface preparation for adhesive, 26:55597 (SC-DC-714099)

BONDS, CHEMICAL
- research on covalently bonded compounds of light elements, 26:55523(R) (COO-3544-1)

BONE MARROW
- radiation dose to human, following whole-body exposure, use of lithium fluoride dosimeters in Alderson Rando phantom for calculation of γ, 26:53406 (NASA-TM-X-2440, pp 974-80)
- radiation dose to, of medical personnel during arteriography, x, 26:53443
- radiation effects on rat, role of thymus gland in recovery from γ, 26:53479
- radiation effects on ratio of erythrocytes to leukocytes in, of mice, evaluation for use as biological dosimeter following whole-body exposure, 26:53473
- radioinduced chromosome aberrations in cells of human, following local therapeutic exposure, effects of dose and time on frequency of γ, 26:53445
- radioinduced leukemic transformations in, of mice following intraperitonal injection of strontium-90, β, 26:53512
- radioinduced suppression of hematopoietic function of, in monkeys following continuous and subsequent fractionated whole-body exposures, effects of dose and dose rate on recovery from γ, 26:53452 (NASA-TM-X-2440, pp 633-40)

BONES
- arsenic-74 uptake and retention by, of mice, rabbits, and rats following oral administration, time dependence of, 26:53538
- homeostatic function of, in relation to calcium

    metabolism, 26:55477 (BNL-50345)
  radiation effects on maxillary, of dogs following exposure of teeth, effects of lead bridges and plastic caps on γ, 26:53480
  radioinduced necrosis of jaw, in man following therapy of neoplasms of head and neck region, 26:53418
  strontium-90 content of samples of human, collected in France during 1970 in relation to stable strontium content, 26:53520 (CEA-N-1535)
  x-ray dose across plane interface with tissue, contribution of photoelectrons to, (T), 26:54896
BORIDES
  fracture toughness of composites of, effects of carbon and nickel on, 26:53581
BORON
  abundance in primary cosmic radiation, (E), 26:53833
  coating with boron nitride, method for surface, 26:53572
  content profile in silicon and silica, determination of, using secondary ion emission, 26:52937
  deposition on carbon monofilament substrate, problems in chemical vapor, 26:53571
  determination in aluminum and aluminum alloys by direct spectrophotometry, 26:52928
  determination in water samples by spark source mass spectroscopy, 26:52914 (ANL-7860(Pt.3), pp 55-63)
  dimensions and mechanical properties of advanced composites of, fabricated by cocuring process, 26:53570
  effects of fiber reinforcements of, on transverse tensile properties of aluminum composites, 26:53687
  effects on sintering and stress-rupture properties of nickel-base alloys, 26:53674
  fabrication of advanced composites of, cocuring method for, 26:53570
BORON CARBIDES
  Al-base--B_4C--TiH_2, radiation effects on tensile properties of, at cryogenic temperatures for use in NERVA Program, fast neutron, 26:53696 (NASA-TM-X-2440, pp 595-602)
BORON IONS
  effects on budding haploid yeast cells, sensitivity to lethal, 26:53368
  effects on silicon at 40 keV, rod-like defects produced in, 26:54995
  implantation in amorphous silicon at 22 keV, secondary-ion mass spectrometric study of profile of, 26:55014
  reactions with copper and tantalum at 10.4 MeV/nucleon, neutron yield from, (E), 26:54881 (NASA-TM-X-2440, pp 520-2)
BORON ISOTOPES B-10
  proton elastic scattering at 15.1 to 22.9 MeV, cross section and depolarization parameter for, (E), 26:54525 (FRNC-TH-191)
BORON ISOTOPES B-12
  nuclear dynamics of, particle--hole description of semileptonic electromagnetic and weak interactions in, (T), 26:54541
BORON NITRIDES
  deposition on boron fibers, method for surface, 26:53572
  radioinduced paramagnetic centers in hexagonal, correlation of EPR, thermally stimulated current, and thermoluminescence of γ, 26:55015
BORON OXIDES
  reactions with alkali metal halides in carrier distillation process for uranium oxide (U_3O_8), 26:52955 (RT/CHI-(72)4)
BORON SYSTEMS
  Al--B, design and fabrication of composites of, for use in aircraft structures, 26:53573
  Al--B, fabrication of resin-bonded composites of, method for, 26:53574
  Al--B, mechanical properties of composites of, for use in aircraft structures, 26:53573
  Al--B, mechanical properties of resin-bonded composites of, 26:53574
  Al--B--SiC, development of aluminum--Borsic composite blades for use in advanced composite engine, 26:53575
  Al--B--SiC, fracture properties of Al--Borsic composites, dynamic, 26:53557 (SC-DC-721080)
  B--graphite, dimensions and mechanical properties of advanced composites of, fabricated by cocuring process, 26:53570
  B--graphite, fabrication of advanced composites of, cocuring method for, 26:53570
  B--polyimide, development of composite blades of, for use in advanced composite engine, 26:53575
  B--SiC, effects of fiber reinforcements of Borsic on transverse tensile properties of aluminum composites, 26:53687
BOROSILICATES
  radiation effects on transmittance of BK-7 glass, electron, 26:54049 (NASA-TM-X-2440, pp 748-55)
BOSONS
  interactions with excited two-level system, mean transverse spin components from, (T), 26:55075
  interactions with excited two-level system, stationary level populations from, (T), 26:55076
  interactions with massive scalar and massless spinor fields, quantum two-dimensional classically solvable model with nontrivial scattering for, (T), 26:54385
  production of pairs of scalar, in threshold region by square-well potential with smooth sides, probability for, (T), 26:54384
  stability of many-body systems with singular attractive potentials, self-consistent Hartree field as limit for Schroedinger equation for, (T), 26:54408 (ITF-72-14-E)
  thermodynamic stability of nonideal Bose--Einstein gas, (T), 26:54432
BOSONS, INTERMEDIATE
  production of W^- in $e^+ + e^-$ colliding-beam interactions, total cross sections and angular and energy distribution for, (T), 26:54277
BRAIN
  arsenic-74 uptake and retention by, of mice, rabbits, and rats following oral administration, time dependence of, 26:53538
  metabolism of palmitic acid in developing rat, tracer study, 26:55620 (UCLA-12-871)
  radiation effects on human, following hypophysectomy using proton beams, 26:53446
  radiation effects on, comparison for rats and sharks, gamma, 26:53487
  radioinduced malformations in, of mice and rats following prenatal exposure, effects of developmental stage at exposure on, 26:53437
  radiosensitivity of rat, relation of content of acetylcholine to, 26:53461(R) (UCB-34-P-82-13)
BRASS
  analysis for copper by amperometric titration, 26:52924
  deuterium-molecule reactions with surfaces of, secondary-electron emission coefficients for, (E), 26:54105
  hydrogen-molecule reactions with surfaces of, secondary-electron emission coefficients for, (E), 26:54105
BREMSSTRAHLUNG
  dose deposition calculations for plane slabs, comparison of methods for 0.5- to 10-MeV, 26:54886 (NASA-TM-X-2440, pp 801-15)
  emission from relativistic particles in turbulent plasma, (T), 26:54774(T) (AEC-tr-7323)
  production in inelastic $\nu + \mu$ interactions, four-component neutrino theory for e and μ polarization effects on form of spectra for, (T), 26:54290
  production in potential scattering, soft-photon theorem for, 26:54737
  production of soft, in $p + p \to \pi^+ + d + \gamma$ interactions, amplitudes of, (T), 26:54250
  reactions $(\gamma,2n)$ with yttrium-89 at 23 to 50 MeV, calculation of isomer ratio in, (T), 26:54725
  reactions (γ,n) with $Z = 13$ to 82 nuclei at 12 to 23 MeV, neutron spectra from, (E), 26:54563
  reactions (γ,xn) with lanthanum-139 and praseodymium-141 at 8 to 24 MeV, cross sections for, (E), 26:54629
  scattering by concrete, iron, and lead at 2.0 to 10.5 MeV, dose albedos of back-angle, (E), 26:54892
  spectra of suprathermal proton cosmic, (E/T), 26:53820
BRICKS
  age of, thermoluminescent method for estimation of, 26:53177
BROMINE
  determination in environmental samples by neutron activation, 26:52897 (CONF-721010-3)
  determination of trace amounts of, in tobacco by neutron activation, 26:52907
  solubility in liquid sodium, tracer studies on, 26:52895 (CONF-710959-, Paper 18)
BROMINE ISOTOPES Br-79
  neutron capture at 25 keV, model analysis of isomeric cross section ratio for, (E/T), 26:54589
BROMINE ISOTOPES Br-80
  half-life of, (E), 26:54595
BROMINE SYSTEMS
  Br--HBr, photolysis of, deuterium isotope effects on reactions of hot hydrogen atoms from, 26:52962
BRONZE
  analysis for copper by amperometric titration, 26:52924
BRUNSWICK POWER REACTOR, UNIT 1
  engineered safeguards for, effects of circulating water system failure on flooding of, 26:55329 (DOCKET-50324-43)
BRUNSWICK POWER REACTOR, UNIT 2
  engineered safeguards for, effects of circulating water system failure on flooding of, 26:55329 (DOCKET-50324-43)
BUBBLES
  thermal equilibrium of vapor, near heated solid surface, model for prediction of, 26:53119 (AREAEE-122)
BUILDING MATERIALS
  damage to distant, from mechanical effects of underground nuclear explosions in granite, (E), 26:53129(T) (UCRL-Trans-10616-2)
BULK SHIELDING FACILITY
  operation during April to June 1972, 26:55408(R) (ORNL-TM-3949)
  operation of PCA in, during April to June 1972, 26:55408(R) (ORNL-TM-3949)
1,3-BUTANEDIONE, 4,4,4-TRIFLUORO-2-METHYL-1-(2-THIENYL)-
  solvent properties for cerium, synergistic effect of tri-n-octylamine on, 26:52952
1,3-BUTANEDIONE, 4,4,4-TRIFLUORO-1-(2-THIENYL)-
  solvent properties for tetravalent plutonium, 26:53034(T) (MLM-1964(tr))

C

CABLES
  power transmission by superconducting, underground, 26:54461 (BNL-50325)
CADARACHE REACTORS (RAPSODIE)
  cooling system of, decontamination of primary, (E), 26:55163 (CONF-710959-, Paper 3)
  cooling system of, post operation inspection and monitoring of, 26:55162 (CONF-710959-, Paper 2)
  fuel burnup in, program for measurement of, 26:55119 (CONF-720901-(Bks.1 and 2), pp 888-904)
  fuel element failures in, radioactive tracer technique for locating, 26:55185 (CONF-710959-, Paper 1)
  fuel elements of, location and effects of rupture of pin, 26:55162 (CONF-710959-, Paper 2)
  pumps of, decontamination of primary coolant, 26:55163 (CONF-710959-, Paper 3)
  rare gas transport in, 26:55185 (CONF-710959-, Paper 1)
CADMIUM
  cyclotron resonance in magnetic field in radio frequency region, Doppler-shifted, (E/T), 26:55044
  determination in environmental samples by neutron activation, 26:52897 (CONF-721010-3)
  determination in lunar, meteoritic, and terrestrial materials by neutron activation following separation from other elements, 26:52906
  determination in minerals by neutron activation and γ spectroscopy, nondestructive, 26:52901 (UJV-2851-F,Ch)
  determination in organometallic compounds using oxine method after combustion, gravimetric or titrimetric, 26:52930
  determination in water samples by spark-source mass spectroscopy, 26:52914 (ANL-7860(Pt.3), pp 55-63)
  distribution in cores from Green Bay, relations with depth, 26:53164 (ANL-7860(Pt.3), pp 64-76)
  effects on exit-tube measurements of neutron spectra, (E), 26:54470 (AREAEE-133)
  separation from indium by ion exchange chromatography, 26:52949
  sorption on diethylaminoethylcellulose in methanol--thiocyanate--hydrochloric acid media, 26:52951
  spectra of, relative isotope shifts in, (E), 26:54625
CADMIUM ALLOYS AND SYSTEMS
  Ag--Cd, phase transformation interfaces in, properties of massive, 26:53644
  Au--Cd, lattice heat capacity of intermetallic AuCd, at 20 to 298°K, 26:53637 (LBL-101)
  Cd--Mg, superconductivity in, (E), 26:54444
  Cd--Zr, phase diagrams for, 26:53663
  Cd--Zr, thermodynamic properties of, 26:53663
CADMIUM ISOTOPES Cd-112
  neutron reactions with, resonance parameters for, (E), 26:54599 (IAE-2116)
CADMIUM ISOTOPES Cd-114
  energy level of, multiple Coulomb interference effects on quadrupole moment of first 2+, (E), 26:54623
  helium-3 inelastic scattering at 10 to 17 MeV, collective model calculation of form factor for, (E/T), 26:54621
CADMIUM ISOTOPES Cd-115
  isomer yield ratios of, relation to excitation energies, (E), 26:54628
CADMIUM ISOTOPES Cd-116
  neutron reactions (n,2n), isomer yield ratio for, (E), 26:54628
CADMIUM SULFIDES
  radiation effects on donor--acceptor pair luminescence of, electron, 26:55002
  radiation effects on orientation of thin films of, electron-diffraction study of 3-MeV electron, 26:54992
  radiation effects on photocurrent--voltage characteristics of films of, γ, 26:54998
CAFFEINE
  effects on recombinational repair mechanisms for uv-radioinduced lesions in Schizosaccharomyces pombe, inhibitory, 26:53371
CALCIUM
  abundance in γ Cap, (E), 26:53888
  determination in geochemical standards by atomic absorption using nitrous oxide--acetylene flame, 26:52921
  electron reactions at 10 to 40 eV with, cross sections for formation of Ca^{2+} in, 26:54103 (FRNC-CONF-51)
  metabolism in small intestine of animals, role of vitamin D in, 26:55498(R) (COO-1668-46)
  neutron capture by, comparison of ENDF/B III and published data for thermal, 26:54501 (ORNL-TM-3910)
  oxygen ion reactions at 7.5 to 40 MeV, cross sections for K x-ray production in, (E), 26:54467(R) (ORO-2972-204)
  oxygen-16 elastic scattering near the Coulomb barrier, incoming wave boundary condition for, (T), 26:54705
  reactions with plutonium tetrafluoride, estimation of minimum temperatures in bomb reduction, 26:53037 (RFP-1455)
  transport to plant roots by diffusion and mass flow, 26:55490 (COO-1495-17)
CALCIUM CARBONATES
  reactions with yellow organic acids in freshwater, 26:55494 (COO-1599-63)
CALCIUM FLUORIDES
  paramagnetic relaxation in cerium-doped, initiated by flux jumping of Type-II superconductors, (E), 26:55029
CALCIUM IONS
  production in PIG source, 26:53752 (FRNC-CONF-54)
CALCIUM ISOTOPES
  energy levels of even, self-consistent Hartree--Fock, Hartree--Fock--Bogolyubov, and spherical BCS calculations using central Yukawa interaction and Hamada--Johnston and Tabskin potentials, (T), 26:54583
CALCIUM ISOTOPES Ca-40
  alpha elastic scattering at 166 MeV, angular distribution for, (E), 26:54547
  deuteron reactions (d,Li-6) at 28 MeV, angular distributions and spectroscopic factors for, (E), 26:54527 (LYCEN-7219)
  deuteron reactions (d,pγ) at 3 MeV, γ-ray angular correlations for, (E), 26:54578
  energy level at 3.74 MeV from proton inelastic scattering, lifetime of, (E), 26:54575
  energy levels from proton inelastic scattering, (E), 26:54582
  energy-level transition from proton inelastic scattering, strength of E3, (E), 26:54575
  meson (π) reactions at 100 to 260 MeV, Coulomb flux corrections to total cross sections for, (T), 26:54609
  muon (μ^-) capture by, polarization of emitted neutron in, (T), 26:54564
  neutron radius of, determination from α elastic scattering, (E), 26:54547
  nuclear ground-state wave function of, multi-configuration calculation of, (T), 26:54577
CALCIUM ISOTOPES Ca-41
  deuteron reactions (d,p) at 12 MeV, DWBA analysis of differential cross sections and spectrum from, (E), 26:54573
  energy level at 3614 keV from calcium-40 (d,pγ) reactions, spin assignment for, (E), 26:54578
CALCIUM ISOTOPES Ca-42
  energy levels from calcium-41 (d,p) reactions, spectroscopic factors for, (E), 26:54573
  proton reactions (p,γ) at 1 to 2 MeV, cross sections for, (E), 26:54567 (INR-1407)
CALCIUM ISOTOPES Ca-43
  proton reactions (p,γ) at 1 to 2 MeV, isomeric cross section ratios for, (E), 26:54567 (INR-1407)
CALCIUM ISOTOPES Ca-44
  alpha elastic scattering at 166 MeV, angular distribution for, (E), 26:54547
  neutron radius of, determination from α elastic scattering, (E), 26:54547
CALCIUM ISOTOPES Ca-45
  metabolism and protein binding of, effects of method of preparation on, 26:53074
  production of, evaluation of complexing in methods for, 26:53074
CALCIUM ISOTOPES Ca-46
  neutron reactions with, resonance activation integrals for, (E), 26:54585
CALCIUM ISOTOPES Ca-48
  alpha elastic scattering at 166 MeV, angular distribution for, (E), 26:54547
  neutron radius of, determination from α elastic scattering, (E), 26:54547
  proton inelastic scattering at 25.11 to 40.21 MeV, differential cross sections for, (E), 26:54582
  proton reactions (p,γ) and (p,n) at 1 to 2 MeV, cross sections for, (E), 26:54567 (INR-1407)
CALIFORNIUM ISOTOPES Cf-252
  calibration of neutron source of, with fast neutron detector, p.38, 26:53066 (ORNL-4794, pp 36-44)
  dose rate tables of implants of, neutron and gamma, (T), 26:54906
  fabrication of neutron sources of, p. 38, 26:53066 (ORNL-4794, pp 36-44)
  fission of, spectra from coincidence measurements of helium-5 emission in spontaneous, (E), 26:54674
  neutron absorption in reactor spectrum, effective cross section for, (E), 26:54668
  neutron-produced recoil ions about implanted needle of, dose distributions from, 26:54902
  relative biological effectiveness for acute lethality following whole-body exposure of mice, comparison of cobalt-60 and radium-226 γ with γ and neutron, 26:53484
  use as neutron source for radiography, 26:53330(R) (BNWL-1308-10)
CALIFORNIUM ISOTOPES Cf-253
  neutron absorption in reactor spectrum, effective cross section for, (E), 26:54668
CALORIMETERS
  development for solution measurements, 26:52923
CALORIMETRY
  developments in solution, review on, 26:52923
CALVERT CLIFFS POWER REACTOR, UNIT 1
  containment structure for, lightning protection for, 26:55327 (DOCKET-50317-58)
  emergency plan for, additional data on, 26:55327 (DOCKET-50317-58)
  site for, radiation monitoring program for, 26:55327 (DOCKET-50317-58)
  steam line isolation valve for, reliability testing of

    actuation system for main, 26:55327 (DOCKET-50317-58)
  transmission lines for, additional information on, 26:55327 (DOCKET-50317-58)
CALVERT CLIFFS POWER REACTOR, UNIT 2
  containment structure for, lightning protection for, 26:55327 (DOCKET-50317-58)
  emergency plan for, additional data on, 26:55327 (DOCKET-50317-58)
  site for, radiation monitoring program for, 26:55327 (DOCKET-50317-58)
  steam line isolation valve for, reliability testing of actuation system for main, 26:55327 (DOCKET-50317-58)
  transmission lines for, additional information on, 26:55327 (DOCKET-50317-58)
CAMERAS
  recording capability of laser far field, use of grating to increase, 26:55624 (UCRL-51255)
CANADA
  geology of Fay Mine uranium deposit in northwest Saskatchewan, 26:53145
  nuclear power development April 1971 to March 1972, 26:55081(R) (AECL-4162)
  nuclear power program in, development of, 26:55195 (AECL-4254)
CARBIDES
  formation energy of, relations with fuel capsule corrosion and deterioration, 26:53330(R) (BNWL-1308-10)
  sorptive properties of, effects of electronic structure on, 26:53593
  structure of refractory, for use in aerospace, defect and electronic, 26:53581
CARBON
  abundance in primary cosmic radiation from 10 to 1000 MeV/N, (E), 26:53835
  abundance in V553 Cen and RT TrA, (E), 26:53899
  activity in stainless steel, 26:55480(T) (BNWL-tr-72)
  activity in stainless steel, 26:55481(T) (BNWL-tr-73)
  cascades in iron due to 30- to 300-GeV/N cosmic, (E), 26:53832
  coating of monofilament substrate of, with boron, problems in chemical vapor deposition, 26:53571
  deposition on Incoloy, stainless steel, and steel reactor cooling system materials, 26:53605(R) (DP-Report-522)
  determination of surface and body concentrations of, in materials by helium-3 activation, 26:52899 (LA-DC-72-809)
  determination of trace amounts in liquid sodium, vacuum distillation method for, 26:55170 (CONF-710959-, Paper 14)
  effects in helium stars, (E/T), 26:53896
  effects on brittleness of molybdenum, 26:53682
  effects on corrosion resistance of zirconium and zirconium alloys in high-temperature water, 26:53614
  effects on metallography of cast tungsten, 26:53681
  effects on neutron radioinduced strengthening of chromium--iron welds, iron, and pressure vessel steel, 26:53710
  effects on sintering and stress-rupture properties of nickel-base alloys, 26:53674
  ionization balance in solar atmosphere, density dependent, (E), 26:53969
  meson (π^+ and π^-) reactions at 0.7 to 2 GeV/c, model analysis of, (E/T), 26:54529 (RPP/NS-8)
  metabolism in plants, photosynthetic mechanisms, 26:55561 (LBL-383)
  metabolism of dissolved and particulate detrital, in temperate hardwater lake, 26:55493 (COO-1599-58)
  neutron reactions up to 20 MeV, γ production cross sections for, (E), 26:54523 (CONF-720901-(Bks.1 and 2), pp 325-34)
  neutron spectra and age in pulsed sphere of, sensitivity to carbon cross sections in calculation of, 26:54474 (CONF-720901-(Bks.1 and 2), pp 409-17)
  neutron transport in, carbon shielding benchmark problem and other calculations for, 26:54939 (CONF-720901-(Bks.1 and 2), pp 397-408)
  radiation effects on mechanical properties of fibers of, fast neutron, 26:53717
  radiation effects on sorptive properties of activated, for radioiodine, γ, 26:53061 (DP-MS-72-14)
  radioinduced reactions with hydrogen, 30- to 45-keV electron beam, 26:53718
  spectral lines in sunspots due to molecular, (E), 26:53952
  spectral lines in sunspots due to molecular, (E), 26:53953
  spectral lines in zeta Oph due to interstellar, (E), 26:53875
  tensile properties of boron-coated monofilament substrate of, 26:53571
CARBON DIOXIDES
  electron reactions with, relation with Mariner Mars ultraviolet data, below 100-eV range, (E/T), 26:54009
  solvent properties for iodine, water, and krypton, pp. 29-31, 26:53083 (ORNL-4794, pp 26-32)
  solvent properties of liquid, for krypton, tracer studies on, 26:53059 (CONF-720823-12)
CARBON IONS
  effects of implanted, on Doppler broadening of positron annihilation photons in silver halide crystals, 26:54097
  effects on budding haploid yeast cells, sensitivity to lethal, 26:53368
  reactions with copper and tantalum at 10.4 MeV/nucleon, neutron yield from, (E), 26:54881 (NASA-TM-X-2440, pp 520-2)
  reactions with gases at 40 to 140 keV, cross sections for charge exchange in, (E), 26:54137
  spectral lines in zeta Oph due to interstellar, (E), 26:53875
CARBON ISOTOPES
  proton reactions at 3 GeV, time-of-flight measurements of neutron spectra from, (E), 26:54528 (NASA-TM-X-2440, pp 523-6)
CARBON ISOTOPES C-12
  alpha elastic scattering at 166 MeV, angular distribution for, (E), 26:54547
  deuteron reactions (d,α) at 7.2 to 14 MeV, analysis of reaction mechanism in isospin-forbidden and -allowed, (E), 26:54539
  deuteron reactions (d,Li-6) at 28 MeV, angular distributions and spectroscopic factors for, (E), 26:54527 (LYCEN-7219)
  deuteron reactions (d,n) and (d,p) with, calculation of spectroscopic factors using weakly bound projectile model, (T), 26:54543
  deuteron reactions (d,np) at 5.99 MeV, triangle graphs and isospin violation in rescattering in, (T), 26:54716
  electron inelastic scattering by, particle--hole-model calculations of form factor for, (T), 26:54541
  electron quasi-elastic scattering by, shell-model calculation of, 26:54526 (ITF-72-25-P)
  energy levels of, calculation using renormalized Brueckner--Hartree--Fock method with Hamada-Johnston potential, (T), 26:54696 (ORNL-TM-3951)
  giant dipole resonance in, inclusion of hole-state widths in particle--hole calculations of, (T), 26:54714
  helium-3 reactions (He-3,p) at 14 MeV with subsequent proton decay, gamma spectra and gamma and proton angular correlations in, (E), 26:54542
  muon (μ^-) capture by, gamma yields, rates, and weak-magnetism coupling constant from, (E), 26:54537
  muon capture by, particle--hole-model calculations of, (T), 26:54541
  neutrino reactions with, cross sections for, (T), 26:54541
  neutron radius of, determination from α elastic scattering, (E), 26:54547
  nuclear dynamics of, particle--hole description of semileptonic electromagnetic and weak interactions in, (T), 26:54541
  oxygen-16 elastic scattering at 5 to 14 MeV, optical-model analysis of effects of quasi-molecular states in cross sections for, (T), 26:54534
  proton scattering at 20 GeV, analysis using Steenberg model, (T), 26:54530
  reactions (C-12,xn) with lead-208 at 60 to 90 MeV, excitation functions for, (E), 26:54651
CARBON ISOTOPES C-13
  effects on microwave spectra of 3-oxetanone, isotope, 26:52960
CARBON ISOTOPES C-14
  determination in cellulose materials for art identification, 26:52898 (COO-3034-2)
  determination in labeled compounds, use of Knobloch elementary microanalyzer for combustion as pre-stage of liquid scintillation, 26:52944
  effects on cells following incorporation into DNA, role of transmutation in lethal and mutagenic, 26:53505
  incorporation in N,N'-bis(3-phenoxyhydroxypropyl)-ethylenediamine hydrochloride, 26:53052
CARBON MONOXIDES
  electron reactions with, impact cross sections and energy degradation from, relation with dayglow-emission observations from atmospheres of Mars and Venus, (E/T), 26:54008
  radiolytic reactions in, kinetic data on, 26:55416(R) (BNWL-1522-5)
  sorption on tungsten, field-emission microscopic study of binding states of, 26:55023
  spectral lines in xi Per due to interstellar, equivalent widths of, (E), 26:53890
CARBON SULFIDES
  spectral lines in xi Per due to interstellar, equivalent widths of, (E), 26:53890
CARBON SYSTEMS
  C--Fe-base, radiation damage in, electric resistivity study of 4.5°K fast-neutron, 26:54989
  C--graphite, properties at high temperatures, tensile and thermal, 26:53581
  C--Mo, thermodynamic properties of liquid solutions of, 26:53588
  C--O--Zr, reactions in, stability of phases produced by, 26:53581
CARBON TETRACHLORIDE
  effects on γ-induced thermoluminescence of cyclohexene, 26:53010
  potassium-atom scattering at thermal energies by, effects of temperature and internal and translational energy on differential cross sections for nonreactive, 26:54136

CARDIAC PACEMAKERS
  heat sources for, fabrication and safety of plutonium-238, 26:53331 (CEA-CONF-2026)
CASCADE SHOWERS
  development from alpha particles incident on iron absorber at 10 to 300 GeV/N, (E/T), 26:53831
  development in iron absorbers due to 30- to 300-GeV/N primary nuclei, (E), 26:53832
CATALYSTS
  circulation rates in catalytic cracking units, sodium-24 tracer method for measuring, 26:53343
CATTLE
  effects of fascioliasis of, on economic loss in Puerto Rico, 26:53498(R) (PRNC-156)
  effects of gamma-irradiated metacercariae of Fasciola hepatica on immune reactions of, 26:53498(R) (PRNC-156)
  immunization against dictyocaulosis using x-irradiated larvae, 26:53503
  radioisotope uptake by, following deposition of fallout on pasture grass, tracer study using lanthanum-140 labeled sand as simulant, 26:53527 (FOA-4-4503-A-3)
CAVITIES
  content and size of underground, formed by nuclear explosions in granite, (E/T), 26:53130(T) (UCRL-Trans-10616-4)
  natural gas storage in underground nuclear, hazards to users from, 26:53132(T) (UCRL-Trans-10617-2)
CAVITY RESONATORS
  power losses in helical, methods of parameter optimization for minimizing, 26:53744
  surfaces of superconducting rf, experimental study of conditions of niobium, 26:53748
  tests of superconducting niobium helix, 8-week, 26:53750
CELL DIVISION
  radiation effects on circadian changes in, in rat gastric glands following oral administration of radon water, effects of dose on α, 26:53514
CELL MEMBRANES
  lectures at Physics Laboratory of Istituto Superiore di Sanita, Rome, July--Dec. 1970, 26:54162 (ISS-71/31)
CELL PHASE
  effects on sensitivity of chromosomes in cultured rat-kangaroo cells to heliotrine, 26:53359
  effects on x-radiosensitivity of chromosomes in cultured rat-kangaroo cells, 26:53359
CELLS
  radiation effects on count of plaque-forming, in spleen of antigen-stimulated mice following whole-body exposure, effects of dose on γ and x, 26:53469
  radiation effects on mitotic activity and survival of, in early mouse embryos in relation to effects on gastrulation, repair of x, 26:53476
  radiation effects on reproduction of epidermal, of swine, dose dependence of fission neutron, thermal neutron, x, and neutron activation of boron-10 in, 26:53450 (LA-4874, pp 126-44)
  radiation effects on, following incorporation of β-emitting radioisotopes into DNA, comparison of effects of external x-ray exposure with lethal and mutagenic β, 26:53505
  radioinduced suppression of antibody-forming, in mouse spleen during response to antigen challenge, acute whole-body x, 26:53464
  spleen colony formation by hemopoietic stem, following transplantation into lethally x-irradiated isogeneic mice, 26:53466
CELLS, CULTURED
  effects of heliotrine on chromosomes in rat-kangaroo, effects of cell phase on sensitivity to, 26:53359
  mutations induced in Chinese hamster, by chemical mutagens, uv radiation, and x radiation, effects of dose and post-exposure culture medium on frequencies of, 26:53362
  mutations induced in mouse lymphoma, by chemical mutagens and x radiation, phenotypic method for comparing frequency of, 26:53361
  radiation effects on generation time, growth, and proliferation of rat hepatoma, γ, 26:53354
  radiation effects on metabolism of rickettsiae in L, gamma, 26:53360
  radiation effects on proliferation and survival of mouse lymphoma, effects of dose on long term uv and x, 26:53356
  radiation effects on survival of Chinese hamster, following low dose rate exposure, effects of temperature on sensitivity to x, 26:53358
  radiation effects on survival of rat hepatoma, as a function of post-exposure cell phase, statistical study of γ, 26:53354
  radiation effects on wallaby, effects of dose on chromosome aberration rate, DNA synthesis, mitosis rate, reproduction, and survival of, uv, 26:53353 (UR-3490-194)
  radioinduced lesions in Chinese hamster, following low dose rate sublethal exposure, effects of temperature on repair of x, 26:53358
  radioinduced lesions in DNA of mammalian, role of repair processes in recovery from lethal and mutagenic γ, uv, and x, review of, 26:53357
  radiosensitivity of chromosomes in rat-kangaroo, effects of cell phase on x, 26:53359
CELLULOSE
  radioinduced oxidation of, and mixtures with poly(methylhydrogensiloxane), rate of, 26:52994
CENTRAL AMERICA
  radioisotope uses in hydrology in, 26:53168
CEREALS
  analysis for mercury by neutron activation, 26:52911
  flour, radiation effects on bread-making and organoleptic properties of wheat, following grain exposure, dose dependence of γ, 26:53381 (CNEA-309)
  wheat, radiation effects on chemical and nutritional characteristics of, effects of dose on γ, 26:53381 (CNEA-309)
  wheat, radiation processing effects on content of nicotinic acid and vitamins of, gamma, 26:53344
CERIUM
  determination in method for measurement of chemical oxygen demand of water, fluorometric, 26:52915 (CONF-720827-2)
  electron band structure of, photoelectron spectral study of core level binding energies, 26:55024
  energy-level transitions and 4d binding energy of, relation between 4d → 4f, 26:54095
  oxidation of, uv photoemission studies of, 26:53611
  photon reactions (γ,xn) with, model analysis of giant dipole resonance in, (E/T), 26:54598 (FRNC-TH-242)
  separation of trivalent, from hydrochloric acid solutions by solvent extraction using TTA, synergistic effect of tri-n-octylamine on, 26:52952
CERIUM ALLOYS AND SYSTEMS
  Ce--Gd--Ru, magnetic properties of Ce/sub 1-x/Gd/sub x/Ru_2, 26:55037
  Ce--Pt--Ru, thermal capacity of CeRu/sub 2-x/Pt/sub x/ at 1.3 to 9°K, 26:55047
  Ce--Ru, thermal capacity of $CeRu_2$ at 1.3 to 9°K, 26:55047
CERIUM ISOTOPES Ce-136
  energy levels of, quasi-band structure in, (E/T), 26:54600 (INSJ-130)
CERIUM ISOTOPES Ce-140
  alpha elastic scattering at 166 MeV, angular distribution for, (E), 26:54547
  gamma transition cascade at 329 to 487 keV, parameters of unperturbed angular correlation of, (E), 26:55060
  meson (π) reactions at 100 to 260 MeV, Coulomb flux corrections to total cross sections for, (T), 26:54609
  neutron radius of, determination from elastic scattering, (E), 26:54547
CERIUM ISOTOPES Ce-141
  content in agricultural products, atmosphere, rainwater, Savannah River, and vegetation in vicinity of Savannah River Plant, 1971, 26:53153(R) (DPSPU-72-30-1)
CERIUM ISOTOPES Ce-142
  deuteron reactions (d,p) and (d,t) at 12.6 MeV, particle spectra and angular distributions for, (E), 26:54618
  deuteron reactions (d,p) at 9 to 13 MeV, proton spectra from, (E), 26:54467(R) (ORO-2972-204)
  proton elastic and inelastic scattering at 9.5 to 12 MeV with isobaric analog excitation, excitation functions for, (E), 26:54618
CERIUM ISOTOPES Ce-143
  energy levels from cerium-142 (d,p) reactions, spectroscopic factors for, (E), 26:54618
CERIUM ISOTOPES Ce-144
  content in agricultural products, atmosphere, rainwater, Savannah River, and vegetation in vicinity of Savannah River Plant, 1971, 26:53153(R) (DPSPU-72-30-1)
  effects on blood of rats following intratracheal administration, β and γ, 26:53516
  sorption by ocean sediments from seawater, (E), 26:53167
CERIUM METAPHOSPHATES
  preparation and structure of, 26:53045
CERIUM OXIDES
  magnetic susceptibilities of nonstoichiometric, 26:55030
  spectra of, 4.2°K far-infrared (E/T), 26:55032
CERMETS
  fabrication of, review on, 26:53592
  production of plate-shaped and rod-shaped fuel elements of, methods for, 26:53592
CERN II SYNCHROTRON
  description of proposed, 26:53745
  experimental facility for, high intensity muon beam, 26:53783 (DNPL/P-131)
CESIUM
  determination in granitic biotites and feldspars by neutron activation and γ spectrometry, 26:52908
  plasma of, shock-wave investigation of equation of state of nonideal, on heated shock tube, (E), 26:54866
  solubility in liquid sodium, tracer studies on, 26:52895 (CONF-710959-, Paper 18)
CESIUM BROMIDES
  radioinduced color centers in, absorption spectral study of 4.2 and 77°K x-, 26:54980
CESIUM BROMOURANATES
  crystal lattice dynamics of Co_2UBr_6, model for calculations of phonon frequencies in, 26:53046
CESIUM ISOTOPES Cs-131
  electron-capture decay of, double k-shell ionization in, (E), 26:54617
CESIUM ISOTOPES Cs-134
  content in atmosphere and Savannah River in vicinity of

- Savannah River Plant, 1971, 26:53153(R) (DPSPU-72-30-1)
- content in Lake Michigan fish, 26:53169 (ANL-7860(Pt.3), pp 141-50)

CESIUM ISOTOPES Cs-137
- content in agricultural products, animals, atmosphere, fish, milk, rainwater, Savannah River, and vegetation in vicinity of Savannah River Plant, 1971, 26:53153(R) (DPSPU-72-30-1)
- content in fallout in East Germany during 1970, (E), 26:53156 (SZS-128)
- content in Florida biosphere during June 1971 to June 1972, 26:53170(R) (ORO-4066-5)
- content in Lake Michigan fish, 26:53169 (ANL-7860(Pt.3), pp 141-50)
- content in Norwegian meats and milk during 1956 to 1970, 26:53161
- design of γ source of, for simulation of spectrum emitted by radioisotope thermoelectric generator, 26:53335 (NASA-TM-X-2440, pp 850-2)
- determination as measure of burnup in spent fuels, 26:52933 (JAERI-Memo-4094)
- distribution and retention in rabbits following intravenous injection, effects of peritoneal dialysis on, 26:53533
- distribution in soils and vegetation in Puerto Rico, 26:53162 (ANL-7860(Pt.3), pp 1-13)
- sorption by ocean sediments from seawater, (E), 26:53167
- uptake by barley and bean plants from surface contaminated soils, effects of clinoptilolite on, 26:53540
- uptake by clover plants from continuously cropped uniformly contaminated soils, effects of clinoptilolite on, 26:53540
- uptake by fish in White Oak Lake in relation to content of stable cesium and potassium and seasonal changes in food consumption, 26:53535
- uptake by plants in Georgia during 1971 in comparison with 1965, fallout, 26:53539(R) (SRO-641-4)

CESIUM ISOTOPES Cs-138
- half-life of, (E), 26:54667

CESIUM ISOTOPES Cs-139
- half-life of, (E), 26:54667

CESIUM ISOTOPES Cs-140
- beta decay endpoint energy of, (E), 26:54601 (IS-T-534)
- energy-level scheme from xenon-140 decay, (E), 26:54601 (IS-T-534)
- half-life of, (E), 26:54667

CESIUM ISOTOPES Cs-141
- beta decay endpoint energy of, (E), 26:54601 (IS-T-534)

CESIUM ISOTOPES Cs-142
- beta decay endpoint energy of, (E), 26:54601 (IS-T-534)

CHALCOGENIDES
- analysis of thin layers of glasses of, for arsenic, germanium, sulfur, and tellurium by proton activation or x-ray fluorescence, 26:52900 (LYCEN-7236)

CHALCOPYRITES
- analysis for bismuth by neutron activation and α scintillation counting, 26:52910

CHARCOAL
- analysis for tritium by bremsstrahlung counting, 26:52934 (MLM-1368)
- iodine retention on beds of, under accident and post-accident conditions, 26:53058 (CONF-720823-10)
- sorptive properties of commercial impregnated, for iodine and methyl iodide, 26:53058 (CONF-720823-10)
- sorptive properties of iodized, for iodine and methyl iodide, 26:53077 (CONF-720823-9)

CHARGED-PARTICLE BEAMS
- transport in first-order achromatic systems, change in beam spot size due to second-order effects in, 26:53764

CHARGED PARTICLES
- detection of minimum ionizing, design and performance of bifilar helical multiwire proportional counter for, 26:53273 (LA-4968)
- detection of ultrarelativistic, design and performance of transition detector for, 26:53277
- dosimetry of high-Z, Apollo astronaut plastic track detector, 26:53231 (NASA-TM-X-2440, pp 149-56)
- effects on human visual response following retinal exposure, effects of particle flux density on helium, 26:53403 (NASA-TM-X-2440, pp 416-22)
- effects on mice, effects on survival of epidermal cells in skin following single local exposure, comparison of RBE for, carbon, helium, and lithium with x radiation, 26:53456 (NASA-TM-X-2440, pp 652-8)
- effects on retina of dark-adapted human eye, use of virtual-quanta method to calculate stimulatory, 26:53405 (NASA-TM-X-2440, pp 767-72)
- energy distribution in plasmasphere during solar eclipse, dependence of equilibrium potential of satellite surface material on, (T), 26:54054
- interaction with geomagnetic dipole field, study of Earth's environmental space from, (E), 26:54056
- motion in solenoids with random magnetic fields, fluxes in, (T), 26:54783
- radiation emission of relativistic, in field of two plane waves, (T), 26:54264
- relation with creation of polar auroras, application in plasma physics of, (E/T), 26:54043
- scattering by nuclei at low energy, forward dispersion relation including Coulomb interaction for elastic, (T), 26:54711
- scattering by system of identical particles, K-matrix solution to coupled inhomogeneous equations for, 26:54414
- scattering of heavy, effects of Coulomb field on type of diffraction, (T), 26:54415
- trajectories in first-order achromatic beam transport systems, second-order effects on, 26:53764

CHEMICAL ENGINEERING
- research in India, 1971--1972, 26:55452(R) (NP-19407)

CHEMICAL REACTIONS
- kinetic measurements by solution calorimetry, 26:52923
- kinetics of, complex and pure rate laws in heterogeneous, 26:55588(T) (ORNL-tr-2394)

CHEMISTRY
- conference on, Joint Southeast--Southwest Regional ACS, New Orleans, Dec. 2-4, 1970, abstracts of papers, 26:53027
- research in India, 1971--1972, 26:55452(R) (NP-19407)
- research progress on, for April 1, 1971 to March 31, 1972, 26:53080(R) (ORNL-4794)

CHERENKOV RADIATION
- properties from proton reactions with potassium sodium tartrate at 660 MeV, (E), 26:54875 (JINR-P1-6552)
- use in monochromatic energy measurement of 665-MeV proton beams, 26:53800
- use to measure transient free carrier absorption in insulators, feasibility of, 26:54968(R) (AD-737312)

CHIMERAS
- determination of hematopoietic and pulmonary origins of alveolar macrophages in, of mice, 26:53492

CHLORAMPHENICOL
- effects on repair of γ-radioinduced double-strand breaks in DNA of Micrococcus radiodurans, inhibitory, 26:53349

CHLORIDES
- corrosive effects of aqueous solutions of, on overaged and underaged niobium--uranium-base alloys, 26:53608 (RFP-1904)

CHLORINE
- determination in environmental samples by neutron activation, 26:52897 (CONF-721010-3)
- determination of trace amounts in liquid sodium, vacuum distillation method for, 26:55170 (CONF-710959-, Paper 14)
- neutron capture by, comparison of ENDF/B III and published data for thermal, 26:54501 (ORNL-TM-3910)
- reactions of trivalent, with tetravalent uranium in presence of phenol in aqueous acid solutions, mechanism and kinetics of oxidation--reduction, 26:53044
- reactions of trivalent, with tetravalent uranium in presence of phenol in aqueous acid solution, kinetics and mechanisms of oxidation--reduction, 26:53051

CHLORINE IONS
- scattering by argon and neon at 8 to 25 keV, total cross sections and interatomic potentials for, (E), 26:54139

CHLORINE ISOTOPES Cl-34
- beta decay of, electromagnetic corrections to ft values for, (T), 26:54713

CHLORINE ISOTOPES Cl-35
- atomic mass of, 26:54495 (EUR-4765, pp 435-55)
- effects on Zeeman effect in chloroacetylene, 26:52969
- reactions with ruthenium-96 and tin-112 up to 270 MeV, delayed proton spectra from, (E), 26:54608(T) (UCRL-Trans-1473)
- scattering by samarium-152 and gadolinium-154 at 100 MeV with Coulomb excitation, gamma spectra from inelastic, (E), 26:54642

CHLORINE ISOTOPES Cl-36
- abundance in iron meteorites, (T), 26:53808(T) (ORNL-tr-2620)

CHLORINE ISOTOPES Cl-37
- atomic mass of, 26:54495 (EUR-4765, pp 435-55)
- effects on Zeeman effect in chloroacetylene, 26:52969

CHLOROPHYLL
- chemiluminescence and fluorescence of, in algae and green plants, methods for measuring delayed, 26:55517 (COO-3162-12)

CHONDRICHTHYES
- Ginglymostoma cirratum (shark), radiation effects on brain of, gamma, 26:53487
- hematopoiesis in, bibliography on, 26:53447 (CONF-720822-2)
- radiation effects on function of hematopoietic tissues in, effects of dose, dose rate, and species on acute and chronic γ, 26:53447 (CONF-720822-2)

CHROMATOGRAPHY
- development of ion exchange, 26:52948

CHROMIUM
- abundance in 21 sharp-lined nonvariable cool peculiar A stars, (E), 26:53882
- abundance in γ Cap, (E), 26:53888
- book: Early Transition Metals, 26:52956
- determination in geochemical standards by atomic absorption using nitrous oxide--acetylene flame, 26:52921
- determination in water samples by spark source mass spectroscopy, 26:52914 (ANL-7860(Pt.3), pp 55-63)
- effects on cohesion and structural stability of aluminum oxide composites with iron and nickel, 26:53589

  - effects on ductility of copper, 26:53669
  - separation from indium by ion exchange chromatography, 26:52949
- CHROMIUM ALLOYS AND SYSTEMS
  - Al--Co--Cr--Mo--Ni-base--Ta--Ti--W, sintering and stress-rupture properties of, effects of boron, carbon, and oxygen additions on, 26:53674
  - Al--Co--Cr--Mo--Ni-base--Ti, sintering and stress-rupture properties of, effects of boron, carbon, and oxygen additions on, 26:53674
  - Al--Cr--Mo--Nb--Ni-base--Ta--W, production and properties of powder metallurgy components of, for use at high temperatures, 26:53631
  - Co--Cr, microstructure and stability of aluminum coated, effects of heat corrosion on, 26:53676
  - Co-base--Cr--Ni--ThO_2, mechanical properties and microstructure of dispersion-hardened, 26:53675
  - Cr--Cu--Fe--Mo--Ni-base--Ti, corrosion by thorium dioxide dissolvent solutions, 26:53604 (BNWL-CC-449)
  - Cr--Fe-base, radiation effects on mechanical properties of, 2.3-MeV electron, 26:53706
  - Cr--Fe-base, radiation effects on strengthening of welds of, effects of carbon, copper, nickel, and vanadium additions on neutron, 26:53710
  - Cr--Mo--steel, corrosion by products of sodium--water reactions, 26:55154 (CONF-710548-, pp 105-28)
  - Cr-base--Mo--Ta, coatings for nitridation resistance of, in air, chromium, hafnium, lanthanum, and yttrium combination cementation, 26:53689
  - Cr-base--W--Y, coatings for nitridation resistance of, in air, chromium, hafnium, lanthanum, and yttrium combination cementation, 26:53689
  - Cr-base--Y, coatings for nitridation resistance of, in air, chromium, hafnium, lanthanum, and yttrium combination cementation, 26:53689
- CHROMIUM ISOTOPES Cr-51
  - content in conversion products of irradiated 300 series stainless steels, 26:55165 (CONF-710959-, Paper 9)
  - content in Savannah River, 1971, 26:53153(R) (DPSPU-72-30-1)
  - distribution in Columbia River, effects of seawater on soluble-suspended, 26:53166 (RLO-2227-T-12-28)
  - use as tracer in biological materials together with iron-59, computerized data processing system for, 26:53544
- CHROMIUM ISOTOPES Cr-52
  - deuteron elastic scattering at 11.9 MeV, vector-polarized, (E), 26:54572
  - deuteron reactions (d,pγ) at 3 MeV, γ-ray angular correlations for, (E), 26:54578
- CHROMIUM ISOTOPES Cr-53
  - energy level at 3618 keV from chromium-52 (d,pγ) reactions, spin assignment for, (E), 26:54578
- CHROMIUM SILICIDES
  - Cr_5Si_3--TiB_2, oxidation resistance and sinterability of, at high temperatures, 26:53594
  - Cr_5Si_3--ZrB_2, oxidation resistance and sinterability of, at high temperatures, 26:53594
  - $CrSi_2$--TiB_2, oxidation resistance and sinterability of, at high temperatures, 26:53594
  - $CrSi_2$--ZrB_2, oxidation resistance and sinterability of, at high temperatures, 26:53594
- CHROMOSOMES
  - effects of heliotrine on, in cultured rat-kangaroo cells, effects of cell phase on sensitivity to, 26:53359
  - radioinduced aberrations of barley seed, combined effects of space flight environment on gamma, 26:53384
  - radioinduced aberrations of, in cultured human lymphocytes, effects of dose on frequency of x, 26:53355
  - radioinduced aberrations of, in human bone marrow cells following local therapeutic exposure, effects of dose and time on frequency of γ, 26:53445
  - radioinduced aberrations of, in human leukocytes, x, 26:53427
  - radioinduced aberrations of, in human leukocytes, evaluation for use as dosimeter following nuclear explosion, 26:53397 (FOA-4-4500-A-3)
  - radioinduced aberrations of, in human lymphocytes, evaluation for use as biological dosimeters, 26:53420
  - radioinduced aberrations of, in lymphocytes of man exposed to residual fallout from atomic bombing of Nagasaki, 26:53414
  - radioinduced aberrations of, in mature oocytes of Drosophila melanogaster, effects of premeiotic breakage and interchanges on types of x, 26:53501
  - radioinduced aberrations of, in mature spermatozoa of Drosophila melanogaster, inhibitory effects of dactinomycin on post-fertilization maternal repair of x, 26:53502
  - radioinduced aberrations of, in mice, strontium-90 β and x, 26:53496
  - radioinduced aberrations of, in peripheral leukocytes of medical radiography personnel, incidence of x, 26:53428
  - radioinduced aberrations of, in rat embryos following exposure in utero, time dependence of fast neutron, 26:53470
  - radioinduced aberrations of, in rye root cell, effects of genetic heterogeneity on frequency of γ, 26:53392
  - radiosensitivity in cultured rat-kangaroo cells, effects of cell phase on x, 26:53359
- CHROMOSPHERE
  - current dissipation in, (T), 26:53937
  - spectra of quite, characteristics of Ca II K-line profiles in, (E), 26:53948
  - spectra of, ionized helium in, (T), 26:53949
- CIRCADIAN CLOCK
  - radiation effects on circadian changes in mitotic index and DNA synthesis in cells of rat gastric glands following oral administration of radon water, effects of dose on α, 26:53514
  - radiation effects on diurnal rhythm of neurosecretory activity in mice following whole-body exposure, x, 26:53478
- CIRCUITS
  - design and performance of radiation-hardened, for gated differential video amplifiers, 26:53307 (SC-DC-721159)
  - design for studying interaction of hf fields and plasma, 26:54775(T) (AEC-tr-7326)
  - design of radiation-tolerant integrated, DIAMOND method for, 26:53309 (SC-DC-721162)
  - design of Universal Digital Integrated, 26:53308 (SC-DC-721161)
  - fabrication of multilayer printed wiring boards, 26:55469 (BDX-613-382(Rev.))
  - ground detectors for ungrounded reactor control, methods for increasing sensitivity of, 26:55135 (DUN-SA-169)
  - radiation effects on integrated, neutron, 26:53309 (SC-DC-721162)
  - radiation effects on Universal Digital Integrated, neutron, 26:53308 (SC-DC-721161)
- CIRENE POWER REACTOR
  - control system for, hydraulic and dynamic testing of two-phase fluid, 26:55133 (CISE-R-268)
  - cooling channels for, steady-state and transient measurements on scale model of, 26:55148 (CISE-R-270)
  - core for, TERMO code for thermohydraulic analysis of, 26:55104 (CISE-R-246)
  - fuel elements for, ESSOR reactor neutron flux measurements on, 26:55105 (CISE-R-258)
  - lattice cell parameters of, RB-1 reactor measurements of, 26:55102 (CISE-R-239)
  - neutron buckling in, lattice mockup measurements of, 26:55106 (CISE-R-283)
- CIVILIAN DEFENSE
  - shelters for, numerical model of effectiveness of quick-access, 26:53135 (ORNL-TM-3485(Vol.1))
- CLAYS
  - age of, thermoluminescent method for estimation of, 26:53177
- CLINOPTILOLITE
  - effects on cesium-137 and strontium-90 uptake by clover plants from continuously cropped uniformly contaminated soils, 26:53540
  - effects on cesum-137 and strontium-90 uptake by barley and bean plants from surface contaminated soils, 26:53540
- CLINTON P. ANDERSON MESON PHYSICS FACILITY
  - academic uses of, promotion of, 26:53796 (LA-4874, pp 92-8)
  - biomedical research programs at, 26:53398 (LA-4874, pp 79-83)
  - development of, status of, 26:53739 (LA-4874, pp 16-20)
  - experimental facilities at, description of secondary pion, 26:53797 (LA-DC-72-881)
  - experimental facilities for, data acquisition system for, 26:53795 (LA-4874, pp 86-9)
  - experimental facilities for, nuclear chemistry, 26:53792 (LA-4874, pp 72-7)
  - experimental facility for, Biomedical Pion Channel, 26:53793 (LA-4874, pp 78)
  - experimental facility for, Energetic Pion Channel and Spectrometer, 26:53787 (LA-4874, pp 51-4)
  - experimental facility for, High Resolution Proton Spectrometer, 26:53791 (LA-4874, pp 67-71)
  - experimental facility for, neutrino, 26:53794 (LA-4874, pp 84-5)
  - experimental facility for, Nucleon Physics Laboratory, 26:53790 (LA-4874, pp 63-6)
  - experimental facility for, proposed low-energy pion channel, 26:53786 (LA-4874, pp 48-50)
  - experimental facility for, status of Pion and Particle Physics, 26:53788 (LA-4874, pp 55-8)
  - experimental facility for, stopped muon channel, 26:53789 (LA-4874, pp 59-62)
  - research program at, review of high-energy physics, 26:54195 (LA-4874, pp 36-44)
  - research proposals for, status of, 26:53785 (LA-4874, pp 45-7)
  - users meeting, Nov. 8-9, 1971, 26:53784 (LA-4874)
- CNIDARIA
  - corals, growth rates of, lead-210 and radium-228 methods for measuring, 26:53179
- COAGULATION
  - efficiency of, using organic flocculants, 26:53040 (SZS-129)
- COATINGS
  - effects of tungsten, on evaporation rate of zirconium carbide--tungsten, 26:55022
  - radiation resistance of selected, evaluation of, p. 98-100, 26:52986 (ORNL-4794, pp 98-101)
- COBALT
  - determination in water, effects of large amounts of

copper on spectrographic, 26:52927
determination of trace amounts of, in soil and plant tissue by instrumental neutron activation, 26:52904
distribution in cores from Green Bay, relations with depth, 26:53164 (ANL-7860(Pt.3), pp 64-76)
effects on cohesion and structural stability of aluminum oxide composites with iron, 26:53589
separation from iron by solvent extraction using Aliquat-336, 26:53076

COBALT ALLOYS AND SYSTEMS
composition and physical properties of composite powders of, 26:53680
preparation of composite powders of, by hydrogen reduction, 26:53680
Al--Co--Cr--Mo--Ni-base--Ta--Ti--W, sintering and stress-rupture properties of, effects of boron, carbon, and oxygen additions on, 26:53674
Al--Co--Cr--Mo--Ni-base--Ti, sintering and stress-rupture properties of, effects of boron, carbon, and oxygen additions on, 26:53674
Co--Cr, microstructure and stability of aluminum coated, effects of heat corrosion on, 26:53676
Co--Pt, microstructure of intermetallic compounds of, methods for ion microscopy imaging of, 26:53655
Co--rare earth, magnetic properties of R_3Co, pulsed-field magnetometer measurements of, 26:55050
Co--transition metal carbides, erosion resistance of anodes of, 26:53568
Co--V, vanadium-51 NMR quadrupole splitting in sigma-phase, effects of composition on intensity of, 26:55056
Co-base--Cr--Ni--ThO_2, mechanical properties and microstructure of dispersion-hardened, 26:53675
Co-base--Ni--ThO_2--Zr, mechanical properties and microstructure of dispersion-hardened, 26:53675
Co-base--ThO_2, mechanical properties and microstructure of dispersion-hardened, 26:53675
Co-base--ThO_2--Zr, mechanical properties and microstructure of dispersion-hardened, 26:53675

COBALT ISOTOPES Co-54
beta decay of, electromagnetic corrections to ft values for, (T), 26:54713

COBALT ISOTOPES Co-58
content in conversion products of irradiated 300 series stainless steels, 26:55165 (CONF-710959-, Paper 9)

COBALT ISOTOPES Co-59
alpha elastic scattering at 166 MeV, angular distribution for, (E), 26:54547
helium-3 reactions (He-3,$d\gamma$) at 18 MeV, gamma spectra from, (E), 26:54587 (FRNC-TH-240)
neutron radius of, determination from α elastic scattering, (E), 26:54547
proton reactions at 3 GeV, time-of-flight measurements of neutron spectra from, (E), 26:54528 (NASA-TM-X-2440, pp 523-6)

COBALT ISOTOPES Co-60
content in atmosphere and Savannah River in vicinity of Savannah River Plant, 1971, 26:53153(R) (DPSPU-72-30-1)
content in conversion products of irradiated 300 series stainless steels, 26:55165 (CONF-710959-, Paper 9)
content in Lake Michigan fish, 26:53169 (ANL-7860(Pt.3), pp 141-50)
design of γ source of, for simulation of spectrum emitted by radioisotope thermoelectric generator, 26:53335 (NASA-TM-X-2440, pp 850-2)
diffusion in α-zirconium, mechanism of, 26:53666
distribution in Columbia River, effects of seawater on soluble-suspended, 26:53166 (RLO-2227-T-12-28)
use as tracer for measuring leakage through dam near Baguio City, Philippines, 26:53175

COINCIDENCE CIRCUITS
design for plastic scintillation detectors for fission neutron detection for interrogation determination of uranium-235, 26:53217

COLCHICINE
effects on Aspergillus niger, mutagenic for citric acid production, 26:53380

COLLECTIVE ACCELERATORS
electric fields in coaxial channel of closed-electron-drift, effects of magnetic field configuration on, 26:53743

COLLISION PROCESSES
book: Excitation in Heavy-Particle Collisions, 26:54118
energy-level transitions in inelastic and reactive, calculation of semiclassical S-matrix elements for, by integration along complex-valued trajectories, 26:54129
resonance states in atomic, finite-difference boundary-value method for calculation of wave functions and energies of shape-, 26:54124
theory of, including rearrangement processes, WKB approximation and classical limit of S matrix in time-dependent, 26:54107

COLLOIDS
reactions of, theoretical model for, 26:53067 (ORNL-4794, pp 88-90)

COLUMBIA RIVER
radioisotope distribution in, effects of seawater on soluble-suspended, 26:53166 (RLO-2227-T-12-28)
water and sediment distribution, properties, and transport in coastal northeast Pacific Ocean, (E), 26:53165(R) (RLO-2225-T-25-6)

COMETS
electron energy deposition in water vapor in water, (E/T), 26:54033

COMPOSITE MATERIALS
conference on, for aerospace material and process engineers, Los Angeles, California, April 11 to 13, 1972, 26:53569
fatigue properties of, data interpretation on static, 26:55619 (UCID-16100)
preparation and properties of powdered, 26:53680

COMPUTATIONAL MODULAR SYSTEMS
description for real-time computer based on CAMAC instrumentation, 26:55464 (AERE-R-6601)

COMPUTER PROGRAMS
ACSAP, for analysis of resonance neutron cross section data, 26:54468 (ANCR-1042)
ANALCOV, for covariance analysis, 26:55567 (MLM-1847)
AUGAT, for design of integrated circuits on wire wrap cards, 26:55563 (LBL-515)
BEHAVE-2, for operating performance of metal clad oxide fuel pins, FORTRAN 4 for GE 635, 26:55418 (GEAP-13788)
CITATION, for reactor in-core fuel cycle analysis, 26:55198 (ORNL-TM-2496(Rev.2)(Suppl.3))
CNTR, for producing contour plots, in FORTRAN IV, 26:55609 (SC-TM-710557)
DASQHE, for thermal reactor physics calculations, FORTRAN 5 for UNIVAC 1108, 26:55421 (BNWL-CC-2274)
DOMINO, general purpose discrete-ordinates-to-Monte-Carlo coupling, for radiation transport, 26:54872 (CONF-720901-(Bks.1 and 2), pp 499-511)
ENEDEP, for gamma-ray energy deposition in laminated materials, Extended Basic for GE-265, 26:54959 (NASA-TM-X-2440, pp 387-91)
EULERO, for visual display of periodical phenomena, for IBM 360/75, 26:55595 (RT/FIMA-(72)1)
for analysis of heat exchanger performance in nuclear-heated gas turbines, 26:53114
for automatic peak identification in analysis of gamma spectra from Ge(Li) detectors, in FORTRAN IV, 26:53257 (RT/FI-(72)14)
for processing clinical scintigraphic data, 26:53228
for processing of ENDF/B data, test using idealized data, 26:54475 (CONF-720901-(Bks.1 and 2), pp 1048-60)
for texture analysis, 26:55501 (COO-2118-35)
for unfolding neutron spectra, evaluation of, 26:53252 (CONF-720901-(Bks.1 and 2), pp 524-40)
GS-1, for analysis of pulsed neutron experiments on bare fast multiplying system by Storrer--Stievenart theory, 26:54483 (JAERI-M-4652)
HEATMESH-71, for generating geometrical data for studying heat transfer in axisymmetric structures, 26:55610 (SCL-DR-720004)
IMAGEN, for image enhancement and display of two-dimensional data, in FORTRAN for CDC-6600 and Univac 1108, 26:55608 (SC-RR-720286)
IONR, for damage profile in ion-bombarded targets, 26:54969 (AECL-4130)
IRT, for providing author proof plots of experimental data, 26:55476 (BNL-17115)
JN-METD2, for solution of neutron transport problems in multilayer slabs with isotropic scattering by J/sub N/ method, 26:54481 (EUR-4839)
KAPER, for core physics analysis in critical assemblies, 26:55396 (EURFNR-1014)
language for, specification of program flow in Madcap VI, 26:55547 (LA-DC-72-141)
MARE, for compound nucleus reaction calculations in the continuum, in FORTRAN IV, 26:54701 (RT/FI-(72)7)
MASH, for mesh generation for two-dimensional finite element and finite difference codes, in FORTRAN IV, 26:55609 (SC-TM-710557)
MOBIDIC, for analysis of reactor continuous axial refueling, for IBM 7040, 26:55196 (CISE-R-241)
MOICANO-1, for reactivity and neutron flux calculations for fog cooled reactors, FORTRAN 4 for IBM 7040, 26:55103 (CISE-R-242)
optimization of, 26:55599 (SC-DC-721376)
ORCOST, for capital costs of nuclear and steam power plants, FORTRAN 4 for IBM 360, 26:55265 (ORNL-TM-3743)
PAD, evaluation for reactor explosive power transients, 26:55441 (LA-DC-72-660)
PIBIMUG, for reactor physics calculations, FORTRAN-2 for IBM-1130, 26:55420 (AREAEE-141)
radiation transport, for calculating dose distributions, 26:54890 (ORNL-TM-3816)
RAS, for calculation of two-group neutron flux in polar geometry, 26:54471 (CISE-R-252)
reliability of Monte Carlo, for criticality calculations, 26:55445 (Y-KC-96)
RELIP, for economics of nuclear power plant mix in power grid, FORTRAN-4 for IBM-360, 26:55266 (RD/B/N-2261)
RELY 4, for Monte Carlo calculations of reactor system reliability, ALGOL, 26:55209 (RISO-M-1500)
REST-1, -2, -3, for decay heat from fission products in boiling water reactors, FORTRAN, 26:55127 (KFK-1579)
SATURN-1, for time history of fast reactor fuel pins, 26:55186(T) (EURFNR-985)
SLIP, for list processing, in FORTRAN for CDC 3300 and ICL 1905, 26:55543 (KFKI-72-32)
SOWACS, for sodium--water reactions, FORTRAN for CDC-

  - 3600, 26:55157 (CONF-710548-, pp 171-86)
  - TERMO, for steady state thermohydraulic analysis of CIRENE type reactors, 26:55104 (CISE-R-246)
  - TRASHP, for program assembly in FORTRAN for Hewlett--Packard minicomputers, 26:55606 (SC-M-720514)
  - TREFACT and TREMISS, for calculating exhaust emissions from transportation vehicles, 26:55467 (ANL/ES-15)
  - TRUD, for calculation of anisotropic neutron diffusion in xy geometry, in FORTRAN IV, 26:54488 (RT/FI-(72)1)
  - VIM-1, for Monte Carlo physics calculations for fast critical assemblies, FORTRAN for CDC 6600 and IBM 360, 26:55378 (AI-AEC-12951)
- COMPUTERS
  - data display system for, perspective transformer for stereomatrix 3-d iterative graphics, 26:55489 (COO-1469-210)
  - history of, trilogy on errors in, 26:55548 (LA-DC-72-243)
  - image restoration by, constrained least-squares estimation method for, 26:55451 (LA-DC-72-626)
  - interfacing for CAMAC systems, 26:53297 (CEA-N-1549)
  - language for Maniac, terminal control language for Madcap, 26:55551 (LA-DC-72-411)
  - languages for, meta-language for describing keyboard-based two dimensional, 26:55550 (LA-DC-72-410)
  - languages for, two-dimensional, 26:55549 (LA-DC-72-331)
  - number representation of exact and inexact quantities in, format and rules for, 26:55553 (LA-DC-72-783)
  - pattern recognition by, model for, 26:55455 (OSU-CISRC-TR-72-8)
  - PL/1 language for, use for interrogation of personnel card files, 26:55450 (CEA-CONF-2005)
  - research in India, 1971--1972, 26:55452(R) (NP-19407)
  - review of 1971 activities at Sydney Univ, 26:53993 (INIS-mf-252)
  - systems research at Illinois University, annual progress report on, 26:55488(R) (COO-1469-208)
  - use for reactor control and monitoring of mini-, compliance with IEEE-279 safety criteria of, 26:55136 (DUN-SA-186)
- CONCRETES
  - photon scattering at 2.0 to 10.5 MeV, dose albedos of back-angle, (E), 26:54892
  - concretes--polymer, development of composite materials of, 26:55473 (BNL-16609)
  - concretes--polymers, preparation and properties of, produced by radioinduced polymerization, 26:53722
- CONNECTICUT YANKEE POWER REACTOR
  - containment structure for, leak rate testing during June 1970 to June 1972, 26:55241 (DOCKET-50213-158)
  - site for, environmental radiation survey during January to June 1972, 26:55240 (DOCKET-50213-157)
- CONSTANTS AND CONVERSION FACTORS
  - relations between cosmological and quantum, 26:54392 (ITF-72-3-P)
- COOLING TOWERS
  - operation of, fog and glazed frost formation from, 26:53117
- COOPER POWER REACTOR
  - engineered safeguards for, effects of equipment failure on possible flooding of, 26:55307 (DOCKET-50298-50)
- COPPER
  - complexes with phthalocyanine, radiation effects on, chemical state of recoil copper-64 from neutron, 26:53032
  - complexes, copper-64 electron capture decay in labeled and neutron-irradiated crystals of phthalocyanine, 26:53032
  - determination in alloys and ore concentrates by amperometric titration, 26:52924
  - determination in liquid sodium by neutron activation, 26:52895 (CONF-710959-, Paper 18)
  - determination in presence of iron using EKCO mineral analyzer, 26:55568 (NIM-1430)
  - determination in samples from boreholes, neutron activation method for, 26:53174
  - determination in water samples by spark source mass spectroscopy, 26:52914 (ANL-7860(Pt.3), pp 55-63)
  - distribution in cores from Green Bay, relations with depth, 26:53164 (ANL-7860(Pt.3), pp 64-76)
  - ductility of, effects of chromium and zirconium additions on, 26:53669
  - effects of large amounts of, on spectrographic determination of heavy elements in natural water, 26:52927
  - effects on neutron radioinduced strengthening of chromium--iron welds, iron, and pressure vessel steel, 26:53710
  - ion reactions at 10.4-MeV/nucleon, neutron yield from, (E), 26:54881 (NASA-TM-X-2440, pp 520-2)
  - meson (K^0) reactions at 500 to 1500 MeV/c, $K_2^0 \to K_1^0$ regeneration amplitude from, (E), 26:54230
  - mixing of powders of, effects of friction on, 26:53617
  - oxygen ion reactions at 7.5 to 40 MeV, cross sections for K x-ray production in, (E), 26:54467(R) (ORO-2972-204)
  - photoelectron emission by, model calculations of angular and energy distributions of, 26:54885 (NASA-TM-X-2440, pp 792-800)
  - photon reactions (γ,n) at 12 to 23 MeV, neutron spectra from, (E), 26:54563
  - radiation damage in, electron microscopic study of 650-kV electron, 26:54972 (COO-2119-2)
  - radiation effects on spherical void growth in, effects of triaxial stress on, (T), 26:53702 (TID-26150)
  - radiation effects on surface microtopography of, argon-ion, 26:55008
  - separation from indium by ion exchange chromatography, 26:52949
  - solubility in liquid sodium, tracer studies on, 26:52895 (CONF-710959-, Paper 18)
  - sorption on diethylaminoethylcellulose in methanol--thiocyanate--hydrochloric acid media, 26:52951
- COPPER ALLOYS AND SYSTEMS
  - composition and physical properties of composite powders of, 26:53680
  - preparation of composite powders of, by hydrogen reduction, 26:53680
  - Au--Cu, lattice heat capacity of intermetallic $AuCu_3$, at 20 to 298ºK, effects of ordering on, 26:53637 (LBL-101)
  - Be--Cu-base, mechanical properties and stress relaxation of Alloy 25 at -320 to 300ºF, 26:53641 (SC-DR-720471)
  - Cr--Cu--Fe--Mo--Ni-base--Ti, corrosion by thorium dioxide dissolvent solutions, 26:53604 (BNWL-CC-449)
  - Cu--Ni--Tb, magnetic structures in TbNi/sub 1-x/Cu/sub x/ below ordering temperature, stability of sinusoidal-wave, 26:55039
  - Cu--Ni--Zn, analysis of nickel silver for copper by amperometric titration, 26:52924
  - Cu--Zn, phase transformation interfaces in, properties of massive, 26:53644
  - Cu-base--Fe, surface resistance of, Kondo anomaly in far-infrared, 26:55508 (COO-3151-4)
  - Cu-base--Ti, hardening of, mechanism of precipitation, 26:55615(R) (TID-26148)
- COPPER BORIDES
  - radiation effects on tensile properties of, at cryogenic temperatures for use in NERVA Program, fast neutron, 26:53696 (NASA-TM-X-2440, pp 595-602)
- COPPER COUPLES
  - Cu/steel, corrosion by water at ambient temperature, fretting, 26:53609 (RT/ING-(72)7)
- COPPER FORMATES
  - structure for antiferroelectric phase of tetrahydrate of, 26:55614 (TID-25974)
- COPPER IONS
  - scattering by argon and neon at 8 to 25 keV, total cross sections and interatomic potentials for, (E), 26:54139
- COPPER ISOTOPES Cu-60
  - beta and electron-capture decay of, γ spectra and log ft value for, (E), 26:54593
- COPPER ISOTOPES Cu-63
  - alpha inelastic scattering at 5.5 and 7 MeV, γ-γ angular correlations for, (E), 26:54594
  - energy-level transitions from alpha Coulomb excitation, probabilities and multipole mixing ratios for, (E), 26:54594
- COPPER ISOTOPES Cu-64
  - chemical state of recoil, in neutron-irradiated copper phthalocyanine, 26:53032
  - electron capture decay in labeled and neutron-irradiated α-copper phthalocyanine crystals, 26:53032
  - meson (π) reactions at 100 to 260 MeV, Coulomb flux corrections to total cross sections for, (T), 26:54609
- COPPER ISOTOPES Cu-65
  - alpha inelastic scattering at 5.5 and 7 MeV, γ-γ angular correlations for, (E), 26:54594
  - energy levels from nickel-64 proton scattering, spin--parity assignments and elastic and inelastic widths for isobaric analog, (E), 26:54590
  - energy-level transitions from alpha Coulomb excitation, probabilities and multipole mixing ratios for, (E), 26:54594
- CORRONEL 230
  - corrosion by thorium dioxide dissolvent solutions, 26:53604 (BNWL-CC-449)
- CORROSION
  - conference on uses of field-ion microscopy in studies of, Atlanta, Georgia, May 15 to 17, 1968, 26:53647
- CORROSION LOOPS
  - corrosion product deposition in liquid sodium, measurement of patterns of, 26:55173 (CONF-710959-, Paper 17)
  - design and operation of, for studies of activated material mass transfer by sodium, 26:53121 (CONF-710959-, Paper 7)
- COSMIC GAMMA SOURCES
  - detection of Libra γ-1, (E), 26:53924
- COSMIC PARTICLES
  - abundance of $Z > 83$ nuclei in, (T), 26:53867
  - acceleration of high Z, in pulsars, (T), 26:53857
  - anisotropies of, effects of solar cycle on narrow-angle, (T), 26:53868
  - anisotropy of medium energy, sidereal, (E), 26:53846
  - anisotropy of primary, components of sidereal, (E/T), 26:53848
  - anisotropy of primary, interpretation of sidereal, (E), 26:53847
  - anisotropy of primary, sidereal and solar, (E), 26:53850
  - anisotropy of primary, spurious, (T), 26:53849
  - anisotropy of ultrahigh-energy, (E/T), 26:53851
  - anisotropy of, limits on magnitude of, (E), 26:53852
  - cascades from Z greater than or equal to 3 primary, in

iron, (E), 26:53832
charge composition of heavy primary nuclei, (E), 26:53842
charge composition of nuclear component of, (T), 26:53854
charge composition of primary nuclei, (E), 26:53839
charge composition of primary, at energies up to 10^{12} eV, (E), 26:53830
charge composition of primary, up to Z = 26, (E), 26:53836
charge composition of Z = 2 to 30 primary, (E), 26:53838
charge composition of, accelerated in pulsars, (T), 26:53858
charge composition to Z = 28 of primary, source, (E), 26:53837
charge of heavy and superheavy nuclei, calculation of delta electrons formed in stopping media as aid in determination of, 26:53805(T) (N-71-30295)
chemical composition of heavy primaries above 5 GeV, (E), 26:53840
chemical composition of low-energy L and M nuclei in primary, (E), 26:53841
confinement in Galaxy, mechanisms for, (T), 26:53865
confinement time of, galactic, (E), 26:53833
doses of secondary particles produced by heavy galactic primary, calculations of, 26:54878 (NASA-TM-X-2440, pp 104-7)
energy spectra of 3- to 15-GeV primary electrons, (E), 26:53821
energy spectra of heavy primary nuclei, (E), 26:53842
energy spectra of primary deuterons and helium-3 nuclei, (E), 26:53828
energy spectra of primary electrons and positrons, (E), 26:53855
energy spectra of primary electrons between 10 and 200 GeV, (E), 26:53823
energy spectra of primary electrons between 10 and 1000 GeV, (E), 26:53822
energy spectra of primary nuclei, effect of ionization loss on, (T), 26:53862
energy spectra of VH and VVH primary nuclei, (E), 26:53843
energy spectrum of primary electrons, 26:53809
eye light flashes induced by Cherenkov radiation from heavy nuclei, calculation of frequency of, 26:54882 (NASA-TM-X-2440, pp 757-66)
flux of anti-alpha particles at 0.3 to 3 GeV/N, (E), 26:53825
flux of primary electrons between 10 and 1000 GeV, (E), 26:53822
flux of transuranic nuclei, (E), 26:53844
intensity profiles of charged, in atmosphere, balloon measurements of flux and ionization, 26:53807 (NASA-TM-X-2440, pp 908-13)
mass of primary nuclei, method for determining, (E/T), 26:53824
mean age of superheavy, (T), 26:53867
neutron spectra measurements in upper atmosphere, 26:54066 (NASA-TM-X-2440, pp 922-5)
origin in Crab Nebula, (E/T), 26:53856
origin in pulsars, (T), 26:53858
origin in stellar flares, (T), 26:53853
origin in white-dwarf stars, (T), 26:53854
properties of neutrino, review of solar neutrinos, Fermi interaction, and stellar evolution for, (E/T), 26:54185 (NEIC-RR-47)
reactions with nuclei, cross sections for, (T), 26:53845
rigidity spectra for Z greater than or equal to 2, (E), 26:53826
rigidity spectrum of 5- to 300-GeV primary nuclei, (E), 26:53834
scattering by hydromagnetic waves, pitch-angle, (T), 26:53863
sources of extragalactic, (T), 26:53859
spectrum of primary, explanation of break in, (T), 26:53869
trapping of superheavy elements in geomagnetic field, possible detection of, 26:54047 (NASA-TM-X-2440, pp 548-55)

COSMIC RADIATION
anisotropy of, effects of source distribution and propagation on, (T), 26:53861
book: Measurement of Radiation in Space, 26:53276
chemical composition of, effects of source distribution and propagation on, (T), 26:53861
composition and energy spectra of primary, survey of, 26:53806 (NASA-TM-X-2440, pp 209-14)
conference on, Hobart 8/71, Vol. I, 26:53814
density in Milky Way, (E/T), 26:53992
detection of soft x-ray, thin polypropylene window proportional counters for, 26:53206
diquark search at 2750-m altitude in, 26:54177
diurnal variation from Deep River meson and neutron data, characteristics of, (E), 26:53811
diurnal variation of primary, modulation of solar, (T), 26:53849
doses to crew and passengers at SST altitudes, 26:54888 (NASA-TM-X-2440, pp 894-901)
effects of finite rest mass of wave quantum, (T), 26:53866
effects on eyes of astronauts during space flight, stimulatory for formation of phosphenes in, 26:53407 (NASA-TM-X-2440, pp 1002-6)
effects on space vehicle components and subsystems, design parameters and test facilities for testing, 26:53695 (NASA-TM-X-2440, pp 570-6)
flux of high-energy gamma rays in Milky Way, (E), 26:53819
galactic component of, upper limits for, (E/T), 26:53851
gamma background, energy spectra of 0.25 to 4.2 MeV, (E), 26:53818
gamma spectra from suprathermal proton bremsstrahlung, (E/T), 26:53820
hazards to astronauts during prolonged space flight, 26:53408 (NASA-TM-X-2440, pp 1007-15)
interaction with interstellar material, x-ray emission from, (E/T), 26:53815
measurements of gamma, behind shield on balloons at high altitudes, 26:54964 (NASA-TM-X-2440, pp 914-21)
modulation following June 8, 1969 Forbush decrease, abrupt change in 11-year variation of, (E), 26:53870
monitoring in stratosphere for SST Concorde flight, hybrid detector system for, 26:53203 (NASA-TM-X-2440, pp 874-83)
parameters of, effects of galactic field line motion on, (T), 26:53864
polar-cap noise absorption by solar flare particles, 26:53927 (NASA-TM-X-2440, pp 193-208)
propagation and source distribution of primary, (T), 26:53861
propagation in atmosphere of galactic, theory of, 26:54067 (NASA-TM-X-2440, pp 926-41)
quark search at 2750-m altitude in, e/3 and 2e/3, 26:54164
radionuclide production in lunar rocks by primary, (E/T), 26:53860
spectra of ultrahigh energy, hadronic interactions of urbaryons for cut-off problem in integral, (T), 26:54313
variations in interplanetary space, modulation effects on anisotropy responsible for solar semidiurnal, (T), 26:53812
variations in interplanetary space, modulation effects on anisotropy responsible for solar semidiurnal, 26:53813

COSMIC RADIO SOURCES
brightness distributions for 11, (E), 26:53914
positions of 11, (E), 26:53914
radiation emission mechanism for extragalactic, (T), 26:53925
rotation measures of, effects of galactic field on, (E), 26:53911
scintillation measurements of small-diameter, solar-wind parameters from analysis of three-station interplanetary, (E/T), 26:54070
scintillation observations of Cygnus A, F-region power-law wavenumber spectrum deduced from ionospheric, (E/T), 26:54029

COSMIC SHOWERS
arrival directions of EAS, (E/T), 26:53851
arrival directions of large E greater than 10^{17} eV, (E), 26:53852

COSMIC X-RAY SOURCES
energy spectra of Cyg X-1, short-period variations of, (E), 26:53921
energy spectra of several, in the 20- to 150-keV range, (E), 26:53920
gamma fluxes from Sco X-1, (E), 26:53818
identification of 2ASE 1253-28 with EX Hydrae, (E), 26:53895
identification of Leo XR-1 with CP0950, (E/T), 26:53907
intensity of several, in the 20- to 150-keV range, (E), 26:53920
intensity variations of Cyg X-1, short-period, (E), 26:53921
luminosity of Sco X-1, optical, (E), 26:53917
model for Sco X-1, featuring white dwarf, (E), 26:53917
optical observations of Sco X-1, (E), 26:53918
spectra of Sco X-1, time variation of, (E), 26:53917
spectral lines and continuum in optically-thick, transfer effects on, (T), 26:53926
spectral lines and continuum in Sco X-1, transfer effects on, (T), 26:53926
x-ray observations of Sco X-1, (E), 26:53918

COSMOLOGY
constants of, relations between quantum constants and, 26:54392 (ITF-72-3-P)
Friedmann models of, exact expressions for properties of zero-pressure, (T), 26:53999
galaxy formation in anisotropic, 26:53980
Hubble constant in, method for estimating, (E), 26:53974
models in scalar--tensor gravitation theory, isotropic, 26:54396 (ITF-72-41-P)
perturbations in expanding universe of free particles, (T), 26:53997
scalar--tensor field equations in, (T), 26:53998

COULOMETERS
design of controlled-potential controlled-current cyclic, engineering drawings for, 26:52957
design of solid-state controlled-potential, engineering drawings for, 26:55642

COUNTING DEVICES
operation of up--down, optimum value of open aperture fraction of chopper for, 26:53323

CRAB NEBULA
  cosmic-particle origin in, (E/T), 26:53856
  gamma emission above 10 MeV from, search for, (E), 26:53816
  gamma emission from, search for pulsed, (E), 26:53922
  x-ray spectra between 2.3 and 9.9 keV, (E), 26:53919
CRACKS
  detection of neutron-induced, detector for, 26:53317
CRITICAL ASSEMBLIES
  control rod mockups in ZPPR, reactivity worths and γ heating of boron and tantalum, (E), 26:55134 (CONF-720901-(Bks.1 and 2), pp 579-98)
  core physics analysis in SNEAK, evaluation of KAPER code for, 26:55396 (EURFNR-1014)
  core physics in, KAPER code for calculation of, 26:55396 (EURFNR-1014)
  correlation function from noise analysis of ZPR-9, 26:55448
  critical parameters of enriched uranium fueled graphite reflected cores in FCA, (E), 26:55401 (JAERI-Memo-3891)
  criticality measurements in MASURCA, program for, 26:55118 (CONF-720901-(Bks.1 and 2), pp 822-38)
  criticality measurements in ZPPR and ZPR-6, program for benchmark, 26:55116 (CONF-720901-(Bks.1 and 2), pp 789-808)
  criticality measurements in ZPPR, benchmark, 26:55117 (CONF-720901-(Bks.1 and 2), pp 809-21)
  criticality measurements in ZPPR-3 for liquid metal fast breeder core mockups, 26:55114 (CONF-720901-(Bks.1 and 2), pp 724-38)
  cross sections for fast, evaluation of ENDF/B data on, 26:55416(R) (BNWL-1522-5)
  Doppler reactivity measurements on uranium-238 in ZPPR-2, effects of core configuration on, 26:55393 (CONF-720901-(Bks.1 and 2), pp 1006-15)
  neutron fraction in plutonium fueled fast, measurement of effective delayed, 26:55389 (CONF-720901-(Bks.1 and 2), pp 700-12)
  operation of STEK, quarterly summary of, 26:55083(R) (EURFNR-1001)
  physics calculations for fast, KFKINR set of group constants for, 26:55397 (EURFNR-1016)
  physics calculations for fast, VIM-1 computer program for, 26:55378 (AI-AEC-12951)
  physics measurements for SNEAK 6A, 6B, and 6D, (E/T), 26:55398 (EURFNR-1029)
  physics measurements in fast, evaluation of neutron cross sections from, 26:55385 (CONF-720901-(Bks.1 and 2), pp 623-35)
  physics measurements in FCA, pulsed neutron techniques for effective delayed neutron fraction, 26:55403 (JAERI-Memo-4004)
  physics measurements in ZPPR-2 and ZPR-6-7, comparison for fuel plates vs. fuel pins of, 26:55395 (CONF-720901-12)
  physics measurements on plutonium fueled cores in SNEAK, (E/T), 26:55387 (CONF-720901-(Bks.1 and 2), pp 645-59)
  reactivity calculations for VINS, using Monte Carlo transport codes, 26:54469 (ANCR-1071)
  reactivity worth measurements in ZPPR-2, heterogeneity effects in sodium void, 26:55392 (CONF-720901-(Bks.1 and 2), pp 973-85)
CRITICALITY
  calculations for reactors, zero variance estimator for Monte Carlo, 26:55431 (CONF-720901-(Bks.1 and 2), pp 229-39)
  calculations for, reliability of Monte Carlo computer programs, 26:55445 (Y-KC-96)
  control parameters for 6 percent or less enriched uranium, 26:53733 (WCAP-2999)
  excursions in large boiling water reactors, analytical method for rod drop super prompt, 26:55353 (NEDO-10527)
  measurements in high burnup plutonium, effects of plutonium isotopic composition in, 26:55416(R) (BNWL-1522-5)
  measurements in plutonium nitrate ($Pu(NO_3)_4$)—polystyrene lattices, 26:55416(R) (BNWL-1522-5)
CRUSTACEA
  Chaetophiloscia sicula, γ radiosensitivity of, 26:53504
  Porcellio dilatus, γ radiosensitivity of, 26:53504
CRYSTAL RIVER POWER REACTOR, UNIT 3
  owners of, antitrust review for, 26:55308 (DOCKET-50302-52)
CRYSTAL STRUCTURE
  lectures at Physics Laboratory of Istituto Superiore di Sanita, Rome, July--Dec. 1970, 26:54162 (ISS-71/31)
CRYSTALS
  defects in lattices of, atomistic computer simulation of, (E), 26:54970 (CEA-CONF-1890)
  electron beam motion through, laser modulation in Schwarz--Hora effect for light production and upper limit for laser emission in, (T), 26:54245 (IS-T-531)
  electronic structure of conductor, in magnetic field, (T), 26:55533 (ITF-72-16-E)
  exciton energy in semiconductor, formulae for longitudinal, (E/T), 26:55065(T) (UCRL-Trans-10643)
  ion channeling in, flux peaking effect in, (T), 26:55007
  phonon frequency distributions of fcc Lennard--Jones harmonic, (T), 26:55515 (COO-3161-3)
  phonon resonant scattering by impurities in, review, 26:55511 (COO-3151-8)
  radiation damage in cubic and diamond lattices, correlated recovery kinetics of anisotropic, (T), 26:55005
  radiation effects on, atomistic computer simulation of, (E), 26:54970 (CEA-CONF-1890)
  transformations in ionic, with triparticle interactions, theory of polymorphous, 26:55538 (ITF-72-50-P)
CULTURE MEDIA
  effects on recovery of γ-irradiated pathogenic bacteria, combined effects of dose and storage temperature on, 26:53369
CURIUM ISOTOPES Cm-242
  content in atmosphere in vicinity of Savannah River Plant, 1971, 26:53153(R) (DPSPU-72-30-1)
CURIUM ISOTOPES Cm-244
  content in atmosphere in vicinity of Savannah River Plant, 1971, 26:53153(R) (DPSPU-72-30-1)
  preparation of high purity, by reduction of curium oxide, p. 41, 26:53066 (ORNL-4794, pp 36-44)
CURIUM OXIDES
  reduction of, preparation of high purity curium metal by, p. 41, 26:53066 (ORNL-4794, pp 36-44)
CURRENT ALGEBRA
  commutation of axial charges with axial divergences for baryon states, 26:54341
  representations of local, general properties of, 26:54239
  SU(3) x SU(3) chiral, for mixing operator for baryons, 26:54370 (NP-19418)
2,4,6-CYCLOHEPTATRIEN-1-ONE, 2-HYDROXY-3-ISOPROPYL-
  solvent properties for tetravalent plutonium, 26:53034(T) (MLM-1964(tr))
CYCLOHEXANE
  radiolysis of gaseous, mass spectrometric studies on ion--molecule reactions produced by γ, 26:52982 (EUR-4765, pp 11-24)
CYCLOHEXENE
  radioinduced thermoluminescence of, effects of additives and dose on γ, 26:53010
CYCLOTRONS
  beam emittance measurements at Cracow U-120, for design of beam transport system, 26:53760
  beam injection systems for, review on, 26:53756 (LBL-654)
  beam oscillations in electron model of isochronous, effects of beam space charge on frequency shift of incoherent axial, 26:53761
  ion source for LBL 88-in., description of Penning-type heavy-, 26:53755 (LBL-644)
  operation of LBL 88-in., review of heavy-ion, 26:53755 (LBL-644)
CYSTEAMINE
  radioprotective effects on mice following fractionated sublethal whole-body exposure, 26:53475
CYSTEINE
  radiolysis of frozen aqueous solutions of, ESR study of free radicals from γ, 26:52995

D

DACTINOMYCIN
  effects on post-fertilization expression of x-radioinduced dominant and recessive lethal mutations in mature spermatozoa of Drosophila melanogaster, 26:53502
  effects on post-fertilization maternal repair of x-radioinduced chromosome aberrations in mature spermatozoa of Drosophila melanogaster, inhibitory, 26:53502
  effects on repair of γ-radioinduced double-strand breaks in DNA of Micrococcus radiodurans, inhibitory, 26:53349
DATA ACQUISITION SYSTEMS
  description for LAMPF experimental facilities, 26:53795 (LA-4874, pp 86-9)
  description of computer-based real time, for nondestructive testing, 26:55607 (SC-R-722879)
  description of Grenoble IBM 360-50 computer, 26:53312
  design and performance for mass spectrometer, 26:53324
DATA PROCESSING SYSTEMS
  buffers in real-time on-line computer, technique for handling, 26:55465 (AERE-R-6623)
  description of computer-based, for clinical scintigraphic data, 26:53228
  description of computer-based, for polarity-correlation noise analysis, 26:55448
  development of computerized, for gamma spectra subtraction during use of chromium-51 and iron-59 as dual tracers in biological systems, 26:53544
  development of digital computer, for analysis of gamma camera radioisotope imaging data for clinical use, 26:55457 (TID-26141)
  operation of computer, for periodic maintenance and calibration of reactor instrumentation, 26:55132 (ANL/EBR-63)
DATA TABULATIONS
  cross sections for excitation in heavy-particle collisions, 26:54118
  cross sections for π^{+-} + d, π^{+-} + n, and π^{+-} + p

- interactions, 26:54201 (CERN/HERA-72-1)
- on gamma rays from fission products, 26:54607 (RD/B/M-2356)
- on γ spectra from fissionable nuclei, 26:54652 (ANCR-1069)

DECAY SCHEMES
- measurement of, review of impact of advances in instrumentation on, 26:53263

DEER
- radioactivity monitoring of, in vicinity of Savannah River Plant, 1971, 26:53153(R) (DPSPU-72-30-1)

DERMATITIS
- radioinduced, in man following local exposure for therapy of underlying neoplasms, γ, 26:53433

DESALTING
- research in India, 1971--1972, 26:55452(R) (NP-19407)

DEUTERIUM
- abundance in Jovian atmosphere, (E), 26:54007
- atomic mass of, 26:54495 (EUR-4765, pp 435-55)
- crystal structure of, 26:55559 (LA-DC-72-903)
- deuteron elastic scattering at 12.305 MeV, differential cross sections for, (E), 26:54497 (LA-DC-72-876)
- deuteron reactions (d,n) at 30 keV to 1.5 MeV, calculation of thick target yields for, (T), 26:54502 (SC-RR-720513)
- deuteron reactions (d,n) at 6 to 14 MeV, differential polarization from, (E), 26:54516
- deuteron reactions (d,p) at 2.0 to 14.0 MeV, differential polarization from, from tritium (p,d) reactions, (E), 26:54517
- effects on ESR spectra of γ-irradiated nitric acid, isotope, 26:53009
- effects on hot hydrogen atom reactions in bromine--hydrobromic acid systems, isotope, 26:52962
- effects on hydrolysis of tetrahydridoborate, isotope, 26:52965
- effects on methane ion molecule reactions with silane, isotope, 26:52961
- effects on potential function for ring puckering vibration of diborane, isotope, 26:52966
- effects on proton transfer to cyanines, solvent isotope, 26:52964
- effects on quenching of tyrosine and tryptophan fluorescence by water, isotope, 26:52958 (UR-3490-193)
- effects on Raman and ir spectra of ammonia polycrystals at 18 to 107°K, isotope, 26:52968
- effects on Raman spectra of cubic and orthorhomic hydrogen chloride at 86 to 104°K, isotope, 26:52971
- effects on triplet lifetimes of anthracene, position dependence of isotope, 26:52972
- effects on variable traps in electronic states of s-triazine, isotope, 26:52963
- exchange between ammonia and hydrogen molecules, heavy water production process based on, 26:53088
- exchange between heavy water and tetrahydridoborate, 26:52965
- exchange between water and N,N'-bis(3-phenoxyhydroxypropyl)ethylenediamine hydrochloride, 26:53052
- exchange equilibria in ammonia, effects of vibrational anharmonicity on self-, 26:52973
- exchange with hydrogen in x-irradiated DL-serine at 300°K, 26:52996
- interactions $\pi^- + d \to 2p + \pi^+ + 3\pi^- + m\pi^0$ at 7 GeV/c in deuterium bubble chamber, cross sections and upper limit for exotic multipion resonance production in, (E), 26:54208 (COO-3065-16)
- neutron elastic scattering at zero energy, method of moments for solution of Faddeev equations for, (T), 26:54715
- nucleon elastic scattering at 10.85 MeV, agreement of exact calculations of polarization in, (T), 26:54509
- phase transitions in, 26:55559 (LA-DC-72-903)
- proton elastic scattering at 600 MeV, differential cross section for, (E), 26:54512
- proton reactions (p,2p) and (p,pn) with small momentum transfer, polar graph interpretation of differences in cross sections for, (T), 26:54510
- proton reactions (p,2p) at 155 MeV, analysis of angular distributions for off-energy-shell effects, (E), 26:54522
- proton reactions (p,2p) at 51.8 MeV, analysis of cross sections and spectra from, (E/T), 26:54505
- proton reactions (p,n) at 16 to 26 MeV, analysis of p - p final state interaction in, (E/T), 26:54503 (UCRL-74069)
- proton reactions (p,pn) and (p,2p) at 20 to 60 MeV, analysis of rescattering effects in, (E/T), 26:54511
- reactions between molecules of, at 50 to 500 eV, angular distributions and total cross sections for production of fast molecular ions in, (E), 26:54105
- reactions with brass surfaces of molecular, secondary-electron emission coefficients for, (E), 26:54105
- separation from hydrogen produced from water vapor, 26:52975(P)
- triton reactions (t,n) at 30 keV to 1.5 MeV, calculation of thick target yields for, (T), 26:54502 (SC-RR-720513)

DEUTERIUM HYDRIDES
- nuclear spin--spin coupling constant of, perturbation calculation using bare-nucleus potential as function of internuclear separation, 26:54092
- spectral lines in xi Per due to interstellar, equivalent widths of, (E), 26:53890

DEUTERIUM SYSTEMS
- D--T, laser beam reactions with solid targets of, fusion reactions from, 26:54830
- D--T, thermonuclear reactions from spherical hot-spot in, (T), 26:54831

DEUTERONS
- breakup in Coulomb field in ISABELLE, cross section for, (T), 26:53776 (BNL-17063)
- dechanneling at 1.5 MeV in diamond lattices, 26:54988
- effects on crosslinking and fading in poly(vinyl chloride) containing 1,4-diaminoanthraquinone, 26:53020
- energy spectra of primary cosmic, (E), 26:53828
- interactions anti p + d → anti p + p + n, Fermi motion and n + p final-state interaction effects on low-momentum transfer cross sections for, (T), 26:54347 (UM-P-72-6)
- interactions anti p + d → p + anything, nonzero orbital momenta of anti pn bound states from recoil proton momentum spectrum in, (T), 26:54334
- interactions α + d at 1 to 200 MeV (cms), optical-potential description of phases for scattering, (T), 26:54532
- interactions e + d → e + d, renormalization and neutron magnetic form factor from analysis of available data on, (E), 26:54169 (JINR-E1-6647)
- interactions $\gamma + d \to p + p + \pi^-$ up to 1 GeV in bubble chamber, angular distributions and total cross sections for, (E/T), 26:54171 (LNF-72/31)
- interactions $K^+ + d$ at 9 GeV/c in deuterium bubble chamber, analysis of Q region of $K^+\pi^+\pi^-$ mass spectra from, (E), 26:54228
- interactions n + d, calculation of breakup cross section with separable potentials, 26:54520
- interactions n + d, calculation of doublet scattering length using Skornyakov--Ter-Martirosyan equations, 26:54344 (ITF-72-10-P)
- interactions ν + d → 2p + e near 50 MeV, cross section calculations for, (T), 26:54233 (LA-DC-72-848)
- interactions p + d → p + d at 10 to 70 GeV, tables of absolute differential cross sections and amplitudes for, (E), 26:54194 (JINR-E1-6615)
- interactions p + d at 10 to 70 GeV, slope parameter of diffraction cone and ratio of real to imaginary parts of amplitude of elastic, (E), 26:54197
- interactions p + d at 800 MeV, calculation of relative neutron and pion yields in, (T), 26:54467(R) (ORO-2972-204)
- interactions π + d, recoil and Fresnel corrections to Glauber multiple-scattering model for, 26:54352
- interactions $\pi^- + d \to 2p + 2\pi^- + m\pi^0$ at 7 GeV/c in deuterium bubble chamber, cross sections and upper limit for exotic multipion resonance production in, (E), 26:54208 (COO-3065-16)
- interactions $\pi^- + d \to 2p + 2\pi^- + \pi^0$ at 7 GeV/c in deuterium bubble chamber, cross sections, upper limit for exotic multipion resonance production, and validity of spectator model for cross sections for Δ^0rho$^-$ channel in, (E), 26:54208 (COO-3065-16)
- interactions $\pi^- + d \to 2p + 2\pi^-$ at 7 GeV/c in deuterium bubble chamber, cross sections, upper limit for exotic multipion resonance production, and π + π scattering phase shifts in, (E), 26:54208 (COO-3065-16)
- interactions $\pi^- + d \to 2p + \pi^+ + 3\pi^- + \pi^0$ at 7 GeV/c in deuterium bubble chamber, cross sections and upper limit for exotic multipion resonance production in, (E), 26:54208 (COO-3065-16)
- interactions $\pi^- + d \to 2p + \pi^+ + 3\pi^-$ at 7 GeV/c in deuterium bubble chamber, cross sections and upper limit for exotic multipion resonance production in, (E), 26:54208 (COO-3065-16)
- interactions $\pi^+ + d \to 2p + \pi^+ + \pi^-$ at 13 GeV/c, I = 0 S-wave phase shift from partial-wave analysis of ππ spectra and rho and f production cross sections in, (E/T), 26:54219
- interactions $\pi^+ + d$, compilation of cross sections for, 26:54201 (CERN/HERA-72-1)
- interactions $\pi^- + d$, compilation of cross sections for, 26:54201 (CERN/HERA-72-1)
- proton elastic scattering at 3.6 to 9.1 MeV, vector to tensor polarization transfer in, (E), 26:54499 (LA-DC-72-905)
- reactions (d,α) and (d,p) with fluorine-19 at 3 MeV, differential cross sections for, (E), 26:54548
- reactions (d,α) with carbon-12 at 7.2 to 14 MeV, analysis of reaction mechanism in isospin-forbidden and -allowed, (E), 26:54539
- reactions (d,α) with iron-57 at 16 MeV, angular distributions for, (E), 26:54584
- reactions (d,α) with neon-20 at 3.5 to 8 MeV, excitation functions for, (E), 26:54467(R) (ORO-2972-204)
- reactions (d,Li-6) with carbon-12, oxygen-16, fluorine-19, and calcium-40 at 28 MeV, angular distributions and spectroscopic factors for, (E), 26:54527 (LYCEN-7219)
- reactions (d,n) and (d,p) with carbon-12, calculation of spectroscopic factors using weakly bound projectile model, (T), 26:54543
- reactions (d,n) with A = 2 to 9 nuclei at 30 keV to 1.5 MeV, calculation of thick target yields for, (T),

26:54502 (SC-RR-720513)
  reactions (d,n) with beryllium-9 at 50 and 54 MeV, biological implications of neutron spectra from, (E/T), 26:53804
  reactions (d,n) with deuterium, at 6 to 14 MeV, differential polarization from, (E), 26:54516
  reactions (d,np) and (d,p) with strontium-88 at 7.5 to 10.0 MeV, coupled-channels Born-approximation calculations of excitation functions for, (E/T), 26:54588
  reactions (d,np) with carbon-12 at 5.99 MeV, triangle graphs and isospin violation in rescattering in, (T), 26:54716
  reactions (d,p) and (d,t) with cerium-142 at 12.6 MeV, particle spectra and angular distributions for, (E), 26:54618
  reactions (d,p) with calcium-41 at 12 MeV, DWBA analysis of differential cross sections and spectrum from, (E), 26:54573
  reactions (d,p) with cerium-142 at 9 to 13 MeV, proton spectra from, (E), 26:54467(R) (ORO-2972-204)
  reactions (d,p) with deuterium at 2.0 to 14.0 MeV, differential polarization from, from tritium (p,d) reactions, (E), 26:54517
  reactions (d,p) with hafnium-179 at 12 and 14 MeV, proton spectra from, (E), 26:54636
  reactions (d,p) with helium-3 at 366 to 1090 keV using polarized beam, analyzing power for, (E), 26:54500 (LA-DC-72-906)
  reactions (d,p) with iron-58 at 10 MeV, angular distributions for, (E), 26:54592
  reactions (d,p) with molybdenum-100 at 3.05 to 3.75 MeV, DWBA analysis of differential cross sections and excitation function for, (E), 26:54614
  reactions (d,p) with nickel-62 and -64 at 12 MeV, angular distributions for, (E), 26:54587 (FRNC-TH-240)
  reactions (d,p) with rhenium-187 at 12 MeV, proton spectra and cross sections for, (E), 26:54637
  reactions (d,p) with silver-109 at 10 MeV, proton spectra from, (E), 26:54467(R) (ORO-2972-204)
  reactions (d,pγ) with calcium-40, chromium-52, and iron-54 at 3 MeV, γ-ray angular correlations for, (E), 26:54578
  reactions (d,t) with dysprosium-164 and gadolinium-160, coupled channel analysis of mixing in, (T), 26:54635 (JINR-P4-6509)
  reactions (d,t) with hafnium-177 at 12 and 14 MeV, triton spectra from, (E), 26:54636
  scattering by deuterium at 12.305 MeV, differential cross sections for elastic, (E), 26:54497 (LA-DC-72-876)
  scattering by helium-4 at 4.8 to 8.6 MeV, polarization transfer in elastic, (E), 26:54498 (LA-DC-72-904)
  scattering by hydrogen at 6.00 to 11.50 MeV, phase-shift analysis of polarized elastic, (T), 26:54513
  scattering by iron-56 and -58 at 10 MeV, angular distributions and optical model parameters for elastic, (E), 26:54592
  scattering by magnesium-24 at 12.1 MeV, coupled-channels and DWBA analyses of differential cross sections and analyzing powers from polarized elastic and inelastic, (E), 26:54557
  scattering of vector-polarized, by titanium-48, -49, -50 and chromium-50 at 11.9 MeV, elastic, (E), 26:54572
DIAMONDS
  radiation effects on optical spectra of Type-I, 17.0- and 18.3-MeV proton, 26:54991
DIELECTRICS
  magnetic splittings in cubic antiferro-, theory of Bethe and Davydov, 26:55536 (ITF-72-32-P)
DIET
  radium-226 content of human, in Poland, 26:53525
DIFFERENTIAL EQUATIONS
  book: Kinetic Equations, 26:54797
DIODES
  fabrication and properties of ion-implanted zinc telluride electroluminescent, 26:54971 (CEA-R-4313)
DISEASES
  hypertension, radioinduced, in rats, effects on distribution and excretion of exchangeable sodium, sodium-22 tracer study of, 26:53463
  thrombocytopenia, radioinduced, in man following intravenous injection of colloidal gold-198 for therapy of liver involvement in Hodgkin's disease, relation of dose fractionation and protraction to β and γ, 26:53507
DISPERSION RELATIONS
  derivation of forward, for low-energy elastic scattering of charged particles by nuclei, (T), 26:54711
  sum rules in axiomatic quantum field theory, spectral Jost--Lehman--Dyson representation for structure of, 26:54377 (ITF-72-54-P)
DISPLACEMENT GAGES
  design of electroacoustical, for signaling sample arrival in pneumatic reactor tubes, 26:55413(P)
DISTILLATION
  thermochemical reactions of alkaline halides in carrier, for uranium oxide purification, 26:53719
DOGS
  radiation dose distribution in respiratory tract tissues of, following inhalation of strontium-90 as fused clay aerosols, β, 26:53536
  radiation effects on maxillary bone of, following exposure of teeth, effects of lead bridges and plastic caps on γ, 26:53480
  radiation effects on thyroid gland of, relation of metabolic rate to carcinogenic and morphologic, x, 26:53462 (UR-3490-183)
DONALD C. COOK POWER REACTOR, UNIT 1
  construction of, authorization for provisional permit for, 26:55323 (DOCKET-50315-79)
  construction of, provisional permit for, 26:55320 (DOCKET-50315-76)
  containment spray system for, design changes for, 26:55322 (DOCKET-50315-78)
  containment system for, evaluation program for ice condenser, 26:55324 (DOCKET-50315-80)
  coolant for, increase in average temperature for, 26:55322 (DOCKET-50315-78)
  effluents from, environmental monitoring programs for chemical and thermal, 26:55326 (DOCKET-50315-82)
  emergency core cooling system for, design changes for, 26:55322 (DOCKET-50315-78)
  safety evaluation of, Division of Reactor Licensing, 26:55318 (DOCKET-50315-74)
  site for, Benton Harbor limnology survey near, 26:55325 (DOCKET-50315-81)
  site for, nonradiological environmental monitoring program for, 26:55326 (DOCKET-50315-82)
  spent fuel pit for, tornado and missile hazard analysis for, 26:55321 (DOCKET-50315-77)
  steam generator for, design changes for isolation valve for, 26:55322 (DOCKET-50315-78)
  valves for, verification of wall thicknesses for nuclear service, 26:55319 (DOCKET-50315-75)
DONALD C. COOK POWER REACTOR, UNIT 2
  construction of, authorization for provisional permit for, 26:55323 (DOCKET-50315-79)
  construction of, provisional permit for, 26:55320 (DOCKET-50315-76)
  containment spray system for, design changes for, 26:55322 (DOCKET-50315-78)
  containment system for, evaluation program for ice condenser, 26:55324 (DOCKET-50315-80)
  coolant for, increase in average temperature for, 26:55322 (DOCKET-50315-78)
  effluents from, environmental monitoring programs for chemical and thermal, 26:55326 (DOCKET-50315-82)
  emergency core cooling system for, design changes for, 26:55322 (DOCKET-50315-78)
  safety evaluation of, Division of Reactor Licensing, 26:55318 (DOCKET-50315-74)
  site for, Benton Harbor limnology survey near, 26:55325 (DOCKET-50315-81)
  site for, nonradiological environmental monitoring program for, 26:55326 (DOCKET-50315-82)
  spent fuel pit for, tornado and missile hazard analysis for, 26:55321 (DOCKET-50315-77)
  steam generator for, design changes for isolation valve for, 26:55322 (DOCKET-50315-78)
  valves for, verification of wall thicknesses for nuclear service, 26:55319 (DOCKET-50315-75)
DOUNREAY FAST REACTOR
  coolant contamination in, mechanisms of, (E), 26:55167 (CONF-710959-, Paper 11)
  cooling systems of, effectiveness of water for decontamination of, (E), 26:55167 (CONF-710959-, Paper 11)
  cooling systems of, mechanisms of fission and corrosion product deposition in, (E), 26:55167 (CONF-710959-, Paper 11)
  fission product transport in NaK coolant of, mechanisms of, (E), 26:55167 (CONF-710959-, Paper 11)
  fuel element corrosion in NaK coolant of, mechanisms of, (E), 26:55167 (CONF-710959-, Paper 11)
  fuel transport in NaK coolant of, mechanisms of, (E), 26:55167 (CONF-710959-, Paper 11)
DRESDEN POWER REACTOR, UNIT 1
  valves for, verification of wall thicknesses for nuclear service, 26:55274 (DOCKET-50010-117)
DRESDEN POWER REACTOR, UNIT 2
  steam line for, low flow in, 26:55244 (DOCKET-50237-258)
  switches for, incorrect scram setpoints for electrohydraulic control oil low pressure, 26:55243 (DOCKET-50237-257)
  valves for, verification of wall thicknesses for nuclear service, 26:55274 (DOCKET-50010-117)
DRESDEN POWER REACTOR, UNIT 3
  hydraulic control system for, incorrect set point for low oil pressure scram switches for electro, 26:55247 (DOCKET-50249-155)
  switches for, incorrect scram setpoints for electrohydraulic control oil low pressure, 26:55243 (DOCKET-50237-257)
  turbine for, malfunction of control valve for, 26:55247 (DOCKET-50249-155)
  valves for, verification of wall thicknesses for nuclear service, 26:55274 (DOCKET-50010-117)
DRILL CORES
  analysis for copper and nickel, by neutron activation using californium-252 source, 26:53174
DRILL HOLES
  exploration of, neutron activation method for, 26:53174

DUANE ARNOLD POWER REACTOR
  valves for, verification of wall thicknesses for nuclear service, 26:55330 (DOCKET-50331-52)
DURALUMIN
  analysis for copper by amperometric titration, 26:52924
DUSTS
  density in solar corona, (T), 26:53938
  infrared radiation from interstellar, (T), 26:53989
DYES
  toxicity of diphenylthiocarbazone, 1,5-diphenyl-3-thiocarbohydrazide, purpurin, quinalizarin, and quinizarin in mammals, bibliography on, 26:55574 (ORNL-TIP/TIRC-72-4)
DYSPROSIUM
  magnetoelastic interaction for magnon--phonon mixing, (T), 26:55026
  oxidation under controlled oxygen partial pressures at 727 to 1327°C, 26:53550 (IS-T-540)
DYSPROSIUM ISOTOPES Dy-153
  electron-capture decay of, conversion-electron and gamma spectra from, (E), 26:54643
DYSPROSIUM ISOTOPES Dy-155
  beta and electron-capture decay of, conversion-electron spectra from, (E), 26:54643
DYSPROSIUM ISOTOPES Dy-160
  neutron reactions (n,α) with, calculation of, (T), 26:54707
DYSPROSIUM ISOTOPES Dy-162
  neutron reactions (n,α) with, calculation of, (T), 26:54707
DYSPROSIUM ISOTOPES Dy-163
  neutron capture up to 200 eV, correlation of partial radiative and neutron widths in resonance, (E), 26:54631(T) (BNL-tr-490)
DYSPROSIUM ISOTOPES Dy-164
  deuteron reactions (d,t) with, coupled channel analysis of mixing in, (T), 26:54635 (JINR-P4-6509)
  neutron capture at 25 keV, model analysis of isomeric cross section ratio for, (E/T), 26:54589
  neutron reactions (n,α) with, calculation of, (T), 26:54707
DYSPROSIUM ISOTOPES Dy-165
  beta decay of, heat-flow analysis of temperature spikes following, (E/T), 26:54646

E

EARTH
  rotation of, relativistic gravitational effects on influence on mechanical vibrations of, 26:54400 (ITF-72-59-P)
EARTHQUAKES
  ground motion from San Fernando, damage to Glendale, Calif. residential buildings from, 26:53137 (JAB-99-96)
ECOSYSTEMS
  cesium-137 content in Florida, during June 1971 to June 1972, 26:53170(R) (ORO-4066-5)
  hazards to aquatic, from surface water-discharge of power plant waste heat, 26:53194
  model of hardwood forest, development of analog, 26:53170(R) (ORO-4066-5)
  nutrient cycling through forest floor-arthropod, tracer studies on calcium and potassium, 26:53539(R) (SRO-641-4)
  phosphorus flux through salt marsh, model for, 26:55612(R) (SRO-639-12)
  plant associations in Whiteshell Nuclear Research Establishment controlled area, 26:55462 (AECL-3957)
  radioisotope content and distribution in Savannah River swamp forest, (E), 26:53171(R) (SRO-708-1)
  radioisotope cycling in, bibliography on, 26:53530 (TID-3915(Suppl.1))
  radioisotope transport in marine, relation of uptake by animals and plants to strontium-90 and zinc-65, 26:53532
  trophic dynamics and niches of salt marsh foraminifera, 26:55520 (COO-3254-6)
  zinc-65 distribution in Oregon and Washington continental shelf, 26:53149 (RLO-2227-T-12-26)
EDDY CURRENT TESTING
  equipment and method for Type 316 stainless steel fuel cladding tubes, 26:53125
EDWIN I. HATCH POWER REACTOR, UNIT 1
  steam line isolation valves for, verification of wall thicknesses for main, 26:55328 (DOCKET-50321-49)
EGYPT
  mineralogy of southwest Aswan radioactive syenite rock in, 26:53142 (AREAEE-138)
ELECTRIC CURRENTS
  effects of pulsed, on crystal structure of tungsten, 26:53668
ELECTRIC DISCHARGE
  blast wave generation in plasma in pulsed, (E), 26:54856
  collision processes in, research on, (E/T), 26:54779(R) (NP-19393)
  oscillations in bounded neon positive column, constant-wavelength, (E/T), 26:54859
  plasma density and skin-layer thickness measurements in strong hf, (E), 26:54768(T) (AEC-tr-7329)
  plasma diffusion coefficients for shf, transverse and longitudinal, (E), 26:54776(T) (AEC-tr-7332)
  plasma oscillations in hf, in magnetic fields, (E), 26:54849
  plasma wave transformation region in shf, localization of, (E), 26:54842(T) (AEC-tr-7339)
  research on low-pressure, Flinders Univ. of South Australia, (E/T), 26:54779(R) (NP-19393)
ELECTRIC FIELDS
  symmetries of nonrelativistic, relativistic, and approximate relativistic Coulomb problem for, radial integrals, relation between parabolic and spherical wave functions, and first-order Stark shifts from, (T), 26:54374
ELECTRIC POWER
  generation in manned space stations, design and requirements of nuclear systems for, 26:53094 (NASA-TM-X-2440, pp 26-33)
  generation in US, evaluation of optional methods for, 26:53097
  generation in US, legal methods for controlling demand for increased, 26:53101
  generation of, survey of options in, 26:55086
  operation and use of, environmentalists' view on growth rates for, 26:53100
  production in Japan, evaluation of hydraulic, fossil fuel, and nuclear methods for, 26:55092
  requirements in US for, during the period 1980 to 2000, 26:53097
  transmission by underground superconducting cable, 26:54461 (BNL-50325)
  transmission of, survey of options in, 26:55086
ELECTRIC PROBES
  plasma flow around, potential measurements for ionospheric applications, 26:54011 (ONERA-Publ.-137)
ELECTROHYDRODYNAMIC GENERATORS
  operation of, description of simulator facility for, 26:53089 (AD-737380)
ELECTROJETS
  lunar variations in Peruvian equatorial, comments on seasonal and daily, (E), 26:54041
  wave generation in ionospheric, potential transverse-current-produced, (T), 26:54027
ELECTROLUMINESCENCE
  diode fabrication and properties, using ion-implanted zinc telluride, 26:54971 (CEA-R-4313)
ELECTROLYTES
  mass transfer in systems of, multicomponent, p. 93, 26:53085 (ORNL-4794, pp 91-5)
ELECTROMAGNETIC FIELDS
  interactions with many-level molecular systems, semiclassical theory of, 26:55468 (AREAEE-136)
  Maxwell equations in presence of electric and magnetic charges for, variational principle and external invariance of, (T), 26:54373 (ITF-72-35-P)
  pair production in strong, with arbitrary spin and magnetic moment, 26:54266
  penetration into nontransparent plasma, traveling hf, (T), 26:54843 (AREAEE-124)
ELECTROMAGNETIC LENSES
  charged-particle trajectories in first-order achromatic, second-order effects on, 26:53764
  coil configurations in superconducting quadrupole, limitations on good field aperture due to use of finite number of ribbons in, 26:53768 (BNL-16980)
  design for producing separated electron beams over 100 GeV by using synchrotron radiation, 26:53801
  field distribution in superconducting, calculation of, 26:53759
ELECTROMAGNETIC WAVES
  absorption in linear plasma layer in hybrid resonance region, extraordinary, (T), 26:54864
  charged-particle radiation emission in field of two plane, relativistic, (T), 26:54264
  excitation in plasma by relativistic electron beams, (T), 26:54837(T) (AEC-tr-7333)
  interactions with collisionless plasma, generation of fast electrons in, (E), 26:54836(T) (AEC-tr-7331)
  propagation in homogeneous magnetosphere, nonlinear theory of monochromatic circularly polarized ulf and vlf, (T), 26:54050
  propagation in magnetosphere of ulf Pc-1 micropulsations, effect of nonlinear phenomena on, (E/T), 26:54050
  reflection at oblique incidence on sharp plasma boundary formed by ionization source moving with constant velocity, (T), 26:54865
  scattering on plasma in flat waveguides, effect of electron charge fluctuations on, (T), 26:54848
ELECTROMETERS
  design for ionization chamber for monitoring normal gamma environmental levels, engineering drawings for, 26:53218
ELECTRON BEAMS
  diffraction by magnetoactive plasma cylinder, (T), 26:54847
  dosimetry of pulsed calorimeter for, 26:53258 (SC-DR-720630)
  effects on alkali halides at 10 to 50 keV, density of color centers from, (E), 26:54973 (FRNC-TH-210)
  effects on carbon--hydrogen reactions at 30 to 45 keV, 26:53718
  focusing by ion beams in transverse gas flow, (E/T),

26:54086
interactions of large-current linear-discharge-produced pulsed, with argon plasma, argon-ion stimulation emission from, (E), 26:54787
interactions with plasma, dispersion equation for multiloop, (T), 26:54793
interactions with plasma, electromagnetic wave excitation by relativistic, (T), 26:54837(T) (AEC-tr-7333)
interactions with plasma, instability control in, (E), 26:54819
interactions with plasma, ion heating by oscillations, (E), 26:54762
interactions with plasma, modulation of lf oscillations from, 26:54782
interactions with plasma, nonlinear interaction of waves from, (T), 26:54795
interactions with plasma, steady-state beam shape in, (T), 26:54794
interactions with proton beams, calculation of luminosity of, 26:53777 (BNL-17067)
monitoring of currents of relativistic, Faraday ring for, 26:53747 (SC-DR-720447)
motion of relativistic, in drift space, self-consistent, 26:53757
motion through crystal, laser modulation in Schwarz--Hora effect for light production and upper limit for laser emission in, (T), 26:54245 (IS-T-531)
penetration in dense gas, (E/T), 26:54763

ELECTRON CAPTURE
book: Beta Processes. Functions for Analyzing Beta Spectra and Electron Capture, 26:54740

ELECTRON GAS
pair-correlation function of degenerate, 26:55532 (ITF-72-2-P)
positron correlation energy in, (T), 26:55066

ELECTRON MICROSCOPES
defect diffusion to surface in foils irradiated by high-voltage, (T), 26:54985
use of high-voltage, for high-flux irradiation of Nimonic PE 16, 26:53708

ELECTRON MICROSCOPY
selected-area diffraction in high-voltage, error distance in, 26:54972 (COO-2119-2)

ELECTRON TUBES
design and performance of magnetrons in production of multicharged ions, 26:54079 (FRNC-CONF-53)
ion density measurement in microwave, probe technique for, 26:55641

ELECTRONIC EQUIPMENT
radiation protection standards for, development of, 26:54925

ELECTRONICS
vacuum technique application to, conference at Versailles, France, Sept. 13, 1971, 26:53138

ELECTRONS
absorbed dose in tumor therapy, integral, (T), 26:54909
configuration diagram of solvated, spectral studies on, 26:53025
detection and measurement of, design and performance of retarding field-cylindrical mirror analyzer for, 26:53310 (SC-DC-721302)
detection at high energies, fabrication of total-absorption detector using condensed xenon for, 26:53272 (JINR-P13-6541)
detection at ISABELLE and PEP storage rings, design of hybrid detector for, 26:53268 (BNL-17066)
diffusion into polar-cap regions of 0.4- to 1.0-MeV solar, from interplanetary space, (E), 26:54069
dose deposition calculations for plane slabs, comparison of methods for 0.5- to 10-MeV, 26:54886 (NASA-TM-X-2440, pp 801-15)
dose distribution perturbation near cavities in tissue-equivalent materials at 10 to 35 MeV, iso-, (E), 26:54903
dose to man during high-energy therapy, use of thermoluminescent dosimeters to determine, 26:53415
dynamics in magnetosphere, conjugate features observed at balloon altitudes of, (E), 26:54020
effects of intense pulses of, on solids, 26:55012
effects of Jupiter-belt, on fly-by space missions, 26:54002 (NASA-TM-X-2440, pp 781-4)
effects of pulsed, on aqueous solutions of potassium hydroxide, kinetics of disappearance of hydrated electron from, 26:53018
effects of pulsed, on gases, determination of short-lived species from, 26:52980(R) (COO-3461-1)
effects of pulsed, on succinonitrile plastic crystals, transient absorption spectra from, 26:53003
effects on aluminum at 150 to 200 keV, effects of helium doping on threshold energy of, 26:54990
effects on cadmium sulfide films at 3 MeV, 26:54992
effects on curing of adhesives by polymerization at room temperature, 26:53716
effects on defect charge state in germanium converted to p-type at 140°K and 1 MeV, 26:55013
effects on dielectric constants and crystal structure of perovskite-type compounds, 26:55020
effects on electric conductivity of naphthalene, (E/T), 26:54968(R) (AD-737312)
effects on gadolinium single-crystal films, dislocation loops produced in, 26:54979
effects on gallium arsenide, (E), 26:54968(R) (AD-737312)
effects on liquid ammonia, preparation of anhydrous hydrazine by, 26:53001(P)
effects on luminescence of cadmium sulfide, 26:55002
effects on mechanical properties of chromium--iron alloys and iron--molybdenum alloys at 2.3 MeV, 26:53706
effects on metals, graphite, and quartz at 650 kV, electron microscopic studies of, 26:54972 (COO-2119-2)
effects on n-type germanium at 85°K, similarity of annealing behavior to p-type germanium, 26:54997
effects on platinum, comparison of stage I annealing with interstitial-migration theories for, 26:55011
effects on platinum, recovery in stage I of annealing of, (E), 26:55010
effects on point defect distribution in quench hardened aluminum at 1.6 MeV, 26:53712
effects on silicon at energies far below threshold, (E/T), 26:55017
effects on silicon, (E/T), 26:54968(R) (AD-737312)
effects on skin of miniature swine, dose and time dependence of pathological, 26:53458 (NASA-TM-X-2440, pp 665-71)
effects on small solid grains, collision processes in heating, (T), 26:54874 (EUR-CEA-FC-647)
effects on solid molecular hydrogen at 1.4 to 8°K, yields and EPR spectra of hydrogen atoms from, 26:52979 (COO-1105-179)
effects on swelling of metals, dose and dose rate dependences of, (T), 26:53707
effects on transmittance of borosilicate glass, 26:54049 (NASA-TM-X-2440, pp 748-55)
effects on vibrational spectra of gallium arsenide containing silicon and boron, 26:54984
emission by copper of secondary photo-, model calculations of angular and energy distributions of, 26:54885 (NASA-TM-X-2440, pp 792-800)
emission by gamma- and x-irradiated materials, Monte Carlo POEM program for calculating, 26:54884 (NASA-TM-X-2440, pp 786-91)
emission by solids bombarded by low-energy ions, surface analysis by, 26:52936 (RT/EL-(72)4)
energy spectra in water irradiated with 10- to 20-MeV electron beams, 26:54894
energy spectra of 3- to 15-GeV primary cosmic, (E), 26:53821
energy spectra of primary cosmic, (E), 26:53855
energy spectra of primary cosmic, between 10 and 1000 GeV, (E), 26:53822
energy spectra of primary cosmic, between 10 and 200 GeV, (E), 26:53823
energy spectrum for primary cosmic, equilibrium, (T), 26:53809
flux measurements at ATS-5 satellite at synchronous altitude of low-energy, effects of magnetic activity on, 26:54045 (NASA-TM-X-2440, pp 530-8)
flux of primary cosmic, between 10 and 1000 GeV, (E), 26:53822
fluxes in Jupiter radiation belt, models of, 26:54001 (NASA-TM-X-2440, pp 556-60)
fluxes of geomagnetically trapped, temporal variations in, 26:54046 (NASA-TM-X-2440, pp 539-47)
fluxes of trapped, in Jovian magnetosphere, (E/T), 26:54006
geomagnetic cutoff-rigidity calculations for Fort Churchill, Canada, daily variations of, (E/T), 26:54065
gyromagnetic ratio of, sixth-order contribution to anomalous, (T), 26:54271
interaction with water vapor, atomic processes and energy deposition, applications in atmospheric sciences of, (E/T), 26:54033
interactions $e + d \to e + d$, renormalization and neutron magnetic form factor from analysis of available data on, (E), 26:54169 (JINR-E1-6647)
interactions $e + N \to \pi + N$ at threshold, method for calculating axial nucleon form factor and pion electromagnetic form factor in, (T), 26:54247 (NP-19417)
interactions e + N at high energies, review of kinematics, scaling, scattering from deuterons and complex nuclei, sum rules, single π^+ production, vector meson diffractive production, and coincidence measurements in inelastic, (E), 26:54173 (RPP/H-97)
interactions e + N at $q^2 = 0.6$ to 1.56 GeV^2, angular distributions for π^0 production in, (E), 26:54268
interactions e + N in quark--parton model, bare quark mass and structure function for, (T), 26:54282
interactions e + N, relation between prominent resonances and limiting scaling data in inelastic, (T), 26:54258
interactions e + N, sum rule and model for S-matrix elements in presence of standing-wave states as shadow quarks in Bjorken limit of deep inelastic, (T), 26:54248 (ORO-3992-106)
interactions $e + p \to e + K^+(K^-)$ + anything at 6.5 GeV, momentum spectra of K in inclusive, (E), 26:54178
interactions $e + p \to e + \mu^+ + \mu^-$ + anything, test of algebra of bilocal operators from, (T), 26:54253
interactions $e + p \to e + p$ + anything at 6.5 GeV, momentum spectra of protons in inclusive, (E), 26:54178
interactions $e + p \to e + \pi^+(\pi^-)$ + anything at 6.5 GeV,

momentum spectra of π in inclusive, (E), 26:54178
interactions $e + p \to e^+ + e^- + e + p$ at 30 GeV, angular distributions, mass spectra, and total cross sections for, (T), 26:54263
interactions $e + p \to \mu^+ + \mu^- + e + p$ at 30 GeV, angular distributions, mass spectra, and total cross sections for, (T), 26:54263
interactions $e + p$ at $q^2 = 1(\mathrm{GeV}/c)^2$ in resonance region, separation of longitudinal contribution from total cross sections of virtual $\gamma + p$ interactions in inelastic, (E), 26:54168 (DESY-72/38)
interactions $e + p$ in spin-$^1/_2$ parton model, two-photon exchange effects in deep inelastic, (T), 26:54269
interactions $e + p$, k^2 dependence of transverse cross section for meson (π^+) production in generalized Born term model, (T), 26:54243 (DESY-72/30)
interactions $e + p$, perturbation theory for $e^+ + e^- \to$ hadrons relation to deep inelastic, (T), 26:54262
interactions $e^+ + e^- \to$ hadrons, perturbation theory for relation to deep inelastic $e + p$ scattering, (T), 26:54262
interactions $e^+ + e^- \to$ hadrons, review of total cross sections, SU(3) ratios, SU(6) quark model predictions, multiplicities, transverse momentum distributions, resonance production, and $\gamma + \gamma$ processes for annihilation, (E/T), 26:54176 (SLAC-PUB-1043)
interactions $e^+ + e^- \to W^- + e^+ + \nu$, total cross section and angular and energy distributions of e^+ and W^- production in, (T), 26:54277
interactions $e^+ + e^- \to W^- + \mu^+ + \nu$, W^- production in, (T), 26:54277
interactions $e^+ + e^-$ in storage rings, test for existence of high-mass vector mesons in, (T), 26:54283
interactions $e^+ + e^-$, angular distributions in annihilation, (T), 26:54281
interactions $e^+ + e^-$, Schwarz inequality for asymptotic behavior of cross sections for annihilation, (T), 26:54287 (LBL-766)
interactions $\gamma + e$, differential cross sections and left--right asymmetry in Compton, (T), 26:54256
interactions $\gamma + e$, hypothesis consistency and relation with behavior of electromagnetic current commutator near light cone for automodel asymptotic of spectral functions of virtual Compton, (T), 26:54246 (JINR-P2-6636)
interactions $\gamma + e$, Schwinger source theory for calculation of spectral forms for invariant amplitudes of order e^4 for Compton, (T), 26:54255
interactions of current-sheet, with electrostatic waves, one-dimensional model of resonant, (T), 26:54052
interactions with hadrons, Regge and scaling limits for inclusive production, (T), 26:54275
isodose curves in lungs, measurement of, 26:54901
measurements on Apollo-15 subsatellite, high-energy solar-wind and interplanetary, (E), 26:54072
penetration of 1-MeV, in aluminum slab, phase-space-time-evolution calculations of, 26:54887 (NASA-TM-X-2440, pp 821-31)
photon Compton scattering by K-shell, nonrelativistic theory with retardation for inelastic, 26:54279
photon Compton scattering by K-shell, nonrelativistic dipole approximation for, (T), 26:54280
production in inelastic $\nu + \mu$ interactions with bremsstrahlung, four-component neutrino theory for e and μ polarization effects on form of spectra for, (T), 26:54290
production of $e^+ - e^-$ pairs in photon reactions with spin-$^1/_2$ point nuclei, differential cross sections and effects of neutral vector mesons an angular dependence of cross sections for, (T), 26:54260
production of relativistic, from solar flares associated with sunspot groups that emit meter type-I noise storms, (T), 26:53968
reaction with carbon dioxide, prediction of distribution of energy among possible loss channels from energetic, (E/T), 26:54009
reactions (e,e'p) with, cross-section calculations for, (T), 26:54496 (ITF-72-24-P)
reactions of hydrated, in radiolysis of aqueous solutions of indole-3-acetic acid and other plant hormones, 26:53015
reactions of radiolytic hydrated, with hydrogen ions and organic compounds, kinetics of, 26:53006
reactions with argon at 25 keV and small angles, determination of optical sums from energy-loss spectra from, 26:54128
reactions with atoms having Z = 23 to 83 at 2.04 MeV, atomic-number dependence of cross sections for K-shell ionization in, (E), 26:54104
reactions with atoms up to few keV, processes of formation of multicharged ions in, 26:54103 (FRNC-CONF-51)
reactions with atoms, distorted-wave approximation for excitation in, 26:54106
reactions with atoms, role of configuration mixing of diabatic states in excitation in, (T), 26:54117
reactions with carbon monoxide, impact cross sections and energy degradation from, relation with dayglow-emission observations from atmospheres of Mars and Venus, (E/T), 26:54008
reactions with helium and hydrogen atoms, adiabatic-approximation calculations of cross sections for excitation and spin change in, 26:54117
reactions with helium and nitrogen molecules, dependence of computed excitation cross sections for, on accuracy of wave functions used, 26:54108
reactions with helium at 200 to 500 eV, second-Born-approximation calculations of 1^1S, 2^1S, and 2^1P transitions in, 26:54138
reactions with helium at 26.5 to 300 eV, distorted-wave calculations of differential and integral cross sections for excitation of ^1p states in, 26:54106
reactions with helium at 30 to 80 eV, relation of momentum transfer to coincidence-measured angular and energy distributions of electrons scattered and ejected in ionization in, 26:54123
reactions with helium at 50 to 200 eV, coincidence measurements of absolute differential cross sections for 1^1S--4^1D transition in, 26:54113
reactions with helium, close-coupling calculations of indirect coupling effects on cross sections for excitation in, 26:54108
reactions with helium, relation between dispersion relation, optical theorem, and second Born scattering amplitude for, (T), 26:54110
reactions with lamellar media and single layers, radiation from 0.25- to 3.7-GeV, (T), 26:54907
reactions with mercury at 25 to 180 eV, distorted-wave calculations of differential cross sections for excitation and spin polarization of emitted electrons from, 26:54106
reactions with nitrogen molecules, calculation of excitation cross sections for, using Gaussian orbitals, 26:54108
reactions with nitrous oxide diluted with ethane, hydrogen, nitrogen, or propane at 278 to 355°K, rate constants for dissociative electron attachment and subsequent electron detachment in, (E), 26:54135
reactions with solids, mass spectra of ions emitted in, 26:54084
scattering by carbon-12, particle--hole-model calculations of form factor for inelastic, (T), 26:54541
scattering by carbon-12, shell-model calculation of quasi-elastic, 26:54526 (ITF-72-25-P)
scattering by lead-208 at 124 and 167 MeV, differential cross sections for inelastic, (E), 26:54649
scattering by lithium-6 with deuteron emission, cross-section calculations using Born approximation, (T), 26:54546
scattering by nitrogen molecules, method of linear combination of scaled atomic charge distributions for calculation of static potential for, 26:54125
scattering by nuclei at high energy, analysis of short-range correlations by, 26:54687 (ISS-71/29)
scattering by nuclei, contributions of time reversal noninvariant terms in elastic, (T), 26:54363 (IS-T-536)
scattering of microwave background by relativistic, (E/T), 26:54000
scattering, Monte Carlo study of catastrophic collisions with delta electrons considered, (T), 26:54898
separation from other particles over 100 GeV by using synchrotron radiation, angle and energy fluctuations in, 26:53801
spatial distribution of greater than equal to 50-keV, in plasma sheet at 24 R/sub E/, (E), 26:54057
spectra of hydrated, in pulse radiolysis of aqueous solutions of potassium hydroxide, 26:53018
spectra of radiolytic solvated, in liquid 3-methylhexane and propane, time dependence of, 26:53007
spectra of trapped radiolytic, in crystalline ice, 26:53002
structure of radiolytic hydrated, calculations of spin density distributions for, 26:52989 (ORO-2968-78, Paper 4)
transport data, parametric fits for spacecraft shielding, 26:54963 (NASA-TM-X-2440, pp 832-41)
ELECTROSTATIC ANALYZERS
  design and performance of retarding field-cylindrical mirror, for Auger and ionization spectroscopy, 26:53310 (SC-DC-721302)
ELECTROSTATIC PRECIPITATORS
  electrode for, vibration analysis of discharge, 26:55591(T) (ORNL-tr-2636)
ELEMENT 104
  properties of, use of Mendeleev periodic law for prediction of, 26:53053
ELEMENT 105
  properties of, use of Mendeleev periodic law for prediction of, 26:53053
ELEMENT 106
  properties of, use of Mendeleev periodic law for prediction of, 26:53053
ELEMENT 107
  properties of, use of Mendeleev periodic law for prediction of, 26:53053
ELEMENT 114
  nuclear binding energy of, Hartree--Fock calculations for, (T), 26:54726
ELEMENTARY PARTICLE MODELS
  diffraction, behavior in nondiffractive regions, 26:54303 (RPP/T-25)

- dual absorptive, helicity-conserving and helicity-nonconserving pomeron-exchange amplitudes in, 26:54419
- dual resonance, calculation of cross sections for inclusive interactions in, 26:54301 (ITF-72-55-P)
- dual resonance, derivation of off-shell N-point amplitude in, 26:54420
- dual resonance, power law fall off of elastic form factor and nonscaling of structure function in, 26:54235 (COO-264-611)
- dual resonance, relation between quantum field theory and zero-slope limit of, 26:54388
- dual resonance, review of fragmentation and pionization in inclusive interactions in, 26:54302 (LBL-1007)
- dual resonance, statistical approach to multiplicity and resonance widths in, (T), 26:54300 (ITF-72-53-E)
- dual resonance, two-particle distribution functions from inclusive reactions at high energies, (T), 26:54307
- dual, calculation of distribution function for resonance spins and dependence of elastic widths of resonances on mass using statistical mechanics methods, 26:54299 (ITF-72-49-P)
- dual, Feynman rules for massive gauge fields with topology of, 26:54381
- dual, for three-particle scattering in double-Regge region, 26:54422
- dual, SL(2,C) symmetry in formulation of, 26:54309
- kappa dominance, bounds on $K \to \pi + l + \nu$ decay parameters from weak, 26:54289
- Lee, infinity suppression due to nonlinearity in generalized, 26:54310
- Lee, unitary renormalization, positivity, and hermiticity of Hamiltonian for four-dimensional, 26:54237 (ITF-72-48-E)
- multiperipheral, interference term effects on cross section energy dependence, pion multiplicities, and correlation function structures in K + p and π + p interactions in, 26:54329 (NYO-3533-265)
- multiperipheral, two-particle distribution function for inclusive interactions, 26:54312
- parton, elastic and inelastic form factors of hadrons in, 26:54311
- pion--muon, linear mass relations from, 26:54272
- spectator, validity for cross sections of Δ^0rho$^-$ channel in $\pi^- + d \to 2p + 2\pi^- + \pi^0$ interactions at 7 GeV/c in deuterium bubble chamber, (E), 26:54208 (COO-3065-16)
- statistical, for conservation of P-, C-, and G-parity, 26:54360
- theory for multiple production based on intuitive picture of hadrons, 26:54314
- urbaryon, test of Nagoya and Hiroshima, 26:54297

ELEMENTARY PARTICLES
- compositeness condition for three-particle bound state, vanishing of vertex-function renormalization constant as, (T), 26:54379
- detection and measurement at high energies, design and performance of helium recoil spectrometer for, 26:53281
- interaction radius of, scaling of, (T), 26:54354
- interactions at high energies, calculation of two-particle distribution function using dual resonance model, (T), 26:54307
- interactions at high energies, design of 4π multiwire proportional counter for high-multiplicity, 25:53267 (BNL-17064)
- interactions in multiperipheral model, two-particle distribution function for inclusive, (T), 26:54312
- interactions of, exotic fragmenting states in inclusive, 26:54304
- interactions of, generalization of semilocal duality for three-particle to three-particle, 26:54422
- interactions of, research at Purdue Univ., June 1971 to May 1972, (T), 26:54236(R) (COO-1428-303)
- interactions of, review of Mueller formalism, SU(3) predictions, angular distributions, dual resonance model for fragmentation and pionization, γ and π^0 distributions, and charged multiplicity for inclusive, (T), 26:54302 (LBL-1007)
- interactions of, unitary renormalization, positivity, and hermiticity of Hamiltonian for four-dimensional Lee model for, (T), 26:54237 (ITF-72-48-E)
- interactions with external fields, Bogoliubov transformation in strong coupling theory for mass squared spectrum for classical relativistic, 26:54383
- interactions with protons at high energies in deuterium targets, proposed experiment using spectator neutrons for determining total cross sections for, (E), 26:54163 (NP-19421)
- mass relations from pion--muon model, linear, 26:54272
- production of pairs with arbitrary spin and magnetic moment in strong electromagnetic field, (T), 26:54266
- strong interactions of, quasi-eikonal approximation with contributions of Regge poles and rescattering for amplitudes of, (T), 26:54306
- strong interactions of, research at Indiana Univ., Dec. 1971 to Nov. 1972, (E), 26:54206(R) (COO-2009-36)
- strong interactions of, s-channel helicity conservation for amplitudes of elastic, (T), 26:54287 (LBL-766)
- strong interactions of, three-dimensional unitary group for unified gauge weak, electromagnetic, and, (T), 26:54364 (NYO-3533-264)
- structure of, review of, (T), 26:54234 (BNL-50342)
- symmetries from one-particle singularities of current matrix elements for, physical, 26:54356
- symmetry group in general relativity for, asymptotically flat space-time, 26:54357
- theory for nuclear currents in nuclear muon capture and π^- capture by lithium-6, (T), 26:54238 (LYCEN-7211)
- weak interactions of, gauge principle for CP-violating, 26:54367

ELEMENTARY PARTICLES, POSTULATED
- urbaryon hadronic interactions for cut-off problem in integral spectra of ultrahigh energy cosmic rays, 26:54313
- urbaryon structure, test of new Nagoya and Hiroshima models for, 26:54297

ELEMENTS
- electron reactions at 2.04 MeV with A = 23 to 83, atomic-number dependence of cross sections for K-shell ionization in, (E), 26:54104
- isotope abundance of, accuracy of determining natural, 26:52916 (EUR-4765, pp 41-75)
- neutron absorption by, survey of data on Doppler effect in fast, 26:54479 (CONF-720901-(Bks.1 and 2), pp 1152-65)

ELK RIVER POWER REACTOR
- deactivation of, status of, 26:55273 (DOCKET-1151-58)

EMBRYOS
- radiation effects on development of chick, phosphorus-32, 26:53517
- radiation effects on survival of mouse, following acute or fractionated exposure in utero, comparison of fast neutron RBE with x rays, 26:53453 (NASA-TM-X-2440, pp 641)
- radioinduced chromosome aberrations in rat, following exposure in utero, time dependence of fast neutron, 26:53470
- radioinduced inhibition of gastrulation in early mouse, x, 26:53476
- radioinduced malformations in developing rat, following exposure in utero, role of chromosome damage and repair errors in incidence of fast neutron, 26:53470

ENERGY
- book: New Energy Technology: Some Facts and Assessments, 26:55085
- consumption and requirements in US for, predictions for 1972 to 2020, 26:53098
- conversion of, efficiency of methods for, 26:53107
- conversion of, systems for, 26:55085
- conversion to electric power, evaluation of optional methods for, 26:53097
- production and consumption of, environmental impact of, 26:53193
- production and requirements predictions, 26:55091
- production, sources, and uses in US, graphic and tabulated data on, 26:53096 (UCRL-51221)

ENGINEERING
- conference on materials review for 1972 for aerospace and process, Los Angeles, California, April 11 to 13, 1972, 26:53569

ENGINEERING TEST REACTOR
- power variations in, analysis of, 26:55379 (ANCR-1085)

ENVIRONMENT
- book: Patient Earth, 26:53191
- impact report, amendment to San Onofre Power Reactor Units 2 and 3, 26:55338 (DOCKET-50361-27)
- impact report, Fort Calhoun Power Reactor Unit 1, 26:55301 (DOCKET-50285-71)
- impact report, Hutchinson Island Power Reactor Unit 1, 26:55331 (DOCKET-50335-33)
- impact report, Quad Cities Power Reactor Units 1 and 2, 26:55285 (DOCKET-50254-120)
- impact report, supplement to Limerick Power Reactor, Units 1 and 2, 26:55335 (DOCKET-50352-28)
- impact report, supplement to Mendocino Power Reactor, Units 1 and 2, 26:55348 (DOCKET-50398-19)
- impact report, supplement to Nine Mile Point Power Reactor Unit 2, 26:55351 (DOCKET-50410-10)
- impact report, William H, Zimmer Power Reactor Unit 1, 26:55337 (DOCKET-50358-41)
- impact statements on, ORNL Chemical Technology Division participation in, p. 100-1, 26:52986 (ORNL-4794, pp 98-101)
- plutonium-239 transport to man through, following release during fast reactor accidents, hazards from, 26:53511 (TID-26142)
- radioisotope transport through, to man, mechanisms for, 26:53521
- radioisotope transport to animals and plants through, bibliography on, 26:53530 (TID-3915(Suppl.1))
- radioisotope transport to man through, 26:53522
- Regional Modeling Abstracts, Vol. III, 26:55573 (ORNL-NSF-EP-23)
- research on, ANL Radiological Physics Div., Jan. to Dec., 1971, 26:53150(R) (ANL-7860(Pt.3))

ENZYMES
- role in repair of uv-irradiated DNA in microorganisms, 26:53350

EPOXY RESINS
- preparation and properties of, for use as filament winding, 26:55628 (UCRL-73773)
- epoxy resins--glass textiles, fiber strength of composites of, under biaxial loading, 26:55627 (UCRL-73772)

EQUIPMENT AND PROCEDURES
  inventory management of plant, 26:55605 (SC-M-68-808)
  standards for hoisting and rigging of reactor components, 26:53112 (RDT-F-8-6-T(8-72))
ERBIUM
  photon reactions (γ,xn) with, model analysis of giant resonance in, (E/T), 26:54598 (FRNC-TH-242)
ERBIUM ALLOYS AND SYSTEMS
  Au--Er, magnetic structure of ErAu$_2$, neutron diffraction study of, 26:55034
ERBIUM CARBIDES
  magnetic structure of ErC$_2$ at 2 to 297°K, neutron-diffraction study of, 26:55035
ERBIUM ISOTOPES Er-158
  beta and electron-capture decay of, branching ratios, conversion-electron spectra, and log-ft values for, (E), 26:54643
ERBIUM ISOTOPES Er-161
  beta and electron-capture decay of, γ singles and coincidence spectra from, (E), 26:54632 (COO-3255-2)
  electron-capture decay of, branching ratios, conversion-electron spectra, and log-ft values for, (E), 26:54643
ERBIUM ISOTOPES Er-165
  electron-capture decay of, double k-shell ionization in, (E), 26:54617
ERBIUM ISOTOPES Er-166
  neutron reactions (n,α) with, calculation of, (T), 26:54707
ERBIUM ISOTOPES Er-167
  alpha inelastic scattering at 7 to 10 MeV, with Coulomb excitation, heat-flow analysis of temperature spikes following, (E/T), 26:54646
  proton inelastic scattering at 4 MeV with Coulomb excitation, heat-flow analysis of temperature spikes following, (E/T), 26:54646
ERBIUM ISOTOPES Er-168
  neutron reactions (n,α) with, calculation of, (T), 26:54707
  proton inelastic scattering at 15 MeV, proton spectra from, (E), 26:54467(R) (ORO-2972-204)
ERYTHROCYTES
  radiation effects on uptake of selenium-75-labeled selenomethionine by rat, following whole-body exposure, dose dependence of γ, 26:53482
ESOPHAGUS
  radioinduced fistulae and perforations in human, following therapy of esophageal carcinomas and gastric sarcomas, surgical treatment of, 26:53438
ESTERS
  toxicity data for imido, bibliography on, 26:55581 (ORNL-TIP/TIRC-72-54)
ETHANOL, 2-CHLORO-
  reactions with radiolytic hydrated electrons, kinetics of, 26:53006
ETHYL SULFATES
  effects on Eremothecium ashbyii (fungi) in relation to riboflavin production, mutagenic, 26:53374
ETHYLENE
  radiolysis of gaseous, G values for acetylene and methane in argon- and xenon-sensitized, 26:53000
ETHYLENE, CHLORO-, POLYMERS
  radiation effects on 1,4-diaminoanthraquinone-containing, crosslinking and fading produced by alpha particle, deuteron, and γ, 26:53020
  radiation stability of bags of, effects of temperature on γ, 26:52992 (RFP-1924)
  thermal stability of bags of, 26:52992 (RFP-1924)
ETHYLENE POLYMERS
  laser beam reactions with deuterated, plasma production by nanosecond and picosecond, 26:54804
  radiation effects on molding properties of, γ, 26:53720
  polyacrylates--polyethylene, radioinduced crosslinking polymerization of nylon grafted on, 26:53013(P)
EUROPE
  radioactive waste storage sites in, development of community-type, 26:53726
EUROPIUM
  solubility in bismuth--thorium solutions, free energies of formation for compounds produced by, 26:53664
  thermal conductivity divergence at Neel point of, (E), 26:55049
EUROPIUM ISOTOPES Eu-151
  effects on ESR spectra of divalent europium in strontium chloride lattices, 26:52970
  neutron capture at 25 keV, model analysis of isomeric cross section ratio for, (E/T), 26:54589
EUROPIUM ISOTOPES Eu-152
  effects on ESR spectra of divalent europium in strontium chloride lattices, 26:52970
EUROPIUM OXIDES
  magnon states in, bound state of two-, (T), 26:55042
  preparation of transparent films of, by oxidation, effects of annealing and oxidizing temperatures on, 26:53567
EVAPORATORS
  heat transfer in individual tube clusters in VTE-X, measurement of, 26:53110 (ORNL-TM-3841)
  performance of vertical tube, comparison of calculated and measured, 26:53110 (ORNL-TM-3841)
EXPERIMENTAL BREEDER REACTOR-II
  data processing system for periodic maintenance and calibration of instrumentation for, 26:55132 (ANL/EBR-63)
  fuel element irradiation testing in, summary of methods for, 26:55120 (CONF-720901-(Bks.1 and 2), pp 905-27)
  fuel elements for, procedures for xenon tagging pin type driver, 26:55184 (ANL/EBR-57)
  fuel irradiation testing in, status of mixed oxide, 26:55189(R) (GEAP-10028-39)
  instrumentation for, data processing systems for periodic maintenance and calibration of, 26:55132 (ANL/EBR-63)
EXPLOSIVES
  analysis of HMX-containing, by semimicro gel permeation chromatography, 26:55625 (UCRL-73334)
  determination of residual, in drainage ditch soil at sump effluent outlets, 26:55545 (LA-4925)
EXPONENTIAL PILES
  criticality measurements in plutonium nitrate (Pu(NO$_3$)$_4$)-polystyrene, 26:55416(R) (BNWL-1522-5)
EXTRACTION APPARATUS
  interface detector for, salt--metal, p. 12, 26:53081 (ORNL-4794, pp 1-14)
EYES
  light flashes induced by Cherenkov radiation from heavy cosmic nuclei, calculation of frequency of, 26:54882 (NASA-TM-X-2440, pp 757-66)
  radiation dose to, of medical personnel during arteriography, x, 26:53443
  radioinduced light flashes on retina of dark-adapted human, use of virtual-quanta method to calculate frequency of charged particle, 26:53405 (NASA-TM-X-2440, pp 767-72)
  radioinduced phosphenes in, of astronauts during space flight, cosmic, 26:53407 (NASA-TM-X-2440, pp 1002-6)
  radioinduced retinal injuries in human, following therapy of nasal cavity and paranasal sinus carcinomas, dose and time dependence of γ and x, 26:53444
  radiotherapy with ^{60}Co applicators, computer calculation of dose distributions from, 26:54900

F

FALLOUT
  monitoring in East Germany during 1970, 26:53156 (SZS-128)
  monitoring in Norwegian atmosphere during 1956 to 1970, 26:53161
  transport to cattle following deposition on pasture grass, tracer study using lanthanum-140 labeled sand as simulant, 26:53527 (FDA-4-4503-A-3)
FAST BURST REACTOR FACILITY
  use in space radiation studies, summary of, 26:55406 (NASA-TM-X-2440, pp 618-19)
FAST CERAMIC REACTOR
  core for, design and kinetics analysis of, 26:55189(R) (GEAP-10028-39)
  core for, design and kinetics analysis of, 26:55190(R) (GEAP-10028-42)
  fuel elements for, development during February to April 1972, 26:55190(R) (GEAP-10028-42)
  fuel elements for, development during May to July 1971, 26:55189(R) (GEAP-10028-39)
  safety of, development of models for analysis of, 26:55190(R) (GEAP-10028-42)
  safety of, transient overpower and coolant flow loss effects on, 26:55189(R) (GEAP-10028-39)
  safety of, transient overpower and coolant flow loss effects on, 26:55190(R) (GEAP-10028-42)
FAST FLUX TEST FACILITY
  cooling systems of, effects of corrosion on radioactivity levels in, 26:55172 (CONF-710959-, Paper 16)
  fuel element assemblies for, design of grid spaced driver, 26:55190(R) (GEAP-10028-42)
  pipe chases in, neutron streaming in sodium filled, (E/T), 26:55394 (CONF-720901-3)
FAST TEST REACTOR
  cooling system for, neutron streaming in outlet and inlet pipe chases of, (E), 26:55382 (CONF-720901-(Bks.1 and 2), pp 431-41)
  neutron generation time in subcritical, transfer and scattering kinetics scheme for determination of, 26:55437 (CONF-720901-(Bks.1 and 2), pp 713-23)
  physics parameters of, effects of delayed neutron data variations on, 26:55388 (CONF-720901-(Bks.1 and 2), pp 660-86)
  physics parameters of, review of programs for determination of, 26:55391 (CONF-720901-(Bks.1 and 2), pp 839-87)
  reactivity coefficients in, mockup measurements of sodium-void, (E/T), 26:55390 (CONF-720901-(Bks.1 and 2), pp 739-67)
  shielding design for, calculation methods for, 26:55383 (CONF-720901-(Bks.1 and 2), pp 445-58)
  vessel head compartment for, neutron and γ dose rates in, (T), 26:55144 (CONF-720901-(Bks.1 and 2), pp 480-98)
FATS
  radiation effects on, ir spectral studies on γ, 26:52983 (EUR-4828)
FEDERAL REPUBLIC OF GERMANY
  applications of radiation in agriculture research in, 26:53459(R) (NP-19403)
  energy market in, review on, 26:55377

  radiation protection programs for nuclear personnel in, 26:55456 (SZS-136)
  reactor safety research projects in, summaries of current, 26:55202(R) (IRS-F-10)
FELDSPARS
  analysis of granitic, for cesium by neutron activation and γ spectrometry, 26:52908
FERMI FAST BREEDER REACTOR
  core subassembly of, shock loading during handling of, 26:53732 (WCAP-1615)
  cover gas of, performance of cleanup system for, 26:55226 (CONF-710959-, Paper 5)
  maintenance during June 1972, 26:55233 (DOCKET-50016-170)
  operations during June 1972, 26:55233 (DOCKET-50016-170)
  site for, environmental radiation survey during June 1972, 26:55233 (DOCKET-50016-170)
FERMI POWER REACTOR, UNIT 2
  valves for, verification of wall thicknesses for nuclear service, 26:55333 (DOCKET-50341-45)
FERMIONS
  excitations in quantum condensated gas of, (T), 26:54443
  interactions with massive scalar and massless spinor fields, quantum two-dimensional classically solvable model with nontrivial scattering for, (T), 26:54385
  interactions with photons, effective differential cross sections for Compton, (T), 26:54278
  stability of many-body systems with singular attractive potentials, self-consistent Hartree field as limit for Schroedinger equation for, (T), 26:54408 (ITF-72-14-E)
FERMIUM ISOTOPES Fm-256
  fission of, average prompt neutron yield from spontaneous, 26:54659 (JINR-P15-6518)
FERROMAGNETIC MATERIALS
  exchange model of weak ferromagnetism of MnB$_2$, (T), 26:55048
FETUSES
  radiation effects on growth of thyroid gland in mouse, following intravenous injection of iodine-131, β and γ, 26:53513
  radioinduced digital malformations in mouse, following whole-body exposure, effects of developmental stage, dose, and dose rate on incidence of γ, 26:53471
  radioinduced malformations in human, following in utero exposure from maternal therapy during pregnancy, radium and x, 26:53437
  radioinduced malformations of brain of developing mouse and rat, following in utero exposure, effects of developmental stage at exposure on, 26:53437
FIELD EMISSION MICROSCOPES
  design of atom probe-type, for metallography, 26:53648
  performance of tubes of, as chamber for studies of tungsten carburization, 26:53560
  use in study of material deformation structures by instrument tip contact with sample specimen, 26:53651
FIELD EMISSION MICROSCOPY
  method for analysis of dislocations and stacking faults, 26:53649
  method for measuring single atom reactions with atomically defined surfaces, 26:53656
  method for solid solution image analysis, 26:53655
  method for studies of stress corrosion cracking, 26:53610
  method for study of dilute alloys and solid solutions, 26:53652
  method for study of ordered alloys, 26:53654
  methods and equipment for radioinduced point defects in alloys and metals, 26:53704
  methods for studies of corrosion and physical metallurgy, 26:53647
  methods for studies of metal grain boundaries, 26:53650
  methods for studies of phase interfaces and dispersion strengthening of two-phase alloys, 26:53653
FILMS
  deposition of thin, ultrahigh vacuum evaporation unit with high-speed cryopump for, 26:53139
  thickness measurement on thin, using proton-excited x rays, 26:52945
FISSION
  book: Atomic Nucleus, 26:54738
  theory of, review on Strutinsky, 26:54676 (CONF-720901-(Bks.1 and 2), pp 1087-110
FISSION FRAGMENTS
  dose to crew from high-impulse gas-core nuclear rocket plume, (T), 26:54967
  tracks in archaeological materials, errors in dating by, (E), 26:53181
  yield in uranium-235 thermal neutron fission, odd-even effect in, (E), 26:54667
FISSION PRODUCTS
  behavior in liquid sodium systems, 26:55166 (CONF-710959-, Paper 10)
  decay heating of fuel elements following coolant loss accidents, effects of fission product escape on, (T), 26:55206 (KFK-1580)
  detection in reactor coolants, methods for, 26:55218(T) (EURFNR-976)
  determination in irradiated reactor fuels by automated mass spectrometry, 26:52917 (EUR-4765, pp 77-89)
  diffusion and gas bubble nucleation in uranium dioxide fuels, 26:53565
  diffusion from irradiated aluminum--uranium foils, mechanisms and measurement of recoil-induced, 26:53694 (JAERI-Memo-3936)
  diffusion into cooling system cover gases, problems of, 26:55171 (CONF-710959-, Paper 15)
  distribution in cooling systems of HTGR type reactors, (E), 26:55207(R) (ORNL-TM-3900)
  gamma ray emission from, table for, 26:54607 (RD/B/M-2356)
  production of gaseous, reactor irradiation method and apparatus for, 26:53075(P)
  release from coated particle fuels, effects of annealing temperatures on, (E), 26:55207(R) (ORNL-TM-3900)
  release from reprocessing of irradiated recycle test elements, pp. 27-31, 26:53083 (ORNL-4794, pp 26-32)
  release from thermionic reactor cores, methods for control of gaseous, (T), 26:55373 (NASA-TM-X-2440, pp 1016-20)
  release in head-end reprocessing of HTGR-type graphite fuel, 26:53078 (CONF-720823-11)
  release to fast reactor sodium coolant, boundary conditions for, (T), 26:55169 (CONF-710959-, Paper 13)
  separation from off-gases from HTGR fuel reprocessing, 26:53059 (CONF-720823-12)
  separation of rare gas, from combustion off-gases by scrubbing with liquid carbon dioxide, 26:53064(T) (ORNL-tr-2621)
  separation of volatile, in reprocessing of LMFBR fuels by voloxidation, pp. 17-20, 26:53082 (ORNL-4794, pp 15-25)
  tracks from heavier transuranium elements in natural glasses and minerals, study of spontaneous, 26:54670
  transport in NaK, mechanisms of, (E), 26:55167 (CONF-710959-, Paper 11)
FISSIONABLE MATERIAL
  neutron absorption by, summary of resonance and Doppler theory for, 26:54480 (CONF-720901-(Bks.1 and 2), pp 1166-82)
FLORIDA
  cesium-137 behavior in ecosystems in, 26:53170(R) (ORO-4066-5)
FLOWMETERS
  design and testing of 6-in-diameter transit time, for water and liquid sodium, 26:53305 (LMEC-72-4)
FLUIDS
  energy states in fluid--gas system, kinetics of weakly inhomogeneous, (T), 26:55535 (ITF-72-29-P)
FLUORIDES
  determination of ionic, in biological fluids, direct, 26:55637 (UR-3490-184)
  formation energy of, relations with fuel capsule corrosion and deterioration, 26:53330(R) (BNWL-1308-10)
FLUORINE
  determination in water samples by spark source mass spectroscopy, 26:52914 (ANL-7860(Pt.3), pp 55-63)
  maximum safe levels of, for animals and man, bibliography on, 26:55580 (ORNL-TIP/TIRC-72-53)
  reactions of atoms of, laser spectral study of, 26:55527 (IPP-IV-38)
FLUORINE ISOTOPES F-18
  energy levels from nitrogen-15 (Li-6,t) reactions, particle--hole structure of, (E), 26:54549
  energy levels of, off-shell effects in two-particle shell-model calculation of, (T), 26:54538
FLUORINE ISOTOPES F-19
  deuteron beams (d,α) and (d,p) at 3 MeV, differential cross sections for, (E), 26:54548
  deuteron reactions (d,Li-6) at 28 MeV, angular distributions and spectroscopic factors for, (E), 26:54527 (LYCEN-7219)
  effects on γ and neutron spectra of molybdenum--plutonium dioxide heat sources, 26:53336 (NASA-TM-X-2440, pp 853-8)
FLUORINE ISOTOPES F-20
  energy levels from fluorine-19 (d,p) reactions, spin-parity assignments and spectroscopic factors for, (E), 26:54548
FOG
  formation from operation of cooling towers, 26:53117
FOILS
  radioinduced point defects from high-voltage electron microscopy, diffusion to foil surface, (T), 26:54985
FOOD
  book: Radiation and Health, 26:53157
  radiation effects on, bibliography on, 26:53342 (AED-C-5-11)
  radiation effects on, ir spectral studies on γ, 26:52983 (EUR-4828)
  radioactivity monitoring of Hungarian, from 1959 to 1971, 26:53172
  radiopreservation of, in Euratom Community, 26:53459(R) (NP-19403)
  radium-226 content of, in Poland, 26:53525
FOOD CHAINS
  iodine-131 transport from atmosphere through grass-cow-milk-man, relation to radiation dose to thyroid gland of children in relation to age, 26:53506(T) (ORNL-tr-2629)
FORBUSH DECREASES
  occurrence of June 8, 1969, followed by abrupt change in functional form of modulation for 11-year variation,

(E), 26:53870
FORENSIC SCIENCE
  activation analysis uses in, neutron, 26:52896 (CONF-720920-2)
  art identification by nuclear methods of analysis in, 26:52898 (COO-3034-2)
FORESTS
  nutrient cycling in, tracer studies on calcium and potassium, 26:53539(R) (SRO-641-4)
FORGING
  standards for low-alloy steel and stainless steel, 26:53640 (RDT-M-2-2-T(8-72))
FORKED RIVER POWER REACTOR, UNIT 1
  safety analysis report for, revised figures for preliminary, 26:55339 (DOCKET-50363-37)
FORMAMIDE
  reactions with radiolytic hydrated electrons, kinetics of, 26:53006
FORMIC ACID, OXYDI-
  diethyl ester, pharmacology and toxicology of, bibliography on, 26:55579 (ORNL-TIP/TIRC-72-52)
FORT CALHOUN POWER REACTOR, UNIT 1
  containment structure for, information on prestressed tendon installation for, 26:55300 (DOCKET-50285-70)
  effluents from, effects on environment of chemical, radioactive, and thermal, 26:55301 (DOCKET-50285-71)
  operation of, cost-benefit analysis for, 26:55301 (DOCKET-50285-71)
  piping system for, additional data on weld specifications for primary pressure boundary, 26:55302 (DOCKET-50285-72)
  site for, ecology, hydrology, and meteorology of, 26:55301 (DOCKET-50285-71)
FRACTURE TESTS
  conference on cryogenic temperature, Toronto, Ontario, Canada, June 21 to 26, 1970, 26:53660
FRANCE
  strontium-90 content of human bone samples collected during 1970 in, 26:53520 (CEA-N-1535)
FREE RADICALS
  spectra of radiolytic, ESR, 26:52993(R) (RRL-3238-398)
  spectra of trapped radiolytic, in organic liquids, 26:52987(R) (ORO-2968-78)
FRUITS
  analysis for mercury by neutron activation, 26:52911
  oranges, radiation processing of, effects on metabolism and respiration, 26:53347
  oranges, radiation processing of, effects on organoleptic properties and wholesomeness, 26:53347
FUEL CAPSULES
  compatibility of materials for, with strontium fluoride impurities and radioactive decay products, 26:53330(R) (BNWL-1308-10)
  fabrication and testing of, for cesium sources, 26:53330(R) (BNWL-1308-10)
FUEL CELLS
  development for electric power generation, 26:55086
FUELS
  availability of competing, in United Kingdom, 26:55088
  conversion of fossil, 26:55085
  conversion using heat from high-temperature reactors, 26:55377
FUNGI
  Aspergillus chevalieri, radioinduced mutations in, for antibiotic production, gamma and uv, 26:53393
  Aspergillus niger, mutations induced in, by colchicine and nitrogen mustards for citric acid production, comparison of, 26:53380
  Aspergillus niger, radioinduced mutations in, for citric acid production, comparison of γ and uv, 26:53380
  Eremothecium ashbyii, mutations induced in, by diethyl sulfate and nitrosoguanidine for increased riboflavin production, 26:53374
  Eremothecium ashbyii, radioinduced mutations in, for increased riboflavin production, uv, 26:53374
  Streptomyces coelicolor, genotypic classification of uv-radiosensitive mutants of, method for, 26:53378
FUSED SALTS
  electrochemical properties of, voltammeter to study, 26:52957

G

GADOLINIUM
  abundance in 21 sharp-lined nonvariable cool peculiar A stars, (E), 26:53882
  magnetic permeability of, effects of plastic deformation and recrystallization on weak-field ac, 26:55040
  oxidation under controlled oxygen partial pressures at 727 to 1327°C, 26:53550 (IS-T-540)
  radioinduced dislocation loops in thin single-crystal films of, electron microscopy of, 26:54979
GADOLINIUM ALLOYS AND SYSTEMS
  Ce--Gd--Ru, magnetic properties of Ce/sub 1-x/Gd/sub x/Ru$_2$, 26:55037
  Gd--Zn, hyperfine fields in GdZn diluted with yttrium or lanthanum, NMR study of, 26:55059
GADOLINIUM BORIDES
  preparation and thermoemission properties of, 26:53582
GADOLINIUM ISOTOPES Gd-149
  energy-level transitions from terbium-149 decay, internal conversion coefficients for, (E), 26:54603 (JINR-P6-6511)
GADOLINIUM ISOTOPES Gd-151
  energy level at 108 keV, g-factor for, (E), 26:54634 (JINR-E6-6479)
GADOLINIUM ISOTOPES Gd-152
  neutron capture by, cross section for thermal, (E), 26:54585
  neutron reactions with, resonance activation integrals for, (E), 26:54585
GADOLINIUM ISOTOPES Gd-154
  chlorine-35 inelastic scattering at 100 MeV with Coulomb excitation, gamma spectra from, (E), 26:54642
  energy levels from Coulomb excitation, Doppler-shift recoil measurements of lifetimes and transition probabilities for, (E), 26:54642
GADOLINIUM ISOTOPES Gd-155
  nuclear magnetic resonance in GdZn diluted with yttrium or lanthanum, 26:55059
GADOLINIUM ISOTOPES Gd-156
  energy levels from Coulomb excitation, Doppler-shift recoil measurements of lifetimes and transition probabilities for, (E), 26:54642
GADOLINIUM ISOTOPES Gd-158
  neutron reactions with, resonance activation integrals for, (E), 26:54585
GADOLINIUM ISOTOPES Gd-160
  deuteron reactions (d,t) with, coupled channel analysis of mixing in, (T), 26:54635 (JINR-P4-6509)
GALAXIES
  age of II Zw 40, (E), 26:53976
  book: Galactic Astronomy, Vol. I, 26:53981
  Cepheid variables in, (T), 26:53986
  distribution of, (E/T), 26:53995
  evolution of, program for, (T), 26:53978
  evolution of, statistical studies of, (E/T), 26:53995
  formation in anisotropic cosmologies, 26:53980
  hydrogen in three, aperture synthesis of observations of neutral, (E), 26:53971
  magnetic fields in, origin and form of, (T), 26:53975
  metal abundance in, as a function of luminosity, (T), 26:53977
  population synthesis of, quadratic programming for, (T), 26:53977
  properties of 5 Scd, from 21-cm observations, (E), 26:53972
  radio source counts on the basis of evolution models for, (T), 26:53996
  spectra of 3 RCB stars in LMC, (E), 26:53904
  spectra of nucleus of NGC 205, composite, (E), 26:53880
  spiral structure in, causes and effects of irregular, (T), 26:53987
  star formation and evolution in, (T), 26:53978
  structure of II Zw 40, (E), 26:53976
  x-ray emission from intergalactic gas in vicinity of, (T), 26:53988
  x-ray emission from Vir A and Andromeda, (T), 26:53988
GALENAS
  analysis for bismuth by neutron activation and α scintillation counting, 26:52910
GALLIUM
  separation from indium by ion exchange chromatography, 26:52949
GALLIUM ALLOYS AND SYSTEMS
  Ga-base--In, superconductivity and ac susceptibility in fast frozen, (E/T), 26:54438
GALLIUM ARSENIDES
  ion implantation damage in single crystals of, krypton-ion channeling study of dose rate dependence of, 26:54993
  radiation damage in, electron, (E), 26:54968(R) (AD-737312)
  radiation effects on electric conductivity of, tunnel-assisted hopping in neutron, 26:54982
  radiation effects on vibrational spectra of boat-grown and pulled crystals of silicon-doped, electron and neutron, 26:54984
GALLIUM PHOSPHIDES
  charged-particle dechanneling at 1.5 MeV, proton, deuteron, and helium-ion, 26:54988
GAMMA CAMERAS
  description of digital stereoscintigraphic, 26:53215
  performance in conjunction with scintiscanning for diagnosis of neoplasms in man, 26:53214
GAMMA RADIATION
  absorption materials for, thickness calculations for, 26:54936
  angular distribution of, in Milky Way, (E/T), 26:53992
  depth-dose distribution of ^{60}Co, under lattice, theoretical calculation of, 26:54908
  dose changes due to shield layer changes, use of perturbation theory to determine, 26:54941 (CONF-720901-(Bks.1 and 2), pp 541-58)
  dose distribution in man following administration of gold-198 colloids for treatment of malignant pleural effusions, time dependence of, 26:53509
  dose distribution in orthogonal plane surrounding iridium-192 wires implanted for interstitial therapy, effects of arrangement, number, and size of implants on, 26:53422
  dose to fingers of medical personnel during injection of

radioisotopes, phantom studies of, 26:53424
dose to human bone marrow following whole-body exposure, use of lithium fluoride dosimeters in Alderson Rando phantom for calculation of, 26:53406 (NASA-TM-X-2440, pp 974-80)
dose to man during intravenous arteriography using metastable technetium-99-labeled pertechnetate, 26:53542
dose to personnel, comparison of results of actual and phantom measurements of, 26:53426
dose to Thermoelectric Outer Planet Spacecraft from radioisotope thermoelectric generator, environmental analysis of, 26:53338 (NASA-TM-X-2440, pp 862-5)
dosimetry in tissues, tissue-equivalent plastic ionization chamber for simultaneous neutron and, 26:53234 (NASA-TM-X-2440, pp 609-13)
dosimetry of ^{60}Co, grid-walled proportional counter study of micro-, 26:54895
dosimetry of, ^{7}LiF thermoluminescent dosimeter for personnel, 26:53249
dosimetry of, properties of silver-activated glass photoluminescent dosimeter for, 26:53242
dosimetry of, real-time spectrum-to-dose conversion system for, 26:53201 (NASA-TM-X-2440, pp 142-8)
dosimetry simultaneously with neutrons, effects of ^{6}Li content in mixture of natural fluorite and LiF for thermoluminescence, 26:53240
effects on aldrin in lipid solutions, effects of irradiation temperature on, 26:52997
effects on aldrin in organic solvents, effects of temperature and solvent on, 26:53014
effects on amino acids in frozen aqueous solutions, ESR spectral studies of free radicals from, 26:52995
effects on ammonium perchlorate single crystals, electron microscopic studies of, 26:52985 (NASA-TM-X-2440, pp 584-94)
effects on anthracene single crystals at 77°K, absorption spectra of color centers produced in, 26:54996
effects on antibacterial activity of 1-bromo-4-nitrobenzene, nitrobenzene, and p-nitrophenol and their mixtures with 2,2-dichloro-N-[2-hydroxy-1-(hydroxymethyl)ethyl]acetamide, 26:52998
effects on Aspergillus niger, mutagenic for citric acid production, 26:53380
effects on Aspergillus, mutagenic for antibiotic production, 26:53393
effects on bacteria, effects of culture media, dose, storage time, and storage temperature on recovery from pathological and lethal, 26:53369
effects on beans following seed exposure, effects on crop quality and photosynthesis and transpiration in plants, dose dependence of, 26:53387
effects on bovine ferrimyoglobin in anoxic and oxygenated solutions, comparison of, 26:53346
effects on brain, comparison for sharks and rats, 26:53487
effects on cation ion exchange resin Zerolit 225, 26:53016
effects on chromosomes in human bone marrow cells following local therapeutic exposure, effects of dose and time on frequency of aberrant, 26:53445
effects on chromosomes in root cells of rye plants, effects of genetic heterogeneity on frequency of aberrant, 26:53392
effects on Clostridium botulinum spores, relation to growth and toxin production following sublethal exposure, 26:53366(R) (ORO-3347-8)
effects on content of nicotonic acid and vitamins of wheat, wheat bread, and wheat flour, 26:53344
effects on count of plaque-forming cells in spleen of antigen-stimulated mice following whole-body exposure, effects of dose on, 26:53469
effects on crosslinking and fading in poly(vinyl chloride) containing 1,4-diaminoanthraquinone, 26:53020
effects on crustacea, species difference in sensitivity to, 26:53504
effects on crystalline ice, spectra of trapped electrons from, 26:53002
effects on crystalline potassium iodide, effects of water vapor on, 26:53017
effects on curing of adhesives by polymerization at room temperature, 26:53716
effects on deuterated and normal nitric acid at 77°K, ESR and ir spectral studies on products of, 26:53009
effects on dielectric constants and crystal structure of perovskite-type compounds, 26:55020
effects on DNA in cultured mammalian cells and microorganisms, role of repair processes in recovery from lethal and mutagenic, review of, 26:53357
effects on DNA in Micrococcus radiodurans, inhibitory effects of chloramphenicol, dactinomycin, and tetracycline on repair of, 26:53349
effects on electric properties of polystyrene capacitors with metal electrodes, (E), 26:54968(R) (AD-737312)
effects on Escherichia coli capacity to support growth of bacteriophage T4, 26:53372
effects on fats, foods, and plastics, ir studies on, 26:52983 (EUR-4828)
effects on free and bound tryptophan in wheat, dose dependence of, 26:53395
effects on gaseous cyclohexane, mass spectrometric studies on ion--molecule reactions produced by, 26:52982 (EUR-4765, pp 11-24)
effects on gaseous hydrogen sulfide, effects of argon, krypton, nitrogen, and xenon on yields from, 26:53011
effects on gastrointestinal tract of germ-free newborn swine following lethal whole-body exposure, effects of artificial colonization with Escherichia coli on pathological, 26:53495
effects on hematopoiesis and immune reactions in mice following whole-body exposure, comparison of RBE with high-intensity pulsed x rays for pathological, 26:53469
effects on hematopoietic tissues in fish, effects of dose, dose rate, and species on pathological, 26:53447 (CONF-720822-2)
effects on hexagonal boron nitride, EPR, thermally stimulated current, and thermoluminescence of paramagnetic centers produced in, 26:55015
effects on human capacity to perform under stress following continuous or protracted fractionated exposures, effectiveness of pulmonary-impedance power spectral analysis for determining, 26:53401 (NASA-TM-X-2440, pp 238-48)
effects on human cervical vertebrae following therapy of laryngeal and pharyngeal carcinomas, delayed pathological, 26:53425
effects on human gastrointestinal tract following continuous or protracted fractionated whole-body exposure, effectiveness of pulmonary-impedance power spectral analysis for determining pathological, 26:53401 (NASA-TM-X-2440, pp 238-48)
effects on human heart following therapy of esophageal carcinomas, electrocardiogram studies of pathological, 26:53439
effects on human skin following local exposure for therapy of underlying neoplasms, pathological, 26:53433
effects on immune reactions in chick embryos to adult allogeneic leukocytes, 26:53477
effects on infectivity of Salmonella typhimurium for chick embryos following exposure of cultures to substerilizing doses, 26:53369
effects on leukocyte count in peripheral blood of rats following whole-body exposure, dose and time dependence of, 26:53483
effects on limbs of fetal mice following whole-body exposure in utero, effects of developmental stage, dose, and dose rate on incidence of teratogenic, 26:53471
effects on liquid ammonia, preparation of anhydrous hydrazine by, 26:53001(P)
effects on liquid methanol, spin trapping studies on primary methoxy radicals from, 26:52988 (ORO-2968-78, Paper 2)
effects on low-temperature thermal conductivity of vanadium- and titanium-doped alumina single crystals, 26:54978
effects on maize following seed exposure, dose dependence of grain weight and water content, 26:53385
effects on maxillary bone of dogs following exposure of teeth, effects of lead bridges and plastic caps on, 26:53480
effects on metabolism of rickettsiae in L cells, 26:53360
effects on metacercariae of Fasciola hepatica for immunization of rats and cattle, 26:53498(R) (PRNC-156)
effects on mice following whole-body exposure, incidence of leukemogenic, 26:53469
effects on mice, combined effects of cortisone on serum protein content and serum albumin-globulin ratio, 26:53490
effects on mice, effects of bathing in thermal spring water on recovery from pathological mixed fast neutron and, 26:53465
effects on molding properties of polyethylene, 26:53720
effects on monkeys, effects on ability to perform learned tasks following continuous whole-body exposure, dose and dose rate dependence of, 26:53452 (NASA-TM-X-2440, pp 633-40)
effects on monkeys, effects on bone marrow hematopoietic function following continuous and subsequent fractionated whole-body exposures, effects of dose and dose rate on recovery from suppressive, 26:53452 (NASA-TM-X-2440, pp 633-40)
effects on okra following seed exposure, dose dependence of germination, growth, fruit quality, and yield, 26:53390
effects on oocytes of grain moth, effects of meiotic stage on sensitivity to, 26:53499
effects on organisms, combined effects of space flight environment on mutagenesis and survival of insects, microorganisms and plants, 26:53365 (N-72-20065)
effects on oxidation of cellulose or poly(methylhydrogensiloxane) and their mixture, 26:52994
effects on oxides, comparison of explosive shock-induced defects with defects produced by, 26:54983
effects on p-dichlorobenzene and sodium chlorate crystals, 26:52984 (FRNC-TH-262)
effects on photocurrent--voltage characteristics of

- cadmium sulfide films, 26:54998
- effects on poly(vinyl chloride) bags, effects of temperature on, 26:52992 (RFP-1924)
- effects on propene polymers, kinetics of reactions of methyl methacrylate with radicals produced by, 26:53019
- effects on rabbits, effects on serotonin uptake by blood platelets in relation to content during acute radiation syndrome, 26:53486
- effects on radioiodine retention by activated carbon, 26:53061 (DP-MS-72-14)
- effects on rat bone marrow, role of thymus gland in recovery of, 26:53479
- effects on rat hepatoma cells in cultures, effects on generation time, growth, and proliferation of, 26:53354
- effects on rat hepatoma cells in cultures, relation of post-exposure cell phase to incidence of lethal, 26:53354
- effects on rats following acute whole-body exposure, comparison with effects of protons for lethal and neoplastic, 26:53455 (NASA-TM-X-2440, pp 647-51)
- effects on rye seeds, effects of genetic heterogeneity on germination and mitotic activity in, 26:53392
- effects on Salmonella typhimurium during space flight, combined effects of weightlessness on growth and prophage induction, 26:53364 (N-72-20063)
- effects on seeds of barley, combined effects of space flight environment on genetic, 26:53384
- effects on semiconductor devices, hardening against, 26:53289 (NASA-TM-X-2440, pp 481-6)
- effects on sheep following various combinations of acute, chronic, continuous, or fractionated dose whole-body exposure, effects of dose and dose rate on pathological, 26:53451 (NASA-TM-X-2440, pp 622-32)
- effects on single crystals of monohydrate and anhydrous thymine, ESR studies on, 26:52999
- effects on single-strand breaks in DNA, 26:52981 (COO-3571-3)
- effects on sintered aluminum oxide, ESR spectral studies on, 26:53699 (RT/FI-(72)10)
- effects on space vehicle components and subsystems, design parameters and test facilities for testing, 26:53695 (NASA-TM-X-2440, pp 570-6)
- effects on spacecraft instruments, program for studying, 26:53294 (NASA-TM-X-2440, pp 866-72)
- effects on Staphylococcus, relation between loss of pathogenicity and decreased sensitivity to lethal dose, 26:53377
- effects on sugar beets following exposure of seeds, dose dependence of agricultural qualities of, 26:53386
- effects on sugar beets following seed exposure, dose dependence of crop yield, plant morphology, and seed germination, 26:53388
- effects on surface color of vacuum packaged beef following exposure to pasteurizing doses, effects of subsequent exposure to air on, 26:53346
- effects on survival of mice following acute lethal whole-body exposure, comparison of RBE for californium-252, cobalt-60, and radium-226, 26:53484
- effects on swine following various combinations of acute, chronic, continuous, or fractionated dose whole-body exposures, effects of dose and dose rate on pathological, 26:53451 (NASA-TM-X-2440, pp 622-32)
- effects on thermoluminescence of cyclohexene, effects of additives and dose on, 26:53010
- effects on thrombocyte count in man following intravenous injection of colloidal gold-198 for therapy of liver involvement in Hodgkin's disease, relation of dose fractionation and protraction to, 26:53507
- effects on Tradescantia, combined effects of space flight environment on cytologic and mutagenic, 26:53382 (N-72-20054)
- effects on uptake of selenium-75-labeled selenomethionine by rat erythrocytes following whole-body exposure, dose dependence of, 26:53482
- effects on vibronic spectra of silicon, 26:54999
- effects on vision, in relation to changes in human optic nerve and retina following therapy of nasal cavity and paranasal sinus carcinomas, dose and time dependence of pathological, 26:53444
- effects on wheat flour, following grain exposure, dose dependence of bread-making and organoleptic properties of, 26:53381 (CNEA-309)
- effects on wheat, effects of dose on chemical and nutritional characteristics of stored, 26:53381 (CNEA-309)
- emission from Crab and anticenter plane of Milky Way, search for, (E), 26:53816
- emission from Crab Nebula, search for pulsed, (E), 26:53922
- emission from molybdenum--plutonium dioxide heat sources, effects of age, fluorine-19, oxygen-17, oxygen-18, plutonium-236, and size on, 26:53336 (NASA-TM-X-2440, pp 853-8)
- emission from NP 0532, (E), 26:53923
- energy deposition in laminated materials, computer code for dosage and attenuated dosage in, 26:54959 (NASA-TM-X-2440, pp 387-91)
- flux from Sco X-1 and galactic center region, (E), 26:53818
- flux of high-energy, in Milky Way, (E), 26:53819
- flux of solar, (E), 26:53967
- galactic background, energy spectra of 0.25 to 4.2 MeV, (E), 26:53818
- galactic background, flux of, (E), 26:53855
- intensity of 0.511-MeV, in atmosphere, (E), 26:53817
- intensity of, in Milky Way, (E/T), 26:53992
- isodose curves in lungs, measurement of, 26:54901
- monitoring of normal environmental, ionization chamber for, 26:53218
- production by neutron capture in space shielding materials, cascade calculation of, 26:54961 (NASA-TM-X-2440, pp 527-8)
- production by neutron reactions in shielding materials for space nuclear systems, cross sections for, (E), 26:54960 (NASA-TM-X-2440, pp 500-11)
- reactions of secondary, in thermonuclear reactors, problems from, 26:54826 (CONF-720901-(Bks.1 and 2), pp 559-73)
- reactions with materials, Monte Carlo POEM program for calculating electron emission in, 26:54884 (NASA-TM-X-2440, pp 786-91)
- spectra from Ge(Li) detectors, computer program for automatic peak identification in analysis of, 26:53257 (RT/FI-(72)14)
- spectra in reactor cores from thermal neutron capture, heat generation from, (T), 26:55444 (TRG-2189)
- spectra measurements at high altitudes behind shield, 26:54964 (NASA-TM-X-2440, pp 914-21)
- spectra of cosmic, from suprathermal proton bremsstrahlung, (E/T), 26:53820

GAMMA SOURCES
- design for simulation of spectrum emitted by radioisotope thermoelectric generator, 26:53335 (NASA-TM-X-2440, pp 850-2)
- dose distribution near implanted mixed β/γ emitters, (T), 26:54897
- preparation for Moessbauer studies, pp. 38-9, 26:53066 (ORNL-4794, pp 36-44)
- radiation dose distribution from sealed radium-226, used for implant therapy, 26:53409 (STI/PUB-295(Vol.4))
- thickness determination from deformation of hard part of energy spectrum, 26:54936
- use in skin cancer therapy, description of equipment for, 26:53341

GAMMA SPECTROMETERS
- advances in, review of impact on nuclear measurements, 26:53263
- background interference with Apollo, identification and control of onboard radiation sources causing, 26:53255 (NASA-TM-X-2440, pp 714-22)
- calibration up to 10 MeV, least square method for, 26:53253 (FRNC-TH-237)
- data analysis method for real-time spectrum-to-dose conversion, 26:53201 (NASA-TM-X-2440, pp 142-8)
- data reduction of Ge(Li), using small computers, 26:53256 (NASA-TM-X-2440, pp 744-6)
- description of Airborne Radiac scintillation, for measuring ground level radiation dose, 26:53195(R) (AD-737993)
- design of Compton scatter attenuation, for high flux intensities, conceptual, 26:53254 (NASA-TM-X-2440, pp 614-17)
- design of NaI, for spent fuel age determination, engineering drawings for, 26:53261
- operation and performance of Ge(Li), at high dose rates, 26:53237 (RD/B/N-2369)
- shield testing on balloon flights for astrophysical, 26:54964 (NASA-TM-X-2440, pp 914-21)
- stabilization of high-resolution Ge(Li), reference pulser for, 26:53262

GAS ANALYZERS
- description of electron-capture ionization detector, for mine air, 26:53287

GAS CENTRIFUGES
- uranium enrichment using, review of developments in, 26:53328

GAS CHROMATOGRAPHY
- equipment for removal of tritium from gas effluents in, 26:53313(P)

GAS FLOW
- calculations for bundle arranged roughened fuel rods, (T), 26:55188 (EURFNR-1020)
- flow distribution and pressure drop in, through tube clusters in vertical tube evaporator, comparison of calculated and measured, 26:53110 (ORNL-TM-3841)
- magnetohydrodynamic shock wave reflection from boundary shock, (T), 26:54159

GASEOUS DIFFUSION PROCESS
- cascades for, method for calculating flow rate of stream fed to separators in step, 26:53329
- uranium enrichment using, review of developments in, 26:53328

GASES
- analysis by coulometry, 26:55633(T) (UCRL-Trans-10640)
- density of, problems in measuring, 26:53300 (EUR-4797)
- diffusion in binary mixtures of, flowing in inhomogeneous medium, inter-, (T), 26:53120 (CEA-R-4318)
- electron-beam penetration in dense, (E/T), 26:54763
- energy states in fluid--gas system, kinetics of weakly inhomogeneous, (T), 26:55535 (ITF-72-29-P)
- flow through dry crushed salt beds, (E), 26:53724 (ORNL-

TM-3815)
- kinetic theory of, derivation of Boltzmann distribution law for, 26:55071 (LA-4868)
- radiolysis of, determination of short-lived species from electron pulse, 26:52980(R) (COO-3461-1)
- reactions with metals, field-ion microscopy studies of, 26:53657

GASTROINTESTINAL TRACT
- arsenic-74 uptake and retention by, of mice, rabbits, and rats following oral administration, time dependence of, 26:53538
- radioinduced injuries to human, following continuous or protracted fractionated whole-body exposure, effectiveness of pulmonary-impedance power spectral analysis for determining γ, 26:53401 (NASA-TM-X-2440, pp 238-48)
- radioinduced lesions in, of germ-free newborn swine following lethal whole-body exposure, effects of artificial colonization with Escherichia coli on γ, 26:53495

GATING SYSTEMS
- design and development of random pulse sampler, for nuclear reaction studies, 26:53321
- design of gateable delay-gate generator, 26:53299 (COO-3058-10)

GENETICS
- use of radiation in research on, 26:53459(R) (NP-19403)

GENTILLY POWER REACTOR
- operation of, shutdowns and problems in, 26:55268

GEOCHEMISTRY
- conference on, American Geophysical Union annual, Washington, D. C., 4/71, 26:54010

GEOLOGY
- conference on, American Geophysical Union annual, Washington, D. C., 4/71, 26:54010

GEOMAGNETIC FIELDS
- activity of, effect on magnetic-field intensity depression in magnetotail near 60 R/sub E/ due to diamagnetic effect of plasma sheet, (E), 26:54058
- configuration of distant, association with solar-particle access to polar-cap regions from interplanetary space, (T), 26:54069
- conjugacy relation to index K/sub p/, auroral photometric observations of, (E), 26:54013
- disturbances in polar cap, daily variations of Sq/sup p/ and DP-2, (E/T), 26:54053
- interactions with flow of charged particles, study of Earth's environmental space from dipole, (E), 26:54056
- pulsations at magnetospheric polar cusp, occurrence of latitude-dependent Pc-4 and Pc-5, (E), 26:54034
- pulsations in low-latitude, polarization studies of hydromagnetic-emission-type Pc-1, relation with ionosphere--Earth waveguide propagation, (E), 26:54021
- pulsations in, interaction of Pc-1 and Pc-2 with Pc-5 micropulsations at synchronous orbit during magnetospheric substorms, (E), 26:54035
- pulsations in, statistical characteristics of storm-associated Pc-5 micropulsations at synchronous equatorial orbit, (E), 26:54036
- solar-particle magnetospheric access to polar-cap regions of, interplanetary 1.2- to 40-MeV proton and 0.4- to 1.0-MeV electron, (E), 26:54069
- superheavy element trapping in, possible detection of, 26:54047 (NASA-TM-X-2440, pp 548-55)

GEOPHYSICS
- conference on, American Geophysical Union annual, Washington, D. C., 4/71, 26:54010

GERMANIUM
- annealing behavior of p-type and electron-converted n-type, similarities in, 26:54997
- determination in thin layers of chalcogenide glasses by proton activation or x-ray fluorescence, 26:52900 (LYCEN-7236)
- radiation effects on electrical properties of n-type doped, fast-neutron, 26:54981
- radioinduced conversion into p-type, charge state of defects produced at 140°K in 1-MeV electron, 26:55013

GERMANIUM IONS
- production in PIG source, 26:53752 (FRNC-CONF-54)

GERMANIUM ISOTOPES Ge-74
- neutron capture at 25 keV, model analysis of isomeric cross section ratio for, (E/T), 26:54589

GERMANIUM SILICIDES
- electrical properties of hot-pressed, effects of dopant precipitation on, 26:55598 (SC-DC-721020)

GLASS
- crystal lattice deformation in, field-ion microscope studies of tip--glass contact, 26:53651
- fatigue properties of strands of S-, data interpretation on static, 26:55619 (UCID-16100)
- positron lifetimes in nitrate, measurement of temperature-dependent, (E), 26:55064
- radiation effects on transmittance of BK-7 borosilicate, electron, 26:54049 (NASA-TM-X-2440, pp 748-55)
- radiophotoluminescence in silver-activated phosphate, as function of electronic stopping, depth distribution of charged-particle, 26:55009

GLASS TEXTILES
- epoxy resins--glass textiles, fiber strength of composites of, under biaxial loading, 26:55627 (UCRL-73772)
- glass textiles--plastics, preparation and properties of, produced by radioinduced polymerization, 26:53722

GLUCOSE
- preparation of labeled, by tritium atom bombardment, 26:53028 (COO-584-50)

GLYCINE
- radiolysis of frozen aqueous solutions of, ESR study of free radicals from γ, 26:52995

GOLD
- fabrication of thin monocrystalline, by epitaxy, 26:55566 (LYCEN-7232)
- ion channeling through thin crystals of, 0.5 to 2-MeV light, 26:54974 (LYCEN-7228)
- location in silicon lattice of diffused dopant atoms of, using helium-ion channeling, 26:54987
- scattering by argon at 5 to 90 eV, interatomic potentials and total cross sections for elastic, (E), 26:54142

GOLD ALLOYS AND SYSTEMS
- Au--Cd, lattice heat capacity of intermetallic AuCd, at 20 to 298°K, 26:53637 (LBL-101)
- Au--Cu, lattice heat capacity of intermetallic $AuCu_3$, at 20 to 298°K, effects of ordering on, 26:53637 (LBL-101)
- Au--Er, magnetic structure of $ErAu_2$, neutron diffraction study of, 26:55034
- Au--Ho, magnetic structure of $HoAu_2$, neutron diffraction study of, 26:55033

GOLD IONS
- implantation in silica layers for gate MOS structure fabrication, 26:53314
- scattering by argon and neon at 8 to 25 keV, total cross sections and interatomic potentials for, (E), 26:54139

GOLD ISOTOPES Au-197
- neutron capture at 24.3 keV, TOF cross-section measurements using iron-filtered beam, (E), 26:54597 (CONF-720901-(Bks.1 and 2), pp 1107-14)
- neutron capture by, survey of cross section data for, 26:54657 (FEI-292)
- neutron capture near 24.3 keV, pulse height spectra and relative cross section for, (E), 26:54656(R) (COO-3058-21)
- neutron transmission at unresolved resonance energies, effect of temperature on, (E/T), 26:54484 (KFK-1519)
- photon reactions (γ,xn) with, model analysis of giant resonance in, (E/T), 26:54598 (FRNC-TH-242)

GOLD ISOTOPES Au-198
- effectiveness of colloidal, for therapy of liver involvement in Hodgkin's disease following fractionated intravenous injection, additive effects of external x-ray exposure on, 26:53507
- radiation dose to fingers of medical personnel during injection of, phantom studies of, 26:53424
- use of colloids of, for treatment of malignant pleural effusions in man, measurement of dose distribution with time following, beta and gamma, 26:53509

GONIOMETERS
- design of two-axis, with sample temperature control for implantation and channeling experiments, 26:53322

GRAIN STRUCTURE
- grain boundary dislocation model for studies of, 26:55513 (COO-3158-10)

GRANITE DEPOSITS
- cavities and fracture zones in Hoggar, from underground nuclear explosions, content and size of, 26:53130(T) (UCRL-Trans-10616-4)
- nuclear explosion effects in Hoggar, distant mechanical, 26:53129(T) (UCRL-Trans-10616-2)
- nuclear explosion effects on Hoggar, close-in mechanical, 26:53131(T) (UCRL-Trans-10616-5)

GRANITES
- temperature distribution in, following underground nuclear explosion, 26:53127 (CEA-R-4288)

GRAPHITE
- corrosion of H327, by high temperature steam, (E), 26:55207(R) (ORNL-TM-3900)
- dimensions and mechanical properties of advanced composites of, fabricated by cocuring process, 26:53570
- fabrication of advanced composites of, cocuring method for, 26:53570
- radiation damage in, electron microscopic study of 650-kV electron, 26:54972 (COO-2119-2)
- radiation effects on, relations of flux density and temperature to pile neutron, 26:53713 (CEA-CONF-1894)

GRAPHITE SYSTEMS
- B--graphite, dimensions and mechanical properties of advanced composites of, fabricated by cocuring process, 26:53570
- B--graphite, fabrication of advanced composites of, cocuring method for, 26:53570
- C--graphite, properties at high temperatures, tensile and thermal, 26:53581

GRAVITATION
- constant in, time variation of, (E), 26:54403
- cosmological models in scalar--tensor theory of, isotropic, (T), 26:54396 (ITF-72-41-P)
- effects of weightlessness on growth and prophage induction in Salmonella typhimurium during space flight, effects of γ irradiation on, 26:53364 (N-72-20063)
- particle motion in circular orbit in direct interaction theory of, stability of two-body, 26:54399 (ITF-72-58-

  - P)
  - potential in canonical formalism, 26:54405
  - theory for, Lie groups in, 26:54402
  - theory of, scalar--tensor, 26:54395 (ITF-72-21-P)
  - two-body problem in Fokker formalism in direct interaction theory of, existence and uniqueness theorem for equations of motion for, (T), 26:54398 (ITF-72-52-P)
- GRAVITATIONAL FIELDS
  - energy--momentum tensor of, spatial localizability of, (T), 26:54393 (ITF-72-5-P)
  - modeling in Einstein theory for solar, (T), 26:54390 (ITF-71-130-P)
  - photon trajectories in, bending of, (T), 26:53866
  - spaces in two-symmetric and two-recurrent, algebraic method for validity for positively definite metric and classes of relativistic, (T), 26:54397 (ITF-72-46-P)
- GRAVITATIONAL RADIATION
  - emission and scattering by relativistic neutron stars, nonradial vibrational modes from, (T), 26:53894
  - interaction with neutrinos in expanding universe, (T), 26:53997
  - propagation of third- and higher-order, for tensor and scalar--tensor fields, (T), 26:54406
- GRAVITY WAVES
  - propagation in ionospheric E region, induction of gradient instabilities in E region from internal atmospheric, (T), 26:54018
- GROSSWELZHEIM SUPERHEAT REACTOR
  - fuel elements for, criteria for defining voids in, 26:55229(T) (EURFNR-975)
- GROUND
  - motion from San Fernando earthquake, damage to Glendale, Calif. residential buildings from, 26:53137 (JAB-99-96)
- GROUP THEORY
  - Lie groups for gravitation theory, 26:54402
  - Lie groups in, Wigner--Eckart theorem extension for continuum unitary and nonunitary representations of semi-simple, 26:54355 (ITF-72-33-E)
  - Lie groups of automorphisms of C* algebra in, continuity in norm topology for covariance of algebra representations for compact, 26:54358
  - Lorentz-covariant bilinear forms and operators in, manifestly covariant formalism for, 26:54359
- GUANIDINE, 1-METHYL-3-NITRO-1-NITROSO-
  - carcinogenicity of, bibliography on, 26:55583 (ORNL-TIP/TIRC-72-60)
  - effects on Eremothecium ashbyii (fungi) in relation to riboflavin production, mutagenic, 26:53374
- GUINEA PIGS
  - radiation effects on immune reactions in, effects of transplants of cells of bone marrow, lymph nodes, and spleen on lethal dose, 26:53474

H

- H.B. ROBINSON POWER REACTOR, UNIT 2
  - auxiliary systems for, final safety analysis of, 26:55286 (DOCKET-50261-106)
  - control rod system for, malfunction of part length, 26:55252 (DOCKET-50261-109)
  - electrical systems for, final safety analysis of, 26:55286 (DOCKET-50261-106)
  - emergency core cooling system for, revised performance requirements for, 26:55287 (DOCKET-50261-108)
  - emergency systems for, final safety analysis of, 26:55286 (DOCKET-50261-106)
  - operation aspects of, final safety analysis of, 26:55286 (DOCKET-50261-106)
  - power conversion system for, final safety analysis of, 26:55286 (DOCKET-50261-106)
  - radiation protection systems for, final safety analysis of, 26:55286 (DOCKET-50261-106)
  - radioactive waste disposal systems for, final safety analysis of, 26:55286 (DOCKET-50261-106)
  - safety analysis for, 26:55286 (DOCKET-50261-106)
  - testing of, final safety analysis of initial, 26:55286 (DOCKET-50261-106)
- HI REGIONS
  - distribution in 5 Scd galaxies, (E), 26:53972
  - distribution in Milky Way, (T), 26:53984
  - distribution in NGC 4236, NGC 2403, and IC10, (E), 26:53971
  - origin of high-velocity, in Milky Way, (T), 26:53983
- HII REGIONS
  - radio fine structure in, synthesis observations at 11 and 3.7 cm, (E), 26:53910
- HADRONS
  - decay into $e^{+} + e^{-}$ + hadron (photon), radiative corrections to invariant mass spectra of Dalitz pair in, (T), 26:54277
  - detection of high energy, development of total absorption liquid argon scintillation detector for, 26:53269 (BNL-17070)
  - detection of, total absorption counters for, 26:53270 (BNL-17071)
  - form factors in parton model, elastic and inelastic, (T), 26:54311
  - interactions at 50 to 1200 GeV, model for multiple production in, (T), 26:54314
  - interactions of, exotic fragmenting states in inclusive, 26:54304
  - interactions of, study using electromagnetic- and strong-interaction experiments at ISABELLE, (T), 26:54298 (BNL-16997)
  - interactions of, thermodynamic model for limiting temperature for, (T), 26:54305
  - interactions of, three-dimensional unitary group for unified gauge weak--electromagnetic, (T), 26:54364 (NYO-3533-264)
  - interactions of, three-dimensional unitary group for unified gauge weak-electromagnetic-strong, (T), 26:54364 (NYO-3533-264)
  - interactions with electrons, Regge and scaling limits for inclusive production, (T), 26:54275
  - interactions with hadrons and nuclei, diffraction emission in, (T), 26:54690 (ITF-72-57-P)
  - interactions with hadrons, quasi-eikonal approximation with contributions of Regge poles and rescattering for amplitudes of, (T), 26:54306
  - interactions with hadrons, research at Indiana Univ., Dec. 1971 to Nov. 1972, (E), 26:54206(R) (COO-2009-36)
  - interactions with hadrons, s-channel helicity conservation for amplitudes of elastic, (T), 26:54287 (LBL-766)
  - model for, Markoffian, 26:54308
  - production of, thermodynamic model for limiting temperature for, 26:54305
- HAFNIUM
  - book: Early Transition Metals, 26:52956
  - deposition by pack cementation on chromium-base alloys for nitridation protection in air, effects of chromium, lanthanum, and yttrium additions on, 26:53689
- HAFNIUM CARBIDES
  - mechanical properties of hot pressed, at high temperatures, 26:53581
- HAFNIUM ISOTOPES Hf-176
  - energy levels from hafnium-177 (d,t) reactions, Nilsson assignments for, (E), 26:54636
- HAFNIUM ISOTOPES Hf-177
  - deuteron reactions (d,t) at 12 and 14 MeV, triton spectra from, (E), 26:54636
- HAFNIUM ISOTOPES Hf-179
  - deuteron reactions (d,p) at 12 and 14 MeV, proton spectra from, (E), 26:54636
- HAFNIUM ISOTOPES Hf-180
  - energy levels from hafnium-179 (d,p) reactions, Nilsson assignments for, (E), 26:54636
- HAFNIUM NITRIDES
  - mechanical properties of hot pressed, at high temperatures, 26:53581
- HAIR
  - arsenic-74 uptake and retention by, of mice, rabbits, and rats following oral administration, time dependence of, 26:53538
  - radioisotope uptake by rat, following intravenous injection, correlation with body burden, 26:53529 (NASA-TM-X-2440, pp 982-8)
- HALLAM POWER REACTOR
  - cooling system of, sodium removal and disposition during dismantling of, 26:55147 (AI-AEC-Memo-12736)
- HANDBOOKS AND MANUALS
  - on health physics, ORAU, 26:53205 (TID-26132)
  - radioisotope uses in medicine, training course, 26:53541 (TID-26128)
- HANFORD POWER REACTOR, UNIT 2
  - auxiliary systems for, requested and revised data on, 26:55346 (DOCKET-50397-32)
  - auxiliary systems for, revised data on, 26:55345 (DOCKET-50397-28)
  - construction of, revised cost estimates for, 26:55261 (DOCKET-50397-27)
  - containment system for, requested and revised data on, 26:55346 (DOCKET-50397-32)
  - containment system for, revised data on, 26:55345 (DOCKET-50397-28)
  - cooling system for, requested and revised data on, 26:55346 (DOCKET-50397-32)
  - cooling system for, revised data on, 26:55345 (DOCKET-50397-28)
  - costs for, revised estimates of construction, 26:55261 (DOCKET-50397-27)
  - electrical system for, revised data on, 26:55345 (DOCKET-50397-28)
  - electrical systems for, requested and revised data on, 26:55346 (DOCKET-50397-32)
  - power conversion system for, requested and revised data on, 26:55346 (DOCKET-50397-32)
  - site for, requested and revised data on, 26:55346 (DOCKET-50397-32)
  - site for, revised data on, 26:55345 (DOCKET-50397-28)
  - structures for, requested and revised data on, 26:55346 (DOCKET-50397-32)
  - structures for, revised data on, 26:55345 (DOCKET-50397-28)
- HASTELLOY X
  - radiation effects on tensile properties of, at cryogenic temperatures for use in NERVA Program, fast neutron, 26:53697 (NASA-TM-X-2440, pp 603-8)
- HAYNES 25 ALLOY
  - creep rupture of, at 910°K, cyclic, 26:53690

- HEALTH PHYSICS
  - personnel training manual for, ORAU, 26:53205 (TID-26132)
- HEART
  - arsenic-74 uptake and retention by, of mice, rabbits, and rats following oral administration, time dependence of, 26:53538
  - measurements of systolic blood volume in, iodine-131 scanning method, 26:53543
  - radioinduced injuries to human, following therapy of esophageal carcinomas, electrocardiogram studies of γ and x, 26:53439
- HEART, MECHANICAL
  - model design for, spacial constraints of calf and human bodies for, 26:55503(R) (COO-2208-1)
- HEAT EXCHANGERS
  - damage to, effects of sodium--water reactions on, 26:55158 (CONF-710548-, pp 187-205)
  - dismantling of sodium cooled reactor, removal of sodium and decontamination during, 26:55147 (AI-AEC-Memo-12736)
  - leaks of water into liquid sodium in, effects on temperature and pressure of, 26:55152 (CONF-710548-, pp 39-56)
- HEAT-RESISTING ALLOYS AND METALS
  - powder metallurgy of, conference on Reutte/Tyrol, Austria, June 21 to 25, 1971, Vol. 4, 26:53603
  - powder metallurgy of, conference on, Reutte/Tyrol, Austria, June 21 to 25, 1971, Vol. 3, 26:53584
  - powder metallurgy of, conference on, Reutte/Tyrol, Austria, June 21 to 25, 1971, Vol. I, 26:53601
  - powder metallurgy of, conference on, Reutte/Tyrol, Austria, June 21 to 25, 1971, Vol. 2, 26:53602
  - powder metallurgy of, electronic mechanism of basic processes in, 26:53632
  - powder metallurgy of, review on, 26:53590
- HEAT SOURCES
  - development and performance of, for space power systems, 26:53093 (NASA-TM-X-2440, pp 13-25)
  - evaluation of plutonium-238 fuel forms for, 26:53333 (MLM-1213)
- HEAT TRANSFER
  - critical heat flux in water cooled systems, critical review on state of the art of, 26:55179 (TID-25887)
  - mechanisms in axisymmetric structures, computer code for studying, 26:55610 (SCL-DR-720004)
- HEAT TRANSFER SYSTEMS
  - corrosion problems in liquid sodium, comparison of model estimates with experimental results on, (E/T), 26:55168 (CONF-710959-, Paper 12)
  - corrosion product release, transport and deposition in liquid sodium, (E), 26:55164 (CONF-710959-, Paper 8)
  - operation characteristics of Japan Low Temperature Fissiochemical, comparison with design parameters of, 26:55400 (JAERI-M-4630)
  - performance of liquid sodium, effects of corrosion and corrosion product deposition on, 26:55166 (CONF-710959-, Paper 10)
  - pressure drop in, effects of rod configuration and spacing on, 26:55174(T) (EURFNR-986)
- HEATED EFFLUENTS
  - effects of power generating station, on meteorological conditions, 26:53188 (ANL-7860(Pt.3), pp 250-69)
  - effects of surface water-discharged power plant, on environment, 26:53194
  - effects on aquatic organisms, 1971 bibliography on, 26:53190 (ORNL-EIS-72-28)
  - effects on environment of power reactor, 26:55337 (DOCKET-50358-41)
  - effects on environment of power reactor, 26:55301 (DOCKET-50285-71)
  - effects on environment of power reactor, 26:55331 (DOCKET-50335-33)
  - effects on environment of power reactor, 26:55338 (DOCKET-50361-27)
  - effects on environment of power reactor, 26:55285 (DOCKET-50254-120)
  - effects on inshore biological communities of Lake Michigan, 26:53184 (ANL-7860(Pt.3), pp 109-17)
  - effects on major nutrients and water quality parameters at Point Beach Nuclear Power Station, 26:53183 (ANL-7860(Pt.3), pp 103-8)
  - monitoring of plumes from, using temperature-induced fading of thermoluminescent dosimeters, 26:53187 (ANL-7860(Pt.3), pp 131-40)
  - monitoring of Point Beach and Big Rock Point Nuclear Power Stations, 26:53182 (ANL-7860(Pt.3), pp 101-2)
  - monitoring program for power reactor, environmental, 26:55326 (DOCKET-50315-82)
  - temperature of, effects on type and quantity of fish near Point Beach Nuclear Power Plant, 26:53185 (ANL-7860(Pt.3), pp 118-20)
  - thermal plumes from, acoustic location method for studying fish distribution relative to, 26:53186 (ANL-7860(Pt.3), pp 121-30)
  - use for urban space heating, industrial and sewage processing, and agricultural purposes, feasibility of, 26:55212 (CONF-720925-2)
- HEATERS
  - performance of electric, for liquid sodium cooled fuel element testing facility, 26:55207(R) (ORNL-TM-3900)
  - performance of filament type electric, for simulation of uranium oxide (UO_2) rods in pressurized water reactors, 26:55183 (ANCR-1038)
- HELIOTRINE
  - effects on chromosomes in cultured rat-kangaroo cells, effects of cell phase on sensitivity to, 26:53359
- HELIUM
  - abundance in blue horizontal-branch stars, (T), 26:53891
  - abundance in extreme Population I stars and Sun, (T), 26:53892
  - abundance in NGC 7662, (E/T), 26:53873
  - abundance in primary cosmic radiation from 10 to 1000 MeV/N, (E), 26:53835
  - abundance in subdwarf HD 49798, (E), 26:53900
  - binding energy of, effects of intense magnetic fields on, 26:54144
  - carbon-ion reactions at 40 to 140 keV with, cross sections for charge exchange in, (E), 26:54137
  - electron reactions at 200 to 500 eV with, second-Born-approximation calculations of 1^1S, 2^1S, and 2^1P transitions in, 26:54138
  - electron reactions at 26.5 to 300 eV with, distorted-wave calculations of differential and integral cross sections for excitation of ^1p states in, 26:54106
  - electron reactions at 30 to 80 eV with, relation of momentum transfer to coincidence-measured angular and energy distributions of electrons scattered and ejected in ionization in, 26:54123
  - electron reactions at 50 to 200 eV with, coincidence measurements of absolute differential cross sections for 1^1S--4^1D transition in, 26:54113
  - electron reactions with, adiabatic-approximation calculations of cross sections for excitation and spin change in, 26:54117
  - electron reactions with, close-coupling calculations of indirect coupling effects on cross sections for excitation in, 26:54108
  - electron reactions with, dependence of computed excitation cross sections for, on accuracy of wave functions used, 26:54108
  - electron reactions with, relations between dispersion relation, optical theorem, and second Born scattering amplitude for, 26:54110
  - electron-beam penetration in dense, (E/T), 26:54763
  - energy of, calculation using Sams--Kouri method for solving integral form of Schroedinger equation, 26:54145
  - energy spectra of primary cosmic, at 50 to 2000 GeV, (E), 26:53829
  - heat transfer from 16 tube fuel assemblies to, measurement of, 26:55227(T) (EURFNR-1000)
  - heat transfer to boiling, from aluminum surfaces, 26:54465
  - helium-ion reactions at 1 to 3 keV with, differential cross sections for excitation and ionization in, (E), 26:54140
  - helium-ion reactions at 1 to 3 keV with, energy distribution of electrons ejected by ionization in, (E), 26:54140
  - helium-ion reactions at 500 to 1500 eV with, time-of-flight measurements of charge-exchange cross sections and energy-loss spectra of neutral excited atoms from, 26:54109
  - hydrocarbon-ion (CH/sub n/$^+$) reactions at 40 to 140 keV with, cross sections for dissociation and production of hydrogen atoms in, (E), 26:54137
  - ionization energy of, effects of intense magnetic fields on, 26:54144
  - isotopic ratio of, mass spectrometric measurement of, (E), 26:54519
  - neutron attenuation in, measurement using manganese activation, (E), 26:54490
  - neutron total cross section at 0.7 to 30 MeV, (E), 26:54656(R) (COO-3058-21)
  - oxygen-ion (O_2^+) reactions with, impulse approximation for vibrational excitation in, using Morse potential, 26:54131
  - photon reactions with triplet metastable, light-intensity dependence of probability of ionization in five-, (E), 26:54094
  - plasma of, collisional--radiative recombination and ionization coefficients for, 26:54788 (EUR-CEA-FC-642)
  - positron reactions at 2 to 20 eV with, total cross sections for, (E), 26:54119
  - pressure drop in 16 tube fuel assemblies, measurement of, 26:55227(T) (EURFNR-1000)
  - proton reactions at 500 to 3000 eV with, differential cross sections for charge exchange, elastic scattering, excitation to autoionizing levels, and simple excitation in, (E/T), 26:54122
  - reactions with hydrogen atoms, calulation of translational absorption spectrum from, 26:54134
  - reactions with hydrogen molecules at 0.14 meV to 2.9 eV, absolute integral total cross sections and interaction potentials for, (E), 26:54130
  - reactions with rare gases at 100 to 5000 eV, angular and energy distributions of electrons from ionization and autoionization in, (E), 26:54141
  - release of injected, from nickel, stainless steels, and Nimonic PE 16, 26:53709
  - scattering by lithium fluoride surfaces, diffraction intensities for, calculated using pairwise interaction,

26:54089

- thermodynamics of mixtures of hydrogen and, in interior of Jupiter, (T), 26:54003

HELIUM, SUPERFLUID
- energy flux between two baths of, separated by thin metallic foil, 26:54434
- film flow transfer in and out of Plexiglas ampoules, 26:54431
- hydrodynamics near lambda point, high-frequency, 26:54424
- ion mobility in, roton-limited, (T), 26:54425
- roton lifetime in, (T), 26:54429
- scintillation of, alpha-particle-induced, 26:54430
- spectra of, application of equation-of-motion method to, (T), 26:54428
- spectra of, application of equation-of-motion method to, (T), 26:54427

HELIUM HYDRIDES
- dipole moment of ground-state, as function of internuclear separation, (T), 26:54134
- potential-energy curves for ground state of, (T), 26:54134

HELIUM IONS
- channeling of, use to locate diffused depant gold atoms in silicon lattice, 26:54987
- dechanneling at 1.5 MeV in diamond lattices, 26:54988
- effects of injected, on creep rupture properties of Type 316 stainless steel, 26:53703
- effects on silver-activated phosphate glass at 200 to 400 keV, depth distribution of photoluminescence induced by, 26:55009
- effects on structure of polycrystalline molybdenum and nickel at 60 keV, x-ray diffraction studies on, 26:53700(T) (SC-T-722540)
- implantation into nickel at low energy, 26:53709
- reactions with copper and tantalum at 10.4 MeV/nucleon, neutron yield from, (E), 26:54881 (NASA-TM-X-2440, pp 520-2)
- reactions with helium at 1 to 3 keV, differential cross sections for excitation and ionization in, (E), 26:54140
- reactions with helium at 1 to 3 KeV, energy distribution of electrons ejected by ionization in, (E), 26:54140
- reactions with helium at 500 to 1500 eV, time-of-flight study of charge-exchange cross sections and energy-loss spectra of neutral excited atoms from, 26:54109
- reactions with rare gases at 100 to 5000 eV, angular and energy distributions of electrons from ionization and autoionization in, (E), 26:54141
- scattering by tungsten polycrystalline surfaces at 150 to 1000 eV, angular and energy distributions and cross sections for, (E), 26:54083
- spectral lines in prominences and chromosphere due to, (E), 26:53949

HELIUM ISOTOPES He-3
- abundance in atmospheric helium, (E), 26:54519
- abundance in primary cosmic radiation, (E), 26:53827
- alpha inelastic scattering at 115 MeV, cross sections and energy spectra from, (E), 26:54515
- deuteron reactions (d,p) at 366 to 1090 keV using polarized beam, analyzing power for, (E), 26:54500 (LA-DC-72-906)
- electrodisintegration of, calculation of two-particle, (T), 26:54496 (ITF-72-24-P)
- energy spectra of primary cosmic, (E), 26:53828
- interactions ^{3}He + ^{3}He, implications for solar neutrino emission of resonance in, (T), 26:54508
- interactions ^{3}He + t at 1 to 200 MeV (cms), optical-potential description of phases for scattering, (T), 26:54532
- nuclear charge radius of, calculations using very-soft-core Riihimaki potential, (T), 26:54504
- nuclear magnetic moment of, calculation using quark model, 26:54494 (COO-3001-15)
- nuclear magnetic moment of, two-body OPE contributions to isovector, (T), 26:54506
- proton elastic scattering at 30 MeV using polarized beam, analyzing power for, (E), 26:54521
- proton elastic scattering at 600 MeV, differential cross section for, (E), 26:54512
- reactions (He-3,αp) with lithium-6 at 1.54 MeV, asymmetric proton yields for, (E), 26:54540
- reactions (He-3,Be-7) with nuclei, DWBA treatment of, (T), 26:54706
- reactions (He-3,dγ) with cobalt-59 at 18 MeV, angular distributions for, (E), 26:54587 (FRNC-TH-240)
- reactions (He-3,nγ) with neon-20 at 4.3 to 11.5 MeV, coincidence and angular correlation measurements for, (E), 26:54559
- reactions (He-3,p) with carbon-12 at 14 MeV with subsequent proton decay, gamma spectra and gamma and proton angular correlations in, (E), 26:54542
- reactions (He-3,p) with nitrogen-14, contributions of rectangular graphs in, (T), 26:54533
- scattering by cadmium-114 at 10 to 17 MeV, collective model calculation of form factor for inelastic, (E/T), 26:54621
- scattering by intermediate nuclei at 10 to 85 MeV, energy dependence in optical-model analysis of elastic, (T), 26:54580
- scattering by iron-56 at 53.4 MeV, differential cross sections and optical-model parameters for elastic, (E), 26:54571
- scintillation of liquid, alpha-particle-induced, 26:54430
- He-3--He-4, osmotic pressure waves in solutions of superfluid, (T), 26:54433
- He-3--He-4, scintillation of liquid, alpha particle induced, 26:54430
- He-3--He-4, thermal capacity near gas--liquid critical point, (E), 26:54426

HELIUM ISOTOPES He-4
- abundance in primary cosmic radiation, (E), 26:53827
- deuteron elastic scattering at 4.8 to 8.6 MeV, polarization transfer in, (E), 26:54498 (LA-DC-72-904)
- energy levels of, calculations using separable nonlocal potential, (T), 26:54683 (FRNC-TH-180)
- interactions with He-4, potential from low-energy cross-section measurements, (E), 26:54514
- nuclear charge form factor of, effects of center-of-mass spuriosity on, (T), 26:54507
- proton elastic scattering at 0 to 50 MeV, forward dispersion relation including Coulomb interaction for, (T), 26:54711
- proton elastic scattering at 600 MeV, differential cross section for, (E), 26:54512
- proton reactions (p,d) at 65 MeV, cross sections and energy spectra from, (E), 26:54515
- He-3--He-4, osmotic pressure waves in solutions of superfluid, (T), 26:54433
- He-3--He-4, scintillation of liquid, alpha particle induced, 26:54430
- He-3--He-4, thermal capacity near gas--liquid critical point, (E), 26:54426

HELIUM SYSTEMS
- He--N, radiolysis of, determination of short-lived species from electron pulse, 26:52980(R) (COO-3461-1)

HEMATOPOIESIS
- radiation effects on, in mice following whole-body exposure, comparison of RBE for γ and high-intensity pulsed x, 26:53469

HEMATOPOIETIC SYSTEM
- pyramidon effect on, of mammal, bibliography on, 26:55582 (ORNL-TIP/TIRC-72-59)
- radiation effects on survival of erythropoietic stem cells in, of mice following sublethal whole-body exposure, protective effects of AET and serotonin against proton, 26:53454 (NASA-TM-X-2440, pp 642-6)
- radioinduced injuries of, in fish, relation of species to repair time for γ, 26:53447 (CONF-720822-2)

HEXANE, 3-METHYL-
- radiolysis of liquid, time dependence of spectra of solvated electrons from, 26:53007

HIGH-ENERGY PHYSICS
- funding and outlook for medium energy, 26:53740 (LA-4874, pp 21-33)
- lectures at Physics Laboratory of Istituto Superiore di Sanita, Rome, July--Dec. 1970, 26:54162 (ISS-71/31)
- research by High Energy Counter Group at State Univ. of New York, Stony Brook, 1971, 26:54212(R) (TID-26138)
- research program at LAMPF, review of, 26:54195 (LA-4874, pp 36-44)

HIGH-TEMPERATURE GAS-COOLED REACTOR EXPERIMENT
- cooling system for, testing of materials for, 26:53605(R) (DP-Report-522)
- fuel reprocessing for, head-end method for, pp. 27-9, 26:53083 (ORNL-4794, pp 26-32)

HIGH-TEMPERATURE LATTICE TEST REACTOR
- operation of, successfully completed program for, 26:55416(R) (BNWL-1522-5)

HIPPURIC ACID, p-AMINO-
- uptake by rat kidneys following injection, effects of uranyl nitrate on, 26:53537

HIROSHIMA
- radiation dose to residents of, comparison for diagnostic radiographic examinations and A-bomb survivors, 26:53434

HOLMIUM ALLOYS AND SYSTEMS
- Au--Ho, magnetic structure of HoAu$_2$, neutron diffraction study of, 26:55033

HOLMIUM ISOTOPES Ho-158
- energy levels from erbium-158 decay, Nilsson and spin--parity assignments for, (E), 26:54643

HOLMIUM ISOTOPES Ho-161
- energy levels from erbium-161 decay, Nilsson and spin--parity assignments for, (E), 26:54643
- energy levels from erbium-161 decay, spin--parity assignments for, (E), 26:54632 (COO-3255-2)
- energy-level transitions from erbium-161 decay, branching ratios and multipolarities for, (E), 26:54643
- energy-level transitions from erbium-161 decay, multipolarities and conversion coefficients for, (E), 26:54632 (COO-3255-2)

HOLMIUM ISOTOPES Ho-165
- alpha inelastic scattering at 10 MeV with Coulomb excitation, heat-flow analysis of temperature spikes following, (E/T), 26:54646
- photon reactions (γ,xn) with, model analysis of giant resonance in, (E/T), 26:54598 (FRNC-TH-242)
- proton inelastic scattering at 4 MeV with Coulomb excitation, heat-flow analysis of temperature spikes following, (E/T), 26:54646

HOLOGRAPHY
  development of ultrasonic, for visualization of flaws in thick walled structures, 26:55222(R) (NP-19338(Vol.2))
HORMONES, ADRENAL
  cortisone, effects on serum protein content and serum albumin-globulin ratio of gamma-irradiated mice, 26:53490
HORMONES, PLANT
  indole-3-acetic acid, radiolysis of aqueous solutions of, rate constants for reaction of hydrogen atom, hydroxyl radicals, and hydrated electrons in, 26:53015
HOT CELLS
  design for post-irradiation examination of plutonium fuels, 26:53728 (JAERI-Memo-4009)
  design of Hot Fuel Examination Facility, for remote disassembly and inspection of fuel failure test loops, 26:53727 (ANL/HFEF-1)
  sample preparation for metallography in, selection of noncorrosive cleaning solutions and lubricants for, 26:53729 (LA-DC-72-230)
HUNGARY
  radioactivity monitoring of foods in, from 1959 to 1971, 26:53172
HUTCHINSON ISLAND POWER REACTOR, UNIT 1
  effluents from, effects on environment of chemical, radioactive, and thermal, 26:55331 (DOCKET-50335-33)
  operation of, cost-benefit analysis for, 26:55331 (DOCKET-50335-33)
  site for, ecology, geology, hydrology, and meteorology of, 26:55331 (DOCKET-50335-33)
HYDRAZINE
  muon (μ^-) depolarization in aqueous solutions of, effects of chemical reactions, hydrogen peroxide concentration, and temperature on, (E), 26:54099
  radioinduced production of anhydrous, by electron or γ radiolysis of liquid ammonia, 26:53001(P)
HYDRIDES
  properties of metal, for storage of hydrogen, evaluation of, 26:53090 (BNL-16889)
HYDROBROMIC ACID
  Br--HBr, photolysis of, deuterium isotope effects on reactions of hot hydrogen atoms from, 26:52962
HYDROCARBONS
  reactions with gases at 40 to 140 keV of ions (CH/sub n/+) of, cross sections for dissociation and production of hydrogen atoms in, (E), 26:54137
  reactions with nitrogen molecules of ions (CH/sub n/+) of, energy spectra of dissociation products from, (E), 26:54102 (EUR-CEA-FC-644)
HYDROGEN
  abstraction from methanol molecules by radiolytic methyl radicals, 26:52990 (ORO-2968-78, Paper 5)
  atomic mass of, 26:54495 (EUR-4765, pp 435-55)
  carbon-ion reactions at 40 to 140 keV with molecular, cross sections for charge exchange in, (E), 26:54137
  determination of trace amounts in liquid sodium, vacuum distillation method for, 26:55170 (CONF-710959-, Paper 14)
  deuteron elastic scattering at 6.00 to 11.50 MeV, phase-shift analysis of polarized, (T), 26:54513
  dissociation on hot tungsten filaments, ESR study of, 26:55036
  distribution in Zircaloy, effects of thermal gradients on, 26:53665
  distribution of atomic, in Milky Way, (T), 26:53979
  effects in helium stars, (E/T), 26:53896
  effects on corrosion resistance of zirconium and zirconium alloys in high-temperature water, 26:53614
  effects on steel, literature review on, 26:53606 (MLM-1355)
  electron reactions with atomic, adiabatic-approximation calculations of cross sections for excitation and spin change in, 26:54117
  energy of ground and first three excited states of atom of, calculation using Sams--Kouri method for solution of integral form of Schroedinger equation, 26:54145
  energy of ground-state one-dimensional atom of, effects of inclusion of repulsive core in Coulomb potential on, 26:54093
  explosion hazards of, analysis of, 26:55524 (DP-1295)
  handling, shipping, and storage of liquid, 26:55552 (LA-DC-72-632)
  helium-atom reactions at 0.14 MeV to 2.9 eV with molecular, absolute integral total cross sections and interaction potentials for, (E), 26:54130
  hydrocarbon-ion (CH/sub n/+) reactions at 40 to 140 keV with molecular, cross sections for dissociation and production of hydrogen atoms in, (E), 26:54137
  lithium-ion reactions with molecular, quantum mechanical calculations of vibrational excitation in, using coupled Volterra equations, 26:54133
  neutron capture by, comparison of ENDF/B III and published data for thermal, 26:54501 (ORNL-TM-3910)
  photon reactions with singly excited molecules of, calculation of cross sections for ionization in, using phase shifts for electron scattering by hydrogen ions (H_2^+), 26:54091
  plasma of, spectral shifts of Stark broadened Lyman-alpha lines of, (T), 26:54796
  production by reduction of water vapor over chromium, iron, or nickel, 26:52975(P)
  properties of frozen and reacting ortho--para mixtures of, thermodynamic and transport, 26:53715 (NASA-TM-X-2440, pp 476-80)
  proton elastic scattering at 600 MeV, differential cross section for, (E), 26:54512
  radiation effects on thermodynamic and transport properties of frozen and reacting ortho--para mixtures of, 26:53715 (NASA-TM-X-2440, pp 476-80)
  radio emission at 21-cm from neutral, (T), 26:53984
  radioinduced reactions with carbon, 30- to 45-keV electron beam, 26:53718
  radiolysis of solid molecular, at 1.4 to 8°K by 160-keV electrons, yields and EPR spectra of atomic hydrogen from, 26:52979 (COO-1105-179)
  reactions between atoms and molecules of, at 5 to 50 keV, cross sections for dissociation, electron capture, electron loss, excitation, and ionization in, (E), 26:54115
  reactions between atoms and molecules of, free-collision-model calculations of cross sections for electron loss in, 26:54121
  reactions between molecules of, at 50 to 500 eV, angular distributions and total cross sections for production of fast molecular ions in, (E), 26:54105
  reactions of atoms of, in radiolysis of aqueous solutions of indole-3-acetic acid and other plant hormones, 26:53015
  reactions of atoms of, with various substrate molecules in gas phase, research progress on elementary reaction rate constants for, 26:55519(R) (COO-3242-4)
  reactions of photolytic hot, deuterium isotope effects on, 26:52962
  reactions with brass surfaces of molecular, secondary-electron emission coefficients for, (E), 26:54105
  reactions with helium of atomic, calculation of translational absorption spectrum from, 26:54134
  reactions with nitrogen and oxygen molecules of atomic, free-collision-model calculations of cross sections for electron loss in, 26:54121
  reactions with sodium from 300 to 450°C, 26:55154 (CONF-710548-, pp 105-28)
  reactions with uranium dioxide pellets during sintering, oxidation, 26:53563
  reactions with uranium trioxide powders, factors affecting reduction, 26:53548 (AREAEE-139)
  solubility in sodium, 26:55154 (CONF-710548-, pp 105-28)
  spectral lines in xi Per due to interstellar molecular, equivalent widths of, (E), 26:53890
  storage in metal hydrides, evaluation of, 26:53090 (BNL-16889)
  thermodynamics of mixtures of helium and, in interior of Jupiter, (T), 26:54003
  effects on crack propagation and embrittlement of aluminum--molybdenum--titanium-base--vanadium alloy, 26:53685
HYDROGEN HALIDES
  wave functions for, complex, 26:54157
HYDROGEN IONS (H^+)
  reactions with argon at moderate energies, excitation by charge-exchange channel in, (T), 26:54120
  reactions with negative ions above 25 keV, calculation of cross sections for electron capture in, using continuum distorted-wave-Born approximation, 26:54116
  reactions with rare gas atoms at 500 to 3000 eV, atomic-number dependence of charge exchange and excitation in, (E/T), 26:54122
  reactions with rare gas atoms at 500 to 3000 eV, differential cross sections for charge exchange, elastic scattering, excitation to autoionizing levels and simple excitation in, (E/T), 26:54122
  scattering by argon at low and moderate energies, partial-wave calculations for elastic, 26:54120
HYDROGEN IONS (H^-)
  binding energy of, effects of intense magnetic fields on, 26:54144
  ionization energy of, effects of intense magnetic fields on, 26:54144
  proton reactions above 25 keV with, calculation of cross sections for electron capture in, using continuum distorted-wave-Born approximation, 26:54116
HYDROGEN IONS (H_2^+)
  channeling through thin gold crystals at 1 MeV, 26:54974 (LYCEN-7228)
HYDROGEN IONS (H_3^+)
  spectra of, observability of dipole-allowed fundamental transition in infrared absorption, (T), 26:54090
HYDROGEN ISOTOPES
  determination in water using distillation column and mass spectroscopy, 26:52913(T) (AEC-tr-7345)
  effects of, theory of kinetic, 26:52959
HYDROGEN PEROXIDES
  effects on depolarization of negative muons in aqueous solutions and water, (E), 26:54099
HYDROGEN SULFIDES
  radiolysis of gaseous, effects of argon, krypton, nitrogen, and xenon on yields from γ, 26:53011
HYDROGEN SYSTEMS
  H--Sc, properties of, structural and thermodynamic, 26:53556 (SC-CR-723158)
HYDROLASES
  radiation effects on activity of alkaline phosphatase in mice, strontium-90 β and x, 26:53496

radiation effects on L-arginine aminohydrolase activity in liver of rats, dose dependence of, 26:53491

HYDROLOGY
radioisotope uses in, in Latin America, 26:53168

HYDROMAGNETIC WAVES
cosmic-ray pitch-angle scattering by, (T), 26:53863
emission of type Pc-1 micropulsations in plane of Earth's surface, polarization studies of, (E), 26:54021
propagation in incompressible beam--plasma systems, theory for, 26:54857

HYDROXYL (HO)
argon-atom reactions with, calculation of cross sections and rate constants for vibration--rotation energy transfer in, using distorted-wave and sudden approximations, 26:54126
energy levels of, reduced eigenvalues for l = 50 resonance states, 26:54124
parametric down-conversion in astrophysical masers, (T), 26:53909
reactions in radiolysis of aqueous solutions of indole-3-acetic acid and other plant hormones, 26:53015

HYPERNUCLEI
decay of Λ-He^4 and Λ-H^4, model with direct transition of Λ into n for probabilities of nonmesic, (T), 26:54293
energy levels of, shell-model calculations of spin--parity assignments and wave functions for, (T), 26:54351
hyperon (Λ) binding energies in p-shell, shell-model analysis of, (T), 26:54351

HYPERONS
decay of, current-algebra approach to octet dominance in nonleptonic, (T), 26:54286 (DNPL/P-130)

HYPERONS (Λ)
binding energies in p-shell hypernuclei, shell-model analysis of, (T), 26:54351
polarization in $\pi^- + p \to \Lambda + K^0$ interactions at 4.5 and 6 GeV/c, (E), 26:54217
production in $\pi + N \to \pi + \Sigma(\Lambda)$ interactions near threshold, cross sections and polarization phenomena from PCAC theory, (T), 26:54335

HYPERONS (Σ)
production in $\pi + N \to \pi + \Sigma(\Lambda)$ interactions near threshold, cross sections and polarization phenomena from PCAC theory, (T), 26:54335

HYPERONS (Σ^-)
decay $\Sigma^- \to p + \mu^- + e^-$, test of lepton number assignments from, (T), 26:54296
mass difference ($^1/_2$ ($\Sigma^+ + \Sigma^-$) $-$ Σ^0), deep inelastic contribution to electromagnetic, (T), 26:54257
mass difference ($\Sigma^- - \Sigma^+$), deep inelastic contribution to electromagnetic, (T), 26:54257

HYPERONS (Σ^0)
mass difference ($^1/_2$ ($\Sigma^+ + \Sigma^-$) $-$ Σ^0), deep inelastic contribution to electromagnetic, (T), 26:54257

HYPERONS (Σ^+)
decay $\Sigma^+ \to p + \gamma$ in pole model, asymmetry parameter and rate of, (T), 26:54292
mass difference ($^1/_2$ ($\Sigma^+ + \Sigma^-$) $-$ Σ^0), deep inelastic contribution to electromagnetic, (T), 26:54257
mass difference ($\Sigma^- - \Sigma^+$), deep inelastic contribution to electromagnetic, (T), 26:54257

HYPERONS (Ξ^-)
decay $\Xi^- \to \Lambda + \pi^-$ in heavy-liquid bubble chamber, Ξ^- lifetime, α parameters, and branching ratio for, (E), 26:54174 (RPP/H-99)
decay $\Xi^- \to \Sigma^+ + \mu^- + e^-$, test of lepton number assignments from, (T), 26:54296
lifetime of, determination from $\Xi^- \to \Lambda + \pi^-$ decay in heavy-liquid bubble chamber, (E), 26:54174 (RPP/H-99)
mass difference ($\Xi^- - \Xi^0$), deep inelastic contribution to electromagnetic, (T), 26:54257

HYPERONS (Ξ^0)
decay $\Xi^0 \to \Lambda + \pi^0$ in heavy-liquid bubble chamber, Ξ^0 lifetime, α parameters, and branching ratios for, (E), 26:54174 (RPP/H-99)
lifetime of, determination from $\Xi^0 \to \Lambda + \pi^0$ decay in heavy-liquid bubble chamber, (E), 26:54174 (RPP/H-99)
mass difference ($\Xi^- - \Xi^0$), deep inelastic contribution to electromagnetic, (T), 26:54257

I

ICE
radiolysis of crystalline, absorption spectra of trapped electrons from γ, 26:53002

IMAGE BRIGHTNESS INTENSIFIERS
development for neutron radiography using californium-252 sources, 26:53330(R) (BNWL-1308-10)
performance during fluoroscopic x ray examination, hazards to man from deficiencies in, 26:53421

IMIDES
polymers, preparation of syntactic foams of, 26:55601 (SC-DC-722297)
B--polyimide, development of composite blades of, for use in advanced composite engine, 26:53575

IMMUNE REACTIONS
effects of gamma-irradiated metacercariae of Fasciola hepatica on, of cattle, 26:53498(R) (PRNC-156)
radiation effects on, in chick embryos to adult allogeneic leukocytes, γ, 26:53477
radiation effects on, in guinea pigs, lethal dose, 26:53474
radiation effects on, in mice following transplantation of allogeneic bone marrow, lethal x, 26:53485
radiation effects on, in mice following whole-body exposure, comparison of RBE for γ and high-intensity pulsed x, 26:53469
radiation effects on, in patients during therapy, 26:53432
radioinduced suppression of, in mice, acute whole-body x, 26:53464

IN-PILE LOOPS
disassembly and inspection of Fuel Element Failure Propagation, design of facility for, 26:53727 (ANL/HFEF-1)
operation characteristics of Japan Low Temperature Fissiochemical, comparison with design parameters of, 26:55400 (JAERI-M-4630)

INCOLOY 800
coating with carbon from carbon monoxide decomposition in argon coolant at 550 to 600°C, 26:53605(R) (DP-Report-522)
fatigue at 800 to 1400°F, effects of hold-time on low-cycle, 26:53658
radiation effects on swelling and mechanical properties of, fast neutron, (E), 26:55189(R) (GEAP-10028-39)

INCONEL 600
fatigue testing of pipes of, failure rates from, 26:55175(R) (GEAP-10207-26)

INCONEL 713C
microstructure and stability of aluminum-coated, effects of heat corrosion on, 26:53676

INCONEL 718
fabrication of composite structures of, spark sintering and bonding method for, 26:53628
radiation effects on tensile properties of, at cryogenic temperatures for use in NERVA Program, fast neutron, 26:53697 (NASA-TM-X-2440, pp 603-8)

INDIA
nuclear power plant operation in, control of airborne contamination from, 26:53154 (INIS-mf-160, pp 22-52)

INDIAN POINT POWER REACTOR, UNIT 1
boron injection pumps for, requested change in testing schedule for high pressure, 26:55232 (DOCKET-50003-125)
steam stop valve for, malfunction of motor operator for main, 26:55231 (DOCKET-50003-124)

INDIAN POINT POWER REACTOR, UNIT 2
construction of, extension of completion date for permit for, 26:55281 (DOCKET-50247-81)

INDIUM
determination in lunar, meteoritic, and terrestrial materials by neutron activation following separation from other elements, 26:52906
determination in phosphate concentrates by titrimetric method following chromatographic separation from some metals, 26:52949
electron reactions up to 1 keV with, cross sections for formation of multicharged ions in, 26:54103 (FRNC-CONF-51)
neutron capture at 24.3 keV, TOF cross-section measurements using iron-filtered beam, (E), 26:54597 (CONF-720901-(Bks.1 and 2), pp 1107-14)
neutron capture near 24.3 keV, pulse height spectra and relative cross section for, (E), 26:54656(R) (COO-3058-21)
sorption on diethylaminoethylcellulose in methanol--thiocyanate--hydrochloric acid media, 26:52951
superconducting transition in, dependence of variation of dislocation electron slowing-down force on stress, temperature, and velocity in, (T), 26:54447

INDIUM ALLOYS AND SYSTEMS
Ga-base--In, superconductivity and ac susceptibility in fast frozen, (E/T), 26:54438
In--Pb, electric conductivity anisotropy of superconducting, near H/sub c3/, (E), 26:54456
In--Pb, lattice heat capacity of intermetallic InSb, at 20 to 298°K, 26:53637 (LBL-101)
In--Pb-base, superconducting transition in, dependence of variation of dislocation electron slowing-down force on stress, temperature, and velocity in, (T), 26:54447
In--Sc, magnetization and field dependence of sound velocity and thermal capacity of Sc$_3$In, low-temperature, 26:55045

INDIUM ISOTOPES In-111
use to label biological macromolecules for perturbed angular correlation studies, 26:55058

INDIUM ISOTOPES In-113
energy levels of, calculation using vibration--hole coupling, 26:54620

INDIUM ISOTOPES In-115
energy levels of, calculation using vibration--hole coupling, 26:54620

INDIUM ISOTOPES In-117
energy levels of, calculation using vibration--hole coupling, 26:54620

INDOLE
radiolysis of aqueous solutions of, rate constants for reaction of hydrogen atoms, hydroxyl radicals, and hydrated electrons in, 26:53015

INDOLE-3-PROPIONIC ACID
radiolysis of aqueous solutions of, rate constants for

reaction of hydrogen atoms, hydroxyl radicals, and hydrated electrons in, 26:53015
INDUSTRIAL MANAGEMENT
job scheduling in maintenance repair shops, effectiveness of priority rules for, 26:55640 (Y-1848)
INFECTIONS
tuberculosis, occurrence in miners in relation to exposure to radon and radon daughters in air, 26:53412
INFORMATION CENTERS
description of American Nuclear Society' Nuclear Standards, 26:54917
operation of Nuclear Safety, during May and June 1972, 26:55207(R) (ORNL-TM-3900)
INSECTA
Drosophila melanogaster (fruit fly), radiation effects on, following acute exposure of mature spermatozoa, dose dependence of genetic, x, 26:53497(R) (COO-1748-12)
Drosophila melanogaster (fruit fly), radiation effects on metabolism in bar gene mutants of, stimulatory low dose, 26:53500
Drosophila melanogaster (fruit fly), radioinduced chromosome aberrations in mature oocytes of, effects of premeiotic breakage and interchanges on types of x, 26:53501
Drosophila melanogaster (fruit fly), radioinduced chromosome aberrations in mature spermatozoa of, inhibitory effects of dactinomycin on post-fertilization maternal repair of x, 26:53502
Drosophila melanogaster (fruit fly), radioinduced dominant and recessive lethal mutations in mature spermatozoa of, effects of dactinomycin on post-fertilization expression of x, 26:53502
radiation effects on, combined effects of space flight environment on mutagenesis and survival of, γ, 26:53365 (N-72-20065)
Sitotroga cerealella (grain moth), radiosensitivity of oocytes of, effects of meiotic stage on γ, 26:53499
INSTRUMENTS
description for control of cryogenic systems, 26:55554 (LA-DC-72-855)
design and operation of radioactive non-contact encoder, 26:53286 (N-71-37956)
design of passive crack detector, engineering drawings for, 26:53317
development and research in South Africa, 1971, 26:55453(R) (NP-19410)
interfacing of CAMAC, to computers, 26:53297 (CEA-N-1549)
radiation dose to space vehicle, from radioisotope thermoelectric generators, γ and neutron, 26:53338 (NASA-TM-X-2440, pp 862-5)
radiation effects on Grand Tour spacecraft, protective design for, 26:53292 (NASA-TM-X-2440, pp 729-34)
radiation effects on spacecraft, program for studying radioisotope thermoelectric generator, 26:53294 (NASA-TM-X-2440, pp 866-72)
specification of amplitude analog signals for CAMAC, 26:53302 (EUR-5100)
standards for, procedures for developing and writing, 26:53248
INTERFEROMETERS
design for direct measurement of plasma electron densities, 26:54770
INTERNAL CONVERSION
coefficients of, description of electron spectrometer for in-beam measurement of, 26:53264
INTERSTELLAR MATERIAL
cosmic-ray interactions with, x-ray emission from, (E/T), 26:53815
light absorption by, (T), 26:53985
models for, grain, (T), 26:53989
INTESTINES
radiation effects on respiration and ultrastructure of mitochondria in epithelial cells of rat, during amino acid absorption, whole-body x, 26:53493
radioinduced fistulae and perforations in human, following therapy of gastric sarcomas or rectal and uterine neoplasms, surgical treatment of, 26:53438
INVARIANCE PRINCIPLES
charge conjugation, statistical model for conservation of, 26:54360
CP violation in anti K^0 and $K^0 \rightarrow \pi^+ + \pi^-$ time decay distributions, (E), 26:54362 (COO-1195-244)
CP violation in anti K^0 and $K^0 \rightarrow \pi^+ + \pi^-$ time decay rates, (E), 26:54361 (COO-1195-242)
CP violation in $K^0 \rightarrow \mu^+ + \mu^-$ decays, lower bound on, (T), 26:54369
CP violation in $K^0 \rightarrow \pi^+ + \pi^- + \pi^0$ decay, (E), 26:54188
CP-violating gauge interactions, Lagrangian for, 26:54367
G-parity, statistical model for conservation of, 26:54360
gauge invariance in relativistic quantum field theory, (T), 26:54387
parity, statistical model for conservation of, 26:54360
scale invariance breaking for low-energy theorems of $\pi\pi$ interactions, contribution of epsilon and S*(980) to, (T), 26:54319
time reversal noninvariant terms in electron elastic scattering by nuclei, (T), 26:54363 (IS-T-536)
time reversed operator for unstable particles, definition for decays in media without intrinsic T violation, (T), 26:54366
IODINE
desorption from iron oxide (Fe_3O_4), effects of steam on, (E), 26:55207(R) (ORNL-TM-3900)
determination in meteoritic and terrestrial materials by neutron activation following separation from other elements, 26:52906
determination in water samples by spark-source mass spectroscopy, 26:52914 (ANL-7860(Pt.3), pp 55-63)
metabolism in dogs, effects of iodine intake on kinetics of, 26:55518(R) (COO-3173-10)
radiation effects on sorption on activated carbon, 26:53061 (DP-MS-72-14)
reactions of gaseous, with iron oxide (Fe_3O_4), kinetics of surface, 26:52953 (CONF-720716-1)
retention on charcoal beds under accident and post-accident conditions, 26:53058 (CONF-720823-10)
separation from fuel reprocessing off-gases, evaluation of silver-containing sorbents for, 26:53077 (CONF-720823-9)
separation from xenon by liquid nitrogen cooling and distillation, 26:53068
separation of fission product, from off-gases in reprocessing of LMFBR fuel, pp. 21-2, 26:53082 (ORNL-4794, pp 15-25)
solubility in liquid carbon dioxide, pp. 29-31, 26:53083 (ORNL-4794, pp 26-32)
solubility in liquid sodium, tracer studies on, 26:52895 (CONF-710959-, Paper 18)
sorption on commercial impregnated charcoals, efficiencies of, 26:53058 (CONF-720823-10)
transport and retention in reactor cooling systems, effects of reactions with iron oxides on, 26:52953 (CONF-720716-1)
IODINE ISOTOPES
removal from emergency reactor off-gas systems, efficiency of filters for, 26:55146
IODINE ISOTOPES I-125
activity of, evaluation of various methods of counting, 26:53056 (AREAEE-129)
incorporation in iodoquine, 26:53029(P)
production by neutron reactions with xenon in reactor loop, 26:53068
production by proton reactions with tellurium-125, 26:53056 (AREAEE-129)
purification of, 26:53056 (AREAEE-129)
IODINE ISOTOPES I-127
photon reactions (γ,xn) with, model analysis of giant dipole resonance in, (E/T), 26:54598 (FRNC-TH-242)
IODINE ISOTOPES I-131
content in atmosphere, rainwater, and Savannah River in vicinity of Savannah River Plant, 1971, 26:53153(R) (DPSPU-72-30-1)
content in Norwegian milk during 1956 to 1970, 26:53161
content of human milk following injection of labeled pharmaceuticals for diagnostic scanning of kidneys, lungs, and placenta, 26:53524
effects on growth of goitrogen-stimulated thyroid gland in mice following intraperitoneal injection in comparison to effects of x rays, effects of dose rate on inhibitory, 26:53472
effects on growth of thyroid gland in fetal and goitrogen-stimulated adult mice following intravenous injection, 26:53513
exchange between solid silver iodide and iodine in p-cymene solution, effects of temperature on, 26:52974
incorporation in iodoquine, 26:53029(P)
production from neutron-irradiated telluric acid, wet distillation method for, 26:53070
radiation dose to fingers of medical personnel during injection of, phantom studies of, 26:53424
scanning in heart for measurement of systolic blood volume, 26:53543
uptake by children from milk, age dependence of, 26:53506(T) (ORNL-tr-2629)
uptake by hair following intravenous injection in rats, correlation with body burden and, 26:53529 (NASA-TM-X-2440, pp 982-8)
uptake by thyroid gland in birds following parenteral injection, dose-response relations following, 26:53515
use as tracer for measuring leakage through dam near Baguio City, Philippines, 26:53175
IODINE ISOTOPES I-132
effects on growth of goitrogen-stimulated thyroid gland in mice following intraperitoneal injection in comparison to effects of x rays, effects of dose rate on inhibitory, 26:53472
IODINE ISOTOPES I-136
yield of 44- and 83-sec, from thermal fission of uranium-235, (E), 26:54626
IODINE ISOTOPES I-137
beta decay of, prediction of β endpoint energy using Way-Wood diagram, 26:54601 (IS-T-534)
IODINE ISOTOPES I-140
beta decay of, prediction of β endpoint energy using Way-Wood diagram, 26:54601 (IS-T-534)
IODOQUINE
preparation of iodine-125- and iodine-131-labeled, 26:53029(P)

ION BEAMS
  heating of plasma ions by, possibility of collisionless, (E/T), 26:54767
  injection into deuterium--tritium magnetic mirror devices, (T), 26:54757
  interactions with plasma, longwave surface-wave instabilities from, (T), 26:54816
ION EXCHANGE
  development for chromatography, review on, 26:52948
  uses of, review on, 26:52948
ION EXCHANGE MATERIALS
  analysis for beta activities retained in, design and performance of Geiger--Mueller counter for, 26:53212
  radiation effects on degradation and crosslinking in Zerolit 225, γ, 26:53016
  separation of materials from spent, method for, 26:53072(P)
  sorptive properties of silver zeolite, for iodine and methyl iodide, 26:53077 (CONF-720823-9)
ION SOURCES
  description of heavy, with confined electron beam, 26:53753 (FRNC-CONF-56)
  design and performance of duoplasmatrons for production of multicharged ions, 26:54079 (FRNC-CONF-53)
  development using laser beam impact on metallic target, (E), 26:54801 (CEA-CONF-2049)
  focusing system for MEBIS, 26:54081 (FRNC-CONF-57)
  performance of MEBIS, 26:54081 (FRNC-CONF-57)
  performance of PIG, for production of Ca, Ge, Kr, and Zn ions, 26:53752 (FRNC-CONF-54)
  performance of PIG, spectroscopic analysis of, 26:54082 (FRNC-CONF-58)
  performance of, with confined electron beams, review of, 26:54080 (FRNC-CONF-55)
  vacuum lock for mass spectrometer, design of, 26:53318
IONOSPHERE
  D region, collision frequency and electron-density distribution measurements with differential absorption and differential-phase partial-reflection experiments, (E/T), 26:54032
  D region, electron density and collision frequency in, simultaneous measurements by partial reflection of, (E), 26:54028
  E region, characteristics of, over Dushanbe during 1964, (E), 26:54017
  E region, correlation of electron density with height of Sun, calculations at Duschanbe, 1964, (E/T), 26:54016
  E region, instability in, induced by internal atmospheric gravity-wave propagation in E region, (T), 26:54018
  electromagnetic-wave propagation in homogeneous, nonlinear theory of monochromatic circularly polarized ulf and vlf, (T), 26:54050
  electron energy transfer rates to neutral gases in, calculations of, (T), 26:54022
  electron-intensity fluctuations observed on Feb. 14, 1970 in, possible correlation with barium-cloud releases, (E), 26:54039
  F region, far-uv airglow intensity at 1304 and 1356 A from atomic oxygen in, theoretical time-dependent behavior of tropical, 26:54031
  F region, ion distribution in, one-dimensional nonisothermal admixture of, (T), 26:54026
  F region, wavenumber spectrum for sizes 4 to 0.6 km in, deduced from ionospheric scintillation observations of Cygnus A, power-law, (E/T), 26:54029
  F2 layer, average behavior of total electron content, peak density, and slab thickness in, during geomagnetic storms, (E), 26:54040
  plasma diagnostics in, cylindrical probe analysis for, (E/T), 26:54011 (ONERA-Publ.-137)
  scintillation observations from Cygnus A, F-region power-law wavenumber spectrum deduced from, (E/T), 26:54029
  solar-wind torque on, calculations of upper limit, (T), 26:54075
  sporadic E, velocities and heights of nighttime association with atmospheric-gravity-wave-induced instability in ionospheric E region, (T), 26:54018
  wave generation in electrojet region of, potential transverse-current-produced, (T), 26:54027
  whistler propagation in, refractive index and attenuation surfaces in vicinity of cross-over level, (T), 26:54015
IONS
  channeling and blocking in single crystals, experimental apparatus for, 26:54977
  channeling of, design of two-axis goniometer with sample temperature control for study of, 26:53322
  channeling of, flux peaking effect in, (T), 26:55007
  detection of stripped, at electron cyclotron resonance, x-ray-spectroscopy unit for, 26:54078 (CEA-CONF-2050)
  dosimetry of heavy, based on particle tracks in silver halide single crystals, 26:53230 (NASA-TM-X-2440, pp 138-41)
  effects on small solid grains, collision processes in heating, (T), 26:54874 (EUR-CEA-FC-647)
  effects on solids, computer program for damage profile of, 26:54969 (AECL-4130)
  effects on swelling of metals, dose and dose rate dependences of, (T), 26:53707
  emission by semiconductors for determination of impurity profiles, secondary, 26:52937
  energy of degenerate levels of, with two perturbations, double perturbation form for second-order, 26:54152
  implantation damage in gallium arsenide, channeling study of, 26:54993
  implantation facility at Orsay, France, 26:54976
  implantation in silicon, electron microscopic observation of surface and depth distribution of damage produced in, 26:55003
  implantation layers in silicon, computer calculations of sheet resistance of, 26:54986
  implantation of, design of two-axis goniometer with sample temperature control for study of, 26:53322
  production of multicharged, research program on duoplasmatrons and magnetrons for use in, 26:54079 (FRNC-CONF-53)
  proton reactions above 25 keV with negative, calculation of cross sections for electron capture in, using continuum distorted-wave-Born approximation, 26:54116
  reactions between very heavy, effective potentials for superheavy molecules formed in, (T), 26:54111
  reactions with atoms of negative, calculation of ejection probability and energy distribution of electrons from, using sudden-switching approximation, 26:54112
  reactions with atoms, ions, and molecules, bibliography and compilation of data on charge exchange, dissociations, excitation, and ionization, in, 26:54118
  scattering by nuclei above Coulomb barrier, coupled-channel analysis of heavy, (T), 26:54736
  scattering by nuclei, analysis of absorptive potentials for elastic heavy, (T), 26:54678 (COO-535-672)
  stopping of heavy, large-depth decrease of range and deposited-energy distributions in, (T), 26:54899
IRIDIUM
  determination in minerals by neutron activation and γ spectroscopy, nondestructive, 26:52901 (UJV-2851-F,Ch)
IRIDIUM ISOTOPES Ir-186
  beta and electron-capture decay of, γ singles and coincidence spectra from, (E), 26:54633 (COO-3255-3)
IRIDIUM ISOTOPES Ir-192
  implantation of wires of, for interstitial therapy, effects of arrangement, number, and size of implants on radiation dose distribution in surrounding tissues, 26:53422
IRON
  abundance in 120 evolved stars, (E), 26:53898
  abundance in 21 sharp-lined nonvariable cool peculiar A stars, (E), 26:53882
  abundance in solar corona, (E), 26:53957
  cascades in iron due to 30- to 300-GeV/N cosmic, (E), 26:53832
  content in rock, γ--γ selective method for determination of equivalence between other heavy element and, 26:52943
  determination in geochemical standards by atomic absorption using nitrous oxide--acetylene flame, 26:52921
  determination in minerals by direct measurement of oxide ratios, spectroscopic, 26:52932
  determination in water, effects of large amounts of copper on spectrographic, 26:52927
  distribution in cores from Green Bay, relations with depth, 26:53164 (ANL-7860(Pt.3), pp 64-76)
  mixing of powders of, effects of friction on, 26:53617
  neutron capture by, comparison of ENDF/B III and published data for thermal, 26:54501 (ORNL-TM-3910)
  neutron cross-section sensitivity analysis for sodium/iron shielding, 26:54940 (CONF-720901-(Bks.1 and 2), pp 512-23)
  neutron distributions behind Fe/plastic/Fe barriers, spatial, angular, and energy, 26:54966
  neutron reactions at 0.8 to 20 MeV, data tabulation on γ production cross sections for, 26:54569 (ORNL-4798)
  neutron reactions at energies up to 16 MeV, cross sections for gamma-ray production in, (E), 26:54960 (NASA-TM-X-2440, pp 500-11)
  neutron reactions up to 20 MeV, γ production cross sections for, (E), 26:54523 (CONF-720901-(Bks.1 and 2), pp 325-34)
  neutron total cross section at 10 to 1000 keV, (E), 26:54566 (CONF-720901-(Bks.1 and 2), pp 1075-86)
  neutron total cross section at 22 to 25 keV, R-matrix fit to, 26:54656(R) (COO-3058-21)
  neutron transport in sodium/iron shield, effect of cross section sensitivity on 300-keV to thermal-range, (T), 26:54943 (CONF-720901-6)
  neutron transport in, analysis of mechanism in fast, 26:54473 (CONF-720901-(Bks.1 and 2), pp 335-48)
  oxygen ion reactions at 30 MeV, Kα x-ray spectra from, (E), 26:54467(R) (ORO-2972-204)
  photon scattering at 2.0 to 10.5 MeV, dose albedos of back-angle, (E), 26:54892
  radiation effects on lower yield strength of, relations of spectra with neutron, 26:53705
  radiation effects on strengthening of, effects of carbon, copper, nickel, phosphorus, and vanadium additions on neutron, 26:53710
  radiation effects on surface microtopography of, argon-ion, 26:55008
  separation from cobalt and manganese by solvent extraction using Aliquat-336, 26:53076
  separation from indium by ion exchange chromatography,

- 26:52949
- separation from uranium by fractional dissolution of crude sodium diuranate, 26:52976 (IEA-250)
- spectral lines in Vega due to, (E), 26:53887

IRON ALLOYS AND SYSTEMS
- Al_2O_3--Fe, cohesion and structural stability of composites of, effects of chromium, cobalt, manganese, molybdenum, nickel, and titanium additions on, 26:53589
- C--Fe-base, radiation damage in, electric resistivity study of 4.5°K fast-neutron, 26:54989
- Cr--Cu--Fe--Mo--Ni-base--Ti, corrosion by thorium dioxide dissolvent solutions, 26:53604 (BNWL-CC-449)
- Cr--Fe-base, radiation effects on mechanical properties of, 2.3-MeV electron, 26:53706
- Cr--Fe-base, radiation effects on strengthening of welds of, effects of carbon, copper, nickel, and vanadium additions on neutron, 26:53710
- Cu-base--Fe, surface resistance of, Kondo anomaly in far-infrared, 26:55508 (COO-3151-4)
- Fe--transition metal carbides, erosion resistance of anodes of, 26:53568
- Fe-base--Mo, radiation effects on mechanical properties of, 2.3-MeV electron, 26:53706
- Fe-base--N, radiation damage in, electric resistivity study of 4.5°K fast-neutron, 26:54989

IRON CHLORIDES $FeCl_2$
- magnetic phase transition at 2 kbar, study using frequency shift of far-infrared-active antiferromagnetic resonance mode, 26:55509 (COO-3151-5)

IRON ISOTOPES Fe-53
- energy levels from neutron pickup reactions, spectroscopic factors and spins for, (T), 26:54576

IRON ISOTOPES Fe-54
- deuteron reactions (d,pγ) at 3 MeV, γ-ray angular correlations for, (E), 26:54578
- energy level at 1.409 MeV from Coulomb excitation, g factor for, (E), 26:54581
- energy levels of, shell-model study of, (T), 26:54570
- neutron reactions at 0.8 to 20 MeV, data tabulation on γ production cross sections for, 26:54569 (ORNL-4798)
- neutron total cross section at 10 to 1000 keV, (E), 26:54566 (CONF-720901-(Bks.1 and 2), pp 1075-86)
- oxygen-16 reactions (O-16,C-12) at 46 MeV, analysis for reaction mechanism in, (E), 26:54579

IRON ISOTOPES Fe-55
- energy level at 3788 keV from iron-54 (d,pγ) reactions, spin assignment for, (E), 26:54578
- energy levels from iron-57 (p,t) reactions, spin--parity assignments for, (E), 26:54584

IRON ISOTOPES Fe-56
- alpha elastic scattering at 166 MeV, angular distribution for, (E), 26:54547
- deuteron elastic scattering at 10 MeV, angular distributions and optical model parameters for, (E), 26:54592
- energy levels of, shell-model study of, (T), 26:54570
- helium-3 elastic scattering at 53.4 MeV, differential cross sections and optical-model parameters for, (E), 26:54571
- neutron radius of, determination from α elastic scattering, (E), 26:54547

IRON ISOTOPES Fe-57
- charge states in solid xenon following cobalt-57 decay, Moessbauer effect study of, 26:55057
- deuteron reactions (d,α) at 16 MeV, angular distributions for, (E), 26:54584
- Moessbauer effect in transition-metal borides, 26:55055 (IS-T-529)
- Moessbauer effect measurements on, in nickel host near Curie point, 26:55572 (NYO-3823-12)
- neutron total cross section at 10 to 1000 keV, (E), 26:54566 (CONF-720901-(Bks.1 and 2), pp 1075-86)
- proton reactions (p,He-3) and (p,t) at 27 MeV, angular distributions for, (E), 26:54584
- triton elastic scattering at 12 MeV, angular distribution and optical model parameters for, (E), 26:54592
- triton reactions (t,p) at 12 MeV, angular distributions for, (E), 26:54592

IRON ISOTOPES Fe-58
- deuteron elastic scattering at 10 MeV, angular distributions and optical model parameters for, (E), 26:54592
- deuteron reactions (d,p) at 10 MeV, angular distributions for, (E), 26:54592

IRON ISOTOPES Fe-59
- diffusion in α-zirconium, mechanism of, 26:53666
- energy levels from (t,p) and (d,p) reactions, spin-parity assignments and spectroscopic factors for, (E), 26:54592
- production of carrier-free, from neutron-irradiated cobalt by solvent extraction using Aliquat-336, 26:53076
- radiation dose to fingers of medical personnel during injection of, phantom studies of, 26:53424
- use as tracer in biological materials together with chromium-51, computerized data processing system for, 26:53544

IRON OXIDES Fe_3O_4
- iodine desorption from, effects of steam on, (E), 26:55207(R) (ORNL-TM-3900)
- reactions with gaseous iodine, kinetics of surface, 26:52953 (CONF-720716-1)

IRRADIATION FACILITIES
- construction and calibration of standard thermal neutron flux, 26:53118
- design for testing space vehicle components and subsystems, 26:53695 (NASA-TM-X-2440, pp 570-6)
- dose distribution in gamma, at the Isotopes Institute, Budapest, 26:53340
- performance of californium-252 neutron source activation, at Savannah River Laboratory, 26:53109 (DP-MS-72-37)

ISOCYANIC ACID
- tert-butyl ester, radiolysis of crystals of, ESR studies on, 26:52991 (ORO-2968-78, Paper 6)

ISOLEUCINE
- radiolysis of frozen aqueous solutions of, ESR study of free radicals from γ, 26:52995

ISOPENTYLAMINE
- toxicology of, bibliography on, 26:55584 (ORNL-TIP/TIRC-72-61)

ISOTHIOCYANIC ACID
- tert-butyl ester, radiolysis of crystals of, ESR studies on, 26:52991 (ORO-2968-78, Paper 6)

ISOTOPE EFFECTS
- theory of kinetic hydrogen, 26:52959

ISOTOPE SEPARATION METHODS
- performance of rotating plasma, 26:53327 (JEN-244)

ISOTOPES
- determination of natural abundance of, accuracy of, 26:52916 (EUR-4765, pp 41-75)

ITALY
- applications of radiation in agriculture research in, 26:53459(R) (NP-19403)

J

JAMES A. FITZPATRICK POWER REACTOR
- owners of, financial data on, 26:55259 (DOCKET-50333-53)

JAPAN
- electric power production in, review on, 26:55092
- legislation regarding nuclear liability in, revision of, 26:55459
- nuclear energy industry in, requirements of, 26:55094
- nuclear industry in, status of development of, 26:55089
- radiation protection legislation in, during 1970, enforcement of, 26:55458
- uses of radiation sources and radioisotopes in medicine, industry, and research in, during 1970, status of, 26:55458

JAPANESE EXPERIMENTAL FAST REACTOR
- experimental facilities in, conceptual design of, 26:55405(T) (JAPFNR-43)
- steam generators for, development of, 26:55155 (CONF-710548-, pp 129-54)
- steam generators for, use of hydrogen detector for detection of small leaks in, 26:55156 (CONF-710548-, pp 155-70)

JAPANESE POWER DEMONSTRATION REACTOR
- fuel element burnup in, FLARE and TERA code calculations of, 26:55264 (JAERI-Memo-4083)

JAPANESE POWER DEMONSTRATION REACTOR II
- control rods for, use of VISTA method for development of, 26:55137 (JAERI-Memo-3893)
- pressure vessel for, cyclic pressure loading of model, 26:55228 (JAERI-Memo-4016)

JINR SYNCHROTRON
- beam extraction by 2/3 nonlinear resonance, (T), 26:53754 (JINR-E9-6538)

JUPITER (PLANET)
- deuterium in atmosphere of, (E), 26:54007
- hydrogen--helium mixtures in interior of, statistical mechanics of, (T), 26:54003
- magnetosphere of, fluxes of trapped electrons and protons in, (E/T), 26:54006
- radiation belt effects on spacecraft, calculations of, 26:54002 (NASA-TM-X-2440, pp 781-4)
- radiation belt of, models of electron and proton fluxes in, 26:54001 (NASA-TM-X-2440, pp 556-60)
- radio emission from, effects of Io on, (T), 26:54004

K

KEWAUNEE POWER REACTOR
- containment system for, revised information on, 26:55309 (DOCKET-50305-48)
- electrical systems for, revised information on, 26:55309 (DOCKET-50305-48)
- engineered safeguards for, revised information on, 26:55309 (DOCKET-50305-48)
- instrumentation for, revised information on, 26:55309 (DOCKET-50305-48)
- protection systems for, revised information on, 26:55309 (DOCKET-50305-48)
- radioactive waste disposal systems for, revised information on, 26:55309 (DOCKET-50305-48)
- safety analysis for, revised information on, 26:55309 (DOCKET-50305-48)
- safety analysis report for, errata sheets for, 26:55311

(DOCKET-50305-51)
- valves for, verification of wall thicknesses for nuclear service, 26:55310 (DOCKET-50305-49)

KIDNEYS
- arsenic-74 uptake and retention by, of mice, rabbits, and rats following oral administration, time dependence of, 26:53538
- radioinduced carcinomas of, in parabiosed rats, whole-body x, 26:53449 (COO-3017-4)
- scintiscanning of human, for diagnosis of neoplasms, use of gamma camera in, 26:53214
- uptake of organic bases by rat, effects of uranyl nitrate on, 26:53537

KRYPTON
- effects on yields from γ radiolysis of gaseous hydrogen sulfide, 26:53011
- electron reactions with, Auger and direct ionization processes in, 26:54103 (FRNC-CONF-51)
- helium-atom and -ion reactions at 100 to 5000 eV with, angular and energy distributions of electrons from ionization and autoionization in, (E), 26:54141
- plasma of, continuum spectra of shock-heated, (E), 26:54777 (BMBW-FBK-72-8)
- proton reactions at 500 to 3000 eV with, differential cross sections for charge exchange, elastic scattering, excitation to autoionizing levels, and simple excitation in, (E/T), 26:54122
- separation from off-gases from HTGR fuel reprocessing, 26:53059 (CONF-720823-12)
- separation of fission product, from combustion off-gases by scrubbing with liquid carbon dioxide, 26:53064(T) (ORNL-tr-2621)
- solubility in liquid carbon dioxide, pp. 29-31, 26:53083 (ORNL-4794, pp 26-32)
- solubility in liquid carbon dioxide, tracer studies on, 26:53059 (CONF-720823-12)

KRYPTON IONS
- channeling of, use to study ion implantation damage in gallium arsenide, 26:54993
- production in PIG source, 26:53752 (FRNC-CONF-54)

KRYPTON ISOTOPES
- abundance in Mokoia and Allende chondrites, (E), 26:53810
- radiation dose to human body and lungs following ingestion, inhalation, or immersion in cloud of, methods for estimation of, 26:53510
- yields in uranium-235 thermal neutron fission, (E), 26:54667

KRYPTON ISOTOPES Kr-85
- content in atmosphere in vicinity of Savannah River Plant, 1971, 26:53153(R) (DPSPU-72-30-1)
- content in natural gas stored in underground nuclear cavities, 26:53132(T) (UCRL-Trans-10617-2)
- release in head-end reprocessing of HTGR-type graphite fuel, 26:53078 (CONF-720823-11)

KRYPTON ISOTOPES Kr-86
- proton elastic and inelastic scattering at 4.8 to 10.1 MeV, excitation functions for, (E), 26:54467(R) (ORO-2972-204)

KRYPTON ISOTOPES Kr-87
- energy levels of, calculation of wave functions and binding energies using weak coupling model, (T), 26:54467(R) (ORO-2972-204)
- half-life of, (E), 26:54667

KRYPTON ISOTOPES Kr-88
- content in atmosphere in vicinity of Savannah River Plant, 1971, 26:53153(R) (DPSPU-72-30-1)
- half-life of, (E), 26:54667

KRYPTON ISOTOPES Kr-89
- half-life of, (E), 26:54667

L

LA CROSSE BOILING-WATER REACTOR
- valves for, verification of wall thicknesses for nuclear service, 26:55350 (DOCKET-50409-13)

LA SALLE COUNTY POWER REACTOR, UNIT 1
- valves for, verification of wall thicknesses for nuclear service, 26:55341 (DOCKET-50373-27)

LA SALLE COUNTY POWER REACTOR, UNIT 2
- valves for, verification of wall thicknesses for nuclear service, 26:55341 (DOCKET-50373-27)

LAKE MICHIGAN
- ecology of, effects of thermal effluents on, 26:53184 (ANL-7860(Pt.3), pp 109-17)
- nutrient enrichment and eutrophication of, 26:55499(R) (COO-2003-17)
- radioisotope content of fish in, 26:53169 (ANL-7860(Pt.3), pp 141-50)
- surface energy budget measurements over, 26:53189 (ANL-7860(Pt.3), pp 270-98)
- trace element content in sediments and core samples from Green Bay area of, 26:53164 (ANL-7860(Pt.3), pp 64-76)

LAKES
- heated effluent and radioisotope effects on Cayuga, predictions of, 26:53192

LAMINATES
- electron reactions with single layers and, radiation from 0.25- to 3.7-GeV, (T), 26:54907
- gamma-ray energy deposition in, computer code for dosage and attenuated dosage in, 26:54959 (NASA-TM-X-2440, pp 387-91)

LANTHANUM
- deposition by pack cementation on chromium-base alloys for nitridation protection in air, effects on chromium, hafnium, and yttrium additions on, 26:53689
- distribution in cores from Green Bay, relations with depth, 26:53164 (ANL-7860(Pt.3), pp 64-76)
- electron band structure of, photoelectron spectral study of core level binding energies, 26:55024
- energy-level transitions and 4d binding energy of, relation between 4d → 4f, 26:54095
- solubility in bismuth--thorium solutions, free energies of formation for compounds produced by, 26:53664

LANTHANUM ALLOYS AND SYSTEMS
- La--Ru, thermal capacity of $LaRu_2$ at 1.3 to 20°K, 26:55047

LANTHANUM BORIDES
- preparation and thermoemission properties of, 26:53582
- BaB_6--LaB_6, preparation, sintering, and thermoemission properties of, 26:53582

LANTHANUM HYDRIDES
- preparation and characterization of, p. 41, 26:53066 (ORNL-4794, pp 36-44)

LANTHANUM ISOTOPES
- proton decay of light, search for, (E), 26:54608(T) (UCRL-Trans-1473)

LANTHANUM ISOTOPES La-131
- beta and electron-capture decay of, conversion-electron and gamma spectra from, (E), 26:54643

LANTHANUM ISOTOPES La-132
- beta and electron-capture decay of isomeric, conversion-electron spectra from, (E), 26:54643
- energy-level transitions from decay of isomeric, multipolarities for, (E), 26:54643
- isomeric transitions in, conversion-electron spectra from, (E), 26:54643

LANTHANUM ISOTOPES La-139
- nuclear magnetic resonance in lanthanum-diluted GdZn, 26:55059
- photon reactions (γ,xn) at 8 to 24 MeV, cross sections for, (E), 26:54629
- photon reactions (γ,xn) with, model analysis of giant dipole resonance in, (E/T), 26:54598 (FRNC-TH-242)

LANTHANUM ISOTOPES La-140
- content in Savannah River, 1971, 26:53153(R) (DPSPU-72-30-1)

LANTHANUM ISOTOPES La-141
- half-life of, (E), 26:54667

LANTHANUM ISOTOPES La-142
- half-life of, (E), 26:54667

LANTHANUM ISOTOPES La-143
- half-life of, (E), 26:54667

LANTHANUM ISOTOPES La-144
- beta decay of, prediction of β endpoint energy using Way--Wood diagram, 26:54601 (IS-T-534)

LANTHANUM OXIDES
- spectra and structure of, vibrational, 26:55031
- vaporization at 1927°C, measurement of isothermal, 26:53549 (EUR-4765, pp 343-63)

LASER RADIATION
- emission in electron beam motion through crystal, laser modulation in Schwarz--Hora effect for upper limit for, 26:54245 (IS-T-531)
- interaction with plasma, kinetic processes in high temperature, (T), 26:54799
- interactions with discharge plasmas, transmission in, (E), 26:54785
- interactions with plasma, electron density determination from refraction of, 26:54769
- pulse duration and intensity of, different order photoelectric effects method for measuring mode-locked ultrashort, 26:55544 (KFKI-72-41)
- reactions with deuterated polyethylene, plasma production from nanosecond and picosecond, 26:54804
- reactions with metallic targets, analysis of heavy ions from, (E), 26:54801 (CEA-CONF-2049)
- reactions with solid deuterium--tritium targets, fusion reactions from, 26:54830
- reactions with solid targets, ion energies from, (E/T), 26:54802
- reactions with solid targets, self-igniting pulsed optical discharges from, (E), 26:54803
- scattering by plasma, induced Compton effect in, (T), 26:54798

LASERS
- feasibility of gamma, based on long-lived Moessbauer isomers, (T), 26:55062
- modulation effects in Schwarz--Hora effect for light production and upper limit for laser emission in electron beam motion through crystal, (T), 26:54245 (IS-T-531)
- spectrum of pulsed discharge-initiated hf hydrogen fluoride, 26:55526 (IPP-IV-31)
- use to heat superdense plasma, (T), 26:54764
- use with magnetic field to heat plasma, (T), 26:54760
- uses in spectrochemical analysis, 26:55590(T) (ORNL-tr-2613-A)
- uses of solid-state, in spectral analysis, 26:55589(T) (ORNL-tr-2603)

LEAD
- alpha elastic scattering near the Coulomb barrier,

incoming wave boundary condition for, (T), 26:54705
content in rock, γ--γ selective method for determination of equivalence between other heavy element and, 26:52943
determination in water samples by spark-source mass spectroscopy, 26:52914 (ANL-7860(Pt.3), pp 55-63)
determination in water, effects of large amounts of copper on spectrographic, 26:52927
diffusion in mercury at 25°C, 26:53636 (IS-T-554)
meson (π^+ and π^-) reactions at 0.7 to 2 GeV/c, model analysis of, (E/T), 26:54529 (RPP/NS-8)
neutron capture by, comparison of ENDF/B III and published data for thermal, 26:54501 (ORNL-TM-3910)
photon reactions (γ,n) at 12 to 23 MeV, neutron spectra from, (E), 26:54563
photon scattering at 2.0 to 10.5 MeV, dose albedos of back-angle, (E), 26:54892
separation from indium by ion exchange chromatography, 26:52949
spectra of monovalent, from x radiolysis of lead acetate monocrystals and powders, ESR, 26:53008
superconducting transition in, dependence of variation of dislocation electron slowing-down force on stress, temperature, and velocity in, (T), 26:54447
superconductivity of single crystals, anisotropy of surface, (E), 26:54440
x-ray attenuation by, 50- to 300-kVp broad-beam, (E), 26:54904

LEAD ACETATES
radiolysis of monocrystals and powders of, ESR studies on Pb$^+$ and PbH^{2+} from x, 26:53008

LEAD ALLOYS AND SYSTEMS
In--Pb, electric conductivity anisotropy of superconducting, near H/sub c3/, (E), 26:54456
In--Pb, lattice heat capacity of intermetallic InSb, at 20 to 298°K, 26:53637 (LBL-101)
In--Pb-base, superconducting transition in, dependence of variation of dislocation electron slowing-down force on stress, temperature, and velocity in, (T), 26:54447

LEAD HYDRIDES
spectra of PbH^{2+}, from x radiolysis of lead acetate monocrystals and powders, ESR, 26:53008

LEAD ISOTOPES
photon reactions (γ,3π) with, test of low-energy theorem for $\gamma + \gamma \to \pi + \pi + \pi$ interactions from, (T), 26:54252

LEAD ISOTOPES Pb-204
energy-level transition from thallium-205 (p,2n) reactions, branching ratio for cross-over, (E), 26:54647

LEAD ISOTOPES Pb-208
alpha elastic scattering at 166 MeV, angular distribution for, (E), 26:54547
carbon-12 reactions (C-12,xn) at 60 to 90 MeV, excitation functions for, (E), 26:54651
electron inelastic scattering at 124 and 167 MeV, differential cross sections for, (E), 26:54649
energy levels from electron inelastic scattering, transition probabilities for, (E), 26:54649
energy-level transitions of muonic atoms of, corrections to long-wavelength approximation for electric multipole, 26:54098
meson (π) reactions at 100 to 260 MeV, Coulomb flux corrections to total cross sections for, (T), 26:54609
neutron capture at 6.2 to 14.7 MeV, cross section for, (E), 26:54662
neutron radius of, determination from elastic scattering, (E), 26:54547
nitrogen-14 reactions (N-14,xn) at 80 to 100 MeV, excitation functions and delayed alpha spectrum from, (E), 26:54651
photon reactions (γ,xn) with, model analysis of giant resonance in, (E/T), 26:54598 (FRNC-TH-242)

LEAD ISOTOPES Pb-209
energy levels from neutron capture by lead-208, (E), 26:54662

LEAD ISOTOPES Pb-210
content ratio to radium-226 in corals, determination of coral growth rates from measurements of, 26:53179

LEAD ISOTOPES Pb-211
energy levels of, shell-model calculations of wave functions for, low-lying, (T), 26:54650

LEAD TITANATES
radiation effects on dielectric properties and crystal structure of, electron, neutron, and γ, 26:55020

LEAD ZIRCONATES
radiation effects on dielectric constants and crystal structure of, electron and γ, 26:55020

LEAK DETECTORS
development of acoustic, for sodium--water, 26:55154 (CONF-710548-, pp 105-28)
use of hydrogen detectors for sodium--water, 26:55156 (CONF-710548-, pp 155-70)

LEPTONS
assignment of lepton number, test of schemes for, (T), 26:54296
field theory of, unified, (T), 26:54294
interactions l + N, asymmetries for models for spin-averaged cross sections and spin effects in Bjorken scaling region for polarization effects in deep inelastic, (T), 26:54244 (DESY-72/36)
interactions of, three-dimensional unitary group for unified gauge weak--electromagnetic, (T), 26:54364 (NYO-3533-264)

LEPTONS, HEAVY
theory for, from unified weak--electromagnetic gauge schemes based on three-dimensional unitary group, 26:54364 (NYO-3533-264)

LEUCINE
radiolysis of frozen aqueous solutions of, ESR study of free radicals from γ, 26:52995

LEUKOCYTES
determination of hematopoietic and pulmonary origins of alveolar macrophages in mouse radiation chimeras, 26:53492
radiation effects on count of human, following whole-body exposure for therapy of leukemias and lymphosarcomas, multifactorial analysis of dose and time dependence of, 26:53400 (NASA-TM-X-2440, pp 233-7)
radiation effects on count of, in peripheral blood of rats following whole-body exposure, dose and time dependence of γ, 26:53483
radioinduced aberrations of chromosomes in human, evaluation for use as dosimeter for populations following nuclear explosion, 26:53397 (FOA-4-4500-A-3)
radioinduced aberrations of chromosomes in, of human peripheral blood following exposure of stomach during diagnostic radiography, x, 26:53427
radioinduced chromosome aberrations in peripheral, of medical radiography personnel, incidence of x, 26:53428

LEVEL INDICATORS
performance of, using time domain reflectometry for liquids in tanks, 26:53306 (RFP-1902)

LIGASES
role of DNA ligase in repair of uv-irradiated DNA in microorganisms, 26:53351

LIGHT
conference on light scattering in solids, Paris, France, 7/71, 26:55041
photoelectric counting statistics of Gaussian, effect of spatial coherence on, 26:55506 (COO-3120-2)
production in electron beam motion through crystal, laser modulation in Schwarz--Hora effect for, (T), 26:54245 (IS-T-531)

LIGHTNING
electron energy deposition in water vapor in, (E/T), 26:54033

LIMERICK POWER REACTOR, UNIT 1
environmental effects of, requested additional data on, 26:55335 (DOCKET-50352-28)

LIMERICK POWER REACTOR, UNIT 2
environmental effects of, requested additional data on, 26:55335 (DOCKET-50352-28)

LINEAR ACCELERATORS
beam instability in traveling wave electron, effects of injection parameters on transverse, 26:53758
beam preinjector system for I-100, power supply for, 26:53751(T) (BNL-tr-498)
cavity resonators for electron, surface condition of niobium for superconducting rf, 26:53748
experimental facility for x radiotherapy at 10-MeV electron, depth dose data and isodose curves for, 26:53799
microwave matching of waveguide and accelerator tubes at Risoe 10-MeV electron, 26:53746 (RISO-M-1518)

LIPIDS
metabolism in Bacillus licheniformis, effects of fatty acid structure and temperature on, 26:55622 (UCLA-12-879)

LIQUID FLOW
magnetohydrodynamic electrically conducting viscous, agitated by oscillating plane in induction field, (T), 26:54161
magnetohydrodynamic incompressible viscous, due to time-varying motion of infinite flat plate, (T), 26:54158
magnetohydrodynamic, electromagnetic coupling of two one-dimensional laminar viscous, (T), 26:54160

LIQUID METAL FAST BREEDER REACTOR
control rods for, reactivity worths and γ heating of boron and tantalum, (E), 26:55134 (CONF-720901-(Bks.1 and 2), pp 579-98)
criticality measurements on ZPPR-3 core mockups of, program for, 26:55114 (CONF-720901-(Bks.1 and 2), pp 724-38)
Doppler reactivity feedback in, measurements of transient, 26:55123 (CONF-720901-(Bks.1 and 2), pp 986-1005
fuel assemblies for, design of Failed Fuel Mockup for thermal and hydraulic testing of, 26:55191 (ORNL-TM-3656)
fuel assemblies for, Fuel Failure Mockup measurements of coolant temperature oscillations in, 26:55192 (ORNL-TM-3761)
fuel element bundles for, effects of configuration and flow blockage area on heat transfer coefficients and temperature distribution in, (E/T), 26:55207(R) (ORNL-TM-3900)
fuel element bundles for, Failed Fuel Mockup facility for testing, 26:55207(R) (ORNL-TM-3900)
fuel elements for, development of stainless steel clad plutonium oxide (PuO_2)--uranium oxide (UO_2), 26:55189(R) (GEAP-10028-39)
fuel reprocessing for, development of aqueous methods

for, 26:53082 (ORNL-4794, pp 15-25)
- fuels for, radiation properties and shielding requirements of, pp. 22-3, 26:53082 (ORNL-4794, pp 15-25)
- physics calculations for, effects of fast neutron multigroup cross section generation methods on, 26:55113 (CONF-720901-(Bks.1 and 2), pp 211-28)
- physics parameters of, benchmark measurements on, 26:55117 (CONF-720901-(Bks.1 and 2), pp 809-21)
- physics parameters of, program for benchmark measurements on, 26:55116 (CONF-720901-(Bks.1 and 2), pp 789-808)
- shielding for, design of experiments for development of, 26:55145(R) (GEAP-13822-1)

LIQUIDS
- levels in tanks, performance of time domain reflectometry for measuring, 26:53306 (RFP-1902)
- pair potential in, from exact Born-Green equation, 26:55516 (COO-3161-4)

LITHIUM
- distribution between liquid bismuth--lithium alloys and molten lithium chloride, p. 4, 26:53081 (ORNL-4794, pp 1-14)
- performance as coolant for fusion reactor blankets, thermodynamic evaluation for, 26:54827 (IPP-4/97)
- performance as toroidal fusion reactor coolant, stress analysis for determining, (T), 26:54825 (CLM-R-116)
- separation from salt solutions by synergistic extraction using β-diketone and trioctylphosphine oxide, p. 57, 26:53084 (ORNL-4794, pp 54-62)
- sodium-ion reactions with, two-state impact-parameter calculations of total cross sections for charge exchange in, 26:54127

LITHIUM CHLORIDES
- LiCl--UCl$_3$--UCl$_4$, melting point diagrams for, 26:53721

LITHIUM FLUORIDES
- helium-atom elastic scattering by, diffraction intensities for, calculated using pairwise interaction, 26:54089
- neon-atom scattering by surfaces of, calculation of angular distributions from, as functions of beam temperature and angle and plane of incidence, 26:54088
- neon-atom scattering by surfaces of, determination of potential parameters from data on, 26:54087
- radioinduced color centers in, by 10- to 50-keV electron beams, (E), 26:54973 (FRNC-TH-210)
- BeF$_2$--LiF, thermodynamic evaluation for use as fusion reactor coolant, 26:54827 (IPP-4/97)

LITHIUM HYDRIDES
- analysis for impurities from production process by activation, 26:52894 (CEA-R-4338)
- fabrication for space-reactor shields, facility for, 26:54949 (NASA-TM-X-2440, pp 92-7)
- neutron transmission measurements in aluminum-clad slabs of, analysis of Shield Test Facility, 26:54944 (NAA-SR-Memo-8597)
- production of single crystals of, tracer and activation studies of impurities occurring in, 26:52894 (CEA-R-4338)

LITHIUM IONS
- effects on budding haploid yeast cells, sensitivity to lethal, 26:53368
- reactions with hydrogen molecules, quantum mechanical calculations of vibrational excitation in, using coupled Volterra equations, 26:54133

LITHIUM ISOTOPES Li-6
- deuteron reactions (d,n) at 30 keV to 1.5 MeV, calculation of thick target yields for, (T), 26:54502 (SC-RR-720513)
- effects on electrophoretic behavior of lithium in sulfuric acid solution, 26:52967
- electron scattering with deuteron emission, cross-section calculations using Born approximation, (T), 25:54546
- helium-3 reactions (He-3,αp) at 1.54 MeV, asymmetric proton yields for, (E), 26:54540
- meson (π^-) capture by, elementary particle theory for nuclear currents in, (T), 26:54238 (LYCEN-7211)
- neutron total cross section at 0.7 to 30 MeV, (E), 26:54656(R) (COO-3058-21)
- nuclear form factors in α--d and ^{3}He--t channels, cluster-model calculations of, (T), 26:54532
- reactions (Li-6,d) with nickel-58 at 38 MeV, DWBA analysis of differential cross sections and spectrum from, (E), 26:54586
- reactions (Li-6,d) with nickel-64 at 38 MeV, cross sections for, (E), 26:54586
- reactions (Li-6,d) with nuclei, DWBA treatment of, (T), 26:54706
- reactions (Li-6,t) with nitrogen-15 at 30 MeV, angular distributions and energy spectra from, (E), 26:54549

LITHIUM ISOTOPES Li-7
- deuteron reactions (d,n) at 30 keV to 1.5 MeV, calculation of thick target yields for, (T), 26:54502 (SC-RR-720513)
- effects on electrophoretic behavior of lithium in sulfuric acid solution, 26:52967
- reactions (Li-7,t) with nitrogen-15 and oxygen-16, finite-range DWBA analysis of, (T), 26:54708
- reactions (Li-7,t) with nuclei, DWBA treatment of, (T), 26:54706

LITHIUM SULFATES
- analysis for impurities, spectrographic, 26:52935(R) (MLM-1888)

LIVER
- arsenic-74 uptake and retention by, of mice, rabbits, and rats following oral administration, time dependence of, 26:53538
- radioisotope retention in, of mammals, mechanisms for americium-241 and plutonium-239, 26:53526(T) (BNWL-tr-71)
- scintiscanning of human, for diagnosis of neoplasms, use of gamma camera in, 26:53214

LUNAR MATERIALS
- analysis for cadmium and indium by neutron activation following separation from other elements, 26:52906
- cosmic-ray production of radionuclides in, (E/T), 26:53860

LUNGS
- arsenic-74 uptake and retention by, of mice, rabbits, and rats following oral administration, time dependence of, 26:53538
- biochemical studies on pulmonary surfactant, 26:55565(T) (LF-tr-72)
- plutonium removal from, of monkeys following inhalation as oxide, effectiveness of pulmonary lavage for, 26:53528(T) (LF-tr-71)
- radiation isodose curves for, cobalt-60 gamma and 35-MeV electron, 26:54901
- sorption of toxic metals, 26:55634 (UR-3490-136)

LUTETIUM
- photon reactions (γ,xn) with, model analysis of giant resonance in, (E/T), 26:54598 (FRNC-TH-242)

LUTETIUM ISOTOPES Lu-175
- proton inelastic scattering at 3 MeV with Coulomb excitation, heat-flow analysis of temperature spikes following, (E/T), 26:54646

LYMPH SYSTEM
- radioinduced injuries of, in young chickens following acute sublethal exposure, proton, 26:53457 (NASA-TM-X-2440, pp 659-64)

LYMPHOCYTES
- radiation effects on count of human, following extracorporeal exposure of blood, effects of dose on, 26:53440
- radiation effects on production of, in patients during therapy of mammary neoplasms, relation of thymus exposure to, 26:53432
- radioinduced aberrations of chromosomes in human, dose response relationships, evaluation for use as biological dosimeters, 26:53420
- radioinduced chromosome aberrations in cultured human, effects of dose on frequency of x, 26:53355

LYSINE
- transport of l, by isolated chick intestinal epithelial cells, 26:55636 (UR-3490-177)

M

MACHINE TOOLS
- bearings for production, design and fabrication of gas, 26:53113 (Y-DA-4541(Rev.1))

MAGNESIUM
- determination in geochemical standards by atomic absorption using nitrous oxide--acetylene flame, 26:52921
- determination in organometallic compounds using oxine method after combustion, gravimetric or titrimetric, 26:52930
- neon-ion reactions at 0.7 to 4 MeV with, neon isotope effects on cross sections for K-shell ionization in, (E), 26:54114
- oxygen ion reactions at 21 MeV, Kα x-ray spectra from, (E), 26:54467(R) (ORO-2972-204)
- spectral lines in Vega due to, (E), 26:53887
- superconducting transition temperature for pure, extrapolated from Mg--Cd data, 26:54444

MAGNESIUM ALLOYS AND SYSTEMS
- Cd--Mg, superconductivity in, (E), 26:54444
- Mg--Sb, lattice heat capacity of intermetallic Mg$_3$Sb$_2$, at 20 to 298°K, 26:53637 (LBL-101)

MAGNESIUM IONS
- scattering by argon and neon at 8 to 25 keV, total cross sections and interatomic potentials for, (E), 26:54139

MAGNESIUM ISOTOPES Mg-22
- energy levels from neon-20 (He-3,nγ) reactions, lifetimes and spin--parity assignments for, (E), 26:54559
- energy-level transitions from neon-20 (He-3,nγ) reactions, branching and multipole mixing ratios for, (E), 26:54559

MAGNESIUM ISOTOPES Mg-24
- alpha elastic scattering at 166 MeV, angular distribution for, (E), 26:54547
- deuteron elastic and inelastic scattering at 12.1 MeV, coupled-channels and DWBA analyses of differential cross sections and analyzing powers from polarized, (E), 26:54557
- energy levels of, projected Hartree--Fock and shell-model calculations of spins of, (T), 26:54553
- muon (μ^-) capture by, γ-ray yields from, (E), 26:54555
- neutron radius of, determination from α elastic scattering, (E), 26:54547
- nuclear deformation from polarized deuteron elastic and

inelastic scattering, (E), 26:54557
proton elastic and inelastic scattering at 9.7 MeV, polarization in, (E), 26:54467(R) (ORO-2972-204)
proton inelastic scattering by, coupled-channel treatment with projected Hartree--Fock wave functions, (T), 26:54565

MAGNESIUM ISOTOPES Mg-25
energy levels from aluminum-27 (p,He-3) reactions, (E), 26:54551 (COO-535-673)

MAGNESIUM ISOTOPES Mg-26
proton reactions (p,t) at 26 MeV, Hauser--Feshback calculation of angular distributions for, (T), 26:54556

MAGNESIUM OXIDES
fabrication by hot isostatic pressing, 26:53578
radioinduced defects in, comparison of explosive shock-induced defects with, 26:54983
sintering of powders of, mechanism of material transport by dislocation motion in, 26:53620

MAGNET COILS
design for fusion reactor technology, summary of conference on, 26:54829 (ORNL-TM-3953)
design of conventional--superconducting 250-kG, for continuous operation, 26:54466
processing evaluation of magnetic products, 26:55470 (BDX-613-518(Rev.))

MAGNETIC FIELDS
atlas of coronal, (E), 26:53955
compression by implosion process, energy-transfer efficiency in, 26:54781
diffusion of solar, in weak-plage regions, (E), 26:53933
direction of interplanetary, relation to polar-cap electric-field distributions, (E), 26:54062
effects of intense, on properties and electronic structure of atoms, (T), 26:54144
effects on electric fields in closed-electron-drift accelerators, 26:53743
effects on plasma heating by laser, (T), 26:54760
intensity depression in magnetotail near 60 R/sub E/ due to diamagnetic effect of plasma sheet, effect of geomagnetic activity on, (E), 26:54058
measurements in extended magnetotail at approximately 1000 R/sub E/, (E), 26:54074
origin of galactic, primordial model for, (T), 26:53975
production of megagauss, methods for, 26:54834
spectral line formation in solar, mean depth of, (T), 26:53944
structure of interplanetary, in solar-flare-associated solar-wind disturbances, (E/T), 26:54076

MAGNETIC MATERIALS
conference, digests of 1971 INTERMAG, Denver, April 13 to 16, 1971, 26:55028

MAGNETIC MIRROR MACHINES
atomic beam injection into deuterium--tritium, penetration properties of, (T), 26:54757
ion beam injection into deuterium--tritium, penetration properties of, (T), 26:54757
plasma confinement in hybrid fields, with quadrupole and quadrupole-cusp geometries, 26:54756
plasma instabilities in, research on, (T), 26:54807(R) (COO-3497-2)
plasma stabilization in, method and apparatus for, 26:54823(P)

MAGNETIC RECORDING SYSTEMS
conference, digests of 1971 INTERMAG, Denver, April 13 to 16, 1971, 26:55028

MAGNETIC STORMS
correlation of expansion phase of magnetospheric substorm with Pc-5 micropulsations at synchronous equatorial orbit, statistical characteristics of, 26:54036
development of magnetospheric substorm, ground-based and satellite coordinated observations of, (E), 26:54061
development of magnetospheric substorms, May 2 and May 5, 1970, (E), 26:54060
development of magnetospheric substorms, physical mechanism for growth and expansion phases, (T), 26:54051
effect on average behavior of total electron content, peak density, and slab thickness in midlatitude F region, (E), 26:54040
morphology of polar substorms in evening high latitudes, relation of partial ring currents with space--time, (E), 26:54023
relation of magnetospheric substorms with interaction of Pc-1 and 2 with Pc-5 micropulsations at synchronous orbit, (E), 26:54035
solar-flare proton-to-alpha ratios during, (E), 26:53966

MAGNETISM
conference, digests of 1971 INTERMAG, Denver, April 13 to 16, 1971, 26:55028

MAGNETOHYDRODYNAMIC GENERATORS
description of low-temperature, for production of electricity, 26:53108(P)
development for electric power generation, 26:55086
electron density relaxation in ducts of non-equilibrium, 26:53104
end power losses in channels, determination of magnetic field extension profile for reducing, (T), 26:53099
performance of liquid metal, effects of Hall current and heterogeneity on, 26:53105
performance of, using cesium--neon working fluid, (T), 26:53091 (IPP-IV-36)
pressure drop in, using liquid mercury working fluid, 26:53106

MAGNETOSHEATH
geomagnetic sudden-impulse propagation in, origin and speed of, (E), 26:54055

MAGNETOSPHERE
bow-shock interaction with interplanetary double-shock ensemble, MHD theory for, 26:54073
charged-particle energy distribution in plasmasphere during solar eclipse, dependence of equilibrium potential of satellite surface material on, (T), 26:54054
charged-particle flux measurements in ATS-5 satellite at synchronous altitude, effects of magnetic activity on low-energy, 26:54045 (NASA-TM-X-2440, pp 530-8)
dynamics and structure of, from solar-wind and interplanetary electron measurements on Apollo-15 subsatellite, (E/T), 26:54072
electric-field distributions in, relation to interplanetary magnetic-field direction, polar-cap, (E), 26:54062
electric-field induction in, by slowly decaying ring current, (T), 26:54063
electromagnetic-wave propagation in homogeneous, nonlinear theory of monochromatic circularly polarized ulf and vlf, (T), 26:54050
electron dynamics observed at balloon altitudes in, conjugate features of, (E), 26:54020
geomagnetic-field pulsations at polar cusp, occurrence of latitude-dependent Pc-4 and Pc-5, (E), 26:54034
magnetic substorms in, manifested by DP-2 mode in polar cap, (E/T), 26:54053
magnetic-storm development in, ground-based and satellite coordinated observations of substorm, E), 26:54061
magnetic-storm development in, physical mechanism for growth and expansion phases of substorm, (T), 26:54051
magnetic-substorm onset in, characteristics of May 2 and May 5, 1970 slowly developing, (E), 26:54060
magnetosonic waves in, nonlinear, (T), 26:53941
particle cutoff-rigidity calculations for Fort Churchill, Canada, daily variations of electron and proton, (E/T), 26:54065
phenomena of, from simulated steady-flow interaction of charged particles with geomagnetic dipole field, (E), 26:54056
phenomena of, relation with creation of polar auroras, (E/T), 26:54043
proton measurements with energies down to 12.4 keV over polar caps following Mar. 21, 1969 solar-particle event, solar-flare, (E), 26:54071
solar-wind plasma in boundary layer of, upper limit of torque exerted in coupling to ionosphere, 26:54075
whistler propagation in, comparison of quasi-monochromatic helical-wave evolution in plasma with monochromatic, (E/T), 26:54868

MAGNETOTAIL
configuration of distant, association with solar-particle access to polar-cap regions from interplanetary space, (T), 26:54069
electric current system in, determination of contributions from magnetization, curvature drift, and gradient drift to total, (T), 26:54064
electron spatial distribution in plasma sheet at 24 R/sub E/, greater than equal to 50-keV, (E), 26:54057
electrostatic-wave interactions with electrons in current sheet, one-dimensional model of resonant, (T), 26:54052
geomagnetic sudden-impulse propagation in, origin and speed of, (E), 26:54055
plasma flow at inner edge of plasma sheet, proposed model of, (T), 26:54051
plasma-sheet characteristics near 60 R/sub E/ in, spatial distributions of averaged magnetic-field magnitude and plasma energy density, (E), 26:54058
plasma-sheet structure in, magnetic balance of stresses in, (T), 26:54059
solar-wind and plasma measurements in expected region at approximately 1000 R/sub E/, Pioneer-7 simultaneous, (E), 26:54074

MAGNETS
design and fabrication of high-performance window frame-type, for magnetic-lens spectrometers, 26:53296 (CEA-N-1539)
design for fusion reactor technology, summary of conference on, 26:54829 (ORNL-TM-3953)
design for TRIUMF, history of, 26:53749
fault protection for ISABELLE, method for, 26:53765 (BNL-16816)
materials for superconducting, review of developments in and radiation effects on, 26:54464 (ORNL-TM-3921)
operation of superconducting, use of liquid helium bath level indicator for observing normalcies in, 26:54463 (ORNL-TM-3886)

MAINE YANKEE POWER REACTOR
coolant loss accidents in, fuel element cladding peak temperature for, 26:55312 (DOCKET-50309-68)
operation of, license for, 26:55313 (DOCKET-50309-69)
technical specifications for, 26:55313 (DOCKET-50309-69)

MALEIMIDE, N-ETHYL-
radiosensitizing effects of, on DNA, review of x, 26:53352

MALFORMATIONS
- radioinduced digital, in fetal mice following whole-body exposure in utero, effects of developmental stage, dose, and dose rate on incidence of γ, 26:53471
- radioinduced, in brain of children following prenatal exposure from maternal therapy during pregnancy, radium and x, 26:53437
- radioinduced, in brain of mice and rats following prenatal exposure, effects of developmental stage at exposure on, 26:53437
- radioinduced, in rat embryos following exposure in utero, role of chromosome damage and repair errors in incidence of fast neutron, 26:53470

MAMMALIA
- radioisotope retention in liver of, mechanisms for americium-241 and plutonium-239, 26:53526(T) (BNWL-tr-71)

MAN
- iodine-131 content of milk in women following injection of labeled pharmaceuticals for diagnostic scanning of kidneys, lungs, and placenta, 26:53524
- iodine-131 uptake from milk by children, age dependence of, 26:53506(T) (ORNL-tr-2629)
- lymphoma incidence in, residing in Hiroshima and Nagasaki in relation to radiation exposure dose, 26:53432
- radiation dose distribution in tissues of, following administration of gold-198 or phosphorus-32 colloids for treatment of malignant pleural effusions, time dependence of beta and gamma, 26:53509
- radiation dose distribution in, as a function of time following inhalation of plutonium-239 oxide aerosols, guidelines for estimation of, 26:53511 (TID-26142)
- radiation dose distribution in, following whole-body exposure, role of quality factors and fluence in calculating, 26:53404 (NASA-TM-X-2440, pp 424-34)
- radiation dose distribution in, from sealed radium-226 sources used for implant therapy, γ, 26:53409 (STI/PUB-295(Vol.4))
- radiation dose to body and lungs of, following ingestion, inhalation, or immersion in cloud of xenon isotopes, methods for estimation of, 26:53510
- radiation dose to body and lungs of, following ingestion, inhalation, or immersion in cloud of krypton isotopes, methods for estimation of, 26:53510
- radiation dose to bone marrow of, following whole-body exposure, use of lithium fluoride dosimeters in Alderson Rando phantom for calculation of γ, 26:53406 (NASA-TM-X-2440, pp 974-80)
- radiation dose to children during diagnostic radiography, methods for reducing x, 26:53417
- radiation dose to gonads and stomach wall of, during diagnostic radiography of stomach, relation to induction of chromosome aberrations in peripheral blood leukocytes, x, 26:53427
- radiation dose to respiratory tract tissues of, following inhalation of radon-222 and radon-220 daughter products as aerosols, use of ICRP lung model for estimation of alpha, 26:53508
- radiation dose to, during diagnostic radiographic examinations, phantom measurements in bone marrow, gonads, and skin, x, 26:53434
- radiation dose to, during diagnostic radiography, phantom studies for predetermination of absorbed x, 26:53416
- radiation dose to, during high-energy therapy, use of thermoluminescent dosimeters to determine electron, 26:53415
- radiation dose to, during intravenous arteriography using metastable technetium-99-labeled pertechnetate, γ, 26:53542
- radiation doses to crew and passengers at SST altitudes from cosmic and solar rays, 26:54888 (NASA-TM-X-2440, pp 894-901)
- radiation effects on ability of, to perform under stress following continuous or protracted fractionated exposure, effectiveness of pulmonary-impedance power spectral analysis for determining γ, 26:53401 (NASA-TM-X-2440, pp 238-48)
- radiation effects on brain of, following hypophysectomy using proton beams, 26:53446
- radiation effects on immune reactions in, during therapy, 26:53432
- radiation effects on leukocyte count in, following whole-body exposure for therapy of leukemias and lymphosarcomas, multifactorial analysis of dose and time dependence of, 26:53400 (NASA-TM-X-2440, pp 233-7)
- radiation effects on lymphocyte production in, during therapy of mammary neoplasms, relation of thymus exposure to, 26:53432
- radiation effects on oral tissues of, during tumor therapy in head and neck region, construction of prosthesis shield for protection against, 26:53410
- radiation effects on rate of recovery from traumatic injuries, whole-body, 26:53419
- radiation effects on survival of neoplastic cells in, relation of anoxia to response to chemical radiosensitizers during fractionated dose therapy, 26:53430
- radiation effects on visual response of, following retinal exposure, effects of particle flux density on charged helium ion, 26:53403 (NASA-TM-X-2440, pp 416-22)
- radiation hazards to, during fluoroscopic radiographic examination, effects of image intensifier performance on, 26:53421
- radiation hazards to, during space flight, extrapolation of clinical data on dose-response-time relations to estimate, 26:53402 (NASA-TM-X-2440, pp 398-415)
- radioinduced aberrations of chromosomes in leukocytes of, evaluation for use as biological dosimeter following nuclear explosion, 26:53397 (FOA-4-4500-A-3)
- radioinduced aberrations of chromosomes in lymphocytes of, evaluation for use as biological dosimeters, 26:53420
- radioinduced chromosome aberrations in bone marrow cells of, following local therapeutic exposure, effects of dose and time on frequency of γ, 26:53445
- radioinduced chromosome aberrations in lymphocytes of, exposed to residual fallout from atomic bombing of Nagasaki, 26:53414
- radioinduced dermatitis in, following local exposure for therapy of underlying neoplasms, γ, 26:53433
- radioinduced gastrointestinal distress in, following continuous or protracted fractionated whole-body exposure, effectiveness of pulmonary-impedance power spectral analysis for determining γ, 26:53401 (NASA-TM-X-2440, pp 238-48)
- radioinduced inflammation of salivary glands of, following therapy, 26:53423
- radioinduced inhibition of spermatogenesis in, following exposure of testes, dose and time dependence of x, 26:53399 (NASA-TM-X-2440, pp 229-32)
- radioinduced injuries in skin of, following chronic therapeutic exposure, relation of DNA and RNA contents and ultrastructural changes in epidermis during x, 26:53441
- radioinduced injuries in tissues of, following therapy of neoplasms, surgical treatment of local, 26:53438
- radioinduced injuries in, clinical aspects of pathogenesis and recovery from, relevance of animal studies to, 26:53411
- radioinduced injuries of skin of, dose-response relationships for, 26:53431
- radioinduced injuries of spinal cord tissues in, following therapy, etiology of, 26:53429
- radioinduced injuries to heart in, following therapy of esophageal carcinomas, electrocardiogram studies of γ and x, 26:53439
- radioinduced injuries to optic nerve and retina of, following therapy of nasal cavity and paranasal sinus carcinomas, dose and time dependence of γ and x, 26:53444
- radioinduced leukemia and other neoplasms in, following exposure in utero, review of epidemiological studies on, 26:53435
- radioinduced light flashes on retina of dark-adapted eye of, use of virtual-quanta method to calculate frequency of charged particle, 26:53405 (NASA-TM-X-2440, pp 767-72)
- radioinduced lymphopenia in, following extracorporal exposure of blood, effects of dose on extent and rate of development of, 26:53440
- radioinduced malformations of brain of children following prenatal exposure from maternal therapy during pregnancy, radium and x, 26:53437
- radioinduced myelopathy in cervical vertebrae of, following therapy, role of vascular changes in pathogenesis of γ, 26:53425
- radioinduced necrosis of jaw bones of, following therapy of neoplasms of head and neck region, 26:53418
- radioinduced neoplasms in, relation of radioisotope content of environment to, 26:53523
- radioinduced neoplasms in, surviving atomic bombing of Nagasaki 10 to 25 years following exposure as children, effects of dose on incidence of, 26:53442
- radioinduced thrombocytopenia in, following intravenous injection of colloidal gold-198 for therapy of liver involvement in Hodgkin's disease, relation of dose fractionation and protraction to β and γ, 26:53507
- radioisotope transport through environment to, 26:53521
- radioisotope transport to, following release to environment, 26:53522
- strontium-90 content of bones of, in France during 1970, age dependence of, 26:53520 (CEA-N-1535)

MANGANESE
- abundance in 21 sharp-lined nonvariable cool peculiar A stars, (E), 26:53882
- determination in geochemical standards by atomic absorption using nitrous oxide--acetylene flame, 26:52921
- determination in minerals by direct measurement of oxide ratios, spectroscopic, 26:52932
- determination in water samples by spark source mass spectroscopy, 26:52914 (ANL-7860(Pt.3), pp 55-63)
- determination in water, effects of large amounts of copper on spectrographic, 26:52927
- effects on cohesion and structural stability of aluminum oxide composites with iron and nickel, 26:53589
- separation from iron by solvent extraction using Aliquat-336, 26:53076

MANGANESE ALLOYS AND SYSTEMS
- Mn--Mo--Ni--steel, mechanical properties of pressure vessel, effects of quenching, tempering, and heat

  treatment on, 26:53646
MANGANESE BORIDES
  ferromagnetism of MnB$_2$, exchange model of weak, (T), 26:55048
MANGANESE FLUORIDES
  superexchange interactions in undoped and ferrous-doped, study using pressure shift of far-infrared-active magnetic mode frequency, 26:55510 (COO-3151-6)
MANGANESE ISOTOPES Mn-50
  beta decay of, electromagnetic corrections to ft values for, (T), 26:54713
MANGANESE ISOTOPES Mn-53
  cosmic-ray production in lunar rocks, (E/T), 26:53860
MANGANESE ISOTOPES Mn-54
  content in conversion products of irradiated 300 series stainless steels, 26:55165 (CONF-710959-, Paper 9)
  content in Savannah River, 1971, 26:53153(R) (DPSPU-72-30-1)
  distribution in Columbia River, effects of seawater on soluble-suspended, 26:53166 (RLO-2227-T-12-28)
  production of carrie-free, from neutron-irradiated iron by solvent extraction using Aliquat-336, 26:53076
  uptake by hair following intravenous injection in rats, correlation with body burden and, 26:53529 (NASA-TM-X-2440, pp 982-8)
MANGANESE ISOTOPES Mn-55
  energy levels from (d,α) and (p,He-3) reactions, spin--parity assignments for, (E), 26:54584
  energy levels in K-mesic atoms, resonance coupling between atomic and nuclear, (E), 26:54568 (LBL-776)
MANGANESE OXIDES
  superexchange interactions in, study using pressure shift of far-infrared-active magnetic mode frequency, 26:55510 (COO-3151-6)
MANY BODY PROBLEM
  energy variational principle in, derivation of explicit equations for linked cluster amplitudes for, (T), 26:54735
  Faddeev equations for three-body, method of moments for solution of, (T), 26:54715
  fermion operators in, transition operator boson expansion of, (T), 26:54682 (COO-3071-10)
  symmetry groups for orbital angular momentum in, orthogonal and unitary, 26:55072
  three-nucleon problem with large-momentum cutoff, solutions of Skornyakov--Ter-Martirosyan equations for, 26:54344 (ITF-72-10-P)
  variational transformation for nuclear, 26:54718
MARITIME NUCLEAR STEAM GENERATOR
  coolant for, radiation dose from oxygen activation in secondary, (T), 26:55356 (CONF-720901-(Bks.1 and 2), pp 471-9)
MARITIME PRESSURIZED-WATER REACTOR
  fire protection procedures for, inadequacies in, 26:55357 (DOCKET-50238-92)
MARS (PLANET)
  dayglow emission from atmosphere of, relation with electron impact excitation cross sections and energy degradation in carbon monoxide, (E/T), 26:54008
  ultraviolet radiation data from Mariner in atmosphere of, relation with electron reactions with carbon dioxide below 100 eV, (E/T), 26:54009
MASERS
  parametric down-conversion in astrophysical, (T), 26:53909
MASS SPECTROGRAPHY
  analysis of solids using ion emission induced by electron beam, 26:54084
  conference on, Ispra, Italy, Sept. 1--3, 1971, 26:52893 (EUR-4765)
MASS SPECTROMETERS
  data acquisition system for, design and performance of, 26:53324
  ion source for, vacuum lock for thermal-ionization, 26:53318
MATERIALS TESTING, NONDESTRUCTIVE
  facility for evaluation of, description of, 26:55221 (NP-19338(Vol.1))
  methods for reactor pressure vessel, development of in-service, 26:55222(R) (NP-19338(Vol.2))
  methods for reactor pressure vessel, development of in-service, 26:55221 (NP-19338(Vol.1))
MATHEMATICAL PHYSICS
  analytic extrapolation from boundary and interior points, functional integration approach to, 26:55079
  Bogolyubov kinetic equations in, method for solution in Banach space, (T), 26:55067 (ITF-72-9-E)
  fermion operators in, transition operator boson expansion of, (T), 26:54682 (COO-3071-10)
MATHEMATICS
  covariance analysis in, computer program for, 25:55567 (MLM-1847)
  gamma distribution, computer programs for significant digit incomplete gamma ratios for, 26:55604 (SC-DR-720303)
  Pade approximant for series expansion, invariance and convergence properties of, 26:55475 (BNL-17110)
  Pade approximant for series expansion, two recent generalizations of, 26:55557 (LA-DC-72-879)
  Pade approximants for Legendre series, nonlinear, 26:55556 (LA-DC-72-873)
  Pade approximants for series expansions, generalizations of, 26:55555 (LA-DC-72-872)
  Pade approximants, effect of random errors in terms of power series on convergence of, 26:55558 (LA-DC-72-880)
MATTER, ANTI-
  flux of cosmic anti-alpha particles at 0.3 to 3.0 GeV/N, (E), 26:53825
MEATS
  analysis for mercury by neutron activation, 26:52911
  beef, radiation processing of vacuum packaged, effects on surface color, effects of subsequent exposure to air on γ, 26:53346
  cesium-137 content of Norwegian, 1956 to 1970, 26:53161
MEDICAL PERSONNEL
  radiation dose to bone marrow and eyes of, during arteriography, x, 26:53443
  radiation dose to fingers of, during injection of radioisotopes, phantom studies of β and γ, 26:53424
  radioinduced chromosome aberrations in peripheral leukocytes of radiography, incidence of x, 26:53428
  training programs for medical physicists, 26:55461 (ACRH-1000-350)
  training programs for medical physicists, 26:55460 (ACRH-1000-349)
MEDICINE
  research in India, 1971--1972, 26:55452(R) (NP-19407)
  uses of radiation and radioisotopes in, IAEA-WHO survey on world-wide, 26:53413
  uses of radioisotopes in, training course manual, 26:53541 (TID-26128)
MEIOSIS
  effects on γ-radiosensitivity of grain moth oocytes, 26:53499
MEMBRANES
  phase transitions in mitochondrial, spin label studies on, 26:55504(R) (COO-2223-1)
MENDOCINO POWER REACTOR, UNIT 1
  auxiliary systems for, revised data on, 26:55347 (DOCKET-50398-18)
  containment system for, revised data on, 26:55347 (DOCKET-50398-18)
  engineered safeguards for, revised data on, 26:55347 (DOCKET-50398-18)
  fire protection system for, revised data on, 26:55347 (DOCKET-50398-18)
  instrumentation for, revised data on, 26:55347 (DOCKET-50398-18)
  piping systems for, stress limits for, 26:55347 (DOCKET-50398-18)
  power conversion system for, requested data on, 26:55347 (DOCKET-50398-18)
  power transmission lines for, environmental impact of, 26:55348 (DOCKET-50398-19)
  pumps for, stress limits for, 26:55347 (DOCKET-50398-18)
  radioactive waste system for, revised data on, 26:55347 (DOCKET-50398-18)
  structures for, earthquake stress limits for Class 1, 26:55347 (DOCKET-50398-18)
  structures for, stress limits for support, 26:55347 (DOCKET-50398-18)
  valves for, stress limits for, 26:55347 (DOCKET-50398-18)
MENDOCINO POWER REACTOR, UNIT 2
  auxiliary systems for, revised data on, 26:55347 (DOCKET-50398-18)
  containment system for, revised data on, 26:55347 (DOCKET-50398-18)
  engineered safeguards for, revised data on, 26:55347 (DOCKET-50398-18)
  fire protection system for, revised data on, 26:55347 (DOCKET-50398-18)
  instrumentation for, revised data on, 26:55347 (DOCKET-50398-18)
  piping systems for, stress limits for, 26:55347 (DOCKET-50398-18)
  power conversion system for, requested data on, 26:55347 (DOCKET-50398-18)
  power transmission lines for, environmental impact of, 26:55348 (DOCKET-50398-19)
  pumps for, stress limits for, 26:55347 (DOCKET-50398-18)
  radioactive waste system for, revised data on, 26:55347 (DOCKET-50398-18)
  structures for, earthquake stress limits for Class 1, 26:55347 (DOCKET-50398-18)
  structures for, stress limits for support, 26:55347 (DOCKET-50398-18)
  valves for, stress limits for, 26:55347 (DOCKET-50398-18)
MERCURY
  determination in environmental samples by neutron activation, 26:52897 (CONF-721010-3)
  determination in minerals by neutron activation and γ spectroscopy, nondestructive, 26:52901 (UJV-2851-F,Ch)
  determination of trace amounts of, in foodstuffs by neutron activation, 26:52911
  determination of trace amounts of, in tobacco by neutron activation, 26:52907
  diffusion of bismuth and lead in, at 25°C, 26:53636 (IS-T-554)
  distribution in cores from Green Bay, relations with depth, 26:53164 (ANL-7860(Pt.3), pp 64-76)

electron reactions at 25 to 180 keV with, distorted-wave calculations of differential cross sections for excitation and spin polarization of emitted electrons from, 26:54106
toxicity in rats following subcutaneous injection as chloride, prophylactic effects of ascorbic acid on, 26:55497 (COO-1630-29)
MERCURY (PLANET)
perihelion advance of, comparison of experiment with general relativistic predictions for, (E/T), 26:54403
MERCURY ALLOYS AND SYSTEMS
Ar--Hg, ionization of gaseous, 26:53196(R) (COO-323-28)
MERCURY ISOTOPES Hg-203
radiation dose to fingers of medical personnel during injection of, phantom studies of, 26:53424
MESIC ATOMS
resonance coupling in manganese-55 K-, between nuclear and atomic energy levels, (E), 26:54568 (LBL-776)
x-ray spectra from niobium-93 μ^-, (E), 26:54605 (KFK-1602)
MESONS
diurnal variation of cosmic, temperature effects on, (E), 26:53811
form factors in parton model, elastic and inelastic, (T), 26:54311
interactions with baryons, effective Lagrangian model for, (T), 26:54333
interactions with baryons, transition amplitudes, cross sections, and partial-wave decompositions for three-particle final state in, 26:54330
reactions with carbon and lead, model analysis of, (E/T), 26:54529 (RPP/NS-8)
reactions with nuclei at 0.7 to 2 GeV/c, π^-/π^+ cross section ratios for, (E), 26:54529 (RPP/NS-8)
MESONS (eta)
decay eta $\to 3\pi$, model satisfying analyticity, crossing symmetry, and approximate unitarity for, (T), 26:54259
decay eta $\to 3\pi$, Moffat model of meson--meson scattering for, (T), 26:54276
decay eta $\to \gamma + e^+ + e^-$, radiative corrections to, (T), 26:54277
production of eta^0 in $\pi^- + p \to p + \pi^+ + 2\pi^- + \pi^0$ interactions at 20 GeV/c, cross sections for, (E), 26:54207 (COO-3064-3)
production of S^*, D^0, and E^0 in anti p + p interactions at 1.2 GeV/c, (E), 26:54199
MESONS (K)
decay $K \to 3\pi$, model satisfying analyticity, crossing symmetry, and approximate unitarity for, (T), 26:54259
decay $K \to 3\pi$, Moffat model of meson--meson scattering for, (T), 26:54276
decay $K \to \pi + l + \nu$, Schwarz inequality for slope parameter relation with spectral function of isovector electromagnetic current for, (T), 26:54287 (LBL-766)
decay $K \to \pi + l + \nu$, weak kappa-dominance model for bounds on parameters for, (T), 26:54289
interactions K + p, interference term effects in multiperipheral model for cross section energy dependence, pion multiplicities, and structures in correlation functions for, (T), 26:54329 (NYO-3533-265)
interactions $K + \pi$ at 0.640 to 1 GeV, dispersion relations for S and P waves for resonance behavior of phase shifts for, (T), 26:54315 (JINR-E2-6525)
production in $p + p \to K$ + anything interactions at 12 to 30 GeV/c, Bose distribution and scaling behavior for, (T), 26:54349
production in p + p and $\pi^- + p$ interactions, multiperipheral-model calculations of cross sections for, (T), 26:54325 (COO-3533-2)
MESONS (K^-)
capture by nuclei, gamma yields for different final states in, (T), 26:54536
decay $K^- \to \mu^- + \pi^0 + \nu$ in hydrogen bubble chamber, branching ratio for, (E), 26:54190
decay $K^- \to \pi^0 + e + \nu$ in hydrogen bubble chamber, branching ratio for, (E), 26:54190
decay $K^- \to \pi^+ + \mu^- + e^-$, test of lepton number assignments from, (T), 26:54296
decay $K^- \to \pi^- + \pi^0 + \pi^0$ in hydrogen bubble chamber, branching ratio for, (E), 26:54190
decay $K^- \to \pi^- + \pi^0$ in hydrogen bubble chamber, branching ratio for, (E), 26:54190
decay $K^- \to \pi^- + \pi^+ + \pi^-$ in hydrogen bubble chamber, branching ratio and slope of Dalitz plot for, (E), 26:54190
interactions $K^- + n \to \Lambda + \pi + K^0$ + anti K^0 at 4.9 GeV/c, total and differential cross sections for, (E), 26:54229
interactions $K^- + n \to \Lambda + \pi^-$ + eta at 4.9 GeV/c, total and differential cross sections for, (E), 26:54229
interactions $K^- + n \to \Lambda + \pi^-$ + missing mass at 4.9 GeV/c, total and differential cross sections for, (E), 26:54229
interactions $K^- + n \to \Lambda + \pi^- + \pi^0$ at 4.9 GeV/c, total and differential cross sections for, (E), 26:54229
interactions $K^- + n \to \Lambda + \pi^-$ at 4.9 GeV/c, total and differential cross sections for, (E), 26:54229
interactions $K^- + n \to \Sigma^0 + \pi^-$ at 4.9 GeV/c, total and differential cross sections for, (E), 26:54229
interactions K^- + N, urbaryon rearrangement diagram for structures in elastic and inelastic, (T), 26:54342
interactions $K^- + p \to$ anti K^0 + n at 1 to 3 GeV/c, scintillation counter study of cross sections and resonance production in, (E/T), 26:54210 (NP-19419)
interactions $K^- + p \to$ anti K^0 + n at 1700 to 2100 MeV, cross sections, polarizations, and angular distributions for, (E), 26:54215
interactions $K^- + p \to$ anti K^0 + n, Regge pole--cut model for, (E/T), 26:54230
interactions $K^- + p \to \Delta^{++} + K^{*-} + \pi^-$ at 10 GeV/c, Veneziano model analysis of, (E/T), 26:54225
interactions $K^- + p \to \Lambda + \pi^0$ at 1700 to 2100 MeV, cross sections, polarizations, and angular distributions for, (E), 26:54215
interactions $K^- + p \to p$ + anti $K^0 + \pi^+ + \pi^- + \pi^- + \pi^0$ at 10 GeV/c, analysis of $K^{*-}(890)$, $\Delta^{++}(1236)$, and ω^0 production in, (E), 26:54225
interactions $K^- + p \to p$ + anti $K^0 + \pi^+ + \pi^- + \pi^-$ at 10 GeV/c, analysis of $K^{*-}(890)$, $\Delta^{++}(1236)$, and rho^0 production in, (E), 26:54225
interactions $K^- + p \to \pi^- + \Sigma^+$, new Regge absorption model for cross sections of, (T), 26:54336
interactions $K^- + p \to \pi^+(\pi^-)$ + anything at 10 GeV/c, differential cross sections and symmetry of π emission in, (E), 26:54222
interactions K^- + p at 6 to 14 GeV/c, evidence for interaction radius scaling from analysis of polarization in, (T), 26:54354
production in $e + p \to e + K^-$ + anything interactions at 6.5 GeV, momentum spectra of, (E), 26:54178
production of K^+--K^- pairs in three- and four-prong anti p + p interactions at 7 GeV/c in deuterium bubble chamber, (E), 26:54218
MESONS (K^0)
decay $K^0 \to \pi^+ + \pi^- + \pi^0$, CP violation in, (E), 26:54188
decay $K^0 \to \pi^+ + \pi^-$, wire spark chamber and scintillation counter study of CP violation in time dependence of rates for, (E), 26:54361 (COO-1195-242)
decay $K^0 \to \pi^+ + \pi^-$, wire spark chamber study of CP violation in time decay distributions of, (E), 26:54362 (COO-1195-244)
decay $K_1^0 \to 2\gamma$ relative to $K_2^0 \to \pi^+ + \pi^-$, use of dispersion relation and unitarity in calculation of rate, (T), 26:54295
decay $K_1^0 \to \mu^+ + \mu^-$, lower bound for CP-nonconservation in, (T), 26:54369
decay $K_2^0 \to 3\pi^0$ in xenon bubble chamber, branching ratio relative to $K_2^0 \to \pi^+ + \pi^- + \pi^0$, (E), 26:54187
decay $K_2^0 \to \mu^+ + \mu^-$, lower bound for CP-nonconservation in, (T), 26:54369
decay $K_2^0 \to \pi + l + \nu$, ν/sub e/ and ν/sub mu/ mass upper limits from double magnetic spectrometer study of, (E), 26:54184 (LBL-4)
decay $K_2^0 \to \pi^+ + \pi^- + \gamma$, SU(3) symmetry-breaking model for rate of, (T), 26:54365
decay of K_2^0, search for neutral vector meson in, (E), 26:54291
decay of, effects of T violation in medium on conclusions from apparent T violation in, (T), 26:54366
regeneration $K_2^0 \to K_1^0$ on copper at 500 to 1500 MeV/c, amplitude for, (E), 26:54230
MESONS (anti K^0)
decay anti $K^0 \to \pi^+ + \pi^-$, wire spark chamber and scintillation counter study of CP violation in time dependence of rates for, (E), 26:54361 (COO-1195-242)
decay anti $K^0 \to \pi^+ + \pi^-$, wire spark chamber study of CP violation in time decay distributions of, (E), 26:54362 (COO-1195-244)
MESONS (K^+)
decay $K^+ \to e^+ + \nu + \gamma$, SU(3) symmetry-breaking parameter for, (T), 26:54365
decay $K^+ \to \mu^+ + \nu$, branching ratio for, (E), 26:54186
decay $K^+ \to \pi^0 + e^+ + \nu$, branching ratio for, (E), 26:54186
decay $K^+ \to \pi^0 + \mu^+ + \nu$, branching ratio for, (E), 26:54186
decay $K^+ \to \pi^0 + \mu^+(e^+) + \nu$ in heavy-liquid bubble chamber, form factors, branching ratios, and Dalitz diagrams for, (E), 26:54170 (LAL-1255)
decay $K^+ \to \pi^+ + \gamma + \gamma$, SU(3) symmetry-breaking model for π spectra and rate of, (T), 26:54365
decay $K^+ \to \pi^- + \mu^+ + e^+$, test of lepton number assignments from, 26:54296
decay $K^+ \to \pi^+ + \pi^0 + \pi^0$, branching ratio for, (E), 26:54186
decay $K^+ \to \pi^+ + \pi^0$, branching ratio for, (E), 26:54186
decay $K^+ \to \pi^+ + \pi^- + e^+ + \nu$, Pais--Treiman determination of π--π phase shift from spark chamber study of, 26:54183 (CEA-N-1553)
decay $K^+ \to \pi^+ + \pi^+ + \pi^-$, branching ratio for, (E), 26:54186
interactions K^+ + d at 9 GeV/c in deuterium bubble chamber, analysis of Q region of $K^+\pi^+\pi^-$ mass spectra from, (E), 26:54228
interactions $K^+ + n \to K^0 + p$, Regge pole--cut model for, (E/T), 26:54230
interactions $K^+ + n \to K^+ + \pi^- + p$ at 3.8 GeV/c in deuterium bubble chamber, cross sections and quasi-two-body interaction cross sections for $K^0(890)$ and $K^0(1420)$ production in, (E), 26:54202 (COO-1195-238)
interactions $K^+ + n \to K^+ + \pi^- + p$ at 9 GeV/c, resonance production in, (E), 26:54203 (COO-1428-308)

  interactions $K^+ + n \to p +$ anything at 9 GeV/c in deuterium bubble chamber, proposed experiment for K(1760) and K(2200) production in, (E), 26:54204 (COO-1428-310)
  interactions $K^+ + N$, urbaryon rearrangement diagram for structures in elastic and inelastic, (T), 26:54342
  interactions $K^+ + p \to K^0 + \pi^0 + \pi^+ + p$ at 5 to 12.7 GeV/c, longitudinal phase space analysis of, (E/T), 26:54226
  interactions $K^+ + p \to K^+ + \pi^- + \pi^+ + p$ at 5 to 12.7 GeV/c, longitudinal phase space analysis of, (E/T), 26:54226
  interactions $K^+ + p \to p + K^0 + \pi^+$ at 1.37 to 2.17 GeV/c, cross sections for, (E), 26:54231
  interactions $K^+ + p \to p + K^+ + \pi^+ + \pi^-$ at 1.37 to 2.17 GeV/c, cross sections for, (E), 26:54231
  interactions $K^+ + p \to \pi^- +$ anything at 12.6 GeV/c, multiperipheral-model calculations of cross sections for, (T), 26:54325 (COO-3533-2)
  interactions $K^+ + p$ at 0.909 to 1.907 GeV/c, differential and total cross sections for elastic, (E), 26:54211 (RPP/H-95)
  interactions $K^+ + p$ at 6 to 14 GeV/c, evidence for interaction radius scaling from analysis of polarization in, (T), 26:54354
  interactions $K^+ + \pi^0$, Schwarz inequality for cross sections for, (T), 26:54287 (LBL-766)
  production in $e + p \to e + K^+ +$ anything interactions at 6.5 GeV, momentum spectra of, (E), 26:54178
  production of K^+--K^- pairs in three- and four-prong anti $p + p$ interactions at 7 GeV/c in deuterium bubble chamber, (E), 26:54218
MESONS (ω)
  coupling constants for $\gamma\omega$, in relativistic extended quark model, 26:54283
  mixing of ω--phi in Odorico bootstrap model for pseudoscalar meson interactions, (T), 26:54323
  production in $\gamma + p$ interactions at 2 to 7.5 GeV in hydrogen bubble chamber, cross sections for, (E), 26:54175 (SLAC-143)
  production of ω^0 in $\pi^- + p \to p + \pi^+ + 2\pi^- + \pi^0$ interactions at 20 GeV/c, cross sections for, (E), 26:54207 (COO-3064-3)
  vertex function of nonrenormalizable ωrhoπ interaction, ladder approximation for, (T), 26:54322
MESONS (phi)
  coupling constant for γ phi, in relativistic extended quark model, 26:54283
  mixing of ω--phi in Odorico bootstrap model for pseudoscalar meson interactions, (T), 26:54323
MESONS (π)
  coupling constant for πN from test of analyticity of forward $\pi + N$ charge-exchange amplitude, (T), 26:54337
  dose computations and treatment planning in, therapy, 26:54876 (LA-4874, pp 145-52)
  dose distribution of, in therapy, treatment planning using, 26:54877 (LA-4874, pp 153-61)
  effectiveness for therapy of carcinomas, research programs on, 26:53398 (LA-4874, pp 79-83)
  form factor in $e + N \to \pi + N$ interactions at threshold, method for calculating electromagnetic, (T), 26:54247 (NP-19417)
  form factor of, Schwarz inequality for electromagnetic, (T), 26:54287 (LBL-766)
  form factors of, absence of zeros for electromagnetic, 26:54273
  interactions $\gamma + \pi \to \pi + \pi$ with soft pions, structure of observable amplitudes for, (T), 26:54265
  interactions $K + \pi$ at 0.640 to 1 GeV, dispersion relations for S and P waves for resonance behavior of phase shifts for, (T), 26:54315 (JINR-E2-6525)
  interactions $\pi + d$, recoil and Fresnel corrections to Glauber multiple-scattering model for, 26:54352
  interactions $\pi + N \to \pi + \Sigma(\Lambda)$ near threshold, cross sections and polarization phenomena from PCAC theory, (T), 26:54335
  interactions $\pi + N$ at 4.8 to 20 GeV, double Regge cuts in Regge pole--cut model for charge exchange, (T), 26:54324 (COO-1428-309)
  interactions $\pi + N$ at low energies, current algebra model with physical pions for scattering and energy dependence of S- and P-phase, (T), 26:54339
  interactions $\pi + N$, inequalities between relative phase of amplitudes and polarization in, (T), 26:54340
  interactions $\pi + N$, nonlocal separable potentials for, (T), 26:54724
  interactions $\pi + N$, πN coupling constant from test of analyticity of forward amplitude of charge-exchange, (T), 26:54337
  interactions $\pi + N$, urbaryon rearrangement diagrams for structures in elastic and inelastic, (T), 26:54342
  interactions $\pi + p$ at high energies with polarized target, design of equipment for measuring polarization of recoil protons in elastic, 26:54232
  interactions $\pi + p$ in colliding beams at ISABELLE, feasibility of, (E), 26:54200 (BNL-17069)
  interactions $\pi + p$, interference term effects in multiperipheral model for cross section energy dependence, pion multiplicities, and structures in correlation functions for, (T), 26:54329 (NYO-3533-265)
  interactions $\pi + \pi$ at low energies, Schwarz inequality for p-wave cross sections of, (T), 26:54287 (LBL-766)
  interactions $\pi + \pi$ in $\pi^- + d \to 2p + 2\pi^-$ at 7 GeV/c in deuterium bubble chamber, s- and d-wave phase shifts for, (E), 26:54208 (COO-3065-16)
  interactions $\pi + \pi$, epsilon and S*(980) contributions to broken scale invariance for low-energy theorems of, (T), 26:54319
  interactions $\pi + \pi$, review of dipion production, analyticity, crossing, unitarity, and inelastic channels for, (E/T), 26:54317 (RPP/T-27)
  mass differences of members of A_1, rho, and π isomultiplets, dynamic chiral symmetry and cancellation of divergences in, (T), 26:54321
  production in dual resonance model, statistical approach to calculation of multiple, (T), 26:54300 (ITF-72-53-E)
  production in $e + N \to \pi + N$ interactions at threshold, method for calculating axial nucleon form factor and pion electromagnetic form factor in, (T), 26:54247 (NP-19417)
  production in $p + p \to \pi +$ anything interactions at 12 to 30 GeV/c, Bose distribution and scaling behavior for, (T), 26:54349
  production in proton reactions with emulsion nuclei at 22.6 GeV/c, velocity distribution of secondary, 26:54196
  production in $\pi + p$ and $K + p$ interactions at 10 GeV/c symmetry of momentum distribution in, (E), 26:54222
  reactions with nuclei at 100 to 280 MeV, Coulomb flux corrections to total cross sections for, (T), 26:54609
  reactions with nuclei below 3 GeV, intranuclear-cascade evaporation calculations for nonelastic, (T), 26:54727
  scattering by nuclei, analysis of nuclear surface properties by elastic, (T), 26:54722
  vertex function of nonrenormalizable ωrhoπ interaction, ladder approximation for, (T), 26:54322
MESONS (π^-)
  capture by lithium-6, elementary particle theory for nuclear currents in, (T), 26:54238 (LYCEN-7211)
  dose distributions for radiobiology and radiotherapy, radiation transport codes for, (T), 26:54890 (ORNL-TM-3816)
  interactions $\pi^- + d \to 2p + 2\pi^- + m\pi^0$ at 7 GeV/c in deuterium bubble chamber, cross sections and upper limit for exotic multipion resonance production in, (E), 26:54208 (COO-3065-16)
  interactions $\pi^- + d \to 2p + 2\pi^- + \pi^0$ at 7 GeV/c in deuterium bubble chamber, cross sections, upper limit for exotic multipion resonance production, and validity of spectator model for cross sections for Δ^0rho-channel in, (E), 26:54208 (COO-3065-16)
  interactions $\pi^- + d \to 2p + 2\pi^-$ at 7 GeV/c in deuterium bubble chamber, cross sections, upper limit for exotic multipion resonance production, and $\pi + \pi$ scattering phase shifts in, (E), 26:54208 (COO-3065-16)
  interactions $\pi^- + d \to 2p + \pi^+ + 3\pi^- + m\pi^0$ at 7 GeV/c in deuterium bubble chamber, cross sections and upper limit for exotic multipion resonance production in, (E), 26:54208 (COO-3065-16)
  interactions $\pi^- + d \to 2p + \pi^+ + 3\pi^- + \pi^0$ at 7 GeV/c in deuterium bubble chamber, cross sections and upper limit for exotic multipion resonance production in, (E), 26:54208 (COO-3065-16)
  interactions $\pi^- + d \to 2p + \pi^+ + 3\pi^-$ at 7 GeV/c in deuterium bubble chamber, cross sections and upper limit for exotic multipion resonance production in, (E), 26:54208 (COO-3065-16)
  interactions $\pi^- + d$, compilation of cross sections for, 26:54201 (CERN/HERA-72-1)
  interactions $\pi^- + n$ at 40 GeV/c, average number of produced π^+--π^- pairs, coefficient of nucleon charge exchange, and identical distribution over charged particle multiplicity for, (T), 26:54327 (JINR-E2-6596)
  interactions $\pi^- + n$, compilation of cross sections for, 26:54201 (CERN/HERA-72-1)
  interactions $\pi^- + p \to$ eta $+ n$, Regge pole--cut model for, (E/T), 26:54230
  interactions $\pi^- + p \to K +$ anti K at 4 to 40 GeV/c, multiperipheral-model calculations of cross sections for, (T), 26:54325 (COO-3533-2)
  interactions $\pi^- + p \to \Lambda + K$ at 4 to 40 GeV/c, multiperipheral-model calculations of cross sections for, (T), 26:54325 (COO-3533-2)
  interactions $\pi^- + p \to \Lambda + K^*(1420)$ at 4.5 and 6 GeV/c, differential cross sections, Λ polarization, and $K^*(1420)$ density matrix elements for, (E), 26:54217
  interactions $\pi^- + p \to \Lambda(1405) + K^0$ at 4.5 and 6 GeV/c, differential cross sections for, (E), 26:54217
  interactions $\pi^- + p \to \Lambda(1520) + K^0$ at 4.5 and 6 GeV/c, differential cross sections for, (E), 26:54217
  interactions $\pi^- + p \to \Lambda(\Sigma^0) + K^*(890)$ at 4.5 and 6 GeV/c, differential cross sections, $\Lambda(\Sigma)$ polarization, and $K^*(890)$ density matrix elements from, (E), 26:54217
  interactions $\pi^- + p \to \Lambda(\Sigma^0) + K^0$ at 4.5 and 6 GeV/c, differential cross sections and $\Lambda(\Sigma)$ polarization for, (E), 26:54217
  interactions $\pi^- + p \to N + 2\pi$ at 1.6 to 2.0 GeV, energy-independent partial-wave analysis of baryon resonance production in, (T), 26:54328 (LBL-544)
  interactions $\pi^- + p \to n +$ anything at 2.4 GeV/c,

scintillation counter study of $M^0(1033)$ production in, (E), 26:54205 (COO-1428-311)

- interactions $\pi^- + p \to n + \pi^+ + \pi^- + m\pi^0 (m = 1$ to $5)$ at 5 GeV/c in propane bubble chamber, resonance production and partial cross sections for, (E), 26:54220
- interactions $\pi^- + p \to n + \pi^+ + \pi^-$ at 2.77 GeV/c, parametrization of nonevasive exchange processes and background contributions in, (E/T), 26:54214
- interactions $\pi^- + p \to p$ + anything at 25 and 40 GeV/c, triple-Pomeranchuk coupling and scaling in inclusive, (E/T), 26:54221
- interactions $\pi^- + p \to p$ + anything, triple-Regge formalism for analysis of, (T), 26:54332
- interactions $\pi^- + p \to p + \pi^+ + 2\pi^- + \pi^0$ at 20 GeV/c in hydrogen bubble chamber, cross sections for resonance production in, (E), 26:54207 (COO-3064-3)
- interactions $\pi^- + p \to p + \pi^-$ at 5.91 to 13.73 GeV/c, extrapolation of asymptotic cross section for baryon-pole coupling in backward, (E/T), 26:54331
- interactions $\pi^- + p \to \pi^0 + n$, new Regge absorption model for cross sections and polarization in, (T), 26:54336
- interactions $\pi^- + p \to \pi^0 + n$, Regge pole--cut model for, (E/T), 26:54230
- interactions $\pi^- + p \to \pi^0$(eta) + n with small momentum transfer, method for determining differential cross sections for, 26:54209 (JINR-P1-6414)
- interactions $\pi^- + p \to \pi^- + p$ at 0.875 to 1.580 GeV/c, differential cross sections for forward, (E/T), 26:54224
- interactions $\pi^- + p \to \pi^- + \pi^+ + n$ at 8 GeV/c, production and decay angular distributions of rho^0, f^0, and g^0 in, (E), 26:54216
- interactions $\pi^- + p \to \pi^+(\pi^-)$ + anything at 16 GeV/c, differential cross sections and symmetry of π emission for, (E), 26:54222
- interactions $\pi^- + p \to \pi^+(\pi^-)$ + anything at very high energies, limiting distributions for, (T), 26:54326 (DESY-72/40)
- interactions $\pi^- + p \to$ rho^0 + n, contribution of unnatural parity exchanges to, (T), 26:54270
- interactions $\pi^- + p \to \Sigma(1385) + K^+$ at 4.5 and 6 GeV/c, differential cross sections for, (E), 26:54217
- interactions $\pi^- + p$ at 0.4 to 0.90 GeV/c, total cross sections for, (E), 26:54213
- interactions $\pi^- + p$ at 40 GeV/c, average number of produced π^+--π^- pairs, coefficient of nucleon charge exchange, and identical distribution over charged particle multiplicity for, (T), 26:54327 (JINR-E2-6596)
- interactions $\pi^- + p$, compilation of cross sections for, 26:54201 (CERN/HERA-72-1)
- interactions $\pi^+ + \pi^-$ from $\pi^+ + p \to \pi^+ + \pi^- + \Delta^{++}$ interactions at 13 GeV/c, phase shift analysis of, (E), 26:54223
- production in $\gamma + n \to \pi^- + p$ interactions at 600 to 1250 MeV, differential cross sections for, (E), 26:54179
- production in inclusive $e + p \to e + \pi^-$ + anything interactions at 6.5 GeV, momentum spectra of, (E), 26:54178
- production in inclusive hadron interactions with protons at very high energies, limiting distributions for, (T), 26:54326 (DESY-72/40)
- production in inclusive interactions, multiperipheral-model calculations of cross sections for, (T), 26:54325 (COO-3533-2)
- production of π^+--π^- pairs in $\pi^- + p$ and $\pi^- + n$ interactions at 40 GeV/c, average number for, (T), 26:54327 (JINR-E2-6596)

MESONS (π^0)
- decay $\pi^0 \to \gamma + e^+ + e^-$, radiative corrections to, (T), 26:54277
- interactions $K^+ + \pi^0$, Schwarz inequality for cross sections for, (T), 26:54287 (LBL-766)
- production in e + N interactions at $q^2 = 0.6$ to 1.56 GeV^2, angular distributions for, (E), 26:54268

MESONS (π^+)
- decay $\pi^+ \to \mu^+ + \nu$, π^+ mass and upper limit on ν mass from μ^+ energy in, (E), 26:54189
- interactions $\pi^+ + d \to 2p + \pi^+ + \pi^-$ at 13 GeV/c, I = 0 S-wave phase shift from partial-wave analysis of $\pi\pi$ spectra and rho and f production cross sections in, (E/T), 26:54219
- interactions $\pi^+ + d$, compilation of cross sections for, 26:54201 (CERN/HERA-72-1)
- interactions $\pi^+ + n$, compilation of cross sections for, 26:54201 (CERN/HERA-72-1)
- interactions $\pi^+ + p \to K^+ + \Sigma^+$, new Regge absorption model for cross sections of, (T), 26:54336
- interactions $\pi^+ + p \to N + 2\pi$ at 1.6 to 2.0 GeV, energy-independent partial-wave analysis of baryon resonance production in, (E), 26:54328 (LBL-544)
- interactions $\pi^+ + p \to p + \pi^+$ at 5.91 to 13.73 GeV/c, extrapolation of asymptotic cross section for baryon-pole coupling in backward, (E/T), 26:54331
- interactions $\pi^+ + p \to \pi^-$ + anything at 7 GeV/c, multiperipheral-model calculations of cross sections for, (T), 26:54325 (COO-3533-2)
- interactions $\pi^+ + p \to \pi^-$ + anything at 8 and 16 GeV/c, differential cross sections and symmetry of π emission for, (E), 26:54222
- interactions $\pi^+ + p \to \pi^+ + p + \pi^+ + \pi^-$ at 5.45 GeV/c, production properties of A_1^+ in, (E), 26:54227
- interactions $\pi^+ + p \to \pi^+ + \pi^- + \Delta^{++}$ at 13 GeV/c, phase shift analysis of $\pi^+\pi^-$ scattering from, (E), 26:54223
- interactions $\pi^+ + p \to \pi^+(\pi^-)$ + anything at very high energies, limiting distributions for, (T), 26:54326 (DESY-72/40)
- interactions $\pi^+ + p$ at 0.4 to 0.90 GeV/c, total cross sections for, (E), 26:54213
- interactions $\pi^+ + p$, compilation of cross sections for, 26:54201 (CERN/HERA-72-1)
- interactions $\pi^+ + p$, identical distribution over charged particle multiplicity for, (T), 26:54327 (JINR-E2-6596)
- interactions $\pi^+ + \pi^-$ from $\pi^+ + p \to \pi^+ + \pi^- + \Delta^{++}$ interactions at 13 GeV/c, phase shift analysis of, (E), 26:54223
- mass from $\pi^+ \to \mu^+ + \nu$ decay, (E), 26:54189
- production in e + p interactions, k^2 dependence of transverse cross section in generalized Born term model, (T), 26:54243 (DESY-72/30)
- production in $\gamma + p \to \pi^+ + n$ interactions at 0.5 to 2.2 GeV, magnetic spectrometer study of structure in target asymmetry in, (E), 26:54172 (NP-19415)
- production in inclusive $e + p \to e + \pi^+$ + anything interactions at 6.5 GeV, momentum spectra of, (E), 26:54178
- production in inclusive hadron interactions with protons at very high energies, limiting distributions for, (T), 26:54326 (DESY-72/40)
- production of π^+--π^- pairs in $\pi^- + p$ and $\pi^- + n$ interactions at 40 GeV/c, average number for, (T), 26:54327 (JINR-E2-6596)

MESONS (rho)
- coupling constants for γ rho, in relativistic extended quark model, 26:54283
- decay rho $\to \pi^+ + \pi^-$, I = 0 S-wave phase shift from partial-wave analysis of $\pi\pi$ spectra and angular distributions for, (E/T), 26:54219
- decay rho$^-$ $\to 2\pi$ in hydrogen bubble chamber, width of, (E), 26:54175 (SLAC-143)
- mass differences of members of A_1, rho, and π isomultiplets, dynamic chiral symmetry and cancellation of divergences in, (T), 26:54321
- production and decay angular distributions from $\pi^- + p \to \pi^- + \pi^+ + n$ interactions at 8 GeV/c, (E), 26:54216
- production in $\pi^+ + d \to 2p + \pi^+ + \pi^-$ interactions at 13 GeV/c, cross sections for, (E), 26:54219
- production of rho^0 and rho$^-$ in $\gamma + p$ interactions at 2 to 7.5 GeV, cross sections for, (E), 26:54175 (SLAC-143)
- production of rho$^-$ and rho^0 in $\pi^- + p \to p + \pi^+ + 2\pi^- + \pi^0$ at 20 GeV/c in hydrogen bubble chamber, cross sections for, (E), 26:54207 (COO-3064-3)
- production of rho$^-$ in $\pi^- + d \to 2p + 2\pi^- + \pi^0$ interactions at 7 GeV/c in deuterium bubble chamber, validity of spectator model for cross sections for, (E), 26:54208 (COO-3065-16)
- vertex function of nonrenormalizable πrhoπ interaction, ladder approximation for, (T), 26:54322

MESONS, PSEUDOSCALAR
- interactions involving vector mesons and photons, ω--phi mixing angle from Odorico bootstrap of, (T), 26:54323
- production in ν + N interactions, quark-model predictions of cross sections for, (T), 26:54285 (DESY-72/32)
- vertex function of nonrenormalizable vector--pseudoscalar--pseudoscalar meson interaction, ladder approximation for, (T), 26:54322

MESONS, RESONANCE
- mass and width of broad S-wave (1305) in $K^+ + n \to K^+ + \pi^- + p$ interactions at 9 GeV/c, (E), 26:54203 (COO-1428-308)
- mass and width of $M^0(1033)$ in $\pi^- + p \to n$ + anything interactions at 2.4 GeV/c, scintillation counter study of, (E), 26:54205 (COO-1428-311)
- production of (2020) enhancement in three- and four-prong anti p + p interactions at 7 GeV/c in deuterium bubble chamber, (E), 26:54218
- production of broad S-wave (1305) in $K^+ + n \to K^+ + \pi^- + p$ interactions at 9 GeV/c, (E), 26:54203 (COO-1428-308)
- production of exotic multipion, in $\pi^- + d$ interactions at 7 GeV/c in deuterium bubble chamber, upper limit for, (E), 26:54208 (COO-3065-16)
- production of F_1 in anti p + p interactions at 1.2 GeV/c, (E), 26:54199
- production of $M^0(1033)$ in $\pi^- + p \to n$ + anything interactions at 2.4 GeV/c, scintillation counter study of, (E), 26:54205 (COO-1428-311)
- properties of 3π, Kanti Kπ, and K$\pi\pi$, relativistic Faddeev-type approach to, (T), 26:54318

MESONS, RESONANCE (eta)
- decay f(1260) $\to \pi^+ + \pi^-$, I = 0 S-wave phase shift from partial-wave analysis of $\pi\pi$ spectra and angular distributions for, (E/T), 26:54219
- decay $f^0 \to K^+ + K^-$, cross sections, branching ratios, and angular distributions for, (E), 26:54218
- effects of epsilon and S*(980) on scale invariance breaking for low-energy theorems for $\pi\pi$ interactions, 26:54319
- interference of f^0 and $A_2{}^0$ in three- and four-prong anti p + p interactions at 7 GeV/c in deuterium bubble chamber, (E), 26:54218
- production and decay angular distributions of $f^0(1260)$ from $\pi^- + p \to \pi^- + \pi^+ + n$ interactions at 8 GeV/c, (E),

- 26:54216
  - production of f(1260) in $\pi^+ + d \to 2p + \pi^+ + \pi^-$ interactions at 13 GeV/c cross sections for, (E), 26:54219
  - production of f^0(1260) and f'(1514) in three- and four-prong anti p + p interactions at 7 GeV/c in deuterium bubble chamber, (E), 26:54218
- MESONS, RESONANCE (K)
  - decay of K(1760) and K(2200) in deuterium bubble chamber, proposed experiment for, (E), 26:54204 (COO-1428-310)
  - decay $Q \to K(890) + \pi^+$ from $K^+ + d$ interactions at 9 GeV/c, (E), 26:54228
  - mass and width of K^0(890) and K^0(1420) in $K^+ + n \to K^+ + \pi^- + p$ interactions at 3.8 GeV/c in deuterium bubble chamber, (E), 26:54202 (COO-1195-238)
  - production of K* in $K^+ + p$ interactions at 1.37 to 2.17 GeV/c, analysis of, (E), 26:54231
  - production of K*(890) and K*(1420) in $\pi^- + p$ interactions at 4.5 and 6 GeV/c, differential cross sections and density matrix elements for, (E), 26:54217
  - production of K(1760) and K(2200) in $K^+ + n \to p +$ anything interactions at 9 GeV/c in deuterium bubble chamber, proposed experiment for, (E), 26:54204 (COO-1428-310)
  - production of K(890) and K(1420) in $K^+ + n \to K^+ + \pi^- + p$ interactions at 9 GeV/c, (E), 26:54203 (COO-1428-308)
  - production of K^0(890) and K^0(1420) in $K^+ + n \to K^+ + \pi^- + p$ interactions at 3.8 GeV/c in deuterium bubble chamber, cross sections for, (E), 26:54202 (COO-1195-238)
  - production of K_1K_1(1440) in three- and four-prong anti p + p interactions at 7 GeV/c in deuterium bubble chamber, (E), 26:54218
  - production of Q in $K^+ + d$ interactions at 9 GeV/c in deuterium bubble chamber, spin--parity analysis of, (E), 26:54228
  - spin density matrix elements of K^0(890) in $K^+ + n \to K^+ + \pi^- + p$ interactions at 3.8 GeV/c in deuterium bubble chamber, (E/T), 26:54202 (COO-1195-238)
- MESONS, RESONANCE (π)
  - decay $A_2^0 \to K^+ + K^-$, cross sections, branching ratios, and angular distributions for, (E), 26:54218
  - interference of f^0 and A_2^0 in three- and four-prong anti p + p interactions at 7 GeV/c in deuterium bubble chamber, (E), 26:54218
  - mass differences of members of A_1, rho, and π isomultiplets, dynamic chiral symmetry and cancellation of divergences in, (T), 26:54321
  - production of A_1^0 and A_2^0 in $\pi^- + p \to p + \pi^+ + 2\pi^- + \pi^0$ interactions at 20 GeV/c, upper limits for cross sections for, (E), 26:54207 (COO-3064-3)
  - production of A_1^+ in $\pi^+ + p \to \pi^+ + p + \pi^+ + \pi^-$ interactions at 5.45 GeV/c, (E), 26:54227
  - production of A_2(1310) in $\gamma + p$ interactions at 2 to 7.5 GeV in hydrogen bubble chamber, (E), 26:54175 (SLAC-143)
  - production of A_2(1310) in three- and four-prong anti p + p interactions at 7 GeV/c in deuterium bubble chamber, (E), 26:54218
  - properties of A_2(1310), spark chamber study of, (E), 26:54206(R) (COO-2009-36)
- MESONS, RESONANCE (rho)
  - production of B^-(1235) in $\pi^- + p \to p + \pi^+ + 2\pi^- + \pi^0$ interactions at 20 GeV/c, cross sections for, (E), 26:54207 (COO-3064-3)
  - production of g^0(1670) in $\pi^- + p \to \pi^- + \pi^+ + n$ interactions at 8 GeV/c, (E), 26:54216
  - production of rho^-(1250) and rho^-(1650) in $\gamma + p$ interactions at 2 to 7.5 GeV in hydrogen bubble chamber, cross sections for, (E), 26:54175 (SLAC-143)
  - production of rho^-(1700) in $\pi^- + p \to p + \pi^+ + 2\pi^- + \pi^0$ interactions at 20 GeV/c, upper limits for cross sections for, (E), 26:54207 (COO-3064-3)
  - production of S(1070), g(1660), and rho(1710) in three- and four-prong anti p + p interactions at 7 GeV/c in deuterium bubble chamber, (E), 26:54218
- MESONS, VECTOR
  - decays into pseudoscalar meson + photons, coupling constants for, (T), 26:54323
  - existence of high-mass, from $e^+ + e^-$ interactions in storage rings, (T), 26:54283
  - role of neutral, in $e^+ - e^-$ pair production in photon reactions with spin-$^1/_2$ point nuclei, angular dependence of cross sections for, (T), 26:54260
  - search for neutral, in K_2^0 decays, (E), 26:54291
  - vertex function of nonrenormalizable vector--pseudoscalar--pseudoscalar meson interaction, ladder approximation for, (T), 26:54322
- METALLOGRAPHY
  - sample preparation for, in hot cells, selection of cleaning solutions and lubricants for, 26:53729 (LA-DC-72-230)
- METALLURGICAL EQUIPMENT
  - description for examination of irradiated uranium dioxide NTR fuel particles, 26:53555 (RD/B/N-2214)
- METALLURGY
  - conference on uses of field-ion microscopy in, Atlanta, Georgia, May 15 to 17, 1968, 26:53647
  - research in India, 1971--1972, 26:55452(R) (NP-19407)
  - research on, compilation of projects on USAEC, 26:53600 (WASH-1181-72)
- METALS
  - abundance in galaxies, (T), 26:53977
  - abundance in globular clusters, (E), 26:53880
  - deformation of, structure dependence of high-temperature, 26:55613(R) (SU-326-P-17-X-2)
  - dislocations and stacking faults in, field-ion microscopy studies of, 26:53649
  - fabrication by rolling at high temperature under vacuum, 26:53630
  - grain boundary structures in, field-ion microscopy studies of, 26:53650
  - impurity distribution in, effects of thermal gradients on, 26:53665
  - positron correlation energy in, (T), 26:55066
  - radiation effects on spherical void growth in, effects of triaxial stress on, (T), 26:53702 (TID-26150)
  - radioinduced point defects in, field-ion microscopy studies of, 26:53704
  - radioinduced swelling of, dose and dose rate dependences of, (T), 26:53707
  - reactions with gases, field-ion microscopy studies of, 26:53657
  - sintering of, review on mechanism of activated, 26:53587
  - spectral lines in prominences and chromosphere due to, (E), 26:53949
  - welding of thick sheets of, equipment and methods for electron beam, 26:53633
  - metals--plastics, preparation and properties of, produced by radioinduced polymerization, 26:53722
- METEORITES
  - analysis for iodine and six metals by neutron activation and separation processes, 26:52906
  - cosmic-ray reactions in iron, (T), 26:53808(T) (ORNL-tr-2620)
  - isotopic abundances in iron, (T), 26:53808(T) (ORNL-tr-2620)
  - rare gases in Mokoia and Allende, isotopic composition of, (E), 26:53810
- METHACRYLIC ACID, METHYL ESTER POLYMERS
  - effects of Plexiglas ampoules on helium II superfluid film flow transfer, 26:54431
  - reactions with radicals produced by γ radiolysis of propene polymers, kinetics of, 26:53019
- METHANE
  - yields from argon- and xenon-sensitized radiolysis of gaseous ethylene, 26:53000
- METHANE, DICHLORODIFLUORO-
  - flow in heated loops, photographic study of post-burnout two-phase, 26:53122
- METHANE, IODO-
  - separation from fuel reprocessing off-gases, evaluation of silver-containing sorbents for, 26:53077 (CONF-720823-9)
  - sorption on commercial impregnated charcoals, efficiencies of, 26:53058 (CONF-720823-10)
- METHANE, NITRO-
  - photolysis of liquid, analysis of products from, 26:52978 (CEA-N-1528)
  - properties of, summary of chemical and physical, 26:52978 (CEA-N-1528)
  - radiolysis of liquid, analysis of products from, 26:52978 (CEA-N-1528)
  - reactions with methyl radicals, 26:52978 (CEA-N-1528)
- METHANESULFONIC ACID
  - hycanthone, effects on cultured mouse lymphoma cells in comparison to effects of EMS and x radiation, phenotypic method for determining frequency of mutagenic, 26:53361
- METHANESULFONIC ACID, ETHYL ESTER
  - effects on cultured mouse lymphoma cells in comparison to effects of hycanthone methane-sulfonate and x radiation, phenotypic method for determining frequency of mutagenic, 26:53361
- METHANOL
  - effects on γ-induced thermoluminescence of cyclohexene, 26:53010
  - radiolysis of glasses of, hydrogen abstraction by methyl radical in, 26:52990 (ORO-2968-78, Paper 5)
  - radiolysis of liquid, spin trapping studies on primary methoxy radicals from γ, 26:52988 (ORO-2968-78, Paper 2)
- METHYL RADICALS
  - reactions of photolytic, with nitromethane, 26:52978 (CEA-N-1528)
  - reactions of radiolytic, with hydrogen from methanol molecules, 26:52990 (ORO-2968-78, Paper 5)
  - thermal decay of radiolytic, in methanol glasses, ESR studies on, 26:52990 (ORO-2968-78, Paper 5)
- MICE
  - arsenic-74 distribution and metabolism in tissues of, following oral administration, time dependence of, 26:53538
  - determination of hematopoietic and pulmonary origins of alveolar macrophages in radiation chimeras of, 26:53492
  - radiation effects on alkaline phosphatase activity and chromosomes of, strontium-90 β and x, 26:53496
  - radiation effects on count of plaque-forming cells in spleen of antigen-stimulated, following whole-body exposure, effects of dose on γ and x, 26:53469
  - radiation effects on diurnal rhythm of neurosecretory activity in, following whole-body exposure, x,

26:53478

radiation effects on growth of goitrogen-stimulated thyroid gland in, effects of dose rate on RBE for internal iodine-131 or iodine-132 β and γ and external x, 26:53472

radiation effects on growth of thyroid gland in fetal and goitrogen-stimulated adult, following intravenous injection of iodine-131, β and γ, 26:53513

radiation effects on hematopoiesis and immune reactions in, following whole-body exposure, comparison of RBE for γ and high-intensity pulsed x, 26:53469

radiation effects on immune reactions to allogenic bone marrow transplants in, age dependence of lethal dose x, 26:53485

radiation effects on phagocytic activity of reticuloendothelial cells in, following whole-body exposure, effects of dose on x, 26:53468

radiation effects on ratio of erythrocytes to leukocytes in bone marrow of, evaluation for use as biological dosimeter, 26:53473

radiation effects on serum protein content and serum albumin-globulin ratio of, combined effects of cortisone on gamma, 26:53490

radiation effects on spleen colony formation by transplanted isogeneic hematopoietic stem cells in, lethal dose x, 26:53466

radiation effects on survival of embryos of, following acute or fractionated exposure in utero, comparison of RBE of fast neutron with x radiation, 26:53453 (NASA-TM-X-2440, pp 641)

radiation effects on survival of epidermal cells in skin of, following single local exposure, comparison of RBE for carbon, helium, and lithium charged particle with x radiation, 26:53456 (NASA-TM-X-2440, pp 652-8)

radiation effects on survival of erythropoietic stem cells in, following sublethal whole-body exposure, protective effects of AET and serotonin against proton, 26:53454 (NASA-TM-X-2440, pp 642-6)

radiation effects on survival of, following acute lethal whole-body exposure, comparison of RBE for californium-252 γ and neutron with cobalt-60 and radium-226 γ, 26:53484

radiation effects on survival of, following lethal whole-body exposure, protective effects of combined AET and pantothenic acid against x, 26:53481

radiation effects on survival of, protective effects of allogeneic bone marrow transplants against lethal x, 26:53485

radioinduced changes in pituitary gland of, following partial- or whole-body exposure, relation of ultrastructural changes to secretory changes in cells of, x, 26:53467

radioinduced digital malformations in fetal, following whole-body exposure in utero, effects of developmental stage, dose, and dose rate on incidence of γ, 26:53471

radioinduced inhibition of gastrulation in early embryos of, x, 26:53476

radioinduced leukemia in, following fractionated sublethal whole-body exposure, protective effects of cysteamine against, 26:53475

radioinduced leukemia in, following fractionated whole-body exposure, incidence and cytological characteristics of x, 26:53512

radioinduced leukemia in, following intraperitoneal injection of strontium-90, incidence and cytological characteristics of β, 26:53512

radioinduced leukemia in, following whole-body exposure, comparison of incidence of γ and x, 26:53469

radioinduced leukemia in, studies on transmission of strontium-90 β and x, 26:53496

radioinduced malformations of brain of, following prenatal exposure, effects of developmental stage at exposure on, 26:53437

radioinduced pathological changes in, effects of bathing in thermal spring water on recovery from mixed fast neutron and γ, 26:53465

radioinduced suppression of antibody-forming cells in spleen of, during response to antigen challenge, acute whole-body x, 26:53464

rotational tracer study using perturbed angular correlation of indium-111, 26:55058

MICROORGANISMS

radiation effects on, combined effects of space flight environment on mutagenesis and survival of, γ, 26:53365 (N-72-20065)

MICROWAVES

cosmic background, Compton scattering by relativistic cosmic electrons, (E/T), 26:54000

MILK

iodine-131 content of human, following injection of labeled pharmaceuticals for diagnostic scanning of kidneys, lungs, and placenta, 26:53524

radioactivity monitoring of, in vicinity of Savannah River Plant, 1971, 26:53153(R) (DPSPU-72-30-1)

radioisotope content of Norwegian, 1956 to 1970, cesium-137, iodine-131, and strontium-90, 26:53161

MILKY WAY

book: Galactic Astronomy, Vol. I, 26:53981

central region of, dynamics of, (T), 26:53983

Cepheid variables in, (T), 26:53986

continuum radiation from, thermal and nonthermal, (T), 26:53984

cosmic-ray confinement mechanisms, (T), 26:53865

dynamics of, (T), 26:53982

electron diffusion in, (T), 26:53809

gamma emission above 10 MeV from anticenter plane of, search for, (E), 26:53816

gamma flux from center region of, (E), 26:53818

gamma flux in, high-energy, (E), 26:53819

gamma-ray density in, (E/T), 26:53992

HI regions in, origin of, (T), 26:53983

hydrogen distribution in, (T), 26:53984

hydrogen in, angular distribution of atomic, (T), 26:53979

interstellar absorption of optical lines in, (T), 26:53985

kinematics of stellar motions in, (T), 26:53982

magnetic-field line wandering in, effects on cosmic-ray parameters, (T), 26:53864

rotation from 21-cm study, (T), 26:53984

spiral structure in, causes and effects of irregular, (T), 26:53987

spiral structure of, 21-cm line study of, (T), 26:53983

star distribution in, (E/T), 26:53992

supernovae in, rate of, (E), 26:53974

x-ray background in, origin of, (E), 26:53973

x-ray brightness of disc of, (T), 26:53853

MILLSTONE POINT POWER REACTOR, UNIT 1

coolant for, abnormal chemistry limits for, 26:55280 (DOCKET-50245-160)

cooling system for, abnormal leak rate for primary, 26:55280 (DOCKET-50245-160)

operation of, application for conversion from provisional to full term license for, 26:55279 (DOCKET-50245-159)

site for, environmental radiation survey during January to June 1972, 26:55246 (DOCKET-50245-158)

MINERALS

analysis by neutron activation and γ spectroscopy, nondestructive, 26:52901 (UJV-2851-F,Ch)

analysis for iron, manganese, niobium, and tantalum by direct measurement of oxide ratios, spectroscopic, 26:52932

fission fragment tracks from heavier transuranium elements in natural, study of spontaneous, 26:54670

reactions of sulfide, with thiol reagents, 26:52954 (NIM-1439)

MINES

air in, electron-capture ionization detector for analyzing, 26:53287

radon daughter products in air of uranium, α-spectrometric method for determining content of, 26:53226

MITOCHONDRIA

radiation effects on respiration and ultrastructure of, in intestinal epithelial cells of rats during amino acid absorption, whole-body x, 26:53493

MOESSBAUER EFFECT

experiments on lifetime of excited nuclei, suggested, 26:55061

gamma laser based on long-lived isomers, feasibility of, (T), 26:55062

polarization effects in, (T), 26:54703

uses in analytical chemistry, 26:52942

uses in art identification, 26:52898 (COO-3034-2)

MOLECULAR STRUCTURE

wave functions in, spin-dependent operators in occupation-branching number representation for open-shell, (T), 26:55077

MOLECULES

atom reactions with diatomic, calculation of semiclassical S-matrix elements for transitions in inelastic and reactive, by integration along complex-valued trajectories, 26:54129

atom reactions with diatomic, effects of attractive Morse potential on quantum mechanical transition probabilities in, (T), 26:54132

atom reactions with diatomic, impulse approximation for vibrational-excitation probabilities in, using Morse potential, 26:54131

electromagnetic-field interactions with system of, semiclassical theory of, 26:55468 (AREAEE-136)

energy of degenerate levels of, with two perturbations, double perturbation form for second-order, 26:54152

expectation values for, calculation using spin-adapted antisymmetrized products, 26:54154

potentials for superheavy, formed in heavy-ion collisions, (T), 26:54111

reactions with atoms, ions, and molecules, bibliography and compilation of data on charge exchange, dissociations, excitation, and ionization, in, 26:54118

study of biological macro-, using indium-111 tracer and perturbed angular correlation, 26:55058

wave functions for, direct diagonalization method for generation of Serber-type simultaneous angular-momentum and spin eigenfunctions for use in expansion of, 26:54156

wave functions for, direct-diagonalization method for generation of Serber-type spin eigenfunctions for use in expansion of, 26:54155

wave functions for, expansion in terms of spin-adapted antisymmetrized products, 26:54154

wave functions for, instabilities associated with complex

and unrestricted Hartree--Fock, 26:54157
wave functions for, review of properties and uses of natural spin orbitals in construction of, 26:54150
MOLLUSCA
Lymnaea columella (snail), role as vector of fascioliasis in Puerto Rico, 26:53498(R) (PRNC-156)
Lymnaea cubensis (snail), role as vector of fascioliasis in Puerto Rico, 26:53498(R) (PRNC-156)
MOLTEN SALT BREEDER REACTOR
fuel reprocessing for, design and construction of molybdenum reductive extraction equipment for, pp. 11-12, 26:53081 (ORNL-4794, pp 1-14)
fuel reprocessing for, research progress on, 26:53081 (ORNL-4794, pp 1-14)
MOLTEN SALT REACTOR EXPERIMENT
control systems of, detailed design of, 26:55138 (ORNL-TM-729(Pt.2B))
coolant for, performance of eutectic mixture sodium fluoroborate and sodium fluoride secondary, (E), 26:55177 (ORNL-TM-3344)
electric circuitry of, detailed design of central and instrumentation, 26:55138 (ORNL-TM-729(Pt.2B))
fuel reprocessing systems for, detailed design of instrumentation for, 26:55138 (ORNL-TM-729(Pt.2B))
instrumentation of, detailed design of, 26:55138 (ORNL-TM-729(Pt.2B))
safety systems of, detailed design of instrumentation of, 26:55138 (ORNL-TM-729(Pt.2B))
MOLYBDENITES
processing of, separation of molybdenum and rhenium from scrubber solutions from, 26:52950(P)
reactions with thiol reagents, 26:52954 (NIM-1439)
MOLYBDENUM
book: Early Transition Metals, 26:52956
compatibility of fuel capsules of, with plutonium-238 oxide fuels, 26:53551(R) (MDC G-3153)
content in rock, γ--γ selective method for determination of equivalence between other heavy element and, 26:52943
deformation of single-crystal, effects of surface orientation on, 26:53645
deposition by hydrogen reduction of chloride or fluoride, method for chemical vapor, 26:53622
determination in steel by potentiometric titration, 26:52924
determination in water, effects of large amounts of copper on spectrographic, 26:52927
determination using carminic acid, spectrophotometric, 26:52931
determinaton of trace amounts of, spectroscopic, 26:52929
effects on cohesion and structural stability of aluminum oxide composites with iron and nickel, 26:53589
embrittlement of, effects of carbon and oxygen on, 26:53682
fabrication by hot isostatic pressing, 26:53578
fabrication by rolling at high temperature under vacuum, 26:53630
fabrication for use as reductive extraction equipment in MSBR fuel reprocessing, pp. 11-12, 26:53081 (ORNL-4794, pp 1-14)
incorporation of reinforcing fibers of, in stainless steel with precise alignment and uniform distribution, method for, 26:53629
muon stopping and diffusion in hot foils of, in vacuum, production of muonium by, (E), 26:54096
photon reactions (γ,n) at 12 to 23 MeV, neutron spectra from, (E), 26:54563
radiation effects on structure of polycrystalline, x-ray diffraction studies on 60-keV helium ion, 26:53700(T) (SC-T-722540)
separation from indium by ion exchange chromatography, 26:52949
separation from molybdenite using thiol reagents, 26:52954 (NIM-1439)
separation from scrubber solutions from roasting of molybdenite by solvent extraction and crystallization, 26:52950(P)
sintering of powders of, at 1200 to 1450°C, kinetics and mechanism of, 26:53621
solvent properties for nitrogen, effects of temperature and pressure on, 26:53580
void lattice model, 26:55052
welding of, effects of contact surface and structure on diffusion, 26:53625
MOLYBDENUM ALLOYS AND SYSTEMS
composition and physical properties of composite powders of, 26:53680
preparation of composite powders of, by hydrogen reduction, 26:53680
Al--Co--Cr--Mo--Ni-base--Ta--Ti--W, sintering and stress-rupture properties of, effects of boron, carbon, and oxygen additions on, 26:53674
Al--Co--Cr--Mo--Ni-base--Ti, sintering and stress-rupture properties of, effects of boron, carbon, and oxygen additions on, 26:53674
Al--Cr--Mo--Nb--Ni-base--Ta--W, production and properties of powder metallurgy components of, for use at high temperatures, 26:53631
Al--Mo--Sn--Ti-base--Zr, creep rupture of, at 755 and 865°K, cyclic, 26:53690
Al--Mo--Ti-base--V, crack propagation and embrittlement by gaseous hydrogen, mechanism of, 26:53685
C--Mo, thermodynamic properties of liquid solutions of, 26:53588
Cr--Cu--Fe--Mo--Ni-base--Ti, corrosion by thorium dioxide dissolvent solutions, 26:53604 (BNWL-CC-449)
Cr--Mo--steel, corrosion by products of sodium--water reactions, 26:55154 (CONF-710546-, pp 105-28)
Cr-base--Mo--Ta, coatings for nitridation resistance of, in air, chromium, hafnium, lanthanum, and yttrium combination cementation, 26:53689
Fe-base--Mo, radiation effects on mechanical properties of, 2.3-MeV electron, 26:53706
Mn--Mo--Ni--steel, mechanical properties of pressure vessel, effects of quenching, tempering, and heat treatment on, 26:53646
Mo--N, degassing at 1200 to 3000°C in, equilibria and kinetics of, 26:53580
Mo--N--Nb, phase studies and thermodynamics of, as function of pressure and temperature, 26:53671
Mo--Nb-base, entropy of vortices in superconducting, (E), 26:54441
Mo--Ni--W-base, mechanical properties of, effects of heat treatments following sintering on, 26:53679
Mo--Ni--W-base, preparation and composition of, 26:53679
Mo--Ni-base, mechanical properties of, at 800 to 1200°C, 26:53667
Mo--O, thermodynamic properties of liquid solutions of, 26:53588
Mo--PuO_2, radiation emission by heat sources of, effects of age, fluorine-19, oxygen-17, oxygen-18, plutonium-236, and size on γ and neutron, 26:53336 (NASA-TM-X-2440, pp 853-8)
Mo--Si, diffusion of silicon in Mo_5Si_3 phase in, at high temperatures, 26:53583
Mo--U-base, corrosion of wires of, ion microscopy studies of stress, 26:53610
Mo--UO_2, fabrication of, review on methods for, 26:53592
Mo--W-base, compatibility of fuel capsules of, with plutonium-238 oxide fuels, 26:53551(R) (MDC G-3153)
Mo--ZrO_2, oxidation of, effects of temperature on rate of, 26:53585
Mo-base--Re, compatibility of fuel capsules of, with plutonium-238 oxide fuels, 26:53551(R) (MDC G-3153)
MOLYBDENUM ISOTOPES Mo-90
beta decay scheme, (E), 26:54613
MOLYBDENUM ISOTOPES Mo-92
alpha elastic scattering at 166 MeV, angular distribution for, (E), 26:54547
neutron radius of, determination from elastic scattering, (E), 26:54547
proton elastic and inelastic scattering at 12.0 MeV, differential cross sections for, (E), 26:54606 (ORNL-TM-3913)
proton elastic scattering at 11.2 to 12.4 MeV, excitation functions for, (E), 26:54467(R) (ORO-2972-204)
MOLYBDENUM ISOTOPES Mo-93
energy level at 1.69 MeV from molybdenum-95 (p,t) reactions, spin--parity assignment for, (E), 26:54612
MOLYBDENUM ISOTOPES Mo-94
proton elastic and inelastic scattering at 12.0 MeV, differential cross sections for, (E), 26:54606 (ORNL-TM-3913)
MOLYBDENUM ISOTOPES Mo-95
proton reactions (p,t) at 31 MeV, DWBA analysis of differential cross sections for, (E), 26:54612
MOLYBDENUM ISOTOPES Mo-96
proton elastic and inelastic scattering at 12.0 MeV, differential cross sections for, (E), 26:54606 (ORNL-TM-3913)
MOLYBDENUM ISOTOPES Mo-100
deuteron reactions (d,p) at 3.05 to 3.75 MeV, DWBA analysis of differential cross sections and excitation function for, (E), 26:54614
proton elastic and inelastic scattering at 12.0 MeV, differential cross sections for, (E), 26:54606 (ORNL-TM-3913)
MOLYBDENUM ISOTOPES Mo-101
energy levels from molybdenum-100 (d,p) reactions, spectroscopic factors and spin--parity assignments for, (E), 26:54614
nuclear spin, parity, and spectroscopic factor from molybdenum-100 (d,p) reactions, (E), 26:54614
MOLYBDENUM OXIDES
growth and hardness of spherical agglomerates of, produced from powders, 26:53577
production of microspheres of, from powders in rotating container, 26:53577
MOLYBDENUM SILICIDES
fabrication by casting of thermoplastic masses, 26:53586
Mo_5Si_3--ZrB_2, oxidation resistance and sinterability of, at high temperatures, 26:53594
$MoSi_2$--ZrB_2, oxidation resistance and sinterability of, at high temperatures, 26:53594
MONKEYS
plutonium removal from lungs of, following inhalation as oxide, effectiveness of pulmonary lavage for, 26:53528(T) (LF-tr-71)
radiation dose distribution in respiratory tract tissues of, following inhalation of strontium-90 as fused clay aerosols, β, 26:53536
radiation effects on ability to perform learned tasks

- following continuous whole-body exposure, effects of dose and dose rate on γ, 26:53452 (NASA-TM-X-2440, pp 633-40)
- radioinduced suppression of bone marrow hematopoietic function in, following continuous and subsequent fractionated whole-body exposures, effects of dose and dose rate on recovery from γ, 26:53452 (NASA-TM-X-2440, pp 633-40)

MONTICELLO POWER REACTOR, UNIT 1
- maintenance during January to June 1972, 26:55253 (DOCKET-50263-149)
- operations during January to June 1972, 26:55253 (DOCKET-50263-149)
- site for, environmental radiation survey during January to June 1972, 26:55253 (DOCKET-50263-149)
- valves for, verification of wall thicknesses for nuclear service, 26:55288 (DOCKET-50263-150)

MOON
- charged-particle shadowing by, (T), 26:53943
- interactions with near magnetic fields and plasmas, Apollo-15 subsatellite observations of, (E), 26:54072
- tides in, effects on seasonal and daily variations in Peruvian equatorial electrojets, (E), 26:54041

MOUTH
- radiation effects on tissues of, in patients during tumor therapy in head and neck region, construction of prosthesis shield for protection against, 26:53410

MUONIC ATOMS
- energy-level transitions of heavy, corrections to long-wavelength approximation for x radiation from electric multipole, 26:54098

MUONIUM
- conversion to antimuonium, method of search for, 26:54096
- production in vacuum by diffusion of muons stopped in hot metal foils, (E), 26:54096

MUONS
- anisotropy of cosmic, sidereal, (E), 26:53846
- betatron oscillations in g - 2 experiment in storage rings, 26:53763
- detection and discrimination from pions using multiwire proportional counters, 26:53282
- gyromagnetic ratio of, sixth-order contribution to anomalous, (T), 26:54271
- intensity variations of cosmic, sidereal, (E), 26:53847
- interactions $\mu + p \to \mu^+ + \mu^- + e + p$ at 30 GeV, angular distributions, mass spectra, and total cross sections for, (T), 26:54263
- interactions $\nu + \mu$ with bremsstrahlung, four-component neutrino theory for e and μ polarization effects on form of photon and electron spectra from inelastic, (T), 26:54290
- magnetic moment of, Schwarz inequality for lower bound on hadronic contribution to, 26:54287 (LBL-766)
- production of intense beams of, CERN II Synchrotron facility for, 26:53783 (DNPL/P-131)
- stopping and diffusion in hot metal foils in vacuum, production of muonium by, (E), 26:54096

MUONS (μ^-)
- capture by carbon-12, gamma yields, rates, and weak-magnetism coupling constant from, (E), 26:54537
- capture by magnesium-24 and silicon-28, γ-ray yields from, (E), 26:54555
- capture by nuclei, elementary particle theory for nuclear currents in, (T), 26:54238 (LYCEN-7211)
- capture by nuclei, polarization of emitted neutron in, (T), 26:54564
- depolarization in aqueous solutions and water in magnetic fields, effects of chemical reactions, hydrogen peroxide concentration, and temperature on, (E), 26:54099
- interactions $\mu^- + p \to \mu^- +$ anything in scaling region, differential cross sections and detection and isolation of neutral weak currents for, (T), 26:54288 (RPP/T-26)
- interactions $\mu^- + p \to \mu^+ + \mu^- + \mu^- + p$ at 30 GeV, angular distributions, mass spectra, and total cross sections for, (T), 26:54263
- production in $e + p \to e + \mu^+ + \mu^- +$ anything interactions, test of bilocal operators from, (T), 26:54253
- production in p + p interactions in colliding beams at ISABELLE, forward, (E/T), 26:54181 (BNL-16977)
- production of μ^+ -- μ^- pairs in $p + p \to \mu^+ + \mu^- +$ anything interactions, neutral weak currents in, (E/T), 26:54182 (BNL-17092)
- production of μ^+ -- μ^- pairs in p + p interactions in colliding beams at ISABELLE, forward, (E/T), 26:54181 (BNL-16977)

MUONS (μ^+)
- energy in $\pi^+ \to \mu^+ + \nu$ decay, (E), 26:54189
- interactions $\mu^+ + p \to \mu^+ + \mu^- + \mu^+ + p$ at 30 GeV, angular distributions, mass spectra, and total cross sections for, (T), 26:54263
- production in $e + p \to e + \mu^+ + \mu^- +$ anything interactions, test of bilocal operators from, (T), 26:54253
- production in p + p interactions in colliding beams at ISABELLE, forward, (E/T), 26:54181 (BNL-16977)
- production of μ^+ -- μ^- pairs in $p + p \to \mu^+ + \mu^- +$ anything interactions, neutral weak currents in, (E/T), 26:54182 (BNL-17092)
- production of μ^+ -- μ^- pairs in p + p interactions in colliding beams at ISABELLE, forward, (E/T), 26:54181 (BNL-16977)

MUSCLES
- arsenic-74 uptake and retention by, of mice, rabbits, and rats following oral administration, time dependence of, 26:53538

MUTATIONS
- Escherichia coli, use of tritium suicide method for selective enrichment of altered acyl CoA synthetase in, 26:53518
- induced in Aspergillus niger by colchicine and nitrogen mustards for citric acid production, comparison of, 26:53380
- induced in cultured Chinese hamster cells by chemical mutagens, uv radiation, and x radiation, effects of dose and post-exposure culture medium on frequencies of, 26:53362
- induced in cultured mouse lymphoma cells by chemical mutagens and x radiation, phenotypic method for comparing frequency of, 26:53361
- induced in Eremothecium ashbyii (fungi) by diethyl sulfate and nitrosoguanidine for increased riboflavin production, 26:53374
- models for selection and, in multi-locus systems, mathematical, 26:55487(R) (COO-1437-8)
- radioinduced dominant and recessive lethal, in mature spermatozoa of Drosophila melanogaster, effects of dactinomycin on post-fertilization expression of x, 26:53502
- radioinduced reversion, in Escherichia coli, effects of tryptophan starvation on uv, 26:53379
- radioinduced reversion, in Saccharomyces cerevisiae, effects of photoreactivation repair mechanism on frequency of uv, 26:53375
- radioinduced, for antibiotic production in Aspergillus, gamma and uv, 26:53393
- radioinduced, in Aspergillus niger for citric acid production, comparison of γ and uv, 26:53380
- radioinduced, in Eremothecium ashbyii (fungi) for increased riboflavin production, uv, 26:53374
- use of radioinduced, for improvement of crops and domestic animals, 26:53459(R) (NP-19403)

MYOGLOBIN
- radiation effects on bovine ferri-, in anoxic and oxygenated solutions, comparison of γ, 26:53346

N

NAGASAKI
- atomic bombing of, incidence of chromosome aberrations in lymphocytes of man exposed to residual fallout from, 26:53414
- radiation dose to residents of, comparison for diagnostic radiographic examinations and A-bomb survivors, 26:53434
- radioinduced neoplasms in human survivors of atomic bombing of, 10 to 25 years following exposure as children, effects of dose on incidence of, 26:53442

NAILS
- arsenic-74 uptake and retention by, of mice, rabbits, and rats following oral administration, time dependence of, 26:53538

NAPHTHALENE
- radioinduced electric conductivity of, electron, (E/T), 26:54968(R) (AD-737312)

NAPHTHALENEACETIC ACID
- radiolysis of aqueous solutions of, rate constants for reaction of hydrogen atoms, hydroxyl radicals, and hydrated electrons in, 26:53015

NATIONAL RADIOACTIVE WASTE REPOSITORY
- radioactive waste storage in, effects of adjacent American Salt Corp. mining activities on high-level, 26:53725 (ORNL-TM-3903)

NATURAL BACKGROUND RADIATION
- monitoring of gamma, ionization chamber for, 26:53218

NATURAL GAS
- radioactivity of, stored in underground nuclear explosion cavities, hazards to commercial users from, 26:53132(T) (UCRL-Trans-10617-2)
- storage in cavities in salt domes, cavity construction for, 26:53115
- tritium content of nuclearly stimulated, development of radiation standard for, 26:53134
- tritium removal from, stored in nuclear cavities, method for, 26:53128 (ORNL-4794, pp 63-4)

NATURAL WATERS
- plutonium in, possibility of pentavalent, 26:52935(R) (MLM-1888)

NAVIGATION
- Geographical Position Locator (GPL) for inertial, equipment and methods for testing mathematical error-reduction techniques for, 26:53311 (UCRL-51130(Vol.8))

NAVIGATIONAL INSTRUMENTS
- accuracy testing of Geographic Position Locator, 26:55631 (UCRL-74039)
- radiation effects on photomultiplier star sensor system for attitude determination for space vehicles, 26:53293 (NASA-TM-X-2440, pp 735-43)

NEBULAE
- spectra of, Z dependence of level intervals in $2s^22p^2$,

- $2s^22p^3$, and $2s^22p^4$, (E), 26:53954
- structure of, (T), 26:53985

NEMATODA
- Dictyocaulus viviparus, radiation effects on infectivity of larvae of, for immunization of cattle, x, 26:53503

NEODYMIUM
- abundance in 21 sharp-lined nonvariable cool peculiar A stars, (E), 26:53882
- ionization of surfaces of, 26:53033 (EUR-4765, pp 117-30)
- magnetoresistance at 1.4 to 20°K, 26:55021
- solubility in bismuth--thorium solutions, free energies of formation for compounds produced by, 26:53664

NEODYMIUM ISOTOPES Nd-138
- energy levels of, quasi-band structure in, (E/T), 26:54600 (INSJ-130)

NEODYMIUM ISOTOPES Nd-141
- beta and electron-capture decay of, β, γ, and conversion electron spectra from, (E), 26:54604 (JINR-P6-6519)

NEODYMIUM ISOTOPES Nd-142
- photon reactions (γ,xn) with, model analysis of giant resonance in, (E/T), 26:54598 (FRNC-TH-242)

NEODYMIUM ISOTOPES Nd-143
- photon reactions (γ,xn) with, model analysis of giant resonance in, (E/T), 26:54598 (FRNC-TH-242)

NEODYMIUM ISOTOPES Nd-144
- photon reactions (γ,xn) with, model analysis of giant resonance in, (E/T), 26:54598 (FRNC-TH-242)

NEODYMIUM ISOTOPES Nd-145
- photon reactions (γ,xn) with, model analysis of giant resonance in, (E/T), 26:54598 (FRNC-TH-242)

NEODYMIUM ISOTOPES Nd-146
- photon reactions (γ,xn) with, model analysis of giant resonance in, (E/T), 26:54598 (FRNC-TH-242)

NEODYMIUM ISOTOPES Nd-148
- photon reactions (γ,xn) with, model analysis of giant resonance in, (E/T), 26:54598 (FRNC-TH-242)

NEODYMIUM ISOTOPES Nd-150
- photon reactions (γ,xn) with, model analysis of giant resonance in, (E/T), 26:54598 (FRNC-TH-242)

NEODYMIUM OXIDES
- spectra and structure of, vibrational, 26:55031

NEON
- abundance in extreme Population I stars and Sun, (T), 26:53892
- abundance in NGC 7662, (E/T), 26:53873
- carbon-ion reactions at 40 to 140 keV with, cross sections for charge exchange in, (E), 26:54137
- electron reactions with, Auger and direct ionization processes in, 26:54103 (FRNC-CONF-51)
- helium-atom and -ion reactions at 100 to 5000 eV with, angular and energy distributions of electrons from ionization and autoionization in, (E), 26:54141
- hydrocarbon-ion (CH/sub n/+) reactions at 40 to 140 keV with, cross sections for dissociation and production of hydrogen atoms in, (E), 26:54137
- ion scattering at 8 to 25 keV by, total cross sections and interatomic potentials for, (E), 26:54139
- ionization balance in solar atmosphere, density dependent, (E), 26:53969
- plasma of, constant-wavelength oscillations in bounded positive column, (E/T), 26:54859
- proton reactions at 500 to 3000 eV with, differential cross sections for charge exchange, elastic scattering, excitation to autoionizing levels, and simple excitation in, (E/T), 26:54122
- scattering by lithium fluoride surfaces, calculation of angular distributions from, as functions of beam temperature and angle and plane of incidence, 26:54088
- scattering by lithium fluoride surfaces, determination of potential parameters from data on, 26:54087

NEON IONS
- reactions with aluminum and magnesium at 0.7 to 4 MeV, neon-isotope effects on cross sections for K-shell ionization in, (E), 26:54114
- scattering by tungsten polycrystalline surfaces at 150 to 1000 eV, angular and energy distributions and cross sections for, (E), 26:54083

NEON ISOTOPES
- abundance in Mokoia and Allende chondrites, (E), 26:53810

NEON ISOTOPES Ne-20
- deuteron reactions (d,α) at 3.5 to 8 MeV, excitation functions for, (E), 26:54467(R) (ORO-2972-204)
- effects on K-shell ionization of aluminum and magnesium by neon-ion bombardment at 0.7 to 4 MeV, (E), 26:54114
- energy levels of, calculation of rotational, (T), 26:54562
- helium-3 reactions (He-3,nγ) at 4.3 to 11.5 MeV, coincidence and angular correlation measurements for, (E), 26:54559
- proton inelastic scattering by, coupled-channel treatment with projected Hartree--Fock wave functions, (T), 26:54565
- reactions with aluminum-27 at 85 to 206 MeV, direct-reaction effects in excitation functions and gamma spectra from, (E), 26:54558

NEON ISOTOPES Ne-22
- effects on K-shell ionization of aluminum and magnesium by neon-ion bombardment at 0.7 to 4 MeV, (E), 26:54114

NEOPLASMS
- carcinoma, radiotherapy of human skin, description of equipment for, 26:53341
- carcinomas, radioinduced, in human survivors of atomic bombing of Nagasaki 10 to 25 years following exposure as children, effects of dose on incidence of, 26:53442
- carcinomas, radioinduced, in kidneys of parabiosed rats, x, 26:53449 (COO-3017-4)
- carcinomas, radiotherapy of human, research programs on use of pion beam for, 26:53398 (LA-4874, pp 79-83)
- electron integral absorbed dose in therapy of, (T), 26:54909
- leukemia, radioinduced in human children following exposure in utero, review of epidemiological studies on, 26:53435
- leukemia, radioinduced, in human survivors of atomic bombing of Nagasaki 10 to 25 years following exposure as children, effects of dose on incidence of, 26:53442
- leukemia, radioinduced, in mice following fractionated sublethal whole-body exposure, protective effects of cysteamine against, 26:53475
- leukemia, radioinduced, in mice following fractionated whole-body exposure, incidence and cytological characteristics of x, 26:53512
- leukemia, radioinduced, in mice following intraperitoneal injection of strontium-90, incidence and cytological characteristics of β, 26:53512
- leukemia, radioinduced, in mice following whole-body exposure, comparison of incidence of γ and x, 26:53469
- leukemia, radioinduced, in mice, studies on transmission of strontium-90 β and x, 26:53496
- lymphomas, occurrence in atomic bomb survivors of Hiroshima and Nagasaki in relation to radiation exposure dose, 26:53432
- radioinduced in human children following exposure in utero, review of epidemiological studies on, 26:53435
- radioinduced mammary, in rats following acute whole-body exposure, comparison of γ and proton, 26:53455 (NASA-TM-X-2440, pp 647-51)
- radioinduced, in respiratory and gastrointestinal tracts of miners in relation to exposure to radon and radon daughters in air, 26:53412
- radiosensitivity of cells of human, relation of anoxia to response to TAN, 26:53430
- sarcomas, implantation in rats, inhibitory effects on regeneration of thyroid gland, effects of whole-body x irradiation on, 26:53494

NEPHELINE SYENITES
- mineralogy of southwest Aswan radioactive, 26:53142 (AREAEE-138)

NEPTUNIUM
- ionization of surfaces of, 26:53033 (EUR-4765, pp 117-30)
- neutron reactions with, in neptunium oxide, production of plutonium-238 by, 26:53073
- separation from plutonium in MILLI laboratory by solvent extraction using TBP, 26:53073
- separation of protactinium from, by anion exchange, 26:52903

NEPTUNIUM ISOTOPES Np-239
- content in Savannah River, 1971, 26:53153(R) (DPSPU-72-30-1)

NERVES
- radioinduced degeneration of human optic, following therapy of nasal cavity and paranasal sinus carcinomas, dose and time dependence of γ and x, 26:53444

NERVOUS SYSTEM
- radiosensitivity of rat, relation of content of acetylcholine to, 26:53461(R) (UCB-34-P-82-13)

NETHERLANDS
- applications of radiation in agricultural research in, 26:53459(R) (NP-19403)
- fast reactor development in, progress on, 26:55083(R) (EURFNR-1001)

NEUTRINOS
- emission from sun, effects of resonance in $^3He + {}^3He$ system on, (T), 26:54508
- interactions $\nu + d \rightarrow 2p + e$ near 50 MeV, cross section calculations for, (T), 26:54233 (LA-DC-72-848)
- interactions $\nu + \mu$ with bremsstrahlung, four-component neutrino theory for e and μ polarization effects on form of photon and electron spectra from inelastic, (T), 26:54290
- interactions $\nu + N \rightarrow \nu + N'$ as test of new Nagoya and Hiroshima models for urbaryons, 26:54297
- interactions ν + N, quark-model predictions of cross sections for production of pseudoscalar mesons in, (T), 26:54285 (DESY-72/32)
- interactions with gravitational radiation in expanding universe, (T), 26:53997
- mass of, weak interaction as origin of, (T), 26:54294
- production of ν--anti ν pairs as energy loss mechanism in stars, Weinberg theory of weak and electromagnetic interactions for, (T), 26:53893
- properties of cosmic, review of solar neutrinos, Fermi interaction, and stellar evolution for, (E/T), 26:54185 (NEIC-RR-47)
- reactions with carbon-12, cross sections for, (T), 26:54541

NEUTRINOS (ANTI ν)
- production of ν--anti ν pairs as energy loss mechanism in stars, Weinberg theory of weak and electromagnetic interactions for, (T), 26:53893

- NEUTRINOS (ν/sub e/)
  - mass upper limits from double magnetic spectrometer study of $K_2^0 \to \pi + l + \nu$ decay, (E), 26:54184 (LBL-4)
- NEUTRINOS (ν/sub μ/)
  - mass from $\pi^+ \to \mu^+ + \nu$ decay, upper limit on, (E), 26:54189
  - mass upper limits from double magnetic spectrometer study of $K_2^0 \to \pi + l + \nu$ decay, (E), 26:54184 (LBL-4)
- NEUTRON BEAMS
  - production of monoenergetic, using ISABELLE in Whiplash mode, feasibility of, 26:53775 (BNL-17057)
  - production using beryllium-9 (d,n) reactions, biological implications of intensity estimates from, (E/T), 26:53804
- NEUTRON CROSS SECTIONS
  - bibliography on thermal, 26:54602 (JAERI-M-4666)
  - computer processing of ENDF/B, test of codes using idealized data, 26:54475 (CONF-720901-(Bks.1 and 2), pp 1048-60)
  - data analysis of, computer program for, 26:54468 (ANCR-1042)
  - data files for, description of ENDF/B III, 26:54478 (CONF-720901-(Bks.1 and 2), pp 1127-51)
  - evaluation of ENDF/B data with fast reactor measurements, 26:55125 (CONF-720901-(Bks.1 and 2), pp 1033-47)
  - evaluation with integral data measurements in fast reactors, 26:55385 (CONF-720901-(Bks.1 and 2), pp 623-35)
  - evaluation with integral data measurements in fast reactors, 26:55384 (CONF-720901-(Bks.1 and 2), pp 613-22)
  - evaluation with integral data measurements in fast reactors, 26:55436 (CONF-720901-(Bks.1 and 2), pp 599-612)
  - measurement of interaction, review of developments in, 26:55140 (CONF-720901-(Bks.1 and 2), pp 295-315)
  - survey on fast, 26:54476 (CONF-720901-(Bks.1 and 2), pp 1063-74)
- NEUTRON DIFFRACTOMETERS
  - crystal mount for, engineering drawings for, 26:53319
- NEUTRON SOURCES
  - composition of matter in, (T), 26:53908
  - design for use in interrogation determination of U-235 in containers, engineering drawings for, 26:53217
  - equation of state for, (T), 26:53908
  - intensity of beryllium-9 (d,n), biological implications of, (E/T), 26:53804
  - neutron spectra from liquid hydrogen and deuterium moderated cold, measurements and Monte Carlo calculations of, (E/T), 26:54493
  - reactivity calculations for VINS, using Monte Carlo transport codes, 26:54469 (ANCR-1071)
  - structure of, internal, (T), 26:53908
- NEUTRON SPECTROMETERS
  - design and operation of stilbene scintillation, with double compensation circuit for gamma discrimination, 26:53251 (AREAEE-137)
  - development for pulsed-beam time-of-flight studies, 26:54467(R) (ORO-2972-204)
  - performance of time-of-flight, for fast neutrons, 26:53260
- NEUTRON SPECTROSCOPY
  - spectral unfolding codes in, evaluation of, 26:53252 (CONF-720901-(Bks.1 and 2), pp 524-40)
- NEUTRON STARS
  - gravitational wave emission and scattering by relativistic, nonradial vibrational modes from, (T), 26:53894
  - x-ray emission from, detection of, (E/T), 26:53907
- NEUTRONS
  - absorption by fissionable materials, summary of resonance and Doppler theory for, 26:54480 (CONF-720901-(Bks.1 and 2), pp 1166-82)
  - attenuation by sodium slabs, benchmark measurements of, (E/T), 26:55142 (CONF-720901-(Bks.1 and 2), pp 418-30)
  - capture by dysprosium-163 up to 200 eV, correlation of partial radiative and neutron widths in resonance, (E), 26:54631(T) (BNL-tr-490)
  - capture by indium, tantalum-181, gold-197, and uranium-238 at 24.3 keV, TOF cross-section measurements using iron-filtered beam, (E), 26:54597 (CONF-720901-(Bks.1 and 2), pp 1107-14)
  - capture by mixed oxide reactor fuels, effects of particle size on resonance, (E/T), 26:55425 (CONF-720901-(Bks.1 and 2), pp 108-13)
  - capture by nuclei, radiative decay of resonant states in, 26:54675 (BNL-17029)
  - capture by silver-107, silver-109, gold-197, thorium-232, and uranium-238, survey of cross section data on, 26:54657 (FEI-292)
  - capture by space shielding materials, cascade calculation of gamma-ray yields from, 26:54961 (NASA-TM-X-2440, pp 527-8)
  - capture by Z = 29 to 79 nuclei at 1 keV to 10 MeV, cross-section calculations using Hauser--Feshbach--Margolis method, (T), 26:54700 (RT/FI-(72)6)
  - cross-section sensitivity analysis for sodium/iron shielding, 26:54940 (CONF-720901-(Bks.1 and 2), pp 512-23)
  - detection of monoenergetic, from radioisotope thermoelectric generator, Monte Carlo calculation of response of silicon detectors for, 26:53291 (NASA-TM-X-2440, pp 708-13)
  - detection of, description of multiwire proportional counter for, 26:53200 (LBL-707(Summ.))
  - diffusion equation for hexagonal reactor lattices, simultaneous line over-relaxation method for solution of, 26:55433 (CONF-720901-(Bks.1 and 2), pp 253-65)
  - diffusion equation in polar geometry, computer code for calculation of two-group, 26:54471 (CISE-R-252)
  - diffusion equations for cylindrical reactors, variational synthesis analysis of two-group, 26:55422 (CISE-R-243)
  - diffusion equations for finite cylindrical reactors, iterative solution of, 26:55423 (CISE-R-273)
  - diffusion in gas cooled fast breeder reactors, calculation of anisotropic, (T), 26:55126 (KFK-1577)
  - diffusion of, computer program for calculation of anisotropic, 26:54488 (RT/FI-(72)1)
  - diurnal variation of cosmic, temperature effects on, (E), 26:53811
  - dose changes due to shield layer changes, use of perturbation theory to determine, 26:54941 (CONF-720901-(Bks.1 and 2), pp 541-58)
  - dose distribution in cylinders similar to rats, rabbits, and humans, effects of secondary components on, (E), 26:54871 (CEA-CONF-1976)
  - dose distributions for radiobiology and radiotherapy, radiation transport codes for, (T), 26:54890 (ORNL-TM-3816)
  - dose to Thermoelectric Outer Planet Spacecraft from radioisotope thermoelectric generator, environmental analysis of, 26:53338 (NASA-TM-X-2440, pp 862-5)
  - dosimetry in tissues in gamma fields, tissue-equivalent plastic ionization chamber for, 26:53234 (NASA-TM-X-2440, pp 609-13)
  - dosimetry simultaneously with gamma rays, effects of ^{6}Li content in mixture of natural fluorite and LiF for thermoluminescence, 26:53240
  - effects on copper phthalocyanine, chemical state of recoil copper-64 from, 26:53032
  - effects on electric conductivity of gallium arsenide, tunnel-assisted hopping in, 26:54982
  - effects on fatigue crack propagation in Types 304 and 316 stainless steel at 427 to 593°C, 26:53698 (NRL-7446)
  - effects on materials, instrument for detecting cracks from, 26:53317
  - effects on mechanical properties and structure of stainless steel, 26:53701 (STU-70-419/U-350(Pt.1.1))
  - effects on p-dichlorobenzene crystals, 26:52984 (FRNC-TH-262)
  - effects on semiconductor devices, hardening against, 26:53289 (NASA-TM-X-2440, pp 481-6)
  - effects on silicon, (E/T), 26:54968(R) (AD-737312)
  - effects on silicon, EPR spectra of defects produced in, 26:55006
  - effects on spacecraft instruments, program for studying, 26:53294 (NASA-TM-X-2440, pp 866-72)
  - effects on strengthening of chromium--iron welds, iron, and pressure vessel steel, effects of carbon, copper, nickel, phosphorus, and vanadium additions on, 26:53710
  - effects on survival of mice following acute lethal whole-body exposure, RBE for californium-252, in comparison with cobalt-60 and radium-226 γ, 26:53484
  - effects on swelling of metals, dose and dose rate dependences of, (T), 26:53707
  - effects on vibrational spectra of gallium arsenide containing silicon and boron, 26:54984
  - emission from molybdenum--plutonium dioxide heat sources, effects of age, fluorine-19, oxygen-17, oxygen-18, plutonium-236, and size on, 26:53336 (NASA-TM-X-2440, pp 853-8)
  - emission time in sodium assembly, 26:54656(R) (COO-3058-21)
  - flux distribution and profile measurements, use of indium, gold, manganese, and depleted uranium foils for, 26:55137 (JAERI-Memo-3893)
  - flux of solar, (E), 26:53967
  - form factor of, analysis of available data on $e + d \to e + d$ interactions for magnetic, (E), 26:54169 (JINR-E1-6647)
  - generation time in subcritical fast reactors, transfer and scattering kinetics scheme for determination of, 26:55437 (CONF-720901-(Bks.1 and 2), pp 713-23)
  - interactions anti $p + n \to \pi^+ + \pi^- + \pi^-$ at 1.2 GeV, Veneziano model with satellites and dual amplitude with Mandelstam analyticity for, (T), 26:54320
  - interactions $\gamma + n \to n + \eta$ at threshold to 1.1 GeV, transition amplitudes and cross sections for N resonance production in, (E), 26:54166 (CALT-68-322)
  - interactions $\gamma + n \to p + \pi^-$ up to 1 GeV in deuterium bubble chamber, spectator-model analysis of differential and total cross sections for, (E/T), 26:54171 (LNF-72/31)
  - interactions $\gamma + n \to \pi^- + p$ at 600 to 1250 MeV, differential cross sections for, (E), 26:54179
  - interactions $\gamma + n \to \pi^- + p$ in 3,3 resonance region, discrepancy between dispersion relation predictions and experiment, 26:54261
  - interactions γ + n, evaluation of J = 0 fixed pole in Compton, 26:54254
  - interactions $K^+ + n \to K^+ + \pi^- + p$ at 3.8 GeV/c in deuterium bubble chamber, cross sections and quasi-two-

body interaction cross sections for K^0(890) and K^0(1420) production in, (E), 26:54202 (COO-1195-238)
interactions $K^+ + n \to K^+ + \pi^- + p$ at 9 GeV/c, resonance production in, (E), 26:54203 (COO-1428-308)
interactions $K^- + n \to \Lambda + \pi + K^0$ + anti K^0 at 4.9 GeV/c, total and differential cross sections for, (E), 26:54229
interactions $K^- + n \to \Lambda + \pi^-$ + eta at 4.9 GeV/c, total and differential cross sections for, (E), 26:54229
interactions $K^- + n \to \Lambda + \pi^-$ + missing mass at 4.9 GeV/c, total and differential cross sections for, (E), 26:54229
interactions $K^- + n \to \Lambda + \pi^- + \pi^0$ at 4.9 GeV/c, total and differential cross sections for, (E), 26:54229
interactions $K^- + n \to \Lambda + \pi^-$ at 4.9 GeV/c, total and differential cross sections for, (E), 26:54229
interactions $K^+ + n \to p$ + anything at 9 GeV/c in deuterium bubble chamber, proposed experiment for K(1760) and K(2200) production in, (E), 26:54204 (COO-1428-310)
interactions $K^- + n \to \Sigma^0 + \pi^-$ at 4.9 GeV/c, total and differential cross sections for, (E), 26:54229
interactions n + d, calculation of breakup cross section with separable potentials, 26:54520
interactions n + d, calculation of doublet scattering length using Skornyakov--Ter-Martirosyan equations, 26:54344 (ITF-72-10-P)
interactions n + n, scattering length from final state, (T), 26:54503 (UCRL-74069)
interactions $n + p \to p + n$, contribution of unnatural parity exchanges to charge-exchange, (T), 26:54270
interactions n + p, effects on low-momentum transfer cross sections for anti $p + d \to$ anti $p + p + n$ interactions from final-state, (E), 26:54347 (UM-P-72-6)
interactions $\pi^- + n$ at 40 GeV/c, average number of produced π^+--π^- pairs, coefficient of nucleon charge exchange, and identical distribution over charged particle multiplicity for, (T), 26:54327 (JINR-E2-6596)
interactions $\pi^+ + n$, compilation of cross sections for, 26:54201 (CERN/HERA-72-1)
interactions $\pi^- + n$, compilation of cross sections for, 26:54201 (CERN/HERA-72-1)
interactions with protons in nuclei, mass number dependence of residual, (T), 26:54739
magnetic moment of, Markoffian model for, 26:54308
mass difference (n - p), deep inelastic contribution to electromagnetic, (T), 26:54257
noise analysis in reactors, state of the art in 1971 of, 26:55442 (RT/FI-(72)11)
orbital momenta of, of anti pn bound states, recoil proton momentum spectrum in anti $p + d \to p$ + anything interactions for nonzero, 26:54334
production by 10.4-MeV/nucleon ions in copper and tantalum, extrapolation to space energies, 26:54881 (NASA-TM-X-2440, pp 520-2)
reactions (n,2n) with cadmium-116, isomer ratios in, (E), 26:54628
reactions (n,α) with tin-118, isomer ratios in, (E), 26:54628
reactions (n,f) at 14.8 MeV with thorium-232 and uranium-238, cadmium-115 isomer ratios in, (E), 26:54628
reactions (n,f) with uranium-235 and plutonium-239, survey of cross section data on, 26:54657 (FEI-292)
reactions with aluminum, iron, tungsten, and uranium-238 at thermal to 16 MeV, cross sections for gamma-ray production in, 26:54960 (NASA-TM-X-2440, pp 500-11)
reactions with bare fast multiplying systems of uranium, Storrer--Stievenart analysis of pulsed, (T), 26:54483 (JAERI-M-4652)
reactions with cadmium-112, resonance parameters for, (E), 26:54599 (IAE-2116)
reactions with calcium-46, strontium-84, barium-130, gadolinium-152, and gadolinium-150, resonance activation integrals for, (E), 26:54585
reactions with carbon, silicon, iron, and tantalum-181 up to 20 MeV, γ production cross sections for, (E), 26:54523 (CONF-720901-(Bks.1 and 2), pp 325-34)
reactions with iron-54, iron-57, and natural iron at 10 to 1000 keV, total cross sections for, (E), 25:54566 (CONF-720901-(Bks.1 and 2), pp 1075-86)
reactions with nuclei, strength function evaluation for a small number of resonances in, (T), 26:54720
reactions with tissues, local dose from neutron-produced recoil ions in therapeutic ^{252}Cf, 26:54902
resonance self-shielding coefficients for, interpolation formula for published data on, 26:54489 (ZJE-124)
scattering by nuclei, optical model calculations for, (T), 26:54677 (CONF-720701-3)
slowing down in pulsed heavy media, Green function coupling method for calculation of time-dependent, 26:55428 (CONF-720901-(Bks.1 and 2), pp 179-94)
slowing down theory for, review on continuous, 26:54472 (CONF-720901-(Bks.1 and 2), pp 143-61)
spectra and age in pulsed carbon sphere, sensitivity to carbon cross sections in calculation of, 26:54474 (CONF-720901-(Bks.1 and 2), pp 409-17)
spectra from homogeneous spheres containing uranium-235 and plutonium-239, benchmark calculations for, 26:54486 (RISO-M-1526)
spectra in reactors, many-resonance approximation of energy, 26:55429 (CONF-720901-(Bks.1 and 2), pp 195-206)
spectra measurements in fast reactor, use of proton-recoil spectrometry for, 26:55122 (CONF-720901-(Bks.1 and 2), pp 959-72)
spectra measurements in upper atmosphere, 26:54066 (NASA-TM-X-2440, pp 922-5)
spectra measurements, use of indium, gold, manganese, and depleted uranium foils for, 26:55137 (JAERI-Memo-3893)
spectra of, exit tube effect on measured, (E), 26:54470 (AREAEE-133)
total cross sections for stainless steel, experimental check for 1.2- to 11-MeV, 26:54965 (ORNL-TM-3871(Rev.))
transmission and self-indication ratio measurements in depleted uranium, time-dependent, (E), 26:54477 (CONF-720901-(Bks.1 and 2), pp 1115-26)
transmission by lithium hydride slabs, analysis of Shield Test Facility measurements of, 26:54944 (NAA-SR-Memo-8597)
transmission in gold at unresolved resonance energies, effect of temperature on, (E/T), 26:54484 (KFK-1519)
transport calculations for reactors, optimum angular segmentations in, 26:55434 (CONF-720901-(Bks.1 and 2), pp 266-74)
transport calculations for, predetermination of statistical errors in Monte Carlo, 26:55430 (CONF-720901-(Bks.1 and 2), pp 207-10)
transport equation in plane geometry, reflection function method analysis of multigroup, 26:55440 (INIS-mf-195)
transport equation with anisotropic scattering, system of elementary solutions for, 26:54492
transport equations for reactors, improved S/sub N/ inner iteration convergence criterion for, 26:55435 (CONF-720901-(Bks.1 and 2), pp 275-92)
transport in air and liquid nitrogen, calculation for evaluation of nitrogen neutron cross section sets, 26:54485 (ORNL-TM-3768)
transport in carbon, carbon shielding benchmark problem and other calculations for, 26:54939 (CONF-720901-(Bks.1 and 2), pp 397-408)
transport in multilayer slabs with isotropic scattering, computer program for J/sub N/ solution of, 26:54481 (EUR-4839)
transport in shielding, integral experiments and philosphy of ''benchmark'' calculations in, 26:54937 (CONF-720901-(Bks.1 and 2), pp 349-84)

NEUTRONS, COLD
attenuation in air and helium, measurement using manganese activation, (E), 26:54490
scattering by deuterium at zero energy, method of moments for solution of Faddeev equations for elastic, (T), 26:54715

NEUTRONS, DELAYED
fraction in plutonium fueled fast critical assemblies, measurement of effective, 26:55389 (CONF-720901-(Bks.1 and 2), pp 700-12)
fraction measurements in FCA, use of pulsed neutron technique and eigenvalue calculations for effective, 26:55403 (JAERI-Memo-4004)

NEUTRONS, FAST
absorption by elements, survey of data on Doppler effect in, 26:54479 (CONF-720901-(Bks.1 and 2), pp 1152-65)
absorption by uranium-238, Doppler effect in, 26:54479 (CONF-720901-(Bks.1 and 2), pp 1152-65)
capture by lead-208 at 6.2 to 14.7 MeV, cross section for, (E), 26:54662
cross section generation methods for, effects on fast reactor physics calculations of multigroup, 26:55113 (CONF-720901-(Bks.1 and 2), pp 211-28)
distributions behind three-layer barriers, spatial, energy, and angular, 26:54966
dose distributions for radiotherapy, 26:54893
dosimetry of, design of tissue-equivalent microcalorimeter for, 26:53250
effects on anthracene crystals for dosimetry, 26:53229 (COO-1105-172)
effects on chromosomes in rat embryos following exposure in utero, time dependence of aberrant, 26:53470
effects on development of rat embryos following exposure in utero, role of chromosome damage and repair errors in teratogenic, 26:53470
effects on electrical properties of n-type doped germanium, 26:54981
effects on Ge(Li) detectors, fission foil detector for flux monitoring for preventing deleterious, 26:53223
effects on Incoloy 800 and stainless steels Type 316, Type 321, and Type 347, 26:55189(R) (GEAP-10028-39)
effects on lower yield strength of iron, relations with spectra, 26:53705
effects on mechanical properties of carbon fibers, 26:53717
effects on mice, effects of bathing in thermal spring water on recovery from pathological mixed γ and, 26:53465
effects on mouse embryos following acute or fractionated exposure in utero, comparison of RBE with x rays for lethal, 26:53453 (NASA-TM-X-2440, pp 641)
effects on silicon and germanium single crystals, proton-channeling study of, 26:55004
effects on space vehicle components and subsystems,

  - design parameters and test facilities for testing, 26:53695 (NASA-TM-X-2440, pp 570-6)
  - effects on structure of lead titanate, 26:55020
  - effects on tensile properties of A-286, aluminum--boron carbide--titanium hydride, beryllium, and copper boride at cryogenic temperatures for use in NERVA Program, 26:53696 (NASA-TM-X-2440, pp 595-602)
  - effects on tensile properties of NERVA structural alloys at cryogenic temperatures, 26:53697 (NASA-TM-X-2440, pp 603-8)
  - energy transfer to soft tissue, microdosimetric studies of, 26:54873 (EUR-4787)
  - radiation effects on stainless steels Type-304, Type-316, Type-321, and Type-321-H, 26:55190(R) (GEAP-10028-42)
  - reactions (n,2nf) with uranium-238 at 14 MeV, method for determining lifetime of compound nucleus in, (E), 26:54669
  - reactions (n,α) with deformed doubly even nuclei, knock-on mechanism for, (T), 26:54707
  - reactions (n,f) with uranium-235, uranium-238, and plutonium-239 at 14 MeV, delayed neutron spectra from, (E), 26:54655 (CONF-720901-(Bks.1 and 2), pp 687-99)
  - reactions in homogeneous spheres, calculation of reaction rate neglecting elastic scattering, 26:54491
  - reactions of D--T produced, in thermonuclear reactors, problems from, 26:54826 (CONF-720901-(Bks.1 and 2), pp 559-73)
  - reactions with helium and lithium-6 at 0.7 to 30 MeV, total cross sections for, (E), 26:54656(R) (COO-3058-21)
  - reactions with iron-54 and natural iron at 0.8 to 20 MeV, data tabulation on γ production cross sections for, 26:54569 (ORNL-4798)
  - spectra in fast reactors, review of measurements of, 26:55438 (CONF-720901-(Bks.1 and 2), pp 943-58)
  - transport in iron, analysis of mechanism in, 26:54473 (CONF-720901-(Bks.1 and 2), pp 335-48)
  - transport in shielding, developments in integral experiments for, 26:54938 (CONF-720901-(Bks.1 and 2), pp 385-96)
- NEUTRONS, FISSION
  - effects on skin of swine, dose dependence of reproductive kinetics of cells, 26:53450 (LA-4874, pp 126-44)
- NEUTRONS, INTERMEDIATE
  - capture by A = 74 to 164 nuclei at 25 keV, model analysis of isomeric cross section ratios for, (E/T), 26:54589
  - capture by indium, tantalum-181, gold-197, and uranium-238 near 24.3 keV, pulse height spectra and relative cross sections for, (E), 26:54656(R) (COO-3058-21)
  - reactions with iron at 22 to 25 keV, R-matrix fit to total cross section for, 26:54656(R) (COO-3058-21)
  - transmission and self-indication ratio in depleted uranium, 26:54656(R) (COO-3058-21)
- NEUTRONS, PILE
  - absorption by californium-252 and -253, effective cross sections for, (E), 26:54668
  - effects on graphite, relations of flux density and temperature to, 26:53713 (CEA-CONF-1894)
  - reactions with heavy actinides, status of cross-section data for, 26:54654 (CONF-720901-(Bks.1 and 2), pp 97-107)
- NEUTRONS, THERMAL
  - capture by gadolinium-152, cross section for thermal, (E), 26:54585
  - capture by rhenium-187, γ singles and coincidence spectra from, (E), 26:54637
  - capture by Z = 1 to 82 nuclei, comparison of ENDF/B III and published data for, 26:54501 (ORNL-TM-3910)
  - capture in reactor cores, γ spectra from, (T), 26:55444 (TRG-2189)
  - detection in gamma fluxes, standard for performance of BF$_3$ proportional counter for, 26:53204 (RDT-C-15-11-T(8-72))
  - effects on Chlorella, in nitrogen-14 media, reaction mechanisms for, 26:53394
  - effects on maize, effects of dose and genotype on sensitivity to, 26:53383
  - effects on skin of swine, dose dependence of reproductive kinetics of cells, 26:53450 (LA-4874, pp 126-44)
  - reactions (n,f) with uranium-235, delayed neutron spectra from, (E), 26:54655 (CONF-720901-(Bks.1 and 2), pp 687-99)
  - reactions (n,f) with uranium-235, delayed neutron spectra from, (E), 26:54660(R) (RLO-2225-T-17-4)
  - reactions (n,f) with uranium-235, independent yields of krypton and xenon isotopes in, (E), 26:54667
  - reactions with heavy nuclei, interpretation of energy-dependent cross sections for, 26:54653 (CONF-720901-(Bks.1 and 2), pp 81-96)
  - scattering by nuclei, bibliography on elastic, 26:54602 (JAERI-M-4666)
  - scattering by phonons in zinc, neutron groups from inelastic, (E), 26:54487 (RT/FI-(71)37)
- NEVADA TEST SITE
  - geologic faults at, effects of eight 1971 underground nuclear explosions on displacement of, 26:53133 (USGS-474-155)
  - surface fractures at, effects of eight 1971 underground nuclear explosions on, 26:53133 (USGS-474-155)
- NEW MEXICO
  - sandstone--uranium deposits in Grants Region of, trend orebody studies on formation of, 26:53144 (GJO-936-2)
- NEWBOLD ISLAND POWER REACTOR, UNIT 1
  - site for, human population distribution surrounding, 26:55336 (DOCKET-50354-28)
- NEWBOLD ISLAND POWER REACTOR, UNIT 2
  - site for, human population distribution surrounding, 26:55336 (DOCKET-50354-28)
- NICKEL
  - abundance in γ Cap, (E), 26:53888
  - abundance in solar corona, (E), 26:53957
  - determination in minerals by neutron activation and γ spectroscopy, nondestructive, 26:52901 (UJV-2851-F,Ch)
  - determination in samples from boreholes, neutron activation method for, 26:53174
  - determination in water samples by spark source mass spectroscopy, 26:52914 (ANL-7860(Pt.3), pp 55-63)
  - determination in water, effects of large amounts of copper on spectrographic, 26:52927
  - effects on cohesion and structural stability of aluminum oxide composites with iron, 26:53589
  - effects on hydrogen reduction of tungsten oxide and sintering of tungsten powders, 26:53579
  - effects on neutron radioinduced strengthening of chromium--iron welds, iron, and pressure vessel steel, 26:53710
  - helium release in annealing of, 26:53709
  - ion emission by electron-bombarded, mass-spectral analysis of, 26:54084
  - ion implantations in, release of low-energy helium, 26:53709
  - radiation damage in, electron microscopic study of 650-kV electron, 26:54972 (COO-2119-2)
  - radiation effects on structure of polycrystalline, x-ray diffraction studies on 60-keV helium ion, 26:53700(T) (SC-T-722540)
  - separation from indium by ion exchange chromatography, 26:52949
  - spectral lines in Vega due to, (E), 26:53887
- NICKEL ALLOY COUPLES
  - Inconel/Zircaloy-2, corrosion by air, nitrogen, and water at ambient temperature, fretting, 26:53609 (RT/ING-(72)7)
- NICKEL ALLOYS AND SYSTEMS
  - composition and physical properties of composite powders of, 26:53680
  - preparation of composite powders of, by hydrogen reduction, 26:53680
  - production and properties of high-density powder metallurgy components of, for use at high temperatures, 26:53631
  - Al$_2$O$_3$--Ni, cohesion and structural stability of composites of, effects of chromium, manganese, and molybdenum additions on, 26:53589
  - Al--Co--Cr--Mo--Ni-base--Ta--Ti--W, sintering and stress-rupture properties of, effects of boron, carbon, and oxygen additions on, 26:53674
  - Al--Co--Cr--Mo--Ni-base--Ti, sintering and stress-rupture properties of, effects of boron, carbon, and oxygen additions on, 26:53674
  - Al--Cr--Mo--Nb--Ni-base--Ta--W, production and properties of powder metallurgy components of, for use at high temperatures, 26:53631
  - Al--Ni-base--W--Zr, production and properties of powder metallurgy components of, for use at high temperatures, 26:53631
  - Co-base--Cr--Ni--ThO$_2$, mechanical properties and microstructure of dispersion-hardened, 26:53675
  - Co-base--Ni--ThO$_2$--Zr, mechanical properties and microstructure of dispersion-hardened, 26:53675
  - Cr--Cu--Fe--Mo--Ni-base--Ti, corrosion by thorium dioxide dissolvent solutions, 26:53604 (BNWL-CC-449)
  - Cu--Ni--Tb, magnetic structures in TbNi/sub 1-x/Cu/sub x/ below ordering temperature, stability of sinusoidal-wave, 26:55039
  - Cu--Ni--Zn, analysis of nickel silver for copper by amperometric titration, 26:52924
  - Mn--Mo--Ni--steel, mechanical properties of pressure vessel, effects of quenching, tempering, and heat treatment on, 26:53646
  - Mo--Ni--W-base, mechanical properties of, effects of heat treatments following sintering on, 26:53679
  - Mo--Ni--W-base, preparation and composition of, 26:53679
  - Mo--Ni-base, mechanical properties of, at 800 to 1200°C, 26:53667
  - Ni--rare earth, magnetic properties of R$_3$Ni, pulsed-field magnetometer measurements of, 26:55050
  - Ni--transition metal carbides, erosion resistance of anodes of, 26:53568
  - Ni--V, ordering transformation in Ni$_2$V, 26:53659
- NICKEL IONS
  - scattering by argon and neon at 8 to 25 keV, total cross sections and interatomic potentials for, (E), 26:54139
- NICKEL ISOTOPES
  - energy levels of even, self-consistent Hartree--Fock, Hartree--Fock--Bogolyubov, and spherical BCS calculations using central Yukawa interaction and Hamada--Johnston and Tabskin potentials, (T), 26:54583
- NICKEL ISOTOPES Ni-56
  - energy levels of, shell-model study of, (T), 26:54570
- NICKEL ISOTOPES Ni-58
  - alpha elastic scattering at 166 MeV, angular distribution

  - for, (E), 26:54547
  - energy levels from proton inelastic scattering, spin--parity assignments and branching ratios for, (E), 26:54587 (FRNC-TH-240)
  - energy levels of, shell-model study of, (T), 26:54570
  - lithium-6 reactions (Li-6,d) at 38 MeV, DWBA analysis of differential cross sections and spectrum from, (E), 26:54586
  - neutron radius of, determination from α elastic scattering, (E), 26:54547
  - proton inelastic scattering at 12 MeV, proton angular distributions and γ spectra from, (E), 26:54587 (FRNC-TH-240)
  - proton reactions at 5 to 56 MeV, cross sections for, (E), 26:54591
- NICKEL ISOTOPES NI-60
  - alpha elastic scattering at 166 MeV, angular distribution for, (E), 26:54547
  - energy level transitions from copper-60 decay, (E), 26:54593
  - energy levels from proton inelastic scattering and cobalt-59 (He-3,dγ) reactions, spin--parity assignments and branching ratios for, (E), 26:54587 (FRNC-TH-240)
  - neutron radius of, determination from elastic scattering, (E), 26:54547
  - proton inelastic scattering at 12 MeV, proton angular distributions and γ spectra from, (E), 26:54587 (FRNC-TH-240)
  - proton reactions at 5 to 56 MeV, cross sections for, (E), 26:54591
- NICKEL ISOTOPES NI-61
  - proton reactions at 5 to 56 MeV, cross sections for, (E), 26:54591
- NICKEL ISOTOPES NI-62
  - alpha elastic scattering at 166 MeV, angular distribution for, (E), 26:54547
  - deuteron reactions (d,p) at 12 MeV, angular distributions for, (E), 26:54587 (FRNC-TH-240)
  - energy levels from proton inelastic scattering, spin--parity assignments and branching ratios for, (E), 26:54587 (FRNC-TH-240)
  - neutron radius of, determination from elastic scattering, (E), 26:54547
  - proton inelastic scattering at 12 MeV, proton angular distributions and γ spectra from, (E), 26:54587 (FRNC-TH-240)
  - proton reactions at 5 to 56 MeV, cross sections for, (E), 26:54591
- NICKEL ISOTOPES NI-63
  - diffusion in polycrystalline α-titanium and α-zirconium, mechanism of, 26:53666
- NICKEL ISOTOPES NI-64
  - deuteron reactions (d,p) at 12 MeV, angular distributions for, (E), 26:54587 (FRNC-TH-240)
  - energy levels from proton inelastic scattering, spin--parity assignments and branching ratios for, (E), 26:54587 (FRNC-TH-240)
  - lithium-6 reactions (Li-6,d) at 38 MeV, cross sections for, (E), 26:54586
  - proton inelastic scattering at 12 MeV, proton angular distributions and γ spectra from, (E), 26:54587 (FRNC-TH-240)
  - proton inelastic scattering at 3.1 to 5.3 MeV, angular distributions and excitation functions for, (E), 26:54590
  - proton reactions at 5 to 56 MeV, cross sections for, (E), 26:54591
- NICOTINAMIDE, N-METHYL-
  - uptake by rat kidneys following injection, effects of uranyl nitrate on, 26:53537
- NICOTINIC ACID
  - radiation effects on content of, in wheat, wheat bread, and wheat flour, gamma, 26:53344
- NIMONIC PE 16
  - helium release in annealing of, 26:53709
  - irradiation using high-voltage electron microscope, high-flux, 26:53708
- NINE MILE POINT POWER REACTOR, UNIT 2
  - site for, additional data on alternate, 26:55351 (DOCKET-50410-10)
  - transmission lines for, additional data on, 26:55351 (DOCKET-50410-10)
- NIOBIUM
  - book: Early Transition Metals, 26:52956
  - complexes with Alizarin Red S, spectrophotometric studies on formation of, 26:52926
  - content in southwest Aswan syenite rock, 26:53142 (AREAEE-138)
  - deposition of thin films of, ultrahigh vacuum evaporation unit with high-speed cryopump for, 26:53139
  - determination in minerals by direct measurement of oxide ratios, spectroscopic, 26:52932
  - determination using Alizarin Red S, spectrophotometric, 26:52926
  - diffusion in aluminum nitride, silicon nitride, and titanium dioxide, 26:53677
  - energy gaps, ultrasonic evidence against multiple, (E), 26:54437
  - fabrication by rolling at high temperature under vacuum, 26:53630
  - performance of superconducting helix resonator cavity of, tests of, 26:53750
  - separation from tantalum, titanium, and zirconium by solvent extraction, hydrolysis, and extraction, 26:52947 (BM-RI-7671)
  - separation of protactinium from, by anion exchange, 26:52903
  - superconducting transition in, use of acoustical measurements for, 26:54439
- NIOBIUM ALLOYS AND SYSTEMS
  - Al--Cr--Mo--Nb--Ni-base--Ta--W, production and properties of powder metallurgy components of, for use at high temperatures, 26:53631
  - Mo--N--Nb, phase studies and thermodynamics of, as function of pressure and temperature, 26:53671
  - Mo--Nb-base, entropy of vortices in superconducting, (E), 26:54441
  - N--Nb-base--Zr, internal friction of, effects of nitrogen content on, 26:53692
  - Nb--Si, diffusion of silicon in Nb_5Si_3 phase in, at high temperatures, 26:53583
  - Nb--Ti, superconducting transition temperature and upper critical field, data on, 26:54464 (ORNL-TM-3921)
  - Nb--U-base, stress corrosion cracking by sodium chloride sprays, protective effects of epoxy-primed polyurethane-painted surface on, 26:53607 (RFP-1891)
  - Nb--U-base, stress corrosion cracking of overaged and underaged, by aqueous chloride solutions, 26:53608 (RFP-1904)
  - Nb--U-base--Zr, tensile properties of polycrystalline, as function of strain rate, 26:53691
- NIOBIUM CARBIDES
  - fabrication by casting of thermoplastic masses, 26:53586
  - mechanical properties and microstructure of, effects of hot working on, 26:53581
  - sorptive properties of, effects of electronic structure on, 26:53593
- NIOBIUM ISOTOPES Nb-90
  - energy levels for zirconium-90 (p,n) reactions, (E), 26:54613
- NIOBIUM ISOTOPES Nb-91
  - energy level of, shell-model calculation of isomeric, (T), 26:54611
- NIOBIUM ISOTOPES Nb-93
  - nuclear electric quadrupole and magnetic dipole moments of, (E), 26:54605 (KFK-1602)
  - photon reactions (γ,xn) with, model analysis of giant resonance in, (E/T), 26:54598 (FRNC-TH-242)
  - x-ray spectra from μ-mesic atoms of, (E), 26:54605 (KFK-1602)
- NIOBIUM ISOTOPES Nb-95
  - content in agricultural products, atmosphere, rainwater, Savannah River, and vegetation in vicinity of Savannah River Plant, 1971, 26:53153(R) (DPSPU-72-30-1)
  - isomer ratios of, formed in fission of bismuth-209, (E), 26:54627
- NIOBIUM NITRIDES
  - sorptive properties of, effects of electronic structure on, 26:53593
- NIOBIUM OXIDES
  - compression of Nb_2O_5, formation of Nb/sub x/O_2 phase by shock, 26:53561
- NITRIC ACID
  - radiolysis of deuterated and normal at 77°K, ESR and ir spectral studies on products of γ, 26:53009
  - $Al(NO_3)_3$--HNO_3--NH_4F, corrosive effects on Corronel 230, HAPO-20 alloy, and Type 304L stainless steel, 26:53604 (BNWL-CC-449)
- NITRIDES
  - formation energy of, relations with fuel capsule corrosion and deterioration, 26:53330(R) (BNWL-1308-10)
  - sorptive properties of, effects of electronic structure on, 26:53593
- NITROGEN
  - abundance in primary cosmic radiation from 10 to 1000 MeV/N, (E), 26:53835
  - carbon-ion reactions at 40 to 140 keV with molecular, cross sections for charge exchange in, (E), 26:54137
  - corrosive effects on copper/steel, Inconel/Zircaloy-2, and Zircaloy-2/Zircaloy-2 couples, fretting, 26:53609 (RT/ING-(72)7)
  - effects of interstitial, on asymmetry of yield stress in single-crystal tantalum, 26:53643
  - effects on corrosion resistance of zirconium and zirconium alloys in high-temperature water, 26:53614
  - effects on yields from γ radiolysis of gaseous hydrogen sulfide, 26:53011
  - electron reactions with molecular, calculation of excitation cross sections for, using Gaussian orbitals, 26:54108
  - electron reactions with molecular, dependence of computed excitation cross sections for, on accuracy of wave functions used, 26:54108
  - electron scattering by molecular, method of linear combination of scaled atomic charge distributions for calculation of static potential for, 26:54125
  - excitation of N_2 in ionosphere, rates for vibrational, (T), 26:54022
  - hydrocarbon-ion (CH/sub n/$^+$) reactions at 40 to 140 keV with molecular, cross sections for dissociation and production of hydrogen atoms in, (E), 26:54137
  - hydrocarbon-ion (CH/sub n/$^+$) reactions with molecular,

  energy spectra of dissociation products from, (E), 26:54102 (EUR-CEA-FC-644)
  hydrogen-atom reactions with molecular, free-collision-model calculations of cross sections for electron loss in, 26:54121
  neutron and secondary gamma spectra in liquid, calulation for evaluation of neutron cross section sets, 26:54485 (ORNL-TM-3768)
  radiolysis of, determination of short-lived species from electron pulse, 26:52980(R) (COO-3461-1)
  reactions of muonic, with hydrogen peroxide in aqueous solutions, (E), 26:54099
  solubility in molybdenum, rhenium, and tungsten, effects of temperature and pressure on, 26:53580
  spectral emission during arc event of Mar. 8--9, 1970, spectroscopy of $N(^2D)$ state, (E), 26:54014
  spectral emission volume of N_2 3371 A in overhead auroral zone, March 19 and 27, 1971, (E), 26:54012 (SC-RR-720543)

NITROGEN IONS
  abundance of N^{7+} in microamp beams of, time-of-flight method for measurement of, 26:54077 (CEA-CONF-2048)
  detection of multicharged, using x-ray-spectroscopy at 1 to 20 A, 26:54078 (CEA-CONF-2050)
  effects of implanted, on Doppler broadening of positron annihilation photons in silver halide crystals, 26:54097
  reactions with copper and tantalum at 10.4 MeV/nucleon, neutron yield from, (E), 26:54881 (NASA-TM-X-2440, pp 520-2)
  spectral lines in zeta Oph due to interstellar, (E), 26:53875

NITROGEN IONS (N_2^+)
  spectral emission volume of 3914 A in overhead auroral zone, March 19 and 27, 1971, (E), 26:54012 (SC-RR-720543)

NITROGEN ISOTOPES N-12
  nuclear dynamics of, particle--hole description of semileptonic electromagnetic and weak interactions in, (T), 26:54541

NITROGEN ISOTOPES N-14
  energy level at 10.81 MeV from carbon-12 (He-3,$p\gamma$) and (He-3,p) N-14 (p') reactions, spin--parity assignments for, (E), 26:54542
  energy-level transitions from carbon-12 (He-3,$p\gamma$) and (He-3,p) N-14 (p') reactions, branching ratios for, (E), 26:54542
  helium-3 reactions (He-3,p) with, contributions of rectangular graphs in, (T), 26:54533
  neutron capture by, comparison of ENDF/B III and published data for thermal, 26:54501 (ORNL-TM-3910)
  reactions (N-14,xn) with lead-208 at 80 to 100 MeV, excitation functions and spectrum from, (E), 26:54651

NITROGEN ISOTOPES N-15
  lithium-6 reactions (Li-6,t) at 30 MeV, angular distributions and energy spectra from, (E), 26:54549
  lithium-7 reactions (Li-7,t) with, finite-range DWBA analysis of, (T), 26:54708
  photon reactions with giant resonance excitation, continuum shell-model calculation of, (T), 26:54545
  proton reactions (p,γ) at 7.4 to 15.0 MeV, analyzing power angular distributions and T-matrix elements for polarized, (T), 26:54531

NITROGEN MUSTARDS
  effects on Aspergillus niger, mutagenic for citric acid production, 26:53380

NITROGEN OXIDES
  radiosensitizing effects of, on DNA, review of x, 26:53352

NITROGEN OXIDES N_2O
  electron reactions at 278 to 355°K with, effects of dilution with ethane, hydrogen, nitrogen, or propane on rate constants for dissociative electron attachment and subsequent electron detachment in, (E), 26:54135

NITROGEN SYSTEMS
  Ar--N, radiolysis of, determination of short-lived species from electron pulse, 26:52980(R) (COO-3461-1)
  Fe-base--N, radiation damage in, electric resistivity study of 4.5°K fast-neutron, 26:54989
  He--N, radiolysis of, determination of short-lived species from electron pulse, 26:52980(R) (COO-3461-1)
  Mo--N, degassing at 1200 to 3000°C in, equilibria and kinetics of, 26:53580
  Mo--N--Nb, phase studies and thermodynamics of, as function of pressure and temperature, 26:53671
  N--Nb-base--Zr, internal friction of, effects of nitrogen content on, 26:53692
  N--Re, degassing at 1200 to 3000°C in, equilibria and kinetics of, 26:53580
  N--W, degassing at 1200 to 3000°C in, equilibria and kinetics of, 26:53580

NORTH ANNA POWER REACTOR, UNIT 1
  transmission lines for, requested additional data on, 26:55332 (DOCKET-50338-51)

NORTH ANNA POWER REACTOR, UNIT 2
  transmission lines for, requested additional data on, 26:55332 (DOCKET-50338-51)

NORTH ANNA POWER REACTOR, UNIT 3
  accident analysis for, requested information on, 26:55349 (DOCKET-50404-22)
  containment depressurization system for, requested information on, 26:55349 (DOCKET-50404-22)
  equipment for, earthquake stress limits for Class 1, 26:55349 (DOCKET-50404-22)
  owners of, financial data on, 26:55263 (DOCKET-50404-24)
  pipes for, mechanical properties of stainless steel, 26:55349 (DOCKET-50404-22)
  quality assurance program for, requested information on, 26:55349 (DOCKET-50404-22)
  service water reservoir for, requested information on, 26:55349 (DOCKET-50404-22)
  transmission lines for, requested additional data on, 26:55332 (DOCKET-50338-51)

NORTH ANNA POWER REACTOR, UNIT 4
  accident analysis for, requested information on, 26:55349 (DOCKET-50404-22)
  containment depressurization system for, requested information on, 26:55349 (DOCKET-50404-22)
  equipment for, earthquake stress limits for Class 1, 26:55349 (DOCKET-50404-22)
  owners of, financial data on, 26:55263 (DOCKET-50404-24)
  pipes for, mechanical properties of stainless steel, 26:55349 (DOCKET-50404-22)
  quality assurance program for, requested information on, 26:55349 (DOCKET-50404-22)
  service water reservoir for, requested information on, 26:55349 (DOCKET-50404-22)
  transmission lines for, requested additional data on, 26:55332 (DOCKET-50338-51)

NORWAY
  radioactivity monitoring in environment of, 1956 to 1970, 26:53161

NOZZLES
  stresses in reactor pressure vessel, effects of attachment configuration on, (E/T), 26:55207(R) (ORNL-TM-3900)
  uranium enrichment using separation, review of developments in, 26:53328

NUCLEAR AUXILIARY POWER SYSTEMS
  development of radioisotope- and reactor-powered, for manned space stations, 26:53094 (NASA-TM-X-2440, pp 26-33)
  radiation dose during constant-velocity motion near reactor, (T), 26:55363 (NASA-TM-X-2440, pp 270-6)
  shielding of thermionic reactor, for integration with manned space station, (T), 26:55365 (NASA-TM-X-2440, pp 299-306)

NUCLEAR BINDING ENERGY
  Hartree--Fock calculations for superheavy nuclei, 26:54726

NUCLEAR ELECTRIC MOMENTS
  theory of quadrupole interactions in terms of irreducible tensors, 26:55063

NUCLEAR EMULSIONS
  description for dosimetry in Skylab space station, 26:53236 (NASA-TM-X-2440, pp 958-73)

NUCLEAR EXPLOSIONS, HIGH-ALTITUDE
  electron belts and effects on Van Allen belts of Starfish and Soviet, 26:54044 (NASA-TM-X-2440, pp 178-92)

NUCLEAR EXPLOSIONS, UNDERGROUND
  blowoff impulse from, development of probe velocity transducer for measuring x-ray-produced, 26:53303 (LA-4999)
  cavities and fracture zones from, in granite, content and size of, (E/T), 26:53130(T) (UCRL-Trans-10616-4)
  cavities from contained, radiological risks to users of natural gas stored in, 26:53132(T) (UCRL-Trans-10617-2)
  chemical uses of, research progress on, 26:53128 (ORNL-4794, pp 63-4)
  effects of close-in, in granite, calculation and measurement of mechanical, 26:53131(T) (UCRL-Trans-10616-5)
  effects of selected 1971 Nevada Test Site, on surface fractures, (E), 26:53133 (USGS-474-155)
  effects on structures beyond close-in zone, measurement of mechanical, 26:53129(T) (UCRL-Trans-10616-2)
  impulse gage for, design of passive, 26:53316
  natural gas production stimulation using, development of radiation standard for tritium contamination of gas from, 26:53134
  radioactivity from March 23, 1971 USSR, Swedish detection and monitoring of airborne, 26:53158 (FOA-4-4502-A-1)
  temperature distribution in granite terrain following, effects of heat transfer properties on, 26:53127 (CEA-R-4288)

NUCLEAR FORCES
  neutron-proton residual interaction in mirror nuclei, 26:54721
  nucleon--nucleon, nucleon form factors in generalized field theory for, 26:54382
  potential for, derivation of separable nonlocal, including phase shifts for S, P, and D waves, (T), 26:54683 (FRNC-TH-180)
  theory of, review of problems in, 26:54688 (ITF-71-77-P)

NUCLEAR MAGNETIC MOMENTS
  calculations for odd-A nuclei, corrections for core polarization and mesonic currents in, (T), 26:54679 (COO-3001-17)

NUCLEAR MATERIALS MANAGEMENT
  safeguards system for, during fuel fabrication, automatic on-line weighing and recording equipment for, 26:53723

NUCLEAR MATTER
- binding energy of, calculations using separable nonlocal potential, (T), 26:54683 (FRNC-TH-180)
- binding energy of, deficiency of OBE potentials for, (T), 26:54744

NUCLEAR MODELS
- collective, algebraic approach to spherical to deformed transition in, 26:54681 (COO-3071-9)
- optical, calculations for neutron scattering by nuclei, (T), 26:54677 (CONF-720701-3)
- optical, energy dependence of helium-3 potential in, (E/T), 26:54580
- particle--hole, inclusion of hole-state widths in calculations in, (T), 26:54714
- rotational, formulation of cranking, 26:54692 (JINR-P4-6543)
- rotational, formulation of governor, 26:54719
- shell, comparison of approximation schemes for continuum, (T), 26:54729
- shell, correlated wave functions and effective operators for, (T), 26:54728
- shell, fractional parentage coefficients for J = 11/2 orbitals in, 26:54686 (INR-1406)
- single-particle, nonlocal potential for, (T), 26:54746
- variable moment of inertia, extension to odd-A nuclei with weak Coriolis coupling, (T), 26:54710
- variable moment of inertia, generalization for phenomenological description of rotational states, (T), 26:54712

NUCLEAR PHYSICS
- book: Atomic Nucleus, 26:54738
- funding and outlook for medium energy, 26:53740 (LA-4874, pp 21-33)
- macroscopic approach to heavy-ion, 26:54694 (LBL-972)
- research in South Africa, 1971, 26:55453(R) (NP-19410)
- research on theoretical, Flinders Univ. of South Australia, 26:54779(R) (NP-19393)
- review of 1971 activities at Sydney Univ, 26:53993 (INIS-mf-252)

NUCLEAR POWER
- book: Conception on Nuclear Energy Till 2000 AD, in Japanese, 26:55090
- development and research in South Africa, 1971, 26:55453(R) (NP-19410)
- development in India, 1971--1972, 26:55452(R) (NP-19407)
- development in Japan, status of, 26:55089
- development in US, 26:55085
- developments in U.K. during 1970-71, survey of, 26:55084(R) (INIS-mf-212)
- growth in United Kingdom, 26:55088
- requirements in Sweden and UK, 26:53102

NUCLEAR POWER PLANTS
- costs for, computer program for calculation of capital, 26:55265 (ORNL-TM-3743)
- development during 1972 to 1985, 26:55267 (WASH-1139(Rev.1))
- development in Japan for domestic use and export, 26:55094
- development in Japan, survey of sites and needs for, 26:55092
- economics of integration in utility system, 26:55197 (ORNL-4794, pp 96-7)
- economics of mix in power grid of, RELIP code for, (T), 26:55266 (RD/B/N-2261)
- maintenance standards for equipment in, development of, 26:55201 (DUN-SA-168)
- safety of Czech, problems of, 26:55210
- testing of U. S., table of, 26:55214 (WASH-1208(9-72))
- thermal efficiency of closed-cycle MHD, using cesium--neon working fluid, (T), 26:53091 (IPP-IV-36)
- thermal efficiency of, calculation of, 26:53107
- thermal effluents from, feasibility of useful heat extraction from, 26:55212 (CONF-720925-2)
- waste heat from, feasibility for use for urban space heating, industrial and sewage processing, and agricultural purposes of, 26:55212 (CONF-720925-2)

NUCLEAR QUADRUPOLE RESONANCE
- theory of pure and Zeeman spectra of, using irreducible tensors, 26:55063

NUCLEAR REACTIONS
- compound nucleus, computer programs for calculation in continuum region, 26:54701 (RT/FI-(72)7)
- Coulomb excitation in inelastic scattering, heat-flow analysis of temperature spikes following, (E/T), 26:54646
- currents for, elementary particle theory for second-class, (T), 26:54238 (LYCEN-7211)
- DWBA analysis of sub-Coulomb multi-transfer, (T), 26:54695 (LYCEN-7213)
- DWBA treatment of cluster transfer reactions, (T), 26:54706
- DWBA treatment of Coulomb deuteron break-up, 26:54743
- giant resonance in, Fermi-fluid drop model for intermediate and heavy nuclei, (T), 26:54689 (ITF-72-12-P)
- heavy-ion induced, macroscopic approach to, 26:54694 (LBL-972)
- high-energy approximation and generalized Huygen's principle in, (T), 26:54690 (ITF-72-57-P)
- isomer ratios from low primary excitation in, method for calculation of, (T), 26:54725
- knock-on mechanism for (n,α) reactions on deformed doubly even nuclei, (T), 26:54707
- nuclear reactions with intermediate and heavy, Fermi-fluid drop model for giant resonance in, (T), 26:54689 (ITF-72-12-P)
- potentials for (p,2p), 26:54699 (ORO-4317-11)
- rescattering in 3-particle-final-state, triangle graphs and isospin violation in, (T), 26:54716
- theory for one-nucleon transfer, semiclassical, 26:54742

NUCLEAR STRUCTURE
- calculations for even--even nuclei using rotational model with rotationally invariant core, 26:54719
- Coriolis anti-pairing transition in, microscopic model for, (T), 26:54680 (COO-3071-7)
- description of band structure in rotating nuclei using rotor-particle coupling, (T), 26:54733
- effect of quadrupole pairing field on 0+ vibrations in shape deformed nuclei, 26:54731
- fermion operators in, transition operator boson expansion of, (T), 26:54682 (COO-3071-10)
- wave functions for, extraction from particle transfer data, (T), 26:54693 (LA-DC-72-954)
- wave functions in, spin-dependent operators in occupation-branching number representation for open-shell, (T), 26:55077

NUCLEAR THEORY
- Hartree--Bogolyubov calculations in, boson expansion method for, 26:54741
- local density approximation in, spurious center-of-mass effect from, 26:54734
- many body problem in, analysis using variationally determined transformation, 26:54718
- many-fermion systems in, intermediate state single-particle energies in two-hole-line approximation for, 26:54717
- nuclear densities in a model well of arbitrary shape, 26:54704
- Strutinsky shell correction method in, 26:54684 (IAE-2115)
- three body systems in, effect of off-shell 2-body t-matrix on, 26:54697 (ORO-4317-7)

NUCLEAR WEAPONS
- effects on aerospace personnel and their task performance, modular analysis of radiobiological, 26:54880 (NASA-TM-X-2440, pp 364-7)
- safeguarding of, equipment and methods for testing mathematical error-reduction techniques for Geographical Position Locator (GPL) for, 26:53311 (UCRL-51130(Vol.8))

NUCLEI
- abundances of light and heavy, in primary cosmic radiation, (E), 26:53835
- abundances of Z = 1 to 26, in primary cosmic radiation, (E), 26:53836
- acceleration of high Z, in pulsar vicinity, (T), 26:53857
- alpha decay of, pulsed-beam technique for measuring half-life for, 26:54651
- book: Atomic Nucleus, 26:54738
- cascades from Z greater than or equal to 3 primary cosmic, in iron absorber, (E), 26:53832
- charge composition of heavy cosmic primary, (E), 26:53842
- charge composition of primary cosmic, (E), 26:53839
- charge composition of primary cosmic, (E), 26:53830
- charge composition of primary cosmic, up to Z = 28, (E), 26:53837
- charge composition of Z = 2 to 30 primary cosmic, (E), 26:53838
- charge composition of Z = 4 to 30 primary cosmic, (E), 26:53840
- charge of heavy and superheavy cosmic, calculation of delta electrons formed in stopping media as aid in determination of, 26:53805(T) (N-71-30295)
- charged-particle elastic scattering at low energy, forward dispersion relation including Coulomb interaction for, (T), 26:54711
- chemical composition of low-energy L and M, in primary cosmic radiation, (E), 26:53841
- cosmic particle reactions with primary cosmic, cross sections for, (T), 26:53845
- decay of, review of impact of advances in instrumentation on measurement of, 26:53263
- electron elastic scattering by, contributions of time reversal noninvariant terms in, (T), 26:54363 (IS-T-536)
- electron scattering at high energy, analysis of short-range correlations by, 26:54687 (ISS-71/29)
- energy levels of single-closed-shell, relations among magnetic moments and rates for M1 transitions of, (T), 26:54702
- energy levels of, generalized variable-moment-of-inertia models for rotatonal, (T), 26:54712
- energy levels of, method for measuring magnetic moments of short-lived, using Coulomb excitation by polarized heavy-ion beams, (E/T), 26:54630
- energy levels of, shell effects on spin determination by spectroscopic factor ratios, (E/T), 26:54612
- energy spectra of heavy cosmic primary, (E), 26:53842
- energy spectra of low-energy L and M, in primary cosmic radiation, (E), 26:53841
- energy spectra of primary cosmic, effects of Fermi

- acceleration on, (T), 26:53862
- energy spectra of VH and VVH primary, (E), 26:53843
- hadron interactions with, diffraction emission in, (T), 26:54690 (ITF-72-57-P)
- heavy-ion elastic scattering by, analysis of absorptive potentials for, (T), 26:54678 (COO-535-672)
- heavy-ion scattering above Coulomb barrier, coupled-channel analysis of, (T), 26:54736
- mass of primary cosmic, method for determining mean, (E/T), 26:53824
- meson (K^-) capture by, gamma yields for different final states in, (T), 26:54536
- meson (π) elastic scattering by, analysis of nuclear surface properties by, (T), 26:54722
- meson (π) reactions below 3 GeV, intranuclear-cascade evaporation calculations for nonelastic, (T), 26:54727
- meson (π^+ and π^-) reactions at 0.7 to 2 GeV/c, cross-section ratios for, (E), 26:54529 (RPP/NS-8)
- muon (μ^-) capture by, elementary particle theory for nuclear currents in, (T), 26:54238 (LYCEN-7211)
- muon (μ^-) capture by, polarization of emitted neutron in, (T), 26:54564
- neutron and proton residual interaction in, mass number dependence of, (T), 26:54739
- neutron capture at 1 keV to 10 MeV by Z = 29 to 79, cross-section calculations using Hauser--Feshbach--Margolis method, (T), 26:54700 (RT/FI-(72)6)
- neutron capture by, radiative decay of resonant states in, 26:54675 (BNL-17029)
- neutron elastic scattering by, bibliography on, 26:54602 (JAERI-M-4666)
- neutron reactions with, strength function evaluation for a small number of resonances in, (T), 26:54720
- nucleon reactions below 3 GeV, intranuclear-cascade evaporation calculations for nonelastic, (T), 26:54727
- photon reactions (γ,π^0) with, calculation of absorption in, 26:54691 (JINR-P2-6539)
- photon reactions with spin-$^1/_2$ point, differential cross sections for $e^+ - e^-$ pair production and effects of neutral vector mesons on angular dependence of cross sections for, (T), 26:54260
- proton reactions at 22.6 GeV/c with emulsion, velocity distribution of secondary π production from, (E), 26:54196
- rigidity spectra of Z greater than or equal to 2 primary cosmic, (E), 26:53826
- rigidity spectra of Z greater than or equal to 3 primary cosmic, at 5 to 300 GeV, (E), 26:53834
- single-particle properties of, nonlocal potential for, (T), 26:54746
- x-ray disintegration of high Z, in pulsar environment, (T), 26:53857
- xenon reactions with, review of experiments on, 26:54658 (JINR-P7-6523)

NUCLEI, EVEN-EVEN
- energy levels of, quasi-band structure in, (E/T), 26:54600 (INSJ-130)
- neutron reactions (n,α) with deformed, knock-on mechanism for, (E), 26:54707

NUCLEI, EVEN-ODD
- energy levels of, extension of variable-moment-of-inertia model to, (T), 26:54710

NUCLEI, HEAVY
- beta decay of neutron-rich Z > 90, half-life calculations based on nuclear potential energy surface from modified harmonic oscillator potential, (T), 26:54663
- density of deformed, (T), 26:54704
- fission of neutron-rich Z > 90, half-life calculations based on nuclear potential energy surface from modified harmonic oscillator potential for neutron-induced and spontaneous, (T), 26:54663
- neutron reactions with, interpretation of energy-dependent cross sections for, 26:54653 (CONF-720901-(Bks.1 and 2), pp 81-96)
- octupole deformations in A > 208, (T), 26:54732

NUCLEI, INTERMEDIATE
- energy levels of odd A = 153 to 177, equilibrium deformations of, (T), 26:54640
- helium-3 elastic scattering at 10 to 85 MeV, energy dependence in optical-model analysis of, (T), 26:54580

NUCLEI, LIGHT
- alpha-cluster structure of ground states for self-conjugate 4n, (T), 26:54723
- binding and separation energies, rms radii, and electric quadrupole moments of, unrestricted Hartree--Fock calculations of, (T), 26:54745
- energy levels of deformed odd--odd, properties of effective neutron--proton interaction in rotational, (T), 26:54747
- energy levels of exotic, shell-model calculations of spin--parity assignments and wave functions for, (T), 26:54351
- giant dipole resonance in, inclusion of hole-state widths in particle--hole calculations of, (T), 26:54714
- hyperon (Λ) binding energies in exotic, shell-model analysis of, (T), 26:54351

NUCLEI, ODD-EVEN
- energy levels of, extension of variable-moment-of-inertia model to, (T), 26:54710

NUCLEI, ODD-ODD
- energy levels of deformed light, properties of effective neutron--proton interaction in rotational, (T), 26:54747

NUCLEIC ACID, DEOXYRIBO-
- preparation and structure of single molecules of, Kleinschmidt's method for, 26:55530 (ISS-71/22)
- radiation effects on circadian changes in synthesis of, in cells of rat gastric glands following oral administration of radon water, effects of dose on α, 26:53514
- radiation effects on content of, in human epidermis during atrophic and dermatitis reactions to chronic therapeutic exposure, x, 26:53441
- radiation effects on metabolism of, in L cells infected with rickettsiae, effects of cycloheximide on gamma, 26:53360
- radiation effects on replication of, in bacteria and bacteriophages, role in molecular repair mechanisms, 26:53348
- radiation effects on sedimentation properties of single-stranded, in bacteriophages in relation to molecular structure, uv, 26:53373
- radiation effects on single-strand breaks in, γ, 26:52981 (COO-3571-3)
- radiation effects on synthesis and degradation of, in liver, spleen, and thymus of rats, x, 26:53489
- radiation effects on, in microorganisms, review of role of enzymes in repair of uv, 26:53351
- radiation effects on, in organisms, comparison of RBE for high with low LET, 26:53345 (NASA-TM-X-2440, pp 222-8)
- radiation effects on, review of effects of sensitizing agents on, 26:53352
- radioinduced double-strand breaks in, of Micrococcus radiodurans, inhibitory effects of chloramphenicol, dactinomycin, and tetracycline on repair of γ, 26:53349
- radioinduced lesions in, following incorporation of β-emitting radioisotopes, repair processes for β, 26:53505
- radioinduced lesions in, of cultured mammalian cells and microorganisms, role of repair processes in recovery from lethal and mutagenic, γ, uv, and x, review of, 26:53357
- radioinduced lesions in, of microorganisms, role of enzymes in repair of uv, 26:53350

NUCLEIC ACID, RIBO-
- radiation effects on content of, in human epidermis during atrophic and dermatitis reactions to chronic therapeutic exposure, x, 26:53441

NUCLEOGENESIS
- γ-process, production of transactinide elements in, (T), 26:53867

NUCLEONS
- coupling constant for πN from test of analyticity of forward π + N charge-exchange amplitude, (T), 26:54337
- form factor in e + N → π + N interactions at threshold, method for calculating axial, (T), 26:54247 (NP-19417)
- form factors in generalized field theory for nuclear forces, 26:54382
- interactions anti N + N, urbaryon rearrangement diagram for structures in elastic and inelastic, (T), 26:54342
- interactions e + N → π + N at threshold, method for calculating axial nucleon form factor and pion electromagnetic form factor in, (T), 26:54247 (NP-19417)
- interactions e + N at high energies, review of kinematics, scaling, scattering from deuterons and complex nuclei, sum rules, single π^+ production, vector meson diffractive production, and coincidence measurements in inelastic, (E), 26:54173 (RPP/H-97)
- interactions e + N at q^2 = 0.6 to 1.56 GeV^2, angular distributions for π^0 production in, (E), 26:54268
- interactions e + N in quark--parton model, bare quark mass and structure function for, (T), 26:54282
- interactions e + N, relation between prominent resonances and limiting scaling data in inelastic, (T), 26:54258
- interactions e + N, sum rule and model for S-matrix elements in presence of standing-wave states as shadow quarks in Bjorken limit of deep inelastic, (T), 26:54248 (ORO-3992-106)
- interactions K^+ + N, urbaryon rearrangement diagram for structures in elastic and inelastic, (T), 26:54342
- interactions K^- + N, urbaryon rearrangement diagram for structures in elastic and inelastic, (T), 26:54342
- interactions l + N, asymmetries for models for spin-averaged cross sections and spin effects in Bjorken scaling region for polarization effects in deep inelastic, (T), 26:54244 (DESY-72/36)
- interactions N + N at 50 to 1200 GeV, model for multiple production in, (T), 26:54314
- interactions N + N, explicit damped phase shifts for one-plus two-pion-exchange and pseudoscalar vector meson models and radiation damping effects on amplitudes and phase parameters of, (T), 26:54350
- interactions N + N, factorization of pair potential by Bateman modified method for behavior of approximated phases of, (T), 26:54345 (JINR-P4-6505)
- interactions N + N, Gelfand--Levitan unitary-transform method for extension of T matrix off the energy shell, 26:54698 (ORO-4317-8)
- interactions N + N, hard-core radius of, 26:54251
- interactions N + N, phase shifts and coupling parameters from damped pseudoscalar- and vector-meson model for

elastic, 26:54348
  interactions N + N, urbaryon rearrangement diagram for structures in elastic and inelastic, (T), 26:54342
  interactions ν + N, quark-model predictions of cross sections for production of pseudoscalar mesons in, (T), 26:54285 (DESY-72/32)
  interactions $\pi + N \rightarrow \pi + \Sigma(\Lambda)$ near threshold, cross sections and polarization phenomena from PCAC theory, (T), 26:54335
  interactions π + N at 4.8 to 20 GeV, double Regge cuts in Regge pole--cut model for charge exchange, (T), 26:54324 (COO-1428-309)
  interactions π + N at low energies, current algebra model with physical pions for scattering and energy dependence of S- and P-phase, (T), 26:54339
  interactions π + N, inequalities between relative phase of amplitudes and polarization in, (T), 26:54340
  interactions π + N, nonlocal separable potentials for, (T), 26:54724
  interactions π + N, πN coupling constant from test of analyticity of forward amplitude of charge-exchange, (T), 26:54337
  interactions π + N, urbaryon rearrangement diagrams for structures in elastic and inelastic, (T), 26:54342
  reactions with nuclei below 3 GeV, intranuclear-cascade evaporation calculations for nonelastic, (T), 26:54727
  scattering by deuterium at 10.85 MeV, agreement of exact calculations of polarization in elastic, (T), 26:54509
  structure functions in parton model, (T), 26:54311
NUCLEONS (anti N)
  interactions anti N + N, urbaryon rearrangement diagram for structures in elastic and inelastic, (T), 26:54342

O

OCEANOGRAPHY
  conference on, American Geophysical Union annual, Washington, D. C., 4/71, 26:54010
OCONEE POWER REACTOR, UNIT 1
  cooling system for, hydraulic stress failures of internal components of, 26:55225 (BAW-10050)
OILS
  analysis of pump, for tritium by bremsstrahlung counting, 26:52934 (MLM-1368)
OLDBURY REACTORS
  performance of, methods for improvement of, 26:55270
OOCYTES
  radioinduced chromosome aberrations in mature, of Drosophila melanogaster, effects of premeiotic breakage and interchanges on types of x, 26:53501
  radiosensitivity of grain moth, effects of meiotic stage on γ, 26:53499
OREGON
  zinc-65 distribution and concentration in benthic fauna from continental shelf of, 26:53149 (RLO-2227-T-12-26)
ORES
  analysis for thorium by neutron activation, anion exchange purification of protactinium for, 26:52903
ORGANIC COMPOUNDS
  radioinduced preparation of, review on methods for, 26:53023
ORGANISMS
  radiation effects on DNA in, comparison of RBE for high with low LET, 26:53345 (NASA-TM-X-2440, pp 222-8)
  radioisotope distribution and metabolism in, development of kinetic models for multi-parameter analysis of, 26:53519
  thermal effects on aquatic, 1971 bibliography on, 26:53190 (ORNL-EIS-72-28)
ORNL HIGH-FLUX ISOTOPE REACTOR
  activation analysis facility at, features and tests of, 26:52897 (CONF-721010-3)
  startup of, model for on-line reactivity balance calculations during, (E/T), 26:55407 (ORNL-TM-3769)
OSMIUM
  determination in minerals by neutron activation and γ spectroscopy, nondestructive, 26:52901 (UJV-2851-F,Ch)
  determination in residues from leaching of mattes by distillation and colorimetry, 26:52919 (NIM-1432)
OSMIUM ISOTOPES Os-184
  energy level from Coulomb excitation, quadrupole moment and transition probability of first 2^+, (E), 26:54638
OSMIUM ISOTOPES Os-185
  electron-capture decay of, γ-γ angular correlations from, (E), 26:54644
OSMIUM ISOTOPES Os-186
  energy level from Coulomb excitation, quadrupole moment and transition probability of first 2^+, (E), 26:54638
  energy levels from iridium-186 decay, spin-parity assignments for, (E), 26:54633 (COO-3255-3)
OSMIUM ISOTOPES Os-188
  energy level from Coulomb excitation, quadrupole moment and transition probability of first 2^+, (E), 26:54638
OSMIUM ISOTOPES Os-190
  energy level from Coulomb excitation, quadrupole moment and transition probability of first 2^+, (E), 26:54638
OSMIUM ISOTOPES Os-192
  energy level from Coulomb excitation, quadrupole moment and transition probability of first 2^+, (E), 26:54638
OSTEICHTHYES
  abundance of, relations with discharge cooling water temperature from Point Beach Power Plant, 26:53185 (ANL-7860(Pt.3), pp 118-20)
  distribution in vicinity of thermal plume, acoustic location method for studying, 26:53186 (ANL-7860(Pt.3), pp 121-30)
  hematopoiesis in, bibliography on, 26:53447 (CONF-720822-2)
  Lepomis macrochirus (bluegill), cesium-137 content of, in White Oak Lake in relation to content of stable cesium and potassium and seasonal changes in food consumption, 26:53535
  radiation effects on function of hematopoietic tissues in, effects of dose, dose rate, and species on acute and chronic γ, 26:53447 (CONF-720822-2)
  radioactivity monitoring of, in vicinity of Savannah River Plant, 1971, 26:53153(R) (DPSPU-72-30-1)
  radioisotope content in Lake Michigan, from Big Rock Point and Point Beach Nuclear Power Plant effluents, 26:53169 (ANL-7860(Pt.3), pp 141-50)
OTTO HAHN REACTOR
  coolant for, radiation dose from oxygen activation in secondary, (T), 26:55356 (CONF-720901-(Bks.1 and 2), pp 471-9)
OXIDES
  formation energy of, relations with fuel capsule corrosion and deterioration, 26:53330(R) (BNWL-1308-10)
  sintering of, review on mechamism of activated, 26:53587
  sorptive properties of, effects of electronic structure on, 26:53593
OXONIUM IONS
  reactions with radiolytic hydrated electrons, kinetics of, 26:53006
OXYFLUOROURANATES
  complexes with organic basic cations, thermogravimetric studies on, 26:53043
OXYGEN
  abundance in NGC 7662, (E/T), 26:53873
  abundance in primary cosmic radiation from 10 to 1000 MeV/N, (E), 26:53835
  chemical demand for, in water, use of perchloratocerate reagent and fluorometric determination of cerium as measure of, 26:52915 (CONF-720827-2)
  determination of surface and body concentrations of, in materials by helium-3 activation, 26:52899 (LA-DC-72-809)
  determination of trace amounts in liquid sodium, vacuum distillation method for, 26:55170 (CONF-710959-, Paper 14)
  effects on brittleness of molybdenum, 26:53682
  effects on corrosion resistance of zirconium and zirconium alloys in high-temperature water, 26:53614
  effects on sintering and stress-rupture properties of nickel-base alloys, 26:53674
  effects on tantalum compatibility with sodium at 600°C, 26:53688
  emission in nightglow, altitude distribution of $O_2(^1\Delta)$ 1.27-μ, (E), 26:54042
  excitation of atomic, ^1D state in ionosphere, calculations of electron, (T), 26:54022
  excitation of O_2 in ionosphere, rates for vibrational, (T), 26:54022
  hydrogen-atom reactions with molecular, free-collision-model calculations of cross sections for electron loss in, 26:54121
  ionization balance in solar atmosphere, density dependent, (E), 26:53969
  light absorption by solid crystals of alpha-, 26:55531 (ITF-71-95-P)
  radiosensitizing effects of, on DNA, review of x, 26:53352
  reactions with dysprosium and gadolinium under controlled partial pressures at 727 to 1327°C, self-diffusion coefficients for, 26:53550 (IS-T-540)
  solubility in sodium, 26:55154 (CONF-710548-, pp 105-28)
  spectral emission at 1304 and 1356 A in tropical ionospheric F region, theoretical time-dependent behavior of far-uv airglow intensity from, 26:54031
  spectral emission during arc event of Mar. 8--9, 1970, spectroscopy of $O(^1D)$ and $O(^1S)$ states, (E), 26:54014
  spectral emission volume of O 5577 A in overhead auroral zone, March 19 and 27, 1971, (E), 26:54012 (SC-RR-720543)
  spectral lines in zeta Oph due to interstellar, (E), 26:53875
OXYGEN IONS
  effects of implanted, on Doppler broadening of positron annihilation photons in silver halide crystals, 26:54097
  effects on silver-activated phosphate glass at 200 to 400 keV, depth distribution of photoluminescence induced by, 26:55009
  reactions with aluminum, calcium, and copper at 7.5 to 40 MeV, cross sections for K x-ray production in, (E), 26:54467(R) (ORO-2972-204)
  reactions with copper and tantalum at 10.4 MeV/nucleon, neutron yield from, (E), 26:54881 (NASA-TM-X-2440, pp 520-2)
  reactions with magnesium at 21 MeV, Kα x-ray spectra from, (E), 26:54467(R) (ORO-2972-204)
  reactions with silicon and iron at 30 MeV, Kα x-ray

    spectra from, (E), 26:54467(R) (ORO-2972-204)
  spectral Lamb shift in $^{16}O^{7+}$, quantum electrodynamics test in, (E), 26:54375(R) (COO-1811-3)
OXYGEN IONS (O_2^+)
  reactions with helium, impulse approximation for vibrational excitation in, using Morse potential, 26:54131
OXYGEN ISOTOPES O-14
  beta decay of, electromagnetic corrections to ft values for, (T), 26:54713
OXYGEN ISOTOPES O-16
  content ratio to oxygen-18 in biogenic silica, 26:53178
  deuteron reactions (d,Li-6) at 28 MeV, angular distributions and spectroscopic factors for, (E), 26:54527 (LYCEN-7219)
  energy levels of, evaluation of Hartree-Fock calculations for, (T), 26:54524 (COO-2171-14)
  lithium-7 reactions (Li-7,t) with, finite-range DWBA analysis of, (T), 26:54708
  neutron capture by, comparison of ENDF/B III and published data for thermal, 26:54501 (ORNL-TM-3910)
  nuclear charge form factor of, effects of center-of-mass spuriosity on, (T), 26:54507
  oxygen-16 elastic scattering by, statistical calculation of adiabatic potential for, (T), 26:54544
  reactions (O-16,C-12) with iron-54 at 46 MeV, analysis for reaction mechanism in, (E), 26:54579
  reactions with aluminum-27 at 96 to 165 MeV, direct-reaction effects in excitation functions and gamma spectra from, (E), 26:54558
  scattering by calcium near the Coulomb barrier, incoming wave boundary condition for elastic, (T), 26:54705
  scattering by carbon-12 at 5 to 14 MeV, optical-model analysis of effects of quasi-molecular states in cross sections for elastic, (T), 26:54534
  scattering by oxygen-16, statistical calculation of adiabatic potential for elastic, (T), 26:54544
OXYGEN ISOTOPES O-17
  effects on γ and neutron spectra of molybdenum--plutonium dioxide heat sources, 26:53336 (NASA-TM-X-2440, pp 853-8)
OXYGEN ISOTOPES O-18
  content in marine sulfates, (E), 26:53180
  content ratio to oxygen-16 in biogenic silica, 26:53178
  effects on γ and neutron spectra of molybdenum--plutonium dioxide heat sources, 26:53336 (NASA-TM-X-2440, pp 853-8)
  energy levels of, calculations using separable nonlocal potential, (T), 26:54683 (FRNC-TH-180)
  energy levels of, off-shell effects in two-particle shell-model calculation of, (T), 26:54538
OXYGEN ISOTOPES O-19
  energy levels of, calculations using separable nonlocal potential, (T), 26:54683 (FRNC-TH-180)
OXYGEN ISOTOPES O-20
  energy levels of, calculations using separable nonlocal potential, (T), 26:54683 (FRNC-TH-180)
OXYGEN SYSTEMS
  C--O--Zr, reactions in, stability of phases produced by, 26:53581
  Mo--O, thermodynamic properties of liquid solutions of, 26:53588
OYSTER CREEK POWER REACTOR, UNIT 1
  maintenance during January to June 1972, 26:55242 (DOCKET-50219-213)
  operations during January to June 1972, 26:55242 (DOCKET-50219-213)

P

PACIFIC OCEAN
  Columbia River water and sediment distribution and transport in northeast, 26:53165(R) (RLO-2225-T-25-6)
PAINTS
  radiation resistance of selected, evaluation of, p. 98-100, 26:52986 (ORNL-4794, pp 98-101)
PALISADES POWER REACTOR
  control rod drives for, test failure of, 26:55251 (DOCKET-50255-99)
  valves for, verification of wall thicknesses for nuclear service, 26:55278 (DOCKET-50155-125)
PALLADIUM
  recovery of fission product, for commercial uses, feasibility of, 26:53330(R) (BNWL-1308-10)
PALLADIUM ALLOYS AND SYSTEMS
  Pd--Ti, diffusion measurements on, at 600 to 1000°C, 26:53677
  Pd--V, diffusion measurements on, at 608 to 1300°C, 26:53677
PALLADIUM CHLORIDES
  $PdCl_2$--W, sintering of powders of, mechanism of material transport by dislocation motion in, 26:53620
PALLADIUM ISOTOPES Pd-108
  energy levels from rhodium-108 decay, collective model analysis of, (E/T), 26:54596 (CEA-R-4286)
PALLADIUM ISOTOPES Pd-110
  energy levels from rhodium-110 decay, collective model analysis of, (E/T), 26:54596 (CEA-R-4286)
PANCREAS
  scintiscanning of human, for diagnosis of neoplasms, use of gamma camera in, 26:53214
PARTICLE TRACK MEASURING EQUIPMENT
  circuits for DOLLY CRT flying spot scanner, digital-to-analog converter, 26:53278
  data processing program for HPD, for bubble chamber film, 26:53274 (RHEL/R-241)
PARTICLE TRACKS
  sizes of proton and alpha-, in sodium chloride monocrystals, (E), 26:55016
PARTICLES
  betatron oscillations in two dimensions in nearly periodic system, perturbed equations for, 26:53763
  time reversal operator for unstable, definition for decays in media without intrinsic T violation, (T), 26:54366
PEACH BOTTOM POWER REACTOR, UNIT 1
  maintenance during January to June 1972, 26:55238 (DOCKET-50171-106)
  operations during January to June 1972, 26:55238 (DOCKET-50171-106)
PEACH BOTTOM POWER REACTOR, UNIT 2
  circulating water system for, possible failure of expansion bellows for, 26:55292 (DOCKET-50277-56)
  containment structure for, effects of coolant loss accidents on atmosphere in, 26:55293 (DOCKET-50277-57)
  cooling system for, vibration testing of components of, 26:55293 (DOCKET-50277-57)
  emergency core cooling system for, requested data on performance evaluation of, 26:55293 (DOCKET-50277-57)
  radioactive effluents from, requested and revised data on, 26:55293 (DOCKET-50277-57)
PEACH BOTTOM POWER REACTOR, UNIT 3
  circulating water system for, possible failure of expansion bellows for, 26:55292 (DOCKET-50277-56)
  containment structure for, effects of coolant loss accidents on atmosphere in, 26:55293 (DOCKET-50277-57)
  cooling system for, vibration testing of components of, 26:55293 (DOCKET-50277-57)
  emergency core cooling system for, requested data on performance evaluation of, 26:55293 (DOCKET-50277-57)
  pressure vessel for, damage report for top fuel guide of, 26:55294 (DOCKET-50278-58)
  radioactive effluents from, requested and revised data on, 26:55293 (DOCKET-50277-57)
PEOPLE'S DEMOCRATIC REPUBLIC OF GERMANY
  fallout monitoring in, during 1970, 26:53156 (SZS-128)
PEROVSKITES
  magnetic moment direction in rare-earth, crystal-field calculation of, 26:55054
PERSONNEL
  card files for, use of PL/1 as interrogation language for, 26:55450 (CEA-CONF-2005)
  management of, universal time administration in real time system for, 26:55541 (KFK-1526)
  mortality of mining, in relation to exposure to radon and radon daughters in air, epidemiological survey of contribution of neoplasms of respiratory and gastrointestinal tract and tuberculosis to, 26:53412
  radiation dose to various body parts of betatron, comparison of actual and phantom measurements of beta and gamma, 26:53426
  radiation dose to, criteria for maximum permissible, 26:53436
  radiation protection programs for, in German Federal Republic, 26:55456 (SZS-136)
PERTURBATION THEORY
  continued-fraction method for Mathieu equation and anharmonic-oscillator equation in, 26:55078
  energy of degenerate levels in Rayleigh--Schroedinger single, expression of second-order, in double perturbation form, 26:54152
  formalism of time-dependent, for quantum-mechanical systems, 26:55073
PETROLEUM
  analysis for vanadium by neutron activation, 26:52905
PHANTOMS
  evaluation for measurement of radiation dose to various body parts of personnel, beta and gamma, 26:53426
  neutron dose distribution in rat, rabbit, and human, effects of secondary components on, (E), 26:54871 (CEA-CONF-1976)
  radiation isodose curves in water, automatic system for measuring, 26:53243
  use for predetermination of absorbed x-ray dose to man during diagnostic radiography, 26:53416
  use of Alderson Rando, with lithium fluoride dosimeters for calculation of γ dose to human bone marrow following whole-body exposure, 26:53406 (NASA-TM-X-2440, pp 974-80)
  x-ray absorbed dose and effective energy distribution under screen filters in tissue-equivalent, 26:54911
  x-ray scattering by tissue-equivalent, from 50 to 300 kVp, (E), 26:54905
PHENIX FAST REACTOR
  fuel element failures in, radioactive tracer technique for locating, 26:55185 (CONF-710959-, Paper 1)
  rare gas transport in, 26:55185 (CONF-710959-, Paper 1)
  steam generator for, effects of sodium--water reactions on, 26:55150 (CONF-710548-, pp 1-16)
PHENOL, p-NITRO-
  radiation effects on antibacterial activity of, and in

    mixtures with 2,2-dichloro-N-[2-hydroxy-1-(hydroxymethyl)ethyl]acetamide, γ, 26:52998
PHONONS
  production in lithium-ion-doped and hydroxide-ion-doped potassium chlorides, with pulsed electric fields, (E/T), 26:55512 (COO-3151-139)
  resonant scattering by impurities in crystals, review, 26:55511 (COO-3151-8)
PHOSPHENES
  radioinduced, in eyes of astronauts during space flight, cosmic, 26:53407 (NASA-TM-X-2440, pp 1002-6)
PHOSPHORIC ACID, TRIBUTYL ESTER
  solvent properties for neptunium and plutonium, 26:53073
PHOSPHORUS
  determination as orthophosphate using molybdenum and carminic acid, spectrophotometric, 26:52931
  determination in water samples by spark source mass spectroscopy, 26:52914 (ANL-7860(Pt.3), pp 55-63)
  effects on neutron radioinduced strengthening of chromium--iron welds, iron, and pressure vessel steel, 26:53710
  ionization in biological materials, relation of energy level transitions to changes in molecular structure, 26:53376
  separation from uranium by fractional dissolution of crude sodium diuranate, 26:52976 (IEA-250)
  toxicity of elemental, bibliography on, 26:55586 (ORNL-TIP/TIRC-72-63)
PHOSPHORUS IONS
  implantation in silicon, precipitation upon annealing after, 26:54994
  scattering by argon and neon at 8 to 25 keV, total cross sections and interatomic potentials for, (E), 26:54139
PHOSPHORUS ISOTOPES P-29
  energy levels from silicon-28 (p,γ) reactions, lifetimes and spin-parity assignments for, (E), 26:54552 (FRNC-TH-227)
  energy-level transitions from silicon-28 (p,γ) reactions, branching and mixing ratios for, (E), 26:54552 (FRNC-TH-227)
PHOSPHORUS ISOTOPES P-32
  effects on cells following incorporation into DNA, role of transmutation in lethal and mutagenic, 26:53505
  effects on embryonic development, hatchability, and growth of chicks, 26:53517
  production from neutron-irradiated sulfur in hot toluene, extraction methods for, 26:53069
  use of colloids of, for treatment of malignant pleural effusions in man, measurement of dose distribution with time following, beta, 26:53509
PHOTOELECTRIC EFFECT
  electron emission by copper, model calculations of angular and energy distributions of secondary, 26:54885 (NASA-TM-X-2440, pp 792-800)
PHOTOGRAPHIC FILM
  radiation shielding on Skylab space station, 26:54049 (NASA-TM-X-2440, pp 748-55)
PHOTOGRAPHY
  performance of high-speed, for studying post-burnout two-phase Freon-12 flow, 26:53122
PHOTOMULTIPLIER TUBES
  radiation effects on star sensor system using, for attitude determination for spacecraft, 26:53293 (NASA-TM-X-2440, pp 735-43)
PHOTONS
  cosmic effects of finite rest mass of, (T), 26:53866
  coupling constant for γ phi, in relativistic extended quark model, 26:54283
  coupling constants for γ rho, in relativistic extended quark model, 26:54283
  coupling constants for $\gamma\omega$, in relativistic extended quark model, 26:54283
  detection at high energies, fabrication of total-absorption detector using condensed xenon for, 26:53272 (JINR-P13-6541)
  detection of pulsed, time response of L-125A Compton diodes for, (E/T), 26:53197 (EGG-1183-2277)
  interactions $\gamma + d \to p + p + \pi^-$ up to 1 GeV in bubble chamber, angular distributions and total cross sections for, (E/T), 26:54171 (LNF-72/31)
  interactions $\gamma + e$, differential cross sections and left--right asymmetry in Compton, (T), 26:54256
  interactions $\gamma + e$, hypothesis consistency and relation with behavior of electromagnetic current commutator near light cone for automodel asymptotic of spectral functions of virtual Compton, (T), 26:54246 (JINR-P2-6636)
  interactions $\gamma + e$, Schwinger source theory for calculation of spectral forms for invariant amplitudes of order e^4 for Compton, (T), 26:54255
  interactions $\gamma + \gamma \to m\pi(m = 2 \text{ or } 3)$ with soft pions, structure of observable amplitudes for, (T), 26:54265
  interactions $\gamma + \gamma \to \pi + \pi + \pi$, photon reactions $(\gamma,3\pi)$ with lead for test of low-energy theorem for, (T), 26:54252
  interactions $\gamma + n \to n + $ eta at threshold to 1.1 GeV, transition amplitudes and cross sections for N resonance production in, (E), 26:54166 (CALT-68-322)
  interactions $\gamma + n \to p + \pi^-$ up to 1 GeV in deuterium bubble chamber, spectator-model analysis of differential and total cross sections for, (E/T), 26:54171 (LNF-72/31)
  interactions $\gamma + n \to \pi^- + p$ at 600 to 1250 MeV, differential cross sections for, (E), 26:54179
  interactions $\gamma + n \to \pi^- + p$ in 3,3 resonance region, discrepancy between dispersion relation predictions and experiment, 26:54261
  interactions $\gamma + n$, evaluation of $J = 0$ fixed pole in Compton, 26:54254
  interactions $\gamma + p \to p + $ eta at threshold to 1.1 GeV, recoil proton polarization, transition amplitudes, and cross sections for N resonance production in, (E), 26:54166 (CALT-68-322)
  interactions $\gamma + p \to p + \pi^+ + \pi^-$ at 2 to 5 GeV in hydrogen bubble chamber, cross sections and resonance production in, (E), 26:54175 (SLAC-143)
  interactions $\gamma + p \to p(n) + \pi^+ + \pi^- + \pi^0(\pi^+)$ at 4.3 to 7.5 GeV, cross sections and resonance production in, (E), 26:54175 (SLAC-143)
  interactions $\gamma + p \to \pi^0(\gamma) + p$ at 3 to 7 GeV, polarization of recoil proton in, (E), 26:54167 (COO-3069-71)
  interactions $\gamma + p \to \pi^- + $ anything at 9.3 GeV/c, multiperipheral-model calculations of cross sections for, (T), 26:54325 (COO-3533-2)
  interactions $\gamma + p \to \pi^+ + n$ at 0.5 to 2.2 GeV, magnetic spectrometer study of structure in target asymmetry in, (E), 26:54172 (NP-19415)
  interactions $\gamma + p \to \pi^+ + n$ in 3,3 resonance region, discrepancy between dispersion relation predictions and experiment, 26:54261
  interactions $\gamma + p \to \pi^+ + n$, contribution of unnatural parity exchanges to, (T), 26:54270
  interactions $\gamma + p \to \pi^+(\pi^-) + $ anything at very high energies, limiting distributions for, (T), 26:54326 (DESY-72/40)
  interactions $\gamma + p$ in $\Delta(1236)$ resonance region, differential cross sections for elastic Compton, (E), 26:54180
  interactions $\gamma + p$, proposed experiment using multiwire proportional chambers and wide-gap spark chambers for charged-particle multiplicity and angular correlations in, (E), 26:54192 (BNL-17141)
  interactions $\gamma + \pi \to \pi + \pi$ with soft pions, structure of observable amplitudes for, (T), 26:54265
  interactions with charged fermions with intrinsic dipole moments, effective differential cross sections for Compton, (T), 26:54278
  interactions with photons, effects of velocity on, (T), 26:53866
  production in inelastic $\nu + \mu$ interactions with bremsstrahlung, four-component neutrino theory for e and μ polarization effects on form of spectra for, (T), 26:54290
  production of soft, in $p + p \to \pi^+ + d + \gamma$ interactions, amplitudes of, (T), 26:54250
  reactions $(\gamma,3\pi)$ with lead, test of low-energy theorem for $\gamma + \gamma \to \pi + \pi + \pi$ interactions from, (T), 26:54252
  reactions (γ,π^0) with nuclei, calculation of absorption in, 26:54691 (JINR-P2-6539)
  reactions (γ,xn) with $Z = 37$ to 79 nuclei, model analysis of giant resonance in, (E/T), 26:54598 (FRNC-TH-242)
  reactions with helium triplet metastable atoms, light-intensity dependence of probability of ionization in, (E), 26:54094
  reactions with nitrogen-15 with giant resonance excitation, continuum shell-model calculation of, (T), 26:54545
  reactions with singly excited hydrogen molecules, calculation of cross sections for ionization in, using phase shifts for electron scattering by hydrogen ions (H_2^+), 26:54091
  reactions with spin-$^1/_2$ point nuclei, differential cross sections for $e^+ - e^-$ pair production and effects of neutral vector mesons on angular dependence of cross sections for, (T), 26:54260
  scattering by K-shell electrons, nonrelativistic dipole approximation for Compton, (T), 26:54280
  scattering by K-shell electrons, nonrelativistic theory with retardation for Compton-type inelastic, 26:54279
  stability against decay, 26:54274
PHOTOSPHERE
  magnetic field distribution in, (E), 26:53947
  magnetic fields in weak-plage regions of, diffusion of, (E), 26:53933
  magnetic fields in, associated with quiescent prominences, (T), 26:53950
  oscillations in, velocity, (E/T), 26:53946
  oscillations of, spatial properties of five-minute, (E/T), 26:53945
  spectroheliograms of, (E), 26:53947
PHYSICS
  research in India, 1971--1972, 26:55452(R) (NP-19407)
PICOLINE
  complexes with oxyfluorouranate ions, thermogravimetric studies on, 26:53043
PILGRIM POWER REACTOR
  equipment for, evaluation of possible flooding of Class 1, 26:55304 (DOCKET-50293-88)
  operation of, license for, 26:55305 (DOCKET-50293-90)
  technical specifications for, 26:55305 (DOCKET-50293-90)
PINCH DEVICES
  plasma confinement in theta-, low-density limit for, (T),

26:54754 (LA-5019)
  plasma halo development in ISAR I linear theta-, properties of, (E), 26:54784 (IPP-1/125)
  plasma stabilization in theta-, transverse dynamic, (T), 26:54808 (LRP-51/72)
  review of Scyllac experiments, 26:54828 (LA-DC-72-896)
PINCH EFFECT
  plasma heating processes in z, gas kinetic relations for, (T), 26:54749(T) (AEC-tr-7330)
PIPE FITTINGS
  rupture studies of long radius elbow, 26:55175(R) (GEAP-10207-26)
PIPES
  design criteria for nuclear service, development program for, 26:55207(R) (ORNL-TM-3900)
  dismantling of sodium cooled reactor, removal of sodium and decontamination during, 26:55147 (AI-AEC-Memo-12736)
  effects of ducts on space nuclear shield, (E/T), 26:54958 (NASA-TM-X-2440, pp 375-82)
  fatigue testing of stainless steel Type-304 and Type-304L, Inconel-600, and carbon steel, fatigue rates from, 26:55175(R) (GEAP-10207-26)
  rupture studies of welded, 26:55175(R) (GEAP-10207-26)
  tees for nuclear service, stress testing of, 26:55207(R) (ORNL-TM-3900)
PISTON ENGINES
  piston ring and ring groove wear in 6-cylinder Diesel, neutron activation measurements of, 26:53339 (KFK-1568)
PITUITARY GLAND
  radioinduced changes in, ultrastructure and secretory activity of cells in mice following partial- or whole-body exposure, γ, 26:53467
PLANETARY NEBULAE
  formation from final phase of mass loss on red-giant branch, (T), 26:53874
  model for NGC 7662, consistent, (E/T), 26:53873
  structure of, (T), 26:53985
PLANETS
  formation from solar nebula, (T), 26:54005
PLANTS
  analysis for trace amounts of cobalt by instrumental neutron activation, 26:52904
  cesium-137 distribution in Puerto Rican, 26:53162 (ANL-7860(Pt.3), pp 1-13)
  cesium-137 uptake by, in Georgia during 1971 in comparison with 1965, fallout, 26:53539(R) (SRO-641-4)
  radioactivity monitoring of, in vicinity of Savannah River Plant, 1971, 26:53153(R) (DPSPU-72-30-1)
  radioisotope uptake and retention in, following release to environment, bibliography on, 26:53530 (TID-3915(Suppl.1))
  radioisotope uptake by marine, from seawater, strontium-90 and zinc-65, 26:53532
  uptake of radioisotopes by, 26:53459(R) (NP-19403)
PLANTS (INDUSTRIAL)
  heat sources for, feasibility of use of power plant waste heat for, 26:55212 (CONF-720925-2)
PLASMA
  bibliography on plasma physics and fusion reactors, 26:54748
  book: Kinetic Equations, 26:54797
  collision frequency during rf heating in Q devices, effective, (E), 26:54750 (CONF-720705-2)
  collision of trapped particles in toroidal, resonant, (T), 26:54792
  confinement in circulary polarized magnetic fields and additional electromagnetic fields, (T), 26:54761
  confinement in FM-1 device, anomalous and pseudoclassical, 26:54753 (CONF-720804-5)
  confinement in hybrid mirror fields with quadrupole and quadrupole-cusp geometries, 26:54756
  confinement in theta pinches, low-density limit for, (T), 26:54754 (LA-5019)
  confinement in toroidal magnetic geometries, effect of laminar flow on, (T), 26:54755
  confinement of ionized residual gas at bottom of potential well, (E), 26:54800(T) (AEC-tr-7350)
  diffusion coefficients for argon in shf discharges, longitudinal and transverse, (E), 26:54776(T) (AEC-tr-7332)
  diffusion during strong turbulence, resonant, (T), 26:54791
  diffusion in afterglows, electron temperature changes in, (E), 26:54786
  electromagnetic field penetration into nontransparent, traveling hf, (T), 26:54843 (AREAEE-124)
  electron beam interactions with, dispersion equation for multiloop, (T), 26:54793
  electron beam interactions with, ion heating by oscillations, (E), 26:54762
  electron beam interactions with, modulation of lf oscillations from, 26:54782
  electron beam interactions with, nonlinear interaction of waves from, (T), 26:54795
  electron beam interactions with, steady-state beam shape in, (T), 26:54794
  electron--ion recombination and ionization coefficients for helium, collisional--radiative, 26:54788 (EUR-CEA-FC-642)
  equilibrium in magnetic configurations with helical axis, toroidality effects on, (T), 26:54815
  heating at cyclotron resonance, asymptotic particle distribution function for, (T), 26:54759
  heating by carbon dioxide laser, effects of magnetic field on, (T), 26:54760
  heating by excited waves near ion cyclotron frequency in ST Tokamak, (E), 26:54752 (CONF-720804-4)
  heating by microwaves in Tuman-2 device, (E), 26:54758
  heating by rf fields in Q devices, effective collision frequency in, (E), 26:54750 (CONF-720705-2)
  heating by parametric instabilities during hf excitation, (E), 26:54751 (CONF-720705-3)
  heating of ions by collisionless shock waves, (E), 26:54766
  heating of ions by ion beam, possibility of collisionless, (E/T), 26:54767
  heating of ions in plasma--beam discharge by oscillations, (E), 26:54762
  heating of superdense, by laser, (T), 26:54764
  heating of turbulent, theory for stochastic, (T), 26:54765
  heating processes in pulsed z discharges, gas kinetic relations for, (T), 26:54749(T) (AEC-tr-7330)
  injection of atomic and cluster ion beams into mirror geometries, (T), 26:54757
  interaction with dipole field magnetic field in presence of radial electric field, simulation of steady-flow, (E), 26:54056
  interactions with high-frequency fields, circuits for studying, 26:54775(T) (AEC-tr-7326)
  ion energies from laser-irradiated solid target, (E/T), 26:54802
  ionization processes in hot, collisional, (T), 26:54778 (CEA-CONF-2047)
  kinetic equations for classical, derivation of, (T), 26:54789 (ITF-71-96-P)
  laser beam interactions in, kinetic processes in high temperature, (T), 26:54799
  laser beam scattering on, induced Compton effect in, (T), 26:54798
  laser beam transmission through high-power discharge, absorptive properties in, (E), 26:54785
  magnetosonic waves in, nonlinear, (T), 26:53941
  motion in toroidal magnetic geometries, laminar flow effects on confinement in, (T), 26:54755
  pinch halo development and properties in ISAR I, (E), 26:54784 (IPP-1/125)
  radiations from laser-produced nonuniform, second harmonic, (T), 26:54790(T) (JPRS-56713)
  radiations from relativistic particles in turbulent, bremsstrahlung, (T), 26:54774(T) (AEC-tr-7323)
  research at Wills Plasma Physics Department, Jan.--June 1972, 26:54780(R) (NP-19414)
  research on discharge, Flinders Univ. of South Australia, 26:54779(R) (NP-19393)
  review of 1971 activities at Sydney Univ, 26:53993 (INIS-mf-252)
  spectra of shock-heated krypton and xenon, continuum, (E), 26:54777 (BMBW-FBK-72-8)
  spectral shifts of Stark broadened Lyman-alpha lines of hydrogen, (T), 26:54796
  thermonuclear reactions from spherical hot-spot in deuterium--tritium, (T), 26:54831
PLASMA ACCELERATORS
  jet diagnostics from pulsed erosive, using high-speed spectrography, 26:54773
PLASMA DIAGNOSTICS
  interferometer measurements of electron density, circuit for direct, 26:54770
  laser-beam refraction measurements for electron density, 26:54769
  measurements of density and skin-layer thickness in strong hf discharges, (E), 26:54768(T) (AEC-tr-7329)
  methods for measuring transient properties of dense aluminum plasmas, (E/T), 26:54771
  spectra analysis for magnetic field determination, hydrogen line contours for, 26:54772
PLASMA INSTABILITIES
  current-driven instabilities in plasma, linear theory for, (T), 26:54810
  dissipative instabilities due to supersonic ion motion, (T), 26:54812
  electron-cyclotron drift instabilities in plasma, growth rates for, (T), 26:54811
  electrostatic instabilities of hot-electron plasma in hf fields, (T), 26:54817
  excitation in beam--plasma system, control using electrodes, (E), 26:54819
  magnetohydrodynamic equilibria of plasma, determination of vacuum magnetic field for two-dimensional, 26:54814
  magnetohydrodynamic instabilities in tokamaks, growth rates for, (T), 26:54813
  magnetohydrodynamic instability in Tokamaks, toroidal effects on, (T), 26:54806 (CONF-720804-6)
  parametric instabilities during hf excitation, effect on heating, (E), 26:54751 (CONF-720705-3)
  parametric instabilities in magnetoplasma, excitation by vhf waves, (E), 26:54809 (NP-19406)
  parametric instabilities near lower hybrid frequency, (E), 26:54805 (CONF-720705-4)
  research in collisionless plasma in magnetic mirrors,

(T), 26:54807(R) (COO-3497-2)
  stabilization in mirror machines, method and apparatus for, 26:54823(P)
  stabilization in theta pinches, transverse dynamic, (T), 26:54808 (LRP-51/72)
  stabilization of beam instabilities in plasma--beam system, nonlinear, (T), 26:54821
  surface-wave instability in ion-beam--plasma system, longwave, (T), 26:54816
  synchrotron instabilities for plasma waves, (T), 26:54820
  tearing instabilities in tokamaks, growth rates for, (T), 26:54813
  transverse instability of hot-electron plasma in cylindrical resonator, (T), 26:54818
  two-stream instabilities in spatially separated plasma beams, quasi-hydrodynamic approximation for, (T), 26:54822
PLASMA JETS
  flow around conducting cylinders, potential measurements for ionospheric applications, (E/T), 26:54011 (ONERA-Publ.-137)
PLASMA PRODUCTION
  electron beam interactions for, heating processes in, (E/T), 26:54763
  ionization and accumulation at bottom of potential well, (E), 26:54800(T) (AEC-tr-7350)
  laser beam irradiation for, self-igniting pulsed optical discharges from, (E), 26:54803
  laser beam irradiation of metallic targets, analysis of heavy ions from, (E), 26:54801 (CEA-CONF-2049)
  laser beam irradiation of solid target for, ion energies from, (E/T), 26:54802
  laser beam reactions with deuterated polyethylene for, nanosecond and picosecond, 26:54804
  laser beam reactions with solid targets of deuterium--tritium, fusion reactions from, 26:54830
PLASMA WAVE PHENOMENA
  Alfven wave propagation in incompressible beam--plasma systems, (T), 26:54857
  blast wave generation in pulsed electric discharges, (E), 26:54856
  electromagnetic wave absorption in linear plasma layer in hybrid resonance region, extraordinary, (T), 26:54864
  electromagnetic wave diffraction by magnetoactive plasma cylinder, (T), 26:54847
  electromagnetic wave excitation in plasma by relativistic electron beams, (T), 26:54837(T) (AEC-tr-7333)
  electromagnetic wave interactions with collisionless plasma, generation of fast electrons in, (E), 26:54836(T) (AEC-tr-7331)
  electromagnetic wave reflection at oblique incidence on sharp plasma boundary formed by ionization source moving with constant velocity, (T), 26:54865
  electromagnetic wave scattering on plasma in flat waveguides, effect of electron charge fluctuations on, (T), 26:54848
  electron wave echoes in plasma, saturation effects of, (E/T), 26:54846 (EUR-CEA-FC-639)
  excitation of quasi-static surface waves by weak high-frequency electric field in semi-finite plasma, theory of parametric, 26:54867
  ion oscillations in, automodulation of, 26:54851
  oscillations in bounded neon positive column, constant-wavelength, (E/T), 26:54859
  oscillations in inhomogeneous plasma, theory of parametric excitation of, (T), 26:54844 (AREAEE-125)
  oscillations in plasma, effect of hf wave potential on, (T), 26:54840(T) (AEC-tr-7337)
  oscillations in weakly ionized plasma in hf discharges in magnetic fields, (E), 26:54849
  shock wave investigation of equation of state of nonideal cesium plasma on heated shock tube, (E), 26:54866
  shock wave propagation in collisionless magnetized plasma, oblique, (T), 26:54852
  shock wave propagation in low-density discharge plasma, turbulence in electrostatic, (E/T), 26:54855
  sound wave propagation in nonisothermal fully ionized gas, dispersion relation for, (T), 26:54858
  wave damping in one- and two-component cold and hot plasmas, formulas for long-, (T), 26:54869
  wave excitation and interactions in beam--plasma system, nonlinear, (T), 26:54795
  wave interactions in cylindrical column of magneto-active plasma, hydrodynamic approximation for nonlinear electromagnetic, (T), 26:54863
  wave interactions with magnetohydrodynamic wave radiation in anisotropic plasma, nonlinear high-frequency, (T), 26:54862
  wave interactions with trapped particles in toroidal plasma, resonant, (T), 26:54792
  wave propagation along magnetized plasma layer, effect of electromagnetic field pressure on, (T), 26:54839(T) (AEC-tr-7336)
  wave propagation in magneto-active plasma near electron gyrofrequency harmonics, relativistic and collision effects on, (T), 26:54860
  wave propagation in plasma along magnetic field, nonlinear evolution of quasi-monochromatic packet of helical, (E/T), 26:54868
  wave propagation in plasma sheath, nonlinear space-charge, (T), 26:54853
  wave propagation in plasma, stability of monochromatic against induced scattering, (T), 26:54854
  wave propagation near lower hybrid resonance frequency, nonlinear effects of, (E), 26:54845 (CONF-720804-3)
  wave transformation conditions for plasma with nonmonotonic longitudinal distributon, (E/T), 26:54841(T) (AEC-tr-7338)
  wave transformation in cylinder with spirally conducting surface, volume and surface, (T), 26:54861
  wave transformation into longitudinal oscillations in surface of plasma waveguides, (T), 26:54838(T) (AEC-tr-7335)
  wave transformation region in shf discharges, localization of, (E), 26:54842(T) (AEC-tr-7339)
  wave--wave interactions in plasma, nonlinear kinetics of, (T), 26:54850
PLASMAPAUSE
  phenomena of, from simulated steady-flow interaction of charged particles with geomagnetic dipole field, (E), 26:54056
PLASTICS
  neutron distributions behind Fe/plastic/Fe barriers, spatial, angular, and energy, 26:54966
  preparation of air-equivalent, for ionization chambers, 26:53196(R) (COO-323-28)
  radiation effects on, ir spectral studies on γ, 26:52983 (EUR-4828)
  glass textiles--plastics, preparation and properties of, produced by radioinduced polymerization, 26:53722
  metals--plastics, preparation and properties of, produced by radioinduced polymerization, 26:53722
  plastics--wood, preparation and properties of, produced by radioinduced polymerization, 26:53722
PLATES
  fusion of semi-infinite, model for dynamic edge, 26:55611 (SCL-RR-710113)
  liquid flow due to time-varying motion of infinite flat, MHD incompressible viscous, (T), 26:54158
PLATING
  performance of high-energy ion method for, 26:53615 (SC-DC-722284)
PLATINUM
  muon stopping and diffusion in hot foils of, in vacuum, production of muonium by, (E), 26:54096
  radiation effects on, comparison of stage I annealing with interstitial-migration theories for electron, 26:55011
  radiation effects on, recovery in stage I of annealing of electron, (E), 26:55010
PLATINUM ALLOYS AND SYSTEMS
  Ce--Pt--Ru, thermal capacity of CeRu/sub 2-x/Pt/sub x/ at 1.3 to 9°K, 26:55047
  Co--Pt, microstructure of intermetallic compounds of, methods for ion microscopy imaging of, 26:53655
PLATINUM ISOTOPES
  proton reactions at 3 GeV, time-of-flight measurements of neutron spectra from, (E), 26:54528 (NASA-TM-X-2440, pp 523-6)
PLATYHELMINTHES
  Fasciola hepatica (liver fluke), determination of life cycle of, in snails, mice, and rats, 26:53498(R) (PRNC-156)
  Fasciola hepatica (liver fluke), radiation effects on metacercariae of, for immunization of cattle and rats, 26:53498(R) (PRNC-156)
PLUMES
  rise of, Tabulation Prediction Technique for determining, 26:53152 (ANL-7860(Pt.3), pp 230-49)
PLUTONIUM
  activity concentrations of aerosols of, generated in processing and producing plutonium, 26:53062 (LA-DC-72-920)
  chemical state in solutions, effects of hydrolysis on, 26:52935(R) (MLM-1888)
  content of pentavalent, in natural waters, possibility of, 26:52935(R) (MLM-1888)
  criticality of high burnup fuel of, effects of plutonium isotopic composition in, 26:55416(R) (BNWL-1522-5)
  determination in soil, sample size for fusion method for, 26:52935(R) (MLM-1888)
  determination in urine by radiochemical methods using ion exchanger filters, 26:52940
  fabrication by rolling at high temperature under vacuum, 26:53630
  hydrolysis of tetravalent, solvent extraction studies on, 26:53034(T) (MLM-1964(tr))
  ionization of surfaces of, 26:53033 (EUR-4765, pp 117-30)
  polymerization of tetravalent, spectrophotometric study of, pp. 81, 26:53036 (ORNL-4794, pp 81-3)
  production by bomb reduction of plutonium tetrafluoride, estimation of minimum temperatures in, 26:53037 (RFP-1455)
  purification by extraction with amines, research progress on, p. 55, 26:53084 (ORNL-4794, pp 54-62)
  removal from lungs of monkeys following inhalation as oxide, effectiveness of pulmonary lavage for, 26:53528(T) (LF-tr-71)
  requirements in power production 1980 to 2000, calculations of, 26:55093
  separation from neptunium in MILLI laboratory by solvent

  extraction using TBP, 26:53073
  separation from uranium, residue adsorption and anion exchange methods for, 26:52935(R) (MLM-1888)
  separation from Zircaloy-clad oxide fuels, head-end pyrochemical Saltex process for, 26:53079 (EUR-4812)
  separation of tetravalent, from aqueous solutions by solvent extraction using isopropyltropolone, 26:53034(T) (MLM-1964(tr))
  shipping of, severe-environment testing of 6M, L-10, and SP5795 containers for, 26:53736 (SC-DR-720597)
  size characteristics of aerosols generated in processing and production of, 26:53062 (LA-DC-72-920)
  storage of, evaluation of PVC bags for, 26:52992 (RFP-1924)

PLUTONIUM CARBIDES
  preparation by carbothermic method, research progress on, p. 86-7, 26:53554 (ORNL-4794, pp 84-7)
  PuC--UC, preparation by carbothermic method, research progress on, p. 86-7, 26:53554 (ORNL-4794, pp 84-7)

PLUTONIUM CARBONITRIDES
  preparation by carbothermic method, research progress on, p. 86-7, 26:53554 (ORNL-4794, pp 84-7)
  PuCN--UCN, preparation by carbothermic method, research progress on, p. 86-7, 26:53554 (ORNL-4794, pp 84-7)

PLUTONIUM FLUORIDES PuF_4
  production by fluorination of plutonium dioxide in fluidized bed reactor, comparison of hydrofluorination process with, 26:53039 (RFP-1890)
  production by fluorination of plutonium dioxide using fluorine in fluidized bed reactor, 26:53038 (RFP-1889)
  reduction using calcium, estimation of minimum temperatures in bomb, 26:53037 (RFP-1455)

PLUTONIUM ISOTOPES Pu-236
  effects on γ and neutron spectra of molybdenum--plutonium dioxide heat sources, 26:53336 (NASA-TM-X-2440, pp 853-8)

PLUTONIUM ISOTOPES Pu-238
  analysis for uranium-232 and uranium-234 by hydrolysis, residue adsorption, and α spectroscopy, 26:52935(R) (MLM-1888)
  content in atmosphere in vicinity of Savannah River Plant, 1971, 26:53153(R) (DPSPU-72-30-1)
  content in off-gases from combustion of HTGR graphite fuels, 26:53060 (CONF-720823-14)
  fabrication and safety of sealed sources of, for cardiac pacemakers, 26:53331 (CEA-CONF-2026)
  fuel forms of, for radioisotope heat sources, evaluation of, 26:53333 (MLM-1213)
  preparation of metallic, equipment and methods for, 26:53332 (MLM-1150)
  production by neutron irradiation of neptunium oxide and TBP solvent extraction in MILLI laboratory, 26:53073
  production, processing, and properties of, for use in space research, 26:53337 (NASA-TM-X-2440, pp 859-61)
  radiation properties of, for use in space research, 26:53337 (NASA-TM-X-2440, pp 859-61)

PLUTONIUM ISOTOPES Pu-239
  content in atmosphere in vicinity of Savannah River Plant, 1971, 26:53153(R) (DPSPU-72-30-1)
  energy level at 57.3 keV from neptunium-239 beta decay, Moessbauer-effect measurement of lifetime of, (E), 26:54661
  Moessbauer effect in plutonium dioxide, spectrum from, (E), 26:54661
  neutron fission at 14 MeV, delayed neutron spectra from, (E), 26:54655 (CONF-720901-(Bks.1 and 2), pp 687-99)
  neutron fission of, survey on cross section data for, 26:54657 (FEI-292)
  neutron spectra from homogeneous sphere containing, benchmark calculations for, 26:54486 (RISO-M-1526)
  release to environment as oxide aerosols during fast reactor accidents, hazards to human population, 26:53511 (TID-26142)
  uptake and retention in liver of mammals, mechanisms for, 26:53526(T) (BNWL-tr-71)
  uptake and retention in tissues of animals following inhalation as oxide aerosols, extrapolation of pathological data to man, 26:53511 (TID-26142)

PLUTONIUM ISOTOPES Pu-240
  decay of, γ-ray energies and intensities from, (E), 26:54652 (ANCR-1069)
  energy levels in isomeric, from uranium-238 (α,2n) reactions, rotation constant for, (E), 26:54664
  energy-level transitions in isomeric, from uranium-238 (α,2n) reactions, intensities of, (E), 26:54664

PLUTONIUM ISOTOPES Pu-241
  decay of, γ-ray energies and intensities from, (E), 26:54652 (ANCR-1069)

PLUTONIUM NITRATES
  purification and concentration by anion exchange using small resins, p. 91-3, 26:53085 (ORNL-4794, pp 91-5)

PLUTONIUM OXIDES PuO_2
  compatibility of plutonium-238 enriched fuels of, with molybdenum, rhenium, tungsten, and their alloys, T-111, and TZM, 26:53551(R) (MDC G-3153)
  fluorination in fluidized bed reactor using fluorine, production of plutonium tetrafluoride by, 26:53038 (RFP-1889)
  fluorination using fluorine and fluidized bed reactor, comparison of plutonium tetrafluoride production by hydrofluorination or, 26:53039 (RFP-1890)
  plutonium-239 Moessbauer effect in, spectrum from, (E), 26:54661
  release of plutonium-239 aerosols of, to environment during fast reactor accidents, hazards to human population, 26:53511 (TID-26142)
  Mo--PuO_2, radiation emission by heat sources of, effects of age, fluorine-19, oxygen-17, oxygen-18, plutonium-236, and size on γ and neutron, 26:53336 (NASA-TM-X-2440, pp 853-8)
  PuO_2--UO_2, corrosive effects on stainless steel of fission products of, effects of burnup on, 26:55187 (EURFNR-989)
  PuO_2--UO_2, oxidation of unirradiated fuels of, p. 84-5, 26:53554 (ORNL-4794, pp 84-7)
  PuO_2--UO_2, preparation of by sol-gel process, research progress on, p. 85-6, 26:53554 (ORNL-4794, pp 84-7)
  PuO_2--UO_2, properties of fuels of, mechanical, physical, and thermal, (E), 26:55189(R) (GEAP-10028-39)
  PuO_2--UO_2, radiation effects testing of fuels of, 26:55189(R) (GEAP-10028-39)
  PuO_2--UO_2, reactivity of fuel elements of, effects of grain size of plutonium oxide in, 26:55416(R) (BNWL-1522-5)
  PuO_2--UO_2-base, deformation and fracture of, effects of temperature and strain rate on, 26:53545 (ANL-7945)

POINT BEACH POWER REACTOR, UNIT 1
  emergency core cooling system for, elimination of hot leg injection, 26:55289 (DOCKET-50266-79)
  radioactive effluents from, effects on radioisotope content in Lake Michigan fish, 26:53169 (ANL-7860(Pt.3), pp 141-50)
  thermal effluents from, correlation of type and quantity of fish collected with temperature of, 26:53185 (ANL-7860(Pt.3), pp 118-20)
  thermal effluents from, ecological studies on effects of, 26:53182 (ANL-7860(Pt.3), pp 101-2)
  thermal effluents from, effects on inshore biological communities of Lake Michigan, 26:53184 (ANL-7860(Pt.3), pp 109-17)
  thermal effluents from, effects on major nutrients and water quality parameters of, 26:53183 (ANL-7860(Pt.3), pp 103-8)
  valves for, verification of wall thicknesses for nuclear service, 26:55290 (DOCKET-50266-80)

POINT BEACH POWER REACTOR, UNIT 2
  emergency core cooling system for, elimination of hot leg injection, 26:55289 (DOCKET-50266-79)
  valves for, verification of wall thicknesses for nuclear service, 26:55290 (DOCKET-50266-80)

POLAND
  radium-226 content of foods, human diet, and urine in, relation between, 26:53525

POLARIMETERS
  design for spin-rotation measurements in elastic $\pi + p$ interactions at high energies, 26:54232

POLONIUM ISOTOPES Po-210
  properties for use in SNAP heat sources, 26:53334 (MLM-1228)

POLONIUM ISOTOPES Po-218
  content in uranium mine air, α-spectrometric method for determining, 26:53226

POLYMERS
  mechanical properties of particulate-filled, 26:55603 (SC-DR-70-617)
  spectra of molecular dimers, vibronic absorption, 26:55534 (ITF-72-27-P)
  concretes--polymer, development of composite materials of, 26:55473 (BNL-16609)
  concretes--polymers, preparation and properties of, produced by radioinduced polymerization, 26:53722

POPULATIONS
  radiation dose to human, following nuclear explosion, evaluation of use of chromosome aberrations in leukocytes to estimate, 26:53397 (FOA-4-4500-A-3)
  radiation dose to human, following release of radioisotopes to environment, criteria for maximum permissible, 26:53523
  radiation dose to human, of Hiroshima and Nagasaki, comparison of, for diagnostic radiographic examinations with A-bomb survivors, 26:53434
  radiation hazards to human, following release of plutonium-239 oxide aerosols to environment during fast reactor accidents, guidelines for estimation of, 26:53511 (TID-26142)
  radioinduced neoplasms in human, following exposure in utero, review of epidemiological studies on, 26:53435

POSITRON BEAMS
  production of 1-eV, by backscattering of sodium-22 positrons by magnesium-oxide-coated gold surface, 26:54119

POSITRONIUM
  formation and lifetime of ortho-, in liquid and solid amides, effects of dipolar electric fields of amide groups on, (E), 26:54100

POSITRONS
  annihilation in ion-implanted silver halide crystals, measurement of Doppler broadening of photons from, using Ge(Li) detector, 26:54097
  correlation energy in metals, (T), 26:55066
  energy spectra of primary cosmic, (E), 26:53855
  interactions $e^+ + e^- \to$ hadrons, perturbation theory for relation to deep inelastic $e + p$ scattering, (T),

26:54262
  interactions $e^+ + e^- \rightarrow$ hadrons, review of total cross sections, SU(3) ratios, SU(6) quark model predictions, multiplicities, transverse momentum distributions, resonance production, and $\gamma + \gamma$ processes for annihilation, (E/T), 26:54176 (SLAC-PUB-1043)
  interactions $e^+ + e^- \rightarrow W^- + e^+ + \nu$, total cross section and angular and energy distributions of e^+ and W^- production in, (T), 26:54277
  interactions $e^+ + e^- \rightarrow W^- + \mu^+ + \nu$, W^- production in, (T), 26:54277
  interactions $e^+ + e^-$ in storage rings, test for existence of high-mass vector mesons in, (T), 26:54283
  interactions $e^+ + e^-$, angular distributions in annihilation, (T), 26:54281
  interactions $e^+ + e^-$, Schwarz inequality for asymptotic behavior of cross sections for annihilation, (T), 26:54287 (LBL-766)
  interactions $e^+ + p \rightarrow e^+ + e^- + e^+ + p$ at 30 GeV, angular distributions, mass spectra, and total cross sections for, (T), 26:54263
  lifetime in liquid and solid amides, effects of dipolar electric fields of amide groups on, (E), 26:54100
  lifetimes in ammonium chloride NH_4Cl and nitrate glasses, measurement of temperature-dependent, (E), 26:55064
  reactions with argon at 8 eV, total cross sections for, (E), 26:54119
  reactions with helium at 2 to 20 eV, total cross sections for, (E), 26:54119
POTASSIUM
  determination of, radiometric, 26:52942
  neutron capture by, comparison of ENDF/B III and published data for thermal, 26:54501 (ORNL-TM-3910)
  scattering by carbon tetrachloride, sulfur hexafluoride, and tin chloride at thermal energies, effects of temperature and internal and translational energy on differential cross sections for nonreactive, (E), 26:54136
  thermal conductivity at 1.5 to 15°K, effects of magnetic field and impurities on, (E/T), 26:55507 (COO-3150-6)
POTASSIUM ALCOHOLATES
  description of low-temperature, for production of electricity, 26:53108(P)
POTASSIUM BROMIDES
  charged-particle dechanneling at 1.5 MeV, proton, deuteron, and helium-ion, 26:54988
  radioinduced color centers in, by 10- to 50-keV electron beams, (E), 26:54973 (FRNC-TH-210)
  radioinduced fast recombination luminescence in, lifetime and temperature dependence of proton-pulse, 26:55000
POTASSIUM CHLORIDES
  charged-particle dechanneling at 1.5 MeV, proton, deuteron, and helium-ion, 26:54988
  phonon generation in Li^+- and OH^--doped, with pulsed electric fields, (E/T), 26:55512 (COO-3151-139)
  radiation effects on spectra of hexacyanocobaltate-doped, x, 26:55001
  radioinduced color centers in, by 10- to 50-keV electron beams, (E), 26:54973 (FRNC-TH-210)
POTASSIUM HYDROXIDES
  properties for use as electrolyte in magnetohydrodynamic generator working fluids, 26:53108(P)
  radiolysis of aqueous solutions of, kinetics of hydrated electron disappearance in pulse, 26:53018
POTASSIUM IODATES
  toxicity in animals and man, bibliography on, 26:55575 (ORNL-TIP/TIRC-72-10)
POTASSIUM IODIDES
  properties for use as electrolyte in magnetohydrodynamic generator working fluids, 26:53108(P)
  radioinduced color centers in, by 10- to 50-keV electron beams, (E), 26:54973 (FRNC-TH-210)
  radioinduced fast recombination luminescence in, lifetime and temperature dependence of proton-pulse, 26:55000
  radiolysis of crystalline, effects of water vapor on γ, 26:53017
POTASSIUM ISOTOPES K-39
  energy levels of, intermediate coupling calculation of, (T), 26:54685 (INP-795)
POTASSIUM ISOTOPES K-40
  abundance in iron meteorites, (T), 26:53808(T) (ORNL-tr-2620)
  content in Lake Michigan fish, 26:53169 (ANL-7850(Pt.3), pp 141-50)
POTASSIUM OXIDES
  K_2O--SiO_2--SrO, diffusion in, electrostatic effects and mobility in, 26:53598
POTASSIUM SODIUM TARTRATES
  proton reactions at 660 MeV, properties of Cherenkov radiation from, (E), 26:54875 (JINR-P1-6552)
POTENTIOMETERS
  design of chrono-, for analysis of molten salts, engineering drawings for, 26:52957
POWDER METALLURGY
  conference on high-temperature materials, Reutte/Tyrol, Austria, June 21 to 25, 1971, Vol. 3, 26:53584
  conference on high-temperature materials, Reutte/Tyrol, Austria, June 21 to 25, 1971, Vol. I, 26:53601
  conference on high-temperature materials, Reutte/Tyrol, Austria, June 21 to 25, 1971, Vol. 2, 26:53602
  conference on high-temperature materials, Reutte/Tyrol, Austria, June 21 to 25, 1971, Vol. 4, 26:53603
  review on high-temperature materials, 26:53590
POWDERS
  mixing of metal and refractory compound, effects of friction on, 26:53617
  production of, Coldstream process for, 26:53591
POWER CYCLES
  efficiency of nonconventional two-phase, for automobile engines, (T), 26:53103
POWER PLANTS
  thermal effluents from, feasibility of useful heat extraction from, 26:55212 (CONF-720925-2)
  waste heat discharges from, to surface waters, environmental effects of, 26:53194
  waste heat from, feasibility for use for urban space heating, industrial and sewage processing, and agricultural purposes of, 26:55212 (CONF-720925-2)
POWER SUPPLIES
  design for beam preinjector of I-100 linac, 26:53751(T) (BNL-tr-498)
PRAIRIE ISLAND POWER REACTOR, UNIT 1
  auxiliary systems for, revised and additional data on, 26:55299 (DOCKET-50282-73)
  containment system for, revised and additional data on, 26:55299 (DOCKET-50282-73)
  cooling system for, revised and additional data on, 26:55299 (DOCKET-50282-73)
  electrical systems for, revised and additional data on, 26:55299 (DOCKET-50282-73)
  engineered safeguards for, revised and additional data on, 26:55299 (DOCKET-50282-73)
  instrumentation for, revised and additional data on, 26:55299 (DOCKET-50282-73)
  operations for, revised and additional data on, 26:55299 (DOCKET-50282-73)
  power conversion system for, revised and additional data on, 26:55299 (DOCKET-50282-73)
  radioactive waste disposal system for, revised and additional data on, 26:55299 (DOCKET-50282-73)
  safety analysis for, revised and additional data on, 26:55299 (DOCKET-50282-73)
  site for, revised and additional data on, 26:55299 (DOCKET-50282-73)
  testing program for, revised and additional data on, 26:55299 (DOCKET-50282-73)
  valve torque switches for, failure of motor operated, 26:55258 (DOCKET-50282-74)
  valves for, verification of wall thicknesses for nuclear service, 26:55298 (DOCKET-50282-72)
PRAIRIE ISLAND POWER REACTOR, UNIT 2
  auxiliary systems for, revised and additional data on, 26:55299 (DOCKET-50282-73)
  containment system for, revised and additional data on, 26:55299 (DOCKET-50282-73)
  cooling system for, revised and additional data on, 26:55299 (DOCKET-50282-73)
  electrical systems for, revised and additional data on, 26:55299 (DOCKET-50282-73)
  engineered safeguards for, revised and additional data on, 26:55299 (DOCKET-50282-73)
  instrumentation for, revised and additional data on, 26:55299 (DOCKET-50282-73)
  operations for, revised and additional data on, 26:55299 (DOCKET-50282-73)
  power conversion system for, revised and additional data on, 26:55299 (DOCKET-50282-73)
  radioactive waste disposal system for, revised and additional data on, 26:55299 (DOCKET-50282-73)
  safety analysis for, revised and additional data on, 26:55299 (DOCKET-50282-73)
  site for, revised and additional data on, 26:55299 (DOCKET-50282-73)
  testing program for, revised and additional data on, 26:55299 (DOCKET-50282-73)
  valves for, verification of wall thicknesses for nuclear service, 26:55298 (DOCKET-50282-72)
PRASEODYMIUM ISOTOPES
  proton decay of light, search for, (E), 26:54608(T) (UCRL-Trans-1473)
PRASEODYMIUM ISOTOPES Pr-141
  energy levels from neodymium-141 decay, properties of quasi-proton, (E), 26:54604 (JINR-P6-6519)
  photon reactions (γ,xn) at 8 to 24 MeV, cross sections for, (E), 26:54629
  photon reactions (γ,xn) with, model analysis of giant resonance in, (E/T), 26:54598 (FRNC-TH-242)
  proton reactions (p,t) at 40 MeV, analysis of angular distributions for collective effects, (E), 26:54615
PRASEODYMIUM ISOTOPES Pr-142
  concentration by (n,γ) reactions in molecular sieves, 26:53067 (ORNL-4794, pp 88-90)
PRASEODYMIUM ISOTOPES Pr-143
  energy levels from cerium-142 proton resonances, isobaric analog, (E), 26:54618
PRASEODYMIUM OXIDES
  spectra of nonstoichiometric, 4.2°K far-infrared, (E/T), 26:55032
PREAMPLIFIERS
  design of high-rate direct-coupled, for Ge(Li) detector, engineering drawings for, 26:53219
PRESSURE DROP
  coefficients in liquid systems, effects of rod

configuration and spacing on, 26:55174(T) (EURFNR-986)

PRESSURE VESSELS
  defects in reactor, capabilities for in-service detection and analysis of, 26:55222(R) (NP-19338(Vol.2))
  defects in reactor, capabilities for in-service detection and analysis of, 26:55221 (NP-19338(Vol.1))
  design of reactor steel, survey of, 26:55224
  fabrication of reactor steel, survey of, 26:55224
  fracture toughness of heavy section steel, (E), 26:55207(R) (ORNL-TM-3900)
  inspection of reactor, development of methods for in-service, 26:55222(R) (NP-19338(Vol.2))
  inspection of reactor, development of methods for in-service, 26:55221 (NP-19338(Vol.1))
  nozzles for, effects of attachment configuration on stresses in, (E/T), 26:55207(R) (ORNL-TM-3900)

PRESSURE WAVES
  propagation in coolant pipe rupture accidents in water cooled reactors, BURST code analysis of, 26:55203 (JAERI-M-4473)

PROCESS EQUIPMENT
  circuits for computer controlled in-line monitoring of radioisotope in chemical process streams, engineering drawings for, 26:53220

PROMETHIUM OXIDES
  properties of, chemical and physical, 26:53596

PROPANE
  radiolysis of liquid, time dependence of spectra of solvated electrons from, 26:53007

1,3-PROPANEDIONE, 1,3-DIPHENYL-
  solvent properties for tetravalent plutonium, 26:53034(T) (MLM-1964(tr))
  uses in spectrophotometric determination of hexavalent uranium, 26:52920 (RT/CHI-(72)3)

PROPENE POLYMERS
  radiolysis of, kinetics of reactions at 300°K of methyl methacrylate with radicals produced by γ, 26:53019

PROSPECTING
  developments in India, for nuclear materials, 26:55452(R) (NP-19407)

PROTACTINIUM
  precipitation as oxide from molten salts, pp. 5-6, 26:53081 (ORNL-4794, pp 1-14)
  separation from actinium, niobium, and neptunium, by anion exchange, 26:52903
  separation from spent molten salt fuel by reductive extraction, 26:53086(P)

PROTEINS
  production of nervous-system-specific (14-3-2), by human neuroblastoma cells in culture, 26:55621 (UCLA-12-877)
  radiation effects on content of, in blood of rats following intratracheal administration of cerium-144, 26:53516
  radiation effects on content of, in serum of mice, combined effects of cortisone on gamma, 26:53490
  radiation effects on metabolism of, in L cells infected with rickettsiae, effects of cycloheximide on gamma, 26:53360
  radioisotope binding by blood, relation to uptake and retention in liver of mammals, americium-241 and plutonium-239, 26:53526(T) (BNWL-tr-71)

PROTON BEAMS
  acceleration in Saturne, method for preserving beam polarization during, 26:53762
  effects on human brain following use for hypophysectomy, 26:53446
  energy measurement of 665-MeV, using Cherenkov radiation, performance of monochromatic method for, 26:53800
  interactions with electron beams, calculation of luminosity of, 26:53777 (BNL-17067)
  production of polarized, using ISABELLE in Whiplash mode, feasibility of, 26:53775 (BNL-17057)

PROTONS
  bremsstrahlung from suprathermal cosmic, (E/T), 26:53820
  cascades in iron due to 30- to 300-GeV/N cosmic, (E), 26:53832
  channeling in thin gold crystals, 26:54974 (LYCEN-7228)
  channeling of 1-MeV, in fast neutron-irradiated silicon and germanium single crystals, 26:55004
  charge radius in nonlinear sigma model, 26:54251
  dechanneling at 1.5 MeV in diamond lattices, 26:54988
  diffusion into polar-cap regions of 1.2- to 40-MeV solar, from interplanetary space, (E), 26:54069
  dose calculations for space missions, using USAF--NASA model man, 26:54883 (NASA-TM-X-2440, pp 773-80)
  dose distributions for radiobiology and radiotherapy, radiation transport codes for, (T), 26:54890 (ORNL-TM-3816)
  effects of 17.0- and 18.3-MeV, on optical spectra of Type-I diamonds, 26:54991
  effects of 2-MeV pulses of, on alkali metal halides, lifetime of fast recombination luminescence transitions induced in, 26:55000
  effects of Jupiter-belt, on fly-by space missions, 26:54002 (NASA-TM-X-2440, pp 781-4)
  effects on lymphatic organs following acute sublethal exposure of young chickens, comparison of RBE for 2.2 GeV with x radiation, 26:53457 (NASA-TM-X-2440, pp 659-64)
  effects on mice, effects on survival of erythropoietic stem cells following sublethal whole-body exposure, protective effects of AET and serotonin against high-energy, 26:53454 (NASA-TM-X-2440, pp 642-6)
  effects on rats following acute whole-body exposure, comparison with effects of γ rays for lethal and neoplastic, 26:53455 (NASA-TM-X-2440, pp 647-51)
  effects on silver-activated phosphate glass at 200 to 400 keV, depth distribution of photoluminescence induced by, 26:55009
  effects on young chickens following acute whole-body exposure, lethal, 26:53457 (NASA-TM-X-2440, pp 659-64)
  energy spectra of primary cosmic, at 50 to 2000 GeV, (E), 26:53829
  flux during energetic storm particle event, (E), 26:53966
  flux measurements at ATS-5 satellite at synchronous altitude of low-energy, effects of magnetic activity on, 26:54045 (NASA-TM-X-2440, pp 530-8)
  fluxes in Jupiter radiation belt, models of, 26:54001 (NASA-TM-X-2440, pp 556-60)
  fluxes of trapped, in Jovian magnetosphere, (E/T), 26:54006
  form factors of, anomalous dimensions for relation of $p + p \rightarrow p + p$ interactions at high energies and large angles with electromagnetic, (T), 26:54343 (DESY-72/35)
  geomagnetic cutoff-rigidity calculations for Fort Churchill, Canada, daily variations of, (E/T), 26:54065
  interactions anti $p + p \rightarrow \pi^-$ + anything at 5.6 to 70 GeV/c, uncorrelated jet model predictions for pion multiplicity distribution in annihilation, (T), 26:54316 (RPP/T-24)
  interactions anti p + p at 1.2 GeV/c, analysis of K anti K and K anti Kπ resonances in annihilation, (E), 26:54199
  interactions anti p + p at 6 to 14 GeV/c, evidence for interaction radius scaling from analysis of polarization in, (T), 26:54354
  interactions anti p + p at 7 GeV/c in deuterium bubble chamber, anti p--p and K^+--K^- pair and resonance production, f^0--A_2^0 interference, and cross sections for three- and four-prong, (E), 26:54218
  interactions anti p + p at very low energy, research proposal for ISABELLE for, 26:53766 (BNL-16818)
  interactions anti p + p, description of annihilation spectrometer for measuring cross sections for, 26:53279
  interactions anti p + p, identical distribution over charged particle multiplicity for, (T), 26:54327 (JINR-E2-6596)
  interactions at high energies, design of 4π Porcupine detector for detecting products from high-multiplicity, 26:53266 (BNL-17020)
  interactions $e + p \rightarrow e + K^+(K^-)$ + anything at 6.5 GeV, momentum spectra of K in inclusive, (E), 26:54178
  interactions $e + p \rightarrow e + \mu^+ + \mu^-$ + anything, test of algebra of bilocal operators from, (T), 26:54253
  interactions $e + p \rightarrow e + p$ + anything at 6.5 GeV, momentum spectra of protons in inclusive, (E), 26:54178
  interactions $e + p \rightarrow e + \pi^+(\pi^-)$ + anything at 6.5 GeV, momentum spectra of π in inclusive, (E), 26:54178
  interactions $e + p \rightarrow e^+ + e^- + e + p$ at 30 GeV, angular distributions, mass spectra, and total cross sections for, (T), 26:54263
  interactions $e + p \rightarrow \mu^+ + \mu^- + e + p$ at 30 GeV, angular distributions, mass spectra, and total cross sections for, (T), 26:54263
  interactions e + p at $q^2 = 1(\mathrm{GeV}/c)^2$ in resonance region, separation of longitudinal contribution from total cross sections of virtual $\gamma + p$ interactions in inelastic, (E), 26:54168 (DESY-72/38)
  interactions e + p in spin-$^1/_2$ parton model, two-photon exchange effects in deep inelastic, (T), 26:54269
  interactions e + p, k^2 dependence of transverse cross section for meson (π^+) production in generalized Born term model, (T), 26:54243 (DESY-72/30)
  interactions e + p, perturbation theory for $e^+ + e^- \rightarrow$ hadrons relation to deep inelastic, (T), 26:54262
  interactions $e^+ + p \rightarrow e^+ + e^- + e^+ + p$ at 30 GeV, angular distributions, mass spectra, and total cross sections for, (T), 26:54263
  interactions $\gamma + p \rightarrow p$ + eta at threshold to 1.1 GeV, recoil proton polarization, transition amplitudes, and cross sections for N resonance production in, (E), 26:54166 (CALT-68-322)
  interactions $\gamma + p \rightarrow p + \pi^+ + \pi^-$ at 2 to 5 GeV in hydrogen bubble chamber, cross sections and resonance production in, (E), 26:54175 (SLAC-143)
  interactions $\gamma + p \rightarrow p(n) + \pi^+ + \pi^- + \pi^0(\pi^+)$ at 4.3 to 7.5 GeV, cross sections and resonance production in, (E), 26:54175 (SLAC-143)
  interactions $\gamma + p \rightarrow \pi^0(\gamma) + p$ at 3 to 7 GeV, polarization of recoil proton in, (E), 26:54167 (COO-3069-71)
  interactions $\gamma + p \rightarrow \pi^-$ + anything at 9.3 GeV/c, multiperipheral-model calculations of cross sections for, (T), 26:54325 (COO-3533-2)
  interactions $\gamma + p \rightarrow \pi^+ + n$ at 0.5 to 2.2 GeV, magnetic spectrometer study of structure in target asymmetry in, (E), 26:54172 (NP-19415)
  interactions $\gamma + p \rightarrow \pi^+ + n$ in 3,3 resonance region,

discrepancy between dispersion relation predictions and experiment, 26:54261
interactions $\gamma + p \to \pi^+ + n$, contribution of unnatural parity exchanges to, (T), 26:54270
interactions $\gamma + p \to \pi^+(\pi^-)$ + anything at very high energies, limiting distributions for, (T), 26:54326 (DESY-72/40)
interactions $\gamma + p$ in $\Delta(1236)$ resonance region, differential cross sections for elastic Compton, (E), 26:54180
interactions $\gamma + p$, proposed experiment using multiwire proportional chambers and wide-gap spark chambers for charged-particle multiplicity and angular correlations in, (E), 26:54192 (BNL-17141)
interactions $K + p$, interference term effects in multiperipheral model for cross section energy dependence, pion multiplicities, and structures in correlation functions for, (T), 26:54329 (NYO-3533-265)
interactions $K^+ + n \to K^0 + p$, Regge pole--cut model for, (E/T), 26:54230
interactions $K^- + p \to$ anti $K^0 + n$ at 1 to 3 GeV/c, scintillation counter study of cross sections and resonance production in, (E/T), 26:54210 (NP-19419)
interactions $K^- + p \to$ anti $K^0 + n$ at 1700 to 2100 MeV, cross sections, polarizations, and angular distributions for, (E), 26:54215
interactions $K^- + p \to$ anti $K^0 + n$, Regge pole--cut model for, (E/T), 26:54230
interactions $K^- + p \to \Delta^{++} + K^{*-} + \pi^-$ at 10 GeV/c, Veneziano model analysis of, (E/T), 26:54225
interactions $K^+ + p \to K^0 + \pi^0 + \pi^+ + p$ at 5 to 12.7 GeV/c, longitudinal phase space analysis of, (E/T), 26:54226
interactions $K^+ + p \to K^+ + \pi^- + \pi^+ + p$ at 5 to 12.7 GeV/c, longitudinal phase space analysis of, (E/T), 26:54226
interactions $K^- + p \to \Lambda + \pi^0$ at 1700 to 2100 MeV, cross sections, polarizations, and angular distributions for, (E), 26:54215
interactions $K^- + p \to p +$ anti $K^0 + \pi^+ + \pi^- + \pi^- + \pi^0$ at 10 GeV/c, analysis of $K^{*-}(890)$, $\Delta^{++}(1236)$, and ω^0 production in, (E), 26:54225
interactions $K^- + p \to p +$ anti $K^0 + \pi^+ + \pi^- + \pi^-$ at 10 GeV/c, analysis of $K^{*-}(890)$, $\Delta^{++}(1236)$, and rho^0 production in, (E), 26:54225
interactions $K^+ + p \to p + K^0 + \pi^+$ at 1.37 to 2.17 GeV/c, cross sections for, (E), 26:54231
interactions $K^+ + p \to p + K^+ + \pi^+ + \pi^-$ at 1.37 to 2.17 GeV/c, cross sections for, (E), 26:54231
interactions $K^+ + p \to \pi^-$ + anything at 12.6 GeV/c, multiperipheral-model calculations of cross sections for, (T), 26:54325 (COO-3533-2)
interactions $K^- + p \to \pi^- + \Sigma^+$, new Regge absorption model for cross sections of, (T), 26:54336
interactions $K^- + p \to \pi^+(\pi^-)$ + anything at 10 GeV/c, differential cross sections and symmetry of π emission in, (E), 26:54222
interactions $K^+ + p$ at 0.909 to 1.907 GeV/c, differential and total cross sections for elastic, (E), 26:54211 (RPP/H-95)
interactions $K^+ + p$ at 6 to 14 GeV/c, evidence for interaction radius scaling from analysis of polarization in, (T), 26:54354
interactions $K^- + p$ at 6 to 14 GeV/c, evidence for interaction radius scaling from analysis of polarization in, (T), 26:54354
interactions $\mu + p \to \mu^+ + \mu^- + e + p$ at 30 GeV, angular distributions, mass spectra, and total cross sections for, (T), 26:54263
interactions $\mu^- + p \to \mu^-$ + anything in scaling region, differential cross sections and detection and isolation of neutral weak currents for, (T), 26:54288 (RPP/T-26)
interactions $\mu^+ + p \to \mu^+ + \mu^- + \mu^+ + p$ at 30 GeV, angular distributions, mass spectra, and total cross sections for, (T), 26:54263
interactions $\mu^- + p \to \mu^+ + \mu^- + \mu^- + p$ at 30 GeV, angular distributions, mass spectra, and total cross sections for, (T), 26:54263
interactions $n + p \to p + n$, contribution of unnatural parity exchanges to charge-exchange, (T), 26:54270
interactions $n + p$, effects on low-momentum transfer cross sections for anti $p + d \to$ anti $p + p + n$ interactions from final-state, (E), 26:54347 (UM-P-72-6)
interactions $p + d \to p + d$ at 10 to 70 GeV, tables of absolute differential cross sections and amplitudes for, (E), 26:54194 (JINR-E1-6615)
interactions $p + d$ at 10 to 70 GeV, slope parameter of diffraction cone and ratio of real to imaginary parts of amplitude of elastic, (E), 26:54197
interactions $p + d$ at 800 MeV, calculation of relative neutron and pion yields in, (T), 26:54467(R) (ORO-2972-204)
interactions $p + p \to e^+(e^-) + \nu$ + anything in colliding beams, test of Fermi theory of weak intractions in parton model for cross sections and counting rates for, (T), 26:54284 (BNL-16978)
interactions $p + p \to e^+(\mu^+) + \nu$ + anything, resolution in mass-squared for lepton pair in, (E/T), 26:54182 (BNL-17092)
interactions $p + p \to K$ + anti K at 10 to 40 GeV/c, multiperipheral-model calculations of cross sections for, (T), 26:54325 (COO-3533-2)
interactions $p + p \to \Lambda + K$ at 10 to 40 GeV/c, multiperipheral-model calculations of cross sections for, (T), 26:54325 (COO-3533-2)
interactions $p + p \to \mu^+ + \mu^-$ + anything, neutral weak currents in, (E/T), 26:54182 (BNL-17092)
interactions $p + p \to p$ + anything, triple-Regge formalism for analysis of, (T), 26:54332
interactions $p + p \to p + p + \gamma$ at 15 to 280 MeV, effects of relativistic spin corrections for angular distributions and excitation functions for, (T), 26:54267
interactions $p + p \to p + p$ at 8 to 70 GeV, tables for absolute differential cross sections and slope and real part parameters for, (E), 26:54193 (JINR-E1-6613)
interactions $p + p \to p + p$ at high energies and large angles, anomalous dimensions for relation of proton electromagnetic form factors with, (T), 26:54343 (DESY-72/35)
interactions $p + p \to \pi(K)$ + anything at 12 to 30 GeV/c, Bose distribution and scaling law for inclusive, (T), 26:54349
interactions $p + p \to \pi^-$ + anything at 28.5 GeV/c, multiperipheral-model calculations of cross sections for, (T), 26:54325 (COO-3533-2)
interactions $p + p \to \pi^-$ + anything with and without strange particle production at 19 GeV/c, comparison of π momentum distributions in, (E), 26:54198
interactions $p + p \to \pi^+ + d + \gamma$, amplitudes of, (T), 26:54250
interactions $p + p \to \pi^+(\pi^-)$ + anything at very high energies, limiting distributions for, (T), 26:54326 (DESY-72/40)
interactions $p + p$ at 6 to 14 GeV/c, evidence for interaction radius scaling from analysis of polarization in, (T), 26:54354
interactions $p + p$ at extremely high energies, fixed-pole Pomeron and shielding branch cuts for, (T), 26:54353
interactions $p + p$ at high energies, Feynman--Wilson two-component theory and independent model for integral and differential data for two-particle correlations between negative pions for diffractive and nondiffractive, (T), 26:54346 (RPP/T-28)
interactions $p + p$ in colliding beams at ISABELLE, forward production of muons and muon pairs in, (E/T), 26:54181 (BNL-16977)
interactions $p + p$ in colliding beams, proposed method for total cross section determination for, (E/T), 26:54191 (BNL-17065)
interactions $p + p$ in thermodynamic model, limiting temperature for production of massive hadron pairs in, 26:54305
interactions $p + p$, identical distribution over charged particle multiplicity for, (T), 26:54327 (JINR-E2-6596)
interactions $p + p$, proposed experiment using multiwire proportional chambers and wide-gap spark chambers for cross sections, charged particle multiplicity, and angular correlations in, (E), 26:54192 (BNL-17141)
interactions $p + p$, scattering length from final state, (E/T), 26:54503 (UCRL-74069)
interactions $\pi + p$ at high energies with polarized target, design of equipment for measuring polarization of recoil protons in elastic, 26:54232
interactions $\pi + p$ in colliding beams at ISABELLE, feasibility of, (E), 26:54200 (BNL-17069)
interactions $\pi + p$, interference term effects in multiperipheral model for cross section energy dependence, pion multiplicities, and structures in correlation functions for, (T), 26:54329 (NYO-3533-265)
interactions $\pi^- + p \to$ eta $+ n$, Regge pole--cut model for, (E/T), 26:54230
interactions $\pi^- + p \to K$ + anti K at 4 to 40 GeV/c, multiperipheral-model calculations of cross sections for, (T), 26:54325 (COO-3533-2)
interactions $\pi^+ + p \to K^+ + \Sigma^+$, new Regge absorption model for cross sections of, (T), 26:54336
interactions $\pi^- + p \to \Lambda + K$ at 4 to 40 GeV/c, multiperipheral-model calculations of cross sections for, (T), 26:54325 (COO-3533-2)
interactions $\pi^- + p \to \Lambda + K^*(1420)$ at 4.5 and 6 GeV/c, differential cross sections, Λ polarization, and $K^*(1420)$ density matrix elements for, (E), 26:54217
interactions $\pi^- + p \to \Lambda(1405) + K^0$ at 4.5 and 6 GeV/c, differential cross sections for, (E), 26:54217
interactions $\pi^- + p \to \Lambda(1520) + K^0$ at 4.5 and 6 GeV/c, differential cross sections for, (E), 26:54217
interactions $\pi^- + p \to \Lambda(\Sigma^0) + K^*(890)$ at 4.5 and 6 GeV/c, differential cross sections, $\Lambda(\Sigma)$ polarization, and $K^*(890)$ density matrix elements from, (E), 26:54217
interactions $\pi^- + p \to \Lambda(\Sigma^0) + K^0$ at 4.5 and 6 GeV/c, differential cross sections and $\Lambda(\Sigma)$ polarization for, (E), 26:54217
interactions $\pi^- + p \to N + 2\pi$ at 1.6 to 2.0 GeV, energy-independent partial-wave analysis of baryon resonance production in, (T), 26:54328 (LBL-544)
interactions $\pi^+ + p \to N + 2\pi$ at 1.6 to 2.0 GeV, energy-independent partial-wave analysis of baryon resonance production in, (E), 26:54328 (LBL-544)

interactions $\pi^- + p \to n +$ anything at 2.4 GeV/c, scintillation counter study of $M^0(1033)$ production in, (E), 26:54205 (COO-1428-311)
interactions $\pi^- + p \to n + \pi^+ + \pi^- + m\pi^0 (m = 1$ to $5)$ at 5 GeV/c in propane bubble chamber, resonance production and partial cross sections for, (E), 26:54220
interactions $\pi^- + p \to n + \pi^+ + \pi^-$ at 2.77 GeV/c, parametrization of nonevasive exchange processes and background contributions in, (E/T), 26:54214
interactions $\pi^- + p \to p +$ anything at 25 and 40 GeV/c, triple-Pomeranchuk coupling and scaling in inclusive, (E/T), 26:54221
interactions $\pi^- + p \to p +$ anything, triple-Regge formalism for analysis of, (T), 26:54332
interactions $\pi^- + p \to p + \pi^+ + 2\pi^- + \pi^0$ at 20 GeV/c in hydrogen bubble chamber, cross sections for resonance production in, (E), 26:54207 (COO-3064-3)
interactions $\pi^- + p \to p + \pi^-$ at 5.91 to 13.73 GeV/c, extrapolation of asymptotic cross section for baryon-pole coupling in backward, (E/T), 26:54331
interactions $\pi^+ + p \to p + \pi^+$ at 5.91 to 13.73 GeV/c, extrapolation of asymptotic cross section for baryon-pole coupling in backward, (E/T), 26:54331
interactions $\pi^- + p \to \pi^0 + n$, new Regge absorption model for cross sections and polarization in, (T), 26:54336
interactions $\pi^- + p \to \pi^0 + n$, Regge pole--cut model for, (E/T), 26:54230
interactions $\pi^- + p \to \pi^0$(eta) + n with small momentum transfer, method for determining differential cross sections for, 26:54209 (JINR-P1-6414)
interactions $\pi^+ + p \to \pi^- +$ anything at 7 GeV/c, multiperipheral-model calculations of cross sections for, (T), 26:54325 (COO-3533-2)
interactions $\pi^+ + p \to \pi^- +$ anything at 8 and 16 GeV/c, differential cross sections and symmetry of π emission for, (E), 26:54222
interactions $\pi^+ + p \to \pi^+ + p + \pi^+ + \pi^-$ at 5.45 GeV/c, production properties of $A_1{}^+$ in, (E), 26:54227
interactions $\pi^- + p \to \pi^- + p$ at 0.875 to 1.580 GeV/c, differential cross sections for forward, (E/T), 26:54224
interactions $\pi^+ + p \to \pi^+ + \pi^- + \Delta^{++}$ at 13 GeV/c, phase shift analysis of $\pi^+\pi^-$ scattering from, (E), 26:54223
interactions $\pi^- + p \to \pi^- + \pi^+ + n$ at 8 GeV/c, production and decay angular distributions of rho^0, f^0, and g^0 in, (E), 26:54216
interactions $\pi^- + p \to \pi^+(\pi^-) +$ anything at 16 GeV/c, differential cross sections and symmetry of π emission for, (E), 26:54222
interactions $\pi^- + p \to \pi^+(\pi^-) +$ anything at very high energies, limiting distributions for, (T), 26:54326 (DESY-72/40)
interactions $\pi^+ + p \to \pi^+(\pi^-) +$ anything at very high energies, limiting distributions for, (T), 26:54326 (DESY-72/40)
interactions $\pi^- + p \to$ rho^0 + n, contribution of unnatural parity exchanges to, (T), 26:54270
interactions $\pi^- + p \to \Sigma(1385) + K^+$ at 4.5 and 6 GeV/c, differential cross sections for, (E), 26:54217
interactions $\pi^+ + p$ at 0.4 to 0.90 GeV/c, total cross sections for, (E), 26:54213
interactions $\pi^- + p$ at 0.4 to 0.90 GeV/c, total cross sections for, (E), 26:54213
interactions $\pi^- + p$ at 40 GeV/c, average number of produced π^+--π^- pairs, coefficient of nucleon charge exchange, and identical distribution over charged particle multiplicity for, (T), 26:54327 (JINR-E2-6596)
interactions $\pi^+ + p$, compilation of cross sections for, 26:54201 (CERN/HERA-72-1)
interactions $\pi^- + p$, compilation of cross sections for, 26:54201 (CERN/HERA-72-1)
interactions $\pi^+ + p$, identical distribution over charged particle multiplicity for, (T), 26:54327 (JINR-E2-6596)
interactions virtual $\gamma + p$ in inelastic e + p interactions at $q^2 = 1(\text{GeV}/c)^2$ in resonance region, separation of longitudinal contribution from total cross sections of, (E), 26:54168 (DESY-72/38)
interactions virtual $\gamma + p$ in inelastic e + p interactions at $q^2 = 1(\text{GeV}/c)^2$ in resonance region, separation of longitudinal contribution from total cross sections of, (E), 26:54168 (DESY-72/38)
interactions with neutrons in nuclei, mass number dependence of residual, (T), 26:54739
interactions with particles at high energies using deuterium targets, proposed experiment using spectator neutrons for determining total cross sections for, (E), 26:54163 (NP-19421)
magnetic moment of, Markoffian model for, 26:54308
mass difference (n - p), deep inelastic contribution to electromagnetic, (T), 26:54257
measurements in extended magnetotail at approximately 1000 R/sub E/, number density and velocity, (E), 26:54074
measurements with energies down to 12.4 keV over polar caps following Mar. 21, 1969 solar-particle event, solar-flare, (E), 26:54071
polarization of recoil, in $\gamma + p \to \pi^0(\gamma) + p$ interactions at 3 to 7 GeV, (E), 26:54167 (COO-3069-71)
production in inclusive $e + p \to e + p +$ anything interactions at 6.5 GeV, momentum spectra of, (E), 26:54178
production of anti p--p pairs in three- and four-prong anti p + p interactions at 7 GeV/c in deuterium bubble chamber, (E), 26:54218
production of more than or equal to 10 MeV solar-flare, short-term prediction of, 26:53931 (NASA-TM-X-2440, pp 356-61)
propagation of primary cosmic, in interstellar space, (E), 26:53828
propagation of solar-flare, Fokker--Planck equation for, (E/T), 26:53932
reactions (p,2n) with thallium-205 at 14 MeV, gamma spectra from, (E), 26:54647
reactions (p,2p) and (p,pn) with deuterium at small momentum transfer, polar graph interpretation of differences in cross sections for, (T), 26:54510
reactions (p,2p) with deuterium at 155 MeV, analysis of angular distributions for off-energy-shell effects, (E), 26:54522
reactions (p,2p) with deuterium at 51.8 MeV, analysis of cross sections and spectra from, (E/T), 26:54505
reactions (p,2p) with heavy nuclei, various potentials for, (T), 26:54699 (ORO-4317-11)
reactions (p,α) with zirconium-92 at 28 MeV, DWBA calculation of form factors for, (T), 26:54467(R) (ORO-2972-204)
reactions (p,d) with helium-4 at 65 MeV, cross sections and energy spectra from, (E), 26:54515
reactions (p,d) with tritium at 6.7 to 14.7 MeV, analyzing power for polarized, (E), 26:54517
reactions (p,γ) and (p,n) with calcium-48 at 1 to 2 MeV, cross sections for, (E), 26:54567 (INR-1407)
reactions (p,γ) with calcium-42 at 1 to 2 MeV, cross sections for, (E), 26:54567 (INR-1407)
reactions (p,γ) with calcium-43 at 1 to 2 MeV, isomeric cross section ratios for, (E), 26:54567 (INR-1407)
reactions (p,γ) with nitrogen-15 at 7.4 to 15.0 MeV, analyzing power angular distributions and T-matrix elements for polarized, (T), 26:54531
reactions (p,γ) with silicon-28 at 0.3 to 3 MeV, γ-ray angular distributions and correlations for, (E), 26:54552 (FRNC-TH-227)
reactions (p,He-3) and (p,t) with iron-57 at 27 MeV, angular distributions for, (E), 26:54584
reactions (p,n) with deuterium at 16 to 26 MeV, analysis of p - p final state interaction in, (E/T), 26:54503 (UCRL-74069)
reactions (p,n) with tellurium-125, iodine-125 production by, 26:53056 (AREAEE-129)
reactions (p,n) with zirconium-90 at 6.9 to 9.5 MeV, gamma spectra and excitation functions for, (E), 26:54613
reactions (p,pn) and (p,2p) with deuterium at 20 to 60 MeV, 26:54511
reactions (p,π^-) and (p,π^+) with beryllium-9 at 600 MeV, cross sections and spectra from, (E), 26:54535
reactions (p,t) and (p,He-3) with aluminum-27 at 27 MeV, angular distributions for, (E), 26:54551 (COO-535-673)
reactions (p,t) with magnesium-26 at 26 MeV, Hauser--Feshback calculation of angular distributions for, (T), 26:54556
reactions (p,t) with molybdenum-95 at 31 MeV, DWBA analysis of differential cross sections for, (E), 26:54612
reactions (p,t) with praseodymium-141 at 40 MeV, analysis of angular distributions for collective effects, (E), 26:54615
reactions (p,t) with terbium-159 at 30 MeV, DWBA analysis of differential cross sections and spectrum from, (E), 26:54645
reactions with aluminum, carbon, cobalt, and platinum at 3 GeV, time-of-flight measurements of neutron spectra from, (E), 26:54528 (NASA-TM-X-2440, pp 523-6)
reactions with emulsion nuclei at 22.6 GeV/c, velocity distribution of secondary π production from, (E), 26:54196
reactions with nickel isotopes at 5 to 56 MeV, cross sections for, (E), 26:54591
reactions with nuclei of primary cosmic, cross sections for, (T), 26:53845
reactions with potassium sodium tartrate at 660 MeV, properties of Cherenkov radiation from, (E), 26:54875 (JINR-P1-6552)
reactions with thorium-232 and uranium-235 at 0.7 GeV, calculation of spallation--fission competition using intranuclear-cascade model, (T), 26:54666
reactions with tungsten at 28 GeV, yields of actinides and transactinides from secondary reactions following, (E), 26:54672
reactions with uranium at 2.25 MeV, x-ray fluorescence spectrum from, (E), 26:53803
reactions with uranium-238 at 0.15 to 3 GeV, calculation of spallation-fission competition using intranuclear-cascade model, (T), 26:54666
reactions with uranium-238 at 12 and 28 GeV, yields of actinides and transactinides from secondary reactions following, (E), 26:54672
scattering by beryllium-9, boron-10, and aluminium-27 at 15.1 to 22.9 MeV, cross sections and depolarization parameters for elastic, (E), 26:54525 (FRNC-TH-191)
scattering by beryllium-9, carbon-12, and aluminum-27 at

    20 GeV, analysis using Steenberg model, (T), 26:54530
  scattering by calcium-48 at 25.11 to 40.21 MeV, differential cross sections for inelastic, (E), 26:54582
  scattering by cerium-142 at 9.5 to 12 MeV with isobaric analog excitation, excitation functions for elastic and inelastic, (E), 26:54618
  scattering by deuterium at 3.6 to 9.1 MeV, vector to tensor polarization transfer in elastic, (E), 26:54499 (LA-DC-72-905)
  scattering by erbium-168 at 15 MeV, proton spectra from inelastic, (E), 26:54467(R) (ORO-2972-204)
  scattering by helium-3 at 30 MeV using polarized beam, analyzing power for, (E), 26:54521
  scattering by helium-4 at 0 to 50 MeV, forward dispersion relation including Coulomb interaction for elastic, (T), 26:54711
  scattering by holmium-165 and erbium-167 at 4 MeV with Coulomb excitation, heat-flow analysis of temperature spikes following inelastic, (E/T), 26:54646
  scattering by hydrogen, deuterium, helium-3, and helium-4 at 600 MeV, differential cross sections for elastic, (E), 26:54512
  scattering by krypton-86 at 4.8 to 10.1 MeV, excitation functions for elastic and inelastic, (E), 26:54467(R) (ORO-2972-204)
  scattering by lutetium-175 at 3 MeV with Coulomb excitation, heat-flow analysis of temperature spikes following inelastic, (E/T), 26:54646
  scattering by magnesium-24 at 9.7 MeV, polarization in elastic and inelastic, (E), 26:54467(R) (ORO-2972-204)
  scattering by molybdenum-92 and zirconium-94 at 11.2 to 12.4 MeV, excitation functions for elastic, (E), 26:54467(R) (ORO-2972-204)
  scattering by molybdenum-92, -94, -96, and -100 at 12.0 MeV, differential cross sections for elastic and inelastic, (E), 26:54606 (ORNL-TM-3913)
  scattering by neon-20 and magnesium-24, coupled-channel treatment with projected Hartree--Fock wave functions for inelastic, (T), 26:54565
  scattering by nickel-58, -60, -62, and -64 at 12 MeV, proton angular distributions and γ spectra from inelastic, (E), 26:54587 (FRNC-TH-240)
  scattering by nickel-64 at 3.1 to 5.3 MeV, angular distributions and excitation functions for inelastic, (E), 26:54590
  scattering by tritium at 19 and 30 MeV using polarized beam, differential cross sections and analyzing power for, (E), 26:54521
  scattering by tritium at 6.7 to 14.7 MeV, differential analyzing power and phase-shift analysis of polarized elastic, (E), 26:54518
  track size in sodium chloride monocrystals, (E), 26:55016
  trajectories of Crab Nebula, arriving at the Earth, (E/T), 26:53856
PROTONS (anti p)
  interactions anti p + d → anti p + p + n, Fermi motion and n + p final-state interaction effects on low-momentum transfer cross sections for, (T), 26:54347 (UM-P-72-6)
  interactions anti p + d → p + anything, nonzero orbital momenta of anti pn bound states from recoil proton momentum spectrum in, (T), 26:54334
  interactions anti p + n → $\pi^+ + \pi^- + \pi^-$ at 1.2 GeV, Veneziano model with satellites and dual amplitude with Mandelstam analyticity for, (T), 26:54320
  interactions anti p + p → π^- + anything at 5.6 to 70 GeV/c, uncorrelated jet model predictions for pion multiplicity distribution in annihilation, (T), 26:54316 (RPP/T-24)
  interactions anti p + p at 1.2 GeV/c, analysis of K anti K and K anti Kπ resonances in annihilation, (E), 26:54199
  interactions anti p + p at 6 to 14 GeV/c, evidence for interaction radius scaling from analysis of polarization in, (T), 26:54354
  interactions anti p + p at 7 GeV/c in deuterium bubble chamber, anti p--p and K^+--K^- pair and resonance production, f^0--$A_2{}^0$ interference, and cross sections for three- and four-prong, (E), 26:54218
  interactions anti p + p at very low energy, research proposal for ISABELLE for, 26:53766 (BNL-16818)
  interactions anti p + p, description of annihilation spectrometer for measuring cross sections for, 26:53279
  interactions anti p + p, identical distribution over charged particle multiplicity for, (T), 26:54327 (JINR-E2-6596)
  orbital momenta of, of anti pn bound states, recoil proton momentum spectrum in anti p + d → p + anything interactions for nonzero, 26:54334
  production of anti p--p pairs in three- and four-prong anti p + p interactions at 7 GeV/c in deuterium bubble chamber, (E), 26:54218
PROTOTYPE FAST REACTOR
  heat exchangers for, description of, 26:55158 (CONF-710548-, pp 187-205)
PROTOZOA
  bioluminescence in marine dinoflagellates, action spectrum for photoinhibition of mechanically stimulable, 26:55521 (COO-3277-14)
  Tintinnopsis beroidea, growth characteristics of, in continuous culture, 26:55522 (COO-3390-2)
PUBLIC HEALTH
  book: Radiation and Health, 26:53157
  effects of radioisotope release to environment during accidents on, 26:53523
PUERTO RICO
  cesium-137 distribution in soils and vegetation in, 26:53162 (ANL-7860(Pt.3), pp 1-13)
  control of fascioliasis in, using radiation vaccines, 26:53498(R) (PRNC-156)
PULSARS
  cosmic nuclei acceleration by, (T), 26:53857
  cosmic particle acceleration by, (T), 26:53858
  cosmic-ray acceleration in, energy cutoff in, (T), 26:53869
  formation in supernovae, (T), 26:53912
  gamma emission from NP 0532, (E), 26:53923
  identification of CP0950 with x-ray source Leo XR-1, (E/T), 26:53907
  radiation emission mechanism for, (T), 26:53925
  scintillation pattern of PSR 0329 + 54, interstellar, (E), 26:53915
  surface density of, calculation using Thomas--Fermi-like model of crushed atoms, 26:54144
  x-ray pulses from NP 0532, (E), 26:53919
PULSE ANALYZERS
  baseband distortion equalization in input channel of, 26:55630 (UCRL-73943)
PULSE CONVERTERS
  design of ultra-linear 16-bit digital-to-analog, engineering drawings for, 26:53278
PULSE GENERATORS (ELECTRONICS)
  design of dual, for high-resolution Ge(Li) gamma spectrometer, engineering drawings for, 26:53262
  design of transistorized, for testing nuclear counting equipment, 26:53295 (AREAEE-132)
PULSE SHAPERS
  design and performance with universal logic for 100 MHz count rates, 26:53320
PUMICE
  age of volcanic, thermoluminescent method for estimation of, 26:53177
PUMPS
  design criteria for nuclear service, development program for, 26:55207(R) (ORNL-TM-3900)
  dismantling of sodium cooled reactor, removal of sodium and decontamination during, 26:55147 (AI-AEC-Memo-12736)
PYROMETERS
  characteristics of germanium resistance, interpolation of, 26:55542 (KFK-1601)

Q

Q DEVICES
  plasma collision frequency during rf heating, (E), 26:54750 (CONF-720705-2)
QUAD CITIES POWER REACTOR, UNIT 1
  core isolation cooling system for, failure of valves for, 26:55250 (DOCKET-50254-117)
  effluents from, effects on environment of chemical, radioactive, and thermal, 26:55285 (DOCKET-50254-120)
  operation of, cost-benefit analysis for, 26:55285 (DOCKET-50254-120)
  pump room for, requested information on possible flooding of condensate, 26:55284 (DOCKET-50254-119)
  site for, ecology, hydrology, and meteorology of, 26:55285 (DOCKET-50254-120)
  technical specifications for, requested data on, 26:55283 (DOCKET-50254-118)
  valves for, verification of wall thicknesses for nuclear service, 26:55274 (DOCKET-50010-117)
QUAD CITIES POWER REACTOR, UNIT 2
  containment structure, failure of suppression chamber to drywell vacuum breaker valves for, 26:55254 (DOCKET-50265-115)
  effluents from, effects on environment of chemical, radioactive, and thermal, 26:55285 (DOCKET-50254-120)
  operation of, cost-benefit analysis for, 26:55285 (DOCKET-50254-120)
  pump room for, requested information on possible flooding of condensate, 26:55284 (DOCKET-50254-119)
  site for, ecology, hydrology, and meteorology of, 26:55285 (DOCKET-50254-120)
  technical specifications for, requested data on, 26:55283 (DOCKET-50254-118)
  valves for, verification of wall thicknesses for nuclear service, 26:55274 (DOCKET-50010-117)
QUALITY CONTROL
  design criteria for confidence and reliability based on small samples, 26:55618 (UCID-16099)
QUANTUM ELECTRODYNAMICS
  test from Lamb shift in $^{16}O^{7+}$, (E), 26:54375(R) (COO-1811-3)
QUANTUM FIELD THEORY
  Bethe--Salpeter equation for scalar particle interactions in ladder approximation, variational Pade solution of, 26:54380
  boson pair production in threshold region by square-well

  potential with smooth sides in, probability for scalar, 26:54384
  current matrix elements in, physical symmetries from one-particle, 26:54356
  dispersion sum rules in axiomatic, spectral Jost--Lehman--Dyson representation for structure of, 26:54377 (ITF-72-54-P)
  dual resonance model relation with, zero-slope limit for, 26:54388
  formalism of generalized, for nuclear and atomic theory, 26:54382
  gauge fields with dual diagram topology in, Feynman rules for massive, 26:54381
  Green's functions of Euclidean, solvability of Schwinger equations for, (T), 26:55070 (ITF-72-45-P)
  interactions of massive scalar with massless spinor fields in, classical and quantum two-dimensional classically solvable model with nontrivial scattering for, 26:54385
  particle interactions with external fields in, Bogoliubov transformation in strong coupling theory for mass squared spectrum for classical relativistic, 26:54383
  renormalization constants for three-particle bound state, vanishing of vertex-function, 26:54379
  S matrix in g(:phi*:)$_2$, equations for elements of, in Euclidean domain, 26:54376 (ITF-72-15-E)
  S-matrix unitarity in nonlocal, 26:54413 (JINR-P2-6586)
  scalar field interactions with fixed source, Hamiltonian as graph limit with infinite renormalization for, 26:54386
  symmetry breaking and gauge invariance in, spontaneous, 26:54387
  Ward identities in axiomatic, spectral Jost--Lehman--Dyson representation for structure of, 26:54377 (ITF-72-54-P)
  Wightman axiomatic approach for concentratable field, global field properties in, 26:54378 (ITF-72-62-E)
QUANTUM MECHANICS
  Bogolyubov kinetic equations in, method for solution in Banach space, (T), 26:55067 (ITF-72-9-E)
  constants of, relations between cosmological constants and, 26:54392 (ITF-72-3-P)
  Feynman path-integral formulation of, 26:55080
  perturbation theory for Mathieu equation and anharmonic-oscillator equation in, continued-fraction method for, 26:55078
  perturbation theory for systems in, time-dependent, 26:55073
  Schroedinger equation for stability of many-body systems with singular attractive potentials in, self-consistent Hartree field as limit for, 26:54408 (ITF-72-14-E)
  Schroedinger equation with singular potential in, approximate methods for solving, 26:55074
  Schroedinger equation with singular potentials in nonrelativistic, total Hamiltonian and semigroup product formula for, 26:55069 (ITF-72-36-E)
  systems with singular attractive potentials in, Hartree one-particle asymtotically exact solutions for, 26:55068 (ITF-72-31-P)
  wave functions in, spin-dependent operators in occupation-branching number representation for open-shell, (T), 26:55077
QUARKS
  mass of, bare, (T), 26:54282
  search for 4e/3 charged di-, in cosmic radiation at 2750-m altitude, 26:54177
  search for e/3 and 2e/3 charged, in cosmic radiation at 2750-m altitude, (E), 26:54164
  search for mass 2 to 7 GeV/c^2, at IHEP 70-GeV accelerator, sensitivity of, 26:54165
  search for, analysis of experiments on, 26:54165
  theory as shadow states in Bjorken limit of deep inelastic e + N interactions, 26:54248 (ORO-3992-106)
QUARTZ
  fission fragment tracks from heavier transuranium elements in natural, study of spontaneous, 26:54670
  radiation damage in, electron microscopic study of 650-kV electron, 26:54972 (COO-2119-2)
  toxicity of particles of, bibliography on, 26:55585 (ORNL-TIP/TIRC-72-62)
QUASARS
  distribution of, space, (E/T), 26:53994
  evolution of, (E/T), 26:53994
  luminosities of, (E/T), 26:53994
  luminosity functions for, optical and radio, (T), 26:53996
  optical positions of, (E), 26:53913
  radio source counts on the basis of evolution models for, (T), 26:53996
  redshift--magnitude relation for, (T), 26:53998
  resonance-line radiation in differentially expanding atmospheres of, transfer of, (T), 26:53879
  resonance-line radiation in differentially expanding atmospheres of, transfer of, (T), 26:53878
  rotation measures of, effects of galactic field on, (E), 26:53911
  spectral indices for 3C2, 3C245, and 3C279, (E), 26:53914
QUINOLINE
  complexes with oxyfluorouranate ions, thermogravimetric studies on, 26:53043

R

RABBITS
  arsenic-74 distribution and metabolism in tissues of, following oral administration, time dependence of, 26:53538
  cesium-137 distribution and retention in, following intravenous injection, effects of peritoneal dialysis on, 26:53533
  radiation effects on serotonin uptake by blood platelets in, in relation to content during acute radiation syndrome, γ, 26:53486
  radioisotope distribution and retention in, following intravenous injection, kinetics of barium-133 and strontium-90, 26:53534
RADAR
  signal propagation retardation for, comparison of experiment with general relativistic predictions for, (E/T), 26:54403
RADIATION
  applications in agricultural research in Euratom Community, 26:53459(R) (NP-19403)
  bibliography of publications and reports issued by BNL Radiation Division, July 1968 through June 1971, 26:53325 (BNL-50335)
  book: Radiation and Health, 26:53157
  conference on natural and manmade, in space, Las Vegas, Nev., 3/71, 26:54870 (NASA-TM-X-2440)
  dose distribution in man following whole-body exposure, role of quality factors and fluence in calculating, 26:53404 (NASA-TM-X-2440, pp 424-34)
  dose from geomagnetically trapped radiation belts, review of, 26:54952 (NASA-TM-X-2440, pp 170-7)
  dose measurements on Apollo missions, 26:54953 (NASA-TM-X-2440, pp 215-19)
  dose rate measurements at SST altitudes during solar flares, 26:54889 (NASA-TM-X-2440, pp 902-7)
  effect on crystalline solids, atomistic computer simulation of, (E), 26:54970 (CEA-CONF-1890)
  effects of pile, on sintered aluminum oxide, ESR spectral studies on, 26:53699 (RT/FI-(72)10)
  effects on acetylenedicarboxylic acid dihydrate monocrystals, ESR studies on, 26:53005
  effects on animals following traumatic injuries, effects on recovery rate of, whole-body, 26:53419
  effects on aqueous solutions of indole-3-acetic acid and other plant hormones, 26:53015
  effects on behavior of animals, review of literature on, 26:53448 (COO-1332-78)
  effects on biological materials, 26:53396
  effects on blood pressure in rats following renal exposure, sodium-22 tracer study of sodium kinetics during development of pathological, 26:53463
  effects on bone marrow in mice, dose response of ratio of erythrocytes to leukocytes, use as biological dosimeter, 26:53473
  effects on brain of mice and rats following prenatal exposure, effects of developmental stage at exposure on teratogenic, 26:53437
  effects on chromosomes in lymphocytes of man exposed to residual fallout from atomic bombing of Nagasaki, aberrant, 26:53414
  effects on crystals, correlated recovery kinetics of anisotropic damage, (T), 26:55005
  effects on DNA in organisms, comparison of RBE for high with low LET, 26:53345 (NASA-TM-X-2440, pp 222-8)
  effects on DNA replication in bacteria and bacteriophages, role in molecular repair mechanisms, 26:53348
  effects on Drosophila, effects of low-dose on metabolism in bar gene mutants of, stimulatory, 26:53500
  effects on human children following exposure in utero, review of epidemiological studies on carcinogenic and leukemogenic, 26:53435
  effects on human leukocyte count following whole-body exposure for therapy of leukemias and lymphosarcomas, multifactorial analysis of dependence of dose and time, 26:53400 (NASA-TM-X-2440, pp 233-7)
  effects on human lymphocyte count following extracorporeal exposure of blood, effects of dose on, 26:53440
  effects on human skin, dose-response relationships for pathological, 26:53431
  effects on human survivors of atomic bombing of Nagasaki 10 to 25 years following exposure as children, effects of dose on incidence of carcinogenic, 26:53442
  effects on human tissues following therapy of neoplasms, surgical treatment of local pathological, 26:53438
  effects on immune reactions in guinea pigs, lethal dose, 26:53474
  effects on L-arginine aminohydrolase activity in liver of rats, dose dependence of, 26:53491
  effects on man following traumatic injuries, effects on recovery rate of, whole-body, 26:53419
  effects on man, clinical aspects of pathogenesis and recovery from, relevance of animal studies to, 26:53411
  effects on mice following fractionated sublethal whole-

body exposure, protective effects of cysteamine against late leukemogenic, 26:53475
  effects on mice for determining origin of alveolar macrophages in chimeras, 26:53492
  effects on oral tissues of patients during tumor therapy in head and neck region, construction of prosthesis shield for protection against, 26:53410
  effects on oranges following exposure for sterilization, effects on organoleptic properties and wholesomeness of, 26:53347
  effects on oranges following exposure for sterilization, effects on metabolism and respiration in, 26:53347
  effects on salivary glands in man following therapy, inflammation induced by, 26:53423
  effects on silica, valence-bond model of x-ray spectra, bond breaking, and point-defect production in, (T), 26:55018
  effects on space vehicles, design considerations for thermoelectric generators for simulated in-flight testing of, 26:53095 (NASA-TM-X-2440, pp 844-9)
  effects on spherical void growth in metals, relation of triaxial stress to, (T), 26:53702 (TID-26150)
  effects on sulfoxidation of alkanes, effects of purity of compounds, dose, and pressure on kinetics of, 26:53012
  effects on thermodynamic and transport properties of frozen and reacting orthohydrogen--parahydrogen mixtures, 26:53715 (NASA-TM-X-2440, pp 476-80)
  hazards to man during space flight, extrapolation of clinical data on dose-response-time relations to estimate, 26:53402 (NASA-TM-X-2440, pp 398-415)
  hazards to space missions from solar proton events, probability analysis of, 26:54955 (NASA-TM-X-2440, pp 310-23)
  hazards to space travel from solar cosmic-ray protons, statistical treatment of, 26:53930 (NASA-TM-X-2440, pp 345-55)
  uses in medicine, IAEA-WHO survey on world-wide, 26:53413

RADIATION CHEMISTRY
  book: Advances in Radiation Chemistry. Vol. 3, 26:53021
  electron spin resonance studies in, 26:52993(R) (RRL-3238-398)
  mechanisms in radiobiology, review on, 26:53024
  research program on ionic and free radical reactions in, 26:52987(R) (ORO-2968-78)
  search for H_3O radical, 26:53026
  short-lived transients in, review on identification and kinetic measurements of, 26:53022
  synthesis of organic compounds in, review on, 26:53023

RADIATION DETECTORS
  advances in, review of impact on nuclear measurements, 26:53263
  book: Measurement of Radiation in Space, 26:53276
  book: Particle Detectors, 26:53208
  circuits for computer controlled in-line monitoring of radioisotope in chemical process streams, engineering drawings for, 26:53220
  design of solenoid--quantameter--hadrometer (calorimeter), for electron detection at ISABELLE and PEP, 26:53268 (BNL-17066)
  development for heavy-ion dosimetry based on damage tracks in silver halide single crystals, 26:53230 (NASA-TM-X-2440, pp 138-41)
  pulse counting statistics for, 26:53207
  time response of L-125A Compton diode, time domain reflectometry measurement of, (E/T), 26:53197 (EGG-1183-2277)

RADIATION DETECTORS, ACTIVATION
  description for dosimetry in Skylab space station, 26:53236 (NASA-TM-X-2440, pp 958-73)
  description for space radiation dosimetry, 26:53235 (NASA-TM-X-2440, pp 944-56)

RADIATION DETECTORS, BUBBLE CHAMBER
  particle tracks in, data processing program for HPD analysis of, 26:53274 (RHEL/R-241)
  particle tracks in, digital-to-analog converter for DOLLY CRT flying spot scanner for measuring, 26:53278

RADIATION DETECTORS, CHERENKOV
  operation and performance for beta counting of radioisotopes in solution with radiator, 26:53209

RADIATION DETECTORS, DIELECTRIC TRACK
  description for dosimetry in Skylab space station, 26:53236 (NASA-TM-X-2440, pp 958-73)
  description for high-Z particle dosimetry during Apollo missions, 26:53231 (NASA-TM-X-2440, pp 149-56)

RADIATION DETECTORS, FISSION FOIL
  development for monitoring of fast neutron flux for preventing radiation damage to Ge(Li) detectors, 26:53223

RADIATION DETECTORS, GEIGER-MUELLER
  design and performance of, for counting beta activities retained in resin columns, 26:53212

RADIATION DETECTORS, HODOSCOPE
  description for investigation of heavy meson spectra from antiproton annihilation, 26:53279

RADIATION DETECTORS, IONIZATION CHAMBER
  calibration of current from, for measuring radon-220 content in atmosphere, 26:53227
  correction factors for x-ray dosimetry, 26:53247
  description for measuring isodose curves in water phantom, 26:53243
  description of open window, for detection below 1 keV, 26:53210(P)
  description of quartz fiber, for dosimetry in Skylab space station, 26:53236 (NASA-TM-X-2440, pp 958-73)
  description of tissue-equivalent, for dosimetry in Skylab space station, 26:53236 (NASA-TM-X-2440, pp 958-73)
  description of tissue-equivalent, for space radiation dosimetry, 26:53241(P)
  design as electronic switch for controlling and recording irradiation times of samples in reactors, 26:53224
  design for monitoring normal gamma environmental levels, engineering drawings for, 26:53218
  development for environmental radiation, 26:53196(R) (COO-323-28)
  development of hybrid, for radiation monitoring on the SST Concorde, 26:53203 (NASA-TM-X-2440, pp 874-83)
  development of macro-subsystem and micro-subsystem of, for dosimetry in tissues, 26:53232 (NASA-TM-X-2440, pp 435-7)
  development of small 0.5-cc air-equivalent, muscle-equivalent, and magnesium, 26:53196(R) (COO-323-28)
  operation and performance of tissue-equivalent plastic, for neutron or gamma plus neutron absorbed dose measurements, 26:53234 (NASA-TM-X-2440, pp 609-13)
  W values for, compared to G values for chemical dosimeters, (T), 26:53244

RADIATION DETECTORS, PROPORTIONAL
  description for muon detection and discrimination from pions, 26:53282
  description of multiwire, for neutron radiography, 26:53200 (LBL-707(Summ.))
  design and performance of bifilar helical multiwire, with delay-line readout for position-sensitive detecton of minimum ionizing particles, 26:53273 (LA-4968)
  design and performance of multiwire, with intermediate high-voltage planes, 26:53213
  design and performance of position-sensitive, for ionizing radiation, 26:53221
  design of 4π multiwire, for high-multiplicity interactions, 26:53267 (BNL-17064)
  design of 4π Porcupine, with 47000 elements for detecting products from high-mulitplicity interactions, 26:53266 (BNL-17020)
  design of gamma compensated flowthrough, for tritium monitoring, engineering drawings for, 26:53216
  development of hybrid moderated, for radiation monitoring on the SST Concorde, 26:53203 (NASA-TM-X-2440, pp 874-83)
  development of rocket-borne thin polypropylene window, for detecting soft cosmic x rays, 26:53206
  gas amplification in low pressure cylindrical, 26:53198 (FRNC-TH-189)
  performance of BF_3, for neutron detection in gamma fluxes, standard for, 26:53204 (RDT-C-15-11-T(8-72))

RADIATION DETECTORS, SCINTILLATION (LIQUID)
  development of total absorption argon, for detecting high energy hadrons, 26:53269 (BNL-17070)
  solvent composition for, quaternary ammonium base, 26:53211(P)

RADIATION DETECTORS, SCINTILLATION (SOLID)
  attenuation coefficients for NaI(Tl), of arbitrary geometry, method for rapid comparison of angular-distribution, 26:53225
  description of Airborne Radiac gamma spectrometer for measuring ground level radiation dose, 26:53195(R) (AD-737993)
  design and operation of stilbene, for neutron spectroscopy with gamma discrimination, 26:53251 (AREAEE-137)
  design for neutron interrogation determination of U-235 in containers, engineering drawings for, 26:53217
  design of NaI, for spent fuel age determination, engineering drawings for, 26:53261
  scintillator materials for alpha detection, properties of thin films of organic fluorescent, 26:53265

RADIATION DETECTORS, SEMICONDUCTOR
  description of telescope, for measuring LET spectrum of space radiation, 26:53241(P)
  performance of high-resolution particle identifier for particles in Van Allen belt, (T), 26:53280

RADIATION DETECTORS, SEMICONDUCTOR (GERMANIUM)
  attenuation coefficients for Ge(Li), of arbitrary geometry, method for rapid comparison of angular-distribution, 26:53225
  fabrication of germanium--silicon alloy, 26:53202 (NASA-TM-X-2440, pp 723-8)
  operation and performance of germanium--silicon alloy, 26:53202 (NASA-TM-X-2440, pp 723-8)
  preamplifier for Ge(Li), high-rate direct-coupled, 26:53219
  radiation damage to Ge(Li), fission foil detector for monitoring fast neutron flux for preventing, 26:53223
  spectra from Ge(Li), computer program for automatic peak identification in analysis of gamma, 26:53257 (RT/FI-(72)14)

RADIATION DETECTORS, SEMICONDUCTOR (SILICON)
  description of telescope counter of Si(Li), for dosimetry in Skylab space station, 26:53236 (NASA-TM-X-2440, pp 958-73)
  fabrication of germanium--silicon alloy, 26:53202 (NASA-TM-X-2440, pp 723-8)
  operation and performance of germanium--silicon alloy,

26:53202 (NASA-TM-X-2440, pp 723-8)
response to monoenergetic neutrons from radioisotope thermoelectric generator, Monte Carlo calculation of, 26:53291 (NASA-TM-X-2440, pp 708-13)
RADIATION DETECTORS, SHOWER
design and operation of total absorption, for hadron detection, 26:53270 (BNL-17071)
fabrication of total-absorption, using condensed xenon for measuring high-energy electrons and photons, 26:53272 (JINR-P13-6541)
light attenuation in large, method for correcting, 26:53285
RADIATION DETECTORS, SPARK CHAMBER
characteristics of current-limited, with electrodes sealed in glass, 26:53283
design and performance of wire, with ferrite core memory, 26:53271 (JINR-P13-6522)
power supply for high pulse rate, 26:53275 (RPP/H-101)
readout system for wire, study of output pulses of sparkostrictive, 26:53222
RADIATION DETECTORS, TELESCOPE
description of multiple detector, for charged particle spectroscopy in space, 26:53235 (NASA-TM-X-2440, pp 944-56)
description of semiconductor, for measuring LET spectrum of space radiation, 26:53241(P)
description of Si(Li), for dosimetry in Skylab space station, 26:53236 (NASA-TM-X-2440, pp 958-73)
performance of high-resolution solid state particle identifier for particles in Van Allen belt, (T), 26:53280
RADIATION DETECTORS, TRANSITION
design and performance for ultrarelativistic charged particles, 26:53277
RADIATION DOSE
calculation for secondary particles produced by heavy galactic cosmic primaries, 26:54878 (NASA-TM-X-2440, pp 104-7)
calculation of human, from domestic uses of nuclearly stimulated natural gas, 26:53134
calculation of integral absorbed, 26:54910
calculation of, and treatment planning in pion therapy, 26:54876 (LA-4874, pp 145-52)
calculations for manned space missions, methods for, 26:54951 (NASA-TM-X-2440, pp 108-16)
calculations of solar-flare, inside space vehicles during interplanetary voyage, 26:54956 (NASA-TM-X-2440, pp 324-8)
isodose curves for, automatic system for producing, 26:53243
maximum permissible, criteria for personnel, 26:53436
maximum permissible, for human population following release of radioisotopes to environment, criteria for, 26:53523
maximum permissible, for thyroid of children following uptake of iodine-131 from milk, 26:53506(T) (ORNL-tr-2629)
maximum permissible, from plutonium-239 oxide aerosol inhalation, guidelines for estimation for human populations, 26:53511 (TID-26142)
tables for californium-252 implants, (T), 26:54906
RADIATION DOSIMETERS
design of, human engineering standards for, 26:53246
development for dosimetry in Skylab space station, 26:53236 (NASA-TM-X-2440, pp 958-73)
development for heavy-ion dosimetry based on damage tracks in silver halide single crystals, 26:53230 (NASA-TM-X-2440, pp 138-41)
development for radiation monitoring in space shuttles and space stations, 26:53235 (NASA-TM-X-2440, pp 944-56)
testing of personnel, critique of standard methods for, 26:53247
RADIATION DOSIMETERS, BIOLOGICAL
evaluation of chromosome aberrations in human lymphocytes for use as, 26:53420
evaluation of chromosome aberrations in leukocytes as, for use for civilian population following nuclear explosion, 26:53397 (FOA-4-4500-A-3)
evaluation of ratio of erythrocytes to leukocytes in bone marrow for use as, 26:53473
RADIATION DOSIMETERS, CALORIMETRIC
design and operation for pulsed electron beam energy measurements, 26:53258 (SC-DR-720630)
design of tissue-equivalent micro-, for fast neutrons, engineering drawings for, 26:53250
RADIATION DOSIMETERS, CHEMICAL
development of, paramagnetic resonance studies for, 26:52979 (COO-1105-179)
G values for, compared to W values for ionization chambers, (T), 26:53244
RADIATION DOSIMETERS, PHOTOGRAPHIC FILM
correction factors for x-ray dosimetry, 26:53247
performance for medical personnel dosimetry, comparison with thermoluminescent dosimeters, 26:53239
RADIATION DOSIMETERS, PHOTOLUMINESCENT
development possibilities of crystalline anthracene, for fast neutron dosimetry, 26:53229 (COO-1105-172)
properties of silver-activated fluoride-based glass, for gamma detection, 26:53242
RADIATION DOSIMETERS, THERMOLUMINESCENT
correction factors for x-ray dosimetry, 26:53247
description for dosimetry in Skylab space station, 26:53236 (NASA-TM-X-2440, pp 958-73)
description for space radiation dosimetry, 26:53235 (NASA-TM-X-2440, pp 944-56)
design of ^{7}LiF, for personnel beta and gamma dosimetry, engineering drawings for, 26:53249
development for long term intrauterine dosimetry, 26:53238
performance for measurement of dose to man during high-energy electron therapy, 26:53415
performance for medical personnel dosimetry, comparison with photographic film dosimeters, 26:53239
performance of LiF, in human phantom for measurement of dose to bone marrow during whole-body exposure, 26:53406 (NASA-TM-X-2440, pp 974-80)
performance testing for high-precision NERVA shielding measurements, reproducibility and spatial resolution, 26:53233 (NASA-TM-X-2440, pp 466-70)
properties of LiF(Mg,Ti) and CaF$_2$:Mn, response and fading, 26:53245
sensitivity to mixed gamma and neutrons of mixture of natural fluorite and LiF, effects of ^{6}Li content on, 26:53240
use for average temperature measurements of aquatic thermal discharges based on fading, 26:53187 (ANL-7860(Pt.3), pp 131-40)
RADIATION DOSIMETRY
calculation of dose distributions of ^{60}Co ophthalmic applicators, computerized, 26:54900
energy deposition theory in, distribution of energy losses in, 26:54879 (NASA-TM-X-2440, pp 157-61)
microdosimetry of beta particles, and γ and x radiation using grid-walled proportional counter, 26:54895
principles of, review of, 26:54891 (SLAC-153)
RADIATION MONITORING
equipment for environmental, at Lawrence Berkeley Lab, 26:53199 (LBL-585)
programs for control of nuclear power plant effluents in India, 26:53154 (INIS-mf-160, pp 22-52)
RADIATION PROTECTION
book: Radiation Protection at High-Energy Accelerators, 26:53742
calculations for crew of high-impulse gas-core nuclear rocket, 26:54967
conference on natural and manmade radiation in space, Las Vegas, Nev., 3/71, 26:54870 (NASA-TM-X-2440)
conference on radiation protection standards, Richland, Wash., 11/71, 26:54914
conference on radiation protection standards, Richland, Wash., 11/71, 26:54922
guides and constraints for space-mission and vehicle-design studies involving nuclear systems, 26:54913
guides for surface contamination by radioactive materials, survey of, 26:54920
lectures at Physics Laboratory of Istituto Superiore di Sanita, Rome, July--Dec. 1970, 26:54162 (ISS-71/31)
legislation in Japan during 1970, enforcement of, 26:55458
methods for reducing x-ray dose to children during diagnostic radiography, 26:53417
programs for personnel in German Federal Republic, 26:55456 (SZS-136)
programs in New South Wales during 1971, 26:55454(R) (NP-19412)
research in India, 1971--1972, 26:55452(R) (NP-19407)
risk versus benefit analysis, broader perspective of, 26:54930
risk versus benefit analysis, criteria for, 26:54932
risk versus benefit analysis, fallacy of ''maximum credible incident'' concept in, 26:54929
risk versus benefits ratios for, control of, 26:54931
Safety and Health Act of 1970, description of Occupational, 26:54926
safety criteria for nuclear power in space, 26:54921
standards for AEC contractor program, application of, 26:54923
standards for electronic products, development of, 26:54925
standards for surface contamination by radioactive materials, criteria for, 26:54919
standards for, AEC regulatory program for, 26:54924
standards for, description of American Nuclear Society's information center on, 26:54917
standards for, development of, 26:55220 (BNL-16965)
standards for, industry's thoughts on, 26:54933
standards for, problems of enforcing state regulatory control programs for, 26:54928
standards for, role of Environmental Protection Agency in developing, 26:54927
standards for, role of Health Physics Society in development of, 26:54918
standards for, use and abuse of, 26:54934
standards in USA for, role of American National Standards Institute in development of, 26:54916
standards in USA for, role of National Council on Radiation Protection and Measurements in development of, 26:54915
RADIATION-SCATTERING ANALYSIS
methods and uses of backscattering spectrometry, review on, 26:52939

RADIATION SOURCES
- preparation of americium-241 alpha--photon, development of sputtering methods for, 26:53330(R) (BNWL-1308-10)
- survey of natural and man-made, 26:53396
- uses in medicine, industry, and research in Japan during 1970, status of, 26:55458

RADIATION STANDARDS AND UNITS
- definition of x-ray exposure rate, variance from ICRU, 26:54935

RADIATION SYNDROME
- serotonin content of blood during acute, in rabbits, relation between reduced uptake by blood platelets following exposure and, 26:53486

RADIATION TARGET CHAMBERS
- description for charged particle-induced x-ray fluorescence studies, 26:53803

RADIO ASTRONOMY
- book: Galactic Astronomy, Vol. I, 26:53981

RADIO GALAXIES
- distribution of, (E/T), 26:53995
- evolution of, statistical studies of, (E/T), 26:53995
- luminosity functions for, optical and radio, (T), 26:53996
- optical positions of, (E), 26:53913
- radio source counts on the basis of evolution models for, (T), 26:53996
- redshifts of 20, (E), 26:53991
- resonance-line radiation in differentially expanding atmospheres of, transfer of, (T), 26:53878
- resonance-line radiation in differentially expanding atmospheres of, transfer of, (T), 26:53879
- rotation measures of, effects of galactic field on, (E), 26:53911
- spectra of Cyg A, emission, (E), 26:53990

RADIO WAVES
- deflection of, comparison of experiment with general relativistic predictions for, (E/T), 26:54403

RADIOACTIVE CONTAMINATION
- book: Radiation and Health, 26:53157
- control at nuclear power plants in India, micrometeorological studies for, 26:53154 (INIS-mf-160, pp 22-52)
- guides for surface, survey of, 26:54920
- standards for surface, criteria for, 26:54919

RADIOACTIVE MATERIALS
- criticality calculations for, reliability of Monte Carlo computer programs for, 26:55445 (Y-KC-96)

RADIOACTIVE MINERALS
- mineralogy of southwest Aswan syenite rock, 26:53142 (AREAEE-138)

RADIOACTIVE WASTE
- book: Radiation and Health, 26:53157
- combustion of plutonium-bearing solid, 26:53063 (ORNL-4794, pp 33-5)
- decontamination of off-gas, from HTGR fuel reprocessing, 26:53059 (CONF-720823-12)
- dilution of gaseous, from combustion of HTGR graphite fuels, calculation of air required for, 26:53060 (CONF-720823-14)
- disposal in salt beds, research progress on, 26:53063 (ORNL-4794, pp 33-5)
- disposal of tritiated water, generated in natural gas reservoirs produced by nuclear explosions, 26:53128 (ORNL-4794, pp 63-4)
- disposal system for reactor off-gas, efficiency of filters for, 26:55146
- fixation in glass or ceramic substances, suitability of vulcanites for, 26:53057(T) (BNWL-tr-75)
- limits for water cooled power reactor, development of reasonable legal, 26:55220 (BNL-16965)
- processing of liquid, estimation of cost of, 26:53065
- processing of uranium-containing, from fuel reprocessing, 26:53079 (EUR-4812)
- processing of, research progress on, 26:53063 (ORNL-4794, pp 33-5)
- separation of iodine and methyl iodide from off-gas, by sorption on charcoal, 26:53058 (CONF-720823-10)
- separation of iodine and methyl iodide from off-gas, by sorption on silver-containing adsorbents, 26:53077 (CONF-720823-9)
- storage in salt mines, gas flow through dry crushed salt during, (E), 26:53724 (ORNL-TM-3815)
- storage of high-level solidified, in Carey salt mine, effects of adjacent American Salt Corp. mining activities on, 26:53725 (ORNL-TM-3903)
- storage sites for, development of European community-type, 26:53726
- thermal stability of alpha, 26:53063 (ORNL-4794, pp 33-5)

RADIOACTIVITY
- book: Atomic Nucleus, 26:54738
- monitoring in Hungarian foodstuffs, from 1959 to 1971, 26:53172
- monitoring in Sweden from March 23, 1971 USSR underground nuclear explosion, 26:53158 (FOA-4-4502-A-1)

RADIOAPPLICATORS
- gamma dose distributions of ^{60}Co ophthalmic, computer-calculated, 26:54900

RADIOBIOLOGY
- book: Advances in Radiation Chemistry. Vol. 3, 26:53021
- energy deposition theory in, distribution of energy losses in, 26:54879 (NASA-TM-X-2440, pp 157-61)
- radioinduced chemical processes in, review on, 26:53024

RADIOCHEMICAL PROCESSING PLANTS
- development of MILLI, in Federal Republic of Germany, 26:53087
- effluent control from, pp. 24-5, 26:53082 (ORNL-4794, pp 15-25)
- radioactive waste from, trapping of iodine from off-gas, 26:53077 (CONF-720823-9)

RADIOCHEMISTRY
- hot atom reactions in, computer simulation of scavenger competition, 26:53030
- hot atom reactions in, effects of scavenger competition on kinetic theory of, 26:53031
- research in India, 1971--1972, 26:55452(R) (NP-19407)

RADIOGRAPHY, BIOMEDICAL
- dose calculation in x and γ, integral absorbed, 26:54910
- facilities for, IAEA-WHO survey on world-wide, 26:53413
- radiation dose to bone marrow and eyes of medical personnel during arteriography, x, 26:53443
- radiation dose to children during, methods for reducing x, 26:53417
- radiation dose to gonads and stomach wall of man during diagnostic, of stomach, relation to chromosome aberration induction in peripheral blood leukocytes, x, 26:53427
- radiation dose to man during diagnostic, phantom measurements in bone marrow, gonads, and skin, x, 26:53434
- radiation dose to man during, phantom studies for predetermination of absorbed x, 26:53416
- radiation hazards to man during fluoroscopy, effects of image intensifier performance on, 26:53421

RADIOGRAPHY, INDUSTRIAL
- equipment and methods for neutron, using californium-252 sources, 26:53330(R) (BNWL-1308-10)
- performance of neutron, with multiwire proportional counter, 26:53200 (LBL-707(Summ.))

RADIOISOTOPE SCANNING
- data from, computer programs for processing, 26:53228
- development of digital computer data processing system for analysis of gamma camera data, 26:55457 (TID-26141)
- training course manual, 26:53541 (TID-26128)
- uses of radiation and radioisotopes in, IAEA-WHO survey on world-wide, 26:53413

RADIOISOTOPES
- content and distribution of, in Savannah River swamp forest ecosystem, (E), 26:53171(R) (SRO-708-1)
- determination in mixtures, data reduction for Ge(Li) gamma spectrometers using small computers for, 26:53256 (NASA-TM-X-2440, pp 744-6)
- development and research in South Africa, 1971, 26:55453(R) (NP-19410)
- distribution and metabolism in biological systems, development of kinetic models for multi-parameter analysis of, 26:53519
- release to environment during accidents, relation to public health, 26:53523
- research in India, 1971--1972, 26:55452(R) (NP-19407)
- separation from spent ion exchange resins, method for, 26:53072(P)
- sorption by soils near Baguio City, Philippines, (E), 26:53175
- transport through ecosystems, bibliography on, 26:53530 (TID-3915(Suppl.1))
- transport to man following release to environment, 26:53522
- uptake by cattle following deposition of fallout on pasture grass, tracer study using lanthanum-140 as simulant, 26:53527 (FOA-4-4503-A-3)
- uptake by man following release to environment, 26:53521
- uses in analytical chemistry, 26:52942
- uses in hydrology in Latin America, 26:53168
- uses in medicine, IAEA-WHO survey on world-wide, 26:53413
- uses in medicine, industry, and research in Japan during 1970, status of, 26:55458
- uses in medicine, training course manual, 26:53541 (TID-26128)

RADIOMETRIC ANALYSIS
- book: Radiometric Methods of Analysis, in Romanian, 26:52942

RADIOPROTECTIVE COMPOUNDS
- bibliography on chemical, 26:53460 (SZS-132)

RADIOSTERILIZATION
- dose during, production and testing of homogeneous sterilization, 26:53340

RADIOTHERAPY
- dose calculation during interstitial radium, integral absorbed, 26:54910
- dose computations and treatment planning in pion, 26:54876 (LA-4874, pp 145-52)
- dose distributions for fast neutron, 26:54893
- dose rate tables for californium-252 implants, neutron and gamma, (T), 26:54906
- effectiveness of radiosensitizers during fractionated dose, of human neoplasms, relation of anoxia to cellular response to, 26:53430
- effects on immune reactions in patients, 26:53432
- equipment for skin cancer, description of, 26:53341
- injuries of human spinal cord exposed during, etiology

  of, 26:53429
  necrosis of jaw bones induced by exposure during head and neck neoplasm, 26:53418
  protection of oral tissues during head and neck, in patients, construction of prosthesis shield for, 26:53410
  treatment planning using pi mesons, 26:54877 (LA-4874, pp 153-61)
  use of sealed radium-226 gamma sources for implant, isodose curves for, 26:53409 (STI/PUB-295(Vol.4))
  uses of radiation and radioisotopes in, IAEA-WHO survey on world-wide, 26:53413
RADIUM
  determination of, radiometric, 26:52942
  effects on children following use for maternal therapy during pregnancy, pathological and teratological, 26:53437
RADIUM ISOTOPES Ra-216
  alpha decay of, half-life and width for, (E), 26:54651
RADIUM ISOTOPES Ra-223
  energy levels from thorium-227 decay, spin-parity assignments for, (E), 26:54673
RADIUM ISOTOPES Ra-226
  content in corals, determination of coral growth rates from measurements of, 26:53179
  content of foods, human diet, and urine in Poland, relation between, 26:53525
  content ratio to lead-210 in corals, determination of coral growth rates from measurements of, 26:53179
  content ratio to radium-228 in corals, determination of coral growth rates from measurements of, 26:53179
  decay of, γ-ray energies and intensities from, (E), 26:54652 (ANCR-1069)
  use as sealed gamma source for implant therapy, 26:53409 (STI/PUB-295(Vol.4))
RADIUM ISOTOPES Ra-228
  content ratio to radium-226 in corals, determination of coral growth rates from measurements of, 26:53179
RADON
  content of mine air, relation to mortality of miners, 26:53412
  effects on circadian changes in mitotic index and DNA synthesis in cells of rat gastric glands following oral administration of, in water, effects of dose on, 26:53514
RADON ISOTOPES Rn-220
  content in atmosphere of Nagoya, Japan in Nov. 1968, 26:53227
  radiation dose to human respiratory tract tissues following inhalation as aerosols, method for estimation of alpha, 26:53508
RADON ISOTOPES Rn-222
  decay products of, content in uranium mine air, α-spectrometric method for determining, 26:53226
  radiation dose to human respiratory tract tissues following inhalation as aerosols, method for estimation of alpha, 26:53508
RAINWATER
  radioactivity monitoring of, in vicinity of Savannah River Plant, 1971, 26:53153(R) (DPSPU-72-30-1)
RANCHO SECO POWER REACTOR
  auxiliary systems for, requested and revised data on, 26:55315 (DOCKET-50312-51)
  containment system for, requested and revised data on, 26:55315 (DOCKET-50312-51)
  cooling system for, requested and revised data on, 26:55315 (DOCKET-50312-51)
  electrical cables for, requested information on quality assurance procedures for installation of, 26:55314 (DOCKET-50312-50)
  engineered safeguards for, requested and revised data on, 26:55315 (DOCKET-50312-51)
  instrumentation for, requested and revised data on, 26:55315 (DOCKET-50312-51)
  owners of, financial data on, 26:55315 (DOCKET-50312-51)
  piping system for, additional data on imperfections in welds for, 26:55316 (DOCKET-50312-52)
  power conversion system for, requested and revised data on, 26:55315 (DOCKET-50312-51)
  quality assurance program for, requested and revised data on, 26:55315 (DOCKET-50312-51)
  radioactive waste disposal system for, requested and revised data on, 26:55315 (DOCKET-50312-51)
  safety analysis for, requested and revised data on, 26:55315 (DOCKET-50312-51)
  testing program for, requested and revised data on, 26:55315 (DOCKET-50312-51)
RAPP POWER REACTOR
  description of, 26:55215
RARE EARTH ALLOYS AND SYSTEMS
  Co--rare earth, magnetic properties of R_3Co, pulsed-field magnetometer measurements of, 26:55050
  Ni--rare earth, magnetic properties of R_3Ni, pulsed-field magnetometer measurements of, 26:55050
  rare earths--Th, solubility in liquid bismuth, pp. 4-5, 26:53081 (ORNL-4794, pp 1-14)
RARE EARTH HYDRIDES
  properties of ternary, literature review on, 26:53558 (UCRL-51244)
RARE EARTH IONS
  magnetic properties of, diamagnetic susceptibility and nuclear magnetic shielding constants, (T), 26:55025
RARE EARTH OXIDES
  magnetic moment direction in perovskites, crystal-field calculation of, 26:55054
  spectra of R_2O_3, 4.2°K far-infrared, (E/T), 26:55032
RARE EARTHS
  abundance in γ Cap, (E), 26:53888
  magnetic properties of, diamagnetic susceptibility and nuclear magnetic shielding constants, (T), 26:55025
  separation by pressurized ion exchange, p. 37, 26:53084 (ORNL-4794, pp 54-62)
  separation from MSBR fuel salt by metal transfer process, contactor studies for, pp. 8-9, 26:53081 (ORNL-4794, pp 1-14)
  separation from MSBR fuel salt by metal transfer process, pp. 7-8, 26:53081 (ORNL-4794, pp 1-14)
  separation from spent molten salt fuel by reductive extraction, 26:53086(P)
  separation from uranium by fractional dissolution of crude sodium diuranate, 26:52976 (IEA-250)
  separation from uranium by ion exchange using diethylaminoethylcellulose, 26:52951
  spin-wave energy fitting to interatomic exchange parameters in ferromagnetic, (T), 26:55053
RARE GASES
  chemistry of, 26:55562 (LBL-416)
  proton reactions at 500 to 3000 eV with, atomic-number dependence of charge exchange and excitation in, (E/T), 26:54122
  separation of fission product, from combustion off-gases by scrubbing with liquid carbon dioxide, 26:53064(T) (ORNL-tr-2621)
  transport in reactor core, tracer method for determining, 26:55185 (CONF-710959-, Paper 1)
RATS
  americium-241 distribution, retention in skeleton and excretion in urine of, following inhalation, time dependence of, 26:53531(T) (UCRL-Trans-1477)
  americium-241 removal from skeleton of, effectiveness of DTPA for, 26:53531(T) (UCRL-Trans-1477)
  arsenic-74 distribution and metabolism in tissues of, following oral administration, time dependence of, 26:53538
  radiation effects of L-arginine aminohydrolase activity in liver of, dose dependence of, 26:53491
  radiation effects on blood cells and protein content of blood of, following intratracheal administration of cerium-144, 26:53516
  radiation effects on bone marrow of, role of thymus gland in recovery from γ, 26:53479
  radiation effects on brain of neonatal, relation of acetylcholine metabolism to pathological, x, 26:53461(R) (UCB-34-P-82-13)
  radiation effects on brain of, relation of glycogen content to pathological, γ, 26:53487
  radiation effects on circadian changes in mitotic index and DNA synthesis in cells of gastric glands, following oral administration of radon water, effects of dose on α, 26:53514
  radiation effects on DNA synthesis and degradation in liver, spleen, and thymus of, x, 26:53489
  radiation effects on leukocyte count in peripheral blood of, following whole-body exposure, dose and time dependence of γ, 26:53483
  radiation effects on motor activity of, following exposure of embryos, dose dependence of x, 26:53488
  radiation effects on regeneration of thyroid gland in, following whole-body exposure, effects of prior implantation of sarcoma on x, 26:53494
  radiation effects on respiration and ultrastructure of mitochondria in intestinal epithelial cells of, during amino acid absorption, whole-body x, 26:53493
  radiation effects on survival of, following acute whole-body exposure, comparison of γ and proton, 26:53455 (NASA-TM-X-2440, pp 647-51)
  radiation effects on uptake of selenium-75-labeled selenomethionine by erythrocytes of, following whole-body exposure, dose dependence of γ, 26:53482
  radioinduced carcinomas in kidneys of parabiosed, whole-body x, 26:53449 (COO-3017-4)
  radioinduced chromosome aberrations in embryos of, following exposure in utero, time dependence of fast neutron, 26:53470
  radioinduced hypertension in, effects on distribution and excretion of exchangeable sodium, sodium-22 tracer study of, 26:53463
  radioinduced malformations in developing embryos of, following in utero exposure, role of chromosome damage and repair errors in incidence of fast neutron, 26:53470
  radioinduced malformations of brain of, following prenatal exposure, effects of developmental stage at exposure on, 26:53437
  radioinduced mammary neoplasms in, following acute whole-body exposure, comparison of γ and proton, 26:53455 (NASA-TM-X-2440, pp 647-51)
  radioisotope content of hair of, following intravenous injection, correlation with body burden, 26:53529 (NASA-TM-X-2440, pp 982-8)
  uptake of organic bases by kidneys of, effects of uranyl nitrate on, 26:53537

- REACTIVITY
  - effects of plutonium oxide (PuO_2) grain size in mixed oxide fuel elements with respect to homogeneity, 26:55416(R) (BNWL-1522-5)
  - measurements in sodium of fuel plates vs. fuel pins, comparison of, 26:55395 (CONF-720901-12)
- REACTOR CONTAINMENT STRUCTURES
  - deformation of fast sodium cooled, effects of excursion pressure loading on, (E/T), 26:55139 (ANL-7911(Suppl.1))
- REACTOR CONTROL ELEMENTS
  - development of cruciform, VISTA-SHE measurements for, 26:55137 (JAERI-Memo-3893)
  - drives for pressurized water power reactor, analysis of discontinuities in motor tube extensions of, 26:55217 (BAW-10047(Rev.1))
  - gamma heating of boron and tantalum, in liquid metal fast breeder core mockup, (E), 26:55134 (CONF-720901-(Bks.1 and 2), pp 579-98)
  - reactivity worths of boron and tantalum, in liquid metal fast breeder core mockup, (E), 26:55134 (CONF-720901-(Bks.1 and 2), pp 579-98)
- REACTOR CONTROL SYSTEMS
  - design of minicomputer, compliance with IEEE-279 safety criteria of, 26:55136 (DUN-SA-186)
  - economics of minicomputer, analysis of, 26:55136 (DUN-SA-186)
  - electric circuits in, ground detectors for ungrounded, 26:55135 (DUN-SA-169)
- REACTOR EXPERIMENTAL FACILITIES
  - rabbit system for, design of ionization chamber as electronic switch for control of, 26:53224
  - sample arrival in pneumatic tubes, system for signaling, 26:55413(P)
- REACTOR FUEL ELEMENTS
  - arrangement of spherical, into spherical core for optimum heat transfer, 26:55131(P)
  - cladding for fast, radiation effects on embrittlement of stainless steels Type 304 and Type 316, 26:55083(R) (EURFNR-1001)
  - cladding for mixed plutonium oxide (PuO_2)--uranium oxide (UO_2) fast, development and testing of stainless steel, 26:55189(R) (GEAP-10028-39)
  - cladding for mixed plutonium oxide (PuO_2)--uranium oxide (UO_2) fast, development and testing of stainless steel, 26:55190(R) (GEAP-10028-42)
  - compatibility of plutonium oxide (PuO_2)--uranium oxide (UO_2) with stainless steel cladding of, effects of burnup on, 26:55187 (EURFNR-989)
  - coolant flow in bundles of rod, effects of Reynolds number in velocity profile, intensity, and scale of, 26:55416(R) (BNWL-1522-5)
  - coolant flow in hexagonal and square rod bundles, pressure drop for laminar, (T), 26:55449 (KFK-1503)
  - coolant flow through 16 tube bundles of, measurements of heat transfer and pressure drop in, 26:55227(T) (EURFNR-1000)
  - coolant flow through hexagonal assemblies of, method for visual study of, 26:55176 (KFK-1548)
  - corrosion of stainless steel clad, effects of stresses on, 26:55166 (CONF-710959-, Paper 10)
  - critical heat flux in rod bundles of, calculation using tube bundles correlation, 26:53123
  - design characteristics for mockup liquid sodium cooled bundles, 26:55207(R) (ORNL-TM-3900)
  - design with moderator and insulating layer, for high negative temperature coefficient of reactivity, 26:55419(P)
  - development of fast, progress in Netherlands on, 26:55083(R) (EURFNR-1001)
  - failure of water cooled and sodium cooled, methods for detection of, 26:55218(T) (EURFNR-976)
  - fission product decay heating following coolant loss accidents, effects of fission product escape on, (T), 26:55206 (KFK-1580)
  - fission products in, migration of cesium and tellurium, 26:55190(R) (GEAP-10028-42)
  - flow distribution in bundle arranged roughened rods, calculation of gas, (T), 26:55188 (EURFNR-1020)
  - friction factors for bundle arranged roughened rods, calculation of gas flow, (T), 26:55188 (EURFNR-1020)
  - fuel distribution in high-temperature, roentgenographic method for studies of, 26:53599
  - gamma scanning of irradiated oxide, self-absorption correction for, 26:53041 (UJV-2867-M,A)
  - handling and shipping of, analysis of shock loading parameters for, 26:53732 (WCAP-1615)
  - heat transfer coefficients in mockup liquid sodium cooled bundles, effects of configuration and flow blockage area on, (E/T), 26:55207(R) (ORNL-TM-3900)
  - heat transfer in water cooled, effects of coolant loss accident conditions on, (E/T), 26:55207(R) (ORNL-TM-3900)
  - heat transfer in, development of model for inclusion in COBRA-3B computer code of, 26:55416(R) (BNWL-1522-5)
  - hydrodynamic effects of configuration and spacing of, 26:55174(T) (EURFNR-986)
  - loading of spherical, design of conveying tube for pneumatic, 26:55194(P)
  - oxygen release during burnup of mixed oxide, corrosive effects on stainless steel cladding of, 26:55187 (EURFNR-989)
  - performance for pin fast, SATURN-1 code for time dependent history of, 26:55186(T) (EURFNR-985)
  - performance of defected mixed plutonium oxide (PuO_2)--uranium oxide (UO_2) fast, in flowing liquid sodium, 26:55189(R) (GEAP-10028-39)
  - performance of defected mixed plutonium oxide (PuO_2)--uranium oxide (UO_2) fast, in flowing liquid sodium, 26:55190(R) (GEAP-10028-42)
  - performance of metal clad oxide pins, BEHAVE-2 computer program for calculation of operating, 26:55418 (GEAP-13788)
  - physics measurements of plate vs. pin, comparison of, 26:55395 (CONF-720901-12)
  - production of plate-shaped and rod-shaped dispersion cermet-type, methods for, 26:53592
  - radiation effects testing of mixed plutonium oxide (PuO_2)--uranium oxide (UO_2) fast, 26:55189(R) (GEAP-10028-39)
  - radiation effects testing of mixed plutonium oxide (PuO_2)--uranium oxide (UO_2) fast, 26:55190(R) (GEAP-10028-42)
  - reactivity of plutonium oxide (PuO_2)--uranium oxide (UO_2), effects of grain size of plutonium oxide on, 26:55416(R) (BNWL-1522-5)
  - reprocessing of graphite, fission product release in head-end, 26:53078 (CONF-720823-11)
  - reprocessing of HTGR, development of head-end methods for, 26:53083 (ORNL-4794, pp 26-32)
  - separation of plutonium from Zircaloy-clad oxide, head-end pyrochemical Saltex process for, 26:53079 (EUR-4812)
  - simulation of uranium oxide (UO_2) rods, performance of filament type electric heater, (E), 26:55183 (ANCR-1038)
  - storage time of spent, design of gamma scanner for measuring, 26:53261
  - tagging procedures for pin type, xenon, 26:55184 (ANL/EBR-57)
  - temperature distribution in mockup liquid sodium cooled bundles, effects of configuration and flow blockage area on, (E/T), 26:55207(R) (ORNL-TM-3900)
  - thermocouples for mockup liquid sodium cooled bundles, arrangement of, 26:55207(R) (ORNL-TM-3900)
  - voids in vibratory compacted, criteria for defining, 26:55229(T) (EURFNR-975)
- REACTOR FUELS
  - analysis of irradiated, for fission products by automated mass spectrometry, 26:52917 (EUR-4765, pp 77-89)
  - burnup analysis of, remote electrophoretic method for, 26:52933 (JAERI-Memo-4094)
  - burnup analysis of, separation of cesium-137 for, 26:52933 (JAERI-Memo-4094)
  - burnup determination by isotope dilution, 26:52917 (EUR-4765, pp 77-89)
  - cladding for, eddy current testing of stainless steel tubing for, 26:53125
  - coolant flow past sphere-type, studies at high Reynolds numbers of gas, 26:55180
  - cycle management of high temperature gas cooled, methods for in-core three-dimensional, 26:55111 (CONF-720901-(Bks.1 and 2), pp 68-80)
  - cycles for, CITATION code for analysis of in-core, 26:55198 (ORNL-TM-2496(Rev.2)(Suppl.3))
  - inspection of irradiated plutonium-bearing, design of hot cell for, 26:53728 (JAERI-Memo-4009)
  - neutron resonance capture in mixed oxide, effects of particle size on, (E/T), 26:55425 (CONF-720901-(Bks.1 and 2), pp 108-13)
  - preparation of particulate oxide, equipment and method for, 26:53566(P)
  - radiation effects on dissolution characteristics of LMFBR, pp. 20-1, 26:53082 (ORNL-4794, pp 15-25)
  - radiation testing in swimming pool reactors, device for control of, 26:55380 (CEA-N-1211)
  - reprocessing in India, 1971--1972, 26:55452(R) (NP-19407)
  - reprocessing of HTGR graphite, air required for dilution of off-gases from combustion in, 26:53060 (CONF-720823-14)
  - reprocessing of HTGR graphite, decontamination of off-gases from, 26:53059 (CONF-720823-12)
  - reprocessing of LMFBR, development of aqueous methods for, 26:53082 (ORNL-4794, pp 15-25)
  - reprocessing of LMFBR, trapping of iodine in off-gases from, 26:53077 (CONF-720823-9)
  - reprocessing of molten salt, axial dispersion in simulated continuous fluorinator for, pp. 9-10, 26:53081 (ORNL-4794, pp 1-14)
  - reprocessing of molten salt, by fluorination and reductive extraction methods, 26:53086(P)
  - reprocessing of molten salt, development of frozen-wall continuous fluorinator for, pp. 10-11, 26:53081 (ORNL-4794, pp 1-14)
  - reprocessing of MSBR, chemistry of fuel reconstitution in, p. 6, 26:53081 (ORNL-4794, pp 1-14)
  - reprocessing of MSBR, research progress on, 26:53081 (ORNL-4794, pp 1-14)
  - reprocessing of, contactor studies for rare earth removal by metal transfer process in, pp. 8-9, 26:53081 (ORNL-4794, pp 1-14)
  - reprocessing of, development of methods for, 26:53088

reprocessing of, engineering studies of burner off-gas decontamination for, pp. 29-32, 26:53083 (ORNL-4794, pp 26-32)
reprocessing of, research progress on solvent extraction of plutonium using amines in, p. 55, 26:53084 (ORNL-4794, pp 54-62)
reprocessing of, review on methods for, 26:52977
reprocessing of, use of modified Purex Process in MILLI laboratory for, 26:53087
requirements for power reactor development during 1972 to 1985, 26:55267 (WASH-1139(Rev.1))
requirements in power production 1980 to 2000, calculations of, 26:55093
thermal conductivity of sheared prototype LMFBR, p. 16, 26:53082 (ORNL-4794, pp 15-25)
uranium dioxide content in, during fuel fabrication, automatic on-line system for weighing and recording, 26:53723

REACTOR SAFETY
development activities during May and June 1972, 26:55207(R) (ORNL-TM-3900)
effects of minicomputerized control systems on, analysis of, 26:55136 (DUN-SA-186)
research program on, review of Japanese, 26:55204 (JAERI-M-4535)
research projects in West Germany, summaries of current, 26:55202(R) (IPP-F-14)

REACTOR SAFETY EXPERIMENTS
coolant loss accident simulation in, instrumentation for, 26:55205 (JAERI-Memo-4041)

REACTOR SIMULATORS
development of analog and digital, for sodium--water reactions, 26:55150 (CONF-710548-, pp 1-16)
performance of hybrid computer, for fast breeder reactor lattice parameter identification, 26:55099 (AD-738874)

REACTORS
burnout in, description of bridge-type detector for detecting, 26:53304(T) (LIB/Trans-431)
components for, standards for hoisting and rigging equipment for, 26:53112 (RDT-F-8-6-T(8-72))
components for, supplement to standards for high temperature requirements of Class 1, 26:55208 (RDT-F-9-1-T(8-72))
cooling system, standards for valves for, 26:53111 (RDT-E-1-13-T(8-72))
core-supporting structure in, equipment for observing position of, 26:55128(P)
cores for, effects of thermal neutron capture γ spectra on, (T), 26:55444 (TRG-2189)
criticality calculations for, reliability of Monte Carlo computer programs for, 26:55445 (Y-KC-96)
criticality calculations for, zero variance estimator for Monte Carlo, 26:55431 (CONF-720901-(Bks.1 and 2), pp 229-39)
description of, for space power systems, (T), 25:54950 (NASA-TM-X-2440, pp 98-102)
development and research in South Africa, 1971, 26:55453(R) (NP-19410)
development in India, 1971--1972, 26:55452(R) (NP-19407)
instrumentation systems for, RELY 4 code for reliability analysis of, 26:55209 (RISO-M-1506)
maintenance standards for, development of equipment, 26:55201 (DUN-SA-168)
neutron diffusion equation for hexagonal lattices, simultaneous line over-relaxation method for solution of, 26:55433 (CONF-720901-(Bks.1 and 2), pp 253-65)
neutron diffusion equations for cylindrical, variational synthesis analysis of two-group, 26:55422 (CISE-R-243)
neutron diffusion equations for finite cylindrical, iterative solution of, 26:55423 (CISE-R-273)
neutron energy spectra in, many-resonance approximation of, 26:55429 (CONF-720901-(Bks.1 and 2), pp 195-206)
neutron flux at cooling system of, standard for BF_3 proportional counter for measuring, 26:53204 (RDT-C-15-11-T(8-72))
neutron multiplication factors for, use of optimal control theory for determination of burnup dependence of infinite, 26:55432 (CONF-720901-(Bks.1 and 2), pp 240-51)
neutron transport calculations for, optimum angular segmentations in, 26:55434 (CONF-720901-(Bks.1 and 2), pp 266-74)
neutron transport equations for, improved S/sub N/ inner iteration convergence criterion for, 26:55435 (CONF-720901-(Bks.1 and 2), pp 275-92)
noise analysis for, bibliography on, 26:55443 (RT/FI-(72)13)
noise analysis in, state of the art in 1971 of, 25:55442 (RT/FI-(72)11)
physics calculations for, use of variational and perturbation methods in, 26:55426 (CONF-720901-(Bks.1 and 2), pp 162-7)
physics of, conference on new developments in, 25:55424 (CONF-720901-(Bks.1 and 2))
power transients in, use of PAD code for calculation of explosive, (T), 26:55441 (LA-DC-72-660)
radioactive waste system for, efficiency of filters for removal of radioactive iodine from off-gas, 25:55146
refueling of, MOBIDIC code for analysis of continuous axial, 26:55196 (CISE-R-241)
shielding calculations for, development of ENDF/B library for, 26:55141 (CONF-720901-(Bks.1 and 2), pp 315-24)
shielding calculations for, measurement and evaluation of neutron cross sections for, 26:55140 (CONF-720901-(Bks.1 and 2), pp 295-315)
shielding of, conference on new developments in, 26:55424 (CONF-720901-(Bks.1 and 2))

REACTORS, AIRCRAFT
shield for, thermal displacements of front island, (T), 26:55374 (CERN-HERA-72-1)

REACTORS, BOILING
cooling systems of, rupture studies on pipes in, 26:55175(R) (GEAP-10207-26)
decay heat from fission products in, REST-1, REST-2, and REST-3 codes for, 26:55127 (KFK-1579)
effluents from, development of legal limits for radioactive, 26:55220 (BNL-16965)
excursions in large, rod drop analysis of super prompt critical, 26:55353 (NEDO-10527)
physics of, review of developments in, 26:55112 (CONF-720901-(Bks.1 and 2), pp 114-40)

REACTORS, BREEDER
cooling systems of sodium cooled, fission and corrosion product behavior in, 26:55166 (CONF-710959-, Paper 10)
cooling systems of, conference on corrosion products in, 26:55417 (CONF-710959)
core design of fast, for decreased coolant void coefficient, 26:55129(P)
cover gas of, economic feasibility of cleanup system for, 26:55226 (CONF-710959-, Paper 5)
design of light-water seed--blanket, 26:55130(P)
design of molten chloride salt fast, (T), 26:55082 (EIR-215)
development for electric power generation, 26:55086
fuel burnup in, program for measurement of, 26:55119 (CONF-720901-(Bks.1 and 2), pp 888-904)
fuels for light-water, preparation of uranium-233 dioxide, 26:53553 (ORNL-4794, pp 52-3)
fuels for, preparation of particulate oxide, 26:53566(P)
lattice parameter identification in, performance of hybrid computer simulator for, 26:55099 (AD-738874)
neutron diffusion in gas cooled fast, calculation of anisotropic, (T), 26:55126 (KFK-1577)
physics of fast, review of, 26:55115 (CONF-720901-(Bks.1 and 2), pp 771-88)
physics parameters of sodium cooled, MASURCA measurements of, 26:55118 (CONF-720901-(Bks.1 and 2), pp 822-38)
physics parameters of, use of integral measurements in analysis of, 26:55121 (CONF-720901-(Bks.1 and 2), pp 928-39)

REACTORS, CANDU-TYPE
cooling systems for, economic effects of valve performance in, 26:55181
development of, status of, 26:55195 (AECL-4254)

REACTORS, FAST
containment structures for sodium cooled, effects of excursion pressure waves on deformation of, (E/T), 26:55139 (ANL-7911(Suppl.1))
coolant for liquid metal cooled, combustion characteristics of liquid sodium and sodium peroxide mixtures, (E), 26:55178 (RD/B/N-2364)
coolant loss accidents in, temperatures during, 26:55083(R) (EURFNR-1001)
cooling systems for sodium cooled, testing of components for secondary, 26:55182
cooling systems for, heat transfer studies in liquid sodium, 26:55083(R) (EURFNR-1001)
cooling systems of sodium cooled, fission and corrosion product behavior in, 26:55166 (CONF-710959-, Paper 10)
cooling systems of, conference on corrosion products in, 26:55417 (CONF-710959)
core design of breeder, for decreased coolant void coefficient, 26:55129(P)
core physics of, effects of fission products on, 25:55083(R) (EURFNR-1001)
cover gas of, economic feasibility of cleanup system for, 26:55226 (CONF-710959-, Paper 5)
design of molten chloride salt breeder, (T), 26:55082 (EIR-215)
development in Netherlands, progress on, 26:55083(R) (EURFNR-1001)
Doppler reactivity effects in, pulsed activation techniques for measurement of, 26:55124 (CONF-720901-(Bks.1 and 2), pp 1016-32)
fuel burnup in, program for measurement of, 26:55119 (CONF-720901-(Bks.1 and 2), pp 888-904)
fuel elements for gas cooled, calculation of friction factors and flow distribution in bundle arranged roughened rods, (T), 26:55168 (EURFNR-1020)
fuel elements for, SATURN-1 code for calculation of time history of pin, 26:55186(T) (EURFNR-986)
kinetics analysis of, survey of developments in, 26:55427 (CONF-720901-(Bks.1 and 2), pp 166-78)
lattice parameter identification in, performance of hybrid computer simulator for, 26:55099 (AD-738874)
neutron diffusion in gas cooled breeder, calculation of anisotropic, (T), 26:55126 (KFK-1577)
neutron generation time in subcritical, transfer and scattering kinetics scheme for determination of, 26:55437 (CONF-720901-(Bks.1 and 2), pp 713-23)
neutron spectra measurements in, proton-recoil spectrometry methods for, 26:55122 (CONF-720901-(Bks.1 and 2), pp 959-72)

neutron spectra measurements in, review of fast, 26:55438 (CONF-720901-(Bks.1 and 2), pp 943-58)
physics calculations for zero power, KFKINR set of group constants for, 26:55397 (EURFNR-1016)
physics calculations for zero power, VIM-1 computer program for, 26:55378 (AI-AEC-12951)
physics measurements for liquid sodium cooled, (E/T), 26:55398 (EURFNR-1029)
physics measurements in, adjustments of neutron cross section data from, 26:55436 (CONF-720901-(Bks.1 and 2), pp 599-612)
physics of breeder, review of, 26:55115 (CONF-720901-(Bks.1 and 2), pp 771-88)
physics parameters of sodium cooled, MASURCA measurements of, 26:55118 (CONF-720901-(Bks.1 and 2), pp 822-38)
physics parameters of, ENDF/B data evaluation for benchmark measurements of, 26:55125 (CONF-720901-(Bks.1 and 2), pp 1033-47)
physics parameters of, use of integral measurements in analysis of, 26:55121 (CONF-720901-(Bks.1 and 2), pp 928-39)
plutonium-239 release to environment as oxide aerosols during accidents involving, hazards to human population from, 26:53511 (TID-26142)
safety of, effects of fuel element cladding rupture and coolant loss accidents on, 26:55083(R) (EURFNR-1001)
shielding calculations for, methods development for, 26:55144 (CONF-720901-(Bks.1 and 2), pp 480-98)
shielding design for, diffusion theory analyses for, 26:55143 (CONF-720901-(Bks.1 and 2), pp 459-70)
REACTORS, FLUID-FUELED
propellant pumping in gas core, performance of bleed-cycle, (T), 26:55358 (N-72-18051)
REACTORS, GAS-COOLED
coolant flow through 16 tube fuel assemblies, measurements of heat transfer and pressure drop in, 26:55227(T) (EURFNR-1000)
fuel elements for fast, calculation of friction factors and flow distribution in bundle arranged roughened rods, (T), 26:55188 (EURFNR-1020)
fuel management in high temperature, methods for three-dimensional, 26:55111 (CONF-720901-(Bks.1 and 2), pp 68-80)
fuel reprocessing for, decontamination factors for gaseous effluents from combustion process in, 26:53060 (CONF-720823-14)
fuel reprocessing for, development of methods for, 26:53083 (ORNL-4794, pp 26-32)
fuels for, preparation of oxide, 26:53552 (ORNL-4794, pp 45-51)
neutron diffusion in fast breeder, calculation of anisotropic, (T), 26:55126 (KFK-1577)
physics of high temperature, review of French studies on, 26:55109 (CONF-720901-(Bks.1 and 2), pp 33-54)
physics of high temperature, review of U.K. studies on, 26:55110 (CONF-720901-(Bks.1 and 2), pp 55-67)
reactivity temperature coefficient of high temperature, determination of, (E/T), 26:55108 (CONF-720901-(Bks.1 and 2), pp 23-32)
REACTORS, HEAVY WATER-MODERATED
physics of, lectures on, 26:55100 (BARC/I-148)
physics parameters of natural uranium fueled, (E), 26:55101 (CISE-R-203)
REACTORS, HETEROGENEOUS
physics parameters of, dipolar formulation of, 26:55447
physics parameters of, dipolar formulation of, 26:55446
REACTORS, LIQUID METAL-COOLED
containment structures for sodium cooled, effects of excursion pressure waves on deformation of, (E/T), 26:55139 (ANL-7911(Suppl.1))
coolant for fast, combustion characteristics of liquid sodium and sodium peroxide mixtures, (E), 26:55178 (RD/B/N-2364)
coolant voids in, effects on core physics of sodium, 26:55395 (CONF-720901-12)
cooling systems for sodium cooled, testing of components for secondary, 26:55182
cooling systems for sodium, problems of impurities in cover gas systems for, 26:55171 (CONF-710959-, Paper 15)
cooling systems for, heat transfer studies in liquid sodium, 26:55083(R) (EURFNR-1001)
cooling systems of sodium, fission and corrosion product behavior in, 26:55166 (CONF-710959-, Paper 10)
cooling systems of, conference on corrosion products in, 26:55417 (CONF-710959)
cooling systems of, corrosion product release, transport, and deposition in, (E), 26:55164 (CONF-710959-, Paper 8)
cooling systems of, effects of corrosion on radioactivity levels in, 26:55172 (CONF-710959-, Paper 16)
core design of fast breeder, for decreased void coefficient, 26:55129(P)
core supporting structure in, equipment for observing position of, 26:55128(P)
cover gas of, economic feasibility of cleanup system for, 26:55226 (CONF-710959-, Paper 5)
fuel element failures in sodium, methods for detection of, 26:55218(T) (EURFNR-976)
physics measurements for fast, (E/T), 26:55398 (EURFNR-1029)
physics parameters of sodium cooled, MASURCA measurements of, 26:55118 (CONF-720901-(Bks.1 and 2), pp 822-38)
standards for, development of engineering, 26:55207(R) (ORNL-TM-3900)
thermowell system for, standards for design and fabrication of, 26:55219 (RDT-C-7-18-T(8-72))
REACTORS, MARINE
development in Japan, status of, 26:55089
REACTORS, MOLTEN-SALT
design of fast breeder, with molten chlorides for fuel and coolant, (T), 26:55082 (EIR-215)
fuel reprocessing for, by fluorination and reductive extraction methods, 26:53086(P)
fuel reprocessing for, chemical engineering studies related to, p. 94-5, 26:53085 (ORNL-4794, pp 91-5)
REACTORS, PEBBLE-BED
coolant flow at high Reynolds numbers in, aerodynamics of, 26:55180
core of, spherical arrangement for optimum heat transfer in, 26:55131(P)
fuel sphere transfer into, design of conveying tube for pneumatic, 26:55194(P)
REACTORS, POWER
accidents in, classification of types of, 26:55211
condenser cooling water distribution at planned Swedish, scale model measurements on, 26:55352 (INIS-mf-205)
control rod drives for pressurized water, analysis of discontinuities in motor tube extensions of, 26:55217 (BAW-10047(Rev.1))
coolant loss accident for 2568 MW(t) pressurized water, safety analysis for, 26:55271 (BAW-10034(Suppl.1))
coolant loss accident for 2762 MW(t) pressurized water, safety analysis for, 26:55272 (BAW-10048(Suppl.1))
coolant loss accidents in pressurized water, model accuracy for safety analysis of, 26:55199(T) (AEC-tr-7319)
cooling systems of sodium cooled, fission and corrosion product behavior in, 26:55166 (CONF-710959-, Paper 10)
cooling systems of, rupture studies on pipes in, 26:55175(R) (GEAP-10207-26)
core of, effect of fuel rod configuration and spacing on coolant pressure drop in, 26:55174(T) (EURFNR-986)
cover gas of, economic feasibility of cleanup system for, 26:55226 (CONF-710959-, Paper 5)
development during 1972 to 1985, 26:55267 (WASH-1139(Rev.1))
development in Canada during April 1971 to March 1972, 26:55081(R) (AECL-4162)
development in Japan, status of, 26:55089
development in U.K., economic and technical problems in, 26:55087
development of fast breeder, 26:55086
economics of dual purpose, for electricity production and district heating in Czechoslovakia, (T), 26:55376 (INIS-mf-172, pp 7-13)
effluents from, development of legal limits for radioactive, 26:55220 (BNL-16965)
energy conversion in, efficiency of, (T), 26:53107
excursions in large, rod drop analysis of super prompt critical, 26:55353 (NEDO-10527)
fuel cycle requirements for, calculations of, 26:55093
fuel element failures in water cooled and sodium cooled, methods for detection of, 26:55218(T) (EURFNR-976)
licensing of U. S., legislative changes and proposals for, 26:55355
plutonium-239 release to environment as oxide aerosols during accidents involving, hazards to human population from, 26:53511 (TID-26142)
pressure vessels for 1200 MW(e) water moderated, survey of design and fabrication of steel, 26:55224
pressure vessels for, development of methods for in-service inspection of, 26:55221 (NP-19338(Vol.1))
pressure vessels for, development of methods for in-service inspection of, 26:55222(R) (NP-19338(Vol.2))
siting requirements for dual purpose, for electricity production and district heating in Czechoslovakia, (T), 26:55375 (INIS-mf-172)
REACTORS, PRESSURIZED-WATER
control rod drives for power, analysis of discontinuities in motor tube extensions of, 26:55217 (BAW-10047(Rev.1))
coolant loss accident for 2568 MW(t), safety analysis for, 26:55271 (BAW-10034(Suppl.1))
coolant loss accident for 2762 MW(t), safety analysis for, 26:55272 (BAW-10048(Suppl.1))
coolant loss accidents in power, model accuracy for safety analysis of, 26:55199(T) (AEC-tr-7319)
coolant loss accidents in, fuel assembly heat transfer characteristics during, (E/T), 26:55207(R) (ORNL-TM-3900)
effluents from, development of legal limits for radioactive, 26:55220 (BNL-16965)
fuel elements for, performance of filament type electric heater simulation of uranium oxide (UO_2) rod, (E), 26:55183 (ANCR-1038)
lattice cells of, group constant generation for resolved resonance region in, 26:55439 (CONF-720901-(Bks.1 and 2), pp 1183-91)
physics of, review of, 26:55107 (CONF-720901-(Bks.1 and 2), pp 3-22)
thermal shielding for, design and evaluation study for replacement with neutron shielding pads of, 26:55223

(WCAP-7870)
  transients without scram in, probability and consequences of, 26:55193 (BAW-10016)
REACTORS, PROCESS HEAT
  economics of dual purpose, for electricity production and district heating in Czechoslovakia, (T), 26:55376 (INIS-mf-172, pp 7-13)
  siting requirements for dual purpose, for electricity production and district heating in Czechoslovakia, (T), 26:55375 (INIS-mf-172)
  use for conversion of fossil fuels, engineering problems in, 26:55377
REACTORS, RESEARCH
  construction of, review of, 26:55402 (JAERI-Memo-4002)
  containment structures for Grenoble HFR, design and construction of, 26:55410
  coolant for Grenoble HFR, tritium removal from, 26:55415
  cooling system for Grenoble HFR, design of, 26:55415
  development in Japan, status of, 26:55089
  development of Berkeley zero energy facility, program for, 26:55409 (RD/B/N-2272)
  experimental facilities in JRR-2, description of, 26:55404 (JAERI-Memo-4052)
  inpile loop for JRR-1, inpile and out-of-pile performance testing of, 26:55381 (CONF-710959-, Paper 6)
  irradiation experiments in JRR-2, summary of, 26:55404 (JAERI-Memo-4052)
  moderator loss from Frankfurt University FRF-2, γ dose rates from water, (T), 26:55399 (IKF-27)
  neutron buckling in ECO uranium oxide (UO_2) fueled heavy water moderated lattices, (E), 26:55106 (CISE-R-283)
  neutron flux measurements on CIRENE fuel element in, 26:55105 (CISE-R-258)
  neutron source in Grenoble HFR, design of liquid deuterium cold, 26:55414
  operation of SAFARI-I, 1971, 26:55453(R) (NP-19410)
  performance of Grenoble HFR, survey of, 26:55412
  physics measurements in CFRMF, evaluation of neutron cross sections from, 26:55384 (CONF-720901-(Bks.1 and 2), pp 613-22)
  physics measurements on uranium oxide (UO_2) fueled heavy water moderated lattices in RB-1, 26:55102 (CISE-R-239)
  safety of Grenoble HFR, design of systems and components for, 26:55411
  shield plug of Frankfurt University FRF-2, γ dose rates from open, (T), 26:55399 (IKF-27)
REACTORS, ROCKET
  propellant pumping in gas core, performance of bleed-cycle, (T), 26:55358 (N-72-18051)
  radiation from, hardening of Saturn 5 components and systems to, 26:55370 (NASA-TM-X-2440, pp 471-5)
  shield weight optimizations for 375- and 600-MW, FASTER-III Monte Carlo program for, 26:54962 (NASA-TM-X-2440, pp 697-705)
  shields for, effects of ducts on effectiveness of, (E/T), 26:54958 (NASA-TM-X-2440, pp 375-82)
REACTORS, SUPERHEATING
  core design of fast breeder, for decreased void coefficient, 26:55129(P)
REACTORS, SWIMMING-POOL
  fuel irradiation in, device for control of, 26:55380 (CEA-N-1211)
  irradiation tubes in, system for signaling sample arrival in pneumatic, 26:55413(P)
REACTORS, THERMAL
  physics calculations for, DASQHE computer program for, 26:55421 (BNWL-CC-2274)
REACTORS, THERMIONIC
  core for, venting of gaseous fission products from, (T), 26:55373 (NASA-TM-X-2440, pp 1016-20)
  physics calculations for in-core, MORSE-K code for Monte Carlo, 26:55386 (CONF-720901-(Bks.1 and 2), pp 636-44)
  shielding of 40 kW(e), for integration with manned space station, (T), 26:55365 (NASA-TM-X-2440, pp 299-306)
  shielding requirements of, for unmanned ion propulsion space vehicles, (T), 26:55364 (NASA-TM-X-2440, pp 292-8)
REACTORS, WATER-COOLED
  coolant loss accidents in, effects of fission product escape on fuel element heating following, (T), 26:55206 (KFK-1580)
  coolant loss accidents in, instrumentation for simulation of, 26:55205 (JAERI-Memo-4041)
  coolant loss accidents in, pressure drops and heat transfer coefficients for, (E/T), 26:55200(R) (COO-2152-4)
  cooling system of, critical review on boiling crisis and critical heat flux in, 26:55179 (TID-25887)
  cooling systems for, pressure wave propagation from pipe ruptures in, (T), 26:55203 (JAERI-M-4473)
  design of breeder seed--blanket, 26:55130(P)
  fuel element failures in, methods for detection of, 26:55218(T) (EURFNR-976)
  neutron flux calculations for fog cooled, MOICANO-1 code for, 26:55103 (CISE-R-242)
  pressure vessels for 1200-MW(e) survey of design and fabrication of steel, 26:55224
  reactivity calculations for fog cooled, MOICANO-1 code for, 26:55103 (CISE-R-242)
  standards for, development of engineering, 26:55207(R) (ORNL-TM-3900)
REACTORS, WATER-MODERATED
  design of breeder seed--blanket, 26:55130(P)
  physics calculations for, PIBIMUG code for, 26:55420 (AREAEE-141)
RECOILS
  reactions of, computer simulation of effect of scavenger competition on, 26:53030
  reactions of, effects of scavenger competition in kinetic theory of, 26:53031
REFRACTORY MATERIALS
  friction coefficients for, 26:53617
  powder metallurgy of, electronic mechanism of basic processes in, 26:53632
  properties at high temperatures for use in areospace, 26:53581
REGGE POLE THEORY
  absorption model in, generalization of weak-cut Regge, 26:54336
  cuts in pole--cut model for π + N charge exchange interactions at 4.8 to 20 GeV, double, 26:54324 (COO-1428-309)
  formalism for inclusive cross sections, triple-Regge, 26:54332
  trajectories in Veneziano-like representations, behavior of, 26:54423
  trajectories of baryon resonances, correlations among, 26:54338
RELATIVITY THEORY, GENERAL
  constants of, relations between quantum constants and, 26:54392 (ITF-72-3-P)
  coordinate transformation from Schwarzchild system to that of local pseudodecart in, 26:54401 (ITF-72-60-P)
  coordinate transformations conserving test-body trajectories in, use of group methods for infinitesimal, 26:54389 (ITF-71-85-P)
  geometry of state space of free particle in gravitational field, 26:54391 (ITF-71-132-P)
  mechanical vibrations in, effects of earth rotation on, 26:54400 (ITF-72-59-P)
  potentials in collapsing systems in, nonlinear generalization of Maxwell equations for static repulsive, 26:54404
  predictions for radar signal propagation retardation, radio wave deflection, and Mercury perihelion advance, comparison with experimental data, 26:54403
  Riessner--Nordstroem problem in presence of scalar field, exact static central-symmetric solution for, 26:54394 (ITF-72-20-P)
  Schwarzchild field in, effects of Einstein theory of gravitation for two-particle vibrations in, 26:54401 (ITF-72-60-P)
RELATIVITY THEORY, SPECIAL
  experimental test of, Trouton--Noble, 26:55540 (JINR-P2-6532)
RELAYS
  book: Radioisotopic Relays, 26:53288
REMOTE-CONTROL EQUIPMENT
  design and objectives of teleoperator, for NERVA, 26:53730 (NASA-TM-X-2440, pp 277-9)
  developments in teleoperator systems for manned space flights, 26:53731 (NASA-TM-X-2440, pp 280-90)
REMOTE-HANDLING EQUIPMENT
  development and uses of, review on, 26:53734
REMOTE-VIEWING EQUIPMENT
  design for positioning core-supporting structure inside reactor, 26:55128(P)
RESPIRATORY TRACT
  radiation dose distribution in, of dogs and monkeys following inhalation of strontium-90 as fused clay aerosols, β, 26:53536
  radiation dose to human, following inhalation of radon-222 and radon-220 daughter products as aerosols, use of ICRP lung model for estimation of alpha, 26:53508
RETICULO-ENDOTHELIAL SYSTEM
  radiation effects on phagocytic activity of cells of, in mice following whole-body exposure, effects of dose on x, 26:53468
RHENIUM
  compatibility of fuel capsules of, with plutonium-238 oxide fuels, 26:53551(R) (MDC G-3153)
  separation from scrubber solutions from roasting of molybdenite by solvent extraction, 26:52950(P)
  solvent properties for nitrogen, effects of temperature and pressure on, 26:53580
RHENIUM ALLOYS AND SYSTEMS
  Mo-base--Re, compatibility of fuel capsules of, with plutonium-238 oxide fuels, 26:53551(R) (MDC G-3153)
  N--Re, degassing at 1200 to 3000°C in, equilibria and kinetics of, 26:53580
  Re--ThO_2--W-base, creep properties of, at 1800 to 2200°C, 26:53678
  Re--W-base, compatibility of fuel capsules of, with plutonium-238 oxide fuels, 26:53551(R) (MDC G-3153)
RHENIUM ISOTOPES Re-185
  energy-level transitions from osmium-185 decay, multipole mixing ratios for, (E), 26:54644
RHENIUM ISOTOPES Re-187
  deuteron reactions (d,p) at 12 MeV, proton spectra and cross sections for, (E), 26:54637
  neutron capture by, γ singles and coincidence spectra

- from thermal, (E), 26:54637
- RHENIUM ISOTOPES Re-188
  - energy-level scheme for, (E), 26:54637
- RHENIUM OXIDES
  - magnetic susceptibility of ReO$_3$ at 77 to 300°K, comparison with sodium tungsten bronze, 26:55046
- RHODIUM
  - recovery of fission product, for commercial uses, feasibility of, 26:53330(R) (BNWL-1308-10)
- RHODIUM ISOTOPES Rh-103
  - neutron capture at 25 keV, model analysis of isomeric cross section ratio for, (E/T), 26:54589
- RHODIUM ISOTOPES Rh-108
  - beta decay of ground-state and isomeric, β and γ singles and coincidence spectra from, (E/T), 26:54596 (CEA-R-4286)
- RHODIUM ISOTOPES Rh-110
  - beta decay of ground-state and isomeric, β and γ singles and coincidence spectra from, (E/T), 26:54596 (CEA-R-4286)
- RHODOPSIN
  - light flashes induced by Cherenkov radiation from heavy cosmic nuclei, calculation of frequency of, 26:54882 (NASA-TM-X-2440, pp 757-66)
- RICHLAND AREA (WASH.)
  - climatography of, 26:55478 (BNWL-1605)
- RICKETTSIA
  - Rickettsia akari, radiation effects on metabolism of, in L cells, gamma, 26:53360
  - Rickettsia typhi, radiation effects on metabolism of, in L cells, gamma, 26:53360
- RING CURRENT
  - decay of, electric-field induction in magnetosphere from slow, (T), 26:54063
  - relation of partial, with space--time morphology of polar magnetic substorms in evening high latitudes, (E), 26:54023
- ROBERT E. GINNA POWER REACTOR, UNIT 1
  - radioactive effluents from, measurements during July 26 to August 25, 1972, 26:55245 (DOCKET-50244-118)
- ROCKET REACTORS (KIWI)
  - radiation environment from B4D and B4E, external gamma, (E), 26:55367 (NASA-TM-X-2440, pp 440-8)
- ROCKET REACTORS (NERVA)
  - development of, summary of program for, 26:55359 (NASA-TM-X-2440, pp 2-12)
  - engine components for, radiation heating in, (T), 26:55369 (NASA-TM-X-2440, pp 460-5)
  - radiation dose rates from flight module, coupling of discrete ordinates and Monte Carlo analyses of, 26:55371 (NASA-TM-X-2440, pp 681-6)
  - radiation dose rates from flight module, MORSE code analysis of, 26:55372 (NASA-TM-X-2440, pp 692-6)
  - radiation environment for rendezvous and docking with space stations, 26:55361 (NASA-TM-X-2440, pp 257-63)
  - radiation environment from reusable nuclear shuttle to orbiting lunar station and lunar surface, (T), 26:55362 (NASA-TM-X-2440, pp 264-9)
  - radiation levels on crew in Reusable Nuclear Shuttle, (T), 26:54945 (NASA-TM-X-2440, pp 40-7)
  - shielding design for, in Reusable Nuclear Shuttle, (E), 26:54954 (NASA-TM-X-2440, pp 251-6)
  - shielding measurements for, selection and use of thermoluminescent dosimeters for, 26:53233 (NASA-TM-X-2440, pp 466-70)
  - shielding of Reusable Nuclear Shuttle from, (T), 26:54946 (NASA-TM-X-2440, pp 48-56)
  - shields for, discrete ordinates analysis of minimum weight shadow, (E/T), 26:55368 (NASA-TM-X-2440, pp 449-59)
  - teleoperator design and objectives for, 26:53730 (NASA-TM-X-2440, pp 277-9)
- ROCKET REACTORS (PHOEBUS)
  - radiation environment from 1B and 2A, external gamma, (E), 26:55367 (NASA-TM-X-2440, pp 440-8)
- ROCKETS
  - components for Saturn 5, radiation hardening of, 26:55370 (NASA-TM-X-2440, pp 471-5)
- ROCKS
  - age of, thermoluminescent method for estimation of, 26:53177
  - analysis for alkaline earth metals and refractory oxides by atomic absorption spectroscopy, 26:52921
  - analysis for iodine and six metals by neutron activation and separation processes, 26:52906
  - barium, iron, lead, and molybdenum content in, γ--γ selective method for determination of equivalence between, 26:52943
  - uranium content of upper Jurassic black bituminous argillite, of West Siberian plate, (E), 26:53146
- ROVER REACTORS
  - radiation environment from Pewee 1, external gamma, (E), 26:55367 (NASA-TM-X-2440, pp 440-8)
- RUBIDIUM
  - photon reactions (γ,xn) with, model analysis of giant resonance in, (E/T), 26:54598 (FRNC-TH-242)
- RUBIDIUM ISOTOPES Rb-85
  - neutron capture at 25 keV, model analysis of isomeric cross section ratio for, (E/T), 26:54589
- RUBIDIUM ISOTOPES Rb-87
  - energy levels from krypton-86 proton resonances, widths and weak coupling coefficients for isobaric analog, (E), 26:54467(R) (ORO-2972-204)
- RUBIDIUM ISOTOPES Rb-89
  - half-life of, (E), 26:54667
- RUBIDIUM ISOTOPES Rb-90
  - half-life of, (E), 26:54667
- RUBIDIUM ISOTOPES Rb-91
  - half-life of, (E), 26:54667
- RUTHENIUM
  - determination in minerals by neutron activation and γ spectroscopy, nondestructive, 26:52901 (UJV-2851-F,Ch)
  - determination in residues from leaching of mattes by distillation and atomic absorption spectroscopy, 26:52919 (NIM-1432)
  - recovery of fission product, for commercial uses, feasibility of, 26:53330(R) (BNWL-1308-10)
- RUTHENIUM ALLOYS AND SYSTEMS
  - Ce--Gd--Ru, magnetic properties of Ce/sub 1-x/Gd/sub x/Ru$_2$, 26:55037
  - Ce--Pt--Ru, thermal capacity of CeRu/sub 2-x/Pt/sub x/ at 1.3 to 9°K, 26:55047
  - Ce--Ru, thermal capacity of CeRu$_2$ at 1.3 to 9°K, 26:55047
  - La--Ru, thermal capacity of LaRu$_2$ at 1.3 to 20°K, 26:55047
- RUTHENIUM ISOTOPES Ru-94
  - energy-level transitions in, shell-model calculations of, (T), 26:54611
- RUTHENIUM ISOTOPES Ru-96
  - chlorine-35 reactions up to 250 MeV, delayed proton spectra from, (E), 26:54608(T) (UCRL-Trans-1473)
  - sulfur-32 reactions up to 270 MeV, delayed proton spectra from, (E), 26:54608(T) (UCRL-Trans-1473)
- RUTHENIUM ISOTOPES Ru-102
  - energy levels from technetium-102 decay, collective model analysis of, (E/T), 26:54596 (CEA-R-4286)
- RUTHENIUM ISOTOPES Ru-103
  - content in atmosphere, rainwater, Savannah River, and vegetation in vicinity of Savannah River Plant, 1971, 26:53153(R) (DPSPU-72-30-1)
- RUTHENIUM ISOTOPES Ru-104
  - energy levels from technetium-104 decay, collective model analysis of, (E/T), 26:54596 (CEA-R-4286)
- RUTHENIUM ISOTOPES Ru-106
  - content in atmosphere, rainwater, Savannah River, and vegetation in vicinity of Savannah River Plant, 1971, 26:53153(R) (DPSPU-72-30-1)

S

- S-MATRIX
  - elements in g(:phi*:)$_2$ theory in Euclidean domain, equations for, 26:54376 (ITF-72-15-E)
  - formulation for Glauber multiple scattering theory, 26:54416
  - meromorphic continuation for elliptic partial differential operators in unbounded domains, method for, 26:54407 (BNL-16752)
  - unitarity in nonlocal quantum field theory, 26:54413 (JINR-P2-6586)
- SACLAY PROTON SYNCHROTRON (SATURNE)
  - beam polarization in, method for preserving, during acceleration, 26:53762
- SAINT LAURENT-DES-EAUX REACTOR (EDF-4)
  - fuel element failure detection system for, modification of, 26:55230
  - fuel meltdown in, radiation protection measures during repair following, 26:55354
- SALEM POWER REACTOR, UNIT 1
  - auxiliary systems for, requested and revised data on, 26:55291 (DOCKET-50272-35)
  - containment system for, requested and revised data on, 26:55291 (DOCKET-50272-35)
  - emergency systems for, requested and revised data on, 26:55291 (DOCKET-50272-35)
  - engineered safeguards for, requested and revised data on, 26:55291 (DOCKET-50272-35)
  - power conversion system for, requested and revised data on, 26:55291 (DOCKET-50272-35)
  - quality assurance program for, requested and revised data on, 26:55291 (DOCKET-50272-35)
  - radiation protection system for, requested and revised data on, 26:55291 (DOCKET-50272-35)
  - radioactive waste disposal system for, requested and revised data on, 26:55291 (DOCKET-50272-35)
  - safety analysis for, requested and revised data on, 26:55291 (DOCKET-50272-35)
  - site for, requested and revised data on, 26:55291 (DOCKET-50272-35)
- SALEM POWER REACTOR, UNIT 2
  - auxiliary systems for, requested and revised data on, 26:55291 (DOCKET-50272-35)
  - containment system for, requested and revised data on, 26:55291 (DOCKET-50272-35)
  - emergency systems for, requested and revised data on, 26:55291 (DOCKET-50272-35)
  - engineered safeguards for, requested and revised data on, 26:55291 (DOCKET-50272-35)
  - power conversion system for, requested and revised data on, 26:55291 (DOCKET-50272-35)

  quality assurance program for, requested and revised data on, 26:55291 (DOCKET-50272-35)
  radiation protection system for, requested and revised data on, 26:55291 (DOCKET-50272-35)
  radioactive waste disposal system for, requested and revised data on, 26:55291 (DOCKET-50272-35)
  safety analysis for, requested and revised data on, 26:55291 (DOCKET-50272-35)
  site for, requested and revised data on, 26:55291 (DOCKET-50272-35)
SALIVARY GLANDS
  radioinduced inflammation of, in man following therapy, 26:53423
SALT DEPOSITS
  cavity construction by leaching in, for natural gas storage, 26:53115
SALTS
  radioisotope diffusion in crushed, 26:53063 (ORNL-4794, pp 33-5)
SAMARIUM
  phase transitions in, at 77 to 300°K, x-ray diffraction technique for study of, (E), 26:55051
  photon reactions (γ,xn) with, model analysis of giant resonance in, (E/T), 26:54598 (FRNC-TH-242)
SAMARIUM ISOTOPES Sm-144
  energy-level scheme from γ resonance scattering, (E), 26:54619
SAMARIUM ISOTOPES Sm-152
  chlorine-35 inelastic scattering at 100 MeV with Coulomb excitation, gamma spectra from, (E), 26:54642
  energy levels from Coulomb excitation, Doppler-shift recoil measurements of lifetimes and transition probabilities for, (E), 26:54642
SAMPLING
  design criteria for confidence and reliability based on small samples, 26:55618 (UCID-16099)
SAN ONOFRE POWER REACTOR, UNIT 1
  safety injection system for, thermal stresses from actuation of, 26:55239 (DOCKET-50206-167)
SAN ONOFRE POWER REACTOR, UNIT 2
  effluents from, effects on environment of radioactive and thermal, 26:55338 (DOCKET-50361-27)
  operation of, requested data on cost-benefit analysis for, 26:55338 (DOCKET-50361-27)
  site for, meteorology and radiation monitoring program for, 26:55338 (DOCKET-50361-27)
SAN ONOFRE POWER REACTOR, UNIT 3
  effluents from, effects on environment of radioactive and thermal, 26:55338 (DOCKET-50361-27)
  operation of, requested data on cost-benefit analysis for, 26:55338 (DOCKET-50361-27)
  site for, meteorology and radiation monitoring program for, 26:55338 (DOCKET-50361-27)
SANDSTONE DEPOSITS
  formation of Grants Region, N. Mex. uranium-bearing, trend orebody studies of, 26:53144 (GJO-936-2)
SATELLITES
  charged-particle flux measurements in ATS-5, at synchronous altitude, low-energy, 26:54045 (NASA-TM-X-2440, pp 530-8)
  effects of Io on Jovian decametric radiation, (T), 26:54004
  radiation dose and LET measurements on OV1-19, April--Dec. 1969, 26:54048 (NASA-TM-X-2440, pp 561-8)
  surface material of, effect of particle energy distribution in plasmasphere during solar eclipse on equilibrium potential of, (T), 26:54054
SAVANNAH RIVER
  ecosystems of swamp forest near, radioisotope content and distribution in, 26:53171(R) (SRO-708-1)
  radioactivity monitoring of, in vicinity of Savannah River Plant, 1971, 26:53153(R) (DPSPU-72-30-1)
SAXTON POWER REACTOR
  decommissioning of, approved technical specifications for surveillance and staffing for, 26:55276 (DOCKET-50146-111)
SCALERS
  driver circuit for, 26:53298 (COO-3058-9)
SCANDIUM
  abundance in γ Cap, (E), 26:53888
SCANDIUM ALLOYS AND SYSTEMS
  H--Sc, properties of, structural and thermodynamic, 26:53556 (SC-CR-723158)
  In--Sc, magnetization and field dependence of sound velocity and thermal capacity of Sc_3In, low-temperature, 26:55045
SCANDIUM ISOTOPES Sc-42
  beta decay of, electromagnetic corrections to ft values for, (T), 26:54713
SCANDIUM ISOTOPES Sc-46
  distribution in Columbia River, effects of seawater on soluble-suspended, 26:53166 (RLO-2227-T-12-28)
SCANDIUM ISOTOPES Sc-50
  energy levels of, calculations using separable nonlocal potential, (T), 26:54683 (FRNC-TH-180)
SCATTERING
  amplitudes free from kinematical singularities, four-fermion, 26:54417
  amplitudes in dual absorptive model, helicity-conserving and helicity-nonconserving pomeron-exchange, 26:54419
  amplitudes of self-energy graphs under analytic regularization, homogeneity violation of renormalized Feynman, 26:54411 (ITF-72-39-P)
  amplitudes of, behavior of Regge trajectories in Veneziano-like representations for, 26:54423
  amplitudes of, derivation of off-shell N-point dual resonance, 26:54420
  amplitudes of, parameter-dependent analytic regularization for renormalized Feynman, 26:54409 (ITF-72-37-P)
  amplitudes of, unitarity constraints on helicity, 26:54418
  amplitudes under scale transformations in scalar field theory, behavior of analytically renormalized Feynman, 26:54410 (ITF-72-38-P)
  amplitudes with Mandelstam analyticity, high-energy behavior of dual, 26:54412 (ITF-72-63-E)
  angular distribution of charged particles in diffraction, diagram for predicting gross structure in, (T), 26:54415
  bremsstrahlung production in potential, soft-photon theorem for, 26:54737
  diffraction, effects of Coulomb field on type of, (T), 26:54415
  Faddeev equations for two- and three-body, factorization of pair potential by Bateman modified method for behavior of approximated phases of, 26:54345 (JINR-P4-6505)
  Glauber theory of, S-matrix approach to, 26:54416
  N/D equations in, Newton--Kantorovich method for coupling constant and convergence conditions for sequence of iterations for Chew--Low, 26:54421
  operators in unbounded domains in, method for meromorphically continuing S-matrix and distorted plane waves associated with elliptic differential, 26:54407 (BNL-16752)
  potential, Hartree one-particle asymptotically exact solutions for quantum mechanical systems with singular attractive, 26:55068 (ITF-72-31-P)
  potential, self-consistent Hartree field as limit for many-body Schroedinger equation for stability of particle systems with singular attractive, 26:54408 (ITF-72-14-E)
  theory for identical-particle, unitarity in inhomogeneous equations method in, 26:54414
SEALS AND GLANDS
  surface flatness of mechanical face, broad source interference method for measuring, 26:55463 (AECL-4208)
SEAWATER
  effects on distribution of soluble-suspended radioisotopes in, 26:53166 (RLO-2227-T-12-28)
  radioisotope transport through, relation of uptake by animals and plants to strontium-90 and zinc-65, 26:53532
  radioisotope uptake from, by ocean sediments, measurements of cerium-144, cesium-137, and thorium-234, 26:53167
SEDIMENTARY DEPOSITS
  analysis of ocean-bed, neutron activation and instrumental methods for, 26:53330(R) (BNWL-1308-10)
SEED
  radiation effects on barley, combined effects of space flight environmental factors on rate of chromosome aberrations, mitosis, and germination of, gamma, 26:53384
SEISMIC WAVES
  propagation from underground nuclear explosions in granite, 26:53131(T) (UCRL-Trans-10616-5)
SELENIUM
  determination in water samples by spark source mass spectroscopy, 26:52914 (ANL-7860(Pt.3), pp 55-63)
  determination of trace amounts of, in tobacco by neutron activation, nondestructive, 26:52907
SELENIUM ISOTOPES Se-75
  uptake of selenomethionine-incorporated, by erythrocytes in γ-irradiated rats, 26:53482
SELENIUM ISOTOPES Se-80
  neutron capture at 25 keV, model analysis of isomeric cross section ratio for, (E/T), 26:54589
SEMICONDUCTOR DEVICES
  radiation effects on, calculations of Jupiter-belt, 26:54002 (NASA-TM-X-2440, pp 781-4)
  radiation hardening of, neutron and gamma, 26:53289 (NASA-TM-X-2440, pp 481-6)
  testing of chips, using electron beam, 26:53315
SEMICONDUCTORS
  analysis for impurity profiles, using secondary ion emission, 26:52937
  exciton energy in crystals of, formulae for longitudinal, (E/T), 26:55065(T) (UCRL-Trans-10643)
  properties of, use of sweeping microscope for studying, 26:55482 (CEA-CONF-2000)
  superconductivity in polar degenerate, (T), 26:54449
  vacuum technique application to, conference at Versailles, France, Sept. 13, 1971, 26:53138
SEPARATION PROCESSES
  reagents for, search for new, pp. 54-5, 26:53084 (ORNL-4794, pp 54-62)
  research progress on, 26:53084 (ORNL-4794, pp 54-62)
SERINE
  radiation effects on single crystals of, at 77 to 340°K, electron nuclear double resonance and ESR studies on x,

  26:52996
  radiolysis of frozen aqueous solutions of, ESR study of free radicals from γ, 26:52995
  radiolysis of single crystals of, at 77 to 340°K, ESR and ENDOR studies on free radicals from x, 26:53004
SEROTONIN
  radiation effects on uptake of, by blood platelets in rabbits in relation to content during acute radiation syndrome, γ, 26:53486
  radioprotective effect on erythropoietic stem cells in mice, proton, 26:53454 (NASA-TM-X-2440, pp 642-6)
SEWAGE
  analysis of aqueous, for tritium by bremsstrahlung counting, 26:52934 (MLM-1368)
  heat sources for processing of, feasibility of use of power plant waste heat for, 26:55212 (CONF-720925-2)
SEYFERT GALAXIES
  resonance-line radiation in differentially expanding atmospheres of, transfer of, (T), 26:53879
  resonance-line radiation in differentially expanding atmospheres of, transfer of, (T), 26:53878
SHEARON HARRIS POWER REACTOR, UNIT 1
  owners of, financial data on, 26:55262 (DOCKET-50400-23)
SHEARON HARRIS POWER REACTOR, UNIT 2
  owners of, financial data on, 26:55262 (DOCKET-50400-23)
SHEARON HARRIS POWER REACTOR, UNIT 3
  owners of, financial data on, 26:55262 (DOCKET-50400-23)
SHEARON HARRIS POWER REACTOR, UNIT 4
  owners of, financial data on, 26:55262 (DOCKET-50400-23)
SHEEP
  radiation effects on, following various combinations of acute, chronic, continuous, and fractionated whole-body exposures, effects of dose and dose rate on γ and x, 26:53451 (NASA-TM-X-2440, pp 622-32)
SHELTERS
  effectiveness of quick-access civil defense, numerical model for, 26:53135 (ORNL-TM-3485(Vol.1))
SHIELDED CONTAINERS
  design and handling criteria for uranium hexafluoride shipping, description of USAEC, 26:53735 (ORO-651(Rev.3))
  design of steel-banded wooden, for shipping slightly enriched uranium metal, billets, ingots, and fuel cores, engineering drawings for, 26:53737
  development for shipping irradiated LMFBR fuel, pp. 15-16, 26:53082 (ORNL-4794, pp 15-25)
  testing of 6M, L-10, and SP5795, under severe environments for shipping plutonium, 26:53736 (SC-DR-720597)
SHIELDING
  calculation for complex space vehicles, SWORD computational techniques for optimal, 26:54957 (NASA-TM-X-2440, pp 368-74)
  calculations for fast reactors, methods development for, 26:55144 (CONF-720901-(Bks.1 and 2), pp 480-98)
  calculations for fast reactors, use of diffusion theory for, 26:55143 (CONF-720901-(Bks.1 and 2), pp 459-70)
  calculations for manned space missions, methods for, 26:54951 (NASA-TM-X-2440, pp 108-16)
  calculations for nuclear rocket internal, discrete ordinates techniques for, (E/T), 26:55368 (NASA-TM-X-2440, pp 449-59)
  calculations for reactors, development of ENDF/B library for, 26:55141 (CONF-720901-(Bks.1 and 2), pp 316-24)
  calculations for reactors, measurement and evaluation of neutron cross sections for, 26:55140 (CONF-720901-(Bks.1 and 2), pp 295-315)
  configuration for Reusable Nuclear Shuttle, (E), 26:54947 (NASA-TM-X-2440, pp 58-64)
  construction of prosthesis, for protection of oral tissues in patients during head and neck radiotherapy, 26:53410
  design for radiation protection, using railway rails, 26:53136(P)
  design for SNAP-8 power system, preliminary, 26:54948 (NASA-TM-X-2440, pp 78-83)
  duct effects on space nuclear, (E/T), 26:54958 (NASA-TM-X-2440, pp 375-82)
  effects on Reusable Nuclear Shuttle design, (E), 26:54954 (NASA-TM-X-2440, pp 251-6)
  electron transport data, parametric fits for spacecraft for 0.1 to 10-MeV, 26:54963 (NASA-TM-X-2440, pp 832-41)
  fabrication of lithium hydride space-reactor, facility for, 26:54949 (NASA-TM-X-2440, pp 92-7)
  gamma dose changes due to layer changes in, use of perturbation theory to determine, 26:54941 (CONF-720901-(Bks.1 and 2), pp 541-58)
  neutron cross-section sensitivity analysis for sodium/iron, 26:54940 (CONF-720901-(Bks.1 and 2), pp 512-23)
  neutron cross-section sensitivity analysis method for, 26:54943 (CONF-720901-6)
  neutron dose changes due to layer changes in, use of perturbation theory to determine, 26:54941 (CONF-720901-(Bks.1 and 2), pp 541-58)
  neutron transport in, developments in integral experiments for fast, 26:54938 (CONF-720901-(Bks.1 and 2), pp 385-96)
  neutron-capture gamma-ray yields of, cascade calculation of, 26:54961 (NASA-TM-X-2440, pp 527-8)
  optimization of, effective multiple-constraint technique for, 26:54942 (CONF-720901-(Bks.1 and 2), pp 574-6)
  optimization of, in design of Reusable Nuclear Shuttle, (T), 26:54946 (NASA-TM-X-2440, pp 48-56)
  radiation dose rate from geomagnetically trapped radiation, 26:54952 (NASA-TM-X-2440, pp 170-7)
  radiation levels on crew in Reusable Nuclear Shuttle, (T), 26:54945 (NASA-TM-X-2440, pp 40-7)
  radiation measurements for NERVA, selection and use of thermoluminescent dosimeters for, 26:53233 (NASA-TM-X-2440, pp 466-70)
  transport problems in, survey of ''benchmark'' integral experiments and reference calculations for, 26:54937 (CONF-720901-(Bks.1 and 2), pp 349-84)
  weight calculation and optimization for rocket reactors, theory used in FASTER-III Monte Carlo program for, 26:54962 (NASA-TM-X-2440, pp 697-705)
  weight requirements for Reusable Nuclear Shuttle, (E), 26:54947 (NASA-TM-X-2440, pp 58-64)
SHIELDING MATERIALS
  testing of beryllium hydride, 26:53714 (NAA-SR-8533)
SHIPPING
  containers and procedures for uranium hexafluoride, USAEC criteria for, 26:53735 (ORO-651(Rev.3))
  containers for plutonium, testing of 6M, L-10, and SP5795, 26:53736 (SC-DR-720597)
  equipment and methods for spent LMFBR fuel elements, pp. 15-16, 26:53082 (ORNL-4794, pp 15-25)
SHOCK WAVES
  interactions of interplanetary double-shock ensemble with Earth's bow shock, MHD theory for, 26:54073
  interactions with plasma, ion heating from collisionless, (E), 26:54766
  observations of Aug. 29, 1966 interplanetary, Pioneer-7 plasma and magnetic-field data for proposal of double-shock ensemble following, (E/T), 26:54068
  phenomena of, from simulated steady-flow interaction of charged particles with geomagnetic dipole field, (E), 26:54056
  production from July 7, 1966 solar flare, piston-driven, (E/T), 26:53970
  propagation in collisionless magnetized plasma, oblique, (T), 26:54852
  propagation in low-density discharge plasmas, turbulence in electrostatic, (E/T), 26:54855
  reflection of MHD, from boundary shock, (T), 26:54159
SILICATE ROCKS
  analysis for vanadium by paper chromatography, neutron activation, and γ spectrometry, 26:52909
SILICIDES
  oxidation resistance of coatings of, on tantalum and its alloys, 26:53613
SILICON
  abundance in 21 sharp-lined nonvariable cool peculiar A stars, (E), 26:53882
  boron content profile determination using secondary ion emission, 26:52937
  charged-particle dechanneling at 1.5 MeV, proton, deuteron, and helium-ion, 26:54988
  determination in water samples by spark source mass spectroscopy, 26:52914 (ANL-7860(Pt.3), pp 55-63)
  dopant location in lattice of, helium-ion channeling study of diffused gold, 26:54987
  ion implantation damage in, electron microscopic observation of surface and depth distribution of, 26:55003
  ion implantation in, precipitation upon annealing of phosphorus-, 26:54994
  ion implantation layers in, computer calculations of sheet resistance of n- and p-type, 26:54986
  ion implantation profile in amorphous, secondary-ion mass spectrometric study of 22-keV boron, 26:55014
  ion implantation-induced expansion of, x-ray topographic study of, 26:55019
  ion implantations in, rod-like defects from 40-keV boron-, 26:54995
  neutron capture by, comparison of ENDF/B III and published data for thermal, 26:54501 (ORNL-TM-3910)
  neutron reactions up to 20 MeV, γ production cross sections for, (E), 26:54523 (CONF-720901-(Bks.1 and 2), pp 325-34)
  oxygen ion reactions at 30 MeV, Kα x-ray spectra from, (E), 26:54467(R) (ORO-2972-204)
  radiation damage in single crystals of, proton-channeling study of fast-neutron, 26:55004
  radiation damage in, neutron and electron, (E/T), 26:54968(R) (AD-737312)
  radiation effects on bulk and thin-film, subthreshold-energy electron, (E/T), 26:55017
  radiation effects on cathodoluminescence spectra of vibronic bands of, γ, 26:54999
  radioinduced defects in, EPR spectra of neutron-, 26:55006
  separation from uranium by fractional dissolution of crude sodium diuranate, 26:52976 (IEA-250)
SILICON CARBIDES
  effects of fiber reinforcements of, on transverse tensile properties of aluminum composites, 26:53687
  fabrication by casting of thermoplastic masses, 26:53586
  Al--B--SiC, development of aluminum--Borsic composite blades for use in advanced composite engine, 26:53575
  Al--B--SiC, fracture properties of Al--Borsic composites,

- dynamic, 26:53557 (SC-DC-721080)
- B--SiC, effects of fiber reinforcements of Borsic on transverse tensile properties of aluminum composites, 26:53687

SILICON IONS
- spectral lines in zeta Oph due to interstellar, (E), 26:53875

SILICON ISOTOPES Si-28
- alpha elastic scattering at 166 MeV, angular distribution for, (E), 26:54547
- alpha inelastic scattering at 10, 12, 14, and 18 MeV, α--γ angular correlations from, (E), 26:54561
- energy levels of, projected Hartree--Fock and shell-model calculations of spins of, (T), 26:54553
- muon (μ^-) capture by, γ-ray yields from, (E), 26:54555
- muon (μ^-) capture by, polarization of emitted neutron in, (T), 26:54564
- neutron radius of, determination from α elastic scattering, (E), 26:54547
- nuclear ground-state deformation from α inelastic scattering, (E), 26:54561
- proton reactions (p,γ) at 0.3 to 3 MeV, γ-ray angular distributions and correlations for, (E), 26:54552 (FRNC-TH-227)

SILICON JUNCTIONS
- electrical parameters of ion-implanted diodes, photovoltaic-effect study of, 26:54975 (RT/EL-(72)2)

SILICON NITRIDES
- diffusion of niobium, tantalum, titanium, and vanadium in, 26:53677
- fabrication by casting of thermoplastic masses, 26:53586

SILICON OXIDES
- boron content profile determination using secondary ion emission, 26:52937
- ion implantation in layers of, for gate MOS structure fabrication, 100-keV gold, 26:53314
- oxygen-16/-18 ratio in biogenic, 26:53178
- radiation damage in, valence-bond model of x-ray spectra, bond breaking, and point-defect production in, (T), 26:55018
- radioinduced defects in, comparison of explosive shock-induced defects with, 26:54983
- spectral lines in xi Per due to interstellar, equivalent widths of, (E), 26:53890
- toxicity of particles of, bibliography on, 26:55585 (ORNL-TIP/TIRC-72-62)
- Al_2O_3--SiO_2, sorptive properties of silver salt-treated, for iodine and methyl iodide, 26:53077 (CONF-720823-9)
- Al_2O_3--SiO_2, viscosity of melts of, 26:55632(T) (UCRL-Trans-1479)
- K_2O--SiO_2--SrO, diffusion in, electrostatic effects and mobility in, 26:53598

SILICON SYSTEMS
- Al-base--Si, tensile properties of boron, Borsic, and silicon carbide fiber-reinforced composites of, transverse, 26:53687
- Mo--Si, diffusion of silicon in Mo_5Si_3 phase in, at high temperatures, 26:53583
- Nb--Si, diffusion of silicon in Nb_5Si_3 phase in, at high temperatures, 26:53583
- Si--Ta, diffusion of silicon in Ta_5Si_3 phase in, at high temperatures, 26:53583
- Si--W, diffusion of silicon in W_5Si_3 phase in, at high temperatures, 26:53583

SILOXANES
- poly(methylhydrogensiloxane), radioinduced oxidation of, and mixtures with cellulose, rate of, 26:52994

SILTS
- characterization of suspended, methods for, 26:55479 (BNWL-SA-4385)
- distribution, properties, and transport of Columbia River, in coastal northeast Pacific Ocean, 26:53165(R) (RLO-2225-T-25-6)
- radioisotope uptake by, from seawater, measurements of cerium-144, cesium-137, and thorium-134, 26:53167
- zinc-65 distribution and concentration in Oregon and Washington continental shelf, 26:53149 (RLO-2227-T-12-26)

SILVER
- determination in meteoritic and terrestrial materials by neutron activation following separation from other elements, 26:52906
- determination in water samples by spark source mass spectroscopy, 26:52914 (ANL-7860(Pt.3), pp 55-63)
- determination in water, effects of large amounts of copper on spectrographic, 26:52927
- diffusion in, grain-boundary self-, 26:55514 (COO-3158-11)

SILVER ALLOYS AND SYSTEMS
- composition and physical properties of composite powders of, 26:53680
- preparation of composite powders of, by hydrogen reduction, 26:53680
- Ag--Cd, phase transformation interfaces in, properties of massive, 26:53644

SILVER BROMIDES
- AgBr--AgCl, positron annihilation in ion-implanted crystals of, measurement of Doppler broadening of photons from, using Ge(Li) detector, 26:54097

SILVER CHLORIDES
- positron annihilation in ion-implanted crystals of, measurement of Doppler broadening of photons from, using Ge(Li) detector, 26:54097
- AgBr--AgCl, positron annihilation in ion-implanted crystals of, measurement of Doppler broadening of photons from, using Ge(Li) detector, 26:54097

SILVER HALIDES
- radioinduced particle tracks in single crystals of, for heavy-ion dosimetry, 26:53230 (NASA-TM-X-2440, pp 138-41)

SILVER IONS
- scattering by argon and neon at 8 to 25 keV, total cross sections and interatomic potentials for, (E), 26:54139

SILVER ISOTOPES Ag-107
- neutron capture by, survey of cross section data for, 26:54657 (FEI-292)

SILVER ISOTOPES Ag-108
- meson (π) reactions at 100 to 260 MeV, Coulomb flux corrections to total cross sections for, (T), 26:54609

SILVER ISOTOPES Ag-109
- deuteron reactions (d,p) at 10 MeV, proton spectra from, (E), 26:54467(R) (ORO-2972-204)
- neutron capture by, survey of cross section data for, 26:54657 (FEI-292)

SINGLE CRYSTALS
- ion channeling and blocking experiments on, apparatus for, 26:54977

SINTERING
- methods for studying initial-stage, review of nonisothermal, 26:53595

SKELETON
- scintiscanning of human, for diagnosis of neoplasms, use of gamma camera in, 26:53214

SKIN
- arsenic-74 uptake and retention by, of mice, rabbits, and rats following oral administration, time dependence of, 26:53538
- radiation effects on cell kinetics of swine, dose dependence of fission neutron, thermal neutron, x, and neutron activation of boron-10 in, 26:53450 (LA-4874, pp 126-44)
- radiation effects on survival of epidermal cells in mouse, following single local exposure, comparison of RBE for carbon, helium, and lithium charged particles with x radiation, 26:53456 (NASA-TM-X-2440, pp 652-8)
- radioinduced atrophy and dermatitis of human, following chronic therapeutic exposure, relation of DNA and RNA contents and ultrastructural changes in epidermis during x, 26:53441
- radioinduced dermatitis in human, following local exposure for therapy of underlying neoplasms, γ, 26:53433
- radioinduced injuries of human, dose-response relationships for, 26:53431
- radioinduced injuries to, of miniature swine, dose and time dependence of electron, 26:53458 (NASA-TM-X-2440, pp 665-71)
- radioinduced ulcers in human, following therapy of mammary carcinomas, surgical treatment of, 26:53438

SODIUM
- analysis of liquid, for copper by neutron activation, 26:52895 (CONF-710959-, Paper 18)
- boiling in, acoustic method for detection of, 26:55083(R) (EURFNR-1001)
- combustion characteristics of mixtures of sodium peroxide and liquid, (E), 26:55178 (RD/B/N-2364)
- compatibility with tantalum at 600°C, effects of oxygen on, 26:53688
- corrosion product release, transport, and deposition in flowing liquid, (E), 26:55164 (CONF-710959-, Paper 8)
- corrosive effects on austenitic stainless steel, effects of temperature on, (E/T), 26:55168 (CONF-710959-, Paper 12)
- corrosive effects on irradiated 300 series stainless steels of flowing liquid, 26:55165 (CONF-710959-, Paper 9)
- corrosive effects on stainless steels of flowing liquid, 26:55166 (CONF-710959-, Paper 10)
- corrosive effects on Type-316 stainless steel of liquid, measurement of, 26:55173 (CONF-710959-, Paper 17)
- cover gas systems for, problems of impurities in, 26:55171 (CONF-710959-, Paper 15)
- decontamination of coolant, procedures during reactor dismantling for, 26:55147 (AI-AEC-Memo-12736)
- determination in environmental samples by neutron activation, 26:52897 (CONF-721010-3)
- disposal of coolant, procedures during reactor dismantling for, 26:55147 (AI-AEC-Memo-12736)
- distribution and excretion of exchangeable, in rats during irradiation hypertension, sodium-22 tracer study of, 26:53463
- flow measurements of liquid, testing of transit time flowmeter for, 26:53305 (LMEC-72-4)
- flow through fuel element assemblies of liquid, effects of partial blockage on distribution of, 26:55176 (KFK-1548)
- impurities in liquid, vacuum distillation method for determination of carbon, chlorine, hydrogen, and oxygen, 26:55170 (CONF-710959-, Paper 14)
- mass transfer of activated material in, test loop for studies of, 26:53121 (CONF-710959-, Paper 7)
- neutron attenuation by slabs of, benchmark measurements of, (E/T), 26:55142 (CONF-720901-(Bks.1 and 2), pp

  418-30)
  neutron cross-section sensitivity analysis for sodium/iron shielding, 26:54940 (CONF-720901-(Bks.1 and 2), pp 512-23)
  neutron emission time in assembly of, 26:54656(R) (COO-3058-21)
  neutron transport in sodium/iron shield, effect of cross section sensitivity on 300-keV to thermal-range, (T), 26:54943 (CONF-720901-6)
  plugging temperature indicator for liquid, design of, 26:53116
  reactions with hydrogen from 300 to 450°C, 26:55154 (CONF-710548-, pp 105-28)
  reactions with sodium hydroxide from 300 to 450°C, 26:55154 (CONF-710548-, pp 105-28)
  reactions with water from 350 to 600°C, effects on rupture of austenitic steel of, 26:55161 (CONF-710548-, pp 221-42)
  reactions with water in steam generators, tube damage from, 26:55150 (CONF-710548-, pp 1-16)
  reactions with water of liquid, design of equipment for studying, 26:55153 (CONF-710548-, pp 57-104)
  reactions with water, brief summary of studies in Italy on, 26:55160 (CONF-710548-, pp 213-20)
  reactions with water, conference on, 26:55149 (CONF-710548)
  reactions with water, effects on temperature and pressure of, 26:55152 (CONF-710548-, pp 39-56)
  reactions with water, kinetics of, 26:55155 (CONF-710548-, pp 129-54)
  reactions with water, pressure wave from, 26:55157 (CONF-710548-, pp 171-86)
  reactions with water, summary of study of large-scale, 26:55158 (CONF-710548-, pp 187-205)
  reactions with water, use of hydrogen detector for detection of, 26:55156 (CONF-710548-, pp 155-70)
  shipping of irradiated, from Hallam Power Reactor, 26:55147 (AI-AEC-Memo-12736)
  solvent properties for cesium, copper, antimony, bromine, and iodine, tracer studies on, 26:52895 (CONF-710959-, Paper 18)
  solvent properties for hydrogen, oxygen, and sodium hydroxide, 26:55154 (CONF-710548-, pp 105-28)
SODIUM BORIDES
  chemical properties of NaB$_6$, 26:55560(T) (LA-tr-72-16)
SODIUM CHLORATES
  radiation effects on crystals of, studies on γ and x, 26:52984 (FRNC-TH-262)
SODIUM CHLORIDES
  charged-particle dechanneling at 1.5 MeV, proton, deuteron, and helium-ion, 26:54988
  corrosive effects of sprays of, on niobium--uranium-base alloys, protective effects of polyurethane-painted surface on stress, 26:53607 (RFP-1891)
  gas-flow properties of dry crushed, (E), 26:53724 (ORNL-TM-3815)
  ion emission by electron-bombarded, mass-spectral analysis of, 26:54084
  particle track sizes in monocrystals of, proton and alpha-, (E), 26:55016
  radiation effects on spectra of hexacyanocobaltate-doped, x, 26:55001
  radioinduced color centers in, by 10- to 50-keV electron beams, (E), 26:54973 (FRNC-TH-210)
  radioinduced fast recombination luminescence in, lifetime and temperature dependence of proton-pulse, 26:55000
SODIUM FLUORIDES
  performance of secondary coolant for molten salt fueled reactor, (E), 26:55177 (ORNL-TM-3344)
SODIUM FLUOROBORATES
  performance of secondary coolant for molten salt fueled reactor, (E), 26:55177 (ORNL-TM-3344)
SODIUM HYDRIDES
  NaH--Na$_2$O--NaOH, physical properties of, 26:55158 (CONF-710548-, pp 187-205)
SODIUM HYDROXIDES
  reactions with sodium from 300 to 450°C, 26:55154 (CONF-710548-, pp 105-28)
  solubility in sodium, 26:55154 (CONF-710548-, pp 105-28)
  NaH--Na$_2$O--NaOH, physical properties of, 26:55158 (CONF-710548-, pp 187-205)
SODIUM IONS
  reactions with lithium, two-state impact-parameter calculations of total cross sections for charge exchange in, 26:54127
  scattering by argon and neon at 8 to 25 keV, total cross sections and interatomic potentials for, (E), 26:54139
SODIUM ISOTOPES Na-20
  beta decay of, resolutions of apparent anomaly in superallowed, (E), 26:54550 (COO-535-671)
SODIUM ISOTOPES Na-22
  abundance in iron meteorites, (T), 26:53808(T) (ORNL-tr-2620)
  effects on electrophoretic behavior of sodium in sulfuric acid solution, 26:52967
  energy levels from resonances in neon-20 (d,α) reactions, (E), 26:54467(R) (ORO-2972-204)
SODIUM ISOTOPES Na-23
  neutron capture by, comparison of ENDF/B III and published data for thermal, 26:54501 (ORNL-TM-3910)
SODIUM ISOTOPES Na-24
  effects on electrophoretic behavior of sodium in sulfuric acid solution, 26:52967
  use as tracer for measuring catalyst circulation rates in catalytic cracking unit, 26:53343
SODIUM NIOBATES
  radiation effects on dielectric constants and crystal structure of, electron and γ, 26:55020
SODIUM NITRITES
  effects on hemopoietic and vascular system of mammal, 26:55577 (ORNL-TIP/TIRC-72-45)
SODIUM OXIDES
  NaH--Na$_2$O--NaOH, physical properties of, 26:55158 (CONF-710548-, pp 187-205)
SODIUM PEROXIDES
  combustion characteristics of mixtures of liquid sodium and, (E), 26:55178 (RD/B/N-2364)
SODIUM URANATES
  processing of crude, by fractional dissolution, production of uranyl nitrate by, 26:52976 (IEA-250)
SOILS
  analysis for plutonium, sample size for fusion method for, 26:52935(R) (MLM-1888)
  analysis for trace amounts of cobalt by instrumental neutron activation, 26:52904
  cesium-137 distribution in Puerto Rican, 26:53162 (ANL-7860(Pt.3), pp 1-13)
  movement of radioisotopes and water in, 26:53459(R) (NP-19403)
  radioisotope release to plants from continuously cropped uniformly contaminated, effects of clinoptilolite on cesium-137 and strontium-90, 26:53540
  radioisotope release to plants from surface contaminated, effects of clinoptilolite on cesium-137 and strontium-90, 26:53540
  sorptive properties for radioisotopes, near Baguio City, Philippines, (E), 26:53175
  tritium transport through, independent test of Argonne model for, 26:53163 (ANL-7860(Pt.3), pp 32-7)
SOL-GEL PROCESS
  microsphere production in, p. 93-4, 26:53085 (ORNL-4794, pp 91-5)
SOLAR CELLS
  radiation damage at synchronous altitudes by solar flares, 26:53927 (NASA-TM-X-2440, pp 193-208)
  radiation effects on silicon, near interface of materials of different atomic number, 26:53290 (NASA-TM-X-2440, pp 577-83)
SOLAR CORONA
  current dissipation in, (T), 26:53937
  dust density in, (T), 26:53938
  electron densities of, (E), 26:53958
  electron density in, (T), 26:53938
  electron density of enhanced region in, (E), 26:53957
  generation of Type III radio bursts in, (E/T), 26:53964
  heating of, Rayleigh--Taylor instability in composite medium, (T), 26:53940
  hydrodynamics of large streamer observed during eclipse of Mar. 7, 1970, (E), 26:53956
  magnetic fields in, atlas of, (E), 26:53955
  model for studying Type III bursts, (E/T), 26:53934
  radio emission sources in, positions of continuum, (E), 26:53935
  spectra of, Z dependence of level intervals in $2s^22p^2$, $2s^22p^3$, and $2s^22p^4$, (E), 26:53954
  temperature of enhanced region in, (E), 26:53957
  ultraviolet observations of holes in, extreme, (E), 26:53939
  x-ray photography of, (E), 26:53958
SOLAR FLARES
  current limitations in, (T), 26:53937
  development of, relation with ejection of keV electrons, (T), 26:53968
  effects on solar-wind disturbances, association with interplanetary magnetic field structure, (E/T), 26:54076
  electron production from, associated with sunspot groups that emit meter type-I noise storms, relativistic, (T), 26:53968
  energy releases from Oct. 4, 1965, Jan. 18 and July 7, 1966, comparison of analytical and numerical techniques for determination of mechanical, (E/T), 26:53970
  gamma flux during, solar, (E), 26:53967
  magnetosonic waves in, nonlinear, (T), 26:53941
  neutron flux during, solar, (E), 26:53967
  particle event of Mar. 21, 1969, polar-cap measurements of solar-flare protons with energies down to 12.4 keV following, (E), 26:54071
  particle flux from, time and distance dependence of, (T), 26:53929 (NASA-TM-X-2440, pp 336-44)
  particle propagation in, Fokker--Planck equation for, (E), 26:53932
  particle radiation from, review, 26:53927 (NASA-TM-X-2440, pp 193-208)
  proton fluxes from, short-term prediction of, 26:53931 (NASA-TM-X-2440, pp 356-61)
  proton-to-alpha ratio during, variations of, (E), 26:53966
  radiation dose and LET measurements on OV1-19 satellite, April--Dec. 1969, 26:54048 (NASA-TM-X-2440, pp 561-8)
  radiation dose rate measurements at SST altitudes, 26:54889 (NASA-TM-X-2440, pp 902-7)
  radiation doses inside space vehicle during

  interplanetary voyage, MCFLARE calculations, 26:54956 (NASA-TM-X-2440, pp 324-8)
  radio observations of, of Oct. 24, 1969, (E), 26:53959
  white-light continuum emission in, mechanism for, (E/T), 26:53961
  x-ray emission during, polarization of, (E), 26:53962
  x-ray observations of, Oct. 24, 1969, (E), 26:53959
SOLAR PARTICLES
  hazards to space missions from proton events, probability analysis of, 26:54955 (NASA-TM-X-2440, pp 310-23)
  hazards to space travel, statistical treatment of, 26:53930 (NASA-TM-X-2440, pp 345-55)
  proton events and doses in 19th and 20th cycles, 1964-70, 26:53928 (NASA-TM-X-2440, pp 329-35)
SOLAR PROMINENCES
  electric currents in quiescent, (T), 26:53950
  magnetic fields in quiescent, (T), 26:53950
  spectra of, ionized helium in, (T), 26:53949
SOLAR RADIATION
  doses to crew and passengers at SST altitudes, 26:54888 (NASA-TM-X-2440, pp 894-901)
  effects on earths heat balance, 26:53193
  monitoring in stratosphere for SST Concorde flight, hybrid detector system for, 26:53203 (NASA-TM-X-2440, pp 874-83)
SOLAR RADIO BURSTS
  acceleration mechanism in Type III, role in soft x-ray source volume, (E/T), 26:53963
  continua during initial stage of Type IV, time behavior of, (E/T), 26:53965
  distribution of Type III, as a function of heliocentric longitude, (E/T), 26:53934
  electron energy losses in, (E/T), 26:53961
  electron temperatures of small 3-cm, (E), 26:53960
  generation mechanism for Type III, (E/T), 26:53964
  observations of, associated with flare of Oct. 24, 1969, (E), 26:53959
  position measurements of Type III sources, (E), 26:53935
  relation of small 3-cm, to transient features on $H\alpha$ films, (E), 26:53960
  visibility of Type III, model for, (E/T), 26:53934
SOLAR SYSTEM
  formation of planets in, (T), 26:54005
SOLAR WIND
  cosmic-ray modulation by, anisotropy responsible for solar semidiurnal variations from, (T), 26:53812
  cosmic-ray modulation by, anisotropy responsible for solar semidiurnal, (T), 26:53813
  disturbances in, magnetic-field structure in solar-flare-associated, (E/T), 26:54076
  electron measurements on Apollo-15 subsatellite, high-energy, (E), 26:54072
  energy transport in, models for, (T), 26:53942
  measurements in extended magnetotail at approximately 1000 R/sub E/, (E), 26:54074
  parameters from analysis of three-station interplanetary scintillation measurements of small-diameter cosmic radio sources, (E/T), 26:54070
  particle shadowing by Moon, (T), 26:53943
  phenomena of, relation with creation of polar auroras, (E/T), 26:54043
  plasma torque on Earth ionosphere, upper limit of magnetospheric boundary-layer, (T), 26:54075
SOLAR X-RAY BURSTS
  electron energy losses in, (E/T), 26:53961
  observations of, associated with flare of Oct. 24, 1969, (E), 26:53959
  polarization of, (E), 26:53962
  source volume of, role of Type III acceleration mechanism in, (E/T), 26:53963
SOLID SOLUTIONS
  crystal structure of, field-ion microscope studies of, 26:53652
  microstructure of, studies of ion microscopy images from, 26:53655
SOLIDS
  analysis of surfaces of, by electron emission induced by low-energy ion bombardment, 26:52936 (RT/EL-(72)4)
  atom elastic scattering by surfaces of, model for, based on pairwise interaction potential, 26:54089
  conference on light scattering in, Paris, France, 7/71, 26:55041
  heating of small grains by electron and ion bombardment, collision processes in, (T), 26:54874 (EUR-CEA-FC-647)
  ion implantation facility at Orsay, France, 26:54976
  light dispersion in absorption region by impurity centers, 26:55539 (ITF-72-67-P)
  radiation damage profiles in, computer program for ion, 26:54969 (AECL-4130)
  radiation effects on, heat-flow analysis of temperature spikes following Coulomb excitation, (E/T), 26:54646
  radioinduced destruction of, pulse electron, 26:55012
  spectra of, surface effects on optical, 26:55537 (ITF-72-40-P)
  vibrational excitations in amorphous and crystalline, high pressure and infrared and Raman spectroscopy methods for studies of, 26:55502(R) (COO-2126-7)
SOLUTIONS
  photolysis of aqueous, search for H_3O radical from, 26:53026
  radiolysis of aqueous, reactions of hydrated electrons in pulse, 26:53006
SOLVENT EXTRACTION PROCESSES
  control of Eurex, mass spectrometric analysis of uranium for, 26:52918 (EUR-4765, pp 91-115)
SOUND
  propagation in nonisothermal fully ionized gas, dispersion relation for, (T), 26:54858
SOUTH AMERICA
  radioisotope uses in hydrology in, 26:53168
SOUTHWEST EXPERIMENTAL FAST OXIDE REACTOR
  Doppler reactivity feedback in, measurements of transient, 26:55123 (CONF-720901-(Bks.1 and 2), pp 986-1005
SPACE
  book: Measurement of Radiation in Space, 26:53276
  conference on natural and manmade radiation in space, Las Vegas, Nev., 3/71, 26:54870 (NASA-TM-X-2440)
  radiation dose analysis for manned missions, methods for, 26:54951 (NASA-TM-X-2440, pp 108-16)
  radiation protection criteria for nuclear power in, 26:54921
  research in India, 1971--1972, 26:55452(R) (NP-19407)
  shock waves in interplanetary, MHD theory for Earth's bow-shock interaction with double-shock ensemble of, 26:54073
  shock-wave observations in interplanetary, Aug. 29, 1966 Pioneer-7 plasma and magnetic-field data for proposal of double-shock ensemble, (E/T), 26:54068
  teleoperators for remote operation in, design and objectives for, 26:53730 (NASA-TM-X-2440, pp 277-9)
SPACE FLIGHT
  effects of environment during, on gamma sensitivity of barley seeds, 26:53384
  effects of environment during, on gamma-irradiated Tradescantia, cytologic and mutagenic, 26:53382 (N-72-20054)
  effects of environment during, on growth of γ-irradiated bacteria, 26:53364 (N-72-20063)
  effects of environment during, on organisms, combined effects of gamma on mutagenesis and survival of insects, microorganisms, and plants, 26:53365 (N-72-20065)
  proton dose calculations using USAF--NASA model man, 26:54883 (NASA-TM-X-2440, pp 773-80)
  radiation dose measurements on Apollo missions, 26:54953 (NASA-TM-X-2440, pp 215-19)
  radiation dosimetry during Apollo, plastic track detector measurements of high-Z particle, 26:53231 (NASA-TM-X-2440, pp 149-56)
  radiation hazards from solar cosmic-ray protons, statistical treatment of, 26:53930 (NASA-TM-X-2440, pp 345-55)
  radiation hazards from solar proton events, probability analysis of, 26:54955 (NASA-TM-X-2440, pp 310-23)
  radiation hazards to astronauts during prolonged, cosmic, 26:53408 (NASA-TM-X-2440, pp 1007-15)
  radiation hazards to man during, extrapolation of clinical data on dose-response-time relations to estimate, 26:53402 (NASA-TM-X-2440, pp 398-415)
  radiation protection guides for, involving nuclear systems, 26:54913
  radioinduced phosphene formation in eyes of astronauts during, cosmic, 26:53407 (NASA-TM-X-2440, pp 1002-6)
  teleoperator systems for manned, developments in, 26:53731 (NASA-TM-X-2440, pp 280-90)
SPACE VEHICLES
  attitude measurements for, radiation effects on photomultiplier star sensor system for, 26:53293 (NASA-TM-X-2440, pp 735-43)
  configuration of Reusable Nuclear Shuttle, impact of radiation dose on, (T), 26:54945 (NASA-TM-X-2440, pp 40-7)
  design of Reusable Nuclear Shuttle for maximum shielding, (E), 26:54954 (NASA-TM-X-2440, pp 251-6)
  electron shielding calculations, parametric, 26:54963 (NASA-TM-X-2440, pp 832-41)
  instruments for Grand Tour, protective design for radiation effects on, 26:53292 (NASA-TM-X-2440, pp 729-34)
  neutron production by ions in walls of, estimates of, 26:54881 (NASA-TM-X-2440, pp 520-2)
  power systems for manned, developments in nuclear, 26:53094 (NASA-TM-X-2440, pp 26-33)
  power systems for, developments in nuclear, 26:53093 (NASA-TM-X-2440, pp 13-25)
  radiation analysis of vehicle and payload configurations for Reusable Nuclear Shuttle, (T), 26:54947 (NASA-TM-X-2440, pp 58-64)
  radiation dose to, from radioisotope thermoelectric generator, environmental analysis of γ and neutron, 26:53338 (NASA-TM-X-2440, pp 862-5)
  radiation doses inside, during interplanetary voyage, MCFLARE calculations, 26:54956 (NASA-TM-X-2440, pp 324-8)
  radiation dosimetry at space stations, advanced dosimetry systems for, 26:53235 (NASA-TM-X-2440, pp 944-56)
  radiation dosimetry in Skylab space station, dosimeters for, 26:53236 (NASA-TM-X-2440, pp 958-73)
  radiation effects on components and subsystems of, design parameters and test facilities for testing, 26:53695 (NASA-TM-X-2440, pp 570-6)

- radiation effects on, calculations of Jupiter-belt, 26:54002 (NASA-TM-X-2440, pp 781-4)
- radiation effects on, design considerations for thermoelectric generator for simulated in-flight testing of, 26:53095 (NASA-TM-X-2440, pp 844-9)
- radiation environment effects on Reusable Nuclear Shuttle system, (T), 26:54946 (NASA-TM-X-2440, pp 48-56)
- radiation environment for rendezvous and docking with nuclear rockets, 26:55361 (NASA-TM-X-2440, pp 257-63)
- radiation environment from reusable nuclear shuttle to orbiting lunar station and lunar surface, (T), 26:55362 (NASA-TM-X-2440, pp 264-9)
- radiation protection for crew of, powered by gas-core nuclear rocket, (T), 26:54967
- radiation safety criteria for, 26:54921
- radiation shielding of experiments on Skylab, 26:54049 (NASA-TM-X-2440, pp 748-55)
- radiation sources on Apollo, identification and control of, 26:53255 (NASA-TM-X-2440, pp 714-22)
- reactor descriptions for, (T), 26:54950 (NASA-TM-X-2440, pp 98-102)
- roll control of, during reentry, fluidically actuated monopropellant hydrazine system for, 26:55600 (SC-DC-722244(RD))
- shielding analysis, SWORD computational techniques for, 26:54957 (NASA-TM-X-2440, pp 368-74)
- shielding calculations, methods for, 26:54951 (NASA-TM-X-2440, pp 108-16)
- shielding for reactor power systems in, (E), 26:54949 (NASA-TM-X-2440, pp 92-7)
- shielding requirements for unmanned, with thermionic reactor ion propulsion system, (T), 26:55364 (NASA-TM-X-2440, pp 292-8)
- shields for, effects of ducts on effectiveness of, (E/T), 26:54958 (NASA-TM-X-2440, pp 375-82)
- sterilization of bacteria and fungi on components of, research program on pre-flight, 26:53367(R) (SC-RR-720516)
- thermal insulation for nuclear powered, data plot for optimization of, (T), 26:55366 (NASA-TM-X-2440, pp 392-6)

SPECTROMETERS
- description of annihilation, for measuring cross sections for anti p + p interactions, 26:53279
- description of charged-particle, for space radiation, 26:53235 (NASA-TM-X-2440, pp 944-56)
- design and performance of helium recoil, for high-energy particles, 26:53281
- design of 2π-steradian magnetic, with low aberration for high-energy physics, 26:53284
- magnets for magnetic-lens, design and fabrication of high-performance window frame-type, 26:53296 (CEA-N-1539)

SPECTROSCOPY
- methods for analysis of very small samples, 26:52929
- principles of micro-emission, using solid-state lasers, 26:55589(T) (ORNL-tr-2603)
- sensitivity of localized, using lasers, 26:55590(T) (ORNL-tr-2613-A)

SPERM
- radioinduced chromosome aberrations in mature, of Drosophila melanogaster, inhibitory effects of dactinomycin on post-fertilization maternal repair of x, 26:53502
- radioinduced dominant and recessive lethal mutations in mature, of Drosophila melanogaster, effects of dactinomycin on post-fertilization expression of x, 26:53502

SPERMATOGENESIS
- radioinduced inhibition of, in man following exposure of testes, dose and time dependence of x, 26:53399 (NASA-TM-X-2440, pp 229-32)

SPHERES
- neutron reaction rates in homogeneous, calculation neglecting elastic scattering in fast, 26:54491

SPINAL CORD
- radioinduced injuries of human, following therapy, etiology of, 26:53429
- radioinduced myelopathy in human, following therapy, role of vascular changes in pathogenesis of γ, 26:53425

SPINELS
- preparation of polycrystalline, by freeze drying method, 26:55564 (LBL-876)

SPLEEN
- arsenic-74 uptake and retention by, of mice, rabbits, and rats following oral administration, time dependence of, 26:53538
- radioinduced suppression of antibody-forming cells in mouse, during response to antigen challenge, acute whole-body x, 26:53464
- scintiscanning of human, for diagnosis of neoplasms, use of gamma camera in, 26:53214

STAINLESS STEEL
- carbon activity and solubility in, 26:55480(T) (BNWL-tr-72)
- carbon activity and solubility in, 26:55481(T) (BNWL-tr-73)
- coating with carbon from carbon monoxide decomposition in argon coolant at 550 to 600°C, 26:53605(R) (DP-Report-522)
- corrosion by fission products, effects of burnup on, 26:55187 (EURFNR-989)
- corrosion by flowing liquid sodium, 26:55166 (CONF-710959-, Paper 10)
- corrosion by flowing sodium of irradiated 300 series, 26:55165 (CONF-710959-, Paper 9)
- corrosion by liquid sodium of austenitic, effects of temperature on, (E/T), 26:55168 (CONF-710959-, Paper 12)
- corrosion by liquid sodium of Type-316, measurement of, 26:55173 (CONF-710959-, Paper 17)
- corrosion of Type 304L, by thorium dioxide dissolvent solutions, 26:53604 (BNWL-CC-449)
- creep and stress relaxation properties of, interrelationship of, 26:53642 (STU-70-419/U-350(Pt.1.2))
- creep behavior and rupture of titanium-stabilized 1515, effects of thermomechanical treatments on, 26:53635(T) (EURFNR-998)
- creep rupture of Type 316, at 980°K, cyclic, 26:53690
- creep rupture of Type 316, effects of injected helium on, 26:53703
- deposition of irradiated 300 series, in flowing liquid sodium, 26:55165 (CONF-710959-, Paper 9)
- fabrication of capsules of Types 304 and 316, for cesium sources, 26:53330(R) (BNWL-1308-10)
- fatigue testing of pipes of Type-304 and Type-304L, failure rates from, 26:55175(R) (GEAP-10207-26)
- helium release in annealing of Type 316 and 18/8, 26:53709
- mass transfer by liquid sodium of Type-316, effects of stresses on, 26:55173 (CONF-710959-, Paper 17)
- mechanical properties of welds in Types 304 and 316, at 900 to 1300°F, literature review on, 26:53638 (ORNL-4781)
- neutron total cross sections at 1.2 to 11 MeV for, experimental check for, 26:54965 (ORNL-TM-3871(Rev.))
- preparation of molybdenum and tungsten fiber-reinforced, with precise alignment and uniform distribution, method for, 26:53629
- radiation damage in Type 304, electron microscopic study of 650-kV electron, 26:54972 (COO-2119-2)
- radiation effects in embrittlement of Type 304 and Type 316, fast neutron, 26:55083(R) (EURFNR-1001)
- radiation effects on fatigue crack propagation in Types 304 and 316, at 427 to 593°C, neutron, 26:53698 (NRL-7446)
- radiation effects on mechanical properties and structure of, neutron, 26:53701 (STU-70-419/U-350(Pt.1.1))
- radiation effects on swelling and mechanical properties of Type 316, Type 321, and Type 347, fast neutron, (E), 26:55189(R) (GEAP-10028-39)
- radiation effects on swelling and mechanical properties of Type-304, Type-316, Type-321, and Type-321-H, fast neutron, 26:55190(R) (GEAP-10028-42)
- radiation effects on tensile properties of Type 347, at cryogenic temperatures for use in NERVA Program, fast neutron, 26:53697 (NASA-TM-X-2440, pp 603-8)
- standards for forgings of, 26:53640 (RDT-M-2-2-T(8-72))
- testing of fuel jacket cladding tubing of Type 316, eddy current method of, 26:53125

STANDARDS
- BF_3 gamma-tolerant neutron detector tubes, 26:53204 (RDT-C-15-11-T(8-72))
- butterfly-type isolation valves, 26:53111 (RDT-E-1-13-T(8-72))
- conference on radiation protection standards, Richland, Wash., 11/71, 26:54922
- development and writing of, procedures for, 26:53248
- development of radiation, for tritium content in nuclear stimulated natural gas, 26:53134
- development of reactor engineering, during May and June 1972, 26:55207(R) (ORNL-TM-3900)
- development of reactor equipment maintenance, 26:55201 (DUN-SA-168)
- for evaluation of radiation dosimeters, critique of, 26:53247
- hoisting and rigging of critical components and related equipment, 26:53112 (RDT-F-8-6-T(8-72))
- manufacturing specification for high-temperature thermocouples for use in nuclear irradiation experiments, 26:53301 (EUR-4807)
- reactor Class 1 components, supplement to high temperature requirements of, 26:55208 (RDT-F-9-1-T(8-72))
- stainless and low-alloy steel forgings (ASME SA-182 with additional requirements), 26:53640 (RDT-M-2-2-T(8-72))
- thermowell systems for liquid metal service, 26:55219 (RDT-C-7-18-T(8-72))

STAR CLUSTERS
- age of NGC 6530, 26:53883
- distance of NGC 6530, (E), 26:53883
- dynamics of, (T), 26:53982
- membership in NGC 6530, (E), 26:53883
- pulsation of main-sequence stars in open, short-period, (E/T), 26:53872
- spectra of five globular, in M31, (E), 26:53880
- spectra of four globular, composite, (E), 26:53880
- variability of A and B stars in Pleiades, (E), 26:53871

STARCHES
- preparation of labeled, by tritium atom bombardment, 26:53028 (COO-584-50)

STARS
  atmospheres of, Rayleigh--Taylor instability in composite medium, (T), 26:53940
  carbon abundance in V553 Cen and RT TrA, (E), 26:53899
  collisions of, dynamics of, (T), 26:53982
  color indices of supergiant and OB, (E), 26:53884
  cosmic particle acceleration by white-dwarf, (T), 26:53854
  element abundances in 21 sharp-lined nonvariable cool peculiar A, (E), 26:53882
  energy loss by neutrino pair production in, Weinberg theory of weak and electromagnetic interactions for, (T), 26:53893
  envelopes of luminous red-giant, relaxation oscillations in, (T), 26:53874
  evolution from formation to main sequence, (T), 26:53903
  evolution from main sequence to death, (T), 26:53978
  evolution of 0.60 solar-mass horizontal-branch, effects of semiconvection on, (T), 26:53885
  evolution of helium, (E/T), 26:53896
  evolution of homogeneous model, (T), 26:53886
  helium abundance in subdwarf HD 49798, (E), 26:53900
  identification of EX Hydrae with x-ray source 2ASE 1253-28, (E), 26:53895
  interpretation of B subdwarf, in halo, (T), 26:53891
  iron abundance in 120 evolved, (E), 26:53898
  light curve of Am CVn, (E), 26:53902
  light variations in supergiant and OB, (E), 26:53884
  luminosity of o Cet B, (E), 26:53901
  magnetic-field variations in 78 Vir, βCBr, and 73 Dra, (E), 26:53876
  model for Am CVn, (E), 26:53902
  model for Sco X-1 featuring white-dwarf, (E), 26:53917
  models for extremely blue horizontal-branch, (T), 26:53891
  motions of, kinematics of, (T), 26:53982
  noble-gas abundances in extreme Population I, (T), 26:53892
  periodic variability of HD 111133, (E), 26:53877
  photometry of Am CVn, (E), 26:53902
  photometry of mira, ultraviolet, (E), 26:53901
  photometry of rapid blue variable EX Hydrae, (E), 26:53895
  photometry of RY Sgr, (E), 26:53905
  photometry of Wolf--Rayet, infrared, (E), 26:53889
  proper motions for 363, in vicinity of NGC 6530, (E), 26:53883
  properties of Cepheid variable, (E/T), 26:53986
  pulsation of main-sequence, in open clusters, (E/T), 26:53872
  pulsation periods for A and B, in Pleiades cluster, (E), 26:53871
  resonance-line radiation in differentially expanding atmospheres of, transfer of, (T), 26:53878
  resonance-line radiation in differentially expanding atmospheres of, transfer of, (T), 26:53879
  spectra of 3 RCB, in LMC, (E), 26:53904
  spectra of homogeneous, secular, (T), 26:53886
  spectra of subdwarf HD 49798, non-LTE analysis of, (E), 26:53900
  spectra of Vega, ultraviolet absorption lines in, (E), 26:53887
  spectra of xi Per, equivalent widths of interstellar molecular lines in, (E), 26:53890
  spectra of zeta Oph, interstellar lines in uv, (E), 26:53875
  spectra of, study of unidentified interstellar diffuse features in, (E), 26:53881
  spectral analysis of γ Cap, (E), 26:53888
  spectroscopy of RY Sgr, (E), 26:53905
  structure of helium, (E/T), 26:53896
  variability of A and B, in Pleiades cluster, (E), 26:53871
STATISTICS
  binomial distribution and Gaussian distribution in radiation measurements, 26:53207
  Boltzmann distribution law for, derivation of, 26:55071 (LA-4868)
  design criteria for confidence and reliability based on small samples, 26:55618 (UCID-16099)
STEAM
  corrosive effects on H327 graphite, (E), 26:55207(R) (ORNL-TM-3900)
  H_2O--steam, flow in turbines, equipment and methods for studying, 26:53124
STEAM POWER PLANTS
  costs for, computer program for calculation of capital, 26:55265 (ORNL-TM-3743)
STEEL
  analysis for molybdenum by potentiometric titration, 26:52924
  analysis for tritium by bremsstrahlung counting, 26:52934 (MLM-1368)
  analysis for uranium by extraction--photometric method, 26:52922
  analysis for uranium by x-ray fluorescence method, photometric method for calibrating, 26:52922
  coating with carbon from carbon monoxide decomposition in argon coolant at 550 to 600°C, 26:53605(R) (DP-Report-522)
  crack tolerance of A533B, effects of strain gradients on gross strain, 26:53634 (CONF-720806-3)
  fabrication by hot isostatic pressing, 26:53578
  fatigue testing of pipes of carbon, failure rates from, 26:55175(R) (GEAP-10207-26)
  fracture toughness of ASTM A553-A, HP 9-4-20, PH 13-8Mo, and 18 Ni maraging, at room and subzero temperatures, measurement of plane strain, 26:53661
  grain structure of annealed, effects of austenite grain size on ferrite banded, 26:55593(T) (RFP-Trans-108)
  mechanical properties of welds in low-alloy, at 900 to 1300°F, literature review on, 26:53638 (ORNL-4781)
  properties of French Cor-Ten, for use in nuclear power plants, 26:53612
  radiation effects on strengthening of Type A302 pressure vessel, effects of copper and vanadium additions on, neutron, 26:53710
  reactions with hydrogen, literature review on, 26:53606 (MLM-1355)
  standards for forgings of low-alloy, 26:53640 (RDT-M-2-2-T(8-72))
  stress in hardened, x-ray methods of measuring residual, 26:55594(T) (RFP-Trans-110)
  Cr--Mo--steel, corrosion by products of sodium--water reactions, 26:55154 (CONF-710548-, pp 105-28)
  Mn--Mo--Ni--steel, mechanical properties of pressure vessel, effects of quenching, tempering, and heat treatment on, 26:53646
STEEL COUPLES
  Cu/steel, corrosion by water at ambient temperature, fretting, 26:53609 (RT/ING-(72)7)
  steel/Zircaloy-2, corrosion by air, nitrogen, and water at ambient temperature, fretting, 26:53609 (RT/ING-(72)7)
STELLAR FLARES
  contribution to primary cosmic radiation, (T), 26:53853
STELLARATORS
  magnetic configuration analysis for, space-periodic, 26:54824(T) (AEC-tr-7334)
STOMACH
  radiation effects on circadian changes in mitotic index and DNA synthesis in glandular cells of rat, following oral administration of radon water, effects of dose on α, 26:53514
STORAGE RINGS
  beam betatron oscillations in muon g - 2 experiment, 26:53763
  beam dynamics in ISABELLE, effects of random magnetic field errors in exciting nonlinear resonances in, 26:53774 (BNL-17056)
  beam dynamics in long insertions of ISABELLE, elimination of momentum mismatch in, 26:53773 (BNL-17051)
  beam dynamics in, variation of betatron frequency across beam due to image fields, 26:53770 (BNL-17016)
  beam luminosity for colliding beams, methods for measuring, 26:53771 (BNL-17019)
  beam luminosity for electron--proton colliding beams, calculation of, 26:53777 (BNL-17067)
  beam luminosity of ISABELLE, method for absolute calibration using $p + p \rightarrow p + \Delta^+(1236)$ interaction, 26:53772 (BNL-17021)
  beam luminosity of, method for determining, using intersection of high β section with low β section, 26:53769 (BNL-16996)
  beam luminosity, lifetime, and size of CERN ISR, 26:53782 (CERN-72-14)
  beam stability in, effects of low-periodicity insertions on, 26:53780 (BNL-17152)
  design of ISABELLE, need for rings of unequal energy in, 26:53778 (BNL-17068)
  design proposal for ISABELLE, incorporating large aperture spectrometer magnet, 26:53779 (BNL-17142)
  deuteron breakup in Coulomb field of ISABELLE, cross section for, (T), 26:53776 (BNL-17063)
  experimental program at ISABELLE, for studying hadron interactions and properties, 26:54298 (BNL-16997)
  experimental program at ISABELLE, muon and muon pair production and detection, 26:54181 (BNL-16977)
  experimental program at ISABELLE, $p + p \rightarrow e + \nu +$ anything interactions, 26:54284 (BNL-16978)
  experimental program at ISABELLE, p + p weak interaction, 26:54182 (BNL-17092)
  experimental program of ISABELLE, feasibility of $\pi + p$ interactions, 26:54200 (BNL-17069)
  importance of colliding beam, for high-energy physics studies, 26:53767 (BNL-16830)
  lectures on intersecting, 26:53782 (CERN-72-14)
  magnets for ISABELLE, method for fault protection for, 26:53765 (BNL-16816)
  operation of ISABELLE in Whiplash mode for producing polarized proton or monoenergetic neutron beams, feasibility of, 26:53775 (BNL-17057)
  research proposal for ISABELLE, for very low energy anti p + p experiments using beams moving in same direction, 26:53766 (BNL-16818)
  vacuum chamber of ISABELLE, eddy current losses in, 26:53781 (BNL-17153)
STRAIN
  design basis for allowable plastic, 26:55500 (COO-2048-7)
  measurement of, evaluation of split Hopkinson pressure bar technique for, 26:55626 (UCRL-73610)

- STRATOSPHERE
  - balloon flights in, history of use for scientific experiments, 26:54019
  - neutron spectra measurements on balloon in, 26:54066 (NASA-TM-X-2440, pp 922-5)
  - radiation dose rate measurements at SST altitudes during solar flares, 26:54889 (NASA-TM-X-2440, pp 902-7)
  - radiation doses to crew and passengers at SST altitudes from cosmic and solar rays, 26:54888 (NASA-TM-X-2440, pp 894-901)
- STRONTIUM
  - determination in geochemical standards by atomic absorption using nitrous oxide--acetylene flame, 26:52921
  - electron reactions at 10 to 40 eV with, cross sections for formation of Sr^{2+} in, 26:54103 (FRNC-CONF-51)
  - oxidation of, uv photoemission studies of, 26:53611
  - photon reactions (γ,xn) with, model analysis of giant resonance in, (E/T), 26:54598 (FRNC-TH-242)
  - transport to plant roots by diffusion and mass flow, 26:55490 (COO-1495-17)
- STRONTIUM FLUORIDES
  - compatibility with fuel capsule materials, effects of impurities and radioactive decay on, 26:53330(R) (BNWL-1308-10)
- STRONTIUM ISOTOPES Sr-84
  - neutron reactions with, resonance activation integrals for, (E), 26:54585
- STRONTIUM ISOTOPES Sr-85
  - uptake by hair following intravenous injection in rats, correlation with body burden and, 26:53529 (NASA-TM-X-2440, pp 982-8)
- STRONTIUM ISOTOPES Sr-87
  - dosimetry of metastable, 26:54912
- STRONTIUM ISOTOPES Sr-88
  - alpha elastic scattering at 166 MeV, angular distribution for, (E), 26:54547
  - deuteron reactions (d,np) and (d,p) at 7.5 to 10.0 MeV, coupled-channels Born-approximation calculations of excitation functions for, (E/T), 26:54588
  - neutron radius of, determination from elastic scattering, (E), 26:54547
- STRONTIUM ISOTOPES Sr-89
  - content in atmosphere, fish, rainwater, and Savannah River in vicinity of Savannah River Plant, 1971, 26:53153(R) (DPSPU-72-30-1)
- STRONTIUM ISOTOPES Sr-90
  - content in agricultural products, atmosphere, fish, milk, rainwater, and Savannah River in vicinity of Savannah River Plant, 1971, 26:53153(R) (DPSPU-72-30-1)
  - content in fallout in East Germany during 1970, (E), 26:53156 (SZS-128)
  - content in Norwegian milk during 1956 to 1970, 26:53161
  - content of human bone, samples collected in France during 1970, in relation to stable strontium content, 26:53520 (CEA-N-1535)
  - distribution and retention in rabbits following intravenous injection, kinetics of, 26:53534
  - distribution in tissues of respiratory tract of dogs and monkeys following inhalation as fused clay aerosols, 26:53536
  - effects on alkaline phosphatase activity and chromosomes of mice, 26:53496
  - effects on mice following intraperitoneal injection in comparison to effects of external x rays, incidence of leukemogenic, 26:53512
  - effects on mice, studies on transmission of leukemogenic, 26:53496
  - uptake by barley and bean plants from surface contaminated soils, effects of clinoptilolite on, 26:53540
  - uptake by clover plants from continuously cropped uniformly contaminated soils, effects of clinoptilolite on, 26:53540
  - uptake by marine animals and plants from seawater, relation of alginic acid to retention, 26:53532
- STRONTIUM ISOTOPES Sr-91
  - half-life of, (E), 26:54667
- STRONTIUM ISOTOPES Sr-93
  - half-life of, (E), 26:54667
- STRONTIUM OXIDES
  - K_2O--SiO_2--SrO, diffusion in, electrostatic effects and mobility in, 26:53598
- STRONTIUM TITANATES
  - radiation effects on dielectric constants and crystal structure of, electron and γ, 26:55020
- STRUCTURAL BEAMS
  - strength of composite, subjected to positive and negative bending, studies of ultimate, 26:55571(T) (NRC-TT-1557)
- STRUCTURES
  - damage to distant, from mechanical effects of underground nuclear explosions in granite, (E), 26:53129(T) (UCRL-Trans-10616-2)
  - damage to Glendale, Calif., from ground motion from San Fernando earthquake, 26:53137 (JAB-99-96)
  - heating of urban and industrial, feasibility of use of power plant waste heat for, 26:55212 (CONF-720925-2)
- STYRENE POLYMERS
  - radioinduced carriers in capacitors of, γ, (E), 26:54968(R) (AD-737312)
- SUCCINONITRILES
  - radiolysis of crystals of, ESR studies on, 26:52991 (ORO-2968-78, Paper 6)
  - radiolysis of plastic crystals of, transient absorption spectra from pulse, 26:53003
- SUGARS
  - accumulation by isolated intestinal epithelial cells, effects of trans-membrane potassium gradients on, 26:55635 (UR-3490-174)
- SULFATES
  - oxygen-18 content of marine, (E), 26:53180
- SULFIDES
  - analysis of residues from leaching of matte, for osmium and ruthenium, 26:52919 (NIM-1432)
- SULFUR
  - determination in thin layers of chalcogenide glasses by proton activation or x-ray fluorescence, 26:52900 (LYCEN-7236)
  - neutron reactions with, production of phosphorus-32 by, 26:53069
- SULFUR FLUORIDES
  - potassium-atom scattering at thermal energies by, effects of temperature and internal and translational energy on differential cross sections for nonreactive, 26:54136
- SULFUR IONS
  - effects of implanted, on Doppler broadening of positron annihilation photons in silver halide crystals, 26:54097
  - spectral lines in zeta Oph due to interstellar, (E), 26:53875
- SULFUR ISOTOPES S-32
  - alpha elastic scattering at 166 MeV, angular distribution for, (E), 26:54547
  - energy levels of, projected Hartree--Fock and shell-model calculations of spins of, (T), 26:54553
  - muon (μ^-) capture by, polarization of emitted neutron in, (T), 26:54564
  - neutron radius of, determination from α elastic scattering, (E), 26:54547
  - reactions with ruthenium-96 and tin-112 up to 270 MeV, delayed proton spectra from, (E), 26:54608(T) (UCRL-Trans-1473)
- SULFUR ISOTOPES S-34
  - alpha reactions (α,γ) at 3.6 to 4.8 MeV, γ angular distributions and γ--γ angular correlations for, (E), 26:54560
- SULFUR ISOTOPES S-35
  - content in Savannah River, 1971, 26:53153(R) (DPSPU-72-30-1)
- SUN
  - atmosphere of, density dependent ionization balance of carbon, neon, and oxygen in, (E), 26:53969
  - atmosphere of, mean depth of line formation in, (T), 26:53944
  - gamma emission from, upper limits on, (E), 26:53967
  - gravitational field of, Einstein theory for modeling of, 26:54390 (ITF-71-130-P)
  - height in summer-winter 1964, correlation with ionospheric E-region electron density, (E/T), 26:54016
  - neutrino emission from, effects of resonance in $^3He + {}^3He$ system on, (T), 26:54508
  - neutron emission from, upper limits on, (E), 26:53967
  - noble-gas abundance in, (T), 26:53892
  - oblateness signal of, fluctuations of, (E), 26:53936
- SUNSPOTS
  - effects of cycle of, on narrow-angle cosmic-ray anisotropies, (T), 26:53868
  - magnetic fields of, Rayleigh--Taylor instability in composite medium, (T), 26:53940
  - spectra of, molecular carbon lines in, (E), 26:53952
  - spectra of, molecular carbon lines in, (E), 26:53953
  - spectra of, π-component splitting in, (T), 26:53951
- SUPERCONDUCTING JUNCTIONS
  - electric conductivity for tunnel, numerical calculation with depairing of zero bias, 26:54462 (LNF-72/27)
  - tunneling in, role of paramagnetic impurities in barrier region for, 26:54442
- SUPERCONDUCTIVITY
  - book: Superconductvity, 26:54460
  - model problems with positive pair interactions, asymptotic expression for, 26:54435 (ITF-72-56-E)
  - statistical mechanics of one-dimensional Ginzburg--Landau fields, (T), 26:54452
  - thermodynamic stability of nonideal Bose--Einstein gas, (T), 26:54432
- SUPERCONDUCTORS
  - acoustic interactions in, low-frequency, 26:54439
  - book: Superconductvity, 26:54460
  - Bose condensation and macroscopic coherence in, effect of dimensionality on, (T), 26:54436 (NP-19425)
  - Cooper pair structure in, 26:54459
  - critical anomalies in external fields in, nonperturbational calculation of, 26:54458
  - electron state densities for two-band, with nonmagnetic impurities, (T), 26:54454
  - energy gap parameter outside core of isolated flux line for T greater than or equal to T/sub c/, 26:54446
  - excitations in quantum condensated fermion gas, (T), 26:54443
  - magnetic flux penetration into thin-film, relaxation time--pick-up voltage frequency relation for, (T), 26:54453

  mixed-state structure near boundary of semi-infinite Type-II, 26:54448
  model of polar degenerate semiconductor, (T), 26:54449
  properties of two-band, effect of Fermi-surface topology change under pressure on, 26:54445
  thermal conductivity in dirty Type-II, near upper critical field, (T), 26:54451
  transition temperature in, effect of metal--dielectric phase transition in, (T), 26:54457
  vortex entropy in, 26:54441
SUPERFLUIDITY
  thermodynamic stability of nonideal Bose--Einstein gas, (T), 26:54432
SUPERNOVA REMNANTS
  contribution to galactic background of synchrotron radiation, (T), 26:53912
  formation of pulsars in, (T), 26:53912
  radio observations of galactic, (E), 26:53974
  rate of formation of, (T), 26:53912
SUPERNOVAE
  disruption of spiral structure in galaxies by super, (T), 26:53987
  nucleosynthesis in, harmonic oscillator-model calculations of termination of r process in, (T), 26:54663
  occurrence in Milky Way, rate of, (E), 26:53974
  spectra of Type II, absorption, (E), 26:53897
SURFACE WATERS
  temperature variations in, from heated effluents, use of temperature-induced fading of thermoluminescent dosimeter for measuring, 26:53187 (ANL-7860(Pt.3), pp 131-40)
SURFACES
  bibliography on surface and vacuum physics, 26:54085
  contamination by radioactive materials, criteria for radiation standards for, 26:54919
  contamination by radioactive materials, survey of guides for, 26:54920
  flatness of mechanical face seal, broad source interference method for measuring, 26:55463 (AECL-4208)
SURGERY
  effectiveness for treatment of local radiation injuries in man following radiotherapy, 26:53438
  effects of cardiac, on hypophosphatemia development in man, 26:55638 (UR-3490-187)
SURRY POWER REACTOR, UNIT 1
  decay heat removal system for, malfunction of steam vent system on, 26:55297 (DOCKET-50280-85)
  personnel for, revised organization of, 26:55295 (DOCKET-50280-82)
  site for, revised temperature monitoring requirements for, 26:55295 (DOCKET-50280-82)
  steam vent system for, malfunction of decay heat release system in, 26:55296 (DOCKET-50280-84)
SURRY POWER REACTOR, UNIT 2
  operation of, notice of return to power, 26:55257 (DOCKET-50280-83)
SWEDEN
  beta activity in atmosphere near ground at Marsta Observatory in, natural, 26:53159 (UUIM-26)
  power requirements in, comparison with UK, 26:53102
  radioactivity monitoring in, from March 23, 1971 USSR underground nuclear explosion, 26:53158 (FOA-4-4502-A-1)
SWINE
  radiation effects on epidermal cell kinetics of, dose dependence of fission neutron, thermal neutron, x, and neutron activation of boron-10 in, 26:53450 (LA-4874, pp 126-44)
  radiation effects on, following various combinations of acute, chronic, continuous, and fractionated whole-body exposures, effects of dose and dose rate on γ and x, 26:53451 (NASA-TM-X-2440, pp 622-32)
  radioactivity monitoring of, in vicinity of Savannah River Plant, 1971, 26:53153(R) (DPSPU-72-30-1)
  radioinduced injuries to skin of miniature, dose and time dependence of electron, 26:53458 (NASA-TM-X-2440, pp 665-71)
  radioinduced lesions in gastrointestinal tract of germ-free newborn, following lethal whole-body exposure, effects of artificial colonization with Escherichia coli on γ, 26:53495
SYMMETRY GROUPS
  breaking in relativistic quantum field theory with gauge fields, spontaneous, 26:54387
  irreducible representations of asymptotically flat space-time, for elementary particles, 26:54357
  orthogonal and unitary groups for orbital angular momentum of N identical particles, 26:55072
  physical symmetries from one-particle singularities of current matrix elements, 26:54356
  SL(2,C), formulation of dual model with, 26:54309
  SU(3) X SU(3) X U(1) X U(1) chiral, unified gauge weak-electromagnetic and weak-electromagnetic-strong interactions in, 26:54364 (NYO-3533-264)
  SU(3) x SU(3), tensors and axial charges for baryon-octet couplings in chiral, 26:54371
  SU(3) X U(1), unified gauge weak-electromagnetic and weak-electromagnetic-strong interactions in, 26:54364 (NYO-3533-264)
  W(3) Schwinger group for relativistic equation for four-particle composite structure of baryons, 26:54372
  W(3) Schwinger group, for relativistic equation for four-particle composite structure of baryons, 26:54368
SYNCHROTRON RADIATION
  emission in vacuum, faster-than-light, (T), 26:53916
  galactic background, contribution of supernova remnants to, (T), 26:53912
  polarization of, vertical angular distribution of intensities for linear, (T), 26:54249
SYSTEMS FOR NUCLEAR AUXILIARY POWER (SNAP)
  development and operating characteristics of radioisotope- and reactor-powered, 26:53093 (NASA-TM-X-2440, pp 13-25)
  heat sources for, preparation of metallic plutonium-238, 26:53332 (MLM-1150)
  heat sources for, properties of polonium-210, 26:53334 (MLM-1228)
  safety criteria for, 26:54921
SYSTEMS FOR NUCLEAR AUXILIARY POWER (SNAP-8)
  shield design for, 26:54948 (NASA-TM-X-2440, pp 78-83)
  shutdown on space stations, fission product γ dose rates following, (T), 26:55360 (NASA-TM-X-2440, pp 84-91)
SYSTEMS FOR NUCLEAR AUXILIARY POWER (SNAP-21)
  design, development, and testing of, for deep-sea applications, 26:53092(R) (MMM-3691-5(Rev.1))

T

T-111 (TANTALUM ALLOY)
  compatibility of fuel capsules of, with plutonium-238 oxide fuels, 26:53551(R) (MDC G-3153)
TANKS
  dismantling of sodium cooled reactor, removal of sodium and decontamination during, 26:55147 (AI-AEC-Memo-12736)
TANTALUM
  analysis for carbon and oxygen by helium-3 activation, 26:52899 (LA-DC-72-809)
  book: Early Transition Metals, 26:52956
  compatibility with sodium at 600ºC, effects of oxygen on, 26:53688
  deformation and recrystallization of, produced by electron-induced fusion and sintering, 26:53623
  determination in alloys using Nile Blue, spectrophotometric, 26:52925
  determination in minerals by direct measurement of oxide ratios, spectroscopic, 26:52932
  diffusion in aluminum nitride, silicon nitride, and titanium dioxide, 26:53677
  fabrication by rolling at high temperature under vacuum, 26:53630
  ion reactions at 10.4-MeV/nucleon, neutron yield from, (E), 26:54881 (NASA-TM-X-2440, pp 520-2)
  muon stopping and diffusion in hot foils of, in vacuum, production of muonium by, (E), 26:54096
  oxidation of silicide-coated, to 1500ºC, 26:53613
  production by electron-induced fusion and sintering, deformation and recrystallization studies on, 26:53623
  separation from niobium, titanium, and zirconium by solvent extraction, hydrolysis, and extraction, 26:52947 (BM-RI-7671)
  superconducting transition in, use of acoustical measurements for, 26:54439
  tensile properties of single-crystal, effects of interstitial nitrogen on asymmetric, 26:53643
TANTALUM ALLOYS AND SYSTEMS
  oxidation of silicide-coated, to 1500ºC, 26:53613
  Al--Co--Cr--Mo--Ni-base--Ta--Ti--W, sintering and stress-rupture properties of, effects of boron, carbon, and oxygen additions on, 26:53674
  Al--Cr--Mo--Nb--Ni-base--Ta--W, production and properties of powder metallurgy components of, for use at high temperatures, 26:53631
  Cr-base--Mo--Ta, coatings for nitridation resistance of, in air, chromium, hafnium, lanthanum, and yttrium combination cementation, 26:53689
  Si--Ta, diffusion of silicon in Ta_5Si_3 phase in, at high temperatures, 26:53583
TANTALUM CARBIDES
  growth on calcium fluoride, magnesium oxide, and sodium chloride substrates, electron beam evaporation method for epitaxial film, 26:53564
  sorptive properties of, effects of electronic structure on, 26:53593
TANTALUM ISOTOPES Ta-181
  neutron capture at 24.3 keV, TOF cross-section measurements using iron-filtered beam, (E), 26:54597 (CONF-720901-(Bks.1 and 2), pp 1107-14)
  neutron capture near 24.3 keV, pulse height spectra and relative cross section for, (E), 26:54656(R) (COO-3058-21)
  neutron reactions up to 20 MeV, γ production cross sections for, (E), 26:54523 (CONF-720901-(Bks.1 and 2), pp 325-34)
  photon reactions (γ,xn) with, model analysis of giant resonance in, (E/T), 26:54598 (FRNC-TH-242)
TANTALUM OXIDES
  films of, use of proton-excited x rays for thickness measurement on, 26:52945

TANTALUM SILICIDES
Ta$_5$Si$_3$--TiB$_2$, oxidation resistance and sinterability of, at high temperatures, 26:53594
Ta$_5$Si$_3$--ZrB$_2$, oxidation resistance and sinterability of, at high temperatures, 26:53594
TaSi$_2$--TiB$_2$, oxidation resistance and sinterability of, at high temperatures, 26:53594
TaSi$_2$--ZrB$_2$, oxidation resistance and sinterability of, at high temperatures, 26:53594
TD-NICKEL
production using poly(methylmethacrylate) as starter, Onera method for, 26:53626
TD-NICKEL CHROMIUM
production by chromium diffusion through halogen carrier in nickel--thorium dioxide grain, 26:53627
TECHNETIUM
recovery of fission product, for commercial uses, feasibility of, 26:53330(R) (BNWL-1308-10)
TECHNETIUM ISOTOPES Tc-93
energy level of, shell-model calculation of isomeric, (T), 26:54611
TECHNETIUM ISOTOPES Tc-99
activity of isomeric, calibration against cobalt-57 for determining, 26:52946
effectiveness of pertechnetate-incorporated metastable, for gamma camera visualization of normal and occluded arteries in human limbs, 26:53542
TECHNETIUM ISOTOPES Tc-102
beta decay of ground-state and isomeric, β and γ singles and coincidence spectra from, (E/T), 26:54596 (CEA-R-4286)
TECHNETIUM ISOTOPES Tc-104
beta decay of, β and γ singles and coincidence spectra from, (E), 26:54596 (CEA-R-4286)
TEETH
arsenic-74 uptake and retention by, of mice, rabbits, and rats following oral administration, time dependence of, 26:53538
TELLURIC ACID
neutron reactions with tellurium-130 in, production of carrier-free iodine-131 from, 26:53070
TELLURIUM
determination in meteoritic and terrestrial materials by neutron activation following separation from other elements, 26:52906
determination in thin layers of chalcogenide glasses by proton activation or x-ray fluorescence, 26:52900 (LYCEN-7236)
TELLURIUM ISOTOPES Te-125
proton reactions (p,n) with, iodine-125 production by, 26:53056 (AREAEE-129)
TELLUROBISMUTHITE
xenon-129, -130, and -131 contents in Swedish, measurement of, 26:53176
TEMPERATURE
effects on repair of sublethal x-radioinduced lesions in cultured Chinese hamster cells, 26:53358
effects on x-radiosensitivity of cultured Chinese hamster cells under conditions of low dose rate exposure, 26:53358
TERBIUM
magnetoelastic interaction for magnon--phonon mixing, (T), 26:55026
spin-wave energy fitting to interatomic exchange parameters in ferromagnetic, (T), 26:55053
TERBIUM ALLOYS AND SYSTEMS
Cu--Ni--Tb, magnetic structures in TbNi/sub 1-x/Cu/sub x/ below ordering temperature, stability of sinusoidal-wave, 26:55039
TERBIUM ISOTOPES Tb-149
alpha, beta, and electron-capture decay of, γ singles and coincidence spectra and α/β branching ratio for, (E), 26:54603 (JINR-P6-6511)
TERBIUM ISOTOPES Tb-153
energy levels from dysprosium-153 electron-capture decay, spin--parity assignments for, (E), 26:54643
TERBIUM ISOTOPES Tb-155
energy levels from dysprosium-155 decay, spin--parity assignments for, (E), 26:54643
energy-level transitions from dysprosium-155 decay, branching ratios and multipolarities for, (E), 26:54643
TERBIUM ISOTOPES Tb-157
energy levels from terbium-159 (p,t) reactions, spin--parity assignments for rotational, (E), 26:54645
TERBIUM ISOTOPES Tb-159
photon reactions (γ,xn) with, model analysis of giant resonance in, (E/T), 26:54598 (FRNC-TH-242)
proton reactions (p,t) at 30 MeV, DWBA analysis of differential cross sections and spectrum from, (E), 26:54645
TERBIUM OXIDES
magnetic moment direction in, crystal-field calculation of, 26:55054
spectra of nonstoichiometric, 4.2°K far-infrared, (E/T), 26:55032
TETRACYCLINE
effects on repair of γ-radioinduced double-strand breaks in DNA of Micrococcus radiodurans, inhibitory, 26:53349
THALLIUM ISOTOPES Tl-205
proton reactions (p,2n) at 14 MeV, gamma spectra from, (E), 26:54647
THALLIUM ISOTOPES Tl-206
beta decay of, β spectra, half-life, and matrix elements for, (E), 26:54648
THERMAL CYCLING
effects on corrosion resistance of zirconium and zirconium alloys in high-temperature water, 26:53614
THERMAL DIFFUSION
column shape factors for, derivation of empirical, 26:53326 (AREAEE-131)
data analysis of pulsed laser-induced, computer-based real-time, 26:55639 (Y-1841)
THERMAL INSULATION
optimization for nuclear powered space vehicles, data plot for, (T), 26:55366 (NASA-TM-X-2440, pp 392-6)
THERMAL RADIATION SHIELDING
replacement in large pressurized water reactors with neutron shielding pads, design and evaluation study for, 26:55223 (WCAP-7870)
THERMOCOUPLES
arrangement for mockup liquid sodium cooled fuel rod bundles, 26:55207(R) (ORNL-TM-3900)
standard for manufacturing of high-temperature rhenium--tungsten, for use in nuclear irradiation experiments, 26:53301 (EUR-4807)
thermowell systems for liquid metal service, standards for design and fabrication of, 26:55219 (RDT-C-7-18-T(8-72))
THERMODYNAMICS
violation of second law of, in black-hole physics, (T), 26:53906
THERMOELECTRIC GENERATORS
design considerations for simulated radiation effects in-flight testing of space vehicles, 26:53095 (NASA-TM-X-2440, pp 844-9)
design, development, and testing of strontium-90-fueled, for SNAP-21, 26:53092(R) (MMM-3691-5(Rev.1))
development and performance of, for space vehicles, 26:53093 (NASA-TM-X-2440, pp 13-25)
gamma emission by, design of γ sources for simulation of, 26:53335 (NASA-TM-X-2440, pp 850-2)
radiation emission from Thermoelectric Outer Planet Spacecraft, environmental analysis of γ and neutron, 26:53338 (NASA-TM-X-2440, pp 862-5)
THERMOMETERS
design of plugging, for liquid sodium, engineering drawings for, 26:53116
THERMONUCLEAR REACTORS
bibliography on plasma physics and fusion reactors, 26:54748
coolants for blankets of, thermodynamic evaluation of lithium and flibe, 26:54827 (IPP-4/97)
coolants for toroidal, stress analysis for determining performance of liquid lithium, (T), 26:54825 (CLM-R-116)
developments in U.K. during 1970-71, survey of, 26:55084(R) (INIS-mf-212)
energy balance of deuterium--tritium-fueled, conditions for self-sustaining reactions in, (T), 26:54833
magnet design for, summary of conference on, 26:54829 (ORNL-TM-3953)
magnetic configuration analysis for, space-periodic, 26:54824(T) (AEC-tr-7334)
magnetic configuration of, toroidality effects on helical magnetic axis, (T), 26:54832
physics problems in D--T fueled low-β toroidal, neutron and γ, 26:54826 (CONF-720901-(Bks.1 and 2), pp 559-73)
plasma confinement in FM-1, anomalous and pseudoclassical, 26:54753 (CONF-720804-5)
plasma confinement in toroidal, effects of laminar flow on, (T), 26:54755
plasma equilibrium in configurations with helical magnetic axis and considering toroidality, (T), 26:54815
plasma heating in Tuman-2, microwave, (E), 26:54758
tritium recovery in blankets of, research on methods for, 26:53085 (ORNL-4794, pp 91-5)
THERMOSPHERE
electron energy deposition in water vapor in, (E/T), 26:54033
plasma variations between 3000 and 5700 km at L = 2 to 4, spatial and temporal thermal-, (E), 26:54037
THORITES
content in southwest Aswan syenite rock, 26:53142 (AREAEE-138)
THORIUM
content in alkali olivine basalt in USSR, (E), 26:53147
content in southwest Aswan syenite rock, 26:53142 (AREAEE-138)
determination in comparison with uranium content in standard samples by γ spectroscopy, 26:52941
determination in ores by neutron activation, anion exchange purification of protactinium for, 26:52903
determination of, radiometric, 26:52942
distribution in cores from Green Bay, relations with depth, 26:53164 (ANL-7860(Pt.3), pp 64-76)
ionization of surfaces of, 26:53033 (EUR-4765, pp 117-30)
separation from ores, review of, 26:52977
separation from uranium by fractional dissolution of crude sodium diuranate, 26:52976 (IEA-250)

  separation of uranium-233 from, 26:52977
  solubility in bismuth--rare earth solutions, free energies of formation for compounds produced by, 26:53664
THORIUM ALLOYS AND SYSTEMS
  rare earths--Th, solubility in liquid bismuth, pp. 4-5, 26:53081 (ORNL-4794, pp 1-14)
THORIUM CARBIDES
  crushing and combustion of TRISO-coated, fission product release in, 26:53078 (CONF-720823-11)
THORIUM ISOTOPES Th-227
  alpha decay of, α-γ coincidence spectra and angular correlations for, (E), 26:54673
THORIUM ISOTOPES Th-230
  triton reactions (t,p) at 15 to 20 MeV, proton spectra and angular distributions for, (E), 26:54671
THORIUM ISOTOPES Th-232
  neutron capture by, survey of cross section data for, 26:54657 (FEI-292)
  neutron reactions (n,f) at 14.8 MeV, cadmium-115 isomer ratios in, (E), 26:54628
  proton reactions at 0.7 GeV, calculation of spallation--fission competition using intranuclear-cascade model, (T), 26:54666
  triton reactions (t,p) at 15 to 20 MeV, proton spectra and angular distributions for, (E), 26:54671
THORIUM ISOTOPES Th-234
  sorption by ocean sediments from seawater, (E), 26:53167
THORIUM METAPHOSPHATES
  preparation and structure of, 26:53045
THORIUM MINERALS
  content in southwest Aswan syenite rock, 26:53142 (AREAEE-138)
THORIUM NITRATES
  properties and structure of aqueous sols of, ir and light scattering studies on, 26:53048
  purification and concentration by anion exchange using small resins, p. 91-3, 26:53085 (ORNL-4794, pp 91-5)
THORIUM NITRIDES
  electric conductivity, thermal conductivity, and thermoelectric power of, (E), 26:55027
  ThN--UN, electric resistivity, thermal conductivity, and thermoelectric power of, (E), 26:55027
THORIUM ORES
  analysis of standard, for thorium and uranium by γ spectroscopy, 26:52941
  processing of, review on, 26:52977
THORIUM OXIDES
  preparation of aqueous solutions of sols of, for light scattering measurements, 26:53050
THORIUM OXIDES ThO$_2$
  dissolution solutions for, corrosion of Corronel 230, HAPO-20 alloy, and Type 304L stainless steel by fluoride-catalyzed nitric acid, 26:53604 (BNWL-CC-449)
  sintering of, nonisothermal method for studying initial-stage, 26:53595
  Co-base--Cr--Ni--ThO$_2$, mechanical properties and microstructure of dispersion-hardened, 26:53675
  Co-base--Ni--ThO$_2$--Zr, mechanical properties and microstructure of dispersion-hardened, 26:53675
  Co-base--ThO$_2$, mechanical properties and microstructure of dispersion-hardened, 26:53675
  Co-base--ThO$_2$--Zr, mechanical properties and microstructure of dispersion-hardened, 26:53675
  Re--ThO$_2$--W-base, creep properties of, at 1800 to 2200°C, 26:53678
  ThO$_2$--UO$_2$, crushing and combustion of BISO-coated, fission product release in, 26:53078 (CONF-720823-11)
THORIUM SILICATES
  crystal structure of, atomic positions in, 26:55038
THREE MILE ISLAND POWER REACTOR, UNIT 1
  auxiliary systems for, requested and revised data on, 26:55303 (DOCKET-50289-66)
  engineered safeguards for, requested and revised data on, 26:55303 (DOCKET-50289-66)
  instrumentation for, requested and revised data on, 26:55303 (DOCKET-50289-66)
  operations for, requested and revised data on, 26:55303 (DOCKET-50289-66)
  personnel for, requested and revised data on, 26:55303 (DOCKET-50289-66)
  radioactive waste disposal system for, requested and revised data on, 26:55303 (DOCKET-50289-66)
  site for, revised data on meteorology of, 26:55303 (DOCKET-50289-66)
  testing program for, requested and revised data on, 26:55303 (DOCKET-50289-66)
THYMINE
  radiolysis of single crystals of anhydrous and monohydrate, ESR studies on radicals from γ, 26:52999
THYMUS GLAND
  radioinduced leukemic transformations in, of mice following fractionated whole-body exposure, x, 26:53512
  role in recovery of bone marrow in γ-irradiated rats, 26:53479
THYROID GLAND
  radiation dose to, in children from iodine-131 ingestion in milk, maximum permissible, 26:53506(T) (ORNL-tr-2629)
  radiation effects on growth of goitrogen-stimulated, in mice, effects of dose rate on RBE for internal iodine-131 or iodine-132 β and γ and external x, 26:53472
  radiation effects on growth of, in fetal and goitrogen-stimulated adult mice following intravenous injection of iodine-131, β and γ, 26:53513
  radiation effects on morphology and physiology of, in birds following parenteral injection of iodine-131, dose-response relations for β and γ, 26:53515
  radiation effects on regeneration of rat, following whole-body exposure, effects of prior implantation of sarcoma on x, 26:53494
  radiation effects on, of dogs following whole-body exposure, relation of metabolic rate to carcinogenic and morphologic, x, 26:53462 (UR-3490-183)
  scintiscanning of human, for diagnosis of neoplasms, use of gamma camera in, 26:53214
TIN
  determination in meteoritic and terrestrial materials by neutron activation following separation from other elements, 26:52906
  determination in minerals by neutron activation and γ spectroscopy, nondestructive, 26:52901 (UJV-2851-F,Ch)
  determination in water samples by spark-source mass spectroscopy, 26:52914 (ANL-7860(Pt.3), pp 55-63)
  determination in water, effects of large amounts of copper on spectrographic, 26:52927
  Josephson effect in superconducting films, evidence for ac and dc, (E), 26:54455
  photon reactions (γ,xn) with, model analysis of giant dipole resonance in, (E/T), 26:54598 (FRNC-TH-242)
  separation from indium by ion exchange chromatography, 26:52949
  superconducting transition in, use of acoustical measurements for, 26:54439
TIN ALLOYS AND SYSTEMS
  Al--Mo--Sn--Ti-base--Zr, creep rupture of, at 755 and 865^{o}K, cyclic, 26:53690
  Al--Sn--Ti-base, radiation effects on tensile properties of, at cryogenic temperatures for use in NERVA Program, fast neutron, 26:53697 (NASA-TM-X-2440, pp 603-8)
TIN CHLORIDES
  potassium-atom scattering at thermal energies by, effects of temperature and internal and translational energy on differential cross sections for nonreactive, 26:54136
TIN ISOTOPES Sn-112
  chlorine-35 reactions up to 250 MeV, delayed proton spectra from, (E), 26:54608(T) (UCRL-Trans-1473)
  sulfur-32 reactions up to 270 MeV, delayed proton spectra from, (E), 26:54608(T) (UCRL-Trans-1473)
TIN ISOTOPES Sn-116
  alpha elastic and inelastic scattering at 166 MeV, angular distributions for, (E), 26:54616
  alpha elastic scattering at 166 MeV, angular distribution for, (E), 26:54547
  neutron radius of, determination from elastic scattering, (E), 26:54547
  nuclear properties of, analysis using high-energy α scattering, (E), 26:54616
TIN ISOTOPES Sn-118
  alpha elastic and inelastic scattering at 166 MeV, angular distributions for, (E), 26:54616
  alpha elastic scattering at 166 MeV, angular distribution for, (E), 26:54547
  neutron radius of, determination from elastic scattering, (E), 26:54547
  neutron reactions (n,α), isomer yield ratio for, (E), 26:54628
  nuclear properties of, analysis using high-energy α scattering, (E), 26:54616
TIN ISOTOPES Sn-119
  energy level at 89 keV, nuclear magnetic moment of, (E), 26:54624
TIN ISOTOPES Sn-120
  alpha elastic and inelastic scattering at 166 MeV, angular distributions for, (E), 26:54616
  alpha elastic scattering at 166 MeV, angular distribution for, (E), 26:54547
  neutron radius of, determination from elastic scattering, (E), 26:54547
  nuclear properties of, analysis using high-energy α scattering, (E), 26:54616
TIN ISOTOPES Sn-124
  alpha elastic and inelastic scattering at 166 MeV, angular distributions for, (E), 26:54616
  alpha elastic scattering at 166 MeV, angular distribution for, (E), 26:54547
  neutron radius of, determination from elastic scattering, (E), 26:54547
  nuclear properties of, analysis using high-energy α scattering, (E), 26:54616
TISSUE EQUIVALENT MATERIALS
  electron isodose distribution perturbation near cavities in, at 10 to 35 MeV, (E), 26:54903
  electron scattering by, Monte Carlo study with catastrophic collisions in, 26:54898
  neutron energy transfer to soft, microdosimetric studies of fast, 26:54873 (EUR-4787)
TISSUES
  gamma depth-dose distribution under lattice in, theoretical calculation of ^{60}Co, 26:54908
  neutron energy transfer to soft, microdosimetric studies of fast, 26:54873 (EUR-4787)

  neutron isodose curves in, normalized to kerma from small tissue volume in free space, 26:54902
  radiation dose distribution in orthogonal plane in, surrounding iridium-192 wires implanted for interstitial therapy, effects of arrangement, number, and size of implants on β and γ, 26:53422
  radiation dosimetry in, system of ionization chambers for, 26:53232 (NASA-TM-X-2440, pp 435-7)
  x-ray dose across plane interface with bone, contribution of photoelectrons to, (T), 26:54896
TITANIUM
  abundance in γ Cap, (E), 26:53888
  book: Early Transition Metals, 26:52956
  content in southwest Aswan syenite rock, 26:53142 (AREAEE-138)
  determination in geochemical standards by atomic absorption using nitrous oxide--acetylene flame, 26:52921
  determination in water, effects of large amounts of copper on spectrographic, 26:52927
  diffusion in aluminum nitride, silicon nitride, and titanium dioxide, 26:53677
  diffusion of nickel-63 in polycrystalline α-, mechanism of, 26:53666
  effects on cohesion and structural stability of aluminum oxide composites with iron, 26:53589
  fabrication by rolling at high temperature under vacuum, 26:53630
  flow stress of, effects of impurities on strain rate sensitivity of, 26:53639(R) (ORO-3262-25)
  mechanical properties of, effects of impurities on, 26:53639(R) (ORO-3262-25)
  photon reactions (γ,n) at 12 to 23 MeV, neutron spectra from, (E), 26:54563
  reactions of ion-refined surfaces of, with hydrogen and oxygen, field-ion microscopy studies of, 26:53657
  separation from niobium, tantalum, and zirconium by solvent extraction, hydrolysis, and extraction, 26:52947 (BM-RI-7671)
  strain aging in, dynamic, 26:53639(R) (ORO-3262-25)
  strain rate sensitivity in, validity of Cottrell--Stokes Law in terms of variation of, 26:53639(R) (ORO-3262-25)
  strain rate sensitivity in, validity of Cottrell--Stokes Law in terms of variation of, 26:53639(R) (ORO-3262-25)
  tensile properties of, at room temperature, effects of prestraining at 77°K on, 26:53639(R) (ORO-3262-25)
TITANIUM ALLOYS AND SYSTEMS
  Al--Co--Cr--Mo--Ni-base--Ta--Ti--W, sintering and stress-rupture properties of, effects of boron, carbon, and oxygen additions on, 26:53674
  Al--Co--Cr--Mo--Ni-base--Ti, sintering and stress-rupture properties of, effects of boron, carbon, and oxygen additions on, 26:53674
  Al--Mo--Sn--Ti-base--Zr, creep rupture of, at 755 and 865°K, cyclic, 26:53690
  Al--Mo--Ti-base--V, crack propagation and embrittlement by gaseous hydrogen, mechanism of, 26:53685
  Al--Sn--Ti-base, radiation effects on tensile properties of, at cryogenic temperatures for use in NERVA Program, fast neutron, 26:53697 (NASA-TM-X-2440, pp 603-8)
  Al--Ti, reactions of ion-refined surfaces of intermetallic Ti_3Al, with hydrogen and oxygen, field-ion microscopy, studies of, 26:53657
  Al--Ti-base--V, fracture toughness of $\alpha + \beta$ and β processed, at room and subzero temperatures, measurement of plane strain, 26:53661
  Cr--Cu--Fe--Mo--Ni-base--Ti, corrosion by thorium dioxide dissolvent solutions, 26:53604 (BNWL-CC-449)
  Cu-base--Ti, hardening of, mechanism of precipitation, 26:55615(R) (TID-26148)
  Nb--Ti, superconducting transition temperature and upper critical field, data on, 26:54464 (ORNL-TM-3921)
  Pd--Ti, diffusion measurements on, at 600 to 1000°C, 26:53677
TITANIUM BORIDES
  oxidation resistance and sinterability of, effects of metal silicide additions on, 26:53594
  Cr_5Si_3--TiB_2, oxidation resistance and sinterability of, at high temperatures, 26:53594
  $CrSi_2$--TiB_2, oxidation resistance and sinterability of, at high temperatures, 26:53594
  Ta_5Si_3--TiB_2, oxidation resistance and sinterability of, at high temperatures, 26:53594
  $TaSi_2$--TiB_2, oxidation resistance and sinterability of, at high temperatures, 26:53594
  TiB_2--Ti_5Si_3, oxidation resistance and sinterability of, at high temperatures, 26:53594
  TiB_2--$TiSi_2$, oxidation resistance and sinterability of, at high temperatures, 26:53594
  TiB_2--W_5Si_3, oxidation resistance and sinterability of, at high temperatures, 26:53594
  TiB_2--WSi_2, oxidation resistance and sinterability of, at high temperatures, 26:53594
TITANIUM CARBIDES
  fabrication by casting of thermoplastic masses, 26:53586
  mechanical properties and microstructure of, effects of hot working on, 26:53581
  sorptive properties of, effects of electronic structure on, 26:53593
TITANIUM CHLORIDES
  production of, separation of niobium, tantalum, titanium, and zirconium from wastes from, 26:52947 (BM-RI-7671)
TITANIUM HYDRIDES
  Al-base--B_4C--TiH_2, radiation effects on tensile properties of, at cryogenic temperatures for use in NERVA Program, fast neutron, 26:53696 (NASA-TM-X-2440, pp 595-602)
TITANIUM IONS
  phonon resonant scattering at, in alumina single crystals, 26:54978
TITANIUM ISOTOPES Ti-48
  alpha elastic scattering at 166 MeV, angular distribution for, (E), 26:54547
  deuteron elastic scattering at 11.9 MeV, vector-polarized, (E), 26:54572
  neutron radius of, determination from α elastic scattering, (E), 26:54547
TITANIUM ISOTOPES Ti-49
  deuteron elastic scattering at 11.9 MeV, vector-polarized, (E), 26:54572
TITANIUM ISOTOPES Ti-50
  deuteron elastic scattering at 11.9 MeV, vector-polarized, (E), 26:54572
TITANIUM NITRIDES
  sorptive properties of, effects of electronic structure on, 26:53593
TITANIUM OXIDES
  diffusion of niobium, tantalum, titanium, and vanadium in, 26:53677
  reactions with alkali metal halides in carrier distillation process for uranium oxide (U_3O_8), 26:52955 (RT/CHI-(72)4)
  sorptive properties of, effects of electronic structure on, 26:53593
TITANIUM SILICIDES
  TiB_2--Ti_5Si_3, oxidation resistance and sinterability of, at high temperatures, 26:53594
  TiB_2--$TiSi_2$, oxidation resistance and sinterability of, at high temperatures, 26:53594
TOBACCO (the commodity)
  analysis for arsenic, bromine, mercury, and selenium by neutron activation, 26:52907
TOKAMAK DEVICES
  plasma instabilities in, growth rates of MHD and tearing-mode, (T), 26:54813
  plasma MHD instabilities in, Toroidal effects on, (T), 26:54806 (CONF-720804-6)
TOKAMAK MODEL ST
  plasma heating by excited waves near ion cyclotron frequency, (E), 26:54752 (CONF-720804-4)
TOWER SHIELDING FACILITY
  neutron attenuation by sodium slabs at, benchmark measurements of, (E/T), 26:55142 (CONF-720901-(Bks.1 and 2), pp 418-30)
  pipe chase mockup in, neutron streaming in sodium filled, (E/T), 26:55394 (CONF-720901-3)
  pipe chase mockup in, neutron streaming in sodium filled, (E), 26:55382 (CONF-720901-(Bks.1 and 2), pp 431-41)
TRACER TECHNIQUES
  development for studies of nutrient cycling in forest floor-arthropod food chains, use of cesium-134 as tracer for potassium and strontium-85 as tracer for calcium, 26:53539(R) (SRO-641-4)
  development of computerized data processing systems for, using chromium-51 and iron-59 together, 26:53544
  facilities for medical, IAEA-WHO survey on world-wide, 26:53413
  method for measuring wear in Diesel engine piston rings and ring grooves using neutron activation, 26:53339 (KFK-1568)
  performance of sodium-24, for measuring catalyst circulation rates in catalytic cracking units, 26:53343
  uses in medicine, training course manual, 26:53541 (TID-26128)
TRANSACTINIDE ELEMENTS
  abundance in primary cosmic radiation, (T), 26:53867
  nuclear binding energies of superheavy, calculation using Hartree--Fock method, (T), 26:54726
  production of superheavy, by xenon reactions with heavy nuclei, 26:54658 (JINR-P7-6523)
  properties of, use of Mendeleev periodic law for prediction of, 26:53053
  search for superheavy, from secondary reactions following proton reactions in tungsten and uranium-238, (E), 26:54672
  synthesis in supernovae, harmonic oscillation-model calculations of termination of r-process, (T), 26:54663
  trapping of superheavy, in geomagnetic field, possible detection of, 26:54047 (NASA-TM-X-2440, pp 548-55)
TRANSDUCERS
  development of probe velocity, for measuring x-ray-produced blowoff impulse from nuclear explosions, 26:53303 (LA-4999)
TRANSFERASES
  isolation and purification of steroid glucuronyl-, from animals and man, 26:55472 (BMBW-FBK-72-9)
  ribonuclease, indium-111 PAC studies of, 26:55058
  role of DNA polymerase in repair of uv-irradiated DNA in microorganisms, 26:53351

TRANSISTORS
fabrication and electrical properties of multilayer gate IGFET, using ion implantation, 26:53314
radiation hardening of bipolar MIS and junction FET, NERVA neutron and gamma, 26:53289 (NASA-TM-X-2440, pp 481-6)
TRANSITION METAL ALLOYS AND SYSTEMS
magnetic properties of, Moessbauer measurements with nickel-61 of, 26:55617 (TID-26159)
TRANSITION METAL BORIDES
nuclear hyperfine interactions in, iron-57 Moessbauer-effect study of, 26:55055 (IS-T-529)
TRANSITION METAL CARBIDES
Co--transition metal carbides, erosion resistance of anodes of, 26:53568
Fe--transition metal carbides, erosion resistance of anodes of, 26:53568
Ni--transition metal carbides, erosion resistance of anodes of, 26:53568
TRANSITION METAL HYDRIDES
properties of ternary and quaternary, literature review on, 26:53558 (UCRL-51244)
TRANSITION METALS
atomic binding energy of 5d, relative to tungsten, 26:53656
compounds, nuclear quadrupole resonance study of halide, 26:55529 (IS-T-526)
crystal lattice deformation in, field-ion microscopy studies of tip--metal contact, 26:53651
magnetic properties of, Moessbauer measurements with nickel-61 of, 26:55617 (TID-26159)
thermal conductivity near upper critical field in dirty superconducting, (T), 26:54451
TRANSPORT THEORY
calculations for dose distributions of π^-, neutrons, and protons, use of computer codes for, 26:54890 (ORNL-TM-3816)
calculations in complex shielding problems, survey of ''benchmark'' needs and problems in, 26:54937 (CONF-720901-(Bks.1 and 2), pp 349-84)
calculations of radiation, discrete-ordinates-to-Monte-Carlo coupling code, DOMINO, for, 26:54872 (CONF-720901-(Bks.1 and 2), pp 499-511)
discrete ordinates method in, effect of singularities in, 26:54482 (INR-P-1405)
TRANSURANIUM ELEMENTS
abundance in primary cosmic radiation, (T), 26:53867
fission fragment tracks from, in natural minerals, study of spontaneous, 26:54670
flux in primary cosmic radiation, (E), 26:53844
phase diagrams of sesquioxides of, p. 42, 26:53066 (ORNL-4794, pp 36-44)
processing of, research on, 26:53066 (ORNL-4794, pp 36-44)
purification of TRU product, pp. 37-8, 26:53066 (ORNL-4794, pp 36-44)
TRANSURANIUM PROCESSING PLANT
operation of, pp. 36-7, 26:53066 (ORNL-4794, pp 36-44)
TRAUMA
radiation effects on recovery from accidental and surgical, in animals and man, whole-body, 26:53419
TRIOCTYLAMINE
effects on solvent extraction of trivalent cerium from hydrochloric acid solution by TTA, synergistic, 26:52952
TRITIUM
content in agricultural products, atmosphere, drinking water, milk, rainwater, and Savannah River in vicinity of Savannah River Plant, 1971, 26:53153(R) (DPSPU-72-30-1)
content in natural gas stored in underground nuclear cavities, 26:53132(T) (UCRL-Trans-10617-2)
content in nuclearly stimulated natural gas, development of radiation standard for, 26:53134
control, handling, and monitoring of, bibliography on, 26:53155 (MLM-1946)
determination by bremsstrahlung counting, polyethylene containers for, 26:52934 (MLM-1368)
determination by liquid scintillation counting, 26:52935(R) (MLM-1888)
deuteron reactions (d,n) at 30 keV to 1.5 MeV, calculation of thick target yields for, (T), 26:54502 (SC-RR-720513)
effects on cells following incorporation into DNA, role of transmutation in lethal and mutagenic, 26:53505
effects on cells following incorporation into DNA, effects of carrier molecule efficiency on RBE in comparison with external x radiation for lethal and mutagenic, 26:53505
effects on Escherichia coli following uptake as labeled oleate, use of lethal, for selective enrichment of altered acyl CoA synthetase mutants, 26:53518
exchange between water and N,N'-bis(3-phenoxyhydroxypropyl)ethylenediamine hydrochloride, 26:53052
incorporation in N,N'-bis(3-phenoxyhydroxypropyl)-ethylenediamine hydrochloride, 26:53052
monitoring in air, gamma compensated flowthrough proportional counter, 26:53216
nuclear magnetic moment of, calculation using quark model, 26:54494 (COO-3001-15)
nuclear magnetic moment of, two-body OPE contributions to isovector, (T), 26:54506
production of, reactor irradiation method and apparatus for, 26:53075(P)
proton elastic scattering at 19 and 30 MeV using polarized beam, differential cross sections and analyzing power for, (E), 26:54521
proton elastic scattering at 6.7 to 14.7 MeV, differential analyzing power and phase-shift analysis of polarized, (E), 26:54518
proton reactions (p,d) at 6.7 to 14.7 MeV, analyzing power for polarized, (E), 26:54517
reactions of atoms of, with glucose and starch, 26:53028 (COO-584-50)
recovery from blankets of controlled thermonuclear reactors, research on methods for, p. 95, 26:53085 (ORNL-4794, pp 91-5)
release in head-end reprocessing of HTGR-type graphite fuel, 26:53078 (CONF-720823-11)
removal from gas streams, design of device for, 26:53313(P)
removal from natural gas stored in nuclear cavities, method for, 26:53128 (ORNL-4794, pp 63-4)
separation from off-gases in reprocessing of LMFBR fuel, pp. 21-2, 26:53082 (ORNL-4794, pp 15-25)
transport through soils, independent test of Argonne model for, 26:53163 (ANL-7860(Pt.3), pp 32-7)
TRITIUM SYSTEMS
D--T, laser beam reactions with solid targets of, fusion reactions from, 26:54830
D--T, thermonuclear reactions from spherical hot-spot in, (T), 26:54831
TRITONS
binding energy, charge radius, and D-state probability of, calculations using very-soft-core Riihimaki potential, (T), 26:54504
interactions ^{3}He + t at 1 to 200 MeV (cms), optical-potential description of phases for scattering, (T), 26:54532
reactions (t,n) with deuterium at 30 keV to 1.5 MeV, calculation of thick target yields for, (T), 26:54502 (SC-RR-720513)
reactions (t,p) with A = 230 to 238 nuclei at 15 to 20 MeV, proton spectra and angular distributions for, (E), 26:54671
reactions (t,p) with iron-57 at 12 MeV, angular distributions for, (E), 26:54592
scattering by iron-57 at 12 MeV, angular distributions and optical model parameters for elastic, (E), 26:54592
TRI-UNIVERSITY MESON FACILITY (TRIUMF)
development of, 1971, 26:53741(R) (NP-19416)
magnet for, history of design of, 26:53749
TROJAN POWER REACTOR, UNIT 1
inspection of, noncompliance activities from, 26:55334 (DOCKET-50344-31)
TRYPTOPHAN
radiation effects on free and bound, in wheat, dose dependence of gamma, 26:53395
TUBES
failure of austenitic steel, effects of sodium--water reactions on, 26:55161 (CONF-710548-, pp 221-42)
failures of sodium--water steam generator, performance and safety aspects of, 26:55159 (CONF-710548-, pp 206-12)
TUNGSTEN
book: Early Transition Metals, 26:52956
compaction of powders of, feasibility of explosive, 26:53619
compatibility of fuel capsules of, with plutonium-238 oxide fuels, 26:53551(R) (MDC G-3153)
creep properties of fine wires of pure, doped, and thoriated, at 2450 to 3000°C, 26:53683
crystal structure of, effects of electric pulses on, 26:53668
deformation texture of polycrystalline, following drawing and swaging, 26:53670
deposition by hydrogen reduction of chloride or fluoride, method for chemical vapor, 26:53622
electron reactions with, Auger and direct ionization processes in, 26:54103 (FRNC-CONF-51)
fracture and structure of cast, effects of carbon on, 26:53681
grain structure of, effects of quench sintering on, 26:53662
growth and hardness of spherical agglomerates of, produced from powders, 26:53577
hydrogen dissociation on hot filaments of, ESR study of, 26:55036
incorporation of reinforcing fibers of, in stainless steel with precise alignment and uniform distribution, method for, 26:53629
ion channeling and blocking in single crystals of, 26:54977
ionization of surfaces of, 26:53033 (EUR-4765, pp 117-30)
muon stopping and diffusion in hot foils of, in vacuum, production of muonium by, (E), 26:54096
neutron capture at thermal to 100 keV, cross sections for gamma-ray production in, (E), 26:54960 (NASA-TM-X-2440, pp 500-11)
neutron distributions behind W/Al$_2$O$_3$/W barriers, spatial,

  angular, and energy, 26:54966
  photon reactions (γ,n) at 12 to 23 MeV, neutron spectra from, (E), 26:54563
  production of microspheres of, from powders in rotating container, 26:53577
  properties of sintered powders of, following hydrogen reduction of oxide at 750 to 1050°C, effects of nickel additions on mechanical and physical, 26:53579
  properties of, effects of porosity on bending resistance, elastic, and electric and thermal conductivity, 26:53684
  proton reactions at 28 GeV, yields of actinides and transactinides from secondary reactions following, (E), 26:54672
  radiation effects on recrystallized grain size and recrystallization temperature of ribbons of, α, 26:53711
  rare-gas-ion scattering at 150 to 1000 eV by polycrystalline surfaces of, angular and energy distributions and cross sections for, (E), 26:54083
  reactions of single atoms of, with atomically defined surfaces, 26:53656
  sintering of powders of, mechanism of material transport by dislocation motion in, 26:53620
  sintering of, reduced by hydrogen at 750 to 1050°C, effects of nickel additions on, 26:53579
  solvent properties for nitrogen, effects of temperature and pressure on, 26:53580
  sorptive properties for carbon monoxide, field-emission microscopic study of binding states of, 26:55023

TUNGSTEN ALLOYS AND SYSTEMS
  preparation of strengthened, by powder metallurgical internal oxidation, 26:53616
  Al--Co--Cr--Mo--Ni-base--Ta--Ti--W, sintering and stress-rupture properties of, effects of boron, carbon, and oxygen additions on, 26:53674
  Al--Cr--Mo--Nb--Ni-base--Ta--W, production and properties of powder metallurgy components of, for use at high temperatures, 26:53631
  Al--Ni-base--W--Zr, production and properties of powder metallurgy components of, for use at high temperatures, 26:53631
  Cr-base--W--Y, coatings for nitridation resistance of, in air, chromium, hafnium, lanthanum, and yttrium combination cementation, 26:53689
  Mo--Ni--W-base, mechanical properties of, effects of heat treatments following sintering on, 26:53679
  Mo--Ni--W-base, preparation and composition of, 26:53679
  Mo--W-base, compatibility of fuel capsules of, with plutonium-238 oxide fuels, 26:53551(R) (MDC G-3153)
  N--W, degassing at 1200 to 3000°C in, equilibria and kinetics of, 26:53580
  $PdCl_2$--W, sintering of powders of, mechanism of material transport by dislocation motion in, 26:53620
  Re--ThO_2--W-base, creep properties of, at 1800 to 2200°C, 26:53678
  Re--W-base, compatibility of fuel capsules of, with plutonium-238 oxide fuels, 26:53551(R) (MDC G-3153)
  Si--W, diffusion of silicon in W_5Si_3 phase in, at high temperatures, 26:53583
  UN--W, preparation of fuels of, method for, 26:53562(P)
  W--ZrC, evaporation rate at 2600 to 2970°K, effects of tungsten coating on, 26:55022

TUNGSTEN CARBIDES
  fabrication by hot isostatic pressing, 26:53578
  formation in field-ion microscope tubes, studies on, 26:53560
  growth and hardness of spherical agglomerates of, produced from powders, 26:53577
  production of microspheres of, from powders in rotating container, 26:53577
  production of powders of, from scrap, Coldstream process for, 26:53591
  sintering of, effects of annealing and ball milling on, 26:53576

TUNGSTEN ISOTOPES W-188
  beta decay of, γ spectra from, (E), 26:54637
  beta decay of, interpretation of forbidden $0^+ \to 0^+$, (E/T), 26:54641

TUNGSTEN OXIDES
  growth and hardness of spherical agglomerates of, produced from powders, 26:53577
  production of microspheres of, from powders in rotating container, 26:53577
  reduction by hydrogen at 750 to 1050°C, effects of nickel additions on, 26:53579

TUNGSTEN SILICIDES
  TiB_2--W_5Si_3, oxidation resistance and sinterability of, at high temperatures, 26:53594
  TiB_2--WSi_2, oxidation resistance and sinterability of, at high temperatures, 26:53594
  W_5Si_3--ZrB_2, oxidation resistance and sinterability of, at high temperatures, 26:53594
  WSi_2--ZrB_2, oxidation resistance and sinterability of, at high temperatures, 26:53594

TUNNELS
  development for utility installations, 26:55484 (CONF-720925-3)

TURBINES
  heat exchangers for nuclear-heated gas, computer program for performance analysis of, 26:53114
  steam--water flow in, equipment and methods for studying, 26:53124

TURKEY POINT POWER REACTOR, UNIT 3
  diesel generator for, failure of required test output for emergency, 26:55249 (DOCKET-50250-94)
  power tilt limits for, revised technical specifications for reduction of, 26:55282 (DOCKET-50250-93)
  pump for, failure of packing for charging, 26:55249 (DOCKET-50250-94)
  residual heat removal system for, failure of packing on gate valve in suction line from, 26:55248 (DOCKET-50250-92)
  safety injection systems for, unplanned simultaneous activation of, 26:55249 (DOCKET-50250-94)

TURKEY POINT POWER REACTOR, UNIT 4
  diesel generator for, failure of required test output for emergency, 26:55249 (DOCKET-50250-94)
  pump for, failure of packing for charging, 26:55249 (DOCKET-50250-94)
  residual heat removal system for, failure of packing on gate valve in suction line from, 26:55248 (DOCKET-50250-92)
  safety injection systems for, unplanned simultaneous activation of, 26:55249 (DOCKET-50250-94)

TZM (MOLYBDENUM ALLOY)
  compatibility of fuel capsules of, with plutonium-238 oxide fuels, 26:53551(R) (MDC G-3153)
  composition, microstructure, and physical properties of forged, 26:53673
  fabrication of 1300 kg powder metallurgy billets of, by forging, 26:53673
  fabrication of sintered, growth and recrystallization studies on, 26:53624
  properties and uses of, review on corrosion resistant, oxidation resistant, and physical, 26:53672

U

UDIMET 700
  production and properties of high-density powder metallurgy components of, for use at high temperatures, 26:53631

ULTRASONIC TESTING
  method for metallic welds, 26:53126(P)
  reliability for in-service inspection of reactor pressure vessels, improvement of conventional, 26:55222(R) (NP-19338(Vol.2))

ULTRAVIOLET RADIATION
  effects on Aspergillus niger, mutagenic for citric acid production, 26:53380
  effects on Aspergillus, mutagenic for antibiotic production, 26:53393
  effects on bacterial spores on space vehicle components, dose dependence of sterilizing, 26:53367(R) (SC-RR-720516)
  effects on cultured Chinese hamster cells in comparison to effects of chemical mutagens and x radiation, effects of dose and post-exposure culture medium on frequency of mutagenic, 26:53362
  effects on DNA in bacteriophages in relation to molecular structure, 26:53373
  effects on DNA in cultured mammalian cells and microorganisms, role of repair processes in recovery from lethal and mutagenic, review of, 26:53357
  effects on DNA in microorganisms, review of role of enzymes in repair of, 26:53351
  effects on DNA in microorganisms, role of enzymes in repair of, 26:53350
  effects on Eremothecium ashbyii (fungi) in relation to riboflavin production, mutagenic, 26:53374
  effects on Escherichia coli, comparison of dose-response kinetics and photoreactivation of 254 nm and 313 nm, 26:53370
  effects on Escherichia coli, effects of tryptophan starvation on mutagenic, 26:53379
  effects on mouse lymphoma cells in cultures, effects of dose on proliferation and survival of, 26:53356
  effects on Saccharomyces cerevisiae, effects of photoreactivation repair mechanism on frequency of mutagenic, 26:53375
  effects on Schizosaccharomyces pombe, correlation between induced mitotic recombination and repair mechanisms for, 26:53371
  effects on Schizosaccharomyces pombe, inhibitory effects of caffeine on recombinational repair mechanisms for, 26:53371
  effects on survival of Streptomyces coelicolor, method for genotypic classification of mutants sensitive to, 26:53378
  effects on wallaby cells in culture, effects of dose on chromosome aberration rate, DNA synthesis, mitosis rate, reproduction, and survival time, 26:53353 (UR-3490-194)
  emission during weak breakup of aurora, sounding-rocket observation on Feb. 18, 1970 of strong extreme, (E), 26:54030

UNITED KINGDOM
  nuclear power growth in, 26:55088
  nuclear power plant development in, 26:55087
  power developments during 1970-71, survey of nuclear and thermonuclear, 26:55084(R) (INIS-mf-212)

- power requirements in, comparison with Sweden, 26:53102

UNITED STATES
- electric power generation in, legal methods for controlling demand for increased, 26:53101
- energy production, sources, and uses in, graphic and tabulated data on, 26:53096 (UCRL-51221)
- energy technology in, assessments of, 26:55085
- nuclear power plants in, complete testing of, 26:55214 (WASH-1208(9-72))
- power reactor development during 1972 to 1985, 26:55267 (WASH-1139(Rev.1))
- radiation protection standards for, role of Health Physics Society in development of, 26:54918
- radiation protection standards in, role of American National Standards Institute in development of, 26:54916
- radiation protection standards in, role of National Council on Radiation Protection and Measurements in development of, 26:54915

UNIVERSE
- models in scalar--tensor gravitation theory for observable, 26:54396 (ITF-72-41-P)
- perturbations in expanding, of free particles, (T), 26:53997
- scalar--tensor field equations in matter, (T), 26:53998

URANIUM
- complexes of tetravalent, preparation of alkyl and aryl, 26:53047
- complexes, formation with nicotinic, picolinic, and α-quinolinecarboxylic acids in water and alcohol, 26:53054
- complexes, spectra of dioxobisbenzoatodiaquouranyl(VI), ir, 26:53042
- content in alkali olivine basalt in USSR, (E), 26:53147
- content in upper Jurassic black bituminous argillites of West Siberian plate, 26:53146
- critical control parameters for 6 percent or less enriched, 26:53733 (WCAP-2999)
- determination in comparison with thorium content in standard samples by γ spectroscopy, 26:52941
- determination in ores by x-ray fluorescence method, photometric method for calibrating, 26:52922
- determination in organometallic compounds using oxine method after combustion, gravimetric or titrimetric, 26:52930
- determination in steels by extraction--photometric method, 26:52922
- determination in water samples by spark-source mass spectroscopy, 26:52914 (ANL-7860(Pt.3), pp 55-63)
- determination of hexavalent, in aqueous and nonaqueous solutions using 1,3-diphenyl-1,3-propanedione, standardization of spectrophotometric, 26:52920 (RT/CHI-(72)3)
- determination of, radiometric, 26:52942
- distribution between liquid bismuth and MSBR fuel salt, pp. 6-7, 26:53081 (ORNL-4794, pp 1-14)
- distribution in cores from Green Bay, relations with depth, 26:53164 (ANL-7860(Pt.3), pp 64-76)
- enrichment by gaseous diffusion process, method for calculation of flow rate in step cascades for, 26:53329
- enrichment of, review of centrifugation, electromagnetic, gaseous diffusion, and thermal diffusion methods of, 26:52977
- ionization of surfaces of, 26:53033 (EUR-4765, pp 117-30)
- neutron reactions with bare fast multiplying systems of, Storrer--Stievenart analysis of pulsed, (T), 26:54483 (JAERI-M-4652)
- neutron transmission and self-indication measurements in depleted, 26:54656(R) (COO-3058-21)
- neutron transmission and self-indication ratio measurements in depleted, temperature-dependent, (E), 26:54477 (CONF-720901-(Bks.1 and 2), pp 1115-26)
- proton reactions at 2.25 MeV, x-ray fluorescence spectrum from, (E), 26:53803
- reactions of tetravalent, with trivalent chlorine in presence of phenol in aqueous acid solution, kinetics and mechanism of oxidation--reduction, 26:53051
- reactions of tetravalent, with trivalent chlorine, in presence of phenol in aqueous acid solutions, mechanism and kinetics of oxidation--reduction, 26:53044
- separation from impurities by fractional dissolution of crude sodium diuranate, 26:52976 (IEA-250)
- separation from molten fluoride salts by oxide precipitation, pp. 12-14, 26:53081 (ORNL-4794, pp 1-14)
- separation from ores in South Africa, 26:55453(R) (NP-19410)
- separation from ores, review on, 26:52977
- separation from phosphoric acid by solvent extraction using DEHPA and TOPO, pp. 55-7, 26:53084 (ORNL-4794, pp 54-62)
- separation from phosphoric acid by solvent extraction using mixture of mono- and dioctylphenyl phosphates, pp. 55-7, 26:53084 (ORNL-4794, pp 54-62)
- separation from plutonium, residue adsorption and anion exchange methods for, 26:52935(R) (MLM-1888)
- separation from spent molten salt fuel by fluorination and reductive extraction methods, 26:53086(P)
- separation from sulfuric acid solutions by solvent extraction using primary amine pp. 57-61, 26:53084 (ORNL-4794, pp 54-62)
- separation of hexavalent, by ion exchange using diethylaminoethylcellulose, 26:52951
- shipping of slightly enriched billets, ingots, and fuel cores of, design of wooden container for, 26:53737
- sorption of hexavalent, on diethylaminoethylcellulose in methanol--thiocyanate--hydrochloric acid media, 26:52951

URANIUM ALLOYS AND SYSTEMS
- Al--U, fission product release from irradiated foils of, mechanisms and measurement of recoil gaseous, 26:53694 (JAERI-Memo-3936)
- Mo--U-base, corrosion of wires of, ion microscopy studies of stress, 26:53610
- Nb--U-base, stress corrosion cracking by sodium chloride sprays, protective effects of epoxy-primed polyurethane-painted surface on, 26:53607 (RFP-1891)
- Nb--U-base, stress corrosion cracking of overaged and underaged, by aqueous chloride solutions, 26:53608 (RFP-1904)
- Nb--U-base--Zr, tensile properties of polycrystalline, as function of strain rate, 26:53691

URANIUM CARBIDES
- crushing and combustion of TRISO-coated, fission product release in, 26:53078 (CONF-720823-11)
- preparation by carbothermic method, research progress on, p. 86-7, 26:53554 (ORNL-4794, pp 84-7)
- PuC--UC, preparation by carbothermic method, research progress on, p. 86-7, 26:53554 (ORNL-4794, pp 84-7)

URANIUM CARBONITRIDES
- preparation by carbothermic method, research progress on, p. 86-7, 26:53554 (ORNL-4794, pp 84-7)
- PuCN--UCN, preparation by carbothermic method, research progress on, p. 86-7, 26:53554 (ORNL-4794, pp 84-7)

URANIUM CHLORIDES
- $LiCl--UCl_3--UCl_4$, melting point diagrams for, 26:53721

URANIUM CHLORIDES UCl_4
- complexes with nicotinic, picolinic, and α-quinolinecarboxylic acids in water and alcohol, spectrophotometric studies of, 26:53054

URANIUM DEPOSITS
- formation in Grants Region, N. Mex. sandstone, trend orebody studies of, 26:53144 (GJO-936-2)
- geology of Fay Mine, in Saskatchewan, 26:53145
- prospecting for south Texas, Conquista Project for, 26:53148
- roll formation and migration in Wyoming, physical and chemical factors responsible for, 26:53143 (GJO-936-1)

URANIUM FLUORIDES UF_4
- analysis for uranium-235, system for neutron interrogation, 26:53217
- reactions with uranium hexafluoride in molten beryllium fluoride--lithium fluoride--thorium fluoride, p. 6, 26:53081 (ORNL-4794, pp 1-14)

URANIUM FLUORIDES UF_6
- handling procedures and container criteria for, description of USAEC, 26:53735 (ORO-651(Rev.3))
- reactions with uranium tetrafluoride in molten beryllium fluoride--lithium fluoride--thorium fluoride, p. 6, 26:53081 (ORNL-4794, pp 1-14)
- uranium-235 concentration in, review of methods for, 26:53328

URANIUM ISOTOPES
- determination in Eurex process solutions by mass spectrometry, 26:52918 (EUR-4765, pp 91-115)

URANIUM ISOTOPES U-232
- determination in plutonium-238 and uranium-234 by hydrolysis, residue adsorption, and α spectroscopy, 26:52935(R) (MLM-1888)

URANIUM ISOTOPES U-233
- purification of, p. 51, 26:53552 (ORNL-4794, pp 45-51)
- separation from thorium,, 26:52977
- storage and distribution of, p. 51, 26:53552 (ORNL-4794, pp 45-51)

URANIUM ISOTOPES U-234
- content in atmosphere in vicinity of Savannah River Plant, 1971, 26:53153(R) (DPSPU-72-30-1)
- determination in plutonium-238 and uranium-232 by hydrolysis, residue adsorption, and α spectroscopy, 26:52935(R) (MLM-1888)
- energy levels from two-nucleon transfer reactions, calculation using quadrupole pairing correlations, 26:54731
- purification of, anion exchange method for, 26:52935(R) (MLM-1888)
- triton reactions (t,p) at 15 to 20 MeV, proton spectra and angular distributions for, (E), 26:54671

URANIUM ISOTOPES U-235
- alpha fission at 24.5 to 28.0 MeV, excitation function for, (E), 26:54665
- alpha reactions (α,3n) and (α,t) at 24.5 to 28.0 MeV, excitation function for, (E), 26:54665
- concentration in uranium hexafluoride, review of methods for, 26:53328
- content in atmosphere in vicinity of Savannah River Plant, 1971, 26:53153(R) (DPSPU-72-30-1)
- determination in containers, system for neutron interrogation, 26:53217
- neutron fission at thermal and 14 MeV energies, delayed neutron spectra from, (T), 26:54655 (CONF-720901-(Bks.1 and 2), pp 687-99)

- neutron fission of, delayed neutron spectra from, (E), 26:54660(R) (RLO-2225-T-17-4)
- neutron fission of, independent yields of krypton and xenon isotopes in thermal, (E), 26:54667
- neutron fission of, survey on cross section data for, 26:54657 (FEI-292)
- neutron fission of, yields for thermal, (E), 26:54626
- neutron spectra from homogeneous sphere containing, benchmark calculations for, 26:54486 (RISO-M-1526)
- proton reactions at 0.7 GeV, calculation of spallation--fission competition using intranuclear-cascade model, (T), 26:54666

- URANIUM ISOTOPES U-236
  - triton reactions (t,p) at 15 to 20 MeV, proton spectra and angular distributions for, (E), 26:54671
- URANIUM ISOTOPES U-238
  - alpha reactions (α,2n) at 25 MeV, conversion-electron spectra from, (E), 26:54664
  - content in atmosphere in vicinity of Savannah River Plant, 1971, 26:53153(R) (DPSPU-72-30-1)
  - decay of, γ-ray energies and intensities from, (E), 26:54652 (ANCR-1069)
  - neutron absorption by, Doppler effect in fast, 26:54479 (CONF-720901-(Bks.1 and 2), pp 1152-65)
  - neutron capture at 24.3 keV, TOF cross-section measurements using iron-filtered beam, (E), 26:54597 (CONF-720901-(Bks.1 and 2), pp 1107-14)
  - neutron capture at thermal to 100 keV, cross sections for gamma-ray production in, (E), 26:54960 (NASA-TM-X-2440, pp 500-11)
  - neutron capture by, survey of cross section data for, 26:54657 (FEI-292)
  - neutron capture near 24.3 keV, pulse height spectra and relative cross section for, (E), 26:54656(R) (COO-3058-21)
  - neutron fission at 14 MeV, delayed neutron spectra from, (E), 26:54655 (CONF-720901-(Bks.1 and 2), pp 687-99)
  - neutron fission at 14 MeV, method for determining lifetime of compound nucleus in, (E), 26:54669
  - neutron reactions (n,f) at 14.8 MeV, cadmium-115 isomer ratios in, (E), 26:54628
  - proton reactions at 0.15 to 3 GeV, calculation of spallation--fission competition using intranuclear-cascade model, (T), 26:54666
  - proton reactions at 12 and 28 GeV, yields of actinides and transactinides from secondary reactions following, (E), 26:54672
  - reactivity worth measurements in ZPPR-2 on, effects of core configuration on Doppler, 26:55393 (CONF-720901-(Bks.1 and 2), pp 1006-15)
  - triton reactions (t,p) at 15 to 20 MeV, proton spectra and angular distributions for, (E), 26:54671
- URANIUM METAPHOSPHATES
  - preparation and structure of, 26:53045
- URANIUM NITRIDES
  - electric conductivity and thermoelectric power of, (E), 26:55027
  - fabrication of high-density, by sintering, 26:53581
  - ThN--UN, electric resistivity, thermal conductivity, and thermoelectric power of, (E), 26:55027
  - UN--W, preparation of fuels of, method for, 26:53562(P)
- URANIUM ORES
  - analysis of standard, for thorium and uranium by γ spectroscopy, 26:52941
  - mining and milling of south Texas, equipment and methods in Conquista Project for, 26:53148
  - processing of, review on, 26:52977
- URANIUM OXIDES UO_2
  - content in reactor fuels during fuel fabrication, automatic on-line system for weighing and recording, 26:53723
  - critical control parameters for 6 percent or less enriched, 26:53733 (WCAP-2999)
  - densification of, review on effects of chemical, physical, physicochemical, and process variables on, 26:53547 (AREAEE-135)
  - dissolution in aqueous solutions, potentiostatic studies on anodic, 26:53035 (NIM-1448)
  - fission gas bubble nucleations and migration in, mechanisms of, 26:53565
  - gamma scanning of irradiated pellets of, self-absorption corrections for, 26:53041 (UJV-2867-M,A)
  - oxidation of colloidal, 26:53067 (ORNL-4794, pp 88-90)
  - oxidation of fuel pellets of, during hydrogen sintering, 26:53563
  - pore migration in, effects of impurity additions on thermal gradient-induced lenticular, 26:53559
  - preparation of microspheres of, sol-gel process development for, p. 45, 26:53552 (ORNL-4794, pp 45-51)
  - preparation of microspheres of, using ion exchange resins, pp. 47-9, 26:53552 (ORNL-4794, pp 45-51)
  - preparation of sinterable powders of, conditions and method for, 26:53546 (AREAEE-134)
  - preparation of uranium-233-enriched, for light-water breeder reactors, research progress on, 26:53553 (ORNL-4794, pp 52-3)
  - production by reduction of uranium trioxide powders, 26:53548 (AREAEE-139)
  - radiation effects on fuel particles of, equipment and methods for studies of, 26:53555 (RD/B/N-2214)
  - sintering kinetics of, effects of green density on initial-stage, 26:53597
  - sintering of, nonisothermal method for studying initial-stage, 26:53595
  - sintering of, review on mechanism of activated, 26:53587
  - Mo--UO_2, fabrication of, review on methods for, 26:53592
  - PuO_2--UO_2, corrosive effects on stainless steel of fission products of, effects of burnup on, 26:55187 (EURFNR-989)
  - PuO_2--UO_2, oxidation of unirradiated fuels of, p. 84-5, 26:53554 (ORNL-4794, pp 84-7)
  - PuO_2--UO_2, preparation of by sol-gel process, research progress on, p. 85-6, 26:53554 (ORNL-4794, pp 84-7)
  - PuO_2--UO_2, properties of fuels of, mechanical, physical, and thermal, (E), 26:55189(R) (GEAP-10028-39)
  - PuO_2--UO_2, radiation effects testing of fuels of, 26:55189(R) (GEAP-10028-39)
  - PuO_2--UO_2, reactivity of fuel elements of, effects of grain size of plutonium oxide in, 26:55416(R) (BNWL-1522-5)
  - PuO_2--UO_2-base, deformation and fracture of, effects of temperature and strain rate on, 26:53545 (ANL-7945)
  - ThO_2--UO_2, crushing and combustion of BISO-coated, fission product release in, 26:53078 (CONF-720823-11)
- URANIUM OXIDES UO_3
  - analysis for uranium-235, system for neutron interrogation, 26:53217
  - reduction of powders of, by ammonia or hydrogen, factors affecting, 26:53548 (AREAEE-139)
- URANIUM OXIDES U_3O_8
  - analysis for uranium-235, system for neutron interrogation, 26:53217
  - purification by carrier distillation using alkaline halides, thermochemical reactions in, 26:53719
  - requirements in power production 1980 to 2000, calculations of, 26:55093
  - spectra of, reactions of alkali metal halides with oxide impurities in carrier distillation process for production of, 26:52955 (RT/CHI-(72)4)
- URANIUM RESERVES
  - estimates in South Africa, 26:55453(R) (NP-19410)
- URANYL COMPOUNDS
  - reactions with hydrofluoric acid and hydroxylamine, production of ammonium uranium pentafluoride by, 26:53049(P)
- URANYL NITRATES
  - analysis for uranium-235, system for neutron interrogation, 26:53217
  - effects on rat kidneys uptake of organic bases, 26:53537
  - preparation of clear solutions of, by fractional dissolution of crude sodium diuranate, 26:52976 (IEA-250)
- UREA, 1-METHYL-1-NITROSO-
  - effects on cultured Chinese hamster cells in comparison to effects of 5-bromodeoxyuridine, uv radiation, and x radiation, effects of dose and post-exposure culture medium on frequency of mutagenic, 26:53362
- URETHAN POLYMERS
  - protective properties of painted surfaces of, against stress corrosion cracking of niobium--uranium-base alloys, 26:53607 (RFP-1891)
- URIDINE, 5-BROMO-2'-DEOXY-
  - effects on cultured Chinese hamster cells in comparison to effects of N-nitrosomethylurea, uv radiation, and x radiation, effects of dose and post-exposure culture medium on frequency of mutagenic, 26:53362
- URINARY TRACT
  - radioinduced fistulas in human, following therapy of rectal and uterine neoplasms, surgical treatment of, 26:53438
- URINE
  - analysis for plutonium by radiochemical methods using ion exchanger filter, 26:52940
- UTERUS
  - radiation dosimetry in, thermoluminescent dosimeter for long term, 26:53238

V

- VACCINES
  - effectiveness of irradiated metacercariae as, for immunization of cattle against fascioliasis, 26:53498(R) (PRNC-156)
  - effectiveness of x-irradiated Dictyocaulus larvae as, for immunization of cattle, 26:53503
- VACUUM
  - bibliography on surface and vacuum physics, 26:54085
  - measurement of ultrahigh, equipment and methods for, 26:53140
  - production of ultrahigh, for industrial and scientific uses, equipment and methods for, 26:53140
- VACUUM GAGES
  - calibration of, methods for, 26:53300 (EUR-4797)
- VACUUM PUMPS
  - design and performance of improved ion-type, 26:53141(P)
  - performance of cryogenic, in ultrahigh vacuum unit for film deposition, 26:53139
- VACUUM SYSTEMS
  - controls for automatic, design of pneumatic logic, 26:55629 (UCRL-73921)
  - design of ultrahigh evaporation unit for deposition of thin films, 26:53139

VACUUM TECHNIQUES
  conference on application to semiconductors and electronics, Versailles, France, Sept. 13, 1971, 26:53138
VALVES
  design criteria for nuclear service, development program for, 26:55207(R) (ORNL-TM-3900)
  standards for butterfly-type isolation, 26:53111 (RDT-E-1-13-T(8-72))
VAN ALLEN RADIATION BELTS
  dose and dose rate from, for space vehicle design and mission planning, 26:54952 (NASA-TM-X-2440, pp 170-7)
  electron fluxes trapped in, temporal variations in, 26:54046 (NASA-TM-X-2440, pp 539-47)
  electron injection and effects from high-altitude nuclear explosions, 26:54044 (NASA-TM-X-2440, pp 178-92)
  particles in, performance of high-resolution particle identifier for detection and measurement of, (T), 26:53280
  radiation dose and LET measurements on OV1-19 satellite, April--Dec. 1969, 26:54048 (NASA-TM-X-2440, pp 561-8)
VAN DE GRAAFF ACCELERATORS
  experimental facilities for EN tandem, pulsed-beam neutron time-of-flight, 26:54467(R) (ORO-2972-204)
VANADIUM
  book: Early Transition Metals, 26:52956
  determination in geochemical standards by atomic absorption using nitrous oxide--acetylene flame, 26:52921
  determination in mineral oil by neutron activation, 26:52905
  determination in silicate rocks by paper chromatography, neutron activation, and γ spectrometry, 26:52909
  determination in water samples by spark source mass spectroscopy, 26:52914 (ANL-7860(Pt.3), pp 55-63)
  determination in water, effects of large amounts of copper on spectrographic, 26:52927
  diffusion in aluminum nitride, silicon nitride, and titanium dioxide, 26:53677
  effects on neutron radioinduced strengthening of chromium--iron welds, iron, and pressure vessel steel, 26:53710
  fabrication by rolling at high temperature under vacuum, 26:53630
  superconducting transition in, use of acoustical measurements for, 26:54439
VANADIUM ALLOYS AND SYSTEMS
  Al--Mo--Ti-base--V, crack propagation and embrittlement by gaseous hydrogen, mechanism of, 26:53685
  Al--Ti-base--V, fracture toughness of $\alpha + \beta$ and β processed, at room and subzero temperatures, measurement of plane strain, 26:53661
  Co--V, vanadium-51 NMR quadrupole splitting in sigma-phase, effects of composition on intensity of, 26:55056
  Ni--V, ordering transformation in Ni_2V, 26:53659
  Pd--V, diffusion measurements on, at 608 to 1300°C, 26:53677
VANADIUM IONS
  phonon resonant scattering at, in alumina single crystals, 26:54978
VANADIUM ISOTOPES V-46
  beta decay of, electromagnetic corrections to ft values for, (T), 26:54713
VANADIUM ISOTOPES V-49
  abundance in iron meteorites, (T), 26:53808(T) (ORNL-tr-2620)
  energy level at 153 keV from titanium-48 (p,γ) reactions, g factor and lifetime of, (E), 26:54574
VANADIUM ISOTOPES V-51
  nuclear magnetic resonance quadrupole splitting in sigma-phase vanadium--cobalt alloys, 26:55056
VANADIUM OXIDES
  phase transition in VO_2 single crystals, Raman-scattering study of phonon spectrum in semiconductor--metal, (E), 26:55043
VEGETABLES
  analysis for mercury by neutron activation, 26:52911
VEHICLES
  exhaust emissions from transportation, computer and manual methods for calculating, 26:55467 (ANL/ES-15)
  propulsion of automotive, nonconventional two-cycle engines for, 26:53103
VELOCITY
  measurement of x-ray-produced blowoff, in nuclear explosions, development of probe velocity transducer for, 26:53303 (LA-4999)
VENUS (PLANET)
  dayglow emission from atmosphere of, relation with electron impact excitation cross sections and energy degradation in carbon monoxide, (E/T), 26:54008
VERMONT YANKEE POWER REACTOR
  operation of, temporary license for, 26:55256 (DOCKET-50271-101)
  site for, environmental radiation survey during January to June 1972, 26:55255 (DOCKET-50271-100)
VIBRATING REED ELECTROMETERS
  improvement of Shonka, 26:53196(R) (COO-323-28)
VIRGIL C. SUMMER POWER REACTOR, UNIT 1
  auxiliary system for, revised and additional data on, 26:55344 (DOCKET-50395-28)
  containment system for, revised and additional data on, 26:55344 (DOCKET-50395-28)
  engineered safeguards for, revised and additional data on, 26:55344 (DOCKET-50395-28)
  instrumentation for, revised and additional data on, 26:55344 (DOCKET-50395-28)
  power conversion system for, revised and additional data on, 26:55344 (DOCKET-50395-28)
  site for, revised and additional data on, 26:55344 (DOCKET-50395-28)
  structures for, revised and additional data on, 26:55344 (DOCKET-50395-28)
VISION
  diagnosis of visual fields, modeling of visual pathway for interactive, 26:55466 (ANL-7858)
  photoinitiated processes in, 26:55495(R) (COO-1627-22)
  photoinitiated processes in, 26:55496(R) (COO-1627-23)
  radiation effects on human visual response following retinal exposure, effects of particle flux density on charged helium ion, 26:53403 (NASA-TM-X-2440, pp 416-22)
  radiation effects on human, following therapy of nasal carcinomas, γ and x, 26:53444
VITAMIN B GROUP
  B_{12}, determination in blood by radiochemical method, 26:52938
  pantothenic acid, radioprotective effects of, in combination with AET on mice, whole-body x, 26:53481
VITAMINS
  radiation effects on content of, in wheat, wheat bread, and wheat flour, gamma, 26:53344

W

WASHINGTON
  zinc-65 distribution and concentration in benthic fauna from continental shelf of, 26:53149 (RLO-2227-T-12-26)
WASPALOY
  production and properties of high-density powder metallurgy components of, for use at high temperatures, 26:53631
WATER
  analysis for heavy metals, effects of large amounts of copper on spectrographic, 26:52927
  analysis for trace elements by spark-source mass spectroscopy, 26:52914 (ANL-7860(Pt.3), pp 55-63)
  analysis of deuterium-depleted, for hydrogen isotopes using distillation column and mass spectroscopy, 26:52913(T) (AEC-tr-7345)
  chemical oxygen demand of, use of perchloratocerate reagent and fluorometric determination of cerium for measurement of, 26:52915 (CONF-720827-2)
  corrosive effects on copper/steel, Inconel/Zircaloy-2, steel/Zircaloy-2, and Zircaloy-2/Zircaloy-2 couples, fretting, 26:53609 (RT/ING-(72)7)
  corrosive effects on zirconium and zirconium alloys at high temperatures, factors controlling, 26:53614
  cosmic secondary particle dose calculations, heavy galactic, 26:54878 (NASA-TM-X-2440, pp 104-7)
  decontamination of radioactively contaminated, by coagulation, use of organic flocculants in, 26:53040 (SZS-129)
  electron energy spectrum in, irradiated with 10- to 20-MeV electron beams, 26:54894
  lectures at Physics Laboratory of Istituto Superiore di Sanita, Rome, July--Dec. 1970, 26:54162 (ISS-71/31)
  mass transfer from sol droplets, p. 93, 26:53085 (ORNL-4794, pp 91-5)
  muon (μ^-) depolarization in aqueous solutions and pure, effects of chemical reactions, hydrogen peroxide concentration, and temperature on, 26:54099
  radioactivity monitoring of, in vicinity of Savannah River Plant, 1971, 26:53153(R) (DPSPU-72-30-1)
  radiolytic reactions in, kinetic data on, 26:55416(R) (BNWL-1522-5)
  reactions with liquid sodium, design of equipment for studying, 26:55153 (CONF-710548-, pp 57-104)
  reactions with sodium from 350 to 600°C, effects on rupture of austenitic steel of, 26:55161 (CONF-710548-, pp 221-42)
  reactions with sodium in steam generators, tube damage from, 26:55150 (CONF-710548-, pp 1-16)
  reactions with sodium, brief summary of studies in Italy on, 26:55160 (CONF-710548-, pp 213-20)
  reactions with sodium, conference on, 26:55149 (CONF-710548)
  reactions with sodium, effects on temperature and pressure of, 26:55152 (CONF-710548-, pp 39-56)
  reactions with sodium, kinetics of, 26:55155 (CONF-710548-, pp 129-54)
  reactions with sodium, pressure wave from, 26:55157 (CONF-710548-, pp 171-86)
  reactions with sodium, summary of study of large scale, 26:55158 (CONF-710548-, pp 187-205)
  reactions with sodium, use of hydrogen detectors for detection of, 26:55156 (CONF-710548-, pp 155-70)
  H_2O--steam, flow in turbines, equipment and methods for studying, 26:53124
WATER-d_2
  production of, advantages of ammonia isotopic exchange process for, 26:53088

  requirements in power production 1980 to 2000, calculations of, 26:55093

WATER-t
  separation from environmental samples by freeze drying, equipment for, 26:53151 (ANL-7860(Pt.3), pp 45-50)

WATER-t$_2$
  disposal of, generated in natural gas reservoirs produced by nuclear explosions, 26:53128 (ORNL-4794, pp 63-4)

WATER VAPOR
  electron interaction with, atomic processes and energy deposition, applications in atmospheric sciences of, (E/T), 26:54033
  radioinduced ionization of undeuterated and deuterated, energy for ion pair formation in beta, 26:53196(R) (COO-323-28)
  reactions on chromium, iron, or nickel, hydrogen production by, 26:52975(P)

WATERFORD POWER REACTOR, UNIT 3
  owners of, financial data on, 26:55260 (DOCKET-50382-36)

WATTS BAR POWER REACTOR, UNIT 1
  auxiliary building crane for, revised and additional data on, 26:55342 (DOCKET-50390-23)
  component cooling water system for, revised and additional data on, 26:55342 (DOCKET-50390-23)
  compressed air system for, revised and additional data on, 26:55342 (DOCKET-50390-23)
  containment purge supply and exhaust system for, revised and additional data on, 26:55342 (DOCKET-50390-23)
  cooling system for, design stress limits for, 26:55342 (DOCKET-50390-23)
  fire protection system for, revised and additional data on, 26:55342 (DOCKET-50390-23)
  flood level maximum for, revised and additional data on, 26:55342 (DOCKET-50390-23)
  instrument room for, fire protection for cables in auxiliary, 26:55342 (DOCKET-50390-23)
  instrumentation display system for, revised and additional data on, 26:55342 (DOCKET-50390-23)
  protection system for, design seismic stresses on, 26:55343 (DOCKET-50390-24)
  safety analysis reports, index to, 26:55213 (FIND-50390(8-72))
  site for, revised and additional data on, 26:55342 (DOCKET-50390-23)

WATTS BAR POWER REACTOR, UNIT 2
  auxiliary building crane for, revised and additional data on, 26:55342 (DOCKET-50390-23)
  component cooling water system for, revised and additional data on, 26:55342 (DOCKET-50390-23)
  compressed air system for, revised and additional data on, 26:55342 (DOCKET-50390-23)
  containment purge supply and exhaust system for, revised and additional data on, 26:55342 (DOCKET-50390-23)
  cooling system for, design stress limits for, 26:55342 (DOCKET-50390-23)
  core support structures for, design stress limits for, 26:55342 (DOCKET-50390-23)
  fire protection system for, revised and additional data on, 26:55342 (DOCKET-50390-23)
  flood level maximum for, revised and additional data on, 26:55342 (DOCKET-50390-23)
  instrument room for, fire protection for cables in auxiliary, 26:55342 (DOCKET-50390-23)
  instrumentation display system for, revised and additional data on, 26:55342 (DOCKET-50390-23)
  protection system for, design seismic stresses on, 26:55343 (DOCKET-50390-24)
  safety analysis reports, index to, 26:55213 (FIND-50390(8-72))
  site for, revised and additional data on, 26:55342 (DOCKET-50390-23)

WEISWEILER POWER REACTOR
  coolant activation in, (T), 26:55169 (CONF-710959-, Paper 13)
  coolant flow in, effects of partial blockage in fuel element assemblies on distribution of, 26:55176 (KFK-1548)
  cooling systems of, corrosion problems in, (E/T), 26:55168 (CONF-710959-, Paper 12)
  cooling systems of, effects of temperature on corrosion product deposits in, (E/T), 26:55168 (CONF-710959-, Paper 12)
  cooling systems of, sources of radioactivity in, (T), 26:55169 (CONF-710959-, Paper 13)
  design basis accidents in, effects of fission product release on, (T), 26:55169 (CONF-710959-, Paper 13)
  design parameters of, summary of, 26:55096
  development of, program for, 26:55098
  development of, program for, 26:55097
  development program for, 26:55095
  fuel element cladding of, effects on coolant contamination of defects in, (T), 26:55169 (CONF-710959-, Paper 13)
  steam generators for, leak testing of straight tube models of, 26:55151 (CONF-710548-, pp 17-38)
  structural materials in, effects on coolant contamination of corrosion of, (T), 26:55169 (CONF-710959-, Paper 13)

WELDING
  equipment and methods for electron beam, of thick metal sheets, 26:53633

WELDS
  inspection of metallic, for defects, ultrasonic method for, 26:53126(P)
  mechanical properties of, in low-alloy steel at 900 to 1300°F, literature review on, 26:53638 (ORNL-4781)
  mechanical properties of, in Types 304 and 316 stainless steel at 900 to 1300°F, literature review on, 26:53638 (ORNL-4781)

WELL LOGGING
  interpretation of data from continuous gamma, differential, 26:53173 (INP-793)

WHISTLERS
  propagation of magnetospheric monochromatic vlf, effect of nonlinear phenomena on, (E/T), 26:54050
  refractive index and attenuation surfaces in vicinity of cross-over level, (T), 26:54015

WHITE OAK LAKE
  cesium-137 cycling in fish in, 26:53535

WILLIAM H. ZIMMER POWER REACTOR, UNIT 1
  effluents from, effects on environment of chemical, radioactive, and thermal, 26:55337 (DOCKET-50358-41)
  operation of, cost-benefit analysis for, 26:55337 (DOCKET-50358-41)
  site for, ecology, geology, hydrology, and meteorology of, 26:55337 (DOCKET-50358-41)

WIND TUNNELS
  Magnus force and moment measurements in NOL Supersonic, 26:55596 (SC-CR-723162)

WIRES
  sparkostriction in, laser-based study output pulses from, 26:53222

WOOD
  plastics--wood, preparation and properties of, produced by radioinduced polymerization, 26:53722

WYLFA REACTORS
  performance during first 18 months operation, summary of, 26:55269

X

X RADIATION
  absorbed dose and effective energy distribution under screen filter in tissue-equivalent phantom, (E), 26:54911
  attenuation by lead, 50- to 300-kVp broad-beam, (E), 26:54904
  cosmic background, intensities of lines in the 0.25- to 1-keV range, (E/T), 26:53815
  cosmic background, inverse Compton models for, (E/T), 26:54000
  detection of soft cosmic, thin polypropylene window proportional counters for, 26:53206
  detection of, design and performance of position-sensitive proportional counter for, 26:53221
  disintegration of high Z nuclei in pulsar environment, (T), 26:53857
  dose across plane bone--tissue interface, contribution of photoelectrons to, (T), 26:54896
  dose to bone marrow and eyes of medical personnel during arteriography, measurement of, 26:53443
  dose to children during diagnostic radiography, methods for reducing, 26:53417
  dose to human gonads and stomach wall during diagnostic radiography of stomach, x, 26:53427
  dose to man during diagnostic radiography, phantom studies for predetermination of absorbed, 26:53416
  dose to man during diagnostic radiography, phantom measurements in bone marrow, gonads, and skin, 26:53434
  dosimetry of 250- and 65-kVp, grid-walled proportional counter study of micro-, 26:54895
  dosimetry of, correction factors for dosimeters for, 26:53247
  effectiveness in combination with internal colloidal gold-198 for therapy of liver involvement in Hodgkin's disease, 26:53507
  effects on alkaline phosphatase activity and chromosomes of mice, 26:53496
  effects on ammonium perchlorate single crystals, electron microscopic studies of, 26:52985 (NASA-TM-X-2440, pp 584-94)
  effects on antibody-forming cells in mouse spleen during response to antigen challenge, acute whole-body, 26:53464
  effects on budding haploid yeast cells, sensitivity to lethal, 26:53368
  effects on carrots following exposure of seeds, dose dependence of growth and yield, 26:53391
  effects on cell volume and DNA content of parent strain and radioresistant mutant of Escherichia coli, 26:53363
  effects on cesium bromide at 4.2 and 77°K, color centers produced in, 26:54980
  effects on chickens, effects on lymphatic organs following acute sublethal exposure of young, 26:53457 (NASA-TM-X-2440, pp 659-64)
  effects on children following use for maternal therapy during pregnancy, pathological and teratological, 26:53437
  effects on chromosomes human lymphocytes in cultures, effects of dose on frequency of aberrant, 26:53355

effects on chromosomes in cultured rat-kangaroo cells, effects of cell phase on sensitivity to, 26:53359
effects on chromosomes in leukocytes of peripheral blood of man following stomach exposure during diagnostic radiography, aberrant, 26:53427
effects on chromosomes in mature oocytes of Drosophila melanogaster, effects of premeiotic breakage and interchanges on types of aberrant, 26:53501
effects on chromosomes in mature spermatozoa of Drosophila melanogaster, inhibitory effects of dactinomycin on post-fertilization maternal repair of aberrant, 26:53502
effects on chromosomes in peripheral leukocytes of medical radiography personnel, incidence of aberrant, 26:53428
effects on count of plaque-forming cells in spleen of antigen-stimulated mice following whole-body exposure, effects of dose on, 26:53469
effects on cultured Chinese hamster cells following low dose rate sublethal exposure, effects of temperature on repair of, 26:53358
effects on cultured Chinese hamster cells in comparison to effects of chemical mutagens and uv radiation, effects of dose and post-exposure culture medium on frequency of mutagenic, 26:53362
effects on cultured mouse lymphoma cells in comparison to effects of chemical mutagens, phenotypic method for determining frequency of mutagenic, 26:53361
effects on developing brain of rats, relation of acetylcholine metabolism to pathological, 26:53461(R) (UCB-34-P-82-13)
effects on Dictyocaulus larvae infectivity for vaccinating cattle, 26:53503
effects on diurnal rhythm of neurosecretory activity in mice following whole-body exposure, 26:53478
effects on DNA in cultured mammalian cells and microorganisms, role of repair processes in recovery from lethal and mutagenic, review of, 26:53357
effects on DNA synthesis and degradation in liver, spleen, and thymus of rats, 26:53489
effects on DNA, review of sensitizing effects of N-ethylmaleimide, N-oxyl radicals, nitric oxide, and oxygen, 26:53352
effects on Drosophila melanogaster following acute exposure of mature spermatozoa, dose dependence of genetic, 26:53497(R) (COO-1748-12)
effects on growth of goitrogen-stimulated thyroid gland of mice in comparison to effects of internal exposure from iodine-131 or iodine-132, effects of dose rate on inhibitory, 26:53472
effects on human heart following therapy of esophageal carcinomas, electrocardiogram studies of pathological, 26:53439
effects on human skin following chronic therapeutic exposure, changes in DNA and RNA contents and ultrastructure of epidermis resulting from pathological, 26:53441
effects on human spermatogenesis following exposure of testes, effects of dose on inhibitory, 26:53399 (NASA-TM-X-2440, pp 229-32)
effects on kidneys of parabiosed rats following whole-body exposure, carcinogenic, 26:53449 (COO-3017-4)
effects on lead acetate monocrystals and powders, ESR studies on, 26:53008
effects on mature spermatozoa of Drosophila melanogaster, effects of dactinomycin on post-fertilization expression of mutagenic, 26:53502
effects on mice following fractionated whole-body exposure in comparison to effects of internal strontium-90, effects of thymectomy on incidence of leukemogenic, 26:53512
effects on mice following lethal whole-body exposure, protective effects of combined AET and pantothenic acid against, 26:53481
effects on mice following whole-body exposure, incidence of leukemogenic, 26:53469
effects on mice, effects on hematopoiesis and immune reactions following high-intensity pulsed whole-body exposure, comparison of RBE with γ rays for pathological, 26:53469
effects on mice, relation to spleen colony formation by transplanted isogenic hemopoietic stem cells in, lethal dose, 26:53466
effects on mice, studies on transmission of leukemogenic, 26:53496
effects on motor activity of rats following exposure of embryos, dose dependence of γ, 26:53488
effects on mouse embryos following acute or fractionated exposure in utero, effects of dose on lethal, 26:53453 (NASA-TM-X-2440, pp 641)
effects on mouse embryos, inhibitory for gastrulation, 26:53476
effects on mouse lymphoma cells in cultures, effects of dose on proliferation and survival of, 26:53356
effects on p-dichlorobenzene and sodium chlorate crystals, 26:52984 (FRNC-TH-262)
effects on phagocytic activity of reticuloendothelial cells in mice following whole-body exposure, effects of dose on inhibitory, 26:53468
effects on pituitary gland in mice following partial- or whole-body exposure, relation of ultrastructural changes to secretory changes induced in, 26:53467
effects on radishes following seed exposure, dose dependence of growth and yield, 26:53391
effects on rats, effects on respiration and ultrastructure of mitochondria in intestinal epithelial cells during amino acid absorption, whole-body, 26:53493
effects on regeneration of thyroid gland in rats following whole-body exposure, effects of prior implantation of sarcoma on inhibitory, 26:53494
effects on serine single crystals at 77 to 340°K, ESR and ENDOR studies on free radicals from, 26:53004
effects on sheep following various combinations of acute, chronic, continuous, or fractionated dose whole-body exposures, effects of dose and dose rate on pathological, 26:53451 (NASA-TM-X-2440, pp 622-32)
effects on single crystals of DL-serine at 77 to 340°K, electron nuclear double resonance and ESR studies on, 26:52996
effects on skin of swine, dose dependence of reproductive kinetics of cells, 26:53450 (LA-4874, pp 126-44)
effects on spectra of hexacyanocobaltate-doped sodium chloride and potassium chloride, 26:55001
effects on sugar beets following seed exposure, effects of ploidy on seed germination and weight of beets, 26:53389
effects on survival of cultured Chinese hamster cells following low dose rate exposure, effects of temperature on sensitivity to, 26:53358
effects on survival of mice following transplantation of allogeneic bone marrow, relation of age and immune reactions to lethal, 26:53485
effects on survival of parent strain and radioresistant mutant of Escherichia coli, 26:53363
effects on survival of spores of Bacillus subtilis, effects of energy level on, 26:53376
effects on swine following various combinations of acute, chronic, continuous, or fractionated dose whole-body exposures, effects of dose and dose rate on pathological, 26:53451 (NASA-TM-X-2440, pp 622-32)
effects on thyroid gland in dogs following whole-body exposure, relation of metabolic rate to carcinogenic and morphologic, 26:53462 (UR-3490-183)
effects on vision, in relation to changes in human optic nerve and retina following therapy of nasal cavity and paranasal sinus carcinomas, dose and time dependence of pathological, 26:53444
effects on young chickens following acute whole-body exposure, lethal, 26:53457 (NASA-TM-X-2440, pp 659-64)
emission during stellar flares, (T), 26:53853
emission from intergalactic gas in neighborhood of galaxies, (T), 26:53988
emission from neutron stars, detection of, (E/T), 26:53907
emission from solar atmosphere, (E), 26:53958
galactic background, 6-keV line in, (E), 26:53918
galactic background, origin of, (E), 26:53973
hazards to man during fluoroscopic radiographic examination, effects of image intensifier performance on, 26:53421
reactions with materials, Monte Carlo POEM program for calculating electron emission in, 26:54884 (NASA-TM-X-2440, pp 786-91)
scattering by tissue-equivalent phantoms from 50 to 300 kVp, (E), 26:54905

X-RAY CAMERAS
design and performance of position-sensitive proportional counter for, 26:53221

X-RAY DIFFRACTOMETERS
crystal mount for, engineering drawings for, 26:53319

X-RAY EMISSION ANALYSIS
methods using excitation of x rays by protons, for thin film measurements, 26:52945

X-RAY EQUIPMENT
description for use in skin cancer thrapy, 26:53341

X-RAY FLUORESCENCE ANALYSIS
radioisotope uses as sources in, 26:52942

X-RAY SPECTROMETERS
background interference with Apollo, identification and control of onboard radiation sources causing, 26:53255 (NASA-TM-X-2440, pp 714-22)
development of high resolution Bragg--Soller, 26:54467(R) (ORO-2972-204)
performance for detection of multicharged ions, 26:54078 (CEA-CONF-2050)

XENON
effects on radiolysis of gaseous ethylene, 26:53000
effects on yields from γ radiolysis of gaseous hydrogen sulfide, 26:53011
helium-atom and -ion reactions at 100 to 5000 eV with, angular and energy distributions of electrons from ionization and autoionization in, (E), 26:54141
iron-57 charge states following cobalt-57 decay in solid, Moessbauer effect study of, 26:55057
plasma of, continuum spectra of shock-heated, (E), 26:54777 (BMBW-FBK-72-8)
plasma of, diffusion effects on electron temperature in afterglows, (E), 26:54786
proton reactions at 500 to 3000 eV with, differential cross sections for charge exchange, elastic scattering, excitation to autoionizing levels, and simple excitation in, (E/T), 26:54122

separation from iodine by liquid nitrogen cooling and distillation, 26:53068
uses of purified fission product, evaluation of large-scale, 26:53330(R) (BNWL-1308-10)
XENON IONS
reactions with nuclei, review of experiments on, 26:54658 (JINR-P7-6523)
XENON ISOTOPES
abundance in Mokoia and Allende chondrites, (E), 26:53810
radiation dose to human body and lungs following ingestion, inhalation, or immersion in cloud of, methods for estimation of, 26:53510
tagging of pin type fuel elements, procedures for, 26:55184 (ANL/EBR-57)
yields in uranium-235 thermal neutron fission, (E), 26:54667
XENON ISOTOPES Xe-124
energy levels of, quasi-band structure in, (E/T), 26:54600 (INSJ-130)
XENON ISOTOPES Xe-126
energy levels of, quasi-band structure in, (E/T), 26:54600 (INSJ-130)
XENON ISOTOPES Xe-129
abundance in Mokoia and Allende chondrites, (E), 26:53810
content in tellurobismuthite from Boliden, Sweden, 26:53176
XENON ISOTOPES Xe-130
content in tellurobismuthite from Boliden, Sweden, 26:53176
XENON ISOTOPES Xe-131
content in atmosphere in vicinity of Savannah River Plant, 1971, 26:53153(R) (DPSPU-72-30-1)
content in tellurobismuthite from Boliden, Sweden, 26:53176
XENON ISOTOPES Xe-133
content in atmosphere in vicinity of Savannah River Plant, 1971, 26:53153(R) (DPSPU-72-30-1)
production of, reactor irradiation method and apparatus for, 26:53075(P)
XENON ISOTOPES Xe-135
content in atmosphere in vicinity of Savannah River Plant, 1971, 26:53153(R) (DPSPU-72-30-1)
XENON ISOTOPES Xe-136
yield in thermal fission of uranium-235, (E), 26:54626
XENON ISOTOPES Xe-137
energy levels of, calculation using core coupling, (T), 26:54467(R) (ORO-2972-204)
half-life of, (E), 26:54667
XENON ISOTOPES Xe-140
beta decay of, β endpoint energy and γ and conversion electron spectra from, (E), 26:54601 (IS-T-534)
XENON ISOTOPES Xe-141
beta decay endpoint energy of, (E), 26:54601 (IS-T-534)
XENON ISOTOPES Xe-142
beta decay endpoint energy of, (E), 26:54601 (IS-T-534)

Y

YANKEE POWER REACTOR
control rods for, measured drop times for, 26:55236 (DOCKET-50029-202)
engineered safeguards for, effects of circulating water system failure on flooding of, 26:55275 (DOCKET-50029-200)
inspection of, March 1972 inservice, 26:55235 (DOCKET-50029-201)
turbine for, effects of revised cooling system low flow trip level on trip requirements for, 26:55234 (DOCKET-50029-199)
YEASTS
Saccharomyces cerevisiae, radioinduced reversion mutations in, effects of photoreactivation repair mechanism on frequency of uv, 26:53375
Saccharomyces cerevisiae, radiosensitivity of budding cells of, effects of LET on heavy ion and x, 26:53368
Schizosaccharomyces pombe, radioinduced lesions in, correlation between induced mitotic recombination and repair mechanisms for uv, 26:53371
Schizosaccharomyces pombe, radioinduced lesions in, inhibitory effects of caffeine on recombinational repair mechanisms for uv, 26:53371
YTTERBIUM ISOTOPES Yb-162
electron-capture decay of, half-life and γ and x-ray spectra for, (E), 26:54639
YTTERBIUM ISOTOPES Yb-163
half-life of, 26:54639
YTTERBIUM ISOTOPES Yb-164
half-life of, 26:54639
YTTERBIUM ISOTOPES Yb-165
half-life of, 26:54639
YTTERBIUM ISOTOPES Yb-167
half-life of, 26:54639
YTTRIUM
abundance in γ Cap, (E), 26:53888
content in southwest Aswan syenite rock, 26:53142 (AREAEE-138)
deposition by pack cementation on chromium-base alloys for nitridation protection in air, effects of chromium, hafnium, and lanthanum additions on, 26:53689
electron band structure of, photoelectron spectral study of core level binding energies, 26:55024
YTTRIUM ALLOYS AND SYSTEMS
Cr-base--W--Y, coatings for nitridation resistance of, in air, chromium, hafnium, lanthanum, and yttrium combination cementation, 26:53689
Cr-base--Y, coatings for nitridation resistance of, in air, chromium, hafnium, lanthanum, and yttrium combination cementation, 26:53689
YTTRIUM BORIDES
preparation and thermoemission properties of, 26:53582
YTTRIUM ISOTOPES Y-89
alpha elastic scattering at 166 MeV, angular distribution for, (E), 26:54547
neutron radius of, determination from elastic scattering, (E), 26:54547
photon reactions (γ,2n) at 23 to 50 MeV, calculation of isomer ratio for, (T), 26:54725
photon reactions (γ,xn) with, model analysis of giant resonance in, (E/T), 26:54598 (FRNC-TH-242)
YTTRIUM ISOTOPES Y-93
half-life of, (E), 26:54667
YTTRIUM ISOTOPES Y-94
half-life of, (E), 26:54667

Z

ZINC
determination in organometallic compounds using oxine method after combustion, gravimetric or titrimetric, 26:52930
determination in presence of iron using EKCO mineral analyzer, 26:55568 (NIM-1430)
determination in water samples by spark source mass spectroscopy, 26:52914 (ANL-7860(Pt.3), pp 55-63)
distribution in cores from Green Bay, relations with depth, 26:53164 (ANL-7860(Pt.3), pp 64-76)
neutron inelastic scattering by phonons in, neutron groups from thermal, (E), 26:54487 (RT/FI-(71)37)
separation from indium by ion exchange chromatography, 26:52949
sorption on diethylaminoethylcellulose in methanol--thiocyanate--hydrochloric acid media, 26:52951
ZINC ALLOYS AND SYSTEMS
Cu--Ni--Zn, analysis of nickel silver for copper by amperometric titration, 26:52924
Cu--Zn, phase transformation interfaces in, properties of massive, 26:53644
Gd--Zn, hyperfine fields in GdZn diluted with yttrium or lanthanum, NMR study of, 26:55059
ZINC IONS
production in PIG source, 26:53752 (FRNC-CONF-54)
ZINC ISOTOPES Zn-62
energy levels from nickel-58 (Li-6,d) reactions, spin--parity assignments for, (E), 26:54586
ZINC ISOTOPES Zn-65
content in Lake Michigan fish, 26:53169 (ANL-7860(Pt.3), pp 141-50)
content in Savannah River, 1971, 26:53153(R) (DPSPU-72-30-1)
distribution in Columbia River, effects of seawater on soluble-suspended, 26:53166 (RLO-2227-T-12-28)
distribution in sedimentary environment and in benthic fauna on Oregon and Washington continental shelf, 26:53149 (RLO-2227-T-12-26)
uptake by hair following intravenous injection in rats, correlation with body burden and, 26:53529 (NASA-TM-X-2440, pp 982-8)
uptake by marine animals and plants from seawater, 26:53532
ZINC ISOTOPES Zn-67
nuclear magnetic resonance in GdZn diluted with yttrium or lanthanum, 26:55059
ZINC ISOTOPES Zn-68
alpha elastic scattering at 166 MeV, angular distribution for, (E), 26:54547
energy levels from nickel-64 (Li-6,d) reactions, spin--parity assignments for, (E), 26:54586
neutron radius of, determination from elastic scattering, (E), 26:54547
ZINC OXIDES
radioinduced defects in, comparison of explosive shock-induced defects with, 26:54983
ZINC TELLURIDES
ion implantation for fabrication of electroluminescent diodes, 26:54971 (CEA-R-4313)
ZION POWER REACTOR, UNIT 1
containment system for, revised data on, 26:55306 (DOCKET-50295-61)
electrical systems for, revised data on, 26:55306 (DOCKET-50295-61)
emergency core cooling system for, revised data on, 26:55306 (DOCKET-50295-61)
emergency plans for, 26:55306 (DOCKET-50295-61)
engineered safeguards for, revised data on, 26:55306 (DOCKET-50295-61)
instrumentation for, revised data on, 26:55306 (DOCKET-50295-61)
operation of, requested data on, 26:55306 (DOCKET-50295-61)

  personnel for, organization of, 26:55306 (DOCKET-50295-61)
  quality assurance program for, revised data on, 26:55306 (DOCKET-50295-61)
  radioactive effluents from, revised data on, 26:55306 (DOCKET-50295-61)
  safety aspects of, analysis of aircraft impact, 26:55306 (DOCKET-50295-61)
  testing program for, post criticality, 26:55306 (DOCKET-50295-61)
  valves for, verification of wall thicknesses for nuclear service, 26:55274 (DOCKET-50010-117)
ZION POWER REACTOR, UNIT 2
  containment system for, revised data on, 26:55306 (DOCKET-50295-61)
  electrical systems for, revised data on, 26:55306 (DOCKET-50295-61)
  emergency core cooling system for, revised data on, 26:55306 (DOCKET-50295-61)
  emergency plans for, 26:55306 (DOCKET-50295-61)
  engineered safeguards for, revised data on, 26:55306 (DOCKET-50295-61)
  instrumentation for, revised data on, 26:55306 (DOCKET-50295-61)
  operation of, requested data on, 26:55306 (DOCKET-50295-61)
  personnel for, organization of, 26:55306 (DOCKET-50295-61)
  quality assurance program for, revised data on, 26:55306 (DOCKET-50295-61)
  radioactive effluents from, revised data on, 26:55306 (DOCKET-50295-61)
  safety aspects of, analysis of aircraft impact, 26:55306 (DOCKET-50295-61)
  testing program for, post criticality, 26:55306 (DOCKET-50295-61)
  valves for, verification of wall thicknesses for nuclear service, 26:55274 (DOCKET-50010-117)
ZIRCALOY
  hydrogen distribution in, effects of thermal gradients on calculation of, 26:53665
ZIRCALOY-2
  fabrication by hot isostatic pressing, 26:53578
ZIRCONIUM
  book: Early Transition Metals, 26:52956
  content in southwest Aswan syenite rock, 26:53142 (AREAEE-138)
  corrosion by water at high temperatures, effects of impurities, thermal cycling, and vibrations on, 26:53614
  crystal orientation and hardness of α, 26:53693
  determination in minerals by neutron activation and γ spectroscopy, nondestructive, 26:52901 (UJV-2851-F,Ch)
  diffusion of cobalt-60, iron-59, and nickel-63 in α-, mechanism of, 26:53666
  distribution between liquid bismuth and MSBR fuel salt, pp. 6-7, 26:53081 (ORNL-4794, pp 1-14)
  effects on ductility of copper, 26:53669
  effects on tensile properties of tungsten, 26:53616
  fabrication by rolling at high temperature under vacuum, 26:53630
  flow stress of, effects of impurities on strain rate sensitivity of, 26:53639(R) (ORO-3262-25)
  mechanical properties of, effects of impurities on, 26:53639(R) (ORO-3262-25)
  radiation damage in, calculated profiles of argon, 26:54969 (AECL-4130)
  separation from niobium, tantalum, and titanium by solvent extraction, hydrolysis, and extraction, 26:52947 (BM-RI-7671)
  strain aging in, dynamic, 26:53639(R) (ORO-3262-25)
  strain rate sensitivity in, validity of Cottrell--Stokes Law in terms of variation of, 26:53639(R) (ORO-3262-25)
ZIRCONIUM ALLOY COUPLES
  Inconel/Zircaloy-2, corrosion by air, nitrogen, and water at ambient temperature, fretting, 26:53609 (RT/ING-(72)7)
  steel/Zircaloy-2, corrosion by air, nitrogen, and water at ambient temperature, fretting, 26:53609 (RT/ING-(72)7)
  Zircaloy-2/Zircaloy-2, corrosion by air, nitrogen, and water at ambient temperature, fretting, 26:53609 (RT/ING-(72)7)
ZIRCONIUM ALLOYS AND SYSTEMS
  corrosion by water at high temperatures, effects of impurities, thermal cycling, and vibrations on, 26:53614
  Al--Mo--Sn--Ti-base--Zr, creep rupture of, at 755 and 865°K, cyclic, 26:53690
  Al--Ni-base--W--Zr, production and properties of powder metallurgy components of, for use at high temperatures, 26:53631
  Al-base--Zr, crystal structure of intermetallic metastable phase Al$_3$Zr in molten, produced by rapid solidification, 26:53686
  C--O--Zr, reactions in, stability of phases produced by, 26:53581
  Cd--Zr, phase diagrams for, 26:53663
  Cd--Zr, thermodynamic properties of, 26:53663
  Co-base--Ni--ThO$_2$--Zr, mechanical properties and microstructure of dispersion-hardened, 26:53675
  Co-base--ThO$_2$--Zr, mechanical properties and microstructure of dispersion-hardened, 26:53675
  N--Nb-base--Zr, internal friction of, effects of nitrogen content on, 26:53692
  Nb--U-base--Zr, tensile properties of polycrystalline, as function of strain rate, 26:53691
ZIRCONIUM BORIDES
  fabrication by casting of thermoplastic masses, 26:53586
  oxidation resistance and sinterability of, effects of metal silicide additions on, 26:53594
  Cr$_5$Si$_3$--ZrB$_2$, oxidation resistance and sinterability of, at high temperatures, 26:53594
  CrSi$_2$--ZrB$_2$, oxidation resistance and sinterability of, at high temperatures, 26:53594
  Mo$_5$Si$_3$--ZrB$_2$, oxidation resistance and sinterability of, at high temperatures, 26:53594
  MoSi$_2$--ZrB$_2$, oxidation resistance and sinterability of, at high temperatures, 26:53594
  Ta$_5$Si$_3$--ZrB$_2$, oxidation resistance and sinterability of, at high temperatures, 26:53594
  TaSi$_2$--ZrB$_2$, oxidation resistance and sinterability of, at high temperatures, 26:53594
  W$_5$Si$_3$--ZrB$_2$, oxidation resistance and sinterability of, at high temperatures, 26:53594
  WSi$_2$--ZrB$_2$, oxidation resistance and sinterability of, at high temperatures, 26:53594
  ZrB$_2$--Zr$_5$Si$_3$, oxidation resistance and sinterability of, at high temperatures, 26:53594
  ZrB$_2$--ZrSi$_2$, oxidation resistance and sinterability of, at high temperatures, 26:53594
ZIRCONIUM BROMIDES
  fabrication by hot isostatic pressing, 26:53578
ZIRCONIUM CARBIDES
  sorptive properties of, effects of electronic structure on, 26:53593
  W--ZrC, evaporation rate at 2600 to 2970°K, effects of tungsten coating on, 26:55022
ZIRCONIUM IONS
  scattering by argon and neon at 8 to 25 keV, total cross sections and interatomic potentials for, (E), 26:54139
ZIRCONIUM ISOTOPES Zr-90
  alpha elastic scattering at 166 MeV, angular distribution for, (E), 26:54547
  energy level at 1.761 MeV from yttrium-89 (He-3,d) reactions, effects of configuration mixing on lifetime of, (T), 26:54610
  energy-level transitions in, shell-model calculations of, (T), 26:54611
  neutron radius of, determination from elastic scattering, (E), 26:54547
  photon reactions (γ,xn) with, model analysis of giant resonance in, (E/T), 26:54598 (FRNC-TH-242)
  proton reactions (p,n) at 6.9 to 9.5 MeV, gamma spectra and excitation functions for, (E), 26:54613
ZIRCONIUM ISOTOPES Zr-92
  proton reactions (p,α) at 28 MeV, DWBA calculation of form factors for, (T), 26:54467(R) (ORO-2972-204)
ZIRCONIUM ISOTOPES Zr-94
  alpha elastic scattering at 166 MeV, angular distribution for, (E), 26:54547
  neutron radius of, determination from elastic scattering, (E), 26:54547
  proton elastic scattering at 11.2 to 12.4 MeV, excitation functions for, (E), 26:54467(R) (ORO-2972-204)
ZIRCONIUM ISOTOPES Zr-95
  content in agricultural products, atmosphere, rainwater, Savannah River, and vegetation in vicinity of Savannah River Plant, 1971, 26:53153(R) (DPSPU-72-30-1)
ZIRCONIUM ISOTOPES Zr-96
  energy level from proton inelastic scattering, lifetime of first-excited, (E), 26:54622
ZIRCONIUM NITRIDES
  sorptive properties of, effects of electronic structure on, 26:53593
ZIRCONIUM OXIDES
  effects on tensile properties of tungsten, 26:53616
  Mo--ZrO$_2$, oxidation of, effects of temperature on rate of, 26:53585
ZIRCONIUM SILICIDES
  ZrB$_2$--Zr$_5$Si$_3$, oxidation resistance and sinterability of, at high temperatures, 26:53594
  ZrB$_2$--ZrSi$_2$, oxidation resistance and sinterability of, at high temperatures, 26:53594

REPORT NUMBER INDEX

Reports, conference papers and proceedings, numbered translations, and patents are included in this index. Each item is listed by report number; this is followed by the abstract number and a brief notation regarding public availability. The index entries show which reports are on file in the institutions listed on the back of the front cover (Dep.), which reports have been published in open-literature journals (journal citation), and which reports can be purchased (source and price). Whenever a report is identified by more than one number, the availability is given under the primary number, and a cross reference is given under the secondary report number.

The report number codes apply to USAEC reports unless designated otherwise. Non-USAEC reports are identified by parenthetical notes after the report codes; e.g., (non-AEC), (British), (Canadian), (French). The note (Misc.) identifies the codes used for both USAEC and non-USAEC reports. Patents are listed under the heading "PATENTS"; the country of origin is included in parentheses.

A comprehensive list of both USAEC and non-USAEC report codes is contained in the latest revision of TID-85, *Report Number Series Used by the USAEC Technical Information Center in Cataloging Reports.* This information is also included in the Cumulative Report Number Index (issued annually).

Availability of USAEC Reports

All USAEC Reports abstracted in *Nuclear Science Abstracts* are available through one or more of the following sources:

(1) University and public libraries in the United States. A list of these organizations appears on the inside front cover of each issue of *NSA*.

(2) NCR Microcard Editions in Microcard and micronegative form. Orders and inquiries should be sent to: Order Processing Department, 365 South Oak Street, West Salem, Wisconsin 54669.

(3) National Technical Information Service, U. S. Department of Commerce, Springfield, Virginia 22151.

(4) Superintendent of Documents, U. S. Government Printing Office, Washington, D. C. 20402.

(5) Microsurance, Inc., P. O. Box 3522, Oak Ridge, Tenn. 37830, in micronegative form. Purchase details available on request.

Availability of Non-USAEC Reports

U. S. Reports. Reports of U. S. Government agencies are available to the public from the National Technical Information Service (NTIS). If specific availability is not shown, inquiries may be directed to NTIS.

Non-U. S. Reports. Reports of atomic energy organizations of other countries are available from NTIS for U. S. sale only. Specific availability in the country of origin is shown, when known, at the report number entry. Otherwise, inquiries should be made to the organizations listed below:

AUSTRALIA

Australian Atomic Energy Commission Research Establishment. Available upon request from the Library, Australian Atomic Research Establishment, Private Mail Bag, Sutherland, New South Wales, Australia.

BELGIUM

Centre d'Étude de l'Energie Nucléaire. Available upon request to individuals and organizations from the Centre d'Etude de l'Energie Nucléaire (C.E.N.), Studiecentrum voor Kernenergie (S.C.K.), Technical Information Dept., MOL-DONK (Belgium).

CERN

CERN European Organization for Nuclear Research. Available without charge from CERN European Organization for Nuclear Research, Geneva 23, Switzerland. Copies are deposited in libraries throughout the world.

FRANCE

Commissariat à l'Energie Atomique. Inquiries for reports numbered 1-2199 should be addressed to Service Central de Documentation du C.E.A., Centre d'Etudes Nucléaires de Saclay, Boîte postale n° 2, 91. GIF-sur-YVETTE, FRANCE. Reports numbered 2200 and above are available from La Documentation Française, 31 quai Voltaire, 75, PARIS (7e), FRANCE.

Service Central de Protection contre les Rayonnements Ionisants. Copies are available from Ministère de la Santé Publique, Service Central de Protection contre les Rayonnements Ionisants, B.P. n° 78 Le Vesinet (France) Telex 25667.

GERMANY

Deutsches Elektronen-Synchrotron DESY. Copies are available from Deutsches Elektronen-Synchrotron DESY, Dokumentation, 2000 Hamburg 52, Notkestieg 1, Germany.

Gesellschaft für Kernforschung mbH (KFK). Copies are available from Gesellschaft für Kernforschung mbH, 75 Karlsruhe, Postfach 947, Germany. Copies are also deposited in many national nuclear centers in the world.

Kernforschungsanlage. Copies may be ordered from Zentralbibliothek der Kernforschungsanlage Jülich, Jülich, Bundesrepublik Deutschland.

Hahn-Meitner-Institute für Kernforschung. Available without charge from Hahn-Meitner-Institute für Kernforschung Berlin, Bibliothek, Glienicker Strasse 100, 1 Berlin 39, Germany. Copies are deposited in many national nuclear centers in the world.

Johann-Wolfgang-Goethe Universität, Frankfurt Am Main, Institut für Kernphysik, (IKF). Copies are available from Gmelin Institut, 40–42 Varrentrappstrasse, Frankfurt (Main), West Germany.

ISRAEL

Israel Atomic Energy Commission. Available without charge from Israel Atomic Energy Commission, Soreq Nuclear Research Centre, Yavne, Israel.

ITALY

Centro Informazioni Studi Esperienze (CISE). For sale at CISE Press Office, Casella Postale 3986, Milano, Italy. Copies are deposited in the libraries of various nuclear centers in Italy and abroad.

Comitato Nazionale per l'Energia Nucleare. Copies are available from Comitato Nazionale per l'Energia Nucleare, Divisione Affari Internazionali e Studi Economici, Ufficio Pubblicazioni, Via Belisario, 15, Roma, Italy.

JAPAN

Japan Atomic Energy Research Institute (JAERI). Available from the Staff Supply Cooperative of Japan Atomic Energy Research Institute (JAERI), Tokai-mura, Naka-gun, Ibaraki-ken, Japan. Copies are deposited in depositories in Tokyo, Nagoya, and Osaka.

Nagoya University. Copies are available from Research Information Center, Institute of Plasma Physics, Nagoya University, Nagoya, Japan.

University of Tokyo. Available free of charge from Institute for Nuclear Study, University of Tokyo, Tanashi-Machi, Kitatama-gun, Tokyo, Japan.

NETHERLANDS

Reactor Centrum Nederland. For sale by Reactor Centrum Nederland, 112 Scheveningseweg, 's-Gravenhage, The Netherlands. Copies are deposited in university libraries in Holland and in many national nuclear centers in the world.

NEW ZEALAND

Institute of Nuclear Sciences. Copies are available from Librarian, N. Z. Institute of Nuclear Sciences, D.S.I.R., Private Bag, Lower Hutt, New Zealand. Copies are deposited in other countries.

PAKISTAN

Atomic Energy Center. Copies are available from Atomic Energy Center, P. O. Box 658, Lahore, (West Pakistan).

POLAND

Reports of the Polish nuclear institutes are published by the Nuclear Energy Information Center of the Government Commissioner for Use of Nuclear Energy. Copies are available free of charge from Nuclear Energy Information Center, Palace of Culture and Science, Warsaw, Poland.

SPAIN

Junta de Energia Nuclear. "JEN" reports are available without charge from Servicio de Documentation, Junta de Energia Nuclear, Ciudad Universitaria, Madrid (3), España.

SWITZERLAND

Eidgenössisches Institut für Reaktorforschung. "EIR" reports are available from Eidgenössisches Institut für Reaktorforschung, c/o Bibliothek, 5303 Würenlingen/Switzerland.

TURKEY

Turkish Atomic Energy Commission. Copies are available free of charge from T.A.E.C., Çekmece Nuclear Research Center, P. O. Box 1, Airport, Istanbul, Turkey.

Conferences

Published conference proceedings as well as individual unpublished papers from conferences are included in this index. A CONF number is assigned to the conference if published proceedings are received and also if only a single paper is received. The base number used is year-month-sequence. Thus, the number CONF-650101 indicates that the conference was held in 1965, in January, and that this was the first January 1965 conference so received. This number would be assigned to complete published proceedings. If individual papers are received, the base number is extended to include a paper number, e.g., CONF-650101-1. As additional papers are received, they will be assigned consecutive numbers in the series, CONF-650101-1, CONF-650101-2, etc. This numbering system ensures that all papers received from a conference will be associated with that conference in this index.

If published proceedings are received after the receipt of individual papers, the complete proceedings will be abstracted and the abstract number will appear in this index with the base CONF number.

Abbreviations Used in Availability Column

AECL	Reports of the Atomic Energy of Canada Limited are for sale by the Scientific Document Distribution Office, Atomic Energy of Canada Limited, Chalk River, Ontario, Canada.
CFSTI	See NTIS
DENM	Reports of the Atomic Energy Commission Research Establishment, Risö, are available on exchange from the Library, Danish Atomic Energy Commission, Risö, Roskilde, Denmark. Also for sale at the price shown from Jul. Gjellerup, Booksellers, 87 Sölvgade, Kobenhavn K., Denmark. Reports of Danatom are available on loan from Research Establishment, Risö, Roskilde, Denmark. Copies are available from Danatom, Aurehojvej 2, Hellerup, Denmark.
Dep.	AEC reports so designated are maintained in the organizations listed on the inside front cover of *NSA*. Prior to July 1, 1965, reports were deposited either in printed copy form or in microform. After that time, all reports have been in the form of micronegatives. Reports from other countries so designated are available in the United States at the organizations listed on the inside front cover of *NSA*.

DTIE	Available from the U. S. Atomic Energy Commission, USAEC Technical Information Center, P. O. Box 62, Oak Ridge, Tennessee 37830. (Conference papers are available on loan only.)
EM	Blueline prints of AEC engineering drawings are available from NTIS, U. S. Department of Commerce, Springfield, Virginia 22151. Current prices of the CAPE-packages may be obtained from this address. TID-4100, available from the USAEC Technical Information Center, P. O. Box 62, Oak Ridge, Tennessee 37830, contains information on all the CAPE-packages for sale.
EUR	For sale by Centrale de vente des publications des Communautés européennes 37, rue Glesener-Luxembourg.
GPO	For sale by the Superintendent of Documents, Government Printing Office, Washington, D. C. 20402.
IAEA	Available from the International Atomic Energy Agency, Vienna, Austria, and from its sales agencies in various countries throughout the world. A list of these agencies is found in each STI/DOC and STI/PUB publication.
INIS	Available on microfiche at $0.65 per document from INIS Section, International Atomic Energy Agency, P. O. Box 590 A-1011, Vienna, Austria
LMEC	Available *only to requesters within the United States* from the Liquid Metal Engineering Center, P. O. Box 1449, Canoga Park, CA 91304
NORW	Reports from Forsvarets Forskningsinstitutt are available from Norwegian Defense Research Establishment, Library, P. O. Box 25, Kjeller, Norway. "KR" reports are available on an exchange basis from the Library, Institutt for Atomenergi, Box 40, Kjeller, Norway. Reports of the Norwegian Reactor School are available from the Library, Institutt for Atomenergi, P. O. Box 40, Kjeller, Norway.
NRC	For sale by the National Research Council of Canada, Ottawa, Ontario, Canada.
NTIS	For sale by the National Technical Information Service (NTIS), U. S. Department of Commerce, Springfield, Virginia 22151 at the following prices for eye legible copy: 1–300 pages $3.00 301–600 pages $6.00 601–900 pages $9.00 Documents over 900 pages have special prices which may be obtained from NTIS. Microfiche copy of each separately bound document can be purchased for $0.95. Reports issued by organizations outside the United States will be sold by NTIS *only to purchasers within the United States.* Purchasers outside the United States may acquire such reports from the sources described elsewhere in these columns.
OECD	Available from O. E. C. D., Publications 2, rue, André-Pascal, 75 Paris 16^e, France, and from its sales agencies in various countries throughout the world. A list of these agencies is found in each OECD publication.
RSO	Available *only to requesters within the United States* from the Reactor Standards Office, Oak Ridge National Laboratory, P. O. Box X, Oak Ridge, TN 37830
SWED	"AE" reports (full size or microcopies) are for sale from Aktiebolaget Atomenergi, Studsvik, Library, Fack, S-611 01 NYKÖPING 1, Sweden. Other series are not generally available to the public. Organizations in the Atomic Energy field may obtain copies from Aktiebolaget Atomenergi.
UK	United Kingdom Atomic Energy Authority reports generally may be purchased from Her Majesty's Stationery Office, P. O. Box 569, London S.E.1. Copies of many UKAEA reports (particularly earlier ones) may be purchased in microcopy form from Micro Methods Ltd., East Ardsley, Wakefield, Yorkshire, England. Copies of UKAEA reports are deposited with the National Lending Library for Science and Technology and 10 public libraries in England; with the USAEC and (through USAEC) with NTIS; and in most national nuclear centers throughout the world. In the USA, UKAEA reports are available on a subscription basis, by subject category, from UNIPUB, Inc., P. O. Box 433, New York, NY 10016, USA; and from Pendragon House, Inc., 1093 Charter Avenue, Redwood City, CA 94063, USA.
UN	Mail orders should be directed to the Sales Section, Room 1059, United Nations Headquarters, New York, New York 10017.
ZAED	Available from ZAED, Kernforschungszentrum, 7501 Leopoldshafen, West Germany

Report No.	Abstract No.	Availability
NUMERICAL		
72-NED-18	26-55353	See NEDO-10527
71-260	26-53089	See AD-737380
ACRH-		
1000-349	26-55460	Dep. NTIS, 3p.
1000-350	26-55461	Dep. NTIS, 10p.
AD-	(Misc.)	
737312	26-54968	NTIS, 140p.
737380	26-53089	NTIS, 59p.
737993	26-53195	NTIS, 16p.
738874	26-55099	NTIS, 87p.
AE-MF-	(Swedish)	
204	26-53701	See STU-70-419/U-350(Pt.1.1)
232	26-53642	See STU-70-419/U-350(Pt.1.2)
AEC-tr-		
7319	26-55199	Dep. NTIS
7323	26-54774	Dep. NTIS
7326	26-54775	Dep. NTIS
7329	26-54768	Dep. NTIS
7330	26-54749	Dep. NTIS
7331	26-54836	Dep. NTIS
7332	26-54776	Dep. NTIS
7333	26-54837	Dep. NTIS
7334	26-54824	Dep. NTIS
7335	26-54838	Dep. NTIS
7336	26-54839	Dep. NTIS
7337	26-54840	Dep. NTIS
7338	26-54841	Dep. NTIS
7339	26-54842	Dep. NTIS
7345	26-52913	Dep. NTIS
7350	26-54800	Dep. NTIS
AECL-	(Canadian)	
3957	26-55462	Dep. NTIS (U. S. Sales Only). AECL $2.00, 77p.
4130	26-54969	Dep. NTIS (U. S. Sales Only). AECL $1.50, 52p.
4162	26-55081	Dep. NTIS (U. S. Sales Only), 48p.
4208	26-55463	Dep. NTIS (U. S. Sales Only). AECL $0.50, 20p.
4254	26-55195	Dep. NTIS (U. S. Sales Only). AECL $0.50, 10p.
AED-C-	(Non-AEC)	
5-11	26-53342	Dep. NTIS (U. S. Sales Only), 127p.
AERE-R-	(British)	
6601	26-55464	Dep. NTIS (U. S. Sales Only). UK 13 pence, 11p.
6623	26-55465	Dep. NTIS (U. S. Sales Only). UK 1s. 9d, 6p.
AI-AEC-		
12951	26-55378	Dep. NTIS, 90p.
AI-AEC-Memo-		
12736	26-55147	Dep. NTIS, 137p.
ANCR-		
1038	26-55183	Dep. NTIS, 40p.
1042	26-54468	Dep. NTIS, 145p.
1069	26-54652	Dep. NTIS, 51p.
1071	26-54469	Dep. NTIS, 18p.
1085	26-55379	Dep. NTIS, 62p.
ANL-		
7858	26-55466	Dep. NTIS, 74p.
7860(Pt.3)	26-53150	Dep. NTIS, 320p.
7911(Suppl. 1)	26-55139	Dep. NTIS, 18p.
7945	26-53545	Dep. NTIS, 39p.
ANL/EBR-		
57	26-55184	Dep. NTIS, 24p.
63	26-55132	Dep. NTIS, 51p.
ANL/ES-		
15	26-55467	Dep. NTIS, 187p.
ANL/HFEF-		
1	26-53727	Dep. NTIS, 117p.
AREAEE-	(Egyptian)	
122	26-53119	Dep. NTIS (U. S. Sales Only), 33p.
124	26-54843	Dep. NTIS (U. S. Sales Only), 20p.
125	26-54844	Dep. NTIS (U. S. Sales Only), 23p.
129	26-53056	Dep. NTIS (U. S. Sales Only), 32p.
131	26-53326	Dep. NTIS (U. S. Sales Only), 19p.
132	26-53295	Dep. NTIS (U. S. Sales Only), 21p.
133	26-54470	Dep. NTIS (U. S. Sales Only), 26p.
134	26-53546	Dep. NTIS (U. S. Sales Only), 28p.
135	26-53547	Dep. NTIS (U. S. Sales Only), 27p.
136	26-55468	Dep. NTIS (U. S. Sales Only), 38p.
137	26-53251	Dep. NTIS (U. S. Sales Only), 58p.
138	26-53142	Dep. NTIS (U. S. Sales Only), 22p.
139	26-53548	Dep. NTIS (U. S. Sales Only), 22p.
141	26-55420	Dep. NTIS (U. S. Sales Only), 20p.
ARL-	(Misc.)	
ASTM-STP-	(Non-AEC)	
496	26-53660	Philadelphia; American Society for Testing and Materials (1971). 86p. $5.00
BARC/I-	(Indian)	
148	26-55100	INIS
BAW-	(Misc.)	
10016	26-55193	
10034 (Suppl.1)	26-55271	
10047(Rev. 1)	26-55217	
10048 (Suppl.1)	26-55272	
10050	26-55225	
BDX-		
613-382 (Rev.)	26-55469	Dep. NTIS, 68p.
613-518 (Rev.)	26-55470	Dep. NTIS, 81p.
BLG-	(Belgian)	
461	26-55471	Dep. NTIS (U. S. Sales Only), 52p.
BM-RI-	(Misc.)	
7671	26-52947	
BMBW-FBK-	(West German)	
72-8	26-54777	Dep. NTIS (U. S. Sales Only), 110p.
72-9	26-55472	Dep. NTIS (U. S. Sales Only), 69p.
BNL-		
16609	26-55473	Dep. NTIS, 18p.
16752	26-54407	Dep. NTIS, 60p.
16816	26-53765	Dep. NTIS, 5p.
16818	26-53766	Dep. NTIS, 9p.
16830	26-53767	Dep. NTIS, 5p.
16889	26-53090	Dep. NTIS, 22p.
16965	26-55220	Dep. NTIS, 25p.
16977	26-54181	Dep. NTIS, 8p.
16978	26-54284	Dep. NTIS, 16p.
16980	26-53768	Dep. NTIS, 9p.
16996	26-53769	Dep. NTIS, 3p.
16997	26-54298	Dep. NTIS, 18p.
17004	26-55474	Dep. NTIS, 6p.
17016	26-53770	Dep. NTIS, 7p.
17019	26-53771	Dep. NTIS, 14p.
17020	26-53266	Dep. NTIS, 18p.
17021	26-53772	Dep. NTIS, 9p.
17029	26-54675	Dep. NTIS, 30p.
17051	26-53773	Dep. NTIS, 5p.
17056	26-53774	Dep. NTIS, 3p.
17057	26-53775	Dep. NTIS, 8p.
17063	26-53776	Dep. NTIS, 1p.
17064	26-53267	Dep. NTIS, 8p.
17065	26-54191	Dep. NTIS, 8p.
17066	26-53268	Dep. NTIS, 17p.
17067	26-53777	Dep. NTIS, 9p.
17068	26-53778	Dep. NTIS, 2p.
17069	26-54200	Dep. NTIS, 6p.
17070	26-53269	Dep. NTIS, 4p.
17071	26-53270	Dep. NTIS, 14p.
17092	26-54182	Dep. NTIS, 14p.
17110	26-55475	Dep. NTIS, 13p.
17115	26-55476	Dep. NTIS, 74p.
17141	26-54192	Dep. NTIS, 29p.
17142	26-53779	Dep. NTIS, 5p.
17152	26-53780	Dep. NTIS, 11p.
17153	26-53781	Dep. NTIS, 6p.
50325	26-54461	Dep. NTIS, 78p.
50335	26-53325	Dep. NTIS, 4p.
50342	26-54234	Dep. NTIS, 10p.
50345	26-55477	Dep. NTIS, 15p.
BNL-tr-		
490	26-54631	Dep. NTIS
498	26-53751	Dep. NTIS
BNLSC-	(British)	
63	26-55409	See RD/B/N-2272
BNWL-		
1308-10	26-53330	Dep. NTIS, 40p.
1522-5	26-55416	Dep. NTIS, 66p.
1605	26-55478	Dep. NTIS, 269p.
BNWL-CC-		
449	26-53604	Dep. NTIS, 10p.
2274	26-55421	Dep. NTIS, 12p.
BNWL-SA-		
4385	26-55479	Dep. NTIS, 18p.
BNWL-tr-		

Report No.	Abstract No.	Availability
71	26-53526	Dep. NTIS
72	26-55480	Dep. NTIS
73	26-55481	Dep. NTIS
75	26-53057	Dep. NTIS
CALT-		
68-322	26-54166	Dep. NTIS, 14p.
CAPE-		
1653	26-52957	EM
2191	26-53317	EM
2192	26-53278	EM
2193	26-53318	EM
2194	26-55642	EM
2204	26-53216	EM
2208	26-53219	EM
2209	26-53250	EM
2210	26-53262	EM
2237	26-53220	EM
2238	26-53261	EM
2239	26-53249	EM
2240	26-53217	EM
2244	26-53319	EM
2251	26-53116	EM
2254	26-53316	EM
2257	26-53218	EM
2259	26-53737	EM
CEA-CONF-	(French)	
1890	26-54970	Dep. NTIS (U. S. Sales Only), 32p.
1894	26-53713	Dep. NTIS (U. S. Sales Only), 3p.
1976	26-54871	Dep. NTIS (U. S. Sales Only), 24p.
2000	26-55482	Dep. NTIS (U. S. Sales Only), 3p.
2005	26-55450	Dep. NTIS (U. S. Sales Only), 9p.
2026	26-53331	Dep. NTIS (U. S. Sales Only), 26p.
2047	26-54778	Dep. NTIS (U. S. Sales Only), 6p.
2048	26-54077	Dep. NTIS (U. S. Sales Only), 6p.
2049	26-54801	Dep. NTIS (U. S. Sales Only), 11p.
2050	26-54078	Dep. NTIS (U. S. Sales Only), 5p.
CEA-N-	(French)	
1211	26-55380	Dep. NTIS (U. S. Sales Only), 18p.
1528	26-52978	Dep. NTIS (U. S. Sales Only), 119p.
1535	26-53520	Dep. NTIS (U. S. Sales Only), 25p.
1539	26-53296	Dep. NTIS (U. S. Sales Only), 71p.
1549	26-53297	Dep. NTIS (U. S. Sales Only), 20p.
1553	26-54183	Dep. NTIS (U. S. Sales Only), 144p.
CEA-R-	(French)	
3633	26-52913	For translation see AEC-tr-7345
4286	26-54596	Dep. NTIS (U. S. Sales Only), 117p.
4288	26-53127	Dep. NTIS (U. S. Sales Only), 38p.
4313	26-54971	Dep. NTIS (U. S. Sales Only), 101p.
4318	26-53120	Dep. NTIS (U. S. Sales Only), 33p.
4338	26-52894	Dep. NTIS (U. S. Sales Only), 34p.
CERN-	(European Organization for Nuclear Research)	
72-14	26-53782	Dep. NTIS (U. S. Sales Only), 53p.
CERN-HERA-	(European Organization for Nuclear Research)	
72-1	26-55374	Dep. NTIS, 51p.
CISE-R-	(Italian)	
203	26-55101	INIS
239	26-55102	INIS
241	26-55196	INIS
242	26-55103	INIS
243	26-55422	INIS
246	26-55104	INIS
252	26-54471	Dep. NTIS (U. S. Sales Only), 95p.
258	26-55105	INIS
268	26-55133	INIS
270	26-55148	INIS
273	26-55423	INIS
283	26-55106	INIS
CLM-R-	(British)	
116	26-54825	Dep. NTIS (U. S. Sales Only). UK 50 pence, 10p.
CNEA-	(Argentinean)	
309	26-53381	Dep. NTIS (U. S. Sales Only), 14p.
CONF-680570-	(Conference on Applications of Field-Ion Microscopy in Physical Metallurgy and Corrosion, Atlanta, GA., May 15-17, 1968)	
	26-53647	Atlanta; Georgia Institute of Technology (1969). 503p
CONF-680571-	(Materials Technology--An Interamerican Approach Conference, Sao Paulo, Brazil, May 1968)	
1	26-52976	See IEA-250
CONF-690565-	(Nuclear Heating Symposium, Tatranska Lomnica, Czechoslovakia, May 13-15, 1969)	
1	26-55375	See INIS-mf-172
[illegible]	26-55376	See INIS-mf-172, pp 7-13

Report No.	Abstract No.	Availability
CONF-700670-	(Fracture Toughness Testing at Cryogenic Temperatures Symposium, Toronto, Ontario, Canada, June 21-26, 1970)	
	26-53660	Philadelphia; American Society for Testing and Materials (1971). 86p. $5.00
CONF-700847-	(Seminar on Pollution and Human Environment, New Delhi, India, Aug. 26-27, 1970)	
5	26-53154	See INIS-mf-160, pp 22-52
CONF-701204-	(Regional Meeting of the American Chemical Society, New Orleans, La., Dec. 2-4, 1970)	
(Absts)	26-53027	Washington, D. C.; American Chemistry Society (1970). 220p
CONF-710304-	(Symposium on Natural and Manmade Radiation in Space, Las Vegas, Nev., Mar. 1-5, 1971)	
	26-54870	See NASA-TM-X-2440
CONF-710408-	(American Geophysical Union National Meeting, Washington, D.C., Apr. 12-16, 1971)	
(Absts.)	26-54010	EOS, Trans. Amer. Geophys. Union; 52: No. 4, 122-392(Apr 1971)
CONF-710436-	(Symposium on Energy for the Future, Washington, D.C., Apr. 26, 1971)	
2	26-55561	See LBL-383
CONF-710446-	(Intermag Conference, Denver, Colo., Apr. 13-16, 1971)	
	26-55028	New York; Institute of Electrical and Electronics Engineers, Inc. (1971). 187p. $4.00
CONF-710548-	(Specialists' Meeting on Sodium-Water Reactions, Melekess, U.S.S.R., May 18-21, 1971)	
	26-55149	Dep. NTIS, 263p.
CONF-710549-	(12th European Conference on Leading, Brussels, Belgium, May 11-13, 1971)	
1	26-55450	See CEA-CONF-2005
CONF-710555-	(VTE-X Symposium, Washington, D.C., May 26, 1971)	
1	26-53110	See ORNL-TM-3841
CONF-710602-	(7th Plansee Seminar on Powder Metallurgy of High Temperature Materials, Reutte, Austria, June 21-25, 1971)	
(Vol.1)	26-53601	Reutte/Tyrol, Austria; Metallwerk Plansee (1971). 214p
(Vol.2)	26-53602	Reutte/Tyrol, Austria; Metallwerk Plansee (1971). 197p
(Vol.3)	26-53584	Reutte/Tyrol, Austria; Metallwerk Plansee (1971). 167p
(Vol.4)	26-53603	Reutte/Tyrol, Austria; Metallwerk Plansee (1971). 326p
CONF-710714-	(Workshop on Personnel Neutron Dosimetry, New York, N.Y., July 8-9, 1971)	
2	26-53229	See COO-1105-172
CONF-710720-	(International Conference on Light Scattering from Fluids, Paris, France, July 15, 1971)	
	26-55041	Portland, Oreg.; International Scholarly Book Services, Inc. (1971). 529p. $45.00
CONF-710730-	(Conference on Microprobe of the National Association on Research Technique, Strasbourg, France, July 3, 1971)	
1	26-55482	See CEA-CONF-2000
CONF-710807-	(12th International Conference on Cosmic Rays, Hobart, Australia, Aug. 16-25, 1971)	
(Vol.1)	26-53814	Hobart, Australia; International Union of Pure and Applied Physics (1971). 436p
CONF-710810-	(Meeting on Particles and Fields, Rochester, N.Y., Aug. 30-Sept. 2, 1971)	
6	26-54184	See LBL-4
CONF-710816-	(International Symposium on Electron and Photon Interactions at High Energies, Ithaca, N.Y., Aug. 23-27, 1971)	
24	26-54166	See CALT-68-322
CONF-710903-	(1st International Conference on Structural Mechanics in Reactor Technology, Berlin, Germany, Sept. 20-24, 1971)	
32	26-55500	See COO-2048-7
CONF-710911-	(4th International Conference on High Energy Physics and Nuclear Structure, Dubna, U.S.S.R., Sept. 7-11, 1971)	
15	26-54687	See ISS-71/29
CONF-710932-	(3rd International Symposium on the Application of Vacuum Techniques in	

Report No.	Abstract No.	Availability
	Semiconductor Industry, Electronic Components and Micro-Electronics, Versailles, France, Sept. 13-18, 1971)	
	26-53138	Paris; Societe Francaise des Ingenieurs et Techniciens du Vide (1971). 467p
CONF-710948-	(International Seminar on Pion-Nucleus Interactions, Strasbourg, France, Sept. 1971)	
2	26-53797	See LA-DC-72-881
CONF-710957-	(2nd Conference on Mass Spectrometry, Ispra, Italy, Sept. 1-3, 1971)	
	26-52893	See EUR-4765
CONF-710959-	(Meeting on Fission and Corrosion Product Behaviour in Primary Systems of LMFBR'S, Bensberg, West Germany, Sept. 20-22, 1971)	
	26-55417	
CONF-710966-	(Meeting of the Society of German Chemists, Karlsruhe, Germany, Sept. 13-18, 1971)	
1	26-53064	See ORNL-tr-2621
CONF-711117-	(2nd JANNAF Propellant Characterization Working Group Meeting, Las Vegas, Nev., Nov. 1, 1971)	
2	26-55625	See UCRL-73334
CONF-711119-	(6th Annual Topical Symposium on Radiation Protection Standards: Quo Vadis, Richland, Wash., Nov. 2-5, 1971)	
(Vol.1)	26-54914	Richland, Wash.; Health Physics Society (1972). 263p
(Vol.2)	26-54922	Richland, Wash.; Health Physics Society (1972). 244p
CONF-711138-	(5th LAMPF Users Meeting, Los Alamos, NM., Nov. 8-9, 1971)	
	26-53784	See LA-4874
CONF-711204-	(Meeting on Radiobiological Applications of Neutron Irradiation, Vienna, Austria, Dec. 6, 1971)	
2	26-54871	See CEA-CONF-1976
CONF-720120-	(Conference on the Sources of Multicharged Ions, Paris, France, Jan. 28, 1972)	
2	26-54778	See CEA-CONF-2047
3	26-54077	See CEA-CONF-2048
4	26-54801	See CEA-CONF-2049
5	26-54078	See CEA-CONF-2050
6	26-54103	See FRNC-CONF-51
7	26-53753	See FRNC-CONF-56
8	26-54080	See FRNC-CONF-55
9	26-54082	See FRNC-CONF-58
10	26-54079	See FRNC-CONF-53
11	26-53752	See FRNC-CONF-54
12	26-54081	See FRNC-CONF-57
CONF-720208-	(2nd Conference on Embryonic and Fetal Antigens in Cancer, Oak Ridge, Tn., Feb. 14-16, 1972)	
3	26-55505	See COO-3012-21
CONF-720321-	(International Cancer Conference, Sydney, Australia, Mar. 13-17, 1972)	
2	26-53341	pp 307-21 of Melanoma and Skin Cancer. /McCarthy, W. H. (ed.). Sydney; Australian Cancer Society (1972)
CONF-720328-	(6th International Congress on New Trends in Radiation Protection, Bordeaux, France, Mar. 27-31, 1972)	
2	26-53199	See LBL-585
CONF-720409-	(3rd International Conference on Experimental Meson Spectroscopy, Philadelphia, PA., Apr. 28-29, 1972)	
14	26-54176	See SLAC-PUB-1043
CONF-720423-	(1st European Conference on Computational Physics, Geneva, Switzerland, Apr. 10-14, 1972)	
4	26-54970	See CEA-CONF-1890
CONF-720435-	(Seminar on Training and Education in Medical Physics, Kiel, Germany, Apr. 10-22, 1972)	
4	26-55460	See ACRH-1000-349
5	26-55461	See ACRH-1000-350
CONF-720437-	(17th National SAMPE Symposium and Exhibit, Los Angeles, CA., Apr. 11-13, 1972)	
	26-53569	Azusa, Calif.; Society of Aerospace Material and Process Engineers (1972). 312p
CONF-720513-	(Applied Superconductivity Meeting, Annapolis, MD., May 1-3, 1972)	
9	26-54463	See ORNL-TM-3886

Report No.	Abstract No.	Availability
CONF-720519-	(2nd International Symposium on Power from Radioisotopes, Madrid, Spain, May 29-June 2, 1972)	
3	26-53331	See CEA-CONF-2026
CONF-720530-	(20th Annual Meeting of the Radiation Research Society, Portland, OR., May 14-18, 1972)	
5	26-53449	See COO-3017-4
CONF-720546-	(Symposium on Detritus and Its Ecological Role in Aquatic Ecosystems, Pallanza, Italy, May 1972)	
1	26-55493	See COO-1599-58
CONF-720607-	(18th Annual American Nuclear Society Conference, Las Vegas, NV., June 18-22, 1972)	
26	26-53200	See LBL-707(Summ.)
CONF-720609-	(International Carbon Conference, Baden-Baden, Germany, June 26-30, 1972)	
4	26-53713	See CEA-CONF-1894
CONF-720612-	(Conference on Pade Approximants and Their Applications, Canterbury, England, June 25-July 25, 1972)	
2	26-55555	See LA-DC-72-872
3	26-55556	See LA-DC-72-873
4	26-55557	See LA-DC-72-879
5	26-55558	See LA-DC-72-880
CONF-720614-	(17th Annual Meeting of the Health Physics Society, Las Vegas, NV., June 12-16, 1972)	
1	26-55220	See BNL-16965
CONF-720624-	(Conference on Precision Electromagnetic Measurements, Boulder, CO., June 26-29, 1972)	
1	26-55630	See UCRL-73943
CONF-720626-	(International Conference on Pade Approximants, Continued Fraction and Related Topics, Boulder, CO., June 22, 1972)	
2	26-55475	See BNL-17110
CONF-720634-	(1st Topical European Nuclear Physics Conference, Aix-En-Provence, France, June 26-July 1, 1972)	
1	26-54694	See LBL-972
CONF-720642-	(10th Annual Meeting of the Caribbean Food Crops Society, Mayaguez, Puerto Rico, June 11-17, 1972)	
1	26-55483	Dep. NTIS, 7p.
CONF-720645-	(Conference on a Re-Examination of Non-Specific Factors Influencing Host Resistance, Bern, Switzerland, June 19-21, 1972)	
1	26-55474	See BNL-17004
CONF-720701-	(International Conference on Nuclear Structure Study with Neutrons, Budapest, Hungary, July 31-Aug. 5, 1972)	
2	26-54675	See BNL-17029
3	26-54677	Dep. NTIS, 56p.
CONF-720705-	(1st Topical Conference on RF Plasma Heating, Lubbock, TX., July 6-8, 1972)	
2	26-54750	Dep. NTIS, 10p.
3	26-54751	Dep. NTIS, 15p.
4	26-54805	Dep. NTIS, 8p.
CONF-720709-	(International Conference on Dynamic Crack Propagation, Bethlehem, PA., July 9-13, 1972)	
1	26-53557	See SC-DC-721080
CONF-720716-	(International Conference and Exhibition on Vacuum Instruments and Methods in Surface Studies, Guildford, Surrey, England, July 10-13, 1972)	
1	26-52953	Dep. NTIS, 31p.
CONF-720717-	(6th International Cyclotron Conference, Vancouver, B.C., July 18-21, 1972)	
5	26-53756	See LBL-654
6	26-53755	See LBL-644
CONF-720803-	(Cryogenic Engineering Conference, Boulder, CO., Aug. 9-11, 1972)	
6	26-55554	See LA-DC-72-855
CONF-720804-	(5th European Conference on Controlled Fusion and Plasma Physics, Grenoble, France, Aug. 21-25, 1972)	
3	26-54845	Dep. NTIS, 4p.

Report No.	Abstract No.	Availability
	(Non-AEC)	
112	26-55283	See DOCKET-50254-118
113	26-55284	See DOCKET-50254-119
114	26-55285	See DOCKET-50254-120
115	26-55254	Dep. NTIS, 3p.
116	26-55274	See DOCKET-50010-117
DOCKET-50266-	(Point Beach Nuclear Plant) (Non-AEC)	
79	26-55289	Dep. NTIS, 2p.
80	26-55290	Dep. NTIS, 7p.
DOCKET-50271-	(Vermont Yankee Nuclear Power Station) (Non-AEC)	
100	26-55255	Dep. NTIS, 13p.
101	26-55256	Dep. NTIS, 12p.
DOCKET-50272-	(Salem Nuclear Generating Station--Formerly Burlington Nuclear Generating Station, See also DOCKET-50311) (Non-AEC)	
35	26-55291	Dep. NTIS, 415p.
DOCKET-50277-	(Peach Bottom Atomic Power Station; See also DOCKET-50171 and DOCKET-50278) (Non-AEC)	
56	26-55292	Dep. NTIS, 2p.
57	26-55293	Dep. NTIS, 35p.
DOCKET-50278-	(Peach Bottom Atomic Power Station; See also DOCKET-50171 and DOCKET-50277) (Non-AEC)	
56	26-55292	See DOCKET-50277-56
57	26-55293	See DOCKET-50277-57
58	26-55294	Dep. NTIS, 3p.
DOCKET-50280-	(Surry Power Station, See also DOCKET-50281) (Non-AEC)	
82	26-55295	Dep. NTIS, 4p.
83	26-55257	Dep. NTIS, 2p.
84	26-55296	Dep. NTIS, 63p.
85	26-55297	Dep. NTIS, 32p.
DOCKET-50282-	(Prairie Island Nuclear Generating Plant, See also DOCKET-50306) (Non-AEC)	
72	26-55298	Dep. NTIS, 6p.
73	26-55299	Dep. NTIS, 438p.
74	26-55258	Dep. NTIS, 2p.
DOCKET-50285-	(Fort Calhoun Station) (Non-AEC)	
70	26-55300	Dep. NTIS, 5p.
71	26-55301	Dep. NTIS, 272p.
72	26-55302	Dep. NTIS, 4p.
DOCKET-50289-	(Three Mile Island Nuclear Station) (Non-AEC)	
66	26-55303	Dep. NTIS, 27p.
DOCKET-50293-	(Pilgrim Nuclear Power Station) (Non-AEC)	
88	26-55304	Dep. NTIS, 4p.
90	26-55305	Dep. NTIS, 257p.
DOCKET-50295-	(Zion Station Nuclear Power Plant. See also DOCKET-50304) (Non-AEC)	
61	26-55306	Dep. NTIS, 454p.
62	26-55274	See DOCKET-50010-117
DOCKET-50298-	(Cooper Nuclear Station) (Non-AEC)	
50	26-55307	Dep. NTIS, 3p.
DOCKET-50301-	(Point Beach Nuclear Plant) (Non-AEC)	
70	26-55289	See DOCKET-50266-79
71	26-55290	See DOCKET-50266-80
DOCKET-50302-	(Crystal River Nuclear Plant; see DOCKET-50303) (Non-AEC)	
52	26-55308	Dep. NTIS, 2p.
DOCKET-50304-	(Zion Station Nuclear Power Plant. See also DOCKET-50295) (Non-AEC)	
61	26-55306	See DOCKET-50295-61
62	26-55274	See DOCKET-50010-117
DOCKET-50305-	(Kewaunee Nuclear Power Plant) (Non-AEC)	
48	26-55309	Dep. NTIS, 113p.
49	26-55310	Dep. NTIS, 8p.
51	26-55311	Dep. NTIS, 9p.
DOCKET-50306-	(Prairie Island Nuclear Generating Plant, See also DOCKET-50282) (Non-AEC)	
69	26-55298	See DOCKET-50282-72
70	26-55299	See DOCKET-50282-73
DOCKET-50309-	(Maine Yankee Atomic Power Company) (Non-AEC)	
68	26-55312	Dep. NTIS, 1p.
69	26-55313	Dep. NTIS, 190p.
DOCKET-50311-	(Salem Nuclear Generating Station--Formerly Burlington Nuclear Generating Station, See also DOCKET-50272) (Non-AEC)	
35	26-55291	See DOCKET-50272-35
DOCKET-50312-	(Rancho Seco Nuclear Generating Station) (Non-AEC)	
50	26-55314	Dep. NTIS, 2p.
51	26-55315	Dep. NTIS, 359p.
52	26-55316	Dep. NTIS, 68p.
DOCKET-50313-	(Arkansas Nuclear One, Unit 1) (Non-AEC)	
50	26-55317	Dep. NTIS, 165p.
DOCKET-50315-	(Donald C. Cook Nuclear Power Plant, See also DOCKET-50316) (Non-AEC)	
74	26-55318	Dep. NTIS, 152p.
75	26-55319	Dep. NTIS, 9p.
76	26-55320	Dep. NTIS, 6p.
77	26-55321	Dep. NTIS, 60p.
78	26-55322	Dep. NTIS, 6p.
79	26-55323	Dep. NTIS, 10p.
80	26-55324	Dep. NTIS, 4p.
81	26-55325	Dep. NTIS, 74p.
82	26-55326	Dep. NTIS, 11p.
DOCKET-50316-	(Donald C. Cook Nuclear Power Plant, See also DOCKET-50315) (Non-AEC)	
74	26-55318	See DOCKET-50315-74
75	26-55319	See DOCKET-50315-75
76	26-55320	See DOCKET-50315-76
77	26-55321	See DOCKET-50315-77
78	26-55322	See DOCKET-50315-78
79	26-55323	See DOCKET-50315-79
80	26-55324	See DOCKET-50315-80
81	26-55325	See DOCKET-50315-81
82	26-55326	See DOCKET-50315-82
DOCKET-50317-	(Calvert Cliffs Nuclear Power Plant, See also DOCKET-50318) (Non-AEC)	
58	26-55327	Dep. NTIS, 57p.
DOCKET-50318-	(Calvert Cliffs Nuclear Power Plant, See also DOCKET-50317) (Non-AEC)	
58	26-55327	See DOCKET-50317-58
DOCKET-50321-	(Edwin I. Hatch Nuclear Plant) (Non-AEC)	
49	26-55328	Dep. NTIS, 156p.
DOCKET-50324-	(Brunswick Steam Electric Plant, Units 1 and 2, See also DOCKET-50325) (Non-AEC)	
43	26-55329	Dep. NTIS, 1p.
DOCKET-50325-	(Brunswick Steam Electric Plant, Units 1 and 2, See also DOCKET-50324) (Non-AEC)	
44	26-55329	See DOCKET-50324-43
DOCKET-50331-	(Daune Arnold Energy Center) (Non-AEC)	
52	26-55330	Dep. NTIS, 3p.
DOCKET-50333-	(James A. Fitzpatrick Nuclear Power Plant) (Non-AEC)	
53	26-55259	Dep. NTIS, 109p.
DOCKET-50335-	(Hutchinson Island Plant) (Non-AEC)	
33	26-55331	Dep. NTIS, 171p.
DOCKET-50338-	(North Anna Power Station; See also DOCKET-50339) (Non-AEC)	
51	26-55332	Dep. NTIS, 52p.
DOCKET-50339-	(North Anna Power Station; See also DOCKET-50338) (Non-AEC)	
45	26-55332	See DOCKET-50338-51
DOCKET-50341-	(Enrico Fermi Atomic Power Plant) (Non-AEC)	
45	26-55333	Dep. NTIS, 7p.
DOCKET-50344-	(Trojan Nuclear Plant) (Non-AEC)	
31	26-55334	Dep. NTIS, 4p.
DOCKET-50352-	(Limerick Generating Station) (See also DOCKET-50353) (Non-AEC)	
28	26-55335	Dep. NTIS, 19p.
DOCKET-50353-	(Limerick Generating Station; See also DOCKET-50352) (Non-AEC)	
28	26-55335	See DOCKET-50352-28
DOCKET-50354-	(Newbold Island Nuclear Generating Station; See also DOCKET-50355) (Non-AEC)	
28	26-55336	Dep. NTIS, 165p.
DOCKET-50355-	(Newbold Island Nuclear Generating Station; See also DOCKET-50354) (Non-AEC)	
27	26-55336	See DOCKET-50354-28
DOCKET-50358-	(Wm. H. Zimmer Nuclear Power Station Units 1 and 2; See also DOCKET-50359) (Non-AEC)	
41	26-55337	Dep. NTIS, 196p.
DOCKET-50361-	(San Onofre Nuclear Generating Station, Units 2 and 3; See also DOCKET-50362 and DOCKET-50206, Unit 1) (Non-AEC)	
27	26-55338	Dep. NTIS, 503p.
DOCKET-50362-	(San Onofre Nuclear Generating Station, Units 2 and 3; See also DOCKET-50361 and DOCKET-50206, Unit 1) (Non-AEC)	

Report No.	Abstract No.	Availability
26	26-55338	See DOCKET-50361-27
DOCKET-50363-	(Forked River Nuclear Station, Unit 1) (Non-AEC)	
37	26-55339	Dep. NTIS, 64p.
DOCKET-50367-	(Bailly Generating Station Nuclear 1), (Non-AEC)	
31	26-55340	Dep. NTIS, 2p.
DOCKET-50373-	(LaSalle County Station, Units 1 and 2; See also DOCKET-50374) (Non-AEC)	
27	26-55341	Dep. NTIS, 3p.
DOCKET-50374-	(LaSalle County Station, Units 1 and 2; See also DOCKET-50373) (Non-AEC)	
26	26-55341	See DOCKET-50373-27
DOCKET-50382-	(Waterford Steam Electric Station; See also DOCKET-50383) (Non-AEC)	
36	26-55260	Dep. NTIS, 100p.
DOCKET-50390-	(Watts Bar Nuclear Plant; See also DOCKET-50391) (Non-AEC)	
23	26-55342	Dep. NTIS, 47p.
24	26-55343	Dep. NTIS, 7p.
DOCKET-50391-	(Watts Bar Nuclear Plant; See also DOCKET-50390) (Non-AEC)	
23	26-55342	See DOCKET-50390-23
24	26-55343	See DOCKET-50390-24
DOCKET-50395-	(Virgil C. Summer Nuclear Station) (Non-AEC)	
28	26-55344	Dep. NTIS, 223p.
DOCKET-50397-	(Hanford No. 2 Nuclear Power Plant-NON-AEC)	
27	26-55261	Dep. NTIS, 5p.
28	26-55345	Dep. NTIS, 103p.
32	26-55346	Dep. NTIS, 103p.
DOCKET-50398-	(Mendocino Power Plant, Units 1 and 2; See also DOCKET-50399) (Non-AEC)	
18	26-55347	Dep. NTIS, 137p.
19	26-55348	Dep. NTIS, 347p.
DOCKET-50399-	(Mendocino Power Plant, Units 1 and 2; See also DOCKET-50398) (Non-AEC)	
18	26-55347	See DOCKET-50398-18
19	26-55348	See DOCKET-50398-19
DOCKET-50400-	(Shearon Harris Nuclear Power Plant; See also DOCKET-50401, 50402, 50403) (Non-AEC)	
23	26-55262	Dep. NTIS, 62p.
DOCKET-50401-	(Shearon Harris Nuclear Power Plant, Units 1, 2, 3 and 4; See also DOCKET-50400, 50402, 50403) (Non-AEC)	
23	26-55262	See DOCKET-50400-23
DOCKET-50402-	(Shearon Harris Nuclear Power Plant, Units 1, 2, 3, and 4; See also DOCKET-50400, 50401, 50403) (Non-AEC)	
23	26-55262	See DOCKET-50400-23
DOCKET-50403-	(Shearon Harris Nuclear Power Plant, Units 1, 2, 3, and 4; See also DOCKET-50400, 50401, 50402) (Non-AEC)	
23	26-55262	See DOCKET-50400-23
DOCKET-50404-	(North Anna Power Station, Units 3 and 4; See also DOCKET-50405) (Non-AEC)	
22	26-55349	Dep. NTIS, 55p.
23	26-55332	See DOCKET-50338-51
24	26-55263	Dep. NTIS, 78p.
DOCKET-50405-	(North Anna Power Station, Units 3 and 4; See also DOCKET-50404) (Non-AEC)	
22	26-55349	See DOCKET-50404-22
23	26-55332	See DOCKET-50338-51
24	26-55263	See DOCKET-50404-24
DOCKET-50409-	(LaCrosse Boiling Water Reactor--Formerly DOCKET-1155) (AEC)	
13	26-55350	Dep. NTIS, 7p.
DOCKET-50410-	(Nine Mile Point Nuclear Station, Unit 2; See Also DOCKET-50220, Unit 1) (Non-AEC)	
10	26-55351	Dep. NTIS, 128p.
DP-		
1295	26-55524	Dep. NTIS, 39p.
DP-MS-		
72-14	26-53061	Dep. NTIS, 14p.
72-37	26-53109	Dep. NTIS, 6p.
DP-Report-	(British)	
522	26-53605	Dep. NTIS (U. S. Sales Only), 82p.
DPSPU-		
72-30-1	26-53153	Dep. NTIS, 21p.
DSR-	(Non-AEC)	
77907-D	26-54167	See COO-3069-71
DUN-SA-		
168	26-55201	Dep. NTIS, 8p.
169	26-55135	Dep. NTIS, 18p.
186	26-55136	Dep. NTIS, 10p.
E-	(Misc.)	
6639	26-55358	See N-72-18051
EGG-		
1183-2277	26-53197	Dep. NTIS, 72p.
EIR-	(Swiss)	
215	26-55082	Dep. NTIS (U. S. Sales Only), 75p.
ENDF-		
170(Rev.)	26-54965	See ORNL-TM-3871(Rev.)
172	26-54501	See ORNL-TM-3910
EUR-	(European Atomic Energy Community)	
4728	26-55188	See EURFNR-1020
4765	26-52893	
4787	26-54873	Dep. NTIS (U. S. Sales Only), 138p.
4797	26-53300	Dep. NTIS (U. S. Sales Only), 34p.
4807	26-53301	Dep. NTIS (U. S. Sales Only). EUR B. Fr. 50.-, 42p.
4812	26-53079	Dep. NTIS (U. S. Sales Only), 45p.
4828	26-52983	Dep. NTIS (U. S. Sales Only), 32p.
4839	26-54481	Dep. NTIS (U. S. Sales Only). EUR B. Fr. 85.-, 57p.
4871	26-55525	Dep. NTIS (U. S. Sales Only). EUR B. Fr. 25.-, 10p.
5100	26-53302	Dep. NTIS (U. S. Sales Only). EUR B. Fr. 25.-, 10p.
EUR-CEA-FC-	(European Atomic Energy Community)	
630	26-54101	Dep. NTIS (U. S. Sales Only), 101p.
639	26-54846	Dep. NTIS (U. S. Sales Only), 220p.
642	26-54788	Dep. NTIS (U. S. Sales Only), 29p.
644	26-54102	Dep. NTIS (U. S. Sales Only), 65p.
647	26-54874	Dep. NTIS (U. S. Sales Only), 23p.
EURFNR-	(European Atomic Energy Community)	
975	26-55229	Dep. NTIS
976	26-55218	Dep. NTIS
985	26-55186	Dep. NTIS
986	26-55174	Dep. NTIS
989	26-55187	Dep. NTIS, 14p.
998	26-53635	Dep. NTIS
1000	26-55227	Dep. NTIS
1001	26-55083	Dep. NTIS (U. S. Sales Only), 78p.
1014	26-55396	Dep. NTIS (U. S. Sales Only), 64p.
1016	26-55397	Dep. NTIS (U. S. Sales Only), 81p.
1020	26-55188	Dep. NTIS (U. S. Sales Only), 24p.
1029	26-55398	Dep. NTIS (U. S. Sales Only), 99p.
FEI-	(Russian)	
292	26-54657	Dep. NTIS (U. S. Sales Only), 29p.
FIND-		
50390(8-72)	26-55213	Dep. NTIS, 18p.
50391(8-72)	26-55213	See FIND-50390(8-72)
FOA-	(Swedish)	
4-4490-A-3	26-53738	Dep. NTIS (U. S. Sales Only), 13p.
4-4500-A-3	26-53397	Dep. NTIS (U. S. Sales Only), 22p.
4-4502-A-1	26-53158	Dep. NTIS (U. S. Sales Only), 18p.
4-4503-A-3	26-53527	Dep. NTIS (U. S. Sales Only), 18p.
FRNC-CONF-	(French)	
51	26-54103	Dep. NTIS (U. S. Sales Only), 21p.
53	26-54079	Dep. NTIS (U. S. Sales Only), 18p.
54	26-53752	Dep. NTIS (U. S. Sales Only), 5p.
55	26-54080	Dep. NTIS (U. S. Sales Only), 17p.
56	26-53753	Dep. NTIS (U. S. Sales Only), 6p.
57	26-54081	Dep. NTIS (U. S. Sales Only), 9p.
58	26-54082	Dep. NTIS (U. S. Sales Only), 2p.
FRNC-TH-	(French)	
180	26-54683	
189	26-53198	Dep. NTIS (U. S. Sales Only), 69p.
191	26-54525	Dep. NTIS (U. S. Sales Only), 68p.
210	26-54973	Dep. NTIS (U. S. Sales Only), 80p.
227	26-54552	Dep. NTIS (U. S. Sales Only), 87p.
237	26-53253	Dep. NTIS (U. S. Sales Only), 90p.
240	26-54587	Dep. NTIS (U. S. Sales Only), 114p.
242	26-54598	Dep. NTIS (U. S. Sales Only), 245p.
262	26-52984	Dep. NTIS (U. S. Sales Only), 109p.
GEAP-	(Misc.)	
10028-39	26-55189	Dep. NTIS, 99p.
10028-42	26-55190	Dep. NTIS, 123p.
10207-26	26-55175	Dep. NTIS, 77p.
13788	26-55418	Dep. NTIS, 84p.
13822-1	26-55145	Dep. NTIS, 26p.
GJO-		

Report No.	Abstract No.	Availability
936-1	26-53143	Dep. NTIS, 132p.
936-2	26-53144	Dep. NTIS, 178p.
GULF-RT-A-		
10870	26-54968	See AD-737312
HDI-	(Non-AEC)	
60-3	26-54968	See AD-737312
IAE-	(Russian)	
2115	26-54684	Dep. NTIS (U. S. Sales Only), 36p.
2116	26-54599	Dep. NTIS (U. S. Sales Only), 24p.
IEA-	(Brazilian)	
250	26-52976	Dep. NTIS (U. S. Sales Only), 8p.
IFVE-	(Russian)	
71-83	26-53751	For translation see BNL-tr-498
IKF-	(German)	
27	26-55399	Dep. NTIS (U. S. Sales Only), 19p.
INIS-mf-	(International Atomic Energy Agency)	
172	26-55375	INIS
195	26-55440	NTIS, 178p.
205	26-55352	INIS
212	26-55084	INIS
252	26-53993	INIS
INP-	(Polish)	
793	26-53173	Dep. NTIS (U. S. Sales Only), 50p.
795	26-54685	Dep. NTIS (U. S. Sales Only), 16p.
INR-	(Non-AEC)	
1406	26-54686	Dep. NTIS (U. S. Sales Only), 6p.
1407	26-54567	Dep. NTIS (U. S. Sales Only), 16p.
INR-P-	(Polish)	
1405	26-54482	Dep. NTIS (U. S. Sales Only), 25p.
INSJ-	(Japanese)	
130	26-54600	NTIS (U. S. Sales Only), 41p.
IPP-	(Non-AEC)	
1/125	26-54784	Dep. NTIS (U. S. Sales Only), 94p.
4/97	26-54827	Dep. NTIS (U. S. Sales Only), 22p.
IPP-IV-	(German)	
31	26-55526	Dep. NTIS (U. S. Sales Only), 50p.
36	26-53091	Dep. NTIS (U. S. Sales Only), 22p.
38	26-55527	Dep. NTIS (U. S. Sales Only), 82p.
IRS-F-	(West German)	
10	26-55202	Dep. NTIS (U. S. Sales Only), 90p.
IS-		
2838	26-55528	Dep. NTIS, 174p.
IS-T-		
526	26-55529	Dep. NTIS, 90p.
529	26-55055	Dep. NTIS, 97p.
531	26-54245	Dep. NTIS, 56p.
534	26-54601	Dep. NTIS, 100p.
536	26-54363	Dep. NTIS, 83p.
540	26-53550	Dep. NTIS, 77p.
554	26-53636	Dep. NTIS, 65p.
ISS-	(Italian)	
71/22	26-55530	Dep. NTIS (U. S. Sales Only), 14p.
71/29	26-54687	Dep. NTIS (U. S. Sales Only), 19p.
71/31	26-54162	Dep. NTIS (U. S. Sales Only), 22p.
ITF-	(Russian)	
71-77-P	26-54688	Dep. NTIS (U. S. Sales Only), 17p.
71-85-P	26-54389	Dep. NTIS (U. S. Sales Only), 21p.
71-95-P	26-55531	Dep. NTIS (U. S. Sales Only), 48p.
71-96-P	26-54789	Dep. NTIS (U. S. Sales Only), 34p.
71-130-P	26-54390	Dep. NTIS (U. S. Sales Only), 16p.
71-132-P	26-54391	Dep. NTIS (U. S. Sales Only), 23p.
72-2-P	26-55532	Dep. NTIS (U. S. Sales Only), 37p.
72-3-P	26-54392	Dep. NTIS (U. S. Sales Only), 10p.
72-5-P	26-54393	Dep. NTIS (U. S. Sales Only), 10p.
72-9-E	26-55067	Dep. NTIS (U. S. Sales Only), 24p.
72-10-P	26-54344	Dep. NTIS (U. S. Sales Only), 11p.
72-12-P	26-54689	Dep. NTIS (U. S. Sales Only), 14p.
72-14-E	26-54408	Dep. NTIS (U. S. Sales Only), 6p.
72-15-E	26-54376	Dep. NTIS (U. S. Sales Only), 14p.
72-16-E	26-55533	Dep. NTIS (U. S. Sales Only), 14p.
72-20-P	26-54394	Dep. NTIS (U. S. Sales Only), 13p.
72-21-P	26-54395	Dep. NTIS (U. S. Sales Only), 37p.
72-24-P	26-54496	Dep. NTIS (U. S. Sales Only), 20p.
72-25-P	26-54526	Dep. NTIS (U. S. Sales Only), 15p.
72-27-P	26-55534	Dep. NTIS (U. S. Sales Only), 16p.
72-29-P	26-55535	Dep. NTIS (U. S. Sales Only), 19p.
72-31-P	26-55068	Dep. NTIS (U. S. Sales Only), 22p.
72-32-P	26-55536	Dep. NTIS (U. S. Sales Only), 68p.
72-33-E	26-54355	Dep. NTIS (U. S. Sales Only), 17p.
72-35-P	26-54373	Dep. NTIS (U. S. Sales Only), 21p.
72-36-E	26-55069	Dep. NTIS (U. S. Sales Only), 22p.
72-37-P	26-54409	Dep. NTIS (U. S. Sales Only), 20p.
72-38-P	26-54410	Dep. NTIS (U. S. Sales Only), 22p.
72-39-P	26-54411	Dep. NTIS (U. S. Sales Only), 11p.
72-40-P	26-55537	Dep. NTIS (U. S. Sales Only), 14p.
72-41-P	26-54396	Dep. NTIS (U. S. Sales Only), 14p.
72-45-P	26-55070	Dep. NTIS (U. S. Sales Only), 35p.
72-46-P	26-54397	Dep. NTIS (U. S. Sales Only), 21p.
72-48-E	26-54237	Dep. NTIS (U. S. Sales Only), 21p.
72-49-P	26-54299	Dep. NTIS (U. S. Sales Only), 8p.
72-50-P	26-55538	Dep. NTIS (U. S. Sales Only), 29p.
72-52-P	26-54398	Dep. NTIS (U. S. Sales Only), 21p.
72-53-E	26-54300	Dep. NTIS (U. S. Sales Only), 8p.
72-54-P	26-54377	Dep. NTIS (U. S. Sales Only), 19p.
72-55-P	26-54301	Dep. NTIS (U. S. Sales Only), 24p.
72-56-E	26-54435	Dep. NTIS (U. S. Sales Only), 11p.
72-57-P	26-54690	Dep. NTIS (U. S. Sales Only), 14p.
72-58-P	26-54399	Dep. NTIS (U. S. Sales Only), 24p.
72-59-P	26-54400	Dep. NTIS (U. S. Sales Only), 12p.
72-60-P	26-54401	Dep. NTIS (U. S. Sales Only), 6p.
72-62-E	26-54378	Dep. NTIS (U. S. Sales Only), 27p.
72-63-E	26-54412	Dep. NTIS (U. S. Sales Only), 16p.
72-67-P	26-55539	Dep. NTIS (U. S. Sales Only), 20p.
JAB-	(Non-AEC)	
99-96	26-53137	Dep. NTIS, 35p.
JAERI-M-		
4473	26-55203	NTIS (U. S. Sales Only), 106p.
4535	26-55204	NTIS (U. S. Sales Only), 41p.
4630	26-55400	NTIS (U. S. Sales Only), 17p.
4652	26-54483	NTIS (U. S. Sales Only), 15p.
4666	26-54602	NTIS (U. S. Sales Only), 17p.
JAERI-Memo-	(Japanese)	
3891	26-55401	NTIS (U. S. Sales Only)
3893	26-55137	NTIS (U. S. Sales Only)
3936	26-53694	NTIS (U. S. Sales Only)
4002	26-55402	NTIS (U. S. Sales Only)
4004	26-55403	NTIS (U. S. Sales Only)
4009	26-53728	NTIS (U. S. Sales Only)
4016	26-55228	NTIS (U. S. Sales Only)
4041	26-55205	Dep. NTIS (U. S. Sales Only), 76p.
4052	26-55404	NTIS (U. S. Sales Only)
4083	26-55264	NTIS (U. S. Sales Only)
4094	26-52933	NTIS (U. S. Sales Only)
JAPFNR-	(Japanese)	
43	26-55405	Dep. NTIS (U. S. Sales Only)
JEN-	(Spanish)	
244	26-53327	Dep. NTIS (U. S. Sales Only), 45p.
JINR-	(Russian)	
E1-6613	26-54193	Dep. NTIS (U. S. Sales Only), 26p.
E1-6615	26-54194	Dep. NTIS (U. S. Sales Only), 17p.
E1-6647	26-54169	Dep. NTIS (U. S. Sales Only), 8p.
E2-6525	26-54315	Dep. NTIS (U. S. Sales Only), 22p.
E2-6596	26-54327	Dep. NTIS (U. S. Sales Only), 11p.
E6-6479	26-54634	Dep. NTIS (U. S. Sales Only), 12p.
E9-6538	26-53754	Dep. NTIS (U. S. Sales Only), 16p.
P1-6414	26-54209	Dep. NTIS (U. S. Sales Only), 8p.
P1-6552	26-54875	Dep. NTIS (U. S. Sales Only), 27p.
P2-6225	26-53808	For translation see ORNL-tr-2620
P2-6532	26-55540	Dep. NTIS (U. S. Sales Only), 7p.
P2-6539	26-54691	Dep. NTIS (U. S. Sales Only), 8p.
P2-6586	26-54413	Dep. NTIS (U. S. Sales Only), 17p.
P2-6636	26-54246	Dep. NTIS (U. S. Sales Only), 37p.
P4-6505	26-54345	Dep. NTIS (U. S. Sales Only), 13p.
P4-6509	26-54635	Dep. NTIS (U. S. Sales Only), 20p.
P4-6543	26-54692	Dep. NTIS (U. S. Sales Only), 15p.
P6-6313	26-54608	See UCRL-Trans-1473
P6-6511	26-54603	Dep. NTIS (U. S. Sales Only), 27p.
P6-6519	26-54604	Dep. NTIS (U. S. Sales Only), 22p.
P7-6523	26-54658	Dep. NTIS (U. S. Sales Only), 28p.
P13-6522	26-53271	Dep. NTIS (U. S. Sales Only), 18p.
P13-6541	26-53272	Dep. NTIS (U. S. Sales Only), 14p.
P15-6518	26-54659	Dep. NTIS (U. S. Sales Only), 9p.
JPRS-	(Non-AEC)	
56713	26-54790	NTIS
KFK-	(German)	
1348	26-55229	For translation see EURFNR-975
1427	26-55174	For translation see EURFNR-986
1452	26-55218	For translation see EURFNR-976
1477	26-55186	For translation see EURFNR-985
1503	26-55449	INIS
1519	26-54484	Dep. NTIS (U. S. Sales Only), 75p.
1526	26-55541	Dep. NTIS (U. S. Sales Only), 17p.
1535	26-53635	For translation see EURFNR-998
1548	26-55176	Dep. NTIS (U. S. Sales Only), 32p.
1549	26-55227	For translation see EURFNR-1000
1557	26-55396	See EURFNR-1014
1568	26-53339	Dep. NTIS (U. S. Sales Only), 104p.
1572	26-55397	See EURFNR-1016
1577	26-55126	Dep. NTIS (U. S. Sales Only), 146p.
1579	26-55127	Dep. NTIS (U. S. Sales Only), 38p.
1580	26-55206	Dep. NTIS (U. S. Sales Only), 188p.
1582	26-53506	For translation see ORNL-tr-2629
1588	26-55188	See EURFNR-1020
1601	26-55542	Dep. NTIS (U. S. Sales Only), 19p.
1602	26-54605	Dep. NTIS (U. S. Sales Only), 177p.

Report No.	Abstract No.	Availability
1612	26-55398	See EURFNR-1029
KFKI-	(Hungarian)	
72-32	26-55543	Dep. NTIS (U. S. Sales Only), 55p.
72-41	26-55544	Dep. NTIS (U. S. Sales Only), 11p.
KHFTI-	(Russian)	
70/49	26-54824	For translation see AEC-tr-7334
70-49	26-54824	See AEC-tr-7334
70-55	26-54838	For translation see AEC-tr-7335
70-57	26-54839	For translation see AEC-tr-7336
70-58	26-54840	For translation see AEC-tr-7337
LA-		
4868	26-55071	Dep. NTIS, 16p.
4874	26-53784	Dep. NTIS, 168p.
4925	26-55545	Dep. NTIS, 7p.
4968	26-53273	Dep. NTIS, 11p.
4973	26-55546	Dep. NTIS, 6p.
4999	26-53303	Dep. NTIS, 6p.
5019	26-54754	Dep. NTIS, 9p.
LA-DC-		
72-141	26-55547	Dep. NTIS, 32p.
72-230	26-53729	Dep. NTIS, 5p.
72-243	26-55548	Dep. NTIS, 30p.
72-331	26-55549	Dep. NTIS, 19p.
72-410	26-55550	Dep. NTIS, 14p.
72-411	26-55551	Dep. NTIS, 10p.
72-626	26-55451	Dep. NTIS, 8p.
72-632	26-55552	Dep. NTIS, 13p.
72-660	26-55441	Dep. NTIS, 14p.
72-783	26-55553	Dep. NTIS, 4p.
72-809	26-52899	Dep. NTIS, 17p.
72-848	26-54233	Dep. NTIS, 4p.
72-855	26-55554	Dep. NTIS, 23p.
72-872	26-55555	Dep. NTIS, 11p.
72-873	26-55556	Dep. NTIS, 5p.
72-876	26-54497	Dep. NTIS, 4p.
72-879	26-55557	Dep. NTIS, 7p.
72-880	26-55558	Dep. NTIS, 4p.
72-881	26-53797	Dep. NTIS, 17p.
72-896	26-54828	Dep. NTIS, 12p.
72-903	26-55559	Dep. NTIS, 12p.
72-904	26-54498	Dep. NTIS, 4p.
72-905	26-54499	Dep. NTIS, 4p.
72-906	26-54500	Dep. NTIS, 4p.
72-920	26-53062	Dep. NTIS, 15p.
72-954	26-54693	Dep. NTIS, 11p.
LA-tr-		
72-16	26-55560	Dep. NTIS
LAL-	(French)	
1255	26-54170	Dep. NTIS (U. S. Sales Only), 194p.
LBL-		
4	26-54184	Dep. NTIS, 13p.
101	26-53637	Dep. NTIS, 74p.
383	26-55561	Dep. NTIS, 26p.
416	26-55562	Dep. NTIS, 18p.
515	26-55563	Dep. NTIS, 22p.
544	26-54328	Dep. NTIS, 95p.
585	26-53199	Dep. NTIS, 25p.
644	26-53755	Dep. NTIS, 8p.
654	26-53756	Dep. NTIS, 12p.
707(Summ.)	26-53200	Dep. NTIS, 3p.
766	26-54287	Dep. NTIS, 76p.
776	26-54568	Dep. NTIS, 9p.
876	26-55564	Dep. NTIS, 70p.
972	26-54694	Dep. NTIS, 14p.
1007	26-54302	Dep. NTIS, 162p.
LF-tr-		
71	26-53528	Dep. NTIS
72	26-55565	Dep. NTIS
LIB/Trans-	(Australian)	
431	26-53304	Dep. NTIS (U. S. Sales Only)
LMEC-		
72-4	26-53305	Dep. NTIS, 84p.
LNF-	(Italian)	
72/27	26-54462	Dep. NTIS (U. S. Sales Only), 13p.
72/31	26-54171	Dep. NTIS (U. S. Sales Only), 33p.
LRP-	(Swiss)	
51/72	26-54808	Dep. NTIS (U. S. Sales Only), 33p.
LYCEN-	(French)	
7211	26-54238	Dep. NTIS (U. S. Sales Only), 103p.
7213	26-54695	Dep. NTIS (U. S. Sales Only), 19p.
7219	26-54527	Dep. NTIS (U. S. Sales Only), 12p.
7228	26-54974	Dep. NTIS (U. S. Sales Only), 37p.
7232	26-55566	Dep. NTIS (U. S. Sales Only), 31p.
7236	26-52900	Dep. NTIS (U. S. Sales Only), 59p.
MDC G-		
3153	26-53551	Dep. NTIS, 41p.
MLM-		

Report No.	Abstract No.	Availability
1150	26-53332	Dep. NTIS, 19p.
1213	26-53333	Dep. NTIS, 10p.
1228	26-53334	Dep. NTIS, 13p.
1355	26-53606	Dep. NTIS, 18p.
1368	26-52934	Dep. NTIS, 12p.
1847	26-55567	Dep. NTIS, 56p.
1888	26-52935	Dep. NTIS, 24p.
1946	26-53155	Dep. NTIS, 44p.
1964(tr)	26-53034	Dep. NTIS
MMM-		
3691-5(Rev. 1)	26-53092	Dep. NTIS, 96p.
N-	(Misc.)	
71-30295	26-53805	NTIS
71-37956	26-53286	NTIS, 20p.
72-18051	26-55358	NTIS, 76p.
72-20054	26-53382	NTIS, 24p.
72-20063	26-53364	NTIS, 16p.
72-20065	26-53365	NTIS, 14p.
NAA-SR-		
8533	26-53714	Dep. NTIS, 25p.
NAA-SR-Memo-		
8597	26-54944	Dep. NTIS, 9p.
NASA-TM-X-	(Misc.)	
2440	26-54870	NTIS $10.00, 1020p.
2517	26-55358	See N-72-18051
65715	26-53286	See N-71-37956
NASA-TT-F-	(Non-AEC)	
13743	26-53805	See N-71-30295
NEDO-	(Non-AEC)	
10527	26-55353	
NEIC-RR-	(Polish)	
47	26-54185	Dep. NTIS (U. S. Sales Only), 129p.
NIM-	(Non-AEC)	
1430	26-55568	Dep. NTIS (U. S. Sales Only), 26p.
1432	26-52919	Dep. NTIS (U. S. Sales Only), 4p.
1439	26-52954	Dep. NTIS (U. S. Sales Only), 9p.
1448	26-53035	Dep. NTIS (U. S. Sales Only), 23p.
NP-	(AEC File No. for Non-AEC Reports)	
18759	26-54774	For translation see AEC-tr-7323
18895	26-54775	For translation see AEC-tr-7326
18912	26-54842	For translation see AEC-tr-7339
18913	26-54841	For translation see AEC-tr-7338
18916	26-54776	For translation see AEC-tr-7332
18946	26-54768	For translation see AEC-tr-7329
18947	26-54749	For translation see AEC-tr-7330
18958	26-54836	For translation see AEC-tr-7331
18982	26-54837	For translation see AEC-tr-7333
19338(Vol. 1)	26-55221	
19338(Vol. 2)	26-55222	
19380	26-52942	Bucharest; Editura Academiei Republicii Socialiste Romania (1971). 346p
19393	26-54779	Dep. NTIS (U. S. Sales Only), 66p.
19403	26-53459	Dep. NTIS (U. S. Sales Only), 153p.
19404	26-55569	Dep. NTIS (U. S. Sales Only), 188p.
19406	26-54809	Dep. NTIS (U. S. Sales Only), 17p.
19407	26-55452	Dep. NTIS (U. S. Sales Only), 192p.
19408	26-55570	Dep. NTIS (U. S. Sales Only), 183p.
19410	26-55453	Dep. NTIS (U. S. Sales Only), 64p.
19412	26-55454	Dep. NTIS (U. S. Sales Only), 17p.
19414	26-54780	Dep. NTIS (U. S. Sales Only), 8p.
19415	26-54172	Dep. NTIS (U. S. Sales Only), 15p.
19416	26-53741	Dep. NTIS (U. S. Sales Only), 58p.
19417	26-54247	Dep. NTIS (U. S. Sales Only), 32p.
19418	26-54370	Dep. NTIS (U. S. Sales Only), 17p.
19419	26-54210	Dep. NTIS (U. S. Sales Only), 167p.
19421	26-54163	Dep. NTIS (U. S. Sales Only), 4p.
19425	26-54436	Dep. NTIS (U. S. Sales Only), 6p.
NRC-TT-	(Canadian)	
1557	26-55571	Dep. NTIS (U. S. Sales Only)
NRL-	(Misc.)	
7446	26-53698	
NRL-MR-	(Non-AEC)	
2391	26-53195	See AD-737993
NTS-		
237	26-53133	See USGS-474-155
NYO-		
3533-264	26-54364	Dep. NTIS, 20p.
3533-265	26-54329	Dep. NTIS, 11p.
3823-12	26-55572	Dep. NTIS, 92p.

Report No.	Abstract No.	Availability
ONERA-Publ.-	(French)	
137	26-54011	Dep. NTIS (U. S. Sales Only), 81p.
ORNL-		
4781	26-53638	Dep. NTIS, 62p.
4794	26-53080	Dep. NTIS, 121p.
4798	26-54569	Dep. NTIS, 67p.
ORNL-EIS-		
72-24	26-55573	See ORNL-NSF-EP-23
72-28	26-53190	Dep. NTIS, 162p.
ORNL-NSF-EP-		
23	26-55573	Dep. NTIS, 331p.
ORNL-TIP/TIRC-		
72-4	26-55574	Dep. NTIS, 9p.
72-10	26-55575	Dep. NTIS, 2p.
72-13	26-55576	Dep. NTIS, 33p.
72-45	26-55577	Dep. NTIS, 4p.
72-49	26-55578	Dep. NTIS, 6p.
72-52	26-55579	Dep. NTIS, 4p.
72-53	26-55580	Dep. NTIS, 3p.
72-54	26-55581	Dep. NTIS, 3p.
72-59	26-55582	Dep. NTIS, 5p.
72-60	26-55583	Dep. NTIS, 3p.
72-61	26-55584	Dep. NTIS, 6p.
72-62	26-55585	Dep. NTIS, 9p.
72-63	26-55586	Dep. NTIS, 13p.
ORNL-TM-		
729(Pt.2B)	26-55138	Dep. NTIS, 439p.
2496(Rev.2)(Suppl.3)	26-55198	Dep. NTIS, 28p.
3344	26-55177	Dep. NTIS, 132p.
3485(Vol.1)	26-53135	Dep. NTIS, 232p.
3656	26-55191	Dep. NTIS, 187p.
3743	26-55265	Dep. NTIS, 83p.
3761	26-55192	Dep. NTIS, 23p.
3768	26-54485	Dep. NTIS, 66p.
3769	26-55407	Dep. NTIS, 16p.
3815	26-53724	Dep. NTIS, 123p.
3816	26-54890	Dep. NTIS, 27p.
3841	26-53110	Dep. NTIS, 42p.
3871(Rev.)	26-54965	Dep. NTIS, 25p.
3886	26-54463	Dep. NTIS, 7p.
3898	26-55587	Dep. NTIS, 93p.
3900	26-55207	Dep. NTIS, 144p.
3903	26-53725	Dep. NTIS, 36p.
3910	26-54501	Dep. NTIS, 29p.
3913	26-54606	Dep. NTIS, 23p.
3921	26-54464	Dep. NTIS, 63p.
3949	26-55408	Dep. NTIS, 23p.
3951	26-54696	Dep. NTIS, 12p.
3953	26-54829	Dep. NTIS, 51p.
ORNL-tr-		
2394	26-55588	Dep. NTIS
2603	26-55589	Dep. NTIS
2613-A	26-55590	Dep. NTIS
2620	26-53808	Dep. NTIS
2621	26-53064	Dep. NTIS
2629	26-53506	Dep. NTIS
2636	26-55591	Dep. NTIS
ORO-		
651(Rev.3)	26-53735	Dep. NTIS, 75p.
2968-71	26-53003	J. Amer. Chem. Soc.; 94: No. 18, 6301-4(6 Sep 1972)
2968-78	26-52987	Dep. NTIS, 106p.
2972-204	26-54467	Dep. NTIS, 174p.
3262-25	26-53639	Dep. NTIS, 35p.
3347-8	26-53366	Dep. NTIS, 111p.
3992-106	26-54248	Dep. NTIS, 51p.
4066-5	26-53170	Dep. NTIS, 55p.
4317-7	26-54697	Dep. NTIS, 18p.
4317-8	26-54698	Dep. NTIS, 28p.
4317-11	26-54699	Dep. NTIS, 20p.
OSU-CISRC-TR-	(Non-AEC)	
72-8	26-55455	
PATENTS	(French)	
2,070,548	26-53136	
2,081,592	26-53029	
2,087,507	26-53001	
2,091,902	26-55128	
2,093,020	26-53108	
2,093,406	26-53126	
2,097,288	26-53141	
2,098,623	26-52975	
PATENTS	(German)	
1,302,274	26-55131	
1,464,645	26-55419	
1,542,344	26-53566	
1,614,404	26-55129	
2,060,673	26-55194	
PATENTS	(U. S.)	
3,662,042	26-53562	
3,668,066	26-54823	
3,668,067	26-54835	
3,669,631	26-53072	
3,671,392	26-55130	
3,672,846	26-53086	
3,677,964	26-53211	
3,678,274	26-53210	
3,678,275	26-53241	
3,679,366	26-53313	
3,680,284	26-53075	
3,681,016	26-52950	
3,681,035	26-53049	
3,681,194	26-55413	
3,681,216	26-53013	
PEL-	(South African)	
220	26-55592	Dep. NTIS (U. S. Sales Only), 13p.
PIB-	(West Germany)	
1-181	26-54172	See NP-19415
PNC-N-	(Japanese)	
141-72-1-13	26-55405	For translation see JAPFNR-43
Pr-	(Non-AEC)	
13	26-53805	For translation see N-71-30295
PR-	(Non-AEC)	
23	26-54780	See NP-19414
PRDC-EF-		
106	26-55233	See DOCKET-50016-170
PRNC-		
156	26-53498	Dep. NTIS, 61p.
RCN-	(Dutch)	
168	26-55083	See EURFNR-1001
RD/B/M-	(British)	
2356	26-54607	Dep. NTIS (U. S. Sales Only), 180p.
RD/B/N-	(British)	
2214	26-53555	Dep. NTIS (U. S. Sales Only), 17p.
2261	26-55266	Dep. NTIS (U. S. Sales Only), 31p.
2272	26-55409	Dep. NTIS (U. S. Sales Only), 26p.
2364	26-55178	Dep. NTIS (U. S. Sales Only), 6p.
2369	26-53237	Dep. NTIS (U. S. Sales Only), 10p.
RDT-C-		
7-18-T(8-72)	26-55219	RSO
15-11-T(8-72)	26-53204	RSO
RDT-E-		
1-13-T(8-72)	26-53111	RSO
RDT-F-		
8-6-T(8-72)	26-53112	RSO
9-1-T(8-72)	26-55208	RSO
RDT-M-		
2-2-T(8-72)	26-53640	RSO
RFP-		
1455	26-53037	Dep. NTIS, 7p.
1889	26-53038	Dep. NTIS, 11p.
1890	26-53039	Dep. NTIS, 21p.
1891	26-53607	Dep. NTIS, 11p.
1902	26-53306	Dep. NTIS, 7p.
1904	26-53608	Dep. NTIS, 6p.
1924	26-52992	Dep. NTIS, 6p.
RFP-Trans-		
108	26-55593	Dep. NTIS
110	26-55594	Dep. NTIS
RHEL/R-	(British)	
241	26-53274	Dep. NTIS (U. S. Sales Only). UK 20 pence, 15p.
RISO-M-	(Danish)	
1500	26-55209	Dep. NTIS (U. S. Sales Only), 78p.
1518	26-53746	Dep. NTIS (U. S. Sales Only), 31p.
1526	26-54486	Dep. NTIS (U. S. Sales Only), 12p.
RLO-		
2225-T-17-4	26-54660	Dep. NTIS, 12p.
2225-T-25-6	26-53165	Dep. NTIS, 12p.
2227-T-12-26	26-53149	Dep. NTIS, 16p.
2227-T-12-28	26-53166	Dep. NTIS, 30p.
RPP/H-	(British)	
95	26-54211	Dep. NTIS (U. S. Sales Only), 27p.
97	26-54173	Dep. NTIS (U. S. Sales Only), 52p.
99	26-54174	Dep. NTIS (U. S. Sales Only), 23p.

Report No.	Abstract No.	Availability
101	26-53275	Dep. NTIS (U. S. Sales Only), 21p.
RPP/NS-	(British)	
8	26-54529	Dep. NTIS (U. S. Sales Only), 10p.
RPP/T-	(British)	
24	26-54316	Dep. NTIS (U. S. Sales Only), 13p.
25	26-54303	Dep. NTIS (U. S. Sales Only), 9p.
26	26-54288	Dep. NTIS (U. S. Sales Only), 17p.
27	26-54317	Dep. NTIS (U. S. Sales Only), 106p.
28	26-54346	Dep. NTIS (U. S. Sales Only), 10p.
RRL-		
3238-398	26-52993	Dep. NTIS, 17p.
RT/CHI-	(Italian)	
(72)3	26-52920	Dep. NTIS (U. S. Sales Only), 39p.
(72)4	26-52955	Dep. NTIS (U. S. Sales Only), 46p.
RT/EL-	(Italian)	
(72)2	26-54975	Dep. NTIS (U. S. Sales Only), 77p.
(72)4	26-52936	Dep. NTIS (U. S. Sales Only), 31p.
RT/FI-	(Italian)	
(71)37	26-54487	Dep. NTIS (U. S. Sales Only), 25p.
(72)1	26-54488	Dep. NTIS (U. S. Sales Only), 273p.
(72)6	26-54700	Dep. NTIS (U. S. Sales Only), 335p.
(72)7	26-54701	Dep. NTIS (U. S. Sales Only), 53p.
(72)10	26-53699	Dep. NTIS (U. S. Sales Only), 49p.
(72)11	26-55442	Dep. NTIS (U. S. Sales Only), 33p.
(72)13	26-55443	Dep. NTIS (U. S. Sales Only), 96p.
(72)14	26-53257	Dep. NTIS (U. S. Sales Only), 79p.
RT/FIMA-	(Italian)	
(72)1	26-55595	Dep. NTIS (U. S. Sales Only), 7p.
RT/ING-	(Italian)	
(72)7	26-53609	Dep. NTIS (U. S. Sales Only), 54p.
S-	(Misc.)	
544-R	26-53197	See EGG-1183-2277
SC-CR-		
723158	26-53556	Dep. NTIS, 17p.
723162	26-55596	Dep. NTIS, 117p.
SC-DC-		
714099	26-55597	Dep. NTIS, 19p.
721020	26-55598	Dep. NTIS, 23p.
721080	26-53557	Dep. NTIS, 16p.
721159	26-53307	Dep. NTIS, 10p.
721161	26-53308	Dep. NTIS, 13p.
721162	26-53309	Dep. NTIS, 11p.
721302	26-53310	Dep. NTIS, 15p.
721376	26-55599	Dep. NTIS, 14p.
722244(RD)	26-55600	Dep. NTIS, 67p.
722284	26-53615	Dep. NTIS, 26p.
722297	26-55601	Dep. NTIS, 17p.
722298	26-55602	Dep. NTIS, 3p.
SC-DR-		
70-617	26-55603	Dep. NTIS, 28p.
720303	26-55604	Dep. NTIS, 21p.
720447	26-53747	Dep. NTIS, 42p.
720471	26-53641	Dep. NTIS, 21p.
720597	26-53736	Dep. NTIS, 72p.
720630	26-53258	Dep. NTIS, 27p.
SC-M-		
68-808	26-55605	Dep. NTIS, 42p.
720514	26-55606	Dep. NTIS, 12p.
SC-R-		
722879	26-55607	Dep. NTIS, 4p.
SC-RR-		
720286	26-55608	Dep. NTIS, 62p.
720513	26-54502	Dep. NTIS, 28p.
720516	26-53367	Dep. NTIS, 100p.
720543	26-54012	Dep. NTIS, 62p.
SC-T-		
722540	26-53700	Dep. NTIS
SC-TM-		
710557	26-55609	Dep. NTIS, 50p.
SCL-DR-		
720004	26-55610	Dep. NTIS, 80p.
SCL-RR-		
710113	26-55611	Dep. NTIS, 36p.
SLAC-		
143	26-54175	Dep. NTIS, 186p.
153	26-54891	Dep. NTIS, 214p.
SLAC-PUB-		
1043	26-54176	Dep. NTIS, 27p.
SRO-	(Misc.)	
639-12	26-55612	Dep. NTIS, 15p.
641-4	26-53539	Dep. NTIS, 32p.
708-1	26-53171	Dep. NTIS, 44p.
STI/PUB-	(International Atomic Energy Agency)	
295(Vol.4)	26-53409	IAEA $20.00
STU-	(Swedish)	
70-419/U-350(Pt.1.1)	26-53701	
70-419/U-350(Pt.1.2)	26-53642	
SU-	(Misc.)	
326-P-17-X-2	26-55613	Dep. NTIS, 66p.
4205-2	26-54325	See COO-3533-2
4205-264	26-54364	See NYO-3533-264
4205-265	26-54329	See NYO-3533-265
SZS-	(German)	
128	26-53156	Dep. NTIS (U. S. Sales Only), 47p.
129	26-53040	Dep. NTIS (U. S. Sales Only), 60p.
132	26-53460	Dep. NTIS (U. S. Sales Only), 52p.
136	26-55456	Dep. NTIS (U. S. Sales Only), 72p.
THTR-	(German)	
56	26-53605	See DP-Report-522
TID-		
3915(Suppl.1)	26-53530	Dep. NTIS, 70p.
25887	26-55179	Dep. NTIS, 89p.
25974	26-55614	Dep. NTIS, 16p.
26128	26-53541	Dep. NTIS, 220p.
26132	26-53205	Dep. NTIS, 213p.
26138	26-54212	Dep. NTIS, 34p.
26141	26-55457	Dep. NTIS, 311p.
26142	26-53511	Dep. NTIS, 99p.
26148	26-55615	Dep. NTIS, 21p.
26149	26-55616	Dep. NTIS, 45p.
26150	26-53702	Dep. NTIS, 30p.
26159	26-55617	Dep. NTIS, 2p.
TRG-	(Misc.)	
2189	26-55444	INIS
UCB-		
34-P-82-13	26-53461	Dep. NTIS, 41p.
UCID-		
16099	26-55618	Dep. NTIS, 17p.
16100	26-55619	Dep. NTIS, 38p.
UCLA-		
12-871	26-55620	Dep. NTIS, 18p.
12-877	26-55621	Dep. NTIS, 11p.
12-879	26-55622	Dep. NTIS, 63p.
34-P-91-48	26-55623	Dep. NTIS, 248p.
UCRL-		
51130(Vol.8)	26-53311	Dep. NTIS, 56p.
51221	26-53096	Dep. NTIS, 129p.
51244	26-53558	Dep. NTIS, 22p.
51255	26-55624	Dep. NTIS, 7p.
73334	26-55625	Dep. NTIS, 15p.
73610	26-55626	Dep. NTIS, 23p.
73772	26-55627	Dep. NTIS, 10p.
73773	26-55628	Dep. NTIS, 8p.
73921	26-55629	Dep. NTIS, 11p.
73943	26-55630	Dep. NTIS, 27p.
74039	26-55631	Dep. NTIS, 40p.
74069	26-54503	Dep. NTIS, 4p.
UCRL-Trans-		
1473	26-54608	Dep. NTIS
1477	26-53531	Dep. NTIS
1479	26-55632	Dep. NTIS
10616-2	26-53129	Dep. NTIS
10616-4	26-53130	Dep. NTIS
10616-5	26-53131	Dep. NTIS
10617-2	26-53132	Dep. NTIS
10640	26-55633	Dep. NTIS
10643	26-55065	Dep. NTIS
UIUCDCS-R-		
72-531	26-55501	See COO-2118-35
72-532	26-55489	See COO-1469-210
UM-P-	(Australian)	
72-6	26-54347	Dep. NTIS (U. S. Sales Only), 31p.
UR-		
387	26-54208	See COO-3065-16
406	26-54524	See COO-2171-14
3490-136	26-55634	Dep. NTIS, 35p.
3490-174	26-55635	Dep. NTIS, 41p.

Report No.	Abstract No.	Availability
3490-177	26-55636	Dep. NTIS, 44p.
3490-183	26-53462	Dep. NTIS, 60p.
3490-184	26-55637	Dep. NTIS, 23p.
3490-187	26-55638	Dep. NTIS, 21p.
3490-193	26-52958	Dep. NTIS, 19p.
3490-194	26-53353	Dep. NTIS, 37p.
USGS-		
474-155	26-53133	Dep. NTIS, 31p.
UUIM-	(Swedish)	
26	26-53159	Dep. NTIS (U. S. Sales Only), 46p.
27	26-53160	Dep. NTIS (U. S. Sales Only), 34p.
WASH-		
1139(Rev.1)	26-55267	Dep. GPO $0.30
1181-72	26-53600	Dep. NTIS, 86p.
1208(9-72)	26-55214	Dep. NTIS, 9p.
WCAP-	(Misc.)	
1615	26-53732	Dep. NTIS, 26p.
2999	26-53733	
7870	26-55223	
X-	(Misc.)	
721-71-349	26-53286	See N-71-37956
Y-		
1841	26-55639	Dep. NTIS, 27p.
1848	26-55640	Dep. NTIS, 160p.
Y-DA-		
4541(Rev.1)	26-53113	Dep. NTIS, 14p.
Y-KC-		
96	26-55445	Dep. NTIS, 14p.
ZJE-	(Czechslovakian)	
124	26-54489	Dep. NTIS (U. S. Sales Only), 90p.

☆U. S. GOVERNMENT PRINTING OFFICE: 1972—746-149/10

UNITED STATES
GOVERNMENT PRINTING OFFICE
DIVISION OF
PUBLIC DOCUMENTS
WASHINGTON, D.C. 20402

OFFICIAL BUSINESS

POSTAGE AND FEES PAID
U S GOVERNMENT PRINTING OFFICE

U.S.MAIL

NUCLEAR SAFETY

A Bimonthly
Technical Progress Review

The United States Atomic Energy Commission publishes *Nuclear Safety* as a bimonthly technical progress review to meet the needs of industry and government for concise summaries of current developments. This journal digests and evaluates the latest findings in its area of nuclear technology and science.

Primary emphasis is on safety in reactor design, construction, and operation. However, safety considerations in reactor fuel fabrication, spent-fuel processing, nuclear waste disposal, handling of radioisotopes, and environmental effects of these operations are also treated.

Nuclear Safety is prepared by the Nuclear Safety Information Center at Oak Ridge National Laboratory for the United States Atomic Energy Commission.

Nuclear Safety may be purchased from the Superintendent of Documents, U. S. Government Printing Office, Washington, D. C. 20402, at $3.50 per year (six issues) or $0.60 per issue.

Postpaid within the United States, Canada, Mexico, and all Central and South American countries except Argentina, Brazil, Guyana, French Guiana, Surinam, and British Honduras. For these Central and South American countries and all other countries: for each annual subscription, add $1.00; for single issues, add one-fourth of the single-issue price. Payment should be by check, money order, or document coupons, and MUST accompany order. Remittances from foreign countries should be made by international money order or draft on an American bank payable to the Superintendent of Documents or by UNESCO book coupons.